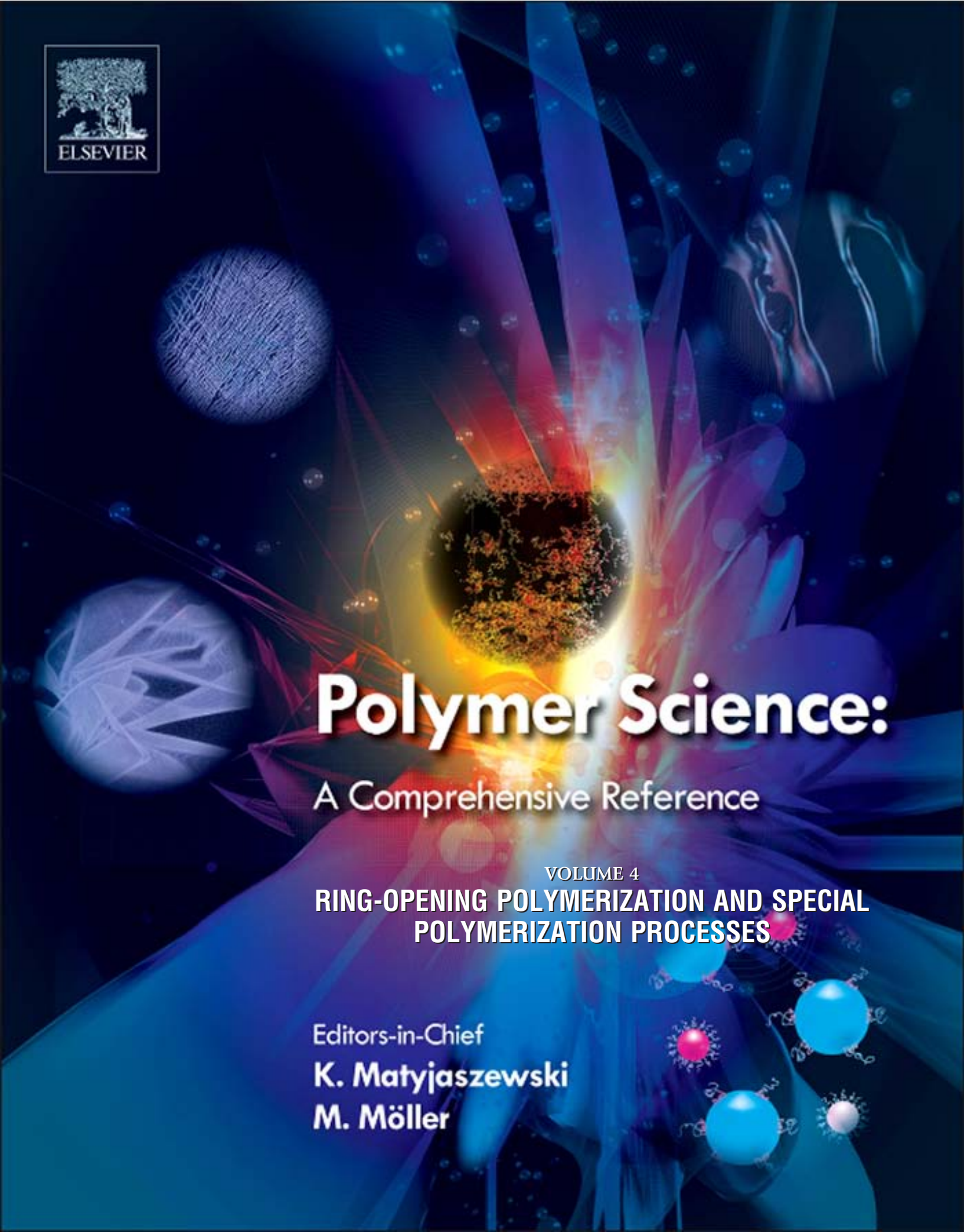
ELSEVIER
Polymer Science:
A Comprehensive Reference
VOLUME 4
RING-OPENING POLYMERIZATION AND SPECIAL POLYMERIZATION PROCESSES
Editors-in-Chief
K. Matyjaszewski
M. Möller

POLYMER SCIENCE: A COMPREHENSIVE REFERENCE

POLYMER SCIENCE: A COMPREHENSIVE REFERENCE

EDITORS-IN-CHIEF

Krzysztof Matyjaszewski

Carnegie Mellon University, Pittsburgh, PA, USA

Martin Möller

RWTH Aachen University, Aachen, Germany

VOLUME 4
RING-OPENING POLYMERIZATION AND SPECIAL POLYMERIZATION PROCESSES

VOLUME EDITORS

S. Penczek

Polish Academy of Sciences, Lodz, Poland

R. Grubbs

California Institute of Technology, Pasadena, CA, USA

ELSEVIER

AMSTERDAM BOSTON HEIDELBERG LONDON NEW YORK OXFORD
PARIS SAN DIEGO SAN FRANCISCO SINGAPORE SYDNEY TOKYO

Elsevier
Radarweg 29, PO Box 211, 1000 AE Amsterdam, The Netherlands
The Boulevard, Langford Lane, Kidlington, Oxford OX5 1GB, UK
225 Wyman Street, Waltham, MA 02451, USA

The following articles are US Government work in the public domain and is not subject to copyright:
Chapter 4.17 Polymerization of Cyclic Siloxanes, Silanes, and Related Monomers
Chapter 7.18 Polymer Dynamics in Constrained Geometries

A catalogue record for this book is available from the British Library

A catalog record for this book is available from the Library of Congress

ISBN: 978-0-444-53349-4

For information on all Elsevier publications
visit our website at books.elsevier.com

Printed and bound in Spain

12 13 14 15 16 10 9 8 7 6 5 4 3 2 1

Editorial: Claire Byrne
Production: Karen East and Kirsty Halterman
Publishing Assistants: Ashlie Jackman and Joanne Williams
Associate Project Manager: Sue Jakeman

CONTENTS OF VOLUME 4

VOLUME EDITORS

Volume 1 – Basic Concepts and Polymer Properties

AR Khokhlov, Moscow State University, Moscow, Russia
F Kremer, University of Leipzig, Leipzig, Germany

Volume 2 – Polymer Characterization

T Hashimoto, Japan Atomic Energy Agency, Ibaraki, Japan
HW Spiess, Max Planck Institute for Polymer Research, Mainz, Germany
M Takenaka, Kyoto University, Kyoto, Japan

Volume 3 – Chain Polymerization of Vinyl Monomers

GW Coates, Cornell University, Ithaca, NY, USA
M Sawamoto, Kyoto University, Kyoto, Japan

Volume 4 – Ring-Opening Polymerization and Special Polymerization Processes

S Penczek, Polish Academy of Sciences, Lodz, Poland
R Grubbs, California Institute of Technology, Pasadena, CA, USA

Volume 5 – Polycondensation

H-W Schmidt, University of Bayreuth, Bayreuth, Germany
M Ueda, Engineering Tokyo Institute of Technology, Tokyo, Japan

Volume 6 – Macromolecular Architectures and Soft Nano-Objects

AHE Müller, University of Bayreuth, Bayreuth, Germany
KL Wooley, Texas A&M University, College Station, TX, USA

Volume 7 – Nanostructured Polymer Materials and Thin Films

E Kumacheva, University of Toronto, Toronto, ON, Canada
TP Russell, University of Massachusetts, Amherst, MA, USA

Volume 8 – Polymers for Advanced Functional Materials

K Müllen, Max Planck Institute for Polymer Research, Mainz, Germany
CK Ober, Cornell University, Ithaca, NY, USA

Volume 9 – Polymers in Biology and Medicine

DA Tirrell, California Institute of Technology, Pasadena, CA, USA
R Langer, Massachusetts Institute of Technology, Cambridge, MA, USA

Volume 10 – Polymers for a Sustainable Environment and Green Energy

JE McGrath, Virginia Polytechnic Institute and State University, Blacksburg, VA, USA
MA Hickner, The Pennsylvania State University, University Park, PA, USA
R Höfer, Editorial Ecosiris, Düsseldorf, Germany

EDITORS-IN-CHIEF: BIOGRAPHIES

Krzysztof Matyjaszewski received his PhD degree in 1976 from the Polish Academy of Sciences under Prof. S. Penczek. Since 1985 he has been at Carnegie Mellon University where he is currently J. C. Warner University Professor of Natural Sciences and director of Center for Macromolecular Engineering. He is also Adjunct Professor at the University of Pittsburgh and at the Polish Academy of Sciences. He is the editor of *Progress in Polymer Science and Central European Journal of Chemistry*. He has coedited 14 books and coauthored more than 70 book chapters and 700 peer-reviewed publications; he holds 41 US and more than 120 international patents. His papers have been cited more than 50 000 times. His research interests include controlled/living radical polymerization, catalysis, environmental chemistry, and advanced materials for optoelectronic and biomedical applications.

Dr. Matyjaszewski has received 2011 Wolf Prize, 2011 Prize of Société Chimique de France, 2009 Presidential Green Chemistry Challenge Award, 2004 Prize from the Foundation of Polish Science, and several awards from the American Chemical Society (including 2011 Hermann Mark Award, 2011 Applied Polymer Science Award, 2007 Mark Senior Scholar Award, 2002 Polymer Chemistry Award, and 1995 Marvel Creative Polymer Chemistry Award). He is a member of US National Academy of Engineering, Polish Academy of Sciences, Russian Academy of Sciences, and received honorary degrees from l'Institut Polytechnique, Toulouse, France; University of Athens, Greece; Russian Academy of Sciences; Lodz Polytechnic, Poland; and University of Ghent, Belgium.

Martin Möller studied chemistry at Hamburg and Freiburg. He received his PhD degree in 1981 from the University of Freiburg.

He was a Feodor-Lynen Research Fellow of the Alexander von Humboldt Foundation at the Polymer Science and Engineering Department, University of Massachusetts, Amherst, USA. After his habilitation in 1989 at Freiburg University he was professor at the universities of Twente, Enschede, The Netherlands and Ulm, Germany. Since 2002 he is professor of Textile and Macromolecular Chemistry at RWTH Aachen University, and since 2003 also the director of DWI-Interactive Materials Research Institute at RWTH Aachen University. He has served on the editorial board of several polymer journals. His fields of interest include polymers self-organization of macromolecules, surface modification and activation, formation of functional nanostructures, and organic–inorganic hybrid structures. Martin Möller has received the the Körber-Prize 2002. He is a member of the Deutsche Akademie der Technikwissenschaften (acatech) and of the Academy of Sciences of the state of North-Rhine Westphalia.

EDITORS: BIOGRAPHIES

Alexei R. Khokhlov was born in 1954 in Moscow, Russia. He graduated from Moscow State University in 1977, received his PhD in 1979 and Doctor of Science in 1983. He is Full Professor and Head of the Chair of Physics of Polymers and Crystals. He is a Member of Russian Academy of Sciences (2000), Chairman of Polymer Council of Russian Academy of Sciences (2002) and Laureate of the Russian National Award (2007).

Friedrich Kremer is Professor of Molecular Physics, Materials Research Spectroscopy, Institute of Experimental Physics I, University of Leipzig, Germany. His research interests include broadband dielectric spectroscopy, time-resolved Fourier transform infrared (FTIR) spectroscopy, and experiments with optical tweezers. In 2005 he was awarded with the Karl Heinz Beckurts – Prize; in 2011 he received the Wolfgang-Ostwald-Prize from the German Colloid Society.

Takeji Hashimoto received his MS degree in 1969 and PhD in 1971 (with Prof. R. S. Stein) from the University of Massachusetts. He was appointed as an assistant professor at Kyoto University, Japan, in 1971, and was promoted as a full professor in 1994. He was director of the Hashimoto Polymer Phasing Project, ERATO (Exploratory Research for Advanced Technology), supported by JST (Japan Science and Technology Agency), from 1993 to 1998. He served as a group leader and invited researcher for the project 'Neutron Scattering and Structure-Functionality of Soft Matters' at the Advanced Science Research Center (ASRC), Japan Atomic Energy Research Institute (JAEA), Tokai, from 2003 to 2005. Since his retirement from Kyoto University in March 2005, he has been a professor emeritus of Kyoto University, and served as a full-time visiting researcher at ASRC, JAEA, Tokai, from 2005 to 2008 and as a group leader for the physical science and life science group. He has been a visiting scientist at JAEA, Tokai, since 2008 and a visiting professor at the School of Science and Technology, Kwansei-Gakuin University, Sanda, Japan, since 2009. He has received several awards including the Society of Polymer Science Japan Award (1986), the High Polymer Physics Award (Ford Prize) from the American Physical Society (1987), the award for Young Rheologist from the Society of Rheology, Japan (1989), the Society of Fiber Science Japan Award (1990), the Osaka Science Award (1992), the Turner Alfrey Award from

Midland Molecular Institute, Midland Section of ACS (1997), the Fraser Price Memorial Award from the University of Massachusetts (1997), the Chemical Society of Japan Award (2003), the Japanese Society for Neutron Science Award (2004), and Society of Polymer Science Japan Award for Outstanding Achievement in Polymer Science and Technology (2006).

Hans Wolfgang Spiess, born in 1942, received his doctoral degree in physical chemistry in 1968 from the University of Frankfurt with H. Hartmann. After a postdoctoral stay at Florida State University (with R. K. Sheline), he returned to Germany in 1970 and joined the Max Planck Institute for Medical Research (with K. H. Hausser), taking part in the rapid development of novel NMR techniques for studying molecular motion in liquids and solids. In 1978, he finished his habilitation in physical chemistry at the University of Mainz in the group of H. Sillescu. Subsequently, he held professorships of physical chemistry at the University of Münster (1981–82) and macromolecular chemistry at the University of Bayreuth (1983–84). In 1984, he was appointed a director of the newly founded Max Planck Institute for Polymer Research in Mainz. His research interests include the development of magnetic resonance techniques for elucidating the structure, dynamics, phase behavior, and order of synthetic macromolecules and supramolecular systems. He applies these methods to the study of new polymer materials to relate their microscopic and macroscopic behavior. Spiess has served as chairman of the European Polymer Federation (1991–92) and as chairman of the Capital Investment Committee of the German Science Foundation (1994–96). From 1999 till 2005, he has been a member of the Scientific Council of the Federal Republic of Germany. His achievements have been honored by several distinctions, including the Leibniz Prize of the German Research Foundation in 1987, the European Ampere Prize, the Liebig Medal of the German Chemical Society, the Award of the Society of Polymer Science (Japan) in 2002, the Walther Nernst Medal of the German Bunsen Society for Physical Chemistry in 2007, and the Paul J. Flory Research Prize in 2010. He is doctor *honoris causa* of the Technical University of Cluj-Napoca, Romania (1997), and of Adam Mickiewicz University, Poznan, Poland (1998).

Mikihito Takenaka received both the master's degree in engineering in 1988 and the doctor's degree in engineering in 1993 with Prof. Takeji Hashimoto from Kyoto University. In 1997, he was appointed as an assistant professor of the Department of Polymer Chemistry in Kyoto University. He was promoted to associate professor in 2011. His research scope includes the dynamics of phase transitions of polymer alloys and the directed self-assembling of block copolymer thin films.

Geoffrey W. Coates was born in 1966 in Evansville, Indiana. He received a BA degree in chemistry from Wabash College in 1989 and a PhD in organic chemistry from Stanford University in 1994. His thesis work, under the direction of Robert M. Waymouth, investigated the stereoselectivity of metallocene-based Ziegler–Natta catalysts. Following his doctoral studies, he was an NSF Postdoctoral Fellow with Robert H. Grubbs at the California Institute of Technology. During the summer of 1997, he joined the faculty of Cornell University as an assistant professor of chemistry. He was promoted to associate professor in 2001 and to professor in 2002. He was appointed to the first Tisch University Professorship in 2008.

The research focus of the Coates Group is the development of new catalysts for the synthesis of macromolecules as well as small molecules. Professor Coates' research concentrates on developing new methods for reacting commodity feedstocks in unprecedented ways. His current research centers on the development of homogeneous catalysts for olefin polymerization, heterocycle carbonylation, epoxide homo- and copolymerization, and utilization of carbon dioxide in polymer synthesis.

Professor Coates is an Alfred P. Sloan Research Fellow and has received awards from the ACS (A. C. Cope Scholar Award, Affordable Green Chemistry Award, A. K. Doolittle Award, Carl S. Marvel – Creative Polymer Chemistry Award, and Akron Section Award), NSF (CAREER), MIT Technology Review Magazine (TR 100 Award), Research Corporation (Innovation Award), Arnold and Mabel Beckman Foundation (Young Investigator Award), David and Lucile Packard Foundation (Fellowship in Science and Engineering), and Dreyfus Foundation (Camille and Henry Dreyfus New Faculty and Camille Dreyfus Teacher-Scholar Awards). In 2006, he received the Stephen and Margery Russell Distinguished Teaching Award at Cornell University and became a member of the American Association for the Advancement of Science. In 2011, he was identified by Thomson Reuters as one of the world's top 100 chemists on the basis of the impact of his scientific research. He is a member of the editorial advisory boards of the *Journal of Polymer Science*, *Chemical Reviews*, and *ChemCatChem*. He is a member of the editorial board of *Dalton Transactions* and is an associate editor for *Macromolecules*.

Mitsuo Sawamoto was born in 1951 in Kyoto, Japan. He received a BS (1974), an MS (1976), and PhD degrees (1979) in polymer chemistry from Kyoto University, Japan. After a postdoctoral research at the Institute of Polymer Science, The University of Akron, Akron, OH, USA (1980–81), he joined the faculty of Department of Polymer Chemistry, Kyoto University, Japan in 1981 as a research instructor and is currently Professor of Department of Polymer Chemistry, Graduate School of Engineering, Kyoto University, Japan since 1994.

He served as President of the Society of Polymer Science, Japan from 2008–10, and is currently an executive member of the Science Council of Japan, a titular member of IUPAC Polymer Division, and one of the Editors of the *Journal of Polymer Science, Part A, Polymer Chemistry*. He is also the principal investigator of a research project "Sequence-Regulated Macromolecules" (2006–10; Grant-in-Aid for Scientific Research: Creation of Novel Academic Disciplines) and the project leader of the Kyoto University Global Center of Excellence (GCOE) Project "Integrated Materials Science" (2007–11), both granted by the Ministry of Education, Science, Culture, and Sports, Japan via the Japan Society for Promotion of Science.

With over 350 original papers and over 30 reviews, he has received, among others, Award of the Society of Polymer Science, Japan (1992), Divisional Research Award of the Chemical Society of Japan (1999), and Arthur K. Doolittle Award of PMSE Division, the American Chemical Society (2002). His research interest includes development of novel precision polymerizations and catalysis (living cationic polymerization with Lewis-acid catalysts (1984) and living radical polymerization with transition metal complex catalysts (since 1995)), the synthesis of designed functional polymers, the nature of polymerization intermediates, and most recently the sequence regulation in chain growth polymerization for single-chain functional macromolecules of carbon-based backbones.

The first paper on his living radical polymerization has been cited thus far over 1600 times and is ranked number two in the most cited papers published in *Macromolecules*; a comprehensive review on this discovery published in *Chemical Reviews* has now been cited over 1200 times and has been selected as one of the ACS 2007 Highly Cited Papers (within top 1%) in the latest ten years (1998–2007); and he was ranked number one in Japan and number three in the world among the most cited scientists in organic and polymer chemistry for the period of 1997–2001.

Stanislaw Penczek is Professor of Polymer Chemistry at the Polish Academy of Sciences (Centre of Molecular and Macromolecular Studies in Lodz). He teaches at the Graduate School of the Jagiellonian University (Krakow) as an honorary professor. He has mostly contributed to the kinetics, thermodynamics, and mechanisms of the ring-opening polymerization, publishing over 300 papers in related areas. He was one of the first to observe living and controlled polymerizations in cationic and anionic ROP, including reversibility of deactivation of propagating species. Among other honors from Belgium, Japan, and Germany (the Warburg Prize), he is a member of the Polish Academy of Sciences and foreign member of German (Nordrhein) Academy, Dr *h.c.* of the Pierre and Marie Curie University in Paris and Dr *h.c.* of the Russian Academy of Sciences. He was a member of the International Union of Pure and Applied Chemistry (IUPAC) Bureau for two terms, and former president of European Polymer Federation.

Robert (Bob) Howard Grubbs' main interests in organometallic chemistry and synthetic chemistry are catalysts, notably Grubbs' catalyst for olefin metathesis and ring-opening metathesis polymerization with cyclic olefins such as norbornene. He also contributed to the development of so-called 'living polymerization'.

Grubbs has received many awards including Alfred P. Sloan Fellow (1974–76), Camille and Henry Dreyfus Teacher-Scholar Award (1975–78), Alexander von Humboldt Fellowship (1975), ACS Benjamin Franklin Medal in Chemistry (2000), ACS Herman F. Mark Polymer Chemistry Award (2000), ACS Herbert C. Brown Award for Creative Research in Synthetic Methods (2001), the Tolman Medal (2002), and the Nobel Prize in Chemistry (2005). He was elected to the National Academy of Sciences in 1989 and a fellowship in the American Academy of Arts and Sciences in 1994.

Hans-Werner Schmidt studied chemistry at the University of Mainz (Germany) and ETH Zürich (Switzerland). He received his diploma in chemistry and Dr. rer. nat. degree in macromolecular chemistry with Prof. Helmut Ringsdorf at the University of Mainz. After a stay at the DuPont Central Research in Wilmington, Delaware (USA), he moved to the University of Marburg to obtain his habilitation. From 1989 to 1994, he was Assistant and Associate Professor of Materials with tenure at the Materials Department, College of Engineering at the University of California, Santa Barbara. Since 1994, he has been Full Professor for Macromolecular Chemistry at the University of Bayreuth. He is director of the Bayreuth Institute of Macromolecular Research and founding member of the Bayreuth Centre for Colloids and Interfaces. Since 2009, he has been Vice President of the University of Bayreuth for research and since 2004 chairman of the 'Elite Study Program Macromolecular Science' (Elite Network Bavaria).

His research interest is focused on the synthesis and development of novel organic functional materials in the area of emerging technologies. This includes multifunctional polymers, molecular glasses, and supramolecular polymer additives and gelators. Combinatorial methods to efficiently synthesize and screen materials properties of polymer and supramolecular materials and functions of devices are an additional aspect.

Mitsuru Ueda received his BS and MS degrees in polymer chemistry from Chiba University in 1970 and 1972, respectively, and a PhD degree from Tokyo Institute of Technology in 1978. He joined Yamagata University in 1972 and was promoted to a professor in 1989. He moved to Tokyo Institute of Technology in 1999. His current research interests are the development of new synthetic methods for condensation polymers, polymer solar cells, fuel-cell membranes, photosensitive materials for microelectronics, and new advanced resist materials.

Axel H. E. Müller obtained his PhD in 1977 from Johannes Gutenberg University in Mainz, Germany, for the work on the kinetics of anionic polymerization with G. V. Schulz. Since 1999, he has been professor and chair of macromolecular chemistry at the University of Bayreuth. In 2004, he received the IUPAC MACRO Distinguished Polymer Scientist Award and since 2011, he has been a Fellow of the Polymer Chemistry Division of the American Chemical Society. He is senior editor of the journal *Polymer*. His research interests focus on the design of well-defined polymer structures by controlled/living polymerization techniques and on self-organized nanostructures and hybrids obtained from them. He has coedited five books and published over 400 research papers.

Karen L. Wooley holds the W. T. Doherty-Welch Chair in the Department of Chemistry at Texas A&M University, with a joint appointment in the Department of Chemical Engineering. She received a BS in chemistry from Oregon State University in 1988 and then studied under the direction of Professor Jean M. J. Fréchet at Cornell University, obtaining a PhD in polymer/organic chemistry in 1993. She began an academic career as an assistant professor of chemistry at Washington University in St. Louis, Missouri; was promoted in 1999 to full professor with tenure; and was installed as a James S. McDonnell Distinguished University Professor in Arts & Sciences in 2006. In 2009, she relocated to Texas A&M University. Research areas include the synthesis and characterization of degradable polymers, unique macromolecular architectures and complex polymer assemblies, and the design and development of well-defined nanostructured materials, for which she has received several awards, including an Arthur C. Cope Scholar Award, a Herman F. Mark Scholar Award, and awards from the National Science Foundation, the Office of Naval Research, and the Army Research Office. Karen serves as an editor for the *Journal of Polymer Science, Part A: Polymer Chemistry*. She directs an NHLBI-supported Program of Excellence in Nanotechnology and also serves on the Scientific Advisory Panel for the NIH Nanomedicine Development Centers and on the International Scientific Advisory Board for the Dutch BioMedical Materials Program.

Professor Eugenia Kumacheva is a Canada Research Chair in Advanced Polymer Materials. Her current research interests are in polymer micro- and nanostructured materials, hybrid materials, biomaterials, inorganic nanoscale materials, and microfluidics.

Thomas Russell is Silvio O. Conte Distinguished Professor, Polymer Science and Engineering Department; Director, Energy Frontier Research Center (EFRC), Polymer-Based Materials for Harvesting Solar Energy. His research interests are polymer-based nanoscopic structures, polymer-based nanoparticle assemblies, electrohydrodynamic instabilities in thin polymer films, surface and interfacial properties of polymers, polymer morphology; kinetics of phase transitions, and supercritical fluid/polymer interactions.

Professor Christopher K. Ober received his BSc in honours chemistry (co-op) from the University of Waterloo, Ontario, in 1978. He received his PhD in polymer science and engineering from the University of Massachusetts (Amherst) in 1982. From 1982 until 1986, he was a senior staff member at the Xerox Research Centre of Canada where he worked on marking materials. Ober joined Cornell University as an assistant professor in the Department of Materials Science and Engineering in 1986. He recently served as Interim Dean of the College of Engineering. He has pioneered new methods in photolithography and studies the biology materials interface. His awards include the 2009 Gutenberg Research Award from the University of Mainz, the 1st Annual FLEXI Award in the Education Category (for flexible electronics) awarded in 2009, the 2007 Humboldt Research Prize, the 2006 ACS Award in Applied Polymer Science, and the Photopolymer Science and Technology Award in 2004. He was elected an ACS Fellow in the 2009 Inaugural Class.

Professor Dr. Klaus Müllen obtained his PhD degree from the University of Basel, Switzerland, in 1972 where he undertook research with Professor F. Gerson on EPR spectroscopy of twisted π-systems. In 1972, he joined the group of Professor J.F.M. Oth at the Swiss Federal Institute of Technology in Zürich where he worked in the field of dynamic NMR spectroscopy and electrochemistry. He received his habilitation from the ETH Zurich in 1977. In 1979, he became a professor in the Department of Organic Chemistry, University of Cologne, and accepted an offer of a chair in organic chemistry at the University of Mainz in 1983. In 1988, he joined the Max-Planck-Society and in 1989 as one of the directors of the Max-Planck Institute for Polymer Research. His current research topics include new polymer-forming reactions, multidimensional polymers with complex shape-persistent architectures, dyes, chemistry and physics of single molecules, polymers for electronic and optoelectronic devices, materials for lithium or hydrogen storage, biosynthetic hybrids, and nanocomposites. In recent years, he has especially focused on the chemistry and physics of carbon-rich materials such as carbon nanotubes, graphenes, and nanographenes. He has received numerous prestigious awards such as the International Award of the Polymer Society of Japan (2009), the ACS Award for Polymer Chemistry (2011), the ERC Advanced Grant (2011), and the Tsungming Tu Award (2011). Since 2006, he acts as Associate Editor of the *Journal of the American Chemical Society* and in 2008 and 2009 he served as President of the German Chemical Society.

David A. Tirrell is the Ross McCollum-William H. Corcoran Professor of chemistry and chemical engineering at the California Institute of Technology. After earning the BS degree in chemistry at MIT in 1974, he enrolled in the Department of Polymer Science and Engineering at the University of Massachusetts, where he was awarded the PhD degree in 1978 for work done under the supervision of Otto Vogl. After a brief stay with Takeo Saegusa at Kyoto University, he accepted an assistant professorship in the Department of Chemistry at Carnegie Mellon University in the fall of 1978. He returned to Amherst in 1984 and served as director of the Materials Research Laboratory at the University of Massachusetts before moving to Caltech in 1998. He chaired the Division of Chemistry and Chemical Engineering at Caltech from 1999 until 2009. His contributions to chemistry and chemical engineering have been recognized by his election to the National Academy of Sciences, the National Academy of Engineering, the Institute of Medicine, and the American Academy of Arts and Sciences.

Robert S. Langer is the David H. Koch Institute Professor (there are 14 Institute Professors at MIT; being an Institute Professor is the highest honor that can be awarded to a faculty member). Dr. Langer has written nearly 1130 articles. He also has approximately 800 issued and pending patents worldwide. Dr. Langer's patents have been licensed or sublicensed to over 220 pharmaceutical, chemical, biotechnology, and medical device companies. He is the most cited engineer in history. He served as a member of the United States Food and Drug Administration (FDA)'s SCIENCE Board, the FDA's highest advisory board, from 1995 to 2002 and as its Chairman from 1999 to 2002.

Dr. Langer has received over 180 major awards including the 2006 United States National Medal of Science; the Charles Stark Draper Prize, equivalent of the Nobel Prize for engineers; the 2008 Millennium Prize, the world's largest technology prize; and the 2012 Priestley Medal, the highest award of the American Chemical Society. He is the also the only engineer to receive the Gairdner Foundation International Award; 72 recipients of this award have subsequently received a Nobel Prize. Among numerous other awards Langer has received are the Dickson Prize for Science (2002); Heinz Award for Technology, Economy and Employment (2003); the Harvey Prize (2003); the John Fritz Award (2003) (given previously to inventors such as Thomas Edison and Orville Wright); the General Motors Kettering Prize for Cancer Research (2004); the Dan David Prize in Materials Science (2005); the Albany Medical Center Prize in Medicine and Biomedical Research (2005), the largest prize in the United States for medical research; induction into the National Inventors Hall of Fame (2006); the Max Planck Research Award (2008); and the Prince of Asturias Award for Technical and Scientific Research (2008). In 1998, he received the Lemelson-MIT Prize, the

world's largest prize for invention for being 'one of history's most prolific inventors in medicine'. In 1989, Dr. Langer was elected to the Institute of Medicine of the National Academy of Sciences, and in 1992, he was elected to both the National Academy of Engineering and the National Academy of Sciences. He is one of very few people ever elected to all three United States National Academies and the youngest in history (at age 43) to ever receive this distinction.

Forbes Magazine (1999) and *Bio World* (1990) have named Dr. Langer as one of the 25 most important individuals in biotechnology in the world. *Discover Magazine* (2002) named him as one of the 20 most important people in this area. *Forbes Magazine* (2002) selected Dr. Langer as one of the 15 innovators worldwide who will reinvent our future. *Time Magazine* and CNN (2001) named Dr. Langer as one of the 100 most important people in America and one of the 18 top people in science or medicine in America (America's Best). *Parade Magazine* (2004) selected Dr. Langer as one of six 'Heroes whose research may save your life'. Dr. Langer has received honorary doctorates from Harvard University, the Mt. Sinai School of Medicine, Yale University, the ETH (Switzerland), the Technion (Israel), the Hebrew University of Jerusalem (Israel), the Universite Catholique de Louvain (Belgium), Rensselaer Polytechnic Institute, Willamette University, the University of Liverpool (England), Bates College, the University of Nottingham (England), Albany Medical College, Pennsylvania State University, Northwestern University, Uppsala University (Sweden), and the University of California–San Francisco Medal. He received his bachelor's degree from Cornell University in 1970 and his ScD from the Massachusetts Institute of Technology in 1974 (both degrees in Chemical Engineering).

James E. McGrath received his BS in chemistry from Siena College in New York (1956) and his MS (1964) and PhD (1967) in polymer science from the University of Akron, where he worked on emulsion and anionic polymerization of synthetic rubbers, ozone cracking, and triblock copolymer thermoplastic elastomers. After 19 years in industry (Rayonier (cellulose), Goodyear (synthetic rubbers), and Union Carbide (engineering thermoplastics, polyolefins)), he joined the Chemistry Department at Virginia Tech in 1975. He is now Ethyl Chair and a University Distinguished Professor. He was director of the first group of NSF Science and Technology Centers from 1989 to 2000 on Structural Adhesives and Composites and focused on high-temperature polymers including polyimides, polysulfones, and toughened epoxy polymeric matrix resins for carbon fiber composites. He has many contributions to the anionic and ring-opening polymerization of dienes, epoxides, and organosiloxanes. His current focus is on polymeric materials for carbon fibers and membranes, including fuel cells, reverse osmosis water purification and gas separation systems. He has 50 patents and over 500 publications and has received numerous awards, including election to the National Academy of Engineers (1994), The International SPE award, the Plastics Hall of Fame, and the ACS awards in Applied Polymer Science (2002) and Polymer Chemistry (2008). He has graduated more than 100 PhD chemists and engineers and remains one of the leaders in polymer science and engineering, with a current group (2011) of 13 students and postdoctoral fellows.

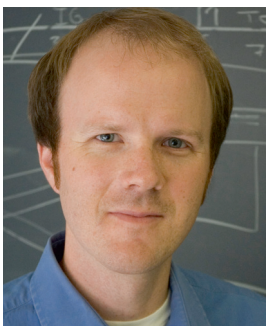

Michael A. Hickner received a BS in chemical engineering from Michigan Tech in 1999 and MEng in 2002 and PhD in chemical engineering from Virginia Tech in 2003. In graduate school, he worked under the direction of James E. McGrath and also spent time in the fuel cell group at Los Alamos National Laboratory developing novel aromatic proton exchange membranes for both hydrogen and direct methanol fuel cells. Before joining the Department of Materials Science and Engineering at Penn State in July 2007, he was a postdoctoral researcher and subsequently became a staff member at Sandia National Laboratories in Albuquerque, NM, where he conducted experimental investigations and modeling studies of liquid water transport in fuel cells and porous media and properties of ion-containing membranes, electrochemical reactors, and nanoporous membranes for water treatment applications. His research group at Penn State is focused on the synthesis and properties of ion-containing polymers, measurement of water–polymer interactions using spectroscopic techniques, and the study of self- and directed assembly of polymeric nanostructures for fast transport. He has ongoing projects in new polymer synthesis, fuel cells, batteries, water treatment membranes, and organic photovoltaic materials. He is currently an assistant professor and the Virginia S. and Philip L. Walker Jr. Faculty Fellow in the Materials Science Department at Penn State. Hickner's work has been recognized by a

Powe Junior Faculty Enhancement Award (2008), Young Investigator Awards from ONR and ARO (2008), a 3M Non-tenured Faculty Grant (2009), and a Presidential Early Career Award for Scientists and Engineers from President Obama in 2009. He has five US and international patents and over 60 peer-reviewed publications since 2001 that have been cited more than 2900 times as of 2011.

Rainer Höfer graduated in Inorganic Chemistry with Professor Oskar Glemser at the Georg-August Universität zu Göttingen in 1973 with work on sulfur–nitrogen–fluorine chemistry. He spent three years at the Technical University of Oran (ENSEP), Algeria, as Maître de Conférences and Directeur de l'Institut de Chimie before joining Henkel in Düsseldorf. With Henkel KGaA and then as Vice President Research & Technology with Cognis GmbH in Monheim, he has assumed global research and development, application technology, technical sales service, strategic business development, and technology scouting responsibilities in oleochemistry, polymer chemistry, and surfactant chemistry for the polymerization, coatings, graphic arts, adhesives, engineering plastics, agrochemical, synthetic lubricants, mining, and pulp and paper markets. He is founder of Editorial Ecosiris with consultancy and publishing activities in the domains of green chemistry, renewable resources, sustainable development, and interculturation.

CONTRIBUTORS OF VOLUME 4

SM Ahmed
Cornell University, Ithaca, NY, USA

H Ajiro
Cornell University, Ithaca, NY, USA

SD Allen
Cornell University, Ithaca, NY, USA

A Barrère
Université Paris, Villetaneuse, France

S Beuermann
University of Potsdam, Potsdam/Golm, Germany

CW Bielawski
The University of Texas at Austin, Austin, TX, USA

D Bogdal
Politechnika Krakowska, Krakow, Poland

M Buback
Georg-August-Universität Göttingen, Göttingen, Germany

MR Buchmeiser
Universität Stuttgart, Stuttgart, Germany; and Institut für Textilchemie und Chemiefasern (ITCF), Denkendorf, Germany

S Carlotti
Université Bordeaux, Pessac, France

E Casazza
Università di Genova, Genova, Italy; and INSTM, Consorzio Interuniversitario Nazionale di Scienza e Tecnologia dei Materiali, Firenze, Italy

GW Coates
Cornell University, Ithaca, NY, USA

O Coulembier
University of Mons, Mons, Belgium

JV Crivello
Rensselaer Polytechnic Institute, Troy, NY, USA

M Cypryk
Polish Academy of Sciences, Lodz, Poland

A Deffieux
Université Bordeaux, Pessac, France

TJ Deming
University of California–Los Angeles, Los Angeles, CA, USA

B Dervaux
Ghent University, Gent, Belgium

I Dimitrov
Bulgarian Academy of Sciences, Sofia, Bulgaria

P Dubois
University of Mons, Mons, Belgium

A Duda
Polish Academy of Sciences, Lodz, Poland

J-Z Du
University of Science and Technology of China, Hefei, Anhui, People's Republic of China

BD Edgecombe
Materia, Inc., Pasadena, CA, USA

T Endo
Kinki University Iizuka, Japan

WJ Feast
Durham University, Durham, UK

H Frey
Johannes Gutenberg University (JGU), Mainz, Germany

M Fèvre
Université de Bordeaux, Pessac, France

Y Gnanou
Université de Bordeaux, Pessac, France

EJ Goethals
Ghent University, Gent, Belgium

RH Grubbs
California Institute of Technology, Pasadena, CA, USA

A Hamielec
McMaster University, Hamilton, ON, Canada

C Jérôme
University of Liège, Liège, Belgium

K Kaluzynski
Centre of Molecular and Macromolecular Studies, Lodz, Poland

LL Kiessling
University of Wisconsin–Madison, Madison, WI, USA

S Kobayashi
Kyoto Institute of Technology, Kyoto, Japan

P Kubisa
Polish Academy of Sciences, Lodz, Poland

G Lapienis
Polish Academy of Sciences, Lodz, Poland

TJA Loontjens
University of Groningen, Groningen, The Netherlands

SL Mangold
University of Wisconsin–Madison, Madison, WI, USA

R Mincheva
University of Mons, Mons, Belgium

JP Moerdyk
The University of Texas at Austin, Austin, TX, USA

A Nickel
Materia, Inc., Pasadena, CA, USA

CD Papaspyrides
National Technical University of Athens, Zographou, Athens, Greece

PG Parzuchowski
Warsaw University of Technology, Warsaw, Poland

S Penczek
Polish Academy of Sciences, Lodz, Poland

S Połowiński
Technical University of Lodz, Lodz, Poland

JA Pojman
Louisiana State University, Baton Rouge, LA, USA

J-M Raquez
University of Mons, Mons, Belgium

G Rokicki
Warsaw University of Technology, Warsaw, Poland

S Russo
Università di Genova, Genova, Italy; and INSTM, Consorzio Interuniversitario Nazionale di Scienza e Tecnologia dei Materiali, Firenze, Italy

C Schüll
Johannes Gutenberg University (JGU), Mainz, Germany

S Slomkowski
Polish Academy of Sciences, Lodz, Poland

R Szymanski
Polish Academy of Sciences, Lodz, Poland

D Taton
Université de Bordeaux, Pessac, France

CB Tsvetanov
Bulgarian Academy of Sciences, Sofia, Bulgaria

JP Vairon
Université Pierre et Marie Curie, Paris, France

J Vignolle
Université de Bordeaux, Pessac, France

SN Vouyiouka
National Technical University of Athens, Zographou, Athens, Greece

J Wang
University of Science and Technology of China, Hefei, Anhui, People's Republic of China

PCB Widger
Cornell University, Ithaca, NY, USA

D Wilms
Johannes Gutenberg University (JGU), Mainz, Germany

Y-Y Yuan
University of Science and Technology of China, Hefei, Anhui, People's Republic of China

S Zhu
McMaster University, Hamilton, ON, Canada

PREFACE

Comprehensive Polymer Science was published in 1989 as a set of seven volumes and then supplemented by two additional volumes. This excellent print collection comprehensively covered the entire field of polymer science at that time. Much of the information is currently still as valuable as it was then, although some aspects are seen differently now. Those differences are important in order to understand the enormous development polymer science has taken since 1989. When we developed the concept for an entirely new edition of *Polymer Science: A Comprehensive Reference*, we intended not only to update and replace the original edition of *Comprehensive Polymer Science*, (we are pleased to announce that it will be soon available in electronic format) but also to focus on a widely observed transition of polymer science, from exploring only macromolecules, polymeric materials, and polymerization processes to become part of a comprehensive study on molecular soft matter science enabling advancements in other related disciplines.

In 1989, polymer science had just started a second stage of development after completing the scientific and technological evolution of its fundamental principles. This second stage has been driven by the continuously increasing understanding of the complexity in the structural organization of polymer materials and the challenge to understand and to master the fundamental underlying structure formation on exceedingly large length scales. Material functions based on molecular organization have been the focus of outstanding and highly recognized achievements, for example, new concepts for macromolecular architectures, self-assembling properties, electronically conductive polymers, ultrathin films, and hybrid structures or bioconjugates.

We are once again at the beginning of another step forward in the development of polymer science. Based on an increasing understanding of molecular processes, for example, advancements in mastering molecular self-assembly and the interfacing of bottom-up and top-down approaches to molecular organization, the tremendous progress in understanding the molecular basis of biological processes, and the growing ability to describe more and more complex systems with the rigorous approaches of physics, the traditional boundaries between these fields of science are being torn down. At the same time, the differentiation between materials and living organisms is becoming more and more indistinct, that is, machines are becoming biological and biology is becoming engineered. Already a new field of biofunctional materials is emerging, where 'biofunctional' represents the ability to activate and control a biological response. As a consequence, polymer science is facing a shift in paradigm from having been focused on itself, toward creating an enabling science that provides an understanding of a much broader base of 'molecular soft matter science' that reaches out and provides important contributions toward biology and information- and energy-related technologies. This development is seen in the increased worldwide interest in bioinspired materials engineering biomimetic materials and in the creation of smart nanostructures, as well as polymeric electronic and photonic devices.

The great progress that has been made in many areas of polymer science since 1989 is reflected in, and aided by, three major developments: (1) the advancements in precision polymerization and synthetic combination of well-defined (bio)macromolecular building blocks, for example, controlled polymerization processes, and new macromolecular architectures; (2) the progress in characterization methods spanning an enormous increase in length- and timescales, for example, single molecule imaging and spectroscopy that provides an improved insight on slow and cooperative relaxation and ordering; and (3) significant improvement in the understanding of complex macromolecular systems like polyelectrolytes and block and graft copolymers amplified

by the dramatically enhanced power of computational simulations. In addition, much interest has been focused on polymers and materials coming from biological sources, or those designed to serve specific functions in a biological system, which is partly driven by environmental and sustainability aspects, but also by the rising interest in smart biomimetic and bioactive materials. Besides the emergence of new biomaterials and biohybrid macromolecules, this also leads to a new interest in waterborne polymers and polymer synthesis in aqueous systems, for example, enzymatic polymerization.

The organization and outline of the ten volumes of this edition of *Polymer Science: A Comprehensive Reference* has been chosen to give consideration to these developments, but also to link the fundamentals of polymer science, as developed over almost 100 years, with the challenges of the ever more complex systems, and introduce connections that will dominate the future development of a polymer-based molecular soft matter science. Besides the classic print edition, this new edition of *Polymer Science: A Comprehensive Reference* is also provided as an e-version, enabled with efficient cross-referencing and multimedia. We invited the top world experts in polymer science to serve as volume editors and this 'dream team' has prepared a ten-volume set with 269 chapters covering both the fundamentals and the most recent advances in polymer science. Volumes 1–5 are directed toward the fundamentals of polymer science, that is, polymer physics and physical chemistry, advanced characterization methods, and polymer synthesis. In spite of the breadth of information collected in these five volumes, it has not been possible to cover all aspects of polymer science. In some cases, the reader must refer to the chapters in volumes 6–10 that address topical developments with a stronger material focus.

The progress in polymer science is revealed in essentially all chapters of this edition of *Polymer Science: A Comprehensive Reference*. In Volume 1, edited by Khokhlov and Kremer, this is reflected in the improved understanding of the properties of polymers in solution, in bulk, and in confined situations such as in thin films. Volume 2, edited by Spiess, Hashimoto, and Takenaka, addresses new characterization techniques that were not covered in the first edition, or did not even exist in 1989, such as high-resolution optical microscopy, scanning probe microscopy, and other procedures for surface and interface characterization. Volume 3, edited by Coates and Sawamoto, presents the great progress achieved in precise synthetic polymerization techniques for vinyl monomers to control macromolecular architecture: the development of metallocene and post-metallocene catalysis for olefin polymerization, new ionic polymerization procedures, atom transfer radical polymerization, nitroxide-mediated polymerization, and reversible addition-fragmentation chain transfer systems as the most often used controlled/living radical polymerization methods. Volume 4, edited by Penczek and Grubbs, is devoted to kinetics, mechanisms, and applications of ring-opening polymerization of heterocyclic monomers and cycloolefins (ROMP), as well as to various less common polymerization techniques. Polycondensation and non-chain polymerizations, including dendrimer synthesis and various 'click' procedures, are covered in Volume 5, edited by Schmidt and Ueda. Volume 6, edited by Müller and Wooley, focuses on several aspects of controlled macromolecular architectures and soft nanoobjects including hybrids and bioconjugates. Many of the achievements would have not been possible without new characterization techniques like atomic force microscopy (AFM) that allowed direct imaging of single molecules and nanoobjects with a precision only recently available. An entirely new aspect in polymer science is based on the combination of bottom-up methods such as molecularly programmed self-assembly with top-down structuring such as lithography and surface templating, as presented in Volume 7, edited by Kumacheva and Russell. It encompasses polymer and nanoparticle assembly in bulk and under confined conditions or influenced by an external field, including thin films, inorganic–organic hybrids, or nanofibers. Volume 8, edited by Muellen and Ober, expands these concepts, focusing on applications in advanced technologies, for example, in electronic industry and centers, in combination with the top-down approach and functional properties like conductivity. Another type of functionality that is rapidly increasing in importance in polymer science is introduced in volume 9, edited by Langer and Tirrell. This deals with various aspects of polymers in biology and medicine, including the response of living cells and tissue to the contact with biofunctional particles and surfaces. Volume 10, edited by Höfer, Hickner, and McGrath, is devoted to the scope and potential provided by environmentally benign and green polymers, as well as energy-related polymers. It discusses new technologies needed for a sustainable economy in our world of limited resources. Common to all approaches in this edition of *Polymer Science: A Comprehensive Reference* is the mastering of an increasing complexity of the polymer material structure needed for a change in focus

from commodities to materials for various advanced applications, related to energy, environment, and biomedicine.

We hope that this new edition of *Polymer Science: A Comprehensive Reference* will provide the readers with state-of-the-art coverage of all important and modern aspects of polymer science. We would like to thank all volume editors, contributing authors, and Elsevier personnel for their efforts, not only in completing the project in a timely fashion but also in ensuring the outstanding quality of the final product.

Krzysztof Matyjaszewski
Martin Möller

FOREWORD

Polymer science has experienced a most impressive expansion in depth, breadth, and diversity through developments in its core domains as well as at the interfaces of polymer chemistry and physics with materials science, supramolecular chemistry, nanoscience, biophysics, and biology. These developments are reflected in the evolution from the original edition of *Comprehensive Polymer Science* to the present edition *Polymer Science: A Comprehensive Reference*. None of these areas can nowadays be envisaged without considering the contributions of polymer science to their own progress. At the same time and with increasing impact, scientists from the other fields contribute new findings and concepts to polymer science and many novel and topical approaches are rooted in the areas mentioned above.

The extension of the concepts and features of supramolecular chemistry from discrete species to polymolecular entities has opened novel perspectives in materials science. It defines a field of supramolecular materials that rests on the explicit implementation of intermolecular interactions and recognition processes for controlling the buildup, the architecture, and the properties of polymolecular assemblies as they emerge from their components through self-organization. Such spontaneous but directed self-assembly is of major interest for the supramolecular design, synthesis, and engineering of novel materials presenting novel properties.

Our own connection with polymer science stems from the introduction and progressive establishment of a supramolecular polymer chemistry built on entities generated by polyassociation between molecular 'monomeric' components through dynamic noncovalent interactions with molecular recognition between the components. The more recent development of dynamic covalent chemistry led to the investigation of dynamic covalent polymers formed by polycondensation through reversible reactions between subunits bearing suitable functional groups. The dynamic features of both these molecular and supramolecular polymers characterize dynamic polymers, dynamers, on both levels. Dynamers may be defined as constitutional dynamic polymers, that is, polymeric entities whose monomeric components are linked through reversible connections and have therefore the capacity to modify their constitution by exchange and reshuffling of their components. They may undergo constitutional variation by incorporation, decorporation, and exchange of components. These dynamic properties confer to dynamers the ability to undergo adaptation and driven evolution in response to physical stimuli or chemical effectors. Dynamers are thus constitutional dynamic materials resulting from the application of the principles of constitutional dynamic chemistry to polymer science. As such, they open wide perspectives toward adaptive materials and technologies.

By the nature and the size of its objects, polymer science plays a very important role in nanoscience and nanotechnology, both areas experiencing a profound mutual fertilization. Polymer science has also been subject to major developments at the interface with biology, by the incorporation of biological components into synthetic polymers, as well as by applying its own principles to the understanding of the features of biological macromolecules.

An extremely rich variety of novel architectures, processes, and properties have resulted and may be expected to further emerge from the blending of polymer science with the other areas of materials chemistry and physics, with ongoing developments in chemistry as well as with the investigation of complex molecular behavior in biological sciences.

Polymer Science: A Comprehensive Reference provides complete and up-to-date coverage of the most important contemporary aspects and fundamental concepts of polymer science. It will become the indispensable reference not only for polymer scientists but also for all researchers in disciplines related to macromolecular systems.

Jean-Marie Lehn
ISIS - Université de Strasbourg, Strasbourg, France

4.01 Introduction

S Penczek, Polish Academy of Sciences, Lodz, Poland
RH Grubbs, California Institute of Technology, Pasadena, CA, USA

Ring-opening polymerization (ROP) encompasses polymerization of cyclic compounds (monomers) with at least one heteroatom or a double bond in the molecules. Polymerization of the latter proceeds by the metathesis mechanism and is called ring-opening metathesis polymerization (ROMP). It has become customary to use the expression 'ROP' mostly for heterocyclic monomers. Both processes belong to the larger family of chain polymerizations. In this volume of Polymer Science: A Comprehensive Reference there are a few chapters that do not entirely belong to ROP.

The first chapters describe the general phenomena of ROP (and ROMP). For the first time, the mechanistic aspects of ROMP are presented, as they were not treated in the first edition of Comprehensive Polymer Science (CPS). These chapters will present a discussion of the history of development of 'living' ROMP and the key features that must be controlled to obtain narrow dispersity polymer samples with the desired molecular weight.

Thermodynamic features of polymerization of both classes of monomers are similar and the ring strain is mostly responsible for conversion of monomer into polymer unit. The origins of the ring strains are similar, namely distortion of the ring angles and stretching bonds. Nevertheless, certain differences in thermodynamics in the two groups of monomers stems from the conversion of the single bonds into single bonds in the former and the conversion of the double bond into a double bond in the repeating units in the latter. Then, if there is a sufficiently short distance, their interaction may influence the enthalpy of the chemical change.

Metathesis can be accomplished with ruthenium-based catalysis in water solvent, whereas ionic processes typical in the ROP exclude water as a reaction medium (there are a few exceptions: the most basic monomers, radical ROP as well as unusual ionic polymerization in water emulsions (cyclic siloxanes)).

Impressive progress has been made in stereospecific polymerization of cyclic ethers and cyclic esters since the first edition of *CPS* was published. A novel ROP phenomenon called stereocomplexation, which is especially important when it involves homochiral macromolecules, poly(*R*)- and poly(*S*)- polylactides, is analyzed in detail (chapter devoted to cyclic esters). A breakthrough in the stereoregulation of methyloxirane (propylene oxide) polymerization is the subject of a chapter on stereospecific polymerization of oxiranes.

Several chapters describe ROP of major classes of monomers such as cyclic ethers, acetals, esters, sulfides, amines, amides, oxazolines, and less common ones, like *N*-carboxyanhydrides (NCAs) of α-amino acids, leading to polypeptides or ROP of cyclic esters of phosphoric acid allowing synthesis of the backbones of DNA.

Novel phenomena are examined such as ROMP (metal-catalyzed ROMP of olefins) involving new classes of initiators (so-called metal free) and phosphorus compounds. Moreover, if one looks at the literature cited in the majority of chapters, then it becomes clear that at least half of the chapters are based on results published after the first edition of *CPS* appeared. Of course, there are established fields, like polymerizations of cyclic sulfides or cationic polymerization of cyclic acetals or several cyclic ethers (e.g., tetrahydrofuran (THF)). Therefore, in the corresponding chapters, the major facts of the past are recalled. However, in the chapters on mechanism of ROMP or cyclic esters, almost exclusively new data are set forth, like the polymerization of biobased monomers (e.g., lactides). The mechanism of the most often used catalytic system, based on $Sn(Oct)_2$, is novel and conditions for living and controlled polymerization of L-lactide polymer (PLA), which is called the 'polymer of the twenty-first century', are discussed in detail.

In the processes of chain ROP/ROMP, there are several phenomena not existing in the vinyl chain polymerizations. These include chain transfer to macromolecules with chain breaking, the most prominent in the polymerization of cyclic acetals (described Chapter **4.10** by Kubisa and Warren), where cationic active species may react with the repeating units of macromolecules with rate constants exceeding the rate constants of propagation.

Similar phenomena, although less effective, take place in the polymerization of all monomers leading to macromolecules with heteroatoms in the chains. A related phenomenon is chain transfer to the same macromolecule, called backbiting and bearing a resemblance to the intramolecular transfer in, for example, polymerization of ethylene. However, in the latter, branching results from 'backbiting' and in ROP/ROMP formation of cyclic molecules is the dominating process.

The theory of chain transfer with chain breaking is presented Chapter **4.11** by Duda. Zwitterionic ROP was studied already in the 1970s (initiation with strong bases – tertiary amines and phosphines), but this work has mostly been forgotten. Related classes of strong nucleophiles and carbenes have appeared and are discussed under the more appealing name 'no metal catalysts'. These are particularly important for cyclic esters due to the value of the final applications of the resulting polymers ranging from medicine to electronics. In addition, strong bases and acids, which perform equally well in some systems, also belong to this category of initiators/catalysts.

The second large group of chapters specifically describes the synthetic aspects of ROP/ROMP. In this section, the architecture of polymers prepared by ROMP, functionalization of poly(ethylene oxide), chain extension by ROP, nonlinear polyethers, as well as ROP in heterogeneous media are discussed. It also describes methods of polymerization that provide regular and mostly spherical particles, and gives for the first time a review of the kinetics and mechanism of this particular system that resembles emulsion vinyl polymerization. The chapter on polymerization in confined space (encompassing matrix polymerization) summarizes results that may open the way to the 'replica polymerization', a process that is typical for the matrix synthesis of biomacromolecules in nature.

Frontal polymerization and solid-state polymerization, which are found in separate chapters, are gaining practical importance. Solid-state polymerization is a useful tool to 'fight against thermodynamics'. Indeed, when polymerization is conducted at a relatively high temperature (e.g., polymerization of L-lactide), there is a high equilibrium monomer concentration. Changing from homogeneous to heterogeneous conditions may not change the equilibrium monomer concentration but changes the volume of the system in which polymer–monomer equilibrium takes place, reducing the amount of monomer left at equilibrium. Ring-chain equilibrium and copolymerization at equilibria are the subjects of separate chapters, giving the necessary theoretical background.

The next group of chapters is devoted to particularly important applications. In this section, a chapter on conducting polymers by ROMP describes advances in this popular area and several chapters are devoted to biomedical applications: biorelated polymers by ROMP, functional surfaces and supports prepared by ROMP, biological applications of polyphosphoesters by ROP, and the already mentioned chapter on functionalized poly(ethylene oxide) (PEO), devoted mostly to the preparation of PEO for further PEGylation, a process making bioactive macromolecules more stable toward biohydrolysis.

The final group of chapters describes either already existing general industrial methods of polymer synthesis (Chapter **4.32**) or polymerization methods specifically related to a given group (Chapters **4.30, 4.36, 4.37** and **4.39**). Under these general titles, there are several important specific ROP polymerizations, like ROP of cyclic ethers, where photochemical initiation converts thermally stable compounds into strong protonic acids initiating fast cationic polymerization. Nevertheless, radical photopolymerization is still the most important area of research, and the introduction of lasers now competes successfully with the ionizing radiation processes. High-pressure polymerization, mostly known as an industrial process of ethylene polymerization, is the subject of the last chapter of this volume. It provides up-to-date analysis of the radical high-pressure polymerization and stresses the importance of the high pressure in supercritical CO_2 (supercritical CO_2).

It could be assumed that the accumulated knowledge would also be used for monomers with structural features preventing them from polymerization under normal conditions (resulting in thermodynamic potentials that indicate 'nonpolymerizability'). Several cyclic compounds that might under high pressure successfully become monomers are considered.

Since the first edition of *CPS*, significant progress has been made in ROP and ROMP; the chapters of this section of the book were designed to emphasize these aspects and to put them in the context of prior work on ring-opening processes.

Biographical Sketches

Stanislaw Penczek is Professor of Polymer Chemistry at the Polish Academy of Sciences (Centre of Molecular and Macromolecular Studies in Lodz). He teaches at the Graduate School of the Jagiellonian University (Krakow) as an honorary professor. He has mostly contributed to the kinetics, thermodynamics, and mechanisms of the ring-opening polymerization, publishing over 300 papers in related areas. He was one of the first to observe living and controlled polymerizations in cationic and anionic ROP, including reversibility of deactivation of propagating species. Among other honors from Belgium, Japan, and Germany (the Warburg Prize), he is a member of the Polish Academy of Sciences and foreign member of the German (Nordrhein) Academy, Dr *h.c.* of the Pierre and Marie Curie University in Paris and Dr *h.c.* of the Russian Academy of Sciences. He was a member of the International Union of Pure and Applied Chemistry (IUPAC) Bureau, and former president of European Polymer Federation.

Professor Robert (Bob) Howard Grubbs' main interests in organometallic chemistry and synthetic chemistry are catalysts, notably Grubbs' catalyst for olefin metathesis and ring-opening metathesis polymerization with cyclic olefins such as norbornene. He also contributed to the development of so-called 'living polymerization'.

Grubbs has received many awards including Alfred P. Sloan Fellow (1974–76), Camille and Henry Dreyfus Teacher-Scholar Award (1975–78), Alexander von Humboldt Fellowship (1975), ACS Benjamin Franklin Medal in Chemistry (2000), ACS Herman F. Mark Polymer Chemistry Award (2000), ACS Herbert C. Brown Award for Creative Research in Synthetic Methods (2001), the Tolman Medal (2002), and the Nobel Prize in Chemistry (2005). He was elected to the National Academy of Sciences in 1989 and a fellowship in the American Academy of Arts and Sciences in 1994.

4.02 Thermodynamic and Kinetic Polymerizability

S Penczek, Polish Academy of Sciences, Lodz, Poland
K Kaluzynski, Center of Molecular and Macromolecular Studies, Lodz, Poland

4.02.1 Introduction

In the first edition of *Comprehensive Polymer Science*[1] the thermodynamics of cationic ring-opening polymerization (CROP) was discussed exclusively. The content of this earlier chapter is to some extent retained, although entirely rewritten, taking into account the IUPAC document 'Glossary of Terms Related to Kinetics, Thermodynamics, and Mechanisms of Polymerization' ('Glossary')[2] published in 2008 as well as some new literature data. In the 'Glossary' enthalpy and entropy of polymerization as well as ceiling and floor temperatures are defined.

Major references are given to monographs, textbooks, and review papers. Nevertheless, papers that mostly contributed to the thermodynamics of polymerization are duly quoted.

Thermodynamics of polymerization does not formally differ from that of any other chemical reaction if by 'polymerization' the propagation step is understood.

Then

$$\mathrm{M} \rightleftarrows 1/n\,\text{–}(\mathrm{m})_n\text{–}$$

where M is a monomer, –(m)– is the repeating unit, and n is the polymerization degree (P_n). Like in any other chemical reaction, the polymerization may occur if the Gibbs energy of polymerization (actually, propagation) is negative ($\Delta G < 0$).

4.02.2 Major Definitions

Thermodynamic functions of polymerization may depend on the polymerization degree (P_n) (length of the polymer chain). If P_n is large enough the influence of the chain ends and the translation entropy of the macromolecule as a whole could be neglected, and the thermodynamic functions practically do not depend on P_n.

According to the IUPAC definition, Gibbs energy (G) is defined as "Enthalpy minus the product of thermodynamic temperature and entropy": $G = H - TS$.[3] The corresponding definitions of enthalpy and entropy related to polymerization are given below and are copied from the 'Glossary'.[2]

4.02.2.1 (Molar) Enthalpy of Polymerization (ΔH_m or $\Delta_{ab}H_m$, SI Unit: J mol^{-1})

Change of enthalpy, in a 'chain polymerization' forming a homopolymer, is associated with the conversion of one mole of monomer into polymer under isobaric and isothermal conditions.

Note 1: Under defined standard conditions the enthalpy of polymerization is designated $\Delta H^\circ{}_m$.

Note 2: The subscripts a and b in $\Delta_{ab}H_m$ denote the state of the monomer and the state of polymer, respectively:
g: gaseous state (hypothetical in the case of polymer);

l: liquid state (must be specified in the case of a mesophase);
s: in solution (solvent and mesophases, if any, must be specified);
c: (condensed) amorphous, glassy states;
c′: crystalline or partly crystalline state;
for example, $\Delta_{lc}H_m$ means: from liquid state to amorphous or glassy state; and
$\Delta_{ss}H_m$ means: from monomer in solvent to polymer in solvent.

Note 3: The symbol ΔH_{ab}, in common usage in polymer chemistry, is discouraged as the IUPAC-recommended symbol is $\Delta_{ab}H_m$.

4.02.2.2 (Molar) Entropy of Polymerization (ΔS_m or $\Delta_{ab}S_m$, SI Unit: J mol^{-1} K^{-1})

Change of entropy, in a 'chain polymerization' forming a homopolymer, is associated with the conversion of 1 mol of monomer into polymer under isobaric and isothermal conditions.

Note 1: Under defined standard conditions, the entropy of polymerization is designated $\Delta S^\circ{}_m$; thus, if the standard state refers to standard concentration, and the monomer behaves ideally, $\Delta S_m = \Delta S^\circ{}_m + R\ln([M]_0/c^\circ)$, where $[M]_0$ denotes the starting monomer concentration and $c^\circ = 1\ \text{mol dm}^{-3}$ is the standard concentration.

Note 2: The a and b subscripts in $\Delta_{ab}S_m$ denote the state of the monomer and the state of polymer, respectively (see Section 4.02.2.1).

In the present chapter the subscript m is omitted and all the values are given for 1 mol. In place of dm^{-3} symbol l (allowed by IUPAC) is used.

To use the accepted IUPAC definitions and notations is necessary, since in many monographs and textbooks, particularly coming from various countries, similar phenomena are described by different terms. For instance, Gibbs energy (IUPAC-preferred term) is still called 'free energy' or 'free enthalpy'.[4] In the authoritative monograph *Kinetics of Polymerization Processes* published in Russia *G* is called 'thermodynamic potential',[5] although this term (not existing in the IUPAC Gold Book) describes all the major thermodynamic functions, namely Gibbs energy $G(T, P, n)$, enthalpy $H(S, P, n)$, internal energy $U(S, V, n)$, and Helmholtz energy $F(T, V, n)$. The letters in brackets have their usual meaning (n is the number of species). The relationship between these thermodynamic potentials is known to be given by Legendre transforms, defining the other thermodynamic potentials in terms of U minus variable as shown above for a given potential.[6] An understanding of the interrelation is important, since in some monographs and textbooks either ΔG or ΔF is used. As it is known, exclusively at constant P and V $\Delta G = \Delta F$.

Thermodynamic potentials should be known, as well as their change when polymerization occurs, in order to properly understand positions of equilibriums (thermodynamic polymerizability). These potentials, like potential energy in mechanics, give information about the most stable state of the system, related to polymerizability.

Moreover, when for a given system, for example, $\Delta_{ss}G > 0$, it does not mean that polymerization in bulk would not also be possible (or vice versa), since it may happen at the same P, V, and T, $\Delta_{lc}G < 0$.

Thermodynamic polymerizability of monomers may be described and compared in various ways. $\Delta_{ab}G$ at a given temperature is one of the possible approaches. However, the ceiling temperature of monomers in bulk (T_c(bulk)) appears as a useful candidate since this is the upper limit at which the polymer of a given monomer is thermodynamically stable.

4.02.3 Equilibrium and Ceiling (Floor) Temperatures (T_e and T_c/T_f)

The history of the term 'ceiling temperature' is described in the paper by Ivin[7] and this term was first used for copolymerization of olefins with SO_2, studied in Phillips Petroleum by Snow and Frey. Copolymerization proceeded only below a certain temperature, which the authors called 'ceiling temperature'.[8]

In several papers and textbooks there is no clear-cut distinction made between equilibrium temperatures (T_e) and this particular temperature – ceiling temperature (T_c) – above which high polymer may not exist.

The statements from some textbooks are for instance as follows: "The temperature at which propagation and depropagation rates are equal is called a ceiling temperature".[9] "The temperature at which this equilibrium occurs is called ceiling temperature".[10] In the Odian's textbook we find "Finally a temperature – the *ceiling temperature* T_c is reached at which propagation and depropagation notes are equal".[11] Actually $\Delta G = 0$ (or $\Delta F = 0$) is a necessary but not a sufficient condition to fulfill the IUPAC definition and the original meaning introduced by Dainton and Ivin.[12] At T_c no high polymer, according to IUPAC definition (cf. below), is formed, and Snow and Frey (*vide supra*) have indeed not observed any polymer formation. To make it clear, let us assume that monomer M is to be polymerized at a certain temperature T_1 in bulk at living polymerization conditions. Then, after addition of an initiator polymerization proceeds until equilibrium monomer concentration $[M]_e$ is reached. Thus the $\Delta_{ss}G = 0$ condition is fulfilled. At this $T_1 = T_e$, however, a certain amount of polymer (P) is produced. The total number of repeating units (P_n) is equal to $[M]_0 - [M]_e$. Polymerization of, for example, tetrahydrofuran (oxolane) in bulk ($[M]_0 = 12.5\ \text{mol l}^{-1}$) and at 298 K would stop eventually at this temperature. Equilibrium monomer concentration $[M]_e$ would be equal to $2.3\ \text{mol l}^{-1}$. When the temperature is increased further, finally at a certain temperature, called, according to the above definition, ceiling temperature, T_c, there will be no high polymer formed, and $[M]_e = [M]_c \approx [M]_0$ (here $\sim 12.5\ \text{mol l}^{-1}$). Thus, there is, when polymerization is conducted in bulk, an infinite number of 'pairs': equilibrium monomer concentration $[M]_e$ paired with the corresponding equilibrium temperatures T_e. For these conditions (bulk), there is, however, only one ceiling temperature T_c(bulk), which for THF ≅ 84 °C.

When polymerization is conducted in solution, in the ideal system, the polymerization started at $[M]_0$ would go to equilibrium at $[M]_e$, characteristic only for the temperature of polymerization: $[M]_e$ does not depend on $[M]_0$ although T_c does depend, as it follows from eqn [1]. If the temperature is

increased further, finally $[M]_e$ becomes equal to $[M]_0$, and only then there would be no high polymer formed. In the nonideal systems (Section 4.02.7) $[M]_e$ is a function of $[M]_0$ (cf. Figure 4). Thus, in these real systems there is an infinite number of pairs of $[M]_e$ and T_e for various $[M]_0$ and an infinite number of T_c for various $[M]_0$. The corresponding equation relating T_c and $[M]_0$ reads

$$\Delta G = 0 = \Delta H - T_c(\Delta S^\circ + R\ln[M]_0) \quad [1]$$

(Since the system is nonideal ΔS° may also depend on $[M]_0$.)

In eqn [1] and in some further equations the subscripts at ΔG, ΔH, and ΔS (existing in the IUPAC document) are omitted. Equations may be valid for any chosen conditions with a pertinent modification. Often the subscript 'p' is used in the literature (e.g., ΔH_p) indicating the polymerization process, particularly when a paper is published in journals of a more general scope. These are also omitted in this chapter. Finally, ΔH can be taken as equal to ΔH°, since practically it depends neither on temperature nor on monomer concentration, in contrast to ΔS.

If the standard conditions are used, when $[M]_0 = 1\ \mathrm{mol\,l^{-1}}$, then

$$\Delta G = 0 = \Delta H - T\Delta S^\circ;\ \text{therefore}\ \Delta H = T\Delta S^\circ\ (\text{in general}) \quad [2]$$

From this relationship, for polymerizations with negative ΔH the exothermicity of polymerization (propagation) is counterbalanced at equilibrium by a negative change of entropy. This simple thermodynamic condition could also be explained by kinetic approach. At any equilibrium (i.e., also at T_c) the forward reaction (propagation) may proceed all of the time, although it is counterbalanced by an equally fast depropagation.

In the present treatment it is assumed that high molar mass polymers are formed; therefore $\ldots(-m-)_n m^* \approx \ldots(-m-)_{n+1} m^*$ $= [P_i^*]$.

The rate constants can be expressed according to the theory of the transition state (rate constants are given at T_c):

$$k_p = A_p \exp(-E_p/RT_c) \quad [3]$$

$$k_d = A_d \exp(-E_d/RT_c) \quad [4]$$

At the ceiling temperature polymer (by definition) is not formed; therefore, at this particular equilibrium $[M]_e = [M]_c = [M]_0$.

The rate of propagation and the rate of depropagation are equal:

$$A_p \exp(-E_p/RT_c)[M]_0[P_i^*] = A_d \exp(-E_d/RT_c)[P_i^*] \quad [5]$$

It follows that

$$T_c = (E_p - E_d)/R\ln\{(A_p/A_d)[M]_0\} = \Delta H/(\Delta S^\circ + R\ln[M]_0) \quad [6]$$

remembering that $E_p - E_d = \Delta H$, $\Delta S^\circ = \Delta^{\neq}S_p^\circ - \Delta^{\neq}S_d^\circ = R\ln(A_p/A_d)$, and $\Delta^{\neq}S_p^\circ$ and $\Delta^{\neq}S_d^\circ$ are entropies of activation and A_p and A_d are probability factors of propagation and depropagation, respectively, and concentrations of species can be omitted.

There is also another strictly thermodynamic way to express T_c as the function of ΔH and ΔS.

As it is known from monographs on thermodynamics,[13,14] it could be shown by methods of chemical thermodynamics or statistical mechanics (both out of scope of this chapter) that Gibbs energy change and equilibrium constant are related in the following way:

$$\Delta G = \Delta G^\circ + RT\ln K;\ \text{at equilibrium}\ \Delta G = 0 \quad [7]$$

$$\Delta G^\circ = -RT\ln K;\ \text{since}\ K = k_p/k_d = 1/[M]_e (\text{for long chains}) \quad [8]$$

$$\Delta G^\circ = RT\ln[M]_e;\ \text{thus, at}\ T_c:\ \Delta G^\circ = RT_c\ln[M]_0 \quad [9]$$

Thus

$$\Delta G^\circ = \Delta H - T_c\Delta S^\circ = RT_c\ln[M]_0 \quad [10]$$

After rearranging

$$T_c = \Delta H/(\Delta S^\circ + R\ln[M]_0)\ (\text{cf. eqns [1] and [6]}) \quad [11]$$

At particular conditions, when $[M]_0 = 1\ \mathrm{mol\,l^{-1}}$

$$T_c = \Delta H/\Delta S^\circ \quad [12]$$

(Superscript over ΔH may be omitted for reasons presented above.)

The higher the ceiling temperature of a given monomer, the higher its thermodynamic polymerizability. T_c could be calculated from ΔH and ΔS° and the extensive scale of T_c for various monomers could thus be tabulated.

Since

$$\ln[M]_e = \Delta H/RT_e - \Delta S^\circ/R \quad [13]$$

the experimentally accessible plot of $\ln[M]_e$ versus $1/T_e$ gives from the intercept and slope ΔS° and ΔH, respectively.

In Figure 1 this plot is shown for polymerization of L-lactide (L-LA).[15] The calculated values are $\Delta H = -22.9\ \mathrm{kJ\,mol^{-1}}$ and $\Delta S^\circ = -25\ \mathrm{J\,mol^{-1}\,K^{-1}}$. In this particular instance, as in many others, T_c is higher than the temperature at which the polymer would start to degrade.

In the extensive paper by Duda and Kowalski, published in 2009, a large number of ΔH, ΔS°, and $[M]_e$ at 298 K are tabulated.[16]

4.02.3.1 The IUPAC Definitions for Ceiling and Floor Temperatures

The IUPAC definitions taken in extenso from the IUPAC 'Glossary'[2] are given below.

4.02.3.1.1 Ceiling temperature (T_c, SI Unit: K)

Temperature above which, in a given 'chain polymerization', polymer of high molar mass is not formed.

Note 1: A ceiling temperature is only observed for enthalpy-driven *chain polymerizations* in which $\Delta H_m < 0$ and $\Delta S_m < 0$, where ΔH_m and ΔS_m are, respectively, the enthalpy and entropy change per mole of monomer reacted.

Note 2: For most *chain polymerizations*, $\Delta H_m < 0$ and $\Delta S_m < 0$.

Note 3: Below T_c, ΔG_m $(= \Delta H_m - T\Delta S_m) < 0$; at T_c, $\Delta G_m = 0$; and above T_c, $\Delta G_m > 0$.

Note 4: Because $\Delta G_m = 0$ at the ceiling temperature, $T_c = \Delta H_m^\circ/\Delta S_m^\circ$. If ΔH_m° and ΔS_m° are the enthalpy and entropy

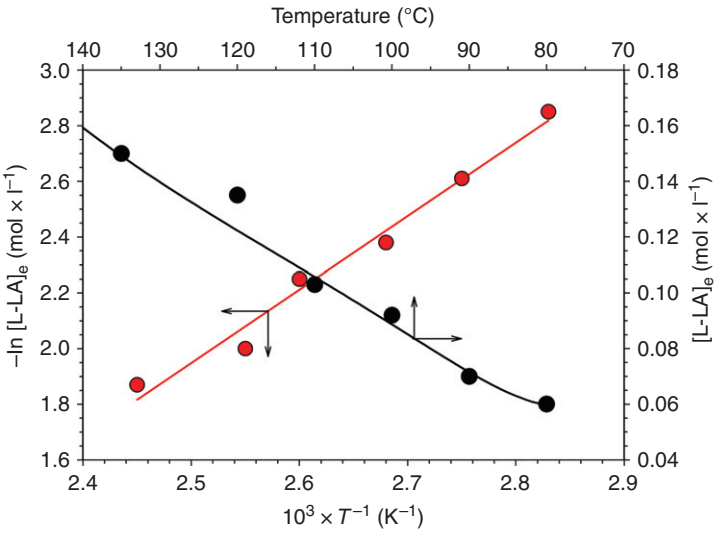

Figure 1 Dependence of the equilibrium concentration of L-lactide on the reciprocal of the absolute temperature.

changes in the standard state, and the monomer behaves ideally, then $T_c = \Delta H_m^\circ / \{\Delta S_m^\circ + R \ln([M]_0/c^\circ)\}$, where $c^\circ = 1$ mol dm^{-3} is the standard concentration and $[M]_0$ is the initial monomer concentration. Thus, T_c depends on the initial monomer concentration.

Note 5: The symbol $T_c(c^\circ)$ is used to denote the ceiling temperature when the initial monomer concentration, $[M]_0$, is equal to c°.

Note 6: The symbol T_c(bulk) is used to denote the ceiling temperature when the initial monomer concentration is equal to its undiluted concentration.

4.02.3.1.2 Floor temperature (T_f, SI Unit: K)

Temperature below which, in a given 'chain polymerization', polymer of high molar mass is not formed.

Note 1: A floor temperature is only observed for entropy-driven 'chain polymerizations' in which $\Delta H_m > 0$ and $\Delta S_m > 0$, where ΔH_m and ΔS_m are, respectively, the enthalpy and entropy change per mole of monomer reacted.

Note 2: Examples of 'chain polymerizations' for which $\Delta H_m > 0$ and $\Delta S_m > 0$ are polymerizations of larger cyclic monomers, for example, elemental sulfur (S_8) and octamethylcyclotetrasiloxane (2,2,4,4,6,6,8,8-octamethyl-1,3,5,7,2,4,6,8-tetraoxatetrasiloxane), proceeding via ring-opening mechanisms.

Note 3: Above T_f, ΔG_m ($= \Delta H_m - T\Delta S_m$) < 0; at T_f, $\Delta G_m = 0$; and below T_f, $\Delta G_m > 0$.

Note 4: Because $\Delta G_m = 0$ at the floor temperature, $T_f = \Delta H_m / \Delta S_m$. If ΔH_m° and ΔS_m° are the enthalpy and entropy changes in the standard state, and the monomer behaves ideally, then $T_f = \Delta H_m^\circ / \{\Delta S_m^\circ + R \ln([M]_0/c^\circ)\}$ where $c^\circ = 1$ mol dm^{-3} is the standard concentration. Thus, T_f depends on the initial monomer concentration.

Note 5: The symbol $T_f(c^\circ)$ is used to denote the floor temperature when the initial monomer concentration, $[M]_0$, is equal to c°.

Note 6: The symbol T_f(bulk) is used to denote the floor temperature when the initial monomer concentration is equal to its undiluted concentration. In this chapter subscript 'm' is omitted.

4.02.4 Methods for Determination of T_c (or $[M]_e$)

For living polymerizations a simple method could be to measure the monomer concentration as a function of temperature (e.g., NMR, GC, SEC) and determine the temperature at which $[M]_e = [M]_0$, that is, there is no polymer in the system. This method may be impractical for several cyclic monomers with highly exothermic polymerization, since their T_c, particularly in bulk, may be too high and decomposition would come first.

Ceiling temperatures T_c and floor temperatures T_f of polymerizations in bulk are usually reported for $\Delta_{lc}G$ or $\Delta_{lc'}G$ for polymerizations of liquid monomers (subscript l) to amorphous (subscript c) or crystalline (subscript c') polymers. Polymerization in solution is usually referred to as the polymerization of a 1 mol l^{-1} monomer solution (subscript s) to a dissolved polymer (subscript s), that is, $\Delta_{ss}G^\circ = 0$. Ceiling temperatures in bulk (T_c(bulk)) are always higher than ceiling temperatures in solution.

Another method would be based on the determination of ΔH and ΔS° first from studies of dependence of $[M]_e$ on $1/T$, as shown in Figure 1.

How large are differences between T_c(bulk) and T_c(25 °C) is shown for a few examples in Table 1.

4.02.5 Factors Affecting Polymerizability: Enthalpy of Polymerization

Any factor that lowers the enthalpy or raises the entropy of a particular species in a system will shift the equilibrium to favor that species.

Table 1 Comparison of ceiling temperatures (T_c): determined for bulk – lc or (lc′) and ss conditions (the former for bulk, the latter for $[M]_c = ([M]_0) = 1\ mol\ l^{-1}$)[17]

	T_c (°C)	
Monomer	*lc*	*ss (solvent)*
 Tetrahydrofuran	80	23 (C_6H_6)
 1,3-Dioxolane	91	1 (CH_2Cl_2)
 1,3-Dioxepane	149 (gc′)	78 (C_6H_6)
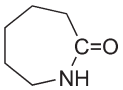 ε-Caprolactam	223	

Table 2 Dependence of ΔH on the ring size for cyclic ethers[19]

Monomer	*Ring size*	*$-\Delta H$ (kJ mol^{-1})*
Ethylene oxide (oxirane)	3	94.5
Trimethylene oxide (oxetane)	4	81
Tetrahydrofuran (oxolane)	5	15
Tetrahydropyran (oxane)	6	~0
1,4-Dioxane	6	~0
Hexamethylene oxide (oxepane)	7	35.5[20]

Table 3 Dependence of ΔH on the ring size for lactams[21]

Monomer	*Ring size*	*$-\Delta H$ (kJ mol^{-1})*
Butano-4-lactam	5	4.6
Pentano-5-lactam	6	7.1
Hexano-6-lactam (ε-caprolactam)	7	13.8
Heptano-7-lactam	8	22.6
Octano-8-lactam	9	35.1
Nonano-9-lactam	10	23.4
Decano-10-lactam	11	11.7
Undecano-11-lactam	12	–2.1
Dodecano-12-lactam	13	2.9

4.02.5.1 Ring Strain

In polymerization at normal pressure, the $P\Delta V$ term in $\Delta H = \Delta E - P\Delta V$ is negligible and the enthalpy change is almost equal to the change in the internal energy of the monomer. Thus, the heat of polymerization may be used as a measure of the strain energy in the cyclic compound, which reflects well the thermodynamic polymerizability of the monomer. The major sources of ring strain are (1) bond-angle distortion (angular strain); (2) bond stretching or compression; (3) repulsion between eclipsed hydrogen atoms (conformational strain, bond torsion, bond opposition); and (4) nonbonded interaction between atoms or substituents attached to different parts of the ring (transannular strain, compression of the van der Waals radii).

In some groups of monomers, there are additional sources of strain, such as inhibition or reduction of amide-group resonance in lactams.[18] The contribution of each type of strain depends on the chemical structure of the cyclic monomer, ring size, and its substitution.

Distortion in bond angles is the major source of the ring strain in three- and four-membered cyclic monomers. In five-membered cyclic compounds, the strain is mostly due to bond opposition forces, arising from eclipsed conformations. Tetrahydrofuran is an example. In medium-sized rings, strain arises primarily from nonbonded interactions and bond oppositions. Any kind of strain, including transannular interactions, can be removed completely in very large rings by arranging the ring atoms into two almost parallel chains.[19]

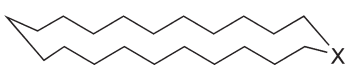

ΔH as a function of the ring size in cyclic ethers and for lactams are given in Table 2 and Table 3, respectively.

The normal angles between the four valences of a tetrahedral carbon atom are assumed to be 109°28′, that is, the valences are equally spaced about the atom: then, in three- and four-membered rings, severe valence angles must be involved. Thus, if rings are considered to be planar (which is, however, not true for majority of heterocyclic monomers), the distortion [0.5 × (normal valence angle minus actual angle between bonds)] from normal valence angle would be the number of atoms in the ring, and distortion, given in this order, is 3, 24°44′; 4, 9°44′; 5, 0°44′; and 6, -5°16′. Thus, the angle strain is quite severe in the three- and four-membered rings. It is much lower for the five- and six-membered rings (minimum of strain). Cyclic esters are exceptions from this rule, due to the presence of the >C=O group. Comparison of conformations of the five- and six-membered lactones and five-membered THF is given in Figure 2. There is a repulsion between the H atoms in the six-membered lactones, which is practically not present in the five-membered rings. Therefore, the six-membered ester is known to polymerize, whereas the five-membered is not. In the same figure a model of tetrahydrofuran, a polymerizable five-membered cyclic ether, is shown and opposition of H atoms is seen.

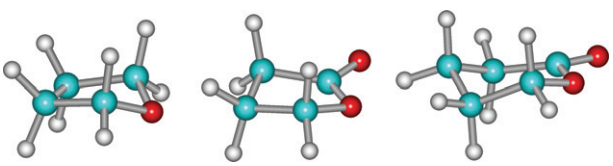

Figure 2 Comparison of conformations of five-membered cyclic ether (tetrahydrofuran) and the five- and six-membered lactones.

4.02.5.2 Side Groups' Interaction

Bulky side groups attached to the polymer chain can destabilize a polymer relative to monomer or cyclic oligomers. The presence of small substituents may have no influence on the repulsion in monomer and polymer, which can be negligible. On the other hand, the presence of large substituents may practically make polymerization impossible. For vinyl monomers the best known example is 1,1-diphenylethene:

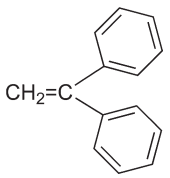

In polymerization of cyclic siloxanes (cf. Chapter 4.17 in this comprehensive), even in poly(dimethylsiloxane), there is 87% of linear polymer at equilibrium and the rest consists of cyclics:

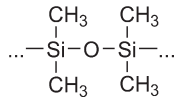

When larger substituents are present, then monomer and cyclic oligomers are further favored and thermodynamic polymerizability is lowered.[22]

Allcock[23] gives corresponding examples for cyclophosphazenes:

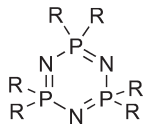

For R = Cl the polymer is stable up to 350 °C whereas when R = OCH_2CF_3 or OC_6H_5 substantial depropagation takes place at much lower temperatures.

In the monograph on ring-opening polymerization (ROP) by Ivin and Saegusa[24] over 170 various cyclic compounds, five-, six-, and seven-membered (plus bridged ones), are tabulated and their ability to polymerize is described in the chapter on polymerization thermodynamics. In another comprehensive treatment ΔH, $\Delta S°$, and $[M]_e$ data for 25 more common monomers (mostly at 298 K) are compiled.[16]

On the other hand, in Allcock's textbook several T_c(bulk) are given and unsaturated monomers are compared, showing that, for example, for tetrafluoroethene T_c(bulk) equals 1100 °C whereas for acetaldehyde it is as low as −40 °C. For cyclic monomers these differences may also be quite high. It is understandable that for a strained ethylene oxide it would have been ~1000 °C whereas for THF it is equal, as mentioned above, to ~84 °C (T_c(bulk)).

4.02.5.3 Independent Determination of ΔH and ΔS

As it follows from the 'Glossary' document,[2] it is necessary for the purpose of tabulation and comparison of, for example, $[M]_e$ to choose standard states such as 25 °C, 1 mol l^{-1} of monomer in the inert solvent, converted to 1 mol l^{-1} of repeating units, that is, to $1/n$ mole of polymer with an average degree of polymerization n in the same solvent.

Standard enthalpies of polymerization $\Delta H°$ (ΔH) are most generally obtained by direct comparison of the results of calorimetric measurements of the amount of monomer converted to polymer with the determined amount of heat evolved. The heat of combustion of monomer and polymer give standard enthalpies of formation for the monomer ($\Delta H_f°(M)$) and polymer unit ($1/n\ \Delta H_f°(P_n)$) respectively. The difference (Eqn 14) is equal to the standard enthalpy of polymerization.

$$\Delta H^\circ = 1/n\Delta H_f^\circ(P_n) - \Delta H_f^\circ(M) \quad [14]$$

Standard entropies of polymerization $\Delta S°$ are generally calculated from the absolute entropies of the monomer and polymer:

$$\Delta S_f^\circ = 1/nS^\circ(P_n) - S^\circ(M) \quad [15]$$

The absolute entropies are determined in turn from calorimetric measurements of the heat capacities of the monomer and polymer over a wide temperature range using the expression

$$S^o(T) = \int_0^T \left(\frac{C_p}{T}\right) dT \quad [16]$$

where C_p is the molar heat capacity at constant pressure and T is the absolute temperature.

Quite often ΔH and ΔS are determined at the temperature of the process and then ΔG has to be known at standard conditions, that is, at $T = 298$ K. Thus, the dependence of ΔH and ΔS on temperature should be known:

$$\Delta H_T = \Delta H_{298} + \int_{298}^T \Delta C_p dT \quad [17]$$

and

$$\Delta S_T = \Delta S_{298} + \int_{298}^T (\Delta C_p/T) dT \quad [18]$$

where ΔC_p is the change of heat capacity.

Although it is generally accepted that ΔH and ΔS do not substantially depend on temperature, Berlin *et al.* calculated this dependence for polymerization of gaseous formaldehyde to crystalline polymer.[5] Such a calculation could seldom be found in the polymer monographs and textbooks.

The experimentally determined $\Delta_{gc}H = 70.4$ kJ mol^{-1}. The temperature range for calculations was chosen from 26 to 72 °C. Values of C_p of monomer and polymer in the given states are known, being equal to 43.2 and 34.8 J mol^{-1}, respectively.

Thus, $\Delta C_p = 8.4$ J mol^{-1} K^{-1} and

$$\int_{298}^T \Delta C_p dT \approx \Delta C_p \Delta T \approx 0.2 \text{ kJ mol}^{-1} \quad [19]$$

The average temperature of experiment is equal to 48 °C, that is, correction for $\Delta T = 23$ °C has to be introduced. The measured value is equal to 70.4 kJ mol^{-1} and the correction for the temperature change would only be 0.2 kJ mol^{-1}. Similar comparison of measured and calculated values of ΔS_T (the measured ΔS_T for the same temperature interval) equals −178.9 J mol^{-1} K^{-1} and correction for every 10 K is equal to ~0.24 J mol^{-1} K^{-1}. Therefore, if T_c is calculated or determined

for a certain monomer at a temperature that differs from 298 K it can be compared with T_c of other monomers, taking as an average corrections as calculated above. However, when $|\Delta H|$ and $|\Delta S|$ have low absolute values this correction may have a much larger influence.

When $\Delta_{gg}H$ is known by calculations (gaseous monomer gives hypothetical gaseous polymer), then, to find, for example, $\Delta_{sc}H$, that is, formation of the crystalline polymer from monomer in solution, it is necessary to calculate heat of monomer dissolution (interaction with solvent), dissolution of polymer, and polymer crystallization.

4.02.6 Entropy-Driven Polymerization

Polymerization driven by entropy may only proceed if $|\Delta H| \leq |T\Delta S|$, that is, $|\Delta H| \leq |T(\Delta S^\circ + R \ln[M])|$ (since $\Delta H > 0$). Thus, $\Delta G < 0$.

The best known example is polymerization of sulfur (cyclooctasulfur). Cyclooctasulfur monomer is an eight-membered, crown compound with restricted rotational and vibrational freedom. The eight-membered ring is not strained; however, polymerization is possible, since at high enough temperature (above the floor temperature T_f) the entropic factor ($T(\Delta S^\circ + R \ln[M])$) outweighs the positive or near to zero ΔH value. Entropy of polymerization is positive as polymer units have more freedom (rotational, vibrational) than in S_8 ring, in spite of losing the translational entropy. The sulfur polymerization and its copolymerization with selenium had been used by Tobolsky and Eisenberg[25,26] for detailed analysis of thermodynamics of homopolymerization and of equilibrium copolymerization. These works, together with works of Dainton and Ivin,[12] are the milestones of polymerization thermodynamics.

Later, a general solution of equilibrium copolymerization in living conditions was developed by Szwarc[27] and Szymanski (cf. Chapter 4.04 in this comprehensive).

In the polymerization of the six-membered cyclic esters of phosphoric acid (dioxaphosphorinanes)

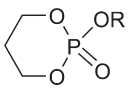

it was observed that polymerization is entropy driven (in contrast to the five-membered cyclic triester, cf. Figure 3). These monomers are puckered and vibration as well as rotation is easier in linear chains. These apparently contribute sufficiently to a positive change of entropy of polymerization. The larger the exocyclic group the higher the contribution to a positive change of entropy as it follows from the dependence of ΔH on ΔS° shown in Figure 3.[28,29]

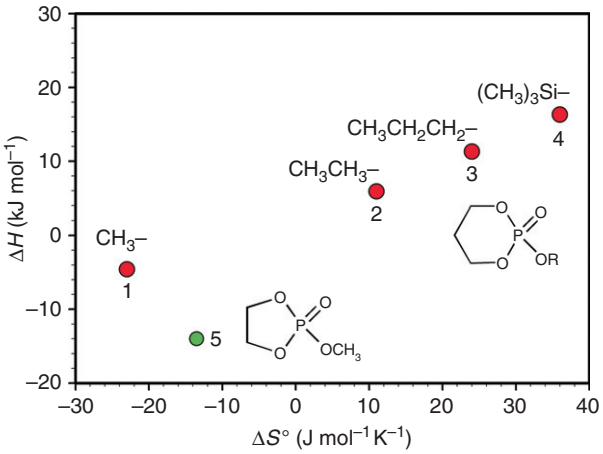

Figure 3 Isoequilibrium dependence for 2-alkoxy-2-oxo-1,3,2-dioxaphosphorinan-2-ones (six-membered) substituted in position 2. Exocyclic substituents are indicated in the figure. Point 5: 2-methoxy-2-oxo-1,3,2-dioxaphospholan-2-one (five-membered) for comparison.[28]

4.02.6.1 Polymerization of Cyclic Oligocarbonates

An interesting case of the entropy-driven reaction is the polymerization of cyclic oligocarbonates.[30] The monomer consisting of a mixture of cyclic oligocarbonates is made by the pseudo-high dilution method (Scheme 1). Bisphenol A bis (chloroformate) was added slowly to a mixture of $(C_2H_5)_3N$, aqueous NaOH, and CH_2Cl_2. The selectivity for cyclics versus linear oligomers was 10 000:1.0.

On polymerization by ring opening at 180 °C a linear polymer is formed containing less than 1% of cyclic oligomers at equilibrium. The actual entropy change depends on the value of n and on the dilution, but at the used conditions $T\Delta S$ is much greater than $-\Delta H$, which is close to zero.

4.02.6.2 Ring-Opening Metathesis Polymerization

Besides the heterocyclic monomers, mostly discussed in this chapter, this volume is also devoted to the ring-opening metathesis polymerization (ROMP). This polymerization is initiated and propagated by metal carbene complexes and metallacyclobutane complexes as shown in Scheme 2.

This reaction is reversible and back reactions can lead to cyclic oligomers as well as the starting monomer. The

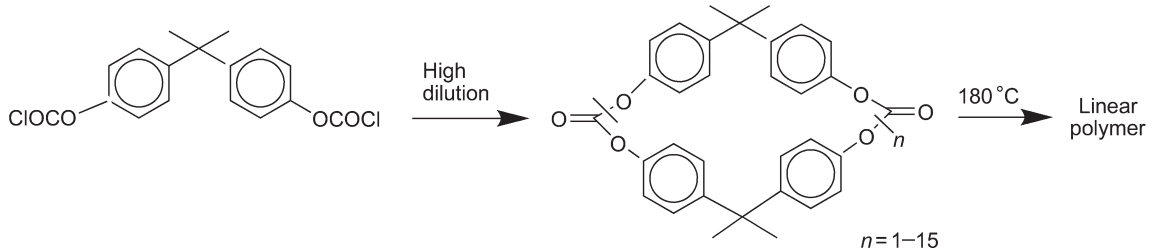

Scheme 1 Formation of cyclic oligocarbonates by the pseudo-high dilution method.

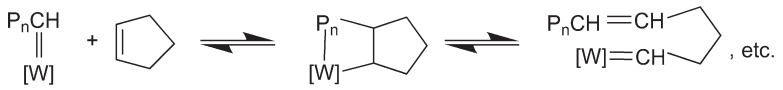

(P_n is a polymer chain, W stands for wolfram)

Scheme 2 Ring-opening metathesis polymerization of cyclopentene.

Table 4 Polymerizability of substituted cyclopentenes[31,32]

High conversion:	
Some conversion:	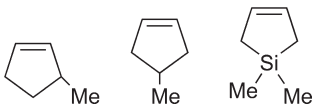
No conversion:	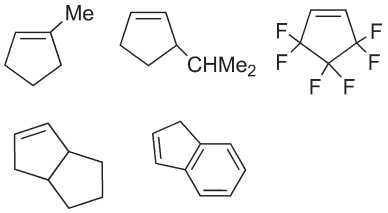

polymerizability of some substituted five-membered cycloalkenes is illustrated in Table 4 taken *in extenso* from Reference 7.

For norbornene and its derivatives, as indicated by Ivin,[7] the opening of the bicyclic structures results in a considerable release of ring strain when double bond is cleaved during polymerization and monomers polymerize to high conversion. The metathesis reaction of the double bonds in the initial monomers is much less thermodynamically favorable but finally could lead to cross-linked polymers (Scheme 3).[7]

4.02.7 Nonideal (Real) Systems

When the conversion of a monomer into a polymer unit is measured in bulk or at high $[M]_0$, the monomer–polymer interaction cannot be neglected. The same is true when the measurements are made in a solvent interacting differently with the monomer and polymer. Under these conditions, the corresponding interactions have to be taken into account. If the molar mass of the polymer is high enough, the following semiempirical equation can be used to determine ΔG:

$$\Delta G = RT[\ln\Phi_1 + 1 + \chi(\Phi_1 - \Phi_2)] \qquad [20]$$

where Φ_1 and Φ_2 are the volume fractions of the monomer and polymer, respectively, and χ is the polymer–monomer interaction parameter according to the Flory–Fox theory. At these conditions either $\Delta_{lc}G$ or $\Delta_{ss}G$ is determined.[33]

The relationship between these two functions is as follows: $\Delta_{lc}G = \Delta_{ss}G + \Delta_1G - \Delta_2G$, where Δ_1G and Δ_2G are the related Gibbs energies of dissolution of the monomer and polymer in the given solution. In an inert solvent $\Delta_1G \approx \Delta_2G$ and then $\Delta_{lc}G \approx \Delta_{ss}G$, indicated above simply as ΔG.

4.02.7.1 Influence of Initial Monomer Concentration

It was observed in the polymerization of THF in benzene solvent that the equilibrium monomer concentration $[THF]_e$ depends linearly on $[THF]_0$. A method was elaborated to determine $\Delta_{lc}H$ and $\Delta_{lc}S°$ from the experimental data for such nonideal thermodynamics.

It has also been observed that the extent of dependence of $[THF]_e$ on $[THF]_0$ is a function of the acidity of the solvent used.[34] This is shown in Figure 4 (Reference 1), where $[THF]_e$ is plotted as a function of $[THF]_0$ for CCl_4, C_6H_6, CH_2Cl_2, and CH_3NO_2 solvents. Some of these solvents interact with THF, making its polymerization more difficult. This is because THF is a stronger base than its open-chain counterpart and, thus, interaction with polymer units is relatively weaker. These dependences can be envisaged: THF behaves as if its actual instantaneous concentration available for polymerization were lowered by a fraction of complexed monomer, provided that the complexed monomer propagates less rapidly and requires preliminary desolvation. Indeed, the heat of mixing of THF with CCl_4 is only $-2.9\ kJ\ mol^{-1}$, whereas the heat of mixing of THF with CH_2Cl_2 is $-5.0\ kJ\ mol^{-1}$.

1,3-Dioxolane (DXL) is much less basic than THF and, besides, in contrast to THF, DXL is slightly less basic than its polymer, although the difference is not as great as in the THF/polyTHF system. It follows that the dependence of its equilibrium

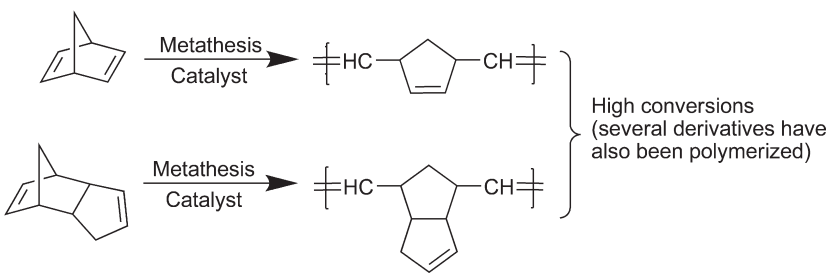

Scheme 3 Ring-opening metathesis polymerization of the bicyclic monomers (norbornene and its derivatives).

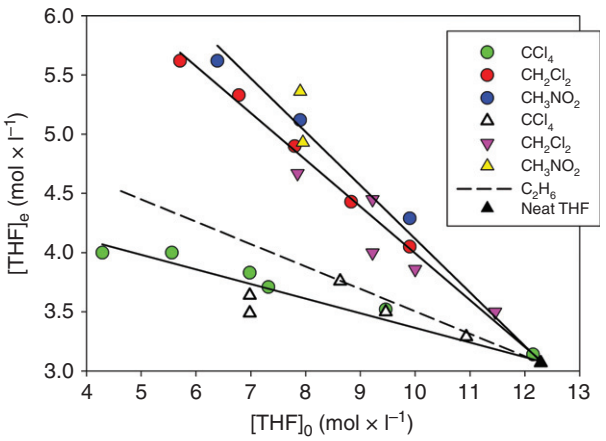

Figure 4 Dependence of the equilibrium monomer concentration $[THF]_e$ on initial monomer concentration $[THF]_0$ at 25 °C; ●, NMR; ▲, gravimetrically. Solvent: CCl_4, C_6H_6, CH_2Cl_2, CH_3NO_2 (References 1 and 34).

concentration $[DXL]_e$ on $[DXL]_0$ and solvent acidity is much smaller than in the polymerization of THF.[35] In the monograph published in 2008 this system is analyzed in great details on the basis of the series of papers published earlier mostly by Berlin *et al.* (cited in the monograph).[36] This is the most comprehensive coverage of the monomer–solvent–polymer system in the ROP (like α-methylstyrene analyzed by Szwarc in the anionic vinyl polymerization).[37] According to these studies the equilibrium monomer concentration $[M]_e$ is practically a linear function of $[M]_0$ (i.e., like for THF as above), although this dependence, at least for CH_2Cl_2 solvent, is indeed much less pronounced than for THF. The dependence of $\ln[M]_e$ on $1/T$ in this series of works agrees well with the earlier data of Plesch[35] and leads to $\Delta_{lc}H = -23.0$ kJ mol^{-1} and $\Delta_{lc}S^\circ = -62.9$ J K mol^{-1}.

Knowledge of the dependence of $[M]_e$ on $[M]_0$ is of primary importance in the studies of kinetics of polymerization. The use of a wrong value of $[M]_e$ may lead to erroneous values of k_p, especially when polymerization is studied starting from $[M]_0$ close to $[M]_e$. Therefore, the studies of equilibrium polymerization, when $[M]_e$ is relatively high, require determination of $[M]_e$ for every run.

4.02.8 Influence of Degree of Polymerization

The equilibrium monomer concentration $[M]_e$ depends on P_n for shorter chains because, in the neighborhood of the end groups, the thermodynamic potentials of the polymer units are different from those in the middle of the chain.

These relationships, described by Tobolsky and Eisenberg,[25] have been confirmed experimentally for THF polymerization by Fukuda and Hirota.[38]

For low polymerization degrees,

$$P_n = \frac{\sum_{n=1}^{\infty} n[P_n^*]_e}{\sum_{n=1}^{\infty}[P_n^*]_e} = \frac{\sum_{n=1}^{\infty} nK_1K_p^{n-1}[I]_e([M]_e)^n}{\sum_{n=1}^{\infty} K_1K_p^{n-1}[I]_e([M]_e)^n} = \frac{1}{1 - K_p[M]_e} \quad [21]$$

(when $K_1 = K_p$, where K_p is an equilibrium constant at any polymerization degree). Fukuda studied the polymerization of THF at high dilution. At these conditions it was observed that $[M]_e$ 'increased' with increasing $[M]_0$ which was contrary to the dependence shown above in Figure 4, when the interaction of the monomer and polymer with solvent has to be taken into account.

This observation is described for the sake of completeness of information, although it is of minor importance, since for $P_n = 10$, K_p differs from $1/[M]_e$ only by 10% and usually $[M]_e$ is determined for much higher P_n. This is true, however, only when the equilibrium constant K is the same for all the propagation/depropagation steps, including the first one, namely, the reaction of initiator with the monomer.

When the equilibrium constants are not the same, they can be determined by Szwarc's treatment, based on the reduction of the number of steps.[39] Heitz *et al.*[40] have studied the cationic oligomerization of THF and established that only the first equilibrium constant K_0 differs from K_n, that is, the equilibrium constant for every next step. Thus, $K_0 = 1.7$ l mol^{-1} and $K_n = 0.25$ l mol^{-1}. This study has been made possible by using high-resolution HPLC, allowing measurements of the concentrations of all of the chains involved. It is also based on the assumption that the distribution of the growing chains is the same as that of the dead macromolecules.

4.02.9 Influence of Phase Separation

When a liquid monomer in solution is converted into an insoluble polymer, the following possibilities arise: (1) solid amorphous polymer precipitates out of the saturated solution; (2) solid crystalline polymer precipitates from the saturated solution; and (3) polymerization proceeds in the crystalline state and the monomer is supplied from solution.

Only polymerization proceeding in the crystalline state differs thermodynamically from the polymerization of the same monomer in homogeneous solution. In the first two instances, the growing species may still remain in solution and $[M]_e$ would be the same for both homogeneous and apparently heterogeneous systems. However, this does not mean that the polymer yield would be the same. Although $[M]_e$ remains the same, in the precipitating system the total volume of the liquid polymer–monomer mixture becomes smaller, so the amount of monomer at equilibrium is smaller anyway when the polymer precipitates.

The change in the Gibbs energy of the polymerization proceeding in the crystalline state differs from that taking place in the homogeneous solution by the heat of crystallization. Therefore, we have

$$[M]_{e,s}/[M]_{e,ss} = \exp\Delta G_{cryst}/RT \quad [22]$$

It follows from this equation that the $[M]_e$ observed in the homogeneous polymerization may be greatly reduced by performing polymerization under conditions when the propagation step proceeds at the crystalline sites of a solid polymer.

Cationic polymerization of 1,3,5-trioxane (TXN) takes place in the crystalline state. The hypothetical equilibrium monomer concentration calculated for the homogeneous polymerization is $[TXN]_e = 2.5$ mol l^{-1} (CH_2Cl_2, 20 °C),[41] whereas $[TXN]_e$ for the polymerization from the dissolved monomer directly to the crystalline polymer is 0.11 mol l^{-1} (at 25 °C). Thus, if one starts from a 30% solution of TXN (~3.3 mol l^{-1}), then, in the homogeneous solution, 72% of the monomer would be

left at equilibrium, whereas the real polymerization, proceeding in the crystalline state, leaves only ~3% of the unreacted monomer.

The only ROP process in industry, using conversion of a liquid monomer into an insoluble, crystalline polymer, is cationic polymerization of TXN. Although in this process no solvent is used, there was also elaborated polymerization of TXN in cyclohexane solvent with the formation of insoluble, crystalline polymer. Therefore, it was of interest to compare the dependence of $[M]_e$ on the solvent properties. Some data[5] (formula of solvent and $[TXN]_e$ in $mol\,l^{-1}$) follow in this order (for 20–30 °C): $C_6H_5NO_2$: 0.14; CH_2Cl_2 : 0.11; C_7H_{16} : 0.03. From the thermodynamic viewpoint the higher the difference between the polarity (dielectric permittivity was taken as a measure) of solvent and monomer the higher then the chemical potential of the system.

Summarizing the thermodynamic polymerizability, some data of ΔH ($kJ\,mol^{-1}$) and $\Delta S°$ ($J\,K^{-1}\,mol^{-1}$) for cyclic monomers are given below, according to Ref. 42 and from the more recent compilation by Duda and Kowalski, giving ΔH and $\Delta S°$ as well as $[M]_e$ at 25 °C.[16]

Ceiling temperatures (T_c) can be calculated from the corresponding values of ΔH and $\Delta S°$ from Table 5.

4.02.10 Final Remarks on the Thermodynamic Polymerizability

It might look like a paradox that in this part of the chapter the thermodynamic polymerizability has mostly been determined by the critical temperature of the given monomer (the best is T_c (bulk)) or the change of enthalpy and entropy as measured in polymerization. This could indicate that the information on the range of polymerizability requires preformation of the polymerization itself. It is true in the sense that in this way the structure and polymerizability of monomers could be correlated, which then allow the prediction of the polymerizability of a novel monomer taken for polymerization. However, in such an instance the thermochemical measurements (calorimetry) may also be of help and a certain model of the not yet existing polymer could be taken as a standard. Then, if the thermodynamic polymerizability is established, the proper mechanism (initiator/catalysts) has to be chosen.

4.02.11 Kinetic Polymerizability

Thermodynamic polymerizability is of major importance. If a monomer to be studied had (for $\Delta H < 0$) a very low T_c(bulk), as determined thermochemically or calculated, then its polymerization is hopeless. If it looks thermodynamically polymerizable then it could be expected that the mechanism would be found for successful polymerization. The accumulated experience allows to reasonably choose the corresponding conditions of polymerization.

A large majority of cyclic monomers polymerize by one of the ionic or coordination (so-called pseudoionic) mechanisms. Moreover, kinetic polymerizability and the difference in the rates of polymerization depend on the used conditions and may vary dramatically. In CROP there is no difference between the reactivities of ions and ion pairs, but in anionic polymerization (e.g., of ethylene oxide) ions are much more reactive than ion pairs. In a solvent (e.g., in 1,4-dioxane, poorly solvating ions) there may occur no polymerization, whereas in, for example, hexamethylphosphorotriamide (HMPTA) (highly solvating, helping dissociation) there could occur a fast polymerization. Cyclic esters, for example, ε-caprolactone (CL) or lactides, polymerize by cationic, anionic, and coordination polymerizations. For the same conditions (monomer concentration, active species concentration, and solvent) the difference between the rates of propagation can be 1000-fold.

In the propagation step some active species could reversibly be converted into the inactive species, like, for instance, in the polymerization of lactides initiated by aluminum alkoxides, when unimers propagate and their aggregates do not. For all these reasons there is no simple way to compare kinetic reactivities of various monomers and construct the table comparing kinetic reactivities – in contrast to the thermodynamic reactivities, when some of the thermodynamic potentials give an absolute measure and could be correlated with monomer structure (ring size, heteroatoms present, substituents). The thermodynamic activation parameters of the rate constants of propagation, namely $\Delta^{\neq}G$, $\Delta^{\neq}H$, and $\Delta^{\neq}S$, also have different values, depending on the structure of the active species (i.e., initiator/catalyst used). Therefore, these parameters can reasonably be compared only for a given monomer and various active species or for a given active species (e.g., anionic pair with a defined cation) for various monomers. This kind of experimental data is almost nonexistent. Besides, some authors determine the dependence of the rate of polymerization (not propagation!) on the reciprocal of the absolute temperature and are erroneously calling the temperature coefficient determined in this way merely temperature coefficient – as activation parameters. For CROP there was an attempt to correlate rate constants of propagation with basicities of different heterocyclic monomers. This dependence taken from Reference 43 is tabulated in Table 6.

Thus, the data above indicate that the highest rate constant is observed for the monomer of lowest basicity. This 'correlation' is rather rough but, indeed, more basic monomers are slower, even if the bridged four-membered ring is compared with the five-membered THF.

The proper correlation analyses of the reactivities of given species (i.e., monomers or active centers) requires comparing additions of various monomers to the same active species as well as the addition of the same monomer to different active species.

The methyloxonium cation derived from THF was used as a model of cationic active centers and triflic ester as a model of the covalent ones (Scheme 4).[43]

The values of the corresponding rate constants determined in this way are given in Table 7. In this series higher rate constants were observed for monomers of higher basicity.

These data indicate that the rate constants for reactions of various monomers and model active species, both ionic and covalent, are the function of monomer basicity.

In order to correlate the reactivities of various onium ions (active species) within their structures, the reaction of ions, modeling different active species, and the highly nucleophilic monomer conidine was studied. The corresponding rate constants are given in Table 8.

Table 5 Summary of thermodynamic polymerizability: ΔH and $\Delta S°$ data for the most often polymerized cyclic monomers

No	*Monomer*	*Conditions*	*ΔH*	*ΔS°*	*Method*
1	 Ethylene oxide	gl	–140	–174	Semiempirical calculation
2	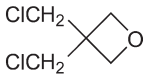 3,3-Bis(chloromethyl)oxetane	lc	–84.5	nd	Experimentally measured heats of polymerization
3	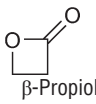 β-Propiolactone	lc	–80.5	nd	Experimentally determined heats of formation
4	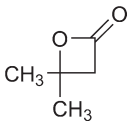 Pivalolactone	lc	–92.0	nd	As above
5	 Tetrahydrofuran	lc	–12.5	–41.0	From $[M]_e = f(l/T_e)$
6	 1,3-Dioxolane	ss	–21.3	–77.8	As above
7	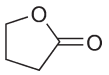 γ-Butyrolactone (butano-4-lactone)	lc	5.1	–29.9	Thermochemical
8	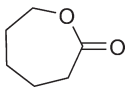 ε-Caprolactone (hexano-6-lactone)	lc′	–28.8	–53.9	From $[M]_e = f(l/T_e)$
9	 1,3,5-Trioxane	lc′	–28	nd	From heats of formation
10	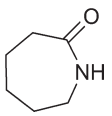 Hexano-6-lactam	lc	–12.5	+5.4	As above
11	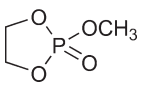 Ethylenemethylphosphate	ss	–14.0	–13.5	From $[M]_e = f(l/T_e)$
12	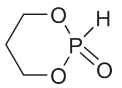 Trimethylene-*H*-phosphonate	ssls	5.4 – 0.64	7.1 – 5.8	As above
13	Sulfur	ls	13.2	19.4	

In this series a reverse order of reactivities is observed: active species from more basic monomers are less reactive. Thus the observed order of reactivities in homopropagation is parallel to the order of reactivities in the reaction of standard monomer with different active species and reverse to that observed in the reaction of different monomers with standard active species.

Table 6 Rate constants of propagation and basicities of different heterocyclics

Monomer				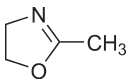	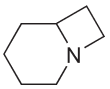
k_p ($mol^{-1}\,l\,s^{-1}$)	$\sim 10^4$	4×10^{-2}	$\sim 10^{-8}$	5×10^{-5}	7×10^{-3}
pK_a	−6.5	−2.0	1.2	3.4	11

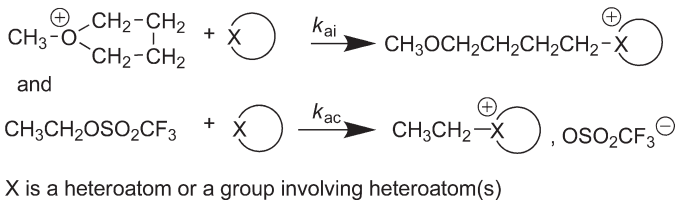

X is a heteroatom or a group involving heteroatom(s)

Scheme 4 Models of cationic and covalent active centers: methyloxonium cation of THF and triflic ester, respectively.

Table 7 Rate constants for the addition of heterocyclic monomers to the model active species ($C_6H_5NO_2$, 35 °C), shown in **Scheme 4**[43]

Monomer	*(Ionic)* k_{ai} *($mol^{-1}\,l\,s^{-1}$)*	(Covalent) k_{ac} *($mol^{-1}\,l\,s^{-1}$)*	*pK_a*
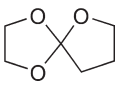	4.5×10^{-3}	4×10^{-5}	−7.3
	10^{-4}	6×10^{-5}	−6.5
	4×10^{-2}	2×10^{-4}	−2.0
	20	4.4×10^{-2}	1.2
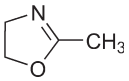	120	4×10^{-1}	3.4
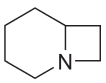	500	170	11

Table 8 Rate constants of addition of conidine to various onium ions, differing in heteroatoms ($C_6H_5NO_2$, 35 °C)[43]

Active center	k_{add} *($mol^{-1}\,l\,s^{-1}$)*
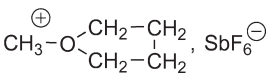	5×10^2
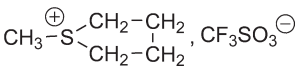	1×10^{-3}
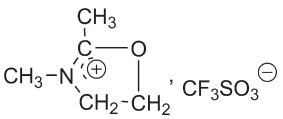	9×10^{-2}
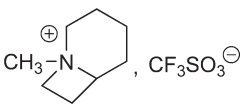	7×10^{-3}

This is a clear demonstration that in passing from the ground state to the transition state the bond-breaking is more advanced than the bond-making.

With a further shift in the direction of still more advanced breaking of the bond within active species this borderline S_N2 mechanism could eventually convert into the S_N1 mechanism. This should be promoted by the presence of a stabilizing group located close to the carbenium ion (like in the polymerization of cyclic acetals) and/or high ring strain (like in the three-membered rings). Indeed, contribution of the S_N1 mechanism in both cases has been postulated for polymerization of 1,3-dioxolane and isobutylene oxide (2,2-dimethyloxirane) but there is still no clear-cut evidence for its operation. This is probably the reason for high kinetic polymerizability of these monomers.

Cationic polymerization of heterocyclic monomers can proceed not only by the S_N2 mechanism involving onium ions located at the chain end, and analyzed in this chapter, but also by another S_N2 mechanism involving an activated monomer, adding to the neutral chain ends.

4.02.12 Kinetic Polymerizability versus Macroions and Macroion Pairs in Propagation

Kinetic polymerizability depends on the actual conditions of polymerization, having no influence on thermodynamic polymerizability. There are a few systems for which equilibrium constants of dissociation (K_D) were determined in order to establish the proportions of macroion pairs and macroions. Then, the rate constants of propagation for these species were determined and in this way the kinetic reactivity of various forms of active species could be compared. In the cationic polymerization of THF, oxepane (OXP), and more recently conidine, it has been shown that $k_p^{\pm} = k_p^{+}$.[44] This was explained by assuming weak interactions of counterions within the ion

Table 9 Rate constants of propagation in anionic polymerization of heterocyclic compounds

Monomer polymerization conditions	*Active species*	$k_p^{\pm}$ *(mol^{-1} l s^{-1})*	k_p^{-} *(mol^{-1} l s^{-1})*	*Reference*
 THF, 20 °C	…–$CH_2CH_2O^-K^+$	4.8×10^{-2}	–	45
	…–$CH_2CH_2O^-Cs^+$	1.22×10^{-1}	–	45
	…–$CH_2CH_2O^-K^+$[2.2.2]-cryptand	2.5×10^{-2}	1.67	45
 THF, –30 °C	…–$CH_2CH(CH_3)S^-Na^+$	2.5×10^{-3}	3.8	45
	…–$CH_2CH(CH_3)S^-Cs^+$	2.3×10^{-1}	–	45
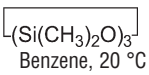 Benzene, 20 °C	…–$Si(CH_3)_2O^-Li^+$[2.1.1]-cryptand	1.4	–	45
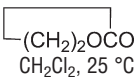 CH_2Cl_2, 25 °C	…–$CH_2CH_2COO^-K^+$DB-18-C6	7.0×10^{-4}	1.6×10^{-1}	46
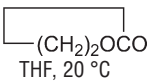 THF, 20 °C	…–$C(O)(CH_2)_5O^-K^+$	4.7	–	47

pairs, due to delocalization of the positive charge in the components of onium ions, as well as by the stereochemical course of the propagation step, in which the approaching monomer hardly requires the pulling apart from the anion.

In the anionic polymerization there are three monomers only that have been studied in more detail, namely ethylene oxide, propylene oxide (methyloxirane), and β-propiolactone (propano-3-lactone). In the anionic active species, like alcoholate anions, the negative charge (in contrast to onium cations) is localized almost exclusively on one atom. Therefore, dissociation constants are much lower and the differences in reactivity of ions and ion pairs are much more pronounced (**Table 9**).

Comparison of kinetic reactivities of the monomers provides interesting observations. Oxirane (EO) is more strained than CL, but $k_p^{\pm}$ for the … $-O^-,K^+$ ion pairs is ~100 times higher for CL than EO. Presumably, this is because the higher ring strain of EO, in comparison with that of CL, outweighs the higher reactivity of the ester linkage (lower bond energy).

The kinetic polymerizability of monomers belonging to the same class of compounds and studied at similar conditions could be compared using thermodynamic activation parameters. Actually, these parameters are determined from the dependence of the rate constants of elementary reactions (ln k_p) on $1/T$; in several instances comparison of k_p could be sufficient. Comparison of $\Delta^{\neq}H$ and $\Delta^{\neq}S$ is more subtle since it provides information on the genuine source of differences in k_p and therefore on kinetic polymerizabilities. A good example of such a comparison for CROP of oxetane, 3-methyloxetane, and 3,3-dimethyloxetane is given in a classical work by Saegusa and Kobayashi.[48]

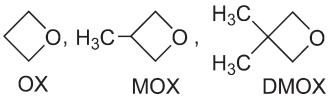

In this work rate constants were determined from the slope of the linear dependence of $\ln([M]_{t1}/[M]_{t2})$ on

$$\int_{t_1}^{t_2}[P^+]dt \qquad [23]$$

and the change in $[P^+]$ was determined by ion trapping. Then, the dependence of ln k_p on $1/T$ provides the thermodynamic parameters of activation. These are given in the following order: monomer, k_p (at –20 °C; in mol^{-1} l s^{-1}), $\Delta^{\neq}H$ (in kJ mol^{-1}), and $\Delta^{\neq}S$ (in J mol^{-1} K^{-1}): OX: 0.18, 44.8 and similarly, –77.9; MOX: 0.92, 47.3, –61.1; DMOX: 3.4, 50.7, –35.6.

Thus cationic polymerizability could only be related to the entropy of activation as described in this chapter for cyclic esters of phosphoric acid. Most probably substituents and the related polymer linear units are getting enhanced statistical probability of states in the transition state. One could expect dependence on basicity, but the known basicities are almost the same and do not change monotonically (given in ΔD_γ (m^{-1})): OX: 103; MOX: 106; DMOX: 99.[48] Thus, like in polymerization of cyclic esters of phosphoric acid, where the thermodynamic reactivity is governed by entropy change, this is the kinetic reactivity depending on the change of entropy of activation.

Summarizing the kinetic ring-opening polymerizability/reactivity it should be stressed that there are a larger number of monomers polymerizing cationically than anionically. This can be understood when the cationic and anionic propagation steps are compared:

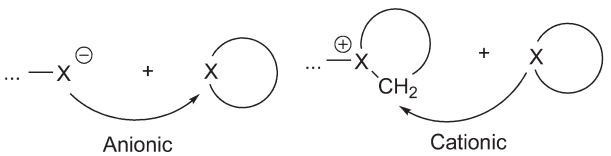

Thus, in the cationic process the (usually) strained onium ion is attacked, whereas in the anionic polymerization the neutral cyclic species is attacked, which is less prone to ring opening. There are a few monomers that are able to polymerize exclusively by cationic mechanism (cyclic amines, phosphazenes) and all monomers polymerizing anionically are also able to polymerize cationically (**Table 10**).

Table 10 Monomers, catalysts, and polymerizability in ROP (taken in part with some modifications) from Reference 49

Class	*Ring structure*	*Ring size*[a]	*Catalyst type*[b]*/mechanism*
Olefin		4, 5, 8	ROMP
Ether		3, 4, 5, 7	Anionic, cationic (including activated monomer)
Thioether		3, 4	Anionic, cationic
Amine		3, 4, 7	Cationic
Lactone	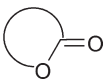	4, 6, 7, 8	Anionic, cationic, coordinate
Thiolactone	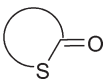	4–8	Anionic, cationic
Lactam	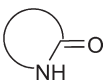	4–8 and higher	Anionic, cationic (including activated monomer)
Disulfide		4–8 and higher	Radical
Anhydride	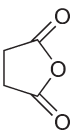	5, 7, 8, and higher	Anionic, cationic
Carbonate	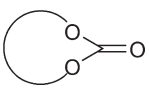	6, 7, 8, 20, and higher	Anionic, cationic, coordinate
Formal		5, 7, 8, and higher	Cationic
Siloxane	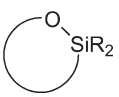	6, 8, 10, and higher	Anionic, cationic
Phosphazene	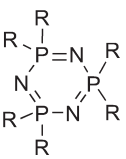	6	Cationic
Oxazole	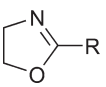	5	Cationic
Phosphonite	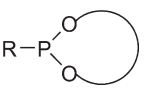	3, 5, 6, 7	Cationic
Dioxaphosphorinanes(cyclic phosphates)	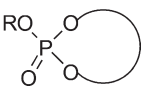	5, 6	Anionic, cationic, coordination

[a]Ring sizes affording high molar mass polymers.
[b]Covalent nucleophilic mechanisms may include alkylating agents (e.g., benzyl chloride) and organometallics (e.g., R_3-Sn-X).

4.02.13 Outlook

Major principles governing thermodynamic and kinetic polymerizabilities in ROP/ROMP are already established. Angular strain, transannular interactions leading to strain, translational, vibrational, and rotational entropies in polymerization, as well as other factors were described in the past for several systems in polymer monographs and handbooks. Principal definitions of thermodynamic parameters and ceiling (and floor) temperatures have been formulated by IUPAC. Nevertheless, the general theory in the form of the algorithm encompassing constitutive elements of monomer structures and polymerizabilities does not exist since the data are scattered and not sufficient. On the other hand, all new monomers are polymerized and thermodynamic equilibrium data as well as thermodynamic activation parameters are being determined for those novel systems.

References

1. Penczek, S.; Goethals, E. In *Comprehensive Polymer Science*; Eastmond, G.C.; Ledwith, A.; Russo, S.; Sigwalt, P., Eds., 1st ed.; Pergamon: Oxford, 1989; Vol. 3, Part I, p 719.
2. Penczek, S.; Moad, G. *Pure Appl. Chem.* **2008**, *80*, 2163.
3. McNaught, A. D.; Wilkinson, A. *Compendium of Chemical Terminology*, 2nd ed.; Blackwell Science, 1997. Copyright 1997–2004 IUPAC.
4. Green Book, IUPAC. *Quantities, Units and Symbols in Physical Chemistry*, 2nd ed.; Blackwell: Oxford, UK, 1993; p 48.
5. Berlin, Al. Al.; Volfson, S. A.; Enikolopyan, N. S. *Kinetics of Polymerization Processes* (in Russian); Khimia: Moscow, Russia, 1978.
6. Alberty, R. *Pure Appl. Chem.* **2001**, *73*, 1349.
7. Ivin, K. J. *J. Polym. Sci.: Part A: Polym. Chem.* **2000**, *38*, 2137.
8. Snow, R. D.; Frey, F. E. *Ind. Eng. Chem.* **1938**, *30*, 176.
9. Stevens, M. P. *Polymer Chemistry. An Introduction*; Addison-Wesley: Massachusetts, 1975; p 20.
10. Cowie, J. M. G. In *Comprehensive Polymer Science*; Eastmond, G.C.; Ledwith, A.; Russo, S.; Sigwalt, P., Eds., 1st ed.; Pergamon: Oxford, 1989; Vol. 3, Part I, p 1.
11. Odian, G. *Principles of Polymerization*, 4th ed.; Wiley: Hoboken, NJ, 2004.
12. Dainton, F. S.; Ivin, K. *J. Q. Rev.* **1958**, *12*, 61.
13. Denbigh, K. *The Principles of Chemical Equilibrium*; Cambridge University Press: Cambridge, 1966.
14. van Ness, H. C. *Understanding Thermodynamics*; McGraw-Hill: New York, 1969.
15. Duda, A.; Penczek, S. *Macromolecules* **1990**, *23*, 1636.
16. Duda, A.; Kowalski, A. In *Handbook of Ring-Opening Polymerization*; Dubois, P.; Coulembier, O.; Raquez, J.M., Eds.; Wiley-VCH Verlag: Weinheim, Germany, 2009;p 1.
17. Elias, H. G. *Macromolecules*: Vol. 1, Chemical Structures and Syntheses; Wiley-VCH: Weinheim, 2005.
18. Brown, H. C. *J. Chem. Soc.* **1956**, 1248.
19. Sawada, H. *J. Macromol. Sci., Rev. Macromol. Chem.* **1970**, *C5* (1), 151.
20. Busfield, W. K.; Lee, R. M.; Merigold, D. *Makromol. Chem.* **1972**, *156*, 183.
21. Sekiguchi, H. In *Ring-Opening Polymerization*; Ivin, K.J.; Saegusa, T., Eds.; Elsevier: New York, 1984; Vol. 2, p 809.
22. Brown, E. D.; Carmichael, J. B. *J. Polym. Sci.: Part B: Polym. Lett.* **1965**, *3*, 473.
23. Allcock, H.; Lampe, F.; Mark, J. *Contemporary Polymer Chemistry*, 3rd ed.; Pearson Education, Prentice Hall, 2004, 546.
24. Ivin, K. J.; Saegusa, T. *Ring-Opening Polymerization*; Elsevier: New York, 1984; Vol. 1.
25. Tobolsky, A. V.; Eisenberg, A. *J. Am. Chem. Soc.* **1960**, *82*, 289.
26. Tobolsky, A. V. *J. Colloid Sci.* **1962**, *17*, 49.
27. Szwarc, M.; Perrin, C. L. *Macromolecules* **1985**, *18*, 528.
28. Lapienis, G.; Penczek, S. *Macromolecules* **1977**, *10*, 1301.
29. Penczek, S.; Biela, T.; Klosinski, P.; Lapienis, G. *Makromol. Chem., Makromol. Symp.* **1986**, *6*, 123.
30. Brunelle, D. J. In *Ring Opening Polymerization*; Brunelle, D.J., Ed.; Hanser: New York, 1993; p 309.
31. Ivin, K. J.; Mol, J. C. *Olefin Metathesis and Metathesis Polymerization*; Academic Press: London, UK, 1997.
32. Fisher, R. A.; Grubbs, R. H. *Macromol. Chem., Macromol. Symp.* **1992**, *63*, 271.
33. Ivin, K. J.; Leonard, J. *Eur. Polym. J.* **1970**, *6*, 331.
34. Penczek, S.; Matyjaszewski, K. *J. Polym. Sci., Polym. Symp.* **1976**, *56*, 255.
35. Plesch, P. H.; Westermann, H. *J. Polym. Sci.* **1968**, *16C*, 3837.
36. Berlin, Al. Al.; Deberdaer, P. J.; Perukhin, Jn. W.; Garipov, R. M. *Polyoxymethylenes* (in Russian); Nauka: Moscow, Russia, 2008.
37. Szwarc, M. *Carbanions Living Polymers and Electron Transfer Processes*; Interscience, Wiley: New York, 1968.
38. Hirota, M.; Fukuda, H. *Makromol. Chem.* **1987**, *188*, 2259.
39. Vrancken, A.; Smid, J.; Szwarc, M. *Trans. Faraday Soc.* **1962**, *58*, 2036.
40. Kress, H. J.; Stix, W.; Heitz, W. *Makromol. Chem., Makromol. Symp.* **1988**, *13/14*, 507.
41. Berlin, Al. Al.; Enikolopian, N. S. *Vysokomol. Soedin., Ser. A.* **1973**, *15*, 555.
42. Allen, P. E. M.; Patrick, C. R. *Kinetics and Mechanisms of Polymerization Reactions*; Harwood: Chichester, UK, 1974; p 210.
43. Penczek, S.; Kubisa, P.; Slomkowski, S.; Matyjaszewski, K. In *Ring-Opening Polymerization*; McGrath, J.E., Ed.; ACS Symp. Ser. 286; ACS: Washington, DC, 1985; p 117.
44. Matyjaszewski, K.; Szymanski, R.; Kubisa, P.; Penczek, S. *Acta Polym.* **1984**, *35*, 14.
45. Boileau, S. In *ACS Symp. Ser. 166*; McGrath, J.E., Ed.; ACS: Washington, DC, 1981; p 283.
46. Slomkowski, S.; Penczek, S. *Macromolecules* **1980**, *13*, 229.
47. Sosnowski, S.; Slomkowski, S.; Penczek, S. *J. Macromol. Sci. Chem.* **1983**, *A20* (9), 979.
48. Saegusa, T.; Fuji, H.; Kobayashi, Sh.; *et al. Macromolecules* **1973**, *6*, 26.
49. Brunelle, D. J. *Ring-Opening Polymerization*; Hanser: New York, 1993; p 2.

Biographical Sketches

Stanislaw Penczek is professor of polymer chemistry at the Polish Academy of Science (Centre of Molecular and Macromolecular Studies in Lodz) and teaches at the Graduate School of the Jagiellonian University (Krakow) as honorary professor. He mostly contributed to the kinetics, thermodynamics, and mechanisms of the ROP, publishing over 300 papers in the related areas. He was a member of the first group to observe living and controlled polymerizations in cationic and anionic ROP, including reversibility of deactivation of propagating species. Among other honors from Belgium, Japan, and Germany (the Warburg Prize), he is a member of the Polish Academy of Science and a foreign member of the German (Nordrhein) Academy, dr *h.c.* of the P. M. Curie University in Paris and dr *h.c.* of the Russian Academy of Science. He was a member of the IUPAC Bureau for two terms, and a former president of European Polymer Federation.

Krzysztof Kaluzynski is currently working in the Center of Molecular and Macromolecular Studies of Polish Academy of Sciences, Lodz, Poland. He received his MS (1969) from the Technical University in Lodz and PhD (1988) from the Center of Molecular and Macromolecular Studies under the supervision of professor Stanislaw Penczek. In 1989–1990 he worked with professor Hisaya Sato in the Graduate School of Bio-Applications and Systems Engineering of Tokyo University of Agriculture and Technology as a scientific researcher. The main research interests of K. Kaluzynski are mechanisms and kinetics of polymerization of cyclic phosphates. He is a co-author of over 50 original papers and reviews and three patents. He has twice received group Awards of Scientific Secretary of Polish Academy of Sciences. Krzysztof Kaluzynski is a longtime co-worker of professor Stanislaw Penczek.

4.03 Living Ring-Opening Olefin Metathesis Polymerization

RH Grubbs, California Institute of Technology, Pasadena, CA, USA

Calderon was the first to find a catalyst system that would initiate both ring-opening polymerization of olefins (subsequently named ROMP by Tim Swager when he was a student at Caltech) and acyclic metathesis of simple olefins.[1] Up until his findings, most catalysts for acyclic metathesis were heterogeneous systems, and metal salts were used to polymerize strained olefins such as norbornenes.[2] Beautiful work was carried out using the poorly defined systems to work out the stereochemistry and mechanism of metathesis. This beautiful work provides an excellent backdrop for the work described here.[3] This section will focus on the use of well-defined complexes as initiators for the living polymerization of cyclic olefins.

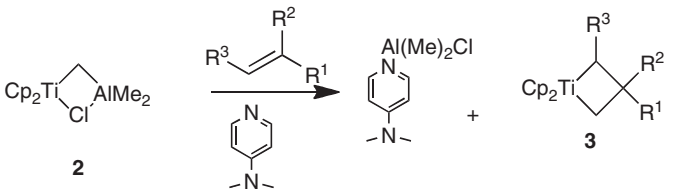

Although metathesis polymerization was well known from previous work using ill-defined catalysts, it was only with the introduction of single component catalysts that well-defined polymerizations using ring-opening metathesis polymerization (ROMP) became possible.

As with any living system, an initiator is needed which will polymerize without termination or chain transfer.[4] In addition, to obtain well-controlled polymer molecular weight and polydispersity, the initiation and quenching of the growing polymer must be controlled. The mechanism of olefin metathesis provides this potential and with an understanding of the mechanistic steps, each of the three requirements can be regulated.

The first use of a well-defined initiator was by Katz[5] in which he used the Fisher-type carbenes as prepared by Casey and Burkhardt[6] for the polymerization of strained olefins such as norbornene and cyclobutenes.

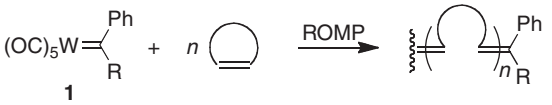

These systems gave poor control of molecular weight, but showed some of the characteristics of a living system such as the ability to prepare blocky polymers and the incorporation of an ill-defined initiator fragment in the resulting polymer.

The work of Fred Tebbe, of Dupont, provided a good starting point for the creation of living ROMP initiators where each of the critical features could be controlled. Tebbe and co-workers[7] demonstrated that the titanocene methylene complex would undergo a metathesis exchange with terminal olefins. This provided one of the earliest examples of a well-defined metal alkylidene complex undergoing a clean exchange with an olefin. The Caltech group demonstrated that a kinetically competent metallacyclobutane could be isolated from this system.[8]

The isolated metallacyclobutane would also undergo exchange with an olefin and provided a model for metathesis and a clean system for systematic mechanistic study.[9] The Tebbe reagent also reacted with carbonyl compounds such as ketones and esters to exchange an oxygen from the organic for the methylene of the complex. This reaction has become an often used transformation for organic synthesis.[10]

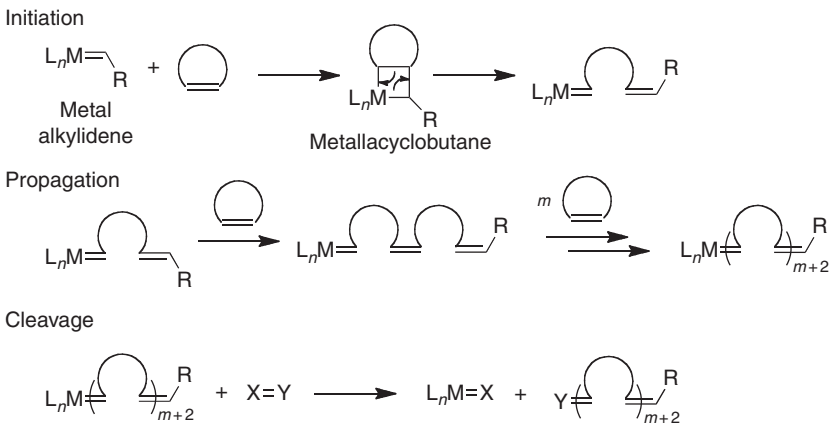

 doi:10.1016/B978-0-444-53349-4.00093-5

Since metathesis is a reversible reaction, monomers must be chosen so that the monomer should be more reactive than the double bond in the polymer. If this is not the case, the polymer will compete with the monomer for reaction and will result in a chain transfer reaction. Consequently, norbornenes have been used in most cases, although other less readily available strained monomers such as cyclobutenes, cyclopropenes, and transcyclooctenes have also been used in living ROMP.[11]

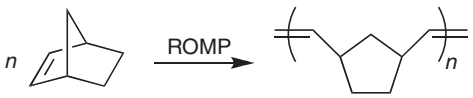

The reaction of the Tebbe reagent with a base and norbornene gave an isolated metallacycle.[12] When the isolated metallacycle was heated with monomer, polymerization initiated at 60 °C and cooling to room temperature stopped the reaction. The resulting polymer containing the metallacycle end group could be isolated and the polymer could be released from the metal by the addition of acetone that undergoes a Wittig-type reaction to replace the metal with a dimethyl group. These polymers were living – that is, termination was much slower than polymerization, and the resulting polymer was relatively stable with the initiator at the terminus. However, the polydispersity was near 1.5.

The titanium initiators were used to demonstrate many of the features of living systems such as the formation of block systems[13] and the ability to use the chain end to initiate other polymerization reactions.

An amusing application of this system was the use of the alkylidene to produce a living polymer that was converted to a system with the polymer attached to the metal through a single bond. This complex could be used to initiate polymerization of ethylene to generate a block[polynorbornene-polyethylene].[14]

Later the Schrock group[15] demonstrated that Ta complex **7** showed similar reactivity to the titanium system.

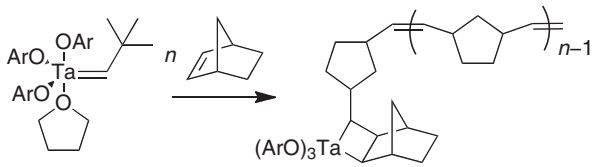

7, Ar = 2,6-diisopropylbenzene

The thermal and functional group sensitivity of these complexes limited their application in functional polymer synthesis

As better initiators became available,[16] there was little further research utilizing these very early Ti and Ta complex initiators. However, these early studies provided the foundation for living ROMP. With the titanium systems, it was demonstrated that:

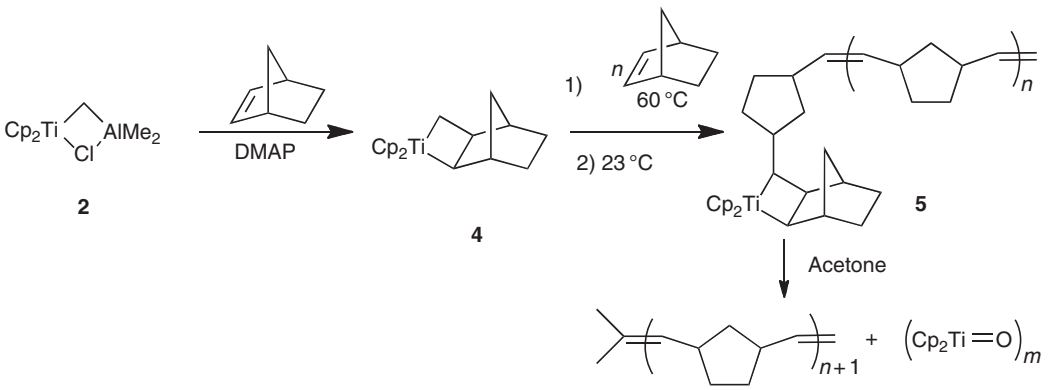

1. Well-defined initiators resulted in a general living metathesis polymerization system with strained olefin (a limited number were known at the time). Stable initiators produced stable propagating species.
2. Control of initiator structure was required to obtain low polydispersity indices (PDIs). Standard organometallic principles could be used to balance the rates of initiation and termination.
3. The 'Wittig'-like activity of these systems provided a clean termination process.

The final feature needed was an increase in the initiation rate. The starting metallacycle is a disubstituted metallacycle, while the propagating metallacycle is trisubstituted. Steric interactions will destablize the trisubstituted metallacycle relative to the disubstituted – that is, propagating species is more reactive than the initiator. To solve this problem, a more reactive initiator was required. It was found that the addition of dimethylcyclopropene to the Tebbe reagent in the presence of a base resulted in the formation of a stable metallacycle. The ring strain of the cyclopropene-derived metallacycle resulted in a very reactive initiator and the polynorbornene resulting from this initiator was near 1.1.

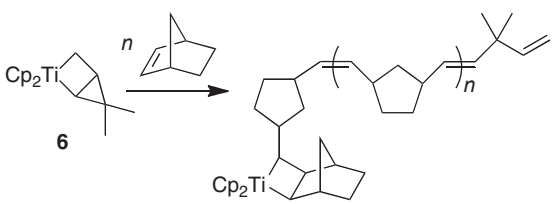

Many new applications were opened with the advent of much more active and stable tungsten and later molybdenum and ruthenium initiators. A number of these applications will be discussed in other sections. In this chapter, we will limit the discussion to those points directly related to the use of these systems in the synthesis of well-defined, low PDI, living polymers.

While Schrock was on sabbatical at Caltech, we initiated a collaboration to examine the living nature of other metathesis active complexes. The highly active tungsten-based metathesis catalysts that were the focus of this study opened the next chapter in living ROMP. The high activity of these systems required the development of additional methods of control. If the catalysts were too active, termination and backbiting reactions destroyed the livingness of the systems. Schrock had found that the activity of these tungsten systems could be controlled by the structure of the alkoxy ligands. The hexafluoro-*t*-butanol complex (**8c**) was much more active than that of the *t*-butoxy complex (**8a**). The less active complex gave lower polydispersities since the more active complex reacted with the polymer in competition with monomer.[17] In addition, the lower activity of the **8a** catalyst resulted in a much better balance in the initiation–propagation rates such that low PDIs of less than 1.1 were produced.

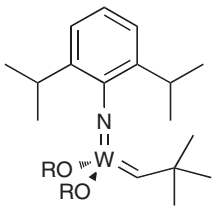

8a, R = *t*Bu
8b, R = $C(CH_3)_2(CF_3)$
8c, R = $C(CH_3)(CF_3)_2$

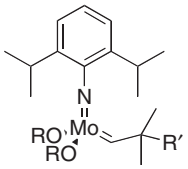

9a,R = *t*Bu
9b,R = $C(CH_3)_2(CF_3)$
9c,R = $C(CH_3)(CF_3)_2$
(R′ = CH_3 or Ph)

By controlling the ligands and additives, these systems opened the way to the synthesis of a wide array of homo and block polymers of well-defined structures. Polymers with PDIs of less than 1.1 that contained a variety of functional groups were routinely prepared using these initiators.

The Mo-based systems are used in a wide variety of applications. However, for the present discussion, the principles developed during these studies were as follows:

1. The activity of the catalyst must be controlled by ligands to prevent backbiting into the growing polymer chains.
2. Systems can be controlled by the addition of reversible inhibitors to control the propagation rate by reversible termination as in ATRP.
3. Highly active, functional group-tolerant initiators can be used to prepare a wide array of functional homo and block polymers with well-controlled structures.[20]

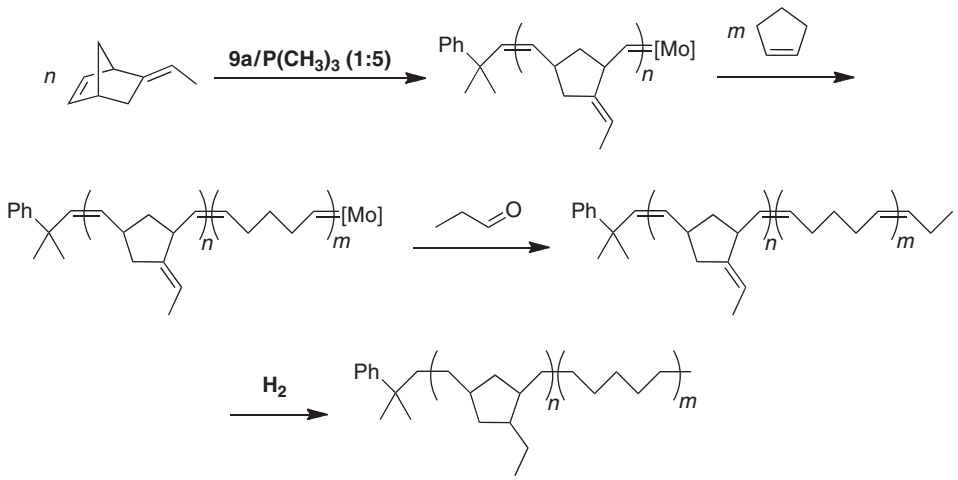

The second method of controlling the polymerization of these systems was the addition of phosphine, an inhibitor, to the system that stabilized the intermediate, decreased the reactivity of the chain end, and resulted in much narrower polydispersity.[18] The additives appeared to operate by the reversible termination principle that is the basis for atom transfer radical polymerization (ATRP). As was the case with the Tebbe systems, the tungsten alkylidenes reacted cleanly with aldehydes or ketones. Consequently, the living systems could be terminated by the addition of an aldehyde or ketone.

A related series of Mo-based complexes were more controlled and functional group tolerant than were the corresponding W-based systems. In a similar way, the structure of the alkoxide ligand controlled the catalyst activity.[19]

Based on work with aqueous ruthenium-based metathesis systems, stable, active, and well-defined ruthenium metathesis catalysts were developed. As will be demonstrated, the early promise of broadly functional group-tolerant and water-tolerant initiators based on ruthenium have been realized. The first complex, **10**, was not particularly reactive, but would polymerize norbornene and its derivatives. These complexes were much more stable to functional groups, water, and oxygen than prior systems. It was demonstrated that these systems would give a living polymer with norbornene and could be used to form block polymers.[21]

The usual quenching conditions that had been developed for earlier metal-based ROMP systems, the addition of an aldehyde, ketone, or acid, did not provide a clean cleavage of the metal from

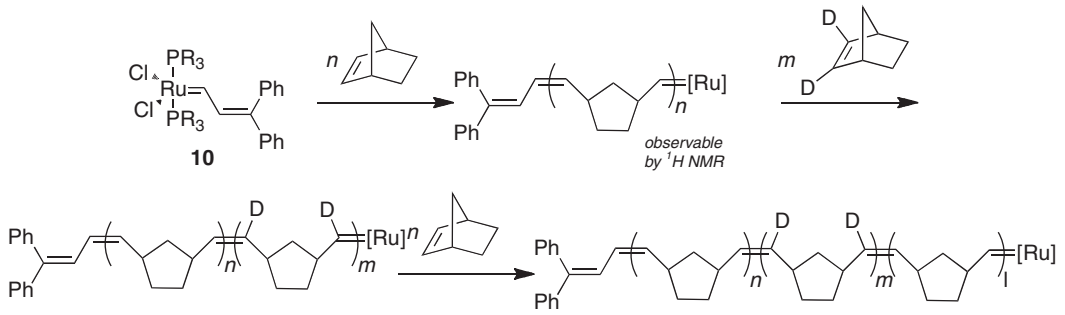

the polymer chain with the Ru initiators. It was found that the addition of a vinyl ether cleaved the chain and produced a 'Fisher' carbene that is less reactive than the initiating complex. Polymers with PDI of less than 1.2 could be obtained with these systems.

In contrast to the Mo and W systems, where electron-withdrawing groups increased the activity of the catalysts, it was found in the ruthenium systems that addition of the more electron-rich tricyclohexylphosphine to the original triphenylphosphine complexes resulted in the formation of a much more reactive complex.[22]

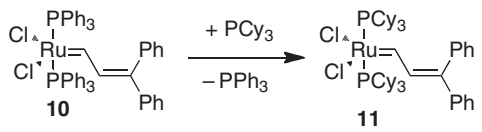

The complex **11** gave low polydispersity polymers, below 1.2, but additives were required to obtain narrow dispersity blocks and homopolymers.[23] As had been demonstrated with the Mo and W systems, a reversible inhibitor could be used to control the system.

The added excess phosphine slows the rate of polymerization. Addition of more than one equivalent gives good control of the PDI without completely shutting down the reaction. To understand the effect of added phosphine and to guide further changes in ligands, the mechanism of the activity of these systems in general metathesis reactions was examined.

The rate of reaction in most cases appears to be controlled by the loss of one of the neutral ligands to produce the active 14-electron species.

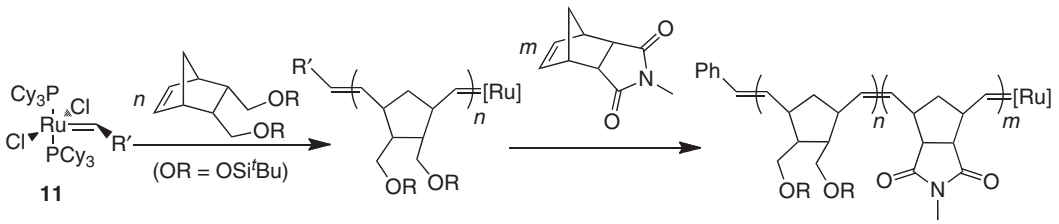

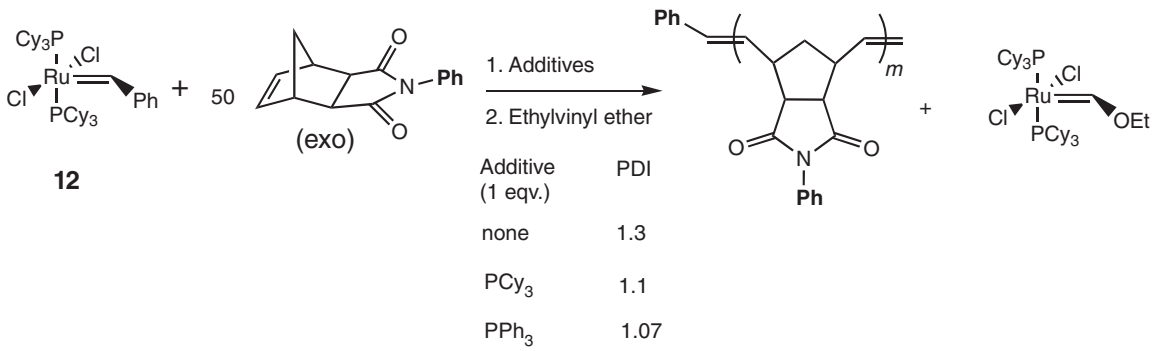

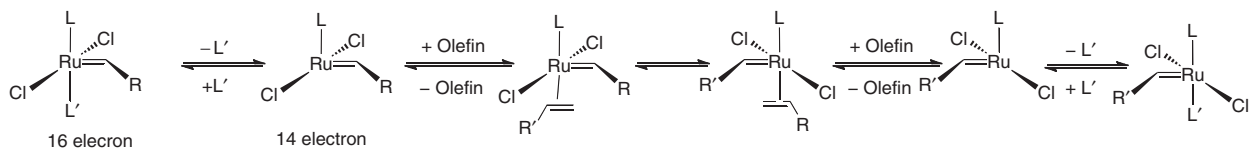

Under normal operating conditions, the 14-electron species is not detected. Only the 16-electron species that are the chain-carrying species in the reaction are observed. Buildup of significant concentrations of the reactive 14-electron complex leads to decomposition. In polymerization terms, the generation of the 14-electron species is initiation and the metathesis step is propagation. The addition of excess phosphine balances the initiation/propagation rates. Using these systems, well-defined homo and block polymers could be prepared. However, to obtain good control and rates, the less available *exo* isomers of the norbornene derivatives were required.

As a result of examining more electron-rich ligands, the *N*-mesityl family of *N*-heterocyclic carbene complexes was developed.[24] These complexes appear to operate by the same basic mechanism as the bisphosphine complexes with the initiation step slower and the propagation faster. As a result, these systems gave polynorbornenes with high PDIs. However, the higher activity did result in excellent rates of polymerizations with endo norbornenes. Attempts to control the PDI by the addition of excess phosphine resulted in some narrowing of the dispersity, but they remained unacceptably broad to be used to prepare well-controlled polymers. Apparently, the initiation of these systems is too slow relative to the propagation rate to be controlled by the addition of phosphine. A new derivative was needed.[25]

As part of a study to explore the role of phosphine structure on initiation, other phosphine derivatives of **12** were prepared from the bispyridine complex **13**. Complex **13** precipitated when **12** was dissolved in a pyridine solution. Mixing **13** with a solution of the desired phosphine and pumping off the solvent and pyridine resulted in the clean production of the desired new complex.[26] Although some of these initiated more rapidly, it was found that the bispyridine complex itself initiated at a very rapid rate.[27] Complex **13** could be used to prepare a wide variety of new well-defined homo and block polymers with PDIs less than 1.1.[28] In some cases, the PDI is lower than the standard polystyrenes used in calibration of gel permeation chromatography (GPC).

Initially, the *meta*-bromopyridine complex **13b** was used since it initiated at a very rapid rate. However, it was found in subsequent studies that the slower initiating pyridine complex **13a** was more stable and still provided good control.[29]

Polymerization with **13a** could be carried out under nitrogen in standard equipment and the reactions to produce well-defined polymers in the 100 K range were completed in tens of minutes.

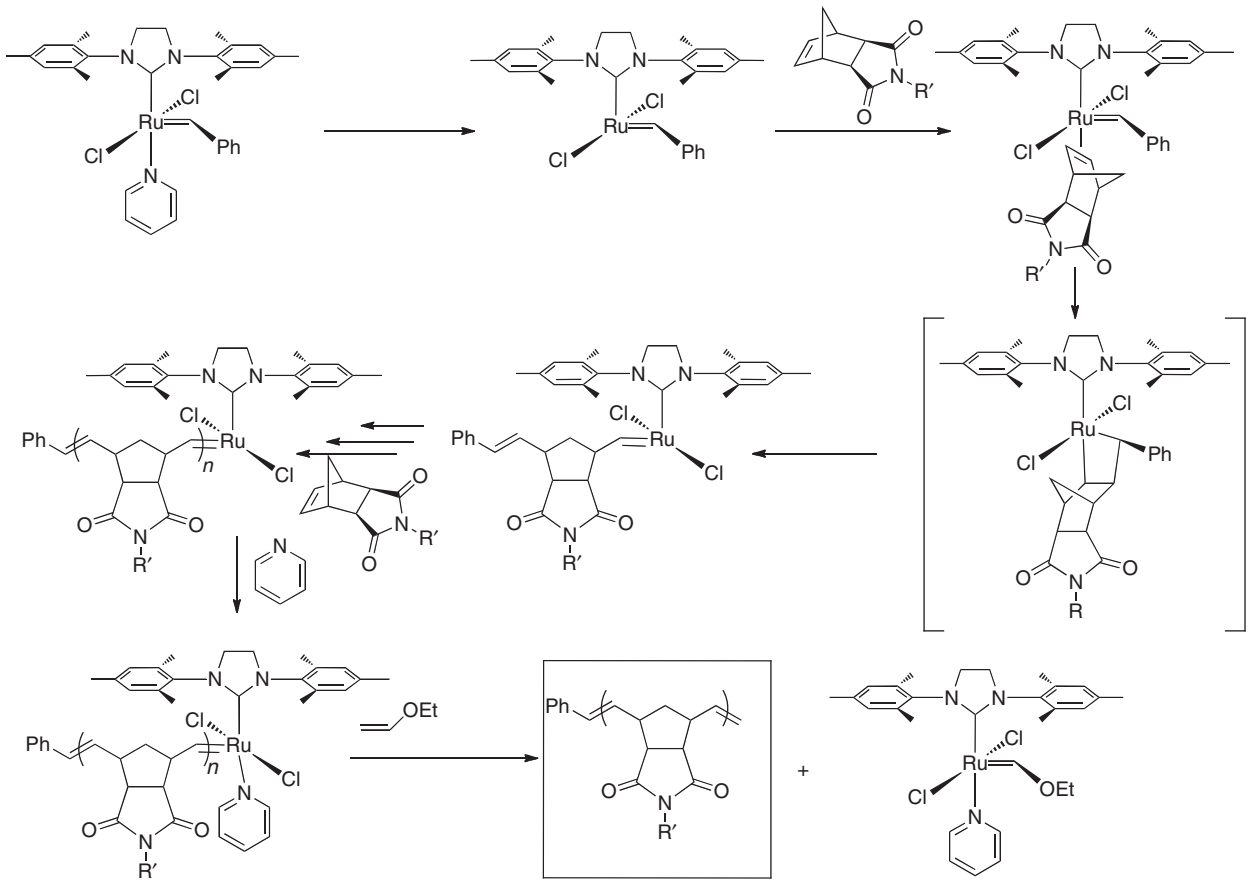

In a recent example of the control of polymer structure that is made possible utilizing these initiators, a family of brush polymers was prepared. Brush polymers have been explored by many groups due to their interesting topology and are prepared using macromers–monomers that are short oligomers containing a polymerizable end group.[30] The special features of these materials

result from the collapse of these macromers along the backbone to produce rigid systems with high persistence lengths. However, it has proven difficult to prepare them with well-controlled structures by other living systems due to the steric hindrance around the end group induced by the high molecular weight of the monomers. Living radical systems are limited due to the instability of the propagating species[31] and the steric congestion resulting from the close proximity of the side groups. The ROMP systems have proven to be particularly useful for the preparation of well-defined brush polymers due to the stability of the propagating alkylidene as well as the broader displacement of the side groups resulting from the greater spacing resulting from opening of a norbornene monomer.[32]

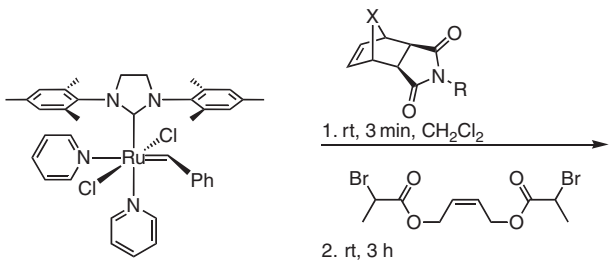

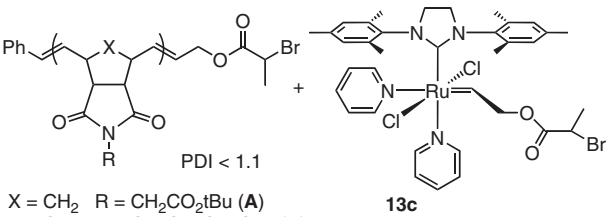

A variety of well-defined macromers with PDIs of less than 1.1 could be prepared by the use of ATRP or the living opening of lactides. Using these macromers, high-molecular-weight polymers could be prepared with PDIs of less than 1.1. Atomic force microscope (AFM) images demonstrated that these polymers dispersed on a surface with highly extended structures. The lengths demonstrated that the backbones were consistent, with all the C–C bonds being fully transoid and extended.[33] Bulk samples of block brush copolymers demonstrated facile and well-defined periodic structures resulting from phase separation of the blocks.[33]

A major limitation of all living systems is the requirement that one initiator produces only one chain. In ROMP, the initiators are rather complex and have high molecular weight. To solve this last limiting problem, pulsed living polymerization was developed. This approach was based on the observation that living systems could be terminated cleanly using *cis*-olefins.[34] The following terminations were carried out to prepare polymers that contained an end functionality that could be used to grow block polymers where the second block was prepared by ATRP.[35]

The key to these reactions was the higher rate of reactivity of the *cis*-olefin relative to the double bonds in the polymer. The predominantly *trans* stereochemistry of the polymer and the allylic substituents slow the reaction of the polymer double bonds relative to those in the *cis* acyclic olefin. In subsequent reactions, it was found that the *cis*-olefin could be present from the beginning of the reaction, that is, the stained norbornene reacted much faster than the *cis*-olefin. Since the complex resulting from the termination of the polymers with the acyclic

Cycles	Mn(GPC)×10^3	PDI
1	13.2	1.10
2	11.3	1.09
3	12.7	1.09
4	12.6	1.08
5	12.6	1.11
6	12.4	1.11
7	14.2	1.12
8	14.3	1.11
9	15.3	1.14
10	13.7	1.13

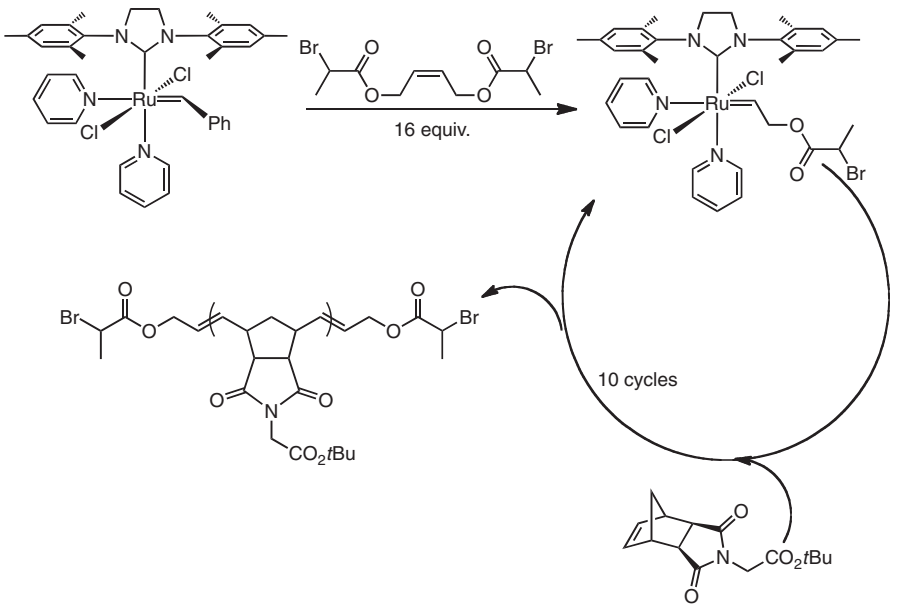

olefin is also an initiator, the system is perfectly set up to continue a second polymerization on addition of a pulsed addition of a new bolus of monomer.

The reaction was carried out in 10 vials using a robot to add more monomer at the appropriate times. Each vial contained monomer, initiator, and an excess of the *cis*-olefin terminator. At the end of each 30 min cycle, a second addition of monomer was added to vials 2–10. On each subsequent monomer addition, another vial was eliminated so that at the last time period, only the 10th vial received an injection of monomer. As can be seen in the table, even after 10 additions of monomer, the polymer was near 1.1 in PDI and near the predicted molecular weight. The increase in PDI and molecular weight are a result of loss of initiator in each step due to decomposition during the slow reaction with the terminator. Subsequent reactions could be run so that the amount of monomer was decreased slightly in each cycle to maintain the appropriate molecular weight and PDI.

At this stage, all of the steps of ROMP were demonstrated to produce polymers of well-defined and low PDI homo and block polymers. The last remaining issue is the control of the stereochemistry of the double bonds in the resulting polymer. Traditional molybdenum- and ruthenium-based catalysts give polymers with high levels of E geometry. However, it had been observed with some special ill-defined catalysts that high E or high Z polymers could be produced depending on the catalyst structure, although most of the ill-defined catalysts gave near equilibrium ratios of E and Z double bonds.[36] Some of the earliest well-defined tungsten catalysts give high Z stereochemistry. No explanations for these observations were given.[15] However, the ability to rationally control the stereochemistry and tacticity of the resulting polymer has recently been demonstrated for a well-defined catalyst. The Schrock and Hoveyda groups[37] have prepared a family of molybdenum- and tungsten-based initiators that produce high percentages of the Z isomer in standard metathesis reactions. Some of these same catalysts will also polymerize norbornenes and cyclopropenes to produce high *cis* polymers. As was found with ill-defined catalysts that gave good control of the double-bond geometry, these catalysts also provided excellent control of the tacticity of the resulting polymers. For example, it was found that the polymerization of the norbornadiene derivative with catalyst **14** gave a stereoregular polymer that was highly *cis* and syndiotactic.[38] The stereochemistry of the polymer is explained by addition of the norbornadiene on the *exo* face with the methylene pointing toward the adamantly group. If the norbornadiene always adds in that direction, *cis* polymer is obtained. The addition of the monomer to opposite faces of the growing polymer as a result of the chirality of the complex results in the *syntio*tactic structure.

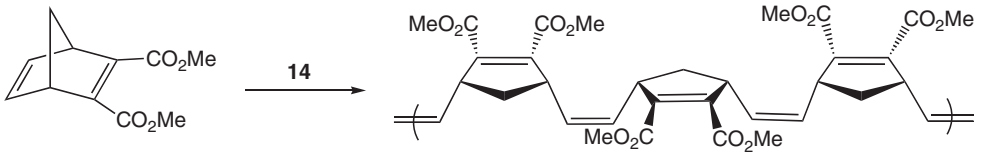

> 99% *cis*, >99% syndiotactic

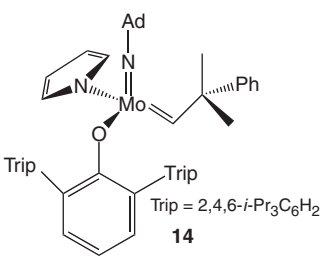

Although ROMP of norbornenes and related strained monomers has been known since the 1960s, the development of well-defined catalysts/initiators for this reaction over the past 25 years has resulted in the ability to prepare polymeric structures that have controlled length and block structures. Only recently have well-defined catalysts been prepared that produce polymers with defined double-bond geometry and tacticity which can be easily assigned based on the catalyst structure.

As a result of this control, the promise of olefin metathesis as a polymerization method has been realized. The controlled ROMP techniques, combined with ATRP and other living polymerization methods, provide the ability to produce polymeric materials of high molecular weight with unprecedented control.

References

1. (a) Calderon, L. N. *Macromol. Sci. Rev. Macromol. Chem.* **1972**, *7*, 105; (b) Calderon, N. *Acc. Chem. Res.* **1972**, *5*, 127; (c) Calderon, N.; Ofstead, E. A.; Judy, W. A. *Angew. Chem. Int. Ed. Engl.* **1976**, *15*, 401.
2. Ivin, K. J.; Mol, J. C. *Olefin Metathesis and Metathesis Polymerization*; Academic Press: San Diego, CA, 1997.
3. (a) Hamilton, J. G. In *Handbook of Metathesis*; Grubbs, R. H., Ed.; Wiley-VCH: Weinheim, Germany, 2003; Vol. 3, p 143; (b) Ivin, K. J.; Laverty, D. T.; Rooney, J. J. *Makromol. Chem.* **1977**, *178*, 1545; (c) Thoi, H. H.; Ivin, K. J.; Rooney, J. J. *Makromol. Chem.* **1982**, *183*, 1629.
4. Szwarc, M. *Nature* **1956**, *178*, 1168.
5. (a) Katz, T. J.; Lee, S. J.; Acton, N. *Tetrahedron Lett.* **1976**, *47*, 4247; (b) Katz, T. J.; Acton, N. *Tetrahedron Lett.* **1976**, *47*, 4251.
6. Casey, C. P.; Burkhardt, T. J. *J. Am. Chem. Soc.* **1973**, *95*, 5833.
7. Tebbe, F. N.; Parshall, G. W.; Reddy, G. S. *J. Am. Chem. Soc.* **1978**, *100*, 3611.
8. Howard, T. R.; Lee, J. B.; Grubbs, R. H. *J. Am. Chem. Soc.* **1980**, *102*, 6876.
9. Lee, J. B.; Ott, K. C.; Grubbs, R. H. *J. Am. Chem. Soc.* **1982**, *1982*, 7491.
10. Pine, S. H.; Zahler, R.; Evans, D. A.; Grubbs, R. H. *J. Am. Chem. Soc.* **1980**, *102*, 3270.
11. Katz, T. J.; Lee, S. J.; Shippey, M. A. *J. Mol. Catal.* **1980**, *8*, 219.
12. Gilliom, L. R.; Grubbs, R. H. *J. Am. Chem. Soc.* **1986**, *108*, 733.
13. (a) Cannizzo, L. F.; Grubbs, R. H. *Macromolecules* **1988**, *21*, 1961; (b) Risse, W.; Grubbs, R. H. *J. Mol. Catal.* **1991**, *65*, 211.

14. Tritto, I.; Grubbs, R. H. In *Catalytic Olefin Polymerization*; Keii, T.; Soga, K., Eds.; Kodansha-Elsevier Publishers: Tokyo, 1990; p 301.
15. Wallace, K. C.; Dewan, J. C.; Schrock, R. R. *Macromolecules* **1987**, *20*, 448.
16. Schrock, R. R.; Feldman, J.; Cannizzo, L. F.; Grubbs, R. H. *Macromolecules* **1987**, *20*, 1169.
17. (a) Schrock, R. R.; Krouse, S. A.; Knoll, K.; *et al. J. Mol. Catal.* **1988**, *46*, 243; (b) Schrock, R. R.; Yap, K. B.; Yang, D. C.; *et al. Macromolecules* **1989**, *22*, 3191; (c) Dounis, P.; Feast, W. J. *Polymer* **1996**, *37*, 2547; (d) Trzaska, S. T.; Lee, L.-B. W. *Macromolecules* **2000**, *33*, 9215.
18. Wu, Z.; Wheeler, D. R.; Grubbs, R. H. *J. Am. Chem. Soc.* **1992**, *114*, 146.
19. (a) Bazan, G. C.; Khosravi, E.; Schrock, R. R.; *et al. J. Am. Chem. Soc.* **1990**, *112*, 8378; (b) Bazan, G. C.; Oskam, J. H.; Cho, H.-N.; *et al. J. Am. Chem. Soc.* **1991**, *113*, 6899; (c) Bazan, G. C.; Schrock, R. R.; Cho, H.-N.; Gibson, V. C. *Macromolecules* **1991**, *24*, 4495.
20. Grubbs, R. H. *Handbook of Metathesis*; Wiley-VCH: Weinheim, Germany, 2003, Vol. 3.
21. (a) Nguyen, S. T.; Johnson, L. K.; Grubbs, R. H.; Ziller, H. W. *J. Am. Chem. Soc.* **1992**, *114*, 3974; (b) Wu, Z.; Benedicto, A. D.; Grubbs, R. H. *Macromolecules* **1993**, *26*, 4975.
22. (a) Nguyen, S. T.; Grubbs, R. H.; Ziller, J. W. *J. Am. Chem. Soc.* **1993**, *115*, 9858; (b) Schwab, P.; France, M. B.; Ziller J. W.; Grubbs, R. H. *Angew. Chem. Int. Ed. Engl.* **1995**, *107*, 2179.
23. Bielawski, C. W.; Grubbs, R. H. *Macromolecules* **2001**, *34* (26), 8838.
24. (a) Scholl, M.; Ding, S.; Lee, C. W.; Grubbs, R. H. *Org. Lett.* **1999**, *1*, 953; (b) Scholl, M.; Trnka, T. M.; Morgan, J. P.; Grubbs, R. H. *Tetrahedron Lett.* **1999**, *40*, 2247; (c) Weskamp, T.; Kohl, F. J.; Herrmann, W. A. *J. Organomet. Chem.* **1999**, *582*, 362; (d) Weskamp, T.; Kohl, F. J.; Hieringer, W.; *et al. Angew. Chem. Int. Ed.* **1999**, *38*, 2416; (e) Ackermann, L.; Furstner, A.; Weskamp, T.; *et al. Tetrahedron Lett.* **1999**, *40*, 4787; (f) Huang, J.; Stevens, E. D.; Nolan, S. P.; Petersen, J. *J. Am. Chem. Soc.* **1999**, *121*, 2674.
25. Bielawski, C. W.; Grubbs, R. H. *Angew. Chem. Int. Ed. Engl.* **2000**, *39* (16), 2903
26. Sanford, M. S.; Love, J. A.; Grubbs, R. H. *Organometallics* **2001**, *20*, 5314.
27. (a) Love, J. A.; Morgan, J. P.; Trnka, T. M.; Grubbs, R. H. *Angew. Chem. Int. Ed.* **2002**, *41*, 4035; (b) Sanford, M. S.; Love, J. A.; Grubbs, R. H. *J. Am. Chem. Soc.* **2001**, *123*, 6543.
28. Choi, T.-L.; Grubbs, R. H. *Angew. Chem. Int. Ed. Engl.* **2003**, *42*, 1743.
29. Matson, J. B.; Grubbs, R. H. *J. Am. Chem.* **2008**, *21* (130), 6731.
30. Milner, S. T.; Witten, T. A.; Cates, M. E. *Macromolecules* **1989**, *22*, 853.
31. (a) Matyjaszewski, K.; Xia, J. *Chem. Rev.* **2001**, *101*, 2921; (b) Lord, S. J.; Sheiko, S. S.; LaRue, I.; *et al. Macromolecules* **2004**, *37* (11), 4235.
32. Xia, Y.; Kornfield, J. A.; Grubbs, R. H. *Maromolecules* **2009**, *42*, 4560.
33. Xia, Y.; Olsen, B. D.; Kornfield, J. A.; Grubbs, R. H. *J. Am. Chem. Soc.* **2009**, *131*, 18525.
34. (a) Matson, J. B.; Grubbs, R. H. *Macromolecule* **2008**, *41* (15), 5626; (b) Matson, J. B.; Virgil, S. C.; Grubbs, R. H. *J. Am. Chem. Soc.* **2009**, *131* (9), 3355.
35. Bielawski, C. W.; Morita, T.; Grubbs, R. H. *Macromolecules* **2000**, *33* (3), 678.
36. Katz, T. J.; Acton, N. *Tetrahedron Lett.* **1977**, *6*, 585–588; see Reference 2, page 264, for further discussion.
37. King, A. J.; Zhao, Y.; Schrock, R. R.; Hoveyda, A. *J. Am. Chem. Soc.* **2009**, *131*, 16630.
38. (a) Flook, M. M.; Gerber, L. C.; Debelouchina, G. T.; Schrock, R. R. *Macromolecules* **2010**, *43*, 7515; (b) McConville, D. H.; Wolf, J. R.; Schrock, R. R. *J. Am. Chem. Soc.* **1993**, *115*, 4413.

Biographical Sketch

Professor Robert (Bob) Howard Grubbs' main interests in organometallic chemistry and synthetic chemistry are catalysts, notably Grubbs' catalyst for olefin metathesis and ring-opening metathesis polymerization with cyclic olefins such as norbornene. He also contributed to the development of so-called 'living polymerization'.

Grubbs has received many awards including Alfred P. Sloan Fellow (1974–76), Camille and Henry Dreyfus Teacher-Scholar Award (1975–78), Alexander von Humboldt Fellowship (1975), ACS Benjamin Franklin Medal in Chemistry (2000), ACS Herman F. Mark Polymer Chemistry Award (2000), ACS Herbert C. Brown Award for Creative Research in Synthetic Methods (2001), the Tolman Medal (2002), and the Nobel Prize in Chemistry (2005). He was elected to the National Academy of Sciences in 1989 and a fellowship in the American Academy of Arts and Sciences in 1994.

4.04 Ring–Chain Equilibria in Ring-Opening Polymerization

R Szymanski, Polish Academy of Sciences, Lodz, Poland

4.04.1 Phenomenon of the Ring–Chain Equilibria in Ring-Opening Polymerization

The general scheme of a ring-opening polymerization (ROP) contains, besides initiation and propagation, additional processes. Putting transfer reactions, termination, and other transformations of active species aside, the most important reaction involved often in polymerization processes of cyclic monomers is depolymerization. Formation of cyclic oligomers and polymers, macrocycles, is chemically similar to this reaction. Macrocycles can act as monomers in polymerization processes and their formation can be regarded as depolymerization of macrocycle polymerization. As all these reactions can in many systems be simultaneously reversible (polymerization and depolymerization of monomer and macrocycles), the ring–chain equilibria are important in many ROPs, playing positive or negative roles, depending on the aim of a given ROP.

Main reactions constituting the ring–chain equilibria in ROP are shown in a simplified scheme (**Scheme 1**).

The interchain segmental exchange reactions were not included in the scheme because they do not directly influence the ring–chain equilibria, although the reactions of the active chain-end (ACE) with the repeating units resulting in breaking of the polymer chain are similar to the backbiting reaction leading to macrocycles. However, although neglected here, they influence the kinetics of attaining the ring–chain equilibria by broadening the dispersity of linear polymer, usually doing it much faster than depolymerization and cyclization alone. Consequently, when the interchain segmental exchange is very effective, the system reaches the equilibrium faster and the kinetic enhancement in cyclic or linear polymer, the phenomena discussed in Section 4.04.5, can be less pronounced or not observed at all.

Cyclic oligomers can be formed mainly in the so-called end- and backbiting reactions shown in the scheme. The first of them is a reaction of active species of polymerization, located on one of the growing chain-ends, with the end group formed in polymerization initiation (or in chain transfer reactions). Quite often reactivities of these end groups in relation to active species are higher than reactivities of repeating units of the growing chain (backbiting reactions – see **Scheme 1**). It can stem from chemical differences of reacting groups (end group differing from the corresponding group of the repeating unit), but steric hindrance alone often also favors endbiting over backbiting. Depending on the considered ROP system, back- and endbiting reactions can lead either directly to macrocycles and shorter living chains (backbiting) or initiator/activator molecule or ion (endbiting), or activated macrocycles are formed first as intermediates (cf. **Scheme 1**). Free macrocycles can next be formed as a result of other reactions, for example, as shown in the scheme via breaking of the exocyclic bond connecting the activating group to the cycle.

If endbiting is very effective, it can be mistaken for ring-expansion reaction, also shown in **Scheme 1**.

Such a situation existed in polymerization of cyclic acetals. After observing in many systems the formation of exclusively cyclic polyacetals, Plesch and Westermann[1] argued that no linear propagation accompanied by cyclization can explain this situation. Consequently, they proposed the ring-expansion mechanism of polymerization of cyclic acetals operating on cationated monomer and macrocycles.

However, as discussed by Szymanski *et al.*,[2] ring-expansion mechanism can be excluded on the basis of the presence of a fraction of linear polymer in polymerization systems as well as on the basis of some model reactions and computer simulations. Arguments presented by the authors prove that endbiting reaction accompanying linear propagation together with other reactions of ring–chain equilibria can explain experimental results and it is not necessary to assume ring-expansion reaction.

Thus, if endbiting is very effective and reversible, and activated macrocycles can react as active species with monomer giving normal linear growing chain, the net result can be very similar to ring expansion. **Scheme 2** shows this possibility, explaining Plesch's results of observing only macrocycles in some polymerizations of cyclic acetals (here 1,3-dioxolane

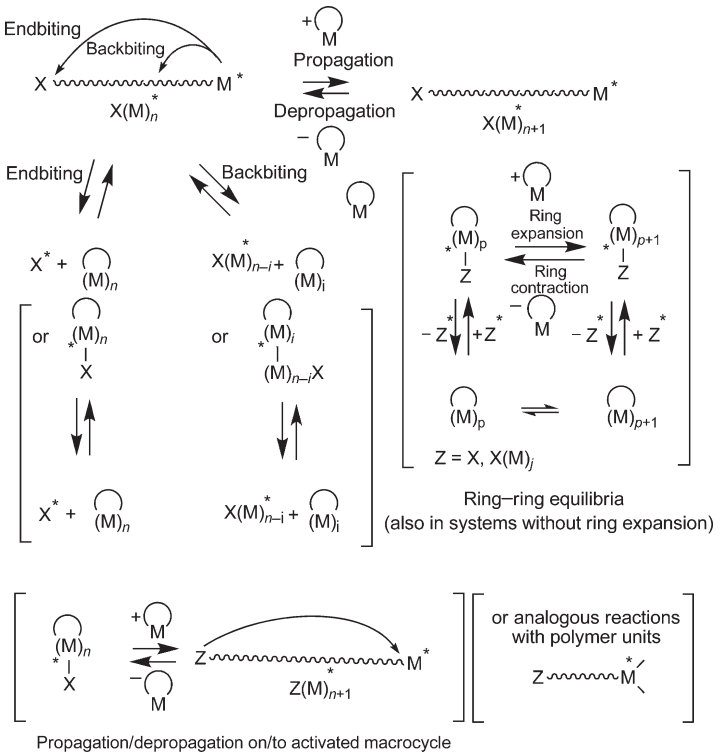

Scheme 1 Reactions constituting ring–chain equilibria in ROP (simplified scheme). In brackets, a variant with hyper-bonded structures, for example, with oxonium cations or catalyst coordinated (activated) compounds, is shown. Z denotes an initiator originated end group (X–) or a linear fragment of polymer (X(M)$_i$–). Reversible ring-expansion/contraction reactions were added to this general scheme, although they are usually possible and/or important only in some coordination ROP polymerizations.

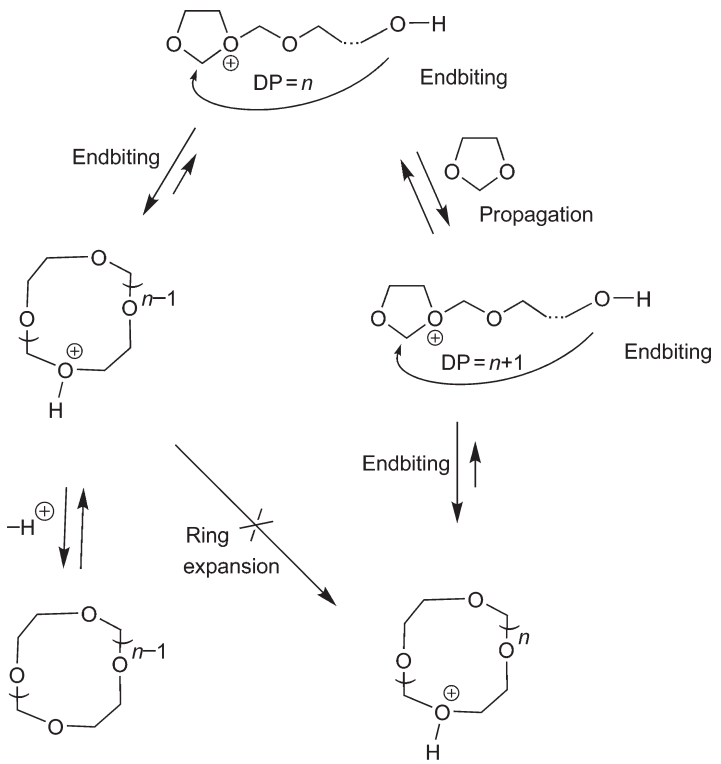

Scheme 2 Formation of macrocycles in polymerization of 1,3-dioxolane initiated with protonic acids. Backbiting neglected, ring expansion route rather improbable.[2]

polymerization system is shown), although ring expansion can be usually excluded.

It is worth stressing that the existence of ring–chain equilibria in polymerization results automatically in the existence of the chain–chain and ring–ring equilibria even if direct routes in some systems are absent (like direct ring interconversions rarely observed in ROP). On the other hand, the ring–chain equilibrium can in some systems be reached faster via the direct ring–ring interconversions if these reaction routes are present and are kinetically favored (fusion/fission reactions – the simplest reactions constituting the ring–ring equilibria).

Nevertheless, the ring-expansion reaction (and generally ring–ring interconversions) are postulated for some systems with heteroatoms having 3d or higher orbitals, including systems with catalyst capable of incorporation itself into the monomer ring. In such systems, ring expansion is possible via concerted reaction of insertion of monomer molecules (and/or macrocycles) into the corresponding bond of the hybrid cycle. Some examples are shown in the following sections.

However, it is worth noting that the equilibrium in real ring-expansion systems, without linear chains, should rather give higher equilibrium concentrations of macrocycles than in systems in which linear chains are formed. It stems from the mass balance not including the absent linear polymer fraction (see a short discussion in the next section), but it has not yet been verified experimentally.

4.04.2 Thermodynamics of the Ring–Chain Equilibria in ROP

Equilibrium in ROP accompanied by macrocyclization reactions is described by an infinite set of equations:

$$-\mathrm{M}_y- \underset{}{\overset{K_x}{\rightleftharpoons}} -\mathrm{M}_{y-x}- + (\mathrm{M}_x) \qquad [1]$$

$$K_x = \frac{[\text{c-M}_x][-\mathrm{M}_{y-x}-]}{[-\mathrm{M}_y-]} \qquad [2]$$

where K_x is the cyclization equilibrium constant for formation of x-size ring (monomer, cyclic oligomers and polymers, cyclo-M_x); x, $y = 1, 2, 3, \ldots$ are the numbers of repeating units in a (macro)cycle and linear polymer (eqn [1]), respectively.

Jacobson and Stockmayer[3] analyzed such types of equilibria and formulated a theory describing dependence of the cyclization equilibrium constants on the ring size.

It is assumed, that K_x is independent of the polymer length, that is, $y > x$ in eqns [1] and [2].

As K_x is a thermodynamic function, it is independent of the reaction routes (see, e.g., **Scheme 1**) leading to the state described by eqns [1] and [2].

Although Jacobson and Stockmayer analyzed mainly the polycondensation systems, their results are also valid for ROP.

In ROP, K_x is equal to the ratio of the rate constants of backbiting and polymerization (addition) of macrocycle

$$-\mathrm{M}_y^* \underset{k_{px}}{\overset{k_{bx}}{\rightleftharpoons}} -\mathrm{M}_{y-x}^* + (\mathrm{M}_x) \qquad [3]$$

$$K_x = \frac{k_{bx}}{k_{px}} \qquad [4]$$

Analogously it can be defined by rate constants of endbiting reactions or any other set of reactions of the full reaction scheme (e.g., reactions of **Scheme 1**).

Because distribution of lengths of linear polymer in equilibrium is usually the most probable one, the ratio of concentrations of chains differing by x repeating units can be expressed as p^x,

$$p^x = \frac{[-\mathrm{M}_{y+x}-]}{[-\mathrm{M}_y-]} \qquad [5]$$

where p is the ratio of concentrations of chains differing by one repeating unit (eqn [6])

$$p = \frac{[\mathrm{M}_{y+1}-]}{[-\mathrm{M}_y-]} = 1 - \frac{1}{\mathrm{DP}_n} \qquad [6]$$

(DP_n is the number average degree of polymerization) being close to unity for a large average length of linear polymer chains.

Consequently, from eqns [2] and [5], we get the equation relating the equilibrium concentration of macrocycle with the corresponding cyclization equilibrium constant and parameter p describing the linear polymer

$$[\text{c-M}_x] = K_x p^x \qquad [7]$$

One can easily observe that the cyclization equilibrium constants are in fact reciprocals of the equilibrium polymerization constants of macrocycles, regarded as monomers of linear homopolymerization.

The sum of monomer units incorporated into cyclics is in the equilibrium dependent on p, that is, in fact on the average length of linear polymer:

$$[-\mathrm{M}-]_{\text{cyclic}} = \sum_{i=1}^{\infty} i[\text{c-M}_i] = \sum_{i=1}^{\infty} iK_i p^i = \sum_{i=1}^{\infty} iK_i \left(1 - \frac{1}{\mathrm{DP}_n}\right)^i \qquad [8]$$

This relationship gives the so-called critical monomer concentration, also called a critical cyclics concentration or a cutoff point (calculated from the above equation for $p = 1$), being the total equilibrium concentration of cyclics (monomer and macrocycles), expressed in monomer units, in the systems with linear polymer of infinite average length. For initial monomer concentration larger than this critical concentration, we can have the linear high-molar-mass polymer and macrocycles, while for lower initial monomer concentrations practically all the monomer above its equilibrium concentration is converted into cyclic oligomers. This critical monomer concentration is not a sharp borderline (cutoff point) because in fact the equilibrium concentrations of macrocycles depend on DP_n of linear polymer (eqn [7]). Consequently, in real systems, with not very low initiator concentrations, the fraction of linear oligomers gradually decreases in equilibrium with decreasing initial monomer concentration from values close above to values below the critical value. The computed dependence of cyclic fraction in equilibrium systems of 1,3-dioxolane polymerization initiated irreversibly with two different concentrations of initiator is shown in **Figure 1**.

For higher initiator concentration ($0.01\ \mathrm{mol\,l^{-1}}$) the maximum fraction of macrocycles in polymerization product at

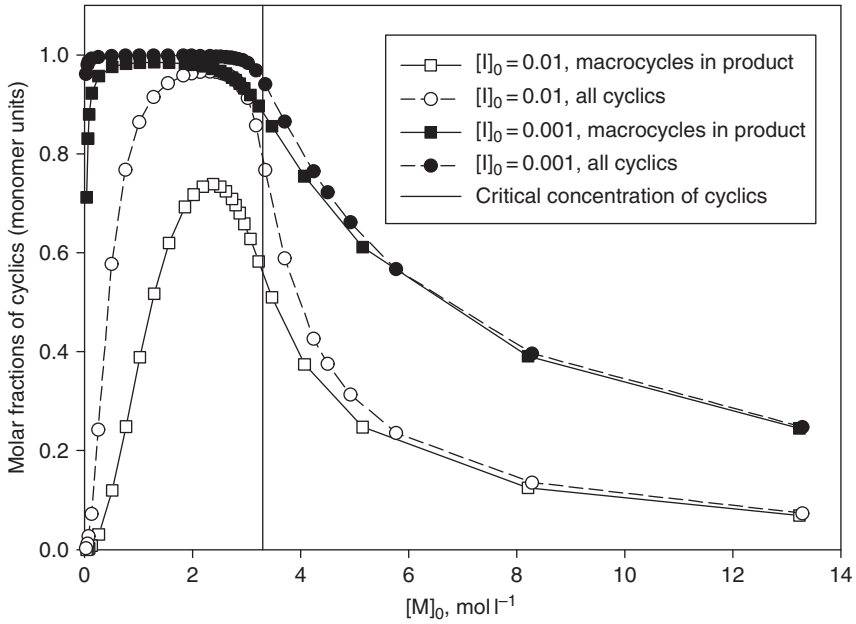

Figure 1 Contributions of cyclics in the equilibrium system of 1,3-dioxolane computed[4] for various initial concentrations of monomer and two concentrations of initiators: 0.01 and 0.001 mol l^{-1}. All-cyclics plots include monomer both in cyclics and in total mass of the systems. Equilibrium constants are taken from Andrews, J. M.; Semlyen, J. A. Polymer, **1972**, *13*, 142.[5]

equilibrium is about 74%, while the maximum fraction of cyclics, including monomer, reaches 96.5%. For 10 times lower concentrations of initiator (0.001 mol l^{-1}), the corresponding numbers are 98% and 99.8% and the critical monomer concentration borderline at about 3.3 mol l^{-1} is pronounced a bit more sharply. It is worth noting that at low initial monomer concentrations close to zero, the fraction of cyclics drops to zero due to the assumed irreversible initiation and decreasing the average length of linear oligomers to unity (consequently, the parameter p from eqns [5]–[8] limiting the equilibrium concentrations of cyclics, attains zero).

Jacobson and Stockmayer[3] analyzing the density of distribution of segments of linear polymer formulated a theory relating the distribution function of the end-to-end vector $\mathbf{r}$ for linear polymer composed of x units ($W_x(\mathbf{r})$), per unit range in $\mathbf{r}$, with the equilibrium constant of cyclization for systems without ring-strain and other enthalpic factors (equilibrium governed only by entropic factors):

$$K_x = \frac{W_x(\mathbf{0})}{N_A \sigma_{Rx}} \qquad [9]$$

where N_A is the Avogadro constant and σ_{Rx} the symmetry number for macrocycle of size x.

The above equation was derived assuming, besides no heat of cyclization, that the probability of cyclization is proportional to the fraction of polymer conformations at which the ends are close to each other and that reactivity of terminal groups are independent of the chain length.

Consequently, Jacobson and Stockmayer came to the conclusion that K_x is proportional to x raised to the power –5/2.

Flory and Semlyen[6] contributed to the original Jacobson–Stockmayer (J-S) theory assuming that for sufficiently long chains $W_x(\mathbf{r})$ should be Gaussian to an adequate approximation, fulfilling the relationship

$$W_x(\mathbf{0}) = \left(3/2\pi \langle r_x^2 \rangle\right)^{3/2} \qquad [10]$$

where $\langle r_x^2 \rangle$ is the mean-square end-to-end length averaged over all configurations of the real linear chain of size x. Additionally, as an approximation, they identified $\langle r_x^2 \rangle$ with the unperturbed mean-square end-to-end length $\langle r_x^2 \rangle_0$ as, for instance, in dilute theta solvent.

The unperturbed mean-square end-to-end length $\langle r_x^2 \rangle_0$ appears to be approximately proportional to the ring size x:

$$\langle r_x^2 \rangle_0 = C_x v x l^2 \qquad [11]$$

where C_x is the characteristic ratio of linear x-mer, l the average length of skeletal bonds, and v the number of these bonds in repeating unit.

For large x, C_x can be replaced with the limiting value of the characteristic ratio

$$C_\infty = \left(\frac{\langle r_x^2 \rangle_0}{v x l^2}\right)_{x \to \infty} \qquad [12]$$

Combining eqns [9]–[11], we get the relationship

$$K_x = \frac{\left[3/(2\pi C_x v x l^2)\right]^{3/2}}{N_A \sigma_{Rx}} \qquad [13]$$

which allows a prediction of the equilibrium constants of macrocyclization for nonstrained macrocycles on the basis of geometric features of polymers.

This equation does not take into account in a visible way the conformational restrictions (although they can be partly accounted for, hidden in the value of the characteristic ratio C_x). Conformational constraints are especially important for rigid chains. For instance, the equilibrium concentration of cyclics in poly(butylene isophthalate) is ~3 times higher than in poly(butylene terephthalate), because the former has a bent rigid structure.[7]

As the symmetry number for macrocycle σ_{Rx} is proportional to the ring size, for instance, cyclic x-mers of poly(dimethylsiloxane) is equal to $2x$, the cyclization equilibrium constant for larger macrocycles is, according to Flory and Semlyen, proportional to the ring size to the power −2.5 ($\sim x^{-5/2}$), similarly as was predicted in the original version of J-S theory.

This relationship was verified experimentally for many systems.

Any deviations from the predicted relationship could be explained by the ring strain of smaller macrocycles, not theta solvent or insufficient dilution, or by other factors.

An example of the experimentally determined dependence of the cyclization equilibrium constants on the ring size, indicating the observed deviation from the J-S theory, is shown in Figure 2.[8]

The fraction of macrocycles in the overall polymer at equilibrium conditions is, however, usually overestimated by the J-S theory and some of its improvements. There are several reasons for that, but the most important, besides the ring strain of smaller macrocycles, is insufficient approximation of the polymer segments distribution by the Gaussian density distribution function. Some factors, such as the polymer excluded volume, important for larger macromolecules, are not taken correctly into account due to lack of sufficiently good models. Also, the geometric restrictions for ring closure (orientational factor) can not always be correctly taken into account. One of the possible solutions to these problems is using Monte Carlo simulations to determine, for instance, the fraction of chain conformations for which both ends meet inside a small sphere and have the correct orientations. One of the models, most often used in these computations, is the rotational isomeric state model.[9]

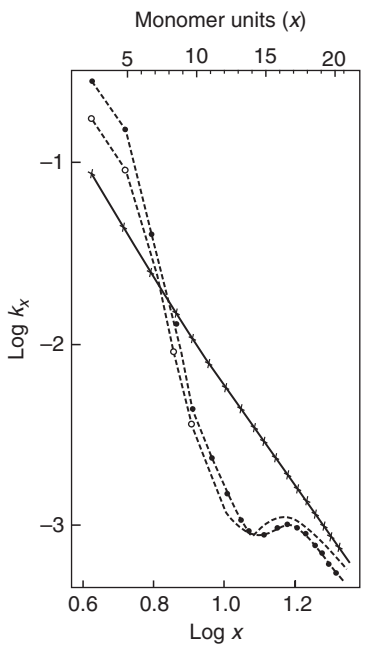

Figure 2 Molar cyclization equilibrium constants K_x for cyclics $((CH_3)_2SiO)_x$ at 383 K for a bulk equilibrate (open circles) are compared with a solution equilibrate (filled circles) and with values calculated (x) according to the J-S theory. K_x values are in mol l^{-1}. Reproduced with permission from Semlyen, J. A. *Adv. Polym. Sci.* **1976**, *21*, 41.[8]

From the formal equilibria for ring–chain interconversions (eqns [2]–[7]), we also get equations for the ring–ring equilibria.

The equilibrium constants for these reactions, derived from the ring–chain equilibria relationships, are also valid, being the real thermodynamic functions, for systems without reaction routes leading to linear polymers. In other words, they are also valid for systems in which ring expansion and ring contraction operate, but there are no reactions for formation of linear polymer.

Taking into account eqn [2], we get the relationships [14]:

$$K_{x,y} = \frac{[\text{c-M}_{x+y}]}{[\text{c-M}_x][\text{c-M}_y]} = \frac{K_{x+y}}{K_x K_y} \qquad [14]$$

indicating that the equilibrium constants of ring–ring equilibria are functions of the macrocyclization equilibrium constants.

Assuming that sufficiently large homogeneous macrocycles are considered (nonstrained and with approximately equal characteristic ratios $C_x \approx C_y \approx C_{x+y} \approx C_\infty$) and that the symmetry numbers for macrocycles are proportional to the ring size, $\sigma_{Rz} = az$, we get, combining eqns [13] and [14], a simple equation relating the ring–ring equilibria constants with the ring sizes

$$K_{x,y} = \frac{K_{x+y}}{K_x K_y} = N_A a \left(\frac{x+y}{xy}\right)^{-5/2} [\, 3/(2\pi C_\infty v l^2)\,]^{-3/2} \qquad [15]$$

where a is a proportion coefficient relating the symmetry number of macrocycles with their size ($\sigma_{Rz} = az$).

This relationship differs from the one given by Kricheldorf, who assumed that the dependence of the equilibrium constants of ring–ring equilibria on the equilibrium constants of ring–chain equilibria can be neglected and that independence of the ring–ring equilibrium constants of the sizes of rings describes the ring–ring equilibrium systems sufficiently well ($K_{x,y} = K_{\text{cyclo}}$, for any x and y).[10]

Moratti[11] criticized the Kricheldorf's paper indicating that this assumption of all ring–ring equilibrium constants being similar is incorrect. Nevertheless, Kricheldorf in the later paper repeats his treatment, extending the simplifying assumption to the kinetically controlled distribution of macrocycles.[12]

One more aspect of ring–ring equilibria can be noted. When no linear polymer can be formed and the system reaches the ring–ring equilibria, the mass–balance relationship without terms for linear polymer has to be held:

$$[\text{M}]_0 = [\text{c-M}_1]_0 = \sum_{i=1}^{\infty} i[\text{c-M}_i] \qquad [16]$$

As can be easily derived from eqn [7], the concentration of any ring at equilibrium is proportional to the ring–chain equilibrium constant and to the corresponding power of the parameter $p = [\text{M}]/K_1$ (defined here on the basis of eqn [7], not in relation to linear polymer as it is not present)

$$[\text{c-M}_i] = K_i \left(\frac{[\text{c-M}_1]}{K_1}\right)^i = K_i \left(\frac{[\text{M}]}{K_1}\right)^i = K_i p^i \qquad [17]$$

Combining eqns [16] and [17], we get the equation relating the initial concentration of monomer to the ring–chain equilibrium constants and the parameter p

$$[\mathrm{M}]_0 = \sum_{i=1}^{\infty} i[\mathrm{c\text{-}M}_i] = \sum_{i=1}^{\infty} iK_i p^i \qquad [18]$$

This parameter p resembles the analogous parameter for equilibrium systems of linear ROP in which p is equal to the ratio of concentrations of chains differing by one repeating unit and is always lower than 1 for such systems.

However, if formation of linear polymer is not possible, and the initial concentration of monomer is above the critical monomer concentration, then the ratio $p = [\mathrm{M}]/K_1$ becomes higher than 1. Otherwise the sum on the right-hand side of eqn [18] would be, at the most, equal to the critical cyclic concentration (cf. eqn [8]), and the eqn [18] would not hold.

Thus, p in systems without linear polymer and initial monomer concentration larger than the critical value is larger than 1 and consequently the total concentration of macrocycles in equilibrium ring-expansion systems without reaction routes leading to linear polymer, is higher than in systems of ring–chain equilibria.

Moreover, we can prove that the J-S theory of ring–chain equilibria, or rather its simplification giving the known dependence of the cyclization equilibrium constants on the ring sizes, is not correct for macrocycles of sizes attaining infinity. Namely, otherwise the infinite sum, defining the total concentration of monomer units in all cyclics (eqn [18]), attains infinity for any $p > 1$

$$[\mathrm{-M-}]_{\mathrm{cyclic}} = \sum_{i=1}^{\infty} i[\mathrm{c\text{-}M}_i] = \sum_{i=1}^{\infty} iK_i p^i = \sum_{i=1}^{\infty} Ai^{-1.5} p^i \qquad [19]$$

where A is a factor stemming from the simplified expression of the macrocyclization equilibrium constants being, according to the J-S theory, proportional to the ring size raised to the power −2.5 (deviation of smaller rings from the general relationship was neglected).

The conclusion is only one: at least for very large macrocycles, the cyclization equilibrium constants have to decrease with the ring size i faster than $i^{-2.5}$. Thus, the slope of log K_x versus log x for at least very large macrocycles has to increase (in absolute value) gradually giving the slope parameter less than −2.5, the value predicted by the J-S theory. This can be associated with not taking correctly into account the exclusion volume factor by the J-S theory or its extensions for very large polymers.

4.04.3 Thermodynamics of Ring–Chain Equilibria in Copolymerization

The J-S theory describing the ring–chain equilibria in systems of nonstrained cyclics can be applied also to copolymerization. However, due to possible differences of comonomers in their structures, including the number and type of atoms, bond lengths, and bond angles, the eqn [13] cannot be applied directly. We have to take into account the equilibrium distribution of comonomer units in copolymer chains of different lengths. Szymanski[13] has proposed relating the copolymerization cyclization equilibrium constants to analogous constants for homopolymerization to simplify the treatment.

Combining the equilibrium constants formulated according to the Flory and Semlyen (eqn [13]) for homo- and copolymeric macrocycles, the following relationship can be obtained:[13]

$$K_{x\mathrm{A}n\mathrm{B}m} = \frac{\sigma_{Rx\mathrm{A}}^{n/x}\sigma_{Rx\mathrm{B}}^{m/x}}{\sigma_{R\mathrm{A}n\mathrm{B}m}K_{x\mathrm{A}}^{n/x}K_{x\mathrm{B}}^{m/x}W} \qquad [20]$$

where $K_{x\mathrm{A}n\mathrm{B}m}$, $K_{x\mathrm{A}}$, and $K_{x\mathrm{B}}$ are the cyclization equilibrium constants for formation of homo- and copolymeric macrocycles composed of x units, $x = n + m$, n, and m are the numbers of A and B units in copolymeric macrocycle, respectively, and σ are the symmetry numbers of macrocycles, W is a function of the mean-square end-to-end lengths of homogeneous and heterogeneous chains of size x

$$W = \left(\frac{\langle r_x^2\rangle_{\mathrm{A}n\mathrm{B}m}}{\langle r_x^2\rangle_{\mathrm{A}x}^{n/x}\langle r_x^2\rangle_{\mathrm{B}x}^{m/x}}\right)^{3/2} \qquad [21]$$

The coefficient W for copolymers of similar monomers can be predicted to be close to 1 and thus can be neglected. For other systems, it can be approximated by computation, for instance, assuming the model of free-joint chain with block distribution of units A and B

$$W = \left(\frac{\langle r_x^2\rangle_{\mathrm{A}n\mathrm{B}m}}{\langle r_x^2\rangle_{\mathrm{A}x}^{n/x}\langle r_x^2\rangle_{\mathrm{B}x}^{m/x}}\right)^{3/2} \approx \left\{\frac{(na-1)L_{\mathrm{A}}^2 + (mb-1)L_{\mathrm{B}}^2 + (L_{\mathrm{A}}^2 + L_{\mathrm{B}}^2)/2}{[(na-1)L_{\mathrm{A}}^2]^{n/x}[(mb-1)L_{\mathrm{B}}^2]^{m/x}}\right\}^{3/2} \qquad [22]$$

where L_{A}^2 and L_{B}^2 are the average squared bond lengths of units A and B, a and b the numbers of bonds in corresponding copolymer units, and the squared AB bond length was approximated by the mean squared length of homogeneous bonds $(L_{\mathrm{A}}^2+L_{\mathrm{B}}^2)/2$. If L_{A} and L_{B} differ much, and the squared length of the A–B bond differs significantly from the assumed value, the real microstructure of the chain corresponding to the given macrocycle (not the block structure assumed above) should be taken into account.

However, unlike in homopolymerization systems, the concentrations of macrocycles are not at equilibrium equal (or approximately equal for not infinitely long linear chains) to the macrocyclization equilibrium constants. It stems from the fact that various compositions and microstructures of chains can usually be obtained depending on the initial monomer feed and copolymerization equilibrium constants (of homo- and crosspropagations). The only exceptions are alternating copolymers for which macrocycle concentrations correspond to macrocyclization equilibrium constants like in homopolymerization systems.

Szymanski[13] formulated the equations for the equilibrium concentrations of copolymer macrocycles as functions of the equilibrium constants of macrocyclizations, homo- and crosspropagations, and equilibrium concentrations of comonomers. For dyad model copolymerization, the derived relationship is the following (eqn [23]):

$$[C_{\mathrm{A}n\mathrm{B}m\mathrm{AB}r}] = K_{\mathrm{A}n\mathrm{B}m\mathrm{AB}r}(K_{\mathrm{AA}}[A])^n(K_{\mathrm{BB}}[B])^m\left(\frac{K_{\mathrm{AB}}K_{\mathrm{BA}}}{K_{\mathrm{AA}}K_{\mathrm{BB}}}\right)^r \qquad [23]$$

where $C_{\mathrm{A}n\mathrm{B}m\mathrm{AB}r}$ denotes a copolymer macrocycle composed of n units A and m units B and containing r AB bonds (and r BA bonds; the number of heterogeneous bonds is $2r$), and with the

distinct symmetry number (depending on microstructure) determining (besides other parameters) the macrocyclization equilibrium constant $K_{AnBmABr}$ (cf. eqn [20]). The brackets are used for denoting the equilibrium concentrations.

Instead of the homo- and crosspropagation equilibrium constants and the equilibrium comonomer concentrations, we can use the experimentally determined ratios of corresponding sequences of linear copolymer. For instance, for dyad model copolymerization, the following equation can be obtained:

$$[C_{AnBmABr}] = K_{AnBmABr}\left(\frac{[-AA-]}{[-A-]}\right)^{n}\left(\frac{[-BB-]}{[-B-]}\right)^{m}\left(\frac{[-AB-][-BA-]}{[-AA-][-BB-]}\right)^{r} \quad [24]$$

Analyzing these equations, we can easily come to the conclusion that linear and cyclic polymers can at equilibrium differ in copolymer units composition and microstructure (e.g., contributions of various triads). Such a phenomenon was observed for some copolymerization systems, for example, the maleic acid units fraction in macrocycles and in linear polymer differ for poly(hexane-1,6-diyl maleate-*co*-hexane-1,6-diyl fumarate).[14]

Equation [24] (after rearrangement) can be used for computing the macrocyclization equilibrium constants in copolymerization on the basis of the determined equilibrium concentrations of macrocycles and linear copolymer microstructure.

The relationships presented for copolymerization systems can also be used for some homopolymerization systems in which polymer with irregular structures is formed, like one containing head-to-head and tail-to-tail sequences. This problem is discussed in Section 4.04.6.2.

When the cyclization equilibrium constants in copolymerization are known, the same eqn [24] can be used to predict the equilibrium concentrations of macrocycles provided the equilibrium composition and microstructure of linear copolymer is known. When the properties of the equilibrium linear copolymer cannot be determined, but the equilibrium constants of macrocyclization and copolymerization are known, the prediction of the equilibrium concentrations of macrocycles can still be accomplished, but only by formulation and solving the set of equations, taking into account besides eqn [23] the mass balance equations for comonomer units in linear and cyclic fractions.[13]

4.04.4 Effects of Pressure and Solvents on the Ring–Chain Equilibria

Smaller cyclic oligomers, due to conformational restrictions as well as changed bond lengths and angles often differ from the high polymer in densities and some other features, like the average dipole moment of repeating units. Consequently, we can expect the dependence of the cyclization equilibrium constants for these cyclics on pressure and the reaction medium, solvent, and dilution.

The effect of pressure on undiluted oligo(dimethylsiloxane) ring–chain equilibria was studied by Wright.[15,16] The author found that at 3500 atm, the weight content of smaller cyclics D_x, where D denotes the dimethylsiloxane unit and $x = 4$, 5, 6, decreases at equilibrium from 6.2, 3.8, 1.6, respectively, at 1 atm to 4.4, 2.8, 1.3, respectively, while the content of larger macrocycles remains unchanged. It is associated directly with the differences of densities of siloxane compounds: at 383 K, the values for cyclic tetramer, pentamer, and high polymer are equal to 0.853, 0.866, and 0.898 g cm^{-3}, respectively.

Wright and Semlyen[17] also observed an increase in the equilibrium constants of cyclization for small-ring cyclic dimethyl-, methyl-, and diethylsiloxanes diluted with diglyme and toluene. For instance, K_x, $x = 4$ and 5, are equal to 0.19 and 0.09 for the undiluted system at 383 K (898 g l^{-1} for dimethylsiloxane compounds) and to 0.21 and 0.13 in diglyme solution (212 g l^{-1}, 333 K), and 0.30 and 0.15 in toluene solution (224 g l^{-1}, 383 K). Consequently, while diluting the systems to the critical concentration (calculated from K_x values for the undiluted systems), the contents of cyclic fraction increases faster than expected.

Solvent also changes the density distribution function of the end-to-end vector $\mathbf{r}$ for linear polymer of x units ($W_x(\mathbf{r})$), influencing in this way directly the ring–chain equilibria. In a good solvent, this effect, associated with the excluded volume, change the power law of the dependence of K_x on the ring size x, making this dependence steeper: instead of −2.5 ($K_x \sim x^{-2.5}$) values −2.8 or even −2.9 are observed.[18,19]

The effect of solvent on the cyclization equilibrium constants was analyzed by Carmichael *et al.*[20] for dimethylsiloxane systems in xylene and diglyme solutions. They explained it from the viewpoint of 'good' (toluene, xylene) and 'poor' solvents (diglyme) and semiempirical parameters of the Flory–Huggins equations for three-component systems.[21]

4.04.5 Kinetics of the Ring–Chain Equilibria in ROP

Looking at the general reaction scheme of the ring–chain equilibria (**Scheme 1**), we can predict that the main factor determining the rates of formation of macrocycles, besides the chemical structures of ROP monomers and initiators/catalysts, is the distance between the reacting entities of linear macromolecule (cyclization).

If diffusion of polymer segments is much faster than the rate of reaction of reacting groups forming the ring closing bond, and the ring strain influencing the activation enthalpy of the reaction can be neglected, the rate of cyclization is proportional to the distribution function of the end-to-end vector $\mathbf{r}$ for linear polymer of x units at $\mathbf{r}$ close to 0 ($W_x(\mathbf{0})$). According to the J-S theory,[3] the chain conformations are governed by the Gaussian distribution of interunit vectors, giving $W_x(\mathbf{0})$ and consequently the rate of cyclization proportional to the ring size raised to the power −3/2 for sufficiently large cyclics.

As there are at least two distinguished routes of macrocycle formation: backbiting and endbiting, that is, the reaction of the ACE of growing macromolecule with the chemical group located inside the chain and with a group located at the second chain-end, the kinetics of macrocycle formation in ROP of the same monomer may differ, depending on composition of the analyzed system, not only quantitatively (different time scales of attaining the equilibrium) but also qualitatively. The groups inside the chains and located at the chain end differ at least in

accessibility (differences in steric hindrance) but often they are also chemically different.

Discussion of one of the possible situations is given in Section 4.04.6.2.

Qualitatively the results of differences in rates of cyclization proceeding via back- and endbiting reactions (the mentioned polymerization of cyclic acetals is just an example) can be described simplifying cyclizations to be one-step reactions.

The differences in end- and backbiting rates result in phenomena known as kinetic enhancement of macrocycles or linear polymer. The former occurs when endbiting is more effective than backbiting and manifests itself in formation of macrocycles during polymerization in concentrations higher than the equilibrium values.

It is observed, for instance, in many ROPs of cyclic acetals and ethers initiated with protonic acids. The hydroxy end group formed in initiation is more effective in cyclization than acetal or ether groups of polymer repeating units, giving as a result a kinetic product with increased concentration of macrocycles, as briefly discussed previously for polymerization of 1,3-dioxolane. When the system can be kept living for a longer time, it eventually reaches the ring–chain equilibrium but for intermediate times the enhancement in macrocycles is observed. Such behavior was modeled by Matyjaszewski *et al.*[22] who have shown, assuming cyclizations to be one-step reactions, that during polymerization in systems with endbiting rate constants larger than those of backbiting, the concentrations of macrocycles after reaching maxima decreases to the equilibrium values. When endbiting can be neglected the concentrations of macrocycles, according to the same paper, steadily increase from zero to the equilibrium concentrations.

Similar simulations were performed by Slomkowski,[23] who assumed that cyclizations via backbiting are one-step reactions while endbiting gives more stable macrocycles with active centers (cf. **Scheme 1**). These activated macrocycles can either react in the reverse reaction giving linear growing chains or react in the exchange reaction of the active center with other cyclics, including monomer. Reactions of activated (e.g., protonated) macrocycle with linear polymer were neglected as well as all reactions leading to its ring opening in reaction with monomer or other compounds.

Nevertheless, such approximation can be justified for some cyclic ethers and acetals, at least for the initial stages of polymerization. The simulations have proved that a high contribution of macrocycles in the kinetic product of polymerization can be expected for systems with effective endbiting, especially for lower initial monomer concentrations, and the ring-expansion mechanism proposed by Plesch and Westermann[1] for cyclic acetals is not necessary to explain the experimental evidence of dominance of cyclics in some polymerizations.

However, the authors of both simulation works mentioned above analyzed systems with high DP_n of linear polymer. When critical concentration (total equilibrium concentration of cyclics for infinite DP_n of linear polymer, expressed in monomer units) for a given monomer is high in comparison to the initial monomer concentration and the concentration of initiator DP_n is also relatively high, the resulting equilibrium linear polymer is of low DP_n. Consequently, the effect of kinetic enhancement of macrocycles, that is, passing of the macrocycle concentrations through maxima, is observed not only for systems with effective endbiting but also for systems with negligible endbiting. This was shown by Szymanski[24] in computer simulations and it stems from changing the molar mass distribution of linear polymer after reaching the maximum monomer conversion. This phenomenon exactly corresponds to the well-known slow decrease in the steady-state (pseudo-equilibrium) concentration of monomer in reversible polymerization, proceeding simultaneously with broadening of the dispersity of polymer chain lengths. The kinetic linear polymer can often have a low dispersity, which means that the concentration of chains of DP close to DP_n can, at these stages of polymerization, be much higher than in the equilibrium product. Consequently, the rates of macrocyclizations leading to rings of those sizes and smaller are much higher than in equilibrium. Consequently, the instantaneous, steady-state concentrations of them can be significantly higher than the equilibrium concentrations. Computer simulations performed for rate constants determined for ε-caprolactone polymerization have shown, for lower initial monomer concentrations, the predicted enhancement of macrocycles, although not confirmed yet experimentally (**Figure 3**).[24]

For systems with propagation rate constants significantly higher than the rate constants of macrocyclization, a phenomenon of kinetic enhancement of linear polymer is observed. When the differences in ring strain and/or other factors influencing reactivity, like steric effect, discriminating monomer from monomer units, are sufficiently large, it is often possible to find an initiator giving active centers of propagation reacting predominantly, almost selectively, with monomer. Reactions with polymer repeating units (macrocyclization or interchain exchange) are much slower. Consequently, in such polymerizations, monomer is converted initially almost exclusively to linear polymer, giving a product of low dispersity. Next, in a different time scale, sometimes practically not attainable, a

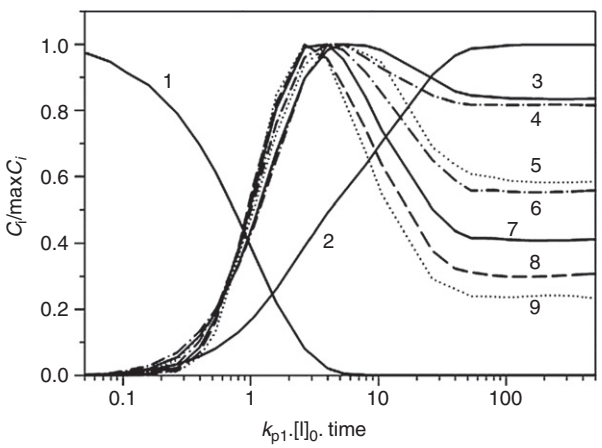

Figure 3 Kinetics of attaining the equilibrium concentrations of macrocycles of the size $x = 2$ to 9 in polymerization of ε-caprolactone computed for $[M]_0/[I]_0 = 22.7$ and the low initial monomer concentration $[M]_0 = 0.08\ mol\ l^{-1}$. The initial condition chosen to get a clearly visible effect of kinetic enhancement of macrocycles despite neglecting the endbiting reaction. Maximum concentrations of cyclics: 0.088 ($C_1 = [M]$), 0.0202 (C_2), 5.29×10^{-3} (C_3), 3.05×10^{-3} (C_4), 1.65×10^{-3} (C_5), 9.15×10^{-4} (C_6), 5.21×10^{-4} (C_7), 3.12×10^{-4} (C_8), 1.88×10^{-4} (C_9), all in $mol\ l^{-1}$. Reproduced with permission from Szymanski, R.; Baran, J. *Polimery (Warsaw)* **2003**, *48*, 758.[24]

macrocyclic product is slowly formed and interchain segmental exchange is also observed. Both these reactions lead to broadening of the molar mass distribution and the ring–chain equilibria can be reached after a much longer time than polymerization.

A special type of kinetic enhancement in linear polymer is observed when the polymerization is carried out via the activated monomer (AM) mechanism. Instead of active species located on the chain ends, the active species is located on some of the monomer molecules. Most often, such an activation proceeds via proton transfer reactions – protonated (cationic process) or deprotonated (anionic process) monomer can further react with the chain ends of linear polymer, increasing their lengths.

As the growing chain does not contain an active center, cyclization reactions are impossible or strongly hindered.

A case of AM polymerization of oxirane is briefly discussed in Section 4.04.6.2.

Specific kinetic enhancement in one type of macrocycle can sometimes be observed in enzymatically catalyzed processes. For instance, in lipase-catalyzed polycondensation of dimethyl terephthalate and diethylene glycol at first a series of cyclic oligomers is formed. Further, due to polymerization/depolymerization of them, almost exclusively a cyclic dimer is obtained[25] while the most stable oligomer is trimer.[26]

4.04.6 Ring–Chain Equilibria in Selected ROP Systems

A few ROP systems in which ring–chain equilibria are important are briefly discussed. No attempt was made to give a comprehensive review of various groups of ROP monomers but peculiarities of the ring–chain equilibria in each of the presented systems are indicated while describing their examples.

4.04.6.1 Ring–Chain Equilibria in Polysiloxane Systems

Polymerizations of cyclic siloxanes are systems in which ring–chain equilibria have been studied in detail for a long time. Following the usage of many authors, the dimethylsiloxane unit is denoted here as D, and consequently cyclic monomers of ring sizes 6, 8, 10, and so on, as D_3, D_4, D_5. Octamethylcyclotetrasiloxane (D_4) is the only significantly strained cyclic monomer of this group, polymerizing readily to a linear polymer (eqn [25]).

$$-P_n^* + D_4 \underset{k_{b4}}{\overset{k_{p4}}{\rightleftharpoons}} -P_{n+4}^* \qquad [25]$$

Depolymerization of poly(dimethylsiloxane) was postulated by Grubb and Osthoff[27] in 1955, but it was Scott[28] in 1946 who first determined the equilibrium concentrations of D_4, as well as of D_3 and several larger macrocycles (a few months earlier, the equilibration reaction between cyclic and linear polysiloxanes was reported by Wilcock[29]).

Polysiloxane systems were the most widely used by several authors to verify the theory of the ring–chain equilibria formulated by Jacobson and Stockmayer. This was because it was relatively easy to determine concentrations of macrocycles up to 200-membered rings and even larger.

Wright and Semlyen[17] have studied the effect of substituents in a polysiloxane system determining the equilibrium cyclization constants for cyclics $[R(CH_3)SiO]_x$, where R = H, Et, Pr, and $CF_3CH_2CH_2$.

There is a significant correlation between equilibrium cyclization constants K_x and the size of the substituent group R. The K_x values for the smallest nonstrained rings ($x = 4$ or 5) increase with the size of R: $H < CH_3 < CH_3CH_2 < CH_3CH_2CH_2 < CF_3CH_2CH_2$. However, the K_x values for the larger macrocycles decrease with increasing size of R and, for example, K_{12} for $[H(CH_3)SiO]_{12}$ is 10 times larger than K_{12} for $[CF_3CH_2CH_2(CH_3)SiO]_{12}$. Such a dependence on the substituent size can be explained by the steric interactions of R, influencing the numbers of possible low-energy conformations of the open-chain molecules. The cyclic tetramer and pentamer can adopt a number of strain-free conformations independently of the size of the studied range of substituents. However, as the group R increases, the number of low-energy conformations, which may be adopted by the corresponding linear chains are drastically reduced, resulting in the increase in the equilibrium cyclization constants K_x in the order of the increasing size of R. For larger macrocycles, which attain the prediction by the J-S theory proportionality of the equilibrium cyclization constants to the ring size in the power – 2.5, the key factor is the decrease in the 'flexibilities' of siloxane chains in the order

$$H > CH_3 > CH_3CH_2 > CH_3CH_2CH_2 > CF_3CH_2CH_2$$

resulting in the parallel decrease in the chain end-to-end vector density $W_{12}(\mathbf{0})$. Consequently, the equilibrium cyclization constants decrease for larger macrocycles with the increase equilibrium in the substituent size.

Similarly, taking into account conformations of linear chains, Wright and Semlyen explain the observed differences in the characteristic minima observed in the log K_x versus log x plots for various R (an example of such a minimum can be seen in **Figure 2**). The minimum is not observed (only a slight inflection point at about $x = 12$) for R = H and for larger R it is shifted to higher values of x with the increase in the substituent size. Consequently, the plots show the limiting slope –2.5 for $x > 12$ and R = H but starting from $x > 25$ for $R = CF_3CH_2CH_2$.

Thomas and Kendrick[30] observed the establishment of the ring–chain equilibria in systems of linear poly(dimethylsiloxane) at high temperatures without catalysts and interpreted their results as the effect of a siloxane-bond interchange reaction involving a four-center transition state. This reaction is in fact a ring-insertion/exclusion reaction (**Scheme 3**) (or ring-expansion/contraction reaction if only cyclic compounds are involved, cf. **Scheme 4**):

Bannister and Semlyen[31] studied an analogous reaction using both linear and cyclic oligo/poly(dimethylsiloxane)s as substrates at temperatures 623–693 K. When cyclic substrates were used, equilibration of the systems gave a product containing a typical cyclic fraction and a high-molar-mass product. The authors believed that the high-molar-mass polymer also had cyclic structure and was formed via siloxane-bond exchange reactions (ring-expansion/contraction reactions) (**Scheme 4**):

If only cyclic compounds are present, the reactions of ring expansion/contraction lead to ring–ring equilibria. However, the authors did not give any evidence that the high-molar-mass product had cyclic structure. Therefore, one cannot exclude that the high-molar-mass product observed by

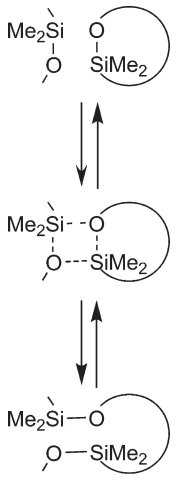

Scheme 3 The ring-insertion/exclusion reaction proposed by Thomas and Kendrick[30] for thermal equilibration of poly(dimethylsiloxane) systems.

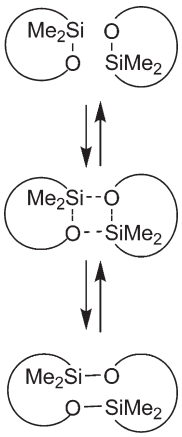

Scheme 4 The ring-expansion/contraction reactions proposed by Bannister and Semlyen[31] for poly(dimethylsiloxane) systems.

the authors is in fact a linear polymer formed from impurities or some degradation products acting as initiators of linear chains, and the ring-expansion/contraction reactions, if really operating in the systems, are only responsible for faster establishing of the ring–chain equilibria. The determined relatively low dispersity of the high-molar-mass polymer may be artificial because of a too low exclusion limit of the used chromatographic columns.

4.04.6.2 Ring–Chain Equilibria in Cyclic Acetals and Ethers Polymerizations

Cyclic acetals are very reactive in cationic conditions and both linear polymer and cyclic compounds are formed. Both types of cyclization (back- and endbiting) are important.

For instance, in polymerization of cyclic acetals the oxonium or oxocarbenium cation acting as the active center of propagation can react with the acetal groups located inside the polymer chain (backbiting) or with the end group, the nature of which depends on the used initiator. If polymerization was initiated with protonic acid, the end group is a hydroxy group. On the other hand, initiation with trialkyloxonium salts gives an ether end group. Both these groups are stronger bases than acetal groups, which causes that cyclization with their participation proceeds faster in comparison to the acetal groups located at the same distance from the active centers. Nevertheless, the kinetics of macrocyclization proceeds in these exemplary systems quite differently. The rates of both types of cyclization decrease with the cycle size proportionally to the probability of formation of the corresponding conformations of linear polymer (as discussed previously $k \sim x^{-3/2}$ for larger cycles). However, besides the relations between the rates of propagation, backbiting, and endbiting, other factors, such as the nature and kinetics of elementary reactions of two- or multistep cyclizations, determine as well the kinetic picture of polymerization.

The effects of the endbiting observed in polymerization of cyclic acetals can be explained as follows (Scheme 5). As an example of cyclic acetals, 1,3-dioxolane was chosen.

Because of low basicity of acetal oxygen atoms in comparison to the end groups in both systems, differing in the initiator used, cyclization involving end groups is faster than the analogous reaction (formation of rings of the same size) involving the acetal groups of polymer repeating groups. However, in order to get a free macrocycle, the intermediate macrocyclic oxonium cation has to react with any nucleophile present in the system (monomer, polymer unit, counter-ion, etc.), converting it to a free macrocycle. If the secondary oxonium cation is considered (protonated macrocycle) deprotonation as a proton transfer reaction is very fast, several orders of magnitude higher than the other possible reactions preventing formation of macrocycle. In Scheme 3, one of these side-reactions is shown, namely the reaction of an activated acetal methylene group (adjacent to the protonated oxygen atom) with monomer. Instead of monomer, shown as an example of a base for the proton transfer reaction, any other nucleophile present in the system, including polymer units or anion of the protonic acid used as initiator, can participate in such reactions. Consequently, as proton transfer reactions are very fast practically any macrocyclization reaction involving the hydroxy end group leads to a macrocycle released to the polymerization medium.

A different situation is when a tertiary macrocyclic oxonium cation involving the ether end group is formed. In order to get a free macrocycle, a reaction of nucleophile (monomer, polymer repeating unit, etc.) with the alkyl group from the end group is necessary. However, the acetal methylene group, also present at the tertiary oxonium atom, is much more reactive. Consequently, most cyclizations involving the ether end group are ineffective from the point of view of macrocycle formation, because predominantly they are followed by reactions of ring opening of the macrocyclic oxonium cation.

If reaction of backbiting is considered, involving the intrachain acetal group, the macrocyclic oxonium cation is about 50% converted to free macrocycle. This is because for nonstrained, sufficiently large cyclic oxonium cations, the reactivities of the two acetal methylene groups at the oxonium oxygen atom – endocyclic and exocyclic – are practically equal, which results in equal probabilities of endo- and exocyclic reactions. The exocyclic attack of monomer leads to free

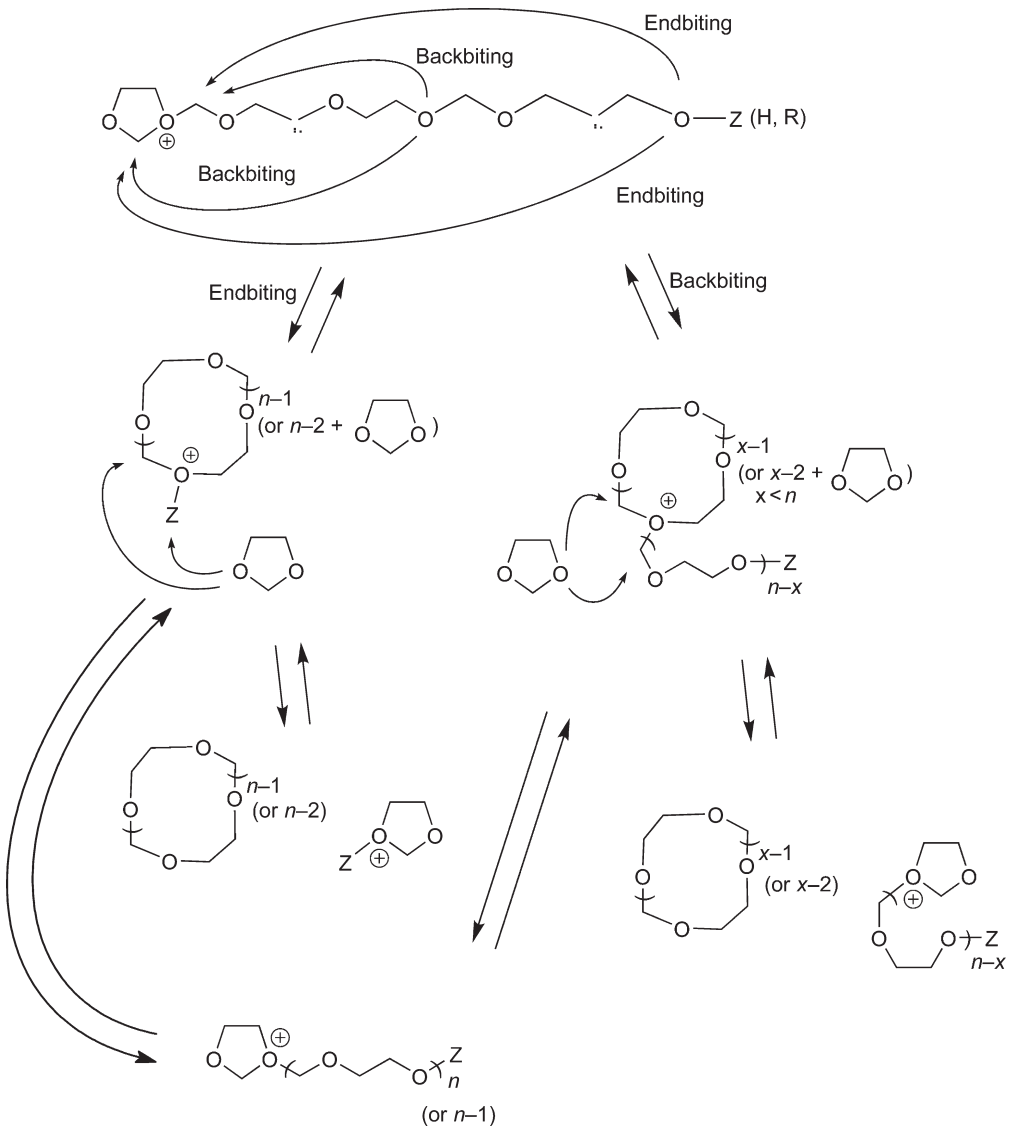

Scheme 5 A simplified reaction scheme for 1,3-dioxolane polymerization initiated with protonic acid (Z=H) or an alkylating agent (Z=R). See text for differences in effectiveness of end- and backbiting in these systems.

macrocycle and a shorter living linear chain, while the analogous endocyclic reaction leads to linear growing chain with the degree of polymerization increased by one unit in comparison to the macromolecule from which the macrocyclic oxonium cation was formed.

It is worth adding that because of at least two bonds (more in compounds with two or more acetal groups) which can be broken in monomer as well as in repeating units of polymer, the redistribution of polymer ends as well as the redistribution of polymer segments has to be considered in polymerization of cyclic acetals. If unsubstituted cyclic acetals with one acetal group, for example, 1,3-dioxolane, are considered only the effect of redistribution of chain ends and reshuffling of polymer segments leading to a faster attainment of the system equilibrium, can be observed. However, when an asymmetrically substituted monomer is polymerized, the effects of head-to-head and tail-to-tail structures and/or tacticity has to be additionally taken into account.

For instance, 4-methyl-1,3-dioxolane can be polymerized at low temperatures[32,33] giving macrocycles differing not only in sizes but also in their structure (structural and geometric isomers).

It is a special case of 1,3,5-trioxepane (TXP) as an example of a cyclic acetal monomer capable of creation of polymer segments as well as cyclic oligomers not being the simple multiplication of monomer units.[34] This monomer contains two acetal groups (and four acetal bonds, easily breakable in cationic conditions) and the real repeating segments in linear polymer and macrocycles, distributed statistically according to polymerization kinetics and the system thermodynamics, are oxymethylene groups (formally formaldehyde monomer units) and 1,3-dioxolane monomer units (Scheme 6).

Both formaldehyde and 1,3-dioxolane can be detected in the equilibrium besides monomer, polymer, and macrocycles. Polymer and macrocycles are composed of the mentioned repeating units, giving various microstructures and

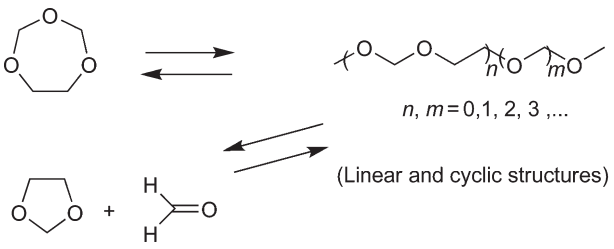

Scheme 6 Equilibria in 1,3,5-trioxepane polymerization.

compositions. TXP can be considered as a composed monomer and the thermodynamic parameters for such a monomer cannot be determined simply on the basis of the measured equilibrium concentrations at several temperatures. Namely, the equilibrium monomer concentration (at high DP_n of linear polymer) is not equal to a reciprocal equilibrium constant of propagation (or to the equilibrium cyclization constant if the ring–chain equilibria are considered) but is also a function of the microstructure of linear polymer. The latter depends, for a given temperature, mainly on initial monomer concentration because the equilibrium concentration of 1,3-dioxolane constitutes a different fraction of the system of 1,3-dioxolane units depending on the system. As it was indicated first by Szwarc and Perrin,[35] and then the corresponding relationship corrected by Szymanski,[13] the equilibrium constant of propagation for 1,3,5-trioxepane K_{TXP} (equal to the reciprocal equilibrium constant of cyclization) can be computed, taking into account, besides the equilibrium concentration of TXP, the polymer composition:

$$K_{TXP} = K_{cTXP}^{-1} = [TXP]^{-1} \frac{[-TXP-]^2}{[-E-]([-M-]-[-E-])} \qquad [26]$$

where K_{TXP} and K_{cTXP} are the equilibrium constants of TXP polymerization and of the corresponding cyclization, while –TXP–, –E–, –M–, denote TXP, oxyethylene, and formaldehyde units, respectively.

The general equation for determination of the equilibrium cyclization constants for the composed cyclics is in fact the one shown previously in Section 4.04.2 (eqn [24]), because the equilibrium in polymerizations of such monomers is the same as in copolymerization of corresponding simpler monomers (e.g., 1,3,5-trioxepane polymerization versus 1:1 copolymerization of 1,3-dioxolane and formaldehyde).

In ROP polymerization of cyclic ethers, oxiranes are the ones with the highest ring strain.[36] They can undergo the ring-opening reactions in anionic and cationic as well as in coordination processes. However, cyclization requires the reaction of the ether groups of linear polymer with active species and the only effective reaction proceeds with cationic species (and some dormant forms of them, like trifluoromethanesulfonate ester groups). As a result of fast cyclization, leading at first to nonstrained oxonium cations (preferably with six-membered rings when without bulky substituents), cyclic oligomers are formed (Scheme 7).

Consequently, linear polymer cannot be usually obtained because of kinetic enhancement in macrocycles connected with conversion of the active center of oxirane propagation to more stable nonstrained oxonium cations. Dale *et al.*[37] have observed that oligomerization of oxirane with BF_3 in

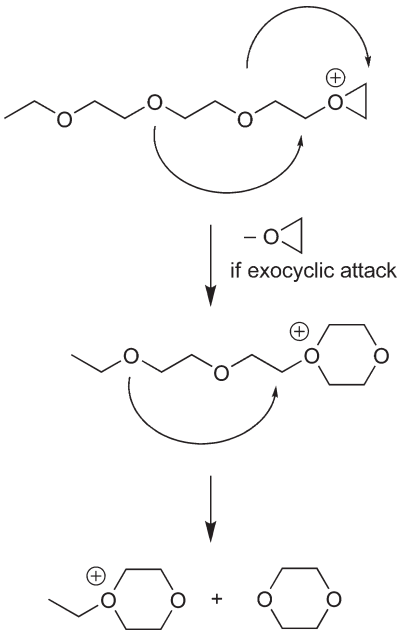

Scheme 7 Formation of 1,4-dioxane in cationic active chain-end (ACE) polymerization of oxirane. Larger cyclics can be formed in a similar way.

dichloromethane containing deuterated 1,4-dioxane gave after 8 h a product containing 85 wt.% of dioxane. Larger identified cyclic oligomers of oxirane were trimer to hexamer, in quantities, respectively: 1, 4, 1, 1 (wt.%), while still 8 wt.% of oxirane was unreacted. Linear product was not observed.

For bulky substituted oxiranes, the kinetic enhancement in cyclics are also observed but the main products of cyclization are tetramers.[38]

However, while applying the method of the AM polymerization, oxiranes can be polymerized to linear oligomers.

For instance, oxiranes in the presence of alcohols giving, as initiators, its hydroxy and alkyl groups to polymer chains can be polymerized via the AM mechanism while catalyzed with strong protonic acids (like $HAsF_6$, also generated *in situ* from, e.g., oxonium salts) (Scheme 8).

AM, reacting with the polymer hydroxy end group, forms intermediate secondary oxonium cation and after deprotonation a linear chain by one monomer unit longer. As the reactivity of hydroxy end groups toward AM is higher than toward ether groups of repeating units, linear oligomers can

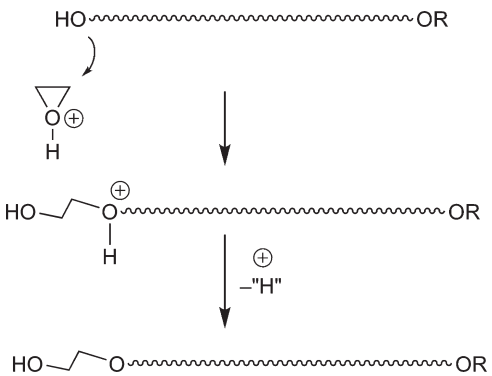

Scheme 8 Activated-monomer polymerization of oxirane.

be obtained and such a polymerization can be treated as a process with kinetic enhancement in the linear polymer – ring–chain equilibria not reached in the polymerization time scale.

Formation of cyclic oligomers in cationic polymerization of highly strained four-membered cyclic ethers, oxetanes, seems to proceed in parallel with propagation and virtually stops when monomer is consumed.[39] The equilibrium is not attained probably because the active species of propagation are not stable and their terminated forms, like protonated polymer, formed after finished polymerization, are not effective in starting any cyclization reactions, unless a new portion of monomer is added.

Nonstrained cyclic ethers are much less reactive. Therefore, attaining the ring–chain equilibria takes much time despite the stability of active species (oxonium cations) in many systems. Nevertheless, formation of cyclic oligomers was reported for all common monomers belonging to this group.

Pruckmayr,[40,41] for instance, reported formation of cyclic oligomers in polymerizations of tetrahydrofuran (THF) initiated with both trialkyloxonium salts and trifluoromethanesulfonic acid (TfOH). As expected, more cyclic oligmers were observed in the systems with TfOH as initiator, although no kinetic enhancement in macrocycles was observed. It stems probably from higher reactivities of ether groups in polymer chain than of terminal hydroxy groups toward the exo- and endocyclic methylene groups of the five-membered oxonium cation – active center of THF polymerization. Additionally, a high effectiveness of backbiting leading to fast re-formation of the active center from the side-chain of the macrocyclic oxonium cation plays an important role in limiting the contribution of endbiting (see Scheme 9). In the scheme, cyclization reactions involve exocyclic methylene groups. However, formation of sufficiently large macrocycles via backand endbiting can also proceed with an attack on endocyclic methylene groups adjacent to oxonium atom (steric hindrance prevents this back attack breaking endocyclic O–C bond only in smaller rings).

4.04.6.3 Ring–Chain Equilibria in Cyclic Ester Polymerizations

In this section some systems of ROP of cyclic esters (of carboxylic acids, including carbonates) are reviewed from the point of view of importance of the ring–chain equilibria. All these monomers are capable of undergoing the ring-opening reactions involving the carbonyl group. The mechanisms of these reactions depend on the reagents used but independently of these mechanisms the eventual equilibria of linear polymer and cyclics, usually monomer and macrocycles, depend only on the structure of monomer and reaction conditions (dependences of the equilibrium concentrations of strained cyclics on temperature and of all cyclics on solvation phenomena). If monomer is significantly more strained than other cyclics, it is often possible to find an initiator creating an active center of polymerization reacting almost selectively only with monomer. Reactions with repeating units, either of its own chain, leading to macrocyclization, or of other macromolecules, resulting in reshuffling of polymer segments in and between chains, is much slower, sometimes negligible. In such systems, we have the kinetic enhancement in linear polymer, usually of low dispersity. The thermodynamic product containing macrocycles and the most probable distribution of chain lengths of linear polymer is not formed in applied polymerization times. An example of such a situation is polymerization of ε-caprolactone, which is strained only moderately ($\Delta H_{lc} = -28.8\ kJ\ mol^{-1}$)[42] and forms macrocycles easily while polymerized with most anionic, cationic, and coordination

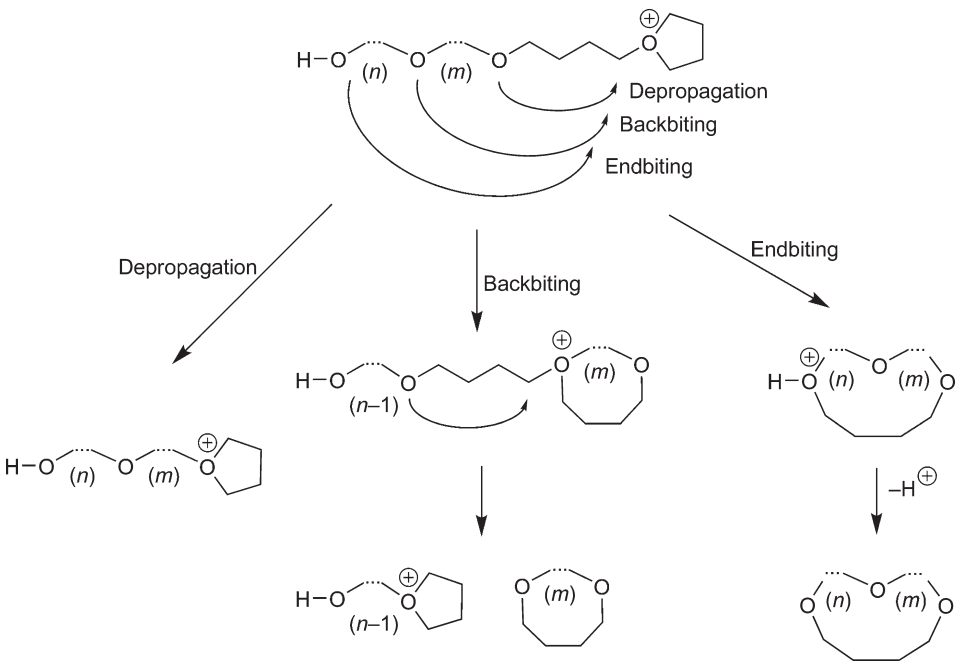

Scheme 9 Macrocyclization in polymerization of THF initiated with strong protonic acids. The suspension points denote a number of repeating units (the numbers indicated in parentheses).

initiators. It can be polymerized to linear polymer of low dispersity when a coordination initiator creating active species with large steric hindrance is used.

Hofman *et al.*[43] presented a system of ε-caprolactone polymerization with suppression of macrocycle formation, observed when using $MeOAlEt_2$ as initiator. The authors explained the results by a high selectivity ratio of active species of propagation, reacting preferably with monomer, while cyclization reactions were much slower due to steric hindrance at the ACE. The following equation for the selectivity ratio, defined as the ratio of the propagation and cyclization rate constants ($k_{p1}/k_{c(n)}$), was derived:

$$\frac{\ln([M]/[M]_0)}{\ln\left(([C_n]_e - [C_n])/[C_n]_e\right)} = \frac{k_{p1}}{k_{c(n)}}[C_n]_e \qquad [27]$$

where k_{p1} is the propagation rate constant and $k_{c(n)}$ is the cyclization rate constant of formation of macrocycle of size n (C_n), brackets indicate concentrations of monomer and macrocycle, subscripts e indicate equilibrium values for high DP_n of linear polymer while 0 initial conditions (the equilibrium concentration of monomer is assumed to be close to zero).

This equation relates the concentrations of macrocycles in the polymerization system to monomer concentration. The higher the selectivity ratio ($k_{p1}/k_{c(n)}$), the lower is concentration of macrocycle at the given monomer concentration

$$[C_n] = [C_n]_e\left\{1-\left(\frac{[M]}{[M]_0}\right)^{\frac{k_{c(n)}}{k_{p1}[C_n]_e}}\right\} \qquad [28]$$

(equation obtained by rearrangement of eqn [27]).

Baran *et al.*[44] analyzed a series of initiators for polymerization of ε-caprolactone and found that for bulky active species in systems initiated with triisopropoxyaluminum the selectivity ratio, defined as the ratio of the propagation rate constant to the sum of cyclization rate constants (depropagation neglected), was equal to 3×10^5 while for anionic polymerization (sodium ethanolate) this ratio was equal only to 1.6×10^3.

Applying zinc octoate as initiator, forming also bulky active species, allowed high-molar-mass poly(ε-caprolactone) ($M_n \sim 4 \times 10^5$) to be obtained with no cyclic oligomers formed.[45]

Florczak and Duda,[46] while using as initiator aluminum alkoxide with a didentate, bulky ligand of the R or S configuration, 2,2′-[(1,1′-binaphthalene-2,2′-diyl)bis(iminomethyl)] diphenoxide, observed negligible formation of macrocycles not only in polymerizations of ε-caprolactone and L,L-lactide, but also in copolymerizations of these monomers. Additionally, applying enatiomerically pure R or S forms of the initiator or their mixtures they could get copolymers of various controlled microstructures.

Kricheldorf published a series of papers indicating that the ring-expansion polymerization of various monomers can be carried out when appropriate initiators are used (e.g., Reference 47 and references therein). Applying cyclic tin alkoxides, he managed to obtain tin-containing cyclic polyesters. For instance, when 2,2-dibutyl-1,3,2-dioxastannepane (2,2-dibutyl-2-stanna-1,3-dioxepane, DSDOP) was used as initiator in polymerization of ε-caprolactone the product was cyclic polymer formed by addition to the initiator ring a number of monomer molecules.[48] Although polymerization

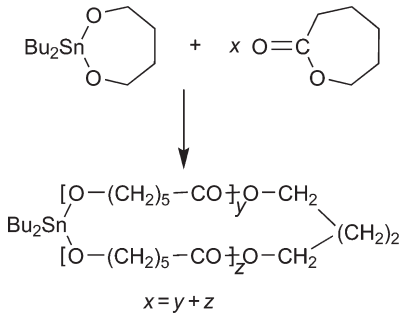

Scheme 10 Polymerization of ε-caprolactone via monomer insertion to cyclic dialkoxydialkyltin species.[48]

resembled a living process, the dispersity of the product was about 1.5, much higher than expected. If the ring–ring equilibrium is considered, the process can be treated as a kinetic enhancement in rings containing one initiator unit (Scheme 10).

The thermodynamic product would contain oligomers of ε-caprolactone as well, formed in ring-contraction reactions (Scheme 11). Cyclics containing more than one tin atom, formed in statistically less frequent reactions of ring-expansion/contraction of tin-containing macrocycles.

If a reaction route leading to linear polymer were available, which cannot be excluded, the ring–chain equilibria should be considered as well. Unfortunately, no equilibrium was established in the studied systems and therefore no comparison with the ε-caprolactone ring–chain equilibria could be performed.

A special case of kinetic enhancement in macrocycles is observed when a zwitterionic polymerization of lactide was carried out. Waymouth and co-workers[49,50] have observed formation of cyclic polymer of M_n up to 3×10^4 and dispersity below 1.3 when polymerization was initiated by heterocyclic carbene (1,3-dimesitylimidazol-2-ylidene). It stems probably from propagation being much faster than cyclization and end-biting being much faster than backbiting. The latter can be explained by the reaction of oppositely charged chain-ends, located close to each other more frequently than can be expected for neutral chains (Scheme 12).

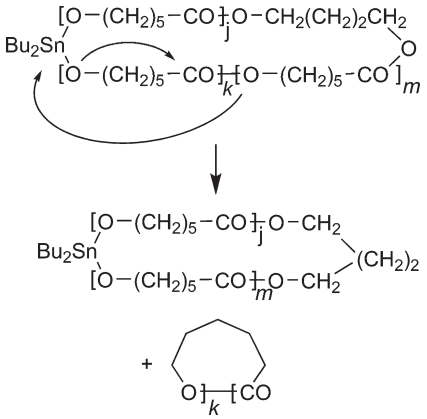

Scheme 11 The ring-contraction reaction of the tin-containing macrocycles of poly(ε-caprolactone) system leading to ε-caprolactone cyclic oligomers.

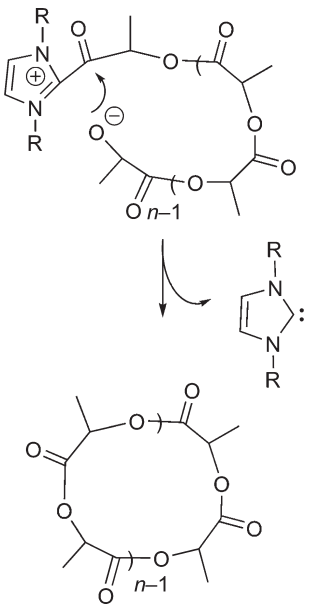

Scheme 12 Formation of macrocycles in zwitterionic polymerization of lactide.[49]

Kinetic enhancement in cyclics was also observed by Kricheldorf *et al.*[51] in polymerization of L-lactide with imidazole. The authors proposed the mechanism of formation of cyclics via endbiting, involving the increased reactivity of the carbonyl group of terminal polymer unit bonded to the imidazole moiety. However, the participation of the zwitterionic structures cannot be excluded here as well.

Macrocyclic oligoesters are often convenient monomers for preparation of high-molar-mass polymer. They have advantages over polycodensation monomers (e.g., diacid/diol monomers) because no by-product has to be removed during polymerization, the process can be carried out usually at lower temperatures, and the viscosity of the polymerization mixture is lower. Polymerization of macrocyclic oligoesters, as an entropy-driven process with often negligible enthalpic effect, has no technological limitations of the polymerization volume because of the heat transfer problems. The only important drawback of polymerization of macrocyclic oligoesters is their limited availability.

Ballone and Jones[52,53] studied ROP of cyclic oligomers of Bisphenol A polycarbonate using density functional calculations of the structure, potential energy surface, and reactivity of species. In their Monte Carlo simulations, the authors demonstrated that entropy in redistribution of interparticle bonds was the driving force for chain formation in the studied polymerization of macrocycles.

Several methods of preparation of such macrocyclic monomers, capable of polymerization to high-molar-mass polymers, were described in literature. Virtually all of them are reviewed in two sections of the 'Cyclic Polymers' book edited by Semlyen.[54,55] The most important two methods of them are:

1. high-dilution polycondensation of corresponding monomers, for example, preparation of macrocyclic carbonates in polycondensation of bis(chloroformate) of 4,4′-isopropylidenediphenol (BPA) with BPA (and its monochloroformate, both formed *in situ* from BPA dichloroformate);[56]
2. depolymerization of linear polyesters, for example, of poly(propane-1,3-diyl succinate) yielding a distillate containing 89% of cyclic dimer and 9% of cyclic monomer.[57]

Cyclic oligomers of poly(ethylene terephthalate) (PET) can be obtained by both mentioned methods.[58] The authors also studied polymerization of cyclic oligomers of PET and found that they readily polymerize if hydroxy-containing compounds are added. Without addition of such initiating species, cyclic tris(ethylene terephthalate) polymerizes extremely slowly even at temperatures up to 300 °C.

Preparation of high-molar-mass polyesters from cyclic oligomers seems to be a promising route. In literature, many such processes were described. For instance, many cyclic carbonates of bisphenols (mixtures of oligomers) could be polymerized to high-molar-mass polymers.[59,60]

Applications of macrocyclic oligomers of engineering thermoplastics (not only oligoesters) were reviewed by Brunelle.[61]

4.04.6.4 Ring–Chain Equilibria in Other ROP Systems

Ring–chain equilibria or reversible formation of cyclic oligomers were observed in ROP polymerizations of all other groups of ROP monomers. However, no detailed descriptions of the corresponding systems will be given in this section of the review, and many monomer groups will not be even mentioned. The interested reader can find the corresponding literature relatively easily.

In this section, only the most important groups of ROP systems, in which the ring–chain equilibria are important, but not discussed previously, are presented.

4.04.6.4.1 Cyclic oligomers of polylamides

The chain–ring equilibria are often observed in systems of polyamides. Independently of the route of preparation of polymers (polycondensation, polymerization of lactams, or other cyclic amides, including cyclic oligomers) the ring–chain interconversions are often important and cannot be neglected. However, the equilibrium conditions usually are not reached and often only kinetic distributions can be observed.

Oligo/macrocyclic polyamides are frequent contaminations of commercial polyamides, like various Nylons, and often have to be removed by extraction with hot water.[62–64]

According to Mori *et al.*,[65] the content of cyclics in polycaprolactam reaches about 10% (8% monomer), while in poly(dodecano-12-lactam) 1.5% (0.3% monomer).

Gupta *et al.*[66] simulated polymerization of caprolactam including all important reactions: reversible ROP, polycondensation, polyaddition, and cyclization reactions as well as the reaction with monofunctional acids and found that reactions constituting the ring–chain equilibria influence the molar mass distribution of product.

4.04.6.4.2 Cyclic poly(aryl ether)s

Cyclic poly(aryl ether)s containing electron-withdrawing groups, enabling nucleophilic substitution in aromatic rings, can be polymerized with nucleophilic initiators.[67–69] These oligomers are usually prepared by condensation, but the proposed mechanisms of polymerization and the often observed presence of cyclic oligomers in product suggest that polymerization is reversible and degradation of high-molar-mass

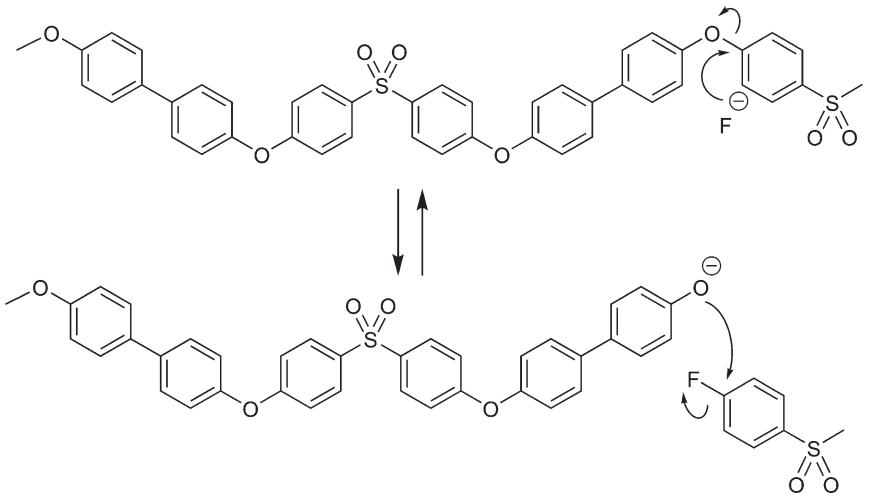

Scheme 13 Reversible initiation of cyclization processes with fluoride anion in poly(aryl ether) systems.[68]

polymer carried out in dilute solution could also give cyclic oligomers if a proper initiator was chosen.

Colquhoun *et al.*[68] managed to obtain cyclic oligomers from poly(ethersulfone), poly(oxybiphenyl-4,4′-diyloxy-1,4-phenylenesulfonyl-1,4-phenylene), by initiating the process with fluoride anion in dilute dimethylacetamide solution (Scheme 13).

After getting cyclic oligomers via cyclodepolymerization, the authors polymerized them using as initiator cesium salt of 4-benzoylbenzene-1-thiol getting linear polymer of rather high dispersity ($M_w = 151\,000$, $M_n = 26\,000$, and a level of residual macrocyclic oligomers of ~4%). Unfortunately, no studies have been performed to determine equilibrium constants of the ring–chain equilibria (Scheme 14).

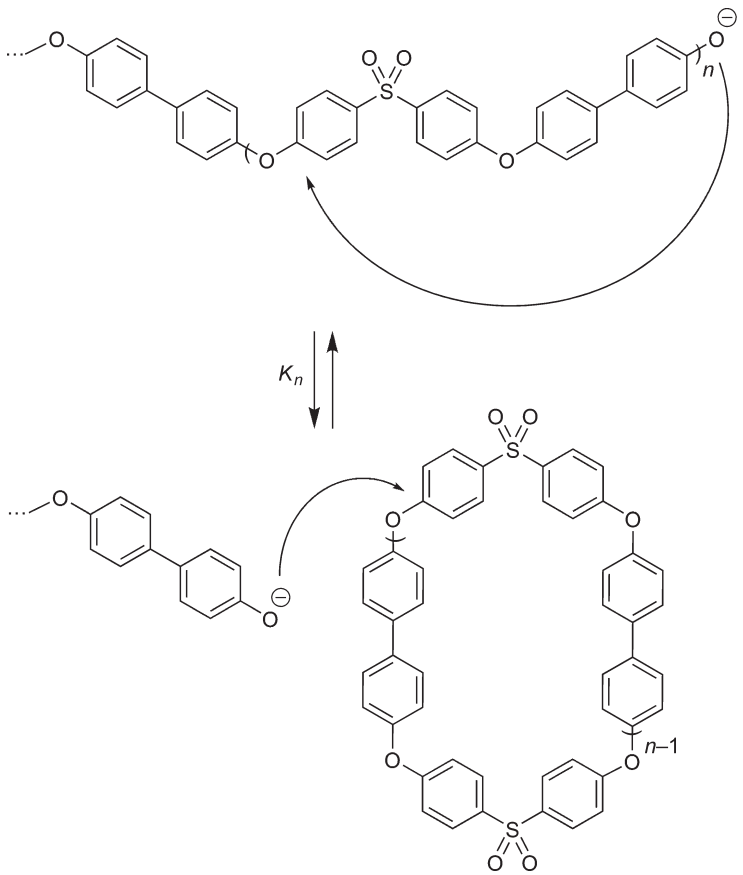

Scheme 14 Cyclizations in poly(aryl ether) systems and polymerization of cyclic oligomers.

4.04.6.4.3 Metathesis ROP systems

Many cyclic hydrocarbons containing unsaturated bonds (double or triple carbon-to-carbon bonds) can undergo ROP via metathesis reaction. These processes are usually reversible and cyclic oligomers are often observed as kinetic or thermodynamic side-products. In this section, no details of polymerization processes will be given. The interested reader can consult some reviews on metathesis polymerizations[70–72] and original papers cited therein. Here, only some specific features of ring–chain equilibria in metathesis ROP (ROMP) are mentioned and briefly discussed.

Cycloolefins as well as resulting linear and cyclic oligomers and linear polymers can have *cis* and *trans* configurations at the C=C bond. Depending on the catalyst used and possible mechanisms of polymerization, we can expect various types of interconversions. Configuration of the C=C bond in monomer may be either preserved after incorporation into polymer chain or changed, or both possible configurations in polymer can be formed. Similar problems can be expected if cyclizations leading to cyclic oligomers are analyzed. Besides, if substituted cycloolefins are polymerized structural isomerism (head-to-tail and head-to-head structures) and/or tacticity has to be taken into account.

All these structural variations imply differences in linear chain conformation distributions depending on chain structure.

The observed dependence of the cyclization rate constants on the number of monomer units was often steeper than expected from the J-S theory ($K_x \sim x^{-2.5}$) and explained by nontheta solvent conditions. The exponent was usually expressed as $-(2+a)$, where a, the exponent of the Mark–Houwink relation between intrinsic viscosity and molecular weight, was found to be, for instance, 0.68 for cyclooctene oligomers in chlorobenzene,[72] 0.67 for poly(1-octene-1,8-diyl)/toluene,[73] and 0.72 for polybutadiene/toluene.[74]

The equilibrium cyclization constants in respect to *cis–trans*, as well as to structural or configurational isomerism in ROMP, was not studied in detail. However, after analyzing the distribution of *cis trans* configurations, Thorn-Csányi and Ruhland[75] observed that the proportion of ttt to ctt trimeric rings in the equilibrium of 1,4-polybutadiene system ($-CH_2CH{=}CHCH_2-$) was about 9 in toluene and 10 in cyclohexane, while the ratio of *trans* to *cis* configurations in linear polymer was 83:17. The exclusively entropically controlled backbiting process should, according to the authors, give the same *cis*/*trans* ratio in cyclics of all sizes. Therefore, these results for cyclic trimers, and the differences also observed for larger cyclics, indicate that some other factors, enthalpic in nature, such as exothermic formation of trimers, influence the ring–chain equilibria as well.[76]

4.04.7 Conclusions and Outlook

The ring–chain equilibration is a phenomenon frequently observed in ROP systems. Most often, it is treated as disadvantage disallowing a high-molar-mass polymerization product to be obtained. Knowledge of mechanism, kinetics, and thermodynamics of the ring–chain equilibria often allows the problems in obtaining a high-molar-mass products with negligible content of macrocycles to be overcome. However, for some systems, ring–chain equilibria can give access to low-molar-mass cyclics allowing the polymerization of them in a more controlled way than in direct polycondensation routes from initial substrates. Moreover, macrocycles, capable of being polymerized or used in other chemical processes, can often be produced from waste polymeric materials. Thus, ring–chain equilibria enable the recycling of such materials, which is becoming more and more important nowadays when environmental issues cannot be neglected.

References

1. Plesch, P. H.; Westermann, P. H. *J. Polym. Sci., Part C: Polym. Symp.* **1968**, *16*, 3837.
2. Szymanski, R.; Kubisa, P.; Penczek, S. *Macromolecules* **1983**, *16*, 1000.
3. Jacobson, H.; Stockmayer, W. H. *J. Chem. Phys.* **1950**, *18*, 1600.
4. Szymanski, R., computed for this review on the basis of eqn [8] and DP_n found from the mass balance equation $[M]_0 = [-M-]_{cyclic} + DP_n \times [I]_0$.
5. Andrews, J. M.; Semlyen, J. A. *Polymer* **1972**, *13*, 142.
6. Flory, P. J.; Semlyen, J. A. *J. Am. Chem. Soc.* **1966**, *88*, 3209.
7. Brunelle, D. J. In *Encyclopedia of Polymer Science and Technology*; Wiley, **2008** (online).
8. Semlyen, J. A. *Adv. Polym. Sci.* **1976**, *21*, 41.
9. Suter, U. W.; Höcker, H. *Makromol. Chem.* **1988**, *189*, 1603.
10. Kricheldorf, H. R. *Macromolecules* **2003**, *36*, 2302.
11. Moratti, S. C. *Macromolecules* **2005**, *38*, 1520.
12. Kricheldorf, H. R.; Lomadze, H. *J. Polym. Sci., Ser. C* **2009**, *51*, 133.
13. Szymanski, R. *Makromol. Chem.* **1989**, *190*, 2903.
14. Mezoul, G.; Lalot, T.; Brigodiot, M.; Maréchа1, M. *Macromol. Chem. Phys.* **1996**, *197*, 3581.
15. Wright, P. V. PhD thesis, University of York, York, UK, **1970**.
16. Wright, P. V.In *Ring-Opening Polymerization*; Ivin, K. J., Saegusa, T., Eds.; Elsevier: London, UK, **1984**; Vol. 2, p 1055.
17. Wright, P. V.; Semlyen, J. A. *Polymer* **1970**, *11*, 462.
18. Brown, J. F.; Slusarczuk, G. M. *J. Am. Chem. Soc.* **1965**, *87*, 932.
19. Cloiseaux, J. des *J. Phys., Colloq.* **1978**, *C2*, 135.
20. Carmichael, J. B.; Gordon, D. J.; Isackson, F. J. *J. Phys. Chem.* **1967**, *71*, 2011.
21. Flory, P. J. *Principles of Polymer Chemistry*; Cornell University Press: Ithaca, NY, **1953**.
22. Matyjaszewski, K.; Zielinski, M.; Kubisa, P.; *et al. Makromol. Chem.* **1980**, *181*, 1469.
23. Slomkowski, S. *Makromol. Chem.* **1985**, *186*, 2581.
24. Szymanski, R.; Baran, J. *Polimery (Warsaw)* **2003**, *48*, 758.
25. Lavalette, A.; Lalot, T.; Brigodiot, M.; Maréchа1, E. *Biomacromolecules* **2002**, *3*, 225.
26. Goodman, I.; Nesbitt, B. F. *Polymer* **1960**, *1*, 384.
27. Grubb, W. T.; Osthoff, R. C. *J. Am. Chem. Soc.* **1955**, *77*, 1405.
28. Scott, D. W. *J. Am. Chem. Soc.* **1946**, *68*, 2294.
29. Wilcock, D. F. *J. Am. Chem. Soc.* **1946**, *68*, 691.
30. Thomas, T. H.; Kendrick, T. C. *J. Polym. Sci., Part A-2* **1969**, *7*, 537.
31. Bannister, D. J.; Semlyen, J. A. *Polymer* **1981**, *22*, 377.
32. Firat, Y.; Plesch, P. H. *Makromol. Chem.* **1975**, *176*, 1179.
33. Goulart, G.; Sanchez, J.-Y.; Armand, M. *Electrochim. Acta* **1992**, *37*, 1589.
34. Schulz, R. C.; Albrecht, K.; Rentsch, C.; Tran Thi, Q. V. *ACS Symp. Ser.* **1977**, *59*, 77.
35. Szwarc, M.; Perrin, C. L. *Macromolecules* **1979**, *12*, 699.
36. Pell, A. S.; Pilcher, G. *Trans. Faraday Soc.* **1965**, *61*, 71.
37. Dale, J.; Daasvatn, K.; Grønneberg, T. *Makromol. Chem.* **1977**, *178*, 873.
38. Sato, A.; Hirano, T.; Suga, M.; Tsuruta, T. *Polym. J.* **1977**, *9*, 209.
39. Dreyfuss, P.; Dreyfuss, M. P. *Polym. J.* **1976**, *8*, 81.
40. McKenna, J. M.; Wu, T. K.; Pruckmayr, G. *Macromolecules* **1977**, *10*, 877.
41. Wu, T. K.; Pruckmayr, G. *Macromolecules* **1978**, *11*, 265.
42. Duda, A.; Penczek, S. In *Polymers from Renewable Resources: Biopolyesters and Biocatalysis*; Scholz, C., Gross, R. A., Eds.; American Chemical Society: Washington, DC, **2001**; p 160.
43. Hofman, A.; Slomkowski, S.; Penczek, S. *Makromol. Chem.* **1987**, *188*, 2027.
44. Baran, J.; Duda, A.; Kowalski, A.; *et al. Macromol. Symp.* **1997**, *123*, 93.
45. Kowalski, A.; Libiszowski, J.; Majerska, K.; *et al. Polymer* **2007**, *48*, 3952.
46. Florczak, M.; Duda, A. *Angew. Chem., Int. Ed.* **2008**, *47*, 9088.
47. Kricheldorf, H. R.; Stricker, A. *Macromolecules* **2000**, *33*, 696.

48. Kricheldorf, H. R.; Eggerstedt, S. *Macromol. Chem. Phys.* **1998**, *199*, 283.
49. Culkin, D. A.; Jeong, W.; Csihony, S.; *et al. Angew. Chem., Int. Ed.* **2007**, *46*, 2627.
50. Jeong, W.; Shin, E. J.; Culkin, D. A.; *et al. J. Am. Chem. Soc.* **2009**, *131*, 4884.
51. Kricheldorf, H. R.; Lomadze, N.; Schwarz, G. *Macromolecules* **2008**, *41*, 7812.
52. Ballone, P.; Jones, R. O. *J. Chem. Phys.* **2001**, *115*, 3895.
53. Ballone, P.; Jones, R. O. *Comput. Phys. Commun.* **2002**, *147*, 325.
54. Brunelle, D. J. In *Cyclic Polymers*; Semlyen, J. A., Ed.; Kluwer: New York, **2000**; p 185.
55. Wood, B. R.; Hamilton, S. C. In *Cyclic Polymers*; Semlyen, J. A., Ed.; Kluwer: New York, **2000**; p 271.
56. Brunelle, D. J.; Shannon, T. G. *Macromolecules* **1991**, *24*, 3035.
57. Spanagel, E. W.; Carothers, W. H. *J. Am. Chem. Soc.* **1935**, *57*, 929.
58. Burch, R. R.; Lustig, S. R.; Spinu, M. *Macromolecules* **2000**, *33*, 5053.
59. Brunelle, D. J. *Makromol. Chem., Macromol. Symp.* **1992**, *64*, 65.
60. Brunelle, D. J.; Boden, E. P. *Makromol. Chem., Macromol. Symp.* **1992**, *54/55*, 397.
61. Brunelle, D. J.In *Encyclopedia of Materials: Science and Technology*; Buschow, K. H. J., Cahn, R. W., Flemings, M. C., Ilschner, B., Kramer, E. J., Mahajan, S., Eds.; Elsevier: Amsterdam, The Netherlands, **2001**; Vol. 5, p 4712.
62. Jacobs, D. B.; Zimmerman, J. In *High Polymers*; Schildknecht, C. E., Skeist, I., Eds.; Wiley: New York, **1977**; Vol. 29, p 424.
63. Sekiguchi, H.In *Ring-Opening Polymerization*; Ivin, K. J., Saegusa, T., Eds.; Applied Science Publishers: London, UK, **1984**; Vol. 2, p 809.
64. Sebenda, J. In *Comprehensive Chemical Kinetics*; Bamford, C. H., Tipper, C. F. H., Eds.; Elsevier: Oxford, UK, **1976**; Vol. 15, p 379.
65. Mori, S.; Furusawa, M.; Takeuchi, T. *Anal. Chem.* **1970**, *42*, 661.
66. Gupta, S. K.; Naik, C. D.; Tandon, P.; Kumar, A. *J. Appl. Polym. Sci.* **1981**, *26*, 2153.
67. Xie, D.; Ji, Q.; Gibson, H. W. *Macromolecules* **1997**, *30*, 4814.
68. Colquhoun, H. M.; Dudman, C. C.; Thomas, M.; *et al. J. Chem. Soc., Chem. Commun.* **1990**, 336.
69. Wang, Y.-F.; Chan, K. P.; Hay, A. S. *J. Polym. Sci., Part A: Polym. Chem.* **1996**, *34*, 375.
70. Ivin, K. J.; Mol, J. C. *Olefin Metathesis and Metathesis Polymerization*; Academic Press: London, UK, **1997**.
71. Bielawski, C. W.; Grubbs, H. R. *Prog. Polym. Sci.* **2007**, *32*, 1.
72. Grubbs, R. H. *Handbook of Metathesis*; Wiley-VCH: Weinheim, Germany, **2003**.
73. Reif, L.; Höcker, H. *Macromolecules* **1984**, *17*, 952.
74. Glenz, W.; Holtrup, W.; Kupper, F. W.; Meyer, H. H. *Angew. Makromol. Chem.* **1974**, *37*, 97.
75. Thorn-Csányi, E.; Ruhland, K. *Macromol. Chem. Phys.* **1999**, *200*, 1662.
76. Brandrup, J.; Immergut, E. H. *Polymer Handbook*; Wiley: New York, **1975**.

Biographical Sketch

Ryszard Szymanski received his MS degree in organic synthesis from the Technical University at Lodz, Poland, in 1972. In the same year, he started his work at the Center of Molecular and Macromolecular Studies of the Polish Academy of Sciences (CMMS), Lodz, Poland, as research assistant. He worked in Professor Stanislaw Penczek's group and earned his PhD in 1980 in polymer chemistry. His PhD thesis was devoted to the reactions of alkoxymethylium cations with ethers and acetals as models of cyclic acetal polymerization. In 1981, he was a postdoc at Professor H.K. Hall's laboratory, in Tucson, Arizona, investigating polymerization of bicyclic orthoesters. After returning to Poland, he continued his work as an adjunct professor in the field of ROP in CMMS with Professor Penczek. His main interests are the mechanisms and kinetics of polymerization of cyclic monomers. In his work, he has developed computer simulation techniques. In 1994, he spent 6 months with Professor K. Matyjaszewski in Pittsburgh, Pennsylvania, where he studied the mechanism of cationic polymerization of styrene using computer simulation methods. After returning to CMMS, he received his DSc degree with the thesis on problems connected with equilibrium in copolymerization. He continues his work in CMMS as an associate professor in the Laboratory for Computer Simulations.

4.05 Equilibrium Copolymerization in Ring-Opening Polymerization

R Szymanski, Polish Academy of Sciences, Lodz, Poland

4.05.1 Phenomenon of the Equilibrium Copolymerization in Ring-Opening Polymerization

The general scheme of a ring-opening (RO) copolymerization contains, besides initiation and propagations (homo- and cross-propagations), additional processes. Among the many RO copolymerizations, the most important are processes that lead to depolymerization, usually homo- and cross-depropagations – the reverse reactions of the corresponding propagations. In many reversible RO copolymerizations, we have to also take into account reversible macrocyclizations, which can be regarded as depropagations and propagations of the composed monomers (built of two or more copolymer repeating units). All these reactions, together with another important reaction in many systems, namely, the segmental exchange leading to redistribution of copolymer repeating units, are shown in the simplified scheme of the reversible RO copolymerization (**Scheme 1**).

Depending on the relationships between the rates of reactions operating in the RO copolymerization shown in **Scheme 1**, we can have either a purely kinetically or thermodynamically controlled product or a copolymer that is neither of these when contributions of kinetic and thermodynamic control do not differ much or change during copolymerization. Similarly, when depropagations are slow but the segmental exchange (reshuffling) fast, a copolymer can resemble a thermodynamic product when the copolymer microstructure is analyzed, although its composition can correspond to the kinetic control.

The overall equilibrium in copolymerization requires attaining in the system the equilibrium composition and microstructure of a copolymer and the equilibrium concentrations of comonomers and all linear and cyclic oligomers and polymers. When the rate constants of all reactions operating in the system are known, the equilibrium conditions (concentrations of all reagents and the average parameters describing a copolymer such as contents of copolymer units and various sequences) can be predicted. As shown in Section 4.05.3, the equilibrium condition depends on the initial composition of the copolymerization system. However, kinetic restrictions can result in not reaching the overall equilibrium. Still, if the copolymer composition and microstructure are thermodynamically controlled, the process can be called an equilibrium copolymerization.

A specific case of the RO equilibrium copolymerization is one that is concerned with systems without a linear polymer, involving only (besides activators/catalysts) RO comonomers and cyclic oligomers and polymers, and in which equilibrium can be reached by ring expansion/contraction and/or ring fusion/fission reactions. Such systems are briefly discussed in one of the sections below.

4.05.2 The Concept of the Equilibrium Copolymerization

In literature the term 'equilibrium copolymerization' has two distinct meanings. The first meaning is copolymerization system at equilibrium, that is, the copolymerization system in the state when all propagation/depropagation reactions have reached their equilibrium (**Schemes 1** and **2**).

The equilibrium in all these reactions ensures that the equilibrium of the segmental exchange (cf. **Scheme 1**) is reached as well, independently of the rates of these reactions.

When the reaction routes leading to macrocyclization are available, the real equilibrium requires equilibration of the ring-chain interconversions (cf. **Scheme 1**) as well.

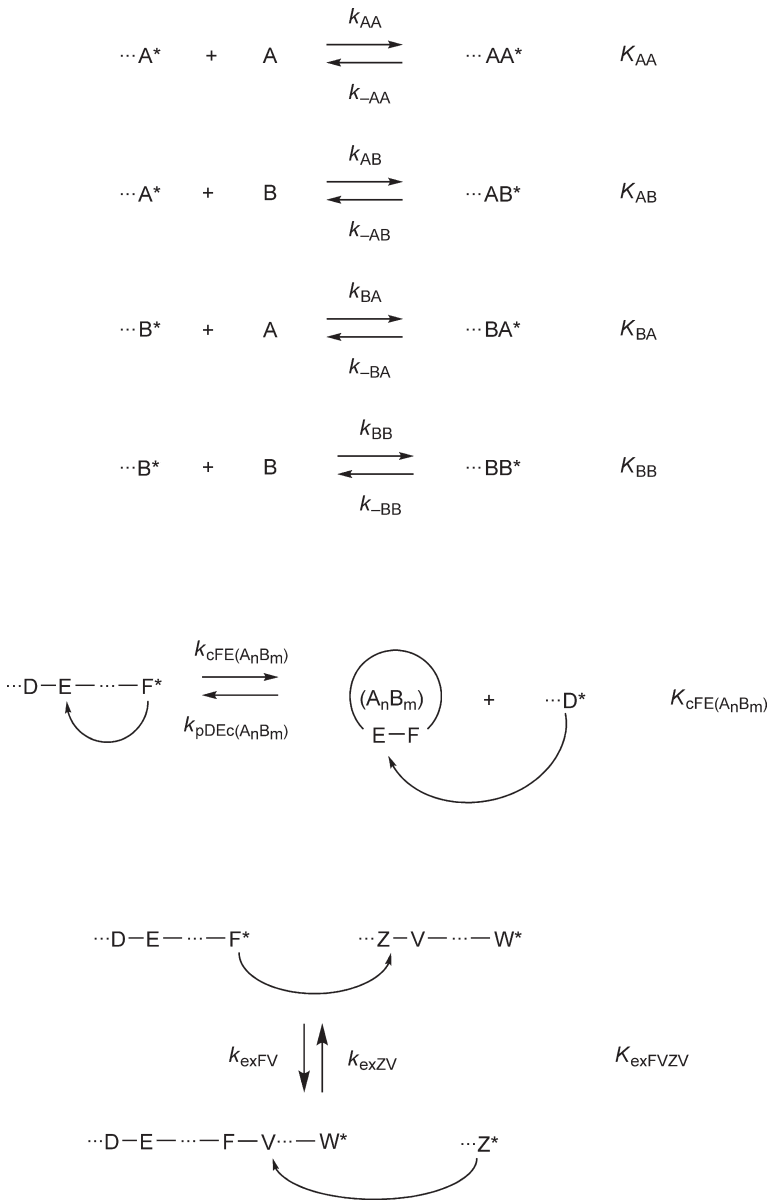

Scheme 1 A simplified scheme of an equilibrium binary RO copolymerization. Only the dyad model of propagation and depropagation reactions, reversible cyclizations, and segmental exchange reactions are shown. Equilibrium constants of the corresponding reactions (denoted with the capital letter *K* with subscripts) are equal to the ratios of the corresponding rate constants. D, E, F, V, W, and Z denote copolymer units A and/or B.

Unfortunately, the timescale of reaching the overall ring-chain equilibrium is usually much larger, and, therefore, most often, macrocyclization is not taken into account when the equilibrium copolymerization is analyzed.

The second meaning of the 'equilibrium copolymerization' is a copolymerization process carried out in conditions when at least one of the reversible propagations is practically at equilibrium, that is, propagation (homo- or cross-propagation) is counterbalanced with the corresponding depropagation. Because other propagations are not at equilibrium, the conversion of all comonomers can proceed and be relatively high and contribution(s) of dyads (sequences) formed in the equilibrated propagation(s) can sometimes be significant. One of these types of the equilibrium copolymerization is shown schematically in **Scheme 3**.

Similarly, to this type of the equilibrium copolymerization belong systems with the equilibrated cross-propagation and systems where the equilibria are maintained for more than one propagation and/or in which all or some of the nonequilibrated propagations are reversible.

Some of the equilibrium copolymerizations of this type were kinetically analyzed by Lowry,[1] Hazell and Ivin,[2] Yamashita *et al.*,[3] and Wittmer,[4] who derived equations for the composition of a copolymer in systems with reversibility of some reactions in triad (or some in dyad) model copolymerizations. Although the analyzed systems are concerned with

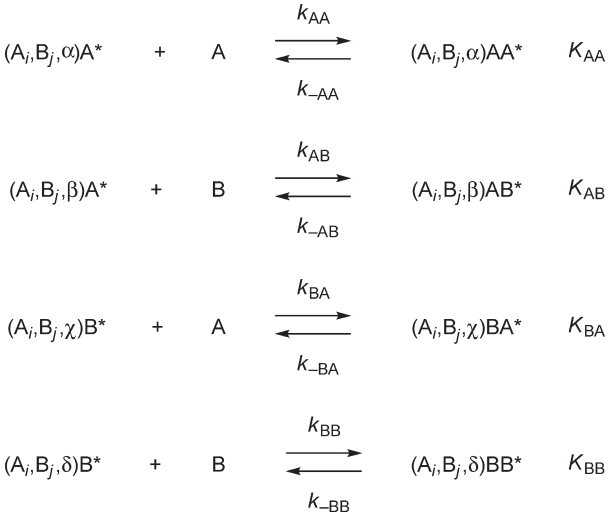

Scheme 2 Equilibria of propagations in copolymerization hold for any chain length and copolymer sequences (i, j = 0, 1, 2, …; α, β, χ, and δ indicate symbolically all possible copolymer unit sequences).

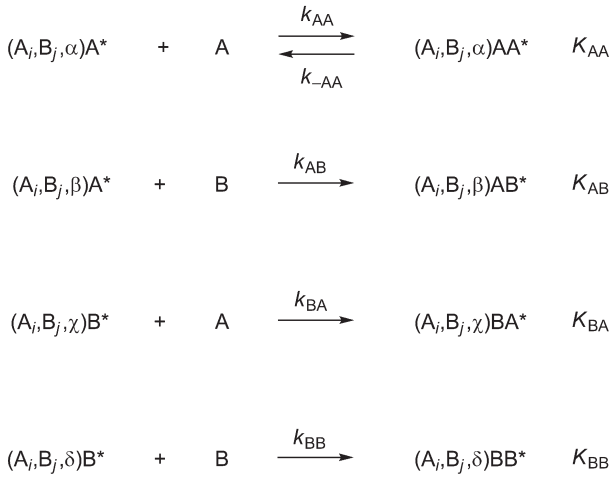

Scheme 3 Equilibrium copolymerization with only one homopropagation being in equilibrium and other propagations being irreversible.

vinyl monomer copolymerizations, the derived equations can also be used for RO polymerization systems.

Because of the decreasing equilibrium concentrations of monomers, the equilibrium copolymerization often allows polymerization of RO monomers, which do not homopolymerize.

Some examples of such processes are shown in the following sections of the chapter.

4.05.3 Copolymerization Equilibrium

The term 'equilibrium copolymerization' was introduced by Alfrey and Tobolsky in 1959,[5] who stated that, mathematically, the equilibrium in copolymerization is identical with the Ising problem in ferromagnetism, which leads to the same solution. Consequently, the authors formulated the most important equation relating the composition of the equilibrium copolymer with the equilibrium constant, at that moment not yet related with chemical reactions:

$$\frac{(N_A - M_{AB})(N_B - M_{AB})}{M_{AB}^2} = K = \left(\frac{f_{AA}f_{BB}}{f_{AB}^2}\right)\exp\left(\frac{\Delta E_{AB}}{RT}\right) \quad [1]$$

where N_A and N_B are the numbers of monomeric units A and B, respectively, and M_{AB} is the number of dyads AB (equal to the number of dyads BA as the infinite chain length approximation was assumed). According to Alfrey and Tobolsky, K is an equilibrium constant expressed in terms of vibrational partition functions f_{AA}, f_{BB}, and f_{AB} and the energy change ΔE_{AB}. ΔE_{AB} is equal to the corresponding differences per mole of bonds AA, BB, and AB ($2E_{AB} - E_{AA} - E_{BB}$).

A few years later, Tobolsky and Owen[6] showed that the equilibrium copolymer composition is related to the propagation equilibrium constants in simple systems such as the copolymerization of sulfur with selenium (the terminal model of copolymerization without any effect of ultimate units, i.e., $K_{AA} = K_{BA}$, $K_{BB} = K_{AB}$; cf. propagation equations of Scheme 1).

It was Izu and O'Driscoll[7] who first formulated the equations describing the relationships between the equilibrium copolymer composition and microstructure, the equilibrium comonomer concentrations, and the equilibrium constants of the dyad model of copolymerization – the model most often used in the analysis of copolymerization processes. On analyzing the probabilities of finding copolymer units at various positions of copolymer chains, the authors obtained the following relationships:

$$[A]_e = \frac{\varepsilon}{K_{AA}} \qquad [B]_e = \frac{\eta}{K_{BB}} \quad [2]$$

$$K_{AB}K_{BA} = \left(\frac{1}{[A]_e} - K_{AA}\right)\left(\frac{1}{[B]_e} - K_{BB}\right) \quad [3]$$

$$\frac{K_{AB}K_{BA}}{K_{AA}K_{BB}} = \left(\frac{1-\varepsilon}{\varepsilon}\right)\left(\frac{1-\eta}{\eta}\right) \quad [4]$$

$$F_A = \frac{1-\eta}{2-\varepsilon-\eta} \qquad F_B = \frac{1-\varepsilon}{2-\varepsilon-\eta} \quad [5]$$

$$F_{AA} = \frac{\varepsilon(1-\eta)}{2-\varepsilon-\eta} \qquad F_{BB} = \frac{\eta(1-\varepsilon)}{2-\varepsilon-\eta} \quad [6]$$

$$F_{AB} = F_{AB} = \frac{(1-\varepsilon)(1-\eta)}{2-\varepsilon-\eta} \quad [7]$$

where F_A, F_B, F_{AA}, F_{BB}, F_{AB}, and F_{BA} are the mole fractions of the indicated copolymer units or dyads in the equilibrium copolymer; ε and η are the conditional probabilities of preceding the unit A and unit B, respectively, by a unit of the same kind.

On analyzing the above equations, which enable us, after adding the mass–balance relationships, to calculate the equilibrium conditions of binary copolymerization, we can easily find that the equilibrium constant K from Alfrey and Tobolsky's equation (eqn [1]) is equal to the ratio of products of cross- and homopropagation equilibrium constants, $(K_{AB}K_{BA})/(K_{AA}K_{BB})$.

In another paper, Howell with Izu and O'Driscoll[8] related the triad model of copolymerization equilibrium constants to the microstructure and composition of the equilibrium copolymer. Also, analysis of a multicomponent equilibrium copolymerization was presented.[9]

Most of the equations, derived by O'Driscoll and co-workers with the assumption of infinite chains, appeared to be valid also for the equilibrium systems with low X_n (number-average degree of polymerization), which was shown by Szymanski[10] in his analysis of equilibrium in copolymerization systems.

4.05.3.1 Comonomer Equilibrium Concentrations

Concentrations of comonomers at the copolymerization equilibrium are lower than those in homopolymerizations, provided no specific interactions/solvation play important roles in distinguishing these systems qualitatively or quantitatively. The decrease in the monomer equilibrium concentration in copolymerization stems from the decrease in the proportion of homosequences. For instance, for the dyad model of copolymerization, when we assume the same value for the equilibrium constant of homopropagation (no specific interactions) as in homopolymerization (cf. **Scheme 2**), the following equation for the equilibrium concentration of monomer A can be formulated, independently if homo- or copolymerization is considered:

$$[A]_{eq} = \frac{[-AA^*]}{[-A^*]K_{AA}} \quad [8]$$

where K_{AA} is the corresponding equilibrium constant of homopropagation; subscript eq refers to the equilibrium conditions (omitted from brackets denoting concentrations of active species); -AA* and –A* denote, respectively, the active chain ends terminated with the indicated dyad or unit; –A* includes the species with terminal dyads (–AA*), but besides them it contains linear unimers (XA*, where X denotes the fragment coming from the initiator) and in the case of copolymerization chains terminated with a heterodyad –BA* ($[-A^*] = [XA^*]+[-AA^*]+[-BA^*]$). Consequently,

$$\begin{aligned} \{[A]_{eq}\}_{homo} &= \frac{[-AA^*]}{[-A^*]K_{AA}} = \frac{[-A^*]-[XA^*]}{[-A^*]K_{AA}} \\ > \{[A]_{eq}\}_{co} &= \frac{[-AA^*]}{[-A^*]K_{AA}} \\ &= \frac{[-A^*]-[XA^*]-[-BA^*]}{[-A^*]K_{AA}} \end{aligned} \quad [9]$$

where subscripts homo and co correspond to homo- and copolymerization, respectively. The decrease in the equilibrium concentration in copolymerization is very large when the equilibrium copolymer resembles the alternating copolymer ($[-A^*] \approx [XA^*] + [-BA^*]$) and very small when the equilibrium copolymer microstructure can be characterized by large blocks, that is, low content of heterodyads and high average lengths of homosequences ($[-BA^*] \approx 0$).

This phenomenon of decreasing the equilibrium concentration of the monomer in copolymerization is essential to understanding why for some monomers it is not possible to obtain homopolymer but copolymers often can be obtained. Simply, the equilibrium constant of polymerization for a non (homo)polymerizing polymer (K_{AA}) is low (because of thermodynamic reasons), and its reciprocal corresponding to the equilibrium monomer concentration ($[A]_{eq(homo)} \approx 1/K_{AA}$) is higher than the concentration of the monomer in bulk. When an appropriate comonomer is found capable of forming effective heterodyads, the equilibrium concentration of a non-homopolymerizing monomer can drop below the bulk (or solution) concentration and the formation of a copolymer is thermodynamically possible. When the formation of heterodyads is strongly favored or the equilibrium constants of homopropagation are not too low (and moderate formation of heterodyads is sufficient), it is possible to form a copolymer from two (or a larger number of) the non-homopolymerizing monomers. The content of heterodyads in such a copolymer formed from non-homopolymerizing comonomers is higher than that in a random copolymer. If specific interactions operate in the system such that the apparent equilibrium constants are dependent on the system composition, then this restriction does not hold, as indicated in Section 4.05.4.1.

However, the dependence of the comonomer equilibrium concentrations on the equilibrium constants of homo- and cross-propagations and on the copolymerization feed is complex.

The aforementioned papers by O'Driscoll and co-workers[7–9] give access to the equilibrium concentrations of comonomers and copolymer sequences for systems when the infinite chain length approximation can be applied. In the next section, the relationships that enable us to compute all equilibrium features of copolymerization without any restrictions of the length of copolymer chains are presented. Quantities such as the equilibrium concentrations of comonomers and chains of any given sequence of copolymer units, X_n (number-average degree of the polymerization of copolymer chains), D_X (dispersity of copolymer chain lengths), and contributions of various sequences can be computed on the basis of the assumed model of copolymerization.

There is also a special case of the equilibrium copolymerization when no linear polymer is formed and the equilibrium is exclusively established between cyclic compounds: comonomers and cyclic homo- and copolymeric oligomers and polymers. Such an equilibrium can be observed only in those

systems in which no initiator of linear polymerization is added and only reactions of ring expansion/contraction and/or ring fusion/fission can operate, often catalyzed by the added catalyst or initiated with a cyclic initiator. A series of papers on the formation of cyclic RO polymers were published by Kricheldorf[11] (and see references listed therein), but there were none in which the equilibrium was quantitatively analyzed. The present author in another contributed chapter (see Chapter 4.30) discussed this problem, arriving at the conclusion that the concentrations of cyclic oligomers and polymers in systems without linear polymers are only slightly larger than those in which the ring-chain equilibrium was established. The reader can also look into that chapter to find the analysis of the ring-chain equilibrium in copolymerization.

4.05.3.2 General Treatment of Copolymerization Equilibrium

The general treatment of the copolymerization equilibrium without restrictions of the chain lengths was first presented by Szwarc and Perrin,[12] who delivered a mathematical solution for any number of comonomers but restricted to the dyad model of propagation. Applying equations derived by Szwarc and Perrin, we can compute the concentrations of chains of any length and the sequence of copolymer units and consequently can compute any statistical feature of the system, such as the equilibrium concentrations of any dyad, triad, or longer sequence of copolymer units. However, their solution cannot be applied to systems in which $K_{AA}K_{BB} = K_{AB}K_{BA}$, which results in singularity of matrixes used in computations.[13] This is an important drawback of the presented treatment, because many copolymerizations can be characterized as ideal, that is, those in which the difference between the Gibbs energies for the addition of any of the two comonomers to the same active center depends only on these comonomers. For such systems, $K_{AA}K_{BB} = K_{AB}K_{BA}$ and the equilibrium copolymer has a random microstructure. Then, a solution of this problem was suggested,[14] which would have, however, to be changed considering that generally $[^0A_1]/[^0B_1] \neq [^0A_2]/[^0B_2]$, where subscripts indicate the length of oligomers with the indicated comonomer unit at the starting position (hence superscripts 0).

Another general treatment of the copolymerization equilibrium was provided by Szymanski,[10] who used, while deriving his relationships, similarly as O'Driscoll and co-workers,[7–9] the 'reverse' conditional probabilities (of a copolymer unit to be preceded by the same or a different unit). This treatment looks simpler than the one proposed earlier by Szwarc and Perrin,[12] and similarly their equations can be applied to the systems of any number of comonomers and any average degree of polymerization. The proposed solution also applies to the systems of ideal copolymerization ($K_{AA}K_{BB} = K_{AB}K_{BA}$). Besides, the method can easily be extended to the triad model of copolymerization (corresponding equations are shown in the appendix of Reference 10).

When the dyad model of copolymerization equilibrium constants and initial conditions are known, the basic features of the equilibrium system (without cyclizations) can be found by solving a set of $4i$ equations, where i is the number of comonomers, denoted below as A, B, …, H:

$$\begin{bmatrix} (1-K_{AA}a) & -K_{AB}b & \dots & -K_{AH}h \\ -K_{BA}a & (1-K_{BB}b) & \dots & -K_{BH}h \\ \vdots & \vdots & \vdots & \vdots \\ -K_{HA}a & -K_{HB}b & \dots & (1-K_{HH}h) \end{bmatrix} \begin{bmatrix} Y_A \\ Y_B \\ \vdots \\ Y_H \end{bmatrix} = \begin{bmatrix} 1 \\ 1 \\ \vdots \\ 1 \end{bmatrix} \quad [10]$$

$$\begin{matrix} A_0 = A_1^* Y_A \\ \vdots \\ H_0 = H_1^* Y_H \end{matrix} \quad [11]$$

$$\begin{matrix} (A) = A_0 + a_0 - a = A^* Y_A \\ \vdots \\ (H) = H_0 + h_0 - h = H^* Y_H \end{matrix} \quad [12]$$

$$\begin{bmatrix} (1-K_{AA}a) & -K_{BA}a & \dots & -K_{HA}a \\ -K_{AB}b & (1-K_{BB}b) & \dots & -K_{HB}b \\ \vdots & \vdots & \vdots & \vdots \\ -K_{AH}h & -K_{BH}h & \dots & (1-K_{HH}h) \end{bmatrix} \begin{bmatrix} A^* \\ B^* \\ \vdots \\ H^* \end{bmatrix} = \begin{bmatrix} A_1^* \\ B_1^* \\ \vdots \\ H_1^* \end{bmatrix} \quad [13]$$

where $a_0 \dots h_0$ and $a \dots h$ denote, respectively, the initial and equilibrium concentrations of comonomers ($[A]_0 \dots [H]_0$, $[A] \dots [H]$), while (P), P_0, P^*, and P_1^* (P = A…H) denote the total concentrations of copolymer units and the initial and equilibrium concentrations of active species and initiated monomers (living linear unimers) of the indicated type. $Y_A \dots Y_H$ denote the copolymer parameters equal to the ratios of copolymer units and active species of the given kind ($Y_A = (A)/A^*$; for homopolymerization, they are equal to X_n). K_{AA}, K_{AB}, …, K_{HH} are the dyad model of copolymerization equilibrium constants.

The solution of eqns [10]–[13] directly gives the equilibrium concentrations of comonomers ($a \dots h$) and the composition of the equilibrium copolymer ($(A) \dots (H)$). Besides, the equilibrium concentrations of living linear unimers and copolymerization parameters $Y_A \dots Y_H$ are found.

The copolymerization parameters Y_P allow computation of the average conditional probabilities of a copolymer unit of the given kind to be followed by a unit of the same (q_{PP}) or a different type (q_{PR}):

$$q_{PR} = K_{PR} r \left(\frac{Y_R}{Y_P} \right) \quad [14]$$

where P, R = A, B, … and $r = a, b, \dots$.

Consequently, the equilibrium concentrations of any copolymer sequence can be computed:

$$(PRS \dots TUV) = (P) q_{PR} q_{RS} \dots q_{TU} q_{UV} \quad [15]$$

where symbols in parentheses denote the equilibrium concentrations of copolymer sequences or copolymer units.

However, computation of the equilibrium concentrations of copolymer chains of a given sequence of copolymer units is more complex and can be found in the cited paper of Szymanski.[10] It stems from the fact that the probabilities of finding a unit of a given kind in a copolymer chain depends, in a general case, on X (degree of polymerization), considered position, and a type of active center. Only for an ideal equilibrium copolymerization ($K_{XX}K_{YY} = K_{XY}K_{YX}$), the probabilities of finding a copolymer unit at any chain position (but the first) are dependent only on the unit type and thus computation of all copolymer equilibrium concentrations is relatively simple.[10]

Another general solution describing relationships between the equilibrium constants of copolymerization and the features of the equilibrium systems, such as copolymer sequence distribution and comonomer equilibrium concentrations, computed for various initial conditions and various

relationships between the equilibrium constants was given by Cai and Yan.[15]

4.05.4 Thermodynamics of Copolymerization

The first comprehensive treatment of copolymerization thermodynamics was provided by Sawada,[16,17] who analyzed the relationships between the thermodynamic parameters of copolymerization and such features of the system as the equilibrium concentrations of comonomers and the sequence distribution. Generally, the (molar) Gibbs energy of copolymerization can be defined, similarly as for homopolymerization, as the difference between the Gibbs energies of 1 base-mole of a copolymer and comonomers (the average value):

$$\Delta_{xy}G = G_y - G_x = \frac{1}{n}G^{(n)}_{\mathrm{co}(y)} - f_{\mathrm{A}}G_{\mathrm{A}(x)} - f_{\mathrm{B}}G_{\mathrm{B}(x)} - \cdots \qquad [16]$$

where x and y describe the standard states of comonomers (A, B, …) and a copolymer, respectively. $G_y = G^{(n)}_{\mathrm{co}(y)}/n$ is the Gibbs energy of a copolymer with the degree of polymerization equal to n and specific composition and microstructure, while $G_x = f_{\mathrm{A}}G_{\mathrm{A}(x)} + f_{\mathrm{B}}G_{\mathrm{B}(x)} + \cdots$ is the average Gibbs energy of comonomers (where f_{A}, f_{B}, … are the molar fractions of different copolymer units and $G_{\mathrm{A}(x)}$, $G_{\mathrm{B}(x)}$, … are the standard Gibbs energies of comonomers). Usually the following notation of copolymer and comonomer states is adopted: c = condensed, c′ = crystalline, s = in solution, and so on. Note the use of, according to the IUPAC recommendation, the symbol delta with the subscript indicating the initial state of (co)monomers and of resulting (co)polymer in notations of the thermodynamic functions of (co)polymerization.

Equation [16] was formulated by assuming the following stoichiometric equation of copolymerization:

$$f_{\mathrm{A}}\mathrm{A} + f_{\mathrm{B}}\mathrm{B} + \cdots \longrightarrow \frac{1}{n}\{\mathrm{A}_{f_{\mathrm{A}}}\mathrm{B}_{f_{\mathrm{B}}}\ldots\}^{(\alpha)}_n \qquad [17]$$

where n denotes X_{n} of the copolymer ($n > 1$), { } contains copolymer composition, and (α) denotes the microstructure specific for the given copolymerization process.

The value of the Gibbs energy of copolymerization, $\Delta_{xy}G$, determines whether copolymerization can be a spontaneous process ($\Delta_{xy}G < 0$) or it can be the reverse reaction, depolymerization ($\Delta_{xy}G > 0$). When $\Delta_{xy}G = 0$, both processes are thermodynamically possible and copolymerization can be in equilibrium.

However, $\Delta_{xy}G = 0$ is not a sufficient condition for copolymerization to be at equilibrium, because $\Delta_{xy}G$ is an average thermodynamic function (averaged over the whole set of copolymer chains) and the equilibrium of copolymerization is reached only when all reactions describing the overall equilibrium are at equilibrium:

$$f_{\mathrm{A}}\mathrm{A} + f_{\mathrm{B}}\mathrm{B} + \cdots \underset{}{\overset{K_{f_{\mathrm{A}},f_{\mathrm{B}},\ldots,\beta,n}}{\rightleftharpoons}} \frac{1}{n}\{\mathrm{A}_{f_{\mathrm{A}}}\mathrm{B}_{f_{\mathrm{B}}}\ldots\}^{(\beta)}_n \qquad [18]$$

where n denotes X_{n} of the copolymer ($n = 1, 2, \ldots$) and (β) is the specific sequence of copolymer units. Here, all possible sequences have to be considered. The K on the arrow denotes the equilibrium constant, which is different for different values of n and (β) (other symbols have the same meaning as in eqn [17]).

Consequently, Gibbs energies for all component equilibrium reactions are (have to be) equal to zero for copolymerization being at equilibrium:

$$\begin{aligned}\Delta_{xy}G_{(f_{\mathrm{A}},f_{\mathrm{B}},\ldots,\beta,n)} &= G_{y\,(f_{\mathrm{A}},f_{\mathrm{B}},\ldots,\beta,n)} - G_{x(f_{\mathrm{A}},f_{\mathrm{B}},\ldots)} \\ &= \frac{1}{n}G^{(n)}_{\mathrm{co}(y,f_{\mathrm{A}},f_{\mathrm{B}},\ldots,\beta,n)} - f_{\mathrm{A}}G_{\mathrm{A}(x)} - f_{\mathrm{B}}G_{\mathrm{B}(x)} - \cdots = 0\end{aligned} \qquad [19]$$

Although there are an infinite number of equilibrium reactions to be considered, the reversibility-of-microstates rule allows us to decrease the number of considered equilibria to a relatively small number, depending on the assumed model of copolymerization (although if considered on the level of Gibbs energies, such models often do not take into account the distribution of chain lengths).

Analyzing thermodynamics of homopolymerization, the monomer polymerizability feature called the ceiling (or floor) temperature is often determined.

The Gibbs energy of polymerization can be expressed as a function of two other thermodynamic functions: enthalpy and entropy of polymerization. For equilibrium conditions, we have

$$\Delta_{xy}G = \Delta_{xy}H - T\Delta_{xy}S = 0 \qquad [20]$$

where $\Delta_{xy}H$ and $\Delta_{xy}S$ denote the enthalpy and entropy of polymerization for the process carried out in a way described by the subscripts, for example, ss denotes solution conditions of substrates and product and lc the liquid mixture of comonomers giving a condensed copolymer. The temperature T is given in absolute scale.

Rearranging this fundamental equation, we get the temperature at which the system is at equilibrium for the given values of enthalpy and entropy of polymerization:

$$T_{\mathrm{c}} = \frac{\Delta_{xy}H}{\Delta_{xy}S} \qquad [21]$$

where the subscript c refers to the ceiling temperature; the subscript f can be used when the equation is used to calculate the floor temperature.

Both terms describe the temperature at which a monomer and a polymer of a high molar mass and negligible quantity coexist at equilibrium and the difference between the ceiling and the floor temperature lies in what is below and above.

One has to keep in mind that the entropy of polymerization depends on the monomer concentration:

$$\Delta_{xy}S = \Delta_{xy}S^{\circ} + R\ln[\mathrm{M}] \qquad [22]$$

where $\Delta_{xy}S^{\circ}$ is the standard entropy of polymerization (where the standard state was assumed to be monomer at a concentration of 1 mol l^{-1}; alternatively, instead of monomer concentration, mole fraction can be used – in that case, the standard state corresponds to a pure monomer).

Because of the dependence of $\Delta_{xy}S$ on the monomer concentration, the ceiling and floor temperatures are dependent on the monomer concentration in feed.

This concept of ceiling/floor temperature formulated for homopolymerization can be applied to copolymerization as well. Similarly as for homopolymerization, the ceiling temperature can be found in these copolymerization systems in which, while increasing the temperature, we get positive $\Delta_{xy}G$ and consequently the depolymerization of a copolymer (provided the active species of the copolymerization are alive). On the other hand, when spontaneous depolymerization occurs

with the decreasing temperature, the equation describes the floor temperature and the subscript f should be used instead of c. The ceiling temperature is observed for exoenthalpic ($\Delta_{xy}H<0$) and exoentropic ($\Delta_{xy}S<0$) copolymerizations (most of RO homo- and copolymerizations), while the floor temperature is observed for endoenthalpic ($\Delta_{xy}H>0$) and endoentropic ($\Delta_{xy}S>0$) systems (e.g., polymerizations and copolymerization of sulfur and selenium). When $\Delta_{xy}H$ and $\Delta_{xy}S$ differ in their signs, no equilibrium is possible: for any temperature, $\Delta_{xy}G$ is either negative (exoenthalpic and endoentropic systems) and copolymers alone are thermodynamically stable or positive (endoenthalpic and exoentropic systems) and comonomers alone are thermodynamically stable.

This analysis is, however, a simplified one. Simplification stems from the fact that the average thermodynamic functions ($\Delta_{xy}G$, $\Delta_{xy}H$, $\Delta_{xy}S$) for copolymerization depend on the composition of the system. Consequently, for any copolymerization feed composition (including the content of solvent determining, besides the comonomer concentrations ratio, the comonomer concentrations), we can compute, using, for instance, the relationships describing equilibrium in copolymerization mentioned in Section 4.05.3, the equilibrium concentrations of comonomers. Consequently, we can determine whether a high-molar-mass copolymer is formed and what is its composition (which is usually different from that of the feed). When the thermodynamic parameters of all homo- and cross-propagations are known, which enables us to calculate the equilibrium constants for any temperature, we can repeat such computations for various temperatures and the copolymerization system compositions, thus finding the ceiling or floor temperatures. These temperatures correspond to conditions when negligibly low amount of a high-molar-mass copolymer is formed.

A simple mathematical analysis of relationships describing the copolymerization system allows us to predict (although not found yet experimentally) that there are possible copolymerization systems having for some compositions ceiling and for other floor temperatures.

For the sake of visualizing the dependence of the ceiling temperature on the composition of the copolymerization system, the author performed, especially for this chapter, some simulations and the computed ceiling temperatures for the copolymerization of 1,3-dioxolane (DXL) with 1,3-dioxane are presented in **Figure 3** (see Section 4.05.6.1.2).

4.05.4.1 Thermodynamics of Copolymerization in Systems with Intercomponent Interactions

Harvey and Leonard[18] were the first who analyzed the thermodynamics of copolymerization from the viewpoint of the Flory–Huggins theory of intercomponent interactions in polymer solutions. Unfortunately, in deriving their equations, Harvey and Leonard assumed the same composition of copolymer chain ends as that of the whole copolymer. Mita[19] provided an analogous solution without this assumption. He formulated the overall equilibrium as the equality of chemical potentials of comonomers and copolymer units ($\mu_x = (\partial G/\partial N_x)_{T,p,N_i(i\neq x)}$, where x, i are comonomer (A, B, …) or comonomer unit, N_i is the number of moles of the system component 'i', G is the Gibbs energy of the system; the partial derivative is determined for constant temperature, pressure, and numbers of moles of components, other than x, in the copolymerization system):

$$\mu_A = \mu_\alpha \qquad \mu_B = \mu_\beta \qquad [23]$$

where α and β refer to the corresponding copolymer units.

Taking into account the Gibbs energy of mixing and the entropy of the copolymer units distribution, he obtained the equations that enable us to predict for any initial conditions the composition of the copolymerization system at equilibrium (for the sake of simplicity, he assumed, while deriving the equations, that molar volumes of solvent, comonomers, and copolymer units are equal):

$$\exp\left(-\frac{\Gamma}{RT}\right) = [\exp(Z_A)-1][\exp(Z_B)-1] \qquad [24]$$

$$\frac{\Phi_{B0}-\Phi_B}{\Phi_{A0}-\Phi_A} = \frac{1-\exp(-Z_A)}{1-\exp(-Z_B)} \qquad [25]$$

$$\Phi_{A0}+\Phi_{B0} = \Phi_A+\Phi_B+\Phi_P = 1-\Phi_S \qquad [26]$$

where

$$\Gamma = \Delta G^\circ_{\alpha B}+\Delta G^\circ_{\beta A}-\Delta G^\circ_{\alpha A}-\Delta G^\circ_{\beta B} \qquad [27]$$

$$Z_A = \Delta G^\circ_{\alpha A}-\ln\Phi_A-1+\chi_{AP}(\Phi_A-\Phi_P)+(\chi_{BP}-\chi_{AB})\Phi_B + (\chi_{SP}-\chi_{AS})\Phi_S \qquad [28]$$

$$Z_B = \Delta G^\circ_{\beta B}-\ln\Phi_B-1+\chi_{BP}(\Phi_B-\Phi_P)+(\chi_{AP}-\chi_{AB})\Phi_A + (\chi_{SP}-\chi_{BS})\Phi_S \qquad [29]$$

and Φ_X (X = A, B, P, S) are volume fractions of comonomers, copolymer, and solvent, respectively and χ_{XY} (X, Y = A, B, P, S) denote the Flory–Huggins interaction parameters for the indicated copolymerization system components (in the above equations, $\chi_{XY}=\chi_{YX}$ because of the assumed equal molar volumes of all components).

The microstructure of the equilibrium copolymer can be predicted on the basis of the randomness parameter ψ, which is defined as the sum of the conditional probabilities of finding copolymer units followed by different units ($\psi = P_{\alpha\beta}+P_{\beta\alpha}$):

$$\psi = \frac{[1-\exp(-Z_A)]}{x_\beta} = \frac{[1-\exp(-Z_B)]}{x_\alpha} \qquad [30]$$

$$P_{\alpha\beta} = \psi x_\beta \qquad P_{\beta\alpha} = \psi x_\alpha \qquad [31]$$

$$P_{\alpha\alpha} = 1-P_{\alpha\beta} \qquad P_{\beta\beta} = 1-P_{\beta\alpha} \qquad [32]$$

where x_α is the molar fraction of copolymer unit A, equal to $(\Phi_{A0}-\Phi_A)/(\Phi_{A0}-\Phi_A+\Phi_{B0}-\Phi_B)$ because of the assumed equality of molar volumes of copolymerization system components; analogously, $x_\beta = 1-x_\alpha$.

Mita's treatment is useful in predicting the composition and microstructure of a copolymer as well as the equilibrium concentrations of comonomers on the basis of known thermodynamic functions characterizing the copolymerization system. When, however, these functions are not known, their determination from the analysis of the copolymerization experimental data is possible only by numerical fitting of the computed quantities to the experimentally determined ones (Φ_A, Φ_B, x_α, x_β, $P_{\alpha\alpha}$, $P_{\beta\beta}$, $P_{\alpha\beta}$, $P_{\beta\alpha}$).

However, the assumption introduced by Mita that the interaction parameters for all components of the copolymerization system are equal can be questioned. The present author[20] provided analogous analysis of the copolymerization equilibrium from the point of view of intercomponent interactions

distinguishing interactions between comonomers (χ_{ab}), giving a relatively simple solution for bulk copolymerization (without solvent) and equal molar volumes of comonomers and copolymer units (the interaction parameters involving copolymer units were assumed to be equal, and denoted as χ). This solution is a set of six equations with six unknowns (volume fractions of comonomers and dyads):

$$\Delta G^{\circ}_{AA} = RT\left[\ln\left(1+\frac{\Phi_{AB}}{\Phi_{AA}}\right)+\ln\Phi_a+\left(1-\frac{1}{DP}\right)-(2\Phi_a+2\Phi_b-1)\chi+\Phi_b\chi_{ab}\right] \quad [33]$$

$$\Delta G^{\circ}_{BB} = RT\left[\ln\left(1+\frac{\Phi_{BA}}{\Phi_{BB}}\right)+\ln\Phi_b+\left(1-\frac{1}{DP}\right)-(2\Phi_a+2\Phi_b-1)\chi+\Phi_a\chi_{ab}\right] \quad [34]$$

$$\Delta G^{\circ}_{AB}+\Delta G^{\circ}_{BA} = RT\left[\ln\left(1+\frac{\Phi_{AA}}{\Phi_{AB}}\right)+\ln\left(1+\frac{\Phi_{BB}}{\Phi_{BA}}\right)+\ln\Phi_a+\ln\Phi_b+2\left(1-\frac{1}{DP}\right)-2(2\Phi_a+2\Phi_b-1)\chi+(\Phi_a+\Phi_b)\chi_{ab}\right] \quad [35]$$

$$\Phi_{a0}=\Phi_a+\Phi_{AA}+\Phi_{AB}\quad \Phi_{b0}=\Phi_b+\Phi_{BB}+\Phi_{BA}\quad \Phi_{AB}=\Phi_{BA} \quad [36]$$

where DP is the average degree of the polymerization of a copolymer. Equations [36] are the mass–balance equations, with Φ_{a0}, Φ_{b0}, Φ_a, Φ_b, Φ_{AA}, Φ_{BB}, Φ_{AB}, and Φ_{BA} being the volume fractions of comonomers, initial and at equilibrium, and of copolymer dyads, respectively. The volume fractions of dyads are defined as

$$\Phi_{XY}=\frac{V_X n_{XY}}{V_a n_a+V_b n_b+V_A n_A+V_B n_B} \quad [37]$$

where V and n with the corresponding subscripts denote the molar volumes of comonomers and copolymer units and the numbers of moles of comonomers, copolymer units, and dyads, respectively.

The above-mentioned equations make it possible to predict the equilibrium conditions for any initial conditions, provided the standard free energies of comonomer additions are known. It is worth adding here that these thermodynamic functions are in fact $\Delta_{ss}G$ parameters referring to comonomers and a copolymer dissolved in the reaction mixture (however, some authors treat homogeneous bulk copolymerization as the lc process: liquid comonomers converted to an amorphous copolymer).

Choosing, however, as standard states for copolymer units the infinite dilution solutions in the corresponding comonomers, we can get an alternative set of equations for bulk copolymerization equilibria:

$$\overline{K}_{AA}=\frac{\Phi_{AA}}{\Phi_A\Phi_a}=K_{AA}\exp[\Phi_b\chi_{ab}+2(1-\Phi_a-\Phi_b)\chi] \quad [38]$$

$$\overline{K}_{BB}=\frac{\Phi_{BB}}{\Phi_B\Phi_b}=K_{BB}\exp[\Phi_a\chi_{ab}+2(1-\Phi_a-\Phi_b)\chi] \quad [39]$$

$$\overline{K}_{AB}\overline{K}_{BA}=\frac{\Phi_{AB}\Phi_{BA}}{\Phi_A\Phi_B\Phi_a\Phi_b}=K_{AB}K_{BA}\exp[(\Phi_a+\Phi_b)\chi_{ab}+4(1-\Phi_a-\Phi_b)\chi] \quad [40]$$

where K_{AA} and so on are the equilibrium constants. The ones with overbars are the apparent equilibrium constants, which are dependent on the system compositions, while the others can be treated as the absolute equilibrium constants, the thermodynamic functions depending only on the nature of comonomers and the temperature:

$$K_{XY}=\exp\left(-\frac{\Delta G^{*}_{XY}}{RT}\right) \quad [41]$$

where ΔG^{*}_{XY} is the $\Delta_{ss}G$-type standard molar Gibbs energy for the addition of the corresponding comonomer Y, leading to the dyad XY with comonomer Y as the solvent. It is worth noting that apparent equilibrium constants become equal to the absolute equilibrium constants when both χ and χ_{ab} are equal to zero. For such cases, eqns [38]–[40] become equivalent to the analogous equations derived for systems without intercomponent interactions (eqns [2]–[4]; however, note the difference in measurement units).

Equations [38]–[40] together with the mass–balance equations allow not only prediction of the equilibrium comonomer concentrations and the composition and microstructure of a copolymer but also relatively easy determination of the interaction parameters χ and χ_{ab} as well as the absolute equilibrium constants when they are not known.

Combining eqns [38]–[40], we can get relationships that allow the determination of χ_{ab} (and the ratio of the absolute equilibrium constants for homoaddition) from a simple linear regression of experimentally measured quantities (linear function of $\Phi_b-\Phi_a$):

$$\ln\frac{\Phi_{AA}\Phi_B\Phi_b}{\Phi_A\Phi_a\Phi_{BB}}=\ln\frac{K_{AA}}{K_{BB}}+(\Phi_b-\Phi_a)\chi_{ab} \quad [42]$$

Next, if χ_{ab} is known, the other interaction parameter (χ) and the absolute equilibrium constant of homoaddition can also be determined via linear regression (rearrangement of eqn [38]):

$$\ln\frac{\Phi_{AA}}{\Phi_A\Phi_a}-\Phi_b\chi_{ab}=\ln K_{AA}+2(1-\Phi_a-\Phi_b)\chi \quad [43]$$

Analogously, K_{BB} and $K_{AB}K_{BA}$ can be determined.

It is worth observing that the ratio of the products of volumes of hetero- and homodyads is equal to the simple functions of the absolute equilibrium constants, resembling (and in fact equal here, as equal molar volumes were assumed) the corresponding relationship derived for systems without intercomponent interactions (see the comment below eqn [7]):

$$\frac{\Phi_{AB}\Phi_{BA}}{\Phi_{AA}\Phi_{BB}}=\frac{\overline{K}_{AB}\overline{K}_{BA}}{\overline{K}_{AA}\overline{K}_{BB}}=\frac{K_{AB}K_{BA}}{K_{AA}K_{BB}} \quad [44]$$

Simulations presented in the original paper of Szymanski[20] have shown that although both interaction parameters χ_{ab} and χ are positive, they decrease the equilibrium comonomer concentrations, the latter being more important in influencing the copolymerization equilibrium. Besides, when comonomers do not homopolymerize (K_{AA}, $K_{BB}<1$; equilibrium constants defined by volume fractions), the copolymer in the system without intercomponent interactions (χ_{ab}, $\chi=0$) can be formed only for $K_{AB}K_{BA}>1$ (heterodyads prevail, a certain tendency of an alternating copolymer). When $K_{AB}K_{BA}>>K_{AA}K_{BB}$, the alternating copolymer is formed in equilibrium. When, however, both interaction parameters are positive, two non-homopolymerization comonomers – both having

absolute homopropagation equilibrium constants less than 1 – can be polymerized even when the absolute cross-propagation equilibrium constants are also less than 1 (cf. Figure 8 in the cited Reference 20, showing simulation for the system with $K_{AA} = 0.98$, $K_{BB} = 0.9$, $(K_{AB}K_{BA})^{0.5} = 0.94$, and $\chi_{ab} = \chi = 0.5$, resulting in the formation of a random copolymer). Without specific interactions, two such non-homopolymerizing comonomers can give a copolymer only when $K_{AB}K_{BA} > K_{AA}K_{BB}$, which results in the alternating tendency of dyad distribution.

4.05.5 Determination of the Equilibrium Constants on the Basis of the Analysis of the Copolymerization Equilibrium

The relationships between the comonomer and copolymer sequence equilibrium concentrations and the equilibrium constants, presented in the previous sections, allow prediction of the equilibrium conditions for any initial conditions, provided the equilibrium constants are known. Therefore, determination of these constants is crucial.

Rearranging eqns [10]–[13], we can get the following relationships,[10] making it possible to determine the equilibrium constants for the dyad model of copolymerization, on the basis of experimentally measurable quantities such as the equilibrium concentrations of comonomers and proportions of various sequences:

$$K_{XX} = \frac{(XX)}{(X)x} \quad [45]$$

$$K_{XY}K_{YX} = \frac{(XY)(YX)}{(X)(Y)xy} \quad [46]$$

$$K_{XY} = \frac{Y^*}{X^*}\frac{(XY)}{(Y)y} \quad [47]$$

where X and Y ($X \neq Y$) denote copolymer units (A, B, …), parentheses indicate the equilibrium concentrations of the corresponding units or dyads, and asterisks indicate the equilibrium concentrations of active species of the given kind. The lowercase x and y denote the equilibrium concentrations of comonomers.

Combining eqns [45] and [46], we can get the relationship that allows determination of the ratio of products of cross- and homopropagation equilibrium constants from experimentally determined contribution of various dyads (previously derived by O'Driscoll[7–9] for systems of infinitely large X_n):

$$\frac{K_{XY}K_{YX}}{K_{XX}K_{YY}} = \frac{(XY)(YX)}{(XX)(YY)} \quad [48]$$

It is more difficult to determine the equilibrium constants for the triad model of copolymerization. Only the equilibrium constants of triad homopropagation and some functions of the cross-propagation equilibrium constants can be determined directly on the basis of the experimentally found equilibrium concentrations of comonomers and proportions of copolymer sequences (notation similar to that in eqns [45]–[47])[21]:

$$K_{XXX} = \frac{(XXX)}{(XX)x} \quad [49]$$

$$K_X = \frac{K_{XXY}K_{YXX}}{K_{YXY}} = \frac{(XXY)(YXX)}{(XX)(YXY)x} \quad [50]$$

$$K_{XYX}K_{YXY} = \frac{(XYX)(YXY)}{(XY)(YX)xy} \quad [51]$$

Determination of other than K_{XXX} individual equilibrium constants is possible when proportions of all types of active species at equilibrium conditions are known:

$$K_{XYZ} = \frac{(XYZ)}{(XY)z}\frac{Y_{XY}}{Y_{YZ}} = \frac{(XYZ)YZ^*}{(YZ)zXY^*} \quad [52]$$

where Y_{XY} and so on are the ratios of concentrations of copolymer dyads and active species of the given kind, that is, the parameters analogous to Y_X obtained from eqns [10]–[13] for the dyad model of systems.

4.05.6 Selected Examples of the Equilibrium Copolymerization

4.05.6.1 Copolymerization of Cyclic Acetals

Cyclic acetals readily polymerize and copolymerize, provided enthalpic (mainly ring strain) or entropic factors make the Gibbs energy negative. From the technological point of view, the most important is the homo- and copolymerization of 1,3,5-trioxane (TXN). Unfortunately, little reliable data exist on the equilibrium conditions for the homogeneous copolymerization of TXN, mainly because products usually readily precipitate (at a higher content of TXN in feed) and the real homogeneous equilibrium is often not reached. One can, however, assume, on the basis of the estimated enthalpies of the homopolymerization of TXN in nitrobenzene (-0.3 ± 0.3 kcal mol^{-1} at 150–180 °C and -1.4 ± 0.1 kcal mol^{-1} at 25–180 °C),[22,23] that the Gibbs energy for homogeneous homoaddition of TXN is close to zero or even positive at higher temperatures and that the driving force for copolymerization is precipitation of the polymer from the solution and/or polymerization in solid state. Only very short active chains can exist in the solution in equilibrium with the dissolved monomer. Therefore, the copolymerization of TXN with other comonomers can often be treated as the equilibrium copolymerization understood as a copolymerization process carried out when some propagations are in equilibrium. The cationic copolymerization of TXN with 1,3-dioxepane (DXP) was investigated by Sharavanan *et al.*,[24] who observed the dependence of the precipitation time on the ratio of comonomer concentrations and no precipitation when the content of DXP was above 20%. Unfortunately, hardly any data on homogeneous systems were given. Copolymerization was carried out at 80 °C, that is, above the ceiling temperature of DXP, making it possible that the homopropagation of DXP (and maybe of TXN as well because of its low concentration) be considered to be at equilibrium (shifted to the monomer side). Consequently, the driving force for copolymerization in the homogeneous systems is the randomization of a copolymer (formation of heterodyads), either directly through cross-propagations or through the segmental exchange reactions.

There are also little data on the thermodynamics of the copolymerization of other acetals. In fact, the only reliable data on the equilibrium in homogeneous copolymerization systems of cyclic acetals are those reported by the present author and described in the following sections.

4.05.6.1.1 Equilibrium copolymerization of 1,3-dioxolane with 1,3-dioxepane

Equations [45]–[47] allow determination of the equilibrium constants on the basis of the experimentally found equilibrium concentrations of comonomers and ratios of contributions of copolymer sequences and concentrations of active species. The author of the paper on copolymerization of DXL with DXP[21] performed these determinations by using ^{1}H NMR (and ^{31}P NMR for the ion-trap determination of active species) analysis of the equilibrium in the copolymerization of DXL with DXP in dichloromethane solution. Examples of the NMR spectra are shown in Figures 1 and 2.

The determined equilibrium constants are listed in Table 1.

The thermodynamic parameters determined for homopropagations are similar to the corresponding parameters determined in homopolymerizations.[25–27] On the other hand, the sum of the thermodynamic parameters for heteroaddition is approximately equal to the sum of the corresponding parameters for homoadditions. This is equivalent to the approximately equal products of the equilibrium constants of homo- and cross-propagations, which results in the formation of a random copolymer. The individual equilibrium constants for cross-propagations were determined for active species only at one temperature, but the similarity of their values to the corresponding equilibrium constants for homopropagations of the same active species seems to indicate that the nature of active species is more important in comonomer additions than is the nature of comonomers.

4.05.6.1.2 Equilibrium copolymerization of 1,3-dioxolane with 1,3-dioxane

The equilibrium of the copolymerization of DXL with 1,3-dioxane (non-homopolymerizing comonomer) is

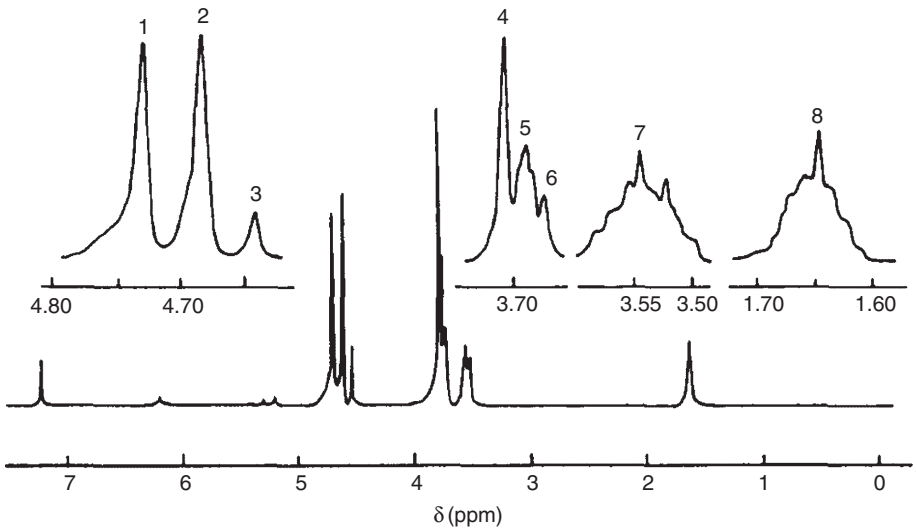

Figure 1 ^{1}H NMR spectrum of the equilibrium copolymerization of DXL (A) and DXP (B). Initial copolymerization conditions: $[A]_0 = 3.15\ mol\ l^{-1}$, $[B]_0 = 1.09\ mol\ l^{-1}$, $[(C_6H_5)_3C^+SbF_6^-]_0 = 5 \times 10^{-3}\ mol\ l^{-1}$ in CH_2Cl_2 at 0 °C. Assignment of signals: 1, 2, 3: $OC\underline{H}_2O$ in dyads AA, AB (and BA), and BB, respectively; 4, 5, 6: $OC\underline{H}_2C\underline{H}_2O$ in triads A$\underline{A}$A, A$\underline{A}$B (and B$\underline{A}$A), and B$\underline{A}$B, respectively; 7: $OC\underline{H}_2CH_2CH_2C\underline{H}_2O$; 8: $OCH_2C\underline{H}_2CH_2C\underline{H}_2O$. Reproduced with permission from Szymanski, R. *Makromol. Chem.* **1991**, *192*, 2943–2959,[21] Copyright Wiley-VCH Verlag GmbH & Co. KGaA.

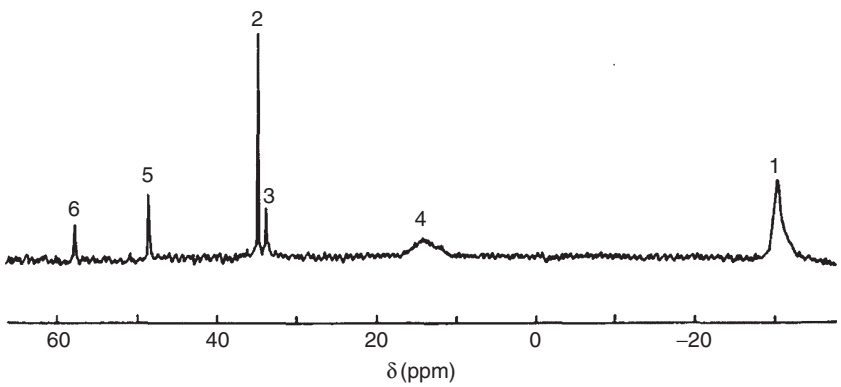

Figure 2 $^{31}P\ \{^{1}H\}$ NMR spectrum of the equilibrium cationic copolymerization system of DXL (A) with DXP (B) reacted with an excess of tributylphosphine. Initial conditions: $[A]_0 = 2.88\ mol\ l^{-1}$, $[B]_0 = 1.36\ mol\ l^{-1}$, $[(C_6H_5)_3C^+SbF_6^-]_0 = 2.2 \times 10^{-2}\ mol\ l^{-1}$ in CH_2Cl_2 at 0 °C. Assignment of signals: 1: P(n-C_4H_9)$C_4H_9)_3$; 2: $OCH_2CH_2OCH_2P^+(n\text{-}C_4H_9)_3$; 3: $O(CH_2)_4OCH_2P^+(n\text{-}C_4H_9)_3$; 4: $HP^+(n\text{-}C_4H_9)_3$; 5: $O{=}P(n\text{-}C_4H_9)_3$; 6: $HOP^+(n\text{-}C_4H_9)_3$. Reproduced with permission from Szymanski, R. *Makromol. Chem.* **1991**, *192*, 2943–2959,[21] Copyright Wiley-VCH Verlag GmbH & Co. KGaA.

Table 1 The determined equilibrium constants of the copolymerization of DXL (A) and DXP (B) in dichloromethane solution and the corresponding thermodynamic parameters

Temperature (K)	K_{AA} (mol^{-1} l)	K_{BB} (mol^{-1} l)	K_{AB} (mol^{-1} l)	K_{BA} (mol^{-1} l)
273	1.43	2.41	1.38[a]; 2.23[b]	2.50[a]; 1.52[b]
295	0.78	1.64	1.87[c]; 1.57[b]	0.81[b]
313	0.60	1.23	1.13[c]; 1.20[b]	0.61[b]
ΔH_{XY} (AA, BB, AB, BA) (kJ mol^{-1})	−15.6 ± 1.7	−11.9 ± 1.5	−14.5 ± 1.2[c] −11.0 ± 1.3[b]	−16.4 ± 1.5[b]
ΔS_{XY} (AA, BB, AB, BA) (J mol^{-1} K^{-1})	−54.5 ± 7.3	−36.3 ± 5.6	−46.6 ± 3.6[c] −33.5 ± 3.7[b]	−56.8 ± 5.7[b]

[a]Determined for active centers.
[b]Determined for methoxy end groups (copolymerization in the presence of dimethoxymethane).
[c]$(K_{AB}K_{BA})^{0.5}$, $(\Delta H_{AB} + \Delta H_{BA})/2$, and $(\Delta S_{AB} + \Delta S_{BA})/2$ determined for active centers.
Based on the data from Szymanski, R. *Makromol. Chem.* **1991**, *192*, 2943.[21]

described in the same paper[21] that previously discussed the copolymerization of DXL with DXP. The observed dependence of the equilibrium concentrations of comonomers and of various dyads on the initial conditions could not be explained assuming the dyad model of copolymerization. The author explained the experimental results assuming the triad model of copolymerization. As an alternative, the analysis of the system from the point of view of the Flory–Huggins interaction parameters was also performed. Consequently, as for the system with DXP, some equilibrium constants and thermodynamic parameters could be determined. The quantities estimated assuming the triad model of copolymerization are listed in **Table 2**.[21]

The known thermodynamic parameters of copolymerization can be used to calculate the ceiling temperatures for the given system. The author made such calculations by using the apparent equilibrium constants for the dyad model reported in the original paper of Szymanski.[21] Assuming the linear dependence of the apparent thermodynamic parameters on the feed content of 1,3-dioxane, it was possible to calculate the apparent thermodynamic parameters for any temperature and any feed composition. As for the ceiling temperature, the content of a copolymer is negligible and consequently the feed concentrations are the equilibrium concentrations. It was sufficient to solve the set of four equations, with four unknowns – T, K_{AA}, K_{BB}, and $K_{AB}K_{BA}$ – to find the ceiling temperature ($T_c = T$) for any feed on the basis of the above-mentioned estimated linear correlations:

$$K_{AA} = \exp\left(\frac{-\Delta H_{AA} + T\Delta S_{AA}}{RT}\right) \quad [53]$$

$$K_{BB} = \exp\left(\frac{-\Delta H_{BB} + T\Delta S_{BB}}{RT}\right) \quad [54]$$

$$K_{AB}K_{BA} = \exp\left[\frac{-(\Delta H_{AB} + \Delta H_{BA}) + T(\Delta S_{AB} + \Delta S_{BA})}{RT}\right] \quad [55]$$

$$\frac{(1 - K_{AA}a)(1 - K_{BB}b)}{K_{AB}K_{BA}ab} = 1 \quad [56]$$

The last equation can be derived from eqns [45] and [46], remembering that for infinitely long copolymer chains the concentrations of units are equal to the sum of the corresponding homo- and heterodyads ($(X) = (XX) + (XY)$ and $(XY) = (YX)$).

Then, when the dependence of the ceiling temperature is computed for any feed the composition of the equilibrium copolymer (mole fraction of 1,3-dioxane units, fr(B)) can be calculated on the basis of the computed equilibrium constants of homopropagation (the equation easily derivable from relationships [45] and [46] assuming the infinite X_n):

$$\mathrm{fr(B)} = \frac{(1 - K_{AA}a)}{(1 - K_{AA}a) + (1 - K_{BB}b)} \quad [57]$$

The computed dependence of the ceiling temperature on the feed and copolymer composition for the bulk copolymerization of DXL with 1,3-dioxane is presented in **Figure 3**.

Table 2 The equilibrium constants and the corresponding thermodynamic parameters governing the bulk copolymerization of DXL (A) with 1,3-dioxane (B)

Temperature (K)	K_{AAA} (mol^{-1} l)	K_A[a] (mol^{-1} l)	K_{BBB} (mol^{-1} l)	K_B[a] (mol^{-1} l)	$(K_{ABA}K_{BAB})^{1/2}$ (mol^{-1} l)
273	1.203	1.642	0.0559	0.0417	0.226
294	0.653	0.969	0.0473	0.0430	0.152
313	0.391	0.715	0.0472	0.0441	0.120
ΔH_Z[b] (kJ mol^{-1})	−20 ± 2	−14.9 ± 0.8	−3 ± 1	1 ± 0.1	−11 ± 1
ΔS_Z[b] (J mol^{-1} K^{-1})	−71 ± 10	−50 ± 5	−36 ± 3	−22.8 ± 0.3	−54 ± 4

[a]$K_X = K_{XXY}K_{YXX}/K_{YXY}$ $(X \neq Y)$.
[b]Z denotes a type of thermodynamic parameter (AAA, A, …) that correspond to the listed equilibrium constants.

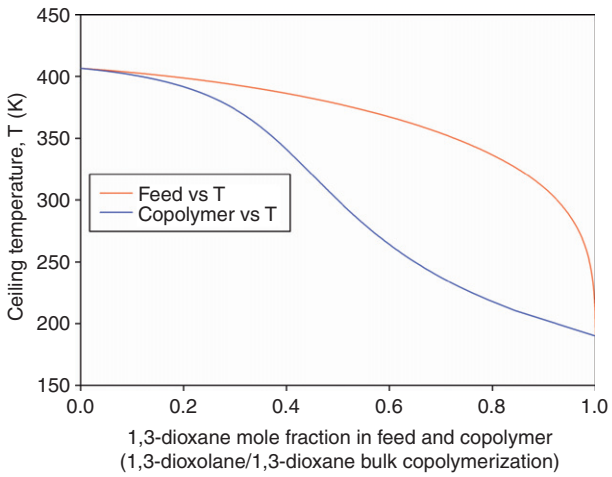

Figure 3 Dependence of the ceiling temperature on the feed and copolymer composition for the bulk copolymerization of DXL with 1,3-dioxane. Computations were performed by neglecting dependences of the comonomer densities on the temperature and melting point of 1,3-dioxane (11.8 °C).

The plot shows a strong nonlinear dependence of the ceiling temperature on the feed composition and the discrepancy between the feed and copolymer compositions for ceiling temperature conditions. As expected, a copolymer is richer in DXL than feed for any ceiling temperature and, on the other hand, the ceiling temperature for any feed composition is higher than for a copolymer of the same composition. The highest difference between the compositions of the feed and the copolymer is observed for the ceiling temperature close to the average value for both comonomers and corresponding to the approximately equal contents of both comonomers in the feed. One would have to compute such dependences for various copolymerization systems in order to check whether these observations are general or only specific for the discussed system.

4.05.6.1.3 Equilibrium in 1,3,5-trioxepane polymerization regarded as an example of the equilibrium copolymerization

1,3,5-Trioxepane (TXP) is a seven-membered cyclic monomer formed from a DXL ring expanded by the insertion of a formaldehyde unit (F). Thus, it is a cyclic monomer containing two adjacent oxymethylene groups and four acetal bonds. Acetal bonds are very labile in cationic polymerization conditions, which results in the formation of a copolymer composed of statistically distributed DXL and F units (Scheme 4).[28]

During the polymerization of TXP formation of cyclic compounds, including DXL, oligomers of DXL and TXN, and other cyclic compounds containing all possible numbers of DXL and F units and characterized by all possible distributions of them

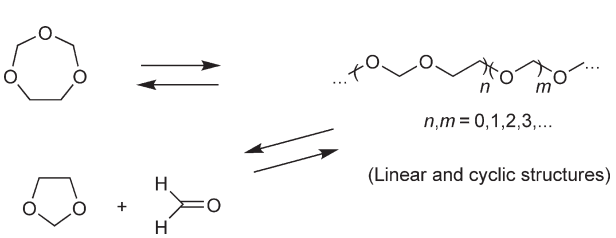

Scheme 4 Polymerization of TXP regarded as copolymerization of DXL with formaldehyde.

is observed. Besides, free formaldehyde is formed. Addition of these compounds to active species and the segmental exchange reaction operating in the system that cause all possible distributions of DXL and F units can also be found in a linear polymer.

The presence of two adjacent oxyethylene units (fragment of DXL unit) was not observed, probably because the nucleophilic attack of acetal oxygen atoms (weak base) on the ether carbon atom ($O\underline{C}H_2CH_2$ group) of oxonium cations (active species of copolymerization or of segmental exchange) is much slower than on the acetal carbon atom ($O\underline{C}H_2O$). Therefore, the equilibrium of the polymerization of TXN can also be regarded as the equilibrium of the copolymerization of DXL with F. Consequently, the method of analysis of a copolymer microstructure, making it possible to determine the thermodynamic parameters of homo- and heteroadditions, can be applied.

It was Szwarc and Perrin,[29] who first made this observation and calculated the correct equilibrium constants of homoaddition of TXN on the basis of the experimental data of Schulz *et al.*[28] and determined the thermodynamic parameters of its polymerization. The corresponding equation, the version modified by Szymanski,[30] that enables us to compute the equilibrium constant of homoaddition of TXN is shown in Chapter 4.30.

The thermodynamic parameters for the polymerization of TXN (to uniform polymer) as computed by Szwarc and Perrin[29] were $\Delta H_{TT} = -6.9\,kJ\,mol^{-1}$ and $\Delta S_{TT} = -31.5\,J\,mol^{-1}\,K^{-1}$ (which corresponds to the equilibrium concentration equal to $2.11\,mol\,l^{-1}$ at 0 °C and $3.66\,mol\,l^{-1}$ at 60 °C, while the observed concentrations by Schulz *et al.*[28] were much lower, equal to 0.23 and $1.36\,mol\,l^{-1}$, respectively, because of the copolymerization nature of the process).

4.05.6.2 Copolymerization of Sulfur with Norbornene Trisulfide

Penczek and Duda studied the copolymerization of sulfur with organic sulfides (cf. Reference 31 and references listed therein). These copolymerizations, when performed below the floor temperature of sulfur, can be regarded as the equilibrium copolymerization because homodepropagation of sulfur counterbalance the homopropagations, and the equilibrium is established determining the average length of blocks of sulfur atoms of the sulfur-terminated anionic active species of copolymerization. However, when alkylene monosulfides are copolymerized with sulfur, cyclic trisulfide is formed as the by-product and then it functions as a comonomer of copolymerization. Besides, homopolymerization of monosulfides is practically irreversible. Therefore, a simpler equilibrium copolymerization system is that when trisulfide is used instead of monosulfide in copolymerization with elemental sulfur.

Penczek and Duda investigated the copolymerization of norbornene trisulfide (NS_3) with sulfur (S_8) and managed to determine the equilibrium concentrations of both comonomers at 25 °C in the bulk. The results are listed in Table 3.[31]

Unfortunately, the authors did not discuss their results from the point of view of the copolymerization equilibrium. However, it is a bit striking that the equilibrium concentration of NS_3 is almost independent of the feed composition. This may indicate that either specific intercomponent interactions influence the values of the apparent equilibrium constants or

Table 3 Dependence of the equilibrium concentrations of norbornene trisulfide (NS_3) and sulfur (S_8) and of the average length of sulfur copolymer segments X_n on the feed composition

$\frac{8[S_8]_0}{8[S_8]_0+[NS_3]}$	$8[S_8]_0$ ($mol\,l^{-1}$)	$[NS_3]_0$ ($mol\,l^{-1}$)	$8[S_8]_{eq}$ ($mol\,l^{-1}$)	$[NS_3]_{eq}$ ($mol\,l^{-1}$)	X_n
0	0	7.0	0	3.70	3.0
0.50	6.3	6.3	1.7	3.17	4.5
0.67	11.5	5.7	3.6	3.30	6.2
0.75	15.8	5.3	6.8	3.15	7.2
0.80	19.6	4.8	11.4	3.20	8.0
0.83	22.4	4.5	15.5	3.20	8.4

the triad (or of higher order) model of copolymerization has to be taken into account, and consequently, while increasing the content of sulfur in the system the fraction of NS_3 dyads does not change significantly (in other words, the proportion of short S_3 segments almost does not change).

4.05.6.3 Equilibrium Copolymerization of γ-Butyrolactone with ε-Caprolactone

Five-membered cyclic ester γ-butyrolactone (BL) does not polymerize under normal conditions. It stems from low ring strain. Linear oligomers can, however, be obtained,[32] which indicates that the formal (apparent) homopolymerization equilibrium concentration of this monomer (equal to the reciprocal of the equilibrium constant of homopropagation) is not too high. Duda and Penczek[32] managed to copolymerize BL with ε-caprolactone (CL) and analyze the resulting copolymer. Unfortunately, because of the inability to determine quantitatively the contributions of various triads, the authors did not analyze their result from the point of view of the equilibrium copolymerization. Nevertheless, assuming the random microstructure of the copolymer for which the content of dyads can be computed on the basis of the Bernoulli statistics ($[-(BL)_2-]/[-BL-] = fr(BL)$, where fr(BL) is the molar fraction of BL units in the copolymer), the formal (apparent) equilibrium concentration of BL can be estimated to be for bulk conditions at 20 °C, equal to about 26 $mol\,l^{-1}$ ($[BL]_{eq(homo)} = [BL]_{eq(co)}/fr(BL)$). This value is close to the apparent monomer equilibrium concentration in the homopolymerization of 1,3-dioxane, discussed previously, and confirms relatively easy copolymerization of BL with CL and other lactones.

4.05.6.4 Equilibrium Copolymerization of Tetrahydropyran with Oxetane

Recently, Bouchékif *et al.*[33] published a paper claiming that they observed pseudoperiodic 'living' and/or controlled nature of cationic copolymerization of oxetane (OXT) with tetrahydropyran (THP). Their kinetic interpretation of the results of the copolymerization is, however, not correct. The authors considered the formation of a copolymer as a pseudoperiodic living and/or controlled cationic RO copolymerization of OXT with THP, as described by Scheme 5.

The kinetic analysis presented in this chapter is incorrect, assuming that the THP exchange reaction (rate constant k_s in Scheme 5) is crucial, which, according to the authors, determines the kinetics of copolymerization. This incorrect assumption (the THP exchange reaction does not influence copolymerization) resulted in an erroneous interpretation of results. The

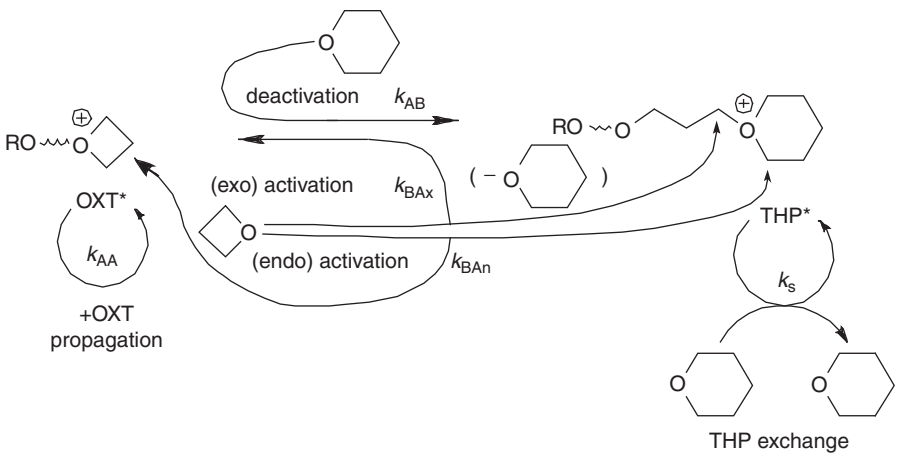

Scheme 5 Copolymerization of OXT with THP as a living process with 1-alkyl-tetrahydropyranium cations regarded as dormant species.

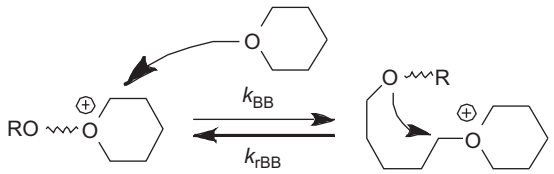

Scheme 6 Equilibrium of homoaddition of THP in copolymerization of OXT with THP.

copolymerization system under consideration can, however, be regarded as the equilibrium copolymerization, understood as a process in which the homoaddition of THP (non-homopolymerizing comonomer) is at equilibrium shifted strongly to the monomer side. The homopropagation of THP is counterbalanced by depropagation, which results in very short THP copolymer segments, the average length being close to unity (Scheme 6).

The authors claimed that only monads are incorporated in a copolymer, simplifying the system description or overlooking formations of dyads (and because of the statistical nature of propagations, also longer sequences, existing in much lower quantities). The ^{13}C NMR spectrum of the carbon atoms of the THP copolymer units, adjacent to the oxygen atoms, clearly indicates the presence of about 17% of the THP dyads (about one sixth of THP carbon atoms in the corresponding magnetic environment) in the total content of the THP segments (Figure 4).

This information is sufficient to estimate the equilibrium constant of the homopropagation of THP and the formal equilibrium concentration of THP for homopolymerization (the reciprocal equilibrium constant) (cf. eqn [45]):

$$K_{BB} = \frac{[-BB-]}{[-B-][THP]_{e(co)}} \approx \frac{1}{6 \times 20} = 8.3 \times 10^{-3}\ \text{mol}^{-1}\ \text{l}$$

$$[THP]_{e(homo)} = K_{BB}^{-1} \approx 120\ \text{mol l}^{-1}$$

The estimated equilibrium constant of the homopolymerization of THP is much lower than the estimated equilibrium constant for another six-membered cyclic monomer 1,3-dioxane (4.73×10^{-2} mol^{-1} l at 294 K); the copolymerization of 1,3-dioxane with DXL was discussed in Section 4.05.6.1.1. Consequently, the formal equilibrium concentration in the homopolymerization of THP (120 mol l^{-1}) is much higher than for 1,3-dioxane (21.1 mol l^{-1}). This can be

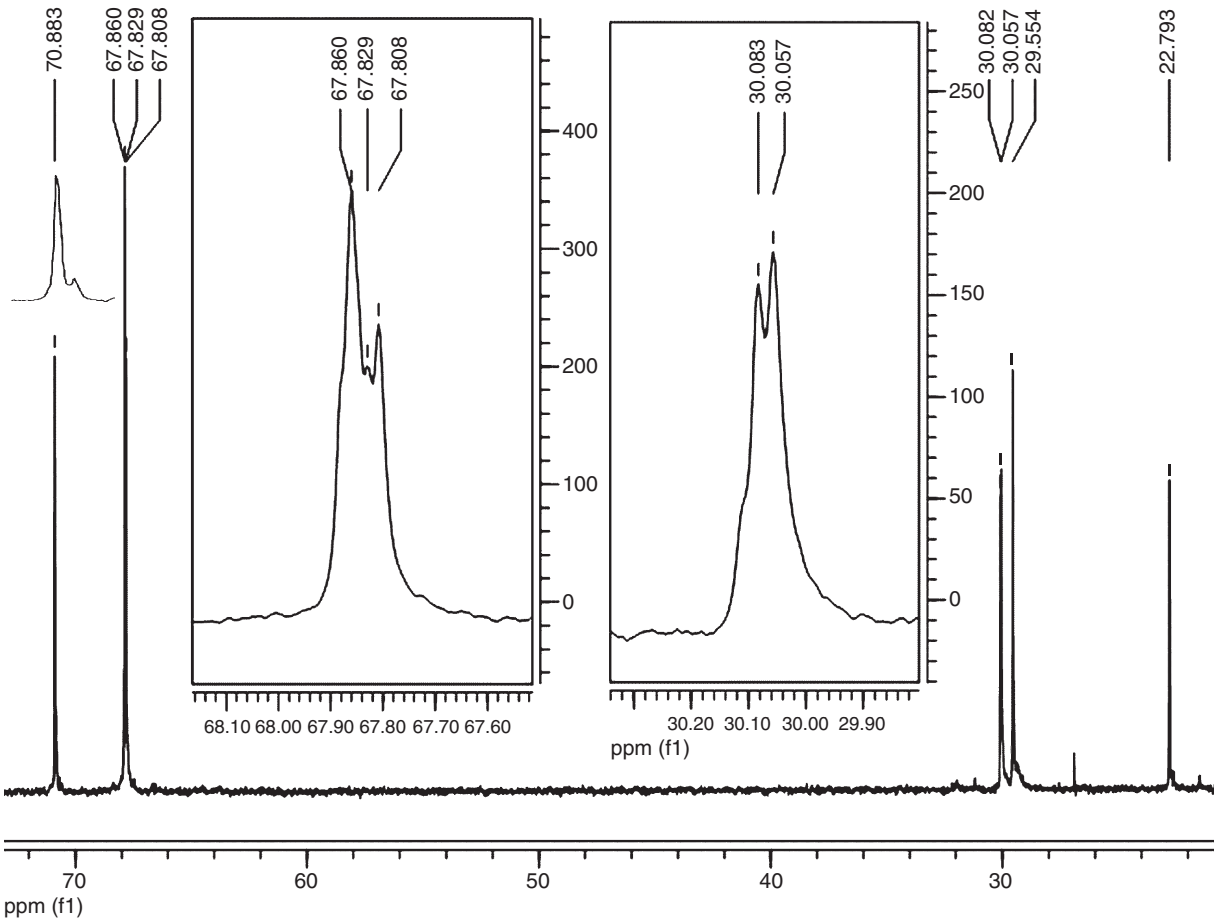

Figure 4 ^{13}C {^1H} NMR spectrum of the copolymerization of THP with OXT, showing expanded fragments of copolymer signals. Note the presence of signals of $O(CH_2)_4\underline{C}H_2OX$ dyads at about 71 ppm and X = OXT (larger peak) and THP (smaller peak). Experimental conditions: $[OXT]_0 = 0.25$ mol l^{-1}, $[THP]_0 = 20$ mol l^{-1}, room temperature, OXT conversion = 4%, THP content in copolymer = 29.2%, $M_{n(SEC)} = 7300$, $Đ_n = 1.6$. Reproduced with permission from the supporting information of Bouchékif, H.; Philbin, M. I.; Colclough, E.; Amass, A. J. *Macromolecules* **2010**, *43*, 845.[33]

explained by the nonexistence of THP monomer interactions that are important in 1,3-dioxane, mainly between oxygen atoms; this increases for 1,3-dioxane the Gibbs energy of the formation of a cyclic compound in comparison to linear one (polymer segment).

4.05.6.5 Equilibrium Copolymerization of Tetrahydrofuran Above Its Ceiling Temperature with Oxetanes

Kubisa and Penczek[34] reported the copolymerization of tetrahydrofuran (THF) above its ceiling temperature (bulk systems at 100 °C, while the ceiling temperature is about 80 °C; $Al(i\text{-}Bu)_3$ used as the catalyst) with a few 3,3-bis-substituted oxetanes. Applying some simplifications, the authors derived equations that enable them to determine the reactivity ratios and the apparent equilibrium constant of the homopropagation of THF in the studied systems. The maximum content of THF in a copolymer was found to be about 50% for copolymers with 3,3-dimethyloxetane and with 3,3-bis(fluoromethyl)oxetane but about 66% for bis(chloromethyl)oxetane (BCMO). This may suggest that the penultimate unit effect can be important for the bulkiest comonomer, causing depropagation of the THF–THF dyad-terminated active species to be slower than the homopolymerization of THF, and consequently the corresponding propagation equilibrium constant is larger. In fact, the apparent equilibrium constant of homopropagation of THF was found to be $K_{AA} = 0.8\ mol^{-1}\ l$ by using the aforementioned equations, which would correspond to the equilibrium concentration of THF being equal to $1.25\ mol\ l^{-1}$ if the dyad model of copolymerization was true for this system. The determined reactivity ratios for this system were $r_{BCMO} = 0.35$ and $r_{THF} = 9$, which corresponds to the product of these values equal to about 3, indicating a certain tendency to block formation. The THF–BCMO system was also studied by Yamashita *et al.*,[3] who had similar observations but studied the system at several temperatures and also observed the dependence of the reactivity ratios and composition of a copolymer on the catalyst used. It may indicate the importance of the nature of active species on their relative reactivities toward different comonomers. For the THF–BCMO system catalyzed with $Et_3O^+BF_4^-$, the determined reactivity ratios were $r_{BCMO} = 0.3$ and $r_{THF} = 1.2$, indicating the tendency to form alternating copolymers contrary to the previously mentioned tendency to block formation.

4.05.7 Conclusions and Outlook

Reversibility of propagation is often observed in RO polymerization systems, including copolymerization. Although attaining equilibrium is rather infrequently the aim of copolymerization, it can be used as a tool not only for obtaining copolymers of thermodynamically defined properties but also for other purposes. The term 'equilibrium copolymerization' means not only the equilibrium in copolymerization but also copolymerization in which one or more of homo- or cross-propagations are counterbalanced by depropagations. Consequently, although the equilibrium is often not reached, equilibrium copolymerization frequently allows us to obtain products containing substantial content of units coming from non-homopolymerizing comonomers. When the real equilibrium is reached, the analysis of copolymer composition and microstructure, combined with determination of the equilibrium concentrations of comonomers, gives access to the equilibrium constants of homopropagation. In this way, equilibrium constants of homoadditions of non-homopolymerizing monomers can be determined as well, and consequently the thermodynamic parameters of the polymerization of such monomers are often not accessible by other methods. When the equilibrium concentrations of active species can be measured, the equilibrium constants and the corresponding thermodynamic parameters of cross-propagations can be additionally determined.

References

1. Lowry, G. G. *J. Polym. Sci.* **1960**, *42*, 463.
2. Hazell, J. E.; Ivin, K. J. *Trans. Faraday Soc.* **1961**, *58*, 176.
3. Yamashita, Y.; Kasahara, H.; Suyama, K.; Okada, M. *Makromol. Chem.* **1968**, *117*, 242.
4. Wittmer, P. In *Multi Component Polymer Systems*; Platzer, N. A. J., Ed.; American Chemical Society: Washington, DC, 1971; p 140.
5. Alfrey, T.; Tobolsky, A. V. *J. Polym. Sci.* **1959**, *38*, 269.
6. Tobolsky, A. V.; Owen, G. D. T. *J. Polym. Sci.* **1962**, *59*, 329.
7. Izu, M.; O'Driscoll, K. F. *Polym. J.* **1970**, *1*, 27.
8. Howell, J.; Izu, M.; O'Driscoll, K. F. *J. Polym. Sci. A-1* **1970**, *8*, 699.
9. Kang, B. K.; O'Driscoll, K. F. *J. Polym. Sci. A-1* **1972**, *10*, 2349.
10. Szymanski, R. *Makromol. Chem.* **1987**, *188*, 2605.
11. Kricheldorf, H. R.; Stricker, A. *Macromolecules* **2000**, *33*, 696.
12. Szwarc, M.; Perrin, C. L. *Macromolecules* **1985**, *18*, 528.
13. Szymanski, R. *Macromolecules* **1986**, *19*, 3003.
14. Szwarc, M. *Macromolecules* **1986**, *19*, 3003.
15. Cai, G.-F.; Yan, D.-Y. *J. Macromol. Sci., Part A* **1987**, *24*, 869.
16. Sawada, H. *Polym. Rev.* **1974**, *10*, 293.
17. Sawada, H. *Polym. Rev.* **1974**, *11*, 257.
18. Harvey, P. E.; Leonard, J. *Macromolecules* **1972**, *5*, 698.
19. Mita, J. J. *J. Macromol. Sci., Part A* **1974**, *A8*, 1273.
20. Szymanski, R. *Makromol. Chem. Theory Simul.* **1992**, *1*, 129.
21. Szymanski, R. *Makromol. Chem.* **1991**, *192*, 2943.
22. Berlin, A. A.; Bogdanova, K. A.; Markevich, M. A.; *et al. Dokl. Akad. Nauk USSR* **1973**, *211*, 874.
23. Berlin, A. A.; Deberdeev, R. Ya.; Perukhin, Yu. V.; *et al. Polioksimetileny*; Nauka: Moscow, 2008.
24. Sharavanan, K.; Ortega, E.; Moreau, M.; *et al. Macromolecules* **2009**, *42*, 8702.
25. Binet, R.; Leonard, J. *Polymer* **1973**, *14*, 355.
26. Kuzub, L. I.; Markovitch, M. A.; Berlin, A. A.; Enikolopyan, N. S. *Vysokomol. Soedin. Ser. A* **1968**, *10*, 2007.
27. Plesch, R. H.; Westermann, P. H. *Polymer* **1969**, *10*, 105.
28. Schulz, R. C.; Albrecht, K.; Rentsch, C.; Tran Thi, Q. V. *ACS Symp. Ser.* **1977**, *59*, 77.
29. Szwarc, M.; Perrin, C. L. *Macromolecules* **1979**, *12*, 699.
30. Szymanski, R. *Makromol. Chem.* **1989**, *190*, 2903.
31. Penczek, S.; Duda, A. *Phosphorus, Sulfur, Silicon* **1991**, *59*, 41.
32. Duda, A.; Penczek, S. *Macromol. Chem. Phys.* **1996**, *191*, 1273.
33. Bouchékif, H.; Philbin, M. I.; Colclough, E.; Amass, A. J. *Macromolecules* **2010**, *43*, 845.
34. Kubisa, P.; Penczek, S. *Rocz. Chem.* **1973**, *47*, 1857.

Biographical Sketch

Ryszard Szymanski received his MS degree in organic synthesis from Technical University at Lodz, Poland, in 1972. In the same year he started his work in the Center of Molecular and Macromolecular Studies of the Polish Academy of Sciences (CMMS), Lodz, Poland, as a research assistant. He worked in Professor Stanislaw Penczek's group and received his PhD in 1980 in polymer chemistry. His PhD thesis was on the reactions of alkoxymethylium cations with ethers and acetals as models of cyclic acetal polymerization. He worked as a postdoc at Professor H.K. Hall's Laboratory in Tucson, AZ, in 1981, and investigated the polymerization of bicyclic orthoesters. After returning to Poland, he continued his work as an adjunct professor in the field of ring-opening polymerization in CMMS with Professor S. Penczek. In 1994 he spent 6 months with Professor K. Matyjaszewski in Pittsburgh, PA, where he studied the mechanism of the cationic polymerization of styrene by using computer simulation methods. After returning to CMMS, he received his DSc degree, with the thesis on problems connected with equilibrium in copolymerization. He continues his work in CMMS as an associate professor in the Laboratory for Computer Simulations. His main research interests are mechanisms and kinetics of the polymerization of cyclic monomers. In his work he develops computer simulation techniques.

4.06 Organocatalyzed Ring-Opening Polymerizations

M Fèvre, J Vignolle, Y Gnanou, and D Taton, Université de Bordeaux, Pessac, France

4.06.1 Introduction

Polymer chemistry has been dominated, in the twentieth century, on the one hand, by radical processes, and, on the other hand, by metal-based catalysis. Besides polymers obtained by radical polymerization, which account for about 50% of polymeric materials produced industrially, most of the other synthetic polymers require metallic species to catalyze, activate, or initiate elementary reactions that bring about their synthesis.[1,2] In most cases, the metallic catalyst (typically, organometallic complexes based on transition metals or metal-based ionic species) represents minute amounts and remains in the final polymer.

A representative example of a metal-based catalysis is the Ziegler–Natta process, which has been gradually improved to such an extent that the monomer-to-catalyst ratio is typically in the range 10^6–10^8.[3] As a matter of fact, removal of the metallic catalyst is not needed and commodity polymers obtained in this way (polyolefins) are directly processed without any purification step. In contrast, the synthesis of specialty polymers used in niche applications requires larger amounts of metallic catalysts (the monomer-to-catalyst ratios being 10^3–10^4). To prevent hazards due to the presence of toxic metallic species that can freely migrate out of the polymeric material when in service, a purification process is sometimes required which adds to the cost of the polymer produced. In sensitive domains such as biomedical, packaging, and microelectronics, metal-based catalysts are prohibited.

Organic and enzymatic catalyses appear today as reliable alternatives to metal-mediated catalysis for polymer synthesis.[4–7] Organocatalysis, in its general sense, is a part of the general concept of catalysis and is categorized as green chemistry. Organocatalysis has been known for a while, since Justus Liebig[8] reported as early as 1859 the synthesis of oxamide employing acetaldehyde as organic catalyst. A few decades later, Emil Fischer[9–11] developed the glycosidation processes using acids as catalysts. Some significant examples of organocatalytic approaches were reported in the 1970s.[12–14] However, not less than a century had passed before organocatalysis could be finally recognized as the third pillar of catalysis,[5] besides metallic catalysis and enzymatic catalysis. The twentieth century has indeed witnessed the dramatic development of transition metal-based catalysts; meanwhile, concepts of organocatalysis have been clearly neglected. While in the last decade, tremendous efforts have been made in molecular chemistry to develop powerful organocatalysts for a variety of transformations, most of the work has been focused on enantioselective processes, using chiral organocatalysts and taking inspiration from the *modus operandi* of enzymes to catalyze reactions in a biomimetic fashion. In this regard,

organocatalysts can be viewed as 'minimal enzymes' possessing advantages of enzymes such as selectivity and mild reaction conditions, without the drawbacks of biocatalysts such as the complexity of their structure/conformation, their lack of availability, and their lack of robustness due to possible deactivation/denaturation.[15] In molecular chemistry, most of the organocatalyzed enantioselective transformations can be classified as follows:

1. asymmetric C–C bond and C–X (X = O, N, H, etc.) forming reactions (e.g., Michael additions, Mannich reactions, aldol additions, vinylogous aldol additions, allylation reactions, α-alkylation of amino acids, α-halogenation or α-amination of carbonyl compounds, protonation, etc.);
2. enantioselective oxidation–reduction processes (epoxidations, sulfoxidations of thioethers, enantioselective reduction processes, and α-hydroxylation of carbonyl compounds).

Several reviews have already reported on the general topic of organocatalysis in molecular chemistry.[16–20] It is not yet viewed as a mature field and it is far from being applied in the chemical industry. A representative example is the synthesis of the Wieland–Miescher ketone developed in 1970 on an industrial scale, via an enantioselective organocatalytic aldol process.[21]

In the last decade, organocatalysis has also been applied to a few polymerization reactions, in an attempt to replace classical catalysts and to enhance the rate of polymerization through activation of monomers and/or polymer chain ends.[5,6]

Use of organocatalysts as promoters of polymerization reactions has actually been known for a while. For instance, the polyurethane synthesis by step-growth polymerization of multihydroxy compounds with multiisocyanates can be catalyzed with tertiary amines such as 1,5-diazabicyclo[5.4.0]undec-5-ene (DBU) or triethylamine. The group transfer polymerization (GTP) of methacrylic monomers can be also categorized, to some extent, as organocatalyzed polymerization when a metal-free nucleophilic catalyst (Lewis base) is employed.[22] One can also mention pioneering works by the group of Penczek[23] in the late 1980s regarding the cationic ROP of cyclic ethers by acids such as BF_3 or HPF_6, which have provided the first metal-free approach for precision polymer synthesis.

However, the (re)emergence of the field of organocatalyzed polymerization dates back to 2001 with the first reports by Hedrick (IBM), Waymouth (Stanford), and co-workers who employed dialkylaminopyridines for the ring-opening polymerization (ROP) of lactones and lactide.[24,25]

This chapter covers past and recent achievements related to ROP reactions employing organic catalysts. This field – including chain and step-growth polymerizations – was reviewed in 2007 and at the beginning of 2010 by Kamber *et al.*[5] and Kiesewetter *et al.*[6] Roughly a hundred papers have been published in peer-reviewed journals in the past 20 years. The introduction of the chapter will present general consideration on the meaning of 'organocatalyzed polymerization', all of the employed catalysts (classified according to the nature of the active center of the catalyst, i.e., its functional group), monomers which have been polymerized, and general polymerization mechanisms encountered. The discussion will then put a special emphasis on the scope and limitations of each family of catalysts as well as on related mechanisms (monomer activation and/or chain end activation), though the latter aspect has not been systematically discussed in the original reports.

4.06.2 Metal-Free Initiated versus Metal-Free Organocatalyzed Polymerizations

Beyond radical processes, the use of organic promoters for the purpose of metal-free polymerization reactions is well documented.[6] A distinction should be made, however, between metal-free polymerizations triggered by organic reagents actually playing the role of initiators and truly organocatalyzed polymerizations, where an organic promoter is used in the presence of a chain length regulator as the other component. For instance, the ROP of *N*-carboxyanhydrides (NCAs) can be readily initiated with amines, as reported in the early 1970s.[26] The ROP of β-lactones can be triggered with amines, phosphines, or tetraalkyl ammonium caboxylates, as organic initiators.[27,28] The same is true for the ROP of epoxides in the presence of organic amino-containing initiators.[27] The cationic ROP of 2-alkyl oxazolines generally employs organic benzyl halides or alkyl tosylates.[29] Initiation of the zwitterionic chain-growth polymerization of cyanoacrylates can be achieved with phosphines,[30] and so on. In all cases, however, the organic initiator is part of the polymer being formed (**Scheme 1**). In contrast, an organic catalyst is supposed to be regenerated on the completion of the polymerization process and, ideally, it is employed in substoichiometric amounts relatively to the initiator. Only studies fulfilling at least the first criterion will be discussed in the following section.

4.06.3 Organocatalytic Platforms, Monomer Candidates, and Related Mechanisms

4.06.3.1 The Different Organic Catalysts

Organic catalysts can be classified according to the nature of the reactive center (its functional group) involved in the activation of monomers and/or chain end (**Figure 1**). Only organocatalysts employed in polymerization reactions will be considered in this chapter. These include Bronsted acids, from weak carboxylic derivatives (e.g., CF_3COOH, lactic acid, and alanine) to stronger acids (e.g., CF_3SO_3H and CH_3SO_3H) and superstrong acids (e.g., $(CF_3SO_2)_2NH$ and $(C_4F_9SO_2)_2NH$), Bronsted bases (e.g., phosphazenes such as *t*-BuP_4, pyridine derivatives, and carbenes), and Lewis bases (mostly phosphines, 4-(dimethylamino) pyridine (DMAP), guanidines, and carbenes). Combination of two amphiphilic catalysts, within the same molecule or not, leads to bifunctional systems, but the strength of each antagonistic reactive center has to be moderate enough so as to not quench the system (e.g., a strong Bronsted acid combined with a strong Bronsted base will react together preventing any monomer activation). Most of the systems reported involved a basic-nucleophilic-type function, associated with a weak acid-electrophile. Note that thiourea (TU) derivatives can be considered as weak electrophiles due to their H-bonding donor ability.[31] Such organic catalytic systems lead to cooperative activation of the monomer and initiator (see Section 4.06.3.3.4). In this respect, bifunctional organocatalysts find analogies with multicentered enzymatic catalysis, which allows synergistic

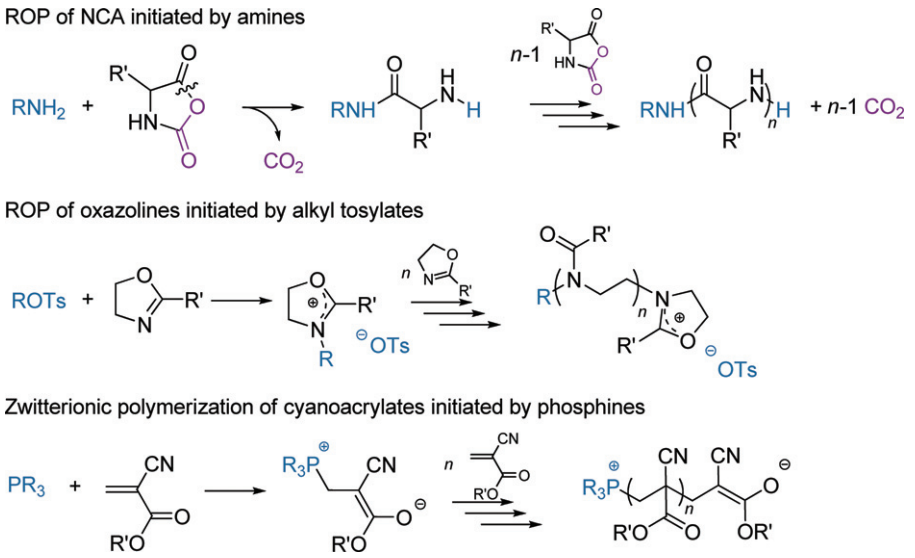

Scheme 1 Examples of metal-free initiated polymerizations.

interactions with the different reaction partners with high selectivities. A typical example of a dual activation by hydrogen bonding is provided by the bicyclic guanidine 1,5,7-triazabicyclo[4.4.0]dec-5-ene (TBD) (Section 4.06.5) or by combination of a TU moiety with an amino group (Section 4.06.6) in a mono- or a bicomponent catalytic system.

Many of the aforementioned organic catalysts provide high rates and selectivities, tolerance to functional groups, easy handling, and environmental friendliness and sometimes offer opportunities for new synthetic strategies.[5,6]

4.06.3.1.1 4-(Dialkylamino)pyridines

4-(Dialkylamino)pyridines (**Figure 1**) behave either as weak bases or as nucleophiles via the sp^2-hybridized nitrogen atom. DMAP and 4-pyrrolidinopyridine (PPY), which are commercially available, are prototypes of such 4-aminopyridine derivatives. In molecular chemistry, these compounds have proven efficient in acylation transesterification reactions.[32,33] Section 4.06.4 will discuss their use for the organocatalyzed ROP of carbonyl-containing heterocycles.

4.06.3.1.2 Guanidines and amidines

The guanidine moiety is present in many natural products where its catalytic activity has been established.[34] Representative examples of these organocatalysts are shown in **Figure 1**. They include 7-methyl-1,5,7-triazabicyclo[4.4.0]dec-5-ene (MTBD), DBU, and the aforementioned TBD. In terms of basicity, TBD is more basic than MTBD and DBU: $pK_a(MTBDH^+) = 25.5$, $pK_a(DBUH^+) = 24.3$, and $pK_a(TBDH^+) = 26.0$, as determined in acetonitrile and where pK_a is given with regard to the cationized conjugated acid of each base. For the sake of comparison, the pK_a value of (−)-sparteine, a base often employed in combination with TU in organocatalysis, is equal to 17.3. TBD is commercially available. The synthesis of specific acyclic guanidines can be performed by reaction of carbodiimides with secondary amines.[35]

Literature in molecular chemistry has shown that TBD can be employed as a strong base for a variety of reactions, including Michael additions,[36] Wittig reactions,[37] enantioselective Strecker synthesis of R-aminonitriles and R-amino acids,[38] or transesterification reactions.[39] Section 4.06.5 will highlight the higher catalytic efficacy of TBD over MTB and DBU for various organocatalyzed polymerizations.

2-Amino-oxazoline and 2-aminothiazoline (**Figure 1**) are organocatalysts whose structure exhibits similarities with that of TBD.[40] Indeed, both 2-aminothiazoline and 2-amino-oxazolines have a three-centered –N=C–NH– moiety, like TBD. These catalysts were shown to provide a dual activation in the organocatalyzed ROP of lactide.

4.06.3.1.3 TU-amino derivatives

Ureas and TUs are hydrogen-donating compounds that can easily activate carbonyl-, sulfoxide-, or nitro-containing substrates[19,35] and can be viewed as weak electrophile.[31] In molecular synthesis, a variety of chiral urea- and TU-based catalysts have been employed for stereoselective C–C bond forming reactions, including the Strecker, Mannich, Pictet–Spengler reactions, and aza-Henry and Michael reactions.[41–53] As mentioned above, bifunctional TU-amino derivatives allow for an activation of carbonyl substrate in a dual manner, when the TU moiety is combined with an amino-functionality in a mono- or a bicomponent catalytic system.[45,46,54,55] The strength of hydrogen bonding can be finely tuned through a proper selection of substituents both on the TU and on the amine.

4.06.3.1.4 Phosphorus-based catalysts: Phosphines and phosphazenes

Tertiary phosphines are known to behave as Lewis bases in acylation reactions that proceed through a nucleophilic activation mechanism (see Section 4.06.7 for possible mechanisms operating in organocatalyzed polymerization).[56,57] Their use as nucleophilic catalysts in enantioselective processes, which include the addition of alcohols to ketenes, the rearrangement of O-acylated azlactones, and the kinetic resolution of alcohols, is also well documented.[58–63]

Surprisingly, and to the best of our knowledge, while phosphines have been used to directly initiate several metal-free

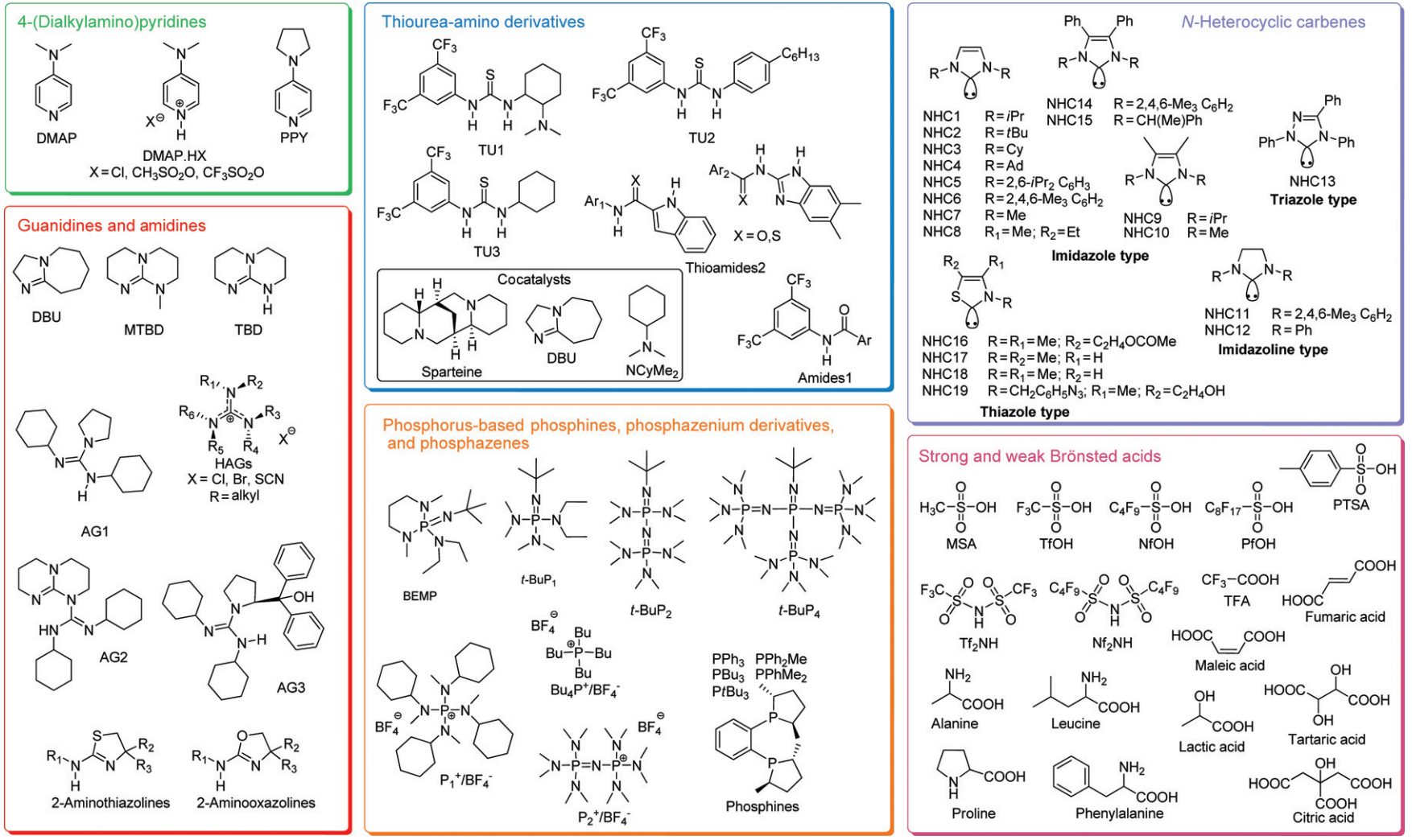

Figure 1 Organic catalysts used for polymerization reactions.

(noncatalyzed) polymerizations (see Section 4.06.2), there is only one report about their use as true organic catalysts (and not as initiators).[64] In these circumstances trialkyl- and triarylphosphines such as PBu_3, PPh_3, $PPheMe_2$, and PPh_2Me have been employed (Section 4.06.7).

Phosphazenes such as (*tert*-butylimino)-tris(dimethylamino)phosphorane (*t*-BuP_1), {[(*tert*-butylimino)bis(dimethylamino)phosphoranyl]imino}tris(dimethylamino)phosphorane (*t*-BuP_2), (*tert*-butylimino)tris{[tris(dimethylamino)phosphoranylidene]amino}phosphorane (*t*-BuP_4), and 2-(*tert*-butylimino)-2-(diethylamino)-1,3-dimethylperhydro-1,3,2-diazaphosphorinane (BEMP) were developed by Schwesinger and Schlemper.[65] They are generally considered as strong, nonnucleophilic, neutral Bronsted bases, high pK_a value characterizing their conjugated acid (pK_a = 27.6, 30.2, and 27.6 for the conjugate acid of *t*-BuP_1, *t*-BuP_4, and BEMP, respectively, as measured in acetonitrile and dimethyl sulfoxide).[66] Generally speaking, phosphazenes are thus more basic by approximately 2–3 pK_a units than guanidines such as DBU and MTBD (pK_a around 24.3–25.5 for the corresponding acids). For this reason, phosphazenes have exclusively served as strongly basic deprotonating agents of acidic OH-, SH-, or CH-containing initiators in metal-free polymerizations (see Section 4.06.7).

4.06.3.1.5 N-heterocyclic carbenes

N-heterocyclic carbenes (NHCs) are a specific subgroup of carbenes, which are neutral divalent species of carbon, possessing six peripheral electrons in their valence shell. Four of them are involved in two σ-bonds while the two nonbonding electrons remain at the central carbon. When the carbene center is not properly substituted, these species are highly reactive with lifetime typically under 1 s (0.1–1 ns).[67] The first isolated stable carbene was a non-NHC acyclic (phosphinosilyl)carbene, synthesized by Igau *et al.* in 1988.[68] A few years later, Arduengo *et al.*[69] succeeded in isolating the first NHC, 1,3-diadamantylimidazol-2-ylidene. Variation of R_1–R_4 substituents of NHCs offers opportunities to tune both the electronic and steric properties, hence modulating their reactivity/nucleophilicity. Since these pioneering works on stable carbenes, these species have received considerable attention in molecular synthesis[70–72] and, more recently, in macromolecular chemistry as well.[5,6] Thanks to their peculiar electronic properties, stable singlet carbenes, and in particular NHCs, have become not only versatile ligands for transition metals[73–77] but also powerful organocatalysts for a variety of organic transformations. Many of these NHC-catalyzed reactions are based on the activation of the carbonyl group (e.g., benzoin condensation, Stetter reaction, and transesterification),[70,72] though other electrophilic groups such as trimethylsilyl can be activated (e.g.,cyanosilylation or (trifluoromethyl)silylation reactions).[78]

NHCs are generally obtained by deprotonation of their conjugate acids, namely imidazoli(ni)um salts, with a strong base. Excellent reviews can be found on the synthesis of carbenes, their electronic properties, their reactivity, and means to manipulate these catalysts.[70,75,79,80]

The pK_a values of some carbenes were determined both experimentally and theoretically and they range between 15 and 30 (pK_a values of corresponding azolium salts in water at 25 °C: NHC2 ~ 25, NHC5 and NHC6 ~ 21, see **Figure 1**).[81]

4.06.3.1.6 Bronsted acids

Besides strong Bronsted acids, such as trifluoromethanesulfonic acid (CF_3SO_3H also denoted TfOH), recent years have witnessed the development of so-called superstrong Bronsted acids as powerful catalysts in organic synthesis. Of particular interest are sulfonimide-type acids, whose prototype bis(trifluoromethanesulfonyl)imide $(CF_3SO_2)_2NH$ (Tf_2NH) allowed significant achievements in molecular chemistry for a variety of C–C bond forming reactions.[82–84] Penczek pioneered the use of Bronsted acids to trigger the ROP of cyclic ethers in the late 1980s (see Section 4.06.9). Among acid-containing catalysts, strong and superstrong acids such as methanesulfonic acid (CH_3SO_3H), CF_3SO_3H, or $(CF_3SO_2)_2NH$ have been the most studied. Nevertheless, not only weak acids such as carboxylic acids (e.g., CF_3CO_2H) but also naturally occurring α-hydroxyacids and α-amino acids can serve as organocatalysts of polymerization (**Figure 1**).

4.06.3.2 Monomer Candidates

Figure 2 shows the different families of monomers that were subjected to an organocatalyzed polymerization pathway, with their name and abbreviation as will be used hereafter. In their vast majority, monomers amenable to organocatalyzed polymerizations are heterocyclics, which are the main focus of this chapter. In particular, carbonyl-containing heterocyclics were subjected to ROP by almost all categories of the aforementioned organic catalysts. Carbonyl heterocycles thus include lactide (both in its racemic and enantiopure versions, *rac*-LA and DD- or LL-LA, respectively), lactones, cyclic carbonates, NCAs, and 1,3-dioxolane-2,4-diones, referred to as *O*-carboxyanhydrides (OCAs). In the two latter cases, the driving force of the polymerization is the evolution of a CO_2 molecule in each propagation step. For instance, the ROP of L-Lac-OCA proved a competitive synthetic route to poly(LA) (=PLA) compared with the ROP of LA.[85] Due to space limitation, the synthesis of specific monomers that were thus polymerized by an organocatalyzed pathway cannot be detailed. Related information can be found in the original reports.

Many of these heterocycles are commercially available. They arise from petroleum as source, except LA. Methyl-substituted seven-membered ring carbonates (7CCs), namely 4-methyl- and 5-methyl-1,3-dioxepan-2-one (R-Me7CC and β-Me7CC), have been synthesized by cyclization of the corresponding α,ω-diols drawn from green renewable acids.[86]

Specific monomers incorporating functional groups in a protected form, for example, protected functional cyclic carbonates or L-Glu-OCA or (3*S*)-3-{2-[(benzyloxy)carbonyl]ethyl}-1,4-dioxane-2,5-dione (BED), were purposely designed, sometimes via multistep synthetic methods.[87–89] Introduction of pendant functional groups in the resulting polymers was aimed at bestowing better degradation properties and greater hydrophilicity of these materials.

Less polar cyclic monomers, such as ethylene oxide (EO), propylene oxide (PO), cyclosiloxanes and cyclocarbosiloxanes, have also been reported to undergo a metal-free ROP, in particular using NHCs as organocatalysts.

Besides, a few examples of polymers grown (or depolymerized) by GTP of (meth)acrylics and step-growth (de)polymerizations, employing NHCs (and more recently TBD), were also described.

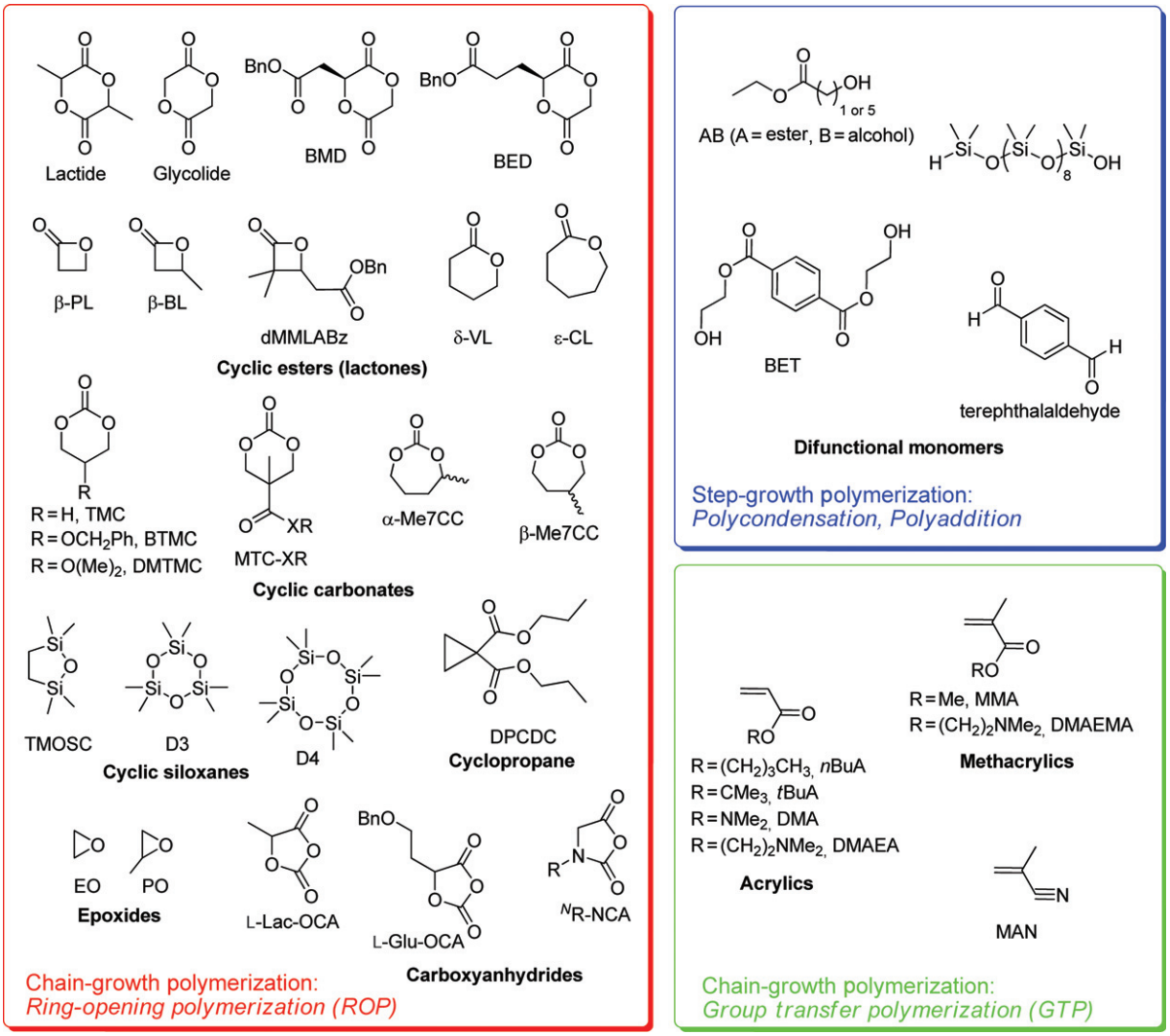

Figure 2 Monomers polymerized via an organocatalytic pathway.

4.06.3.3 General Polymerization Mechanisms

Since organic catalysts may operate differently as compared with metal-based ones, they may offer a diversity of mechanistic pathways to control the polymerization. In the particular case of the ROP of heterocycles, four distinct mechanisms can be singled out, depending upon the nature of the active center of the organocatalyst (acid vs. base and/or electrophilic vs. nucleophilic) used.[6] In the presence of a purposely added 'chain regulator', that is, an initiator controlling the resulting polymer chain length (typically an alcohol in the following examples), the organocatalyst can activate either the latter initiator and then the polymer chain ends after repetitive propagation steps or the monomer substrate or both via a cooperative dual activation.

Polymerization proceeding by activation of the monomer is referred to as the 'activated monomer mechanism' (AMM) – both nucleophilic and electrophilic – whereas polymerization by activation of the initiator/polymer chain ends is referred to as the 'active chain end mechanism' (ACEM). Note that, in the context of true organocatalysis, only basic catalysts are able to promote ACEM. Although out of the main focus of this chapter, the so-called dissociative versus associative polymerization mechanism operating in the GTP of (meth)acrylic monomers mediated by organic catalysts (e.g., ammonium fluoride, strong acids, or NHCs) is another example of initiator/polymer chain end activation. In some cases, it is unclear whether polymerization occurs solely by monomer activation, initiator activation, or both. Sometimes, one mechanism is exclusive (as in the case of bulky nonnucleophilic phosphazenes, which operate as strong bases to activate the initiator), but in general, different mechanisms may be operative concomitantly.

4.06.3.3.1 Nucleophilic AMM

AMM has been suggested in the early 1970s for several polymerizations involving organometallic species. A typical example is the ROP of ε-caprolactam by lithium amides, as illustrated in Scheme 2.[90] With the recently developed nucleophilic organic catalysts, the nucleophilic AMM proceeds by a direct attack of the cyclic monomer by the catalyst Nu (Scheme 3). This ring opening generates a zwitterionic intermediate, typically an alkoxide featuring a bulky and soft countercation, for example,

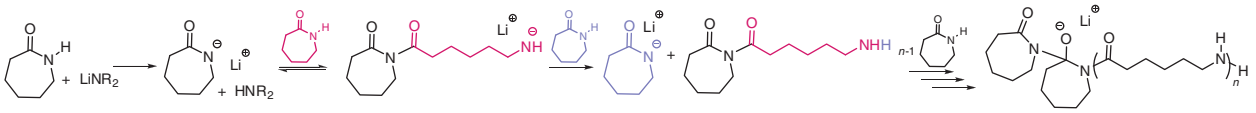

Scheme 2 ROP of ε-caprolactam by lithium amides (nucleophilic activated monomer).[90]

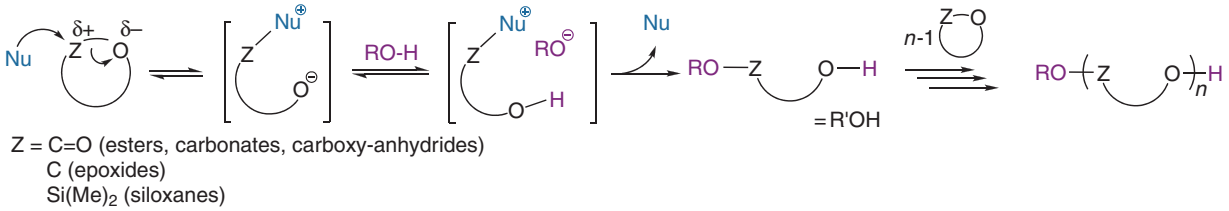

Scheme 3 AMM via nucleophilic monomer activation.

pyridinium and imidazolinium when DMAP or a NHC is used. Protonation of this zwitterionic 'activated monomer' by the alcohol initiator (ROH), and subsequent displacement of the bound catalyst by the alkoxide arising from the initiator (RO^-), generates a ring-opened alcohol monoadduct, with concomitant release of the organic catalyst. The next propagation step proceeds in the same way, that is, by activation of the monomer, except that this is the alcohol monoadduct which reacts with the activated monomer. This nucleophilic AMM mechanism has been proposed for miscellaneous nucleophilic organocatalysts, including DMAP, PPY, trialkyl- and triarylphosphines, and NHCs (Scheme 3).

4.06.3.3.2 Electrophilic AMM

As already mentioned, the AMM induced by Lewis or Bronsted acids has been established, in particular by the group of Penczek *et al.*,[91,92] for the ROP of cyclic ethers. In this case, the electrophilic (acidic) catalyst activates the cyclic monomer through protonation of the heteroatom (e.g., the oxygen of the carbonyl group for cyclic esters or the oxygen atom of cyclic ethers, Scheme 4). The resulting activated monomer undergoes ring opening by nucleophilic attack of the oxygen of the alcohol initiator (or polymer chain end), leading to the formation of the monoadduct alcohol, while the acidic catalyst is regenerated. Strong and weak acids have been reported to induce such an electrophilic AMM in the case of the ROP of epoxides, LA, lactones, or cyclic carbonates (Scheme 4, see also Section 4.06.9).

4.06.3.3.3 Active chain end mechanism

ACEM occurs in the anionic or ionic coordinated ROP of many heterocycles mediated by organometallic species. Propagation occurs by the direct attack of the active chain end (an alkoxide, a carboxylate, a silanolate, and a thiolate, depending on the cyclic monomer involved) on the cyclic monomer. With metal-free organic catalysts, a similar mechanism can operate but under milder conditions, where the basic catalyst typically activates the initiator (or the polymer chain end), most often by hydrogen bonding thereby increasing its nucleophilicity, which favors the attack on the cyclic monomer (Scheme 5). Note that depending on the pK_a difference between the initiating alcohol and the Bronsted base, the RO–H proton can be completely transferred to the basic site, thus generating an alkoxide. In fact, the extent of proton transfer will greatly vary with the nature of the alcohol and the basicity of the catalyst.

4.06.3.3.4 Dual activation of monomer and initiator/chain end

Cooperative dual activation of both the monomer and the initiator/polymer chain ends can be operative with specific catalysts (e.g., TU-amino derivatives, TBD, or even DMAP) as a means to trigger the ROP of cyclic esters. Here also, analogies can be found with some metal-based catalysts which have been suggested to behave by such a dual activation (Scheme 6).[27] Using true organic catalysts for ROP implies that an electrophilic moiety (typically proton) activates the heteroatom of the

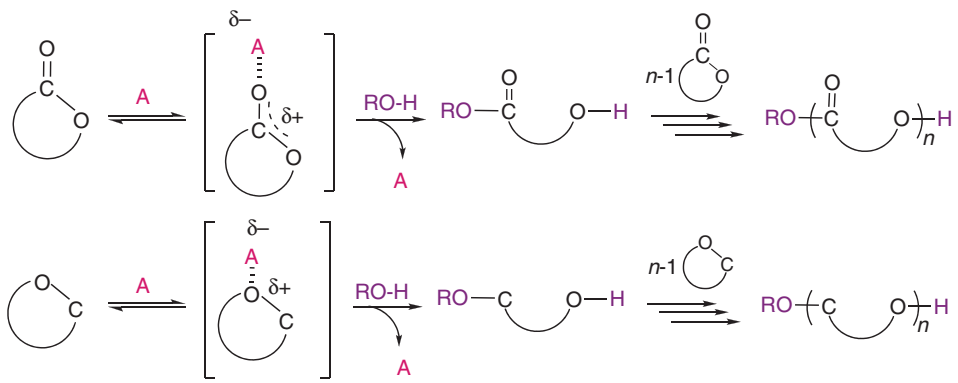

Scheme 4 AMM via acid (A) monomer activation.

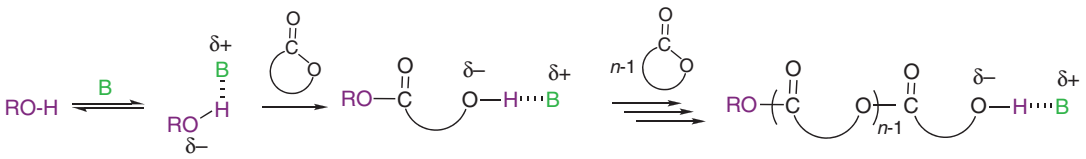

Scheme 5 Basic active initiator/chain end mechanism (ACEM).

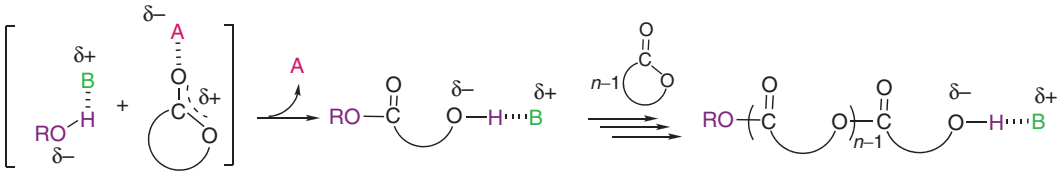

Scheme 6 Acid-basic bifunctional activation.

cyclic monomer, while a base interacts with the proton of the alcohol initiator, increasing its nucleophilicity.

4.06.4 Polymerizations Catalyzed by 4-(Dialkylamino) pyridines

An overview of the main monomers polymerized from these organocatalysts and related formed polymers is shown in Figure 3. Table 1 summarizes the different works employing DMAP or PPY for the ROP of a few heterocycles, including trimethylene carbonate (TMC), LA, ε-CL, and OCAs, in the presence of hydroxy- or amino-containing initiators.

Kricheldorf *et al.*[97] have reported that pyridines can be directly used as organic nucleophilic initiators for the metal-free – but noncatalyzed – zwitterionic ring-opening polymerization (ZROP) of pivalolactone (Scheme 7). Linear zwitterionic aliphatic polyesters, with a pyridinium and a carboxylate group, in α- and ω-position respectively, are formed in this way.

In polymer synthesis, DMAP is among the first employed organocatalyst. In 2001, Nederberg *et al.*[24] indeed reported the 'first organocatalytic living polymerization' of LA mediated either by DMAP or PPY, in the presence of ethanol, isopropanol, or benzyl alcohol as initiator (Table 1, entry 1). PLAs with a predictable degree of polymerization (from 5 to 120) and a dispersity below 1.2 could be achieved under relatively mild

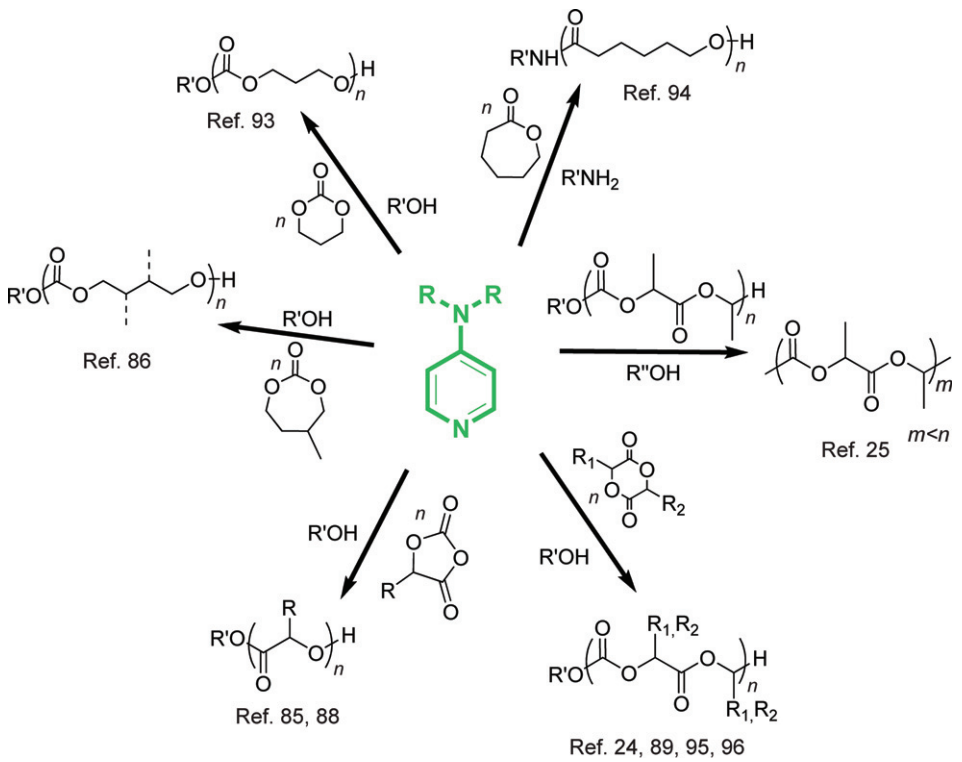

Figure 3 Overview of main polymers obtained from 4-(dialkylamino)pyridines as catalysts.

Table 1 Representative examples of ROP catalyzed by 4-(dialkylamino)pyridines

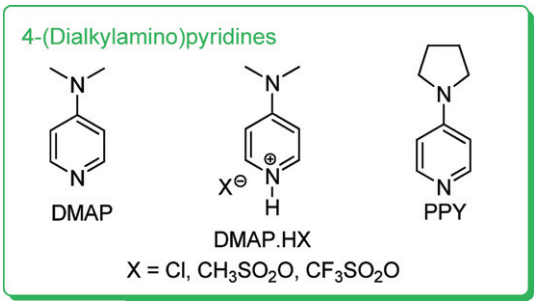

Entry	*Catalyst*	*Monomer*	*Bulk/solvent*	*Initiator*	*[C]/[I]$_0$*	*t*	*T (°C)*	*Conv (%)*	*M_n (g mol^{-1})*	*D*	*Reference*
1	DMAP, PPY	Lactide	Dichloromethane	EtOH, BnOH, *i*-PrOH	0.1–4	20–96 h	35	17–100	720–11 000	<1.16	24
			Bulk	BnOH	2–4	6–20 min	135–185	70–100	4 200–17 000		
2	DMAP	Lactide	Bulk	Ru-complex OH-pendant groups	3.5–7	10 min	135	<50	6 600–57 000 (stars)	<1.26	95
3	DMAP	ε-CL	Water	Chitosan NH_2-pendant groups	2	24 h	120	17–64	NM	NM	94
4	DMAP	L-lac-OCA	Dichloromethane	*neo*-pentanol/2° alcohols	1	<5–1140 min	25	>96	1 200–63 000	<1.22	85
5	DMAP	L-glu-OCA	Dichloromethane	*n*-pentanol/*neo*-pentanol	1	<5–90 min	25	>96	3 000–18 000	<1.25	88
6	DMAP	BED	Dichloromethane	*n*-pentanol	1–5	7–24 h	30	>98	3 000–19 000	<1.27	89
7	DMAP 5 000–42 000	TMC	Bulk 1.18–1.62	BnOH 93	0.05–0.2	5– 150 min				60–150	50–98
8	DMAP	β-Me7CC	Bulk	BnOH	1	1 h	110	87	8 500	1.21	86
9	DMAP/DMAP.HX (1/5–5/1)	Lactide	Dichloromethane	1° and 2° alcohols	1–5	24–48 h	25 or 40	30–100	900–13 000	<1.17	96

NM, not mentioned.

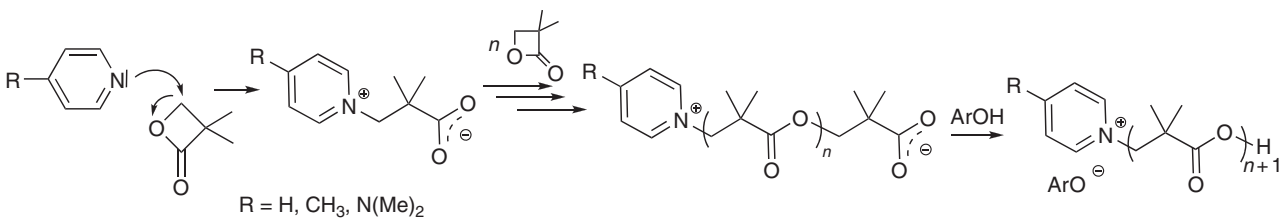

Scheme 7 Metal-free initiated ZROP of pivalolactone.[97]

conditions (bulk at 135 °C or in CH_2Cl_2 at 35 °C), though 0.1–4 equiv. of amine relative to the initiating alcohol was employed. It was also possible to immobilize DMAP onto cross-linked polystyrene particles and thus perform the ROP of LA from such polymer-supported organocatalysts, allowing its easy recovery by simple filtration.

A significant advantage of DMAP is its high selectivity of propagation in the ring opening of cyclic esters and resistance to adverse intra and/or intermolecular transesterifications (chain reshuffling).

DMAP was also found compatible with a metal-centered tris-hydroxylated initiator, namely $[Ru(bpyPLA_2)_3](PF_6)_2$, so as to produce three-arm PLA stars with luminescent tris(2,2′-bipyridine)ruthenium centers (**Table 1**, entry 2).[95]

In 2006, Feng and Dong[94] applied the DMAP-induced ROP to prepare a series of biodegradable graft copolymers consisting of a naturally occurring chitosan backbone and poly(ε-caprolactone) (PCL) grafts (entry 3). They employed 2 equiv. of DMAP relative to the amino groups carried by chitosan and water as swelling agent. The grafting density could be finely tuned through the [ε-CL]/[chitosan] molar feed ratio. It was shown that initiation took place from the primary amino-functions of chitosan rather than from the hydroxyl groups, in agreement with the higher nucleophilicity of

amino versus alcohol functions. However, the extent of amino groups participating in the initiation was found to decrease, as the [ε-CL]/[chitosan] ratio increased, which was ascribed to the progressive heterogeneity of the aqueous reaction mixture.

Relatively slow reaction times characterize the DMAP-catalyzed ROP of cyclic esters, in spite of a catalyst concentration in the order of that of initiator (**Table 1**). LA could be polymerized by both DMAP and PPY as organic catalysts, either in solution or in the melt.[24,25]

In contrast, the lactide equivalent *O*-carboxyanhydride (L-Lac-OCA) was polymerized much more rapidly than LA, in the presence of DMAP and an equivalent of either primary or secondary alcohols as initiators (**Table 1**, entry 4) typically within a few minutes at room temperature (vs. a few days at 35 °C for LA) for the [L-Lac-OCA]/[*n*-pentanol]/[DMAP] ratio equal to 20/1/1.[85]

The attack of DMAP at the more electrophilic carbonyl group of the monomer was postulated, followed by an exchange of proton with the hydroxyl-containing initiator or polymer chain end and decarboxylation (**Scheme 8**), the polymerization thus occurring through an AMM. The same group also reported the DMAP-mediated ROP of OCA derived from glutamic acid (L-Glu-OCA, **Figure 2**).[88] This functional monomer was found to exhibit a much higher reactivity compared with its 1,4-dioxane-2,5-dione homolog. Here also, 1 equiv. of DMAP relative to the initiator was employed (entry 5). Metal-free aliphatic (co)polyesters featuring pendant protected carboxylic acid groups in the form of benzyl esters could thus be obtained. Such polymers were prepared with degree of polymerization (DP) up to 100 in dichloromethane at room temperature, using *n*- or 2,2-bis(hydroxymethyl)propane-1,3-diol (*neo*-pentanol) as initiator, with a good polymer chain end fidelity. Complete deprotection of the pendant COOH groups could be readily achieved by hydrogenolysis. Synthesis of both random and block copolymerization of L-Glu-OCA and L-Lac-OCA was also investigated. Block copolymers were synthesized by the DMAP-catalyzed sequential ROP of both monomers, whereas access to various statistical copolymers was possible by varying the L-Glu-OCA to L-Lac-OCA ratios from 1:10 to 1:1. The random character of these copolymers was supported by analysis using ^{13}C NMR spectroscopy. A comparative study finally showed that the functionalized monomer, L-Glu-OCA, was slightly more reactive than L-Lac-OCA.

DMAP-induced ROP of (3*S*)-3-{2-[(benzyloxy)carbonyl] ethyl}-1,4-dioxane-2,5-dione (BED, **Figure 2**) was also recently investigated by du Boullay *et al.*[89] Well-defined polymers of molar masses up to 36 000 g mol^{-1} were obtained at 30 °C in dichloromethane ([BED]$_0$ = 1 mol l^{-1}) and *n*-pentanol as initiator (entry 6). Complete conversion was achieved in a few hours. Under these conditions, BED showed a slightly higher reactivity compared with LA. Deprotection of the pendant carboxylic groups was achieved by hydrogenolysis (**Scheme 9**). However, a bicomponent catalytic system based on TU and (−)-sparteine was found significantly more active than DMAP (see Section 4.06.6).

Two recent studies by Brignou *et al.*[86] and Helou *et al.*[93] showed that substoichiometric amounts of DMAP relative to the alcoholic initiator could be employed to polymerize six-membered cyclic carbonates (entry 7). Polymerizations were performed in bulk (solvent-free conditions) in a range of temperatures between 60 and 150 °C. The ROP of the seven-membered cyclic carbonates (entry 8) was conducted with equimolar amounts of DMAP relative to the OH-containing initiator which also required higher temperature (110 °C) compared with organometallic complexes used as catalysts.

An AMM was originally put forward to account for the ROP of LA, via a direct nucleophilic attack of DMAP onto the carbonyl function of the cyclic ester (see **Scheme 1**).[24,85] However, on the basis of computational investigations of model reactions in the case of DMAP-catalyzed ROP of LA and Lac-OCA, Bonduelle *et al.*[98] suggested that an ACEM, where DMAP activates the alcohol through hydrogen bonding, was energetically more favorable (**Scheme 10**). The ACEM provided, indeed, the lower energy profile compared with the AMM involving *N*-acylpyridinium intermediates.[98] The authors demonstrated the key role of multiple hydrogen bonding, as well as the possibility of DMAP to act not only as a base but also as a

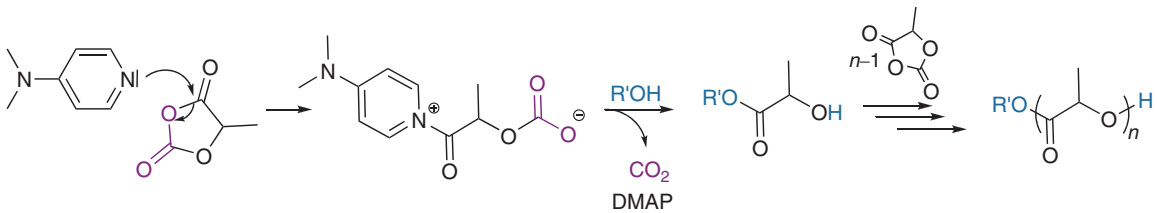

Scheme 8 Polymerization of L-Lac-OCA initiated by ROH and catalyzed by DMAP (AMM).[85]

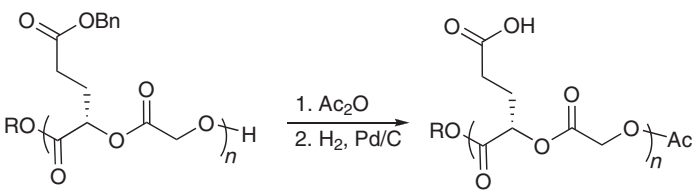

Scheme 9 Deprotection of PBED pendant carboxylic groups by hydrogenolysis.[89]

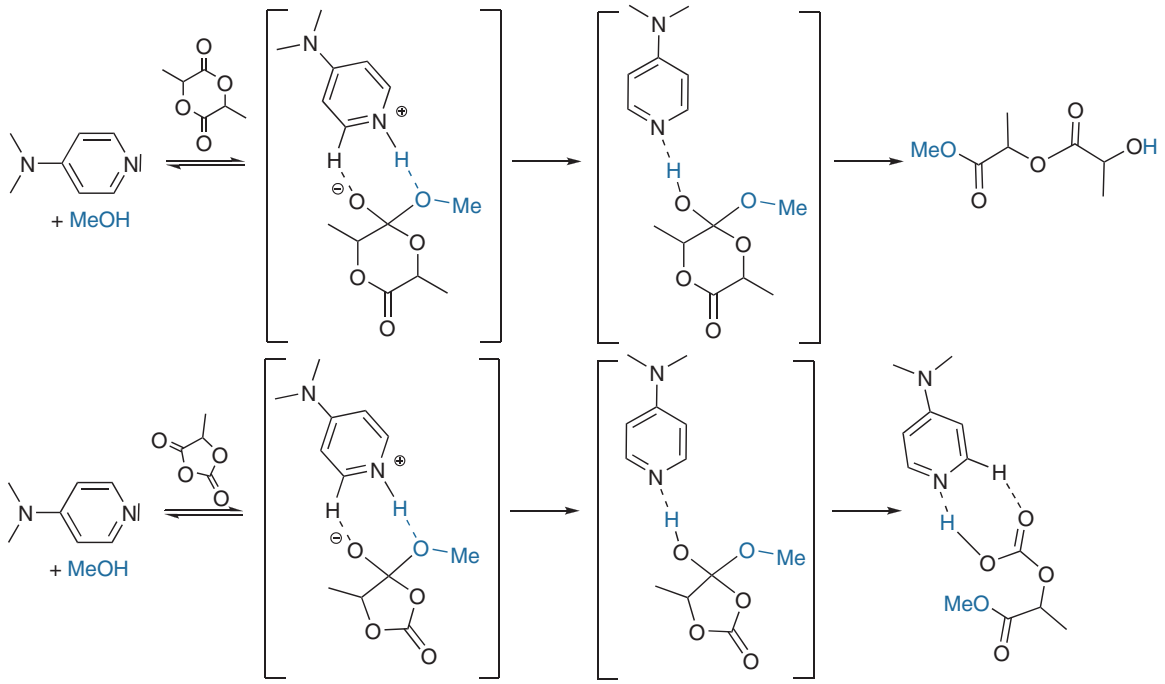

Scheme 10 Mechanism proposed for DMAP-catalyzed ROP of LA and L-lac-OCA on the basis of computational studies by Bonduelle *et al.*[98]

bifunctional catalyst, through its basic nitrogen center and an acid ortho-hydrogen atom.

In 2010, Kadota *et al.*[96] employed DMAP coexisting with equimolar amounts of its conjugate acid, that is, in its protonated form (DMAP/HX), to trigger the organocatalyzed ROP of LA in the presence of various alcohols as initiators. Such a combination provided cooperative activation by H-bondings of both the PLA chain end and the monomer (Scheme 11). Such bicomponent catalytic systems should thus be also categorized as dual catalysts (see Section 4.06.3.3.4). These organocatalytic systems, where the counteranion X^- could be varied, were found significantly more active than DMAP alone, with a rate enhancement in the order $X = CF_3SO_3 > CH_3SO_3 > Cl$. Control of molar masses up to 13 000 g mol^{-1} and PLA with relatively narrow dispersities were obtained at room temperature after 24–48 h (entry 9).

4.06.5 Polymerizations Catalyzed by Amidines

Representative examples of amidines are shown in Figure 1; see also Table 2 and Figure 4 for a summary of potentials offered by these organocatalysts. First attempts to polymerize ε-CL, LA, and glycolide using hexaalkylguanidinium salts (HAGs) as direct initiators – not catalysts – were reported by Li *et al.*[102] These metal-free polymerizations were performed in bulk at 120 °C. However, a relatively poor control over molar masses and dispersities was obtained (Table 2, entry 1).

Both MTBD and DBU efficiently catalyze the ROP of LA, leading to well-defined PLAs with a DP up to 500, a dispersity lower than 1.1 in less than 1 h, and a turnover frequency (TOF) ~0.05 s^{-1} (entry 2).[103] However, broadening of molar mass distribution due to transesterification was observed at high conversions. Attempts to catalyze the ROP of other heterocyclic

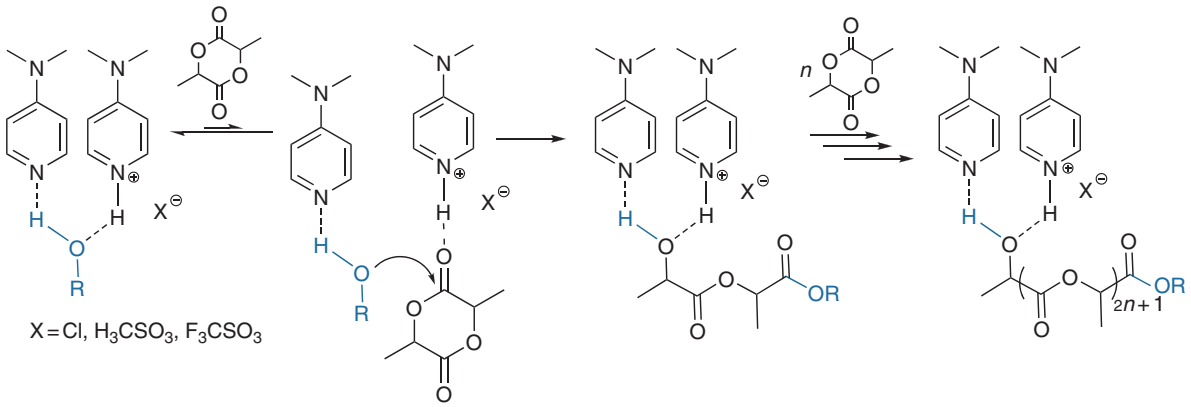

Scheme 11 Cooperative activation by H-bondings proposed for the ROP of LA catalyzed by DMAP+DMAP/HX.[96]

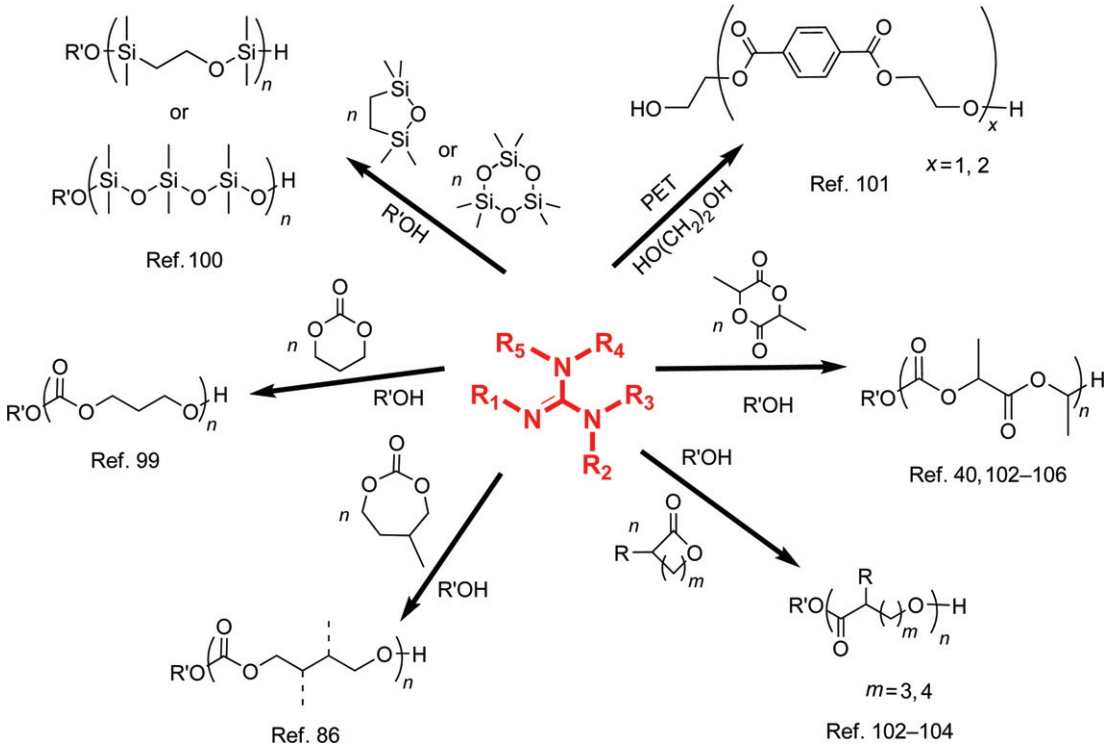

Figure 4 Overview of polymers obtained from amidines as catalysts.

substrates including ethylene oxide (EO), β-butyrolactone (βb-BL), δ-valerolactone (δ-VL), or ε-caprolactone (ε-CL) or carbosiloxanes by MTBD and/or DBU met with very limited success.[100,103] Improvements were observed when employing these organocatalysts in combination with TU (see next section).

In contrast, TBD proved highly active in the ROP of LA, δ-VL, ε-CL, methylcarboxytrimethylene carbonate (MTC), TMC, and even noncarbonyl monomers such as carbosiloxanes with exceptionally high rates, rivaling the carbene organocatalysts (Section 4.06.8) in TOF.[99,104,107] TBD exhibited a much higher reactivity toward the ROP of LA and TMC than its substituted analog, MTBD (TOF = 81 vs. 0.002 s^{-1} and TOF = 0.1 s^{-1} vs. 0.1 h^{-1} for the ROP of LA and TMC, respectively). For instance, polymerization of LA in CH_2Cl_2 using 0.1% catalyst relative to monomer and 1% of 4-pyrenebutanol (PBuOH) gave a well-defined PLA in seconds at room temperature (entries 2 and 3, **Table 2**). At the completion of these polymerizations, however, TBD also catalyzed transesterification reactions of the resulting aliphatic polyester, as indicated by the broadening of the molar mass distribution. As a matter of fact, poor reliability of the presence of end groups was noted. Yet, TBD could be quenched, before it catalyzed transesterification of PLA chains, simply by adding benzoic acid.

Note that ROP of β-BL cannot be performed at room temperature by TBD due to the formation of a stable hydrogen-bonded intermediate with the catalyst (**Scheme 12**).[106] In contrast, TBD-catalyzed ROP of δ-VL was carried out in benzene solution and was found more slowly than that of LA, leading to poly(δ-valerolactone) (PVL) with a molar mass of 14 500 g mol^{-1} and a dispersity of 1.09. A significant increase in dispersity was noted for PCL prepared by ROP of ε-CL catalyzed by TBD.[103]

Use of monohydroxy-functionalized polymers as macroinitiators (e.g., poly(ethylene oxide), PEO; poly(styrene), PS; and poly(*N*,*N*-dimethylacrylamide), PDMA) allowed the synthesis of block copolymers with PLA, P(δ-VL), and P(ε-CL) as second block. Interestingly, sequential ROP of cyclic esters of different reactivity employing TBD could be achieved at room temperature. Aliphatic block copolyesters could thus be obtained, by polymerizing first the slower propagating monomer to high conversion and subsequently adding the second monomer.[103]

No transetherification was noted at full conversion in the case of the TBD-catalyzed ROP of carbosiloxanes (entry 6), in contrast to the situation prevailing for NHCs (see Section 4.06.8).[100] Bulk polymerization at 65 °C or solution polymerization (2.0 M in CH_2Cl_2) at room temperature of TMC was also efficiently accomplished in the presence of MTBD, TBD, and DBU organocatalysts, providing good control over molar mass and dispersity (entries 4 and 5, **Table 2**).[99] Polycarbonates with M_n up to 40 000 g mol^{-1} and dispersity below 1.08 were obtained in this way. Random copoly(ester-*co*-carbonate)s were also prepared by copolymerizing TMC and δ-VL in bulk. Synthesis of block copolymers featuring biodegradable PTMC blocks could also be achieved by combining distinct polymerization techniques, for example, nitroxide-mediated polymerization (NMP) or reversible addition fragmentation chain transfer (RAFT) polymerization with TBD-catalyzed ROP of TMC.

Whereas DBU and MTBD seem to only activate the alcohol initiator by ACEM (**Scheme 13**),[99,103] the unique activity of TBD catalyst was explained by its bifunctionality during ROP of LA, involving a H-bonding mechanism (**Scheme 14**). This was supported by computational studies which provided the lower

Table 2 Representative examples of the ROP catalyzed by amidines

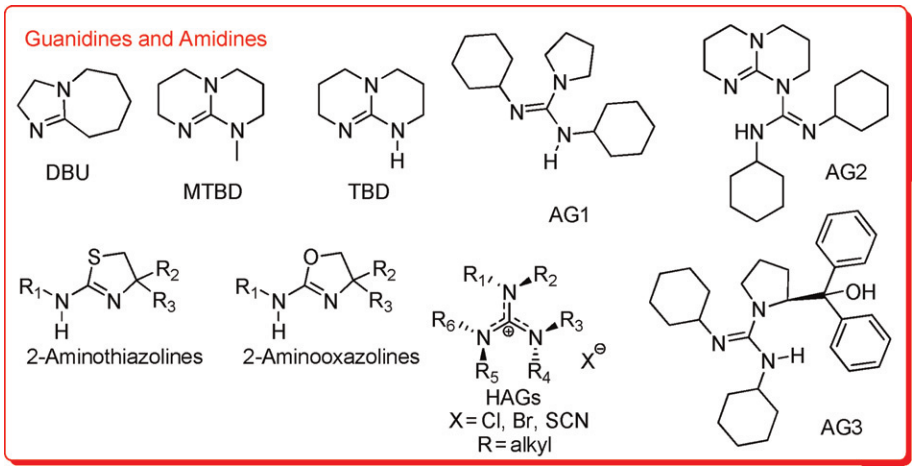

Entry	Catalyst	Monomer	Bulk/solvent	Initiator	$[C]/[I]_0$	t	T (°C)	Conv (%)	M_n (g mol^{-1})	D	References
1		Lactide, ε-CL, glycolide	Bulk	HAGs[a]		72–336 h	120	> 90	2 000–21 000	1.6–2.2	102
2	TBD, MTBD, DBU	Lactide	Dichloromethane	PBuOH	0.1–5	20 s to 1 h	RT	92–99	18 000–85 000	1.05–1.19	103
3	TBD	Lactide	Dichloromethane, chloroform	PBuOH	0.1–0.6	20 s to 8 h	RT	52–99	4 000–62 000	1.05–1.19	103, 104
		ε-CL, δ-VL	Benzene								
4	TBD, MTBD, DBU	TMC	Dichloromethane	BnOH	0.01	15–480 min	RT	> 99	4 000–38 000	1.04–1.32	99
5	DBU		Bulk			30 min	65		3 000	1.09–1.15	
6	TBD	TMOSC	Toluene	PBuOH	0.7–1	30 min to 26 h	RT	> 76	7 000–23 000	< 1.05	100
		D3			1	NM		NM	NM	< 1.2	
7	AG1, AG2, AG3	Lactide	Dichloromethane	PBuOH	1	20–40 min	RT	50–99	17 600–37 000	1.04–1.49	107
8	TBD	Lactide	Dichloromethane	PCN OH-pendant groups	~0.07	80 min	0		305 000 (grafted)	2.34	105
9	TBD	TMC	Bulk	BnOH	0.005–0.2	5 min to 15 h	60–150	82–99	5 000–45 000	1.52–1.85	93
			Dichloromethane		1	6 h	RT	99	43 000	1.31	
10	TBD	β-Me7CC	Bulk	BnOH	1	60 min	110	100	10 000	1.4	86
			Toluene			75 min			7 000	1.23	
11	Amino-oxazolines	Lactide	Dichloromethane	*neo*-pentanol	0.7–7	8–48 h	22–60	11–98	1 000–20 000	1.04–1.33	40

[a] Terminated with H_2O.

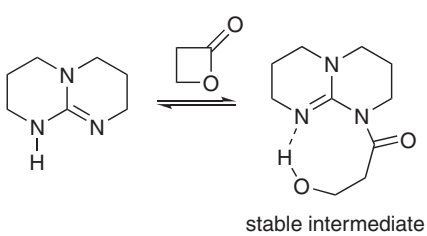

Scheme 12 Stable intermediate between TBD and β-BL.[106]

energy profile in the case of such a dual activation, relatively to a nucleophilic AMM involving an acyl–TBD intermediate.[106,108] TBD would thus simultaneously activate both the alcohol and the carbonyl group of the cyclic ester by H-bonding. In molecular chemistry, bicyclic guanidine catalysts were also found to provide such hydrogen bonding for the enantioselective Strecker reaction of R-aminonitriles and R-amino acids.[35]

The acyclic guanidines synthesized by reaction of carbodiimides with secondary amines were also shown to catalyze the

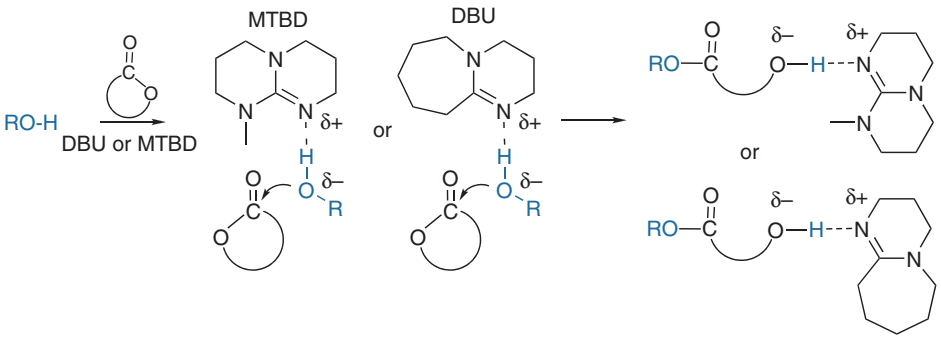

Scheme 13 Proposed mechanism (ACEM) for the ROP of cyclic esters catalyzed by MTBD or DBU.[99,103]

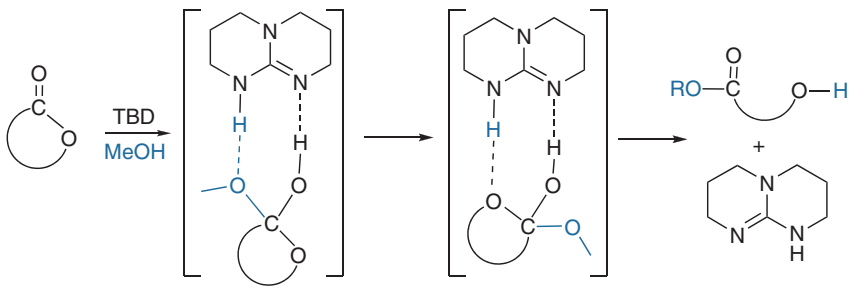

Scheme 14 Proposed mechanism (bifunctional activation) for the ROP of cyclic esters catalyzed by TBD (computational study).[106,108]

ROP of LA (Table 2, entry 7), though providing lower rates of reactions as compared with TBD under the same conditions.[107] Polymerizations were performed in CH_2Cl_2 (2 M) with equimolar amounts of catalyst relative to initiator (4-pyrenebutanol), corresponding to 1 mol.% relative to monomer. PLAs were obtained in approximately 40 min in nearly quantitative yield and high end-group fidelity was demonstrated. The molar masses were varied from 17 600 to 37 000 g mol^{-1} with a dispersity lower than 1.1. Though less basic than TBD, these guanidines were also found to be hydrogen donors and, similarly to TBD, could catalyze the reaction by activation of the alcohol initiator through hydrogen bonding.

TBD-catalyzed ROP of LA was recently applied by Theryo *et al.* to the synthesis of graft copolymers consisting of a rubbery backbone ($T_g \approx -80$ °C) and PLA grafts.[105] A statistical copolymer was first synthesized by ring-opening metathesis copolymerization (ROMP) of 1,5-cyclooctadiene and 5-norbornene-2-methanol in the presence of the second-generation Grubbs' catalyst. The PLA grafts were then grown from the statistically distributed pendant primary hydroxyl groups by TBD-catalyzed ROP of LA, following a grafting from approach (entry 8). A chain transfer agent, namely (*Z*)-1,4-diacetoxybut-2-ene, was used to control the chain length of the ROMP-derived rubbery copolymer. Despite a large compositional asymmetry, these graft copolymers exhibited a microphase-separated morphology and an improved tensile ductility compared with neat PLA homopolymer.

Works by Brignou *et al.*[86] and Helou *et al.*[93] showed that very low amounts (as low as 10 ppm) of TBD could efficiently catalyze the ROP of six- and seven-membered cyclic carbonates (TMC, 3,3-dimethoxytrimethylene carbonate (DMTMC), 3-benzyloxytrimethylene carbonate (BTMC), or methyltetramethylene carbonate (Me7CC) in Figure 2) in bulk, in the presence of benzyl alcohol, though relatively high temperatures (60–150 °C) were required to counterbalance the low catalyst loading (entries 9 and 10, Table 2). At 110 °C, for instance, 500 equiv. of monomer was converted within 5 min (vs. 30 min at 60 °C). Interestingly, 10 000 equiv. of the technical-grade unpurified TMC monomer could be almost quantitatively polymerized in the presence of 200 equiv. of alcohol, in contrast to organometallic catalytic systems. The highest activity was obtained for TBD-catalyzed ROP of purified TMC at 150 °C: TOF = 49 200–55 800 h^{-1}. The molar mass distribution of polycarbonates prepared in bulk was slightly larger than that observed for solution polymerization, owing to the higher probability of side reactions such as transesterification and/or transcarbonation reactions.

As mentioned above, 2-amino-oxazoline and 2-aminothiazoline show structural analogies with TBD (see Figure 1). The ROP of LA at room temperature in CH_2Cl_2 mediated by these organocatalysts (7 mol.% loading relative to monomer), in the presence of *neo*-pentanol (2,2-dimethylpropan-1-ol) as initiator, was found to be well controlled (entry 11), as described by Becker *et al.*[40] The more active catalysts were the more electron-rich derivatives, in particular that featuring a 2-cyclohexylamino substitution on the thiazoline ring. The polymerization kinetics was found to be first order with respect to monomer, initiator, and catalyst. Significant interactions between the three components were also noted, suggesting that these catalysts, like TBD, provide a dual activation of both the monomer substrate and initiator by hydrogen bonding (Scheme 15). Upon increasing the reaction time, however, transesterification side reactions were observed.

As reported by Fukushima *et al.*,[101] TBD was used as catalyst to depolymerize polyethylene terephthalate (PET) leading to bis(2-hydroxyethyl)terephthalate (BHET) (Scheme 16). The

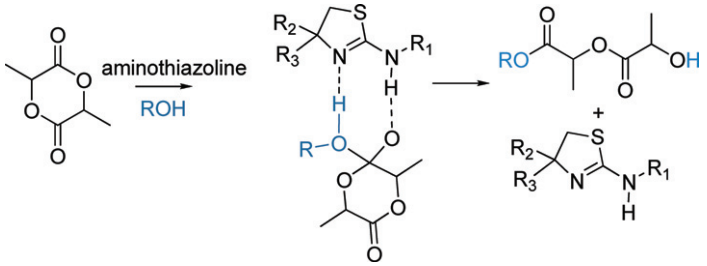

Scheme 15 Dual activation proposed for the ROP of LA catalyzed by aminothiazolines.[40]

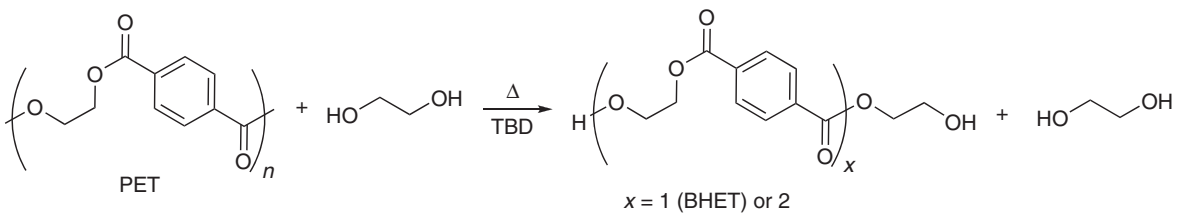

Scheme 16 Depolymerization of PET catalyzed by TBD.[101]

high efficiency of this catalyst was highlighted since 0.5 mol.% is sufficient to achieve complete glycolysis at 190 °C. These results are comparable with the one obtained for commonly used metal catalysts. With a large excess of ethylene glycol to decrease the content of final BHET dimers, TBD (10 mol.%) allowed complete depolymerization of PET within 150 min even after nine consecutive catalyst cycles.

4.06.6 Polymerizations Catalyzed by TUs and TU-Amino Derivatives

As mentioned above, TU derivatives easily activate carbonyl-containing substrates by hydrogen bonding. Such organocatalysts have thus logically served to trigger the ROP of various cyclic esters, as illustrated in **Figure 5** (see also **Table 3** for the most representative results). For instance, mono- and bicomponent TU-amino catalysts (**Figure 1**) allowed good control of the ROP of LA in solution in CH_2Cl_2 (1 M) at 25 °C in the presence of 4-pyrenebutanol as initiator (entries 1 and 2 in **Table 3**).[103,111] In the former case, a PLA with $M_n = 23\,000\,g\,mol^{-1}$ and a dispersion of 1.05 was obtained for 97% monomer conversion, which required, however, long reaction times (48 h). These organocatalysts exhibited a high selectivity toward polymerization of LA relative to transesterification of in-chain esters, as indicated by the invariance of molar mass distribution even after prolonged reaction times (several days). Analysis by ^{13}C NMR of PLAs thus obtained showed that racemization did not occur.

Use of a monohydroxy PDMA macroinitiator to initiate the TU-amino-catalyzed ROP of LA allowed the authors to prepare PDMA-*b*-PLA diblock copolymers (**Scheme 17**). Double-headed initiators were also used for the purpose of block copolymer synthesis, by combining controlled radical polymerization (RAFT or NMP) and organocatalysis by TUs.[112]

Catalytic systems based on the combination of MTBD or DBU with TU3 were found to control the ROP of δ-VL, yielding PVL with DP up to 200 and TOF around $5\,h^{-1}$ (entry 3). When applied to the ROP of ε-CL, however, several days were required to reach 80% conversion.[103]

The high selectivity of TU organocatalysts toward ring opening of cyclic esters relative to side transesterification reactions can be explained by the higher H-binding capacity of TU with the more basic cyclic esters (**Scheme 18**). The strength of the hydrogen bonding can be manipulated through the proper design of the catalyst, which allows a shortening of the reaction times and a better control of the polymerization.[112] For instance, TUs bearing the most electron-withdrawing substituents (arising from the starting isothiocyanate) exhibited the highest activity, due to its enhanced acidity toward activation of the lactide. A proper selection of the amine Bronsted base is also crucial, however, for an efficient polymerization. Thus, pyridine and *N*,*N*-dimethylaniline were ineffective, likely because of their too weak basic character, to activate the alcohol initiator. In contrast, combination of TU with DMAP or (cyclohexyl)dimethyl amine, triethylamine, 1,4-diazabicyclo[2.2.2]octane (DABCO), and *N*,*N*,*N*′,*N*′-tetramethylethylenediamine (TMEDA) in a bicomponent catalytic system led to complete conversion of LA. The chiral (−)-sparteine was found to be the most effective amine, 95% conversion being achieved in only 2 h, with an excellent control over molar mass and dispersity of the resulting PLAs. This base also allowed some stereocontrol of the ROP of *rac*-LA. Characterization by NMR indicated that isotactic enrichment in such organocatalyzed ROP occurred by a chain end control.

The mechanism of TU-amino-mediated ROP thus occurs by a dual activation via a hydrogen bonding between the TU group and the carbonyl group of the monomer and, in the meantime, activation of the initiating/propagating alcohol by the basic amino-functionality group of the catalytic system (**Scheme 19**). Hence, the presence at the same time of both the TU and the amino-functions is necessary for an efficient catalysis of polymerization, as demonstrated in control experiments. The implication of hydrogen bonding in the activation process was supported by studying the polymerization in various solvents. While nonhydrogen bonding solvents, such as

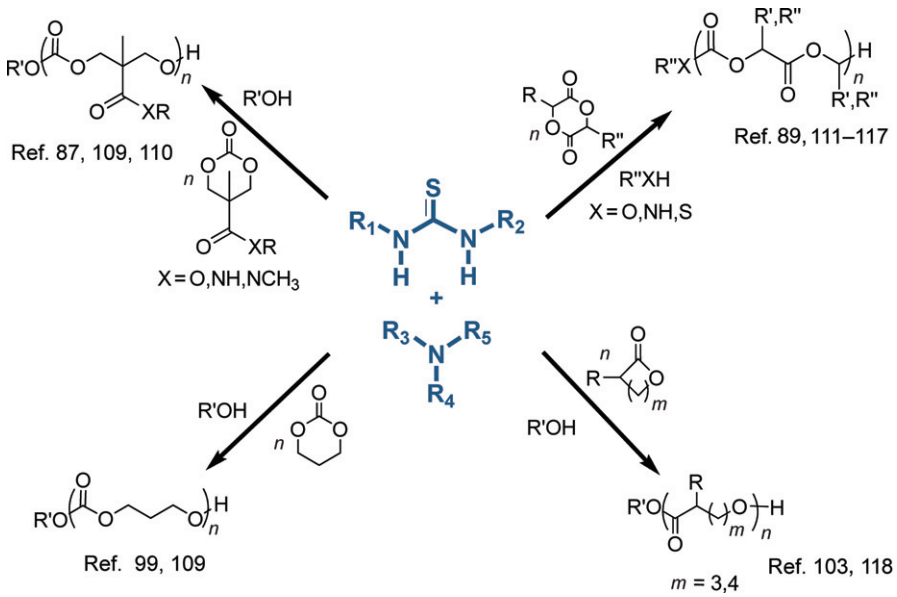

Figure 5 Overview of polymers obtained from TU-amino derivatives as catalysts.

$CHCl_3$, CH_2Cl_2, and toluene led to well-defined PLAs, no polymerization was observed in tetrahydrofuran (THF) and dimethylformamide (DMF), owing to a competitive hydrogen bonding of these solvents by the TU moiety.[112]

Middleton *et al.*[113] recently employed astaxanthin as bifunctional hydroxy-containing initiator for the ROP mediated by the monocomponent bifunctional TU/tertiary amine catalyst (**Table 3**, entry 4). Astaxanthin is a conjugated pink-colored carotenoid that is present in plants, phytoplankton, or algae. It can serve as an antioxidant. It aids in light absorption during photosynthesis. For these reasons, carotenoids in general possess antiinflammatory properties that can be exploited in the treatment of cardiovascular diseases. PLAs with a central astaxanthin moiety were synthesized with molar masses up to 30 000 g mol^{-1}. In this case, prolonged time periods of polymerization of LA (up to 36 days) revealed the occurrence of transesterification, compared with polymerizations utilizing 4-pyren-1-ylbutan-1-ol as initiator.

Combining TU with MTBD and DBU favored an efficient polymerization of various heterocycles, including δ-VL, ε-CL, TMC, and MTC, whereas, as highlighted in previous sections, MTBD alone or TU combined with other amines can only activate the ROP of LA.[87,99,103] For instance, the DBU/TU combination used for the ROP of the cyclic carbonates MTC bearing an -OR functional group (MTC-OR) gave a higher TOF (19 h^{-1}) than for TMC.[109] This catalytic system also allowed random copolymerizations of these MTC-OR cyclic carbonates with TMC. The MTC-OR monomers were more rapidly incorporated in the copolymer than TMC, suggesting the formation of gradient copolymers, in accordance with their higher reactivities in homopolymerization (entries 5–7).[99,109] Block copolymer synthesis by sequential ROP of six-membered cyclic carbonates was also possible. The functionalized cyclic carbonates were polymerized using the organocatalyst combination TU/DBU.[87] Miscellaneous polycarbonates with predictable molar masses and dispersities close to unity could thus be obtained.

In order to introduce pendant functionalities in aliphatic polyesters, Pounder and Dove[114] took advantage of the selectivity of the TU/DBU catalytic system for the ROP of six-membered cyclic carbonates, namely (3*S*)-3-{[(benzyloxy) carbonyl]methyl}-1,4-dioxane-2,5-dione (BMD) and (3S,6*S*)-3,6-bis{[di(benzyloxy)carbonyl]methyl}-1,4-dioxane-2,5-dione (malide) both derived from malic acid (**Figure 2**). The resulting polymers thus consisted of glycolic acid and benzyl L-(alkylamino)malate units. The TU/(−)-sparteine-mediated ROP of BMD, in the presence of benzylamine or primary or secondary alcohol initiators, led to structurally well-defined polyesters (entry 8). OH-containing initiators included monohydroxy poly(ethylene oxide) (PEO) and L-PLA used for the preparation of block copolymers. In contrast, the ROP of malide with the same catalytic system was ineffective. The poly(glycolic acid-*co*-malic acid)s (PGMAs) generated by deprotection of the benzyl groups of poly(BMD)s by hydrogenation were found to undergo autocatalytic degradation in dilute H_2O, with complete degradation within 6 days.

In addition to DMAP (see Section 4.06.4), du Boullay *et al.*[89] employed the bicomponent TUCy/(−)-sparteine organocatalyst to trigger the ROP of (3*S*)-3-{2-[(benzyloxy) carbonyl]ethyl}-1,4-dioxane-2,5-dione (BED, **Figure 2**) in CH_2Cl_2 solution at 30 °C (**Table 3**, entry 9). Neither interference of the pendant functional group nor transesterification reactions in the polymerization were noted. Ring opening of BED was shown to occur indifferently on either of the endocyclic ester groups. As a matter of fact, the resulting poly(BED)s exhibited a random distribution of glycolic and *O*-{2-[(benzyloxy)carbonyl]ethyl}glycolic units. Deprotection by hydrogenolysis led to well-defined poly(*R*-hydroxyacids).

Fukushima *et al.*[110] applied TU-mediated organocatalyzed polymerization to macromolecular engineering. For instance, they reported the synthesis of 'comb-shaped block copolymers' made of PEO as the hydrophilic component and a statistical copolycarbonate as hydrophobic backbone carrying

Table 3 Representative examples of the ROP catalyzed by TU-amino derivatives

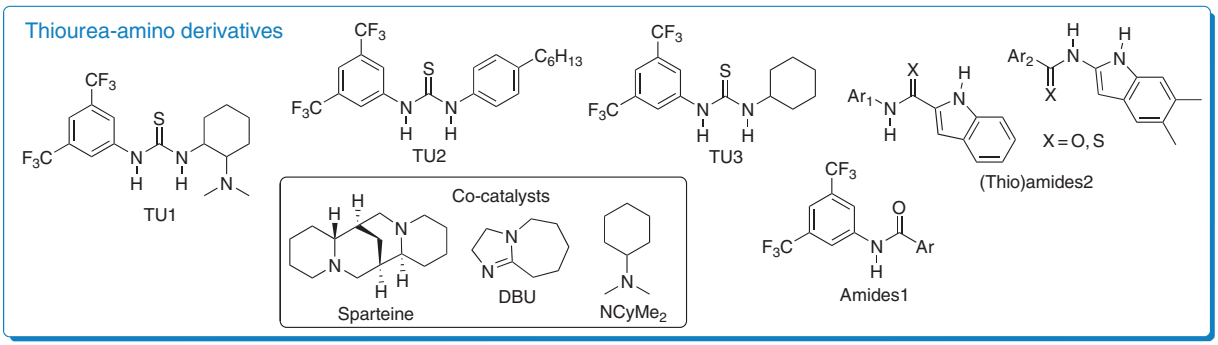

Entry	Catalyst	Monomer	Bulk/solvent	Initiator	$[C]/[I]_0$	t	T (°C)	Conv (%)	M_n (g mol^{-1})	D	Reference
1	TU1	Lactide	Dichloromethane	PBuOH	0.05	24–105 h	25	> 97	5 200–42 000	< 1.08	111
2	TU2/$NCyMe_2$ (1/1), TU3/$NCyMe_2$ (1/1)	Lactide	Dichloromethane, chloroform	PBuOH	10	72 h	25	98	~18 000	< 1.09	112
	TU1		Chloroform	ROH, RNH_2, RSH	2.8–10	20–72 h	25	80–99	8 000–24 000	< 1.12	
3	TU3/DBU (1/1), TU3/MTBD (1/1)	ε-CL, δ-VL	Benzene	PBuOH	2.5–10	3–120 h	RT	78–95	4 100–16 200	< 1.06	103
4	TU1	Lactide	Dichloromethane	astaxanthin	0.1	NM	25	> 95	2 200–36 000	1.02–1.33	113
5	TU3/sparteine (1/1), TU1	TMC	Dichloromethane	BnOH	2.5	720 min to 6 days	25	88–> 99	~4 000	< 1.09	99
6	TU3/DBU (1/1)	MTC-XR	Dichloromethane	Bn-MPA, PBuOH	2.2–5	2 h to 5/6 days	RT	60–86	4 400–17 000	1.24–1.42	87
7	TU3/DBU (1/1)	TMC MTC-OR	Dichloromethane	PBuOH	2.5	3 h 30 min	20	90 93	8 600 11 600	1.03 1.12	109
8	TU3/sparteine (5/1 or 7/1)	BMD	Chloroform	$BnNH_2$, I and II alcohols	0.25–0.35	5–50 min	25	> 96	3 500–13 300	< 1.19	114
9	TU3/sparteine (1/1), TU1	BED	Dichloromethane	*n*-Pentanol	1 or 2	20–60 min	30	> 98	8 000–36 000	< 1.22	89
10	TU3/DBU (1/1)	MTC-OEt + MTC-O$(CH_2)_2$OTHP[a]	Dichloromethane	PEO_{5000}-OH	1.25	1 h	25	90	~7 000	< 1.13	110
11	TU3/sparteine (1/1)	Lactide	Dichloromethane	Difunctionalized PEO[b]	0.87	Overnight	25	NM	~2 000–~7 000	< 1.16	115
12	TU3/DBU (1/1)	δ-VL	Toluene	$N_3(CH_2)_6OH$	1.5–5	2–5 h	25	> 99	2 600–9 900	< 1.11	118
13	Amides1/sparteine (1/1)	Lactide	Dichloromethane	4-Phenylbenzyl alcohol	1	2–24 h	20	22–100	3 400	1.08	116
14	(Thio)amides2/ sparteine or / $NCyMe_2$ (1/1)	Lactide	Dichloromethane	4-Phenylbenzyl alcohol	1	2–72 h	20	20–100	600–15 000	< 1.12	117

[a] Both incorporated at the beginning of the polymerization.
[b] Leading to branched polymer.
NM, not mentioned.

stereoregular L-PLA or D-PLA grafts (Scheme 20).[110] The latter backbone was prepared by copolymerizing two different cyclic carbonates, as discussed above, including a latent (tetrahydropyranyl)oxy-initiating group. After formation of the amphiphilic backbone, followed by deprotection under acidic conditions and ROP of LA in the presence of TU organocatalyst, relatively well-defined copolymers were obtained, with up to eight PLA grafts. Mixtures of the enantiomerically pure copolymers of L-LA and D-LA showed that stereocomplexation occurred, as evidenced by a significant increase in the melting point. The stereocomplexes were found to form micelle-like structures at very low concentrations.

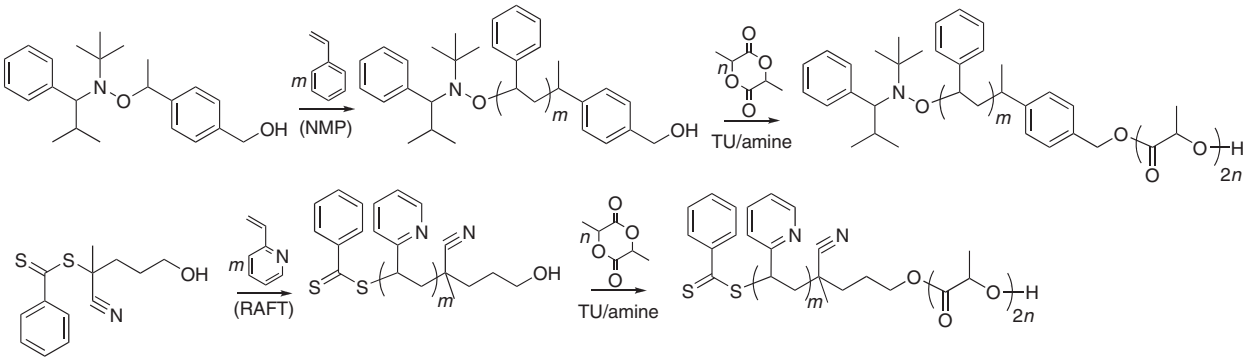

Scheme 17 Block copolymer synthesis: first block PS (by NMP) or PDMA (by RAFT), second block: PLA (by organocatalyzed ROP).[112]

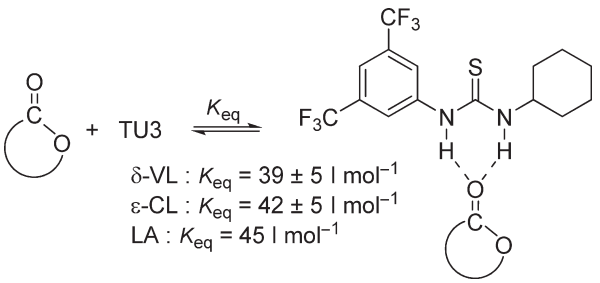

Scheme 18 Binding constants of TU3 with some cyclic esters.[103]

The same group reported a synthetic strategy utilizing a carboxylic acid-containing cyclic carbonate derived from 2,2′-bis(hydroxymethyl)propanoic acid and the TU-mediated organocatalysis to prepare ABC-type miktoarm copolymers.[115] The functional carbonate was first coupled onto a monohydroxy PEO. Subsequent ring opening of the cyclic carbonate using a functional amine (RNH_2) generated a carbamate group carrying a functional moiety in the R group, namely an alkoxyamine or a protected hydroxyl group aimed at triggering NMP or ROP, respectively, together with a primary hydroxyl group (**Scheme 21**). The two additional polymer arms of the ABC-type miktoarm stars were then grown by tandem polymerization. The amphiphilic miktoarm star copolymers featuring poly(D- and L-LA) were found to form stereocomplexes in the bulk. Micelle-like structures with narrow size distribution were observed in aqueous solution from the stereocomplex mixture of Y-shaped miktoarm stars, PEO-poly(D-LA)-poly(D-LA) and PEO-poly(L-LA)-poly(L-LA), or the stereoblock miktoarm PEO-poly(D-LA)-poly(L-LA). The critical micelle concentrations of these micelles were significantly lower than the values generally obtained from traditional stereoregular linear or branched (Y-shaped) amphiphiles. Such polymer micelles exhibited a high loading capacity of the anticancer drug paclitaxel, leading to a near-zero ordered release of the drug, without a significant initial burst.

In 2009, Misaka *et al.*[118] reported the synthesis of macrocyclic PVLs (**Scheme 22**) by ring closure of an α-azido, ω-alkynyl-PVL by the Huisgen 1,3 dipolar cycloaddition (referred to as 'click chemistry'). The heterodifunctionalized PVL precursors (M_n from 2600 to 9900 g mol^{-1}) were first obtained by ROP of δ-VL in toluene at 25 °C, using the bicomponent TU/DBU catalytic system in the presence of 6-azidohexan-1-ol (**Table 3**, entry 12), followed by post-functionalization of the thus formed ω-end of α-N_3,ω-OH PVL with hex-5-ynoyl chloride. The 'click cyclization' was achieved in 60–80% yield in DMF, under highly diluted conditions, in the presence of the Cu(I)Br/2,2′-bipyridine catalytic system.

(Thio)amidoindoles and (thio)amidobenzimidazoles show structural similarities with TU-amino derivatives (**Figure 1**). These bifunctional organocatalysts were employed by Koeller *et al.*[116] to polymerize LA. These authors first showed that amidoindole combined with (−)-sparteine could efficiently catalyze the ROP of LA (entry 13), yielding PLAs of controlled dispersity and molar mass.[116] It was first shown that both NH groups of the amide and the indole moieties provided activation of the LA substrate by hydrogen bonding, as supported by the X-ray structure of the hydrogen-bonded 1:1 complex between the catalyst and LA. Complete conversion

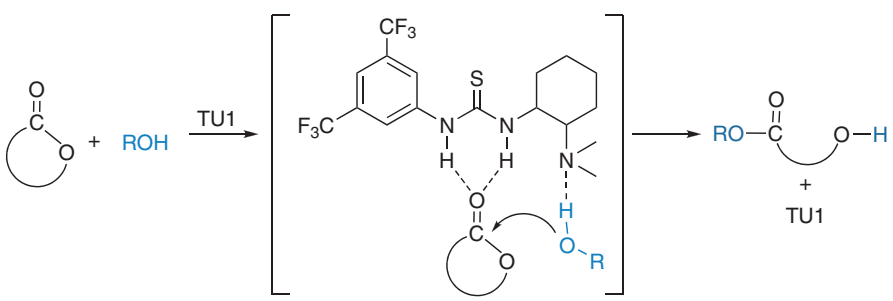

Scheme 19 Proposed mechanism (dual activation) for the ROP of cyclic esters catalyzed by the TU/tertiary amine system.[103,112]

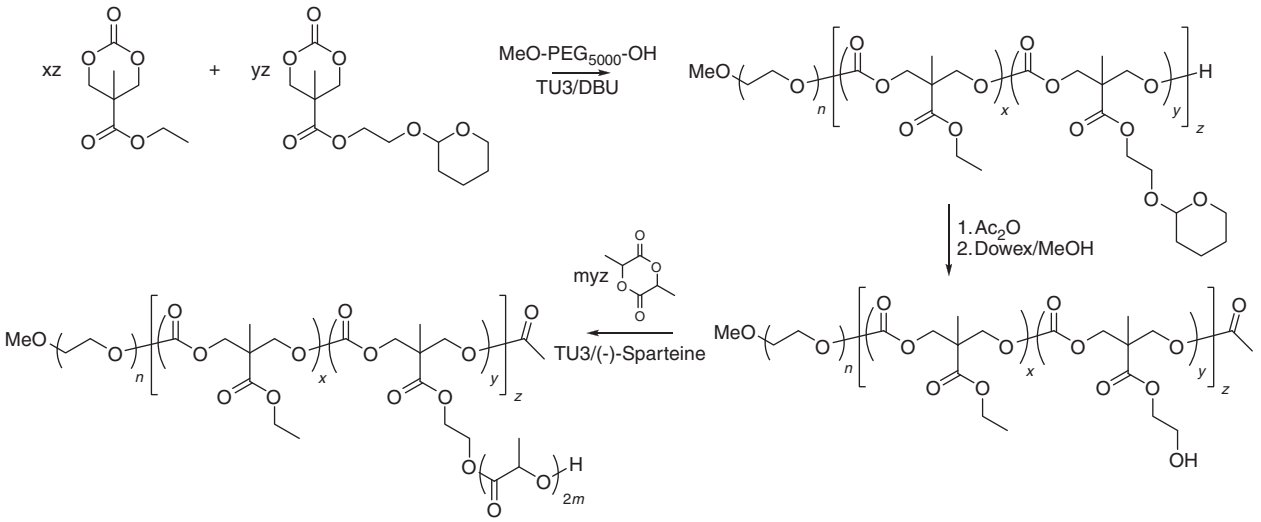

Scheme 20 Synthesis of comb block copolymer (backbone: PEO-*b*-polycarbonate, grafts: PLA) via organocatalyzed ROP.[110]

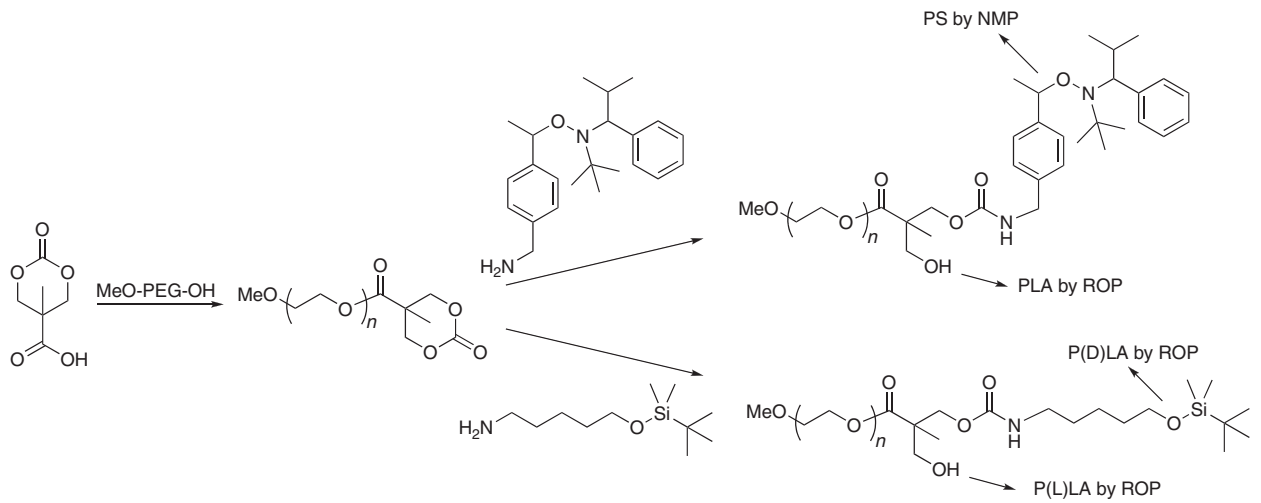

Scheme 21 Synthesis of ABC-miktoarms combining NMP and organocatalyzed ROP.[115]

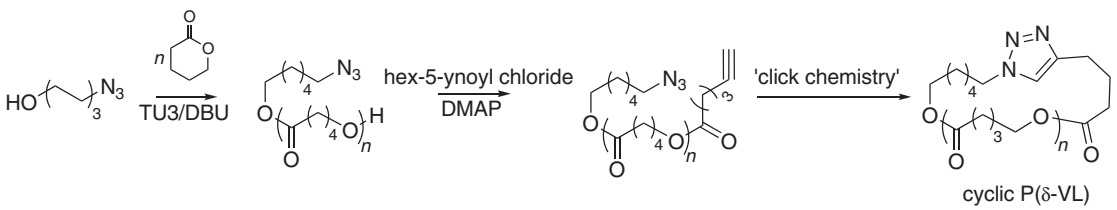

Scheme 22 Synthesis of macrocyclic PVLs via organocatalyzed ROP and click chemistry.[118]

was achieved within 2 h at 20 °C in 0.7 M CH_2Cl_2 solution. In a subsequent contribution, the same group investigated more systematically the catalytic activity of amides and related thioamides carrying either an indole or a benzimidazole moiety, toward the ROP of LA when used in the presence of a tertiary amine as cocatalyst (entry 14).[117] These molecules tended to form dimeric species by self-assembling, making the NH group less available for monomer activation. Therefore, the proper selection of the two partners in such bicomponent catalytic systems proved crucial for the outcome and the control of the

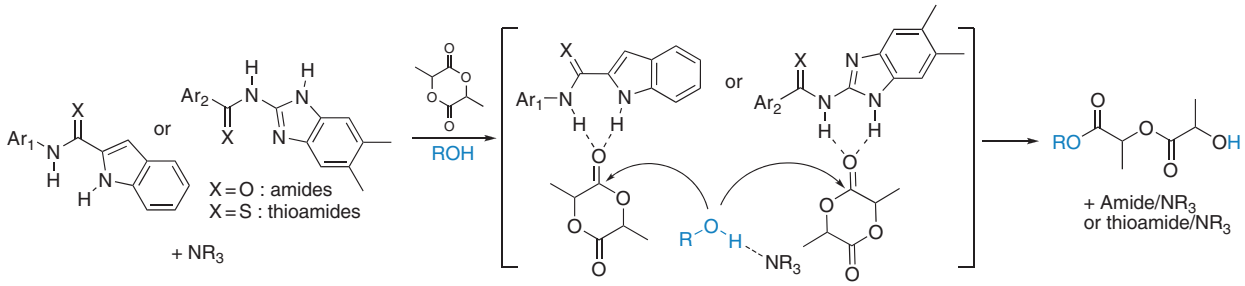

Scheme 23 Proposed mechanism for ROP of LA catalyzed by amides and thioamides.[117]

polymerization. For instance, catalytic activity could be enhanced by introducing electron-withdrawing groups in the aromatic ring and using an amide rather than a thioamide moiety. In the latter case, indeed, the catalytic activity of (thio) amides was inhibited owing to the development of hydrogen bondings between the two partner catalyst (Scheme 23).

4.06.7 Polymerizations using Phosphorus-Based Catalysts: Phosphines and Phosphazenes

As already mentioned, although the use of commercially available phosphines as acylation nucleophiles is well documented, their potential for organocatalyzed polymerizations has been certainly underexploited so far. There is only one report in 2002, by Myers *et al.*[64] where phosphines, such as PBu_3, $PPhMe_2$, PPh_2Me, and PPh_3, were employed as true catalysts for the ROP of LA in the presence of an alcohol initiator.[64] The catalytic efficacy was found to depend on the substitution pattern of the phosphine: for instance, trialkylphosphines proved more active (being more basic and more nucleophilic) than the triaryl phosphines. Polymerizations could be carried in bulk at 135 °C, yielding well-defined PLAs with a TOF of 0.01 s^{-1} (Table 4, entry 1).

In the context of ROP of heterocycles, phosphazenes were reported to operate mainly as deprotonating agents of alcohols or thiols, or even of CH-acid compounds serving as initiators. The main polymers obtained in this way are shown in Figure 6, and the main results are summarized in Table 4. Upon protonation, the resulting phosphazenium cation is soft and bulky enough to induce controlled/living polymerization of several monomers, including EO, cyclosiloxanes, ε-CL, δ-VL, LA, and cyclic carbonates. In addition, when associated with enolate precursors, the 'controlled/living' metal-free anionic polymerization of (meth)acrylates was also reported.[128,129]

Using phosphazenes in the context of polymerization was pioneered by the group of Molenberg and Möller[119] who first demonstrated their utility for the metal-free anionic ROP of octamethylcyclotetrasiloxane in bulk or in toluene, in the presence of methanol as initiator (Table 4, entry 2). The base *t*-BuP_4 allowed shortening reaction times and gave rise to homogeneous reaction mixtures, compared with metal-based alkoxide initiators. However, quite a broad molar mass distribution was observed. The same group reported the metal-free anionic ROP of EO with $[t\text{-}BuP_4H]^+$ as countercation, performed at 80 °C in a glass autoclave or at room temperature in solution in THF or in toluene.[120] Methanol or octan-1-ol served as initiators, leading to well-defined PEOs with M_n values ranging from 4400 to 6600 g mol^{-1} and a dispersity < 1.13 (Table 4, entry 3). In addition, pentaerythritol and poly[ethylene-*co*-(vinyl alcohol)] as tetrafunctional initiator and multifunctional polymer, respectively, were successfully employed to access tetra-arm star PEOs and poly{[ethylene-*co*-(vinyl alcohol)]-*graft*-PEO} graft copolymers. The soft cation $[t\text{-}BuP_4H]^+$ associated was found to improve the solubility of the multifunctional alkoxide-type initiators, in comparison to metal-based alkali alkoxides. Initiation of ROP of EO from pentaerythritol occurred from a heterogeneous dispersion in THF, owing to the poor solubility of the initiator. After 30% monomer conversion, however, a homogeneous solution was obtained, and the resulting star polymer proved relatively well defined. As for the poly[ethylene-*co*-(vinyl alcohol)] precursor used for synthesis of the graft copolymers, it also gave a heterogeneous reaction mixture at room temperature, but homogeneous conditions were achieved in xylene at 80 °C. Complete solubilization at room temperature occurred in the former case after 25% conversion (2–3 h).

The contribution by Schlaad *et al.*[121] in 2001 described the synthesis of heterobifunctional PEOs using a similar strategy. In this case, either (R)-(α-methylbenzyl) cyanide or *p*-cresol was employed as CH- and OH-initiating precursors to be deprotonated by equimolar amounts of *t*-BuP_4 (Scheme 24). Anionic ROP of EO was conducted in THF at 45 °C for 20 h, leading to well-defined PEOs (M_n < 3000 g mol^{-1}; D < 1.1). Postfunctionalization of α-PEO chain ends of each of the PEO products allowed the authors to access α-amino-ω-hydroxy and α-bromo-ω-hydroxy-PEOs.

Rexin and Mülhaupt[122] investigated the effect of the bulky tetrakis[cyclohexyl(methyl)amino]-phosphonium (P_1^+), where the positive charge is delocalized over five atoms in the phosphazenium countercations, during the ROP of PO. The challenge with this monomer is to avoid side reactions, in particular, the transfer reaction to monomer, restricting the molar mass and forming allyl end groups. P_1^+ was thus compared with cations K^+, $P_2{}^+$, Bu_4P^+, and *t*-BuP_4H^+ (Scheme 25). Furthermore, the polymerization with Bu_4P^+ whose positive charge is not delocalized was investigated. A series of alkoxides derived from dipropylene glycol (DPG) serving as initiators with different organic countercations ($P_1{}^+$, $P_2{}^+$, Bu_4P^+, *t*-BuP_4H^+) were first prepared by reacting phosphonium or phosphazenium methoxide with DPG. An extent of

Table 4 Representative examples of the ROP catalyzed by phosphorus-based catalysts

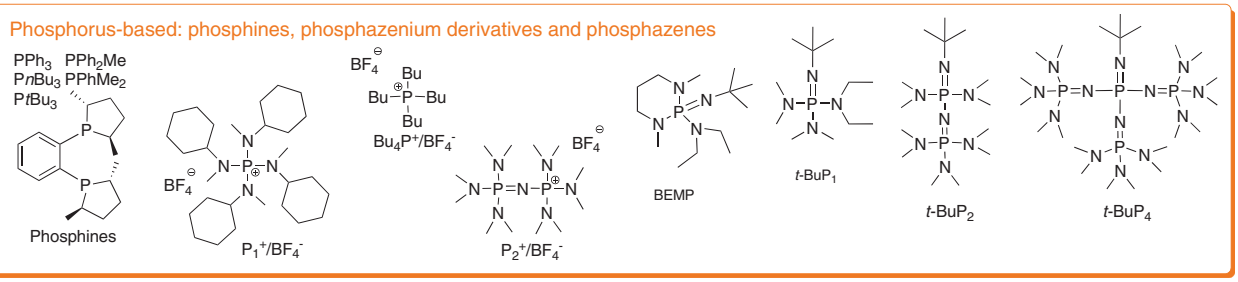

Entry	Catalyst	Monomer	Bulk/ solvent	Initiator	[C]/[I]$_0$	t	T (°C)	Conv (%)	M_n (g mol^{-1})	D	References
1	Phosphines	Lactide	Bulk	BnOH	1	10 min–50 h	135 or 180	40–92	3 000–13 000	1.11–1.4	64
2	*t*-BuP$_4$	D4	Toluene or bulk	MeOH	1		RT	43–80	117 000–440 000	1.7–1.9	119
3	*t*-BuP$_4$	EO	THF or toluene	MeOH, octanol, pentaerythritol	1	48 h	RT	75–> 90	4 400–6 600	< 1.13	120
4	*t*-BuP$_4$	EO	THF	α-Methylbenzylcyanide, *p*-cresol	1	20 h	45	> 90	2 500	< 1.1	121
5	Bu$_4$P$^+$ BF$^-_4$, P$_1^+$BF$^-_4$, P$_2^+$BF$^-_4$, *t*-BuP$_4$	PO	Bulk	DPG	1[a]	1.4–108 h	95–110	24–79	1 700–3 500	< 1.15	122
6	BEMP, *t*-BuP$_1$	Lactide ε-CL, δ-VL	Toluene Bulk	PBuOH, BnOH	0.5–2	23–70 h 45–240 h	25 25 or 80	48–97 14–93	3 600–18 000	1.05–1.23	123
7	*t*-BuP$_2$	Lactide	Toluene	PBuOH, PS-OH	1	0.17–220 min	–75 to 20	84–> 99	13 000–27 000	1.06–1.23	124
8	*t*-BuP$_1$, *t*-BuP$_2$, *t*-BuP$_4$	dMMLABz	THF	Cinnamic acid, PEO-COOH	1	6–768 h	25	81–> 99	4 800–1 500 000	1.13–1.55	125
9	BEMP	TMC, BTMC, DMTMC	Bulk	BnOH, propane-1,4-diol, glycerol	0.005–0.2	5 min–26 h	60–150	81–100	850–46 000	1.26–1.66	93
10	BEMP	β-Me7CC	Bulk	BnOH	1	60 min	110	100	7 800	1.20	86
11	*t*-BuP$_4$	DPCDC	THF	RSH, ROH, RR′NH, R$_2$CH$_2$[b]	1	15–156 h	60 or 100	> 97	3 000–42 000	< 1.1	126, 127

[a] 5% of I is actually deprotonated.
[b] Terminated with alkyl halides.

deprotonation of only 5% was chosen, owing to the fast exchange occurring between propagating (secondary) alkoxides of poly(propylene oxide) (PPO) and dormant hydroxylated PPO chains. ROP of PO was performed at 100 °C at atmospheric pressure (Table 4, entry 5). It was found that propagation rates increased in the following order: Bu$_4$P$^+$ < K$^+$ < P$_1^+$ < P$_2^+$ < *t*-BuP$_4$H$^+$. The DP of the resulting poly (PPO)s was in the range of 20–64 and dispersities were between 1.03 and 1.09. Unsaturations at polymer chain ends were observed, however, in a range 13–60 mmol kg^{-1}, with larger contents by increasing polymerization rates.

Phosphazenes such as *t*-BuP$_1$ and BEMP were also successfully employed as basic catalysts for the ROP of lactones and LA in the presence of alcohol initiators, BEMP being the most effective.[123] The BEMP-mediated ROP of L-LA was studied in dry toluene at room temperature, in the presence of 4-pyren-1-ylbutan-1-ol as initiator (entry 6). The higher activity of BEMP came at the expense of the control of the polymerization, since transesterification of the polymer backbone was noted at high conversion. As for ε-CL, it was polymerized very slowly since only 14% of monomer conversion was obtained after 10 days.

An ACEM involving the sole activation of the alcohol by hydrogen bonding (and subsequently the activation of the hydroxyl polymer chain end) and favoring a nucleophilic attack on the monomer substrate by the active initiator was proposed (Scheme 26).[123] The resulting aliphatic polyesters exhibited high reliability of the presence of end groups, narrow dispersities, and a linear relationship between conversion and molar mass.

The same group reported that the ROP of *rac*-LA catalyzed by the dimeric phosphazene *t*-BuP$_2$ exhibited a high

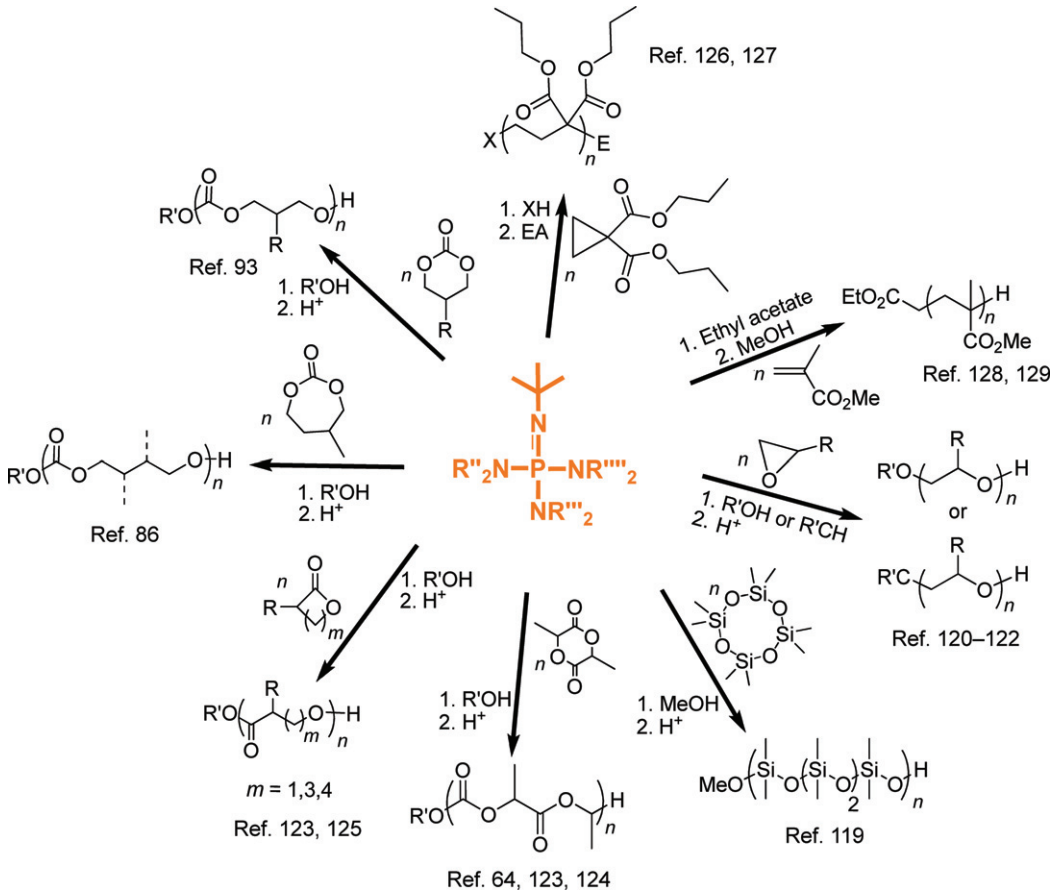

Figure 6 Overview of polymers obtained from phosphazene-based catalysts.

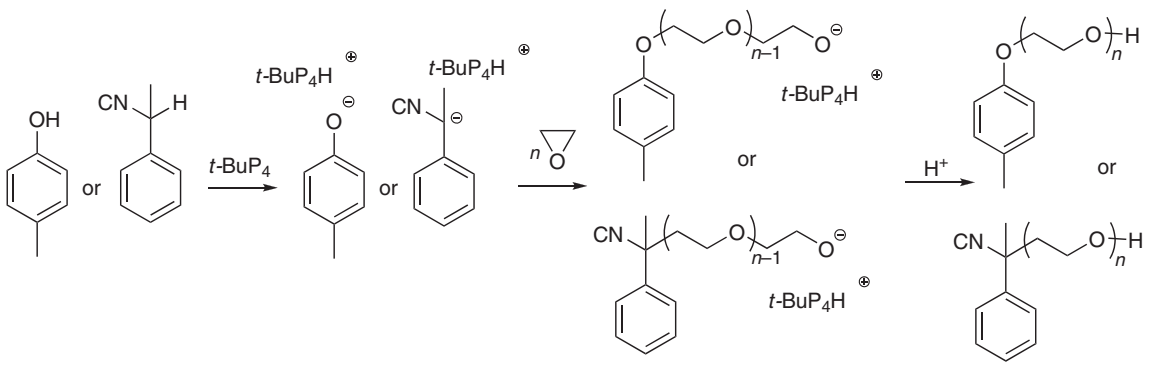

Scheme 24 Metal-free anionic polymerization of EO initiated by *t*-BuP$_4$/-CH or -OH compounds.[119]

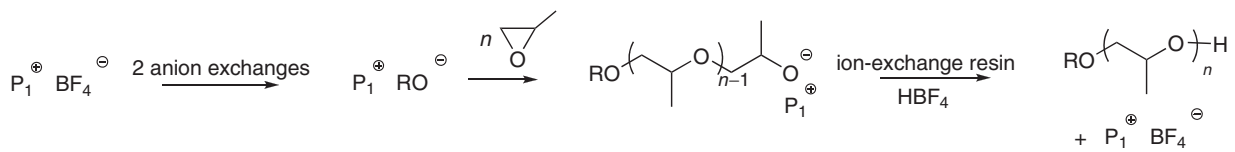

Scheme 25 Metal-free ROP of PO using P_1^+ as countercation.[122]

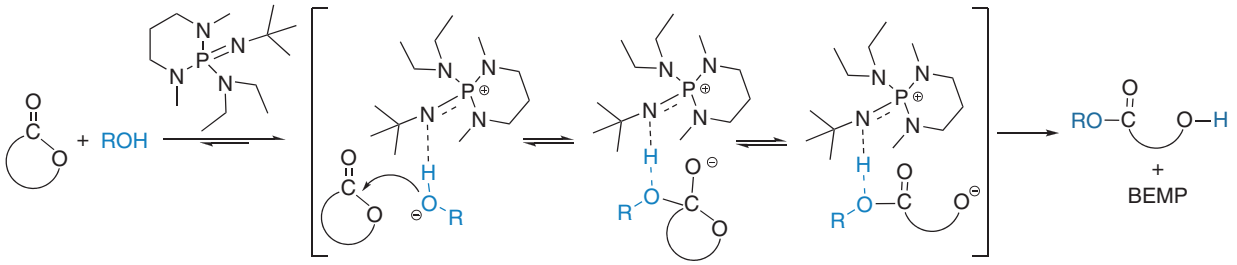

Scheme 26 Putative mechanism (ACEM) for the ROP of cyclic esters with BEMP.[123]

stereoselectivity at low temperature.[124] Catalysis of polymerization by *t*-BuP$_2$ was first studied in toluene at room temperature with enantiomerically pure L-LA, in the presence of 4-pyren-1-ylbutan-1-ol as initiator. Complete monomer conversion was achieved within 10 s using a monomer-to-initiator-to-catalyst molar ratio of 100:1:1 (entry 7). The ROP of *rac*-LA was accomplished at room temperature under dilute conditions (0.08 M) or at lower temperature, which yielded 99% conversion after 3 h. A *rac*-PLA was also prepared at –75 °C for comparison purpose and was found to be a crystalline polymer with a melting peak at 201 °C, which was much higher than that of L-PLA (163 °C). No transesterification was observed at such a low temperature. Analysis by NMR of the microstructure of the different PLAs formed, combined with DSC data, established the formation of a stereocomplex morphology of the *rac*-PLA at –75 °C, with long isotactic poly(*S*) segments and poly(*R*) segments. Cocrystallization of L-PLA and D-PLA blocks could explain the high melting peak of the thus-formed *rac*-PLA. In contrast, the *rac*-PLA obtained at room temperature was an amorphous polymer. The stereoselectivity of the *t*-BuP$_2$-catalyzed polymerization was explained by a chain end control mechanism whereby the terminal alkoxide of the last inserted monomer in the growing chain selectively attacked the monomer of the same configuration, leading to isotactic enchainment (**Scheme 27**). The bulky *t*-BuP$_2$ catalyst presumably influences the steric hindrance around the catalytic site, enhancing the stereoselectivity, in particular at low temperature.

(*RS*)-4-[(benzyloxy)carbonyl]-3,3-dimethyloxetan-2-one (dMMLABz, **Figure 2**) was subjected to ROP in THF at room temperature catalyzed by *t*-BuP$_1$, *t*-BuP$_2$, and *t*-BuP$_4$, as reported by De Winter *et al.*[125] Such a substituted

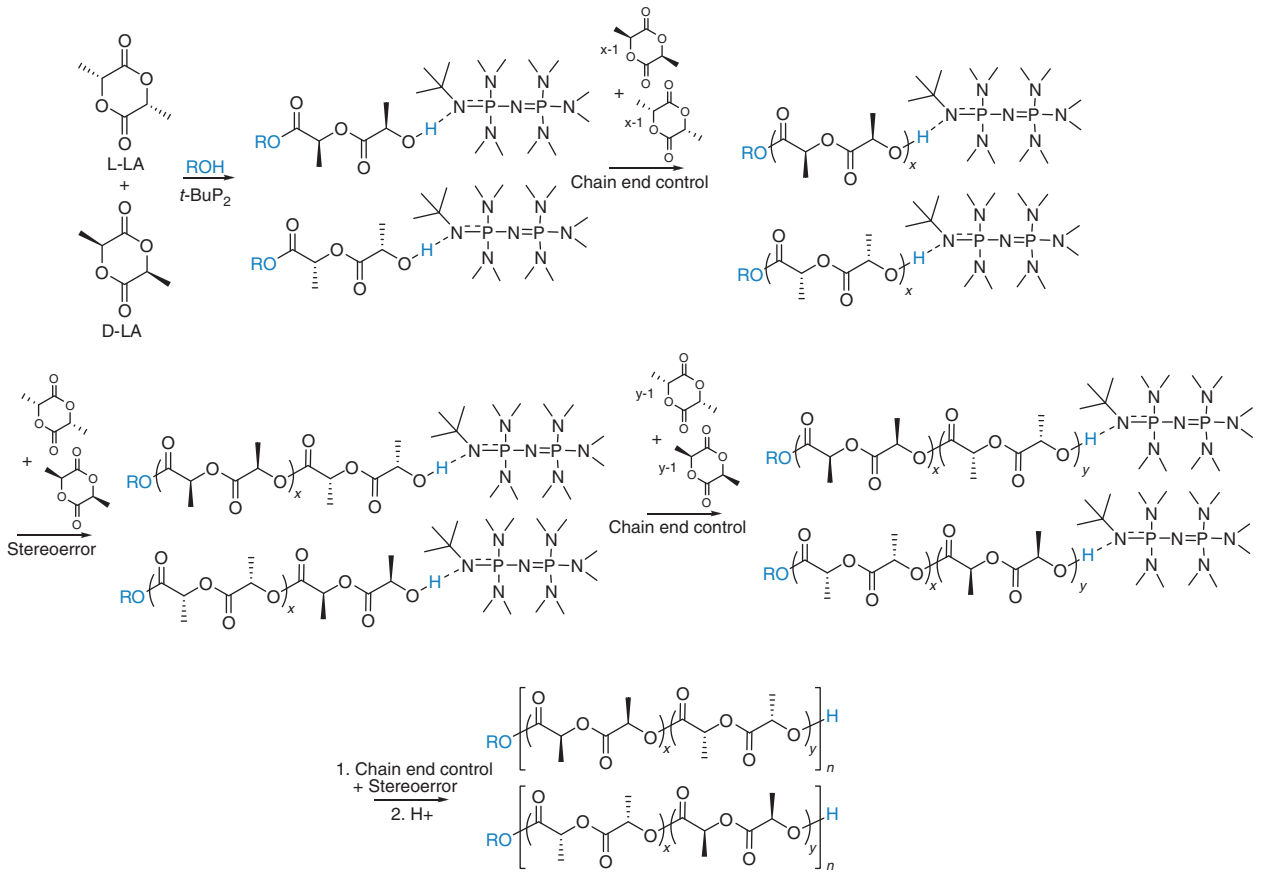

Scheme 27 Stereoselectivity of PLA during the ROP of *rac*-LA with *t*-BuP$_2$.[124]

four-membered β-lactone was also polymerized using these phosphazenes in the presence of ω-COOH-containing precursors, namely cinnamic acid or a purposely designed ω-carboxylic acid PEO used as a macroinitiator. Good control over the molar masses, dispersities, and reliability of the end-group presence in the resulting polyesters was achieved with all catalysts, the catalytic activity increasing in the order *t*-BuP$_1$ < *t*-BuP$_2$ < *t*-BuP$_4$. In the latter case, the poly(dMMLABz) of molar mass as high as 1.5×10^6 g mol^{-1} could be prepared (Table 4, entry 8). As indicated by the molecular characteristics of the obtained polyesters, the mechanism of this polymerization involved deprotonation of the COOH-functionality and ring opening of the β-lactone via an *O*-alkyl scission forming phosphazenium carboxylate active species.

In two recent reports, the group of Carpentier and Guillaume showed that six- and seven-membered cyclic carbonates such as TMC, DMTMC, BTMC,[93] as well as R-Me7CC and β-Me7CC[86] could undergo a 'controlled/living' ROP under relatively mild conditions (bulk, 60–150 °C), in the presence of BEMP as organocatalyst and a mono- or a multifunctional hydroxylated initiator (entries 9 and 10, Table 4). For instance, 100 000 equiv. of TMC was fully converted using only 10 ppm of BEMP, providing PTMCs of high molar mass. Very high activities (e.g., 55 800 h^{-1} in the case of the ROP of TMC) thus characterize these polymerizations. Well-defined α-hydroxy-ω-alkoxy, α,ω-dihydroxytelechelic linear, or three-arm star polycarbonates of controlled molar masses were obtained in this way, using benzyl alcohol, propane-1,3-diol, or glycerol as initiator, respectively. PTMCs with a molar mass as high as 45 800 g mol^{-1} could be obtained from a technical-grade, unpurified TMC, with a BEMP loading as low as 10 ppm (i.e., 2 mg of BEMP used to polymerize, quantitatively, 74.4 g of TMC). In comparison with other organocatalysts employed by the authors, BEMP could be ranked as follows regarding the ROP of TMC in bulk within 30 min at 60 °C: TOF: TBD (990 h^{-1}) > BEMP (800 h^{-1}) > DMAP (500 h^{-1}) and within 5 min at 110 °C: TOF: TBD (5940 h^{-1}) > DMAP (5220 h^{-1}) > BEMP (4800 h^{-1}). Both BTMC and DMTMC were also subjected to ROP initiated with a [BEMP]$_0$/[alcohol]$_0$ ratio of 1:5 at 60 or 90 °C. For instance, 500 equiv. of monomer was readily converted into the polycarbonates within 240 min.

In 2009, Illy *et al.*[126] reported that *t*-BuP$_4$ could successfully deprotonate mono- or difunctional thiol precursors such as benzenethiol and bis(2-sulfanylethyl)ether for the subsequent ROP of dipropyl cyclopropane-1,1-dicarboxylate, via malonate carbanions featuring phosphazenium as active species. Stoichiometric amounts of *t*-BuP$_4$ were employed (Table 4, entry 11), affording polymers with a narrow dispersity (< 1.08) under milder conditions (THF at 60 °C), in comparison with conventional processes utilizing alkali metal benzenethiolates as initiators. Upon quenching the living polymeric malonates with allyl bromide, the authors could introduce functional allylic groups in ω-position of the polymer formed. The scope of this metal-free polymerization of cyclopropane-1,1-dicarboxylates was further extended to a range of OH-, SH-, NH-, and CH-containing initiating precursors, including aromatic and aliphatic thiols, a phenol, a carbazole, and a malonate precursor.[127] Polymerizations could be performed in a nonpolar solvent such as toluene as a substitute to THF, which allowed the authors to control the polymerization at 100 °C.

4.06.8 Polymerizations Catalyzed by NHCs

Among organocatalysts, carbenes were the most investigated in the last decade for the purpose of polymerization (Figure 7). As already mentioned, both the electronic and steric properties of carbenes, hence their reactivity/nucleophilicity, can be finely tuned through variation of their substituents R_1–R_4 pattern. In particular, NHCs have served to catalyze different polymerization reactions, including step-growth and chain-growth polymerizations. Interestingly, not only carbonyl-containing monomer substrates but also epoxides as well as silicon-containing initiators or monomers could be activated.

It is worth mentioning that the first attempt to synthesize polymers via a NHC organocatalysis was reported by Jones *et al.* in the late 1990s.[158,159] These authors applied the principle of the so-called Stetter reaction to diformylarenes and bis-Mannich bases used as bifunctional monomers (Scheme 28) in the presence of a thiazolylidene catalyst. Polymeric 1,4-diketones were synthesized in this way. Subsequent ring closure of these polymer precursors by the Paal–Knorr reactions led to conjugated alternating copolymers bearing pyrroles, furan, or thiophene moieties.

In the course of their investigations into NHC-catalyzed transesterification reactions occurring in the corresponding ROP, Nyce *et al.*[137] reported the synthesis of PET. This could be achieved using a two-step procedure with NHCs as single catalytic components for the preparation of BHET, followed by its self-condensation (Scheme 29). The reaction proved reversible in the presence of methanol. Interestingly, the same NHCs were also effective for chemical degradation of PET under mild conditions (typically at 80 °C or even less), representing the first example of a depolymerization reaction utilizing organocatalysis.[136,138] The same group described the synthesis of PCL and poly(glycolide) by self-condensations of ethyl 6-hydroxyhexanoate and ethyl glycolate.[136] The reactions were performed in bulk at 60 °C under vacuum for 24 h, leading to aliphatic polyesters with molar masses M_n ranging from 8000 to 20 000 g mol^{-1}. In addition, a copolymer was also obtained from the condensation of the two monomer types.

By taking inspiration of the mechanism of benzoin condensation, which consists in reacting two aldehyde functions through a resonance-stabilized enaminol-type intermediate called the Breslow intermediate, Pinaud *et al.*[134] employed a commercially available bis-aldehyde, namely terephthaldehyde. The latter monomer was polymerized by a NHC-catalyzed step-growth polymerization (Scheme 30), leading to the formation of poly(1,4-phenylene-1-oxo-2-hydroxyethylene)s referred to as polybenzoins under relatively mild conditions (THF or dimethylsulfoxide (DMSO) at 40 °C). Out of the four organocatalysts employed in this study, 1,3,4-triphenyl-1,2,4-triazol-5-ylidene was the most active. Formation of cyclic polymers during the polymerization was also noticed, and the cyclic content was found to vary depending on the reaction media used and the monomer conversion reached.

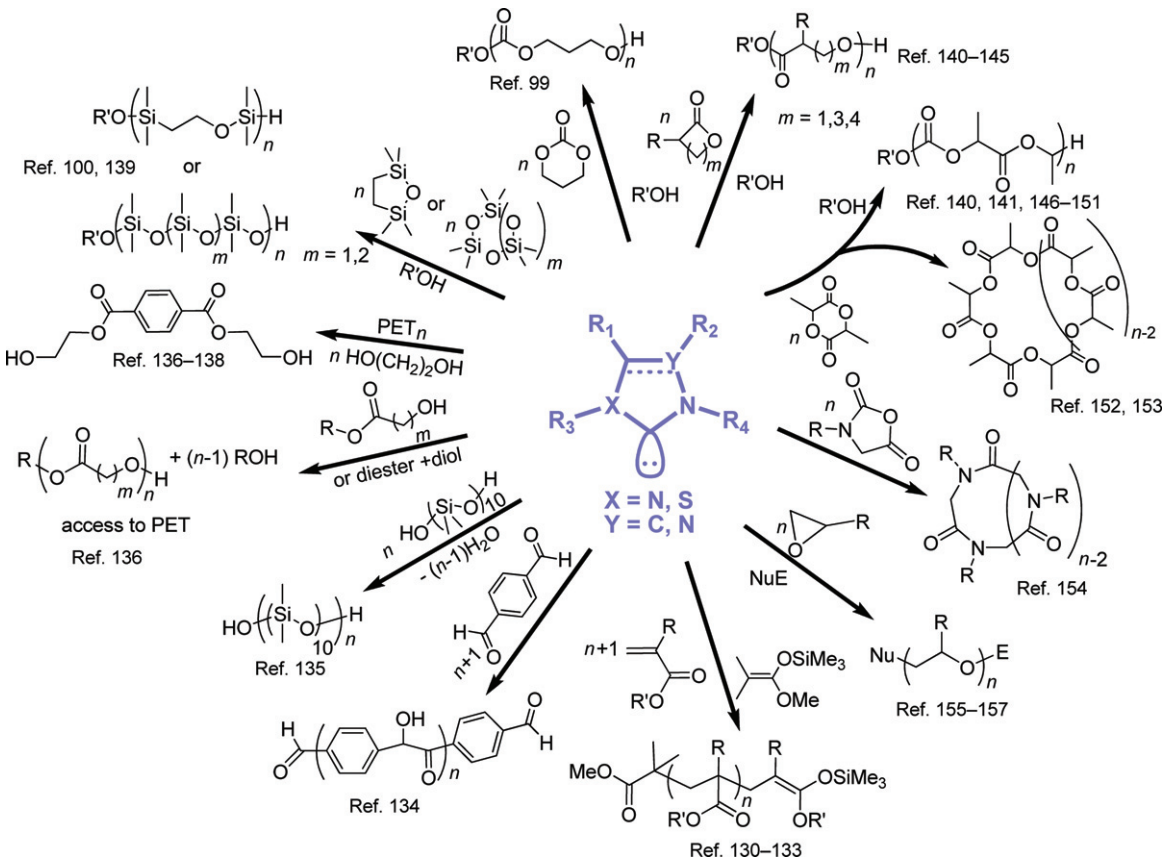

Figure 7 Overview of polymers obtained from NHCs.

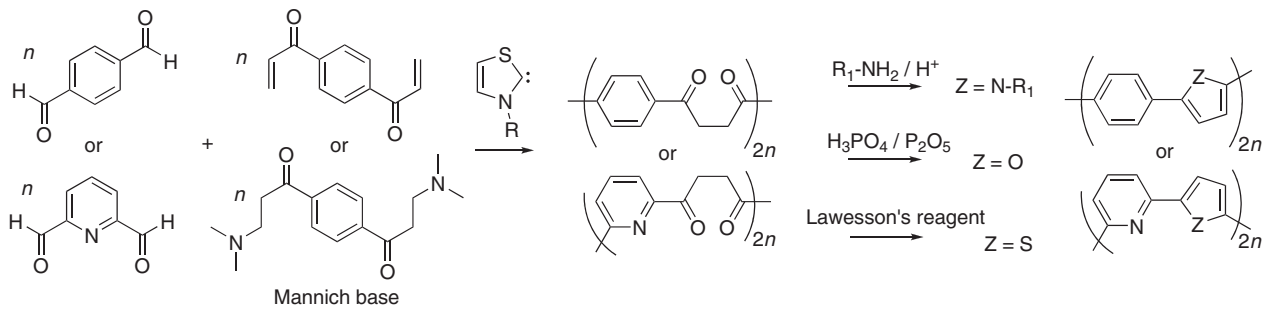

Scheme 28 Synthesis of polymeric 1,4-diketones by thiazolylidene-catalyzed step-growth polymerization and subsequent ring closure.[128,129]

Another example of a NHC-catalyzed step-growth polymerization was reported by Marrot *et al.*[135], concerning the polycondensation of α,ω-dihydroxy disilanol oligomers, forming polydimethylsiloxane (PDMS). What was unexpected here was the dehydration of the disilanol precursors by NHCs, in spite of their moisture sensitivity. This was explained by the fact that the as-formed H_2O was not miscible with PDMS. HO $[(SiMe_2)O]_{10}$-H was heated at 80 °C for 16 h, in the presence of 2500 ppm of NHCs, causing an increase in viscosity of the reaction mixture and a modification of the signals in the ^{1}H NMR spectrum of the recovered PDMS.

Besides their use to trigger step-growth polymerization reactions, NHCs were mainly used as organic catalysts in chain-growth ROP of cyclic esters to produce linear as well as cyclic aliphatic polyesters, as summarized in **Table 5**.[5,6]

The first report dates back to 2002 and exploited the ability of NHC6 (IMes) to catalyze transesterification reactions. PLA, PCL, poly(β-butyrolactone) (PBL), and PVL with controlled molar masses, high chain end fidelity, and a dispersity close to unity were synthesized by the ROP of corresponding cyclic esters in THF solution (1–2 M) at 25 °C, in the presence of benzyl alcohol or 4-(pyren-1-yl)butan-1-ol playing the role of initiator (chain regulator controlling the molar mass of the polyesters) (**Table 5**, entry 1).[140] A chain extension experiment employing a PLA precursor yielded a PLA of molar mass of 39 500 g mol^{-1} and a dispersity of 1.17. A well-defined star PCL was even synthesized from six-arm poly(propylene glycol), PPG (M_n = 3000 g mol^{-1}), as macromolecular hexafunctional initiator. Compared with DMAP, the ROP of LA catalyzed by IMes proved much faster (TOF ~ 18 s^{-1}).

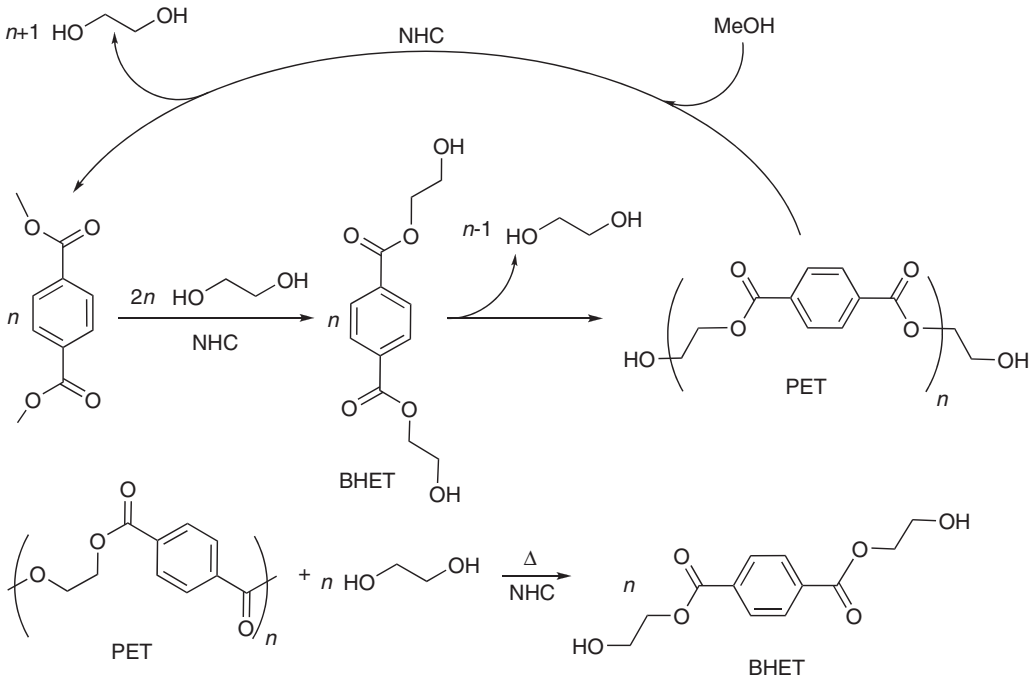

Scheme 29 Synthesis of PET by step-growth polymerization and depolymerization of PET via transesterification with a NHC.[136–138]

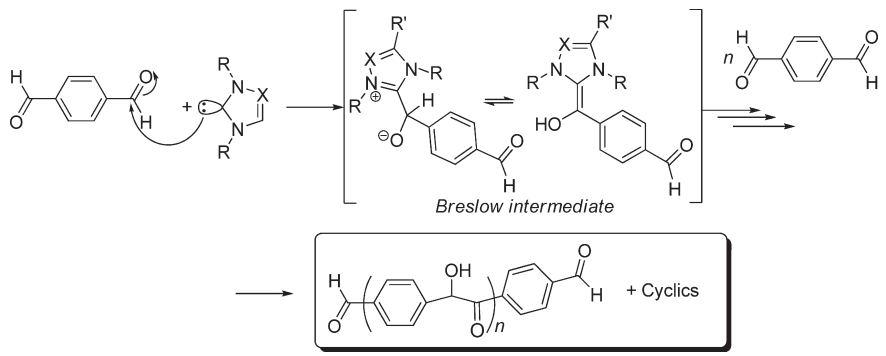

Scheme 30 NHC-catalyzed benzoin condensation in step-growth polymerization.[136]

Since this first report, several other NHCs, in their naked or under their masked form, were tested for the ROP of cyclic esters. In most cases, OH-containing precursors were employed as initiators which control the chain length of the final polymer.[5,6]

In a more systematic study, Nyce *et al.*[141] reported that NHCs derived from imidazolium- and thiazolium ionic liquid salts (precatalysts) could be generated *in situ* using a strong Bronsted base. This allowed screening different precatalysts and thus correlating the catalytic activity of NHCs toward the polymerization rate and the quality of control of these polymerizations with their structure. LA, β-PL, δ-VL, and ε-CL were investigated (**Table 5**, entry 2). For instance, imidazole-based NHC catalysts (e.g., NHC6) exhibited a higher reactivity than thiazole-based catalysts. Imidazol-2-ylidene and imidazolin-2-ylidene catalysts showed similar catalytic activity. IMes was found the most active for the ROP of LA. This particular NHC proved quite active even with low catalyst loading (0.5 mol.%), and molar masses could be targeted by varying the monomer to initiator ratio (DP = [M]/[I]) without changes in dispersity ($D < 1.2$).

In the same report, the authors developed an attractive interfacial polymerization process where the ionic liquid precatalyst served as reservoir forming a two-phase reaction mixture with THF solution containing both the monomer and the initiator. Subsequent *in situ* activation of the ionic liquid allowed generating the NHC that was able to migrate to the THF phase so as to trigger repetitive ROPs. Treatment under acid conditions on the completion of the reaction allowed regeneration and ready recovery of the ionic liquid precatalyst. The use of cross-linked polymer-supported precatalysts was also developed to trigger the ROP of cyclic esters. The versatility of this approach was demonstrated through the synthesis of well-defined homopolyesters, macromonomers, as well as block and graft copolymers.

As described in the literature on molecular chemistry,[160] alternatives to *in situ* generation of NHCs imply the thermolysis of NHC monoadducts, serving as masked NHCs. Upon

Table 5 Representative examples of the ROP catalyzed by NHCs

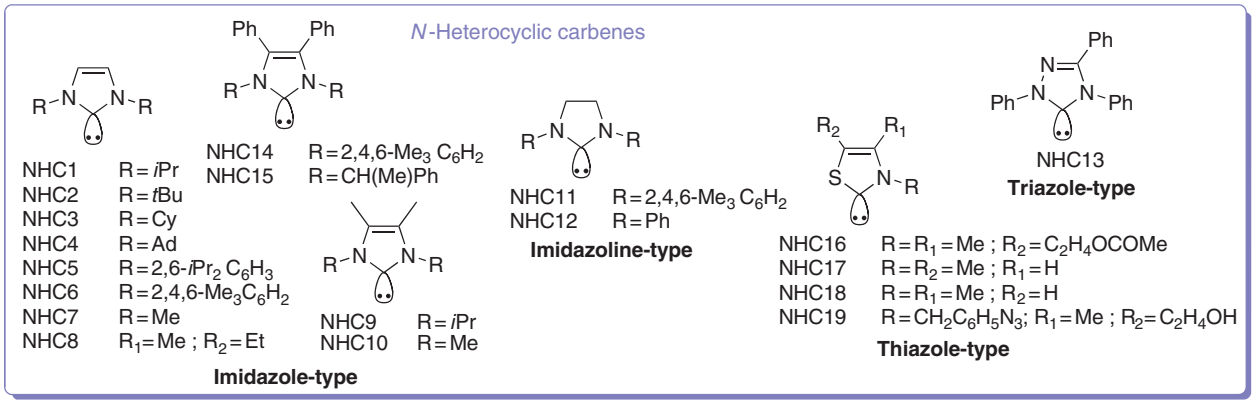

Entry	*Catalyst (NHC)*	*Monomer*	*Bulk/solvent*	*Initiator*	*[C]/[I]$_0$*	*t*	*T (°C)*	*Conv (%)*	*M_n (g mol^{-1})*	*D*	*References*
1	6	Lactide, ε-CL, β-BL	THF	BnOH, PBuOH	0.0083–1.5	2 h	25	60–99	1 600–17 000	1.05–1.33	140
2	10, 7[a], 12[a]	ε-CL, δ-VL, β-BL	THF	BnOH	0.5–1.8	0.5–6 h	25	> 98	2 900–28 000	1.04–1.55	141
	5[a], 6[a], 7[a], 8[a], PS-8[a], 11[a], 12[a]	Lactide		BnOH	0.25–1.5	0.25–1 h	25	60–99	17 700–28 000	1.15–1.52	
	16[a], 17[a], PS-18[a], 19[a]	Lactide		BnOH, PBuOH	< 0.005	48–72 h	25–38	80–85	6 900–14 400	1.07–1.35	
3	11 adducts[b]	Lactide	THF	$R(OH)_x$	*x*	10 min	RT	84–99	12 000–25 500	1.16–1.34	146
4	13[c]	Lactide	Toluene	MeOH/PBuOH/PEO-OH/bis-MPA=$R(OH)_x$	*x*	19–113 h	90	35–97	2 600–19 000	1.06–1.36	147
5	13[c,d]	β-BL	THF Toluene	PBuOH	NM	3–24 h	50 90	81–95	4 400–15 500	1.09–1.19	142
6	13[c,d]	dMMLABz+β-BL[e]	Toluene/*t*-BuOH mixture	Ethylene glycol	2	2 days	80	< 95	~10 000 $f_{dMMLABz}$ = 0.1–0.58	< 1.27	143
7	13[c]	Lactide	Benzene	$R(OH)_x$ or $R(NH_2)_y$	*x* or 2*y*	18–71 h	90	70–100	8 000–18 000	1.07–1.24	148
8	11, 12 adducts[f]	Lactide	THF, toluene, or o-xylene	BnOH	1.5	3–24 h	65–144	30–83	3 200–10 000	1.10–1.52	149
9	2, 5, 6	D,L-Lactide	Dichloromethane	BnOH	0.5–2	20–30 min	–20 to 25	71–98	7 000–17 000	1.23–1.39	150
10	14, 15	*rac*- or *meso*-Lactide[g]	Dichloromethane	PBuOH	1	1–240 min	–70 to 25	> 88	~14 000	1.18–1.48	151
11	9, 10	ε-CL	THF	BnOH	0.5–1	2 min–5 h	RT	18–77	1 000–14 500	1.11–1.3	144
12	5, 9	TMC	Benzene	BnOH	0.05	0.1–30 min	25	> 99	4 500	1.04–> 2	99
13		Lactide	THF	NHC6[h]		10–900 s	25	32–92	7 000–26 000	1.15–1.35	152, 153
14		(*R*)β-BL[h]	THF, benzene	NHC11		4 h	RT	24	4 900	1.42	145

(*Continued*)

Table 5 (*Continued*)

Entry	*Catalyst (NHC)*	*Monomer*	*Bulk/solvent*	*Initiator*	*[C]/[I]$_0$*	*t*	*T (°C)*	*Conv (%)*	*M_n (g mol^{-1})*	*D*	*References*
		β-BL[h]				10 min			5 800	1.16	
15		^{N}Bu-NCA	THF	NHC5[i]		16 h	50	79–100	3 000–27 000	< 1.12	154
16	2, 3	D4	Bulk	BnOH/MeOH/*t*-BuOH	0.014–1	16 h	80	∼85	20 000–220 000	∼1.6	139
17	6, 9	TMOSC	Benzene	PBuOH	1	1–30 min	RT	80–99	10 000–13 000	1.14–1.19	100
	9	D3	Toluene	NM	1	NM	NM	NM	NM	> 1.4	
18		EO	DMSO	NHC1[j]		3 days	50	100	2 400–13 000	< 1.14	155
19	1, 2	EO	DMSO	Chain regulator NuE	0.1	4 days	50	> 90	2 000–12 000	< 1.15	156
20	1	PO	Bulk	Chain regulator NuE	0.1	3 days	50	30–40	1 800–7 300	< 1.18	157

[a] *In situ* generated with *t*-BuOK (triethylamine for thiazole-based carbenes).
[b] Adducts with $R(OH)_x$ ($R(OH)_x$ is further used as the initiator) (equilibrium between NHC and adduct at RT).
[c] Forms adducts with alcohols and amines (stable at RT).
[d] *t*-BuOH used to decrease the NHC activity (by adduct formation).
[e] dMMLABz + β-BL both incorporated at the beginning of the polymerization.
[f] Adducts with $CHCl_3$ or $C_6H_xF_{(6-x)}$ ($x > 1$) (stable at RT).
[g] *rac*-Lactide leading predominantly to isotactic polymers (*RRR* or *SSS*); *meso*-L-lactide leading predominantly to heterotactic polymers (*RRSSRRSS*).
[h] Terminated with CS_2, leading to cyclics.
[i] Terminated with Dithranol, leading to cyclics.
[j] Terminated with NuE, leading to α,ω difunctionalized PEO.
NM, not mentioned.

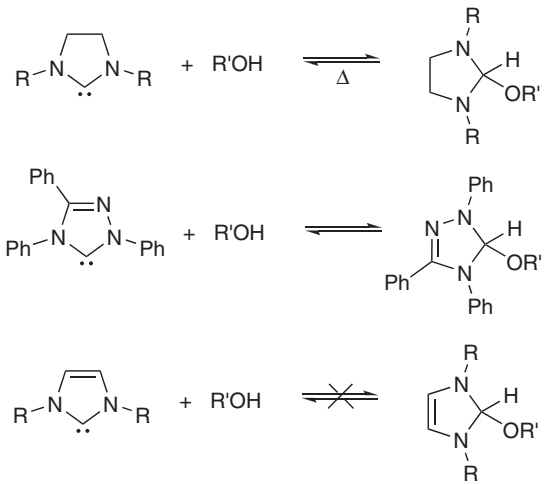

Scheme 31 Reaction of alcohol with free NHCs.[131,146]

heating, such precursors undergo an α-elimination reaction, affording NHCs without the need for a strong base. This method was used by Enders *et al.*[161] to obtain the first commercially available NHC in the late 1990s.

For instance, upon heating the NHC13-alcohol monoadduct at 80 °C under vacuum (0.1 mbar) methanol is released, forming the corresponding 1,2,4-triazol-5-ylidene. This strategy can also be applied to produce imidazolin-2-ylidenes.[70,146] Other adducts, obtained from a 1:1 reaction between imidazolin-2-ylidene and alcohols, can also be cleaved to release the free NHC, as illustrated in **Scheme 31**.[146,162] However, masking NHCs with alcohols cannot be applied to generate imidazol-2-ylidenes (unsaturated NHCs).

The above methods were exploited by the group of Hedrick and Waymouth in the generation of NHCs for the organocatalyzed ROP of various esters.[141–143,146–149] For instance, they reported the synthesis of a series of primary and secondary alcohol adducts of imidazolin-2-ylidenes, as single-component latent catalyst/initiators for the ROP of LA, giving PLA of controlled molar masses, in THF solution at room temperature within 10 min (**Table 5**, entry 3).[146] These adducts were stable as solids at room temperature, but they readily released alcohol and a free saturated NHC in solution. Di- and trifunctional adducts were also prepared to access, respectively, two-arm linear and three-arm star (**Scheme 32**) based on PLA.

Similarly, and on the basis of observations made by Enders *et al.*,[161] the group of Dubois designed alkoxytriazolines derived from the commercially available 1,3,4-triphenyl-4,5-dihydro-1*H*-1,2,4-triazol-5-ylidene carbene, as latent unimolecular catalyst/initiator systems.[142,147] When used at room temperature to carry out the ROP of LA, such triazole carbenes exhibited a low reactivity, owing to the reversible formation of alcohol adducts. Polymerizations of either LA or β-BL were thus performed at 90 °C in the presence of a variety of initiating alcohols in 1 M toluene solution, which gave nearly quantitative monomer conversion in ~50 h and PLAs of controlled molar masses and low dispersities (entries 3 and 4). An interesting feature of polymerization utilizing these alkoxytriazolines was that the hydroxy-terminated PLA and the free triazole carbene reacted together in a reversible manner, forming a dormant polymer adduct. Such a reversible termination process helped in minimizing the concentration of propagating alkoxides, thus preventing the occurrence of side transesterification reactions between polymer chains. In this way, activation/deactivation cycles of polymer chain ends were possible simply by heating/cooling the reaction mixture on demand. This high level of control also facilitated chain extension experiments: after full conversion of a first load of monomer, the NHC-catalyzed ROP of a second monomer readily occurred, even after precipitation.

This strategy was next applied to macromolecular engineering, through the design of block copolymers and 'hybrid dendrimer/star' copolymer made of a dendritic core surrounded by 24 PLA branches. For block copolymer synthesis, adducts of hydroxy-functionalized oligomers or bifunctional 'double-headed' initiators were employed, by combining disparate polymerization techniques (typically NMP or RAFT with the NHC-catalyzed ROP). A multifunctional hydroxylated three-generation dendrimer derived from 2,2′-bis(hydroxymethyl)propanoic acid served as thermolabile multifunctional macroinitiator to access the hybrid dendrimer/star copolymer.

In another contribution, the same group reported the synthesis of amphiphilic ABA-type triblock copolymers based on PLA and poly(dimethyl malic acid) (poly(dMMLA)), via the triazole carbene organocatalysis.[143] A statistical poly(dMMLABz-*co*-β-BL) was first prepared by carrying out the NHC-catalyzed ring-opening copolymerization of dMMLABz and β-BL in a toluene/*t*-BuOH solvent mixture at 80 °C, in the presence of ethylene glycol as initiator (**Table 5**, entry 3). Under such conditions, the dMMLABz monomer was preferentially incorporated in the resulting aliphatic polyester chains, both monomers being polymerized via a selective *O*-acyl ring opening. This precursor was further employed as a difunctionalized macroinitiator for the ROP of LA at 90 °C. After a deprotection step by catalytic hydrogenation of the pendant benzylic ester groups of poly(dMMLABz), the expected PLA-*b*-poly(dMMLA-*co*-β-BL)-*b*-PLA triblock copolymer was obtained (**Scheme 33**). Investigations into the self-assembling

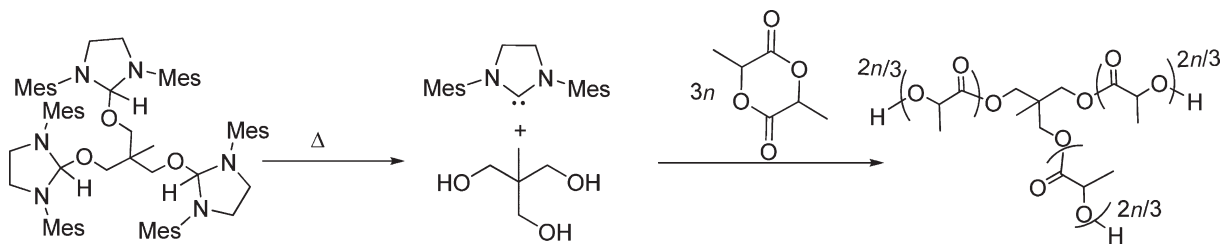

Scheme 32 ROP of LA employing a tri-NHC-alcohol adduct and leading to three-arm star PLAs.[146]

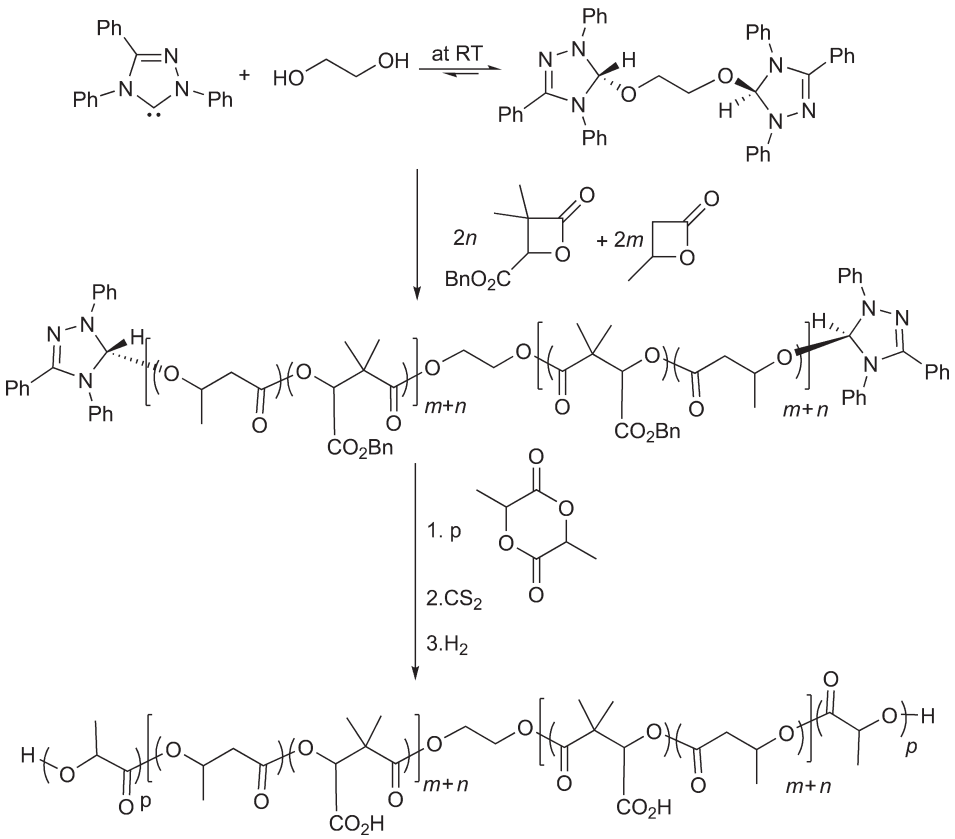

Scheme 33 Synthesis of PLA-*b*-poly(dMMLA-*co*-β-BL)-*b*-PLA triblock copolymer via the triazole carbene organocatalysis.[143]

properties in aqueous solutions of these amphiphilic compounds revealed the formation of 'flower-like' micelles at 4 °C. Increasing the temperature to 25 °C induced the microgelation of the above micelles, which upon further increase in temperature to 40 °C led to a disruption of the microgel. This demonstrated the temperature-dependent reversible sol–gel transition of these self-assembled triblock copolymers.

In addition to alcohols, the same triazole carbene was employed in the presence of primary amino-containing precursors serving as initiators.[148] In this case, however, the primary amino-function was shown to act as a bifunctional initiating site in the ROP of LA in the presence of the triazole carbene (**Table 5**, entry 7). By making use of multifunctional (macro) initiators based on PEO and featuring multiple primary amino-functionalities, 'H-shaped' and 'super-H-shaped' architectures based on PEO/PLA could be synthesized. Initiation from each primary amine indeed created imide-type functions corresponding to branching points (two chains per initiating amine).

In other words, polymerization occurred from all four N–H-bonds of the PEO macroinitiator (**Scheme 34**). A model primary amine initiator, namely 1-aminomethylpyrene, was

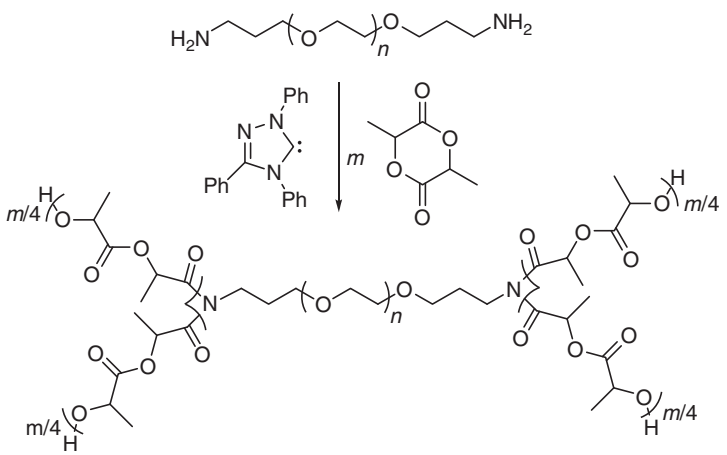

Scheme 34 Synthesis of H-shaped PEO/PLA-based block copolymers by NHC-catalyzed ROP of LA.[148]

first employed for the ROP of LA using triazole carbene as catalyst in benzene. Initiation of LA at both N–H groups of the initiator (i.e., both the amine and resulting amide functionality) was established. For instance, ROP of LA from a 1:1 mixture of PEO-$(OH)_2$ and PEO-$(NH_2)_2$ at 90 °C catalyzed by the triazole NHC led to a mixture of diblock copolymers of $M_n = 20\,000$ and $9000\ g\ mol^{-1}$, corresponding to the formation of a mixture of the H-shaped architecture derived from PEO-$(NH_2)_2$ and having twice the molar mass of the linear block copolymer grown from PEO-$(OH)_2$. The ability for an amido-group to initiate the ROP of LA was then verified using ε-caprolactam as initiator. Using a telechelic tetrakis-amino-functionalized PEO precursor allowed the authors to synthesize the 'super-H-shaped' copolymers.

Nyce *et al.*[149] also developed the synthesis of NHC adducts featuring substituents with a good leaving group ability in C-1 position, by condensation of diamines with fluorinated benzaldehydes. In the solid state, these adducts were found to cleave at temperatures between 80 °C and 165 °C, depending on the fluorinated substituent and the carbene used, as investigated by thermal analysis and spectroscopic techniques. In contrast to adducts derived from chloroform, the adducts from pentafluorobenzene were stable at room temperature. Such adducts were successfully employed as organic precatalysts for the ROP of LA (**Scheme 35**) carried out in THF, toluene, or *o*-xylene solution (**Table 5**, entry 8), though elevated temperatures were required to release the carbene catalyst (between 60 °C and 144 °C, as a function of the structure of the precatalyst).

In 2004, Jensen *et al.*[150] discovered that the free achiral NHC, 1,3-dimesitylimidazol-2-ylidene, triggered the stereoselective polymerization of *rac*-LA (**Table 5**, entry 9). While the bimetallic Zn-based complex formed by addition of benzyl alcohol to the complex (1,3-dimesitylimidazol-2-ylidene)$ZnEt_2$ produced heterotactic PLA, the metal-free catalyzed ROP of *rac*-LA mediated by the same NHC led to isotactic enriched PLA under similar conditions (CH_2Cl_2, 25 °C). Actually, other NHCs, namely 1,3-di-*tert*-butylimidazol-2-ylidene and 1,3-bis(2,6-diisopropylphenyl)imidazol-2-ylidene, also formed isotactic enriched PLA, showing semicrystalline properties. No clear explanation, however, was provided by the authors to differentiate the behavior of the free NHCs and the metal-based complex.

Dove *et al.*[151] reported that sterically hindered unsaturated free NHCs catalyzed the polymerization of *rac*-LA, leading to highly isotactic PLA or *meso*-LA to give heterotactic PLA at low temperature (from −70 °C to −15 °C). Both the chiral and achiral versions of these NHCs were purposely designed. It was first noted that these catalysts exhibit a very high activity ($95\ min^{-1}$) at room temperature, providing PLA of controlled molar mass and low dispersity (entry 10). Highly isotactic PLA, with blocks of (*R*,*R*)-LA and (*S*,*S*)-LA in the PLA chain, as suggested by NMR characterization of these materials, was next generated at low temperature, with an increase in the probability of isotactic enrichment (P_i), from 0.59 at room temperature to 0.90 at −70 °C. The high level of stereoselectivity with this NHC was ascribed to the steric hindrance brought by the phenyl groups at the back of this catalyst. The ROP of *rac*-LA using the chiral NHC also formed highly isotactic PLAs at low temperature. It was, however, suggested that the stereocontrol was mainly dominated by the steric congestion of the active site (**Scheme 36**) rather than by the chirality of the catalyst. The polymerization of *meso*-LA mediated by a chiral NHC yielded a heterotactic PLA. All these observations (highly isotactic polymer formed from *rac*-LA and heterotactic polymer with *meso*-LA) were in agreement with a chain end control mechanism for both achiral and chiral NHCs, despite the presence of chiral groups close to the active site. In the case of *rac*-LA, both D- and L-LA should be subjected to a stereoselective attack by the terminal alkoxide of the last inserted monomer unit, leading to isotactic enrichment. In the case of heterotactic-enriched PLA obtained from *meso*-LA, the oxygen adjacent to the last chiral center of the PLA chain end (either *R* or *S*) might attack the activated monomer with the same stereogenic configuration adjacent to it.

While NHCs are highly active in the ROP of LA, they are much less efficient in the ROP of ε-CL.[140,141] However, the more electron-rich and sterically unhindered carbenes 1,3-diisopropyl-4,5-dimethylimidazol-2-ylidene (NHC9) and 1,3,4,5-tetramethylimidazol-2-ylidene (NHC10) proved to be active organocatalysts for the synthesis of well-defined PCL, again corroborating that the catalytic activity is sensitive to the steric and electronic nature of the carbene (entries 1, 2, and 11 in **Table 5**).[144] The ROP of ε-CL was performed at room temperature in THF solution (0.5–2.0 M), in the presence

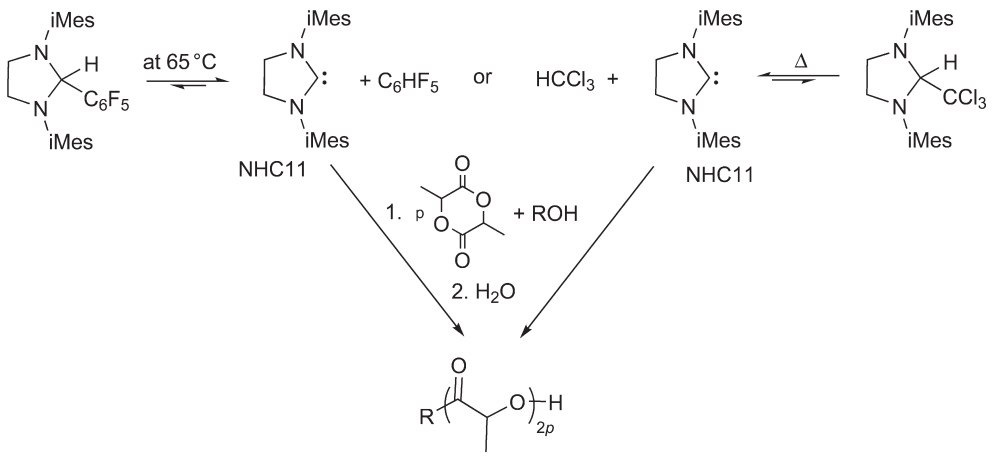

Scheme 35 Synthesis of PLA catalyzed by fluorinated or chlorinated NHC adducts.[149]

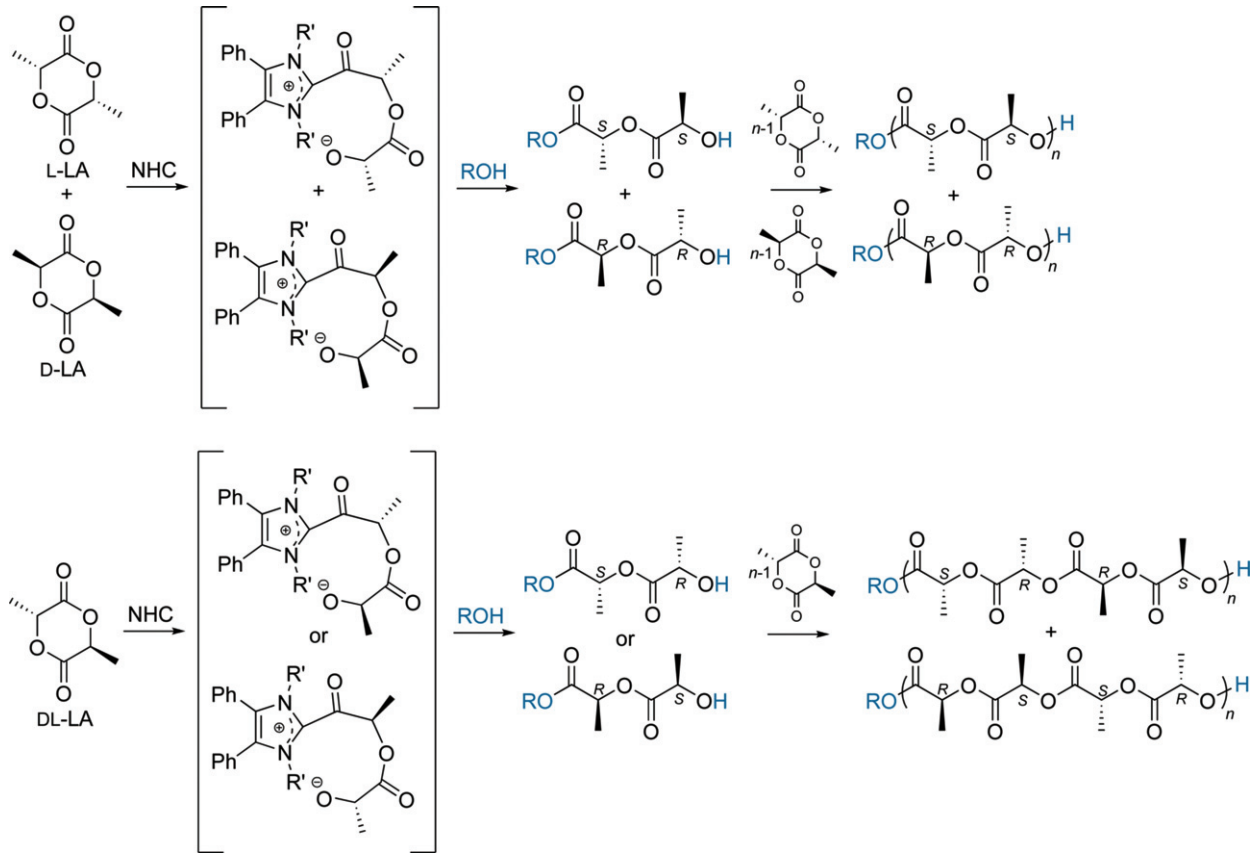

Scheme 36 Stereoselectivity of PLA during the ROP of *rac*-LA or *meso*-LA (controlled chain end mechanism).[151]

of BnOH and 4-pyren-1-ylbutan-1-ol as a monofunctional initiator, or using multihydroxylated initiators such as ethylene glycol, 1,1,1-tris(hydroxymethyl)propane, and pentaerythritol. Heterodifunctionalized PCL and three- and tetra-arm poly (ε-CL) stars were thus generated. Low NHC/ε-CL ratios were required to obtain PCL of low molar masses, so as to avoid side transesterification reactions and formation of cyclic oligomers.

The NHC-catalyzed ROP of TMC was also shown to be a controlled process (**Table 5**, entry 12).[99] NHC catalysis (5 mol.%) allowed fast conversion (> 99% after 30 min), yielding polymers with dispersity as low as for the best of the other organocatalysts used. However, the use of a more reactive NHC did not allow a good control.

The two mechanisms already discussed above for other organocatalysts were eventually proposed to account for the 'controlled/living' character of NHC-catalyzed ROPs of cyclic esters, in general. In the AMM, the carbonyl group of the cyclic ester substrate is first subjected to a nucleophilic attack by the carbene catalyst (Path A, **Scheme 37**). The activate initiator/chain end mechanism (ACEM) involves interaction of the O–H group of the alcohol initiator with the NHC lone pair (Path B, **Scheme 37**) and the nucleophilic attack of the monomer by the oxygen of this alcohol.

Evidence for both mechanisms was discussed, according to the nature of the NHC catalyst. First, Connor *et al.*[140] argued that NHCs were unable to deprotonate alcohols and initiate an anionic polymerization from the corresponding iminium alkoxide. However, theoretical calculations predicted that the ACEM involving H-bond had a lower barrier than the AMM.[163] Interactions involved in alcohol complexes of IMes (NHC6) were studied by NMR spectroscopy and by X-ray crystallography. Such adducts were greatly sensitive to the solvent and to the structure/nature of the alcohol:[164] the more sterically hindered the alcohol, the weaker the interaction with the carbene. A more acid alcohol thus led to greater involvement of imidazolium alkoxides in equilibrium with other hydrogen-bonded complexes.

Evidence of a direct attack of the nucleophilic NHC IMes to the cyclic ester was given by polymerizing LA in total absence of an alcohol initiator.[152,153] In this case, cyclic PLAs could be obtained by a kinetically controlled zwitterionic ROP mechanism (referred to as the ZROP mechanism). In this case, deactivation of polymeric zwitterionic species occurred intramolecularly (**Scheme 38**), even at relatively high monomer concentrations (0.6–1.0 M in THF). Under such conditions, molar masses were directly controlled by the initial ratio of the monomer to the NHC (**Table 5**, entry 13). In other words, NHC played in this case the role of initiator, though it was released after intramolecular cyclization (macrolactonization reaction). These polymerization reactions proved to be very fast ($k_p = 48.7\,l\,mol^{-1}\,s^{-1}$), yielding high molar mass cyclic PLAs ($M_n = 5000$ and $30\,000\,g\,mol^{-1}$) with narrow dispersities ($D < 1.32$) in only a few seconds (5–900 s). Polymerization reactions were quenched by adding carbon disulfide trapping the NHC by forming an irreversible zwitterionic NHC–CS_2 adduct.

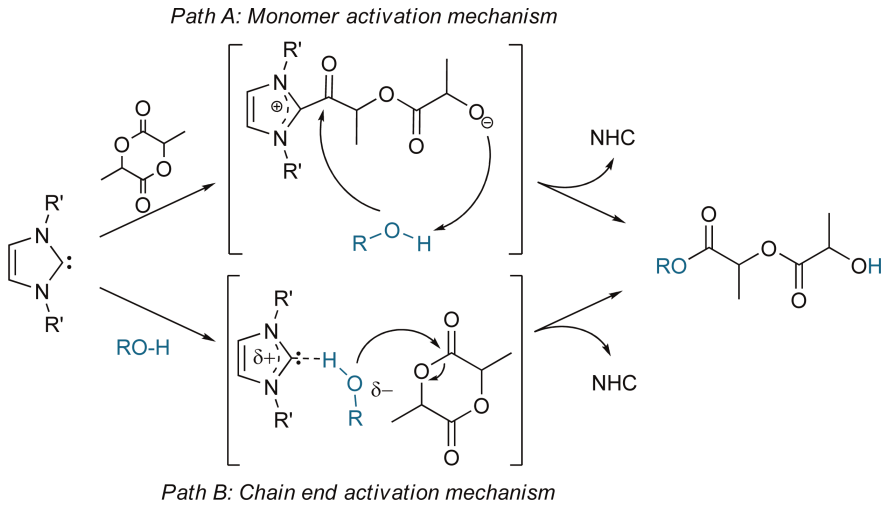

Scheme 37 Initiation of the ROP of LA and subsequent propagation to form PLA.

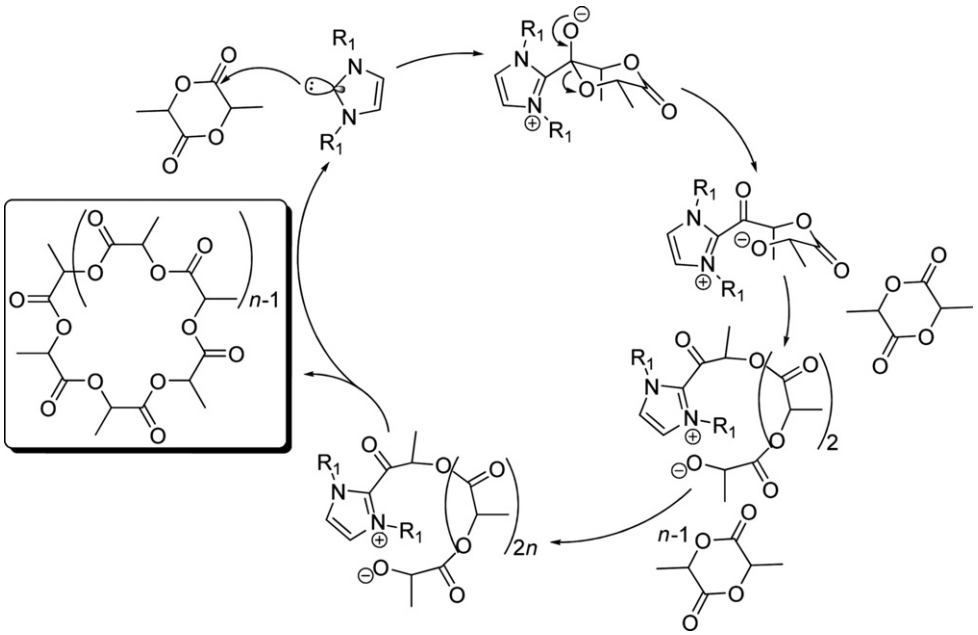

Scheme 38 ZROP of LA catalyzed by IMes and synthesis of cyclic PLAs.[152,153]

The cyclic architecture was supported by a combination of techniques, including NMR, MALDI-TOF MS, and viscometry of the cyclic polymers in comparison with the linear homologs of the same molar mass (prepared in the presence of alcohol initiators). In addition, thermogravimetric analysis (TGA) suggested that cyclic PLAs were more thermally stable than the respective linear polymers. When IMes-mediated ROP was applied to optically pure L-LA, a crystalline isotactic cyclic PLA was formed, indicating that the polymerization occurred without epimerization of the chiral center.

Investigations into the kinetics of these ZROPs mediated by NHC6 (IMes) allowed the authors to account for these experimental observations.[153] If the rate of cyclization is of the same order than the rate of propagation, cyclization would be the result of an intramolecular chain transfer, releasing NHC that would create new chains. In the latter case, the molar masses should not evolve linearly but should remain constant with monomer conversion, while the dispersity should be equal to 2.0. Since this was not observed experimentally, it was proposed that the IMes-mediated ZROP involved a slow initiation step (which was second order in monomer concentration, $k_i = 0.274\ l^2\ mol^{-2}\ s^{-1}$), a propagation step (first order in monomer concentration) that was found much faster than initiation, cyclization ($k_c = 0.0575\ s^{-1}$), and depropagation ($k_d = 0.208\ s^{-1}$). As a matter of fact, few chains could be reinitiated by the carbenes released upon cyclization. The very fact that the dispersity increased at high conversions was explained by the occurrence of either competitive transesterification reactions of the propagating zwitterions or transesterification reactions of the cyclic polymers by the zwitterions or the carbene molecules. These kinetic data were supported by numerical and stochastic simulations.

In complement to the previous studies on IMes-mediated cyclization of PLA, the reaction of the saturated homologue of IMes, that is, 1,3-dimesitylimidazolin-2-ylidene (NHC11), with four-membered lactones (β-butyrolactone and β-propiolactone) was investigated (Table 5, entry 14).[145] Equimolar amounts of that carbene generated zwitterionic species by nucleophilic attack of the carbene on the lactone, which was followed by ring closure. This led to the formation of a neutral and stable imidazolidine spirocycle which was isolated and characterized by crystallography. Interestingly, this spirocyclic intermediate could serve as a latent initiator that did undergo propagation steps in the presence of excess β-BL monomer. In other words, the controlled ROP of both β-PL and β-BL operated by reversible opening and closure of labile spirocyclic imidazolidine intermediates, affording well-defined aliphatic poly(β-BL) and poly(β-PL), as illustrated in Scheme 39. The use of CS_2 allowed quenching of these polymerizations and release of the cyclic polyesters.

If other organocatalysts were capable of catalyzing mostly the polymerization of carbonyl-containing monomers (see previous sections), NHCs were found advantageous to polymerize a variety of monomers, including not only heterocycles such as lactones, lactide, cyclic carbonates, cyclic siloxanes, epoxides, NCAs but also bis-aldehydes and both acrylates and methacrylates.

For instance, Guo *et al.*[154] reported the synthesis of poly(α-peptoid)s that are structural mimics of poly(α-peptide)s, via the direct NHC-initiated ROP of *N*-substituted NCAs (^{N}R-NCA) (Table 5, entry 15). In contrast to poly(α-peptide)s whose well-defined secondary structures are stabilized through hydrogen bonding interactions, poly(α-peptoid)s are free of such interactions. As with regular NCA monomers, ^{N}R-NCA can be polymerized through a nucleophilic chain-growth pathway that entails regioselective insertion of a nucleophilic initiator (e.g., primary amine) into the anhydride carbonyl group, followed by elimination of CO_2 reforming an amino propagating chain end. These ^{N}R-NCA monomers could be polymerized in the presence of various amounts of NHC used as a direct initiator, thus controlling the polymer chain length (ZROP mechanism). It is interesting to note that the activated functional group (i.e., anhydride) of the ^{N}R-NCA monomer is different from that of the polymer backbone (i.e., amide). As NHCs have not been reported to trigger transamidation reactions, it is likely that inter- and intrachain transfer (side) reactions, if existing, are *de facto* reduced. This situation differs from that of aliphatic polyesters discussed above, which can be subjected to NHC-catalyzed transesterifications.

Analysis by mass spectroscopy revealed that the carbene moiety was retained as spirocycle adduct when precipitated in hexane. Thus, after complete conversion of the initial monomer, chain extension could be performed upon addition of a second batch of ^{N}R-NCA monomer, confirming the living nature of the polymerization. Analysis by MALDI-TOF MS showed that the resulting polymers mainly consisted of cyclic poly(α-peptoid)s formed by ZROP, followed by intramolecular cyclization and release of the NHC moiety (Scheme 40). The cyclic architecture was confirmed by viscometric measurements. Interestingly, control over polymer molar mass and dispersity could be maintained even at relatively high concentrations of monomer, in contrast to common synthetic strategies for cyclic polymers that generally require dilute conditions. Cyclic diblock copoly(α-peptoid)s could even be obtained by sequential ZROP of ^{N}Me-NCA and ^{N}Bu-NCA monomers.

NHCs were also employed to catalyze the ROP of cyclosiloxanes (hexamethylcyclotrisiloxane and octamethyltetracyclosiloxane referred to as D_3 and D_4, respectively) and carbosiloxanes in the presence of initiating alcohols. For instance, Rodriguez *et al.*[139] reported the ROP of D_4 in THF solution at 25 °C, using NHC2 or NHC3 as catalyst, in the presence of methanol, *tert*-butyl alcohol, or benzyl alcohol as initiator. PDMS of relatively broad molar mass distribution (dispersity 1.58–1.70) was obtained (Table 5, entry 16), likely due to undesirable intra- (back-biting) and intermolecular transfer reactions. The authors also observed faster polymerization as the amount of NHC catalyst increased. This was attributed to the affinity of carbenes to the silicon atom and the propensity of Si to hypervalency,[78] favoring ring opening of D_4. Thus, either the AMM or the ACEM is plausible in these polymerizations, detailed mechanistic investigations being necessary.

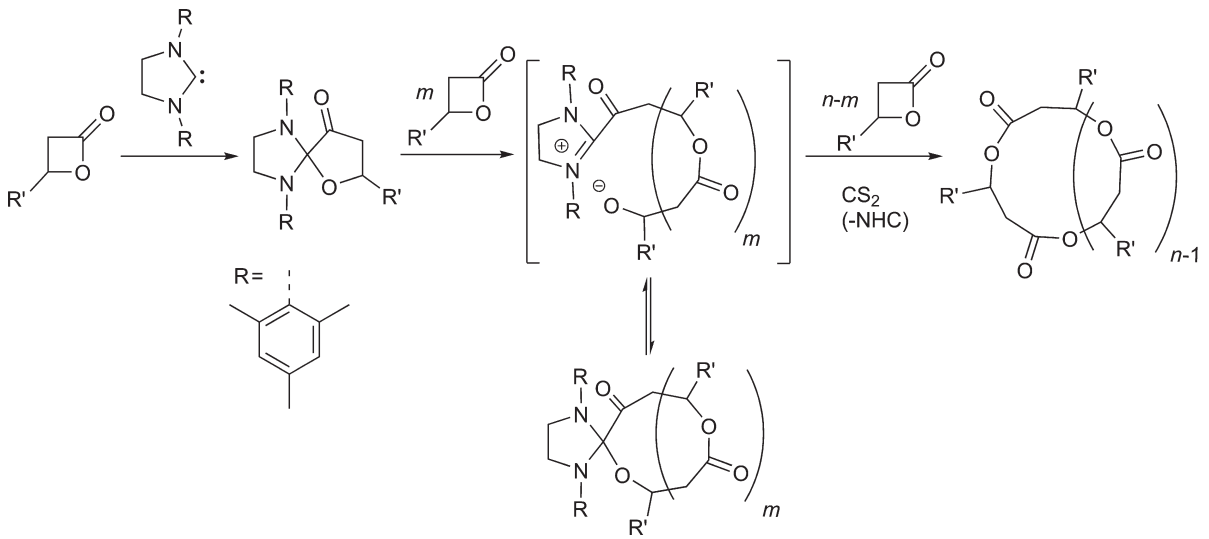

Scheme 39 Formation of a spirocycle from β-butyrolactone (R′= CH_3) and the saturated NHC 1,3-dimesitylimidazolin-2-ylidene (R = mesityl; NHC11).[145]

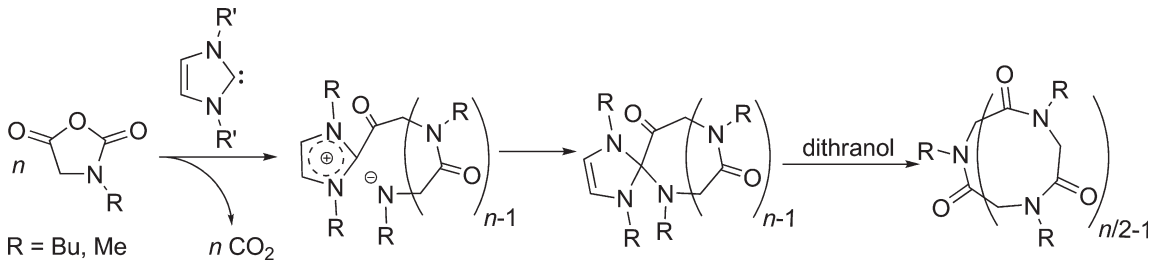

Scheme 40 NHC-catalyzed ROP of carboxylic anhydrides.[154]

The ROP of 2,2,5,5-tetramethyl-1-oxa-2,5-disilacyclopentane (TMOSC, Figure 2) catalyzed by the strongly basic NHC9 in the presence of the initiating alcohol was found to be very fast (99% conversion in 1 min, $k = 1.65\ s^{-1}$), forming poly(carbosiloxane) having a molar mass 10 200 g mol^{-1} and a dispersity equal to 1.19 (Table 5, entry 17).[100] The polymerization was slower with the NHC IMes (80% after 30 min, $k = 0.044\ s^{-1}$). An initiator (of the alcohol-type)/chain end (of the silanol-type) activation mechanism was proposed. However, activation of the silicon atoms of the monomer could be also envisaged in this case.

Raynaud *et al.*[155] reported that NHCs could directly open EO, a less polar monomer substrate than any of the aforementioned heterocycles. NHCs could serve not only as direct initiators (via a ZROP mechanism) but also as organocatalysts when used in conjunction with chain regulators of the NuE type, where Nu and E are the nucleophilic and electrophilic moieties, respectively (e.g., Nu = $PhCH_2O$, $HC{\equiv}CCH_2O$, and N_3 and E = H and $SiMe_3$). In both cases, linear α,ω-heterodifunctionalized PEOs could be synthesized (entries 18 and 19). For instance, 1,3-diisopropylimidazol-2-ylidene (NHC1) directly initiated the metal-free ROP of EO at 50 °C in DMSO, in the absence of any other reagents. In other words, the latter polymerization proceeded via ZROP. Without any other reagent added in the beginning, the PEO chain length was strictly controlled by the EO to the NHC molar ratio (typically, [EO]/[NHC] = 100/1). No competitive intra- or intermolecular transfer reactions are expected during anionic ROP of EO, the possible side reactions being transfer reactions to protic impurities or cyclization of the growing zwitterionic PEO chains. The resulting polymer, namely 1,3-diisopropylimidazol-2-ylidinium alkoxide, was quenched on the completion of ZROP by the NuE functionalizing terminator, leading exclusively to linear α-Nu,ω-OH (or α-Nu,ω-$OSiMe_3$)-difunctionalized PEOs, unlike the zwitterionic polymerization of LA described above. The quantitative introduction of the Nu moiety in α-position and of OH (or $OSiMe_3$) in ω-position of PEO chains occurred through the nucleophilic substitution of the imidazolium moiety by $Nu^{\delta-}$ and the concomitant reaction of the ω-growing alkoxide of PEO chain with $H^{\delta+}$ (or $Me_3Si^{\delta+}$), as illustrated in Scheme 41. In particular, difunctionalized α,ω-dihydroxy-telechelic, α-benzyl, ω-hydroxy, and α-azido, ω-hydroxy-PEOs were synthesized by NHC-initiated ZROP, using H_2O, $PhCH_2OH$, and N_3SiMe_3 as terminating agents. A well-defined PEO-*b*-PCL diblock copolymer could also be directly synthesized by sequential ZROP in DMSO, using the same NHC as organic initiator, without isolation of the zwitterionic PEO block intermediate.

Instead of using NHCs as direct initiators, the same group also reported the ROP of EO with NHCs as real organocatalysts (instead of initiators), in conjunction with not only alcohol but also trimethylsilylated initiators (the same NuE-type compounds mentioned above) introduced at the beginning.[156] Typical amounts of NHC catalyst equal to 10 mol.% relative to NuE were employed in this case, leading to PEOs with molar masses in the range 1800–10 500 g mol^{-1} and dispersities lower than 1.15.

Similarly to ROP of cyclic esters, two distinct mechanisms of initiation and chain growth were proposed (Scheme 42). NHCs might be nucleophilic and silicophilic enough to activate the electrophilic part (E = H or $SiMe_3$) of NuE chain regulators. Thus, both trimethylsilylated and hydroxylated chain regulators can be activated by NHCs, followed by monomer insertion (ACEM, path B). However, a nucleophilic attack by the NHC catalyst on the monomer is also plausible (AMM, path A). Protonation (or silylation) of the zwitterionic intermediate species by an alcohol (or a silyl ether), followed by addition of the resulting

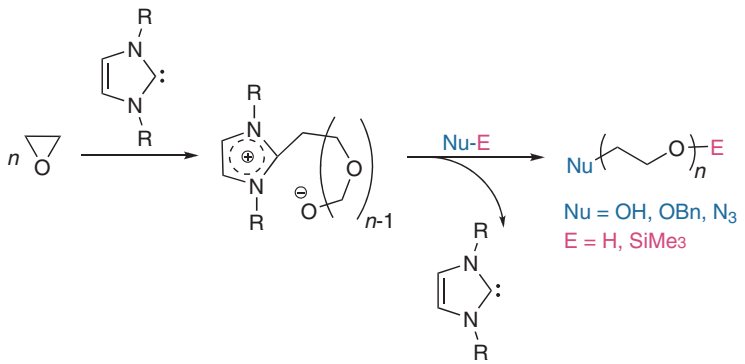

Scheme 41 Functionalizing terminators in the ZROP of EO.[155]

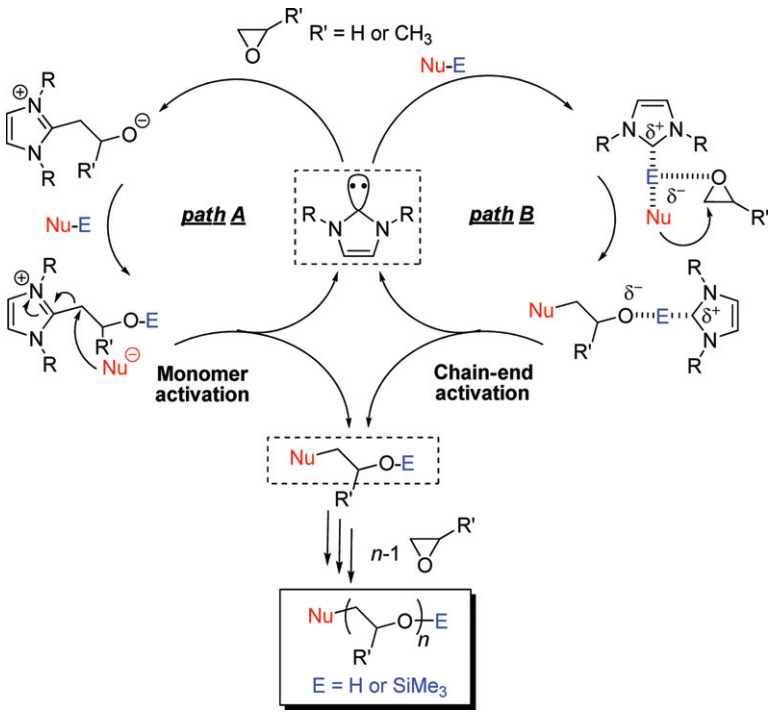

Scheme 42 AMM (path A) and ACEM (path B) in ROP of EO (R′ = H) and PO (R′ = CH_3) catalyzed by NHCs.[155,156]

alkoxide on the activated azolium, generates a new alcohol (or silyl ether) with an incorporated monomer unit. In the meantime, the NHC catalyst is released and can activate another EO molecule. The monoadduct, Nu-CH_2CH_2O-E, can serve for subsequent chain propagation. At this stage of their investigations, the authors acknowledged that it was unclear whether the NHC directly attacks the monomer, forming a zwitterionic intermediate, or activates the E moiety of the chain regulator, then the ω-OE moiety of the PEO chain. The fact that Tris(dimethylamino)sulfonium difluorotrimethylsilicate ($TASF_2SiMe_3$) did not yield any polymer in the presence of an *O*-TMS reagent might favor the AMM, as it was expected that this catalyst could generate benzylic alkoxide to initiate the ROP of EO by activation of the initiator. However, no polymer was formed under these conditions. Likewise, when used with EO in the absence of any other reagent, no PEO was obtained, $TASF_2SiMe_3$ being a too weak nucleophile to directly attack EO.

In a subsequent contribution, the same group applied the two methods discussed above, that is, with NHCs employed either as direct initiator in ZROP or as true organocatalyst in the presence of the aforementioned NuE-type reagents to the ROP of PO.[157] Both methods allowed the authors to derive α,ω-difunctionalized PPOs using NHC1 under metal-free and solvent-free conditions, whereas PPO is generally obtained by anionic ROP in low polar media from alkali metal-based initiators.[27] When NHC was used as a direct organic initiator, the polymerization was simply quenched by H_2O, leading to dihydroxytelechelic PPOs with molar masses up to 4500 g mol^{-1} (**Table 5**, entry 20). Targeting PPO of higher molar masses, however, showed the presence of a small extent of allyl-ended PPO chains, as observed by ^{1}H NMR, which was characteristic of the occurrence of the chain transfer to monomer of active PPO chains. With NHC as catalyst and the hydroxylated or trimethylsilylated reagents as initiators, the ROP of PO at 50 °C permitted the synthesis of PPOs of molar masses up to 8000 g mol^{-1} with a dispersity lower than 1.18. Both routes implied PO polymerization in bulk and incomplete monomer conversion (≤ 40% in all experiments), allowing an easy removal – and possible recycling – of the residual low-boiling monomer by simple evaporation.

Although focusing mainly on organocatalyzed ROP, this chapter underscores that organocatalysis has much broader scope and has been used in other chain polymerizations. For instance, Scholten *et al.*[130] on the one hand and Raynaud *et al.*,[131] on the other hand, reported that the GTP of (meth) acrylic monomers can advantageously be catalyzed by NHCs. GTP was proposed in the mid-1980s as a convenient method to control the polymerization of (meth)acrylic monomers at ambient temperature and above.[165] It is based on the repetition of Mukaiyama–Michael reactions[166] involving the addition of silyl ketene acetal (SKA) onto an incoming (meth)acrylic monomer. GTP is generally catalyzed by a metal-free nucleophile (Lewis base) or a metal-based Lewis acid, for methacrylic or acrylic monomers, respectively.[167] The absence of a unique catalytic system that could be generalized for both families of monomers did not permit, however, the synthesis of block copolymers featuring both monomer units by sequential GTP.[168] However, new developments in GTP via an organocatalysis pathway have been recently disclosed.

Webster[168] originally suggested the name 'group transfer polymerization' to account for the fact that the trimethylsilyl group remained at the end of the 'chain it created with throughout polymerization'. In other words, an associative (concerted) mechanism of GTP involving the transfer of the trialkylsilyl group from the polymer chain end to the inserted monomer was originally put forward. However, this pathway was further

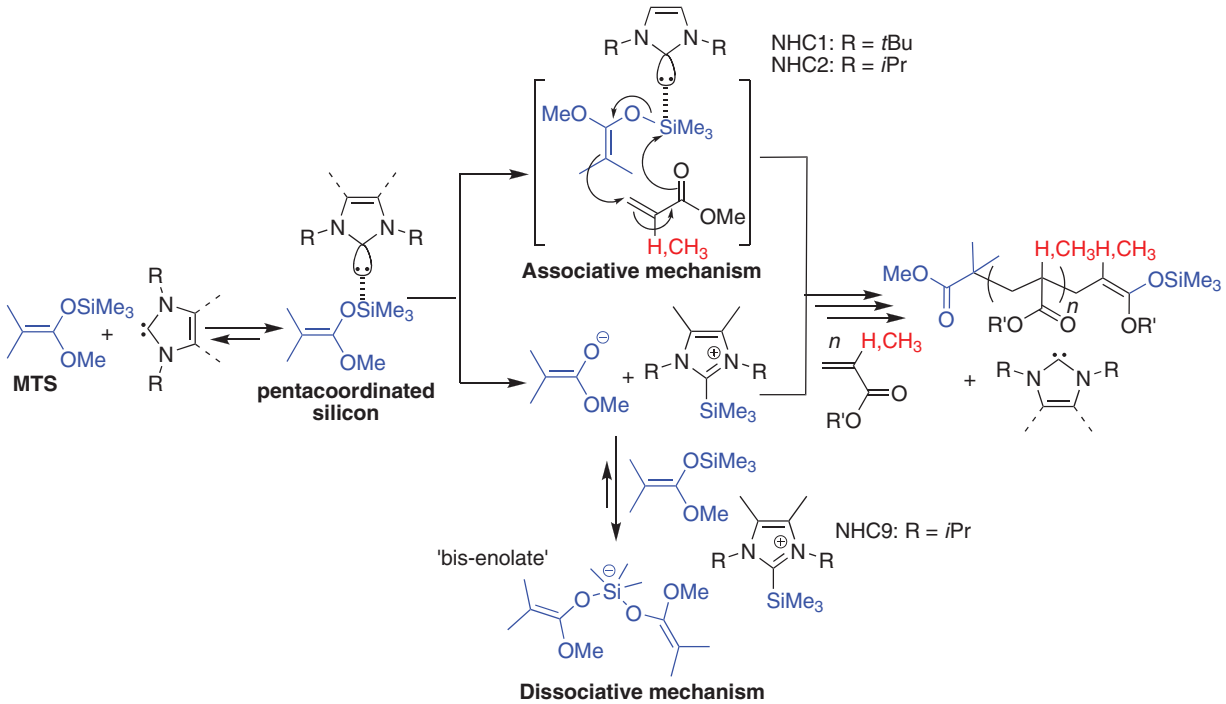

Scheme 43 Associative and dissociative mechanisms for NHC-mediated GTP.[130,132]

questioned. In particular, Quirk proposed that GTP occurred by a dissociative mechanism through minute amounts of propagating enolates.[169] These anionic species would be the real active centers and be temporarily trapped by the SKAs, forming dormant trimethylsilyl bis-enolates (Scheme 43). In fact, the mechanism of GTP seems to strongly depend on the overall polymerization conditions and, in particular, on the nature of the catalyst.[170] NHCs were themselves reported to induce either the dissociative or the associative mechanism, depending upon the one used (Scheme 43).

While Scholten *et al.*[130] postulated a dissociative mechanism forming enolate-type species using NHC9 as catalyst, Raynaud *et al.*[132] provided a series of experimental evidences suggesting that GTP occurred by an associative (concerted) mechanism, when catalyzed by NHC1 or NHC2 (Scheme 43). This difference was explained by the varying nucleophilicity/silicophilicity of the different NHCs used. NHC9 is indeed slightly more nucleophilic than NHC1 and NHC2. Though the two mechanisms lead to the same polymer, the polymerization kinetics and the properties of the final polymers associated with each of them are yet different.[167,170] These NHC-catalyzed GTPs were further applied to the synthesis of all-acrylic block copolymers.[133]

The NHC-catalyzed GTP of (meth)acrylic monomers was typically performed at room temperature, using 1-methoxy-2-methyl-1-[(trimethylsilyl)oxy]prop-1-ene (MTS) as initiator, in polar (THF) or nonpolar (toluene) medium. In this way, polymethacrylates and polyacrylates with molar masses in the range 10 000–300 000 g mol^{-1}, corresponding to the initial [monomer]/[MTS] ratio and with dispersities lower than 1.2, were obtained in quantitative yields. Several features were observed with NHC1 and NHC2 as GTP catalysts, supporting the existence of the associative mechanism involving the formation of hypervalent siliconate intermediates:

- Though the first-order kinetic plot $\ln[M]_0/[M]$ versus time deviated from linearity at high monomer conversions, no inhibition period was noted at low monomer conversion. Moreover, the polymerization rate dramatically increased as the concentration of initiator increased, with first-order kinetic dependence of the initiator.
- When mixed in 1:1 molar ratio, MTS and NHC1 did not reveal the formation of enolate-type species by ^{29}Si or ^{13}C NMR spectroscopy.
- The production of well-defined poly(methyl methacrylate)s (PMMAs) using the 1:1 adducts of NHC1 and MTS as initiating system.
- The controlled polymerization of butyl and *tert*-butyl acrylates in the presence of NHC1 or NHC2, suggesting that back-biting and internal isomerization could be minimized, presumably because no enolates were generated.
- The preparation of block copolymers based on acrylate-type and methacrylate-type monomer units, irrespective of the order of addition of the two monomers, which would not be possible from pure enolates formed by a dissociative mechanism.

It is very likely, however, that the more slightly nucleophilic NHC9 used by Scholten *et al.*[130] brought about the GTP of (meth)acrylics via a dissociative pathway.

In a subsequent contribution, Raynaud *et al.*[133] exploited the potential of NHC1 and NHC2 to catalyze the MTS-initiated GTP of a variety of monomers in THF or toluene at room temperature. Monomers include not only acrylics (i.e., butyl acrylate, *tert*-butyl acrylate, and 2-(dimethylamino)ethyl acrylate) and methacrylics (methyl methacrylate (MMA) and 2-(dimethylamino)ethyl methacrylate), but also an

acrylamide-type monomer, namely, *N*,*N*-dimethylacrylamide. The NHC-catalyzed MTS-initiated GTP of methacrylonitrile using DMF as solvent was also reported for the first time. Like in the case of MMA, the GTP of *tert*-butyl acrylate showed a first-order kinetics and a direct dependence of the rate of polymerization on the concentration in MTS, again suggesting the occurrence of the associative mechanism.

4.06.9 Polymerization Catalyzed by Weak, Strong, and 'Super Strong' Bronsted Acids

Cationic ROP of cyclic ethers occurring in the ACEM consists, first, in the protonation of the monomer oxygen generating a secondary oxonium ion, followed by ring opening of the latter species by the oxygen atom of another cyclic ether molecule (Figure 8). The resulting tertiary oxonium ion propagates the polymerization by successive ring opening by the incoming monomer (Scheme 44).

Chain transfer to polymer, either by intramolecular (back-biting) or intermolecular reaction, characterizes many cationic ROPs.[27,91,92] This is due to the nucleophilicity of heteroatoms along the polymer backbone which compete with that of the monomer (Scheme 45). For instance, 1,4-dioxane is predominantly formed as the cyclic dimer in the cationic ROP of EO. Cyclic trimers or tetramers are also generated by cationic ROP of PO or epichlorohydrin. Under optimal conditions, the cationic ROP of THF can proceed, however, in a 'controlled/living' manner,[195,196] because the rates of back-biting and intermolecular transfer are slow relative to the rate of propagation.

In the late 1980s, Penczek *et al.*[27,91,92] unveiled AMM and applied it to the cationic ROP of oxiranes. These early works utilizing acid catalysts such as BF_3 or HPF_6 paved the way for precision polymer synthesis of a metal-free approach. This

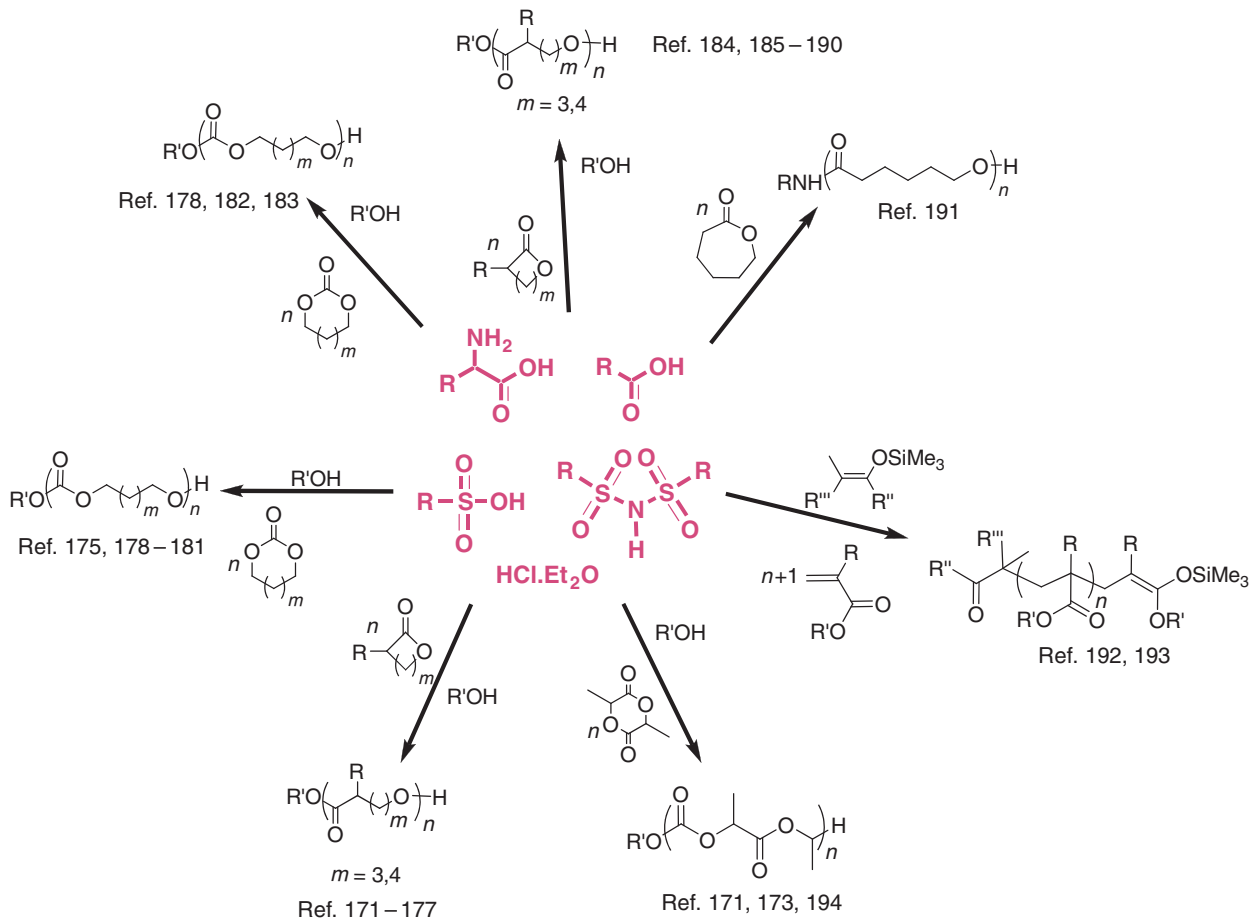

Figure 8 Overview of polymers obtained from acids as catalysts.

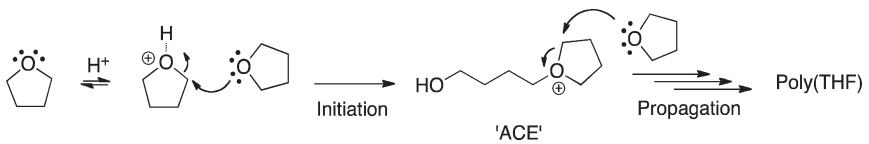

Scheme 44 Cationic ROP of THF initiated by acids.

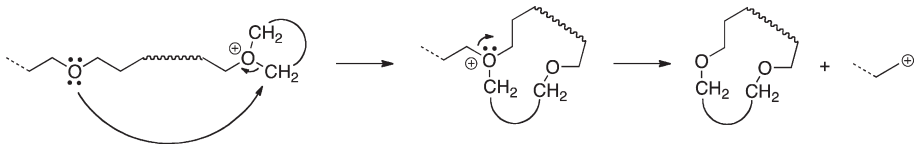

Scheme 45 Intramolecular side reactions in cationic ROPs of cyclic ethers.

could be achieved using a protic reagent (typically ROH) and a catalytic amount of strong acid, while maintaining a low instantaneous concentration of monomer (by its continuous slow addition). The amount of cyclic oligomers can indeed be reduced thanks to the presence of the alcohol, playing the role of a chain transfer agent/initiator, which controls the polymer chain length.[27,91,92] The AMM involves, in this case, oxonium-type active centers that are located on the monomer, whereas the polymer chain exists in a (neutral) dormant form with a terminal OH-functionality (see **Scheme 4**). Under such conditions, back-biting is minimized, allowing for the synthesis of well-defined polyethers, including telechelics and macromonomers derived from ethylene and POs, epichlorohydrin and glycidol, and cyclic acetals. However, a relatively limited molar mass could be achieved by this synthetic strategy.

To favor AMM over ACEM, a slow monomer addition process is beneficial as the instantaneous concentration of monomer is kept low. In the ideal case where the ACEM is totally suppressed, the molar mass of the final polymer is controlled by the initial [ROH]/[monomer] ratio and a linear relationship is observed between M_n and [ROH]/[monomer]. However, exclusive AMM is rarely observed.

In recent years, a few groups revisited such Bronsted acid-mediated ROP which was applied to heterocycles other than cyclic ethers. In particular, organic acid catalysts were employed, mainly to polymerize cyclic esters. A better insight into the influence of the catalyst on the kinetics of the reaction was gained through a combination of experimental and theoretical studies. It turns out that the catalyst efficiency does not simply correlate with its acidity, suggesting a more complicated situation. Nevertheless, and for the sake of clarity, Bronsted organocatalysts will be divided into three subgroups in the following sections according to their acidity, that is, according to the nature of the acid group: sulfonic (RSO_3H), sulfonimide $(RSO_2)_2NH$, and carboxylic acids (RCOOH). Although HCl is not an organic catalyst, this metal-free polymerization system nonetheless shares common features with Bronsted organocatalysts, and so it may be included in this section for comparison.

4.06.9.1 Sulfonic Acid-Mediated ROP

In the past 10 years, efforts were devoted to the controlled polymerization of not only lactones such as δ-VL, ε-CL, and LA but also cyclic carbonates, using strong sulfonic acid catalysts, in the presence of an alcohol initiator.

Both methanesulfonic acid (MSA) and HOTf permitted a 'controlled/living' ROP of ε-CL, at 30 °C, in the presence of primary or secondary alcohol as initiators (entries 1 and 2, **Table 6**).[171,172] Polymerizations proceeded within hours for a typical [ROH]/[cat] ratio comprised between 0.5 and 1. The activity of MSA was similar to that of TfOH, despite a difference in pK_a of more than 10 units (MSA: $H_0 = -1$; TfOH: $H_0 = -14$; H_0: Hammett acidity). For comparison, HCl proved far less active than the two sulfonic acids, in spite of its intermediate acidity ($H_0 = -8$). A faster reaction was observed in toluene than in chlorinated solvents, which was thought to result from a slightly tighter interaction between the acid catalyst and the monomer in a less polar solvent. With both acids, the experimental M_n values varied linearly with the monomer-to-initiator ratio and agreed well with those calculated from the monomer feed. Molar masses up to 11 000 g mol^{-1}, narrow distribution ($1.07 < M_w/M_n < 1.21$), and reliability of the end-group presence were reported. The controlled character of the MSA- and TfOH-catalyzed polymerizations was further supported by chain extension experiments; expected M_n and narrow dispersity M_w/M_n were obtained. Interestingly, increasing the concentration of MSA induced faster polymerization, while a higher concentration of TfOH slowed down the reaction. It was proposed that the difference in behavior between the two acids could result from the competition between the activation of the monomer and the deactivation of the initiating/propagating alcohol (**Scheme 46**).

The stronger TfOH acid would deactivate the alcohol, while MSA would lead to more efficient monomer activation. ROP of ε-CL, catalyzed by sulfonic acid, was investigated by density functional theory (DFT), using a model reaction involving the nucleophilic addition of MeOH to ε-CL, followed by ring opening.[197] For both elementary steps, the sulfonic acid was actually predicted to behave as a bifunctional catalyst, operating as a proton shuttle via its acid hydrogen atom and basic oxygen atoms. The computed activation barriers were consistent with the relatively fast polymerizations observed experimentally at room temperature.

Other sulfonic acids such as p-toluenesulfonic acid (PTSA), 1,1,2,2,3,3,4,4,4-nonafluoro-1-butanesulfonic acid (NfOH), and 1,1,2,2,3,3,4,4,5,5,6,6,7,7,8,8,8-heptadecafluoro-1-octanesulfonic acid (PfOH), whose Hammett acidity ranged from −2.3 to −12.3, also proved efficient catalysts for the ROP of ε-CL. Although the control and livingness of the polymerization were not investigated, low catalyst loading (0.1 mol.% relative to the initiator) led to complete monomer conversion within 3–5 h at 50 °C in toluene (**Table 6**, entry 3).[174]

Controlled polymerization of LA catalyzed by TfOH, in the presence of an alcohol initiator (ROH), was also described by Bourissou *et al.*[194] and Baśko and Kubisa.[171] The solvent for polymerization was somewhat restricted to dichloromethane, toluene being a poor solvent of PLA and THF being polymerized by TfOH.[194] In dichloromethane, polymerization proceeded at 25–35 °C within hours for a typical [ROH]/[cat] between 0.5 and 1, with various initiators, including H_2O, *i*-PrOH, PrOH, and pentan-1-ol (entries 7 and 8). Other catalysts such as CF_3COOH and HCl in the presence of *i*-PrOH were found completely ineffective for LA polymerization, under identical conditions. LA was thus found much less

Table 6 Representative examples of the ROP catalyzed by weak, strong, and 'super strong' Bronsted acids

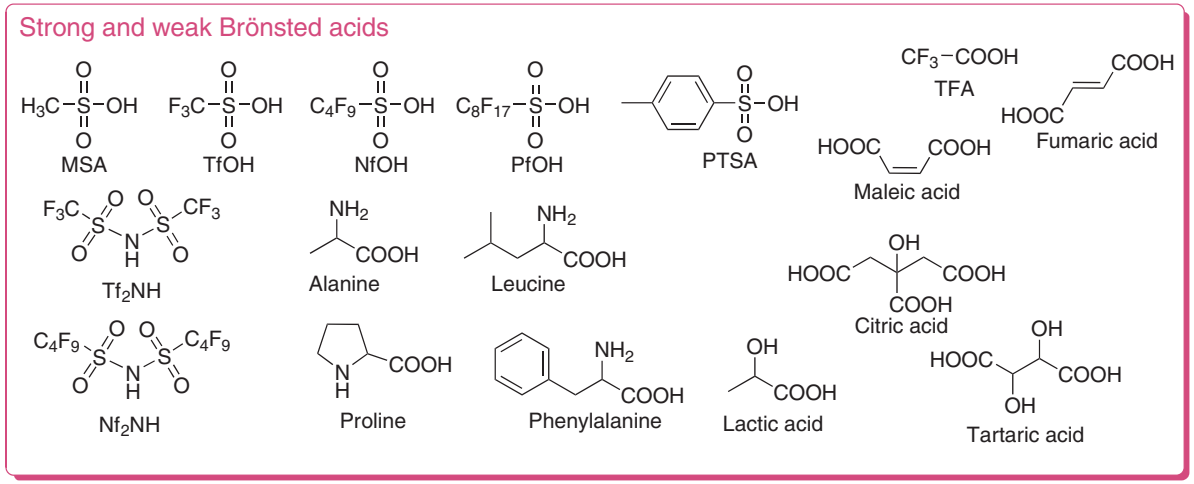

Entry	*Catalyst*	*Monomer*	*Bulk/solvent*	*Initiator*	*[C]/[I]$_0$*	*t*	*T (°C)*	*Conv (%)*	*M_n (g mol^{-1})*	*I_p*	*References*
1	TfOH, MSA	ε-CL	Dichloromethane, toluene	Prim. and sec. alcohols	1–3	12–140 min	30	> 98	1 200–10 000	1.07–1.21	172
2	TfOH	ε-CL	Dichloromethane	*i*-PrOH, ethylene glycol	0.4		35	> 95	3 500 (^{1}H NMR)	1.05	171, 173
3	PTSA, TfOH, NfOH, PfOH	ε-CL	Toluene	EtOH	0.001	3–18 h	25–50	90–> 99	4 800–6 900 (SEC, PS, $CHCl_3$)/ 2 400–3 200 (^{1}H NMR)	1.16–1.45	174
4	HCl/Et_2O	ε-CL	Dichloromethane	BuOH	1–10	24 h	25	> 94	2 600–14 000	< 1.17	175
5	HCl/Et_2O	δ-VL	Dichloromethane	BuOH	1.5	0.5 h	–40 or 25	77–86	2 400–3 700	< 1.27	175
6	HCl/Et_2O	δ-VL	Dichloromethane	Prim. alcohols	3	1.5–14.5 h	0	65–98	5 000–50 000	1.02–1.15	176
7	TfOH	Lactide	Dichloromethane	H_2O/*i*-PrOH/pentan-1-ol	1	150–1680 min	25	> 96	1 700–16 000	< 1.48	194
8	TfOH	Lactide	Dichloromethane	*i*-PrOH, ethylene glycol	0.4		35	> 95	1 800–1 900 (^{1}H NMR)	1.38	171, 173
9	HCl/Et_2O	7CC	Dichloromethane	BuOH, H_2O	1.5	4–24 h	25	95–99	1 900–12 400	1.12–1.23	175, 178, 179
10	MSA	5,5-Dimethyl-1,3-dioxane-2-one	Toluene	BuOH	0.5	3–10 h	50	> 96	2 300–9 300	1.13–1.24	180
11	TfOH, MSA	TMC	Toluene	H_2O/pentan-1-ol	1–6	0.75–3.5 h	30/80	> 96	1 100–8 600	1.08–5.31	181
12	Tf_2NH	δ-VL	Dichloromethane	$Ph(CH_2)_3OH$	0.1	2–48 h	27	77–85	4 200–12 700	< 1.16	177
13	Tf_2NH, Nf_2NH	ε-CL	Toluene, chloroform	EtOH	0.001	1.5–30 h	25–50	> 99		1.10–1.48	174

									5 000–13 500 (SEC, PS, $CHCl_3$)/2 000–6 400 (^{1}H NMR)		
14	Amino acids, α-hydroxy acids, carboxylic acids	ε-CL	Bulk	BnOH	10/3	2–7 h	120	< 5–> 95	450–2 700	< 1.3	184
15		ε-CL	Bulk	Amino acids[a]	0.5–3.3% to M	24–48 h	160	> 96	3 600–26 800	1.5–1.86	191
16	L-lactic acid	ε-CL	Bulk	$R(OH)_6$	0.1	1 h	120	100	12 400	1.48	185
17	L-lactic acid	ε-CL	Bulk	Saccharides	1–4	1.5–21 h	120	100	1 600–6 500	< 1.5	186
18	$HCl.Et_2O$, CF_3COOH, CCl_3COOH, maleic acid, fumaric acid	ε-CL	THF,	dichloromethane, bulk	1,1,1-Tris			(hydroxymethyl) propane, pentaerythritol	6–20	6–75	20–90
	35–95	4 800–15 800	1.06–1.98	187							
19	Oxalic, succinic, fumaric acids	ε-CL	Bulk	*threo*-9,10-Dihydroxyoctadecanoic acid	1–10	24 h	70–150	28–97	7 500–15 200	1.11–1.48	188
20	DL-lactic acid	ε-CL	Bulk	Macroalcohol (M_n = 2 770)	0.1–1	1.5–24 h	140	44–79	2 900–13 030 M_n of the diblock copolymer	1.54–2.74	189
21	Tartaric acid	δ-VL	Bulk	BnOH	10/3	7 h	120	> 95	M_w = 2 608 Da		184
22	Fumaric acid	δ-VL	Bulk	Dipentaerythritol	6–10	18 h	100	96	6 150–99 100	1.07–1.36	190
23	TFA	6CC, 7CC	Dichloromethane, toluene	H_2O, prim. alcohols	0.5	24–30 h	0 or 50	77–98	2 500–6 800	1.16–1.24	178, 182
24	Fumaric acid	BTMC	Bulk	Macrodiols	0.02 wt.%	24 h	150	41–91 yield of A-B-A triblock copolymer	8 200–27 200 M_n of the A-B-A triblock copolymer	1.54–1.86	183

[a]Initiation by $–NH_2$ group.

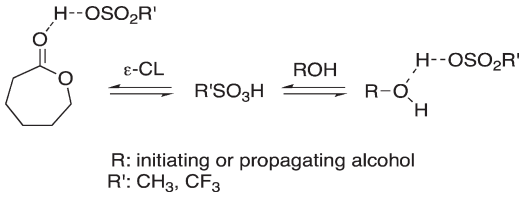

Scheme 46 Competitive monomer activation and alcohol deactivation.[171,172]

reactive than ε-CL or δ-VL, in sharp contrast to the situation prevailing with Bronsted bases (see previous sections); both ε-CL and δ-VL could indeed be polymerized with HCl at room temperature.[175,176] PLAs with molar masses ranging from 1500 to 20 000 g mol^{-1} and relatively low dispersity ($1.13 < D < 1.50$) were obtained. The controlled character of these polymerizations was demonstrated by the linear evolution of experimental M_n values with the monomer conversion. This was supported by a second feed experiment, a quantitative reinitiation of chain ends being observed. Both ^{1}H NMR and mass spectra analyses evidenced quantitative initiation of the polymerization by the alcohol, without a trace of adverse transesterification reactions up to 93–96% conversion. However, prolonged reaction times caused the formation of odd and even numbers of lactate units, as seen by MALDI-TOF MS, owing to the occurrence of transesterification.[171]

Investigations into the kinetics of polymerization revealed a first-order kinetics dependence on LA concentration, with a k_{obs} of 6.8×10^{-3} min^{-1} at room temperature, which was comparable with the activity of DMAP, although a temperature of 35 °C and longer reaction times were required.[24]

From a mechanistic viewpoint, protonation of LA and its subsequent ring opening by the alcohol initiator or the growing polymer chain were shown to occur selectively. The chain growth involved an acyl cleavage of LA rather than alkyl cleavage, as could be deduced from the presence of isopropyl ester chain ends in the NMR spectra of the resulting PLAs (Scheme 47).

No configuration change on the chiral carbon atom was observed during the L-LA polymerization in dichloromethane at room temperature, a perfectly isotactic PLA being obtained.

Baśko and Kubisa[171,173] studied the copolymerization of ε-CL and L-LA catalyzed by TfOH in dichloromethane at 35 °C, in the presence of an alcohol initiator such as PrOH or ethylene glycol. L-LA was preferentially incorporated into the copolymer, despite its slower rate of homopolymerization (relative to that of ε-CL), a situation reminiscent of that observed for the homo- and copolymerization of LA and ε-CL by anionic or coordination mechanism.[198,199] This apparent discrepancy was explained by the twice higher probability of protonation of LA which contains two ester groups compared with ε-CL. Analysis by ^{13}C NMR of the copolymer microstructure was found to depend on the alcohol initiator (PrOH vs. ethylene glycol), on the LA to ε-CL ratio and the conversion. Thus the microstructure of the copolymer might be governed either by the relative reactivity of the comonomers[171] or by transesterification, regardless of the kinetics of comonomer incorporation.[173]

Shibasaki *et al.*[179] reported, in 1999, the use of HCl/H_2O as initiating system for the cationic ROP of 1,3-dioxepan-2-one (7CC) following an AMM (Table 6, entry 9). Polycarbonates with M_n ranging from 3000 to 12 400 g mol^{-1} and low dispersity (1.15–1.23) could be quantitatively obtained by ROP of 7CC in dichloromethane at room temperature. M_n values could be controlled by the initial amount of water; they were found to increase linearly with monomer conversion, regardless of the initial [M]/[I] ratio. According to NMR spectroscopy, no decarboxylation was noted under these conditions, a side reaction commonly observed during cationic ROP of cyclic carbonates.[200]

At the same time, Nakano[180] reported the organocatalytic ROP of a six-membered cyclic carbonate, namely 5,5-dimethyl-1,3-dioxan-2-one, catalyzed by MSA in the presence of BuOH as initiator (entry 10). Polymerization proceeded homogeneously at 50 °C in toluene within 3–10 h, yielding polycarbonates with M_n ranging from 2300 to 9300 g mol^{-1} and a relatively narrow dispersity (1.13–1.24). However, GPC profiles proved unimodal only for [M]/[I] < 20 but bimodality was observed for the ratios higher than 30. Although some polymer chains were effectively initiated by BuOH, according to ^{1}H NMR spectroscopy, side reactions such as back-biting occurred to a significant extent.

In 2010, Delcroix *et al.*[181] revisited the ROP of cyclic carbonates catalyzed by sulfonic acids and investigated the scope and limitations of such an organocatalysis (Table 6, entry 11). Both MSA and TfOH were employed and compared, for the ROP of TMC, with water or pentan-1-ol as protic initiators. In contrast to TfOH, MSA yielded a PTMC free of ether linkage, even under forcing conditions. Increasing the catalyst concentration induced a faster polymerization in the case of MSA, while the

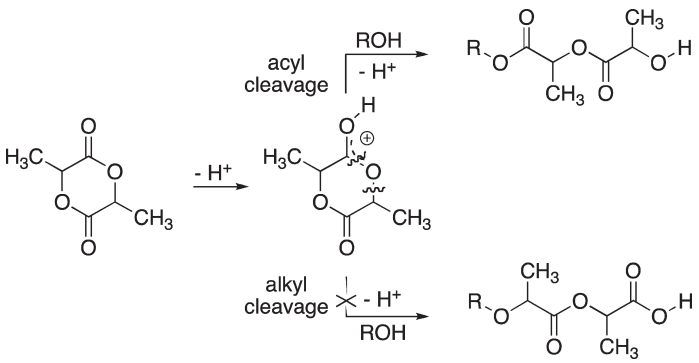

Scheme 47 ROP of LA in the presence of sulfonic acid.

kinetics slowed down with TfOH, in line with the observations made for the ROP of ε-CL. In the case of the MSA-catalyzed pentan-1-ol-initiated ROP of TMC, the molar mass of PTMC was only controlled for [M]/[I] < 20. For higher ratios, lower M_n experimental values were obtained, owing to the occurrence of competitive AMM and ACEM. Importantly, no cyclic structures could be identified, suggesting the absence of back-biting reactions. It is noteworthy that such a competition between the AMM and the ACEM is unprecedented for the polymerization of carbonyl-containing monomers by strong Bronsted acids, but is similar to that observed during the ROP of cyclic ethers.[27,91,92] By analogy with the aforementioned works by Penczek with oxiranes, ACEM could be minimized, by decreasing the instantaneous concentration of TMC, using multifeed experiments or a continuous slow monomer addition. Controlled M_n values up to 4000 g mol^{-1} were obtained with the multifeed approach, while M_n values up to 9000 g mol^{-1} were reached with the continuous addition of the monomer. In the latter case, SEC analysis revealed a unimodal but slightly asymmetric distribution of molar masses, due to a small contamination of polycarbonate chains grown by the ACEM, besides the main population of chains derived from AMM. Under these optimized conditions, the molar mass of PTMC increased linearly with monomer conversion.

4.06.9.2 Sulfonimide-Based Catalysts for ROP

Introduction of these organocatalysts in polymer chemistry was reported by Kakuchi *et al.*[192] in 2009 who reported the GTP of (meth)acrylic monomers (see below). Bis(perfluoroalkanesulfonyl)imides such as Tf_2NH and Nf_2NH were also found particularly active in the Bronsted acid-catalyzed ROP of δ-VL and ε-CL.[174,177]

PVL with molar mass up to 9400 g mol^{-1} (reaction time: 9 h) and low dispersity (M_w/M_n = 1.09) could be obtained in dichloromethane at 27 °C, with a catalyst loading of 0.1 mol.% (relative to the initiator) and 3-phenylpropan-1-ol as initiator (**Table 6**, entry 12).[177] The controlled nature of the polymerization was demonstrated: the M_w/M_n remained low (1.09–1.16), molar masses increased linearly with increasing the initial [M]/[I] ratios, and a chain extension experiment was successfully performed. In addition, PVL featuring functionalized chain ends could be prepared using a heterodifunctional alcohol initiator, incorporating an azido, pentafluorophenyl, or maleimido group.

In 2011, Oshimura *et al.*[174] reported that Tf_2NH and Nf_2NH efficiently catalyzed the ROP of ε-CL (entry 13). PCL with M_n ranging from 2000 to 6400 g mol^{-1} and relatively narrow dispersities (1.10–1.48) was synthesized in toluene, using a low catalyst loading (0.1 mol.% relative to the initiator). Quantitative monomer conversion could be obtained in 8–10 h at 25 °C, while the reaction time could be shortened to 2.5–3 h by increasing the temperature to 50 °C. When THF was used as solvent, its incorporation into PCL was observed, by analogy with the ability of TfOH to initiate THF polymerization. Although a postpolymerization experiment was performed, no evidence of the controlled/living character of the polymerization was provided. Interestingly, Nf_2NH could be recycled for a subsequent polymerization by simple extraction of the reaction mixture with water. Several reaction parameters such as rate constants, activation energies, enthalpy of activation, entropy, and Gibbs energy for the ROP of ε-CL were determined, but no clear relationship between the catalyst acidity and rate of polymerization, on the one hand, and the solvent polarity and rate of polymerization, on the other hand, was established.

The group of Kakuchi applied the organocatalysis based on Tf_2NH to the GTP of (meth)acrylate derivatives such as MMA[192] and *N*,*N*′-dimethylmethacrylamide (DMA)[193] (**Scheme 48**; see also Section 4.06.8 for a general discussion about GTP and recent developments employing NHCs as catalysts).

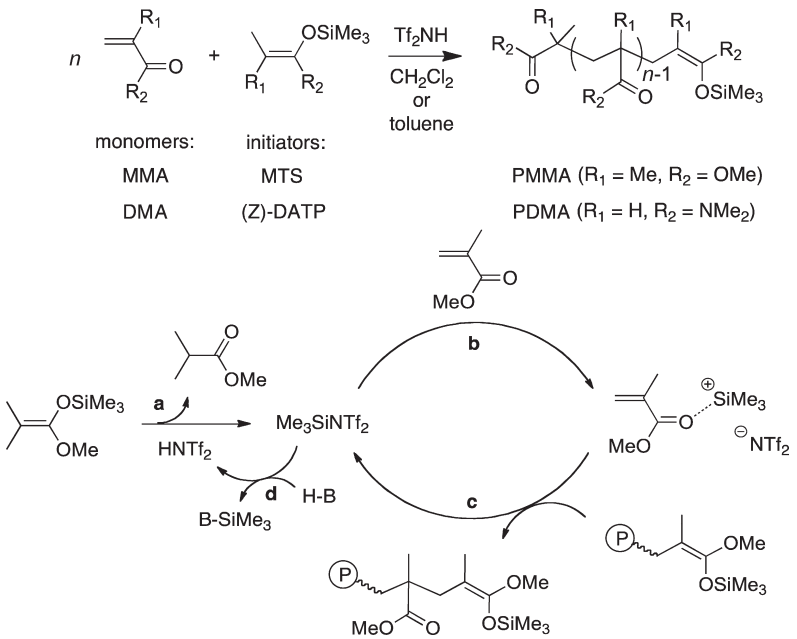

Scheme 48 GTP of (meth)acrylics using $HNTf_2$ (MTS: $R_1 = CH_3$, $R_2 = OCH_3$; (Z)-DATP: $R_1 = H$, $R_2 = NMe_2$).[192,193]

In contrast to traditional metal-based Lewis acid-mediated GTP,[170] only 5 mol.% of $HNTf_2$ (relative to the initiator) was required for quantitative monomer conversion to be reached. PMMA with M_n up to 17 000 g mol^{-1} and low dispersity ($M_w/M_n = 1.04–1.08$) could be obtained in dichloromethane solution with MTS as initiator, in 24 h at 27 °C. Polymers with M_n values ranging from 6000 to 54 000 g mol^{-1} in dichloromethane solution and dispersity from 1.06 to 1.20 were synthesized by GTP of DMA in toluene solution, at 0 °C, within 3–9 h. In the latter case, (*Z*)-1-(dimethylamino)-1-trimethylsiloxy-1-propene, (*Z*)-DATP, was found more appropriate as initiator than MTS (**Scheme 48**). The controlled character of the GTP of both MMA and DMA was evidenced through (1) the increase in molar mass with increasing the [MMA]/[MTS] ratio, (2) the increase in molar mass with increasing monomer conversion, (3) the reliability of the presence of end groups, and (4) postpolymerization experiments. From a mechanistic viewpoint, the polymerization presumably proceeded in a similar way as the Mukaiyama aldol molecular reaction catalyzed by strong Bronsted acids, as described by the groups of Yamamoto and List[82–84,201] First, $HNTf_2$ reacts with the initiator to generate the actual catalytically active species Me_3SiNTf_2 (step a, **Scheme 48**). Coordination of Me_3SiNTf_2 to MMA increases the electrophilicity of the monomer (step b), which can thus undergo nucleophilic addition of the propagating SKA chain end (step c). This results in the formation of PMMA containing $(n + 1)$ units while the catalyst is regenerated. Note that this Tf_2NH-mediated reaction is also characterized by a 'self-repair' mechanism (step d), which further consumes MTS to regenerate Me_3SiNTf_2 due to the presence of a very low amount of impurities (BH). This mechanism was consistent with the slightly higher molar mass observed for PMMA synthesized by the Tf_2NH-catalyzed GTP of MMA. These results contrasted with those reported for the $CF_3SO_3SiR_3$-catalyzed GTP, which was found to lose livingness ($M_w/M_n = 2.35$) and to yield incomplete monomer conversion.[202]

Interestingly, the Tf_2NH-catalyzed GTP produced a predominantly syndiotactic PMMA at room temperature (*mm*/*mr*/*rr* = 1/27/72). Lowering the temperature to −55 °C allowed the author to reach 90% syndiotacticity (*mm*/*mr*/*rr* = 0/10/90), which compared with *t*-BuLi/AlR_3, one of the most established transition metal-based synthetic pathways to syndiotactic PMMA. In the case of PDMA, the dyad tacticity (*m*/*r*) was influenced by both the solvent polarity and the temperature of polymerization: the (*m*/*r*) values determined vary from 35/65 in dichloromethane to 44/56 in toluene at 0 °C and from 27/73 in dichloromethane to 38/62 in toluene at −78 °C.

4.06.9.3 Carboxylic Acid-Mediated Polymerizations

Various carboxylic acids, including not only trifluoroacetic acid (TFA) but also naturally occurring α-hydroxyacids and α-amino acids, have attracted great interest in polymer chemistry over the last 10 years. This is due to their broad availability from renewable resources as well as their air and moisture stability.[15] Unlike enzymes, these small molecules display a higher thermal stability and better solubility in organic solvents. Compared with stronger acids, the carboxylic acid derivatives with pK_a around 3–5 usually lead to few side reactions, while providing high chemoselectivity.[15] Moreover, these catalysts allow the polymerization to be performed under solvent-free conditions, which is of prime relevance in the context of green chemistry. Most lactones have been polymerized so far, including ε-CL, δ-VL, and LA. The polymerization of cyclic carbonates was also briefly investigated.

Naturally occurring α-hydroxyacids such as lactic acid, citric acid, mandelic acid, tartaric acid, and other α-amino acids proved efficient for the ROP of ε-CL. Complex polymer architecture such as dendrimer-like PCLs could be obtained via such an organocatalyzed pathway. The selective modification of saccharides and even cellulose fibers was also described. In most cases, the ROP of ε-CL catalyzed by carboxylic acids was performed in bulk at 120 °C. α-Hydroxyacids such as lactic, tartaric, and citric acids proved more efficient than nonhydroxylated carboxylic acids (hexanoic and propionic acids), which was thought to result from the higher acidity of the former catalysts (pK_a = 3.8 vs. 4.5). Casas *et al.*[184] showed that high monomer conversion (80–90%) was obtained in 4 h with tartaric acid as catalyst ([I]/[cat] = 3) and benzyl alcohol as initiator (**Table 6**, entry 14). PCLs with molar masses up to 2700 g mol^{-1} and dispersity around 1.3 could be synthesized. In contrast, with aliphatic carboxylic acids such as propionic and hexanoic acids, low monomer conversions (10%) were observed and only oligomers (M_n = 450 g mol^{-1}) were formed. In the absence of an external alcohol initiator, α-hydroxyacids were also found to initiate the polymerization. This situation is reminiscent of the amino acid-mediated ROP of ε-CL described by Liu *et al.*, which afforded PCL terminated with an amino acid (entry 15).[191] L-Alanine, L-proline, L-phenylalanine, and L-leucine could serve as both catalysts and initiators for the bulk ROP of ε-CL at 160 °C, quantitative monomer conversion being reached in 24–48 h. PCL of relatively well-controlled molar mass, ranging from 3700 to 26 800 g mol^{-1}, but of rather high dispersity (1.50–1.89), could be obtained by varying the initial [ε-CL]/[amino acid] feed ratio.

In contrast to strong Bronsted acids, the softer carboxylic acids were expected to display a high functional group tolerance which could provide the opportunity to readily access polymers incorporating multifunctional groups. A difunctional initiator featuring two types of OH groups (phenol and alkanol) was shown to exclusively initiate via its alkanol group the tartaric acid-catalyzed ROP of ε-CL.[185] Increasing the [I]/[cat] ratio from 0.7 to 3.5 led to a slight decrease in the PCL molar mass from 10 300 to 8900 g mol^{-1}, suggesting initiation by tartaric acid itself. PCLs with a dendrimer-like architecture were also prepared using, in this case, a hexahydroxy-functional initiator in the presence of lactic acid ([I]/[cat] = 0.125) as catalyst (entry 16).[185] The polymerization was carried out at 120 °C for 1 h under solvent-free conditions, affording dendrimer-like structures with molar mass M_w = 12 550 g mol^{-1} and a dispersity of 1.4. According to ^{1}H NMR spectroscopy, however, the dendritic structures were found to be contaminated with linear PCL chains that were directly initiated by tartaric acid. Interestingly, the lactic acid catalyst could be recycled twice, without affecting the yield of the dendrimer-like PCLs. Upon subsequent recycling, however, the molar mass decreased from 12 550 to 10 800 g mol^{-1}, while the dispersity broadened significantly (from 1.4 to 2.1 in the first and third run, respectively). Although it was claimed that the high chemoselectivity of this system prevented the aryl ester functions of the initiator from being transesterified by

growing chain end of PCL, the transesterification involving PCL alkyl ester groups likely occurred.

Persson *et al.*[186] showed that various sugars such as methyl-β-D-glucopyranoside, sucrose, and raffinose could initiate the ROP of ε-CL in bulk at 120 °C, in the presence of L-lactic acid catalyst ([I]/[cat] = 1–4) (**Table 6**, entry 17). Depending on the initiator used, PCLs with molar mass ranging from 1600 to 6500 g mol^{-1} and relatively narrow dispersity (1.3–1.5) were obtained in high yields (up to 95% based on consumed ε-CL). It was found that these sugar-initiated PCLs were contaminated with some lactic acid-initiated PCL, in line with previous observations made with other initiators (*vide supra*). Interestingly, the first direct catalytic ROP from cellulose fibers was described with the mild, tartaric acid-catalyzed bulk polymerization of ε-CL at 120 °C, initiated by cotton and paper cellulose. Such an organocatalytic pathway to polyester–polysaccharide composites might be suitable biomaterials for various applications.[203]

Three- and four-arm star PCL polymers have been prepared by Sanda *et al.*[187] by ROP of ε-CL with a triol (1,1,1-tris(hydroxymethyl)propane) and a tetrol (pentaerythritol) initiator respectively, in the presence of various acid catalysts such as HCl.Et_2O, TFA, CCl_3COOH, maleic, and fumaric acids (entry 18). With carboxylic acids, the polymerization was carried out in bulk at 70–90 °C for 6–24 h; star PCL (61–95% yield) of molar mass ranging from 4400 to 15 800 g mol^{-1} could be obtained (M_w/M_n = 1.07–1.98).[187]

The synthesis of lipid-functionalized PCL was recently described by Oledzska *et al.*[188] by ROP of ε-CL in bulk at 70–150 °C, initiated with *threo*-9,10-dihydroxyoctadecanoic acid and catalyzed by oxalic, succinic, or fumaric acids (entry 19). Functionalized PCL of molar mass ranging from 7500 to 15 200 (M_n/M_w = 1.11–1.48) was obtained in 28–95% yield.

Block copolymers based on pseudo-poly(amino acid) and PCL have been prepared by Lee *et al.*[189] by ROP of ε-CL in bulk, using an OH-terminated pseudo-poly(L-proline) derivative as initiator and DL-lactic acid as catalyst (**Table 6**, entry 20). Within 1.5–24 h, block copolymers of 2900–13 030 g mol^{-1} could be obtained at 140 °C, with a low catalyst loading ([C]/[M] = 0.1–1). The ability of these amphiphilic copolymers to form micelles in aqueous media was also studied.

The feasibility of a carboxylic acid-mediated ROP of δ-VL was first reported by the group of Córdova in 2004 (**Table 6**, entries 21 and 22).[184,190] PVLs with molar mass of 2600 g mol^{-1} were obtained in 7 h (conversion > 95%) by ROP of δ-VL in bulk at 120 °C, using tartaric acid ([I]/[cat] = 0.33) as catalyst and benzylalcohol as initiator. Further development of this methodology by Zeng *et al.*[190] allowed the polymerization to be controlled, giving an access to complex polymer structures, such as six-arm star PVL and some star-block copolymer derivatives. The polymerization of δ-VL in bulk at 60–70 °C, in the presence of fumaric acid as catalyst and dipentaerythritol as hexafunctional initiator, yielded hexa-arm star PVL exhibiting higher molar masses than expected, owing to the poor initiator efficiency (less than 0.3). Raising the temperature to 100 °C allowed the authors to increase the initiator efficiency to 0.9 and to synthesize PVLs with molar mass ranging from 6150 to 99 100 g mol^{-1} and a dispersity of 1.07–1.36, using a relatively high catalyst loading ([I]/[cat] = 0.1). The molar masses calculated from the ^{1}H NMR spectra were in good agreement with the theoretical values.

The group of Endo[175,182] investigated the organocatalytic ROP of six- and seven-membered cyclic carbonates (6CC and 7CC, respectively) in the presence of a protic initiator (entry 23). In particular, among a variety of organic acids screened, only TFA proved efficient in the ROP of both carbonates. High monomer conversion (77–98%) was reached for the polymerizations of 6CC and 7CC in dichloromethane at 0 °C and in toluene at 50 °C, respectively, using a low catalyst loading ([I]/[cat] = 2) and a primary alcohol (BnOH or BuOH) as initiator. Polycarbonates with molar masses ranging from 2500 to 6800 g mol^{-1} and relatively narrow dispersities (M_w/M_n = 1.16–1.24) could be synthesized in 24–30 h. It was shown that molar masses of poly(6CC) and poly(7CC) increased with conversion, indicating a controlled character of the polymerization. This situation contrasted with the HCl-catalyzed ROP of 7CC, where the molar mass of the resulting polymers increased linearly with increasing the initial [M]/[I] feed ratio, a good agreement between calculated and theoretical molar masses being observed.[175] These differences might arise from the inability of HCl to mediate ROP of cyclic carbonates in the absence of a protic initiator, while TFA was shown to induce an ACEM when used as direct initiator, in spite of higher acidity of HCl. Importantly, no decarboxylation occurred in these two systems, in contrast to what was observed under typical cationic polymerization conditions.[200] In dichloromethane, the rate of polymerization of 7CC is ca. 30 times higher than that observed for the polymerization of 6CC, which is thought to result from the higher ring strain of 7CC. Interaction of TFA with both 6CC and 7CC in $CDCl_3$ could be established by ^{1}H and ^{13}C NMR spectroscopy, following a polymerization by AMM, as proposed by the authors.

A further development of the carboxylic acid-mediated ROP of cyclic carbonates was reported in 2009 by Zhang *et al.*[183] for the synthesis of triblock polycarbonates (**Table 6**, entry 24). The authors showed that the polymerization of 2-(benzyloxy) propane-1,3-diyl carbonate could be conducted at 150 °C under solvent-free conditions, with 2.0 wt.% of the fumaric acid catalyst, using a dihydroxylated macroinitiator. Under these conditions, A-B-A triblock copolymers of predictable molar mass could be synthesized with moderate to excellent yields (41–91%), by varying the initial feed ratio of comonomers. The molar mass of the A blocks could be varied from 2650 to 9450 g mol^{-1}, while only a slight increase in the dispersity of the triblock copolymer, compared with that of the macroinitiator for B-block, was observed.

4.06.10 Conclusion

Tremendous research efforts are currently being made in organic synthesis, focusing on the development of more sustainable processes, taking into account mild conditions, energy savings, high selectivities, reduced by-products, and wastes. In this regard, both enzymatic catalysis and organocatalysis offer new opportunities for activating various substrates and accessing functional building blocks. General concepts of organocatalysis have been applied to polymer synthesis, allowing significant breakthroughs such as enhancement of polymerization rates and high selectivity of propagation relative to adverse chain breaking by termination or transfer reactions. Organocatalysis has also allowed the preparation of

polymeric structures that would be hard to access by a metal-mediated polymerization. Moreover, this metal-free approach has led to the production of biocompatible polymers without metal residues, which could be used in biomedical applications. It might be anticipated that organocatalysis could be applied in the near future to the synthesis of polymer for optoelectronic applications, where metallic impurities are also problematic.

The field of organocatalyzed polymerization, however, is still in its infancy. Since organic catalysts may operate differently as compared with metal-based ones, they offer a diversity of mechanistic pathways to control the polymerization. In some cases, it has not been clearly established whether the organic catalysts activate the monomer or the initiator/polymer chain ends or operate by cooperative dual activation. It turns out that the polymerization mechanism dramatically depends on the catalyst structure/reactivity. In this context, DFT calculations appear as a complementary tool to better understand the polymerization mechanism.

Thus, challenges still remain in macromolecular synthesis by an organocatalyzed pathway. For instance, only a few monomer candidates have actually been investigated so far, carbonyl-containing monomers such as cyclic esters and cyclic carbonates being the most studied in the context of ROP. This can be explained by the relatively high reactivity of polar carbonyl group. Also polymer molar masses of polymers are somehow limited in most of the examples reported. On the other hand, asymmetric polymerizations using chiral catalysts have to be investigated in much more detail, since they are far from competing with organometallic catalysts.[204]

References

1. Odian, G. In *Principles of Polymerization*, Fourth Edition, John Wiley & Sons, Inc., Hoboken, NJ, USA, 2004, pp i–xxiv.
2. Percec, V. *Chem. Rev.* **2009**, *109*, 4961–4962.
3. Soga, K.; Shiono, T. *Prog. Polym. Sci.* **1997**, *22*, 1503–1546.
4. Kobayashi, S.; Makino, A. *Chem. Rev.* **2009**, *109*, 5288–5353.
5. Kamber, N. E.; Jeong, W.; Waymouth, R. M.; *et al. Chem. Rev.* **2007**, *107*, 5813–5840.
6. Kiesewetter, M. K.; Shin, E. J.; Hedrick, J. L.; *et al. Macromolecules* **2010**, *43*, 2093–2107.
7. Platel, R. H.; Hodgson, L. M.; Williams, C. K. *Polym. Rev.* **2008**, *48*, 11–63.
8. *J. Prakt. Chem.* **1873**, *8*, 428–458.
9. Fischer, E. *Ber. Dtsch. Chem. Ges.* **1893**, *26*, 2400–2412.
10. Fischer, E. *Ber. Dtsch. Chem. Ges.* **1895**, *28*, 1145–1167.
11. Fischer, E.; Beensch, L. *Ber. Dtsch. Chem. Ges.* **1894**, *27*, 2478–2486.
12. Steglich, W.; Höfle, G. *Angew. Chem., Int. Ed.* **1969**, *8*, 981.
13. Eder, U.; Sauer, G.; Wiechert, R. *Angew. Chem., Int. Ed.* **1971**, *10*, 496–497.
14. Overberger, C. G.; Dixon, K. W. *J. Polym. Sci.: Polym. Chem. Ed.* **1977**, *15*, 1863–1868.
15. Domínguez de María, P. *ChemCatChem* **2010**, *2*, 487–492.
16. Dalko, P. I.; Moisan, L. *Angew. Chem., Int. Ed.* **2004**, *43*, 5138–5175.
17. Barbas, C. F. *Angew. Chem., Int. Ed.* **2008**, *47*, 42–47.
18. Seayad, J.; List, B. *Org. Biomol. Chem.* **2005**, *3*, 719–724.
19. Zhang, Z.; Schreiner, P. R. *Chem. Soc. Rev.* **2009**, *38*, 1187–1198.
20. Bertelsen, S.; Jorgensen, K. A. *Chem. Soc. Rev.* **2009**, *38*, 2178–2189.
21. Hajos, Z. G.; Parrish, D. R. DE 2102623, 1971.
22. Chattopadhyay, D. K.; Raju, K. V. S. N. *Prog. Polym. Sci.* **2007**, *32*, 352–418.
23. Penczek, S.; Kubisa, P.; Matyjaszewski, K. *Adv. Polym. Sci.* **1980**, *37*, 1–144.
24. Nederberg, F.; Connor, E. F.; Möller, M.; *et al. Angew. Chem., Int. Ed.* **2001**, *40*, 2712–2715.
25. Nederberg, F.; Connor, E. F.; Glausser, T.; *et al. Chem. Commun.* **2001**, (*20*) 2066–2067.
26. Kricheldorf, H. R. *Angew. Chem., Int. Ed.* **2006**, *45*, 5752–5784.
27. Penczek, S.; Cypryk, M.; Duda, A.; *et al. Prog. Polym. Sci.* **2007**, *32*, 247–282.
28. Odian, G. In *Principles of Polymerization*, Fourth Edition, John Wiley & Sons, Inc., Hoboken, NJ, USA, 2004, pp 544-618.
29. Aoi, K.; Okada, M. *Prog. Polym. Sci.* **1996**, *21*, 151–208.
30. Cronin, J. P.; Pepper, D. C. *Makromol. Chem. Macromol. Chem. Phys.* **1988**, *189*, 85–102.
31. Schreiner, P. R.; Wittkopp, A. *Org. Lett.* **2002**, *4*, 217–220.
32. Otera, J. *Chem. Rev.* **1993**, *93*, 1449–1470.
33. Ie, Y.; Fu, G. C. *Chem. Commun.* **2000**, (*2*) 119–120.
34. Jen, W. S.; Wiener, J. J. M.; MacMillan, D. W. C. *J. Am. Chem. Soc.* **2000**, *122*, 9874–9875.
35. Doyle, A. G.; Jacobsen, E. N. *Chem. Rev.* **2007**, *107*, 5713–5743.
36. Ye, W.; Xu, J.; Tan, C.-T.; *et al. Tetrahedron Lett.* **2005**, *46*, 6875–6878.
37. Simoni, D.; Rossi, M.; Rondanin, R.; *et al. Org. Lett.* **2000**, *2*, 3765–3768.
38. Corey, E. J.; Grogan, M. J. *Org. Lett.* **1999**, *1*, 157–160.
39. Schuchardt, U.; Vargas, R. M.; Gelbard, G. *J. Mol. Catal. Chem.* **1995**, *99*, 65–70.
40. Becker, J. M.; Tempelaar, S.; Stanford, M. J.; *et al. Chem. Eur. J.* **2010**, *16*, 6099–6105.
41. Curran, D. P.; Kuo, L. H. *J. Org. Chem.* **1994**, *59*, 3259–3261.
42. Fuerst, D. E.; Jacobsen, E. N. *J. Am. Chem. Soc.* **2005**, *127*, 8964–8965.
43. Hoashi, Y.; Okino, T.; Takemoto, Y. *Angew. Chem., Int. Ed.* **2005**, *117*, 4100–4103.
44. Joly, G. D.; Jacobsen, E. N. *J. Am. Chem. Soc.* **2004**, *126*, 4102–4103.
45. Okino, T.; Hoashi, Y.; Takemoto, Y. *J. Am. Chem. Soc.* **2003**, *125*, 12672–12673.
46. Okino, T.; Nakamura, S.; Furukawa, T.; *et al. Org. Lett.* **2004**, *6*, 625–627.
47. Schreiner, P. R. *Chem. Soc. Rev.* **2003**, *32*, 289–296.
48. Sigman, M. S.; Vachal, P.; Jacobsen, E. N. *Angew. Chem., Int. Ed.* **2000**, *39*, 1279–1281.
49. Taylor, M. S.; Jacobsen, E. N. *J. Am. Chem. Soc.* **2004**, *126*, 10558–10559.
50. Vachal, P.; Jacobsen, E. N. *Org. Lett.* **2000**, *2*, 867–870.
51. Vachal, P.; Jacobsen, E. N. *J. Am. Chem. Soc.* **2002**, *124*, 10012–10014.
52. Wenzel, A. G.; Jacobsen, E. N. *J. Am. Chem. Soc.* **2002**, *124*, 12964–12965.
53. Yoon, T. P.; Jacobsen, E. N. *Angew. Chem., Int. Ed.* **2005**, *44*, 466–468.
54. Berkessel, A.; Cleemann, F.; Mukherjee, S.; *et al. Angew. Chem., Int. Ed.* **2005**, *44*, 807–811.
55. Hoashi, Y.; Okino, T.; Takemoto, Y. *Angew. Chem., Int. Ed.* **2005**, *44*, 4032–4035.
56. Vedejs, E.; Bennett, N. S.; Conn, L. M.; *et al. J. Org. Chem.* **1993**, *58*, 7286–7288.
57. Vedejs, E.; Diver, S. T. *J. Am. Chem. Soc.* **1993**, *115*, 3358–3359.
58. Qiao, S.; Fu, G. C. *J. Org. Chem.* **1998**, *63*, 4168–4169.
59. Vedejs, E.; Daugulis, O.; Diver, S. T. *J. Org. Chem.* **1996**, *61*, 430–431.
60. Tanaka, K.; Qiao, S.; Tobisu, M.; *et al. J. Am. Chem. Soc.* **2000**, *122*, 9870–9871.
61. Vedejs, E.; Daugulis, O. *J. Am. Chem. Soc.* **1999**, *121*, 5813–5814.
62. Vedejs, E.; Rozners, E. *J. Am. Chem. Soc.* **2001**, *123*, 2428–2429.
63. Marinetti, A.; Voituriez, A. *Synlett* **2010**, (*2*) 174–194.
64. Myers, M.; Connor, E. F.; Glauser, T.; *et al. J. Polym. Sci., Part A: Polym. Chem.* **2002**, *40*, 844–851.
65. Schwesinger, R.; Schlemper, H. *Angew. Chem., Int. Ed.* **1987**, *26*, 1167–1169.
66. Kaljurand, I.; Kütt, A.; Sooväli, L.; *et al. J. Org. Chem.* **2005**, *70*, 1019–1028.
67. Smith, M. B.; March, J. In *March's Advanced Organic Chemistry: Reactions, Mechanisms, and Structure*, Sixth Edition, John Wiley & Sons, Inc., Hoboken, NJ, USA, 2006, pp 234–295.
68. Igau, A.; Grutzmacher, H.; Baceiredo, A.; *et al. J. Am. Chem. Soc.* **1988**, *110*, 6463–6466.
69. Arduengo, A. J.; Harlow, R. L.; Kline, M. *J. Am. Chem. Soc.* **1991**, *113*, 361–363.
70. Enders, D.; Niemeier, O.; Henseler, A. *Chem. Rev.* **2007**, *107*, 5606–5655.
71. Marion, N.; Díez-González, S.; Nolan, S. P. *Angew. Chem., Int. Ed.* **2007**, *46*, 2988–3000.
72. Moore, J.; Rovis, T. In *Asymmetric Organocatalysis*; List, B., Ed.; Springer: Berlin, Heidelberg, Germany, 2009; Vol. 291, pp 77–144.
73. Díez-González, S.; Marion, N.; Nolan, S. P. *Chem. Rev.* **2009**, *109*, 3612–3676.
74. Poyatos, M.; Mata, J. A.; Peris, E. *Chem. Rev.* **2009**, *109*, 3677–3707.
75. Dröge, T.; Glorius, F. *Angew. Chem., Int. Ed.* **2010**, *49*, 6940–6952.
76. Crabtree, R. H. *Coord. Chem. Rev.* **2007**, *251*, 595.
77. Glorius, F. In *N-Heterocyclic Carbenes in Transition Metal Catalysis*; Springer: Berlin, Heidelberg, Germany, 2007; Vol. 21, pp 1–20.
78. Fuchter, M. J. *Chem. Eur. J.* **2010**, *16*, 12286–12294.
79. Delaude, L. *Eur. J. Inorg. Chem.* **2009**, *2009*, 1681–1699.
80. de Frémont, P.; Marion, N.; Nolan, S. P. *Coord. Chem. Rev.* **2009**, *253*, 862–892.
81. Higgins, E. M.; Sherwood, J. A.; Lindsay, A. G.; *et al. Chem. Commun.* **2011**, *47*, 1559–1561.
82. Akiyama, T. *Chem. Rev.* **2007**, *107*, 5744–5758.
83. Cheon, C. H.; Yamamoto, H. *Chem. Commun.* **2011**, *47*, 3043–3056.
84. Yamamoto, H. *Tetrahedron* **2007**, *63*, 8377–8412.

85. Thillaye du Boullay, O.; Marchal, E.; Martin-Vaca, B.; *et al. J. Am. Chem. Soc.* **2006**, *128*, 16442–16443.
86. Brignou, P.; Priebe Gil, M.; Casagrande, O.; *et al. Macromolecules* **2010**, *43*, 8007–8017.
87. Sanders, D. P.; Fukushima, K.; Coady, D. J.; *et al. J. Am. Chem. Soc.* **2010**, *132*, 14724–14726.
88. Thillaye du Boullay, O.; Bonduelle, C.; Martin-Vaca, B.; *et al. Chem. Commun.* **2008**, (*15*) 1786–1788.
89. du Boullay, O. T.; Saffon, N.; Diehl, J.-P.; *et al. Biomacromolecules* **2010**, *11*, 1921–1929.
90. Hashimoto, K. *Prog. Polym. Sci.* **2000**, *25*, 1411–1462.
91. Kubisa, P.; Penczek, S. *Prog. Polym. Sci.* **1999**, *24*, 1409–1437.
92. Penczek, S. *J. Polym. Sci., Part A: Polym. Chem.* **2000**, *38*, 1919–1933.
93. Helou, M.; Miserque, O.; Brusson, J.-M.; *et al. Chem. Eur. J.* **2010**, *16*, 13805–13813.
94. Feng, H.; Dong, C.-M. *J. Polym. Sci., Part A: Polym. Chem.* **2006**, *44*, 5353–5361.
95. Johnson, R. M.; Fraser, C. L. *Biomacromolecules* **2004**, *5*, 580–588.
96. Kadota, J.; Pavlović, D. E.; Desvergne, J.-P.; *et al. Macromolecules* **2010**, *43*, 8874–8879.
97. Kricheldorf, H. R.; Garaleh, M.; Schwarz, G. *J. Macromol. Sci., Part A: Pure Appl. Chem.* **2005**, *42*, 139–148.
98. Bonduelle, C.; Martín-Vaca, B.; Cossío, F.; *et al. Chem. Eur. J.* **2008**, *14*, 5304–5312.
99. Nederberg, F.; Lohmeijer, B. G. G.; Leibfarth, F.; *et al. Biomacromolecules* **2006**, *8*, 153–160.
100. Lohmeijer, B. G. G.; Dubois, G.; Leibfarth, F.; *et al. Org. Lett.* **2006**, *8*, 4683–4686.
101. Fukushima, K.; Coulembier, O.; Lecuyer, J. M.; *et al. J. Polym. Sci., Part A: Polym. Chem.* **2011**, *49*, 1273–1281.
102. Li, H.; Wu, J.; Brunel, S.; *et al. Ind. Eng. Chem. Res.* **2005**, *44*, 8641–8643.
103. Lohmeijer, B. G. G.; Pratt, R. C.; Leibfarth, F.; *et al. Macromolecules* **2006**, *39*, 8574–8583.
104. Pratt, R. C.; Lohmeijer, B. G. G.; Long, D. A.; *et al. J. Am. Chem. Soc.* **2006**, *128*, 4556–4557.
105. Theryo, G.; Jing, F.; Pitet, L. M.; *et al. Macromolecules* **2010**, *43*, 7394–7397.
106. Nederberg, F.; Trang, V.; Pratt, R. C.; *et al. Biomacromolecules* **2007**, *8*, 3294–3297.
107. Zhang, L.; Pratt, R. C.; Nederberg, F.; *et al. Macromolecules* **2010**, *43*, 1660–1664.
108. Simón, L.; Goodman, J. M. *J. Org. Chem.* **2007**, *72*, 9656–9662.
109. Pratt, R. C.; Nederberg, F.; Waymouth, R. M.; *et al. Chem. Commun.* **2008**, (*1*) 114–116.
110. Fukushima, K.; Pratt, R. C.; Nederberg, F.; *et al. Biomacromolecules* **2008**, *9*, 3051–3056.
111. Dove, A. P.; Pratt, R. C.; Lohmeijer, B. G. G.; *et al. J. Am. Chem. Soc.* **2005**, *127*, 13798–13799.
112. Pratt, R. C.; Lohmeijer, B. G. G.; Long, D. A.; *et al. Macromolecules* **2006**, *39*, 7863–7871.
113. Middleton, H.; Tempelaar, S.; Haddleton, D. M.; *et al. Polym. Chem.* **2011**, *2*, 595–600.
114. Pounder, R. J.; Dove, A. P. *Biomacromolecules* **2010**, *11*, 1930–1939.
115. Nederberg, F.; Appel, E.; Tan, J. P. K.; *et al. Biomacromolecules* **2009**, *10*, 1460–1468.
116. Koeller, S.; Kadota, J.; Deffieux, A.; *et al. J. Am. Chem. Soc.* **2009**, *131*, 15088–15089.
117. Koeller, S.; Kadota, J.; Peruch, F.; *et al. Chem. Eur. J.* **2010**, *16*, 4196–4205.
118. Misaka, H.; Kakuchi, R.; Zhang, C.; *et al. Macromolecules* **2009**, *42*, 5091–5096.
119. Molenberg, A.; Möller, M. *Macromol. Rapid Commun.* **1995**, *16*, 449–453.
120. Eßwein, B.; Steidl, N. M.; Möller, M. *Macromol. Rapid Commun.* **1996**, *17*, 143–148.
121. Schlaad, H.; Kukula, H.; Rudloff, J.; *et al. Macromolecules* **2001**, *34*, 4302–4304.
122. Rexin, O.; Mülhaupt, R. *J. Polym. Sci., Part A: Polym. Chem.* **2002**, *40*, 864–873.
123. Zhang, L.; Nederberg, F.; Pratt, R. C.; *et al. Macromolecules* **2007**, *40*, 4154–4158.
124. Zhang, L.; Nederberg, F.; Messman, J. M.; *et al. J. Am. Chem. Soc.* **2007**, *129*, 12610–12611.
125. De Winter, J.; Coulembier, O.; Gerbaux, P.; *et al. Macromolecules* **2010**, *43*, 10291–10296.
126. Illy, N.; Boileau, S.; Penelle, J.; *et al. Macromol. Rapid Commun.* **2009**, *30*, 1731–1735.
127. Illy, N.; Boileau, S.; Buchmann, W.; *et al. Macromolecules* **2010**, *43*, 8782–8789.
128. Pietzonka, T.; Seebach, D. *Angew. Chem., Int. Ed.* **1993**, *32*, 716–717.
129. Börner, H. G.; Heitz, W. *Macromol. Chem. Phys.* **1998**, *199*, 1815–1820.
130. Scholten, M. D.; Hedrick, J. L.; Waymouth, R. M. *Macromolecules* **2008**, *41*, 7399–7404.
131. Raynaud, J.; Ciolino, A.; Baceiredo, A.; *et al. Angew. Chem., Int. Ed.* **2008**, *47*, 5390–5393.
132. Raynaud, J.; Gnanou, Y.; Taton, D. *Macromolecules* **2009**, *42*, 5996–6005.
133. Raynaud, J.; Liu, N.; Gnanou, Y.; *et al. Macromolecules* **2010**, *43*, 8853–8861.
134. Pinaud, J.; Vijayakrishna, K.; Taton, D.; *et al. Macromolecules* **2009**, *42*, 4932–4936.
135. Marrot, S.; Bonnette, F.; Kato, T.; *et al. J. Organomet. Chem.* **2008**, *693*, 1729–1732.
136. Kamber, N. E.; Tsujii, Y.; Keets, K.; *et al. J. Chem. Educ.* **2010**, *87*, 519–521.
137. Nyce, G. W.; Lamboy, J. A.; Connor, E. F.; *et al. Org. Lett.* **2002**, *4*, 3587–3590.
138. Hedrick, J. L.; Nyce, G. W.; Waymouth, R. M. U.S. Patent 7053221, 2006.
139. Rodriguez, M.; Marrot, S.; Kato, T.; *et al. J. Organomet. Chem.* **2007**, *692*, 705–708.
140. Connor, E. F.; Nyce, G. W.; Myers, M.; *et al. J. Am. Chem. Soc.* **2002**, *124*, 914–915.
141. Nyce, G. W.; Glauser, T.; Connor, E. F.; *et al. J. Am. Chem. Soc.* **2003**, *125*, 3046–3056.
142. Coulembier, O.; Lohmeijer, B. G. G.; Dove, A. P.; *et al. Macromolecules* **2006**, *39*, 5617–5628.
143. Coulembier, O.; Mespouille, L.; Hedrick, J. L.; *et al. Macromolecules* **2006**, *39*, 4001–4008.
144. Kamber, N. E.; Jeong, W.; Gonzalez, S.; *et al. Macromolecules* **2009**, *42*, 1634–1639.
145. Jeong, W.; Hedrick, J. L.; Waymouth, R. M. *J. Am. Chem. Soc.* **2007**, *129*, 8414–8415.
146. Csihony, S.; Culkin, D. A.; Sentman, A. C.; *et al. J. Am. Chem. Soc.* **2005**, *127*, 9079–9084.
147. Coulembier, O.; Dove, A. P.; Pratt, R. C.; *et al. Angew. Chem., Int. Ed.* **2005**, *44*, 4964–4968.
148. Coulembier, O.; Kiesewetter, M.; Mason, A.; *et al. Angew. Chem., Int. Ed.* **2007**, *46*, 4719–4721.
149. Nyce, G. W.; Csihony, S.; Waymouth, R. M.; *et al. Chem. Eur. J.* **2004**, *10*, 4073–4079.
150. Jensen, T. R.; Breyfogle, L. E.; Hillmyer, M. A.; *et al. Chem. Commun.* **2004**, (*21*) 2504–2505.
151. Dove, A. P.; Li, H.; Pratt, R. C.; *et al. Chem. Commun.* **2006**, (*27*) 2881–2883.
152. Culkin, D.; Jeong, W.; Csihony, S.; *et al. Angew. Chem., Int. Ed.* **2007**, *46*, 2627–2630.
153. Jeong, W.; Shin, E. J.; Culkin, D. A.; *et al. J. Am. Chem. Soc.* **2009**, *131*, 4884–4891.
154. Guo, L.; Zhang, D. *J. Am. Chem. Soc.* **2009**, *131*, 18072–18074.
155. Raynaud, J.; Absalon, C.; Gnanou, Y.; *et al. J. Am. Chem. Soc.* **2009**, *131*, 3201–3209.
156. Raynaud, J.; Absalon, C.; Gnanou, Y.; *et al. Macromolecules* **2010**, *43*, 2814–2823.
157. Raynaud, J.; Ottou, W. N.; Gnanou, Y.; *et al. Chem. Commun.* **2010**, *46*, 3203–3205.
158. Alan Jones, R.; Karatza, M.; Voro, T. N.; *et al. Tetrahedron* **1996**, *52*, 8707–8724.
159. Jones, R. A.; Civcir, P. U. *Tetrahedron* **1997**, *53*, 11529–11540.
160. Arduengo Iii, A. J.; Calabrese, J. C.; Davidson, F.; *et al. Helv. Chim. Acta* **1999**, *82*, 2348–2364.
161. Enders, D.; Breuer, K.; Raabe, G.; *et al. Angew. Chem., Int. Ed.* **1995**, *34*, 1021–1023.
162. Wanzlick, H. W. *Angew. Chem., Int. Ed.* **1962**, *1*, 75–80.
163. Lai, C.-L.; Lee, H. M.; Hu, C.-H. *Tetrahedron Lett.* **2005**, *46*, 6265–6270.
164. Schmidt, M. A.; Müller, P.; Movassaghi, M. *Tetrahedron Lett.* **2008**, *49*, 4316–4318.
165. Webster, O. W.; Hertler, W. R.; Sogah, D. Y.; *et al. J. Am. Chem. Soc.* **1983**, *105*, 5706–5708.
166. Mukaiyama, T. *Angew. Chem., Int. Ed.* **2004**, *43*, 5590–5614.
167. Brittain, W. J. *Rubber Chem. Technol.* **1992**, *65*, 580–600.
168. Webster, O. W. *J. Polym. Sci., Part A: Polym. Chem.* **2000**, *38*, 2855–2860.
169. Quirk, R. P.; Kim, J.-S. *J. Phys. Org. Chem.* **1995**, *8*, 242–248.
170. Webster, O. W. In *New Synthetic Methods*; Springer: Berlin, Heidelberg, Germany, 2004; Vol. 167, pp 257–266.
171. Baśko, M.; Kubisa, P. *J. Polym. Sci., Part A: Polym. Chem.* **2006**, *44*, 7071–7081.
172. Gazeau-Bureau, S. P.; Delcroix, D.; Martín-Vaca, B.; *et al. Macromolecules* **2008**, *41*, 3782–3784.
173. Baśko, M.; Kubisa, P. *J. Polym. Sci., Part A: Polym. Chem.* **2007**, *45*, 3090–3097.
174. Oshimura, M.; Tang, T.; Takasu, A. *J. Polym. Sci., Part A: Polym. Chem.* **2011**, *49*, 1210–1218.

175. Shibasaki, Y.; Sanada, H.; Yokoi, M.; *et al. Macromolecules* **2000**, *33*, 4316–4320.
176. Lou, X.; Detrembleur, C.; Jérôme, R. *Macromolecules* **2002**, *35*, 1190–1195.
177. Kakuchi, R.; Tsuji, Y.; Chiba, K.; *et al. Macromolecules* **2010**, *43*, 7090–7094.
178. Shibasaki, Y.; Sanda, F.; Endo, T. *Macromolecules* **2000**, *33*, 3590–3593.
179. Shibasaki, Y.; Sanda, F.; Endo, T. *Macromol. Rapid Commun.* **1999**, *20*, 532–535.
180. Nakano, S. *Prog. Org. Coat.* **1999**, *35*, 141–151.
181. Delcroix, D.; Martín-Vaca, B.; Bourissou, D.; *et al. Macromolecules* **2010**, *43*, 8828–8835.
182. Matsuo, J.; Nakano, S. L.; Sanda, F.; *et al. J. Polym. Sci., Part A: Polym. Chem.* **1998**, *36*, 2463–2471.
183. Zhang, X.; Mei, H.; Hu, C.; *et al. Macromolecules* **2009**, *42*, 1010–1016.
184. Casas, J.; Persson, P.; Iversen, T.; *et al. Adv. Synth. Catal.* **2004**, *346*, 1087–1089.
185. Persson, P. V.; Casas, J.; Iversen, T.; *et al. Macromolecules* **2006**, *39*, 2819–2822.
186. Persson, P. V.; Schröder, J.; Wickholm, K.; *et al. Macromolecules* **2004**, *37*, 5889–5893.
187. Sanda, F.; Sanada, H.; Shibasaki, Y.; *et al. Macromolecules* **2001**, *35*, 680–683.
188. Oledzka, E.; Narine, S. S. *J. Appl. Polym. Sci.* **2011**, *119*, 1873–1882.
189. Lee, R.-S.; Li, H.-R.; Yang, J.-M.; *et al. Polymer* **2005**, *46*, 10718–10726.
190. Zeng, F. Q.; Lee, H.; Chidiac, M.; *et al. Biomacromolecules* **2005**, *6*, 2140–2149.
191. Liu, J.; Liu, L. *Macromolecules* **2004**, *37*, 2674–2676.
192. Kakuchi, R.; Chiba, K.; Fuchise, K.; *et al. Macromolecules* **2009**, *42*, 8747–8750.
193. Fuchise, K.; Sakai, R.; Satoh, T.; *et al. Macromolecules* **2010**, *43*, 5589–5594.
194. Bourissou, D.; Martin-Vaca, B.; Dumitrescu, A.; *et al. Macromolecules* **2005**, *38*, 9993–9998.
195. Matyjaszewski, K.; Słomkowski, S.; Penczek, S. *J. Polym. Sci.: Polym. Chem. Ed.* **1979**, *17*, 69–80.
196. Matyjaszewski, K.; Słomkowski, S.; Penczek, S. *J. Polym. Sci.: Polym. Chem. Ed.* **1979**, *17*, 2413–2422.
197. Susperregui, N.; Delcroix, D.; Martin-Vaca, B.; *et al. J. Org. Chem.* **2010**, *75*, 6581–6587.
198. Jacobs, C.; Dubois, P.; Jerome, R.; *et al. Macromolecules* **1991**, *24*, 3027–3034.
199. Kuran, W. *Prog. Polym. Sci.* **1998**, *23*, 919–992.
200. Rokicki, G. *Prog. Polym. Sci.* **2000**, *25*, 259–342.
201. García-García, P.; Lay, F.; García-García, P.; *et al. Angew. Chem., Int. Ed.* **2009**, *48*, 4363–4366.
202. Ute, K.; Ohnuma, H.; Kitayama, T. *Polym. J.* **2000**, *32*, 1060–1062.
203. Hafrén, J.; Córdova, A. *Macromol. Rapid Commun.* **2005**, *26*, 82–86.
204. Chuma, A.; Horn, H. W.; Swope, W. C.; *et al. J. Am. Chem. Soc.* **2008**, *130*, 6749–6754.

Biographical Sketches

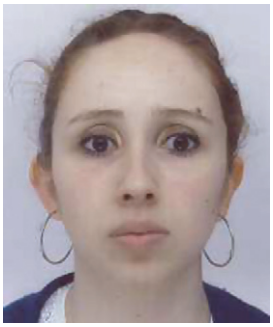

Maréva Fèvre received her masters degree from the National Graduate School of Physics and Chemistry of Bordeaux in 2009. During her undergraduate education, she worked at Schering Plough (Holland) as an intern on solid state characterization of APIs. She performed her master's thesis in the team of Prof. J.-C. Leroux at the ETH Zürich working on liposomal formulations. She then started her PhD under the supervision of Prof. D. Taton at the Laboratoire de Chimie des Polymères Organiques (CNRS-Université de Bordeaux). Her work is mainly focused on organic catalytic systems for polymerization reactions.

Joan Vignolle was born in Biarritz (France) in 1979. He studied biology at the Université de Pau (France) and chemistry at the Université de Toulouse (France). He then started his PhD (2003–2006), working under the supervision of Prof. G. Bertrand and Dr. D. Bourissou both at the University of Toulouse and at the University of California, Riverside. After a 2-year postdoctoral stay at the University of California, Berkeley (Prof. T. D. Tilley), he joined the LCPO-CNRS-Université de Bordeaux 1 (France) as a research associate (Prof. D. Taton). He is presently working as a *Chargé de Recherches CNRS* on organocatalyzed polymerization reactions.

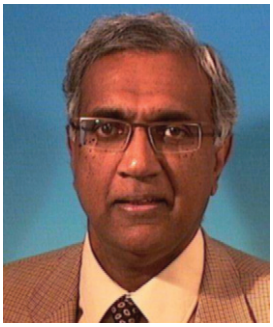

Dr. Yves Gnanou is a director of research for the 'Centre National de la Recherche Scientifique' and currently the vice-president for Education at Ecole Polytechnique. He has coauthored more than 160 publications in peer-reviewed journals, 40 book chapters, and 25 patents. He has published two textbooks coauthored by Prof. M. Fontanille and coedited a four-volume book along with Dr. L. Leibler and Prof. K. Matyjaszewski. His research interests include the design of complex polymeric architectures, the investigation of 'living' chain and step-growth polymerizations, the study of the self-assembling properties of copolymers in selective media leading to nanostructured morphologies, and the synthesis of polymers in dispersed media. Of late, he has developed an activity in the area of polysaccharide-based block copolymers, nanostructured assemblies based on polymeric ionic liquids, and the design of environmental-friendly processes through the study of organocatalyzed polymerizations.

Pr. Daniel Taton is 42 years old and received his PhD in polymer chemistry in 1994 at the University Pierre et Marie Curie (Paris VI). He has been appointed as an assistant professor at the University of Bordeaux in 1995. He develops his research activities at the Laboratoire de Chimie des Polymères Organiques (LCPO). From 2000 to 2002, he was temporarily attached to the research center of Rhodia, where he contributed to the research and development of synthetic specialty polymers.

He has been appointed as a full professor at the University of Bordeaux 1 in 2008. He has published 91 articles in peer-reviewed journals and 12 patents. His contributions are in the field of macromolecular engineering, through the development of original methodologies based on controlled radical or ionic polymerizations for the synthesis of 'complex' macromolecular architectures, including star-like polymers, dendrimer-like polymers, nanogels, and for the design of block copolymers featuring specific blocks (oligosaccharides, polypeptidic, or polymeric ionic liquids). More recently, he has launched a research program on the development of multitask organic catalysts based on *N*-heterocyclic carbenes for different chain-growth and step-growth polymerization reactions.

4.07 Anionic Ring-Opening Polymerization of Epoxides and Related Nucleophilic Polymerization Processes

A Deffieux and S Carlotti, Université Bordeaux, Pessac, France
A Barrère, Université Paris, Villetaneuse, France

4.07.1 Introduction

Among cyclic ethers, three-membered ring epoxides – with the exception of some four-membered ring oxetanes – are the only ones that can be polymerized by an anionic or a related nucleophilic polymerization mechanism. Larger cyclic ethers polymerize exclusively by a cationic or electrophilic ring-opening mechanism.

The conventional anionic ring-opening polymerization of epoxides can be described by the set of reactions shown in Scheme 1 for a monosubstituted epoxide.

Initiation is a bimolecular nucleophilic substitution that leads to the formation of an alkoxide species more or less ionized according to the nature of the associated counterion Mt provided by the initiating species AMt. The alkoxide must have a high enough nucleophilicity to attack a new epoxide molecule and propagate. Initiation and propagation of the ring-opening polymerization by nucleophilic species involving a preliminary complexation of the monomer can be considered as related processes.

The polymerizability of epoxides is determined by the negative change of Gibbs energy in the polymerization reaction, ΔG_p.

$$\Delta G_p = \Delta H_p - T\,\Delta S_p < 0$$

with ΔH_p and ΔS_p the enthalpy and entropy changes in the polymerization, respectively, and T the absolute temperature (in kelvin). For the small epoxide ring, the polymerizability is mainly under the control of the enthalpy term and the important ring strain. Repulsion between substituents is also an effective parameter.

Epoxide reactivity and polymerization kinetics are also influenced by electronic and steric factors associated with the ring substituents, as well as by the initiator nature, the solvent, and reaction conditions, which determine the characteristics of the active species of polymerization. The ability of epoxide monomers to be activated by complexation with an electrophile may also strongly facilitate nucleophilic ring opening.

In this chapter, the anionic and related nucleophilic polymerizations of epoxides are reviewed. The elementary mechanisms involved in the presence of different initiators and catalysts and the main synthetic strategies developed for the preparation of epoxide homopolymers and copolymers are described. In the second section, the anionic polymerization of epoxides involving alkali metal derivatives is described. The use of organic derivatives as counterions or catalysts is presented in the third section. The fourth section is devoted to epoxide-coordinated polymerization. Finally, in the last section, monomer-activated epoxide polymerization is described. The cationic polymerization of epoxides is described in another chapter.

4.07.2 Anionic Epoxide Polymerization Initiated by Alkali Metal Derivatives

Alkali metal derivatives, including hydrides, alkyls and aryls, hydroxides, alkoxides, and amides, have been used as initiators for the anionic polymerization of epoxides. Sodium, potassium, and to a lesser extent cesium are the most often used alkali metals.[1] Lithium derivatives are generally avoided since after the insertion of the first epoxide unit, they yield alkoxide species that are unable to properly propagate the polymerization, due to strong association. Anionic polymerization of

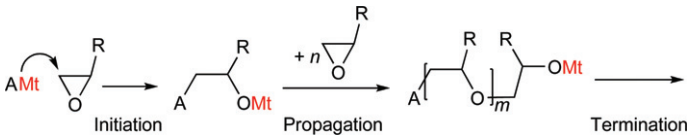

Scheme 1 Ring-opening polymerization of epoxides involving nucleophilic species AM.

epoxides can be conducted in aprotic solvents such as dioxane, tetrahydrofuran (THF), hexamethylphosphoramide (HMPA), and dimethyl sulfoxide (DMSO), or in the bulk monomer.

Alkali metal dispersions can also be used to initiate the polymerization of epoxides via electron transfer, but these systems show very poor efficiency. For an almost similar reason, initiation by alkali metal hydrides, which proceeds mostly at the surface of metal hydride particles, is slow and not controlled.[2,3] Addition of complexing agents such as crown ethers to alkali metal hydrides in THF was found to strongly accelerate epoxide polymerization.[4,5] However, the initiation mechanism seems unclear; instead of the expected hydrogen as the initiator fragment, most of the polyethers possess a hydroxyl head group. This suggests the reaction of residual water with the alkali metal hydride to form a metal hydroxide, which is the true initiating species.[5,6]

Detailed studies on the mechanisms of initiation and propagation of epoxide polymerization have been conducted using well-defined and stable initiators. Ethylene oxide (EO) was generally chosen as the reference monomer, owing to the living character of its polymerization,[7,8] whereas the anionic polymerization of most other epoxides, including propylene oxide (POx),[9] is subject to side reactions.

4.07.2.1 Ethylene Oxide

Anion radicals such as sodium naphthalene can react with monomers in two ways, via electron transfer to monomer or by direct addition of the monomer to the anion radical. The second addition mechanism applies to EO.[10] Indeed the reaction of EO with naphthalene results in the formation of a bifunctional initiator through addition of two monomer molecules on a same naphthalene molecule (Scheme 2).

The kinetics and mechanisms of initiation of EO polymerization by alkali metal salts of carbanions (polystyryl (PS^-), cumyl, and fluorenyl (F^-)[11,12]) and of nitranions (carbazyl (N^-) and dibenzocarbazyl (DBN^-) derivatives[13]) (Scheme 3) have been investigated in detail in ethereal solvents.

The intrinsic reactivity of ion pairs and free ions in EO addition was determined. In the case of weakly delocalized anions, illustrated by PS^- and N^-, free ions are more reactive than ion pairs. In contrast, for more delocalized anions (F^-, DBN^-), the reactivity order was opposite. For instance, the rate of cleavage of EO by alkali salts of 9-methylfluoren-9-yl[12] decreases from tight ion pairs to solvated ion pairs and free ions. It was suggested that electrophilic activation of the epoxide by the metallic counterion (step 1 of Scheme 4) makes an important positive contribution to the ring-opening reaction (step 2) which overcomes the energy required for ion-pair dissociation. For more localized N^- or PS^- anions, the interaction of the anion with the cation is stronger and the energy required for separating the charges lowers the reactivity of ion pairs compared to free ions.

Initiation of the EO polymerization by alkali metal alkoxides has also been investigated in detail since the structure of these derivatives is close to that of alkoxide propagating species. In aprotic solvents of low-to-medium polarity, such as ethers, alkali metal alkoxides show a strong tendency to aggregate and yield complex reaction kinetics. This is particularly significant for small metals such as lithium or sodium. If the reactions follow a monomer order of 1, the order in alkoxide propagating species varies according to the counterion and

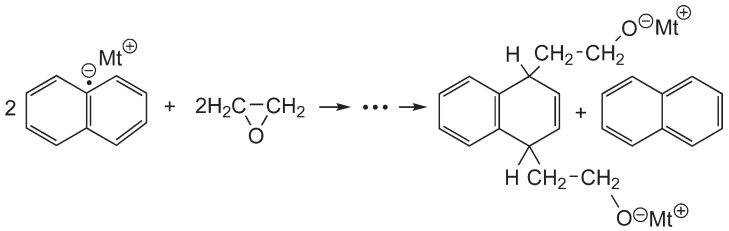

Scheme 2 Initiation of EO polymerization by naphthalene alkali metal salts (for a detailed mechanism, see Reference 10).

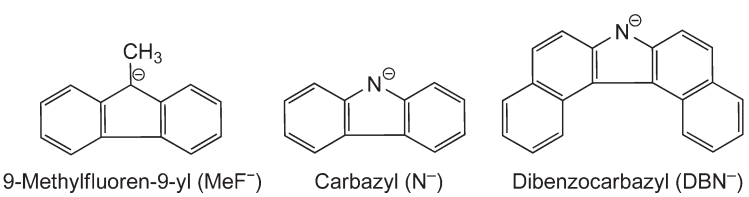

Scheme 3 Stable alkali metal salts used as initiator for EO polymerization.

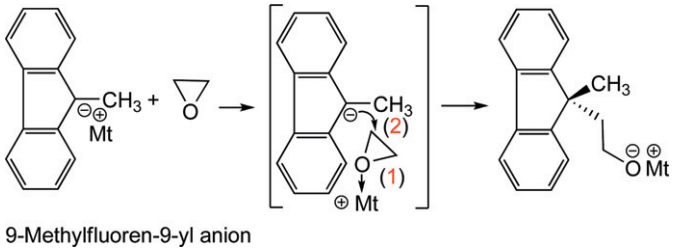

Scheme 4 Mechanism of initiation of EO polymerization by alkali salts of 9-Methylfluoren-9-yl.

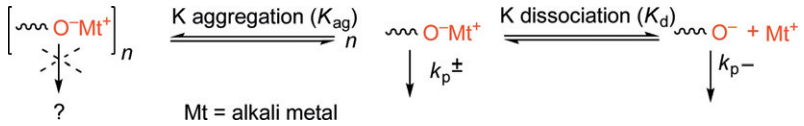

Scheme 5 Aggregates, ion pairs, and free ions in EO polymerization and their ability to contribute to propagation.

the solvent. This can be related to the presence of various amounts of aggregates, ion pairs, and free ions of different intrinsic reactivity. The main types of poly(EO) ends and their corresponding propagation rate constants are indicated in Scheme 5. EO polymerization within alkoxide aggregates is extremely slow and negligible in most cases.

The kinetics of EO propagation reactions have been investigated in media of various polarities. In HMPA ($\varepsilon = 30$, 20 °C) using the sodium, potassium,[7] and cesium[14] salts of the monomethylether of diethylene glycol as initiators, the reaction rates were found to be first order in monomer, zeroth order with respect to sodium alkoxide, and between zero and unity with respect to potassium alkoxide. This is explained by association of alkoxide chain ends as shown by viscometric measurements performed on living and dead polymerization mixtures. With cesium as counterion, aggregates are absent and the propagation rate constant, k_p, is a linear function of 1/[propagating species]$^{1/2}$, indicating that propagation proceeds by ion pairs and free ions.[14] Although the latter are present in very low proportion (see K_D value in Table 1), they are of much higher reactivity.[15] At 40 °C, k_p^- is approximately 100 times higher than $k_p^{\pm}$ of Cs ion pairs.

Several papers report studies on the anionic polymerization of EO in DMSO. The use of potassium *tert*-butoxide (*t*-BuOK) as initiator was reported to yield living poly(EO)s with molar masses controlled by the ratio [monomer]/[initiator][14,16,17] although dimsyl ion resulting from transfer to the solvent (Scheme 6) has been considered by some authors as the principal polymerization initiator.[18,19]

In the case of K and Cs salts, EO polymerization in DMSO proceeds almost exclusively by free ions[17] in agreement with a higher dissociation constant in this solvent ($K_d = 9.4 \times 10^{-2}$ mol l^{-1} at 50 °C for Cs counterion), in line with the high permittivity of DMSO (dielectric constant; $\varepsilon = 48$, 20 °C). With Na counterion, both ion pairs and free ions contribute to the propagation.[17] The estimated $k_p^{\pm}$ and k_p^- values are given in Table 1. It is worth noting the much higher propagation rate constants are observed in HMPA (at 40 °C) compared to DMSO (at 50 °C); if we neglect the difference in reaction temperatures, which would increase the gap, the ratio of about 1800 is observed between k_p^- in the two solvents. This large difference may be accounted for by an important stabilization of the free anion via hydrogen interaction with DMSO.

The kinetics of polymerization of EO have also been investigated in pure ethereal solvents.[20,22,24] In THF ($\varepsilon = 7.6$, 25 °C) in the presence of sodium, potassium, and cesium naphthalene as initiators, a living polymerization takes place,[20,22] the rate of propagation increasing with the size of the counterion.[1] The kinetics are however complicated by strong association of alkoxide end groups manifesting itself by the low fractional kinetic order of the reactants, that is, 0.25 for Na alkoxide and 0.33 for K and Cs salts.[20] Dissociation constants are very low (see Table 1).

Table 1 Dissociation constant and ion-pair and free ion propagation rate constants for EO polymerization in different solvents

Solvent	*T (°C)*	*Counterion*	K_D *(mol l^{-1})*	$k_p^{\pm}$ *(l mol^{-1} s^{-1})*	k_p^- *(l mol^{-1} s^{-1})*	*Reference*
THF	20	K	1.8×10^{-10}	0.05	-	20
	20	K + 222	3.0×10^{-7}	0.03	1.7	21
	20	Cs	2.7×10^{-10}	0.12	1.7	22
	20	Cs + Sphere	1.0×10^{-6}	0.09	1.7	23
HMPA	40	Cs	5.0×10^{-5}	0.2	22	14
DMSO	50	Na	6.1×10^{-4}	0.63×10^{-2}	1.2×10^{-2}	17
	50	K	4.7×10^{-2}			17
	50	Cs	9.4×10^{-2}			17

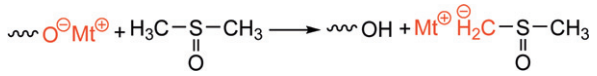

Scheme 6 Formation of dimsyl ion through transfer to DMSO.

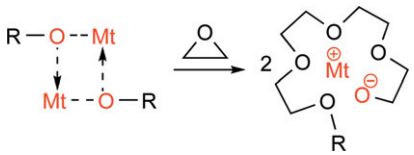

Scheme 7 Solvation of the alkoxide propagating species by the polyether growing chain.

The presence of an acceleration period at the beginning of the polymerization in ether solvents was interpreted as the increasing solvation by the polyether growing chain of alkoxide aggregates, until the chain reaches up to 4–6 EO units (Scheme 7).[22]

Addition of complexing agents of alkali metal cations, such as crown ethers or cryptands,[13,21,23] was shown to drastically increase the EO propagation rate in ether solvents. They both reduce the aggregation of alkoxide polymer ends and increase the proportion of free ions. For example, at 20 °C in THF, the dissociation constant of poly(EO)$^-$K$^+$ (Table 1) is 1700 times higher when K$^+$ is complexed by cryptand 222 (see Scheme 8). In this system, the reactivity of free ions is about 60 times higher than that of cryptated ion pairs. Surprisingly, the reactivity of cryptated ion pairs was found to be very close to or even lower than that of the corresponding noncomplexed ion pairs, though the charges are more separated.[21] A similar tendency was reported for cryptated Cs.[23] This has been explained by partial insertion of the oxygen anion in the cavity of the complexing agent.[1,25]

Early studies of EO polymerization in ether solvents dealt with initiating systems involving alkoxides, RO$^-$Mt$^+$, associated with their parent alcohol ROH to improve their solubility and limit the aggregation phenomenon.[15] Indeed, these systems are composed of two types of chains: growing chains with an alkoxide end and dormant chains possessing a -CH_2CH_2OH terminus. Since alcohols act as efficient chain transfer agents, true living poly(EO) is not formed in these conditions. However, the reversibility of the transfer process resulting from rapid exchanges between the two chain ends ensured the growth of both chains allowing control of the molar mass of poly(EO) ($M_n = [EO]/([RO^-Mt^+] + [ROH])$). The propagation and reversible transfer reactions are illustrated in Scheme 9.

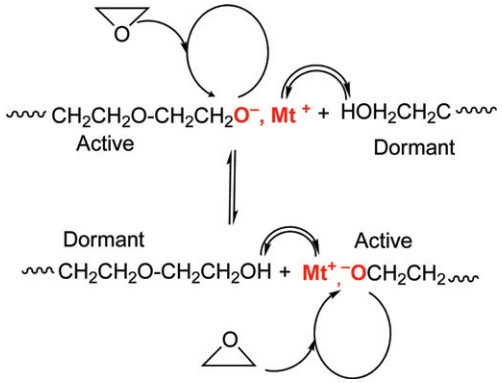

Scheme 9 Exchange reactions between active and dormant species in ROMt/ROH polymerization systems.

The presence of alcohol in the medium leads to a reduction of the apparent polymerization rate; the greater the proportion of alcohol introduced into the reaction medium, the lower the EO polymerization rate.[26,27] It was proposed that the hydroxy-terminated chains contribute to decrease the polymerization rate by hydrogen-bonding interactions with alkoxide ends. The combination of alkoxide with the parent hydroxy compound has been used to initiate EO polymerization in various media (THF, DMSO). This was used for the preparation of multibranched poly(EO). Typically, a polyhydroxy compound to be used as multifunctional initiator is partially deprotonated by the addition of 0.2–0.8 molar equivalent of an alkali metal derivative.[28,29] This limits aggregation of alkoxide species and preserves solubility, thus allowing a better control of the initiation and propagation of EO polymerization, but to the detriment of reaction kinetics.

Poly(EO), also often referred to as poly(ethylene glycol) (PEG), is a reference biocompatible polymer used in the biomedical field[30] as a result of its unique properties, namely, its chemical stability, solubility in both organic and aqueous media, nontoxicity, low immunogenicity, and low antigenicity.[31] PEG derivatives have been widely used as conjugates (PEGylation reaction) to increase the circulation half-life of biologically active molecules (e.g., enzymes, peptides, proteins), to improve the solubility of various anticancer agents (e.g., taxol or camptothecin), to impart enhanced permeability and retention, and to increase passive targeting of anticancer drugs.[32–35] PEG is also used as an efficient spacer in delivery systems such as PEG-grafted liposomes and nanoparticles. Several PEG-conjugated proteins are already available as clinical therapeutics.[36] Applications of PEO often require α,ω-heterodifunctional PEO-based oligomers possessing

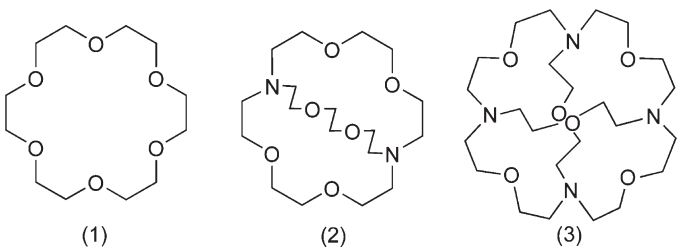

Scheme 8 Crown ether 18C6 (1) and cryptands 222 (2), and sphere (3) used to complex alkali metal cations in EO polymerization.

tailored reactive end functions to react with a variety of ligands.[28,36–39] Their preparation can be achieved readily owing to the living character of anionic EO polymerization.

In addition to these biomedical applications, PEG also serves as an inert support in liquid-phase organic synthesis[40] or as a polyelectrolyte in the presence of salts.[41–45]

4.07.2.2 Monosubstituted Epoxides

For monosubstituted epoxides such as POx, the monomer ring opening can proceed in two ways: attack on the methylene (1) or methine (2) carbons, leading respectively to the break of the CH_2–O or R–CH–O bond (Scheme 10). Indeed, in contrast to cationic polymerization, the nucleophilic attack of the alkoxide proceeds selectively on the methylene carbon (1). The secondary alkoxide generated by ring opening attacks a new monomer following the same mechanism. As a result of the high selectivity in the ring opening, polyethers with only head-to-tail enchainment are obtained.

The ring-opening mechanism is of the S_N2 type with inversion of the configuration at the methylene carbon atom of the epoxide ring where it is cleaved. This was shown using deuterated POx (Scheme 11).

Since racemic (*RS*)-POx monomer mixtures are most generally utilized, the resulting polymers are atactic and amorphous. Proportions of isotactic, heterotactic, and syndiotactic triads can be determined through resolution of the stereosensitive asymmetric carbon signal by ^{13}C NMR.[46] However, anionic polymerization of (*R*)- or (*S*)-epoxides yields the corresponding isotactic polyethers. This is the case for polymerization of the (–)-(*S*)-POx by potassium hydroxide, which yields a crystalline poly(POx).[47]

In the presence of K^+ as counterion (*t*-BuOK as initiator, 40 °C) and on the basis of overall polymerization rates, the reactivity of racemic POx in HMPA is about one-fourth that of EO.[48]

In contrast to the living character of the polymerization of EO, the anionic polymerization of substituted epoxides like POx[16,49] initiated by alkali metal derivatives is subject to transfer reactions to the monomer. Indeed, the highly basic alkoxide propagating species can pull out a proton of the monomer substituent, leading to chain termination and the formation of a new growing chain bearing a terminal double bond, as indicated in Scheme 12 in the case of POx.

Bulk polymerization of POx at 90–150 °C yields poly(POx) with molar masses limited to about 6000 g mol^{-1}, which corresponds to the ratio of the apparent rate constant and the rate constant of chain transfer to monomer (k_p/k_{trM}) of 100.[49] In HMPA at 40 °C, this ratio is equal to 75. Indeed, several factors influence the extent of this chain transfer reaction:[50] temperature, initiator, and nature of the counterion. Chain transfer to monomer decreases in the order $Na^+ > K^+ > Cs^+$, in agreement with interactions between the metal cation and the oxygen of the monomer.

The reactivity of other monosubstituted epoxides depends on both electronic and steric factors associated with the substituent attached to the epoxide ring.[6] For instance, the reactivity of 2,2-dimethyloxirane (DMO) is 10 times lower than that of POx, whereas glycidyl ethers such as *tert*-butyl glycidyl ether (*t*-BuGE) are more readily polymerized than POx[48] (see also Table 2). The complexation of the counterion by crown ethers significantly increases the reactivity. This can be explained both by a reduction of aggregates and by a larger charge separation of ion pairs accompanied by an increase in ion dissociation constant.

In relation to the different acidic character of the hydrogens on the α-carbon of the monomer, the nature of the epoxide substituent plays an important role in the chain transfer process.[3,27,51] For instance, the anionic polymerization of long-chain alkylene oxides employing potassium and cesium alkoxides as initiators is much less subject to chain transfer processes than that of POx. This is shown by the higher poly(2-butyloxirane) molar masses obtained at temperatures ranging between 20 and 80 °C (see Table 3).[52]

Owing to the increase in reactivity in the presence of crown ethers, the polymerization temperature of 2-butyloxirane (BO) and of higher 2-alkyloxiranes could be reduced below 0 °C. This allowed the elimination of side reactions almost completely (Table 4). However, very long reaction times were required (4–8 days). The best results were obtained with potassium alkoxides and 18-crown-6 in toluene at –10 to –23 °C (Table 4). Poly(2-ethyloxirane), poly(2-butyloxirane), and poly(2-hexyloxirane) homopolymers with molar masses of up to 50 000–100 000 g mol^{-1}, close to theoretical values, and $M_w/M_n < 1.1$ were synthesized in this way.

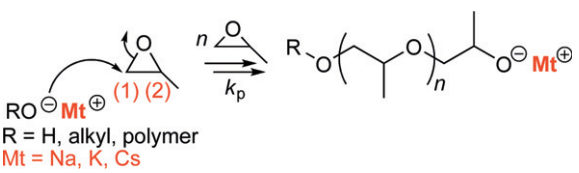

Scheme 10 Mechanism of initiation and propagation of anionic polymerization of POx.

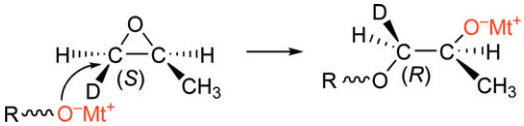

Scheme 11 S_N2 ring-opening mechanism with inversion of the configuration at the cleaved methylene carbon atom of the epoxide ring.

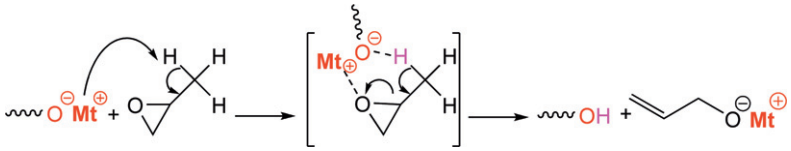

Scheme 12 Chain transfer to monomer during POx polymerization.

Table 2 Influence of addition of crown ether 18C6 on polymerization time and rate constant of POx, phenyl glycidyl ether (PGE), and *t*-butylglycidyl ether (*t*-BuGE)

Monomer	*Initiator*	r[a]	*Solvent*	*T (°C)*	*Polymerization time (h)*	*Conv. (%)*	$k_{p(18C6)}/k_p$	*Reference*
POx	$MeOCH_2CH(CH_3)OK$	1.5	Bulk	60	92	95	13	51
PGE	*t*-BuOK	1	THF	25	7	81	14	27
t-BuGE	*t*-BuOK	1	THF	25	6	95	7	3
t-BuGE	*t*-BuOK	2	THF	25	6	95	13	3

[a] *r* = [complexing agent]/[initiator].

Table 3 Polymerization conditions and characteristics of poly(2-butyloxirane) synthesized in the presence of K or Cs *tert*-butoxide in toluene without or with crown ether 18C6[52]

Counterion	*Polymerization temperature (°C)*	*Reaction time (h)*	*Conv. (%)*	$\bar{M}_n$ theor.[a]	$\bar{M}_n$ exp.[b]	$\bar{M}_w/\bar{M}_n$[c]
K	80	40	96	14 700	11 200	1.15
Cs	80	18	97	14 800	11 700	1.11
Cs	60	38	94	13 800	14 400	1.06
K/18C6	20	19	92	47 000	43 600	1.11
Cs/18C6	20	68	81	39 600	28 000	1.13

[a] Calculated from the amount of initiator and polymerized monomer.
[b] From SEC with triple detection.
[c] From SEC, PS calibration. Molar ratio 18C6/metal = 3.
Reprinted with permission from Allgaier, J.; Willbold, S.; Taihyun, C. Macromolecules 2007, 40, 518–525.[52] Copyright 2011 American Chemical Society.

Table 4 Optimized conditions for the polymerization of BO, 2-hexyl oxirane (HO), and 2-octyl oxirane (OO) in the presence of *t*-BuOK with crown ether 18C6 and characteristics of the polymers[52]

Monomer	*Polymerization temperature (°C)*	*Reaction time (h)*	*Conv. (%)*	$\bar{M}_n$ theor.[a]	$\bar{M}_n$ exp.[b]	$\bar{M}_w/\bar{M}_n$[c]
BO	20	19	92	47 000	43 600	1.11
HO	20	92	99	67 800	52 500	1.18
HO	–23	187	84	56 500	52 700	1.09
OO	–23	189	73	61 600	50 000	1.09
OO	–14	187	98	51 300	48 900	1.05

[a] Calculated from the amount of initiator and polymerized monomer.
[b] From SEC (size exclusion chromatography) with triple detection.
[c] From SEC, PS calibration. Molar ratio 18C6/K = 3. Solvent used is toluene.
Reprinted with permission from Allgaier, J.; Willbold, S.; Taihyun, C. Macromolecules 2007, 40, 518–525.[52] Copyright 2011 American Chemical Society.

Another mechanism of chain transfer to the monomer has been highlighted by Stolarzewicz[27] in the case of phenyl glycidyl ethers (PGEs). As shown in Scheme 13, it involves abstraction of a proton from the methine carbon of the ring and the formation of new carbonylated initiating species. The author argues that this reaction could also occur during the polymerization of propylene and styrene oxides.

The world market for poly(alkylene oxide)s, which is mainly based on poly(POx), is estimated to be over 4 million tons since 2007.[53] Poly(POx) is mainly produced as a telechelic oligomer for polyurethane industry and as a di- and triblock copolymer

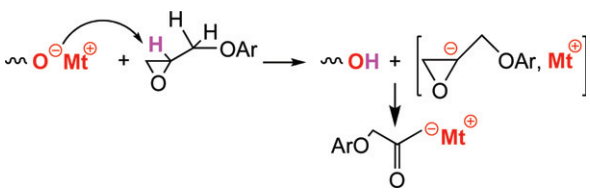

Scheme 13 Second type of chain transfer to the monomer in glycidyl ether polymerizations.[27]

with EO for surfactant applications. Poly(alkylene oxide)s are usually produced worldwide, according to the same anionic process using sodium, potassium, or cesium hydroxide in the presence of glycerol or other triol or tetrol in a discontinuous batch process. The use of multihydroxy compounds as initiators allows compensation of the loss of OH functionality of the chain due to chain transfer to monomer. Commonly, a small amount of EO is added at the end of the reaction to convert the secondary hydroxyl end group to primary hydroxyl end group, which has a higher reactivity in urethane formation.[54] Cesium hydroxide, which allows faster polymerization and reduces the amount of mono-ol resulting from transfer by half, is also used. Recently, a competitive process based on multimetal cyanide (MMC) catalyst,[55] which yields poly(POx) with almost no chain unsaturation, has also been used industrially.

4.07.3 Initiation by Organic Bases as Initiators

Complexation of alkali metal counterions was shown to significantly increase the reactivity of propagating species in anionic polymerization. Besides the use of crown ethers or cryptands, the use of large organic molecules as metal-complexing agents or directly as organic counterions has been studied.

4.07.3.1 Organic Bases as Counterions

The use of tetraalkyl ammonium as counterions was explored but remains limited due to the low thermal stability of the compound. As an example, didodecyldimethylammonium hydroxide was employed by Maitre *et al.*[56] to polymerize PGE. The polymerization was performed in bulk at 60 °C and complete conversions were obtained for short polymerization times, but molar masses of poly(PGE) did not exceed 3000 g mol^{-1}. Transposition of this system to miniemulsion leads to several oligomeric populations, with the highest polymerization degree of 8.[56]

Phosphonium salts and phosphazene bases developed by Schwesinger and Schlemper[57] and Schwesinger *et al.*[58] (**Scheme 14**) are of broader interest for epoxide polymerization. These soft and highly delocalized organic compounds reduce aggregation phenomena and favor ionic dissociation by increasing the interdistance between charges in ion pairs.

Phosphonium and phosphazene bases have been successfully used as counterions for polymerizing siloxanes,[59] lactones, and (meth)acrylates.[60–62] Their use in the synthesis of poly(EO)[63,64] and poly(POx)s[53,65,66] and in the preparation of linear and branched copolymers with polyether blocks has been reported.

The polyaminophosphazene base *t*-BuP$_4$ was used in combination with alkyllithium as initiator for the anionic polymerization of EO[67] (**Scheme 15(a)**). The space inside the molecule is sufficient to host the compact lithium cation and the base works as a cryptand for Li$^+$ ions with the polar amino and imino groups located inside the globular molecule and the outer shell formed by alkyl substituents. The equilibrium between complexed lithium alkoxide ion pairs and reactive free anions is thus shifted allowing polymerization.

One major interest in these organic bases is the activation of living polymer chains with lithium counterions toward epoxide polymerization. This is of particular interest for the synthesis of poly(EO)-containing block copolymers by sequential anionic

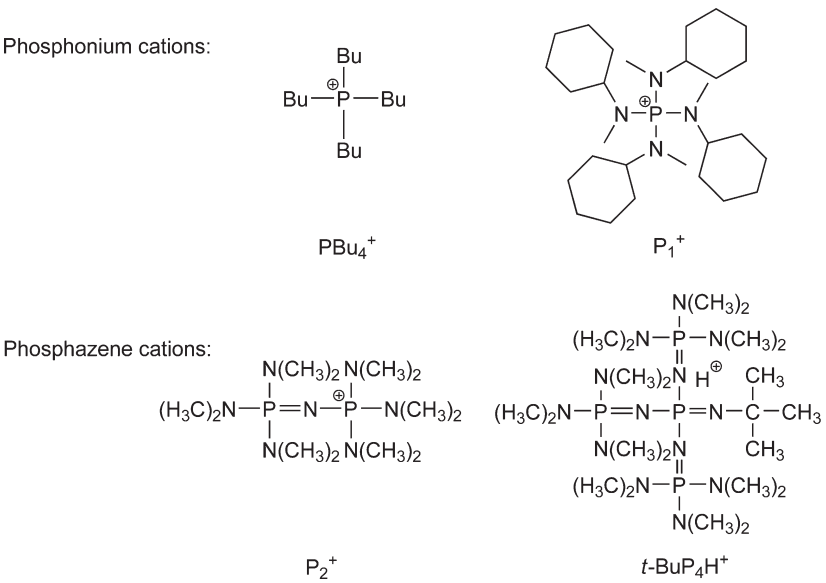

Scheme 14 Phosphonium and phosphazene cations used as counterions for the anionic polymerization of oxiranes.

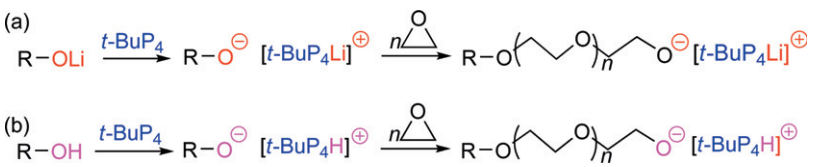

Scheme 15 Initiation of EO polymerization involving activation of lithium alkoxide (a) and alcohol (b) by phosphazene *t*-BuP$_4$.

polymerization. Using *t*-BuP_4 as an additive to living polymers prepared using organolithium initiators has the advantage that the block poly(EO) can be prepared without an exchange of the cation. This strategy was successfully applied to the synthesis of polystyrene-*block*-poly(EO), although the presence of an induction period resulting from the slow disaggregation of the lithium alkoxide ends complicates the EO polymerization.[68]

Additionally, Esswein *et al.*[63] have directly used the strong poly(aminophosphazene) base *t*-BuP_4 in the presence of mono- and plurifunctional alcohols without any metallic cation to generate the alkoxide of the protonated base and initiate the anionic polymerization of EO (**Scheme 15(b)**). Using methanol as initial alcohol, poly(EO) oligomers, with M_n up to 6000 g mol^{-1} and low polydispersity ($M_w/M_n \approx 1.1$), were obtained in THF or toluene after 48 h reaction at 80 °C. Graft copolymers of poly[ethylene-*graft*-(vinyl alcohol)] (PEVA) with poly(EO) were synthesized in high yields in this way.[64]

Anionic ring-opening polymerization of POx initiated by partially deprotonated dipropyleneglycol (DPG) in the presence of the phosphonium cation tetrakis[cyclohexyl(methyl) amino]phosphonium as counterion (P_1^+; **Scheme 14**) has been reported by Rexin and Mülhaupt.[65,66] An alcohol/phosphonium alkoxide mixture (95/5) was utilized to control reactivity, making use of a fast proton exchange reaction between dormant hydroxy compounds and active phosphonium alkoxide ends (**Scheme 16**).

The reaction was performed at 100 °C in pure POx under reflux. Polymerization rates and hydroxyl functionalities of poly(POx)s prepared in the presence of K^+ and other phosphonium and phosphazene base counterions were compared (**Table 5**).[66] Polymerization rates of POx vary in the following order: $PBu_4^+ < K^+ < P_1^+ < t\text{-}Bu_4PH^+ < P_2^+$. These differences were explained by a more or less pronounced delocalization of the charge inside the counterion. Indeed, for a similar steric

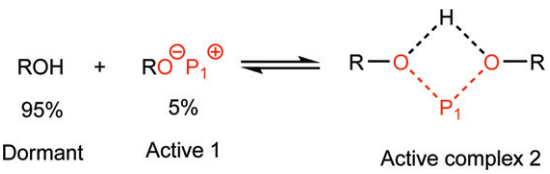

Scheme 16 Equilibrium between active and dormant species.

Table 5 Influence of various nonmetallic counterions on the rate of polymerization (Rp) of POx initiated by dipropylene glycol deprotonated at 5% and on the formation of terminal unsaturation; Bulk, 100 °C[66]

Counterion	V_p *(h^{-1})*	*C=C (mmol kg^{-1})*
PBu_4^+	0.3	27
K^+	0.6	13
P_1^+	1.8	38
t-BuP_4H^+	40.2	60
P_2^+	42.8	55

Rexin, O.; Mülhaupt, R. J. Polym. Sci., Part A: Polym. Chem. 2002, 40, 864–873.[66]

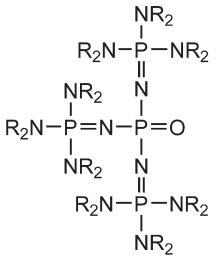

tris(Phosphazenyl) phosphine oxide (PZO)

Scheme 17 Tris(phosphazenyl) phosphine oxide(PZO) used in presence of glycerol for POx polymerization.

hindrance, P_1^+ involves a 6 times faster polymerization than PBu_4^+, whose charge is not delocalized. Similarly, phosphazenes, whose delocalization is more pronounced than the delocalization of P_1^+, lead to a better separation of the charge and consequently to a faster polymerization.

Polyether polyols were produced also at varied temperatures in the presence of DPG and bulky iminophosphonium counterions $R_4P_1^+$, whose substituents, R, were varied as propyl, octyl, and cyclohexyl (denoted as P_1^+ in **Scheme 14**).[66]

All polyols show unimodal and narrow molar mass distributions with values for M_w/M_n of about 1.20 without any subdistribution. The varied substituents, propyl, octyl, and cyclohexyl, have no influence on the propagation rate or on the total degree of unsaturation. The equilibrium between active alkoxide and dormant species, depicted in **Scheme 16**, permits the control of molar masses and the maintenance of a low poly (POx) dispersity. Indeed, in spite of faster polymerization, a better control of POx polymerization is not achieved compared to K^+; the increase of polymerization rate is accompanied by an increase in the proportion of carbon–carbon double bonds, and only poly(POx) oligomers can be synthesized.

In a recent paper, Nobori *et al.*[53] claimed an increase of the POx polymerization rate (450 times) and a reduction of the transfer to monomer corresponding to the reduction of mono-ols by a factor of 5 and the formation of poly(POx) up to 20 000 g mol^{-1} using glycerol in the presence of *t*-BuP_4 or tris (phosphazenyl) phosphine oxide (PZO) (**Scheme 17**).

4.07.3.2 Organic Bases as Nucleophilic Initiators

Tertiary amines like benzyldimethylamine, pyridine, and imidazole have been widely used as a base to initiate the anionic polymerization of PGE and its derivatives as well as for the synthesis of epoxy resins of diglycidyl ether of bisphenol A (DGEBA). Even if initiation occurs with amine alone, the introduction of an alcohol is a common procedure to suppress the observed induction period and increase the polymerization rate.[69] Two initiation mechanisms have been proposed[70,71] (**Scheme 18**): (1) direct nucleophilic attack of the amine onto the cyclic monomer to yield the zwitterion (a); and (2) formation of alkoxide (b) via proton transfer in the presence of alcohol. Fast exchange between dormant alcohol and active alkoxide allows chain growth from both initial amine (a) and alcohol (b).[72] Poly(PGE) oligomers whose degree of polymerization does not exceed 5 are obtained. The presence of terminal double bonds indicates significant transfer to the monomer via

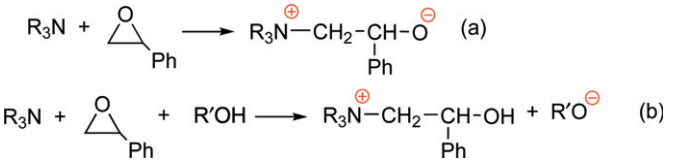

Scheme 18 Initiation steps in the PGE polymerization initiated by tertiary amines in the presence of an alcohol.

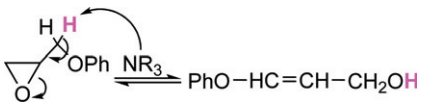

Scheme 19 Formation of allylic alcohol from PGE in the presence of tertiary amine.

hydride abstraction. This may involve alkoxide chain ends or direct proton abstraction by the amine initiator (Scheme 19).[70]

4-(Dimethylamino)pyridine can initiate readily the anionic polymerization of PGE.[71] This is explained by its conjugated structure in which the tertiary amine has a positive charge while the pyridine nitrogen brings a negative charge which can attack the epoxide monomer (Scheme 20). PGE conversions are complete in 1 h at 80 °C or in 10 min at 110 °C. However, only low-molar-mass poly(PGE) polymers ($< 1000\,g\,mol^{-1}$) were obtained due to an intramolecular transfer reaction involving attack of the pyridine ring by the terminal alkoxide (Scheme 20).

Recently, N-heterocyclic carbenes (NHCs), such as 1,3-diisopropylimidazol-2-ide (**1**), were found to initiate the ring-opening polymerization of EO at 50 °C in DMSO.[73] In the presence of **1**, poly(EO)s of narrow dispersity and molar masses perfectly matching the [monomer]/[**1**] ratio are obtained, attesting to the controlled/living character of such carbene-initiated EO polymerizations. However, long reaction times are needed. It is argued that NHC adds to EO via nucleophilic attack onto one methylene group of EO to form a zwitterionic species, namely 1,3-diisopropylimidazolidin-2-ylium alkoxide, which further propagates by a zwitterionic ring-opening polymerization (ZROP) mechanism (Scheme 21). In this process, the attached imidazolidinylium moiety at the chain head also plays the role of the counter cation.

End-functionalized poly(EO) chains were generated by adding at the end of the polymerization a functional terminating agent Nu-E, in which Nu and E represent a nucleophilic and electrophilic moiety respectively (Scheme 21). Nu was found to substitute the imidazolium head group (see above), whereas E terminates the chain. α,ω-Dihydroxy, α-benzyl-ω-hydroxy, and α-azido-ω-hydroxy difunctionalized poly(EO)s were obtained in this way.

Controlled EO polymerization was found to proceed also with catalytic amounts of the NHC in the presence of Nu-E as polymerization additives in DMSO at 50 °C, typically in molar proportions [NHC]/[Nu-E]/[EO] = 0.1/1/100.[74] In this case, the poly(EO) molar masses match the [EO]/[Nu-E] ratio. Characterization of poly(EO)s confirmed the quantitative introduction of the nucleophilic moiety (Nu) and of its electrophilic component (E = H or $SiMe_3$) in the α- and ω-positions, attesting that Nu-E controls the poly(EO) molar masses and functionality.

Two possible mechanisms are considered (Scheme 22): (a) nucleophilic attack of the NHC catalyst onto EO and the formation of a zwitterionic intermediate; or (b) activation of the E moiety by the NHC followed by EO polymerization initiated by the Nu moiety. In the second case, the NHC behaves similarly to phosphazene bases. Reversible exchanges with Nu-E molecules involving the formation of active and dormant chains then yield α-Nu-ω-E poly(EO)s.

Access to α,ω-difunctionalized poly(POx) (PPO) oligomers based on a metal-free and solvent-free polymerization using an NHC serving as either direct initiator or organocatalyst has also been recently described by the same group.[75] Dihydroxytelechelic poly(POx) oligomers were synthesized by quenching the NHC-initiated ring-opening polymerization of POx with water,

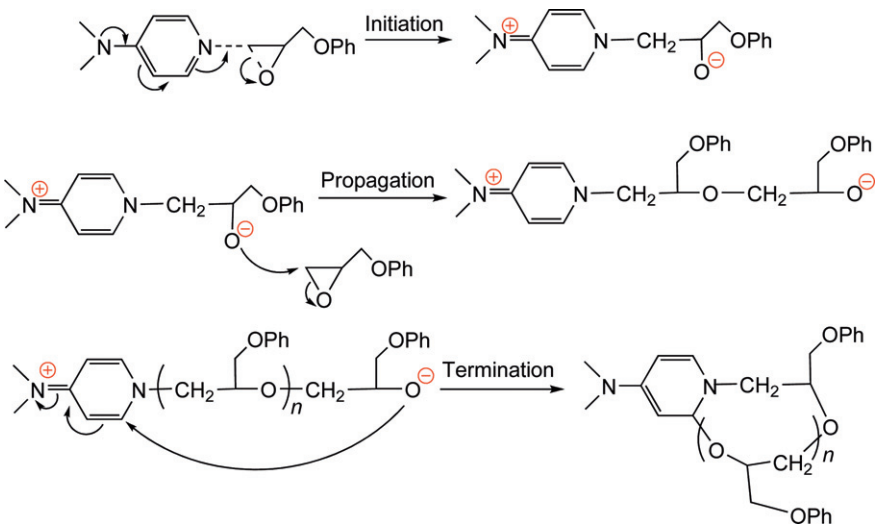

Scheme 20 Polymerization of PGE initiated by 4-(dimethylamino)pyridine.

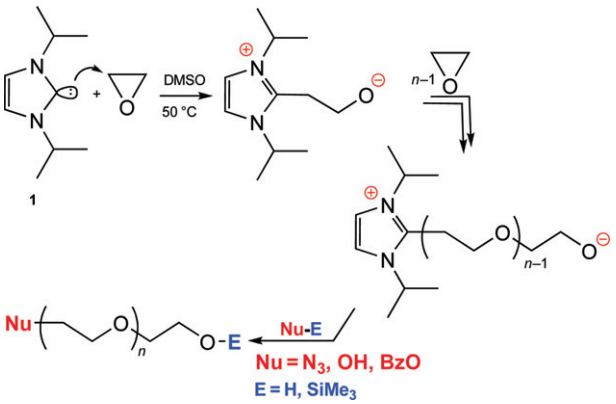

Scheme 21 Proposed mechanism of ZROP of EO initiated by 1,3-diisopropyl-2,3-dihydroimidazol-2-ide.

whereas α-benzyl-ω-hydroxy and α-propargyl-ω-hydroxy difunctionalized PPOs were prepared via an NHC-catalyzed ring-opening polymerization, using $PhCH_2OH$, $PhCH_2OSiMe_3$, and $HC{\equiv}CCH_2OH$ as functionalizing agents. Characterizations of all α,ω-difunctionalized poly(POx)s attest to the quantitative introduction of functional groups at both α- and ω-positions and the formation of narrow-molar-mass oligomers.

4.07.4 Coordination Anionic Polymerization

Coordination organometallic polymerization catalysis can be considered as borderline to anionic polymerization processes since epoxide ring opening involves a nucleophilic-like mechanism, which is assisted by monomer coordination on a metal atom of the catalytic system. In this preliminary coordination step ascribed to the Lewis acidity of the metal, the epoxide ring is activated for a nucleophilic attack, while the catalyst metal–X bond is weakened, increasing the nucleophilic character of the X moiety.

These systems can yield high-molar-mass polyethers, which could not be obtained using conventional anionic polymerization except for poly(EO). The possibility to synthesize stereoregular and/or optically active polyethers with crystalline properties is also an important particularity of these coordination processes.

4.07.4.1 Monometallic Coordinating Catalytic Systems

The first coordination epoxide polymerization catalytic system was reported by Pruitt and Baggett[76] in 1955. It was based on iron trichloride. Since that time, metal-based catalysts have been widely exploited for epoxide polymerization. The most studied systems are those based on zinc or aluminum derivatives. A first group consists of diethylzinc or trialkylaluminum associated to a 'cocatalyst', which is generally water or an organic compound (alcohol, amine, and other compounds) that reacts with the alkyl metal to form *in situ* new metal derivatives as the true catalytic system exploited (see **Table 6**). For a detailed review on the coordination polymerization of epoxides, see Kuran.[77]

Trialkylaluminum and dialkylzinc when used alone yield very low epoxide conversions with long polymerization times.[90] Addition of water[91,92] results in the formation of active metal oxides containing Mt–O–Mt bonds. Indeed these catalysts yield a mixture of several polymer populations that are produced according to different mechanisms.[93] For example, POx polymerization in the presence of $AlEt_3/H_2O$ yields three polymer fractions: (1) the first fraction constituted by isotactic high-

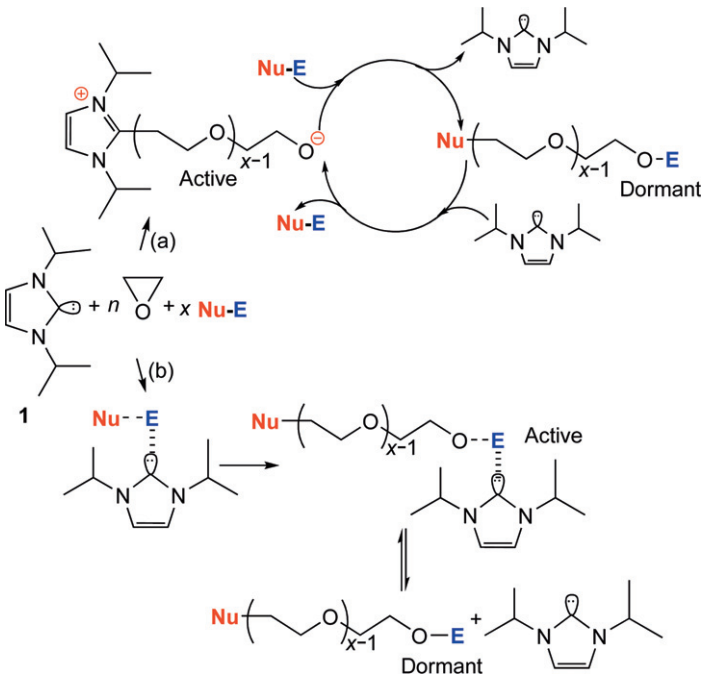

Scheme 22 Proposed mechanism for epoxide polymerization in the presence of NHC and additives constituted of nucleophilic and electrophilic parts.

Table 6 Main catalytic systems used for the coordination polymerization of epoxides[78]

Monomer	*Catalysts*	*Reference*
Methyloxirane	$FeCl_3$/POx, $ZnEt_2/H_2O$, $AlEt_3/H_2O$/pyridine, and others	47,76,79–81
Phenyloxirane	$ZnEt_2(H_2O)$	82,83
(Haloalkyl)oxiranes (e.g., ECH)	$FeCl_3$/POx, $AlEt_3/H_2O$(/pyridine)	84
Oxiranes substituted with acetal groups	$ZnEt_2$/MeOH, $ZnEt_2$/cyclohexanol	78
Oxiranes substituted with ester groups	$AlEt_3/H_2O$/acetylacetone	85
Oxiranes substituted with organosilane or organosiloxane	$ZnEt_2/H_2O$	86
Oxiranes substituted with nitrile	$Al(i\text{-}Bu)_3/H_2O$/acetylacetone	87
2,3-Dimethyloxirane	$Al(i\text{-}Bu)_3/H_2O$, $ZnEt_2/H_2O$	78
bis(Chloromethyl)oxirane	$Al(i\text{-}Bu)_3/H_2O$	88
1,2-Epoxycyclohexane	$ZnEt_2$, $(EtZnOMe)_4$, $Al(i\text{-}Bu)_3/H_2O$, $AlEt_3/H_2O$/acetylacetone, and others	89
Others (ethyl, *tert*-butyl, neopentyl, allyl amines, sulfones, ether, amides)	$ZnEt_2/H_2O$	78

molar-mass chains arising from a living-like coordination polymerization mechanism;[92] (2) the second fraction corresponding to low-molar-mass amorphous chains; and (3) the last fraction composed mainly of tetramers. The last two populations are attributed to a cationic polymerization process associated with the presence of highly acidic metal sites as indicated by the presence of irregular head-to-head and tail-to-tail enchainments and the presence of oligocyclic structures.

Isotacticity of poly(POx) chains corresponding to the crystalline fraction is explained by steric constraints and orientation of the complexed monomer, which induces stereoselectivity in the nucleophilic attack by the chain end. It was demonstrated that monomer insertion proceeds by attack at the carbon atom of the epoxide ring where it is cleaved with inversion of the carbon configuration. This necessitates an attack of the complexed monomer by the nucleophile from the back, which requires the participation of two adjacent aluminum atoms and chain transfer from one aluminum atom to the other one at each monomer addition. The coordination polymerization mechanism proposed by Vandenberg[94] for the trialkylaluminum/water system is shown in **Scheme 23**.

The complexation results in partial electron transfer from the epoxide to the metal, rendering the methylene carbon atom of the ring more prone to nucleophilic attack. Coordination also induces a concerted electron transfer between the two adjacent aluminum atoms, which weakens the polymer–aluminum bond, increasing reactivity of the corresponding alkoxide moieties toward the electrophilic carbon of the neighboring epoxide.

The cationic polymerization mechanism that takes place aside from the coordinative process is illustrated in **Scheme 24** in the case of the $ZnEt_2/H_2O$ catalytic system;[84] coordination of an epoxide molecule to a highly acidic metal atom leads to the formation of 'oxonium'-like species making the two-ring carbon atoms strongly electrophilic, thus allowing nonregiospecific ring opening by attack of another epoxide molecule.

Additives such as pyridine, tertiary amines, or acetylacetone have been used to modulate the metal acidity and improve the selectivity toward high-molar-mass polymers. As an example, the addition of acetylacetone as chelating agent to AlR_3/H_2O or ZnR_2/H_2O systems permits, by limiting the cationic process, to

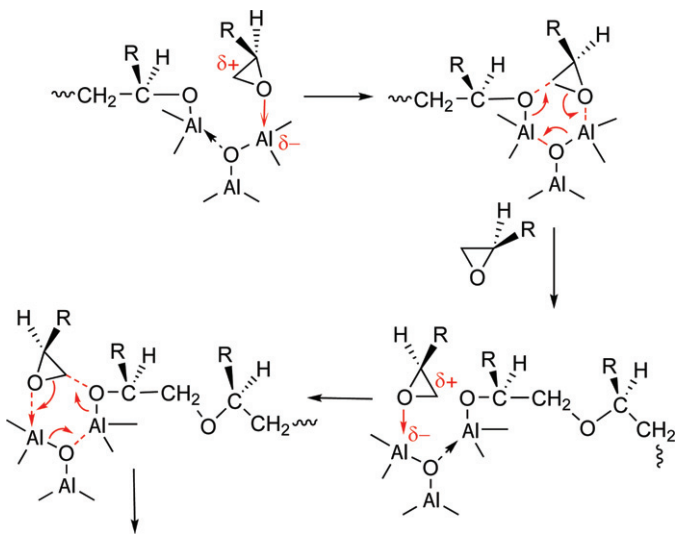

Scheme 23 Mechanism proposed for epoxide activation and polymerization by AlR_3/H_2O.[94]

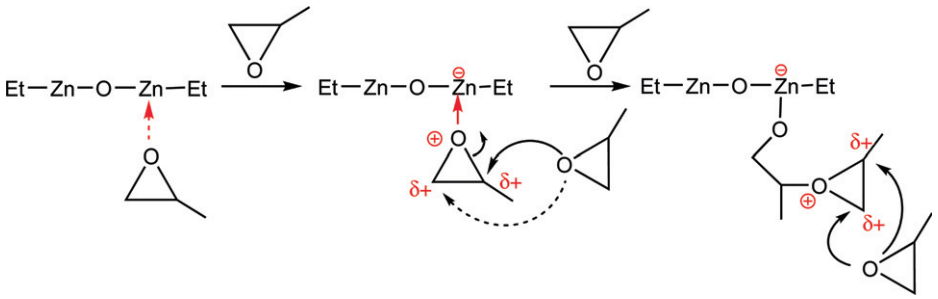

Scheme 24 Mechanism proposed for cationic polymerization of epoxide by the ZnR_2/H_2O system. Electron transfer to the epoxide rendering the two-ring carbon atoms highly electrophilic is illustrated by δ+ charges.

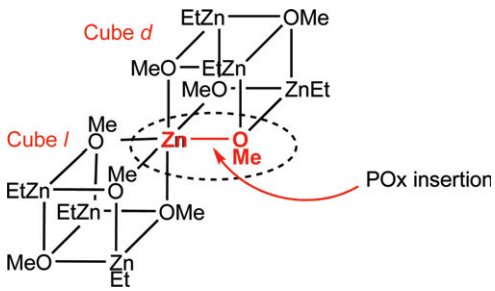

Scheme 25 Structure of $[Zn(OMe)_2{\cdot}(EtZnOMe)_6]$.

increase the proportion of crystalline polymer.[94] Also by decreasing the amount of the most acid sites, addition of pyridine or tertiary amines leads to the same effect.[81,95] As a consequence, the crystalline polymer fraction is higher but the overall polymerization rate is decreased.

Tsuruta *et al.* have investigated diethylzinc/alcohol systems for the polymerization of epoxides. Several well-defined active complexes such as $[Zn(OMe)_2 \cdot (EtZnOMe)_6]$[96–98] (Scheme 25) and $[Zn(OCH(Me)CH_2OMe)_2 \cdot (EtZn(OCH(Me)CH_2OMe))_2]$ have been identified as initiating species[99] for the coordinated POx polymerization.

Initiation takes place at the central zinc–internal methanolate bond,[100,101] represented in red in Scheme 25. Indeed the diethylzinc/alcohol systems may lead to the formation of two polymer fractions: one essentially isotactic with high molar masses and a second one atactic with lower molar masses. Both contain 95% of head-to-tail enchainments, which suggests that the amorphous fraction is not formed by cationic polymerization. The high molar masses, typically 10^5 g mol^{-1}, result from a slow initiation and only 10^{-4}–10^{-3} mol of polymer is obtained per 1 mol of initiator. On the basis of a continuous increase in molar mass with conversion, the polymerization of POx was qualified as living-like by Ishimori *et al.*[97] and Tsuruta.[100]

In contrast to the above-reported coordinated polymerization mechanisms, it was proposed that oxirane molecules coordinate to the same zinc atom prior to undergoing a nucleophilic attack on their less substituted carbon (Scheme 26).[102,103]

4.07.4.1.1 Stereoselective and stereoelective coordination polymerizations: tacticity control

Complexes such as $[Zn(OMe)_2 \cdot (EtZnOMe)_6]$, shown in Scheme 25, possess a centrosymmetric structure consisting of two enantiomorphic cubes whose common vertex is a zinc atom.[102] According to Tsuruta,[104] these cubes constitute enantioselective *d* and *l* sites, which in the presence of racemic monomer mixtures, such as POx, favor the incorporation of either the (*R*) or the (*S*) enantiomer and yield isotactic and crystalline chains constituted of either (*R*) or (*S*) monomer units. For instance, when the nucleophilic attack is achieved by a methanolate of the *d* cube, the insertion of *l* enantiomers will be favored. Similarly when methanolate of *l* cubes are involved the formation of *d* enantiomers is privileged.[104] Since in this complex the two enantioselective sites are in equal proportion, the two enantiomeric forms of the monomer will be incorporated selectively into distinct isotactic chains. This corresponds to a stereoselective polymerization. This interpretation was confirmed later by Furukawa *et al.*[80] and Kuran and Listos,[103] who used a chiral amino acid and a chiral alcohol, respectively, for the alcoholysis of diethylzinc. In this case, the enantioselective sites are not equivalent and one of the two enantiomers of the monomer is preferentially polymerized. This yields an optically active polymer while the residual monomer is enriched in the opposite enantiomer, corresponding to the stereoelective polymerization.

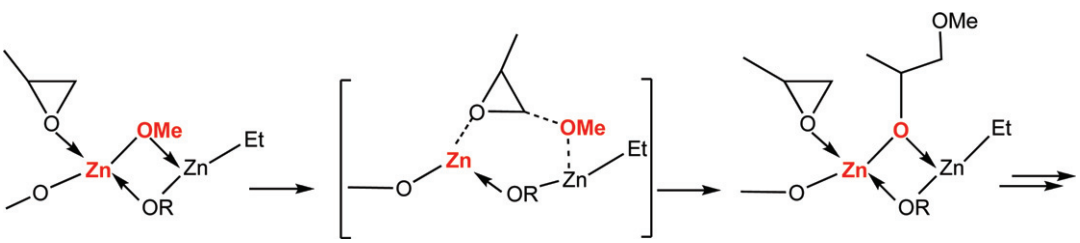

Scheme 26 Mechanism proposed for POx polymerization initiated by the $ZnEt_2$–MeOH system. Other interactions between Zn and oxygen atoms, not directly involved in POx insertion, are omitted.

4.07.4.2 Porphyrin Salts

Epoxide polymerization catalysts of quite different characteristics are those constituted by the metalloporphyrins of aluminum and zinc, such as (5,10,15,20-tetraphenylporphinato)aluminum chloride ((TPP)AlCl), (5,10,15,20-tetraphenylporphinato) aluminum methoxide ((TPP)AlOMe) (see Scheme 27), and (5,10,15,20-tetraphenyl-21-methylporphinato)zinc methoxide ((MTPP)ZnOMe).[105–109]

The covalent nature of the aluminum–X bond suggests that polymerization occurs following a coordination process. This hypothesis is reinforced by the exclusive presence of regular head-to-tail enchainments[109] and tacticity which is dependent on porphyrin structure.[110] Indeed the substituents in ortho positions of peripheral phenyl groups affect the reactivity of the Al–X bond; polar groups lead to a very high initiation activity, whereas nonpolar substituents result in an opposite effect.

When compared to the abovementioned highly associated multinuclear coordination catalysts of very low initiation efficiency, metalloporphyrins with mononuclear Mt–X species have been reported to be excellent catalysts for the living polymerization of epoxides.[105,111,112] The molar mass distribution of the polyethers obtained is narrow, and their molar mass can be controlled by changing the epoxide-to-catalyst mole ratio. As illustrated in Figure 1, poly(POx) chains with molar masses up to 70 000 g mol^{-1}, in good agreement with theoretical ones, have been synthesized, with a unimodal distribution and dispersity lower than or equal to 1.5.[109] Absence of chain transfer reactions allowed the synthesis of a series of block copolymers, including POx-*b*-EO, BO-*b*-POx, POx-*b*-ECH (ECH, epichlorohydrin), lactone-*b*-POx, and lactone-*b*-EO.[113,114]

Aluminum porphyrins are also effective polymerization catalysts for lactones[114,115] and acrylates.[116] Porphyrins based on manganese or zinc, for example, present similar characteristics.[117]

Although EO polymerization can be achieved quite rapidly (reaction half-time is about 30 min at room temperature for [EO]/[(TPP)AlCl] = 400 in dichloromethane), other epoxides show a lower reactivity. In similar conditions, it requires several hours for POx and 1,2-epoxybutane (BOx),[105] whereas for styrene oxide or 1,2-epoxy-2-methylpropane conversions do not exceed 15% after 8 days of reaction (Table 7).[109]

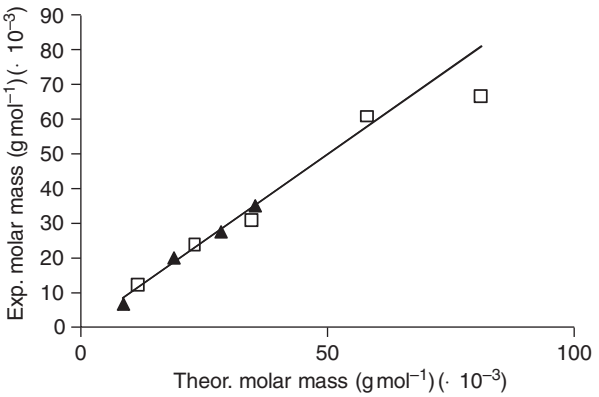

Figure 1 Evolution of experimental molar masses as a function of theoretical ones in the bulk polymerization of POx (□) and of EO (▲) initiated by (TPP)AlCl[109] at 20 °C in CH_2Cl_2.[105]

Table 7 Polymerization of epoxides in the presence of (TPP)AlCl, in CH_2Cl_2, at room temperature

Monomer	$\bar{M}_n$ theor. (g mol^{-1})	*Time (days)*	*Conv. (%)*
EO	8 800	6	100
1,2-Epoxybutane	14 400	6	100
ECH[a]	37 000	3	80
Cyclohexene oxide	19 600	6	85
Epoxypentene	16 800	6	70
Styrene oxide	24 000	8	13
1,2-Epoxy-2-methylpropane	14 400	8	15

[a]Bulk polymerization.

In contrast to conventional anionic polymerizations, in which epoxide insertion involves an inversion of the configuration at the carbon atom of the epoxide ring where cleaved, some porphyrin systems were shown to operate by a nondissociative reaction mechanism, with retention of configuration at the carbon atom of the epoxide ring where cleaved (Scheme 28).

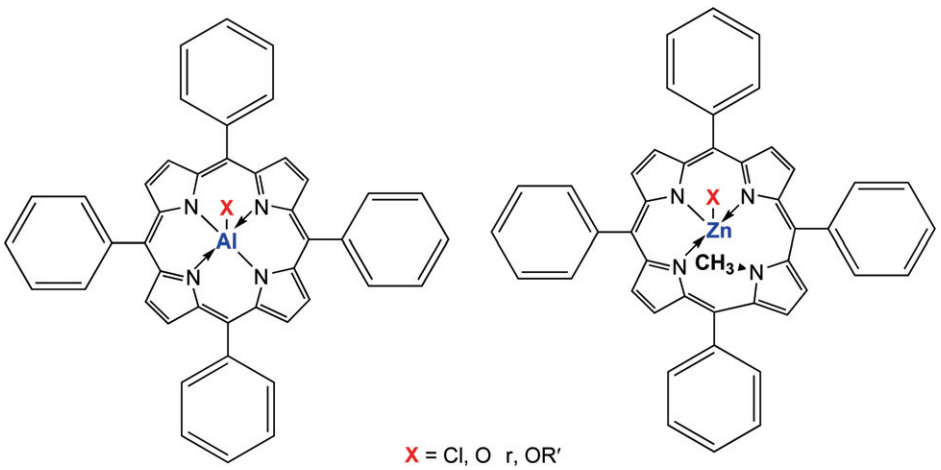

Scheme 27 (Tetraphenylporphinato)aluminum (TPP)AlX and *N*-methyltetraphenylporphinatozinc (*N*-(MTPP)ZnX) derivatives.

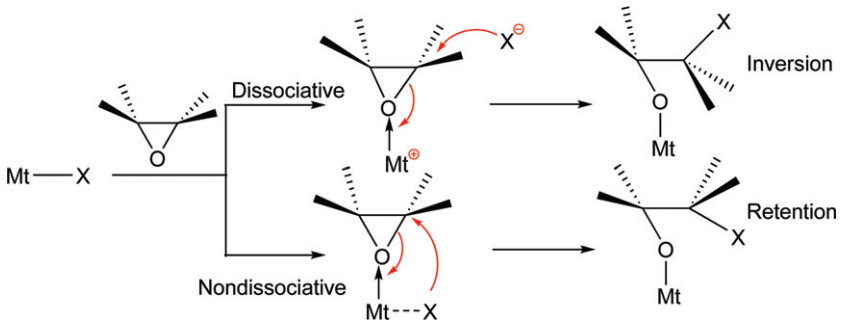

Scheme 28 Inversion and retention of configuration during monomer insertion into mononuclear active species operating via a dissociative and a nondissociative mechanism.

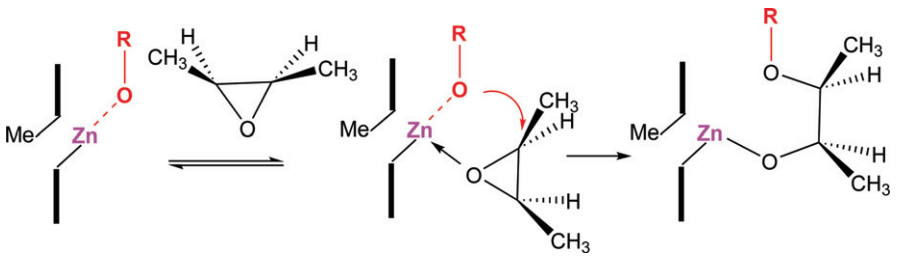

Scheme 29 Proposed mechanism for insertion of (*Z*)-2,3-epoxybutane with retention of configuration into *N*-(MTPP)ZnOR.

Indeed systems that proceed in this way are mostly zinc derivatives in which the monomer and the growing polymer end are located on the same side of the porphyrin plane (Scheme 29). It was also suggested that retention of configuration may result from a double-inversion mechanism.[118]

Indeed the polymerization of 2,3-epoxybutane with aluminum porphyrin revealed a coordinative process with inversion of configuration,[119] which counters the above nondissociative reaction. Aida and Inoue proposed a mechanism involving two porphyrin molecules, one activating the monomer via coordination on the opposite face of the X group while the other proceeds as nucleophilic attack of the activated monomer (see Scheme 30).[107] Initiation results from the insertion of the monomer into the Al–X bond leading to an aluminum alkoxide which becomes the propagating species. Consequently, the synthesized polyether chains possess an X and a hydroxyl group at their extremities.[112]

Aluminum porphyrins were shown to be active toward epoxides in the presence of protic compounds, like alcohol, carboxylic acid, or hydrochloric acid, which act as reversible chain transfer agents. The polymerization pathway is described in Scheme 31. When an active chain reacts with a protic species, either a chain transfer agent or a dormant chain, a new initiating species and a new dormant chain are created. In turn, each 'transferred' species can initiate a new chain or undergo a new chain transfer reaction, whereas no termination occurs. The rate constants of chain transfer reactions were found to be about 8–10 times larger than the propagation rate constants, thus leading to relatively low polydispersity of the polyethers[108] and a number of polyether chains corresponding to the total amount of initiator and transfer agent. Inoue named this polymerization reaction as 'immortal'. Chain ends are constituted by the nucleophilic fragment X coming from the porphyrin initiator and a hydroxyl group after hydrolysis of the Al–O bond.[106]

Addition of protic agents allows control of the polymer molar masses and chain end functionality but at the same time drastically slows down the polymerization rate. As can be seen in Table 8, increasing the number of methanol equivalents with respect to the initiator from 10 to 50 necessitates an extremely long reaction time to achieve monomer conversion.

An increase in the reactivity of metalloporphyrin systems via monomer activation involving a Lewis acid additive will be discussed in the following section.

Other systems have been examined as porphyrin substitutes, such as chiral Schiff bases[120] or calixarene complexes[121] (Scheme 32). In all cases, no significant improvement was made in comparison to porphyrins, and molar masses of the polyethers obtained remained quite low ($< 5000\ g\ mol^{-1}$).

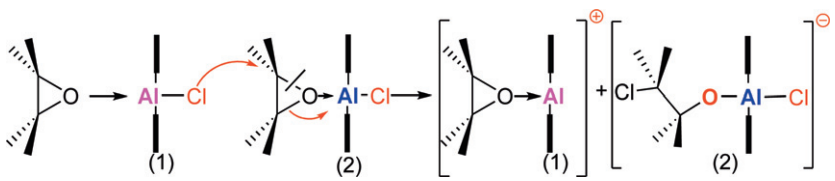

Scheme 30 Bimolecular process proposed for coordination polymerization of epoxide by (TPP)AlX (X = Cl).

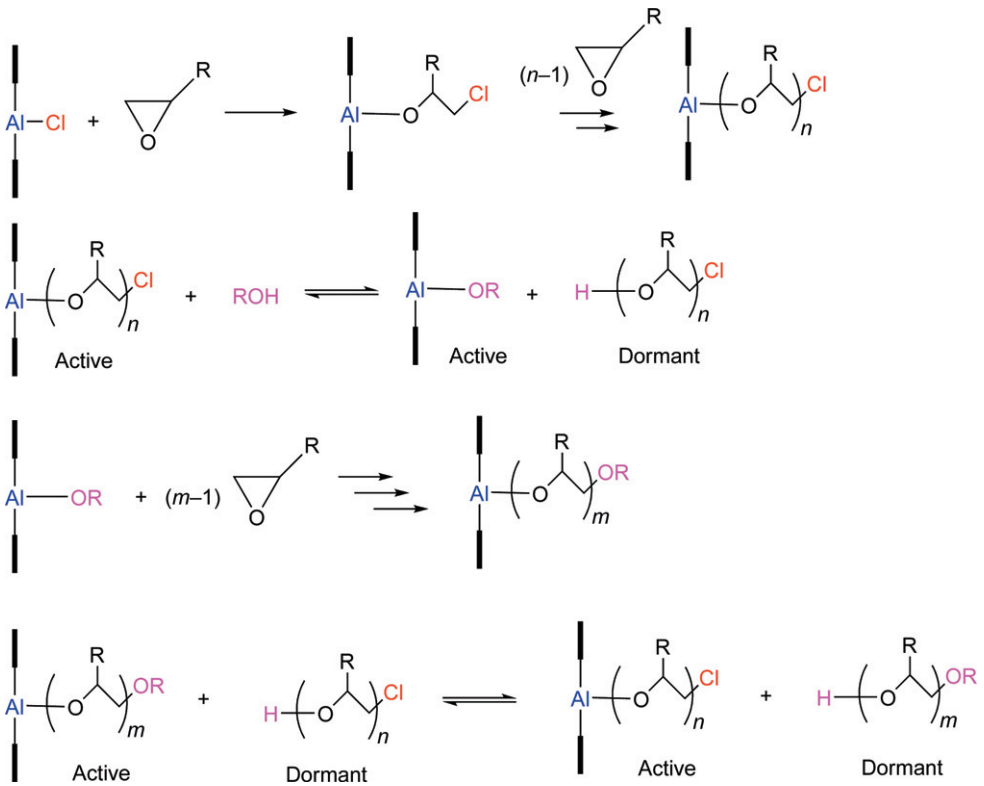

Scheme 31 Reaction pathway of immortal epoxide polymerization.

Table 8 Bulk polymerization of epoxides with (TPP)AlCl/MeOH at room temperature[106,108]

Epoxide	*[MeOH]/ [TPPAlCl]*	*Time (h)*	*Conv. (%)*	$\bar{M}_n$ theor. *(g mol^{-1})*	$\bar{M}_n$ exp. *(g mol^{-1})*	$\bar{D}$
EO	9	48	100	980	700	1.05
POx	9	0.5	70	810	780	1.10
	9	48	100	1160	1300	1.08
	49	600	75	890	900	1.09
Epoxybutane	9	96	100	1600	1200	1.10
Glycidyl methyl ether[a]	9	168	60	1100	610	1.07
ECH	9	4	90	1660	1050	1.08

[a] 70 °C.
$\bar{D}$, dispersity.

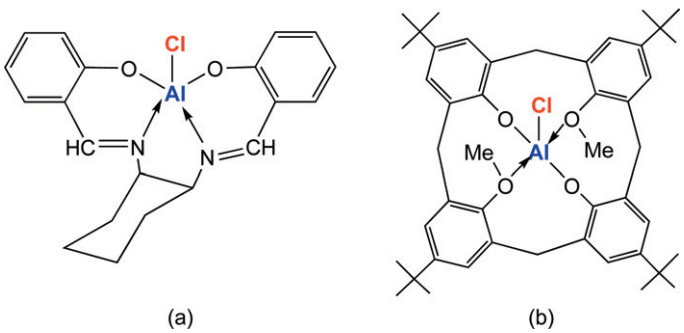

Scheme 32 Organoaluminum compounds used as substitute of aluminum porphyrins: Schiff base (a) and calixarene aluminum complexes (b).

Table 9 Polymerization of epoxides, initiated by $(i\text{-PrO})_3Al$ and $(i\text{-PrO})_3Al/ZnCl_2$ (1:1) in bulk, at 80 °C

Monomer	Catalyst	Time (days)	Conv. (%)	$\bar{M}_v$ ($g\,mol^{-1}$)	Reference
POx	$(i\text{-PrO})_3Al$	2	13	41 000	124
POx	$(i\text{-PrO})_3Al/ZnCl_2$ (1:1)	1	98	739 000	124
EO	$(i\text{-PrO})_3Al$	6	15	21 300	125
EO	$(i\text{-PrO})_3Al/ZnCl_2$ (1:0.55)	6	85	322 000	125

4.07.4.3 Bi- and Plurimetallic Coordination Catalytic Systems

To improve the characteristics of coordination polymerization catalysts, the combinations of different metal derivatives have been investigated. The association of zinc chloride to aluminum alcoholates improves the reactivity significantly and results in higher conversions (see **Table 9**). However, two polymer fractions are still obtained: an isotactic and crystalline polymer of high molar mass and an amorphous and atactic polymer (mole fraction of isotactic dyads is less than 0.6). In contrast to AlR_3/H_2O or ZnR_2/H_2O, the latter consists of regular head-to-head and tail-to-tail enchainments.[122,123]

Several μ-oxo-bimetallic complexes with Mt_1–O–Mt_2 bonds were prepared by condensing a metal (Mt_1) alkoxide and a metal (Mt_2) ester derivative[126,127] (**Scheme 33**), and investigated as coordination catalysts.

These systems, soluble in hydrocarbons, exhibit characteristics that depend on metals Mt_1 and Mt_2, on the R group, and on the association degree *n*. The combination of Al and Zn as Mt_1 and Mt_2 leads to the best results.[126] Comparative polymerization experiments show that EO and POx are the most reactive monomers.[128] Other oxiranes investigated have an intermediate reactivity, with ECH being less reactive.

In most cases, three polymer populations are obtained:[129] a highly isotactic and crystalline fraction, ranging from 25% to 95%, whose molar masses reach $10^6\,g\,mol^{-1}$; a second one amorphous with high molar masses; and a third one constituted of oligomers. According to Kohler *et al.*,[128] oligomers are not formed by a cationic process since THF, which polymerizes only by a cationic mechanism, does not react with these complexes. The catalyst composition and the reaction conditions strongly influence the relative proportion of these different populations. Oligomer formation is favored by the presence of protic additives, owing to reversible exchanges between growing chains and protic compound.[130]

Scheme 33 General formula for μ-oxido-dinuclear complexes.

A mechanism close to the one proposed by Vandenberg was proposed by Teyssié and co-workers[126–128] for the polymerization of epoxide in the presence of dinuclear μ-oxoalkoxides (**Scheme 34**). Polymerization proceeds by the insertion of the monomer into a metal–oxygen bond with inversion of configuration. The growing chain is between the two metals.

4.07.4.4 Double Metal Cyanide Complexes

Originally discovered by General Tire Inc.[131] in the 1960s, double metal cyanide (DMC) complexes are important catalytic systems for the polymerization of epoxides and in particular for the synthesis of POx oligomers. DMC (**Scheme 35**) catalysts are obtained by the reaction of potassium hexacyanocobaltate (III) ($K_3[Co(CN)_6]_2$) and zinc chloride ($ZnCl_2$) in the presence of an alcohol, *tert*-BuOH, as complexing reagent. This is worthy of mention in this review even though some authors have proposed that the polymerization of epoxides may proceed by a cationic coordination mechanism.[132] Compared to conventional anionic catalysts, DMC catalysts give high-quality poly(POx) products that have low levels of unsaturation, narrow molar mass distribution, and low viscosity. ^{13}C NMR analysis showed that the polyols have head-to-tail regiosequence and a random distribution of the configurational sequences with an amount of [rr] triads larger than that of polyol obtained with conventional KOH catalyst. The presence

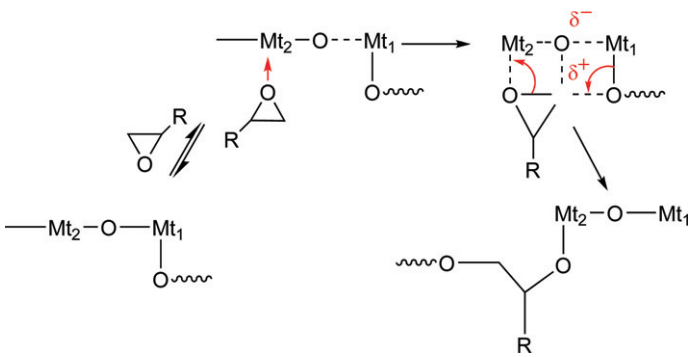

Scheme 34 Mechanism of POx polymerization initiated by μ-oxido-dinuclear complexes.

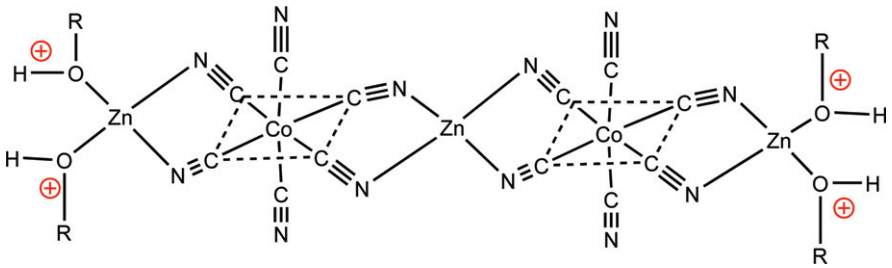

Scheme 35 Structure proposed for DMC catalysts.[132]

of some regioirregular sequences supports some cationic character of the active sites.[132]

While DMC catalysts offer significant advantages compared to KOH, first-generation catalysts required long activation times, increasing polymerization cycles, which has undercut the economic advantages of these systems. DMC catalysts should be activated over 2 h before the epoxide is continuously added to the reactor at high temperature (> 100 °C). Usually, a polyol initiator (or starter) and a DMC catalyst are combined and heated under vacuum prior to the addition of a small proportion of monomer.[133] In addition, heating the catalyst for a prolonged period at a temperature above 100 °C reduces its activity or deactivates it completely.[134]

DMC preparation and composition were revisited in the middle of the 1980s, with significant improvements made by some companies, including ARCO, Shell, and Asahi Glass, making DMC catalysts much more attractive for commercial manufacture of polyether polyols,[135–138] which are useful in a wide range of polyurethane applications.

Highly active catalysts with reduced induction periods are obtained by adding a polyether, poly(butane-1,4-diol), as a co-complexing agent[134] or using $CaCl_2$-modified Zn–Co(III) DMC.[139] The resulting poly(POx) shows a very low unsaturation level (0.003–0.006 mequiv. g^{-1}) and a narrow molar mass distribution ($\bar{D}$ = 1.02–1.04).

4.07.5 Polymerization Involving Monomer Activation by a Lewis Acid Additive

Anionic and anionic coordination polymerizations of epoxides are often slow processes that require long reaction times to achieve high monomer conversions. Moreover, as reported in previous sections, a majority of these polymerizations suffer from side reactions, illustrated by the chain transfer reaction to monomer in alkali metal anionic polymerization and by a very low initiation efficiency and the formation of several polyether populations in coordination polymerizations.

Anionic and related nucleophilic epoxide polymerizations involving an activated monomer have appeared to be of great interest in this context since they allow the nucleophilic ring-opening reaction to be speeded up drastically and the living character of the polymerization to be improved. Activation of epoxides toward nucleophilic attacks can be achieved by introducing in the reaction media an appropriate Lewis acid that will complex with the oxygen of the monomer, rendering it more prone to react with initiating and propagating nucleophilic species. Strategies developed so far are based on the association of aluminum porphyrin to highly encumbered aluminum phenoxides or on the use of alkali metal or tetraalkylammonium derivatives as initiators in the presence of trialkylaluminum.

4.07.5.1 Aluminum Porphyrins Associated with Lewis Acids

Inoue and co-workers were the first to report the use of bulky Lewis acid as additives to aluminum porphyrin initiators to enhance the polymerization rate. This was shown in particular for methacrylic esters[107,140,141] and POx.[107,141,142] For instance, in the presence of methylaluminum bis(2,4,6-trialkylphenolate) (MAlBP) as Lewis acid (**Scheme 36**), POx polymerization initiated by (TPP)AlCl (**Scheme 30**) is drastically accelerated. This is explained by coordination of the epoxide to the acid aluminum center of MAlBP. Electron transfer from the oxygen to the metal makes the ring carbon atoms electron-deficient, favoring an attack by even weak nucleophilic species[142] (**Scheme 37**, path 1).

The competitive complexation that could occur between the epoxide and the acidic aluminum center of MAlBP is minimized by the steric hindrance around the aluminum atom (**Scheme 37**, path 2).

Owing to the monomer activation, polymerization undergoes a drastic acceleration while keeping a good control of molar masses and distributions. For instance, the polymerization rate of POx is multiplied by a factor of 460 after the addition of 0.25% methylaluminum bis(2,4,6-tri-*tert*-butylphenolate).[142]

The living/controlled and high-speed nature of the ring-opening polymerization of POx with aluminum porphyrin/a bulky organoaluminum compound was further demonstrated by the successful synthesis of block copolymers from POx and BOx.[142]

As reported earlier for porphyrin salts, protic reversible chain transfer agents, generally alcohols, can be used in association with aluminum porphyrin/bulky organoaluminum compound systems, reducing significantly the amount of aluminum in the polymer. Coordination of the Lewis acid to the alcohol increases alcohol acidity and accelerates exchange

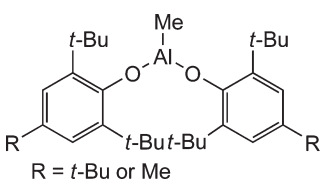

Scheme 36 Bulky Lewis acid (MAlBP) used with aluminum porphyrin initiators for the monomer-activated polymerization of epoxides.

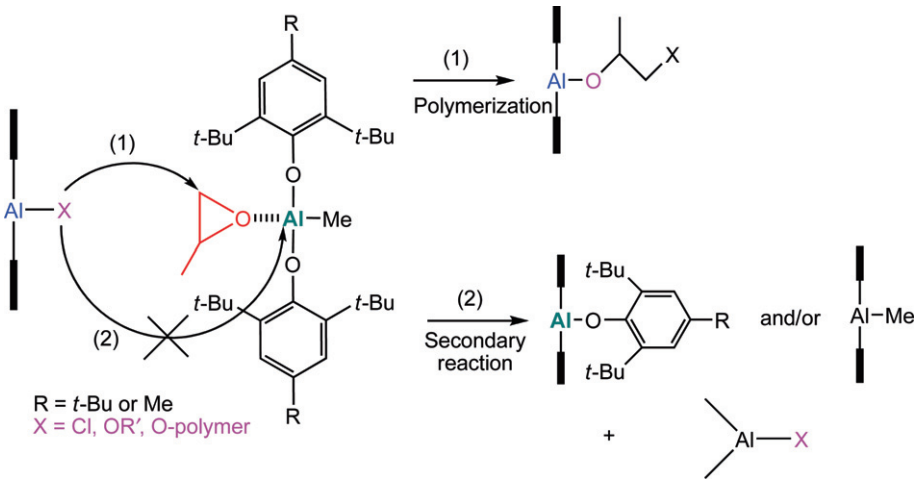

Scheme 37 Epoxide polymerization with porphyrin/bulky Lewis acid (MAlBP) systems involving monomer activation.

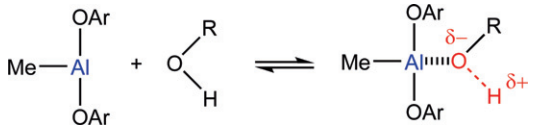

Scheme 38 Coordination of Lewis acid and alcohol.

reactions[143] (Scheme 38), thus allowing a good control of polymer molar masses and keeping the 'immortal' characteristics of the polymerization in high-speed conditions.[144]

4.07.5.2 Other Aluminum Derivatives

Based on the same monomer activation strategy, aluminum phthalocyanine and Schiff bases[142] have been used in association with MAlBP to initiate POx polymerization. Although the rate and control of polymerization are lower than those observed with aluminum porphyrins, the acceleration in the presence of MAlBP derivatives is extremely marked for all initiating systems.

Mixtures of trialkylaluminum and highly hindered di- or tetraphenol compounds have also been investigated recently as catalytic systems for the polymerization of EO and POx.[145] Ligands bearing four phenol groups form particularly active catalysts when combined with an excess of triisobutylaluminum (2 equiv.) and triethylamine (1 equiv.) as initiator. Productivities of $> 100\,g\,mmol^{-1}$ Al have been achieved in both EO and POx polymerizations. Chain transfer to alcohol (propan-2-ol or benzyl alcohol) has been demonstrated for porphyrin systems. A dinuclear insertion process was proposed. However, molar masses of the poly(POx) produced are not controlled and, moreover, the highly regioirregular structure observed with some of these catalytic systems suggests that the mechanism involved differs from the ones so far described.[145]

4.07.5.3 Alkali Metal Derivatives and Quaternary Onium Salts

Braune and Okuda[146] have shown that in the presence of some bulky diphenoxyaluminum compounds it is possible to replace aluminum porphyrins by cesium alkoxides or tetrabutylammonium salts as initiators for POx polymerization. The ring-opening polymerization proceeds under the synergic interaction of a phenolate–aluminum–oxirane complex forming an activated monomer with the corresponding 'ate' complex, which serves as initiator (Scheme 39). Ring opening takes place by transfer of an alkoxy group from the 'ate' complex regenerating an aluminate. The synthesis of poly(POx) with a molar mass up to $4000\,g\,mol^{-1}$ was reported.

Using relatively similar systems based on quaternary ammonium and quaternary phosphonium halides in conjunction with sterically hindered methyl(diphenoxy)aluminum, anionic coordination polymerization of the less reactive four-membered ring oxetane was shown to occur,[147] giving low-dispersity polyoxetanes with M_n up to $17\,000\,g\,mol^{-1}$, owing to strong monomer activation by complexation with the aluminum derivatives.

Simpler initiating systems based on the association of conventional anionic initiators, typically sodium or potassium alkoxides (ROMt), with trialkylaluminum (R_3Al) behave very similarly to porphyrin salts associated to bulky Lewis acid systems. For instance, sodium isopropoxide in combination with triisobutylaluminum in hydrocarbon solvents yields rapid POx polymerization at room temperature or below.[148] The chain transfer reactions are also strongly reduced in these conditions, thus allowing the synthesis of regioregular atactic poly(POx), with relatively high molar masses (up to $50\,000\,g\,mol^{-1}$).

The exclusive presence of head-to-tail enchainments in the polymer is indicative of an anionic coordination type mechanism. Increasing trialkylaluminum concentration, at constant monomer and alkali metal alkoxide concentrations, was shown to lead to a drastic increase in the polymerization rate (Figure 2), whereas the number of poly(POx) chains remained unchanged. In these systems, the trialkylaluminum derivative is involved in the formation of two distinct complexes (Scheme 40): one 1:1 'ate' complex with the alkali metal alkoxide; which serves as initiator; and the other one, at $[AlR_3]/[ROMt]$ ratio (r) higher than unity, with the POx monomer. Polymerization proceeds only at r higher than unity, indicating that only complexed POx molecules are susceptible to ring opening in these conditions, owing to

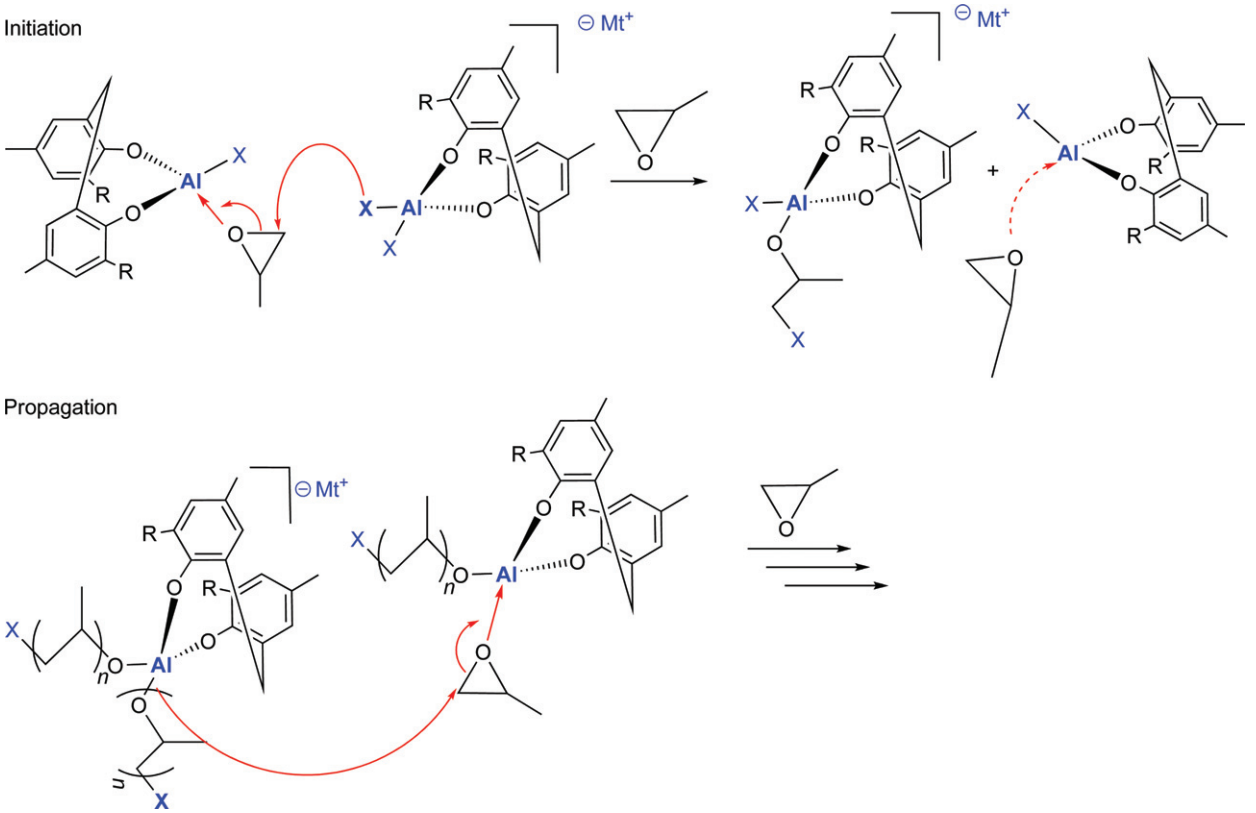

Scheme 39 Activated anionic polymerization of POx involving cesium or ammonium salts and diphenoxyaluminum compounds.

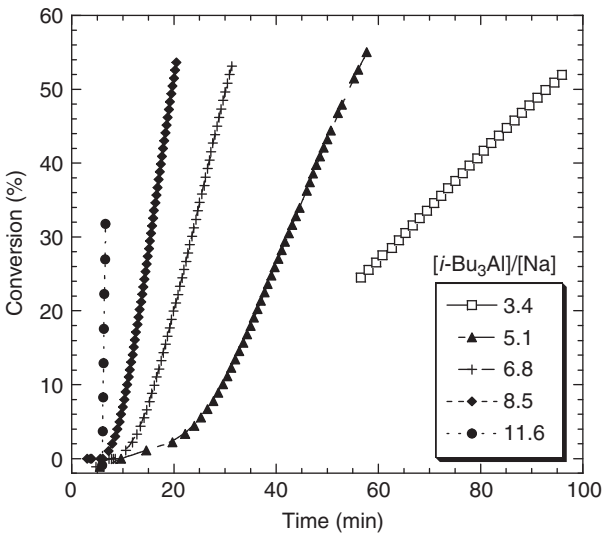

Figure 2 Conversion vs. time curves of POx polymerizations initiated by *i*-PrONa in the presence of increasing amounts of *i*-Bu_3Al in cyclohexane at 0 °C. [POx]/[*i*-PrONa] = 189. Reprinted with permission from Billouard, C.; Carlotti, S.; Desbois, P.; Deffieux, A. *Macromolecules* **2004**, 37, 4038–4043.[148] Copyright 2011 American Chemical Society.

significant electron withdrawing, which renders the ring carbon atoms much more electrophilic. Moreover, since the withdrawing effect is less pronounced on the POx methyl group, the complexation also results, advantageously, in a higher selectivity toward the ring-opening reaction, to the detriment of the proton abstraction process responsible for chain transfer to monomer. The polymerization mechanism is shown in Scheme 40.

Initiation was shown to proceed mainly by attack of the alkoxide moieties of the aluminate complex, thus yielding poly-(POx) with an alkoxide head group and, after hydrolysis, a hydroxy chain end. The presence of small fractions of poly-(POx) with hydrogen or alkyl head groups indicates the minor contribution of other initiation mechanisms involving ligand reorganization in the initial complex (see Scheme 41), as well as some, but limited, chain transfer to monomer.

The possibility of using a similar strategy to initiate EO polymerization in the presence of alkyllithium associated to triisobutylaluminum was recently demonstrated with the synthesis of poly(EO) with molar masses up to 10 000 g mol^{-1}, at low temperature and in nonpolar media.[149] The presence of AlR_3 in excess with respect to the lithium initiator permits disaggregation of lithium alkoxide species by forming lithium aluminate complexes able to ring-open the AlR_3-complexed EO molecules. However, ligand exchanges in the lithium aluminate complex lead to slow deactivation of the propagating species during the polymerization, which limits the access to high-molar-mass poly-(EO) (Scheme 42).

The replacement in the above systems of the alkali metal initiators by onium salts, typically tetraalkylammonium or tetraalkylphosphonium halides, drastically improves the synthesis of polyethers. For instance, poly(POx)s of controlled molar masses, up to 150 000 g mol^{-1},[150] are obtained in very short reaction times using tetrabutylammonium chloride and bromide as initiating species in the presence of a slight excess of

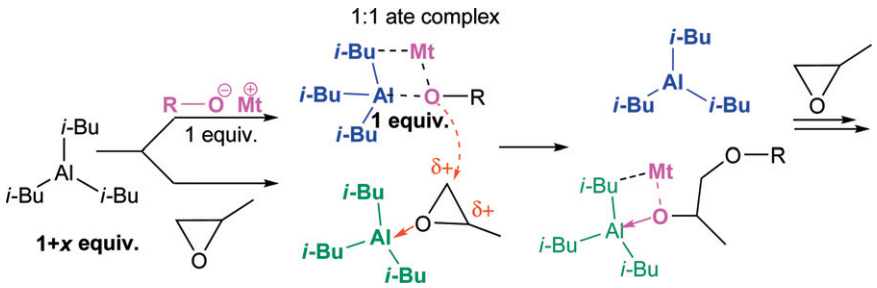

Scheme 40 Mechanism proposed for the POx polymerization involving alkali metal alkoxide in the presence of *i*-Bu_3Al.

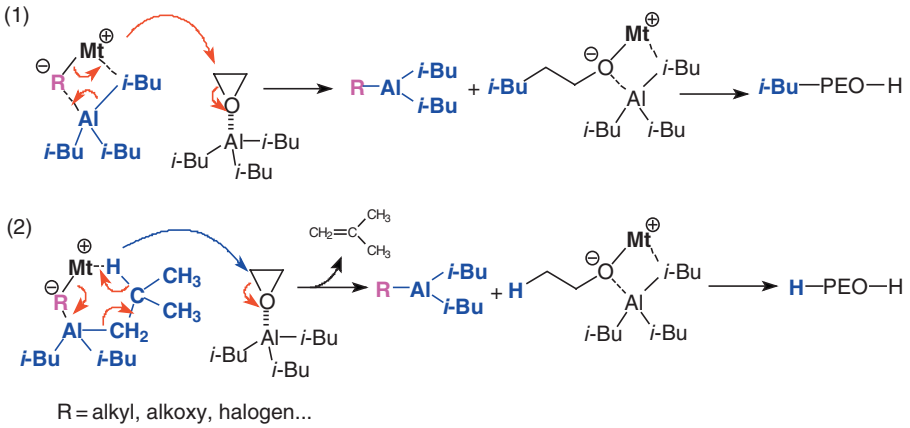

Scheme 41 Secondary initiation processes involving ligand exchanges in aluminate complexes.

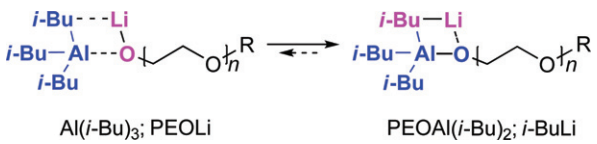

Scheme 42 Proposed ligand exchanges in lithium aluminate complexes leading to slow deactivation during the EO polymerization.

i-Bu_3Al (*i*-$Bu_3Al/NR_4X \sim 1.2$). The polymerization rate was shown to increase with the size of the counter cation (Figure 3).

These initiating systems have been applied to the polymerization of a wide range of epoxides and to the design of telechelic polyethers. Compared to conventional alkali metal initiators, the tetraoctylammonium bromide/*i*-Bu_3Al initiating system strongly enhances the rate of EO polymerization keeping the living character of the reaction.[151] At the ratio [*i*-Bu_3Al]/[$NOct_4Br$] = 1.5, the synthesis of poly(EO) of molar mass (MM) 20 000 g mol^{-1} with bromide and hydroxyl end groups is completed in 2 h at room temperature in dichloromethane. Monomer-activated anionic polymerization of ECH under similar conditions has also been described.[152] In contrast to conventional anionic polymerization, the aluminate species that ensures propagation in the AlR_3/onium systems selectively reacts with the activated ECH ring, leaving the chloromethyl function untouched.[152] The synthesis of poly(glycidyl methyl ether),[153] linear poly(2-ethoxyethyl glycidyl ether), and poly(*t*-BuGE)[154] with narrow chain dispersity and controlled molar masses has also been reported. The amount of Lewis acid required to trigger the reaction and achieve quantitative monomer conversions was shown to increase with the number of oxygen atoms in the monomer.

This approach allowed the direct synthesis from the corresponding ammonium salts of a broad series of heterofunctional polyethers bearing for instance a chloride, bromide, or azide head group[38] (Scheme 43) and a hydroxy-terminated chain. Poly(EO)- and poly(POx)-protected polyglycidol and poly(ECH) have been prepared in this way with a high functionalization efficiency.

The living/controlled character of the monomer-activated anionic polymerization involving onium salt/triisobutylaluminum systems has been applied to the synthesis of a series of random and block copolymers. EO/POx random copolymers with a gradient structure, molar masses up to 70 000 g mol^{-1}, and narrow dispersity have been synthesized by Rejsek *et al.*[151] Poly(POx-*co*-ECH) and amphiphilic poly(alkylene oxide-*co*-glycidol) were also prepared via the synthesis of poly(POx-*co*-EEGE) and poly(BOx-*co*-*t*-BuGE) copolymers, after deprotection of hydroxyl groups.[154] Interestingly, despite the

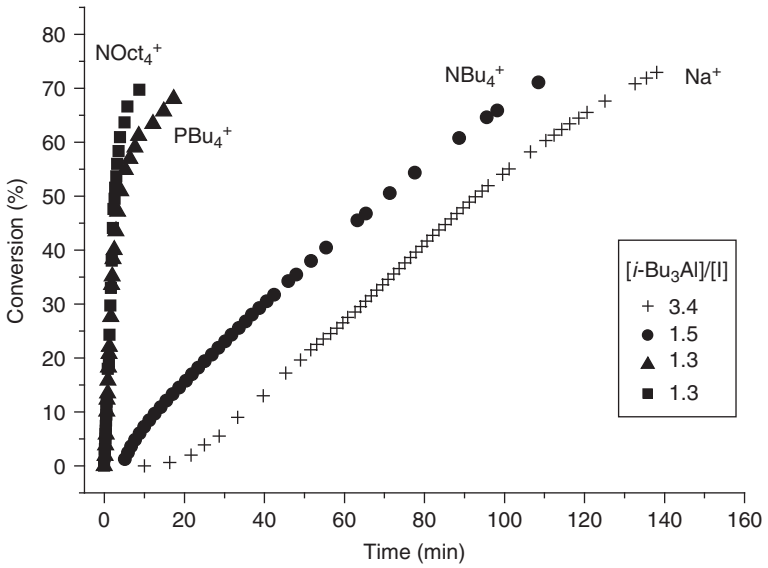

Figure 3 Conversion vs. time curves of POx polymerization initiated by *i*-PrONa (+), NBu_4Cl (●), $NOct_4Br$ (■), and PBu_4Cl (▲) in the presence of *i*-Bu_3Al at 0 °C in cyclohexane. Reprinted with permission from Labbé, A.; Carlotti, S.; Billouard, C.; *et al. Macromolecules* **2007**, 40, 7842–7847.[150] Copyright 2011 American Chemical Society.

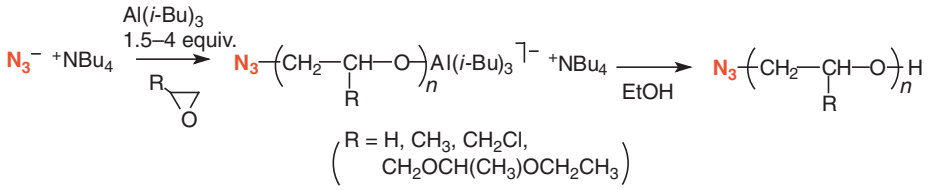

Scheme 43 Synthesis of α-azido-ω-hydroxy polyethers using the tetrabutylammonium azide/*i*-Bu_3Al initiating system.

determining role of the monomer complexation in this polymerization process, the copolymerization ratios remain close to those reported for conventional anionic copolymerization.

Different diblock and triblock copolymers of various compositions and lengths have also been prepared by sequential monomer addition, as illustrated by the Size Exclusion Chromatography (SEC) trace reported in the synthesis of poly(EO-*b*-POx-*b*-PEO) triblock copolymers with $NOct_4Br$/*i*-Bu_3Al (Figure 4).[151]

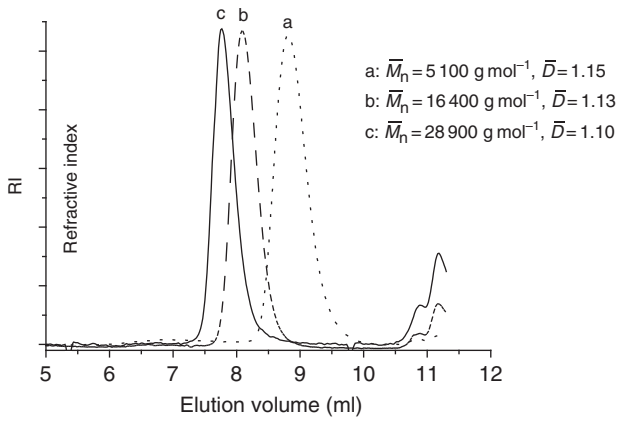

Figure 4 SEC traces corresponding to different stages of the synthesis of a poly(EO-*b*-POx-*b*-PEO) triblock copolymer with $NOct_4Br$/*i*-Bu_3Al system: (a) poly(EO) first block; (b) poly(EO-*b*-POx) diblock; and (c) poly (EO-*b*-POx-*b*-EO) triblock. Reprinted with permission from Rejsek, V.; Sauvanier, D.; Billouard, C.; et al. Macromolecules 2007, 40, 6510–6514.[151] Copyright 2011 American Chemical Society.

Poly(POx-*b*-ECH) block copolymers with MM ranging from about 6000 up to 30 000 g mol^{-1} and with various poly(POx) and poly(ECH) block lengths[152] were also prepared by sequential addition of the two monomers. The reinitiation efficiency starting from either poly(POx) or poly(ECH) as first block was shown to be quantitative.

Finally, block copolymerization of EO initiated by living polymer chains with lithium counterion was also recently described.[149] Although it is known that EO polymerization could not proceed properly when lithium alkoxide species are involved,[155,156] in the presence of AlR_3 it was shown that living polystyryllithium (PSLi) and polyisoprenyllithium (PILi) chains can play the role of a macroinitiator for EO polymerization, thus yielding in hydrocarbon solvent in short reaction times poly-(S-*b*-EO) and poly(I-*b*-EO) with poly(EO) block molar masses up to 10 000 g mol^{-1}.

In conclusion, epoxide derivatives constitute an important group of monomers that can be readily prepared by epoxidation of olefins. Their polymerization allows the synthesis of a broad series of polyethers, ranging from hydrophilic to highly hydrophobic, with biocompatible characteristics. Owing to the recent progress in their ring-opening polymerization, in particular via the use of an appropriate combination of weakly nucleophilic initiators and catalysts or activators, functional oligomers and block copolymers of a much broader series of epoxides can now be prepared, opening new application opportunities in several important areas.

4.07.6 Summary

Epoxide derivatives constitute an important group of monomers that can be readily prepared by epoxidation of natural and synthetic alkenes. Their polymerization by anionic and by related nucleophilic ring-opening reactions is described and discussed in this chapter. The mechanisms of initiation, propagation, and transfer reactions in the presence of ionic initiators, typically alkali metal derivatives, and their impact on the polyether characteristics are first examined. Following this, the recent use of organic derivatives as counterion or catalyst is presented. The last sections of the chapter are devoted to epoxide polymerizations involving a preliminary coordination/activation of the monomer before insertion. The recent progress achieved in the polymerization control of a broad series of epoxide monomers, including functional ones, via the monomer-activated polymerization is highlighted in particular since it opens interesting opportunities in the preparation and design of new polyether materials.

References

1. Boileau, S. In *Comprehensive Polymer Science*; Sir Allen, G., Sigwalt, P., Eds.; The Synthesis, Characterization, Reactions & Applications of Polymers - Chain Polymerization Part I; Pergamon Press: Oxford, UK, 1989; Vol. 3(I), p 467.
2. Stolarzewicz, A.; Neugebauer, D.; Grobelny, Z. *Macromol. Chem. Phys.* **1995**, *196*, 1301–1306.
3. Stolarzewicz, A.; Neugebauer, D.; Grobelny, Z. *Macromol. Chem. Phys.* **1995**, *196*, 1295–1300.
4. Stolarzewicz, A.; Grobelny, Z. *Die Makromol. Chem.* **1992**, *193*, 531–538.
5. Stolarzewicz, A.; Neugebauer, D.; Grobelny, Z. *Macromol. Rapid Commun.* **1996**, *17*, 787–793.
6. Stolarzewicz, A.; Neugebauer, D. *Macromol. Chem. Phys.* **1999**, *200*, 2467–2470.
7. Figueruelo, J. E.; Worsfold, D. J. *Eur. Polym. J.* **1968**, *4*, 439–444.
8. Boileau, S.; Champetier, G.; Sigwalt, P. *Makromol. Chem.* **1963**, *69*, 180.
9. Gee, G.; Higginson, W. C. E.; Taylor, K. J.; Trenholme, M. W. *J. Chem. Soc. (Resumed)* **1961**, 4298–4303.
10. Richards, D. H.; Szwarc, M. *Trans. Faraday Soc.* **1959**, *55*, 1644–1650.
11. Lassalle, D.; Boileau, S.; Sigwalt, P. *Eur. Polym. J.* **1977**, *13*, 591–597.
12. Lassalle, D.; Boileau, S.; Sigwalt, P. *Eur. Polym. J.* **1977**, *13*, 587–589.
13. Boileau, S.; Deffieux, A.; Lassalle, D.; *et al. Tetrahedron. Lett.* **1978**, *20*, 1767–1770.
14. Nenna, S.; Figueruelo, J. E. *Eur. Polym. J.* **1975**, *11*, 511–513.
15. Szwarc, M. *Carbanions, Living Polymers and Electron Transfer Processes*; Interscience: New York, 1968.
16. Price, C. C.; Carmelite, D. D. *J. Am. Chem. Soc.* **1966**, *88*, 4039–4044.
17. Solov'yanov, A. A.; Kazanskii, K. S. *Polym. Sci. U.S.S.R* **1972**, *14*, 1196–1206.
18. Bawn, C. E. H.; Ledwith, A.; McFarlane, N. *Polymer* **1969**, *10*, 653–659.
19. Blanchard, L. P.; Hornof, V.; Moinard, J.; Tahiani, F. *J. Polym. Sci.: Polym. Chem. Ed.* **1972**, *10*, 3089–3102.
20. Kazanskii, K. S.; Solovyanov, A. A.; Entelis, S. G. *Eur. Polym. J.* **1971**, *7*, 1421–1433.
21. Deffieux, A.; Boileau, S. *Polymer* **1977**, *18*, 1047–1050.
22. Solov'yanov, A. A.; Kazanskii, K. S. *Polym. Sci. U.S.S.R.* **1972**, *14*, 1186–1195.
23. Deffieux, A.; Graf, E.; Boileau, S. *Polymer* **1981**, *22*, 549–552.
24. Solov'yanov, A. A.; Kazanskii, K. S. *Polym. Sci. U.S.S.R.* **1970**, *12*, 2396–2408.
25. Boileau, S. In *Anionic Polymerization, Kinetics, Mechanisms, and Synthesis;* Comstock, M. J., Ed.; Anionic Polymerization Series. American Chemical Society: Washington, DC, 1985; Vol. 166, pp 283–305.
26. Stolarzewicz, A.; Grobelny, Z.; Kowalczuk, M. *J. Organomet. Chem.* **1995**, *492*, 111–113.
27. Stolarzewicz, A. *Die Makromol. Chem.* **1986**, *187*, 745–752.
28. Knischka, R.; Lutz, P. J.; Sunder, A.; *et al. Macromolecules* **2000**, *33*, 315–320.
29. Feng, X. S.; Taton, D.; Chaikof, E. L.; Gnanou, Y. *J. Am. Chem. Soc.* **2005**, *127*, 10956–10966.
30. Zalipsky, S. *Adv. Drug Deliv. Rev.* **1995**, *16*, 157–182.
31. Thompson, M. S.; Vadala, T. P.; Vadala, M. L.; *et al. Polymer* **2008**, *49*, 345–373.
32. Zalipsky, S. *Bioconjug. Chem.* **1995**, *6*, 150–165.
33. Roberts, M. J.; Bentley, M. D.; Harris, J. M. *Adv. Drug Deliv. Rev.* **2002**, *54*, 459–476.
34. Akiyama, Y.; Nagasaki, Y.; Kataoka, K. *Bioconjug. Chem.* **2004**, *15*, 424–427.
35. Hiki, S.; Kataoka, K. *Bioconjug. Chem.* **2007**, *18*, 2191–2196.
36. Vadala, M. L.; Thompson, M. S.; Ashworth, M. A.; *et al. Biomacromolecules* **2008**, *9*, 1035–1043.
37. Lapienis, G.; Penczek, S. *Biomacromolecules* **2005**, *6*, 752–762.
38. Gervais, M.; Labbé, A.; Carlotti, S.; Deffieux, A. *Macromolecules* **2009**, *42*, 2395–2400.
39. Pfister, A.; Fraser, C. L. *Biomacromolecules* **2006**, *7*, 459–468.
40. Lapienis, G. *Prog. Polym. Sci. (Oxford)* **2009**, *34*, 852–892.
41. Basumallick, I.; Roy, P.; Chatterjee, A.; *et al. J. Power Sources* **2006**, *162*, 797–799.
42. Siqueira, L. J. A.; Ribeiro, M. C. C. *J. Chem. Phys.* **2006**, *125*, 214903.
43. Siva Kumar, J.; Subrahmanyam, A. R.; Jaipal Reddy, M.; Subba Rao, U. V. *Mater. Lett.* **2006**, *60*, 3346–3349.
44. Wang, Y. J.; Pan, Y.; Wang, L.; *et al. J. Appl. Polym. Sci.* **2006**, *102*, 4269–4275.
45. Marzantowicz, M.; Dygas, J. R.; Krok, F.; *et al. J. Power Sources* **2009**, *194*, 51–57.
46. Oguni, N.; Lee, K.; Tani, H. *Macromolecules* **1972**, *5*, 819–820.
47. Price, C. C.; Osgan, M. J. *Am. Chem. Soc.* **1956**, *78*, 4787–4792.
48. Price, C. C.; Akkapeddi, M. K. *J. Am. Chem. Soc.* **1972**, *94*, 3972–3975.
49. St Pierre, L. E.; Price, C. C. *J. Am. Chem. Soc.* **1956**, *78*, 3432–3436.
50. Gagnon, S. D. In *Encyclopedia of Polymer Science and Engineering*; 2nd ed.; Kruschwitz, J. I., Ed.; Wiley-Interscience: New York, 1985; Vol. 6, pp 273–307.
51. Ding, J.; Heatley, F.; Price, C.; Booth, C. *Eur. Polym. J.* **1991**, *27*, 895–899.
52. Allgaier, J.; Willbold, S.; Taihyun, C. *Macromolecules* **2007**, *40*, 518–525.
53. Nobori, T.; Hayashi, T.; Shibahara, A.; *et al. Catal. Surv. Asia* **2010**, *14*, 164–167.
54. De Lucas, A.; Rodriguez, L.; Perez-Collado, M.; Sanchez, P. *Polym. Int.* **2002**, *51*, 1041–1046.
55. Lee, S. H.; Byun, S. H.; Baek, S. T.; *et al. Catal. Today* **2008**, *132*, 170–177.
56. Maitre, C.; Ganachaud, F.; Ferreira, O.; *et al. Macromolecules* **2000**, *33*, 7730–7736.
57. Schwesinger, R.; Schlemper, H. *Angew. Chem., Int. Ed. Engl.* **1987**, *26*, 1167–1169.
58. Schwesinger, R.; Schlemper, H.; Hasenfratz, C.; *et al. Liebigs Ann.* **1996**, *1996*, 1055–1081.
59. Molenberg, A.; Möller, M. *Macromol. Rapid Commun.* **1995**, *16*, 449–453.
60. Reetz, M. T.; Knauf, T.; Minet, U.; Bingel, C. *Angew. Chem., Int. Ed. Engl.* **1988**, *27*, 1373–1374.
61. Pietzonka, T.; Seebach, D. *Angew. Chem., Int. Ed. Engl.* **1993**, *32*, 716–717.
62. Baskaran, D.; Möller, A. H. E. *Macromol. Rapid Commun.* **2000**, *21*, 390–395.
63. Esswein, B.; Molenberg, A.; Möller, M. *Macromol. Symp.* **1996**, *107*, 331–340.
64. Esswein, B.; Steidl, N. M.; Möller, M. *Macromol. Rapid Commun.* **1996**, *17*, 143–148.
65. Rexin, O.; Mülhaupt, R. *Macromol. Chem. Phys.* **2003**, *204*, 1102–1109.
66. Rexin, O.; Mülhaupt, R. *J. Polym. Sci., Part A: Polym. Chem.* **2002**, *40*, 864–873.
67. Esswein, B.; Möller, M. *Angew. Chem., Int. Ed. Engl.* **1996**, *35*, 623–625.
68. Schmalz, H.; Lanzendörfer, M. G.; Abetz, V.; Müller, A. H. E. *Macromol. Chem. Phys.* **2003**, *204*, 1056–1071.
69. Berger, J.; Lohse, F. *Eur. Polym. J.* **1985**, *21*, 435–444.
70. Han, J. L.; Hsieh, K. H.; Chiu, W. Y. *J. Appl. Polym. Sci.* **1993**, *50*, 1099–1106.
71. Dell'Erba, I. E.; Williams, R. J. J. *Polym. Eng. Sci.* **2006**, *46*, 351–359.
72. Tanaka, Y.; Tomio, M.; Kakiuchi, H. *J. Macromol. Sci.* **1967**, *3*, 471.
73. Raynaud, J.; Absalon, C.; Gnanou, Y.; Taton, D. *J. Am. Chem. Soc.* **2009**, *131*, 3201–3209.
74. Raynaud, J.; Absalon, C.; Gnanou, Y.; Taton, D. *Macromolecules* **2010**, *43*, 2814–2823.
75. Raynaud, J.; Ottou, W. N.; Gnanou, Y.; Taton, D. *Chem. Commun.* **2010**, *46*, 3203–3205.
76 Pruitt, M.E.; Jackson, L.; Baggett, J. M. U.S. Patent 2,706,181, 1955.
77. Kuran, W. *Prog. Polym. Sci.* **1998**, *23*, 919–992.
78. Inoue, S.; Aida, T. In *Handbook of Polymer Synthesis (Part A)*; Kricheldorf, H. R., Ed.; Marcel Dekker: New York, 1992; Vol. 78, pp 481–543.
79. Colclough, R. O.; Gee, G.; Higginson, W. C. E.; *et al. J. Polym. Sci.* **1959**, *34*, 171–179.
80. Furukawa, J.; Tsuruta, T.; Sakata, R.; *et al. Die Makromol. Chem.* **1959**, *32*, 90–94.
81. Imai, H.; Saegusa, T.; Furukawa, J. *Die Makromol. Chem.* **1965**, *82*, 25–31.
82. Kern, R. J. *Die Makromol. Chem.* **1965**, *81*, 261–263.
83. Kasperczyk, J.; Jedlinski, Z. J. *Die Makromol. Chem.* **1986**, *187*, 2215–2221.
84. Saegusa, T.; Ueshima, T.; Tomita, S. *Die Makromol. Chem.* **1967**, *107*, 131–141.
85. Hu, L.; Vogl, O. *Die Makromol. Chem., Macromol. Symp.* **1986**, *3*, 193–202.
86. Tsuruta, T.; Inoue, S.; Hideomi, K. *Die Makromol. Chem.* **1968**, *112*, 58–65.
87. Cantor, S. E.; Brindell, G. D.; Brett, T. J. *J. Macromol. Sci.* **1973**, *A7*, 1483–1508.
88. Vandenberg, E. J. *Pure Appl. Chem.* **1976**, *48*, 295–306.

89. Hasabe, Y.; Tsuruta, T. *Die Makromol. Chem.* **1987**, *188*, 1403–1414.
90. Ebert, P. E.; Price, C. C. *J. Polym. Sci.* **1959**, *34*, 157–160.
91. Garty, K. T.; Gibb, T. B.; Cendinning, R. A. *J. Polym. Sci., Part A* **1963**, *1*, 85–102.
92. Booth, C.; Higginson, W. C. E.; Powell, E. *Polymer* **1964**, *5*, 479–497.
93. Ueyama, N.; Araki, T.; Tani, H. *Macromolecules* **1974**, *7*, 153–160.
94. Vandenberg, E. J. *J. Polym. Sci.* **1960**, *47*, 486–488.
95. Vandenberg, E. J. *J. Polym. Sci.: Part A-1* **1969**, *7*, 525–567.
96. Ishimori, M.; Tsuruta, T. *Die Makromol. Chem.* **1963**, *64*, 190–206.
97. Ishimori, M.; Hsiue, G.; Tsuruta, T. *Die Makromol. Chem.* **1969**, *124*, 143–151.
98. Ishimori, M.; Hagiwara, T.; Tsuruta, T. *Die Makromol. Chem.* **1978**, *179*, 2337–2342.
99. Kageyama, H.; Kai, Y.; Kasai, N.; *et al. Die Makromol. Chem., Rapid Commun.* **1984**, *5*, 89–93.
100. Tsuruta, T. *J. Polym. Sci., Part D* **1972**, *6*, 179–250.
101. Chisholm, M. H.; Gallucci, J. C.; Yin, H.; Zhen, H. *Inorg. Chem.* **2005**, *44*, 4777–4785.
102. Hagiwara, T.; Ishimori, M.; Tsuruta, T. *Die Makromol. Chem.* **1981**, *182*, 501–511.
103. Kuran, W.; Listos, T. *Macromol. Chem. Phys.* **1994**, *195*, 401–411.
104. Tsuruta, T. *J. Polym. Sci.: Polym. Symp.* **1980**, *67*, 73–82.
105. Aida, T.; Inoue, S. *Macromolecules* **1981**, *14*, 1162–1166.
106. Asano, S.; Aida, T.; Inoue, S. *J. Chem. Soc., Chem. Commun.* **1985**, (17), 1148–1149.
107. Aida, T.; Inoue, S. *Acc. Chem. Res.* **1996**, *29*, 39–48.
108. Aida, T.; Maekawa, Y.; Asano, S.; Inoue, S. *Macromolecules* **1988**, *21*, 1195–1202.
109. Aida, T.; Mizuta, R.; Yoshida, Y.; Inoue, S. *Die Makromol. Chem.* **1981**, *182*, 1073–1079.
110. Sugimoto, H.; Aida, T.; Inoue, S. *Macromolecules* **1990**, *23*, 2869–2875.
111. Inoue, S. *J. Polym. Sci., Part A: Polym. Chem.* **2000**, *38*, 2861–2871.
112. Aida, T.; Inoue, S. *Macromolecules* **1981**, *14*, 1166–1169.
113. Aida, T.; Wada, K.; Inoue, S. *Macromolecules* **1987**, *20*, 237–241.
114. Yasuda, T.; Aida, T.; Inoue, S. *Macromolecules* **1984**, *17*, 2217–2222.
115. Endo, M.; Aida, T.; Inoue, S. *Macromolecules* **1987**, *20*, 2982–2988.
116. Kuroki, M.; Aida, T.; Inoue, S. J. *Am. Chem. Soc.* **1987**, *109*, 4737–4738.
117. Kuroki, M.; Aida, T.; Inoue, S. *Die Makromol. Chem.* **1988**, *189*, 1305–1313.
118. Inoue, M.; Sugita, T.; Kiso, Y.; Ichikawa, K. *Bull. Chem. Soc. Jpn.* **1976**, *49*, 1063–1071.
119. Watanabe, Y.; Yasuda, T.; Aida, T.; Inoue, K. *Macromolecules* **1992**, *25*, 1396–1400.
120. Vincens, V.; Le Borgne, A.; Spassky, N. *Die Makromol. Chem., Rapid Commun.* **1989**, *10*, 623–628.
121. Kuran, W.; Listos, T.; Abramczyk, M.; Dawidek, A. *J. Macromol. Sci. – Pure Appl. Chem.* **1998**, *3*, 427–439.
122. Jedlinski, Z.; Dworak, A.; Bero, M. *Die Makromol. Chem.* **1979**, *180*, 949–952.
123. Haubenstock, H.; Panchalingam, V.; Odian, G. *Die Makromol. Chem.* **1987**, *188*, 2789–2799.
124. Osgan, M.; Price, C. C. *J. Polym. Sci.* **1959**, *34*, 153–156.
125. Miller, R. A.; Price, C. C. *J. Polym. Sci.* **1959**, *34*, 161–163.
126. Osgan, M.; Teyssié, P. *Polym. Lett.* **1967**, *5*, 789–792.
127. Osgan, M.; Pasero, J. J.; Teyssié, P. *Polym. Lett.* **1970**, *88*, 319–321.
128. Kohler, N.; Osgan, M.; Teyssié, P. *Polym. Lett.* **1968**, *6*, 559–564.
129. Teyssié, P.; Bioul, J. P.; Condé, P.; *et al. Polym. Prepr.* **1984**, *25* (1), 218–219.
130. Taquet, A.; Jérôme, R.; Teyssié, P.; *et al. J. Polym. Sci., Part A: Polym. Chem.* **1995**, *33*, 1169–1176.
131 Herold, R. J. U.S. Patent 5,158,922, 1966.
132. Kim, I.; Ahn, J. T.; Ha, C. S.; *et al. Polymer* **2003**, *44*, 3417–3428.
133. Lee, S. H.; Lee, I. K.; Ha, J. Y.; *et al. Ind. Eng. Chem. Res.* **2010**, *49*, 4107–4116.
134. Kim, I.; Ahn, J.-T.; Lee, S.-H.; *et al. Catal. Today* **2004**, *93–95*, 511–516.
135 Harper S. D. EP Patent 0,283,148, 1988.
136 Harper S. D.; Harris S. H. US Patent 4,721,818, 1988.
137 Hinney, H.R.; Wardius, D. S. U.S. Patent 5,158,922, 1992.
138 Van der Hulst, H.; Pogany, G.A.; Kuyper, J. U.S. Patent 4,477,589, 1984.
139 Huang, Y.-J.; Zhang, X.-H.; Hua, Z.-J.; *et al. Macromol. Chem. Phys.* **2010**, *211* (11), 1229–1237.
140. Sugimoto, H.; Kuroki, M.; Watanabe, T.; *et al. Macromolecules* **1993**, *26*, 3403–3410.
141. Sugimoto, H.; Inoue, S. *Adv. Polym. Sci.* **1999**, *146*, 41–119.
142. Sugimoto, H.; Kawamura, C.; Kuroki, M.; *et al. Macromolecules* **1994**, *27*, 2013–2018.
143. Inoue, S. *J. Polym. Sci., Part A: Polym. Chem.* **2000**, *38*, 2861–2871.
144. Akatsuka, M.; Aida, T.; Inoue, S. *Macromolecules* **1994**, *27*, 2820.
145. Tang, L.; Wasserman, E. P.; Neithamer, D. R.; *et al. Macromolecules* **2008**, *41*, 7306–7315.
146. Braune, W.; Okuda, J. *Angew. Chem., Int. Ed.* **2003**, *42*, 64–68.
147. Takeuchi, D.; Aida, T. *Macromolecules* **1996**, *29*, 8096–8100.
148. Billouard, C.; Carlotti, S.; Desbois, P.; Deffieux, A. *Macromolecules* **2004**, *37*, 4038–4043.
149. Rejsek, V.; Desbois, P.; Deffieux, A.; Carlotti, S. *Polymer* **2010**, *51*, 5674–5679.
150. Labbé, A.; Carlotti, S.; Billouard, C.; *et al. Macromolecules* **2007**, *40*, 7842–7847.
151. Rejsek, V.; Sauvanier, D.; Billouard, C.; *et al. Macromolecules* **2007**, *40*, 6510–6514.
152. Carlotti, S.; Labbé, A.; Rejsek, V.; *et al. Macromolecules* **2008**, *41*, 7058–7062.
153. Labbé, A.; Carlotti, S.; Deffieux, A.; Hirao, A. *Macromol. Symp.* **2007**, *249–250*, 392–397.
154. Gervais, M.; Brocas, A.-L.; Cendejas, G.; *et al. Macromolecules* **2010**, *43*, 1778–1784.
155. Quirk, R. P.; Ma, J. J. J. *Polym. Sci., Part A: Polym. Chem.* **1988**, *26*, 2031–2037.
156. Quirk, R. P.; Guo, Y.; Wesdemiotis, C.; Arnould, M. A. *Polymer* **2004**, *45*, 3423–3428.

Biographical Sketches

Dr. Alain Deffieux, born in Libourne, France, did his PhD in polymer science in the group of Pierre Sigwalt at the University Pierre and Marie Curie, Paris VI, and then spent 2 years as associate researcher in the laboratory of Professor Vivian Stannett at North Carolina University. He joined the Centre National de la Recherche Scientifique (CNRS) in 1974 at Paris VI University and then moved to Bordeaux University in 1986 in the newly created Laboratoire de Chimie des Polymères Organiques where he became research professor. His research activities are focused on precision polymer synthesis ranging from studying the mechanisms of elementary reaction processes and reactivity control to the design and characterization of polymers with complex chain architecture such as combs, stars, dendrigrafts, and macrocycles.

Dr. Stéphane Carlotti has been an associate professor at the University of Bordeaux 1 since 2007. He completed his PhD course in the field of polymer science in 1998 at the University of Montpellier. After a postdoctoral stay at the Loker Hydrocarbon Research Institute (University of Southern California, Los Angeles, CA, USA), supervised by Pr. T. Hogen-Esch, he joined the Laboratoire de Chimie des Polymères Organiques (LCPO) in 1999 at the University of Bordeaux 1 as assistant professor. He worked mainly on the synthesis of polymers and copolymers with controlled architecture. He studied the living anionic polymerizations of ethylenic monomers in bulk at high temperature and cyclic ethers by an activated mechanism. Other interests are in the fields of ring-opening metathesis polymerization and chemical modification of polymers.

Dr. Amélie Barrère is associate professor at the University of Paris 13, France. Previously, she graduated from the University of Bordeaux 1, France, and obtained a PhD in 2007 on the activated anionic polymerization of epoxides under the supervision of Dr. A. Deffieux. She joined the laboratory 'Bio-ingénierie des Polymères Cardiovasculaires', supervised by Dr. D. Letourneur where her research area is oriented toward the development of coatings of cardiovascular devices based on natural polymers such as polysaccharides.

4.08 Cationic Ring-Opening Polymerization of Cyclic Ethers

P Kubisa, Polish Academy of Sciences, Lodz, Poland

4.08.1 General Considerations

Cyclic ethers constitute an important class of heterocyclic monomers that polymerize by ionic mechanisms. Studies of the mechanism, kinetics, and thermodynamics of cyclic ether polymerization were essential in establishing basic principles of ionic ring-opening polymerization (ROP). There are several book chapters and reviews summarizing this field and although some of them date back to early 1980s, the main conclusions are still valid and provide a basis for more recent developments.[1–12]

Cyclic ethers are the class of heterocyclic monomers that provide suitable models for mechanistic studies. Polymerization of several monomers of this class leads to polymeric materials that are produced on an industrial scale. The most prominent examples are polymers of ethylene oxide (EO), propylene oxide (PO), epichlorohydrin (ECH), or tetrahydrofuran (THF). Cationic ring-opening polymerization (CROP) of cyclic ethers is thus interesting from both an academic and industrial point of view.

In this chapter, the basic features of CROP of cyclic ethers will be briefly outlined on the basis of published earlier chapters and reviews, mainly the first edition of *Comprehensive Polymer Science,*[6] and then more recent developments will be discussed based on the original literature.

4.08.1.1 Thermodynamic Polymerizability of Cyclic Ethers

Polymerizability in a thermodynamic sense is related to the Gibbs energy change (ΔG) associated with a conversion of monomer into polymer unit. More detailed analysis of the thermodynamics of polymerization is given in Chapter 4.02; in this section (4.08.1.1), the simplified description is provided to show the relationship between equilibrium monomer concentration ($[M]_e$), enthalpy of polymerization (ΔH) (closely related to the ring strain), and temperature. Gibbs energy of polymerization is a function of enthalpy (ΔH) and entropy (ΔS) of polymerization.

$$\Delta G_p = \Delta H_p - T\Delta S_p \qquad [1]$$

In the polymerization of heterocyclic monomers, the driving force of polymerization is provided by the release of the strain of the ring upon its opening.[13]

In the process of polymerization, many monomer molecules are incorporated into a polymer chain thus translational entropy decreases. This may be partly counterbalanced by the increase in rotational and vibrational entropy resulting from converting a rigid monomer molecule into a more flexible chain unit. Thus, the entropy of polymerization of heterocyclic monomers is typically lower than entropy of polymerization of vinyl monomers. Although entropy of polymerization depends on the ring size, $-\Delta S$ values for polymerization of cyclic ethers are typically not higher than 80 J (~20 cal)/ °C × mol.[13] Thus, at ambient temperatures (~300 K), the term $-T\Delta S$ usually does not exceed the value 25 kJ mol^{-1} (~6 kcal mol^{-1}). This sets a borderline between polymerization that is practically irreversible and polymerization that proceeds reversibly because in order to make polymerization possible from the thermodynamic point of view ($\Delta G < 0$), enthalpy (ΔH) must outweigh the entropy term ($T\Delta S$). Thus, the thermodynamic polymerizability is governed by the enthalpy of polymerization closely

Table 1 Ring strains of cycloalkanes[14]

Number of atoms in the ring	*Bond angle distortion*	*Strain energy (kJ mol^{-1})*
3	24°44′	115 (27.6 kcal mol^{-1})
4	9°44′	110 (26.2 kcal mol^{-1})
5	0°44′	26 (6.3 kcal mol^{-1})
6	–5°16′	1 (0.2 kcal mol^{-1})
7	–9°33′	27 (6.4 kcal mol^{-1})
8	–12°46′	42 (9.9 kcal mol^{-1})

related to the ring strain of the monomer. Polymerization of highly strained three- and four-membered cyclic ethers is practically irreversible while polymerization of five-membered THF is a typical example of reversible polymerization in which a significant amount of monomer remains in equilibrium with polymer.

Enthalpy of polymerization is related mainly (but not exclusively) to the ring strain. As the bond lengths and the bond angles for C–O and C–C bonds are similar, the ring strains of cycloalkanes provide a good approximation for ring strains of cyclic ethers. Ring strains of cycloalkanes are listed in **Table 1**.

For nonsubstituted cyclic ethers, the following values of ring strain are given in the literature (**Table 2**).[15] The geometry of cyclic ethers is governed mainly by the number of atoms in the ring. Ring strain is caused mainly by the difference between the angles resulting from orbital overlap and the angles imposed by the ring size. The additional strain may arise from the interactions of the nonbonded atoms located in close proximity.

Molecules of cyclic ethers, with the exception of EO, are not planar although the deviation from planarity in the four- and five-membered rings is small. The free electron pairs on the oxygen atoms behave sterically like medium-sized substituents.

As already mentioned, polymerization of highly strained three- and four-membered cyclic ethers is practically irreversible, while polymerization of five-membered THF is a typical example of reversible polymerization.

Reversibility of propagation in simplified form may be represented by eqn [2]:

$$\cdots - M_n^* + \mathrm{M} \rightleftharpoons \cdots - M_{n+1}^* \qquad [2]$$

Equilibrium constant for reversible propagation is equal to:

$$K = [\cdots - M_{n+1}^*]/[\cdots - M_n^*][\mathrm{M}]_e \text{ and assuming that } [\cdots - M_{n+1}^*] = [\cdots - M_n^*] \qquad [3]$$

$K = 1/[\mathrm{M}]_e$, where $[\mathrm{M}]_e$ denotes concentration of monomer at equilibrium.

There is the following relationship between Gibbs energy of polymerization and equilibrium constant K:

$$\Delta G^o = RT \ln K \qquad [4]$$

Thus,

$$RT \times \ln 1/[\mathrm{M}]_e = \Delta H - T\Delta S \quad \text{and} \quad \ln 1/[\mathrm{M}]_e = \Delta H/RT - \Delta S/R \qquad [5]$$

A more detailed description of thermodynamics of polymerization is given in Chapter 4.02; in this section, the simplified analysis is provided to show the relationship between equilibrium monomer concentration ($[\mathrm{M}]_e$), enthalpy of polymerization (ΔH) (closely related to the ring strain), andtemperature.

Table 2 Ring strains of cyclic ethers[15]

Cyclic ether	*Ring strain (kJ mol^{-1})*
Oxirane (three membered)	114
Oxetane (four membered)	107
Tetrahydrofuran (oxolane) (five membered)	23
Tetrahydropyran (oxane) (six membered)	5
Oxocane (eight membered)	42

In simple terms

1. the lower is the enthalpy of polymerization (ring strain) the higher is the equilibrium monomer concentration;
2. the higher the temperature the higher the equilibrium monomer concentration; and
3. for each initial concentration of monomer ($[\mathrm{M}]_0$), there is a temperature at which $[\mathrm{M}]_e$ becomes equal to $[\mathrm{M}]_0$ meaning that for a given $[\mathrm{M}]_0$ at this and higher temperatures polymerization is not possible. This temperature is denoted as a ceiling temperature for polymerization (T_c). Ceiling temperature is typically given in the literature either for standard conditions (i.e., for $[\mathrm{M}]_0 = 1\ \mathrm{mol\,l^{-1}}$) or for bulk polymerization. For practical purposes, the value of T_c for bulk polymerization is of interest because above this temperature the monomer will not polymerize under any conditions.

There are the following practical consequences that are important for understanding of behavior of cyclic ethers in ROP.

Gibbs energy of polymerization is strongly negative for the polymerization of strained three- and four-membered cyclic ethers; therefore, polymerization is practically irreversible, which means that there are no thermodynamic barriers for reaching quantitative conversions even at low $[\mathrm{M}]_0$ and higher temperatures. It should be remembered, however, that kinetic factors may prevent quantitative conversion if a termination reaction occurs.

In contrast, polymerization of weakly strained cyclic ethers containing five or more atoms in the ring is highly reversible, which means that there are thermodynamic limits on the ultimate conversion. The highest conversion that may be achieved is equal to:

$$\text{Ultimate conversion} = ([\mathrm{M}]_0 - [\mathrm{M}]_e)/[\mathrm{M}]_0 \times 100\% \qquad [6]$$

Thus, to reach the highest monomer conversion in reversible polymerization, polymerization should be conducted at high $[M]_0$ and low temperature (to reduce $[M]_e$ value). This latter requirement is in conflict with kinetic requirements. In the system with reversible propagation, polymerization is faster at higher temperatures but because of higher $[M]_e$, the highest attainable conversion is lower. Thus, it should be remembered that the term 'polymerizability' does not have an unequivocal meaning and one should clearly distinguish between kinetic and thermodynamic polymerizability. The former is governed by rate constants of elementary reactions while the latter by the equilibrium constant of propagation. Thus, typically, with increasing temperature kinetic polymerizability will be enhanced (higher rate of propagation) but thermodynamic polymerizability will be lowered (equilibrium position will be less favorable for the formation of polymer).

It should be pointed out that the presented picture applies to homopolymerization. Monomers that do not undergo homopolymerization at particular conditions may still be able to undergo copolymerization. It should also be remembered that thermodynamic parameters of polymerization are valid for the transformation of monomer into relatively high-molecular-weight polymer. Therefore, even at the conditions when monomer does not polymerize due to the thermodynamic restrictions, some low-molecular-weight oligomers may still be formed.

4.08.1.2 Nucleophilicity and Basicity of Cyclic Ethers

Propagation in the cationic polymerization of cyclic ethers proceeds as a nucleophilic attack of an oxygen atom on the carbon atom in α-position in an oxonium ion (Scheme 1).

If the oxygen atom (-O-) is a part of monomer molecule, this scheme represents chain propagation. If, however, it is a part of polymer unit, such a reaction is a chain transfer to polymer. Chain transfer to polymer (either intermolecular or intramolecular) is a typical feature in CROP of cyclic ethers. Its significance in particular cases will be discussed in subsequent sections (Section 4.08.1.5 and 4.08.2.1).

As the reaction shown in the scheme above is a nucleophilic substitution reaction, nucleophilicity of oxygen atoms in monomers and polymer units is an important factor governing the competition between chain propagation and chain transfer to polymer.

Nucleophilicity is often expressed in terms of basicity. Nucleophilicity and basicity reflect the same property, namely the ability to share the lone electron pair with an electron acceptor. Nucleophilicity is determined at kinetically controlled conditions whereas basicity is determined at the conditions controlled thermodynamically (from the studies of equilibria).

Linear and cyclic ethers belong to the group of weak organic bases.[16,17]

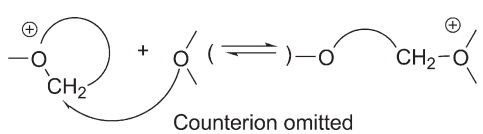

Scheme 1

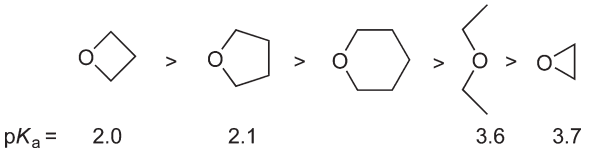

Scheme 2

Basicity of cyclic ethers decreases in the order as shown in Scheme 2.

Knowledge of the order of basicities of cyclic and linear ethers is important for understanding certain phenomena in cyclic ether polymerization. As indicated earlier, chain transfer to polymer is a general feature of the cationic polymerization of cyclic ethers because the nucleophilic site of the monomer molecule (oxygen atom) is transferred to the polymer unit. To what extent chain transfer to polymer competes with propagation depends on the relative nucleophilicity of monomer and polymer unit. Thus, for five-membered THF, the polymer unit is a weaker base than the monomer. This makes the polymer less reactive than the monomer in nucleophilic substitution type reactions. Consequently, for this monomer, chain transfer to polymer is slow as compared to propagation. In contrast, in the polymerization of three-membered EO, the polymer unit is more basic than monomer. Therefore, reactions involving the polymer chain are important in this system. Practical consequences will be discussed in the subsequent sections devoted to polymerization of different classes of cyclic ethers.

4.08.1.3 Mechanism of Cationic Polymerization of Cyclic Ethers

Cyclic ethers polymerize by ionic mechanism. Three-membered cyclic ethers (oxiranes) polymerize by both cationic and anionic mechanisms. Four-membered and higher cyclic ethers polymerize by cationic mechanism only (although examples of anionic polymerization are occasionally mentioned in the literature). Thus, cationic mechanism is a general mechanism of cyclic ether polymerization.

The growing species on which propagation occurs are typically tertiary oxonium ions (although the mechanism involving secondary oxonium ions, the activated monomer (AM) mechanism may also operate as it will be discussed in the following sections). Those tertiary oxonium ions are located at the growing chain end; thus, the typical mechanism of cyclic ethers polymerization is called the active chain end (ACE) mechanism.

Propagation by the ACE mechanism is represented in Scheme 3.

Propagation proceeds by nucleophilic attack of an oxygen atom in a monomer molecule on a carbon atom in α-position to an oxygen atom bearing formally the positive charge in a tertiary oxonium ion located at the chain end. Even such a simplified scheme indicates the possibility of a side reaction that is a typical feature of cationic polymerization of cyclic ethers. A nucleophilic center (oxygen atom) is present not only in monomers but also in polymer chains. Therefore, the attack of an oxygen atom from the chain on a carbon atom in a

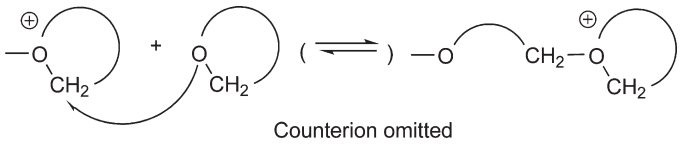

Scheme 3

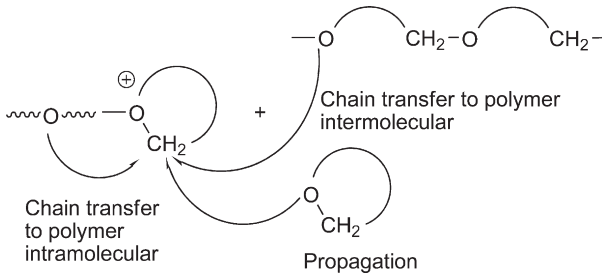

Scheme 4

growing center may occur and compete with propagation, as shown in Scheme 4.

It should be stressed that the fact that the monomer molecule is strained while the polymer chain is essentially strainless is not relevant from the point of view of competition between both the processes. In both the cases, it is the ring in the growing center that is opened while the attacking molecule remains intact. Thus, the competition is governed mainly by nucleophilicity of an oxygen atom in cyclic and linear structures (with a possible contribution of steric effects). Therefore, chain transfer to polymer is a typical feature in CROP of cyclic ethers. Intermolecular reaction leads to segmental exchange (so-called scrambling), while intramolecular reaction leads to cyclization as shown in Scheme 5.

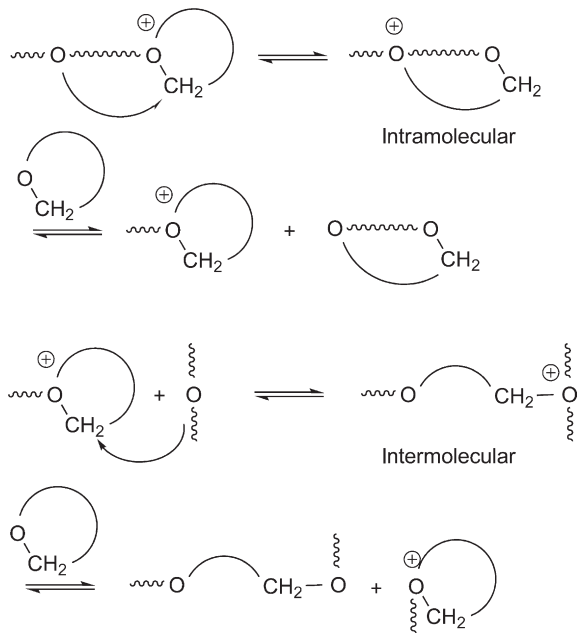

Scheme 5

As a result of intramolecular chain transfer to polymer, a certain number of cyclic oligomers may be formed in addition to linear polymers. This is a serious limitation for synthetic applications of CROP of cyclic ethers because a fraction of the polymer may have a distinctly different molecular weight (thus broadening molecular weight distribution) and will not contain end-groups (which is especially disadvantageous for the synthesis of reactive, telechelic polymers). In some systems (as in the cationic polymerization of THF), chain transfer to polymer is slow as compared to propagation and polymerization may be terminated before cyclic oligomers start to form. In other systems, however, especially in the cationic polymerization of oxiranes, cyclization in polymerization proceeding by the ACE mechanism cannot be avoided. As will be discussed, cyclization may be eliminated if polymerization is conducted at conditions where the AM mechanism of propagation dominates.

Intermolecular chain transfer to polymer is less harmful because the number of macromolecules does not change and the number-average degree of polymerization (DP) is not affected. Segmental exchange leads, however, to a broadening of molecular weight distribution. Another effect may be disproportionation of polymer end-groups as shown in Scheme 6.

Chain transfer to polymer is the major side reaction in CROP of cyclic ethers. If it could be avoided, the system would approach conditions required for living polymerization. According to the recent IUPAC definition, living polymerization is: "A chain polymerization from which irreversible chain transfer and irreversible chain termination (deactivation) are absent."[18]

Tertiary oxonium ions that are active species in CROP of cyclic ethers are inherently stable (trialkyloxonium salts with stable counterions are commercially available and may be stored without special precautions for prolonged periods of time). Thus, if basic impurities are avoided in CROP of cyclic ethers, there is essentially no irreversible termination. Those polymerization are, however, not classified as living because reversibility of propagation and reversible chain transfer to polymer cause deviations from the ideal situation observed for, for example, anionic vinyl polymerization in which $DP_n = [M]_0/[I]_0$, molecular weight distribution is close to Poisson distribution and the nature of end-groups may be strictly controlled. As will be discussed in subsequent sections, conditions of living polymerization may be more closely approached if polymerization proceeds by the AM mechanism.

4.08.1.4 Elementary Reactions in Cationic Polymerization of Cyclic Ethers

4.08.1.4.1 Initiation

There are three possible routes of initiation of cyclic ether polymerization, by:

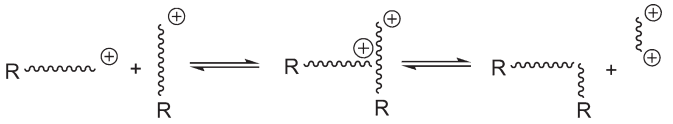

Scheme 6

1. direct addition of initiator to monomer molecule;
2. abstraction of hydride ion (H^-) from monomer molecule; and
3. formation of zwitterions between monomer and initiator.

Most commonly initiation proceeds as direct addition of initiator to monomer molecule (route 1). Cationic polymerization of cyclic ethers may be initiated by both Bronsted and Lewis acids. Most commonly used initiators include strong protic acids such as trifluoromethanesulfonic (triflic) acid (also its anhydride or esters), fluorosulfonic acid, perchloric acid, or heteropolyacids, oxonium salts such as triethyloxonium (e.g., $Et_3O^+A^-$), carbenium (e.g., $Ph_3C^+A^-$), or carboxonium (e.g., $C_6H_5CO^+A^-$) salts where A^- should be stable, weakly nucleophilic counterion (e.g., BF_4^-, PF_6^-, and SbF_6^-) or Lewis acids (most commonly used is $BF_3 \cdot Et_2O$). Several other initiation systems have been used (e.g., rare earth triflates) but the advantages over typically used simple and easily available initiators have not always been shown.

The mechanism of initiation is relatively simple in the case of initiation by protic acids. There is a fast protonation of monomer molecule with formation of secondary oxonium ion followed by reaction of this ion with another monomer molecule forming tertiary oxonium ion. This step may be slower than subsequent propagation steps because reactivity of secondary oxonium ions is generally lower than that of tertiary oxonium ions (Scheme 7).

Oxonium, carbenium, or oxocarbenium salts generate tertiary oxonium ions in single step, as shown in Scheme 8 for initiation with triethyloxonium salt.

Some carbenium salts that form sterically hindered addition product, that is, triphenylmethylium (trityl) salts may initiate through hydride ion abstraction as shown in Scheme 9 (route b).[19,20] Oxocarbenium ions thus formed serve as actual

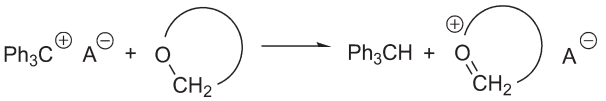

Scheme 9

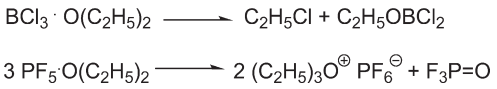

Scheme 10

initiator (although proton expulsion and formation of double bonds is also possible).

Less obvious is the mechanism of initiation in the case of Lewis acid initiators. First of all, the behavior of different Lewis acids in similar systems may be different. Thus, complexes of BF_3 with ethers are stable while BCl_3 may react with ethers[21] and complexes of PF_5 with ethers may undergo disproportionation (Scheme 10).[22]

There is no evidence supporting the view that the most commonly used Lewis acid, that is, BF_3 (typically as a complex with Et_2O) may generate ionic species directly. Thus, it is generally accepted that the presence of coinitiator is necessary and (unless coinitiator is purposely added) this role is most often played by adventitious water. In a related system, that is, in the cationic polymerization of cyclic acetals, it was conclusively proved that if water is rigorously excluded, BF_3 does not initiate polymerization.[23] In less thoroughly dried systems, addition of a proton trap effectively prevented initiation by BF_3.[24]

It has been claimed, however, that some of the cyclic ethers, particularly the strained ones, may directly produce a zwitterion with a tertiary oxonium ion at one of its ends, when initiated with BF_3, as shown in Scheme 11.[25]

It has also been claimed that PF_5 may directly initiate polymerization of THF and, on the basis of ^1H and ^{31}P NMR

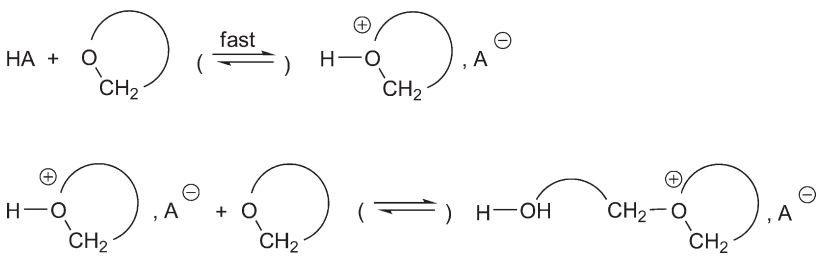

Scheme 7

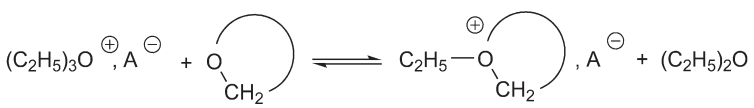

Scheme 8

Scheme 11

spectra, formation of transient zwitterions has been postulated.[26] On the other hand, BF_3 forms a complex with THF which does not initiate the polymerization of THF in the absence of coinitiator.[27]

4.08.1.4.2 Propagation

As already discussed, propagation in cationic polymerization of cyclic ethers by the ACE mechanism proceeds on tertiary oxonium ion active species. Ionic species in general may exist in the form of ion-pairs (contact or solvent separated) and free ions. The fraction of each form is governed by a corresponding equilibrium constant that depends on the polarity of the medium. The knowledge of the fraction of different ionic forms, which is essential for the proper analysis of kinetics of anionic vinyl polymerization in which different forms show different reactivity, is less crucial in analyzing the kinetics of cationic polymerization of cyclic ethers because available data point out to equal reactivity of ion-pairs and free ions in propagation.

This has been shown for cationic polymerization of five-membered THF[28,29] and seven-membered oxepane.[30] The difference between situations encountered in anionic vinyl polymerization and cationic polymerization of cyclic ethers stems from the solvating ability of the latter class of monomers. Cyclic ethers solvate cationic centers and solvation of free oxonium cation is much stronger than solvation of ion-pairs, which provides a counterbalance for the inherent differences in reactivity of different ionic species.

Analysis of polymerization kinetics and the determination of the true values of propagation rate constants require the knowledge of the concentration of growing species. If it can be proved that initiation is fast and quantitative (e.g., by showing that $DP_n = ([M]_0 - [M]_t)/[I]_0$), the concentration of active species may be simply taken as equal to the starting concentration of the initiator. The concentration of active species can also be measured. It should be noted that propagation rate constants in the cationic polymerization of cyclic ethers are relatively low (in the range 10^{-4} to $1\,mol^{-1}\,l\,s^{-1}$); thus, to achieve reasonable rates of polymerization, the concentration of active species is typically much higher (at the level 10^{-4}–$10^{-2}\,mol\,l^{-1}$) than that in the cationic vinyl polymerization.

In the cationic polymerization of THF, the concentration of active species was measured by capping the growing chain with sodium phenoxide and the determination of phenoxy groups in polymers by UV spectroscopy.[31] More general methods have been developed in the Lodz group.[32,33] Active species of cationic polymerization of cyclic ethers (and other heterocyclic monomers) were trapped by reaction with tertiary phosphine. It was shown that oxonium ions are fast and irreversibly converted to corresponding phosphonium ions that could be quantitatively analyzed by ^{31}P NMR using a known excess of phosphine as an internal standard without the need for polymer isolation. The principle of the method, which allows determination not only of concentration but also of the structure of active species, is outlined in Scheme 12.

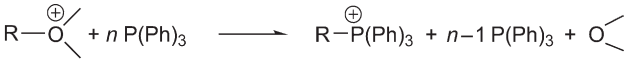

Concentration: integration of signal of R-$P^+(Ph)_3$ vs $P(Ph)_3$
Structure: ^{31}P NMR chemical shift of R-$P^+(Ph)_3$

Scheme 12

For several monomers, propagation rate constants have been determined (the extensive list can be found in Reference 3). For polymerization of THF, the values between 3×10^{-3} and $1 \times 10^{-2}\,mol^{-1}\,l\,s^{-1}$ are given by different authors for different conditions for polymerization of oxepanes values between 10^{-4} and $10^{-5}\,mol^{-1}\,l\,s^{-1}$ and for polymerization of oxetanes values between 10^{-1} and $1\,mol^{-1}\,l\,s^{-1}$ (at 0 °C in different solvents at different monomer and initiator concentrations).

4.08.1.4.3 Termination

Due to the lower reactivity of oxonium ions and the basic character of monomers, chain transfer (other than chain transfer to polymer) and/or termination is less critical in CROP of cyclic ethers than in vinyl polymerization (either cationic or anionic). The best documented system not involving any termination is polymerization of five-membered THF in the presence of stable counterions (SbF_6^-, AsF_6^-, and PF_6^-) or noncomplex anions like $CF_3SO_3^-$ for which recombination occurs but is fully reversible. For these systems, the DP is equal to the calculated value up to the high DP_n values.[29,34]

$$DP_n = ([THF]_0 - [THF]_e)/[I]_0 \qquad [7]$$

The H^+ transfer, that is a typical route of transfer in cationic vinyl polymerization, is not important in the polymerizations proceeding with the participation of tertiary oxonium ions as active species. This type of transfer may, however, occur in special cases where the presence of carbenium ions cannot be excluded. Such situations may appear in the cationic polymerization of suitably substituted oxiranes when the presence of low concentration of carbenium ions in equilibrium with oxonium ions has been postulated (Scheme 13).

Unsaturated end-groups were indeed observed in cationic copolymerization of nitroglycidyl ether or ECH with THF.[35]

4.08.1.5 Macrocyclization in the CROP of Cyclic Ethers

In CROP, electrophilic active centers can react with heteroatoms in their own chains. This reaction, called 'backbiting', leads to the formation of cyclic oligomers. Formation of cyclic oligomers is a reversible process; monomers and macrocycles react with active centers in a similar way.

Competition between backbiting and propagation depends on the relative nucleophilicity of oxygen atoms in monomer and polymer units. In the polymerization of EO, the basicity of the polymer unit is higher than that of the monomer (cf. Section 4.08.1.2); thus, macrocyclization proceeds concurrently with propagation, and formation of cyclic oligomers cannot be avoided in the polymerization

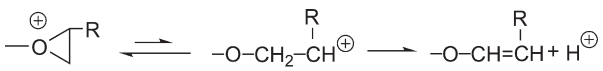

Scheme 13

proceeding by the ACE mechanism. On the other hand, in the cationic polymerization of THF, the basicity of oxygen in polymer units is considerably lower than that of oxygen in monomer molecules. Therefore, cyclization by backbiting is relatively slow as compared to propagation. Thus, in cationic polymerization of THF, there is a kind of window when high conversion is already attained but the concentration of macrocyclics is still negligible. If polymerization is terminated at this stage, a linear polymer free of cyclic fractions may be obtained. If, however, the system is kept nonterminated for a prolonged period of time, a build-up of cyclic fractions is gradually observed until a final equilibrium distribution of cyclic and linear polymer is attained.[36] Thus, this system provides a good example of the distinction between the kinetic and thermodynamic distribution of cyclic and linear fraction in CROP. Unfortunately, cationic polymerization of THF is rather an exception. In the polymerization of oxiranes or oxetanes, the kinetic factor does not disfavor backbiting and cyclic oligomers are formed parallel to the formation of linear polymer.

What factor governs the distribution of cyclic and linear fractions? Distribution of unstrained cyclic oligomers in equilibrium is described by the dependence

$$[M_n] = A \times n^{-5/2} \qquad [8]$$

(where n is a polymerization degree and A is preexponencial factor) derived theoretically by Jacobson and Stockmayer (JS theory) for polymers with unperturbed chain conformation.[37] The JS theory describes an idealized situation because it assumes that all macrocycles are strainless and that polymer chain conformation is described by Gaussian statistics. For some systems in CROP, distribution of cyclic oligomers close to that predicted by the JS theory was indeed observed. This is the case of cationic polymerization of cyclic siloxanes[38] and cyclic acetals[39] because in those systems, due to the flexibility of polymer chains, deviations from the assumptions of the JS theory are relatively small.

In most systems, however, more complicated situations are encountered. Due to different strains of rings in cyclic oligomers, their distribution is different from that predicted by the JS theory and those oligomers that may assume conformation minimizing the strain are preferentially formed. This is the case of cationic polymerization of oxiranes. In the polymerization of oxirane (EO), predominantly six-membered cyclic dimer (1,4-dioxane) is formed.[40,41] Polymerization of substituted oxiranes yields products containing not only the cyclic dimers but also higher cyclic oligomers. This was observed for polymerization of methyloxirane (propylene oxide),[42,43] (chloromethyl)oxirane (ECH),[42,44] 2,2-dimethyloxirane (isobutylene oxide),[45] or phenyloxirane (styrene oxide)[46] where mainly cyclic trimers or tetramers were observed.

4.08.2 CROP of Oxiranes

4.08.2.1 Mechanism of Polymerization

The mechanism of cationic polymerization of three-membered cyclic ethers (oxiranes) was studied mostly in the 1960s and 1970s and the major findings have been summarized in several monographs and reviews published since then.[1–12] Thus, in this chapter, the basic features of CROP of oxiranes will be outlined only briefly and then the recent developments, mainly related to various synthetic applications, will be presented.

Three-membered rings are highly strained; ring strain arises because it is not possible for the atom orbitals to overlap at their optimum angles in rings composed of only three atoms. Thus, ring strain for EO is equal to 26.8 kcal mol^{-1}.[47–49] Due to relatively large ring strain, the enthalpy factor significantly outweighs the entropy factor in the equation $\Delta G = \Delta H - T\Delta S$ and polymerization of oxiranes is practically irreversible.

CROP of oxiranes may be initiated by typical cationic initiators including strong protic acids (e.g., $HOSO_2CF_3$), Lewis acids (e.g., BF_3 and its complexes), or oxonium salts (e.g., R_3O^+, A^-).

Of practical importance is photoinitiated cationic polymerization of oxiranes, this subject will be discussed in more detail later on in this section.

Secondary or tertiary oxonium ions formed upon initiation react with another monomer molecule generating tertiary oxonium ions as growing species as shown schematically for polymerization of EO initiated by $HOSO_2CF_3$ (**Scheme 14**).

Propagation proceeds by nucleophilic attack of an oxygen atom in a monomer molecule on a carbon atom in α-position to an oxygen atom bearing formally the positive charge in tertiary oxonium ion located at the chain end. Such a mechanism is known thus as ACE mechanism.

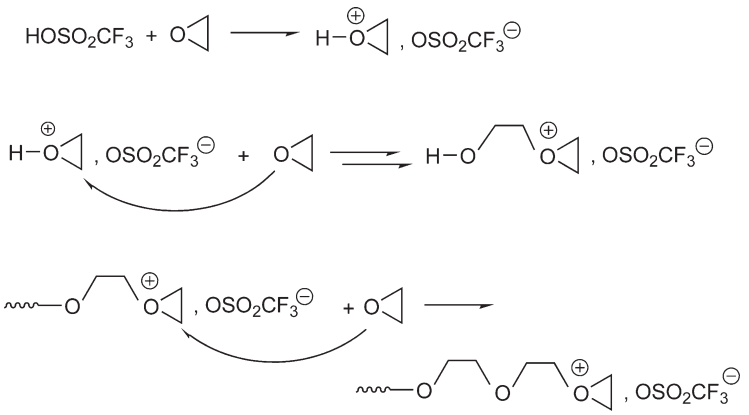

Scheme 14

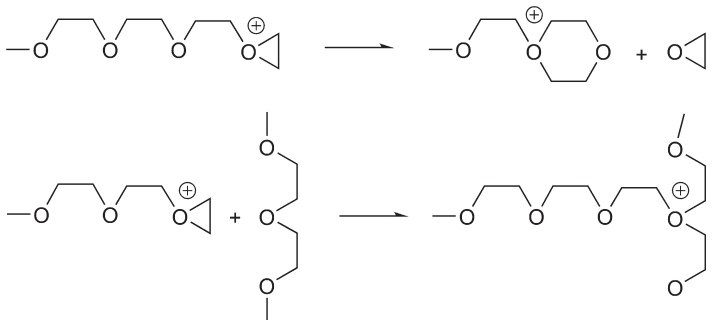

Scheme 15

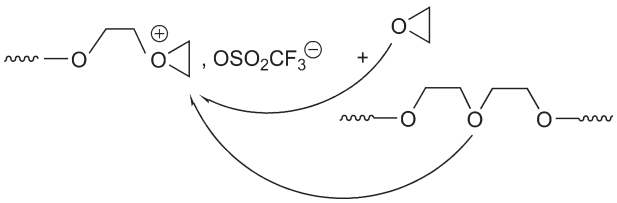

Scheme 16

The oxiranium cation has not been observed directly. It has been shown, however, on the basis of ^{1}H and ^{13}C NMR spectra that the strained oxonium ion is partly converted into a less strained oxonium ion involving a six-membered ring and to a strainless branched oxonium ion (**Scheme 15**).[50]

In CROP of cyclic ethers, a nucleophilic center (oxygen atom) is also present in a polymer chain. Therefore, the attack of this oxygen on the carbon atom in the growing center may occur and compete with propagation, as shown in **Scheme 16**.

As discussed in the previous section, the competition between propagation and chain transfer to polymer is governed mainly by the nucleophilicity of oxygen atoms in cyclic and linear structures (with a possible contribution of steric effects). Thus, chain transfer to polymer is important in the case of CROP of cyclic ethers. The intermolecular reaction leads to segmental exchange ('scrambling') while the intramolecular reaction leads to cyclization. The intramolecular reaction is especially pronounced in CROP of three-membered cyclic ethers because the basicity of the polymer unit is higher than that of the cyclic oxirane monomers (cf. Section 4.08.1.2). Cyclization of oxirane may occur at the stage when the product is a strainless cyclic dimer (1,4-dioxane). Cationic polymerization of unsubstituted oxirane (EO) leads to a mixture of rather low-molecular-weight linear polymer and cyclic oligomers (predominantly cyclic dimer, i.e., 1,4-dioxane).[40,41] Similar behavior was observed for monosubstituted oxiranes such as PO[42] or ECH,[44] although in those cases cyclic trimers or tetramers were the main components of cyclic fraction. Therefore, CROP of oxiranes proceeding by the ACE mechanism is of little synthetic value for the synthesis of high-molecular-weight polymers, although the tendency to cyclization has been ingeniously applied in the synthesis of crown ethers. CROP of EO in the presence of suitable cations, due to the template effect, leads to crown ethers of a given ring size in good yields. Thus, in the presence of large Rb^{+} and Cs^{+} cations, the cyclic fraction contains almost exclusively 18-crown-6 (cyclic hexamer), while in the presence of small lithium cation a mixture containing 30% of cyclic tetramer and 70% of cyclic pentamer is formed.[51]

Cyclization by backbiting cannot be avoided if active species of propagation are tertiary oxonium ions located at the chain end. Several years ago, we proposed that if acid-catalyzed polymerization of oxiranes is conducted in the presence of hydroxyl-group-containing compounds, the other mechanism competes with the ACE mechanism. This mechanism is based on the established mechanism of acid-catalyzed hydrolysis of oxiranes.[52] In analogy to the hydrolysis mechanism, if an excess of oxirane (e.g., EO) is present, successive reactions of protonated monomer molecules with hydroxyl groups lead to extension of the chain as shown in **Scheme 17**.[53]

According to this mechanism, charged species are protonated (activated) monomer molecules, thus the term 'activated monomer mechanism' has been applied in analogy to the term introduced by Szwarc and Bamford for anionic polymerization of *N*-carboxyanhydrides (NCA).[54] It should be noted that in polymerization proceeding by the AM mechanism, hydroxyl-group-containing compounds act as initiators, being incorporated into polymer chains as end-groups, while strong protic acids are catalysts. It should also be stressed that introduction of hydroxyl-group-containing compounds does not simply shift the mechanism of polymerization from ACE mechanism to AM mechanism. In the absence of intentionally added hydroxyl-group-containing compounds, the only propagation reaction possible is reaction of protonated monomer with another monomer molecule leading to the formation of tertiary oxonium ion on which further propagation proceeds by ACE mechanism (in fact, some hydroxyl end-groups are formed as a result of initiation, but their concentration is low as compared to concentration of monomer).

When a hydroxyl-group-containing compound is introduced into the system, protonated monomer may react either with monomer or with hydroxyl group as shown in **Scheme 18** for polymerization of EO.

Competition between ACE and AM mechanisms in CROP of oxiranes was discussed in a series of original papers[55,56] and reviews;[9,53,57] therefore, in this chapter, only a general picture will be presented.

The contribution of two competing reaction pathways depends on the ratio of corresponding rate coefficients and the ratio of concentrations. Rate coefficients depend on nucleophilicity of both competing nucleophiles, that is, hydroxyl groups and cyclic ether. Although the pK_B values reported in the literature differ depending on the measurement method, it

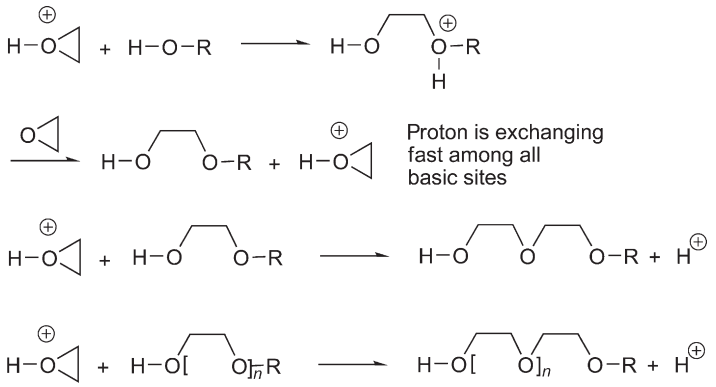

Scheme 17

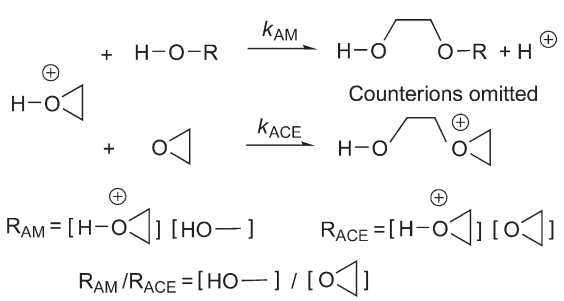

Scheme 18

may be estimated that basicities of hydroxyl groups and cyclic ethers are not much different. Indeed for CROP of ECH, the ratio of k_{AM}/k_{ACE} was found to be close to 5.[58] Because in AM polymerization, hydroxyl-group-containing compound (R–OH) is an initiator, the DP (if side reactions were excluded) should be equal to $DP_n = [M]_0/[I]_0$ (where M denotes cyclic ether and I denotes R–OH). At the conditions when $[M] \gg [I]$ required for the formation of polymer, the AM-type of propagation may play only a minor role considering that k_{AM} is not very much higher than k_{ACE}.

Suitable conditions for AM-type polymerization may be created, however, by applying the overall ratio of [M]/[I] high enough to allow the formation of polymer chain with desired length, but at the same time keeping instantaneous concentration of monomer low to ensure low instantaneous ratio of [M]/[I]. Thus, polymerization should be conducted by slow feeding of monomer to reaction mixture, that is, at monomer-starved conditions.

What are the advantages of conducting CROP of oxiranes by AM mechanism? First of all, because there is no charged species at the growing chain ends, chain transfer to polymer is eliminated and linear polymers free of cyclic fraction may be formed. This was shown conclusively for polymerization of EO, PO, and ECH. In **Table 3**, the dependence of content of cyclic dimer on [EO]/[HO^-] ratio is shown.[59] The same effect was observed for polymerization of PO (**Table 4**).[60]

Secondly, hydroxyl-group-containing compounds, acting as initiator, are incorporated into chain ends. As shown in **Scheme 19**, depending on the nature of initiator, different types of functional polymers can be obtained.

Table 3 Yield of 1,4-dioxane formed in the oligomerization of ethylene oxide (EO) in the presence of CH_3OH

[EO]/[CH_3OH]	*Yield of 1,4-dioxane (%)*
2.0	1.1
4.2	13.4
6.0	39.5
7.8	43.0
17.0	66.5
120	~100

$[EO]_0 = 1.1$ mol l^{-1}, $BF_3{\cdot}Et_2O = 0.03$ mol l^{-1}, CH_2Cl_2, 25 °C, complete conversion of EO. From Penczek, S.; Kubisa, P.; Szymański, R. *Makromol. Chem., Macromol. Symp.* **1986**, *3*, 203.[59]

Telechelic oligodiols and macromonomers with M_n close to calculated values, narrow-molecular-weight distribution, and required functionality were prepared by AM CROP of PO and ECH.[59–62]

Block or star copolymers can be obtained by AM polymerization if polymers containing hydroxyl groups are used as macroinitiators. Application of poly(ethylene glycol) as initiator in cationic AM polymerization of glycidyl methacrylate (GM) led to block copolymers containing hydrophilic poly(oxyethylene) block and poly(GM) block in which methacrylic double bonds were fully preserved. The resulting amphiphilic block copolymers formed core-shell micelles in water that could be stabilized by cross-linking involving double bonds of poly(GM) block.[63]

Cationic AM polymerization of EO initiated by a multihydroxy core obtained by cationic polymerization of 3-ethyl-3-(hydroxymethyl)oxetane (as described in Section 4.08.3.3) in the presence of acid catalyst allowed preparation of star polymers.[64]

Although polymerization of oxiranes by the AM mechanism offers several advantages, there are also some limitations. Instantaneous [M]/[HO] ratio should be kept low thus monomer should be fed slowly into reaction mixture. The reaction is, therefore, slow and to achieve higher molecular weights, long reaction times are required. Moreover, the proton from a catalyst is exchanged quickly between all basic sites and only its fraction participates in the activation of the monomer. At the

Table 4 Influence of instantaneous monomer concentration (PO) on the amount of cyclic tetramer formed.

Conditions	*$[PO]_{total}$ ($mol\,l^{-1}$)*	*$[HO^-]_0$ ($mol\,l^{-1}$)*	*$[PO]_{inst}$ ($mol\,l^{-1}$)*	*PO conversion (%)*	*Tetramer (wt.%)*
PO introduced in the beginning	2.0	4×10^{-1}	$2.0 \rightarrow 0$	100	4.0
Faster feeding	2.0	4×10^{-1}	0.3–0.7	82	2.35
Slower feeding	2.0	4×10^{-1}	0.05–0.14	100	0.95

$[HBF_4{\cdot}Et_2O] = 2.5–5 \times 10^{-3}$ mol l, CH_2Cl_2, 25 °C. From Wojtania, M.; Kubisa, P.; Penczek, S. *Makromol. Chem., Macromol. Symp.* **1986**, *6*, 201.[60]

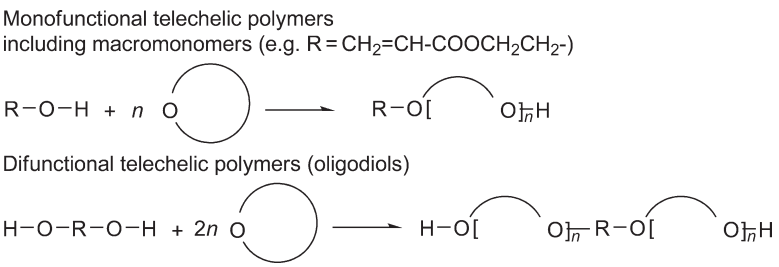

Scheme 19

early stages, proton is involved in protonation of HO groups and oxygen atoms in monomer molecule, while in the later stages an increasing fraction of protons is involved in protonation of oxygen atoms in the polymer chain thus the fraction of protons activating monomer decreases in the course of polymerization. For these reasons, AM CROP of oxiranes is a suitable method of synthesis of medium-molecular-weight telechelic polymers (M_n up to $\sim$5000) rather than high-molecular-weight polymers.

If both functions, that is, oxirane group and hydroxyl group, are present in the same molecule than propagation by AM mechanism leads to branched structures.[65] The simplest monomer of this class is (hydroxymethyl)oxirane (glycidol). Polymerization of glycidol by ACE mechanism should lead to polymers composed entirely of 1,3-units. Analysis of ^{13}C NMR spectra of the relatively high-molecular-weight polymers (M_n up to 10^4) prepared with $HPF_6 \cdot Et_2O$ as a catalyst in bulk revealed the presence of both 1–4 and branched units providing direct proof for the participation of the AM mechanism. It was not possible, however, to resolve sufficiently the ^1H and ^{13}C NMR spectra and to thus obtain quantitative information on the relative contributions of both the mechanisms.[66]

The formation of 1–4 units (containing secondary hydroxyl groups), resulting from AM propagation, was confirmed, however, by analysis of ^{29}Si NMR spectra of a silylated polymer (**Scheme 20**). In subsequent attempts to analyze the contributions of the AM and ACE mechanisms in the polymerization of glycidol, it was observed that the structure of the polymer formed depends to some extent on the nature of the catalyst.[67] The content of 1–3, 1–4, and branched units was measured by ^{13}C and ^{29}Si NMR, and on this basis the following contribution of the AM mechanism was estimated: $SnCl_4 \sim 80\%$, $BF_3 \cdot Et_2O \sim 50–70\%$, and $CF_3SO_3H \sim 50\%$.

Hyperbranched polyethers were also obtained by cationic copolymerization of glycidol with alkyl glycidyl ethers.[68]

Glycidol polymerizes also by anionic mechanism. Anionic polymerization leading to hyperbranched multihydroxyl polyethers has been studied extensively and possible applications of polymers obtained by anionic polymerization have been indicated.[69–71]

Properties of hyperbranched polyethers prepared by cationic polymerization of glycidol have also been studied. Cationically prepared polyglycidol after esterification of hydroxyl end-groups with palmitoyl chloride showed an interesting self-assembly behavior. Depending on the solvent and content

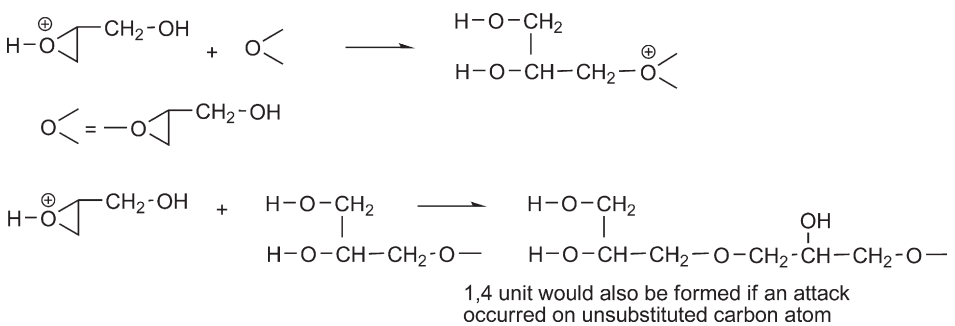

Scheme 20

of hydrophobic arms, regular unimolecular micelles or vesicles of different size were observed.[72] Block copolymers containing polystyrene (formed by atom transfer radical polymerization (ATRP)) and polyglycidol block (formed by cationic polymerization) in combination with lithium salts have been applied as polymer electrolytes.[73]

Although anionic polymerization of glycidol leading to hyperbranched multihydroxyl polyethers, as reviewed recently,[71] has been studied much more extensively than the cationic process, cationic polymerization of hydroxyl-group-containing cyclic ethers provides a more general approach to the synthesis of branched multifunctional polyethers because, as discussed in Sections 4.08.3.3 and 4.08.4.3, it may be extended to four- and five-membered cyclic ethers that polymerize only by cationic mechanism.

4.08.2.2 Cationic Photopolymerization of Oxiranes

Photopolymerization of various classes of monomers is covered in more detail in Chapter 4.37; therefore, in this section, only the major findings related specifically to oxirane photopolymerization are briefly outlined.

The advantage of photoinitiated cationic polymerization is its lack of sensitivity to atmospheric oxygen and substantial dark polymerization, that is, the chain reaction continues to proceed effectively after UV exposure is terminated, due to the fact that the propagating polymer cations, in contrast to radicals, do not mutually react. On the other hand, the rate of cationic photopolymerization of difunctional epoxides is by 1 order of magnitude lower than that of radical photopolymerization of diacrylate monomers, most probably because of a lower propagation rate constant.[74] Nevertheless, in recent years, cationic photopolymerization of oxiranes have found many applications, for example, in coatings, adhesives, and printing inks.[75]

Cationic photopolymerization is typically initiated by onium salts, for example, diaryliodonium salts $Ar_2I^+ MtX_n^-$ or triarylsulfonium salts Ar_3S^+, MtX_n^- ($MtX_n^- = PF_4^-$, BF_6^-, SbF_6^-, etc.). The irradiation of photoinitiator generates a number of reactive species that subsequently react with solvent or monomer to give protonic acid $HMtX_n$.

Although in photocurable formulations, difunctional oxirane derivatives are employed; for mechanistic studies, monofunctional oxiranes are used including cyclohexene oxide, styrene oxide, or phenyl glycidyl ether. These studies indicate that the cationic polymerizations proceeding as a result of photoinitiation by onium salts have typical characteristics of polymerizations initiated by strong protonic acids. Thus, initiation involves protonation of oxirane ring while propagation proceeds on tertiary oxonium ions as active species, that is, by the ACE mechanism.[76,77]

Photoinitiated cationic polymerization may also proceed by the AM mechanism if an HO-containing compound is present in the system. AM polymerization of cyclohexene oxide was used to prepare polymer/clay nanocomposite by photopolymerization of cyclohexene oxide in the presence of montmoryllonite modified with ammonium salts containing $-CH_2CH_2OH$ groups and $(Ph)_2I^+ PF_6^-$ as photoinitiator. Upon irradiation protic acid was formed that catalyzed AM propagation on HO groups. As a result, polymer chains were attached to clay surfaces and exfoliated structures were obtained.[78]

AM photopolymerization of epoxy monomers bearing hydroxyl groups has also been studied. In analogy to the earlier described AM polymerization of simplest monomer of this class, that is, glycidol, AM photopolymerization of cyclohexene oxide and norbornene oxide substituted with hydroxyl group led to highly branched polyethers containing several hydroxyl end-groups. The rates of photopolymerization of those monomers were significantly higher than the rates of photopolymerization of analogous epoxy monomers bearing methoxy groups, which was attributed to inherently more rapid kinetics of the AM mechanism that the former monomers undergo as compared to the conventional epoxide ROP for the latter compounds.[79]

4.08.3 CROP of Oxetanes

4.08.3.1 Mechanism of Polymerization

In contrast to three-membered cyclic ethers, oxiranes, and four-membered cyclic ethers, oxetanes polymerize only by cationic mechanism (although anionic polymerization of oxetanes has been occasionally reported[80]). Polymerization of oxetanes, due to the relatively high ring strain is practically irreversible.

First reports on the cationic polymerization of oxetanes appeared in the open literature in the 1950s,[81,82] but the process had been studied earlier because at that time Hercules Inc. had developed the industrial production of polymer of 3,3-bis (chloromethyl)oxetane (poly-BCMO) and had been marketing the polymer for about 15 years under the Trade Name Penton®.

On the basis of studies of the parent monomer of this class (unsubstituted oxetane), the basic features of cationic polymerization of oxetanes (including substituted oxetanes) have been established. Typically, polymerization was initiated by BF_3 (in the form of complex with, e.g., Et_2O) and the necessity of water cocatalysis was well documented.[81–86]

Another system especially suited for the synthesis of high-molecular-weight poly(BCMO) is the R_3Al/H_2O initiating system.[87–89] Kinetic studies revealed that for this system the rate of polymerization increases by increasing the ratio $[H_2O]/[R_3Al]$ up to 1/1. This indicates clearly that polymerization is initiated by protic acid generated by interaction of water with Lewis acid.

Cationic polymerization of oxetanes provided examples of the influence of the number and size of substituents on the tendency to cyclization. The steric hindrance caused by the presence of substituents can make it more difficult for the macromolecule to assume conformation suitable for the ring closure. Thus, in the cationic polymerization of unsubstituted oxetane, up to 50% of cyclic tetramer was formed (at 100 °C with $BF_3 \cdot Et_2O$ initiator). The content of cyclic fraction was lower at lower temperatures.[82] In the polymerization of 3,3-dimethyloxetane, the content of cyclic fraction was considerably lower (~20%).[90] In the polymerization of 3,3-bis-(chloromethyl)oxetane containing still larger substituents, only 2% of cyclic oligomers were formed in polymerization initiated with the R_3Al/H_2O system even at high temperature (180 °C).[91]

Cyclization occurs by intramolecular chain transfer to polymer. Intermolecular reaction leads to the formation of branched polymeric tertiary oxonium ion of low reactivity,

thus such a reaction leads to termination. Although the two possible modes of chain transfer to polymer (intra- or intermolecular reaction) are not necessarily related, in the cationic polymerization of oxetanes for those groups of monomers that have stronger tendency to cyclization, generally lower molecular weights of linear fraction were observed. Thus, in the polymerization of unsubstituted oxetane, polymers with M_n in the range $\sim 3.5 \times 10^4$ and broad-molecular-weight distribution were obtained at −20 °C[92] while in polymerization of 3-methyl-3-(chloromethyl)oxetane and BCMO initiated with a R_3Al/H_2O system polymers with M_n exceeding 5×10^5 and $M_w/M_n < 1.3$ could be prepared.[88,89]

More recently, cationic polymerization of oxetane has been studied in the presence of an ether additive that converts strained tertiary oxonium ion active species into strain-free tertiary oxonium ion (dormant species) that may be reactivated by monomer addition as shown in **Scheme 21**.[93–95]

The concept of polymerization involving reversible deactivation of growing species had been applied earlier to a number of systems in the field of radical as well as ionic polymerization. The authors stress that "unlike conventional quasi-living polymerization based on reversible end-capping reactions, the dormant species is reactivated by a monomer addition"[92–94] (the term 'quasi-living' is discouraged in IUPAC terminology). This, however, is not an entirely new concept. In the cationic polymerization of THF in the presence of $CF_3SO_3^-$ counterion, deactivation of growing species occurred by the formation of covalent macroester that could be reactivated mainly by reaction with monomer molecules (see Section 4.08.4.1). Cationic polymerization of oxetane in the presence of a suitable additive (1,4-dioxane, tetrahydropyran) indeed proceeds as a living/controlled process and side reactions resulting from chain transfer to polymer such as cyclization or chain segment redistribution may be eliminated. Polymers with M_n up to 1.6×10^5 and a narrow-molecular-weight distribution ($M_w/M_n = 1.18–1.28$) were obtained.[95]

Cationic polymerization of oxetanes has been more recently exploited to prepare a variety of functional polymer materials including functional polymer networks and energetic binders for solid rocket propellants. Polymerization of BCMO has been studied extensively in the past because of the industrial application of this process. After the production of Penton® was discontinued the interest in polymers of BCMO ensued from the fact that they may serve as a precursor for various functional polyoxetanes.

Polymers used as energetic binders should act not only as a binder but also as a real propellant component. Thus most frequently azido groups having a tendency to highly exothermic decomposition are introduced into a side chain. Oxetane

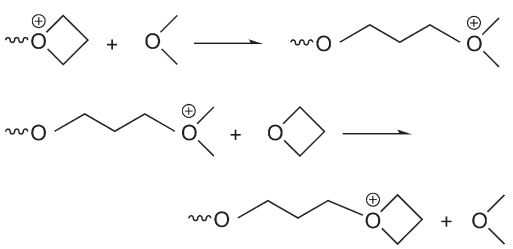

Scheme 21

polymers are used because by replacement of $-CH_2Cl$ groups in BCMO (or its polymer) two $-CH_2N_3$ groups may be introduced into each repeating unit, which results in a high nitrogen content (50 wt.%), considerably higher than in polymers derived from oxirane derivative, for example, glycidyl azide (42.5 wt.%). Two approaches are used to synthesize azido-group-containing oxetane polymers; azido groups are introduced by the reaction of suitable substituents ($-CH_2Cl$, $-CH_2Br$, and $-CH_2OTs$) in the monomer with NaN_3 (with subsequent cationic polymerization) or in polymer. The disadvantage of the former route is a necessity of handling and storage of azide-containing monomers that are considerably more shock sensitive than the corresponding polymers.[96] Frequently, to decrease crystallinity, other monomer units are introduced along the chain by copolymerization.[97–99]

Side-chain liquid-crystalline polyoxetanes showing smectic polymorphism were obtained by cationic polymerization of oxetanes substituted with two mesogenic groups connected by a flexible spacer.[100]

Oxetane polymers containing perfluorinated substituents are also studied. Cationic polymerization of 3,3-bis[(2,2,2-trifluoroethoxy)methyl]oxetane leads to polymers showing oleophobicity that compare favorably with that of more highly fluorinated acrylates.[101]

Telechelic oxetane polymers containing hydroxyl end-groups at both ends were synthesized by cationic polymerization of substituted oxetanes in the presence of diols.[102,103] Although the mechanism of polymerization was not discussed, it may be expected that polymerization proceeded by the AM mechanism. These telechelics containing fluorinated substituents after converting hydroxyl end-groups into ammonium salts showed unusually low surface tensions.[104] Telechelics containing fluorinated and alkylammonium substituents along the chain were also obtained by cationic copolymerization of suitably substituted oxetanes and were incorporated into polyurethanes in order to modify their surface properties.[105]

Oxetanes containing fluorinated substituents are employed for preparation of oligodiols, which may be used for the synthesis of polyurethanes having more hydrophobic surfaces.[106] Oxetanes containing pentafluoropropoxy or heptafluorobutoxy groups in position 3 were polymerized with $BF_3 \cdot Et_2O$ as initiator in the presence of a butandiol giving telechelic polymers with M_n in the range $4–12 \times 10^3$ and rather high polydispersity ($M_w/M_n \sim 2–3$). There was no simple relationship between the reported M_n values and [monomer]/[HO] ratio as observed for polymerization of oxiranes in the presence of HO-containing compounds and proceeds by the AM mechanism which may indicate that some chain transfer and/or termination reaction operate in this system.[103] Characterization of poly(perfluorooxetane)s by matrix-assisted laser desorption/ionization (MALDI) mass spectrometry, size exclusion chromatography, and NMR spectroscopy has been reported.[107]

Dioxetane monomers containing two oxetane rings coupled with short poly(oxyethylene) chains (as shown in **Scheme 22**) were polymerized with $BF_3 \cdot Et_2O$ to network polymers that showed activity as phase-transfer catalysts.[108]

Polymerization of such dioxetanes could be initiated by lithium salts (e.g., $LiN(SO_2CF_3)_2$) giving polyoxetane-lithium salt complexes that could be applied as solid polymer electrolytes.[109]

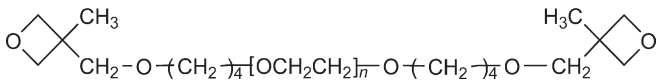

Scheme 22

4.08.3.2 Cationic Photopolymerization of Oxetanes

Photopolymerization of various classes of monomers is covered in more detail in Chapter 4.37; thus in this section, only the major findings related specifically to oxetane photopolymerization are briefly outlined.

In comparison with epoxides, the photoinitiated cationic polymerization of oxetane monomers is relatively slow and proceeds with an extended induction period.[110] The origin of the induction period is still a matter of discussion.[111] The induction period may be considerably shortened by conducting photopolymerization in the presence of more reactive epoxide monomers. Due to relatively low reactivity of propagating tertiary oxonium ions, photopolymerization of oxetane monomers is rather slow but the polymerization continues during the dark storage of a sample.[112] Cationic photopolymerization of di- and trifunctional oxetanes, including those containing mesogenic groups, proceeds with a low volume shrinkage.[113,114] The volume shrinkage can be further reduced by copolymerization with spiro orthocarbonates.[115] An oxetane monomer, 3-ethyl-3-[(methacryloyloxy)methyl]oxetane, was polymerized by ATRP on the surface of monodisperse silica particles. The polymeric layer thus obtained was cross-linked by cationic polymerization of oxetane groups and after removal of silica core, uniform polymeric hollow spheres were obtained.[116]

Fabrication of solution-processed multilayered organic light-emitting diodes (OLEDs) from oxetane-functionalized precursors, which are commonly photochemically cross-linked by UV radiation in the presence of a photoinitiator, has been reported recently.[117] The reaction proceeds via CROP. Insoluble cross-linked polymer networks were obtained using precursors that contain two or more oxetane units per molecule. This novel approach simplifies OLED fabrication, and is generally compatible with various deposition/printing techniques.

4.08.3.3 CROP of Oxetanes Leading to Hyperbranched Polyethers

Synthesis of highly branched polyethers by cationic polymerization of hydroxymethyl-substituted oxetanes is a relatively recent development, not covered by earlier reviews, therefore this subject will be discussed in more detail.

As discussed in previous section, cationic polymerization of cyclic ethers (e.g., glycidol) containing hydroxyl groups as substituents leads to highly branched multihydroxy polyethers by the process involving propagation by the ACE and AM mechanisms. Polymerization of three-membered glycidol (either cationic or anionic) leads to branched polyethers containing both primary and secondary hydroxyl groups. In contrast, polymerization of oxetane monomers substituted with CH_2OH groups leads to branched polyethers containing exclusively primary hydroxyl groups, irrespectively of contribution of ACE and AM mechanisms. Typical monomers of this class are shown in Scheme 23.

Vandenberg *et al.* reported that cationic polymerization of those monomers leads to branched polymers, but they did not investigate the process in more detail because their interest at that time was in the synthesis of linear polymers.[118] More recently, there has been an increasing interest in the synthesis of highly branched polymers, which in some applications may perform certain functions of dendrimers but being much easier to synthesize.

Studies of cationic polymerization of 3-ethyl-3-(hydroxymethyl)oxetane (EOX), conducted by us[119,120] and by other groups[121,122] showed that this monomer can be polymerized to medium-molecular-weight polymers (molecular weights amounts to few thousands). There seems to be a certain upper limit of molecular weights that can be achieved, although it has been reported that somewhat higher-molecular-weight polymers are formed at higher temperatures.[123]

The polymers contain three types of units shown in Scheme 24.

The contents of terminal, linear, and branched units can be determined by ^{13}C NMR. The signals of quaternary carbon atoms in those units (after acetylation of HO groups) are well separated allowing integration. The number of branched units in poly(EOX) is limited. In polymers with DP_n of about 15, there are on an average about three branched units per macromolecule.[119,120] The degree of branching increases with increasing conversion[123] and with increasing temperature.[124] It was shown that in the cationic polymerizatization of 3-ethyl-3-(hydroxymethyl)oxetane

3-alkyl-3-(hydroxymethyl)oxetane

3,3-bis(hydroxymethyl)oxetane

Scheme 23

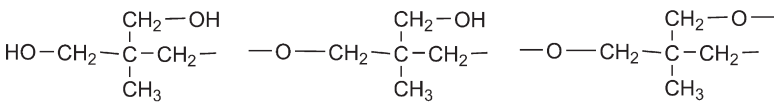

Terminal unit

Linear unit

Branched unit

Scheme 24

(EOX) M_n of the polymer is essentially independent of conversion. Analysis of MALDI time-of-flight (MALDI-TOF) spectra of polymers revealed that one kind of macromolecules is present and that the molar masses of macromolecules are exact multiples of molar mass of monomeric units.[120] This indicates that the macromolecules are cyclic or contain cyclic fragment. The cyclic fragment may be formed by the reaction of either a protonated oxetane ring or a tertiary oxonium ion with any HO group of the same macromolecule (**Scheme 25**).

Also, 3,3-bis(hydroxymethyl)oxetane (BHMO) polymerizes by cationic mechanism. Every unit in BHMO polymers contains two HO groups; therefore, the probability of branching should be enhanced. Poly(BHMO) is, however, insoluble in common organic solvents, thus the structure of polymer cannot be easily determined. Copolymerization of BHMO with EOX leads to soluble polymers with molecular weights similar to those of poly(EOX), that is, $2–3 \times 10^3$ with a considerably higher fraction of branched units as shown by ^{13}C NMR. MALDI-TOF analysis indicates that also in this system cyclic macromolecules are formed.[125]

In view of the proposed polymerization mechanism, the fact that M_n is rather low and does not increase with conversion is a little unexpected. Branched units are formed by reactions involving HO groups. The question arises why at a certain stage of growth of macromolecules the HO groups are no longer able to participate in growth of the macromolecule (M_n does not change significantly with conversion).

Analysis of IR and NMR spectra of polymers provided indication of hydrogen bonding of HO groups.[65] Hydrogen bonding may strongly reduce the nucleophilic reactivity of HO groups.[126] With an increasing number of HO-containing units within the macromolecule, intramolecular hydrogen bonding may force the macromolecule into conformation facilitating intramolecular chain transfer to polymer (cyclization) as shown in **Scheme 26**.

Poly(EOX) and its copolymers with BHMO are either amorphous with $T_g \sim 40\ ^\circ C$ (at high degree of branching) or

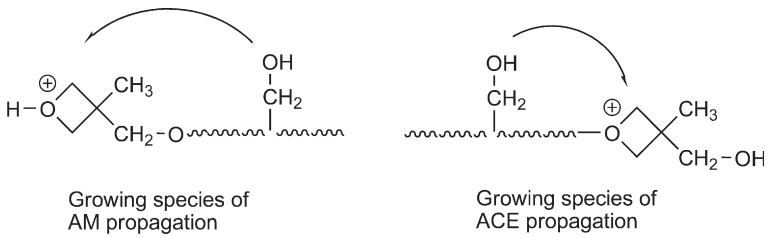

Scheme 25

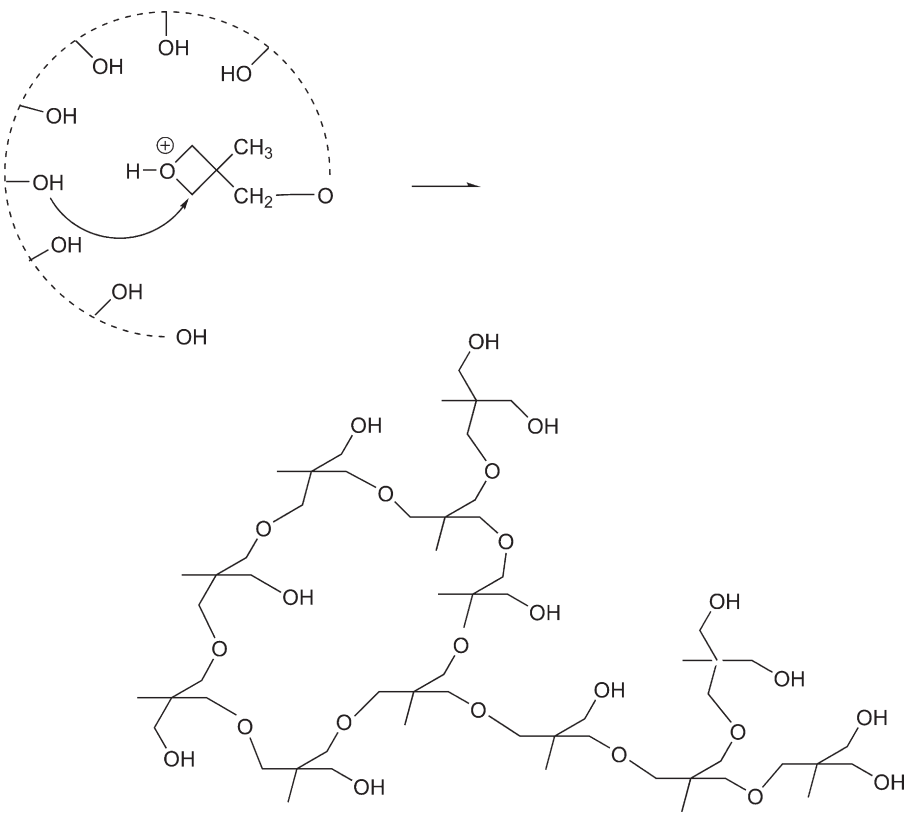

Scheme 26

semicrystalline with $T_m \sim 100–130$ °C (at low degree of branching).

Although these materials may find applications that are predicted for hyperbranched polymers, they are used rather as precursors allowing (either by using hydroxyl groups directly or after their transformation into required initiating groups) the synthesis of multiarm star polymers of different structures.[127,128] Star polymers containing poly(EOx) core may also be prepared by a one-pot procedure. Thus, in cationic copolymerization of EOX with THF, EOX polymerized first and, after it was essentially exhausted, the resulting hyperbranched species acted as a macroinitiator and initiated the cationic polymerization of THF.[129] More recently, dumb-bell polymers consisting of linear poly(EO) middle block and two outer branched poly(EOX) blocks were synthesized by bulk cationic polymerization via dropwise addition of EOX to poly (ethylene glycol) (PEG, $M_n \sim 1900$) in the presence of $BF_3 \cdot Et_2O$. Polymers containing up to ~ 14 EOX units per PEG chain were obtained (Scheme 27).[130]

Copolymerization of 3-(hydroxymethyl)-3-methyloxetane (MeOx) with oxetane containing in position 3 the $-[OCH_2CH_2]_3OCH_3$ substituent (MEMO) led to branched polymers with short oligo(ethylene oxide) chains. These materials were tested as potential solid polymer electrolytes.[131]

A one-pot procedure was developed for the synthesis of star polymers containing poly(EOx) core and poly(ethylene oxide),[132,133] poly(propylene oxide)[134] or poly(tetrahydrofuran) (PTHF) arms.[129]

EOX was polymerized first with $BF_3 \cdot Et_2O$ as initiator in CH_2Cl_2 solution. EO was then added dropwise at –20 °C. Star polymers with M_n in the range $1–2 \times 10^4$ and M_w/M_n between 1.5 and 1.9 were obtained. In acetone solution, these products underwent self-organization to multiwalled tubes with diameters of the order of millimeters and lengths of the order of centimeters. In water solution, large vesicles having a high (> 60%) hydrophilic fraction were formed. Star polymers containing poly(propylene oxide) arms also self-assembled into large spherical micelles (> 120 nm) with the size depending on the molar ratio of arms to core.[134] Multiarm star polymers containing poly(EOX) core with different degrees of branching (DB) and polyoxyethylene (POE) arms can self-assemble into vesicles, wormlike micelles, and spherical micelles depending on DB of the core.[135,136]

It was reported recently that hyperbranched multifunctional polyethers can be advantageously used as coatings of capillary columns for separation of proteins showing reduced adsorption of basic proteins and excellent separation efficiency.[137] EOX was also polymerized in the presence of solid materials containing hydroxyl groups on the surface. In this way, hyperbranched polyethers were attached to surfaces of carbon black,[138] carbon nanotubes,[139] or montmoryllonite.[140]

Cationic polymerization of oxetane-containing polymeric precursor obtained by anionic polymerization of 3-ethyl-3-[(oxiranylmethoxy)methyl]oxetane led to ladder polymers containing 15-crown-4 units as shown in Scheme 28.

Gel-free polymers showed the metal binding selectivity similar to 14-crown-4. Possible applications as polymer electrolytes were indicated.[141]

It should be noted that although generally oxetanes polymerize only by a cationic mechanism, there are a few reports on the anionic polymerization of (hydroxymethyl)oxetanes.[142,143]

4.08.4 CROP of THFs (Oxolanes)

Three- and four-membered cyclic ethers are highly strained (ring strain > 20 kcal mol^{-1}) thus their polymerization is practically irreversible. When there are five- and more atoms in the ring, the ring strain is considerably lower; thus polymerization of five- and seven-membered cyclic ethers is highly reversible while six-membered cyclic ethers do not polymerize.

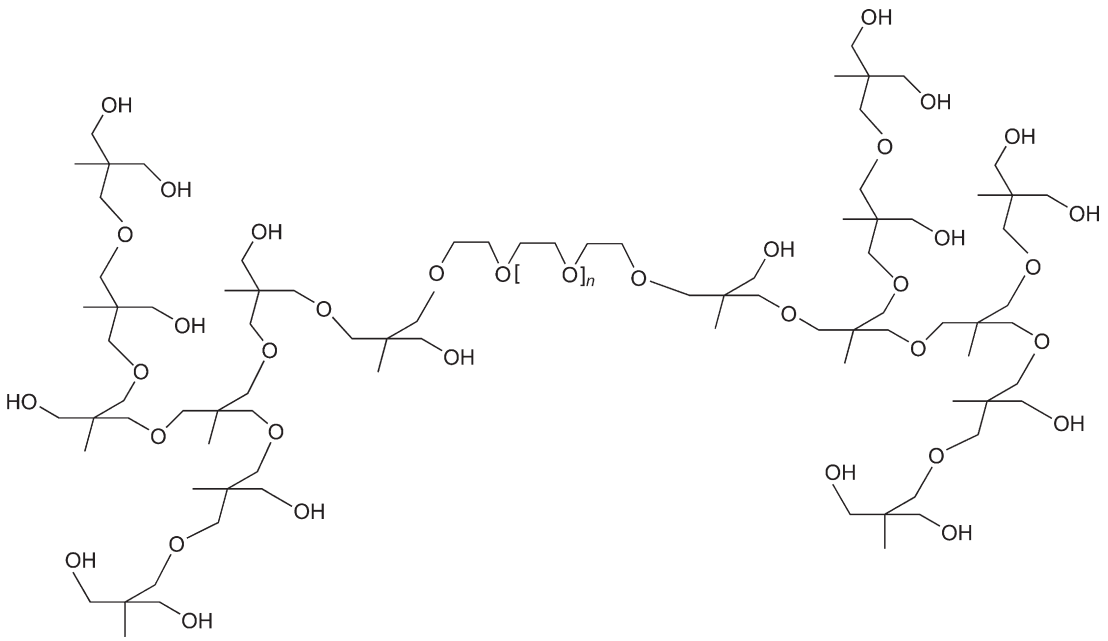

Scheme 27

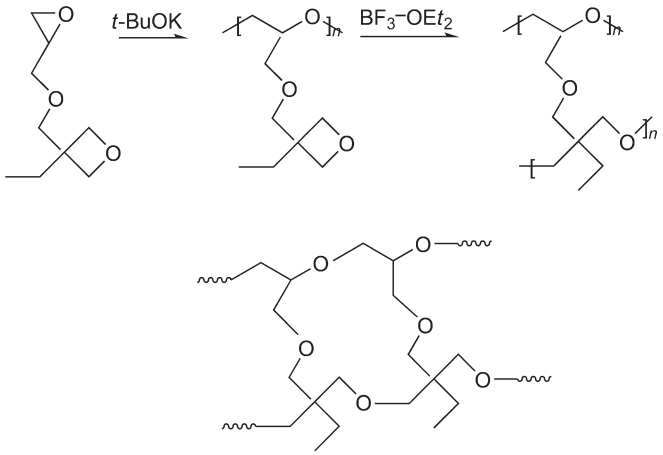

Scheme 28

Practical consequences of reversibility of propagation have been already discussed (cf. Section 4.08.1.1). They may be summarized as follows:

1. The highest conversion that can be achieved is equal to $([M]_0 - [M]_e)/[M]_0 \times 100\%$. Thus, to reach the highest monomer conversion in reversible polymerization, it should be conducted at high $[M]_0$ and low temperature ($[M]_e$ decreases with decreasing temperature).
2. Active centers of polymerization should be deactivated at the temperature at which polymerization is conducted. Otherwise changes of temperature or concentration in the course of polymer isolation and/or purification may cause depolymerization.

For polymerization of unsubstituted five-membered cyclic ether – THF – the ceiling temperature for bulk polymerization is ~80 °C (the values reported in the literature differ slightly, see Reference 13, p 168), which means that above this temperature THF cannot be polymerized even in bulk. The equilibrium monomer concentration $[M]_e$ at room temperature is close to 3.3 mol l^{-1},[144] but it may vary depending on the solvent. This means that the highest conversion allowed by thermodynamics for bulk polymerization at room temperature is close to 75%.

It should be remembered that the equilibrium constant of propagation is dependent on the chain length becoming constant only after reaching a certain DP_n value. Thus, short oligomers may be still formed at conditions when polymerization to a high-molecular-weight polymer is prohibited by thermodynamics. It should also be remembered that at the conditions when monomer cannot undergo homopolymerization, it may participate in copolymerization.

4.08.4.1 Mechanism of Cationic Polymerization of THF

The discoverer of living polymerization, M. Szwarc, discussed cationic polymerization of THF as an example of living polymerization.[145,146] Indeed, in early studies of this system, it had been pointed out that polymerization may proceed as a terminationless process.[147–150] Thus, cationic polymerization of THF has been studied in detail and many fundamental issues related to the kinetics and mechanism of polymerization of cyclic ethers in general have been resolved on the basis of studies of this system.

In the book *Cationic Ring Opening Polymerization* published in 1985,[5] a whole chapter was devoted to temporary (reversible) termination. Polymerizations proceeding with reversible deactivation of active species are now widely studied because they offer the possibility of controlling molecular weights, molecular weight distribution, and the structure of end-groups in a variety of radical and ionic polymerizations (living/controlled polymerizations).

Cationic polymerization of THF provided the first thoroughly studied example of polymerization with reversible deactivation of active species. In the polymerization initiated by trifluoromethanesulfonic acid (or its derivatives such as anhydride or ester), the active species are involved in the following equilibria (**Scheme 29**).[151–156]

Ionic and covalent active species have been directly observed by ^{1}H NMR. Methylene groups in α-position to oxygen bearing a positive charge in ionic species give a triplet at 4.86 ppm (δ) while methylene groups in covalent species ($-CH_2OSO_2CF_3$) give a triplet at 4.58 ppm. Both signals can be independently observed in polymerizing mixture and their fractions depend on the polarity of solvent as shown in **Figure 1**.[151]

In highly polar nitromethane almost exclusively, ionic species are present in moderately polar methylene chloride, both types of species are observed in similar concentrations while in nonpolar tetrachloromethane covalent species predominate with only ~5% of ionic species.

In the original publications, these two routes of ionization were described as internal ionization and covalent propagation (although the latter could also be considered as external ionization).

The full kinetic scheme (**Scheme 30**) including rate constants of ionization and deactivation (temporary termination), rate constants of propagation and all involved equilibrium constants have been resolved, as discussed in detail in several reviews.[1–12]

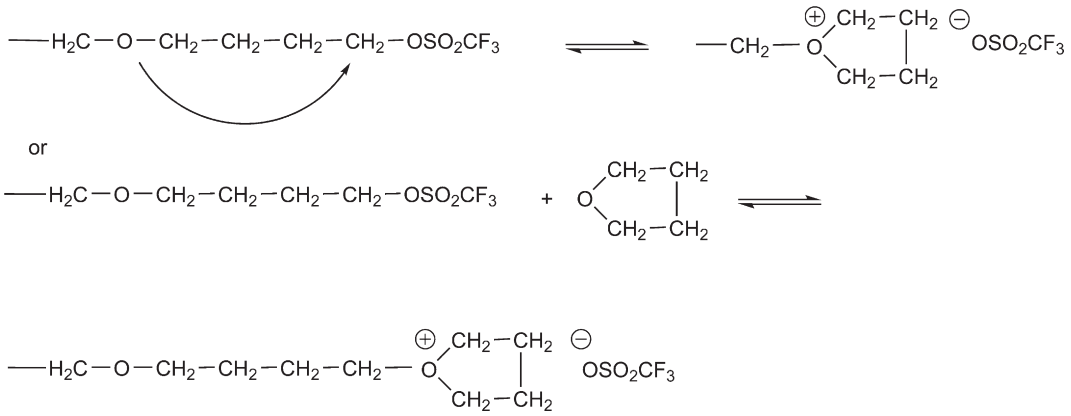

Scheme 29

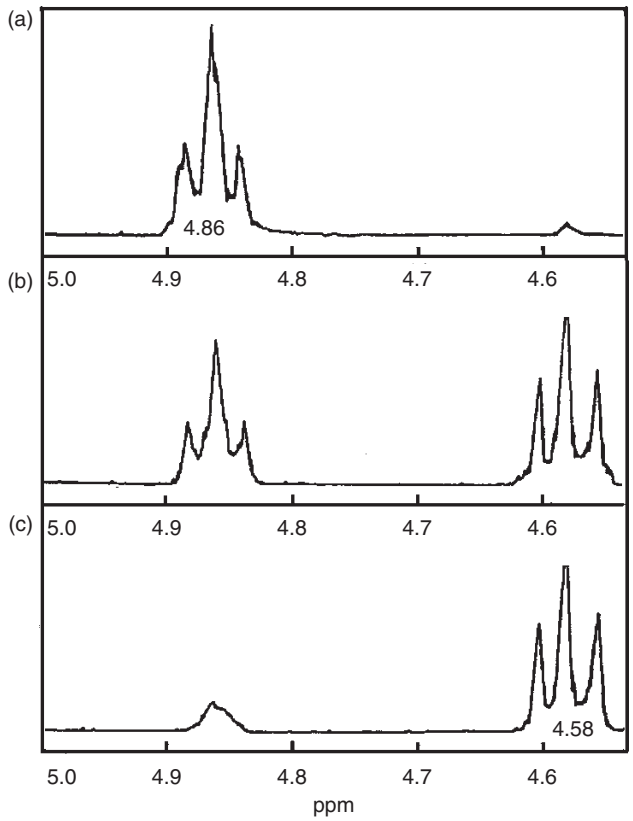

Figure 1 300 MHz ^{1}H NMR spectra (4.5–5.0 ppm region only) of living poly(THF) with $CF_3SO_3^-$ anion at 17 °C. $[M]_0 = 8.0\,mol\,l^{-1}$, $[initiator]_0 = 0.05\,mol\,l^{-1}$ in (a) CD_3NO_2, (b) CH_2Cl_2, and (c) CCl_4. Reprinted with permission from Matyjaszewski, K.; Penczek, S. *J. Polym. Sci. Polym. Chem. Ed.* **1974**, *12*, 1905.[151]

All involved rate constants (and also equilibrium constants) have been determined. For a $7\,mol\,l^{-1}$ solution of THF in CH_3NO_2 at 25 °C, the following values were obtained: $k_{pc} = 5 \times 10^{-4}\,mol^{-1}\,l\,s^{-1}$, $k_{p+/-} = k_{p+} = 2.4 \times 10^{-2}\,mol^{-1}\,l\,s^{-1}$, $k_{ii} = 12 \times 10^{-2}\,s^{-1}$, $k_{tt} = 0.3 \times 10^{-2}\,s^{-1}$.

The major findings can be summarized as follows:

- Ionization of covalent species proceeds predominantly by intramolecular ionization ($k_{ii} \gg k_{pc}$). Covalent species are essentially dormant (k_{pc} is very low) but may be reactivated by intramolecular ionization. Thus, formally the situation resembles that encountered in more recently studied processes of controlled radical polymerization (ATRP and nitroxide-mediated polymerization (NMP)) and the system can be described as polymerization with reversible deactivation of growing species.
- Propagation rate constants for ion-pairs and free ions are the same ($k_p^+ = k_p^{\pm}$); the reactivity of ion-pairs does not depend on the structure of counterion. This is a general feature of

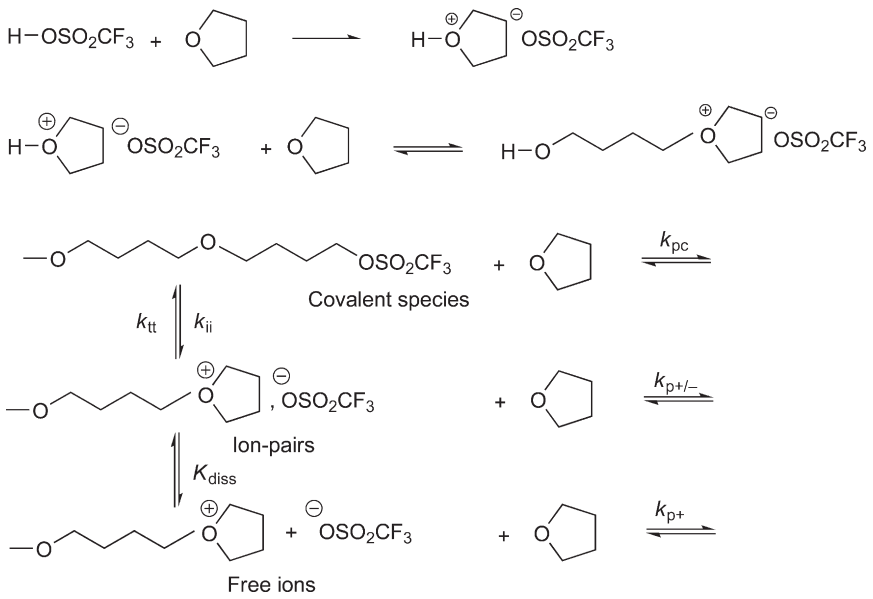

Scheme 30

CROP, in contrast to anionic vinyl and anionic ROP polymerizations.[157,158] In anionic polymerization the charge is localized on the terminal atom while in CROP the charge is delocalized between the oxygen and neighboring carbon atoms in cyclic oxonium ion; thus the interaction of cation and anion is rather weak. Free cations may be more strongly solvated, which may counterbalance the interaction with anion in ion-pair. Additionally, according to the steric course of S_N2 reactions, propagation on ion-pair may not require complete separation of ion-pair. All these factors account for equal reactivity of free ions and ion-pairs in CROP of THF.[28,29] The same reactivity of ion-pairs and free ions was found also for CROP of seven-membered cyclic ethers – oxepanes.[30,159]

4.08.4.2 Synthetic Applications of Cationic Polymerization of THF

Cationic polymerization of THF proceeds without chain transfer or termination and in principle it can be considered as living polymerization (although it is highly reversible). Thus, this process is well suited for the synthesis of telechelic polymers. Tetrahydrofuran oligodiols (poly(butane-1,4-diol) known under the trivial name poly(tetramethylene glycol) (PTMEG)) are used for the preparation of polyurethanes and polyester thermoplastic elastomers with outstanding hydrolytic stability at elevated temperatures and desirable mechanical properties.[160] The world capacity for PTMEG amounted to $\sim 300\,000\,t\,yr^{-1}$ in 2001 and since then has increased further, mainly due to new production facilities in China (overall China PTMEG capacity has expanded to $230\,000\,t\,yr^{-1}$).[161]

Earlier processes employed strong protic acids (e.g., fluorosulfonic acid) as initiators with subsequent hydrolysis of ester end-groups. Newer processes use catalytic amounts of immobilized acids. THF is polymerized over a heterogeneous catalyst in the presence of acetic anhydride to form polymer diacetate which is converted to PTMEG by transesterification with an excess of methanol in the presence of a basic catalyst. Such an approach reduces considerably the amount of waste. Unreacted THF (being in equilibrium with polymer) is recovered and recycled to the reactor.[162]

It should be pointed out that AM polymerization of THF would be the most straightforward route to poly(THF) diols (PTMEG used in polyurethane and polyester technology). THF, however, does not polymerize in the presence of hydroxyl-containing compounds (alcohols and diols) used in quantities required to obtain polymers with molecular weights in the range of few thousands. At first sight, this seems a little unexpected because strong protic acids (e.g., trifluoromethanesulfonic acid) initiate polymerization of THF, although the initiation is slow as compared to propagation. This may be related to lower reactivity of secondary oxonium ions as compared to tertiary oxonium ion. Initiation with strong protic acids generates HO head groups and further polymerization proceeds in the presence of those hydroxyl groups. It should be pointed out, however, that PTMEG used to introduce soft blocks into polyurethanes or block copolyesters has M_n in the range $1–2 \times 10^3$. To obtain such polymers by AM polymerization, the ratio [THF]/[diol] should not exceed 40 (considering limited conversion of THF due to reversibility of propagation). Thus, the ratio [THF]/[HO] should not be higher than 20, which corresponds to 5 mol.% with respect to THF. In the polymerization initiated by acids, concentration of initiator (and thus concentration of HO head groups) is considerably lower. Thus, cationic polymerization of THF is possible in the presence of minute amounts of HO groups but is prohibited if the concentration of HO groups is in the range that would be needed for AM polymerization giving PTMEG in the required range of molecular weights.

THF may be incorporated into oligodiols by the process involving both the AM and ACE mechanisms if a highly strained cyclic ether (e.g., EO or ECH) is continuously fed into the reaction mixture containing THF and the diol as

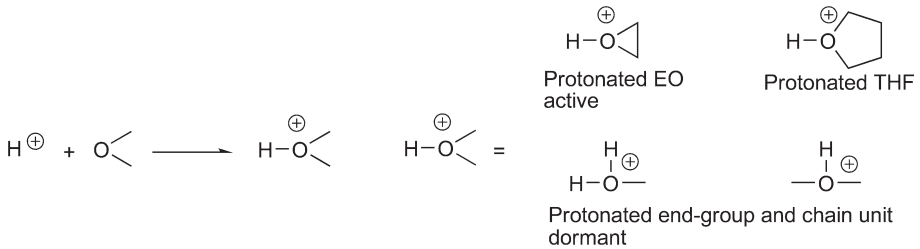

If [THF] >>[EO], [HO-] then protonated EO reacts preferentially with THF

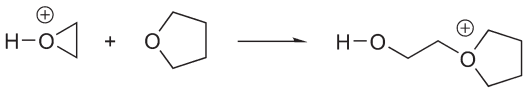

A few propagation steps by ACE mechanism may occur before the whole segment is incorporated into the growing macromolecule by reaction with HO- group.

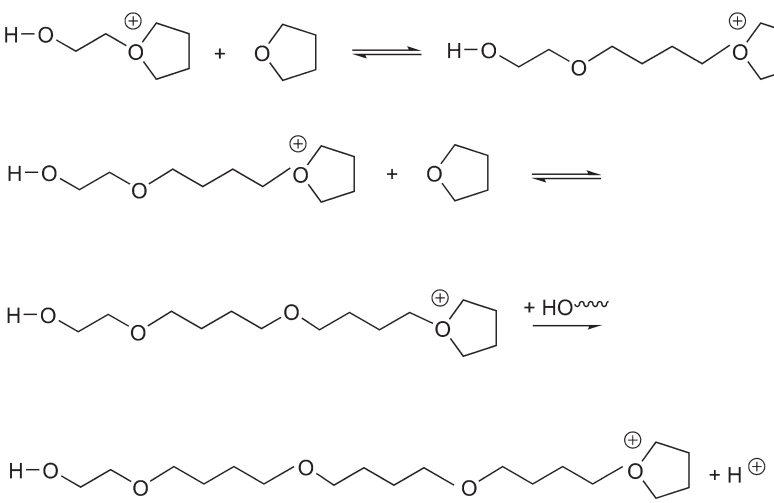

Scheme 31

reagent and strong protic acid as catalyst. The reaction proceeds by the mechanism outlined in **Scheme 31**.[163,164]

Although PTMEG is by far the most important commercial product (and one of the prominent examples of industrial application of CROP), there is a considerable research activity concerning other synthetic applications of CROP of THF.

Active species of CROP of THF are long-living, which makes possible their quantitative conversion to a variety of functional polymers that may be used for synthesis of polymers with complex architectures, such as star polymers or block copolymers.[165]

Star polymers of THF were prepared by the reaction of living poly(THF) with multifunctional amines. Stars containing up to seven arms were prepared using this approach.[166,167]

A similar approach was based on the coupling of bifunctional living poly(THF) and dendrimers containing iminopropane-2,3-diyl units or grafting of living poly(THF) onto an amino dendrimer to form a star, acrylate-terminated poly(THF) multimacromonomer with the dendrimer as core. Subsequent addition of unreacted amino groups of the dendrimer onto acrylate end-groups led to the formation of a segmented polymer network containing amino dendrimers (**Scheme 32**).[168]

Cationic polymerization of THF followed by termination of living chain ends with 2,2′-bipyridine led to ionene elastomers.[169] Another approach to the synthesis of poly(THF) ionenes was based on the chain extension reaction of living poly(THF) chains with (dimethylamino)trimethylsilane.[170] Hydrolysis of block copolymers containing 2-methyl-4,5-dihydroimidazole (2-methyl-2-oxazoline) and THF blocks gave block copolymers containing linear poly(ethylenimine) blocks. Addition of $CuCl_2$ to these block copolymers led to the formation of the corresponding complexes, which resulted in dramatic changes in their physical properties. Depending on the relative length of each block, the complexed polymers were soft and ductile materials or tough thermoplastic elastomers.[171]

Developments in controlled radical polymerization led to novel block copolymers involving poly(THF) blocks.[172] ATRP was used to polymerize radically polymerizable monomers to polymers containing reactive chain ends (e.g., halogen end-groups in the case of ATRP) and, after transforming end-groups into groups that can initiate cationic polymerization of THF, a second block was obtained by CROP. In this way, block copolymers containing polystyrene and poly(THF) blocks,[173–175] poly(methyl methacrylate) (PMMA), and poly

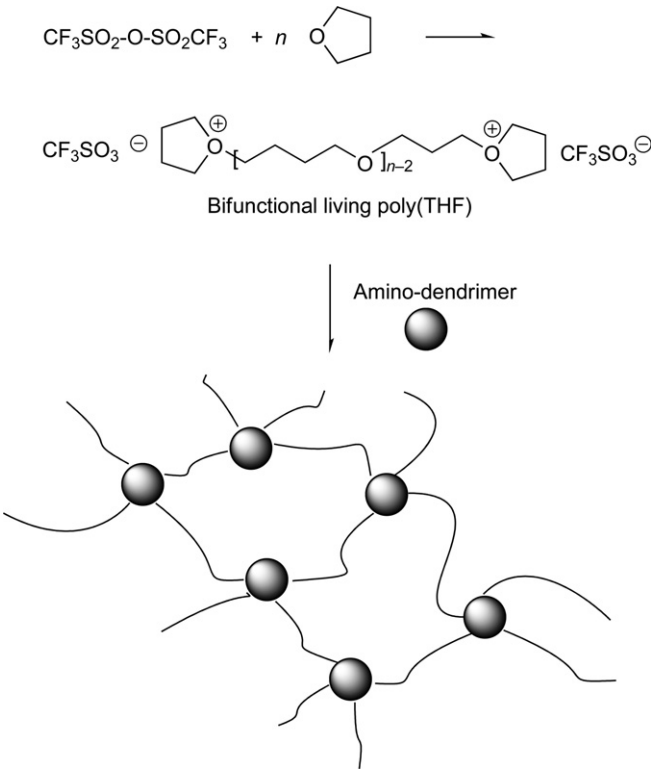

Scheme 32

(THF) blocks,[176,177] or polacrylate and poly(THF) blocks[178] as well as star block copolymers with PTHF core and poly(*tert*-butyl acrylate) (PtBA) shell[178] were obtained.

Reversible addition-fragmentation chain transfer polymerization (RAFT) polymerization of methyl acrylate was combined with cationic polymerization of THF to synthesize comb copolymers.[179] Asymmetric star block copolymers based on polystyrene (PS), PTHF, and PMMA were synthesized by a combination of CROP and redox polymerization methods.[180] Miktoarm star polymers containing poly(THF) and polystyrene arms were also obtained by combining CROP and ATRP methods.[181] Another approach for the synthesis of block copolymers involving poly(THF) blocks is based on transformation of cationic active species of THF polymerization into species initiating anionic[182] or radical polymerization.[183] Copolymerization of poly(THF) macromonomers with *N*-isopropylacrylamide (NIPAA) led to segmented polymer networks acting as polymer membranes with thermoresponsive permeability.[184] Conducting THF copolymers were obtained by capping living poly(THF) with a thiophene or pyrrole derivative and subsequent electropolymerization.[185,186]

By applying cationic polymerization of tetrahydrofuran starting from the carbonyl chloride group-functionalized multiwalled carbon nanotubes (MWNT)[187] with silver perchlorate as a catalyst poly-THF was chemically anchored to MWNT surfaces affecting their properties.[126]

4.08.4.3 CROP of Substituted THFs

THF as a five-membered cyclic ether is only weakly strained. Substitution decreases thermodynamic polymerizability of heterocyclic monomers; thus substituted THFs do not polymerize (although their oligomerization to low-molecular-weight products is possible).[188] It should be remembered, however, that the enthalpy of polymerization (ΔH) is not exclusively related to ring strain (although ring strain provides a major contribution to the ΔH value). If the ring is substituted, it does not affect significantly the ring strain in the monomer but steric repulsion between substituents may introduce strain into the polymer chain as shown in **Scheme 33**.

An interesting example of the influence of the number and positions of substituents on the thermodynamic polymerizability was provided by studies of cationic polymerization of 3,4-dialkoxy-THF.[189] When two substituents were in *cis*-position, polymers with DP_n up to ~ 35 could be obtained while *trans*-monomer essentially did not polymerize. As shown in **Scheme 34**, if substituents in cyclic monomer are in *cis*-position, there is a considerable additional strain due to their steric repulsion; this strain is partly released when a rigid cyclic monomer is converted to a polymer chain in which, due to free rotation around carbon–carbon and carbon–oxygen bonds, the strain can be minimized. In *trans*-monomers, steric repulsion is considerably lower; thus the gain in enthalpy is less significant.

More recently, it has been shown that disubstituted THF derivatives containing two hydroxymethyl groups

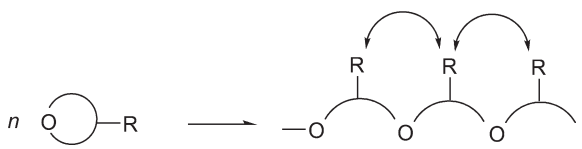

Scheme 33

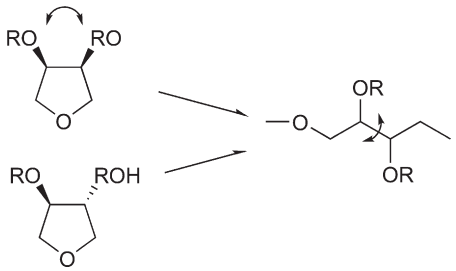

Scheme 34

Scheme 35

(anhydrosugars) can be polymerized to medium-molecular-weight highly branched polymers in analogy to hydroxymethyl-substituted three- and four-membered cyclic ethers (cf. Section 4.08.3.3) and an AM mechanism of propagation was suggested.[190–193] It was shown, however, that in addition to ROP, dehydration reaction occurs; thus the structure of polymers is more complex than suggested.[194]

Although this chapter deals with ROP of cyclic ethers, it should be mentioned that 2,3-dihydrofurans and their derivatives (cyclic vinyl ethers) polymerize cationically through opening of the double bond as shown in Scheme 35.[195–198]

4.08.5 Outlook

Cyclic ethers constitute an important class of heterocyclic monomers that polymerize by ionic mechanism. Studies of the mechanism, kinetics, and thermodynamics of cyclic ether polymerization were essential in establishing basic principles of ionic ROP. Cyclic ethers are the class of heterocyclic monomers that provide suitable models for mechanistic studies. On the other hand, polymerization of several monomers of this class leads to polymeric materials that are produced on an industrial scale. The most prominent examples are polymers of EO, PO, ECH, or THF. CROP of cyclic ethers is thus interesting from both the academic and industrial point of view.

Investigations of CROP of cyclic ethers (mainly THF) provided the first thoroughly studied examples of polymerization with reversible deactivation of growing species involving equilibria between ionic and covalent (dormant) species. Studies of polymerization kinetics led to determination of rate constants of elementary reactions and in several cases equal reactivity of ions and ion-pairs in propagation was observed, which seems to be a general phenomenon in CROP of heterocyclic monomers.

More recent developments of cationic polymerization proceeding by the AM mechanism have opened new horizons for the synthetic application of ROP of cyclic ethers. By using this approach, main side reaction (intramolecular chain transfer to polymer leading to the formation of cyclic fraction) can be minimized and control over molecular weight, molecular weight distribution, and the structure of end-groups can be achieved under kinetic control. AM polymerization is especially suited for the synthesis of telechelic (functional) oligomers such as oligodiols or macromonomers and several examples of successful application of AM polymerization to the synthesis of such materials can be found in recent literature. AM polymerization of cyclic ethers containing hydroxyl functionality offers also a convenient synthetic route to hyperbranched multihydroxy polyethers and this area was also explored recently.

Thus, there is steady, although not very intensive, progress in the field of CROP of cyclic ethers. It can be expected that this trend will continue and new specialty polymers or oligomers will be created by combining the knowledge accumulated over several decades with new developments such as the AM polymerization mechanism.

Acknowledgment

This chapter is based on the chapter *Cationic Ring-Opening Polymerization: Ethers* coauthored by S. Penczek and P. Kubisa from the first edition of *Comprehensive Polymer Science*, Vol. 3, Part I. The author wishes to express his gratitude to Professor Stanislaw Penczek for the permission to use large parts of the text from the first edition.

References

1. Kubisa, P.; Penczek, S. In *Encyclopedia of Polymer Science and Technology*; Gaylord, N. G., Bikales, N. M., Mark, H. F., Eds.; Interscience Publishers: New York; London; Sydney; Toronto, 1977; *Suppl. Vol. II*, pp 161–197.
2. Dreufuss, P. *Poly(tetrahydrofuran)*. Gordon and Breach: New York, 1982.
3. Penczek, S.; Kubisa, P.; Matyjaszewski, K. *Cationic Ring-Opening Polymerization of Heterocyclic Monomers, Part I: Mechanisms*. Springer: Berlin, Germany, 1980.
4. Ivin, K. J.; Saegusa, T., Eds. *Ring-Opening Polymerization*. Elsevier: London, UK, 1984; *Vol. I, II*.
5. Penczek, S.; Kubisa, P.; Matyjaszewski, K. *Cationic Ring-Opening Polymerization of Heterocyclic Monomers, Part II: Synthetic Applications*. Springer: Berlin, Germany, 1985.
6. Penczek, S.; Kubisa, P. In *Comprehensive Polymer Science*; Allen, G., Bevington, J. C., Eds.; Pergamon Press: Oxford, UK, 1989; *Vol. 3*, p 751.
7. Dreyfuss, P.; Dreyfuss, M. P. In *Comprehensive Polymer Science*; Allen, G., Bevington, J. C., Eds.; Pergamon Press: London, UK, 1989; *Vol. 3*, p 851.
8. Kubisa, P.; Penczek, S. In *Encyclopedia of Polymer Science and Technology*, 2nd ed.; Mark, H. F., Bikales, N. M., Overberger, C. G., Menges, G., Eds.; Wiley Interscience: New York, 1989; *Suppl. Vol. II*, p 380.
9. Penczek, S.; Kubisa, P. In *Ring-Opening Polymerization*; Brunelle, D. J., Ed.; Carl Hanser Verlag: Munich, Germany, 1993; p 13.
10. Kubisa, P. In *Cationic Polymerizations*; Matyjaszewski, K., Ed.; Marcel Dekker: New York, 1996; p 437.
11. Penczek, S. *J. Polym. Sci., Part A: Polym. Chem.* **2000**, *38*, 1919.
12. Hoogenboom, R. In *Handbook of Ring-Opening Polymerization*; Dubois, Ph., Coulembier, O., Raquez, J.-M., Eds.; Wiley-VCH: Weinheim, Germany, 2009.
13. Sawada, H. *Thermodynamics of Polymerization*. Marcel Dekker: New York, 1976.
14. Kubisa, P. In *Cationic Polymerizations*; Matyjaszewski, K., Ed.; Marcel Dekker: New York, 1996; p 137.
15. Pell, A. S.; Pilcher, G. *Trans. Faraday Soc.* **1965**, *61*, 71.
16. Searless, E. M., Jr.; Tamres, M. In *The Chemistry of Ether Linkage*; Patai, S., Ed.; Wiley: New York, 1967; p 243.
17. Arnett, E. M. In *Progress in Physical Organic Chemistry*; Streitwieser, A., Taft, R. W., Eds.; Interscience: New York, 1963; *Vol. 7*.
18. Penczek, S. *J. Polym. Sci., Part A: Polym. Chem.* **2002**, *40*, 1665.
19. Kuntz, J. *J. Polym. Sci., Polym. Chem.* **1967**, *5*, 193.
20. Dreyfuss, M. P.; Westphal, J. C.; Dreyfuss, P. *Macromolecules* **1968**, *1*, 437.
21. Olah, G. A., Ed. *Friedel-Crafts and Related Reactions*. Interscience Publishers: New York, 1965; *Vol. I*, p 702.

22. Olah, G. A.; Surya Prakash, G. K.; Sommer, J. *Superacids*. Wiley-Interscience: New York, 1985; p 184.
23. Collins, G. L.; Greene, R. K.; Berardinelli, F. M.; *et al. J. Polym. Sci., Polym. Lett. Ed.* **1979**, *17*, 667.
24. Stasiński, J.; Dmowska, G. *Makromol. Chem., Rapid Commun.* **1987**, *8*, 535.
25. Entelis, S. G.; Korovina, G. V. *Makromol. Chem.* **1974**, *175*, 1523.
26. Hoene, R.; Reichert, K.-H. W. *Makromol. Chem.* **1976**, *177*, 3545.
27. Browstein, S.; Eastham, A. M.; Latremouille, G. A. *J. Phys. Chem.* **1963**, *67*, 1028.
28. Matyjaszewski, K.; Słomkowski, S.; Penczek, S. *J. Polym. Sci., Polym. Chem. Ed.* **1979**, *17*, 69.
29. Matyjaszewski, K.; Słomkowski, S.; Penczek, S. J. *Polym. Sci., Polym. Chem. Ed.* **1979**, *17*, 2413.
30. Brzezińska, K.; Matyjaszewski, K.; Penczek, S. *Makromol. Chem.* **1978**, *179*, 2387.
31. Saegusa, T.; Matsumoto, S. *J. Polym. Sci., Part A1: Polym. Chem.* **1968**, *6*, 1559.
32. Brzezińska, K.; Chwialkowska, W.; Kubisa, P.; *et al. Makromol. Chem.* **1977**, *178*, 2491.
33. Matyjaszewski, K.; Penczek, S. *Makromol. Chem.* **1981**, *182*, 1735.
34. Franta, E.; Reibel, L.; Lehman, J.; *et al. Polym. Sci., Polym. Symp.* **1976**, *56*, 139.
35. Grinevitch, T. V.; Shupik, A. N.; Korovina, G. V.; *et al. Eur. Polym. J.* **1981**, *17*, 1107.
36. Pruckmayr, G.; Wu, T. K. *Macromolecules* **1978**, *11*, 265.
37. Jacobson, H.; Stockmayer, W. H. *J. Chem. Phys.* **1950**, *18*, 1600.
38. Chojnowski, J.; Ścibiorek, M.; Kowalski, J. *Makromol. Chem.* **1977**, *178*, 1.
39. Andrews, J. M.; Semlyen, J. A. *Polymer* **1972**, *13*, 142.
40. Worsfold, D. V.; Eastham, A. M. *J. Am. Chem. Soc.* **1957**, *79*, 900.
41. Kobayashi, S.; Morikawa, K.; Saegusa, T. *Polym. J.* **1979**, *11*, 405.
42. Kern, R. J. *J. Org. Chem.* **1968**, *33*, 388.
43. Katnik, R. J.; Schaefer, J. *J. Org. Chem.* **1968**, *33*, 384.
44. Ito, K.; Usami, N.; Yamashita, Y. *Polym. J.* **1979**, *11*, 171.
45. Yamashita, Y.; Ito, K. *Polym. Bull.* **1978**, *1*, 173.
46. Summerbell, R. K.; Kland-English, M. J. *J. Am. Chem. Soc.* **1955**, *77*, 5095.
47. Eigenmann, H. K.; Golden, D. M.; Benson, S. W. *J. Phys. Chem.* **1973**, *77*, 1687.
48. Dudev, T.; Lin, C. *J. Am. Chem. Soc.* **1988**, *120*, 4450.
49. Berthelot, M.; Besseau, F.; Laurence, Ch. *Eur. J. Org. Chem.* **1998**, *5*, 925.
50. Libiszowski, J.; Szymański, R.; Penczek, S. *Makromol. Chem.* **1989**, *190*, 1225.
51. Dale, J.; Daasvatn, K. *J. Chem. Soc. Chem. Commun.* **1976**, 295.
52. Parker, R. E.; Isaacks, N. S. *Chem. Rev.* **1959**, *59*, 737.
53. Kubisa, P.; Penczek, S. *Progr. Polym. Sci.* **1999**, *24*, 1409.
54. Goodman, M.; Peggion, E.; Szwarc, M.; *et al. Macromolecules* **1977**, *10*, 1299.
55. Brzezinska, K.; Szymanski, R.; Kubisa, P.; *et al. Makromol. Chem., Rapid Commun.* **1986**, *7*, 1.
56. Kubisa, P.; Bednarek, M.; Biedroń, T.; *et al. Macromol. Symp.* **2000**, *153*, 217.
57. Penczek, S.; Sekiguchi, H.; Kubisa, P. In *Macromolecular Design of Polymeric Materials*, Hatada, K., Kitayama, T., Vogl, O., Eds.; Marcel Dekker: New York, 1997.
58. Biedroń, T.; Szymański, R.; Kubisa, P.; *et al. Makromol. Chem., Macromol. Symp.* **1990**, *32*, 155.
59. Penczek, S.; Kubisa, P.; Szymański, R. *Makromol. Chem., Macromol. Symp.* **1986**, *3*, 203.
60. Wojtania, M.; Kubisa, P.; Penczek, S. *Makromol. Chem., Macromol. Symp.* **1986**, *6*, 201.
61. Biedroń, T.; Kubisa, P.; Penczek, S. *J. Polym. Sci., Part A: Polym. Chem. Ed.* **1991**, *29*, 619.
62. Biedroń, T.; Brzezinska, K.; Kubisa, P.; *et al. Polym. Int.* **1995**, *36*, 73.
63. Huang, W.; Zhou, Y. F.; Yan, D. Y. *J. Polym. Sci., Part A: Polym. Chem. Ed.* **2005**, *43*, 2038.
64. Bednarek, M.; Kubisa, P. *Polimery (Warsaw)* **2004**, *49*, 719.
65. Kubisa, P. *J. Polym. Sci., Part A: Polym. Chem. Ed.* **2003**, *41*, 457.
66. Tokar, R.; Kubisa, P.; Dworak, A.; *et al. Macromolecules* **1994**, *27*, 320.
67. Dworak, A.; Walach, W.; Trzebicka, B. *Macromol. Chem. Phys.* **1995**, *196*, 1963.
68. Royappa, A. T.; McDaniel, R. L. *J. Appl. Polym. Sci.* **2005**, *97*, 1462.
69. Sunder, A.; Mulhaupt, R.; Haag, R.; *et al. Adv. Mater.* **2000**, *12*, 235.
70. Wilms, D.; Wurm, F.; Nieberle, J.; *et al. Macromolecules* **2009**, *42*, 3239.
71. Wilms, D.; Stiriba, S. E.; Frey, H. *Acc. Chem. Res.* **2010**, *43*, 129.
72. Cheng, H. X.; Wang, S. G.; Yang, J. T.; *et al. J. Colloid Interface Sci.* **2009**, *337*, 278.
73. Peng, Y.; Liu, H. W.; Zhang, X. Y. *J. Polym. Sci., Part A: Polym. Chem. Ed.* **2009**, *47*, 949.
74. Decker, C. *Progr. Polym. Sci.* **1996**, *21*, 593.
75. Falk, B.; Zonca, M. R.; Crivello, J. V. *Macromol. Symp.* **2005**, *226*, 97.
76. Crivello, J. V. In *Ring-Opening Polymerization*; Brunelle, D. J., Ed.; Hanser Publishers: Munich, Germany, 1993.
77. Bulut, U.; Crivello, J. V. *Macromolecules* **2005**, *38*, 3584.
78. Oral, A.; Tasdelen, M. A.; Demirel, A. L.; *et al. J. Polym. Sci., Part A: Polym. Chem. Ed.* **2009**, *47*, 5328.
79. Crivello, J. V.; Liu, S. *J. Polym. Sci., Part A: Polym. Chem. Ed.* **2000**, *38*, 389.
80. Hirano, T.; Nakayama, S.; Tsuruta, T. *Makromol. Chem.* **1975**, *176*, 1897.
81. Farthing, A. C.; Reynolds, R. J. W. *J. Polym. Sci.* **1954**, *12*, 503.
82. Rose, J. B. *J. Chem. Soc.* **1956**, 542.
83. Farthing, A. C. *J. Chem. Soc.* **1955**, *130*, 3648.
84. Penczek, I.; Penczek, S. *Makromol. Chem.* **1963**, *130*, 186.
85. Dreyfus, P.; Dreyfus, M. P. *Polym. J.* **1976**, *8*, 81.
86. Goethals, E. J. *Adv. Polym. Sci.* **1977**, *23*, 101.
87. Saegusa, T.; Imai, H.; Hirai, S.; *et al. Makromol. Chem.* **1962**, *53*, 203.
88. Kubisa, P.; Penczek, S. *Makromol. Chem.* **1969**, *130*, 186.
89. Aleksiuk, G. P.; Shamanin, V. V.; Podolsky, A. F.; *et al. Polym. J.* **1981**, *13*, 23.
90. Bucquoye, M. R.; Goethals, E. J. *Makromol. Chem.* **1978**, *179*, 1681.
91. Arimatsu, Y. *J. Polym. Sci., Part A1: Polym. Chem.* **1966**, *4*, 728.
92. Black, P. E.; Worsfold, D. J. *Can. J. Chem.* **1976**, *54*, 3325.
93. Bouchekif, H.; Philbin, M. I.; Colclough, E.; *et al. Chem. Commun.* **2005**, *41*, 3870.
94. Bouchekif, H.; Philbin, M. I.; Colclough, E.; *et al. Macromolecules* **2008**, *41*, 1989.
95. Bouchekif, H.; Philbin, M. I.; Colclough, E.; *et al. Macromolecules* **2010**, *43*, 845.
96. Barbieri, U.; Polacco, G.; Massimi, R. *Macromol. Symp.* **2006**, *234*, 51.
97. Jutier, J. J.; de Gunzbourg, A.; Prudhomme, R. E. *J. Polym. Sci., Part A: Polym. Chem. Ed.* **1999**, *37*, 1027.
98. Pisharath, S.; Ang, H. G. *Polym. Degrad. Stab.* **2007**, *92*, 1365.
99. Barbieri, U.; Keicher, T.; Polacco, G. *E-polymers* **2009**, *203*, 046.
100. Del Campo, A.; Bello, A.; Perez, E. *Macromol. Chem. Phys.* **2002**, *203*, 975.
101. Zheng, Y.; Zhang, W.; Gupta, M.; *et al. J. Polym. Sci., Part B: Polym. Phys.* **2010**, *48*, 1022.
102. Desai, H. J.; Cunliffe, A. X.; Hamid, J.; *et al. Polymer* **1996**, *15*, 3461.
103. Fujiwara, T.; Makal, U.; Wynne, K. J. *Macromolecules* **2003**, *36*, 9383.
104. Kausch, C. M.; Leising, J. E.; Medsker, R. E.; *et al. Langmuir* **2002**, *18*, 5933.
105. Kurt, P.; Wynne, K. J. *Macromolecules* **2007**, *40*, 9537.
106. Kim, Y. S.; Lee, J. S.; Ji, Q.; *et al. Polymer* **2002**, *43*, 7161.
107. Wesdemiotis, C.; Pingitore, F.; Polce, M. J.; *et al. Macromolecules* **2006**, *39*, 8369.
108. Ueyama, A.; Mizuno, M.; Kanoh, S.; *et al. Polym. J.* **2002**, *34*, 944.
109. Miwa, Y.; Tsutsumi, H.; Oishi, T. *Polym. J.* **2001**, *33*, 568.
110. Crivello, J. V.; Sasaki, H. *J. Macromol. Sci., Pure Appl. Chem.* **1993**, *30*, 189.
111. Bulut, U.; Crivello, J. V. *J. Polym. Sci., Part A: Polym. Chem. Ed.* **2005**, *43*, 3205.
112. Sangermano, M.; Malucelli, G.; Bongiovanni, R.; *et al. Eur. Polym. J.* **2004**, *40*, 353.
113. Nuyken, O.; Bohner, R.; Erdmann, C. *Macromol. Symp.* **1996**, *107*, 125.
114. Lub, J.; Recaj, V.; Puig, L.; *et al. Liq. Cryst.* **2004**, *41*, 1627.
115. Nagai, D.; Nishida, M.; Nagasawa, T.; *et al. Macromol. Rapid Commun.* **2006**, *27*, 921.
116. Morinaga, T.; Ohkura, M.; Ohno, K.; *et al. Macromolecules* **2007**, *40*, 1159.
117. Kohnen, A.; Riegel, N.; Kremer, J. H.-W. M.; *et al. Adv. Mater.* **2009**, *21*, 879.
118. Vandenberg, E. J.; Mulis, J. C.; Juvet, R. S. *J. Polym. Sci., Part A: Polym. Chem.* **1989**, *27*, 3083.
119. Bednarek, M.; Biedroń, T.; Heliński, J.; *et al. Macromol. Rapid Commun.* **1999**, *20*, 369.
120. Bednarek, M.; Kubisa, P.; Penczek, S. *Macromolecules* **2001**, *34*, 5112.
121. Magnusson, H.; Malmstrom, E.; Hult, A. *Macromol. Rapid Commun.* **1999**, *20*, 453.
122. Yan, D.; Hou, J.; Zhu, X.; *et al. Macromol. Rapid Commun.* **2000**, *21*, 557.
123. Magnusson, H.; Malmstrom, E.; Hult, A. *Macromolecules* **2001**, *34*, 5786.
124. Mai, Y.; Zhou, Y.; Yan, D.; *et al. Macromolecules* **2003**, *36*, 9667.
125. Chen, T.; Bednarek, M.; Kubisa, P.; *et al. J. Polym. Sci., Part A: Polym. Chem. Ed.* **2002**, *40*, 1991.
126. Bednarek, M.; Kubisa, P.; Penczek, S. *Macromolecules* **1999**, *32*, 5257.
127. Biela, T.; Duda, A.; Penczek, S.; *et al. J. Polym. Sci., Part A: Polym. Chem. Ed.* **2002**, *40*, 2884.
128. Bednarek, M.; Kubisa, P. *J. Polym. Sci., Part A: Polym. Chem. Ed.* **2004**, *42*, 608.
129. Hou, J.; Yan, D. Y. *Macromol. Rapid Commun.* **2002**, *23*, 456.
130. Rahm, M.; Westlund, R.; Eldsater, C.; *et al. J. Polym. Sci., Part A: Polym. Chem. Ed.* **2009**, *47*, 6191.
131. Ye, L.; Gao, P.; Wu, F.; *et al. Polymer* **2007**, *48*, 1550.
132. Yan, D.; Zhou, Y.; Hou, J. *Science* **2004**, *303*, 65.
133. Zhou, Y.; Yan, D. *Angew. Chem., Int. Ed.* **2004**, *43*, 4896.
134. Mai, Y.; Zhou, Y.; Yan, D. *Macromolecules* **2005**, *38*, 8679.
135. Zhou, Y. F.; Yan, D. Y.; Dong, W. Y.; *et al. J. Phys. Chem. B* **2007**, *111*, 1262.
136. Cheng, H. X.; Yuan, X. J.; Sun, X. Y.; *et al. Macromolecules* **2010**, *43*, 1143.

137. Shou, C. Q.; Song, N. J.; Zhang, Z. L. *J. Appl. Polym. Sci.* **2010**, *116*, 2473.
138. Yang, Q.; Wang, L.; Xiang, W. D.; *et al. J. Appl. Polym. Sci.* **2007**, *103*, 2086.
139. Wang, X. H.; Liu, H. W.; Qiu, L. Z. *Mater. Lett.* **2007**, *61*, 2350.
140. Bednarek, M.; Pluta, M. *Macromol. Symp.* **2010**, *287*, 119.
141. Satoh, T.; Ishihara, H.; Sasaki, H.; *et al. Macromolecules* **2003**, *36*, 1522.
142. Smith, T. J.; Mathias, L. J. *Polymer* **2002**, *43*, 7275.
143. Morita, A.; Kudo, H.; Nishikubo, T. *J. Polym. Sci., Part A: Polym. Chem. Ed.* **2004**, *42*, 3739.
144. Dreyfuss, M. P.; Dreyfuss, P. *J. Polym. Sci., Part A-1* **1966**, *4*, 2179.
145. Szwarc, M. *Ionic Polymerization Fundamentals*. Hanser: Munich, Germany, 1996.
146. Szwarc, M.; van Beylen, M. *Ionic Polymerization and Living Polymers*. Chapman & Hall: New York, 1993.
147. Meerwein, H.; Delfs, D.; Morschel, M. *Angew. Chem.* **1969**, *72*, 927.
148. Rosenberg, B. A.; Lyudvig, E. B.; Gantmacher, A. R.; *et al. J. Polym. Sci., Part C: Polym. Symp.* **1967**, *16*, 1917.
149. Dreyfuss, P.; Dreyfuss, M. P. *Adv. Polym. Sci.* **1967**, *4*, 528.
150. Vofsi, D.; Tobolsky, A. V. *J. Polym. Sci.* **1965**, *A3*, 3361.
151. Matyjaszewski, K.; Penczek, S. *J. Polym. Sci., Polym. Chem. Ed.* **1974**, *12*, 1905.
152. Kobayashi, S.; Danda, H.; Saegusa, T. *Macromolecules* **1974**, *7*, 415.
153. Buyle, A. M.; Matyjaszewski, K.; Penczek, S. *J. Polym. Sci., Polym. Chem. Ed.* **1976**, *14*, 125.
154. Buyle, A. M.; Matyjaszewski, K.; Penczek, S. *Macromolecules* **1977**, *20*, 269.
155. Matyjaszewski, K. *J. Macromol. Sci., Rev.* **1986**, *C26*, 1.
156. Penczek, S.; Szymanski, R.; Duda, A. *Macromol. Symp.* **1995**, *98*, 193.
157. Szwarc, M. *Adv. Polym. Sci.* **1969**, *91*, 236.
158. Szwarc, M. *Carbanions, Living Polymers and Electron Transfer Processes*. Interscience: New York, 1968.
159. Baran, T.; Brzezińska, K.; Matyjaszewski, K.; *et al. Makromol. Chem.* **1983**, *184*, 2497.
160. Dreyfuss, P. In *Handbook of Elastomers*; Bhowmick, A. K., Stephens, H. L., Eds.; Marcel Dekker Inc.: New York; Basel, 2001; p 723.
161. Research and Markets. http://www.researchandmarkets.com/reports/1195472.
162. Conser S.p.A. Consulting Engineers. http://www.conserspa.com/page_pr-de10.htm.
163. Bednarek, M.; Biedron, T.; Kubisa, P.; *et al. Makromol. Chem., Macromol. Symp.* **1991**, *42/43*, 475.
164. Bednarek, M.; Kubisa, P. *Macromol. Symp.* **1998**, *132*, 349.
165. Goethals, E. J.; Dubreuil, M.; Wang, Y.; *et al. Macromol. Symp.* **2000**, *153*, 209.
166. VanCaeter, P.; Goethals, E. J. *Macromol. Rapid Commun.* **1997**, *18*, 393.
167. Van Renterghem, L. M.; Goethals, E. J.; Du Prez, F. E. *Macromolecules* **2006**, *39*, 528.
168. Tanghe, L. M.; Goethals, E. J.; Du Prez, F. *Polym. Int.* **2003**, *52*, 191.
169. Ikeda, Y.; Murakami, T.; Yuguchi, Y.; *et al. Macromolecules* **1998**, *31*, 1246.
170. Ikeda, Y.; Murakami, T.; Urakawa, H.; *et al. Polymer* **2002**, *43*, 3483.
171. Wang, Y.; Goethals, E. J. *Macromolecules* **2000**, *33*, 808.
172. Matyjaszewski, K. *Macromol. Symp.* **1998**, *132*, 85.
173. Xu, Y. J.; Pan, C. Y. *J. Polym. Sci., Part A: Polym. Chem.* **2000**, *38*, 337.
174. Guo, Y. M.; Pan, C. Y. *Polymer* **2001**, *42*, 2863.
175. Yenice, Z.; Tasdelen, A.; Oral, G.; *et al. J. Polym. Sci., Part A: Polym. Chem.* **2009**, *42*, 2190.
176. Chagneux, N.; Camerlynck, S.; Hamilton, E.; *et al. Macromolecules* **2007**, *40*, 3183.
177. Narita, M.; Nomura, R.; Tomita, I.; *et al. Macromolecules* **2000**, *33*, 4979.
178. Erdogan, T.; Bernaerts, K. V.; Van Renterghem, L. M.; *et al. Des. Monomers Polym.* **2005**, *8*, 705.
179. Wang, W. P.; You, Y. Z.; Hong, C. Y.; *et al. Polymer* **2005**, *46*, 9489.
180. Arslan, H.; Hazer, B.; Higashihara, T.; *et al. Appl. Polym. Sci.* **2006**, *102*, 516.
181. Guo, Y. M.; Pan, C. Y.; Wang, J. *J. Polym. Sci., Part A: Polym. Chem.* **2001**, *39*, 2134.
182. Nomura, R.; Shibasaki, Y.; Endo, T. *J. Polym. Sci., Part A: Polym. Chem.* **1998**, *36*, 2209.
183. Yoshida, E.; Sugita, A. *J. Polym. Sci., Part A: Polym. Chem.* **1998**, *36*, 2059.
184. Lequieu, W.; Du Prez, F. E. *Polymer* **2004**, *45*, 749.
185. Unur, E.; Toppare, L.; Yagci, Y.; *et al. J. Appl. Polym. Sci.* **2005**, *95*, 1014.
186. Kizilyar, N.; Toppare, L.; Onen, A.; *et al. Polym. Bull.* **1998**, *40*, 639.
187. Guo, Y. M.; Zou, Y. F.; Pan, C. Y. *Macromol. Chem. Phys.* **2001**, *202*, 1094.
188. Guzman, J.; Garrido, L.; Riande, E. *Macromolecules* **1984**, *17*, 2005.
189. Thiem, J.; Strietholt, W. A.; Haring, T. *Macromol. Chem.* **1989**, *190*, 1737.
190. Imai, T.; Satoh, Y.; Kaga, H.; *et al. Macromolecules* **2004**, *37*, 3113.
191. Satoh, T.; Imai, T.; Ishihara, H.; *et al. Macromolecules* **2003**, *36*, 6364.
192. Satoh, T.; Imai, T.; Ishihara, H.; *et al. Macromolecules* **2005**, *38*, 4202.
193. Satoh, T.; Kakuchi, T. *Macromol. Biosci.* **2007**, *7*, 999.
194. Bednarek, M.; Kubisa, P. *J. Polym. Sci., Part A: Polym. Chem.* **2006**, *44*, 6484.
195. Ogawa, Y.; Sawamoto, M.; Higashimura, T. *Polym. J.* **1984**, *16*, 415.
196. Nuyken, O.; Aechtner, S. *Polym. Bull.* **1992**, *28*, 117.
197. Naumov, S.; Janovsky, I.; Knolle, W.; *et al. Macromol. Chem. Phys.* **2004**, *205*, 1530.
198. Yonezumi, M.; Kanaoka, S., Aoshima, S. *J. Polym. Sci., Part A: Polym. Chem.* **2008**, *46*, 4495.

Biographical Sketch

Przemyslaw Kubisa received his MSc degree in 1963 from Warsaw University of Technology. From 1963 until 1969, he was employed in the Institute of Plastics in Warsaw as a research associate and in 1969, he joined the Center of Molecular and Macromolecular Studies (CMMS) of the Polish Academy of Sciences in Lodz. In 1972, he received his PhD (under the guidance of Prof. S. Penczek) and in 1978 his habilitation from the Technical University in Lodz. P. Kubisa was a postdoc in the University of Masschussetts (group of Prof. Otto Vogl) (1974) and a visiting scientist in the University of Masschussetts (6 months in 1979) and the Institut Ch. Sadron in Strasbourg (1 year in 1984).

The research interests of P. Kubisa cover various aspects of ionic (mostly cationic) ring-opening polymerization of oxygen-containing heterocyclic monomers. He is an author or coauthor of 140 original papers and 40 book chapters or review papers. From 1991 until 2007, he held a position of the Deputy Director of CMMS and in 2005, he succeeded Prof. S. Penczek as the Head of Polymer Chemistry Department (until 2009). He is presently a Titular Member of IUPAC Polymer Division.

4.09 Stereoselective Ring-Opening Polymerization of Epoxides

H Ajiro, PCB Widger, SM Ahmed, SD Allen, and GW Coates, Cornell University, Ithaca, NY, USA

4.09.1 Introduction

4.09.1.1 Background

In the 1950s, Baggett and Pruitt[1–4] reported that iron (III) chloride was capable of polymerizing racemic propylene oxide to give a polymeric material that could be separated into amorphous as well as crystalline materials using solvent fractionation. Shortly thereafter, Natta *et al.*[5] and Price *et al.*[6,7] provided evidence that the crystalline material was isotactic poly(propylene oxide), in which the main-chain stereogenic centers were of the same relative configuration. This finding marked the first discovery of a stereoselective catalyst for epoxide polymerization. This chapter highlights the significant advances made in the field of stereoselective epoxide polymerization and copolymerization using discrete catalysts.

4.09.1.2 Scope

Many of the important contributors to the field of stereoselective epoxide polymerization have written accounts of their research;[8–20] we have recently written a comprehensive review which forms the basis for this review.[21] This chapter focuses on discrete catalysts for the stereoselective polymerization of racemic (chiral) and meso (prochiral) epoxides. Due to space limitations, catalysts bearing at least one ancillary ligand that is not likely to react with epoxides are discussed; catalysts only bearing ligands that are well known to react with epoxides are not covered. A discussion of strategies for controlling the relative configuration of main-chain stereogenic centers of epoxide polymers is included. The polymerization of optically active epoxides[6] is not covered as the emphasis of this chapter is on stereochemical control of polymerization by the catalyst or initiator.

4.09.2 Basic Concepts in Stereoselective Epoxide Polymerization

4.09.2.1 Regiochemistry

Both the ancillary ligands (L_n) surrounding the active metal center (M) and the growing polymer chain (OR) influence the regiochemistry and stereochemistry of epoxide polymerization (**Scheme 1**(a)).[22] When the epoxide is unsymmetrically substituted (i.e., propylene oxide), enchainment commonly can occur in two ways: (1) S_N2 attack by the polymer's alkoxide chain-end at the less-substituted methylene with retention of the configuration of the substituted carbon to give a secondary metal alkoxide; or (2) S_N2 attack at the substituted methine with inversion of configuration to give a primary metal alkoxide (**Scheme 1**). The polymer is regioregular when only one

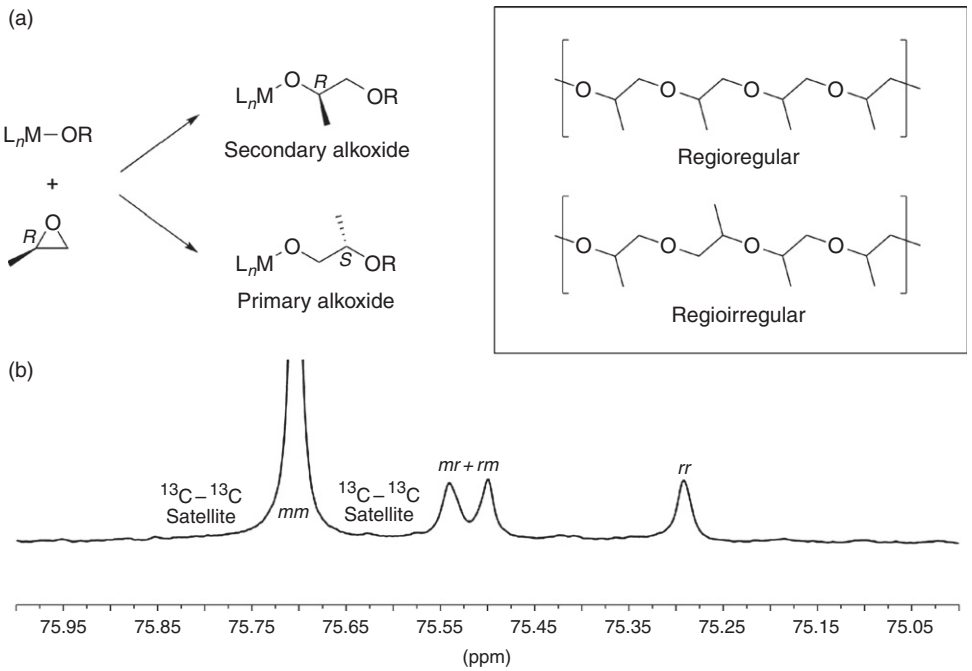

Scheme 1 Methine region of the ^{13}C NMR spectrum of partially isotactic poly(propylene oxide) showing triad stereoerrors.

process dominates; the polymer is regioirregular when both processes occur. The regiochemistry of a polyether (such as poly(propylene oxide)) can be readily determined by ^{13}C NMR spectroscopy.[23–25]

4.09.2.2 Analysis of Polymer Stereochemistry

NMR spectroscopy is the most useful method for determining polymer tacticity.[26,27] In many cases, the chemical shifts for the various polymer nuclei are sensitive to adjacent stereogenic centers, resulting in fine structure that can provide quantitative information about the polymer microstructure once the shift identities are assigned. For example, the methyl, methylene, and methine regions of a high-resolution ^{13}C NMR spectrum of regioregular atactic poly(propylene oxide) display several resonances, each of which represents a different set of consecutive stereocenters. As each resonance in the spectrum has been assigned (**Scheme 1(b)**),[23,24,28] a routine ^{13}C NMR experiment can reveal both the tacticity and the degree of stereoregularity of a sample of poly(propylene oxide).

4.09.2.3 Chain-End Control and Enantiomorphic Site Control of Stereochemistry

In a chain-growth polymerization reaction, one end of the polymer chain remains at the active metal center during monomer enchainment. Thus, the stereogenic center in the polymer chain from the last enchained monomer unit will have an influence on the stereochemistry of monomer enchainment. If this influence is significant, the mode of stereochemical regulation is referred to as 'polymer chain-end control' (**Scheme 2(a)**). If the active site is chiral and overrides the influence of the polymer chain end, the mechanism of stereochemical direction is termed 'enantiomorphic site control' (**Scheme 2(b)**).[9–11] The Bovey formalism is a convenient way to describe polymer tacticity, where an '*m*' for *meso* (same configuration), or an '*r*' for *racemic* (opposite configuration) describes relationships between adjacent stereogenic centers (dyads). These dyads are seen as unique signals in ^{13}C NMR. The monomer enchainment mechanism can be easily identified by observing the stereochemical errors propagated in a polymer chain. The ratio of the signals in a ^{13}C NMR spectrum can be used to determine the mechanism of stereocontrol. In the case of an isotactic polymer, a 'chain-end control' mechanism produces polymers in which stereoerrors are propagated (i.e., would display primarily *mm*, *mr*, and *rm* triads, **Scheme 2(a)**). In the 'enantiomorphic site control' mechanism, correction of stereoerrors occurs because the ligands direct the stereochemical events, leading to an isolated error (i.e., produces a polymer which would display primarily *mm*, *mr*, *rm*, and *rr* triads, **Scheme 2(b)**).

Optically active catalysts can kinetically resolve racemic monomers (**Scheme 2**) via enantioselective polymerization producing optically active polymers as well as enantiomerically enriched monomers. The nonpreferred enantiomer remains unreacted in the reaction mixture after the preferred enantiomer of monomer has been enchained as a polymer. The quantitative measure of stereocontrol in such a system is given by the selectivity factor (s-factor, *s*), which is the ratio of the rate constants for the polymerization of the fast enantiomer converted to polymer with respect to the slow enantiomer enchained [$s = k_{fast}/k_{slow} = \alpha/(1-\alpha)$] ($\alpha$ is the probability that the preferred enantiomer will be selected by the catalyst).[29] A racemic enantioselective catalyst can polymerize both enantiomers of racemic monomer via isoselective polymerization to give racemic isotactic polymer.

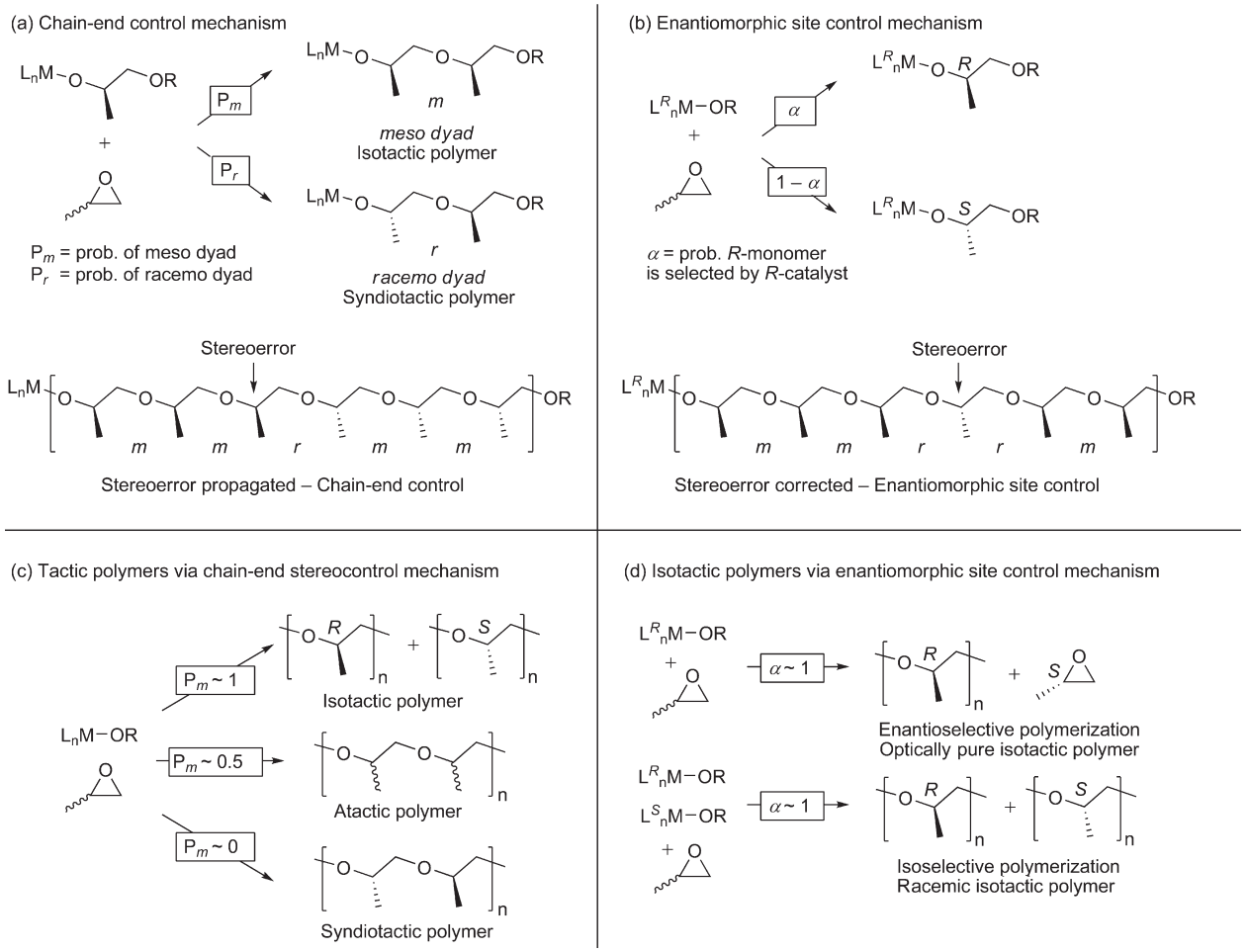

Scheme 2 (a) Chain-end stereocontrol mechanism. (b) Enantiomorphic site stereocontrol mechanism. (c) Tactic polymers via chain-end control mechanism. (d) Isotactic polymers via enantiomorphic site control mechanism. L^R_nM–OR is an enantiomerically pure metal alkoxide complex that prefers *R*-monomer; L^R_n is an enantiomerically pure, chiral ligand.

4.09.3 Stereoselective Epoxide Polymerization

The vast majority of papers reporting stereoselective epoxide polymerization focus on the isoselective polymerization of propylene oxide using different metal-based catalysts. Thus, this chapter is organized based on the metal of the active center of the catalyst. Aluminum, zinc, cobalt, tin, and chromium are the most commonly used metals for discrete stereoselective epoxide polymerization catalysts and their use in this field of research forms the foundation of this review.

4.09.3.1 Aluminum-Based Catalysts

Although aluminum alkoxide- and aluminoxane-based catalysts have shown promise for the isoselective polymerization of epoxides, the poorly defined nature of these species has significantly hampered their use in such polymerizations due to the formation of large amounts of atactic polyether.[30] Some examples of discrete aluminum complexes have been reported herein.

4.09.3.1.1 Aluminum–acetylacetonate complexes

The prevailing theory for the mechanism of epoxide polymerization has been that epoxide coordination to the metal center precedes insertion. To support this mechanism, Vandenberg proposed that the addition of chelating agents such as acetylacetonate (acac) to an R_3Al/H_2O (R = alkyl) polymerization system would block potential coordination sites on the metal center, thus hindering the reaction. Instead, these additives enhanced the polymerization rate and ushered in a new class of versatile and highly active catalysts.[12,31–33] The presumed structure of the active aluminum–acac catalyst is shown in Scheme 3. Although the precise structure of the active catalyst is unknown, a few structural features have been determined: (1) an oxygen atom bridges two aluminum centers (although the presence of multiple linkages, such as those in oligomeric aluminoxanes, cannot be ruled out); (2) alkyl groups are present on the aluminum atoms; and (3) the acac ligand is chelated to the aluminum center.[20]

Tuning the AlR_3/H_2O/acac catalyst (R = alkyl) composition by varying the R groups and the ratio of components creates systems that conduct epoxide polymerizations to give high conversions, in many instances achieving >90% conversion to give high-molecular-weight, acetone-insoluble polyethers. The fraction of acetone-insoluble, isotactic polymer produced varies according to the exact composition of the catalyst system used, and is ~30% of the total mass of the ether-insoluble material, while the remaining 70% is acetone-soluble atactic polymer.[32,33]

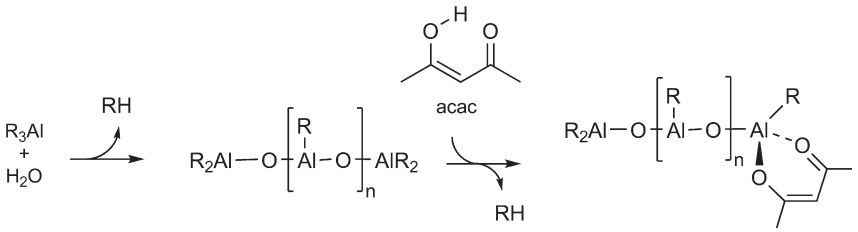

Scheme 3 Synthesis of AlR_3/H_2O/acac epoxide polymerization catalysts (R = alkyl).

In work investigating the mechanism of this system, Vandenberg used AlR_3/H_2O catalysts to polymerize *cis*- and *trans*-2,3-epoxybutane. Mechanistic information for the polymerization was obtained from the properties of the resultant polymers and the examination of the diol decomposition products. These results are summarized in Scheme 4.[12,20,34–36]

The AlR_3/H_2O catalysts polymerize both *cis*- and *trans*-2,3-epoxy butane instantaneously at −78 °C, consistent with a cationic process for monomer enchainment. The polymer isolated from the *cis* isomer is an amorphous rubber, whereas the polymer isolated from the *trans* isomer is crystalline with a melting temperature (T_m) of 100 °C. This finding is in contrast to the AlR_3/H_2O/acac system, which only slowly polymerizes the same monomers at 65 °C, presumably through a much slower coordination–insertion mechanism. The coordination polymerization of the *cis* isomer yields a crystalline polymer with a T_m of 162 °C, whereas the *trans* isomer polymerizes extremely slowly, producing only trace amounts of a crystalline polymer with a T_m similar to that obtained with the cationic polymerization. Vandenberg attributes the extremely slow polymerization of the *trans* isomer to its increased steric bulk compared to the *cis* isomer at the metal coordination site. The steric bulk hinders the required precoordination to the metal center for monomer insertion.

Through the controlled degradation of the polyethers to diol dimers using *n*-butyllithium, the stereochemistry of the monomer units in the polymer chain was determined.[34] The decomposition of all four polymers showed that inversion of configuration at the site of attack on the epoxide ring occurred in both cationic and coordination–insertion polymerization mechanisms. The *cis* epoxides (*RS* stereocenters) produce monomeric units in the polymer chain with *RR* and *SS* stereocenters, and the *trans* epoxides (either *RR* or *SS*) produce monomeric units in the polymer chain with only *RS* units.

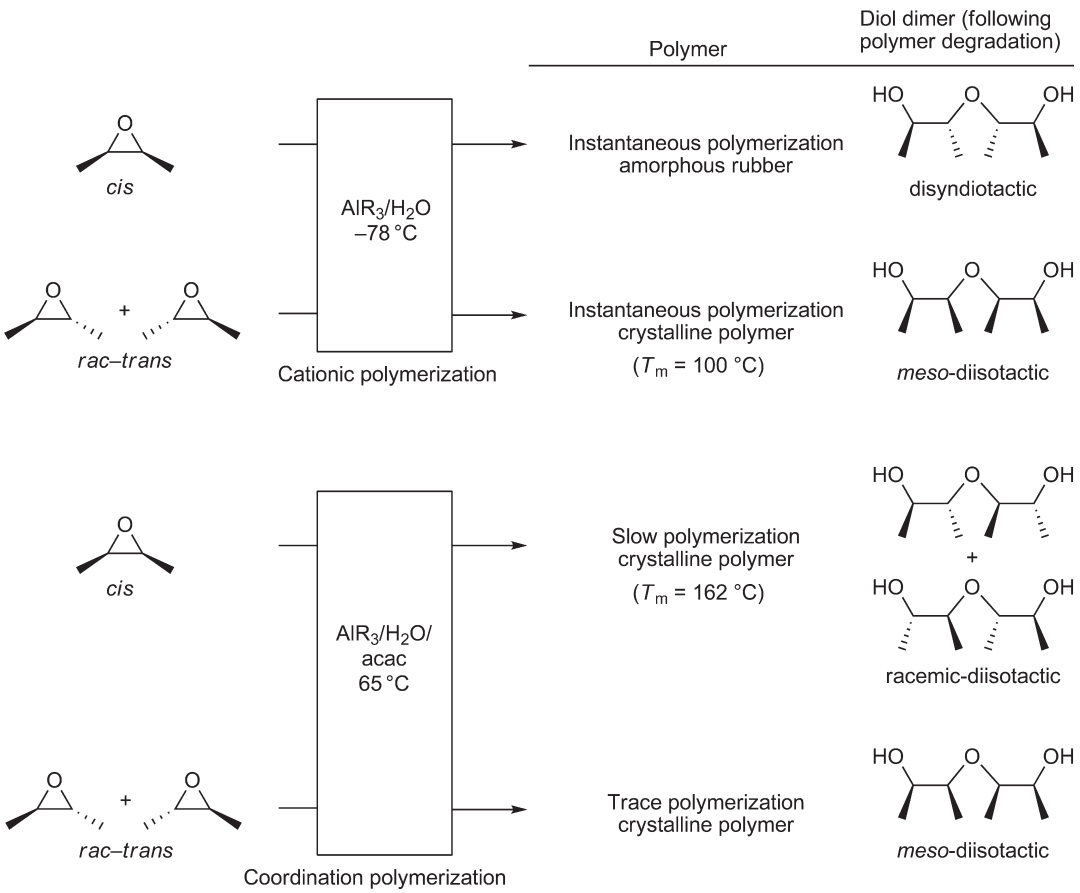

Scheme 4 Stereoselectivity of polymerization of *cis*- and *trans*-2,3-epoxybutane using AlR_3/H_2O catalysts (R = alkyl).

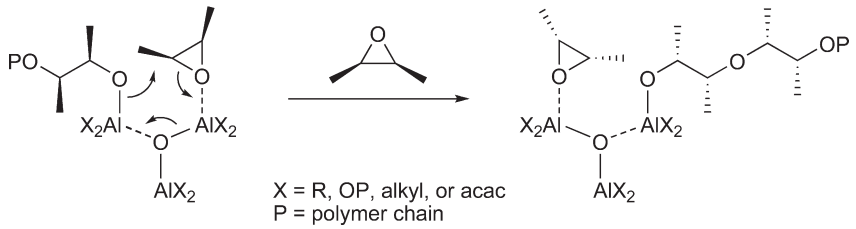

Scheme 5 Proposed bimetallic enchainment of epoxides using (acac)Al complexes. acac, acetylacetonate; P, polymeryl.

This observation shows that both polymerizations are stereospecific, with inversion of configuration occurring at the site of attack, regardless of the polymerization mechanism.

In order to obtain the geometry required for an S_N2 attack in a coordination–insertion mechanism, Vandenberg proposed the transition-state structure shown in Scheme 5. In this scheme, an epoxide is activated by coordination to an aluminum center, while the adjacent aluminum center delivers the growing polymer chain. During this process, coordination bonds are exchanged to keep the charges balanced. Although a bimetallic mechanism for epoxide ring opening is claimed, there is scant evidence for this proposal.[37–39]

4.09.3.1.2 Aluminum systems featuring chiral alkoxides

Haubenstock and co-workers[40] synthesized chiral aluminum alkoxides for the stereoselective polymerization of propylene oxide. Addition of 1.5 equiv. of (−)-(*R*)-3,3-dimethylbutane-1,2-diol ((*R*-dmbd)H_2) to AlH_3 generated the active complex $[(R\text{-dmbd})_{1.5}/Al]_n$. Alone, $[(R\text{-dmbd})_{1.5}/Al]_n$ displayed very low activity for the polymerization of propylene oxide, achieving 85% conversion in 3 weeks with negligible optical activity in the unreacted monomer. The addition of $ZnCl_2$ (Al:Zn = 1:1) to the $[(R\text{-dmbd})_{1.5}/Al]_n$ initiator generated a much more active catalyst, as shown in Scheme 6. Furthermore, the optical activity of the unreacted propylene oxide was observed to increase with increasing conversion to polymer, and based on the optical rotation of the unreacted monomer, Haubenstock and co-workers[40] determined that the catalyst system preferentially reacted with (*R*)-propylene oxide because the reaction solution became enriched in the (*S*) enantiomer, although with modest selectivity ($s = 1.05$). On fractionation, 10% of the total mass of the isolated polymer was acetone insoluble and highly isotactic (>99% *m*-dyads), whereas the remainder of the polymer was acetone soluble and atactic. Although a slight enantiomeric enrichment of monomer was achieved, this system did not significantly improve the yield of isotactic poly(propylene oxide) compared to similar systems,[41–43] and it is unclear whether the selective enchainment of the *R*-enantiomer was contributing to the formation of the 10% of crystalline polymer as opposed to it arising from a different mechanism.

4.09.3.1.3 Aluminum–porphyrin complexes

Inoue[44–46] first reported that 5, 10, 15, 20-tetraphenylporphyrin (tpp) aluminum chloride (Figure 1, **1**) was active for the living polymerization of propylene oxide. Although the polymer microstructure was not studied in great detail, ^{13}C NMR spectra showed the polymers to be highly regioregular and slightly isotactic.[44,45] The activity of (tpp)AlCl was relatively low, requiring 6 days to achieve 100% conversion. The addition of Cl or OMe substituents on the porphyrin ligand, as in (*p*-Cl-tpp)AlCl (**2**) and (*p*-OMe-tpp)AlCl (**3**), increased the activity by a factor of 2, but the tacticity of the resulting polymers was not discussed.[45] More detailed ^{13}C NMR analyses by Le Borgne and co-workers[24] showed that the poly(propylene oxide) derived from **1** was slightly isotactic, with an *m*-dyad content of 69% and an *mm*-triad content of 45%, confirming the initial results reported by Inoue.

4.09.3.1.4 Aluminum–Schiff base complexes

Well-defined [*N*,*N*′-bis-(2-hydroxybenzylidene)-(1*R*,2*R*)cyclohexane-1,2-diamine] (*R*,*R*-salcy) aluminum complexes (Figure 1, **4**) have been used as enantioselective epoxide polymerization catalysts.[47–49] Polymerization of racemic propylene oxide in the presence of 5 mol.% **4** yields ~70% conversion to poly(propylene oxide) after 62 h. The remaining unreacted monomer exhibits an optical rotation of +1.85°, which corresponds to an *ee* of 15% (Scheme 7). The modest s-factor of 1.3 obtained in this system is slightly higher than that observed for the previously discussed heterogeneous aluminum systems.[50] Examination of the isolated polymer reveals both chloro and hydroxyl end groups, suggesting that each metal center produces a single polymer chain since each chain bears a Cl atom from initiation and a hydroxyl group from terminiation.[48]

4.09.3.1.5 Aluminum–calixarene complexes

Kuran and co-workers synthesized a dimethylcalixarene-based system (Figure 1, **5**) that exhibited low activity for propylene

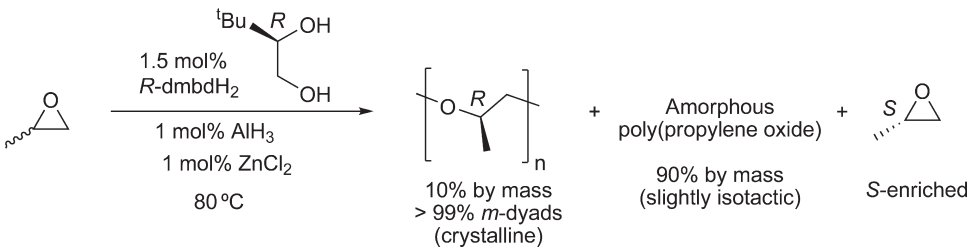

Scheme 6 Polymerization of propylene oxide with $[(R\text{-dmbd})_{1.5}Al]_n/ZnCl_2$ catalysts. dmbd, 3,3-dimethyl-1,2-butanediolate.

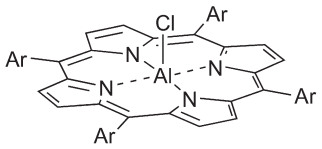

Ar = C_6H_5 (tpp); **1**
Ar = *p*-C_6H_4Cl (*p*-Cl-tpp); **2**
Ar = *p*-C_6H_4OMe (*p*-OMe-tpp); **3**

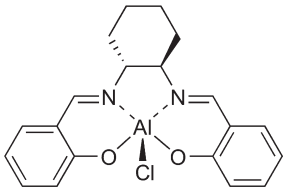

(*R*,*R*-salcy)AlCl; **4**

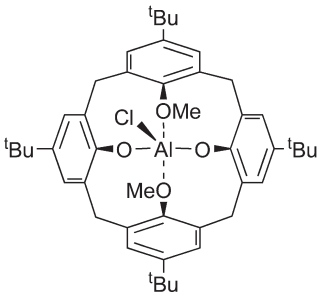

(dmca)AlCl; **5**

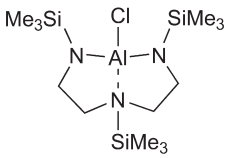

6

Figure 1 Well-defined complexes for the polymerization of epoxides. tpp, 5,10,15,20-tetraphenylporphyrin; *R*,*R*-salcy, *N*,*N*′-bis-(2-hydroxybenzylidene)-(1*R*,2*R*)-1,2-cyclohexanediamine; dmca, dimethylcalixarene.

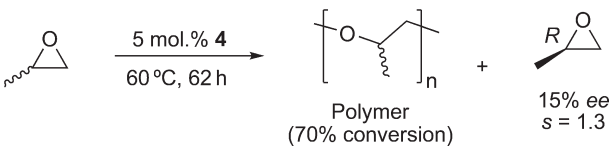

Scheme 7 Attempted enantioselective polymerization of racemic propylene oxide using **4**.

oxide polymerization (TOF = 0.06 h^{-1}).[51] The polymerization of propylene oxide produced predominantly isotactic poly(propylene oxide) with an *m*-dyad content of ~74%.

4.09.3.1.6 Other well-defined aluminum systems

N,*N*′,*N*″-Tris(trimethylsilyl)diethylenetriamine complexes of aluminum have been shown to be active oligomerization catalysts for propylene oxide.[52] Over the course of 2 days, catalyst **6** (**Figure 1**) produces low-molecular-weight poly(propylene oxide) (M_n < 500 g mol^{-1}) with predominantly head-to-tail linkages and an *m*-dyad content of 60%.

4.09.3.2 Zinc-Based Catalysts

During research on aluminum catalysts for the stereoselective polymerization of epoxides, it was discovered that the addition of zinc cocatalysts to these systems greatly enhanced catalyst activity.[41] These enhancements prompted a number of studies focusing on the design of zinc-based catalyst systems.

4.09.3.2.1 Zinc alkoxide catalysts

Furukawa and co-workers[53] explored catalysts derived from the addition of methanol or ethanol to diethylzinc as epoxide polymerization systems, and found that both the yield and crystallinity of the resulting polymers were inferior to those for polymers synthesized with the $ZnEt_2/H_2O$ system. The use of achiral alcohols as cocatalysts was revisited in 1994 when Kuran and Listos[54] reported the polymerization of propylene oxide and cyclohexene oxide (a *meso* substrate) with $ZnEt_2$/polyhydric phenol (such as 4-*tert*-butylcatechol), phenol, or 1-phenoxypropan-2-ol. The poly(propylene oxide) formed from these systems contained mostly isotactic dyads (72% *m*), while the poly(cyclohexene oxide) contained mostly syndiotactic dyads (80% *r*) (**Scheme 8**).

4.09.3.2.2 Chiral zinc alkoxide catalysts

Sigwalt and co-workers noted higher stereoselectivity during the polymerization of propylene sulfide using a (*R*)-3,3-dimethylbutane-1,2-diol/$ZnEt_2$ system when compared with a similar chiral alcohol/$ZnEt_2$ system. Based on these results, they applied this system to propylene oxide, but noticed that stereoselectivity was actually lower than that for the polymerization of propylene sulfide.[16,55,56] This lower stereoselectivity was attributed to the weaker coordination of the 'harder' epoxide oxygen atom to zinc, as compared to the 'softer' coordination of the episulfide sulfur atom.

Sepulchre and co-workers investigated the polymerization of cyclohexene oxide using $ZnEt_2$ activated with water, alcohols, and chiral alcohols. In their study, a mixture of $ZnEt_2$ and 1-methoxypropan-2-ol or (1*S*,2*R*)-ephedrine simultaneously afforded a mixture of isotactic and syndiotactic poly(cyclohexene oxide) that was characterized using ^1H and ^{13}C NMR spectroscopies (**Scheme 9**).[57,58] They proposed a 'flip-flop' mechanism (similar to that proposed by Vandenberg[20] as shown in **Scheme 5**) involving neighboring zinc centers to explain this observation.

4.09.3.2.3 Zinc alkoxide clusters

Tsuruta and co-workers[59–68] synthesized and investigated the epoxide polymerization activity of several well-defined zinc clusters (**Figure 2**). Complexes $[Zn(OMe)_2 \bullet (EtZnOMe)_6]$ (**7**), $[Zn(OCH_2CH_2OMe)_2 \bullet (EtZnOCH_2CH_2OMe)_6]$ (**8**), and

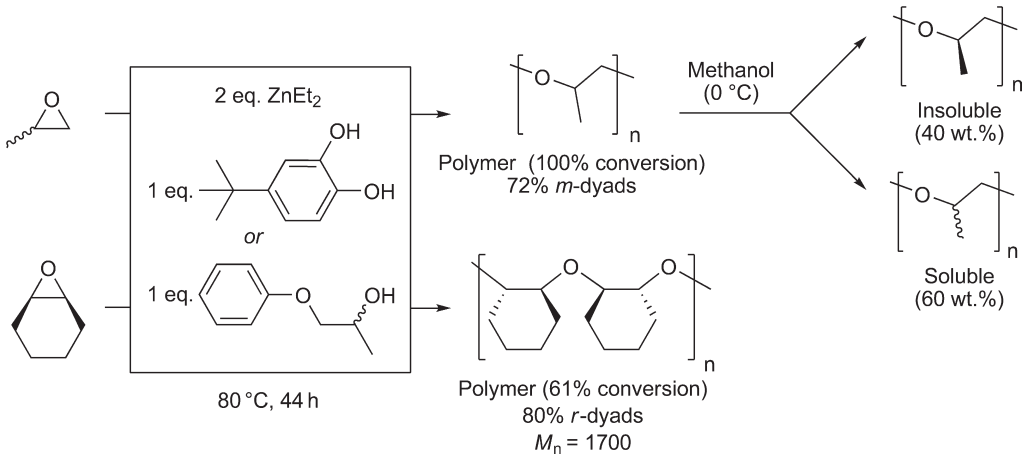

Scheme 8 Polymerization of epoxides with $ZnEt_2$/1-phenoxy-2-propanol or 4-*tert*-butylcatechol.

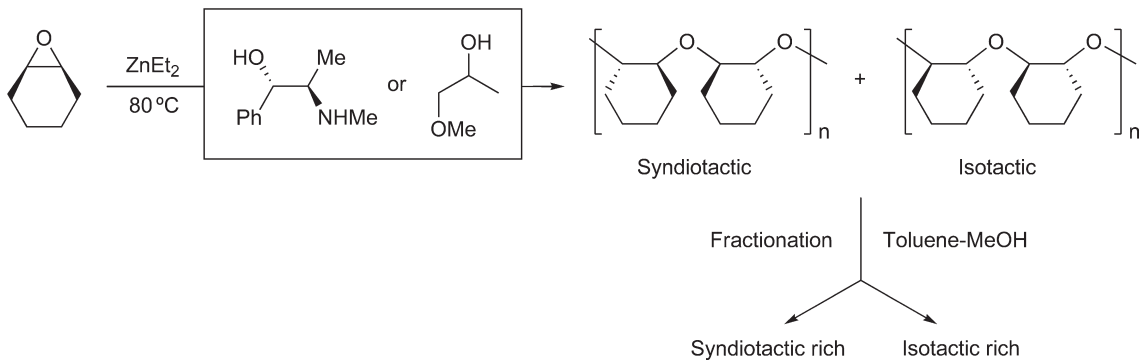

Scheme 9 Preparation of a mixture of isotactic and syndiotactic poly(cyclohexene oxide) using chiral zinc alkoxide catalysts.

$[\{CH_3OCH_2CH(Me)OZnOCH(Me)CH_2OCH_3\}_2 \bullet \{EtZnOCH(Me)CH_2OCH_3\}_2]$ (**9**), were synthesized by the dropwise addition of 1.1 equiv. of the corresponding alkoxyalcohols to $ZnEt_2$ in heptanes at 5 °C. Each complex was crystalline, and its molecular structure was determined using X-ray crystallography (**Figure 2**).[59,62,68]

The polymerization activity for each complex is shown in **Scheme 10**. Surprisingly, isostructural complexes **7** and **8** had significantly different polymerization activities; **7** achieved 91% conversion in 216 h, while **8** attained only 22% conversion in 240 h. Catalyst **9**, however, was twice as active as complex **7**. This catalyst has a different molecular structure, as shown in **Figure 2**. Complex **9** bears six 1-methoxypropan-2-yl groups in a chair-like structure in three different coordination environments; the methoxy groups are either endo- and exo-coordinated to the central zinc atoms, or noncoordinated.

Studies using a deuterated version of **9** revealed that the non-coordinating 1-methoxypropan-2-olate groups initiated the polymerization by attack on the propylene oxide monomer, whereas the coordinated 1-methoxypropan-2-olate groups provided the chiral structure, which remained unchanged during the polymerization.[63] When these

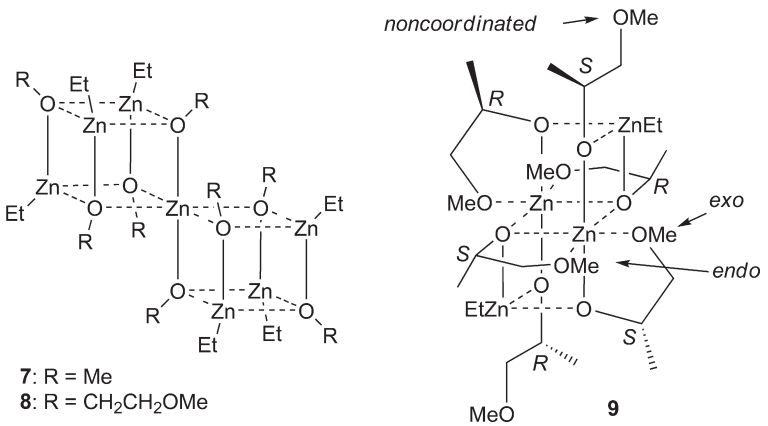

Figure 2 Structures of zinc cluster catalysts **7**, **8**, and **9**.

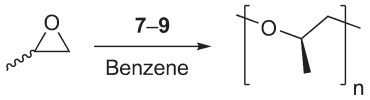

Catalyst	Temp. (°C)	Time (h)	Yield (%)	*m*-Dyads (%)
7	80	216	91	63
8	80	240	22	59
9	80	100	93	79
9	35	240	9	81

Scheme 10 Polymerization of racemic propylene oxide with zinc alkoxide cluster catalysts **7**–**9**.

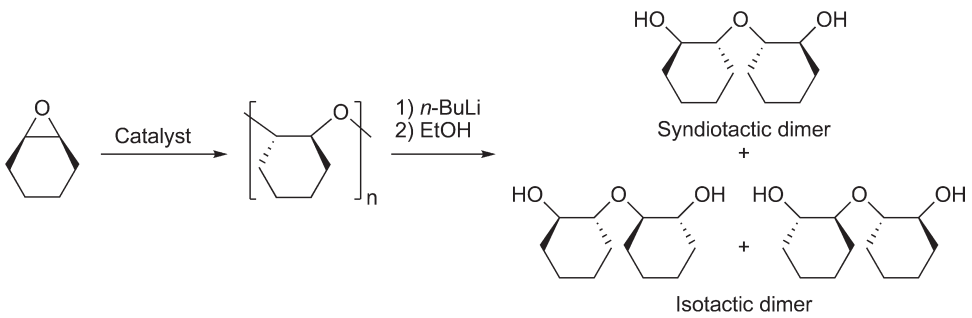

Catalyst	Syndiotactic dimer (%)	Isotactic dimer (%)
$ZnEt_2$	66	34
$(EtZnOMe)_4$	66	34
9	81	19

Scheme 11 Syndioselective polymerization of cyclohexene oxide with **9** and subsequent degradation.

complexes were screened for cyclohexene oxide polymerization, only 9 was found to be active.[69,70] Through ^{1}H NMR analysis of polymer decomposition products (using Vandenberg's[34] method), Tsuruta and co-workers determined that the poly(cyclohexene oxide) obtained was predominantly syndiotactic (Scheme 11).

4.09.3.2.4 Zinc porphyrin-based catalysts

Inoue and co-workers reported that the polymerization of propylene oxide at 20 °C with the zinc porphyrin catalyst (Et_2Zn/*N*-methyl-5, 10, 15, 20-tetraphenylporphyrin, **10**) produced syndiotactic poly(propylene oxide) (M_w = 31 000, 60% *r*) (Scheme 12). This result was in contrast to those seen for all other zinc-based systems, which afford isotactic poly (propylene oxide). The authors attributed the unexpected syndiotactic microstructure of the polymer to the planar ligand and the isolated nature of the zinc center, which is different from that present in most other zinc aggregate systems.[44]

4.09.3.2.5 Zinc catalysts for asymmetric cyclohexene oxide/CO_2 copolymerization

There is significant interest in controlling the absolute stereochemistry of ring opening in epoxide/CO_2 copolymerization. Cyclohexene oxide, a *meso* molecule, is an ideal substrate for desymmetrization using chiral catalysts. In 1999, Nozaki *et al.*[71] reported that a 1:1 mixture of $ZnEt_2$ and (*S*)-diphenyl (pyrrolidine-2-yl)methanol (**11**) (Scheme 13) was active for stereoselective cyclohexene oxide/CO_2 copolymerization at 40 °C and 30 atm. CO_2 (Scheme 14). The resultant polycarbonate contained 100% carbonate linkages, had an M_n of

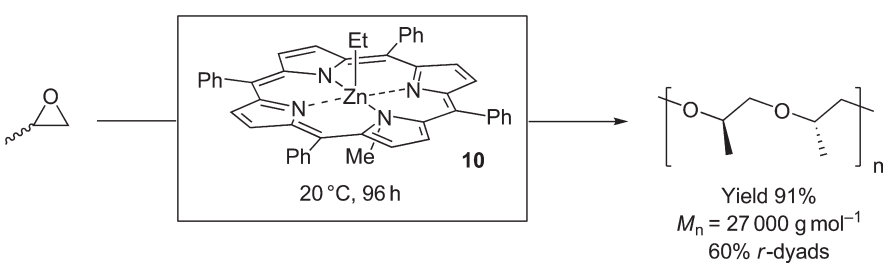

Scheme 12 Syndioselective polymerization of propylene oxide with **10**.

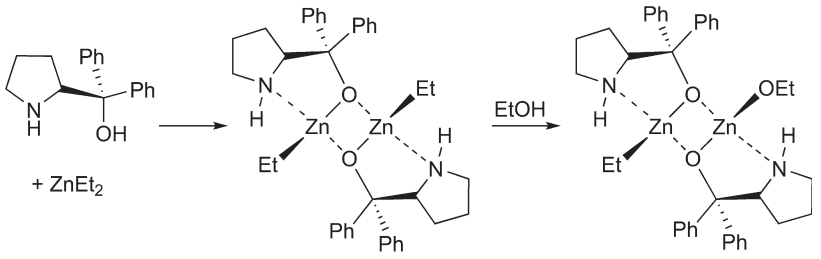

Scheme 13 Chiral zinc catalysts for the asymmetric, alternating copolymerization of cyclohexene oxide and CO_2.

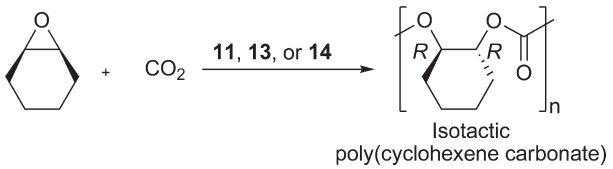

Scheme 14 Enantioselective copolymerization of cyclohexene oxide and CO_2 with **11**, **13**, or **14**.

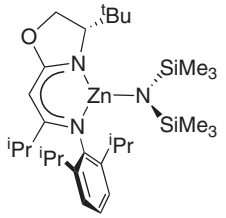

14

Figure 3 Chiral zinc catalyst **14** for the asymmetric, alternating copolymerization of cycloalkene oxides and CO_2.

8400 g mol^{-1}, and had a M_w/M_n of 2.2. Hydrolysis of this poly(cyclohexane-1,2-diyl carbonate) with base produced the corresponding *trans*-cyclohexane-1,2-diol with 73% *ee*. ^{13}C NMR spectroscopy studies of model polycarbonate oligomers afforded spectral assignments for the isotactic (153.7 ppm) and syndiotactic dyads (153.3–153.1 ppm) of poly(cyclohexene oxide),[72] which agreed with those proposed by Cheng *et al.*[73] Finally, the ring-opening polymerization proceeded stereospecifically via complete inversion of configuration (S_N2 mechanism) of one carbon of each repeat unit; hence, no *cis*-cyclohexane-1,2-diol was observed after base-catalyzed degradation of the polycarbonate.

In a 2003 report, Nozaki and co-workers[74] isolated presumed intermediates in the asymmetric alternating copolymerization of cyclohexene oxide with CO_2. Reaction of a 1:1 mixture of $ZnEt_2$ and (*S*)-α,α-diphenylpyrrolidine-2-yl-methanol (**11**, **Scheme 13**) yielded dimeric **12**, which was structurally characterized by X-ray diffraction studies. At 40 °C and 30 atm. CO_2, **12** catalyzed the formation of isotactic poly(cyclohexane-1,2-diyl carbonate) (M_n = 11 800 g mol^{-1}, M_w/M_n = 15.7) with a turnover frequency of 0.6 h^{-1}. Hydrolysis of the resulting poly(cyclohexene carbonate) yielded the *trans*-cyclohexane-1,2-diol of 49% *ee*, which was lower than that seen with catalyst **11**. When copolymerization was attempted using a catalyst system consisting of **12** and 0.2–1.0 equiv. EtOH (**12**/EtOH), the *ee* of the hydrolyzed cyclohexane diol increased up to 80%. The catalyst and EtOH combination resulted in better control of polymer molecular weights and molecular weight distributions in comparison to polymerization using only **12**. Compound **13** (**Scheme 13**) was proposed to be the active initiating species in this polymerization. End-group analysis of the poly(cyclohexane-1,2-diyl carbonate)s prepared with **12** and **12**/0.2 EtOH by matrix-assisted laser desorption/ionization time-of-flight (MALDI-TOF) mass spectrometry revealed that in the absence of ethanol or in the presence of 0.2 equiv. ethanol end-group signals assignable to an aminoalcohol-initiated polymerization were identified. However, as EtOH addition was increased from 0.2 to 1.0 equiv., signals corresponding to the aminoalcohol-initiated polycarbonate disappeared as signals corresponding to end-group structures for EtOH-initiated poly(cyclohexane-1,2-diyl carbonate) emerged. This result was further confirmed by end-group analysis using ^{1}H NMR spectroscopy. Finally, mechanistic studies suggested that the dimeric form of the catalyst, **13**, was in fact the active species.

In 2000, Cheng and co-workers[73] developed C_1-symmetric imine-oxazoline ligated zinc compounds (**Figure 3**, **14**) for the isoselective, alternating copolymerization of cyclohexene oxide and CO_2 (**Scheme 14**). Through multiple electronic and steric manipulations of the imine-oxazoline ligand framework, compound **14** was found to exhibit the highest enantioselectivity for polymerization (*RR*:*SS* ratio in polymer was 86:14; 72% *ee*). Poly(cyclohexane-1,2-diyl carbonate) prepared with this catalyst possessed 100% carbonate linkages, an M_n of 14 700 g mol^{-1}, and an M_w/M_n of 1.35. This poly(cyclohexane-1,2-diyl carbonate) was crystalline with a glass transition temperature (T_g) of 120 °C, and a melting temperature (T_m) of 220 °C. Furthermore, stereocontrol was also achieved in the alternating copolymerization of cyclopentene oxide and CO_2, producing poly(cyclopentane-1,2-diyl carbonate) with an *RR*:*SS* ratio of 88:12 (76% *ee*). As revealed by ^{13}C NMR spectroscopy, the experimental carbonyl tetrad concentrations of this material matched the predicted tetrad concentrations for an enantiomorphic site control mechanism.[73]

4.09.3.3 Cobalt-Based Catalysts

Tsuruta found that the optically pure complex [(*R*,*R*-salcy)Co] (**15**) was active for epoxide polymerization (**Scheme 15**) when activated with $AlEt_3$. Although the system exhibited no enantioselectivity for the polymerization of propylene oxide, it was moderately selective ($s \sim 1.5$) for the enantioselective polymerization of *tert*-butyl ethylene oxide and epichlorohydrin (**Scheme 15**).[75]

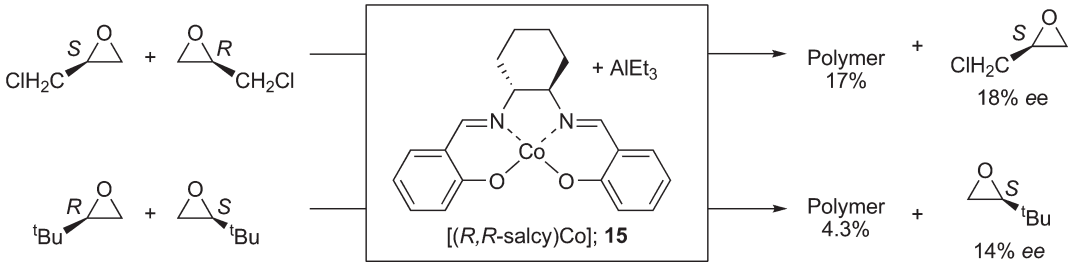

Scheme 15 Enantioselective polymerization of racemic *tert*-butyl ethylene oxide and epichlorohydrin using **15**/$AlEt_3$.

4.09.3.3.1 Epoxide-carbon dioxide copolymerization systems

Qin and co-workers[76] reported that [(*R*,*R*-salcy-^{t}Bu)CoOAc] (**16**) copolymerizes propylene oxide and CO_2 (**Scheme 16**). Novel features of the catalyst are high regioregularity and alternation, coupled with high selectivity for polycarbonate formation (cyclic propylene carbonate is not formed). (*S*)-Propylene oxide is consumed faster than (*R*)-propylene oxide with a modest s-factor of 2.8. Given the same absolute monomer configuration and similar s-factor observed by Tokunaga *et al.*[39] for the cobalt-catalyzed ring opening of aliphatic epoxides with benzoic acid, a related mechanism was proposed to occur for polymerization with [(*R*,*R*-salcy-^{t}Bu)CoOAc], giving a cobalt-alkoxide catalyst resting state to produce the regioregular structure shown in **Scheme 16**.

Lu and co-workers[77] found that the addition of quaternary ammonium salts increased the s-factor to 3.5. The use of cobalt–salen complexes (in conjunction with an ionic organic ammonium salt or a sterically hindered strong organic base) allowed for the stereoselective alternating copolymerization of CO_2 and racemic aliphatic epoxides. By using a 7-methyl-1,5,7-triazabicyclo[4.4.0]dec-5-ene (MTBD) cocatalyst with the cobalt catalyst, it was possible to produce poly(propylene carbonates) with a s-factor of 5.6, with >95% head-to-tail units and >99% carbonate linkages. The same catalytic system was also used for the copolymerization of cyclohexene oxide and CO_2 to produce polycarbonates with an *ee* of 36.6% and greater than 99% carbonate linkages.[78] More recently, Cohen and Coates[79] have reported that a combination of complex **17** and bis(triphenylphosphine)iminium chloride ([PPN]Cl) exhibits an s-factor of 9.7 for the copolymerization of propylene oxide and CO_2 at −20 °C (**Scheme 16**).

Cohen and co-workers[80] also reported the first syndioselective copolymerization of cyclohexene oxide and CO_2 (**Scheme 17**). Using complex [*rac*-(salpr-^{t}Bu)CoBr] (**18**), poly(cyclohexane-1,2-diyl carbonate) was formed with 80% *r*-dyads, as determined by ^{13}C NMR spectroscopy. The carbonyl

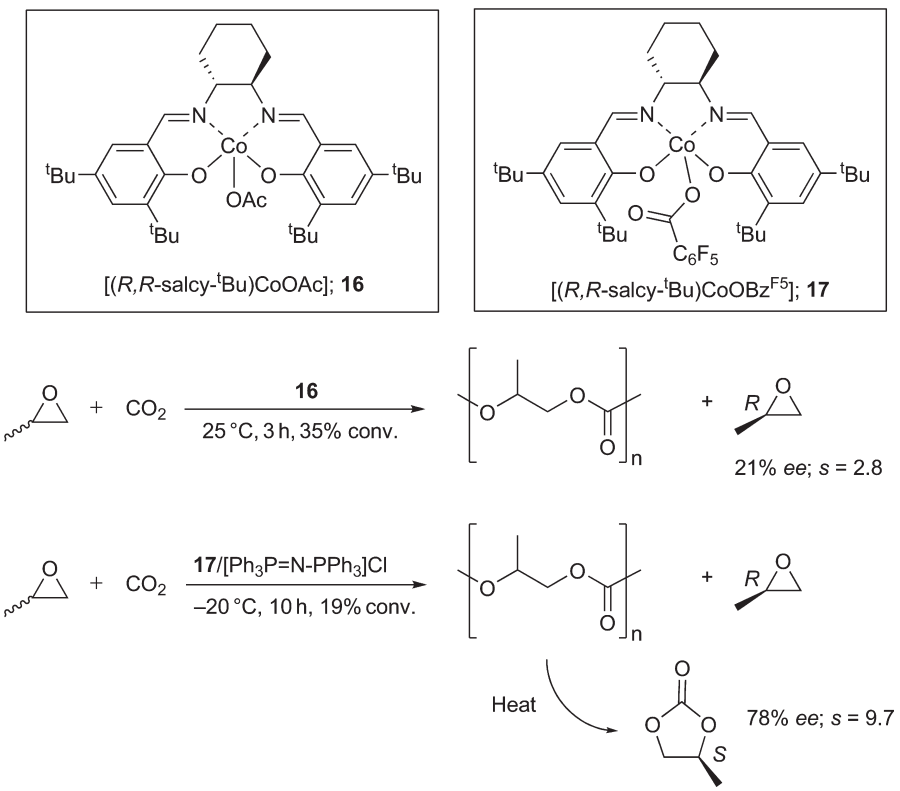

Scheme 16 Enantioselective polymerization of racemic propylene oxide using **16** and **17**/[Ph_3P=N-PPh_3]Cl.

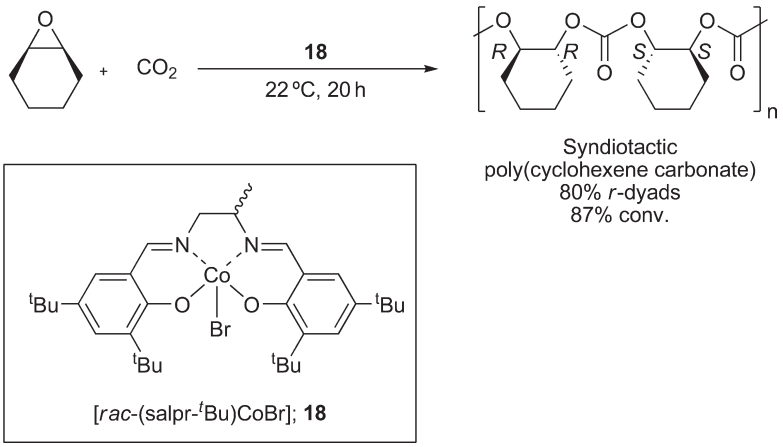

Scheme 17 Syndioselective copolymerization of cyclohexene oxide and CO_2 with **18**.

and methylene regions were best simulated using Bernoullian statistical methods, supporting a chain-end stereochemical control mechanism.

4.09.3.3.2 Recent stereoselective epoxide homopolymerization systems

In 2005, Peretti and co-workers[81] reported a highly active and isoselective (TOF = 220 h^{-1}, *mm* > 99%) cobalt complex, [(salph-^{t}Bu)CoOAc] **19** (**Scheme 18(a)**) for the polymerization of racemic propylene oxide. This is the first example of highly isotactic poly(propylene oxide) generation from racemic propylene oxide without concomitant atactic byproduct. 1-Butene oxide and 1-hexene oxide, though structurally similar to propylene oxide, displayed only trace activity with **19**, while all other substituted epoxides screened showed no activity. Though suitable crystals of **19** were not obtained, the crystal structure of the methoxide analog **20**, revealed the formation of chiral clefts that are proposed to facilitate its isoselective nature. Adjacent cobalt atoms were separated by 7.13 Å with the salen planes oriented 52° to each other, as shown in **Scheme 18(b)**.[82] Studies found that samples of crystalline **20** that had been ground mechanically displayed significantly higher activity than unground **20**. This large increase in polymerization activity of **20** with increased surface area supports that polymerization occurs on

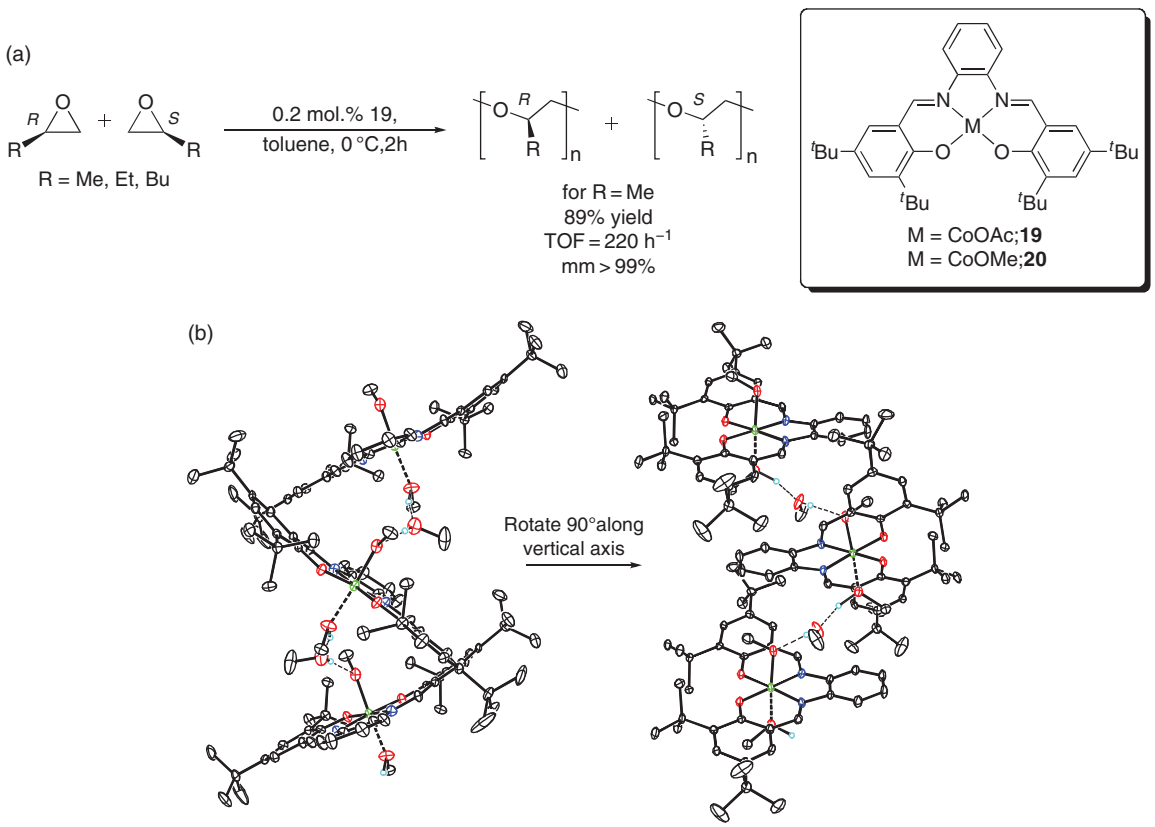

Scheme 18 (a) Isoselective polymerization of propylene oxide using **19**; (b) Molecular structure of methoxide analog **20**.

the surface of crystalline **19** and crystalline **20**. The supramolecular structure of **19** and **20** limits any attempts at catalyst optimization through substituent modification due to the inability to accurately predict structural packing, leading to desire for a soluble modular system to synthesize isotactic polyethers.

Mechanistic studies of **19** and **20** lead to the design of the complex **21**, which was reported by Coates and co-workers[83,84] in 2008. An axially chiral binaphthol linker covalently oriented the cobalt centers in the appropriate geometry and maintained the ideal distance between metal centers for epoxide polymerization (**Scheme 19**). The catalytic system consisting of **21** and a cocatalyst, [PPN]OAc, can enantioselectively polymerize propylene oxide with s-factor greater than 300 and TOF of 5400 h^{-1}. The system displayed enantiomorphic site control as determined by ^{13}C NMR. A variety of monosubstituted racemic monomers including alkyl, glycidyl, vinyl, styrenic, and fluorinated epoxides were shown to be enantioselectively polymerized to form highly isotactic enantiopure polyethers. This left valuable enantiopure epoxides in the starting material with s-factors ranging from 20 to 300. Racemic catalyst was shown to isoselectively polymerize epoxides in quantitative yield at low (0.1 mol.%) catalyst loading. Many of the isotactic polyethers synthesized were crystalline unlike their atactic analogs and nearly all had high M_n values.

Subsequent work developed a simplified isoselective variant of the catalyst (**22**) by substituting the cyclohexanediamine bridge for ethylenediamine and using a racemic binapthol linker (**Scheme 20**).[85] This complex displayed low activity and selectivity for TOF when combined with [PPN]OAc. The identity of the cocatalyst was found to dramatically affect reactivity, the bulkier [PPN]OPiv cocatalyst gave the highest rates and isoselectivities for a broad range of epoxides. This system displays the highest rate reported for isoselective TOF (=1000 h^{-1}) and high tacticity (*mm* = 97%).

Studies of these bimetallic systems have shown that the axial chirality of the binapthol linker determines the enantiopreference for epoxide enchainment,[85] rather than the stereochemistry of the diamine, unlike related cobalt salen systems.[39,79] Complexes **21** and **22** are currently believed to exist as mixtures of exo/endo chloride diastereomers. Addition of cocatalyst leads to an active anionic complex as shown in

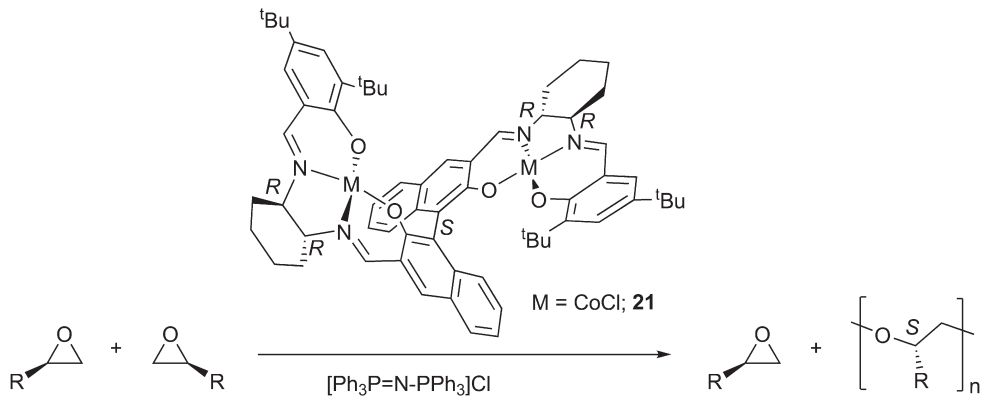

Epoxide	TOF (min^{-1})	M_n (kg mol^{-1})	*s*-Factor	Epoxide	TOF (min^{-1})	M_n (kg mol^{-1})	*s*-Factor
	91	26	>300		760	140	>70
	16	61	>300	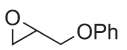	960	130	>70
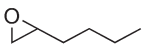	6	77	>100		14	79	>20
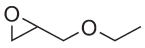	10	8	>50	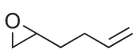	21	46	>300
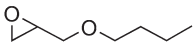	14	33	>50	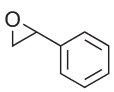	11	50	>70
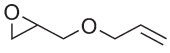	130	110	>100				
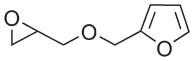	230	69	>80		190	20	>300

Scheme 19 Enantioselective polymerization of epoxides with **21**.

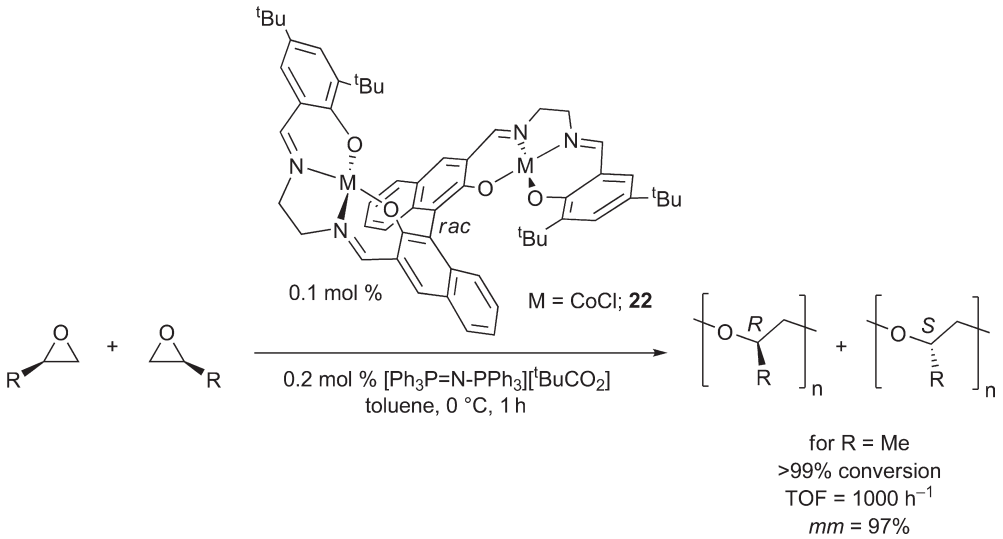

Scheme 20 Isoselective polymerization of epoxides with **22**.

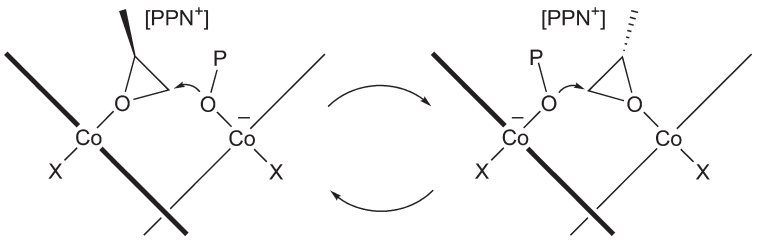

Scheme 21 Proposed mechanism of polymerization for **21** and **22**.

Scheme 21 where X can be either a chloride or a carboxylate. These bimetallic cobalt catalysts display induction periods and poor agreement between theoretical and experimental M_n values likely due to slow initiation relative to propagation. Polydispersities (M_w/M_n) were ~2, consistent with a single-site mechanism.[84]

4.09.3.4 Tin-Based Catalysts

In 1993, Miura and co-workers[86] studied the use of organotin-alkyl phosphate condensates derived from dibutyltin oxide and tributyl phosphate to catalyze the polymerization of propylene oxide (Figure 4). They observed that the polymeric product could be fractionated into benzene–hexane soluble and insoluble fractions. On studying the stereoerrors of the product by ^{13}C NMR, they determined that the insoluble fraction was isotactic poly(propylene oxide) with 94% *m*-dyads (91% *mm*-triads). A direct correlation was found between increasing the molecular weights of the tin condensate initiators with increasing molecular weight and stereoregularity of the polyethers synthesized. Schütz and co-workers[87] later demonstrated the further use of organotin phosphate coordination polymers to synthesize isotactic poly(propylene oxide). The tin phospate polymers were made by the condensation of tributyl phosphate and butyl tin trichloride. Propylene oxide was polymerized with high activity (TOF = 100 h^{-1}). After fractionation of the polymeric product, 10% was found to be insoluble in acetone and highly isotactic with 88% *m*-dyads. No allyl end groups were detected; these polymerizations have been proposed to undergo a bimetallic mechanism for enchainment.

4.09.3.5 Chromium-Based Catalysts

A significant contribution toward developing regioregular polycarbonates has been made by the Lu research group, including developing a saturated salicylaldimine chromium(III) catalyst ([SalanCr(III)], Figure 5), which in conjunction with

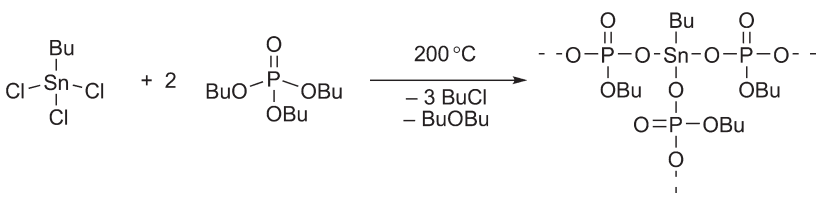

Figure 4 Preparation of organotin phosphate condensates.

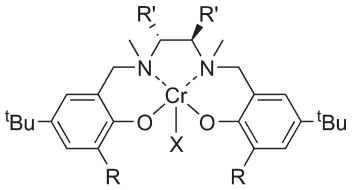

(Salan)Cr(III)

Figure 5 Structure of Salan Cr(III) complex.

quaternary ammonium salts can produce high-molecular-weight poly(propylene carbonate) with regiochemical control (>95% head-to-tail linkages) while also displaying moderate enantioselectivity ($2 < s < 8$) depending on the quaternary ammonium cocatalyst used.[88]

4.09.4 Conclusion/Outlook

Although significant advances in stereoselective epoxide polymerization have been achieved over the last half-century, only recently have catalysts been developed that are capable of high levels of stereocontrol. Historically, most catalysts for stereoselective epoxide polymerization have been heterogeneous and have exhibited poor selectivity. Current work in the development of well-defined, homogeneous, multimetallic catalysts with controlled spatial orientation of the active catalyst centers could lead to new generations of improved stereoselective epoxide polymerization catalysts. Major frontiers in stereoselective epoxide polymerization have yet to be explored – these include the development of new systems that are highly stereoselective for epoxide/CO_2 copolymerization, highly selective for polymerization of polysubstituted epoxides, as well as living and stereoselective, allowing for the formation of block copolymers. New catalysts are still needed to accomplish the challenge of synthesizing precisely defined highly tactic polyethers and polycarbonates.

References

1. Pruitt, M.E.; Baggett, J. M. U.S. Patent 2,706,181, 1955.
2. Pruitt, M.E.; Baggett, J.M.; Bloomfield, R.J.; Templeton, J. H. U.S. Patent 2,706,182, 1955.
3. Pruitt, M.E.; Baggett, J. M. U.S. Patent 2,706,189, 1955.
4. Booth, C.; Jones, M. N.; Powell, E. *Nature* **1962**, *196*, 772.
5. Natta, G.; Corradini, P.; Dall'Asta, G. *Atti Acad. Nazl. Lincei Rend., Cl. Sci., Fis., Mat. Nat.* **1956**, *20*, 408.
6. Price, C. C.; Osgan, M. *J. Am. Chem. Soc.* **1956**, *78*, 4787.
7. Price, C. C.; Osgan, M.; Hughes, R. E.; Shambelan, C. *J. Am. Chem. Soc.* **1956**, *78*, 690.
8. Vandenberg, E. J. *Polymer* **1994**, *35*, 4933.
9. Spassky, N.; Dumas, P.; Le Borgne, A.; *et al. Bull. Soc. Chim. Fr.* **1994**, *131*, 504.
10. Spassky, N.; Momtaz, A.; Kassamaly, A.; Sepulchre, M. *Chirality* **1992**, *4*, 295.
11. Spassky, N. *Makromol. Chem., Macromol. Symp.* **1991**, *42/43*, 15.
12. Vandenberg, E. J. In *Coordination Polymerization*; Vandenberg, E. J., Price, C. C., Eds.; Plenum Publishing Corp.: New York, 1983; p 11.
13. Tsuruta, T. *Pure Appl. Chem.* **1981**, *53*, 1745.
14. Spassky, N.; Leborgne, A.; Sepulchre, M. *Pure Appl. Chem.* **1981**, *53*, 1735.
15. Spassky, N. *ACS Symp. Ser.* **1977**, *59*, 191.
16. Sigwalt, P. *Pure Appl. Chem.* **1976**, *48*, 257.
17. Price, C. C. *Acc. Chem. Res.* **1974**, *7*, 294.
18. Tsuruta, T. *J. Polym. Sci., Part D: Macromol. Rev.* **1972**, *6*, 179.
19. Duda, A. *Polimery* **2004**, *49*, 469.
20. Vandenberg, E. J. *J. Polym. Sci., Polym. Chem. Ed.* **1969**, *7*, 525.
21. Ajiro, H.; Allen, S. D.; Coates, G. W. *Stereoselective Polymerization with Single-Site Catalysts*; CRC Press: Boca Raton, FL, 2007; p 627.
22. Farina, M. *Top. Stereochem.* **1987**, *17*, 1.
23. Schilling, F. C.; Tonelli, A. E. *Macromolecules* **1986**, *19*, 1337.
24. Le Borgne, A.; Spassky, N.; Jun, C. L.; Momtaz, A. *Makromol. Chem.* **1988**, *189*, 637.
25. Ugur, N.; Alyuruk, K. *J. Polym. Sci., Part A: Polym. Chem.* **1989**, *27*, 1749.
26. Cheng, H. N. In *Modern Methods of Polymer Characterization*; Barth, H. G., Mays, J. W., Eds.; Wiley: New York, 1991; p 409.
27. Bovey, F. A.; Mirau, P. A. *NMR of Polymers*; Academic Press: San Diego, CA, 1996.
28. Chisholm, M. H.; Navarro-Llobet, D. *Macromolecules* **2002**, *35*, 2389.
29. Gawley, R. E. *J. Org. Chem.* **2006**, *71*, 2411.
30. Wu, B.; Harlan, C. J.; Lenz, R. W.; Barron, A. R. *Macromolecules* **1997**, *30*, 316.
31. Vandenberg, E. J. *J. Polym. Sci.* **1960**, *47*, 486.
32. Vandenberg, E. J. U.S. Patent 3,135,705, 1964.
33. Vandenberg, E. J. U.S. Patent 3,219,591, 1965.
34. Vandenberg, E. J. *J. Polym. Sci., Part B: Polym. Lett.* **1964**, *2*, 1085.
35. Vandenberg, E. J. *J. Am. Chem. Soc.* **1961**, *83*, 3538.
36. Vandenberg, E. J. *J. Polym. Sci.* **1960**, *47*, 489.
37. Braune, W.; Okuda, J. *Angew. Chem., Int. Ed.* **2003**, *42*, 64.
38. Moore, D. R.; Cheng, M.; Lobkovsky, E. B.; Coates, G. W. *J. Am. Chem. Soc.* **2003**, *125*, 11911.
39. Tokunaga, M.; Larrow, J. F.; Kakiuchi, F.; Jacobsen, E. N. *Science* **1997**, *277*, 936.
40. Haubenstock, H.; Panchalingam, V.; Odian, G. *Makromol. Chem.* **1987**, *188*, 2789.
41. Osgan, M.; Price, C. C. *J. Polym. Sci.* **1959**, *34*, 153.
42. Kasperczyk, J.; Dworak, A.; Jedlinski, Z. *Makromol. Chem., Rapid Commun.* **1981**, *2*, 663.
43. Dworak, A.; Jedlinski, Z. *Polymer* **1980**, *21*, 93.
44. Takeda, N.; Inoue, S. *Makromol. Chem.* **1978**, *179*, 1377.
45. Aida, T.; Inoue, S. *Macromolecules* **1981**, *14*, 1166.
46. Aida, T.; Inoue, S. *Macromolecules* **1981**, *14*, 1162.
47. Vincens, V.; Le Borgne, A.; Spassky, N. *Makromol. Chem., Rapid Commun.* **1989**, *10*, 623.
48. Vincens, V.; Le Borgne, A.; Spassky, N. *Makromol. Chem., Macromol. Symp.* **1991**, *47*, 285.
49. Le Borgne, A.; Vincens, V.; Jouglard, M.; Spassky, N. *Makromol. Chem., Macromol. Symp.* **1993**, *73*, 37.
50. Matsuura, K.; Inoue, S.; Tsuruta, T. *Makromol. Chem.* **1965**, *86*, 316.
51. Kuran, W.; Listos, T.; Abramczyk, M.; Dawidek, A. *J. Macromol. Sci., Pure Appl. Chem.* **1998**, *A35*, 427.
52. Emig, N.; Nguyen, H.; Krautscheid, H.; *et al. Organometallics* **1998**, *17*, 3599.
53. Furukawa, J.; Tsuruta, T.; Sakata, R.; *et al. Makromol. Chem.* **1959**, *32*, 90.
54. Kuran, W.; Listos, T. *Macromol. Chem. Phys.* **1994**, *195*, 401.
55. Coulon, C.; Spassky, N.; Sigwalt, P. *Polymer* **1976**, *17*, 821.
56. Kassamaly, A.; Sepulchre, M.; Spassky, N. *Polym. Bull. (Berlin)* **1988**, *19*, 119.
57. Sepulchre, M.; Kassamaly, A.; Spassky, N. *Polym. Prepr. (Am. Chem. Soc., Div. Polym. Chem.)* **1990**, *31*, 91.
58. Sepulchre, M.; Kassamaly, A.; Spassky, N. *Makromol. Chem., Macromol. Symp.* **1991**, *42/43*, 489.
59. Ishimori, M.; Hagiwara, T.; Tsuruta, T.; *et al. Bull. Chem. Soc. Jpn.* **1976**, *49*, 1165.
60. Tsuruta, T. *J. Polym. Sci., Polym. Symp.* **1980**, *67*, 73.
61. Tsuruta, T. *Macrmol. Chem. Phys., Supp.* **1981**, *5*, 230.
62. Kageyama, H.; Miki, K.; Tanaka, N.; *et al. Makromol. Chem., Rapid Commun.* **1982**, *3*, 947.
63. Hasebe, Y.; Tsuruta, T. *Makromol. Chem.* **1988**, *189*, 1915.
64. Yoshino, N.; Suzuki, C.; Kobayashi, H.; Tsuruta, T. *Makromol. Chem.* **1988**, *189*, 1903.
65. Tsuruta, T. *Makromol. Chem., Macromol. Symp.* **1991**, *47*, 277.
66. Tsuruta, T.; Hasebe, Y. *Macromol. Chem. Phys.* **1994**, *195*, 427.
67. Tsuruta, T. *Makromol. Chem., Macromol. Symp.* **1986**, *6*, 23.
68. Kageyama, H.; Kai, Y.; Kasai, N.; *et al. Makromol. Chem., Rapid Commun.* **1984**, *5*, 89.
69. Hasebe, Y.; Tsuruta, T. *Makromol. Chem.* **1987**, *188*, 1403.
70. Hasebe, Y.; Izumitani, K.; Torii, M.; Tsuruta, T. *Makromol. Chem.* **1990**, *191*, 107.
71. Nozaki, K.; Nakano, K.; Hiyama, T. *J. Am. Chem. Soc.* **1999**, *121*, 11008.
72. Nakano, K.; Nozaki, K.; Hiyama, T. *Macromolecules* **2001**, *34*, 6325.
73. Cheng, M.; Darling, N. A.; Lobkovsky, E. B.; Coates, G. W. *Chem. Commun.* **2000**, 2007.
74. Nakano, K.; Nozaki, K.; Hiyama, T. *J. Am. Chem. Soc.* **2003**, *125*, 5501.
75. Tezuka, Y.; Ishimori, M.; Tsuruta, T. *Makromol. Chem.* **1983**, *184*, 895.
76. Qin, Z. Q.; Thomas, C. M.; Lee, S.; Coates, G. W. *Angew. Chem., Int. Ed.* **2003**, *42*, 5484.
77. Lu, X. B.; Wang, Y. *Angew. Chem., Int. Ed.* **2004**, *43*, 3574.

78. Lu, X.-B.; Shi, L.; Wang, Y.-M.; *et al. J. Am. Chem. Soc.* **2006**, *128*, 1664.
79. Cohen, C. T.; Coates, G. W. *J. Polym. Sci., Part A: Polym. Chem.* **2006**, *44*, 5182.
80. Cohen, C.; Thomas, C.; Peretti, K.; *et al. Dalton Trans.* **2006**, 237.
81. Peretti, K.; Ajiro, H.; Cohen, C.; *et al. J. Am. Chem. Soc.* **2005**, *127*, 11566.
82. Ajiro, H.; Peretti, K. L.; Lobkovsky, E. B.; Coates, G. W. *Dalton Trans.* **2009**, 8828.
83. Hirahata, W.; Thomas, R. M.; Lobkovsky, E. B.; Coates, G. W. *J. Am. Chem. Soc.* **2008**, *130*, 17658.
84. Thomas, R. M.; Widger, P. C. B.; Ahmed, S. M.; *et al. J. Am. Chem. Soc.* **2010**, *132*, 16520.
85. Widger, P. C. B.; Ahmed, S. M.; Hirahata, W.; *et al. Chem. Commun.* **2010**, *46*, 2935.
86. Miura, K.; Kitayama, T.; Hatada, K.; Nakata, T. *Polym. J.* **1993**, *25*, 685.
87. Schütz, C.; Dwars, T.; Schnorpfeil, C.; *et al. J. Polym. Sci., Part A: Polym. Chem.* **2007**, *45*, 3032.
88. Li, B.; Wu, G.-P.; Ren, W.-M.; *et al. J. Polym. Sci., Part A: Polym. Chem.* **2008**, *46*, 6102.

Biographical Sketches

Hiroharu Ajiro received his Bachelor's degree in 1999, Master's degree in 2001, and PhD degree in 2004 from Nagoya University under the direction of Professor Yoshio Okamoto. He received a Research Fellowship for Young Scientists of the Japan Society for the Promotion of Scientists (2003–04). In 2004–05, he was a Postdoctoral Associate with Prof. Geoffrey W. Coates at Cornell University. He joined Osaka University, the Center for Advanced Medical Engineering and Informatics, as a specially appointed lecturer in 2006. He received the CSJ Presentation Award 2010 and the Award for Encouragement of Research in Polymer Science from SPSJ in 2010.

Peter C. B. Widger received his BS degree in chemistry from the University of New Hampshire in 2006. He then went on to study polymer chemistry at Cornell University with Professor Geoffrey Coates and received his PhD degree in 2011. He is currently a researcher at E Ink Corporation.

Syud Momtaz Ahmed received his BA degree in chemistry and mathematics from Wabash College in 2007, and is currently pursuing his PhD degree in organic materials at Cornell University. His research, conducted under the supervision of Professor Geoffrey W. Coates, focuses on the development of catalysts to synthesize polyethers and polycarbonates with controlled stereo- and regiochemistry. Ahmed has been recognized with multiple awards for academic excellence, was inducted to Phi Lambda Upsilon, the national chemistry honors society, and also received an award for excellence in teaching. Aside from chemistry, he has also established himself as a respectable musician and released commercial albums under reputable music labels in his home country of Bangladesh.

Scott Allen obtained his BS degree in chemistry from Virginia Commonwealth University in 1999 and moved to Cornell University to pursue his PhD degree on the design of catalysts for epoxide/CO_2 copolymerization under the supervision of Geoffrey Coates. After receiving his PhD degree in 2004, he cofounded Novomer to commercialize catalyst technology discovered at Cornell. Currently, he is the Vice President of Catalyst Development at Novomer.

Geoffrey W. Coates received his PhD degree in organic chemistry with Robert Waymouth at Stanford University in 1994 and was an NSF Postdoctoral Fellow with Robert Grubbs at the California Institute of Technology. He joined the Cornell University faculty in 1997, where he is now the Tisch University Professor. Professor Coates has received many awards, including the A. C. Cope Scholar Award, ACS Affordable Green Chemistry Award, and the Carl S. Marvel Creative Polymer Chemistry Award. In 2011, he was identified by Thomson Reuters as one of the world's top 100 chemists on the basis of the impact of his scientific research and was inducted into the American Academy of Arts & Sciences. He is the scientific cofounder of Novomer Inc., is a member of the Editorial Board of *Dalton Transactions*, and is an Associate Editor for *Macromolecules*.

4.10 Ring-Opening Polymerization of Cyclic Acetals

P Kubisa, Polish Academy of Sciences, Lodz, Poland
JP Vairon, Université Pierre et Marie Curie, Paris, France

4.10.1 Introduction

Homogeneous polymerization of cyclic acetals had been studied mostly before the first edition of *Comprehensive Polymer Science* was published and since then there has been limited activity in this area. Therefore, the first part of this chapter is based (sometimes *in extenso*) on the chapter 'Cationic Ring-Opening Polymerization: Acetals' from the first edition.[1] There are several reviews and book chapters in which cationic polymerization of cyclic acetals (including bicyclic acetals) has been discussed.[2–12]

Important progress has been made only in the field of heterogeneous polymerization of 1,3,5-trioxane (TOX) and this subject will be treated more extensively on the basis of more recent data in the second part of this chapter.

Cyclic acetals are five- and higher-membered monomers with at least one unit in which two oxygen atoms flank an unsubstituted or substituted methylene group. The bridge connecting two acetal oxygen atoms may be either an all-carbon chain (e.g., $-(CR^1R^2)_n-$) or may contain additional heteroatoms (e.g., $-(CR^1R^2)_nX(CR^1R^2)_m-$, where X is oxygen). Some typical monomers belonging to this class are shown in **Scheme 1**.

TOX, the six-membered cyclic trimer of formaldehyde, belongs to this group but its polymerization shows several distinct features and, therefore, it will be discussed separately in the last section of this chapter.

Polyacetals were among the first synthetic polymers studied by Staudinger[13] in the 1920s. Polyformaldehydes prepared by both anionic polymerization of formaldehyde and cationic polymerization of TOX were, however, thermally unstable. Thus, they were not commercialized until the late 1950s when the reasons for the thermal instability were better understood and the stabilization methods were developed. The DuPont process, based on anionic formaldehyde polymerization, involves esterification of unstable hemiacetal end groups from which degradation starts, while in the Celanese-Hoechst process TOX is copolymerized with a few percent of

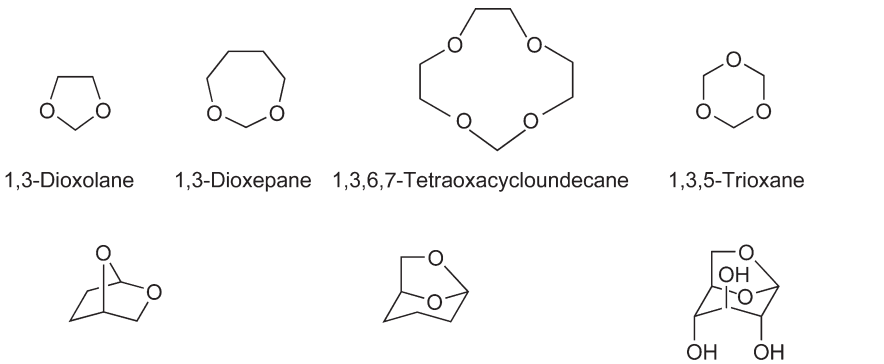

Scheme 1 Typical cyclic acetals.

comonomer, for example, ethylene oxide (EO) or 1,3-dioxolane (DXL). Randomly distributed -OCH_2CH_2- units interrupt the sequences of -OCH_2- units, which prevents depolymerization (unzipping). Polyformaldehyde (also called polytrioxane) is the only polyacetal made on an industrial scale (over 500×10^3 tons a year worldwide at the end of twentieth century).[14]

It should be noted that ring-opening polymerization of cyclic acetals is not the only route to polyacetals. Polyacetals are also formed by ionic polymerization of aldehydes,[15] by polycondensation of aldehydes and diols,[16] or by polyaddition of divinyl ethers to diols.[17–19] In this chapter, however, only cationic ring-opening polymerization of cyclic acetals will be discussed.

Cationic polymerization of cyclic acetals yields polyacetals, that is, polymers containing acetal bonds -OCR^1R^2O- in the main chain (the class name polyacetals should not be confused with the name poly(vinyl acetal)s, which is the class name for a group of polymers that are products of the reaction between poly(vinyl alcohol) and an aldehyde). Homopolymers of cyclic acetals are at the same time perfectly alternating copolymers composed of oxymethylene and oxyalkylene units, as shown for DXL polymerization in Scheme 2.

Acetal bonds appears also in some anhydrosugars. Anhydrosugars are monosaccharide derivatives that in addition to five-membered furanose ring or six-membered pyranose ring contain another oxygen-containing ring formed through elimination of water from two hydroxy groups of sugar. Anhydrosugars containing acetal bonds may have skeletons shown in Scheme 3.

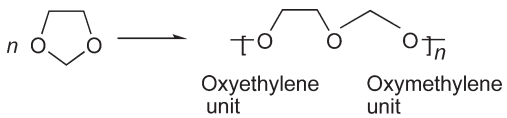

Scheme 2 Structure of the repeating unit of polyDXL.

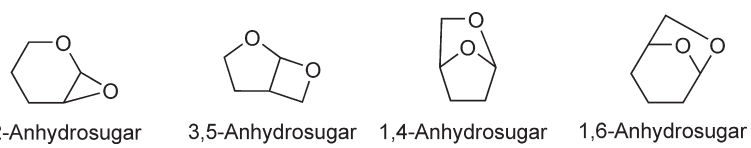

Scheme 3 Skeletons of typical anhydrosugars.

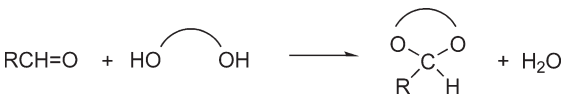

Scheme 4 Synthesis of acetals by condensation of diols with aldehydes.

The remaining hydroxy groups in anhydrosugars have to be blocked prior to polymerization.[20] Synthetic polysaccharides prepared by polymerization of the acetal ring in anhydrosugars cannot compete with inexpensive products isolated from natural sources for use on a large scale such as food additives, paper additives, adhesives, and coatings. Thus, research on synthetic polysaccharides is stimulated mainly by their potential biomedical applications. It is expected that it will be easier to meet the high requirements for standardization with synthetic products than with natural ones.

4.10.1.1 Monomers

Cyclic acetals are usually prepared by condensation of formaldehyde (conveniently in the form of paraformaldehyde or TOX) or higher aldehydes with diols in the presence of 1–2 wt.% of an acid catalyst; *p*-toluenesulfonic acid or ion-exchange resins are most frequently used for this purpose (Scheme 4).[21]

TOX, the cyclic trimer of formaldehyde, is prepared by heating aqueous solutions of formaldehyde in the presence of strong acids. Water/TOX azeotrope (~ 70% TOX) is distilled off and pure TOX is isolated. The simplest purification method involves fractionation (b.p. 115 °C), often in the presence of a solvent that forms azeotrope with water, for example, *n*-heptane.

Synthesis of bicyclic acetals is more complex; thus, for example, 6,8-dioxabicyclo[3.2.1]octane (6,8-DBO) is prepared in three steps from acrolein as shown in Scheme 5.

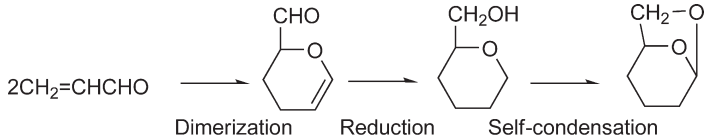

Scheme 5 Synthesis of bicyclic acetal: 6,8-dioxabicyclo[3.2.1]octane.

4.10.1.2 Polymerizability of Cyclic Acetals

Polymers are formed from the corresponding monomer when

1. polymerization is thermodynamically possible,
2. a suitable mechanism exists.

The smallest ring of a cyclic acetal contains five atoms. Ring-opening polymerization of cyclic monomers with rings composed of more than four atoms is a reversible process due to a relatively low negative ΔH_p (enthalpy of polymerization) value (Table 1) (*see* Chapter 4.02). Thus, monomer–polymer equilibrium is established, and if the equilibrium monomer concentration $[M]_e$ is higher than its starting concentration, polymerization is not possible. This is the case with the six-membered cyclic acetal 1,3-dioxane.

Cyclic acetals are weak bases and require strong acids to initiate polymerization. The acetal bond is highly reactive and is easily opened in the presence of acid catalyst; thus, cationic polymerization provides a suitable mechanism for converting a cyclic acetal into a linear polymer.

4.10.1.3 Thermodynamics of Polymerization

For reversible polymerization, two interrelated parameters characterize the system: equilibrium monomer concentration $[M]_e$ (at a given temperature) and ceiling temperature T_c (for a given initial monomer concentration $[M]_0$, usually equal to 1 mol l^{-1} or in bulk concentration). The smaller the negative ΔG° (Gibbs free energy) value, the higher the $[M]_e$ value and the lower the T_c value:

$$\Delta G^\circ = \Delta H - T\Delta S \qquad [1]$$

$$\ln\left(\frac{1}{[M]_e}\right) = \frac{-\Delta G^\circ}{RT} \qquad [2]$$

where H is enthalpy, T is temperature, S is entropy, and R is gas constant. Selected thermodynamic parameters for polymerization of cyclic acetals are listed in Table 1.

It was not always recognized in the past that in order to make polymerization of some cyclic acetals feasible, the highest possible $[M]_0$ and the lowest possible temperature should be used. This led to some unsuccessful attempts to prepare high polymers from substituted cyclic acetals. However, when suitable conditions were used, substituted cyclic acetals such as 4-phenyl-1,3-dioxolane[25] or 2-butyl-1,3,6-trioxocane[26] gave reasonably high yields of high-molecular-weight polymers.

For bicyclic (i.e., disubstituted) acetals, the thermodynamic polymerizability is usually enhanced due to additional strain introduced by the presence of the second ring; thus, for example, 6,8-DBO at concentrations of ca. 2.5 mol l^{-1} can be polymerized up to 95% conversion at −78 °C in CH_2Cl_2, which means that $[M]_e < 1.25 \times 10^{-1}$ mol l^{-1} under these conditions.[27]

The influence of the additional strain on the thermodynamic polymerizability may be illustrated by the polymerization of 7,9-dioxabicyclo[4.3.0]nonane. *Trans*-monomer gives high-molecular-weight polymer in high yield while under the same conditions *cis*-monomer gives only a cyclic dimer (Scheme 6).[28]

In some instances, the excess strain can even lead to the opening of the six-membered ring instead of the five-membered one. Thus, 2,7-dioxabicyclo[2.2.1]heptane, in which the six-membered ring is forced into an unfavorable boat conformation, gives polymers containing both five- and six-membered rings (Scheme 7).[10]

The thermodynamics of TOX polymerization, studied extensively by Enikolopyan and reviewed recently in a book by Berlin *et al.*[29] entitled *Polyoxymethylenes* (in Russian), is more complex. This is due to the fact that propagation proceeds simultaneously with phase transition; phase transition of the monomer molecule from liquid phase to crystalline phase occurs simultaneously with its incorporation into a polymer chain. Thus, the overall Gibbs free energy (ΔG°) for the propagation step is the sum of the energy changes associated with chemical reaction and phase transition. Consequently, equilibrium is shifted more toward polymer and TOX

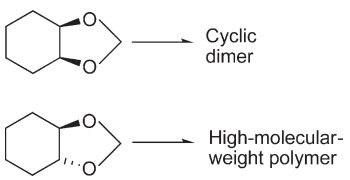

Scheme 6 Polymerization of cis- and trans-7,9-dioxabicyclo[4.3.0] nonane.

Table 1 Thermodynamic parameters of homogeneous polymerization of unsubstituted cyclic acetals in CH_2Cl_2 solution

Monomer	ΔH^o (kJ mol^{-1})	ΔS^o (J mol^{-1} K^{-1})	T_c (°C) for $[M]_0$ = 1 mol l^{-1}	*References*
DXL	−21.7	−77.7	1	22
1,3-Dioxepane	−15.0	−48.1	27	22
1,3,5-Trioxepane	−6.9	−31.5		23
1,3,6-Trioxocane	−16.7	−34.3		23
1,3,6,9-Tetraoxa-cycloundecane	−13.4	−13.0		24

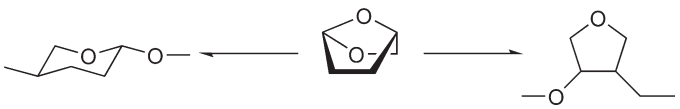

Scheme 7 Repeating units containing either 6-membered or 5-memebered ring formed in the polymerization of bicyclic acetal: 2.7-dioxabicyclo[2.2.1.] heptane.

(six-membered ring of low strain) can be polymerized with high conversions.

The thermodynamics of trioxane polymerization is discussed in more detail in the chapter on Thermodynamic and Kinetic Polymerizability (Chapter 4.02) (by S. Penczek and K. Kałużyński).

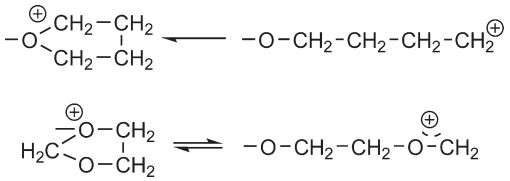

Scheme 9 Unimolecular opening of oxonium ion in the cationic polymerization of cyclic ether (THF) and cyclic acetal (DXL).

4.10.2 Mechanism of Homogeneous Polymerization of Cyclic Acetals

4.10.2.1 General Considerations

Although the chemistry of acetal and ether bonds is quite different, cyclic acetals bear some resemblance to cyclic ethers; thus the polymerization of both groups of monomers shows some similarities. Essentially the same groups of initiators that initiate cationic polymerization of cyclic ethers (i.e., strong protonic acids, Lewis acids, or oxonium, carbenium, or oxocarbenium salts) are also effective in the polymerization of cyclic acetals. On the other hand, there are distinct differences.

An acetal group readily participates in hydride transfer reactions because the resulting carboxonium ion is stabilized by electron pairs of the two neighboring oxygen atoms. Thus if compounds capable of acting as hydride ion acceptors, such as (triphenylmethyl)carbenium ions, are used as initiators, initiation of DXL polymerization proceeds through intermediate 1,3-dioxolan-2-ylium ion, which is a real initiator, as shown in Scheme 8.[30,31]

The presence of two oxygen atoms in an acetal bond raises also the question of the nature of active species and the mechanism of propagation. It is generally accepted that active species in the cationic polymerization of cyclic ethers are oxonium ions and propagation proceeds by S_N2 mechanism as an attack of oxygen atom of monomer molecule on α-carbon atom in cyclic oxonium ion (for active chain end (ACE)-type polymerization). An alternative pathway involving unimolecular opening of oxonium ion ring with formation of carbenium ion and subsequent reaction of this ion with monomer is excluded because conversion of relatively stable oxonium ion to highly reactive primary carbenium ion would be energetically very unfavorable. However, the situation is different in the cationic polymerization of cyclic acetals because unimolecular opening of oxonium ion ring generates stabilized carboxonium ion as shown in Scheme 9.

There was a long-lasting controversy concerning the participation of both types of ions in propagation. By studying a suitable model system it was eventually shown that carboxonium ions do exist in equilibrium although at typical polymerization conditions their fraction is low (< 0.1% of all ionic species, depending however on conditions such as temperature and solvent). In spite of low concentration of carboxonium ions their role in propagation is not negligible because the rate constant of propagation on carboxonium species is 2 orders of magnitude higher than the rate constant of propagation on an oxonium ion active species.[32]

In contrast to tetrahydrofuran (THF) polymerization, where chain transfer to polymer is slow compared to propagation, in the polymerization of cyclic acetals chain transfer to polymer is fast compared to propagation. Intramolecular chain transfer to polymer leads to the formation of a cyclic fraction. It was shown that cyclic oligomers are always formed in the cationic polymerization of DXL and this observation even led to the hypothesis that polymerization proceeds by ring-expansion mechanism and polymers are exclusively cyclic.[33] Detailed studies of this system revealed, however, that in the polymerization initiated with Lewis acids the content and distribution of the cyclic oligomer fraction agree well with those predicted by the Jacobson–Stockmayer (J-S) theory based on equilibrium between linear and cyclic macromolecules.[34]

In the polymerization initiated with protic acids, cyclic oligomers may be formed not only by random backbiting (i.e., according to the J-S theory) but also by end-to-end coupling. This type of initiation introduces the HO- head group,

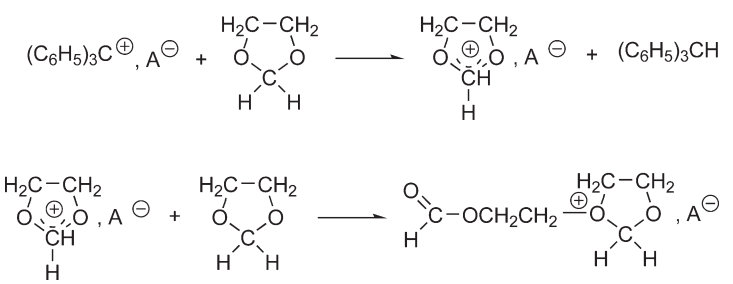

Scheme 8 Initiation of DXL polymerization via intermediate formation of 1,3-dioxolan-2-ylium cation.

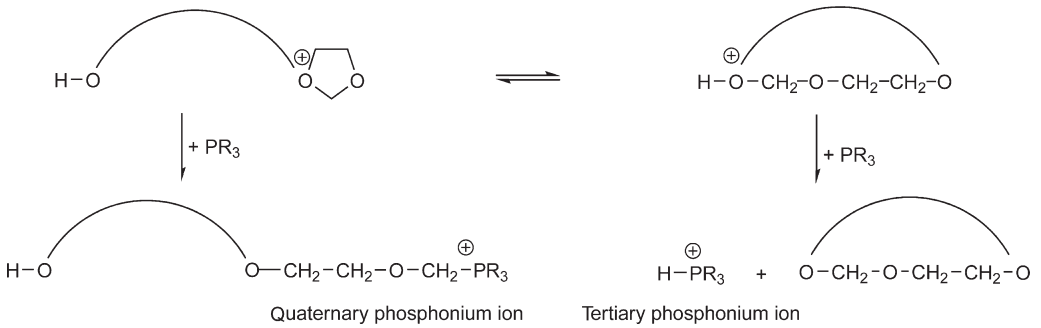

Scheme 10 Phosphine ion-trapping in the cationic polymerization of DXL.

which is considerably more nucleophilic than acetal oxygen atoms along the chain. Thus especially at the early stages, when relatively short chains can easily assume conformation in which HO- head group and tertiary oxonium ion at the end of a macromolecule are in close proximity, end-to-end closure may be favored over random backbiting, leading to kinetic enhancement in macrocycles. With increasing chain length this effect disappears as shown for cationic polymerization of 1,3,6,9-tetraoxacycloundecane (triethylene glycol formal).[35]

In the polymerization of DXL, using the phosphine end-capping method (the principle of the method is outlined in Scheme 10), it was shown that secondary oxonium ions exist in equilibrium with tertiary ones and the position of equilibrium is shifted toward tertiary oxonium ions with increasing chain length.[36]

The major conclusions stemming from these studies are the following:

- both tertiary oxonium ions and secondary oxonium ions (i.e., 'protons') are present in the system; therefore, propagation can take place on the linear active macromolecules (this is not excluding propagation on the cyclic ones);
- the proportion of tertiary oxonium ions on linear macromolecules is higher for longer chains, as can be expected.

4.10.2.2 Initiation

Cyclic acetals polymerize almost exclusively by a cationic mechanism. Most typical cationic initiators will initiate polymerization of cyclic acetals. Examples are (1) strong protonic acids, for example, $HClO_4$ and CF_3SO_2OH and their derivatives, esters (CF_3SO_2OR), anhydrides [$(CF_3SO_2)_2O$] but also tungsten or molybdenum heteropolyacids, for example, $H_3PMo_{12}O_{40}$; (2) organic salts: carbenium, for example, $Ph_3C^+A^-$, oxonium, for example, $Et_3O^+A^-$, or oxycarbenium, for example, $PhCO^+A^-$; and (3) Lewis acids (Friedel–Crafts catalysts), for example, BF_3, $SbCl_5$, and PF_5, and their complexes with, for example, ethers.

The (co)polymerization of TOX can also be mediated by transition metal complexes, for example, molybdenum or palladium.[37,38]

4.10.2.2.1 Influence of the counterion structure

Organic cations (carbenium, carboxonium, oxycarbenium, and oxonium) are coupled with complex counterions of MX^-_{n+1} type, for example, SbF_6^-, $SbCl_6^-$, or BF_4^-, or with noncomplex counterions, for example, ClO_4^- or $CF_3SO_2O^-$. It has been shown for DXL polymerization that only those initiators that contain the most stable and the least nucleophilic counterions, such as SbF_6^- and AsF_6^-, lead to the quantitative formation of stable active species.[39–41]

The unstable $SbCl_6^-$ and BF_4^- counterions, due to their fragmentation, give rise to side reactions, resulting in incomplete initiation and a decrease in active species concentration.

The fragmentation of counterions and the resulting decay of active species have been studied in detail for DXL polymerization in the presence of $SbCl_6^-$.[31]

Noncomplex counterions, derived from protonic acids (e.g., ClO_4^- or $CF_3SO_2O^-$), react with active species, forming covalent esters. However, this reaction being reversible does not lead to irreversible termination of the polymer chain:

$$-OCH_2^+ + CF_3SO_2O^- \rightleftharpoons CF_3SO_2OCH_2O- \qquad [3]$$

In eqn [5] and subsequent reaction schemes, ionic active species are shown for simplicity in the form of alkoxycarbenium (carboxonium) ions, although in reality a large majority of active species exist in the form of oxonium ions. There are several types of oxonium ions coexisting in the system (see Section 4.10.2.3.1) and, due to their multiplicity, schematic representation is difficult.

For DXL and 1,3-dioxepane (DXP) polymerizations initiated with $(CF_3SO_2)_2O$, the degree of polymerization is given by

$$DP_n = \frac{[M]_0 - [M]_e}{[(CF_3SO_2)_2O]_0} \qquad [4]$$

Equation [4] indicates that the number of growing macromolecules is equal to the number of initiator molecules used. Some representative data are given in Table 2.[42]

The overall rates of polymerization are ca. 10^2 times lower than the polymerization rates initiated with $PhCO^+SbF_6^-$. This indicates that active species exist predominantly in the form of

Table 2 Calculated and measured molecular weights in the polymerization of DXL and DXP initiated with $(CF_3SO_2)_2O$[42]

Monomer	M_n *calculated*	M_n *found (membrane osmometry)*
DXL	19 350	18 250
	21 300	21 100
	35 000	44 500
DXP	13 250	10 700
	55 600	57 100
	76 500	78 000

$[M]_0 = 1–3$ mol l^{-1}, $[(CF_3SO_2)_2O]_0 = 10^{-3}–10^{-2}$ mol l^{-1}, CH_2Cl_2, –50 to –78 °C.

less reactive covalent species. However, the agreement between the observed and calculated molecular weights clearly shows that there is an efficient exchange between covalent (dormant) and active ionic species.

4.10.2.2.2 Addition versus hydride transfer

The first fast step in initiation is the protonation or alkylation (acylation) of the monomer molecules. This leads to the formation of secondary or tertiary oxonium ions, as shown for DXL in Scheme 11.

The subsequent slower step involves nucleophilic attack of another monomer molecule, leading to the ring opening and formation of active species (Scheme 12).

Initiation proceeds according to Scheme 12 for the majority of initiators used, although the rate of initiation depends on the nature of R. In the polymerization of DXL initiated with $Et_3O^+SbF_6^-$ and $PhCO^+SbF_6^-$, the corresponding initiator fragments are incorporated quantitatively as the end groups.[40]

For some initiators, however, an alternative route of initiation is possible. For triphenylmethylium (tritylium) salts, the preinitiation step is highly reversible (Scheme 13).[43]

The equilibrium constant of this reaction is equal to $K = 3.2 \times 10^{-2}\,mol^{-1}\,l$ (CH_2Cl_2, 25 °C).[43] Thus, under typical polymerization conditions, a significant amount of carbenium ions exists in equilibrium and they participate in hydride transfer reactions. Carbenium ions are efficient hydride ion (H^-) acceptors. This reaction is relatively fast ($k = 8.3 \times 10^{-3}\,mol^{-1}\,l\,s^{-1}$, CH_2Cl_2, 25 °C), while an attack of another monomer molecule on an oxonium ion is apparently slow. Thus, instead of simple initiation by addition, as shown in Scheme 13, hydride transfer takes place and 1,3-dioxolan-2-ylium salt and triphenylmethane are formed quantitatively as shown in Scheme 8. 1,3-Dioxolan-2-ylium salts, which are relatively stable and can be isolated as pure crystalline compounds, are thus the true initiators, formed *in situ* in the DXL-$Ph_3C^+A^-$ system.

4.10.2.2.3 Friedel–Crafts-type initiators: Direct initiation versus coinitiation

The mechanism of initiation with Friedel–Crafts-type initiators is generally obscure. For BF_3, the most commonly used initiator of this type, two mechanisms, namely direct initiation and initiation by coinitiator (e.g., water present as impurity), have been proposed (Scheme 14).[44]

For polymerization of TOX in media of low polarity, it has been shown that in a rigorously dried system BF_3 alone is not able to initiate polymerization. There are, however, some indirect indications that in polar solvents such as nitrobenzene, which facilitate charge separation and formation of zwitterions, initiation may proceed even in the absence of a coinitiator.[45]

A mechanism of direct initiation, involving the formation of a zwitterion, has been proposed for polymerization of the bicyclic monomer 1,6-anhydro-2,3,4-tri-*O*-benzyl-β-D-glucopyranose initiated with PF_5. All the proposed species, for

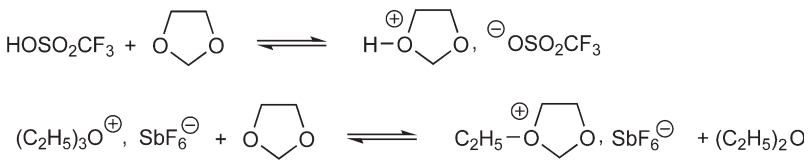

Scheme 11 Formation of oxonium ions in the initiation of cationic polymerization of DXL.

Scheme 12 Nucleophilic attack of DXL molecule on the oxonium ion formed in initiation reaction.

Scheme 13 Reversible addition of DXL to triphenylmethylium salt.

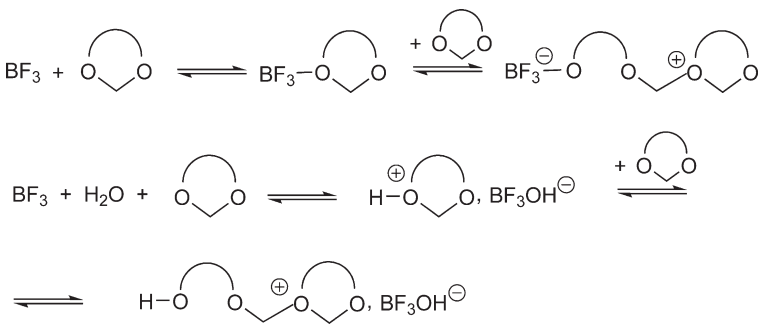

Scheme 14 Two possible mechanisms of initiation of cationic polymerization of cyclic acetals by BF_3.

example, $PF_5{}^-O<$, PF_4O^-, and PF_6^-, were identified on the basis of ^{31}P and ^{19}F nuclear magnetic resonance (NMR) spectra. In addition, formation of POF_3 was observed, indicating that terminal $-CH_2-OPF_4$ groups undergo decomposition to $-CH_2F$ and POF_3.[46] This reaction path is similar to the one observed for the THF/PF_5 system.[47]

It may be concluded that unlike protonic acids and organic salts, which under suitable conditions give clean quantitative initiation, Friedel–Crafts-type initiators lead to poorly defined systems. The efficiency of initiation, structure of counterions, and the structure of end groups are generally not known with any certainty for these initiators. The overall polymerization rates are usually lower than with other initiators, indicating the low efficiency of initiation.

4.10.2.3 Propagation

4.10.2.3.1 Structure of active species

4.10.2.3.1(i) Oxonium–alkoxycarbenium ion equilibria

The simplest structure of active species in the polymerization of cyclic acetals, by analogy with the polymerization of other heterocyclic monomers, is an oxonium ion holding the monomer molecule (Scheme 15).

Already in the 1960s–1970s it was assumed, but not proven, that these species may coexist in equilibrium with carbenium (carboxonium) ion species.[48–51] Later studies of the model systems have revealed that indeed oxonium ions coexist in equilibrium with their alkoxycarbenium counterparts, in which the positive charge is delocalized between the carbon and α-oxygen atoms (Scheme 16).[32]

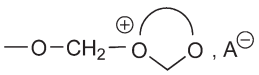

Scheme 15 Structure of oxonium ion in the cationic polymerization of cyclic acetals.

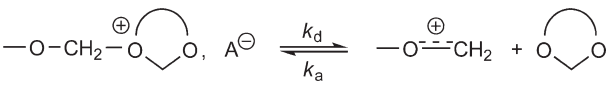

Scheme 16 Oxonium-carboxonium ion equilibrium in the cationic polymerization of cyclic acetals.

Equilibrium constants for the model reaction between methoxymethylium cation and dimethoxymethane (simple linear model of acetal) have been determined by dynamic ^1H NMR studies and were found to be $K_{ea} = k_a/k_d = 3 \times 10^3\ mol\,l^{-1}$ (SO_2, −70 °C).[32] This value indicates that active species in cyclic acetal polymerization exist predominantly in the form of oxonium ions, although a small proportion exist in the form of alkoxycarbenium ions.

4.10.2.3.1(ii) Structure of oxonium active species

The rate constants for formation (k_a) and dissociation (k_d) of oxonium ions are high: $k_a = 2 \times 10^6\ mol^{-1}\,l\,s^{-1}$ and $k_d = 6.7 \times 10^2\ s^{-1}$ (SO_2, −70 °C). Thus, the system is in a fast dynamic equilibrium. This leads to very fast isomerization of oxonium active species, proceeding via alkoxycarbenium ions.

When DXL was used instead of dimethoxymethane in the studies of equilibria, it was observed by ^1H NMR that the predominant structure was not the five-membered ring oxonium ion but the corresponding cyclic ion involving the seven-membered ring (Scheme 17).

The ratio of equilibrium constants K_7 and K_5, corresponding to the ratio of concentrations of seven-membered oxonium ions to five-membered ones, is equal to 3×10^2.

When the six-membered (1,3-dioxane) or the seven-membered (DXP) cyclic acetals were used in the studies of related equilibria, isomerization to the expanded ring structures (eight- or nine-membered, respectively) was negligible because the starting rings were less strained than the expanded ones.[52] All these reactions proceed with high rates; therefore, at any stage of polymerization, the equilibrium between alkoxycarbenium ions and various cyclic (formed by intramolecular reaction) and branched (formed by intermolecular reaction) oxonium ions is quickly established (Scheme 18).

4.10.2.3.1(iii) Secondary versus tertiary oxonium ions

Polymerization of cyclic acetals initiated with protonic acids may lead to kinetic enhancement in macrocycles. This effect is due to the efficient end-to-end cyclization of the short growing macromolecules (Scheme 19).

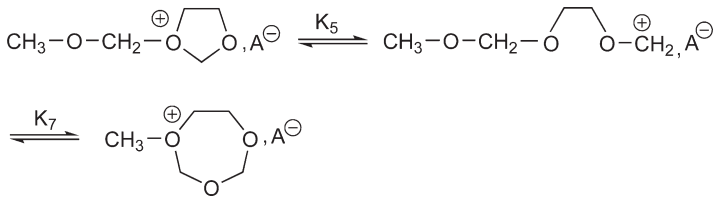

Scheme 17 Formation of seven-membered oxonium ion in the cationic polymerization of DXL.

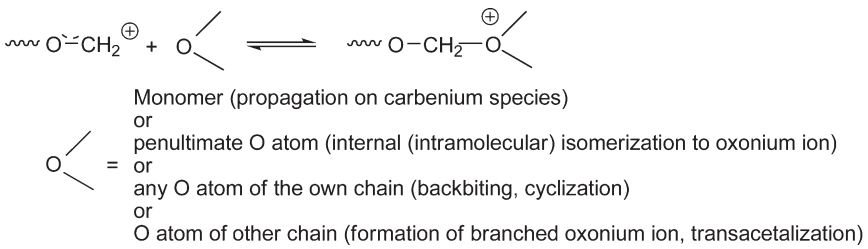

Scheme 18 Equilibria between alkoxycarbenium ions and cyclic or branched oxonium ions.

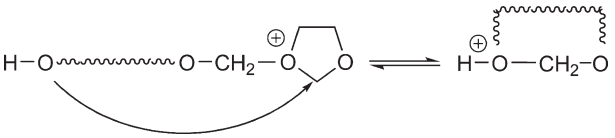

Scheme 19 End-to-end cyclization in the cationic polymerization of DXL.

Thus, tertiary oxonium ion active species are converted to secondary oxonium ions in this process. These equilibria have been studied by ion-trapping methods for the polymerization of DXL initiated with $HOSO_2CF_3$. The principle of the method is shown in Scheme 10.[36] Analysis of ^{31}P NMR spectra, based on the different chemical shifts of the tertiary ($\delta = 11.9$ ppm) and quaternary ($\delta = 31.4$ ppm) phosphonium ions, allows the determination of the relative concentrations of the secondary and tertiary oxonium ions. It was shown that in agreement with the end-to-end cyclization scheme, the concentration of the secondary oxonium ions is high for short growing chains, but decreases gradually with increasing chain length. This conclusion was later confirmed by studies of the ^1H NMR spectra of the same system. Protons in HO- end groups and H-O$^+$ < species exchange fast, giving one narrow signal. The averaged chemical shift of this signal allows determination of the relative contribution of both species.[53]

These observations prove that secondary oxonium ions are indeed formed by end-to-end cyclization, as shown in Scheme 19.

4.10.2.3.2 Reactivity of active species

It follows from the preceding discussion that in the polymerization of cyclic acetals (at least DXL) small but definite concentrations of alkoxycarbenium active species exist in equilibrium with oxonium active species. The equilibrium constant, measured for a model system, indicates that alkoxycarbenium ions constitute ca. 10^{-2}% of all active species in the polymerization of DXL at −78 °C in CH_2Cl_2. This proportion may vary substantially with the conditions applied and, of course, depends on the structure of the monomer. To estimate to what extent the alkoxycarbenium ions participate in propagation, the rate constants of model reactions have been measured (Scheme 20).

The corresponding values, determined using dynamic NMR line broadening, are $k_{oc} = 2 \times 10^6\ mol^{-1}\,l\,s^{-1}$ and $k_{ox} = 1.9 \times 10^4\ mol^{-1}\,l\,s^{-1}$ (both in SO_2 at −70 °C).[32] Thus, oxonium ions are only ca. 10^2 times less reactive than alkoxycarbenium species. Since the ratio of concentrations is ca. 10^4, it may be concluded that propagation proceeds predominantly on the oxonium ions.

4.10.2.4 Transfer and Termination

4.10.2.4.1 Chain transfer to polymer – transacetalization

Intermolecular chain transfer to polymer is well documented in the cationic polymerization of cyclic acetals. In the polymerization of TOX, as will be discussed in Section 4.10.3, chain transfer to polymer is essential for the preparation of thermally stable polyacetal. Intermolecular chain transfer to polymer is detrimental to the synthesis of monofunctional polymers such as macromonomers because segment exchange (scrambling) leads to disproportionation and formation of products having two, one, and none of the functional groups (Scheme 21).[54,55]

Intermolecular chain transfer to polymer prohibits also the synthesis of block copolymers by sequential polymerization of two cyclic acetals. Addition of DXP to a solution of living polyDXL resulted in further polymerization but the copolymer formed had a nearly statistical distribution of units.[42]

Chain transfer to polymer in cyclic acetal polymerization is a special case of transacetalization reaction which is well known in organic chemistry. By studying the model system it was found that in a mixture of DXL with alcohols in the presence of an acid, fast equilibration occurs as shown in Scheme 22.[56]

Active species in the polymerization of cyclic acetals undergo fast isomerization. This results in chain transfer to polymer, that is, formation (by intramolecular reaction) of cyclic structures or formation (by intermolecular reaction) of branched oxonium ions, followed by exchange of the linear fragments of the chain (transacetalization) (cf. Scheme 18).

Chain transfer to polymer is facilitated by the higher basicity of oxygen atoms in the polymer chain than in the monomer molecule; this is a general feature of polyacetals. Backbiting (and/or end-biting) leads to the formation of macrocycles. Formation of branched structures results in transacetalization (also called scrambling). In branched ions, two (or all three for TOX) of the bonds between carbon and oxygen atoms bearing the positive charge are identical. Further reaction of branched oxonium ions may thus lead to redistribution of polymer segments, as shown in Scheme 23 for TOX polymerization.

This reaction, which is fast, results in continuous transfer of the monomer units or longer sequences between the chains.

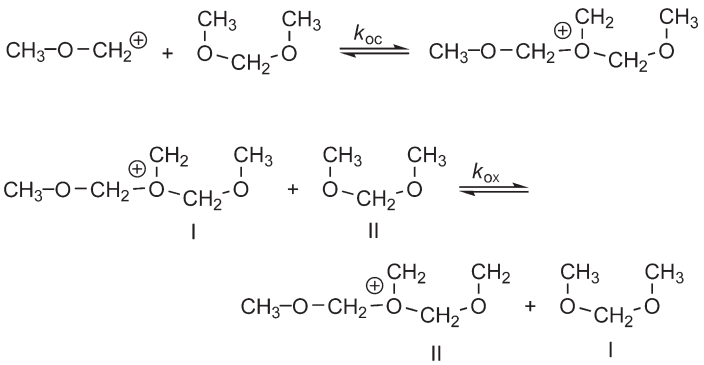

Scheme 20 Model reaction of alkoxycarbenium ions with acetals.

Scheme 21 Disproportionation of end-groups by intermolecular chain transfer to polymer.

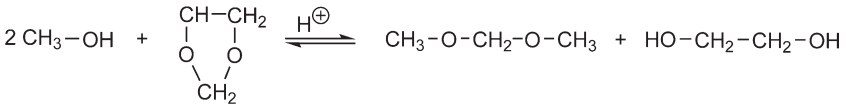

Scheme 22 Equilibration of a mixture of DXL with alcohol in the presence of acid.

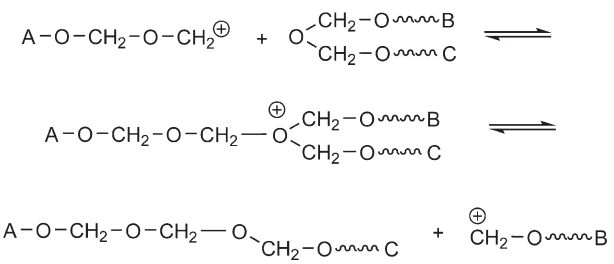

Scheme 23 Redistribution of segments by intermolecular chain transfer to polymer in the cationic polymerization of TOX.

Thus, when sequential polymerization of cyclic acetals was performed by introducing DXP into a solution of living polyDXL or vice versa, the copolymer isolated after longer reaction times showed DXL-DXL/DXL-DXP/DXP-DXP dyad distribution (determined by ^{13}C NMR) in ratios of 1:2:1, characteristic of random copolymers. When copolymerization was terminated after shorter reaction times, the proportion of heterodyads was lower, but at no stage of copolymerization could pure block copolymer be isolated.[42]

Transacetalization plays an important role in the copolymerization of TOX and DXL.[57] In these systems, due to the different reactivities of both comonomers, DXL polymerizes first. Therefore, at the early stages of polymerization, the soluble polymer, consisting essentially of DXL units, is formed. Nevertheless, the distribution of DXL units in the final product is close to random. This indicates that the originally formed polyDXL blocks undergo further fast and efficient scrambling. Thus, due to the transacetalization, thermally stable polymers containing randomly distributed oxyethylene units derived from DXL are formed. A small amount of the unstable fraction (< 5%) corresponds to oxymethylene units at the end of the chain. This fraction is removed by heating before processing the polymer (see Section 4.10.3).

4.10.2.4.2 Termination

In the absence of impurities, and when stable counterions (SbF_6^-, AsF_6^-, $OSO_2CF_3^-$) are used, polymerization of simple cyclic acetals, namely DXL and DXP, proceeds without termination at least within the time needed to reach equilibrium. It has been shown (Table 2) that molecular weights in these systems are described by eqn [4] and the only end groups, identified quantitatively, are those coming from initiator and intentionally added terminating agent. It has to be remembered, however, that eventually, due to the presence of carboxonium ions in equilibrium with oxonium ions (cf. Scheme 16), hydride transfer reaction from monomer molecule to carboxonium ion may lead to the formation of macromolecules terminated with $-OCH_3$ groups while the 1,3-dioxolan-2-ylium cation may start a new chain (cf. Scheme 8). Also in the polymerization of TOX, hydride transfer to apparently living active species has been observed even several hours after equilibrium conversion of monomer had been reached. Some of this long-lived species may, however, become unavailable for propagation as a result of occlusion within the polymer particles.[57,58]

4.10.2.5 Formation of Cyclic Oligomers

4.10.2.5.1 Backbiting

Chain transfer to polymer leads to the formation of macrocyclic oxonium ions, which on further reaction may release a cyclic fragment (Scheme 24).

A thermodynamic approach to the ring-chain equilibria has been developed by Jacobson and Stockmayer (J-S theory),

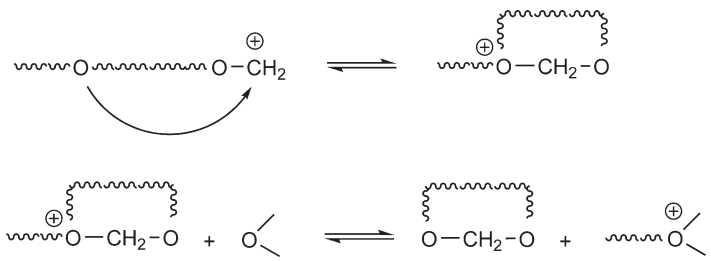

Scheme 24 Intermolecular chain transfer to polymer leading to formation of cyclic fraction in the cationic polymerization of cyclic acetals.

discussed in more detail in the pertinent chapter of this volume. According to this approach, the concentration of each cyclic oligomer in equilibrium with a linear chain is related to the probability of the required conformation of linear chain being achieved and can be calculated using the rotational isomeric state model.

For DXL polymerization, these 'theoretical' equilibrium concentrations of cyclic oligomers have been calculated and compared with the values measured for real systems by gas–liquid chromatography (GLC).[34] The experimental curve shows a typical deviation from theory for oligomers with $n = 2$–4, which are still strained. (J-S theory is valid only for the strainless rings.)

DXL and macrocyclic formals are the only cyclic acetals for which cyclization has been studied quantitatively.[24,34,59] The formation of cyclic fraction may, however, be expected in the polymerization of any cyclic acetal. It has been indicated that cyclic oligomers are formed in the polymerization of TOX. Nonstabilized homopolymer always contains some amount (up to 25%) of a stable fraction,[58] which, at least partially, is assumed to be cyclic (instability is related to the hemiacetal groups, which are absent in cyclic macromolecules). Cyclic oligomers are also believed to be responsible for the bimodal molecular weight distribution observed by GPC.[60]

4.10.2.5.2 End-to-end cyclization

It has been shown that in certain systems, for example, in the protonic acid-initiated polymerization of DXL[36] or 1,3,6,9-tetraoxacycloundecane,[35] end-to-end cyclization may dominate over random backbiting at the early stages of polymerization, that is, when the growing chains are still relatively short (Scheme 25).

This leads to kinetic enhancement of cyclic macromolecules. This means that at the early stages of polymerization the concentration of a given cyclic oligomer is higher than when the final equilibrium is attained. This results from the contribution of the end groups of short chains, which essentially vanish when the high polymer is finally formed. Thus, the concentration of small cyclics grows, goes through a maximum when the end-to-end cyclization aids their formation most, and then decreases with increasing chain length, falling to the equilibrium concentration.

4.10.2.5.3 Proportions of cyclic and linear fractions

Reactions involving polyacetal chains, including intramolecular reactions, are fast compared to propagation, resulting in the simultaneous formation of macrocycles and linear polymers.

Therefore, the preparation of purely linear polymers is virtually impossible. The equilibrium concentration of individual cyclic oligomers is, however, not very high (ca. 10^{-2} mol l^{-1} for the cyclic dimer and similar values for oligomers with $n = 3$–5 in DXL polymerization).[34] The sum of the thus-calculated equilibrium concentrations of cyclics from $n = 2$ to infinity gives a relatively high value, 0.85 mol l^{-1}, for DXL polymerization. The actual measured values are somewhat lower than the calculated ones; thus the value 0.85 mol l^{-1} should be taken as an upper limit. The concentration of DXL in bulk equals 12.75 mol l^{-1} (at 25 °C). Thus, the lowest proportion of cyclic oligomers, starting from dimer, that can be attained for this monomer is close to 7.5 wt.%.

The fraction of cyclic oligomers at equilibrium is expressed as

$$f = \frac{\sum[\text{monomer units in cyclics}]}{[\text{monomer}]_0 - [\text{monomer}]_e} \quad [5]$$

Thus at low $[M]_0$, polyacetals at equilibrium may contain a considerably high proportion of the cyclic fraction. At the conditions when eqn [6] holds, almost all of the polymer can be cyclic.

$$\sum[\text{monomer units in cyclics}] > [\text{monomer}]_0 - [\text{monomer}]_e \quad [6]$$

Some authors observed almost exclusively cyclic polymers and concluded, without considering the consequences of the J-S theory, that the chain growth must proceed by ring expansion.[33] With our present knowledge of the mechanism of cyclization however, all experimental observations can be interpreted in terms of the conventional propagation mechanism (involving linear active species) coupled with backbiting and/or end-to-end cyclization.

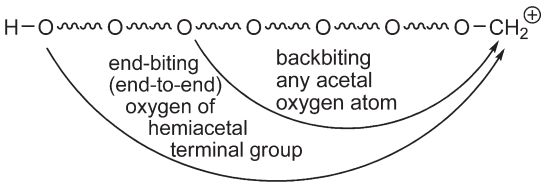

Scheme 25 End-to-end cyclization and back-biting in the cationic polymerization of cyclic acetals.

4.10.2.6 Bicyclic Acetals

The acetal bond appears in some anhydrosugars. Anhydrosugars are monosaccharide derivatives that in addition to five-membered furanose ring or six-membered pyranose ring contain another oxygen-containing ring formed through elimination of water from two hydroxy groups of sugar. Anhydrosugars containing acetal bonds may have skeletons shown in Scheme 26.

The bicyclic acetal, 6,8-DBO, possesses the structural skeleton of the 1,6-anhydrosugars and, because it is readily prepared from acrolein dimer, its cationic polymerization has been investigated. Mostly Lewis acids (BF_3, PF_5) were used as initiators, and at low temperature (−78 °C) polymers with M_n up to 10^5 could be obtained although dispersity was broad.[61–63]

Better control over molecular weights and dispersity was obtained using the 2-chloroethyl isobutyl ether/ZnI_2 initiating system. At −16 °C, the molecular weight increased linearly with conversion up to $M_n \sim 5 \times 10^3$ and dispersity was relatively low ($M_w/M_n \sim 1.3$).[64] In anhydrosugars, the ring is formed by condensation of two hydroxy groups, and the remaining hydroxy groups have to be blocked before polymerization.[65,66]

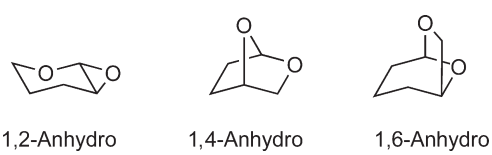

Scheme 26 Skeletons of typical anhydrosugars containing acetal bonds.

Cationic polymerization of anhydrosugars has been reviewed[20,67] and since then there has been little activity in this area. More recent studies revealed, however, that cationic polymerization of anhydrosugars displayed many of the elements of controlled polymerization: a linear increase in molecular weights with conversion and block copolymer formation.

In the polymerization of 1,4-anhydrosugar with blocked hydroxy groups initiated with $BF_3 \cdot Et_2O$, a linear increase in molecular weight with conversion was observed although dispersity was not narrow ($M_w/M_n \sim 1.6–1.7$). Block copolymers composed of two different polysaccharides could be obtained in sequential polymerization.[68]

Cationic polymerization of 1,6-anhydrosugar with blocked hydroxy groups initiated by the cumyl chloride (2-chloro-2-phenylpropane)/ZnI_2 initiating system gave polysaccharides with relatively low dispersity ($M_w/M_n \sim 1.25$). The kinetic plots of ln[M] versus time were linear and a linear increase in M_n with conversion was observed at least up to $M_n \sim 6 \times 10^3$. There was evidence of slow chain transfer at these polymerization temperatures, although a majority of polymer chains contained the initiator fragment. The authors concluded that through a proper combination of monomer structure, protecting groups, and initiators, other anhydrosugars may be polymerized with control over the molecular weights and end-group structures.[69]

There are also reports on the cationic polymerization of anhydrosugars having free hydroxy groups. Anhydrosugars shown in Scheme 27 were polymerized at high temperatures (>130 °C) with sulfonium salts as initiators to highly branched polysaccharides with M_w in the range between 3×10^4 and 8×10^4.

The presence of branched units, as confirmed by ^{13}C NMR analysis, indicates that free HO groups participate in propagation.[70,71]

4.10.2.6.1 Stereochemistry of polymerization

Unsubstituted monocyclic acetals (symmetrical molecules) are not suitable for studies of the stereochemistry of polymerization. Because there are no reliable data on the stereochemistry of polymerization of the substituted monocyclic acetals, the only available information relating to the steric course of polymerization comes from studies of bicyclic acetals. This subject has been reviewed.[72]

For polymerization of 6,8-DBO, it has been shown that at −78 °C inversion of configuration occurs in nearly 100%. This result is in full agreement with the oxonium ion mechanism involving S_N2 substitution and an attack of the incoming monomer molecule from the 'opposite' side, along the carbon–oxygen bond as shown in Scheme 28.

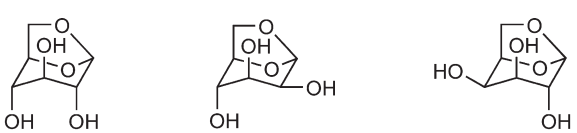

Scheme 27 Anhydrosugars containing free hydroxyl groups that have been polymerized by cationic mechanism.

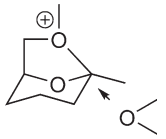

Scheme 28 Direction of nucleophilic attack leading to inversion of configuration in cationic polymerization of bicyclic acetal.

At higher temperatures, the stereospecificity of reaction is lower. It has been argued, however, that this effect is only apparent, that is, propagation proceeds with inversion of configuration, while racemization is due to the side reactions involving polymer chains (transacetalization).

The steric course of polymerization of anhydrosugars depends on the size of the fused rings.[65,66] Thus, for polymerization of 1,2- and 1,4-anhydrosugars, racemization has been observed and explained by participation of alkoxycarbenium ions in the propagation step (e.g., for 1,2-anhydrosugars, see Scheme 29).

1,6-Anhydrosugars, which have a 6,8-DBO skeleton, polymerize mainly with inversion of configuration; thus α-monomers give β-polymers and vice versa. For example, 1,6-anhydro-2,3,4-tri-*O*-benzyl-β-D-glucose (Scheme 30) polymerizes at −60 °C in CH_2Cl_2 with PF_5 initiator (1 mol.%) to give a high-molecular-weight polymer (M_n up to 7×10^5) in 50% yield. The polymer, after debenzylation, has a specific rotation up to 197° and is identical to a naturally occurring polysaccharide (dextran) for which a highly specific α-structure has been established.[73] Natural dextran has $[\alpha]_D^{25}$ values between + 196° and + 199°.

For the polymerization of 6,8-DBO, it has also been shown that stereoselection operates to some extent. Thus, polymer formed from racemic monomer is enriched in isotactic dyads (up to 85%). Polymerization of a racemic mixture enriched in one of the enantiomers has also been studied, and it was shown that selection of the enantiomer present in excess leads to polymers with an enhanced proportion of this enantiomer.[27,74]

On the basis of these observations, the mechanism of enantiomer selection by growing chain ends has been proposed. According to this theory, steric repulsion is minimized when

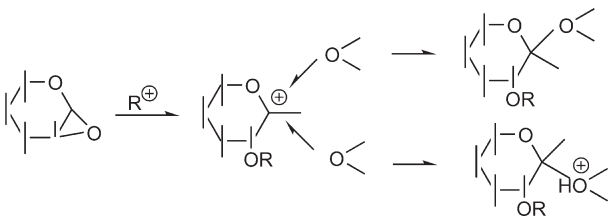

Scheme 29 Participation of alkoxycarbenium ions in the propagation step for cationic polymerization of 1,2-anhydrosugars.

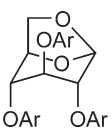

Scheme 30 1,6-anhydro-2,3,4-tri-*O*-benzyl-β-D-glucose.

the monomer incorporated into the growing species and the incoming monomer molecule have the same chirality.

4.10.2.7 Microstructure of Polymer Chain

Polymerization of cyclic acetals proceeds by opening one of the -O–CH_2–O- bonds; thus polyacetals are built up as shown in Scheme 31.

This was confirmed by ^{1}H and ^{13}C NMR spectroscopy; thus, for example, the ^{1}H NMR spectrum of polyDXL consists of two sharp singlets at $\delta = 4.76$ ppm (OCH_2O) and 3.73 ppm (OCH_2CH_2O).[75] For substituted cyclic acetals, breaking of either the O(1)–C(2) or the O(3)–C(2) bond may lead to a polymer of irregular structure. Indeed, by analyzing the methylene group signals in ^{1}H NMR spectra of poly(4-ethyl-1,3-dioxolane), it has been shown that the polymer is composed of both types of units (Scheme 32).[76]

4.10.2.8 Functional Polyacetals

Polyacetals containing functional groups were prepared by cationic copolymerization of cyclic acetals with methyl 2-oxopropanoate (methylglyoxylate (GM)) (Scheme 33).

In the copolymerization of DXL with GM, a large amount of mixed cyclic dimer (containing one DXL and one GM unit) was formed (up to 70%).[77]

Cyclization was eliminated when DXP was used instead of DXL and linear copolymers with M_n up to 2×10^4 containing 30–70 mol.% of GM units were obtained.[78] Partial replacement of the ester groups in GM-DXP copolymers with amide groups by reaction with α-amino-ω-methoxypoly(oxyethylene) (Jeffamine) led to graft copolymers in which the remaining ester groups were hydrolyzed to carboxylate groups. The resulting water-soluble graft copolymers containing hydrophilic side chains and carboxylate groups along the main chain belong to the class of double-hydrophilic graft copolymers used as modifiers of crystallization of inorganic salts.

Extensive transacetalization proceeding parallel to propagation essentially precludes the possibility of the synthesis of perfectly monofunctional polymers or block copolymers by cationic polymerization of cyclic acetals. Transacetalization is not that detrimental to synthesis of difunctional telechelic polyacetals and several such products have been obtained. Because polyacetals such as polyDXL readily undergo depolymerization in the presence of acids, telechelic polyacetals were used to synthesize degradable polyurethanes[79–81] or degradable polymer networks.[82–84]

Such networks that can be easily solubilized under mild conditions may be useful as materials. Besides, the possibility to study the residual material after hydrolysis of linear chains may provide more insight into the mechanism of network formation.[81]

PolyDXL bis-macromonomers were prepared by cationic polymerization of DXL initiated by triflic anhydride, end-capping of the resulting bifunctional living polymers with triethylamine, and nucleophilic substitution of ammonium end groups by a methacrylate anion.[85]

Another approach involved cationic polymerization of DXL in the presence of dialkylformals containing methacryloyl groups as chain-transfer agents (shown in Scheme 34).

Efficient transacetalization led to the formation of polymers containing polymerizable groups at both ends, as shown by ^{1}H NMR. Their degree of polymerization was governed by the ratio [monomer]/[chain-transfer agent] and the measured values were close to the calculated values up to $M_n \sim 10^4$.

Copolymerization of bis-macromonomers gave polymer networks which could be de-cross-linked at mild conditions in the presence of an acid. Analysis of degradation products indicated that polyDXL bis-macromonomers were quantitatively incorporated into the network structure.[85]

Polyacetals containing polymerizable acrylate groups at both ends were also prepared (but not fully characterized) by cationic polymerization of DXL initiated with triflic anhydride in the presence of HEMA (hydroxyethyl methacrylate). Radical copolymerization of those bis-macromonomers with acrylic acid led to degradable pH-sensitive networks.[86]

Block copolymers containing polyacetal blocks have been prepared by a combination of reversible addition-fragmentation chain-transfer (RAFT) polymerization and cationic ring-opening polymerization. Polystyrene (PSt) containing end groups with hydroxy and dithiobenzoate functions (as shown in Scheme 35) were obtained and used as macroinitiator for subsequent cationic polymerization of DXP and RAFT polymerization of methyl methacrylate (MMA). The product was mikto-arm ABC star copolymer containing PSt, PDXP, and PMMA arms.[87]

Water-soluble polyacetals are also used as drug carriers. Therapeutic application of some drugs is hindered by very low solubility in aqueous media. Water solubility may be greatly improved by the coupling of a hydrophobic drug to a hydrophilic polymer carrier. Water-soluble polyacetals were used as suitable carriers but these polymers were not made by ring-opening polymerization but by polyaddition of diols with divinyl ethers[88–91] or by controlled degradation of corresponding polysaccharides.[92] The application of polyacetals for drug delivery has been recently reviewed.[93]

The possibility of applying polyacetals as host polymers for polymer electrolytes has been explored.[94] Although completely amorphous polymer matrices were obtained for some

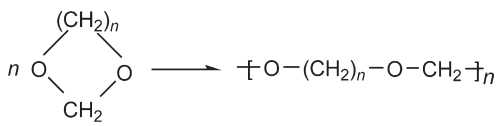

Scheme 31 Structure of repeating unit in polymers of cyclic acetals.

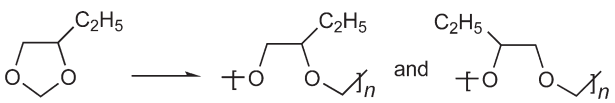

Scheme 32 Structure of repeating units in polymer of 4-ethyl-1,3-dioxolane.

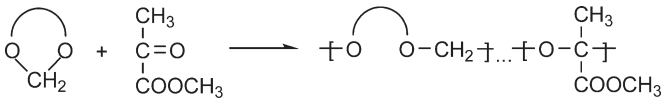

Scheme 33 Copolymerization of cyclic acetal with methyl-2-oxopropanoate.

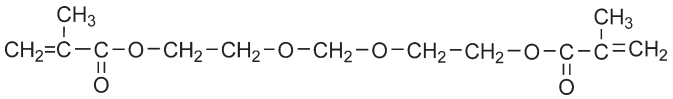

Scheme 34 End-functionalized formal effective as chain transfer agent in the cationic polymerization of DXL.

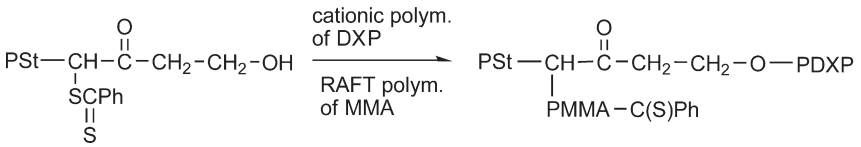

Scheme 35 Formation of triblock copolymer by combination of cationic polymerization of DXP and RAFT polymerization of methyl methacrylate using polystyrene containing hydroxyl and dithiobenzoate groups as macroinitiator.

concentrations of dissolved lithium salts, the systems were not stable due to salt desolvation and polymer degradation.

4.10.3 Heterogeneous Polymerization of 1,3,5-Trioxane

As indicated in Section 4.10.1, in recent years there has been significant research activity in the field of heterogeneous polymerization of TOX. Therefore, this topic is presented in a more detailed way.

4.10.3.1 General Features of Heterogeneous Polymerization of 1,3,5-Trioxane

As noted earlier in this chapter, poly(oxymethylene) (POM) is thermally unstable and tends to depolymerize starting at the unstable hemiacetal hydroxy group releasing formaldehyde (methanal) by an 'unzipping' mechanism. The early strategy to prevent this depolymerization, used for the homopolymers prepared anionically, consisted in stabilizing the polymer chain ends by a suitable capping method. Industrially, a widely developed alternative way to obtain thermally stable POMs is to copolymerize cationically TOX with a few percent of EO or cyclic acetals (DXL, DXP).

POM also known as polyformaldehyde, the product of TOX polymerization, is insoluble in common organic solvents, including molten monomer. Thus, polymerization of this monomer proceeds as a heterogeneous process and conclusions based on the model studies of homogeneous systems cannot be directly adopted in TOX polymerization. The studies of the topochemical aspects of polymerization carried out by Mateva *et al.*[95] and Wegner *et al.*[96] strongly indicate that the active species in TOX polymerization are located on the surface of the growing polymer crystal. Thus, they cannot be directly observed or identified by spectroscopic methods.

It is known that in this polymerization, even in the rigorously purified systems, the molecular weights corresponding to the lengths of the kinetic chains cannot be attained. This was attributed to the hydride transfer reaction shown in Scheme 36.[97]

As a result, the polymer would acquire -OCH_3 end groups and the 1,3,5-trioxan-2-ylium cation would start a new chain.[98] The stable -OCH_3 end groups may be responsible, at least partially, for the presence of ca. 25% of the thermally stable fraction in otherwise unstabilized polymers.[58] It has to be remembered, however, that this may also be due to the presence of a cyclic fraction.

The fact that hydride transfer reactions occur in TOX polymerization indicates that the fraction of the alkoxycarbenium active species may be significant, because only these species can participate in hydride transfer; no hydride transfer reaction was observed with oxonium ions.

Active species in TOX polymerization are located on the surface of the growing polymer crystals. Thus, monomer molecules, when being incorporated into the polymer chain, are at the same time transferred from the liquid into the crystalline phase. This affects the thermodynamics of polymerization and introduces an additional factor in the mechanism of chain growth.

The (co)polymerization of TOX, conducted in the bulk molten monomer, a monomer–comonomer mixture, or in solution (with precipitation of polymer), presents very specific features as propagation is essentially heterophasic at the interface between the liquid medium and the precipitated crystalline (co)polymer. The reaction starts by a short so-called 'induction' period during which the medium remains homogeneous and the conversion limited, followed by a rapid heterogeneous propagation–crystallization process going to complete conversion as soon as the -$(CH_2\text{-}O)_n$- sequences are long enough to nucleate the crystallization. Since the pioneering work of Jaacks and Kern[44,99] and Jaacks[100] (induction period), Wegner *et al.*[96] (heterophasic propagation), and Berlin *et al.*[101] (thermodynamics), several papers and patents have been devoted to the (co)polymerization of TOX either in bulk or in the presence of a polar or nonpolar diluent. Several sound reviews[1,3,5,102] summarized all the approaches, pointing out the numerous unclear aspects of this very complex

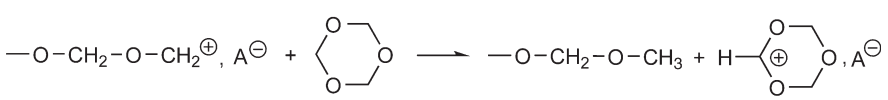

Scheme 36 Hydride transfer reaction in the polymerization of TOX.

polymerization, in particular the key role of the induction period in the understanding of the overall process and in the control of the stability of the final product.

4.10.3.2 The 'Induction' Period in the Homo- and Copolymerization of 1,3,5-Trioxane

The literature devoted to the homogeneous stage or 'clear' or 'induction' period of both homo- and copolymerization of TOX has been covered until the 1990s in the exhaustive reviews of Penczek and Kubisa[1] and Masamoto[102] and will not be reconsidered in detail here. We will rather focus on some more recent studies that afford new light on the complex processes. In the past two decades, high-field ^{1}H, ^{13}C, and 2D NMR techniques allowed to follow accurately the *in situ* formation and evolution of the intermediates and products involved during the homogeneous period, leading thus to the composition of the reaction medium at the onset of the precipitation stage. This composition could hardly be attained in the former studies and is a key factor governing as well the processes involved in this second stage such as the stability and properties of the final polyacetal.

The (co)polymerization can be initiated either by Friedel–Crafts-type initiators, essentially BF_3 and its etherates, or by strong protic acids ($HClO_4$, $HOSO_2CF_3$) and was previously studied generally in solution with solvents of various polarities (saturated hydrocarbons, halogenated hydrocarbons, benzene, nitrobenzene, etc.) in order to increase considerably the duration of the induction period to experimentally reach the concentrations of products and intermediates. For the $BF_3{\cdot}OR_2$ initiating system, after an early controversy there is now a general agreement that the reaction is initiated by the Brönsted acid resulting, in very low concentration, from the equilibrated reaction of the Lewis acid with residual water (coinitiation).[103–108] Few basic studies were devoted to initiation by protic acids. Nevertheless, it was reported that even with acid concentrations 100–300 times lower than those when using $BF_3{\cdot}OR_2$, the rates of polymerization were noticeably higher.[109] The observed induction periods when protic acid initiation is used are much shorter, indicating a higher initiation efficiency but making the experimental approach of the induction stage much more difficult.

4.10.3.2.1 Homopolymerization of 1,3,5-trioxane

The bulk homopolymerization of TOX, performed at the melting temperature of TOX (~63 °C) and initiated by $BF_3{\cdot}OEt_2$ in the absence (undetectable by the Karl Fischer method) and in the presence of a controlled amount of water, has been carefully examined using the *in situ* ^{1}H NMR technique.[110] It was shown that in the absence of added water, no significant amount of formaldehyde is formed and the polymerization does not proceed. In the presence of added water (0.13 mol.%, 20 times the amount of $BF_3{\cdot}OEt_2$), this water is rapidly consumed and the formation of formaldehyde is observed. Then further reaction of the HO-CH_2^+ cation with TOX leads, by direct insertion and/or backbiting, to higher cyclics, essentially 1,3,5,7-tetraoxane (TEOX) but also some 1,3,5,7,9-pentaoxane, which agrees with the earlier qualitative observations for solution and bulk polymerizations (Scheme 37).[111,112] The appearance of the -$(CH_2$-$O)_3$- (MMM) triads characteristic of TOX polymerization is delayed for about 60–100 s until the formaldehyde and TEOX concentrations reach their maximum values (Figure 1).

Then, at the end of the induction period, ca. 300 s, the POM sequences develop until they are long enough to allow the crystallization (Scheme 37) whereas the concentrations of formaldehyde and TEOX level off to constant values.

The rapid precipitation process shifts all equilibria toward the formation of the high polymer. Thus, it is concluded that formaldehyde formation does not essentially result, as considered in earlier studies, from the unzipping of short POM sequences but essentially from the opening of the protonated TOX ring.

As the system is initially far from equilibrium, it was proposed[110] that the decomposition of the carboxonium intermediate is favored, allowing a rapid buildup of formaldehyde until a steady-state concentration of 4×10^{-2} mol l^{-1} is reached, a value that is comparable with that reported (6×10^{-2} mol l^{-1}) in the early study of Jaacks and Kern[99] in the case of polymerization of TOX at 30 °C in CH_2Cl_2 solution (a much longer induction period). The subsequently formed TEOX is then protonated and releases formaldehyde and longer oxymethylene sequences, which favor the formation of the polymer and shorten the induction period.[110,111]

A recent study of the bulk polymerization of TOX initiated by perchloric acid at 80 °C has shown that the nature of the diluent of the initiator, even though present at very low concentration in the molten monomer, may have a strong effect on the duration of the induction period, varying from 1 to 3 s in the case of 1,4-dioxane to 20–30 s in the case of triglyme (Figure 2).[113]

This was explained by a very low concentration of reactive unsolvated initiating hydronium ions and propagating carboxonium when triglyme is used rather than when using dioxane, and thus by both slower initiation and propagation (Scheme 38).

This agrees with a much higher proton-binding ability of triglyme compared with dioxane, even though their reported pK_b (~6) values are close.[105,106,114] Even if the overall rate of propagation is decreased by the solvation of active centers, the rapid exchange between solvated and unsolvated species causes the rate of growth of each individual chain to be the same and also the time for the POM sequences to reach their critical crystallization length to be the same for all chains irrespective of their number. In other words, the duration of the induction period should be independent of the total concentration of propagating species but dependent on their average reactivity. Figure 2 confirms that the induction period is not much dependent on the initiator concentration but highly sensitive to potential solvation of propagating centers.

Water, necessary as coinitiator at low concentration for the Lewis acid-initiated polymerizations, becomes a strong retarder when used in excess, increasing the induction period. It acts as a transfer agent leading to hydroxy-terminated oligomers until it is sufficiently consumed.[110,115.]

For the polymerization initiated by perchloric acid diluted with either triglyme or 1,4-dioxane, a dramatic effect of water on the induction period is observed when using triglyme whereas this effect almost disappears when using dioxane (Table 3).[113]

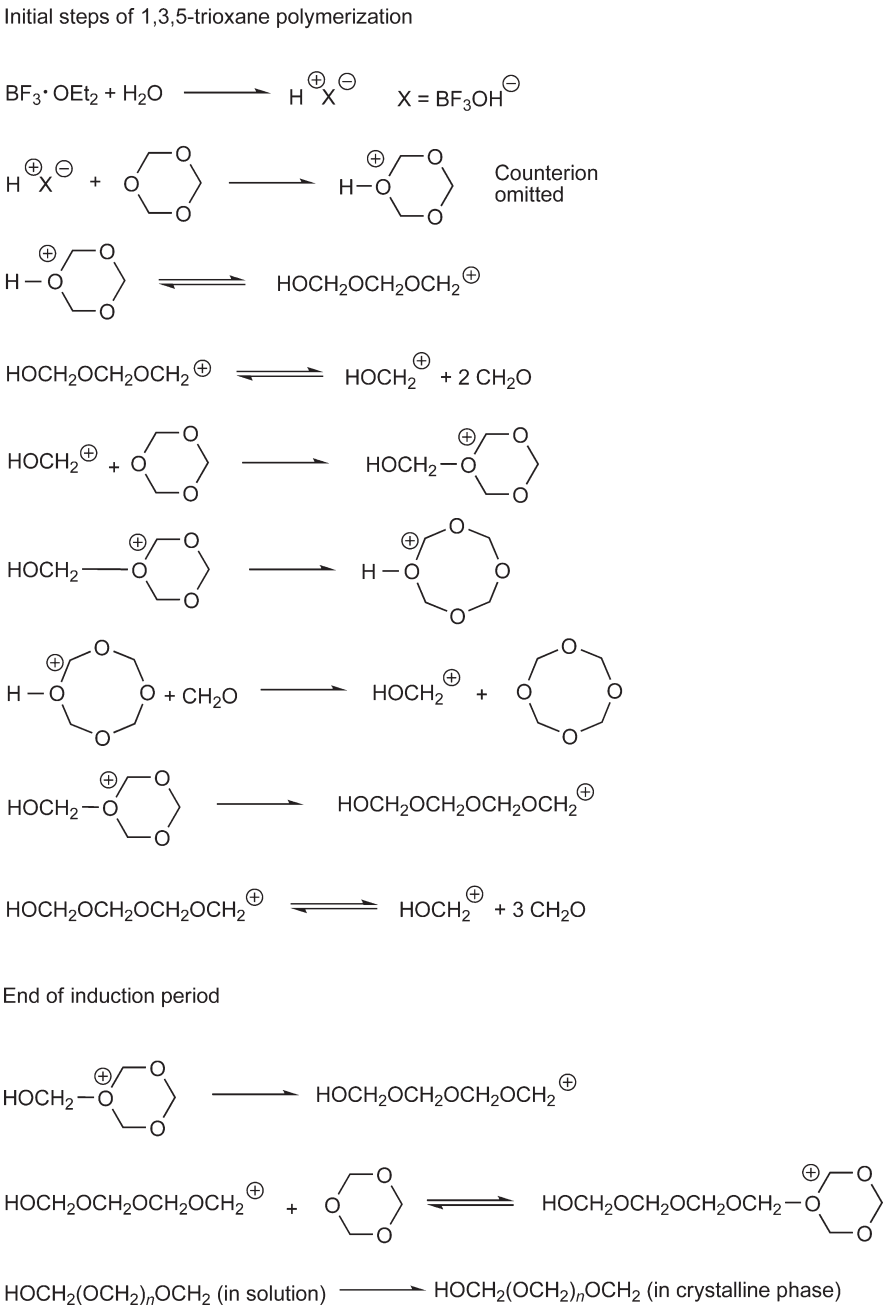

Scheme 37 Chemical processes during the induction period of bulk polymerization of TOX[110].

This can again be explained by a very low concentration of unsolvated active centers when triglyme is used as a diluent of the initiator.

As previously considered in this chapter, propagation proceeds via oxonium and/or carboxonium ions, and these species are reasonably assumed to remain stable and active. The formation of formaldehyde during the process, resulting from thermodynamic depolymerization of trioxane and to a lesser extent from unzipping of open-chain active ends, indicates that carboxonium ions are in equilibrium with oxonium ions. This is also supported by the observation of methoxy and formate end groups resulting from hydride shift processes in transfer reactions to monomer or polymer, as oxonium ions do not abstract hydride anions.[1,5,58,97,100,102,116–118]

4.10.3.2.2 Copolymerization of 1,3,5-trioxane

The bulk and solution copolymerizations of TOX were extensively studied with EO and DXL but paradoxically not that much with DXP even though the copolymers issued from this last comonomer are also of major industrial importance. The higher basicities (by 3–4 orders of magnitude)[105,106] of the usual comonomers (EO, cyclic acetals) with respect to TOX lead essentially to protonation of the comonomer and to subsequent initiation of copolymerization consuming this comonomer more rapidly until its concentration becomes

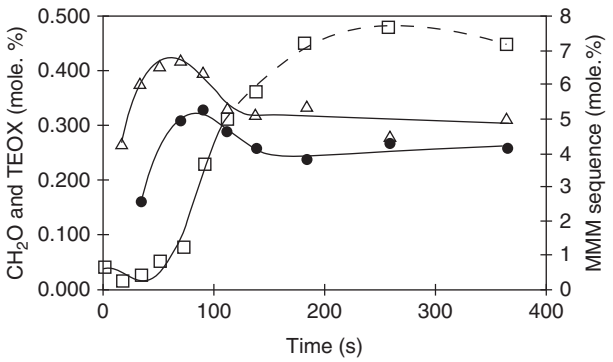

Figure 1 Kinetic profiles for each component in the course of trioxane homopolymerization in bulk at 63 °C, $[BF_3{\cdot}OEt_2] = 0.0073$ mol.%, and $[H_2O] = 0.13$ mol.%. HCHO (Δ), TEOX (●), MMM sequences (□). Reproduced with permission from Lu, N.; Collins, G. L.; Yang, N. L. *Macromol. Symp.* **1991**, *42/43*, 425,[110] figure 2.

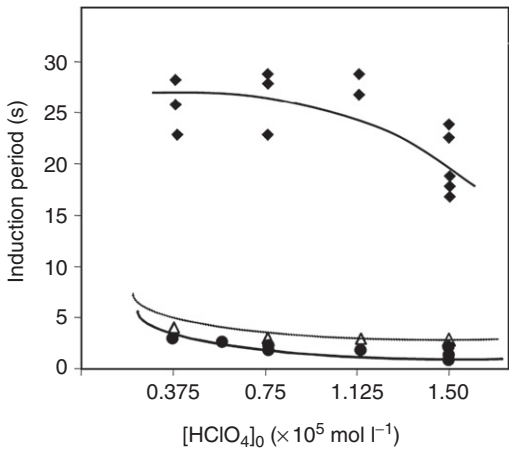

Figure 2 Bulk homopolymerization of TOX at 80 °C initiated by perchloric acid. Dependence of the induction period on the initiator concentration and diluent.[113] (◆) triglyme, (Δ) toluene, (●) dioxane. Reproduced with permission from Sharavanan, K.; Ortega, E.; Moreau, M.; *et al. Macromolecules* **2009**, *42*, 8702,[113] figure 1.

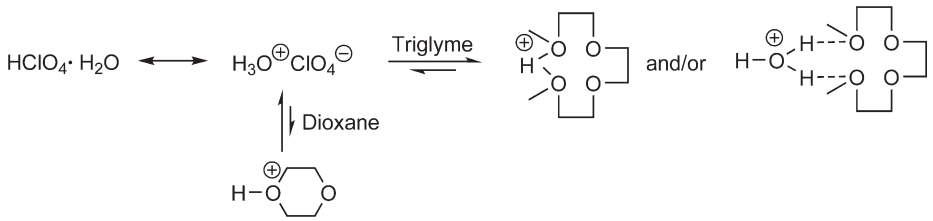

Scheme 38 Perchloric acid complexation using either 1,4-dioxane or triglyme as diluents for the initiator solution.[113]

low enough to allow the progressive incorporation of the trioxane units -$(CH_2\text{-}O)_3$- (MMM triad) and longer sequences. Thus the composition of the homogeneous medium during the induction period should comprise comonomer-enriched soluble chains together with formaldehyde, and higher cyclics, including those resulting from the comonomer. The further transacetalization processes, at the end of the induction period when TOX incorporation starts and then essentially during the heterogeneous stage, ensure the randomization of the distribution of the comonomer units along the POM chain and thus lead to the required thermal stability of the copolymer.

The duration of the induction stage in copolymerization is generally longer than in the case of homopolymerization of TOX. It also varies widely depending on the conditions of the reaction (comonomer and concentration, temperature, residual water, initiating system and its possible diluent, use of a solvent, purities of reactants, etc.). It is still very short (from a few seconds to minutes) in the case of the industrial copolymerization of TOX with low amounts (typically ~2–3 wt.%) of comonomer in bulk at the usual temperature (above T_m of the monomer). Therefore, many of the basic studies on mechanisms or kinetics were conducted either in solution at lower temperatures or in the melt with high comonomer concentration, in order to sufficiently extend the induction period or even to avoid the precipitation stage.

Table 3 Bulk homopolymerization of 1,3,5-trioxane initiated by perchloric acid at 80 °C. Dependence of the induction period on the amount of water present in the medium using triglyme and dioxane initiator solution[113]

Initiator diluents	*$[H_2O]/[H^+]$*	*Induction period (s)*
Triglyme	2.34[a]	26
	3.01	128
	5.30	180
	5.58	277
1,4-Dioxane	2.34[a]	1
	63.6	2
	186.4	4

$[H^+]_0 = 1.5 \times 10^{-5}$ mol.L^{-1}
[a] H_2O from ($HClO_4$, 2.4 H_2O).

The bulk copolymerization of TOX with EO has been considered in detail by the researchers of Hoechst Celanese and of Asahi Chemical Industry Co. One of the main features, observed by Weissermel *et al.*[58] in the 1960s, is that EO is converted into DXL during the first homogeneous stage of the reaction, and it was later confirmed that the TOX (co)polymerization does not start until complete EO transformation into DXL and higher cyclics, that is, that the comonomer is entirely consumed during the induction period.[102,119,120] Using quenching experiments during the copolymerization of 2 mol.% (~ 0.5 mol l^{-1}) of EO in molten TOX initiated at 70 °C (or 80 °C) by 1.25×10^{-3} mol l^{-1} $BF_3{\cdot}OBu_2$, it was confirmed that the rapid decrease in EO in the homogeneous stage of the reaction was accompanied by the formation of both DXL and 1,3,5-trioxepane (TXP) (**Figure 3**).[119]

Due to the difference in basicity between EO ($pK_b \sim 7.3$) and trioxane ($pK_b \sim 10$),[105] the cyclic oxonium resulting from protonation of EO was considered to be largely predominant. It has been assumed that its reaction with the formaldehyde from trioxane depolymerization should lead to the ring-expanded cyclic oxonium and then to DXL by proton exchange with EO. Further insertion of formaldehyde into the DXL-cyclic oxonium would then lead to TXP (**Scheme 39**).[119,120]

As long as EO is present, similar processes can also take place via backbiting of the terminal carboxonium ions of the possible EO or EO-rich oligomeric chains that are in equilibrium with their relevant cyclic oxonium ions. When all EO is consumed, both TXP and DXL copolymerize with TOX and then a POM copolymer with a random distribution of isolated -(CH_2-CH_2-O)- units is formed during the short heterogeneous second stage of the reaction.

The above proposal prevailed until the early 1990s even though some aspects remained unclear. First, it was assumed that owing to its very low basicity, TOX could not undergo nucleophilic attack onto the EO-cyclic oxonium; second, that the TXP results from initially formed DXL (which might be questioned from the plots in **Figure 3**); and third, that further ring expansion to higher cyclic formals was discarded due to the significant strain expected for 8–12-membered rings.

Masamoto and co-workers[121–125] reconsidered the homogeneous stage of the bulk copolymerization in similar conditions as above but using a broader range of EO

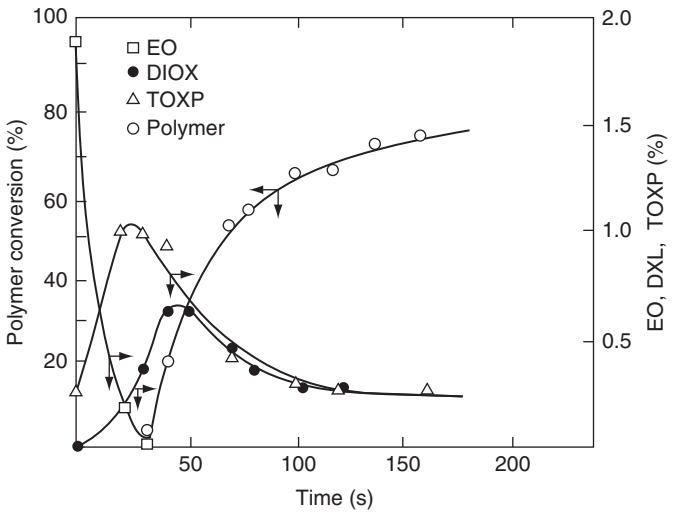

Figure 3 Concentration profile of reactants and intermediates in the bulk copolymerization of TOX with EO at 80 °C. Reproduced with permission from Collins, G. L.; Greene, G.; Berinardelli, F. M.; Ray, W. H. *J. Polym. Sci., Part A: Polym. Chem. Ed.* **1981**, *19*, 1597,[119] figure 3.

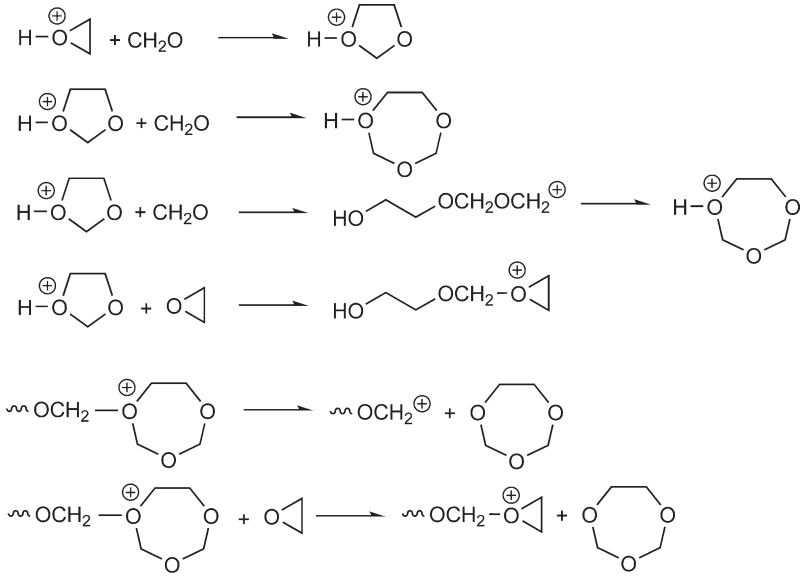

Scheme 39 Formation of DXL and TXP by insertion of formaldehyde in the EO- and DXL-cyclic oxonium ion.[119]

concentrations and proposed an alternative mechanism. A series of extracted aliquots versus time, analyzed by gas chromatography (GC) and NMR, clearly showed that higher cyclic formals, 1,3,5,7-tetraoxacyclononane (TOCN) and 1,3,5,7,10-pentaoxacyclododecane (POCD), appear first, as long as EO is still present, and then are consumed, whereas TXP and DXL develop progressively at the end of the induction period (**Figure 4**).[121–126]

These authors focused on the homogeneous period of copolymerization with different initial EO concentrations. The observed intermediates were isolated by microdistillation and preparative GC, and then characterized by NMR, EI-MS (electron impact mass spectrometry), and determination of their physical properties.[122,125,126]

At the lowest EO concentration (EO/TOX ~ 1 mol.%), the TOCN resulting from the insertion of the -CH_2CH_2O- grouping of EO into the trioxane ring was the only high cyclic formal observed, whereas at the highest concentration ($[EO]_0$ ~ 4 mol.%/TOX) two further intermediates POCD and 1,3,5,7,10,13-hexaoxacycloheptadecane (HOCP), issued from the insertions of two and three -CH_2CH_2O- groupings, could be quantitatively identified (**Figures 5(a)** and **5(b)**).[125]

It was concluded that the ring expansion resulting from successive insertions of EO units (-CH_2CH_2O-) into cyclic formals issued from TOX is the main initial process of the reaction during the induction period. The appearance of TXP and then DXL is delayed until most of EO is consumed. This conflicts with the previously proposed mechanism involving the prior formation of dioxolane by reaction of formaldehyde with the EO oxonium followed by the reversible insertion of formaldehyde unit (OCH_2) into the DXL oxonium leading to TXP.

The higher cyclic formals do exist exclusively in the presence of EO, which indicates that (1) their formation implies the reaction of TOX with EO oxonium (or EO carboxonium) and ring closure, and (2) their consumption generates formaldehyde in equilibrium with more stable lower cyclic formals, essentially TXP and then DXL, at the end of the homogeneous period (**Scheme 40**).[123]

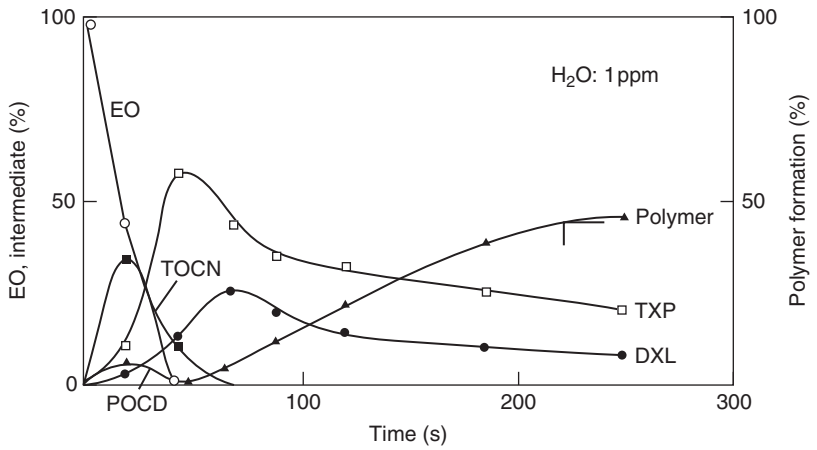

Figure 4 Concentration profiles of reactants and intermediates in TOX-EO bulk copolymerization at 70 °C. EO/TOX = 4.5×10^{-2} mol mol^{-1} TOX, $BF_3{\cdot}Bu_2O$/TOX = 7×10^{-5} mol mol^{-1} TOX, $[H_2O]$ = 1 ppm. Reproduced with permission from Nagahara, H.; Kagawa, K.; Iwaisako, T.; Masamoto, J. *Ind. Eng. Res.* **1995**, *34*, 2515,[121] figure 4.

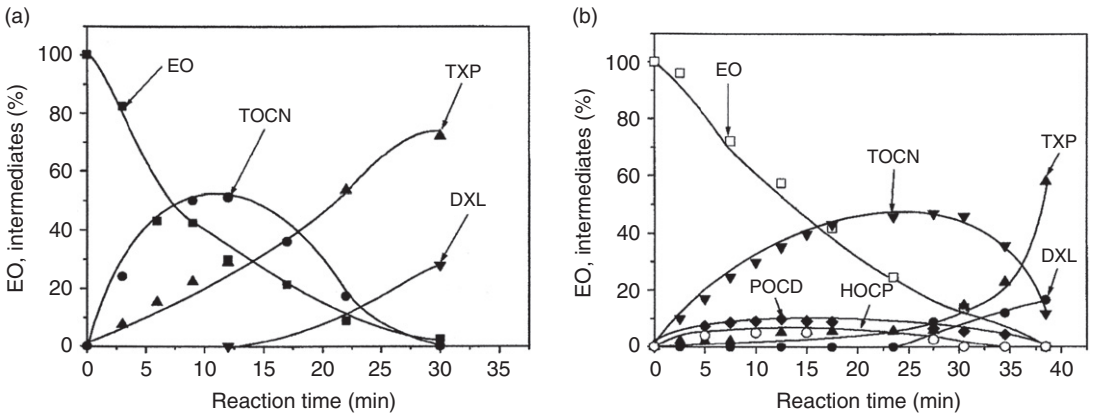

Figure 5 Concentration profiles of reactants and intermediates in TOX-EO bulk copolymerization at 70 °C: (a) EO/TOX = 0.95 mol.%, $BF_3{\cdot}Et_2O$/TOX = 8.4×10^{-5} mol mol^{-1}. Reproduced with permission from Yamasaki, N.; Masamoto, J. *J. Polym. Sci., Part A: Polym. Chem. Ed.* **2004**, *42*, 520,[125] figure 2; (b) EO/TOX = 3.9 mol.%, $BF_3{\cdot}Et_2O$/TOX = 3.9×10^{-5} mol mol^{-1}. Reproduced with permission from Yamasaki, N.; Masamoto, J. *J. Polym. Sci., Part A: Polym. Chem. Ed.* **2004**, *42*, 520,[125] figure 6.

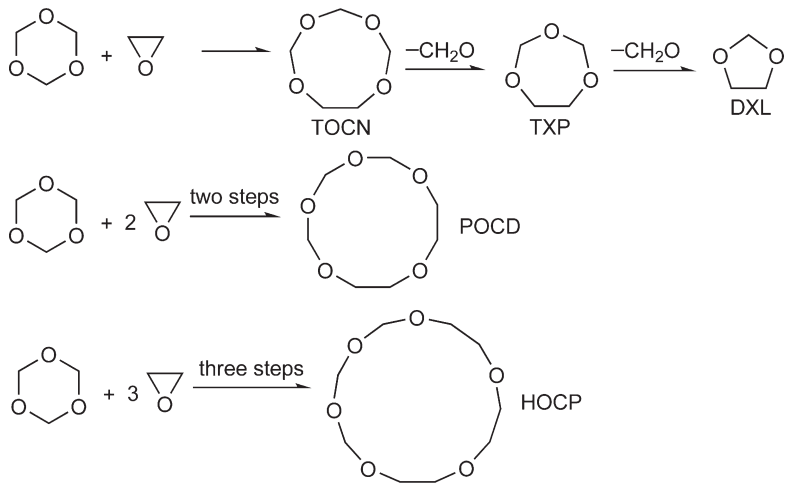

Scheme 40 Intermediates formed during the homogeneous stage of EO-TOX copolymerization.[123]

Owing to the long duration of the homogeneous period in the given experimental conditions, the reactions involving formaldehyde are thermodynamically controlled and TXP and DXL should be in equilibrium. The disappearance of the higher cyclic formals during this homogeneous period can also result from their copolymerization and insertion in the EO-rich soluble chains of the already formed EO-TOX copolymer. In that case, the final POM copolymer should exhibit a random distribution of EO single units and of $(EO)_{2\rightarrow n}$ sequences along the POM chain. Accurate pyrolysis/GC and hydrolysis analyses of the sequence distributions in models and commercial EO-based polyacetals unambiguously showed that for an EO/TOX fraction of 1–2 mol.%, the final copolymer presents an $(EO)_1/(EO)_2/(EO)_3$ composition of approximately 75/20/5 whereas further sequences can be quantitatively identified when EO content increases (up to $(EO)_7$ for 9 mol.% of comonomer).[123,125,127] Table 4 clearly shows that whatever the EO content the main sequences observed in the resulting copolymer are the isolated EO units issued from the TXP, DXL, and possibly tetraoxacyclononane together with the $(EO)_2$ sequences issued from the pentaoxacyclododecane, in accordance with the copolymerization pathway proposed by Yamasaki and Masamoto.[125]

A most important feature of the EO-TOX copolymerization is that at the onset of the heterogeneous phase of the reaction that generates most of the polyacetal, the bulk medium is essentially composed of TXP and DXL dissolved in the molten TOX, together with EO-rich soluble oligomers, which are the reservoirs of longer $(EO)_2\ldots(EO)_n$ sequences. Scrambling by chain transfer onto -$(CH_2$-O)- units (transacetalization) during this second stage leads to the final expected randomization.

The solution and bulk copolymerizations of TOX with DXL have also been extensively studied and present common features with both the TOX homopolymerization and the TOX-EO copolymerization considered above. The early works showed that due to its much higher basicity, DXL is preferentially protonated with respect to TOX and essentially consumed during the homogeneous period to give soluble polyDXL and DXL-rich copolymers of DXL with formaldehyde.[57] Higher cyclic formals like tetraoxane and trioxepane were also formed during the induction period and were supposed to result from the backbiting of the oxymethylium ends of the soluble copolymer chains. A later quantitative approach performed in 1,2-dichloroethane solution led to the conclusion that the

Table 4 Sequence distributions of polyacetal EO-TOX copolymers estimated by pyrolysis-GC (Py-GC) and hydrolysis methods[127]

	POM-EO-1 [98.6/1.4]		*POM-EO-2 [95.3/4.7]*		*POM-EO-3 [91.1/8.9]*	
Sequence	*Py-GC*[a]	*Hydrolysis*[b]	*Py-GC*[a]	*Hydrolysis*[b]	*Py-GC*[a]	*Hydrolysis*[b]
-FEF-	70.1 (74.5)	79.3	60.0	59.0	44.3	47.1
-FE_2F-	255 (22.3)	17.2	33.0	31.6	37.1	322
-FE_3F-	4.4 (3.2)	3.5	5.6	8.7	9.5	14.9
-FE_4F-			1.4	0.7	5.2	4.9
-FE_5E-					2.7	0.9
-FE_6E-					0.9	
-FE_7F-					0.3	
Total	100.0	100.0	100.0	100.0	100.0	100.0

[a]Sequence distribution obtained by Py-GC through the reactive pyrolysis at 400 °C in the presence of 5 wt.% cobalt sulfate. The values in parentheses are obtained in the presence of 1 wt.% cobalt sulfate.
[b]Sequence distribution obtained from hydrolysis followed by GC.
E, -[CH_2-CH_2-O]-; F, -[CH_2-O]-.
Reproduced with permission from Ishida, Y.; Ohtani, H.; Abe, K.; *et al. Macromolecules* **1995**, *28*, 8702,[127] table 4.

formation of TXP by insertion of formaldehyde (OCH_2) into the protonated DXL was more likely.[120]

In situ ^{1}H NMR experiments, based on previous assignment of the different M (oxymethylene) and E (oxyethylene) centered sequences,[128,129] were used to identify and follow quantitatively the intermediates formed during the induction period of the bulk copolymerization initiated by $BF_3{\cdot}OEt_2$ at 63 °C with different initial TOX/DXL ratios.[110] When TOX is in large excess, formaldehyde, tetraoxane (TEOX), and TXP are generated a long time before the appearance of the MMM, MEM/EME, and MME triads, characteristic of the poly(TOX), polyDXL, and copolymer sequences, respectively (**Figure 6**).[110] This confirms that the TXP formed during the induction period results from formaldehyde insertion into the protonated DXL rather than from a backbiting process. Formation of tetraoxane can be identified only when the instantaneous concentration of formaldehyde resulting from TOX depolymerization is significant, that is, for the higher TOX/DXL ratio. The duration of the induction period was not specified but, owing to the delayed appearance of the POM sequences, it was probably in the minutes timescale. When DXL is used in large excess (TOX/DXL 0.3/1), the protonation of TOX is less likely and formaldehyde is undetectable by NMR, indicating that it is immediately consumed to generate trioxepane. In this case, the only polymer sequences observed are those of the homopolymers of DXL and TXP (or their copolymers).

The events occurring during the homogeneous period of the bulk copolymerization of trioxane with DXL have been recently reexamined in conditions as above but using the pairs of labeled comonomers, TOX-d_6/DXL and TOX/DXL-2,2-d_2.[130,131] In both cases, ^{1}H NMR allowed to track the pathways of the -(CH_2-O)- oxymethylene (M) and -(CH_2-CH_2-O)- oxyethylene (E) units originating from the comonomers, and the fact that the -(CD_2-O)- (M′) units were undetectable drastically improved the spectral resolution. Detailed analyses of the evolution of the complex sets of pentad sequences involving E, M, and M′ units confirmed the previous general observations of Lu *et al.*[110] but the successive occurrence of the reactions in the course of the induction period was more precisely identified, which lead to a deeper insight into the complex mechanistic route of the copolymerization. Owing to the high initial DXL concentration in these experiments, the duration of the homogeneous period was drastically increased (hours), and most of DXL was consumed. Thus the medium at the onset of the heterogeneous period should be essentially composed of molten TOX and soluble E-rich copolymers together with some remaining comonomers

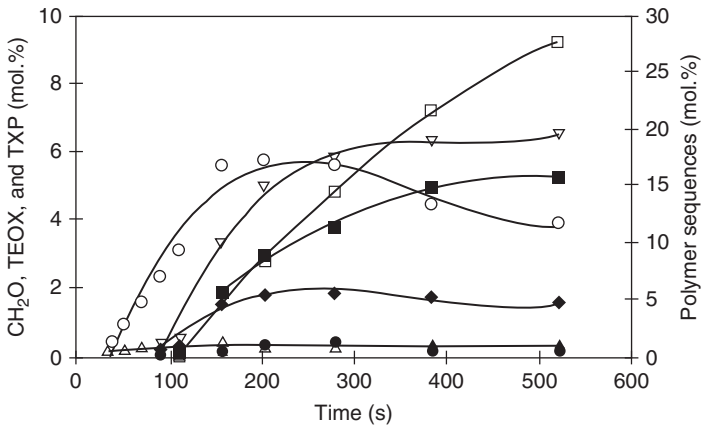

Figure 6 Kinetic profiles for each component during the course of the bulk copolymerization of TOX and DXL, mole ratio 2:1, at 63 °C. [$BF_3.OEt_2$] = 0.028 mol.%, [H_2O] = 0.05 mol.%. MMM (□), MME (■), EME (◆), MEM (▽), OCH_2 (Δ), TXP (○), TEOX (●). Reproduced with permission from Lu, N.; Collins, G. L.; Yang, N. L. *Macromol. Symp.* **1991**, *42/43*, 425,[110] figure 6.

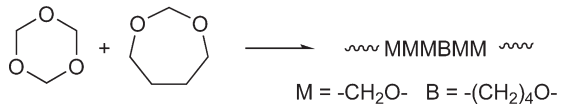

Scheme 41 Copolymerization of TOX and DXP.

and cyclics (TEOX), which does not necessarily reflect the situation of the industrial process involving only a few wt.% of comonomer and exhibits much shorter induction periods.

The copolymerization of TOX with DXP is the third process of industrial importance.[102] It was mentioned in the early works on polyacetals, but few specific studies were devoted until recently to this copolymerization (**Scheme 41**).[113,132–134]

The first detailed approach to the mechanisms involved during the homogeneous stage of the reaction was again based on *in situ* analyses using high-field ^{13}C NMR techniques in order to identify the intermediates in real time.[133,134] As B units from DXP cannot be adjacent, the sequences are limited to six M-centered (MMMMM, BMMMM, BMMMB, MBMMM, MBMMB, MBMBM) and three B-centered (MMBMM, BMBMM, BMBMB) pentads and their assignment to the relevant chemical shifts was established based on 2D NMR experiments and by comparison with the data from pentads of TOX/DXL copolymer (**Table 5**). Heptads and nonads could also be identified for some M-centered sequences.

The experiments were conducted in bulk at 70 °C and the M/B ratio was 9/1 (ca. 27 mol.% of DXP). In such conditions of high comonomer concentration, the reaction was slowed down and the crystallization of the copolymer was considerably delayed, allowing accurate measurements during the homogeneous stage.

The evolutions of the M-centered pentads are shown in **Figure 7**. After the injection of initiator, the MBMBM pentad characteristic of the homopolymer of DXP grows quickly. It is observed to incorporate 50% of the DXP during the first 15 min. Then it goes through a maximum, declines, and transforms into sequences bearing two adjacent M units, which progressively turn into pentads with three and four adjacent M units until the MMMMM sequence from the TOX-rich copolymer develops.

In contrast to DXL, no cyclic formal resulting from DXP ring expansion was observed during the homogeneous period. This could result from thermodynamics (instability of higher cyclics) but a significant difference of ring strain between the 1,3,5-trioxacyclononane expected from formaldehyde insertion into DXP and the 1,3,5,7-tetraoxacyclonane identified as intermediate in TOX/EO copolymerization is questionable. An alternative explanation could be the higher basicity of DXP with respect to DXL,[105,106,135] which makes the early formation of formaldehyde from protonated TOX much less likely when DXP is used as a comonomer. Thus the homopoly(DXP) is essentially produced at the beginning of the reaction whereas the copolymer appears progressively when the concentration of DXP is low enough to allow a significant formation of formaldehyde and its further incorporation in the growing chains. In these experimental conditions, most of the comonomer is consumed before the heterogeneous stage starts, which might not be verified in conditions of the industrial processes involving much lower comonomer concentrations.

The TOX/DXP bulk copolymerization initiated by perchloric acid at 80 °C has been recently reexamined over a broader range of comonomer concentration (from TOX/DXP 97/3 w/w, DXP 2.7 mol.% to TOX/DXP 80/20, DXP 18 mol.%).[113] Increasing the concentration of the comonomer in the molten trioxane increases significantly the induction period as shown in **Figure 8**.

In the conditions of the industrial copolymerization (DXP ~ 2–3 wt.%), the induction period is very short (a few seconds) but a dramatic effect of the initial DXP concentration on the duration of this induction period, that is, on the buildup of long $(-CH_2-O-)_n$ sequences, can be expected from extrapolation above ~ 25 wt.% of comonomer from the plots of **Figure 8**. This agrees with the very long induction period observed for an initial DXP concentration close to 30 wt.%.[133,134]

Table 5 ^{1}H and ^{13}C NMR chemical shifts of pentad sequences from TOX/DXP and TOX/DXL copolymers[134]

Pentad sequence	*^{1}H (ppm)*	*^{13}C (ppm)*	*Pentad sequence*	*^{1}H (ppm)*	*^{13}C (ppm)*
MMMMM	4.84	90.04	MMMMM	4.84	90.04
BMMMM	4.82	89.60	EMMMM	4.83	90.74
BMMMB	4.80	89.18	EMMME	4.82	89.34
MBMMM	4.72	92.74	MEMMM	4.75	92.92
MBMMB	4.70	92.24	MEMME	4.74	92.62
MBMBM	4.59	95.14	MEMEM	4.66	95.56
MMB_1[a]	3.54	68.70	MMEMM	3.67	67.72
BMB_1[a]	3.50	68.04	EMEMM	3.66	67.14
B_2[a]	1.59	26.13 26.07	EMEME	3.64	67.22

[a]'B_1' and 'B_2' denote '$OCH_2CH_2CH_2CH_2$' and '$OCH_2CH_2CH_2CH_2$', respectively.
The ^{1}H NMR chemical shift data were obtained at 140 °C with DMSO-d_6 as solvent and referenced to 2.49 ppm of DMSO; the ^{13}C chemical shift data were obtained at 50 °C with a solution of ca. 20 vol.% of 1,1,1,3,3,3-hexafluoropropan-2-ol in $CDCl_3$ as solvent and referenced to chloroform triplet 77.00 ppm. Reproduced with permission from Cui, M.-H.; Zang, Y.; Werner, M.; *et al. ACS Symp. Ser.* **2003**, *834*, 228,[134] table 1.

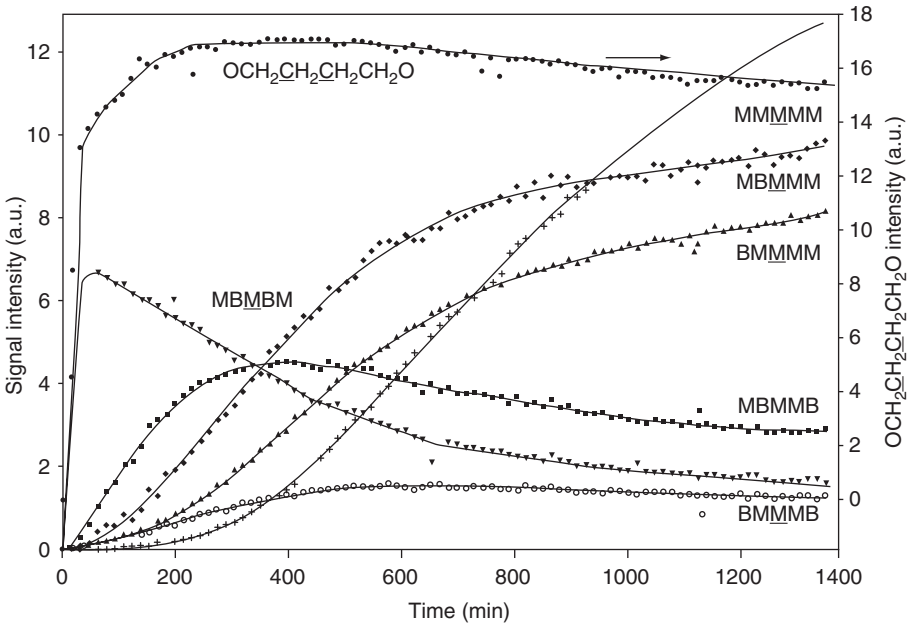

Figure 7 TOX/DXP bulk copolymerization at 70 °C: kinetic profiles of pentad sequences and central carbon of -$CH_2CH_2CH_2CH_2O$- unit, B_2. Molar ratio M/B = 9 (i.e., DXP ~27 mol.%), [$BF_3{\cdot}OEt_2$] = 30 ppm. Reproduced with permission from Cui, M.-H.; Zang, Y.; Werner, M.; *et al. ACS Symp. Ser.* **2003**, *834*, 228,[134] figure 2.

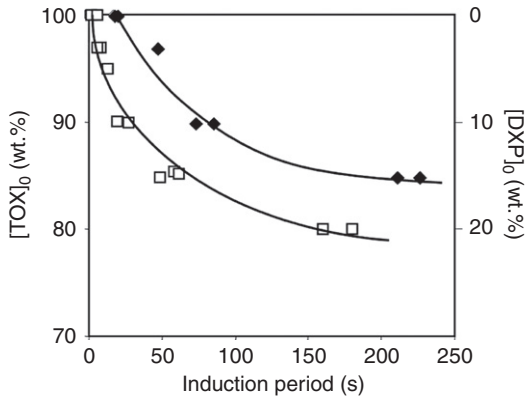

Figure 8 Copolymerization of TOX with DXP in bulk at 80 °C. The figure demonstrates variation of the induction period depending on the initial DXP content, using triglyme (♦) and dioxane (□) as diluents for the perchloric acid solution.Reproduced with permission from Sharavanan, K.; Ortega, E.; Moreau, M.; *et al. Macromolecules* **2009**, *42*, 8702,[113] figure 2.

Kinetic profiles of the components during the induction period (≤ 40 s) for a series of copolymerizations in the range TOX/DXP 80/20 to 97/3 w/w have been determined.

For the highest DXP concentration (ratio 80/20), the results agree well with the previous observations of Cui *et al.*[133] The DXP is rapidly consumed, essentially producing its homopolymer during the first half of the induction period. When the concentration of DXP is significantly lowered, TOX units are more and more incorporated, whereas the DXP homopolymer progressively disappears due to simultaneous depolymerization and transacetalization. For the lowest initial concentrations of DXP, the conversion during the induction period is drastically slowed down and leveled off, as shown for the 90/10 comonomer ratio in Figure 9 and Table 6. For the 95/5 and 97/3 ratios, the induction periods were too short and the (co)polymers were formed in a too low concentration to be accurately identified and followed with time but the concentration of the remaining DXP at the end of the induction period could be estimated by NMR.

The remaining comonomer concentration at the end of the induction period appears roughly constant (≈ 0.5–0.7 mol l^{-1}) and it represents the critical value below which the TOX sequences of the copolymer are long enough to spontaneously crystallize in bulk at 80 °C. The conversion of DXP at the end of the homogeneous period appears clearly dependent on its initial concentration and is very limited for the lowest initial concentrations (3–5 wt.%). Furthermore, the DXP homopolymerization is equilibrated. The value of the equilibrium concentration $[DXP]_{eq,ss}$ at 80 °C was estimated between 1 and 2 mol l^{-1} from literature data.[22,136] Even though the value is not fully reliable as in the present case, the DXP equilibrium concentration should be dependent on DXP-TOX, poly(DXP-TOX), and poly(DXP-DXP) interactions presently not quantified, and it was assumed to be definitely higher than the $[DXP]_0$ for the 95/5 and 97/3 TOX/DXP ratios. Thus a DXP homopolymer can hardly be formed and the copolymerization with TOX takes place from the very beginning producing copolymer chains with isolated DXP units. This agrees with the very short induction periods observed in the industrial processes.

It was concluded that at the onset of the heterogeneous stage, the composition of the medium could be radically different depending on the amount of the comonomer used. For high initial DXP concentrations, most of the comonomer has already been incorporated in a noticeable amount of soluble DXP-rich copolymer chains bearing $(BM)_n$ sequences, whereas for the lowest concentrations most of the comonomer still remains. The preformed copolymer, in low amount, is essentially TOX-rich with isolated comonomer units. In the latter case, the final polyacetal obtained after the further copolymerization–crystallization

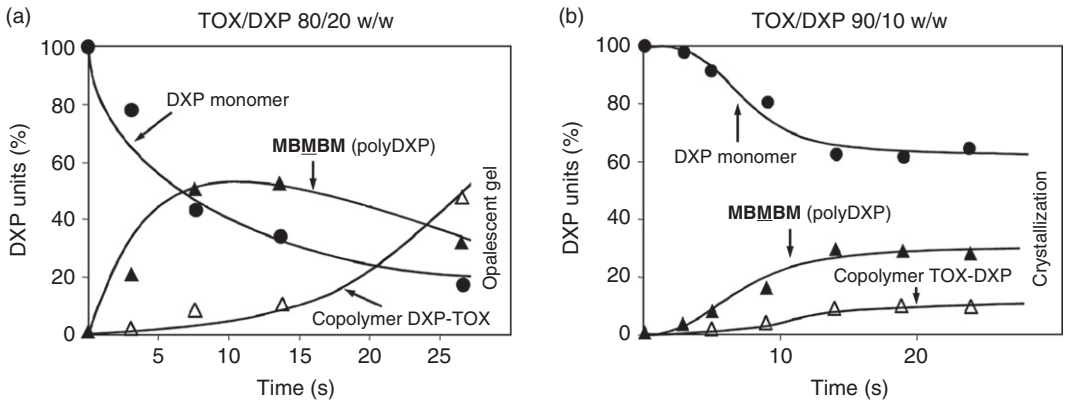

Figure 9 Copolymerization of TOX with DXP at 80 °C in bulk. Kinetic profiles of components during the induction period for TOX/DXP ratios (a) 80/20 w/w and (b) 90/10 w/w. DXP monomer (●), poly(DXP) pentad (▲), DXP-TOX copolymer (Δ). Reproduced with permission from Sharavanan, K.; Ortega, E.; Moreau, M.; *et al. Macromolecules* **2009**, *42*, 8702,[113] figure 6.

Table 6 Copolymerization of 1,3,5-trioxane with 1,3-dioxepane at 80 °C in bulk. DXP concentration at the end of the induction period depending on the initial TOX/DXP ratio.[113]

TOX/DXP (w/w)	*$[DXP]_0$ (mol l^{-1})*	*DXP conversion during the induction period (%)*	*[DXP] at the end of the induction period (mol l^{-1})*
80/20	2.20	80	0.44 ± 0.05[a]
90/10	1.12	35	0.72 ± 0.1[b]
95/5	0.57	18	0.48 ± 0.05[b]
97/3	0.33	10[c]	

[a]Just before turbid gel.
[b]Just before crystallization.
[c]Extrapolated.
$[H^+]_0 = 1.5 \times 10^{-5}$ mol l^{-1}.

stage should contain exclusively isolated BM units randomly distributed by transacetalization, allowing the highest crystallinity and the optimal stability.

4.10.3.3 The Polymerization–Crystallization Stage in the (Co)polymerizations of 1,3,5-Trioxane

In the usual conditions of (co)polymerization of TOX (low comonomer to monomer ratio), the first homogeneous stage or 'induction' period of the reaction is very short and ends as soon as the sequences $-(CH_2O)_n-$ $(M)_n$ are long enough to nucleate the crystallization. The final polyacetal is essentially produced during the second heterogeneous stage.

When crystallized from solution or from the melt, the POM is obtained as a stable trigonal form involving the packing of extended chains with a 9/5 helical conformation (space group $P3_1$) and a threefold screw symmetry.[137]

A metastable orthorhombic modification with a 2/1 helical conformation exists but it is transformed above 69 °C into the trigonal form.[138,139] Hexagonal lamellar single crystals are formed with chain axis orthogonal to the lamella surface (**Figures 10(a)** and **10(d)**).[95] It must be stressed that in the case of this TOX heterogeneous polymerization the relative rates of polymerization and crystallization are the key factor governing the final morphology and crystallinity. When the rate of polymerization R_p is much higher than the rate of crystallization R_c, the system behaves similarly as from crystallization from solution or melt of already formed coiled polymer chains, whereas if the rates are of the same order of magnitude ($R_c \geq R_p$) the polymerization and the crystallization take place simultaneously.[141] The latter case leads to extended-chain crystals and a higher crystallinity of the final polyacetal.

The crystallization of POM during the polymerization of TOX has been extensively studied by the Wegner group.[95,140,142,143] At the cloud point corresponding to the end of the induction period, small flat hexagonal crystals are formed with a narrow distribution of diameters. At first, a lateral tangential growth is observed and is explained by monomer insertion and chain transfer of soluble oligomers to active centers located at the side wall of the crystal (**Figures 10(b)** and **10(c)**).

Then, when polymerization is progressing, the crystal thickening starts by monomer insertion or chain transfer at the fold interface leading to a spiral growth due to a screw dislocation on the base surface of the lamella. The proposed explanation involves protonation of a terminal hydroxy group located at the interface or of an oxygen of the strained fold followed by TOX attack on the resulting oxonium and chain expansion along the chain axis. The actual mechanism probably involves a multistep process (**Scheme 42**).

Thus, the size of the crystals increases when the reaction progresses; at the same time the degree of crystallinity increases. This process does not stop even after equilibrium conversion is reached. This is explained in terms of dissolution (by depolymerization) of the smaller, less perfect crystals in favor of the thermodynamically preferred larger, more perfect crystals. The changes of crystal size and degree of crystallinity in the polymerization of TOX are illustrated by the data in **Table 7**.[95]

A low-M_n (ca. $1–3 \times 10^3$) fraction is observed in the generally bimodal size-exclusion chromatography (SEC) curves of POM. It was assigned to linear oligomers bearing -OH, -CHO, and $-OCH_3$ end groups and/or to macrocycles resulting from backbiting processes. The analysis of this fraction using hyphenated techniques (SEC/gradient polymer elution chromatography (GPEC)/NMR/matrix-assisted laser desorption/ionization-time of flight (MALDI-TOF), etc.) is extremely complex[144] and the question of macrocycles remained open for a long time. Hasegawa *et al.*[145] submitted a POM sample to heat

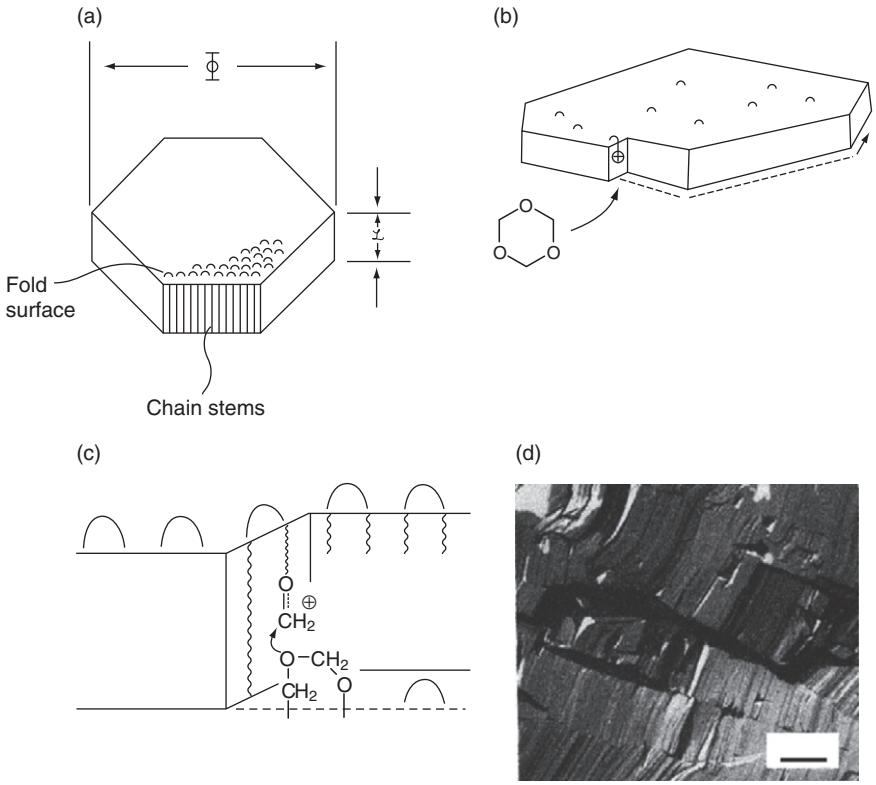

Figure 10 Crystallization of POM during the heterogeneous second stage of the polymerization of TOX: (a) extended-chain stems and folded interface. Reproduced with permission from Mateva, R.; Wegner, G.; Lieser, *G. J. Polym. Sci., Polym. Lett. Ed.* **1973**, *11*, 369,[95] figure 3; (b) monomer insertion at the crystal lateral front and tangential growth. Reproduced with permission from Wegner, G.; Rodriguez-Baeza, M.; Lucke, A.; Lieser, *G. Makromol. Chem.* **1980**, *181*, 1763,[96] figure 16a; (c) chain transfer at the crystal lateral front. Reproduced with permission from Wegner, G.; Rodriguez-Baeza, M.; Lucke, A.; Lieser, *G. Makromol. Chem.* **1980**, *181*, 1763,[96] figure 22; (d) fracture surface of extended-chain crystals. Reproduced with permission from Rodriguez-Baeza, M. *Polym. Bull.* **1991**, *26*, 521–528, 142,[140] figure 5.

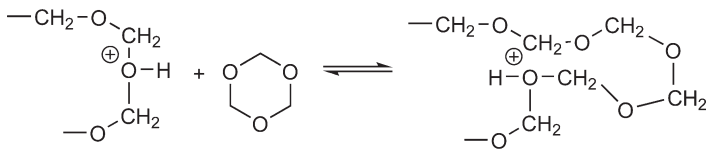

Scheme 42 Chain expansion with monomer insertion at the fold interface.

Table 7 Growth of POM crystals during cationic polymerization of TOX in nitrobenzene at 35 °C[95]

Time (h)	*Conversion (%)*	*M_n ($\times 10^{-3}$)*	*Crystal diameter (μm)*	*Crystal thickness (μm)*	*Degree of crystallinity (%)*
0.5	20	17.5	14	0.01	79.1
1.0	55	40	27	0.03	84.3
3.0	75	50	37		88.2
6.0	75	53	57	0.18	88.2
12.0	75	53	70	0.20	88.8

$[BF_3{\cdot}OEt_2] = 7.8 \times 10^{-4}$ mol l^{-1}, [TOX] = 1.8 mol l^{-1}.

and alkaline degradations and isolated a low-molecular-weight fraction with a narrow distribution which should include only the linear oligomers with stable -OCH_3 groups at both ends and the possible macrocycles. It was shown (1) that the content of this fraction with methoxy end groups was very low, and (2) that the measured M_n was close to twice the calculated M_n for two 9/5 helical extended-chain stems of the crystal lamella. A backbiting involving the neighboring loop at the fold interface was proposed to explain both the narrow distribution and the dependence of the M_n of the formed macrocycles on the crystal morphology (Figure 11).

In the case of copolymerization of trioxane with a low amount of EO, DXL, or DXP, most generally used to obtain thermal stability, the localization of the comonomer units

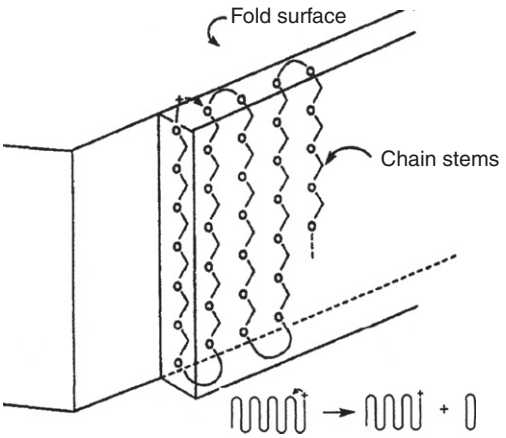

Figure 11 Formation of POM macrocycles by backbiting of an active center on the neighboring loop at the fold interface of the crystal lamella. Reproduced from Hasegawa, M.; Yamamoto, K.; Shiwaku, T.; Hashimoto, T. *Macromolecules* **1990**, *23*, 2629, scheme 4.[145]

within the semicrystalline organization of the copolymer is a central feature, and a major question to be addressed is the possibility of these comonomer units to be inserted randomly within the POM crystalline domains.

Dröscher *et al.*[143] prepared copolymers of trioxane and dioxolane which were almost completely crystalline for low comonomer concentrations. Even if a segregation was observed with an enrichment of the amorphous phase in comonomer units, an insertion of the -(CH_2-CH_2-O)- (E) segments in the crystalline -(O-CH_2)$_n$- domain was demonstrated. With respect to the trioxane homopolymer lattice, a lateral expansion (cell parameter *a*) and a contraction along the chain axis (cell parameter *c*) roughly proportional to the amount of comonomer were observed up to a mole fraction of 0.1. The density and melting point of the lattice decreased accordingly. It was also shown that for the same comonomer amount, the lattice cell of these 'extended-chain' copolymer crystals was larger than the one observed as-crystallized from the melt or solution.

The possible insertion of longer -O-(CH_2)$_4$- (B) segments in the crystalline -(O-CH_2)$_n$- lattice was recently examined in a solid-state NMR, wide-angle X-ray spectroscopy (WAXS), and differential scanning calorimetry (DSC) study of trioxane-dioxepane copolymers with a comonomer weight fraction from 0.03 to 0.3.[146] It has been shown that in these semicrystalline TOX-DXP copolymers, a part of the single dioxepane units, involved in isolated MMMBM and MBMMM pentads, is located in the crystalline phase and in the crystalline/amorphous interfacial regions. The sequences composed of more than one dioxepane unit should be rejected into the amorphous phase. The fraction *r* of B units to the total number of B and M units in the crystalline phase, including the noncrystalline/crystalline interfaces, was estimated, as well as the corresponding partitioning coefficient $P_{CI/CR}$. The latter corresponds to the ratio of *r* to the fraction *j* of B units in the copolymer and thus indicates the propensity for the dioxepane comonomer to be inserted in the crystallites and at their immediate interfaces. The variations of *r* and $P_{CR/CI}$ with the overall molar fraction φ of B units in the copolymers are presented in **Figure 12(a)**. For the lowest TOX/DXP ratio (97/3), $P_{CR/CI}$ equals 1. This means that the concentration of B units is the same in both amorphous and crystalline phases, that is, 3 wt.%, but the distribution of these B units along the POM chain should be quite different for the macromolecules of the two phases. As the initial concentration of dioxepane is increased in the feed, the partitioning coefficient $P_{CR/CI}$ decreases to a plateau value, indicating that the relative amount of B units inserted in the crystalline (and interfacial) regions gets lower and lower. A decrease in the average crystallite size occurs simultaneously with this progressive rejection of dioxepane in the amorphous phase (**Figure 12(b)**).

It was concluded that the isolated B unit which results from copolymerization of trioxane with a low concentration (ca. 3–5 wt.%) of dioxepane can be inserted in the crystal lattice and/or at its immediate interface. If an active center located on the crystal adds several successive units of DXP, the sequence cannot enter the crystal, and the active chain grows outside until either the formation of a TOX sequence long enough to allow a further crystalline accommodation or the occurrence of a transfer event. These results are in general agreement with the conclusions of the chemical approach of the induction period

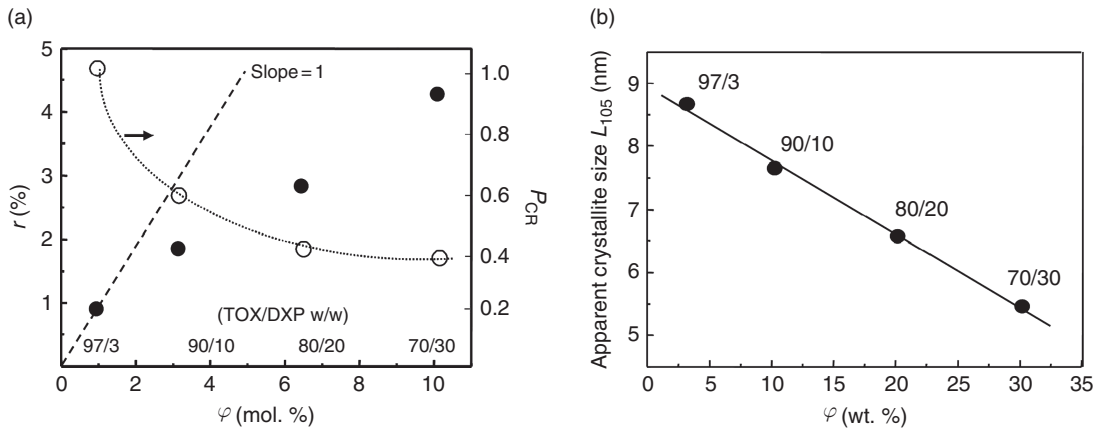

Figure 12 Insertion of isolated oxybutane-1,4-diyl (tetramethylene oxide) units (B) in the crystalline phase of trioxane-dioxepane copolymers:[145,146] (a) variation of the concentration *r* of units (B) in the interfacial and crystalline regions, and the partitioning coefficient P_{CR} of the B units with the overall molar fraction φ of B units in the TOX/DXP copolymers; (b) influence of the DXP content on the apparent crystallite size, L_{105}, estimated from WAXS measurements. Reproduced with permission from Sharavanan, K.; Ortega, E.; Moreau, M.; *et al. Macromolecules* **2009**, *42*, 8702,[113] figure 10a-b.

developed in the previous section for the trioxane-dioxepane copolymerization.

4.10.3.4 Radiation-Initiated Solid-State Polymerization of 1,3,5-Trioxane

Solid-state polymerization of TOX can be initiated by different kinds of radiation, including γ-rays, X-rays, electron beams, or α-particles.[147–149] The mechanism of initiation is not well understood. It is, however, generally accepted that radiation induces cationic polymerization. Ions or radical ions are generated by electron transfer, the loss of hydrogen ions, or the heterolytic cleavage of TOX rings.

Radiation-induced solid-state polymerization of TOX was studied intensively in the past because it was believed that it could lead to large-scale production. The process is, however, highly irreproducible and extremely sensitive to impurities.[150] Thus, although high-molecular-weight polymers can be obtained in high yields (~80%) by direct irradiation of the crystalline monomer, interest in radiation-induced polymerization is vanishing.

4.10.3.5 Properties of Poly(oxymethylene)

The only polyacetal that is made on an industrial scale (>500 × 10^3 tons per year) is POM also known as polyformaldehyde. This is a highly crystalline polymer (50–60% crystallinity for commercial products) with a crystalline melting point of ca. 180 °C and a density of 1.42 g cm^{-3} (both density and melting point, however, decrease with increasing content of oxyethylene units). The polymer is insoluble in common organic solvents; it dissolves well only in strongly hydrogen-bonded solvents (e.g., phenols) at above 100 °C, or in hexafluoroacetone at room temperature.

Polyformaldehyde is perfectly stable in even strongly basic media and moderately stable in acidic media; it is a high-performance engineering plastic.

Outlook

There are certain similarities between cationic ring-opening polymerization (CROP) of cyclic acetals and cyclic ethers. Essentially the same group of initiators may start the polymerization and in both cases the major growing species are tertiary oxonium ions of similar structure as shown below for polymerization of five-membered cyclic ether and cyclic acetal:

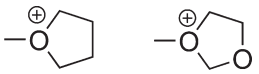

There are also, however, distinct differences between CROP of these two groups of oxygen-containing heterocyclic monomers. CROP of cyclic acetals is a ring-opening polymerization. In some respect, however, it may be considered as a borderline case between typical ring-opening and vinyl polymerization. The growing species in the CROP of cyclic acetals are mostly tertiary oxonium ions as in typical CROP of cyclic ethers. The presence of carboxonium ions in equilibrium with their oxonium counterparts and their not-negligible (due to much higher reactivity) role in propagation have been clearly established. As shown in the scheme below, carboxonium growing species of cyclic acetal polymerization bear some resemblance to growing species of vinyl ether polymerization:

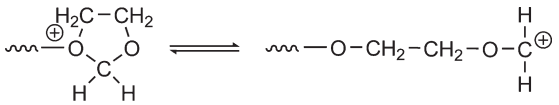

cyclic acetals

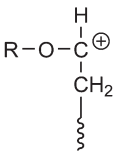

vinyl ethers

The other characteristic feature of CROP of cyclic acetals is reversibility of propagation and the high extent of chain transfer to polymer.

The smallest ring of cyclic acetal is a five-membered (weakly strained) ring; therefore, polymerization of cyclic acetals is a reversible process. Thus, an understanding of polymerization thermodynamics is important for designing workable polymerization process. Certain limitations stemming from reversibility of propagation may be overcome if polymerization, as in the case of CROP of TOX (cyclic formaldehyde trimer), proceeds with precipitation of polymer (insoluble in any solvent). Additional contribution of enthalpy of crystallization shifts the equilibrium toward polymer and polymerization of six-membered monomer, which in solution would be highly reversible, proceeds to high conversion. This is of practical importance because CROP of TOX is one of the two routes used in industry to manufacture polyacetal (polyformaldehyde).

The other characteristic feature of CROP of cyclic acetals is the high extent of chain transfer to polymer. These processes occur in many ring-opening polymerizations but because linear acetals (chain units) are more basic than cyclic acetals (monomers) they are especially pronounced in the case of cyclic acetal polymerizations. Chain transfer to polymer may be detrimental, leading to the formation of cyclic fractions or precluding the formation of block copolymers, but it may also be beneficial. In order to improve thermal stability of polyformaldehyde the sequence of -O-CH_2- units has to be from time to time interrupted by -CH_2-CH_2- units, which are introduced by copolymerizing TOX with few mole% of EO or DXL. To achieve an optimum effect, comonomer units should be distributed randomly along the chain. Due to efficient transacetalization coupled with reversibility of propagation step, this is achieved irrespective of propagation kinetics. These factors as well as the high rate of polymerization make the cationic copolymerization of TOX an industrially attractive route to polyacetal thermoplastics.

Acknowledgments

This chapter is based on large fragments of the chapter 'Cationic Ring-Opening Polymerization: Acetals' coauthored by

S. Penczek and P. Kubisa from the first edition of *Comprehensive Polymer Science,* Vol. 3, Part I. The authors of this chapter wish to express their gratitude to Professor Stanislaw Penczek for the permission to use large fragments of the text from the first edition in the present chapter.

References

1. Penczek, S.; Kubisa, P. In *Comprehensive Polymer Science*; *Vol. 3*; Allen, G., Bevington, J. C., Eds.; Pergamon Press: Oxford, UK, 1989, Part 1, p 787.
2. Kubisa, P.; Penczek, S. In *Encyclopedia of Polymer Science and Technology.* Gaylord, N. G., Bikales, N. M., Mark, H. F., Eds.; Interscience Publishers: New York, London, Sydney, Toronto, 1977; Suppl, *Vol. II*, p 161.
3. Penczek, S.; Kubisa, P.; Matyjaszewski, K. *Cationic Ring-Opening Polymerization of Heterocyclic Monomers, Part I: Mechanisms*; Springer: Berlin, Germany, 1980.
4. Schulz, R. C.; Hellerman, W.; Nienburg, J. In *Ring in Ring-Opening Polymerization*; Ivin, K. J., Saegusa, T., Eds.; Elsevier: London, UK, 1984, *Vol. I*, p 369.
5. Penczek, S.; Kubisa, P.; Matyjaszewski, K. *Cationic Ring-Opening Polymerization of Heterocyclic Monomers, Part II: Synthetic Applications*; Springer: Berlin, Germany, 1985.
6. Kubisa, P.; Penczek, S. In *Concise Encyclopedia of Polymer Science and Technology*; Kroschwitz, J. I., Ed.; Wiley-Interscience: New York, 1990; p 559.
7. Gorissen, H. In *Handbook of Polymer Synthesis*; Kricheldorf, H. R., Ed.; Marcel Dekker Inc.: New York, 1992; p 617.
8. Penczek, S.; Kubisa, P. In *Ring-Opening Polymerization*; Brunelle, D. J., Ed.; Carl Hanser: Munich, Germany, 1993.
9. Kubisa, P. In *Cationic Polymerizations*; Matyjaszewski, K., Ed.; Marcel Dekker: New York, 1996.
10. Schuerch, C. *Adv. Polym. Sci.* **1972**, *10*, 173.
11. Sumitomo, H.; Okada, M. In *Ring-Opening Polymerization*; Ivin, K. J., Saegusa, T., Eds.; Elsevier: London, UK, 1984, *Vol. I*, p 299.
12. Yokoyama, Y.; Hall, H. K. *Adv. Polym. Sci.* **1982**, *42*, 107.
13. Staudinger, H. *Die Hochmolekularen Organischen Verbindungen*; Springer: Berlin, Germany, 1922.
14. Brydson, J. A. *Plastic Materials*, 7th ed.; Butterworth-Heinemann: Oxford, UK, 1999; Chapter 19.
15. Vogl, O. *J. Polym. Sci., Part A: Polym. Chem. Ed.* **2000**, *38*, 2293.
16. Bailey, W. J.; Volpe, A. A. *J. Polym. Sci., Part A-1: Polym. Chem.* **1970**, *8*, 2109.
17. Heller, J.; Penhale, D. W. H.; Hellwing, R. F. *J. Polym. Sci., Part C: Polym. Lett.* **1980**, *18*, 293.
18. Zhang, H.; Ruckenstein, E. *J. Polym. Sci., Part A: Polym. Chem. Ed.* **2000**, *38*, 3751.
19. Hashimoto, T.; Ishizuka, K.; Umehara, A.; Koidara, T. *J. Polym. Sci., Part A: Polym. Chem. Ed.* **2002**, *40*, 4053.
20. Okada, M. *Prog. Polym. Sci.* **1991**, *16*, 1027.
21. Frisch, K. C. *Cyclic Monomers*; Wiley Interscience: New York, 1972.
22. Plesch, P. H.; Westermann, P. H. *Polymer* **1969**, *10*, 105.
23. Szwarc, M. *Makromol. Chem.* **1979**, *3*, 327.
24. Yamashita, Y.; Mayumi, J.; Kawakami, Y.; Iyo, K. *Macromolecules* **1980**, *13*, 1075.
25. Krummenacher, B.; Elias, H. G. *Makromol. Chem.* **1971**, *150*, 271.
26. Xu, B. B.; Lillya, C. P.; Chien, J. C. W. *Macromolecules* **1987**, *20*, 271.
27. Okada, M.; Sumitomo, H.; Komada, H. *Macromolecules* **1979**, *12*, 395.
28. Kops, J. *Makromol. Chem.* **1975**, *176*, 229.
29. Berlin, Al. Al.; Deberdeev, R. J.; Perukhin, Yu. W.; Garipov, R. M. *Polyoxymethylenes (in Russian)*; Nauka: Moscow, Russia, 2008.
30. Kubisa, P.; Penczek, S. *Makromol. Chem.* **1971**, *144*, 169.
31. Penczek, S.; Kubisa, P. *Makromol. Chem.* **1973**, *165*, 121.
32. Penczek, S.; Szymański, R. *Polym. J.* **1980**, *12*, 617.
33. Plesch, P. H.; Westermann, P. H. *J. Polym. Sci.* **1968**, *16*, 3837.
34. Andrews, M.; Semlyen, J. A. *Polymer* **1972**, *13*, 142.
35. Rentsch, C.; Schulz, R. C. *Makromol. Chem.* **1977**, *178*, 2535.
36. Kubisa, P.; Penczek, S. *Makromol. Chem.* **1979**, *180*, 1821.
37. Lim, N. K.; Yaccato, K. J.; Dghaym, R. D.; Arndsen, B. A. *Organometallics* **1999**, *18*, 3953.
38. Lindner, E.; Henes, M.; Wieland, W.; *et al. Organomet. Chem.* **2003**, *681*, 12.
39. Jones, F. R.; Plesch, P. H. *Chem. Commun.* **1969**, 1230.
40. Kubisa, P.; Penczek, S. *Makromol. Chem.* **1978**, *179*, 445.
41. Kubisa, P.; Penczek, S. *Macromolecules* **1977**, *10*, 216.
42. Chwiałkowska, W.; Kubisa, P.; Penczek, S. *Makromol. Chem.* **1982**, *183*, 753.
43. Słomkowski, S.; Penczek, S. *J. Chem. Soc., Perkin Trans.* **1974**, *2*, 1718.
44. Jaacks, V.; Kern, W. *Makromol. Chem.* **1963**, *62*, 1.
45. Okamura, S.; Higashimura, T.; Miki, T. *Prog. Polym. Sci. Jpn.* **1972**, *3*, 97.
46. Uryu, T.; Ito, K.; Kobayashi, K.; Matsuzaki, M. *Makromol. Chem.* **1979**, *180*, 1509.
47. Hoene, R.; Reichert, K.-H. W. *Makromol. Chem.* **1976**, *177*, 3545.
48. Kucera, M.; Pichler, Y. *Vysokomol. Soedin.* **1965**, *7*, 3.
49. Yamashita, Y.; Okada, M.; Kasahara, K. *Makromol. Chem.* **1968**, *117*, 256.
50. Rosenberg, B. A.; Irzhak, W. J.; Enikolopyan, N. S.*Interchain Exchange in Polymers (in Russian)*; Khimiya: Moscow, Russia, 1975.
51. Ledwith, A.; Sherrington, D. C. In *Comprehensive Chemical Kinetics*; Bamford, C. H., Tipper, C. F. H., Eds.; Elsevier: Amsterdam, The Netherlands, 1976, *Vol. 15*, p 67.
52. Szymański, R.; Penczek, S. *Makromol. Chem.* **1982**, *183*, 1587.
53. Kubisa, P. *J. Polym. Chem. Part A: Polym. Chem. Ed.* **1987**, *25*, 873.
54. Kruger, H.; Pasch, H.; Much, H.; *et al. Makromol. Chem.* **1992**, *193*, 1975.
55. Franta, E.; Reibel, L. *Makromol. Chem. Macromol. Symp.* **1991**, *47*, 141.
56. Franta, E.; Kubisa, P.; Ould Kada, S.; Reibel, L. *Makromol. Chem. Macromol. Symp.* **1992**, *60*, 145.
57. Weissermel, K.; Fischer, E.; Gutweiler, K.; Hermann, H. D. *Kunststoffe* **1964**, *54*, 410.
58. Weissermel, K.; Fischer, E.; Gutweiler, K.; *et al. Angew. Chem. Int. Ed.* **1967**, *6*, 526.
59. Rentsch, C.; Schulz, R. C. *Makromol. Chem.* **1978**, *179*, 1403.
60. Ischigaki, I.; Morita, Y.; Nishimura, K.; Ito, A. *J. Appl. Polym. Sci.* **1974**, *18*, 1927.
61. Kops, J. *J. Polym. Sci., Part A-1* **1972**, *10*, 1275.
62. Sumitomo, H.; Okada, M.; Hibino, Y. *J. Polym. Sci., Polym. Lett.* **1972**, *10*, 871.
63. Hall, H. K.; Steuck, M. J. *J. Polym. Sci., Polym. Chem. Ed.* **1973**, *11*, 1035.
64. Torres, L. F.; Patten, T. E. *Macromolecules* **1999**, *32*, 6958.
65. Schuerch, C. *Adv. Carbohydr. Chem.* **1981**, *39*, 157.
66. Schuerch, C. In *Encyclopediaof Polymer Science*; Mark, H. F.; Bikales, N. M.; Overberger C. G.; Menges, G., Eds.; Wiley: New York, 1985; *Vol. 13*, pp 147–162.
67. Uryu, T. In *Models of Biopolymers by Ring-Opening Polymerization*; Penczek, S., Ed.; CRC Press: Boca Raton, FL, 1990; p 133.
68. Choi, Y. S.; Uryu, T.; Yoshida, T. *Macromol. Chem. Phys.* **1997**, *198*, 2875.
69. Liang, Y. Z.; Franz, A. H.; Newbury, C.; *et al. Macromolecules* **2002**, *35*, 3402.
70. Satoh, T.; Imai, T.; Kitajyo, Y.; *et al. Macromol. Symp.* **2004**, *217*, 39.
71. Satoh, T.; Imai, T.; Ishihara, H.; *et al. Macromolecules* **2003**, *36*, 6364.
72. Okada, M.; Sumitomo, H. *Makromol. Chem. Suppl.* **1985**, *14*, 29.
73. Uryu, T.; Tachikawa, H.; Ohaku, K. I.; *et al. Makromol. Chem.* **1977**, *178*, 1929.
74. Komada, H.; Okada, M.; Sumitomo, H. *Macromolecules* **1979**, *12*, 5.
75. Fleischer, D.; Schulz, R. C. *Makromol. Chem.* **1975**, *176*, 677.
76. Okada, M.; Mita, K.; Sumitomo, H. *Makromol. Chem.* **1976**, *177*, 895.
77. Basko, M.; Kubisa, P.; Penczek, S.; *et al. Macromolecules* **2000**, *33*, 294.
78. Basko, M.; Kubisa, P. *Macromolecules* **2002**, *35*, 8948.
79. Franta, E.; Lutz, P.; Reibel, L.; *et al. Macromol. Symp.* **1994**, *85*, 167.
80. Goethals, E. J.; Walraedt, S. R.; Han, X. H.; *et al. Macromol. Symp.* **1996**, *107*, 111.
81. Declerq, R. R.; Goethals, E. J. *Macromolecules* **1992**, *25*, 1109.
82. Declerq, R. R.; Trossaert, T. G.; Hartmann, P. J.; *et al. Macromol. Symp.* **1994**, *77*, 395.
83. Wallraedt, S. R.; Goethals, E. J. *Polym. Int.* **1995**, *38*, 89.
84. Goethals, E. J.; Walraedt, S. R.; Han, X. H.; *et al. Macromol. Symp.* **1996**, *107*, 111.
85. Van Meirvenne, D.; Goethaps, E. J. *Makromol. Chem. Suppl.* **1989**, *15*, 61.
86. Du, J.; Peng, Y.; Ding, X. *Colloid Polym. Sci.* **2003**, *281*, 90.
87. Li, Y. G.; Wang, Y. M.; Pan, C. Y. *J. Polym. Sci., Part A: Polym. Chem. Ed.* **2003**, *41*, 1243.
88. Tomlison, R.; Klee, M.; Garrett, S.; *et al. Macromolecules* **2002**, *35*, 473.
89. Tomlison, R.; Heller, J.; Brocchini, S.; Duncan, R. *Bioconjug. Chem.* **2003**, *14*, 1096.
90. Rickerby, J.; Prabhakar, R.; Ali, M.; *et al. Mater. Chem.* **2005**, *15*, 1849.
91. Garipelli, K.; Kim, J.-K.; Namburg, R.; *et al. Acta Biomater.* **2010**, *6*, 477.
92. Yurkovetskiy, A. V.; Hiller, A.; Syed, S.; *et al. Mol. Pharm.* **2004**, *1*, 375.
93. Falco, E. E.; Patel, M.; Fisher, J. P. *Pharm. Res.* **2008**, *25*, 2348.
94. Goulart, G.; Sanchez, J. Y.; Armand, M. *Electrochim. Acta* **1992**, *37*, 1589.
95. Mateva, R.; Wegner, G.; Lieser, G. *J. Polym. Sci., Polym. Lett. Ed.* **1973**, *11*, 369.
96. Wegner, G.; Rodriguez-Baeza, M.; Lucke, A.; Lieser, G. *Makromol. Chem.* **1980**, *181*, 1763.
97. Hermann, H. D.; Fischer, E.; Weissermel, K. *Makromol. Chem.* **1966**, *90*, 1.
98. Kern, W.; Deibig, H.; Giefer, A.; Jaacks, V. *Pure Appl. Chem.* **1966**, *12*, 371.
99. Jaacks, V.; Kern, W. *J. Polym. Sci.* **1960**, *48*, 399.
100. Jaacks, V. *Adv. Chem. Ser.* **1969**, *91*, 371.
101. Berlin, A. A.; Bogdanova, K. A.; Rakova, G. V.; Yenikolopyan, N. S. *Vysokomol. Soedin.* **1975**, *A17* (*3*), 643.

102. Masamoto, J. *Prog. Polym. Sci.* **1993**, *18*, 1.
103. Leese, L.; Baumber, M. W. *Polymer* **1965**, *6*, 269.
104. Iguchi, M. *Br. Polym. J.* **1973**, *5*, 195.
105. Collins, G. L.; Greene, R. K.; Berardinelli, F. M.; Garruto, W. V. *J. Polym. Sci., Polym. Lett. Ed.* **1979**, *17*, 667.
106. Iwatsuki, S.; Takigawa, N.; Okada, M.; *et al. J. Polym. Sci., Polym. Lett. Ed.* **1964**, *2*, 549.
107. Chandrashekara, M. N.; Desai, D.; Chanda, M. *Eur. Polym. J.* **1985**, *21* (*9*), 833.
108. Stasinski, J.; Dmowska, G. *Makromol. Chem., Rapid Commun.* **1987**, *8*, 535.
109. Burg, K.; Schlaf, H.; Cherdron, H. *Makromol. Chem.* **1971**, *145*, 247.
110. Lu, N.; Collins, G. L.; Yang, N. L. *Macromol. Symp.* **1991**, *42/43*, 425.
111. Miki, T.; Higashimura, T.; Okamura, S. *J. Polym. Sci. A-1* **1967**, *5*, 95.
112. Burg, K. H.; Hermann, H. D.; Rehling, H. *Makromol. Chem.* **1968**, *111*, 181.
113. Sharavanan, K.; Ortega, E.; Moreau, M.; *et al. Macromolecules* **2009**, *42*, 8702.
114. Ballistreri, F. P.; Fortuna, C. G.; Musumarra, G.; *et al. ARKIVOC* **2002**, *11*, 54.
115. Baader, H.; Jaacks, K. W. *Makromol. Chem.* **1965**, *82*, 213.
116. Penczek, S. *Makromol. Chem.* **1974**, *175*, 1217.
117. Jaacks, V.; Franck, H.; Grünberger, E.; Kern, W. *Makromol. Chem* **1968**, *115*, 290.
118. Shieh, Y.-T.; Yeh, M.-J.; Chen, S.-A. *J. Polym. Sci., Part A: Polym. Chem. Ed.* **1999**, *37*, 4198.
119. Collins, G. L.; Greene, G.; Berinardelli, F. M.; Ray, W. H. *J. Polym. Sci., Part A: Polym. Chem. Ed.* **1981**, *19*, 1597.
120. Mengoli, G.; Furlanetto, F. *Makromol. Chem.* **1975**, *176*, 143.
121. Nagahara, H.; Kagawa, K.; Iwaisako, T.; Masamoto, J. *Ind. Eng. Chem. Res.* **1995**, *34*, 2515.
122. Masamoto, J.; Yamasaki, N.; Itoh, T.; *et al. Chem. Commun.* **1998**, 1809.
123. Yamasaki, N.; Kanaori, K.; Masamoto, J. *J. Polym. Sci., Part A: Polym. Chem. Ed.* **2001**, *39*, 3239.
124. Yamasaki, N.; Nagahara, H.; Masamoto, J. *Tetrahedron Lett.* **2001**, *42*, 2371.
125. Yamasaki, N.; Masamoto, J. *J. Polym. Sci., Part A: Polym. Chem. Ed.* **2004**, *42*, 520.
126. Yamasaki, N.; Masamoto, J.; Kanaori, K. *Appl. Spectrosc.* **2000**, *54*, 1069.
127. Ishida, Y.; Ohtani, H.; Abe, K.; *et al. Macromolecules* **1995**, *28*, 8702.
128. Fleischer, D.; Schulz, R. *Makromol. Chem.* **1975**, *176*, 677.
129. Opitz, G. *Plaste Kautsch.* **1975**, *22*, 951.
130. Dunn, P.; Yang, N.-L.; Grates, J. A. *Polym. Prepr.* **2000**, *41* (*1*), 381.
131. Dunn, P.; Werner, M.; Yang, N.-L.; *et al. Polym. Prepr.* **2001**, *42* (*1*), 4.
132. Fejgin, J.; Tomaszewicz, M.; Cieslak, J. *Polimery* **1976**, *21*, 298.
133. Cui, M.-H.; Zang, Y.; Werner, M.; *et al. Polym. Prepr.* **2001**, *42* (*1*), 21.
134. Cui, M.-H.; Zang, Y.; Werner, M.; *et al. ACS Symp. Ser.* **2003**, *834*, 228.
135. Frisch, K.; Reegen, S. In *Ring Opening Polymerizations (Kinetics and Mechanisms of Polymerization)*; Marcel Dekker: New York, 1969; *Vol. 2*, pp 168–169.
136. Yamashita, Y.; Okada, M.; Suyama, K.; Kasahara, H. *Makromol. Chem.* **1968**, *114*, 146.
137. Tadokoro, H.; Yasumoto, T.; Murahashi, S.; Nitta, I. *J. Polym. Sci.* **1960**, *44*, 266.
138. Carazzolo, G. A.; Putti, G. *Chim. Ind. (Milan)* **1963**, *45*, 771.
139. Kobayashi, M.; Morishita, H.; Shimonura, M.; Iguchi, M. *Macromolecules* **1987**, *20*, 2453.
140. Rodriguez-Baeza, M. *Polym. Bull.* **1991**, *26*, 521–528.
141. Wunderlich, B. *Angew. Chem.* **1968**, *24*, 1009.
142. Dröscher, M.; Wegner, G. *Ind. Eng. Prod. Res. Dev.* **1979**, *18* (*4*), 259–263.
143. Dröscher, M.; Lieser, G.; Reimann, H.; Wegner, G. *Polymer* **1975**, *16*, 4950.
144. Rittig, F.; Fandrich, N.; Urtel, M.; *et al. Macromol. Chem. Phys.* **2006**, *207*, 1026.
145. Hasegawa, M.; Yamamoto, K.; Shiwaku, T.; Hashimoto, T. *Macromolecules* **1990**, *23*, 2629.
146. Lorthioir, C.; Lauprêtre, F.; Sharavanan, K.; *et al. Macromolecules* **2007**, *40*, 5001.
147. Chapiro, A. In *Encyclopedia of Polymer Science and Technology*; Mark, H. F., Gaylord, G., Eds.; Wiley: New York, 1969, *Vol. 11*, p 702.
148. Eastmond, C. G. In *Progress in Polymer Science*; Jenkins, A. D., Ed.; Pergamon Press: Oxford, UK, 1970, *Vol. II*, p 3.
149. Chatani, Y. *Prog. Polym. Sci. Jpn.* **1974**, *7*, 149.
150. Kiss, G.; Kiss, K.; Kovacs, A. J. *J. Appl. Polym. Sci.* **1981**, *26*, 2485.

Biographical Sketches

Przemysław Kubisa, born in 1940, received MSc degree in 1963 from Warsaw University of Technology. From 1963 until 1969 he was employed in the Institute of Plastics in Warsaw as a research associate and in 1969 he joined the Center of Molecular and Macromolecular Studies (CMMS) of the Polish Academy of Sciences in Lodz. In 1972 he received his PhD (under the guidance of Prof. S. Penczek) and in 1978 his habilitation from Technical University in Lodz. P. Kubisa was a post doc in the University of Massachusetts (group of Prof. Otto Vogl) (1974) and a visiting scientist in the University of Massachusetts (1979, for a period of 6 months) and Institute Ch. Sadron in Strasbourg (1984).

P. Kubisa's research interest covers various aspects of ionic (mostly cationic) ring-opening polymerization of oxygen-containing heterocyclic monomers. He is the author or coauthor of 140 original papers and 40 book chapters or review papers. From 1991 until 2007 he was the Deputy Director of CMMS and in 2005 he succeeded Prof. S. Penczek as Head of Polymer Chemistry Department (until 2009). Presently, he is a Titular Member of IUPAC Polymer Division.

Prof. Jean-Pierre Vairon, born in 1937, studied chemistry and chemical engineering in Bordeaux (ENSCB) and got his doctoral degree in Paris (Sorbonne, 1968) in the field of mechanisms and kinetics of polymerization. He was successively associate and full professor of polymer chemistry at the University P. and M. Curie (UPMC). He became director of the polymer unit UMR 7610 associated to CNRS in 1992. He was also in charge of the polymer section and the materials program (PIRMAT) at the Department of Chemistry of CNRS (1982–90), chairman of the Scientific Council of Chemistry at UPMC (1994–97), chairman of the Theses and Habilitations Committee for Chemistry (1993–98) at UPMC, chairman of the French Polymer Group, chairman of the Polymer Division of the French Chemical Society (1994–97), and in charge of the European ERA program in chemistry at CNRS-INC (2004–10). He is a member of the French National Committee for Chemistry, a titular member of the Polymer Division of IUPAC, and French representative at the IUPAC Council. Emeritus since 2003, he is still active in polymer chemistry research. He has about 170 scientific publications and patents, and has been the supervisor of about 45 PhD students. He is Dr. h.c. of the Russian Academy of Sciences and Honorary member of the Polish Chemical Society.

4.11 ROP of Cyclic Esters. Mechanisms of Ionic and Coordination Processes

A Duda, Polish Academy of Sciences, Lodz, Poland

4.11.1 Introduction

Ring-opening polymerization (ROP) of aliphatic cyclic esters leads to aliphatic polyesters, a rediscovered class of polymers important in practice that show compatibility with natural environment (including human body) and are able to undergo hydrolytic and biological degradation after desired exploitation time.[1]

Two important discoveries that are related to mechanisms of the ROP of cyclic esters, and were made during the mid-1950s, were the following: (1) realization of a living polymerization system by Szwarc;[2] and (2) a thermodynamic description of the reversible chain-growth polymerization by Dainton and Ivin.[3] In contrast to polyesterification, living ROP provided a precise tool for the synthesis of polyesters having required molar masses and fitted with desired end groups. At this point, it should be remembered that Carothers was the first to study the polymerization mechanisms of lactones and lactides (LAs) in a more systematic way:[4,5]

where R = $(CH_2)_x$ (lactones) or $CH(CH_3)C(=O)OCH(CH_3)$ ((di)lactides).

Initially, thermodynamic polymerizability of aliphatic cyclic esters was analyzed in qualitative terms by Hall and Schneider.[6] Later, at the Gorki University, enthalpies and entropies of polymerization were determined for the most important cyclic esters.[7–12]

Until about 1975, the major effort in studies of polymerization of cyclic esters was directed toward finding an efficient initiator and/or catalyst leading eventually to the living process. Commercial availability of β-lactones and of ε-caprolactone (CL) was one of the reasons that already started extensive research programs on their polymerization at Goodrich in 1948[13] then at Union Carbide,[14] Dutch Shell,[15] and Japanese companies.[16,17] Some attempts to elucidate the polymerization mechanisms in these studies were also undertaken, particularly taking into account the ambident structure of cyclic ester monomers. Hall[18] and later Lenz and co-workers[19] carried out extensive kinetic measurements of the anionic polymerization of β-lactones, but the determined apparent

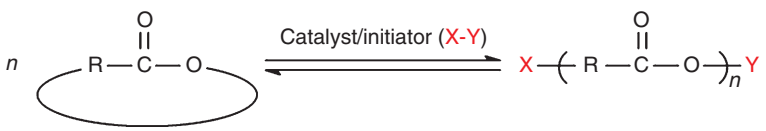

[1]

rate constants of propagation were not related to the elementary reactions.

Successful application of alumoxanes by Vanderberg[20] in stereospecific polymerization of oxiranes prompted several research groups to use these initiators for synthesis of stereoregular polyhydroxyalkanoates by polymerization of β-substituted β-lactones.[21–24] A serious drawback of this system was an unknown concentration of the actually propagating species; eventually, it was impossible to control molar masses of the resulting polyesters.

Teyssie, looking for the structurally similar but better defined initiators, introduced bimetallic alkoxido-μ-oxido compounds (e.g., $(BuO)_2Al\text{-}O\text{-}Zn\text{-}OAl(OBu)_2$) and polymerized CL in a controlled manner.[25] Similar results have been obtained with a much simpler and commercially available aluminum triisopropoxide ($Al(O^iPr)_3$).[26]

Two research groups (Slomkowski and Penczek[27] and Deffieux and Boileau[28]) applied in β-propiolactone (PL) polymerization anionic initiators bearing alkaline metal countercations complexed with crown ethers or cryptands. Concentration and structure of the involved active species have been determined, either by their direct spectroscopic observations[29,30] or by ^{31}P nuclear magnetic resonance (NMR) measurements of the polymerizing mixtures after end-capping with a phosphorus-containing reagent.[31]

Studies of cationic polymerization, carried out in parallel, solved an initial controversy concerning the nature of active species, that is, acylium versus tertiary oxonium cations, in favor of the latter ones.[32,33] Attempts of several laboratories to prepare high-molar-mass aliphatic polyesters in the controlled cationic process eventually failed.[34–39] The first example of a controlled cationic process involving cyclic ester is the activated monomer (AM) polymerization of CL, conducted in the presence of an alcohol.[40] More recently, Basko and Kubisa[41–44] published a series of papers that confirm applicability of the AM mechanism to the controlled synthesis of aliphatic polyesters. Interestingly, it has been also shown for the first time that triflic acid initiation of L,L-lactide (L,L-LA) polymerization, without a purposely introduced alcohol, leads to the living process proceeding in agreement with the AM mechanism.[44]

In spite of the living character of the anionic polymerization of PL, it was revealed that in the case of β-substituted β-lactones or medium-size cyclic esters (LA and CL) this process suffers from various side reactions such as chain transfer to monomer, racemization, segment exchange, or formation of macrocyclic esters.[45–48] Finally, it has been concluded that in the so-called coordination-insertion (pseudoanionic) polymerization, initiated with covalent metal alkoxides ($R_nMtOR'_{n-x}$, where Mt is Zn, Al, Sn, Ti, etc.), these side reactions can be kinetically suppressed or even eliminated.[25,49–52] Correlation of the selectivity parameters, defined as the ratio of rate constants of propagation and transfer (k_p/k_{tr}), with the reactivity of active species (k_p) showed that these polymerizing systems conform to the reactivity–selectivity principle.[53,54]

Systematic kinetic measurements, carried out during the past decade[55–62] revealed the importance of aggregation phenomena in the pseudoanionic polymerizations. The solution of the pertinent kinetic scheme involving aggregation[55–57] allowed determination of the absolute rate constants of propagation on the covalent species. Then, it has been shown that aluminum trialkoxide initiators of various degrees of aggregation may differ considerably in their reactivity toward cyclic esters.[26,63–66]

Application of bulky ligands that fill the space around the 'countercation' metal atom in covalent initiators prevent the aggregation – initially by Inoue and co-workers[67–69] and then by Spassky and co-workers[70,71] – resulted in new mechanistic implications. Inoue introduced a notion of 'immortal' polymerization for the already known processes with reversible chain transfer (the use of this expression is discouraged by IUPAC[72]). Polymerizations initiated with bulky chiral Schiff base Al alkoxides revealed a possibility of the stereoelective polyester synthesis starting from the chiral cyclic ester monomers.[71]

Another possibility of accelerating kinetics of the coordination polymerization of slowly polymerizing monomers (e.g., LAs) has been indicated by the DuPont team[73,74] and then explored by Feijen and co-workers[75,76] and Spassky *et al.*[77] Application of rare earth metal (La, Y, Sm, etc.) alkoxides as initiators resulted in polymerization rates characteristic for ionic active species but with kinetic suppression of side reactions on the level similar to that obtained with covalent alkoxides. The actual structure of the growing species is not yet known. Later, the use of initiators based on Zn alkoxides, which bear bulky ligands, gave a similar kinetic effect in polymerization of LA and β-butyrolactone (β-BL).[78,79]

ROP of CL and LAs seems to be a mature field. Controlled polymerization methods elaborated for these monomers allow preparation of the corresponding aliphatic polyesters in an impressively broad range of M_n: from $\approx 10^2$ up to $\approx 10^6$ g mol^{-1} (see, e.g., Reference 61). Living and controlled polymerization conditions have been established for PL already in 1976,[27,28] but the controlled polymerization of the corresponding β-substituted monomers (e.g., β-BL) still pose a serious challenge[45,46,79,80] due to chain transfer and termination side reactions. It is worth noting, however, that systematic studies carried out among others by Carpentier[81] with various ligand/metal alkoxide combinations led recently to a remarkable progress, particularly in the stereocontrolled polymerization of the racemic β-BL.

Catalyst, which is still the most important in the practical, synthetic, and industrial applications, is tin(II) 2-ethylhexanoate (tin octoate, $Sn(Oct)_2$).[82–84] Therefore, $Sn(Oct)_2$-catalyzed polymerizations of cyclic esters have been systematically studied since 1980s.[85–90] The detailed mechanism of this process remained obscure for a long time. Complementary kinetic, mass spectrometric, and NMR measurements revealed that the initiating and then growing species have the tin(II) alkoxide structure and are formed from the starting carboxylate in the exchange reaction with hydroxy-group-containing compounds (ROH).[91–96] The results coming then from other laboratories, thus, confirmed the formulated polymerization mechanism in the cyclic ester/$Sn(Oct)_2$/ROH system.[97–102]

Finally, in these introductory remarks, the metal-free organocatalytic polymerization of cyclic esters should also be mentioned (see, e.g., References 103–105 and the corresponding papers cited therein). Actually, this area has a long history that has been recently given a new life. Polymerization of β-lactones initiated, for example, with phosphines was already described in the early 1980s, including stereoselective

polymerization of unsymmetrically substituted monomers with optically active phosphines (References 106 and 107 and preceding papers cited therein). In the new series of organocatalytic polymerizations, usually the molar masses are limited and it is not convincing that polymerizations are living indeed, even if this expression is used throughout the papers. Initiation with phosphines or other organic bases leads to zwitterions, and the anionic part, alkoxide anion, is becoming active species known to lead to the chain transfer in CL and LA polymerization.

The same may happen in polymerization initiated with carbenes, providing as well alkoxide anions, at least according to the reaction scheme given by the authors of the pertinent papers (e.g., References 105 and 108). Also, in this process, molar masses are rather moderate and do not exceed $M_n \approx 3 \times 10^4\,g\,mol^{-1}$.

The metal-free, organocatalytic polymerizations encompassing anionic and cationic processes are also thoroughly reviewed in Chapter 4.06 and, therefore, are omitted in this chapter.

Mechanisms of ionic and coordination processes of aliphatic cyclic esters polymerizations have been reviewed systematically since the late 1960s (see, e.g., References 109–116), also including chapters in the first edition of the *Comprehensive Polymer Science*.[117,118] This chapter is based on the previous reviews coauthored by the present author;[111,114,119–122] however, it is supplemented by additional and more recent data (until the beginning of 2011).

4.11.2 Thermodynamics of ROP of Cyclic Esters

A more general description of the thermodynamics of ROP of cyclic monomers is given by Penczek in Chapter 4.02. The ability of a cyclic ester to polymerize by the ring-opening mechanism is determined by two equally important factors – conversion of monomer molecules to macromolecules (of linear or more complex topologies) must be allowed both thermodynamically and kinetically. Practically, this means that (1) the monomer–macromolecule equilibrium has to be shifted to the right-hand side (macromolecule), and (2) the corresponding polymerization mechanism should exist that could enable conversion of monomer molecules to polymer repeating units, within an operable polymerization time.

An elementary reaction of the macromolecular chain growth can be written as

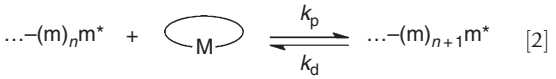

[2]

where M = $(CH_2)_xC(O)O$ (lactone) or $[CH(CH_3)C(O)O]_2$ (lactide); m* denotes the active species, and k_p and k_d are the rate constants of propagation and depropagation, respectively.

The formal thermodynamic criterion of a given monomer polymerizability is related to a sign of the Gibbs energy of polymerization (cf. eqn [3]):

$$\Delta G_p(xy) = \Delta H_p(xy) - T\Delta S_p(xy) \qquad [3]$$

where x and y denote monomer and polymer states, respectively (i.e., x and/or y = l, liquid; g, gaseous; c, solid amorphous; c′, solid crystalline; s, solution), $\Delta H_p(xy)$ and $\Delta S_p(xy)$ the corresponding enthalpy and entropy of polymerization, and T the absolute temperature.

In agreement with general rules of thermodynamics of chemical processes, only for $\Delta G_p(xy) < 0$ the polymerization is possible. It has to be stressed, however, that the $\Delta G_p(xy)$ values usually depend on the monomer and polymer states. Further discussion will be related to ROP carried out in solution or in the monomer/polymer melt and at constant temperature and pressure.

Gibbs energy of polymerization (ΔG_p) may be expressed as a sum of standard enthalpy of polymerization (ΔG_p^o) and a term related to instantaneous concentrations of monomer ([M]) and growing polymer ([…-m*]):

$$\Delta G_p = \Delta G_p^o + RT \ln \frac{[\ldots\text{–}(m)_{i+1}m^*]}{[M][\ldots(m)_i m^*]} \qquad [4]$$

where R denotes the gas constant and T the absolute temperature.

Following Flory's assumption that the reactivity of the active center, located at a sufficiently long polymer chain, does not depend on its polymerization degree (P_i), and taking into account that $\Delta G_p^o = \Delta H_p^o - T\Delta S_p^o$ (where ΔH_p^o and ΔS_p^o denote a standard polymerization enthalpy and entropy, respectively), we obtain:

$$\Delta G_p = \Delta H_p^o - T(\Delta S_p^o + R \ln[M]) \qquad [5]$$

In contrast to polymerization of a large majority of unsaturated monomers, ROP of cyclic monomers is often accompanied by the presence of a relatively high concentration of the unreacted monomer when the process comes to equilibrium. This feature is related to pronounced reversibility of the propagation step (i.e., relatively high k_d in comparison to k_p, eqn [2]). Thus, the value of the equilibrium monomer concentration ($[M]_{eq}$) at a given temperature is usually taken as a measure of the thermodynamic polymerizability of the monomer. The corresponding thermodynamic formalism has been developed by Dainton and Ivin in 1948–1958[3,123] and then by Tobolsky and Eisenberg.[124–126]

At equilibrium ($\Delta G_p = 0$), that is, after the polymerization does not occur, the monomer concentration ($[M]_{eq}$) assumes a value determined by standard polymerization parameters (enthalpy, ΔH_p^o and entropy, ΔS_p^o) and polymerization temperature (see, e.g., References 123–133):

$$\ln[M]_{eq} = \left(\frac{\Delta H_p^o}{RT}\right) - \left(\frac{\Delta S_p^o}{R}\right) \qquad [6]$$

Depending on the starting monomer concentration ($[M]_0$), or actually on the $([M]_0 - [M]_{eq})/\Sigma[\ldots\text{–}m_i^*]$ ratio, for a given concentration of active species ($\Sigma[\ldots\text{–}m_i^*]$), polymers of various number-average polymerization degrees (P_n) could be formed (note that eqn [5] is valid only under Flory's assumption that the reactivity of the active center, located on a sufficiently long macromolecule, does not depend on its polymerization degree (P_i)).

Thus, the polymerization is possible only when $[M]_0 > [M]_{eq}$. For shorter, oligomeric chains ($P_n \leq 20$), not conforming to the Flory's assumption in the expressions for $[M]_{eq}$, reactivities of active species have to be taken into account (see Appendix in Reference 134):

$$\ln\left(\frac{P_n}{P_n - 1}[M]_{eq}\right) = \frac{\Delta H_p^o}{RT} - \frac{\Delta S_p^o}{R} \qquad [7]$$

Figure 1 gives an example of application of relationship [7] for determination of the standard thermodynamic parameters in the ROP of 1,4-dioxan-2-one (DX) using the experimentally determined $[M]_{eq}$'s at various temperatures.

The slope and intercept of this dependence gives an access to ΔH_p^o and ΔS_p^o values, respectively.[134] Another typical method of ΔH_p^o and ΔS_p^o determination is based on the monomer and polymer combustion and specific heat measurements.[7–12] In turn, the thus determined thermodynamic parameters allow estimation of the corresponding $[M]_{eq}$ values, which is particularly useful when $[M]_{eq}$ is close to 0.

The values of thermodynamic parameters characterizing the polymerization ability of representative cyclic esters are compared in Table 1.

The driving force for the polymerization of the majority of cyclic esters is their ring strain, reflecting the deviation from the non-distorted bond angle values, bond stretching and/or compression, repulsion between eclipsed hydrogen atoms, and nonbonding interactions between substituents (angular, conformational, and transannular strain). For systems in which the specific monomer–polymer–solvent interactions can be neglected, enthalpy of polymerization is a measure of the ring strain.

Polymerization of the majority of monomers is accompanied by an entropy decrease, mostly due to the loss of the translational degrees of freedom. In this situation, polymerization is thermodynamically allowed only when the enthalpic contribution to ΔG_p prevails (thus when $\Delta H_p < 0$ and $\Delta S_p < 0$, the inequality $|\Delta H_p| > -T\Delta S_p$ is required; cf. eqn [5]). Therefore, the higher the ring strain, the lower the resulting monomer concentration at equilibrium (eqn [6]).

Although the formation of the three-membered α-lactone intermediates in the nucleophilic substitution of α-substituted carboxylate anions was postulated on the basis of quantum mechanical calculations,[138] these cyclic esters have never been isolated. The four-membered PL ranks among the most strained cyclic monomers and its equilibrium monomer concentration is unmeasurably low, namely, about 10^{-11} mol l^{-1} at room temperature. However, the six-membered monomers, namely, L,L-LA or DX, have relatively high equilibrium monomer concentrations that cannot be neglected in practical considerations. Thus, the equilibrium concentration appeared considerably high, especially at elevated temperatures (at which L,L-LA is usually polymerized). For the temperature range from 80 to 133 °C, $[L,L\text{-LA}]_{eq}$ changes from 0.058 to 0.151 mol l^{-1}. This six-membered cyclic diester (dilactone) assumes irregular skew-boat conformation, in which two ester groups can adopt planar conformation, and has, therefore, a relatively high enthalpy of polymerization equal to 22.9 kJ mol^{-1}. This is very close to the ring strain of δ-valerolactone (VL) and CL, equal to 27.4 and 28.8 kJ mol^{-1}, respectively. Strain comes in these compounds from C–H bond interactions and from distortion of the bond angles. The carbonyl group introduces a certain extent of strain into six-membered rings due to the flat geometry of the ester grouping (…–CH_2–C(=O)–O–…). In contrast, high ring strain in the four-membered PL is mostly due to the bond angle distortion and bond stretching.

In the five-membered cyclics, ring strain comes almost exclusively from the conformational interactions. It is known, however, that the five-membered lactones are not strained because of the reduced number of the C–H bond oppositions, caused by the presence of the carbonyl group in the monomer ring. Indeed, for γ-butyrolactone (γ-BL) we have $\Delta H_p^o = 0.4$ kJ mol^{-1} and $\Delta S_p^o = -0.4$ J mol^{-1} K^{-1}. These give $[\gamma\text{-BL}]_{eq} \approx 5.1 \times 10^3$ mol l^{-1}, whereas the monomer concentration in bulk does not exceed 13 mol l^{-1}. Therefore, in the majority of polymer chemistry textbooks it is stated that γ-BL is not able to polymerize.[127,139–143] γ-BL is indeed not able to give a high-molar-mass homopolymer, but this feature is sometimes incorrectly identified with the inability of BL to undergo the ring-opening reaction at all.

Interestingly enough, introduction of the double bond into the five-membered lactone ring introduces some extent of strain and makes its polymerization feasible as it was observed for α-angelicalactone (Structure 1).[144]

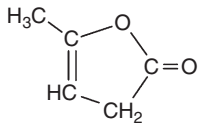

1

Hall and co-workers[145,146] explained some of these thermodynamic features in terms of comparison of the

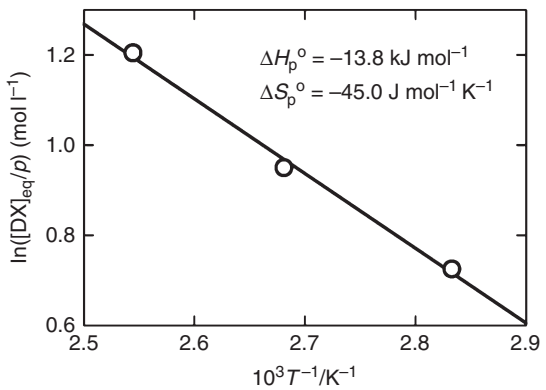

Figure 1 Plot of $\ln([DX]_{eq}/p)$ (where $p = (P_n - 1)/P_n$) on the reciprocal of the absolute temperature (eqn [7]). Bulk oligomerization of 1,4-dioxan-2-one (DX) initiated with a butan-1-ol/tin(II) octoate mixture.[134]

Table 1 Standard thermodynamic parameters of polymerization of some cyclic monomers

Monomer	Ring size	xy	$\Delta H_p^{o\,a}$ (kJ mol^{-1})	$\Delta S_p^{o\,a}$ (J mol^{-1} K^{-1})	$[M]_{eq}^{b}$ (mol l^{-1})	Reference
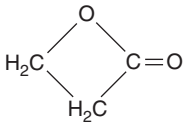 β-Propiolactone (PL)	4	lc′	–82.3	–74	3×10^{-11}	7
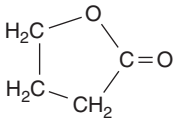 γ-Butyrolactone (γ-BL)	5	lc	5.1	–29.9	3.3×10^{3}	8
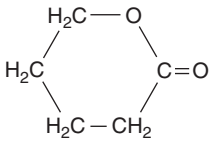 δ-Valerolactone (VL)	6	lc′	–27.4	–65.0	3.9×10^{-1}	9
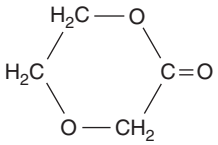 1,4-Dioxan-2-one (DX)	6	ls	–13.8[c]	–45[c]	2.5[d]	134
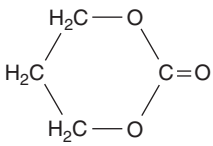 Trimethylene carbonate (TMC)	6	ss	–26.4[e]	–44.8[e]	5.1×10^{-3}	135
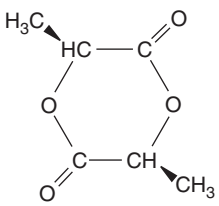 L,L-Lactide (L,L-LA)	6	ss	–22.9[f]	–41.1[f]	1.2×10^{-2}	136
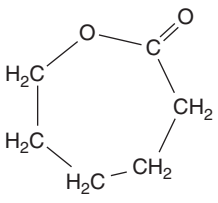 ε-Caprolactone (CL)	7	lc′	–28.8	–53.9	5.1×10^{-2}	12
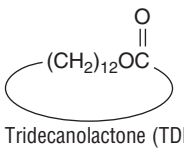 Tridecanolactone (TDL)	14	ll	–8	26	2.3×10^{-2}[g]	137

(*Continued*)

Table 1 (*Continued*)

Monomer	Ring size	xy	$\Delta H_p^{o\,a}$ (kJ mol^{-1})	$\Delta S_p^{o\,a}$ (J mol^{-1} K^{-1})	$[M]_{eq}^{b}$ (mol l^{-1})	Reference
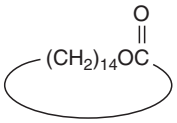 Pentadecanolactone (PDL)	16	II	3	23	0.70[h]	10

[a]At 298 K, if not indicated otherwise.
[b]If not indicated otherwise, calculated from eqn [6], ΔHp^0 and ΔSp° determined thermochemically; standard state: weight fraction = 1; concentrations recalculated from weight fractions to mol l^{-1}.
[c]ΔHp^0 and ΔSp° determined from the experimental $[M]_{eq}$ vs. T^{-1} dependence in monomer/polymer melt, using eqn [7]; standard state: 1 mol l^{-1}.
[d]At 373 K.
[e]ΔHp^0 and ΔSp° determined from the experimental $[M]_{eq}$ vs. T^{-1} dependence in THF solution, using eqn [6]; standard state: 1 mol l^{-1}.
[f]ΔHp^0 and ΔSp° determined from the experimental $[M]_{eq}$ vs. T^{-1} dependence in 1,4-dioxane solution, using eqn [6]; standard state: 1 mol l^{-1}.
[g]At 430 K.
[h]At 370 K.

exergonic character of the ring-opening processes and stability of the coiled conformation of compounds modeling the corresponding polyester chain by means of quantum mechanical calculations.

The thermodynamic data in Table 1 characterizing large lactones (tridecanolactone and pentadecanolactone) suggest that an increase in the ring size leads to a rather small ring strain (if any) and to an increase in the polymerization entropy. The latter is due to a relatively high flexibility of the long polymethylene sequences in the resulting polymer chains.

Figure 2 illustrates characteristic changes of the standard thermodynamic parameters with increasing ring size of lactones shown on the example of bulk polymerization of lactones. Similar dependencies were also observed for other monomers, with only slight changes of positions of the local minima or maxima on the thermodynamic parameter – ring size (n) dependences.[128,133,139] Although ΔG_p^o is temperature dependent, this figure gives at least a qualitative picture of ΔG_p^o versus n changes.

It has also to be stressed that analysis of a given polymerization process, based on the values of the corresponding thermodynamic parameters available in the literature, requires some caution. First of all, ΔH_p^o and ΔS_p^o depend substantially on the monomer and polymer states. For example, thermochemical measurements (heats of combustion and specific heats) gave for 16-membered pentadecanolactone in the liquid phase $\Delta H_p^o = 3$ kJ mol^{-1} and $\Delta S_p^o = 23$ J mol^{-1} K^{-1}, whereas in the crystalline phase $\Delta H_p^o = -39$ kJ mol^{-1} and $\Delta S_p^o = -86$ J mol^{-1} K^{-1}.[10] The difference between these two sets of parameters is caused by the contribution of enthalpies and entropies of phase transitions (crystallization/melting).

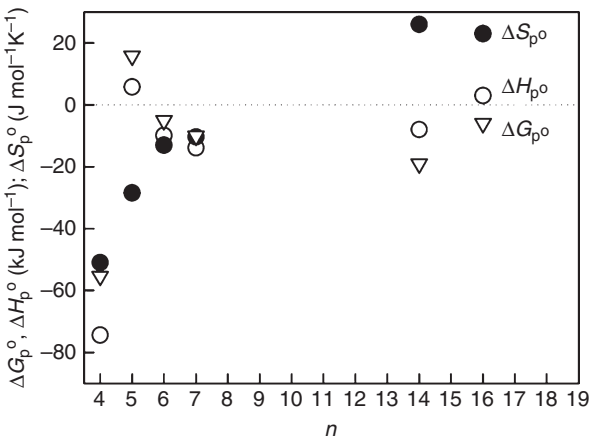

Figure 2 Dependences of standard Gibbs energy (ΔG_p^o, ▽), enthalpy (ΔH_p^o, ○), and entropy (ΔS_p^o, ●) of lactone polymerization on the ring size (n). Temperatures from 350 to 430 K, monomer and polymer liquid. Data taken from References 7–10, 12, and 137.

4.11.2.1 Thermodynamics of ROP of Cyclic Esters: Some Particular Cases

4.11.2.1.1 Thermodynamics of γ-BL (co)polymerization

As already mentioned, several polymer chemistry textbooks claimed that polymerization of γ-BL and/or its ring opening at ambient conditions is not possible.[128,139–143]

Actually, in polymerization of γ-BL initiated with $Al(O^iPr)_3$, a series of short-chain oligomers are formed:

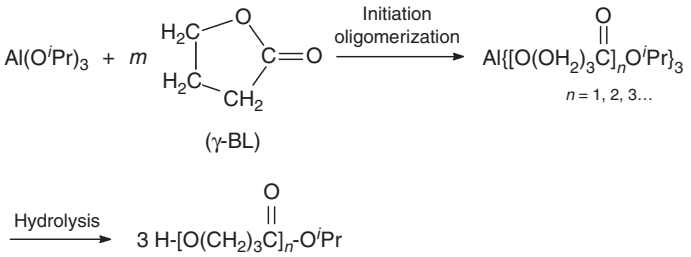

[8]

Both gel permeation chromatography (GPC) and mass spectroscopy show that oligomers are indeed formed (Figure 3).

These results indicate again that the equilibrium constants for the first few monomer additions (K_0, K_1, …) are not the same, as those for addition to a high polymer (K_n). Apparently, there is an influence of the head end group and the conformational flexibility of the macromolecule. Formally, the contribution to the Gibbs energy of the simple concentration term, $RT\ln[M]$ is based on the assumed equality $[\ldots\text{-}(m)_n\text{-}\ldots] \approx [\ldots\text{-}(m)_n\text{+}1\text{-}\ldots]$. For short poly(γ-BL) (Pγ-BL) chains, when this equality does not hold, the expression for the Gibbs energy should read

$$\Delta G_n = \Delta H_n - T\left(\Delta S_n^{\circ} - R\ln\frac{[\text{poly}(\gamma\text{-BL})_{n+1}]}{[\gamma\text{-BL}][\text{poly}(\gamma\text{-BL})_n]}\right) \qquad [9]$$

For mostly short chains, the inequality takes place, $[\text{poly}(\text{BL})_n] > [\text{poly}(\gamma\text{-BL})_{n+1}]$, and the entropic term may outweigh the $\Delta H_n \geq 0$, making $\Delta G_n < 0$ and, thus, allowing shorter chains to be formed.

γ-BL also copolymerizes with other lactone monomers, giving high-molar-mass copolymers.[147–151] For example,

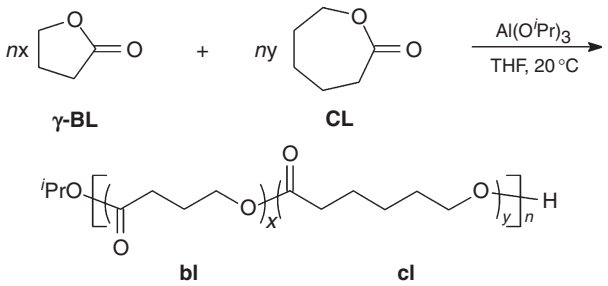

[10]

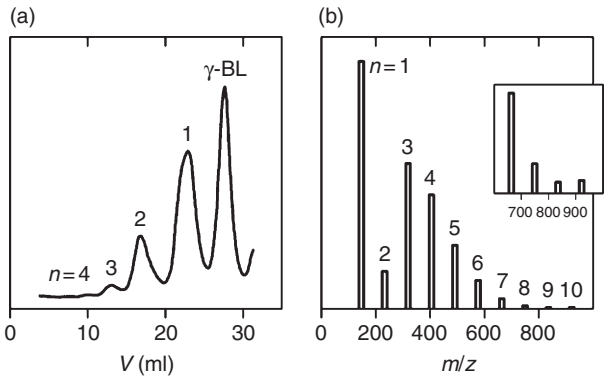

Figure 3 Oligomerization of γ-butyrolactone (γ-BL) initiated with $Al(O^iPr)_3$. (a) GPC trace and (b) mass spectrum (chemical ionization) of the isolated series of linear oligomers: H-[O(CH$_2$)$_3$C(O)]$_n$-O^{i}Pr. Conditions of oligomerization: $[\gamma\text{-BL}]_0 = 3.8\ \text{mol l}^{-1}$, $[Al(O^iPr)_3]_0 = 0.2\ \text{mol l}^{-1}$, THF, 80 °C.[148]

The dependence of the bl polymer units content in the copolymer (X_{bl}), on the γ-BL monomer content in the feed (X_{BL}) is shown in Figure 4. As it could be expected from copolymerization of a monomer unable to give high polymers, even at the high excess of γ-BL in the feed the bl content in copolymer should not exceed 50 mol-%. Thus, one could expect formation of the copolymer close to alternating at a sufficiently large excess of γ-BL. Actually, ^{13}C NMR spectra analysis pointed to the pseudoperiodic copolymer structure.[149] The γ-BL/CL copolymer synthesis was successful because the γ-BL monomer addition to its own …–bl* active chain ends is highly reversible, whereas γ-BL is winning in additions to …–cl* active chain ends since γ-BL is taken in a high excess over CL ([γ-BL] > [CL]) (Figure 4).

4.11.2.1.2 Copolymerization of LA after reaching polymer–monomer equilibrium

The situation of a monomer incapable of giving high polymers at a certain temperature and in a certain monomer concentration range is similar to a monomer that does homopolymerize, but is reaching its polymer–monomer equilibrium. At these conditions, no further increase in conversion takes place. Introduction of another monomer at this moment, capable of homopolymerizing (and copolymerizing), leads to formation of the block copolymer with a junction unit following the first homopolymer block and buildup of a graded copolymer. This was observed when LA has been brought to the polymer–monomer equilibrium and then CL was introduced into the system.[153]

The actual process is illustrated by the kinetic data in Figure 5. Thus, homopolymerization of LA has been brought to equilibrium and reached $[LA]_{eq} = 0.06\ \text{mol l}^{-1}$. Then CL was introduced at $[CL]_0 = 0.84\ \text{mol l}^{-1}$ and copolymerization started. LA was virtually consumed when less than $0.2\ \text{mol l}^{-1}$ of CL remained and finally homopolymerization of CL proceeded. One could imagine that the proper choice of a monomer and other conditions would give even a lower proportion of comonomer needed for complete conversion of LA.

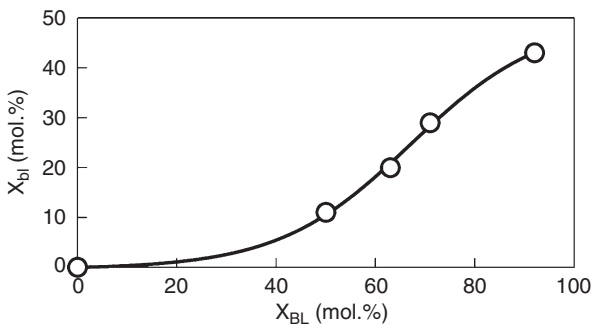

Figure 4 Dependence of the γ-butyryl (bl) unit content in the γ-butyrolactone (γ-BL)/ε-caprolactone (CL) copolymer ($X_{bl} = 100[bl]/([bl] + [cl])$) on the γ-BL monomer content in the feed ($x_{BL} = 100[BL]_0/([BL]_0 + [CL]_0)$).[152]

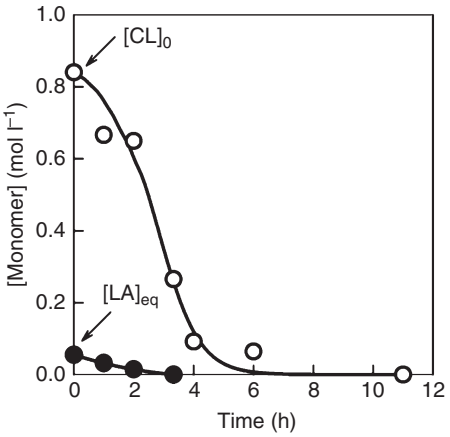

Figure 5 Kinetics of copolymerization of L,L-lactide (LA) (•) and ε-caprolactone (CL) (○). Conditions: $[CL]_0/[LA]_{eq} = 15.3$, $[CL]_0 = 0.89\ mol\ l^{-1}$; 80 °C, THF, M_n (living PLA) = 4780.[153]

This phenomenon is of interest since it allows a polymer to be produced with complete conversion of a monomer below its $[M]_{eq}$.

$$([LA]_{eq})_{co} = \frac{1}{1 + ([\ldots\text{–cl–la}^*]_{eq}/[\ldots\text{–la–la}^*]_{eq})} \times ([LA]_{eq})_{homo} \qquad [11]$$

Equation [11], derived in Reference 153, shows that except $[\ldots\text{–cl–la}^*] = 0$, the equilibrium concentration of LA in copolymerization would always be lower than that in homopolymerization. The research should, thus, be directed toward comonomers giving an as-high-as-possible ratio of active centers resulting from cross- and homopropagations: $[\ldots\text{–cl–la}^*]/[\ldots\text{–la–la}^*]$.

4.11.2.1.3 Polymerization in heterogeneous systems

Polymerization of industrially important monomers, such as DX or LA, is usually carried out above the melting temperature of their polymers in homogeneous melt. Under these conditions (i.e., above 110 °C for poly(DX) and 180 °C for poly(LA)), the equilibrium monomer concentrations are relatively high, namely, $[DX]_{eq} > 2.5\ mol\ l^{-1}$ and $[LA]_{eq} > 0.32\ mol\ l^{-1}$, because of the moderate ring strain in the six-membered monomers. The molar fraction of the unreacted monomers can be, however, reduced by aging the living polymerization mixtures below the melting temperature of the polyesters formed. Under these modified conditions, poly(DX) and poly(LA) crystallize, and the volume of the liquid phase, in which the unreacted monomer still remains, decreases. Then, [M] increases temporarily above the $[M]_{eq}$ and then an additional polymerization of the monomer proceeds, leading to an apparent decrease in $[M]_{eq}$ (actually molar fraction of M), resulting eventually in almost complete monomer consumption. This result is achieved despite the conclusions that could be drawn from the values of the thermodynamic parameters in Table 1 for both discussed monomers.[154,155] This problem has already been discussed for the example of 1,3,5-trioxane bulk polymerization, in the first edition of the *Comprehensive Polymer Science*.[156] Similar phenomena may also take place in other heterogeneous polymerizing systems (see also Chapter 4.25).

4.11.3 Kinetics of the ROP of Cyclic Esters

4.11.3.1 Kinetic Polymerizability

Polymerizability, in the frame of the formalism of propagation kinetics, is related to the sign of the molar Gibbs energy of activation ($\Delta G_p^{\neq}$) – a measure of the energy barrier in the elementary act of propagation (eqn [2]), for which $\Delta G_p^{\neq}$ assumes exclusively positive values. The instance for which $\Delta G_p^{\neq} < 0$ means that a given reaction is more complex and does not exclusively corresponds to the elementary act of the polymer chain growth. The resulting rate constant of propagation (k_p, eqn [12], Reference 157) for a given mechanism and structure of active centers should assume values assuring operable polymerization times at a given temperature.

$$k_p = \frac{k_b T}{h} \exp\left(-\frac{\Delta G_p^{\neq}}{RT}\right) = \frac{k_b T}{h} \exp\left(-\frac{\Delta H_p^{\neq}}{RT} + \frac{\Delta S_p^{\neq}}{R}\right) \qquad [12]$$

where k_b, h, $\Delta H_p^{\neq}$, and $\Delta S_p^{\neq}$ denote the Boltzmann constant, Planck constant, enthalpy, and entropy of activation, respectively.

As it is already stressed in the Introduction, the fulfillment of thermodynamic requirements is a necessary but not sufficient prerequisite for a polymerization to occur. In general, the 'thermodynamic polymerizability' cannot be taken as a direct measure of monomer reactivity. For instance, the rate constants of alkaline hydrolysis of γ-BL and CL at comparable conditions are close to each other (1.5×10^{-4} and $2.6 \times 10^{-4}\ l\ mol^{-1}\ s^{-1}$, respectively)[158] although the corresponding ring strains differ considerably (cf. Table 1).

The difference in ring strain of β-lactones and higher lactones could also suggest that the polymerization rate of the former should be much higher than, for example, that of CL. However, the opposite is true: for example, in the $Al(O^iPr)_3$ – initiated polymerization, k_p(β-BL) = 4×10^{-3} and $k_p(CL) \approx 30\ l\ mol^{-1}\ s^{-1}$ ($[M]_0 = 2\ mol\ l^{-1}$, 80 °C, THF);[159] see also a similar difference in PL and CL reactivities[160–162] in ionic polymerization. This observation can, possibly, be explained by two effects (Scheme 1).[29,33,163,164]

Steric hindrance that hampers the attack of active species on the acyl carbonyl is much more pronounced in the flat β-BL molecule compared with the folded CL molecule. Moreover, the nucleophile addition leads to a change in hybridization of the attacked carbon atom from sp^2 to sp^3. In the β-BL case, an

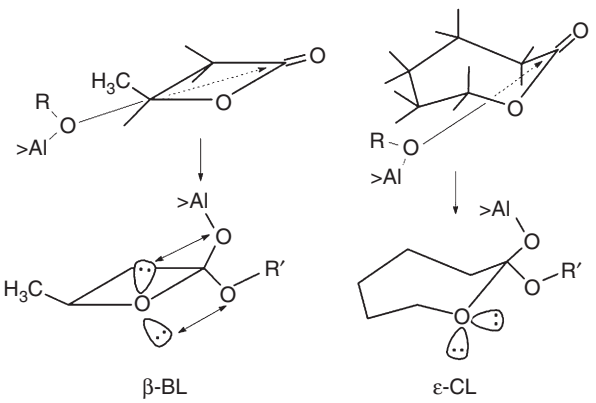

Scheme 1

additional strain appears caused by interaction of the free electron pair of the endocyclic oxygen atom with the exocyclic C=O group in the *cis* conformation forced by the ring topology. The gauche conformation in the CL case does not produce any additional energy barrier of that kind.

The order of monomer reactivities may also depend on the polymerization mechanism as has been revealed, for example, by kinetic studies of polymerization of the 6-, 7-, 9-, 12-, 13-, 16, and 17-membered lactones initiated with the zinc 2-ethylhexanoate/butan-1-ol system[165] or catalyzed enzymatically.[165,166] For the resulting Zn alkoxide propagating species, the following relative rates have been measured: 2500, 330, 21, 0.9, 1, 0.9, and 1, respectively (bulk polymerization, 100 °C). Since the active species operating in polymerization of various lactones in this system are structurally identical, namely,….–C(O)$(CH_2)_{m-1}CH_2O$–Zn–…, the order of the resulting polymerization rates is equivalent to the order of lactone reactivities. Comparison of the lactone ring sizes with the relative polymerization rates shows that the larger the lactone ring, the lower is its reactivity (reactivities of the 12-, 13-, 16-, and 17-membered lactones are practically identical taking into account the experimental error). It can be expected that in the transition state of propagation this strain is partly released and the resulting $\Delta H_p^{\neq}$ is lower for strained monomers in comparison with the nonstrained ones. Probably, this is the main reason why the lactone reactivities decrease with increasing their sizes and eventually reach a constant value for larger rings. Other factors, such as the electrophilicity of the monomer acyl or steric hindrance hampering the approach of the active species to the lactone ester group, probably play a minor role.

Interestingly, the relative rate order of the enzymatic polymerization shows an inverse dependence on the ring size, namely, 0.10:0.13:0.19:0.74:1.0 for the 7-, 12-, 13-, 16-, and 17-membered lactones, respectively.[165] This kinetic behavior can be explained assuming that in enzymatic polymerization, the rate-determining step involves formation of the lactone–enzyme complex. The latter reaction is promoted by hydrophobicity of the lactone monomer, which is higher for large lactone rings. Concluding, thermodynamic and kinetic polymerizabilities for enzymatic processes with regard to the monomer ring sizes are in the opposite order.

The reaction of initiator with monomer (eqn [13a]) should lead to active species capable of adding new monomer molecules (eqn [13b]) faster than they undergo any side reactions (e.g., termination (eqn [13c]) or transfer to monomer (eqn [13d])).

$$\mathrm{I} + \text{M} \xrightarrow{k_i} \text{I-m}^* \qquad [13a]$$

$$\text{…–(m)}_n\text{m}^* + \text{M} \underset{k_d}{\overset{k_p}{\rightleftharpoons}} \text{…–(m)}_{n+1}\text{m}^* \qquad [13b]$$

$$\text{…–(m)}_n\text{m}^* + \text{X} \xrightarrow{k_t} \text{…–(m)}_n\text{m-X} \qquad [13c]$$

$$\text{…–(m)}_n\text{m}^* + \text{M} \xrightarrow{k_{tr}} \text{…–(m)}_n\text{m} + \text{m}^* \qquad [13d]$$

where I denotes the initiator molecule, X the terminating agent, and k_p, k_d, k_t, and k_{tr} the rate constants of propagation, depropagation, termination, and chain transfer to monomer, respectively.

For an ideal living polymerization, $k_t = 0$ and $k_{tr} = 0$ (however, a transfer could occur though reversible[72]). ROP of cyclic esters, the subject of this chapter, could also proceed as living processes. However, the molar mass and end group control of the resultant polymer are possible only when $k_i \geq k_p$ and $k_{tr} = 0$.

4.11.3.2 Initiators and Active Centers: Structures and Reactivities

Extensive lists of initiators and catalysts used in anionic and coordination polymerizations can be found in several reviews (see, e.g., References 111, 167, and 168). In spite of the fact that dozens of 'new' initiators were reported every year in the past decades, for the purpose of this discussion, it is enough to say that, for the four-membered PL, ionic metal carboxylates (most often with K^+, Li^+, or Na^+ counterions) can be used, whereas for higher lactones and LAs, exclusive initiation with the alkoxides is possible. Multivalent metal (e.g., Zn, Sn(II), Al, Sn(IV), Ti, or Zr) alkoxides, giving a good compromise between reactivity and selectivity, lead to propagation on the covalent metal–alkoxide polarized bonds, presumably by a coordination mechanism. In turn, multivalent metal carboxylates or acetylacetonates require the presence of a coinitiator, such as hydroxy or primary amino group for initiating cyclic ester polymerization.

Initiation of β-lactone polymerization with ionic alkoxides proceeds in such a way that it initially results in acyl–oxygen and alkyl–oxygen bond scission in *c*. 1:1 proportion (**Scheme 2**). However, independent of the chemistry at earlier stages, the eventual active species are carboxylate anions.[29–31]

The observed inversion of configuration if the substituted β-carbon is attacked (e.g., in the enantiomerically enriched β-BL) points to the S_N2 mechanism in the active species attack.[169]

The alkyl–oxygen bond scission is known only for β-lactones, whereas for higher lactones and LAs exclusively the acyl–oxygen bond scission proceeds and the active species are alkoxide anions.

Anions of high basicity and, due to steric hindrance, low nucleophilicity (e.g., *tert*-butoxide) initiate the polymerization mostly by proton transfer and in the irreversible (e.g., PL) or reversible (e.g., CL) mode (**Scheme 3**).[170]

The idea of the –C–C– bond breaking in initiation of the four-membered lactone polymerization has recently been shown to be wrong.[171] Actually, Szwarc himself expressed some doubts about this unusual hypothesis much earlier (p 69 in Reference 172).

In contrast to PL, which polymerizes by the action of soft and moderately reactive carboxylate anions, less strained cyclic esters (e.g., CL or LA) require stronger nucleophiles to propagate and, as a consequence, are usually plagued by side reactions. On the other hand, it has been found that coordination ROP of CL or LA initiated with covalent metal alkoxides may proceed in a perfectly controlled way due to a high selectivity, as is quantitatively expressed by high k_p/k_{tr} ratios.[50,53,54,173,174] This feature provides a flexible way not only for synthesis of linear homopolymers, but also for a great

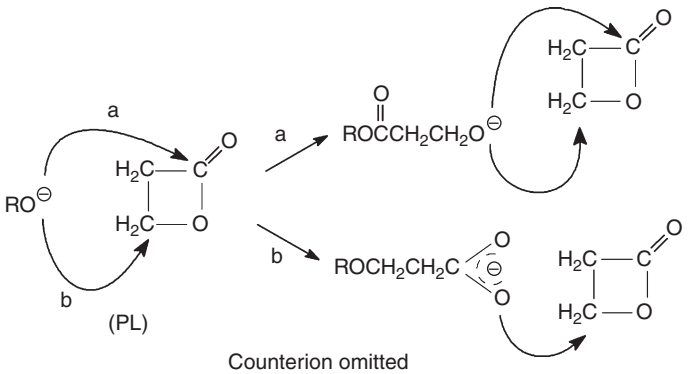

Scheme 2

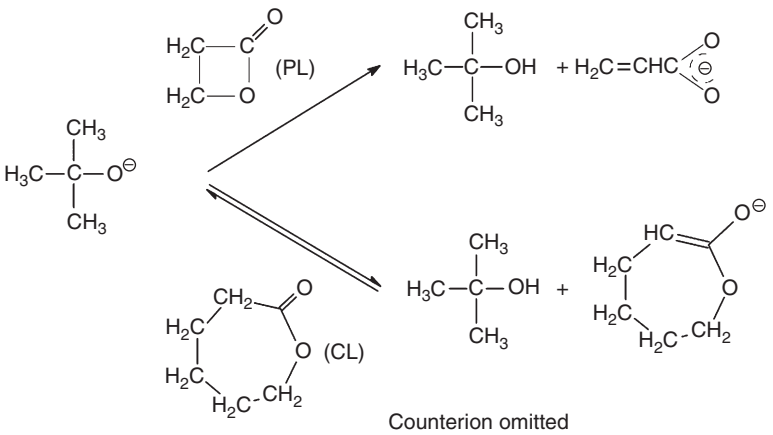

Scheme 3

variety of macromolecules differing in architecture. Polymerization of CL initiated with dialkylaluminum alkoxide is a typical example. The initiation proceeds by a simple monomer insertion, mechanistically identical with the subsequent propagation steps. A comparison of ^{1}H NMR spectra of the initiator and those of the reacting mixture (**Figure 6**) suggests the quantitative initiation and absence of side reactions during the PCL chain growth (eqn [14]).

The related monomer/active species coordination/complexation phenomena and possible chelation effects are discussed in more detail by Lewinski *et al.*[177,178] on the examples of CL and LA polymerization.

Whenever the alkoxides exist in different aggregated forms, it may happen that one form is more reactive than the other one. If, in addition, the exchange between these forms is slow, in comparison with the rate of initiation, then only this reactive form is engaged in initiation, leaving the other form(s) intact, when the polymerization is over. This is the case of initiation of CL with $Al(O^iPr)_3$, consisting of a trimer (reactive) and tetramer (unreactive) at least at ambient temperatures (**Scheme 5**).[65,66]

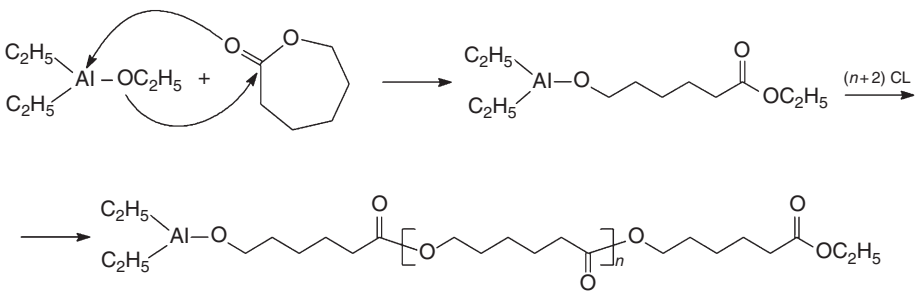

[14]

The monomer insertion may be preceded by the monomer coordination. The elementary reaction of the Al alkoxide active species with the CL monomer proceeds then analogously to the $B_{AC}2$ mechanism, however, with the participation of polarized covalent bonds (**Scheme 4**).[176]

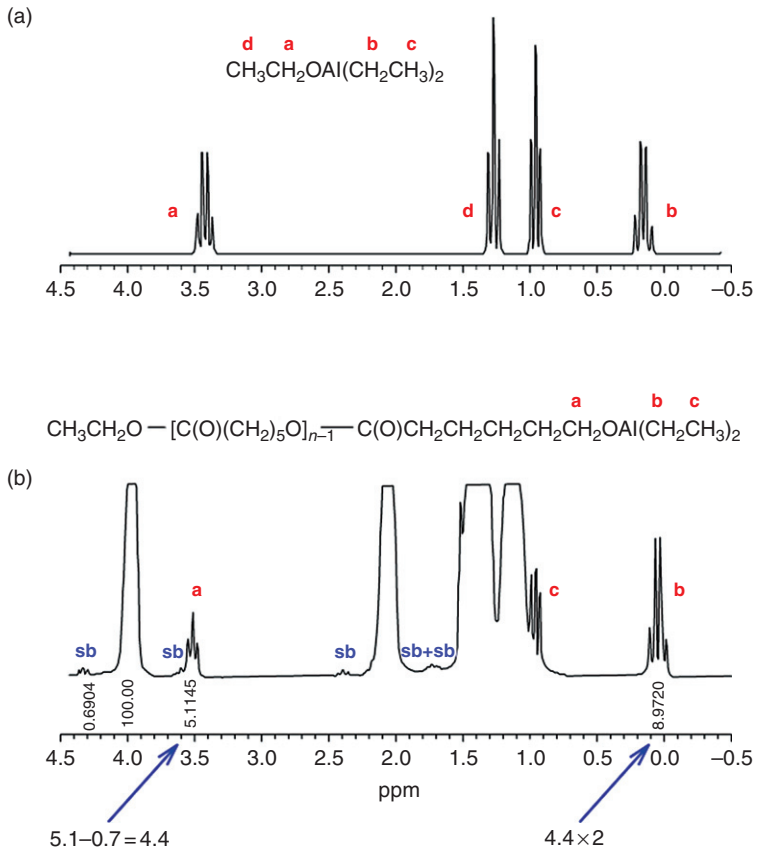

Figure 6 Selective initiation with $(C_2H_5)_2AlOC_2H_5$ (I) of the polymerization of ε-caprolactone (CL). ^1H NMR (200 MHz) spectra of (a) initiator and (b) living PCL. Conditions of polymerization: $[CL]_0 = 2.0$ mol l^{-1}, $[I]_0 = 0.097$ mol l^{-1}, C_6D_6 as solvent, 25 °C (sb = side bands).[175]

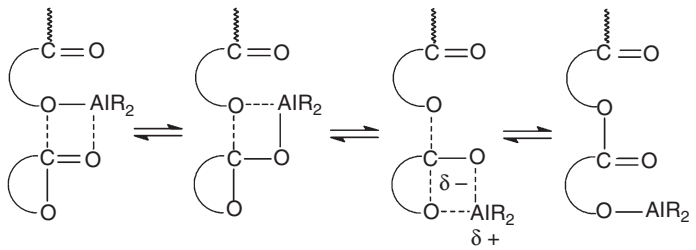

Scheme 4

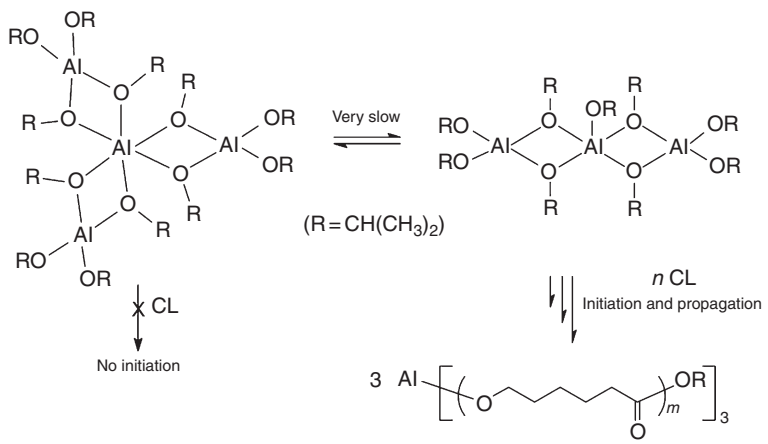

Scheme 5

At higher temperatures (e.g., above 100 °C), the rate of trimer-tetramer exchange may approach the rate of initiation since the temperature coefficient of the rate of exchange is higher than that of initiation.[60]

4.11.3.3 Initiation with Covalent Carboxylates

For a long time, the initiation of polymerization of higher lactones and LAs with covalent (Sn or Zn) carboxylates was under dispute. Leenslag and Pennings[84] and later Zhang *et al.*[88] proposed a mechanism involving reaction of $Sn(Oct)_2$ with a coinitiator, thus leading to the corresponding alkoxide. The hydroxy group may be present as an impurity or may be deliberately added in a compound to the system (e.g., water, alcohol, or hydroxy acid (ROH)), (eqn [15]):

$$\begin{aligned} &Sn(Oct)_2 + ROH \rightleftharpoons OctSn\text{-}OR + OctH \\ &OctSn\text{-}OR + ROH \rightleftharpoons RO\text{-}Sn\text{-}OR + OctH \end{aligned} \qquad [15]$$

where Oct stands for $O(O{=})CCH(C_2H_5)C_4H_9$ (2-ethylhexanoate (octoate)) group and OctH for 2-ethylhexanoic (octanoic) acid.

Then, the resulting tin(II) mono- and/or dialkoxide initiates polymerization in the same manner as the other metal alkoxides. However, there was, at that time, no direct proof of such a mechanism and several other mechanisms have been proposed.[84–90] The most often cited was the 'trimolecular' mechanism[86] in which first the catalyst–monomer complex is formed. This mechanism has conclusively been shown not to operate since it excludes the presence of Sn atoms covalently bonded to the growing macromolecules. The matrix-assisted laser desorption ionization (MALDI) time-of-flight (TOF) mass spectral measurements of the cyclic ester/ROH/$Sn(Oct)_2$ system revealed the presence of tin(II) alkoxides in the growing polyester chains.[92] Moreover, the kinetic studies also clearly supported this sequence of the exchange reactions.[91,93–96]

In Figure 7, the LA polymerization rates in two systems are compared, namely, that initiated with $Sn(Oct)_2$/BuOH and with $Sn(OBu)_2$/OctH.[93] Polymerization at $[Sn(Oct)_2]_0$ = 0.05 mol l^{-1} with no alcohol added is very slow (plot 1). It is certainly co-initiated by compounds containing hydroxy groups, adventitiously present in the system as impurities. Polymerization initiated at $[Sn(OBu)_2]_0 = 0.05$ mol l^{-1} was 2.4×10^2 times faster than that with $Sn(Oct)_2$ alone (plot 4). In the next two experiments, $[Sn(Oct)_2]_0$ and $[Sn(OBu)_2]_0$ were equal (0.05 mol l^{-1}) and 0.1 mol l^{-1} of BuOH and OctH were added.

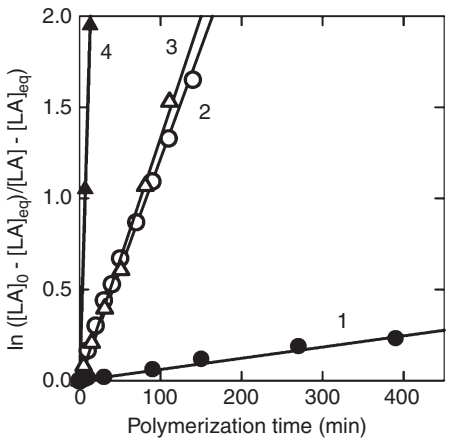

Figure 7 Comparison of kinetics of L,L-lactide (L,L-LA) polymerization initiated by $Sn(Oct)_2$ (1), $Sn(Oct)_2$/BuOH (2), $Sn(OBu)_2$/octanoic acid (OctH) (3), and $Sn(OBu)_2$ (4). Conditions: $[LA]_0 = 1.0$ mol l^{-1}, $[Sn(OBu)_2]_0 = [Sn(Oct)_2]_0 = 0.05$ mol l^{-1}, $[OctH]_0 = [BuOH]_0 = 0.10$ mol l^{-1}, THF, 50 °C.[93]

As it is seen in Figure 7 (plots 2 and 3), polymerization rates in the $Sn(Oct)_2$/BuOH and $Sn(OBu)_2$/OctH systems are practically the same, which strongly supports the proposed mechanism of the actual initiator formation (eqn [15]).

Therefore, these other views could be left aside. Besides hydroxy-group-containing compounds, primary amines can also play a role of the initiator in the $Sn(Oct)_2$-catalyzed polymerizations giving eventually tin(II) alkoxides as the growing species[95] (it has to be stressed that the distinction between initiator and catalyst in such binary systems is not always straightforward and those terms are frequently used interchangeably).

4.11.3.4 Propagation in Anionic ROP of Lactones

Ionic (e.g., alkoxide or carboxylate) active species can participate in the polymerization in different physical forms – ions, ion pairs, and ionic aggregates – which are interchanged slower or faster (Scheme 6).

For example, equilibrium constants of dissociation (K_D) in polymerization of CL and PL change typically at room temperature in the range from $\leq 10^{-10}$ (for $Cat^+ = K^+$) to 10^{-5} mol l^{-1} ($Cat^+ = K^+$ complexed with dibenzo-18-crown-6 (DBC)).[111]

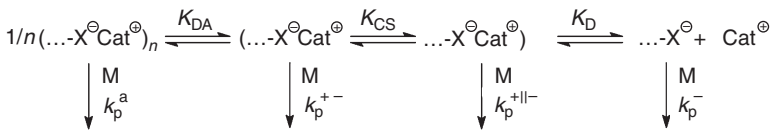

$Cat^{\oplus}$ - countercation
M - monomer
K_{DA}, K_{CS}, and K_D - equilibrium constants of deaggregation, between contact and separated ion pairs, and of dissociation, respectively
k_p^a, k_p^{+-}, $k_p^{+||-}$ and k_p^- - the corresponding rate constants of propagation

Scheme 6

Quantitative studies of the elementary reactions in polymerization of cyclic esters were started by converting or 'upgrading' polymerization of PL from the nonliving to the living conditions. This happened in the mid-1970s when two papers appeared in the same issue of *Macromolecules* revealing that application of crown ethers[27] or cryptands[28] leads to a large increase in the observed rate of polymerization and suppression of transfer reactions. This increase in the rate of polymerization when initiated with crowned potassium acetate was more than 100-fold. In agreement with the knowledge existing at that time on the influence of crown ethers and cryptands on the behavior of ionic reactions, it was assumed that these additives break aggregates of ion pairs, converting the otherwise unreactive aggregates into the unimeric ion pairs with complexed cations. A further consequence was the increase in concentration of the free ions due to a much higher dissociation constant of the crowned ion pairs.

Polymerization was first-order in the monomer; the apparent rate constant increased with the independently determined degree of ionization (α). Besides, molar masses were linear functions of conversion up to $M_n = 2 \times 10^4$. From the corresponding plots of the apparent rate constants of propagation (k_p^{app}) on α (Szwarc plot), both k_p^- and $k_p^{\pm}$ have been determined.[160,161]

Results of these measurements have led to the observation of an unexpected phenomenon. The ion pairs behave in a 'normal' way; at $[PL]_0 = 1.0$ and $3.0\,mol\,l^{-1}$, their reactivity was the same (**Figure 8(c)**), which means that the crowned ion pairs are not specifically solvated by components of the system. This is because ion pairs are electrically neutral and their cation is not easily accessible due to its crowned character. On the contrary, the reactivities (rate constants) of the ions depend on $[PL]_0$, that is, on the solvating power of the reaction medium (it has been assumed that the monomer can solvate ions).

Comparison of k_p^- and $k_p^{\pm}$ at various temperatures is given in **Figure 8**. At low temperature, the reactivity of ions approaches the reactivity of the ion pairs in both CH_2Cl_2 and dimethylformamide (DMF) solvents. In DMF, a temperature could be found at which an inversion of reactivities of both species takes place (isokinetic point). Apparently at this low temperature, the solvation of ions is so strong that an additional energy is required to remove solvating molecules from their immediate environment. Thus, the ions are becoming relatively less reactive. Similar phenomena were also observed in the polymerization of CL.[162]

Thus, one can assume that solvent (S) and monomer (M) molecules (**Scheme 7**) are packed in a disorderly way in the available space around the macroion pair (–, +) being not oriented in any specific way. On the contrary, macroions are specifically solvated, and the thermodynamic potential of the monomer molecules solvating the active species differs from that of the monomer in solution.

The lower the temperature, the more perfect becomes the solvation shell around ions; removal of solvent and/or monomer molecules, a necessary step preceding propagation, becomes more and more difficult. Thus, the activity of ions decreases faster with lowering temperature than the reactivity of ion pairs, where the solvation is not important. Then, at a certain temperature, the reactivities become equal, which is followed by their inversion after a further temperature decrease. van Beylen and Szwarc discussed this system in their book,[179] and expressed some doubts on the above-presented picture. Particularly they say on p 112 (Szwarc and van Beylen[179]): "Since the solvated ions contribute to the electric conductance but not to the propagation and the fraction of the free ions was determined by conductance, the propagation rate constant, k_p, is too low". This statement points to another possible explanation than that given in the original papers.[161,162] It has been assumed there that all of the 'free' ions are solvated, and that there are no two distinct populations, solvated, of low reactivity if any and nonsolvated, of higher reactivity. In the next part of

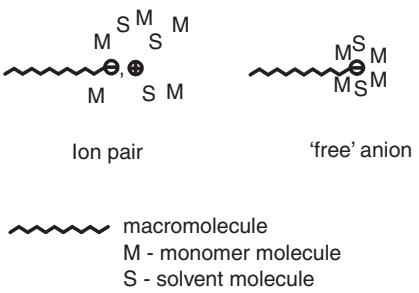

Scheme 7

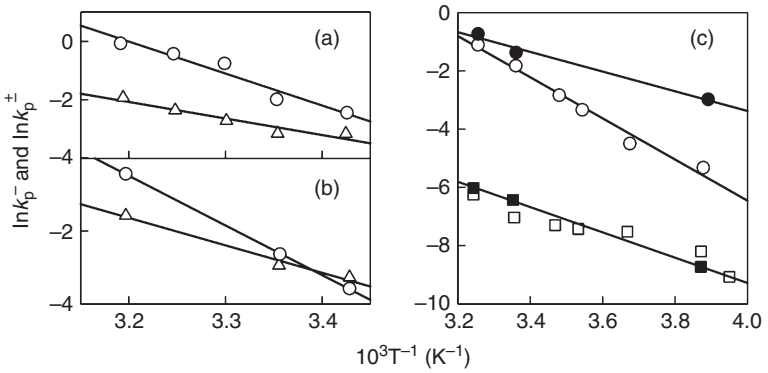

Figure 8 Semilogarithmic dependences of the rate constants of propagation on ions (k_p^-) and ion pairs ($k_p^{\pm}$) vs. reciprocal of the absolute temperature in the polymerization of PL. (a) k_p^- (○), $k_p^{\pm}$ (Δ), $[PL]_0 = 5 \times 10^{-1}\,mol\,l^{-1}$ in DMF; (b) k_p^- (○), $k_p^{\pm}$ (Δ), $[PL]_0 = 1\,mol\,l^{-1}$ in DMF; (c) k_p^- (●), $[PL]_0 = 1\,mol\,l^{-1}$; k_p^-(○), $[PL]_0 = 3\,mol\,l^{-1}$; and $k_p^{\pm}$ (■), $[PL]_0 = 1\,mol\,l^{-1}$; $k_p^{\pm}$ (□), $[PL]_0 = 3\,mol\,l^{-1}$ in CH_2Cl_2.[160,161]

the cited monograph, however, it is added (Szwarc and van Beylen[179]): "If, however, its (of the monomer) orientation in the solvation shell is improper for its insertion and its presence hinders the addition of another monomer, the reactivity of the solvated ion might indeed be very low". This is very close to the explanation given by the authors of the original work.

4.11.3.5 Propagation in Coordinated ROP of Cyclic Esters

The quantitative data on k_p in coordination polymerization are available almost exclusively for cyclic esters. A more detailed analysis of the reactivity–selectivity relationships has been presented in the already published papers.[50,53,54,173,174] Among the first works when coordination initiators were used, the works of Teyssie *et al.* on $Al(O^iPr)_3$[26,180] and the dinuclear μ-oxo-alkoxido compounds have to be mentioned.[25] The actual step of propagation on the >Al–O–… bond has been described in terms close to our present understanding of this reaction. The living character of polymerization has also been demonstrated. Some time later, Kricheldorf *et al.*[64] revealed a similar behavior for the other multivalent metal (Sn(IV), Ti, Zr) alkoxides.

4.11.3.5.1 Dialkylaluminum alkoxide active species

Depending on the structure of the resulting active centers (mostly on the number of growing polyester chains at one metal atom), propagation may also be accompanied by aggregation of the alkoxide species. In the trimeric $Al(O^iPr)_3$ aggregate/CL system, the macroalkoxide species assume exclusively the three-arm unimeric structure,[66] whereas for R_2AlOR'/CL, dimeric and trimeric aggregates prevail at higher concentrations of active centers.[55,56,58,181] Similar phenomena have been observed for ionic centers earlier.[48]

Aggregation may be diagnosed from the external kinetic order in active centers[55,56,58,60,181] and from the $^{27}A1$ NMR data.[185] In the majority of the reported cases, aggregates are not reactive. The corresponding kinetic scheme reads (Scheme 8):

The $(P_i^*)m$ species are dormant and 'retain their ability to grow'[182] and, therefore, polymerization involving these species is living, providing that the aggregation and deaggregation rates are high enough compared with that of propagation.

$$P_i^* + M \xrightarrow{k_p} P_{i+1}^*$$

$$m\,P_i^* \underset{}{\overset{K_a}{\rightleftharpoons}} (P_i^*)_m$$

$$(P_i^*)_m + M \xrightarrow{\text{no reaction}} \times$$

P_i^* - nonaggregated, unimeric active centers
$(P_i^*)_m$ - aggregated species
m - aggregation degree
M - monomer molecule
k_p - rate constant of propagation
K_a - equilibrium constant of aggregation

Scheme 8

Solution of the kinetic Scheme 8 gives two useful dependences, eqns [16] and [17],[55,56,58]

$$\ln r_p = \ln k_p (mK_a)^{-1/m} + \frac{1}{m}\ln[I]_0 \qquad [16]$$

$$r_p^{1-m} = -mK_a k_p^{1-m} + k_p[I]_0 r_p^{-m} \qquad [17]$$

where $r_p = d[M]/[M]dt = t^{-1}\ln([M]_0/[M])$, $[M]_0$ and $[M]$ denoting the starting and instantaneous concentrations of monomer, $[I]_0$ the starting concentration of initiator (being equal at the properly chosen (living) conditions to the total concentration of active species – growing and dormant), and t the polymerization time.

Fitting the experimental data (i.e., r_p and $[I]_0$) available from the kinetic measurements to eqn [16] allows determination of the degree of aggregation (m). However, this approach does not allow determination of K_a and k_p, but merely their product.

The way of determining both k_p and K_a is possible especially when the degree of aggregation can be estimated as described above.[55,56] Equation [17] gives a direct access to both k_p and K_a.

Figure 9 shows example of the r_p versus $[I]_0$ dependences (eqn [16]) obtained in polymerization of CL initiated with Et_2AlOEt and carried out in CH_3CN, THF, and C_6H_6 as solvents.[58] The resulting plots reveal that the order in initiator decreases in all solvents from 1 to 1/3 with increasing total concentration of active centers (equivalent to $[I]_0$ in the living polymerization conditions). This behavior clearly points to the aggregation of the active centers of unimeric aluminum alkoxide (…–C(=O)$CH_2CH_2CH_2CH_2CH_2OAlEt_2$) into the unreactive trimers.

Although it has been known that the degree of aggregation is equal to 3 for polymerization conducted with diethylaluminum alkoxide, but it was decided to test the equation for the known value equal to 3 and to see the results by introducing for the aggregation number an incorrect value equal to 2. The former value gives indeed the straight line as required whereas

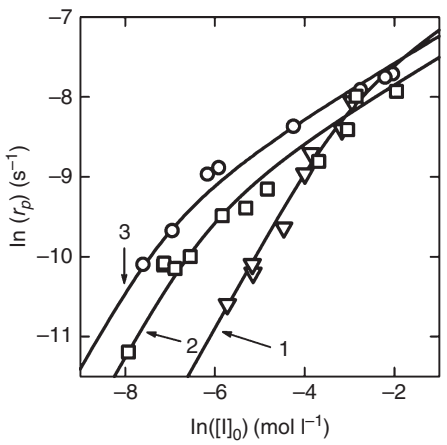

Figure 9 The external order in initiator dependences (eqn [16]) obtained in polymerization of ε-caprolactone (CL) initiated with Et_2AlOEt. Conditions: $[CL]_0 = 2$ mol l^{-1}; solvents – CH_3CN (1), THF (2), and C_6H_6 (3); 25 °C. Points, experimental; lines, computed numerically assuming kinetic Scheme 8.[58]

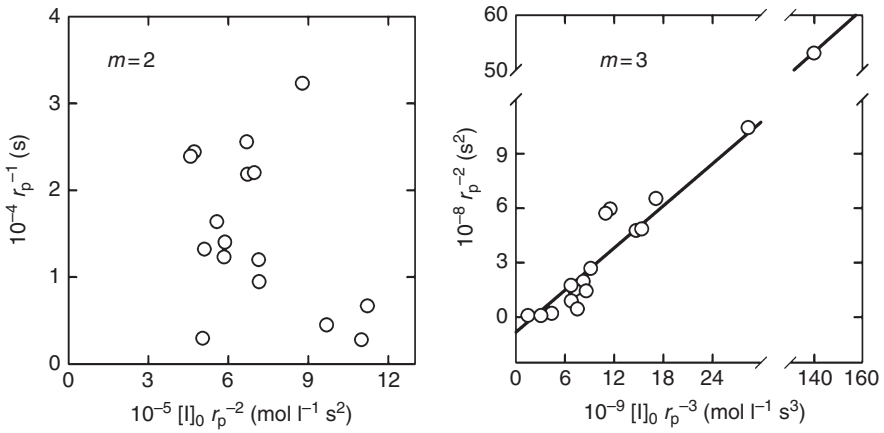

Figure 10 Polymerization of ε-caprolactone (CL) initiated with Et_2AlOEt (THF, 25 °C). Test of eqn [17] for the degree of aggregation *m*. Only for $m = 3$, a straight line was obtained as required. Primary kinetic data taken from Duda, A.; Penczek, S. *Macromol. Rapid Commun.* **1994**, *15*, 559.[56]

assuming the incorrect value gives highly dispersed points (Figure 10).

In Table 2, the values of k_p and K_a determined for the CL/Et_2AlOEt system in solvents of various polarities and solvating power are collected.

These data reveal that the higher the dielectric permittivity of solvent, the lower are both k_p and K_a. Namely, the increase in ε of 2.3–37 causes a decrease in k_p of 8.6×10^{-2}–7.5×10^{-3} l mol^{-1} s^{-1} (i.e., 11 times) and a simultaneous decrease in K_a of 2.4×10^5–7.7×10^1 mol^{-2} l^2. Therefore, for lower total concentrations of active centers, when the nonaggregated, actually growing species dominate (Figure 9), the polymerization rate order, measured for a given $[I]_0$, is as follows: r_p (C_6H_6) > r_p (THF) > r_p (CH_3CN). However, for higher $[I]_0$, when concentration of the unreactive aggregates increases and this increase is higher for the less polar solvents, the polymerization rates tend to converge and, at $[I]_0 = 0.1$ mol l^{-1}, r_p's measured in C_6H_6, THF, and CH_3CN become almost identical (Figure 9). CH_3CN is the most polar of the three used solvents and it apparently breaks down the aggregates. Thus, in the studied range of concentrations, the active species are mostly unimeric (i.e., reactive). In both THF and C_6H_6, the equilibrium between aggregated (unreactive, dormant) and not aggregated species persists although, at a sufficiently low concentration for a given system, the fraction of aggregated species may be negligibly small and no longer important. Both the alkoxide active center and the lactone molecule have dipolar structures. An analysis of the influence of the solvent dielectric permittivity, as a macroscopic parameter, on the k_p of the dipolar molecule–dipolar molecule reaction in terms of the electrostatic effects shows that an increase in ε should lead to a higher k_p. In the analyzed case, the reverse order is observed, namely, k_p in CH_3CN is lower than that in THF and benzene. Such behavior may be related to specific solvation of the growing dialkylaluminum alkoxide by dipolar solvents (THF, CH_3CN), strong enough already in the ground state, thus increasing $\Delta H_p^{\neq}$. Apparently, the specific solvation effects predominate over the electrostatic field effects and, as the net result, the k_p decreases with increasing polarity and solvating power of the solvent.

Table 2 Propagation rate constants (k_p) and equilibrium constants of aggregation (K_a) for polymerization[a] of ε-caprolactone initiated by diethylaluminum ethoxide[58]

Solvent	*Dielectric permittivity (ε)*	k_p *(mol^{-1} l s^{-1})*	K_a *(mol^{-2} l^2)*
CH_3CN	37	7.5×10^{-3}	7.7×10^1
THF	7.3	3.9×10^{-2}	5.5×10^4
C_6H_6	2.3	8.6×10^{-2}	2.4×10^5

[a] $[CL]_0 = 2$ mol l^{-1}, 25 °C.

In studies of CL polymerization, the kinetically determined proportion of the actual growing unimeric species P_i^* was compared with the proportion of P_i^* measured by ^{27}Al NMR spectrometry.[183] The corresponding spectrum is in Figure 11(a). It shows two peaks – for tetracoordinate (Al(4) in unimeric P_i^* species) and for pentacoordinate (Al(5) in $(P_i^*)_3$ aggregated species) aluminum atoms.[184,185] The interconverting species are depicted in Scheme 9. The concentration of the Al(4) propagating species, estimated from the spectrum in Figure 11(a), is set equal to ≈10% of the total, thus being comparable with that determined from the kinetics (Figure 11(b)).

The exchange rates of aggregated (dormant) and unimeric (propagating) species in the CL/R_2AlOR system are high enough to govern an even growth of all macromolecules, as can be judged from M_w/M_n values determined for the resulting poly(CL) and ranging from 1.03 to 1.13.[51]

4.11.3.5.2 Aluminum trialkoxide active species

Propagation on aluminum trialkoxide active species was a matter of controversy concerning the question how many chains grow from one Al atom in that species. Eventually, it has been revealed that, independently of the monomer used, three polyester chains grow from one Al atom (see Scheme 4 for CL polymerization).[66] It was shown[65,66] that an early assumption of Kricheldorf[64] was correct in that all three alkoxide groups in $Al(O^iPr)_3$, if properly used, are active in building the chains.

However, the structure of the living PCL given in Scheme 5 is an oversimplification because the ^{27}Al NMR spectra of the growing species show that an additional coordination takes place.[63,66] In Figure 12, an ^{27}Al NMR spectrum of $Al(O^iPr)_3$

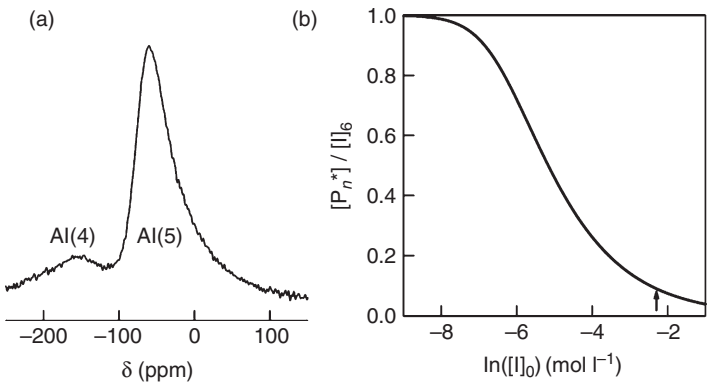

Figure 11 (a) ^{27}Al NMR spectrum of polymerizing mixture: CL/Et_2AlOEt/THF + 10 vol.% of C_6D_6. Conditions: $[CL]_0 = 2$ mol l^{-1}, $[Et_2AlOEt]_0 = 0.1$ mol l^{-1}, 25 °C. (b) Dependence of the mole fraction of the unimeric, nonaggregated active centers ($[P_n^*]/[I]_0$) on their total concentration ($[I]_0$) as determined from the kinetic measurements for the CL/Et_2AlOEt/THF system. Conditions: $[CL]_0 = 2$ mol l^{-1}, THF, 25 °C. The arrow indicates the $[P_n^*]/[I]_0$ obtained for $[I]_0 = 0.1$ mol l^{-1}.[183]

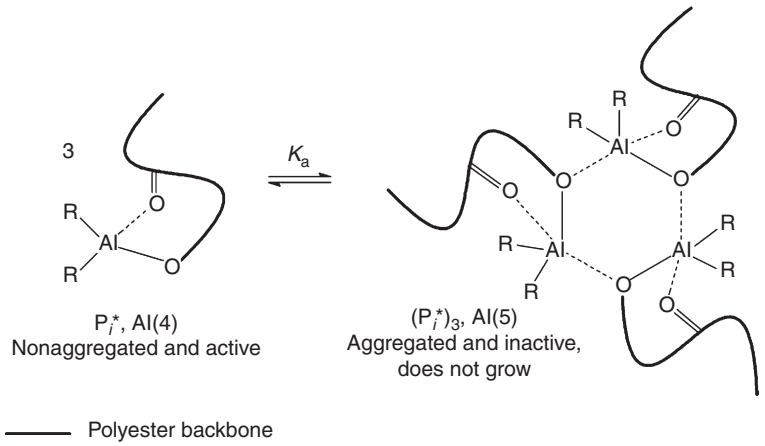

Scheme 9

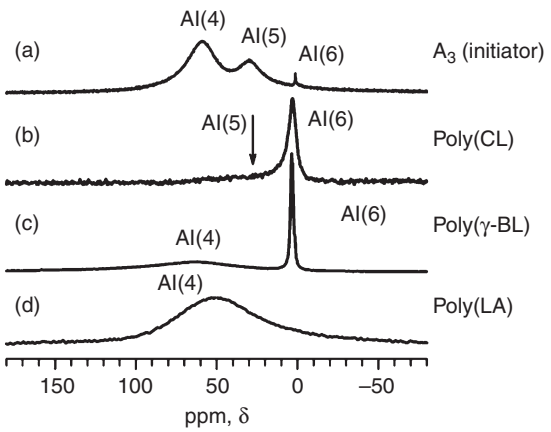

Figure 12 ^{27}Al NMR (75 MHz ^{27}Al, 70 °C, benzene-d_6) spectra of the aluminum triisopropoxide trimer (A_3) and the living polyesters prepared with A_3. (a) A_3; (b) living poly(ε-caprolactone); (c) living poly(γ-butyrolactone); and (d) living poly(L-lactide). Polymerization conditions (concentrations in mol l^{-1}): $3[A_3]_0 = 0.1$, $[CL]_0 = 2.0$, $[\gamma\text{-BL}]_0 = 3.8$, $[LA]_0 = 1.0$, 80 °C, benzene-d_6.[186]

trimer (A_3) is compared with those of the living poly(ε-caprolactone) (PCL), living poly(γ-butyrolactone), and living poly(L-lactide) (PLA); all three polyesters were prepared with A_3 as an initiator. In the initiator itself the tetra- and pentacoordinated Al atoms are present (see the formula in Scheme 4). The spectrum of A_3 exhibits signals at $\delta \approx 60$ and 30 ppm in the expected proportion (2:1), marked in Figure 12(**a**) as Al(4) and Al(5). A small signal in the vicinity of $\delta = 0$ ppm is due to the presence of ≈1.5 mol.% admixture of the tetramer (A_4). In the PCL spectrum, a strong peak at $\delta \approx 4$ ppm due to the hexacoordinated Al atoms (Al(6)) prevails but a small shoulder in the field characteristic of Al(5) is also apparent (Figure 12(**b**)). The spectrum of Pγ-BL shows, apart from the sharp peak of Al(6), a broad signal coming from Al(4) (Figure 12(**c**)), whereas in PLA the Al(4) atoms are present (Figure 12(**d**)).

The observed additional coordination of Al atoms in growing species could result from the intramolecular complexation by the acyl oxygen atoms from the polyester repeating units, as it was originally proposed by the Liege group.[63] Some of the structures are illustrated schematically below (Al(4)1, Al(4)2, Al(5), and Al(6)).

Polymerization of CL exhibited approximately first-order propagation both in monomer (internally) and in active species. The apparent k_p value (encompassing both five- and six-coordinate species) is equal to $0.62\,l\,mol^{-1}\,s^{-1}$ (25 °C, THF).[66] Most probably, propagation proceeds on the more labile five-coordinate species in intramolecular dynamic equilibrium with the hexacoordinate one. Thus, the absolute k_p could be considerably higher.

In PLA, according to the ^{27}Al NMR spectrum (Figure 12(**d**)), hexacoordinated species are not present. This may result from the steric hindrance caused by methyl groups. Moreover, the fractional kinetic orders of active species, observed by Kowalski *et al.*[60] in the polymerization of LA initiated with A_3, suggest that the aggregation–deaggregation equilibrium 2 Al(4)1 ⇆ Al(4)2 (see structures **2**) takes place and the propagation proceeds on the nonaggregated species Al(4)1. Therefore, kinetics of LA polymerization was analyzed in terms of Scheme 8. $K_a = 92\,mol^{-1}\,l$ and $k_p = 8.2 \times 10^{-3}\,l\,mol^{-1}\,s^{-1}$ (80 °C, THF) were determined in this way.

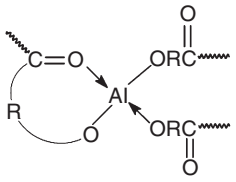

Al(4)1 **2a**

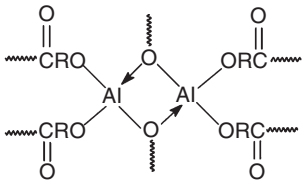

Al(4)2 **2b**

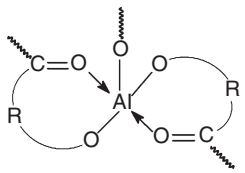

Al(5) **2c**

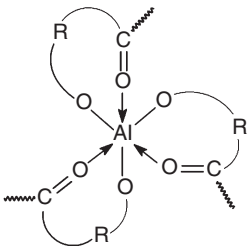

Al(6) **2d**

4.11.4 Livingness of Polymerization in Processes Initiated with Multivalent Metal Alkoxides

Despite the relatively complex kinetics, polymerizations of CL, LA, and other cyclic esters initiated with a number of metal alkoxide initiators fulfill the criteria required for the living process.[114] Figures 13 and 14 show, on the example of CL and LA polymerizations initiated with $R_nAl(OR')_{3-n}$, $R_nSn(OR')_{3-n}$, $Fe(OR)_3$, and $Ti(OR)_4$ alkoxides, the dependencies of ln $\{([M]_0 - [M]_{eq})/([M] - [M]_{eq})\}$ on time and of M_n on the monomer conversion, respectively.[148] Both dependences are linear. Thus, Figure 13 indicates that the polymerization is devoid of termination whereas Figure 14 points to the absence of chain transfer. The lines in Figure 14 correspond to the M_n – conversion dependences calculated assuming that each alkoxide group starts growth of one macromolecule whereas points are experimental.

Good agreement between the calculated and experimental plots suggests that the functionality of multivalent metal alkoxide initiators is equal to the number of alkoxide groups. Some of these initiators, such as $Sn(OBu)_2$ allowed preparation of PLA in the controlled way,[61] with M_n as high as $\approx 10^6$.

It should be added that in the vast majority of the recently reported kinetic studies of the ROP of cyclic esters, the first-order kinetic internal order in the monomer was observed, that is, the experimental plots $\ln\{([M]_0 - [M]_{eq})/([M]_0 - [M])\}$ versus time were linear. Atypically, in LA polymerization initiated with Zn alkoxide bearing 2-[(2-methoxyphenyl) amino]-4-[(2-methoxyphenyl)imino]pent-2-ene bidendate ligand, the second-order kinetics was observed for LA (based on the linearity of the $(1/[LA]) - (1/[LA]_0)$ vs. time plot). A mechanistic explanation of this result, however, has not been given.[187]

In a discussion of the coordination polymerization of cyclic esters, the rare earth metal (e.g., La, Sc, Sm, Y, Yb) alkoxides must also be mentioned. These initiators applied first at the DuPont[73,74] and then in other laboratories[75–77] provided much higher polymerization rates when compared with Sn or Al alkoxides. For example, in the polymerizing system LA/Y $(OAr)_3/^i$PrOH (where Ar = 2,6-di-*tert*-butylphenyl), the value of

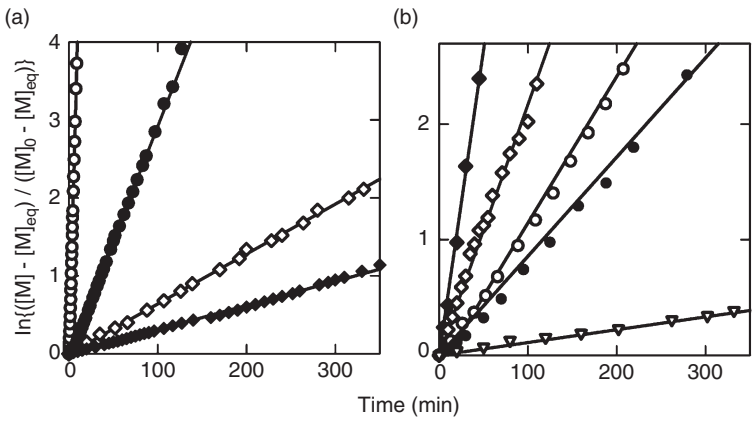

Figure 13 Kinetics of ε-caprolactone (a) and L,L-lactide (b) polymerization initiated with metal alkoxides ($R_nMt(OR')_{x-n}$). Conditions (concentrations in mol l^{-1}): (a, ○) $3[A_3]_0 = 3 \times 10^{-3}$, 25 °C; (a, ◊) $[Sn(OBu)_2]_0 = 3.3 \times 10^{-3}$, 80 °C; (a, ♦) $[Et_2AlOEt]_0 = 8 \times 10^{-3}$, 25 °C; (a, ♦) $[Bu_3SnOEt]_0 = 9.9 \times 10^{-2}$, 80 °C; (b, ◊) $[Ti(O^iPr)_4]_0 = 10^{-2}$, 80 °C; (b, ○) $[Fe(OEt)_3]_0 = 1.4 \times 10^{-3}$, 80 °C; (b, •) $3[A_3]_0 = 2 \times 10^{-2}$, 80 °C; (b, ∇) $[Sn(OBu)_2]_0 = 3 \times 10^{-3}$, 50 °C; (b, ∇) $[Bu_3SnOEt]_0 = 5 \times 10^{-2}$, 80 °C; $[CL]_0 = 2$, $[LA]_0 = 1.0$; THF.[148]

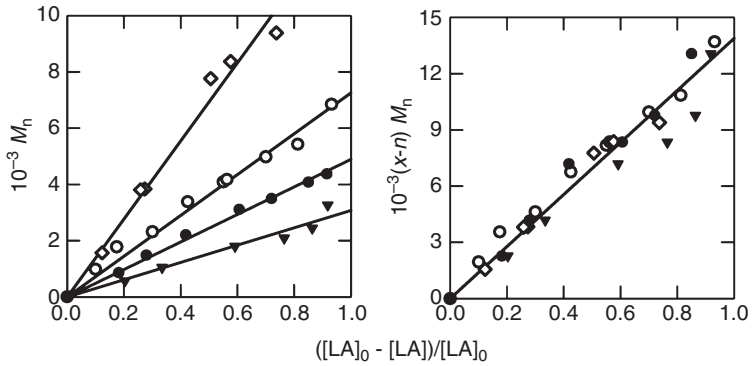

Figure 14 Dependence of M_n of poly(L-lactide) on the monomer conversion. Polymerization of L,L-lactide initiated with metal alkoxides ($R_nMt(OR')_{x-n}$): Bu_3SnOEt (◊), $Sn(OBu)_2$ (○), $Al(O^iPr)_3$ trimer (A_3) (•), and $Ti(O^iPr)_4$ (▼). Conditions: $[LA]_0 = 1.0$ mol l^{-1}, $[R_nMt(OR')_{x-n}]_0 = 10^{-2}$ mol l^{-1}, THF, 80 °C (for $Sn(OBu)_2$ at 25 °C).[148]

$k_p^{app} \geq 10$ l mol^{-1} s^{-1} (CH_2Cl_2, 22 °C) can be estimated.[75] This means that the polymerization proceeds with the rate more typical for the ionic polymerization of cyclic esters.

4.11.5 Extent of Molar Mass Control in Processes Initiated with Multivalent Metal Alkoxides

A number of well-defined macromolecules with well-controlled size and end groups were prepared with Al and Sn (II) initiators. As it is seen in **Figure 15(a)**, M_n's of PCL could be controlled up to $\leq 5 \times 10^5$ with dialkylaluminum alkoxide initiators.[188]

After understanding the difference between $Al(O^iPr)_3$ trimer and tetramer (cf. **Scheme 4**), the isolated trimer has become the most versatile initiator for the controlled polymerization of cyclic esters. It provides fast and quantitative initiation, moderately fast propagation ($k_p = 0.6$ l mol^{-1} s^{-1} compared with 0.039 l mol^{-1} s^{-1} for Et_2AlOEt (25 °C, THF)),[56,66] and relatively good selectivity (with regard to transesterification, see Section 4.11.7).[54] Thus, $Al(O^iPr)_3$ in the form of a trimer seems to be ideally suited for the synthesis of aliphatic polyesters. Apart from good selectivity, it provides a direct control of polymerization degree of the resulting polyester by simply adjusting the $([LA]_0 - [LA]_{eq})/3[Al(O^iPr)_3]_0$ ratio. On the other hand, there is an upper limit of $M_n \approx 3 \times 10^5$ of PLA and PCL, which can be obtained with $Al(O^iPr)_3$,[66,189] whereas with $Sn(OBu)_2$, $M_n \approx 10^6$ has been reached (see **Figure 15(b)**).[61] The reasons for such a limitation are not yet well understood, but they could be related to the concentration of impurities and/or the intramolecular complexation of Al atoms in the active centers by the acyl oxygen atoms from a growing polyester chain.[60,66]

$Sn(Oct)_2$ is probably the most often used catalyst in the polymerization of cyclic esters. This is mostly due to its commercial availability, physical state (liquid), and higher chemical stability in comparison with alkoxides. P_n of the polyester formed in the cyclic ester (M)/$Sn(Oct)_2$/initiator (ROH or RNH_2) systems is determined by the $([M]_0 - [M])/[initiator]_0$ ratio due to the fast initiation and exchange reactions – chain transfer to water, alcohol, or amine and then to the resulting macroalcohol. Using the standard high-vacuum technique and $Sn(Oct)_2$ of 99.0 mol.% purity, it was possible

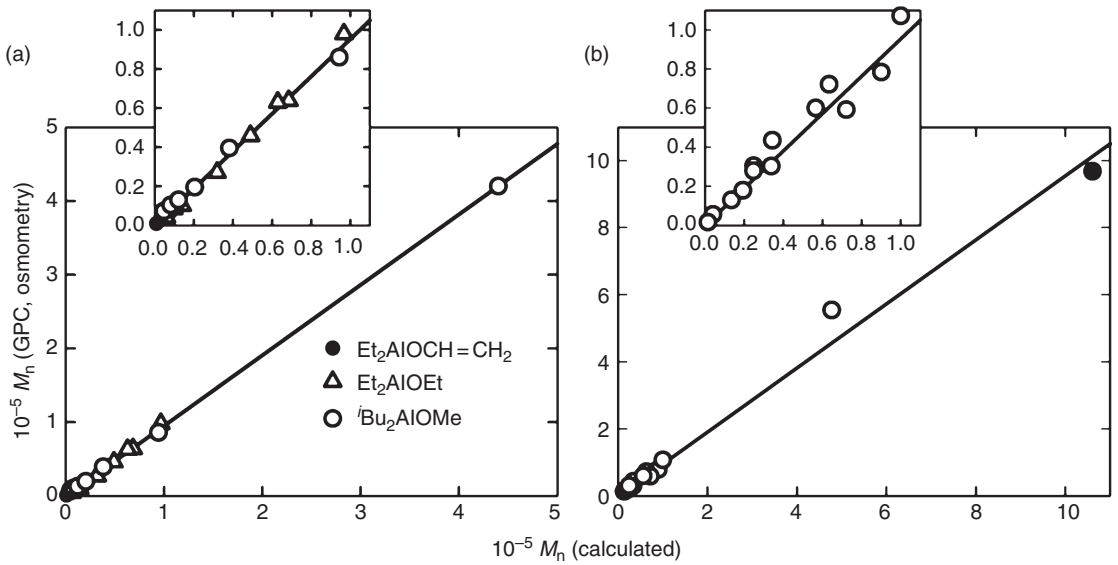

Figure 15 Measured vs. calculated (predicted) molar masses of polyesters obtained by (a) polymerization of ε-caprolactone initiated with R'_2AlOR (THF, 25 °C) and (b) polymerization of (L,L)-lactide initiated with $Sn(OBu)_2$ (○, THF, 80 °C) and (•, bulk, 120 °C).[61,188]

to obtain both PCL and PLA with M_n up to $\approx 9 \times 10^5$. Thus, $M_n \approx 10^6$ seems to be a limit of M_n for the aliphatic polyesters prepared by ROP using the usual techniques, and this limit is, most probably, related to the concentration of impurities. A similar threshold value ($M_v \approx 9 \times 10^5$) was reported by Pennings and co-workers[87] some time before. It is not known whether there is a true termination reaction in these polymerizations.

4.11.6 Controlled Polymerization of Cyclic Esters Initiated with Single-Site Metal Alkoxides

In the group of Al-based initiators, the successful application of aluminum porphyrins in polymerization of cyclic esters should be mentioned. The structure of a typical initiator Al tetraphenylporphyrin (Al-TPP) is shown in structure **3**.

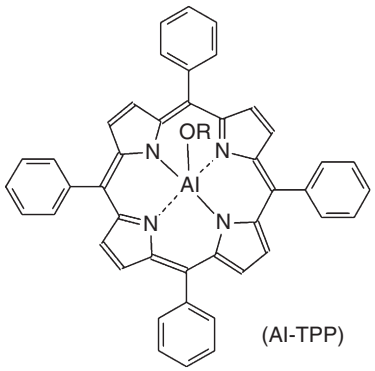

(Al-TPP)

3

The reason for quoting this structure is not only the fact that this class of initiators, developed by Inoue and Aida,[190,191] lead to living processes, but also because more than 20 years later the structurally related 'single-site' initiators became important in the stereocontrolled polymerization of LAs and β-substituted β-lactones (e.g., β-BL). The discovery of the Japanese researchers seems almost forgotten.

Application of single-site catalysts/initiators may also be of interest since it might remove the mechanistic complexity resulting from the aggregation–deaggregation exchange reactions, in which multiple-site alkoxides are usually engaged (see, e.g., References 78, 192–194, and the papers cited therein). According to the definition given by Chamberlain *et al.*:[193] "Single-site catalysts are those polymerization catalysts where enchainment of monomer occurs at a metal center (Mt, the active site) which is bound by an organic ligand (L). This ancillary ligand remains bound throughout the catalytic reaction, modifying the reactivity of the metal center. Typical single-site catalysts for lactone polymerization are of the form L_nMtOR, where the alkoxide group (OR) is capable of propagation".

This concept and definition comes from the studies of olefins polymerization, where the first generations of catalysts were heterogeneous and provided several catalytic sites on the surface of catalysts. Using the same expression in the polymerization of cyclic esters is somehow ambiguous. Indeed, studied in Lodz, the dialkylaluminum alkoxides (R'_2AlOR)[51,55,56,58] belong, in principle, to this category since, at the properly chosen conditions, R′ ligands remain unreactive and the propagation proceeds on the alkoxide group. With R′ being the lower alkyl group, aggregation of active centers takes place. However, deaggregation could be observed, when simple ligands, such as *N,N,N′*-trimethylethylenediamine, were attached to the otherwise aggregated species.[55] Besides, application of the bulky ancillary ligands L in the employed catalysts hampers chain transfer to macromolecules slowing down both intra- and intermolecular transesterification,[53,190,191] which manifests itself in the decreasing M_w/M_n values for the prepared polyesters.

The new generation of the single-site catalysts explored until now in CL polymerization do not show any particular advantage over the multiple-site ones, like $Al(O^iPr)_3$, with respect to the molar mass control as well as molar mass distribution (MMD) or the end group control in the resulting PCL.[187,195–198] Results reported for polymerization of LAs[78,187,193,199] and β-substituted β-lactones[200] initiated with Zn or Mg aminoalkoxides or β-diiminates; point to a considerable rate increase of this process compared with the polymerizations initiated with $Al(O^iPr)_3$.[60,201] For example, for L,L-LA, $k_p = 2.2\,l\,mol^{-1}\,s^{-1}$ at 25 °C ($t_{1/2} = 2.5$ min at $[I]_0 = 10^{-2}\,mol\,l^{-1}$) has been determined.[78]

With regard to β-BL polymerization, two interesting facts were noted: (1) in spite of the single-site structure of the resulting active species, which bear a bulky bidentate ligand, dimer–monomer equilibria were observed and (2) in contrast to the ionic process, exclusive nucleophilic attack on the acyl carbon atom, resulting in the retention of configuration, was observed (**Scheme 10**).[200]

Application of discrete (single-site) catalysts based on the rare earth metals, magnesium, calcium, or zinc, leading to fast propagation, creates an opportunity of synthesis of aliphatic polyesters with a minute content of the metal-based catalyst and alcohol (ROH) as coinitiator/transfer agent controlling the molar mass and structure of end groups.[202,203]

4.11.7 Transfer Processes in the Anionic and Coordination Polymerizations of Cyclic Esters

Transfer processes in polymerization can be divided into at least two categories: irreversible and reversible ones. The irreversible transfer leads inevitably to a remarkable departure from livingness. A typical example is polymerization of β-lactones (**Scheme 11**).

Anionic polymerization of PL with alkali metal counterions as growing species has, perhaps, a measurable transfer to monomer (**Scheme 11**, R = H) as it could be estimated from M_n of the resulting PPL being not higher than $10^5\,g\,mol^{-1}$ even at room temperature.[161] Thus, the question arises whether this system 'fully' conforms to the living polymerization definition (*vide infra*).

β-BL (**Scheme 11**, R = H) is a much better proton donor and the departure from livingness for this monomer is much more pronounced.[45,46] Application of Bu_4N^+ as counterion resulted in enhancement of the k_p/k_{tr} ratio and allowed preparation of poly(β-BL) (Pβ-BL) with $M_n \leq 2 \times 10^5$ but its molar masses could hardly be controlled.[80] Kinetic studies, supported by

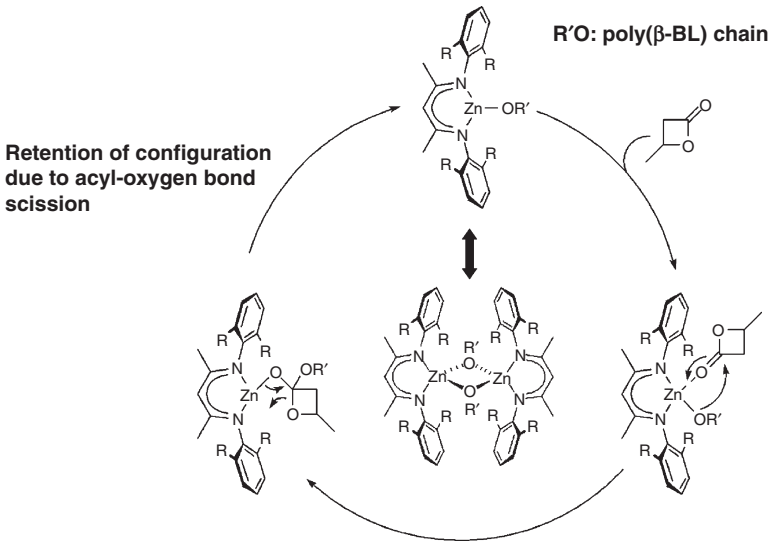

Scheme 10

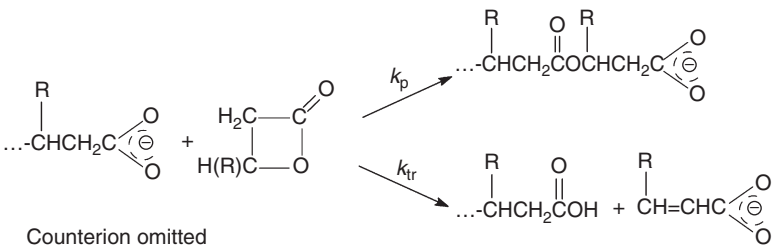

Scheme 11

M_n measurements, allowed to determine the selectivity parameter $k_p/k_{tr} = 4 \times 10^4$ for PL (K^+/DBC, CH_2Cl_2, 20 °C), and $k_p/k_{tr} = 2.0 \times 10^2$ for BL (K^+/DBC, THF, 20 °C).[46] The latter ratio is equal to the maximal number-average degree of β-BL polymerization that can be achieved at these conditions. Both electronic and steric effects of the methyl group are responsible for a lower value of the k_p/k_{tr} ratio for β-BL, when compared with PL. This is at least partly due to differences in the rate constants of propagation (10^{-6} and 4×10^{-3} l mol^{-1} s^{-1} at 20 °C, respectively).

On the other hand, in the purely anionic polymerization of five- or higher-membered cyclic esters, the carbonyl carbon of the monomer is attacked with subsequent acyl–oxygen bond scission and reformation of the alkoxide anion. In the coordination polymerization, this is also the carbonyl carbon that is now first coordinated with alkoxide species and then the acyl–oxygen bond is broken with reforming of the covalent alkoxide chain end. In the already formed macromolecular chains, the same ester bonds are present as those being the site of the nucleophilic attack in the monomer molecules. These processes are illustrated in Scheme 12, where the active centers are shown as …–OMt, for both anionic and covalent centers.

Investigations in this area started from the early work of the Nagoya group[47,204] and have been further quantitatively developed in Lodz.[48,50,53,54,174] Derivation of the corresponding kinetic equations giving access to the rate constant of transfer is based on the kinetic Scheme 13.

The intramolecular process is relatively easy to study quantitatively. This is because the products of the chain transfer (by unimolecular transesterification) are cyclic compounds and their concentration can be measured, for example, by standard chromatographic methods. Thus, propagation and formation of cyclic oligomers are competitive reactions taking place simultaneously.

The solution of the kinetic Scheme 13 (taking into account propagation and intramolecular transfer only) for some monomers (e.g., CL) for which propagation is practically irreversible gives eqn [18].[50]

$$\beta = \frac{k_p}{k_{tr1}(x)} = \frac{\ln([M(1)]_0/[M(1)])}{[M(x)]_{eq} \cdot \ln\{[M(x)]_{eq}/([M(x)]_{eq} - [M(x)])\}} \quad [18]$$

where $\beta = k_p/k_{tr1}(x)$ is the selectivity parameter showing how many elementary acts of propagation (at $[M(1)] = 1$ mol l^{-1}) are accompanied by one macrocyclization (M(1) stands for monomer and M(x) for cyclic oligomer of polymerization degree x).

Thus, the value of β is a direct measure of selectivity of a given active species. In Reference 50, GPC traces recorded for polymerizing mixtures CH_3O^-Na/CL and $(C_2H_5)_2AlOC_2H_5$/CL (THF, 20 °C) are compared. With alkoxide anions, before the monomer is consumed, there is already a large proportion of cyclics, whereas when the aluminum-based covalent active

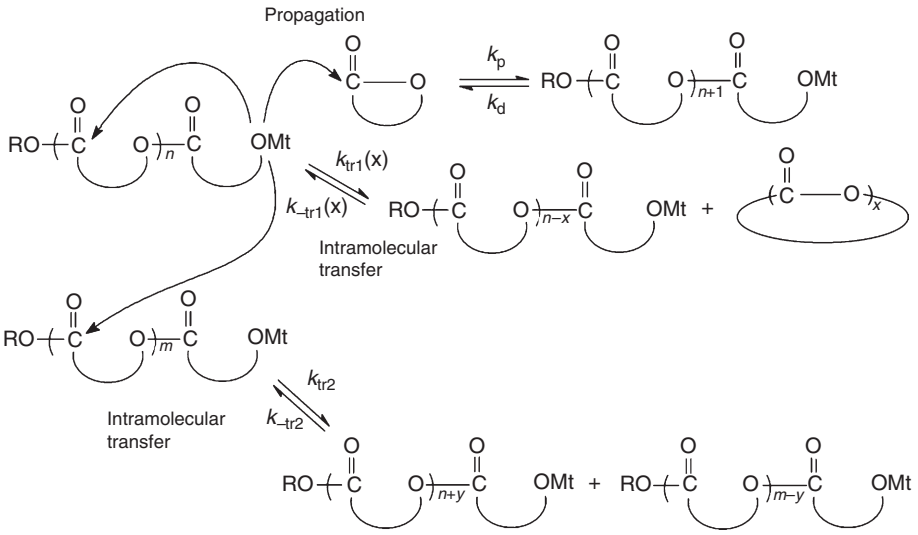

$k_{tr1}(x)$ - rate constant of intramolecular transfer
$k_{-tr1}(x)$ - rate constant of macrocycle propagation
k_{tr2}, k_{-tr2} - rate constants of intermolecular transfer

Scheme 12

species are used there are no detectable cyclics when full monomer conversion is reached. Naturally, at equilibrium, the composition of both systems should be the same, but it takes a long time in the covalent process to attain the equilibrium.

Using the described kinetic approach, the ratios k_p/k_{tr1} were determined for a few initiating systems. This ratio can differ by a factor as large as 10^3. The corresponding data are collected in Table 3. There are two phenomena involved, namely, reactivity and steric hindrance. The higher the reactivity of a species of comparable steric hindrance around growing species, such as Sm trialkoxide and Al trialkoxide, the lower the selectivity. This is often the case for other chemical reactions. If, on the other hand, the reactivity in propagation is the same but steric hindrance differs, then the more sterically hindered species is more selective. This is the case for dialkylaluminum alkoxides. The highest selectivity, however, was observed for a low-reactive Al alkoxide that bears a bulky bidentate (+)-(*S*)-2,2′-[1,1′-binaphthalene-2,2′-diylbis(nitrilomethylidyne)]

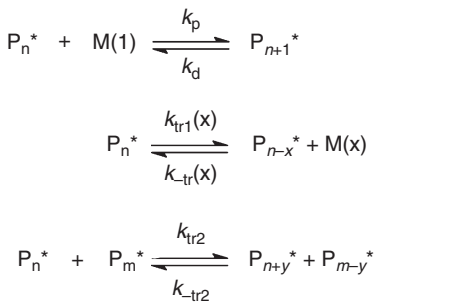

P_n^* - growing polyester chain with $DP = n$
M(1) - monomer, M(x) - macrocycle with $DP = x$

Scheme 13

Table 3 Propagation rate constants (k_p) and the selectivity parameters ($\beta = k_p/k_{tr1}$) for the polymerization[a] of ε-caprolactone[54]

Active species	k_p *(l mol^{-1} s^{-1})*	$\beta = k_p/k_{tr1}$ *(l mol^{-1})*
…–$(CH_2)_5O^-Na^+$	≥1.70	1.6×10^3
…–$(CH_2)_5O$–Sm[$O(CH_2)_5$–…]$_2$	2.00	2.0×10^3
…–$(CH_2)_5O$–Al(C_2H_5)$_2$	0.03	4.6×10^4
…–$(CH_2)_5O$–Al[$CH_2CH(CH_3)_2$]$_2$	0.03	7.7×10^4
…–$(CH_2)_5O$–Al[$O(CH_2)_5$–…]$_2$	0.50	3.0×10^5
…–$(CH_2)_5O$–AlO_2SB[b]	5.8×10^{-3}	≈10^6

[a]Polymerization conditions: 20 °C,THF.
[b]Polymerization conditions: 80 °C, THF, SBO_2: (+)-(*S*)-2,2′-[1,1′-naphthalene-2,2′-diylbis(nitrilomethylidyne)]diphenolate ligand, SB = Schiff base (Duda, A.; Kowalski, A. unpublished results).

diphenolate ligand. The plausible explanation is that more bulky substituents do not affect propagation whereas in macrocyclization, the chains have more problems in achieving the conformation needed for the reaction to occur.

In the intermolecular transfer (by bimolecular transesterification), one active polyester macromolecule reacts with another, also active, and possibly two active ones are reproduced.[173,174,205] Thus, in the intermolecular transfer, the only change that is observed is broadening of the MMD. At a certain conversion, bimodal MMD appears. This is a novel and general phenomenon that was not considered earlier in macromolecular chemistry. It is generally accepted that in polymerization bimodality appears exclusively when two species are propagating with different rate constants and these species do not exchange fast enough.

The rate constant of intermolecular transfer (k_{tr2}) or the k_p/k_{tr2} ratio can be determined on the basis of the change of a function of monomer conversion $\{([M]_0 - [M])/[M]_0\}$.

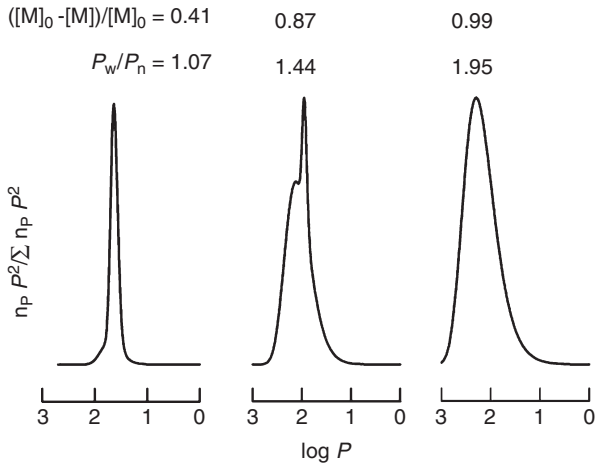

Figure 16 Computed (Monte Carlo method) chain length distributions (P_w/P_n) as a function of the monomer conversion ((($[M]_0 - [M]$)/$[M]_0$). Conditions: $[M]_0/[I]_0 = 10^2$, $k_p >> k_d$.[173]

Figure 16 shows a simulation of the MMD for high k_p/k_{tr2}, that is, for a relatively slow transfer, numerical simulations were based on the kinetic Scheme 13, omitting the intramolecular transfer. Thus, chains are initiated at once and they grow giving in the beginning a distribution close to the Poissonian.

They undergo transfer all the time, but approximately only once for 100 steps of propagation. A new population of macromolecules that participated in transfer reacts slowly with the populations with Poisson distribution. The M_n of the populations participating in the segmental exchange (i.e., intermolecular transfer) is the same, but M_w differs and this appears on the size-exclusion chromatography (SEC) traces, resulting in bimodal and broader distribution. Finally at equilibrium, the M_w/M_n value equal to 2, typical for the most probable distribution, independently of the initiator used, is reached.

Thus, numerical simulation of $M_w/M_n = f((([M]_0 - [M])/[M]_0)$ plots for various assumed k_p/k_{tr2} was applied up to the best fit with the experimental dependence. A typical result is shown in Figure 17 for various covalent alkoxides. The lines were

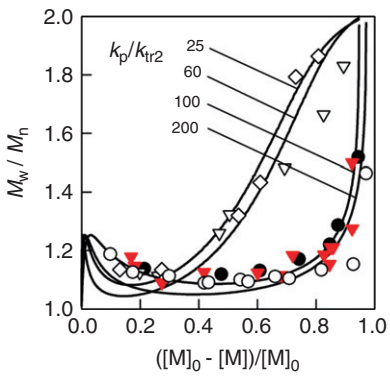

Figure 17 Dependences of M_w/M_n on $([M]_0 - M])/[M]_0$ determined for L,L-lactide polymerization initiated with: (◊) Bu_3SnOEt, (▽) $Fe(OEt)_3$, (▼) $Al(O^iPr)_3$, (●) $Sn(Oct)_2$/BuOH, (○) $Sn(OBu)_2$, THF solvent, 80 °C (for $Sn(OBu)_2$, 20 °C). Points, experimental; lines, computed assuming $k_p/k_{tr2} = 200$, 100, 60, and 25, respectively.[206]

generated for a given ratio of k_p/k_{tr2} and the points are experimental. On this basis, it was possible to determine k_p/k_{tr2} for a given system.[173,174,205]

As it follows from Figure 17, the M_w/M_n ratio in some systems is close to the value expected for a Poisson distribution even for conversions as high as over 80%. Divalent tin has particularly good selectivity. Recently, even better selectivity was observed for >AlO^iPr with bidendate, bulky phenolate-type ligands, similarly as used for the studies of intramolecular transfer (Table 3). It is also worth noting that comparing the extent of transesterification for a different initiator/monomer system on the basis of the M_w/M_n values measured for the resultant polyester is reliable only for the same monomer conversion and $[M]_0/[I]_0$ ratio.

Figure 18 compares, thus, the obtained $\gamma = k_p/k_{tr2}$ with propagation rate constants (k_p) and with the atomic number of metal atoms involved in active species. It is remarkable that for a series of similar alkoxides as growing centers, this dependence conforms to the rules of the reactivity–selectivity principle. Moreover, the larger the size of the metal atom in the growing species, the higher the rate constant of propagation, as it could be expected in the case of lower alkoxide bond energies for larger atomic radii.

Although we are looking for the ways of getting the best possible selectivities, in practice, it is not much important for a homopolymer to have a narrow distribution. Slowing down chain transfer is, however, important for the well-controlled block copolymers and other controlled architectures. Indeed, due to high selectivity of alkoxido {(+)-(*S*)-2,2′-[1,1′-binaphthalene-2,2′-diylbis(nitrilomethylidyne)]diphenolato}aluminum (for the structure, see Figure 19), well-defined LA/CL block copolymers could be prepared by initiating CL polymerization with the living PLA block, which was earlier impossible even with an also highly selective Al trialkoxide.[207]

Thus, in the vast majority of papers reporting on attempts to synthesize the CL/LA block copolymer (PCL-*b*-PLA or PLA-*b*-PCL), the importance of the order in which both the comonomers are polymerized was stressed. When the CL monomer was polymerized first, the living PCL* macromolecules were then able to initiate the PLA chains growth, giving eventually the PCL-*b*-PLA copolymers. On the other hand, numerous attempts of initiating CL polymerization with living PLA* were unsuccessful.[208]

Such a situation had important practical implications since the well-defined multiblock [PLA-*b*-PCL]$_n$ copolymers could be only prepared by coupling of the reactive α,ω-ditelechelic oligomers.

The impossibility of preparing the PLA-*b*-PCL copolymers in the previous works, when starting with polymerization of CL from the living PLA*, was, most probably, related to the rates of the elementary reactions as shown in Scheme 14.

Thus, whenever the …–cl* active species are formed, their attack on the PLA chain is faster than CL propagation ($k_{tr2} > k_{clCL}$). Therefore, in order to prepare the block copolymer, the ratios of the rate constants have to be reversed, that is, k_{clCL} has to be larger than k_{tr2}. Eventually, in agreement with GPC, ^{1}H and ^{13}C NMR evidence, this was possible due to application of a highly selective Al alkoxide initiator supported

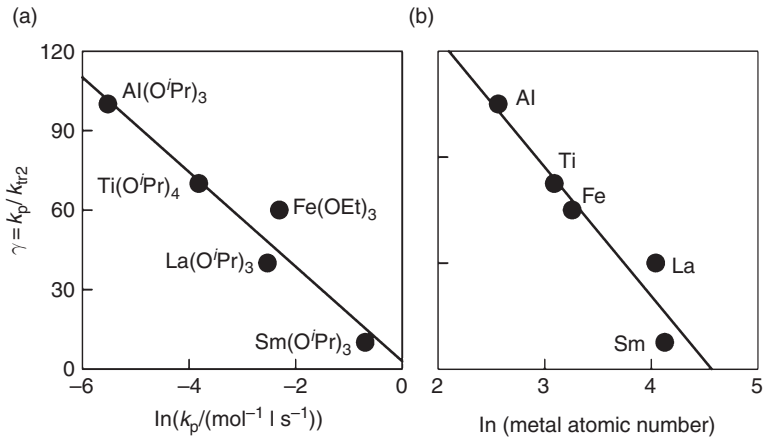

Figure 18 Dependences of $\gamma = k_p/k_{tr2}$ on ln k_p (a) and on the atomic number of the metal atoms involved in active species (b), determined in polymerizations of L,L-lactide initiated by the covalent metal alkoxides (THF, 80 °C).[54,174]

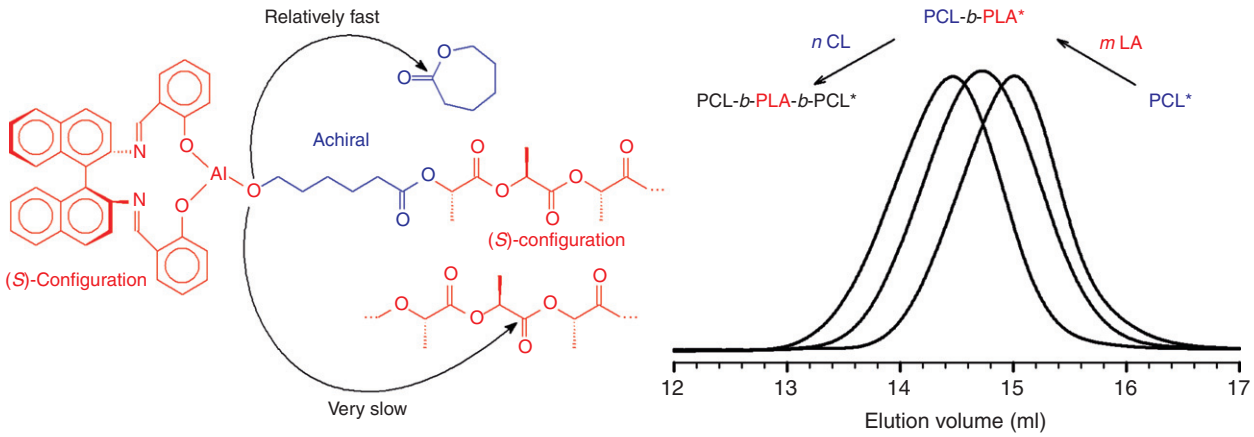

Figure 19 Synthesis of poly(ε-caprolactone)-*b*-poly(L,L-lactide)-*b*-poly(ε-caprolactone) triblock copolymer employing the 'polylactide-first' route.[207]

la and cl denote the C(=O)CH(CH$_3$)O and C(=O)(CH$_2$)$_5$O repeating units
la* and cl* - the corresponding active species
k_{laCL}, k_{clCL}, k_{tr2} - the corresponding rate constants

Scheme 14

by a bulky ligand (see Figure 19). In addition, CL macrocyclization was completely eliminated.

In spite of the fact that polymerization of cyclic esters with anionic or covalent active centers proceeds with inevitable chain transfer (intra- and/or intermolecular) to macromolecules, these processes should not be considered as departing from the living conditions. The proper choice of initiator coupled with kinetic control can exclusively provide macromolecules retaining the ability to grow and eliminate formation of macrocyclics at the kinetically controlled conditions.

4.11.8 Stereochemically Asymmetric ROP of Cyclic Esters

Stereochemically asymmetric ROP polymerizations of cyclic esters (hereafter 'stereocontrolled' processes) involve chiral monomers. There are two major cyclic esters that bear centers of chirality: β-BL and LAs (see structures 4). In this section, a notion of the absolute configuration will be used; thus, the relative configurations D and L correspond to the absolute configurations *R* and *S*, respectively.

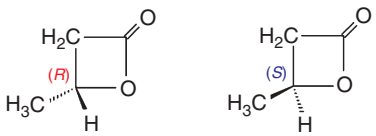

(*R*)-β-BL **4a** (*S*)-β-BL **4b**

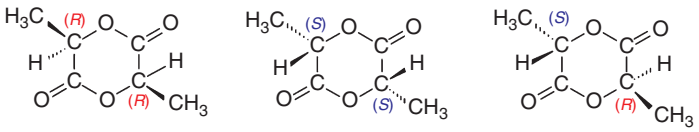

(*R,R*)-LA **4c** (*S,S*)-LA **4d** (*R,S*)-LA **4d**

In agreement with IUPAC recommendations,[209] two types of processes, involving chiral monomers can be distinguished: (1) 'asymmetric enantiomer-differentiating polymerization', an asymmetric polymerization in which, starting from a mixture of enantiomeric monomer molecules, only one enantiomer is polymerized; and (2) a polymerization in which, starting from the racemate of a chiral monomer, two types of polymer molecules, each containing monomer units derived from one of the enantiomers, form in equal amounts is termed 'racemate-forming enantiomer-differentiating polymerization' (see also Figure 20).

In the literature concerning the ROP of heterocyclic monomers, the 'asymmetric, enantiomer-differentiating polymerization' and 'racemate-forming enantiomer-differentiating polymerization'[209] are informally named as 'stereoelective' and 'stereoselective' processes. Stereoelective means that from a racemic monomer mixture only one enantiomer is 'elected' to be enchained into the polymer chain; stereoselective process initiated with racemic (site control) or achiral (chain-end control) initiator gives different populations of macromolecules (poly(*R*) and poly(*S*)) growing separately. In these processes, either the site-control mechanism (SCM), for chiral initiators, or chain-end control mechanism (CEM), for achiral initiators, can operate. Thus, in the latter case, the first addition (initiation) of (*R*)- or (*S*)-monomer decides on a given chain configuration.

β-BL monomers are, in principle, available in the form of pure enantiomers (*R*)-β-BL and (*S*)-β-BL (only in the laboratory-scale quantities) or as the equimolar (*R*)-β-BL/(*S*)-β-BL racemic mixture (*rac*-β-BL). Since LA monomers

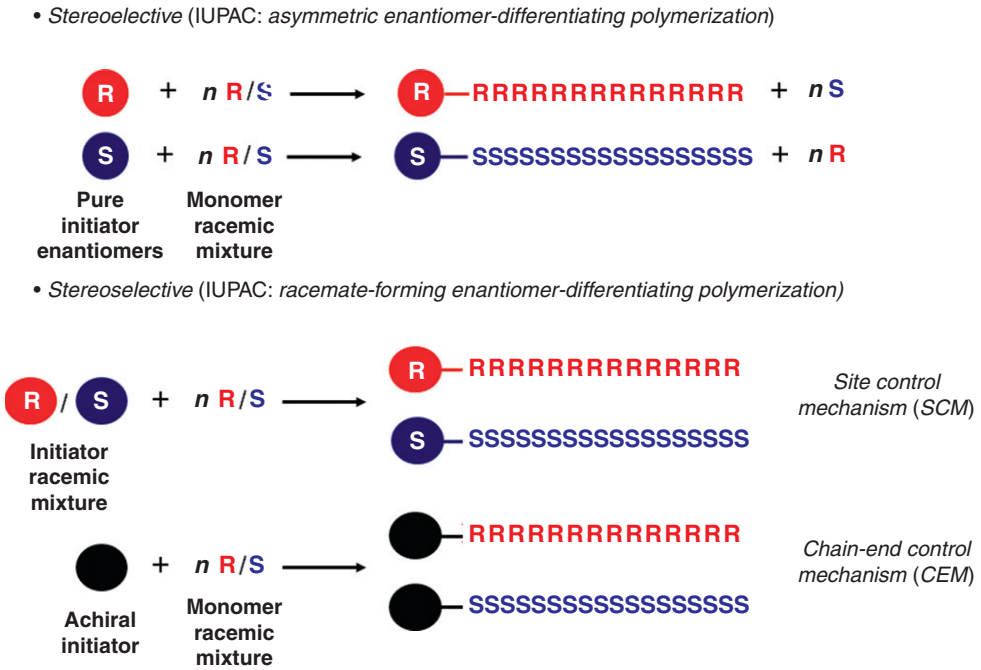

Figure 20 Classification of the stereocontrolled polymerization processes studied in the ROP of racemic cyclic esters and leading to isotactic (homochiral) macromolecules starting from racemic monomer.

contain two centers of chirality, they can be present in a higher number of the stereochemical forms, namely, (*R*,*R*)-LA, (*S*,*S*)-LA, (*R*,*S*)-LA (*meso*-LA), and racemic equimolar (*R*,*R*)-LA/(*S*,*S*)-LA mixture (*rac*-LA).

The preparation of isotactic, enantiomerically pure polymers from the enantiomerically pure heterocyclic monomers is easy if the corresponding monomers are available. Typically, however, the optically pure monomers are not available in large quantities and their synthesis is much more complicated compared with their racemic counterparts. So far, the only exception has been (*S*,*S*)-LA, a monomer synthesized from (*S*)-lactic acid, which in turn is produced on industrial scale by fermentation from carbohydrates of agricultural origin.[82] The resultant high-molar-mass poly[(*S*,*S*)-lactide] is a crystalline (up to ≈70%) polymer melting at 180 °C, whereas poly[(*R*,*R*)-lactide-*co*-(*S*,*S*)-lactide], prepared from the racemic LA, with a random distribution of *R* and *S* repeating units is amorphous.[82,210] Similar difference in properties was observed for, for example, poly[(*R*)-β-BL] and poly[(*R*)-β-BL-*co*-(*S*)-β-BL] with a random distribution of *R* and *S* units. Therefore, stereocontrolled polymerization of *racemo* or *meso* monomers is of particular interest from the practical point of view, since polymer properties depend strongly on the distribution of chirality centers of opposite configuration along the macromolecular chain. This process also provides a useful tool in studies of the polymerization mechanisms of cyclic esters.

Figure 20 illustrates idealized classification of the stereocontrolled polymerizations of a racemic monomer that bears one center of chirality (β-BL case). For the sake of simplicity, only formation of isotactic (…–RRRRRRRR–… or …–SSSSSSSS–…) polymer formation is shown. In principle, this scheme conforms also to the *rac*-LA (containing two identical centers of chirality in one molecule) polymerization. In a more general case, formation of the syndiotactic (…–RSRSRSRS–…) and heterotactic (…–RRSSRRSS–…) polyester chains (see, e.g., structures 5) should additionally be considered (*vide infra*).

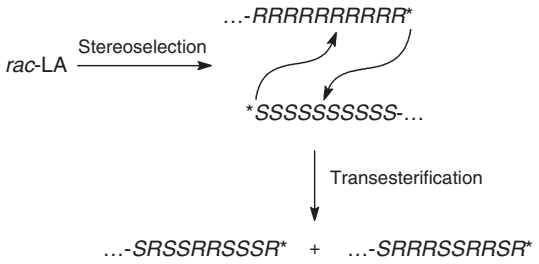

(*R* and *S* stand for (*R*)-and (*S*)-(C=O)CH(CH$_3$)O units, respectively)

Scheme 15

transesterification will lead to the atactic stereocopolymer (Scheme 15).

It seems that the stereocontrolled ROP of chiral aliphatic cyclic esters became recently an emerging field of research in polymer science. Until the mid-1990s, the progress was rather modest. In a review on asymmetric polymerization,[211] only one paper on *rac*-β-BL polymerization has been cited reporting that the enantiomerically pure initiator [(–)-(*R*)-(CH$_3$)$_3$CC*H(OH)CH$_2$O]ZnEt$_2$ gave $k_p(R)/k_p(S)$ ratios not higher than 1.7.[212] Similar $k_p(R)/k_p(S)$ values were obtained in the polymerizations of other chiral β-lactones initiated with optically active phosphines.[106,107]

4.11.8.1 Stereocontrolled ROP of LA

Research on *rac*-LA polymerization has been much more dynamic and successful, especially in the past decade. Suppression or even elimination of the segmental exchange turned out to be possible by applying metal alkoxide initiators with bulky ligands. Steric hindrance at the active center decreases the transesterification rate due to an increase in entropy of activation, while the propagation rate remains constant.[53]

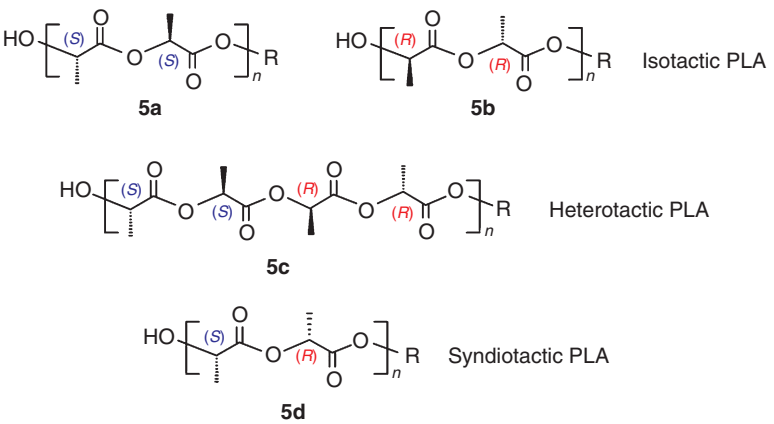

Stereocontrolled polymerization requires elimination of the intermolecular transfer (segmental exchange) between the homochiral chains containing repeating units of opposite configuration. Otherwise, even if initially stereoselective polymerization proceeds giving the homochiral chains,

An efficient enantioelective or enantioselective polymerization, based on single-site initiators of *rac*-LA, has been realized by Spassky and co-workers, who applied achiral and chiral aluminum alkoxides of general structure O$_2$Al–OR, bearing Schiff base ligands.[70,71,213]

The chirality of (*R*)- and (*S*)-SBO_2Al–OR (structures **6c** and **6d**) derivatives has its origin in the hindered rotation of the 2- and 2′-substituted 1,1′-binaphthalene moieties.

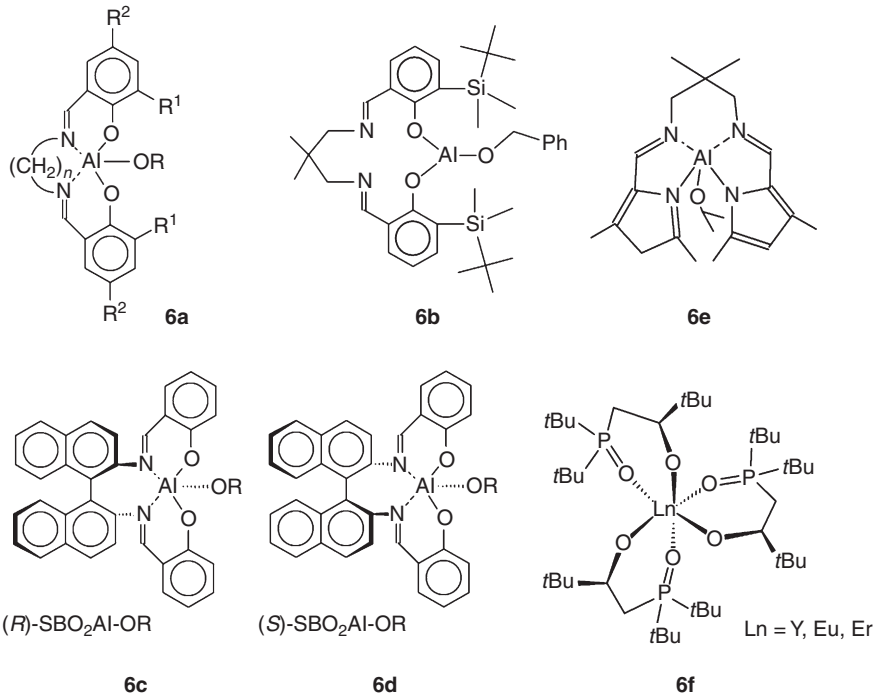

This method, originally developed by Spassky and co-workers, was then followed up by the groups of Radano *et al.*,[214] Ovitt and Coates,[215,216] Zhong *et al.*,[217,218] and Nomura *et al.*[219,220] It was revealed that polymerization of *rac*-LA mediated with either achiral or chiral but racemic initiators led to the multiblock copolymers {poly[(*S*,*S*)-LA]-*b*-poly[(*R*,*R*)-LA]}$_p$, resulting from a CEM or an enantiomorphic SCM of the monomer addition, respectively. Initially, formation of the isotactic polymer composed of an equimolar mixture of (*R*)- and (*S*)-PLA macromolecules was expected.[214]

However, Ovitt and Coates,[215,216] after repeating these experiments, came to the conclusion that the polymer obtained cannot be a mixture of the exclusively homochiral (*R*)- and (*S*)-PLA macromolecules (**Scheme 16**).

Comparison of the recorded and simulated ^{1}H NMR spectra and the assumption that polyester chain growth is accompanied by exchange of chiral macromolecules on alien active centers indicated that the resulting macromolecules were composed of stereoblocks with 11 repeating units derived from LA monomer of a given kind (toluene, 70 °C). Enantiomerically pure (*R*)- or (*S*)-SBO_2Al–OR initiators have been shown to polymerize preferentially one of the enantiomers of *rac*-LA, that is, (*R*,*R*)- or (*S*,*S*)-LA, respectively.[71,221] This enantiospecific preference was indicated by the stereoselectivity ratio $k_p(R/RR)/k_p(R/SS)$ (or $k_p(S/SS)/k_p(S/RR)$) equal to 28, what corresponds to $P_m = 0.96$ (i.e., probability of isotactic enchainment formation, equal to *m* diad content in the resulting polymer).

One of the most important practical consequences of the results described above, with regard to mechanical and thermal properties of PLA, is the possibility of stereocomplex formation by sufficiently long stereoblocks of the opposite configuration. The T_m of the (*R*)-PLA/(*S*)-PLA stereocomplex composed of an equimolar mixture of high-molar-mass *R*- and *S*-macromolecules is 230 °C,[210] whereas the highest T_m of the stereocomplex prepared initially by the stereoselective polymerization with achiral initiator was 192 °C,[219] and later on

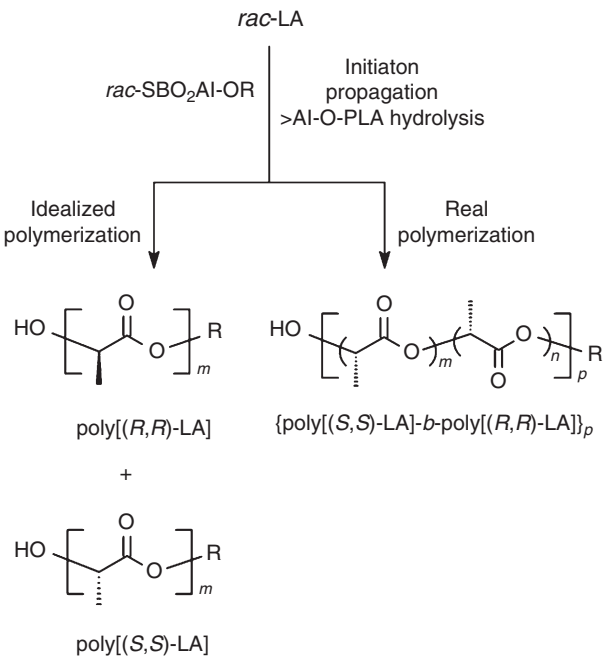

Scheme 16

it was upgraded up to 210 °C by Nomura *et al.*, who applied achiral salen-Al complexes with (*tert*-BuMe$_2$Si)phenoxide ligands (structure **6b**).[220]

In another approach, a combination of the stereoelective polymerization and chiral ligand exchange resulted in the formation of a stereocomplex showing also $T_m = 210$ °C.[221] This was realized by two-step polymerization of *rac*-LA initiated by a (+)-(*S*)-2,2′-[1,1′-binaphthalene-2,2′-diylbis(nitrilomethylidyne)] diphenol [(*S*)-SB(OH)$_2$]–Al(O^{i}Pr)$_3$ trimer mixture, in which the actual initiator (SBO$_2$Al–O^{i}Pr) was formed *in situ* (**Scheme 17**).

First, an (*S*)-SB(OH)$_2$–Al(O^{i}Pr)$_3$ mixture was reacted in THF at 80 °C and then *rac*-LA was introduced. Progress of the polymerization was followed using polarimetry and by GPC.

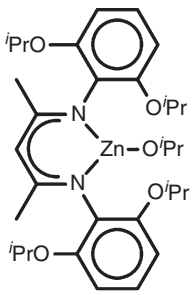

7a

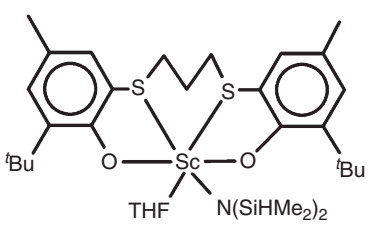

7b

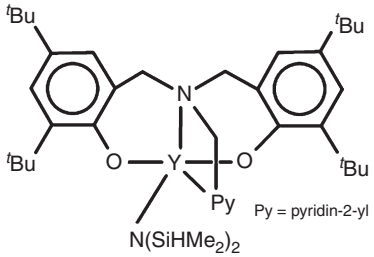

7c

Optical rotation (OR) readings increased with polymerization time and eventually leveled off. GPC measurement showed approximately 50 mol.% consumption of *rac*-LA. In the second step, an equimolar quantity of (*R*)-SB(OH)$_2$ (with respect to the *S* enantiomer) was introduced. In subsequent polymerization, a gradual decrease in OR was observed. Taking into account the determined stereoelectivity coefficient, $P_m = 0.96$, for the final poly(*rac*-LA), the gradient poly[(*S*,*S*)-LA-*grad*-(*R*,*R*)-LA] rather than the block copolymer structure was expected. Indeed, homodecoupled ^{1}H NMR spectra showed, apart from the strong signal of the isotactic *mmm* tetrad, also peaks of lower intensity, which can be ascribed to the *mmr*, *rmm*, and *rmr* tetrads.[223]

Thus, in stereoelective or stereoselective polymerizations of *rac*-LA initiated with salen-Al (e.g., structures **6a–6d**) or Al-pyrrole Schiff base complexes **6e**,[222] predominantly isotactic PLA has been formed. Similar results were obtained with lanthanide L3 complexes of a chiral alkoxides (e.g., structure **6f**).[223]

Surprisingly, different behavior has been observed more recently for other metals and other type of ligands complexing the metal-alkoxide moiety, such as β-diimidate-Zn complex **7a**,[193,224–226] or diphenolate complexes of group III metals **7b**[227] and **7c**.[228] For these initiators, the chain-end-controlled ROP of *rac*-LA afforded highly heterotactic PLA characterized by P_r (i.e., probability of syndiotactic linkages formation, equal to *mr* or *rm* triad content in the resulting polymer) reaching 0.99.

It is worth noting that ROP of *rac*-LA initiated with lithium *tert*-butoxide, as it was reported by Kasperczyk and co-workers,[229,230] gives syndiotactic PLA, thus also with retention of configuration.

Some of the results reported for site-controlled ROP of *meso*-LA initiated with chiral initiators are also striking. For example, enantiomerically pure salen-Al complex **6d** led to syndiotactic chains ($P_r = 0.99$), whereas a **6c**/**6d** racemic mixture afforded heterotactic chains.[216] On the other hand, in the chain-end-controlled ROP initiated with imidozinc complex **7a**, formation of predominantly syndiotactic PLA was observed.[193]

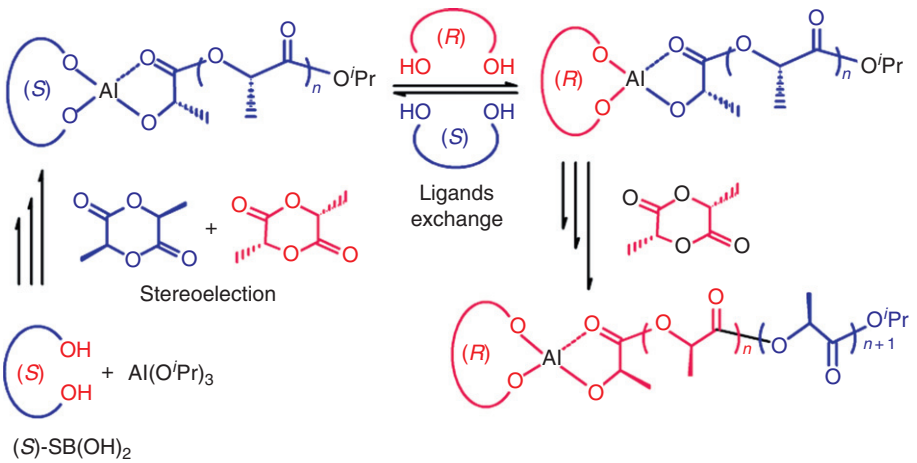

Scheme 17

The determination of the PLA chains microstructure is based mostly on ^{13}C or ^{1}H NMR spectral analysis: for the former in the carbonyl ($\delta \approx 169–170$ ppm) or methine region ($\delta \approx 68.5–69.5$ ppm), whereas for the latter in the region of methine protons ($\delta \approx 5.1–5.25$ ppm) with selective decoupling of methyl protons (chemical shifts are given for $CDCl_3$ as a solvent at room temperature). Systematic studies in this area have been initiated in the mid-1970s[231,232] and subsequently continued by several research groups (Chabot and Vert,[233] Schindler and Gaetano,[234] Bero *et al.*,[235] Dubois *et al.*,[236] Kricheldorf *et al.*,[237] Kasperczyk and co-workers,[229,230,238] Spassky and co-workers,[71,213,239] Stevels *et al.*,[240] Coudane *et al.*,[241] Kricheldorf and Lossin,[242] Thakur *et al.*,[243,244] Ovitt and Coates,[215,216] and Radano *et al.*[214]). Heteronuclear correlated {^{1}H,^{13}C} (HETCOR) two-dimensional spectroscopy was also employed in the analysis of the methine region.[245–247]

Attempts of β-BL polymerization with the multi-site metal alkoxides (e.g., $Al(O^{i}Pr)_3$[201]) were rather unsuccessful since the process was extremely slow (see, e.g., discussion in Section 4.11.3.1). Due to the impressively intensive research, carried out mostly by Coates[200] and Carpentier[81] and their co-workers on new effective ligands combined with properly chosen metals for β-BL ROP catalysis, considerable progress has been made in this area in the 2000–10 decade. Moreover, the new catalysts/initiators lead to remarkable stereochemical effects. In the stereocontrolled polymerization of *rac*-β-BL, two kinds of effects regarding the polymer structure can be expected: either isotactic or syndiotactic poly[(*R*)-β-BL] or poly[(*S*)-β-BL] formation (structures **8**)

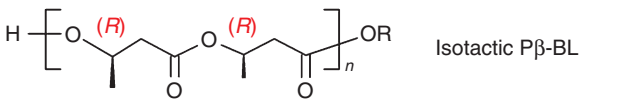

8a Isotactic Pβ-BL

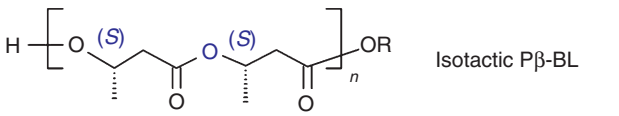

8b Isotactic Pβ-BL

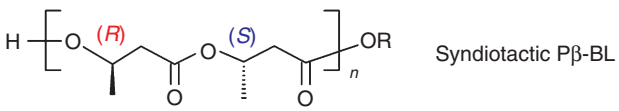

8c Syndiotactic Pβ-BL

4.11.8.2 Stereocontrolled ROP of β-BL

As mentioned in the Introduction, controlled ROP of β-substituted β-lactones is still a serious challenge. Their relatively fast ionic polymerization suffers from chain transfer to monomer and, due to the carboxylic chain-end formation (eqn [20]) followed by carboxylic acid complexation, the polymerization slows down and complete monomer conversion could hardly be achieved.[45,46]

Stereocontrolled ROP of *rac*-β-BL, leading to the homochiral polymer and – which is also important – to the monomer of opposite configuration or to an equimolar mixture of chains with opposite configurations (poly[(*R*)-β-BL] or poly[(*S*)-β-BL]), is still a problem. For example, Rieger and co-workers[248] reported application of highly active achiral Cr(III) salophen complexes, **9a**, giving high-molar-mass Pβ-BLs but with high dispersities ($M_w/M_n = 5.2–9.6$) and with only modest isotacticities (P_r up to 0.66).

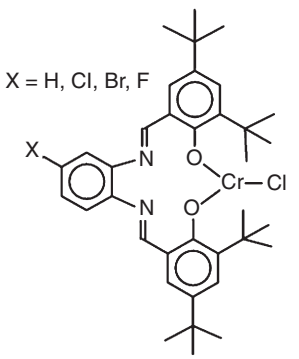

9a

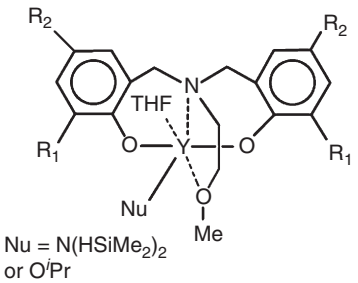

9b

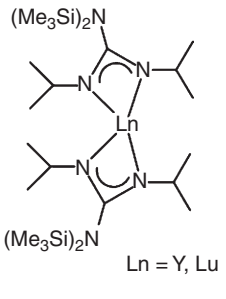

9c

On the contrary, the synthesis leading to a syndiotactic polymer and the corresponding studies of the polymerization mechanism are substantially advanced. Structures **9b** and **9c** are typical examples of catalysts, which afford poly[(*R*,*S*)-β-BL],

predominantly syndiotactic polymers (P_r up to 0.94). R^1 *ortho*-substituents in phenoxide ring in complex **9b** can finely tune the stereocontrol, but the electronic effects (e.g., R^1 in the substituent in the repeating unit C–H…π interactions) can also be important. Thus, depending on the monomer (e.g., *rac*-LA vs. β-BL), the influence of the R^1 bulkiness on the polyester stereoregularity (heterotacticity or syndiotacticity) can act in the opposite direction.[249] For larger substituents, ^{13}C NMR studies of the syndiotactic Pβ-BLs led to the conclusion that in this system the CEM operates.[250,251] Similar results have been obtained with guanidine complexes with group III metals.[252] In addition to high polymerization rates ('complete' monomer consumption in minutes or hours at room temperature!), these systems show typical features of living polymerization (e.g., it was revealed that one molecule of initiator starts, the growth of exactly one macromolecule and the linear dependences M_n vs. monomer conversion were observed).

More detailed information on the stereocontrolled polymerizations of racemic LA and β-BL monomers has been collected in the recently published review papers.[81,253–255]

Microstructure of the *rac*-β-BL polymerization products was resolved in a similar way as in the LAs polymerization case. However, the detailed analysis of the NMR spectra of PLAs and Pβ-BLs is out of the scope of this chapter.

4.11.8.3 Stereocontrolled Copolymerization of L,L-LA with CL

Homopolymerization rates of CL and LA are substantially different. For instance, the ratio of the absolute rate constants of propagation k_p(CL)/k_p(LA) proceeding on aluminum trialkoxide active species is as high as 6.7×10^3 (THF, 20 °C).[60] Surprisingly, in the CL/LA copolymerization, the LA comonomer with this initiating system is consumed first and, typically, block PLA-*b*-PCL or gradient poly(LA-*grad*-CL) copolymers are obtained (see **Figure 21(a)** and References 256–260). Thus, the net reactivities of CL and LA in copolymerization are reversed compared with those in the homopolymerizations. Despite the fact that the first reports describing this puzzling phenomenon were published in the mid-1980s,[256,257] its plausible explanation, on the molecular level, is still under debate.

However, there is at least one report[261] showing that in the CL/LA copolymerization the net reactivities of CL and LA comonomers can be reversed by altering the active center configuration to such an extent that the CL comonomer is consumed first. This new and striking phenomenon is of general importance, since it provides a useful tool for tuning the resultant copolymer microstructure and properties. This concept is depicted in **Scheme 18**.

The described kinetic behavior can be expressed quantitatively in terms of the corresponding reactivity ratios ($r_{CL} = k_{clCL}/k_{clLA}$ and $r_{LA} = k_{laLA}/k_{laCL}$) determined using the numerical integration method; $r_{CL} = 7.2$ and $r_{LA} = 112$ were obtained. Reactivity ratios $r_{CL} = 0.58$ and $r_{LA} = 17.9$ in the copolymerization initiated with neat Al(O^iPr)$_3$ were determined some time ago in the Liege laboratory.[256] Both sets of data, although showing different values, reflect favorable incorporation in the copolymer chain of the repeating units derived from the LA comonomer. A difference between r_{CL}'s and r_{LA}'s obtained for Al(O^iPr)$_3$ and **6d**/Al(O^iPr)$_3$ initiators is not only due to different methods used for their determinations (Mayo–Lewis and numerical integration, respectively) but also, more probably, due to the fact that only with the metal alkoxides that bear bulky substituents can the segmental exchange, modifying the …–cl* and …–la* active species proportions, be avoided.

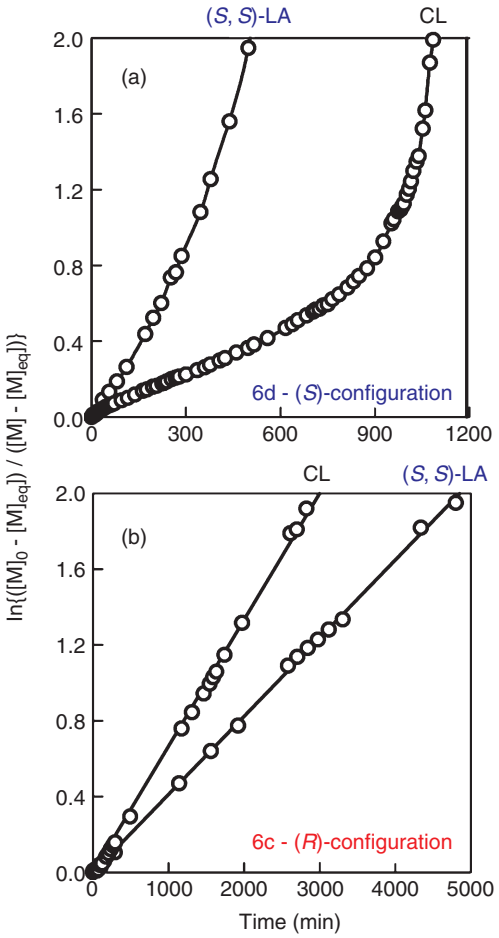

Figure 21 Kinetics of ε-caprolactone (CL)/L,L-lactide [(*S*,*S*)-LA] copolymerization initiated with structure **6d** (a) and structure **6c** (b). Polymerization conditions (concentrations in mol l^{-1}): $[CL]_0 = 2.0$, $[(S,S)\text{-LA}]_0 = 1.0$, $[\mathbf{6c}]_0 = 2 \times 10^{-3}$, $[\mathbf{6d}]_0 = 2.5 \times 10^{-3}$; THF solvent, 80 °C.[261]

Then, kinetic measurements performed for the LA/CL copolymerization initiated with structure **6c** (**Figure 21(b)**) reveal that CL is consumed slightly faster compared with the LA comonomer under the applied polymerization conditions. The determined reactivity ratios are close to each other within the calculated experimental error, namely, $r_{CL} = 3.1$ and $r_{LA} = 4.6$.

According to the ^{13}C NMR spectra, microstructures of the CL/LA copolymers prepared with **6d** and **6c** initiators were substantially different. The corresponding kinetic measurements allow to predict the poly(LA-*grad*-CL)-*b*-poly(CL) or poly(CL-*stat*-LA) copolymer structures obtained with the initiating system of (*S*)- or (*R*)-configuration, respectively.

Finally, it has to be mentioned that later Nomura *et al.*[262] observed a similar copolymer randomization effect in the copolymerization of *rac*-LA and CL initiated with an achiral salen Al-alkoxide complex **6b**, thus by the CEM in contrast to the SECM operating in the **6c**/L,L-LA/CL system.

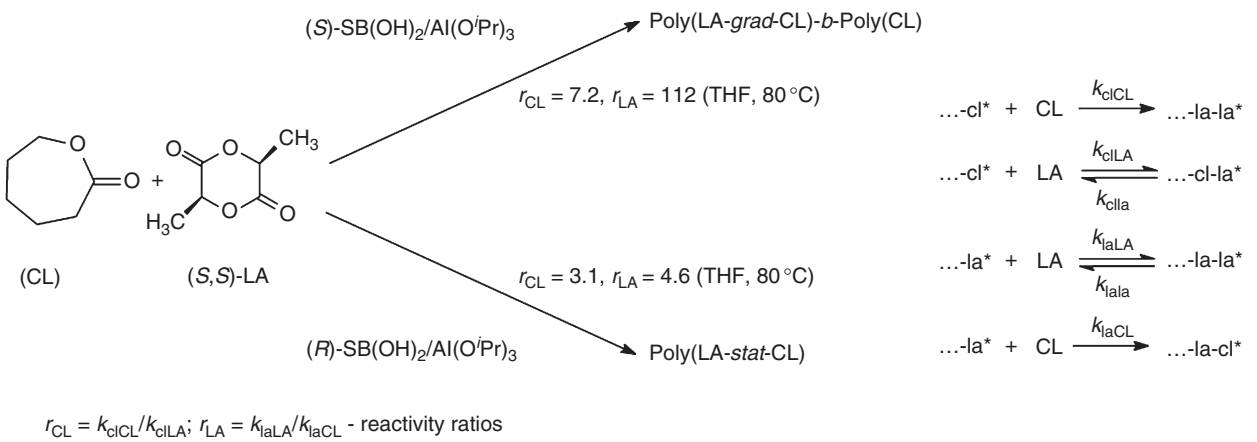

$r_{CL} = k_{clCL}/k_{clLA}$; $r_{LA} = k_{laLA}/k_{laCL}$ - reactivity ratios

Scheme 18

4.11.9 Conclusions

ROP of aliphatic cyclic esters is a continuously and dynamically developing research field. Initially, fundamental aspects of polymerization, such as thermodynamics, kinetics, and mechanisms of the elementary reactions, were explored. The best understood systems encompass polymerization of lactones and LAs. Determination of the standard thermodynamics parameters of polymerization for a majority of the most important monomers now allows the estimation of the equilibrium monomer concentration at given polymerization conditions. For a few polymerizing systems, such as anionic polymerization of PL, CL, or coordinated (proceeding on polarized covalent bonds) polymerizations of CL and LAs, the absolute rate constants have been determined. However, in a majority of the polymerizations, only the net reactivities have usually been determined which does not provide direct access to absolute rate constants of propagation. Nonetheless, the ROP of cyclic esters seems to be a convenient model system for studies of mechanism of cyclic monomers, in general.

Studies leading to depression of even practical elimination of the transfer to monomer or to macromolecule side reactions were also undertaken. Two important factors were recognized that increase the selectivity (i.e., favoritizing propagation over the side reactions): lowering the active species reactivity and increasing the steric hindrance created by ligands located at the active species. Later, precise stereochemical tools were also developed, allowing polylactides and poly(β-substituted β-lactone)s of various stereostructures to be prepared at will.

On that fundamental studies basis, the most convenient conditions for synthesis of aliphatic polyesters were elaborated, controlled with regard to their molar masses, molar mass dispersities, end groups structure, macromolecular architecture, and chain microstructure. One of the most important parameters allowing determination of the polymerization control is the prepared polyester molar mass, theoretically predicted on the starting monomer and initiator concentrations and that measured, most often by GPC. Fortunately, there are numerous examples that can be found in the literature showing the astonishing agreement between M_n determined by GPC employing RI detector and polystyrene standards and that predicted by the starting monomer and initiator concentrations. In parallel, more practical works that aimed to afford either (bio)degradable thermoplastic polyester for high-tonnage applications or specialty polymers for biomedicine or (opto)electronics were carried out. Typically, these are nonsolvent bulk processes, performed at elevated temperatures, above the resultant polyester melting point – under these conditions chain-breaking, transfer, racemization, and transesterification side reaction are particularly advanced. On the contrary, a majority of the mechanistic and stereospecific polymerization studies were carried out in solvent at moderate or low temperatures. Thus, some hopes of transferring results of these studies into the technological polymerization conditions seem to be exaggerated at present.

It can be concluded that studies of a subtle elements of propagation, particularly in the coordinated processes, are still needed. Perhaps the advanced quantum mechanical calculations methods would be very helpful for this purpose. The β-substituted β-lactones are still waiting for the stereospecific initiator allowing the stereoelective and/or stereoselective polymerizations to be carried out. Finally, initiators of the stereocontrolled polymerization operating in bulk, high-temperature processes are also wanted.

References

1. (a) Steinbüchel, A., Doi, Y., Eds. *Biopolymers: Vol. 3a, 3b, 4: Polyesters I–III*; Wiley-VCH: Weinheim, 2002; (b) Nair, L. S.; Laurencin, C. T. *Prog. Polym. Sci.* **2007**, *32*, 762.
2. Szwarc, M. *Nature* **1956**, *178*, 1168.
3. Dainton, F. S.; Ivin, K. J. *Q. Rev., Chem. Soc.* **1958**, *12*, 61.
4. Carothers, W. H.; Dorough, G. L.; van Natta, F. J. *J. Am. Chem. Soc.* **1932**, *54*, 761.
5. van Natta, F. J.; Hill, J. W.; Carothers, W. H. *J. Am. Chem. Soc.* **1934**, *57*, 455.
6. Hall, H. K., Jr.; Schneider, H. K. *J. Am. Chem. Soc.* **1958**, *80*, 6409.
7. Evstropov, A. A.; Lebedev, B. V.; Kulagina, T. G.; *et al. Vysokomol. Soedin., Ser. A* **1979**, *21*, 2038.
8. Evstropov, A. A.; Lebedev, B. V.; Kiparisova, E. G.; *et al. Vysokomol. Soedin., Ser. A* **1980**, *22*, 2450.
9. Evstropov, A. A.; Lebedev, B. V.; Kulagina, T. G.; Lebedev, N. K. *Vysokomol. Soedin., Ser. A* **1982**, *24*, 568.
10. Evstropov, A. A.; Lebedev, B. V.; Kiparisova, E. G. *Vysokomol. Soedin., Ser. A* **1983**, *25*, 1679.

11. Lebedev, B. V.; Evstropov, A. A.; Kiparisova, E. G.; Belov, V. I. *Vysokomol. Soedin., Ser. A* **1978**, *20*, 29.
12. Lebedev, B. V.; Evstropov, A. A.; Lebedev, N. K.; *et al. Vysokomol. Soedin., Ser. A* **1978**, *20*, 1974.
13. Gresham, T. L.; Jansen, J. E.; Shaver, F. W. *J. Am. Chem. Soc.* **1948**, *70*, 998.
14. Cox, E.F.; Hostettler, F., U.S. Patent 3,021,309, 1962.
15. Cherdron, H.; Ohse, H.; Korte, F. *Makromol. Chem.* **1962**, *56*, 187.
16. Tada, K.; Saegusa, T.; Furukawa, J. *Makromol. Chem.* **1964**, *71*, 71.
17. Fukui, K.; Kato, H.; Yonezawa, T.; Okamura, S. *Bull. Chem. Soc. Jpn.* **1964**, *37*, 904.
18. Hall, H. K., Jr. *Macromolecules* **1969**, *2*, 488.
19. (a) Bigdeli, E.; Lenz, R. W. *Macromolecules* **1978**, *11*, 493; (b) Eisenbach, C. D.; Lenz, R. W.*Makromol. Chem.* **1976**, *177*, 2539.
20. Vanderberg, E. J. *J. Polym. Sci.* **1960**, *47*, 489.
21. Agostini, D. E.; Lando, J. B.; Shelton, J. R. *J. Polym. Sci., Polym. Chem. Ed.* **1971**, *6*, 2775.
22. Bloembergen, S.; Holden, D. A.; Bluhm, T. L.; *et al. Macromolecules* **1989**, *22*, 1656.
23. Iida, M.; Araki, T.; Teranishi, K.; Tani, H. *Macromolecules* **1977**, *10*, 275.
24. Zhang, Y.; Gross, R. A.; Lenz, R. W. *Macromolecules* **1990**, *23*, 3206.
25. Hamitou, A.; Ouhadi, T.; Jerome, R.; Teyssie, Ph. *J. Polym. Sci., Polym. Chem. Ed.* **1977**, *15*, 865.
26. Ouhadi, T.; Stevens, Ch.; Teyssie, Ph. *Makromol. Chem., Suppl.* **1975**, *1*, 191.
27. Slomkowski, S.; Penczek, S. *Macromolecules* **1976**, *9*, 367.
28. Deffieux, A.; Boileau, S. *Macromolecules* **1976**, *9*, 369.
29. Hofman, A.; Slomkowski, S.; Penczek, S. *Makromol. Chem.* **1984**, *185*, 91.
30. Sosnowski, S.; Slomkowski, S.; Penczek, S. *Macromolecules* **1993**, *26*, 5526.
31. Sosnowski, S.; Duda, A.; Slomkowski, S.; Penczek, S. *Makromol. Chem., Rapid Commun.* **1984**, *5*, 551.
32. Hofman, A.; Szymanski, R.; Slomkowski, S.; Penczek, S. *Makromol. Chem.* **1984**, *185*, 655.
33. Hofman, A.; Slomkowski, S.; Penczek, S. *Makromol. Chem.* **1987**, *188*, 2027.
34. Cherdron, H.; Ohse, H.; Korte, F. *Makromol. Chem.* **1962**, *56*, 179.
35. Ito, K.; Inoue, T.; Yamashita, Y. *Makromol. Chem.* **1968**, *117*, 279.
36. Kricheldorf, H. R.; Dunsing, R. *Makromol. Chem.* **1986**, *187*, 1611.
37. Kricheldorf, H. R.; Dunsing, R.; Serra, A. *Macromolecules* **1987**, *20*, 2050.
38. Khomyakov, A. K.; Lyudvig, E. B.; Gorelikov, A. T.; Shapetko, N. N. *Vysokomol. Soedin., Ser. A* **1977**, *19*, 867.
39. Rangel, I.; Ricard, M.; Ricard, A. *Macromol. Chem. Phys.* **1994**, *195*, 3095.
40. Okamoto, Y. *Makromol. Chem., Macromol. Symp.* **1991**, *42/43*, 117.
41. Basko, M.; Kubisa, P. *J. Polym. Sci., Part A: Polym. Chem.* **2006**, *44*, 7071.
42. Basko, M.; Kubisa, P. *J. Polym. Sci., Part A: Polym. Chem.* **2007**, *45*, 3090.
43. Basko, M.; Kubisa, P. *J. Polym. Sci., Part A: Polym. Chem.* **2008**, *46*, 7919.
44. Basko, M.; Kubisa, P. *J. Polym. Sci., Part A: Polym. Chem.* **2010**, *48*, 2650.
45. Kricheldorf, H. R.; Scharnagl, N. *J. Macromol. Sci. Chem.* **1989**, *26*, 951.
46. Duda, A. *J. Polym. Sci., Part A: Polym. Chem.* **1992**, *30*, 21.
47. Ito, K.; Yamashita, Y. *Macromolecules* **1978**, *11*, 68.
48. Sosnowski, S.; Slomkowski, S.; Penczek, S.; Reibel, L. *Makromol. Chem.* **1983**, *184*, 2159.
49. Dubois, Ph.; Jerome, R.; Teyssie, Ph. *Polym. Bull.* **1989**, *22*, 475.
50. Hofman, A.; Slomkowski, S.; Penczek, S. *Makromol. Chem., Rapid Commun.* **1987**, *8*, 387.
51. Duda, A.; Florjanczyk, Z.; Hofman, A.; *et al. Macromolecules* **1990**, *23*, 1640.
52. Kricheldorf, H. R.; Scharnagl, N.; Kreiser-Sanders, I. *Makromol. Chem., Macromol. Symp.* **1990**, *32*, 285.
53. Penczek, S.; Duda, A.; Slomkowski, S. *Makromol. Chem., Macromol. Symp.* **1992**, *54/55*, 31.
54. Baran, J.; Duda, A.; Kowalski, A.; *et al. Macromol. Symp.* **1997**, *123*, 93.
55. Duda, A.; Penczek, S. *Makromol. Chem., Macromol. Symp.* **1991**, *47*, 127.
56. Duda, A.; Penczek, S. *Macromol. Rapid Commun.* **1994**, *15*, 559.
57. Duda, A.; Penczek, S. *Macromolecules* **1994**, *27*, 4867.
58. Biela, T.; Duda, A. *J. Polym. Sci., Part A: Polym. Chem.* **1996**, *34*, 1807.
59. Duda, A. *Macromolecules* **1996**, *29*, 1399.
60. Kowalski, A.; Duda, A.; Penczek, S. *Macromolecules* **1998**, *31*, 2114.
61. Kowalski, A.; Libiszowski, J.; Duda, A.; Penczek, S. *Macromolecules* **2000**, *33*, 1964.
62. Dubois, Ph.; Degee, Ph.; Jerome, R.; Teyssie, Ph. *Macromolecules* **1996**, *29*, 1965.
63. Ropson, N.; Dubois, Ph.; Jerome, R.; Teyssie, Ph. *Macromolecules* **1993**, *26*, 6378.
64. Kricheldorf, H. R.; Berl, M.; Scharnagl, N. *Macromolecules* **1998**, *21*, 286.
65. Duda, A.; Penczek, S. *Macromol. Rapid Commun.* **1995**, *16*, 67.
66. Duda, A.; Penczek, S. *Macromolecules* **1995**, *28*, 5981.
67. Yasuda, T.; Aida, T.; Inoue, S. *Macromolecules* **1983**, *16*, 1792.
68. Trofimoff, L.; Aida, T.; Inoue, S. *Chem. Lett.* **1987**, 991.
69. Endo, M.; Aida, T.; Inoue, S. *Macromolecules* **1987**, *20*, 2982.
70. Le Borgne, A.; Vincens, V.; Jouglard, M.; Spassky, N. *Makromol. Chem., Macromol. Symp.* **1993**, *67*, 37.
71. Spassky, N.; Wisniewski, M.; Pluta, Ch.; Le Borgne, A. *Macromol. Chem. Phys.* **1996**, *197*, 2627.
72. Penczek, S.; Moad, G. *Pure Appl. Chem.* **2008**, *80*, 2163.
73. McLain, S. J.; Drysdale, N. E. *Polym. Prepr. (Am. Chem. Soc., Div. Polym. Chem.)* **1992**, *33*(1), 174.
74. McLain, S. J.; Ford, T. M.; Drysdale, N. E. *Polym. Prepr. (Am. Chem. Soc., Div. Polym. Chem.)* **1992**, *33*(2), 463.
75. Stevels, W. M.; Ankone, M. J. K.; Dijkstra, P. J.; Feijen, J. *Macromolecules* **1996**, *29*, 6132.
76. Stevels, W. M.; Ankone, M. J. K.; Dijkstra, P. J.; Feijen, J. *Macromolecules* **1996**, *29*, 8296.
77. Simic, V.; Spassky, N.; Hubert-Pfalzgraf, E. G. *Macromolecules* **1997**, *30*, 7338.
78. Williams, C. K.; Breyfogle, E.; Choi, S. K.; *et al. J. Am. Chem. Soc.* **2003**, *125*, 11350.
79. Schmidt, J. A. R.; Mahadevan, V.; Yutan, D. Y. L.; *et al. J. Am. Chem. Soc.* **2002**, *124*, 15239.
80. Kurcok, P.; Smiga, M.; Jedlinski, Z. *J. Polym. Sci., Part A: Polym. Chem.* **2002**, *40*, 2184.
81. Carpentier, J.-F. *Macromol. Rapid Commun.* **2010**, *31*, 1696.
82. Kharas, G. B.; Sanchez-Riera, F.; Severson, D. K. In *Plastics from Microbes*; Mobley, D. P., Ed.; Hanser Publishers: Munich, Germany; New York, 1994; p 93.
83. Hartmann, M. H. In *Biopolymers from Renewable Resources*; Kaplan, D. L., Ed.; Springer Verlag: Berlin; Heidelberg, 1998; p 367.
84. Leenslag, J. W.; Pennings, A. J. *Makromol. Chem.* **1987**, *188*, 1809.
85. Kricheldorf, H. R.; Kreiser-Saunders, I.; Boettcher, C. *Polymer* **1995**, *36*, 1253.
86. Kricheldorf, H. R.; Kreiser-Saunders, I.; Stricker, A. *Macromolecules* **2000**, *33*, 702.
87. Nijenhuis, A. J.; Grijpma, D. W.; Pennings, A. J. *Macromolecules* **1992**, *25*, 6419.
88. Zhang, X.; MacDonald, D. A.; Goosen, M. F. A.; McAuley, K. B. *J. Polym. Sci., Part A: Polym. Chem.* **1994**, *32*, 2965.
89. Schwach, G.; Coudane, J.; Engel, R.; Vert, M. *J. Polym. Sci., Part A: Polym. Chem.* **1997**, *35*, 3431.
90. In't Veld, P. J. A.; Velner, E. M.; van de Witte, P.; *et al. J. Polym. Sci., Part A: Polym. Chem.* **1997**, *35*, 219.
91. Kowalski, A.; Duda, A.; Penczek, S. *Macromol. Rapid Commun.* **1998**, *19*, 567.
92. Kowalski, A.; Duda, A.; Penczek, S. *Macromolecules* **2000**, *33*, 689.
93. Kowalski, A.; Duda, A.; Penczek, S. *Macromolecules* **2000**, *33*, 7359.
94. Majerska, K.; Duda, A.; Penczek, S. *Macromol. Rapid Commun.* **2000**, *21*, 1327.
95. Libiszowski, J.; Kowalski, A.; Biela, T.; *et al. Macromolecules* **2005**, *38*, 8170.
96. Kowalski, A.; Libiszowski, J.; Majerska, K.; *et al. Polymer* **2007**, *48*, 3952.
97. Ryner, M.; Stritsberg, K.; Albertsson, A. C.; *et al. Macromolecules* **2001**, *34*, 3877.
98. Storey, R. F.; Sherman, J. W. *Macromolecules* **2002**, *35*, 1504.
99. Messman, J. M.; Storey, R. F. *J. Polym. Sci., Part A: Polym. Chem.* **2004**, *42*, 6238.
100. Pack, J. W.; Kim, S. H.; Park, S. Y.; *et al. Macromolecules* **2003**, *36*, 8923.
101. Bratton, D.; Brown, M.; Howdle, S. M. *Macromolecules* **2005**, *38*, 1190.
102. Xian, C.-S.; Wang, Y.-C.; Du, J.-Z.; *et al. Macromolecules* **2006**, *9*, 6825.
103. Kamber, N. E.; Jeong, W.; Waymouth, R. M.; *et al. Chem. Rev.* **2007**, *107*, 5813.
104. Bourissou, D.; Moebs-Sanchez, S.; Martin-Vaca, G. *C. R. Chim.* **2007**, *10*, 775.
105. Coulembier, O.; Degee, P.; Hedrick, J. L.; Dubois, P. *Prog. Polym. Sci.* **2006**, *31*, 723.
106. Corley, L. S.; Vogl, O.; Biela, T.; *et al. Makromol. Chem. Rapid. Commun.* **1981**, *2*, 47.
107. Biela, T.; Penczek, S.; Slomkowski, S. *Makromol. Chem.* **1983**, *184*, 811.
108. Coulembier, O.; Lohmeijer, B. G. G.; Dove, A. P.; *et al. Macromolecules* **2006**, *39*, 5617.
109. Lundberg, R. D.; Cox, E. F. *Ring-Opening Polymerization*; Frish, K. C.; Reegen, S. L., Eds.; Marcel Dekker: New York; London, 1969; p 247.
110. Johns, D. B.; Lenz, R. W.; Luecke, A. In *Ring-Opening Polymerization*; Ivin, K. J.; Saegusa, T., Eds.; Elsevier Applied Science: London; New York, 1984; Vol. 1, p 461.
111. Slomkowski, S.; Duda, A. In *Ring-Opening Polymerization: Mechanisms, Catalysis, Structure, Utility*; Brunelle, D. J., Ed.; Hanser Publishers: Munich; Vienna; New York; Barcelona, 1993; p 87.
112. Loefgren, A.; Albertsson, A.-Ch.; Dubois, P.; Jerome, R. *J. Macromol. Sci., Rev. Macromol. Chem. Phys.* **1995**, *C35*, 379.
113. Mecerreyes, D.; Jerome, R.; Dubois, P. *Adv. Polym. Sci.* **1998**, *147*, 1.
114. Duda, A.; Penczek, S. In *Biopolymers*; Steinbüchel, A., Doi, Y., Eds.; Wiley-VCH: Weinheim, 2002; Vol. 3b, p 371.

115. Dechy-Cabaret, O.; Vaca, B. M.; Bourisou, D. *Chem. Rev.* **2004**, *104*, 6147.
116. Dubois, Ph.; Coulembier, O.; Raquez, J.-M., Eds. *Handbook of Ring-Opening Polymerization*; Wiley-VCH: Weinheim, 2009.
117. Jerome, R.; Teyssie, Ph. In *Comprehensive Polymer Science*; Allen, G.; Bevington, J. C.; Eastmond, G. C.; *et al*., Eds.; Pergamon Press: Oxford, UK, 1989; Vol. 3, Part 1, p 501.
118. Penczek, S.; Slomkowski, S. In *Comprehensive Polymer Science*; Allen, G.; Bevington, J. C.; Eastmond, G. C.; *et al*., Eds.; Pergamon Press: Oxford, UK, 1989; Vol. 3, Part 1, p 813.
119. Penczek, S.; Cypryk, M.; Duda, A.; *et al. Prog. Polym. Sci.* **2007**, *32*, 247.
120. Penczek, S.; Duda, A.; Kubisa, P.; Slomkowski, S. In *Macromolecular Engineering, Precise Synthesis, Material Properties, Applications*; Matyjaszewski, K.; Gnanou, Y.; Leilbler, L., Eds.; Wiley-VCH: Weinheim, 2007; Vol. 1, p 103.
121. Duda, A.; Kowalski, A. In *Handbook of Ring-Opening Polymerization*; Dubois, Ph.; Coulembier, O.; Raquez, J.-M.; Eds.; Wiley-VCH: Weinheim, 2009; p 1.
122. Penczek, S.; Cypryk, M.; Duda, A.; *et al*. In *Controlled and Living Polymerizations. From Mechanisms to Applications*; Matyjaszewski, K.; Mueller, A. H. E., Eds.; Wiley-VCH: Weinheim, 2009; p 241.
123. Dainton, F. S.; Ivin, K. J. *Nature* **1948**, *162*, 705.
124. Tobolsky, A. V. *J. Polym. Sci.* **1957**, *25*, 220.
125. Tobolsky, A. V. *J. Polym. Sci.* **1958**, *31*, 126.
126. (a) Tobolsky, A. V.; Eisenberg, A. *J. Am. Chem. Soc.* **1959**, *81*, 780. (b) Tobolsky, A. V.; Eisenberg, A. *J. Am. Chem. Soc.* **1960**, *82*, 289.
127. Odian, G. In *Principles of Polymerization*, 4th ed.; Wiley: Hoboken, NJ, 2004.
128. Sawada, H. *Thermodynamics of Polymerization*; Marcel Dekker: New York, 1976.
129. Ivin, K. J.; Busfield, W. K. In *Concise Encyclopedia of Polymer Science and Engineering*; Mark, H. F.; Bikales, N. M.; Overberger, C. G.; Menges, G.; Kroschwitz, J. I., Eds.; Wiley: New York, 1988; p 845.
130. Penczek, S.; Kubisa, P. In *Ring-Opening Polymerization. Mechanisms, Catalysis, Structure, Utility*; Brunelle, D. J., Ed.; Hanser Publishers: New York, 1993; p 13.
131. (a) Penczek, S.; Kubisa, P.; Matyjaszewski, K. *Adv. Polym. Sci.* **1980**, *37*, 1. (b) Penczek, S.; Kubisa, P.; Matyjaszewski, K. *Adv. Polym. Sci*. **1985**, *68/69*, 1.
132. Saiyasombat, W.; Molloy, W.; Nicholson, T. M.; *et al. Polymer* **1998**, *39*, 5581.
133. Elias, H.-G. In *Macromolecules Vol. 1: Chemical Structures and Syntheses*; Wiley-VCH: Weinheim, 2005.
134. Libiszowski, J.; Kowalski, A.; Szymanski, R.; *et al. Macromolecules* **2004**, *37*, 52.
135. Matsuo, J.; Aoki, K.; Sanda, F.; Endo., T. *Macromolecules* **1998**, *31*, 4432.
136. Duda, A.; Penczek, S. *Macromolecules* **1990**, *23*, 1636.
137. Evstropov, A. A.; Lebedev, B. V.; Kiparisova, E. G.; Sheveleva, M. G. *Vysokomol. Soedin., Ser. B* **1981**, *23*, 551.
138. Antolovic, D.; Shiner, V. J.; Davidson, E. R. *J. Am. Chem. Soc.* **1988**, *110*, 1375.
139. Stevens, M. P. *Polymer Chemistry*; Addison-Wesley: Reading, MA, 1975.
140. Kucera, M. *Mechanism and Kinetics of Addition Polymerization*; Academia: Prague; Elsevier Science: Amsterdam, 1992.
141. Johns, D. B.; Lenz, R. W.; Luecke, A. In *Ring-Opening Polymerization*; Ivin K. J.; Saegusa, T., Eds.; Elsevier Applied Science: London, 1984; Vol. 1, p 467.
142. Seymour, R. B.; Carraher, Ch. E., Jr. *Polymer Chemistry. An Introduction*, 3rd ed.; Marcel Dekker: New York, 1992.
143. Allcock, H. R.; Lampe, F. W.; Mark, J. E. *Contemporary Polymer Chemistry*, 3rd ed.; Pearson Education: Upper Saddle River; New York, 2003.
144. Chen, T.; Qin, Z.; Qi, Y.; *et al. Polym. Chem.* **2011**, *2*, 1190.
145. Houk, K.; Jabbari, A.; Hall, H. K., Jr.; Aleman, C. *J. Org. Chem.* **2008**, *73*, 2674.
146. Aleman, C.; Betran, O.; Casanovas, J.; *et al. J. Org. Chem.* **2009**, *74*, 6237.
147. Duda, A.; Biela, T.; Libiszowski, J.; *et al. Polym. Degrad. Stab.* **1998**, *59*, 215.
148. Duda, A.; Penczek, S. *ACS Symp. Ser.* **2000**, *764*, 160.
149. Duda, A.; Penczek, S.; Dubois, Ph.; *et al. Macromol. Chem. Phys.* **1996**, *197*, 1273.
150. Ubaghs, L.; Waringo, M.; Keul, H.; Hoecker, H. *Macromolecules* **2004**, *37*, 6755.
151. Agarwal, S.; Xie, X. *Macromolecules* **2003**, *36*, 3545.
152. Duda, A.; Libiszowski, J.; Mosnacek, J.; Penczek, S. *Macromol. Symp.* **2005**, *226*, 109.
153. Mosnacek, J.; Duda, A.; Libiszowski, J.; Penczek, S. *Macromolecules* **2005**, *38*, 2027.
154. Shinno, K.; Mijamoto, M.; Kimura, Y.; *et al. Macromolecules* **1997**, *30*, 6438.
155. Raquez, J.-M.; Degee, P.; Narayan, R.; Dubois, Ph. *Macromolecules* **2001**, *34*, 8419.
156. Penczek, S.; Kubisa, P. In *Comprehensive Polymer Science*; Allen, G.; Bevington, J. C.; Eastmond, G. C.; *et al*., Eds.; Pergamon Press: Oxford, UK, 1989; Vol. 3, Part 1, p 787.
157. (a) Eyring, H. *J. Chem. Phys.* **1935**, *3*, 107. (b) Laidler, K. J.; King, M. C. *J. Phys. Chem.* **1983**, *87*, 2657.
158. (a) Gol'dfarb, Ya. I.; Belen'kii, L. I. *Russ. Chem. Rev.* **1960**, *29*, 214. (b) Huisgen, R.; Ott, H. *Tetrahedron* **1959**, *6*, 214.
159. Duda, A., unpublished results.
160. Slomkowski, S.; Penczek, S. *Macromolecules* **1980**, *13*, 229.
161. Slomkowski, S. *Polymer* **1986**, *27*, 71.
162. Sosnowski, S.; Slomkowski, S.; Penczek, S. *Makromol. Chem.* **1991**, *192*, 735.
163. Burgi, H. B.; Dunitz, J. D.; Lehn, J. M.; Wipf, G. *Tetrahedron* **1974**, *34*, 1563.
164. Blackburn, G. M.; Dodds, H. L. H. *J. Chem. Soc., Perkin* **1977**, *2*, 3773.
165. Duda, A.; Kowalski, A.; Penczek, S.; *et al. Macromolecules* **2002**, *35*, 4266.
166. van der Mee, L.; Helmich, F.; de Bruin, R.; *et al. Macromolecules* **2006**, *39*, 5021.
167. (a) Gupta, A. P.; Kumar, V. *Eur. Polym. J.* **2007**, *43*, 4053. (b) Platel, R. H.; Hodgson, L. M.; Williams, C. K. *Polym. Rev.* **2008**, *48*, 11.
168. Arbaoui, A.; Redshaw, C. *Polym. Chem.* **2010**, *1*, 801.
169. Jedlinski, Z.; Kurcok, P.; Lenz, R. W. *Macromolecules* **1998**, *31*, 2027.
170. Dale, J.; Schwarz, J. E. *Acta Chem. Scand., Ser. B* **1986**, *40*, 559.
171. Grobelny, Z.; Stolarzewicz, A.; Morejko, B.; *et al. Macromolecules* **2006**, *39*, 6832.
172. Szwarc, M. *Ionic Polymerization Fundamentals*; Hanser Publishers: Munich, Germany, 1996.
173. Baran, J.; Duda, A.; Kowalski, A.; *et al. Macromol. Rapid Commun.* **1997**, *18*, 325.
174. Penczek, S.; Duda, A.; Szymanski, R. *Macromol. Symp.* **1998**, *132*, 441.
175. Penczek, S.; Duda, A. *Macromol. Symp.* **1996**, *107*, 1.
176. Jones, R. A. Y. *Physical and Mechanistic Organic Chemistry*; Cambridge University Press: Cambridge, UK, 1984.
177. Lewinski, J.; Horeglad, P.; Tratkiewicz, E.; *et al. Macromol. Rapid Commun.* **2004**, *25*, 1939.
178. Lewinski, J.; Horeglad, P.; Wojcik, K.; Justyniak, I. *Organometallics* **2006**, *24*, 4588.
179. Szwarc, M.; van Beylen, M. *Ionic Polymerization and Living Polymers*; Chapman & Hall: New York, 1993.
180. Jacobs, C.; Dubois., P.; Jerome, R.; Teyssie, P. *Macromolecules* **1991**, *24*, 3027.
181. Penczek, S.; Duda, A. *Makromol. Chem., Macromol. Symp.* **1991**, *42/43*, 135.
182. Khanna, S. N.; Levy, M.; Szwarc, M. *Trans Faraday Soc.* **1962**, *58*, 2159.
183. Penczek, S.; Duda, A.; Szymanski, R.; Biela, T. *Macromol. Symp.* **2000**, *153*, 1.
184. Benn, R.; Rufinska, A. *Angew. Chem., Int. Ed. Engl.* **1986**, *25*, 861.
185. Kriz, O.; Casensky, B.; Lycka, A.; *et al. J. Magn. Reson.* **1984**, *60*, 375.
186. Florczak, M.; Kowalski, A.; Libiszowski, J.; *et al. Polimery (Warsaw)* **2007**, *52*, 722.
187. Chen, H.-Y.; Huang, B.-H.; Lin, C.-C. *Macromolecules* **2005**, *38*, 5400.
188. Biela, T.; Kowalski, A.; Libiszowski, J.; *et al. Macromol. Symp.* **2006**, *240*, 47.
189. Degée, Ph.; Dubois, Ph.; Jerome, R. *Macromol. Chem. Phys.* **1997**, *198*, 1973.
190. Aida, T. *Prog. Polym. Sci.* **1994**, *19*, 469.
191. Aida, T.; Inoue, S. *Acc. Chem. Res.* **1996**, *29*, 39.
192. O'Keefe, B. J.; Hillmyer, M. A.; Tolman, W. B. *J. Chem. Soc., Dalton Trans.* **2001**, 2215.
193. Chamberlain, B. M.; Cheng, M.; Moore, D. R.; *et al. J. Am. Chem. Soc.* **2001**, *123*, 3229.
194. O'Keefe, B. J.; Breyfogle, L. E.; Hillmyer, M. A.; Tolman, W. B. *J. Am. Chem. Soc.* **2002**, *124*, 4384.
195. Ko, B.-T.; Lin, C.-C. *Macromolecules* **1999**, *32*, 8296.
196. Liu, Y.-C.; Ko, B.-T.; Lin, C.-C. *Macromolecules* **2001**, *34*, 6196.
197. Liao, T.-C.; Huang, Y.-L.; Huang, B. H.; Lin, C.-C. *Macromol. Chem. Phys.* **2003**, *204*, 885.
198. Nomura, N.; Aoyama, T.; Ishii, R.; Kondo, T. *Macromolecules* **2005**, *38*, 5363.
199. Chen, H.-Y.; Tang, H.-Y.; Lin, C.-C. *Macromolecules* **2006**, *39*, 5400.
200. Rieth, L. R.; Moore, D. R.; Lobkovsky, E. B.; Coates, G. W. *J. Am. Chem. Soc.* **2002**, *124*, 15239.
201. Kurcok, P.; Dubois, Ph.; Jerome, R. *Polym. Int.* **1996**, *41*, 479.
202. Ajellaj, N.; Carpentier, J.-F.; Guillame, C.; *et al. Dalton Trans.* **2010**, *39*, 8363.
203. Poirier, V.; Roisnel, T.; Carpentier, J.-F.; Sarazin, Y. *Dalton Trans.* **2011**, *40*, 523.
204. Ito, K.; Hashizuka, Y.; Yamashita, Y. *Macromolecules* **1977**, *10*, 821.
205. Szymanski, R. *Macromol. Theory Simul.* **1998**, *7*, 27.
206. Penczek, S.; Biela, T.; Duda, A. *Macromol. Rapid Commun.* **2000**, *21*, 941.
207. Florczak, M.; Libiszowski, J.; Mosnacek, J.; *et al. Macromol. Rapid Commun.* **2007**, *28*, 1385.
208. (a) Song, C. X.; Feng, X. D. *Macromolecules* **1984**, *17*, 2764. (b) Stevels, W. M.; Ankone, J. K.; Dijkstra, P. J.; Feijen, J. *Macromol. Chem. Phys.* **1995**, *196*, 1153. (c) Shen, Y.; Shen, Z.; Zhang, Y.; Yao, K. *Macromolecules* **1996**, *32*, 8289. (d) Deng, X.; Zhu, Z.; Xiong, Ch.; Zhang, L. *J. Polym. Sci., Part A: Polym. Chem.* **1997**, *35*, 703. (e) Pensec, S.; Leroy, M.; Akkouche, H.; Spassky, N. *Polym. Bull. (Berlin)* **2000**, *45*, 373. (f) Cui, D.; Tang, T.; Bi, W.; *et al. J. Polym. Sci., Part A: Polym. Chem.* **2003**, *41*, 2667. (g) Zhang, L.; Shen, Z.; Yu, C.; Fan, L. *J. Macromol. Sci., Part A: Pure Appl. Chem.* **2004**, *41*, 927. (h) Stassin, F.; Jerome, R. *J. Polym. Sci., Part A: Polym. Chem.* **2005**, *43*, 2777. (i) Fan, L.; Xiong, Y.-B.; Xu, H.; Shen, Z. Q. *Eur. Polym. J.* **2005**, *41*, 1647. (j) Chmura, A. J.; Davidson, M. G.; Jones, M. D.; *et al. Macromolecules* **2006**, *39*, 7250.

209. Hatada, K.; Kahovec, J.; Baron, M.; *et al. Pure Appl. Chem.* **2002**, *74*, 915.
210. Sodergard, A.; Stolt, M. *Prog. Polym. Sci.* **2002**, *27*, 1123.
211. Okamoto, Y.; Nakano, T. *Chem. Rev.* **1994**, *94*, 349.
212. Le Borgne, A.; Spassky, N. *Polymer* **1989**, *30*, 2312.
213. Wisniewski, M.; Le Borne, A.; Spassky, N. *Macromol. Chem. Phys.* **1997**, *198*, 1227.
214. Radano, C. P.; Baker, G. L.; Smith, M. R. *J. Am. Chem. Soc.* **2000**, *122*, 1552.
215. Ovitt, T. M.; Coates, G. W. *J. Polym. Sci., Part A: Polym. Chem.* **2000**, *38*, 4686.
216. Ovitt, T. M.; Coates, G. W. *J. Am. Chem. Soc.* **2002**, *124*, 1316.
217. Zhong, Z.; Dijkstra, P. J.; Feijen, J. *Angew. Chem., Int. Ed.* **2002**, *41*, 4510.
218. Zhong, Z.; Dijkstra, P. J.; Feijen, J. *J. Am. Chem. Soc.* **2003**, *125*, 11291.
219. Nomura, N.; Ishi, R.; Akakura, M.; Aoi, K. *J. Am. Chem. Soc.* **2002**, *124*, 5938.
220. Nomura, N.; Ishi, R.; Yamamoto, Y.; Kondo, T. *Chem. Eur. J.* **2007**, *13*, 4433.
221. Majerska, K.; Duda, A. *J. Am. Chem. Soc.* **2004**, *126*, 1026.
222. Du, H.; Velders, A. H.; Dijkstra, P. J.; *et al. Macromolecules* **2009**, *42*, 1058.
223. Arnold, P. L.; Buffet, J.-C.; Blaudeck, R.; *et al. Chem. Eur. J.* **2009**, *15*, 8241.
224. Cheng, M.; Attygale, A. B.; Lobkowski, E. B.; Coates, G. W. *J. Am. Chem. Soc.* **1999**, *121*, 11583.
225. Chisholm, M. H.; Gallucci, J.; Phomphrai, K. *Inorg. Chem.* **2002**, *41*, 2785.
226. Chisholm, M. H.; Gallucci, J.; Phomphrai, K. *Inorg. Chem.* **2005**, *44*, 8004.
227. Ma, H.; Spaniol, T. P.; Okuda, J. *Angew. Chem., Int. Ed.* **2006**, *45*, 7818.
228. Ko, B.-T.; Woo, C.-C.; Lin, C.-C. *Macromolecules* **2001**, *34*, 8851.
229. Bero, M.; Dobrzynski, P.; Kasperczyk, J. *J. Polym. Sci., Part A: Polym. Chem.* **1999**, *37*, 4038.
230. Kasperczyk, J.; Bero, M. *Polymer* **2000**, *41*, 391.
231. Lillie, E.; Schulz, R. C. *Makromol. Chem.* **1975**, *176*, 1901.
232. Schindler, A.; Harper, D. *J. Polym. Sci., Polym. Lett. Ed.* **1976**, *14*, 729.
233. Chabot, F.; Vert, M. *Polymer* **1983**, *24*, 53.
234. Schindler, A.; Gaetano, K. D. *J. Polym. Sci., Part C: Polym. Lett.* **1988**, *26*, 47.
235. Bero, M.; Kasperczyk, J.; Jedlinski, Z. J. *Makromol. Chem.* **1990**, *191*, 2287.
236. Dubois, P.; Jacobs, C.; Jerome, R.; Teyssie, P. *Macromolecules* **1991**, *24*, 2266.
237. Kricheldorf, H. R.; Boettcher, C.; Toennes, K.-U. *Polymer* **1992**, *33*, 2817.
238. Kasperczyk, J. E. *Macromolecules* **1995**, *28*, 3937.
239. Spassky, N.; Simic, V.; Montaudo, M. S.; Hubert-Pfalzgraf, L. G. *Macromol. Chem. Phys.* **2000**, *201*, 2432.
240. Stevels, W. M.; Bernard, A.; van de Witte, P.; *et al. J. Appl. Polym. Sci.* **1996**, *6a*, 1295.
241. Coudane, J.; Ustariz-Peyret, C.; Schwach, G.; Vert, M. *J. Polym. Sci., Part A: Polym. Chem.* **1997**, *35*, 1651.
242. Kricheldorf, H. R.; Lossin, M. *J. Macromol. Sci., Pure Appl. Chem.* **1997**, *34*, 179.
243. Thakur, K. A. M.; Kean, R. T.; Hall, E. S.; *et al. Macromolecules* **1997**, *30*, 2422.
244. Thakur, K. A. M.; Kean, R. T.; Hall, E. S.; *et al. Macromolecules* **1998**, *31*, 1487.
245. Thakur, K. A. M.; Kean, R. T.; Zell, M. T.; *et al. J. Chem. Commun.* **1998**, 1913.
246. Chisholm, M. H.; Iyer, S. S.; McCollum, D. G.; *et al. Macromolecules* **1999**, *32*, 963.
247. Kasperczyk, J. E. *Polymer* **1999**, *40*, 5455.
248. Zintl, M.; Molnar, F.; Urban, T.; *et al. Angew. Chem., Int. Ed.* **2008**, *47*, 3458.
249. Bouyahyi, M.; Ajellal, N.; Kirillov, E.; *et al. Chem. Eur. J.* **2011**, *17*, 1872.
250. Amgoune, A.; Thomas, C. M.; Ilinca, S.; *et al. Angew. Chem., Int. Ed.* **2006**, *45*, 2782.
251. Ajellal, N.; Bouyahyi, M.; Amgoune, A.; *et al. Macromolecules* **2009**, *42*, 987.
252. Ajellal, N.; Lyubov, D. M.; Sinenkov, M. A.; *et al. Chem.-Eur. J.* **2008**, *14*, 5440.
253. Amgoune, A.; Thomas, C. M.; Carpentier, J.-F. *Pure Appl. Chem.* **2007**, *79*, 1831.
254. Stanford, M. J.; Dove, A. P. *Chem. Soc. Rev.* **2010**, *39*, 486.
255. Thomas, C. M. *Chem. Soc. Rev.* **2010**, *39*, 165.
256. Vion, J. M.; Jerome, R.; Teyssie, P.; *et al. Macromolecules* **1986**, *19*, 1828.
257. Vanhoorne, P.; Dubois, P.; Jerome, R.; Teyssie, P. *Macromolecules* **1992**, *25*, 37.
258. Kasperczyk, J.; Bero, M. *Makromol. Chem.* **1991**, *192*, 1777.
259. Kasperczyk, J.; Bero, M.; Adamus, G. *Makromol. Chem.* **1993**, *194*, 907.
260. Kasperczyk, J.; Bero, M.; Adamus, G. *Makromol. Chem.* **1993**, *194*, 913.
261. Florczak, M.; Duda, A. *Angew. Chem., Int. Ed.* **2008**, *47*, 9088.
262. Nomura, N.; Akita, A.; Ishii, R.; Mizuno, M. *J. Am. Chem. Soc.* **2010**, *132*, 1750.

Biographical Sketch

Andrzej Duda is head of the Department of Polymer Chemistry at the Center of Molecular and Macromolecular Studies of the Polish Academy of Sciences in Lodz, Poland and currently chairman of the Polymer Section of the Polish Chemical Society as well as a member of the Polish National Science Center. He received his MSc degree from Lodz University of Technology (1975), his PhD (1984, under the supervision of Stanislaw Penczek), and his DSc (1997) from the Polish Academy of Sciences. Since 2004, he has been a full professor in chemistry with the title conferred by the President of Republic of Poland. His research interests focus on thermodynamics, kinetics, and mechanisms of the ring-opening and ionic polymerizations, reactivity–selectivity relationships in polymerization, methods of controlled/living polymerization, macromolecular engineering, and polymers and monomers available from renewable resources. He is the author and coauthor of more than 100 scientific papers (including 5 book chapters).

4.12 ROP of Cyclic Carbonates and ROP of Macrocycles

G Rokicki and PG Parzuchowski, Warsaw University of Technology, Warsaw, Poland

4.12.1 Introduction

Polycarbonates (PCs) are polyesters of diols or diphenols and carbonic acid containing –OC(O)O– groups in their backbone chains and, therefore, can be divided into aliphatic and aromatic ones. Taking into account the low stability and reactivity of carbonic acid, such polymers cannot be obtained by the polycondensation reaction of H_2CO_3 with diols or diphenols, and therefore, more reactive derivatives of carbonic acid such as phosgene are usually used as starting materials. However, due to the phosgene high toxicity and formation of stoichiometric amounts of sodium chloride as an environmentally burdensome by-product, alternative methods have been developed in which carbon dioxide or low-molecular linear or cyclic carbonate esters are applied.

An alternative method for PC synthesis is ring-opening polymerization (ROP) of cyclic carbonates, both aliphatic and aromatic. The chemistry of PCs is extensive and well developed. A comprehensive study of PCs was reported by Brunelle in 1993, 1997, and 2005.[1–3] A review of aliphatic cyclic carbonate synthesis and chemistry was presented by Rokicki.[4]

Nowadays, aromatic and aliphatic PCs are used in a broad range of applications, for example, as elastomers, sealants, elastoplastics, foams, coatings, and adhesives.[1,5–8] Global consumption of aromatic PC has risen by 9% annually on average over the past decade, and producers see this trend as set to continue along the same lines over the next several years. The outstanding properties of PC include transparency, heat resistance up to 130 °C, high toughness, and excellent dimensional stability. It can be sterilized, welded, or glued and is self-extinguishing. PC is easily blended with other polymers. Some 15% of consumption is for blends – especially popular are blends with styrene-based polymers such as acrylonitrile-butadiene-styrene terpolymer (ABS) or styrene-acrylonitrile copolymer (SAN). Electrical engineering is the most important market for PC, taking 30% of production for housings and covers for products such as distribution boxes, lights, and household appliances, among other applications. Optical storage media such as CDs and DVDs continue to be fast-growing

applications for PC. The main applications are solid and hollow chamber sheeting for canopies and greenhouses, as well as conservatory and swimming pool roofing.

Aliphatic PCs and copolycarbonates, due to their biocompatibility and biodegradability, are valuable biomaterials and stimulate intensive efforts to develop new synthetic methods. Incorporation of the carbonate structure provides flexibility and toughness to the otherwise rigid and brittle polyesters.

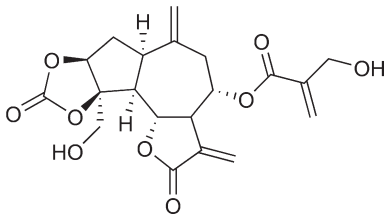

Scheme 2 Natural five-membered cyclic carbonate isolated from *Centaurea hololeuca* (Boiss) plant.

4.12.2 Synthesis of Cyclic Carbonates

4.12.2.1 Synthesis of Aliphatic Cyclic Carbonates

The first information concerning the synthesis of cyclic carbonates was revealed by Carothers *et al.* in the early 1930s.[9–11] Cyclic carbonates were obtained by the depolymerization of respective linear oligocarbonates at high temperature in the presence of various catalysts combined with distillation under reduced pressure. The products (yields of 40–80%) consisted of a mixture of volatile cycles (mostly monomeric and dimeric cyclic carbonates).[12–14] The most effective catalysts in this process were Sn(II), Mn(II), Fe(II), and Mg(II) chlorides, carbonates, and oxides. This method is still applied in the synthesis of six- and seven-membered and of larger size aliphatic cyclic carbonates.

4.12.2.1.1 Synthesis of five-membered cyclic carbonates

The synthesis of five-membered alkylene carbonates (1,3-dioxolan-2-ones) of the structure presented in Scheme 1 has been the subject of considerable research. Two of them, ethylene carbonate (EC) ($R^{1-4} = H$) and propylene carbonate (PC) ($R^{1-3} = H$, $R^4 = CH_3$), have been available commercially for over 45 years.[15,16]

Recently, it has been found that five-membered cyclic carbonate exists in nature. Rosselli and co-workers[17] have presented the first example of natural origin cyclic carbonate terpenoid. They isolated a new guaiane sesquiterpene (Scheme 2), carrying a carbonate ring, from the aerial parts of the *Centaurea hololeuca* (Boiss) plant.

There are two main synthetic routes leading to five-membered cyclic carbonates: the reaction of a respective oxirane with carbon dioxide or 1,2-diol with dialkyl or diphenyl carbonate. Instead of carbonic acid esters, phosgene or its derivatives can also be used.[18]

The alkylene carbonates are easily available through transesterification of dialkyl carbonates (usually dimethyl or diethyl carbonate) or diphenyl carbonate with appropriate 1,2-diols in the presence of alkaline catalysts.[19] This approach for the preparation of five-membered cyclic carbonates also was described in the 1950s by Ludwig and Piech[20] and Sarel *et al.*[18]

Venturello and D'Aloisio[21] also proposed a nonphosgene method for the five-membered synthesis of disubstituted cyclic

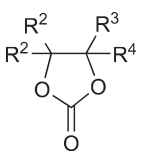

Scheme 1 Chemical structure of five-membered cyclic carbonates.

carbonates. In this method tetraalkylammonium hydrogen carbonate salt is reacted with disubstituted halohydrins such as $R^1CH(OH)CH(Cl)R^2$ ($R^1 = CH_3$ or Ph; $R^2 = H$, CH_3, or Ph) at 20 °C to give the corresponding disubstituted cyclic carbonates (Scheme 3).

Soga *et al.*[22,23] used alkali metal carbonates activated by crown ethers as an alternative source of carbonate linkages in the reaction with dihalo compounds. When epihalohydrin is used instead of the dihalo compound in the reaction with K_2CO_3, corresponding five-membered cyclic carbonates containing an epoxy group are formed.[24,25] In contrast, potassium bicarbonate reacts with epihalohydrin yielding 4-hydroxymethyl-1,3-dioxolan-2-one (glycerol carbonate, GC) (Scheme 4).[24]

Pd(0)-catalyzed arylation of the aryl-substituted α-allenic alcohols with hypervalent iodonium salts afforded substituted *trans*-epoxides.[26] Alternatively, arylation of the alkyl-substituted α-allenic alcohols in the presence of K_2CO_3 afforded *syn*-diol cyclic carbonates and *trans*-epoxides in the presence of Cs_2CO_3 (Scheme 5).

The treatment of carbonyl compounds with SmI_2 and methyl chloroformate in the presence of molecular sieves affords the cyclic carbonates or biscarbonates of pinacols. This one-pot reaction proceeds rapidly even with aliphatic ketones. The stereochemistry of the reaction run by this procedure is different from that of conventional pinacolic couplings.[27]

Trifluoromethylated five-membered cyclic carbonates were prepared through the palladium-promoted reaction of tertiary trifluoromethylated propargylic alcohols and sodium carbonate (Scheme 6).[28]

Tomishige *et al.*[29,30] found that cyclic carbonates such as EC and PC could be selectively synthesized over CeO_2–ZrO_2 catalysts, via the reactions of CO_2 with the respective glycol. No PC or dipropylene glycol was detected under the optimum reaction conditions. The 1,2-propylene glycol conversion was 2% and was much dependent on the composition and calcination temperature of the catalysts.

Organic bases were also used as effective catalysts for the synthesis of PC from propylene glycol and carbon dioxide in the presence of acetonitrile. With 1,5,7-triazabicyclo[4.4.0]dec-5-ene (TBD) as the catalyst, the yield of PC could reach 15.3% with the selectivity of 100% under optimal conditions.[31]

A much more convenient method of obtaining five-membered cyclic carbonates is the insertion of gaseous carbon dioxide into the appropriate oxirane ring (Scheme 7).[32–46]

The catalyst development and the reaction mechanisms over alkali metal halides,[37,39,47,48] organic bases,[49–51] metal oxides,[36,43,35,52] zeolite,[42,53] titanosilicates,[54] and metal complexes[44,55–64] have been reported for the synthesis of cyclic carbonates from CO_2 and epoxides.

Transition metal complexes are effective in the fixation of CO_2. Organotin compounds such as methyltin tribromide and

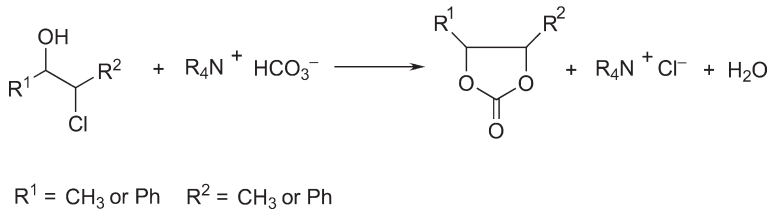

Scheme 3 Synthesis of five-membered cyclic carbonates from disubtituted halohydrins and tatraalkylammonium hydrogen carbonates.

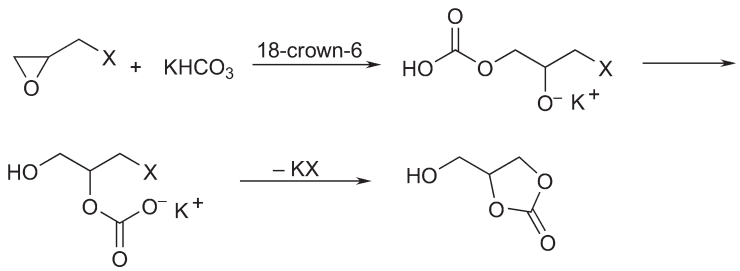

Scheme 4 Synthesis of glycerol carbonate from epihalohydrins and potassium bicarbonate.

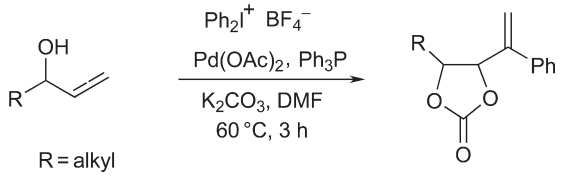

Scheme 5 Synthesis of five-membered cyclic carbonates by Pd(0)-catalyzed arylation of the α-allenic alcohols with hypervalent iodium salts in the presence of K_2CO_3.

butanestannoic acid have a good catalytic effect for EC formation under mild conditions.[65] It was found that pentavalent organoantimony compounds such as Ph_nSbX_{5-n} catalyze the reaction more effectively than tin compounds.[32,66] Additionally, in contrast to tin compounds, the pentavalent organoantimony compounds do not initiate oxirane polymerization. In the case of nickel(0) phosphine complexes cyclic carbonates are produced in high yields. The rate of carbonate formation is dependent on the structure of the epoxide and decreases in the order epichlorohydrin > ethylene oxide (EO) > propylene oxide (PO) > 2,3-epoxybutane.[55]

Quaternary ammonium salts,[67] as well as an anion exchange resin containing those groups, are used in the industrial-scale preparation of five-membered cyclic carbonates.[68,69]

Polyfluoroalkyl phosphonium iodides, Rf_3RPI (Rf = $C_4F_9C_2H_4$, $C_6F_{13}C_2H_4$, and $C_8F_{17}C_2H_4$; R = Me, Rf), catalyzed PC synthesis from PO and carbon dioxide under supercritical carbon dioxide ($scCO_2$) conditions, where PC was spontaneously separated out of the $scCO_2$ phase. The Rf_3RPI catalyst could be recycled with maintaining a high CO_2 pressure and temperature by separating the PC from the bottom of the reactor followed by supplying PO and CO_2 to the upper $scCO_2$ phase in which the Rf_3RPI remained.[70]

Although alkali metal salts appeared to be active catalysts for the CO_2–epoxide reaction, the introduction of crown ethers or phase-transfer agents to the system enhanced their catalytic activities.[71] In the presence of a crown ether, the respective nucleophilic anion is activated to such an extent that the cyclic carbonate is produced in a high yield under mild conditions. In the system studied the intermediate product of the reaction of the halide anion with the oxirane ring – alkoxide ion – does not undergo further reaction with oxirane and no poly(alkylene oxide) is formed. This results from the greater stability of the alkyl carbonate anion than that of the initial alkoxide one. Under these conditions no poly(alkylene carbonate) was formed. Due to anchimeric assistance (kinetic factor) and relatively high thermodynamic stability, the five-membered 1,3-dioxolan-2-one ring is more easily formed from the cyclization of that anion with respect to linear poly(alkylene carbonate) when no coordination catalyst is present. Relatively high pressures of CO_2 (> 8 bar) and temperatures above 100 °C are needed for an acceptable reaction rate. Nevertheless, it was

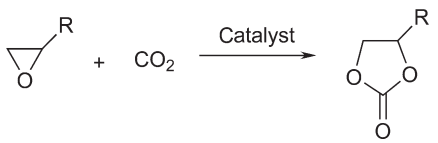

Scheme 7 Synthesis of five-membered cyclic carbonates from oxiranes and CO_2.

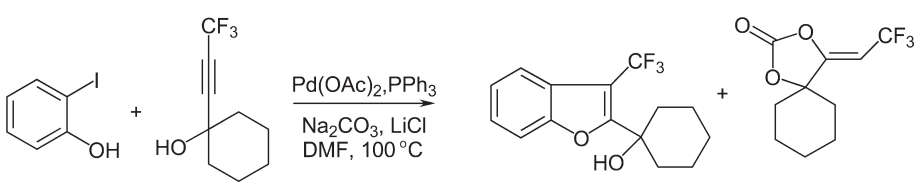

Scheme 6 Synthesis of trifluoromethylated five-membered cyclic carbonate from appropriate propargylic alcohol and Na_2CO_3.

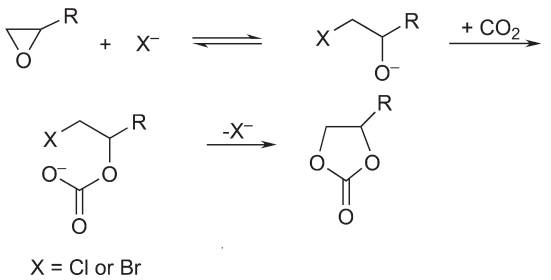

Scheme 8 Synthesis of five-membered cyclic carbonates from CO_2 and oxiranes containing ammonium group in β-position.

found that oxiranes with ammonium groups at the β-position to the oxirane ring, due to the lowering of the activation energy of nucleophilic substitution, are able to fix carbon dioxide at room temperature and low CO_2 pressures (**Scheme 8**, R = CH_2–NR_3^+).[72–74]

The CO_2 insertion into the oxirane ring also proceeds under atmospheric pressure when the reaction is carried out in NMP as a solvent and catalyzed with LiBr at 100 °C.[75]

Cyclic carbonates can also be obtained in good yields under mild conditions from oxiranes and carbon dioxide using an electrochemical procedure.[76] The cyclic carbonate formation is catalyzed by Ni(cyclam)Br and is carried out in single-compartment cells fitted with a magnesium anode.

Chemical fixation of carbon dioxide with oxiranes to form cyclic carbonates proceeds very effectively under mild conditions using immobilized ionic liquid (IL) catalyst in conjunction with zinc chloride without any organic solvents. The optimum reaction conditions were 110 °C and 1.5 MPa, and the catalyst system was recycled and reused.[77] The reaction of carbon dioxide with oxiranes can be catalyzed by typical ILs (1-alkylmethylimidazolium salts).[78,79]

Very recently North's group revealed that the bimetallic aluminum(salen) complex **1** (**Scheme 9**) when used in conjunction with tetrabutylammonium bromide constitutes the only catalyst system capable of catalyzing the insertion of carbon dioxide into oxirane at 1 atm (760 mmHg) and at ambient temperature (25–30 °C).[80–82]

Another promising investigation was done by Li *et al.* They found that CO_2 and olefins can be directly converted into cyclic carbonates with water as solvent.[83]

4.12.2.1.2 Synthesis of six-membered cyclic carbonates

The synthesis of six-membered cyclic carbonates by transesterification of propane-1,3-diols (PPDs) with diethyl carbonate catalyzed with sodium ethanolate described by Carothers and Van Natta[19] gives a yield of 40%. Also Pohoryles and Sarel[18,84,85] reported on the synthesis of various six-membered cyclic carbonates from PPDs with different substituents (**Table 1**).

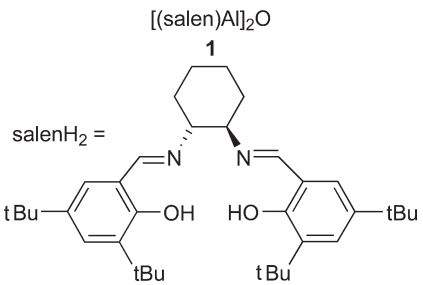

Scheme 9 Bimetallic aluminum(salen) complex.

Thus, when 2,2-dimethyl-, 2-methyl-2-*n*-propyl- and 2-methyl-2-*iso*-amylpropane-1,3-diol were treated with diethyl carbonate in the presence of catalytic amounts of sodium methoxide, only PCs were produced in high yield. On the other hand, six-membered cyclic carbonates are exclusively produced when 2,2-diethyl-, 2-ethyl-2-phenylpropane-1,3-diol, pentane-2,4-diol, 2-methylpentane-2,4-diol,[90] and butane-1,3-diol were subjected to the transesterification reaction (**Scheme 10**).

Table 1 Synthesis and polymerization of six-membered cyclic carbonates

	Chemical structure	*References*
	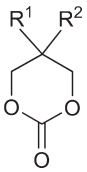	
1	$R^1 = R^2 = H$	6,9–11,18,84–89
2	$R^1 = H$; $R^2 = CH_3$	90
3	$R^1 = H$; $R^2 = C_4H_9$	88
4	$R^1 = R^2 = CH_3$	6,9,10,11,88,91
5	$R^1 = R^2 = C_2H_5$	6
6	$R^1 = Ph$; $R^2 = CH_3$	6,92
7	$R^1 = Ph$; $R^2 = C_2H_5$	6
8	$R^1 = R^2 = Ph$	92
	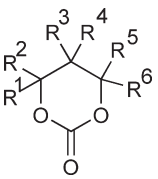	
9	$R^1 = CH_3$; $R^2 = R^3 = R^4 = R^5 = R^6 = H$	9,10,11,12,14,18,84,85,93
10	$R^1 = R^2 = CH_3$; $R^3 = R^4 = R^5 = R^6 = H$	
11	$R^1 = R^5 = CH_3$; $R^2 = R^3 = R^4 = R^6 = H$	
12	$R^1 = R^2 = R^5 = CH_3$; $R^3 = R^4 = R^6 = H$	
13	$R^3 = R^4 = R^5 = CH_3$; $R^1 = R^2 = R^6 = H$	
14	$R^3 = R^4 = CH_3$; $R^5 = CH(CH_3)_2$; $R^1 = R^2 = R^6 = H$	
15	$R^1 = R^2 = R^5 = R^6 = CH_3$; $R^3 = R^4 = H$	
	Spirocyclic carbonates	
16	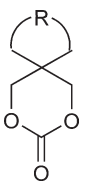	
17	-R- = 	94
18	-R- = 	95

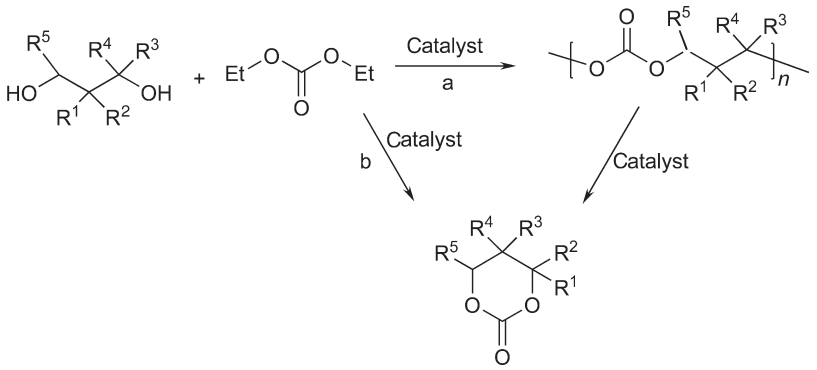

Scheme 10 Synthesis of six-membered cyclic carbonates from 1,3-diols and diethyl carbonate.

A similar method reported by Albertsson and Sjoeling[87] in which equimolar amounts of PPD and diethyl carbonate with stannous 2-ethylhexanoate as the transesterification catalyst were used afforded a yield of 53%. In this method reactants were refluxed for 8 h before ethanol was removed. It is postulated that stannous 2-ethylhexanoate can act both as a polymerization (at lower temperature) and as a depolymerization agent (at higher temperature).[96–99]

In the method proposed by Rokicki *et al.*, the synthesis of trimethylene carbonate (TMC) from PPD and dimethyl carbonate was carried out in three steps. First, bis(methylcarbonate) trimethylene was obtained using high excess of dimethyl carbonate and K_2CO_3 as a catalyst. In the second step bis (methylcarbonate)trimethylene was reacted with equimolar amounts of PPD to afford high-molecular-weight poly(trimethylene carbonate) (PTMC). The only volatile compound present in the reaction system in this step was methanol, easy to remove by distillation. Thus, it was possible to maintain an equimolar ratio of the monomers which resulted in a relatively high molecular weight of the PC. In the third step depolymerization combined with vacuum distillation was proceeded to afford TMC in 75% yield.[89]

Matsuo *et al.*[6] have revealed another universal method of cyclic carbonate synthesis from PPDs and ethyl chloroformate in the presence of a stoichiometric amount of triethylamine. The formation of a specific ammonium salt as an intermediate seems to be the driving force for the reaction proceeding at low temperatures favoring six-membered cycles (yields up to 60%) (**Scheme 11**).

Other phosgene derivatives (di- and triphosgene) also give cyclic products with good yields. The reaction of 2,2-disubstituted PPDs carried out with phosgene dimer affords the cyclic carbonate quantitatively in the reaction of 2-ethyl-2-phenylpropane-1,3-diol and 2,2-diphenylpropane-1,3-diol, while the corresponding oligocarbonates were formed in the reaction of 2,2-diethylpropane-1,3-diol in 24% yield, apart from the corresponding cyclic carbonate.[6]

4.12.2.1.3 Synthesis of seven-membered and of larger ring size cyclic carbonates

Seven-membered and larger ring size cyclic carbonates can be synthesized according to the same transesterification reaction pathways as those leading to five- and six-membered rings[9,18] or in the reaction of appropriate diol with phosgene (or its derivative) in the presence of antipyrine.[100,101]

However, due to the low stability of seven-membered cyclic carbonates, the polymerization of its cyclic dimers (**Scheme 12**) is a better method for synthesis of the corresponding PCs.[102,103] The same concerns 8-, 9- and 13-membered cyclic carbonates.[102,104,105]

Dimers are also easier to obtain in larger quantities. In the transesterification-depolymerization method they are formed almost exclusively when the expected monomer cycle size is from 7 to 12; both monomer and dimer are formed when its size is 13 and 14 and monomers almost exclusively when the cycle size is more than 14.[9]

Typically, the transesterification is carried out at 120–130 °C in the presence of a catalyst (e.g., K_2CO_3, dibutyltin

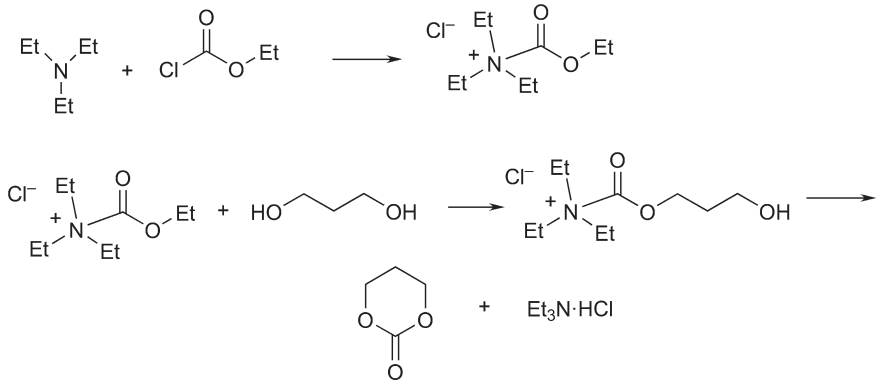

Scheme 11 Synthesis of six-membered cyclic carbonate from 1,3-propanediol and ethyl chloroformate.

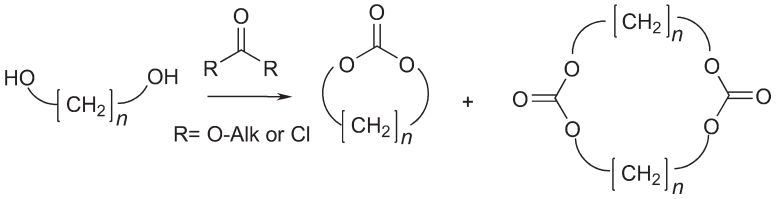

Scheme 12 Formation of monomeric and dimeric large ring size cyclic carbonates.

dimethoxide) under reduced pressure (0.07–11 mbar). The resultant PC subjected to ring-closing depolymerization at 260–300 °C affords cyclic products collected after distillation over a heated column.[102,106] Since 1,5-, 1,6-, and 1,10-diols have high boiling points, a more reactive diphenyl carbonate can be used instead of dimethyl- or diethyl carbonate for the transesterification and higher yields of the respective intermediate polymers can be obtained. The 18-membered cyclic carbonates cyclobis(hexamethylene carbonate) and its fluorinated analog representing the smallest ring carbonates based on hexane-1,6-diol were obtained in this way.[106]

Seven-membered cyclic carbonate – 1,3-dioxepan-2-one – can be obtained in its monomeric form in the reaction of butane-1,4-diol with triphosgene in the presence of antipyrine in anhydrous chloroform. This method does not involve polymerization. The product is purified by column chromatography.[100,101] It is a versatile method that allowed the synthesis of seven-membered cyclic carbonates bearing phenyl, methyl, or cyclic acetal side-groups.[107,108]

4.12.2.2 Synthesis of Aromatic Cyclic Carbonates

The smallest possible five-membered aromatic cyclic carbonate is a derivative of catechol: benzo-1,3-dioxolan-2-one (*o*-phenylene carbonate) (**1**, **Scheme 13**). It was synthesized using three different methods: the reaction of catechol with phosgene (or its dimer or trimer),[109] the reaction of catechol with chloroformate,[110] or by transesterification of catechol with diphenyl carbonate.[111]

The seven-membered aromatic cyclic carbonates were obtained from 2,20-biphenol and 1,10-bi(2-naphthol), *p*-nitrophenyl chloroformate, and a tertiary amine as a base.[112] They could be isolated with 80% yield (**2**, **3**, **Scheme 13**). As was shown by Kricheldorf and Jenssen,[113] disproportionation of 2,20-bis(methoxycarbonyloxy)biphenyl catalyzed by $Sn(Oct)_2$ can also be utilized for obtaining the seven-membered aromatic cyclic carbonate.

The possibility of obtaining aromatic polycyclic carbonates was also reported by Prochaska[114] from *o,o′*-bisphenols and Mandal and Hay[115] from novolac resin. A novolac-type phenol-formaldehyde resin (*ortho*-coupled through methylene group 4-*tert*-butylphenol resins) was reacted with an excess of triphosgene under high-dilution conditions. Because of the relatively low steric hindrance in these systems, the formation of cyclic carbonates was possible and oligomeric polycyclic carbonates were obtained (**4**, **Scheme 13**). The polycyclic carbonates were used for the modification of commercial aromatic PCs. They were mixed with the linear PC in different proportions and cured at different temperatures by using lithium stearate as a catalyst. The curing of a mixture which contained 10 wt.% of the polycyclic carbonates at 350 °C for 30 min resulted in a highly cross-linked system.

Besides the small ring size cyclic carbonates, cyclic oligocarbonates and PCs are known which are obtained in the reaction of bisphenol A (BPA) with phosgene (**5**, **Scheme 13**).[1] They were first found in the commercial condensation polymers such as PC, where they were present at levels of 0.25–2.0%.

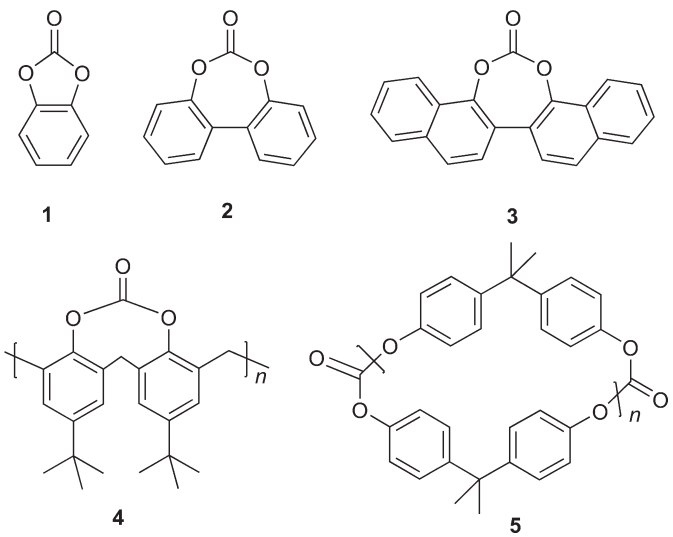

Scheme 13 Aromatic cyclic carbonates.

The attraction of using this type of cyclic oligomers as precursors to engineering thermoplastics is based on the expectation that the oligomers would have significantly lower melt viscosity than the ultimate high-molecular-weight polymers and, therefore, be amenable to reactive processing techniques. Furthermore, since cyclic oligomers would contain no end-groups, very high molecular weights should be achievable without the formation of reaction by-products typically formed in melt polycondensation reactions.

The cyclic aromatic oligocarbonates have been separated from the polymers and characterized by several groups.[116] First attempts to synthesize cyclic BPA oligocarbonates were performed using classical high-dilution techniques.[117] For example, Schnell and Bottenbruch[15,118] reported that the cyclic tetrameric carbonate (**5**, $n = 3$, **Scheme 13**) of BPA could be formed in about 21% yield via slow addition of equimolar amounts of bisphenol and its bischloroformate to pyridine in dichloromethane at a final monomer concentration of 0.05 M.

Currently it is possible to obtain low-molecular-weight cyclic oligomers completely selectively with respect to linear oligomers by applying pseudo-high-dilution conditions to a hydrolysis/condensation reaction of BPA bischloroformate, catalyzed by Et_3N in biphasic dichloromethane/$NaOH_{aq.}$ (**Scheme 14**).

After 1 h of reaction, the HPLC analysis of the crude product clearly shows a range of cyclic oligomers from dimer to docosamer (22 bisphenol units).[119] Selective formation of low-molecular-weight cyclic oligomers occurs even though the final product concentration is 0.2 M, much higher than usually used in cyclization reactions.

To form cyclic oligocarbonate from BPA–bischloroformate starting material, both hydrolysis and condensation reactions must occur (**Scheme 15**).[116] The selectivity of cyclic versus linear products and by-product polymer formation depends on the structure and concentration of the amine catalyst, reaction time and temperature, and pH of the interfacial medium.

In the hydrolysis–condensation reaction, the first step that must occur is the hydrolysis of at least one end of the bischloroformate molecule to form a phenoxide. Maintaining good pH control is important to ensure that highly reactive phenoxides, rather than protonated phenols, are present. Excessive pH can be destructive, since hydrolysis of the cyclic product could additionally occur. After chloroformate hydrolysis, the condensation with fresh bischloroformate entering the reaction can occur, leading to dimeric bischloroformate. As the dimeric bischloroformate itself undergoes hydrolysis, a key intermediate is formed, an oligomer with one phenoxide and one chloroformate end-group. This species can either form a cyclic oligomer or undergo further intermolecular reaction with incoming bischloroformate to form a trimer-bischloroformate which can undergo cyclization or be an intermediate in higher-molecular-weight oligomer formation.

The structure of the amine catalyst and its concentration proved to be critical to selective formation of cyclic carbonates. Application of Et_3N at 0.1 M concentration led to nearly exclusive formation of cyclic oligomers (90%). Examination of other

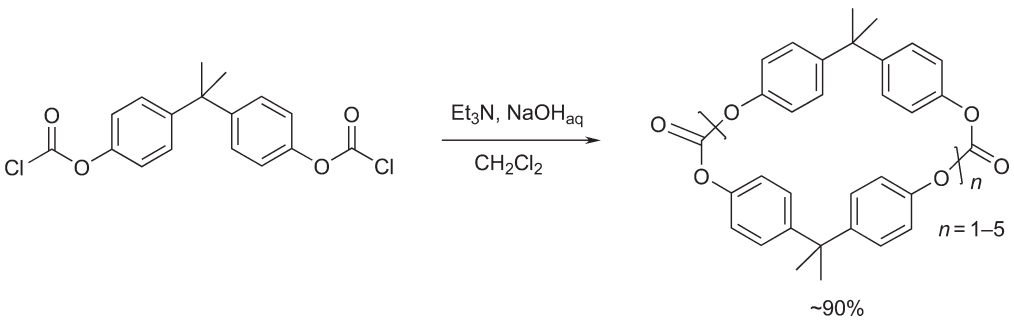

Scheme 14 Synthesis of low-molecular-weight cyclic oligocarbonates.

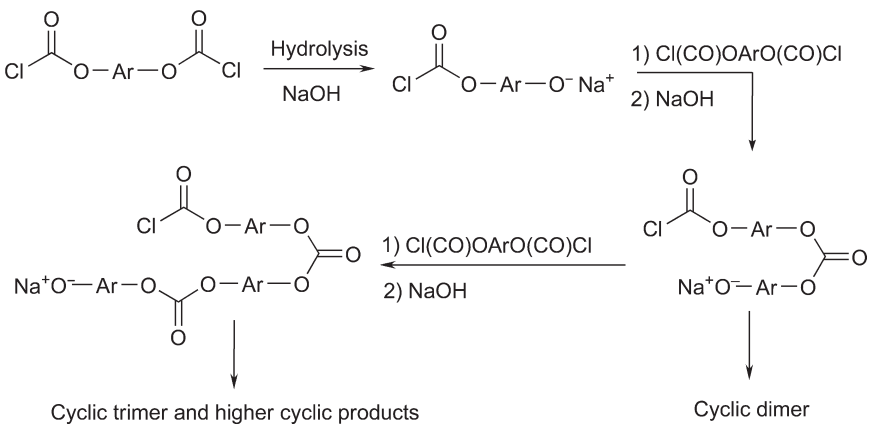

Scheme 15 Hydrolysis and condensation reactions leading to the formation of cyclic oligomers.

amines showed that amines less hindered than Et_3N (e.g., methyldiethylamine) led to mainly linear oligomer formation or mixtures of cyclics and linears. The use of very unhindered amines such as quinuclidine, 1,4-diazabicyclo[2.2.2]octane (DABCO), dimethylethylamine, or pyridine gave almost exclusively linear oligomers, or complete hydrolysis to BPA under more severe conditions. It is interesting to note that each of the five possible reaction outcomes is possible under the same reaction conditions, simply by changing the catalyst (cyclic and linear oligomers, polymer, complete hydrolysis, or no reactions).[116]

4.12.3 Polymerization of Aliphatic Cyclic Carbonates

The ability of cyclic monomers for ROP depends on both thermodynamic and kinetic factors. From the thermodynamic point of view the Gibbs energy (free enthalpy) change [ΔG_p] should be negative.[120–122] The Gibbs energy change in the polymerization is determined by the enthalpy and entropy changes (ΔH_p and ΔS_p) and temperature (T) according to the equation

$$\Delta G_p = \Delta H_p - T\Delta S_p$$

In this equation the monomer and polymer states and crystallinity should also be considered.

For most cyclic monomers of a small ring size ΔH_p and ΔS_p are both negative so they can polymerize only below a temperature known as the ceiling temperature (T_c).[122] The driving force for the polymerization of such monomers is their ring strain, which reflects the deviation from nondistorted bond angle values, bond stretching or compression, crowding repulsion between hydrogen atoms, and other substituents. The Gibbs energy of polymerization may also be expressed as

$$\Delta G_p = \Delta H_p^0 - T(\Delta S_p^0 + R \cdot \ln[M])$$

where ΔH_p^0 and ΔS_p^0 denote a standard polymerization enthalpy and entropy, respectively, [M] denotes monomer concentration, and R is the gas constant.

At equilibrium ($\Delta G_p = 0$) when polymerization is complete, the unreacted monomer concentration ($[M]_{eq}$) is determined by standard polymerization parameters ΔH_p^0 and ΔS_p^0 and polymerization temperature T. Thus, polymerization can occur only when $[M]_0 > [M]_{eq}$.

The angle and bond deformations are most pronounced for the three- and four-membered cyclic monomers and as a result $[M]_{eq}$ is very small. The five- and six-membered cyclic monomers are the least strained, and some of them are unable to polymerize. The introduction of a carbonyl group into the five-membered cycle makes the resultant compounds incapable of high polymer formation under normal conditions. This is caused by sp^2 hybridization of the carbon atom in the >C=O group. The six-membered cycloalkanes and cyclic ethers accept the most convenient chair conformation in which the energy of the conformational interactions is negligible and the hypothetical $[M]_{eq}$ is above any possible monomer concentration ($[M]_0$). In contrast, the presence of carbonate group in the six-membered cycle increases the strain, and cyclic carbonates can be easily polymerized. The carbonyl group introduces strain into six-membered rings due to the flat geometry of the carbonate moieties.

4.12.3.1 Polymerization of Five-Membered Cyclic Carbonates

Cyclic carbonates of the smallest ring size (aliphatic five-membered cyclic carbonates), such as EC (1,3-dioxolan-2-one) and PC (4-methyl-1,3-dioxolan-2-one), behave exceptionally in ROP. Their ceiling temperatures are below 25 °C and ΔH_p^0 is positive (above 120 kJ mol^{-1}), and so no ROP is possible leading to poly(alkylene carbonate), but they can be polymerized at high temperatures (above 150 °C) resulting in poly(ether-carbonate)s.[123] ΔH_{pd}^0 (standard enthalpy of polymerization with simultaneous decarboxylation) for EC becomes negative at 170 °C. The repeated units of the resultant polymers are a mixture of alkylene carbonate and the corresponding alkylene oxide units, which means that CO_2 is lost during the polymerization. Probably in this case the decarboxylation and small carbon dioxide molecules evolution make the ΔS_p^0 value positive and consequently, polymerization becomes thermodynamically possible at higher temperatures. Thus the polymerization of five-membered cyclic carbonates fails to produce thermodynamically disfavored poly(alkylene carbonate)s but leads to poly(alkylene ether-carbonate)s with contents of carbonate units lower than 50 mol.% (**Scheme 16**).[12,13,123–127]

Vogdanis and Heitz used a variety of catalysts for the polymerization of EC, ranging from dibutyltin dimethoxide to butyllithium and found that the retention of CO_2 decreased as the alkalinity of the catalyst increased. When a more basic catalyst was used, the resultant polymers contained 10–20 mol.% of EC units (reaction temperature was about 150 °C and reaction time was 72–98 h).[123,128]

Soga *et al.* proposed the mechanisms in which the polymerization of PC proceeded via spiroorthocarbonate species (2,7-dimethyl-1,4,6,9-tetraoxaspiro[4.4]nonane). To conform this mechanism the authors polymerized the spiroorthocarbonate in the presence of diethylzinc as a catalyst and obtained poly(propylene ether-carbonate) of similar chemical structure.[124] It means that in the first reaction step the monomer decarboxylation takes place. The decarboxylation involves most probably metal carbonate species formation due to the 1,3-dioxolan-2-one ring opening via the alkyl carbon–oxygen bond cleavage.[129]

Detailed investigations of the mechanism of five-membered cyclic carbonate polymerization initiated with tin and zirconium alkoxides were carried out by Kricheldorf *et al.*.[130,131]

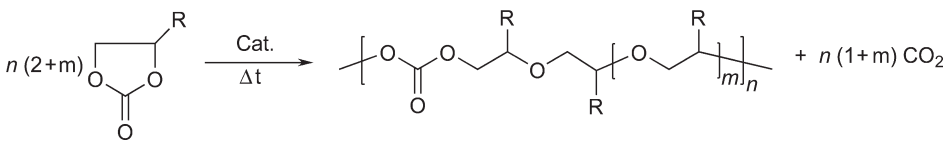

Scheme 16 Polymerization of five-membered cyclic carbonates.

Harris has reported the use of sodium stannate trihydrate as a heterogeneous catalyst in EC polymerization.[125,132] The structures of obtained oligomers have been studied by alkaline degradation to the oligo(oxyethylene) glycols, which make up their backbone, followed by GC analysis. Based on the analytical techniques, it was possible to establish the composition of a given poly(ethylene ether-carbonate) diol. Harris and McDonald[126] have found that 2-hydroxyethyl carbonate and 2-hydroxyethyl ether end-groups are present at the beginning in the polymerization mixture. However, only 2-hydroxyethyl ether end-groups were present during the latter stages of polymerization. When poly(ethylene ether-carbonate) diols were heated at temperatures above 180 °C under reduced pressure, volatile by-product – diethylene glycol (DEG) – was removed, followed by molecular weight advancement. Under such conditions the transesterification process proceeds in which $-OC(O)OCH_2CH_2OCH_2CH_2OH$ end-groups of one molecule react with carbonate moieties of a second molecule with loss of DEG (**Scheme 17**).

Poly(ethylene ether-*co*-ethylene carbonate) diols obtained in this manner had a relatively low dispersion index.[133] Sodium stannate is a preferred catalyst for the preparation of poly(ethylene ether-carbonate) diols. The rate of advancement to 3000 molecular weight products increased together with CO_2 retention when the tin catalyst concentration level was 100–500 ppm. At higher catalyst concentration levels, the product decomposition to 1,4-dioxane became more intensive.[134,135] The same authors also applied dibutyltin diacetate, dilaureate, and dimethoxide as catalysts for EC polymerization.

The process of EC polymerization with an alkaline initiator was analyzed and discussed in more detail by Lee and Litt.[136] They polymerized EC in bulk at 150–200 °C using various amounts of KOH as the initiator. The products were analyzed by gel permeation chromatography (GPC) and NMR spectroscopy. Maximal molecular weights of the polymers did not exceed 7000 after about 3–5 h of heating at 200 °C for the EC/KOH molar ratio = 1000/1. It was shown that the ratio of the rate of polymerization to that of chain scission increased as temperature rose. The EO sequences in the polymer backbone were converted to oligo(oxyethylene) glycols by alkaline hydrolysis of the copolymer. Under such conditions the carbonate linkages easily and fully degrade. Taking the above results into account the authors suggested that in the early stage of the polymerization a major polymer structure comprises one EC unit per two EO units. For longer reaction times the content of EO units increases. The content of EC units, even in the earliest stage of the reaction, was not higher than 32 mol.%. They claimed that polymerization proceeds in two stages. During the first stage EC conversion takes place and molecular weight increases. In the second stage, when no EC is present in the reaction mixture, both the number of EC units and molecular weight decrease with time. The latter indicates that chain cleavage and decarboxylation take place. There are two possible reaction pathways between the alkoxide ion and EC monomer (**Scheme 18**).

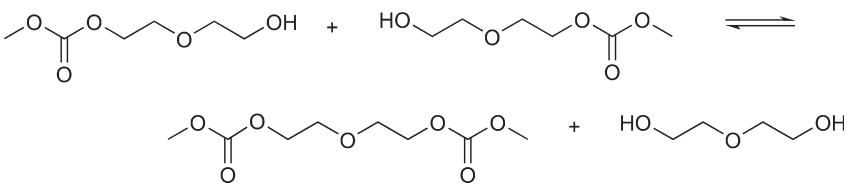

Scheme 17 Homocondensation of 5-hydroxy-3-oxapentylcarbonate groups.

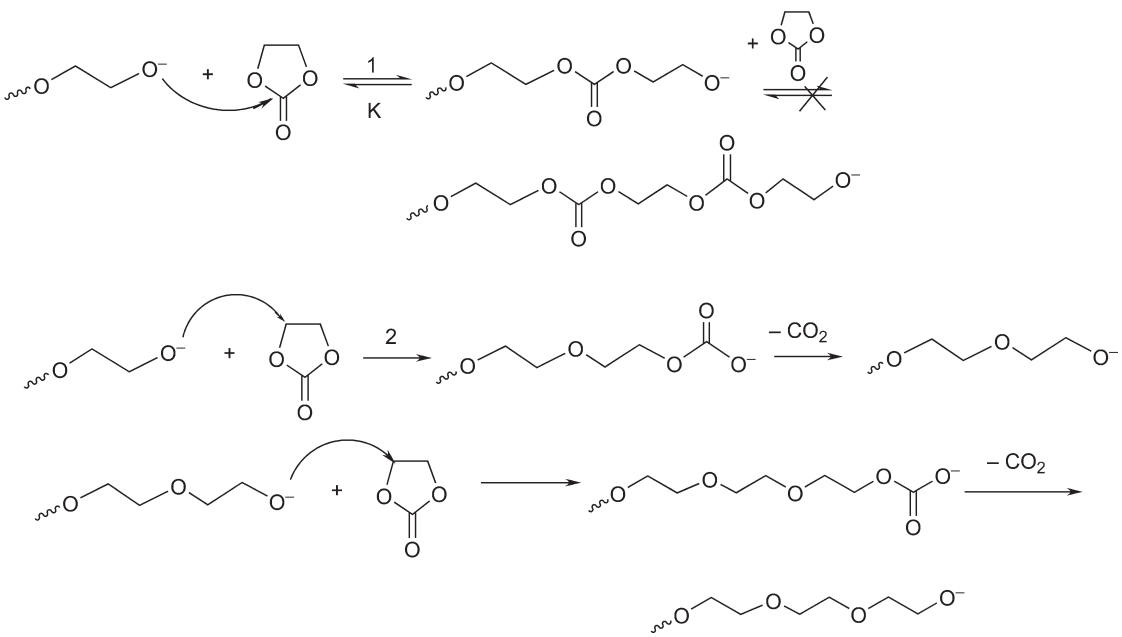

Scheme 18 Formation of poly(ethylene ether-carbonate)s.

According to pathway 1 (Scheme 18), the carbonyl carbon atom in EC is attacked by the alkoxide ion and 2-hydroxyethyl carbonate group is formed. On the other hand, the alkyl carbonyl atom is subjected to nucleophilic attack (2), resulting in decarboxylation and irreversible formation of a DEG unit. Rokicki *et al.*[137] reported the loss of CO_2 from alkyl-potassium carbonate such as 2-(1-phenoxy)propyl potassium carbonate above 150 °C. It should be mentioned that the reaction with carbonyl group (1) is reversible. Kinetically, the carbonyl attack is favored over the alkylene one.

Lee and Litt suggested that the most probable EC polymerization mechanism under basic conditions should be a combination of an alkylene carbon attack (2) and a carbonyl carbon attack (1). However, it should be underlined that the product of reaction (1) cannot react with another EC molecule in the same manner because the formation of the EC–EC sequence is thermodynamically forbidden. Rokicki and Pawlowski investigated the reaction of EC with different diols catalyzed by various alkali metal salts (NaCl, K_2CO_3). The reaction was carried out in xylene with azeotropic distillation of ethylene glycol formed as a side product. They found that to suppress the reaction proceeding according to pathway (2), the diol with long hydrocarbon chain (e.g., 1,6-hexanediol) and less basic catalyst such as NaCl should be used; the reaction temperature should be lower than 145 °C. The products were analyzed by MALDI-TOF mass spectrometry and NMR spectroscopy. The molecules of the resultant oligomer had no more than two EC units (as two terminal 2-hydroxyethylcarbonate groups). It means that terminal –O–(C=O)–OCH_2CH_2O– alkoxide groups cannot react with EC molecule according to pathway (1) (Scheme 19) as well as the transesterification reaction between two 2-hydroxyethylcarbonate groups is not possible (Scheme 20).

Thus, the most plausible reaction mechanism illustrating the formation of EC–EO–EO sequence comprises the formation of tri(ethylene oxide) fragments according to reaction pathway (2) and reaction with EC applying the carbonyl carbon atom attack (pathway 1) (Scheme 18).

Lee and Litt have also observed that in the second stage (after 19 h heating at 180 °C) vinyl ether groups were formed. In the ^{1}H NMR spectra of the product characteristic signals at 6.47 ppm were present which could be assigned to methine protons of vinyl ether. Their intensity increased with the reaction time. The authors discussed two possible elimination reaction mechanisms: pyrolytic (Ei) and bimolecular (E2) eliminations (Scheme 21).

However, taking into account that Ei elimination is a first-order intramolecular reaction and vinyl ether groups formation started in the second stage, bimolecular elimination (E2) is more plausible. In this process proceeding in the presence of a strong base such as alkoxide, proton abstraction from EC unit may occur leading to the vinyl ether formation, chain scission, and decarboxylation. A relationship between carbonate content and degree of polymerization was derived using both decarboxylation and bimolecular elimination reactions for the kinetic equations. The authors indicated that this reaction sequences fit the experimental data.

The process of PC oligomerization in the presence of less alkaline catalyst system was also investigated by Keki *et al.*[138,139] The ring-opening oligomerization of PC was initiated with *tert*-butylphenol/$KHCO_3$. The resultant oligomers were analyzed by means of MALDI-TOF and ESI-TOF mass spectrometries. It was found that in addition to the chain extension reaction with the PO units, the oligomers of all of the PO units and oligomers containing carbonate end-groups condensed. However, the proposed mechanism is less plausible. The alkyl carbonate anion is unstable under the reaction conditions, so fast decarboxylation should take place.

Elmer and Jannasch[140] prepared poly(ethylene oxide-*co*-ethylene carbonate)s by the anionic polymerization of EC with CH_3OK as an initiator. Reaction mixtures composed of EC and CH_3OK in the CH_3OK/EC molar ratio of 1:1000 containing 50 ppm of an antioxidant – triethylene glycol bis-3-(30-*tert*-butyl-40-hydroxy-50-methylphenyl)propionate – was heated at 180 °C. An oligomer having a number-average molecular weight of 2650 and an EC content of 28 mol.% was obtained. This cooligomer was used as a raw material for the preparation of solid polyelectrolyte in lithium batteries.

Recently, Wu *et al.* reported that the polymerization of PC carried out in the presence of BPA initiated with organic bases such as DABCO, 1,8-diazabicyclo[5.4.0]undec-7-ene

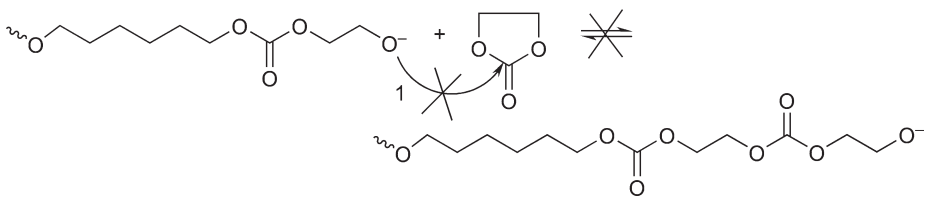

Scheme 19 Forbidden reaction of 2-hydroxyethylcarbonate groups with ethylene carbonate.

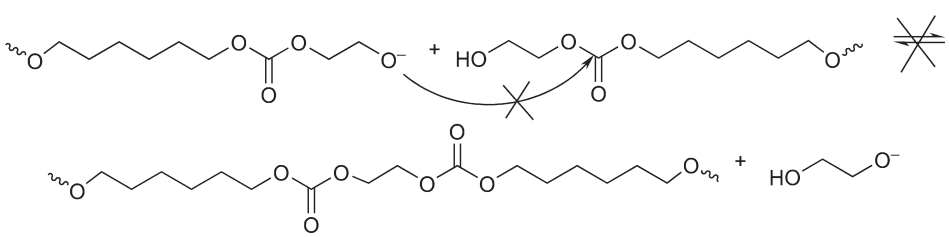

Scheme 20 Forbidden homocondensation of 2-hydroxyethylcarbonate groups.

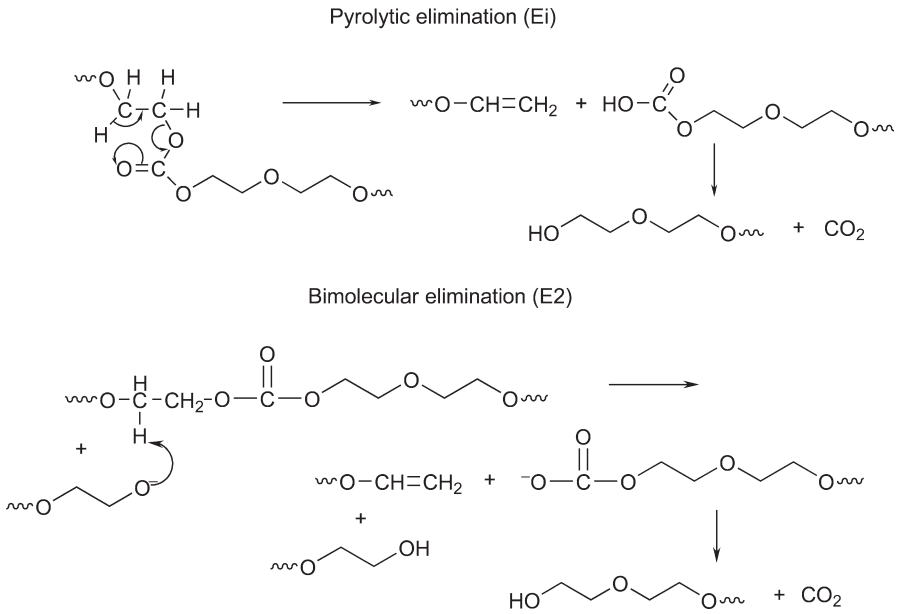

Scheme 21 Formation of vinyl groups after heating poly(ethylene ether-carbonate) at 180 °C.

(DBU), 1,5-diazabicyclo[4.3.0]non-5-ene (DBN), and *N*, *N*-dimethylaminopyridine (DMAP) afforded polyether diols containing BPA moiety.[141] It was shown by MALDI-TOF spectrometry and ^{1}H and ^{13}C NMR spectroscopies that the product obtained from 4-*tert*-butylphenol and PC at 150 °C contained some amount of oligomers with carbonate linkages. The authors suggested that phenols were ionized by an organic base to form an active phenol anion which attacked cyclic carbonate monomer to generate intermediate ions that could further capture proton and react with phenol itself to yield polyether or poly(ether-carbonate).

Another approach was presented by Kadokawa *et al.*[142] They proceeded with the ROP of EC using two ILs, 1-butyl-3-methylimidazolium chloroaluminate ([bmim]Cl-$AlCl_3$) and 1-butyl-3-methylimidazolium chlorostannate ([bmim]Cl-$SnCl_2$), as polymerization catalysts. Although polymerization in the presence of [bmim]Cl-$AlCl_3$ took place even at temperatures below 100 °C, frequent decarboxylation occurred to give polymers with low content of EC units. When the polymerization was performed in the presence of [bmim]Cl-$SnCl_2$ higher reaction temperatures were required. In this case the maximal amount of carbonate units present in the copolymer was 33.9 mol.%.

4.12.3.1.1 Polymerization of five-membered cyclic carbonates with a strained ring

In contrast to typical five-membered cyclic carbonates, which polymerize at high temperatures ($T > 150$ °C) leading to poly(ether-carbonate)s, five-membered cyclic carbonates obtained from methyl 4,6-*O*-benzylidene-glucopyranoside can be polymerized at relatively low temperatures, without elimination of carbon dioxide, to produce homopolycarbonates.[143–145] The polymerization of such a monomer was carried out at 60 °C in tetrahydrofuran (THF) or dimethylformamide (DMF) yielding a polymer exclusively consisting of carbonate repeating units (Scheme 22). Two types of initiators were used: DBU and potassium *tert*-butoxide. It was shown that the polymerization proceeded smoothly even at 30 °C to give the PC of $M_n = 14\,000$ in 93% yield.

To confirm the homopolycarbonate structure, Haba *et al.* hydrolyzed the resulting polymer using KOH in ethanol. The hydrolysis product and the model compound prepared by them from methyl *R*-D-glucopyranoside and benzaldehyde dimethyl acetal were the same.[146] It means that no elimination of carbon dioxide during the anionic polymerization took place and no etherification occurred. The authors presumed that the ring strain was the driving force of ROP of this five-membered cyclic carbonate. The ring strain may result from the connection of two hydroxyl groups in E (*trans*) position by the carbonate linkage. In addition, the carbonate ring is connected on one side to the rigid bicyclic structure of methyl 4,6-*O*-benzylidene-glucopyranoside. The acetal groups in the resulting polymer can be removed by acidic hydrolysis. The presence of two hydroxyl groups in the monomeric units activates such PC to hydrolytic degradation (Scheme 22). Taking

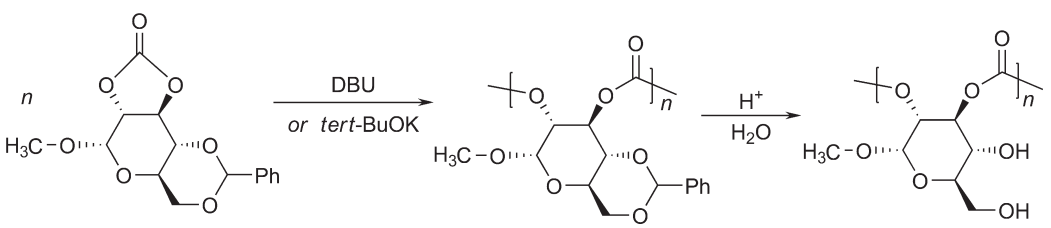

Scheme 22 Polymerization of the five-membered cyclic carbonate with the strained ring.

into account that the monomer was obtained from natural sugar the resultant PC can find application in biomedicine, where fast hydrolityc decomposition is the most important factor.

As far as cationic polymerization concerns, it was shown by Kricheldorf and Jenssen that EC did not react with a cationic-type catalyst such as methyl triflate.[147] No polymer or oligomer was found after 48 h of reaction carried out in nitrobenzene at 100 °C.

The aromatic five-membered cyclic carbonate (benzo-1,3-dioxolan-2-one) appeared inert in anionic polymerization initiated with *sec*-BuLi and potassium dihydronaphthalide.[111]

On the other hand, the high-molecular-weight aliphatic PC with an alternating sequence of the monomeric alkylene units can be obtained by copolymerization of oxiranes with CO_2 using coordination catalysts under appropriate reaction conditions. In 1969, Inoue and co-workers[148] made the remarkable discovery that a mixture of $ZnEt_2$ and H_2O was active as a catalyst system of the alternating copolymerization of PO and CO_2 (Scheme 23), initiating epoxide–CO_2 coupling chemistry. Since the 1970s, a great number of publications dealing with copolymerization of CO_2 with oxiranes and oxetanes have appeared. The reviews concerning CO_2 copolymerization and catalysts used are also available, especially prepared by Inoue, Kuran and Rokicki, Darensbourg and Holtcamp, Super and Beckman, Kuran, Coates and Moore, and very recently by Darensbourg.[33,143,149–153]

4.12.3.1.2 Polymerization of five-membered cyclic carbonates containing functional groups

Aside from the simple alkyl-substituted five-membered cyclic carbonates many derivatives of EC have been developed in recent years that contain added functionality, that is, derivatives bearing reactive groups in addition to the carbonate ring itself.[154] Among them, there are vinyl moieties, esters, ethers, and alcohols (Scheme 24).

Of these, only GC (1, Scheme 24) has been commercialized so far. GC is a stable, colorless liquid that is used as a solvent, additive, and chemical intermediate. As a chemical intermediate it reacts readily with alcohols, phenols, and carboxylic acids with loss of CO_2 as well as with aliphatic amines with carbon dioxide recovery and β-hydroxyurethane bond formation. GC can be obtained according to various methods, using epoxy compounds as well as glycerol as raw materials.[155–158] It was reported that GC can be formed in the reaction of epichlorohydrin with $KHCO_3$ carried out at 80 °C in the presence of 18-crown ether.[24] Nevertheless, more attractive methods are those utilizing glycerol as a renewable and cheap raw material. A typical method of obtaining carbonate derivatives of glycerol is its transesterification with EC or dialkyl carbonate. In the reaction with EC carried out at 125 °C in the presence of sodium bicarbonate the product was formed in a yield of 81%.[159] Very promising methods of GC preparation comprise the reaction of glycerol with CO_2 or carbon monoxide and oxygen in the presence of Cu(I) catalysts.[160] The reaction of

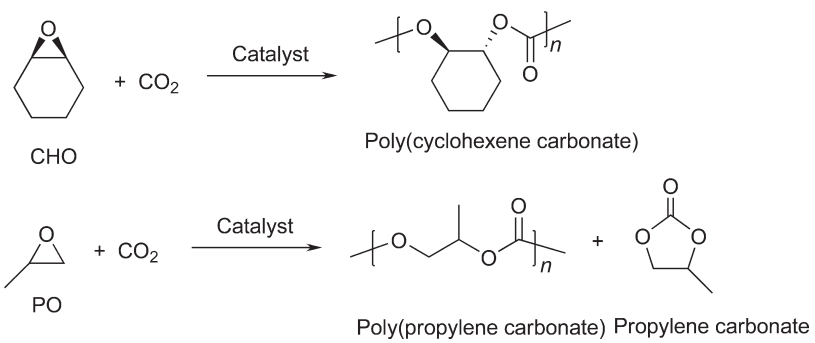

Scheme 23 Copolymerization of cyclohexene oxide and propylene oxide with CO_2.

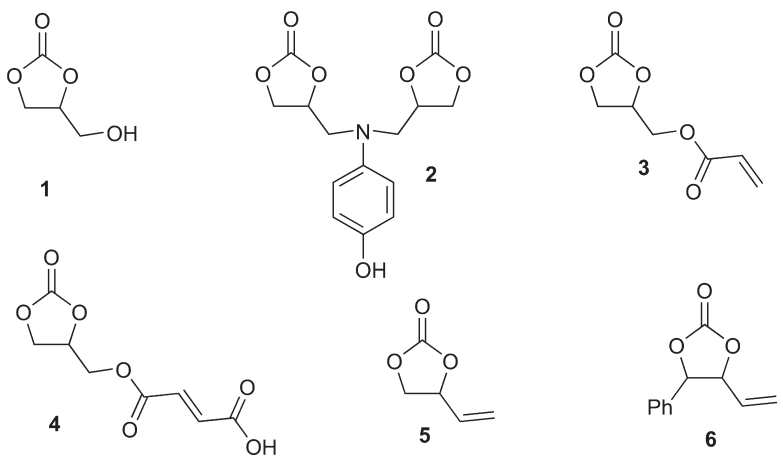

Scheme 24 Five-membered cyclic carbonates containing functional groups.

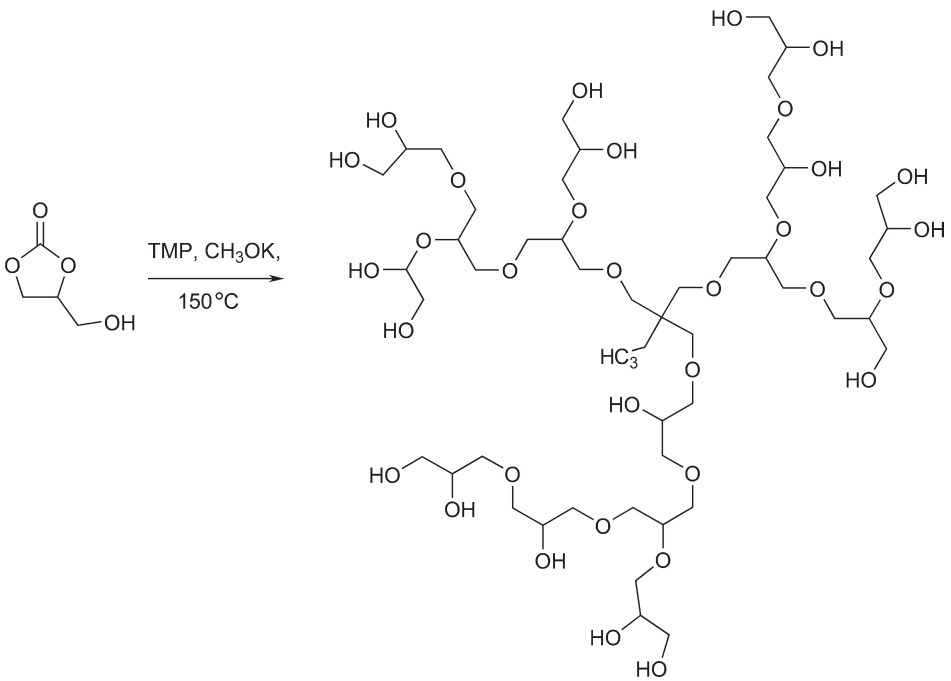

Scheme 25 Anionic polymerization of glycerol carbonate.

glycerol with carbon dioxide was carried out in a $scCO_2$ medium in the presence of zeolite and EC as a cosource of carbonate groups.[161] However, according to all the above-mentioned methods GC should be purified by distillation under reduced pressure at a relatively high temperature (125–150 °C).

Rokicki *et al.* showed that the GC synthesis can be carried out under mild conditions without any solvent, using glycerol and dimethyl carbonate as environmentally benign and renewable reagents.[162] Due to the almost quantitative reaction yield there was no need for the product purification by distillation at high temperature and recovery of unreacted glycerol.

GC alone can be a valuable monomer for the synthesis of hyperbranched poly(hydroxyether)s (**Scheme 25**).[158] In case of polymerization, GC, containing a 1,3-dioxolan-2-one ring and hydroxyl group in a single molecule, is considered a latent cyclic AB_2-type monomer. The anionic ROP of the GC, which proceeds with CO_2 liberation, leads to a branched polyether. 1,1,1-Tris(hydroxymethyl)propane or other multihydroxyl molecules are usually used as a initiator-starter and central core of the polyether. The hyperbranched polyglycerol structure is obtained by slow addition of the cyclic carbonate monomer at above 150 °C. Such polymers are characterized by a flexible polyether core and a multihydroxyl outer sphere. They are suitable for preparation of acrylic resins for dental applications or additives for polyurethane foams. Hyperbranched poly (hydroxyether)s from biscyclic carbonate with phenol group (**2**, **Scheme 24**) were also reported.[162,163]

Because it contains a hydroxy group, GC can be reacted with anhydrides,[164,165] acyl chlorides,[166] isocyanates,[167] and the like. For instance, GC reacted with the multifunctional isocyanate polymeric methylene diphenyl diisocyanate (MDI) in the presence of potassium acetate gave a multifunctional alkylene carbonate.[168] The reaction of GC with isocyanates occurs at room temperature or with slight heating and is generally accompanied by an exotherm such that the controlled addition of one component into the other is desired. The multifunctional carbonates prepared by means of the above process are useful as blow promoters in the preparation of polymeric foams,[168] or they can be reacted with aliphatic diamines to prepare polyurethane resins.

Five-membered cyclic carbonate rings can be also generated on existing polymeric species. For example, hyperbranched polyglycerol was reacted with dimethyl carbonate yielding multifunctional alkylene carbonate.[169] In contrary, soybean oil-based multifunctional alkylene carbonate was prepared via epoxidation of double bonds followed by a pressure reaction with CO_2 catalyzed with KI-crown ether system.[170] Such carbonate derivatives were applied as toughening agents for amine-cured epoxides. Although not yet commercially available, multialkylene carbonates can also be prepared from epoxy resins via CO_2 insertion.[171]

Vinyl-functional alkylene carbonates, useful in the preparation of polymers that contain alkylene carbonate pendant groups, can also be prepared from GC. Two examples are the reaction of GC with maleic anhydride and acryloyl chloride to produce the acrylate-functional cyclic carbonates (**3** and **4**, respectively, **Scheme 24**).[164] Although the transesterification of alkyl esters such as dimethyl maleate or methyl acrylate by reaction with GC represents an obvious means of obtaining the above materials, the temperatures required of such processes (> 100 °C) result in unwanted polymerization of both the reactant and product species, even in the presence of well-known radical inhibitors such as 2,6-di-*tert*-butyl-*p*-cresol or phenothiazine.[164] In addition, the synthesis of vinyl-functional alkylene carbonates is greatly complicated by the fact that such materials cannot be purified by distillation and must be stored at temperatures < 0 °C in the presence of a

polymerization inhibitor.[172] In fact, these and similar species are known to undergo polymerization much more readily than the analogous underivatized vinyl monomers.[173,174]

Vinyl-functional alkylene carbonates can also be prepared from the corresponding epoxides in a manner similar to the commercial manufacture of ethylene and PCs via CO_2 insertion. The most notable examples of this technology are the syntheses of 4-vinyl-1,3-dioxolan-2-one (vinyl ethylene carbonate, VEC) (**5**, Scheme 24) from 3,4-epoxy-1-butene[175] or 4-phenyl-5-vinyl-1,3-dioxolan-2-one[176] (**6**, Scheme 24) from analogous aromatic derivative 1-phenyl-2-vinyl oxirane. Although the homopolymerization of both vinyl monomers produced polymers in relatively low yield, copolymerizations effectively provided cyclic carbonate-containing copolymers. It was found that VEC can be copolymerized with readily available vinyl monomers, such as styrene, alkyl acrylates and methacrylates, and vinyl esters.[175] With the exception of styrene, the authors found that VEC will undergo free-radical solution or emulsion copolymerization to produce polymeric species with a pendant five-membered alkylene carbonate functionality that can be further cross-linked by reaction with amines. Polymerizations of 4-phenyl-5-vinyl-1,3-dioxolan-2-one also provided cyclic carbonate-containing copolymers.

4.12.3.2 Polymerization of Six-Membered Cyclic Carbonates

Six-membered cyclic carbonates such as TMC and neopentyl carbonate, in contrast to thermodynamically unfavorable five-membered cyclic carbonate, easily polymerize to afford PCs without ether sequences. Taking into consideration that the ROP of cyclic carbonates is an equilibrium reaction, six-membered cyclic carbonates show a strong substitution effect on the equilibrium monomer concentration. The anionic ROP of TMC and 5,5-disubstituted 1,3-dioxan-2-ones (dimethyl, methyl-phenyl, diethyl, ethyl-phenyl) in THF solution using potassium *tert*-butoxide initiator exhibited an increasing monomer concentration at equilibrium, with an increasing bulkiness of the substituents. This correlates with the yields obtained in monomer synthesis: the higher the steric effect of the substituents, the higher the selectivity toward the cyclic monomer in comparison to the linear oligomers. An estimation of the thermodynamic parameters reflected the polymerizability of the monomers ($\Delta H_p^0 = -26.37$ to $-5.02\ kJ\ mol^{-1}$); a decrease in the absolute value of ΔH_p^0 is observed for monomers with increased bulkiness of the substituents. The reason for the decrease in polymerizability of the six-membered cyclic carbonates with increased bulkiness of the substituents lies in the conformational distortion of the polymer backbone, rather than in the change of conformation of the monomer caused by the substituents.[6,145]

4.12.3.2.1 Cationic polymerization of six-membered cyclic carbonates

In ROP of aliphatic cyclic carbonates proceeding according to the cationic mechanism, electrophilic reagents are used as initiators. Brønsted and Lewis acids, as well as alkyl esters of strong organic acids (e.g., methyl trifluoromethanesulfonate) are most often involved. Cyclic carbonates contain polarized bonds (C=O)–O, in which carbonyl oxygen atom has a lone electron pair so that it can act as a Lewis base in reaction with an electrophilic initiator. As a result, an alkoxy-substituted carbon atom (trialkoxycarbenium cation) becomes a cationic center. In this mode the ring-opening reaction of the monomer will be caused by the nucleophilic attack of a lone electron pair of a carbonyl group oxygen toward the electrophilic initiator. The resulting cationic species of a cyclic structure can be attacked by another molecule of the monomer to undergo a ring-opening reaction according to S_N2 mechanism (Scheme 26).[6,177]

In contrast, cyclic carbonate with an *exo*-methylene substituent in the ring polymerizes via an S_N1 mechanism. Such a monomer can undergo ring-opening reaction spontaneously to produce a linear product with allyl cation that will be attacked by the carbonyl oxygen atom of the next monomer molecule according to the S_N1 mechanism (Scheme 27). It should be noticed that allyl carbocation is stabilized by an electron delocalization.

The stability of the cation, in this case trialkoxycarbenium cation versus allyl one, decides which of these two mechanisms predominates.[177–179] The selective ROP of 5-methylene-1,3-dioxan-2-one to the linear PC can be explained by assuming that the competitive vinyl polymerization is suppressed by neighboring electron-withdrawing carbonate group.[178]

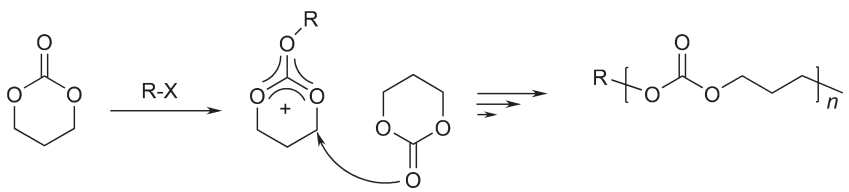

Scheme 26 Cationic polymerization of six-membered cyclic carbonate in accordance with S_N2 mechanism.

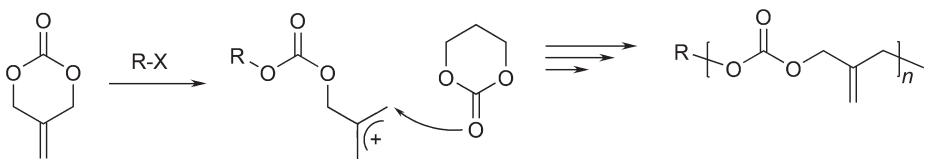

Scheme 27 Cationic polymerization of six-membered cyclic carbonate in accordance with S_N1 mechanism.

It is well known that cationic polymerization of heterocyclic monomers such as oxiranes can proceed according to two mechanisms: activated monomer (AM) and active chain end (ACE) ones. In the polymerization proceeding according to an AM mechanism, the active centers are located on the monomer molecule, while the growing polymer chain is neutral. Taking into account that in the cationic AM mechanism there is no active species at the chain end, the backbiting is to a large extent reduced. In order to suppress the reaction proceeding according to ACE mechanism the instantaneous concentration of monomer in the reaction mixture should be kept very low (e.g., by continuous very slow monomer addition).[122,180,181]

The ROP of TMC initiated with several alcohols was examined by Endo's group.[86] It was found that the reactions proceeded without acidic catalyst in low conversions. However, when the polymerization was carried out in the presence of alcohol/trifluoroacetic acid (ROH/TFA) catalyst system the corresponding PCs with $M_n = 2500–6800$ were formed. The molecular weights increased with an increase of the monomer conversion. Mechanistic aspects studied by NMR spectroscopy indicated that carbonate rings are activated by TFA. The signals of the methylene protons shifted to lower fields by 0.06–0.11 ppm in the ^{1}H NMR spectra after the addition of TFA. Downfield shifts of the carbonyl carbon atom signals in TMC were observed by 3.94–4.15 ppm in the ^{13}C NMR spectra.

Recently, Hyun *et al.*[182] have revealed that TMC can be polymerized according to the AM mechanism when a poly (oxyethylene) glycol/HCl · OEt_2 system was used as a cationic initiator. The polymerization of TMC in the presence of HCl · OEt_2 gave triblock or diblock copolymers composed of poly(ethylene glycol) (PEG) and PTMC units depending on the used PEG or monomethyl-PEG. The obtained PTMC had molecular weights close to the theoretical values calculated from TMC/PEG molar ratios (e.g., 920-2000-920) and exhibited a monomodal GPC curve without any trace of dead polymer. The terminal hydroxy group of PEG served as an initiator in this polymerization system.

The mechanism of cationic polymerization of six-membered cyclic carbonates was also investigated and discussed by Kricheldorf *et al.*[183] Using IR and ^{1}H NMR spectroscopies it was shown that methyl triflate initiated the polymerization of six-membered cyclic carbonates by alkylation of the *exo*-cyclic oxygen atom of the carbonate linkage, generating a trialkoxycarbenium ion, **A** (**Scheme 28**). The reaction equilibrium is established after ring opening by the counterion (eqn [2]). Another molecule of cyclic carbonate can attack the trialkoxycarbenium ion leading to the alkyl–oxygen bond cleavage and the *exo*-cyclic oxygen atom of the nucleophile is alkylated (eqn [3]). The second possible propagation reaction is between the covalent triflate and monomer (eqn [4]).

When an excess of methyl triflate was used it was possible to establish that the covalent initiator is slightly more reactive than the trialkoxycarbenium ion.[147,183] Thus, the propagation reaction involves the cleavage of the alkyl–oxygen bond in the monomer. The active cationic chain end and the dead methyl-carbonate end-groups were identified by means of ^{1}H NMR spectroscopy.

However, the main disadvantage of the cationic polymerization of six-membered cyclic carbonates is the decarboxylation as a side reaction resulting in the formation of ether linkages. The

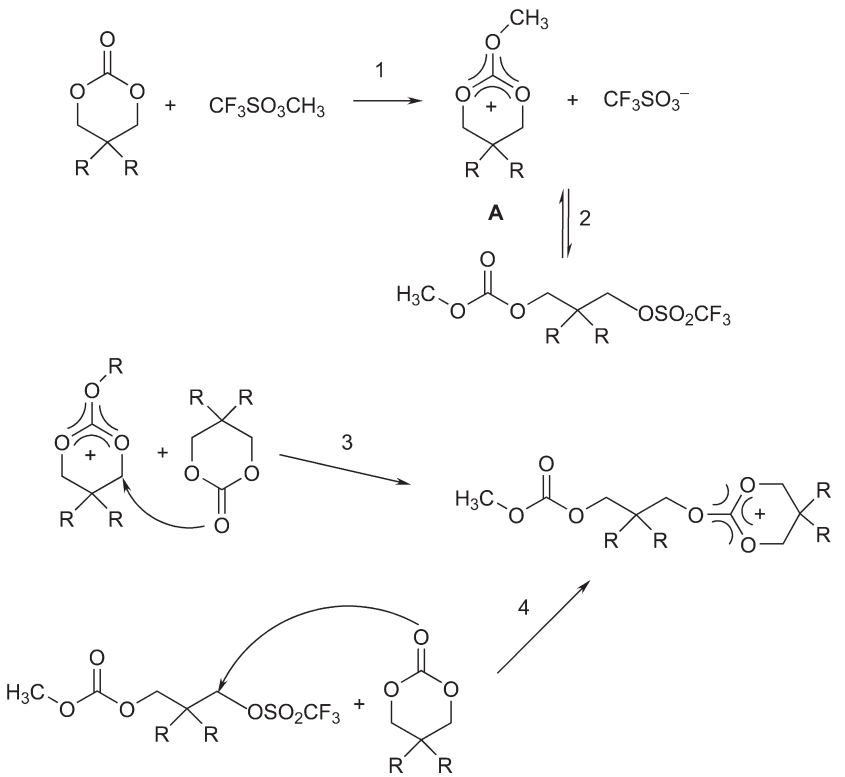

Scheme 28 Cationic polymerization of six-membered cyclic carbonates initiated with methyl triflate.

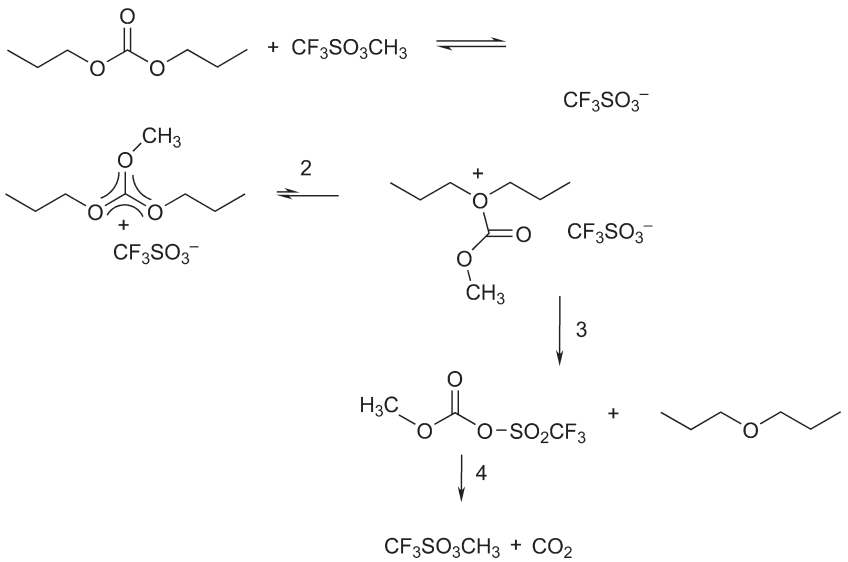

Scheme 29 Formation of ether linkages in cationic polymerization of six-membered cyclic carbonates.

concentration of the ether groups, depending on the chemical structure of the monomer, cationic initiator, and temperature, is in the range of 3–10 mol.% relative to carbonate groups. Molecular weights of the polymers obtained according to this mechanism do not exceed 6000, owing to side reactions such as backbiting and formation of ether groups. The intramolecular migration of an alkyl group is proposed to explain the formation of ether linkages (Scheme 29). The equilibrium 2 is shifted to the trialkoxycarbenium ion due to its better stabilization. But still intramolecular migration is possible and the initiator can be regenerated as shown in eqn [4]. The decarboxylation of carbonates catalyzed by cationic initiators was confirmed by the reaction of diethyl carbonate with 5 mol.% of methyl triflate carried out under reflux. Slow CO_2 evolution and ether formation were observed. After 16 h, 30 mol.% conversion of carbonate groups was found. The ^{1}H NMR spectra of the reaction mixture also revealed the formation of methyl carbonate groups and ethyl triflate that support the proposed reaction mechanism illustrated by eqns [1–4] (Scheme 29).

Other Lewis acids such as $BF_3 \cdot OEt_2$, BCl_3, and BBr_3 were used by Kricheldorf and Weegen-Schulz for the polymerization of neopentyl carbonate and TMC under various conditions. It was found that the six-membered cyclic carbonates and boron halogenides formed crystalline complexes. Depending on the reaction conditions, BCl_3 and BBr_3 react with both cyclic carbonates by ring opening and halogen transfer without initiating polymerization. In contrast, $BF_3 \cdot OEt_2$ initiates polymerizations to give high yields (> 95%) and high molecular weights (M_w > 100 000). However, the resulting PCs contained ether linkages. The molar fraction of ether groups increased with the reaction temperature. Moreover, kinetic data and ^{1}H NMR end-group analyses suggested that a cationic polymerization mechanism involved cyclic trialkoxycarbenium ions in analogy to methyl triflate-initiated polymerizations of six-membered cyclic carbonates (Scheme 29). However, backbiting degradation is much more efficient in the case of the methyl triflate-initiated polymerizations presumably due to the reactivity of a covalent triflate end-group.[147]

Also tin(IV) halogenides ($SnCl_4$, $SnBr_4$, and SnI_4) afforded PCs by cationic ROP.[184] The highest molecular weight (M_w = 150 000) was obtained when the polymerization of six-membered cyclic carbonate (TMC) had been conducted in bulk at 60 °C in the presence of SnI_4. In contrast, $SnCl_4$ and $SnBr_4$ caused partial decarboxylation even at 60 °C (~ 2 mol.%). Both $SnCl_4$ and $SnBr_4$ can form crystalline 1:2 complexes with TMC.[185] IR and ^{1}H ^{13}C NMR spectroscopies indicated complexation at the carbonyl oxygen. Additionally, CH_2OH, CH_2Cl, and CH_2Br end-groups were detected by ^{1}H NMR spectroscopy. Kinetic measurements of polymerization in solvents of different polarity suggested cationic polymerization proceeding according to the AM mechanism.

Organotin(IV) compounds such as $BuSnCl_3$, Bu_2SnCl_2, and Bu_3SnCl were also used for polymerizations of TMC.[186] The polymer yields above 90% were obtained with all three compounds, but their reactivities decreased in the order $BuSnCl_3 > Bu_2SnCl_2 > Bu_3SnCl$. The maximum molecular weights decreased in the same order. The PC of the highest molecular weight (M_w = 250 000) was obtained for $BuSnCl_3$. By means of ^{1}H and ^{13}C NMR spectroscopies the authors revealed that $BuSnCl_3$ forms complexes with the carbonyl group of TMC. In the ^{1}H NMR spectra signals corresponding to CH_2OH and CH_2Cl polymer end-groups were present regardless of the used initiator. Kinetic studies and a comparison with Bu_3SnOMe suggest that at least $BuSnCl_3$ initiates the polymerization proceeding according to a cationic mechanism. It should be noticed that, in contrast to $SnCl_4$, $BuSnCl_3$ did not cause decarboxylation.

Also Albertsson and Sjoeling[87] have reported that bulk polymerization of TMC, especially at higher temperatures (80–100 °C), and preferably when using $BF_3 \cdot OEt_2$ as initiator, afforded PTMC with high molecular weight (~ 100 000). At higher reaction temperatures higher molecular weight could be obtained, but thermal degradation of PTMC and ether group formation were observed. The polymer obtained with this cationic initiator contained about 3 mol.% of ether linkages. Other cationic initiators such as $AlCl_3$ gave a polymer

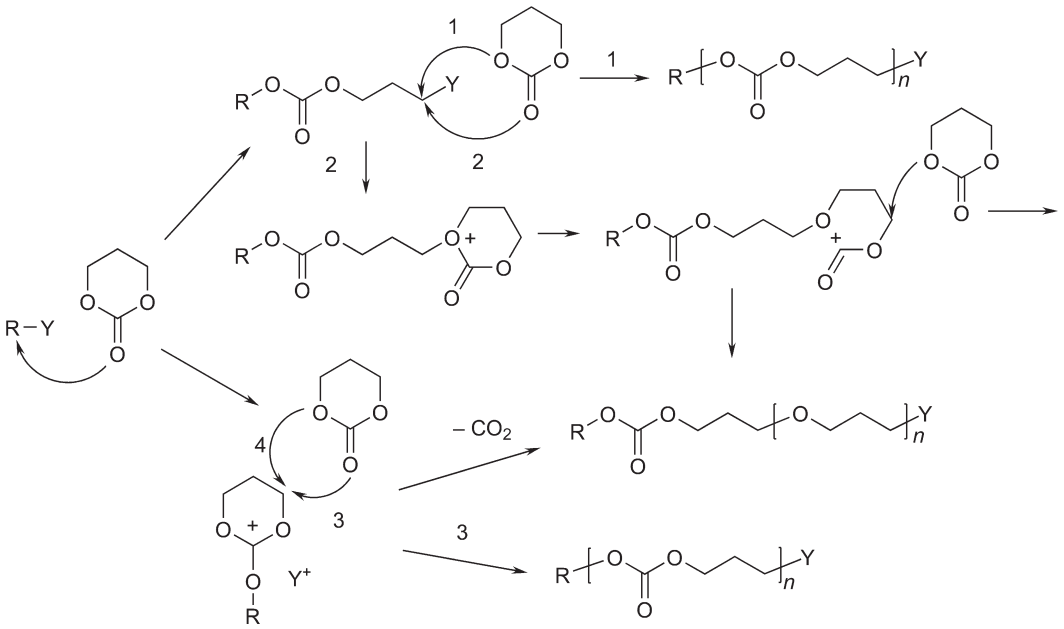

Scheme 30 Polymerization of six-membered cyclic carbonate with alkyl halide – possible reaction pathways.

of much lower molecular weight. Polymerization in solution gave mostly oligomers.

Ariga *et al.*[88,187] have revealed that when alkyl halides were used as cationic initiators for six-membered cyclic carbonates the ROP proceeded without decarboxylation and the corresponding homopolycarbonates, but of rather low molecular weights, were formed. The reactions of PTMC with several cationic initiators including methyl iodide were monitored by ^{1}H NMR and GPC. Both a decrease in the polymer molecular weight and the ether units content strongly depended on the kind of initiator. PM3 molecular orbital calculations using model compounds confirmed that the decarboxylation occurred mainly in the propagation step (**Scheme 30**).

The reaction of TMC with an excess of alkyl halide such as methyl iodide and benzyl bromide at 120 °C afforded the corresponding 1:1 adducts. The yield of the adduct from methyl iodide was only 10%, while the yield of that from benzyl bromide was 78%. The cationic polymerizations of different cyclic carbonates with alkyl halides such as methyl iodide (RY = CH_3I), benzyl bromide (RY = $C_6H_5CH_2Br$), and allyl iodide (RY = $CH_2=CHCH_2I$) carried out under various conditions led to the corresponding PCs without any ether units (pathway 1 in **Scheme 30**). The polymerization with ethyl 3-iodopropyl carbonate as a model compound was examined to prove the structure of the propagation active site. The decarboxylation seems to occur by the attack of the monomer at the propagating end more preferably than that of the polymer at the propagating end. This is because of the better nucleophilic properties of a monomer than those of a polymer, as was postulated from PM3 molecular orbital calculation. The comparison of the HOMO level of cyclic carbonate (TMC) and linear carbonate (dimethyl carbonate) indicates that a cyclic carbonate is more nucleophilic than a linear one. On the other hand, the heat of the formation of cationic intermediates suggests that the stabilization energy of the formation of the cyclic oxonium cation is 7.4 kcal mol^{-1} greater than that of the linear oxonium cation. Therefore, Endo *et al.* suggested that decarboxylation from the monomer should be thermodynamically and kinetically predominant over that from the linear carbonate. Taking into consideration that decarboxylation competes with the propagation process, to suppress the decarboxylation Endo *et al.* proposed to use propagating species of lower reactivity. It is well known that less reactive compounds give products with higher selectivity.[88] Thus, the authors used a less reactive halide ion instead of the triflate one. Less reactive neopentyl carbonate did not polymerize in the presence of alkyl halides, due to unfavorable nucleophilic substitution at the sterically hindered neopentyl position. In contrast to methyl triflate-initiated polymerization (RY = $CH_3OSO_2CF_3$ in **Scheme 30**), in which the resultant polymer contained hydroxyl end-groups, the PC molecules obtained using alkyl halides as a cationic initiator were terminated by haloalkyl groups.

A haloalkyl carbonate structure is formed by the initial ring-opening reaction of the monomer with alkyl halide, which was shown by using ethyl 3-iodopropyl carbonate as the initiator for cyclic carbonate polymerization. The obtained polymer contained both ethyl and iodopropyl end-groups.

According to this mechanism, alkyl halopropylcarbonate is attacked by cyclic carbonate at the carbon atom neighboring the carbonate linkage to afford biscarbonate via ring opening and PC with alkyl and iodopropyl end-groups is formed (Y = I; **Scheme 30**). Since the polymerization initiated by ethyl 3-iodopropyl carbonate is faster than that initiated by methyl iodide, it is suggested that ethyl 3-iodopropyl carbonate is more reactive than methyl iodide and the halopropyl carbonates are the actual propagating species.

The polymerization of cyclic carbonate with alkyl halide proceeds according to pathway 1 (**Scheme 30**) and owing to the higher nucleophilicity of the halide anion, the covalent macrohalide is more favored than the trioalkxycarbenium ion. However, when a solvent of higher polarity is used as the reaction medium, partial decarboxylation takes place due to

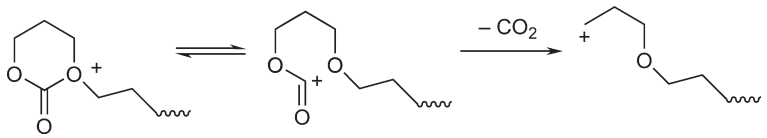

Scheme 31 Mechanism of decarboxylation of terminal oxonium groups.

the shifting of the balance to the carbenium ion species, and a nucleophilic attack along pathway 4 (Scheme 30), causing the decarboxylation, is more probable.

The reaction pathways of TMC during cationic ROP have been explored by Holder and Liu[188,189] applying Austin Model 1 (a semi-empirical method for the quantum calculation) (AM1) semiempirical calculations. They established a species evolution diagram, and the propagation chain ends on the ether oxygen atom have been identified as the species that ultimately lead to decarboxylation (Scheme 31).

Three factors were proposed and evaluated to reduce the degree of decarboxylation based on theoretical calculations: increasing the monomer concentration; decreasing the solvent polarity; and introduction of such ring substituents to bypass the decarboxylation route.

Rare earth halogenides, such as neodymium bromide or iodide, can catalyze TMC and ε-caprolactone (CL) bulk polymerization quickly with small amounts of catalyst ([TMC]/[Ln] = 3000 molar ratio) at 80 °C. The reason why the catalytic activity of TMC polymerization is higher than that of CL polymerization has been studied and it is shown that the difference arises from different polymerization mechanisms of TMC and CL with rare earth halides.[190] Rare earth halogenide single component also can catalyze the copolymerization of TMC and D,L-lactide (LA) and the catalytic activity sequence of various rare earth chlorides is as follows: $LaCl_3 > YCl_3$, $PrCl_3 > NdCl_3 \gg DyCl_3$.[191]

Agarwal *et al.*[192] reported the polymerization of TMC and its copolymerization with L-LA using the SmI_2/Sm initiator system. SmI_2 was prepared by reacting Sm powder with diiodoethane. The reactions proceeded at 70 °C without significant decarboxylation during polymerization.

4.12.3.2.2 Anionic polymerization of six-membered cyclic carbonates

The anionic polymerization of six-membered cyclic carbonates was first reported in the 1930s by Carothers and Van Natta.[19,193] The PCs were obtained by heating TMC in the presence of K_2CO_3.

Generally, six-membered cyclic carbonates easily polymerize with anionic initiators affording high-molecular-weight polymers. In contrast to cationic ROP of cyclic carbonates, these polymers do not contain ether linkages. This feature is especially important when the PCs or their derivatives are utilized in biomedical practice. The presence of ether linkages make such polymers susceptible for oxidation and loss of good mechanical properties.

The ROP of six-membered cyclic carbonates with nucleophilic initiators is a chain reaction in which, besides initiation and propagation reactions, transesterification reactions can also take place (Scheme 32).[194,195] Intramolecular nucleophile (e.g., alkoxide) attacks on carbonyl carbon atom (backbiting) lead to cyclic oligomers, while intermolecular transesterification leads to a change of the macromolecule length with the consequence that, at equilibrium, the most probable distribution of the molecular weight is obtained (Scheme 32).

The initiation reaction comprises the nucleophilic attack of the initiator on the carbonyl carbon atom, followed by an acyl-oxygen cleavage and formation of the active species, an alkoxide.[196] The initiation process depends on the nucleophilicity of the initiator and on the electron affinity of the monomer. A slow initiation in comparison to the propagation process leads to a broadening of the molecular weight distribution and a loss of molecular weight control.[197]

The stereochemistry and mechanism of reversible polymerization of 2,2-disubstituted TMCs were discussed in the 1950s by Sarel and Pohoryles.[84] The anionic mechanism was discussed by Kühling *et al.*[196,198] According to them, a good control of the reaction course can be attained when the ratio of the rate constants of propagation (k_p) and of backbiting (k_b) and transesterification (k_{te}) are large, and there are no termination and transfer reactions. Thus, a high polymer yield and a narrow molecular weight distribution are obtained. The polymerization conditions such as temperature, reaction medium

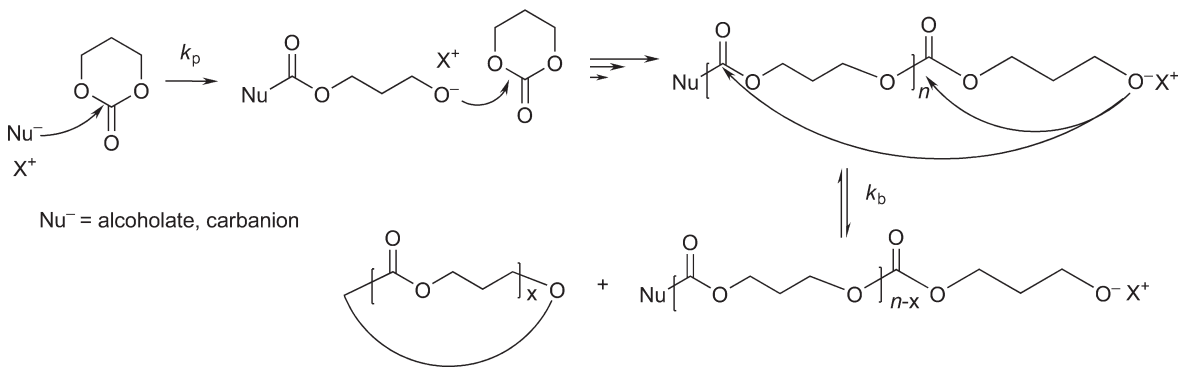

Scheme 32 Anionic polymerization of six-membered cyclic carbonate with nucleophilic initiators.

(solvent polarity), monomer concentration, and the nature of the active site also are important for the polymerization control.

The homopolymerization of the most popular six-membered cyclic carbonates (TMC and neopentyl carbonate) using nucleophilic initiators based on Li-, K-, Mg-, Al-, Zn-, and Sn-containing compounds were also studied. The systems containing alkali metals, Mg and Sn, were found to afford during polymerization, besides linear, also cyclic oligomers.[195,199,200] This shows that for this group of initiators the rate of backbiting reaction (k_b) is of the same order of magnitude as the rate of propagation (k_p).[201] For Al- and Zn-based catalysts no oligomers were detected, so the backbiting reaction is much slower than the chain-growth reaction.[199] With former mentioned initiators the intramolecular and intermolecular transesterification reactions take place. High-molecular-weight polymer is formed when the reaction is kinetically controlled. In the regime of thermodynamic control ring-chain equilibrium takes place.[195]

It is known that the anionic polymerization of dimethyl trimethylene carbonate (DTC) in toluene with lithium cation as a counterion proceeds slower than that with potassium one due to the more covalent character of the lithium–oxygen bond compared with the potassium-oxygen bond; this leads to a lower nucleophilicity of the lithium alkoxide and also the low tendency for complexation with PEG favors lithium as counterion.[91]

Other initiators based on alkali metals such as *sec*-butyllithium (*sec*-BuLi) as well as sodium and potassium naphthalene were also surveyed.[195] Sodium and potassium naphthalene, when used as electron-transfer reagents for the initiation of styrene polymerization, react with neopentyl carbonate as a nucleophile. The investigation of oligomers obtained in the initial stages of the polymerization by means of GPC using a UV-detector revealed naphthalene to be incorporated into the growing chain.

Rokicki and Jezewski[202] showed that when potassium naphthalene reacts with cyclic carbonate (1:2 molar ratio) dialkoxide species are formed. After reaction with α,ω-dibromo-*p*-xylene the resultant product containing aromatic-aliphatic ester and aliphatic linkages was confirmed by ^{1}H NMR spectroscopic analysis.

Macroinitiators such as polymeric Li, Na, and K alkoxides can also be used for the initiation of the six-membered cyclic carbonate polymerization. Thus, besides living vinyl polymers,[203] hydroxyl group-terminated polymers of poly (tetrahydrofuran) (PTHF),[204] poly(oxyethylene),[205] and poly(dimethylsiloxane) (PDMS)[206] were transformed to alkoxides by treatment with *sec*-BuLi or K-naphthalene and used as initiators. The use of these macroinitiators enables the identification of side reactions, as shown by Keul and Höcker for polystyrene lithium (PS^-Li^+).[203] The addition of the macroinitiator to the monomer, to maintain a high excess of monomer, minimizes side reactions. Transformation of the polystyryl carbanion to a less nucleophilic alkoxide to avoid the side reaction was another approach proposed by the authors. They used EO as a reagent for lowering the nucleophilicity of the macroinitiator. Polymerization of neopentyl carbonate initiated by such macroalkoxide ($PS\text{-}CH_2CH_2O^-Li^+$) led to high yields of AB-block-copolymers (**Scheme 33**).

It was found that the polymerization of neopentyl carbonate initiated by PTHF alkoxides with different counterions such as Li^+, K^+, and Bu_4N^+ proceeds slower than that initiated by poly(ethylene oxide) (PEO) alkoxides, which can be explained by the lower solvation ability of PTHF. It was also shown that the nucleophilicity of the active species is significantly reduced by exchanging potassium counterion with lithium one. As a result, high PC yields were obtained after several minutes. The lower nucleophilicity of the lithium alkoxide was ascribed to the more covalent character of the lithium–oxygen bond, compared with the potassium–oxygen one. Moreover, Li^+ exhibits lower tendency for complexation withPEO; self-association prevails, compared with the corresponding potassium alcoholates.[207]

When lithium alkoxide of hydroxyl telechelic PDMS of different molecular weights (M_n = 900–46 000) was used as initiator for the neopentyl carbonate polymerization, the time needed for the complete monomer conversion was significantly longer than that with initiators based on polyethers with the Li^+ counterion.[206] Moreover, a dependence of the polymerization rate on the PDMS molecular weight was observed. For a given concentration of the active species the polymerization rate decreased with increasing molecular weight of the initiating macroinitiator. The low polymerization rate of neopentyl carbonate with PDMS-based macroinitiators has its origins in a decrease of the nucleophilicity of the active species being complexed by the PDMS chain. Such complexation of an alkoxide has been reported, for example, in the reaction of diphenyl-diethoxy silane with potassium ethoxide. The dependence of the polymerization rate of neopentyl carbonate on the molecular weight of the initiator might be explained by the locally larger concentration of complexing $(CH_3)_2SiO$ units.

Anionic metal-free initiation was successfully applied to both aliphatic and aromatic cyclic carbonates.[208] This method is based on the reaction of a silyl ether with fluoride anions, for example, tetrabutyl ammonium fluoride (Bu_4NF) or tris (dimethylamino)sulfonium trimethylsilyl difluoride (TASF, $[(CH_3)_2N]_3\ SSi(CH_3)_3F_2$), to produce an anion with a tetrabutyl ammonium or tris(dimethylamino)sulfonium counterion. The metal-free system is an efficient initiator for neopentyl carbonate polymerization.[209]

An important aspect for materials with applications in the biomedical field is the use of nontoxic catalysts. Biologically nontoxic magnesium and calcium complexes have been successfully employed for the ROP of TMC; however, the toxicity of the salen ligands has not been assessed, and polymerization

Scheme 33 Transformation of the polystyryl carbanion to alkoxide.

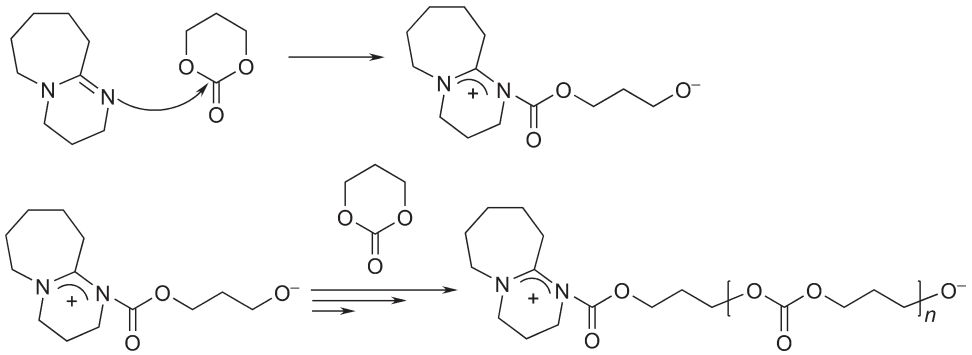

Scheme 34 Anionic polymerization of six-membered cyclic carbonate initiated with DBU.

control was limited as judged from the dispersities of the polymers (~ 1.6).[210]

Thus, instead of using ionic and coordination initiators it is possible to use organic initiators for the polymerization of six-membered cyclic carbonates. Murayama *et al.*[211] have found that polymerization carried out in the presence of tertiary amines such as DBU, DABCO, and DMAP afforded the corresponding PC (Scheme 34). A cyclic carbonate of a norbornene (5,5-(bicyclo[2.2.1]hept-2-en-5,5-ylidene)-1,3-dioxan-2-one) (NBC) initiated by DBU at 120 °C yielded in short time (1 h) a polymer with relatively low molecular weight (6400). However, no polymer was obtained when triethylamine, aniline, *N*,*N*-dimethylaniline, or pyridine were used for the polymerization. The much lower activity of triethylamine than that of DABCO might be caused by the steric hindrance around the nitrogen atom, while aromatic amines showed low activities due to the aromatic resonance effect decreasing their nucleophilicities. The authors proposed the zwitterionic polymerization mechanism (Scheme 34), which was confirmed by FD-MS mass spectrum analysis of the polymerization products. In the spectrum the signals which can be assigned to cyclic oligomers and a linear polymer with DBU end-group were found. Thus, the reaction between DBU and cyclic carbonate to form an alkoxide anion is the initiating step of the polymerization. In the propagation reaction the alkoxide anion attacks the carbonyl group of cyclic carbonate to yield the corresponding PC.

A similar mechanism comprising the formation of the zwitterion intermediate was proposed by Kricheldorf *et al.*[212]

Recently, Nederberg *et al.*[213] reported results on the ROP of TMC using several organocatalysts such as N-heterocyclic carbenes (NHC), guanidine and amidine bases, and the bifunctional thiourea–tertiary amine system. Good polymerization control was found for several of these catalysts yielding well-defined PCs with molecular weights up to 50 000, dispersity index below 1.08, and high end-group fidelity. The authors surveyed the following catalysts: guanidines (TBD, **1**, $pK_a = 26.0$ and 7-methyl-1.5.7-triazabicyclo-[4.4.0]dec-5-ene, MTBD, **2**, $pK_a = 25.5$), amidine base (DBU, **3**, $pK_a = 24.3$), NHCs with either alkyl or aryl substituents (1,3–diisopropyl-4,5-dimethyl-imidazol-2-ylidene, **4**, $pK_a = 30.4$; 1,3-bis(2,6-diisopropylphenyl)-imidazol-2-ylidene, **5**, $pK_a = 22.0$), bifunctional thiourea-tertiary amine catalyst (**6**) and catalyst mixture (**7**) (Scheme 35).

To avoid autoinitiation, the bulk polymerization was carried out at 65 °C. When DBU was used as a catalyst in the presence of benzyl alcohol, TMC was polymerized within minutes, yielding polymers with controlled molecular weight and small dyspersity index (1.09–1.15). To demonstrate the living nature of the polymerization carried out under bulk conditions, the chain extension experiment was conducted. Resultant polymer growth proceeded in a linear fashion. It was demonstrated that the intermediate chains can be employed for further growth, by the addition of more

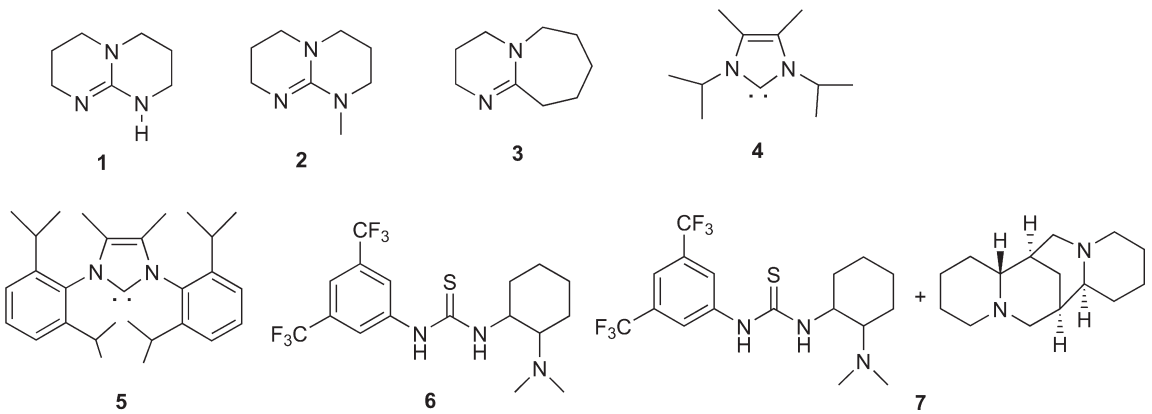

Scheme 35 Organocatalysts for anionic polymerization of six-membered cyclic carbonates.

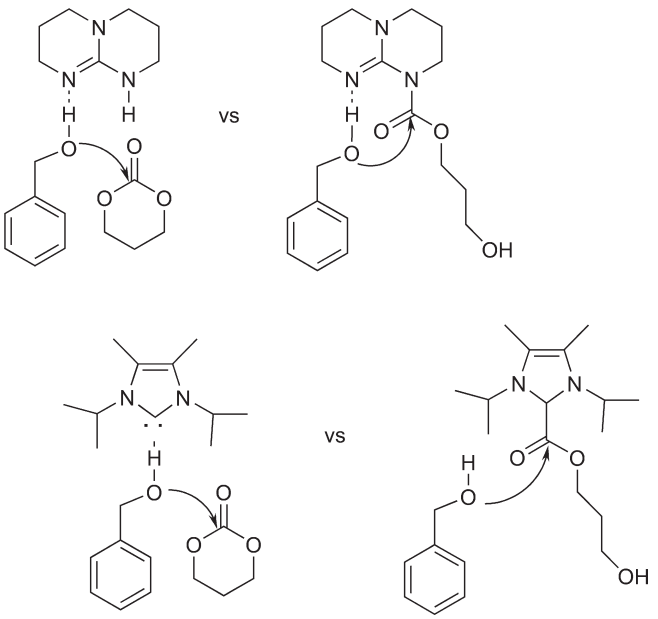

Scheme 36 Hydrogen bond activation of cyclic carbonate monomer and initiator/propagating species.

monomer. The molecular weight distribution remained narrow and monomodal.

These catalysts were used for random ester-carbonate bulk copolymerizations. Furthermore, by combining sequential polymerization techniques using bifunctional initiators, the mild polymerization conditions allow for the preparation of block copolymers. Hydrogen bond activation of monomer and initiator/propagating species was proposed as the underlying mechanism, which can be tuned to mitigate adverse side reactions (Scheme 36).

Liu *et al.*[214] used natural amino acids such as L-alanine, L-valine, L-proline, L-leucine, and L-phenylalanine as initiators of the ROP of DTC and TMC. PTMC and poly(dimethyl trimethylene carbonate) (PDTC) with different M_n were obtained at 80 and 120 °C, respectively, in bulk by changing the molar ratio of [monomer]/[amino acid]. Among these polymers, the maximum values of M_n of the PCs reached 17 800–18 900 and the dispersity index was 1.67 for [monomer]/[L-phenylalanine] molar ratio of 200. ^{1}H NMR spectroscopic analysis demonstrated that amino acid was incorporated into the polymer chain.

A similar approach was presented by Mindemark and coworkers.[215] According to this novel concept a controlled self-catalyzed polymerization reaction yields well-defined α,ω-heterotelechelic polymer chains and at the same time the elimination of low-molecular-weight catalyst residues in the final polymer product. The tertiary amine 2-(dimethylamino) ethanol (DMAE) was used as an efficient initiator/catalyst for the ROP of TMC. The catalytic behavior of DMAE was investigated in bulk polymerizations of TMC at temperatures of 46–48 °C. By carrying a tertiary amine as well as an alcohol functionality, in the initiating step DMAE is bifunctional, acting both as the catalyst and as the initiator (Scheme 37). There are two possible reaction pathways for the initiation step: a monomer-activating and an alcohol-end-group-activating mechanism (Scheme 37).

By ^{1}H NMR spectroscopy the authors have confirmed that the DMAE catalyst is attached to the growing polymer chain. The ROP of TMC catalyzed and initiated by DMAE yields the polymer chains bearing the same functional end-groups as the DMAE initiator molecule. This provides a good opportunity for creating new functional macromolecular architectures.

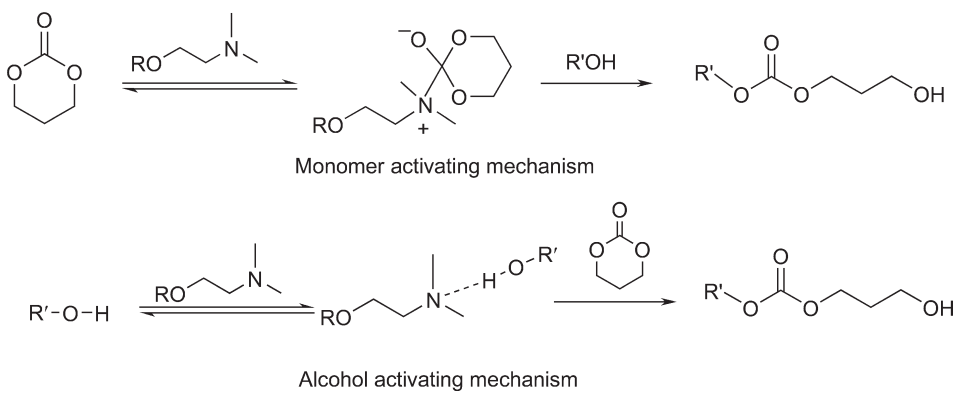

Scheme 37 Two possible reaction pathways for the initiation step of six-membered cyclic carbonate.

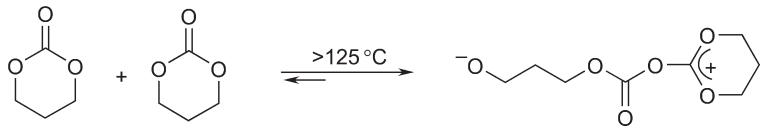

Scheme 38 Thermal spontaneous polymerization of TMC.

It should be noticed that pure TMC undergoes spontaneous polymerization in bulk at above 100 °C. In the plausible formulation of a TMC cleavage, a zwitterion intermediate with the trialkoxycarbenium ion, well stabilized by delocalization, and an alkoxide ion are formed (Scheme 38).[212] The alkoxide ion can initiate chain growth according to the anionic mechanism.

However, less reactive neopentyl carbonate did not undergo spontaneous polymerization. A similar observation concerning thermal ROP of substituted six-membered cyclic carbonate 5-benzyloxy-1,3-dioxan-2-one (BTMC) in bulk in the absence of any catalyst was reported by Feng *et al.*[216] Polymerization carried out at 150 °C for 6 h yielded high-molecular-weight poly (BTMC) (PBTMC) ($M_n = 80\,300$) and subsequent catalytic hydrogenolysis resulted in functional PTMC with pending OH groups (PHTMC). Similar spontaneous polymerization of BTMC in the presence of PEG ($M_n = 2000$) as a macroinitiator provided amphiphilic block polymers. An evaluation of the degradation and cytotoxicity of PHTMC demonstrated enhanced degradability compared with PTMC and similar toxicity compared with poly[(d,l-lactide)-*co*-glycolide] (PLGA), showing PHTMC to be a promising biomaterial.

Pawlowski *et al.* demonstrated that TMC can be polymerized using various diols as initiators but without any catalyst at moderate high temperatures (110–120 °C). The oligocarbonate diols were obtained by the thermal polymerization of TMC using PPD and the reaction products of aliphatic diamines with EC [1,2-bis(2-hydroxyethoxycarbonylamino)ethane and 1,6-bis(2-hydroxyethoxycarbonylamino)hexane] as the initiators.[217] The authors also applied microwave radiation for TMC polymerization in the presence of the alcohol initiator to afford oligocarbonates in a very short time (10–15 min).

Recently, Liao *et al.*[218] have used the same procedure, namely microwave radiation, for the ROP of TMC. The polymerizations were carried out in a single-mode microwave oven using ethylene glycol as an initiator. It was shown that the molecular weight of the resulting PTMC and TMC monomer conversion by the microwave method is higher than those by the conventional method.

Very recently, Okada and co-workers[219] revealed that the polymerization reaction of TMC proceeded rapidly in the aqueous solution and high conversion was achieved in a relatively short time. PPD formed by hydrolysis of TMC played the role of an initiator. The TMC oligomer obtained by ROP had a TMC unit backbone with terminal 3-hydroxypropyl groups at both chains ends. The oligomer underwent transesterification reaction with elimination of PPD, resulting in a gradual increase in the molecular weight of the product. Polymerization of the homogeneous TMC aqueous solution was then performed for up to 16 h at 145 °C with nitrogen bubbling through the solution. The molecular weight was affected by the concentration of TMC.

4.12.3.2.2(i) Site transformation from group transfer polymerization to anionic metal-free polymerization

'Living' poly(methyl methacrylate) (PMMA) prepared by group transfer polymerization (GTP) can be used as a macroinitiator for the ROP of cyclic carbonates. For this purpose the silyl ketene acetal was transformed into an alkoxide (anionic ROP mechanism) with a metal-free counterion (Scheme 39).[220] Hovestadt *et al.*[201] reported that the polymerization of DTC took place under GTP conditions: 1-methoxy-2-methyl-1-trimethylsiloxypropene used as initiator and tetrabutylammonium fluoride as catalyst. A quaternary ammonium alkoxide seems to be the likely propagating species for DTC polymerization.[221] In this way, good yields of the respective block copolymers were obtained.

The fluoride anion promotes desilylation of the silyl ketene acetal with formation of an enolate, which reacts as a carbon-centered nucleophile with the carbonyl carbon of DTC.[222]

4.12.3.2.3 Coordination-insertion ROP of six-membered cyclic carbonates

The pseudo-anionic ROP is often referred to as coordination-insertion ROP, since the propagation is thought to proceed by coordination of the monomer to the active species, followed by insertion of the monomer into the metal–oxygen bond by rearrangement of the electrons (Scheme 40).

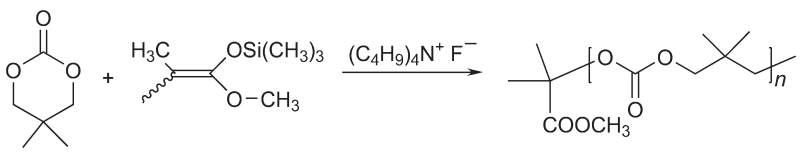

Scheme 39 Polymerization of DTC initiated with 1-methoxy-2-methyl-1-trimethylsiloxypropene in the presence of tetrabutylammonium fluoride.

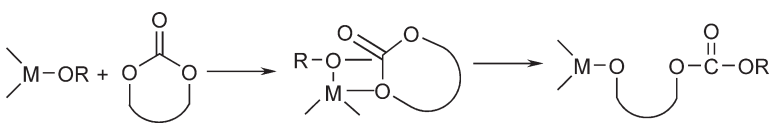

Scheme 40 Coordination-insertion ROP of six-membered cyclic carbonate.

The growing chain remains attached to the metal through an alkoxide bond during the propagation. The covalent metal alkoxides with free p- or d-orbitals react as coordination initiators and not as anionic or cationic initiators. The ring cleavage during the polymerization of the cyclic carbonates in the presence of typical coordination catalysts was found to occur at the C(O)–O bond, resulting in the formation of metal alkoxide propagating species. The reaction is terminated by hydrolysis forming a hydroxy end-group. With functional alkoxy-substituted initiators, macromonomers with end-groups active in postpolymerization reactions are produced.

4.12.3.2.3(i) Tin-based catalysts

Tin(II) 2-ethylhexanoate, commonly referred to as stannous octoate ($Sn(Oct)_2$), is the most frequently used catalyst in the ROP and copolymerization of cyclic heterocyclic monomers including cyclic carbonates due to a high activity as well as an approval by the American Food and Drug Administration (FDA) as a food additive. The mechanism of polymerization with its contribution has been widely discussed. $Sn(Oct)_2$ is not thought to be the actual initiator since the molecular weight does not depend on the monomer/$Sn(Oct)_2$ molar ratio.

Investigations of the coordination-insertion mechanism have resulted in two slightly different reaction pathways. Kricheldorf and co-workers[223,224] have proposed a mechanism in which the initiating alcohol functionality and the monomer are both coordinated to the $Sn(Oct)_2$ complex during propagation (**Scheme 41**, eqn [1]). Penczek and Duda groups have presented a mechanism in which the $Sn(Oct)_2$ is converted into a tin alkoxide before complexation and ring-opening of the monomer (**Scheme 41**, eqn [2]).[122,225–227]

The $Sn(Oct)_2$ catalyst is an active transesterification agent, especially at high temperatures, and the resulting copolymers usually have a randomized microstructure.[228] An increase in reaction temperature or reaction time increases the extent of transesterification reactions.

Kricheldorf and Stricker[229] presented results of ROP of TMC catalyzed with $Sn(Oct)_2$ which enabled understanding the mechanistic aspects of the TMC polymerizations. The temperature range of 100–120 °C seems to play an important role as a borderline for the polymerization mechanism. At lower temperatures an alcohol-type initiator is needed for sufficiently rapid polymerizations. This initiator is incorporated into the chain and formed alkyl carbonate end-groups. Both initiation and propagation follow the pattern of the normal coordination-insertion mechanism (**Scheme 42**). At above 120 °C the TMC can obviously undergo direct insertion into the Sn-O(O)CR bond. The consequences are PTMC chains having one octanoate ester end-group per chain. Furthermore, the molecular weight can be controlled via the M/I ratio and high-molecular-weight PTMC can be obtained with short reaction times at 160 °C.

Applying $Sn(Oct)_2$ as a catalyst, PTMC of exceptionally high molecular weight ($M_n = 450\,000$) can be obtained by TMC polymerization at 130 °C for 3 days.[230] To regulate the molecular weight of PTMC appropriate amounts of alcohol should be added as initiator (e.g., hexanol).

Liao *et al.*[231] applied microwave irradiation for ROP of TMC carried out in the presence of IL (1-*n*-butyl-3-methylimidazolium tetrafluoroborate, [bmim]BF_4) using $Sn(Oct)_2$ as a catalyst. In the presence of 5 wt.% of [bmim]BF_4, PTMC with a molecular weight $M_n = 36\,400$ was obtained after only 60 min. The M_n of PTMC synthesized in the presence of [bmim]BF_4 was much higher than that obtained in bulk for the same reaction time.

Other tin-based catalysts can also be applied for the polymerization of six-membered cyclic carbonates. Kricheldorf and Stricker[232] showed that $Bu_2Sn(Oct)_2$ could be used for the ROP of TMC. Its reactivity was comparable with that of $Sn(Oct)_2$, but details of the initiation process and of the kinetic course of the polymerization were quite different. Polymerizations carried out below 100 °C were initiated by alcohols that accelerated the entire polymerization process and allowed for a control of the molecular weights. The resulting PCs contained alkyl carbonate end-groups derived from the initiator, but no octanoate end-groups. Above 120 °C the polymerizations proceeded with rapid esterification of octanoate residues yielding PCs containing nearly stoichiometric amounts of octanoate

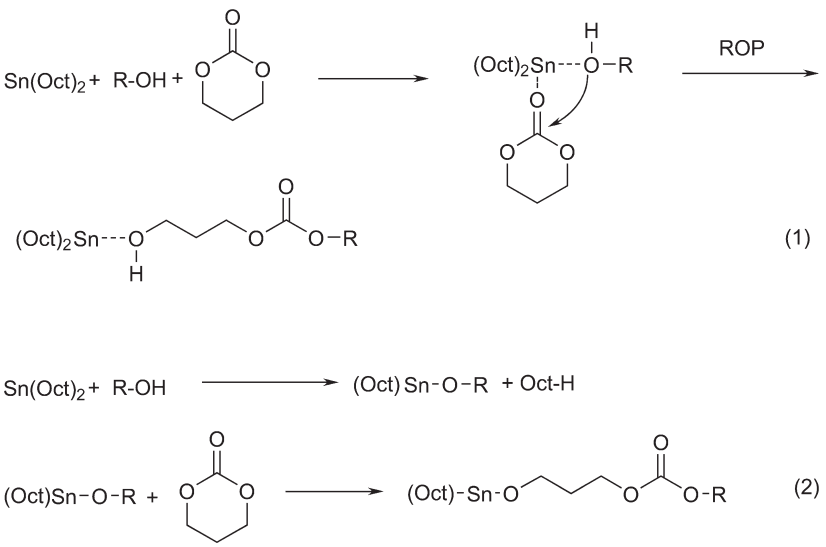

Scheme 41 Mechanisms of coordination-insertion polymerization of six-membered cyclic carbonates.

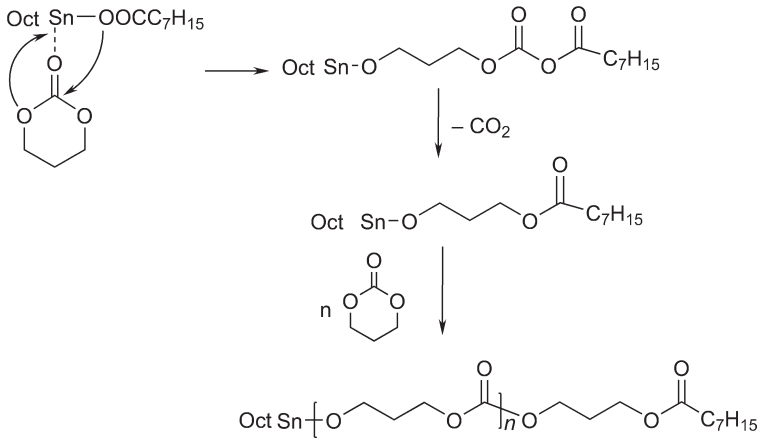

Scheme 42 Polymerization of TMC initiated with $Sn(Oct)_2$.

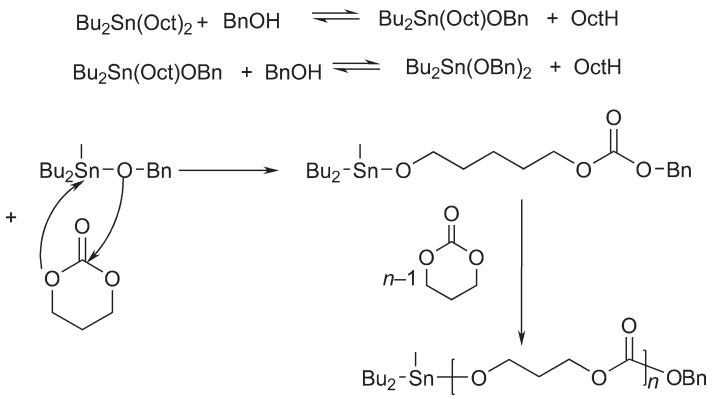

Scheme 43 Polymerization of TMC initiated with $Bu_2Sn(Oct)_2$ in the presence of benzyl alcohol.

end-groups. Model reactions between $Bu_2Sn(Oct)_2$ and benzyl alcohol suggested that no exchange occurs at temperatures below 60 °C. However, at 100 °C a slow esterification process yielding benzyl octanoate and Sn–OH groups takes place (Scheme 43). $Bu_2Sn(Oct)_2$ is a little less reactive than $Sn(Oct)_2$, but polymerization of TMC can be carried out even at 80 °C.

Kricheldorf's group demonstrated that 2,2-dibutyl-2-stanna-1,3-dioxepane (DSDOP) could be used as cyclic initiator for the polymerization of TMC (Scheme 44).[233,234] The polymerizations were either conducted in concentrated chlorobenzene solution at 50 and 80 °C or in bulk at 60 and 120 °C. With monomer/initiator ratios < 100 the conversion was complete within 2 h at 80 °C and within 12 h at 50 °C.

Variation of the reaction time revealed that the rapid polymerization was followed by a relatively rapid (backbiting) degradation even at 80 °C. With optimized reaction time the molecular weight (M_n) roughly paralleled the monomer/initiator ratio and M_ns up to 100 000 were obtained. In contrast to a classical living polymerization broader dispersity indexes (1.5–1.7) were found. In the case of neopentyl carbonate, rapid degradation and chain transfer reactions prevented the formation of high-molecular-weight polymers.

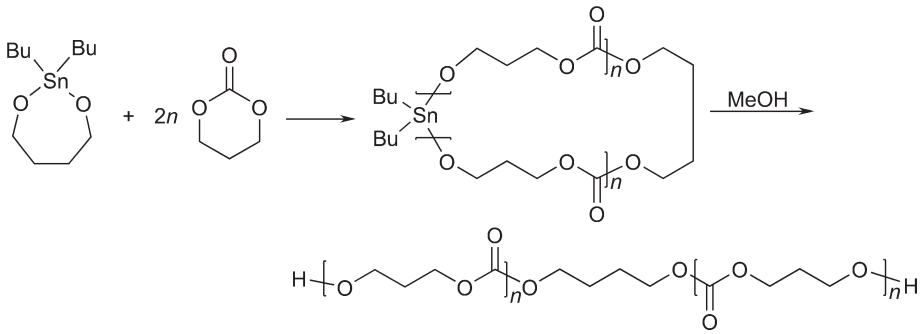

Scheme 44 Polymerization of TMC initiated with 2,2-dibutyl-2-stanna-1,3-dioxepane.

Kricheldorf's group reported that macrocyclic crystalline dibutyltin dicarboxylates (dibutyltin succinate (Bu_2SnSuc) and adipate (Bu_2SnAd)) could be prepared in high yields from Bu_2SnO and respective dicarboxylic acid.[235] It was found that these macrocycles initiated polymerization of TMC at 80 °C which proceeded faster than for $Sn(Oct)_2$ or $Bu_2Sn(Oct)_2$. The resulting PTMC did not contain succinate or adipate groups, and the molecular weight (M_n) was independent of the monomer to initiator ratio (M/I). A complete esterification and incorporation of the dicarboxylic acids took place above 120 °C, and the identification of CH_2OH end-groups suggests that a ring-expansion polymerization proceeded via the insertion of TMC into the Sn–OCH_2 bonds.

The mechanistic aspects of the coordination-insertion polymerization of six-membered neopentyl carbonate (DTC) initiated by tin(II) alkoxide-based catalysts were discussed by Rokicki *et al.*[236] ^{1}H NMR and MALDI-TOF mass spectrometric analyses of the DTC polymerization products revealed that in the presence of the stannane catalyst macrocyclic oligocarbonates are formed predominantly (**Scheme 45**). It was found that the addition of a small amount of water or diol suppresses the macrocyclization and linear PCs could be obtained. The authors suggested a plausible mechanism of macrocyclization in which the reaction proceeds via orthocarbonate species. The reaction pathway involves monomer coordination through the oxygen atom of the carbonyl group (1), cleavage of the C(O)–O bond leading to orthocarbonate species (2), and then after the rearrangement, the formation of a new tin–alkoxide bond (3) (**Scheme 45**).

4.12.3.2.3(ii) Al-based catalysts

Due to high selectivity aluminum alkoxides are frequently used for obtaining well-defined PCs. The propagation reaction is much faster than transesterification in the ROP and molecular weight is very well controlled. There are a number of aluminum alkoxides which can be prepared by reaction of triethylaluminum with selected alcohol ROH (**Scheme 46**). Thus, the choice of the end-group is very flexible. Usually an excess of triethylaluminum is used to form the monoalkoxide catalyst since the di- and trialkoxides aggregate and are less useful in the aliphatic PC or polyester synthesis. The groups involved in coordinative aggregation are not active in propagation. Significant advances in the understanding of the coordination-insertion ROP mechanism have been made through the kinetic studies by Duda and Penczek.[237,238]

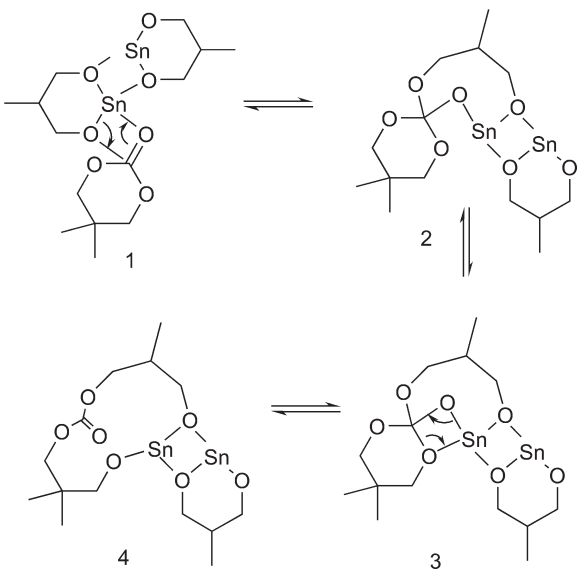

Scheme 45 Formation of cyclic oligocarbonates in the polymerization of DTC initiated with a tin(II) alkoxide-based catalyst.

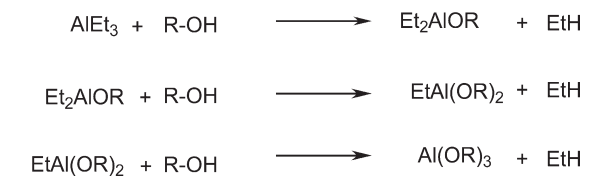

Scheme 46 Reaction of $AlEt_3$ with alcohols.

For safety reasons, residual aluminum must be removed from the material before use in food or biomedical applications. Aluminum can be efficiently extracted by ethylenediaminetetraacetic acid (EDTA) complexation.

The polymerization of neopentyl carbonate with tri-*sec*-butoxyaluminum ($Al(O\textit{sec}\text{-}Bu)_3$), diethyl zinc ($ZnEt_2$), and dibutyldimethoxytin ($Bu_2Sn(OMe)_2$) in toluene as a solvent revealed a clear distinction between the aluminum- and zinc-based catalysts on the one hand and the tin-based catalysts on the other. For the tin-based catalyst, the rates of backbiting reactions (intramolecular transesterification) and intermolecular transesterification reactions are as high as the rate of the propagation reaction, while for aluminum- and zinc-based catalysts, the rate of the propagation reaction is much higher than that of transesterification.[200] Hence, within the scope of a kinetic treatment of the polymerization of DTC with $Al(O\textit{sec}\text{-}Bu)_3$ as a catalyst, only propagation reaction must be considered.[239]

An interesting example of using an Al-based catalyst in ROP was reported by Carter *et al.*[240] Catalysts of the formula $AlEt_{3-x}(OR)_x$, where $x = 1–2$; $R = (CH_2)_2PhNO_2$, were efficient for the solution polymerization of TMC, and it was possible to obtain polymers with each chain terminated by a single nitrophenyl group ($M_n = 9500$) (**Scheme 47**). These nitro groups after reduction under mild conditions afforded amino-terminated PCs.

Florjanczyk *et al.*[241] applied a commercially available methylaluminoxane/$AlMe_3$ system for ROP of cyclic carbonates, ethers, and esters. The analysis of the end-groups by means of MALDI-TOF indicated that the polymerization was

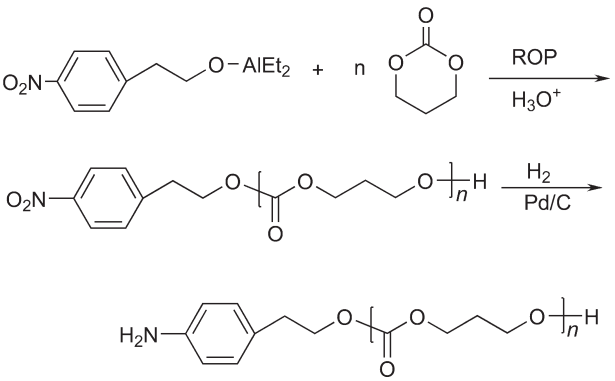

Scheme 47 Formation of amine-terminated poly(trimethylene carbonate).

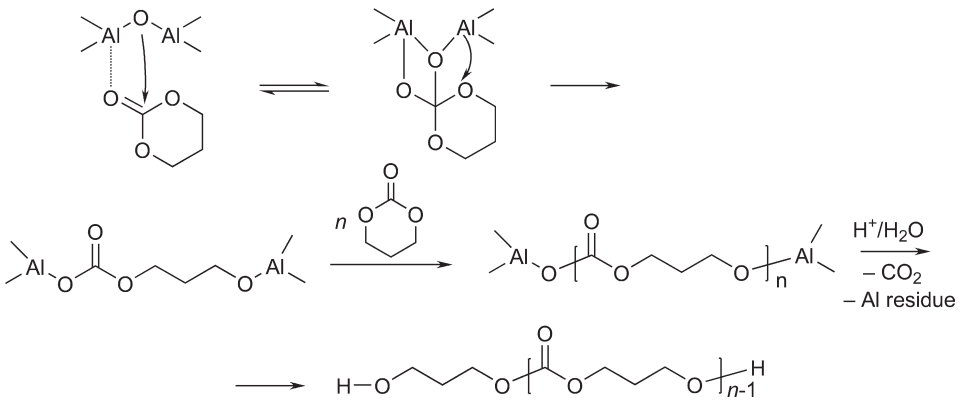

Scheme 48 Polymerization of six-membered cyclic carbonates in the presence of methylaluminoxane/$AlMe_3$ system.

initiated by insertion of a monomer into the Al–O–Al bond, generating alkoxide species, which were active sites in the coordination-insertion polymerization. The final hydrolysis of Al–O bonds was accompanied by elimination of CO_2 from the terminal carbonate units (Scheme 48). The polymerization of six-membered carbonates proceeded selectively, forming linear PC diols with high yields at moderate temperatures.

It is worth mentioning that the interaction of oxiranes with aluminoxane electrophilic sites caused also the formation of cationic species, which initiated the polymerization of THF. To prove the formation of cationic species in those systems, triphenylphosphine was used for their trapping and identification by means of ^{31}P NMR spectroscopy.

Kuran and co-workers[242] used catalysts prepared in the reaction of water with triethylaluminum or diethylzinc for the polymerization of DTC and TMC. The ROP of six-membered cyclic carbonates catalyzed with the above-mentioned compounds was an efficient method for the synthesis of low-molecular-weight PCs terminated from both sides by hydroxyl groups. The very low ether linkage content in the obtained macrodiols indicated that the propagation step occurred practically without any decarboxylation.

Darensbourg's group and Yang *et al.* have reported the use of effective salen complexes of aluminum as catalysts for six-membered cyclic carbonate polymerization.[243,244]

Yang *et al.*[244] tested two aluminum complexes with salen ligands prepared from trimethyl aluminum ($AlMe_3$), methanol, and (*R,R*)-*N,N'*-bis(salicylidene)-1,2-diaminocyclohexane as catalysts for the ROP of TMC and DTC as well as cyclic esters (Scheme 49).

The synthetic results indicated that both metal complexes efficiently catalyzed ROP at 100 °C in an anisole solution, and **2** showed much better controlled characteristics of ROP than **1** (Scheme 49).

Hovestadt *et al.*[201] indicated that the polymerization of six-membered cyclic carbonates catalyzed with porphinatoaluminum compounds like (TPP)AlOR (Scheme 50) exhibited a living character.

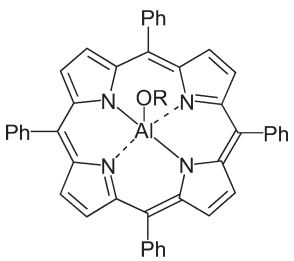

Scheme 50 Porphinatoaluminium (TPP)AlOR) catalyst used for polymerization of six-membered cyclic carbonates.

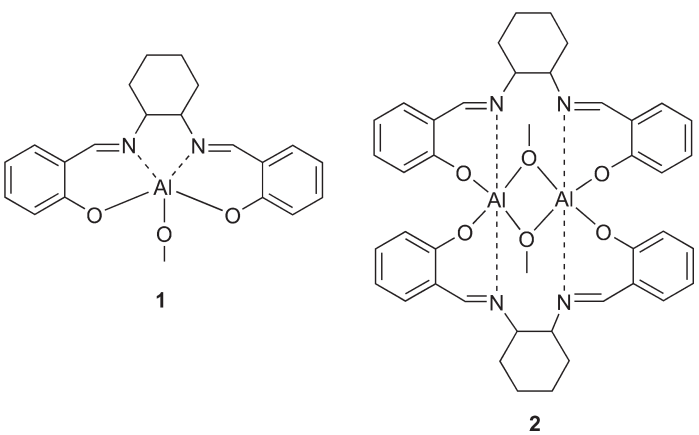

Scheme 49 Aluminum complexes with salen ligands used for polymerization of six-membered cyclic carbonates.

4.12.3.2.3(iii) Biocompatible metal-based catalysts

Taking into account that materials prepared from PTMC are mainly directed for use in medicine (tissue scaffolds, nerve regeneration) the catalyst applied for their preparation must not be toxic and harmful for a human being. Recently, special attention has been given to develop biocompatible metal-based catalysts, for example, calcium-based complexes for the ROP of cyclic carbonates or cyclic esters.[210,245]

Darensbourg *et al.*[246,247] reported that calcium, zinc, and magnesium complexes with tridentate Schiff base ligands showed good catalytic activity for ROP of TMC to produce high-molecular-weight polymers with narrow dispersity index (**Scheme 51**). In addition, these catalysts can be used for effective copolymerization of TMC with L-LA.

It is worth noticing that in these processes a cocatalyst must be present in the reaction system since these M(II) salen derivatives do not possess internal nucleophiles for the chain initiation step as is present in the M(III) derivatives, for example, (salen)AlCl.[243] For this purpose the authors applied anions (e.g., N_3^-) derived from μ-nitrido-bis(triphenylphosphine)$^+$ (PPN^+) or n-Bu_4N^+ salts. It was shown that the catalytic activity depends on a metal used in the order $Ca^{2+} \gg Mg^{2+} > C_2H_5Al^{2+} > Zn^{2+}$. The optimal appeared to be a system containing a calcium(II) salen ligand with *tert*-butyl substituents in the 3,5-positions of the phenolate rings and an ethylene backbone for the diimine grouped together with $PPN^+N_3^-$ (**Scheme 52**).

The kinetic studies revealed the polymerization reaction to be quasi-living. The activation parameters for the ROP of TMC catalyzed by (salen)Ca(II)/n-$Bu_4N^+Cl^-$ in TCE were found to be $\Delta H_p^0 = 20.1 \pm 1.0\ kJ\ mol^{-1}$ and $\Delta S_p^0 = 128 \pm 3\ J\ mol^{-1}\ K$. The ΔG_p^0 value of $58.2\ kJ\ mol^{-1}$ observed for the calcium-catalyzed process was $24.5\ kJ\ mol^{-1}$ lower in energy than that for the reaction catalyzed by an aluminum derivative ($82.7\ kJ\ mol^{-1}$).[243] This is consistent with the latter process occurring much slower under similar reaction conditions. In both instances, these activation parameters are in accordance with a reaction mechanism involving the addition of a nucleophile to a metal-bound cyclic carbonate. The mechanism involves insertion of the monomer into the growing polymer chain by breaking the acyl–oxygen bond instead of the alkyl–oxygen bond (**Scheme 53**).

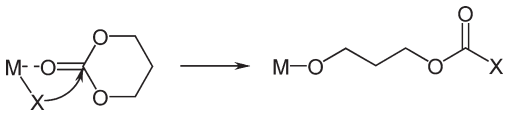

Scheme 53 Insertion of the monomer into the growing polymer chain by breaking the acyl-oxygen bond.

Also zinc lactates can be used as catalysts for ROP of TMC.[248] To shorten the reaction time the polymerization was carried out under microwave radiation and afforded PTMC of high molecular weight ($M_n = 75\,400$) after 30 min at 120 °C.

4.12.3.2.3(iv) Immortal polymerization of cyclic carbonates

Interesting results concerning ROP of TMC have been recently presented by Helou *et al.*[249] The polymerization of six-membered cyclic carbonate carried out in the presence of binary catalyst system based on Coates' zinc complex supported by a β-diiminate ligand and benzyl alcohol as a transfer agent indicated an immortal character. It was shown that this catalytic system is extremely effective; high amounts of TMC can be fully converted into PC in a controlled manner from very small catalytic amounts of the zinc complex combined with large quantities of benzyl alcohol under mild reaction conditions.

The concept of immortal polymerization was first proposed and developed in the 1980s by Inoue for the ROP of oxiranes by an Al-porphyrin/alcohol system.[250,251] In this type of polymerization, the resulting polymers are characterized by a narrow molecular distribution, even in the presence of a chain transfer reaction, because of the reversibility, which leads to the revival of the polymers once dead. As a result, immortal polymerization can afford polymers with a controlled molecular weight. The compound that plays a leading role, in the case of Inoue's system, is metalloporphyrin, in which the metal–axial ligand bond shows unusually high reactivity. Immortal polymerization was carried out in the ROP of oxiranes, by using an appropriate metalloporphyrin as the initiator and a protic compound acting as the chain transfer agent.

Helou *et al.* revealed that TMC can be efficiently polymerized in bulk at 60–110 °C in the presence of [Zn(BDI){$(SiMe_3)_2$}] (BDI = CH($CMeNC_6H_3$-2,6-iPr$_2$)$_2$) as the catalyst precursor and

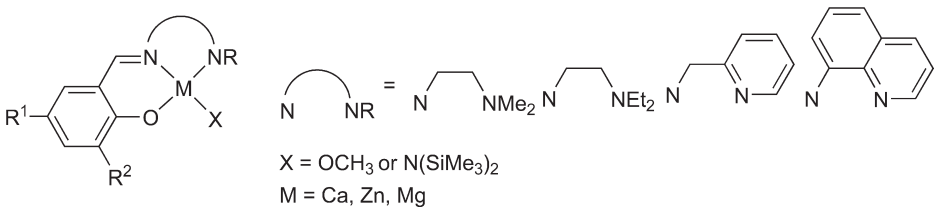

Scheme 51 Calcium, zinc, and magnesium complexes with tridentate Schiff base ligands used for polymerization of six-membered cyclic carbonates.

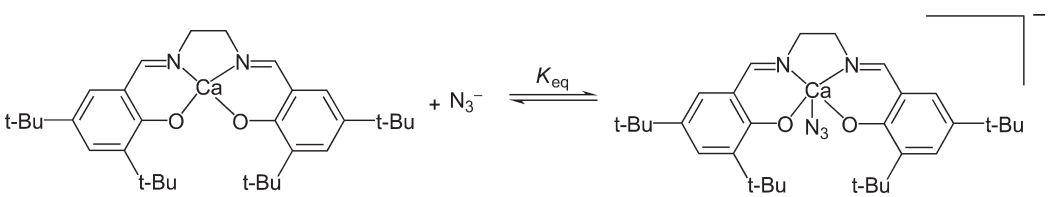

Scheme 52 Formation of the complex of calcium(II) with the salen ligand in the presence of N_3^- cocatalyst.

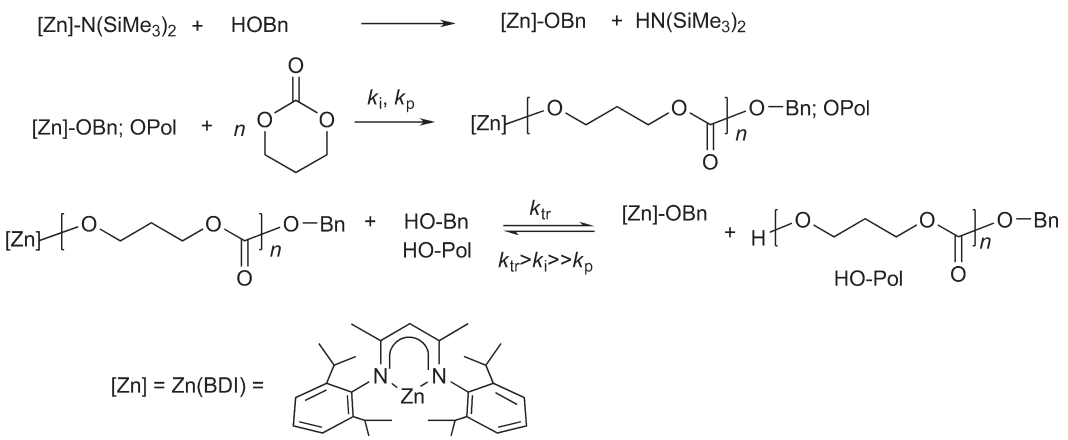

Scheme 54 Mechanism of immortal polymerization of TMC in the presence of the zinc-based binary catalyst.

benzyl alcohol (BnOH) as the transfer agent, with an initial alcohol/zinc ratio varying from 0 to 50 and a monomer/zinc loading ranging from 500 up to 50 000.[249,252,253] It was shown that this binary catalyst system was generated *in situ*, within 15 min, and there was no need for the prior synthesis of this derivative, which is a significant advantage of this method (Scheme 54).

The molecular weights determined by size exclusion chromatography (SEC) were in quite good agreement with the calculated ones, assuming that all the added alcohol molecules contribute to the immortal polymerization.

PTMC terminated with hydroxyl groups (HO-PTMC-OH) was synthesized according to the controlled immortal ROP of TMC under mild conditions (in bulk, 60 °C), using $ZnEt_2$ or $[(BDI)Zn(N(SiMe_3)_2)]$ (BDI = $CH(CMeNC_6H_3$-2,6-$iPr_2)_2$) as a catalyst precursor, in the presence of a diol HO-R-OH (R = $(CH_2)_2$ or $CH_2C_6H_4CH_2$; 0.5–10 equiv. vs. Zn) acting both as coinitiator and as chain transfer agent.[253] The versatility of this immortal ROP also allowed the preparation of star polymers such as the glycerol-based PTMC$(OH)_3$ (Scheme 55). Due to the renewable character of PPD or glycerol used as starting materials, and biometal zinc catalyst used in very small amounts, PTMC obtained according to this method can be considered a 'green' PC.

Dobrzynski *et al.*[254] tested less toxic metal acetylacetonates (Zn(II), Fe(III), and Zr(IV)) as efficient catalysts of trimethylene and neopentyl carbonate polymerization. The reaction carried out at 110 °C with the use of these catalysts was very rapid and of high yield. Using both zinc(II) and iron(III) acetylacetonates, as well as the zirconium(IV) one, at high temperatures it was possible to obtain PC of high molecular weight (M_n = 190 000). It should be underlined that zirconium derivatives are 10 times less toxic than their tin counterparts and Zr-containing drugs and cosmetics are accepted by the FDA.[255] A disadvantage of this method may be a strong influence of thermal degradation on the course of the reaction, particularly at 160 °C. The DTC polymerization proceeded much slower when catalyzed by iron and zinc acetylacetonates. The relation between the molecular weight of the PC and the conversion of the monomer is directly proportional, indicating the living polymerization mode. Dobrzynski explained the reason for low-molecular-weight PTMC formation at 110 °C when $Zr(Acac)_4$ was used as a catalyst. In contrast to cyclic carbonates, at the stage of the initiation of lactide polymerization, the reaction of deprotonation of the monomer and charge transfer of the proton to the acetylacetonate ligand take place. As a result, the exchange of ligands with the release of free acetylacetone occurs. The complex obtained in this way is the

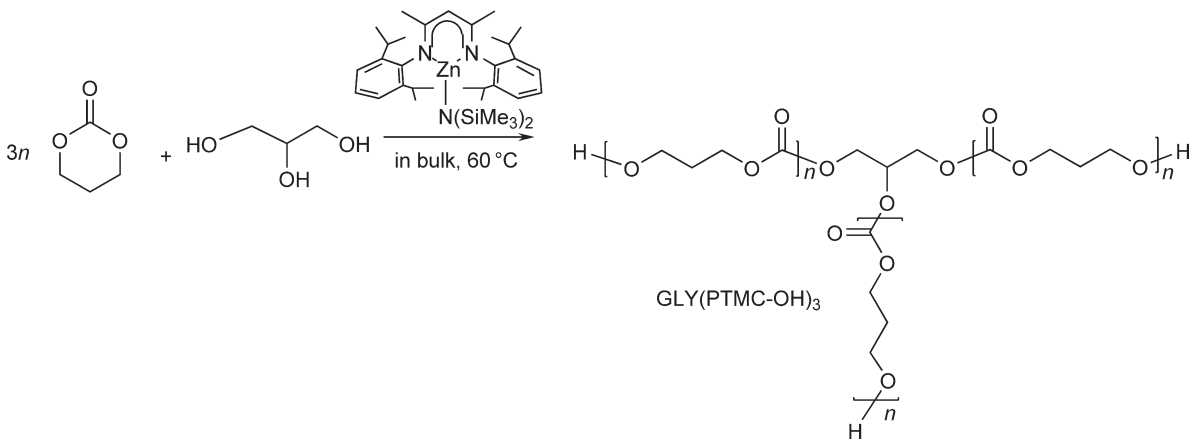

Scheme 55 Preparation of glycerol-based poly(trimethylene carbonate) star polymer by the immortal polymerization of TMC.

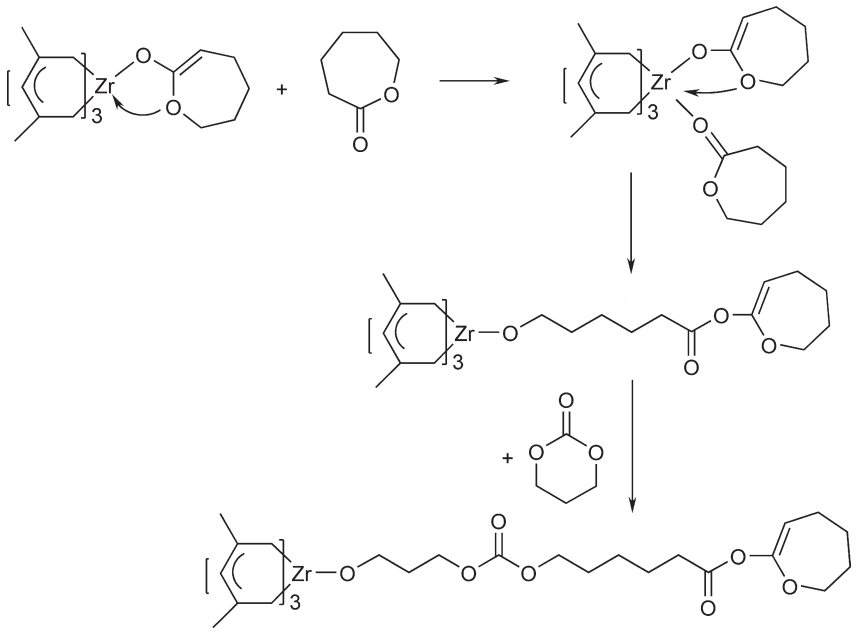

Scheme 56 ε-CL acting as coinitiator in ROP of TMC in the presence of $Zr(Acac)_4$.

actual initiator of the polymerization. In the case of polymerization of TMC, the deprotonation of the monomer does not occur as easily as it does during the polymerization of lactide or glycolide (GL). The author indicated that when CL was added to the system containing TMC and $Zr(Acac)_4$ CL monomer acted as a coinitiator in ROP of TMC and high-molecular-weight PTMC could be obtained at 120 °C (Scheme 56).[256,257]

As was presented by Darensbourg *et al.*,[258] chromium(III) Schiff base catalyst was also active in TMC polymerization. Moreover, chromium(III) salen derivatives in the presence of anionic initiators have been shown to be very effective catalytic systems for the alternating copolymerization of oxetane and carbon dioxide to provide the corresponding PC with a minimal amount of ether linkages. The best results were achieved for the salen ligand with *tert*-butyl groups in the 3,5-positions of the phenolate rings and a cyclohexylene backbone for the diimine along with an azide ion initiator (Scheme 57).

For the reaction catalyzed by (salen)CrCl in the presence of $n\text{-}Bu_4N^+N_3^-$ as the initiator, both MALDI-TOF spectrometry and infrared spectroscopy revealed an azide end-group in the copolymer.[259,260] The formation of the copolymer is shown to proceed in part by way of the intermediacy of TMC (pathway 2, Scheme 58), which was observed as a minor product of the coupling reaction, and by the direct enchainment of oxetane and CO_2.

The determined free energies of activation for these two reactions, namely 101.9 kJ mol^{-1} for ROP of TMC and 107.6 kJ mol^{-1} for copolymerization of oxetane and carbon dioxide, support this conclusion.

4.12.3.2.3(v) Rare earth catalysts

A large variety of rare earth derivatives have been used to initiate ROP of cyclic carbonates. Their usually high reactivity must be emphasized, as exemplified by the polymerization of TMC with $Ln(OAr)_3$ (Ln = Lanthanide = f-block elements) under mild conditions, in contrast to the long reaction time and high temperature required when tin-based or aluminum-based catalysts were used. As rare earth metals La (lanthanum), Ce (cerium), Nd (neodymium), Sm (samarium), Gd (gadolinium), Dy (dysprosium), Er (erbium), Yb (ytterbium), Sc (scandium), and Y (yttrium) are most often applied.[261]

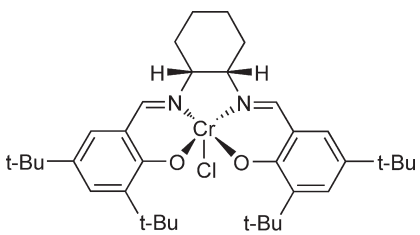

(salen)CrCl catalyst

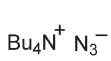

cocatalyst

Scheme 57 Structure of salen-based catalyst.

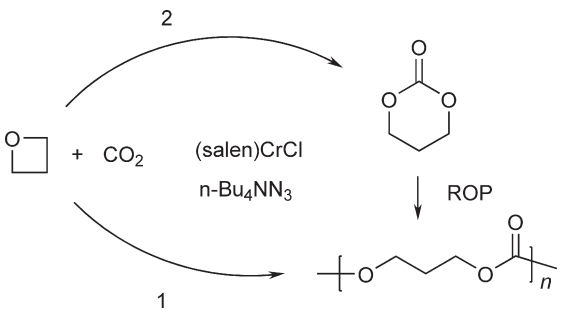

Scheme 58 Copolymerization of an oxetane and CO_2 catalyzed by a (salen)CrCl catalyst.

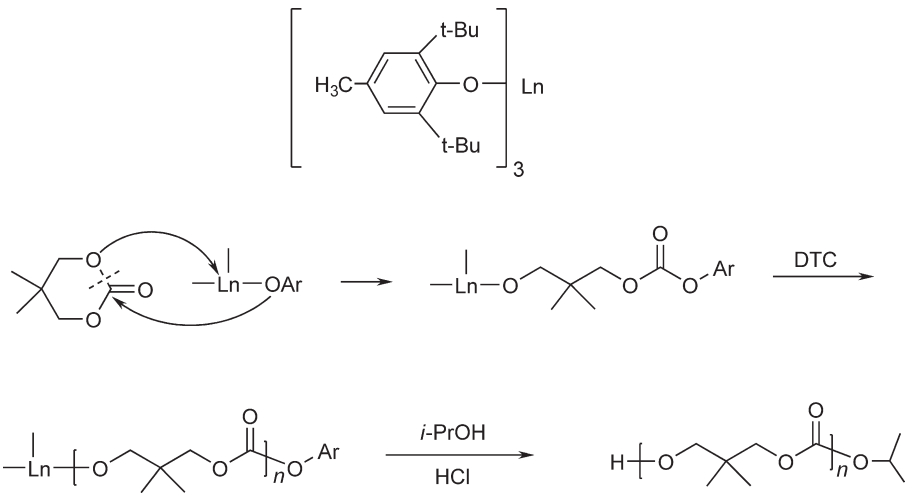

Scheme 59 Polymerization of DTC via an acyl–oxygen bond cleavage in the presence of a lanthanide catalyst.

ROP of cyclic carbonates using lanthanide alkoxide-based initiators is a relatively recent discovery. The first example of lactone polymerization by lanthanide alkoxide complexes was reported in a DuPont patent written by McLain and Drysdale in 1991.[118] Polymers of relatively high molecular weight and narrow dispersity index were formed. However, the disadvantage of these catalysts is the formation of macrocycles.

Shen *et al.*[262] first used lanthanide catalyst for the polymerization of TMC in 1996. Most often rare earth tris(2,6-di-*tert*-butyl-4-methylphenolate)s [$Ln(OAr)_3$] isopropoxide [$Ln(OiPr)_3$] were used as single-component catalysts for the cyclic carbonate and lactone polymerization (**Scheme 59**).[263–265]

The catalysts were highly active in both homopolymerizations of DTC, TMC, and CL and random copolymerizations of DTC with CL and TMC. The polymerization of these monomers proceeded via the same route of an acyl–oxygen bond cleavage in heterocyclic rings (**Scheme 59**). The catalytic activities of various $Ln(OAr)_3$ systems decreased in the following order: La > Nd > Dy ≈ Y.

Very recently, Zhang *et al.*[266,267] investigated single-component rare earth aryl oxides substituted by various alkyl groups such as methyl, isopropyl, and *tert*-butyl used to initiate the ROP of neopentyl carbonate. The experimental results revealed that the catalytic activity of $Ln(OAr)_3$ changes in good concordance with variation of ligands' structure and number of alkyl groups on benzene ring. The greater the ability of electron donation of alkyl groups, the greater the catalytic activity. Moreover, the greater the number of substituted alkyls on benzene ring, the greater the catalytic activity. Thus, the rare earth tris(2,4,6-tri-*tert*-butylphenolate)s [$Ln(OTTBP)_3$] exhibits greatest activity in all lanthanide aryl oxides. The catalytic activity was in the order La > Sm > Gd > Dy > Er, which is in accordance with the results obtained for one-component rare earth metal catalysts.

Bisphenolate lanthanide (Ln = Nd or Yb) methoxide complexes (**Scheme 60**) were also active in ROP of cyclic carbonates as was revealed by Xu *et al.*[268]

In polymer synthesis, calixarenes – cyclic phenol–formaldehyde oligomers – are rarely studied and reported. There are two main applications of calixarenes in polymer synthesis: use of metal calixarene complexes as catalysts for polymerization and star-shaped polymers with a calixarene core.

Calixarene complexes with lanthanides have been developed to catalyze the homopolymerization of TMC and DTC. The complexes were synthesized from lanthanide isopropoxide and appropriate *p-tert*-butylcalix[*n*]arene (*n* = 4, 6, and 8). Based on the polar solvent effect, the end-group examination of the polymers, and NMR analyses of the growing chain, it could be concluded that the polymerizations of TMC and DTC initiated by p-*tert*-butylcalix[*n*]arene (*n* = 4, 6, and 8) complexes of Nd, La, and Y proceeded by a coordination-insertion mechanism.[269–271] Gou *et al.*[272] used scandium p-*tert*-butylcalix[6]arene complex as a single-component catalyst for ROP of cyclic carbonates. The polymerization of neopentyl carbonate using this complex proceeded under mild

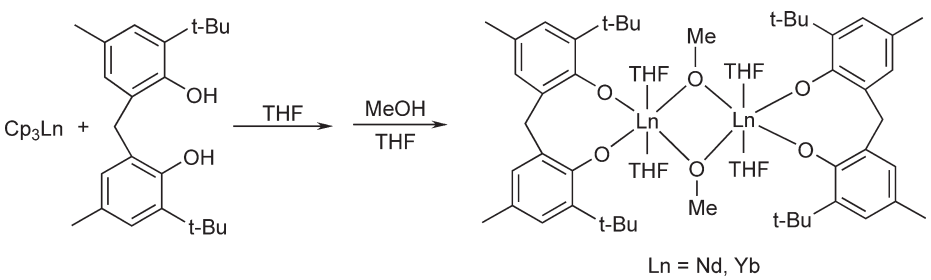

Scheme 60 Structure of bisphenolate lanthanide methoxide complexes active in ROP of cyclic carbonates.

conditions. Poly(neopentyl carbonate) with $M_w = 33\,700$ and dispersity index of 1.21 was prepared. Kinetics study indicated that the polymerization rate was of first order with respect to both monomer and initiator concentrations, and the apparent activation energy of the polymerization was 22.7 kJ mol^{-1}. Instead of phenolate, Li *et al.*[273] applied samarium thiolate derivatives as catalysts for neopentyl carbonate polymerization.

Sheng *et al.*[274] proposed to use the anionic lanthanide-sodium-2,6-di-*tert*-butylphenoxide complexes $[Ln(OAr)_4][Na(DME)_3]\cdot DME$ (Ln = Nd, Sm, or Gd; DME = dimethoxyethane) for the polymerization of cyclic carbonate (TMC) and lactone (CL). The anionic lanthanide complexes were synthesized by the reaction of anhydrous $LnCl_3$ with 4 equiv. of sodium-2,6-di-*tert*-butylphenoxide in high yields. These complexes showed high catalytic activity in the ROPs of TMC and CL. The catalytic activity significantly depended on the lanthanide metals. The active order of Nd > Sm > Gd for the polymerization of TMC was observed. It is worth noting that the anionic complex was more efficient than the corresponding neutral complex, $Ln(OAr)_3(THF)_2$.

Also other alkoxide clusters of lanthanide and sodium, $Ln_2Na_8(OCH_2CF_3)_{14}(THF)_6$, $LnNa_8[OC(CH_3)_3]_{10}(OH)$, and $[Ln_2Na_8(OCH_2CH_2NMe_2)_{12}(OH)_2]$ (Ln = Sm, Y, Nd, Yb), were found to be highly active single-component catalysts for the ROP of TMC.[275–277] These cluster activities were much higher than monometallic alkoxide lanthanides. Homoleptic lanthanide amidinate complexes also indicated high activity for the ROP of TMC, giving polymers with $M_w/M_n = 1.41–1.73$.[278–280] There are two methods of obtaining a homoleptic guanidinate lanthanide complex. The samarium guanidinate complex $[Sm\{Ph_2NC(NCy)_2\}_3]\cdot 2C_7H_8$ was synthesized by the metathesis reaction of lithium guanidinate with anhydrous samarium trichloride in a 3:1 molar ratio. The analogous complexes $[Ln\{Ph_2NC(NCy)_2\}_3]\cdot 2C_7H_8$ [Ln = Yb, Nd] were synthesized by the insertion reaction of *N,N′*-dicyclohexylcarbodiimide into the Ln–N bond of $[(THF)_4Li][Ln(NPh_2)_4]$ in a 3:1 molar ratio in good yield.

Palard *et al.*[281] used samarium borohydride complexes $[Sm(BH_4)_3(THF)_3]$ for the ROP of TMC. This catalyst showed high activity to give high-molecular-weight PTMC with M_w/M_n ranging from 1.2 to 1.4 and with a regular structure without ether linkages (Scheme 61). The rare earth borohydride complex $[Sm(BH_4)_3(THF)_3]$ was an efficient initiator for the controlled ROP of TMC at ambient temperature to form α-formate-ω-hydroxy telechelic PTMC. ^{1}H and ^{13}C NMR analyses, especially of the PC chain ends, idicated that the synthesis of such a formate end-functionalized polymer relies on the intrinsic reactivity of the samarium-bound borohydride ligand, which does not reduce the –O–C(O) – carbonyl and which is eliminated as $BH_3\cdot THF$ (Scheme 61).

Agarwal and Puchner[282] used commercially available, easy to synthesize rare earth cyclopentadiene (CP_3) complexes as catalysts for TMC and cyclic ester polymerization to afford high-molecular-weight polymers. Using these catalysts the PC was obtained in a quantitative yield with moderate dispersity index (1.6–2.1). Rare earth metal cyclopentadienyl complexes ($LnCp_3$; Ln = Ce, Pr, Sm, Gd, and Er) irrespective of their size acted as ROP catalysts for TMC polymerization giving high-molecular-weight PTMC ($M_n \approx 20\,000$) at 78 °C for 1 h. The ^{1}H NMR spectrum of PTMC showed the presence of only two peaks at 4.2 and 1.95 ppm. The absence of peaks between 3.1 and 3.3 ppm clearly indicated the absence of ether units which are generally formed as defects in the polymer structure by cationic polymerization of TMC by elimination of CO_2.

4.12.3.2.4 Enzymatic polymerization of aliphatic cyclic carbonates

Many bacteria synthesize, accumulate, and deposit aliphatic polyesters in their cells. The high stereoselectivity of the enzymatic synthesis produces as a rule polyesters with high crystallinity which have attracted a great deal of attention during the last few years.[81,283,284] The enzymatic ROP of δ-valerolactone (VL) and CL was first conducted using lipase as a catalyst.[285]

On the other hand, it is known that the introduction of carbonate groups into the polymer chain leads to improving the mechanical properties of biodegradable polyesters.[286] The carbonate linkage in the aliphatic polymer chain may be expected to be enzymatically hydrolyzable and more hydrolytically stable than an ester linkage. The copolymerization of

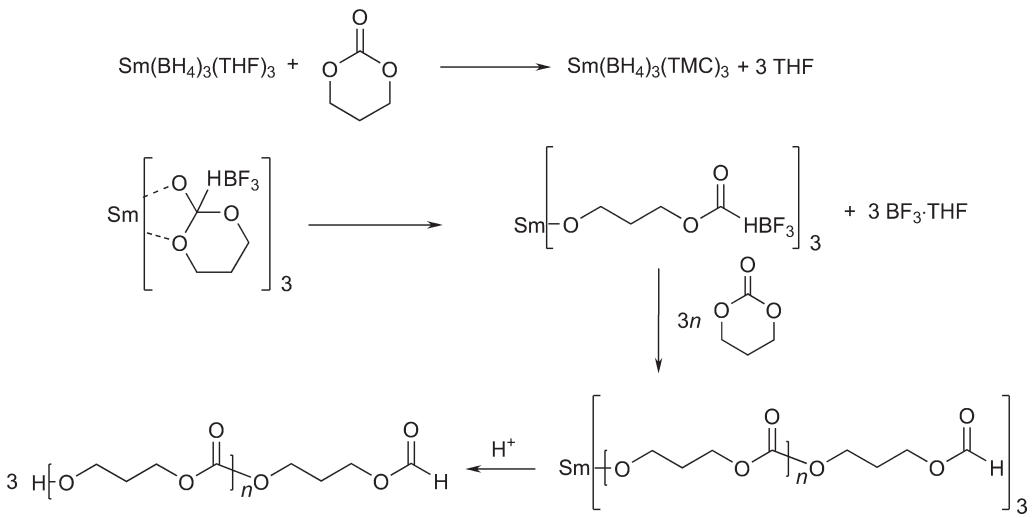

Scheme 61 Polymerization of TMC initiated with samarium borohydride complexes.

cyclic lactones and carbonates needs pure monomers and anhydrous conditions as well as organometallic catalysts, which must be completely removed before use in medical applications.

In contrast to chemical methods, enzyme-catalyzed polymerization of six-membered cyclic esters and carbonates seems to be the practicable method avoiding the above-mentioned difficulties. Kobayashi *et al.*[287] for the first time have shown that lipase not only catalyzes the hydrolysis of esters and carbonates[288] but can initiate ROP. Enzymatic ROP of a six-membered cyclic carbonate, 1,3-dioxan-2-one, was investigated by using lipase as catalyst in bulk.

Similarly, supported lipase derived from *Candida antarctica* catalyzes the polymerization to give the corresponding aliphatic PC. Bisht *et al.*[289] have also directed studies on extending the use of lipase-catalyzed ROP to cyclic carbonate monomers. From several lipases screened for bulk TMC polymerization (70 °C, 120 h), Novozym-435 (*C. antarctica*) gave almost quantitative monomer conversion (97%) and PTMC with a $M_n = 15\,000$ ($M_w/M_n = 2.2$) and with no decarboxylation during propagation. The lipases from *Pseudomonas* species (AK and PS-30) and 'porcine pancreas' (PPL) also exhibited high monomer conversions (80%, 120 h) but gave lower molecular weight polymers with broad dispersity. Analyses by ^{1}H NMR spectroscopy suggested that PTMC prepared by Novozym-435-catalyzed polymerization had terminal $-CH_2OH$ functionalities at both chain ends. Novozym-435-catalyzed TMC bulk polymerization at 70 °C has chain-type propagation kinetics. The highest PTMC molecular weight $M_n = 24\,400$ was obtained by conducting the polymerization at 55 °C. The reaction temperature increase led to lower molecular weight (at 85 °C, 6000). Increasing the water content resulted in enhanced polymerization rates and decreased molecular weights. It is proposed that the polymerization rates increase due to an increase in the number of propagating chain ends.[290] Separation of the oligomeric products from the polymerizations of TMC in dried dioxane and toluene catalyzed by PPL led to the isolation of di- and triaducts of TMC.

Bisht *et al.*[289] proposed a mechanism for chain initiation and propagation for lipase-catalyzed TMC polymerization, based on the symmetrical structure of these products and the end-group structure of high-molecular-weight chains (**Scheme 62**).

In contrast to the results obtained by Bisht and co-workers, Matsumura *et al.*[291] asserted that no polymerization of TMC took place when lipase Novozym-435 was used at 100 °C, while PPL showed the best results with respect to the monomer conversion and the molecular weight of the PC. TMC readily polymerized in bulk in the presence of PPL yielding a PC with M_w of up to 170 000 at 100 °C after 24 h. The enzymatic polymerization of TMC was significantly enhanced by the immobilization of PPL on diatomaceous earth (Celite).

This apparent contradiction is probably caused by the different reaction temperatures applied and different water content.[287] At 100 °C the lipase Novozym-435 seemed to be inactive and at lower temperatures (55–60 °C) exhibited the highest activity in the ROP of TMC among the tested enzymes.

The higher activity of lipase Novozym-435 over PPL was also confirmed by Deng *et al.*[292] in the study of lipase-catalyzed ring-opening copolymerization of CL and TMC. An increase in the lipase concentration in CL and TMC polymerization led to higher initial rates of conversion. In contrast, the M_n decreased at the same level of conversion with increasing catalyst concentration.

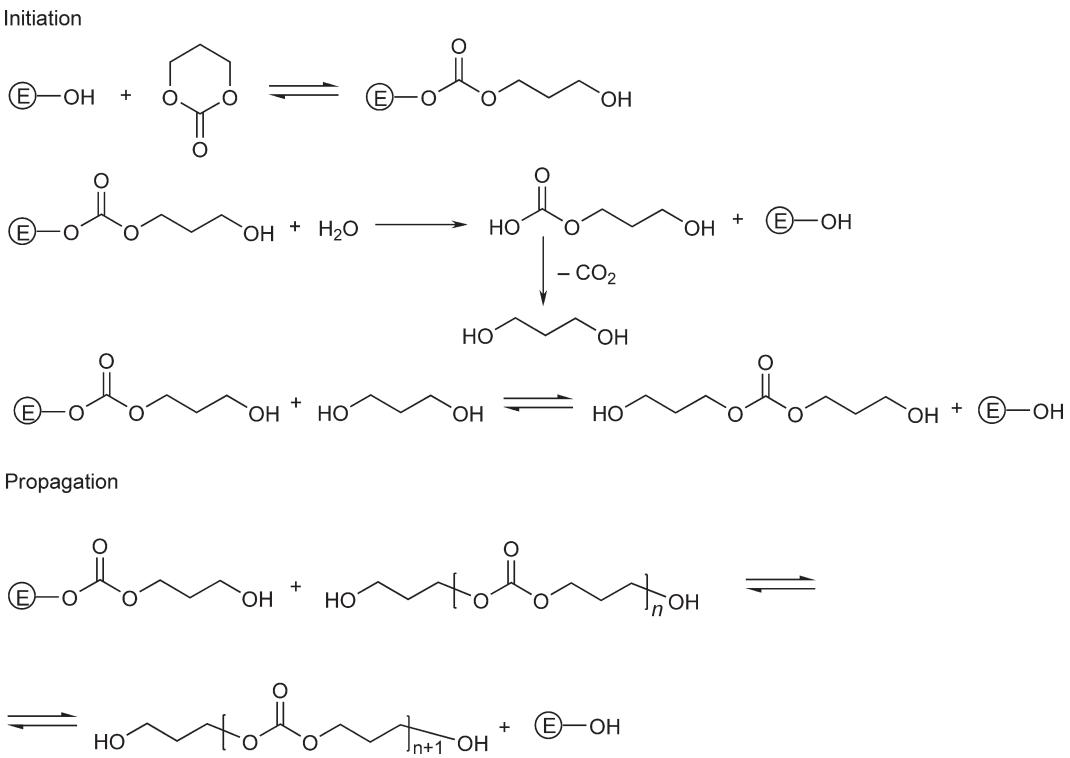

Scheme 62 Mechanism of chain initiation and propagation for lipase-catalyzed TMC polymerization.

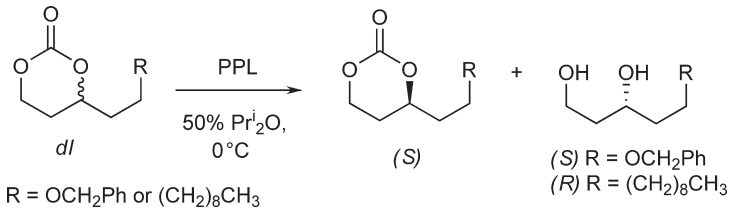

Scheme 63 Enantioselective hydrolysis of substituted cyclic carbonate in the presence of PPL and water.

It is suggested that for higher activity some amount of water should be present in lipase.[289,290,293] However, higher concentration of water and suitable pH leads to enantioselective hydrolysis of substituted cyclic carbonate. The reaction of a six-membered cyclic carbonate, 4-(2-benzyloxyethyl)-1,3-dioxan-2-one, with PPL in phosphate buffer containing 50% of iPr$_2$O at 0 °C proceeded enantioselectively to afford optically active (*S*)-4-(2-benzyloxyethyl)-1,3-dioxan-2-one and (*S*)-5-benzyloxypropane-1,3-diol (**Scheme 63**).[288]

As earlier mentioned, catalytic activity of an enzyme can be increased by immobilization. According to Feng *et al.*,[294] synthesis of PTMC using PPL immobilized on silica particles gave polymers of M_n = 87 400 with M_w/M_n = 2.06. PPL and PPL immobilized on narrow distributed micron-sized glass beads were also employed successfully for the ROP of DTC.[295] Immobilized PPL exhibited higher activity than native PPL. Along with the increasing enzyme concentration, the molecular weight of resulting polymer decreased. Immobilized PPL showed outstanding recyclability even after the fifth recycle time for the synthesis of PDTC. The ^{1}H NMR spectra showed no evidence of decarboxylation during the ROP. Similar results were obtained by the ROP of DTC with free and silica-immobilized PPL. Heating of the monomer with the immobilized catalyst (1 wt.%) at 120 °C for 4 days gave a polymer of M_n = 15 700 (M_w/M_n = 1.4) with 85% yield.[296] Even better results including higher molecular weight (M_n = 26 200, M_w/M_n = 1.33) and PC yield (97.6%) could be achieved by second recycling of supported catalyst.

Large ring size cyclic carbonate cyclobis(decamethylene carbonate) was also polymerized using Novozym-435 as a catalyst in toluene.[297] Novozym-435 exhibited higher catalytic activity compared with Sn(Oct)$_2$ and high molecular weight (M_n) up to 54 100 was easily obtained. ^{1}H NMR spectra clearly demonstrated the existence of a terminal hydroxyl group, suggesting that the trace water may act as a substrate in the initiation process during the polymerization. Also solid phase polymerization in the absence of toluene unexpectedly took place at 75 °C below the melting point of macrocyclic monomer. Compared with six-membered TMC, much lower reaction activity was observed.

In addition to homopolymers a number of copolymers of cyclic carbonates were synthesized by enzymatic ROP. Among them are amphiphilic block copolymers of PBTMC and PEG which were synthesized through enzymatic polymerization using immobilized *porcine pancreas* lipase (IPPL).[298] The copolymerization of ω-pentadecalactone (PDL) and TMC was also studied by using lipase catalysts.[299] Of the six lipases evaluated for PDL/TMC copolymerizations in toluene at 70 °C, an immobilized form of lipase-B from *C. antarctica* (Novozym-435) was preferred. Changing the PDL/TMC comonomers feed ratio from 1:10 to 10:1 (mol:mol) provided copolymers that ranged in M_n and PDL mol.% from 7300 to 25 200 and 28–88, respectively. It was also noticed that in contrast to the chemical catalyst systems, Novozym-435 catalysis showed that PDL was consumed more rapidly than TMC. Also copolymers from Novozym-435 catalysis were characterized by random distribution of the repeating units at extended reaction times. Enzymatic ring-opening copolymerization of 5-methyl-5-benzyloxycarbonyl-1,3-dioxan-2-one (MBC) with TMC performed in the presence of *Pseudomonas fluorescens* (AK) gave polymers of random distribution of repeating units.[300] This copolymer was further used for the preparation of aliphatic PCs with pendant carboxylic acid groups.

Poly(TMC-*co*-ethylene ethyl phosphate) was prepared by ring-opening copolymerization catalyzed by lipase enzymes (pancreas lipase, PPL and *Candida rugosa* lipase, CL) as catalysts in bulk at 100 °C with molecular weight (M_n) from 3200 to 10 200.[301] Degradation experiments showed that introducing phosphate groups into the TMC chain increases the hydrolysis rate of the copolymer.

Taking into consideration that aliphatic PCs and poly (ester-carbonate)s seem to be potential biodegradable or bioabsorbable materials, special interest has been devoted to the so-called biocompatible initiators, which are part of the human metabolism. Hematin, an insoluble pigment formed from the breakdown of hemoglobin, is an example of an enzyme-type initiator used in the polymerization of heterocyclic monomers. In 1993, Kricheldorf and Boettcher[302] used hematin in the polymerization of cyclic esters: L, L- and L,D-dilactides. Hematin was also utilized in the polymerization of TMC and DTC.[212] The polymerization was conducted in bulk at 100 °C, but high yield and high molecular weights (up to 75 000) were obtained only for unsubstituted 1,3-dioxan-2-one. No polymerization was observed for the reaction carried out in toluene, even at 100 °C. The hematin molecule possesses two types of functional groups: the Fe–OH group and three carboxyl groups, which can react with cyclic carbonate. The postulated insertion mechanism involves initiation by the Fe–OH group and subsequent alkoxide formation with CO_2 evolution (**Scheme 64**).

From the point of view of biodegradability it is important that enzymes can be useful both in the synthesis of polymers and their degradation back to cyclic carbonate monomers. TMC was produced by the enzymatic degradation of PTMC using lipase as the chemical recycling product.[303] The enzymatic degradation of PTMC having an M_n of 3000–48 000 using *C. antarctica* lipase (CAL) in acetonitrile at 70 °C afforded the corresponding cyclic monomer, TMC, in a yield of up to 80%. Thus the obtained TMC was readily polymerized again by lipase (**Scheme 65**). This method may be useful in establishing a novel methodology for sustainable polymer recycling.

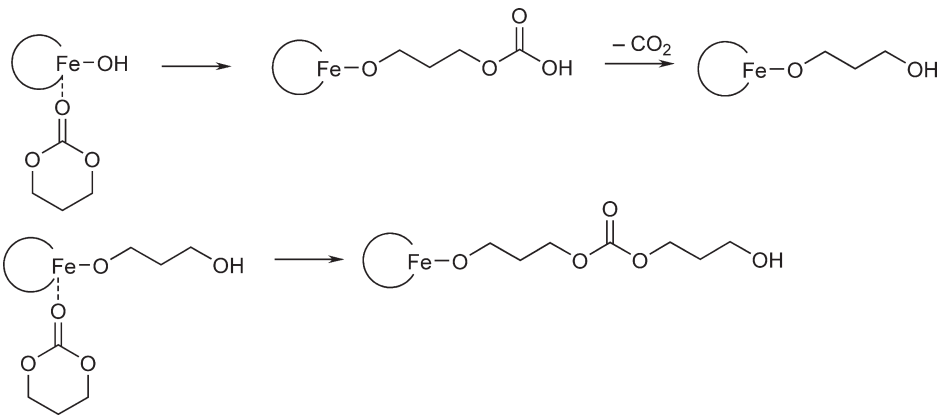

Scheme 64 Postulated TMC polymerization mechanism involving initiation with the hematin Fe–OH group and subsequent alkoxide formation with CO_2 evolution.

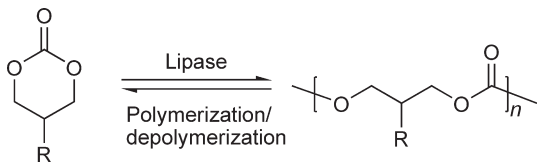

Scheme 65 Lipase-catalyzed reactions of preparation of polycarbonates and their depolymerization.

The ROP of cyclic carbonates initiated by enzyme or enzyme-like species in which PCs terminated by hydroxyl groups are obtained seems very attractive, especially for the production of polyurethanes for medical application.

4.12.3.2.5 Polymerization of six-membered cyclic carbonates bearing functional groups

Polymerization of six-membered cyclic carbonates bearing functional groups, due to great reactivity and lack of CO_2 elimination, is the preferable way for preparation of functionalized PCs. Table 2 collects recently synthesized cyclic carbonates with respective literature references.

There are several methodologies used in the preparation of functionalized six-membered cyclic carbonates. The first one uses 2,2-bis(hydroxymethyl)propionic acid as a starting material[304–307] or its longer chain analogs (Scheme 66).[317]

Table 2 Chemical structures of six-membered cyclic carbonates bearing functional groups

	Chemical structure	*References*
1	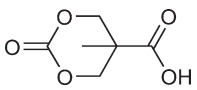	304
2	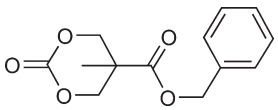	305
3	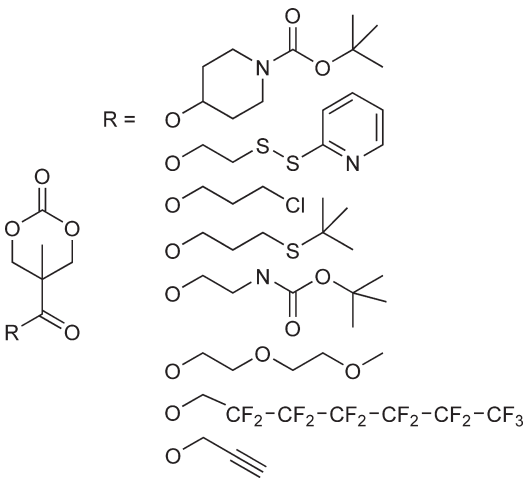	306

(*Continued*)

Table 2 (*Continued*)

	Chemical structure	*References*
4	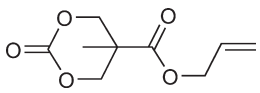	307
5	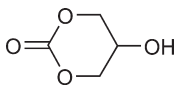	308
6	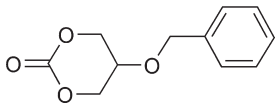	216,309,310
7	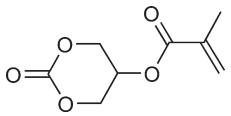	308
8	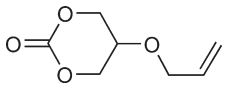	311,312
9	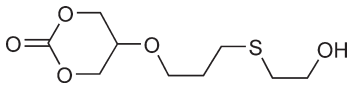	313
10	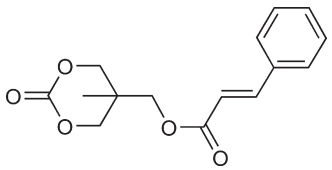	314
11	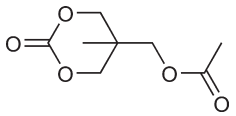	103
12	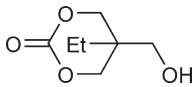	315
13	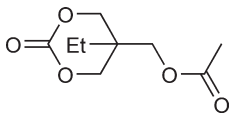	103
14	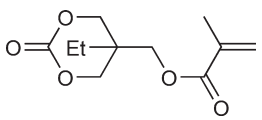	316
15	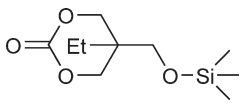	315
16	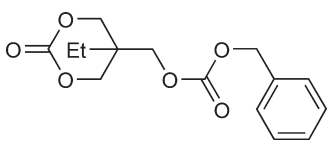	315

(*Continued*)

Table 2 (*Continued*)

	Chemical structure	*References*
17	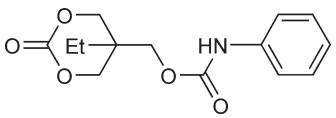	315
18	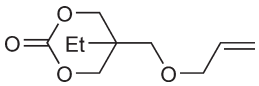	198
19	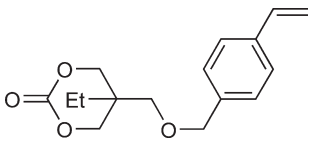	317
20	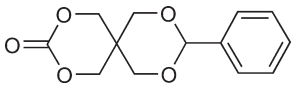	318
21	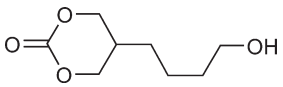	308,319
22	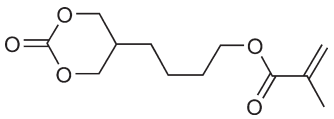	308
23	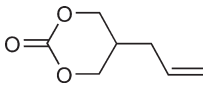	320
24	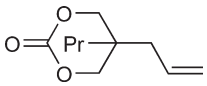	321
25	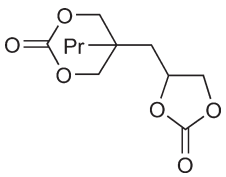	321
26	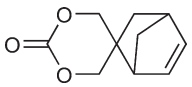	322–324
27	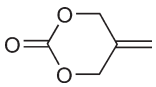	322

Scheme 66 shows a method of synthesis of a versatile synthon for a family of functionalized carbonated monomers. In the first step the benzyl ester of 2,2-bis(hydroxymethyl) propionic acid is formed, which is then converted into cyclic carbonate with triphosgene. Debenzylation is performed using hydrogen with palladium catalyst. Two procedures for the coupling of cyclic carbonate bearing carboxylic group to alcohols are used: either direct coupling using dicyclohexane carbodiimide (DCC) or conversion to the acyl chloride using oxalyl chloride followed by reaction with the alcohol or amine in the presence of base. The latter method has the advantage that the salt by-products are easily removed. Compared with methods wherein the functional group is attached prior to carbonate formation, the inverse sequence shown here more generally requires only a single unique reaction and purification step. Using these methods, a range of functional groups could be incorporated to generate new ROP carbonate monomers offering opportunities for coupling via substitution, cycloaddition, and amide or disulfide linkages or for introducing strongly hydrophilic or hydrophobic groups (Table 2).

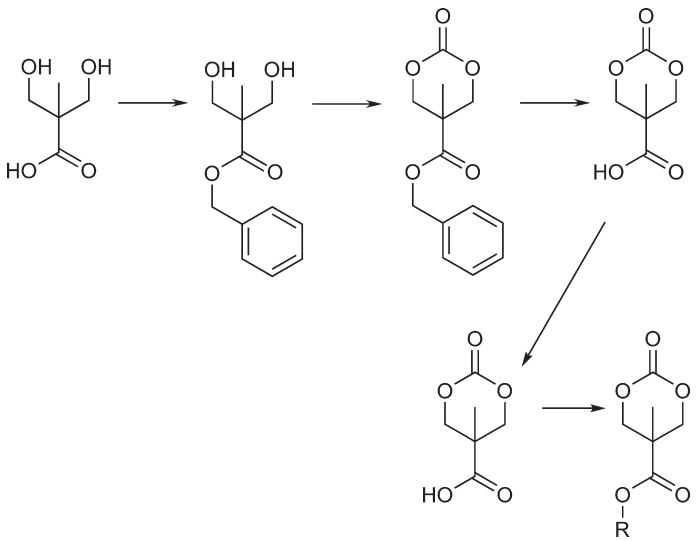

Scheme 66 Synthetic pathway towards 2,2-bis(hydroxymethyl)propionic acid-based functionalized cyclic carbonates.

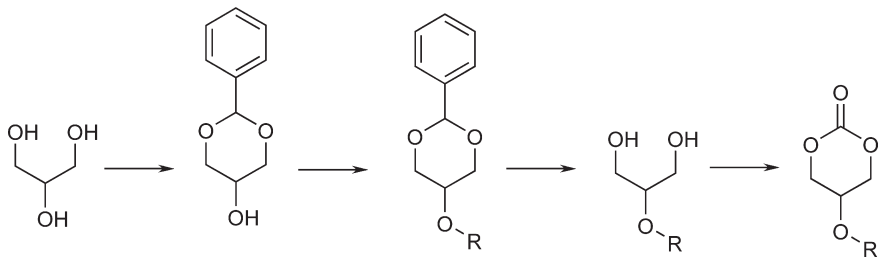

Scheme 67 Synthetic pathway towards glycerol-based functionalized cyclic carbonates.

In the second methodology glycerol is used as a starting material. Differentiation of glycerol hydroxyl groups can be achieved by cyclic acetal formation (Scheme 67).[216,308–313]

In this process benzaldehyde is commonly used in the reaction with glycerol. Acetal (5-hydroxy-2-phenyl-1,3-dioxan) can be isolated from a mixture of products by crystallization from cold ethyl ether. It crystallizes in the *cis* conformation. Then the secondary hydroxyl group can be transformed to the desired functional group. In the end, the protective acetal group is removed under acidic conditions and the cyclic carbonate is formed in the reaction with alkyl chloroformate. Because of the high reactivity of carbonate bonds in the cyclic structure, any further modifications should be carried out under mild reaction conditions.[313] This methodology was also used for other multihydroxyl compounds: 1,1,1-tris(hydroxymethyl)ethane, 1,1,1-tris (hydroxymethyl)propane, and pentaerythritol.[198,314,316,318]

1,1,1-Tris(hydroxymethyl)ethane and 1,1,1-tris(hydroxymethyl)propane were also used for direct carbonate bond formation with use of dialkyl carbonate followed by modification of the remaining hydroxyl group by esterification and carbonate or urethane bond formation (Scheme 68).[103,315]

In another method alkyl malonates are used as starting materials (Scheme 69). This approach uses rather harsh reaction conditions. However, it allows the introduction of allyl-[320,321] or hydroxyl-terminated[308] substituents and further modification.

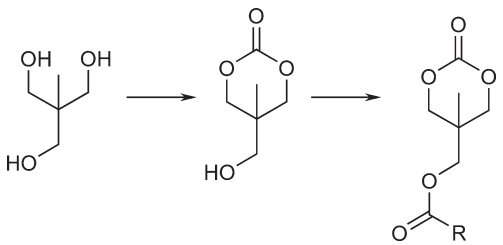

Scheme 68 Synthesis of six-membered cyclic carbonates with ester group.

Other cyclic carbonates were synthesized directly by a one-pot reaction from appropriate dihydroxyl compounds.[322–324]

A number of functionalized PCs and copolycarbonates can be obtained by direct polymerization of cyclic monomers bearing functional groups. Among the functional side-chain groups introduced into PCs are carboxylic group and their derivatives, hydroxyl, allyl, acrylate, methacrylate, styrene, and stilbene derivatives, and even five-membered cyclic carbonates (Table 2).

A series of COOH-functionalized PCs were synthesized via an organocatalytic ROP pathway under mild conditions.[305] The polymers exhibited moderate molecular weight (M_w = 3100–9700) and were very narrowly distributed (dispersity index = 1.07–1.15). Aliphatic amines with different chain lengths (triethylenetetraamine, tetraethylenepentamine, or pentaethylenehexamine)

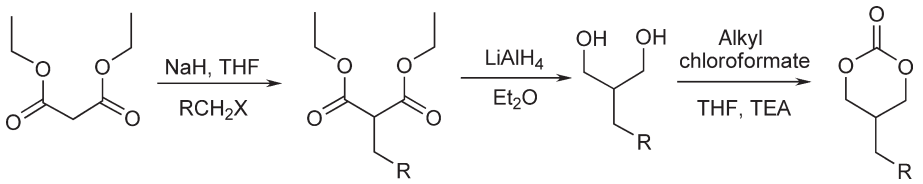

Scheme 69 Synthetic path towards diethyl malonate-based functionalized cyclic carbonates.

were then conjugated onto the PC backbone using *N*, *N*′-diisopropylcarbodiimide/*N*-hydroxysuccinimide (DIC/NHS) chemistry. These amine-functionalized PCs could form nanoparticles upon simple dissolution in water and were able to condense DNA; therefore, they have the potential to be a useful nonviral vector for gene therapy. Polymers of similar properties capable of drug delivery and gene delivery were presented by Frechet's group.[304] The authors used the cyclic carbonate with pendant COOH group to build dendritic molecules which were then eventually reacted with the appropriate amine. They used DCC chemistry for this purpose.

A simple way of preparation of PCs with side-chains terminated with hydroxyl groups is polymerization of cyclic carbonates bearing benzyl protecting group. The polymers were synthesized by ROP in bulk at 150 °C using aluminum isobutoxide [Al(O*i*Bu)$_3$], aluminum isopropoxide, and stannous octanoate as an initiator or by thermal polymerization of 5-benzyloxy-1,3-dioxan-2-one in the absence of any catalyst.[216,309,310] In all cases polymerization resulted in high-molecular-weight PCs (M_n = 80 000). Subsequent catalytic hydrogenolysis resulted in functional poly(5-benzyloxy-1,3-dioxan-2-one). After deprotection the pendant hydroxyl group resulted in an enhancement of the hydrophilicity of the PC. Furthermore, an evaluation of the degradation and cytotoxicity of synthesized polymers demonstrated better degradability compared with PTMC and similar toxicity compared with poly(lactide-*co*-GL).

A similar effect was obtained by polymerization and deprotection of 9-phenyl-2,4,8,10-tetraoxaspiro[5,5]undecan-3-one.[318] The poly(ester-carbonate)s were synthesized by the ROP of L-LA and functionalized pentaerythritol-based carbonate monomer with diethyl zinc as a catalyst (Scheme 70). The protecting benzylidene groups in the copolymer poly(L-LA-*co*-9-phenyl-2,4,8,10-tetraoxaspiro[5,5]undecan-3-one) were removed by hydrogenation with palladium hydroxide on activated charcoal as a catalyst to give a functional copolymer, poly(L-LA-*co*-5,5-bis (hydroxymethyl)-1,3-dioxan-2-one), containing pendant primary hydroxyl groups. The cell morphology and viability on a copolymer film evaluated with ECV-304 cells showed that such poly(ester-carbonate)s derived from 9-phenyl-2,4,8,10-tetraoxaspiro[5,5]undecan-3-one are good biocompatible materials suitable for biomedical applications.

Direct anionic ROP of six-membered cyclic carbonate bearing hydroxyl group, 5-hydroxyl-1,3-dioxan-2-one, was not effective in the preparation of PCs due to the preferable isomerization reaction to inert five-membered GC (Scheme 71).[308] However, six-membered cyclic carbonates bearing free hydroxyl group attached to the ring via aliphatic spacer yielded hyperbranched PCs under anionic, coordination-insertion, or enzymatic ROP reaction conditions.[308,313]

In many cases, reactive double bonds were introduced into the cyclic carbonate structure for subsequent cross-linking, epoxidation, or addition reactions.[307,311,312] Polymers of six-membered cyclic carbonate with pendant allyl ether group

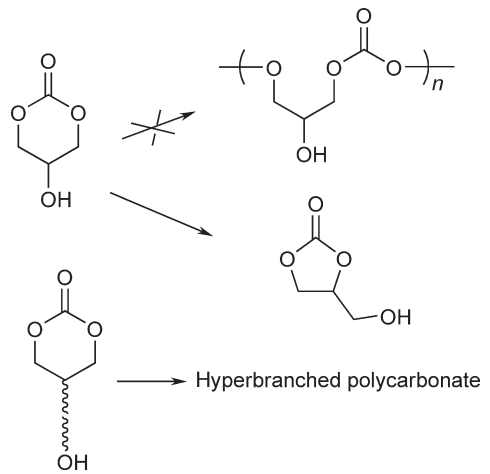

Scheme 71 Preferable isomerization reaction of six-membered cyclic carbonate bearing hydroxyl group to inert five-membered cyclic carbonate (a); formation of hyperbranched polycarbonates in case on monomers with hydroxyl group linked via a spacer (b).

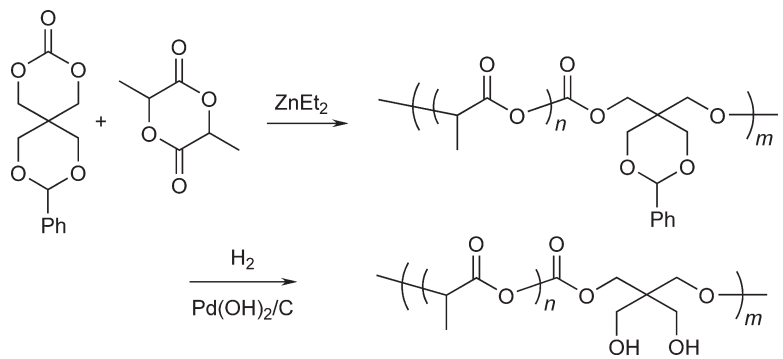

Scheme 70 Synthesis of poly(ester-carbonate)s by the ROP of L-LA and functionalized pentaerythritol-based carbonate monomer with diethyl zinc as a catalyst.

were synthesized by ROP in bulk at 120 °C. Two kinds of catalysts $Sn(Oct)_2$ and IPPL on silica particles were applied. Postpolymerization oxidation reactions carried out with *m*-chloroperoxy benzoic acid afforded polymers with epoxide groups placed randomly along the backbone (random copolymer) or in every repeating unit (homopolymer). The epoxide-containing polymers could afford facilities for further modification. A functionalized cyclic carbonate monomer containing a cinnamate moiety, 5-methyl-5-cinnamoyloxymethyl-1,3-dioxan-2-one, was polymerized and copolymerized with L-LA with diethyl zinc ($ZnEt_2$) as initiator/catalyst.[314] The cinnamate-carrying copolymer was further photo-cross-linked.

In other works the authors performed the ring-opening metathesis polymerization (ROMP) of norbornene functional group with a typical ruthenium catalyst [bis(tricyclohexylphosphine)benzylidene ruthenium(IV) dichloride], to smoothly obtain the corresponding polyalkenamers.[323,324] In addition, the $Sc(OTf)_3$-mediated cationic ring-opening reaction of the cyclic carbonate moiety of polyalkenamer proceeded along with volume expansion or nearly zero volume shrinkage to yield the corresponding networked polymer. Introduction of styrene moiety into the cyclic carbonate structure (**19**, **Table 2**) gave opportunity for the anionic polymerization of a six-membered cyclic carbonate and the anionic depolymerization of the obtained polymer, radical cross-linking, and anionic decross-linking of the cross-linked polymer.[317] The monomer 5-ethyl-5-[(*p*-vinylphenyl)methoxymethyl]-1,3-dioxan-2-one (St6CC) underwent anionic polymerization with potassium *tert*-butoxide (*t*-BuOK) as an initiator in THF to afford the corresponding PC [poly(St6CC)]. It was confirmed that this polymerization was an equilibrium process by the relationships between the polymerization temperature and monomer conversion. Poly(St6CC) underwent anionic depolymerization with *t*-BuOK as a catalyst in THF at 20 °C for 24 h to recover St6CC in 60% yield. Treatment of poly(St6CC) with a radical initiator afforded the cross-linked polymer. Employment of styrene as the comonomer satisfactorily afforded the corresponding cross-linked polymer. It underwent anionic decross-linking with *t*-BuOK in THF at 50 °C for 24 h to afford a THF-soluble polymer. The yield of the THF-soluble part increased as the styrene composition in the cross-linked polymer increased. It was suggested that the decross-linking efficiency depended on the cross-linking density.

In case of selective anionic ROP of a bifunctional cyclic carbonate consisting of both five- and six-membered rings a PC remaining a five-membered cyclic carbonate group in the side-chain (**Table 2**) has been afforded.[321] The equilibrium nature of the polymerization allowed the efficient depolymerization of the polymer by a catalytic amount of DBU to recover the monomer in high yield, in which the five-membered cyclic carbonate ring also remained unreacted.

4.12.3.3 Polymerization of Seven-Membered Cyclic and Larger Ring Size Cyclic Carbonates

4.12.3.3.1 Polymerization of seven-membered cyclic carbonates

The ROP of seven-membered cyclic carbonate (1,3-dioxepan-2-one, tetramethylene carbonate, TeMC), due to relatively high ring strain, proceeds easier than that of the six-membered one. However, the number of reports concerning the polymerization of seven-membered cyclic carbonate is rather limited, mainly because of difficulty in the synthesis of the monomer. In contrast to TMC, seven-membered TeMC is thermally unstable and difficult to isolate and purify. It is easier to obtain the double size cyclic monomer – cyclobis(TeMC) – than the monomeric form.[325] It is worth to underline that the polymerization of seven-membered cyclic carbonate can be proceeded in a controlled manner.

Several attempts have been made to achieve controlled ROP of six-membered cyclic carbonates by the combination of bulky substituents and Lewis acids.[326–328]

Hayakawa *et al.*[329] for the first time reported cationic ROP of seven-membered cyclic carbonates in 1997. Living ROP of the TeMC was achieved when the cationic zirconocene complex $[Cp_2ZrMe]^+[B(C_6F_5)_4]^-$ was used as a catalyst. The authors observed a linear relation between the conversion and molecular weight of the obtained polymer when the reaction was carried out at room temperature. The molecular weight distribution was maintained narrow during the polymerization. The authors claimed that the polymerization proceeds according to an active chain end (ACE) monomer mechanism (**Scheme 72**).

Earlier, Kricheldorf *et al.* examined in detail the polymerization of lactones with several Lewis acids. The authors suggested that some metal bromides with vacant p- or d-orbitals react with lactones to give bromoalkanoic acids via complexation at the *exo*-cyclic oxygen and cleavage of the alkyl–oxygen bond. Especially in the cases of the metal bromide with energetically favorable d-orbitals like $SnBr_4$ and $ZnBr_2$, metal–oxygen bonds are formed leading to polymerization reactions via an insertion mechanism at 60 °C, where M_w/M_n of the obtained polymers is about 1.7.[330] The same group investigated ROP of a TeMC using $BCl_3/HCl \cdot OEt_2$ as an initiator system.[331] It was found that the addition of $HCl \cdot Et_2O$ promoted the polymerization even at low temperature (0 °C) to produce the corresponding PC with controlled molecular weight and narrow dispersity

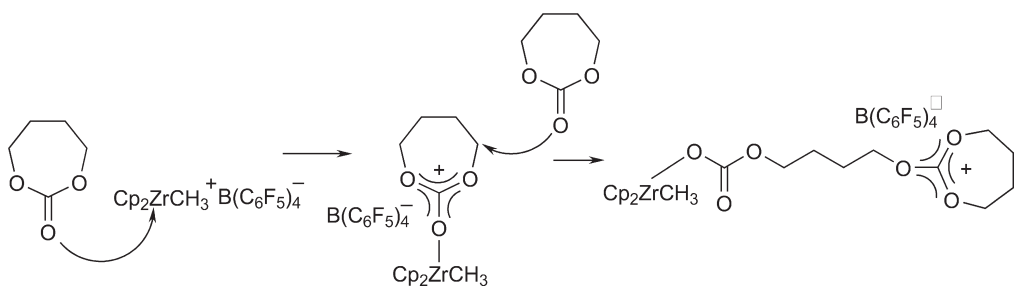

Scheme 72 Cationic polymerization of 1,3-dioxepan-2-one.

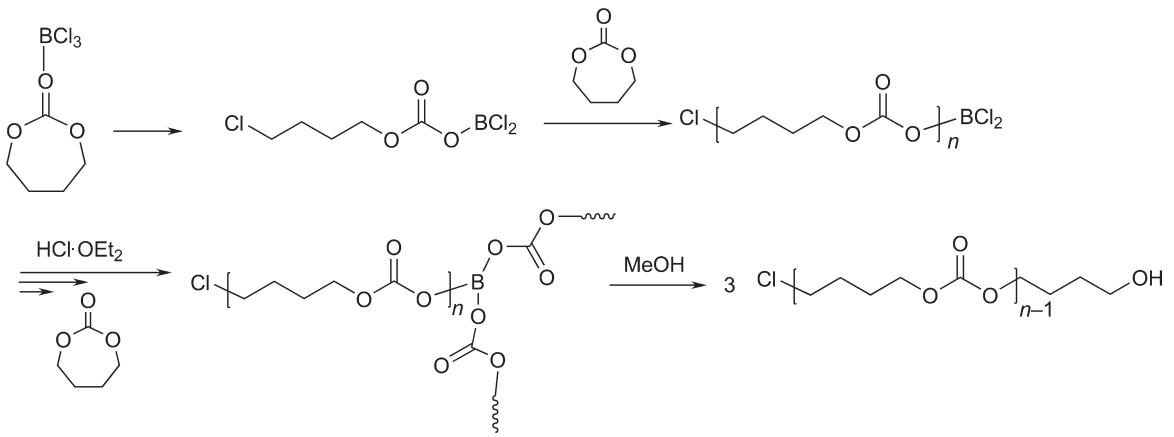

Scheme 73 Polymerization of TeMC initiated with BCl_3/HCl·Et_2O.

index ($M_w/M_n < 1.2$), but relatively low molecular weight ($M_n = 6600$). The authors suggested that the presence of $HCl \cdot OEt_2$ may promote the sequential insertion reaction of TeMC between the boron-oxygen bond by the activation of the monomer and/or loosening the boron-carbonate bond by coordination to the carbonate oxygen in the polymer propagating end (Scheme 73).

It was found that a titanium-based catalyst, 2,2′-methylene-bis(6-*tert*-butyl-4-methylphenolate)titanium dichloride, also initiated the living polymerization of TeMC to afford polymers with narrow molecular weight distributions (Scheme 74). The molecular weight of the poly(TeMC) obtained can be controlled by changing the initial cyclic carbonate/catalyst mole ratio. It is characteristic that the PC macromolecules formed in the presence of this catalyst had hydroxytetramethylene terminal units at both ends.[326,332]

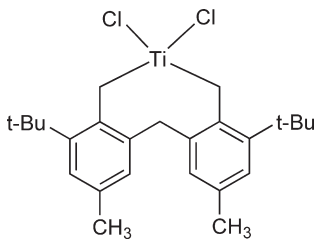

Scheme 74 Structure of titanium catalyst.

Endo *et al.* also found that TeMC underwent polymerization according to an AM mechanism in the presence of alcohol and Brønsted acid as the initiator and activator, respectively (Scheme 75).[333–335]

The first step consists of the protonation of the monomer carbonyl oxygen to produce the AM, which reacts readily with OH groups. The corresponding ring-opening reaction produces a linear carbonate with a terminal hydroxyl group. In the next step another activated molecule of cyclic carbonate reacts with a hydroxyl end-group leading to chain extension. The resulting PC has an R residue which is derived from the initiator alcohol and a hydroxyl group at the chain ends (Scheme 75).

The authors have found that the ROP of TeMC initiated with H_2O or a primary alcohol (e.g., butyl alcohol) in the presence other Brønsted acids such as $HCl \cdot Et_2O$ proceeded without decarboxylation to give linear poly(TeMC) with $M_n = 1000–10\,000$ and a narrow dispersion index (~ 1.15). They postulated that the key feature of this polymerization is the appropriate acidity of the protonic acid, which should be not as high to polymerize the monomer by itself but sufficient to activate the monomer.[333,334]

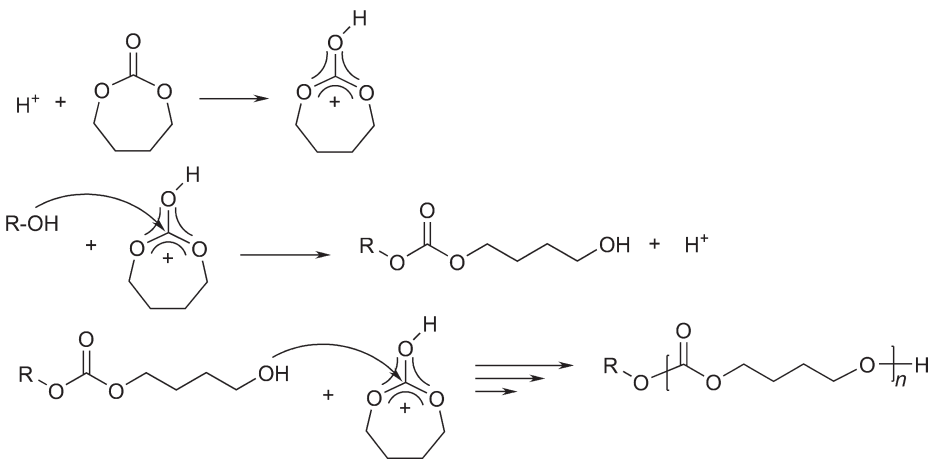

Scheme 75 Mechanism of AM polymerization of TeMC.

It is worth noticing that in contrast to a six-membered cyclic carbonate, the cationic polymerization of seven-membered cyclic carbonate leads to the corresponding polymer without ether linkages.[101] The polymerization of TeMC carried out in the presence of typical cationic initiators like $CH_3OSO_2CF_3$, $C_2H_5OSO_2CF_3$, $HOSO_2CF_3$, and $SnCl_4$ proceeds at 20 °C about 100 times faster than that of TMC and is not accompanied by elimination of carbon dioxide. The decarboxylation, in the case of the polymerization of seven-membered cyclic carbonate, may be suppressed, since the propagation reaction dominates over backbiting degradation. The activation energies in the polymerizations of TeMC and TMC were estimated to be 6.27 and 8.52 kcal mol^{-1}, respectively.[86,101]

Trifluoromethane sulfonic acid was also used as a catalyst in ring-opening copolymerization of a seven-membered cyclic carbonate and trioxane.[336] However, the carbonate monomer was consumed faster than trioxane and the decarboxylation took place to afford corresponding polyacetal–PC type copolymers containing poly(oxytetramethylene) units.

Similarly, the copolymerization of TeMC with glycidyl phenyl ether initiated by $CH_3OSO_2CF_3$ yielded polymers rich in cyclic carbonate-derived units when compared with the corresponding feed ratio and containing oxytetramethylene units as a result of five-membered cyclic carbonate formation.[337]

Similarly to TMC, TeMC undergoes spontaneous polymerization in bulk at above 100 °C affording the corresponding PC.[212]

As far as anionic polymerization of seven-membered cyclic carbonate is concerned, it was found that a ring strained monomer easily undergoes ring-opening reaction. The polymerization of TeMC initiated with *sec*-BuLi and carried out in THF afforded the corresponding PC in a relatively high yield in a short time.[100] It was shown that the polymerization carried out at higher temperature and with a lower initial monomer concentration led to a lower yield, lower molecular weight of the polymer, and a higher content of cyclic oligomers. These results can be explained by the formation of cyclic oligomers via backbiting reaction proceeding in addition to the propagation reaction, which is characteristic for equilibrium polymerizations. However, the relative polymerization rate of TeMC is about 35 times faster than that of TMC. This significant difference in the polymerization rates is caused by the larger ring strain. The negatively larger ΔH_p for TeMC in comparison with that of TMC was estimated by the MO calculations.[325]

Recently, Wu *et al.*[108] have presented enzymatic polymerization of a novel seven-membered cyclic carbonate monomer, (5*S*,6*S*)-dimethyl-5,6-*O*-isopropylidene-1,3-dioxepin-2-one (ITC), derived from naturally occurring L-tartaric acid. The monomer was obtained in three steps (**Scheme 76**).

The polymerization was carried out with four commercially available lipases (*C. antarctica*, CAL-B) immobilized on acrylic resin, Novozyme-435, *P. fluorescens* (AK), and *Pseudomonas cepacia* (PS-30) at 80 °C, in bulk (**Scheme 77**).

The highest molecular weight (M_n = 15 500 with M_w/M_n = 1.7) of the optically active PC ($[\alpha]_D^{20} = +77.8$) was obtained with immobilized *C. antarctica* lipase-B (Novozyme-435). Deprotection of the ketal groups caused minimal polymer chain degradation (M_n = 10 000, M_w/M_n = 2.0) and resulted in optically pure PC ($[\alpha]_D^{20} = +56$) bearing two hydroxy functional groups in the polymer repeating unit. The presence of the pendant hydroxyl groups enhanced the biodegradability of the polymer.

4.12.3.3.2 Polymerization of cyclobis(alkylene carbonate)s

As was mentioned earlier (Section 4.12.3.3.1), it is more convenient to obtain poly(TeMC) using cyclobis(TeMC) instead of its monomeric form: 1,3-dioxepan-2-one.[325] Cyclobis(TeMC) is easy to isolate and purify by recrystallization. The polymerization with *n*-$BuSnCl_3$ or $Sn(Oct)_2$ as an initiator is usually carried out in bulk, because the polymerization in solution (CH_2Cl_2) at lower temperatures proceeds very slowly. The monomer's high melting point (m.p. 172–174 °C) impels that the polymerization of cyclobis(TeMC) in bulk requires a high temperature (180 °C). However, despite high polymerization temperature no ether group formation was observed. In the case of using $Sn(Oct)_2$ the ^1H NMR studies revealed that these PCs contained octoate and OH terminal groups.

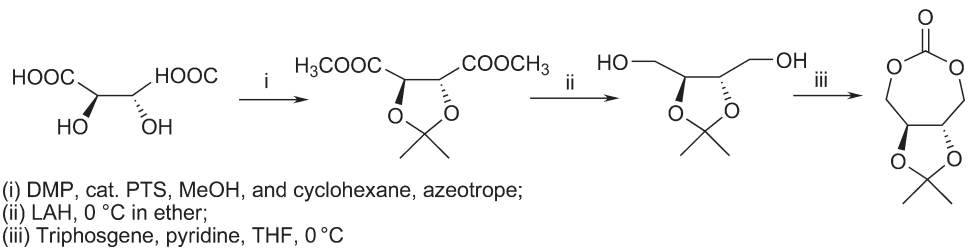

Scheme 76 Synthesis of monomer, ITC derived from naturally occurring L-tartaric acid.

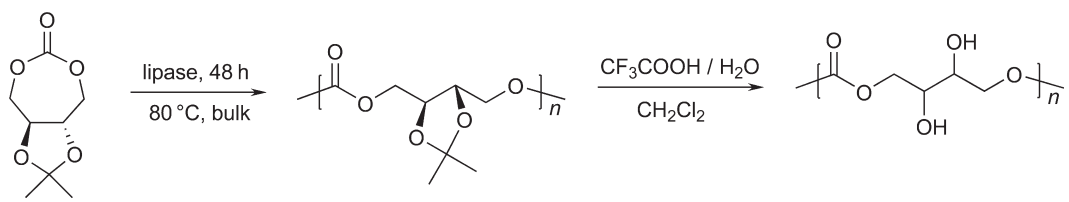

Scheme 77 Enzymatic polymerization of ITC.

It is particularly interesting that poly(TeMC) crystallizes upon annealing, whereas PTMC does not crystallize despite higher concentration of polar carbonate groups. The susceptibility to degradation at relatively low temperatures is a second interesting feature of this aliphatic PC. The degradation to CO_2 and THF is complete at approximately 340 °C without leaving any residue. The material exhibiting such a complete degradation at below 350 °C may be applied for the production of solid foams, when heated together with a thermostable polymer.[338]

Similarly, cyclobis(hexamethylene carbonate), a dimer of nine-membered cyclic carbonate, was subjected to polymerization in bulk at 140 °C using $BuSnCl_3$ or $Sn(Oct)_2$ as a catalyst.[102] The best results were obtained with $BuSnCl_3$ affording polymer yields up to 89% and weight-average molecular weight of $M_w = 200\,000$. In all cases the M_w/M_n ratio was of the order of 2. DSC measurements showed that the PC rapidly crystallizes even at a cooling rate of 40 °C min^{-1}.

Also Weilandt *et al.*[106] have reported the synthesis, polymerization, and copolymerization of cyclobis(hexamethylene carbonate) and its fluorinated analog using anionic initiators and tin-based catalysts such as *sec*-butyllithium (in toluene), dibutylmagnesium (in THF), and dibutyltin dimethoxide (in melt). The resultant poly(hexamethylene carbonate) with molecular weight of $M_n = 48\,000$ ($M_w/M_n = 1.7$) was a semicrystalline polymer with a melting point of 54 °C and a glass transition temperature of − 51.3 °C, while poly (2,2,3,3,4,4,5,5-octafluorohexamethylene carbonate) was obtained either as a semicrystalline material with molecular weight of $M_n = 12\,800$ ($M_w/M_n = 1.94$) and a melting point of 40.8 °C or as an amorphous material with a glass transition temperature of − 39.8 °C.

It was found that the other cyclic dimer, cyclobis(diethylene glycol carbonate), is more stable and easier to isolate than the corresponding cyclic monomer, similarly as in the case of cyclic carbonates derived from α,ω-dihydroxyalkanes with 6, 7, and 8 methylene groups in a molecule. A comparison of the polymerizations of cyclobis(diethylene glycol carbonate) in bulk conducted at 145 °C catalyzed by $BuSnCl_3$, $Sn(Oct)_2$, or Bu_2SnO under similar conditions suggests that Bu_2SnO appeared to be the most reactive catalyst, but $Sn(Oct)_2$ is more attractive for preparative purposes because of higher molecular weights of the resultant polymers. Both ^1H and ^{13}C NMR spectra proved that all poly(diethylene glycol carbonate)s prepared possess an alternating sequence of ether and carbonate linkages. Despite a regular sequence, the amorphous character of poly(ethylene oxide-*co*-ethylene carbonate) was proven by DSC and WAXS measurements. The highest yields and molecular weights were obtained in the shortest time, whereas prolonged times caused rapid depolymerization. The thermal degradation of poly(ethylene oxide-*co*-ethylene carbonate) begun slowly at above 200 °C reached its maximum rate at 320 °C and yielded CO_2 and 1,4-dioxane as the main degradation products (**Scheme 78**).[104]

Polymerization of the largest (26-membered) cyclobiscarbonate, cyclobis(decamethylene carbonate), was conducted in bulk at 120 °C with $BuSnCl_3$ and $Sn(Oct)_2$ as catalysts.[105] Both catalysts showed almost equal reactivities, but the highest yields (up to 98%) and the highest molecular weights (M_w up to 88 000) were obtained with $BuSnCl_3$. Both catalysts yielded poly(decamethylene carbonate) not containing ether groups.

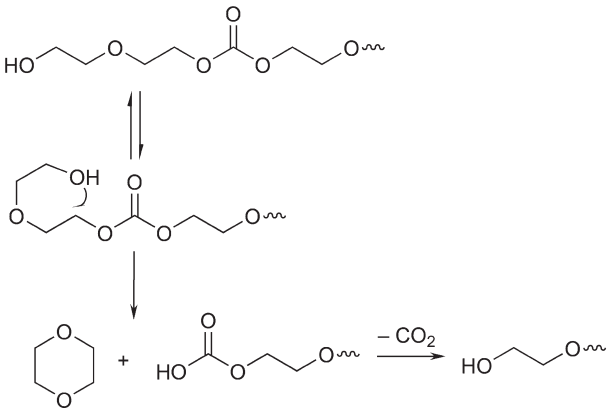

Scheme 78 Thermal degradation of poly(ethylene ether-carbonate).

DSC measurements revealed that poly(decamethylene carbonate) is a rapidly crystallizing material with $T_m = 67$ °C. A comparison with PCs having less CH_2 groups in the repeating unit demonstrated that the rate of crystallization increases with an increasing number of CH_2 groups between carbonate linkages.

As was earlier mentioned, 26-membered macrocyclic carbonate, cyclobis(decamethylene carbonate), was attempted to undergo ROP by lipase catalysis in toluene.[297] Novozym-435 exhibited even higher catalytic activity toward cyclic decamethylene carbonate dimer polymerization compared with $Sn(Oct)_2$, while high molecular weight (M_n) of 54 000 and yield of 99% were still achieved at ultra-low enzyme/substrate (E/S) weight ratio of 1/200.

4.12.4 Copolymerization of Cyclic Carbonates with Other Heterocyclic Monomers

4.12.4.1 Copolymerization of Five-Membered Cyclic Carbonates

Five-membered cyclic carbonates such as ethylene and PCs, as earlier mentioned (Section 4.12.3.1), do not homopolymerize to afford poly(alkylene carbonate)s due to unfavorable thermodynamic characteristics. However, they can undergo copolymerization with other more reactive heterocyclic monomers. It has been found that such carbonate monomers could undergo copolymerization with oxiranes in the presence of organometallic catalysts formed in the diethylzinc-phenol and/or polyfunctional phenol system.[129,339] The authors postulated that the initiation step of the copolymerization involves most likely the epoxide reaction. Zinc alkoxide species formed in this reaction can easily propagate the copolymer chain, coordinating and enchaining both the epoxide and cyclic carbonate comonomers. However, in the case of cyclic carbonate, its ring opening may also proceed according to the reaction outlined in **Scheme 79** (via alkyl-oxygen bond cleavage) leading to decarboxylation. For the sake of clarity, participation of the adjacent zinc atom as the nucleophilic attack carrier is omitted. Thus, the poly(ether-carbonate)s obtained are characterized by a lower content of carbonate units with respect to ether units.[129,340]

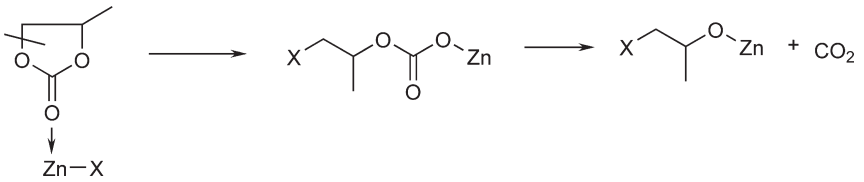

Scheme 79 Ring opening reaction *via* alkyl-oxygene bond cleavage leading to decarboxylation.

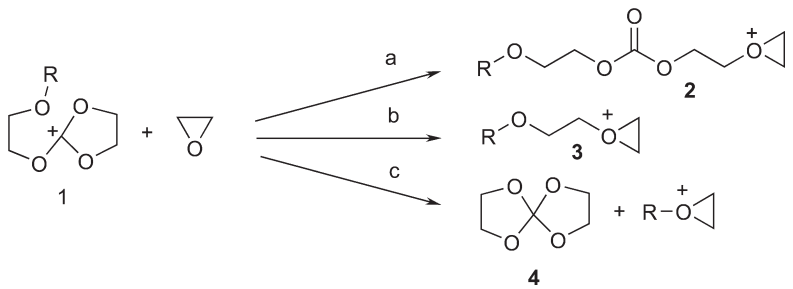

Scheme 80 Possible products of the reaction of five-membered cyclic carbonates with oxiranes in the presence of cationic initiator.

Rokicki and Nguyen[341,342] described that the reaction of oxiranes with five-membered cyclic carbonates in the presence of $BF_3 \cdot OEt_2$ as a cationic initiator led to spiroorthocarbonates, poly(ether-carbonate), or polyether, depending on the oxirane ring substituent. It was found that the copolymerization proceeded through a trialkoxycarbenium cation stabilized by adjacent three oxygen atoms, being thermodynamically favored. A negative charge located on the oxygen atom of the carbonate carbonyl group is twice as large as that located on the oxygen atom of the oxirane, so the reaction with the carbonate monomer is more probable than that with the oxirane one. Trialkoxycarbenium ion (**1**, **Scheme 80**) can react according to three possible reaction pathways.

When *exo*-cyclic carbon atom of **1** is attacked by oxirane the product with ether-carbonate group **2** is formed (reaction pathway **a**). On the other hand as a result of oxirane attack on *endo*-cyclic carbon atom of **1** both the ether group **3** and cyclic carbonate are formed (pathway **b**). The intramolecular reaction between the carbocation and an oxygen atom of linear ether leads to spiroorthocarbonate **4** (pathway **c**). It was shown that the reaction proceeded partially according to pathway **a** in the case of using cyclic carbonates bearing phenoxymethyl and chloromethyl substituents, but for other five-membered cyclic carbonates the reaction pathway **b** dominated. Due to higher stability of the trialkoxycarbenium cation the polymerization rate is slower than that of oxirane homopolymerization.

Recently, a similar system was investigated by Cervellera *et al.*[343] They copolymerized mixtures of diglycidyl ether of bisphenol A (DGEBA) or a cycloaliphatic epoxy resin with PC using lanthanide triflates or $BF_3 \cdot MEA$ as a cationic initiator and DMAP as an anionic initiator. However, they observed that the carbonate was not incorporated into the network and acted like a plasticizer, lowering the T_g values of the cured materials. The same authors also used 4-phenoxymethyl-1,3-dioxolane-2-one (PGEC) and aromatic five-membered cyclic carbonate, 1,3-benzodioxolane-2-one (CC), for copolymerization with DGEBA.[344] Lanthanum(III) triflate used as cationic initiator allowed to copolymerize DGEBA with an aromatic five-membered cyclic carbonate, CC. However, PGEC remained entrapped in the cured material. The authors assigned the different reactivities of these two carbonates to the different electrophilicity of the carbonyl group.

Evans and Katsumata[345] showed that the copolymerization of EC and CL is possible when samarium(II) compounds were used as catalysts. In the presence of samarium complexes such as $(C_9H_7)_2Sm(THF)_{1.5}$, $(C_{13}H_9)_2Sm(THF)_2$, $SmI_2(THF)_2$, and $(C_5Me_5)_2Sm(THF)_2$ polymers containing EC units were formed. The copolymerization carried out in the presence of $[(Me_3Si)_2N]_2Sm(THF)_2$ afforded polymers with up to 23.5 mol.% of EC content, but the molecular weights of these polymers were lower than those produced using the $(C_5Me_5)_2Sm(THF)_2$ catalyst.

Copolymers of EC with CL or VL were also synthesized by Shirahama *et al.*[346] using $(C_5Me_5)_2SmMe(THF)$ as catalyst. It is worth noticing that the copolymerization carried out using samarium catalyst yielded a polymer of really high molecular weight ($M_n = 140\,000$). The EC/CL copolymers contained up to 30 mol.% of carbonate units and were obtained in better yield compared with that of EC/VL copolymers. Chen and co-workers used another lanthanide such as neodymium tris (2,6-di-*tert*-butyl-4-methylphenolate) $[Nd(DBMP)_3]$ as a single-component catalyst for EC/CL copolymerization.[347] Copolymers containing up to 22 mol.% of EC with high molecular weights (140 000) and moderate molecular weight distributions ($M_w/M_n = 1.66–2.03$) were obtained at room temperature. Compared with homopoly(CL), the copolymers with EC units exhibited increased glass transition temperatures (−35.6 °C), reduced melting temperatures (44.5 °C), and greatly enhanced elongation percentage at break. It was found that the crystallinity of the copolymers decreased with the increasing EC molar percentage in the products.

Höcker's group reported that unreactive five-membered cyclic carbonates such as EC and PC can be successfully copolymerized with tetramethylene urea (TeU) to afford polyurethanes.[348–350] It is to be underlined that such polyurethanes were synthesized via nonisocyanate methods. The result of all

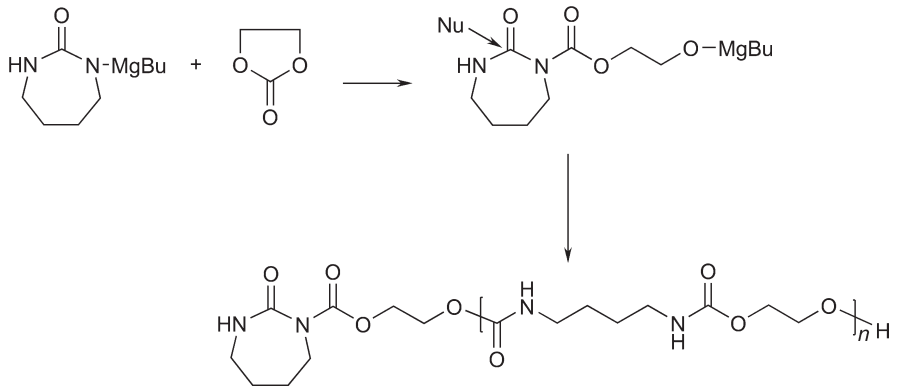

Scheme 81 Copolymerization of five-membered cyclic carbonates with tetramethylene urea leading to polyurethanes.

copolymerization reactions was the polyurethane with alternating carbonyl-amino-tetramethylene-amino and EC, or PC repeating units. The resulting polyurethane was characterized by relatively high molecular weight (~ 20 000) and dispersity index of 2. According to the mechanism proposed by the authors, the butylmagnesium salt of TeU reacts with EC. The resultant butylmagnesium alkoxide reacts with another TeU molecule leading to an intermediate (Scheme 81). The intermediate adduct of EC and TeU represents an A–B-type monomer suitable for a polyaddition reaction.

The polyurethanes with randomly distributed TeU–EC and TeU-PC units, containing up to 54 mol.% of PC repeating units, were obtained. Studies on the copolymerization of TeU with mixtures of EC and PC showed that the reactivity of EC is approximately 5 times higher than that of PC. The authors proposed a new mechanism for the copolymerization based on ^{1}H NMR spectroscopic investigations of a blocked isocyanate model compound, indicating that the TeU ring is not opened to form an isocyanate under the reaction conditions applied.

The same authors successfully copolymerized EC or PC with mixtures of TeU and γ-butyrolactone (BL) at 100 °C in the presence of Bu_2Mg as a catalyst.[351] From NMR spectroscopic data of the terpolymers obtained ($8100 < M_n < 19\,300$) with up to 62.4 mol.% of BL, it was shown that the reactivity of the five-membered cycles used increases in the following order: EC ≫ PC ≈ BL. ^{13}C NMR spectroscopy revealed that TeU–EC or TeU–PC and TeU–BL units were randomly distributed in the polymer chain.

4.12.4.2 Copolymerization of Six-Membered Cyclic Carbonates

Six-membered cyclic carbonates easily copolymerize with different cyclic carbonates (five-, six-, and seven-membered) as well as with other heterocyclic monomers. The majority of copolymerizations proceed according to the coordination-insertion or anionic mechanisms and most of the copolymers were obtained with the participation of TMC or neopentyl carbonate.

4.12.4.2.1 Copolymerization of TMC and neopentyl carbonate with other cyclic carbonates

As was mentioned in Section 4.12.4.1, six-membered TMC is more reactive, copolymerized with five-membered EC, but still the content of EC units in the resulting copolymer was rather small, not exceeding a few mol.%.

TMC and DTC can be used for the copolymerization with a less reactive six-membered cyclic carbonate such as 5,5-diphenyl-1,3-dioxan-2-one.[92] The copolymerization proceeded according to an anionic mechanism to afford a polymer containing 5,5-diphenyl-1,3-dioxan-2-one units, but in lower ratio than that in the monomer feed. DTC was also copolymerized with other six-membered cyclic carbonates to furnish random as well as block copolymers upon addition of the initiator (*sec*-butyllithium) to a mixture of the monomers or upon consecutive addition of the monomers to the initiator, respectively.[198]

4.12.4.2.2 Copolymerization of six-membered cyclic carbonates with cyclic esters and ethers

Aliphatic polyesters have a leading position among the various biodegradable polymers, due to the hydrolytic chain cleavage catalyzed by enzyme yielding hydroxyacids, which are in many cases metabolized. The modification of the properties of the brittle biodegradable polyesters such as poly(hydroxyalkanoate), polylactide, and polyglycolide has been intensively investigated.[291,352]

Usually biodegradable or biocompatible elastomers were introduced to toughen the brittle polyester. Maxon®, a bioabsorbable suture material, is produced by the copolymerization of GL with approximately 32.5 mol.% of the softer TMC.[353] The addition of TMC decreases the brittleness of pure polyglycolide. The incorporation of carbonate linkages into the polyester constitutes an additional route for improvement of the performance of polyesters. Because the carbonate linkages are more stable to hydrolysis *in vitro* (no autocatalytic effect of acid groups) the material has prolonged shelf life. However, the hydrolysis of the carbonate proceeds faster *in vivo* and the copolymer can be used as a bioabsorbable material.[354,355] In relation to this, the copolymerizations of cyclic carbonates with lactones and lactides have been widely explored. Depending on the comonomer reactivity and reaction procedure, the copolymerization may result in random or block copolymers.

DTC has been copolymerized with CL, pivalolactone (PVL), [(R)-β-BL], and L,L-lactide (LLA).

Höcker and co-workers used CL for the copolymerization with DTC. The reaction was carried out using *sec*-BuLi as an anionic initiator in toluene resulting in the formation of a copolymer containing carbonate and CL block fractions.[91] It

was shown that the reactivity of the cyclic carbonate is higher than that of CL.[356]

The copolymerization of a mixture of DTC and CL at low temperatures resulted in A–X–B-type copolymers, where A was a PDTC block, B a PCL block, and X a random DTC and CL block. As a consequence, DTC–CL and CL–DTC heterodiads were observed in the ^{13}C NMR spectra. The concentration of heterodiads was seen to increase with temperature such that, at 80 °C, a random copolymer was obtained. From a mechanistic point of view, the active species of each monomer would be eligible to react with both DTC and CL. In case of using Mg-, Al-, and Zn-based catalysts, transesterification plays a minor role, and the microstructure of the copolymers prepared is determined by the nucleophilicity of the active species and the electrophilicity of the monomer alone. For alkoxide (Li^+, K^+) initiators and Sn-based catalyst, transesterification takes place and determines the final polymer microstructure, besides the copolymerization parameters, especially at higher temperatures.[357]

The copolymerization of DTC and CL was also initiated by polystyryllithium and lithium polystyrylethoxide, leading to a linear copolymer and a cyclic oligomer mixture.[196]

The copolymerization of DTC with another four-membered cyclic ester, PVL, initiated with potassium dihydronaphthalide at – 10 °C in toluene afforded block copolymers in a yield of about 90% (Scheme 82).[91,357,358]

The explanation for this block formation is based on the large difference in the rate of polymerization of DTC and PVL, combined with the incompatibility of the active species of homopolymerizations (potassium carboxylate, active with PVL, does not react with DTC). It is important that no transesterification occurs between the ester and carbonate groups.

The random copolymer of TMC with another four-membered cyclic ester, [(R)-β-BL], exhibits interesting properties (Scheme 83).[359] The presence of ester segments susceptible to enzymatic hydrolysis causes that such poly (ester-carbonate) containing even 80% of TMC easily undergoes biodegradation, while pure PTMC does not degrade under the same conditions.

The sequential copolymerization of DTC and LLA revealed different polymer microstructures, depending on the order in which the monomer was polymerized first.[357,360] When LLA was polymerized first, a random copolymer was formed, whereas the addition of LLA to a 'living PDTC resulted in a block copolymer. The copolymerization of a mixture of LLA and DTC also resulted in a random copolymer. Based on these results, the following mechanism was proposed by the authors. The PLLA active centers are well stabilized by the adjacent carbonyl group (enol formation) and by the formation of a five-membered cyclic complex including the metallic species. After reaction of the PLLA active centers with DTC, the newly formed active site has a reduced capability of stabilization (Scheme 84).

The most electrophilic species in the system capable of reacting with the active centers is the ester group of a LLA–LLA diad in the polymer chain. Hence, by this reaction, the active LLA site is regenerated and an LLA–DTC–LLA triad is formed.

Poly(1,4-dioxan-2-one-*co*-TMC) can also be included to the group of synthetic biodegradable carbonate copolymers.

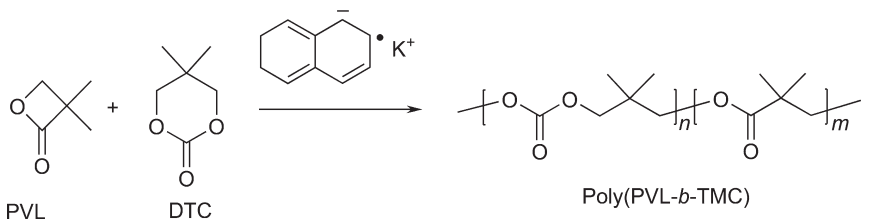

Scheme 82 Copolymerization of DTC with four-membered cyclic ester initiated by potassium dihydronaphthalide.

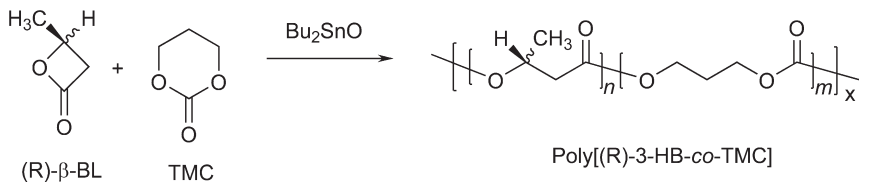

Scheme 83 Random copolymerization of TMC with four-membered cyclic ester leading to polymer susceptible to enzymatic hydrolysis.

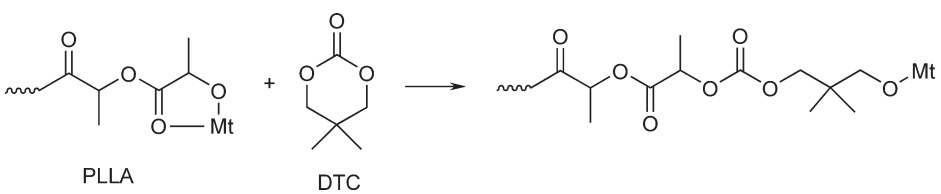

Scheme 84 Sequential copolymerization of LLA and DTC.

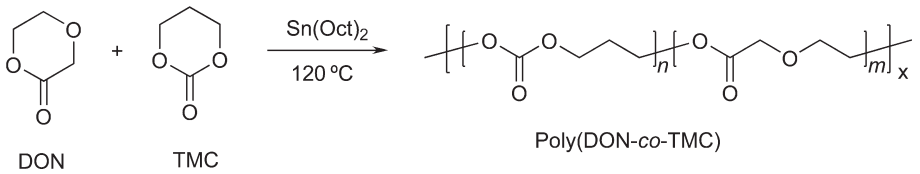

Scheme 85 Copolymerization of 1,4-dioxan-2-one and TMC initiated with $Sn(Oct)_2$.

Polymers with different compositions were synthesized by copolymerizations of 1,4-dioxan-2-one (DON) with TMC at 120 °C in the presence of $Sn(Oct)_2$ (Scheme 85).[361]

These copolymers can be used as a matrix for a sustained drug delivery system.

4.12.4.2.3 Copolymerization of six-membered cyclic carbonates with cyclic anhydrides

PTMC degrades slowly in aqueous solution, showing little molecular weight loss, sample weight loss, or change in morphology after several months which may not be desirable for use in medical implants and for drug delivery applications.[355] In contrary, poly(adipic anhydride) (PAA) attracts increasing attention as a new biomaterial due to its rapid degradation rate.[362] Ring-opening copolymerization of TMC with cyclic anhydrides is a feasible method to adjust the degradation rate of PTMC and to enhance polyanhydride mechanical strength. Attempts were made to alter the chemical composition of PTMC by copolymerization of TMC with adipic anhydride (AA). TMC and AA were copolymerized in bulk and solution with aluminum isopropoxide, $Sn(Oct)_2$, *n*-BuLi, $BF_3 \cdot OEt_2$, and Et_3N as catalysts to obtain block copolymers and random copolymers.[363] No formation of a copolymer was detected, although the synthesis conditions were varied over a broad range in terms of temperature (0–100 °C), solvent, reaction time, and type of initiator. No peaks from AA–TMC or TMC–AA heterolinkages were detected in ^{13}H NMR spectra. FTIR analysis sustained that the product consists of a mixture of homopolymers rather than a copolymer.

Polymerizations of TMC with sebacic anhydride or AAs were also studied at 180 °C with quinoline and $BF_3 \cdot OEt_2$ as catalysts. Either most of the TMC did not react or incomplete homopolymerization of TMC was observed.[364]

Several polymerizations of TMC with succinic anhydride (SA) or glutaric anhydride (GA) were conducted in bulk.[364] All experiments based on SA failed; however, polymerization of TMC and GA was successful when quinoline, 4-(*N*,*N*-dimethylamino)pyridine, or $BF_3 \cdot OEt_2$ were used as catalysts. It was shown that the reaction proceeded with CO_2 evolution. MALDI-TOF mass spectra revealed the formation of cyclic oligoesters by backbiting degradation. However, the main chain of the copolymer did not contain anhydride bonds. The monomer mixtures containing an excess of TMC yielded poly(ester-*co*-carbonate)s with number-average molecular weights up to 16 000. Analogous poly(ester-*co*-carbonate)s were obtained from TMC and 3,3′-tetramethylene GA.

Recently, Ling *et al.* revealed that a THF-soluble block copolymer of neopentyl carbonate with AA containing 64.7/35.3 DTC/AA in molar ratio with M_n of 123 000 and M_w/M_n of 1.64 could be synthesized at 25 °C in 32 min when the lanthanum tris(2,6-di-*tert*-butyl-4-methylphenolate) catalyst was used[365] (Scheme 86). Copolymers with AA block from 8.5 to 50.8% were prepared by changing the solvent and feeding ratio of DTC/AA.

4.12.4.2.4 Copolymerization of six-membered cyclic carbonates with N- and P-containing heterocyclic monomers

In the 1980s, it was reported in the patent literature that lactams can be anionically copolymerized with cyclic carbonates to give a polymer containing urethane and ester groups besides carbonate groups.[366] Similar groups were identified when PCs were treated with ε-caprolactam in the presence of sodium lactamate.[367] In the early 1990s, Wurm *et al.*[368] found that the copolymerization of DTC with ε-caprolactam afforded a copolymer with alternating ester and urethane groups. From mechanistic investigation it was revealed that the polymer is formed in two reaction steps: first the PC is formed, then insertion of the ring-opened lactam moiety into the carbonate group occurs, which leads to ester and urethane groups (Scheme 87).

Similarly, the copolymerization of equimolar amounts of DTC with TeU in the presence of *sec*-butyllithium, dibutylmagnesium, or diethylzinc as a catalyst in melt and in solution with *N*,*N*′-dimethylpropylene urea as a solvent at 120 °C resulted in an almost alternating copolymer (Scheme 88).[348]

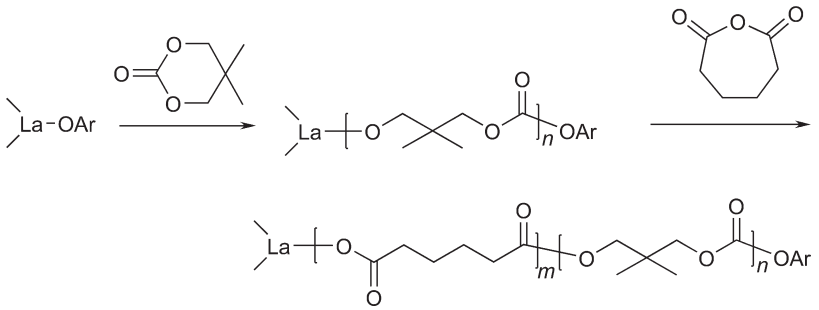

Scheme 86 Copolymerization of adipic anhydride with DTC.

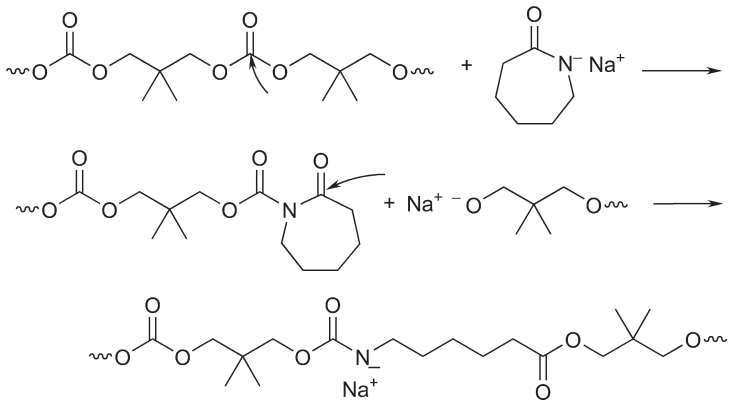

Scheme 87 Copolymerization of ε-caprolactam and DTC leading to the copolymer with carbonate, ester, and urethane groups.

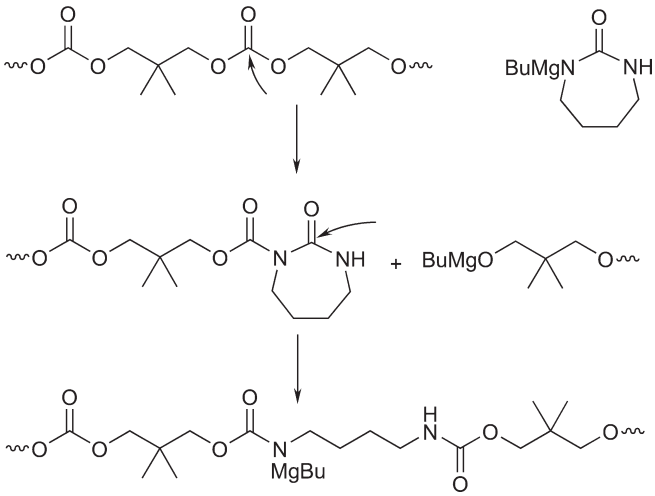

Scheme 88 Copolymerization of tetramethylene urea with DTC leading to the alternating copolymer.

In contrast to the copolymerization with EC (see Section 4.12.3.1), it was revealed that sequences of the PC are formed first. Later, when TeU is consumed, the concentration of carbonate groups in the polymer decreases and that of urethane group concentration increases.[349] After 24 h both monomers were consumed. Bu_2Mg initiates the polymerization of DTC, which is followed by a transfer of the active species to cyclic urea. This nucleophilic TeU species reacts with a carbonate moiety of the PC chain, resulting in chain cleavage and formation of two ACEs. The intermolecular reaction of these two fragments generates a new molecule in which a TeU is inserted formally into a DTC–DTC diad with the formation of two urethane groups. At the same time a new TeU active species is generated by the deprotonation of TeU. In contrast, the copolymerization of DTC with TeU in the presence of dibutyldimethoxytin, tris(*sec*-butoxy)aluminum, or tetrakis (*iso*-propoxy)titanium as a catalyst leads to copolymers with carbonate, urea, and urethane groups.[348] The polyurethane obtained in such a way is an amorphous material with $T_g = 23.3\,^{\circ}C$.

High-molecular-weight poly(ester-urethane)s with an M_w of 103 000 were also produced by the enzymatic ROP of the cyclic ester-urethane monomer.[369] However, this method did not involve polymerization of TMC, but its reaction with aliphatic diamine and then enzymatic cyclization followed by lipase-assisted ROP of cyclic macromonomer (**Scheme 89**).

It is known that poly(phosphoester)s have a great potential as a class of biomedical polymers because of their promising applications in tissue engineering and controlled drug release.[370] The ROP is one of the methods to get high-molecular-weight poly(phosphoester)s. The synthesis of poly (2-hydro-2-oxo-1,3,2-dioxaphosphorinane) and its application as a drug carrier was reported, in the 1970s, by Kaluzynski *et al.*[371] Recently, a new type of synthetic biodegradable copolymer has been synthesized by ring-opening copolymerization of TMC with 2-hydro-2-oxo-1,3,2--dioxaphosphorinane (TMP) in the presence of $Al(iBu)_3$ as a catalyst (**Scheme 90(a)**).[99] The highest molecular weight of the random copolymer was up to 16 000. Conversion studies showed that the composition of the copolymer is in agreement with the feed composition at high conversions, since TMC is more reactive than TMP.

Also, the novel enzymatic ring-opening copolymerization of ethyl ethylene phosphate (EEP) and TMC was performed in bulk at 100 °C using PPL or *C. rugosa* lipase to yield random copolymers having molecular weights ranging from 3200 to

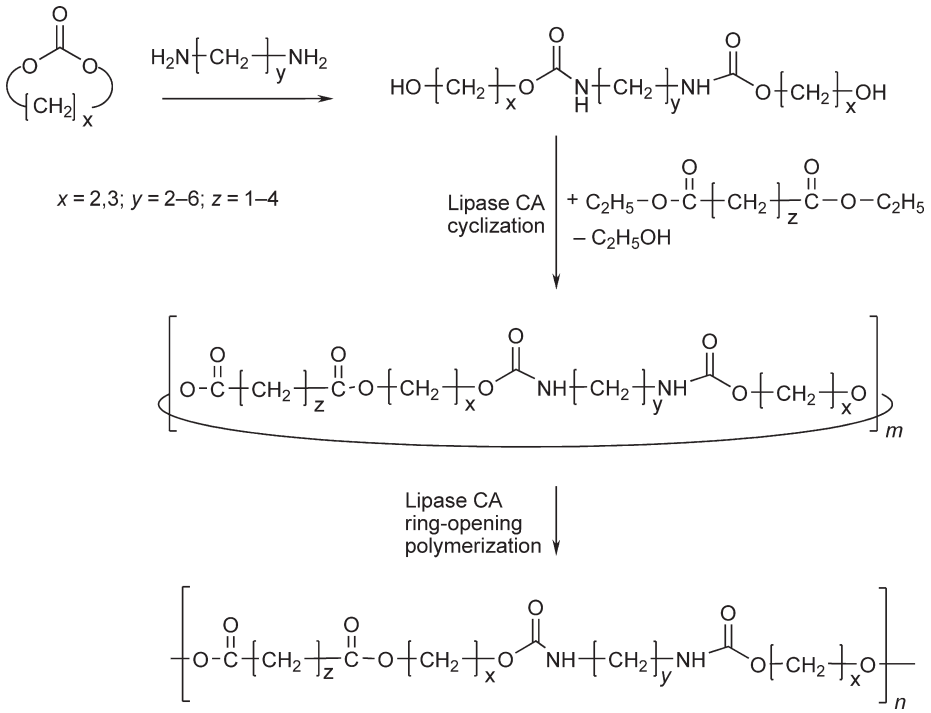

Scheme 89 Enzymatic ROP of a cyclic ester-urethane monomer obtained from cyclic carbonate and diamine.

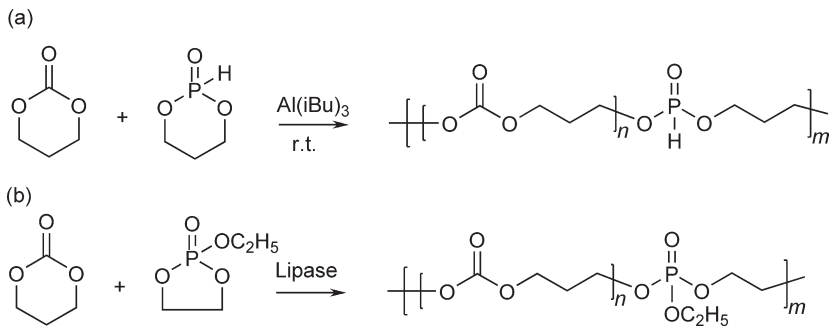

Scheme 90 Copolymerization of TMC with TMP in the presence of Al(*i*Bu)$_3$ as a catalyst (a); enzymatic ring-opening copolymerization of EEP and TMC in the presence of PPL or *C. rugosa* lipase.

10 200 (**Scheme 90(b)**).[301] The degradability of the copolymers was improved by the introduction of an EEP unit to the copolymer chain.

4.12.4.2.5 Cyclic carbonate block copolymers

Nowadays, block copolymers and terpolymers containing PC segments are of interest of many research groups producing biomaterials of special applications. Changing the composition of polymeric blocks as well as the block length, it is possible to tune the properties of the polymeric material such as biodegradation rate, hydrophilic–hydrophobic balance, and temperature sensitivity.

Copolymers containing aliphatic PC blocks can be synthesized according to two main strategies. The first one consists of sequential monomer polymerization proceeding without transformation of the active center. To obtain the copolymer of narrow molecular weight distribution, the order in which the monomers are introduced into reaction system must be adjusted to their reactivity. Additionally, the nature of the active center must be chosen in such a way to eliminate or reduce transesterification as well as backbiting reactions.

It was found that ROP of TMC (first step) and LLA (second step) allowed for the preparation of A–B–A triblock copolymers without significant transesterification. The optimization of the temperature and reaction time were decisive for the success of this approach.[372]

The PC block copolymer can also be obtained using the macroinitiator which constitutes one of the blocks. For the polymerization of cyclic carbonates, hydroxyl telechelic polymers usually are used. First, hydroxyl terminal groups are transformed into alkoxide ones to initiate the anionic ROP. The monofunctional macroinitiators result in A–B or A–B–C block copolymers and the difunctional macroinitiators in B–A–B block copolymers, where A represents the macroinitiator block, B the PC block(s), and C other polymeric blocks. Copolymerization also can proceed in the presence of

insertion-coordination catalysts. Difunctional macroinitiators based on PEO,[205,373–380] PTHF,[204] and PDMS[206] were applied for the ROP of cyclic carbonate.

Hyun *et al.*[182] have decribed synthesis of PTMC–PEG–PTMC triblock and methyl polyethylene glycol (MEPEG)–PTMC diblock copolymers according to the cationic polymerization mechanism using PEG or monomethoxy-PEG and $HCl \cdot OEt_2$ as an initiation system for TMC polymerization.

The syntheses of triblock PEG–CL–TMC copolymers {methoxypoly[(ethylene oxide)-*b*-(CL)-*b*-(trimethylene carbonate)]} were reported by Ould-Ouali *et al.* and Danhier and co-workers.[381,382] These copolymers spontaneously formed micelles and significantly increased the solubility of poorly water-soluble drugs.

Feijen's group synthesized carbonate block copolymers by the ROP of DL-lactide (DLLA), CL, and TMC in the presence of zinc bis-[bis(trimethylsilyl)amide] (97%) and monomethoxy polyethylene glycol (mPEG, 5800 and 1200) at room temperature.[383] In this case zinc bis[bis(trimethylsilyl)amide] combined with mPEG initiated the ROP of heterocyclic monomers with high conversion, affording block copolymers of controlled molecular weight and low dispersity index. Due to its high activity and low toxicity the zinc-based catalyst could be attractive for the synthesis of copolymers for biomedical applications. A similar catalytic system but based on calcium bis[bis(trimethylsilyl)amide] was presented also by Feijen's group.[384]

Hydroxytelechelic PCs are valuable building blocks to access linear A–B–A triblock copolymers incorporating a soft PC segment, such as for instance in PC/polyester, PC/polypeptide, or PC/polyurethane architectures.[385–388]

The synthesis of temperature-responsive poly[(TMC)-*b*-(L-glutamic acid)] copolymer was investigated by Sanson and coworkers.[389] PTMC–PGA diblock copolymer was synthesized by ROP of γ-benzyl-L-glutamate *N*-carboxyanhydride initiated by a primary amine end-functionalized PTMC macroinitiator.

Krogman *et al.*[390] presented the synthesis of blocked poly(phosphazene-*b*-carbonate)s. First, amino-terminated PTMC was synthesized via ROP. In the synthesis of block copolymers of polyphosphazenes linked to PCs the amino terminus was used to form a covalent link to poly(dichlorophosphazene).

Triblock copolymers containing TMC segments and behaving like a thermoplastic elastomer were presented by Feijen's group.[385,391] Such materials were prepared by sequential ROPs of TMC and L-LA as well as TMC and D-LA under argon at 130 °C using 1,6-hexanediol and $Sn(Oct)_2$ as an initiator/catalyst system. First, a hydroxyl group-terminated PTMC was synthesized. These polymers containing polylactide blocks long enough to crystallize exhibited good tensile strenght and excellent resistance to creep. In equimolar blends of these enantiomeric copolymers, stereocomplexation between the enantiomeric polylactide segments occurred. Due to the enhanced phase separation, the specimens of stereocomplex had better resistance to creep than the enantiomeric block copolymers.

It is worth mentioning that instead of homopolymers also random copolymers may constitute the blocks. Feijen's group used a hydroxyl group-terminated random copolymer – poly(TMC-*co*-caprolactone) – instead of homopolycarbonate.[392]

Especially interesting properties exhibited triblock poly{[(CL)-*co*-(TMC)]-*b*-(ethylene oxide)-*b*-[(CL)-*co*-(TMC)]} (PCTC–PEG–PCTC) obtained by Park *et al.*[393] By incorporating up to 25–40 wt.% of the TMC comonomer in the poly(CL) block, the resulting PCTC–PEG–PCTC triblock copolymer achieved sol stability while keeping the thermogelling property in a physiologically important temperature range of 10–50 °C. Thermogelling aqueous solutions of biodegradable polymers can be used as an implantable depot for sustained drug release and tissue engineering. The aqueous polymer solution was a low viscous sol at room temperature (20 °C) and formed a gel at body temperature (~37 °C). The authors assumed that the copolymerization of the TMC and CL would increase the amorphous character of the material and thus avoided the precipitation problem shown in the previously prepared PCL–PEG–PCL triblock copolymer aqueous solution. The PCTC–PEG–PCTC triblock copolymer was prepared according to a classical mode – by random ring-opening copolymerization of CL and TMC in the presence of PEG as a macroinitiator and $Sn(Oct)_2$ as a catalyst.

The first example of biodegradable segmented copolymers introduced in 1980s as a monofilament suture was Maxon™ (Syneture), also containing a random poly(TMC-*co*-GL) middle block. The copolymer was prepared by ring-opening copolymerization of GL and TMC, the final composition being defined by a 67.5 wt.% of GL (**Scheme 91**).[394]

The synthesis of amphiphilic diblock copolymers with various block compositions on the basis of poly(2-ethyl-2-oxazoline) (PEtOz) as a hydrophilic block and PTMC as a hydrophobic block was reported by Kim *et al.*[395] TMC was polymerized in the presence of hydroxyl-terminated PEtOz and $Sn(Oct)_2$ in chlorobenzene under reflux for 39 h.

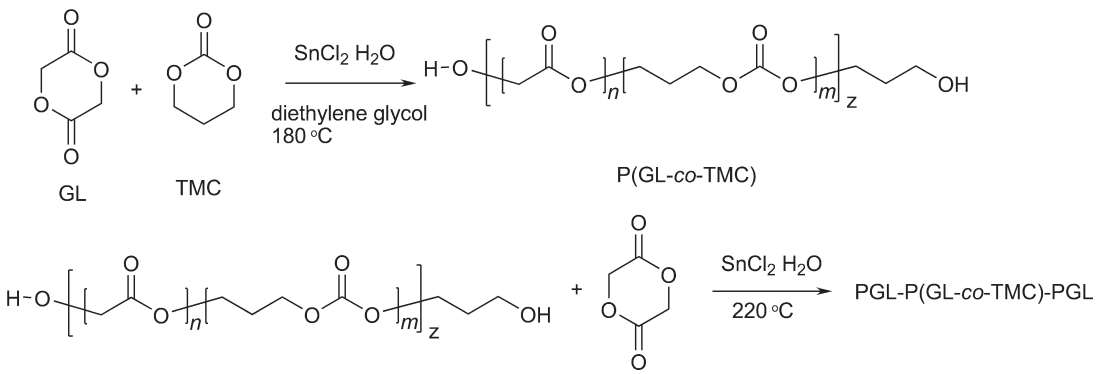

Scheme 91 Biodegradable segmented copolymers of TMC and glycolide.

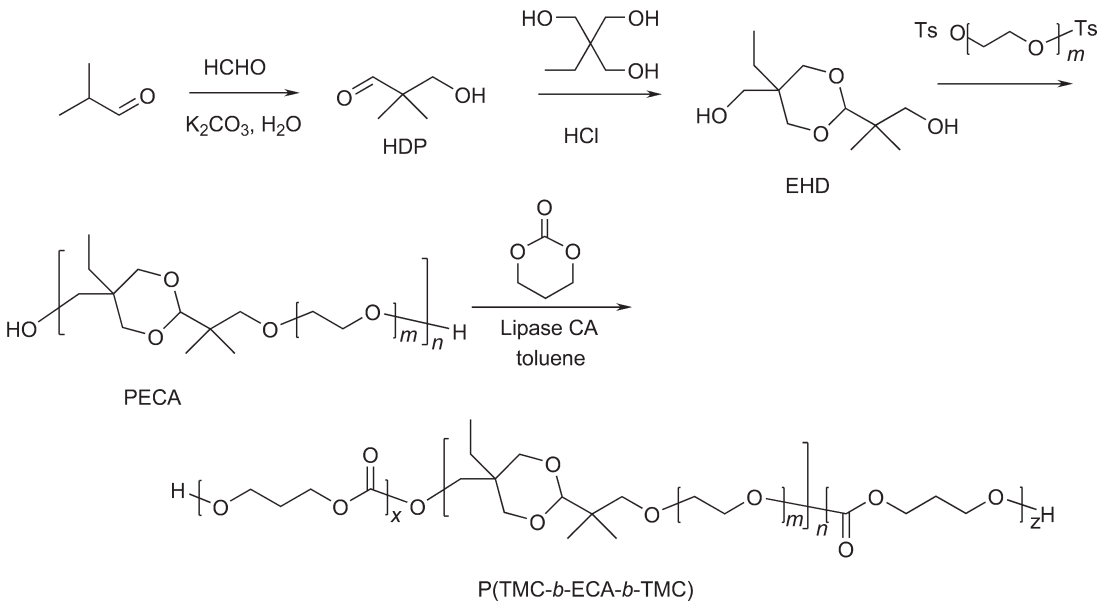

Scheme 92 Chemoenzymatically synthesized degradable triblock copolymers (PTMC-*b*-PECA-*b*-PTMC).

Kaihara *et al.*[396] described chemoenzymatically synthesized degradable triblock poly[(TMC)-*b*-(ethylene oxide-*co*-cyclic acetal)-*b*-(TMC)] (PTMC-*b*-PECA-*b*-PTMC) (**Scheme 92**). Cyclic acetal was introduced into a PEG segment as a degradable segment to impart a pH-dependent degradation nature and to prevent the formation of acidic degradation products. Amphiphilic polymeric micelles were successfully prepared from such a triblock copolymer.

According to the second method of carbonate block copolymer synthesis, sequential monomer polymerization is proceeded with transformation of the active center. The block copolymers are prepared in three steps. First, the polymerization of one monomer is carried out. After complete conversion of the first monomer the transformation of active centers is performed, and the initiation of the polymerization of the second monomer is proceeded. For example, this approach was applied for obtaining poly(styrene-*b*-neopentyl carbonate).[203] After completion of the styrene living polymerization, carbanionic centers were transformed into alkoxide ones via reaction with EO and then the ROP of neopentyl carbonate polymerization was performed. In the case of block copolymers of methyl methacrylate with neopentyl carbonate living PMMA, prepared according to GTP, was used as a macroinitiator for DTC polymerization. A silyl keteneacetal active center was transformed to an alkoxide one.[222] Depending on the functionality of the macroinitiator (A) used for cyclic carbonate polymerization, two types of block copolymers can be obtained: A-B or B-A-B.

An inverse manner of copolymerization was proposed by Watanabe *et al.*[397] First, they polymerized TMC using 4-(chloromethyl)benzyl alcohol (CBA) as an initiator and DBU as an organocatalyst. The benzyl chloride group was involved in the incorporation of dithiocarbamate for pseudo-living radical polymerization of vinyl monomers. The authors applied *N*-isopropylacrylamide, acrylamide glycolic acid, and 2-hydroxyethyl methacrylate as vinyl monomers for the second step of copolymerization (**Scheme 93**). The resulting block copolymers were water soluble due to incorporation of hydrophilic segment into hydrophobic PTMC.

The synthesis of multiblock cyclic carbonate copolymers was presented by Kricheldorf and Rost.[398] First, telechelic random copolymers were prepared by copolymerization of CL and TMC in bulk using bismuth(III) hexanoate [$Bi(OHex)_3$] as an initiator. A-B-A triblock copolymers were synthesized by chain extension of these random copolymers with L-LA. Finally, the triblock copolymers were transformed into multiblock copolymers by chain extension with 1,6-hexamethylene diisocyanate. It is worth mentioning that all three synthetic steps were performed in a 'one-pot procedure'.

Kricheldorf's group also proposed another approach to multiblock copolymers of TMC and LLA synthesis.[234] Sequential copolymerizations of TMC and LLA were performed with 2,2-dibutyl-2-stanna-1,3-oxepane as a bifunctional cyclic initiator. The cyclic triblock copolymers were transformed *in situ* into multiblock copolymers by ring-opening polycondensation with sebacoyl chloride (**Scheme 94**).

4.12.4.2.5(i) Nonlinear carbonate block copolymers

As Hyun has recently revealed, the precise nature of the block copolymer architectures plays an important role in determining their hydrophilic–hydrophobic properties – nonlinear asymmetric (AB_2- or AB_3-type) block copolymers exhibit different micellization behavior compared with the corresponding linear AB diblocks.[399] Taking the above into account Zhang *et al.* prepared the Y-shaped (AB_2-type) amphiphilic copolymers of PEG with TMC, PEG-*b*-$(PTMC)_2$. The block copolymer was synthesized by the ROP of TMC with dihydroxy-modified monomethoxy-PEG [$mPEG(OH)_2$] initiator using $ZnEt_2$ as a catalyst.[400] First, a dihydroxy functional ROP macroinitiator was synthesized by esterification of acryloyl bromide with mPEG, followed by Michael addition using excess of diethanolamine (**Scheme 95**).

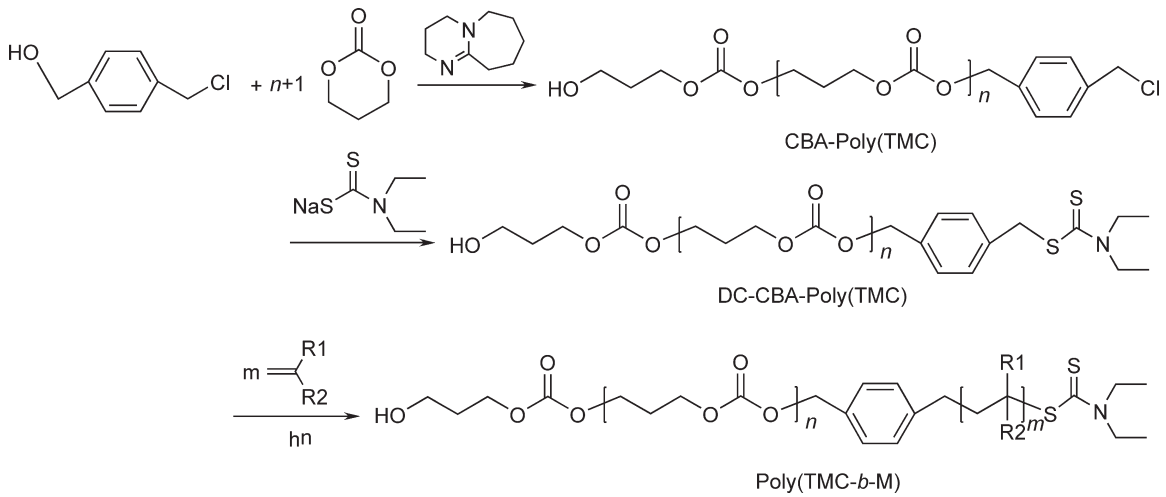

Scheme 93 Preparation of polycarbonates with dithiocarbamate groups for pseudo-living radical polymerization of vinyl monomers.

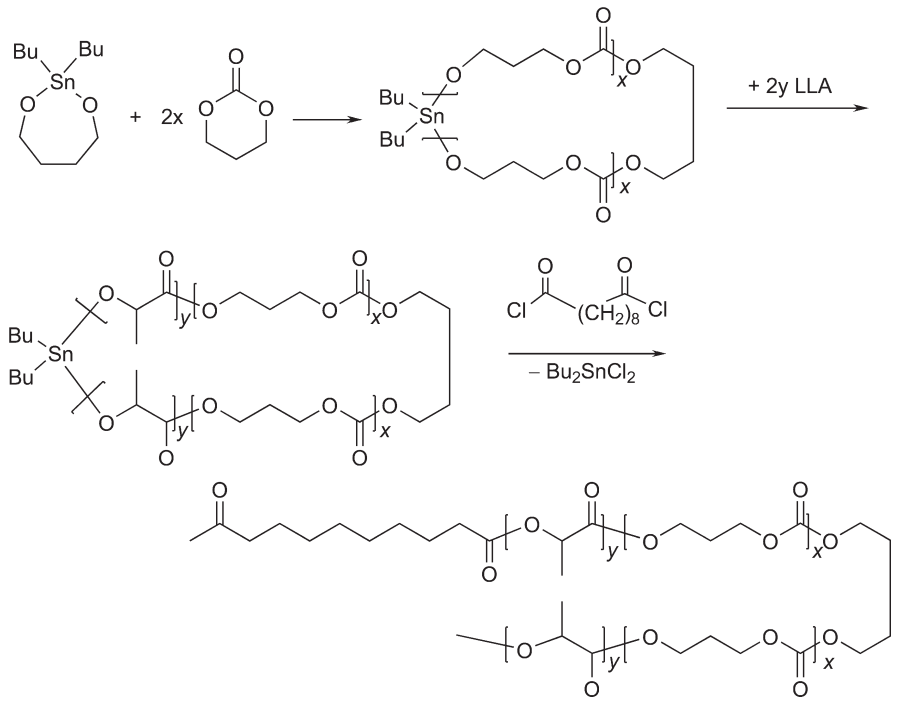

Scheme 94 Sequential copolymerizations of TMC and LLA with 2,2-dibutyl-2-stanna-1,3-oxepane as a bifunctional cyclic initiator.

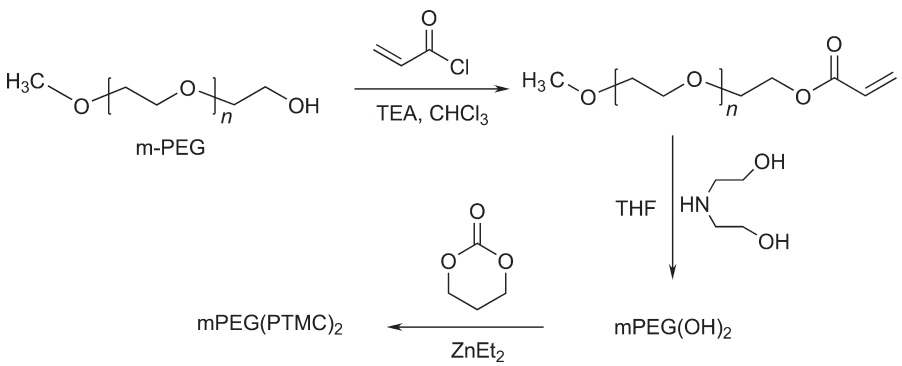

Scheme 95 Synthesis of Y-shaped amphiphilic PEG(PTMC)$_2$ block copolymers via ROP of TMC using mPEG with bishydroxyl end-groups as macroinitiator and $ZnEt_2$ as a catalyst.

A series of Y-shaped amphiphilic PEG(PTMC)$_2$ block copolymers were obtained via ROP of TMC using this mPEG with bishydroxyl end-groups as macroinitiator and $ZnEt_2$ as a catalyst. It was shown that the Y-shaped copolymer mPEG(PTMC)$_2$ could self-assemble into micelles in aqueous medium and the critical micelle concentration values of the micelles decreased with an increase in the hydrophobic PTMC block length of mPEG(PTMC)$_2$.

4.12.4.2.5(ii) Star-shaped carbonate block copolymers

Morinaga *et al.*[401] reported star-shaped, amphiphilic block copolymers prepared by the polymerizations of TMC initiated with a three-armed, PEG-based surfactant (Tween 20) without any catalysts. The metal- and solvent-free polymerization was proceeded at 150 °C to afford star-shaped poly[(ethylene oxide)-*b*-(TMC)] with a sorbitan monolaurate core of molecular weights of 4500–11 900 in good yields (**Scheme 96**).

Similar star-shaped poly[(TMC)-*co*-(CL)] and its block copolymers with lactide/GL were investigated by Joziasse *et al.*[402] When dipentaerythritol was used as a six-functional initiator, cross-linked rubbers were obtained, swelling in chloroform. Star-shaped lactide/GL block copolymers with a poly[(TMC)-*co*-(CL)] rubber core based on D-sorbitol exhibited good mechanical properties.

4.12.5 Polymerization of Cyclic Thiocarbonates

The polymerization of ethylene monothiocarbonate (1,3-oxathiolan-2-one) was carried out in the presence of metal alkyls such as $ZnEt_2$ or $CdEt_2$ and metal alkoxides like $Mg(OCH_3)_2$, $Al(OBu)_3$, or $Ti(OBu)_4$. The polymerization with these catalysts was accompanied by carbon dioxide elimination and the polymers obtained appeared to be poly(ethylene sulfide-monothiocarbonate)s. The content of ethylene monothiocarbonate (oxycarbonylthioethylene) units and ethylene sulfide (thioethylene) units in the produced polymers depended on the catalysts used, but all the polymers yielded from the ethylene monothiocarbonate polymerization at 80 °C contained less than 50 mol.% of monothiocarbonate units.[403] As compared with the EC polymerization, the ethylene monothiocarbonate polymerization with coordination catalysts proceeds easier and also may involve decarboxylation to a lesser extent. The decarboxylation during the ethylene monothiocarbonate polymerization seems to involve the metal–monothiocarbonate species that are analogous to those formed in the system with EC. However, the ethylene monothiocarbonate decarboxylation leads to metal thiolate species, which may be outlined schematically as in **Scheme 97**.

The metal thiolate species are more reactive toward coordinating the monothiocarbonate monomer during the polymerization (**Scheme 98**) than the corresponding metal alkoxide species operating in the EC polymerization.

The relatively highest efficiency of the diethylcadmium catalyst in the ethylene monothiocarbonate polymerization (at 80 °C), as regards the high content of ethylene monothiocarbonate units in the polymer obtained, results probably from the softness of both cadmium and sulfur atoms fitting one to the other, to participate in the covalent bonding. Thus, decarboxylation occurs to the lowest extent. Moreover, the propagation according to **Scheme 99**, involving the formation of the cadmium–sulfur bond leading to the metal thiolate species of relatively high activity, occurs more likely than that which might involve the formation of the less reactive metal alkoxide species.

1,3-Dioxane-2-thione (trimethylene thiocarbonate (**1**), **Scheme 99**) was prepared by the reaction of PPD with

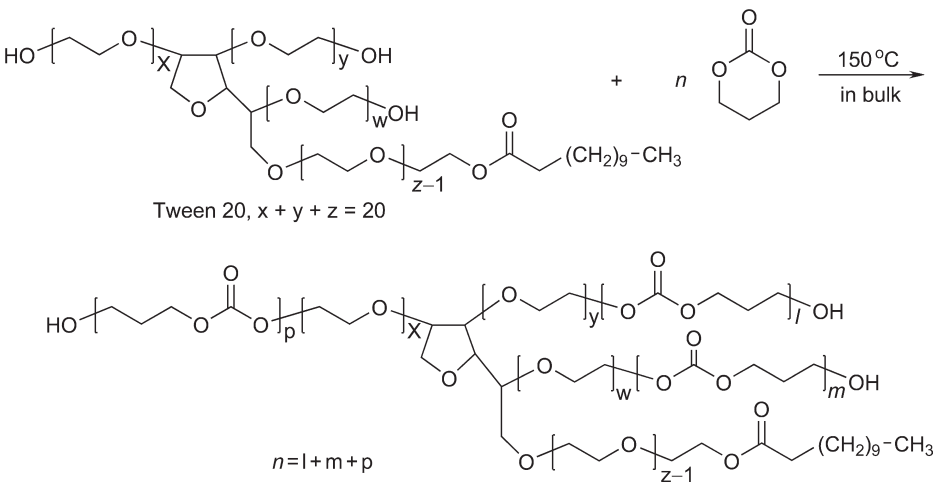

Scheme 96 Star-shaped, amphiphilic block copolymers prepared by the polymerizations of TMC initiated with a three-armed PEG-based surfactant.

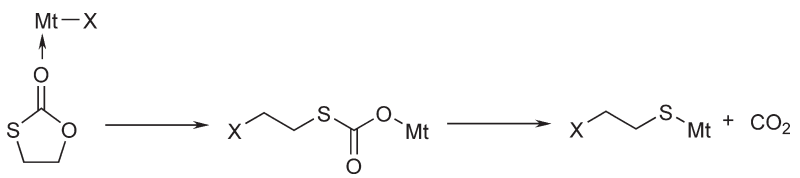

Scheme 97 Decarboxylation during the ethylene monothiocarbonate polymerization in the presence of the metal alkyls and metal alkoxides.

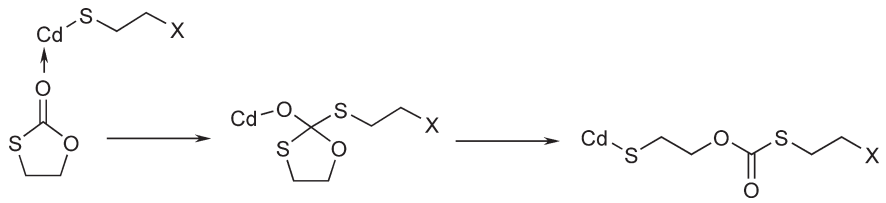

Scheme 98 Polymerization of ethylene monothiocarbonate in the presence of metal thiolates.

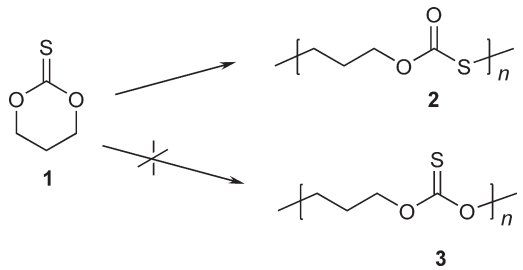

Scheme 99 Cationic polymerization of 1,3-dioxane-2-thione.

thiophosgene and a tertiary amine.[404] This monomer is unstable at >25 °C due to spontaneous oligomerization. Its cationic polymerization in chloroform yielded a relatively high-molecular-weight poly(trimethylene thiocarbonate). IR, ^{1}H, and ^{13}C NMR spectroscopy proved that the oligomers of the spontaneous polymerization and the polymers resulting from the cationic polymerizations possess the structure of a poly (mercaptopropanol carbonate), poly(MPOC) (**2**, **Scheme 99**). All attempts to prepare a polythiocarbonate of isomeric structure (**3**, **Scheme 99**) by anionic polymerizations failed. In contrast to the amorphous PTMC, the poly(MPOC) proved to be a rapidly crystallizing polymer. The cationic polymerization of substituted six-membered cyclic monothiocarbonates such as 5,5-dimethyl-1,3-dioxane-2-thione has also been performed, yielding the corresponding poly(monothiocarbonate)s of the same chain structure.[34]

Similarly, anionic polymerization of six-membered cyclic thiocarbonate derivatives, 5,5-(bicyclo[2.2.1]hept-2-en-5,5-ylidene)-1,3-dioxane-2-thione and 5,5-(bicyclo[2.2.1]heptan-5,5-ylidene)-1,3-dioxane-2-thione, initiated by DBU afforded poly(MPOC) derivatives.[405] It is worth mentioning that those polymers were characterized by a significant 12.3 and 12.6% volume expansion during polymerization, respectively.

The cationic ROP of a seven-membered cyclic monothiocarbonate, 1,3-dioxepan-2-thione, produced a polymer through the selective isomerization of thiocarbonyl to a carbonyl group as well.[406] The molecular weights of the polymer could be controlled by the feed ratio of the monomer to the initiators or the conversion of the monomer during the polymerization, although some termination reactions occurred after the complete consumption of the monomer.

In contrast to five-membered cyclic carbonates, dithiocarbonates undergo cationic ROP to afford corresponding poly (dithiocarbonate)s without evolution of gaseous compounds.[407,408] A five-membered cyclic dithiocarbonate containing a benzyloxymethyl group exhibits interesting features.[409] The monomer, 5-benzyloxymethyl-1,3-oxathiolane-2-thione, subjected to cationic polymerization initiated by CF_3SO_3H or $CF_3SO_3CH_3$ at 60 °C afforded corresponding poly (dithiocarbonate) with $M_n = 9000–25\,000$ in 60–100% yields (**Scheme 100**). The narrow dispersity of the poly(dithiocarbonate)s (1.09–1.29) and the M_n increase in direct proportion to monomer conversion indicate living cationic polymerization based on neighboring group participation. The formation of a carbenium cation stabilized by neighboring benzyloxymethyl group participation, as observed by NMR spectroscopy, might result in the living polymerization.[409]

4.12.6 Polymerization of Macrocycles

4.12.6.1 Polymerization of Macrocyclic Aromatic Carbonates

Aromatic PCs are produced technically from bisphenols via transesterification or interfacial phosgenation. In addition,

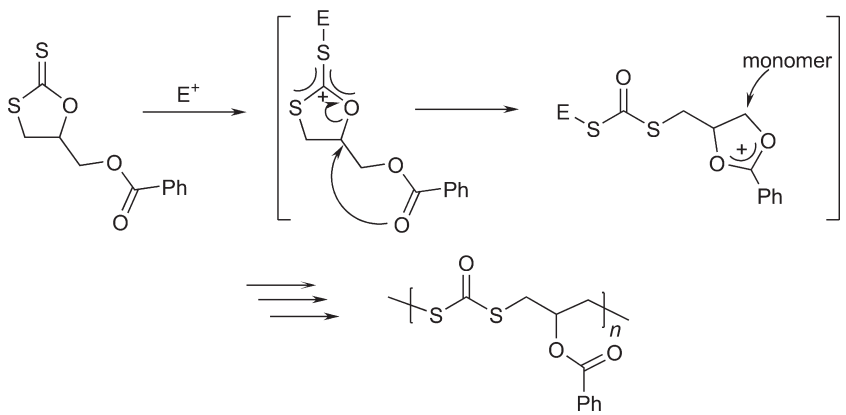

Scheme 100 Cationic polymerization of 5-benzoxymethyl-1,3-oxathiolane-2-thione.

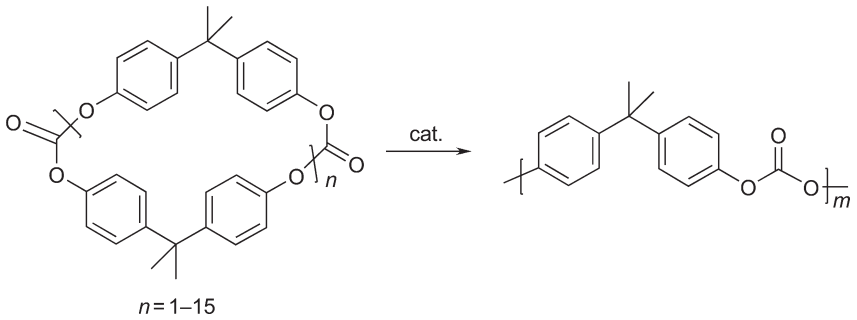

Scheme 101 Polymerization of macrocyclic aromatic carbonates.

ROP in the melt and solid-state polymerization has been developed.

Reactions of ROP can be divided into three groups: those with large reaction exotherms, such as epoxide of large ring strain polymerization; those with moderate exotherms, such as ε-caprolactam or TMC polymerization; and those that are driven by entropy, rather than enthalpy, such as certain cyclic siloxane polymerizations and the polymerizations of oligomeric aromatic cyclic carbonates described in this chapter.[1] Molecular simulation studies on certain cyclic monomers have been carried out by Stewart.[410] He verified that cyclic dimer (**Scheme 101**, $n = 1$) is a tightly packed molecule with a ring strain of 16 kcal mol^{-1}. However, the cyclic tetramer of 48-membered ring size (**Scheme 101**, $n = 3$) is already stress free and the polymerization of such molecule is driven solely by entropy. It is also characterized by a large (12 Å) cavity inside the ring.

Due to their low molecular weight, the cyclic oligomeric carbonates have melt viscosities significantly lower than that of conventionally prepared PCs. This lowered melt viscosity is one of the most useful properties in several applications. At their melting point the mixture of cyclic oligomers have significant flow and have a greater penetration and wetting of fibers in composite applications. There also exists a great potential for the preparation of inorganic organic hybrid materials starting with these cyclic aromatic carbonates.

Fundamental studies on the polymerization of BPA cyclic oligomers have been reported by Evans *et al.*[411] As a starting material they used cyclic oligomers of $M_w = 1300$ determined by GPC with the dispersity index of 1.5. Blank experiment of polymerization performed in glass tubes at 300 °C under nitrogen without addition of catalyst showed modest increase in molecular weight up to 17 000. However, the addition of various catalysts (lithium stearate and Tyzor AA) yielded very high-molecular-weight PCs ($M_w = 117\,000$–$300\,000$). HPLC of the fraction soluble in acetone indicated that only 0.25% of cyclic monomers remained after polymerization. The heat measured with DSC was found to be − 1.2 kJ mol. This slight exotherm can be correlated to the release of ring strain in opening the previously mentioned cyclic dimer. Thus, in general, the reaction seems to be driven by entropy toward formation of linear PC.

Moreover, the dispersity index of the polymers approximately equals 2.0, which indicates that ring-chain and chain–chain equilibration are achieved during the polymerization. Total equilibration is a result of nearly equal energies of the attack on a monomer ring and a carbonate bond in a polymer chain. Due to the size and conformation of the monomer, very few rings are present at equilibrium.

The ROP of BPA-based cyclic carbonates has some of the characteristics of a living polymerization.[1] Upon initiation, the propagation reactions continue until all the cyclic monomers are consumed and the chain ends remain active. Addition of additional portions of a cyclic monomer gives continued reaction and a higher molecular weight as the ratio of monomer to initiator increases. Moreover, the molecular weight of the polymer can be controlled by use of bisphenols or diphenyl carbonate as chain transfer agents.

Stewart has studied the melt polymerization of BPA cyclic oligocarbonates using a rheokinetic method.[412] The reactor was equipped to measure changes in melt viscosity as the reaction proceeded. Despite the fact that melt viscosity is a function of many variables, it was possible to obtain the relative polymerization rates by plotting the viscosity (stirrer torque) as a function of time over the portions of curve where steepest increases were seen. The relative reaction rates for sodium phenoxide-initiated polymerization were measured at five temperatures, in order to construct the Arrhenius plot. The activation energy calculated from the plot (12.5 kcal mol^{-1}) corresponded with the activation energy typical for diaryl carbonate transesterification.[413] Since the activation energy of viscous flow of PC resin is about 23.4 kcal mol^{-1}, it can be concluded that the polymerization of cyclic oligomers is not limited by the diffusion of the reactive end-groups in the polymer melt. In fact, each phenoxide active end-group is surrounded by large excess of carbonate groups coming from cyclic monomers, as well as linear PCs. In such an environment, transesterification reactions are indiscriminate and do not require diffusion over long distances. High-molecular-weight PCs with dispersities lower than those obtained by conventional methods were obtained by Keul *et al.*[208] Polymerizations were performed in THF solution, using potassium dihydronaphthylide as the initiator.

The cyclization and polymerization procedures developed and optimized for the BPA system are fairly general and have been successfully applied to a variety of other bisphenols.[16] Functional groups such as ester, amide, ketone, sulfone, and urethane have been incorporated into the PCs via the cyclic oligomer approach. Brunelle and Shannon[414,415] reported the synthesis of a number of such cyclic monomers and their subsequent polymerization yielding high-molecular-weight PCs. In all cases the reported carbonate functionality played a critical

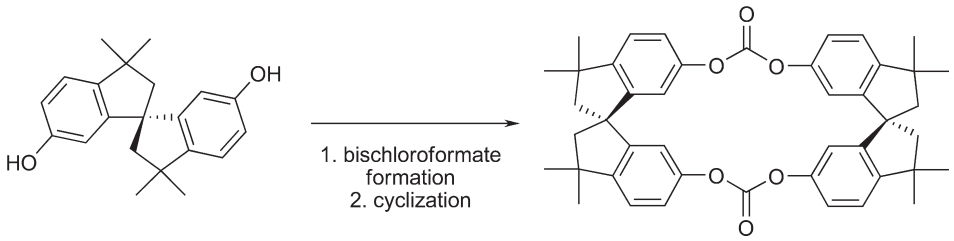

Scheme 102 Spirobiindane bisphenol-based cyclic carbonate.

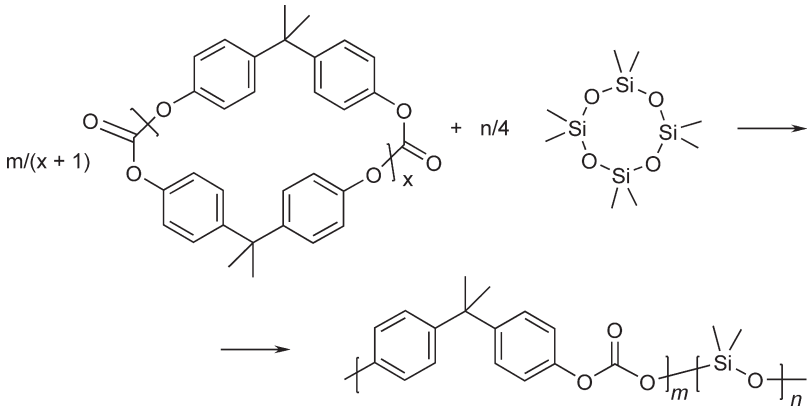

Scheme 103 Direct copolymerization of macrocyclic carbonates with cyclic dimethylsiloxane.

role in cyclic oligomer formation and further in ROP. There were also some bizarre structures, such as spirobiindane bisphenol, used for the preparation of cyclic oligomers (Scheme 102).[416] This rigid molecule favored the formation of cyclic structures, which were isolated with 95% yield. Moreover, the polymerization of such a monomer gave PCs of increased glass transition temperature up to 200 °C. The drawback of the rigid structure of the bisphenol was the higher amount of cyclic products at equilibrium; however, it was eliminated by copolymerization of spirobiindane bisphenol cyclic carbonate with a regular, BPA-based one.

There are numerous reports of the uses of cyclic oligomeric carbonates for copolymerization. Evans and Carpenter[417] reported the preparation of PC/PDMS copolymers (Scheme 103). Two approaches were used in the preparation of the copolymers: the first one used direct reaction of macrocyclic carbonates with cyclic siloxanes, the second one reaction of hydroxy-terminated linear PCs with chlorosilane-terminated PDMSs.

In case of direct copolymerization (Scheme 103) only 52–58% of the siloxane was incorporated into the polymer structure. The PC glass transition temperature (148 °C) was not altered by incorporation of siloxanes. Alternatively, either 'living' PC or 'living' polysiloxane was used to initiate ROP of cyclic siloxane or cyclic carbonate, respectively. Block copolymers were obtained by ROP of cyclic carbonate with BPA, which resulted in hydroxy-terminated PCs, followed by reaction of chlorosilane-terminated polysiloxane. Block copolymers showed good optical clarity and lowered glass transition temperature (110 °C).

Besides siloxane copolymers, poly(phenylene oxide)/PCs,[418] epoxide/PCs,[419] polyimidecarbonates,[420] polyamidecarbonates,[421] polyurethanecarbonates,[422] and copolymers with aliphatic lactones such as pivalactone and CL were also reported.[423]

Cyclic carbonate chemistry has also proven to be useful for the preparation of branched or cross-linked polymers. First branched (hyperbranched) PCs were synthesized by Bolton and Wooley.[424] In one of the published methods of synthesis of hyperbranched PCs they used chloroformate-type 1,1,1-tris(4-hydroxyphenyl) ethane (THPE)-based monomers (Scheme 100).[13] The authors synthesized hyperbranched aromatic PCs by the polymerization of A_2B and AB_2 monomers, which involved the condensation of chloroformate (Scheme 104) functionalities with *tert*-butyldimethylsilyl-protected phenols (Scheme 104), facilitated by reactions with silver fluoride.

The same structure of THPE was used as initiator for ROP of cyclic aromatic carbonates by Krabbenhoft *et al.*[425] The polymerization in the system containing 0.3–1.5 mol.% of THPE resulted in branched resins with enhanced shear sensitivities by as much as 660% when compared with linear PC.

Cross-linked aromatic PCs could be obtained from cyclic oligomers according to three methods. The first one, presented by Rosenquist, is based on the application of biscyclic carbonate (1, Scheme 105) containing two eight-membered rings.[426] Mixtures of small amounts of the biscyclic carbonate with cyclic oligomers were polymerized to give highly cross-linked PC resins characterized by low swelling factor (5.5%) using only 2% of cross-linking agent. The second method utilized multifunctional epoxy compounds. One of the most effective

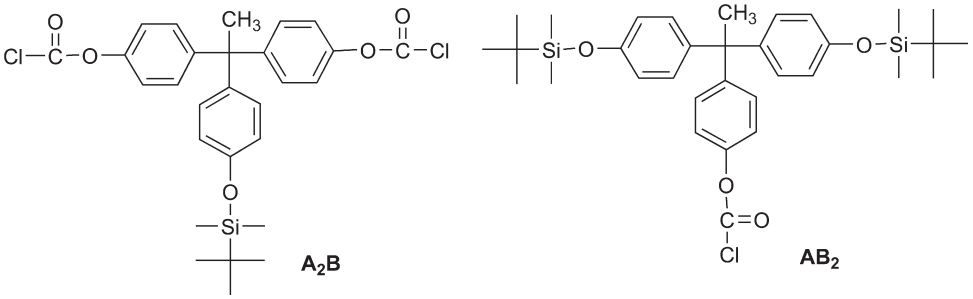

Scheme 104 Chloroformate monomers used in the synthesis of hyperbranched polycarbonates.

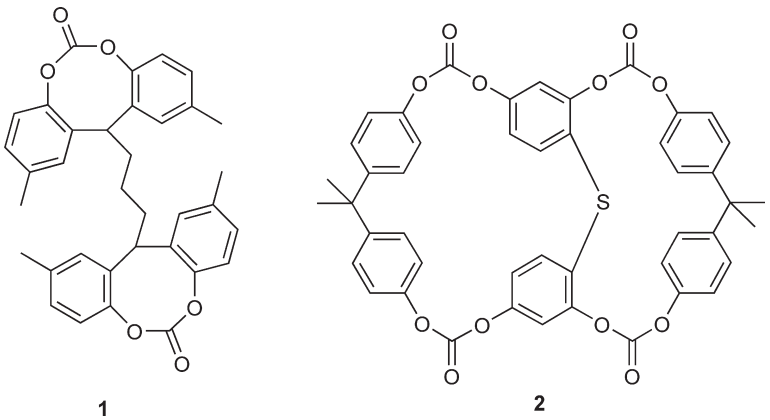

Scheme 105 Biscyclic cross-linking agents for aromatic cyclic carbonates.

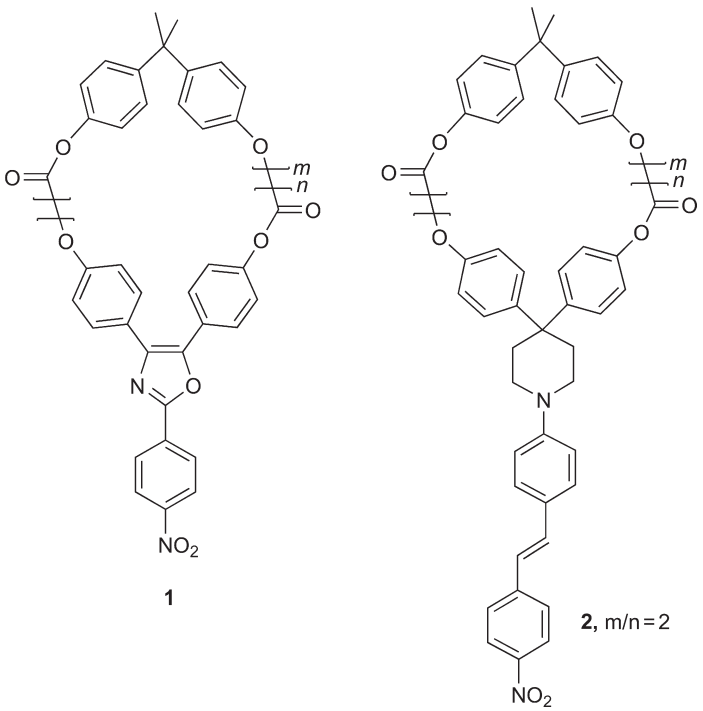

Scheme 106 Mixed type macrocyclic oligocarbonates.

were copolymers of glycidyl methacrylate/styrene resins. The third method uses oligomeric oligocarbonates based on tri- or tetraphenols such as resorcinol sulfide (**2**, **Scheme 105**) as cross-linkers.[427] Again ROP of cyclic oligomers with addition of such compounds yielded highly cross-linked PCs.

The preparation of nonlinear optical (NLO) PCs via macrocyclic prepolymers has the advantage that the low viscosity oligomer mixtures make reactive processing possible. The conversion of macrocycles to polymer occurs with nonvolatile by-products or very little change in volume and can be done simultaneously with electric field poling and, if desired, chemical cross-linking. Kulig *et al.*[428] prepared such PCs based on a triphenyloxazole monomer (**1**, **Scheme 106**). This monomer contained a required NLO material-conjugated system with electron donating and accepting groups. Moreover, it showed good thermal stability to withstand ROP conditions (15–30 min at 250 °C) and structural similarity to BPA. The cyclic oligocarbonates were obtained from the corresponding bis(chloroformates), which were prepared by the reaction of a bisphenol molecule with phosgene. Attempts to prepare the homopolymer produced intractable materials. Therefore, a mixture of BPA and triphenyloxazole derivative was used in the reaction feed (**1**, **Scheme 106**). ROP yielded polymers of $M_w = 69\,000$. The T_g of the final polymer could be controlled by the molar ratio of the triphenyloxazole to BPA. The incorporation of triphenyloxazole increased the T_g of copolycarbonate up to 214 °C (30 mol.% of oxazole).

Another NLO chromophore based on 4-*N*, *N*-dimethylamino-4′-nitrostilbene which contained bisphenol functionality for PC preparation was synthesized in the same manner (**2**, **Scheme 106**).[429] It was used to make macrocyclic carbonate oligomers and the oligomers were converted to PC via ROP in solution.

4.12.7 Conclusions

PCs are usually synthesized by a step-growth process, that is, polycondensation, from phosgene or its derivatives and dihydroxy compounds. Instead of phosgene's method dialkyl- or diphenylcarbonate can also be applied for PC production. The ROP of cyclic carbonates is an alternative method for the synthesis of both aliphatic and aromatic PCs. A comparison of these two methods is in favor of chain-growth process. The polycondensation affords rather limited molecular weight polymers, while high-molecular-weight PCs can be prepared in the ROP of cyclic monomers.

Cyclic carbonate monomers with a variety of functional groups have been prepared and polymerized by means of ROP. Not only the polymer microstructure and architecture but also the molecular weight and molecular weight distribution may be well controlled. A variety of carbonate copolymers comprising blocks of different chemical structures were also prepared. By changing the chemical character of the blocks as well as block lengths mechanical as well as chemical and biochemical properties can be tuned in accordance with target applications. The unique property of six- and seven-membered cyclic carbonates concerning volume expansion during polymerization additionally makes this class of compounds valuable prospective monomers. Recent developments in organocatalysts for the ROP of cyclic carbonate allow processes, which proceed without transesterification, to create polymers that are metal-free and, therefore, good candidates for biomedical and microelectronic applications.

References

1. Brunelle, D. J. In *Ring-Opening Polymerization*;Brunelle, D. J., Ed.; Hanser Verlag: Munich, Germany, 1993; p 309.
2. Brunelle, D. J. In *Macromolecular Design of Polymeric Materials*; Hatada, K., Tatsuki, K., Vogl, O., Eds.; Marcel Dekker: New York, NY, 1997; p 295.
3. Brunelle, D. J.; Smigelski, P. M.; Boden, E. P. In *Advances in Polycarbonates*; Brunelle, D. J., Korn, M. R., Eds.; American Chemical Society: Washington, DC, 2005; p 8.
4. Rokicki, G. *Prog. Polym. Sci.* **2000**, *25*, 259.
5. Kuran, W. *Prog. Polym. Sci.* **1998**, *23*, 919.
6. Matsuo, J.; Aoki, K.; Sanda, F.; *et al. Macromolecules* **1998**, *31*, 4432.
7. Pego, A. P.; Zhong, Z.; Dijkstra, P. J.; *et al. Macromol. Chem. Phys.* **2003**, *204*, 747.
8. Albertsson, A.-C.; Eklund, M. *J. Polym. Sci., Part A: Polym. Chem.* **1994**, *32*, 265.
9. Hill, J. W.; Carothers, W. H. *J. Am. Chem. Soc.* **1933**, *55*, 5031.
10. Carothers, W. H.; Hill, J. W. *J. Am. Chem. Soc.* **1933**, *55*, 5043.
11. Spanagel, E. W.; Carothers, W. H. *J. Am. Chem. Soc.* **1935**, *57*, 929.
12. Soga, K.; Hosoda, S.; Tazuke, Y.; *et al. J. Polym. Sci., Polym. Lett. Ed.* **1976**, *14*, 161.
13. Penco, M.; Donetti, R.; Mendichi, R.; *et al. Macromol. Chem. Phys.* **1998**, *199*, 1737.
14. Inoue, S. *Chem. Tech.* **1976**, *6*, 588.
15. Schnell, H.; Bottenbruch, L. *Makromol. Chem.* **1962**, *57*, 1.
16. Brunelle, D. J.; Shannon, T. G. *Polym. Prepr., ACS Div. Polym. Chem.* **1992**, *33*, 1198.
17. Rosselli, S.; Maggio, A.; Bellone, G.; *et al. Tetrahedron Lett.* **2006**, *47*, 7047.
18. Sarel, S.; Pohoryles, L. A.; Ben-Shoshan, R. *J. Org. Chem.* **1959**, *24*, 1873.
19. Carothers, W. H.; Van Natta, F. J. *J. Am. Chem. Soc.* **1930**, *52*, 314.
20. Ludwig, B. J.; Piech, E. C. *J. Am. Chem. Soc.* **1951**, *73*, 5779.
21. Venturello, C.; D'Aloisio, R. *Synthesis* **1985**, 33.
22. Soga, K.; Toshida, Y.; Hosoda, S.; *et al. Makromol. Chem.* **1977**, *178*, 2747.
23. Soga, K.; Toshida, Y.; Hosoda, S.; *et al. Makromol. Chem.* **1978**, *179*, 2379.
24. Rokicki, G.; Kuran, W. *Bull. Chem. Soc. Jpn.* **1984**, *57*, 1662.
25. Fianz, G.; Gallot, Y.; Parrod, J.; *et al. J. Polym. Sci., Polym. Chem. Ed.* **1962**, *58*, 1363.
26. Kang, S. K.; Yamaguchi, T.; Pyun, S. J.; *et al. Tetrahedron Lett.* **1998**, *39*, 2127.
27. Lu, L.; Fang, J. M.; Lee, G. H.; *et al. J. Chin. Chem. Soc.* **1997**, *44*, 279.
28. Jianga, Z.-X.; Qing, F.-L. *J. Fluorine Chem.* **2003**, *123*, 57.
29. Tomishige, K.; Yasuda, H.; Yoshida, Y.; *et al. Catal. Lett.* **2004**, *95*, 45.
30. Tomishige, K.; Yasuda, H.; Yoshida, Y.; *et al. Green Chem.* **2004**, *6*, 206.
31. Huang, S.; Ma, J.; Li, J.; *et al. Catal. Commun.* **2008**, *9*, 276.
32. Nomura, R.; Ninagawa, A.; Matsuda, H. *J. Org. Chem.* **1980**, *45*, 3735.
33. Darensbourg, D. J.; Holtcamp, M. W. *Coord. Chem. Rev.* **1996**, *153*, 155.
34. Nemoto, N.; Sanda, F.; Endo, T. *Macromolecules* **2000**, *33*, 7229.
35. Yano, T.; Matsui, H.; Koike, T.; *et al. Chem. Commun.* **1997**, *12*, 1129.
36. Yamaguchi, K.; Ebitani, K.; Yoshida, T.; *et al. J. Am. Chem. Soc.* **1999**, *121*, 4526.
37. Zhao, T.; Han, Y.; Sun, Y. *Phys. Chem. Chem. Phys.* **1999**, *1*, 3047.
38. Kim, H. S.; Kim, J. J.; Lee, B. G.; *et al. Angew. Chem., Int. Ed.* **2000**, *39*, 4096.
39. Iwasaki, T.; Kihara, N.; Endo, T. *Bull. Chem. Soc. Jpn.* **2000**, *73*, 713.
40. Ji, D.; Lu, X.; He, R. *Appl. Catal. A* **2000**, *203*, 329.
41. Kawanami, H.; Ikushima, Y. *Chem. Commun.* **2000**, 2089.
42. Tu, M.; Davis, R. J. *J. Catal.* **2001**, *199*, 85.
43. Bhanage, B. M.; Fujita, S.; Ikushima, Y.; *et al. Appl. Catal. A* **2001**, *219*, 259.
44. Paddock, R. L.; Nguyen, S. T. *J. Am. Chem. Soc.* **2001**, *123*, 11498.
45. Peng, J.; Deng, Y. *New J. Chem.* **2001**, *25*, 639.
46. Aresta, M.; Dibenedetto, A. *J. Mol. Catal. A* **2002**, *182–183*, 399.
47. Kihara, N.; Hara, N.; Endo, T. *J. Org. Chem.* **1993**, *58*, 6198.
48. Zhu, H.; Chen, L. B.; Jiang, Y. Y. *Polym. Adv. Technol.* **1996**, *7*, 701.
49. Gomes, C. R.; Ferreira, D. M.; Constantino, C. J. L.; *et al. Tetrahedron Lett.* **2008**, *49*, 6879.
50. Barbarini, A.; Maggi, R.; Mazzacani, A.; *et al. Tetrahedron Lett.* **2003**, *44*, 2931.
51. Shen, Y. M.; Duah, W. L.; Shi, M. *Adv. Synth. Catal.* **2003**, *345*, 337.
52. Yasuda, H.; He, L. N.; Sakakura, T. *J. Catal.* **2002**, *209*, 547.
53. Doskocil, E. J.; Bordawekar, S. V.; Kaye, B. C.; *et al. J. Phys. Chem. B* **1999**, *103*, 6277.

54. Srivastava, R.; Srinivas, D.; Ratnasamy, P. *Catal. Lett.* **2003**, *91*, 133.
55. De Pasquale, R. J. *J. Chem. Soc. Chem. Commun.* **1973**, 157.
56. Jutz, F.; Grunwaldt, J. D.; Baiker, A. *J. Mol. Catal. A: Chem.* **2009**, *297*, 63.
57. Jutz, F.; Grunwaldt, J. D.; Baiker, A. *J. Mol. Catal. A: Chem.* **2008**, *279*, 94.
58. Chen, S. W.; Kawthekar, R. B.; Kim, G. J. *Tetrahedron Lett.* **2007**, *48*, 297.
59. Kim, H. S.; Kim, J. J.; Kwon, H. N.; *et al. J. Catal.* **2002**, *205*, 226.
60. Shen, Y. M.; Duan, W. L.; Shi, M. *J. Org. Chem.* **2010**, *68*, 1559.
61. Li, F. W.; Xia, C. G.; Xu, L. W.; *et al. Chem. Commun.* **2003**, *16*, 2042.
62. Srivastava, R.; Srinivas, D.; Ratnasamy, R. *Catal. Lett.* **2003**, *89*, 81.
63. Paddock, R. L.; Hiyama, Y.; McKay, M. J.; *et al. Tetrahedron Lett.* **2004**, *45*, 2023.
64. Darensbourg, D. J.; Bottarelli, P.; Andreatta, J. R. *Macromolecules* **2007**, *40*, 7727.
65. Matsuda, H.; Ninagawa, A.; Nomura, R.; *et al. Chem. Lett.* **1979**, 573.
66. Matsuda, H.; Ninagawa, A.; Nomura, R. *Chem. Lett.* **1979**, 1261.
67. Fukuoka, S.; Kawamura, M.; Komiya, K.; *et al. Green Chem.* **2003**, *5*, 497.
68. Pepple, W. J. *Ind. Eng. Chem.* **1958**, *50*, 767.
69. Annesini, M. C.; Fumasoni, S.; Giona, A. R.; *et al. Chim. Ind.* **1983**, *65*, 149.
70. He, L.-N.; Yasuda, H.; Sakakura, T. *Green Chem.* **2003**, *5*, 92.
71. Rokicki, G.; Kuran, W.; Pogorzelska-Marciniak, B. *Monatsh. Chem.* **1984**, *115*, 205.
72. Rokicki, G.; Czajkowska, J. *Polimery* **1989**, *34*, 141.
73. Kihara, N.; Kushida, Y.; Endo, T. *J. Polym. Sci., Part A: Polym. Chem.* **1996**, *34*, 2173.
74. Kihara, N.; Endo, T. *J. Polym. Sci., Part A: Polym. Chem.* **1993**, *31*, 2765.
75. Sudo, A.; Morishita, H.; Endo, T. *J. Polym. Sci., Part A: Polym. Chem.* **2010**, *48*, 3896.
76. Tascedda, P.; Dunach, E. *Heterocycl. Commun.* **1997**, *3*, 427.
77. Xiao, L.-F.; Li, F.-W.; Peng, J.-J.; *et al. J. Mol. Catal. A: Chem.* **2006**, *253*, 265.
78. Sun, J.; Fujita, S.-I.; Arai, M. *J. Organomet. Chem.* **2005**, *690*, 3490.
79. Lee, E.-H.; Ahn, J.-Y.; Dharman, M. M.; *et al. Catal. Today* **2008**, *131*, 130.
80. Meléndez, J.; North, M.; Pasquale, R. *Eur. J. Inorg. Chem.* **2007**, 3323.
81. Varma, I. K.; Albertsson, A.-C.; Rajkhowa, R.; *et al. Prog. Polym. Sci.* **2005**, *30*, 949.
82. Clegg, W.; Harrington, R. W.; North, M.; *et al. Chem. Eur. J.* **2010**, *16*, 6828.
83. Eghbali, N.; Li, C.-J. *Green Chem.* **2007**, *9*, 213.
84. Sarel, S.; Pohoryles, L. A. *J. Am. Chem. Soc.* **1958**, *80*, 4596.
85. Pohoryles, L. A.; Sarel, S. *Compt. Rend.* **1957**, *245*, 2321.
86. Matsuo, J.; Nakano, S. L.; Sanda, F.; *et al. J. Polym. Sci., Part A: Polym. Chem.* **1998**, *36*, 2463.
87. Albertsson, A.-C.; Sjoeling, M. *J. Macromol. Sci., Pure Appl. Chem.* **1992**, *A29*, 43.
88. Ariga, T.; Takata, T.; Endo, T. *Macromolecules* **1997**, *30*, 737.
89. Rokicki, G.; Kowalczyk, T. Polish Patent 193,838, 2007.
90. Rokicki, G.; Kowalczyk, T.; Glinski, M. *Polym. J.* **2000**, *32*, 381.
91. Keul, H.; Höcker, H.; Leitz, E.; *et al. Makromol. Chem.* **1988**, *189*, 2303.
92. Matsuo, J.; Sanda, F.; Endo, T. *Macromol. Chem. Phys.* **1998**, *199*, 2489.
93. Cai, J.; Zhu, K. J.; Yang, S. L. *Polymer* **1998**, *39*, 4409.
94. Yu, C.; Zhang, L.; Shen, Z. *Polym. Int.* **2004**, *53*, 1485.
95. Chen, X. H.; McCarthy, S. P.; Gross, R. A. *Macromolecules* **1998**, *31*, 662.
96. Dahlmann, J.; Rafler, G.; Fechner, K.; *et al. Br. Polym. J.* **1990**, *23*, 235.
97. Gilding, D. K.; Reed, A. M. *Polymer* **1979**, *29*, 1459.
98. Kricheldorf, H. R.; Serra, A. *Polym. Bull.* **1985**, *14*, 497.
99. Hu, B.; Zhuo, R. X.; Fan, C. L. *Polym. Adv. Technol.* **1998**, *9*, 145.
100. Matsuo, J.; Sanda, F.; Endo, T. *J. Polym. Sci., Part A: Polym. Chem.* **1997**, *35*, 1375.
101. Matsuo, J.; Sanda, F.; Endo, T. *Macromol. Chem. Phys.* **1998**, *199*, 97.
102. Kricheldorf, H. R.; Mahler, A. *Polymer* **1996**, *37*, 4383.
103. Weilandt, K. D.; Keul, H.; Höcker, H. *Macromol. Chem. Phys.* **1996**, *197*, 3851.
104. Kricheldorf, H. R.; Lossin, M.; Mahler, A. *Macromol. Chem. Phys.* **1997**, *198*, 3559.
105. Kricheldorf, H. R.; Mahler, A.; Lee, S. R. *J. Macromol. Sci., Pure Appl. Chem.* **1997**, *A34*, 417.
106. Weilandt, K. D.; Keul, H.; Höcker, H. *Macromol. Chem. Phys.* **1996**, *197*, 2539.
107. Matsuo, J.; Sanda, F.; Endo, T. *Macromol. Chem. Phys.* **2000**, *201*, 585.
108. Wu, R.; Al-Azemi, T. F.; Bisht, K. S. *Biomacromolecules* **2008**, *9*, 2921.
109. Hanslick, R. S.; Bruce, W. F.; Mascith, A. *Org. Synth.* **1953**, *33*, 74.
110. Ohme, R.; Gründemann, C. DDR Patent 57,856, 1967.
111. Bialas, N. J.; Kühling, S.; Keul, H.; *et al. Makromol. Chem.* **1990**, *191*, 1165.
112. Takata, T.; Matsuoka, H.; Hirasa, T.; *et al. Kobunshi Ronbunshu* **1997**, *54*, 974.
113. Kricheldorf, H. R.; Jenssen, J. *Eur. Polym. J.* **1989**, *25*, 1273.
114. Prochaska, R. J. Belgium Patent 630,530, 1963.
115. Mandal, H.; Hay, A. S. *High Perform. Polym.* **1997**, *9*, 215.
116. Brunelle, D. J. *J. Polym. Sci., Part A: Polym. Chem.* **2008**, *46*, 1151.
117. Schnell, H. *Chemistry and Physics of Polycarbonates*; Wiley: New York, NY, 1964.
118. Schnell, H.; Bottenbruch, L. German Patent 1,229,101, 1966.
119. Brunelle, D. J.; Boden, E. P.; Shannon, T. G. *J. Am. Chem. Soc.* **1990**, *112*, 2399.
120. Odian, G. *Principles of Polymerization*; Wiley: New York, NY, 1991.
121. Slomkowski, S.; Duda, A. In *Ring-Opening Polymerization*; Brunelle, D. J., Ed.; Hanser Publisher: New York, NY, 1993; p 87.
122. Duda, A.; Kowalski, A. In *Handbook of Ring-Opening Polymerization*; Dubois, P., Coulembier, O., Raquez, J.-M., Eds.; Wiley-VCH Verlag: Weinheim, Germany, 2009; p 1.
123. Vogdanis, L.; Martens, B.; Uchtmann, H.; *et al. Makromol. Chem.* **1990**, *191*, 465.
124. Soga, K.; Hosoda, S.; Tazuke, Y.; *et al. J. Polym. Sci., Part A: Polym. Chem.* **1977**, *15*, 219.
125. Harris, R. F. *J. Appl. Polym. Sci.* **1989**, *37*, 183.
126. Harris, R. F.; McDonald, L. A. *J. Appl. Polym. Sci.* **1989**, *37*, 1491.
127. Storey, R. F.; Hoffman, D. C. *Macromolecules* **1992**, *25*, 5369.
128. Vogdanis, L.; Heitz, W. *Makromol. Chem., Rapid Commun.* **1986**, *7*, 543.
129. Kuran, W.; Listos, T. *Makromol. Chem.* **1992**, *193*, 945.
130. Kricheldorf, H. R.; Berl, M.; Scharnagl, N. *Macromolecules* **1988**, *21*, 286.
131. Kricheldorf, H. R.; Jonte, J. M.; Berl, M. *Makromol. Chem., Suppl.* **1985**, *12*, 25.
132. Harris, R. F. *Polym. Prepr., ACS Div. Polym. Chem.* **1988**, *29*, 418.
133. Harris, R. F. *J. Appl. Polym. Sci.* **1989**, *38*, 463.
134. Harris, F. R. *J. Appl. Polym. Sci.* **1990**, *40*, 1265.
135. Storey, R. F.; Hoffman, D. C. *Polymer* **1992**, *33*, 2807.
136. Lee, J.-C.; Litt, M. H. *Macromolecules* **2000**, *33*, 1618.
137. Rokicki, G.; Pawlicki, J.; Kuran, W. *Polym. J.* **1985**, *17*, 509.
138. Keki, S.; Torok, J.; Deak, G.; *et al. Macromolecules* **2001**, *34*, 6850.
139. Keki, S.; Torok, J.; Deak, G.; *et al. Macromol. Symp.* **2004**, *215*, 141.
140. Elmer, A. M.; Jannasch, P. *J. Polym. Sci., Part A: Polym. Chem.* **2006**, *44*, 2195.
141. Wu, M.; Guo, J.; Jing, H. *Catal. Commun.* **2008**, *9*, 120.
142. Kadokawa, J.; Iwasaki, Y.; Tagaya, H. *Macromol. Rapid Commun.* **2002**, *23*, 757.
143. Doane, W. M.; Shasha, B. S.; Stout, E. I.; *et al. Carbohydr. Res.* **1967**, *4*, 445.
144. Haba, O.; Tomizuka, H.; Endo, T. *Macromolecules* **2005**, *38*, 3562.
145. Keul, H. In *Handbook of Ring-Opening Polymerization*; Dubois, P., Coulembier, O., Raquez, J.-M., Eds.; Wiley-VCH Verlag: Weinheim, Germany, 2009; p 307.
146. Evans, M. E. In *Methods in Carbohydrate Chemistry*; Whistler, R. L., BeMiller, J. N., Eds.; Academic Press: New York, NY, 1980; p 313.
147. Kricheldorf, H. R.; Jenssen, J. *J. Macromol. Sci., Pure Appl. Chem.* **1989**, *A26*, 631.
148. Inoue, S.; Koinuma, H.; Tsuruta, T. *Makromol. Chem.* **1969**, *130*, 210.
149. Rokicki, A.; Kuran, W. *J. Macromol. Sci., Rev. Macromol. Chem. C* **1981**, *21*, 135.
150. Super, M. S.; Beckman, E. J. *Trends Polym. Sci.* **1997**, *5*, 336.
151. Coates, G. W.; Moore, D. R. *Angew. Chem., Int. Ed.* **2004**, *43*, 6618.
152. Sugimoto, H.; Inoue, S. *Pure Appl. Chem.* **2006**, *78*, 1823.
153. Darensbourg, D. J. *Chem. Rev.* **2007**, *107*, 2388.
154. Clements, J. H. *Ind. Eng. Chem. Res.* **2003**, *42*, 663.
155. Sugita, A. Japan Patent 6,329,663, 1994.
156. Claude, S.; Zephirin, M.; Yoo, J.; et al. U.S. Patent 6,025,504, 2000.
157. Okutsu, M.; Kitsuki, T. European Patent 1,156,042, 2001.
158. Rokicki, G.; Rakoczy, P.; Parzuchowski, P.; *et al. Green Chem.* **2005**, *7*, 529.
159. Bell, J.B.; Currier, V.A.; Malkemus, J. D. U.S. Patent 2,915,529, 1959.
160. Teles, J.H.; Rieber, N.; Harder, W. U.S. Patent 5,359,094, 1994.
161. Vieville, C.; Yoo, J. W.; Pelet, S.; *et al. Catal. Lett.* **1998**, *56*, 245.
162. Rokicki, G.; Parzuchowski, P. G.; Maciejewski, D.; *et al. Polimery* **2007**, *52*, 648.
163. Tomasik, A.; Biernat, M.; Parzuchowski, P. *Polimery* **2010**, *55*, 35.
164. Grahe, G.; Lachowicz, A. European Patent 328,150, 1989.
165. D'Alelio, G.; Huemmer, T. *J. Polym. Sci. A* **1967**, *5*, 307.
166. Hamaguchi, S.; Yamamura, H.; Hasegawa, J.; *et al. Agric. Biol. Chem.* **1985**, *49*, 1509.
167. Whelan, J.; Hill, M. U.S. Patent 3,072,613, 1963.
168. Gillis, H.; Stanssens, D.; Postema, A.; et al. U.S. Patent 5,703,136, 1997.
169. Parzuchowski, P. G.; Kizlinska, M.; Rokicki, G. *Polymer* **2007**, *48*, 1857.
170. Parzuchowski, P. G.; Jurczyk-Kowalska, M.; Ryszkowska, J.; *et al. J. Appl. Polym. Sci.* **2006**, *102*, 2904.
171. Rokicki, G.; Wojciechowski, C. *J. Appl. Polym. Sci.* **1990**, *41*, 647.
172. Kihara, N.; Endo, T. *Makromol. Chem.* **1992**, *193*, 1481.
173. Decker, C.; Moussa, K. *Makromol. Chem. Rapid Commun.* **1990**, *11*, 159.
174. Decker, C.; Moussa, K. *Makromol. Chem.* **1991**, *192*, 507.
175. Webster, D.; Crain, A. *Am. Chem. Soc. Symp.* **1998**, *704*, 303.
176. Ochiai, B.; Matsuki, M.; Nagai, D.; *et al. J. Polym. Sci., Part A: Polym. Chem.* **2005**, *43*, 584.
177. Endo, T. In *Handbook of Ring-Opening Polymerization*; Dubois, P., Coulembier, O., Raquez, J.-M., Eds.; Wiley-VCH Verlag: Weinheim, Germany, 2009; p 53.
178. Takata, T.; Igarashi, M.; Endo, T. *J. Polym. Sci., Part A: Polym. Chem.* **1991**, *29*, 781.

179. Sanda, F.; Fueki, T.; Endo, T. *Macromolecules* **1999**, *32*, 4220.
180. Penczek, S.; Kubisa, P. In *Ring Opening Polymerization*; Brunelle, D. J., Ed.; Hanser Publishers: Munich, Germany, 1993; p 54.
181. Penczek, S.; Kubisa, P.; Szymanski, R. *Makromol. Chem., Macromol. Symp.* **1986**, *6*, 201.
182. Hyun, H.; Kim, M. S.; Khang, G.; *et al. J. Polym. Sci., Part A: Polym. Chem.* **2006**, *44*, 4235.
183. Kricheldorf, H. R.; Dunsing, R.; Serra, A.; *et al. Makromol. Chem.* **1987**, *188*, 2453.
184. Kricheldorf, H. R.; Weegen-Schulz, B. *Polymer* **1995**, *36*, 4997.
185. Kricheldorf, H. R.; Weegen-Schulz, B. *Makromol. Chem., Rapid Commun.* **1993**, *14*, 405.
186. Kricheldorf, H. R.; Weegen-Schulz, B. *J. Polym. Sci., Part A: Polym. Chem.* **1995**, *33*, 2193.
187. Ariga, T.; Takata, T.; Endo, T. *J. Polym. Sci., Part A: Polym. Chem.* **1993**, *31*, 581.
188. Holder, A. J.; White, D. A.; Harris, C. D.; *et al. J. Mol. Struct. (Thoechem.)* **2001**, *541*, 159.
189. Holder, A. J.; Liu, Y. *J. Polym. Res.* **2010**, *17*, 759.
190. Shen, Y.; Shen, Z.; Zhang, Y.; *et al. J. Appl. Polym. Sci.* **1997**, *64*, 2131.
191. Huang, Q. H.; Shen, Z. Q.; Zhang, Y. F.; *et al. Polym. J.* **1998**, *30*, 168.
192. Agarwal, S.; Puchner, M.; Greiner, A.; *et al. Polym. Int.* **2005**, *54*, 1422.
193. Carothers, W. H.; Dorough, G. L.; Van Natta, F. J. *J. Am. Chem. Soc.* **1932**, *54*, 761.
194. Hocker, H.; Keul, H. In *The Polymeric Materials Encyclopedia: Synthesis, Properties and Applications*; Salomone, J. C., Ed.; CRC Press: Boca Raton, FL, 1996; p 1647.
195. Keul, H.; Bächer, R.; Höcker, H. *Makromol. Chem.* **1986**, *187*, 2579.
196. Kühling, S.; Keul, H.; Höcker, H. *Makromol. Chem. Suppl.* **1989**, *15*, 9.
197. Keul, H.; Müller, A. J.; Höcker, H. *Makromol. Chem., Macromol. Symp.* **1993**, *67*, 289.
198. Kühling, S.; Keul, H.; Höcker, H. *Makromol. Chem.* **1990**, *191*, 1611.
199. Wurm, B.; Keul, H.; Höcker, H.; *et al. Makromol. Chem., Rapid Commun.* **1992**, *13*, 9.
200. Kühling, S.; Keul, H.; Höcker, H. *Makromol. Chem.* **1992**, *193*, 1207.
201. Hovestadt, W.; Keul, H.; Höcker, H. *Polymer* **1992**, *33*, 1941.
202. Rokicki, G.; Jezewski, P. *Polym. J.* **1988**, *20*, 499.
203. Keul, H.; Höcker, H. *Makromol. Chem.* **1986**, *187*, 2833.
204. Müller, A. J.; Keul, H.; Höcker, H. *Eur. Polym. J.* **1993**, *29*, 1171.
205. Müller, A. J.; Keul, H.; Höcker, H. *Eur. Polym. J.* **1991**, *27*, 1323.
206. Müller, A. J.; Keul, H.; Höcker, H. *Polym. Int.* **1994**, *33*, 197.
207. Penczek, S.; Slomkowski, S. In *Recent Advances in Anionic Polymerization*; Hogen-Esch, T. E., Smid, J., Eds.; Elsevier: New York, NY, 1987; p 275.
208. Keul, H.; Deisel, F.; Höcker, H.; *et al. Makromol. Chem., Rapid Commun.* **1991**, *12*, 133.
209. Hovestadt, W.; Müller, A. J.; Keul, H.; *et al. Makromol. Chem., Rapid Commun.* **1990**, *11*, 271.
210. Darensbourg, D. J.; Choi, W.; Ganguly, P.; *et al. Macromolecules* **2006**, *39*, 4374.
211. Murayama, M.; Sanda, F.; Endo, T. *Macromolecules* **1998**, *31*, 919.
212. Kricheldorf, H. R.; Lee, S.-R.; Weegen-Schulz, B. *Macromol. Chem. Phys.* **1996**, *197*, 1043.
213. Nederberg, F.; Lohmeijer, B. G. G.; Leibfarth, F.; *et al. Biomacromolecules* **2007**, *8*, 153.
214. Liu, J.; Zhang, C.; Liu, L. *J. Appl. Polym. Sci.* **2008**, *107*, 3275.
215. Mindemark, J.; Hilborn, J.; Bowden, T. *Macromolecules* **2007**, *40*, 3515.
216. Feng, J.; Wang, X.-L.; He, F.; *et al. Macromol. Rapid Commun.* **2007**, *28*, 754.
217. Pawlowski, P.; Szymanski, A.; Kozakiewicz, J.; *et al. Polym. J.* **2005**, *37*, 742.
218. Liao, L.; Zhang, C.; Gong, S. *Eur. Polym. J.* **2007**, *43*, 4289.
219. Okada, T.; Imamura, Y.; Matsuda, T. *J. Polym. Sci., Part A: Polym. Chem.* **2010**, *48*, 1485.
220. Müller, A. H. E. In *Recent Advances in Mechanistics and Synthetic Aspects of Polymerization*; Fontanille, M., Guyot, A., Eds.; Reidel: Dordrecht, The Netherlands, 1987; p 23.
221. Reetz, M. T.; Knauf, T.; Minet, U.; *et al. Makromol. Chem.* **1988**, *100*, 1422.
222. Hovestadt, W.; Keul, H.; Höcker, H. *Makromol. Chem.* **1991**, *192*, 1409.
223. Kricheldorf, H. R.; Kreiser-Saunders, I.; Stricker, A. *Macromolecules* **2000**, *33*, 702.
224. Kricheldorf, H. R.; Kreiser-Saunders, I.; Boettcher, C. *Polymer* **2010**, *36*, 1253.
225. Kowalski, A.; Duda, A.; Penczek, S. *Macromol. Rapid Commun.* **1998**, *19*, 567.
226. Majerska, K.; Duda, A.; Penczek, S. *Macromol. Rapid Commun.* **2000**, *21*, 1327.
227. Penczek, S.; Duda, A.; Kowalski, A.; *et al. Macromol. Symp.* **2000**, *157*, 61.
228. Bero, M.; Czapla, B.; Dobrzynski, P.; *et al. Macromol. Chem. Phys.* **1999**, *200*, 911.
229. Kricheldorf, H. R.; Stricker, A. *Macromol. Chem. Phys.* **2000**, *201*, 2557.
230. Zhang, Z.; Kuijer, R.; Bulstra, S. K.; *et al. Biomaterials* **2006**, *27*, 1741.
231. Liao, L.; Zhang, C.; Gong, S. *J. Polym. Sci., Part A: Polym. Chem.* **2007**, *45*, 5857.
232. Kricheldorf, H. R.; Stricker, A. *Polymer* **2000**, *41*, 7311.
233. Kricheldorf, H. R.; Stricker, A.; Lossin, M. *J. Polym. Sci., A: Polym. Chem.* **1999**, *37*, 2179.
234. Pospiech, D.; Komber, H.; Jehnichen, D.; *et al. Biomacromolecules* **2005**, *6*, 439.
235. Kricheldorf, H. R.; Stricker, A.; Gomurashvili, Z. *Macromol. Chem. Phys.* **2001**, *202*, 413.
236. Rokicki, G.; Piotrowska, A.; Pawlowski, P. *Polym. J.* **2003**, *35*, 133.
237. Duda, A.; Penczek, S. *Macromolecules* **1994**, *27*, 4867.
238. Duda, A. *Macromolecules* **1996**, *29*, 1399.
239. Wurm, B.; Keul, H.; Höcker, H. *Macromol. Chem. Phys.* **1994**, *195*, 3489.
240. Carter, K. R.; Richter, R.; Kricheldorf, H. R.; *et al. Macromolecules* **1997**, *30*, 6074.
241. Florjanczyk, Z.; Plichta, A.; Sobczak, M. *Polymer* **2006**, *47*, 1081.
242. Kuran, W.; Sobczak, M.; Listos, T.; *et al. Polymer* **2000**, *41*, 8531.
243. Darensbourg, D. J.; Ganguly, P.; Billodeaux, D. *Macromolecules* **2005**, *38*, 5406.
244. Yang, J.; Yu, Y.; Li, Q.; *et al. J. Polym. Sci., Part A: Polym. Chem.* **2005**, *43*, 373.
245. Westerhausen, M.; Schneiderbauer, S.; Kneifel, A. N.; *et al. Eur. J. Inorg. Chem.* **2003**, 3432.
246. Darensbourg, D. J.; Choi, W.; Richers, C. P. *Macromolecules* **2007**, *40*, 3521.
247. Darensbourg, D. J.; Choi, W.; Karroonnirun, O.; *et al. Macromolecules* **2008**, *41*, 3493.
248. Zhang, C.; Liao, L.; Gong, S. *J. Appl. Polym. Sci.* **2008**, *110*, 1236.
249. Helou, M.; Miserque, O.; Brusson, J.-M.; *et al. Chem. Eur. J.* **2008**, *14*, 8772.
250. Asano, S.; Aida, T.; Inoue, S. *J. Chem. Soc., Chem. Commun.* **1985**, 1148.
251. Inoue, S. *J. Polym. Sci., Part A: Polym. Chem.* **2000**, *38*, 2861.
252. Helou, M.; Miserque, O.; Brusson, J.-M.; *et al. Adv. Synth. Catal.* **2009**, *351*, 1312.
253. Helou, M.; Miserque, O.; Brusson, J.-M.; *et al. Macromol. Rapid Commun.* **2009**, *30*, 2128.
254. Dobrzynski, P.; Pastusiak, M.; Bero, M. *J. Polym. Sci., Part A: Polym. Chem.* **2005**, *43*, 1913.
255. Bero, M.; Dobrzynski, P.; Kasperczyk, J. *Polym. Bull.* **1999**, *42*, 131.
256. Dobrzynski, P. *Polymer* **2007**, *48*, 2263.
257. Dobrzynski, P.; Kasperczyk, J. *J. Polym. Sci., Part A: Polym. Chem.* **2006**, *44*, 3184.
258. Darensbourg, D. J.; Moncada, A. I.; Choi, W.; *et al. J. Am. Chem. Soc.* **2008**, *130*, 6523.
259. Darensbourg, D. J.; Ganguly, P.; Choi, W. *Inorg. Chem.* **2006**, *45*, 3831.
260. Darensbourg, D. J.; Moncada, A. I. *Macromolecules* **2010**, *43*, 5996.
261. Zhiquan, S. *Front. Chem. China* **2006**, *3*, 247.
262. Shen, Y. Q.; Shen, Z. Q.; Shen, J. L.; *et al. Macromolecules* **1996**, *29*, 3441.
263. Ling, J.; Shen, Z. *Macromol. Chem. Phys.* **2002**, *203*, 735.
264. Ling, J.; Shen, Z.; Huang, Q. *Macromolecules* **2001**, *34*, 7613.
265. Ling, J.; Dai, Y.; Zhu, Y.; *et al. J. Polym. Sci., Part A: Polym. Chem.* **2010**, *48*, 3807.
266. Zhang, L.; Wang, Y.; Wang, P.; *et al. Sci. China, Ser. B: Chem.* **2010**, *53*, 599.
267. Yu, C.; Zhang, L.; Shen, Z. *J. Mol. Catal. A: Chem.* **2004**, *212*, 365.
268. Xu, X.; Yao, Y.; Zhang, Y.; *et al. Chin. Sci. Bull.* **2007**, *52*, 1623.
269. Ling, J.; Shen, Z. Q.; Zhu, W. P. *J. Polym. Sci., Part A: Polym. Chem.* **2003**, *41*, 1390.
270. Zhu, W.; Ling, J.; Xu, H.; *et al. Polymer* **2005**, *46*, 8379.
271. Zhu, W.; Gou, P.; Shen, Z. *Macromol. Symp.* **2008**, *261*, 74.
272. Gou, P.-F.; Zhu, W.-P.; Shen, Z.-Q. *Sci. China, Ser. B: Chem.* **2007**, *50*, 648.
273. Li, H.; Yao, Y.; Yao, C.; *et al. J. Polym. Sci., Part A: Polym. Chem.* **2005**, *43*, 1312.
274. Sheng, H.; Zhou, L.; Zhang, Y.; *et al. J. Polym. Sci., Part A: Polym. Chem.* **2007**, *45*, 1210.
275. Sheng, H.; Xu, F.; Yao, Y.; *et al. Inorg. Chem.* **2007**, *46*, 7722.
276. Sheng, H.-T.; Li, J.-M.; Zhang, Y.; *et al. Polyhedron* **2008**, *27*, 1665.
277. Sheng, H.; Li, J.; Zhang, Y.; *et al. J. Appl. Polym. Sci.* **2009**, *112*, 454.
278. Zhou, L.; Yao, Y.; Zhang, Y.; *et al. Eur. J. Inorg. Chem.* **2004**, 2167.
279. Li, C.; Wang, Y.; Zhou, L.; *et al. J. Appl. Polym. Sci.* **2006**, *102*, 22.
280. Zhou, L.; Sun, H.; Chen, J.; *et al. J. Polym. Sci., Part A: Polym. Chem.* **2005**, *43*, 1778.
281. Palard, I.; Schappacher, M.; Belloncle, B.; *et al. Chem. Eur. J.* **2007**, *13*, 1511.
282. Agarwal, S.; Puchner, M. *Eur. Polym. J.* **2002**, *38*, 2365.
283. Matsumura, S. *Adv. Polym. Sci.* **2006**, *194*, 95.
284. Albertsson, A.-C.; Srivastava, R. K. *Adv. Drug Deliv. Rev.* **2008**, *60*, 1077.
285. Uyama, H.; Kobayashi, S. *Chem. Lett.* **1993**, 1149.
286. Vert, M.; Feijen, J.; Albertsson, A. C.; *et al. Biodegradable Polymers and Plastics*; Royal Society: London, 1992.
287. Kobayashi, S.; Kikuchi, H.; Uyama, H. *Macromol. Rapid Commun.* **1997**, *18*, 575.
288. Matsumoto, K.; Shimojo, M.; Kitajima, H.; *et al. Synlett* **1996**, 1085.

289. Bisht, K. S.; Svirkin, Y. Y.; Henderson, L. A.; *et al. Macromolecules* **1997**, *30*, 7735.
290. Bisht, K. S.; Henderson, L. A.; Gross, R. A.; *et al. Macromolecules* **1997**, *30*, 2705.
291. Matsumura, S.; Tsukada, K.; Toshima, K. *Macromolecules* **1997**, *30*, 3122.
292. Deng, F.; Henderson, L.; Gross, R. A. *Polym. Prepr., ACS Div. Polym. Chem.* **1998**, *39*, 144.
293. Zaks, A.; Klibanov, A. M. *J. Biol. Chem.* **1988**, *263*, 3194.
294. Feng, J.; He, F.; Zhuo, R. *Macromolecules* **2002**, *35*, 7175.
295. He, F.; Wang, Y. X.; Zhuo, R. X. *Chin. J. Polym. Sci.* **2003**, *21*, 5.
296. Yu, X.-H.; Zhuo, R.-X.; Feng, J.; *et al. Eur. Polym. J.* **2004**, *40*, 2445.
297. Feng, J.; Wang, H.; Zhang, W.; *et al. Eur. Polym. J.* **2009**, *45*, 523.
298. Wang, Y. X.; Feng, J.; He, F.; *et al. Chin. Chem. Lett.* **2007**, *18*, 1528.
299. Kumar, A.; Garg, K.; Gross, R. A. *Macromolecules* **2001**, *34*, 3527.
300. Al-Azemi, T. F.; Harmon, J. P.; Bisht, K. S. *Biomacromolecules* **2000**, *1*, 493.
301. Jun, F.; Renxi, Z.; Feng, H. *Sci. China, Ser. B* **2003**, *46*, 160.
302. Kricheldorf, H. R.; Boettcher, C. *Makromol. Chem.* **1993**, *194*, 463.
303. Matsumura, S.; Harai, S.; Toshima, K. *Macromol. Rapid Commun.* **2001**, *22*, 215.
304. Goodwin, A. P.; Lam, S. S.; Frechet, J. M. J. *J. Am. Chem. Soc.* **2007**, *129*, 6994.
305. Seow, W. Y.; Yang, Y. Y. *J. Controlled Release* **2009**, *139*, 40.
306. Pratt, R. C.; Nederberg, F.; Waymouth, R. M.; *et al. Chem. Commun.* **2008**, 114.
307. Mullen, B. D.; Tang, C. N.; Storey, R. F. *Polym. Prepr., ACS Div. Polym. Chem.* **2003**, *44*, 767.
308. Tryznowski, M. Ph.D. thesis, Warsaw University of Technology, Warsaw, Poland, 2008.
309. Feng, J.; Zhuo, R.; He, F.; *et al. Macromol. Symp.* **2003**, *195*, 237.
310. Wang, X.-L.; Zhuo, R.-X.; Liu, L.-J.; *et al. J. Polym. Sci., Part A: Polym. Chem.* **2002**, *40*, 70.
311. Liu, G.; He, F.; Wang, Y. P.; *et al. Chin. Chem. Lett.* **2006**, *17*, 137.
312. He, F.; Wang, Y.-P.; Liu, G.; *et al. Polymer* **2008**, *49*, 1185.
313. Parzuchowski, P. G.; Jaroch, M.; Tryznowski, M.; *et al. Macromolecules* **2008**, *41*, 3859.
314. Hu, X.; Chen, X.; Cheng, H.; *et al. J. Polym. Sci., Part A: Polym. Chem.* **2009**, *47*, 161.
315. Kühling, S.; Keul, H.; Höcker, H.; *et al. Makromol. Chem.* **1991**, *192*, 1193.
316. Miyazaki, K.; Endo, T.; Sanda, F.; *et al. Polym. Prepr., ACS Div. Polym. Chem.* **1997**, *38*, 165.
317. Miyagawa, T.; Shimizu, M.; Sanda, F.; *et al. Macromolecules* **2005**, *38*, 7944.
318. Xie, Z.; Lu, C.; Chen, X.; *et al. J. Polym. Sci., Part A: Polym. Chem.* **2007**, *45*, 1737.
319. Tryznowski, M.; Tomczyk, K.M.; Rokicki, G., Unpublished data.
320. Tomita, H.; Sanda, F.; Endo, T. *Macromolecules* **2001**, *30*, 7601.
321. Endo, T.; Kakimoto, K.; Ochiai, B.; *et al. Macromolecules* **2005**, *38*, 8177.
322. Ariga, T.; Takata, T.; Endo, T. *J. Polym. Sci., Part A: Polym. Chem.* **1993**, *41*, 319.
323. Hino, T.; Inoue, N.; Endo, T. *Macromolecules* **2004**, *37*, 9660.
324. Hino, T.; Inoue, N.; Endo, T. *J. Polym. Sci., Part A: Polym. Chem.* **2006**, *44*, 395.
325. Kricheldorf, H. R.; Mahler, A. *J. Polym. Sci., Part A: Polym. Chem.* **1996**, *34*, 2399.
326. Takeuchi, D.; Aida, T.; Endo, T. *Macromol. Rapid Commun.* **1999**, *20*, 182.
327. Okuda, J.; Rushkin, I. L. *Macromolecules* **1993**, *26*, 5630.
328. Endo, T.; Aida, T.; Inoue, S. *Macromolecules* **1987**, *20*, 2982.
329. Hayakawa, M.; Mitani, M.; Yamada, T.; *et al. Macromol. Rapid Commun.* **1996**, *17*, 865.
330. Kricheldorf, H. R.; Sumbel, M. V. *Makromol. Chem.* **1988**, *189*, 317.
331. Shibasaki, Y.; Sanda, F.; Endo, T. *Macromol. Rapid Commun.* **2000**, *21*, 489.
332. Takeuchi, D.; Aida, T.; Endo, T. *Macromol. Chem. Phys.* **2000**, *201*, 2267.
333. Shibasaki, Y.; Sanda, F.; Endo, T. *Macromol. Rapid Commun.* **1999**, *20*, 532.
334. Shibasaki, Y.; Sanada, H.; Yokoi, M.; *et al. Macromolecules* **2000**, *33*, 4316.
335. Endo, T.; Shibasaki, Y.; Sanda, F. *J. Polym. Sci., Part A: Polym. Chem.* **2002**, *40*, 2190.
336. Nagai, D.; Yokota, K.; Ogawa, T.; *et al. J. Polym. Sci., Part A: Polym. Chem.* **2008**, *46*, 733.
337. Morikawa, H.; Sudo, A.; Nishida, H.; *et al. Macromol. Chem. Phys.* **2005**, *206*, 592.
338. Carter, K. R.; Richter, R.; Hedrick, J. L.; *et al. Polym. Prepr., ACS Div. Polym. Chem.* **1996**, *37*, 607.
339. Kuran, W.; Listos, T.; Iwaniuk, R.; *et al. Polimery* **1993**, *38*, 405.
340. Kuran, W.; Listos, T. *Pol. J. Chem.* **1994**, *68*, 1071.
341. Rokicki, G.; Nguyen, X. T. *Macromol. Rep.* **1995**, *A32*, 265.
342. Rokicki, G.; Nguyen, T. X. *Polym. Compos.* **1996**, *4*, 45.
343. Cervellera, R.; Ramis, X.; Salla, J. M.; *et al. J. Appl. Polym. Sci.* **2006**, *102*, 2086.
344. Cervellera, R.; Ramis, X.; Salla, J. M.; *et al. J. Appl. Polym. Sci.* **2007**, *103*, 2875.
345. Evans, W. J.; Katsumata, H. *Macromolecules* **1994**, *27*, 4011.
346. Shirahama, H.; Kanetani, A.; Yasuda, H. *Polym. J.* **2000**, *32*, 280.
347. Chen, F.; Zhu, W.; Xu, N.; *et al. J. Polym. Sci., Part A: Polym. Chem.* **2008**, *46*, 4050.
348. Schmitz, F.; Keul, H.; Höcker, H. *Polymer* **1998**, *39*, 3179.
349. Schmitz, F.; Keul, H.; Höcker, H. *Macromol. Rapid Commun.* **1997**, *18*, 699.
350. Ubaghs, L.; Novi, C.; Keul, H.; *et al. Macromol. Chem. Phys.* **2004**, *205*, 888.
351. Ubaghs, L.; Waringo, M.; Keul, H.; *et al. Macromolecules* **2004**, 6755.
352. Dawes, E. A. In *Novel Biodegradable Microbial Polymers*; Dawes, E. A., Ed.; Kluwer Academic Publishers: The Netherlands, 1990.
353. Katz, A. R.; Mukherjee, D. P.; Kagonov, A. L.; *et al. Surg. Gynecol. Obstet.* **1985**, *161*, 213.
354. Zhu, K. J.; Hendren, R. W.; Jensen, K.; *et al. Macromolecules* **1991**, *24*, 1736.
355. Albertsson, A.-C.; Eklund, S. *J. Appl. Polym. Sci.* **1995**, *57*, 87.
356. Gerhard-Abozari, E.; Keul, H.; Höcker, H. *Macromol. Chem. Phys.* **1994**, *195*, 2371.
357. Keul, H.; Schmidt, P.; Robertz, B. *Macromol. Symp.* **1995**, *92*, 243.
358. Keul, H.; Höcker, H.; Leitz, E.; *et al. Makromol. Chem.* **1990**, *191*, 1975.
359. Hori, Y.; Gonda, Y.; Takahashi, Y.; *et al. Macromolecules* **1996**, *29*, 804.
360. Schmidt, P.; Keul, H.; Höcker, H. *Macromolecules* **1996**, *29*, 3674.
361. Wang, H.; Dong, J. H.; Qiu, K. Y.; *et al. J. Polym. Sci., Part A: Polym. Chem.* **1998**, *36*, 1301.
362. Kumar, N.; Langer, R. S.; Domb, A. *J. Adv. Drug Deliv. Rev.* **2002**, *54*, 889.
363. Edlund, U.; Albertsson, A.-C. *J. Appl. Polym. Sci.* **1999**, *72*, 227.
364. Kricheldorf, H. R.; Petermann, O. *J. Polym. Sci., Part A: Polym. Chem.* **2002**, *40*, 4357.
365. Ling, J.; Ren, S.; Shen, Z. *e-Polymers* **2010**, *27*, 1.
366. Krimm, H.; Buysch, H.-J.; Botta, A. European Patent Appl. 0,050,811, 1981.
367. Bayer, A.; Krimm, H.; Buysch, H.-J.; et al. European Patent Appl. 0,050,810, 1981.
368. Wurm, B.; Keul, H.; Höcker, H. *Macromolecules* **1992**, *25*, 2977.
369. Soeda, Y.; Toshima, K.; Matsumura, S. *Macromol. Biosci.* **2005**, *5*, 277.
370. Penczek, S.; Lapienis, G.; Klosinski, P. *Pure Appl. Chem.* **1984**, *56*, 1300.
371. Kaluzynski, K.; Libiszowski, J.; Penczek, S. *Makromol. Chem.* **1977**, *178*, 2943.
372. Kricheldorf, H. R.; Andrea Stricker, A. *Macromol. Chem. Phys.* **1999**, *200*, 1726.
373. Wang, H.; Dong, J. H.; Qiu, K. Y. *J. Polym. Sci., Part A: Polym. Chem.* **1998**, *36*, 695.
374. Feng, Y.; Zhang, S. *J. Polym. Sci., Part A: Polym. Chem.* **2005**, *43*, 4819.
375. Zhang, Y.; Zhuo, R.-X. *Biomaterials* **2005**, *26*, 2089.
376. Zhang, Z.; Grijpma, D. W.; Feijen, J. *J. Controlled Release* **2006**, *111*, 263.
377. Kim, S. Y.; Kim, H. J.; Lee, K. E.; *et al. Macromolecules* **2007**, *40*, 5519.
378. Kim, S. Y.; Lee, K. E.; Han, S. S.; *et al. J. Phys. Chem. B* **2008**, *112*, 7420.
379. Fan, L.; Ni, X.-F.; Shen, Z.-Q. *Colloid Polym. Sci.* **2008**, *286*, 327.
380. Liao, L.; Zhang, C.; Gong, S. *React. Funct. Polym.* **2008**, *68*, 751.
381. Ould-Ouali, L.; Noppe, M.; Langlois, X.; *et al. J. Controlled Release* **2005**, *102*, 657.
382. Danhier, F.; Magotteaux, N.; Ucakar, B.; *et al. Eur. J. Pharm. Biopharm.* **2009**, *73*, 230.
383. Meng, F.; Hiemstra, C.; Engbers, G. H. M.; *et al. Macromolecules* **2003**, *36*, 3004.
384. Zhong, Z. Y.; Dijkstra, P. J.; Birg, C.; *et al. Macromolecules* **2001**, *34*, 3863.
385. Zhang, Z.; Grijpma, D. W.; Feijen, J. *Macromol. Chem. Phys.* **2004**, *205*, 867.
386. Le Hellaye, M.; Fortin, N.; Guilloteau, J.; *et al. Biomacromolecules* **2008**, *9*, 1924.
387. Schappacher, M.; Soum, A.; Guillaume, S. M. *Biomacromolecules* **2006**, *7*, 1373.
388. Dankers, P. Y. W.; Zhang, Z.; Wisse, E.; *et al. Macromolecules* **2006**, *39*, 8763.
389. Sanson, C.; Le Meins, J.-F.; Schatz, C.; *et al. Soft Matter* **2010**, *6*, 1722.
390. Krogman, N. R.; Lee Steely, L.; Hindenlang, M. D.; *et al. Macromolecules* **2008**, *41*, 1126.
391. Zhang, Z.; Grijpma, D. W.; Feijen, J. *J. Mater. Sci., Mater. Med.* **2004**, *15*, 381.
392. Zhang, Z.; Grijpma, D. W.; Feijen, J. *J. Controlled Release* **2006**, *116*, 29.
393. Park, S. H.; Choi, B. G.; Joo, M. K.; *et al. Macromolecules* **2008**, *41*, 6486.
394. Bezwada, R. S.; Jamiolkowski, D. D.; Lee, I. Y.; *et al. Biomaterials* **1995**, *16*, 1141.
395. Kim, C.; Lee, S. C.; Shin, J. H.; *et al. Macromolecules* **2000**, *33*, 7448.
396. Kaihara, S.; Fisher, J. P.; Matsumura, S. *Macromol. Biosci.* **2009**, *9*, 613.
397. Watanabe, J.; Amemori, S.; Akashi, M. *Polymer* **2008**, *49*, 3709.
398. Kricheldorf, H. R.; Rost, S. *Macromolecules* **2005**, *38*, 8220.
399. Hyun, H.; Cho, J. S.; Kim, B. S.; *et al. J. Polym. Sci., Part A: Polym. Chem.* **2008**, *46*, 2084.
400. Zhang, H.-H.; Huang, Z.-Q.; Sun, B.-W.; *et al. J. Polym. Sci., Part A: Polym. Chem.* **2008**, *46*, 8131.
401. Morinaga, H.; Ochiai, B.; Endo, T. *J. Polym. Sci., Part A: Polym. Chem.* **2006**, *44*, 6633.
402. Joziasse, C. A. P.; Grablowitz, H.; Pennings, A. J. *Macromol. Chem. Phys.* **2000**, *201*, 107.
403. Soga, K.; Imamura, H.; Ikeda, S. *Makromol. Chem.* **1975**, *176*, 807.
404. Kricheldorf, H. R.; Damrau, D.-O. *Macromol. Chem. Phys.* **1998**, *199*, 2589.
405. Kakimoto, K.; Nemoto, N.; Sanda, F.; *et al. Chem. Lett.* **2002**, 156.
406. Ochiai, B.; Yoshii, K.; Nagai, D.; *et al. J. Polym. Sci., Part A: Polym. Chem.* **2005**, *43*, 1014.

407. Choi, W.; Sanda, F.; Kihara, N.; *et al. J. Polym. Sci., Polym. Chem. Ed.* **1997**, *35*, 3853.
408. Ochiai, B.; Endo, T. *Prog. Polym. Sci.* **2005**, *30*, 183.
409. Endo, T.; Choi, W.; Sanda, F. In Preprints of IUPAC World Polymer Congress, Gold Coast, Queensland, Australia, 1998; p 275.
410. Stewart, K. R. *Polym. Prepr., ACS Div. Polym. Chem.* **1989**, *30*, 140.
411. Evans, T. L.; Berman, C. B.; Carpenter, J. C.; *et al. Polym. Prepr., ACS Div. Polym. Chem.* **1989**, *30*, 573.
412. Stewart, K. R. *Polym. Prepr., ACS Div. Polym. Chem.* **1989**, *30*, 575.
413. Bartmess, J. E.; Hays, R. L.; Caldwell, G. *J. Am. Chem. Soc.* **1981**, *103*, 1338.
414. Brunelle, D. J.; Shannon, T. G. *Polym. Prepr., ACS Div. Polym. Chem.* **1990**, *31*, 14.
415. Brunelle, D. J.; Shannon, T. G. *Makromol. Chem., Macromol. Symp.* **1991**, *42/43*, 155.
416. Brunelle, D.J.; Evans, T.L.; Shannon, T. G. U.S. Patent 4,736,016, 1988.
417. Evans, T. L.; Carpenter, J. C. *Polym. Prepr., ACS Div. Polym. Chem.* **1990**, *31*, 18.
418. Evans, T.L.; Shea, T.J.; Wasserman, C. B.; *et al.* U.S. Patent 5,010,143, 1991.
419. Evans, T.L.; Rosenquist, N.R.; Bostick, E. E. U.S. Patent 4,746,724, 1988.
420. Evans, T. L. European Patent Appl. 257,469, 1988.
421. Evans, T. L. European Patent Appl. 249,809, 1987.
422. Takeoshi, T.; Anderson, P. P. U.S. Patent 4,766,199, 1988.
423. Evans, T. L. U.S. Patent 4,699,974, 1987.
424. Bolton, D. H.; Wooley, K. L. *Macromolecules* **1997**, *30*, 1890.
425. Krabbenhoft, H. O.; Boden, E. P. *Polym. Prepr., ACS Div. Polym. Chem.* **1990**, *31*, 16.
426. Rosenquist, N. R.; Fontana, L. P. *Polym. Prepr., ACS Div. Polym. Chem.* **1989**, *30*, 577.
427. Brunelle, D.J.; Shannon, T. G. U.S. Patent 4,972,039, 1990.
428. Kulig, J. J.; Brittain, W. J.; Glimour, S.; *et al. Macromolecules* **1994**, *27*, 4838.
429. Moore, C. G.; Brittain, W. J. *Polym. Bull.* **1996**, *37*, 573.

Biographical Sketches

Gabriel Rokicki is a chemistry professor at the Faculty of Chemistry, Warsaw University of Technology, Poland, where he received all his academic education (MSc in 1971, PhD in 1989, and tenure professor in 2002). His current scientific activities include synthesis, structure, and properties of polymer materials, such as aliphatic polycarbonates, polyurethanes, epoxy resins, and biodegradable polymers. He has devoted a special interest to the use of functional polymers in obtaining specialty ceramic materials as well as to polymer recycling. Earlier major interests included the utilization of carbon dioxide and cyclic carbonates in the synthesis of condensation polymers. Another topic of interest was polymeric ion-sensors based on modified calixarenes. He is the author and coauthor of 160 scientific papers and holds more than 50 patents in the above-mentioned areas. At the Faculty of Chemistry of Warsaw University of Technology, he conducts lectures on polymer chemistry and technology.

Paweł G. Parzuchowski received his MS degree in chemical technology from the Faculty of Chemistry of Warsaw University of Technology (WUT), Warsaw, Poland, in 1996. He received his PhD degree in chemistry from the same university in 1999. During his PhD studies he worked on a variety of projects related to design and synthesis of improved ion-sensory materials. He developed a method of covalent binding of calixarene ionophores to acrylic polymer matrix as well as methodology of preparation of dendrimers based on calixarene units. Part of this work was carried out at the Department of Chemistry of Johannes Gutenberg University in Mainz, Germany. He then worked as a postdoctoral research scientist at the University of Michigan, Ann Arbor, USA, until March 2002 in the area of nitric oxide-releasing materials and ionophores for optical and electrochemical sensors. He is presently an assistant professor of chemistry at the Warsaw University of Technology, Poland. His current research interests include development of new bio-based and biocompatible materials, hyperbranched polymers and drug delivery systems, as well as recycling of plastics and development of technologies of production of biodegradable polymers.

4.13 ROP of Cyclic Amines and Sulfides

EJ Goethals and B Dervaux, Ghent University, Gent, Belgium

4.13.1 Introduction

Cyclic amines and cyclic sulfides represent two large families of monomers. The variety of structures, and hence variety of physical properties of the corresponding polymers, stems from the variation of ring size and from the possibility of placing one or more substituents on the heterocycle. In the case of sulfides, this is only possible on carbons; in the case of amines, substituents can be added to nitrogen as well.

Three- and four-membered cyclic amines and sulfides possess high ring strains ranging from 80 to 100 kJ mol^{-1}. From these high values it can be deduced on thermodynamic grounds that the polymerizations of these monomers should lead to high conversions. The five- and six-membered rings have ring strains in the order of 0–20 kJ mol^{-1}, which is not sufficient for polymerization.

The possibility of preparing well-defined polymers from these monomers depends on the operating polymerization mechanism, more particularly on control of the initiation reaction and the occurrence or absence of transfer and/or termination reactions. In this chapter, the mechanism of polymerization of different monomer types will be described, with emphasis on control of the polymer structures formed. This control applies not only to molecular weight and molecular weight distribution (MWD) but also to the stereochemistry and the nature of the polymer end groups.

4.13.2 Cyclic Amines

The three- and four-membered rings (aziridines and azetidines) of this group can be polymerized by cationic initiators. Anionic polymerization has not been reported and is probably impossible. The five-membered ring, pyrrolidine, and the six-membered ring, piperidine, have not enough ring strain to be polymerizable.

The polymerization mechanisms display different characteristics depending on the presence or absence of a substituent on the nitrogen atom, that is, whether the monomer is a tertiary or a secondary amine. Furthermore, as in most cationic ring-opening polymerizations (ROPs), the presence of substituents on the carbon atoms of the monomer plays a role in its 'polymerizability'.

4.13.2.1 Aziridines

4.13.2.1.1 Ethylenimine

The polymerization of the parent compound of this group, ethylenimine, has been known since the early 1940s,[1] and the polymer, polyethylenimine (PEI), is produced commercially in several countries. The polymerization mechanism is complicated due to the occurrence of transfer of a proton from the active species to other amino functions present in the reaction mixture. As a consequence, the first reaction products are oligomeric compounds. The usual initiation reaction is protonation of the monomer. If an alkylating agent is used as initiator, very soon the initiation reaction becomes protonated due to this proton transfer, as shown in **Scheme 1**.

The oligomers formed in the first stages of the polymerization can react in three ways:

1. After protonation of the aziridine end group, a new monomer molecule can be added to form the linear $n+1$ mer (**Scheme 2**).

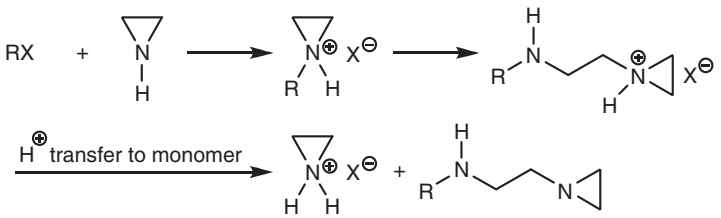

Scheme 1 Polymerization of ethylenimine: initiation, propagation and transfer to monomer.

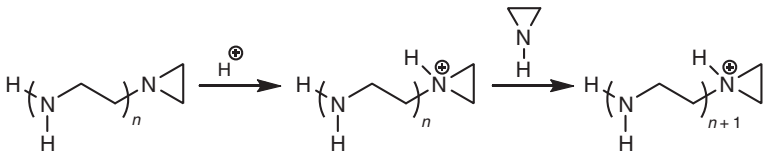

Scheme 2 Polymerization of ethylenimine: re-activation of terminal aziridine polymer end group.

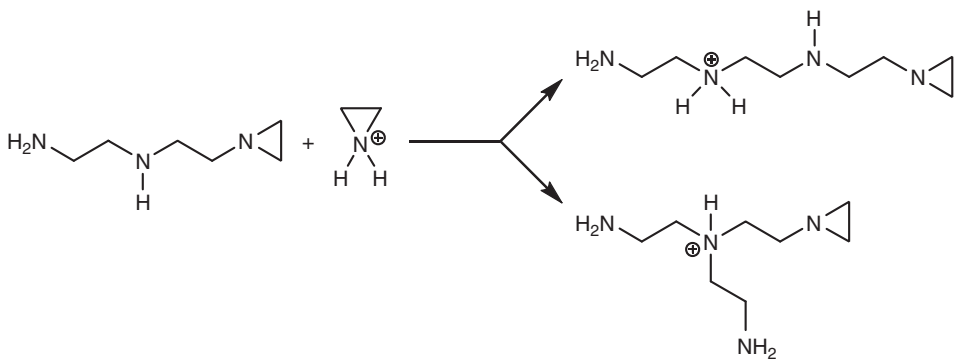

Scheme 3 Polymerization of ethylenimine: formation of linear and branched units.

2. One of the linear amine functions reacts with an aziridinium ion, for example, the protonated monomer, to form a linear or a branched (tertiary amine) structure (Scheme 3).
3. The amino function of the terminal tertiary aziridine reacts as a nucleophile with an aziridinium ion to produce a quaternary aziridinium ion. This will eventually react with an amine also producing a branched (tertiary amine) structure (Scheme 4).

The final polymer has a highly branched structure containing primary, secondary, and tertiary amines (see below) and probably also a small fraction of quaternary ammonium ions formed when a tertiary amine reacts with an aziridinium ion. By this reaction an unreactive cation is formed which means that it is a termination reaction.

The concentrations of the oligomers formed in the first stages of the polymerization have been monitored.[2] The results are shown in Figure 1.

Linear polyethylenimine (LPEI), which contains only secondary amino functions, has been prepared in different ways. The one most used is the hydrolysis of poly(*N*-acyl ethylenimine), which is obtained by cationic polymerization of the corresponding *N*-alkyl or aryl oxazoline[3] (see Chapter 4.24),[4] (Scheme 5). This type of polymerization exhibits living characteristics so that polymers with controlled molecular weight and narrow distribution can be obtained. Consequently, the LPEI obtained from such a polymer will also have a

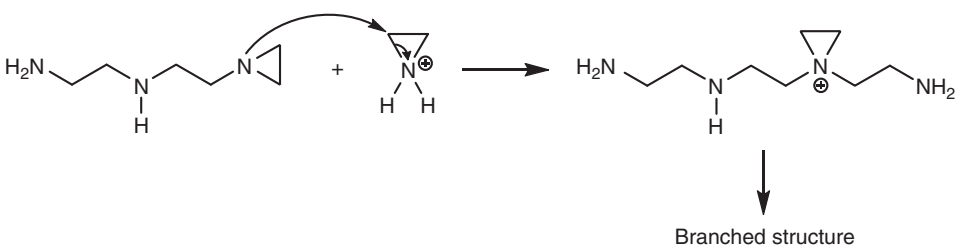

Scheme 4 Polymerization of ethylenimine: formation of quaternary aziridinium ion.

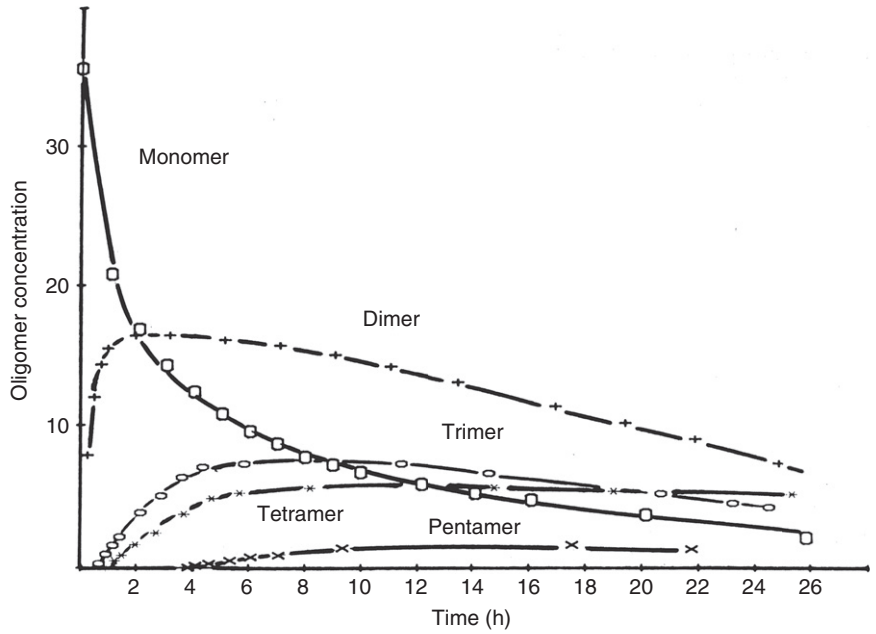

Figure 1 Formation and subsequent reaction of oligomers in the polymerization of ethylenimine.

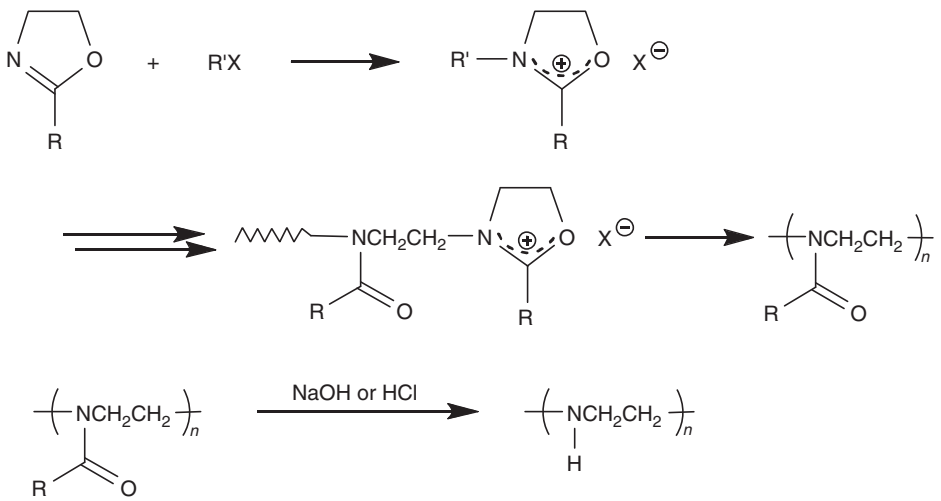

Scheme 5 Polymerization of *N*-alkyl oxazoline and subsequent hydrolysis to LPEI.

well-defined structure. The hydrolysis of the *N*-acyl-PEI can occur in alkaline or in acidic medium.[5]

Two other methods for the synthesis of LPEI have been described. The first method[6] starts from ethylenimine and proceeds in two steps. The first step is the preparation of a mixture of low-molecular-weight oligomers containing predominantly dimer and trimer as described above. The second step is the proton-initiated head-to-tail coupling of these oligomers in the presence of a well-specified amount of water. The role of water is to form a crystalline hydrate with the polyamine as soon as it is formed, thus preventing the reaction between the aziridinium ions in solution and the secondary amino functions in the polymer chain, which is the main cause of the branching (Scheme 6).

The last method[7] consists of polymerizing an N-substituted aziridine in which the substituent can be removed after the

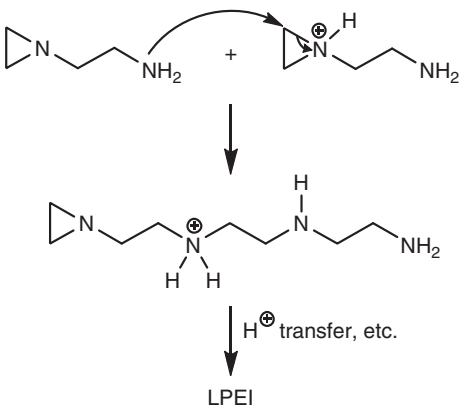

Scheme 6 Formation of LPEI by head-to-tail coupling of ethylenimine oligomers.

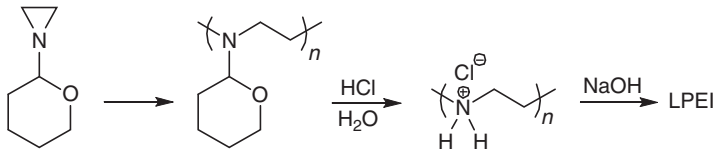

Scheme 7 Polymerization of *N*-(*a*-tetrahydropyranyl) aziridine and subsequent hydrolysis to LPEI.

polymerization. Such a monomer is *N*-(α-tetrahydropyranyl) aziridine. The tetrahydropyranyl group is removed by acid-catalyzed hydrolysis (Scheme 7).

The last two methods have the inconvenience that they start from EI monomer that is not easily available due to its high toxicity. Therefore, the most used route for the LPEI synthesis is via polyoxazoline.

The physical properties of branched PEI and LPEI are quite different. The linear polymer is crystalline (m.p. 58.5 °C) and forms several crystalline hydrates with water, whereas the branched polymer is amorphous. In contrast with the branched form, LPEI is insoluble in cold water but dissolves above its melting point.

The microstructure of PEI, more particularly the relative amounts of primary, secondary, and tertiary amino functions, can be deduced from ^{13}C-NMR spectroscopy. In the spectrum of a branched PEI polymer, eight lines can be distinguished according to the nature of the neighboring amino functions.[8,9] The spectrum of LPEI shows only one peak. The constitution of the polymers has also been analyzed by ^{15}N-NMR spectroscopy.[10]

The Mark–Houwink molecular weight–viscosity relation for LPEI in methanol at 25 °C has been determined.[11]

$$[\eta] = (1.04) \times 10^{-2} \bar{M}_w^{\,0.95}$$

The high value of the exponent in the equation indicates that in this solvent the polymer has a relatively rigid structure. This is in contrast with the values of < 0.5 determined for the branched polymer,[12,13] indicating a compact structure.

4.13.2.1.2 C-substituted aziridines

The polymerization of 2-methylaziridine (propylenimine) has been reported briefly.[14] The structure of the polymer may be expected to be complicated by the presence of head-to-tail, tail-to-tail, and head-to-head diads, tacticity, and branching. Linear head-to-tail polypropylenimine has been produced by isomerization polymerization of 4-methyloxazoline followed by hydrolysis.[15] Starting from optically active monomer, pure head-to-tail, isotactic, optically active polypropylenimine was obtained.[16] The ^{13}C-NMR spectrum of this polymer exhibited only three signals[17] (Scheme 8).

The polymerization of 2-phenylaziridine with several initiator systems has been described. The corresponding polyamines had relatively low molecular weights. The kinetics of the polymerization were studied with perchloric acid and methyl triflate as initiators.[18]

4.13.2.1.3 N-substituted aziridines

The polymerization of N-substituted aziridines is less complicated than that of the N-unsubstituted monomers. The active species are quaternary aziridinium ions so that proton transfer is not possible. The propagation is a nucleophilic attack of the monomer nitrogen on the α-carbon of the aziridinium ion.

The nitrogens of the formed polymer can perform the same reaction, which leads to an unreactive quaternary ammonium ion so that this reaction is a termination. As a consequence, the polymerizations of *N*-alkylaziridines usually stop at limited conversions. This was first observed for the polymerization of *N*-methylaziridine by Jones *et al.*[19] The maximum conversions are determined by the concentration of initiator and by the ratio of the rate constant of the propagation over the rate constant of the termination reaction. This ratio, k_p/k_t, has been taken as a measure of the living character of the polymerization.[20] From kinetic studies and from molecular weight determinations, it was deduced that this termination is predominantly intramolecular, that is, the terminated polymer chains contain a cyclic, nonstrained ammonium ion as an end group (Scheme 9).

As shown in Table 1, the ratio k_p/k_t dramatically increases with the bulkiness of the N substituent. Also, the introduction

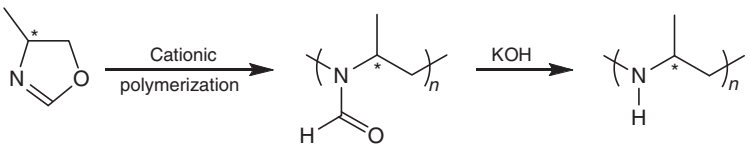

Scheme 8 Synthesis of isotactic, optically active polypropylenimine.

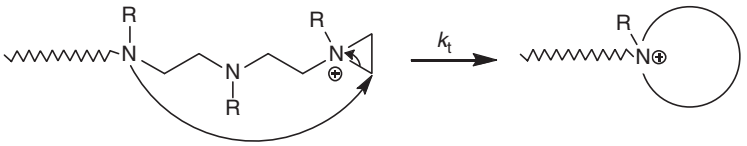

Scheme 9 Intramolecular termination reaction in the polymerization of *N*-substituted aziridines.

Table 1 Values of k_p/k_t for the polymerization[a] of *N*-alkylaziridines

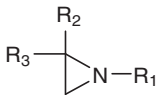

R_1	R_2	R_3	k_p/k_t ($l\,mol^{-1}$)	References
C_2H_5	H	H	6	22
$CH(CH_3)_2$	H	H	20	22
$C(CH_3)_3$	H	H	12 000	22,23
$CH_2C_6H_5$	H	H	85	22
$CH_2CH_2C_6H_5$	H	H	14	22
CH_2CH_2CN	H	H	82	22
$CH_2C_6H_5$	CH_3	H	1 100	20
$CH_2CH_2C_6H_5$	CH_3	H	10 000	20
CH_2CH_2CN	CH_3	H	~5 000	20
$CH_2C_6H_5$	CH_3	CH_3	0	21

[a] Polymerizations carried out in CH_2Cl_2 with Et_3OBF_4 as initiator at 20 °C.

of a substituent on a ring carbon results in a marked increase of the living character. If two substituents are present on one of the ring carbons, the monomer becomes unreactive for (homo) polymerization.[21]

Due to 'steric shielding' of the amino functions in the polymer chains by their own and two adjacent *t*-butyl groups, the polymerization of *N*-*t*-butylaziridine (TBA) has a very high k_p/k_t ratio so that this polymerization may be regarded as being a 'temporary living' one.[22,23] This means that, although there is a termination reaction, its rate is so slow compared with the rate of the propagation that, at almost quantitative conversion, almost every polymer chain in the reaction mixture still contains an active species. The shielding effect is illustrated in Scheme 10.

Thus, end-capping and coupling reactions of living polyTBA can be carried out successfully, provided these reactions are done immediately after the polymerization. These reactions can be performed by addition of a nucleophilic reagent. Table 2 gives an overview of end-capping reactions that have been performed leading to various end group-functionalized polyTBAs or, in case of macromolecular nucleophiles, to graft or block copolymers.

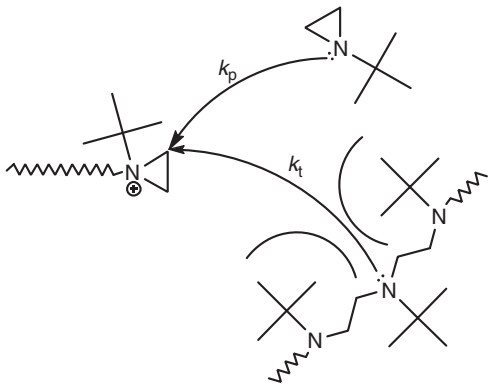

Scheme 10 Schematic representation of 'steric shielding' in TBA polymerization.

Another method for the synthesis of block copolymers is the sequential monomer addition method. In this method, the polymerization of TBA is initiated by the cationic living chain end of another cationic polymerization. This has been carried out with perchlorate-terminated polystyrene[31] and with cationic living polyTHF as the initiating polymer. The polyTHF can be mono-, di-, or trifunctionally living leading to AB, BAB, and three-arm star-shaped block copolymers, respectively.[32]

The copolymerization of polyTBA macromonomers with hydrophilic and hydrophobic comonomers has been reported.[29]

TBA is easily obtained in a two-step reaction from *N*-*t*-butyl-2-aminoethanol.[23] PolyTBA is a crystalline polymer with a melting point of 142 °C. It is soluble in aqueous acid.

Also the bicyclic aziridine monomer, 1-aza-[1,3,0]-bicyclohexane, has been reported to give a living polymerization.[33] Polymerization of one enantiomer of this monomer, synthesized from L-proline, leads to the corresponding chiral polymer[34] (Scheme 11).

When the polymerization of N-substituted aziridines is initiated with a proton acid having a nonnucleophilic anion, a nonnegligible fraction of cyclic oligomers is formed.[35] This is due to the fact that the secondary amino head group formed by the proton initiation is more reactive toward an aziridinium ion than is a tertiary amino function. The probability that this reaction occurs intramolecularly is highest when the secondary amine and the aziridinium end group are separated by three monomer units, leading to cyclic tetramer. The intermolecular reaction results in a coupling between two polymer molecules, leading to higher molecular weights than calculated from monomer consumption and initiator concentration. Moreover, the molecular weight of the polymer continues to increase after all monomer is consumed[36] (Scheme 12).

In the case of TBA, the only cyclic oligomer formed is the pentamer.

If the initiating acid has an anion with a nucleophilicity equal to or higher than the nucleophilicity of the monomer, such as a halide, and if the reaction is carried out in a nonpolar solvent, the main reaction product is the corresponding *N*,*N*′-dialkylpiperazine,[37] formed as in Scheme 13.

In a polar solvent, the intermediate alkyl halide is not formed and the end product is the polymer.

The synthesis and polymerization of 2-(1-aziridinyl)ethyl methacrylate has been reported. This monomer can be polymerized via the methacrylate group or via the aziridine group leading to cross-linkable polymers[38] (Scheme 14).

Poly-*N*-(2-aminoethyl)aziridine has been prepared by polymerization of the corresponding formamide derivative followed by hydrolysis[39] (Scheme 15).

4.13.2.2 Azetidines

4.13.2.2.1 Azetidine

The polymerization of this four-membered secondary amine is similar to the polymerization of ethylenimine.[40] In the first stages of the polymerization, oligomeric products are formed due to the possibility of transferring a proton from the original active species to monomer. In the case of azetidine, this transfer is even more pronounced than in the case of ethylenimine because the basicity of the monomer is higher than that of a substituted azetidine. When all monomer has reacted, 70% of

Table 2 End-capping reactions of living polyTBA

Terminator	*End group*	*Remarks*	*References*
$^{\ominus}OH$	~~OH		24
NH_3	~~NH_2		24
RNH_2	~~NHR		24
RCOOH	~~O–C(=O)–R		24
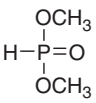	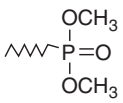		25
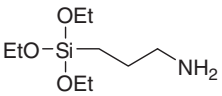	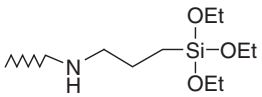	Macromonomer	26
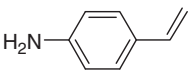	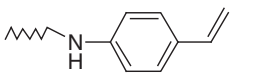	Macromonomer	27
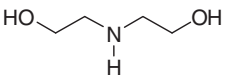	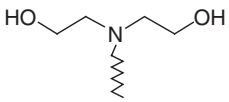	Macromonomer	28
$H_2NCH_2CH_2OH$	~~$HNCH_2CH_2OH$		25
$NaOCH_2CH_2NH_2$	~~$OCH_2CH_2NH_2$		25
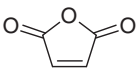	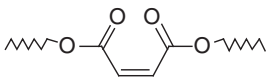		25
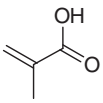	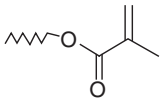	Macromonomer	27
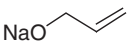	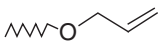	Macromonomer	29
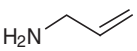	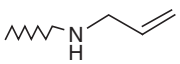	Macromonomer	29
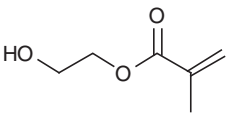	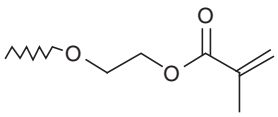	Macromonomer	29
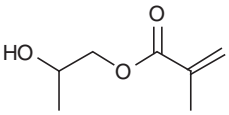	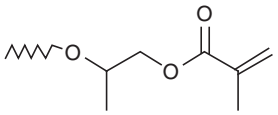	Macromonomer	29
H_2N–polyethyleneoxide–NH_2	~~N(H)–polyEO–N(H)~~	ABA block copolymer	30
HOOC–polybutadiene–COOH	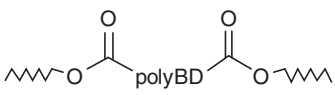	ABA block copolymer	30

(*Continued*)

Table 2 (*Continued*)

Terminator	*End group*	*Remarks*	*References*
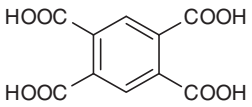	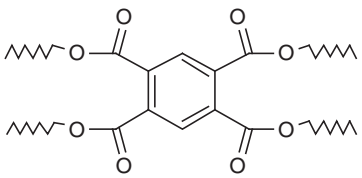	Star-shaped polymer	24
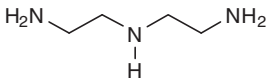	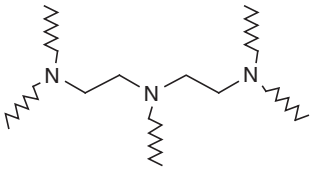	Star-shaped polymer	24

Scheme 11 Polymerization of 1-aza-[1,3,0]-bicyclohexane.

the reaction mixture consists of dimer. This dimer has two nucleophilic sites that can react with an activated (protonated) azetidine group: the primary amine, leading to a linear structure, and the tertiary, leading to a quaternary azetidinium ion (Scheme 16).

Further reaction of the quaternary azetidinium ion with any amine leads to a tertiary amine. Another route to a tertiary amine group is attack of a secondary amine in a polymer chain on an azetidinium ion. Finally, a polymer containing 20% primary, 20% tertiary, and 60% secondary amino functions is formed.

Linear polytrimethylenimine has been synthesized by isomerization polymerization of 1,3-oxazine to the corresponding *N*-formyl polytrimethylenimine, followed by hydrolysis[41] (Scheme 17).

The linear polymer is a crystalline solid with melting point between 74 and 84 °C, depending on the content of water of

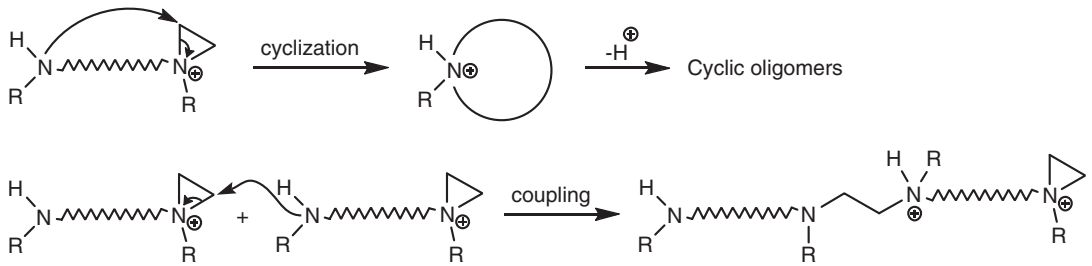

Scheme 12 Intra- and intermolecular end group coupling in proton-initiated polymerization of *N*-alkyl aziridines.

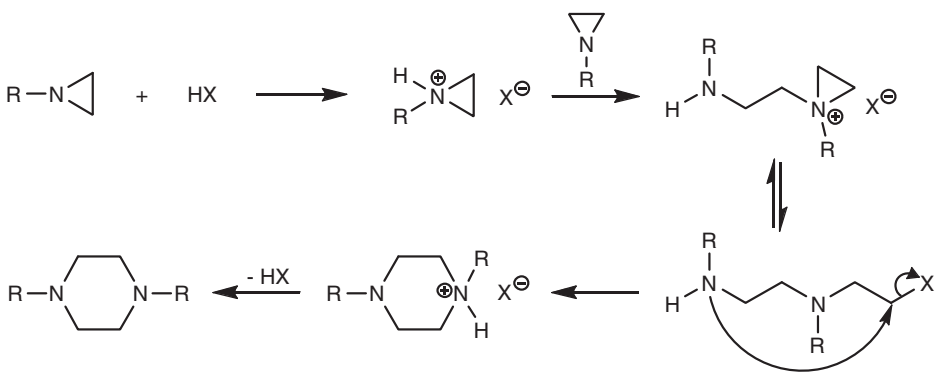

Scheme 13 Cyclic dimer formation in acid catalyzed polymerization of *N*-alkyl aziridines.

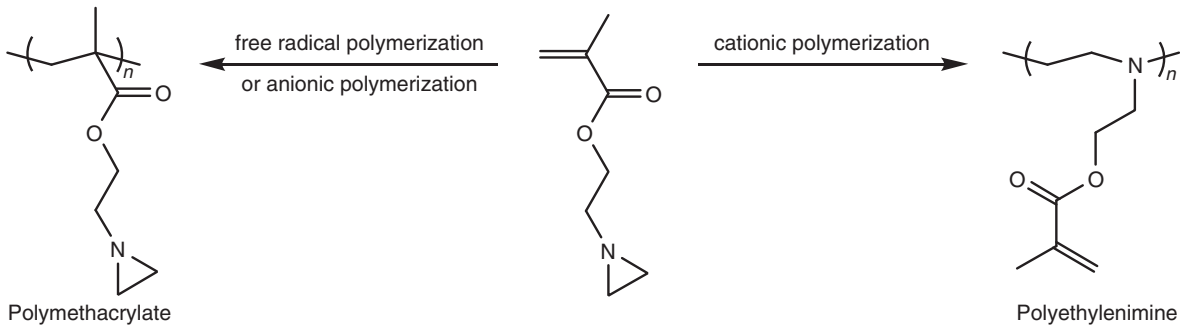

Scheme 14 Two modes of polymerization of 2-(1-aziridinyl)ethyl methacrylate.

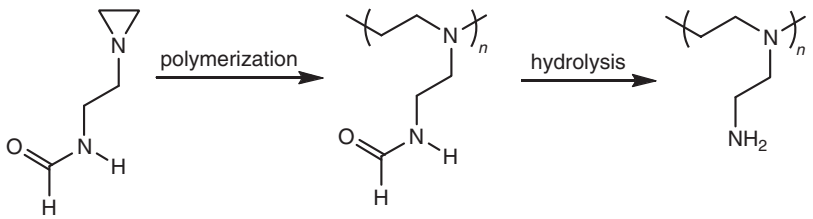

Scheme 15 Synthesis of poly-*N*-(2-aminoethyl)aziridine.

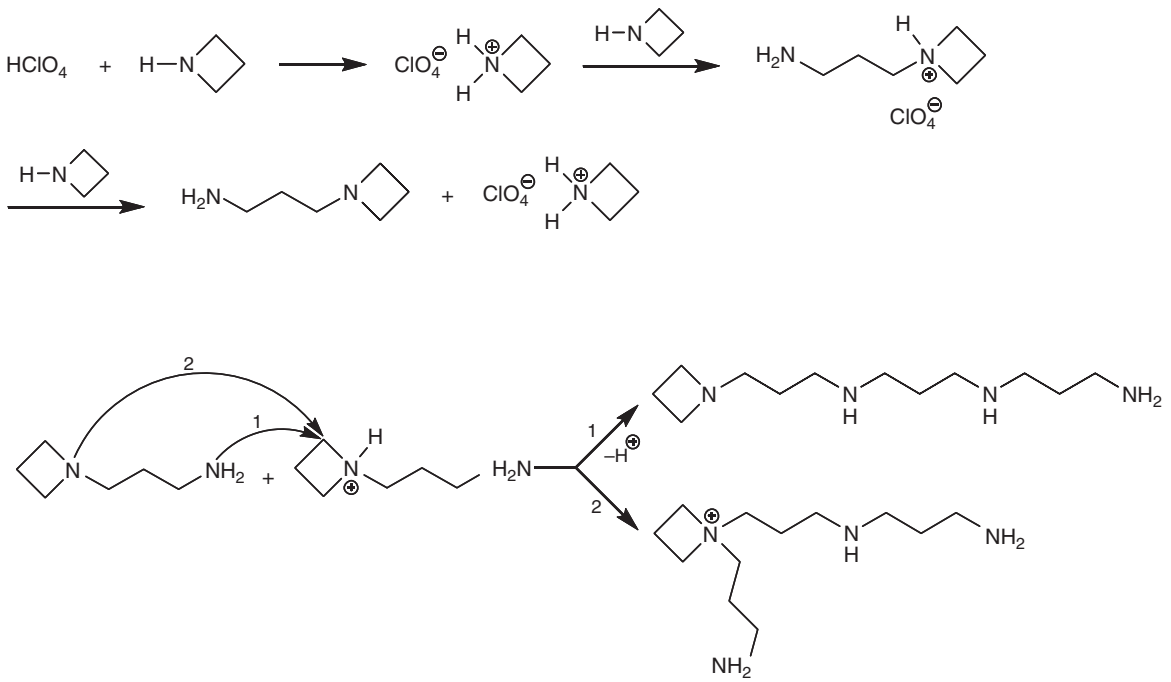

Scheme 16 Proton-initiated polymerization of azetidine.

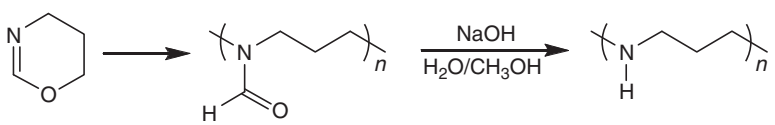

Scheme 17 Synthesis of linear polytrimethylenimine.

crystallization. The branched polymer is a noncrystallizable viscous material.

4.13.2.2.2 N-substituted azetidines

As with the aziridines, the polymerization of *N*-alkyl-substituted azetidines is not complicated by proton transfer and the mechanism can be described by initiation, propagation, and termination. Three monomers have been studied in detail: conidine (1-azabicyclo[4.2.0]octane), 1,3,3-trimethylazetidine, and *N*-phenylazetidine (NPA) (Figure 2).

Conidine contains a chiral carbon atom and can be separated into its enantiomers. The polymerization of an enantiomer leads to polymers having a strong optical rotation of a sign opposite to that of the monomer.[42] These results show that the attack of monomer occurs exclusively at the methylene carbon atom of the azetidinium ion. The polymers are crystalline with a melting point of 94 °C. The mechanism of polymerization of conidine has been studied for polymerizations initiated with the tertiary or quaternary ammonium salts derived from the monomer by reaction with a proton acid or an alkyl halide. Kinetic studies led to the conclusion that with the quaternary ammonium salt initiators, the concentration of the active species remained constant during the polymerization and the degrees of polymerization were proportional to the conversion. Therefore, it was concluded that this polymerization shows a living behavior.[43] The nature of the active species in the polymerization of conidine has been discussed, more particularly the reactivity of the ion pairs and the free ions.[44] It was found that, in nitrobenzene solution, the rate constant of propagation by free ions was equal to that of propagation by ion pairs for a variety of counterions.

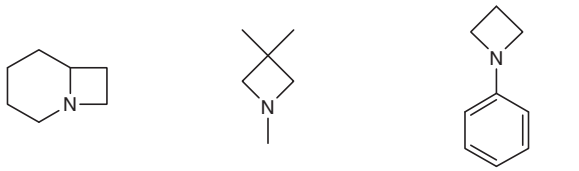

Figure 2 Structure of conidine, 1,3,3-trimethylazetidine, and NPA.

The living character of the polymerization of 1,3,3-trimethylazetidine was demonstrated by kinetic measurements[45] and confirmed by ^{1}H-NMR spectroscopy.[46] With this method it was possible to detect the concentration of the active chain ends during and after the polymerization: the active species concentration remained constant even after all monomer was consumed.

Comparison of the polymerization behavior of 1-methylazetidine with that of 1,3,3-trimethylazetidine shows the importance of the *gem*-dimethyl substituents in the 3-position. With the former monomer, a termination reaction occurring between the active species and an amino function of the polymer, leading to branched or macrocyclic ammonium salts, was observed,[47] whereas with the latter this termination is virtually nonexistent as a consequence of 'steric shielding' of the amino functions in the polymer chain.

The polymerization of NPA with methyl triflate as initiator follows a similar mechanism with a predominantly intermolecular termination reaction by nucleophilic attack of the polymer nitrogens on the active species.[48] At 30 °C, the ratio k_p/k_t is approximately 30.

NPA reacts with living polyTHF to produce an azetidinium-terminated polymer that can be used as macroinitiator for the polymerization of NPA whereby THF–NPA block copolymers are formed.[48] Due to the intermolecular termination, the end products have branched structures.

N-phenylazetidinium ions react with nucleophilic reagents such as carboxylate anions to form the corresponding amino-ester derivatives. This reaction has been used extensively by the group of Tezuka to produce a large variety of cyclic and polycyclic polymer structures by the so-called electrostatic self assembly – covalent fixation method.[49,50]

N-alkyl-3-azetidinols, obtained from epichlorohydrin and a primary amine, have been polymerized to low-molecular-weight hydroxy-substituted polyamines.[51] Transesterification of an azetidinol with methyl acrylate or methacrylate leads to the corresponding azetidinyl esters which can be polymerized or copolymerized with other vinyl monomers to produce reactive, cross-linkable polymers[52] (Scheme 18).

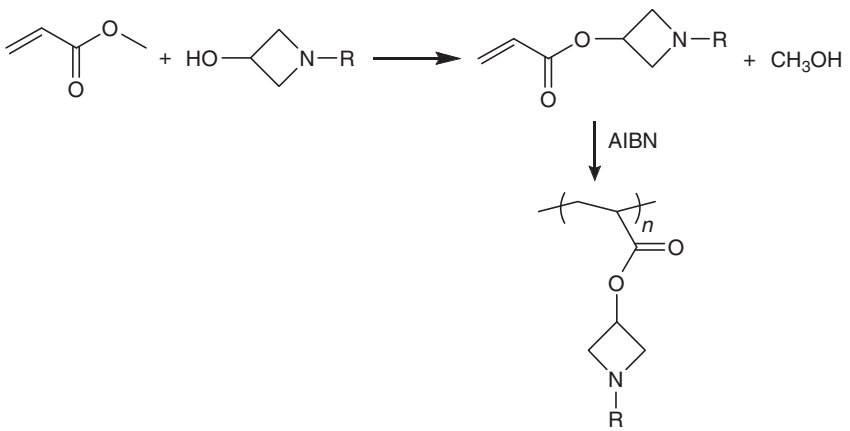

Scheme 18 Synthesis and free radical initiated polymerization of azetidinyl acrylate.

4.13.3 Cyclic Sulfides

4.13.3.1 Thiiranes

The parent compound, thiirane (ethylene sulfide), produces a crystalline polymer with a melting point of 205 °C that is insoluble in most solvents.[53] As a consequence, the polymerizations of this monomer are heterogeneous and mechanistic studies are difficult. The most studied monomer is methylthiirane (MT) often referred to as propylene sulfide. However, other substituted thiiranes have also been described extensively in the literature. The polymerizations can occur by cationic, anionic, coordinative, and 'monomer insertion' mechanisms.

4.13.3.1.1 Cationic polymerization

The cationic polymerization of thiiranes is initiated by proton acids, Lewis acids, and alkylating agents.[54] The counterions of the cationic propagating species must have a nucleophilicity lower than that of the monomer in order to prevent termination reaction with the counterion. Typical nonnucleophilic counterions are tetrafluoroborate, hexafluorophosphate, trifluoromethanesulfonate, and perchlorate.

The propagation reaction is a nucleophilic attack of the monomer on the thiiranium ion (ring substituents omitted) (Scheme 19).

The polymerization is characterized by a rapid (temporary) termination reaction occurring between the active species and a sulfide function in the polymer chain. This termination appears to be reversible so that these terminated groups are 'dormant' rather than 'dead' species.[54,55] The reinitiation reaction can result in the same starting structures; however, as shown in the next scheme, it is equally possible that a neighboring sulfide of another polymer chain produces the thiiranium ion. In that case, polymer P^1 is connected to P^2 and the active species is transferred to polymer P^3 (counterion and substituents omitted) (Scheme 20).

Scheme 19 Propagation reaction in cationic ROP of thiiranes (ring substituents omitted).

This leads to broadening of the MWD of the polymers.

If the termination occurs with a sulfide of the same polymer chain, the subsequent reinitiation results in the formation of a cyclic oligomer. With most monomers, a mixture of cyclic oligomers is formed but the most abundant are the dimers and the 12-membered tetramers, which are formed as in Scheme 21(substituents omitted).

The degradation of polythiiranes leads not only to cyclic oligomers but also to seven-membered trithiepane rings, that is, rings containing a disulfide bond, whereby an olefin is eliminated. The mechanism proposed for this trithiepane formation from poly(*trans*-2,3-dimethylthiirane) is as shown in Scheme 22.[56]

The stereochemistry of this reaction has been studied in detail and has led to the elucidation of the reaction mechanism of the degradation to trithiepanes.

Finally, in cases where the thiiranium ions can form stabilized carbenium ions (e.g., phenylthiirane and 2,2-dimethylthiirane), isomerized five-membered cyclic dimers (1,3-dithiolanes) have been found. These are formed by a mechanism including a hydride transfer in the carbenium ion intermediate.[57]

This cyclic oligomer formation continues after all monomer has been consumed. Therefore, the final end product of the cationic 'polymerization' of thiiranes consists of a mixture of low-molecular-weight polymer and cyclic degradation products.

These degradation products are also obtained when polythiiranes, prepared by other polymerization mechanisms, are treated with cationic (photo-)initiators.[56] The degradations occur rapidly at room temperature. The kind of oligomers formed depends on the nature of the monomer and on the concentration of the initiator. At high initiator concentrations, the smaller rings, that is, dimer or trithiepane, are favored and at lower concentrations, the larger rings, mainly tetramer, are favored.[58]

The occurrence of the intermolecular termination followed by reinitiation is the reason why the formation of block

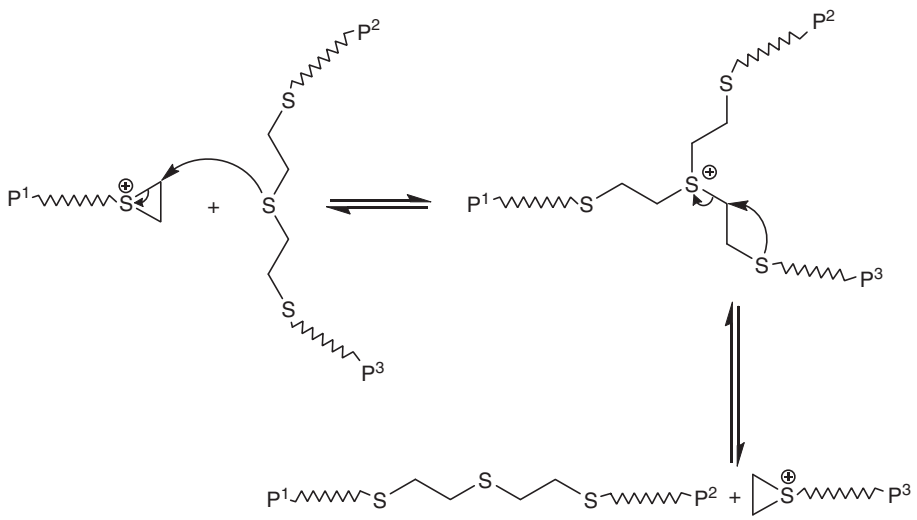

Scheme 20 Termination and re-initiation in cationic ROP of thiiranes (counterion and ring substituents omitted).

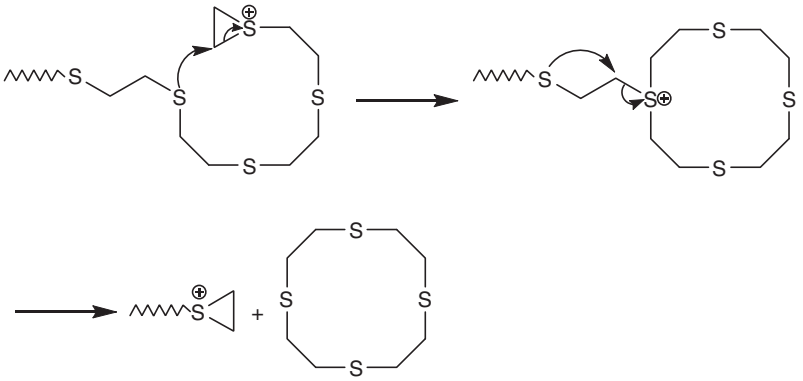

Scheme 21 Formation of cyclic tetramer in cationic ROP of thiiranes (counterion and ring substituents omitted).

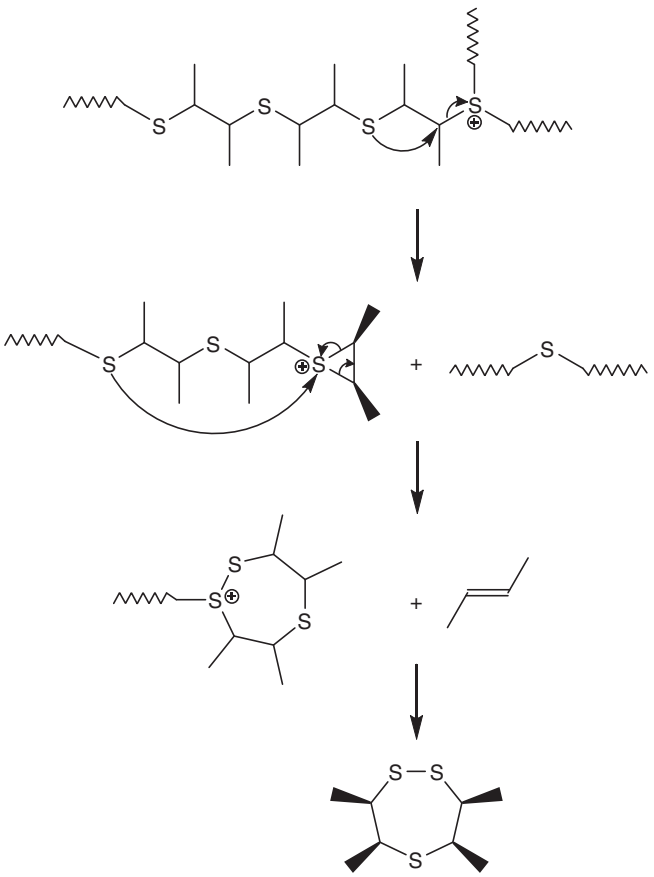

Scheme 22 Formation of trithiepane in cationic ROP of thiiranes.

copolymers of different thiiranes by sequential monomer addition is not possible: these reactions are so rapid that a scrambling of the two monomer units along the polymer chains occurs during the polymerization of the second monomer.[59,60]

The cationic polymerization of 9-carbazolylmethyl- and 10-phenothiazinylmethyl thiiranes initiated by several photoinitiators has been reported.[61] Here also, the end products were a mixture of low-molecular-weight polymers and cyclic oligomers.

4.13.3.1.2 Anionic polymerization

The anionic polymerization of thiiranes had been studied in detail during the 1960s and 1970s by Boileau, Sigwalt, and their co-workers.[53,62,63] Thiirane and various substituted thiiranes, especially MT, have been polymerized to high-molecular-weight polymers by various anionic initiators. The active species of the polymerization are of the thiolate type (Scheme 23).

The attack of the thiolate ion on the monomer proceeds exclusively at the methylene carbon so that the polymers are

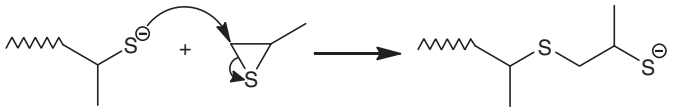

Scheme 23 Propagation reaction in anionic ROP of MT.

pure head-to-tail structures. There is no stereoselectivity in the propagation step, so that polymers with a random Bernoullian tacticity are obtained.

With a number of initiators, such as naphthylsodium, the polymerizations were found to be of the living type. With this particular initiator, the degree of polymerization was governed by the equation

$$\overline{DP}_n = \frac{2[M]}{[In]}$$

indicating that in this case the polymer chains grow at both chain ends. The initiation reaction was proposed to consist of a desulfurization process producing ion radicals that combine to form dithiolates.[64]

A detailed kinetic study of monofunctionally growing polymerization obtained by initiation with carbazylsodium permitted the calculation of the propagation rate constants and of the thermodynamic parameters for propagation via free ions and ion pairs. It was found that the free ions are about 1000 times more reactive than the ion pairs.[65] However, when the sodium counterion was complexed by cryptants, the ion pair rate constant was found to be a factor of about 3 higher than the rate constant for free ions, resulting in a global rate constant increasing with living end concentration.[66]

The anionic polymerization of thiiranes is also initiated by tertiary amines, of which 1,4-diazabicyclo[2.2.2]octane ('DABCO') is the most effective.[67] The polymerization is believed to occur through zwitterionic structures (**Scheme 24**).

PolyMTs containing thiol groups at both chain ends have been prepared by polymerization of MT in the presence of a dithiol as transfer agent[68] and trifunctional polymers were obtained with a trithiol.[69]

With some anionic initiators, such as lithium alcoholates, zinc thiolates, and triethylaluminum, the polymers contain considerable fractions of disulfide linkages with the formation of the corresponding olefin.[70–72]

Quaternary ammonium salts of thioacids or dithioacids have also been used as initiators but the initiation is slower than the propagation, resulting in broad polydispersities and uncontrollable molecular weights.[73]

The thiolate function being the active species of the polymerization, it is evident that thiolates should be the ideal initiators. This has been investigated by Nicol *et al.*[74] who described the polymerization of MT initiated by various mono- and dithiolates. The deprotonation of the thiols was accomplished by addition of a strictly stoichiometric amount of a bulky strong organic base: 1,8-diazabicyclo[5,4,0]undec-7-ene (DBU) (**Scheme 25**).

The polymerizations were found to be of the living type producing polymers with molecular weights that were in accordance with the used monomer/initiator ratios.

It was found that the thiolate end group reacts with disulfide functions which results in a transfer reaction.[75] This

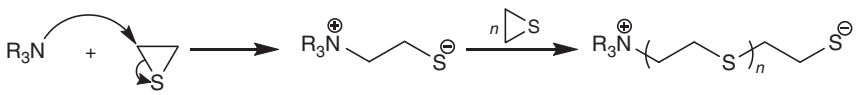

Scheme 24 Anionic ROP of thiiranes initiated by a tertiary amine.

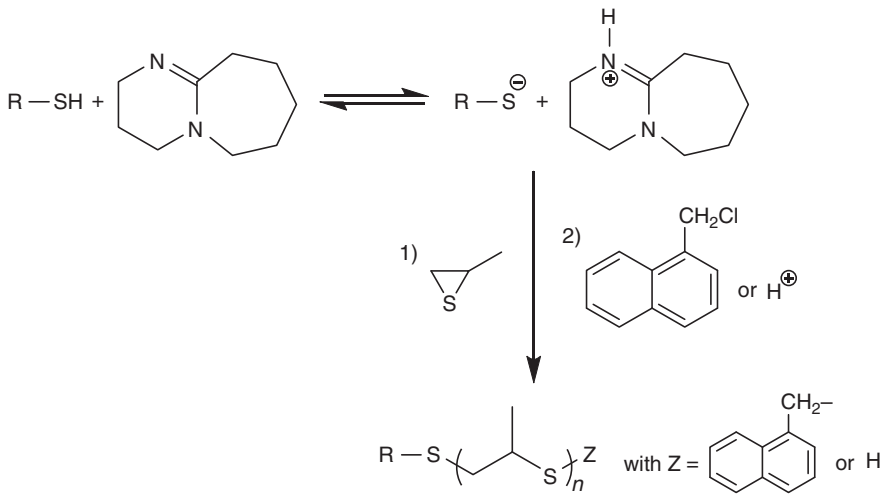

Scheme 25 Anionic polymerization of MT initiated by *in situ* formed thiolates.

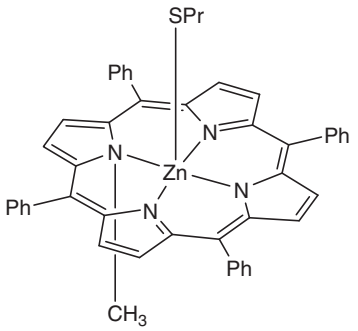

Figure 3 Structure of (NMTPP)ZnSPr.

transfer reaction occurs not only with low-molecular-weight disulfides (leading to a decrease of the molecular weight) but also with disulfide functions present in the polymer chains, leading to a broadening of the MWD. Low-molecular-weight disulfides may be present in the polymerization mixture as a result of oxidation of the initiating thiol. Therefore, several authors describe the use of protected thiols which are deprotected just before polymerization. Examples are the use of thioester, which is transformed into thiolate by the addition of sodium methanolate, and the ring opening of cyclic dithiocarbonates by an amine (see below).

A special kind of living polymerization of MT was developed by Inoue *et al.* Using (*N*-methyl-5,10,15,20-tetraphenylporphinato)zinc propanethiolate ((NMTPP)ZnSPr) as initiator, polymers with predictable molecular weights and with M_w/M_n values of 1.1 were obtained[76] (**Figure 3**).

In the presence of a thiol such as propanethiol or thiophenol, this polymerization exhibits 'immortal' character, that is, the number of polymer molecules exceeds that of the initiator molecules without affecting, however, the narrow MWD. This was attributed to an exchange of the thiol end groups of the polymer chains with the thiolate active species occurring at a rate that is much higher than the propagation rate.

Since the anionic polymerization of thiiranes can be of the living type, it is possible to prepare block copolymers by the sequential monomer addition method. Thus, various AB and ABA block copolymers of thiirane, MT, and 2,2-dimethylthiirane have been obtained by adding the thiirane to a solution of a mono- or bifunctional anionic living polymer. With the (NMTPP)ZnSPr initiator, MT–methyloxirane block copolymers were obtained by first polymerizing the thiirane and then the oxirane, the second-stage polymerization starting on irradiation with visible light.[77] **Table 3** gives a survey of block copolymers that have been obtained via sequential anionic polymerization.

Napoli *et al.*[84] developed a 'one-pot' synthetic method for the preparation of amphiphilic polyethylene glycol (PEG)-*b*-polymethylthiirane (PMT) block copolymers. Their method implies initiation of the MT polymerization by *in situ* generated PEG thiolates, obtained from the corresponding thioacetate PEG end group. Symmetric ABA triblock copolymers were obtained by exposing the thiolate-terminated diblock copolymers to air, to achieve disulfide linking. Asymmetric ABA triblock copolymers were generated by chain coupling by Michael-type addition of the thiolate terminal groups of PMT with PEG monoacrylates.

Table 3 Thiirane block copolymers formed by sequential living anionic polymerizations

First monomer	*Second monomer*	*Number of blocks*	*References*
MT	Thiirane	3	78
Styrene	Thiirane	2,3	79
Methyl methacrylate	Thiirane	2,3	79
Oxirane	Thiirane	2	80
Styrene	MT	2,3	78,79
α-Methylstyrene	MT	3	79,81
Methyl methacrylate	MT	2,3	79
Isoprene	MT	2,3	82
Butadiene	MT	3	82
Oxirane	2,2-Dimethylthiirane	2	80
MT	Methyloxirane	2	77
HydroxyMT	MT	2,3	83

The synthesis of star-shaped polythiiranes, based on the living anionic polymerization mechanism, has been reported by several authors. Nicol *et al.*[85] reported the synthesis of star-shaped PMT by polymerization with tri- and tetrathiol initiators and by end-capping of monofunctionally living polymers with tetrakis(bromomethyl)naphthalene. The latter method produced mixtures of di-, tri-, and tetra-arm polymers. Suzuki *et al.*[86] described the formation of star-shaped PMT by using trifunctional thiol **2** that was formed *in situ* from a tri(cyclic dithiocarbonate) **1** and an amine, as shown in **Scheme 26**.

The initiator system **2a**/DBU was formed by addition of DBU ([**2a**]/[DBU] = 1:1), which leads to the thiolate/thiol equilibrium through proton exchange. The polymerization of MT using this initiator system was carried out in DMF at 0 °C and was quenched by 1-(chloromethyl)naphthalene, which has been reported to be effective for termination of thiirane polymerization. With a feed ratio of $[MT]_0/[\mathbf{2a}/DBU]_0 = 30$, the reaction was complete within 5 min to afford the corresponding star-shaped polymer the number-average molecular weight (M_n) and MWD (M_w/M_n), which were 3500 and 1.05, respectively.

Recently, the same group reported the synthesis of star-shaped poly(phenoxymethyl thiirane) using the same methodology.[87]

Wang *et al.*[88] reported the synthesis of a series of initiators characterized by the presence of one, two, three, or four thioacetates, which, when deprotected with sodium methanolate, produce the corresponding number of thiolates. These initiating systems were used to produce linear monofunctional or difunctional growing polymers and three-arm or four-arm star-shaped thiol-terminated PMTs. In the same paper, the synthesis (and some properties) of star-shaped amphiphilic block copolymers based on PMT and PEG are described. In a subsequent paper by the same group, the role of disulfides in MT polymerization and the methods to minimize their presence and their effect on the final polymer structures are described.[89]

The thiolate chain ends in thiirane polymerizations are unreactive toward hydroxyl groups and even toward water,

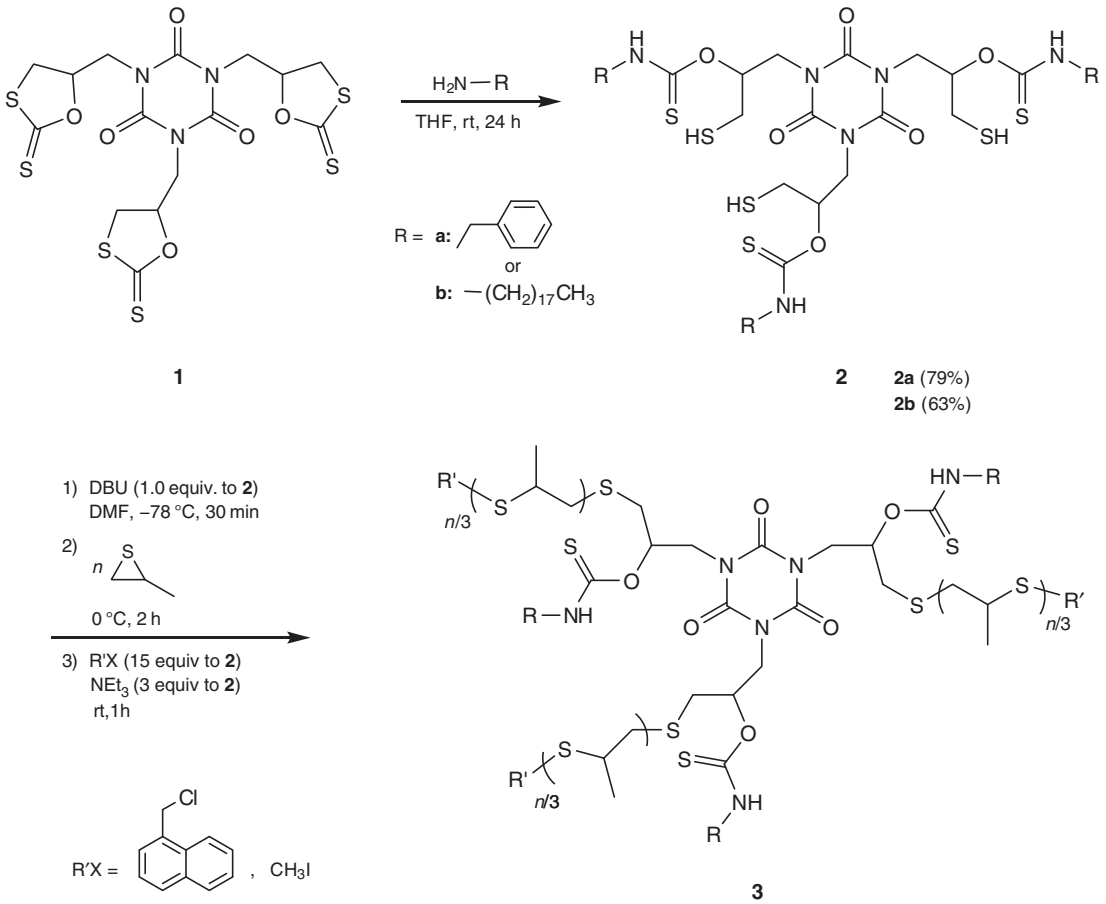

Scheme 26 Formation of star-shaped PMT by using a trifunctional thiol.

and it is, therefore, possible to produce living polymerizations in the presence of alcohols and in aqueous medium. It is also possible to polymerize hydroxyl-containing monomers such as hydroxymethyl thiirane (HMT) in a living fashion.[90] Block copolymers of MT and HMT could be prepared by sequential monomer addition on the condition that the PHMT was the first sequence.[83]

'Living' emulsion polymerization of MT in water, initiated by the system propane-1,3-dithiol/DBU, has been reported, but the polymerization stopped at limited conversions producing polymers with molecular weights lower than predicted from the used M_o/In ratios.[91] Although these observations are in contradiction with a living mechanism, it was shown, by end-capping reactions, that all polymer chains conserved thiolate anions as end groups. The limited conversions were attributed to physical causes rather than to chemical.

A similar chemistry was applied by Morinaga *et al.*[92] to use human hair, which contains thiol functions, in combination with DBU to graft-polymerize MT.

Other examples of functionalized monomers are polyoxyethylene (POE) chains linked to the thiirane with monothioacetal or ester functions (macromonomers),[93] POE chains containing a thiirane group at both chain ends (bis-macromonomer),[94] and stilbene mesogen and other side chain liquid crystalline-substituted thiiranes.[95,96]

The polymerization of 2,3-epithiopropyl methacrylate either by (controlled) free radical polymerization or by anionic ROP has been described[97] (**Scheme 27**).

End-capping of monofunctionally or bifunctionally living polyMT with 2-(bromoacetoxy)ethyl methacrylate leads to the corresponding polyMT mono- or α,ω-dimethacrylate.[98] The latter has been photo-polymerized to yield materials with controlled cross-linking densities.

4.13.3.1.3 Coordinative polymerization

Mono- or unsymmetrically substituted thiiranes exist as two enantiomers. The polymerization of a racemic mixture can occur in different ways:

1. Both enantiomers are incorporated randomly in the polymer chains leading to atactic polymers.
2. Stereoselective propagation leading to a mixture of two enantiomeric polymer chains, that is, a mixture of poly-*R* and poly-*S* chains. This propagation is called enantiosymmetrical.
3. The propagation rate constant for one enantiomer is larger than that of the other enantiomer. This type of propagation is called stereoelective or enantioasymmetrical. This type leads to optically active polymers and to an enrichment of

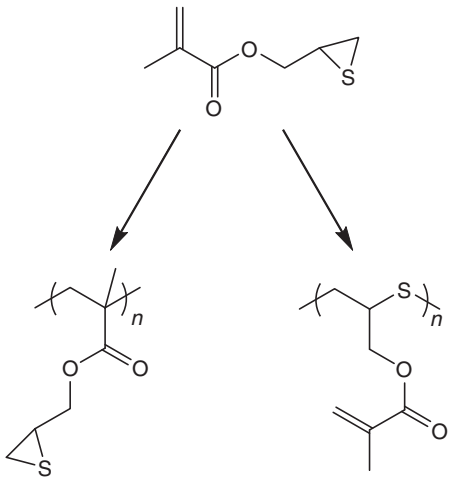

Scheme 27 Two modes of polymerization of 2,3-epithiopropyl methacrylate.

one of the enantiomers in the residual monomer mixture. The enantiomeric composition of the polymer is then governed by the equation

$$\frac{d[R]}{d[S]} = r\left(\frac{[R]}{[S]}\right)$$

where r is the ratio of the propagation rate constants for the *R* enantiomer and the *S*-enantiomer.

The anionic polymerizations of racemic mixtures of thiiranes described above generally lead to atactic polymers. When one pure enantiomer is polymerized, the asymmetric center remains unchanged and the resulting polymer is isotactic. This polymer is optically active and has quite different physical properties compared with the atactic analog. Isotactic polyMT, for example, is a crystalline material with a melting point of up to 63 °C,[53] whereas the atactic polymer is an amorphous material.

A number of initiating systems have been found to produce enantiosymmetrical polymerizations, leading to a racemic mixture of poly-*RR* and poly-*SS*. Typical initiators are the reaction products of alkylmetal compounds with water or with an alcohol. Thus, Machon and Sigwalt[99] have shown that the system diethylzinc/water produces crystalline polyMT. From comparison of the crystal structure of the crystalline fraction of the polymer with that of pure isotactic optically active polymer, it was proposed that the crystalline fraction obtained with that system consists of two kinds of optically active crystallites of *RR* and *SS* types.

Also diethylzinc/alcohol systems are efficient initiators giving high-molecular-weight polymers. High degrees of crystallinity are observed when dihydroxyl compounds are used.[100] PolyMT with high stereoregularities are obtained with cadmium tartrate as initiator. The high-molecular-weight compounds have a melting point of 53–54 °C and contain more than 85% isotactic triads.[101]

When an optically active alcohol is used for the preparation of the initiator, the polymerizations become of the enantioasymmetrical type. The system diethylzinc/(*R*)-(-)-3,3-dimethyl-1,2-butanediol (1:1) has a high stereoelective nature for the polymerization of MT.[102]

Other thiiranes that have been polymerized with stereoselective and/or stereoelective initiator systems include isopropylthiirane,[103] *t*-butylthiirane,[104] and *cis*- and *trans*-2,3-dimethylthiirane.[105,106] The polymerization of *t*-butylthiirane gives pure isotactic chains with most stereospecific initiators. An exceptionally high stereoelection was observed in the polymerization of methyl- or ethylthiirane with optically active atropisomeric initiator systems. For example, zinc (*S*)-1,1-bi-2-naphtholate gave an *r*-value of 15–20.[107,108] At 67% conversion a residual monomer with an optical activity of [α]D24 = 51.77° (neat, 1 dm) was obtained (**Scheme 28**).

Most of the stereoselective initiators are heterogeneous systems that have a low efficiency, and therefore a precise control of molecular weight and polydispersity is not possible. A number of stereoselective and stereoelective polymerizations of MT have also been studied in a homogeneous phase using chiral cadmium thiolates of cysteine esters and cadmium carboxylates of cysteine and methionine (**Figure 4**).

The most studied of these was the (*S*)-cysteine derivative with *R* = isopropyl. The polymerization of MT with this initiator is of the living type.[109] The molecular weights obey the relationship DP = [M]/[Cd], showing that the main propagation is taking place on one valency of cadmium. The stereospecificity appears only for molecular weights higher than 6000 and also depends on the temperature. The stereospecific propagation is proposed to involve cadmium thiolates associated with 'dimeric species' and coordinated by both the monomer and an oligomer or polymer chain.[110] By means of ^{13}C-NMR studies it was found that during the stereospecific polymerization of MT in homogeneous phase initiated by bis (isopropyl-(*S*)-cysteinato)cadmium, an interconversion between active sites occurred, leading to the formation of stereoblocks with an estimated DP_n of 12–14[111] (**Scheme 29**).

Enantiomer-selective polymerization of *RS*-(phenoxymethyl)thiirane with $ZnEt_2$/L-α-amino acid has been reported.[112] The *S*-enantiomer was consumed preferably and isotactic-rich polymers were obtained. With $ZnEt_2$/L-Leu, a high enantiomer selectivity ($r = 5.36$) was observed.

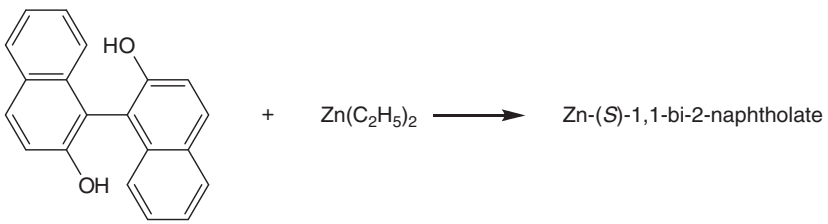

Scheme 28 Formation of Zn-(*S*)-1,1-bi-2-naphtholate.

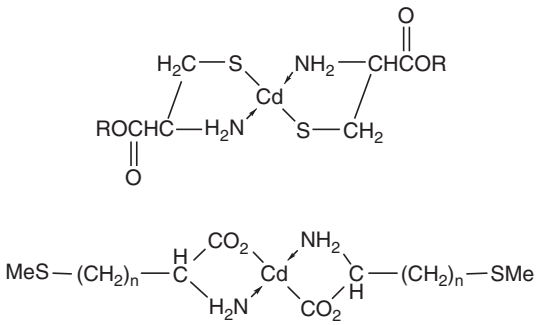

Figure 4 Structure of a cadmium thiolate of cysteine ester and a cadmium carboxylate of methionine.

4.13.3.1.4 Other ROP mechanisms for thiiranes

Acyl-group transfer polymerization of thiiranes using carboxylic acid derivatives and quaternary onium salts is a relatively new method for controlled polymer synthesis from various thiiranes.[113] In this mechanism, an acyl-group is transferred in each propagating step to give the corresponding polythiirane with an *S*-acyl end group (Scheme 30).

When the acyl transfer polymerization method was used with a cyclic dithioester as initiator, cyclic polysulfides are obtained[114] (Scheme 31).

A similar mechanism operates when dithioester such as benzyl dithiobenzoate (BDB) or benzyl 1-pyrrolecarbodithioate (BPC) is used as initiator, resulting in a polysulfide terminated with a RAFT (reversible addition fragmentation chain transfer) agent (Scheme 32).

RAFT polymerization of styrene or dimethylacrylamide with the same compounds in conjunction with AIBN as initiator leads to the corresponding polymers provided with end groups that are capable of initiating the MT polymerization with the formation of well-defined block copolymers[115] (Scheme 33).

Recently, the same group reported the 'living' insertion polymerization of MT with *p*-tolylcarbamothioate (PTCT) as initiator and tetrabutylammonium chloride as catalyst[116] (Figure 5).

4.13.3.2 Thietanes

4.13.3.2.1 Cationic polymerization

The mechanism of the cationic polymerization of thietanes differs from the mechanism described for the thiiranes by the fact that the reaction between the active species and a sulfur atom of the polymer chain appears to be irreversible so that it is a real termination reaction. As a consequence, the polymerizations of thietanes stop before all monomer is consumed and there is no formation of cyclic oligomers.[117] The maximum conversions obtained depend on the amount of initiator used and on the ratio of the rate constant of propagation, k_p, to the rate constant of the termination reaction, k_t (Scheme 34).

The ratio k_p/k_t has been taken as a measure of the living character of the polymerization.[118] This ratio is greatly affected by the presence and the nature of substituents on the thietane ring. Substituents decrease the reactivity of the active species toward the sulfide function but, as shown in Table 4, this decrease is more pronounced for the termination reaction than for the propagation reaction. Thus, thietane polymerizes

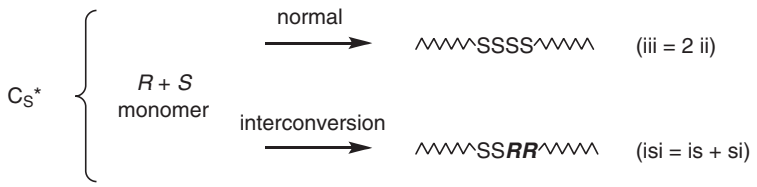

Scheme 29 Stereoblock formation in the polymerization of MT initiated by cadmium thiolate of isopropyl cysteine.

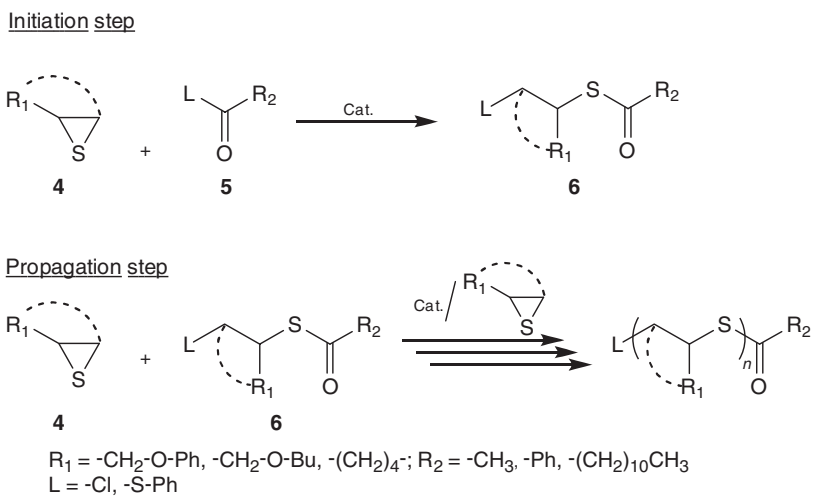

Scheme 30 Acyl transfer polymerization of thiiranes (the dotted line designates the cycloaliphatic monomer cyclohexene sulfide).

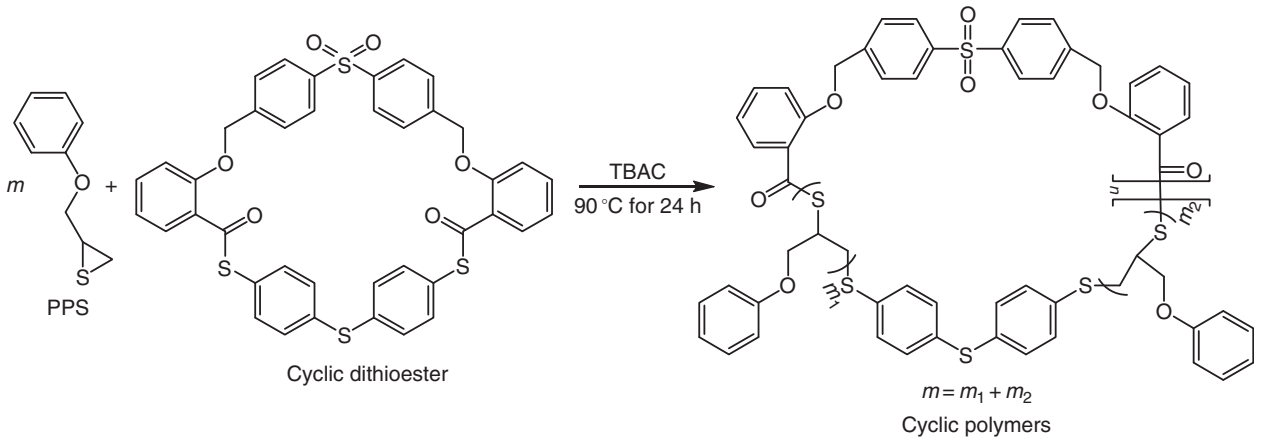

Scheme 31 Formation of cyclic polythiirane by acyl transfer polymerization.

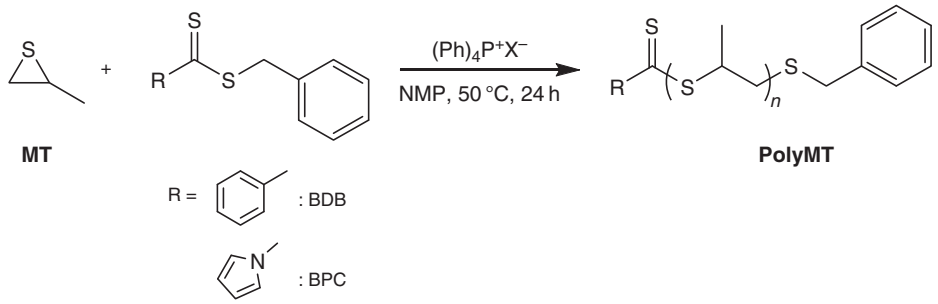

Scheme 32 Formation of PMT provided with a dithioester end group.

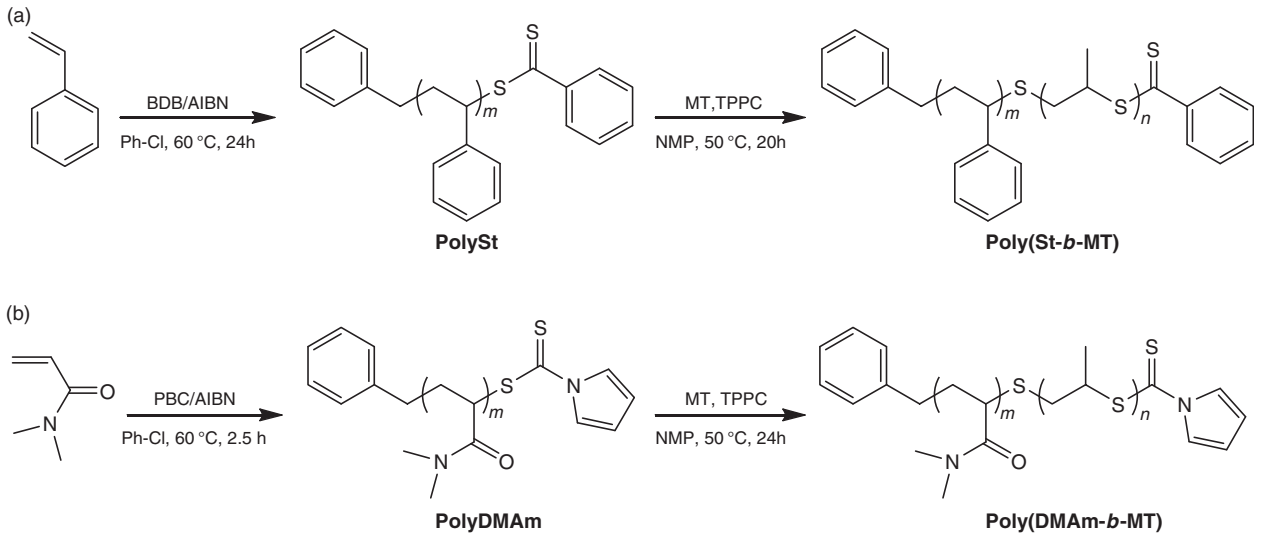

Scheme 33 Formation of poly(St-*b*-MT) and poly(DMAm-*b*-MT) using RAFT strategy.

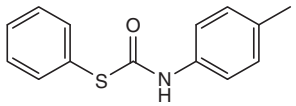

PTCT

Figure 5 Structure of PTCT.

at a high rate but the polymerization stops at low conversions, whereas 3,3-diethylthietane polymerizes very slowly but to almost quantitative conversions. This behavior has been explained by steric shielding of the sulfide functions by two adjacent substituted units in the polymer chain, which reduces the nucleophilic reactivity of the sulfide compared with the sulfide in the monomer.

The occurrence of a termination reaction in the thietane polymerization leads to the formation of branched polymer structures, and therefore it is not possible to control the molecular weight or the MWD, except for the 3,3-diethyl derivative, which shows a relatively high living character.

The occurrence of an intermolecular termination reaction in the polymerization of thietane has been used to prepare star-shaped segmented copolymers.[119] Oxonium ions are excellent initiators for the polymerization of cyclic sulfides and therefore addition of thietane to a living polyTHF solution results in the formation of a block copolymer. Since the thietane polymerization gives the termination reaction described above, the end result of this sequential monomer addition is a

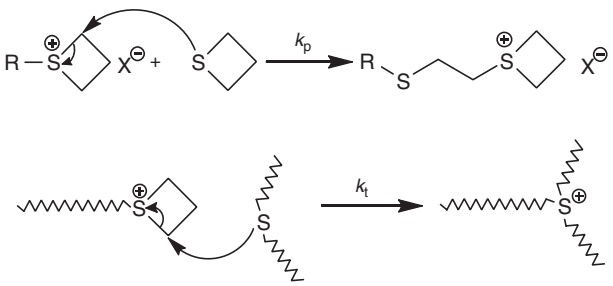

Scheme 34 Propagation and termination in the cationic ROP of thietanes.

Table 4 Ratio of rate constants for propagation and termination for the polymerization of various thietanes[117]

Monomers	*Maximum conversion (%)*[a]	k_p/k_t
	19	1.1
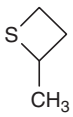	22	2.4
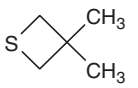	72	28
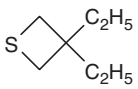	96	450

[a] $m_0 = 1\ \text{mol l}^{-1}$ [In] = 0.02 mol l^{-1} in CH_2Cl_2 at 20 °C. Initiator: Et_3OBF_4.

structure consisting of a branched polythietane core with a linear polyTHF shell (**Scheme 35**).

If the polymerization of the THF was initiated by a bifunctional initiator, such as trifluoromethane sulfonic acid anhydride, the addition of thietane leads to a segmented polymer network consisting of linear polyTHF segments connected to each other by branched polythietane segments.[119]

Similar results have been obtained by combining the living cationic polymerization of vinyl ethers and the ROP of thietane.[120] In this case, the thietane acts as growing species stabilizer for the vinyl ether polymerization by reversible formation of an α-alkoxy-thietanium ion. This ion can, however, also be attacked at an endocyclic methylene by another thietane molecule leading to an alkyl-thietanium ion. This ion is incapable of reacting with a vinyl ether but is the active species for the thietane polymerization. Also in this case the end product is a star-shaped segmented polymer.

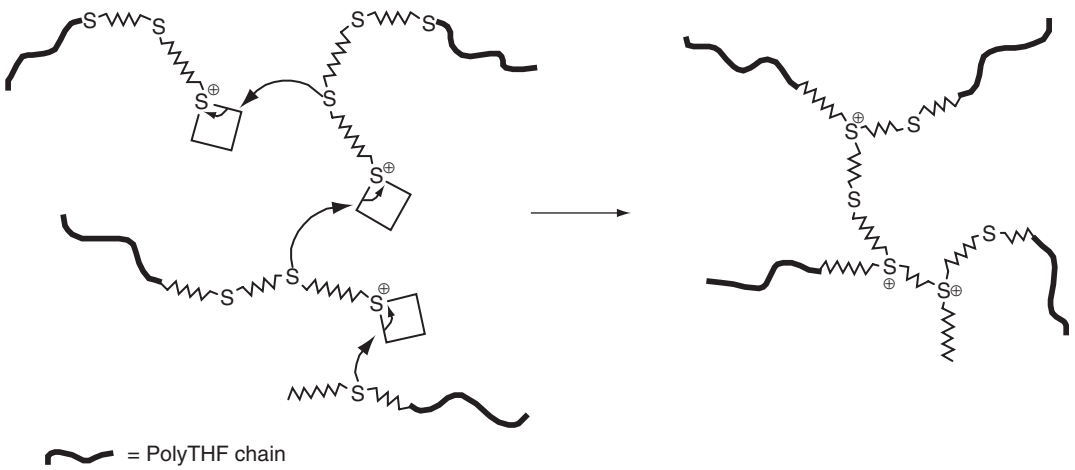

Scheme 35 Formation of star-shaped segmented copolymers by sequential polymerization of THF and thietane.

4.13.3.2.2 Anionic polymerization

Thietane[121,122] and 3,3-dimethylthietane[123,124] have been polymerized to high-molecular-weight polymers by initiation with naphthylsodium or butyllithium. The polymerizations were shown to occur with carbanions as active species (instead of thiolate as in the case of thiiranes).

4.13.3.3 Cyclic Disulfides

The polymerization of cyclic disulfides to polydisulfides has been reported in the 1940s and 1950s. In some cases the polymerizations occur spontaneously.[125] Tobolsky *et al.*[126] reported that 1-oxa-4,5-dithiacycloheptane and 1,3-dioxa-6,7-dithiacyclononane are polymerized by cationic initiators such as sulfuric acid or boron trifluoride. Davis and Fettes[127] reported the anionic polymerization of various cyclic disulfides. In the same period it was also described that cyclic disulfides can copolymerize with vinyl monomers such as styrene and butyl acrylate with AIBN as initiator.[128] That the incorporation of the disulfide was due to copolymerization and not by chain transfer was established by comparing the thermal polymerization of styrene in the presence of dibutyl disulfide and in the presence of 1-oxa-4,5-dithiacycloheptane. In the first case, the polymer contained 2 sulfur atoms per macromolecule as a result of transfer reactions and in the second case 4–20 sulfur atoms depending on the ratio of monomers.

More recently, the polymerization of several cyclic disulfides has been investigated by Endo *et al.* The thermal polymerization of 1,2-dithiane (DT) did not proceed at monomer concentrations below 4.0 mol l^{-1}. The polymerization was inhibited by addition of radical inhibitors, indicating that the propagation proceeds by a radical intermediate. The molecular weight of the polymers increased with reaction time. It was proposed that the cyclic polymer is formed mainly by back-biting reaction mechanism during the polymerization (**Scheme 36**).[129]

The bulk polymerization of DT proceeds readily without initiators above its melting point, giving a polymer in high yield. The molecular weight of polymers obtained could be controlled by the addition of benzyl mercaptan (BM). The ^{13}C- and ^{1}H-NMR spectra suggest that the poly(DT) has a macrocyclic structure in contrast to the linear polymers that were obtained from polymerization in the presence of thiols. Redox reactions could be used to transform the linear in cyclic structures and *vice versa* (**Scheme 37**).

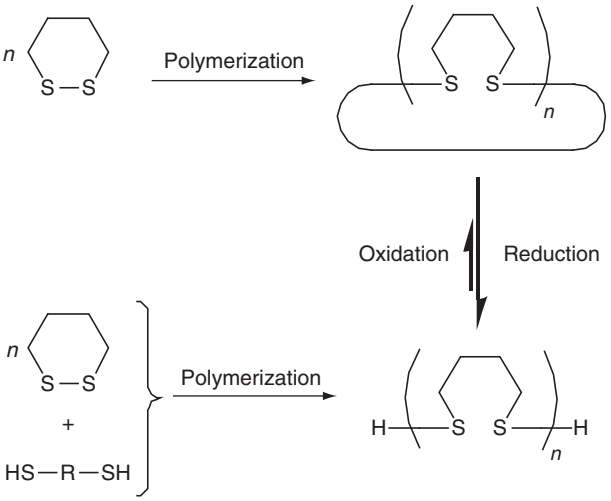

Scheme 37 Two mechanisms for the formation of thiol terminated poly (DT).

When the polymerization of DT was performed in the presence of cyclic poly(oxyethylene) (CPO), the product included a catenane structure of cyclic poly(DT) and CPO entangled with each other. It was concluded that the poly(DT) obtained from polymerization of DT includes a polycatenane structure.[130]

Copolymerization of lipoic acid (LPA) and DT to high-molecular-weight polymers has been reported by the same group.[131] Also in this case, the formation of polycatenane structures was postulated (**Scheme 38**).

The polymerization of *o*-xylylenedisulfide (XDS) proceeds at temperatures above the melting point of XDS to give high-molecular-weight polymers[132] (**Figure 6**).

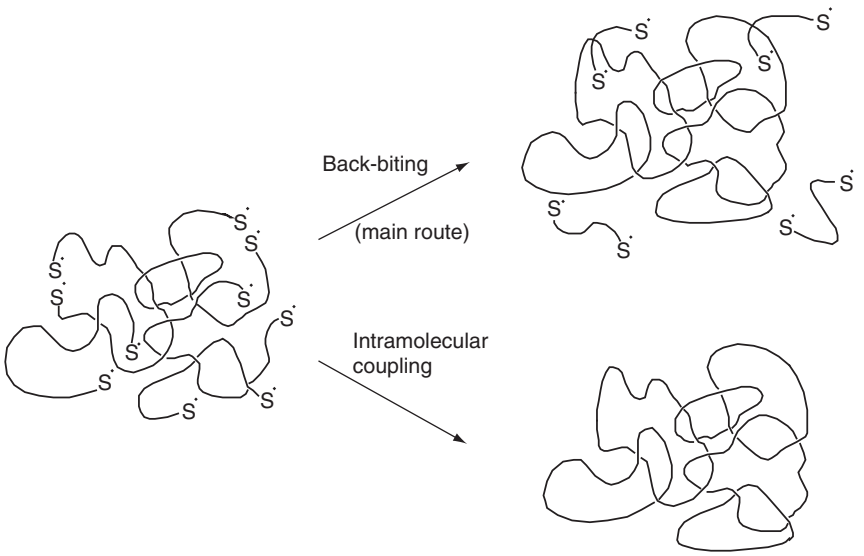

Scheme 36 Free radical polymerization DT leading to cyclic polymers.

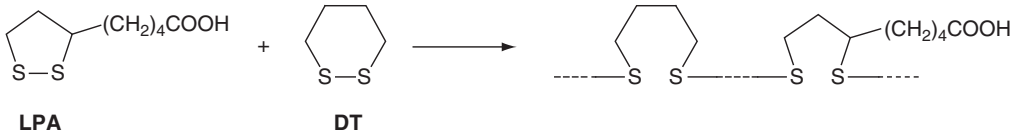

Scheme 38 Copolymerization of LPA and DT.

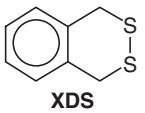

Figure 6 Structure of XDS.

The polymers were characterized to have cyclic structures containing polycatenane structures in contrast to the linear structures obtained in the presence of thiol-containing chain transfer compounds.

4.13.4 Conclusions and Outlook

Polymeric amines in general continue to attract attention in many application fields and several of these products are commercially available. In recent years polyamines have found new applications as gene transfer agents due to the fact that they form interpolymer complexes with nucleic acids. PEI (branched as well as linear) is one of the most studied polymers in this field. It seems, however, that the pure polyamines have several drawbacks and in the latest developments the polyamine is modified with other polymers, such as PEG. Moreover, it is of importance to be able to introduce targeting groups on these macromolecules.[133] Therefore, any method that produces well-defined polyamine structures containing appropriate functional groups for coupling with other polymer chains or with targeting groups is of potential interest in these applications.

Poly(alkylene sulfides) such as those obtained by ROP do not, at the authors knowledge, have widespread applications. However, recently there seems to be some interest in such polymers for biological applications.[134] Here also, the interest stems from the fact that different types of well-defined polymers with well-defined functional end groups as well as polymers with functional groups substituted on the polymer chain can be prepared by relatively simple synthetic techniques. ROP is such a technique. ROP of cyclic disulfides by free radical mechanism has recently gained interest for the production of cyclic polymers containing polycatenane structures.

References

1. Kern, W.; Brenneisen, E. *J. Prakt. Chem.* **1941**, *159*, 193 and 219.
2. Dick, C. R.; Ham, G. E. *J. Macromol. Sci., Chem.* **1970**, *A4*, 1301.
3. Kobayashi, S.; Uyama, H. *J. Polym. Sci., Part A: Polym. Chem.* **2002**, *40*, 192.
4. Kobayashi, S.
5. Lambermont-Thijs, H. M. L.; Bonami, L.; Du Prez, F. E.; *et al. Polym. Chem.* **2010**, *1*, 747.
6. Gembitskii, P. A.; Chmarin, A. I.; Klescheva, N. A.; *et al. Vysokomol. Soedin., Ser. A* **1978**, *A20*, 1505.
7. Weyts, K. F.; Goethals, E. J. *Polym. Bull.* **1988**, *19*, 13.
8. Lukovkin, G. M.; Pshezhetsky, V. S.; Murtazaeva, G. A. *Eur. Polym. J.* **1973**, *9*, 559.
9. St. Pierre, T.; Geckle, M. *ACS Polym. Prepr.* **1981**, *22*, 128.
10. Axelson, D. E.; Blake, S. L. *J. Polym. Sci., Polym. Chem. Ed.* **1985**, *23*, 2507.
11. Weyts, K. F.; Goethals, E. J.; Bunge, W. M.; *et al. Eur. Polym. J.* **1990**, *4*, 445.
12. Horn, D. In *Polymeric Amines and Ammonium Salts*; Goethals, E. J., Ed.; Pergamon Press: Oxford, UK, 1980; p 333.
13. von Harpe, A.; Petersen, H.; Li, H.; *et al. J. Controlled Release* **2000**, *69*, 157.
14. Rivas, B. L.; Barria, B. *Polym. Bull.* **1996**, *36*, 157.
15. Kobayashi, S.; Shimizu, N.; Saegusa, T. *Polym. Bull.* **1984**, *11*, 247.
16. Saegusa, T.; Kobayashi, S.; Ishiguro, M. *Macromolecules* **1974**, *7*, 958.
17. Hamilton, J. G.; Ivin, K. J.; Kuan-Essig, L. C.; *et al. Polymer* **1975**, *16*, 763.
18. Baklouti, M. *Polym. Bull.* **1989**, *21*, 24.
19. Jones, G. D.; MacWilliams, D. C.; Braxtor, N. A. *J. Org. Chem.* **1965**, *30*, 1994.
20. Goethals, E. J.; Schacht, E. H.; Bruggeman, P.; *et al. ACS Symp. Ser.* **1977**, *59*, 1.
21. Goethals, E. J.; Bossaer, P.; Deveux, R. *Polym. Bull.* **1981**, *6*, 121.
22. Bossaer, P.; Goethals, E. J. *Makromol. Chem.* **1977**, *178*, 2983.
23. Munir, A.; Goethals, E. J. In *Polymeric Amines and Ammonium Salts*; Goethals, E. J., Ed.; Pergamon Press: Oxford, UK, 1980; p 19.
24. Munir, A.; Goethals, E. J. *J. Polym. Sci., Polym. Chem. Ed.* **1981**, *19*, 1965.
25. Christova, D. C.; Velichkova, R. S.; Panayotov, I. M. *Makromol. Chem.* **1993**, *194*, 2975.
26. Munir, A.; Goethals, E. J. *Makromol. Chem., Rapid Commun.* **1981**, *2*, 693.
27. Goethals, E. J.; Vlegels, M. *Polym. Bull.* **1981**, *4*, 521.
28. Kazama, H.; Hoshi, M.; Nakajima, H.; *et al. Polymer* **1990**, *31*, 2207.
29. Christova, D. C.; Velichkova, R. S. *Macromol. Chem. Phys.* **1995**, *196*, 3253.
30. Goethals, E. J.; Van de Velde, M.; Munir, A. In *Cationic Polymerization and Related Processes*; Goethals, E. J., Ed.; Academic Press: London, UK, 1984; p 387.
31. Bossaer, P.; Goethals, E. J.; Hackett, P. H.; *et al. Eur. Polym. J.* **1977**, *13*, 489.
32. Goethals, E. J.; Toncheva, V.; Hosteaux, F.; *et al. Makromol. Chem., Makromol. Symp.* **1992**, *64*, 113.
33. Razvodovskii, E. F.; Berlin, A. A.; Nekrasov, A. V.; *et al. Vysokomol. Soedin., Ser. A* **1973**, *A15*, 2233.
34. Yamashita, T.; Nigo, M.; Nakamura, N. *Makromol. Chem.* **1979**, *180*, 1145.
35. Hansen, G. R.; Burg, T. E. *J. Heterocycl. Chem.* **1968**, *5*, 304.
36. Goethals, E. J.; Deveux, R.; Vandenberghe, L. *Makromol. Chem., Rapid Commun.* **1982**, *3*, 515.
37. Dick, C. R. *J. Org. Chem.* **1967**, *32*, 72.
38. Ishizone, T.; Tanaka, T.; Kobayashi, M. *J. Polym. Sci., Part A: Polym. Chem.* **2003**, *41*, 1335.
39. Koper, G. M.; van Duijvenbode, R. C.; Stam, D. D.; *et al. Macromolecules* **2003**, *36*, 2500.
40. Schacht, E. H.; Goethals, E. J. *Makromol. Chem.* **1974**, *175*, 3447.
41. Saegusa, T.; Nagura, Y.; Kobayashi, S. *Macromolecules* **1973**, *6*, 495.
42. Toy, M. S.; Price, C. C. *J. Am. Chem. Soc.* **1960**, *82*, 2613.
43. Razvodovskii, E. F.; Nekrasov, A. V.; Berlin, A. A.; *et al. Dokl. Akad. Nauk. SSSR* **1971**, *198*, 894.
44. Matyjaszewski, K. *Makromol. Chem.* **1984**, *185*, 51.
45. Schacht, E. H.; Goethals, E. J. *Makromol. Chem.* **1973**, *167*, 155.
46. Goethals, E. J.; Schacht, E. H. *J. Polym. Sci., Polym. Lett. Ed.* **1973**, *11*, 497.
47. Schacht, E. H.; Bossaer, P.; Goethals, E. J. *Polym. J.* **1977**, *9*, 329.
48. Oike, H.; Washizuka, M.; Tezuka, Y. *Macromol. Chem. Phys.* **2000**, *201*, 1673.
49. Yamamoto, T.; Tezuka, Y. *Eur. Polym. J.* **2011**, *47*, 535.
50. Tezuka, Y. *J. Polym. Sci., Part A: Polym. Chem.* **2003**, *41*, 2905.
51. Banthia, K.; Schacht, E. H.; Goethals, E. J. *Makromol. Chem.* **1978**, *179*, 841.
52. Bogaert, Y.; Goethals, E. J.; Schacht, E. H. *Makromol. Chem.* **1981**, *182*, 2687.
53. Sigwalt, P.; Spassky, N. In *Ring Opening Polymerization*; Ivin, K. J., Saegusa, T., Eds.; Elsevier Applied Sciences: London, UK, New York, 1984; p 603.
54. Van Ooteghem, D.; Goethals, E. J. *Makromol. Chem.* **1976**, *177*, 3389.
55. Van Ooteghem, D.; Goethals, E. J. *Makromol. Chem.* **1974**, *175*, 1513.
56. Goethals, E. J.; Van Meirvenne, D.; De Clercq, R. *Makromol. Chem., Macromol. Symp.* **1988**, *13/14*, 176.
57. Bhatti, A.; Goethals, E. J. *Makromol. Chem.* **1985**, *186*, 317.
58. Simonds, R. P.; Goethals, E. J. *Makromol. Chem.* **1978**, *179*, 1689.

59. Simonds, R. P.; Goethals, E. J.; Spassky, N. *Makromol. Chem.* **1979**, *179*, 1851.
60. Vancraeynest, W. M.; Goethals, E. J. *Makromol. Chem.* **1978**, *179*, 2613.
61. Andruleviciute, V.; Lazauskaite, R.; Grazulevicius, J. V.; *et al. J. Photochem. Photobiol., A: Chem.* **2002**, *147*, 63.
62. Boileau, S.; Coste, J.; Raynal, J. M.; *et al. Compt. Rend.* **1962**, *254*, 2774.
63. Boileau, S.; Champetier, G.; Sigwalt, P. *Makromol. Chem.* **1963**, *69*, 180.
64. Favier, J. C.; Boileau, S.; Sigwalt, P. *Eur. Polym. J.* **1968**, *4*, 3.
65. Guerin, P.; Hemery, P.; Boileau, S.; *et al. Eur. Polym. J.* **1971**, *7*, 1581.
66. Hemery, P.; Boileau, S.; Sigwalt, P. *J. Polym. Sci.* **1975**, *52*, 189.
67. Morgan, D. R.; Williams, G. T.; Wragg, R. T. *Eur. Polym. J.* **1970**, *6*, 309.
68. Cooper, W.; Morgan, D. R.; Wragg, R. T. *Eur. Polym. J.* **1969**, *5*, 71.
69. Cooper, W. *Br. Polym. J.* **1971**, *3*, 28.
70. Cooper, W.; Morgan, D. R. *Eur. Polym. J.* **1970**, *19*, 71.
71. Aliev, A. D.; Krentsel, B. A.; Alieva, S. L. *Eur. Polym. J.* **1983**, *19*, 71.
72. Dumas, P.; Spassky, N.; Sigwalt, P. *J. Polym. Sci., Polym. Chem. Ed.* **1976**, *14*, 1015.
73. Bonnans-Plaisance, C.; Levesque, G.; Midrak, A. *Eur. Polym. J.* **1994**, *30*, 239.
74. Nicol, E.; Bonnans-Plaisance, C.; Levesque, G. *Macromolecules* **1999**, *32*, 4485.
75. Kilcher, G.; Wang, L.; Tirelli, N. *J. Polym. Sci., Part A: Polym. Chem.* **2008**, *46*, 2233.
76. Aida, T.; Kawaguchi, K.; Inoue, S. *Macromolecules* **1990**, *23*, 3887.
77. Watanabe, Y.; Aida, T.; Inoue, S. *Macromolecules* **1990**, *23*, 2612.
78. Boileau, S.; Sigwalt, P. *Compt. Rend.* **1965**, *261*, 132.
79. Nevin, R. S.; Pearce, E. M. *J. Polym. Sci., Polym. Lett.* Ed. **1965**, *3*, 487.
80. Boileau, S.; Sigwalt, P. *Makromol. Chem.* **1973**, *171*, 11.
81. Morton, M.; Kammereck, R. F.; Fettes, L. J. *Macromolecules* **1971**, *4*, 11.
82. Gourdenne, A.; Sigwalt, P. *Eur. Polym. J.* **1967**, *3*, 481.
83. Bonnans-Plaisance, C.; Guerin, P.; Levesque, G. *Polymer* **1995**, *36*, 201.
84. Napoli, A.; Tirelli, N.; Kilcher, G.; *et al. Macromolecules* **2001**, *34*, 8913.
85. Nicol, E.; Bonnans-Plaisance, C.; Dony, C.; *et al. Macromol. Chem. Phys.* **2001**, *202*, 2843.
86. Suzuki, A.; Nagai, D.; Ochiai, B.; *et al. Macromolecules* **2004**, *37*, 8823.
87. Hirata, M.; Ochiai, B.; Endo, T. *J. Polym. Sci., Part A: Polym. Chem.* **2010**, *48*, 525.
88. Wang, L.; Kilcher, G.; Tirelli, N. *Macromol. Biosci.* **2007**, *7*, 987.
89. Wang, L.; Kilcher, G.; Tirelli, N. *Macromol. Chem. Phys.* **2009**, *210*, 447.
90. Bonnans-Plaisance, C.; Levesque, G. *Macromolecules* **1989**, *2*, 2020.
91. Rehor, A.; Tirelli, N.; Hubbell, J. A. *Macromolecules* **2002**, *35*, 8688.
92. Morinaga, H.; Ochiai, B.; Mori, H.; *et al. J. Polym. Sci., Part A: Polym. Chem.* **2006**, *44*, 3778.
93. Bonnans-Plaisance, C.; Rétif, P. *React. Funct. Polym.* **1999**, *39*, 9.
94. Bonnans-Plaisance, C.; Rétif, P.; Levesque, G. *Polym. Bull.* **1995**, *34*, 141.
95. Bonnans-Plaisance, C.; Corvasier, L.; Emery, J.; *et al. Polym. Bull.* **1998**, *41*, 525.
96. Bonnans-Plaisance, C.; Corvasier, L.; Skoulios, A. *Polymer* **1997**, *38*, 3843.
97. Tebaldi de Sordi, M. L.; Ceschi, M. A.; Petzhold, C. L.; *et al. Macromol. Rapid Commun.* **2007**, *28*, 63.
98. Kilcher, G.; Wang, L.; Duckham, C.; *et al. Macromolecules* **2007**, *40*, 5141.
99. Machon, J. P.; Sigwalt, P. *Compt. Rend.* **1965**, *260*, 549.
100. Spassky, N.; Sigwalt, P. *Eur. Polym. J.* **1971**, *7*, 7.
101. Sepulchre, M.; Spassky, N.; Van Ooteghem, D.; *et al. J. Polym. Sci., Polym. Chem.* **1974**, *12*, 1683.
102. Sepulchre, M.; Spassky, N.; Sigwalt, P. *Macromolecules* **1971**, *5*, 92.
103. Spassky, N.; Dumas, P.; Moreau, M.; *et al. Macromolecules* **1975**, *8*, 956.
104. Dumas, P.; Spassky, N.; Sigwalt, P. *Makromol. Chem.* **1972**, *156*, 55.
105. Momtaz, A.; Spassky, N.; Sigwalt, P. *Nouv. J. Chim.* **1979**, *3*, 669.
106. Goethals, E. J.; Simonds, R.; Spassky, N.; *et al. Makromol. Chem.* **1980**, *181*, 2481.
107. Sepulchre, M.; Spassky, N.; Mark, C.; *et al. Makromol. Chem., Rapid Commun.* **1981**, *2*, 261.
108. Sepulchre, M. *Makromol. Chem.* **1987**, *188*, 1583.
109. Dumas, P.; Sigwalt, P.; Guerin, P. *Makromol. Chem.* **1981**, *182*, 2225.
110. Dumas, P.; Sigwalt, P. *Makromol. Chem.* **1992**, *193*, 1709.
111. Boucard, V.; Moreau, M.; Ph, D. *Macromol. Chem. Phys.* **2001**, *202*, 1974.
112. Imai, Y.; Hayakawa, K.; Satoh, T.; *et al. J. Polym. Sci., Part A: Polym. Chem.* **2002**, *40*, 3443.
113. Kameyama, A.; Shimotsuma, K.; Nishikubo, T. *Polym. J.* **1996**, *25*, 68.
114. Kudo, H.; Makino, S.; Kameyama, A.; *et al. Macromolecules* **2005**, *38*, 5964.
115. Nagai, A.; Koike, N.; Kudo, H.; *et al. Macromolecules* **2007**, *40*, 8129.
116. Kudo, H.; Sato, K.; Nishikubo, T. *Macromolecules* **2010**, *43*, 9655.
117. Goethals, E. J.; Drijvers, W. *Makromol. Chem.* **1970**, *136*, 73.
118. Goethals, E. J. *J. Polym. Sci., Polym. Symp.* **1976**, *56*, 271.
119. Goethals, E. J.; Trossaert, G. G.; Hartmann, P. J.; *et al. Makromol. Chem., Makromol. Symp.* **1993**, *73*, 77.
120. Haucourt, N.; Peng, L. B.; Goethals, E. J. *Macromolecules* **1994**, *27*, 1329.
121. Machon, J. P.; Nicco, A. *Eur. Polym. J.* **1971**, *7*, 353.
122. Morton, M.; Kammereck, R. F. *J. Am. Chem. Soc.* **1970**, *92*, 3217.
123. Lazcano, S.; Marco, C.; Fatou, J. G.; *et al. Eur. Polym. J.* **1989**, *25*, 1213.
124. Lazcano, S.; Bello, A.; Marco, C.; *et al. Polym. Bull.* **1989**, *21*, 571.
125. Affleck, J. G.; Dougherty, J. *J. Org. Chem.* **1950**, *15*, 864.
126. Tobolsky, A. V.; Leonard, F.; Roeser, G. P. *J. Polym. Sci.* **1948**, *3*, 604.
127. Davis, F. O.; Fettes, E. M. *J. Am. Chem. Soc.* **1948**, *70*, 2611.
128. Tobolsky, A. V.; Baysal, B. *J. Am. Chem. Soc.* **1953**, *75*, 1757.
129. Endo, K.; Shiroi, T.; Murata, N. *Polym. J.* **2005**, *37*, 512.
130. Endo, K.; Shiroi, T.; Murata, N.; *et al. Macromolecules* **2004**, *37*, 3143.
131. Endo, K.; Yamanaka, T. *Macromolecules* **2006**, *39*, 4038.
132. Ishida, H.; Kisanuki, A.; Endo, K. *Polym. J.* **2009**, *41*, 110.
133. Park, J. H.; Lee, S.; Kim, J.-H.; *et al. Prog. Polym. Sci.* **2008**, *33*, 113.
134. Vo, C. D.; Kilcher, G.; Tirelli, N. *Macromol. Rapid Commun.* **2009**, *30*, 299.

Biographical Sketches

Eric Goethals graduated from Ghent University (Belgium) in 1958 and obtained his PhD degree in organic chemistry at the same university in 1963. After a postdoctoral year at the Gütenberg University in Mainz (Germany), where he worked with Prof. Rolf Schulz, he returned to Ghent where he started a research group on polymer chemistry. He was appointed associate professor in 1970 and full professor in 1980. He was head of the department of organic chemistry from 1996 till 2002, the year of his retirement from the university. He has lectured organic chemistry to medical students and polymer science to chemists. His research was in polymer synthesis, cationic polymerization, ring-opening polymerization, telechelic polymers, polymer networks, and reactive polymers. He is the editor of 4 books and coauthor of over 400 publications in international scientific journals.

Bart Dervaux was born in 1983 and studied from 2001 to 2005 at Ghent University where he received a master's degree in chemistry. From 2006 till 2010, he did a PhD under the supervision of Prof. F. Du Prez with a fellowship of the Research Foundation – Flanders (FWO), focusing on the synthesis and characterization of block and block-like copolymers and the preparation of block-like copolymers by continuous processes using column reactors. In the framework of his PhD research, he did scientific short-time visits in the research groups of Prof. I. Galaev (Lund, Sweden), Prof. V. Zubov (Moscow, Russia), and Prof. C. Barner-Kowollik (Karlsruhe, Germany). Since 2010, he has been working in the group of Prof. Du Prez as a postdoctoral FWO fellow on the stabilization of polymer nanocomposites. This research is in close collaboration with the research group of Prof. P. Dubois (Mons, Belgium). He is the coauthor of 14 scientific publications and 1 book chapter.

4.14 Ring-Opening Polymerization of Cyclic Amides (Lactams)

S Russo and E Casazza, Università di Genova, Genova, Italy; INSTM, Consorzio Interuniversitario Nazionale di Scienza e Tecnologia dei Materiali, Firenze, Italy

4.14.1 Introduction

Among the heterocyclic compounds able to polymerize, lactams represent one of the most versatile families of monomers. At present, their ring-opening polymerization (ROP) constitutes a very relevant method for the obtainment of polyamides and copolyamides entailing a wide range of properties, covering a large number of applications, and having a crucial industrial interest.

Indeed, even without taking into account the additional contribution of ring substituents, the ring size as such strongly affects not only the lactam reactivity but also the final characteristics of the resultant polyamide; in this respect, the broad range of their behaviors goes from a close similarity with polypeptides for polyamides derived from four-membered lactams to the analogy to polyolefins for polyamides obtained from higher members of the lactam series (e.g., 13-membered lactams).

Before the late 1930s of the last century, the entire class of lactams did not play a role whatsoever in the chemical industry; neither seemed to offer any interesting problem in the domain of scientific research. Carothers,[1] in his famous 1931 work on ring formation and polymerization, for the first time made an extensive and critical investigation on the transformation of cyclic monomers, especially lactones, into linear polymers. He pointed out that, differently from lactones, the five- and six-membered lactams, that is, 2-pyrrolidone and 2-piperidone, were entirely stable substances. On these grounds, the latter lactam resulted quite in counterposition to the easily polymerizable oxygen isologue. Starting from the above misleading findings, Carothers accepted without much hesitation the odd result found together with Berchet[2] that also the seven-membered ε-caprolactam (CL) was not polymerizable, even in the presence of catalysts.

The recognition of the first lactam polymerization should undoubtedly be attributed to Schlack,[3] who polymerized CL using the hydrochloride of ε-aminocaproic acid, replaced by small amounts of water later on, as initiator for the industrial production of polyamide 6 (PA6) for fibers, which started in 1940s in Germany. Since then, the large-scale manufacture of the most important lactam-based polyamide, that is, poly(CL) (PCL), commercially named PA6, has been mostly carried out by what has been identified as the hydrolytic process.[4] It is worth to emphasize here that the hydrolytic mechanism, apart from the initiation step involving the water-catalyzed opening of the lactam ring and the subsequent polyreactions, is also based on polycondensation steps. As a consequence, it cannot be regarded as strictly pertinent to a neat ROP process and will not be deepened in the present chapter. Actually, the water-initiated polymerization is only one of the possible routes to convert some lactams to polyamides inasmuch that the presence of an initiator is essential, with the spontaneous polymerization being presumably attainable only at very high temperatures and for a limited number of lactams. Indeed, due to the amphiprotic character of the amide group, the lactam ROP may be initiated by a base (anionic process), or an acid (cationic process), or simply water (hydrolytic process). Besides the ionic routes, the enzymatic polymerization of four-membered lactams has also been recently accomplished for the preparation of poly (β-peptides), that is, unsubstituted and substituted polyamide 3.

At the end of the 1930s, the cationic polymerization as well has been attempted by Schlack,[5] who discovered that anhydrous hydrogen chloride was capable of initiating the polymerization of CL. However, for reasons unknown at that time, the acid-initiated reaction did not yield high-quality PA6 and was therefore considered to be of no interest for commercial purposes. As a matter of fact, the cationic mechanism of lactam polymerization has always found very limited applications, if any, not only because of the low conversions and the low molar masses of the resultant polyamides but also for the extensive occurring of side reactions.

The anionic polymerization of lactams has been discovered shortly after the cationic polymerization by Joyce and Ritter,[6] who in 1941 patented the conversion of CL to PA6 in the presence of alkali or alkaline earth metals. The reaction was named 'rapid polymerization' by Joyce and Ritter in view of the fact that equilibrium conversion could be attained in a few minutes.

Unlike the abandoned cationic process, the anionic ring-opening polymerization has soon been able to develop several industrial strategies in many fields where hydrolytic polyamides, namely hydrolytic PA6, could not enter because of their inferior mechanical properties and unsuitable synthetic conditions. Indeed, anionic ROP of lactams has shown to be the most versatile process for obtaining, with almost no by-products, polyamides and copolyamides characterized by distinctive properties. Moreover, the possibility of performing polymerization by the activated anionic mechanism by using activators in combination with initiators, soon after Joyce and Ritter's discovery, allowed to pursue very fast reaction kinetics at lower temperatures and reach very high monomer conversions, as well as higher molar masses and higher crystallinity of the resultant PA6.

In more recent years, anionic ROP of CL has also enabled to perform polymerizations directly in the mold and has been found uniquely suited to form thermoplastic composites, such as fiber-reinforced products, by *in situ* reaction injection molding (RIM) and pultrusion processes. The low viscosity and the low melting temperature of the monomer (~70 °C) let to run the reaction at low polymerization temperatures (below T_m of PA6), allowing for a superior fiber wetting and impregnation of reinforced PA6. Additionally, recent studies support the idea that anionic polymerization of some lactams can be efficiently carried out not only in the bulk but also in dispersion, emulsion, and suspension, allowing for a convenient production of polyamides as fine powders and opening new fields of application (e.g., powder coating and cosmetics). In general, for its

versatility, the anionic mechanism of lactam polymerization looks very appealing and still continues to attract the interest of many research groups from both academia and industry.

In the last decades, excellent general reviews have been published on the ROP of lactams,[7–10] with specific attention to their anionic polymerization. Besides, it is worth mentioning here some surveys on PCL by Reimschuessel,[11,12] including outlines of industrial processes and description of all kinds of polymerization mechanisms (i.e., hydrolytic, cationic, and anionic).

4.14.2 Lactams and Their Polymerizability

4.14.2.1 Lactam Family

4.14.2.1.1 Overview

Lactams (contraction of lactone + amide) are the cyclic amides of aliphatic amino acids and form an extensive homologous series of monomers, showing a large variety of unsubstituted examples whose size so far ranges from 4 to 21 ring atoms. They consist of a polar amide group and a nonpolar hydrocarbon moiety formed by a sequence of $-(CH_2)-$ groups.

The various members may be characterized by either the number of ring carbon atoms, n, or the ring size, $n+1$, and are usually symbolized as Ln:

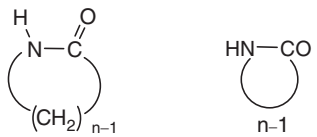

Ln

In this respect, nonuniform notation rules still exist and some authors identify n with the total number of ring atoms. Therefore, it must always be clarified which type of notation is used. Greek prefixes are often used in trivial names and define how many carbon atoms apart from the carbonyl moiety are present in the ring. Thus, excluding the carbonyl, in β-lactam, there are two other carbon atoms (four ring atoms in total); in γ-lactam, three carbon atoms; in δ-lactam, four carbon atoms; in ε-lactam, five carbon atoms, and so on up to L9 (θ-pelargonolactam). Then after, a generic denomination of ω-lactam is adopted. Hence, ω-laurolactam may be referred to, instead of L12, C_{12}-lactam or 13-membered lactam. The synthesis, structure, and properties of lactams have been extensively studied and reviewed.[8,13,14]

The lactam family may be very widely extended if members carrying substituents on C and/or N atom are considered. Moreover, a large variety of other types of lactam analogues exist: heteroatom-containing lactams (e.g., oxalactams), dilactams (containing two amide groups per ring), bicyclic lactams (bislactams, containing two lactam rings bound together by simple linkage or bivalent groups, and bridgehead bicyclic lactams), thiolactams, bicyclic oxalactams, etc. Apart from their industrial utilization for the production of a few aliphatic polyamides (PA6 from L6, PA12 from L12, PA4 from L4, in decreasing order of relevance), some lactams find very significant applications in medicine, in particular for antibiotics preparation (β-lactam antibiotic chemistry).[15] Indeed, the β-lactam ring is a part of the structure of several antibiotic families, mainly the penicillins, cephalosporins, carbapenems, and monobactams. Substituted β-lactams have recently arisen a lot of interest centered on the synthesis of β-polypeptides (PA3 family),[16] which exhibit an important biological activity.

4.14.2.1.2 Nomenclature

Several systems of chemical nomenclature are adopted to designate lactams. The most common systems are reported in **Table 1**, referred to the family of unsubstituted lactams from 3 to 15 ring atoms. Accordingly, the five-membered lactam may be identified by its trivial names as γ-butyrolactam or

Table 1 Nomenclature of the principal unsubstituted lactams

			IUPAC organic nomenclature	
Symbol	*Ring size*	*Trivial name*	*Official*	*Heterocyclics*[a]
L2	3	α-Acetolactam	Ethane-2-lactam	Aziridin-2-one
L3	4	β-Propiolactam	Propane-3-lactam	Azetidin-2-one
L4	5	γ-Butyrolactam α-Pyrrolidone	Butane-4-lactam	2-Pyrrolidinone 2-Pyrrolidone
L5	6	δ-Valerolactam α-Piperidone	Pentane-5-lactam	2-Piperidinone 2-Piperidone
L6	7	CL	Hexane-6-lactam	azepan-2-one
L7	8	ζ-Enantholactam	Heptane-7-lactam	azocan-2-one
L8	9	η-Capryl lactam η-Caprylolactam	Octane-8-lactam	azonan-2-one
L9	10	θ-Pelargonolactam	Nonane-9-lactam	
L10	11	ω-Caprinolactam	Decane-10-lactam	
L11	12	ω-Aminoundecanoic acid lactam	Undecane-11-lactam	
L12	13	ω-Lauryl lactam ω-Laurolactam	Dodecane-12-lactam	
L13	14	ω-Aminotridecanoic acid lactam	Tridecane-13-lactam	
L14	15	ω-Aminotetradecanoic acid lactam	Tetradecane-14-lactam	

[a] Nomenclature adopted by *Chemical Abstracts*.

α-pyrrolidone, by the IUPAC nomenclature as butano-4-lactam, or by the IUPAC heterocyclic nomenclature as 2-pyrrolidone or pyrrolidon-2-one. The seven-membered lactam may be named as CL, hexano-6-lactam or hexahydro-2*H*-azepin-2-one, etc.

In the present chapter, the trivial nomenclature will be generally preferred, with the exemption of the smaller rings up to L5, which will be identified by the IUPAC heterocyclic system. It is convenient to divide lactams into three groups entailing similar properties. Thus, aziridin-2-one, azetidin-2-one, 2-pyrrolidone, and 2-piperidone are grouped as 'lower lactams', CL, ζ-enantholactam, and η-caprylolactam are classified as 'medium-sized lactams', and all the other higher sized lactams are considered as 'higher lactams'.

All 'lower lactams' have strained rings but with some differences among them: aziridin-2-one and azetidin-2-one are highly strained, while 2-pyrrolidone and 2-piperidone have weakly strained rings. The stability of the highly strained lactams may be increased by substitution; in fact, aziridin-2-one is known only in the substituted form.

4.14.2.1.3 Structure and properties

A distinctive aspect characterizing lactams is the high mobility of the electronic structure of their amide group, resulting from several factors: π-electron delocalization, rearrangement of electron lone pairs on both heteroatoms, inductive effects, changes in atomic hybridization, dipole–dipole interactions, and hydrogen bond formation.

The amide group is traditionally described in terms of resonance between Lewis structures:

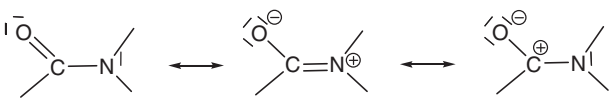

1 2 3

[1]

In general, only the first two structures (**1** and **2**) have been taken into consideration.[17] However, by calculations of C, N, O electron densities of planar and twisted amides, it has been shown[18,19] that while distortion of the amide linkage introduces large variations in the C–N bond length, the bond length of the carbonyl group is hardly changed. Thus, the third resonance structure (**3**) has been introduced in order to rationalize these results, with the two ionic structures becoming the predominant ones in representing the amide group. Furthermore, the methylene groups (as well as methyl groups) linked to nitrogen and carbonyl can enhance the resonance stabilization by hyperconjugation with C=O and C=N bonds. The hyperconjugation effects have also been invoked to justify the higher stability of *N*-alkyl-substituted lactams, for example, *N*-methyl-CL,[20] as compared to their unsubstituted counterparts.

The polarity of the amide bond and also the interaction of the $2p_z$ electrons of N with the π-electrons of the carbonyl group are functions of the ring size and are manifested by different ionization potentials obtained by photoelectron (PE) spectroscopy.[21,22] The map of the spatial electron distribution of *N*-methylacetamide, obtained by CNDO/2 (COMPLETE NEGLECT OF DIFFERENTIAL OVERLAP – SECOND VERSION) and *ab initio* molecular orbital calculations,[23] has already evidenced that the lone pair on the oxygen atom in the amide group is predominant, with the lone pair on nitrogen being involved in the delocalized π system, thus a nonbonding orbital. This result has also given a quite a good explanation for the higher basicity of oxygen, as compared with nitrogen.

However, contrary to unstrained lactams and amides, it has been demonstrated by *ab initio* molecular orbital calculations optimized at the 6-31G* level that the protonation site is a function of the distortion of the amide linkage.[24] Indeed, in aziridin-2-one (**4**) and in bridgehead bicyclic lactams, for example, 1-azabicyclo[2.2.2]octan-2-one (2-quinuclidone) (**5**) and 1-azabicyclo[3.3.1]nonan-2-one (**6**), N-protonation is favored over O-protonation. In particular, in **5**, N-protonation is favored by 100 kJ mol^{-1}:

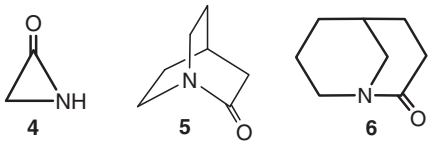

4 5 6

Of interest is the prediction that N-protonated aziridin-2-one spontaneously undergoes ring opening giving a linear aminoacylium ion. Conversely, for azetidin-2-one, the O-protonated form is more stable than the N-protonated one even if the energy gap is reduced.

In the conventional less strained lactams, protonation of the oxygen atom or its coordination to Lewis acids raises the electrophilicity of both the carbonyl and the carbon atom linked to nitrogen ($C_ω$), and increases the nucleophilicity of the carbon linked to the carbonyl ($C_α$); accordingly, the nucleophilicity of nitrogen is decreased. The O-protonated amide group is characterized by a lower energy compared to the N-protonated one; consequently, O-protonation is preferred as the initiation step in the cationic polymerization (see Section 4.14.5).

The sp^2 hybridization of nitrogen and carbonyl carbon and the partial double bond character of the C–N bond, derived from the delocalization of the nitrogen lone pair electrons (p_z-electrons) into the π system of C=O, require a coplanar displacement for all atoms connected to C and N of the amide group (six atoms, in total). Twisting or other distortion of the amide group inhibits this delocalization and thus modifies the electronic structure and the chemical properties of the group, such as, for example, the spectroscopic properties.[25]

Out-of-plane deformations of the amide group from the stable planar form involve the pyramidalization of the amine group and/or twisting around the CO–N bond, which may be accompanied by pyramidalization of the carbonyl carbon atom. The structure and properties of nonplanar amides and lactams have been recently reviewed.[26]

The overlap of the p-π electrons in the O–C–N system brings about the high rotational barrier around the C–N bond, resulting in the two possible configurational isomers: *cis* (**7**) and *trans* (**8**):

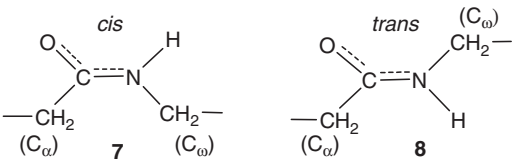

7 8

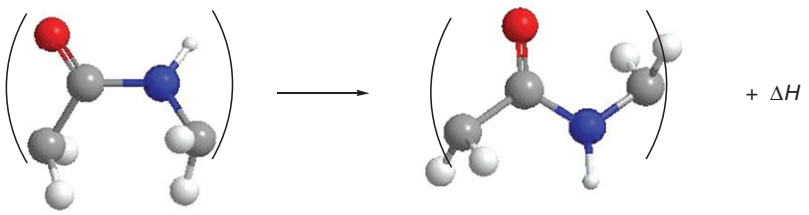

Figure 1 Conversion from the less stable *cis*-amide to *trans*-amide, with liberation of enthalpic energy (approx. 6 kJ mol^{-1}).

Cis-amide group is ~6 kJ mol^{-1} less stable than *trans*-amide group,[7] that is, the *trans* configuration results to be thermodynamically preferred. As a matter of fact, the configuration adopted by the amide group in lactams strictly depends on their size,[27–29] since the physical capability of ring closure and the imposed ring strain must also be taken into account and balanced with previous considerations. In linear polyamides, the amide group can adopt the more stable *trans* form; thus, the ROP of the lactams having *cis*-amide group implies the conversion from a *cis* to a *trans* displacement (**Figure 1**).

In small lactam rings, the amide group is constrained to adopt exclusively the *cis* form. Indeed, in lower lactams and up to the eight-membered ζ-enantholactam, only the *cis* isomer is present. The amide group can adopt the more stable *trans* form only when the ring is large enough to accommodate a torsion angle of approximately 180° around one of its bonds. The crossover point occurs at the nine-membered ring, ζ-caprylolactam, which exhibits a *transoid*-amide form in the crystalline state and an equilibrium mixture of *cis* and *transoid* form in solution, in approx. 4:1 ratio, with the *cis* isomer form having the lowest energy (~4 kJ mol^{-1}).[27,30] The *transoid* form is a distorted structure midway between *cis* and *trans*, derived from the impossibility for this ring size to adopt a strainless planar *trans* configuration.

Discrepancies between the configurations found in the crystalline state and in solution are attributed to the possibility of the molecule to be, in the crystal, more energetically stabilized by hydrogen bonding. Indeed, while the *cis* form of η-caprylolactam is favored in dilute solution, the *trans* form originates a more stable crystal structure where hydrogen bonds link molecules to each other building infinite chains.

In the 'higher lactams', the constraint of the hydrocarbon moiety becomes less and less significant. Thus, the thermodynamically more stable (by ~10 kJ mol^{-1}) *trans* configuration is preferred. The lactam population having the *cis* form decreases with the increasing ring size, not considering the effect of N-substitution, which may alter the configuration.

For example, the 10-membered θ-pelargonolactam in solution at 25 °C consists mainly of the *trans* isomer with only 5–10% of the *cis* isomer,[31] while in crystals, it exists as a mixture of *cis* and *trans* isomers.[27] Conversely, in solutions of the 11-membered lactam, only the *trans* isomer is present.[32] Interestingly, in protonated lactams, the amide configuration is sometimes different from that of the neutral lactams, as shown by the analysis of the hydrochlorides.[27] Drastic is the effect of protonation on η-caprylolactam, which changes its configuration from the nonplanar *transoid* form to a nearly planar *cisoid* form.

The amount of energy relative to the difference between *cis*- and *trans*-amide, released in the conversion from the *cis*-lactams to the *trans*-amide of the polymer chain, significantly contributes to the Gibbs energy of polymerization. In fact, the main driving force in the polymerization of the unstrained 2-piperidone is given by the enthalpic factor related to the above transformation and its polymerization enthalpy has been estimated[33] to be –7.1 kJ mol^{-1}, not very far from the value of approx. –6 kJ mol^{-1}, attributed to *cis–trans* isomerization. The maximum strain energy should be released in the polymerization of bicyclic and tricyclic lactams with the nitrogen at the bridgehead (tertiary amides), in which the amide group is inevitably distorted and less stabilized.

It is noteworthy that in *N*-alkyl-substituted lactams, the resonance stabilization of the amide group is the same as in the open polymer chain, irrespective of the ring size. As a consequence, the polymerization enthalpies of the N-substituted lactams up to ζ-enantholactam are ~6 kJ mol^{-1} lower than those of unsubstituted ones.[7] For instance, the ΔH_p values of CL and *N*-methyl-CL are –15.9 and –9.6 kJ mol^{-1}, respectively (a difference of 6.3 kJ mol^{-1}), and those of ζ-enantholactam and *N*-methyl-ζ-enantholactam are –22.6 and –16.3 kJ mol^{-1} (again a difference of 6.3 kJ mol^{-1}).[8] On the contrary, for higher lactams displaying *trans*-amide groups, similar polymerization enthalpies for unsubstituted and N-substituted lactams are observed.

The overall lactam ring conformation varies greatly as a function of the length of the hydrocarbon sequence, as well.[21,28,29] In the strained lactams, that is, aziridin-2-one and azetidin-2-one, the ring is planar[34] with distortion of the amide group. The aziridin-2-one ring is highly strained (the calculated ring strain being 171 kJ mol^{-1}) and has been predicted, by 6-31G* *ab initio* molecular orbital calculations, to have a pyramidal nitrogen and only 53.2 kJ mol^{-1} of 'operational' resonance.[24] The azetidin-2-one ring (**Figure 2**) is less strained (~109–121 kJ mol^{-1})[35] and has been estimated to have an

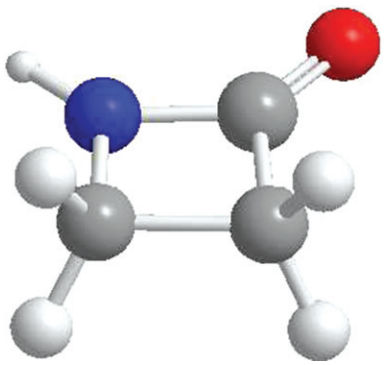

Figure 2 Molecular structure of azetidin-2-one.

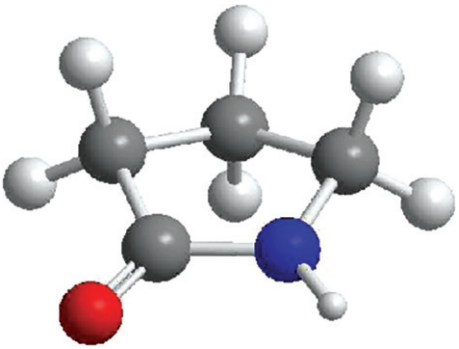

Figure 3 Molecular structure of 2-pyrrolidone.

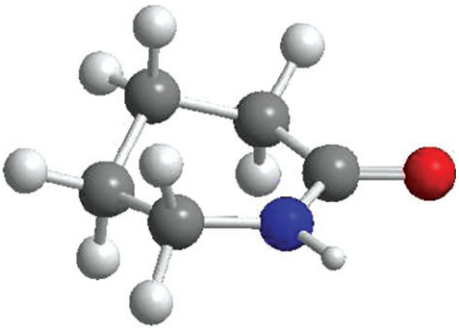

Figure 4 Molecular structure of 2-piperidone, extended chair (envelope) conformation.

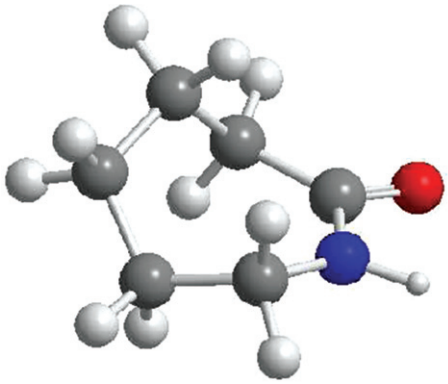

Figure 5 Molecular structure of CL, extended chair conformation.

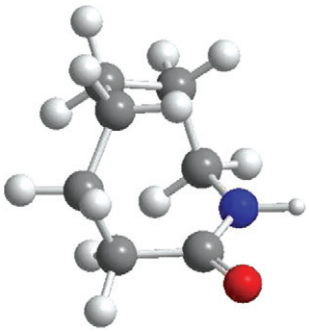

Figure 6 Molecular structure of ζ-enantholactam, a *cis* conformer.

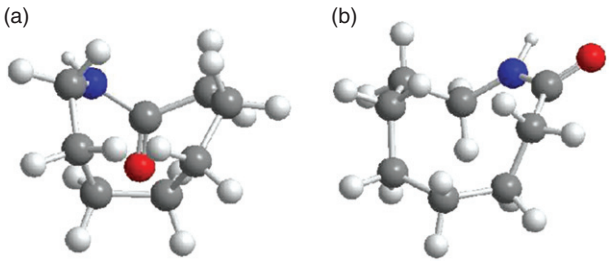

Figure 7 Molecular structure of ζ-caprylolactam: (a) a *transoid* conformer and (b) a *cis* conformer.

'operational' and 'pure' resonance energies of 80.4 and 104.3 kJ mol^{-1}, respectively. For comparison, the 'operational' and the 'pure' resonance energies of acetamide have been reported[24] to be 85.8 and 111 kJ mol^{-1}, respectively.

Since the highest resonance stabilization may be achieved only when the amide group is planar, any departure from planarity results in a higher polymerizability. On the other hand, the preference for coplanarity may render the lactams less stable, introducing some strain into their rings. Contrary to three-and four-membered lactams, the five-membered 2-pyrrolidone is only slightly strained and shows a nearly planar conformation (Figure 3).[36] The impossibility to adopt a fully planar conformation, as it would impose more strain, results in a lower resonance stabilization.

The *cis*-amide group of the six-membered 2-piperidone can easily attain a planar conformation. This lactam displays a nearly strainless ring and for the most part assumes a distorted chair conformation, due to the tendency of the amide group to planarity, and for a minor part an extended chair (envelope) conformation (Figure 4).[14,21]

The most commonly used lactam, CL, exists in only a single conformation (an extended chair type), in both solution[37] and crystals[38] (Figure 5), while the eight-membered ζ-enantholactam (Figure 6), as already mentioned the highest lactam constrained in the *cis* form only, may adopt two different conformations[39] (boat type and puckered ring in crystals).[14]

Going on in the homologous series, the number of existing conformations increases. For example, by X-ray analysis, the crystals of the nine-membered ζ-caprylolactam show two conformers with the *cis*-amide (puckered and boat type) and two conformers with a *transoid*-amide group[30] (Figure 7). In solution, a mixture of *cis* and *trans* isomers with two *trans* conformations has been observed by dynamic nuclear magnetic resonance (NMR) spectroscopy.[40] The 10-membered θ-pelargonolactam has been reported to exist, in the crystalline state, in six *trans* conformers,[41] and 11-membered and 14-membered lactams have been reported to exist, in solutions, in several *trans* conformers.[42] Potentially, the amide group displays three nucleophilic sites, O, N, and C in α position to carbonyl (C_α), and two electrophilic ones, C of carbonyl and C linked to nitrogen (C_ω), which all together give rise to a number of possible reaction routes. As a consequence, lactams are weak acids in terms of –NH and very weak acids relative to $-C_\alpha H$, with the acidity of $C_\alpha H$ being extremely low.[14]

The values of the amide –NH acidity (in terms of pK_a) for the most relevant lactams are given in Table 2, where a few

Table 2 Some physical properties of the most relevant lactams

Code	Lactams	Amide configuration	Acidity (pK_a)[a]	Dipole moment (μ)[b]		Permittivity (ε_r)		Melting point (°C)	Boiling point[c] (°C)	H-bond energy (kJ mol^{-1})		Basicity (pK_a)
				Monomer	Dimer							
				(D)		[e]	[f]			Cis	Trans	
L3	Azetidin-2-one	*Cis*	22.7[g]	–	–	34.8	–	–	–			–0.96
L4	2-Pyrrolidone	*Cis*	24.5	3.55	2.2	22.3	27.1 (31 °C)	25.9	245	34.9	–	0.65
N-MeL 4			–	–		23.6	–	–24	203	–	–	–
L5	2-Piperidone	*Cis*	26.7	3.83	2.4	16.1	17.5 (45 °C)	38	256	30.5	–	0.18
N-MeL 5			–	–		–	–	–	225		–	–
L6	CL	*Cis*	27.2	3.88	2.6	13.5	13.1 (120 °C), 12.5 (150 °C)	69.2	263	29.7	–	0.46 (0.27)[h]
N-MeL 6	*N*-Methyl-CL		–	4.23	–	21.3	–	–	249	–	–	
L7	ζ-Enantholactam	*Cis*	27.2	3.86	2.5	12.1	–	37.1	–	29.1	(15.5)	0.38 (0.42)[h]
L8	η-Caprylolactam	*Cis + transoid*	27.3	3.85	–	27.0	–	73	–	29.5	(21.1)	0.18 (0.37)[h]
L9	θ-Pelargonolactam	*Trans (+cis)*	–	3.79	–	–	–	–	–		16.0	
L10	ω-Caprinolactam	*Trans*	26.9	3.78	–	70.1[i]	–	162	–		16.0	(0.57)[h]
L12	ω-Laurolactam	*Trans*	27.2	3.64	–	70.2[i]	35 (160 °C)	153	–		15.7	(0.52)[h]
N-MeL 12			–	–	–	12.6	–	–	–			
L16	ω-hexadecanoic acid lactam	*Trans*	–	–	–	–	–	124	–			
L20	ω-Icosanoic acid lactam	*Trans*	–	–	–	–	–	83	–			

[a] Measured in DMSO by a spectrophotometric method.
[b] In benzene at 25 °C (values in Debye).
[c] At 760 Torr.
[d] Data from Wan, P.; Modro, T. A.; Yates, K. *Can. J. Chem.* **1980**, *58*, 2423.[43]
[e] At 100 °C.
[f] In molten lactams (at different temperatures).
[g] Estimated from pK_a of 3,3-dimethylazetidin-2-one.
[h] Data from Huisgen, R.; Brade, H.; Walz, H.; *et al. Chem. Ber.* **1957**, *90*, 1437.[44]
[i] Extrapolated value.
N-MeLn, *N*-methyl lactam.
Data from Sekiguchi, H. In *Ring-Opening Polymerizations*; Ivin, K. J.; Saegusa, T., Eds.; Elsevier: London, UK, 1984; Vol. 2, Chapter 12, p 809;[8] Šebenda, J. In *Comprehensive Polymer Science*; Eastmond, G.; Ledwith, A.; Russo, S.; Sigwalt, P., Eds.; Pergamon Press: Oxford, UK, 1989; Vol. 3, Chapter 35, p 511;[9] Puffr, R. In *Lactam-Based Polyamides*; Puffr, R.; Kubánek, V., Eds.; CRC Press: Boca Raton, FL, 1991; Vol. 1, Chapter 1, p 1.[14]

physical properties have also been collected. It can be observed that the highly strained rings show a higher acidity than do medium-sized and higher lactams (displaying similar pK_a data) and that the *cis* or *trans* configuration has no influence on this property.

Due to their –NH acidity, lactams can react with strong bases, giving the corresponding lactam salts that may be more or less dissociated, for example, in alkali metal cations and lactam anions, the latter being the active species initiating the anionic lactam polymerization (see Section 4.14.7). Lactams are weak bases, protonated by strong protic acids, and their basicity can be estimated from the values of the conjugate acid using different methodologies, which can originate contradictory data, as often obtained.[43,44] With the exemption of aziridin-2-ones and some other highly strained lactams, as previously mentioned, protonation occurs essentially at the oxygen atom since N-protonation would destroy the resonance stabilization.[45] Not considering the basicity value calculated for azetidin-2-one, 2-pyrrolidone has been shown to be the least basic and 2-piperidone the most basic of the series (**Table 2**). The values for larger lactams are close to those for linear amides (the pK_a of *N*-ethylacetamide is reported to be –0.49).[43]

Lactams, as weak bases, may act as hydrogen-bonding acceptors with weak protic acids and as Lewis acid acceptors with strong dissociated acids, forming various types of molecular complexes.[8,14] The amide group itself may function as both proton donor and proton acceptor (with the oxygen of the carbonyl); hence, in the absence of stronger electron donors or hydrogen acceptors, lactams form hydrogen-bonded structures by self-association. Lactams with *cis* configuration mainly form cyclic dimeric associates, while *trans*-lactams can form only linear chain structures (**Scheme 1**).

The energy of formation of intermolecular H bonds for the *cis*-lactams is higher than those for *trans*-lactams, the average values being ~30.7 and 16.7 kJ mol^{-1}, respectively (**Table 2**). In addition to self-association, lactams may form molecular complexes with various hydrogen donor molecules (e.g., water, alcohols, amines, phenols, carboxylic acids, inorganic acids, hydrogen halides, and halogenated hydrocarbons). By using the oxygen atom as donor, lactams may form complexes with polar molecules (e.g., I_2, Br_2, ICl, and SO_2) and coordination compounds with inorganic salts where lactams form the ligand field surrounding the metal cation, with the latter behaving as the acceptor. In this respect, the number of lactam complexes that have been synthesized and fully characterized is remarkably large, since the cation of almost any element can be coordinated to the lactam carbonyl giving rise to very ample possibilities.[14] Relevant effects of complexes between CL and LiCl[46] and CL and $CaCl_2$[47] in both the anionic polymerization of the above lactam and the properties of the resultant PA6 have been found by Russo *et al*. and will be summarized later on (Section 4.14.10).

Compared to other homologous series of monomers, lactams possess high values of dielectric permittivity (ε_r), largely varying as a function of ring size (**Table 2**). It is useful to mention here that in lactams containing a *cis*-amide group, a great change of permittivity occurs during polymerization as a consequence of the transformation from *cis* to *trans* configuration; this change may imply differences in polymerization kinetics and can be employed in monitoring the course of the polymerization.[48]

In the lactam series, melting temperatures vary as a function of ring size in a nonuniform manner, as evident from T_m data of **Table 2**. These latter data show the lowest value for 2-piperidone (25.9 °C) reaching a maximum for L10, ω-caprinolactam (162 °C), and then decreasing down to 83 °C for L20. The rather low melting points of the main lactam rings enable to perform bulk polymerization, for example, by the anionic route, at temperatures well below the melting point of the resultant polyamide.

4.14.2.2 Polymerizability

Polymerizability, which should properly be considered a thermodynamic parameter related to Gibbs energy change, is sometimes associated with the polymerization rate, or with the ability to polymerize in milder conditions, or with the capacity to give high polymer yields. Such ambiguity arises from the actual fact that the change in Gibbs energy cannot be the only criterion to describe the aptitude of cyclic monomers, namely lactams, to polymerize.

As a matter of fact, the change of Gibbs energy is only connected to the difference of thermodynamic stability between the monomer ring and the linear chain, regardless of the various ring-opening mechanisms; a negative value of ΔG_p points to whether lactam polymerization is possible and not that it really occurs, since other types of hindrances may take place, such as the absence of a suitable reaction pathway or the existence of more favorable competitive reactions. Therefore, it is obviously affirmed that the thermodynamic polymerizability is a necessary but not sufficient prerequisite and cannot be separated from the kinetic feasibility. On the basis of these two complementary aspects, it must be remarked that the

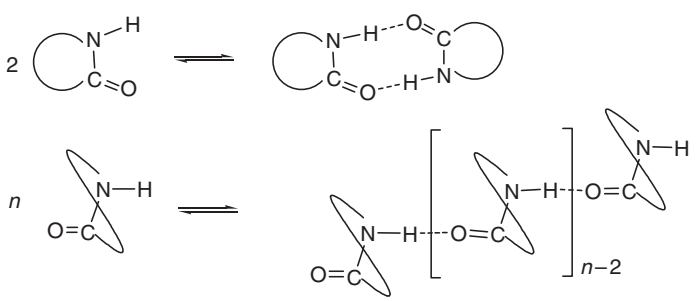

Scheme 1 Hydrogen-bonded structures of *cis*- and *trans*-lactams by self-association.

kinetic polymerizability of lactams states the ease or the difficulty to transform a cyclic monomer into a linear chain unit in specific polymerization conditions, defining the chemical reactivity of the monomer in a selected elementary reaction. Unfortunately, the ring-opening mechanisms are more than one; thus, more than one polymerization rates exist for each specific lactam. The actual capability to polymerize is primarily a function of the type of initiation (e.g., hydrolytic, anionic, or cationic) and involves many parameters. The slower cationic and hydrolytic polymerizations give rise to a wider range of reactivities than does the fast anionic polymerization. The initiation type may have some relevance to the conformation of lactam ring, the main factor related to its reactivity; for example, the conformation of the lactam anion in anionic polymerization may differ from that of the protonated lactam in cationic polymerization, resulting in a different reactivity order. Moreover, when considering, for instance, the activated anionic polymerization (Section 4.14.7.4), in addition to ring strain and substitution as well as acidity and permittivity of monomer and its polymer, the nucleophilicity of the lactam anion and the electrophilicity of the *N*-acyl lactam (activator) must also be included. The correlation of all these parameters is extremely difficult and only partial data may be obtained under specific conditions.

Additionally, even when both the thermodynamic and the chemical feasibilities are assured, the conversion to polymer may not occur because of other competitive reactions that are more favored thermodynamically or kinetically (e.g., N-substituted aziridin-2-ones decompose before polymerizing).

The chemical, thermodynamic, and kinetic aspects of lactam polymerizability have been the subjects of many papers mainly published in the 1960s and 1970s.[9,33,49–54] Remarkably elegant has been the study of Korshak *et al.*,[33] who intended to examine the general capability of lactams to polymerize as a function of their structure, by both a thermodynamic and a kinetic approach. However, being fully aware of the many reasons previously mentioned, it can now be concluded that it is impossible to define a generally applicable classification of the chemical reactivity of lactams toward ROP; as a matter of fact, no more attempts on this issue have been made in recent years. For all these reasons, just a few indications on the thermodynamic feasibility connected to the ring structure and only some general kinetic considerations will be hereafter reported.

4.14.2.2.1 Thermodynamic feasibility

The main relationship in lactam polymerization is the equilibrium established between the monomer and the open-chain amide groups [2]:

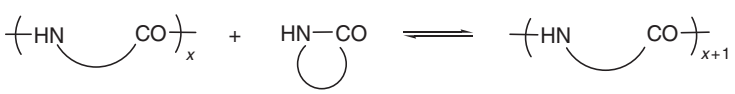

[2]

The displacement of this equilibrium strongly depends on not only ring size and substituents but also the type of initiation and the reaction conditions. In other words, residual monomer concentration, often interpreted as equilibrium monomer concentration [M_e], is always present in ROP. This concentration may be an extremely small value in nonequilibrated polymers, obtained by very fast, kinetically controlled polymerization processes (e.g., in the activated anionic polymerization of CL, Section 4.14.10).

Assuming that all open-chain *trans*-amide groups are of the same reactivity, thermodynamic parameters have to be considered independent of the reaction mechanism and the polymerizability may be described considering the equilibrium between monomer opening into a linear chain and its reforming.

The molar Gibbs energy change accompanying the incorporation of a mole of lactam monomer in the polymer may be expressed as[55]

$$\Delta G_p = \Delta G_p^0 - RT \ln[M] = \Delta H_p^0 - T\Delta S_p^0 - RT \ln[M] \qquad [3]$$

Thus, ΔG_p and ΔH_p can be calculated starting from the [M] values. At equilibrium ($\Delta G_p = 0$, i.e., when polymerization is completed), the monomer concentration is given by

$$[M]_e = \exp\left(\frac{\Delta H_p^0}{RT} - \frac{\Delta S_p^0}{R}\right) \qquad [4]$$

At standard conditions, lactams for which $\Delta H_p^0 > 0$ and $\Delta S_p^0 < 0$ cannot be converted into linear macromolecules. In the case that both enthalpy and entropy terms are negative, namely for the five- and six-membered lactams, formation of high polymer cannot occur at or above a limiting polymerization temperature (ceiling temperature, T_c) [5]:

$$T_c = \frac{\Delta H_p^0}{\Delta S_p^0 + R \ln[M]_0} \qquad [5]$$

where $[M]_e = [M]_0$, initial monomer concentration.

Significantly low is the so-called ceiling temperature of the six-membered 2-piperidone ($T_c = 60\,^\circ C$). Equilibrium monomer concentration can be obtained by analyzing the equilibrated polymer, but reliable $[M]_e$ data are effectively accessible only in a few cases. For instance, the polymerization of 2-pyrrolidone cannot be regarded as an equilibrium reaction due to the irreversible crystallization during polymerization; thus, only a so-called limiting polymerization temperature has been kinetically extrapolated by experimental data. By this way, the actual temperature limit has been found to depend upon the type of initiation, being ~66 °C for its nonactivated anionic polymerization and ~76 °C for the activated anionic polymerization.[56]

In **Table 3**, some examples of equilibrium monomer concentrations at the polymerization temperatures are reported for unsubstituted and substituted CL and substituted ζ-enantholactam.[57] It is notable that the presence of substituents generally shifts the polymer–monomer equilibrium to higher M_e values.

Table 3 Equilibrium monomer content (bulk polymerization)

Lactam	$[M]_e$[a,b] (mol kg^{-1})
CL	0.72
α-Methyl-CL	0.81
β-Methyl-CL	1.51
δ-Methyl-CL	1.76
N-Methyl-ζ-enantholactam	1.35[c]

[a] Data from Šebenda, J. In *Lactam-Based Polyamides*; Puffr, R.; Kubánek, V., Eds.; CRC Press: Boca Raton, FL, 1991; Vol. 1, Chapter 2, p 29.[57]
[b] At 250 °C.
[c] At 260 °C.

Table 4 Equilibrium monomer concentration calculated at 25 °C

Ring size	Lactam	$[M]_e$ at 25 °C[a,b] (mol l^{-1})
5	2-Pyrrolidone	6.3
6	2-Piperidone	1.2
7	CL	2.4×10^{-3}
8	ζ-Enantholactam	1.4×10^{-5}
9	η-Caprylolactam	4.3×10^{-9}
10	θ-Pelargonolactam	4.0×10^{-8}
11	ω-Caprinolactam	3.6×10^{-7}
13	ω-Laurolactam	8.2×10^{-8}

[a] Calculated from the equation $\ln[M]_e = \Delta H_p^0/RT - \Delta S_p^0/R$.
[b] Data from Korshak, V. V.; Kotel'nikov, V. A.; Kurashev, V. V.; *et al. Russ. Chem. Rev. (Engl. Transl.).* **1976**, *45*, 853; *Usp. Khim.* **1976**, *45*, 1673.[33]

M_e values, calculated from eqn [4] at 25 °C for the most relevant lactams, are listed in Table 4. Considerably higher values are shown for 2-pyrrolidone and 2-piperidone (Table 4).

4.14.2.2.1(i) Enthalpy of polymerization

The ΔH_p of cyclic compounds is always associated with the strain of their rings; additionally, in the case of lactam monomers, other factors must be taken into account. The sources of ring strain in lactams are as follows:

- angular strain (bond angle distortion), accompanied by bond stretching or compression;
- repulsion between eclipsed hydrogen atoms or substituents on neighboring atoms (conformational strain, bond torsion, and bond opposition) and interaction of atoms/substituents in different parts of the cycle (transannular strain);
- amide deformation;
- different resonance stabilization of monomer and polymer due to uneven conjugation or hyperconjugation;
- difference between the energies of hydrogen bonds or dipole–dipole interactions in the monomer and the polymer.

These additional factors may account, at least in part, for the lower (i.e., less negative) enthalpies of polymerization of the lactam rings compared to those of the corresponding cycloalkanes (e.g., −4.6 kJ mol^{-1} for 2-pyrrolidone and −21.2 kJ mol^{-1} for cyclopentane).[33]

Assuming that the enthalpy change is almost equivalent to the internal energy of lactam monomer and due to the fact that in polymerizations at normal pressure, the $P\Delta V$ term in $\Delta H = \Delta U - P\Delta V$ is negligible, it is reasonable to consider the heat of polymerization as a measure of the strain energy of the ring. However, it is worth underlining that in some cases, ΔH_p does not reflect the actual ring strain, since polymerization does not necessarily release all the strain of the cyclic monomer (e.g., in highly substituted lactams).

Lactam polymerizations usually imply a volume contraction and, at very high pressures, the effect of the $P\Delta V$ term on equilibrium cannot be neglected. Lactams that have a low T_c or are prevented from polymerizing at normal pressure for thermodynamic reasons can polymerize at high pressures. T_c increases with pressure in accordance with the Clausius–Clapeyron equation.[58]

Since the ΔH_p may be obtained in different ways (e.g., measured by calorimetric techniques, estimated by comparing the experimental combustion heats of lactams and of the corresponding polymers in the amorphous state, or calculated from the enthalpies of cyclization), discordant data are found in literature. For instance, values reported for the enthalpy of CL polymerization range from −13.8[33,59] to −15.4 kJ mol^{-1}.[7,60]

The polymerization heats of the most representative lactams have been collected in Table 5. The data vary with ring size from practically 0 up to the most negative value attributed to substituted azetidin-2-ones, for example, −81.9 kJ mol^{-1} for 3,3-methyl-butyl-azetidin-2-one.[61] Indeed, aziridin-2-ones cannot polymerize and the ΔH_p data for unsubstituted azetidin-2-one are not available.

With increasing ring size, the heat of polymerization (absolute values) goes through a minimum for the five-membered lactam, reaches a maximum for the nine-membered lactam, and again approaches zero for larger lactams (12- and 13-membered lactams) (Figure 8).

The high ring strain is the cause of the high (i.e., more negative) enthalpies of substituted azetidin-2-ones. Conversely, its absence is the origin of the low values encountered for 2-piperidone and 2-pyrrolidone and large lactams. In the nine-membered η-caprylolactam, the *transoid*-amide reduces the resonance stabilization and a higher enthalpy is found.

4.14.2.2.1(ii) Entropy of polymerization

The entropy of polymerization depends on the difference between the probability of monomer existence in the cyclic form and that in the form of repetition unit of the linear polymer. As in all cyclic monomer polymerizations, the decrease in translational entropy is in part counterbalanced by the increase in rotational and vibrational entropy acquired in the conversion of a strained ring into a more or less flexible monomer unit inside the polymer chain. For this reason, the absolute value of the entropy of polymerization for the seven-membered CL is rather low.[7,53]

Beyond the four- and five-membered lactams, the highest rigidity is expected for medium-sized rings (8–11 ring atoms). In these latter cases, the enhanced flexibility of the open-chain monomer unit inside the polymer results in a large increase in the rotational and vibrational entropy.

Table 5 Thermodynamic data of unsubstituted lactams

Monomer	Ring size	ΔH_p° (kJ mol^{-1})	ΔS_p° (J °K^{-1} mol^{-1})	ΔG_p° (kJ mol^{-1})	References
3,3-Methyl-butyl-azetidin-2-one	4	–81.9			61
2-Pyrrolidone	5	–4.6	–30.5	4.6	8, 33
		0.4	–30.1	9.4	55, 62
2-Piperidone	6	–7.1	–25.1	0.4	8, 33
		–7.1	–27.6	1.1	55, 62
CL	7	–13.8	4.6	–15.1	8, 33, 63
			(–13.3)[a]		64
		–15.4			57
ζ-Enantholactam	8	–22.6	16.7	–27.6	8, 33
		–21.8			57
η-Caprylolactam	9	–35.1	(41.8)[b]	(–47.7)[c]	8, 33
		–32.7			57
θ-Pelargonolactam	10	–23.4	(62.8)[b]	(–42.3)[c]	8, 33
ω-Caprinolactam	11	–11.7	(83.7)[b]	(–36.8)[c]	8, 33
ω-Aminoundecanoic lactam	12	2.1	(104.6)[b]	(–29.3)[c]	8, 33
ω-Laurolactam	13	–2.9	(125.5)[b]	(–40.6)[c]	8, 33
			(13.4)[a]		53

[a] Calculated from $[M]_e$.
[b] Extrapolated data.
[c] Calculated using extrapolated entropies.

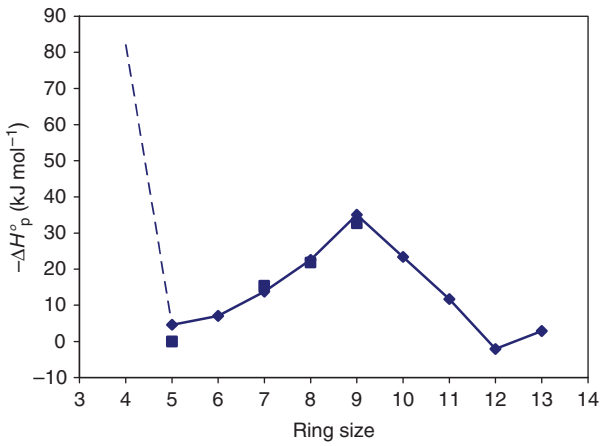

Figure 8 Heat of polymerization of unsubstituted lactams as a function of their size (from data in **Table 5**).

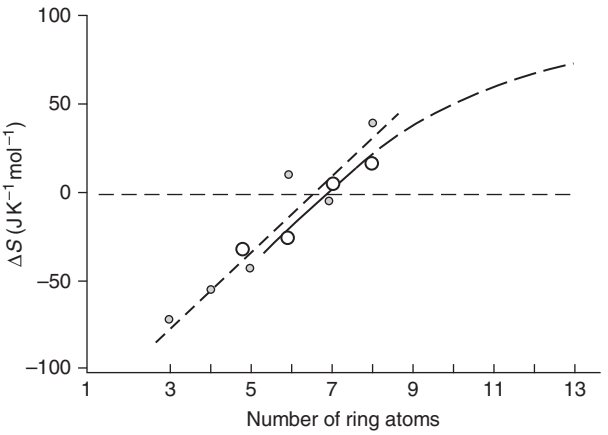

Figure 9 Entropy of polymerization as a function of ring size for unsubstituted lactams (○) and cycloalkanes (●). Reproduced from Sekiguchi, H. In *Ring-Opening Polymerizations*; Ivin, K. J.; Saegusa, T., Eds.; Elsevier: London, UK, 1984; Vol. 2, Chapter 12, p 809.[8]

Indeed, the entropy of polymerization increases roughly linearly from the five-membered to the eight-membered lactam together with the decreased rigidity of the monomer (**Table 5**). It must again be emphasized here that many methods exist for determining the polymerization entropy[33] and they provide discordant values to be found in the literature. Calculated ΔS_p° from the absolute entropy values of monomer and polymer derived from specific heat measurements at low temperature have shown[63] negative entropies only for 2-pyrrolidone and 2-piperidone and a linear increase passing from the five-membered to the eight-membered lactam.[7,53] Notably, these values are of the same order as those of cycloalkanes (**Figure 9**).

However, it is worth noting that incongruent data have been often reported for the entropy of polymerization: for example, the calculated ΔS_p° for CL was found to be 4.6 J K^{-1} mol^{-1}, but a value estimated[64] from the monomer–polymer equilibrium has been found to be equal to –13.3 J K^{-1} mol^{-1} (**Table 5**).

An attempt to obtain the entropy of polymerization for 9–13-membered lactams has been accomplished by operating a linear extrapolation of the values for 5–8-membered lactams,[62] which stay on a straight line, but the results are overestimated and, thus, not very reliable. These data revealed a very sharp increase of ΔS with ring size and are significantly higher compared to those obtained by using equilibrium monomer concentration. For example, for ω-laurolactam, a value of 13.4 J K^{-1} mol^{-1} has been found from the monomer–polymer equilibrium, while a value of 125.5 J K^{-1} mol^{-1} has been derived by extrapolation.[53]

In any case, it can be asserted that the entropy change becomes progressively more important with the increasing

ring size. It is noteworthy to underline that ΔS_p may be more favorable in copolymer formation, that is, in the copolymerization of lactams. Indeed, a lactam may be copolymerized even at a temperature at which homopolymerization cannot proceed. This is the case of the copolymerization of 2-pyrrolidone and CL.[65]

4.14.2.2.1(iii) Gibbs energy

The ΔG_p values calculated from the enthalpy and entropy data in **Table 5** have been plotted to give the approximate trace of **Figure 10**. The Gibbs energy change varies from a small positive value (five-membered ring) and a value close to zero (six-membered ring) to negative values, reaching a minimum for the nine-membered lactam. For five- and six-membered lactams, both the enthalpic and entropic terms are negative; consequently, their polymerization is favorable from the enthalpic standpoint, but not on entropic grounds; the loss of translational degrees of freedom is not well balanced by the gain in rotational and vibrational motions in the polymer. For seven- and eight-membered lactams, the main contribution to ΔG_p comes from the enthalpy factor, while for 9-, 10-, and 11-membered lactams, the contributions of ΔH_p and ΔS_p are approximately the same. For 12- and 13-membered lactams, the enthalpy change is negligible and the entropic factor governs the Gibbs energy.

Taking into account thermodynamic factors only, one may conclude that lactams having ≥ 7 ring atoms are allowed to polymerize. The small positive values of ΔG_p for the polymerization of 2-pyrrolidone and 2-piperidone are surely due to the large errors in the determination of the thermodynamic characteristics, since these two lactams, although long believed to be unable to polymerize, can do it under anionic conditions[66–69] (Section 4.14.11). Taking into account only the Gibbs energies discussed above, it is possible to set up a theoretical series of thermodynamic feasibilities as a function of the ring size:

$$9 > 10 > 13 > 11 > 12 > 8 > 7 >> 6 \sim 5$$

4.14.2.2.2 Kinetic aspects

A few attempts have been made[8,9] to describe the kinetic polymerizability of lactams, but rather poor results have been obtained and contradictory conclusions on reactivities and, in particular, on substituent effects have been published.[49,50,70–73] Sekiguchi and Coutin[51] proposed a criterion for estimating the chemical polymerizability of lactams under anionic conditions, modifying an idea of Carothers,[74] who suggested that polymerizability and rate of hydrolysis for a cyclic monomer should run parallel (in this parallelism, the acid-catalyzed hydrolysis would simulate cationic ring opening and the base-catalyzed hydrolysis would simulate the anionic ring opening).[8] They hypothesized, for the activated anionic mechanism, that the kinetic polymerizability, identified with the propagation rate, might be described by a parameter π, which was assumed proportional to the rate constant of the base-catalyzed endocyclic hydrolysis of the *N*-acyl lactam and inversely proportional to the rate constant of lactam hydrolysis (this latter supposed to be inversely proportional to the basicity of lactam anion). However, scarce and doubtful results have been achieved on these grounds.

As previously mentioned, the complexity of the aspects influencing contemporarily and differently the course of lactam polymerization, in particular under anionic conditions, makes impossible to discriminate between the lactam structural properties (e.g., ring size and substitution) and all other factors. Thus, only limited comparisons under a restricted range of polymerization conditions can be accomplished.

The order of reactivities as a function of ring size, derived from the thermodynamic feasibility, is often modified for the same monomer in a quite different manner, depending on the type of initiation. The slower cationic (Section 4.14.5) and hydrolytic polymerizations (Section 4.14.4) give rise to a wider spread of reactivities than does anionic polymerization.

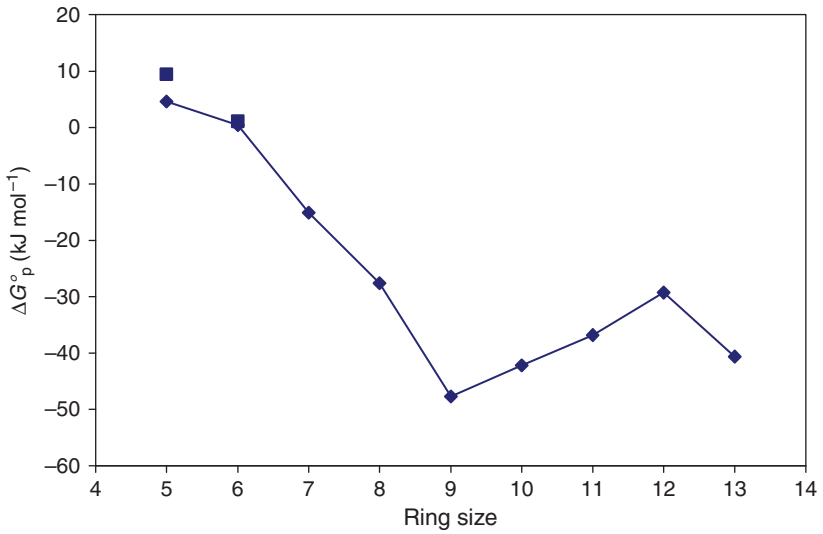

Figure 10 Free-energy change for the polymerization of unsubstituted lactams as a function of the ring size (data from **Table 5**).

Generally speaking, the chemical structure of a lactam monomer influences the kinetic possibilities of polymerization by several aspects, such as the following:

1. configuration of the molecule (e.g., presence of *cis*- or *trans* isomers);
2. resonance stabilization of amide group (presence of mesomeric, inductive, and hyperconjugation effects);
3. basicity and acidity;
4. permittivity and polarity (e.g., presence of hydrogen bonds and dipole–dipole interactions); and
5. substitution (position and nature of substituents).

Surely, five- and six-membered lactams are much more reactive in the anionically initiated mechanism (Section 4.14.7.1), where a nucleophilic attack on the lactam ring is implied, as compared to the polymerization in the presence of water or acids, involving an electrophilic attack and proceeding at a significantly lower rate.

In the anionic polymerization, the monomer structure may have indirect effects as well, influencing, for example, the dielectric properties of the reaction medium and, thus, the course of the polymerization. Since lactam monomers and the resultant polyamides have polar amide bonds, their bulk polymerization rate is strongly affected by the changes in medium permittivity during polymerization. In anionic polymerization, high dielectric permittivities strongly favor the dissociation of the lactam salt (initiator) releasing the free lactam anion (Section 4.14.7.1).

The permittivity of lactams with less than ten ring atoms is lower than that of the corresponding polyamides[48] owing to the different configuration of the amide group: *cis* form in lactams and *trans* form in the polyamide.[75] This effect, for example, is important in the case of CL where polymer permittivity is much higher than that of monomer; this have been invoked to explain the increasing polymerization rate, expressed by an auto acceleration in the propagation step of anionic polymerization in bulk. On the contrary, for the 13-membered laurolactam, the two dielectric permittivities are almost identical (**Figure 11**) and the autoacceleration effect is not shown.

The much higher permittivity of 2-pyrrolidone compared to 2-piperidone (**Table 2**), combined with the lower resonance stabilization of the amide group deriving from the not fully planar conformation, is the main factor contributing to its higher reactivity, although the six-membered lactam is, thermodynamically speaking, slightly more polymerizable.

In higher lactams (carrying a *trans*-amide group), the ring strain is considerably reduced and the reactivity of their amide group is similar to that of the polymer chain (e.g., the acidity of the higher lactams is equal to that of a linear amide group). As a consequence, the rate of the propagation reaction may be reduced. Hence, ω-laurolactam, thermodynamically expected to be more polymerizable than the medium-sized lactams (seven-, eight-, and nine-membered rings), is less reactive than CL.

Strained lactams (in particular, azetidin-2-one rings) are much more acidic than the corresponding linear amide; thus, in all reactions involving the lactam anions, the equilibrium is shifted to the side of these latter species.[9]

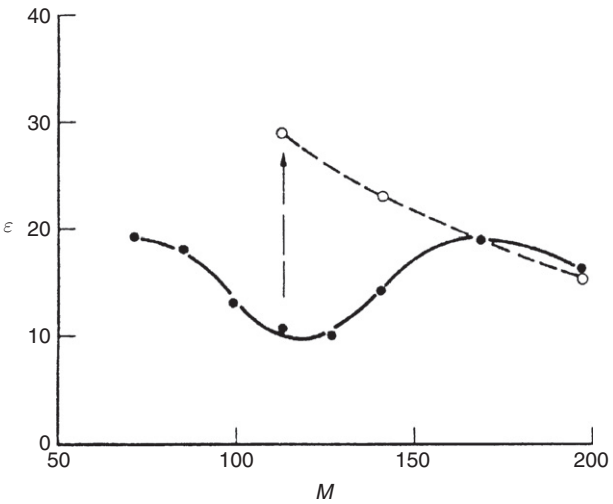

Figure 11 Dielectric permittivity (ε) of lactams (•) and the corresponding polyamides (°) as a function of the molar mass *M*. Reproduced from Šebenda, J. In *Comprehensive Polymer Science*; Eastmond, G.; Ledwith, A.; Russo, S.; Sigwalt, P., Eds.; Pergamon Press: Oxford, UK, 1989; Vol. 3, Chapter 35, p 511.[9]

4.14.2.2.2(i) Substitution effects

Lactam polymerizability is significantly affected by the number, size, and location of substituents, acting in general differently on kinetic and thermodynamic factors. Substituted lactams generally show lower reactivity as compared to the corresponding unsubstituted ones, due to the steric hindrance at the reaction site. This fact has allowed the synthesis of highly strained aziridin-2-one rings, in contrast to the unsubstituted aziridin-2-one, which is too reactive to be isolated. Starting from the isolation of the first α-lactam, 1-*tert*-butyl-3-phenylaziridin-2-one (**9**)[76]

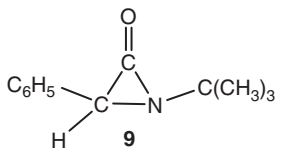

9

a number of aziridin-2-ones have been isolated. A structural requirement for the existence of an α-lactam is the presence of a bulky substituent (e.g., *tert*-butyl, trityl, and 1-adamantyl) on nitrogen and the ability to sterically shield the carbonyl group, to slow down the rate of nucleophilic reaction, and thus to stabilize the lactam from a kinetic point of view.

4.14.2.2.2(i)(a) C substitution Kinetically speaking, the presence of substituents on the methylene groups in the lactam ring may drastically decrease their reactivity since they can both modify the electron density of the amide group, that is, its nucleophilicity, and create steric hindrance. Substituents affect polymerizability in a complex manner since not only their position but also their size and polarity play an important role.[7] From a thermodynamic point of view, substituents affect both the enthalpy and the entropy of polymerization, essentially due to conformational effects. Although the enthalpy and the entropy of a lactam are little influenced by C substitution, the presence of substituents creates new interactions in the

linear monomer unit of the polymer, which may result in a higher enthalpy of the latter and a reduced $|\Delta H_p|$ value.[77] Also from an entropic standpoint, substituents significantly reduce the possibility of free rotation in the polymer chain. In this respect, substituents facilitate ring closure, shifting the monomer–polymer equilibrium toward the monomer side; these effects are relevant in the case of small rings, that is, for the five- and six-membered lactams.[8]

2-Pyrrolidone and 2-piperidone entirely lose their capability to polymerize even in the presence of only one alkyl substituent at the ring carbon atom. However, C substitution does not prevent them from copolymerizing.[8] Thus, C-methyl-substituted 2-pyrrolidones may be copolymerized to a certain extent with 2-pyrrolidone, being mainly incorporated as chain terminators.[78,79]

Since C-alkyl substitution enhances ring closure, the polymerizability of a given lactam is expected to decrease with the increase of substituent length. However, steric repulsions between large substituents and ring atoms (transannular interactions) may result in a relatively higher polymerizability. For example, on the basis of the equilibrium polymer content, the following order of polymerizability for ε-alkyl-substituted CL has been reported:[7]

unsubstituted ε-caprolactam > ε-methyl- ≅ ε-hexyl - > ε-ethyl- >> ε-dodecyl-ε-caprolactam

In the case of 3,3-dialkyl-substituted azetidin-2-ones (α,α-disubstituted β-lactams), other factors must be taken into account to explain, in some reaction conditions, the favorable effect of bulky substituents. Indeed, contrary to previously published data,[70] the propagation rate constant in the anionic polymerization of 3-alkyl-3-methyl-azetidin-2-one, conducted in dimethyl sulfoxide (DMSO) at 22 °C using potassium (or tetramethylammonium) 2-oxopyrrolidin-1-ide and *N*-acetyl-2-pyrrolidone, has been found to be approximately twofold enhanced by increasing the length of R from methyl to *n*-butyl[71,72] (following the order shown in Scheme 2 and being in any case much lower than that for the 4,4-dimethyl derivative).

This effect, not encountered in other lactams (e.g., CL and 2-pyrrolidone) or in lactones, has been attributed to the large hydrophobic R group that inhibits the contact, or intimate ion-pair formation, between the counter ion (K^+ or Me_4N^+) and the lactam N anion. Such phenomenon occurs in polar DMSO solvent, where the 3-butyl-3-methyl-substituted lactam may probably exist as an almost free ion having enhanced reactivity. Indeed, subsequent studies[73] conducted in tetrahydrofuran (THF) revealed, as expected, a decrease in the polymerization rate with the size of substituents.

From a kinetic standpoint, the rate-determining step in the ROP mechanisms is more sensitive to steric effects in the

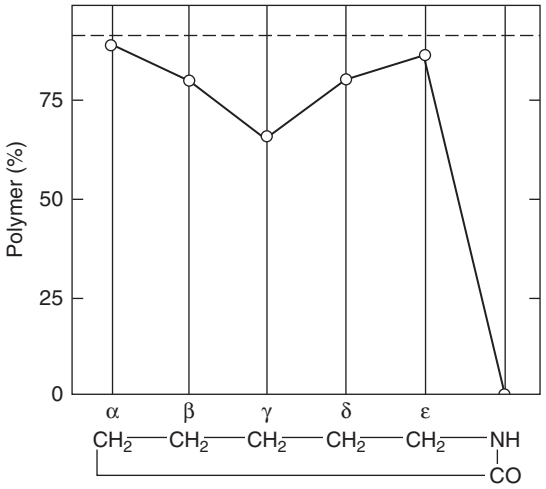

Figure 12 Equilibrium polymer content for methyl-CL isomers at 250 °C as a function of the position of the methyl substituent. The dashed line represents the unsubstituted lactam. Reproduced from Šebenda, J. In *Comprehensive Chemical Kinetics*; Bamford, C. H.; Tipper, C. F. H., Eds.; Elsevier: Amsterdam, The Netherlands, 1976; Vol. 15, Chapter 6, p 379.[7]

vicinity of the amide group (i.e., substituents at the C_α and C_ω atoms), while, thermodynamically speaking, the Gibbs energy of polymerization is more affected by the substitution on the mid-chain methylene groups, favoring ring closure. An example of this fact is given by the monomer–polymer equilibria of the methyl-substituted CL isomers,[7,53] as illustrated in Figure 12. The α-methyl- and the ε-methyl-ε-CL show a lower polymerization rate but a more negative Gibbs energy (i.e., a higher equilibrium polymer yield) as compared to γ-methyl-CL. Moreover, α,α-dimethyl- and ε,ε-dimethyl derivatives are also polymerizable. Namely, the γ-position (position 4) is very sensitive to the increase of the substituent size; thus, γ-*n*-propyl-, γ-phenyl-, γ-*n*-heptyl-CL show an extremely low reactivity or do not polymerize.[7]

The influence of substituents on the Gibbs energy of polymerization decreases with increasing ring size, becoming negligible for higher lactams. It is noteworthy that substitution of both hydrogen atoms in the vicinity of the carbonyl group prevents, in the anionic polymerization, the rise of secondary reactions that destroy active species. This fact is a prerequisite for maintaining a steady concentration of growth centers and obtaining a quasi-living polymerization (see Section 4.14.11.4).

4.14.2.2.2(i)(b) N-substitution The most important feature related to N-substitution is the impracticality of the anionic polymerization, because of the obvious impossibility of forming the lactam anion. Consequently, polyamides from

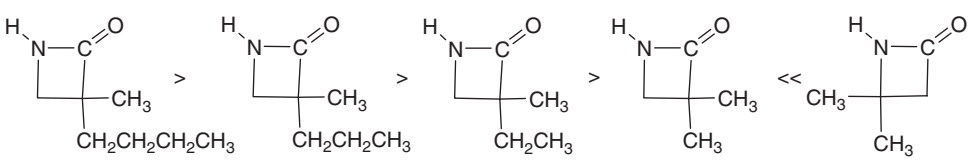

Scheme 2 Order of propagation rate constants for disubstituted b-lactams.

N-substituted 2-pyrrolidone and 2-piperidone cannot be obtained. N-substituted lactams are more or less easily polymerized through the cationic or acidolytic mechanism[80] (Sections 4.14.5 and 4.14.6).

N-substitution affects polymerizability of the *cis*-lactams much more than does C-substitution. The largely reduced reactivity given by substituents with +I effect on nitrogen has been attributed to the loss of resonance stabilization[50] and the *cis* character of the amide bond.[81]

As a consequence, the influence of N-substitution also decreases with increasing ring size. The more strained and reactive four-membered rings (N-substituted azetidin-2-ones) are still able to polymerize, while the five-, six-, and seven-membered lactams generally do not polymerize. Actually, the polymerization feasibility of *N*-methyl-CL, at very low temperature, has not been completely excluded, while it has been ruled out for *N*-methyl-2-piperidone.[80]

For larger lactams, N-substitution does not prevent polymerization; thus, the 8-membered up to 13-membered lactams are polymerizable by the acidolytic and/or hydrolytic route (e.g., *N*-methyl-η-caprylolactam and the *N*-alkyl-ω-laurolactams are hydrolytically polymerizable).[61]

4.14.3 Outline of Lactam Polymerization Routes

The ROP of lactams is based on reversible transamidation/transacylation reactions in which the ring amide groups are converted into linear ones. Due to the amphoteric character of the amide group, the cleavage of the amide bond may proceed by both nucleophilic and electrophilic attack in a number of different transamidation reactions (e.g., aminolysis, acidolysis, and transacylation). Indeed, lactams are versatile monomers that may be polymerized by various polymerization routes with different initiation and propagation mechanisms, namely solvolytic (hydrolytic, acidolytic, and aminolytic), anionic, and cationic. Moreover, even within the same process, polymerization mechanisms and kinetics are functions of the type of initiating species.

The opening of the lactam ring by cleavage of the resonance-stabilized amide group is achieved by hydrolysis or, more easily, by ionic reactions, using lactam anions or protonated lactams. The basic polymerization reactions for lactams having the hydrogen at the amidic nitrogen (N-unsubstituted lactams), in relation to the cationic, hydrolytic, and anionic initiation, are summarized in **Scheme 3**.

Looking at these reactions, a specularity between the anionic and the cationic mechanism is observable. Different from conventional ionic polymerizations, the growth center in cationic and anionic lactam polymerizations is always neutral, and it is the lactam monomer that carries the ionic charge. Such polymerizations follow what is sometimes referred to as 'activated monomer mechanism',[82] since the reactive species are lactam cations/anions, thus activated monomers. However, in order to avoid misunderstandings, it must be well clear that this definition has nothing to do with the term activated

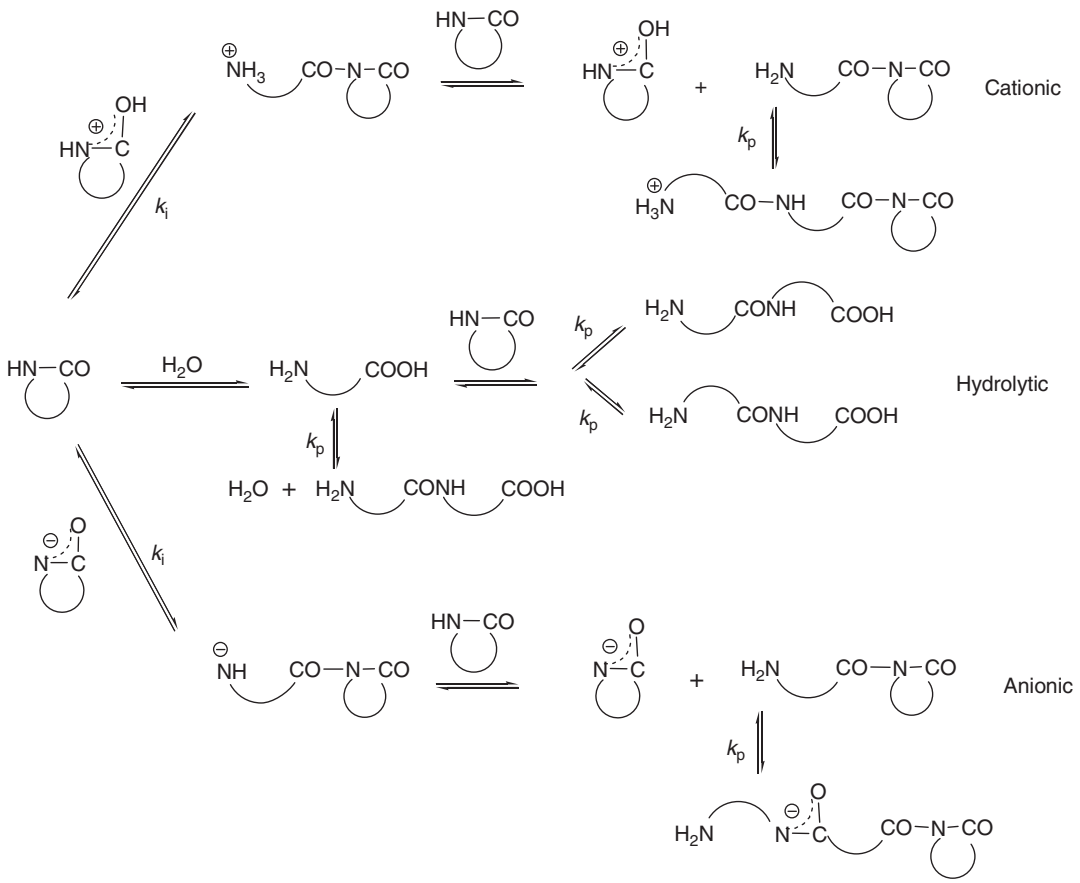

Scheme 3 Opening of the lactam ring by cationic, hydrolytic and anionic initiation mechanisms.

anionic polymerization, which designates a mechanism implying the use of activators (Section 4.14.7.4).

Propagation proceeds essentially by acylation reactions between a nucleophile (donor) and the cyclic carbonyl group of the lactam or the N-acylated lactam (acceptor). Depending on the type of initiation (e.g., hydrolytic, cationic, and anionic), different donors and acceptors may be involved. Some examples are summarized in **Table 6**, where the main reacting donor–acceptor pairs are related to the various polymerization mechanisms.

The order of reactivity of the most important species, as nucleophilic agents (with respect to oxygen or nitrogen atom), is given below (**Scheme 4**):[8]

and the order of the carbonyl acylating strength is (**Scheme 5**)

Not all these active species can coexist simultaneously. However, more than a single type of propagation reactions is possible with a given initiator. In general, under specific polymerization conditions, one of the many feasible reactions predominates. The most probable acylation reactions occur by consuming the most reactive species in the system (the most nucleophilic ones and those with the highest acylating ability). Actually, the anionic mechanism that involves the strongest nucleophile and the most powerful acylating agent is characterized by the highest propagation rate.

Due to the reversibility of the transamidation/transacylation reactions involved in lactam polymerization, several equilibria of linear chains, cyclic molecules, and initiators are established. Linear polymer chains are thermodynamically in equilibrium with monomer (monomer–polymer equilibrium) and with cyclic structures in general (ring-chain equilibria).

The ring-chain equilibria are governed by the ability of the chain segments and the active species to achieve the favorable conformation for ring closure. Indeed, backbiting reactions involving the active terminal group (–COOH, $-NH_2$, RCO–, RNH–, etc.) as well as intramolecular transamidations give rise to monomer, cyclic dimer, or higher cyclic oligomers (an example of backbiting is illustrated in **Scheme 6**).

The reaction of an initiator with an amide group of the polymer chain, instead of that of the monomer, may result in the breaking of the macromolecule. Intermolecular transamidations can also modify the length of the polyamide chains and may generate cyclic structures. These exchange reactions result in a modification of the molar mass distribution.

4.14.4 Hydrolytic Polymerization

The term hydrolytic polymerization refers to the polymerization initiated by water or other substances able to generate water at the reaction conditions. Namely, the above term is widely adopted for the production, at 240–300 °C, of PCL (PA6) and poly(ω-laurolactam) (PA12).

The hydrolytic route is the most important industrial process for the production of the above polyamides, due to the severe drawbacks that have characterized so far both anionic and cationic polymerizations. They have made almost impossible for the latter routes to be employed in various fields, for example, for textile uses. The mechanism and kinetics of the

Table 6 Principal nucleophiles and acylating species involved in the different types of polymerization

Nucleophile (donor) \ *Acylating species (acceptor)*		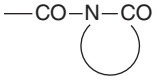	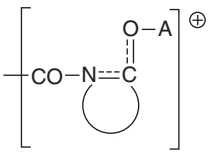	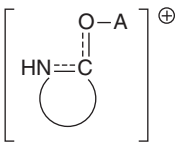
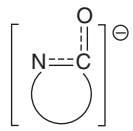	Anionic	Anionic		
—NH_2	Hydrolytic, aminolytic	Anionic, cationic		Cationic, hydrolytic
			Cationic	Cationic, hydrolytic
–$COO^{\ominus}$				Hydrolytic, acidolytic

A, Proton or Lewis acid.

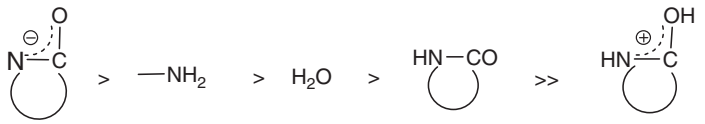

Scheme 4 Order of nucleophile reactivity.

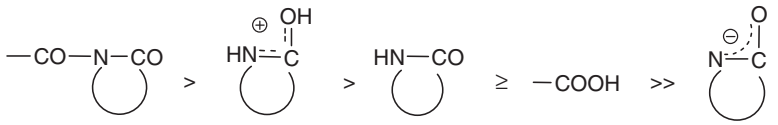

Scheme 5 Order of carbonyl acylating strength.

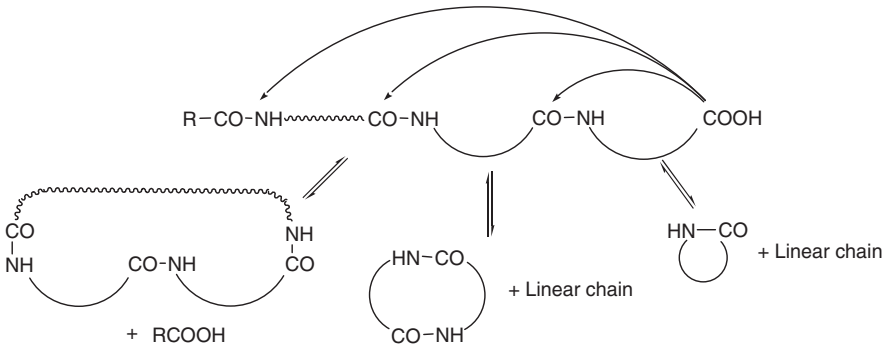

Scheme 6 Examples of the backbiting reaction.

water-initiated polymerization have been studied in detail in the past decades and are now well established.[7,11,12,54,83,84] More recently, the investigations have been focused on both the modeling and the optimization of the industrial polymerization process for PA6[85–87] and the modeling of its higher cyclic oligomer formation.[88] In recent years, some studies on novel polymerization processes for synthesizing hydrolytic PA6, for example, by microwave irradiation, have been reported. The ring opening of CL has been performed in a microwave oven[89] in the presence of ω-aminocaproic acid as initiator for periods of 1–3 h at temperatures varying from 250 to 280 °C.

Both unsubstituted and substituted lactams may be polymerized by the hydrolytic process, provided that the monomer ring size is ≥7. Smaller rings, such as those of 2-pyrrolidone and 2-piperidone, are not polymerizable by the hydrolytic mechanism and, because of this, the above lactams have been long believed to be not polymerizable.

4.14.4.1 Reaction Mechanism

Since the hydrolytic polymerization proceeds as both a stepwise addition and a condensation reaction, it cannot be classified as pure ROP and will not be treated in detail in the present chapter. Only the most relevant aspects of the reaction are hereafter briefly reported.

The water-initiated polymerization is governed by three main equilibrium reactions:

1. Hydrolytic ring opening, with formation of the ω-amino acid:

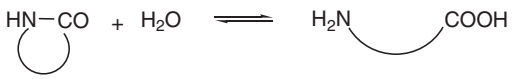

[6]

At high temperatures, the lactam amide is hydrolyzed to give the ω-amino acid [6], which then acts as the initiator. Of course, the introduction of a preformed ω-amino acid at the very beginning of the polymerization achieves the same results. This ring-opening reaction is endothermic and, thus, favored by a temperature increase.[90]

The same reaction, at a later stage, is catalyzed by the carboxyl groups. Indeed, the ring-opening step may be considered an autocatalytic process in which the catalytic function is exerted by the carboxyl groups. The overall rate constant, therefore, is given by the rate constant of the uncatalyzed reaction plus that of the catalyzed reaction. The above polymerization may also be initiated by the addition of phosphoric acid or its alkylammonium salts, as will be mentioned later on.

The acid-catalyzed hydrolysis of the amide group takes place after protonation of the oxygen atom [7]. The rate-determining step is the attack of water and the formation of a tetrahedral intermediate; then, rapid N-protonation and C–N bond cleavage occur:[57]

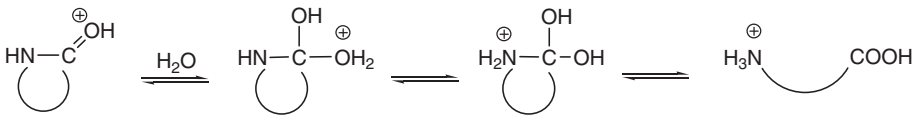

[7]

2. Condensation between amine-terminated and acid-terminated chains with formation of amide groups (polycondensation reactions):

[8]

This reaction contributes to the increase of polymer chain length. In this respect, the presence of water negatively affects the obtainment of high molar masses and must be removed in the final steps of polymerization. The condensation reactions occur even in the solid state and allowing their occurrence is an easy method to increase polyamide molecular masses. In that case, the rate-controlling step is the diffusion of reactive end groups.

3. Stepwise addition of lactam molecules to either amine or carboxyl groups (aminolytic and acidolytic polyreactions):

[9]

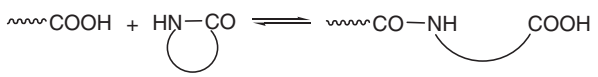

[10]

It has been proven that the polyreaction occurs mainly at amine end groups and the reaction can be catalyzed by the carboxyl groups.[91] In reaction [9], a tetrahedral intermediate, similar to that occurring in the acid-catalyzed hydrolysis, is involved (see Section 4.14.5.1.1, **Scheme 7**). Intermediate amidine groups may also be generated. As a matter of fact, amidines are reported to be present in the polymerization of CL and η-caprylolactam initiated by the corresponding amino acids.[92]

In the simplified reaction schemes given above, the formation of cyclic oligomers has not been considered, although it plays an important role in the industrial production of PA6. Namely, the cyclic dimer formation and its relevance in both the polymerization process and the properties of the resultant polyamide cannot be neglected.[93]

Since the dimer is the major component among the cyclic by-products, in addition to the aforementioned reactions, other equilibrium reactions have to be considered as well: the ring opening of the dimer to (aminocaproyl)aminocaproic acid (hydrolytic ring opening) and the polyreactions, involving the dimer instead of the lactam.

The contribution of the individual processes to the overall lactam consumption depends on both the type of monomer and the reaction conditions. In CL polymerization, the stepwise addition is prevailing[94] and only a small fraction of the monomer is incorporated in the polymer chain through hydrolysis and subsequent condensation.

The reaction is often carried out in the presence of carboxylic acids and/or primary amines (e.g., acetic acid and hexane-1,6-diamine), which act as chain length regulators. Consequently, the concentration of functional end groups is modified.

4.14.5 Cationic Polymerization

The cationic ROP of unsubstituted lactams has been studied in detail, mostly by Rothe *et al.*[95–97] and Bertalan *et al.*,[98–101] between the late 1960s and the late 1980s of the past century, essentially for mechanistic purposes only, since this type of polymerization found very limited applications in practice. At present, cationic polymerization is considered industrially unimportant among the various lactam polymerization processes and has been nearly abandoned. However, it is interesting to point out that, contrary to the anionic route, which obviously is possible only for N-unsubstituted lactams, both N-unsubstituted and N-substituted lactam may be polymerized by the cationic process. Indeed, this latter has been successfully employed for the polymerization of several N-substituted lactams.[80]

The cationic polymerization is initiated under anhydrous conditions by species capable of being coordinated by the lactam molecule to give a lactam cation, which is the reactive species in the polymerization. A variety of compounds may be used as cationic initiators operating with different action mechanisms: strong protic inorganic acids[100] and their salts with ammonia or primary and secondary amines,[99] Lewis acid and metal halides (e.g., $AlCl_3$, $TiCl_4$, WCl_4, WCl_6, $FeCl_3$, $CaCl_2$, and $CrCl_3$), carbenium ions[80] (e.g., $Ph_3C \cdot AsFe_6$ and $PhCO \cdot SbFe_6$), salts of complexing cations (e.g., $(RCOO_2)Zn$), phosphoric and metaphosphoric acids, arsenic acid, sulfonic acids (e.g., CF_3SO_3H), acyl chlorides, and carboxylic acids[102] (giving rise to what is referred to as acidolytic polymerization, Section 4.14.6).

4.14.5.1 Reaction Mechanism

The reaction mechanisms can be very complex since they are functions of both the initiating system and the lactam substitution. Among the various mechanisms, the polymerization initiated by protic inorganic acids, such as hydrogen chloride or bromide, will be those mainly considered and described in detail in the present section.

Strong protic acids act through an easy protonation of the lactam amide group, while several metal halides, such as chromium, iron, aluminum, tungsten, and calcium chlorides, can form complexes with lactams.[8] It has been assumed that the O-coordination with Lewis acids activates lactam

polymerization similarly to the initiation with strong protic acids, yielding to a similar mechanism.[80]

Polymerization initiated by phosphoric or metaphosphoric acid, or their alkylammonium salts, in the absence of water, proceeds probably through a hydrolytic mechanism. Indeed, phosphoric acid at the polymerization temperatures undergoes dehydration and the lactam amide group is then hydrolyzed.[8] The resultant diphosphoric acid catalyzes both hydrolysis and propagation.

4.14.5.1.1 N-unsubstituted lactams

Two potential sites of protonation exist in unsubstituted amides: the nitrogen atom and the oxygen atom. Protonation occurs preferentially at the oxygen (structure **11**), but a small amount of N-protonated lactam (structure **10**) is present.

It is generally assumed that a tautomeric equilibrium [11] between the two protonated forms is established, shifted to the oxygen-protonated one:

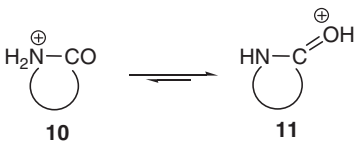

10 **11** [11]

In fact, although nitrogen would be inherently more basic than oxygen, there is an important contribution from three resonance structures in O-protonation [12], particularly the form **14** with the double bond between C and N:

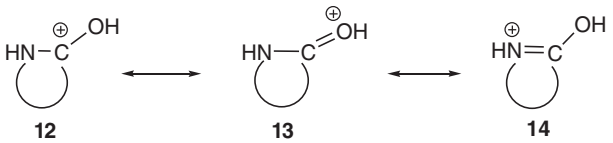

12 **13** **14** [12]

Due to the lack of resonance stabilization, the nitrogen-protonated lactam has a high acylating capability and is the most active species capable of reacting with a lactam molecule at the nitrogen atom.

4.14.5.1.1(i) Initiation

In a reaction mixture where the initiators are strong acids, such as HCl, the strongest nucleophile is the monomer. Indeed, the neutral lactam is more nucleophilic than the chlorine anion; thus, initiation occurs by attack of the monomer on the N-protonated amide. Fast acylation of the monomers with the protonated lactam results in the formation of aminoacyl lactam cations as ammonium salts [13]:

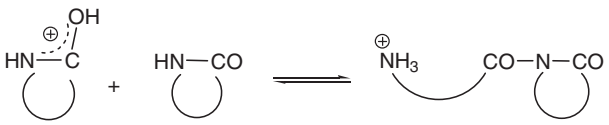

[13]

Indeed, in the above reaction, N-acylated lactams with amine hydrochloride terminal groups are generated. According to the most probable mechanism,[103] the reaction involves several steps: attachment of N atom to the positively charged C, proton transfer from one to the other N, and ring opening with proton transfer from –OH to $-NH_3^+$.

Bertalan[98,100,104] was the first to suggest the formation of a tetrahedral intermediate via stereoelectronic control: the nucleophile approaches the protonated amide group perpendicularly to its plane so that the lone pair orbitals of the amide heteroatoms are oriented antiperiplanar to the direction of the newly formed C–N bond.

Mechanisms based on tetrahedral intermediates apply well for protic acid-initiated polymerization, amine salt-initiated polymerization, and also for hydrolytic polymerization, being in good agreement with experimental data. The existence of a tetrahedral intermediate implies a two-way reaction (**Scheme 7**), which fully accounts for the formation of amidine groups (reported as positively charged amidine hydrochloride). If cleavage of the carbon–nitrogen bond takes place, the lactam monomer is incorporated in the polymer chain (pathway 14); if cleavage of carbon–oxygen bond occurs, amidine groups **16** are formed and water is split off (pathway 15).

This two-way cleavage of the tetrahedral intermediate may be well explained by the theory of stereoelectronic effects:[105]

The protonated *N*-(aminoacyl)lactam **15** is characterized by two reactive sites: the *N*-acyl lactam group and the ammonium ion. As a consequence, it can participate in chain growth reactions that pertain to two different propagation mechanisms.

4.14.5.1.1(ii) Propagation

4.14.5.1.1(ii)(a) Chain growth by acylation The ammonium cation **15** is involved in the equilibrium reaction [16], due to proton transfer to monomer with regeneration of the

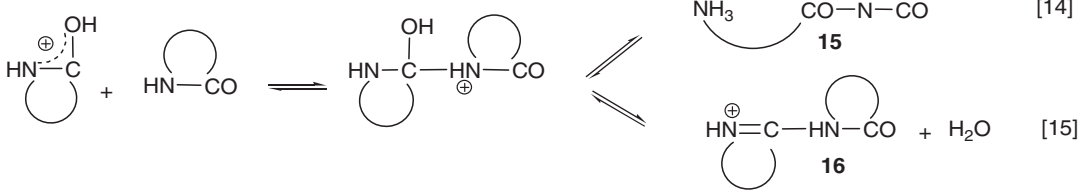

15 [14]

16 [15]

Scheme 7 Formation of a tetrahedral intermediate in the initiation reaction.

protonated lactam plus an electrically neutral molecule carrying the amine end group:

15 [16]

The formation of a certain amount of protonated lactam is allowed by the higher concentration of monomer, despite the higher basicity of the amine group compared to lactam amide. Since the neutral amine group is the strongest nucleophile, it is immediately acylated by the lactam cations, thus incorporating one more monomer unit and giving rise to a chain growth by acylation [17]. As such, the propagation may proceed in a manner similar to the initiation step, by nucleophilic attack of the primary amine group on the protonated monomer:

[17]

A complete agreement does not yet exist about the pathway of this reaction. In fact, some authors support the addition of the neutral lactam to the ammonium cation, justified by the higher basicity of $-NH_2$, as compared to lactam amide group. However, it seems reasonable to take into account the predominant concentration of the neutral monomer, thus shifting the equilibrium in reaction [16].

Actually, the reaction mechanism to be considered is more complex if, in analogy to the initiation reaction (**Scheme 7**), the participation of a tetrahedral intermediate is taken into account (**Scheme 8**). In fact, in this case also, the two-pathway decomposition of such intermediate results in the formation of either the protonated (aminoacyl)lactam (**17**) or the *N*-acylamidine groups (**18**).

Bertalan *et al.*[100] considered the reactions [18] and [19] to occur between neutral lactams and terminal ammonium groups ($-NH_3^+$), but giving the same products. The ammonium site undergoes proton exchange with the monomer, as in reaction [16], reforming the neutral amine group [20] that can react again with lactam cations, similarly to [17]:

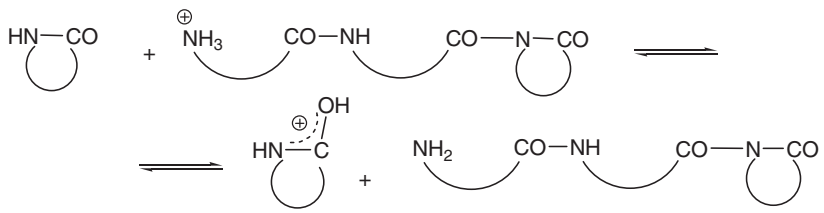

[20]

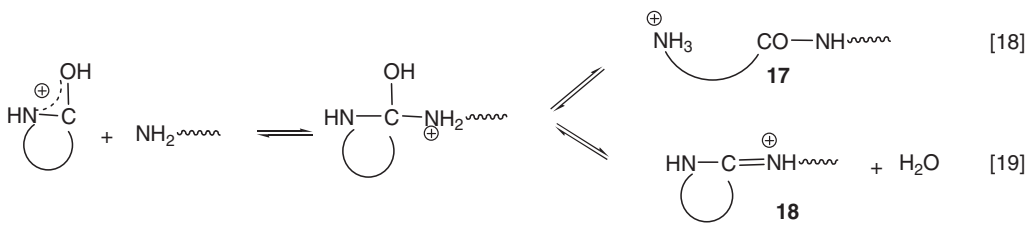

[18]

[19]

Scheme 8 Formation of a tetrahedral intermediate in the propagation reaction.

The above reactions attain equilibrium very rapidly.

4.14.5.1.1(ii)(b) Chain growth by aminolysis The second propagation mechanism is characterized by the interaction of the *N*-acyl lactam moiety with the neutral or the protonated amine group, linking two polymer molecules (aminolysis of aminoacyl lactam). Indeed, protonation of the *N*-acyl lactam moiety in the already formed polyamide molecule provides a strong acylating group (**19**), which can react with the terminal amine groups of another chain:

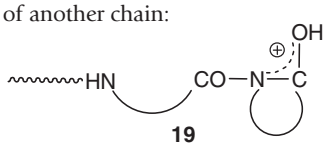

19

Actually, this acylation reaction may involve the endo- as well as the exocyclic carbonyl of the terminal acyl lactam; consequently, two propagation pathways are possible. Moreover, since the bimolecular aminolysis of *N*-acyl lactam may be schematized via formation of a tetrahedral intermediate, four pathways [21]–[22]–[23]–[24] are possible and amidine structures (**21, 23**) may be obtained as well (**Scheme 9**).

These reactions destroy amine groups, which are regenerated by the initiation equilibrium of disproportionation between lactam and protonated amide [13]. The sequence of the disproportionation reaction [13] and the bimolecular aminolysis [21] contributes to the total lactam consumption with the formation [25] of new aminoacyl lactam molecules (**20**).[57,106] Hence, the incorporation of lactam units into the polymer chain proceeds by the reaction of a protonated lactam with amine groups [18] as well as by the sequence of reactions [13] and [21].

In the literature, in this case also, the detailed description of this type of reaction, in relation to the nature and the role of the species involved, has not been unanimous. Sekiguchi[8] described this reaction as occurring between neutral amine groups and neutral acyl lactams. Rothe and Bertalan[97] assumed, as reported here in **Scheme 9**, the bimolecular condensation of neutral amino groups and protonated *N*-acyl lactams, entailing the two possible tetrahedral intermediates and the corresponding elimination products, even taking into account the imide groups in the polymer chain. Bertalan *et al.*,[100] in their study on the mechanism and kinetics of CL cationic polymerization, regarded reactions [23] and [24] as occurring between neutral *N*-acyl lactams and terminal ammonium groups ($-NH_3^+$). Additionally, the reaction between neutral amine groups and *N*-acyl lactam was taken into account as well, yielding amide groups plus neutral lactams (instead of protonated lactams) together with amidines plus water.

4.14.5.1.1(iii) Deactivation of the active species

In spite of the fact that the cationically activated polymerization reactions proceed at high rates, they generally stop at rather low conversions and low molar masses, indicating the relevant presence of side reactions with deactivation of the active species.

For instance, in the case of CL, the initially fast cationic polymerization slows down well before reaching the monomer–polymer equilibrium. Namely, after a short reaction time, particularly at temperatures above 200 °C, both ammonium and acyl lactam groups disappear, resulting in a large decrease of the polymerization rate.

It has been reported[107–109] that all basic groups are essentially represented by the strongly basic amidine functions, while

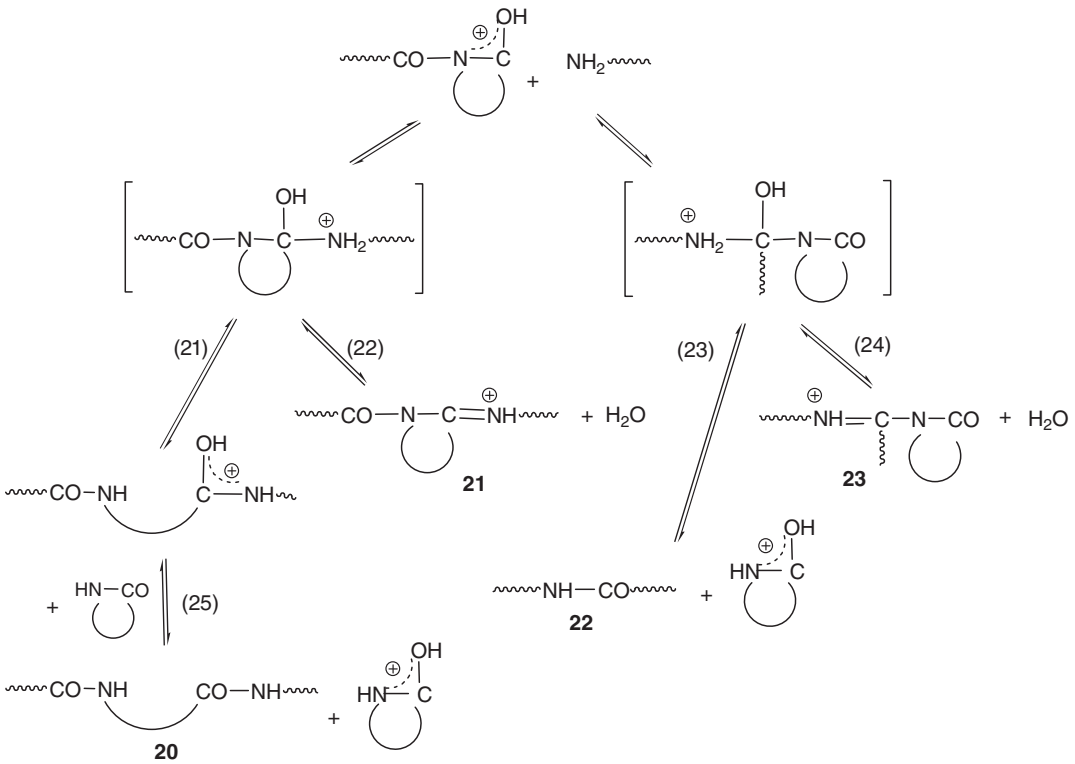

Scheme 9 Possible propagation pathways and structures originated therefrom in lactam cationic polymerizations.

primary amine groups are practically absent. Protonated amidine groups, described by the two resonance forms

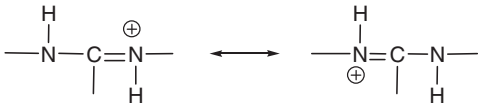
[26]

are assumed to be generated, together with water, by the dehydration of the tetrahedral intermediate, as illustrated in the Schemes 7–9.

As a result, polymerization does not stop completely because of the water and the carboxylic acid groups formed, which are capable of initiating a new slow polymerization. Indeed, the time–conversion curve exhibits an inflexion point that more or less corresponds to the highest concentrations of amidine groups, coinciding with the minimum concentration of amine groups. For example, carboxylic groups may react rapidly with amidine structures restoring the catalytically active strong acid and increasing again the rate of the polymerization process:

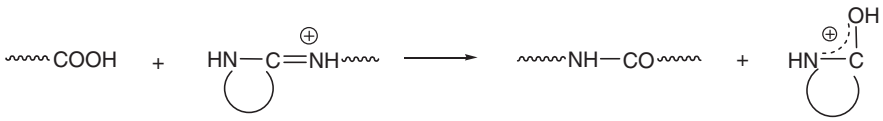
[30]

Furthermore, polymer amide and imide (diacylamines) groups may undergo reaction with terminal NH_2 as well, according to the same reaction pathways depicted in Schemes 8 and 9, respectively. The result is the formation of amidine and acylamidine structures (24 and 25) inside the polymer chain, representing points of branching:

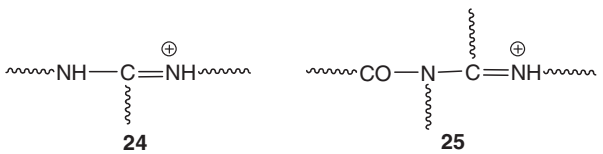
24 25

Due to their high basicity, amidines are capable of neutralizing the acidic initiator and deprotonating the lactam cations, strongly reducing the formation of new propagation centers. Moreover, the terminal amidine groups (18) are unable to react with the monomer and, therefore, stop the chain growth. Consequently, the rate of polymerization, especially at low initiator concentrations and high temperatures, is reduced long before the monomer–polymer equilibrium is attained.

In addition, irrespective of the fact that polymerization has started under anhydrous conditions, water is always generated during amidine formation. Water may give rise to hydrolytic reactions, in particular with acyl lactams and acylamidine structures, yielding carboxylic end groups (Scheme 10), which take part in the polymerization process as well.

Consequently, different active species and more than a single polymerization mechanism are operating in the second stage of the cationic lactam polymerization.

4.14.5.1.2 N-substituted lactams

Polymerization of *N*-alkyl lactams,[80] as already mentioned not polymerizable anionically, can be accomplished cationically by protic and Lewis acids, carbenium and oxocarbenium salts of complex acids, primary and secondary amines, and water.

As compared to the acidolytic, aminolytic, and hydrolytic routes, entailing the same reactions involved for unsubstituted lactams (excluding amidine formation), the polymerization initiated by protic acids, such as HCl, differs for the most part. The most relevant aspects characterizing the cationic polymerization of N-substituted lactams are, as said already, the absence of the detrimental formation of amidines and a much simpler mechanism compared to that pertaining to N-unsubstituted lactams.

4.14.5.1.2(i) Initiation

The free lactam cannot be acylated to give the (aminoacyl) lactam owing to the N-substituent. On the other hand, the anion of the initiating acid (e.g., Cl^-) can undergo acylation by the O-protonated lactam giving rise, for example, as described in reaction [31], to the acyl chloride of the amino acid:

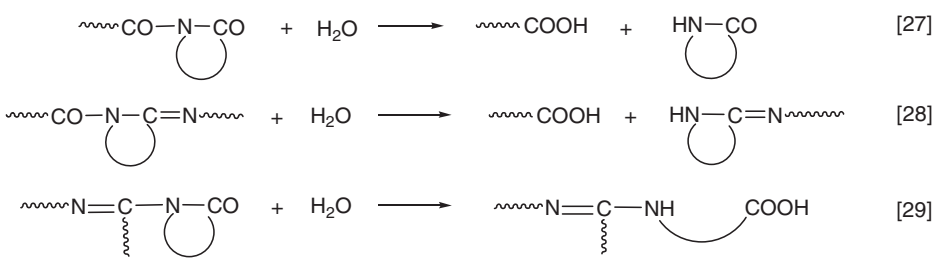
[27] [28] [29]

Scheme 10 Formation of carboxylic end groups by hydrolytic reactions.

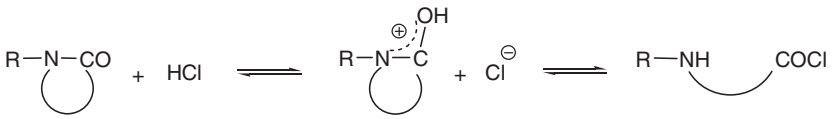

[31]

The formation of the aminoacyl chloride represents the kinetically controlling step of the process.

4.14.5.1.2(ii) Propagation

Propagation then proceeds by fast bimolecular condensation, similar to the bimolecular aminolysis previously described, with a molecule acting as the acceptor and the other as the donor [32]:

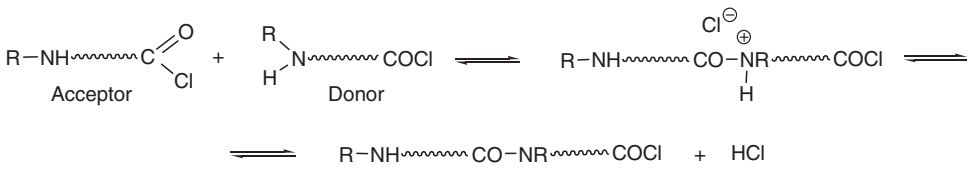

[32]

The regenerated hydrogen chloride enters again into the initiation reaction [31]. Besides this main growth reaction, other competitive propagations are present.[80] In fact, the acyl chloride group may react directly with the lactam monomer; in this case, the aminoacyl chloride acts as the acceptor and the monomer as the donor [33]:

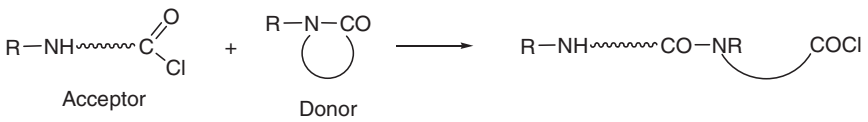

[33]

Additionally, the O-protonated lactam may undergo a nucleophilic attack [34] by the terminal nitrogen of the amino acid (the donor), this reaction nonetheless being an order of magnitude slower than the condensation of the aminoacyl chlorides [34]:

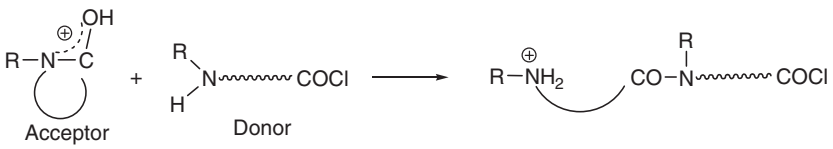

[34]

It is worth underlining that, depending on polymerization time and temperature, the added HCl may result differently distributed in –COCl groups or in acid–base equilibria to give –NHR·HCl [34] and –NRCO·HCl [32]. Hence, not every initiator molecule, in contrast to what happens in the acidolytic polymerization, necessarily yields a polymer chain.

4.14.6 Acidolytic and Aminolytic Polymerizations

Lactam polymerizations initiated under anhydrous conditions by carboxylic acids and primary/secondary amines are referred to as acidolytic or aminolytic polymerizations, respectively. Actually, these terms do not clearly identify different polymerization mechanisms, since their basic reactions simultaneously participate in the cationic and the hydrolytic processes.

The conversion–time curves of amine- and carboxylic acid-initiated polymerization of CL have been reported to show a sigmoidal shape analogous to that given by water initiation.[102] The curves exhibit an initial period during which the rate of conversion increases up to a maximum and, afterward, is constant for some time before decreasing (**Figure 13**).

Acidolytic polymerization is a very slow process, with acids being less efficient than amines in initiating the polymerization. When CL and monocarboxylic acids are considered, the reaction rates have been proven to be inversely proportional to the pK_a of the acid. By extrapolating the experimental data, it has been suggested that acids having pK_a higher than 6–7 are not effective in initiating the polymerization.[102]

The acylation of the monomer by carboxylic acid (acidolysis), or of the protonated monomer by carboxylate anion, is assumed[8,80] to proceed via a transient four-center intermediate. The subsequent acyl exchange and opening of the lactam ring, by splitting of the CO–N bond, gives rise to an amide group and a terminal carboxylic group (reaction [35]):

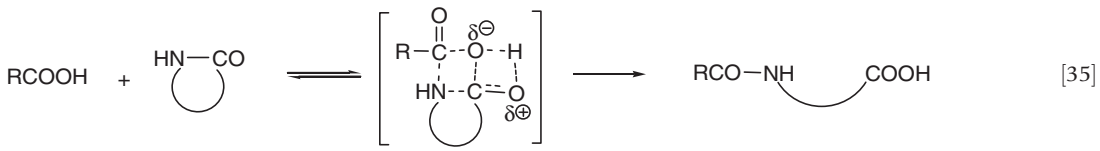

[35]

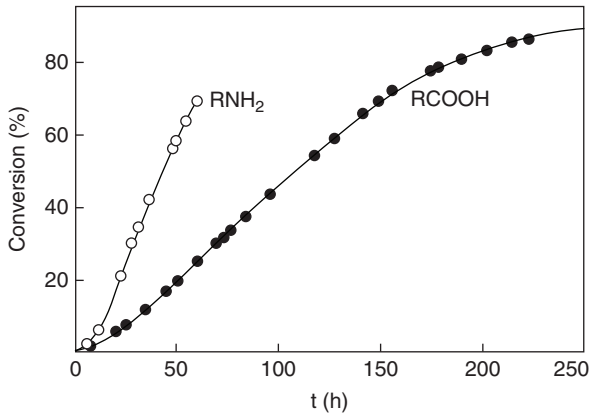

Figure 13 Acidolytic and aminolytic polymerization of CL conducted at 230 °C. Initiator: RNH_2, benzylamine (0.106 mol kg^{-1}) and RCOOH, caproic acid (0.120 mol kg^{-1}). Reproduced from Šebenda, J. In *Lactam-Based Polyamides*; Puffr, R.; Kubánek, V., Eds.; CRC Press: Boca Raton, FL, 1991; Vol. 1, Chapter 2, p 29.[57]

Chain growth then proceeds by reaction of lactam units with the polymer carboxylic groups (reaction [36]):

It is remarkable that in polymerizations initiated by carboxylic acids, the acid is incorporated in the polymer chain, differently from the reaction initiated by strong acids, where the strongest nucleophile is the amide group. An alternative mechanism involving the formation of a mixed anhydride of the acid and the amino acid and subsequent intramolecular rearrangement has been hypothesized.[7] This reaction pathway has been invoked in order to account for the experimental data showing the presence of basic groups (i.e., amine groups) in polymers of seven-, eight-, and nine-membered lactams.[110,111] The proposed mechanism,[54] indeed, implies the formation of anhydride functionality and a terminal amine group:

As soon as basic amine groups are produced, the aminolytic polyreaction between the $-NH_2$-terminated chain and the monomer, described in [9], may compete with the acidolytic reaction as propagation reaction. To a minor extent, the anhydride would also contribute to chain growth by bimolecular aminolysis:

A detailed investigation[110] on the polymerization of ε-capro-, ζ-enantho-, η-caprylo-, and ω-lauro lactam initiated by aliphatic carboxylic acids has shown that propagation prevailingly proceeds via the reaction of the lactam with the carboxyl group and that CL polymerization is characterized by an induction period, unlike the polymerization of eight-, nine-, and thirteen-membered lactams. It has been proven that, with the exemption of CL, the reaction rate of the first lactam with the initiating carboxylic acid is the same as the rate of further lactam molecules to the carboxylic groups of the polymer. On the contrary, in the case of the seven-membered lactam, the first reaction proceeds much slower than the reactions of the second and further molecules. For instance, in lauric acid-initiated polymerizations, the ratio of the rate constants relative to eqns [35] and [36], k_n/k_1, has been found to be 8.4 for the seven-membered lactam and 1.1 and 1.0 for the eight- and nine-membered lactams, respectively. This can be rationalized by the statement that in the case of *trans*-lactams, the rates of initiation and propagation are comparable, while for *cis*-lactams (i.e., CL), they are not.

The presence of the induction period with CL has also been explained[57] by taking into account two propagation reactions, the acidolysis (reaction [35]) and the reaction with amine groups (reaction [9]), and has been related to the formation of basic groups. As a matter of fact, the generation of amine groups increases to a certain level but with very different rates. In the case of ε-capro-, ζ-enantho-, and η-caprylolactam, their concentration attains a constant level at low conversion and the aminolytic polyreaction becomes significant with increasing extent of polymerization. On the other hand, in the seven-membered lactam, due to the existence of the induction period, the formation of basic groups proceeds even at 50% conversion.[110]

Namely, the acidolytic polymerization of η-caprylolactam at 220–280 °C not only proceeds at high rates, much higher than that shown by CL, but also is a little dependent on the acidity of the initiator. Since the hydrolytic process proceeds at comparable rates, the major contribution to monomer consumption has been attributed to the acidolytic reaction [35], neglecting reaction [9].[112]

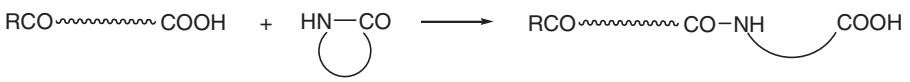

[36]

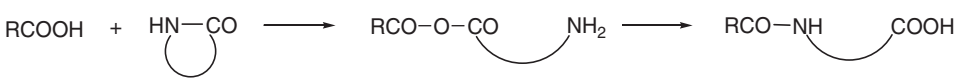

[37]

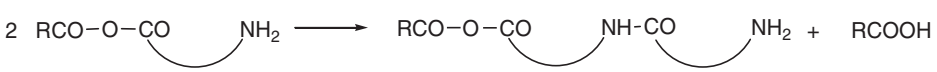

[38]

N-substitution slows down the polymerization rate even in the acidolytic mechanism, as a consequence of the lower rates of transacylation of the lactam as compared to the linear amide, due to the insufficient flexibility of the lactam ring in the formation of the activated complex. Only *N*-benzoyl lactams, together with highly strained rings, raise the rate of acidolytic polymerization by more than three orders of magnitude.[80]

The polymerization initiated by amines is faster than the acidolytic process remaining, in any case, rather slow.[113] For example, the polymerization of CL at 230 °C, initiated by benzylamine (0.106 mol kg^{-1}), is faster than that initiated by caproic acid (0.120 mol kg^{-1}), affording the conversions of 70% and 20%, respectively, after 50 h (**Figure 13**).[83]

The initiating activity of amines increases linearly with their pK_b, but it is also a function of their structure (e.g., secondary amines are less efficient than primary amines). The aminolytic polymerization proceeds by nucleophilic attack of the amine group on the lactam molecule:

[39]

[40]

However, the process is not so simple, implying several types of reactions. The aminolytic CL polymerization exhibits an induction period and its initial rate is proportional to the amine concentration, while the maximum rate of polymerization is proportional to the square root of the amine concentration. The decomposition of the tetrahedral intermediate in this case as well as in the cationic and hydrolytic polymerization, affords amidine and water. The presence of the induction period has been assumed to be associated with slow amidine formation, while the progressive increase of the polymerization rate has been related to the further contribution of the formed carboxylic groups.[57]

4.14.7 Anionic Polymerization

After the early description of Joyce and Ritter,[6] Hanford and Joyce[114] were the first to discuss in 1948 the mechanism of the anionic polymerization of lactams assuming a chain growth via amide anions, which had to be abandoned later on. Only in the early 1960s of the last century, the teams of both Wichterle *et al.*[115] and Champetier and Sekiguchi[116] established the true mechanism involved in these lactam polymerizations.

Since then, the anionic polymerization of lactams has been studied in depth and excellent and exhaustive works have been published; among them are the fundamental reviews of Šebenda, Sekiguchi, and Reimschuessel, already mentioned in part in Section 4.14.1.[7–9,12,117]

The anionic route is the fastest process for producing polyamides, its activation energy being rather low. In bulk polymerizations, the lower temperature limit is the lactam melting temperature, together with the solubility limit of the polymer into the molten monomer. The anionic synthesis, performed in molten lactam, may be accomplished either below or above the melting point of the polymer (i.e., 220 °C for PA6 and 185 °C for PA12). In the first conditions, the reaction mixture, initially liquid, turns turbid at the cloud point and then solidifies in the course of the polymerization. The beginning of solidification is considered the moment at which the growing chains attain a critical length that enables their crystallization, forming spherulites insoluble in the monomer.

The anionic process is the only method allowing the ROP of the stable five- and six-membered lactam rings, 2-pyrrolidone and 2-piperidone. Obviously, as already mentioned, only N-unsubstituted lactams can be polymerized by the anionic mechanism because of the required presence of the hydrogen atom on the amide group.

A great confusion sometimes arises from the literature owing to the nonuniform terminology adopted for the various reactive species. Thus, the terms catalyst, cocatalyst, chain initiator, initiator, coinitiator, precursor, activator, coactivator, and accelerator are indifferently used. In the present chapter, the notation 'initiators' will be used for identifying the ionic lactam salts (i.e., the alkali metal lactamates) capable of starting the anionic polymerization of lactams in suitable conditions. Their 'precursors' will be the basic compounds (e.g., the alkali metals) capable of producing the initiators, while the term 'activators' will be used to denote the species, acting as the source of nonionic growth centers able to run the polymerization in more favorable conditions (high rates and lower temperatures).

4.14.7.1 Reaction Mechanism

The anionic polymerization of lactams is initiated, under anhydrous conditions, by generation of the lactam anion. Any strong base capable of producing the N anion of lactam may be effective in initiating polymerization. The polymerization process carried out in the presence of initiator only, that is, a basic substance providing the lactam anion, is regarded as 'nonactivated polymerization' (or 'nonassisted polymerization'), while polymerization process carried out by adding an activator (e.g., *N*-acyl lactam) is designated as 'activated polymerization' (or 'assisted polymerization').

4.14.7.1.1 Preinitiation

This step involves the formation of the free lactam anion by ionization of the alkali metal salt of the lactam (lactamate), generally produced by treatment of the lactam with a strong base, such as an alkali metal M [41] (see Section 4.14.7.2):

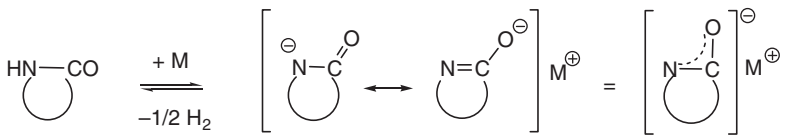

[41]

The negative charge in the lactamate and in the free lactam anion is, as in the case of the lactam cation, delocalized on the amide group in virtue of the resonance stabilization by conjugation with the carbonyl group. The lactamate acts as the source of free lactam anion, which is the active species of the polymerization. The concentration of such free lactam anion is a function of the dissociation constant of the lactam salt [42] and [43], being equal to the concentration of this latter only under conditions of complete dissociation:

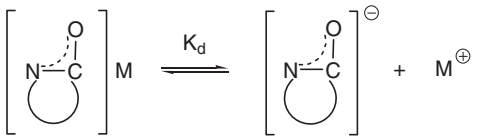

[42]

$$K_d = \frac{[L^-][M^+]}{ML} \qquad [43]$$

Lactamates, and also the salts of polymer amide groups, may be involved in complex equilibria with formation of various aggregates, ion pairs, free ions, and triple ions.[9] In virtue of this fact, the dissociation constant must take into account the participation of the various types of ions. Thus, the concentration of the free lactam anion $[L^-]$ may be written as

$$[L^-] = \left(K_d[ML]_0 + \frac{K_d^2}{4}\right)^{1/2} - \frac{K_d}{2} \qquad [44]$$

where $[ML]_0$ is the initial lactamate concentration.

The contribution of the free lactam anion increases with temperature, starting to be predominant above 150 °C. Only at higher temperatures, the alkali metal lactamates can be considered completely dissociated. When the lactamate is weakly dissociated, the concentration of active species $[L^-]$ may be approximated to vary with the square root of the salt concentration,[118] as in [45]:

$$[L^-] \approx \left(K_d[ML]_0\right)^{1/2} \qquad [45]$$

In the molten lactam medium, without other solvating or complexing species, the lactamate dissociation depends on both the lactam properties (i.e., acidity, dielectric permittivity, donor–acceptor capability, substituents) and the electropositivity of the metal as well (Section 4.14.7.2). For example, higher lactam permittivity, such as in ω-laurolactam as compared to CL, makes easier the salt dissociation (see **Table 7**).[119]

4.14.7.1.2 Initiation in nonactivated polymerization

The lactamate (i.e., the lactam anion) is a very strong nucleophile (see **Scheme 4**). Thus, it is easily acylated by the lactam, although the acylating ability of the latter is poor, with the amide group being stabilized by resonance. The lactam anion reacts with the monomer by a ring-opening transamidation reaction forming *N*-acyl lactam structures carrying primary amine anions (disproportionation reaction).

Assuming a free ion mechanism,[117] the imide anion is formed, in the first slow step, by nucleophilic attack of the lactam anion on the carbonyl of the lactam molecule, via formation of a tetrahedral intermediate [46]:

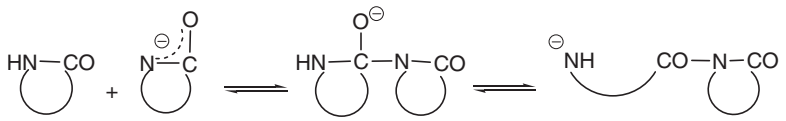

[46]

Table 7 Dissociation constants (K_d) of lactam salts in their respective lactams with different acidity (pK_a at 25 °C) and relative permittivity (ε)

Ring size	Lactam	pK_a	$\varepsilon_r(T)$	T (°C)	$-LogK_d$ $Li^+ L^-$	$Na^+ L^-$	$K^+ L^-$	$Me_3N^+ L^-$	References
5	2-Pyrrolidone	24.5	27.10	31			0.80		14
6	2-Piperidone	26.7	17.49	45		3.89	3.58		14, 57
			13.14	120	7.5	6.31	4.44	3.35	14, 57
7	CL	27.2	12.55	150	4.25	3.98	3.73		14, 57
13	ω-Laurolactam	27.2	35.00	160		2.38			14, 57

The amine anion is highly reactive, unlike the lactam anion, as it is not stabilized by resonance, and rapidly undergoes proton exchange with a lactam molecule, yielding an imide dimer (*N*-acyl lactam) and regenerating a lactam anion [47]:

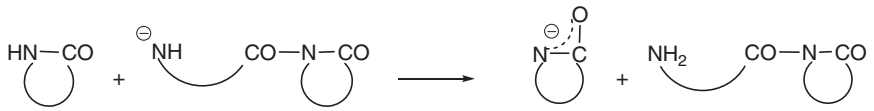

[47]

The result of these two combined reactions is the disproportionation between two amide groups (present in lactam and in lactam anion) to give an amine and an acyl lactam moiety (in the *N*-acyl lactam species). Since the neutralization reaction is extremely fast, the initial rate of disproportionation may be written as

$$v_d = \frac{d[NH_2]}{dt} = K_d[L]\left(K_d[ML]_0\right)^{1/2} \qquad [48]$$

The rate of disproportionation depends on several factors: nature of counter ion and reaction medium, lactam ring size, substituents, and structure of the resulting linear monomeric unit. An N-substituted lactam, for instance, may react with the lactam anion with a rate significantly higher than that of the initial reaction [46], depending on the size and the electrophilicity of the substituent (e.g., *N*-benzoyl lactams are very reactive). As a consequence, specific types of N-substituted lactams are used as activators in the activated anionic polymerization (see Section 4.14.7.4).

On this basis, the *N*-acyl lactam (imide dimer) formed in [47] is highly reactive toward the lactam anion and represents the initiating species necessary for the onset of the polymerization. In fact, while the amide linkage in the lactam monomer is not sufficiently reactive (i.e., not enough electron deficient), the presence of the exocyclic carbonyl group in the *N*-acyl lactam increases the electron deficiency of the amide group and, thus, the acylating ability.

Since the concentration of imide dimers builds up slowly, an initial induction period of very low, if any, polymerization rate is observed. As a consequence, the use of rather high reaction temperatures (255–285 °C) is required and only the more reactive lactams, such as CL, undergo polymerization by strong bases alone in a nonactivated process. As a matter of fact, the formation of the imide growing centre is the controlling step of the polymerization process. In this respect, the nonactivated polymerization can be considered as having an autocatalytic character.[48] When an acyl lactam is added at the very beginning of the polymerization, the induction period is absent[7] and the anionic ROP can be performed at much lower temperatures (e.g., for CL at 130–180 °C)

4.14.7.1.3 Propagation

The *N*-acyl lactam embodies the strongest electrophilic group in the system and the most susceptible site to be attacked by the nucleophilic lactam anion. Thus, the neutral N-acyl lactam acts as the growth centre at the chain end. Propagation proceeds, according to the free ion mechanism, by repeated nucleophilic attack of the lactam anion on the endocyclic carbonyl of the imide group, via formation of the tetrahedral bicyclic intermediate [49]:

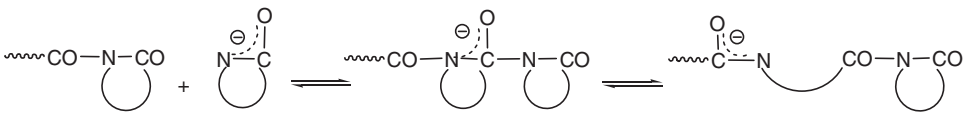

[49]

In contrast to the imide anion formed at the slow initial stage [46], the amide anion is more stable and reaction [49] is appreciably faster. The polymer amide anion participates in the ionization equilibrium with the lactam molecule, thus regenerating the lactam anion [50]:

The combination of these two reactions results in the incorporation of a monomer unit into the polymer and the regeneration of both the active end group and the lactam anion. As soon as the polyamide chain is formed, additional reversible reactions occur. The polymer amide groups may be involved in disproportionation reactions as well, forming acyl lactams and amine end groups [51]:

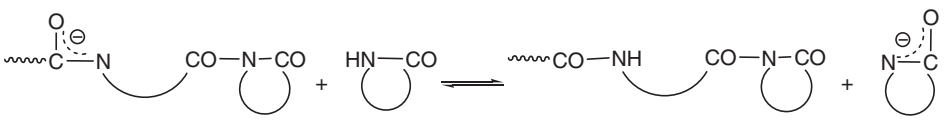

[50]

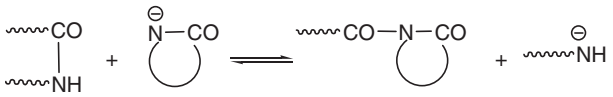

[51]

Furthermore, the presence of amide N anions along the polymer chain, derived from equilibrium reactions with lactam anions in the strongly basic medium [52], may produce diacylamines [53] and polymer branching [54]:

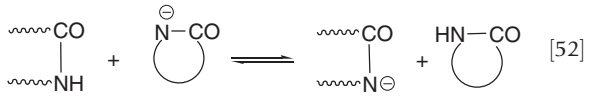

[52]

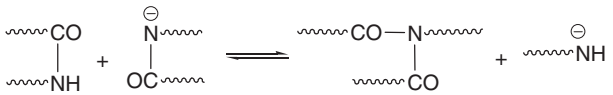

[53]

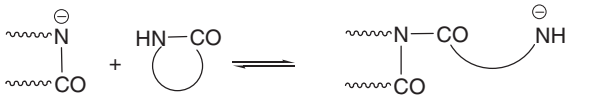

[54]

Transacylation reactions between polymer amide anions and acyl lactams (N-acylations) (Scheme 11) may cause depolymerization or incorporation of a lactam unit when the exocyclic [55] or the endocyclic carbonyl groups [56] are involved, respectively.

4.14.7.1.4 Role of counter ion

The nature of counter ion does affect not only the degree of dissociation of the corresponding lactamates but also the whole polymerization rate, entering in the propagation reactions and influencing also the extent of side reactions.[120] Indeed, aside from the free ion mechanism described above, alternative propagation pathways have been proposed involving the cation participation in ion pairs and complexes: the lactamolytic mechanism put forward by Sekiguchi[116,121,122] and the ion-coordinative mechanism suggested by Frunze *et al.*[123,124]

The lactamolytic mechanism (Scheme 12) assumes a transfer of the alkali metal cation from the activated monomer species to the imide group at the end of the growing chain and its coordination to the carbonyls of the imide [57]. The reaction proceeds via formation of an alokoxide-type anion by nucleophilic attack of the lactam anion on the endocyclic carbonyl, proton exchange with monomer, and, as the final step, rearrangement with ring opening [58]. Sekiguchi derived this mechanism from some experimental evidences. Indeed, he studied the conductivity behavior of the polymerization mixtures of CL,[125] 2-piperidone, and 2-pyrrolidone[126] and found

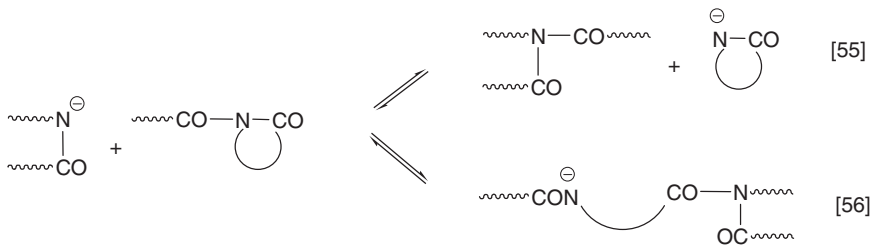

[55]

[56]

Scheme 11 Transacylation reactions between polymer amide anions and acyl lactams.

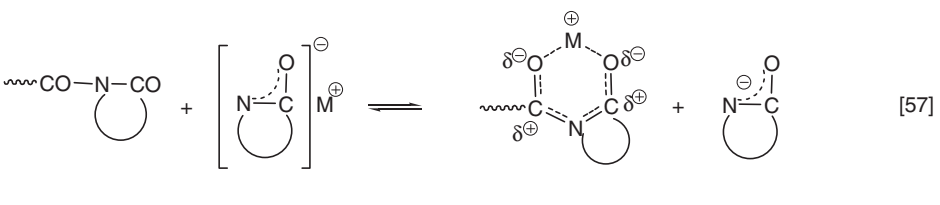

[57]

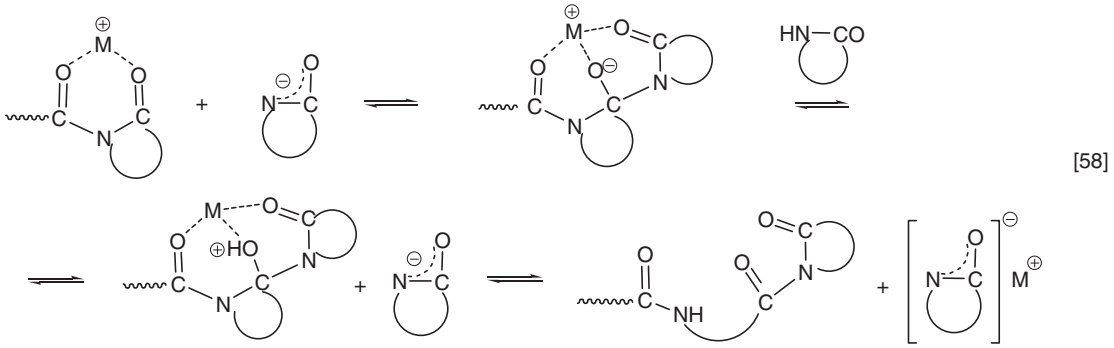

[58]

Scheme 12 Propagation pathways based on lactamolytic mechanism.

that, after the addition of *N*-acyl lactams to the lactam salts, the conductivity increased for CL and 2-piperidone and decreased for 2-pyrrolidone. The increase in conductivity has been attributed to a higher concentration of free ions resulting from reaction [57]. The coordination of the cation would increase the concentration of the free lactam anion and enhance the reactivity of the imide group to nucleophilic attack [58].

Since the ion-pair bonding is fairly weak, lactams with high dielectric permittivities (e.g., 2-pyrrolidone) are incapable of forming the complex by reaction [57]. Moreover, every condition entailing a high degree of dissociation of the lactam salts determines this reaction to be less and less important.[8] However, there are probably no simple relationships between conductivity and interaction of lactamates with growing centers, since dissimilar behaviors have been observed for different lactams.[9]

Frunze *et al.*[123] proposed the participation of ion pairs of lactam salts in the propagation step and suggested an ion-coordination mechanism. According to this mechanism, a complex between the lactamate and the two carbonyl groups of the growing center is formed (**Scheme 13**).

The contribution of free lactam anions and ion pairs would vary as a function of reaction conditions, nature of counter ion, and structure of monomer and chain end. The mechanism hypothesized by Frunze *et al.*[123] is somehow similar to that suggested by Sekiguchi, from which it differs by the fact that it does not necessarily assume free lactam anions besides ion pairs. Arguments may be formulated in support of each mechanism. However, both of them have some difficulties to accommodate all the observed phenomena in a satisfactory way. For instance, as a matter of fact, the occurring of side reactions greatly alters the course of the polymerization reaction, also preventing the formation of living polymers, which would be implied by all assumed mechanisms.

In any case, it may be asserted that free ions play a decisive role at high temperatures and in media of high permittivity, while at low temperatures and in low polar media, the involvement of ion pairs is more influential. A significant increase in dissociation (i.e., conductivity) and in the rate of polymerization of some lactams has been observed[8] by addition of the cryptand Kryptofix[2.2.2], namely 4,7,13,16,21,24-hexaoxa-1,10-diazabicyclo[8.8.8]-hexacosane (**26**) to 2-pyrrolidone and 2-piperidone:

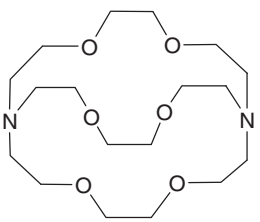

26

This effect has been shown to be more effective in media of low permittivity, which are more sensitive to a gain in dissociation. Indeed, addition of cryptand has only doubled the rate of polymerization for 2-pyrrolidone,[127] while it has enhanced the rate by two orders of magnitudes for 2-piperidone.[126] The same influence has been found in the anionic polymerization of CL conducted in THF at low temperature (25 °C).[128]

4.14.7.2 Side Reactions

Due to the high reactivity of the species involved in the anionic polymerization, a series of side reactions can take place, namely when using high polymerization temperatures and long polymerization times. The lactam anion and the propagation centers, *N*-acyl lactams and diacylamines, can initiate a variety of reversible and irreversible side reactions in which both the growth centers and the monomer anions are consumed. The strongly basic conditions, as described in this section, promote polymer branching and β-keto compounds, yielding to a considerable number of side products and chain irregularities.

The presence of side products and structural irregularities in the final polymer can be monitored by UV spectrophotometry, as most of them are able to strongly absorb in the UV region. As pointed out by Šebenda,[117] in the case of anionic PCL, the absorption maxima in the ultraviolet region between 250 and 300 nm are directly proportional to the total amount of products derived from the imide groups. Namely, most of the irregular structures arising from keto compounds are responsible for the UV absorption in that region. Therefore, an easy method to have a rough idea of the extent of side reactions in the anionic polymerization of CL is to measure the UV absorption spectra of anionic PA6, as often adopted in the literature.[46,129] It is worth emphasizing here that the fast kinetics involved in the activated anionic polymerization of CL at low temperatures, when adopting the 'very fast' activating compounds explored in the last two decades, is capable of drastically limiting the formation of by-products. In this case, indeed, the UV spectra performed on formic acid solutions of anionic PCL samples have shown the structural irregularities to be almost absent.[130]

The origin and the evolution of structures derived from side reactions have been extensively reviewed by Šebenda,[7] studying essentially the polymerization of CL in slow activated conditions. A survey of them is hereafter reported.

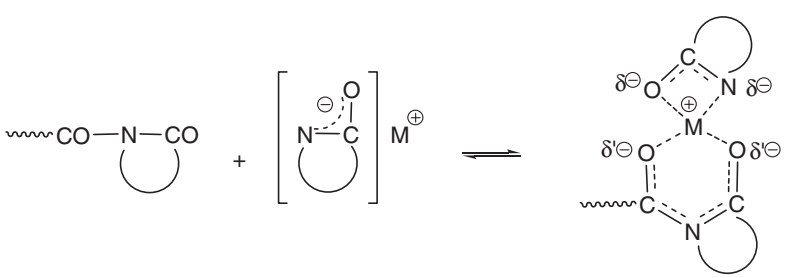

Scheme 13 Propagation pathway based on the ion-coordinative mechanism.

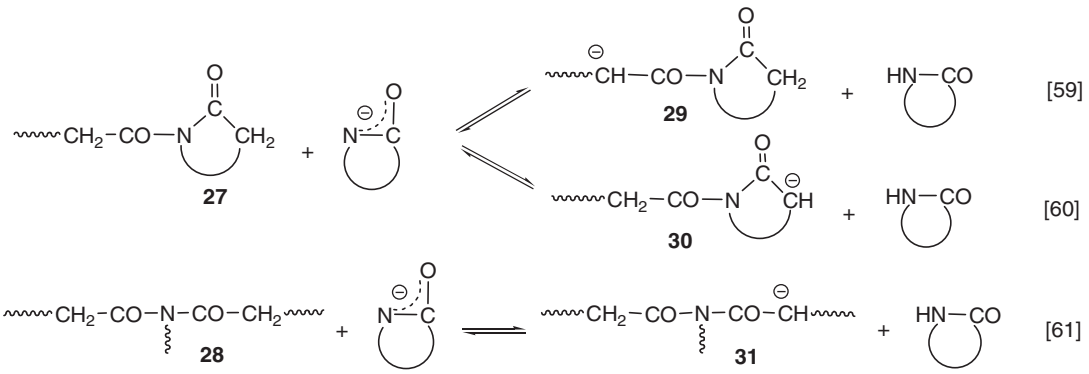

Scheme 14 Formation of carbanions.

4.14.7.2.1 Formation of carbanions

The acidity of the hydrogen atoms in α position, to the carbonyls of the imide group in the *N*-acyl lactam growth center, is comparable to that of hydrogen in the amide group. As a consequence, in the presence of a strong base (e.g., the lactam anion), the ring imide group (**27**) having at least an α-hydrogen to carbonyl, after the established equilibrium with the lactam anion (**Schemes 14**), can undergo Claisen-type condensation reactions, similar to the condensation of esters and ketones.

Analogous behavior is given by diacylamine branching points (**28**), as shown in [61]. The concentration of these carbanions is low. Nevertheless, C-acylations and, only in some specific cases, O-acylations[9] are competitive reactions with regard to the propagation step [49].

4.14.7.2.2 Formation of β-ketoimides and β-ketoamides

As shown in **Scheme 14**, three types of acid hydrogens exist, yielding to three reactive sites for C-acylation. In this respect, two are the most relevant carbonyl sites: the exo- and the endocyclic carbonyl in *N*-acylated lactams (**29** and **30**), respectively, not considering the branched structure (**31**). As a result, six (in total) or, more probably, four possibilities arise, originating six (four) different β-ketoimide structures.

The C-acylation reactions on the exo- and endocarbonyls are illustrated in **Schemes 15** and **16**, respectively. In the

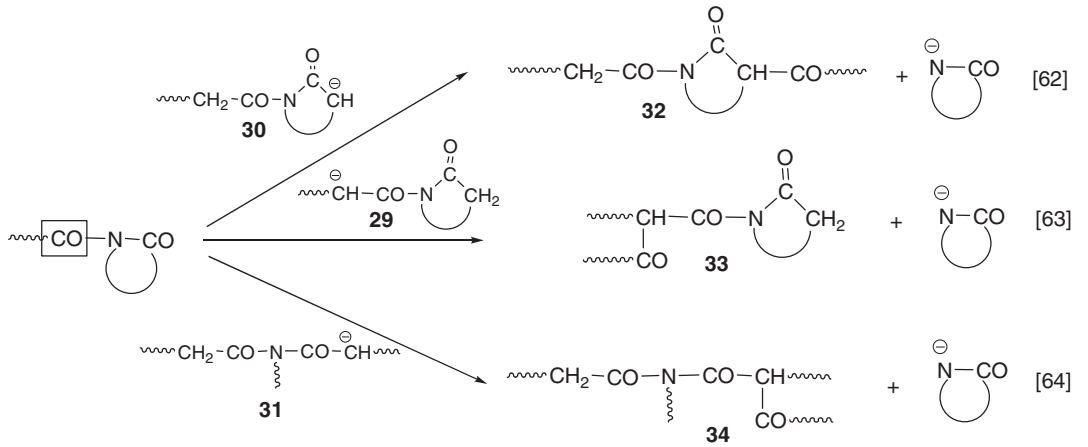

Scheme 15 C-acylation reactions on the exocyclic carbonyl group.

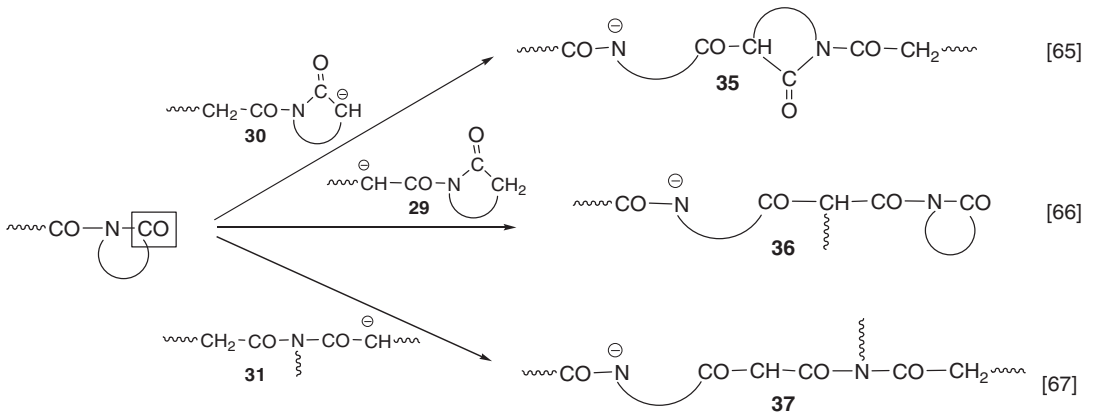

Scheme 16 C-acylation reactions on the endocyclic carbonyl group.

case of CL, the acylation of the exocyclic methylene on the endocyclic carbonyl has been reported to be the fastest.[131] Reactivities of the different acid methylenes and those of carbonyls are related to many factors:[9,127] the lactam properties (e.g., ring size and substituents), the presence and the nature of activator, the initial ratio of initiator and activator concentrations, the permittivity of the reaction medium, and the reaction temperature. The nature of counter ion may play an important role too.

The concentration of the keto groups in the polyamide depends on the initial concentrations of the catalytic components (and, thus, on the basicity of the medium), temperature, and the polymerization time. In the anionic polymerization of CL at high temperatures (250–280 °C), it has been reported[132] that approx. 0.5–1 keto groups per activator molecule (*N*-benzoyl-CL) are formed very quickly. At a low effective basicity, the majority of keto groups are formed during the first minutes, while at higher medium basicity, most of the keto groups are formed in the latter stages of the process.

For the activated polymerization of CL, conducted in THF at 25 °C (using equimolar concentration of potassium ε-caprolactamate and *N*-propionyl-CL (EtCOCL)), it has been found[131] that the rates of C-acylation ([62], [63], [65], [66]) are comparable to those of propagation [49] and the rates of N-acylation ([55], [56]) are slightly lower.

Indeed, the overall activation energies of polymerization and C-acylation reactions have been estimated to be very close (40 and 30 kJ mol^{-1}, respectively)

Neutral β-ketoimides are strong acylating agents and may be involved in a number of complex reactions, acting as growth centers and leading to either branched or linear chains. β-Ketoimides may be converted to β-ketoamides (2-oxoamides), by nucleophilic attack of the N anion on the carbonyl of the imide group, following the general scheme of eqn [68]:

[68]

In the case of reaction with the lactam anion, the *N*-acyl lactam growth centre is regenerated [69]:

β-Ketoimides and β-ketoamides decrease the concentration of active species present in the initiating system. The formation of a ketoimide structure by the Claisen-type condensation reaction consumes two molecules of the initial growth centers (*N*-acyl lactams). Moreover, both β-ketoimides and β-ketoamides having an α-hydrogen are many orders of magnitude more acid than the amide groups, due to the high resonance stabilization given by conjugation with two carbonyls. Thus, they contribute to a decrease in the concentration of lactamates (**Scheme 17**)

The final result is a decrease in both active species and the polymerization rate. As a consequence, a decrease in the rate of the imide C-acylation is observed as well. Indeed, C-acylations are initially very fast, until subsequent side reactions start to consume the β-ketoimides and a temporary equilibrium is attained.

The presence of ketoimide/ketoamide groups has been demonstrated using model experiments and also isolation of aminoketones formed by total hydrolysis of the polymer. It is noteworthy that α,α-disubstituted lactams, lacking α-hydrogens, cannot undergo this type of secondary reactions. In the case of α-monosubstituted lactams, the pattern of side reactions is fairly different: for example, the ketoimide structures obtained by the Claisen-type condensation (see **32** and **35** in **Schemes 15** and **16**) have no acid hydrogens; thus, the concentration of lactam anions is decreased at a lower rate.

4.14.7.2.3 Condensation and decomposition of β-keto compounds

Like other β-carbonyl derivatives, the β-ketoimides and β-ketoamides are very reactive under basic conditions and at high temperatures, and are considered as the key intermediates in a series of complex secondary reactions with formation of water, carbon dioxide, ketones, amines, and rather stable heterocyclic structures (**Scheme 18**).[9] Indeed, condensation reactions involving β-ketoamides [72] may lead to uracil structures (**38**), while β-ketoimides may give hydroxypyridinone structures (**39**) [73]. It is remarkable that these heterocyclic

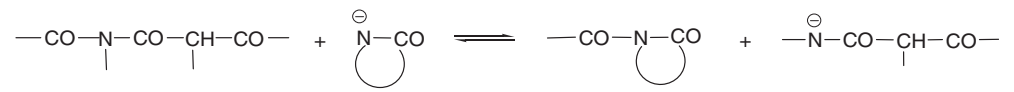

[69]

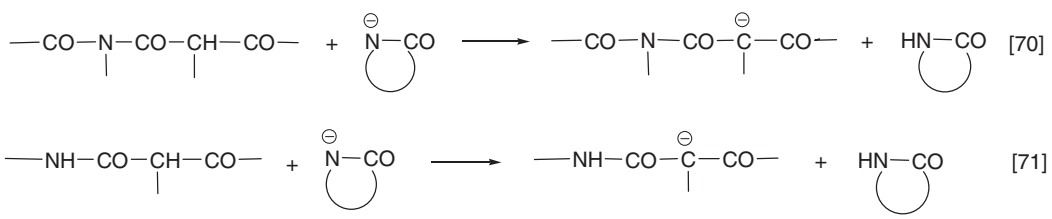

[70]

[71]

Scheme 17 Reaction of b-ketoimides and b-ketoamides with lactamate anions.

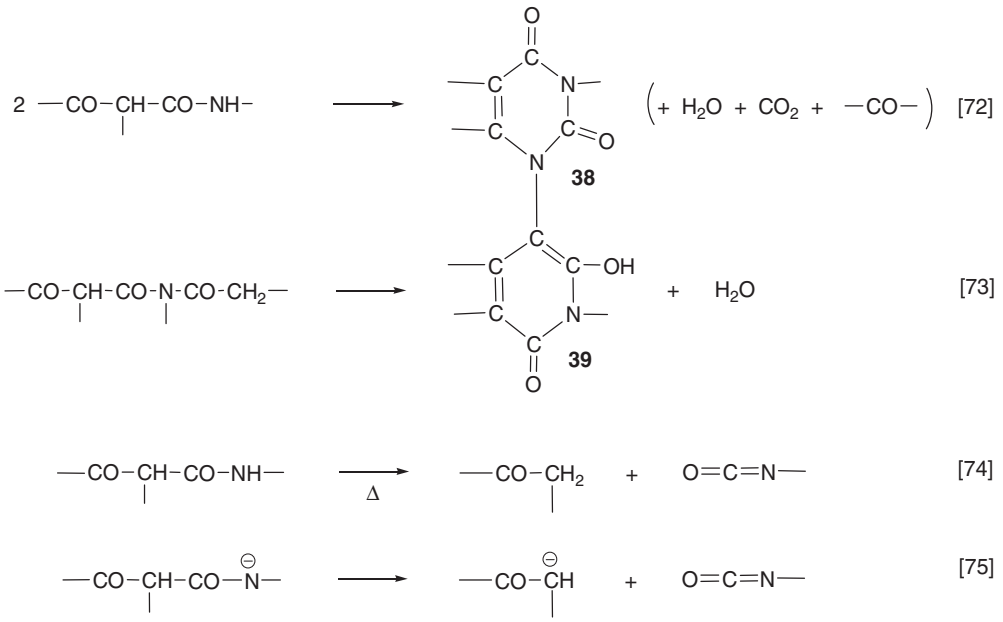

Scheme 18 Condensation and decomposition reactions of b-ketoimides and b-ketoamides.

compounds may act as branching and cross-linking points. On the other hand, the thermal [74] or base-catalyzed decomposition [75] of β-ketoamides can afford ketones and isocyanates. Isocyanates may act as efficient precursors yielding, in subsequent reactions, additional growth centers, such as *N*-acyl lactams (see Section 4.14.7.5).

4.14.7.2.4 Hydrolytic reactions

An important consequence of these side reactions is the presence of water, irrespective of the fact that anionic polymerization starts in anhydrous conditions. Water is able to hydrolyze *N*-acyl lactams, β-ketoamides, β-ketoimides, and the imide branching points via fast base-catalyzed reactions.[7] During these hydrolytic reactions, carboxylates, amine groups, ketones, carbon dioxide, and carbonate are formed (Scheme 19).

4.14.7.3 Initiators

The lactam anion in the form of lactam salt (lactamate) can be obtained by *in situ* reaction with alkali metal compounds, or prepared *ex situ* and then introduced in the polymerization mixture. Some confusion may arise about the terms often used in the literature to identify the various compounds mentioned in previous sections (initiators, or catalysts, or precursors). In this chapter, we prefer to consider the lactamate as the true initiator and the alkali metal compound as the precursor. A great number of precursors are able to generate

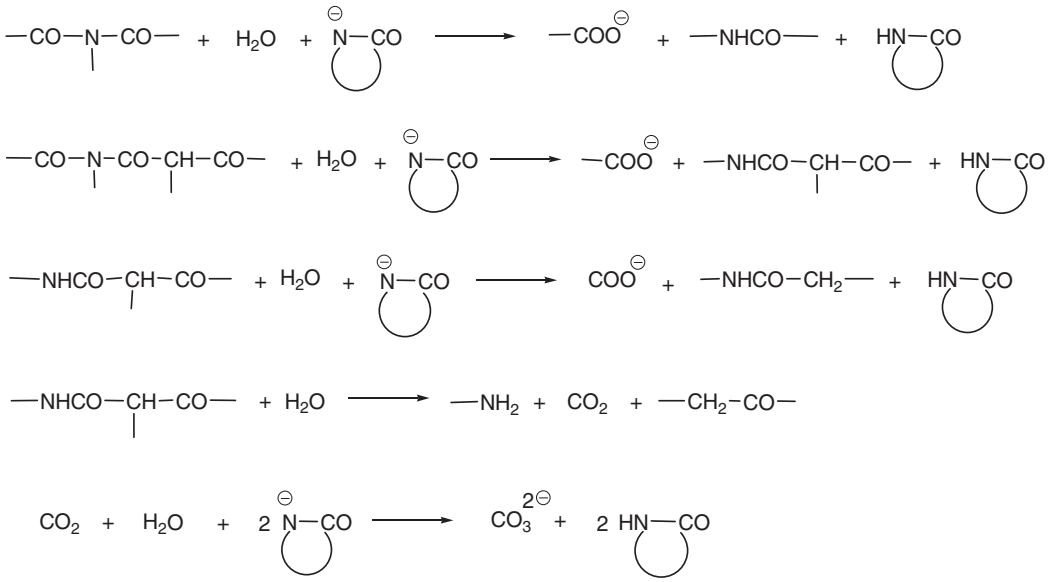

Scheme 19 Hydrolytic reactions as a consequence of side reactions.

M = Na, Li, K, MgBr, 1/2Mg
BM = NaH, CH_3ONa, $(CH_3)_3CONa$, Na_2CO_3, NaOH, KOH,
C_2H_5MgBr, $(i\text{-}C_4H_9)_2Mg$,
$NaAlH_2(OCH_2CH_2OCH_3)_2$, $LiAlH_4$, $LiAlH_n(OR)_{4-n}$, $NaAlH_nR_{4-n}$, $HAlR_2$
BH = H_2, CH_3OH, RH

Scheme 20 Initiator precursors.

lactamates (Scheme 20) and have been widely described in the literature,[8,10] essentially with reference to the polymerization of CL.

As already highlighted in the partial list of Scheme 20, various groups of compounds may act as precursors:[8] alkali metals; alkali metal hydrides, oxides, hydroxides, alkoxides, halides, carbonates; alkali metal salts of organic acids; alkyl aluminums; alkali aluminum hydrides and their alkoxides; quaternary ammonium salts; guanidium salts of lactams, etc.

The nature and concentration of the initiator play a crucial role in the nonactivated anionic polymerization, where the growing centers are formed in the slow reaction [46] between the monomer and the lactam anion bringing about the presence of some induction periods. On the other hand, the evaluation of the specific action of a given initiator in the activated lactam polymerization is more complex, since it cannot be taken in consideration apart from the activator used. It is necessary to consider here the dual system initiator/activator. It seems that the activation energy for the anionic ring-opening polymerization of CL is almost independent of the activator used,[133–135] whilst it is probably a function of the initiator nature.

At high temperatures (150–200 °C), the initial rate of activated polymerization of CL is proportional to the concentration of free lactam anions, increasing with the square root of the dissociation constant (K_d) of the lactamate.[57] For alkali metal lactamates, the value of K_d increases as a function of the electronegativity of cation. At higher temperatures (above 200 °C), the dissociation of the alkali metal lactamates (e.g., caprolactamates) is considered complete; consequently, the rate of polymerization becomes independent of the nature of the cation. Cations of transition metals (e.g., Cr^{3+}) and other metals (e.g., Al^{3+}), exhibiting high values of electronegativity, have very low dissociation constants. Thus, the corresponding lactamates hardly dissociate even at high temperatures.

Accordingly, the activity of the alkali metals follows the order of electropositivity, with the only exception of Li:

$$Na^+ < Li^+ < K^+ < Cs^+, \text{ and } Me_4N^+$$

In fact, lithium, despite its highest ionization energy, shows[46] a higher activity than does sodium as lactamate in initiating CL anionic polymerization. All quaternary ammonium salts of a given lactam exhibit more or less the same activities, decreasing only slightly with the increasing dimensions of the alkyl and/or phenyl substituents, due to restricted mobility and decreased ionization potentials:[8]

$$Me_4N^+ \geq Et_4N^+ Me_3PhN^+ > Bu_4N^+ > (PhCH_2)Et_3N^+$$

The use of sodium salt of the lactam (e.g., Na ε-caprolactamate) has been the most common choice of initiator in lactam polymerization and the most widely reported in literature. In order to prepare the sodium salt, it is possible to have the monomer reacting with Na metal or with strong bases yielding lactamates in irreversible (with NaH) or reversible reactions (e.g., with CH_3ONa, $t\text{-}C_4H_9ONa$, and NaOH). The use of the strong hydride NaH is the fastest way, implying only liberation of molecular hydrogen from the reaction mixture [76]. The use of alkoxides and hydroxides requires the removal of alcohol or water by distillation:

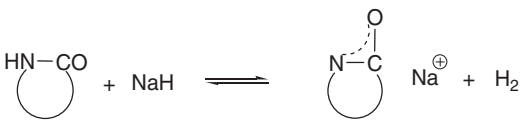

[76]

It has been reported[136] that in the nonactivated polymerization of CL, the sodium salt (CLNa) prepared *in situ* by reaction of the lactam with sodium methoxide (CH_3ONa) is less active than the sodium caprolactamate prepared *ex situ*. Heterogeneous precursor/initiator systems may be used and have been experimented. A potassium–graphite intercalate (KC24) has been compared to the potassium caprolactamate, showing that the nonactivated polymerizations with KC24 were slower, proceeded with an induction period, and gave a polyamide with low molar mass.[137]

The organomagnesium compounds, that is, the Grignard reagents, proved[138–140] to be very effective in the deprotonation of the lactam monomer giving rise to lactam magnesium bromides. They have been specifically tested in the activated polymerization and copolymerization of CL using 'fast' *N*-acyl lactam activators.[141] In recent years, CL magnesium bromide (CLMgBr) has been used more and more as initiator, for a variety of reasons, the most relevant being its stability and ease of handling as compared to sodium metal or sodium hydride as precursors of NaCL. Moreover, its lower nucleophilicity related to the $MgBr^+$ cation ends up in a better processability window, lower

level of side products, and marked suppression of cyclization reactions during polymerization that, in addition, is less sensitive to the presence of water. For these reasons, lactam magnesium bromides are widely adopted in RIM (referred to as Nylon-RIM),[142] reactive extrusion,[143] and centrifugal molding.[144]

CLMgBr can be easily prepared in laboratory by reaction of the lactam with ethylmagnesium bromide:

[77]

Due to their large use, both ClNa and CLMgBr are, at the present time, commercially available. Explanation of the activity of CLMgBr takes into account the capability of $MgBr^+$ to be coordinated to the growing center (*N*-acyl lactam, see Section 4.14.7.1.4) and form a complex with the polymer functional groups. Indeed, the complex formation between magnesium cations and amide anions in the polyamide chain minimizes or prevents cyclic oligomer formation, presumably hindering some polymer chain conformations favorable to the cyclization reaction. Namely, the formation of cyclic dimer is strongly limited or suppressed.[145] Studies on model compounds[146] seem to support the formation of coordination sites stable up to 200 °C. The coordination capability of some counterions and the complex formation between them and the monomers, on the one hand, or between them and the growing chains, on the other hand, have already been suggested in literature.[46,51,122,147]

Chemistry and kinetics of adiabatic homopolymerization and copolymerization of CL using CLMgBr, in combination with isophthaloyl-bis-caprolactam as activator, has been studied in depth.[140,148] It has been shown[148] that the value of the activation energy for homopolymerization using CLMgBr is much lower than that using sodium caprolactamate (30 vs. 73–61 kJ mol^{-1}).

By varying the lactamate counterion in the polymerization of CL, a comparison regarding the formation of side products has been made.[9] At high temperatures, the content of diaminoketone units formed during C-acylation side reactions is almost the same for sodium, potassium, and lithium ε-caprolactamate but much lower when CLMgBr has been used (**Table 8**).

When the presence of side reactions has been studied[10] in the two systems, CLNa/*N*-benzoyl-CL and CLMgBr/*N*-benzoyl-CL with or without the addition of α,ω-dibenzamido-poly (propylene oxide) (PPO), it has been shown that, in the absence of PPO, the content of side structures using CLMgBr is slightly less as compared to CLNa, while in the presence of 20 wt.% of polyether, the side reactions are almost completely suppressed.

More recently, sodium bis(2-methoxyethoxy) aluminum hydride ($NaAlH_2(OCH_2CH_2OCH_3)_2$, structure **40**, available in toluene solution under the commercial name of Synhydride©), has been extensively used in replacement of the more dangerous lithium aluminum hydride as reduction agent in the chemical industry and, specifically, in the polymerization of CL at temperatures below 170 °C:

Table 8 Content of the diaminoketone units anionic PA6 prepared at 225 °C with 0.051 mol kg^{-1} of various lactamates and 0.153 mol kg^{-1} of *N*-benzoyl caprolactam

Diaminoketone units (mol kg^{-1})				
Lactamate	*CLK*	*CLNa*	*CLLi*	*CLMgBr*
	0.044	0.043	0.040	0.019

Data from Šebenda, J. In *Comprehensive Polymer Science*; Eastmond, G.; Ledwith, A.; Russo, S.; Sigwalt, P., Eds.; Pergamon Press: Oxford, UK, 1989; Vol. 3, Chapter 35, p 511.[9]

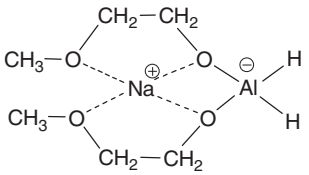

40
Synhydride

While other strong bases, such as $LiAlH_4$ and BuLi, behave similarly to NaH in the deprotonation of monomer, yielding the classical anionic mechanism previously illustrated, lithium dialkoxyaluminum hydrides behave differently. The anion obtained by the reaction of CL with lithium dialkoxyaluminum hydrides is less nucleophilic than the classical lactamate anions.[149,150] A new mechanism has been suggested[151] for this type of polymerization where different active species are involved.

According to the proposed mechanism (see **Scheme 21**), the reaction of CL with sodium dialkoxyaluminum hydride gives rise to the sodium lactamate and dialkoxyaluminum hydride $AlH(OR)_2$ [78]. Then, the reduction of the carbonyl function by the latter produces the sodium salt of 2-(dialkoxyaluminoxy)-l-azacycloheptane (**41**) [79]. The initiation [80] in the presence of *N*-acyl lactam (in activated polymerization) proceeds by nucleophilic attack of the acylated carbonyl leaving the 2-(dialkoxyaluminoxy)-l-azacycloheptane moiety at the chain end (**42**). After proton exchange with the monomer [81], the reduction of the lactamate anion immediately proceeds by displacement and concerted transfer of both the hydride and dialkoxyaluminum groups from the terminal function [82]. Following this process, the initiating species **41** is regenerated, while an acyl lactam function is reformed at the chain end (**43**). This pathway has been regarded as a new propagation step, but it is still open to discussion.

A similar mechanism has been encountered with the family of initiating species derived from metal dialkylaluminum hydrides and strong bases (NaH, BuLi) associated with reducing agents [R_2AlH, R_2BH, RMgBr, R = alkyl].[152] A few nonionic bases have been reported to initiate the ROP of lactams via the anionic mechanism. Pentamethylguanidine, in combination with the *N*-benzoyl lactam activator, is able to start polymerization of CL and η-caprylolactam.[153] Differently from what occurs using standard initiating systems, an induction period is observed. At 175 °C, the polymerization rates are appreciably lower than those

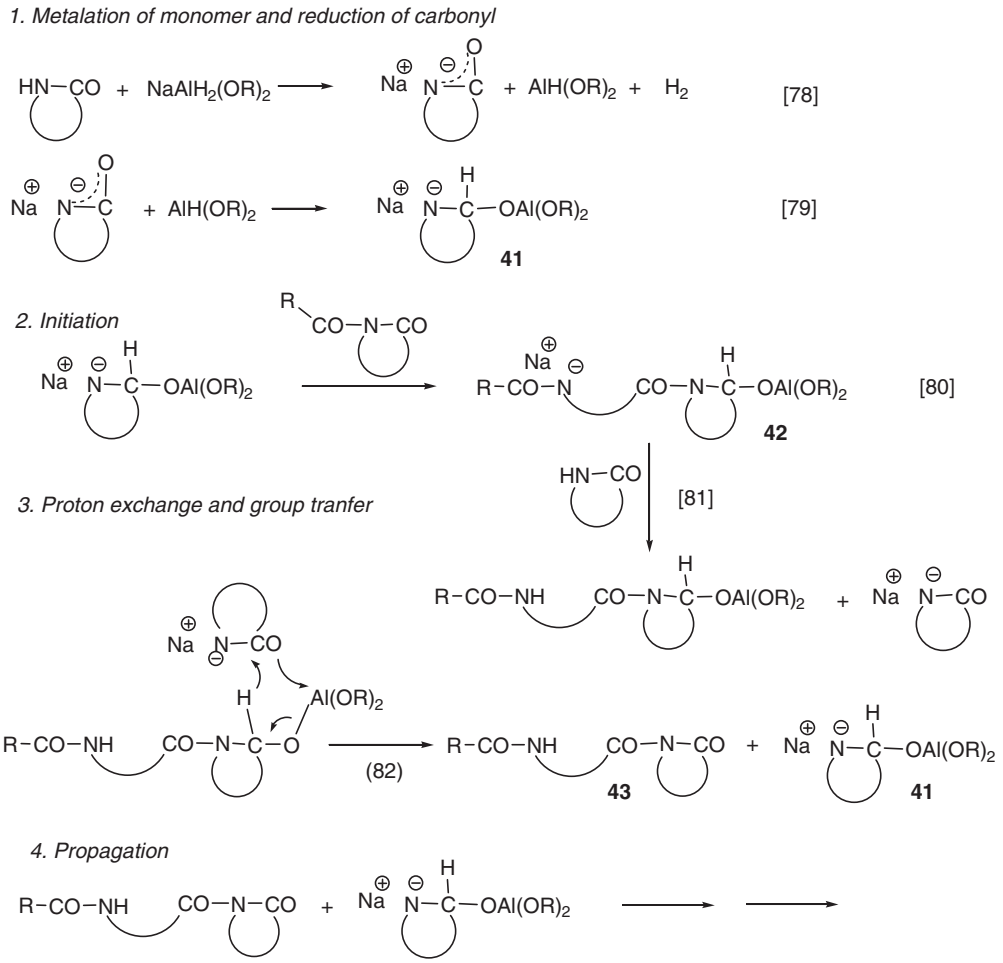

Scheme 21 Mechanism of e-caprolactam anionic polymerization initiated by Synhydride.

found in the activated polymerization of these lactams initiated by their alkali metal salts.

The unconventional nonionic species, poly(aminophosphazene)s (e.g., P4-*t*-Bu, 44) and the bicyclic 'superbase' protophosphatranes, $N[CH_2CH_2N(CH_3)]_3P$ (45), discovered recently,[154,155] have been reported to mimic the classical strong base precursors in lactam polymerization with the added advantage of the tolerance to moisture:[156]

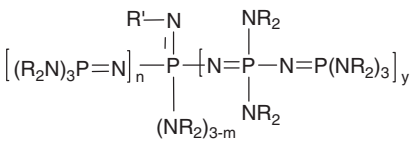

P4-t-Bu 44

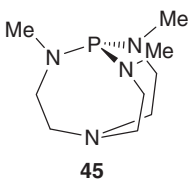

45

A detailed investigation on the ROP of CL using a poly (aminophosphazene) (the P4-*t*-Bu 44) carried out using solid-state cross-polarization magic angle spinning ^{13}P NMR (CP-MAS) showed the conversion to the protonated form of P4-*t*-Bu and the similtaneous formation of the CL anion (46):[156]

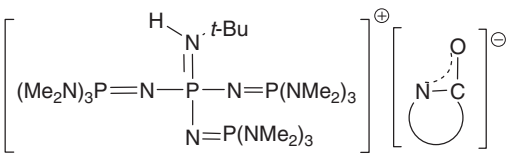

46

4.14.7.4 Activated Anionic Polymerization

The use of strong bases alone is a limiting factor in the anionic lactam polymerization since high polymerization temperatures and relatively slow reaction rates are necessarily implied; side reactions are, therefore, unavoidable. Moreover, only the more reactive lactams, such as CL and ζ-enantholactam, readily polymerize in nonactivated reaction conditions. The less reactive lactams, such as 2-pyrrolidone and 2-piperidone, are much harder to polymerize because the formation of the imide dimer is more difficult. These limitations can be overcome if the imide is generated by reaction of

the lactam with an acylating agent (e.g., an acyl chloride, anhydride, isocyanate, or monocarbodiimide).

When *N*-acyl lactam structures are introduced in the system from the very beginning of the reaction or formed *in situ* from appropriate precursors, the anionic polymerization is defined 'activated'; the rate of the initiation step is much higher and the reaction temperature can be considerably lowered.

Indeed, as already described, reaction [49] is much faster than reaction [46] by virtue of the higher reactivity of imide as compared to the amide group. When introducing *N*-acyl lactam activators, reaction [46] is no longer necessary and an immediate chain initiation is obtained:

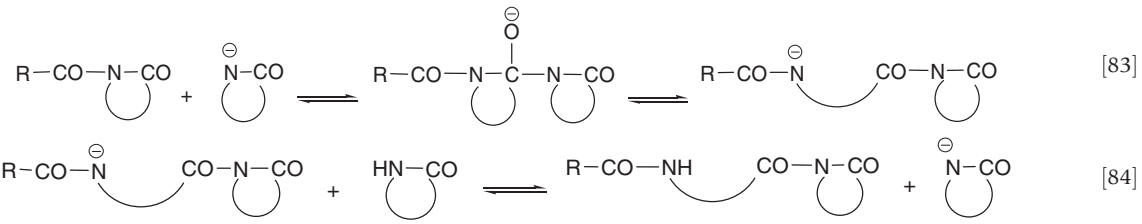

Indeed, apart from some specific effects linked to the different nature of R substituents in the acylated lactam, reaction [83] is the same as reaction [49]; consequently, the activator addition allows to avoid the slow self-initiation step, obtaining immediately the fast propagation reaction. In other words, the initiation of activated polymerization corresponds to the fast propagation step in the nonactivated lactam polymerization.

Working in milder conditions for shorter times brings about the relevant advantage to reduce or even minimize the side reactions, yielding more regular macromolecular chains. Of course, the structural quality of the resultant polymer is also a function of the specific type of activator used (Section 4.14.7.5).

In the activated anionic ROP of CL in the bulk, the short cycle times make the reaction amenable to RIM processing (Section 4.14.13.3). Furthermore, fast polymerization conditions more advantageously offer the possibility of operating in quasi-isothermal conditions using, for instance, emulsion or suspension processes where a good dispersion of the reaction heat can be easily achieved (Section 4.14.13.2).

As mentioned above, in the activated anionic ROP of lactams, the induction period is suppressed and the polymerization rates are enhanced,[7] as shown for CL in **Figure 14**. The rate of the reaction between the *N*-acyl derivatives and the corresponding lactamates significantly varies as a function of the lactam ring size. There is, for example, a remarkable difference between the activation energies relative to the reaction of CL derivatives and those pertaining to higher lactams.[131] The parameters of the Arrhenius equation for the overall consumption of *N*-propionyl lactam in the reaction with the potassium salt of the given lactam, with reference to CL, η-caprylolactam, and ω-laurolactam, are reported in **Table 9**.[127]

In general, in CL polymerization, an equivalent concentration of activator (A) (*N*-acyl lactam or *N*-carbamoyl lactam) and initiator (I), in terms of its functional groups, is the best compromise among polymerization rate, overall conversion, degree of polymerization, high polymer yield, and polyamide properties (see Section 4.14.10.3).

Monomer conversion increases with the concentration of the activator, provided that a suitable initiator concentration is chosen.[144,148,157,158] A relevant difference between nonactivated and activated processes pertains to molar masses and their distribution. In the nonactivated polymerization, the number of growth centers and polymer chains increases as long as lactam anions are present. Since the growth centers formed at the very beginning attain a higher molar mass compared to those formed in the final stage, the molar mass distribution is expected to be quite broad. At sufficiently high temperatures, at which the lactamates are completely dissociated, the final molar mass is the consequence of both the polymerization–depolymerization equilibrium and the presence of side reactions, approaching a value proportional to the square root of initiator concentration.[7]

In the activated polymerization, the number of polymer chains (N) is determined by the concentration of the activator, with the formation of additional growth centers by disproportionation being much slower [46]. In theory, apart from some deviations caused by reversibility of the reaction, the number of polymer chains would be equal to the number of activator molecules. For CL, this number can be expressed in mol kg^{-1} and calculated by

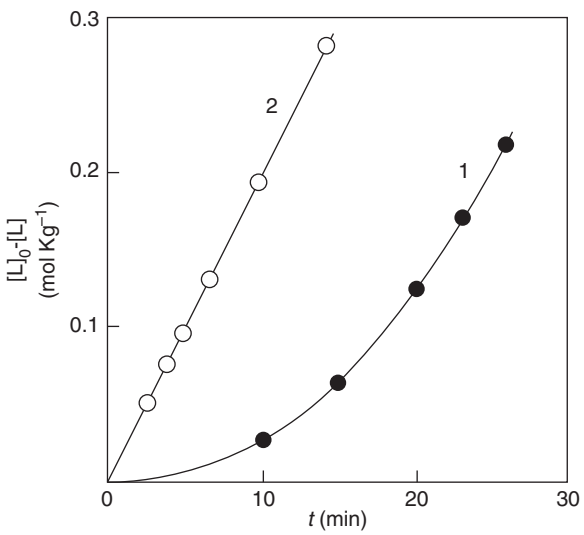

Figure 14 Anionic polymerization of CL with sodium caprolactamate (0.083 mol kg^{-1}) at 160 °C (curve 1) or with equimolar concentration of sodium caprolactamate and *N*-acetyl-caprolactam (0.0177 mol kg^{-1}) at 100 °C (curve 2). Reproduced from Šebenda, J. In *Comprehensive Chemical Kinetics*; Bamford, C. H.; Tipper, C. F. H., Eds.; Elsevier: Amsterdam, The Netherlands, 1976; Vol. 15, Chapter 6, p 379.[7]

Table 9 Activation energy (E) and pre-exponential factor (A) for the overall consumption of *N*-propionyl lactam (for L6, L9, and L12) in the given reaction with the potassium salt of lactams, at equimolar concentration (0.70 mmol l)

	E_a (kJ mol^{-1})	A
CL	40	2.8×10^4
η-Caprylolactam	107	1.2×10^{16}
ω-Laurolactam	103	9.1×10^{15}

Data from Coutin, B.; Sekiguchi, H. *J. Polym. Sci. Polym. Chem.* **1977**, *15*, 2539.[127]

$$N = 10 \cdot \gamma/\mathrm{DP}\cdot 113 \qquad [85]$$

or

$$N = 10 \cdot \gamma/M_n \qquad [86]$$

where γ is the polymer yield (in %), M_n is the number-average molar mass (in g mol^{-1}), DP is the degree of polymerization, and 113 is the CL molar mass.

Actually, the polyamide molar masses are almost always higher than the predicted values. This is mainly due to the lowering of the number of growth centers due to side reactions and to the cross-linking between polymer chains, for example, by Claisen-type condensation reactions, which are more and more relevant as the medium basicity and the polymerization temperature increase.[129] In **Figure 15**, taking the 'slow' activated anionic polymerization of CL as an example, the number of polymer molecules formed per initial activator molecule, $[N]/[A]_0$, is plotted as a function of the initiator (sodium ε-caprolactamate) concentration. This ratio has been found always to be lower than unity, that is, polymer molar masses are higher than expected on the basis of the above assumption, sharply decreasing with the increasing basicity of the reaction medium.[129] The dependence of the $[N]/[A]_0$ ratio on [I] is a straight line, which when extrapolated gives the theoretical value of 1 at the origin.

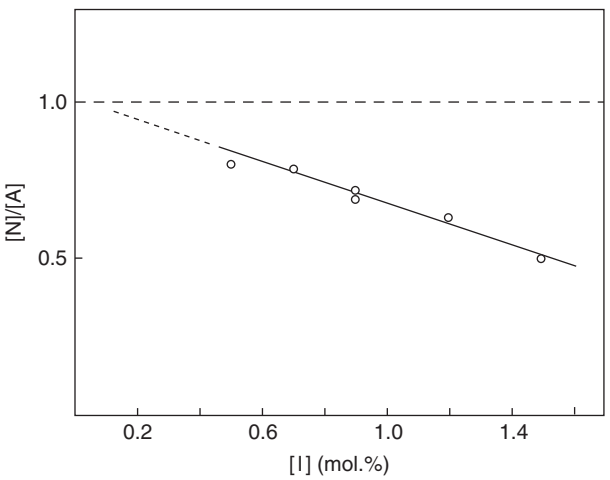

Figure 15 Number of polymer molecules (M) formed per activator molecule (A), as a function of initiator concentration, in the polymerization of CL conducted at 155 °C using equimolar concentrations of sodium ε-caprolactamate (I) and AcCL (A). Reproduced from Alfonso, G. C.; Chiappori, C.; Razore, S.; Russo, S. In *Reaction Injection Molding, Polymer Chemistry and Engineering*; Kresta, J. E., Ed.; ACS Symposium Series No. 270; American Chemical Society: Washington, DC, 1985; Chapter 11, p 163.[129]

A peculiar situation is met in the polymerization at temperatures below the melting point of the polyamide when depolymerization and side reactions are largely reduced and the disproportionation reaction is appreciably slower. In this case, even at equimolar concentrations of initiator and activator, the polymerization proceeds essentially by the reaction of lactam anions with a constant number of growth centers, resulting in a narrower molar mass distribution ($M_w/M_n < 2$).[159] Moreover, since bifunctional activators may be safely used under specific conditions without any formation of cross-linked structures, very high molar masses can be obtained.[140,159,160]

Of course, the monomer conversion, the degree of polymerization, the molar mass distribution, the presence of side reactions, and, thus, the microstructure of the resultant polymer, as already mentioned, are strictly related to the nature of the activator used (Section 4.14.7.4). It has been estimated that the rates of the first steps of propagation, C-acylation, and N-acylation of polymer amide groups (Section 4.14.7.2) depend on the nature of the exocyclic acyl group (i.e., the type of *N*-acyl lactam). In fact, it has been found[131] that, in CL polymerization in THF at 25 °C using an equimolar concentration of potassium ε-caprolactamate and EtCOCL (0.081 mol l^{-1}), the initial rate of propagation is 8.9×10^{-6} mol l^{-1} s^{-1}, that of C-acylation is 4.7×10^{-6} mol l^{-1} s^{-1}, and that of N-acylation is 3.0×10^{-7} mol l^{-1} s^{-1}. On the contrary, when using *N*-benzoyl-CL (0.055 mol l^{-1}) instead of EtCOCL, both the initial propagation and the N-acylation reactions are significantly faster, by two orders of magnitude, being 2.3×10^{-4} and 2.9×10^{-5} mol l^{-1} s^{-1}, respectively, while the rate of C-acylation remains lower (4.0×10^{-7} mol l^{-1} s^{-1}).

The introduction of 'very fast' activators, that is, *N*-carbamoyl lactams, in the above system (Section 4.14.7.5.3) has allowed to drastically reduce the polymerization time:[157,160] by choosing the appropriate initiator/activator ratio, 20–30 s is sufficient to reach polymerization completion with the attainment of a very high polymer yield. The overall polymerization time is obviously linked to the concentration of the specific activator used. Working at low temperatures for shorter times brings about the relevant advantage of reducing or even minimizing the side reactions, yielding more regular PA6 chains when compared to the use of slow activators.[160] The activated anionic polymerization, taking place in very short times, has also opened other opportunities in the vast panorama of polymer modifications. In recent years, attempts have been made to use this polymerization technique for the preparation of compatibilized blends of PA6 with other polymers (*in situ* polymerization and *in situ* compatibilization), as well as grafted copolymers starting from premade polymers with pendant functionalities such as ester, imide, maleic, or isocyanate groups acting as macroactivators (see Section 4.14.7.5.5). The main role of these functional groups on the macroactivator chain is to act as growing centers, forming *N*-acyl lactams by reaction with the lactam monomer and, subsequently, producing a graft copolymer that may be used as compatibilizer.

4.14.7.5 Activators

4.14.7.5.1 Overview

As mentioned in the previous section, an activator has the function to increase the polymerization rate supplying from the very beginning of the polymerization reaction the nonionic growth centers that start a faster initiation [83]. The activator significantly influences not only this initiation step but also the overall course of the polymerization and the whole polymerization rate.

As a matter of fact, the effects triggered by the activator are complex and hardly predictable *a priori*. Surely, remaining linked to the growing polymer chain, it can affect the reaction medium (e.g., its dielectric permittivity, and the dissociation of the initiator) and can change its basicity during polymerization favoring or limiting the side reactions (e.g., Claisen-type condensation and transamidation reactions, causing branching and cross-linking). All characteristics of the resultant polyamide can be considered strictly dependent on the nature and concentration of the activator or, better, of the dual system initiator/activator, influencing the polymer yield, the molar mass distribution, the presence of structural irregularities, the extent of cross-linking, the degree of crystallinity, and, as in the case of PA6, the polymorphism.

The number of possible activators for the lactam anionic polymerization is extraordinarily large. In Scheme 22, some examples of the various types of activators are reported. The activators can be monofunctional or multifunctional and can be divided in two main categories:

1. *Direct activators*. Compounds bearing the *N*-acyl lactam structure, that is, *N*-acyl-substituted lactams with electronegative substituents capable of increasing with the acylation ability of the endocyclic acyl group. Direct activators are essentially the *N*-acyl lactams (of general structure **47**) and *N*-carbamoyl lactams (**48**).
2. *Precursors*. Substances forming the *N*-acyl lactam functionality *in situ* by the reaction with lactam or lactam anion, thus generating the growth centers (e.g., anhydrides, acyl halides, esters, and isocyanates).

It is noteworthy that, very often, the CL derivatives (e.g., *N*-acyl-CLs) are employed as activators also in the homopolymerization of other lactams (e.g., ω-laurolactam). The activity of the activators based on N-substituted lactams generally increases with the increasing electronegativity of the substituent and is decreased by steric effects (Figure 16).

The number of polymer molecules that are formed (*N*) differs substantially for each specific activator, being much lower than the expected value of 1, due to the reduction of growth center concentration caused by side reactions (Section 4.14.7.2) When the polymerization is carried out below the polyamide melting temperature, this decrease of growth centers takes place for the most part at the beginning of the process, in the homogeneous stage. In CL polymerization initiated by 0.044 mol kg^{-1} of sodium ε-caprolactamate, $[N]/[A]_0$ is 0.82 with benzoyl-CL (BzCL) and 0.091 with phenyl-carbamoyl-CL (PCCL).[9]

4.14.7.5.2 N-acyl lactams

The *N*-acyl lactams (**47**), e.g., *N*-acetyl-CL (AcCL), N-propionyl-CL (EtCOCL), and *N*-bis-isophthaloyl-CL (IPBCL), are the first type of activators that have been used and their role on chemistry and kinetics has been examined in depth, essentially in the anionic polymerization of CL, in combination with sodium ε-caprolactamate or CLMgBr as initiator.[127,131,133,134,138,140,144,148,161–163] Obviously, the structure of the *N*-acyl lactam has a relevant influence on the polymerization rate, the side reactions, and the polymer yield. Typically, the activation energy for CL polymerization is about 70 kJ mol^{-1}.[10]

Highly electronegative substituents (e.g., benzoyl) increase the reaction rate of the lactam anion, while bulky acyl (e.g., 2,2-dimethylpropanoyl) groups decrease the reaction rate due to steric hindrance. For example, in CL polymerization, the rate of the reaction [83] with BzCL proceeds 40 times faster than that with EtCOCL.

4.14.7.5.3 N-carbamoyl lactams

By far, the *N*-carbamoyl lactams (**48**) have proved to be the most efficient activators among those investigated, acting much more rapidly than do the *N*-acyl lactams.[160] A reason is the acidity of the carbamoyl group, significantly higher than that of lactam. Examples of monofunctional activators are PCCL and cyclohexyl carbamoyl-CL (CCCL), and examples of bifunctional ones are isophorone-bis(carbamoyl-CL) (IBCCL), 4,4′-methylene-bis(cyclohexyl carbamoyl-CL) (MBCCL), 2,4-toluene-bis(carbamoyl-CL) (TBCCL), and hexamethylene-1,6-bis (carbamoyl-CL) (HBCCL) (see Scheme 22).

The *N*-carbamoyl lactam can be prepared by reaction of lactam (generally CL) with carbamoyl precursors, e.g., the corresponding isocyanates [87]:

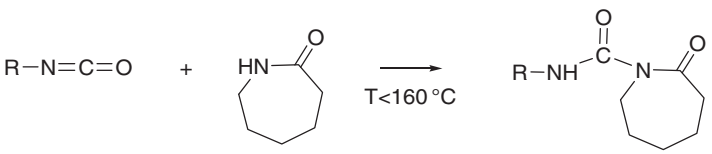

[87]

For instance, CCCL can be easily synthesized by reacting cyclohexyl isocyanate with CL under reflux in boiling anhydrous toluene and then removing the solvent by vacuum distillation. It is important to take into account that, contrary to the thermally more stable *N*-acyl-CLs, *N*-carbamoyl-CLs are

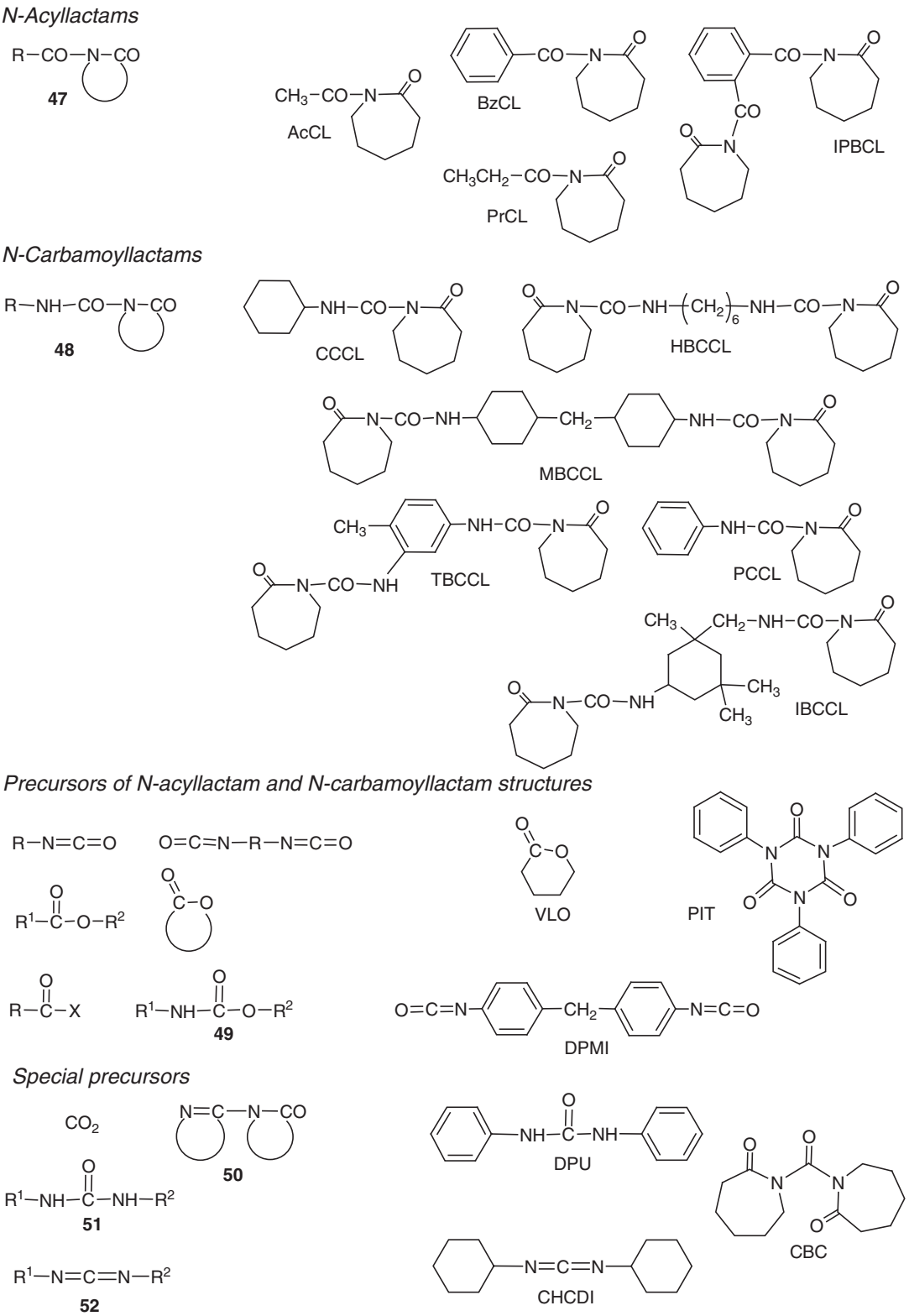

Scheme 22 Some examples of activators and precursors.

cleaved to give again free isocyanates and CL upon heating at 160–180 °C.[164,165]

Actually, it must be remarked that the isocyanate precursors (monofunctional, bifunctional, and also the trimer, PIT) can be used even directly without previous blocking with lactam, as they can react *in situ* with the monomer.[138] The propagation reaction using *N*-carbamoyl derivatives differs from that with *N*-acyl lactams in the first step (eqns [88] and [89]):

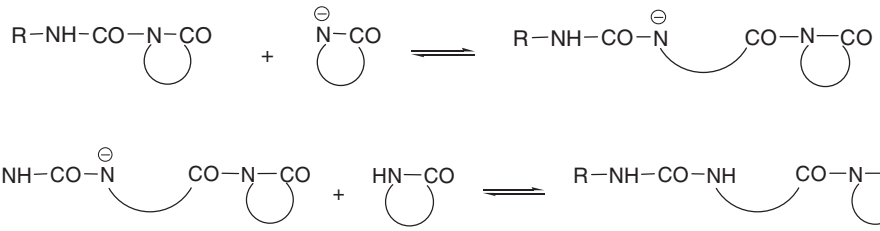

[88]

[89]

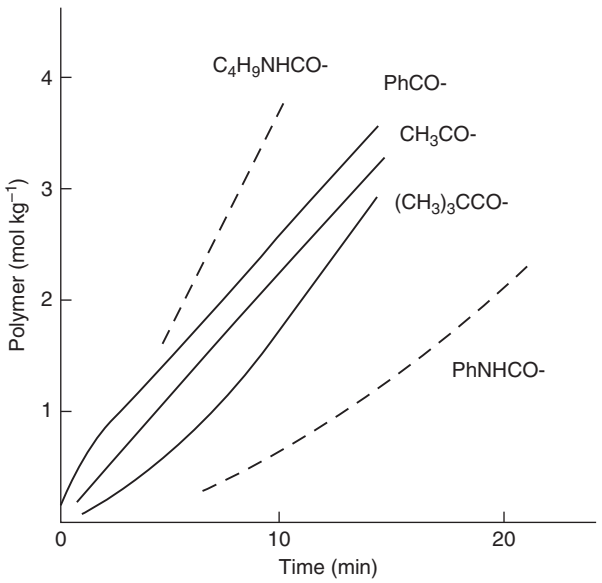

Figure 16 Effect of substituents in some *N*-acyl lactam (plain line) and *N*-carbamoyl lactam (dashed line) activators in the polymerization of CL with equimolar concentration of sodium ε-caprolactamate (0.0177 mmol kg^{-1}). Reproduced from Šebenda, J. In *Comprehensive Polymer Science*; Eastmond, G.; Ledwith, A.; Russo, S.; Sigwalt, P., Eds.; Pergamon Press: Oxford, UK, 1989; Vol. 3, Chapter 35, p 511,[9] with little modifications.

In fact, the resulting polyamide chain has a propagating end with an *N*-acyl lactam moiety and the other end with the structure of a disubstituted urea. On the contrary, using *N*-acyl lactams, the end groups are amides.

In general, aliphatic *N*-carbamoyl lactams (or aliphatic isocyanates) are more efficient activators than are their aromatic counterparts, using alkali metal ε-caprolactamates as initiators.[10] The cyclohexyl isocyanate and CCCL are indeed considered among the fastest ones.

The carbamoyl lactams can be successfully used in the 'very fast' anionic polymerization performed at relatively low temperatures, below the melting point of the resultant polyamide, in quasi-adiabatic or quasi-isothermal conditions (see Section 4.14.10 for the synthesis of PA6).

Several aliphatic carbamoyl-CLs are very fast activators and are able to reduce the polymerization time to less than 60 s for CL, even down to 18 s,[166] when the reaction conditions are optimized. With bifunctional activators, the increase of activator concentration brings about an increase of polymerization rate and conversion, as well as a major content of the cross-linked fraction.[157,167,168]

Indeed, at temperatures exceeding 160 °C, the deblocking reaction takes place, resulting in free isocyanate groups that can react with an amide functionality in the polymer chain to form a branch point (**Scheme 23**). Although these types of reactions occur for both mono- and difunctional carbamoyl-CL activators, the effect is more significant with difunctional activators owing to the fact that all chain ends remain active after

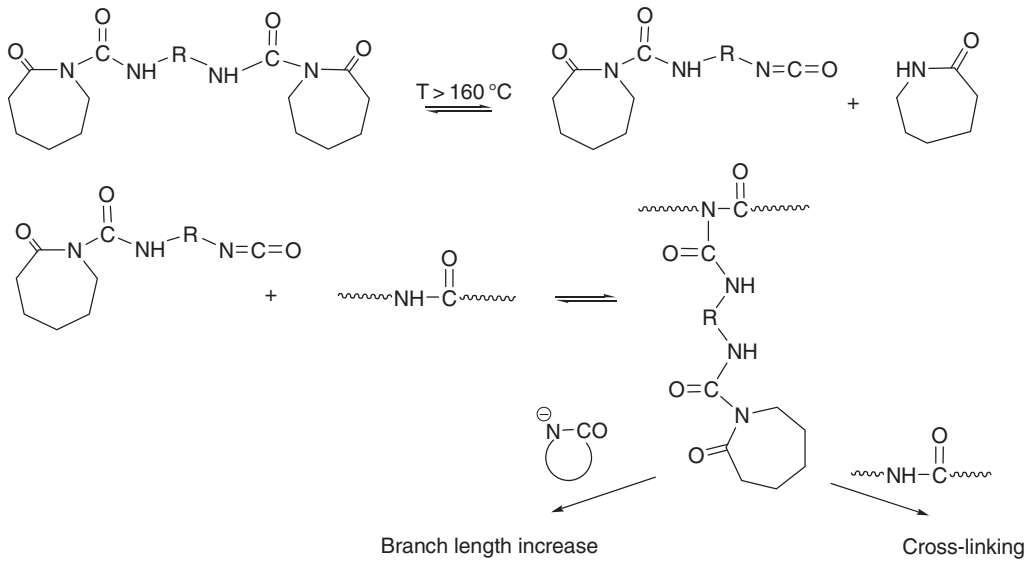

Scheme 23 Deblocking reaction and branch point formation.

branching enabling a further branch growth and a second branching reaction, resulting at the end in a 3D network structure.

The cross-linked fraction in anionic PA6 (determined as the percentage of polymer insoluble in 2,2,2-trifluoroethanol) increases with the increasing concentration of the bifunctional activator and with the [A]/[I] ratio, for example, when using the system HBCCL/CLNa. At the concentration ratio 0.60/0.30 (in mol.%), ~85% of cross-linked PA6 has been found, while at 0.45/0.90 and 0.15/0.60, the values were 9.7% and 3.5%, respectively.[157]

CCCL has been found to be particularly suitable for the anionic polymerization of CL in isothermal conditions at 150–170 °C, resulting in a PA6 in very high yields and almost completely free of structural defects (Section 4.14.10).[130] Indeed, the UV absorbance of PA6 prepared using CCCL as activator has shown a much lower content of structural irregularities and side products compared to those synthesized with other *N*-carbamoyl-type activators (**Figure 17**).

4.14.7.5.4 Precursors and special activators

4.14.7.5.4(i) Carbonyl bis-caprolactam

An isocyanate-free route to obtain carbamoyl derivatives implies the use of carbonyl bis-caprolactam (CBC®), a nontoxic solid compound commercialized by DSM and generally used as chain extender, coupling, and cross-linking agents.[169,170]

At temperatures around 100 °C, carbonyl bis-caprolactam can react with a primary amino group to give CL and *N*-carbamoyl-CL:[171]

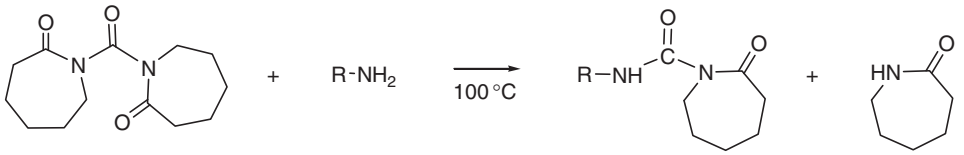

[90]

The carbonyl bis-caprolactam has been successfully employed for the first time as activator in CL polymerization in the 1990s by Mateva *et al.*[172–174] in combination with sodium ε-caprolactamate as initiator, for the production of PA6 and its copolymers. CBC capability as coupling agent also allows the preparation of hybrids, for example, inserting polyhedral oligomeric silsesquioxanes (POSS) in the PA6 matrix (POSS-PA6) by anionic polymerization.[175]

4.14.7.5.4(ii) Carbon dioxide

Carbon dioxide too has been used as activator in anionic lactam polymerization. In particular, it has been successfully employed in the polymerization of 2-pyrrolidone by Roda *et al.*[176,177] The introduction of gaseous CO_2 into the polymerization feed containing monomer and initiator causes the formation of two possible carboxylate growth centers, an N-carboxylate or an O-carboxylate (carbonate) [91], being not yet clarified which one has to be considered the most probable:

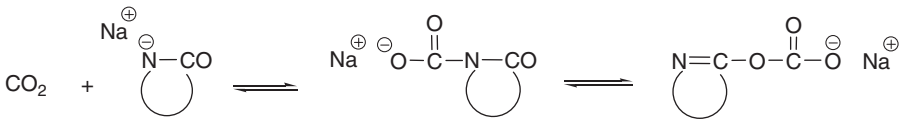

[91]

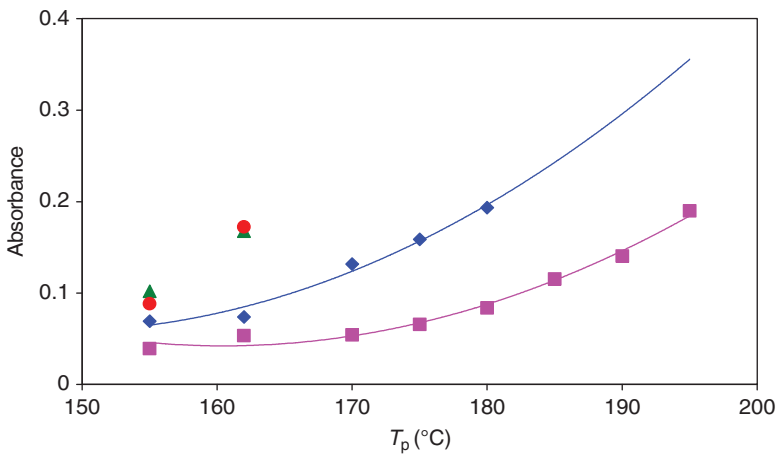

Figure 17 UV absorbance at the band maximum (270–280 nm) for polyamide samples polymerized using the following: ■, CCCL; ◆, HBCCL; ●, MBCCL; and ▲, IBCCL. Reproduced from Ricco, L.; Russo, S.; Orefice, G.; Riva, F. *Macromolecules* **1999**, *32*, 7726.[130]

4.14.7.5.4(iii) N-iminolactams

Lactam anionic polymerization can be accelerated also by the addition of *N*-iminolactams (**50**), which have proved to exert a more efficient activity compared to carbon dioxide. A number of derivatives containing the acylamidine structure have been synthesized and tested, such as 1-(1-pyrrolin-2-yl)-2-pyrrolidone (**53**), 1-(1-azacyclohept-1-en-2-yl)-2-pyrrolidone (**54**), 1-(1-azacyclohept-1-en-2-yl)-1-azacycloheptan-2-one (**55**), and 1-(1-azacyclonon-1-en-2-yl)-2-pyrrolidone (**56**):

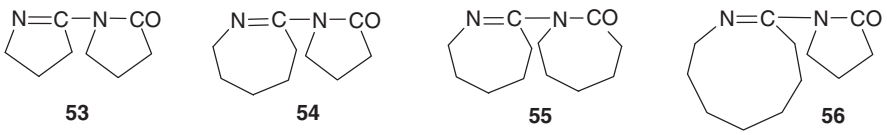

53 **54** **55** **56**

All of them have been studied in the anionic polymerization of CL, initiated with alkali metal lactam salts,[178] and have found a more suitable application in the polymerization of 2-pyrrolidone at 30–50 °C, initiated by potassium 2-oxopyrrolidin-1-ide.[179,180]

4.14.7.5.4(iv) Carbamates

Carbamates (**49**) can also be used as activators, yielding the *N*-carbamoyl lactam structure by reaction with lactamate (**Scheme 24**). The reaction has shown to hold an activation energy of 90 kJ mol^{-1}, comparable to that of *N*-acyl lactam and an order of magnitude lower than that of *N*-carbamoyl lactams.[10]

4.14.7.5.4(v) Esters and lactones

Aliphatic and aromatic esters show an activation effect in the anionic lactam polymerization[161,181] through a fast acylation of the lactam anion (already at 150 °C) with the formation of the corresponding *N*-acyl lactam growth center and of an alkoxy anion as by-product [92]. The reaction is followed by neutralization of the alkoxy anion [93]:

[93]

Similarly, lactones behave as efficient activators [94],[182] generally more active than the linear esters, with an apparent activation energy of about 80 kJ mol^{-1}:

[94]

However, it must be taken into account that, in this case, the *N*-acyl lactam moiety acts as a growth center for the lactam polymerization, while the oxy-anion can initiate the lactone polymerization. Indeed, some lactones behave as activators if present at concentrations of up to 5 mol.%, while they act as comonomers at higher concentrations yielding copolymers poly(ester-co-amide)s (**57**) (Section 4.14.12.3):

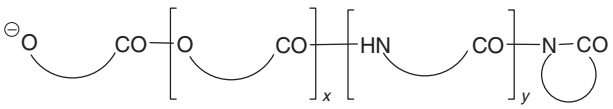

57

It has been demonstrated[181] that δ-valerolactone (VLO) and ε-caprolactone (CLO) are converted into the corresponding

[92]

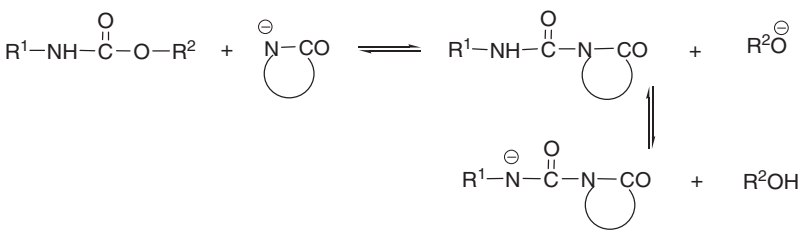

Scheme 24 Reaction of carbamates and lactamates.

homopolymers in the first stage of the polymerization process and it is the ester group of the polyester chain that reacts with CL generating the growth centers for the formation of polyamide chains. Indeed, it is possible to accomplish the CL polymerization in the presence of poly(ε-caprolactone), acting with the esters groups in the macromolecular chain acting as indirect activators via transacylation reactions:[183]

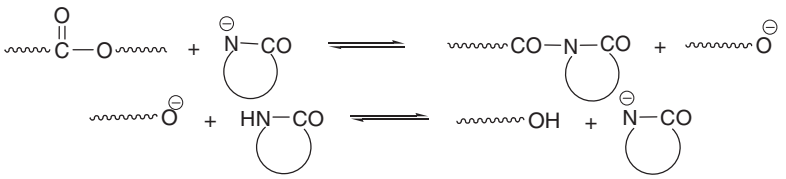

[95]

[96]

With VLO and CLO, the polymerization has been shown[181] to proceed via a pseudo-living character (proved by the linear dependence of the degree of polymerization on the degree of conversion) and has been explained by the unusual balance between growth center formation, chain propagation, and side reactions. It has been calculated that less than 15% of the originally introduced lactone was responsible for the growth center formation.

A different behavior is correlated with the use of γ-butyrolactone, which does not homopolymerize and acts as a classical activator leading to a slower polymerization, lower polymer yield, and lower degrees of polymerization, mainly due to the presence of side reactions and the absence of transacylation reactions.[181]

It is noticeable that using the above lactones (e.g., VLO and CLO) as activators in the polymerization of CL, high degrees of conversion and high degrees of polymerization are achieved even for a 10-fold excess of activator over initiator (e.g., CLMgBr).[181]

4.14.7.5.4(vi) *N,N′-disubstituted ureas*

Disubstituted ureas (**51**), such as *N,N′*-diphenylurea (DPU), *N*-butyl-*N′*-phenylurea, and *N,N′*-dibutylurea, can be present in the anionic polymerization of CL either as additional activators referred to *N*-acyl lactams or as individual activators.[184]

As a matter of fact, urea moieties, as already mentioned, are present in anionic polymerizations activated by *N*-carbamoyl lactams or their precursors and in the synthesis of block copolymers when NH_2-terminated prepolymers are functionalized by isocyanates. When the substituted ureas are used as activators, two initiation mechanisms are possible. In the first route (**Scheme 25**), the thermal dissociation of the urea gives amine and isocyanate, followed by addition of the latter to lactam:

while in the second route (**Scheme 26**), the urea directly produces acylation of the lactam (or the lactam anion):

The number of reactions involved by *N,N′*-disubstituted ureas in the anionic polymerization of CL is relevant and their effects on the resulting polyamide are complex. The rate of the urea-activated process is an order of magnitude lower than that activated by *N*-acyl lactams.

It has been found[184] that in the case of CL, using its sodium salt as initiator and ureas as activators, the polymerization rate increases with the increasing relative acidity of the latter. The acidities of the dialkylureas are similar to that of the monomer, while those of aromatic ureas are much higher. Thus, the polymerization rates change following the sequence: *N,N′*-diphenylurea > *N*-phenyl-*N′*-butylurea > *N,N′*-dibutylurea.

It is remarkable that, contrary to what typically happens when using *N*-acyl lactams and *N*-carbamoyl lactams, the number of polymer chains formed from each urea molecule has been found to be in all cases higher than unity, being approximately 1.3, thus showing that additional growth centers are generated.

Interesting results have been attained using urea as an additive in the anionic polymerization of CL activated by AcCL: a strong acceleration of the polymerization rate has been

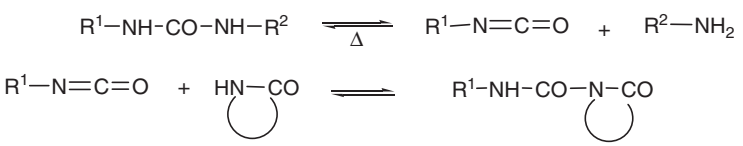

Scheme 25 Thermal dissociation of substituted ureas and subsequent blocking of isocyanate group.

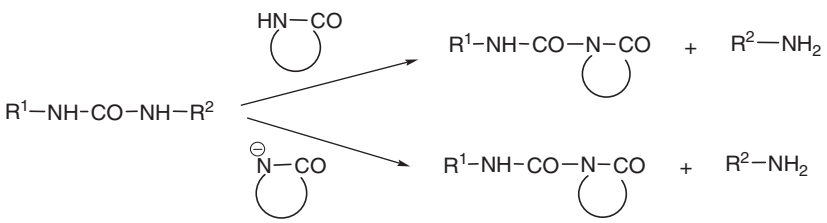

Scheme 26 Direct acylation of lactam or lactamate by substituted ureas.

observed, more than would have been expected from their independent activity. This synergistic effect has been ascribed to both the suppression of side reactions by controlling the system basicity (due to the urea intrinsic acidity) and the formation of additional growth centers.[184]

4.14.7.5.4(vii) Carbodiimides

Carbodiimides (**52**) have been used in a stable liquid system[185] in which the activator (e.g., the N-cycloalkyl carbodiimide, CHCDI) and the initiator (e.g., sodium ε-caprolactamate) are present in an aprotic solvent (e.g., 4,4,5-trimethylimidazolidin-2-one) and mixed with the monomer during processing. Such a system has the major advantage of permitting prolonged storage of the reactants and is particularly well suited for the liquid molding of polyamide composites. It has been successfully employed in the polymerization of ω-laurolactam (Section 4.14.11.3).[186]

The reaction between the above carbodiimides and the sodium caprolactamate takes place in part in the liquid system, producing a resonance-stabilized guanidine anion (Scheme 27). In the initiation of the polymerization, the guanidine anion reacts with the lactam monomer by a proton exchange reaction giving the lactam anion, the actual polymerization initiator. Then, acylation of lactamate occurs, causing cleavage of the CO–N bond with ring opening and reformation of the N anion in the guanidine derivative. The strong resonance stabilization of N anions favors the addition of monomer. Then, repeated proton exchange reactions and nucleophilic additions constitute the subsequent propagation step.

4.14.7.5.5 Macroactivators

When a functional group capable of behaving as an activator or a precursor is linked to a polymer chain, the latter is identified as macroactivator or polymeric activator. The anionic polymerization of lactams using macroactivators is a suitable method for the synthesis of block copolymer (Section 4.14.12.4) incorporating, for example, soft blocks in the main polyamide block. Hydroxy-terminated polymers, such as polyethers (e.g., PPO) with terminal –OH groups, can be reacted with diisocyanates (e.g., isophorone diisocyanate) leaving a free isocyanate group linked to the polymer. This isocyanate-terminated polymer can be used directly as macroactivator or may be previously blocked by reaction with CL to obtain the carbamoyl lactam derivative (**60**):

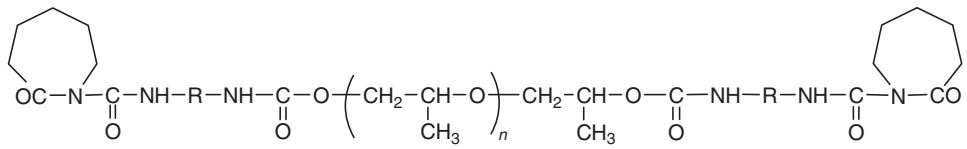

60

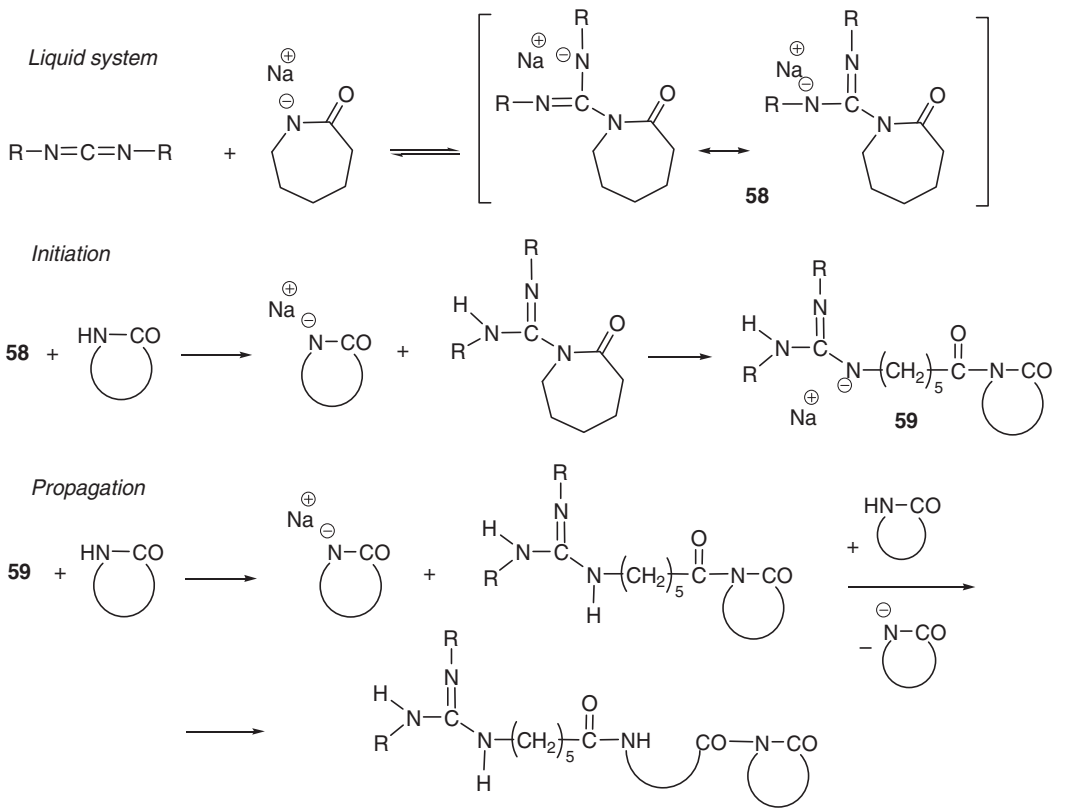

Scheme 27 Reaction pathway of the carbodiimide – sodium caprolactamate liquid system.

Following a similar approach, various polymeric activators bearing pendant functionalities can be synthesized in order to give rise to graft copolymers. For example, a macroactivator with pendant ester,[187,188] or imide,[189] or isocyanate,[190] or maleic anhydride groups[191] can be prepared in order to obtain the growth of grafted polyamide chains onto the macroactivator backbone. In another example, in order to obtain a PS-*g*-PA6 graft copolymer, a macroactivator formed by an isocyanate-bearing polystyrene (PS) backbone has been prepared using a copolymer of styrene and 3-isopropenyl-α,α-dimethylbenzene isocyanate, synthesized by radical polymerization.[192] To overcome the drawbacks associated with to the use of isocyanates, the synthesis of a macroactivator with pendant *N*-carbamoyl lactam moieties seems a better method. Following this approach, poly(methyl methacrylate) (PMMA)- or PS-based macroactivators have been prepared by copolymerization with comonomers bearing *N*-carbamoyl caprolactam functionalities **(61)**:[193]

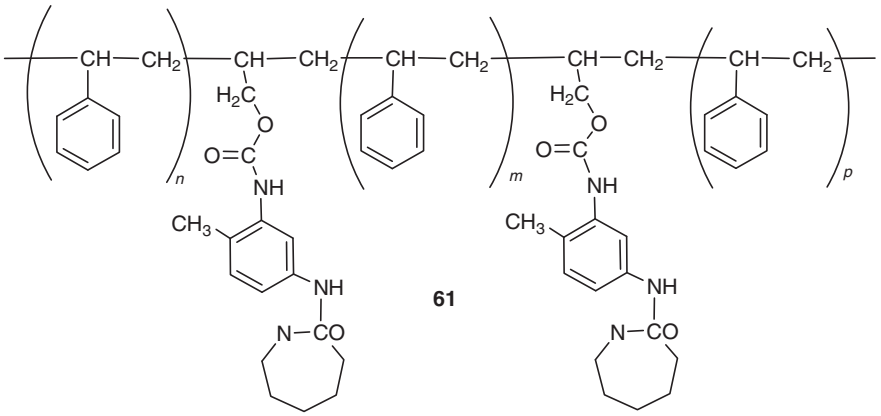

61

4.14.8 Enzymatic Polymerization

Poly(β-alanine) (PA3) cannot be obtained by chemically initiated ROP of the unsubstituted azetidin-2-one (β-lactam), but only by anionic isomerization polymerization of acrylamide.[194] The latter synthesis, however, generally leads to structurally irregular polyamide 3.[195] On the contrary, the polymerization of β-lactams may be accessible by novel enzymatic routes.

Enzymatic polymerization has emerged in the last few decades as a field of considerable interest and commercial promises. It proceeds with high regio-, enantio-, and chemoselectivity under relatively mild conditions. So far, enzymes have been used to synthesize polyesters, polysaccharides, polycarbonates, polyphenols, polyanilines, vinyl polymers, and poly(amino acid)s.[196,197] Namely, the lipase B of *Candida antarctica* (Cal-B, a serine hydrolase) immobilized on polyacrylic resin (Novozyme 435) has proven to be a very versatile catalyst in terms of reaction conditions and acceptance of various substrates. For example, this enzyme has been successfully used to synthesize polyesters.[198–202] However, little has been reported so far on the synthesis of polyamides catalyzed by enzymes.[203]

The enzyme-catalyzed ROP of azetidin-2-one to give unbranched poly(β-alanine) has only recently been achieved.[204] The synthesis has been conducted in toluene at 90 °C using Cal-B, immobilized on Novozyme 435 [97]:

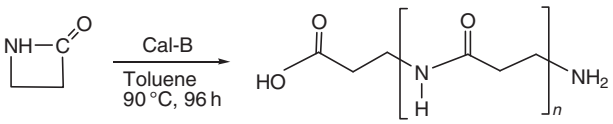

[97]

Linear poly(β-alanine) of low molar mass has been obtained. The rather low-average DP of the polymer (DP = 8) has been related to its poor solubility in the reaction medium. The proposed mechanism (**Scheme 28**) involves the participation of water. Indeed, although the reaction is carried out under essentially anhydrous conditions, water is never removed completely, as it is always present as the structural water of the enzyme.

The polyamide formation initially follows the enzymatic acylation of Ser105 by β-lactam. The reaction of the acyl-enzyme intermediate with water releases β-alanine, and the reaction with the growing oligomer yields poly (β-alanine). It has been shown that this mechanism is applicable only to ß-lactam and not to ß-alanine polymerization.[205]

4.14.9 Spontaneous Polymerization

The spontaneous polymerization of lactams, also referred to as 'autopolymerization', identifies the process in which no initiator is intentionally added. It has been observed to occur only at high temperatures and proceed at very low reaction rates. Purified anhydrous CL has been reported to start a slow polymerization after heating for a considerable time above 250 °C.[206]

The same is valid also for η-caprylolactam at 240 °C[207] and ω-laurolactam at 280 °C.[208] The polymerization mechanism has not been completely clarified and many doubts yet remain on the consistency of the hypothesis that has been postulated. Amine groups and structures easily hydrolyzable to carboxyl groups (e.g., imides) have been found to be present in the polymerization product.[207] A considerable amount of cyclic oligomers have also been detected. Aminoacyl lactams, formed

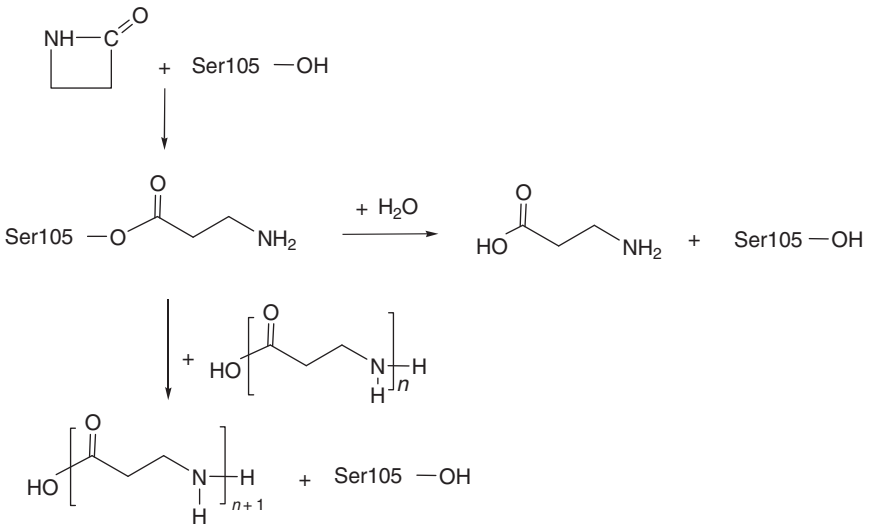

Scheme 28 Reaction pathway in the enzymatic formation of poly(b-alanine) from unsubstituted azetidin-2-one.

by a disproportionation reaction similar to that occurring in the cationic polymerization, have been assumed to be present.[209] Polymerization has been suggested to proceed by bimolecular aminolysis of aminoacyl lactams and/or aminolysis of lactams. The intramolecular cyclization of the aminoacyl lactams has been assumed to give rise to the cyclic oligomers. The activation energies for the autopolymerization of CL, η-caprylolactam, ω-laurolactam, and for the autocopolymerization of the pair CL–ω-laurolactam have been calculated.[210]

However, it must be underlined that a small amount of water still remains in lactam monomers even after a drying procedure. This content of residual water may be the agent able to initiate lactam polymerization.[211]

4.14.10 Anionic Polymerization of CL

4.14.10.1 Overview

The anionic lactam polymerization will be herein described with reference to the most important and most studied member of the class, CL. Since its discovery, CL anionic polymerization has been explored in depth under a great variety of experimental conditions that very strongly affect the development of the reaction and the characteristics of the resultant polymer. The complexity of the role played by the various reacting species and their mutual influence, together with the effects of both the polymerization temperature and the reaction rate on kinetic evolution and established equilibria, has not enabled so far to draw a clear and general picture of CL anionic polymerization, especially when it is carried out in bulk. A first classification of its polymerization can be based on the overall kinetics of the reaction, which can be depicted as 'very fast', 'fast', or 'slow' depending on somewhat arbitrary evaluations. Generally speaking, it can be assumed that a 'very fast' polymerization reaches completion in less than 60 s, while a 'slow' process can take several minutes and even some tens of them. 'Fast' polymerizations are those running for intermediate times, that is, ~1–2 min. Several factors can influence the polymerization rate of CL in the bulk: (1) nature of activator and its concentration; (2) nature and concentration of initiator; (3) initial polymerization temperature T_0; and (4) isothermal, nonisothermal, or adiabatic conditions, with the specific temperature profiles of these latter. 'Very fast', 'fast', or 'slow' processes, on the other hand, strongly affect structure and properties of the resultant anionic PA6. Namely, a proper choice of the initiating pair (activator and initiator), together with suitable experimental parameters ($T_0 \leq 170\,^{\circ}C$, quasi-isothermal conditions), allows to obtain PCL almost completely free of structural defects, such as branching or cross-linking, and color centers.

The activated polymerization of CL, carried out in the bulk, can run almost adiabatically due to the high rates and the poor heat exchange with the surroundings. A temperature rise of up to 52 °C is theoretically predicted and experimentally observed when polymerization starts at 150–155 °C and is followed by crystallization.[11] In quasi-adiabatic conditions, with 'very fast' activators and a starting temperature of ~155 °C (increasing up to ~205 °C), low residual monomer content, low cyclic oligomers, and high molar masses of the resultant polyamide have been achieved.[160] Since the occurrence of side reactions, such as Claisen-type condensations (Section 4.14.7.2), is not only caused by the strong basicity of the reaction medium but also highly favored by the temperature increase due to the lack of dispersion of the polymerization heat, much more interesting results have been obtained by the 'very fast'-activated polymerization run in quasi-isothermal conditions.[130]

Indeed, in quasi-isothermal polymerization processes carried out at relatively low temperatures (150–160 °C) with 'very fast' activators, the presence of side reactions is minimized. A comparison of different polymerization processes, using various types of activators is shown in **Table 10**. The polymerization times and the UV absorbances (Section 4.14.7.2) of polymers synthesized using various types of activators (i.e., slow, fast, and very fast) are reported.

The high reaction rates derived from the use of 'very fast' activators made it possible to realize a quasi-isothermal

Table 10 Polymerization times and UV absorbances referred to PCL synthesized under different polymerization conditions

Process	Activator (A)		Polym. Temperature (°C)	Polym. Time (s)	Absorbance[a]	[I][b] (mol/100 mol CL)	[A]	References
	Type of activity	Name						
Hydrolytic			270	8.4×10^5	0.044			160
Anionic quasi-adiabatic	Slow	AcCL	155 → 205	356	1.160	0.2	0.6	160
Anionic quasi-adiabatic	Very fast	CCCL	155 → 205	36	0.520	0.6	0.6	160
Anionic quasi-adiabatic	Fast[c]	HBCCL	155 → 205	60		0.6	0.3	157
Anionic quasi-adiabatic	Fast[c]	HBCCL	155 → 205	24		0.9	0.45	157
Anionic quasi-isothermal	Slow	AcCL	160	~300	0.940	0.8	0.8	160
Anionic quasi-isothermal	Slow	PIT	160	160	0.500	0.8	0.8	160
Anionic quasi-isothermal	Very fast	CCCL	160	~30	0.071	0.8	0.8	160
Anionic quasi-isothermal	Very fast	CCCL	160	d	0.070	0.6	0.6	160
Anionic quasi-isothermal	Very fast	CCCL	160	d	0.141	0.6	1.0	160
Anionic quasi-isothermal	Very fast	CCCL	170	d	0.129	0.6	0.6	160
Anionic quasi-isothermal	Very fast	CCCL	180	d	0.211	0.6	0.6	160
Anionic quasi-isothermal	Very fast[c]	HBCCL	155	d	0.069	0.6	0.3	130
Anionic quasi-isothermal	Very fast	CCCL	155	d	0.039	0.6	0.6	130

[a] Optical density at Imax in the region 270–280 nm.
[b] Initiator (I): NaCL.
[c] Bifunctional.
[d] Overall experiment time set at 600 s. AcCL, *N*-acetyl-CL; CCCL, cyclohexyl carbamoyl caprolactam; HBCCL, hexamethylene-1,6-bis-carbamoyl caprolactam; PIT, phenylisocyanate cyclic trimer.

polymerization of CL in suspension or in emulsion with a good dissipation of the reaction heat. This topic will be described in detail in Section 4.14.13.2.

Furthermore, the fast cycle times of the activated anionic ROP made this latter amenable to RIM processing, where the anionic PCL and its copolymers have foreseen for several years the potential for their most widespread industrial applications (Section 4.14.13.3). In the following sections, a description of what now appears well established will be provided, with some specific mention of the most reliable kinetic approaches to describe anionic bulk polymerization of CL, as well as the relevant role of initiator and activator concentrations in terms of monomer conversion, high polymer yield, content of cyclic oligomers, and side products. Namely, the formation of cyclic oligomers and higher cyclic species during the anionic polymerization will be described in detail in the light of very recent findings.

4.14.10.2 Kinetic Approaches in the Bulk Polymerization

As shown in other sections of the present chapter, the anionic ROP of CL in the bulk involves a great number of reversible and irreversible reactions (including side reactions) in which, depending on the chosen experimental conditions, the active species are continuously destroyed and reformed. Therefore, any kinetic approach, based on an oversimplified scheme of the reaction chemistry involved in order to model the polymerization pattern, will lead to very questionable conclusions.

So far, after many attempts to apply mechanistic models to interpret anionic polymerization kinetics of CL with very limited success,[148] the above models have been almost completely abandoned in favor of phenomenological approaches, among which the most successful has been the autocatalytic model of Malkin *et al.*[212]

Malkin's model has been put forward to describe the nonisothermal kinetics of both CL and ω-laurolactam anionic polymerizations in bulk, monitoring the temperature rise inside the reactor. The heat balance is given by the following differential equation:

$$\frac{dT}{dt} + \left(\frac{UA}{cm}\right)(T - T_w) + \left(\frac{\Delta H_p}{c}\right)\frac{d\lambda}{dt} = 0 \qquad [98]$$

where T is the temperature inside the reactor; T_w is the wall temperature; U is the overall heat transfer coefficient; A is the surface of the reactor available for heat exchange; c is the specific heat of the reacting system; m is the total mass; ΔH_p is the enthalpy of polymerization ($-140\ kJ\ kg^{-1}$ for CL); and λ is the degree of conversion.

Hence

$$\frac{d\lambda}{dt} = -\left(\frac{c}{\Delta H_p}\right)\left[\left(\frac{dT}{dt}\right) + \frac{(T - T_w)}{\tau}\right] \qquad [99]$$

$\tau\ (= cm/UA)$ is the time constant of the system and is evaluated from a separate set of experiments. For strictly adiabatic conditions, the term $(T - T_w)$ of eqn [99] is equal to zero. Applied to both nonisothermal and quasi-adiabatic polymerization conditions, Malkin's model fits a more or less large amount of data for the activated CL polymerization in bulk, on the basis of the following equation:

$$\frac{d\lambda}{dt} = k\frac{[A]^2}{[M]}(1 - \lambda)\left(1 + \frac{b\lambda}{[A]}\right)\exp\left(-\frac{E_a}{RT}\right) \qquad [100]$$

where $[A]$ is the activator concentration; $[M]_0$ is the initial monomer concentration; E_a is the activation energy ($63 \pm 6\ kJ\ mol^{-1}$); k is the front factor reflecting the reaction rate; and b is the autocatalytic term characterizing the intensity of the self-acceleration effect during chain growth.

Both k and b depend on the chosen activator. For $\lambda << 1$, that is, at the initial stage of polymerization, the value of k can be easily evaluated. Namely, Macosko *et al.*[135] have found that Malkin's model was in very good agreement with their data for both neat CL polymerization and its copolymerization with 16 wt.% of OH-terminated poly(propylene oxide) (PPG) end-capped with hexane-1,6-diyl diisocyanate (HDI).

A summary of Macosko's results is given in **Table 11**, adapted from Reference 213, while **Figure 18**, also taken from Reference 213, shows the adiabatic temperature rise data for the block copolymer formation and the excellent agreement with Malkin's model. The additional temperature rise at longer times is due to polymer crystallization, underlining that the two phenomena, polymerization and crystallization, can be kept well separated by choosing proper experimental setup, thus, avoiding any superposition effect.

The analysis of the thermal balance in transient conditions can be performed with acceptable accuracy on the basis of the simple equation [99] only when the Biot number, a dimensionless parameter used in transient heat transfer calculations, is much smaller than 1.[214] In that case, heat conduction inside the body is implied to be much faster than convection away from its surface, and thermal gradients in the body are negligible.

The autoacceleration in the activated anionic polymerization of CL has been tentatively attributed, as already mentioned (Section 4.14.2.2.2), to the much higher dielectric permittivity of the resultant polymer (PA6), as compared to that of the monomer.[75] This difference is not present in the anionic polymerization of ω-laurolactam. The permittivity difference seems to be linked to the different configurations of the amide group in the monomer (*cis*) and in the polymer (*trans*) for lactams having less than ten ring atoms.

4.14.10.3 Role of Activator and Initiator Concentrations

In the anionic ROP of CL, the influence of activator and initiator concentrations [A] and [I], respectively, as well as their ratio [A]/[I], has been extensively explored by Russo *et al.* both in 'slow'[129,215] and 'very fast'[157,160] polymerizations. Regardless of the chosen conditions, a 1:1 equivalent ratio between the functional groups of the activator and the initiator has always been found as a necessary prerequisite for optimizing high polymer yield and properties, as well as minimizing the formation of oligomers and side products.

As an example, kinetic data obtained from 'slow', quasi-adiabatic CL polymerization, using *N*-acetyl-CL as activator and sodium ε-caprolactamate as initiator, are given in **Table 12** taken from Reference 129, in terms of overall polymerization time t_p and the initial as well as the maximum rate of polymerization. For [A] = [I], an asymtotic decrease of t_p down to slightly more than 3 min for I = 0.9–1.5 mol. % was observed.

For the same 'slow' system and the same equimolar conditions, **Figure 19**, taken from Reference 215, shows additional data in terms of monomer conversion, high polymer yield, and content of both cyclic oligomers and side products. It is evident that the best balance is provided by A = I = 0.6–0.7 mol.% and that their nonequimolar ratios (filled circles in the figure) determine a lowering of the high polymer yield.

Table 11 Kinetic constants for the polymerization of CL with sodium ε-caprolactamate (I) and HDI (A), with [I] = 2[A]

	T_0 (°C)	M_0 (mol l^{-1})	[I] = [NCO] (mol l^{-1})	E_a (kJ mol^{-1})	k (l mol^{-1} s^{-1}) 10^{-8}	b (mol l^{-1})	ΔH (kJ mol^{-1})	References
Homopolymer	131 (139)	8.84	0.18	63.8 ± 0.5	2.23 ± 0.1	1.15 ± 0.5	16	135, 213
Block copolymer[a]	126	7.42	0.15	63.8	2.23	1.15		135, 213

[a] PA6–PPO–PA6 copolymer.

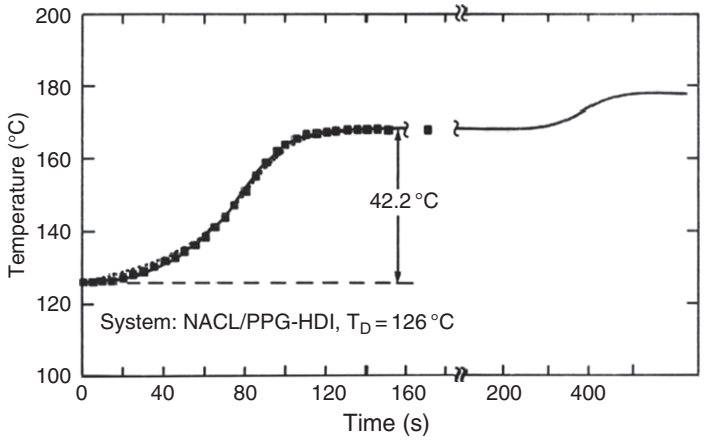

Figure 18 Adiabatic temperature rise in the anionic polymerization of CL followed by polymer crystallization. Initiator, sodium caprolactamate; bifunctional activator, HDI-end capped PPG ($M_n \sim 2000$), 16 wt.%. Dotted line is the temperature rise predicted using Malkin's model with the kinetic constants of **Table 11**. Reproduced from Macosko, C. W. *RIM Fundamentals of Reaction Injection Molding*; Hanser Publication: Munich, Germany, 1989.[213]

Table 12 Polymerization time (t_p) and initial and maximum polymerization rates (expressed by the derivative of monomer conversion λ) in runs with different concentrations of activator (AcCL) and initiator (CLNa)

[A]/[I] (mol/100 mol CL)	*Overall polym. time, t_p (min)*	*Initial rate $(d\lambda/dt) \times 10^2$ (min^{-1})*	*Maximum rate $(d\lambda/dt)_m \times 10^1$ (min^{-1})*
0.3/0.3	12.05	1.95	3.38
0.3/0.3	11.05	1.41	3.74
0.5/0.5	8.10	3.39	5.17
0.7/0.7	4.90	6.98	8.01
0.7/0.7	5.40	7.40	8.28
0.9/0.9	3.80	9.41	10.04
1.2/1.2	3.70	19.28	13.64
1.5/1.5	3.15	23.63	15.82
0.6/0.4	6.50	3.69	5.69
0.7/0.4	9.30	3.37	4.30
0.8/0.4	7.85	4.54	5.06
0.7/0.6	6.05	5.61	6.77
0.8/0.6	5.60	7.10	6.90
0.9/0.6	5.40	4.78	8.21
1.0/0.6	3.95	8.64	9.43
0.8/0.7	5.15	7.49	9.90
0.9/0.7	5.70	6.11	7.77
1.0/0.7	4.70	11.12	10.96
0.7/0.9	5.15	8.57	8.48
1.2/0.9	5.40	9.77	7.96

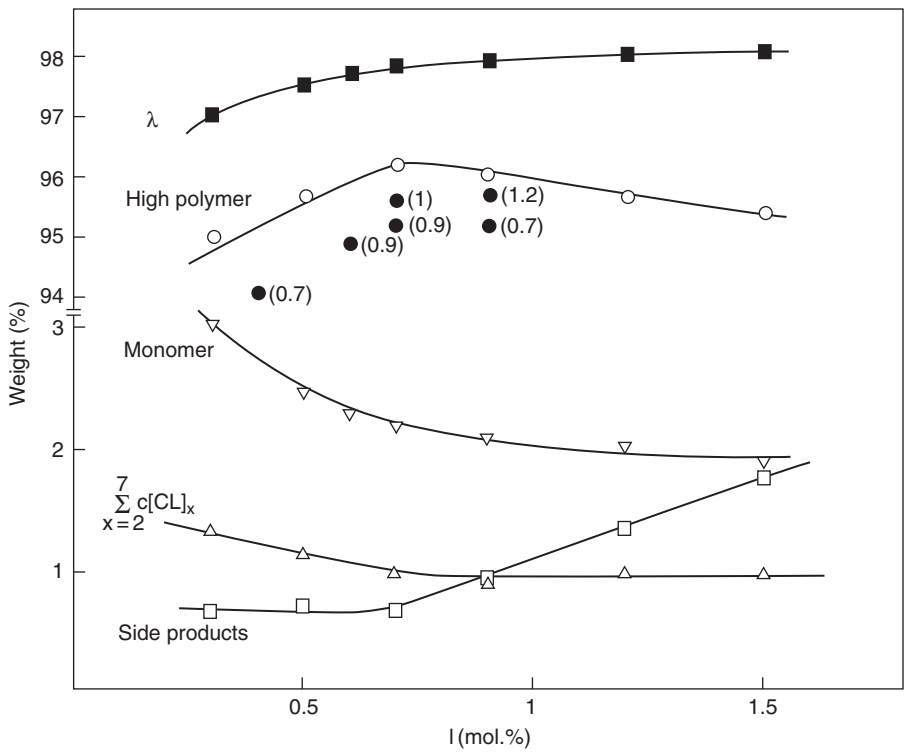

Figure 19 Monomer conversion (λ), high polymer yield, and methanol extractable fraction (wt.%) as functions of initiator concentration ([I], in mol.% referred to 100 mol of CL); I, CLNa; A, AcCL. Figures near • indicate the activator molar concentrations A, in mol. %, in nonequimolar experiments. Reproduced from Biagini, E.; Costa, G.; Russo, S.; *et al. Makromol. Chem., Macromol. Symp.* **1986**, *6*, 207.[215]

Analogously, UV-absorbing species, which can be considered a useful indication of the relevance of side reactions, are already present to a much greater extent in the anionic PA6 samples prepared from nonequivalent concentrations of activator and initiator (**Figure 20**, lines a, b, c, d).[129] The red straight line in the same figure represents

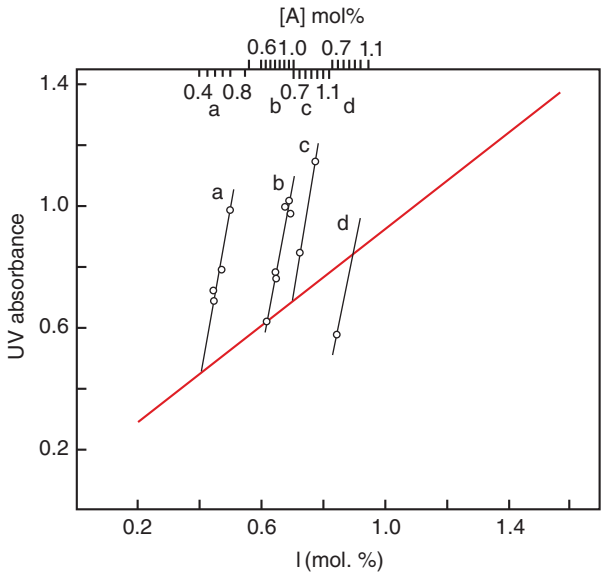

Figure 20 Effect of activator (AcCL) concentration, as constant I (I = CLNa), on polymer UV absorbance at λ = 276 nm. (a) I = 0.4; (b) I = 0.6; (c) I = 0.7; and (d) I = 0.9 mol. %. Reproduced from Alfonso, G. C.; Chiappori, C.; Razore, S.; Russo, S. In *Reaction Injection Molding, Polymer Chemistry and Engineering*; Kresta, J. E., Ed.; ACS Symposium Series No. 270; American Chemical Society: Washington, DC, 1985; Chapter 11, p 163.[129]

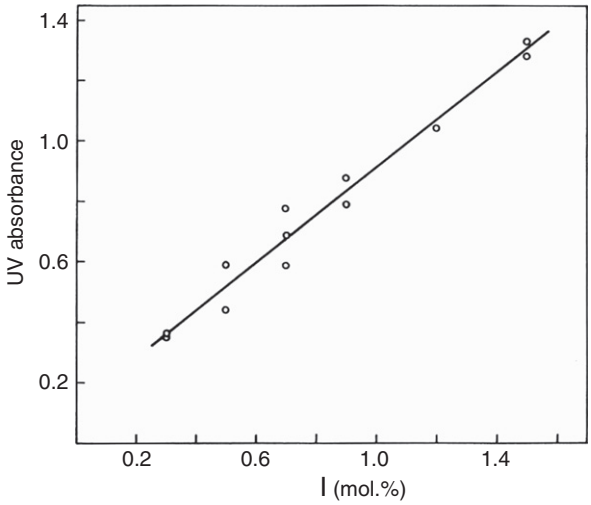

Figure 21 Optical density of PCL samples at 276 nm as a function of initiator concentration, in the case of [I] = [A]; I, CLNa; A, AcCL. Reproduced from Alfonso, G. C.; Chiappori, C.; Razore, S.; Russo, S. In *Reaction Injection Molding, Polymer Chemistry and Engineering*; Kresta, J. E., Ed.; ACS Symposium Series No. 270; American Chemical Society: Washington, DC, 1985; Chapter 11, p 163.[129]

UV absorption of anionic PA6 samples prepared with [A] = [I].

Similar results have been obtained[157] in 'very fast' polymerizing systems, using a bifunctional activator (HBCCL). For a molar ratio of [A]/[I] = 1:2 and I = 0.9 mol.%, t_p as low as 24 s has been found (see **Table 10**). Obviously, by increasing the concentration of initiator, that is, by increasing the basicity of the medium, a higher extent of side reactions is observed (**Figure 21**).[129]

4.14.10.4 Cyclic Oligomers and Cyclic Species

Besides linear homologs and high polymer chains, in polycondensation reactions and in the ring-opening polymerization of heterocyclic monomers, sizeable amounts of cyclic oligomeric species are frequently found in the polymerization products. Namely, in CL polymerization, the formation of low-mass cyclic species has great relevance in terms of reaction kinetics and mechanism, as well as polymer properties. Irrespective of the polymerization mechanism, the linear oligomer content is an order of magnitude lower than the corresponding value for each cyclic species and its formation is usually not taken into consideration.[216]

In contrast to CL hydrolytic polymerization, in which a thermodynamic equilibrium is established in most cases among linear macromolecular chains, monomer, and higher (cyclic and linear) oligomers, the anionic route is very often under stringent kinetic control. In this respect, the residual monomer content, which is ~7–8 wt.% in hydrolytic polymerization, can be far below the value predicted on the basis of thermodynamic considerations (~3 wt.%) and, depending on the reaction conditions chosen, found to be as low as ~1 wt.%[217] or even less,[160] as shown in **Figure 22**.

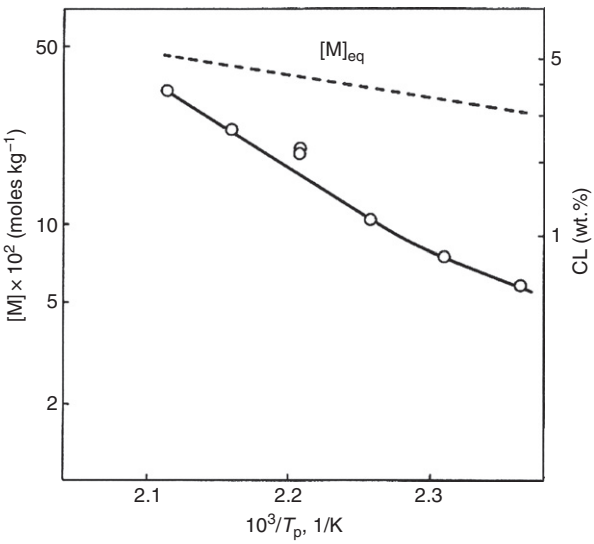

Figure 22 Residual CL content (experimental points) and equilibrium monomer concentration ($[M]_{eq}$, data from Reimschuessel, H. K. In *Ring-Opening Polymerization*; Frisch, K. C.; Reegen, S. L., Eds.; Dekker: New York, 1969; Chapter 7, p 303.[11]) as functions of $1/T_p$. Reproduced from Russo, S.; Biagini, E.; Bontà, G. *Makromol. Chem. Macromol. Symp.* **1991**, *48/49*, 31.[160]

Analogously, as far as higher cyclic oligomers are concerned, the most relevant reaction parameters able to affect their formation are the following:

1. quasi-adiabatic polymerization conditions or controlled polymerization temperature;
2. 'very fast' or 'slow' activators;
3. type and concentration of both initiator and activator; and
4. stoichiometric ratio of their active groups.

Each of the above parameters, alone or in combination with some of the others, can widely modify the overall content of cyclic oligomers and their relative composition. As pointed out by Roda,[10] when the total amount of extractables made of monomer, higher oligomers, and other low-mass species derived from side reactions (quite often present in anionic runs) exceeds 2–3 wt.%, both the processing and the end properties of PCL are negatively affected. Under suitable conditions, the anionic polymerization of CL can be performed in such a way to keep the above amount below that limit, thus avoiding expensive post-treatments of PA6 purification. As mentioned above and described in detail in Section 4.14.7.2, several side products in more or less relevant amounts are usually formed during the anionic polymerization of CL and contribute to make the description of the whole polymerization process very complex. Indeed, the concurrent presence of side reactions can not only affect the isolation, detection, and proper evaluation of cyclic oligomers but also interfere with their formation and reactivity.[7,9] It has been described in Section 4.14.7.2 that relevant amounts of low-molar-mass side species are produced if one or more of the following reaction conditions are established: (1) the reaction temperature exceeds ~170 °C irrespective of the polymerization conditions (isothermal, nonisothermal, or quasi-adiabatic runs); (2) the basicity of the reaction medium is too high due to the type and concentration of initiator; and (3) the polymerization rate is rather 'slow'. At present, the prevailing opinion is that the production of side products can be strongly limited only when the anionic polymerization of CL is carried out in the presence of both 'very fast' activators and quasi-isothermal conditions at $T_p \leq 170$ °C (preferably, at ~150 °C). Only the data from the above set of reaction parameters allow to evaluate the absolute and relative amounts of the main polymerization products (linear PA6 chains and rings) in a very accurate manner and in more detail, without the strong negative interference of side reactions.

As will be seen in the following, even the most recent studies on cyclic oligomer formation in CL anionic polymerization have been quite often carried out without considering the drawbacks and limitations outlined above and caused by experimental conditions, far from the optimum, that have been chosen. Only a few studies on cyclic oligomer formation during the anionic polymerization of CL have explored the role of activators and initiators, with specific attention to the kinetics and mechanism of individual cycle formation.[11,12,145,217] The above studies have attempted to correlate the extent of cyclics and some of the following parameters: (1) type and duration of the anionic polymerization (i.e., activated or nonactivated, 'very fast', 'fast', or 'slow'); (2) thermal histories during and after polymerization (e.g., annealing temperatures and times); (3) crystallinity degree of the resultant polymer; and (4) cyclization constants from equilibrium considerations.[218] However, a further word of caution is necessary, as the various interpretations of the experimental results have been based so far on extraction procedures and extractable analyses that have been questioned in recent years.[219] Following the recent findings of the latter researchers, the most widely used extraction techniques (by boiling water or boiling methanol) are not able to quantitatively remove the whole oligomeric fraction but only the lowest molar-mass species (monomer, dimer, and trimer). Of course, the extraction efficiency has been found to be progressively reduced as a function of the cycle size. Therefore, the content of cycles higher than the trimer, when evaluated by extraction techniques, can be underestimated and their relative ratios, namely those customarily referred to the cyclic dimer, affected by more or less relevant errors. Even the seldom used and time-consuming dissolution/precipitation methods do not allow a full recovery of cyclic oligomers except for cycles up to hexamer/heptamer. A sizeable amount of higher oligomers is retained, with the net result to remarkably affect conclusions and comparisons often present in the literature (kinetically driven processes vs. thermodynamic equilibrium data; agreement or disagreement with Jacobson–Stockmayer theory,[218,220,221] etc.). On these grounds, published data on cyclic oligomer formation during the anionic polymerization of CL, in addition to the role of the chosen conditions of synthesis ('slow' or 'fast' or 'very fast' polymerization, quasi-adiabatic vs. quasi-isothermal conditions), are also strongly dependent on the analytical procedure used (extraction, dissolution/precipitation, direct high-performance liquid chromatographic (HPLC) methods without sample isolation, etc.), as well as the upper limit of ring size chosen by the analytical setup.

No studies able to draw a general and conclusive picture of the relevant aspect of cyclic oligomer formation have been published so far. Ueda *et al.*[217] performed an HPLC analysis only up to the cyclic hexamer, after a 'slow' activated anionic polymerization carried out for very long times (between ~6.5 and 60 h) at 150 °C in conditions approaching the isothermal ones, followed by boiling water extraction for 5 h. Roda's group[145] performed a 'very slow' nonactivated polymerization at 190 °C for times between ~3 and 400 h in quasi-isothermal conditions, followed by repeated boiling methanol extraction and HPLC analysis up to the pentamer only. In previous years, Russo's group carried out both a 'slow' anionic polymerization of CL in quasi-adiabatic conditions[215] (initial T_p 155 °C; final T_p ~205 °C) and a 'fast' one in quasi-isothermal conditions at 160 °C, in bulk and in suspension, followed by boiling water extraction and HPLC up to the nonamer.[160] Most of the above studies and the few others already existing in the literature have shown a monotonic decrease of the individual cyclic oligomer content from the dimer to the highest species detected. However, in more recent years, when the new analytical procedures enabling to determine the exact content of individual oligomers have been applied to anionic PCL, a completely different trend has been found, at least for quasi-isothermally synthesized polymers.[222,223] Instead of a regular, monotonic decrease of the cyclic oligomer content as a function of its size, it has been found[223] that, as given by the matrix-assisted laser desorption/ionization time-of-flight (MALDI-TOF) spectrum of **Figure 23** for a specific sample of anionic PCL, a sharp increase in the higher oligomer content from the hexamer up to the undecamer occurs with a maximum for this latter. After this maximum, higher cyclic oligomers up to $(CL)_{19}$ have been detected and their content follows a more or less regular decrease.

The cyclic undecamer (molecular mass 1244,8), present as the most abundant species in MALDI-TOF, has also been detected by Size Exclusion Chromatography (SEC) (**Figure 24**) as the maximum of a distinct peak in the low-molar-mass region, well separated from the high polymer trace. HPLC analysis of the cyclic oligomer fraction up to the undecamer for another anionic PA6 sample not previously

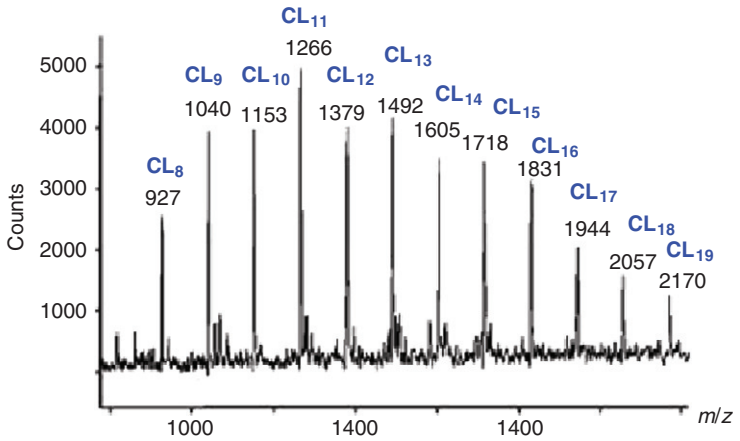

Figure 23 MALDI-TOF spectrum of an anionic PCL sample in the low-molar-mass region. The series of peaks at *m/z* values *n*113 + 23 corresponds to the Na^+ ions of the cyclic oligomers (C_x). Reproduced from Ricco, L.; Casazza, E.; Mineo, P.; *et al. Macromolecules* **2008**, *41*, 3904,[223] with little modification.

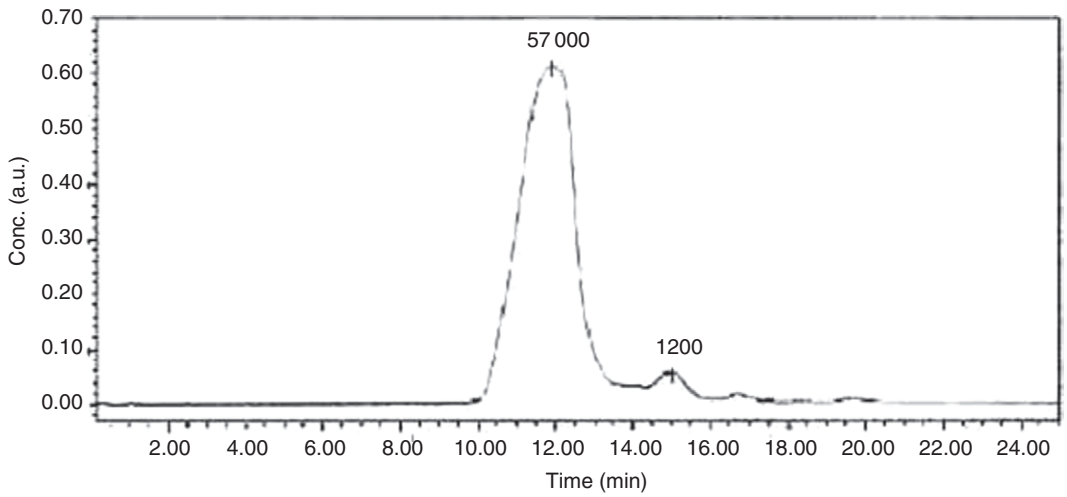

Figure 24 SEC trace of an anionic PCL sample. Reproduced from Casazza, E.; Ricco, L.; Russo, S.; Scamporrino, E. *Macromolecules* **2007**, *40*, 739.[222]

washed with methanol confirms the presence of unpredicted high concentrations of cyclics with a peak maximum corresponding for this sample to the nonamer, as given in Table 13 and Figure 25.

The series of intense peaks at *m/z* values *n*113 + 23 in MALDI-TOF spectrum corresponds to Na^+ ions of cyclic oligomers of PA6 from hexamer (peak at *m/z* 701) up to nonadecamer (at *m/z* 2170). Peaks due to species with higher molar mass are also present, but with very low intensity. The peaks indicated in the spectrum with # (at *m/z* values *n*113 + 39) are due to cyclic oligomers detected as K^+ species.

From the above data it is evident that, depending on the experimental conditions chosen for the anionic polymerization, the low-molar-mass peak, always present in anionic PA6 at 2–3 wt.% concentration and made of macrocycles from the octamer up to approx. $(CL)_{25}$, has a maximum that can be slightly displaced toward other mass values. The finding of the above peak just in recent years is probably linked to the experimental difficulties in the realization of SEC analyses of

Table 13 Cyclic oligomer content M_x in an anionic PCL sample, obtained by HPLC measurements

x	M_x *(wt.%)*	M_x *(mol/100 mol of PCL repeating units)*
1	1.51	1.515
2	0.40	0.200
3	0.13	0.042
4	0.09	0.023
5	0.08	0.017
6	0.11	0.018
7	0.11	0.016
8	0.19	0.023
9	0.27	0.030
10	0.09	0.009
11	0.09	0.008

Reproduced from Casazza, E.; Ricco, L.; Russo, S.; Scamporrino, E. *Macromolecules* **2007**, *40*, 739.[222]

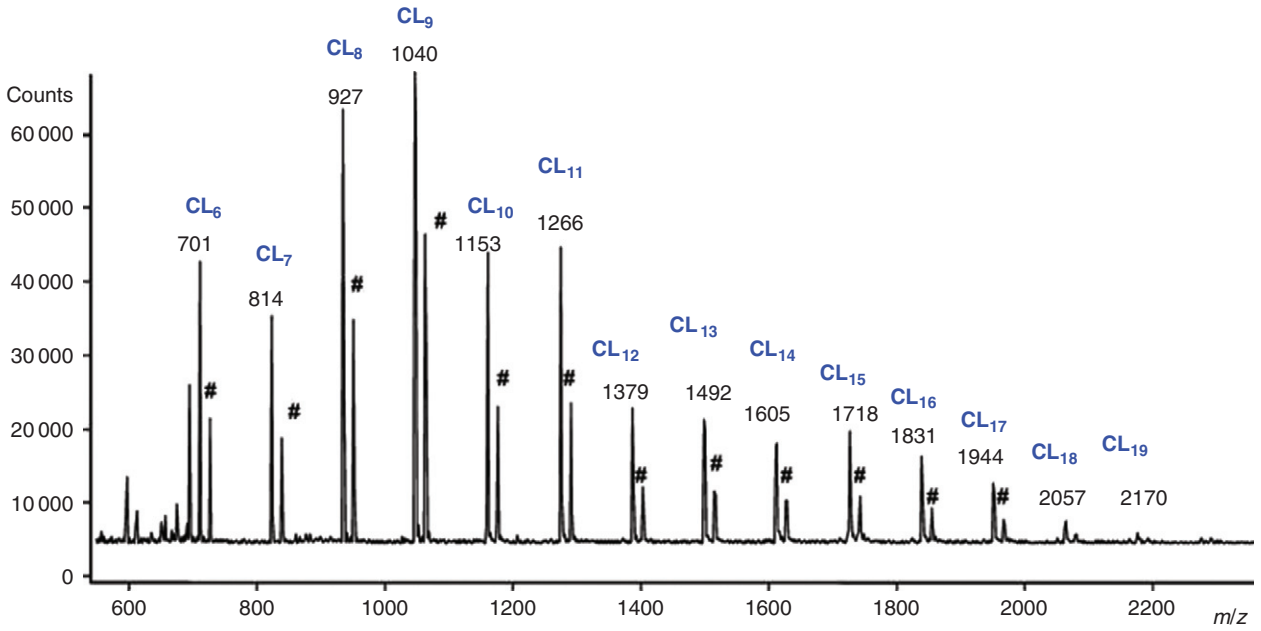

Figure 25 MALDI-TOF spectrum of the low-molar-mass species separated from the high polymer fraction in an anionic PCL. Reproduced from Casazza, E.; Ricco, L.; Russo, S.; Scamporrino, E. *Macromolecules* **2007**, *40*, 739,[222] with little modifications.

PCL, which were strongly affecting its molecular characterization for decades. Only in the last few years, the SEC problem of PA6 was satisfactorily solved by some groups, as described in Reference 159. For comparison, it may be useful to state that SEC analysis of hydrolytic PCL does not show any low-molar-mass peak but a relatively large plateau on the lower mass side of the high polymer peak. Future studies on the nature of this plateau, the masses of which more or less correspond to the anionic peak found by Russo's group, may be attempted in order to evaluate analogies and differences between the two mechanisms of ROP of CL. At present, thanks to MALDI-TOF data on 'fast' anionic PCL in quasi-isothermal conditions[222,223] without any previous oligomer separation from the high polymer fraction, together with SEC and HPLC results, it has been possible to find out a regularly decreasing trend of cyclic oligomer content up to the hexamer, together with a previously unknown peak made of macrocyclics rising from $(CL)_{7-9}$ up to $(CL)_{20-25}$ and with a maximum positioned as a function of the reaction parameters.

Among the first members of the cyclic oligomer series (up to the hexamer), which can be safely considered almost exempt from the extraction and/or analytical biases mentioned above, it may be interesting to describe how the cyclic dimer content depends on the different mechanisms of polymerization and the experimental conditions chosen. As compared to hydrolytic polymerization,[12] the cyclic dimer content in the extractables, derived from a 'slow' adiabatic polymerization,[215] increases from 10.2 wt.% (hydrolytic) to 23.5–44.5 wt.% depending on the experimental conditions, while in 'fast' quasi-isothermally polymerizing systems,[222] it has an intermediate value (17.2 wt.%). Referring to higher cyclics in the different experimental conditions of CL anionic polymerization, for instance, to the cyclic trimer, the $(CL)_3/(CL)_2$ molar ratio in 'fast' quasi-isothermal polymerizing systems[222,223] is almost the double (0.21), as compared to the 'slow' ones, either quasi-isothermal[217] (0.13) or quasi-adiabatic[220] (0.09–0.12). The corresponding value of the same ratio in hydrolytic polymerization, as given by Reimschuessel,[11,12] is 0.46. It is evident that the anionic polymerization of CL favors the cyclic dimer formation over higher cyclic oligomers. $(CL)_2$ is a very stable compound with a melting temperature (347 °C) much higher than that of the other cyclic homologs, a very poor solubility in most solvents, and strong intermolecular hydrogen bonds between NH protons and CO groups in the solid state.[15,16] Its formation in the anionic polymerization of CL is suspected to follow a different mechanism as compared to that of higher oligomers, as its final content in the reaction product is strongly influenced by activator and initiator concentrations, unlike those of the other cyclic oligomers.[224,225]

Ueda *et al.*[217] have recently suggested, as the most probable mechanism of cyclic oligomer formation in anionic PCL prepared by activated polymerization, a unimolecular backbiting reaction, depicted in **Scheme 29**,[223] as follows: an ionized amide bond is produced by proton abstraction along the polyamide growing chain, which is a highly probable event especially in the latter stages of anionic polymerization, invoked also to explain transamidation reactions, branching, and cross-linking, if any. If chain conformation allows the $-N^{\theta}-$ anion to approach its chain end (cyclic imide), it is possible to envisage its nucleophilic attack on the cyclic imide group in competition with that of CL anion. The generated loop, after the attack by the monomer anion, would form a cyclic oligomer and a linear chain. The segmental mobility of the growing chain in the more and more viscous reaction medium will control the formation of the individual cyclic species. So far it has been unclear, however, why formation of larger cycles, that is, $(CL)_{9-11}$, is favored over the smaller ones $(CL)_{4-8}$, although the cyclic dimer (to a greater extent) and cyclic trimer (to a lower extent) remain the most favored cyclic structures formed in the course of CL anionic polymerization.

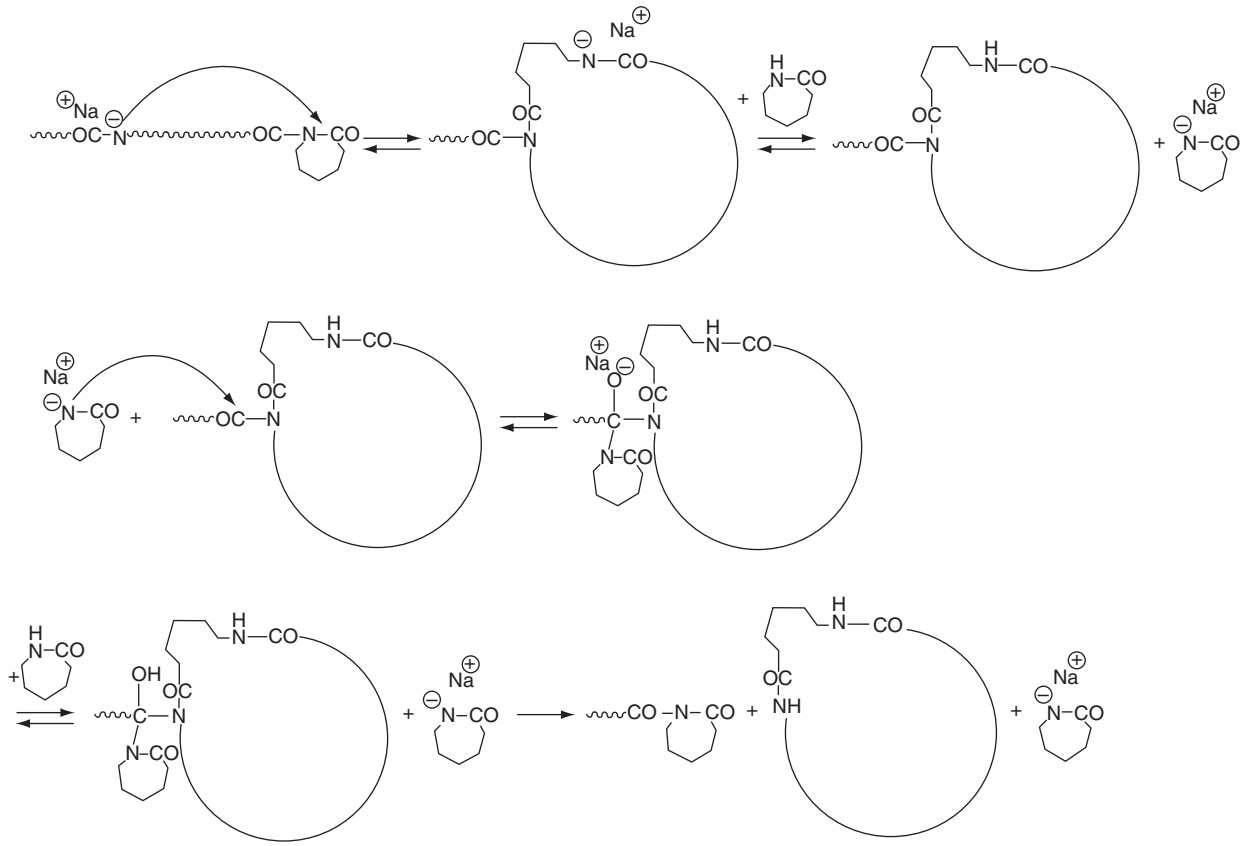

Scheme 29 Possible mechanism of cyclic oligomer formation.

The role of LiCl[46,214,226] and $CaCl_2$[227] in the activated anionic polymerization of CL has been studied in detail by Russo *et al*. As far as cyclic oligomer formation is concerned,[226] a strong decrease in the cyclic dimer content as a function of added LiCl has been found. Higher cyclic oligomers, on the contrary, showed an increasing overall yield. A possible explanation is based on the extensive formation of complexed amide bonds, due to the strong ion–dipole interactions between the carbonyl oxygen atoms of the polyamide chains and Li^+, able to coordinate up to four C=O groups. The possibility of cyclic dimer formation necessarily needs to find pairs of adjacent amide bonds free of complexation, which is less and less probable as the LiCl concentration in the reacting system increases. Conversely, the formation of higher oligomers is not subject to such heavy restriction and is favored by the counterbalancing effect of system densification because of the salt. However, the overall effects of LiCl on the activated anionic polymerization of CL have a negative influence on both the kinetics and the thermodynamics.[46,214] $CaCl_2$,[227] on the contrary, does not show the above pitfalls but only a slight reduction of the high polymer yield and a much lower negative effect on polymerization enthalpy and entropy. Here again, strong ion–dipole interactions between Ca^{2+} and amide groups are responsible for the peculiar properties of the resultant PA6 (e.g., a higher Young's modulus), retained also in the present of moisture, at variance with LiCl.

4.14.11 Anionic Polymerization of Other Lactams

Out of the five to thirteen rings of unsubstituted lactams that can undergo polymerization, the only lactams, besides CL, intensively studied in terms of anionic ROP are 2-pyrrolidone and ω-laurolactam. Also 2-piperidone deserves some considerations in this respect, although it has been much less studied than the other two lactams.

4.14.11.1 2-Pyrrolidone

The potential industrial interest for poly(2-pyrrolidone) (PA4) in relevant fields of application (namely, textiles) arises from its excellent mechanical properties combined with a hydrophilic behavior similar to that of cotton. Other areas of applied interest may be those of membranes and biomedical devices. However, its industrial production has not yet been developed to any appreciable extent because of the many drawbacks existing in both its synthesis and its processing.

2-Pyrrolidone can be polymerized only by an anionic mechanism either in the bulk or in suspension, but so far the polymerization reaction has been less successful than that of CL and ω-laurolactam. First of all, a rather low ceiling temperature (~70 °C) allows the polymerization to be carried out at low T only. Optimum temperatures are in the range 40–50 °C. Within this set of temperatures, in the activated anionic polymerization in the bulk, after a very high rate

developing in a homogeneous system in the first few minutes, further monomer conversion has been found to be strongly limited by the phase separation of the polymer, its nucleation, and crystallization,[228,229] with predominant occlusion of the growth centers in the crystalline regions. As a consequence, the significant decrease of the polymerization rate has made impossible to reach very high conversions in a reasonable time.

Better results in the polymerization of 2-pyrrolidone have been obtained by Sekiguchi *et al.*,[230] when using quaternary ammonium salts as initiators. At 30 °C, PA4 of high intrinsic viscosity in high yields (>80%) has been obtained after prolonged polymerization time (24 h), using tetramethylammonium pyrrolidonate as initiator and *N*-acetyl-2-pyrrolidone as activator. The activity of the alkylammonium salts of the lactam has been found higher than that of alkali metal salts, and the following order has been drawn:

$$NMe_4^+ > K^+ > Na^+ > Li^+$$

Various alkylammonium pyrrolidine salts have been tested and the best results have been found with NMe_4NPy, while $BuEt_3NPy$ was the worst in terms of polymer yield and degree of polymerization. To explain these results, it has been suggested that the use of a sufficiently bulky counter ion allows the breaking of hydrogen bonds between polymer chains and creates local irregularities of the crystalline structure in the neighborhood of the reaction sites, assuring the access of the lactam anion.

Interesting additional results have been reported in polymerizations conduced at 25 °C for 72 h using esters, such as γ-valerolactone and *n*-butyl acetate, as slow activators.[230] Some lactones and polylactones have given PA4 with improved thermal stability. Indeed, upon heating, the ω-hydroxy acyl residue of the activator is cleaved forming again the lactone ring and liberating an amine group at the chain end, which can act as a chain-coupling agent giving rise to condensation reactions with the other chains.

The anionic polymerization of 2-pyrrolidone has also been accomplished employing carbon dioxide as activator.[177] The use of this gaseous activator has made possible to prepare a PA4 possessing a satisfactory thermal stability for fiber preparation and melt spinning.[231] Nonactivated anionic polymerization, on the contrary, enables high molar masses of poly (2-pyrrolidone) to be obtained, but at the expenses of much longer polymerization times.[232]

In general, a severe drawback is caused by the intrinsic thermal instability of the polymer that, at *T* close to the melting temperature, depolymerizes to its monomer. Although several thermal stabilizers have been suggested in the patent literature, the problem is still far from being satisfactorily solved. As far as the synthesis of the polymer is concerned, much better results have been obtained when 2-pyrrolidone has been anionically polymerized in suspension,[233] using its potassium salt as initiator, silicon tetrachloride as activator, possibly a surfactant (sodium dodecylsulfate), and *n*-heptane as the suspending medium. Limiting conversions and polymer molar masses have shown significant improvements (yield ~70%, intrinsic viscosity increase 45%) after 4 h reaction at 43 °C. The most relevant advantage has been the polymer shape, which, in contrast to the products of the bulk polymerization – a compact, rigid block of horny polymer-, was the bulk polymerization- a very fine powder, easily removable from the reactor.

A relevant aspect deserving attention is that both the bulk and suspension methods have been found to provide PA4 free of structural irregularities. This result is a clear indication that side reactions, responsible for the strong UV absorption and widely present in anionic PCL synthesized in the bulk (Section 4.14.10), are here minimized due to both the low polymerization temperature and limited conversions.

4.14.11.2 2-Piperidone

Thermodynamically speaking, 2-piperidone is slightly more polymerizable than 2-pyrrolidone, but kinetically less reactive.[8] The low kinetic polymerizability has been attributed to the concurrent crystallization of the growing chains and consequent physical termination as well as the relevance of side reactions, allowed to extensively occur because of the slowness of the polymerization. Activators have been found to be always essential for the polymerization of 2-piperidone. Relatively high molar masses of poly(2-piperidone) have been achieved only when quaternary ammonium salts have been used as initiators.[128] The resultant polyamide has a T_m of ~283 °C, higher than that of poly(2-pyrrolidone), ~260 °C, and is thermally much more stable than the latter. Therefore, melt spinning can be safely carried out and fibers with good characteristics are obtained.

4.14.11.3 ω-Laurolactam

In recent years, the anionic polymerization and copolymerization of ω-laurolactam has gained increasing attention for a well-balanced set of properties of the resultant polymers and copolymers. The main advantages of ω-laurolactam anionic polymerization are its low level of absorbed moisture, easily removable during heating and melting of the monomer at 150 °C, and the low content of residual ω-laurolactam due to a favorable monomer–polymer equilibrium.

A novel catalytic pair, made of an alicyclic carbodiimide as the activator and sodium caprolactamate as the initiator, has been recently developed[186]. It allows very long-term storage of the initiating species mixed together, an efficient control of the polymerization rate, and an accurate tailoring of polyamide molar masses. A time–temperature–transformation (TTT) diagram, very similar to that of thermosets, has been drawn[234] with the aim of studying the influence of their initiating species on polymerization kinetics and limiting conversions. At variance with the traditional set of initiators (e.g., sodium ε-caprolactamate) and activators (e.g., *N*-acetyl-CL) used by other authors, the novel catalytic pair is able to *in situ* generate a guanidine anion, which reacts very fast with the first molecule of ω-laurolactam, thus performing to the initiation stage of ROP. Propagation is then based on the subsequent reaction of monomer molecules with the active centers. A simplified scheme of the polymerization mechanism has already been described (**Scheme 27**, Section 4.14.7.5.4). Initial concentrations of patented activator and initiator species,[185] as well as their molar ratios, are able to control poly(ω-laurolactam) molar mass and, in general, end properties of the polyamide.

An interesting aspect that has been investigated[174] is the relationship between the anionic polymerization process and

PA12 structure formation in terms of polymorphic modifications α and β, the latter being the more stable one. Different initiators and different types of activation have been found to exert a deep influence on not only polymerization kinetics and thermodynamics but also the degree of crystallinity and the physical structure of anionic PA12.

Significant changes of PA12 properties are achieved by copolymerization of ω-laurolactam with lactams of different ring size[235] or other monomers. The topic is covered in Section 4.14.12.

4.14.11.4 Substituted β-Lactams and Their Living Polymerization

The present status of the studies on β-lactam living polymerization has been described in great detail in a recent review of Hashimoto,[236] with specific attention to the anionic growth mechanism. Both Šebenda *et al.*[237,238] and Hashimoto *et al.*[239–241] have successfully synthesized uniform (i.e., the so-called monodisperse) polyamides from the substituted β-lactams (**62**, **63**, and **64**). Hashimoto *et al.*[242,243] have also obtained a uniform polyamide from the bicyclic oxalactam (**65**):

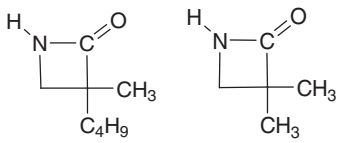

62 **63**

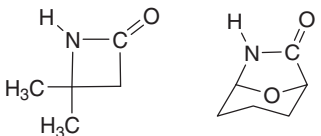

64 **65**

Šebenda *et al.*[237,238] have been the first to discover that the activated anionic polymerization of **62** has a living character, giving a polyamide of molar mass very close to the theoretical, predicted on the basis of the ratio monomer consumed/of activator added.

The roles of both the monomer structure and the reaction parameters in the achievement of living polymerization conditions for lactams have been analyzed by Hashimoto,[236] who found that a stringent control of the proton transfer reaction, restricted to that occurring from the lactam monomer to the anion of the growing chain, as given in [50], is essential for the attainment of living conditions.

No other active hydrogens, apart from that on the nitrogen atom, should in principle be present in the lactam molecule to avoid side reactions. The choice of mild polymerization conditions (e.g., room T_p, homogeneous solution, and low polymerization rates) goes in that direction too. Because of such experimental conditions, it is necessary to have highly reactive lactams, that is, those characterized by a high ring strain. Substituted β-lactams are very suitable in this respect. Furthermore, in order to carry out a homogeneous solution polymerization, selected polyamide solvents, capable of not interfering with the living species, are required. Hashimoto[239,240] made use of aprotic polar solvents (N,N-dimethyl acetamide, DMF, and DMSO) added with LiCl or LiCBr as the reaction media able to act as good solvents for polyamides derived from **63** and **64**. The activated anionic polymerization[239] of **63** in dilute solutions of DMAc + LiCl (5 wt.%) at 25 °C, keeping the initiator (K pyrrolidonate) concentration as low as 0.5 mol.% in order to decrease the polymerization rate and avoid the broadening of molar mass distribution, was completed in less than 20 min. M_w/M_n of the poly(β-lactam) was found to be < 1.1 and M_n was almost linearly proportional to monomer conversion (**Figure 26**).

Also the activated anionic polymerization[240] of **64**, under similar experimental conditions, gave a uniform polyamide, despite the α-active hydrogens of that monomer. The living character of the resultant polyamide has been proved[241] by adding further monomer to the reacting medium for a second-stage polymerization. The gel permeation chromatography (GPC) traces of the above poly(β-lactam) after the first and the second polymerization runs are depicted in **Figure 27** and fully support the living character of this polymerization. Therefore, it can be inferred that, by choosing sufficiently mild polymerization conditions, living polyamides can be obtained from monomers having α-active hydrogens also. The relatively low basicity of the lactamate anions in the chosen experimental conditions would prevent proton withdrawal from the neighboring carbon atom.

In general, several factors have to be taken into account in order to attain a living or a quasi-living polymerization of β-lactams. Monomers having a low rate constant of propagation are preferable for the synthesis of uniform polyamides. Drawbacks in the preparation of uniform polyamides from β-lactams are the very frequent occurrence of depolymerization and transamidation (at the acyl lactam chain end and on the polyamide chain), both causing broadening of molar mass distribution of the resultant polyamide. The latter reaction occurs more frequently at high conversion. Therefore, it is advisable to stop the polymerization at low to intermediate

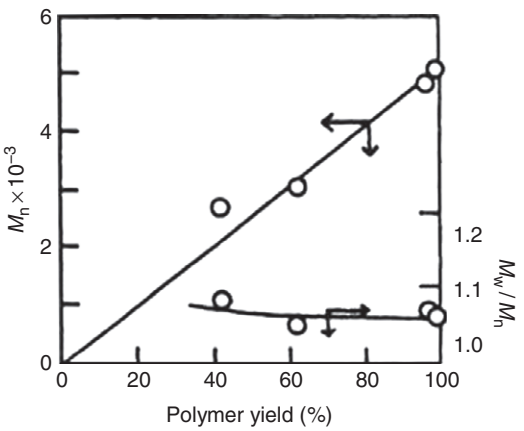

Figure 26 Values of M_n and M_w/M_n of the polyamide samples obtained from the anionic polymerization of **63**. Reproduced from Hashimoto, K. *Prog. Polym. Sci.* **2000**, *25*, 1411,[236] with slight modification.

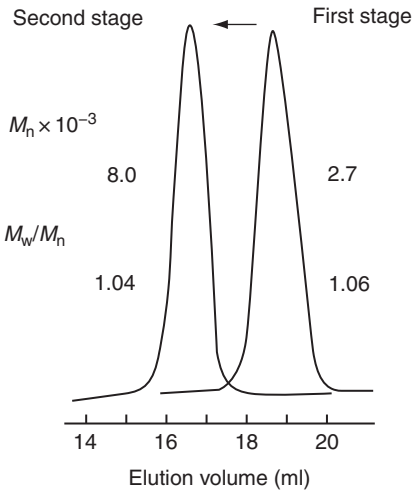

Figure 27 SEC profile of the polyamide obtained in two-stage polymerization of **64** at 258 °C. Reproduced from Hashimoto, K. *Prog. Polym. Sci.* **2000**, *25*, 1411.[236]

conversions in order to get a living or a quasi-living polyamide. Block and graft copolymers, macromonomers, telechelics, and multicomponent polymeric materials, all with well-defined design, have been prepared taking advantage of the living character of the above polymerizations. The excellent review of Hashimoto[236] exhaustively covers also these topics.

An interesting application of the above living polymerization has been suggested by Šebenda *et al*.[238] It takes advantage of the fact that the copolymerization of **62** with other lactams is still running in homogeneous solution even after enchainment of some monomer units of the second lactam, the polymer of which is insoluble in that medium. In this way, the rate of enchainment of any polymerizable lactam can in principle be evaluated under identical conditions.

Quite recently,[242] the anionic homopolymerization of a few substituted β-lactams and the copolymerization of some of the above pairs have been studied in order to prepare polyamide 3-derived polypeptides displaying biological properties. The solution polymerization or copolymerization, initiated by Li amide disubstituted with trimethylsilyl groups and activated with 4-*tert*-butylbenzoyl chloride, does not have living character. From that study,[242] some insights emerged into the reactivity of the above β-lactams in terms of their acidities, as well as electrophilicity of the imide end groups.

So far, apart from β-lactams, the other members of the lactam family characterized by larger rings have been unable to perform a living polymerization. The many stringent requirements that are necessary to fulfill for the development of a living system, that is, high ring strain, low polymerization temperature, solution homogeneity, low rates of polymerization, highly controlled proton transfer, no side reactions, limited conversions, and absence of depolymerization and transamidation reactions, have been so far satisfied only for some β-lactams (**62**, **63**, and **64**) and the bicyclic oxalactam (**65**). The latter is a racemic mixture of the corresponding enantiomers and can be anionically polymerized (e.g., in dimethyl sulfoxide at 25 °C) to ~80% yield of the resultant high-molar-mass polyamide,[243,244]

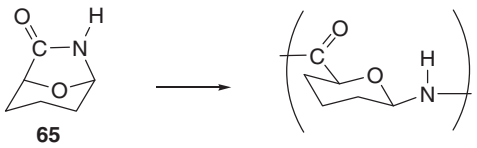

[101]

which should be considered a random copolymer of the above enantiomers. The intermolecular hydrogen bonds between the amide groups may be weakened to the point that justifies its very high solubility in several organic media. The kinetic polymerizability of **65** is very high, due to the high strain of internal bond angles, and its anionic solution polymerization[243] provides a living polyamide at least up to monomer conversions < 60% ($M_w/M_n = 1.1$, M_n directly proportional to conversion), with some broadening of molar mass distribution to ~1.2 at high conversions.

Also the corresponding optically active **65** has been polymerized under conditions similar to those outlined above.[236] The optically active polyamide has shown higher molar mass, higher melting point, and higher degradation temperature as compared to the polyamide prepared from the racemic **65**. Both polyamides are highly hygroscopic. They have been utilized for the preparation of hydrophilic membranes characterized by high water permeability and permselectivity, as well as for the design of multicomponent polymeric materials containing the polyamide block. In future, if proper experimental conditions (e.g., suitable solvents, temperatures, reaction rates, and conversions) would be chosen, other homo- and heterobicyclic lactams might yield living or quasi-living polyamides, opening interesting fields of application in many different areas.

4.14.12 Anionic Copolymers

4.14.12.1 Introduction

Copolymers with at least one component that is a lactam are an interesting family of polymeric materials, whose properties strongly depend on the routes chosen for their synthesis. In this respect, anionic mechanisms offer unique opportunities to control sequence distribution and microstructure of the resultant copolymers. For some specific pairs, the anionic copolymerization is the only way to synthesize materials with tailor-made characteristics. In the following, some relevant examples of anionic copolymers will be given.

4.14.12.2 Copolymerization of CL and ω-Laurolactam

So far, the most studied lactam pair undergoing anionic copolymerization has been that based on CL and ω-laurolactam, the only other lactam industrially accessible. As already mentioned, the main aim has been to extend the range of PCL applications by tailored modifications of its properties, some of which (e.g., low impact strength at low T and high moisture uptake) show characteristics that need to be improved. In this respect, matching PA6 properties with those pertaining to PA12 by suitable copolymerization of the two monomers can lead to material improvement.

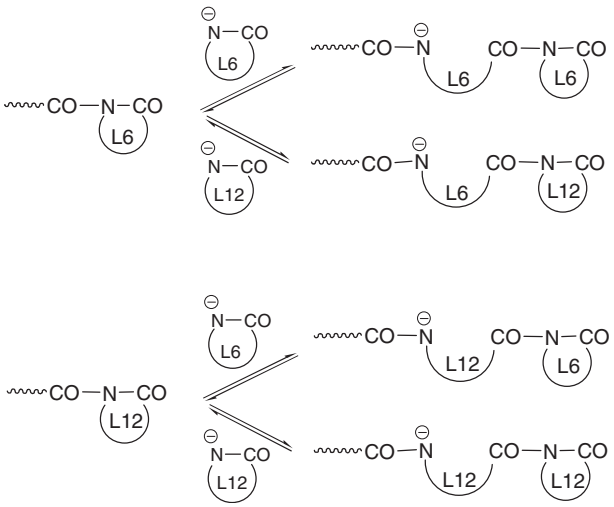

Scheme 30 Propagation stage of CL – w-laurolactam anionic copolymerization.

The anionic copolymerization kinetics of CL and ω-laurolactam, as well as the microstructure and the morphology of the resultant copolymers, is largely dependent on the reaction parameters, such as choice of initiator and activator, their stoichiometric ratio, quasi-adiabatic or quasi-isothermal conditions, and (initial) polymerization temperature. In the propagation stage, four competitive reactions (**Scheme 30**) of the two activated monomers (CL and ω-laurolactam anions) and the two nonionic growth centers (cyclic imides derived from CL and ω-laurolactam, respectively) are present[245] in competition with transacylation (exchange reactions) occurring between the amide groups of copolymer chains (**Scheme 31**).

Therefore, both thermodynamics and kinetics exert a control on copolymer formation, as well as its overall composition and microstructure. As mentioned before, initial temperature and possible temperature increase during polymerization, reaction time (often very high when slow or no activation is present), crystallization occurring after the end of polymerization or during it, absolute and relative concentrations of all reactants (lactams, initiator, activator, growing chains, and ionic species), complex equilibria of the various species, extent of Claisen-type side reactions, and so on make impossible to give a general, quantitative picture of the copolymerization reaction. Notwithstanding that, some relevant achievements have been obtained in recent years[144,245] and some findings well established. The most impressive kinetic information acquired is linked to the striking difference in the polymerization activity and in the role of the following two initiators: CLNa and CLMgBr. Roda's research group in Prague[245] found that the activated anionic copolymerizations (activator *N*-benzoyl-CL), initiated by CLNa, give rise to random copolymers, while those initiated by the Grignard reagent show a heterogeneous character. Indeed, a single melting

Scheme 31 Transacylation reaction between the amide groups of the copolymer chains.

endotherm and a single crystalline form have been found for the former initiating system in the whole range of copolymer compositions, while two melting endotherms and two types (α and β) of crystalline forms are displayed in the copolymers formed from 30 to 70 mol.% of CL in the feed with the latter set of catalytic species. The unusual behavior of the Grignard reagent has been explained on the basis of accurate analyses of copolymer microstructure composed by PA6 blocks (with a minor ω-laurolactam content) linked to sequences of CL/ω-laurolactam random copolymer. Most probably, PA6 is preferentially formed at the beginning of the polymerization, due to the much higher reactivity of CL as compared to ω-laurolactam. Only later on, random copolymers are formed from the remaining CL and the slowly reacting ω-laurolactam. Transamidation reactions, occurring to a very large extent when the polymerization is catalyzed by strong bases (CLNa), cause full randomization of the sequences and formation of a statistical copolymer only. CLMgBr is a much weaker base as compared to CLNa and, on the contrary, allows a much lower extent of transamidation reactions to occur. Long PA6 sequences are preserved and only a few links per chain with the copolymers are possible. The specific role of the Grignard reagent CLMgBr as initiator in anionic lactam polymerizations has been extensively discussed in Section 4.14.7.3. Its relevance is also under consideration in RIM applications, as mentioned in Section 4.14.13.3.

4.14.12.3 Copolymerization of Lactams and Lactones

The anionic ring-opening copolymerization of lactams and lactones has been studied in great detail by several research groups with the main aim to synthesize polyesteramides having potential biodegradable characteristics. Indeed, as remarked by Roda,[10] this is a rare example of copolymerization of rings obeying different mechanisms of homopolymer formation and giving rise to a copolymer using peculiar synthetic pathways.

Indeed, some lactones (such as CLO and VLO) can act as both activators of lactam anionic polymerization (up to ~5 mol.%) and comonomers at higher concentrations, while others (e.g., γ-butyrolactone) are only activators. Acylation of the lactone ring by the lactam anion (eqn [94]) is the initiation step, followed by a very rapid formation of polyester chains by growth reactions of the alkoxy groups and suitable lactone molecules. Taking into consideration the most studied monomer pair (CLO and CL), random or multiblock copolymer structures have been found, depending on the experimental conditions chosen for the synthesis. Copolymerizations initiated by CLMgBr and carried out in quasi-isothermal conditions (reactive casting in a 4-mm-thick mold at 150 °C) have been very successful in terms of copolymer yield, with a very low content of extractables (≤4%),[182,246] at variance with copolymerization runs initiated by CLNa giving extractable yields up to 40%. All copolymers with compositions ranging from 3 to 90 mol.% of CLO showed a random distribution of comonomer units, as supported by the close agreement of experimental T_g values and those calculated from the Fox equation.[247]

The exchange (transacylation) reactions between ester and amide groups in the copolymer chains have been considered responsible for the copolymer randomness, as they are very fast

and occur simultaneously with initiation and propagation steps under the experimental conditions chosen for the reaction. Once again, as we have seen in other sections of the chapter, the use of the Grignard reagent CLMgBr as initiator brings relevant advantages in both the synthesis and the properties of the resultant polymers.

As already mentioned, it is now well ascertained that at the beginning of the anionic copolymerization of CL and CLO, irrespective of the initiating system, it is the latter monomer that is more rapidly consumed, with the formation of poly (ε-caprolactone) homopolymer.

An interesting copolymerization experiment of the above monomers has been published by Scola et al.,[248] who applied a microwave process to convert them in the corresponding copolymers. The two monomers are suitable to effectively absorb the microwave energy due to the high values of their dielectric permittivities (∼14 at 100 °C for CL and ∼42 for CLO at the same temperature) and the additive dielectric properties of their mixtures. The rate of copolymerization is increased by the microwave process as compared to the purely thermal reaction because of more effectively activated molecular collisions and/or lower activation energy. Also in this case, only random copolymers have always been obtained, as supported by a single T_g found by Dynamic Mechanical Thermal Analysis (DMTA). The relevant yield increase and the much higher amide-to-ester ratios in the copolymers synthesized by the microwave-assisted process seem to suggest that a direct interaction between microwaves and molecular dipole moments more efficiently delivers the energy to amide groups (3–4 D) than to ester units (1–2 D), enhancing the reactivity of the former. Surprisingly, the microwave-assisted anionic homopolymerization of CL has not been mentioned in the literature so far, while its hydrolytic variant initiated by ω-aminocaproic acid has been studied.[89]

In more recent years, the anionic copolymerization of various lactams and lactones has been performed under reactive processing conditions, using a twin-screw extruder. By suitable sequential monomer feeding and temperature profiles, it has been possible to get diblock or triblock copolymers, while the simultaneous feeding of monomers always produced random copolymers.[249,250] In sequential feeding, the block lengths and, hence, the molar masses could be adjusted by controlling the feed rate.[251]

4.14.12.4 Block Copolymers and Other Copolymers

The anionic route is particularly suitable for synthesizing lactam-based block copolymers. CL and, to a much lower extent, ω-laurolactam have been the lactams more often used for the purpose. Polymeric activators (macroactivators) (Section 4.14.7.5.5) obtained from appropriately terminated prepolymers can give rise to di- and triblock copolymers or, when other functional groups acting as additional activating centers are present along the prepolymer backbone, even multiblock structures. The latter approach has been found particularly useful in RIM technology and will be discussed in detail in Section 4.14.13.3.

In order to obtain a good combination of end properties, numerous copolymers with a variety of nonpolyamide blocks have been prepared using polymeric activators and accomplishing the *in situ* anionic lactam polymerization. The main aim for synthesizing block copolymers of PA6 has been to improve its toughness, which is rather inadequate especially at low temperatures. Therefore, polymers, such as, polyethers,[252–255] poly(butadiene) (PBu),[256–259] and poly (dimethylsiloxane)[260,261] with suitably modified end groups, can be prepared and transformed into the corresponding polymeric activators. For instance, triblock copolymers with a soft PPO block in the main chain of PA6 or PA12 can be synthesized starting from macroactivators prepared, for example, by reaction of a PPG with isophorone diisocyanate. Further blocking with CL gives the *N*-carbamoyl-CL growth centers at the PPO chain ends.[262] Di- or triblock OH-terminated poly(ethylene oxide)/PA6 copolymers (PEO–PA6) have been synthesized along similar routes, using different macroactivators bearing tolylene-bis-carbamoyl-CL, or HBCCL, or cyclohexyl carbamoyl-CL growth centers, and the resultant morphological, thermal, and mechanical properties related to the conditions of synthesis have been studied.[255] PEO segments in the block copolymers showed amorphous characteristics, whereas a large fraction of unreacted PEO segments was crystallized in as-polymerized samples, with the notable exception of the products obtained using cyclohexyl carbamoyl activator. Among the various products obtained, the triblock copolymers showed the smallest PEO domains and the highest impact strength. Formation of chemical bonds at the interphase has been found as a necessary prerequisite for reaching optimum toughness. Similarly, a telechelic α–ω dihydroxy-poly(butadiene) reacting with a diisocyanate (e.g., 2,4- or 2,6-tolylene diisocyanate), blocked or not with CL, can be used as the polymeric activator to produce a triblock PA6–PBu copolymer, for example, by anionic casting polymerization in the presence of potassium ε-caprolactamate.[256–259] The final properties of the triblock PA6–PBu copolymer depend mostly on the length of the PBu block. A phase separation and an increased toughness (up to an order of magnitude higher as compared to unmodified PA6), as well as decreased Young's moduli and yield strengths, were generally found, together with higher contents of PA6 amorphous phase (and, thus, modified permeation properties).

Also cross-linked block copolymers, arising from three *N*-acyl lactam growth centers per PBu molecule, have been prepared and characterized.[263] Optimum values of impact strength, six times higher than the impact strength of PA6 homopolymer, have been found when 10 wt.% of PBu was used.

Diblock copolymers made of hydrogenated PBu and PA6 units (HPBu–PA6) have been synthesized in a similar manner (but hydrogenating the hydroxyl-terminated PBu) and used as compatibilizers in low-density poly(ethylene)/PA6 blends (PE/PA6).[264] The diblock copolymer exhibited a very relevant interfacial activity, with a reduction of particle size and an improvement of the interfacial adhesion between the incompatible phases. Also hydroxyl-terminated styrene–butadiene rubber (SBR) or poly(ε-caprolactone), after reaction with diisocyanates, were anionically copolymerized with CL in order to get block copolymers with improved mechanical properties.[265]

Graft copolymers can be obtained using macroactivators bearing pendant functionalities (Section 4.14.7.5), mainly for an end use as compatibilizers or to attain the *in situ* compatibilization in reactive blending. In this way, copolymers formed by a backbone of poly(propylene) (PP), PMMA, or PS, grafted

with polyamide chains, are easily obtained by the *in situ* anionic polymerization of lactams.

Thus, for instance, PP-*g*-PA6 copolymers have been obtained by reaction of isocyanate-bearing PP with CL (using, e.g., sodium caprolactamate as initiator),[266–269] and PS-*g*-PA6 have been anionically produced starting from macroactivators synthesized by copolymerization of isocyanate[192] bearing comonomers.

4.14.13 Industrial Applications

4.14.13.1 Introduction

Since the initial applications, essentially limited to the field of 'cast nylon' technology and centered on CL polymerization, the anionic polymerization of lactams has found in recent years several new industrial applications and many other fields have been tentatively explored or foreseen. In the 1980s, RIM and reinforced RIM (R-RIM) processes, previously involving for the most part polyurethane chemistry, seemed very suitable for the *in situ* anionic polymerization of CL in the mold.[270] The initial enthusiasm, however, had to face the complexity of the chemistry involved and the careful control necessary for keeping all reaction parameters under rigorous processability windows. Despite these difficulties, the extensive technological know-how acquired has provided new approaches, which may be extended in the near future to other fields, such as rapid prototyping. In general, in more recent years, some of the above processes, together with modern technologies, opened the route to new ideas, new applications, and new products. Some of them will be briefly outlined in the following.

4.14.13.2 Powdered Polyamides

The obtainment of fine powders of PCL, poly(ω-laurolactam), and their copolymers has attracted relevant attention in recent years for possible commercial utilizations in several fields. Cosmetic formulations, coating and graphic art applications, protein or enzyme immobilization techniques, rotational molding and sintering processes, and filtration devices in food and beverage industry are the major industrial fields where powdered polyamides are currently applied. Their use as stationary phase in chromatography has also been envisaged and introduced for some specific systems.

As compared to the other two techniques industrially utilized for the obtainment of polyamide powders, that is, low-temperature grinding and polymer dissolution/precipitation, anionic ROP of lactams (and, namely, of CL) offers great advantages in terms of much higher particle porosity, total absence of irregular edges and sinterized zones, controlled particle size, very narrow size distribution, and wide range of specific surface areas. Besides CL, ω-laurolactam has been so far the only other lactam considered in this respect, in terms of both ring-opening homopolymerization to polyamide 12 and its copolymerization with CL (PA6/12).

The anionic ROP of the above lactams has been carried out following three different approaches:

1. solution polymerization with phase-separated polymer avoiding its coagulation (dispersion polymerization);[271–276]
2. suspension polymerization in nonaqueous media as the continuous phase;[277] and
3. miniemulsion polymerization in hydrocarbons.[278]

Other, less common approaches can also been found in the open literature.[279] Due to the great potential of the above methods for the obtainment of polyamide powders, it is not surprising that many patents have been issued on these topics and several commercial products are already on the market.

The dispersion polymerization method, which in general needs suitable dispersants in order to avoid polymer coagulation, has been described in detail[271–276] and can be summarized as follows: the powdered PA6 formation is the result of very rapid steps governed by both the chemistry (initiation and growth of the polymer chains) and the physics of the polymerization process (precipitation, aggregation, and, finally, crystallization of the polyamide), steps that in part overlap. As a consequence, polymerization temperature; nature of the solvent; concentration of monomer, initiator, and activator; chemical nature and functionality degree of this latter; and molar ratio of the components of the catalytic pair all strongly affect not only the polymerization rate, the final conversion, and the chain length but also the polymer structure (linear, branched, and cross-linked) and its morphology.[280]

Studies on the suspension polymerization, focused on CL, have mainly been performed in oligo(isobutene) oils of different molar masses (and, therefore, viscosities) as the continuous phase.[277] CL was found partially soluble in the lower molar-mass oils and completely insoluble in intermediate- and high-molar-mass oils. Pure suspension polymerization without additional contributions from solution (dispersion) polymerization has been carried out using the oils of intermediate molar masses, which represent the optimum compromise between monomer insolubility and medium fluidity. Very high monomer conversions in very short times, excellent microstructural regularity of the polymer chain (evaluated by the UV method mentioned below), accurate control of its molar mass and fine-tuning of particle shape, size, and size distribution have been successfully achieved by fast activated anionic polymerization, using the blocked cyclohexyl isocyanate/sodium ε-caprolactamate pair in equimolar concentrations. A typical SEM micrograph is given in **Figure 28**.

By suitably tuning the reaction parameters, the particle coalescence phenomena can be minimized and particle size distribution becomes rather narrow. Also by this method, it is possible to strongly reduce the amount of microstructural defects, as evidenced by the sharp lowering of the UV absorbance peak between 270 and 280 nm, usually assumed to be linked to the presence of structural irregularities in the PA6 chain and roughly proportional to their overall content. The absorbance of the UV absorption peak maximum is as low as ~0.04, almost the same as that for hydrolytic PA6.

As mentioned above, a miniemulsion process has also been successful for the obtainment of powdered PA6.[278] The optimum conditions in terms of miniemulsion stability have been achieved by dissolving CL in polar solvents, such as DMSO, followed by *in situ* formation of sodium ε-caprolactamate and subsequent dispersion in an apolar phase, typically in a branched saturated hydrocarbon (e.g., Isopar M©), with the aid of a suitable surfactant. The anionic ROP starts when the initiator (*N*-acetyl-CL) is added to the reaction medium and

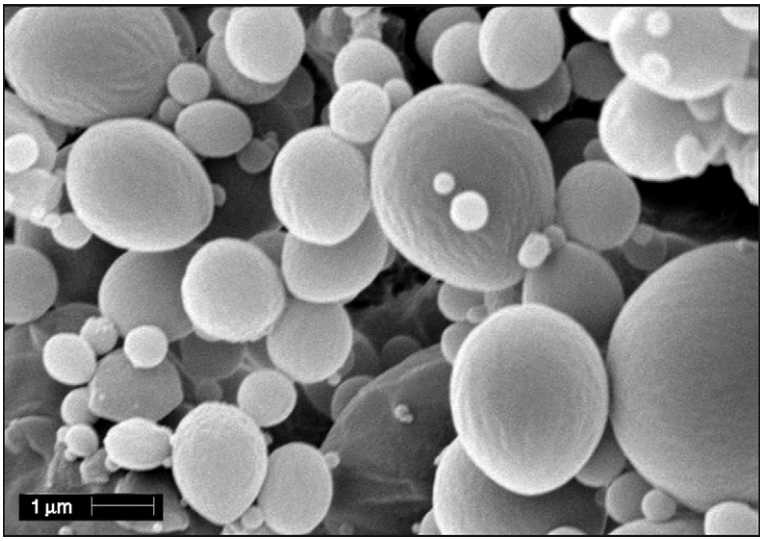

Figure 28 SEM micrograph of the PA6 particles obtained by suspension polymerization, as described in Ricco, L.; Monticelli, O.; Russo, S.; *et al. Macromol. Chem. Phys.* **2002**, *203*, 1436.[277]

polymerization T is reached. Ellipsoidal nanoparticles of PA6, obtained from the precipitation polymerization of CL inside the monomer/DMSO miniemulsion droplets, have been characterized by TEM. Their typical size is in the range of ~30 nm.

On the basis of the results obtained so far using the three methods mentioned above, a relevant conclusion can be drawn: the accurate temperature control (≤ 170 °C) permits to run polymerizations of CL in quasi-isothermal conditions and very efficiently contribute to the minimization of side reactions, the other relevant factor in this respect being the use of very fast activator/initiator pairs. Only the simultaneous effect of both factors, that is, temperature control and very fast catalytic systems, allows to reach both optimum process conditions and excellent polymer properties. The use of slow activators, such as *N*-acetyl-CL, on the contrary, strongly limits possible advantages of the method. Moreover, it should be taken into account that, in general, solution polymerizations (methods 1 and 3) are characterized by lower reaction rates as compared to suspension processes (method 2). On the other hand, these latter methods have to face more difficult and expensive purification procedures of the polyamide from the reaction mixture. The only other lactam-based polyamide synthesized in powder form in laboratory by a suspension process[233] is poly(2-pyrrolidone). A description of its synthesis is given in Section 4.14.11.1.

4.14.13.3 RIM, RTM, Rotational Molding, and Reactive Extrusion

As already mentioned in Section 4.14.13.1, the activated anionic polymerization of CL has undergone interesting industrial developments in the field of well-established monomer casting process, as well as in the more recent areas of RIM (RIM and R-RIM), resin transfer molding (RTM), and rotational molding. In addition, reactive extrusion processes, already explored since 1968,[281] are now gaining renewed attention for the easy preparation of nanocomposites and nanoblends, as described in the following.

Monomer casting, already described in some German and US patents prior to WWII, has been fully developed only since 1956, when several families of new initiators and activators allowed the anionic process to be industrially viable.[115] Due to its high crystallinity and high molar mass, cast PA6 has considerably greater modulus and strength, better wear, higher heat deflection temperature, better solvent resistance, better hygroscopic characteristics, and better dimensional stability as compared to the extruded or molded PA6 and PA6,6 materials. Additionally, a large variety of fillers can be easily added for more demanding applications. The very short polymerization times (2–20 min), as compared to those necessary to perform hydrolytic polymerization runs (12–24 h or more), the very low cyclic oligomer content (~2 vs. 8–12 wt.%), and the much lower initial polymerization temperature (130–170 °C vs. 230–280 °C) are the main advantages of this process.

Additional assets are the low cost of the mold, an almost unlimited range of shapes, and the weights of cast PA6 pieces up to several hundred kilograms. The anionic polymerization of CL in the bulk runs under increasing temperature profiles, even in quasi-adiabatic conditions for large cast volumes. For these latter systems, it is necessary to reduce the rate of polymerization by using slow initiating species and lower initial temperatures in order to avoid incomplete mold filling. To prevent sedimentation of fillers, when present, the reaction mixture is usually added with some polymeric thickener.

Like polyurethanes, in more recent years, PA6 has developed from monomer casting technology to RIM and R-RIM. So far, its only relevant commercial application and products are under the NyRIM© trade name. Indeed, this product is a multiblock copolymer formed from an oligooxypropylene or other elastomer and end functionalized with *N*-acyl lactam groups acting as polymeric activators (chain initiators) for the fast anionic polymerization of CL in the mold. The elastomeric blocks considerably improve the impact strength of the polyamide, thus making end products with the best combination of modulus, impact strength, and use temperature in comparison to any other unfilled RIM polymer. However, some disadvantages are also present: longer demold times and higher temperatures as compared to polyurethanes (PUs), the necessity of anhydrous conditions, and higher production prices.

Essentially, the process shows close similarities to polyurethane and polyurea RIM. Therefore, the machinery developed for these latter polymers and well known in the industrial practice can be readily adapted to NyRIM. The specific requirements of the RIM process applied to CL anionic polymerization have been summarized by Macosko[213] in terms of unit operations. The initiators typically used are sodium ε-caprolactamate or magnesium bromide ε-caprolactamate.

RTM applied to the anionic polymerization of CL is a result of implementation of RIM. A preformed reinforcing mat is placed into the mold where the reacting liquid mixture is injected. The continuous fiber or long fiber reinforcement is easily and fully impregnated by the reactants, which very quickly give rise to molded parts. These latter are characterized by stiffness and toughness much higher than the corresponding values coming from RIM or casting processes with short fiber reinforcement. Moreover, large percentages of fiber reinforcement are allowed by the RTM process.

Rotational molding (or rotational casting) provides hollow parts. The reactant mixture is introduced into a closed mold and rotation around one or two axes produces a uniform layer of PA6 on the inner surface of the cavity. Both RTM and rotational molding processes are advantageously realized with anionic PA6, while they are not practiced with polyurethanes.

Another potentially useful application is the continuous anionic polymerization of CL, which can be performed in twin screw extruders, taking advantage of both the very fast reaction kinetics and the broad limits of reactive system formulations. Recent findings[282] extended these potential applications to the field of nanocomposites, preparing organically modified montmorillonite (MMT) particles almost completely exfoliated and well dispersed in the polyamide matrix, with a sharp improvement of the mechanical properties (elastic modulus inserted up to +60% and tensile stress up to +15%). Another relevant application of CL anionic polymerization under reactive extrusion conditions is related to the *in situ* preparation of compatibilized nanoblends from immiscible/incompatible polymer pairs. For the system PP/PA6, as an example, the average size of the dispersed PA6 particles has been found in the 10–100 nm range.[283] No other blending method can achieve the same level of dispersion.

In general, *in situ* blending by reactive extrusion has been mainly explored in recent years in order to develop toughened PA6, although some studies have also been dealing with PA12 toughening[284,285] by anionic polymerization of ω-laurolactam in the presence of various rubbers. The results obtained so far are very promising and open wide possibilities of technically and economically feasible industrial applications.

4.14.13.4 Composites and Nanocomposites of Anionically Synthesized Polyamides

The anionic polymerization of lactams (mainly, CL) is less suitable than the hydrolytic process for the *in situ* preparation of their composites and nanocomposites. This is particularly the case when clays are used as reinforcing agents due to the presence of sizable amounts of water associated with clay as well as of mobile cations in most clay galleries and surfaces. Both agents contribute to the deactivation of the anionic active groups of the growing polyamide chains or, at least, exert a negative interference with them. In the field of clay-based nanocomposites, pristine MMTs cannot be well dispersed in CL because of the weak hydrogen-bonding interactions between the above components preventing intercalation or exfoliation. On the other hand, organically modified MMTs, which are very successful in the preparation of exfoliated nanocomposites based on clays and other polymers, seem to exert a severe inhibiting effect on the anionic ROP of CL, in addition to a rather poor interaction with it. Quite recently,[286] anionic PA6/MMT nanocomposites have been prepared by a novel two-step procedure able to overcome the above drawbacks, thus allowing full exfoliation of the pristine clay and large improvement of the nanocomposite thermal stability.

Another interesting field of application for PA6-based nanocomposites is that dealing with functionalized carbon nanotubes (CNTs), homogeneously dispersed in the polyamide matrix by *in situ* anionic ROP of CL. Usually, multiwalled carbon nanotubes (MWNTs), suitably functionalized on the surface to enhance hydrogen bonding with CL[287] or to create activators for its anionic ROP ('grafting from' method),[288] are characterized by a uniform and stable dispersion in the anionic PA6 matrix, thus increasing the crystallization temperature and enhancing the degree of crystallinity of the latter. Also single-walled carbon nanotubes (SWNTs) can be easily functionalized by CL attachment on their surface and subsequent anionic bulk polymerization using the above 'grafting from' technique.[289]

A third field where the anionic polymerization of CL has been applied to advantage is the *in situ* preparation of nanocomposites from nanosilica, uniformly dispersed in the monomer. Some recent publications[290–292] describe the fundamental steps of the synthesis and underline the most significant property improvements, especially when chemical bonds between surface-functionalized silica particles and anionic PA6 chains are formed.[291]

References

1. Carothers, W. H. *Chem. Rev.* **1931**, *8*, 353.
2. Carothers, W. H.; Berchet, G. J. *J. Am. Chem. Soc.* **1930**, *52*, 5289.
3. Schlack, P. Ger. Patent 748,253, 1938.
4. Odian, G. *Principles of Polymerization*, 4th ed.; Wiley: Hoboken, NJ, 2004; Chapter 7, p 544.
5. Schlack, P. *Pure Appl. Chem.* **1967**, *15*, 507.
6. Joyce, R. M.; Ritter, D. M. U.S. Proper U.S. Patent: 2,251,519 1941.
7. Šebenda, J. In *Comprehensive Chemical Kinetics*; Bamford, C. H.; Tipper, C. F. H., Eds.; Elsevier: Amsterdam, The Netherlands, 1976; Vol. 15, Chapter 6, p 379.
8. Sekiguchi, H. Ivin, K. J.; Saegusa, T., Eds.; *Ring-Opening Polymerizations*; Elsevier: London, UK, 1984; Vol. 2, Chapter 12, p 809.
9. Šebenda, J. In *Comprehensive Polymer Science*; Eastmond, G.; Ledwith, A.; Russo, S.; Sigwalt, P., Eds.; Pergamon Press: Oxford, UK, 1989; Vol. 3, Chapter 35, p 511.
10. Roda, J. In *Handbook of Ring-Opening Polymerization*; Dubois, P.; Coulembier, O.; Raquez, J.-M., Eds.; Wiley–VCH: Weinheim, Germany, 2009; Chapter 7, p 165.
11. Reimschuessel, H. K. In *Ring-Opening Polymerization*; Frisch, K. C.; Reegen, S. L., Eds.; Dekker: New York, 1969; Chapter 7, p 303.
12. Reimschuessel, H. K. *J. Polym. Sci. Part D Macromol. Rev.* **1977**, *12*, 65.
13. Millich, F.; Seshadri, K. V. In *High Polymers*; Frisch, K. C., Ed.; Wiley: New York, 1972; Vol. 26, Chapter 3, p 179.
14. Puffr, R. In *Lactam-Based Polyamides*; Puffr, R.; Kubánek, V., Eds.; CRC Press: Boca Raton, FL, 1991; Vol. 1, Chapter 1, p 1.
15. Jones, J. H.; Stachulsky, A. V. *Amino Acid Pept.* **1987**, *19*, 251.
16. Zhang, J.; Kissounko, D. A.; Lee, S. E.; *et al. J. Am. Chem. Soc.* **2009**, *131*, 1589.

17. Pauling, L. *The Nature of the Chemical Bond*; Cornell University Press: Ithaca, NY, 1960.
18. Wiberg, K. B.; Laidig, K. E. *J. Am. Chem. Soc.* **1987**, *109*, 5935.
19. Wiberg, K. B.; Breneman, C. M. *J. Am. Chem. Soc.* **1992**, *114*, 831.
20. Ogata, N. *Bull. Chem. Soc. Jpn.* **1959**, *32*, 813.
21. Treschanke, L.; Rademacher, P. *J. Mol. Struct.* (THEOCHEM) **1985**, *122*, 47.
22. Kirby, A. J.; Komarov, I. V.; Kowski, K.; *et al. J. Chem. Soc. Perkin Trans.* **1999**, *2*, 1313.
23. Hagler, A. T.; Lapiccirella, A. *Biopolymers* **1976**, *15*, 1167.
24. Greenberg, A.; Hsing, H.-J.; Liebman, J. F. *J. Mol. Struct.* (THEOCHEM) **1995**, *338*, 83.
25. Yamada, S. *J. Org. Chem.* **1996**, *61*, 941.
26. Greenberg, A.; Breneman, C. M.; Liebman, J. F. *The Amide Linkage: Structural Significance in Chemistry, Biochemistry and Material Science*; Wiley: New York, 2003.
27. Dunitz, J. D.; Winkler, F. K. *Acta Crystallogr.* **1975**, *B31*, 251.
28. Montaudo, G.; Caccamese, S.; Libraudo, V.; Recca, A. *J. Mol. Struct.* **1975**, *27*, 303.
29. Williamson, K. L.; Roberts, J. D. *J. Am. Chem. Soc.* **1976**, *98*, 5082.
30. Winkler, F. K.; Dunitz, J. D. *Acta Crystallogr.* **1975**, *B31*, 276.
31. Borgen, G.; Dale, J.; Rise, F.; Gundersen, L.-L. *Magn. Reson. Chem.* **1995**, *33*, 25.
32. Borgen, G.; Dale, J.; Rise, F.; Gundersen, L.-L. *Magn. Reson. Chem.* **1996**, *34*, 289.
33. Korshak, V. V.; Kotel'nikov, V. A.; Kurashev, V. V.; Frunze, T. M. *Russ. Chem. Rev. (Engl. Transl.).* **1976**, *45*, 853; *Usp. Khim.* **1976**, *45*, 1673.
34. Yang, Q. C.; Seiler, P.; Dunitz, J. D. *Acta Crystallogr.* **1987**, *C43*, 565.
35. Page, M. I.; Laws, A. P.; Slam, M. J.; Stone, J. R. *Pure Appl. Chem.* **1995**, *67*, 711.
36. Warshel, A.; Levitt, M.; Lifson, S. *J. Mol. Spectrosc.* **1970**, *33*, 84.
37. Borgen, G.; Rise, F. *Magn. Reson. Chem.* **1993**, *31*, 51.
38. Winkler, F. K.; Dunitz, J. D. *Acta Crystallogr.* **1975**, *B31*, 268.
39. Borgen, G.; Dale, J.; Rise, F. *Magn. Reson. Chem.* **1993**, *31*, 855.
40. Borgen, G. *Magn. Reson. Chem.* **1991**, *29*, 805.
41. Winkler, F. K.; Dunitz, J. D. *Acta Crystallogr.* **1975**, *B31*, 281.
42. Borgen, G.; Dale, J.; Gundersen, L.-L.; *et al. Acta Chem. Scand.* **1998**, *52*, 1110.
43. Wan, P.; Modro, T. A.; Yates, K. *Can. J. Chem.* **1980**, *58*, 2423.
44. Huisgen, R.; Brade, H.; Walz, H.; Glogger, I. *Chem. Ber.* **1957**, *90*, 1437.
45. Olah, G. A.; White, A. M. *Chem. Rev.* **1970**, *70*, 561.
46. Bontà, G.; Ciferri, A.; Russo, S. In *Ring-Opening Polymerization*; Saegusa, T.; Goethals, E., Eds.; ACS Symposium Series No. 59; American Chemical Society: Washington, DC, 1977; Chapter 16, p 216.
47. Alfonso, G. C.; Cirillo, G.; Russo, S.; Turturro, A. *Eur. Polym. J.* **1983**, *19*, 949.
48. Provaznik, M.; Puffr, R.; Šebenda, J. *Eur. Polym. J.* **1988**, *24*, 511.
49. Ogata, N. *Bull. Chem. Soc. Jpn.* **1961**, *34*, 245.
50. Ogata, N. *Bull. Chem. Soc. Jpn.* **1961**, *34*, 248.
51. Sekiguchi, H.; Coutin, B. *J. Polym. Sci. Polym. Chem. Ed.* **1973**, *11*, 1601.
52. Andrews, J. M.; Jones, F. R.; Semlyen, J. A. *Polymer* **1974**, *15*, 420.
53. Šebenda, J. *Pure Appl. Chem.* **1976**, *48*, 329.
54. Šebenda, J. *Prog. Polym. Sci.* **1978**, *6*, 123.
55. Duda, A.; Kowalski, A. In *Handbook of Ring-Opening Polymerization*; Dubois, P.; Coulembier, O.; Raquez, J.-M., Eds.; Wiley–VCH: Weinheim, Germany, 2009; Chapter 1, p 1.
56. Fries, T.; Belohlavkova, J.; Roda, J.; Králiček, J. *Polym. Bull.* **1984**, *12*, 87.
57. Šebenda, J. In *Lactam-Based Polyamides*; Puffr, R.; Kubánek, V., Eds.; CRC Press: Boca Raton, FL, 1991; Vol. 1, Chapter 2, p 29.
58. Ivin, K. J. *J. Polym. Sci. A Polym. Chem.* **2000**, *38*, 2137.
59. Brill, R. *Z. Phys. Chem. Abt. B* **1943**, *53*, 61.
60. Wichterle, O.; Tomka, J.; Šebenda, J. *Collect. Czech. Chem. Commun.* **1964**, *29*, 610.
61. Šebenda, J.; Hauer, J.; Biroš, J. *J. Polym. Sci. Polym. Chem.* **1976**, *14*, 2357.
62. Bonetskaya, A. K.; Skuratov, S. M. *Vysokomol. Soedin. Ser. A* **1969**, *11*, 532.
63. Kolesov, V. P.; Paukov, I. E.; Skuratov, S. M. *Zh. Fiz. Khim.* **1962**, *36*, 770.
64. Bukač, Z.; Cefelin, P.; Doskočilová, D.; Šebenda, J. *Collect. Czech. Chem. Commun.* **1964**, *29*, 2615.
65. Schirawski, G. *Makromol. Chem.* **1972**, *161*, 69.
66. Ney, W. O.; Nummy, W. R.; Barnes, C. E. U.S. Patent 2,638,463, 1953; *Chem. Abs.* **1953**, *47*, 9624.
67. Ney, W. O.; Crowther, M. U.S. Patent 2,739,959, 1956; *Chem. Abs.* **1956**, *50*, 13504.
68. Barnes, C. E.; Nummy, W. R., Ney, W. O., Jr U.S. Patent 2,806,841, 1957; *Chem. Abs.* **1958**, *52*, 3405.
69. Sekiguchi, H.; Coutin, T. *Makromol. Synth.* **1977**, *6*, 57.
70. Graf, R.; Lohaus, G.; Börner, K.; *et al. Angew. Chem.* **1962**, *74*, 523 (*Angew. Chem. Int. Ed.* **1962**, *1*, 481).
71. Eisenbach, C. D.; Lenz, R. W. *Macromolecules* **1976**, *9*, 227.
72. Eisenbach, C. D.; Lenz, R. W.; Sekiguchi, H. *J. Polym. Sci. Polym. Lett. Ed.* **1977**, *15*, 83.
73. Šebenda, J. *Makromol. Chem. Macromol. Symp.* **1986**, *6*, 1.
74. Mark, H.; Whitby, G. S. *Collected Papers of W.H. Carothers on High Polymeric Substances*; Interscience: New York, 1940; p 148.
75. Russel, R. A.; Thompson, H. W. *Spectrochim. Acta* **1956**, *8*, 138.
76. Baumgarten, H. E. *J. Am. Chem. Soc.* **1962**, *84*, 4975.
77. Cubbon, R. C. P. *Makromol. Chem.* **1964**, *80*, 44.
78. Deratani, A.; Carrière, F.; Sekiguchi, H. *Chem. Zvesti* **1976**, *30*, 292.
79. Deretani, A.; Sekiguchi, H. *Makromol. Chem.* **1979**, *180*, 189.
80. Puffr, R.; Šebenda, J. *Makromol. Chem. Makromol. Symp.* **1986**, *3*, 249.
81. Gutowski, H. S.; Holm, C. H. *J. Chem. Phys.* **1956**, *25*, 1228.
82. Kubisa, P.; Penczek, S. *Prog. Polym. Sci.* **1999**, *24*, 1409.
83. Hermans, P. H.; Heikens, D.; van Velde, P. F. *J. Polym. Sci.* **1958**, *30*, 81.
84. Korshak, V. V.; Frunze, T. M. *Synthetic Heterochain Polyamides*; Israel Program for Scientific Translation: Jerusalem, Israel, 1964; p 157.
85. Srivastava, D.; Gupta, S. K. *Polym. Eng. Sci.* **1991**, *31*, 596.
86. Ramesh, G. M.; Gupta, S. K. *Polymer* **1993**, *34*, 1716.
87. Seavey, K. C.; Khare, N. P.; Liu, Y. A.; *et al. Ind. Eng. Chem. Res.* **2003**, *42*, 3900.
88. Kumar, V. S.; Gupta, S. K. *Ind. Eng. Chem. Res.* **1997**, *36*, 1202.
89. Fang, X.; Simone, C. D.; Vaccaro, E.; *et al. J. Polym. Sci. A Polym. Chem.* **2002**, *40*, 2264.
90. Reimschuessel, H. K. *J. Polym. Sci.* **1959**, *41*, 457.
91. Heikens, D.; Hermans, P. H.; van der Want, G. M. *J. Polym. Sci.* **1960**, *44*, 437.
92. Bertalan, G.; Rusznák, I.; Anna, P. *Makromol. Chem.* **1984**, *185*, 1285.
93. Arai, Y.; Tai, K.; Teranishi, H.; Tagawa, T. *Polymer* **1981**, *22*, 273.
94. Heikens, D.; Hermans, P. H. *J. Polym. Sci.* **1960**, *44*, 429.
95. Rothe, M. *Angew. Chem.* **1968**, *80*, 245.
96. Rothe, M.; Mazánek, J. *Makromol. Chem.* **1971**, *145*, 197.
97. Rothe, M.; Bertalan, G. In *Ring-Opening Polymerization*; Saegusa, T.; Goethals, E., Eds.; ACS Symposium Series No. 59; American Chemical Society: Washington, DC, 1977; Chapter 9, p 129.
98. Bertalan, G.; Rusznák, I.; Ercsényi, Á.; Anna, P. *Makromol. Chem.* **1980**, *181*, 1807.
99. Bertalan, G.; Nagy, T. T.; Rusznák, I.; *et al. Makromol. Chem.* **1987**, *188*, 317.
100. Bertalan, G.; Rusznák, I.; Anna, P.; *et al. Polym. Bull.* **1988**, *19*, 539.
101. Bertalan, G.; Nagy, T. T.; Valkó, P.; *et al. Polym. Bull.* **1988**, *19*, 547.
102. Burnett, G. M.; MacArthur, A. J.; Hay, J. N. *Eur. Polym. J.* **1967**, *3*, 321.
103. Lowry, T. H.; Richardson, K. S. *Mechanism and Theory in Organic Chemistry*, 3rd ed.; Harper & Row: New York, 1987; p 715.
104. Bertalan, G. Ph.D. Thesis, Moscow, Russia, 1967.
105. Deslongschamps, P. *Stereoelectronic Effects in Organic Chemistry*; Pergamon Press: Oxford, UK, 1983; p 101.
106. Doubravszky, V. S.; Geleji, F. *Makromol. Chem.* **1968**, *113*, 270.
107. Schlack, P. *Z. Gesamte. Textilind.* **1963**, *65*, 1052.
108. Schlack, P. *Chemiefasern* **1965**, *15*, 64.
109. Schlack, P.; Rieker, J. *Angew. Makromol. Chem.* **1971**, *15*, 203.
110. Lánská, B.; Šebenda, J. *Eur. Polym. J.* **1974**, *10*, 841.
111. Lánská, B.; Šebenda, J. *Collect. Czech. Chem. Commun.* **1975**, *40*, 1524.
112. Puffr, R.; Šebenda, J. *J. Polym. Sci. C* **1973**, *42*, 21.
113. Burnett, G. M.; Hay, J. N.; MacArthur, A. J. *Soc. Chem. Ind. (London) Monogr.* **1966**, *20*, 139.
114. Hanford, W.; Joyce, R. M. *J. Polym. Sci.* **1948**, *3*, 167.
115. Wichterle, O.; Šebenda, J.; Králiček, J. *Adv. Polym. Sci.* **1961**, *2*, 578.
116. Champetier, G.; Sekiguchi, H. *J. Polym. Sci.* **1960**, *48*, 309.
117. Šebenda, J. *J. Macromol. Sci.* **1972**, *A6*, 1145.
118. Šittler, E.; Šebenda, J. *Collect. Czech. Chem. Commun.* **1968**, *33*, 3182.
119. Stehliček, J.; Šebenda, J. *Eur. Polym. J.* **1987**, *23*, 237.
120. Čefelin, P.; Stehlíček, J.; Šebenda, J. *Coll. Czech. Chem. Commun.* **1974**, *39*, 2212.
121. Sekiguchi, H. *Bull. Soc. Chim. Fr.* **1960**, 1835.
122. Sekiguchi, H. *J. Polym. Sci.* **1963**, *A1*, 1627.
123. Frunze, T. M.; Kotel'nikov, V. A.; Volkova, T. V.; *et al. Eur. Polym. J.* **1981**, *17*, 1079.
124. Frunze, T. M.; Kotel'nikov, V. A.; Volkova, T. V.; *et al. Acta Polym.* **1981**, *32*, 31.
125. Sekiguchi, H. *Nippon Kagaku Zasshi* **1967**, *88*, 577.
126. Coutin, B.; Sekiguchi, H. *1st European Discussion Meeting on Polymer Science: New Developments in Ionic Polymerization*, Strasbourg, France, 1978; Abstracts, p 88.
127. Coutin, B.; Sekiguchi, H. *J. Polym. Sci. Polym. Chem.* **1977**, *15*, 2539.
128. Stehlíček, J.; Šebenda, J. *Eur. Polym. J.* **1986**, *22*, 769.
129. Alfonso, G. C.; Chiappori, C.; Razore, S.; Russo, S. In *Reaction Injection Molding, Polymer Chemistry and Engineering*; Kresta, J. E., Ed.; ACS Symposium Series No. 270; American Chemical Society: Washington, DC, 1985; Chapter 11, p 163.

130. Ricco, L.; Russo, S.; Orefice, G.; Riva, F. *Macromolecules* **1999**, *32*, 7726.
131. Stehlíček, J.; Šebenda, J. *Eur. Polym. J.* **1986**, *22*, 5.
132. Cefelin, P.; Stehlíček, J.; Šebenda, J. *Polym. Sci. C.* **1973**, *42*, 79–88.
133. Malkin, A. V.; Frolov, V. G.; Ivanova, A. N.; Andrianova, Z. S. *Polym. Sci. U.S.S.R.* **1979**, *21*, 691.
134. Bolgov, S. A.; Begishev, V. P.; Malkin, A. Y.; Frolov, V. G. *Polym. Sci. U.S.S.R.* **1981**, *23*, 1485.
135. Sibal, P. W.; Camargo, R. E.; Macosko, C. W. *Polym. Process Eng.* **1983–1984**, *1*, 147.
136. Havlice, J.; Brožek, J.; Šáchová, M.; *et al. Macromol. Chem. Phys.* **1999**, *200*, 1200.
137. Puffr, R.; Vladimirov, N. *Makromol. Chem.* **1993**, *194*, 1765.
138. Greenley, R. Z.; Stauffer, J. C.; Kurz, J. E. *Macromolecules* **1969**, *2*, 561.
139. Gabbert, J. D.; Hedrick, R. M. *Polym. Process Eng.* **1986**, *4*, 359.
140. Udipi, K.; Davé, R. S.; Kruse, R. L.; Stebbins, L. R. *Polymer* **1997**, *38*, 927.
141. Stehlíček, J.; Puffr, R. *Makromol. Chem.* **1992**, *193*, 2539.
142. Hedrick, R. M.; Gabbert, J. D.; Wohl, M. H. In *Reaction Injection Molding, Polymer Chemistry and Engineering*; Kresta, J. E., Ed.; ACS Symposium Series No. 270; American Chemical Society: Washington, DC, 1985; p 135.
143. Buskirk, B. V.; Akkapeddi, M. K. *Polym. Prepr. (Am. Chem. Soc. Div. Polym. Chem.)* **1988**, *29*, 557.
144. Rusu, G.; Ueda, K.; Rusu, E.; Rusu, M. *Polymer* **2001**, *42*, 5669.
145. Arnoldová, P.; Prokopova, I.; Bernat, P.; Roda, J. *Angew. Makromol. Chem.* **1999**, *269*, 25.
146. Arnoldová, P.; Brus, J.; Prokopová, I.; Brožek, J. *e-Polymers* **2006**, *68*, 1618.
147. Sekiguchi, H.; Rapakoulia Tsourkas, P.; Coutin, B. *J. Polym. Sci. C* **1973**, *11*, 1601.
148. Davé, R. S.; Kruse, R. L.; Stebbins, L. R.; Udipi, K. *Polymer* **1997**, *38*, 939.
149. Veith, C. A.; Cohen, R. E. *Polym. Prepr. (Am. Chem. Soc. Div. Polym. Chem.)* **1990**, *31*, 42.
150. Veith, C. A.; Cohen, R. E. *Makromol. Chem. Macromol. Symp.* **1991**, *42/43*, 241.
151. Mougin, N.; Veith, C. A.; Cohen, R. E.; Gnanou, Y. *Macromolecules* **1992**, *25*, 2004.
152. Mougin, N.; Rempp, P.; Gnanou, Y. *Macromolecules* **1992**, *25*, 6739.
153. Fiala, F.; Králíček, J. *Angew. Makromol. Chem.* **1978**, *71*, 29.
154. Schwesinger, R.; Hasenfratz, C.; Schlemper, H.; *et al. Angew. Chem. Int. Ed.* **1993**, *32*, 1361.
155. Tang, J.; Dopke, J.; Verkade, J. G. *J. Am. Chem. Soc.* **1993**, *115*, 5015.
156. Memeger, W., Jr.; Campbell, G. C.; Davidson, F. *Macromolecules* **1996**, *29*, 6475.
157. Russo, S.; Imperato, A.; Mariani, A.; Parodi, F. *Macromol. Chem. Phys.* **1995**, *196*, 3297.
158. Rached, R.; Hoppe, S.; Fonteix, C.; *et al. Chem. Eng. Sci.* **2005**, *60*, 2715.
159. Mendichi, R.; Russo, S.; Ricco, L.; Giacometti Schieroni, A. *J. Sep. Sci.* **2004**, *27*, 637.
160. Russo, S.; Biagini, E.; Bontà, G. *Makromol. Chem. Macromol. Symp.* **1991**, *48/49*, 31.
161. Stehlíček, J.; Šebenda, J.; Wichterle, O. *Collect. Czech. Chem. Commun.* **1964**, *29*, 1236.
162. Rigo, A.; Fabbri, G.; Talamini, G. *J. Polym. Sci. Polym. Lett. Ed.* **1975**, *13*, 469.
163. Stehlíček, J.; Labský, J.; Šebenda, J. *Collect. Czech. Chem. Commun.* **1967**, *32*, 545.
164. Wicks, Z. W., Jr *Prog. Org. Coat.* **1975**, *3*, 733.
165. Engbert, T.; König, E.; Jürgens, E. *Farbe Lack* **1996**, *102*, 51.
166. Russo, S.; Bontà, G.; Imperato, A.; Parodi, F. In *Integration of Fundamental Polymer Science Technology*; Lemstra, P. J.; Kleintjens, L. A., Eds.; Elsevier: London, UK, 1988; Vol. 2, p 17.
167. Mateva, R.; Petrov, P.; Rousseva, S.; *et al. Eur. Polym. J.* **2000**, *36*, 813.
168. Van Rijswijk, K.; Bersee, H. E. N.; Beukers, A.; *et al. Polym. Test.* **2006**, *25*, 392.
169. Maier, S.; Loontjens, T.; Scholtens, B.; Mülhaupt, R. *Macromolecules* **2003**, *36*, 4727.
170. Loontjens, T. *J. Polym. Sci. A Polym. Chem.* **2003**, *41*, 3198.
171. Maier, S.; Loontjens, T.; Scholtens, B.; Mülhaupt, R. *Angew. Chem. Int. Ed.* **2003**, *42*, 5094.
172. Mateva, R.; Delev, O. *Polym. J.* **1995**, *27*, 449.
173. Mateva, R.; Delev, O.; Kaschcieva, E. *J. Appl. Polym. Sci.* **1995**, *58*, 2333.
174. Mateva, R.; Delev, O.; Rousseva, S. *Eur. Polym. J.* **1997**, *33*, 1377.
175. Ricco, L.; Russo, S.; Monticelli, O.; *et al. Polymer* **2005**, *46*, 6810.
176. Roda, J.; Brožek, J.; Králíček, J. *Makromol. Chem., Rapid Commun.* **1980**, *1*, 165.
177. Daniel, L.; Brožek, J.; Roda, J.; Králíček, J. *Makromol. Chem.* **1982**, *183*, 2719.
178. Brožek, J.; Marek, M., Jr.; Roda, J.; Králíček, J. *Makromol. Chem.* **1988**, *189*, 17.
179. Brožek, J.; Rehak, P.; Roda, J.; Králíček, J. *Polym. Bull.* **1984**, *11*, 353.
180. Brožek, J.; Rehak, P.; Marek, M., Jr.; *et al. Makromol. Chem.* **1988**, *189*, 9.
181. Merna, J.; Chromcová, D.; Brožek, J.; Roda, J. *Eur. Polym. J.* **2006**, *42*, 1569.
182. Goodman, I.; Vachon, R. N. *Eur. Polym. J.* **1984**, *20*, 529.
183. Bernášková, A.; Chromcová, D.; Brožek, J.; Roda, J. *Polymer* **2004**, *45*, 2141.
184. Marelová, J.; Roda, J.; Stehlíček, J. *Eur. Polym. J.* **1999**, *35*, 145.
185. Schmid, E.; Eder, R. Ger. Patent DE 19602684 C1, 1997.
186. Luisier, A.; Bourban, P.-E.; Månson, J.-A. E. *J. Polym. Sci. A Polym. Chem.* **2002**, *40*, 3406.
187. Ji, Y.; Ma, J.; Liang, B. *Mater. Lett.* **2005**, *59*, 1997.
188. Pae, Y. *J. Appl. Polym. Sci.* **2006**, *99*, 292.
189. Pae, Y. *J. Appl. Polym. Sci.* **2006**, *99*, 309.
190. Hu, G.-H.; Li, H.; Feng, L.-F. *Macromolecules* **2002**, *35*, 8247.
191. Mohammadian-Gezaz, S.; Ghasemi, I.; Oromiehie, A. *Polym. Test.* **2009**, *28*, 534.
192. Zhang, C.-L.; Feng, L.-F.; Hoppe, S.; Hu, G.-H. *J. Polym. Sci. A Polym. Chem.* **2008**, *46*, 4766.
193. Liu, Y.-C.; Xu, W.; Xiong, Y.-Q.; *et al. Mater. Lett.* **2008**, *62*, 1849.
194. Breslow, D. S.; Hulse, G. E.; Matlack, A. S. *J. Am. Chem. Soc.* **1957**, *79*, 3760.
195. Kennedy, J. P.; Otsu, T. *J. Macromol. Sci. Polym. Rev.* **1972**, *6*, 237.
196. Kobayashi, S.; Ritter, H.; Kaplan, D., Eds. *Enzyme-Catalyzed Synthesis of Polymers* (Adv. Polym. Sci., vol. 194); Springer: Berlin, Germany, 2006.
197. Kobayashi, S.; Makino, A. *Chem. Rev.* **2009**, *109*, 5288.
198. Gross, R. A.; Kumar, A.; Kalra, B. *Chem. Rev.* **2001**, *101*, 2097.
199. Kumar, A.; Mei, Y.; Gross, R. A. *Macromolecules* **2003**, *36*, 5530.
200. Loeker, F. C.; Duxbury, C. J.; Kumar, A.; *et al. Macromolecules* **2004**, *37*, 2450.
201. Thurecht, K. J.; Heise, A.; deGeus, M.; *et al. Macromolecules* **2006**, *39*, 7967.
202. van der Mee, L.; Helmich, F.; de Bruijn, R.; *et al. Macromolecules* **2006**, *39*, 5021.
203. Gu, Q.-M.; Maslanka, W. W.; Cheng, H. N. *Polym. Prepr. (Am. Chem. Soc. Div. Polym. Chem.)* **2006**, *47*, 234.
204. Schwab, L. W.; Kroon, R.; Schouten, A. J.; Loos, K. *Macromol. Rapid Commun.* **2008**, *29*, 794.
205. Baum, I.; Haller, L. A.; Schwab, L. W.; *et al. Chem. Centr. J.* **2009**, *3* (Suppl. 1), p 57; *4th German Conference on Chemoinformatics*, Goslar, Germany, Nov. 9–11, 2008.
206. Hermans, P. H. *J. Appl. Chem.* **1955**, *5*, 493.
207. Falgová, I.; Kondelíková, J.; Králíček, J. *Angew. Makromol. Chem.* **1976**, *49*, 75.
208. Gorbukova, E. V.; Deev, J. S.; Ryabov, Y. A. *Vysokomol. Soedin. Ser. A* **1980**, *22*, 2457.
209. Prokopová, I.; Černý, J.; Kondelíková, J.; *et al. Angew. Makromol. Chem.* **1983**, *112*, 183.
210. Alijev, R.; Kondelíková, J.; Králíček, J.; Kříž, O. *Angew. Makromol. Chem.* **1982**, *108*, 219.
211. Prokopová, I.; Tuzar, Z.; Kondelíková, J.; Králíček, J. *Angew. Makromol. Chem.* **1987**, *147*, 199.
212. Malkin, A.; Ivanova, Ya.; Frolov, V. G.; *et al. Polymer* **1982**, *23*, 1791.
213. Macosko, C. W. *RIM Fundamentals of Reaction Injection Molding*; Hanser Publication: Munich, Germany, 1989.
214. Alfonso, G. C.; Bontà, G.; Russo, S.; Traverso, A. *Makromol. Chem.* **1981**, *182*, 929.
215. Biagini, E.; Costa, G.; Russo, S.; *et al. Makromol. Chem. Macromol. Symp.* **1986**, *6*, 207.
216. Mori, S.; Takeuchi, T. *J. Chromatogr.* **1970**, *50*, 419.
217. Ueda, K.; Hosoda, M.; Matsuda, T.; Tai, K. *Polym. J.* **1998**, *30*, 186.
218. Jacobson, H.; Stockmayer, W. H. *J. Chem. Phys.* **1950**, *18*, 1600.
219. Mengerink, Y.; Peters, R.; Kerkoff, M.; *et al. J. Chromatogr. A* **2000**, *876*, 37.
220. Semlyen, J. A. *Adv. Polym. Sci.* **1976**, *21*, 41.
221. Suter, U. In *Comprehensive Polymer Science*; Eastmond, G. G.; Ledwith, A.; Russo, S.; Sigwalt, P., Eds.; Pergamon Press: Oxford, UK, 1989; Vol. 5, p 91.
222. Casazza, E.; Ricco, L.; Russo, S.; Scamporrino, E. *Macromolecules* **2007**, *40*, 739.
223. Ricco, L.; Casazza, E.; Mineo, P.; *et al. Macromolecules* **2008**, *41*, 3904.
224. Di Silvestro, G.; Sozzani, P.; Bruckner, S.; *et al. Makromol. Chem.* **1987**, *188*, 2745.
225. Kržan, A.; Miertus, S. *Macromol. Chem. Phys.* **2002**, *203*, 1643.
226. Biagini, E.; Pedemonte, B.; Pedemonte, E.; *et al. Makromol. Chem.* **1982**, *183*, 2131.
227. Turturro, A.; Russo, S.; Antolini, E.; Cirafici, S. *Polymer* **1989**, *30*, 1099.
228. Sekiguchi, H. *Bull. Soc. Chim. Fr.* **1960**, 1831.
229. Schirawski, G. *Makromol. Chem.* **1972**, *161*, 57.
230. Sekiguchi, H.; Rapacoulia, P.; Coutin, B. *Nuova Chim.* **1973**, *49*, 32.
231. Roda, J.; Králíček, J. U.S. Patent 4,343,933, 1982.
232. Roda, J.; Votrubcová, Z.; Králíček, J.; *et al. Makromol. Chem.* **1981**, *182*, 2117.
233. Costa, G.; Nencioni, M.; Russo, S.; *et al. Makromol. Chem.* **1981**, *182*, 1399.
234. Luisier, A.; Bourban, P.-E.; Månson, J.-A. E. *J. Appl. Polym. Sci.* **2001**, *81*, 963.
235. Budín, J.; Roda, J.; Brožek, J.; Kříž, J. *Macromol. Symp.* **2006**, *240*, 78.
236. Hashimoto, K. *Prog. Polym. Sci.* **2000**, *25*, 1411.
237. Šebenda, J., Hauer, J., *Polym. Bull.* **1981**, *5*, 529.
238. Šebenda, J.; Hauer, J.; Svetlik, J. *J. Polym. Sci. Polym. Symp.* **1986**, *74*, 303.
239. Hashimoto, K.; Hotta, K.; Okada, M.; Nagata, S. *J. Polym. Sci. A Polym. Chem.* **1995**, *33*, 1995.

240. Hashimoto, K.; Oi, T.; Yasuda, J.; *et al. J. Polym. Sci. A Polym. Chem.* **1997**, *35*, 1831.
241. Hashimoto, K.; Yasuda, J.; Kobayashi, M. *J. Polym. Sci. A Polym. Chem.* **1999**, *37*, 909.
242. Zhang, J.; Gellman, S. H.; Stahl, S. S. *Macromolecules* **2010**, *43*, 5618.
243. Hashimoto, K.; Sumitomo, H.; Washio, A. *J. Polym. Sci. A Polym. Chem.* **1989**, *27*, 1915.
244. Hashimoto, K.; Sugata, T.; Imanishi, S.; Okada, M. *J. Polym. Sci. A Polym. Chem.* **1994**, *32*, 1619.
245. Budin, J.; Brožek, J.; Roda, J. *Polymer* **2006**, *47*, 140.
246. Chromcová, D.; Baslerová, L.; Roda, J.; Brožek, J. *Eur. Polym. J.* **2008**, *44*, 1733.
247. Fox, T. G. *Bull. Am. Phys. Soc.* **1956**, *1*, 123.
248. Fang, X.; Hutcheon, R.; Scola, D. A. *J. Polym. Sci. A Polym. Chem.* **2000**, *38*, 1379.
249. Kim, B. J.; White, J. L. *J. Appl. Polym. Sci.* **2003**, *88*, 1429.
250. Kim, I.; White, J. L. *J. Appl. Polym. Sci.* **2005**, *96*, 1875.
251. Kim, I.; White, J. L. *J. Appl. Polym. Sci.* **2003**, *90*, 3797.
252. Coutinho, F. M. B.; Barbosa Sobrinho, A. A. *Eur. Polym. J.* **1991**, *27*, 105.
253. Stehlíček, J.; Chauhan, G. S.; Znášiková, M. *J. Appl. Polym. Sci.* **1992**, *46*, 2169.
254. Yeh, J.-L.; Kuo, J.-F.; Chen, C.-Y. *J. Appl. Polym. Sci.* **1993**, *50*, 1671.
255. Kim, K. J.; Hong, D. S.; Tripathy, A. R.; Kyu, T. *J. Appl. Polym. Sci.* **1999**, *73* (1), 285.
256. Roda, J. In *Block Copolymers*; Baltá-Calleja, F. J.; Roslaniec, Z., Eds.; Marcel Dekker: New York, 2000; p 93.
257. Nováková, V.; Sobotík, R.; Mat⊠nová, J.; Roda, J. *Angew. Makromol. Chem.* **1996**, *237*, 123.
258. Sobotík, R.; Šruba⊠, R.; Roda, J. *Macromol. Chem. Phys.* **1997**, *198*, 1147.
259. Brožek, J.; Budín, J.; Roda, J. *J. Therm. Anal. Cal.* **2007**, *89*, 211.
260. Owen, M. J.; Thompson, J. *Br. Polym. J.* **1972**, *4*, 297.
261. Mateva, R.; Filyanova, R.; Dimitrov, R.; Velichkova, R. *J. Appl. Polym. Sci.* **2004**, *91*, 3251.
262. Zhilkova, Kr.; Mateva, R. *J. Univ. Chem. Technol. Metall.* **2008**, *43*, 291.
263. Petrov, P.; Jankova, K.; Mateva, R. *J. Appl. Polym. Sci.* **2003**, *89*, 711.
264. Harrats, C.; Fayt, R.; Jérôme, R. *Polymer* **2002**, *43*, 5347.
265. Allen, W. T.; Eaves, D. E. *Angew. Macromol. Chem.* **1977**, *58*, 321.
266. Hu, G.-H.; Cartier, H.; Feng, L.-F.; Li, B.-G. *J. Appl. Polym. Sci.* **2004**, *91*, 1498.
267. Teng, J.; Otaigbe, J. U.; Taylor, E. P. *Polym. Eng. Sci.* **2004**, *44*, 648.
268. Hu, G.-H.; Li, H.; Feng, L.-F. *Polymer* **2005**, *46*, 4562.
269. Hu, G.-H.; Li, H.; Feng, L.-F. *J. Appl. Polym. Sci.* **2006**, *102*, 4394.
270. Hedrick, R. M.; Gabbert, J. D.; Wohl, M. H. in Reaction Injection Molding, Polymer Chemistry and Engineering, Kresta, J. E., Ed.; ACS Symposium Series No. 270; American Chemical Society; Washington, DC, 1985; Chapter 10, p. 135.
271. Biernacki, P.; Chrzczonowicz, S.; Wlodarczyk, M. *Eur. Polym. J.* **1971**, *7*, 739.
272. Biernacki, P.; Wlodarczyk, M. *Eur. Polym. J.* **1975**, *11*, 107.
273. Biernacki, P.; Wlodarczyk, M. *Eur. Polym. J.* **1980**, *16*, 843.
274. Vasiliu-Oprea, Cl.; Dan, F. *J. Appl. Polym. Sci.* **1996**, *62*, 1517.
275. Vasiliu-Oprea, Cl.; Dan, F. *J. Appl. Polym. Sci.* **1997**, *64*, 2575.
276. Dan, F.; Vasiliu-Oprea, Cl. *J. Appl. Polym. Sci.* **1998**, *67*, 231.
277. Ricco, L.; Monticelli, O.; Russo, S.; *et al. Macromol. Chem. Phys.* **2002**, *203*, 1436.
278. Crespy, D.; Landfester, K. *Macromolecules* **2005**, *38*, 6882.
279. Pei, A.; Liu, A.; Xie, T.; Yang, G. *Macromolecules* **2006**, *39*, 7801.
280. Dan, F.; Vasiliu-Oprea, Cl. *Colloid Polym. Sci.* **1998**, *276*, 483.
281. Illing, G. *Mod. Plast.* **1969**, *46*, 70.
282. Rothe, B.; Elas, A.; Michaeli, W. *Macromol. Mater. Eng.* **2009**, *294*, 54.
283. Hu, G.-H.; Cartier, H.; Plummer, C. *Macromolecules* **1999**, *32*, 4713.
284. Wollny, A.; Nitz, H.; Faulhammer, H.; *et al. J. Appl. Polym. Sci.* **2003**, *90*, 344.
285. Du, L.; Yang, G. *Polym. Eng. Sci.* **2010**, *50*, 1178.
286. Liu, A.; Xie, T.; Yang, G. *Macromol. Chem. Phys.* **2006**, *207*, 701.
287. Yan, D.; Xie, T.; Yang, G. *J. Appl. Polym. Sci.* **2009**, *111*, 1278.
288. Yan, D.; Yang, G. *J. Appl. Polym. Sci.* **2009**, *112*, 3620.
289. Qu, L.; Veca, L. M.; Lin, Y.; *et al. Macromolecules* **2005**, *38*, 10328.
290. Rusu, G.; Rusu, E. *High Perform. Polym.* **2006**, *18*, 355.
291. Yang, M.; Gao, Y.; He, J. P.; Li, H. M. *Express Polym. Lett.* **2007**, *1*, 433.
292. Cai, L. F.; Lin, Z. Y.; Qian, H. *Express Polym. Lett.* **2010**, *4*, 397.

Biographical Sketches

Saverio Russo is a senior professor of industrial chemistry at Genoa University, Italy. He has been, and still is, project leader of several research programs supported by the European Union, Italian Ministry of University, and Chemical Companies. He has been working for more than 40 years in the field of macromolecular science and technology, mainly on *advanced polymeric materials: synthesis, characterization and applications.* Polyamide 6 by the anionic routes has been one of the major topics of his research. He is author of more than 250 scientific publications, mostly in international journals, and six patents. Prof. Russo has been member of the Scientific Committee of INSTM (Interuniversity Consortium of Materials Science and Technology) and director of its Section on Functional and Structural Polymeric Materials. He was the co-editor of four volumes of *Comprehensive Polymer Science*, Pergamon, 1989 and two supplement volumes (1992 and 1996). He was the organizer and co-chairman of two *IUPAC Symposia of Free Radical Polymerization: Kinetics and Mechanism*, in 1987 and 1996.

Elena Casazza studied organic chemistry and polymer science at University of Genoa, Italy, where she received her master's degree in chemistry and the PhD in chemical sciences and technology.

For a few years, she worked as a postdoc at Genoa University on macromolecular systems in the research group of Prof. Russo. Afterward, she joined industry in the field of the plastic materials where she has been working for more than 10 years within the Research and Development Department with managerial duties.

At present, she is involved in close scientific collaboration with Italian Universities and acts as a consultant for several chemical companies.

4.15 Polymerization of Oxazolines

S Kobayashi, Kyoto Institute of Technology, Kyoto, Japan

4.15.1 Introduction

Oxazolines are a family of cyclic imino ethers having a five-membered structure. Among the oxazoline family, 2-oxazolines (OZOs; IUPAC name: 4,5-dihydrooxazoles) with an *endo*-imino ether group (–C=N–O–) are most extensively studied so far in the polymerization chemistry. 2-Substituted-2-oxazolines (ROZO, reaction 1, **Scheme 1**) were first derived in the peptide chemistry of α-amino acid derivatives. In the polymer synthesis, pioneering works on the ring-opening polymerization of ROZOs were achieved in the mid-1960s by four independent groups.[1] A cationic catalyst or initiator induced the cationic ring-opening polymerization (CROP) of ROZOs to give poly(*N*-acylethylenimine)s (PROZOs) (reaction 1), during which the isomerization took place from the imino ether group of the monomer to a more thermally stable *N*-acyl group of the polymer.

After the above early studies, ring-opening polymerizations of OZOs have been conducted very actively and continuously for more than four decades, and various types of monomers and catalysts as well as polymerization modes have been developed. These results have been reviewed from time to time by several polymer scientists.[2] **Scheme 1** outlines the six reaction modes found, in which structures of monomers and product polymer units are given in a general form. Reaction 1 shows the CROP involving an isomerization of the –C=N–O– bond to an amide group –C(=O)–N– to produce an ethylenimine (EI) unit, the most well-known reaction mode. This mode of reaction constitutes a major part of the present chapter. Reaction 2 gives an amide unit, which is a mode of ring-opening polyaddition (ROPA) involving isomerization. Bis-ROZO monomers are often used in combination with bifunctional phenols or carboxylic acids for ROPA. Reaction 3 is a unique monomer as well as reaction mode involving isomerization found in polysaccharide synthesis with an enzyme catalyst (enzymatic ROPA (EROPA)) or a cationic catalyst (cationic ROPA (CROPA)). As shown in reaction 4,

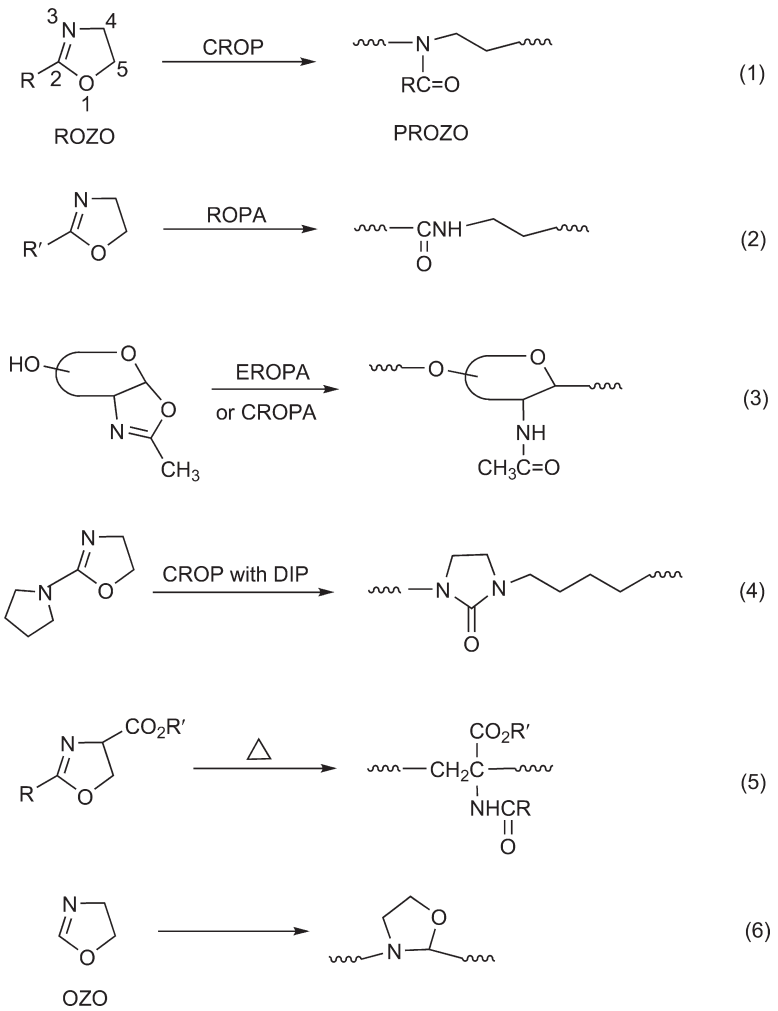

Scheme 1 Major reaction types of oxazoline (OZO) monomers and their product polymer units in OZO polymerizations shown in general expression of structures.

depending on the nature of the monomer substituent and catalyst (initiator), CROP induces a double isomerization polymerization (DIP) during the polymerization to produce a new polymer unit. Reaction 5 involves ring opening of the monomer but affords a different polymer unit like a vinyl polymer under thermal reaction conditions. Reaction 6 does not involve the ring opening, undergoing the C=N reaction. Modes of reactions 5 and 6 are rather rare cases.

The polymers from the reaction (1) possess a PROZO structure, which can often be regarded as 'pseudopeptides' owing to the structure analogy and also to their nontoxic nature.[2,3] These characteristics often lead to 'smart' polymer materials like those quickly responding to external stimuli.

At the early stage of research, PROZOs were paid much attention as a convenient starting polymer for deriving linear polyethylenimine (LPEI), which is otherwise very difficult to prepare. It is because CROP of EI does not give LPEI but branched polyethylenimine (BPEI) (R = H, Scheme 2).[2,4]

This chapter is a comprehensive review dealing with polymerization of various OZO monomers to give a variety of polymers, polymerization reaction characteristics, and properties as well as applications of the product polymers.

4.15.2 Cationic Ring-Opening Polymerization

4.15.2.1 Monomers, Catalysts (Initiators), Reaction Mechanism, and Monomer Reactivity

Typical examples of oxazoline monomers to be polymerized via CROP mode are shown in Scheme 3. Not only five-membered monomers of ROZO and 5-oxazolones (4,5-dihydro-1,3-oxazol-5-one, ROZLO) but also six-membered analogs (5,6-dihydro-4*H*-1,3-oxazines, ROZI) and seven-membered ones (4,5,6,7-tetrahydro-4*H*-1,3-oxazepine, ROXP) have been polymerized. 2-Iminotetrahydrofurans (ITHFs) are known as an *exo*-cyclic imino ether derivative of ROZO. CROP of ITHF was reported in 1963,[5] which was preceded by the studies on the CROP of OZOs.[1] Preparations of these monomers have been well known and documented.[2]

Concerning the structure of substituent R, numerous functional group-containing substituents have been investigated, functional groups being, that is, olefinic-, acetylenic-, phenolic-, hydroxyalkyl-, mercaptoalkyl-, carboxyalkyl-, amino-, aminoalkyl-, haloalkyl-, and other groups.[2,6] Some of these monomers act as a reactive or functional monomer.

As to catalysts or initiators, a variety of acid catalysts (protonic and Lewis acids), cationic species, and electrophiles have been

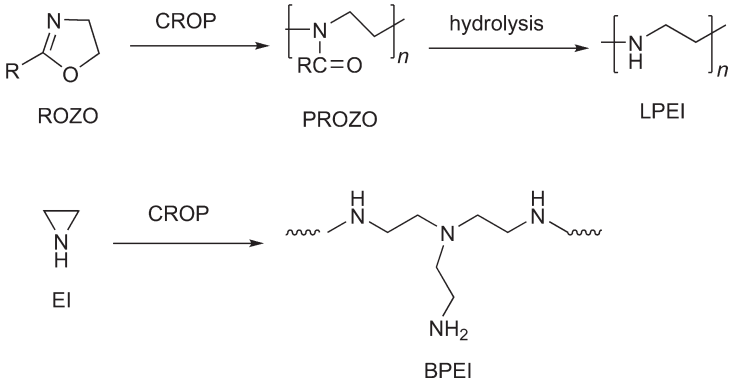

Scheme 2 Synthesis of linear polyethylenimine (LPEI) and branched polyethylenimine (BPEI).

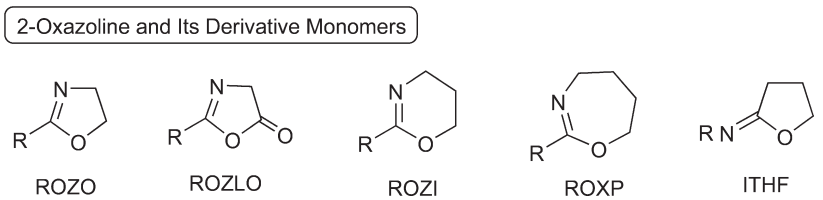

Scheme 3 Monomer structures of 2-oxazoline family.

utilized and examined: typically, X of an electrophile RX = Cl, Br, I, *p*-toluenesulfonate (TsO), trifluoromethanesulfonate (TfO), etc. The nature of X affects the stability of oxazolinium ions and alters the polymerization mode (*vide infra*).[2]

Since the imino nitrogen of OZOs is basic and nucleophilic, they readily react with an electrophile (E^+) to form oxazolinium species. Although the resulting cationic species are stabilized by resonance, they are reactive enough to be attacked by a nucleophile including OZO monomers (Scheme 4).

CROP of OZOs is generally given by using an initiator of R′X (Scheme 5). The nucleophlic attack to the 2-oxazolinium ion occurs selectively at its 5-position, which results in the isomerization of the imidate functional group (–C=N–O–) to a more stable amide group (–C(=O)–N–). Thus, CROP of ROZO is of 'cationic ring-opening isomerization polymerization' type. The CROP often proceeds in a living fashion due to a stable oxazolinium ion. The stable nature of the ions readily brings about the living CROP system.

The isomerization of the functional group gives an important feature on the CROP of ROZOs. The driving force for ROP of well-known monomers such as cyclic ethers, cycloalkene, lactones, and lactams is the release of ring strain (bond strain and tortional strain) during the polymerization.[7] However, the isomerization from the imino ether functional group to the more stable amide group gives an extra enthalpy gain, which was calculated to be 14 kcal mol^{-1}.[8a] This value seems even greater than the ring stain of the monomer since the ring strain of tetrahydrofuran is estimated as 5.5 kcal mol^{-1}.[8b] This enthalpy gain by the isomerization enables the ROP of a six-membered homolog of OZO, ROZI, although its ring strain is small.

Depending upon the nature of X^- (from a cationic catalyst or initiator) and of substituents R (R = H, alkyl, aryl, amino group, alkoxy group, etc., not only at 2-position but also at other positions), the polymerization mode becomes much varied. These affect the stability of the oxazolinium ion, and hence the reaction solvent also influences the reaction mode.

When OZO is allowed to react with an alkyl halide, an *N*-alkylated oxazolinium ion is once produced.[2] If the counter anion X^- is less stable (more nucleophilic), the ion receives a nucleophlic attack of the halide anion to produce the covalent *N*-2-haloethylamide. Therefore, a propagating species is of covalent type (Scheme 6). In the 1970s, from the results of polymerization mechanism studies, the covalent-type species was actually observed by ^{1}H NMR spectroscopy and confirmed as a stable propagating end.[2a–2e] The propagation reaction is a dipole (covalent-type species)–dipole (monomer) S_N2 reaction. This was supported by comparison of activation parameter values of the reaction with those of Menschutokin reaction like $Et_3N + EtI \rightarrow Et_4\ N^+\ I^-$, a similar dipole–dipole S_N2

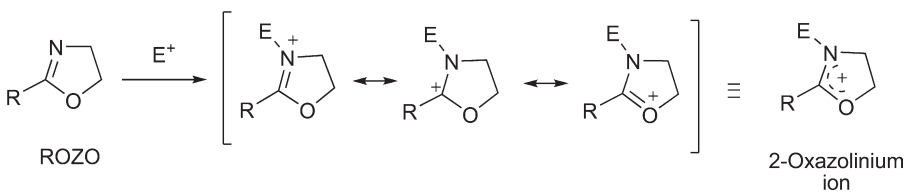

Scheme 4 Structure and properties of 2-oxazolinium ion species.

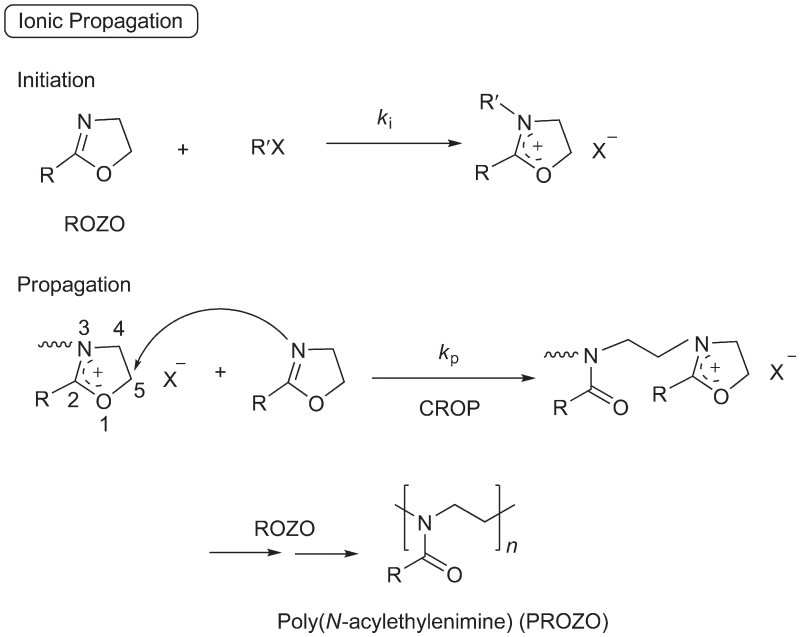

Scheme 5 A general scheme of cationic ring-opening polymerization (CROP) via ionic propagating species.

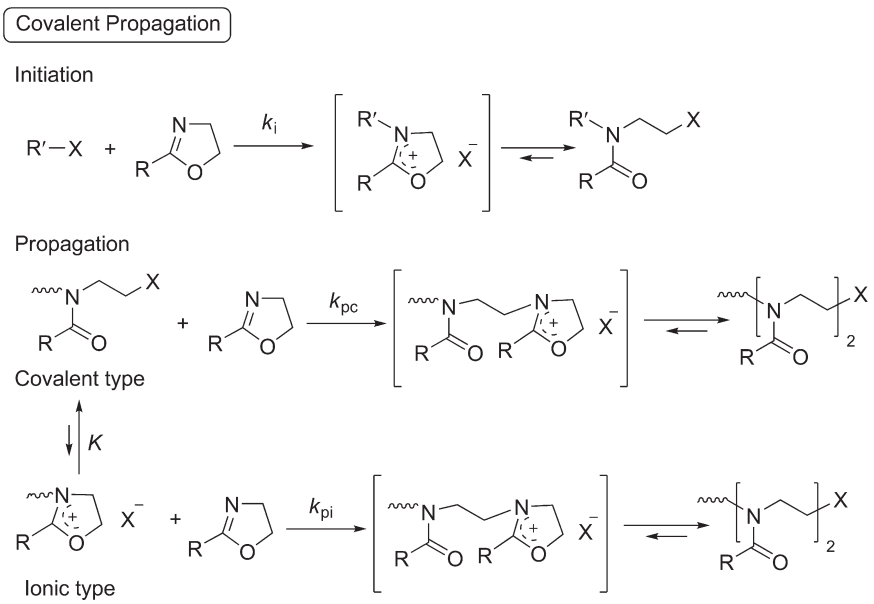

Scheme 6 A general scheme of cationic ring-opening polymerization (CROP) involving covalent propagating species in equilibrium with ionic propagating species.

reaction to form an ion, where the characteristics were indicated by both relatively lower enthalpy and entropy values of the reaction. In contrast to the covalent-type propagation, the ionic propagation is of an ion–dipole S_N2 reaction (Scheme 5), where relatively higher enthalpy yet higher entropy values of the reaction are normally observed. It is also highly possible that an equilibrium exists between the covalent type and the ionic type, the latter being formed via backbiting ionization of the former. The respective propagation reactions are given in Scheme 6; the propagation rate constants are denoted as k_{pc} (propagation due to covalent type) and k_{pi} (propagation due to ionic-type), respectively. An ionic type is normally much higher in reactivity than a covalent type. So, even though the covalent-type species is significant in amount, a major part of monomer may be consumed via the ionic-type propagation, because the rate of interconversion between the covalent type and the ionic type of the propagation end is much faster than the rate of propagation reaction[8c] (see also Scheme 8). If both propagations are involved, the propagation rate constants are in the following relationship:

$$k_{pap} = k_{pc} \times x_c + k_{pi} \times x_i$$

where k_{pap} denotes the apparent rate constant of propagation, and x_c and x_i are the molar fractions of covalent type and ionic type, respectively, that is, $x_c + x_i = 1$.[2a–2e]

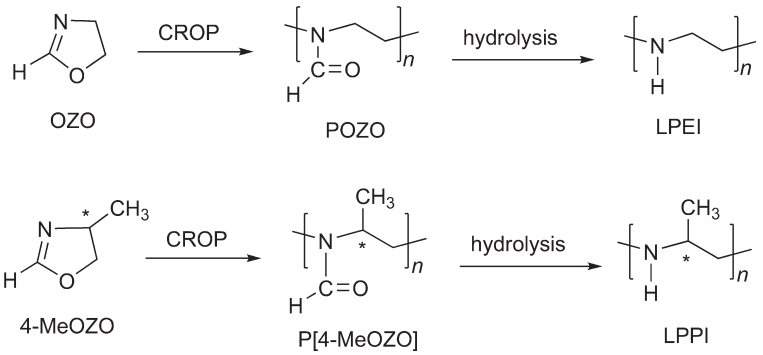

Scheme 7 CROP of 2-unsubstituted OZOs and synthesis of LPEI as well as optically active linear poly(propylenimine) (LPPI) via hydrolysis of the *N*-formyl polymers.

Although ROZOs were extensively studied in the mid-1960s as shown in Scheme 5,[1] preparation of unsubstituted OZO was first reported in 1938,[9] and its CROP was achieved in 1972 (Scheme 7).[4] The OZO polymerization suggested the significance of POZO as a starting polymer for LPEI, due to the much easier hydrolysis of *N*-formyl group compared with that of *N*-acyl group.

This method was extended to the preparation of optically active linear poly(propylenimine) (LPPI) via the CROP of 4-methyl-2-oxazoline (4-MeOZO) followed by the hydrolysis of the product polymer P[4-MeOZO] (Scheme 7).[10] The specific rotation of LPPI was $[\alpha]^{26}_{D}$ +105° (CH_3OH). 5-MeOZO also led to linear LPPI.[11]

So far, many mechanistic and kinetic studies have been reported to elucidate the monomer reactivity and type of CROP. Some of these data are shown in Table 1. The substituents at 2-position of monomers influence the type of the propagation species (ionic or covalent) and the monomer reactivity reflected by k_p values (rate constant of propagation given in Schemes 5 and 6). When the propagation species is ionic, k_p value is very different in the following order: H > Me > Ph. And, the nature of the counteranion (I^- or TsO^-) does not affect the CROP of MeOZO; the propagation is a reaction between an ionic propagating species and a dipole of monomer (Scheme 5). From the initiation reaction, the order Me > H > Ph > R_f accords with the basic strength of the monomer, which is reflected by the rate constant k_i values (data not shown) in Schemes 5 and 6, and also with the type of the propagating species; the higher the basic strength, the more ionic propagating species. However, the k_p value order is not simply in the basicity order of the monomer.

In the OZO polymerization, depending upon the counteranion, the covalent-type species by X = I showed a reduced k_p (about one-hundredth) compared with the ionic-type species by TsO^-, because the propagation is a dipole (covalent-type species)–dipole (monomer) reaction, formation of an oxazolinium ion is a rate-determining step (Scheme 6).

With a very strong nucleophilic Cl anion, propagation species of CROP of all monomers are of covalent type, whereas with the TfO anion, all the monomers proceed in the ionic propagation species, even though the monomers have a very strong electron-withdrawing perfluoroalkyl group. For reference, p*K*a of 2-methyl-2-oxazoline (MeOZO) is ~5, while that of 2-perfluoroethyl-2-oxazoline (R_fOZO) is ~2.[15]

Sometimes, equilibrium in the propagating ends exists between the covalent-type species and the ionic-type species, as they are interconvertible depending on the reaction conditions. The equilibrium is influenced by both the nucleophilicity and the leaving ability of halide ion and those of amide moiety, which are strongly influenced by the substituent of OZO. Actually, CROP of 5-methyl-2-oxazoline (5-MeOZO) with MeI initiator provided an interesting system, where the propagation species is present as both ionic and covalent species in equilibrium (*K*) as indicated in Scheme 8.[16] Concentration of both species much changed with temperature, and the ionic species were present around in one-third

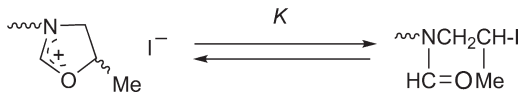

Scheme 8 Both ionic and covalent propagating species are involved in equilibrium.

Table 1 Type of propagating species and propagation rate constants (k_p) of four counteranions

	Counteranion X⁻				
Monomer	*Cl* (k_p)[a]	*I* (k_p)[a]	*TsO* (k_p)[a]	*TfO*	*Reference*
OZO	covalent	covalent (0.18)	ionic (19)	ionic	12
MeOZO	covalent (0.03)[b]	ionic (1.14)	ionic (1.17)	ionic	13
PhOZO	-	covalent	ionic (0.02)[b]	ionic	14
R_fOZO[c]	-	covalent	covalent	ionic	15

[a] In 10^{-4} l mol^{-1} s^{-1} at 40 °C in CD_3CN.
[b] Calculated value from the experimental data.
[c] R_f: perfluoroalkyl group.

at 35 °C. Propagations occur from both species; at 40 °C in CD_3CN, k_p values due to the ionic type (k_{pi}) and covalent type (k_{pc}) were evaluated as 0.059 and 0.022×10^{-4} l mol^{-1} s^{-1}, respectively. With methyl *p*-toluenesulfonate (MeOTs) initiator, on the other hand, CROP of 5-MeOZO proceeded in all ionic propagating species.

Substituent effects on the monomer reactivity was quantitatively examined by performing CROP of 2-[*p*-(substituted) phenyl]-2-oxazolines by MeOTs initiator, where the substituents were H, CH_3, OCH_3, Cl, and NO_2. The k_p values of the monomers was in the following order: $OCH_3 > CH_3 > H > Cl > NO_2$. Hammett plots of the k_p values versus σ^+ values of the substituent gave a linear relationship, indicating that the monomer reactivity is governed by that of the oxazolinium propagating end.[14]

4.15.2.2 CROP: Various Reaction Modes

4.15.2.2.1 Monomers having heteroatom-containing substituents

Alkoxy or dialkylamino substituents were introduced into the 2-position (Scheme 9).[17–23] These OZO derivatives are not one of the classes of cyclic imino ethers, but 2-alkoxy-2-oxazoline is classified into a cyclic imino carbonate and *N,N*-dialkylamino-2-oxazoline into a cyclic pseudo-urea. These monomers polymerized to yield pseudo-polyurethane and pseudo-polyurea, respectively.

Contrary to the general living character of CROP of OZO, the polymerization of 2-ethoxy-2-oxazolines yields an oligomeric product (DP ~ 10) in a high yield as the chain transfer reaction involving the *exo*-attack of the propagating species occurs during CROP (Scheme 10).[17] The chain transfer was suppressed with a monomer having a bulky alkoxy substituent.

4.15.2.2.2 Double isomerization polymerization

All the above-mentioned CROPs involve isomerization one time during the polymerization (single isomerization polymerization (SIP)). However, the equilibrium in the propagating species between an oxazolinium halide and an *N*-haloethylamide brings an interesting yet complicated feature in the polymerization of OZO derivatives. A pseudo-urea is a compound having an –N=C(NR^2)–O– functional group, which is an isomeric form of urea. Then *N,N*-dialkylamino-2-oxazolines undergo CROP which was expected to give a pseudo-polyurea. However, the cationic polymerization of *N,N*-dialkylamino-2-oxazolines showed a unique polymerization behavior.

The cationic polymerization of 2-(1-pyrrolidinyl)-2-oxazoline (PyOZO) gave two different polymers by the selection of initiator.[18] With methyl trifluoromethanesulfonate (triflate) (MeOTf) or methyl *p*-toluenesulfonate (tosylate) (MeOTs), the polymerization of PyOZO yielded poly(*N*-(1-pyrrolidinecarbonylimino)ethylene) according to the usual CROP (SIP). On the other hand, the polymerization of PyOZO with RX gave poly ((1,3-diazolidin-2-one-1,3-diyl)tetramethylene) via DIP (Scheme 11).[19] In the latter polymerization, the OZO ring was opened and rearranged to a five-membered cyclic urea unit.

The polymerization mechanism of the SIP and DIP is explained as follows: In the initiation, *N*-alkylated oxazolinium salt is first formed. With the sulfonate initiator, the propagation via the oxazolinium species occurs to induce the SIP process, as the nucleophilicity of the counteranion is weak. When the counteranion of the salt is sufficiently nucleophilic as in the case of halides (X = Br, Cl), it catalyzes the rearrangement of the oxazolinium ion to 3-methyl-1-azonia-3-azaspiro[4.4] nonan-2-one salt, a spiro-structure, via a covalent-type alkyl halide species as an intermediate. This isomerization to form the spiro-intermediate is the key step of the DIP. Its formation is preferred since it is more thermodynamically stable than the oxazolinium ion, due to the more stable C=O bond than the C=N bond (Scheme 12). This spiro salt is sufficiently electrophilic to suffer the attack of the counteranion or the monomer. The attack of the counteranion exclusively occurs at the pyrrolidinium ring, and a covalent ethyleneurea species is generated selectively.[20]

The DIP has been extended to a bifunctional monomer, 1,4-bis(2-oxazolin-2-yl)piperazine (BOP), which yielded a linear polyurea, poly((1,3-diazolidin-2-one-1,3-diyl)ethylene) (PBOP).[21] When BOP was heated to 100 °C or above with methyl iodide or benzyl bromide in benzonitrile, the DIP proceeded and PBOP was obtained as brown needles whose melting point is 210 °C (Scheme 13).

It is very unusual that the polymerization of the bifunctional monomer of cyclic rigid structure gives linear polymer. The polymerization mechanism for DIP of BOP can be explained as shown in Scheme 14.

The polymerization of BOP with 2 mol% of MeOTf in benzonitrile at 150 °C, on the other hand, quantitatively produced an insoluble gel-like product after 100 h, whose IR spectrum showed the presence of urea and oxazoline groups. Obviously, two oxazoline moieties in BOP polymerized independently, which results in the branching and cross-linking of polymer.

A polymer having a high solubility was prepared from the SIP of 2-(1,3,3-trimethyl-6-azabicyclo[3.2.1]oct-6-yl)-2-oxazoline (TAOZO), although its DIP did not proceed. This polymer

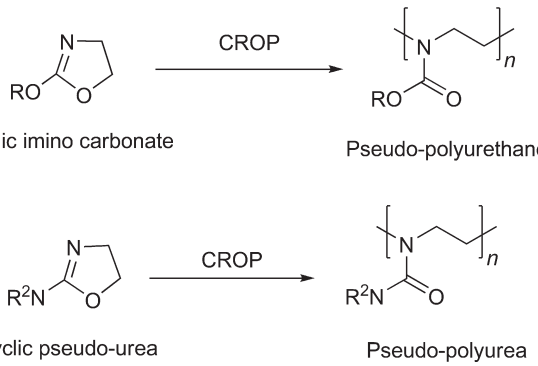

Scheme 9 Formation of pseudo-polyurethane and pseudo-polyurea.

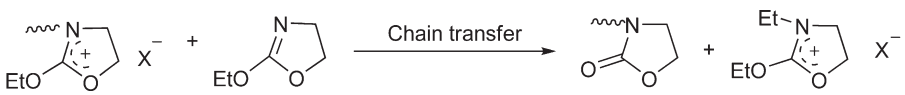

Scheme 10 A chain transfer reaction of 2-ethoxy-2-OZO propagation.

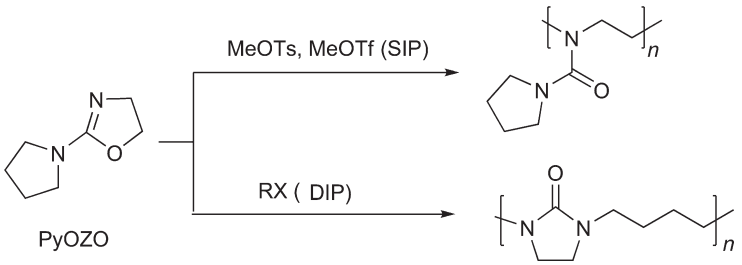

Scheme 11 Normal polymerization and double isomerization polymerization (DIP) of PyOZO monomer.

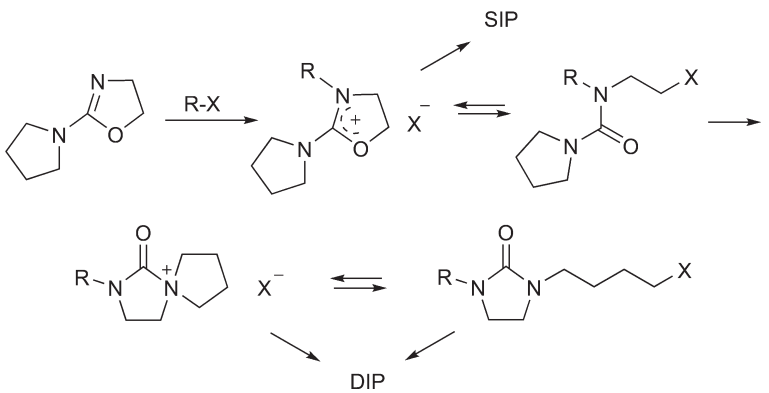

Scheme 12 Mechanism proposed for DIP of PyOZO monomer.

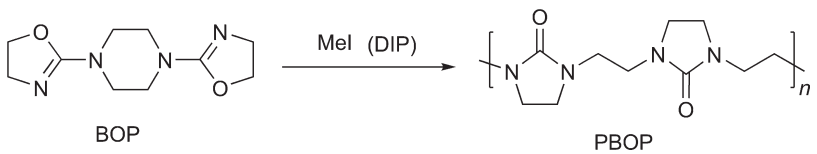

Scheme 13 DIP of a bis-oxazoline monomer of BOP.

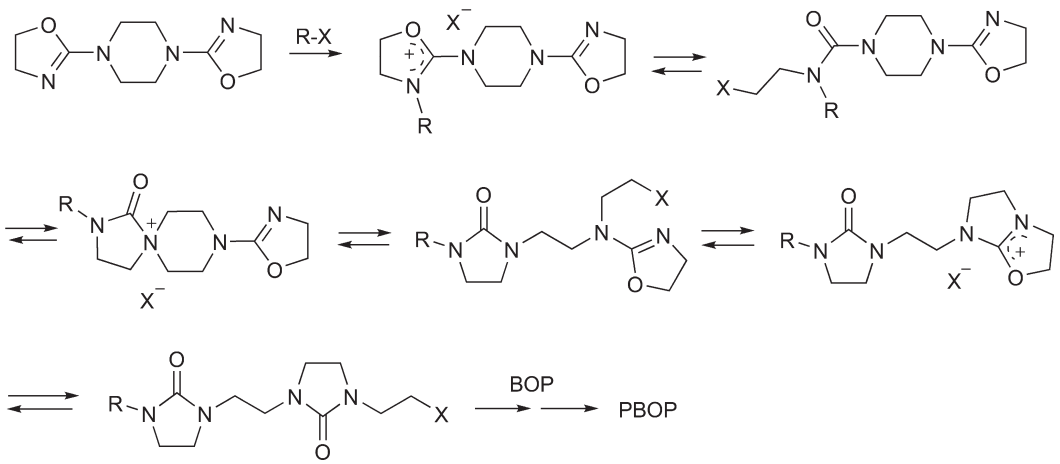

Scheme 14 Mechanism proposed for DIP of BOP monomer.

was soluble in water as well as in common organic solvents.[22] The introduction of *o*-phenylene ring into the polymer main chain strongly reduced its solubility. The DIP of 2-(2-isoindolinyl)-2-oxazoline (IIOZO) with MeI produced an ethyleneurea-type polymer, which was partly soluble in chloroform.[23]

4.15.2.3 Microwave-Assisted CROP Reaction

Microwave irradiation is known to enhance the rate of various reactions. Normally, CROP reactions of ROZOs proceed relatively slowly, by taking some hours to complete the reaction. To accelerate the reaction, microwave irradiation method was applied and found very effective for the reaction, which has been extensively developed recently.[2j]

The first paper in 2004 reported that in comparison with the conventional thermal heating, CROP of 2-ethyl-2-oxazoline (EtOZO) by MeOTs catalyst in acetonitrile at 80–180 °C proceeded very fast under microwave irradiation to give PEtOZO in a living manner; rate acceleration was a factor of 350 (reaction time 6 h→ 1 min) with M_n up to 9000 and a polydispersity index (PDI) of 1.1–1.2. Side reactions were suggested by a slightly yellow coloration of the product solution. The homogeneous microwave irradiation allowed conducting the CROP in bulk or drastically reducing the solvent amount giving an opportunity of undertaking 'green chemistry'.[24]

The reaction rate of CROP of 2-phenyl-2-oxazoline (PhOZO) was similarly accelerated with MeOTs catalyst at 125 °C, showing a living nature to give PPhOZO almost quantitatively with M_n 10700 (PDI = 1.02) after 90 min. A strong microwave effect was suggested for a large rate enhancement. It is considered that microwave-assisted polymerization is a rapid, environmentally friendly method.[25] Whether or not the microwave effect actually exists was investigated by CROP of PhOZO initiated by MeOTs carried out under both microwave irradiation and conventional thermal heating. Then, it was concluded that the rate acceleration of CROP of PhOZO by microwave irradiation results from only the thermal effects.[26,27]

CROP on four monomers, MeOZO, EtOZO, PhOZO, and 2-nonyl-2-oxazoline (NonOZO), was studied by microwave irradiation with MeOTs initiator in acetonitrile at 80–200 °C. Rate enhancement was up to 400-folds, yielding the polymers whose degree of polymerization (DP) is higher than 300 with PDI < 1.20, exhibiting the living nature of the reaction. The fast, direct, and noncontact heating by the microwave irradiation permitted the CROP to be carried out in a highly concentrated solution or in bulk, which is a huge benefit.[28]

Microwave-assisted CROP of two monomers, EtOZO and PhOZO, was kinetically studied in acetonitrile with four initiators, benzyl chloride (BnCl), benzyl bromide (BnBr), benzyl iodide (BnI), and benzyl *p*-toluenesulfonate (BnOTs), to examine the effect on the reaction rate of the four different counteranions.[29] Values of the rate constant of propagation at 160 °C (k_p 10^{-3} l mol^{-1} s^{-1}) were for EtOZO: BnCl (2), BnBr (114), BnI (434), and BnOTs (350); and for PhOZO: BnCl (0), BnBr (2), BnI (7), and BnOTs (98). Percentages (%) of cationic propagating species were also determined by ^{1}H NMR for EtOZO: BnCl (0), BnBr (96), BnI (100), and BnOTs (100); and for PhOZO: BnCl (–), BnBr (0), BnI (25), and BnOTs (100). Namely, the CROP of EtOZO with BzCl and of PhOZO with BzBr proceeded via covalent propagating species in 100%. The nucleophilicity of X^- is in the order: $Cl^- > Br^- > I^- > TsO^-$ (see **Scheme 6**).

A variety of monomers were prepared by changing the structure of 2-substituent R, and their CROP was carried out with MeOTs initiator under microwave irradiation to give the corresponding polymers.[30] Table 2 demonstrates the structure of 12 substituents (R of ROZO) and the results of their kinetic study by k_p values (l mol^{-1} s^{-1}) in the parenthesis carried out at 140 °C in dichloromethane. The k_p values are in the range from 1×10^{-3} to 241×10^{-3} depending on the structure and substituent of ROZOs. An electron-rich aromatic group (furan) shows a higher polymerizability close to an alkyl substituent, whereas bulky groups decrease the k_p values. For reference as to temperature effect, the k_p values of MeOZO (2050×10^{-4} at 140 °C) can be interestingly compared with that (1.17×10^{-4} at 40 °C) in acetonitrile.[31]

4.15.2.4 Copolymerization via CROP-Mode Reaction

When the copolymerization between two ROZO monomers having a close reactivity is conducted, the reaction produces normally random copolymers. In such cases, copolymers with the average properties are expected, but production of copolymers with specific properties is less expected.

4.15.2.4.1 Block copolymerization

The living characteristic nature of CROP led to the development of a new concept in block copolymerization. Actually, AB-type block copolymers were first prepared with an appropriate combination of ROZOs and the product block copolymers were found to be an excellent nonionic polymer surfactant (**Scheme 15**).[3] This finding of amphiphilic copolymers from ROZOs for the new surfactants was based on employing MeOZO and EtOZO as monomers for hydrophilic segments, and 2-propyl (PrOZO), 2-butyl (BuOZO), 2-octyl (OcOZO), 2-dodecyl (DoOZO), and PhOZO as monomers

Table 2 Twelve substituents R of ROZOs and values of propagation rate constant k_p given in parenthesis in 10^{-3} l mol^{-1} s^{-1} by MeOTs initiator at 140 °C in CH_2Cl_2.

Me-	(205)	*n*-Undecyl-	(138)	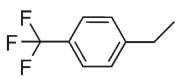	(241)
Et-	(128)	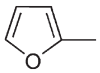	(201)	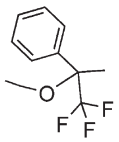	(1)
i-Bu-	(115)	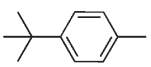	(32)		
n-Octyl-	(132)				
n-Heptyl-	(122)	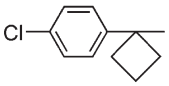	(20)	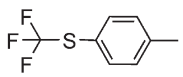	(21)

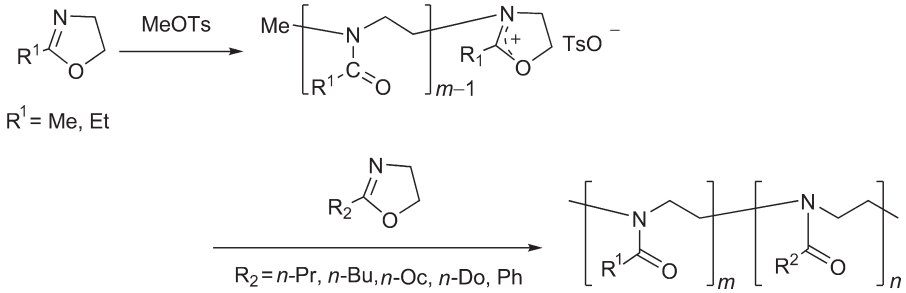

Scheme 15 Synthesis of nonionic amphiphilic block copolymers via living CROP of ROZO monomers giving a hydrophilic segment at 1st stage and a hydrophobic segment at 2nd stage.

for hydrophobic segments. Typically, at the first stage, a living CROP of MeOZO was induced by MeOTs initiator for a hydrophilic A block, and at the second stage, BuOZO was polymerized from the MeOZO living end for a hydrophobic B block, to produce P[MeOZO-*block*-BuOZO] (one-pot, two-stage sequential method). All the products were soluble in water. The surfactant nature was evaluated by the surface tension value (γ, dyn cm^{-1}), for example, a block copolymer with R^1 = Me (m = 19) and R^2 = Bu (n = 5) exhibits γ = 27.5 in contrast to γ of pure water = 71.3. In addition, by using mono- and bifunctional initiators, surfactants of triblock copolymer (BAB type) were prepared and the copolymer P[$OcOZO_6$-*block*-$MeOZO_6$-*block*-$OcOZO_5$] showed the lowest γ value of 23.7 dyn cm^{-1}. The critical micelle concentration (CMC) of these copolymers was lower than 1.0 wt%. It is important to note that PMeOZO segment is so far the most powerful as a nonionic hydrophilic polymer segment due to the polar amide structure, which is more powerful than poly(ethylene glycol) (PEG) segment. Not only ROZO monomers but six-membered ROZI monomers were used for an A block or B block.

In the usual copolymerization between the two monomers of different reactivity, the polymerization of the less reactive monomer should be conducted first. Then, the second monomer is to be added to the system to complete the two stages. Contrary to this general tendency, the cationic copolymerization between MeOZO and RfOZO produced AB-type block copolymers of well-controlled block lengths; R^2 = Rf (fluoroalkyl group) in **Scheme 16**. The employed initiator MeOTs selectively reacts with the more nucleophilic MeOZO, which is followed by the homopolymerization of MeOZO until almost all MeOZO was consumed. Then, the second propagation proceeds slowly to form RfOZO diblock to produce P[MeOZO-*block*-RfOZO] (**Scheme 16**).[15] The monomer reactivity of MeOZO should be more than a hundred times higher than RfOZO, if estimating from values like 205:1 in **Table 2**. This copolymerization provided a one-pot, two-stage method by the simultaneous feeding of two monomers.

Microwave-assisted CROP was utilized extensively for the synthesis of block copolymers, because of the higher rate of reaction and the living nature of CROP of OZOs. Diblock copolymers were prepared from four monomers, MeOZO, EtOZO, PhOZO, and NonOZO, in acetonitrile at 140 °C, which gave a library of 4 chain-extended homo-PROZOs and 12 diblock co-PROZOs. The CROP reaction to yield a total number of 100 (50 + 50) monomer units was designed and thus-obtained 16 polymers showed a narrow PDI (< 1.30). All polymers were stable up to 300 °C.[32]

Furthermore, microwave-assisted polymerization was extended to prepare amphiphilic triblock terpolymers to prepare a library of desired 30 terpolymers via CROP of the above four monomers. The polymerization was performed in a three-step sequential procedure to complete the monomer consumption ranged from 13.2 to 61.6 min. The terpolymers exhibited narrow PDI (~ 1.3) near the targeted monomer ratio of 33:33:33. The T_g values ranged from 50 to 100 °C depending on the incorporated monomers. Some amphiphilic terpolymers containing two hydrophilic and one hydrophobic blocks formed micelles, whose size ranged between 7 and 18 nm.[33] Similarly, tetrablock ter- and quarter-polymers were prepared from the same four monomers to design the polymers having the monomer units as all 25. Well-defined tetrablock polymers were obtained, having the structures of ABCA, ABCB, ABCD, and ABDC, where A is MeOZO block, B EtOZO block, C PhOZO block, and D NonOZO block. These block polymers showed amphiphilic nature found by the surface energy measurement and formed aqueous micelles whose size varied around 5–40 nm.[34]

Tri- and tetrablock polymers prepared from these four monomers formed micelles, whose morphologies were investigated in binary water–ethanol mixtures.[35] The solvophilic/

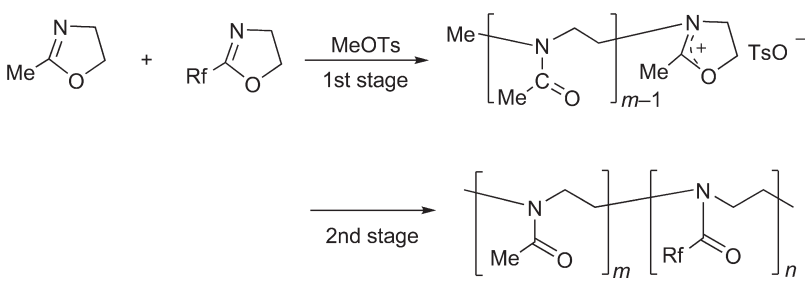

Scheme 16 Block copolymer synthesis via one-pot, two-stage method.

solvophobic balance of these block polymers was tuned owing to the solubility dependence of the PPhOZO block on the solvent composition. Solubility of the four polymer blocks for the solvent composition: For EtOH/water (60/40) wt%: PMeOZO (s), PEtOZO (s), PPhOZO (s), and PNonOZO (ns), whereas for EtOH/water (40/60) wt%: PMeOZO (s), PEtOZO (s), PPhOZO (ns), and PNonOZO (ns), where s and ns mean 'soluble' and 'not soluble', respectively. Dynamic light scattering (DLS) and transmission electron microscopy (TEM) measurements revealed that when the solvophobic fraction consists of both the PPhOZO and PNonOZO blocks, spherical and cylindrical micelles as well as vesicles were observed; the size of spherical micelles was of some 10 nm. The block order in the polymers much affected the final micellar morphology.

In the simultaneous copolymerization of PhOZO with MeOZO or with EtOZO under microwave irradiation, a block-like copolymerization took place to give quasi-diblock copolymers.[36] This is because of a big difference in the monomer reactivity ratio previously reported as $r_{MeOZO} = 10$ and $r_{PhOZO} = 0.02$, the situation of which is similar as mentioned in Scheme 16.

CROP of EtOZO and 2-'soy alkyl'-2-oxazoline (SoyOZO) was performed with microwave irradiation by MeOTs initiator, where SoyOZO monomer was derived from soybean fatty acids (Scheme 17).[37,38] Copolymers obtained were of statistical structure, since both monomers possessed close monomer reactivity ratios: $r_{EtOZO} = 1.4$ and $r_{SoyOZO} = 1.7$. The copolymers showed M_n values of $6–13 \times 10^3$ with PDI of 1.2–1.5. UV irradiation gave a cross-linked material via the reaction of the unsaturated soy alkyl group in the copolymer.

In the random and block copolymer formation from EtOZO and NonOZO monomers, structure–property relationships were investigated.[39] Synthesis of the random copolymers were conducted with microwave irradiation in acetonitrile and synthesis of the block copolymers with the conventional heating, both by MeOTs initiator. Under microwave irradiation, both monomers showed close monomer reactivity ratio values: $r_{EtOZO} = 1.07$ and $r_{NonOZO} = 1.05$. All the product copolymers were shown to have well-defined structure. The organization of the monomer units in the copolymers involves a significant effect on the surface energy, thermal transition, and mechanical properties of the copolymer material, showing that the structural control over monomer distributions is an excellent way to control these properties. Microwave-assisted one-step synthesis of EtOZO/2-(*m*-difluorophenyl)-2-oxazoline (F_2PhOZO) and EtOZO/PhOZO copolymers was conducted via CROP with MeOTs initiator in acetonitrile at 140 °C.[40] The CROP reaction produced the well-defined statistical gradient copolymers, which are good surfactants and formed micelles having a diameter of 9–13 nm determined by atomic force microscopy (AFM). Ionic liquids could be used as solvent at 140 °C for microwave-assisted CROP of PhOZO and F_2PhOZO.[41]

When bifunctional initiators are used, a variety of telechelic PROZO polymers are to be prepared via the nucleophilic reaction of the di-oxazolinium living species for introducing target functionality.

Block polymers using blocks other than PROZO chain were prepared. As a typical example, polytetrahydrofuran (PTHF) was introduced to AB-type and BAB-type block copolymer as shown in Scheme 18.[42] For the synthesis of the diblock copolymer, ethyl trifluoromethanesulfonate (EtOTf) was used as initiator, while for the triblock copolymer, anhydride of TfOH was employed, where a living CROP of THF end, an oxonium species, is involved. PTHF is a hydrophobic chain; both copolymers showed very good surfactant properties, when MeOZO or EtOZO was used, as observed by the surface tension value reaching to $\gamma = 30.1–28.2$.

In place of PTHF, PEG was used for triblock copolymers [PMeOZO-*block*-PEG-*block*-PMeOZO] and the deacetylated copolymer exhibited good anti-electrostatic properties. Also, poly(propylene glycol) chain acted as the block segment.[43] A vinyl ether segment was used as a hydrophobic block, whose copolymer was prepared as shown in Scheme 19.[44] The iodine-catalyzed polymerization of vinyl ether proceeds in a living fashon, whose propagating end causes the CROP of ROZO to give an AB-type diblock copolymer. When R^1 group is *n*-Bu, *i*-Oct, or *n*-Cet, the vinyl ether segment is hydrophobic, whereas the ROZO segment is hydrophilic when R^2 is Me or Et. The block copolymers showed good properties as nonionic polymer surfactant (γ value < 30). The copolymer was readily cleavable under weakly acidic conditions due to the labile bond connecting the two blocks. The cleavage mechanism is considered as also shown in Scheme 19. This property can be conveniently utilized depending on the way of the usage as a 'smart' surfactant.

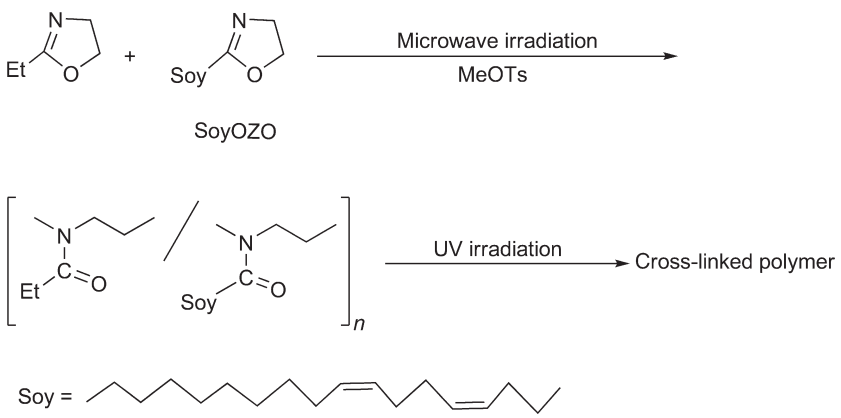

Scheme 17 Microwave assisted copolymerization between EtOZO and SoyOZO.

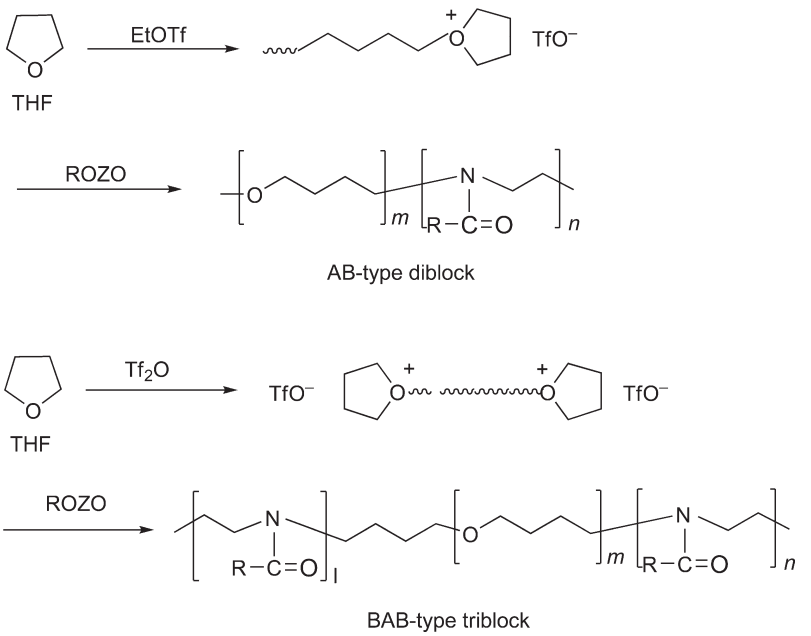

Scheme 18 Synthesis of AB-type and BAB-type block copolymers via CROP of ROZO and tetrahydrofuran (THF).

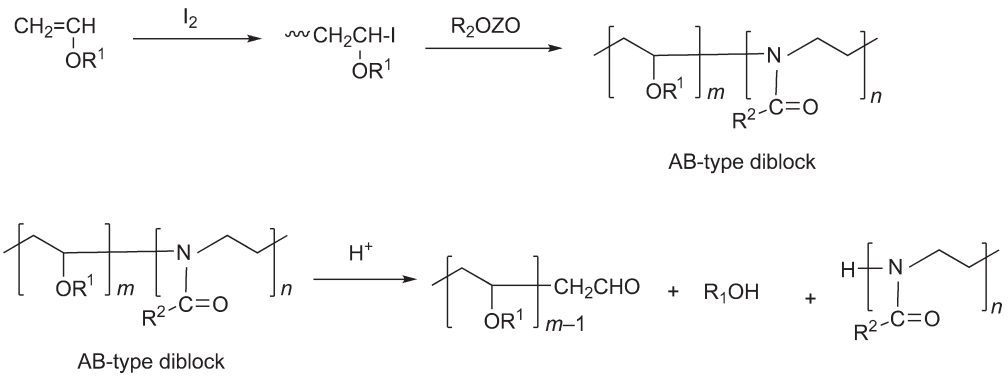

Scheme 19 A block copolymer from a vinyl ether and ROZO, showing readily cleavable nature.

Other examples of polymer chains for the block component are cited such as polystyrene,[45] polyisobutylene for three-armed star-block copolymers,[46] poly(ε-caprolactone),[47] and glycopeptides.[48]

4.15.2.4.2 Graft copolymerization

A variety of graft polymers have been prepared via different methods.

Initiator method: CROP of MeOZO was initiated from chloromethylated polystyrene and the hydrolysis of the PMeOZO produced poly(styrene-*g*-ethylenimine). The graft copolymer (PSt-*g*-LPEI) is an efficient chelating resin for the absorption and recovery of heavy metal ions such as Cu^{+2}, Hg^{+2}, and Cd^{+2} (Scheme 20).[49]

MeOZO and EtOZO were grafted onto cellulose (Cell-OH) and cellulose diacetate, in which CROP of ROZO was initiated

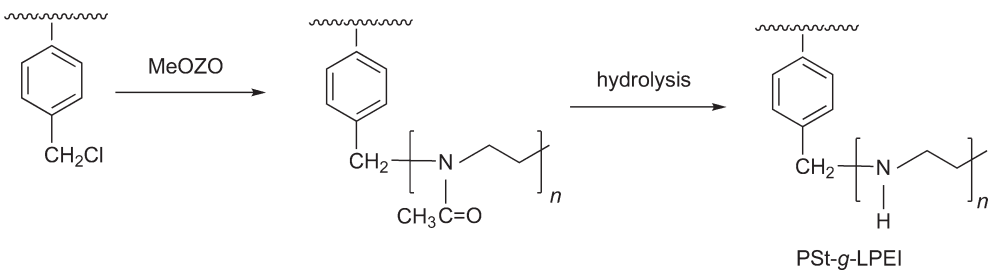

Scheme 20 Synthesis of LPEI-grafted polymer initiated from chloromethylated polystyrene.

from the tosylated group (Scheme 21).[50a] Since the PROZO chains are weakly basic and compatible (miscible) with commodity polymers like poly(vinyl chloride) (PVC) and polystyrene confirmed by measurements using a rheovibron, the graft copolymers (Cell-*g*-PROZO) made cellulose and cellulose diacetate derived from natural polymers well compatible with a commodity polymer.[50b] Therefore, the application of these natural polymers has become widely used.

Terminator method: Another polysaccharide of chitin was used for CROP grafting of ROZO, where the *N*-acetyl group was to be converted to amino group for the next reaction as a deacetylated chitin. Then propagating oxazolinium species was terminated by the reaction with the amino group to produce the graft copolymer (chitin-*g*-PROZO) (Scheme 22).[51] The chitin-based graft copolymer was miscible with poly(vinyl alcohol) (PVA) over a wide range of their composition, whereas chitin and PVA gave a binary blend. The graft copolymer was also miscible with PVC, indicating that PROZO chain functions as the compatiblizer.

Pullulan-*graft*-poly(2-isopropyl-2-OZO) (PiPrOZO) copolymer was obtained by terminating the activated ends of PiPrOZO chain with hydroxy groups of pullulan at room temterature in dimethyl sulfoxide (DMSO). Around one PiPrOZO chain (molecular weight ~3200) was introduced per 100 glucose units.[52]

Macromonomer method: Macromonomers are conveniently used for the graft copolymer synthesis. A macromonomer of PEG chain having an oxazoline polymerizable group was prepared and used for a graft copolymer synthesis (Scheme 23).[53] The macromonomer has a hydrophilic PEG segment, and hence its CROP-type copolymerization with PhOZO proceeded randomly to give an amphiphilic graft copolymer PPhOZO-*g*-PEG, showing good surfactant nature with a γ value of 28.8 dyn cm^{-1}.

Radical copolymerization of an acryl- or methacryl-type PROZO macromonomer (see Scheme 49) with a vinyl monomer of methyl methacrylate (MMA), styrene (St), or acrylamide (AM) produced graft copolymers (Scheme 24).[54] The surface property of the film from the graft copolymer (R = Me) was made hydrophilic due to the character of PMeOZO chain verified by the contact angle measurement. Such behaviors were also observed in the solution of the graft copolymer of PSt-*g*-PMeOZO via ^{1}H NMR measurement.

4.15.2.4.3 Alternating and periodic copoplymerizations

An alternating copolymerization involving a zwitterionic intermediate was widely investigated.[55] When two kinds of monomers, nucleophilic (M_N) and electrophilic (M_E), are combined without catalyst or initiator, they form a zwitterion (genetic zwitterion), which is responsible for both initiation and propagation (Scheme 25). Two molecules of the zwitterion produce a dimeric zwitterion, which further reacts with genetic, dimeric, or polymeric zwitterion of different molecular weight to afford a product alternating copolymer.

Based on this concept, various combinations of M_N and M_E monomers were explored. As M_E monomers, various lactones, (meth)acrylic acid, and acrylates were often employed. Oxazolines were widely used as reactive M_N monomers.[56] An

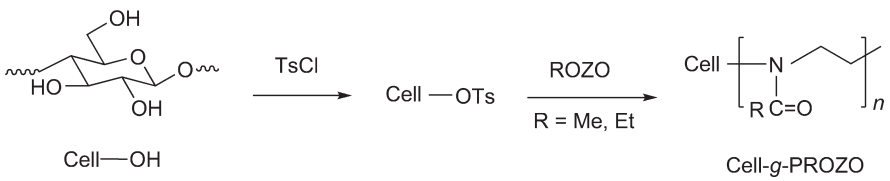

Scheme 21 Synthesis of PROZO-grafted cellulose initiated from tosylated cellulose.

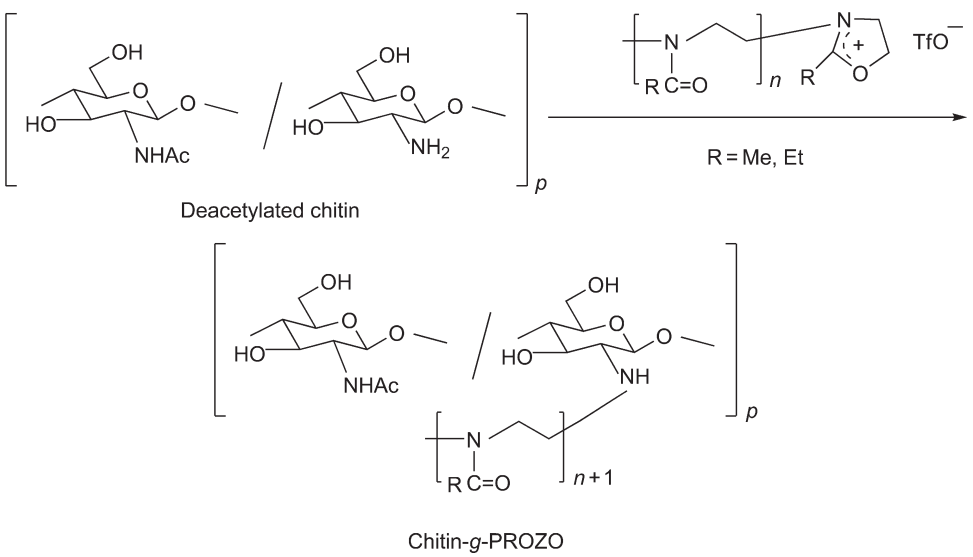

Scheme 22 Synthesis of PROZO-grafted chitin by termination of living CROP end of PROZO with the amino group.

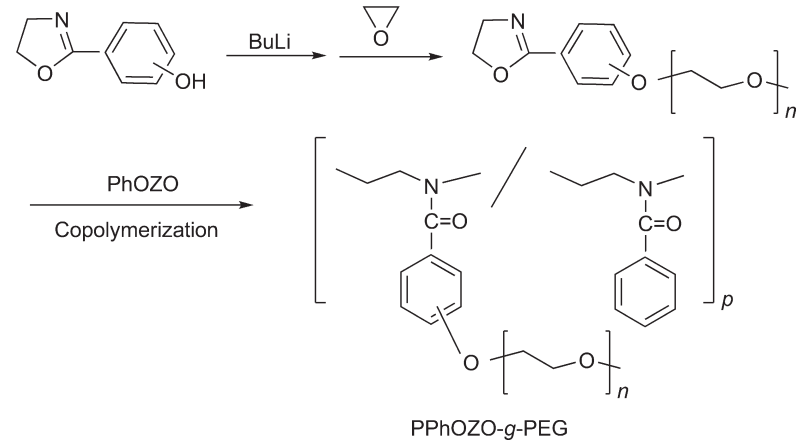

Scheme 23 A hydrophilic OZO macromonomer for synthesis of an amphiphilic graft copolymer.

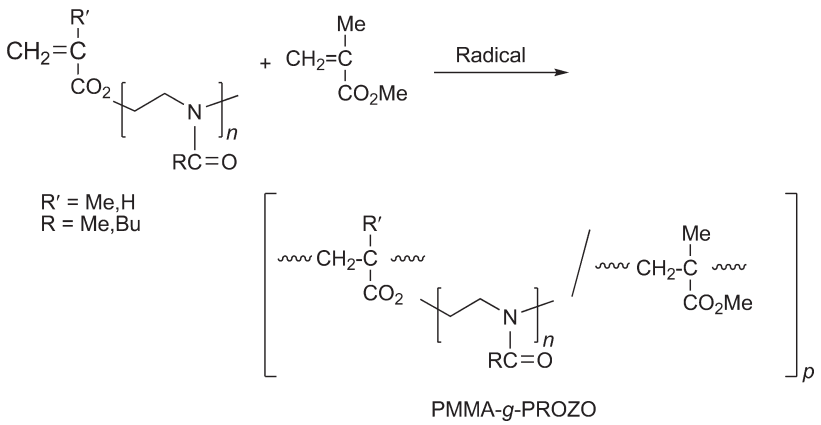

Scheme 24 A radically polymerizable PROZO macromonomer for synthesis of a graft copolymer.

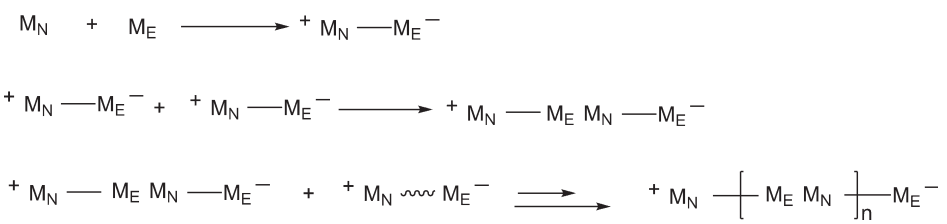

Scheme 25 General scheme of initiation and propagation of alternating copolymerization via zwitterionic intermediates from nucleophilic monomer (M_N) and electrophilic monomer (M_E).

example reaction in the combination of OZO and acrylic acid is shown in Scheme 26, where a proton transfer step of acrylic acid is involved. Hence, the product polymer has the same repeating unit structure of the copolymer from OZO and β-propiolactone.

Ring-opening-closing alternating copolymerization involving a zwitterionic intermediate was found as indicated in Scheme 27, where MeOZO ring was opened, whereas *N*-methyldiacrylamide gave a five-membered ring-closed unit having $M_n = 5600$.[57] The ring closure was at most 65%, the others being of a vinyl-type unit.

Depending on the combination of M_N and M_E monomers, alternating and periodic copolymers were synthesized in various structures such as AB_2, BA_2, $A_{1/2}B$, and ABC types. A periodic A_2B-type copolymer (2:1 monomer composition) having an ABC-type periodic terpolymer structure was produced from OZO and glutaric anhydride (Scheme 28).[58] From OZO, a unit structure of reaction 6 (Scheme 1) is formed.

4.15.3 Ring-Opening Polyaddition

A fundamental reaction mode in this section is generally given in Scheme 29, where a compound having reactive proton (Y-H) adds to ROZO with ring opening (ROPA). The reaction involves a protonated oxazolinium intermediate. As reactive Y-H, RCO_2H-, RSH-, and ArOH-type compounds are normally employed.[2h]

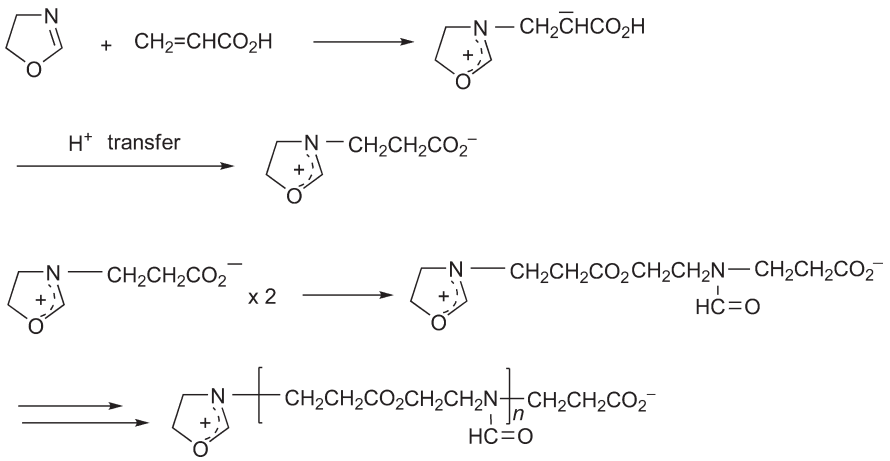

Scheme 26 Alternating copolymerization of OZO (MN) with acrylic acid (ME) involving a proton transfer.

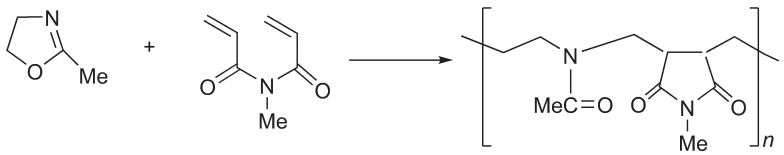

Scheme 27 A ring-opening-closing alternating copolymerization.

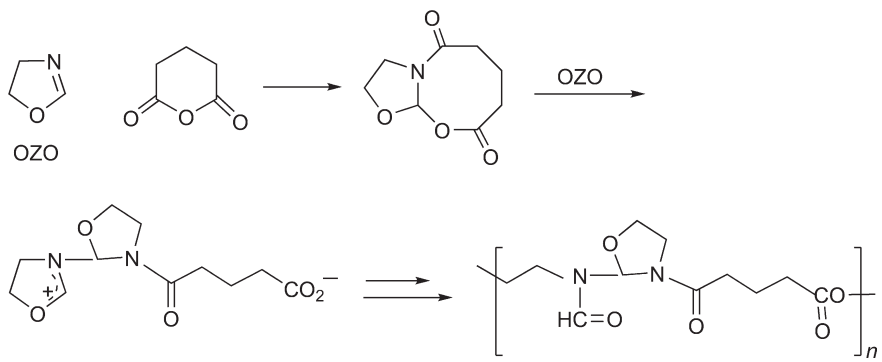

Scheme 28 Periodic copolymerization of OZO (MN) with glutaric anhydride (ME) having a 2:1 periodic structure.

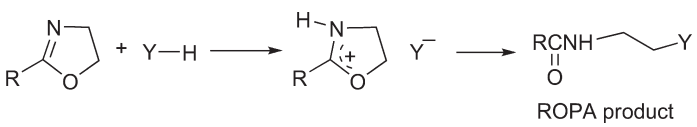

Scheme 29 Reaction mode of ring-opening addition.

4.15.3.1 ROPA Reaction between A-A-Type Monomer and B-B-Type Monomer

Reaction of 2,2′-ethylene-bis(2-oxazoline) (EBOZO, A-A-type monomer) and adipic acid (B-B-type monomer) produced an amide-ester polymer with melting range 145–155 °C (Scheme 30).[1c]

A thermoplastic of an amide-ether type was prepared from an aromatic bis(2-oxazoline) (BOZO) and a bis-phenol at 180 °C. It is an amber, transparent, and brittle solid with molecular weight $M_w \sim 114\,000$ showing melting point 150–160 °C (Scheme 31).[2h]

Also, poly(amide-thioether)s were prepared from a BOZO and a bisthiol (see Scheme 32).[59]

Application of ROPA reaction for chain extender: The highly reactive nature of ROZO toward carboxylic acid group was applied for a chain extender. Poly(ethylene terephthalate) (PET) is an important plastics as it is widely used in daily life. The annual consumption is over 10 million tons worldwide,

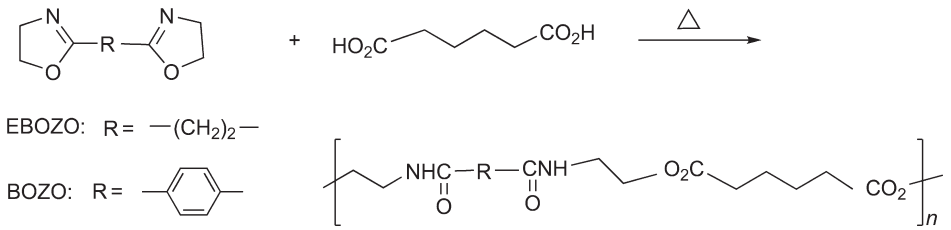

Scheme 30 ROPA reaction between A-A-type monomer and B-B-type monomer.

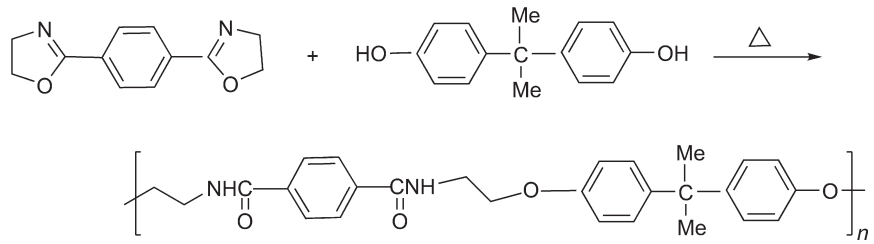

Scheme 31 ROPA reaction between bis(2-oxazoline) and bis-phenol.

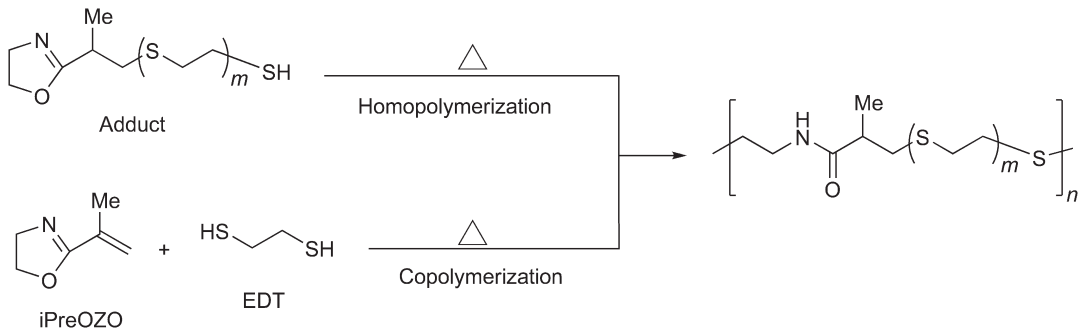

Scheme 32 ROPA reactions using thiol containing monomers.

and its recycling is an important subject in view of environmental aspects. The hydrolytic degradation of recycled PET due to moisture as well as its thermal degradation reduces molecular weight, which lowers the mechanical properties of recycled material. The use of a chain extender and solid-state polymerization (SSP) has been a good method to improve the chain length of recycled PET.[60] Recycled PET contains carboxyl end groups. One of the representative examples of carboxyl-reactant chain extenders is BOZO (Scheme 30). For example, the intrinsic viscosity of PET whose [η] increased from 0.66 to >1.0 after the reaction with 1.0 wt% of BOZO at 280 °C after 5 min.[61] Obviously, BOZO is an effective chain extender of high reactivity to increase the PET molecular weight.

Another example is concerned with poly(L-lactic acid) (PLLA). It is already used in packaging, consumer goods, and many other applications. For PLLA, the usage of a BOZO as chain extender is very adequate as T_m of PLLA (~170 °C) is lower than that of PET, in which the chain extender was used for oligo(lactic acid) prepared by the direct polycondensation.[62] To prepare PLLA sample with two carboxyl ends, L-lactic acid (LLA) was condensed with itself in the presence of 2 mol% of succinic anhydride (SA) and 0.05 wt% of tin(II) octoate. Then the chain extension reaction with BOZO was carried out at 190–210 °C.[63] Thus, high-molecular-weight poly(ester-amide) (PEA) was produced from the PLLA prepolymer only at 200 °C for 10 min with BOZO/SA = 1.2/1.0; value of M_w becomes higher from 1×10^4 to 19×10^4. The resulting PEA was thermoplastic and could be processed by injection molding. The mechanical properties of the resulting PEA specimen were substantially better than those of untreated PLLA. The PEA sample had higher tensile strength and modulus than PLLA as well as other commodity polymers such as polystyrene, poly(butylene terephthalate), and nylon-6. The strain of PEA was slightly higher than that of polystyrene and PLLA.

4.15.3.2 ROPA Reaction of AB-Type Monomers

As AB-type monomers, carboxyl group-containing oxazolines are well known and their polymer formation reaction is the same as shown in Scheme 30. From an aromatic carboxylic acid derivative, a commercial resin was developed. Phenol group-containing oxazolines were reacted similarly as given in Scheme 31.[2h]

Poly(amide-thioether)s were prepared from a BOZO and a bisthiol.[59] A 2-(thiomercaptoalkyl)-2-oxazoline adduct (AB-type monomer) was obtained from a reaction of

2-(*i*-propenyl-2-oxazoline, *i*PreOZO) and 1,2-ethanedithiol (EDT), and the adduct was homopolymerized thermally to produce a poly(amide-thioether) having molecular weight range 4100–43 000 (Scheme 32), where the polymerization is considered to proceed involving a zwitterion intermediate.[64] *i*PreOZO and EDT were copolymerized to produce a similar poly(amide-thioether).

4.15.4 ROPA for Polysaccharide Synthesis

For the polysaccharide synthesis, 'enzymatic polymerization' has been developed as a new *in vitro* synthesis method of natural and unnatural polysaccharides having complicated structures.[65] The method utilizes a hydrolysis enzyme to catalyze the bond formation for the polymer construction, a reverse direction of the hydrolysis to cleave the bond. This catalysis is due to the enzymatic characteristics, where enzymes catalyze the reverse reaction involving a common intermediate in both forward and backward reactions. In nature, there are many polysaccharides having *N*-acetyl groups called 'mucopolysaccharides' such as chitin, hyaluronic acid (HA), and chondroitin (Ch).

4.15.4.1 Enzymatic ROPA of Sugar Oxazolines

It has been found that various sugar oxazoline derivatives serve as monomers for enzymatic catalysis to produce natural and unnatural mucopolysaccharides, in which the monomers were designed and synthesized on the basis of the transition-state analogue substrate (TSAS) concept (*vide infra*).[65] All the sugar oxazoline monomers are of AB-type structure mentioned in Section 4.15.3.2.

Polysaccharide synthesis requires a repetition of a controlled glycosylation reaction, connecting two sugar units in a regioselective and stereocontrolled manner. The synthesis is achieved only when the repetition of the reaction is achieved multiple times. The glycosylation is a reaction between a glycosyl donor and a glycosyl acceptor; a simple example to form a $\beta(1\rightarrow4)$ glycosylation product via condensation is given in Scheme 33. The anomeric C-1 carbon of the donor is to be activated by introducing X.

4.15.4.1.1 Synthesis of chitin and chitin derivatives

The first successful *in vitro* synthesis of chitin was achieved in 1995 by the enzymatic ROPA (EROPA) of a chitobiose OZO monomer catalyzed by chitinase enzyme, affording 'synthetic chitin' in high yields with DP value 10–20 (Scheme 34), in which the stereochemistry and regioselectivity are perfectly controlled.[66] A general reaction mode is that of reaction 3 in Scheme 1. In the reaction of Scheme 34, the chitobiose OZO monomer (without protection) acted as a donor as well as an acceptor, where the oxazoline structure activates the anomeric C-1 carbon of the monomer as donor and it attacks regioselctively the 4′-OH of the acceptor. The oxazoline ring opens with isomerization and affords an *N*-acetyl group, leading to the structure of $\beta(1\rightarrow4)$ glycosidic linkage. To understand and explain the reaction to occur, a new concept of a 'transition-state analog substrate' (TSAS) monomer was proposed.[66] The concept implies that the *in vivo* chitinase-catalyzed hydrolysis of chitin involves an oxazoline or oxazolinium ion intermediate (or transition state), which has actually been confirmed.[67] The TSAS concept also suggests the fundamentally important characteristics of enzymatic reactions, in which an enzyme stabilizes the transition state to lower the activation energy, accelerating the reaction in tremendous rate enhancement.[68]

The enzymatic chitin synthesis together with the TSAS concept provided with a new way for the synthesis of mucopolysaccharides having *N*-acetyl group at the 2-position of the sugar unit, which are widely found polysaccharides in nature. Scheme 35 explains that the MeOZO moiety in the monomer

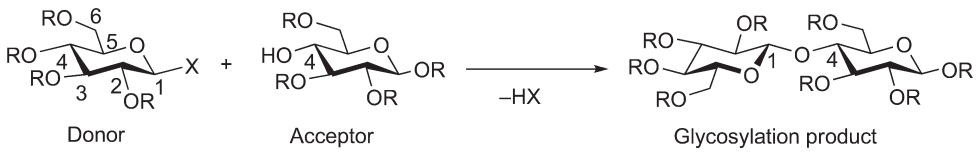

Scheme 33 A glycosylation reaction to form b(1®4) linkage in carbohydrate chemistry.

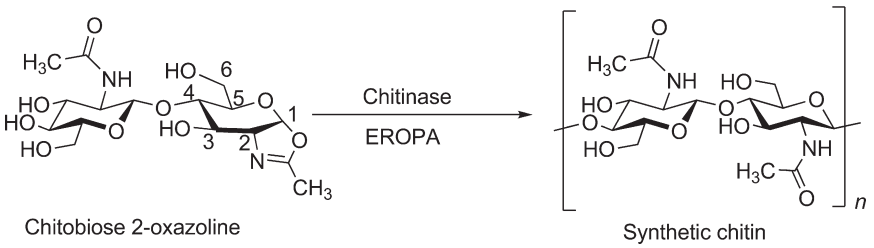

Scheme 34 Synthetic chitin is produced via enzymatic ROPA (EROPA) reaction.

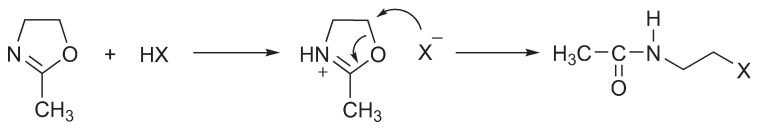

Scheme 35 MeOZO serves as a latent N-acetyl group.

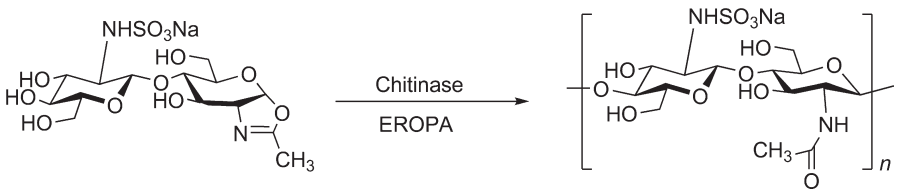

Scheme 36 Chitinase-catalyzed synthesis of a chitin derivative via EROPA reaction.

is a latent *N*-acetyl group generator with ring-opening isomerization leading to the product chitin, as shown by a simple general reaction of MeOZO with an electrophile HX.

In addition, a monomer having a bulky and ionic *N*-sulfonate group at the 2′-position was also catalyzed by chitinase and gave corresponding chitin derivative of the weight-averaged molecular weight (M_w) 4990 in 62% yield (Scheme 36).[69] These results indicate that chemical structure at C-2′ of chitobiose oxazoline is less influential for chitinase recognition in catalysis.

Monomers substituted with fluorine atom at the 6-position(s), whose covalent radius (0.64 Å) is almost the same with that of oxygen (0.66 Å), showed good polymerizability.[70]

4.15.4.1.2 Synthesis of chitin hybrids

With the appropriate design of monomers, the following three hybrid polymers, chitin–cellulose hybrid with DP value 22 in 79% yields,[71] chitin–chitosan hybrid with M_w 4280 in 75% yields,[72] and a water-soluble chitin–xylan hybrid with M_w 2730 in 80% yields,[73] have successfully been synthesized (Scheme 37). In all EROPA reactions, structural control is perfect, having a $\beta(1\rightarrow4)$ glycosidic linkage.

4.15.4.1.3 Synthesis of hyaluronic acid (hyaluronan, HA) and chondroitin (Ch)

HA (hyaluronan) and Ch belong to glycosaminoglycans (GAGs), biomacromolecular heteropolysaccharides, which are normally linked to various proteins to form proteoglycans. Together with collagens, fibronectins, and others, proteoglycans fill the interstitial space between living cells, and they are called extracellular matrices (ECMs). GAGs include HA, chondroitin sulfate (ChS), dermatan sulfate, heparin/heparan sulfate, and keratin sulfate (KS). All GAGs contain hexosamine unit such as *N*-acetyl-D-glucosamine (GlcNAc), *N*-acetyl-D-galactoamine (GalNAc), and their sulfated derivatives. HA is a linear polysaccharide having a repeating unit of β(1 → 3)-GlcNAc-β(1 → 4)-GlcA. Ch is nonsulfated ChS whose repeating unit structure is β(1 → 3)-GalNAc-β(1 → 4)-GlcA.[65i,65j]

Hyaluronidase (HAase) is known to hydrolyze β(1 → 4)-linked GlcNAc (or GalNAc) and GlcA bond in HA and Ch chains. Based on the TSAS concept, *N*-acetylhyalobiuronate (GlcAβ(1 → 3)GlcNAc) oxazoline derivative and an *N*-acetylchondrosine oxazoline derivative are designed as TSAS monomers for the HAase-catalyzed polymerization. Both monomers were effectively catalyzed by ovine or

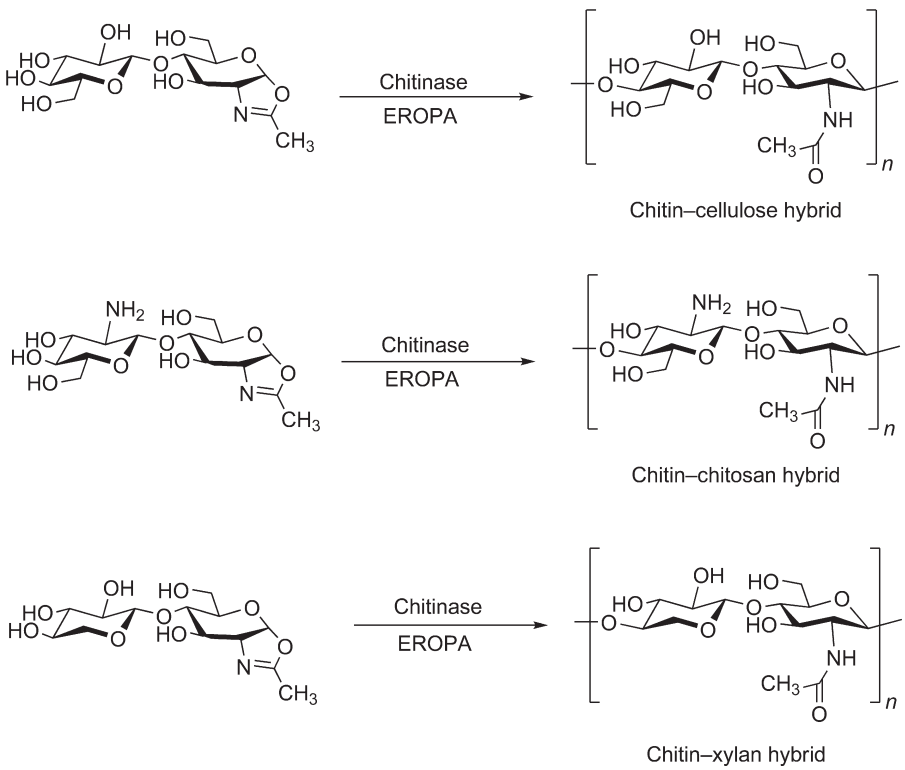

Scheme 37 Chitinase-catalyzed three polymerizations to lead to chitin hybrids via EROPA reactions.

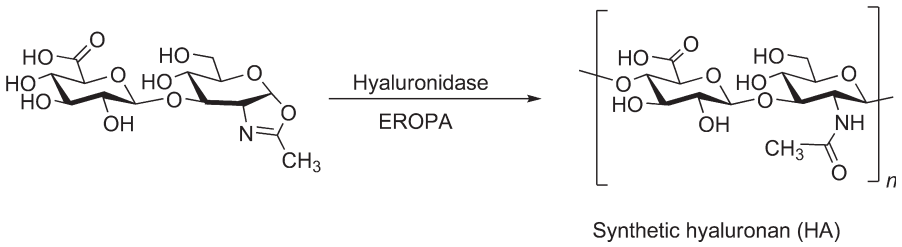

Scheme 38 Synthetic hyaluronan (HA) is obtained via hyaluronidase-catalyzed EROPA reaction.

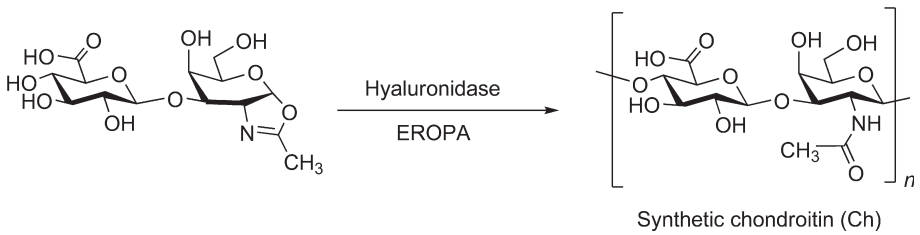

Scheme 39 Synthetic chondroitin (Ch) is produced via hyaluronidase-catalyzed EROPA reaction.

bovine testicular derived HAase, giving rise to the corresponding polysaccharides of 'synthetic HA' (Scheme 38)[74] and 'synthetic Ch' (Scheme 39).[75] The M_w of HA and Ch reached to 25 000 and 6800, respectively. The molecular weight value of Ch corresponds to that of natural Ch. Synthetic HA and Ch provide the first examples having the complicated structure of heteropolysaccharides ever synthesized *in vitro*.

At the catalytic domain of the HAase, there is a conserved DXE(D) motif stabilizing an oxazolinium-ion intermediate (or transition state), and hence the hydrolysis reaction mechanism is considered to be similar to that of chitinases. These observations are in accord with the concept of TSAS monomer, strongly suggesting that two EROPA reactions of Schemes 38 and 39 occur via an oxazolinium transition state.

4.15.4.1.4 Synthesis of HA and Ch derivatives

Variously substituted oxazoline monomers, 2-ethyl, 2-*n*-propyl, and 2-vinyl oxazoline monomers for HA, were newly prepared and polymerized with HAase catalysis. The reactions proceeded with total control of regioselectivity and stereochemistry, to afford the corresponding HA and Ch derivatives (unnatural polysaccharides) possessing *N*-propionyl, *N*-butyryl, and *N*-acryloyl group in every hexosamine unit (Scheme 40).[75,76] Similarly, Ch derivatives were also achieved. The resulting *N*-acryloyl HA and Ch are functional polymers having a reactive vinyl group.

These substituted oxazoline monomers were copolymerized by HAase catalyst to proceed in a regio- and stereoselective manner, producing the corresponding copolymers. Composition of the *N*-acyl group units could be easily controlled by varying the comonomer feed ratio.[77]

HAase-catalyzed copolymerization of an *N*-acetylhyalobiuronate oxazoline monomer and an *N*-acetylchondrosine oxazoline monomer also gave an unnatural intramolecularly hybridized HA–Ch copolymer, which conventional methods can hardly achieve (Scheme 41).[78]

Ch is found in the ECMs and on cell surfaces. Ch is normally sulfated and biological activities of ChS are due to the sulfated pattern. Depending on the major sulfation pattern, natural ChS is classified into the following five types: ChS-A, ChS-C, ChS-D, ChS-E, and ChS-K. None of them is composed of a single repeating unit; all are of mixed type. For example, in a whale cartilage, the so-called ChS-A contains ~20% of ChS-C as a minor component besides the major ~80% of ChS-A. Preparation of ChS to have a well-defined sulfation pattern is, therefore, important for the fundamental investigation of the correlation between the polysaccharide structure and the bioactivities. *N*-Acetylchondrosine oxazoline monomer having a 4-sulfate group at GlcNAc unit was successfully polymerized by HAase, giving rise to ChS in high yields having the sulfate group only at C-4 position on all GlcNAc residues (Scheme 42).[79] The product is a 'pure' ChS-A with M_w values ranging from 5600 to 36 500. Biological activity examination of the synthetic pure ChS-A will be a future study of interest.

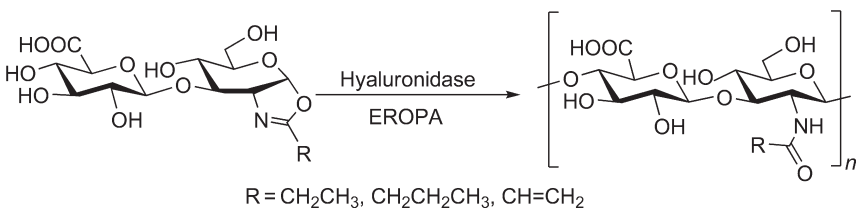

Scheme 40 Hyaluronidase-catalyzed synthesis of HA derivatives.

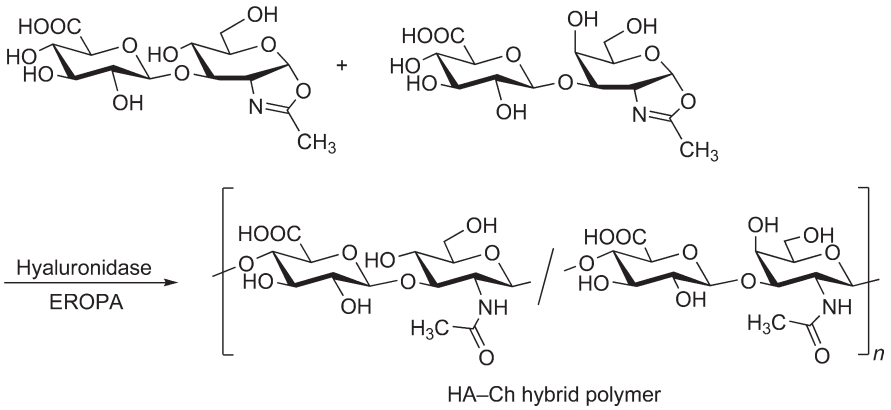

Scheme 41 Hyaluronidase-catalyzed synthesis of HA-Ch hybrid.

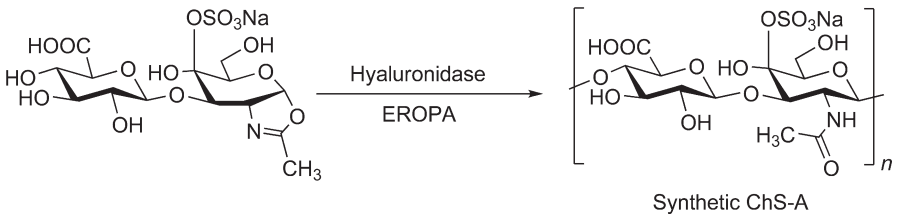

Scheme 42 Synthesis of chondroitin sulfate via hyaluronidase-catalyzed EROPA reaction.

4.15.4.2 Cationic ROPA of Sugar Oxazolines

Polysaccharide synthesis using sugar oxazoline monomers was carried out via cationic ROPA (CROPA) reaction; CROPA of 3,6-di-*O*-benzylated chitin-oxazoline monomer (AB-type monomer) was induced by 10-camphorsulfonic acid (CSA) catalyst to produce di-*O*-benzylated chitin (**Scheme 43(a)**).[80] The CROPA was carried out at a reflux temperature in 1,2-dichloroethane and proceeded involving stereoregular glycosylation, giving rise to a dibenzylchitin product having $\beta(1\rightarrow4)$-grucopyranan structure with M_n up to 4900 in around 50% yields. The debenzylation of the products via the catalytic hydrogenation was incomplete. It is important that the OH groups not to be reacted must be protected! The acid-catalyzed ROPA was extended to the synthesis of the dibenzylchitin having $\beta(1\rightarrow6)$-grucopyranan structure.[81] The product is of unnatural-type structure, whose yield was at most 32% and M_n reached 13 100. The debenzylation of the products took place perfectly to produce the corresponding free aminopolysaccharide of unnatural type.

The principle of the reaction was applied for the preparation of a hyperbranched polymer from an A-B_2-type monomer. In the latter, 3- and 4-positions have free OH groups (**Scheme 43(b)**).[82] The product polymer possessed M_n up to 6600 (PDI < 2), whose detosylation gave a free hyperbranched aminopolysaccharide.

The reaction mode of these CROPA is similar to that of EROPA; both employ sugar oxazoline monomers for the

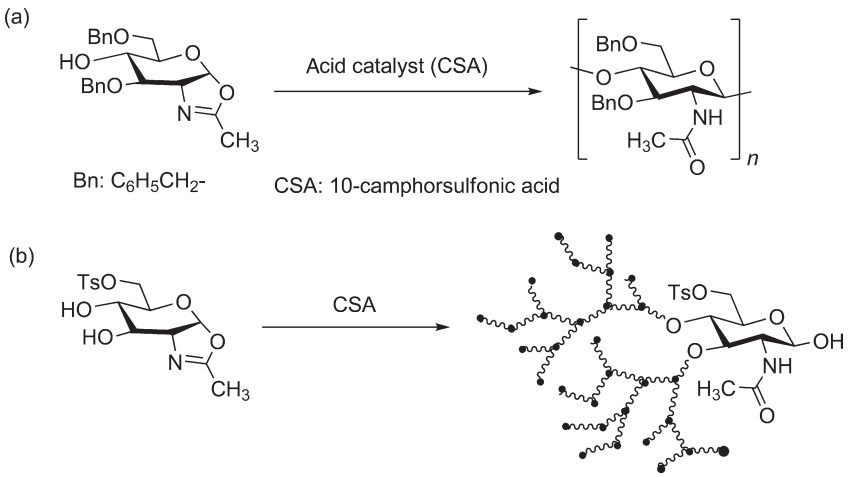

Scheme 43 Acid-catalyzed ROPA reactions to give a chitin derivative (a) and a hyperbranched chitin type polymer (b).

synthesis of various mucopolysaccharides. The exception is the monomer structure, where CROPA needs protection of OH groups at necessary positions, but in the EROPA the reaction takes place regioselectively at the unprotected OH groups.

4.15.5 Ring-Opening Polymerizations of Other Oxazoline Derivative Monomers

In addition to ROZO monomers, the monomers to be mentioned are listed in Scheme 3. They are 5-oxazolones (4,5-dihydro-1,3-oxazol-5-one, ROZLO), six-membered analogs (5,6-dihydro-4*H*-1,3-oxazines, ROZI), and seven-membered ones (4,5,6,7-tetrahydro-4*H*-1,3-oxazepine, ROXP) as well as *exo*-cyclic imino ether derivatives of ROZO, ITHFs which are not mentioned here.

4.15.5.1 Polymerization of 5-Oxazolone

Introduction of a carbonyl group at the 5-position of OZO ring leads to 2-oxazolin-5-one or an 'azlactone' termed by Erlenmeyer (ROZLO). The first paper on CROP reaction of ROZLO was reported in 1986, describing the production of a poly(*N*-formyl-α-peptide) at 60 °C in diglyme in high yields (R = H, R′ = Me, Scheme 44).[83] The peptide is a white powdery material with molecular weight of 5100. The monomer (R = R′ = H) gave the corresponding poly(*N*-formyl-α-peptide) having molecular weight 2400. When the monomer was prepared from L-alanine, optically active poly(*N*-formyl-L-alanine) (R = H, R′ = Me) was derived; the specific rotation value $[\alpha]_D^{22}$ –3.60.

2-Alkoxy derivatives (ROOZLO) were polymerized by MeOTf via CROP mode since its polymerization yields polypeptide derivatives.[84,85] The CROP of (*S*)-4-isopropyl-2-ethoxy-5-oxazolone (R = EtO, R′ = *i*-Pr) (Scheme 44) yields poly(*N*-ethoxycarbonyl-L-valine), which was converted to poly(L-valine) by basic hydrolysis.[84] Contrary to poly(L-valine), poly(*N*-ethoxycarbonyl-L-valine) is soluble in many organic solvents probably due to the lack of amide hydrogen bonding, which is expected to expand the availability of polypeptide derivatives.[85]

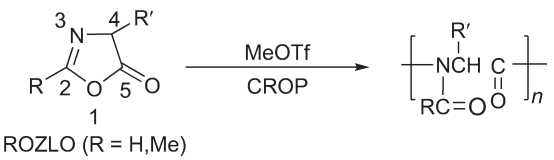

Scheme 44 CROP of an OZO derivative, 5-oxazolone, to produce a poly(α-peptide).

ROZLO (R = H, R′ = H, Me) monomers behaved as electrophilic monomer (M_E) in the combination of M_N monomers according to Scheme 25.[86] As M_N monomer, acrylamide and 2-hydroxyethyl acrylate were employed to produce alternating copolymers, involving zwitterionic intermediate. In these reactions, a proton transfer step was involved.

A corresponding six-membered 'azlactone' (1,3-oxazine-6-one) was polymerized via CROP-mode reaction to produce a poly(*N*-acyl-β-peptide), whose molecular weight reached 5400.[87]

4.15.5.2 Polymerization of 1,3-Oxazine

2-Unsubstituted 1,3-oxazines (R = H, ROZI) were first prepared and polymerized via CROP mode in 1973, whose alkaline hydrolysis gave linear poly(trimethylenimine) (LPTMI) for the first time (Scheme 45).[88] The molecular weight M_n was up to 4840.

Kinetic studies on the ROZI monomer reactivity were examined in detail.[89] All CROP reactions of OZI, MeOZI, and PhOZI monomers with MeOTs initiator proceeded involving oxazinium propagating species in a similar way to Scheme 5 of the ROZO case. For comparison of the monomer polymerizability, rough values are given in $k_p \times 10^4$ values (with MeOTs at 100 °C in acetonitile* or in nitrobenzene#) in $l\,mol^{-1}\,s^{-1}$: OZO (13000*), MeOZO (120*), PhOZO (13*), OZI (110#), MeOZI (19#), and PhOZI (2.5#). With MeI initiator, OZI and MeOZI had oxazinium propagating species, whereas PhOZI showed covalent alkyl iodide propagating species.

Polymerization of ROZI monomers behaved in almost all cases similarly to ROZO monomers in many respects, except for the product polymer structures with a trimethylenimine chain of PROZI instead of an EI chain of PROZO.[2] Many similar behaviors in both monomers of ROZI and ROZO include a living character of CROP, various copolymer syntheses, DIP, and an M_N monomer in zwitterionic alternating copolymerizations. It may be important to mention, however, that ROZI is a little more basic than ROZO from the initiation reaction studies; for example, pK_a value for iPrOZI and iPrOZO are 7.1 and 5.4 in water at 25 °C, respectively.

4.15.5.3 Polymerization of 1,3-Oxazepine

Only one paper appeared on the CROP reaction of 1,3-oxazepine (ROXP).[90] With expected DIP of ROXP, however, it was polymerized to afford the product polyamide according to normal CROP mode; DIP did not occur with MeOTf initiator. With benzyl chloride initiator, only isomerization of the monomer took place to produce a urea without giving a polymer (Scheme 46).

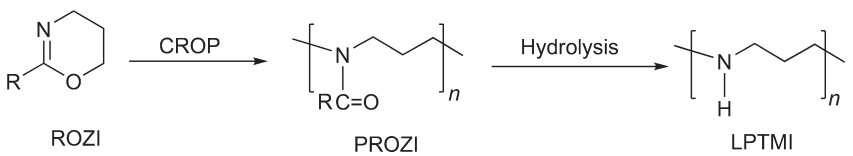

Scheme 45 CROP reaction of 1,3-oxazine (ROZI) to lead to linear poly(trimethylenimine).

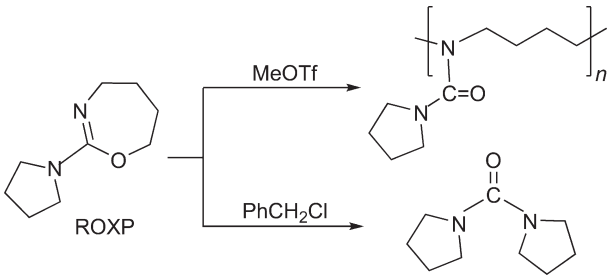

Scheme 46 CROP reaction of 1,3-oxazepine (POXP) gives different products depending on the initiator.

4.15.6 Sythesis of Functional Polymers via CROP Process and Their Applications

The fundamental chemistry of oxazoline polymerization has been extensively accomplished over the past four decades. The main trend of oxazoline polymerization, therefore, is currently and will be in the future toward application studies by utilization of the unique properties of the PROZO polymers.

4.15.6.1 Synthesis of End-Functionalized Polymers

End-functionalized polymers include macromonomers, telechelics, and polymers having functional groups pending to the main chain, for example, employed for click chemistry. End-functional groups can be introduced at the initiating step ('initiator method'), at the terminating step ('terminator method'), or during the polymerization like the copolymerization.

4.15.6.1.1 Synthesis of macromonomer and telechelics

Macromonomers and telechelics are important starting materials for the synthesis of functional polymers. The former was extensively used for graft copolymer synthesis as seen in Section 4.15.2.4.2. They are normally produced via a couple of methods.

Initiator method: An oxazoline-CROP polymerizable macromonomer was first prepared from 2-(hydroxyphenyl)-oxazolines leading to a ROZO macromonomer having a PEG chain as given in **Scheme 24**.[53a] Styryl-type macromonomers were synthesized by using iodomethylstyrene as initiator (**Scheme 47**).[53b]

Numerous types of macromonomers were prepared using various halides as shown in **Scheme 48**.[91] These halides include not only monohalides (a–c) for, for example, a vinyl ester macromonomer, but also dihalides (d–i) and a tetrafunctional halide (j). Allyl-type halides, acetylene-containing halides, and benzyl-type halides are activated and exhibited a higher reactivity than a simple alkyl halide. These halides gave a number of macromonomers and telechelics from ROZO monomers with molecular weights up to several thousand. Compound (j) produced a star-shaped polymer. Polymers derived from these initiators contain reactive olefin, acetylene, diene, and diacetylene groups and can be used not only for macromonomers and telechelics but also further for cross-linking, modification, and so on.

As a typical example of surfactant synthesis via initiator method, 2-(perfluorooctyl)ethyl trifluoromethanesulfonate (RfOTf for R′X in **Schemes 5** and **6**) was used as initiator for CROP of ROZO, then the product polymer was a very efficient surfactant, showing the lowest γ value of 23.9 dyn cm^{-1} (R = Et, DP = 5.7) due to the specific fluoroalkyl group hydrophilicity.[92]

Pluritriflate initiators, derived from mono-, di-, tri-, and tetrafunctional alcohols, were used for CROP of MeOZO for preparing hydrophilic star polymers. It was shown that the propagation of the each arm proceeded in a similar rate in the reaction of these initiators (k_p value = ~ 5×10^{-3} l mol^{-1} s^{-1} at 85 °C).[93]

Scheme 47 Synthesis of styryl-type macromonomer via CROP of MeOZO using initiator method.

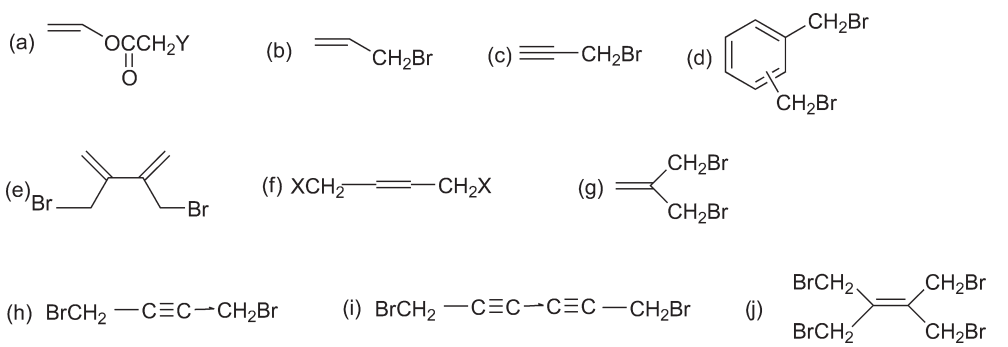

Scheme 48 Various reactive halide initiators for synthesizing macromonomers, telechelics, and a tetra-arm PROZO via initiator method.

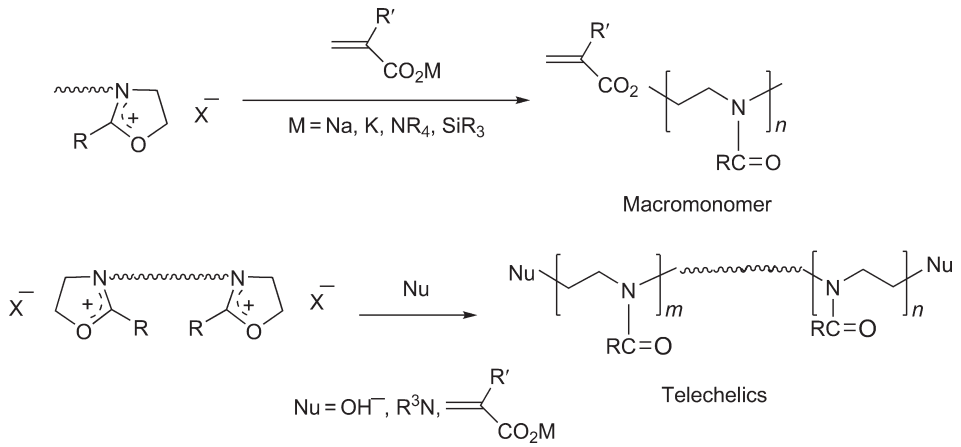

Scheme 49 Synthesis of macromonomers and telechelics via terminator method.

Terminator method: A (meth)acryl-type macromonomer or telechelics can be obtained by the reaction of the POZO living end terminated with a (meth)acrylate salt (Scheme 49).[94] Thus, various functional groups are introduced at one or both terminals.

When a higher fatty acid as a hydrophobic group was introduced at one or both end(s) ($X = RCO_2$ or $Nu = RCO_2^-$) of PMeOZO or PEtOZO of a hydrophilic segment, the products showed excellent surfactant properties.[95] This method seems to be the simplest and economical way for the PROZO surfactants. In addition, a dihalide initiated living POZO and a diamine reacted to afford PROZO ionen polymers.[96]

4.15.6.1.2 Polymer modification via click chemistry

Combination of click chemistry and polymer chemistry leads to new materials. A functional group for click chemistry can be introduced via the CROP of the functional group-containing monomers. A pendant alkyne group-containing PROZO was prepared by CROP of 2-(4-pentynyl)-OZO (PynOZO) monomer, both via its homopolymerization and copolymerization with MeOZO or EtOZO. The copolymer (unit composition; PynOZO: MeOZO = 5:45) was reacted with an azide compound ($R\text{-}N_3$) in aqueous solution via copper-catalyzed Huisgen 1,3-dipolar cycloaddition (click chemistry) to form the 1,2,3-triazole ring (Scheme 50(**a**)).[97]

It was suggested that this type of polymer modification reaction may lead to attached peptidic cell recognition sites for targeted drug delivery system. Another example of click chemistry is a 'thio-click' modification of 3-butenyl (But) group of PButOZO unit with a mercaptan (RS-H) under UV light (Scheme 50(**b**)).[98] Further, to prepare a clickable PROZO, propargyl or 3-butynyl *p*-toluenesulfonate was employed for initiating CROP of MeOZO, EtOZO, NonOZO, and PhOZO monomers under microwave irradiation at 140 °C in acetonitrile. The product PROZOs contain the alkyne end group and the click chemistry reaction of the group with an azide via a copper-catalyzed Huisgen 1,3-cycloaddition to form a 1,2,3-triazole. Reactions of these alkyne end-functionalized PROZOs and various azides will produce new materials for block and graft copolymers.[99]

4.15.6.2 Synthesis of Amphiphilic Copolymers

Amphiphilic copolymers are mentioned above for block and graft copolymers in Section 4.15.2.4. Hence, some specific cases are included mainly for applications here.

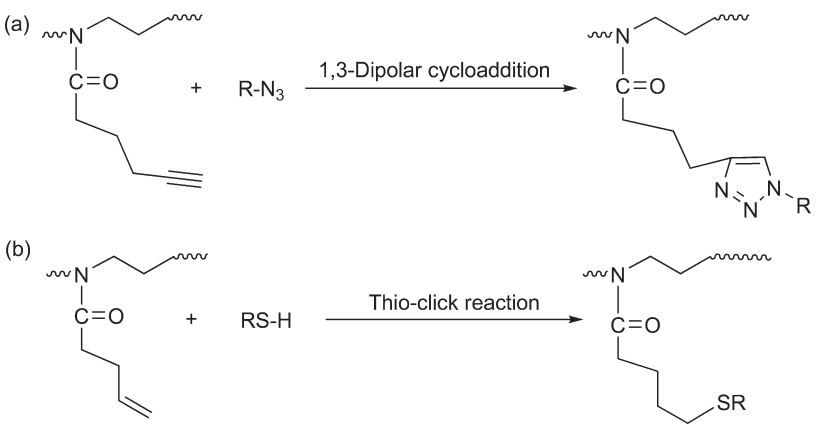

Scheme 50 PROZO polymer modifications via click reactions using an azide (a) and a thiol (b).

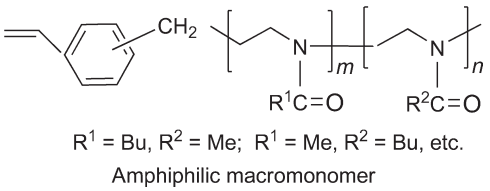

Scheme 51 Styryl-type amphiphilic macromonomers.

A styryl-type macromonomer having a water-soluble ROZO segment (Scheme 47) or having an amphiphilic ROZO block copolymer (Scheme 51) was extensively used as surfactant for the emulsion or dispersion polymerization.[100] Polymerization of St or MMA in the presence the macromonomer as stabilizer (less than ~3 wt% for the total monomer) in water took place with a radical initiator to give stable monodisperse polymer particles with a micron-size diameter. The macromonomer acted as both comonomer and stabilizer; actually the copolymerization occurred. Therefore, the system is micelle forming but soap-free. Hydrophilic PMeOZO segments are preferential on the particle surface.

A vinyl ester-type amphiphilic macromonomer was also employed for emulsion copolymerization of vinyl acetate with the macromonomer to yield polymer particles.[101]

Polymer catalyst ligands utilized an amphiphilic block copolymer, which is bound to the metal catalyst site and forms micelles in aqueous solution reaction. An example is a Ru-containing Hoveyda–Grubbs catalyst (Scheme 52(**a**)).[102] The copolymer uses PMeOZO for hydrophilic segments and PNonOZO for hydrophobic segments. Ru-catalyst (a) was used for the ring-closing metathesis reaction of diethyl diallylmalonate to produce diethyl 3-cyclopentene-1,1′-dicarboxylate plus ethylene (Scheme 52(**b**)), in which the reaction proceeded in micelles effectively, showing a turnover number reaching to 390 in water. A Rh-catalyst with a polymer ligand containing amino group was employed as micellar catalyst for the 1-octene reaction of hydroformylation and hydroxyaminomethylation.[103]

4.15.6.3 Synthesis of Stimuli-Responsible Polymers

Stimuli-responsible polymers are well known, as exemplified by poly(*N*-isopropylacrylamide) (PNIPAM) of vinyl-type polymer, which is a smart thermosensitive polymer (Scheme 53).[104]

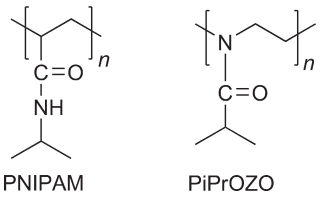

Scheme 53 Two typical thermosensitive polymers, PNIPAM and PiPrOZO.

By using an oxazoline chain, PiPrOZO was first found to be excellent thermosensitive polymer, as well as a smart material (Scheme 53).[105] PiPrOZO ($M_n = 16\,700$, $M_w/M_n = 1.13$) showed a clouding point (CP) of 36.0 °C in water with 0.5 wt% of the polymer, in which the polymer was soluble below CP. It is to be noted that the CP value is near human body temperature. The CP value decreased with increasing the polymer concentration. The value was also affected by an additive; by adding 0.1 and 0.5 mol l^{-1} of NaCl, the value was decreased to 35.6 and 31.5 °C, respectively, whereas by adding 0.01 and 0.05 mol l^{-1} of sodium dodecyl sulfate (SDS), the value was increased to 76.7 °C and >100 °C, respectively. It was explained that in the former, NaCl breaks the hydrogen bonding between the polymer and the water, and in the latter, a nonionic polymer PiPrOZO is complexed with an ionic surfactant of SDS. As an application, the thermosensitive hydrogel was prepared by radical copolymerization of a PiPrOZO macromonomer[106] with ethylene glycol dimethacrylate in an aqueous methanol solution.[105] Further, the hydrogel of PiPrOZO was prepared, whose swelling transition is around human body temperature. This is a good situation for the application of thermosensitively functional biomaterials. Applying the above results to biomedical materials, end-functionalized PiPrOZOs were synthesized, giving the polymers with structures of Me-PiPrOZO-OH, Me-PiPrOZO-NH_2, and acetal-PiPrOZO-OH. A polymer showing the CP near 37 °C was derived.[2i]

Via cationic living copolymerization, iPrOZO as hydrophobic monomer and EtOZO as hydrophilic monomer produced a copolymer P[iPrOZO-*co*-EtOZO]. Monomer reactivity ratios were determined as $r_{iPrOZO} = 0.79$ and $r_{EtOZO} = 1.78$, respectively. These values allowed the development of gradient copolymers (M_n 8000–10 000) with varying compositions and narrow PDI (≤1.02). Lower critical solution temperature (LCST, corresponding to CP) of the copolymers could be precisely tuned over a broad range of 38.7–67.3 °C by varying

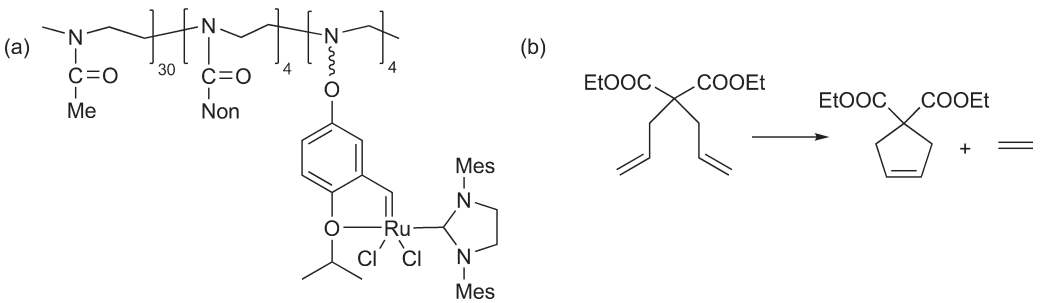

Scheme 52 PROZO-Ru catalyst (a) for a ring-closing metathesis reaction (b).

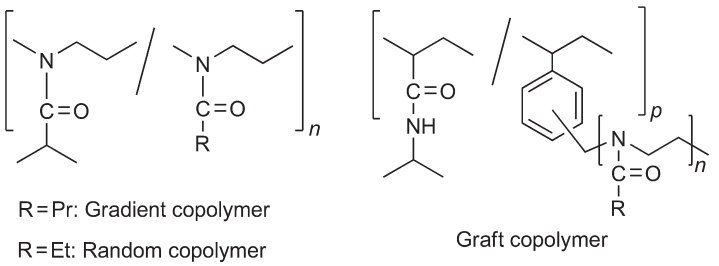

Scheme 54 Thermosensitivity-tuned gradient, random, and graft copolymers containing PROZO chains.

the molar ratio of iPrOZO to EtOZO, showing a linear increase in LCST with an increasing molar percent of EtOZO (Scheme 54).[107]

Thermosensitivity of the ROZO polymers was accurately tuned by using three monomers, PrOZO, iPrOZO, and EtOZO, by designing the reaction to combine PrOZO with either iPrOZO or EtOZO.[108] Cationic copolymerization of PrOZO and iPrOZO ($r_{PrOZO} = 3.15$ and $r_{iPrOZO} = 0.57$, respectively) gave gradient copolymers P[PrOZO-*grad*-iPrOZO], whereas that of PrOZO and EtOZO ($r_{PrOZO} = 1.28$ and $r_{EtOZO} = 1.04$, respectively) produced random copolymers P[PrOZO-*ran*-EtOZO]. The LCST of both the gradient and random copolymers could be tuned over a wide range of temperatures by varying the molar ratio of the two monomers. Most of the random copolymers of M_n around 10 000–14 000 ($M_w/M_n < 1.1$) showed a rapid and modulated response to the temperature change from 23.8 to 75.1 °C. This is good for an ideal system for tuning the LCST around the physiological conditions. In addition, PPrOZO was found to show a sharp LCST behavior near room temperature.

For the investigation of thermosensitive behaviors, gradient and graft copolymers consisting of PNIPAM chain and PiPrOZO as well as PROZO (R = Me, Et) chains were prepared (Scheme 54).[109] The turbidity temperature was tuned by the hydrophilic ROZO chain content from 28 to 42 °C; with increasing the content of ROZO chain, the CT value became higher. Thermosensitive polymers of P[iPrOZO-*block*-3-butenylOZO] with thiol groups were synthesized. A glucose moiety was introduced to the olefinic side chain via 'click' addition of a glucose thiol. Then, the CP of these copolymers was changed from 10 to 85 °C as a function of composition and hydrophilicity of the side chain.[110]

Macromonomer method was used for the synthesis of comb and graft polymers and their LCST behavior was examined, where a hydrophilic oligoEtOZO was utilized as side chains and a hydrophobic methacrylate as backbone (Scheme 55).[111] First, CROP of EtOZO was carried out under microwave irradiation using MeOTs initiator and the living end was terminated with ammonium methacrylate to form macromonomers (M_n 900–3300, $M_w/M_n < 1.1$). Second, homopolymerization of the macronomomer via the reversible addition–fragmentation chain transfer (RAFT) method gave comb polymers (M_n 7000–24 000, $M_w/M_n \leq 1.31$). Copolymerization of the macromonomer with MMA was performed similarly, to produce graft copolymers (MMA, 40–80 mol%, M_n 12000–26 000, $M_w/M_n < 1.3$). The LCST of the graft polymers measured in aqueous solutions was tuned from 35 to 80 °C depending on the MMA content. The LCST value of the comb polymer was significantly decreased when compared to that of linear PEtOZO, which was correlated with microdomain formation due to the crowded comb structure. The solution properties and LCST behaviors of random and block copolymers from EtOZO and NonOZO were also investigated.[112]

4.15.6.4 Archtecture of New Polymeric Systems

An organic–inorganic hybrid was obtained by using a hydrophilic PMeOZO silane coupling agent (Scheme 56).[113] A mixture of the coupling agent and silica gel showed the PMeOZO chain concentrated on the silica gel surface after heating in acetonitrile. The modified gel became more hydrophilic than the untreated gel. The acid-catalyzed hydrolysis of the agent in the presence of tetraethoxysilane (the so-called sol-gel method) afforded a homogeneous and transparent silica gel. The homogeneity of the composite gel is due to the

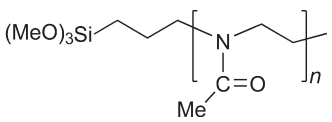

Scheme 56 An organic-inorganic hybrid using PMeOZO chain.

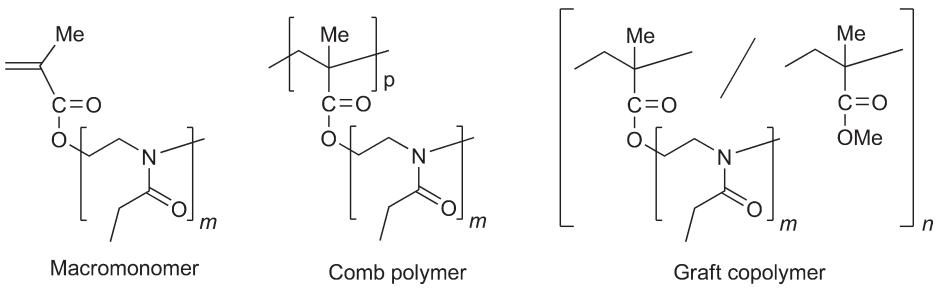

Scheme 55 Macromonomer, comb polymer, and graft copolymer, all containing EtOZO chain for the examination of LCST behaviors.

chemical bonding of the PMeOZO ends and the interaction between the amide group in PMeOZO and the silica through hydrogen bonding, thus giving an organic–inorganic polymer hybrid.

By utilizing an excellent hygroscopic nature of PMeOZO chain, nonionic hydrogels were prepared. Solvent philicity can be tuned by the combination of monomers. CROP mode copolymerization of MeOZO with 2,2′-tetramethylenebis (2-oxazoline) (TBOZO, R = -$(CH_2)_4$- in **Scheme 30**) produced a hydrogel, showing swelling property in water and an aqueous solution. The water uptake was up to 45 multiples of the dry gel. From EtOZO and TBOZO, a characteristic amphiphilic gel (amphigel) was obtained, swelling both in water and in organic solvents. A lipogel (organogel) derived from hydrophobic ROZO (R = Pr, Bu, or Oct) and TBOZO is swollen in less polar organic solvents such as toluene and 1,2-dichloroethane. A ROZO monomer with a photo-cross-linkable group of coumarin was CROP type copolymerized with MeOZO, giving rise to a hydrogel, uptaking water up to 20 times the weight of the dried gel. The cross-linking could be controlled by irradiation of Hg lamp with different wavelength, that is, cross-linking with hν > 300 nm, whereas cleavage of the gel with hν 253 nm.[114]

A new comb-burst dendrimer was synthesized via termination reaction of the living PEtOZO polymerization ends with LPEI, followed by the acid hydrolysis to remove the propionyl group. These reactions were repeated to give dendritic polyethylenimine (PEI).[115]

Self-assembling synthetic polymers are currently an important, widely conducted topic of research; they form a unique architecture in bulk and in solution to give a new material. The following are some examples of self-assembling systems from PROZO chains.

Glycosylated PROZO chains self-assembled into nanotubes in water through intermolecular hydrogen bonding interactions (**Scheme 57**).[116] The driving force for the nanotube formation is considered to be due to the unique polymer structure of the tertiary polyamide backbone (hydrogen-accepting) and glucose side chains (hydrogen-donating), first forming and bending a two-dimensional (2D) hydrogen-bonded layer of interdigitated polymer chains and then closing to form a tube. Rough values of outer and inner radii (r_o and r_i) and wall thickness ($r_o - r_i$) from three polymers are as follows (given in nanometers): a (2.0, 0.8, and 1.2); b (3.0, 2.0, and 1.0); and c (4.5, 1.0, and 3.5).

Langmuir monolayers were prepared at the air–water interface from amphiphilic polymers derived from hydrophilic PMeOZO and hydrophobic stearyl ether groups. A large lowering of the stretching frequencies was detected within the plateau region by IR analysis, probably due to a condensed packing.[117] An ultrathin film grew on the basal plane of graphite via polymerization-induced epitaxy by using PhOZO as monomer. STM observation confirmed the crystalline layer formation.[118] Living CROP of EtOZO was induced from triflate group (TfO) attached to a self-assembled monolayer on planer gold substrates. The resulting polymer was capped with a dialkylamine to show a uniform layer.[119]

The architecture of molecular brushes was developed. They are linear macromolecules having graft polymer side chains with high graft density. The side-chain crowding causes a strong stretching of backbone, resulting in a cylindrical molecular brush structure (**Scheme 58**, neglecting glassy carbon (GC)). First, radical or anionic vinyl polymerization of 2-isopropenyl-2-oxazoline (IPOZO) (a) was carried out to form a backbone polymer with $n = 88$ via radical process and 220 via anionic process (b). Then pendant OZO groups were methylated by MeOTf to form oxazolinium ions that served as macroinitiators (c), and CROP of ROZO monomer was initiated, to give rise to cylindrical molecular brushes P[IPOZO-*graft*-ROZO] (oxazoline units, $m = 18–23$) (d). The substituents R used were Me, Et, and *i*Pr. The LCST was determined by turbidity measurements of a 1.0 wt% aqueous solution, being 63 °C for the brush ($n = 88$, EtOZO, $m = 23$), 30 °C for the brush ($n = 88$, iPrOZO, $m = 18$), and 27 °C for the brush ($n = 220$, iPrOZO, $m = 18$), respectively.[120]

The molecular brush synthesis was extended to synthesize brushes of bottle brushes of PROZO on polished GC substrates (**Scheme 58**).[121] First, UV-induced vinyl polymerization of IPOZO monomer at room temperature was directly initiated from the GC surface (a) and gave PIPOZO-grafted brush layers with thickness up to 160 nm (b). The pendant oxazoline ring of the PIPOZO was used, followed by the oxazolinium-ion formation (c) to perform a second CROP of ROZO monomers to result in bottle-brush brushes (d). It was possible to functionalize the bottle-brush brushes' side-chain end groups with a steric-demanding molecule.

Alkoxy-substituted benzoyl-PEIs having $C_8–C_{13}$ alkyl groups formed self-assembly of hexagonal, columnar, 2D phase.[122] Molecular structures of self-assembling from poly (2-(3,4-bis(*n*-alkoxy)phenyl)-2-oxazoline)s were systematically investigated with regard to the DP and alkoxy chain

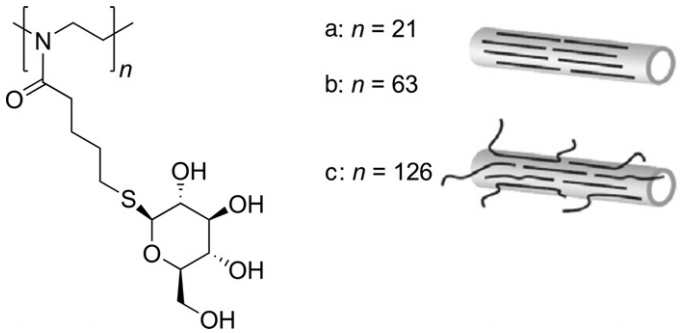

Scheme 57 A nanotube is formed via self-assembling of glycosylated PROZO chains.

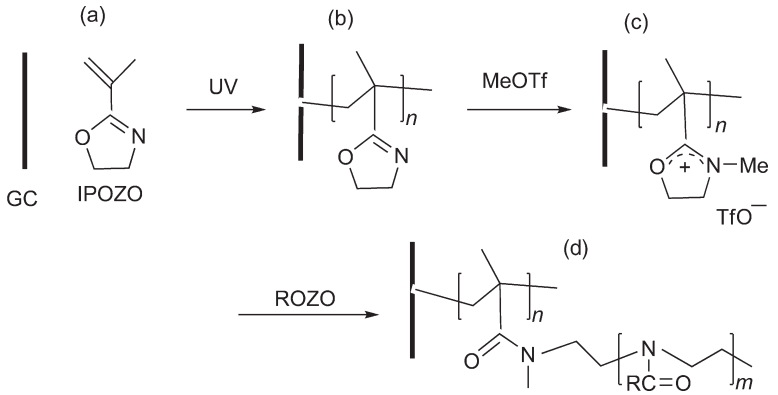

Scheme 58 Architecture of molecular brushes via vinyl polymerization of IPOZO monomer and subsequent CROP processes.

length.[123] The polymers with alkoxy chain length C_8–C_{13} formed columnar hexagonal lattices, whereas polymers with C_{14} and C_{15} alkoxy chains underwent a transition from a three-dimensional (3D) cubic phase for a low DP to a 2D hexagonal columnar phase.

PEtOZO and PiPrOZO bearing a C_{18} alkyl group at the end(s) are effective surfactants, with M_n 7000–13 000. These telechelics self-assembled into micelle aggregates, below the clouding temperature. Further heating brought about the formation of clusters of the micelles, whereas PROZO chains were flexible. When the temperature exceeded 2 °C above the clouding temperature, rigid objects were formed and their size remained constant. These behaviors of PROZO surfactants are quite different, compared with those of PNIPAM or PEG chains. This is considered to be due to different chain conformation of the amide main chain of PROZO involving hydration/dehydration of the chain through hydrogen bonding.[124]

4.15.6.5 Sythesis of Bio-Related Polymers

Applications of PROZO chains in the biomedical and pharmacological areas have been much increasing in recent years.[2k,2l,2m,125] This is mainly because CROP of ROZOs is easily able to achieve the living polymerization to lead to facile design of various polymer structures, PROZOs are of no or low toxicity, and the hydrophilic/hydrophobic nature of the polymers can be tuned readily. Furthermore, PROZO polymers produced from CROP are viewed as 'pseudopeptides' as mentioned in Section 4.15.1. The following are only few examples among many studies for such applications of PROZOs.

PMeOZO-coupled bovine liver catalase was prepared and enabled the enzyme to be used in organic solvents (Scheme 59).[126] The modified enzyme showed catalytic activity in water as well as in benzene and chloroform.

An aggregate of a block copolymer (Scheme 16, R^1 = Me, R^2 = Bu, m = 9, n = 36) and horseradish peroxidase (HRP) were obtained by mixing them in buffer solution as a new

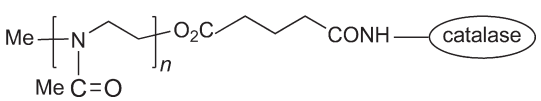

Scheme 59 Bovine liver catalase linked to PMeOZO chain to be used in organic solvents.

biocatalyst. With the formation of the aggregates, the catalytic activity was significantly enhanced.[127] Adducts from PROZO and human protein C retained catalytic avidity for the monoclonal antibody.[128]

Biocompatibility studies of PROZOs using a radio-labeled polymer found that when PMeOZO and PEtOZO were administrated in mice, they were excreted without accumulation from the bloodstream. These results suggest that the polymers possess the 'stealth' nature, meaning the suppression of all interactions with the body, being free from the immune system.[129] This is beneficial for application as drug carriers and other biomedical purposes.

For the application as drug carriers, micelles were prepared from PEtOZO-*block*-poly(ε-caprolactone), which were loaded with an anticancer drug with a poor solubility in water. The micelles were of low cytotoxicity. The loaded micelles were effective *in vitro* inhibition of the proliferation of a human carcinoma cells.[130] Similarly, a triblock copolymer, [PLA-*b*-PEtOZO-*b*-PLA], was employed for micelle roading, and also a diblock copolymer, [PEtOZO-*b*-PEI], for nonviral gene carriers.[131]

LPEI was used for DNA complexation. Novel two triblock copolymers, LPEI-*b*-PEG-*b*-LPEI (M_w 2100-3400-2100 and 4000-3400-4000) (Scheme 60(a)), were shown to condense plasmid DNA effectively to give polymer/DNA complexes (polyplexes) of small sizes (< 100 nm) and moderate ζ-potentials (~ +10 mV) at polymer/plasmid weight ratios ≥ 1.5/1. These polyplexes efficiently transfected COS-7 cells and primary bovine endothelial cells *in vitro* and are a novel class of nonviral gene delivery systems.[132] Lipopolymers were prepared as a potential candidate for constructing tailored model cell membranes. A lipid triflate was used as initiator for CROP of hydrophilic monomers, MeOZO and EtOZO, to produce an amphiphilic polymer as the model (Scheme 60(b)).[133]

Ammonium group-containing PEtOZO and PMeOZO chains showed efficient antimicrobial properties (Scheme 61).[134] Antimicrobial potential of the polymers was evaluated by determining the minimal inhibitory concentration (MIC) of the polymer against the ubiquitous Gram-positive bacterium. MIC is defined as the minimal required concentration to inhibit the growth of 99% of the bacterial cells in a suspension. For example, MIC value of the MeOZO polymer chain (R = Me, n = 53 in Scheme 15) was 1.0 mg ml^{-1}, which is 9 times more effective than the corresponding PEG polymer chain. Also, effect of

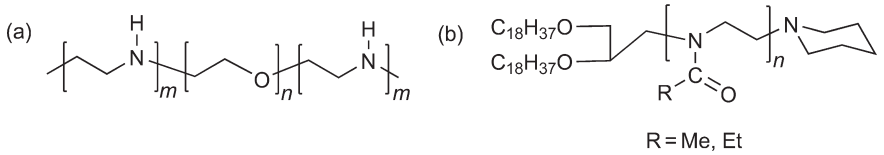

Scheme 60 DNA forms a complex with LPEI triblock copolymers (a) and an amphiphilic polymer model consisted from a hydrophilic PROZO chain and a lipid component (b).

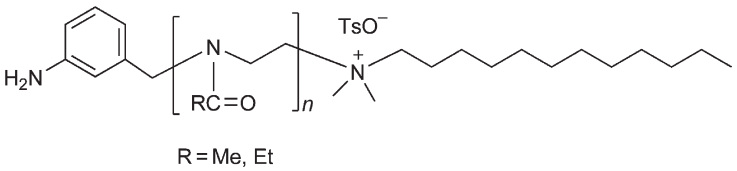

Scheme 61 Ammonium-containing PROZO chain showing antimicrobial properties.

end-group structures on the antimicrobial activity was investigated.[135]

A glycoprotein plays important roles in areas such as bioadhesion, cell–cell interactions, and recognition phenomena. A glycoprotein analog was prepared by combining a linear polysaccharide block and a PROZO block ('psuedopeptide'), for which HA (hyaluronan) and PEtOZO were employed, respectively. A lower molecular-weight HA ($M_w = 2700$) was reacted with an amino group-containing PEtOZO to produce HA-*block*-PEtOZO ($M_w = 10\,200$).[136] Preliminary experiments showed that the anionic copolymer formed colloidally stable particles ($R_h \sim 130$ nm) with a cationic drug diminazene.

References

1. (a) Seeliger, W. Ger. Patent DE 1,206,585, 1965. (b) Litt, M.H.; Levy, A.J.; Bassiri, T. G. Berg. Patent 666,828, 1965. (c) Kagiya, T.; Narisawa, S.; Maeda, T.; Fukui, K. *J. Polym. Sci. Part B: Polym. Lett.* **1966**, *4*, 257. (d) Kagiya, T.; Narisawa, S.; Maeda, T.; Fukui, K. *J. Polym. Sci. Part B: Polym. Lett.* **1966**, *4*, 441. (e) Tomalia, D. A.; Sheetz, D. P. *J. Polym. Sci. Part A: Polym. Chem.* **1966**, *4*, 2253. (f) Seeliger, W.; Aufderha, E.; Diepers, W.; Feinauer, R.; Nehring, R.; Their, W.; Hellmann, H. *Angew. Chem. Int. Ed. Engl.* **1966**, *5*, 874. (g) Levy, A.; Litt, M. *Polym. Lett.* **1967**, *5*, 881.
2. (a) Saegusa, T.; Kobayashi, S. *Macromolecular Science, International Review of Science*, Physical Chemistry Series Two, Butterworths: London, 1975; Vol. 8, Chapter 4, pp 153–190. (b) Kobayashi, S.; Saegusa, T. In *Ring-Opening Polymerization*; Ivin, K. J., Saegusa, T., Eds.; Elsevier Applied Science Publishers Ltd.: London, 1984; Chapter 11, pp 761–807. (c) Kobayashi, S.; Saegusa, T. *Encyclopedia of Polymer Science and Engineering*, 2nd edn; Wiley: New York, 1986; Vol. 4, pp 525–537. (d) Kobayashi, S. *Prog. Polym. Sci.* **1990**, *15*, 751. (e) Aoi, K.; Okada, M. *Prog. Polym. Sci.* **1996**, *21*, 151. (f) Uyama, H.; Kobayashi, S. In *Catalysis in Precision Polymerization*; Kobayashi, S., Ed.; Wiley: Chichester, England, 1997, pp 399–415. (g) Kobayashi, S.; Uyama, H. *J. Polym. Sci. Part A: Polym. Chem.* **2002**, *40*, 192. (h) Culbertson, B. M., *Prog. Polym. Sci.* **2002**, *27*, 579. (i) Park, J.-S.; Akiyama, Y.; Winnik, F. M.; Kataoka, K. *Macromolecules* **2004**, *37*, 6786. (j) Hoogenboom, R. *Macromol. Chem. Phys.* **2007**, *208*, 18. (k) Hoogenboom, R. *Angew. Chem. Int. Ed.* **2009**, *48*, 7978. (l) Makino, A.; Kobayashi, S. *J. Polym. Sci. Part A: Polym. Chem.* **2010**, *48*, 1250. (m) Schlaad, H.; Diehl, C.; Gress, A.; Meyer, M.; Demirel, A. L.; Nuf, Y.; Bertin, A. *Macromol. Rapid Commun.* **2010**, *31*, 511.
3. Kobayashi, S.; Igarashi, T.; Moriuchi, Y.; Saegusa, T. *Macromolecules* **1986**, *19*, 535.
4. Saegusa, T.; Ikeda, H.; Fujii, H. *Polym. J.* **1972**, *3*, 35.
5. Mukaiyama, T.; Sato, K. *Bull. Soc. Chem. Jpn.* **1963**, *36*, 99.
6. (a) Cesana, S.; Auernheimer, J.; Jordan, R.; Kessler, H.; Nuyken, O. *Macromol. Chem. Phys.* **2006**, *207*, 183. (b) Cesana, S.; Kurek, A.; Baur, M. A.; Auernheimer, J.; Nuyken, O. *Macromol. Rapid Commun.* **2007**, *28*, 608.
7. Ivin, K. J.; Saegusa, T. In *Ring-Opening Polymerization*; Ivin, K. J., Saegusa, T., Eds.; Elsevier Applied Science Publishers Ltd.: London, 1984; Chapter 1, pp 1–81.
8. (a) Beak, P. B.; Bonham, J.; Lee, J. T. Jr. *J. Am. Chem. Soc.* **1968**, *90*, 1569. (b) Inoue, S.; Aida, T. In *Ring-Opening Polymerization*; Ivin, K. J., Saegusa, T., Eds.; Elsevier Applied Science Publishers Ltd.: London, 1984; Chapter 4, pp 185–298. (c) Dworak, A. *Macromol. Chem. Phys.* **1998**, *199*, 1843.
9. Wenker, H. *J. Am. Chem. Soc.* **1938**, *60*, 2152.
10. Saegusa, T.; Kobayashi, S.; Ishiguro, M. *Macromolecules* **1974**, *7*, 958.
11. Kobayashi, S.; Shimizu, N.; Saegusa, T. *Polym. Bull.* **1984**, *11*, 247.
12. Saegusa, T.; Ikeda, H.; Fujii, H. *Macromolecules* **1973**, *6*, 315.
13. Saegusa, T.; Ikeda, H.; Fujii, H. *Macromolecules* **1972**, *5*, 359.
14. Kobayashi, S.; Tokuzawa, T.; Saegusa, T. *Macromolecules* **1982**, *15*, 707.
15. (a) Miyamoto, M.; Aoi, K.; Saegusa, T. *Macromolecules* **1988**, *21*, 1880. (b) Miyamoto, M.; Aoi, K.; Saegusa, T. *Macromolecules* **1991**, *24*, 11.
16. Kobayashi, S.; Morikawa, K.; Shimizu, N.; Saegusa, T. *Polym. Bull.* **1984**, *11*, 253.
17. Miyamoto, M.; Aoi, K.; Morimoto, M.; *et al. Macromolecules* **1992**, *25*, 5878.
18. Miyamoto, M.; Aoi, K.; Yamaga, S.; Saegusa, T. *Macromolecules* **1992**, *25*, 5111.
19. Miyamoto, M.; Shimakura, M.; Tsutsui, K.; *et al. Macromolecules* **1993**, *26*, 7116.
20. Miyamoto, M.; Morimoto, M.; Saegusa, T. *Polym. J.* **1993**, *25*, 1133.
21. Miyamoto, M.; Amii, H.; Aoi, K.; Saegusa, T. *Macromolecules* **1993**, *26*, 1474.
22. Miyamoto, M.; Shimakura, M.; Shimoda, S.; Hasegawa, K. *Polym. J.* **1995**, *27*, 469.
23. Miyamoto, M.; Watanabe, T.; Kimura, Y. *Macromol. Chem. Phys.* **1998**, *199*, 2237.
24. Wiesbrock, F.; Hoogenboom, R.; Abeln, C. H.; Schubert, U. S. *Macromol. Rapid Commun.* **2004**, *25*, 1895.
25. Sinnwell, S.; Ritter, H. *Macromol. Rapid Commun.* **2005**, *26*, 160.
26. Hoogenboom, R.; Leenen, M. A. M.; Wiesbrock, F.; Schubert, W. S. *Macromol. Rapid Commun.* **2005**, *26*, 1773.
27. Hoogenboom, R.; Fijten, M. W. M.; Paulus, R. M.; *et al. Polymer* **2006**, *47*, 75.
28. Wiesbrock, F.; Hoogenboom, R.; Leenen, M. A. M.; *et al. Macromolecules* **2005**, *38*, 5025.
29. Fijten, M. W. M.; Hoogenboom, R.; Schubert, U. S. *J. Polym. Sci. Part A: Polym. Chem.* **2008**, *46*, 4804.
30. Kempe, K.; Lobert, M.; Hoogenboom, R.; Schubert, U. S. *J. Polym. Sci. Part A: Polym. Chem.* **2009**, *47*, 3829.
31. Saegusa, T.; Kobayashi, S.; Yamada, A. *Makromol. Chem.* **1976**, *177*, 2271.
32. Wiesbrock, F.; Hoogenboom, R.; Leenen, M.; *et al. Macromolecules* **2005**, *38*, 7957.
33. Hoogenboom, R.; Wiesbrock, F.; Huang, H. Y.; *et al. Macromolecules* **2006**, *39*, 4719.
34. Hoogenboom, R.; Wiesbrock, F.; Leenen, M. A. M.; *et al. Macromolecules* **2007**, *40*, 2837.

35. Hustin, C. A.; Thijs-Lanbermont, H. M. L.; Hoeppener, S.; *et al. J. Polym. Sci. Part A: Polym. Chem.* **2010**, *48*, 3095.
36. Hoogenboom, R.; Thijs, H. M. L.; Fijten, M. W. M.; *et al. J. Polym. Sci. Part A: Polym. Chem.* **2007**, *45*, 416.
37. Hoogenboom, R.; Thijs, H. M. L.; Fijten, M. W. M.; Schubert, U. S. *J. Polym. Sci. Part A: Polym. Chem.* **2007**, *45*, 5371.
38. Hoogenboom, R.; Schubert, U. S. *Green Chem.* **2006**, *8*, 895.
39. Fijten, M. W. M.; Kranenburg, J. M.; Thijs, H. M. L.; *et al. Macromolecules* **2007**, *40*, 5879.
40. Lobert, M.; Hoogenboom, R.; Fustin, C. A.; *et al. J. Polym. Sci. Part A: Polym. Chem.* **2008**, *46*, 5859.
41. Guerrero-Sanchez, C.; Lobert, M.; Hoogenboom, R.; Schubert, U. S. *Macromol. Rapid Commun.* **2007**, *28*, 456.
42. Kobayashi, S.; Uyama, H.; Ihara, E.; Saegusa, T. *Macromolecules* **1990**, *23*, 1586.
43. (a) Miyamoto, M.; Sano, Y.; Saegusa, T.; Kobayashi, S. *Eur. Polym. J.* **1983**, *19*, 955. (b) Miyamoto, M.; Aoi, K.; Yamanaka, H.; Saegusa, T. *Polym. J.* **1992**, *24*, 405.
44. Kobayashi, S.; Uyama, H.; Liu, D. R.; Saegusa, T. *Macromolecules* **1990**, *23*, 5075.
45. Seung, S. L. N.; Young, R. N. *Polym. Bull.* **1979**, *1*, 481.
46. Percec, V.; Guhaniyogi, S. C.; Kennedy, J. P.; Ivan, B. *Polym. Bull.* **1982**, *8*, 25.
47. Sinai-Zingde, G.; Liu, Q.; Brink, A.; *et al. Makromol. Chem. Macromol. Symp.* **1991**, *42/43*, 329.
48. Tsutsumiuchi, K.; Aoi, K.; Okada, M. *Macromol. Rapid Commun.* **1995**, *16*, 749.
49. Saegusa, T.; Kobayashi, S.; Yamada, A. *Macromolecules* **1975**, *8*, 390.
50. (a) Kobayashi, S.; Kaku, M.; Saegusa, T. *Macromolecules* **1988**, *21*, 1921. (b) Kobayashi, S.; Kaku, M.; Saegusa, T. *Macromolecules* **1988**, *21*, 334.
51. (a) Aoi, K.; Takasu, A.; Okada, M. *Macromol. Rapid Commun.* **1995**, *16*, 53. (b) Aoi, K.; Takasu, A.; Okada, M. *Macromol. Rapid Commun.* **1995**, *16*, 757.
52. Morimoto, N.; Obeid, R.; Yamane, S.; *et al. Soft Matter* **2009**, *5*, 1597.
53. (a) Kobayashi, S.; Kaku, M.; Mizutani, T.; Saegusa, T. *Polym. Bull.* **1983**, *9*, 169. (b) Kobayashi, S.; Kaku, M.; Sawada, S.; Saegusa, T. *Polym. Bull.* **1985**, *13*, 447.
54. Shoda, S.-I.; Masuda, E.; Furukawa, M.; Kobayashi, S. *J. Polym. Sci. Part A: Polym. Chem.* **1992**, *30*, 1489.
55. Kobayashi, S.; Saegusa, T. In *Alternating Copolymers*; Cowie, J. M., Ed.; Plenum: New York, 1985; pp 185–238.
56. (a) Saegusa, T.; Ikeda, H.; Fujii, H. *Macromolecules* **1972**, *5*, 354. (b) Saegusa, T.; Kobayashi, S.; Kimura, Y. *Macromolecules* **1974**, *7*, 1. (c) Saegusa, T.; Kimura, Y.; Kobayashi, S. *Macromolecules* **1977**, *10*, 239.
57. Kadokawa, J.; Matsumura, Y.; Kobayashi, S. *Macromol. Chem. Phys.* **1994**, *195*, 3689.
58. Kobayashi, S.; Isobe, M.; Saegusa, T. *Macromolecules* **1982**, *15*, 703.
59. Nishikubo, T.; Iizawa, T.; Watanabe, M. *J. Polym. Sci. Polym. Lett.* **1980**, *18*, 761.
60. (a) Zhi-Lian, T.; Gao, Q.; Nan-Xun, H.; Sironi, C. *J. Appl. Polym. Sci.* **1995**, *57*, 473. (b) Mallon, F. K.; Ray, W. H. *J. Appl. Polym. Sci.* **1998**, *69*, 1775.
61. (a) Inata, H.; Matsumura, S. *J. Appl. Polym. Sci.* **1987**, *33*, 3069. (b) Nascimento, C. R. Azuma, C.; Bretas, R.; Farah, M.; Dias M. L. *J. Appl. Polym. Sci.* **2010**, *115*, 3177.
62. (a) Shinno, K.; Miyamoto, M.; Kimura, Y.; Hirai, Y.; Yoshitome, H. *Macromolecules* **1997**, *30*, 6438. (b) Moon, S.-I.; Lee, C.-W.; Taniguchi, I.; Miyamoto, M.; Kimura, Y. *Polymer* **2001**, *42*, 5059.
63. Maharana, T.; Mohanty, B.; Negi, Y. S. *Prog. Polym. Sci.* **2009**, *34*, 99.
64. (a) Gunatillake, P. A.; Odian, G.; Tomalia, D. A. *Macromolecules* **1987**, *20*, 2356. (b) Gunatillake, P. A.; Odian, G.; Tomalia, D. A. *Macromolecules* **1988**, *21*, 1556.
65. (a) Kobayashi, S.; Shoda, S.; Uyama, H. *Adv. Polym. Sci.* **1995**, *121*, 1. (b) Kobayashi, S.; Shoda, S.; Uyama, H. In *Catalysis in Precision Polymerization*; Kobayashi, S., Ed.; John Wiley: Chichester, England, 1997; pp 417–441. (c) Kobayashi, S. *J. Polym. Sci. Part A: Polym. Chem.* **1999**, *37*, 3041. (d) Kobayashi, S.; Uyama, H.; Ohmae, M. *Bull. Chem. Soc. Jpn.* **2001**, *74*, 613. (e) Kobayashi, S.; Uyama, H.; Kimura, S. *Chem. Rev.* **2001**, *101*, 3793. (f) Kobayashi, S.; Uyama, H. In *Encyclopedia of Polymer Science and Technology*, 3rd ed.; Kroschwitz, J. I., Ed.; John Wiley: New York, 2003; pp 328–364. (g) Kobayashi, S.; Ohmae, M. *Adv. Polym. Sci.* **2006**, *194*, 159. (h) Kobayashi, S.; Ohmae, M. In *Macromolecular Engineering: Precise Synthesis, Materials Properties, Applications*; Matyjaszewski, K., Gnanou, Y., Leibler, L., Eds.; Wiley-VCH: Weinheim, 2007; Chapter 10, pp 400–477. (i) Kobayashi, S. *Proc. Jpn. Acad. B* **2007**, *83*, 215. (j) Kobayashi, S.; Makino, A. *Chem. Rev.* **2009**, *109*, 5288. (k) A part of 5.10 in this *Polymer Science: A Comprehensive Reference* describes ring-opening polymerization of sugar oxazoline derivatives catalyzed by enzymes.
66. (a) Kiyosada, T.; Shoda, S.; Kobayashi, S. *Polym. Prepr. Jpn.* **1995**, *44*, 1230. (b) Kobayashi, S.; Kiyosada, T.; Shoda, S. *J. Am. Chem. Soc.* **1996**, *118*, 13113.
67. Tews, I.; van Scheltinga, A. C. T.; Perrakis, A.; *et al. J. Am. Chem. Soc.* **1997**, *119*, 7954.
68. (a) Pauling, L. *Chem. Eng. News* **1946**, *24*, 1375. (b) Kollman, P. A.; Kuhn, B.; Donini, O.; Perakyla, M.; Stanton, R.; Bakowies, D. *Acc. Chem. Res.* **2001**, *34*, 72.
69. Makino, A.; Nagashima, H.; Ohmae, M.; Kobayashi, S. *Biomacromolecules* **2007**, *8*, 188.
70. Makino, A.; Ohmae, M.; Kobayashi, S. *Macromol. Biosci.* **2006**, *6*, 862.
71. Kobayashi, S.; Makino, A.; Matsumoto, H.; *et al. Biomacromolecules* **2006**, *7*, 1644.
72. Makino, A.; Kurosaki, K.; Ohmae, M.; Kobayashi, S. *Biomacromolecules* **2006**, *7*, 950.
73. Kobayashi, S.; Makino, A.; Tachbana, N.; Ohmae, M. *Macromol. Rapid Commun.* **2006**, *27*, 781.
74. Kobayashi, S.; Morii, H.; Itoh, R.; *et al. J. Am. Chem. Soc.* **2001**, *123*, 11825.
75. Kobayashi, S.; Fujikawa, S.; Ohmae, M. *J. Am. Chem. Soc.* **2003**, *125*, 14357.
76. Ochiai, H.; Ohmae, M.; Mori, T.; Kobayashi, S. *Biomacromolecules* **2005**, *6*, 1068.
77. Ochiai, H.; Ohmae, M.; Mori, T.; Kobayashi, S. *Biomacromolecules* **2007**, *8*, 1327.
78. Ochiai, H.; Fujikawa, S.; Ohmae, M.; Kobayashi, S. *Biomacromolecules* **2007**, *8*, 1802.
79. Fujikawa, S.; Ohmae, M.; Kobayashi, S. *Biomacromolecules* **2005**, *6*, 2935.
80. Kadokawa, J.; Watanabe, Y.; Karasu, M.; *et al. Macromol. Rapid Commun.* **1996**, *17*, 367.
81. Kadokawa, J.; Kasai, S.; Watanabe, Y.; *et al. Macromolecules* **1997**, *30*, 8212.
82. Kadokawa, J.; Sato, M.; Karasu, M.; *et al. Angew. Chem. Int. Ed.* **1998**, *37*, 2373.
83. Kobayashi, S.; Bryant, L. L., Jr.; Tsukamoto, Y.; Saegusa, T. *Macromolecules* **1986**, *19*, 1547.
84. Miyamoto, M.; Itoh, Y.; Lee, C. W.; *et al. Macromolecules* **1997**, *30*, 1863.
85. Miyamoto, M.; Itoh, Y.; Kanayama, R.; *et al. Polym. J.* **1997**, *29*, 854.
86. Bryant, L. L., Jr.; Kinstle, J. E.; Saegusa, T.; Kobayashi, S. *Polym. Bull.* **1986**, *15*, 227.
87. Kobayashi, S.; Tsukamoto, Y.; Saegusa, T. *Macromolecules* **1990**, *23*, 2609.
88. Saegusa, T.; Nagura, Y.; Kobayashi, S. *Macromolecules* **1973**, *6*, 657.
89. (a) Saegusa, T.; Kobayashi, S.; Nagura, Y. *Macromolecules* **1974**, *7*, 265. (b) Saegusa, T.; Kobayashi, S.; Nagura, Y. *Macromolecules* **1974**, *7*, 272. (c) Saegusa, T.; Kobayashi, S.; Nagura, Y. *Macromolecules* **1974**, *7*, 713.
90. Miyamoto, M.; Aoi, K.; Saegusa, T. *J. Polym. Sci. Part A: Polym. Chem.* **1997**, *35*, 933.
91. (a) Uyama, H.; Kobayashi, S. *Macromolecules* **1991**, *24*, 614. (b) Kobayashi, S.; Uyama, H.; Mori, T.; Narita, Y. *Chem. Lett.* **1991**, *1771. (c) Kobayashi, S.; Uyama, H.; Narita, Y.* Makromol. Chem. Rapid Commun. **1992**, 13, *337. (d) Kobayashi, S.; Uyama, H.; Narita, Y.* Macromolecules **1990**, 23, *353. (e) Kobayashi, S.; Uyama, H.; Narita, Y.* Macromolecules **1992**, 25, *3232.*
92. Kobayashi, S.; Iijima, S.; Igarashi, T.; Saegusa, T. *Macromolecules* **1987**, *20*, 1729.
93. Luxenhofer, R.; Bezen, M.; Jordan, R. *Macromol. Rapid Commun.* **2008**, *29*, 1509.
94. (a) Kobayashi, S.; Masuda, E.; Shoda, S.; Shimano, Y. *Macromolecules* **1989**, *22*, 2878. (b) Kobayashi, S.; Uyama, H.; Shirasaka, H. *Makromol. Chem. Rapid Commun.* **1990**, *11*, 11. (c) Kobayashi, S.; Uyama, H.; Higuchi, N.; Saegusa, T. *Macromolecules* **1990**, *23*, 54.
95. Kobayashi, S.; Uyama, H. *Macromolecules* **1991**, *24*, 5473.
96. Kobayashi, S.; Uyama, H. *Polym. J.* **1990**, *22*, 175.
97. Luxenhofer, R.; Jordan, R. *Macromolecules* **2006**, *39*, 3509.
98. Gress, A.; Volkel, A.; Schlaad, H. *Macromolecules* **2007**, *40*, 7928.
99. Fijten, M. W. M.; Haensch, C.; van Lankvelt, B. M.; *et al. Macromol. Chem. Phys.* **2008**, *209*, 1887.
100. (a) Kobayashi, S.; Uyama, H.; Choi, J. C.; Matsumoto, Y. *Proc. Acad. Jpn. Ser. B* **1991**, *67*, 140. (b) Uyama, H.; Matsumoto, Y.; Kobayashi, S. *Chem. Lett.* **1992**, *2401. (c) Kobayashi, S.; Uyama, H.; Lee, S. W.; Matsumoto, Y.* J. Polym. Sci. Part A: Polym. Chem. **1993**, 31, *3133. (d) Kobayashi, S.; Uyama, H.; Choi, J. C.; Matsumoto, Y.* Polym. Int. **1993**, 30, *265.*
101. Uyama, H.; Honda, Y.; Kobayashi, S. *J. Polym. Sci. Part A: Polym. Chem.* **1993**, *31*, 123.
102. Zarka, M. T.; Nuyken, O.; Weberskirch, R. F. *Macromol. Rapid Commun.* **2004**, *25*, 858.
103. Bortenschlager, M.; Schollhorn, N.; Wittmann, A.; Weberskirch, R. *Chem. Eur. J.* **2007**, *13*, 520.
104. Aoshima, S.; Kanaoka, S. *Adv. Polym. Sci.* **2008**, *210*, 169.
105. Uyama, H.; Kobayashi, S. *Chem. Lett.* **1992**, 1643.
106. Kobayashi, S.; Saegusa, T. *Macromol. Chem. Suppl.* **1985**, *12*, 11.
107. Park, J.-S.; Kataoka, K. *Macromolecules* **2006**, *39*, 6622.
108. Park, J.-S.; Kataoka, K. *Macromolecules* **2007**, *40*, 3599.

109. (a) David, G.; Alupei, V.; Simionescu, B. C.; Dincer, S.; Piskin, E. *Eur. Polym. J.* **2003**, *39*, 1209. (b) Rueda, J.; Zschoche, S.; Komber, H.; Schmaljohann, D.; Voit, B. *Macromolecules* **2005**, *38*, 7330.
110. Diehl, C.; Schlaad, H. *Macromol. Biosci.* **2009**, *9*, 157.
111. Weber, C.; Becer, C. R.; Hoogenboom, R.; Schubert, U. S. *Macromolecules* **2009**, *42*, 2965.
112. Lambermont-Thijs, H. M. L.; Hoogenboom, R.; Fustin, C. A.; *et al. J. Polym. Chem. Part A: Polym. Chem.* **2009**, *47*, 515.
113. (a) Chujo, Y.; Ihara, E.; Ihara, H.: Saegusa, T. *Macromolecules* **1989**, *22*, 2040. (b) Chujo, Y.; Ihara, E.; Kure, S.; Saegusa, T. *Macromolecules* **1993**, *26*, 5681.
114. (a) Chujo, Y.; Sada, K.; Matsumoto, K.; Saegusa, T. *Macromolecules* **1990**, *23*, 1234. (b) Chujo, Y.; Sada, K.; Matsumoto, K.; Saegusa, T. *Polym. Bull.* **1989**, *21*, 353. (c) Chujo, Y.; Sada, K.; Saegusa, T. *Macromolecules* **1990**, *23*, 2693.
115. Tomalia, D. A.; Hedstrand, D. M.; Ferritto, M. S. *Macromolecules* **1991**, *24*, 1435.
116. Gress, A.; Heilig, A.; Smarsly, B. M.; *et al. Macromolecules* **2009**, *42*, 4244.
117. Baekmark, T. R.; Wiesenthal, T.; Kuhn, P.; *et al. Langmuir* **1997**, *13*, 5521.
118. Sandberg, M.; Sano, M.; Yoshimura, S. *Chem. Lett.* **1995**, 1148.
119. Jordan, R.; Ulman, A. *J. Am. Chem. Soc.* **1998**, *120*, 243.
120. Zhang, N.; Huber, S.; Schulz, A.; *et al. Macromolecules* **2009**, *42*, 2215.
121. Zhang, N.; Steenackers, M.; Luxenhofer, R.; Jordan, R. *Macromolecules* **2009**, *42*, 5345.
122. Seitz, M.; Plesnivy, T.; Schimossek, K.; *et al. Macromolecules* **1996**, *29*, 6560.
123. (a) Percec, V.; Holerca, M. N.; Magonov, S. N.; Yeardley, D. J. P.; Unger, G.; Duan, H.; Hudson, S. D. *Biomacromolecules* **2001**, *2*, 706. (b) Percec, V.; Holerca, M. N.; Uchida, S.; Yeardley, D. J. P.; Unger, G. D. *Biomacromolecules* **2001**, *2*, 729.
124. Obeid, R.; Maltseva, E.; Thuenemann, A. F.; *et al. Macromolecules* **2009**, *42*, 2204.
125. (a) Schazlein, A. G. *Anti-Cancer Drugs* **2001**, *12*, 275. (b) Adams, N.; Schubert, U. S. *Adv. Drug Deliv.* **2007**, *59*, 1504.
126. Miyamoto, M.; Naka, K.; Shiozaki, M.; *et al. Macromolecules* **1990**, *23*, 3201.
127. Naka, K.; Ohki, A.; Maeda, S. *Chem. Lett.* **1991**, 1303.
128. Velander, W. H.; Madurawe, R. D.; Kumar, G.; *et al. Biotechnol. Bioeng.* **1992**, *39*, 1024.
129. (a) Goddard, P.; Hutchinson, L. E.; Brown, J.; Brookman, L. J. *J. Controll. Rel.* **1989**, *10*, 5. (b) Gaertner, F. C.; Luxenhofer, R.; Blechert, B.; Jordan, R.; Essler, M. *J. Controll. Rel.* **2007**, *119*, 291.
130. (a) Lee, S. C.; Kim, C.; Kwon, I. C.; Chung, H.; Jeong, S. Y. *J. Controll. Rel.* **2003**, *89*, 437.
131. (a) Hsiue, G. H.; Wang, C. H.; Lo, C. L.; Li, J. P.; Yang, J. L. *J. Controll. Rel.* **2006**, *114*, 69. (b) Hsiue, G. H.; Chiang, H. Z.; Wang, C. H.; Juang, T. M. *Bioconjugate Chem.* **2006**, *17*, 781.
132. Zhong, Z. Y.; Feijen, J.; Lok, M. C.; *et al. Biomacromolecules* **2005**, *6*, 3440.
133. Ludtke, K.; Jordan, R.; Hommes, P.; *et al. Macromol. Biosci.* **2005**, *5*, 384.
134. Waschinski, C. J.; Tiller, J. C. *Biomacromolecules* **2005**, *6*, 235.
135. (a) Waschinski, C. J.; Herdes, V.; Schueler, F.; Tiller, J. C. *Macromol. Biosci.* **2005**, *5*, 149. (b) Waschinski, C. J.; Barnett, S.; Theobald, A.; *et al. Biomacromolecules* **2008**, *9*, 1764.
136. Yang, Y. L.; Kataoka, K.; Winnik, F. M. *Macromolecules* **2005**, *38*, 2043.

Biographical Sketch

Shiro Kobayashi studied organic chemistry and polymer chemistry at Kyoto University. After the PhD course, he was a postdoctoral fellow at stayed at Case Western Reserve University for 2 years and investigated cationic reaction mechanisms. He joined Kyoto University and restarted polymer synthesis studies. He was a Humboldt fellow at Mainz University in 1976. Then he was appointed as a full professor of Tohoku University in 1986. He moved to Kyoto University in 1997 and officially retired in 2005 to become a professor emeritus. Since then, he has been a distinguished professor at Kyoto Institute of Technology. His research interests include polymer synthesis, enzymatic polymerizations, organic reactions, and materials chemistry. He has been studying the polymerization of oxazolines for many years. He received the Award of the Chemical Society of Japan for Young Chemists (1976), the Award of the Society of Polymer Science Japan (1987), the Humboldt Research Award (1999), the Chemical Society of Japan Award (2001), the John Stauffer Distinguished Lecture Award (2002), the Medal with Purple Ribbon (2007), and others. He has been a foreign member of the Northrhine Westfalian Academy of Science since 1999. He currently serves as a member of (executive) advisory board and editorial (advisory) board for 14 international journals.

4.16 Ring-Opening Polymerization of Amino Acid *N*-Carboxyanhydrides

TJ Deming, University of California–Los Angeles, Los Angeles, CA, USA

4.16.1 Introduction

Peptide polymers have many advantages over conventional synthetic polymers since they are able to hierarchically assemble into stable ordered conformations.[1] Depending on the amino acid side-chain substituents, polypeptides are able to adopt a multitude of conformationally stable regular secondary structures (e.g., helices, sheets, turns), tertiary structures (e.g., the β-strand-helix-β-strand unit found in β-barrels), and quaternary assemblies (e.g., collagen microfibrils).[1] There is considerable interest in developing synthetic routes for preparation of polypeptide materials to make products for applications in biotechnology (artificial tissues, implants), biomineralization (resilient, lightweight, ordered inorganic composites), and analysis (biosensors, medical diagnostics).[2] To be successful in these applications, it is important that the polypeptides possess precisely defined compositions, sequences, and structures.

Synthetic peptide-based polymers are not new materials: homopolymers of polypeptides have been available for many decades, yet have only seen limited use in materials applications.[3] However, new methods in chemical synthesis have made possible the preparation of increasingly complex polypeptide sequences of controlled molecular weight that display properties far superior to ill-defined homopolypeptides.[4] Examination of the different methods for polypeptide synthesis reveals the limitations of these techniques for preparation of well-defined copolymers. Conventional solid-phase peptide synthesis is neither useful nor practical for direct preparation of large polypeptides (> 100 residues) due to unavoidable deletions and truncations that result from incomplete deprotection and coupling steps. The most economical and expedient process for synthesis of long polypeptide chains is the polymerization of α-amino acid *N*-carboxyanhydrides (NCAs) (eqn [1]).[5] This method involves the simplest reagents and high-molecular-weight polymers can be prepared in good yield and large scale with no detectable racemization at the chiral centers. The considerable variety of NCAs that have been synthesized (> 200) allows exceptional diversity in the types of polypeptides that can be prepared.[5]

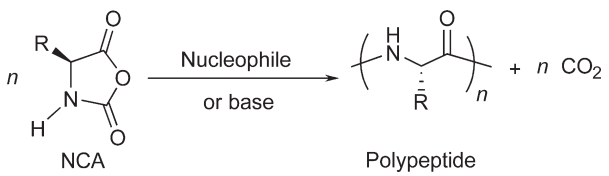

[1]

Since the late 1940s, NCA polymerizations have been the most common technique used for large-scale preparation of high-molecular-weight polypeptides.[6] However, these materials have primarily been homopolymers, random copolymers, or graft copolymers that lack the sequence specificity and monodispersity of natural proteins. Only in recent decades has the level of control in NCA polymerizations been able to rival that found in other synthetic polymerizations (e.g., vinyl addition polymerizations) where sophisticated polymer architectures have been prepared (e.g., stereospecific polymers and block copolymers).[7] Early attempts to prepare block copolypeptides and hybrid block copolymers using NCAs resulted in polymers whose compositions did not match monomer feed compositions and that contained significant homopolymer contaminants.[8] Block copolymers could only be obtained in pure form by extensive fractionation steps, which significantly lowered the yield and efficiency of this method.

Historical limitations of NCA polymerizations have been the presence of side reactions (chain termination and chain transfer) that restrict control over molecular weight, give broad molecular weight distributions, and prohibit formation of well-defined block copolymers.[9] Recent progress in elimination of these side reactions has been a major breakthrough for the polypeptide materials field. This chapter will cover background and recent developments in methods for the ring-opening polymerization (ROP) of NCAs. It will also cover applications of these methods for preparation of block, star, brush, and branched copolypeptides, side-chain functional polypeptides, and poly-β-peptides. Finally, methods for removal of protecting groups and purification of polypeptides will be reviewed. Polypeptide containing hybrid copolymers, where considerable work and progress has been made in recent years,[10] are not covered in this chapter.

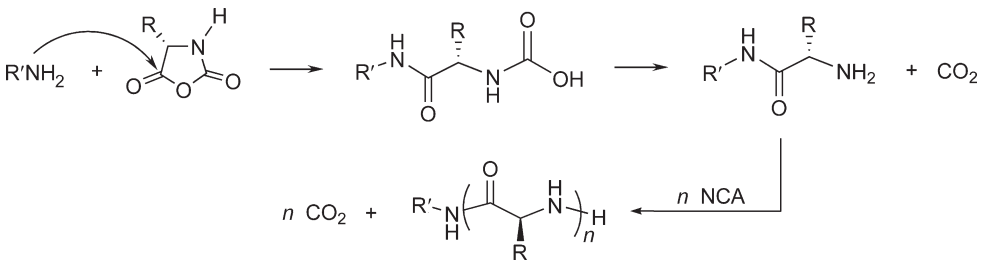

[2]

4.16.2 Polypeptide Synthesis using NCAs

4.16.2.1 Conventional Methods

NCA polymerizations have been initiated using many different nucleophiles and bases, the most common being primary amines and alkoxide anions.[5] Primary amines, being more nucleophilic than basic, are good general initiators for polymerization of NCA monomers. Tertiary amines, alkoxides, and other initiators that are more basic than nucleophilic have found use since they are in some cases able to prepare polymers of very high-molecular-weight where primary amine initiators cannot. Optimal polymerization conditions have often been determined empirically for each NCA, and thus there have been no universal initiators or conditions by which to prepare high polymers from any monomer. This is in part due to the different properties of individual NCAs and their polymers (e.g., solubility) but is also strongly related to the side reactions that occur during polymerization.

The most likely pathways of NCA polymerization are the so-called 'amine' and the 'activated monomer' (AM) mechanisms.[5] The amine mechanism is a nucleophilic ring-opening chain growth process where the polymer could grow linearly with monomer conversion if side reactions were absent (eqn [2]). On the other hand, the AM mechanism is initiated by deprotonation of an NCA, which then becomes the nucleophile that initiates chain growth (eqn [3]). It is important to note that a polymerization can switch back and forth between the amine and AM mechanisms many times: a propagation step for one mechanism is a side reaction for the other, and vice versa. It is because of these side reactions that block copolypeptides and hybrid block copolymers prepared from NCAs using amine initiators have structures different than predicted by monomer feed compositions and most likely have considerable homopolymer contamination. These side reactions also prevent control of chain-end functionality desirable for many applications.

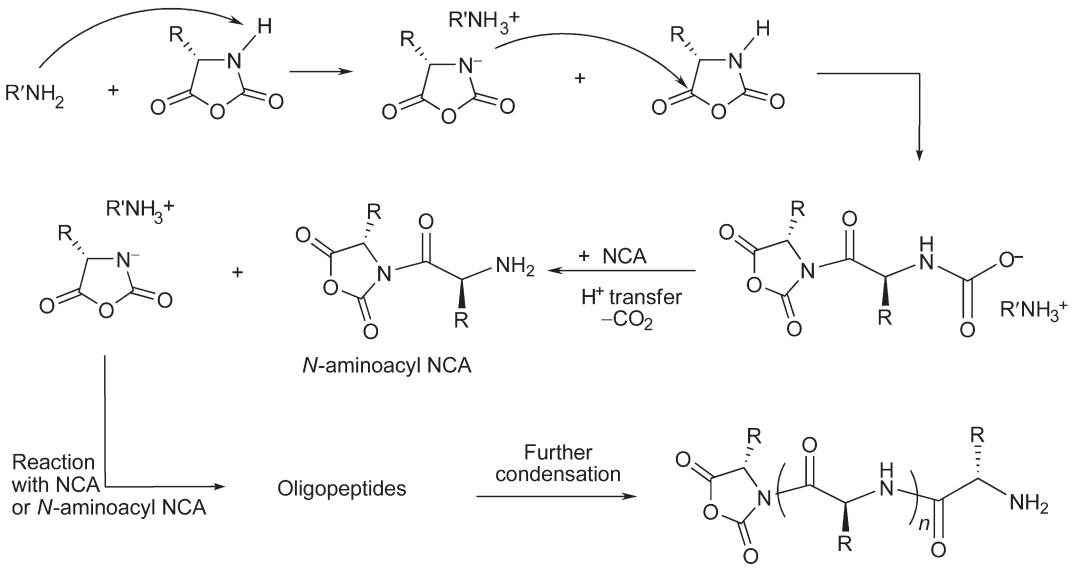

[3]

One inherent problem in conventional NCA polymerizations is that there is no control over the reactivity of the growing polymer chain end during the course of the polymerization. Once an initiator reacts with an NCA monomer, it is no longer involved in the polymerization and the resulting primary amine, carbamate, or NCA anion end group is free to undergo a variety of undesired side reactions. Another problem is one of purity. Although most NCAs are crystalline compounds, they typically contain minute traces of acid, acid chlorides, or isocyanates that can quench propagating chains. The presence of other adventitious impurities, such as water, can cause problems by acting as chain-transfer agents or even as catalysts for side reactions. Overall, the abundance of potential side reactions present in reaction media makes it difficult to achieve a living polymerization system where only chain propagation occurs.

4.16.2.2 Transition Metal Initiators

A successful strategy to eliminate side reactions in NCA polymerizations has been the use of transition metal complexes as active species to control addition of NCA monomers to polymer chain ends. The use of transition metals to control reactivity has been proven in organic and polymer synthesis as a means to increase reaction selectivity, efficiency, and rate.[11] Using this approach, a significant advance in controlled NCA polymerization was realized in 1997. Highly effective zero-valent nickel and cobalt initiators (i.e., bpyNi(COD) and $(PMe_3)_4Co$)[12,13] were developed by Deming that allow the living polymerization of NCAs into high-molecular-weight polypeptides by an unprecedented activation of the NCAs to generate covalent propagating species. The metal ions can be conveniently removed from the polymers by simple precipitation or dialysis of the samples after polymerization.

Mechanistic studies on the initiation process showed that both these metals react identically with NCA monomers to form metallacyclic complexes by oxidative addition across the anhydride bonds of NCAs.[12,13] These oxidative-addition reactions were followed by addition of a second NCA monomer to yield complexes identified as six-membered amido-alkyl metallacycles (eqn [4]). These intermediates were found to further contract to five-membered amido-amidate metallacycles upon reaction with additional NCA monomers. This ring contraction is thought to occur by migration of an amide proton to the metal-bound carbon, which liberates the chain end from the metal (eqn [5]).[14] The resulting amido-amidate complexes were thus proposed as the active polymerization intermediates. Propagation through the amido-amidate metallacycle was envisioned to occur by initial attack of the nucleophilic amido group on the electrophilic C_5 carbonyl of an NCA monomer (eqn [6]). This reaction would result in a large metallacycle that can contract by elimination of CO_2. Proton transfer from the free amide to the tethered amidate group further contracts the ring to regenerate the amido-amidate propagating species, while in turn liberating the end of the polymer chain.

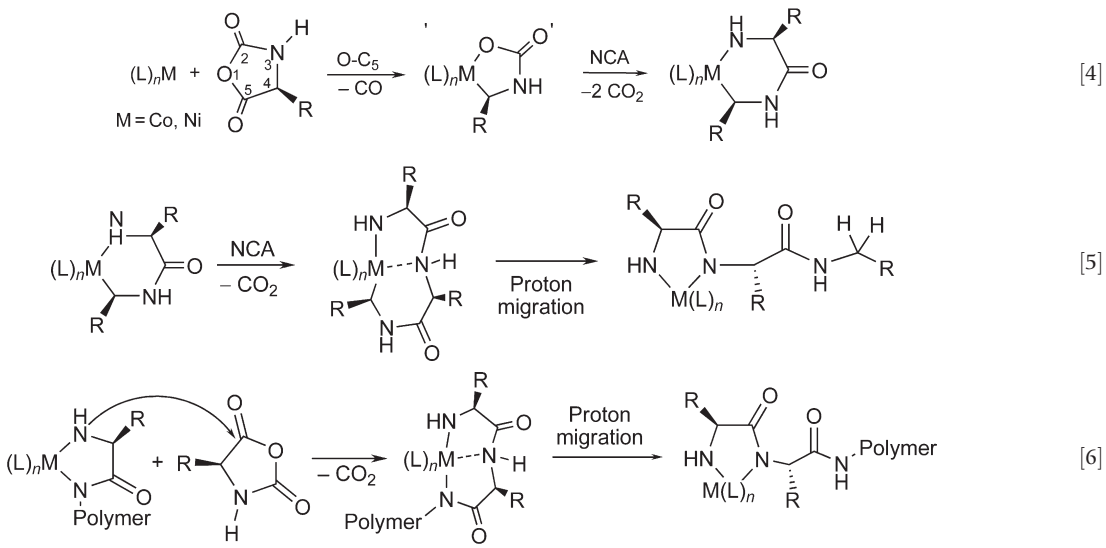

In this manner, the metal is able to migrate along the growing polymer chain, while being held by a robust chelate at the active end. The formation of these chelating metallacyclic intermediates appears to be a general requirement for obtaining living NCA polymerizations using transition metal initiators. These cobalt and nickel complexes are able to produce polypeptides with narrow chain length distributions ($M_w/M_n < 1.20$) and controlled molecular weights ($500 < M_n < 500\,000$).[15] This polymerization system is very general, and gives controlled polymerization of a wide range of NCA monomers as pure enantiomers (D or L configuration) or as racemic mixtures. These polymerizations can be

conducted in a variety of solvents (e.g., tetrahydrofuran (THF), dimethylformamide (DMF), ethyl acetate (EtOAc), dioxane, and acetonitrile (MeCN)) and over a broad range of temperatures (i.e., 10–100 °C) with no loss of polymerization control. By addition of different NCA monomers, the preparation of block copolypeptides of defined sequence and composition is feasible.[4,16]

One potential limitation of using zero-valent metal complexes as initiators is that the active propagating species are generated *in situ*, where the C-terminal end of the polypeptide is derived from the first NCA monomer. Consequently, this method does not allow attachment of functionality (e.g., polymer or small molecule) to the carboxyl chain end. For this reason, Deming and co-workers pursued alternative methods for direct synthesis of the amido-amidate metallacycle propagating species and developed allyloxycarbonylaminoamides as universal precursors to amido-amidate nickelacycles. These simple amino acid derivatives undergo tandem oxidative additions to nickel(0) to give active NCA polymerization initiators (eqn [7]).[17] These complexes were found to initiate polymerization of NCAs yielding polypeptides with defined molecular weights, narrow molecular weight distributions, and with quantitative incorporation of the initiating ligand as a C-terminal end group. This chemistry provides a facile means to incorporate diverse molecules such as polymers, peptides, oligosaccharides, or other ligands onto the chain ends of polypeptides by a robust amide linkage, and was further elaborated by Witte and Menzel[18] to grow polypeptides off polystyrene particles.

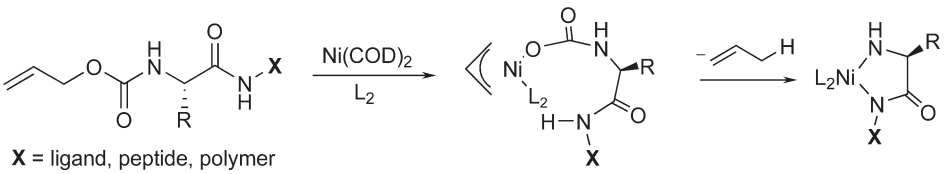

[7]

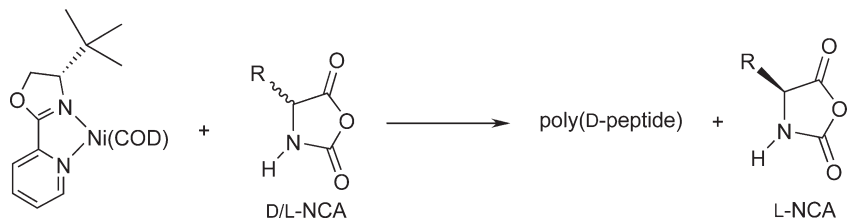

[8]

By knowing the active intermediates in these polymerizations, Cheng and Deming[19] were also able to use chiral donor ligands to prepare optically active nickel initiators for the enantioasymmetric polymerization of NCAs. Since polypeptides are chiral polymers, the ability to control stereochemistry during polymerization is a feature worth pursuing. This is especially true since the self-assembly and properties of polypeptides are critically dependent on the stereochemistry of the amino acid components. Due to constraints imposed by the initial oxidative-addition reactions and the stability of zero-valent cobalt and nickel complexes, only a limited pool of chiral ligands could be used. For example, common chiral aryl-substituted bisphoshines were completely ineffective in promoting oxidative additions of NCAs with nickel(0). Using optically active 2-pyridinyl oxazoline ligands that were mixed with bis(1,5-cyclooctadiene)nickel in THF, it was found that the resulting chiral nickel complexes were able to selectively polymerize one enantiomer of an NCA over the other.[19] The highest selectivity was observed with the nickel complex of (*S*)-4-*tert*-butyl-2-pyridinyl oxazoline, which gave a ratio of enantiomer polymerization rate constants (k_D/k_L) of 5.2(0.1) (eqn [8]). This initiator also gave a 17% enantiomeric excess of the D-antipode in the copolymer formed at 16% conversion in the polymerization of racemic NCA. It was found that subtle modification of this ligand by incorporation of additional substituents had a substantial impact on initiator selectivities. These results were a first step toward the ability to readily synthesize optically pure polypeptides from inexpensive racemic monomer pools. The main limitation of this system, however, is the fluxional coordination geometry around nickel(II), which hinders the development of a rigid, chiral environment at the metal center.

Subsequently, Deming identified new initiating systems based on amido-sulfonamide metallacycles prepared by deprotonation of the corresponding amine complexes. Seidel and Deming[20] studied a ruthenium(II) amido-sulfonamide complex, which although not an amido-amidate metallacycle, was recognized to possess all the required features for controlled NCA polymerization (eqn [9]). This complex contains a nucleophilic alkyl amido group, stabilized by a rigid chelate, and a proton-accepting sulfonamide group on the other end of the metallacycle that allows the chain end to migrate off the metal. This ruthenium complex and the corresponding isoelectronic Cp*iridium(III) (Cp* = C_5Me_5) complex were found to initiate living polymerizations of NCAs,[20] which shows that effective initiators can also be prepared with second and third

row metals.[21] Furthermore, these initiators were found to give much higher enantiomeric selectivities, as well as polymerization activities, in polymerizations of racemic NCAs compared to the nickel systems studied earlier. This work was elaborated by Peng *et al.*[22] who prepared similar amido-sulfonamide metallacycles using platinum(II), and found that these complexes give controlled polymerization of ε-carbobenzyloxy-L-lysine NCA, Z-Lys NCA (eqn [9]).

4.16.2.3 Controlled Polymerization using Amine Initiators

In the past 7 years, a number of new approaches have been reported to give controlled NCA polymerizations. These approaches share a common theme in that they are all improvements on the use of conventional primary amine polymerization initiators. This approach is attractive since primary amines are readily available and since the initiator does not need to be removed from the reaction after polymerization. In

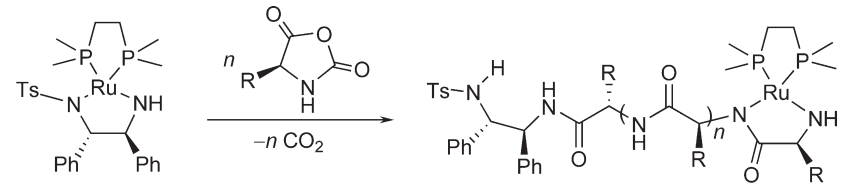

[9]

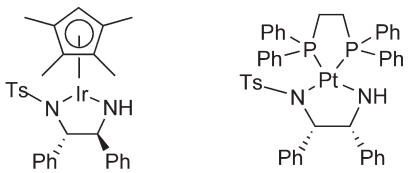

Further extending this work, Deming also developed a means to end-cap living polypeptide chains with electrophilic reagents. When a macromolecular electrophile is used, the resulting product is a polypeptide hybrid block copolymer. It is well known in NCA polymerizations that electrophiles, such as isocyanates, act as chain-terminating agents by reaction with the propagating amine chain ends.[5] Brzezinska *et al.*[23] reported that the reactive living nickelacycle polypeptide chain ends could be quantitatively capped by reaction with excess isocyanate, isothiocyanate, or acid chloride. Using this chemistry, they prepared isocyanate end-capped poly(ethylene glycol) (PEG), and reacted this, in excess, with living poly(γ-benzyl-L-glutamate) (poly (Bn-Glu)) to obtain poly(Bn-Glu)-*b*-PEG diblock copolymers (eqn [10]). Overall, it can be seen that the use of transition metal-initiated NCA polymerization allows formation of well-defined copolymer architectures that rival those prepared using any polymerization system.

fact, if the polymerization proceeds without any chain-breaking reactions, the amine initiator becomes the C-terminal polypeptide end group. In this manner, there is potential to form chain-end-functionalized polypeptides or even hybrid block copolymers if the amine is a macroinitiator. The challenge in this approach is to overcome the numerous side reactions of these systems without the luxury of a large number of experimental parameters to adjust.

In 2004, Aliferis *et al.*[24] reported the primary amine-initiated polymerization of NCAs under high-vacuum conditions. The strategy here was to determine if a reduced level of impurities in the reaction mixture would lead to fewer polymerization side reactions. Unlike the vinyl monomers usually polymerized under high-vacuum conditions, NCAs cannot be purified by distillation. Consequently, it is unclear if NCAs can be obtained in higher purity by high-vacuum recrystallization than by recrystallization under a rigorous inert atmosphere. However, the high-vacuum method does allow for better purification of polymerization

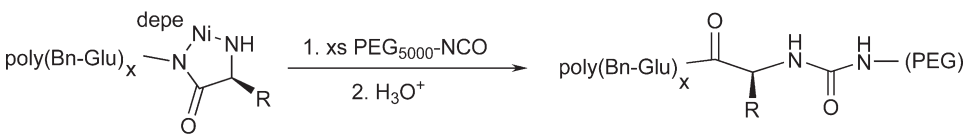

[10]

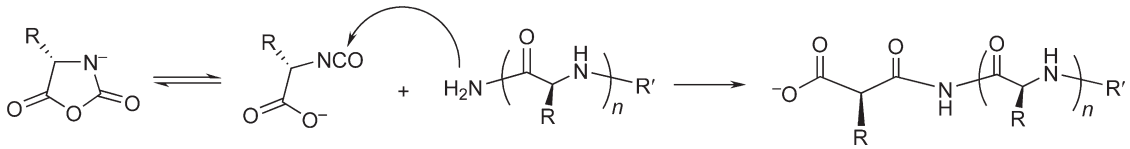

[11]

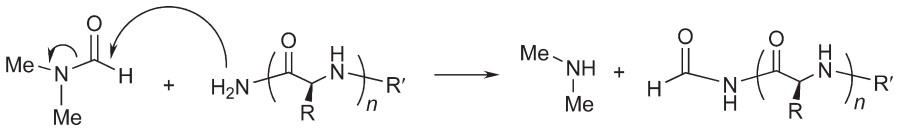

[12]

solvents and the *n*-hexylamine initiator. It was found that polymerizations of Bn-Glu NCA and Z-Lys NCA under high vacuum in DMF solvent displayed all the characteristics of a living polymerization system.[24] Polypeptides could be prepared with control over chain length, chain length distributions were narrow, and block copolypeptides were prepared.

The authors concluded that the side reactions normally observed in amine-initiated NCA polymerizations are simply a consequence of impurities. Since the main side reactions in NCA polymerizations do not involve reaction with adventitious impurities such as water, but instead reactions with monomer, solvent, or polymer (i.e., termination by reaction of the amine end with an ester side chain, attack of DMF by the amine end, or chain transfer to monomer),[5] it appears removal of water suppresses these side reactions. A possible explanation for the polymerization control observed under high vacuum is that impurities (e.g., water) act to catalyze side reactions of growing chains with monomer, polymer, or solvent. In this scenario, it is reasonable to speculate that polar species such as water can bind to monomers or the propagating chain end and thus influence their reactivity. Recently, in polymerizations of *O*-benzyl-L-tyrosine NCA (Bn-Tyr NCA) in DMF, it was determined that although most side reactions are insignificant in the high-vacuum polymerization, some termination of chains by reaction with DMF solvent does occur.[25]

Further insights into amine-initiated NCA polymerizations were also reported in 2004 by Vayaboury *et al.*[26] This group studied the polymerization of ε-trifluoroacetyl-L-lysine NCA (TFA-Lys NCA) in DMF using *n*-hexylamine initiator at different temperatures. Contrary to the high-vacuum work, the solvent and initiator were purified using conventional methods and the polymerizations were conducted under a nitrogen atmosphere on a Schlenk line. After complete consumption of NCA monomer, the crude polymerization mixtures were analyzed by gel permeation chromatography (GPC) and nonaqueous capillary electrophoresis (NACE). A unique feature of this work was the use of NACE to separate and quantify the amount of polymers with different chain ends, which corresponded to living chains (amine end groups) and 'dead' chains (carboxylate and formyl end groups from reaction with NCA anions and DMF solvent, respectively, eqns [11] and [12]). Not surprisingly, at 20 °C, the polymer products consisted of 78% dead chains, and only 22% living chains, which illustrates the abundance of side reactions in these polymerizations under normal conditions.

An intriguing result was found for polymerizations conducted at 0 °C, where 99% of the chains had living amine chain ends, and only 1% were found to be dead chains. To verify that these were truly living polymerizations, additional NCA monomer was added to these chains at 0 °C, resulting in increased molecular weight and no increase of the amount of dead chains. While TFA-Lys NCA was the only monomer studied, this work showed that most common NCA polymerization side reactions can also be eliminated by lowering temperature. The effect of temperature is not unusual, as similar trends can be found in cationic and anionic vinyl polymerizations.[27] At elevated temperature, the side reactions have activation barriers similar to chain propagation. When the temperature is lowered, the activation barrier for chain propagation becomes lower than that of the side reactions and chain propagation dominates kinetically. A key limitation of this method is that these polymerizations are very slow at 0 °C, often requiring numerous days to obtain polypeptide chains of modest length. A remarkable feature of this system is that increased impurity levels, as compared to the high-vacuum method, did not result in side reactions at low temperature. This result further substantiates the idea that the growing chains do not react with the adventitious impurities, but that impurities mainly affect these polymerizations by altering the rates of discrete reaction steps.

4.16.2.4 Amine Hydrochloride-Initiated Polymerizations

An innovative approach to controlling amine-initiated NCA polymerizations was reported in 2003 by Dimitrov and Schlaad.[28] Their strategy was to avoid formation of NCA anions, which cause significant chain termination after rearranging to isocyanocarboxylates,[5] through use of primary amine hydrochloride salts as initiators. The reactivity of amine hydrochlorides with NCAs was first explored by the group of Knobler, who found that they can react with NCAs to give single NCA addition products.[29] Use of the hydrochloride salt takes advantage of its diminished reactivity as a nucleophile compared to the parent amine, which effectively halts the reaction after a single NCA insertion by formation of an inert amine hydrochloride in the product. The reactivity of the hydrochloride presumably arises from formation of a small amount of free

amine by reversible dissociation of HCl (eqn [13]). This equilibrium, which lies heavily toward the dormant amine hydrochloride species, allows for only a very short lifetime of reactive amine species. Consequently, as soon as a free amine reacts with an NCA, the resulting amine end group on the product is immediately protonated and is prevented from further reaction. The acidic conditions also assist elimination of CO_2 from the reactive intermediate, and more importantly, suppress formation of unwanted NCA anions.

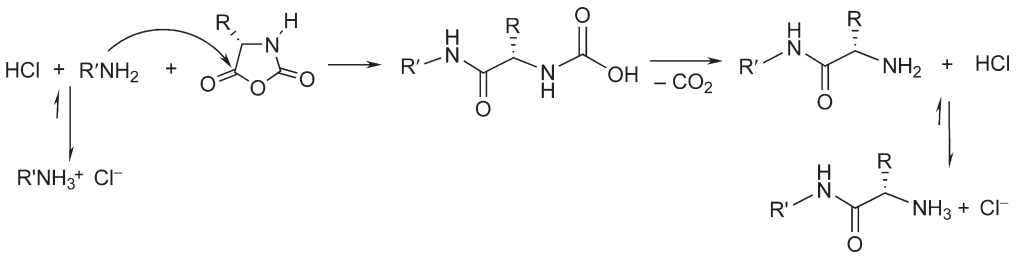

[13]

To obtain controlled polymerization, and not just single NCA addition reactions, Schlaad's group increased the reaction temperature (40 to 80 °C), which was known from Knobler's work to increase the equilibrium concentration of free amine, as well as increase the exchange rate between amine and amine hydrochloride.[29] Using primary amine hydrochloride end-capped polystyrene macroinitiators to polymerize Z-Lys NCA in DMF, Schlaad's group obtained polypeptide hybrid copolymers in 70–80% yield after 3 days at elevated temperature. Although these polymerizations are slow compared to amine-initiated polymerizations, the resulting polypeptide segments were well defined with very narrow chain length distributions ($M_w/M_n < 1.03$). These distributions were much narrower than those obtained using the free amine macroinitiator, which argues for diminished side reactions in the polypeptide synthesis. The molecular weights of the resulting polypeptide segments were found to be *c.* 20–30% higher than would be expected from the monomer to initiator ratios. This result was attributed to termination of some fraction of initiator species by traces of impurities in the NCA monomers, although the presence of unreacted polystyrene chains was not reported. Recently, this methodology was extended to the preparation of new hybrid copolymers of poly(Bn-Glu) from poly(2-isopropyl-2-oxazoline)[30] and PEG-amine hydrochloride[31] macroinitiators.

The use of amine hydrochloride salts as initiators for controlled NCA polymerizations shows tremendous promise. The concept of fast, reversible deactivation of a reactive species to obtain controlled polymerization is a proven concept in polymer chemistry, and this system can be compared to the persistent radical effect employed in all controlled radical polymerization strategies.[32] Like those systems, success of this method requires a carefully controlled matching of the polymer chain propagation rate constant, the amine/amine hydrochloride equilibrium constant, and the forward and reverse exchange rate constants between amine and amine hydrochloride salt. This means it is likely that reaction conditions (e.g., temperature, halide counterion, and solvent) will need to be optimized to obtain controlled polymerization for each different NCA monomer, as is the case for most vinyl monomers in controlled radical polymerizations. Within these constraints, it is possible that controlled NCA polymerizations utilizing simple amine hydrochloride initiators can be obtained.

4.16.2.5 *N*-Trimethylsilyl Amine Initiators

A very promising approach to obtain controlled NCA polymerization using silylated amines was reported in 2007 by Cheng. Hexamethyldisilazane (HMDS) was used to initiate polymerizations of either Z-Lys NCA or Bn-Glu NCA in DMF at ambient temperature and was found to give well-defined polypeptides of controlled chain length and low polydispersity in high yield.[33] Addition of a second batch of monomer to completed chains afforded block copolymers. Chain growth in this system does not appear to show any of the common side reactions found in amine-initiated NCA polymerization, which is attributed to the unique properties of the *N*-trimethylsilyl (N-TMS) groups. The HMDS is proposed to transfer a TMS group to the NCA followed by addition of the silylamine to the resulting intermediate (eqn [14]). This process yields a ring-opened monomer with a TMS-carbamate active end group on the growing chain, similar to processes that occur in group transfer polymerization of vinyl monomers.[34] The TMS-carbamate mediates NCA addition in a way that suppresses side reactions. This system has an advantage in that it proceeds at much higher rates (*c.* 12–24 h at ambient temperature) compared to low-temperature or amine hydrochloride-initiated polymerizations, yet still is slower than transition metal-initiated systems (*c.* 30–60 min at ambient temperature).

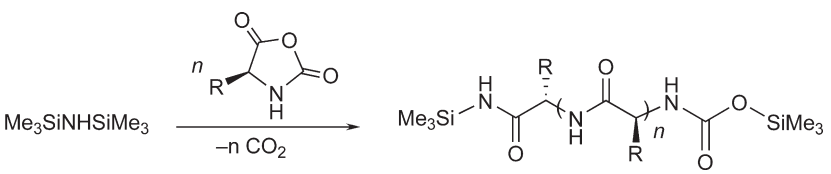

[14]

Cheng elaborated this method by showing that a variety of N-TMS amines can be used as initiators in place of HMDS to give controlled polymerizations by a similar process. These initiators also provide defined C-terminal end groups on the polypeptides from the N-TMS amine initiator (eqn [15]).[35] This chain-end functionalization was found to work well for both Z-Lys NCA and Bn-Glu NCA as well as for block copolymers of these monomers. The TMS-carbamate active chain ends are highly moisture sensitive, yet this is not much of an issue since NCAs themselves are moisture sensitive and must be polymerized in an anhydrous environment. This methodology was used to prepare polypeptide-poly(norbornene diimide) brush copolymers by both 'grafting-from' and 'grafting-through' approaches (eqn [16]).[36] In the grafting-from approach, poly(norbornenes) bearing N-TMS amine functionalities were used as macroinitiators to grow polypeptide brush segments. In the grafting-through approach, N-TMS amine-functionalized norbornene monomers were used to prepare end-functionalized polypeptide segments that were then linked by ring-opening metathesis polymerization (ROMP) of the norbornene end groups.

4.16.3 Copolypeptide Synthesis via ROP

4.16.3.1 Block Copolypeptides

For assembly of novel three-dimensional (3D) structures, block copolypeptides are required that have structural domains (i.e., amino acid sequences) whose size and composition can be precisely adjusted. Such materials have proven elusive using conventional techniques. Strong base-initiated NCA polymerizations are very fast. These polymerizations are poorly understood and well-defined block copolymers cannot be prepared. Primary amine-initiated NCA polymerizations are also not free of side reactions. Even after fractionation of the crude preparations, the resulting polypeptides are relatively ill-defined, which may complicate unequivocal evaluation of their properties and potential applications. Nevertheless, there are many reports on the preparation of block copolypeptides using conventional primary amine initiators.[37] Examples include many hydrophilic–hydrophobic and hydrophilic–hydrophobic–hydrophilic di- and triblock copolypeptides (where hydrophilic residues were glutamate and lysine, and hydrophobic residues were leucine,[38,39] valine,[40] isoleucine,[41] phenylalanine,[42] and alanine[43]) prepared to study

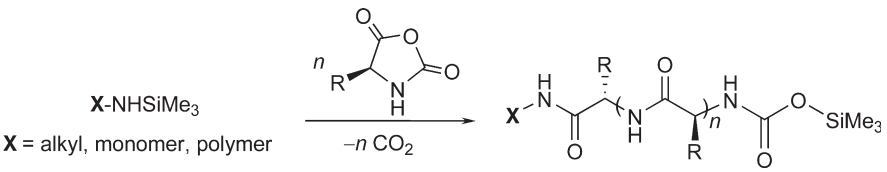

[15]

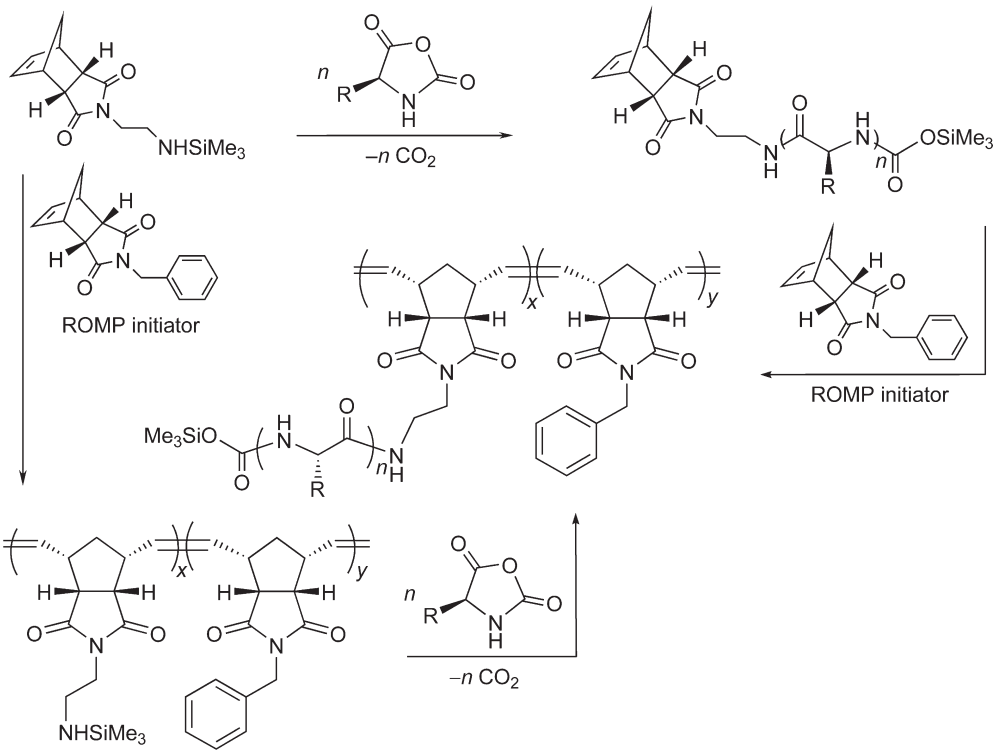

[16]

conformations of the hydrophobic domain in aqueous solution. More recently, Gibson and Cameron[44] reported the synthesis of novel (α-helix)-*b*-(β-sheet) block copolypeptides using amine initiation. These polymers were reported to have polydispersities ranging from 1.47 to 1.60.

The majority of amine-initiated block copolypeptides were often subjected to only limited characterization (e.g., amino acid compositional analysis) and, as such, their structures, and the presence of homopolymer contaminants, were not conclusively determined. Some copolymers, which had been subjected to chromatography, showed polymodal molecular weight distributions containing substantial high- and low-molecular-weight fractions.[42] The compositions of these copolymers were found to be different from the initial monomer feed compositions and varied widely for different molecular weight fractions. It appears that most, if not all, block copolypeptides prepared using amine initiators have structures different than predicted by monomer feed compositions and likely have considerable homopolymer contamination due to the side reactions described above.

Polypeptide block copolymers prepared by transition metal-mediated NCA polymerization are well defined, with the sequence and composition of block segments controlled by order and quantity of monomer added to initiating species, respectively. These block copolypeptides can be prepared with the same level of control found in anionic and controlled radical polymerizations of vinyl monomers, which greatly expands the potential of polypeptide materials. The N-TMS amine initiators and amine initiators under high vacuum have recently also been used to prepare well-defined diblock copolypeptides.[24,34] The unique chemistry of NCAs allows these monomers to be polymerized in any order, which is a challenge in most vinyl copolymerizations, and the robust chain ends allow the preparation of copolypeptides with many block domains (e.g., > 2). The robust nature of transition metal initiation was shown by the linear, stepwise synthesis of tri- and pentablock copolypeptides (eqn [17]).[45] The self-assembly of block copolypeptides has also been investigated, for example, to direct the biomimetic synthesis of ordered silica structures,[46] to form polymeric vesicular membranes,[47,48] to stabilize oil droplets in emulsions,[49] or to prepare self-assembled polypeptide hydrogels.[50] Furthermore, poly(L-lysine)-*b*-poly(L-cysteine) block copolypeptides have been used to generate hollow, organic/inorganic hybrid microspheres composed of a thin inner layer of gold nanoparticles surrounded by a thick layer of silica nanoparticles.[51] In emulsion formation, the use of a racemic hydrophobic segment in poly(L-lysine)-*b*-poly(D/L-leucine) was found to greatly stabilize the oil–water interface allowing the formation of stable water-in-oil-in-water double nanoemulsions.[49]

4.16.3.2 Star Copolypeptides

Star copolymers can be prepared by two main synthetic routes: the 'arm-first' and 'core-first' methodologies. In the first case, living, or end-reactive, polymer chains are coupled to a multifunctional core. In the second case, a multifunctional core molecule is used to initiate the polymerization of the arms. Most of the star polypeptides reported so far have been obtained following the core-first strategy and were prepared using conventional primary amine-initiated NCA polymerization. In this way, Daly *et al.*[52,53] successfully prepared a series of 3-, 4-, 6-, and 9-arm poly(γ-stearyl-L-glutamate) star polypeptides. Inoue *et al.*[54,55] have used hexakis(4-aminophenoxy) cyclotriphosphazene as initiator for the synthesis of 6-arm poly(β-benzyl-L-aspartate), poly(Bn-Asp), and poly(Bn-Glu) stars. These authors used the ability of 5-(4-(dimethylamino) phenyl)-2,4-pentadienal (DMAPP) to selectively react with aromatic primary amines under the formation of the corresponding Schiff bases to quantify the efficiency of the initiation step. For the poly(Bn-Asp) stars, complete consumption of all aromatic primary amine-initiating groups, that is, the formation of well-defined 6-arm star polymers, was observed at sufficiently high monomer/initiator ratios (≥ 100) and high conversions.[54] In a subsequent paper, Inoue *et al.* reported the synthesis of oligo(ethylene glycol)-modified 6-arm poly (L-glutamate) star polymers. These polymers were prepared by transesterification of the benzyl ester groups of 6-arm poly (Bn-Glu) stars with di- or triethylene glycol monomethyl ether in the presence of *para*-toluenesulfonic acid.[56] Depending on the reaction time and temperature, degrees of substitution of 52–63% could be achieved.

Klok and coworkers[57,58] have prepared several water-soluble, fluorescent and near-infrared absorbing 4-arm star polypeptides based on L-lysine and L-glutamic acid. The synthesis of these star polymers started with the ROP of Bn-Glu NCA or Z-Lys NCA using perylene-, terrylene-, or quaterrylene-based multifunctional primary amine initiators. Subsequent removal of the side-chain protective groups afforded the corresponding water-soluble star polypeptides. The experimentally determined peptide arm lengths were in good agreement with those expected based on the monomer/initiator ratio. Furthermore, for the lower-molecular-weight star polymers, ^{1}H NMR spectra indicated complete consumption of all initiator groups, which provided additional evidence for the structural integrity of the star polypeptides.

A first example of the use of controlled NCA polymerization for the preparation of star polypeptides was reported by Aliferis *et al.*[59] Using high-vacuum techniques, these authors first prepared several linear poly(Bn-Glu), poly(Z-Lys), poly(Bn-Glu)-*b*-poly(Z-Lys), and poly(Z-Lys)-*b*-poly(Bn-Glu) precursors, which

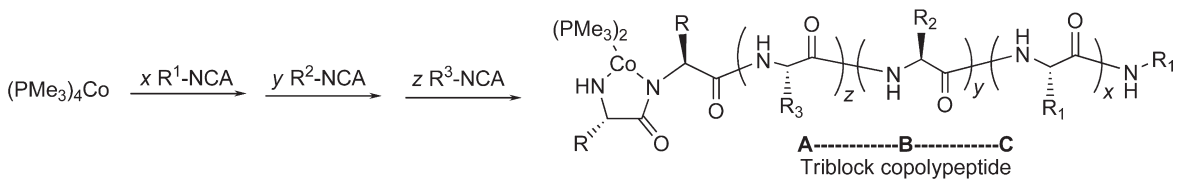

[17]

were subsequently coupled to a trifunctional core, triphenylmethane-4,4′,4″-triisocyanate (Scheme 1). An excess of the linear precursor and reaction times of up to 4 weeks were needed to drive the coupling reaction to completion. Although the excess of the linear precursor could be removed by an additional precipitation step and well-defined star polypeptide could be obtained, this example illustrates the main drawbacks of the arm-first method as compared to the core-first method that has been most widely used for the synthesis of star polypeptides.

To address this issue, Hadjichristidis developed the synthesis of 3- and 4-arm star copolypeptides by high-vacuum polymerization using the core-first method. They prepared 3-arm stars containing poly(Z-Lys) and poly(Bn-Glu) block copolymers that were simultaneously grown off of a 2(aminomethyl)-2-methyl-1,3-propanediamine initiator core (Scheme 2).[60] This method produced well-defined star copolymers with narrow molecular weight distributions. Attempts to prepare 4-arm star copolymers using initiators containing four primary amine groups as well as two tertiary amine groups gave only ill-defined star polymers with bimodal molecular weight distributions.[60] The high polydispersity in these samples was likely due to initiation from both the primary and tertiary amine groups, which have different polymerization characteristics.

4.16.3.3 Brush and Branched Copolypeptides

Most early reports on brush and branched polypeptides utilized conventional NCA polymerization techniques. The first graft polypeptides were published in 1956 by Sela *et al.*[61] Using poly(L-lysine) or poly(D/L-ornithine) as a multifunctional initiator for the ROP of a number of different NCAs, these authors prepared a variety of graft polypeptides, which they termed multichain poly(amino acids) (eqn [18]). Since the NCA polymerizations were carried out in aqueous dioxane,

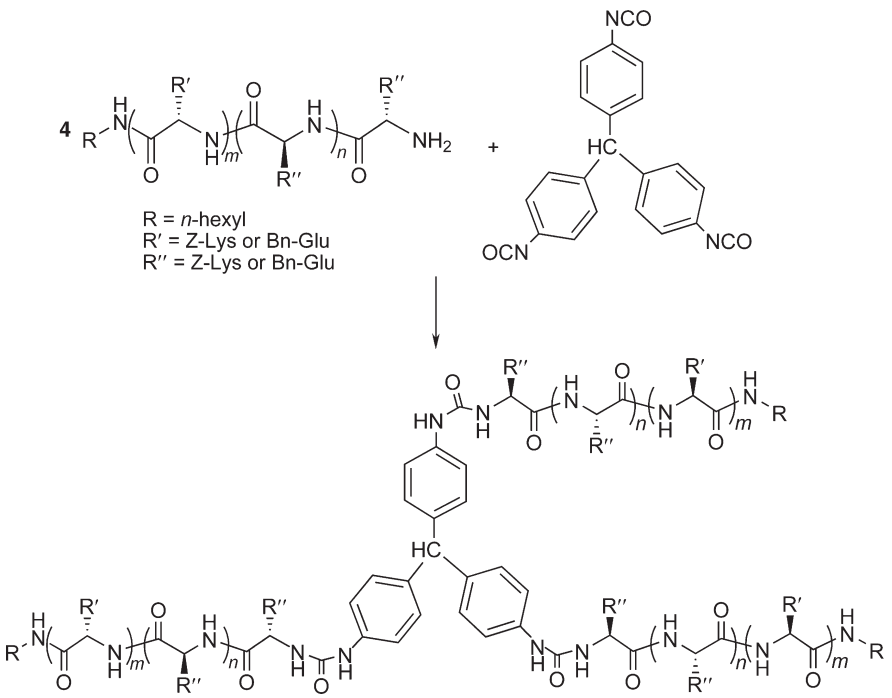

Scheme 1 Preparation of star polypeptides using the "arm-first" method.

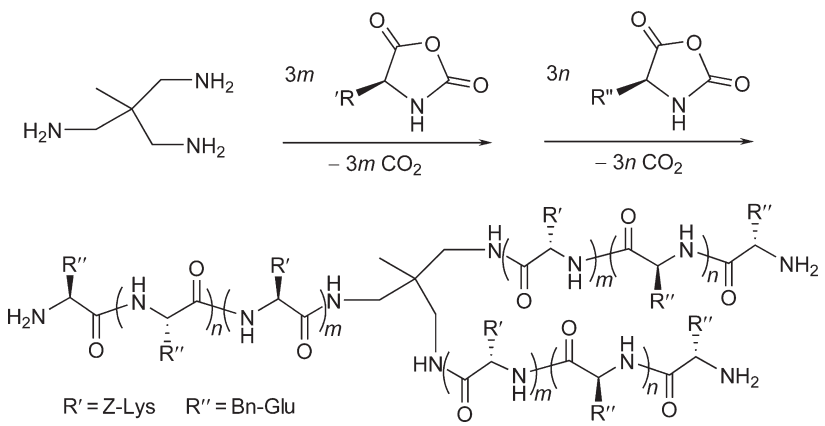

Scheme 2 Preparation of star polypeptides using the "core-first" method.

the synthesis of the graft polypeptides was accompanied by the formation of short linear polypeptides. These by-products, however, could be removed by dialysis. For the graft polymerization, multifunctional poly(L-lysine) or poly(D/L-ornithine) initiators with degrees of polymerization between 20 and 200 were used. The number of amino acid residues per graft was determined by chromatographic analysis of the hydrolyzed product or by end-group titrations. Depending on the length of the poly(L-lysine) or poly(D/L-ornithine) initiator, the number of amino acids per graft varied from 3 to 25. In a subsequent paper, Sela *et al.*[62] used this procedure to prepare a family of multichain copolymers with grafts containing L-tyrosine, L-glutamic acid, and L-alanine residues. The interest in these polymers was due to their potential application as synthetic polypeptide antigens. In this case, in addition to poly(L-lysine) homopolymer, copolymers of D/L-alanine and L-lysine were also used as multifunctional initiators for the NCA graft copolymerization. Furthermore, the grafts of the multichain copolymers were not only simple homopolypeptides, but, in most cases, block-type sequences.

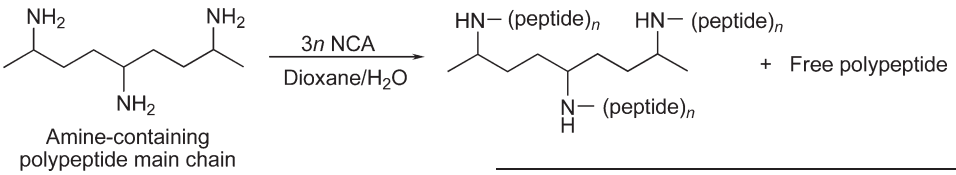

[18]

Since in the examples discussed above, the polymerizations were carried out in the presence of water, the formation of linear polypeptide by-products was inevitable. To overcome this problem, attempts have been made to synthesize multichain polypeptides in anhydrous, polar aprotic solvents such as DMF and dimethyl sulfoxide (DMSO). Sakamoto and co-workers[63–65] prepared different multichain polypeptides using random copolymers of L-lysine and γ-methyl-L-glutamate as initiators for the graft copolymerization of Z-Lys NCA, Bn-Glu NCA, and Bn-Asp NCA. These random copolymers had degrees of polymerizations ranging from 82 to 118 and contained 12–36 lysine residues. The NCA graft copolymerizations were carried out in DMF containing 3 or 9% (v/v) DMSO. However, under these conditions, linear homopolypeptide by-products were also generated, which had to be removed by reprecipitation in diethyl ether (poly(Z-Lys)), methanol (poly(Bn-Glu)), or acetone (poly(Bn-Asp)). The number-average degree of polymerization of the polypeptide grafts was estimated by osmometric molecular weight determination and amino acid analysis and ranged from 20 to 60 amino acids, depending on the initiator and the relative amounts of monomer and initiator that were used.

The findings by Sakamoto are in agreement with earlier observations by Yaron and Berger,[66] who also identified linear homopolypeptide by-products when NCA graft copolymerizations were carried out in dry dioxane or DMF. Tewksbury and Stahmann,[67] in contrast, reported that the synthesis of multichain poly(amino acids) using poly(L-lysine) initiator and D/L-phenylalanine NCA, L-leucine NCA, or Bn-Glu NCA in anhydrous DMSO was not accompanied by the formation of linear by-products. These contradictory observations are characteristic for primary amine-initiated NCA polymerizations, where the success of the polymerization, that is, the homogeneity of the reaction product, can vary significantly depending on the specific monomers and polymerization conditions that are used.

More complex, higher branched polypeptide architectures can be obtained when functional groups in the side chains of the polypeptide grafts are used to initiate a subsequent NCA ROP step. Repetition of this graft-on-graft strategy leads to highly branched, so-called dendrigraft, polypeptides.[68] This is illustrated in **Scheme 3**, which shows the synthesis of dendrigraft polylysine by a repetitive sequence of ROP and deprotection steps using two orthogonally protected L-lysine NCA derivatives. Following this strategy, dendrigraft polylysines containing up to ~160 amino acids, corresponding to a number-average molecular weight of ~40 kDa, could be prepared in just four ring-opening copolymerization–deprotection cycles.[68]

Another approach to prepare polylysine dendrigrafts was reported by Tsogas *et al.*[69] Here, TFA-Lys NCA was oligomerized in aqueous buffer, followed by removal of the TFA groups at pH 11 to give an oligolysine macroinitiator. This process was then repeated by adding more TFA-Lys NCA to the macroinitiator to give a second-generation branched polymer. This cycle was then repeated to give third-generation dendrigraft polylysine (**Scheme 4**). Simultaneous NCA polymerization and side-chain deprotection have also been used to prepare hyperbranched copolypeptides. Vlasov *et al.*[70] reported the ROP of Z-Lys NCA in the presence of H_2/activated Pd, which removes the side-chain protecting groups during polymerization, allowing simultaneous branching and chain growth (**Scheme 5**). Here, the side-chain amine groups that are revealed after hydrogenation serve as polymerization initiation sites. Hyperbranched copolypeptides of lysine containing alanine and glutamic acid were also prepared using this process. Although neither of these processes are controlled polymerizations, branched copolymers with properties substantially different from the linear chains could be prepared.

In addition to the graft-on-graft strategies discussed above, highly branched polypeptides can also be prepared by an iterative sequence of NCA ROP and end-functionalization reactions as illustrated in **Scheme 6**.[71] Each NCA ROP step is followed by an end-functionalization reaction with an appropriate N^{α},N^{ε}-diprotected lysine derivative. Deprotection of the lysine amine groups doubles the number of end groups that can be used to initiate a subsequent NCA ROP step and leads to branching of the polymer architecture. The strategy outlined in **Scheme 6** has been used to prepare highly branched polylysines with number-average molecular weights of up to 33 kDa in only a small number of reaction steps. Birchall and North[72] have used a related approach to prepare highly branched block copolypeptides. In this case, however, relatively hydrophobic

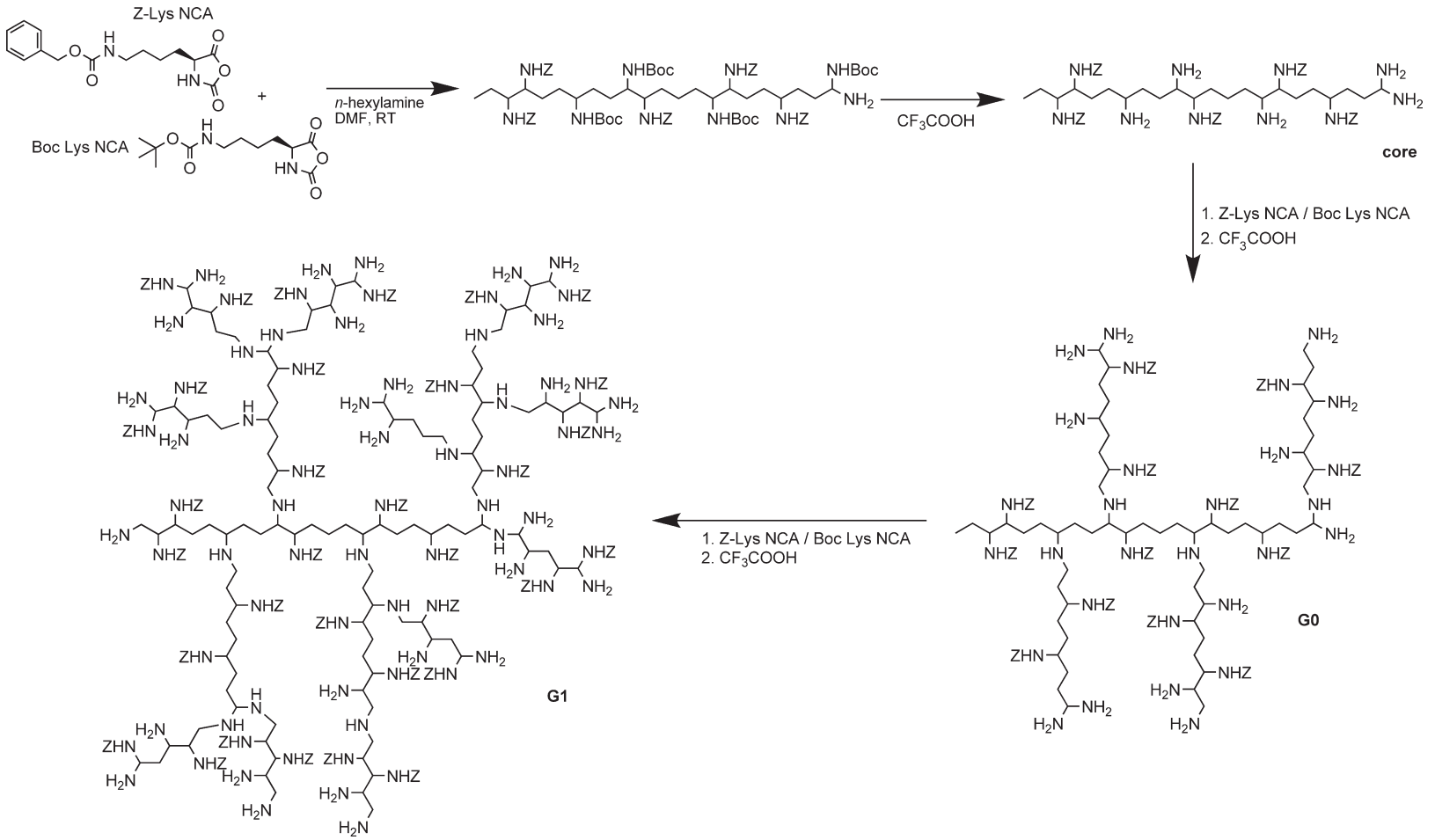

Scheme 3 Preparation of dendrigraft polylysine in a stepwise process.

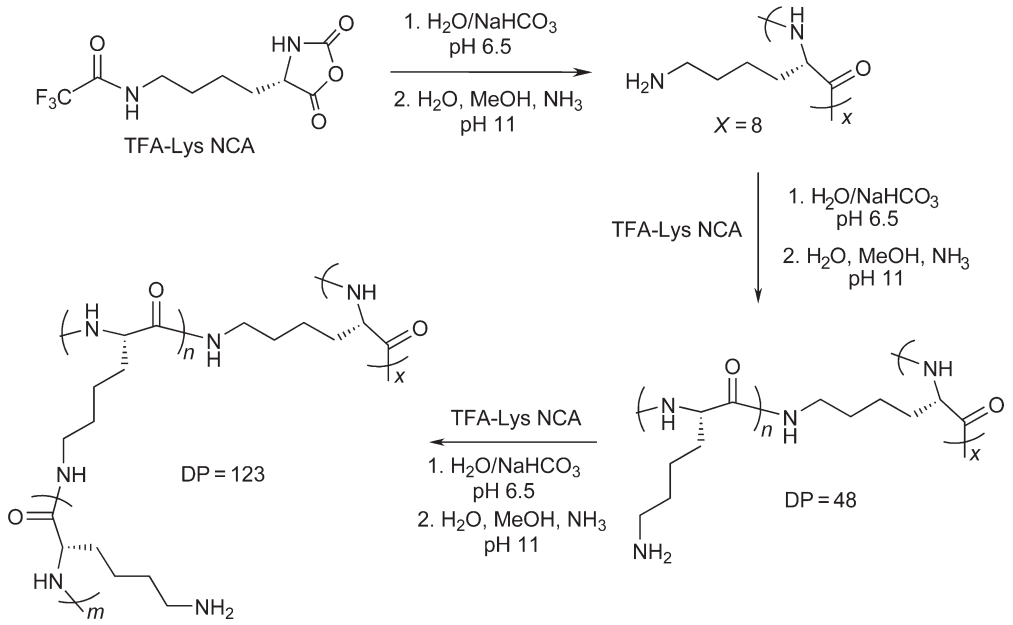

Scheme 4 Preparation of dendrigraft polylysine using *in situ* base deprotection.

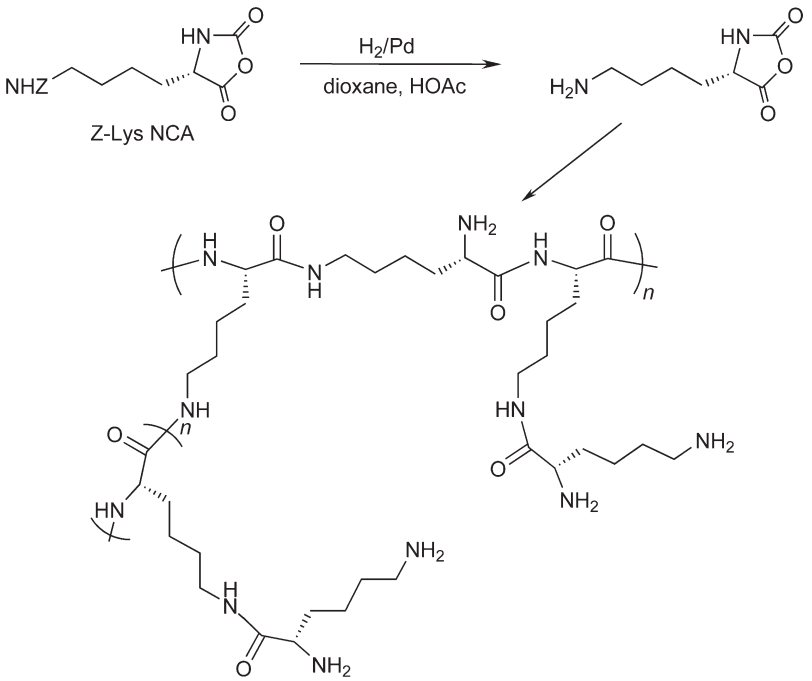

Scheme 5 Preparation of dendrigraft polylysine using *in situ* hydrogenation deprotection.

water-insoluble amino acids such as alanine, leucine, and phenylalanine were used, which made it necessary to keep the polymer chains relatively short (~5 to 10 amino acid repeat units) in order to avoid solubility problems.

4.16.4 Side-Chain Functionalized Polypeptides

There have been many examples where polypeptides were chemically modified to improve their properties for biomedical applications. Typically, this strategy involves the hydrophobic modification of poly(lysine) or poly(glutamate/aspartate) side chains by covalent attachment of lipophilic groups.[73] These modifications are akin to polymer grafting reactions and thus result in random placement of these hydrophobic substituents (typically long alkyl chains) along the polypeptide chains. These modifications were performed in order to increase the polypeptide's ability to bind hydrophobic drugs, aggregate in aqueous solution, and/or penetrate the lipid bilayers of cell walls. The random placement of the hydrophobes along the

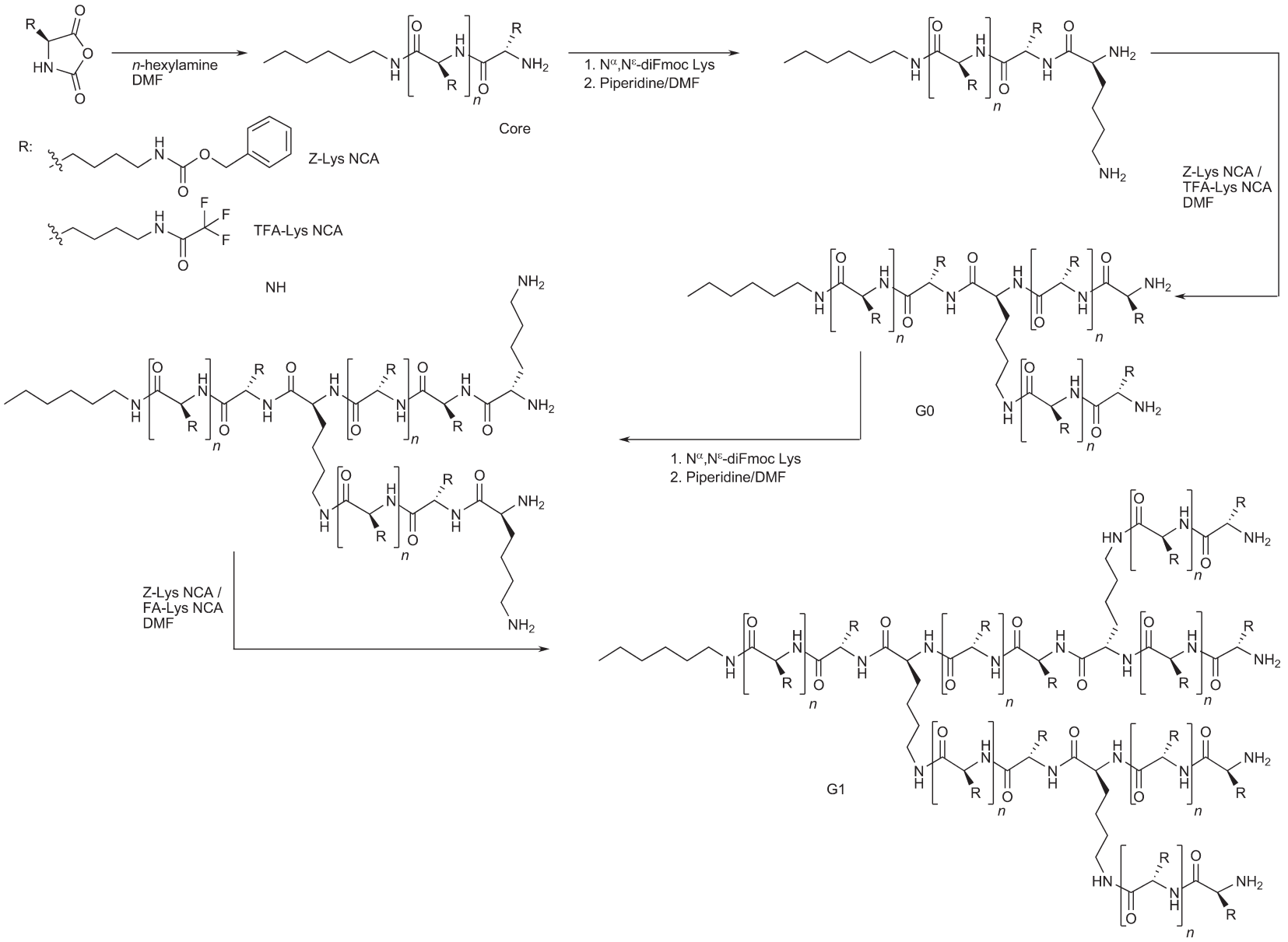

Scheme 6 Preparation of chain-end branched polylysine in a stepwise process.

chain meant that they cannot act as distinct domains in supramolecular assembly, as in a block copolymer, thus limiting their ability to organize.

Other types of chemical polypeptide modification include the addition of nonionic, polar groups to increase solubility and blood circulation lifetime, addition of mesogenic groups, addition of linker groups to allow efficient functionalization of preformed polypeptides by 'click' reactions, and the addition of sugars. Increasing bioavailability and biofunctionality are major goals for development of useful synthetic polypeptide materials.

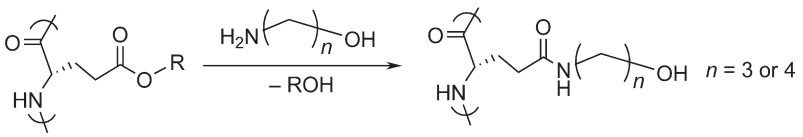

[19]

4.16.4.1 Nonionic Water-Soluble Polypeptides

The amino acid functionalities that provide water solubility (e.g., the amino group of lysine, or the carboxylates of glutamate and aspartate) are also detrimental for biomedical applications in that their polymers behave as polyelectrolytes. As such, they bind strongly to oppositely charged biomolecules (i.e., proteins, polynucleic acids, polysaccharides, and lipids) resulting in aggregation and either rapid removal from the bloodstream or rapid digestion within cells.[74] To circumvent this issue, nonionic, water solubilizing polypeptide residues have long been sought for biomedical uses.[75,76] Following the discovery that optically pure poly(serine) is not water soluble at chain lengths greater than 20 residues,[77] there have been many attempts to prepare nonionic polypeptides that would have good water solubility. The simplest of these approaches is the grafting of PEG chains ($1000 < M_n < 5000$) onto side-chain functionalities, which results in highly heterogeneous materials that retain considerable charge.[78] A more sophisticated solution was the development of hydroxyalkylglutamine polymers, prepared by the reaction of poly (alkyl-L-glutamate) esters with α,ω-amino alcohols (eqn [19]). These polypeptides, poly(hydroxypropyl-L-glutamine) and poly (hydroxybutyl-L-glutamine), in particular, were found to be nonionic and soluble in water over a wide pH range.[79] The major detriments of these materials, however, were that they are recognized as foreign and rapidly degraded *in vivo*, they are difficult to prepare without significantly degrading the polypeptide chains, and they lack ordered secondary structures in solution.[79] The last property is important since a main reason for using polypeptide scaffolds in biomedical applications is to take advantage of their ordered chain conformations to mimic protein structures.

Deming and, more recently, Klok have taken a different approach toward the development of nonionic, water-soluble polypeptides. They incorporated the solubilizing and protective properties of PEG into polypeptides by conjugation of short ethylene glycol (EG) repeats onto amino acid monomers as opposed to the well-documented approach of grafting PEG to the ends or side chains of polypeptides. This strategy avoided both the need for expensive amino- or carboxylato-functionalized PEG molecules necessary for coupling, as well as difficulties associated with derivatization of polymers. In particular, the presence of short EG repeats on every residue resulted in a high density of EG around polymer chains. In effect, the polypeptides are surrounded by an EG sheath that mimics the physical properties of PEG,[80] which did not destabilize the secondary structure of the polypeptide core. The molecular weights of these 'PEG-mimic' polymers could also be easily adjusted by controlling the degree of polymerization of the amino acid.

EG-functionalized monomers and polymers of lysine were first prepared by Deming as shown in **Scheme 7**.[81] Lysine was chosen as the amino acid component for the ease of coupling

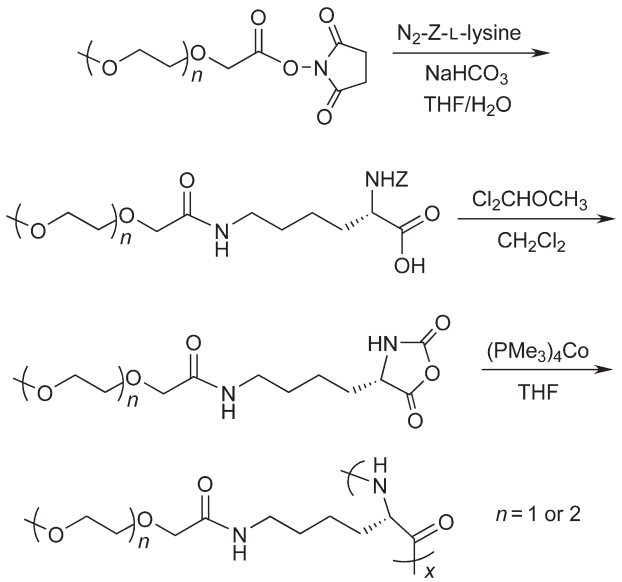

Scheme 7 Preparation of poly(EG_n-Lys).

of the side-chain amine with inexpensive EG-containing carboxylates and for its propensity to form stable α-helical conformations. The formation of EG-L-lysine NCAs allowed facile polymerization into high-molecular-weight polymers by transition metal catalysis. Both poly(N_ε-2-[2-(2-methoxyethoxy)ethoxy]acetyl-L-lysine), poly(EG_2-Lys), and poly(N_ε-2-(2-methoxyethoxy)acetyl-L-lysine) were found to be water soluble, although the greater solubility of poly(EG_2-Lys), which is completely miscible with water in all proportions, led to studies being focused on this polypeptide.

Circular dichroism (CD) analysis revealed that poly(EG_2-Lys) is essentially 100% α-helical in pH 7 water at 25 °C.[81] This conformation was unaffected by many environmental factors. The helical structure of poly(EG_2-Lys) was stable in water over a pH range of 2–12. It was also stable in solutions containing up to 3 M NaCl, 1 M urea, or 1 M guanidinium-HCl. Poly(EG_2-Lys) is soluble and helical in many organic solvents as well (e.g., THF, methanol (MeOH), and $CHCl_3$). The thermal stability of the helical conformation of poly(EG_2-Lys) was also very high. It was found that poly(EG_2-Lys) retains 75% of its helicity at 85 °C in water as compared to only 17% helicity for poly(hydroxypropyl-L-glutamine). Poly(EG_2-Lys) was not digested by hydrolytic enzymes that readily digest poly(L-lysine) (e.g., papain and trypsin),[74] indicative of the PEG-like properties imparted by the EG sheath. Poly(EG_2-Lys) is a polymer with surface properties similar to unstructured PEG, but also possesses a rodlike backbone due to its α-helical character. Similar monomers and polymers were prepared by Klok using succinate linkages between the EG segments and lysine (eqn [20]).[82] In these polymers, the ester linkages to the EG segments are potentially degradable in water, and the polymers were found to prevent nonspecific protein adsorption when used to coat surfaces.

structures upon solvent evaporation or by controlled addition of a solvent that stabilizes the β-conformation. The synthesis of the EG-modified serine is shown in **Scheme 8**, where the EG repeats were coupled onto the amino acid using an ether linkage.[83] The modified amino acids were then converted to their corresponding NCA monomers to allow subsequent polymerization. Of these polymers, only poly(*O*-(2-(2-methoxyethoxy) ethyl)-L-serine), poly(EG_2-Ser), was found to be soluble in water. CD analysis of this polymer in pH 7, deionized water revealed that it was in a 'random coil' conformation.[83] The CD spectra of this polymer were also invariant with solution pH and buffer strength consistent with this result. Films cast from aqueous solutions of this polymer from a variety of buffers all gave CD spectra indicative of the β-sheet conformation. Wide-angle X-ray scattering data from films of poly(EG_2-Ser) revealed reflections that were also commensurate with the antiparallel β-sheet structure.

To probe the interaction of water with poly(EG_2-Ser), CD spectra of this polymer were recorded a function of solvent composition. As solution composition was varied from pure water to increasing percentages of MeOH or MeCN, a random conformation to β-sheet transformation was observed.[83] Aggregation of the polymer with increasing fractions of organic solvents, coincident with β-sheet formation, indicated that it was the strong interaction of poly(EG_2-Ser) with water that destabilizes the β-sheet conformation. The solvent-dependent conformational properties of poly(EG_2-Ser) provide a means for convenient processing of this polymer. Concentrated aqueous solutions can be cast into polypeptide films of high β-sheet content, or can be treated with MeOH to assemble the β-strands. These features allow facile processing of β-sheet domains without use of strong denaturants or pH adjustments that may

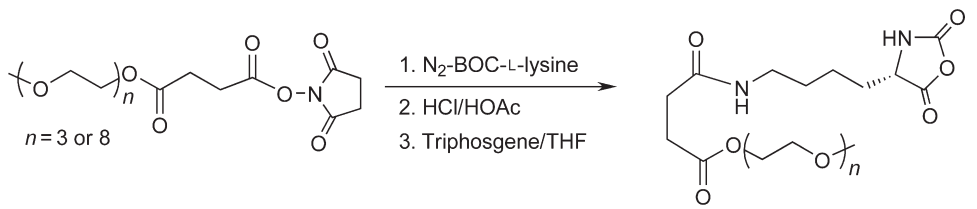

[20]

Similar EG modifications to the β-sheet preferring amino acids L-serine and L-cysteine were also studied by Deming to allow facile aqueous processing of their corresponding β-forming polymers. The EG side chains should provide good water solubility to the polymers, which could then form β-sheet

disrupt or precipitate other secondary structures present. Overall, these EG-modified polypeptides provide 'PEG-like' α-helix- and β-sheet-forming segments that can be incorporated into block copolypeptides for biomedical and biotechnology applications. Such domains provide not only improved

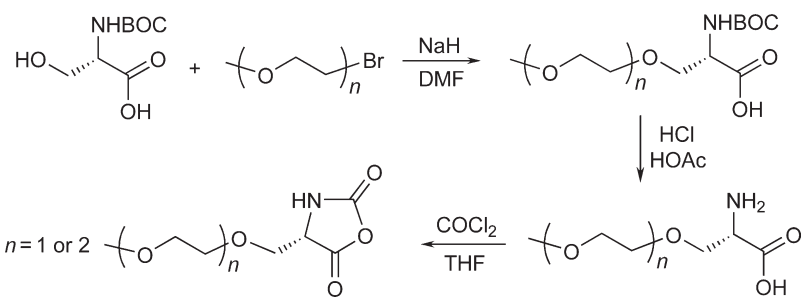

Scheme 8 Preparation of poly(EG_n-Ser).

solubility and bioavailability, but allow incorporation of secondary structure to control self-assembly of the polymers.

4.16.4.2 Mesogen-Functionalized Polypeptides

The polypeptide materials field has grown tremendously in recent years. However, a drawback of polypeptides has been the difficulty in using melt processing with these materials, since the abundant H-bonds and consequent poor chain flexibility prevent melting before decomposition. Although solution-based methods allow processing of these materials for most applications,[84] melt processing, or even capability for thermal annealing, would greatly expand the utility of polypeptides.

Pioneering studies on thermotropic polypeptides were done by Watanabe's group, where poly(glutamates) were derivatized either with long alkyl chains[85] or by end-on attachment of biphenyl mesogens (eqn [21]).[86] Polypeptides with short alkyl side chains were not thermotropic, yet side chains greater than 10 carbons long gave melting transitions from −26 to 54 °C. These samples formed cholesteric liquid crystalline phases above the melting transition, but formed layered structures at low temperatures driven by crystallization of the side chains. Furthermore, poly(γ-octadecyl-L-glutamate) was found to form a columnar hexagonal phase at temperatures above 200 °C, where the rodlike helices make up the two-dimensional (2D) lattice.[85] When biphenyl mesogens were attached end-on to poly(glutamate) side chains by six carbon alkyl spacers, layered structures were observed in the crystalline and liquid crystalline states, followed by transition into a cholesteric structure at higher temperatures.[86] Similar results were found when mesogens were attached end-on to poly(lysine) chains.[87] In these examples, the liquid crystalline mesophases were dominated either by the side-chain group (layered structure) or by the rodlike nature of the polypeptide backbone (hexagonal phase), but in no case was coexistence of both types of ordering observed.

Deming developed mesogen-functionalized polypeptides in which liquid crystalline ordering exists concurrently with backbone ordering. To obtain this coexistence between mesogen and main-chain ordering, 'side-on' mesogen[88] modification of the polypeptides was used to allow facile parallel orientation of mesogens and the peptide backbones. Since it is known that varying the length of flexible spacers connecting polymer backbones and mesogens affects the mesophase behavior of side-chain liquid crystalline polymers,[89] NCA monomers with spacers of 3, 5, and 10 methylene units between the lysine side chains and the mesogens were prepared. The mesogen used for this study was a well-known three-ring aromatic ester molecule,[90] which was derivatized from a central carboxylic acid group by ester coupling to attach linkers of 3, 5, and 10 methylene units to enable attachment to L-lysine (**Scheme 9**). Mesogen-derivatized polypeptides were prepared by polymerization of the corresponding NCAs using $(PMe_3)_4Co$ initiator in THF solvent in high yield.[91] The polypeptides were soluble in THF and were found to adopt α-helical conformations in solution by CD and Fourier transform infrared (FTIR) spectroscopy. These polymers displayed an unusual thermotropic mesophase where both side-chain mesogens and polymer backbones are ordered and coexist in a nematic hexagonal structure.

4.16.4.3 Polypeptides Functionalized for 'Click' Reactivity

The Huisgen [3 + 2] cycloaddition between organic azides and alkynes and the radical-mediated coupling of thiols and alkenes ('click' reactions) are both selective and highly efficient coupling processes.[92] These reactions have had a vast impact in polymer chemistry since they allow multiple site modifications of polymers in high yields, and typically do not interfere with other functional groups. However, use of these reactions for modification of polypeptides has only been demonstrated recently.

Engler *et al.* published the first example of a click coupling onto polypeptides obtained from NCA polymerization in 2009.[93] PEG-azides were coupled using copper catalysis to alkyne functional homopolypeptides synthesized from γ-propargyl-L-glutamate NCA to yield PEG-grafted polypeptide brushes (eqn [22]). The alkyne functional polyglutamate precursors were prepared using conventional amine polymerization and found to be α-helical and soluble in DMF. Coupling of PEG-azides to alkyne groups in DMF at ambient temperature was found to proceed at >95% conversion when two equivalents of azide per alkyne were used. Using the same NCA monomer, Xiao *et al.*[94] reported coupling of

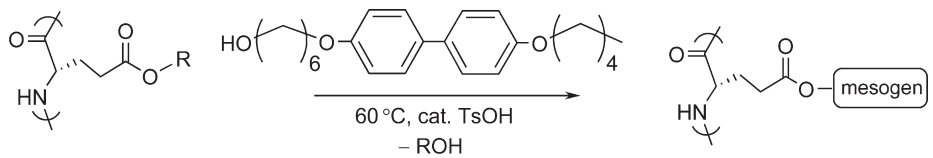

[21]

three different azide-functionalized monosaccharides to this polypeptide using copper catalysis in DMSO. The coupling chemistry was found to proceed in high yield, and these sugar-functionalized polypeptides were found to all be α-helical and soluble in water after removal of protecting groups. In a related strategy, Tang and Zhang[95] reported the preparation of γ-3-chloropropyl-L-glutamate NCA and its corresponding polymer using HMDS-initiated polymerization (eqn [23]). This organic soluble, α-helical polypeptide was further modified by conversion of chloro to azide groups, which were then coupled to alkyne functionalized D-mannose using copper catalysis in DMF.

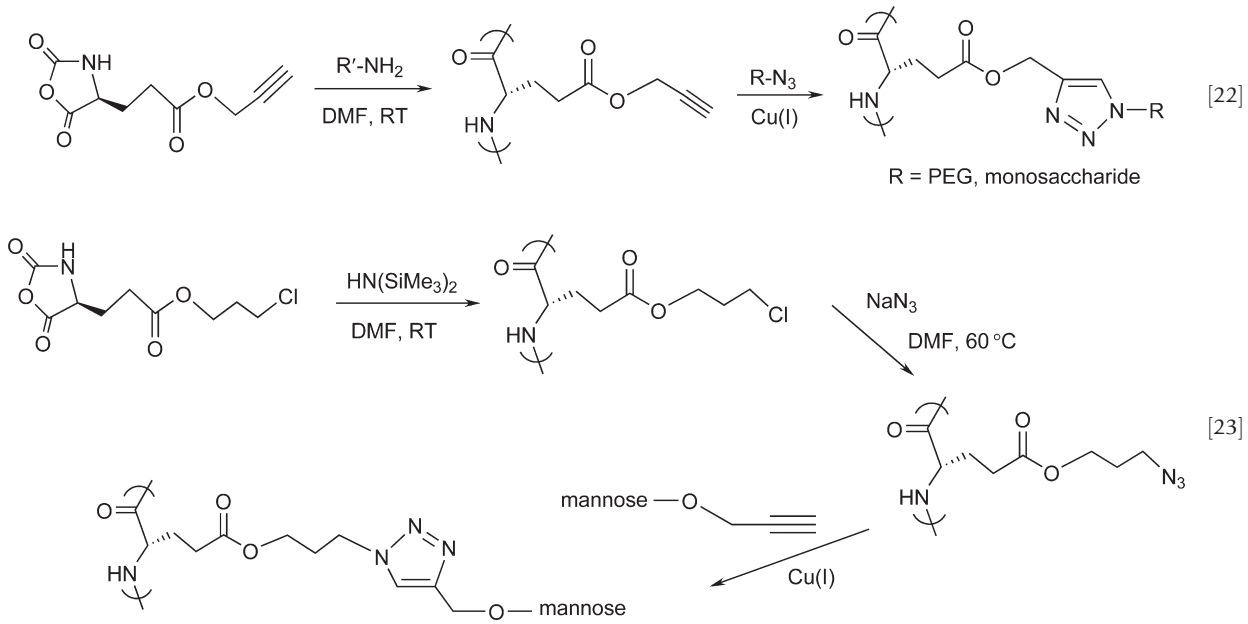

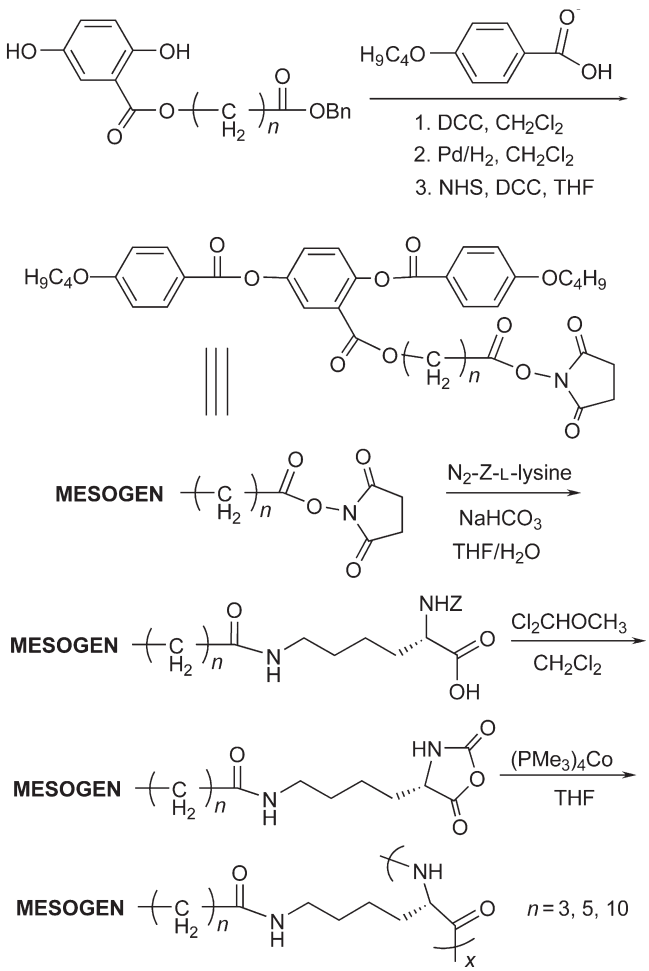

Scheme 9 Preparation of side-on mesogen functionalized polylysines.

While high degrees of click functionalization were obtained using these methods, a potential limitation is the hydrolytic instability of the glutamate ester linkages, which may lead to possible loss of the 'clicked' on functionality by hydrolysis over time. To overcome this issue, Huang *et al.*[96] synthesized poly(D/L-propargylglycine) from the NCA of the commercially available amino acid to directly incorporate alkyne groups into the polypeptides (eqn [24]). This NCA was polymerized at 0 °C in DMF using amine initiation in the presence of LiBr to give soluble low-molecular-weight polymers ($M_n < 3000$ Da). Higher-molecular-weight homopolymers were poorly soluble, yet statistical copolymers of D/L-propargylglycine NCA with Bn-Glu NCA in a 1:2 ratio was found to give higher-molecular-weight polymers that were soluble in DMF. Azide-functionalized galactose was then coupled to these polypeptides in high yield using copper catalysis in DMSO (eqn [24]).

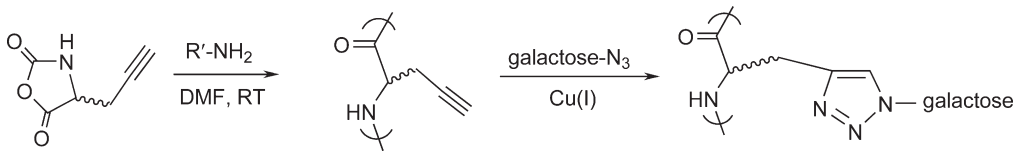

[24]

Utilizing a different type of click reaction, Sun and Schlaad[97] have prepared poly(D/L-allylglycine) from the commercially available amino acid to directly incorporate alkene groups into polypeptides for thiol-ene coupling (eqn [25]). The NCA of D/L-allylglycine was polymerized using hexylamine in DMF to give soluble low-molecular-weight oligomers ($M_n < 2000$ Da). End-functional PEG-NH_2 was also used as a macroinitiator to prepare PEG-poly(D/L-allylglycine) block copolymers. Radical addition of a variety of thiols, catalyzed by 2,2′-azobisisobutyronitrile (AIBN) at elevated temperature using two equivalents of thiol per alkene gave polymers with degrees of alkene functionalization varying greatly with reaction conditions. Using this methodology, ester and monosaccharide functionality was added to the poly(D/L-allylglycine) segments (eqn [25]). Limitations of these last two approaches are the use of racemic amino acids, which prohibit formation of regular polypeptide conformations, and the low molecular weights of the polymers obtained.

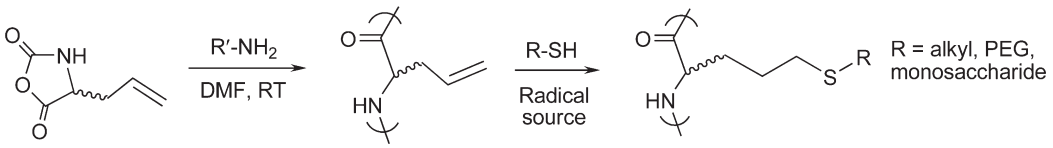

[25]

4.16.4.4 Sugar-Functionalized Polypeptides

Glycosylated peptides and proteins are ubiquitous in nature and display a wide range of biological functions, including mediation of recognition events, protection from proteases, and lubrication in eyes and joints.[98–101] Similarly, synthetic glycopolypeptides are also expected to show great potential as biomedical materials (e.g., scaffolds for tissue repair and drug carriers), as well as serve as valuable tools for probing carbohydrate–protein interactions.[102,103] Although well-defined block copolypeptides are readily prepared using NCA polymerization,[4] the synthesis of well-defined glycopolypeptide materials has been challenging. Rude first prepared *O*-linked glyco-serine NCAs by an inefficient synthesis in 1966, and performed initial studies their polymerization using amine initiators.[76,104] Polymerization of these monomers was studied in more detail by Okada who found they give mainly short, oligomeric products where chain growth is likely inhibited by steric and H-bonding interactions between the sugar substituents and the NCA rings.[105–108] Gibson *et al.*[109] have recently reported an improved synthesis of *O*- and *S*-linked glyco-serine as well as glyco-threonine NCAs; however, these were not sufficiently purified to allow polymerization.

Aside from direct polymerization of glycosylated NCAs, other strategies to prepare glycopolypeptides rely primarily on the addition of sugars to existing polypeptides. Tian *et al.*[110,111] have prepared glyconamidated polypeptides by reaction of D-gluconolactone or lactobionolactone with poly(L-lysine) to attach ring-opened carbohydrates by amide linkages. Also using polypeptide precursors, Xiao *et al.*,[94] Huang *et al.*,[96] Tang and Zhang,[95] and Sun and Schlaad[97] have separately reported glycopolypeptide synthesis using either copper-catalyzed azide-alkyne or thiol-ene click chemistry (eqns [22–25]). While promising, these methods can suffer from incomplete sugar functionalization,[96,97] presentation of sugars in nonnative forms (i.e., ring opened),[110,111] or incorporation of triazole groups[94,95] that may limit biological uses. The propargylglycine and allylglycine polypeptide precursors are somewhat limiting as they were only prepared in racemic form and at low molecular weights. The polyglutamate derivatives of Xiao and Zhang contain ester groups in the linkage, which may result in loss of sugar functionality over time in water.

4.16.5 Poly(β-Peptides)

β-Peptides have received considerable interest in recent years due to their ability to resist proteases, mimic α-peptides, and potential as biomedical materials.[112] For drug delivery applications, polymers of β-amino acids are attractive as analogs of the poly(α-peptides) described above. Poly(β-peptides) have been prepared by condensation of short peptides,[113]

polymerization of β-amino acid *N*-carboxyanhydrides (β-NCAs),[114] and polymerization of β-lactams.[115] However, the ring opening of β-lactams has been the only method shown to yield high-molecular-weight polymers (eqn [26]).[115,116] NCA ROP has not been well explored for the synthesis of poly(β-peptides), primarily since general methods for efficient synthesis of optically pure β-NCAs from amino acids were unavailable until recently. Deming successfully synthesized optically pure β-NCAs from the cyclization of N_{β}-*t*-Boc- or N_{β}-*t*-Cbz-β-amino acids (eqn [27]).[117] Polymerizations of β-NCAs were attempted in THF using either a strong base initiator (NaO*t*Bu) or transition metal initiators.[118] For both types of initiation, the yields of polymers bearing small hydrophobic side chains were high. However, the molecular weights of these polymers were low due to precipitation of the chains during synthesis. NCAs bearing larger substituents did not polymerize well, likely since the bulky substituents hinder access of the propagating chain ends to the monomer anhydride groups, thus slowing the polymerizations.[118] When polymerization of β-NCAs was carried out in DMF solution at elevated temperature, polymers were obtained with slightly larger chain lengths. Under all conditions studied, polymerizations of β-NCAs gave polymers with low molecular weights likely due to precipitation of the polymers from the reaction mixtures. This appears to be a general phenomenon, since no high-molecular-weight poly(β-peptides) have been synthesized by the polymerization of β-NCAs.[118] As with the poly(α-peptides) described above, poly(β-peptides) will only realize their potential if they can be prepared with well-defined sequences and compositions.

large chain length distributions, these samples are ideally also fractionated to give samples of well-defined composition. An additional purification issue arises from the amphiphilic nature of many of these copolymers, for example, PEG-*b*-poly(Bn-Glu). Such polymers tend to associate in most solvents leading to trapped solvents or solutes in the copolymer sample, which can complicate analytical studies. In the case of transition metal-initiated polymerizations, removal of the metal from the sample is also important for most applications. For rigorous purification of these amphiphilic copolymers, Deming has shown that exhaustive dialysis of the samples against deionized water to be very effective at removing small molecule contaminants. In cases where a polymer segment can bind strongly to metals such as Co^{2+} and Ni^{2+}, the addition of a potent metal chelator, such as EDTA, in the early stages of dialysis was found to be sufficient to remove all traces of the metal ions.[119]

A highly useful feature of copolypeptide materials is their functionality. The common naturally occurring amino acids contain numerous acidic and basic functional groups that provide interesting pH-responsive character to these materials. These functional groups are masked by protecting groups before synthesis of the NCA monomers, since they will typically interfere with polypeptide synthesis or NCA stability.[5] Consequently, these protecting groups must be removed after polymerization if one is to utilize the functional group chemistry. The first concern with polypeptide deprotection is whether or not all the protecting groups have been removed. Small amounts of residual protecting groups can significantly influence the resulting polypeptide properties, especially since the protecting groups are typically hydrophobic and the deprotected chain is typically hydrophilic. Fortunately, most of the

[26]

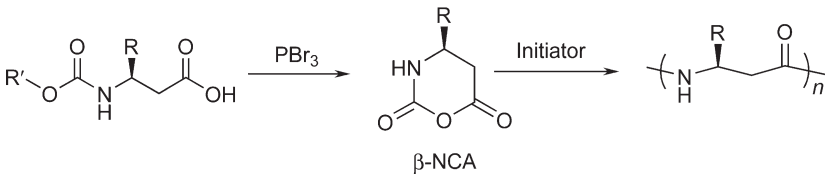

[27]

4.16.6 Polypeptide Deprotection and Purification

Although quite complex copolypeptide architectures can now be synthesized, obtaining these materials in a state of high purity typically requires additional measures. As discussed above, many of the copolypeptides contain homopolymer impurities, which must be removed by selective solvent extractions or fractional precipitation when possible. Since conventional NCA polymerizations also usually give polypeptide segments with common protecting groups are removed without difficulty, and deprotection levels greater than 97% are readily attained. The more serious consequence of deprotection is cleavage of the peptide chain, or racemization of the optically pure amino acid residues.

Basic polypeptides, such as polylysine or polyarginine, are readily deprotected without much difficulty.[5,120] Acidic polypeptides, such as polyglutamic acid or polyaspartic acid, require more care in deprotection reactions due to an abundance of

potential side reactions. Poly(Bn-Glu), for example, can be debenzylated using strong acid, aqueous base, or catalytic hydrogenation. Strong acid (e.g., gaseous HBr or HBr in acetic acid) avoids any racemization, but is known to lead to significant chain cleavage arising from protonation of side-chain ester groups that react with the amide backbone.[121] Basic conditions avoid this reaction, but can lead to significant racemization unless the amount of base is carefully controlled.[122] Hydrogenation would appear to be the most attractive method, however, it is only effective for chains less than 10 kDa in molar mass. Larger poly(Bn-Glu) chains adopt a stable helical conformation that prevents access of the hydrogenation catalyst to the ester groups.[122] Ester cleavage using TMS iodide was found to give clean conversion to the readily hydrolyzed TMS ester, without any racemization or chain cleavage.[123] The major drawbacks of this reagent are its expense and its reactivity with most other functional groups, such as the ether linkages in PEG. The deprotection of poly(Bn-Asp) shows less side reactions under acidic conditions compared to poly(Bn-Glu). However, it has been reported that the polymer backbone undergoes partial rearrangement to β-peptide linkages under basic conditions, presumably through an imide intermediate.[124] The degree of racemization in these samples was not discussed.

4.16.7 Conclusions

The synthesis of polypeptides by ROP is an area that has been under study for more than five decades. Initially, this field suffered from limitations that necessitated excessive sample purification and fractionation to obtain well-defined polypeptides. In recent years, vast improvements in NCA polymerizations now allow the synthesis of a variety of block copolymers of controlled dimensions (molecular weight, sequence, composition, and molecular weight distribution). Many well-defined, side-chain functionalized polypeptides have now been prepared, and efficient conjugation methods now allow high-fidelity postpolymerization modification to polypeptide side chains or chain ends. Such well-defined materials will greatly assist in the identification of new self-assembled structures possible using ordered polypeptide segments, as well as yield new materials with a wide range of tunable properties.

References

1. Voet, D.; Voet, J. G. *Biochemistry, 2nd Ed.*; *Wiley*: New York, NY, 1995.
2. van Hest, J. C. M.; Tirrell, D. A. *Chem. Commun.* **2001**, 1897.
3. (a) Fasman, G. D. *Poly α-Amino Acids*; Dekker: New York, NY, 1967. (b) Fasman, G. D. *Prediction of Protein Structure and the Principles of Protein Conformation*; Plenum Press: New York, NY, 1989.
4. Deming, T. J. *J. Polym. Sci., Polym. Chem. Ed.* **2000**, *38*, 3011.
5. (a) Kricheldorf, H. R. *α-Amino acid-N-Carboxyanhydrides and Related Materials*; Springer: New York, NY, 1987. (b) Kricheldorf, H. R. In *Models of Biopolymers by Ring-Opening Polymerization*; Penczek, S., Ed., CRC Press: Boca Raton, FL, 1990.
6. Woodward, R. B.; Schramm, C. H. *J. Am. Chem. Soc.* **1947**, *69*, 1551.
7. Webster, O. *Science* **1991**, *251*, 887.
8. Howard, J. C.; Cardinaux, F.; Scheraga, H. A. *Biopolymers* **1977**, *16*, 2029.
9. (a) Sekiguchi, H. *Pure Appl. Chem.* **1981**, *53*, 1689. (b) Sekiguchi, H.; Froyer, G. *J. Poly. Sci. Symp.* **1975**, *52*, 157.
10. (a) Hadjichristidis, N.; Iatrou, H.; Pitsikalis, M.; Sakellariou, G. *Chem. Rev.* **2009**, *109*, 5528. (b) Deming, T. J. *Adv. Polym. Sci.* **2006**, *202*, 1.
11. Collman, J. P.; Hegedus, L. S.; Norton, J. R.; Finke, R. G. *Principles and Applications of Organotransition Metal Chemistry, 2nd ed.*; University Science: Mill Valley, CA, 1987.
12. (a) Deming, T. J. *Nature* **1997**, *390*, 386. (b) Deming, T. J. *J. Am. Chem. Soc.* **1998**, *120*, 4240.
13. Deming, T. J. *Macromolecules* **1999**, *32*, 4500.
14. Deming, T. J.; Curtin, S. A. *J. Am. Chem. Soc.* **2000**, *122*, 5710.
15. Deming, T. J. *Adv. Drug Delivery Rev.* **2002**, *54*, 1145.
16. Deming, T. J. *Soft Matter* **2005**, *1*, 28.
17. Curtin, S. A.; Deming, T. J. *J. Am. Chem. Soc.* **1999**, *121*, 7427.
18. Witte, P.; Menzel, H. *Macromol. Chem. Phys.* **2004**, *205*, 1735.
19. Cheng, J.; Deming, T. J. *Macromolecules* **1999**, *32*, 4745.
20. Seidel, S. W.; Deming, T. J. *Macromolecules* **2003**, *36*, 969.
21. Goodwin, A. A.; Bu, X.; Deming, T. J. *J. Organomet. Chem.* **1999**, *589*, 111.
22. Peng, Y.-L.; Lai, S.-L.; Lin, C.-C. *Macromolecules* **2008**, *41*, 3455.
23. Brzezinska, K. R.; Curtin, S. A.; Deming, T. J. *Macromolecules* **2002**, *35*, 2970.
24. Aliferis, T.; Iatrou, H.; Hadjichristidis, N. *Biomacromolecules* **2004**, *5*, 1653.
25. Pickel, D. L.; Politakos, N.; Avgeropoulos, A.; Messman, J. M. *Macromolecules* **2009**, *42*, 7781.
26. Vayaboury, W.; Giani, O.; Cottet, H.; *et al. Macromol. Rapid Commun.* **2004**, *25*, 1221.
27. Odian, G. *Principles of Polymerization, 3rd ed*; Wiley: New York, NY, 1991.
28. Dimitrov, I.; Schlaad, H. *Chem. Commun.* **2003**, 2944
29. (a) Knobler, Y.; Bittner, S.; Frankel, M. *J. Chem. Soc.* **1964**, 3941. (b) Knobler, Y.; Bittner, S.; Virov, D.; Frankel, M. *J. Chem. Soc. C* **1963**, 1821.
30. Meyer, M.; Schlaad, H. *Macromolecules* **2006**, *39*, 3967.
31. Lutz, J.-F.; Schütt, D.; Kubowicz, S. *Macromol. Rapid Commun.* **2005**, *26*, 23.
32. Fischer, H. *Chem. Rev.* **2001**, *101*, 3581.
33. Lu, H.; Cheng, J. *J. Am. Chem. Soc.* **2007**, *129*, 14114.
34. Webster, O. W. *J. Polym. Sci., Polym. Chem. Ed.* **2000**, *38*, 2855.
35. Lu, H.; Cheng, J. *J. Am. Chem. Soc.* **2008**, *130*, 12562.
36. Lu, H.; Wang, J.; Lin, Y.; Cheng, J. *J. Am. Chem. Soc.* **2009**, *131*, 13582.
37. Uralil, F.; Hayashi, T.; Anderson, J. M.; Hiltner, A. *Polym. Eng. Sci.* **1977**, *17*, 515.
38. Auer, H. E.; Doty, P. *Biochemistry* **1966**, *5*, 1708.
39. Ostroy, S. E.; Lotan, N.; Ingwall, R. T.; Scheraga, H. A. *Biopolymers* **1970**, *9*, 749.
40. Epand, R. E.; Scheraga, H. A. *Biopolymers* **1968**, *6*, 1551.
41. Kubota, S.; Fasman, G. D. *Biopolymers* **1975**, *14*, 605.
42. Cardinaux, F.; Howard, J. C.; Taylor, G. T.; Scheraga, H. A. *Biopolymers* **1977**, *16*, 2005.
43. Ingwall, R. T.; Scheraga, H. A.; Lotan, N.; *et al. Biopolymers* **1968**, *6*, 331.
44. Gibson, M. I.; Cameron, N. R. *Angew. Chem., Int. Ed.* **2008**, *47*, 5160.
45. (a) Nowak, A. P.; Sato, J.; Breedveld, V.; Deming, T. J. *Supramol. Chem.* **2006**, *18*, 423. (b) Li, Z.; Deming, T. J. *Soft Matter* **2010**, *6*, 2546.
46. Cha, J. N.; Stucky, G. D.; Morse, D. E.; Deming, T. J. *Nature* **2000**, *403*, 289.
47. Bellomo, E. G.; Wyrsta, M. D.; Pakstis, L.; *et al. Nat. Mater.* **2004**, *3*, 244.
48. Holowka, E. P.; Pochan, D. J.; Deming, T. J. *J. Am. Chem. Soc.* **2005**, *127*, 12423.
49. Hanson, J. A.; Chang, C. B.; Graves, S. M.; *et al. Nature* **2008**, *455*, 85.
50. Nowak, A. P.; Breedveld, V.; Pakstis, L.; *et al. Nature* **2002**, *417*, 424.
51. Wong, M. S.; Cha, J. N.; Choi, K.-S.; *et al. Nano Lett.* **2002**, *2*, 583.
52. Daly, W. H.; Poche, D.; Russo, P. S.; Negulescu, I. *Polym. Prepr. (Abstr. Am. Chem. Soc.)* **1992**, *33(1)*, 188.
53. Daly, W. H.; Poche, D.; Russo, P. S.; Negulescu, I. *J. Macromol. Sci., Pure Appl. Chem.* **1994**, *A31*, 795.
54. Inoue, K.; Sakai, H.; Ochi, S.; *et al. J. Am. Chem. Soc.* **1994**, *116*, 10783.
55. Inoue, K.; Horibe, S.; Fukae, M.; *et al. Macromol. Biosci.* **2003**, *3*, 26.
56. Inoue, K.; Miyahara, A.; Itaya, T. *J. Am. Chem. Soc.* **1997**, *119*, 6191.
57. Klok, H.-A.; Rodriguez-Hernandez, J.; Becker, S.; Müllen, K. *J. Polym. Sci., Polym. Chem. Ed.* **2001**, *39*, 1572.
58. Rodriguez-Hernandez, J.; Qu, J.; Reuther, E.; *et al. Polym. Bull.* **2004**, *52*, 57.
59. Aliferis, T.; Iatrou, H.; Hadjichristidis, N. *J. Polym. Sci., Polym. Chem. Ed.* **2005**, *43*, 4670.
60. Aliferis, T.; Iatrou, H.; Hadjichristidis, N.; *et al. Macromol. Symp.* **2006**, *240*, 12.
61. Sela, M.; Katchalski, E.; Gehatia, M. *J. Am. Chem. Soc.* **1956**, *78*, 747.
62. Sela, M.; Fuchs, S.; Arnon, R. *Biochem. J.* **1962**, *85*, 223.
63. Sakamoto, M.; Kuroyanagi, Y. *J. Polym. Sci., Polym Chem. Ed.* **1978**, *16*, 1107.
64. Sakamoto, M.; Kuroyanagi, Y.; Sakamoto, R. *J. Polym. Sci., Polym. Chem. Ed.* **1978**, *16*, 2001.
65. Sakamoto, M.; Kuroyanagi, Y. *J. Polym. Sci., Polym. Chem. Ed.* **1979**, *17*, 2577.
66. Yaron, A.; Berger, A. *Biochim. Biophys. Acta* **1965**, *107*, 307.
67. Tewksbury, D. A.; Stahmann, M. A. *Arch. Biochem. Biophys.* **1964**, *105*, 527.
68. Klok, H.-A.; Rodriguez-Hernandez, J. *Macromolecules* **2002**, *35*, 8718.
69. Tsogas, I.; Theodossiou, T.; Sideratou, Z.; *et al. Biomacromolecules* **2007**, *8*, 3263.

70. Vlasov, G. P.; Tarasenko, I. I.; Valueva, S. V.; *et al. Polym. Sci., Ser. A* **2005**, *475*, 731.
71. Rodriguez-Hernandez, J.; Gatti, M.; Klok, H.-A. *Biomacromolecules* **2003**, *4*, 249.
72. Birchall, A. C.; North, M. *Chem. Commun.* **1998**, 1335.
73. Pratten, M. K.; Lloyd, J. B.; Hörpel, G.; Ringsdorf, H. *Makromol. Chem.* **1985**, *186*, 725.
74. Sela, M.; Katchalski, E. *Adv. Protein Chem.* **1959**, *14*, 391.
75. Kwon, G. S. *Crit. Rev. Ther. Drug Carrier Syst.* **1998**, *15*, 481.
76. Rüde, E.; Westphal, O.; Hurwitz, E.; *et al. Immunochem.* **1966**, *3*, 137.
77. (a) Bohak, Z.; Katchalski, E. *Biochemistry* **1963**, *2*, 228. (b) Quadrifoglio, F.; Urry, D. W. *J. Am. Chem. Soc.* **1968**, *90*, 2760.
78. (a) Yokoyama, M.; Kwon, G. S.; Okano, T.; *et al. Bioconjugate Chem.* **1992**, *3*, 295. (b) Thünemann, A. F.; Beyermann, J.; Kukula, H. *Macromolecules* **2000**, *33*, 5906.
79. (a) Lupu-Lotan, N.; Yaron, A.; Berger, A.; Sela, M. *Biopolymers* **1965**, *3*, 625. (b) Pytela, J.; Kotva, R.; Rypácek, F. *J. Bioact. Compat. Polym.* **1998**, *13*, 198.
80. Prime, K. L.; Whitesides, G. M. *J. Am. Chem. Soc.* **1993**, *115*, 10714.
81. Yu, M.; Nowak, A. P.; Pochan, D. J.; Deming, T. J. *J. Am. Chem. Soc.* **1999**, *121*, 12210.
82. Wang, J.; Gibson, M. I.; Barbey, R.; *et al. Macromol. Rapid. Commun.* **2009**, *30*, 845.
83. Hwang, J.; Deming, T. J. *Biomacromolecules* **2001**, *2*, 17.
84. Schlaad, H.; Antonetti, M. *Eur. Phys. J. E* **2003**, *10*, 17.
85. (a) Watanabe, J.; Fukuda, Y.; Gehani, R.; Uematsu, I. *Macromolecules* **1984**, *17*, 1004. (b) Watanabe, J.; Ono, H.; Uematsu, I.; Abe, A. *Macromolecules* **1985**, *18*, 2141. (c) Watanabe, J.; Takashina, Y. *Macromolecules* **1991**, *24*, 3423.
86. Watanabe, J.; Tominaga, T. *Macromolecules* **1993**, *26*, 4032.
87. (a) Gallot, B.; Fafiotte, M. *Macromol. Rapid. Commun.* **1996**, *17*, 4931. (b) Guillermain, C.; Gallot, B. *Macromol. Chem. Phys.* **2002**, *203*, 1346.
88. (a) Hessel, F.; Finkelmann, H. *Polym. Bull. (Berlin)* **1986**, *14*, 375. (b) Zhou, Q.-F.; Li, H.-M.; Feng, X.-D. *Macromolecules* **1987**, *20*, 233.
89. Mayer, S.; Zentel, R. *Curr. Opin. Solid State Mater. Sci.* **2002**, *6*, 545.
90. Thomsen, D. L.; III; Keller, P.; Naciri, J.; *et al. Macromolecules* **2001**, *34*, 5868.
91. Schaefer, K. E.; Keller, P.; Deming, T. J. *Macromolecules* **2006**, *39*, 19.
92. Wu, P.; Feldman, A. K.; Nugent, A. K.; *et al. Angew. Chem., Int. Ed.* **2004**, *43*, 3928.
93. Engler, A. C.; Lee, H.; Hammond, P. T. *Angew. Chem., Int. Ed.* **2009**, *48*, 9334.
94. Xiao, C.; Zhao, C.; He, P.; *et al. Macromol. Rapid Commun.* **2010**, *31*, 991.
95. Tang, H.; Zhang, D. *Biomacromolecules* **2010**, *11*, 1585.
96. Huang, J.; Habraken, G.; Audouin, F.; Heise, A. *Macromolecules* **2010**, *43*, 6050–6057. DOI: 10.1021/ma101096h
97. Sun, J.; Schlaad, H. *Macromolecules* **2010**, *43*, 4445.
98. Dwek, R. A. *Chem. Rev.* **1996**, *96*, 683.
99. Carlstedt, I.; Davies, J. R. *Biochem. Soc. Trans.* **1997**, *25*, 214.
100. Wu, A. M.; Csako, G.; Herp, A. *Mol. Cell. Biochem.* **1994**, *137*, 39.
101. Jentoft, N. *Trends Biochem. Sci.* **1990**, *15*, 291.
102. Gestwicki, J. E.; Cairo, C. W.; Strong, L. E.; *et al. J. Am. Chem. Soc.* **2002**, *124*, 14922.
103. Cairo, C. W.; Gestwicki, J. E.; Kanai, M.; Kiessling, L. L. *J. Am. Chem. Soc.* **2002**, *124*, 1615.
104. Rude, E.; Meyer-Delius, M. *Carbohydr. Res.* **1968**, *8*, 219.
105. Aoi, K.; Tsutsumiuchi, K.; Okada, M. *Macromolecules* **1994**, *27*, 875.
106. Tsutsumiuchi, K.; Aoi, K.; Okada, M. *Macromol. Rapid Commun.* **1995**, *16*, 749.
107. Aoi, K.; Tsutsumiuchi, K.; Aoki, E.; Okada, M. *Macromolecules* **1996**, *29*, 4456.
108. Tsutsumiuchi, K.; Aoi, K.; Okada, M. *Macromolecules* **1997**, *30*, 4013.
109. Gibson, M.; Hunt, G.; Cameron, N. *Org. Biomol. Chem.* **2007**, *5*, 27567.
110. Tian, Z.; Wang, M.; Zhang, A.; Feng, Z. *Front. Mater. Sci. China* **2007**, *1*, 162.
111. Tian, Z.; Wang, M.; Zhang, A.; Feng, Z. *Polymer* **2008**, *49*, 446.
112. (a) Gellman, S. H. *Acc. Chem. Res.* **1998**, *31*, 173. (b) Gademann, K.; Ernst, M.; Hoyer, D.; Seebach, D. *Angew. Chem., Int. Ed.* **1999**, *38*, 1223.
113. Kovacs, J.; Ballina, R.; Rodin, R.; *et al. J. Am. Chem. Soc.* **1965**, *87*, 119. (b) Fernández-Santin, J. M.; Muñoz-Guerra, S.; Rodríguez-Galán, A.; *et al. Macromolecules* **1987**, *20*, 62.
114. Birkofer, L.; Modic, R. *Liebigs Ann. Chem.* **1959**, *628*, 162.
115. (a) Ilarduya, A. M.; Alaman, C.; Garcia-Alvarez, M.; *et al. Macromolecules* **1999**, *32*, 3257. (b) Hashimoto, K.; Yasuda, J.; Kobayashi, M. *J. Polym. Sci., Polym. Chem.* **1999**, *37*, 909.
116. Cheng, J.; Deming, T. J. *J. Am. Chem. Soc.* **2001**, *123*, 9457.
117. Cheng, J.; Ziller, J. W.; Deming, T. J. *Org. Lett.* **2000**, *2*, 1943.
118. Cheng, J.; Deming, T. J. *Macromolecules* **2001**, *34*, 5169.
119. Bellomo, E. G.; Davidson, P.; Impéror-Clerc, M.; Deming, T. J. *J. Am. Chem. Soc.* **2004**, *126*, 9101.
120. Ben-Ishai, D.; Berger, A. *J. Chem. Soc.* **1952**, 1564.
121. Blout, E. R.; Idelson, M. *J. Am. Chem. Soc.* **1956**, *78*, 497.
122. (a) Hanby, W. E.; Waley, S. G.; Watson, J. *Nature* **1948**, *161*, 132. (b) Hanby, W. E.; Waley, S. G.; Watson, J. *J. Chem. Soc.* **1950**, 3239.
123. Subramanian, G.; Hjelm, R. P.; Deming, T. J.; *et al. J. Am. Chem. Soc.* **2000**, *122*, 26.
124. (a) Saudek, V.; Pivcová, H.; Drobník, J. *Biopolymers* **1981**, *20*, 1615. (b) Yokoyama, M.; Kwon, G. S.; Okano, T.; *et al. Bioconjugate Chem.* **1992**, *3*, 295.

Biographical Sketch

Timothy J. Deming received a BS in chemistry from the University of California, Irvine, in 1989, and graduated with a PhD in chemistry from the University of California, Berkeley, under Bruce Novak in 1993. After a National Institutes of Health (NIH) postdoctoral fellowship at the University of Massachusetts, Amherst, with David Tirrell, he joined the faculty in the Materials Department at the University of California, Santa Barbara, in 1995. Here he held a joint appointment in the materials and chemistry departments, where he was promoted to associate professor in 1999 and to full professor in 2003. His appointment is now as the chairman of the Bioengineering Department at the University of California, Los Angeles, where he is professor of bioengineering and professor of chemistry and biochemistry. He is a leader in the fields of polypeptide synthesis, self-assembly of block copolypeptides, and biological activity of polypeptides, for which he has received awards from the National Science Foundation, the Office of Naval Research, the Arnold and Mabel Beckman Foundation, the Alfred P. Sloan Foundation, the Camille and Henry Dreyfus Foundation, the Materials Research Society, and the IUPAC Macromolecular Division. He was recently named a fellow of the American Institute for Medical and Biological Engineering.

4.17 Polymerization of Cyclic Siloxanes, Silanes, and Related Monomers

M Cypryk, Polish Academy of Sciences, Lodz, Poland

Published by Elsevier B.V.

4.17.1 Monomers Polymerizable by Breaking the Siloxane Bonds

4.17.1.1 Cyclosiloxanes

Cyclosiloxanes are the ring structures built of alternating silicon and oxygen atoms. They are useful and important monomers for the ionic ring-opening polymerization (ROP) leading to polysiloxanes. ROP of cyclic siloxanes involves transformation of cyclosiloxanes into a linear polymer by cleavage of the Si–O bond in the monomer ring and the subsequent regeneration of this bond in a polymer chain, according to eqn [1].

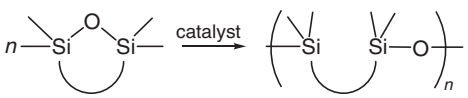

[1]

This process offers a synthetic route to high-molecular-weight (MW) polysiloxanes with a better control of the reaction and of the product structure than the polycondensation methods. A great variety of known cyclic siloxane structures makes this method fairly universal. From the point of view of the polymerization mechanism, the term cyclosiloxane monomer may be extended to a wider class of heteroorganic rings. Cyclic compounds, such as carbosiloxanes (5), arylenesiloxanes (6), oxysilylenes (silaethers) (7), azasiloxanes (8), borasiloxanes (9), and others, may also be considered cyclic siloxane monomers, since they undergo polymerization by the same mechanism.

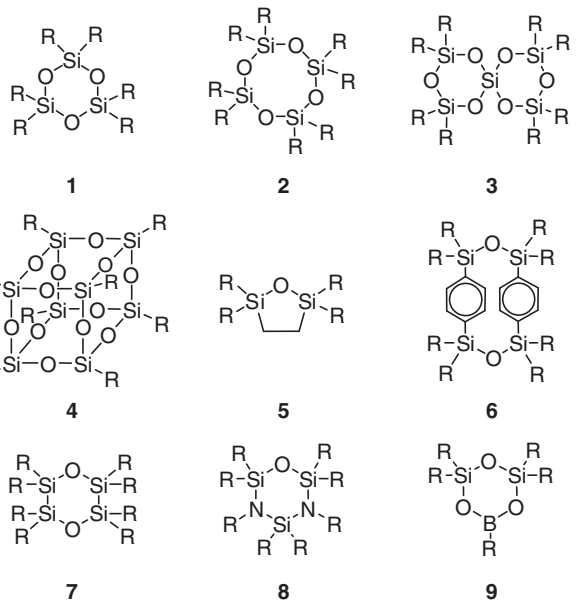

Two cyclic siloxane monomers, octamethylcyclotetrasiloxane, $(Me_2SiO)_4$ (D_4), and hexamethylcyclotrisiloxane, $(Me_2SiO)_3$ (D_3) (structures 2 and 1, where R = Me), are technically the most important as the source of poly (dimethylsiloxane) (PDMS) and various siloxane copolymers. Cyclosiloxanes derived from these monomers by replacement of methyls with various organic groups, such as fluoroalkyl,

vinyl, and phenyl, are used to produce copolymers having more specialized properties. Recently, three-dimensional multicyclic siloxane structures like 3 and 4 have attracted growing attention.

Cyclic organosiloxanes are usually prepared by hydrolytic polycondensation of dichlorodimethylsilane (DDS) or a mixture of α,ω-dichlorooligosiloxanes, $Cl(R_2SiO)_{n-1}R_2SiCl$.[1] This is the synthetic process used in industrial scale (eqn [2]).[2,3]

$$R_2SiCl_2 \xrightarrow[-HCl]{H_2O} \overbrace{(R_2SiO)_n} + —(R_2SiO)_m— \qquad [2]$$

Alternative routes of nonhydrolytic conversion of chlorosilanes into siloxanes are also known. The most common one uses dimethyl sulfoxide (DMSO) as the oxygen source.[4–6] Another useful method of the siloxane bond formation is the reaction of dichlorodiorganylsilanes with some metal oxides, such as ZnO (eqn [3]).[7] The reaction is particularly useful for the synthesis of cyclotrisiloxanes, which are rather difficult to prepare in any other way. By this method they can be obtained with the yield 30–60%.[8,9] The mechanism of this transformation was recently studied by theoretical methods indicating that the reaction involves insertion of –Zn–O– into the Si–Cl bond. An alternative pathway involving transient silanone was shown to be much less thermodynamically feasible.[10]

$$nR_2SiCl_2 + nZnO \rightarrow (R_2SiO)_n + nZnCl_2 \qquad [3]$$

Cyclotrisiloxanes can also be obtained with good yields by the reaction with $NaHCO_3$ in ethyl acetate (eqn [4]).[11,12] The reaction was recently repeated for a series of dichlorosilanes. The content of cyclotrisiloxanes in the resulting mixtures of cyclosiloxanes was 30–67%, depending on the organic substituents at silicon and on the solvent used.[13]

$$nR_2SiCl_2 + 2nNaHCO_3 \rightarrow (R_2SiO)_n + 2nNaCl + 2CO_2 \qquad [4]$$

4.17.1.1.1 Ring-opening polymerization of cyclosiloxanes

As a consequence of the strength and polarity of the siloxane bond, its heterolytic cleavage proceeds much more easily than the homolytic process. ROP of cyclosiloxanes can be effected by both basic and acid catalysts. Thus, the reaction may proceed by an anionic or cationic mechanism, depending on the initiator and on the structure of the active propagation center. The essential features of these processes have been comprehensively reviewed in a number of books and reviews.[1,2,14–24] Recent developments in the field have been summarized by Ganachaud and Boileau.[25] This section is partially based on the previously published chapter.[24]

There are two general methods of ROP of cyclosiloxanes. One of them is equilibrium polymerization; however, its applicability is limited to those systems where the polymer yield in equilibrium is relatively high (see section 4.17.1.1.1(i)). The alternative route is nonequilibrium polymerization, quenched before the equilibrium is attained, when the yield of polymer reaches maximum.[16,17,26–28]

4.17.1.1.1(i) Equilibrium polymerization of cyclosiloxanes

Equilibrium polymerization of cyclic siloxanes (also called equilibration or thermodynamically controlled polymerization), is carried out to the equilibrium state of the process.[20] This state is, by definition, independent of the starting siloxane substrates and of the initiator used (either anionic or cationic). The polymer yield and its characteristics are not related to the polymerization kinetics. Instead, the knowledge of the thermodynamics of the process is essential. The final state of the reaction involves complex equilibria between the polymeric species of two homologous series, cyclic and linear polysiloxanes. The equilibrium state may be described by general eqn [5].

$$—(R_2SiO)_m— \rightleftharpoons \overbrace{(R_2SiO)_n} + —(R_2SiO)_{m-n}— \qquad [5]$$

Since the starting material is usually a mixture of unstrained cyclic siloxanes and the resulting products are also unstrained polysiloxane chains, the net enthalpy effect is close to zero. The driving force for equilibration in this case is the change in entropy of the system. The equilibrium position results from the balance between two opposite tendencies: the formation of small molecules, which is favored because the greater number of molecules corresponds to the increase in entropy of the system, and the formation of polymer chains which shows higher conformational entropy than small molecules. Obviously, the polymer yield depends on initial concentration of siloxane units, as dilution promotes cyclization. To any type of polysiloxane, a critical concentration threshold is related below which only cyclics exist in equilibrium. The entropy gain upon polymerization decreases with the increase in size and polarity of the organic substituents at silicon. Consequently, the yield of polymer at equilibrium becomes smaller upon this change. For example, the equilibrium amount of polymer in bulk dimethylsiloxanes is ~82 wt.%, in methylsiloxanes ~88 wt.%, while in methyl(3,3,3-trifluoropropyl)siloxanes only 17 wt.%.[29]

4.17.1.1.1(i)(a) Ring-chain equilibria There is a direct relationship between equilibrium ring concentrations in equilibrates and the statistical conformations of the corresponding open-chain molecules.[30–32] The cyclization equilibrium constant of an individual cyclic is given by eqn [6].

$$K_n = \frac{[-(R_2SiO)_{m-n}-][(R_2SiO)_n]}{[-(R_2SiO)_m-]} \qquad [6]$$

With a most probable distribution of chain species in the linear polymer, the relationship derived by Flory can be applied (eqn [7]).[33]

$$K_n = \frac{[(R_2SiO)_n]_e}{p^n} \qquad [7]$$

The factor p can be obtained experimentally from the number-average molar mass of the polymer.[33] When molar masses are large enough, p approaches unity, so for many practical purposes, K_n values for cyclic molecules may be assumed equal to their concentrations (eqn [8]).

$$K_n \cong [(R_2SiO)_n]_e \qquad [8]$$

Assuming that conformations of polymer chains obey the Gaussian statistics, the Jacobson and Stockmayer cyclization theory[34] predicts that the cyclization equilibrium constants decrease proportionally to the power 2.5 of the ring size (or chain length) giving the following expression for the

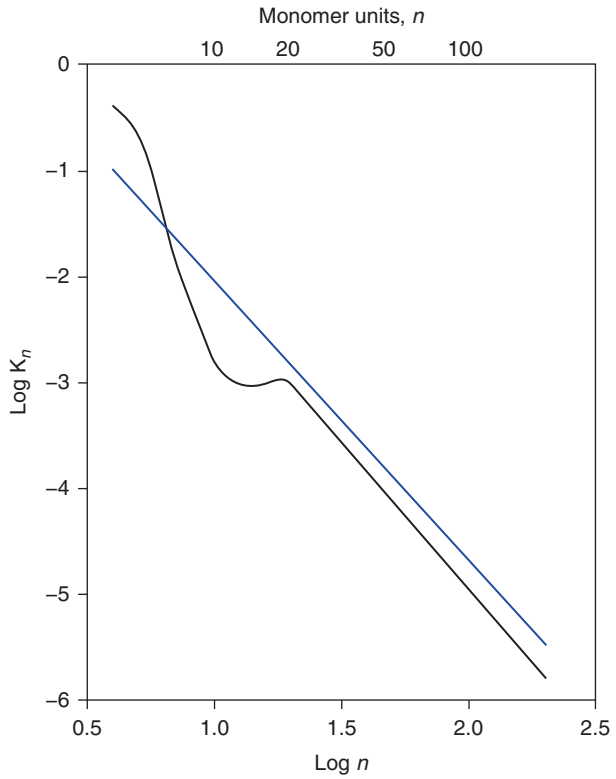

Figure 1 Cyclization constants K_n (mol dm^{-3}) for cyclosiloxanes $(Me_2SiO)_n$ in a ring-chain equilibrate in toluene (black line); compared to theoretical values calculated according to eqn [9] (blue line).[32] Adapted from Flory, P.; Semlyen, J. A. J. *Am. Chem. Soc.* 1966, *88*, 3209, with kind permission of Springer Science and Business Media and ACS, respectively.

cyclization equilibrium constant K_n of an n-membered ring in the ring-chain equilibrate (eqn [9]).

$$K_n \propto n^{-5/2} \qquad [9]$$

A rigorous comparison of theory with experiment in the dimethylsiloxane series was carried out by Semlyen and Wright.[35] They found K_n to be independent of dilution for cyclic species D_n where n lies in the range 11–40. For cyclic species where $n = 4$–10, K_n does increase with dilution. There is a critical dilution beyond which only cyclics are present in equilibrate. **Figure 1** presents the dependence of experimental cyclization equilibrium constants for cyclosiloxanes D_n compared with theoretical values calculated using the Jacobson and Stockmayer cyclization theory (eqn [9]). The deviation from theory in the range $n = 3$–18 reflects the fact that the probabilities of end-to-end closure of short chains, perturbed by excluded volume effects, do not obey the Gaussian statistics.[32]

The equilibration reaction is catalyzed by strong acids and bases. The choice of catalyst depends on the chemical sensitivity of the substituents at silicon. Thus, for example, vinylsiloxanes are usually equilibrated using basic catalysts, while hydrosiloxanes require acid catalysts to preserve the SiH groups. The reaction is usually carried out at elevated temperatures. The chain transfer agent (functional disiloxane or a mixture of α,ω-difunctional oligosiloxanes) is often applied to regulate the MW and to introduce the functional groups into the chain ends (eqn [10]) where X may be H, Me, vinyl, OR, Cl, and so on.

$$m(R_2SiO)_n + pXMe_2SiOSiMe_2X \rightleftharpoons pXMe_2SiO(R_2SiO)_{\frac{n-m}{p}}SiMe_2X \qquad [10]$$

The average MW of the resulting polymer is defined by eqn [11], where $[R_2SiO]_e$ is the equilibrium concentration of R_2SiO units in linear chains, M is the MW of R_2SiO unit, and $[M_2^x]$ is the concentration of terminating agent.[37] Since equilibration is a random process, the polymer usually has the normal Flory MW distribution of 2.[38,39] The association phenomena may result in broader distribution.[40]

$$\overline{M}_n = \frac{[(R_2SiO)_n]_e \times M}{[M_2^X]} \qquad [11]$$

4.17.1.1.1(i)(b) Practical considerations The equilibrium polymerization of cyclosiloxanes is often used for the synthesis of polysiloxanes both in industry and in research laboratories as it has many advantages which are summarized briefly below:

1. This method itself does not impose any restriction on the initiator. Both anionic and cationic initiators may be used. Thus, it is possible to find an initiator, which is tolerated by the functional groups in the polymer. Such an initiator makes it possible to reach the equilibrium state in a sufficiently short time under mild conditions; it may be easily removed from the polymer.
2. There are no rigorous requirements for the moment of quenching the reaction.
3. There are no restrictions concerning the size of the monomer ring. Identical results are obtained using various monomers of the same homologous series. A mixture of cyclics or a mixture of cyclic and linear polysiloxanes may be used as well.
4. Molecular weight may be controlled by using chain blockers such as disiloxanes or short-chain oligosiloxanes. The initial concentration of the initiator, which is also a source of the end groups, must be much lower than that of the blocker. Using functionalized blocking agents results in functionalization of both chain ends. If the blocker is an organic polymer containing the SiOSi grouping, an organic–siloxane–organic triblock copolymer may be obtained.
5. The equilibrium ROP of cyclosiloxanes is a convenient route to siloxane copolymers of random composition. It is possible to introduce functional groups pendant to polysiloxane chain, which are randomly distributed along the polymer chain.

The equilibrium ROP of cyclosiloxanes has also some limitations.[28] The main restraint concerns the formation of cyclic oligomers. Since the polymer yield in equilibrium depends dramatically on the size and polarity of substituents at silicon, the process is usually applied to the synthesis of dimethylsiloxane and methylsiloxane polymers and (their) copolymers. The equilibrium ROP is carried out in bulk as the dilution of the system favors formation of cyclics. The reaction cannot be used for the synthesis of polysiloxanes with a narrow MW

distribution and precisely functionalized at the a single end of the polymer chain. It is not suitable for the synthesis of copolymers with specific distribution of siloxane units, such as alternating or gradient copolymers.[22]

4.17.1.1.1(ii) Nonequilibrium (kinetically controlled) ROP of cyclosiloxanes

The ROP of strained cyclotrisiloxanes and their unstrained homologs, for example, cyclotetrasiloxanes, both lead to the same equilibrium state, however, by different routes. Polymerization of unstrained cyclosiloxanes leads to simultaneous formation of the polymer and of cyclic oligomers. The polymer concentration increases monotonically achieving finally its equilibrium value. In contrast, strained cyclotrisiloxanes in the first, rapid step of the process are transformed mainly into linear polymers, which are randomized and partially decomposed to cyclics in the second, slower step. The system attains the equilibrium state according to general Scheme 1.

Separation of the two stages of polymerization is possible because the propagation of strained monomers is much faster than the backbiting and chain transfer. In contrast to the entropy-driven polymerizations of unstrained cyclosiloxanes, the driving force for the polymerization of cyclotrisiloxanes is the enthalpy of the ring-strain release. If the polymerization is quenched at a proper moment, a high yield of polymer may be obtained even in the case when the equilibrium concentration of linear polysiloxane is very low.

There are some inconsistencies in thermodynamic estimation of the ring strain in cyclotrisiloxanes reported by various authors. For example, the ring strain in D_3 was measured by different authors to be 13–17 and 23 kJ mol^{-1},[14] 50–63 kJ mol^{-1},[37] and as high as 80 kJ mol^{-1}.[41] According to *ab initio* calculations, the ring strain in $(H_2SiO)_3$ is 19 kJ mol^{-1}, which suggests that the lower values of those reported for D_3 are more likely.[42] Slightly higher enthalpy values, 22 and 25 kJ mol^{-1}, were measured for the ring strain in $[Me(CF_3CH_2CH_2)SiO]_3$ and $(MePhSiO)_3$, respectively.[14] The apparent activation energies of anionic polymerization of cyclotrisiloxanes are by about 13–17 kJ mol^{-1} lower than those for basically unstrained cyclotetrasiloxanes, which would suggest almost full strain release in the transition state.[14] These data also agree with the results of quantum chemical calculations of strain energy for $(H_2SiO)_3$.[42]

The kinetically controlled ROP of cyclotrisiloxanes is more difficult to perform than the equilibrium process. It requires more expensive monomers, selected initiators, and more rigorous conditions in terms of purity of the system. On the other hand, it allows polymers of controlled structures to be obtained and is the method of choice for those polymers that cannot be obtained with a reasonable yield by the equilibrium polymerization due to the low equilibrium concentration of linear fraction.

4.17.1.1.1(iii) Anionic ring-opening polymerization of cyclosiloxanes

4.17.1.1.1(iii)(a) General mechanism The anionic ring-opening polymerization (AROP) of cyclic siloxanes is initiated by strong inorganic, organic, or organometallic bases.[16,17,19,20,27,37] The initiation involves the formation of a silanolate anion (eqn [12]), which is the active propagation center, capable of breaking the siloxane bond in a cyclic monomer. Then the monomer is added to the growing chain and the active center is restored (eqn [13]). Cat^+ is usually an alkali metal, tertiary ammonium, or phosphonium cation.

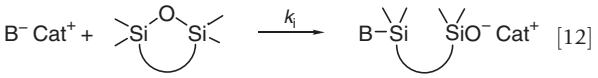

[12]

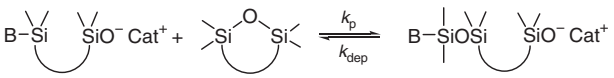

[13]

Reversibility of the propagation step is a consequence of the reaction of the active propagation centers with siloxane bonds in the chain (backbiting). The backbiting process generates a series of monomer homologues of various ring size. The silanolate center may attack another chain as well, leading to the chain transfer (eqn [14]), which results in chain scission and randomization. In the absence of any acid contaminants, the reaction proceeds without termination. Thus, the polymerization must be quenched to deactivate the silanolate centers.

[14]

Initiators may be mono- or bifunctional. A mixture of bifunctional oligo(dimethylsiloxane)diolates can easily be prepared according to eqn [15], removing water from the reaction system.[43] For $n > 2$, the oligo(dimethylsiloxane)diolates are soluble in PDMS and in typical solvents, in contrast to alkali metal hydroxides, which were used as initiators in earlier works.[20]

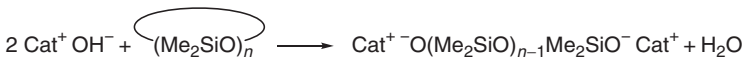

[15]

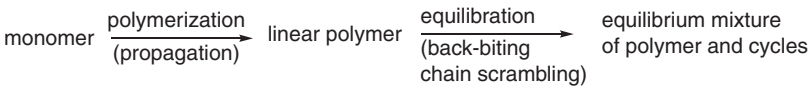

Scheme 1 Ring-opening polymerization of strained cyclic siloxane monomers.

4.17.1.1.1(iii)(b) Kinetics of polymerization The rate of polymerization depends on the initiator, monomer, and solvent. Although the reactive center has the anionic structure, the role of the cation is very important.[1,15,20] In most systems, free silanolate ion does not appear in a kinetically significant concentration and the ion pairs are true active propagating species.[20] In the reaction medium they exist in equilibrium with higher aggregates.[1,15,20,44,45] Since these complexes are much less reactive (or even inactive) in propagation, the association strongly reduces the polymerization rate and affects the kinetic law, leading to the fractional order in silanolate (eqn [16]).

$$-\frac{d[\text{Monomer}]}{dt} = \left(\frac{1}{nK_n}[\text{SiO}^-\text{Cat}^+]\right)^{1/n}(k_p[\text{Monomer}]-k_{dep}) \quad [16]$$

For typical polymerization systems, ~Me_2SiOK in bulk PDMS and ~Me_2SiOLi in THF, the multiplicity of the complex n is[15] 2 and 3 (or 4 if $[SiOLi] > 10^{-2}$ mol dm^{-3}).[45] The aggregation is almost unaffected by temperature, which indicates that it is mostly controlled by entropy factors.[45] Silanolates with bulky cations, where the charge is delocalized, show little tendency to aggregation. Thus, for example, the polymerization of D_3 initiated by trimethylammonium silanolate shows the first-order kinetics in silanolate.[46]

The rate of polymerization of cyclosiloxanes in bulk strongly increases in the series of silanolates $SiOLi < SiONa < SiOK < SiORb < SiOCs \approx SiO^-N^+Me_4 \approx SiO^-P^+Bu_4 < SiO^-P^+(NHtBu)[NP(NMe_2)_3]_3$ due to the loosening of the anion–cation interaction with the increase in cation size, which shifts the equilibrium toward more reactive nonaggregated ion pairs.[14,15,45,47]

Phosphazene superbases (structures **10** and **11**) have recently been explored as extremely effective initiators of the ROP of cyclosiloxanes.[48–54] Neutral phosphazene bases (**10**, **11**) require a proton donor, such as methanol, to form the true initiator, phosphazenium alkoxide (eqns [17] and [18]). Bulky phosphazenium cations are able to very effectively stabilize a positive charge by the resonance effect.[48] The existence of the bare silanolate anion in such systems is very probable. They are also well soluble in the polymerization system.

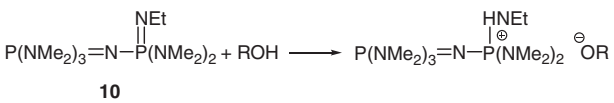

10

[17]

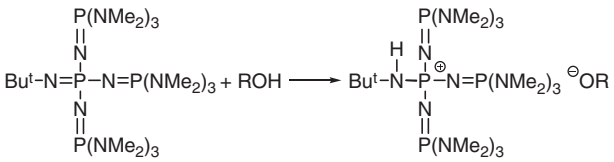

11

[18]

Another class of initiators are amino-substituted oligophosphazenium hydroxides, which do not require any coactivation. Kinetics of the polymerization of D_4 and D_3 initiated by a model hexapyrrolidinodiphosphazenium hydroxide **12** was systematically studied.[53] As expected from low degrees of association of active centers, first-order kinetics with respect to the initiator is observed. More interestingly, the formation of larger cyclics *via* backbiting process is retarded, which is rationalized by the lack of multicenter interactions of the siloxane chain with the bulky cation. Such types of interactions are known to promote formation of cyclics when alkali metal counterions are used.[20]

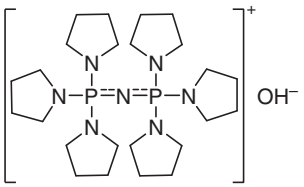

12

Silazane lithium salts $(RMe_2Si)_2NLi$, R = Me, vinyl, Ph, in the presence of promoters such as DMSO were shown to initiate nonequilibrium ROP of D_4 at elevated temperatures. The polymerization leads to high yields (> 90%) of polysiloxane, while MW distributions of the obtained polymers are relatively narrow, $M_w/M_n = 1.25–1.33$, and broaden gradually with time.[55] These data suggest that the propagation in this system is faster than the redistribution reactions, which lead to equilibration. The ROP of D_3 using organodilithium compound as the initiator leads to narrowly dispersed polysiloxane, which may be functionalized at both chain ends.[56]

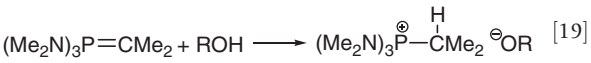

[19]

Looking for the catalytic systems, which may be easily deactivated and removed from the polymer, other nonionic base/alcohol-initiating systems have been examined. Phosphorus ylides, $R_3P=CMe_2$ (eqn [19]), show the activity similar to phosphazene bases in polymerization of D_4. They are thermolabile and easy to remove from the polymer.[57] Promising initiators are also stable (*N*-hetaryl)carbenes (eqn [20])[58,59] and guanidine derivatives.[58] The MWs of the silicone polymers in case of carbenes can be regulated simply by varying the quantity of the alcohol co-initiator.

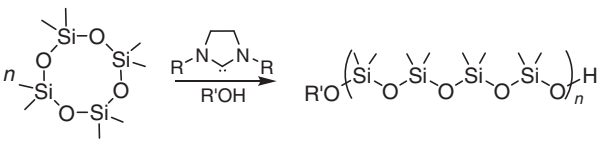

[20]

Uncharged nucleophiles, such as hexamethylphosphorotriamide (HMPT), DMSO, and dimethylformamide (DMF), strongly interacting with metal cations, largely release the anion–cation interaction in the ion pair and, consequently, enhance the polymerization rate.[14,44,45,60] These additives are referred to as the polymerization promoters or activators. The supramolecular complexes of silanolates with crown ethers[61,62]

and cryptands[63,64] also show very high reactivity in polymerization of cyclic siloxanes.

The rate of polymerization depends on the ring size of the monomer and on the substituents at silicon. Cyclotrisiloxanes are particularly reactive, due to their ring strain. A significant increase in the reactivity toward the alkali metal silanolate centers was observed in the series of unstrained cyclodimethylsiloxanes $D_4 < D_5 < D_6 < D_7 < D_8$, when the reaction was performed in bulk or in a nonpolar acid–base inert solvent.[61,65] D_7 and larger cycles were opened faster than D_4 by the factor of 200 and twice as fast as the strained D_3. Similar reactivity enhancement was observed for the backbiting process. An analogous behavior was noted for the cleavage of linear siloxane series $Me_3Si(OSiMe_2)_nOSiMe_3$ by the oligosiloxanolates.[61] The reaction rate increased by more than 3 orders of magnitude, going from $n = 1$ to 10. That behavior was explained by the multidentate interaction of the siloxane chain with metal cation, lowering the energy barrier of reaction (eqn [21]).[20]

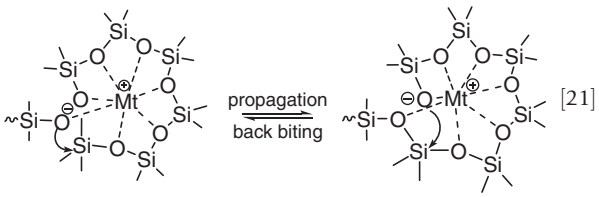

[21]

This mechanism does not operate when the interactions of the siloxane chain with the counterion are suppressed, as in the presence of a nucleophilic additive, basic solvent, or promoter strongly interacting with cation, or when a large, stabilized cation is used.[61] The elimination of the mechanism involving the cation–siloxane interaction largely suppresses backbiting and chain transfer during polymerization of D_3, which allows for a better control of the polymerization process.[26] The multidentate interaction does not affect the rate of polymerization of D_3, since rigid, almost flat six-membered ring is unable to interact in a multidentate way with a cation. This has recently been confirmed by *ab initio* calculations.[66,67] Recent results on the multidentate crown-like interactions of cyclosiloxanes with metal cations have been reviewed.[68]

The rate of the AROP of cyclosiloxane depends also on the organic substituents at silicon. In general, electron-withdrawing substituents at silicon increase the reactivity of monomers by enhancing the electrophilicity of silicon atoms. On the other hand, the reduced electron density on silicon lowers the nucleophilicity of the silanolate ion making weaker its interactions with the counterion.[44] Therefore, the net effect of polar substituents may be difficult to predict. The relative reactivity of cyclosiloxanes in copolymerization was observed to rise strongly with the increasing electronegativity of substituents. For example, in copolymerization of octaphenylcyclotetrasiloxane with octamethylcyclotetrasiloxane, the former monomer is almost fully converted before the latter begins to polymerize.[65]

The AROP of cyclosiloxanes may be accelerated by nucleophilic functional groups in the polymer, such as $-(CH_2)_2CN$[69] or $-(CH_2)_3P(O)Ph_2$,[70] which can directly interact with the counterion resulting in activation of an anion, analogously to promoters.

4.17.1.1.1(iii)(c) Effect of water, alcohol, and silanols Anionic ROP systems often contain small amounts of protic impurities such as water or alcohols. These contaminants do not suppress polymerization unless they are more acidic than silanols themselves, although they may affect the reaction rate. They participate in the polymerization process, forming reactive end groups and reducing the MW of polymer. The presence of water results in formation of silanol groups which, undergoing fast interconversion with silanolate anions, play a role of the dormant centers in propagation.[71,72] Silanol groups strongly accelerate the terminal siloxane unit exchange (eqn [22]), leading to the broadening of the MW distribution.[72] They also undergo homofunctional polycondensation, although this reaction under basic conditions is much slower than the terminal unit exchange.[72,73]

[22]

Water participates also in chain transfer, producing polymer chains growing in two directions. In polymerization systems using monofunctional initiator, the competition of unidirectional and bidirectional chain growth leads to the broad or bimodal MW distribution of polymer.[71]

4.17.1.1.1(iii)(d) Applications of AROP of cyclosiloxanes The first patents on the AROP of cyclosiloxanes appeared in the late 40s. Since that time, this reaction has become widely used in industrial synthesis of polysiloxanes and the interest in development and optimization of this process is still vivid.[74,75]

It may be applied to the synthesis of polysiloxanes with various substituents, provided they do not react with initiator or with the silanolate center. Thus, monomers having groups susceptible to the base substitution or deactivating the active centers, such as $Si–CH_2Cl$ and $Si–(CH_2)_nCOOH$, cannot be polymerized in this way. Some polymers bearing groups, which had been believed to be unstable under basic conditions, were recently obtained by anionic nonequilibrium polymerization of the corresponding cyclotrisiloxanes, for example, poly[(3-chloropropyl)methylsiloxane][12] and poly(methylsiloxane)s.[76–78]

The industrial process of the anionic equilibration of cyclic siloxanes is usually carried out in bulk at elevated temperature. The choice of initiator is critical. Some contaminations, originating from the initiator, particularly those of acid, basic, or ionic nature, dramatically reduce thermal stability of polysiloxanes. Thermolabile silanolates, such as $Me_4N^{+-}OSi\equiv$ or $Bu_4P^{+-}OSi\equiv$, are convenient initiators, because they can be easily removed from polymer by thermal decomposition.[79–81] Silanolate centers must be neutralized to avoid decomposition of polymer. Me_3SiCl is commonly used for this purpose, as it introduces the inert Me_3Si groups to the chain ends; however, it may not react sufficiently fast with strongly aggregated silanolates.

The nonequilibrium AROP of the reactive strained cyclotrisiloxanes as monomers allows to obtain high MW polymer with good yields (>95%). The polymerization must be

quenched before the monomer is totally consumed to minimize the role of backbiting and chain randomization.[26] In contrast to the equilibrium polymerization in this reaction, polymer may be obtained even in a dilute system. The kinetically controlled ROP is used when the linear polymer is thermodynamically disfavored, for example, in the case of poly[methyl(3,3,3-trifluoropropyl)siloxane],[82] poly[methyl (phenyl)siloxane],[83] or poly(diphenylsiloxane).[84–86]

Elimination of the multidentate interaction of a counterion with the siloxane chain is crucial. Otherwise, as mentioned before, the equilibration reactions would make the precision polymerization impossible. Specific initiator–solvent systems used for this purpose may be divided into three groups: (1) basic solvent and a hard counterion, which interacts with solvent stronger than with siloxane, for example, lithium/THF; (2) bulky and soft counterions, for example, Me_4N^+, Bu_4P^+, and phosphazenium cations, which weakly interact with nucleophiles; (3) basic promoters strongly interacting with counterions, such as HMPT, DMSO, DMF, cryptands, and crown ethers.[20]

The AROP of cyclotrisiloxanes is extensively studied in research laboratories,[87–90] as this process makes possible the controlled synthesis of functionalized polysiloxane polymers and copolymers.[22] The precise nonequilibrium AROP is commonly used for the synthesis of end-functionalized polysiloxanes, in particular polysiloxane macromonomers[91,92] and macroinitiators.[93] It provides a high control of MW, MW distribution, and functionalization.[26] Usually, the polydispersity M_w/M_n lower than 1.1 can be achieved.[94] Functionalization of chain ends is effected by using a functionalized initiator,[95] a functionalized terminator,[96] or both.[97] Introduction of functional groups to both ends of the polysiloxane chain by the initiator method is also possible using the stoichiometric amounts of bifunctional terminator, such as Me_2SiCl_2.[98] Polysiloxanes functionalized in the end groups are widely used in polymer engineering for the synthesis of block copolymers,[64,99] graft copolymers,[91,100] regular star polymers,[45,95,101] regular polymer networks,[96] and interpenetrating networks.[23,98,102] Quenching polymerization with the stoichiometric amount of a multifunctional terminator, such as $MeSiCl_3$ or $(Cl_2MeSiCH_2)_2$, gives a star polymer.[45,95,101,103]

4.17.1.1.1(iii)(e) Stereoselectivity and regioselectivity in nonequilibrium anionic polymerization The unsymmetrically substituted polysiloxanes exhibit stereoisomerism. Subsequent cross-linking of polymers with enhanced stereoregularity gives siloxane elastomers, which may have properties superior to their atactic analogs.[104] The synthesis of stereoregular polysiloxanes was reviewed by Saam.[105] The cyclic trisiloxanes with two different substituents at each silicon atom $(RR'SiO)_3$ exist as two isomers, *cis* and *trans* (**13** and **14**).

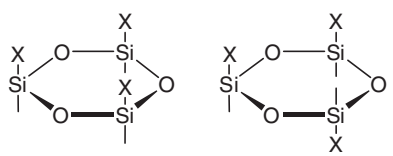

13 **14**

The regioselective course of the polymerization of cyclosiloxanes containing different siloxane units would lead to alternating copolymers. The preparation of such copolymers by nonequilibrium polymerization of some cyclotrisiloxanes with mixed units was reported.[83,106] A detailed sequence analysis of copolymers obtained by anionic polymerization of 3,3,5,5-tetramethyl-1,1-diphenylcyclotrisiloxane has shown that the monomer ring was opened at both nonequivalent siloxane linkages, $-Me_2SiOSiMe_2-$ and $-Me_2SiOSiPh_2-$.[107] The proportion of both openings strongly depends on the counterion. On the other hand, polymerization of pentamethylvinylcyclotrisiloxane at −30 °C gave almost regular polymer with 90% of opening at vinyl-substituted silicon atom.[108] Regular polymers were also obtained by AROP of some hydridocyclotrisiloxanes.[76]

4.17.1.1.1(iv) Cationic ring-opening polymerization of cyclosiloxanes

Cyclic siloxanes can also be transformed into linear polymers by both Bronsted and Lewis acid catalysts.[16,17,19,20,22,27,28] The cationic ring-opening polymerization (CROP) of cyclosiloxanes is a convenient route to linear polysiloxanes, as it may be performed with a suitable rate at room temperature and the catalyst may be easily removed from the polymer. This is the method of choice for the synthesis of siloxane polymers and copolymers with substituents, which are unstable in the presence of strong bases, such as SiH, SiCl, $SiCH_2Cl$, $Si(CH_2)_nCOOH$. The main disadvantage of the cationic process is the simultaneous formation of significant amounts of cyclic oligomers along with the polymer. This general feature seriously limits the application of the process for the kinetically controlled synthesis of polysiloxanes.

Strong protic acids, such as H_2SO_4,[109] sulfonic acids RSO_3H,[109–112] and $HClO_4$,[113] are effective initiators of the cationic polymerization of cyclosiloxanes. Solid acids, such as ion exchange resins, for example, sulfonated polystyrene (PS),[114] acid minerals and acid-activated clays[115–118] are used, since they can be easily removed from polymer by filtration.

There is a continuous search for new superacid catalysts. The kinetics of ROP of D_3 and D_4 initiated by protic borate complex (tetrakis(pentafluorophenyl)boric acid hydrate), HB $(C_6F_5)_4 \cdot 3H_2O$, revealed that the reaction is first-order in monomer and first-order in initiator.[119] The formation of cyclic oligomers typical for CROP of cyclosiloxanes initiated by protic acids was observed.

Lewis acids, such as $FeCl_3$[120] and $SnCl_4$,[121,122] initiate polymerization in cooperation with protic acids, resulting from the reaction of those species with traces of water or other acid contaminations present in the system. Indeed, some Lewis acid–protic acid combinations are very effective as initiators.[120] The question whether Lewis acids alone are capable of initiating ROP of siloxanes is still open. Studies of the polymerization of D_3 in the presence of sterically hindered substituted pyridine used as a proton trap proved that some nonprotic species, such as $RC(O)Cl–SbCl_5$ complex,[123] ethylboron sesquitriflate $(Et_3B_2(OTf)_3)$,[124] and certain metal triflates,[125] can initiate polymerization of this monomer. Trimethylsilyl triflate was considered to be inactive without addition of free trifluoromethanesulfonic (triflic) acid CF_3SO_3H (TfOH).[126] However, Jallouli and Saam[127] reported that, after a long induction period, TMSOTf initiated the polymerization of some

cyclotrisiloxanes, such as D_3, even in the presence of 2,6-di-*tert*-butylpyridine used as the acid scavenger. Silyloxonium ions are effective catalysts of the polymerization of cyclosiloxanes.[128] Various onium salts, such as oxonium, sulfonium, iodonium, acylium, and others, having nonnucleophilic complexed counterions were also reported to initiate the cationic polymerization of siloxanes and other heterocyclic monomers.[129–131] Recently, phosphonitrile halides[117,132] and bis (trifluoromethanesulfonyl)imide, $(CF_3SO_2)_2NH$,[133] have been proved to be very efficient catalysts of the CROP of cyclosiloxanes, even more active than commonly used trifluoromethanesulfonic (triflic) acid.

4.17.1.1.1(iv)(a) Mechanism of the polymerization initiated by protic acids Protic acids are the most common initiators used in the CROP of siloxanes. Their initiating power increases with the acid strength. Thus, CF_3SO_3H and $HClO_4$ are particularly effective, whereas CF_3CO_2H initiates only a slow polymerization of D_3.[27] The process is very sensitive to additives. Some of them, like the basic solvents, reduce the reaction rate, whereas others, like weaker acids, accelerate the process. Water shows an ambivalent behavior, being able to act either as a promoter or as an inhibitor of polymerization.[17,28] Sonification significantly enhances the polymerization rate and reduces the polydispersity of the polymer.[134]

Most of kinetic investigations have been performed on the polymerization of D_3 and D_4, initiated by trifluoromethanesulfonic acid. The studies on the polymerization of larger rings, D_5, D_6, and D_7 are scarce.[135] The mechanism of CROP of siloxanes has been comprehensively presented in earlier reviews.[16,20,136,137] Much higher reactivity of cyclotrisiloxanes, compared to larger cyclics, is the reason for several important kinetic differences between these two classes of monomers. Some concurrent reactions, like backbiting and chain scrambling, which are important in the polymerization of D_4, are negligible in the polymerization of D_3, as long as the monomer is present in the reaction medium. Nonetheless, large amounts of cyclic oligomers, D_{3n}, are produced under these conditions.[122] The kinetic distribution of D_{3n} cyclic oligomers is proportional to $n^{-3/2}$ pointing to the end closure mechanism of their formation, as it was shown in the fundamental work of Chojnowski *et al.*[122]

The mechanism of the cationic polymerization of cyclosiloxanes is very complex and has been controversial for a long time. Some mechanistic details still remain unclear. The most important features of the cationic polymerization of cyclosiloxanes are collected below:[16,20,138,139]

1. Considerable amounts of cyclic oligomers are formed simultaneously with polymer.
2. In the kinetically controlled (nonequilibrium) stage of polymerization of cyclotrisiloxanes, the cycles being the multiples of monomer, $(R_2SiO)_{3n}$, dominate.
3. The activity of the initiator (protic acid) maintains throughout the entire process (permanent initiation).
4. Complex kinetic dependences and complex influence of water indicate the importance of the association phenomena.
5. The number-average molecular weight of polymer increases proportionally with monomer conversion.

- **Initiation**

Protic acids cleave the siloxane bond in monomer with formation of the corresponding oligosiloxane, $H(OSiR_2)_nA$, terminated by the hydroxy group at one end and by the ester group at the other end. High order of the initiation reaction in acid (>3) was interpreted in terms of higher homocomplexes (or hydrates) of acid being the true active species (see other example structures **15, 16**).[139,140] Indeed, the charge separation in such complexes is more effectively stabilized than in the reaction involving a single molecule of acid. This assumption has been supported by quantum chemical calculations.[141]

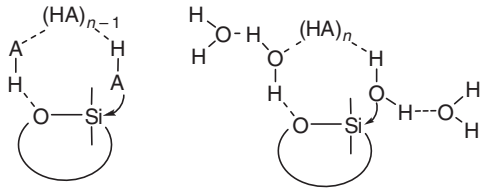

15 **16**

Silanol and ester end groups undergo fast exchange and, as a result, polymer chains grow in both directions (eqn [23]).[142,143]

[23]

- **Cyclization**

The excess of $(R_2SiO)_{3n}$ cyclics in the kinetic stage of polymerization of cyclotrisiloxanes allows to reject backbiting as the main mechanism. The kinetic features of the process point to the end-to-end coupling mechanism.[122] Extensive formation of cyclic products indicates that homo- and/or heterofunctional condensations of the end groups are fast on the propagation time-scale. Intramolecular condensation might be faster than the intermolecular process, as the fraction of end groups bound together intramolecularly via hydrogen bonding is likely to be high, which increases the local concentration of the end groups.[144,145] Cyclization, intermolecular condensation, as well as the silanol–ester group exchange, and the formation of acid hydrates lead to establishing the stationary concentrations of water and acid, which are able to permanently initiate new polymer chains. Thus, the important condition of the living polymerization system, that is, fast and quantitative initiation causing polymer chains to grow simultaneously, is not fulfilled.

The kinetics of formation of D_6 in the polymerization of D_3 is different from that of the other cyclic. Its formation is not suppressed by addition of silyl triflate as the co-initiator. Therefore, Sigwalt *et al.* proposed a special kind of ring expansion involving the oxonium ion, as the main route of D_6 formation (eqn [24]).[146]

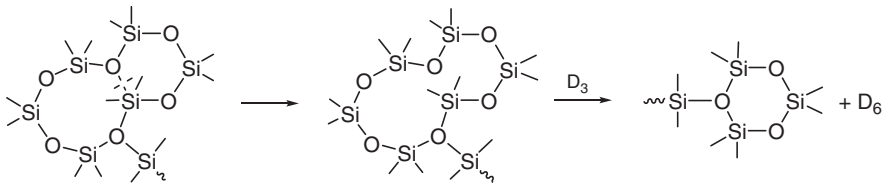

[24]

- **Propagation**

In analogy to the polymerization of cyclic ethers and acetals, it is usually assumed that the active propagation center is a tertiary silyloxonium ion, resulting from the attack of monomer on the ester chain end. Kinetic data suggest that the ester group must be activated by acid, because the basicity of the siloxane monomer is too low to be able to attack the inactivated ester[139] or it requires a very long time to proceed.[127] Alternatively, Toskas *et al.*[126] proposed a mechanism involving propagation on acid-activated ester groups and/or silyloxonium ions (eqn [25]).

[25]

The strongly electrophilic tertiary silyloxonium cation reacts with every nucleophile present in solution: another molecule of monomer, counterion, silanol or water.

The concept of trisilyloxonium ion received strong support from Olah *et al.*,[147] who observed such ions directly by low-temperature ^{29}Si NMR. He also proved that such ions can induce polymerization of D_3 and D_4. Since the time when the tertiary silyloxonium ions were detected by ^{29}Si NMR in the presence of extremely low-nucleophilic counterion (eqn [29]) and proved to initiate the polymerization of cyclic siloxanes, D_3, and D_4, their role as the active centers of propagation has become commonly accepted.[128]

However, kinetic studies led Toskas *et al.*[148] to the conclusion that silyloxonium ions may not be the dominating propagation species in the polymerization initiated by protic acids. Using Olah's initiator and the more nucleophilic monomer, octamethyltetrasila-1,4-dioxane ($^2D_2$) **7**, the transformation of the primary silyloxonium ions formed in the reaction of monomer with initiator into silyloxonium ions at the end of the polymer chain was observed directly by ^{29}Si NMR (eqns [30] and [31]).[149]

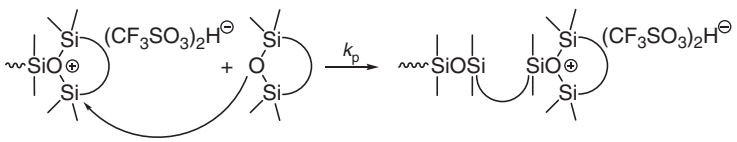

[26]

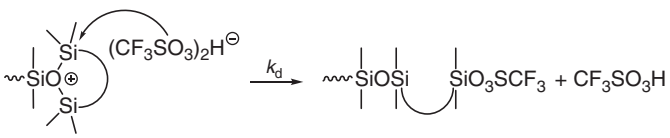

[27]

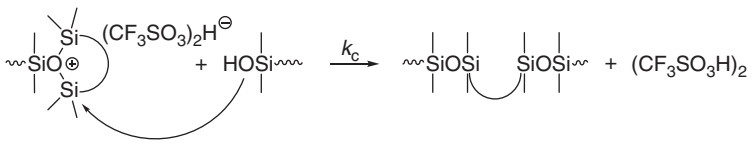

[28]

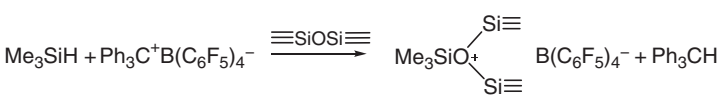

[29]

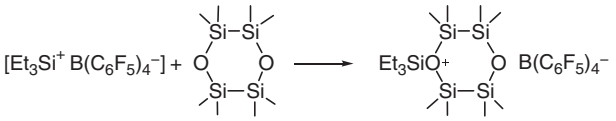

[30]

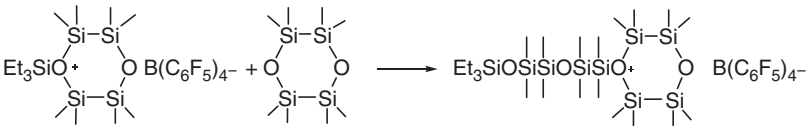

[31]

Studies of the microstructure of polymers obtained by cationic polymerization of tetramethyl-2,2-diphenylcyclotrisiloxane showed that all observed features of the CROP of cyclosiloxanes may be rationalized assuming silyloxonium active centers being in equilibrium with dormant ester end groups.[150] Due to continuous initiation, fast exchange of end groups and extensive chain transfer to the terminal trimethylsiloxy unit, cationic polymerization of cyclosiloxanes is not suitable for the precise synthesis of well-defined polymers and copolymers.

In a series of works, Gädda *et al.*[151] and Paulasaari *et al.*[152] compared the regioselectivity of AROP and CROP of various functional cyclotrisiloxanes (**17a–c**). In all cases, the AROP appeared to be significantly more regioselective than the cationic process.

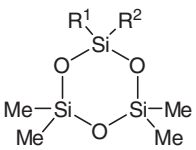

17

(**a**) $R^1 = R^2 = (CH_2)_2(CF_2)_5CF_3$; (**b**) $R^1 = Ph$, $R^2 = m\text{-}C_6H_4CF_3$; (**c**) $R^1 = Ph$, $R^2 = m\text{-}C_6H_4(CF_3)_2$.

- **Chain transfer**

Chain transfer in CROP of cyclosiloxanes was extensively studied and the following reactivity order was established: $D_3 > MM > MDM > MD_2M > D_4$.[15,153] Thus, the terminal siloxane bonds are more reactive than the bonds inside the chain and can significantly contribute in the chain transfer and growth, which has been recently confirmed by the NMR analysis of sequencing near the chain ends of methyl(phenyl) siloxane copolymer (**Scheme 2**).[150]

4.17.1.1.1(iv)(b) Activated monomer mechanism An alternative to the tertiary oxonium ion mechanism of the chain formation (**Scheme 3**) is the activated monomer mechanism assuming the addition of protonated monomer to the silanol end group and the simple condensation mechanism involving the acid-catalyzed silanol–silylester or silanol–silanol condensation without intermediacy of the tertiary oxonium ion. Statistical chain sequencing analysis in CROP of tetramethyl-2,2-diphenylcyclotrisiloxane led to the conclusion that the activated monomer mechanism is not very probable as it neither explains the observed sequence distribution nor the formation of cyclic products in a consistent way.[150,154] Nevertheless, its participation in the overall cationic process as the side reaction cannot be excluded.

4.17.1.1.1(iv)(c) Role of water and silanol Water has a crucial role in the acid-catalyzed polymerization of cyclosiloxanes. Small amounts of water strongly accelerate the initiation and propagation reactions and change the kinetic law of the reaction. Large amounts of water show an inhibiting effect on ROP.[110,111,138,143] An analogous effect is observed when silanol is added to the polymerization system.[111,155,156] Model studies proved the importance of hydrogen bond association in acid–base equilibria.[27] The inhibition effect of excess of water was explained in terms of formation of the strongly

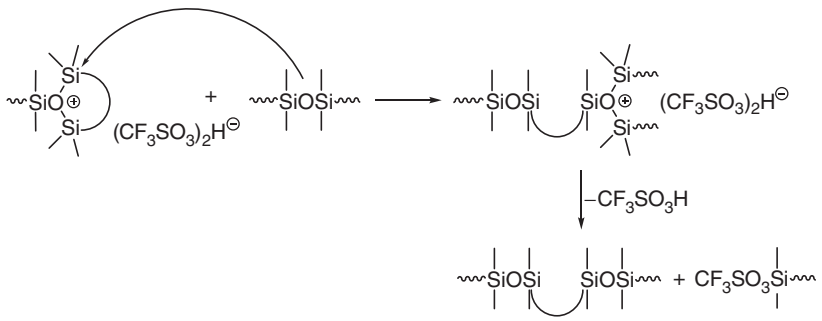

Scheme 2 Mechanism of chain transfer in cationic ROP of cyclosiloxanes.

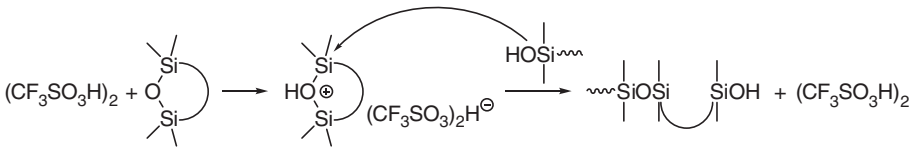

Scheme 3 Activated monomer mechanism in cationic ROP of cyclosiloxanes.

bound triflic acid hydrates that are either inactive or insoluble in the polymerization system.[139,145]

4.17.1.1.1(iv)(d) Application of the CROP of cyclosiloxanes In the industry, the cationic initiators are typically used for the equilibration of cyclosiloxanes in the presence of a chain stopper, which is used to control the MW and to introduce the desired functional groups to the chain ends.[20] Telechelic polysiloxanes prepared in this way are further applied to the synthesis of siloxane–siloxane and siloxane–organic block copolymers. The cationic process appears to be more efficient than the anionic one for the polymerization of cyclotrisiloxanes substituted with large alkyl groups.[157] Cationic polymerization is the method of choice when monomers contain functional groups that are sensitive to bases.[1,20] However, a serious drawback of the CROP of siloxanes is the formation of significant amounts of cyclic oligomers at early stage of the reaction and the extensive chain transfer that makes controlled synthesis of copolymers impossible.

4.17.1.1.1(v) New polymerization processes

Reactions of D_3 with 1,1,3,3-tetramethyldisiloxane, $^{H}MM^{H}$, 1,1,1,3,3-pentamethyldisiloxane, ^{H}MM, dimethyl(phenyl) silane, and methyl(phenyl)silane catalyzed by $B(C_6F_5)_3$ result in ring opening of D_3 by the SiH reactant, producing open-chain oligomers with hydrosilane functionality at one or both chain ends.[158] Unfortunately, the reaction is not selective. Consecutive and competitive processes lead to a series of various oligo homologs (**Scheme 4**).

4.17.1.1.2 Other methods of polymerization of cyclosiloxanes

4.17.1.1.2(i) Polymerization in solid state

Solid-state polymerization of cyclotrisiloxanes may be induced by both acid and basic initiators. Thus, D_3 polymerizes in the presence of gaseous HBr chemisorbed at the surface of the monomer crystal, giving polymer of an MW of 1.5×10^5 to 3×10^5 with up to 80% yield.[159] Anionic nonequilibrium polymerizations of cyclic siloxanes, initiated by KOH, crushed and mixed with the monomer, or by potassium silanolates, were reported to give high MW materials with high yields.[160,161] Poly (diphenylsiloxane) obtained in reaction of the crystalline monomer with KOH showed an MW of 4.4×10^4 and a very broad polydispersity, $M_w/M_n = 21.7$.[162] Polymers having much higher MWs ($M_n > 5 \times 10^5$) and polydisperities of about 2 were obtained when potassium oligomethyl(phenyl)silanolate was used as the initiator. Polymerization proceeds inward from the surface of the monomer crystals, producing a highly crystalline material. The highly ordered crystalline state of hydroxycyclosiloxanes provides a possibility of solid-state synthesis of stereoregular polysiloxanes.[163]

4.17.1.1.2(ii) Radiation polymerization

Radiation-induced polymerization of D_3, D_4, and D_5 was studied in both liquid and solid state.[164,165] Propagation occurs primarily via the cationic mechanism. In contrast to the polymerization initiated by acids, all the monomers show very similar reactivities. This was tentatively explained assuming that the mechanism involved the formation of highly reactive free silylium ions, which reacted in the same way with various monomers. The silylium ions are generated as a result of methide cleavage. The reaction proceeds at the surface. The polymer chains grow on the interface of the formed polymer and the D_3 crystal surface. The reaction requires the use of an extremely pure and dry monomer. The impurities capable of generating negative ions upon irradiation as well as crystal defects strongly decrease the reaction rate and MW of the polymer.

4.17.1.1.2(iii) Polymerization in emulsion

Polymerization of siloxanes in water emulsion attracts still growing interest and has recently been reviewed by Ganachaud and Boileau.[25] Hyde and Wehrly[166] were the first to demonstrate a possibility of ROP of cyclosiloxanes in water emulsion. High MW polymer may be obtained, either in the presence of anionic initiator and cationic emulsifier or using

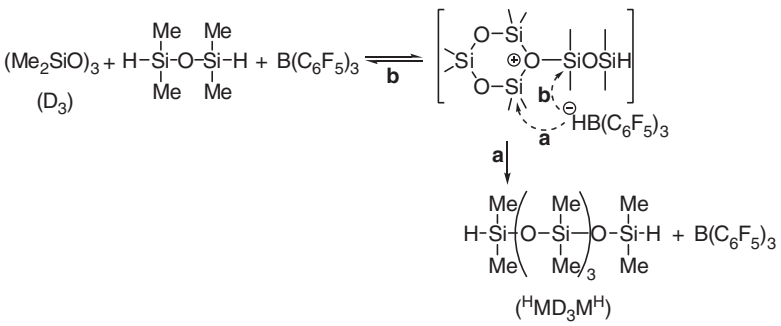

Scheme 4 Ring opening of D_3 by hydrosiloxane catalyzed by $B(C_6F_5)_3$.

the cationic initiator and anionic emulsifier.[167] The use of emulsifier capable of initiating the polymerization, such as dodecylbenzenesulfonic acid (DBSA) or benzyldodecyldimethylammonium hydroxide, permits an effective stabilization of the siloxane emulsion and ensures a high polymerization rate under mild conditions (25–80 °C). The diameter of the particles obtained by cationic polymerization is 0.05–0.5 μm and the MW is higher than 2×10^5. The polymer contains about 15% of cyclic oligomers, D_4–D_{10}.[168] The anionic emulsion ROP of D_4 gave the polymer of somewhat lower MW, $M_n = 50\,000$, with the particle size of 0.2–2 μm.[169]

The proposed mechanisms of the polymerization are complex. The yield and characteristics of resulting polymers are controlled both by chemical reactivity and by physicochemical phenomena, such as diffusion of monomer, phase equilibria, and the nature of the interface. Since these factors depend on the composition of the reaction mixture, the mechanism may change with the extent of the reaction. Polymerization proceeds by combination of the addition and condensation mechanism involving redistribution reactions.[169,170] The first stage of the anionic polymerization process occurs at the siloxane–water interface or in the siloxane phase close to the surface. Once the chains reach a critical degree of polymerization corresponding to their loss of surface tension activity, they penetrate into the particles where side reactions such as redistribution and condensation hardly occur.[170] Thus, the rate is strongly dependent on the size of the surface, which is the function of the concentration of emulsifier. Polycondensation is responsible for a rapid increase in MW, observed at high monomer conversions.

The condensation mechanism of the chain growth seems to be still more important in the cationic emulsion ROP of cyclosiloxanes. Although this process is very efficient for the synthesis of linear polymethylhydrogensiloxanes (PMHS) from D_4^H, these conditions do not seem suitable for the polymerization of D_4.[171–173]

An anionic miniemulsion process was also used for polymerization of cyclosiloxanes with substituents other than methyl. Polymerization of 2,4,6-trimethyl-2,4,6-tris(3,3,3-trifluoropropyl)cyclotrisiloxane (F_3) produced well-defined α,ω-dihydroxy-terminated polymer in very high yields and with molar masses ranging from 2500 to 3500.[174] A kinetic study showed that polymerization occurs in two stages. During the first stage, which corresponds to the anionic nonequilibrium ROP of F_3, the maximum yield is close to 100% and the polydispersity remains around 1.3. The second stage involves condensation and backbiting reactions. MW of the polymer increases up to 30 000–60 000 and polydispersity approaches 2.0.[174] Polymerization of methyl(phenyl)cyclosiloxanes, P_3 and P_4, was also reported. The narrow MW of the obtained α,ω-dihydroxypoly(methylphenylsiloxane)s and a dramatic reduction of backbiting reactions were observed.[175] Copolymerization of D_4 with tetramethyltetravinylcyclotetrasiloxane (V_4) gave a random copolymer with MW up to 50 000. On the other hand, polymerization of V_4 in the presence of linear PDMS led to multiblock copolymers.[176]

4.17.1.1.3 Siloxane functional polymers and copolymers

This section is dedicated to all-siloxane copolymers. Siloxane-organic copolymers constitute a separate, very broad class of macromolecular structures, and the reader is referred to more specialized reviews.[22,23,177–180]

The copolymers often have properties that are superior to those of homopolymers.[17,181] Thus, for example, introduction of methylphenyl- or diphenylsiloxane units to PDMS significantly improves thermal stability of the polymer as well as the resistance to oxidation and radiation. Fluorosilicones containing fluoroalkyl groups are a very important class of polysiloxanes. Extremely low surface tensions; very good resistance to fuels, oils, and hydrocarbon solvents; and good performance at low temperatures down to −70 °C make them unrivalled materials for numerous applications.[182] Therefore, a considerable effort has, in recent years, been concentrated on the synthesis of new fluoroorganylsiloxane monomers and polymers by ROP.[151,183–186] Cyanoalkyl groups in the siloxane chain increase the chemical and solvent resistance and reduce swelling.[187] Due to the ability to bind metals, cyanoalkylpolysiloxanes are explored as possible carriers for magnetic fluids, catalysts, and electrolytes.[188–190] Diethylsiloxane with methylphenyl- or diphenylsiloxane copolymers do not crystallize, which results in lowering of glass transition temperature T_g of the copolymers down to −137 °C giving them excellent low-temperature properties.[191] The character of side groups has a distinct impact on the conformation and behavior of the polymer in solution.[192] Hydrophilic groups give the siloxane copolymers excellent surfactant properties.[193–195]

ROP of functional cyclosiloxanes is a convenient route to all-siloxane copolymers.[16,17,19,181] This may be realized in several ways. Sequential ring-opening copolymerization involves polymerization of one cyclosiloxane monomer to the desired chain length, then the second monomer is introduced, which adds to the growing chains. Diblock and triblock copolymers in the case of bifunctional initiator are produced provided the process is kinetically controlled. Otherwise, a copolymer with random or partly ordered sequencing is obtained. The kinetic control of the copolymerization process imposes the use of cyclotrisiloxanes as monomers. Thus, sequential copolymerization of two or more cyclotrisiloxanes is a good method for the precise synthesis of all-siloxane block copolymers.[12,22,196]

Simple ROP of a cyclosiloxane containing different substituents at silicon atoms is a special case, where homopolymerization of a single monomer results in the copolymer with different siloxane units uniformly distributed along the chain.[76,77,90,107,150,197,198] Again, the use of cyclotetrasiloxanes results in some degree of randomness of the formed copolymers. Using cyclotrisiloxane in which silicon atoms have diverse reactivity due to different substitution, it is possible to prepare polymers of highly regular structure.[76,77,90,108] The applicability of anionic and cationic processes for the synthesis of siloxane copolymers of regular distribution of functional groups has been extensively studied.[51,52,89,107,150,151] In general, the anionic process leads to copolymers of more regular microstructure.

Simultaneous polymerization of a mixture of cyclosiloxanes gives polymers whose microstructure is not easily predictable. Typically, the kinetics of ring-opening copolymerization is analyzed in terms of the Mayo–Lewis copolymerization equations (Scheme 5).[16,181] The aim of such analysis is to determine the Mayo–Lewis reactivity ratios $r_D = k_{DD}/k_{DX}$ and $r_X = k_{XX}/k_{XD}$, which define the composition of a copolymer.[199] The task is relatively easy when the propagation reactions are irreversible.

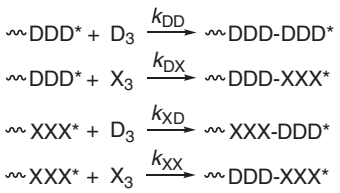

Scheme 5 Copolymerization equations for cyclotrisiloxanes according to terminal model.

It becomes very difficult when monomer addition is reversible. Thus, the applicability of this model is also limited to the copolymerization of cyclotrisiloxanes where, in the kinetically controlled stage, the polymerization may be assumed irreversible.

Even in the case of cyclotrisiloxanes, the analysis of the copolymerization system according to Scheme 5 is oversimplified. The important difficulty in analyzing ionic copolymerization systems is the effect of strong intermolecular interactions, including solvation and association phenomena. As a consequence of these processes, the reaction rate constants may change with variations in the medium and in the concentrations of participating species. If these changes are large, the reactivity ratios lose their physical sense.

Controlled AROP of cyclotrisiloxanes is particularly important, as it allows well-defined silicone structures to be obtained. Controlled synthesis of methyl(vinyl)siloxane-dimethylsiloxane gradient, block and alternate copolymers by AROP of cyclotrisiloxanes has been reported.[108] If cyclotrisiloxane monomer reactivities are different but not too different, simultaneous copolymerization of their mixture gives gradient copolysiloxanes, whose composition continuously changes along the chain. Some copolymerization systems leading to gradient copolymeric siloxanes have recently been studied.[186,200–202]

Equilibrium copolymerization of unstrained cyclosiloxanes leads to random copolymers.[203,204] Thus, for example, equilibrium copolymerization of diethylcyclotetrasiloxane with cyclotetrasiloxanes having various R^1R^2SiO units ($R^1 = R^2$ = methyl or phenyl, or R^1 = methyl, and R^2 = phenyl) gave copolymer of units randomly distributed along the chain.[205] The regioselectivity of the ROP of unsymmetrically substituted cyclotetrasiloxanes such as 2,2,4,4,6,6-hexamethyl-8,8-divinylcyclotetrasiloxane[51] and 2,2,4,4,6,6-hexamethyl-8,8-diphenylcyclotetrasiloxane[52] was studied using P_4-*t*-Bu phosphazene superbase **11** and triflic acid as the initiators. For both monomers, the polymer microstructures indicate that superbase-initiated AROP leads to copolymers with a random microstructure, whereas triflic acid-initiated ROP occurs in a regioselective manner. The preferred directions of ring-opening are shown in Scheme 6, which is explained by the inductive electron-withdrawing effect of a phenyl group that makes the oxygen between a dimethylsilyl and a diphenylsilyl groups less basic than an oxygen between two dimethylsilyl groups. This more stable silyloxonium ion can open in two ways by nucleophilic attack on the dimethylsilyl centers of the oxonium ion by one of the more basic oxygens of another monomer molecule.

The explanation of a lack of regioselectivity in AROP of cyclosiloxanes is more complex as the way of addition of a monomer to a growing chain depends on the electronic character of different substituents at silicon atoms, on the relative

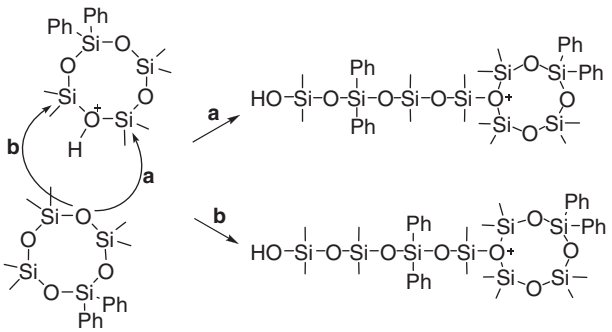

Scheme 6 Regioselectivity of cationic ring opening of 2,2,4,4,6,6-hexamethyl-8,8-diphenylcyclotetrasiloxane.

reactivity of different silanolate centers, and on the interaction of a counterion with monomer.[107]

4.17.1.1.4 New macromolecular architectures by ROP of cyclosiloxanes

4.17.1.1.4(i) Hyperbranched, star-shaped, and dendritic polysiloxanes

Functionalized polysiloxanes of star, comb, and dendritic topologies were described in a series of papers by Chojnowski *et al.*[200,206,207] The branched macromolecules were generated by coupling of the reactive blocks, made via anionic polymerization of vinylcyclotrisiloxanes and their copolymerization with D_3, using a grafting technique. Gradient copolymers were also used to obtain a variable density of branches. First and second-generation dendritic polysiloxanes were obtained using star polysiloxanes functionalized with SiCl groups, as the core.[200] The same methodology was used for the synthesis of 3-chloropropyl-functionalized dendrigraft polysiloxanes and dendritic polyelectrolytes (Scheme 7).[207] The 3-chloropropyl groups on the dendrigraft were further used for the quaternization of dimethyloctylamine, 2-hydroxyethyldimethylamine, and triethylamine producing quaternary ammonium salt groups. Dendrigrafts having an ionic corona and relatively hydrophobic core were synthesized. Preliminary investigations of the behavior of these polymers in aqueous media indicated their strong tendency toward aggregation and the ability to drive solubilization of organic compounds.

Vinyl- and 3-chloropropyl-functionalized branched polysiloxanes of various structures obtained by this method were also grafted on functionalized silica. Silica modified with vinylsiloxane groups was used for the immobilization of transition metal catalysts.[208] 3-Chloropropyl groups on the graft polymer were used to quaternize *N*,*N*-dimethyloctan-1-amine. Silica particles with grafted polysiloxane having quaternary ammonium salt groups pendant to polymer chains were shown to have strong bactericidal properties.[209]

The terminal Si–H bonds have been modified by Pt-catalyzed hydrosilylation with 1,2-epoxy-4-vinylcyclohexane to yield a tetrabranched star PDMSs with terminal epoxy groups (Scheme 8).[210]

An interesting example of a regioselective cationic ring-opening of a cyclotrisiloxane in the presence of a cyclotetrasiloxane has been presented (Scheme 9). The obtained linear siloxane copolymers contain randomly distributed

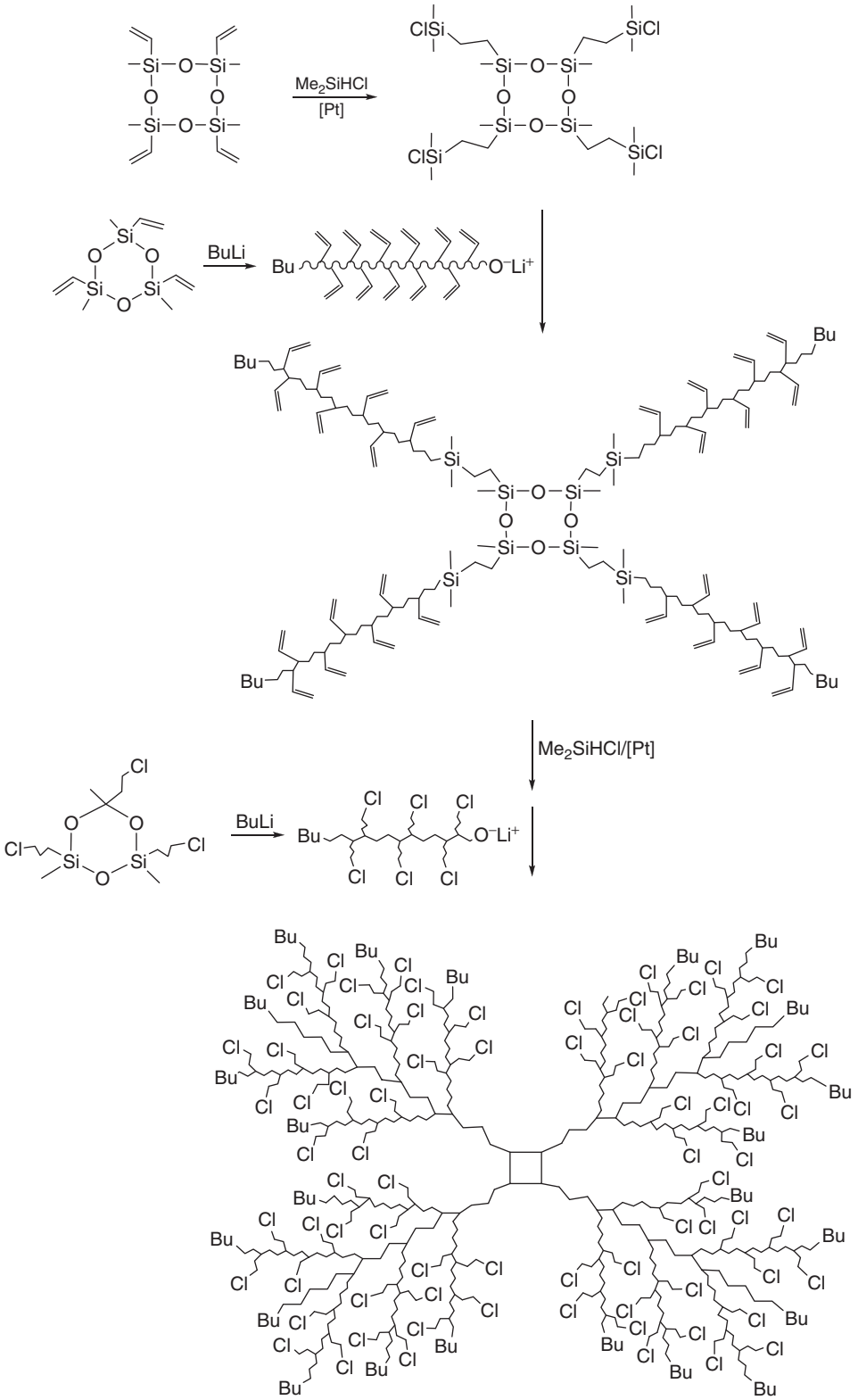

Scheme 7 Synthesis of dendritic polysiloxanes using a grafting technique.

cyclotetrasiloxane pendant groups that may be polymerized at a later stage to give cross-linked materials.[211]

AROP of cyclotrisiloxanes was employed in the synthesis of a series of well-defined A_2B_2, A_2BC, and A_2B_2C miktoarm star polymers, where A is PDMS, B is polystyrene (PS), and C is polyisoprene (PI), by linking functionalized PDMS with living centers of PS or PI copolymers (Scheme 10).[212]

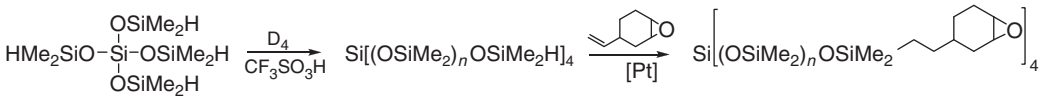

Scheme 8 Synthesis of tetrabranched star polysiloxane.

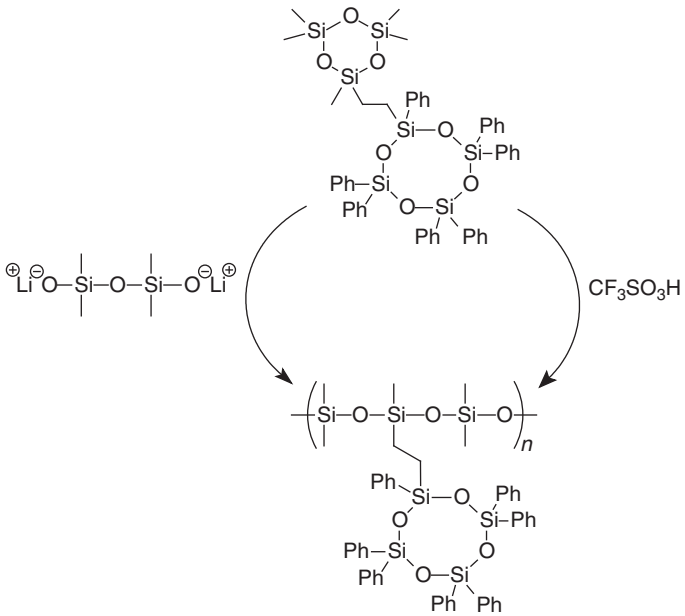

Scheme 9 Synthesis of polysiloxane with cyclosiloxane pendant groups.

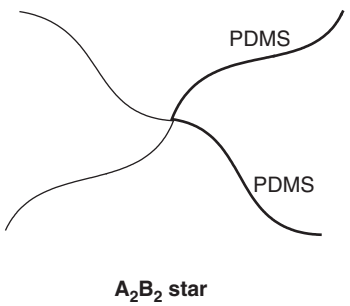

A_2B_2 star

Scheme 10 Miktoarm star copolymers of polydimethysiloxane (A) with polystyrene or polyisoprene (B).

The cross-linkable poly[(3-cyanopropyl)methylsiloxane] was synthesized by ROP of cyclotetra[(3-cyanopropyl) methylsiloxane] using H_2SO_4–SO_3 in the presence of 1,3-di (3-cyanopropyl)tetramethyldisiloxane as a chain stopper. The polysiloxane was then cross-linked by UV irradiation. The pendant cyano groups in the network enhance the solubility of lithium salt and accelerate the migration of lithium ions making this material a useful solid polymer electrolyte.[188,213]

Linear, graft, hyperbranched, and star copolymeric siloxanes obtained via anionic ring-opening copolymerization of functional cyclotrisiloxanes were used as supports for transition metal catalysts.[214,215]

4.17.1.1.4(ii) Silsesquioxanes

Silsesquioxanes represent a wide class of more or less ordered three-dimensional structures of the empirical formula $RSiO_{3/2}$; by their O/Si proportion taking the intermediate position between siloxanes (O/Si = 1) and silica (O/Si = 2). Example of this class (commonly denoted as T_8) is shown as structure **4**.

They are usually generated by hydrolytic condensation of trialkoxy- or trichlorosilanes. Although the regular structures seem to be highly entropically unfavorable, they may be prepared with a reasonable yield by quasi-equilibration, taking advantage of their low solubility in certain solvent systems. However, thermodynamics of this process in acid media must be more complex, since large amounts of cage-like products were identified in solution before they start to crystallize.[216]

There is a lot of literature on their preparation, properties, and applications, including a number of comprehensive reviews.[216–223] Silsesquioxanes are often used as models of silica surfaces, silica-supported catalysts, and so on. Heterosilsesquioxanes, in which one or more silicon atom is replaced by metal (aluminium, titanium, vanadium, etc.) attract much attention as the potential catalysts. Functional poly- and oligosilsesquioxanes are applied as resin additives and cross-linkers improving the properties of coatings. There is also a great number of silsesquioxane–organic copolymers of various architecture. Silsesquioxanes due to their multifunctionality are often used as the core for dendrimer copolymers.[216,224]

Examples of the ROP of silsesquioxanes are sparse as they lead to irregular highly branched or cross-linked structures. The anionic ring-opening copolymerization of D_4 and octaphenylcyclotetrasiloxane, $(Ph_2SiO)_4$, with polyhedral oligomeric silsesquioxanes (POSS) dodecaphenyl-POSS $(PhSiO_{1.5})_{12}$ (eqn [32])[225] and D_4 with octaisobutyl-POSS $(i\text{-}BuSiO_{1.5})_8$ (eqn [33])[226] under the base catalysts was explored.

Copolymerization leads to cross-linked polysiloxanes. The DSC and TG results indicate that the cross-linked polysiloxanes exhibit distinct glass transition temperatures (T_g) and excellent thermal stability.

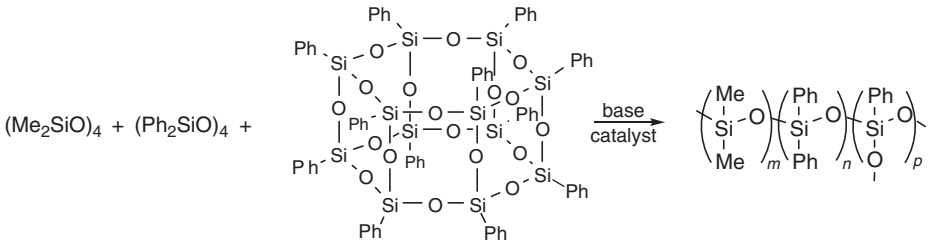

[32]

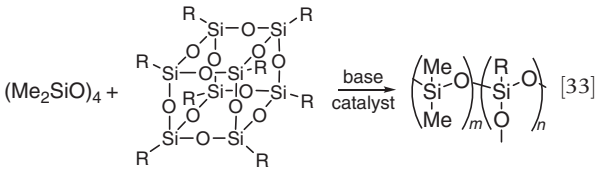

[33]

4.17.1.2 Cyclooxysilylenes (Cyclosilaethers)

While siloxanes are silicon analogs of acetals, oxysilylenes are analogs of ethers. An example of this class of compounds is shown as structure 7. Having a structure of alternating disiloxane–oligosilylene copolymers, they may be considered as a combination of two most important classes of organosilicon polymers, polysiloxanes and polysilanes. Consequently, they are expected to combine some of the corresponding chemical and physical properties of these homopolymers. Close analogies in the kinetics of the generation of siloxane-oligosilylene copolymers and polysiloxanes by ROP suggests a close similarity between the mechanisms involved in these processes. However, poly(oxysilylene)s show some inherent properties that strongly distinguish them from both polysiloxanes and polysilanes.[227]

The common method for synthesis of these monomers is hydrolytic intramolecular condensation of the corresponding α,ω-dichloro-oligo(dimethylsilanediyl)s.[228–230]

4.17.1.2.1 Ring-opening polymerization of cyclic silaethers

Cyclic silaethers can be polymerized via cationic and anionic routes. However, while the cationic polymerization involves exclusively the cleavage and reformation of the siloxane bond, the anionic centers may also open the Si–Si bond, which leads to the polymer of an irregular structure and finally, at equilibrium, a mixture of polysiloxanes and polysilanes is obtained.[231]

Cationic polymerization of cyclic silaethers is initiated by strong protic acids, such as CF_3SO_3H.[232,233] The polymerization leads to both linear polymers and cyclic and macrocyclic silaether oligomeric homologs. All these mechanistic features of the CROP of $^2D_2$ (7) show close similarity to the ROP of D_4 and may be best understood on the basis of a mechanism involving formation of cyclic tertiary oxonium ion propagation centers (see eqns [30] and [31]). These ions of various ring size undergo fast interconversion by a ring expansion-contraction mechanism.[227]

Anionic polymerization of cyclic silaethers is a more complex process than the CROP of these monomers.[231] The ability of anionic propagation centers to cleave both the Si–O and Si–Si bonds[234,235] has two important consequences. First, polymer chain microstructure becomes irregular as the oligosilylene sequences of different lengths are formed. Second, two types of active propagation centers appear in the polymerization system: silanolates and silyl anions, which exhibit different reactivities. The silanolate anion is a hard nucleophilic center, while silyl anion is a soft nucleophile capable of initiating the olefin polymerization. A silaether monomer could serve as a pump changing alkoxide centers into the carbanion centers.[235] Finally, the rearrangement of a polysilaether, in which both types of skeletal bonds in the polymer chain take part, Si–O and Si–Si, leads to a mixture of PDMS and poly(dimethylsilanediyl) exclusively (eqn [34]). This indicates that polysilaether is thermodynamically unstable, which has been confirmed by quantum chemical calculations.[236]

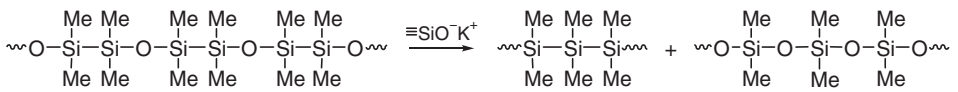

[34]

4.17.1.2.2 Cyclic carbosiloxanes

Poly(carbosiloxane)s having carbosilane and silyloxy linkages in the backbone are attractive materials since they combine useful properties of polysiloxanes and poly(carbosilane)s. A convenient route to poly(carbosiloxane)s is an AROP of 1-oxa-2,5-disilacyclopentanes (see structure 5).

1-Oxa-2,5-disilacyclopentanes with methyl and phenyl substituents at silicon were prepared by Piccoli *et al.*[237] by hydrolytic condensation of 1,4-dichloro-1,4-disilabutanes $ClSiR^1R^2CH_2CH_2R^1R^2SiCl$, where R^1,R^2 = Me or Ph, followed by base-catalyzed thermal decomposition of the hydrolysates. High reactivity of 1-oxa-2,5-disilacyclopentanes (5) has two reasons. First, the five-membered ring is strained. The ring strain for this series of monomers was estimated to range from 33 to 50 kJ mol^{-1}. Second, 5 is also much more nucleophilic than regular siloxanes. High nucleophilicity of 5 results from the unusually narrow SiOSi angle and from the lack of negative

hyperconjugation $[p(O)\rightarrow\sigma^*(Si\text{-}O)]_\pi$, which is largely responsible for the reduced basicity and nucleophilicity of siloxanes.[236]

Anionic polymerization of 2,2,5,5-tetramethyl-1-oxa-2,5-disilacyclopentane and mixed methyl(phenyl) analogs initiated by lithium butyldiphenylsilanolate was studied in the presence of THF as the promoter. The effects of variable concentrations of THF, initiator, and water on polymerization rate and on polydispersity of the polymer were investigated.[71,238] The polymerization process shows similar features to the D_3/lithium silanolate/water system. The kinetics of this process has been studied in detail using sodium dimethyl(phenyl)silanolate as initiator in heptanes and heptane/dioxane media.[44] The evidence of aggregation of active centers and solvation of propagating centers by the monomer in the absence of stronger solvating agent, dioxane, was observed.

Examples of AROP of various substituted 1-oxa-2,5-disilacyclopentanes have been recently reported. These compounds having one to three (trimethylsilyl)oxy groups at Si undergo AROP in the presence of dilithium diphenylsilanediolate. Chain transfer to (trimethylsilyl)oxy group apparently limits the MW of the polymers (**Scheme 11**).[239] Narrowly dispersed poly(carbosiloxane)s with controlled MW and identified end groups can be obtained by ROP of cyclic carbosiloxanes using strongly basic *N*-heterocyclic carbenes and guanidine derivative (1,5,7-triazabicyclo[4.4.0]dec-5-ene) catalysts in the presence of alcohols or other hydrogen bond donors. The pK_b of the catalyst is important in preventing adverse transetherification reactions and obtaining well-defined polymers.[58]

While optically active all-siloxane polymers may be obtained by the AROP only[240] (if the monomer bears a chiral center), the controlled AROP of a cyclocarbosiloxane with a chiral center in the ring skeleton may lead to an optically active polymer. An example of highly stereospecific polymerization of an optically active enantiomer of 1-oxy-2,5-disilacyclopentane (Np = 1-naphthyl) is shown in eqn [35].[241,242]

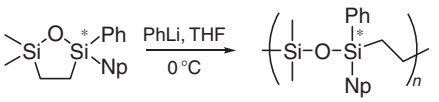

[35]

ROP of 2,2,5,5-tetramethyl-1-oxa-2,5-disilacyclopentane is also catalyzed by a ruthenium cluster in the presence of hydrosilane (eqns [36] and [37]). The preinitiation step involves activation of hydrosilane by a ruthenium complex followed by a nucleophilic attack of the monomer on the so-activated silane. Polymerization proceeds according to the cationic or coordination mechanism.[243] The obtained polymers have MWs in the range 6300–780 000 and very broad polydispersities 1.5–3.

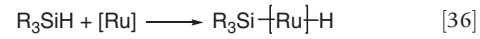

[36]

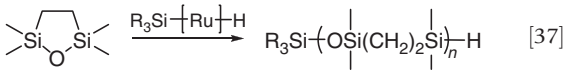

[37]

Polymerization of 1,1,3,3,5,5,7,7-octamethyl-2,6-dioxa-1,3,5,7--tetrasilacyclooctane catalyzed by triflic acid gave an alternating copolymer of dimethylsiloxane and (dimethylsilanediyl)methylene units. Interestingly, the attempts to polymerize this monomer by using anionic catalysts, such as BuLi and KOH, were unsuccessful.[244]

4.17.2 Ring-Opening Polymerization of Cyclic Organosilicon Monomers Not Involving Si–O Bond Cleavage

4.17.2.1 Cyclosilanes

Cyclopolysilanes have been known since the fundamental work of Kipping in 1921, who synthesized the four-, five- and six-membered perphenylcyclosilanes from dichlorodiphenylsilane and sodium. Organic cyclopolysilanes are usually made by the dehalogenative coupling of dialkyl- or diaryldichlorosilanes with alkali metals. The cyclopolysilane yield and the preferred ring size obtained depend strongly on the alkali metal, solvent, and reaction conditions.[245–249] The preferred ring size in the equilibrium mixture obtained from dichlorodiorganylsilanes and alkali metals is additionally governed by the bulkiness of the organic substituents attached to silicon. For small substituents like methyl, the six-membered ring is favored, while five- and four-membered rings are preferentially obtained with larger substituents like phenyl or isopropyl. Even larger substituents like mesityl or *tert*-butyl lead to the formation of three-membered rings.

The electrochemical formation of Si–Si bonds by cathodic reduction of dichlorosilanes provides an alternative access to cyclopolysilanes.[250] Catalytic dehydrogenation coupling of organylhydrosilanes, a common method for the formation of linear polysilanes, can also be applied to cyclopolysilane synthesis. However, long reaction times are required and only moderate yields are obtained.[251]

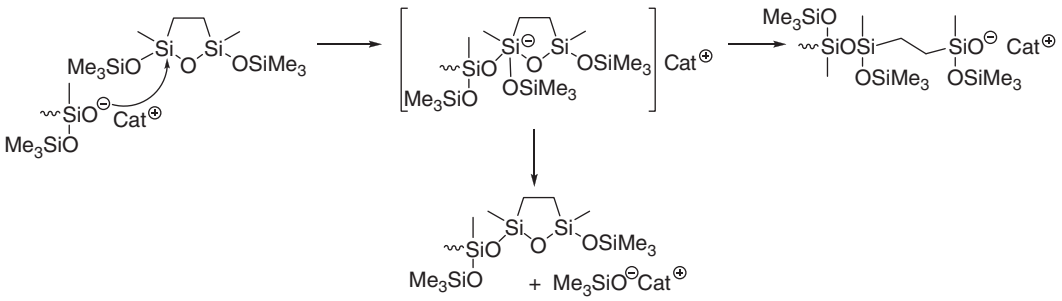

Scheme 11 Anionic polymerization of 2,5-dimethyl-2,5-bis(trimethylsilyloxy)-1-oxa-2,5-disilacyclopentane.

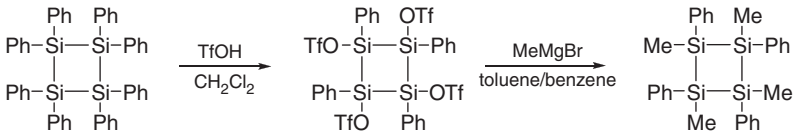

Scheme 12 Synthesis of 1,2,3,4-tetramethyl-1,2,3,4-tetraphenylcyclotetrasilane.

4.17.2.1.1 Ring-opening polymerization of cyclosilanes

Strained cyclosilanes are expected to undergo ROP. ROP, first explored by Matyjaszewski, is an alternative procedure to Wurtz coupling for the synthesis of high MW polysilanes.[252,253] AROP of 1,2,3,4-tetramethyl-1,2,3,4-tetraphenylcyclotetrasilane is effectively initiated by butyllithium or silylpotassium initiators (eqn [38]). Strained and polymerizable cyclotetrasilanes $Si_4Me_nPh_{8-n}$ ($n = 3,4,5,6$) were prepared by partial dearylation of octaphenylcyclotetrasilane with triflic acid and subsequent displacement of triflate groups with MeMgBr (**Scheme 12**). Three of the four possible stereoisomers are obtained in a ratio of **18a**:**18b**:**18c** = 45:15:40, whereas the all-*cis*-isomer **18d** has not been observed (methyl groups in structures **18a, 18b, 18c, 18d** are omitted for clarity).

The *trans*-isomer **18a** can be isolated with 95% purity by recrystallization.[254] The stereochemical control leading to the formation of syndiotactic, heterotactic, or isotactic polymers is poor in all cases. In order to improve the stereoselectivity of the polymerization reaction, less active initiators like silylcuprates are very effective.[255,256]

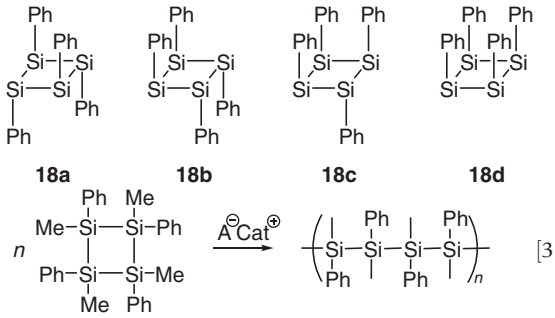

[38]

ROP of the all-*trans* isomer of 1,2,3,4-tetramethyl-1,2,3,4-tetraphenylcyclotetrasilane (**18a**) using silylcuprate $(PhMe_2Si)_2Cu(CN)Li_2$ gives nearly quantitative conversion to polymer with 75% heterotactic and 25% isotactic triads as determined by ^{29}Si NMR spectroscopy. Polymerization of a mixture of the stereoisomers of **18** leads to a polymer with 58% heterotactic, 15% syndiotactic, and 27% isotactic triads. The polymerization initiated with silylcuprates is postulated to occur with inversion of configuration at both the attacked silicon atom and the newly formed active center.

ROP of **18** was also examined using various transition metal catalysts.[257] Some Pd and Pt catalysts led to the formation of large amounts of ring-expanded isomers, $(MePhSi)_8$. The yields of the polymer were in each case very low. The ring expansion most likely proceeds according to a metathesis-type mechanism.[258]

Diblock PS–polysilane copolymers were prepared using living PS to initiate the ROP of 1,2,3,4-tetramethyl-1,2,3,4-tetraphenylcyclotetrasilane (eqn [39]) in the presence of 12-crown-4 to enhance the reactivity of polystyryllithium in the ROP of the cyclotetrasilane. Morphology of the copolymers was studied using TEM and SEM techniques showing a phase separation with the relatively large domain sizes of both the cylinders and the globular micelles, which can be explained by stretching the polymer blocks in the core and in the shell.[259]

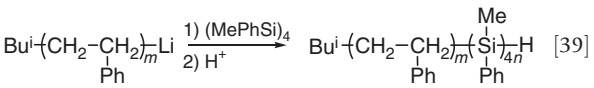

[39]

Poly(methylphenylsilane)–poly(ferrocenyldimethylsilane) block copolymers of various monomer compositions were prepared via thermal ROP of a mixture of cyclotetrasilane $(MePhSi)_4$ (**18**) and the silicon-bridged ferrocene $Fe(\eta\text{-}C_5H_4)_2SiMe_2$ (**19**). Attempts to initiate anionic copolymerization of **18** and **19** were unsuccessful and led exclusively to a mixture of homopolymers (eqn [40]).[260,261]

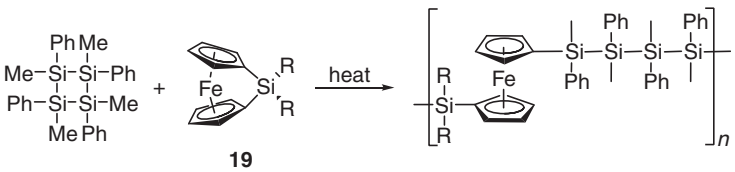

[40]

The AROP of nonamethyl(phenyl)cyclopentasilane was achieved using tetrabutylammonium fluoride and silyl potassium as initiators (eqn [41]).[262] The strong affinity of fluoride anion to silicon promoted the generation of silyl anion in the initiation without any additives. The potassium initiator required the use of HMPA or 18-crown-6 promoters, which solvate the potassium cation and enhance the reactivity of the silyl anion. The polymerization was performed in THF or DME at –78 to –20 °C. The temperature control was exceptionally important for the successful polymerization. The lower the temperature, the higher the polymer yield reaching 80% at –78 °C. At room temperature, no polymer is formed, but mainly

five- and six-membered cyclosilanes. The polymer obtained at low temperatures, if not quenched, also depolymerizes upon warming by backbiting reaction. This observation indicates that the polymer is a kinetic product and cyclic oligosilanes are thermodynamically more stable.[262]

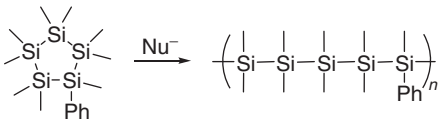

[41]

AROP was also used for the synthesis of a silole-incorporated polysilane (and poly(germasilane)) as shown in eqn [42]. The polymerization was initiated by BuLi at −40 °C. Under these conditions, the polymer with narrow MW distribution ($M_n = 17\,000$, $M_w/M_n = 1.3$) is formed in ~40% yield. The structure of the polymer was highly ordered, as evidenced by NMR spectroscopy.[263]

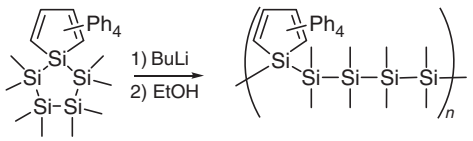

[42]

4.17.2.2 Cyclocarbosilanes

Polycarbosilanes, a class of polymers containing silicon–carbon bonds in the backbone, have many attractive features, and their applications as advanced materials have been widely explored.[264] The major reason for the growing interest in polycarbosilanes has been their potential as precursors to silicon carbide, used mainly as a source of ceramic fibers.

4.17.2.2.1 Ring-opening polymerization of silacyclobutanes

ROP of cyclic carbosilanes is one of the most promising methods for the synthesis of well-defined polycarbosilanes. Four-membered ring compounds, silacyclobutanes and 1,3-disilacyclobutanes, are highly strained (the ring strain of the methyl-substituted cyclics was estimated to 92 and 80 kJ mol^{-1}, respectively), which makes them suitable monomers for ROP.[265] Indeed, polymerization as well as copolymerization of these monomers have been widely investigated in last decades.[264,266–269]

ROP of 1,3-silacyclobutanes may be initiated thermally or catalytically. Most effective transition metal catalysts are hexachloroplatinic acid, H_2PtCl_6, platinum metal, and platinum and rhodium complexes (eqn [43]). Polymerization of silacyclobutanes is accompanied by dimerization, which is the dominant process in the presence of phosphine–platinum complexes.[270]

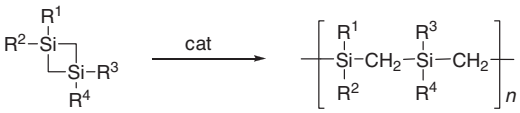

R^1, R^2, R^3, R^4 = Me, Et, Pr, Bu, *n*-C_5H_{11}, *n*-C_6H_{13}, Cl. OEt, Ph
cat = H_2PtCl_6, $Pt(acac)_2$, $Pt(1,5\text{-cod})_2$, $Rh(1,5\text{-cod})_2$, $Rh_2(1,5\text{-cod})_2Cl_2$
(cod = cyclooctadiene)

[43]

1,1,2,2-Tetramethyl-1,2-disilacyclobutane undergoes spontaneous ROP and copolymerization with styrene at room temperature giving linear polymers.[271] A series of poly[(silanediyl)oligomethylene]s with different substituents at the silicon atom, as well as the new poly[(dimethylsilanediyl)oligomethylene]s, were synthesized by the ROP of the corresponding sila- and disilacyclobutanes. For the first time, copolymerization of dimethylsila- and tetramethyldisilacyclobutanes was carried out affording permethylsilalkylene elastomers (25–100 °C, polymer yields 95–100%) (eqns [44] and [45]).[272]

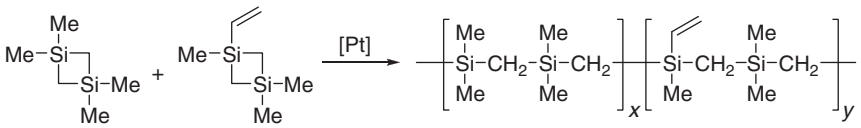

[44]

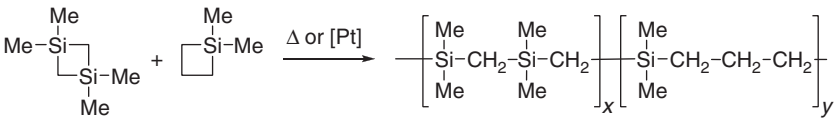

[45]

Copper compounds were found to be effective catalysts of polymerization of 1,3-dimethyl-1,3-diphenyl-1,3-disilacyclobutane and 1,1,3,3-tetraphenyl-1,3-disilacyclobutane. The cationic rhodium(I) complexes $[Rh(1,5\text{-cod})_2]^+A^-$ (A = OTf, PF_6) have been shown to exhibit high catalytic activity for the transition metal-mediated ROP of 1,1,3,3-tetramethyl-1,3-disilacyclobutane.[273]

1,1,3,3-Tetramethyl-1,3-disilacyclobutane undergoes copolymerization with silicon-bridged ferrocene catalyzed by platinum complex (eqn [46]).[274] Block copolymers of silacyclobutane with **19** (where R = Me) can also be obtained on the anionic route.[275]

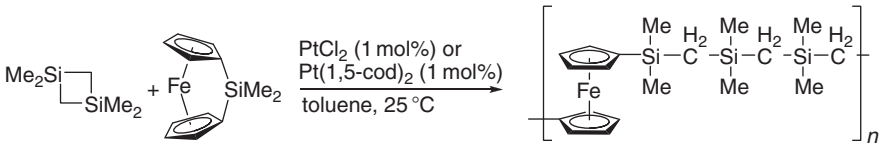

[46]

(cod = cyclooctadiene)

Strong nucleophiles such as organolithium compounds also initiate the ROP of silacyclobutanes, according to the anionic mechanism.[276] The polymerization yields high MW poly(silanediylmethylene)s with a strictly alternating SiR_2/CH_2 backbone structure.[276–281] Polymerizations initiated by butyllithium and silyllithium may proceed in a living manner, depending on the substituents in the ring and on the initiator system. MWs of the polymers were approximately controlled by the monomer-to-initiator ratio (**Scheme 13**).[272,282] On the other hand, polymerization of 1-methyl-1-phenyl-1-silacyclobutane in THF at −78 °C did not show a living nature.[280]

Polymerization of optically pure 1-methyl-1-(1-naphthyl) benzosilacyclobut-2-ene by these initiators gives optically active poly{[methyl(1-naphthyl)silanediyl](1,2-phenylene) methylene} with rather low stereoselectivity (**Scheme 14**, where Np = 1-naphthyl). Although the regioselectivity of the ring-opening of the monomer is high, the stereoselectivity of the ring opening in propagation step is low.[283]

Nucleophilic attack of carbanions on silicon in silacyclobutane rings results in breaking of the ring Si–C bond and the carbanionic center is recovered. Disilacyclobutane **20** was polymerized by alkyllithium as initiator in THF at −78 °C in the presence of HMPA acting as an activator (eqn [47]).[276]

Silacyclobutanes play an important role in the formation of block copolymers. For example, the relatively low-nucleophilic anion of poly(ethylene oxide) cannot initiate the polymerization of vinyl monomers, which require more nucleophilic carboanionic initiators. Silacyclobutane may serve as the nucleophile-transfer agent, which transforms a weaker nucleophilic center into a more nucleophilic one ('anionic pump', **Scheme 15**). This makes possible the copolymerization of heterocyclics with vinyl monomers.[284]

4.17.2.3 Cyclosilazanes

In contrast to polysiloxanes, polysilazanes, that is, polymers that contain –Si–N– repeating units in the backbone, have received much less attention. This is mainly a result of the high reactivity of the Si–N bond (with water, protic acids, and oxygen). Moreover, ROPs of cyclosilazanes usually lead to oligomers or low MW polysilazanes only. Nevertheless, over the past decades, poly(organylsilazane)s have gained increasing attention as precursors to SiN and SiCN ceramics through high-temperature pyrolysis.[266,285,286] Therefore, a search for optimal conditions of the ROP of cyclic silazanes and their copolymerization with siloxanes and organic monomers continues.

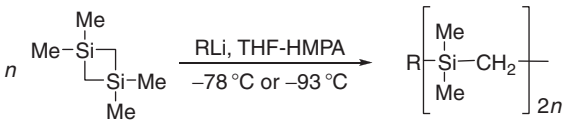

20 R = Bu, Ph, Me_3SiCH_2

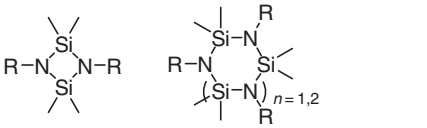

21 **22** (*a* *n* = 1, *b* *n* = 2)

[47]

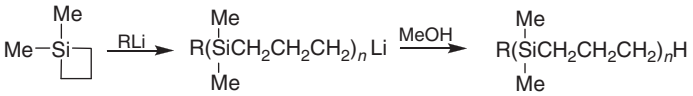

Scheme 13 Polymerization of 1,1-dimethylsilacyclobutane.

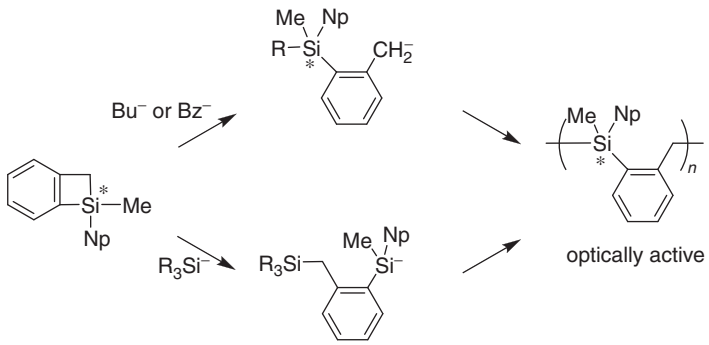

Scheme 14 Polymerization of chiral 1-methyl-1-(1-naphthyl)benzosilacyclobut-2-ene, Np = 1-naphthyl.

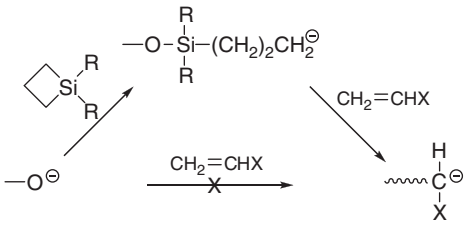

Scheme 15 Silacyclobutane as a nucleophile-transfer reagent ("anionic pump").

Cyclosilazanes **22** are usually prepared by ammonolysis of bifunctional halosilanes. Cyclodisilazanes **21** are obtained by coupling of dilithium derivatives of diaminosilanes with dichlorosilanes.[286]

ROP of cyclosilazanes may be accomplished using both cationic and anionic routes. The catalysts for the cationic process are strong protic acids, such as TfOH, and Lewis acids like alkyl and silyl triflates.[287] The typical initiators of the anionic process are organolithium and organosodium compounds.[288,289] The ionic polymerization of cyclosilazanes is kinetically controlled, first, by the ring strain (which is greater in **21** than in **22**) and, second, by the steric hindrance around the nitrogen atom and/or the electronic effects of the R substituent on the Si–N bond.[286,290] AROP of model cyclodisilazanes, initiated with both organosodium and organolithium initiators exhibits all the characteristics of a living process.[288] Polymers with MWs as high as 100 000 have been prepared. Examination of the cationic polymerization of these monomers shows that the reaction is fast, the monomer conversion is always quantitative, but, in this case, besides the polymer, cyclic compounds $(R_2SiNR')_n$, $n = 3,4$, appear.[290]

Several reports on copolymerization of cyclosilazanes with other monomers have been published. A series of new poly(siloxane)s and poly(silazane)s were synthesized by cationic ring-opening copolymerization of the cyclic monomers, octamethylcyclotetrasiloxane and hexamethylcyclotrisilazane, obtaining PDMS–poly(dimethylsilazane) copolymers with different concentrations of the comonomer units. The polymers were thermally cured and pyrolyzed, producing ceramic materials.[291]

Novel styrene–silazane block copolymers were synthesized via living anionic polymerization (**Scheme 16**). Block copolymer micelles having a polysilazane core or polysilazane shell were prepared in solvents selective for each segment. SiN-based ceramic nanoparticles were successfully synthesized by the cross-linking and pyrolysis of the micelles.[292]

Cyclosiloxazanes are synthesized using the reaction of dichlorosiloxanes with ammonia or amines. The AROP of heptamethyl-1,3-dioxa-5-aza-2,4,6-trisilacyclohexane initiated by organolithium compounds in the presence of DMF as activator has shown to be the controlled process. Backbiting reactions are limited and give only a small amount of a unique specific cyclic compound. Thermodynamic and kinetic studies indicate that the polymerization is equilibrated. The apparent rate constants of propagation and depolymerization along with the thermodynamic parameters (enthalpy and entropy) of the polymerization have been estimated. The active species are ion pairs solvated by DMF in equilibrium with unreactive aggregated ion pairs.[293]

4.17.2.4 Cyclostannasiloxanes

The recent progress in the chemistry of cyclostannasiloxanes and their potential in ROP reactions has been critically evaluated and compared with that of related cyclic borasiloxanes, germasiloxanes, and siloxanes.[294] The ROP of cyclostannasiloxanes is completely reversible upon dilution, which is due to the lability of the Sn–O bond.

4.17.2.5 Ferrocenylsilanes

Strained ferrocenylsilanes (and, more generally, metallocenylsilanes) having Mt–Cp bonding between the cyclopentadienyl rings were studied by Manners *et al.* They have been proven to be easily polymerizable using the anionic route. They make possible incorporation of transition metals and main group elements into the main chain, which provides new interesting self-assembled materials. The examples of such polymers are poly(ferrocenylsilane) (PFS) and its block copolymers. PFS materials are prepared by ROP of 1,1′-silanediylferrocenes (eqn [48]).[295,296]

[48]

4.17.3 Final Remarks

Among all organosilicon heterocycles, cyclic siloxanes are the most important. ROP of cyclic diorganylsiloxanes is an alternative to the polycondensation method of manufacturing siloxane polymers. The most important commercially is the equilibrium polymerization of unstrained octamethylcyclotetrasiloxane (D_4) in the presence of strong acids or bases and, usually, a chain stopper (MW regulator). However, because all bonds in the monomer and polymer are approximately thermodynamically equivalent, this process leads to an

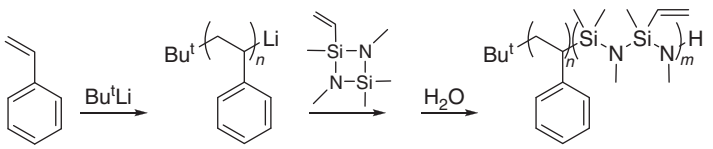

Scheme 16 Synthesis of styrene-silazane block copolymer.

equilibrium mixture of cyclics and linear polymer. The need for new, high-performance materials requires the synthesis of well-defined, having narrow MW distribution, cyclic-free, homo- and copolymers. This can be accomplished by the kinetically controlled polymerization of the strained monomers, hexaalkylcyclotrisiloxanes. In the presence of the proper initiator and under the favorable reaction conditions, the polymerization of cyclotrisiloxanes can proceed as a classical living polymerization. Properly selected anionic initiators, in the presence of cation-interacting promoters, if needed, provide fast and quantitative initiation and propagation that is free of depolymerization or chain-scrambling processes. In this way, siloxane polymers and copolymers of highly regular structure can be obtained with almost quantitative yields. These processes are likely to gain a growing interest in the future. There is also a growing interest in 3D cyclic siloxane structures, that is, silsequioxanes and dendritic or hyperbranched structures which find an increasing number of applications in the synthesis of nanohybrids. Hybrid inorganic–organic composites are an emerging class of new materials that hold significant promise for the electronics, photonics, and other materials technologies.

The silicon chemistry, however, is still developing and new structures, new reactions, and new interesting materials are being continuously discovered. Therefore, it seemed reasonable to mention in this chapter also the other, less frequently reviewed, polymerizable organo silicon monomers and processes leading to the corresponding polymers and copolymers.

References

1. Noll, W. *The Chemistry and Technology of Silicones*; Academic Press: New York, NY, 1968.
2. Butts, M.; Cella, J. A.; Wood, C. D.; *et al. Encyclopedia of Polymer Science and Technology*, 3rd ed.; Mark, H. F., Kroschwitz, J. I., Eds., Wiley-Interscience: Hoboken, NJ, 2004; p 765.
3. Moretto, H.-H.; Schulze, M.; Wagner, G. *Ullmann's Encyclopedia of Industrial Chemistry*; VCH Publishers: Weinheim, Germany, 1993; p 57.
4. Voronkov, M. G.; Basenko, S. V. *J. Organomet. Chem.* **1995**, *500*, 325.
5. Lu, P.; Paulasaari, J. K.; Weber, W. P. *Organometallics* **1996**, *15*, 4649.
6. Le Roux, C.; Yang, H.; Wenzel, S.; *et al. Organometallics* **1998**, *17*, 556.
7. Takiguchi, T.; Sakurai, M.; Kishi, T.; *et al. J. Org. Chem.* **1960**, *25*, 310.
8. Shen, Q.; Interrante, L. V. *Macromolecules* **1997**, *30*, 5485.
9. Unno, M.; Kishimoto, Y.; Matsumoto, H. *Organometallics* **2004**, *23*, 6221.
10. Borisov, Y. A.; Papkov, V. S.; Rabkina, A. Y.; Zavin, B. G. *J. Mol. Struct. Theochem.* **2003**, *664*, 157.
11. UK Patent 683,182, 1952.
12. Fortuniak, W.; Chojnowski, J.; Sauvet, G. *Macromol. Chem. Phys.* **2001**, *202*, 2306.
13. Zuev, V. V.; Kalinin, A. V. *Phosphorus Sulfur Silicon Relat. Elem.* **2003**, *178*, 1289.
14. Voronkov, M. G.; Mileshkevich, V. P.; Yuzhelevskii, Yu. A. *The Siloxane Bond*; Consultants Bureau: New York, NY, 1978.
15. Wright, P. V. *Ring Opening Polymerization*; Ivin, K. J., Saegusa, T., Eds.; Elsevier: London, UK, 1984; p 1055.
16. Kendrick, T. C.; Parbhoo, B. M.; White, J. W. *Comprehensive Polymer Chemistry*; Eastmond, G. C., Ledwith, A., Russo, S., Sigwalt, P., Eds; Pergamon Press: Oxford, UK, 1989; p 459.
17. Kendrick, T. C.; Parbhoo, B. M.; White, J. W. *The Chemistry of Organic Silicon Compounds*; Patai, S., Rappoport, Z., Eds.; Wiley: Chichester, UK, 1989; p 1289.
18. Clarson, S. J.; Semlyen, J. A. *Siloxane Polymers*; Ellis Horwood/PTR Prentice Hall: Englewood Cliffs, NJ, 1993.
19. Drake, R.; MacKinnon, I.; Taylor, R. *The Chemistry of Organic Silicon Compounds*; Rappoport, Z., Apeloig, Y. Eds.; Wiley-Interscience: New York, NY, 1998, Vol. 2; p 2217.
20. Chojnowski, J.; Cypryk, M. *Silicon-Containing Polymers*; Jones, R. G., Ando, W., Chojnowski, J., Eds.; Kluwer Academic Publishers: Dordrecht, The Netherlands, 2000; p 3.
21. Jones, R. G., Ando, W., Chojnowski, J., Eds. *Silicon-Containing Polymers: The Science and Technology of Their Synthesis and Applications*; Kluwer Academic Publishers: Dordrecht, The Netherlands, 2000.
22. Chojnowski, J. *Silanes and Silicones* (Gelest Catalog 2004); Arkles, B., Larson, G., Eds.; Gelest, Inc.: Morrisville, PA, 2004; p 389.
23. Mazurek, M. H. *Comprehensive Organometallic Chemistry III*; Crabtree, R. H., Mingos, M. P., Housecroft, C., Eds.; Elsevier Ltd: Oxford, UK, 2006; 651.
24. Cypryk, M. *Inorganic Polymers*; DeJaeger, R., Gleria, M., Eds.; NOVA Science Publishers: New York, NY, 2007; p 1.
25. Ganachaud, F.; Boileau, S. *Ring-Opening Polymerization*; Dubois, P., Coulembier, O., Raquez, J.-M., Eds.; Wiley-VCH: Weinheim, Germany, 2009; p 65.
26. Chojnowski, J. *J. Inorg. Organomet. Polym.* **1991**, *1*, 299.
27. Chojnowski, J. *Siloxane Polymers*; Clarson, S. J., Semlyen, J. A., Eds.; PTR Prentice Hall: Englewood Cliffs, NJ, 1993; p 1.
28. Chojnowski, J.; Cypryk, M. *Polymeric Materials Encyclopedia*; Salamone, J. C., Ed.; CRC Press: Boca Raton, FL, 1996; 1682.
29. Wright, P. V.; Semlyen, J. A. *Polymer* **1970**, *11*, 462.
30. Semlyen, J. A. *Adv. Polym. Sci.* **1976**, *21*, 43.
31. Semlyen, J. A. *Siloxane Polymers*; Clarson, S. J., Semlyen, J. A., Eds.; PTR Prentice Hall: Englewood Cliffs, NJ, 1993; p 135.
32. Semlyen, J. A. *Cyclic Polymers*, 2nd ed.; Semlyen, J. A., Ed.; Kluwer Academic Publishers: New York, NY, 2000; p 1.
33. Flory, P. *Principles of Polymer Chemistry*; Cornell University Press: Ithaca, NY, 1953.
34. Jacobson, H.; Stockmayer, W. H. *J. Chem. Phys.* **1950**, *18*, 1600.
35. Semlyen, J. A.; Wright, P. V. *Polymer* **1969**, *10*, 543.
36. Flory, P.; Semlyen, J. A. *J. Am. Chem. Soc.* **1966**, *88*, 3209.
37. Brook, M. A. *Silicon in Organic, Organometallic, and Polymer Chemistry*; Wiley: New York, NY, 2000.
38. Carmichael, J. B.; Winger, R. *J. Polym. Sci. A* **1965**, *3*, 971.
39. Scott, D. W. *J. Am. Chem. Soc.* **1946**, *68*, 2294.
40. Mazurek, M.; Ścibiorek, M.; Chojnowski, J.; *et al. Eur. Polym. J.* **1980**, *16*, 57.
41. Voronkov, M. G.; Klyuchnikov, V. A.; Mironenko, E. V.; *et al. J. Organomet. Chem.* **1991**, *406*, 91.
42. Cypryk, M.; Apeloig, Y. *Organometallics* **1997**, *16*, 5938.
43. Grubb, W. T.; Osthoff, R. C. *J. Am. Chem. Soc.* **1955**, *77*, 1405.
44. Chojnowski, J.; Mazurek, M. *Makromol. Chem.* **1975**, *176*, 2999.
45. Wilczek, L.; Kennedy, J. P. *Polym. J.* **1987**, *19*, 531.
46. Kopylov, V. M.; Prikhodko, P. L.; Kovyazin, V. A. *Vysokomol. Soedin. A* **1982**, *24*, 1751.
47. Hurd, D. T.; Osthoff, R. C.; Corrin, M. L. *J. Am. Chem. Soc.* **1954**, *76*, 249.
48. Molenberg, A.; Möller, M. *Macromol. Chem. Rapid Commun.* **1995**, *16*, 449.
49. Van Dyke, M. E.; Clarson, S. J. *J. Inorg. Organomet. Polym.* **1998**, *8*, 111.
50. Hupfield, P. C.; Taylor, R. G. *J. Inorg. Organomet. Polym.* **1999**, *9*, 17.
51. Teng, C. J.; Weber, W. P.; Cai, G. P. *Macromolecules* **2003**, *36*, 5126.
52. Teng, C. J.; Weber, W. P.; Cai, G. P. *Polymer* **2003**, *44*, 4149.
53. Grzelka, A.; Chojnowski, J.; Fortuniak, W.; *et al. J. Inorg. Organomet. Polym.* **2004**, *14*, 85.
54. Pibre, G.; Chaumont, P.; Fleury, E.; Cassagnau, P. *Polymer* **2008**, *49*, 234.
55. Su, S. X.; Zhang, Z. J.; Zheng, Z. M.; Xie, Z. M. *Polym. Int.* **2004**, *53*, 149.
56. Saxena, A.; Rajaraman, S.; Leatherman, M. *Macromolecules* **2007**, *40*, 752.
57. Bessmertynkh, A.; Ben, F.; Bacereido, A.; Mignani, G. *J. Organomet. Chem.* **2003**, *686*, 281.
58. Lohmeijer, B. G. G.; Dubois, G.; Leibfarth, F.; *et al. Org. Lett.* **2006**, *8*, 4683.
59. Rodriguez, M.; Marrot, S.; Kato, T.; *et al. J. Organomet. Chem.* **2007**, *692*, 705.
60. Yuzhelevskii, Yu. A.; Kagan, E. G.; Fedosieeva, N. N. *Polym. Sci. USSR* **1970**, *12*, 1800.
61. Mazurek, M.; Chojnowski, J. *Makromol. Chem.* **1977**, *178*, 1005.
62. Terman, L. M.; Klapshina, L. G.; Kurskii, Yu. A.; Zislina, S. S. *Vysokomol. Soedin. A* **1988**, *30*, 2042.
63. Hubert, S.; Hémery, P.; Boileau, S. *Makromol. Chem. Macromol. Symp.* **1986**, *6*, 247.
64. Molenberg, A.; Siffrin, S.; Moller, M.; *et al. Makromol. Chem. Macromol. Symp.* **1996**, *102*, 199.
65. Laita, Z.; Jelinek, M. *Polym. Sci. USSR* **1962**, *4*, 535.
66. Kress, J. D.; Leung, P. C.; Tawa, G. J.; Hay, P. J. *J. Am. Chem. Soc.* **1997**, *119*, 1954.
67. Kress, J. D.; Leung, P. C.; Tawa, G. J.; Hay, P. J. *ACS Symp. Ser.* **2000**, *729*, 81.
68. Ritch, J. S.; Chivers, T. *Angew. Chem. Int. Ed.* **2007**, *46*, 4610.
69. Yuzhelevskii, Yu. A.; Dmokhovskaya, E. B.; Klebanskii, Al.; Kozlova, N. V. *Vysokomol. Soedin. A* **1969**, *11*, 432.

70. Chojnowski, J.; Rózga, K. *J. Inorg. Organomet. Polym.* **1992**, *2*, 297.
71. Suryanarayanan, B.; Peace, B. W.; Mayhan, K. G. *J. Polym. Sci. Polym. Chem. Ed.* **1974**, *12*, 1089.
72. Suzuki, T. *Polymer* **1989**, *30*, 333.
73. Chojnowski, J.; Kaźmierski, K.; Rubinsztajn, S.; Stańczyk, W. *Makromol. Chem.* **1986**, *187*, 2039.
74. Graiver, D.; Fearon, G. *Silicon-Containing Polymers*; Jones, R. G., Ando, W., Chojnowski, J., Eds.; Kluwer Academic Publishers: Dordrecht, The Netherlands, 2000; p 233.
75. White, J. W. *Organosilicon Chemistry VI: From Molecules to Materials*; Auner, N., Weis, J., Eds.; Wiley-VCH: Weinheim, Germany, 2005; p 602.
76. Cai, G. P.; Weber, W. P. *Macromolecules* **2000**, *33*, 8976.
77. Paulasaari, J. K.; Weber, W. P. *Macromolecules* **1999**, *32*, 6574.
78. Paulasaari, J. K.; Weber, W. P. *Macromolecules* **1999**, *32*, 5217.
79. Andrianov, K. A.; Nogaideli, A. I.; Khubulava, E. I.; *et al. Polym. Sci. USSR* **1976**, *18*, 2987.
80. Brandt, P. J. A.; Elsbernd, C. L. S.; Patel, N.; *et al. Polymer* **1990**, *31*, 180.
81. Gilbert, A. R.; Kantor, S. W. *J. Polym. Sci.* **1959**, *40*, 35.
82. Veith, C. A.; Cohen, R. E. *J. Polym. Sci. A* **1989**, *27*, 1241.
83. Clarson, S. J.; Stuart, J. O.; Selby, C. E.; *et al. Macromolecules* **1995**, *28*, 674.
84. Grigoras, S.; Qian, C.; Crowder, C.; *et al. Macromolecules* **1995**, *28*, 7370.
85. Harkness, B. R.; Tachikawa, M.; Mita, I. *Macromolecules* **1995**, *28*, 8136.
86. Lee, G. J.; Kang, K. K. *J. Org. Chem.* **1988**, *53*, 3634.
87. Molenberg, A.; Klok, H. A.; Moller, M.; *et al. Macromolecules* **1997**, *30*, 792.
88. Molenberg, A.; Michalke, D.; Moller, M.; Pieper, T. *J. Polym. Sci. A* **1998**, *36*, 169.
89. Weber, W. P.; Cai, G. P. *Macromolecules* **2001**, *34*, 4355.
90. Weber, W. P.; Paulasaari, J. K.; Cai, G. P. *ACS Symp. Ser.* **2003**, *838*, 72.
91. Suzuki, T.; Lo, P. Y. *Macromolecules* **1991**, *24*, 460.
92. Suzuki, T.; Yamada, S.; Okawa, T. *Polymer J.* **1993**, *25*, 411.
93. Chang, T. C.; Chen, Y. C.; Ho, S. Y.; Chiu, Y. S. *Polymer* **1996**, *37*, 2963.
94. Maschke, U.; Wegner, T.; Coqueret, X. *Makromol. Chem.* **1992**, *193*, 2453.
95. Dickstein, W. H.; Lillya, P. C. *Macromolecules* **1989**, *22*, 3882.
96. Kazama, H.; Tezuka, Y.; Imai, K. *Macromolecules* **1991**, *24*, 122.
97. Kumar, A.; Eichinger, B. E. *Macromolecules* **2005**, *23*, 5358.
98. Yin, R.; Hogen-Esch, T. E. *Macromolecules* **1993**, *26*, 6952.
99. Tezuka, Y.; Nobe, S.; Shiomi, T. *Macromolecules* **1995**, *28*, 8251.
100. Aoyagi, T.; Takamura, Y.; Nakamura, T.; Nagase, Y. *Polymer* **1992**, *33*, 1530.
101. Hammouch, S. O.; Beinert, G. J.; Ziliox, J. G.; Herz, J. E. *Polymer* **1995**, *36*, 421.
102. Mazurek, M. *Silicon-Containing Polymers*; Jones, R. G., Ando, W., Chojnowski, J., Eds.; Kluwer Academic Publishers: Dordrecht The Netherlands, 2000; p 113.
103. Wilczek, L.; Rubinsztajn, S.; Fortuniak, W.; *et al. Bull. Pol. Acad. Sci. Chem.* **1989**, *37*, 91.
104. Clarson, S. J. *Silicon-Containing Polymers*; Jones, R. G., Ando, W., Chojnowski, J., Eds.; Kluwer Academic Publishers: Dordrecht, The Netherlands, 2000; p 139.
105. Saam, J. C. *J. Inorg. Organomet. Polym.* **1999**, *9*, 3.
106. Baratova, T. N.; Mileshkevich, V. P.; Gurari, V. I. *Vysokomol. Soedin. A* **1983**, *25*, 2497.
107. Cypryk, M.; Kaźmierski, K.; Fortuniak, W.; Chojnowski, J. *Macromolecules* **2000**, *33*, 1536.
108. Chojnowski, J.; Cypryk, M.; Fortuniak, W.; *et al. Polymer* **2002**, *43*, 1993.
109. Patnode, W.; Wilcock, D. F. *J. Am. Chem. Soc.* **1946**, *68*, 358.
110. Sauvet, G.; Lebrun, J. J.; Sigwalt, P. *Cationic Polymerisation and Related Processes*; Goethals, E., Ed.; Academic: London, UK, 1984; p 237.
111. Chojnowski, J.; Wilczek, L. *Makromol. Chem.* **1979**, *180*, 117.
112. Bordone, C.; Desmurs, J.-R.; Ghosez, L.; *et al.* U.S. Patent 6,737,495, 2002.
113. Andrianov, K. A.; Shkolnik, M. I.; Kopylov, V. M.; Bravina, N. *Vysokomol. Soedin. B* **1974**, *16*, 893.
114. Schindler, S.; Rühlmann, K. *Plaste Kautsch.* **1978**, *25*, 384.
115. Elms, R. A. U.S. Patent 4,831,174, 1989.
116. Rashkov, I. B.; Gitsov, I. *J. Polym. Sci. A* **1986**, *24*, 155.
117. Razzano, J.S.; Anderson, P.P.; Perry, R. J. U.S. Patent 5,670,596, 1997.
118. Chen, B.; Zhan, X. L.; Yi, L. M.; Chen, F. Q. *Chin. J. Chem. Eng.* **2007**, *15*, 661.
119. Grzelka, A.; Chojnowski, J.; Fortuniak, W.; *et al. J. Inorg. Organomet. Polym.* **2004**, *14*, 101.
120. Kendrick, T. C. *J. Chem. Soc.* **1965**, 2027.
121. Chernyshev, A. I.; Yastrebov, V. V. *Vysokomol. Soedin. A* **1969**, *11*, 525.
122. Chojnowski, J.; Ścibiorek, M.; Kowalski, J. *Makromol. Chem.* **1977**, *178*, 1351.
123. Sigwalt, P.; Nicol, P.; Masure, M. *Makromol. Chem. Suppl.* **1989**, *15*, 15.
124. Jordan, E.; Lestel, L.; Boileau, S.; *et al. Makromol. Chem.* **1989**, *190*, 267.
125. Yashiro, T.; Kricheldorf, H. R.; Schwarz, G. *Macromol. Chem. Phys.* **2010**, *211*, 1311.
126. Toskas, G.; Besztercey, G.; Moreau, M.; *et al. Macromol. Chem. Phys.* **1995**, *196*, 2715.
127. Jallouli, A.; Saam, J. C. *J. Inorg. Organomet. Polym.* **1998**, *8*, 179.
128. Wang, Q.; Zhang, H.; Prakash, G. K. S.; *et al. Macromolecules* **1996**, *29*, 6691.
129. Farooq, O. U.S. Patent 5,124,417, 1992.
130. Lamanna, W.M.; Palazzotto, M.C.; DeVoe, R. J.; *et al.* U.S. Patent 5,514,728, 1996.
131. Belfield, K.; Zhang, G. *Polym. Bull.* **1997**, *38*, 165.
132. Meliani, A.; Vaugeois, Y.; Bali, H.; *et al. Phosphorus Sulfur Silicon Relat. Elem.* **2000**, *166*, 283.
133. Desmurs, J.-R.; Ghosez, L.; Martins, J.; *et al. J. Organomet. Chem.* **2002**, *646*, 171.
134. Price, G. J.; Hearn, M. P.; Wallace, E. N. K.; Patel, A. M. *Polymer* **1996**, *37*, 2303.
135. Gobin, C.; Masure, M.; Sauvet, G.; Sigwalt, P. *Makromol. Chem. Macromol. Symp.* **1986**, *6*, 237.
136. Stark, F. O.; Falender, J. R.; Wright, A. P. *Comprehensive Organometallic Chemistry*; Wilkinson, G., Stone, F. G. A., Abel, E. W., Eds.; Pergamon Press: Oxford, UK, 1982; p 305.
137. Hardman, B.; Torkelson, A. *Encyclopedia of Polymer Science and Engineering*; Frank, H. F., Bikales, N. M., Overberger, C. G., Menges, G. Eds.; Wiley-Interscience: New York, NY, 1989; p 204.
138. Wilczek, L.; Rubinsztajn, S.; Chojnowski, J. *Makromol. Chem.* **1986**, *187*, 39.
139. Sigwalt, P. *Polym. J.* **1987**, *19*, 567.
140. Wilczek, L.; Chojnowski, J. *Macromolecules* **1981**, *14*, 9.
141. Cypryk, M.; Apeloig, Y. *Organometallics* **2002**, *21*, 2165.
142. Wilczek, L.; Chojnowski, J. *Makromol. Chem.* **1983**, *184*, 77.
143. Sigwalt, P.; Gobin, C.; Nicol, P.; *et al. Makromol. Chem. Macromol. Symp.* **1991**, *42/43*, 229.
144. Chojnowski, J.; Rubinsztajn, S.; Wilczek, L. *Macromolecules* **1987**, *20*, 2345.
145. Cypryk, M.; Sigwalt, P. *Macromolecules* **1994**, *27*, 6245.
146. Nicol, P.; Masure, M.; Sigwalt, P. *Macromol. Chem. Phys.* **1994**, *195*, 2327.
147. Olah, G. A.; Li, X.-Y.; Wang, Q.; *et al. J. Am. Chem. Soc.* **1995**, *117*, 8962.
148. Toskas, G.; Moreau, M.; Masure, M.; Sigwalt, P. *Macromolecules* **2001**, *34*, 4730.
149. Cypryk, M.; Kurjata, J.; Chojnowski, J. *J. Organomet. Chem.* **2003**, *686*, 373.
150. Chojnowski, J.; Cypryk, M.; Kaźmierski, K. *Macromolecules* **2002**, *35*, 9904.
151. Gädda, T. M.; Nelson, A. K.; Weber, W. P. *J. Polym. Sci. A* **2004**, *42*, 5235.
152. Paulasaari, J. K.; Weber, W. P. *Polym. Prepr.* **2000**, *41*, 133.
153. Chojnowski, J.; Scibiorek, M. *Makromol. Chem* **1976**, *177*, 1413.
154. Cypryk, M.; Chojnowski, J.; Kaźmierski, K.; Kurjata, J. *Polimery* **2004**, *49*, 491.
155. Bischoff, R.; Sigwalt, P. *Polym. Int.* **1996**, *40*, 99.
156. Bischoff, R.; Sigwalt, P. *Polym. Int.* **1999**, *48*, 217.
157. Out, G. J.; Klok, H.-A.; Möller, M.; Oelfin, D. *Macromol. Chem. Phys.* **1995**, *196*, 195.
158. Chojnowski, J.; Rubinsztajn, S.; Fortuniak, W.; Kurjata, J. *J. Inorg. Organomet. Polym. Mat.* **2007**, *17*, 173.
159. Chawla, A. S.; St-Pierre, L. E. *J. Appl. Polym. Sci.* **1975**, *19*, 353.
160. Andrianov, K. A.; Hananashvili, L. M.; Zavin, B. G.; *et al. Vysokomol. Soedin. B.* **1969**, *11*, 637.
161. Andrianov, K. A.; Godovskii, Yu. A.; Svistunov, V. S.; *et al. Dokl. Akad. Nauk SSSR* **1977**, *234*, 1326.
162. Buzin, M. I.; Gerasimov, M. V.; Obolonkova, E. S.; Papkov, V. S. *J. Polym. Sci. A* **1997**, *35*, 1973.
163. Unno, M.; Takada, K.; Kawaguchi, Y.; Matsumoto, H. *Mol. Cryst. Liq. Cryst.* **2005**, *440*, 259.
164. Chawla, A. S.; St-Pierre, L. E. *J. Polym. Sci.* **1972**, *10*, 2691.
165. Naylor, D. M.; Stannett, V. T.; Deffieux, A.; Sigwalt, P. *Polymer* **1994**, *35*, 1764.
166. Hyde, J.F.; Wehrly, J. R. U.S. Patent 2,891,920, 1959.
167. De Gunzbourg, A. Ph.D. thesis, Pierre et Marie Curie University-Paris VI, Paris, France, 1993.
168. Graiver, D.; Huebner, D. J.; Saam, J. C. *Rubber Chem. Technol.* **1983**, *56*, 918.
169. De Gunzbourg, A.; Favier, J. C.; Hémery, P. *Polym. Int.* **1994**, *35*, 179.
170. Barrere, M.; Ganachaud, F.; Bendejacq, D.; *et al. Polymer* **2001**, *42*, 7239.
171. De Gunzbourg, A.; Maisonnier, S.; Favier, J. C.; *et al. Makromol. Chem. Macromol. Symp.* **1998**, *132*, 359.
172. Maisonnier, S.; Favier, J. C.; Masure, M.; Hémery, P. *Polym. Int.* **1999**, *48*, 159.
173. Palaprat, G.; Ganachaud, F.; Mauzac, M.; Hémery, P. *Polymer* **2005**, *46*, 11213.
174. Barrere, M.; Maitre, C.; Dourges, M. A.; Hémery, P. *Macromolecules* **2001**, *34*, 7276.
175. Caille, J. R.; Teyssie, D.; Bouteiller, L.; *et al. Makromol. Chem. Macromol. Symp.* **2000**, *153*, 161.
176. Ivanenko, C.; Maitre, C.; Ganachaud, F.; Hémery, P. *e-Polymers* **2003**, *010*.
177. Yilgor, I.; McGrath, J. E. *Adv. Polym. Sci.* **1988**, *86*, 1.
178. Simionescu, B. C.; Harabagiu, V.; Simionescu, C. I. *Polymeric Materials Encyclopedia*; Salamone, J. C. Ed.; CRC Press: Boca Raton, FL, 1996; 7751.
179. Belorgey, G.; Sauvet, G. *Silicon-Containing Polymers, The Science and Technology of Their Synthesis and Applications*; Jones, R. G., Ando, W., Chojnowski, J., Eds.; Kluwer Academic Publishers: Dordrecht, The Netherlands, 2000; p 43.

180. Moretto, H.-H.; Schulze, M.; Wagner, G. *Industrial Polymer Handbook*; Wilks, E. S. Ed.; Wiley-VCH: Weinheim, Germany, 2001; p 1349.
181. Kennan, J. J. *Siloxane Polymers*; Clarson, S. J., Semlyen, J. A., Eds.; Ellis Horwood/PTR Prentice Hall: Englewood Cliffs, NJ, 1993; p 72.
182. Romenesko, D. J.; Chorvath, I.; Olsen, Jr., C.; *et al. Encyclopedia of Chemical Technology*, 5th ed.; Wiley: New York, NY, 2005; p 239.
183. Teng, C. J.; Cai, G. P.; Weber, W. P. *J. Fluorine Chem.* **2004**, *125*, 1451.
184. Grunlan, M. A.; Lee, N. S.; Cai, G. P.; *et al. Chem. Mater.* **2004**, *16*, 2433.
185. Shamaev, A. E.; Ignatenko, A. V.; Krukovsky, S. P. *Russ. Chem. Bull.* **2004**, *53*, 2229.
186. Cypryk, M.; Delczyk, B.; Juhari, A.; Koynov, K. *J. Polym. Sci. A* **2009**, *47*, 1204.
187. Williams, T. C.; Pike, R. A.; Fekate, F. *Ind. Eng. Chem. Res.* **1959**.
188. Lee, Y. S.; Song, G. S.; Kang, Y.; Suh, D. H. *Electrochim. Acta* **2004**, *50*, 311.
189. Li, C. Ph.D. thesis, Virginia Polytechnic Institute and State University, Blacksburg, VA, 1996.
190. Rutnakornpituk, M. Ph.D. thesis, Virginia Polytechnic Institute and State University, Blacksburg, VA, 2002.
191. Liu, L. H.; Yang, S. Y.; Zhang, Z. J.; *et al. J. Polym. Sci. A* **2003**, *41*, 2722.
192. Villegas, J. A.; Olayo, R.; Cervantes, J. *J. Inorg. Organomet. Polym.* **2003**, *13*, 205.
193. Owen, M. J. *Silicon-Containing Polymers*; Jones, R. G., Ando, W., Chojnowski, J., Eds.; Kluwer Academic Publ: Dordrecht, The Netehrlands, 2000; 213.
194. Bauer, J.; Hüsing, N.; Kickelbick, G. *Chem. Commun.* **2001**, 137.
195. Kickelbick, G.; Bauer, J.; Hüsing, N. *Silicon Chemistry. From the Atom to Extended Systems*; Jutzi, P., Schubert, U., Eds.; Wiley-VCH: Weinheim, Germany, 2003; p 439.
196. Ścibiorek, M.; Gladkova, N. K.; Chojnowski, J. *Polym. Bull.* **2000**, *44*, 377.
197. Gädda, T. M.; Nelson, A. K.; Weber, W. P. *J. Polym. Sci. A* **2004**, *42*, 5235.
198. Rózga-Wijas, K.; Chojnowski, J.; Zundel, T.; Boileau, S. *Macromolecules* **1996**, *29*, 2711.
199. Odian, G. *Principles of Polymerization*, 4th ed.; Wiley-Interscience: Hoboken, NJ, 2004.
200. Chojnowski, J.; Cypryk, M.; Fortuniak, W.; *et al. Macromolecules* **2003**, *36*, 3890.
201. Cypryk, M.; Delczyk, B. *Polimery* **2006**, *51*, 499.
202. Cypryk, M.; Delczyk-Olejniczak, B. *Polimery* **2010**, *55*, 503.
203. Cancouët, P.; Daudet, E.; Hélary, G.; *et al. J. Polym. Sci. A* **2000**, *38*, 826.
204. Ziemelis, M.; Saam, J. C. *Macromolecules* **1989**, *22*, 2111.
205. Liu, L. H.; Yang, S. Y.; Zhang, Z. J.; *et al. J. Polym. Sci. A* **2003**, *41*, 2722.
206. Chojnowski, J.; Cypryk, M.; Fortuniak, W.; *et al. ACS Polym. Prepr.* **2001**, *221*, 346.
207. Chojnowski, J.; Fortuniak, W.; Scibiorek, M.; *et al. Macromolecules* **2007**, *40*, 9339.
208. Rózga-Wijas, K.; Chojnowski, J.; Fortuniak, W.; *et al. J. Mater. Chem.* **2003**, *13*, 2301.
209. Rózga-Wijas, K.; Mizerska, U.; Fortuniak, W.; *et al. J. Inorg. Organomet. Polym. Mat.* **2007**, *17*, 605.
210. Cai, G. P.; Weber, W. P. *Polymer* **2004**, *45*, 2941.
211. Gädda, T. M.; Weber, W. P. *J. Polym. Sci. A* **2006**, *44*, 137.
212. Fragouli, P.; Iatrou, H.; Hadichristidis, N.; *et al. J. Polym. Sci. A* **2006**, *44*, 6587.
213. Lee, I. J.; Song, G. S.; Lee, W. S.; Suh, D. H. *J. Power Sources* **2003**, *114*, 320.
214. Kowalewska, A.; Delczyk, B. *Silicon Based Polymers*; Boileau, S., Boury, B., Ganachaud, F., Eds.; Springer: Berlin, Germany, 2008; p 99.
215. Cypryk, M.; Pospiech, P.; Strzelec, K.; *et al. J. Mol. Catal. A* **2010**, *319*, 30.
216. Feher, F. Silanes and Silicones *(Gelest Catalog 2000)*; Arkles, B., Larson, G., Eds.; Gelest, Inc.: Morrisville, PA, 2004; p 55.
217. Baney, R. H.; Itoh, M.; Sakakibara, A.; Suzuki, T. *Chem. Rev.* **1995**, *95*, 1409.
218. Feher, F. J.; Budzichowski, T. A. *Polyhedron* **1995**, *14*, 3239.
219. Loy, D. A.; Shea, K. J. *Chem. Rev.* **1995**, *95*, 1431.
220. Lichtenhan, J. D. *Polymeric Materials Encyclopedia*; Salamone, J. C., Ed.; CRC Press: Boca Raton, FL, 1996; 7768.
221. Baney, R. H.; Cao, X. *Silicon-Containing Polymers*; Jones, R. G., Ando, W., Chojnowski, J., Eds.; Kluwer Academic Publishers: Dordrecht, The Netherlands, 2000; p 157.
222. Abe, Y.; Gunji, T. *Prog. Polym. Sci.* **2004**, *29*, 149.
223. Cordes, D. B.; Lickiss, P. D.; Rataboul, F. *Chem. Rev.* **2010**, *110*, 2081.
224. Li, G.; Wang, L.; Ni, H.; Pittman, C. U., Jr *J. Inorg. Organomet. Polym.* **2002**, *11*, 123.
225. Li, H. Y.; Yu, D. S.; Zhang, J. Y. *Polymer* **2005**, *46*, 5317.
226. Li, H. Y.; Zhang, J. Y.; Xu, R. W.; Yu, D. S. *J. Appl. Polym. Sci.* **2006**, *102*, 3848.
227. Chojnowski, J.; Cypryk, M.; Kurjata, J. *Prog. Polym. Sci.* **2003**, *28*, 691.
228. Chojnowski, J.; Kurjata, J.; Rubinsztajn, S. *Makromol. Chem. Rapid Commun.* **1988**, *9*, 469.
229. Stüger, H.; Eibl, M.; Hengge, E.; Kovacs, I. *J. Organomet. Chem.* **1992**, *431*, 1.
230. Chojnowski, J.; Fortuniak, W.; Gladkova, N. K.; *et al. J. Inorg. Organomet. Polym.* **1995**, *5*, 7.
231. Chojnowski, J.; Kurjata, J. *Macromolecules* **1995**, *28*, 2996.
232. Kurjata, J.; Chojnowski, J. *Makromol. Chem.* **1993**, *194*, 3271.
233. Chojnowski, J.; Kurjata, J. *Macromolecules* **1994**, *27*, 2302.
234. Steward, O. W.; Williams, J. L. *J. Organomet. Chem.* **1988**, *341*, 199.
235. Zundel, T.; Baran, J.; Mazurek, M.; *et al. Macromolecules* **1998**, *31*, 2724.
236. Cypryk, M. *Macromol. Theory Simul.* **2001**, *10*, 158.
237. Piccoli, W. A.; Haberland, G. G.; Merker, R. L. *J. Am. Chem. Soc.* **1960**, *82*, 1883.
238. Suryanarayanan, B.; Peace, B. W.; Mayhan, K. G. *J. Polym. Sci. A* **1974**, *12*, 1109.
239. Ziatdinov, V. R.; Cai, G. P.; Weber, W. P. *Macromolecules* **2002**, *35*, 2892.
240. Rózga, K.; Chojnowski, J.; Boileau, S. *J. Polym. Sci. A* **1997**, *35*, 879.
241. Li, Y.; Kawakami, Y. *Macromolecules* **1999**, *32*, 548.
242. Li, Y.; Kawakami, Y. *Macromolecules* **2000**, *33*, 1560.
243. Matsubara, K.; Nagashima, H. *J. Synth. Org. Chem. Jpn.* **2005**, *63*, 122.
244. Interrante, L. V.; Shen, Q.; Li, J. *Macromolecules* **2001**, *34*, 1545.
245. Hengge, E.; Janoschek, R. *Chem. Rev.* **1995**, *95*, 1495.
246. Hengge, E.; Stuger, H. *The Chemistry of Organic Silicon Compounds*; Rappoport, Z., Apeloig, Y. Eds.; Wiley-Interscience: Chichester, UK, 1998, Vol. 2; p 2177.
247. Jones, R. G.; Holder, S. J. *Silicon-Containing Polymers*; Jones, R. G., Ando, W., Chojnowski, J., Eds.; Kluwer Academic Publ: Dordrecht, The Netherlands, 2000; p 353.
248. Sakurai, H.; Yoshida, M. *Silicon-Containing Polymers*; Jones, R. G., Ando, W., Chojnowski, J., Eds.; Kluwer Academic Publ: Dordrecht, The Netherlands, 2000; p 375.
249. Jones, R. G. *Silicon Chemistry*; Jutzi, P., Schubert, U., Eds.; Wiley-VCH: Weinheim, Germany, 2003; p 139.
250. Hengge, E.; Litscher, G. *Angew. Chem. Int. Ed.* **1976**, *15*, 370.
251. Li, H.; Butler, I. S.; Harrod, J. F. *Organometallics* **1993**, *12*, 4553.
252. Cypryk, M.; Gupta, Y.; Matyjaszewski, K. *J. Am. Chem. Soc.* **1991**, *113*, 1046.
253. Cypryk, M.; Chrusciel, J.; Fossum, E.; Matyjaszewski, K. *Makromol. Chem. Macromol. Symp.* **1993**, *73*, 167.
254. Fossum, E.; Gordon-Wylie, S. W.; Matyjaszewski, K. *Organometallics* **1994**, *13*, 1695.
255. Fossum, E.; Chrusciel, J.; Matyjaszewski, K. *ACS Symp. Ser.* **1994**, *572*, 32.
256. Fossum, E.; Matyjaszewski, K. *Macromolecules* **1995**, *28*, 1618.
257. Chrusciel, J.; Matyjaszewski, K. *J. Polym. Sci. A* **1996**, *34*, 2243.
258. Sakurai, H.; Kamiyama, Y.; Nakadaira, Y. *J. Organomet. Chem.* **1977**, *131*, 147.
259. Fossum, E.; Matyjaszewski, K.; Sheiko, S. S.; Moller, M. *Macromolecules* **1997**, *30*, 1765.
260. Fossum, E.; Matyjaszewski, K.; Rulkens, R.; Manners, I. *Macromolecules* **1995**, *28*, 401.
261. Rulkens, R.; Resendes, R.; Verma, A.; *et al. Macromolecules* **1997**, *30*, 8165.
262. Suzuki, M.; Kotani, J.; Gyobu, S.; *et al. Macromolecules* **1994**, *27*, 2360.
263. Sanji, T.; Sakai, T.; Kabuto, C.; Sakurai, H. *J. Am. Chem. Soc.* **1998**, *120*, 4552.
264. Interrante, L. V.; Shen, Q. *Silicon-Containing Polymers*; Jones, R. G., Ando, W., Chojnowski, J., Eds.; Kluwer Academic Publishers: Dordrecht, The Netherlands, 2000; p 247.
265. Liao, C. X.; Weber, W. P. *Polym. Bull.* **1992**, *28*, 281.
266. Birot, M.; Pillot, J. P.; Dunogues, J. *Chem. Rev.* **1995**, *95*, 1443.
267. Babich, E. D. *Polymeric Materials Encyclopedia*; Salamone, J., Ed.; CRC Press: Boca Raton, FL, 1996; p 7621.
268. Kozytska, M. V.; Dudley, G. B. *Heterocyclic Chemistry III*; Katritzky, A. R., Ramsden, C. A., Scriven, E. F. V., Taylor, R. J. K., Stevens, C., Eds.; Elsevier: Amsterdam, The Netehrlands, 2008; p 513.
269. Cypryk, M.; Jóźwiak, A. *Heterocyclic Chemistry III*; Katritzky, A. R., Ramsden, C. A., Scriven, E. F. V., Taylor, R. J. K., Stevens, C., Eds.; Elsevier: Amsterdam, The Netehrlands, 2008; p 907.
270. Yamashita, H.; Tanaka, M.; Honda, K. *J. Am. Chem. Soc.* **1995**, *117*, 8873.
271. Ogawa, T. *Polymer* **1998**, *39*, 2715.
272. Finkelshtein, E. Sh.; Ushakov, N. V.; Krasheninnikov, E. G.; Yampolskii, Yu. P. *Russ. Chem. Bull.* **2004**, *53*, 2604.
273. Temple, K.; Dziadek, S.; Manners, I. *Organometallics* **2002**, *21*, 4377.
274. Sheridan, J. B.; Elipe, P. G.; Manners, I. *Macromol. Rapid Commun.* **1996**, *17*, 319.
275. Kloninger, C.; Rehahn, M. *Macromolecules* **2004**, *37*, 1720.
276. Matsumoto, K.; Nishimura, M.; Yamaoka, H. *Macromol. Chem. Phys.* **2000**, *201*, 805.
277. Theurig, M.; Weber, W. P. *Polym. Bull.* **1992**, *28*, 17.
278. Koopmann, F.; Frey, H. *Macromolecules* **1996**, *29*, 3701.
279. Ogawa, T.; Lee, S. D.; Murakami, M. *J. Polym. Sci. A* **2002**, *40*, 416.
280. Matsumoto, K.; Shimazu, H.; Deguchi, M.; Yamaoka, H. *J. Polym. Sci. A* **1997**, *35*, 3207.

281. Matsumoto, K.; Shinohata, M.; Yamaoka, H. *Polym. J.* **2000**, *32*, 354.
282. Kawahara, S.; Nagai, A.; Kazama, T.; *et al. Macromolecules* **2004**, *37*, 315.
283. Kakihana, Y.; Uenishi, K.; Imae, I.; Kawakami, Y. *Macromolecules* **2005**, *38*, 6321.
284. Sheikh, M.; Tharanikkarasu, K.; Imae, I.; Kawakami, Y. *Macromolecules* **2001**, *34*, 4384.
285. Soum, A.; Billon, L.; Bouquey, M.; *et al. Polymeric Materials Encyclopedia*; Salamone, J. C. Ed.; CRC Press: Boca Raton, FL, 1996; p 6747.
286. Soum, A. *Silicon-Containing Polymers*; Jones, R. G., Ando, W., Chojnowski, J., Eds.; Kluwer Academic Publishers: Dordrecht, The Netherlands, 2000; p 323.
287. Duguet, E.; Schappacher, M.; Soum, A. *Polym. Int.* **1994**, *33*, 129.
288. Bruzaud, S.; Soum, A. *Macromol. Chem. Phys.* **1996**, *197*, 2379.
289. Cazalis, C.; Mingotaud, A. F.; Soum, A. *Macromol. Chem. Phys.* **1997**, *198*, 3441.
290. Duguet, E.; Schappacher, M.; Soum, A. *Macromolecules* **1992**, *25*, 4835.
291. Rodriguez-Baeza, M.; Neira, C. A.; Aguilera, J. C. *Polym. Bull.* **2003**, *50*, 25.
292. Matsumoto, K.; Nakashita, J.; Matsuoka, H. *J. Polym. Sci. A* **2006**, *44*, 4696.
293. Brochon, C.; Mingotaud, A. F.; Schappacher, M.; Soum, A. *Macromolecules* **2007**, *40*, 3547.
294. Beckmann, J.; Jurkschat, K. *Coord. Chem. Rev.* **2001**, *215*, 267.
295. Rider, D.; Manners, I. *Polym. Rev.* **2007**, *47*, 165.
296. Bellas, V.; Rehahn, M. *Angew. Chem. Int. Ed.* **2007**, *46*, 5082.

Biographical Sketch

Marek Cypryk was born in Łódź, Poland. He received his MSc degree in 1974 in polymer chemistry from the Technical University in Łódź and PhD in 1982 from the Center of Molecular and Macromolecular Studies of the Polish Academy of Sciences under the supervision of Professor Julian Chojnowski. He worked as a postdoctoral fellow at the Carnegie-Mellon University in Pittsburgh, PA, in 1990–1991 in the group of Professor Krzysztof Matyjaszewski. In 2002, he completed his DSc (habilitation) in polymer chemistry. He is currently an associate professor and a head of the Department of Computer Modeling in the Center of Molecular and Macromolecular Studies. His research interests are organosilicon polymer chemistry; reaction mechanisms in organometallic chemistry, computational chemistry, and molecular modeling. He is an author and co-author of over 80 research papers and reviews.

4.18 Ring-Opening Polymerization of Cyclic Phosphorus Monomers

G Lapienis, Polish Academy of Sciences, Lodz, Poland

4.18.1 Scope of the Chapter

This chapter describes the ring-opening polymerization (ROP) of cyclic phosphorus-containing (P-containing) monomers. Phosphorus can be introduced into the polymer backbones and/or to the side chains in a variety of chemical methods. Phosphorus bound to hydrogen, carbon, sulfur, or nitrogen atoms will impart properties that differ so much from each other that any generalization is hazardous. There are two fields where the presence of the phosphorus atoms in the chains is essential, namely, biopolymers and their models and flame retardants. A few percent of P in the polymer is needed, although synergism with halogens allows it to be reduced to 1–2% to have an nonflammable product.

The most prominent phosphorus polymers are nucleic acid (NA) and teichoic acid (TA); these naturally occurring polymers are not covered in this chapter. Backbones of NA and TA are composed of hydrolytically stable diesters of phosphoric acids. The major functions of DNA (and several types of RNA) are related to storing and transferring information, genetic code, synthesis of proteins with a given microstructure, and contribution to the function of memory. Less known TA (mainly polyphosphates of glycerol or ribitol) with molar mass up to 2.5×10^4 are present in cell walls in Gram-positive bacteria. The main function of TAs is to provide rigidity to the cell wall by attracting cations such as magnesium and sodium. TAs also assist in regulation of cell growth and are mostly responsible for the transport of divalent ions (Mg^{2+}) through the cell walls from surrounding medium. Only some of the NA- and TA-related synthetic polymers are discussed in the ring-opening and polyaddition reactions sections.

The chapter consists of two parts. In the first part, the ROP of cyclic organophosphorus compounds is described. The second part is devoted to the synthesis of polymers having inorganic backbones, mainly phosphazenes.

4.18.2 Polymerization of Cyclic Organophosphorus Compounds

There are a number of comprehensive reviews devoted to the synthesis and properties of polymers containing phosphorus atoms in the main and/or side chains.[1–8]

The following methods are usually used for the synthesis of P-containing polymers:

1. Polymerization of cyclic monomers
2. Polycondensation
3. Polyaddition.

Polycondensation and polyaddition, as methods of the synthesis of organophosphorus polymers, have been described in more detail elsewhere.[1,4–7]

In this chapter, mainly the ROP of cyclic P-containing monomers is discussed. The synthesis of P-containing polymers by the polyaddition is discussed only for the reaction of phosphoric acid derivatives with diepoxides.

Discussed polymers are derived from the phosphorus atoms at two different level of oxidation, namely, pentavalent (P^V) and trivalent (P^{III}). Structurally, these compounds can be penta-, tetra-, or tricoordinated with direct bonding of phosphorus with oxygen or carbon atoms.

The following groups of monomers are described: spirophosphoranes (**1**) (pentavalent, pentacoordinated), cyclic phosphates (**2**) and phosphonates (**3**) (pentavalent, tetracoordinated), cyclic phosphites (**4**), phosphonites (**5**), phosphinates (**6**), and phosphines (**7**) (tervalent, tricoordinated). As mentioned above, polymerization of cyclic phosphazenes (**8**) is described in Section 4.18.6.

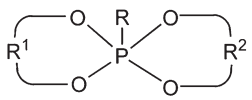

1

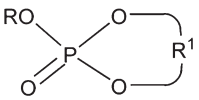

2

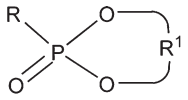

3

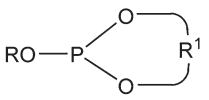

4

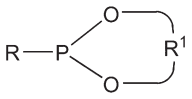

5

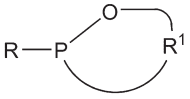

6

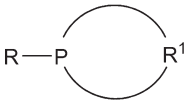

7

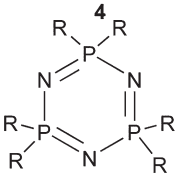

8

4.18.2.1 Introduction

In this section, only the main features of the ROP of cyclic organophosphorus (P^{III} and P^V) compounds are presented. More details on the properties of cyclic monomers were given in the previous chapters.[1,3,4] Copolymerization of cyclic trivalent phosphorus monomers[1,3] and polymerization of spirophosphoranes[1,9] have been reviewed elsewhere.

Some of the freshly distilled monomeric cyclic P^{III} compounds polymerize spontaneously at room temperature in bulk or in solution; for example, 2-methyl-1,3,2-dioxaphospholane (**9**) could not be isolated because of its fast oligomerization.[10,11]

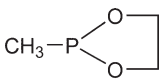

9

Spontaneous polymerization was observed for substituted and unsubstituted cyclic compounds containing pentavalent[12–16] as well as trivalent phosphorus atom in five-,[10,11,17–20] six-,[21–24] seven-,[25] and eight-membered rings.[26–28] It appears that these polymerizations were induced by the presence of the unknown impurities.

The high-vacuum technique[29–32] or the polymerization under the prepurified nitrogen or argon in sealed ampoules[33–36] is the necessary condition for the preparation of high molar mass polymers. As is usually the case in ionic chain processes, the purity of the monomers and solvents used is particularly important. This is clearly seen when the results reported by three different research groups on the polymerization of 2-methoxy-2-oxo-1,3,2-dioxaphospholane (**10**) and 2-ethoxy-2-oxo-1,3,2-dioxaphospholane (**11**) are compared.[31,36,37] Thus, when sodium mirrors were used for the final purification of monomers and solvents, the molar masses of polyphosphates were 3–4 times higher[31] than those reported by Vogt and Pflüger[37] and by Yasuda *et al.*[36]

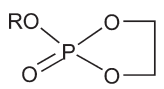

10: R = CH_3

11: R = C_2H_5

The monomers discussed in this chapter are soluble in the majority of common organic solvents such as benzene, methylene chloride, and acetone. Solvents with high solvating power must be used in order to avoid precipitation of the forming polymer, particularly when high polymers are prepared. Polymers have usually high polarity.[30]

The collected data concerning the structure of monomers, conditions of polymerization, and properties of the resulting polymers have been reported previously.[1,3,4,7]

4.18.2.2 Anionic Polymerization

Anionic polymerization of cyclic phosphate esters was studied for 2-alkoxy-2-oxo-1,3,2-dioxaphospholanes (**12**)[31,37–40] and its 2-thiono derivatives (**13**).[41]

poly-**12** (**13**) [1]

12: X = O; R = CH_3, C_2H_5, *n*-C_3H_7, *i*-C_3H_7, *n*-C_4H_9, *t*-C_4H_9

13: X = S; R = CH_3, CH_2CH_2Cl, C_6H_5

2-Methoxy-2-oxo-1,3,2-dioxaphospholanes (**10**) and 2-ethoxy-2-oxo-1,3,2-dioxaphospholanes (**11**) were polymerized over a wide range of temperatures, namely, from −20 to 120 °C

in bulk, in methylene chloride, or in tetrahydrofuran (THF) solutions with Et_2Mg, $(Bu^i)_3Al$, $(Bu^sO)_3Al$, $(Pr^iO)_3Al$, Bu^tOK, and Li metal as initiators.[31,37,38,42,43] The highest molar mass (1.5×10^5) was obtained in the polymerization of structure **10** with Et_2Mg at –20 °C in methylene chloride solution.[31] On the other hand, only oligomers of structure **13** ($M_n \leq 3 \times 10^3$) were formed with Na metal,[44–46] NH_3, or amines[47] as catalysts. Alkyl metals (particularly trialkylaluminums) are the preferred initiators to obtain high molar mass polymers. It is possible that, as mentioned previously, these initiators serve not only as initiators but also as purification agents, removing potentially chain-breaking impurities before the polymerization starts.[48]

It appears that polymerization of structure **10** with $(Pr^iO)_3Al$ (for the concentration range from 10^{-3} to 10^{-2} mol l^{-1}) is a living process.[38]

The ability of structures **12** and **13** to form high molar mass polymers may be attributed to the high strain of the five-membered rings: ~29 kJ mol^{-1} (data from heat of hydrolysis[49,50]) and 15 ± 2 kJ mol^{-1} (data from the heat of polymerization[39]), which presumably lowers the probability of the side reactions.

Cyclic phosphates (**12**) were also polymerized using alcohol and/or macroinitiators with hydroxy end groups as the initiators and tin(II) 2-ethylhexanoate (stannous octoate ($Sn(Oct)_2$)) as catalyst, usually in THF at 30–40 °C or in bulk at 90 °C.[51–59] In long-term polymerization of structure **12** with $Sn(Oct)_2$, some branched structures appeared with high conversion.[52] In addition, side reactions might occur in ROP of five-membered cyclic phosphates at high temperature (130 °C).[60]

There is only one report on the polymerization of structure **12** (R = Pr^i) at 0 °C using 1,8-diazabicyclo[5.4.0]undec-7-ene (DBU) and 1,5,7-triazabicyclo[4.4.0]dec-5-ene (TBD) as organocatalysts.[61]

Enzymatic polymerization of structure **12** (R = Bu^i)[62] and (R = Pr^i)[63] carried out in bulk at temperature ≤ 120 °C (with porcine pancreas lipase) gave polymers with M_n up to 5800.

The presence of substituents in the five-membered rings usually decreases the enthalpy of polymerization[64] (cf. lactams and acetals[65]) and leads to the lowering of the degree of polymerization (DP) of the resulting polymers.[31,36,40,42,66,67] Polymerization of structures **14** and **15** leads to polymers with $M_n = 2–3.5 \times 10^3$.[42] Some substituents may be a site of chain transfer, which will also lower the DP. But in the polymerization of structure **16** (Et_2Mg in benzene) polymers with M_n up to 2.5×10^4 were obtained.[40]

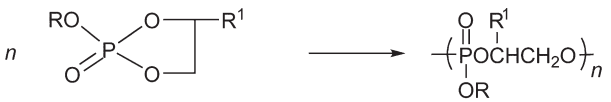

14: R = CH_3; R^1 = CH_3

15: R = C_2H_5; R^1 = CH_3

16: R = t-C_4H_9; R^1 = H, CH_3

poly-**14** (**15**, **16**)

[2]

Identical molar mass (2.5×10^4) was reported for poly-**17a** obtained in the polymerization of structure **17a** initiated by $(Bu^i)_3Al$ (25 °C, in methylene chloride). Because of the different openings of the ring (cleavage of α and/or β bond) of unsymmetrical substituted **17a**, in polymer chain three different units: head-to-head (H–H), head-to-tail (H–T), and tail-to-tail (T–T) were observed.[66]

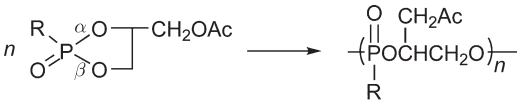

17

a: R = OCH_3

b: R = H

poly-**17**

[3]

Poly-**17b** after oxidation and hydrolysis gave polyphosphate (**18**), the analogue of TA.[66]

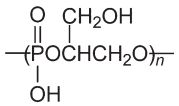

18

Gehrmann and Vogt[68] obtained poly-**17** (R = alkoxy) with much lower M_n (5×10^3).

4,5-Dimethyl-substituted **10** gave oligomer with molar mass equal to 3×10^2 (mostly tetramer), which is about 3 orders of magnitude lower than that of unsubstituted analog (poly-**12**, R = CH_3).[31,36] It is possible that the crowding of substituents in the ring is responsible for increasing the transfer involving the exocyclic group.

Only oligomers with DP not exceeding 7 were obtained in the anionic polymerization of the six-membered esters, 2-methoxy-2-oxo-1,3,2-dioxaphosphorinane (**19a**) and 2-ethoxy-2-oxo-1,3,2-dioxaphosphorinane (**19b**), carried out in bulk or in diglyme solution at 120–155 °C with Na metal, EtONa, Pr^iOK, and $(Bu^sO)_3Al$ as initiators.[30,44,45,69] Similar observations have been made for 5,5-dimethyl-substituted **19b**.[69]

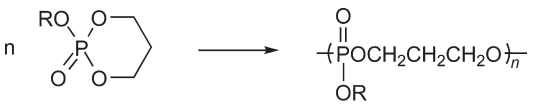

19

a: R = CH_3

b: R = C_2H_5

c: R = n-C_3H_7, i-C_3H_7, n-C_4H_9, $Si(CH_3)_3$

poly-**19**

[4]

Monomers were thoroughly purified in the cited works and the observed phenomena could not be ascribed to transfer or termination by impurities. It was concluded that low ring strain in six-membered cyclic phosphates (~4 kJ mol^{-1}), calculated from the hydrolysis data and confirmed by us in the studies of polymerization thermodynamics,[29] favors the transfer reactions leading to the removal of the exocyclic group from monomer, lowering their molar mass.[70]

It was also reported that fluorosubstituted phosphates (**20a**) undergo thermally, anionically, or cationically catalyzed ROP in bulk at 220–270 °C, giving rubberlike polymers poly-**20a** with intrinsic viscosity ~0.9 dl g^{-1}.[34]

The molar mass of the resulted poly-**20a** depended on the applied initiator. The relative effectiveness of initiators was as follows: KOH > Bu^nLi = $C_3F_7CH_2ONa$ > Et_3N. The presence of

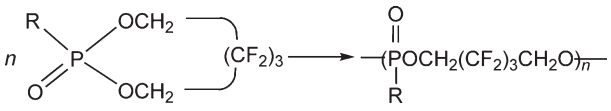

20 poly-**20**

a: R = R_FCH_2O, where R_F = CF_3, C_2F_5, C_3F_7, C_4F_9, $CF_3O(CF_2)_2$
b: R = CH_3, C_3H_7, C_6H_5, $N(CH_3)_2$

[5]

polar agents (e.g., THF, diethyl ether, and dimethylformamide (DMF)) considerably lower the temperature (~100 °C) required for polymerization.[34] The rate of polymerization of structure **20b** initiated by $C_3F_7CH_2ONa$ at 220 °C depends on the substituent (R) in the following way: C_3F_7 > Me > Ph > Me_2N, and is probably connected with some steric interactions.[71]

Five-, six-, seven-, and eight-membered cyclic phosphonates **21** and **20b** also undergo anionic polymerization initiated by sodium or alkyl metals, for example, $(Bu^n)_2Zn$, Me_2Cd, and $(Bu^i)_3Al$, and giving viscous or rubberlike products with reduced viscosity ≤ 0.7 dl g^{-1}.[71,72]

Cyclic unsaturated phosphonates (**21**) (R = CH_2 = CH–), after heating at 140 °C with water for < 80 h, gave telechelic oligomer as starting material for further radical polymerization.[73]

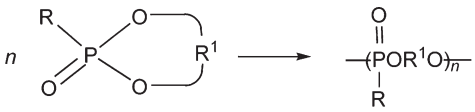

21 poly-**21**

[6]

R = CH_3, $ClCH_2$, C_6H_5

R^1 = $(CH_2)_m$, *m* = 2, 3, 4, 5; $CH_2CH(CH_3)$, $CH(CH_3)CH(CH_3)$, $(CH_2)_2O(CH_2)_2$

The reversible anionic polymerization of 2-hydro-2-oxo-1,3,2-dioxaphosphorinane (**22**) in bulk or in CH_2Cl_2 solution, initiated by EtONa, Bu^tOK, Bu^nLi, or $(Bu^i)_3Al$ at 25–45 °C led to the high molar mass linear polymer with M_n up to 10^5.[74] The best results were obtained with trialkylaluminiums as the initiators. Poly-**22** was easily converted into polyacid **23** by oxidation with N_2O_4.[75]

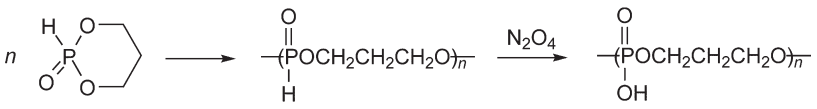

22 poly-**22** **23**

[7]

Another polymer, bearing only sugar in the chain, namely oligo(H-phosphonate) (DP = 9) (poly-**27** with glucose moieties) was obtained in the polymerization of structure **27** initiated with $(Bu^i)_3Al$.[82,83]

In the case of trivalent phosphorus cyclic compounds, only the anionic polymerization of 2-(diethylamino)-1,3,2-dioxaphosphorinane (**28**)[84,85] and methyl 2-deoxy-

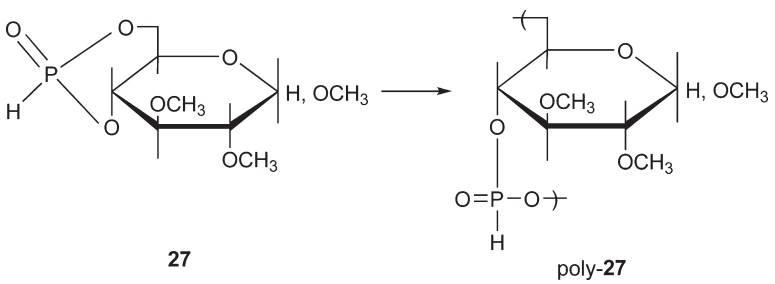

27 poly-**27**

[10]

D-ribofuranoside cyclic *N,N*-diethylphosphoramidite (**29**)[86] was studied. The anionic polymerization of structure **28** is living and fully reversible. The position of equilibrium was determined by ^{31}P NMR.[84]

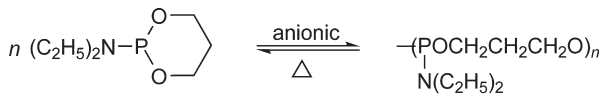

28 poly-**28**

[11]

Poly-**28** obtained by anionic polymerization of structure **28** and initiated with potassium or cesium alcoholates and/or potassium trimethylsilanolate had a linear structure, according to the ^{1}H, ^{13}C, and ^{31}P NMR spectra.[84] Alcoholates with smaller cations (Na^+ or Li^+), forming stronger multicomplexes, were not active in the initiation of the polymerization.

Poly-**28** after acetolysis gave the corresponding poly (H-phosphonate) (poly-**22**) with characteristic P–H coupling. Its further oxidation led to the polyphosphate **23**.[75,84]

[12]

Poly-**29** ($M_n = 9 \times 10^3$) was obtained in polymerization of structure **29** at 25 °C in THF solution with Bu^{t}OK as initiator.[86]

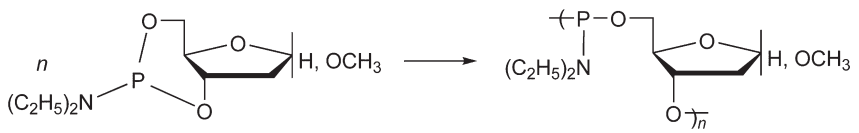

29 poly-**29**

[13]

The further transformation of poly-**29** (acetolysis and oxidation) gave structure **30**, the analog of the NA devoid of base.[86]

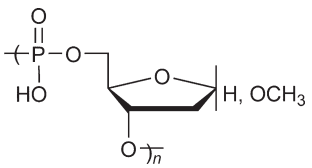

30

4.18.2.3 Cationic Polymerization

Cationic polymerization of the cyclic P-containing monomers gave polymers with lower molar mass than that obtained in anionic polymerization.

Polymerization of cyclic phosphates was studied in detail only for 2-alkoxy-2-oxo-1,3,2-dioxaphospholanes (**12**)[31,44,87–89] and 1,3,2-dioxaphosphorinanes (**19**)[29,44,48] with different exocyclic groups: R = Me, Et, Pr^n, Pr^i, Bu^n, and so on. Reaction was carried out in bulk at 100–155 °C with CF_3SO_3Me, CF_3SO_3Et, $Ph_3C^+A^-$ (A = PF_6, AsF_6, SbF_6) as initiators.[29,31,48] The resulting polymers had rather low molar mass ($M_n \leq 2 \times 10^3$), because of the chain transfer to monomer with simultaneous removal of the exocyclic alkoxy group from the growing tetraalkoxyphosphonium ions (cf. Section 4.18.2.5).[29]

The cationic polymerization of bicyclic phosphate **31**, initiated by traces of water at −78 °C, gave the insoluble cross-linked polymer (poly-**31**) containing five- and six-membered rings in the chain. That polymer after hydrolysis, under the controlled conditions, transformed into a linear polymer **32** without cyclic structures.[68]

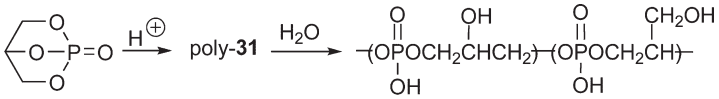

31 **32**

[14]

Shalaby *et al.*[90] described the synthesis and polymerization of 4-methyl-4,7-dioxo-1,4-azaphosphepane (**33**). The resulting poly-**33**, obtained in polymerization conducted with $SnCl_4$, H_3PO_4, or H_2O at 205 °C, had $\eta_{red} \leq 0.33$. Copolymerization of **33** with ε-caprolactam at 255 °C, in the presence of ε-aminocaproic acid (7-aminoheptanoic acid) as a catalyst, gave copolymers with higher viscosities ($\eta_{red} \sim 1.90$).[91]

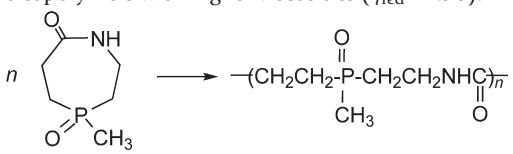

33 poly-**33**

[15]

Cationic polymerization of cyclic trivalent phosphorus compounds, initiated by alkyl halides, Lewis acids, Friedel–Crafts catalysts, and/or esters, was reported for various cyclic phosphites (**34**),[92–94] phosphonites (**35**),[17,21,23,35,95–97] phosphoramidites (**36**),[98] cyclic phosphanols (**37**),[99–101] and cyclic phosphanethiols (**38**).[100,102] MeI, $PhCH_2Br$, and CF_3SO_3Me were mainly used as initiators. The resulting polymers had molar mass not exceeding 5×10^3.

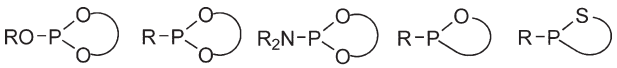

34 **35** **36** **37** **38**

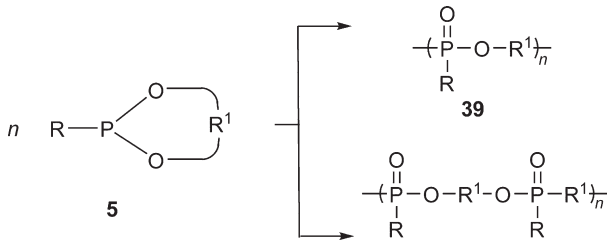

Scheme 1 Michaelis–Arbuzov (M-A) type of rearrangement in cationic polymerization of cyclic phosphonites.

These polymerizations proceed mostly by a Michaelis–Arbuzov (M-A) type of rearrangement (Scheme 1), involving cyclic phosphonium intermediates to produce polyphosphinates or polyphosphonates (39). The presence of isomerized repeating units (40) was the result of the occurrence of side reactions. Sometimes the proportion of the isomerized units was higher than that of the 'normal' units (39).[21,35,96]

Structures 39 and 40 were established on the basis of the analysis of their hydrolysis and chlorination products.[21,35]

Shimidzu *et al.*[93,94] first described the influence of the polymerization conditions of 2-alkoxy-1,3,2-dioxaphospholanes (41) on the structure of the resulting polymers (cf. Scheme 2). Usually polymers containing mixed units were formed. Nevertheless, the conditions for the formation of predominantly one structure were also reported. Thus, structure 42 was obtained by spontaneous oligomerization or by using lithium (or sodium) in liquid ammonia at −78 °C.[93] Structure 43 was formed in the polymerization catalyzed by alkyl halides or Et_3Al,[35,92,93] and structure 44 was formed with Lewis acids as initiators.[93]

There are only a few papers discussing the mechanism and kinetics of cationic polymerization of cyclic tricoordinated phosphorus compounds.

The cyclic phosphoramidites 45a (28) and 45b, initiated by alkyl halides (R^1X), undergo cationic polymerization by M-A rearrangement, giving polymers containing tetracoordinated phosphorus (46).[98] In the anionic polymerization initiated by Bu^tOK, no M-A rearrangement was observed[84,85] and polymers with tricoordinated phosphorus 47 (poly-28) were obtained.

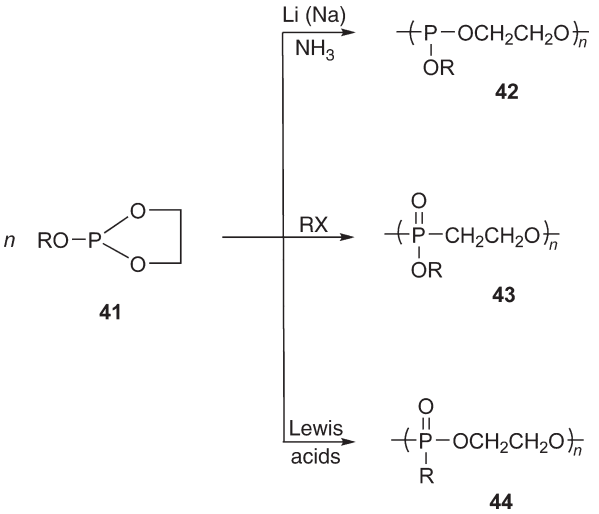

Scheme 2 Influence of the polymerization conditions of 2-alkoxy-1,3,2-dioxaphospholanes (**41**) on the structure of the resulting polymers.

3-Methyl-2-phenyl-1,3,2-oxazaphospholane (48a) initiated by MeI, Me_2SO_4, or $BF_3 \cdot OEt_2$ gave polymers with the structure poly-48;[103] likewise for 48b.

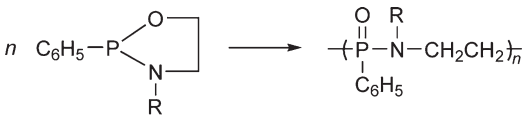

[17]

a: R = CH_3

b: R = C_6H_5

Polymer with the prevailing structure of poly(phosphine oxide) (poly-49; $M_n = 3.9 \times 10^3$) was obtained in the cationic polymerization of 2-phenyl-1,2-oxaphospholane (49). Poly-49 was next reduced to the corresponding polyphosphine to confirm its structure.[99] Structure 49 was also polymerized with chloro- and/or iodomethylated polystyrene, giving graft copolymers.[104]

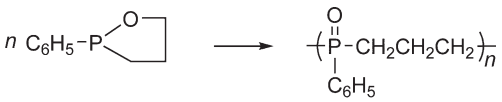

[18]

Ogata and Saito[105] described the synthesis and cationic polymerization of 7-oxo-4-phenyl-1,4-azaphosphepane (50a) and its 3,3,5,5-tetramethyl derivative (50b) with Et_2AlCl and $SnCl_4$ as catalysts. The resulting polymers have $\eta_{sp/c} = 0.08$ dl g^{-1}.

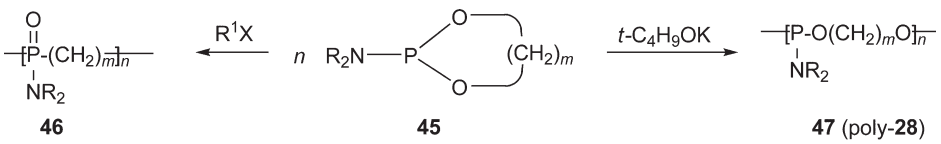

[16]

a: R = C_2H_5; m = 3 (**28**)

b: R = CH_3, C_2H_5; m = 2

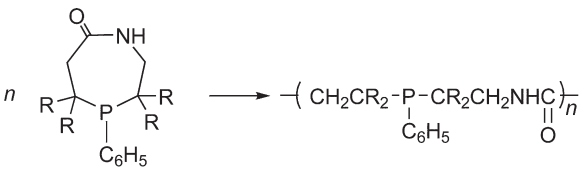

50

a: R = H

b: R = CH_3

[19]

4.18.2.4 Polymerization of Other Cyclic P-Containing Monomers

2-(2-(2-Hydroxyethoxy)ethoxy)-2-oxo-1,3,2-dioxaphospholane (**51**) was polymerized in bulk at temperature ≤ 60 °C without a catalyst.[60,106] As a result, a water-soluble hyperbranched polyphosphate (poly-**51**), having many hydroxyl groups and degree of branching equal to 0.47, was formed.[60]

4.18.2.5 Thermodynamics, Kinetics, and Mechanism of Polymerization

The thermodynamics of polymerization was studied mainly for tetra-[29,30,32,39,48,107] and tricoordinated[84] phosphorus compounds. The reported data are collected in **Table 1**. A plot of ΔH_p against ΔS_p for dioxaphosphorinanes, listed in **Table 1**, gives a straight line [82,108–110](cf. Plot in this volume; in the chapter written by Penczek and Kalużynski). It is apparent that the size of the exocyclic group in the ester series does influence monotonically ΔH_p and ΔS_p. Larger substituents decrease polymerizability of cyclic phosphates. The entropy change is only slightly negative for structure **19a** (with methyl substituent) and starting from the ethyl monomer (**19b**), polymerization becomes driven by a positive entropy change. Conversion of six-membered cyclic phosphates into a polymer results in a considerable increase in the rotational and vibrational entropy, because of the enhanced flexibility of the exocyclic group in the open-chain polymer unit.

The kinetics, mechanism, and thermodynamics of polymerization of cyclic phosphorus monomers were studied for cyclic phosphates[29,30,34,37,38,48,69,107] and trivalent phosphorus

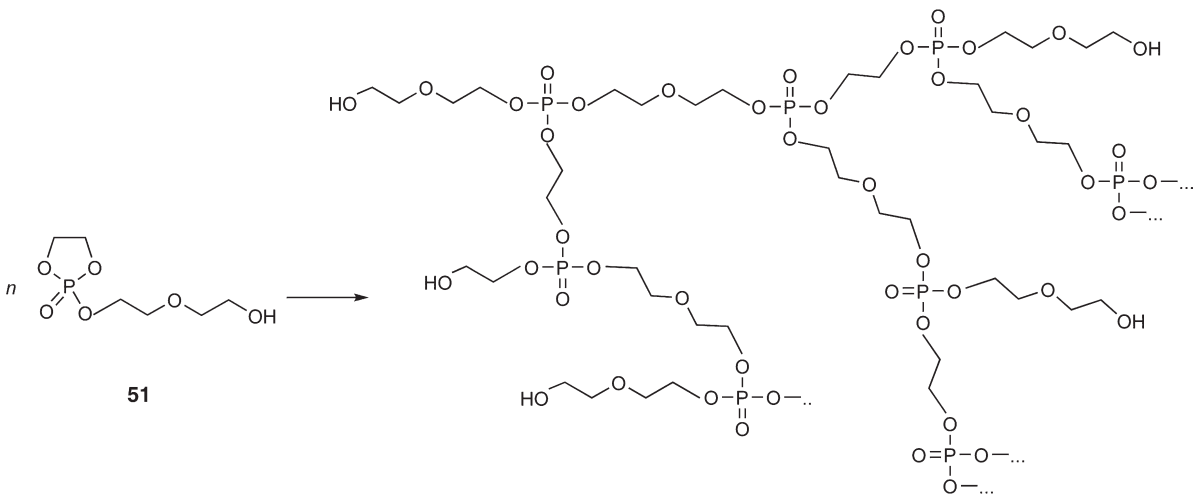

51

poly-**51**

[20]

Photocrosslinkable macromonomers ($M_n \leq 5.4 \times 10^3$) were synthesized in the polymerization of structure **12** (R = CH_2 = C(CH_3)CO, X = O).[55,58] Poly(ethylene glycol) (PEG) as the initiator and Sn(Oct)$_2$ as the catalyst were applied.[58]

The synthesis of star polymers (**53**) with ω-methylpoly (oxyethylene) (MPEG; M_n = 5000) arms and a core formed from di(cyclic phosphate) (**52**) has been recently reported.[59]

compounds: phosphoramidites (**28**),[85] phosphites (**34**),[96] phosphonites (**35**),[97] and cyclic phosphanols (**37**),[100,101] and were described in detail in the previous chapters.[3,4,82,111]

Cyclic phosphates and cyclic phosphites polymerize with anionic or pseudoanionic (e.g., trialkoxyaluminum) initiators. Anionic initiators have been shown to react with monomers by a nucleophilic attack on the phosphorus atom, giving alcoholate anions as the growing species.[39,85,113]

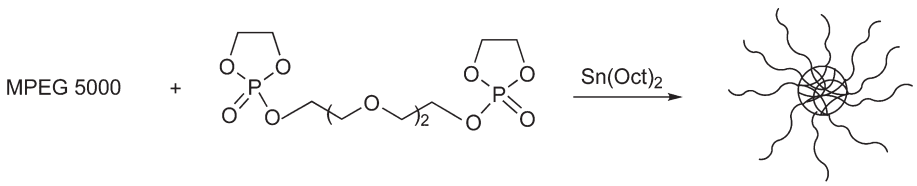

52 **53**

[21]

Table 1 Thermodynamic parameters of polymerization of 2-methoxy-2-oxo-1,3,2-dioxaphospholane (**10**) and 2-R-2-X-1,3,2-dioxaphosphorinanes (**19, 22, 28**)

	Monomer					
Polymerization	*No.*	*R*	*X*	ΔH_p *(kJ mol^{-1})*	ΔS_p *(J mol^{-1} K^{-1})*	*Reference*
Anionic	**10**	MeO	O	-14 ± 2	-13.5 ± 0.8	39
	28	Et_2N	Lone pair	6.3 ± 0.8	19 ± 3	82
	22	H	O	6.3 ± 0.8	19 ± 3	112
	19a	MeO	O	-2.9 ± 2.1	-12 ± 6	30
Cationic	**19a**	MeO	O	-4.6 ± 0.4	-23 ± 0.5	29
	19b	EtO	O	5.9 ± 2.5	11 ± 6	29
	19	Pr^nO	O	11.3 ± 1.6	24 ± 5	29
	19	Me_3SiO	O	16.3 ± 5.4	36 ± 14	29

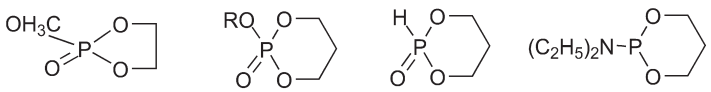

10 **19** **22** **28**

Reproduced from Penczek and Lapienis[4] with permission of Copyright Clearance Center.

Initiation of polymerization of cyclic phosphates (**10** and **19**) with EtO^-Na^+ involves an attack by the ethanolate on the electrophilic phosphorus atom in the monomer molecule and generating a growing alcoholate anion arranged in a trigonal bipyramid (**54**).[30,107,114] The six-membered ring in structure **54** occupies the axial–equatorial position.[115] The apical bond in structure **54** is broken, and the new alcoholate anion (**55**) is produced. In propagation, the growing anionic center (**56**) attacks the phosphorus atom in the next monomer molecule reproducing a structure similar to structure **54**. In anionic polymerization of the six-membered ring phosphates, only low molar mass oligomers were obtained because of the chain transfer to monomer. Instead of ring opening, the exocyclic alkoxy group is leaving (another apical bond in **54** is broken) and the polymer **56** with cyclic end group is formed (eqn [23]).[3,30,110]

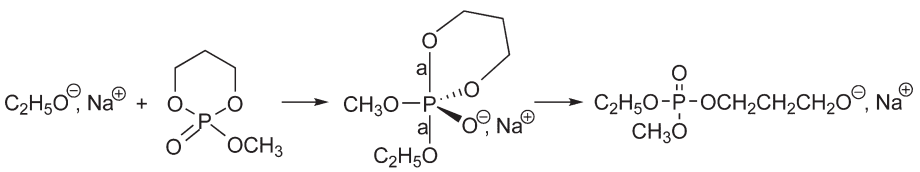

19a **54** **55**

[22]

A chain-transfer reaction was not observed when structure **58** (having the But exocyclic group) was polymerized with 1:0.9 Et_3Al–H_2O mixture in benzene. The resulting poly-**58**

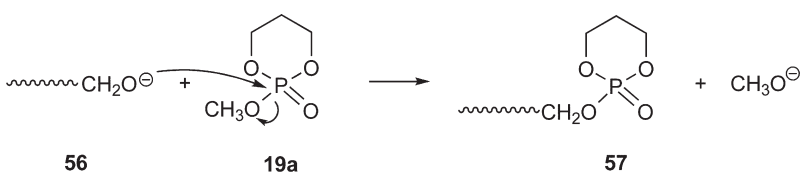

56 **19a** **57**

[23]

was transformed into structure **59** ($M_n = 2.5 \times 10^4$). During heating at 130 °C, *tert*-butyl group was removed as gaseous isobutylene.[40]

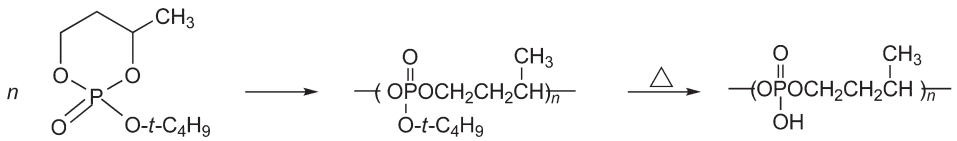

58 poly-**58** **59** [24]

The mechanism of anionic polymerization of 2-methoxy-2-oxo-1,3,2-dioxaphospholane (**10**), initiated by $(Pr^iO)_3Al$, was discussed in detail previously.[38] Polymerization proceeds through the formation of the polymeric Al–OCH_2CH_2–… bond. The proposed mechanism of polymerization can be visualized through the successive reactions (cf. eqn [25]).[38]

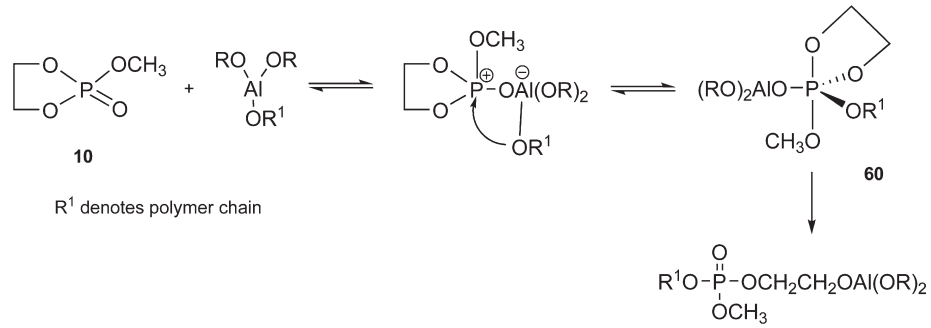

10

R^1 denotes polymer chain

60 [25]

Propagation occurs similar to initiation by macroion pairs and is nearly living; for example, at room temperature for every 250 propagation steps, there is only one termination.[85] The highest measured molar mass of poly-**28** (cf. eqn [11]) was 3.2×10^4.[116] Polymer chain is linear without any isomerization detected.[84]

Termination consists of the alcoholate anion attack on P atom in either polymer or molecule with expulsion of the Et_2N^- anion and formation of P–O bond. The diethylamide anion **61** cannot reinitiate polymerization.[85]

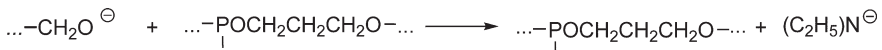

poly-**28** **61** [27]

The intermediate pentacoordinate phosphorus compound exists probably in the trigonal bipyramid structure (**60**), facilitating the –$Al(OR)_2$ group transfer.

Polymerization of structure **28** was initiated by potassium and cesium alcoholates and involves alkoxy anion attack on phosphorus atom. In this reaction, a new alcoholate anion is formed, capable of the further propagation step.

The kinetic parameters determined for structures **9**, **19**, and **28** are shown in **Table 2**.

The mechanism of cationic polymerization of cyclic phosphorus compounds was studied for a larger group of monomers.

Among the tetracoordinated cyclic esters of phosphoric acid, 2-alkoxy-2-oxo-1,3,2-dioxaphosphorinanes (**19**) have been studied in detail.[29,48,107] Trityl salts ($Ph_3C^+A^-$, where $A = PF_6$, AsF_6, SbF_6) and/or triflic esters (CF_3SO_3Me and

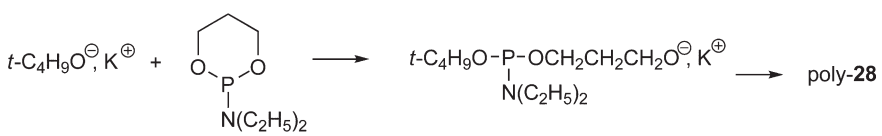

28 [26]

Table 2 Rate constants and activation parameters in the anionic and cationic polymerization of 2-methoxy-2-oxo-1,3,2-dioxaphospholane (**10**),[38] 2-alkoxy-2-oxo-1,3,2-dioxaphosphorinanes (**19**),[29,30,48] and 2-(diethylamino)-1,3,2-dioxaphosphorinanes (**28**)[85]

	Anionic			*Cationic*		
	10[a]	***19a***[b]	***28***[c]	***19a***[d]	***19b***[d]	***19c***[e]
k_i	6.5×10^{-3}	–	–	1.3×10^{-4}	–	–
k_p	4.5×10^{-1}	8.0×10^{-9}	3.4×10^{-4}	1.1×10^{-5}	6.2×10^{-6}	8.5×10^{-6}
k_t	–	–	1.3×10^{-6}	6.0×10^{-7}	8.9×10^{-8}	–
$\Delta H_i^{\neq}$	–	–	–	78 ± 12	–	–
$\Delta S_i^{\neq}$	–	–	–	-109 ± 33	–	–
$\Delta H_p^{\neq}$	42	112 ± 6	55.8	82 ± 12	86 ± 15	77 ± 6
$\Delta S_p^{\neq}$	−105	-26 ± 22	−135	-65 ± 30	-51 ± 38	-83 ± 51
$\Delta H_t^{\neq}$	–	–	–	49 ± 3	39 ± 20	–
$\Delta S_t^{\neq}$	–	–	–	-201 ± 8	-248 ± 51	–

[a] For $(Pr^iO)_3Al$ as initiator.
[b] For EtONa as initiator.
[c] For Me_3SiOK as initiator.
[d] For $Ph_3C^+PF_6^-$ and $Ph_3C^+AsF_6^-$ as initiators.
[e] R = $OSiMe_3$; for CF_3SO_3Et as initiator.
k_i, k_p, and k_t in l mol^{-1} s^{-1} (at 25 °C); $\Delta H^{\neq}$ in kJ mol^{-1}; $\Delta S^{\neq}$ in J K^{-1} mol^{-1}.

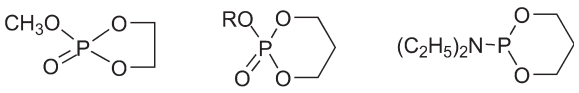

10 **19** **28**

Reproduced from Penczek and Lapienis[4] with permission of Copyright Clearance Center.

CF_3SO_3Et) were used as initiators.[29,48] The structure of tetraalkoxyphosphonium ion (**62**) – the active center in polymerization – was confirmed by ^1H and ^{31}P NMR.

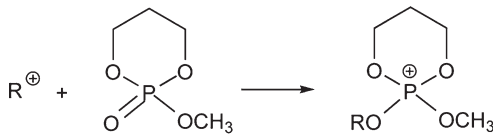

19a **62** (anion omitted) [28]

In polymerization of structure **19** only oligomers were obtained, because of the competition between propagation and chain-transfer processes (cf. **Scheme 3**).

The chain termination occurs analogously to propagation, involving chain transfer to polymer molecule.[29,48,107] Kinetic parameters are given in **Table 2**.

Cationic ROP of cyclic monomers, containing trivalent phosphorus atom,[96,100,101,117] proceeds by two mechanisms of propagation: ionic and/or covalent. These both can be visualized best for the polymerization of structure **49**.[117] Monomer **49** polymerizes by CF_3SO_3Me initiator

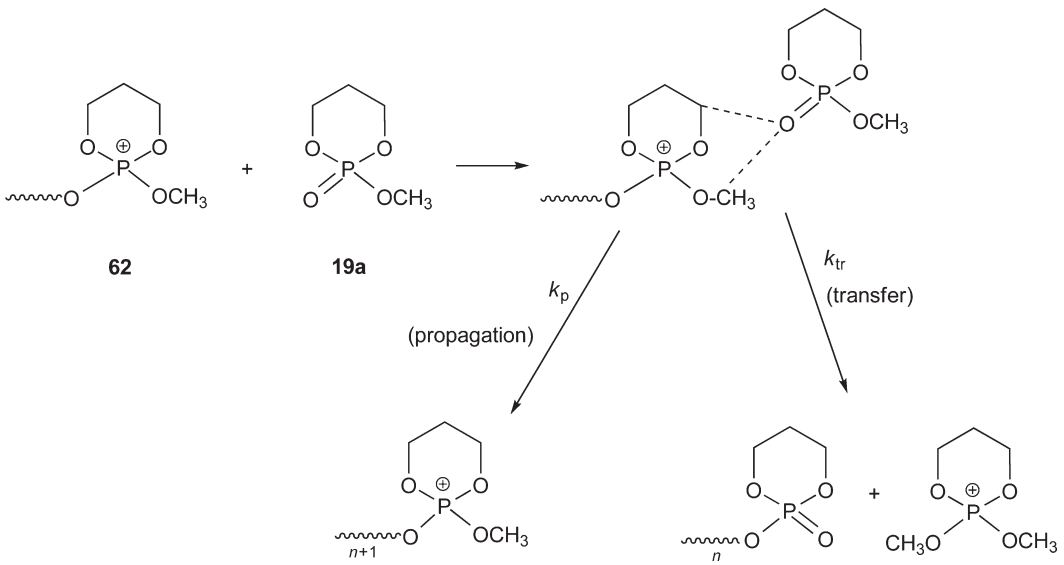

62 **19a**

Scheme 3 Propagation and chain-transfer processes in cationic polymerization of structure **19**.

through an ionic propagating species of a cyclic phosphonium ion structure (eqn [29]), whereas the same monomer, initiated with alkyl chloride initiator, propagates with covalent species of an alkyl chloride structure (eqn [30]).

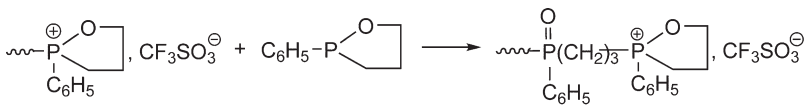

49

[29]

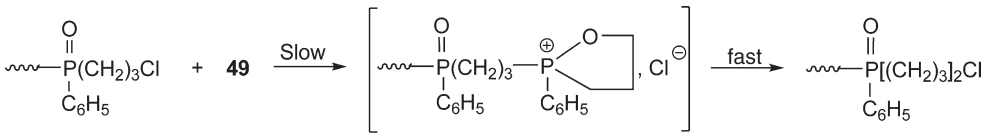

[30]

Polymerization of 2-phenyl-1,3,6,2-trioxaphosphocane (**63**) with CF_3SO_3Me proceeds with isomerization (cf. **Scheme 1**; 34% isomerized units were detected), whereas with $PhCH_2Cl$ nonisomerized structure of polymer has been obtained.[96,100,117] In polymerization of structure **63**, initiated by CF_3SO_3Me, the propagating species have a cyclic phosphonium structure (as in eqn [29]).[96,100,101,117] This structure of ionic propagating species has been proposed also in the polymerization of structures **64**, **65**, and **66**.[100] The calculated rate constants and activation parameters for polymerization of tricoordinated cyclic phosphorus monomers are collected in **Table 3**.

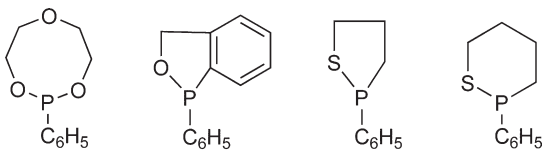

63 **64** **65** **66**

Table 3 Propagation rate constants and activation parameters in the polymerization of tricoordinated cyclic phosphorus compounds

Monomer	*Initiator (solvent)*	*Temp. (°C)*	k_p *(l mol s^{-1})*	$\Delta H_p^{\neq}$ *(kJ mol^{-1})*	$\Delta S_p^{\neq}$ *(J K^{-1} mol^{-1})*	*Ref.*
49	CF_3SO_3Me	50	3.52×10^{-4}	73.3	−84.8	101
	MeI	50	4.53×10^{-4}	66.7	−103	
	$PhCH_2Br$	50	4.75×10^{-5} [a]	63.5	−132	
	$PhCH_2Cl$	50	5.38×10^{-7} [a]	74.3	−136	
63	CF_3SO_3Me	60	7.2×10^{-5}	–	–	96
	$PhCH_2Cl$	150	2.8×10^{-4}	–	–	
64	MeI (MeCN)	35	7.3×10^{-5} [b]	–	–	100
	MeI (PhCN)	35	7.6×10^{-4} [b]	–	–	
	MeI (PhCl)	35	$>1 \times 10^{-2}$ [b]	–	–	
67	MeI ($CHCl_3$)	95	1.34×10^{-3}	–	–	100
68	MeI ($CHCl_3$)	95	2.48×10^{-3}	79.5	−61.6	100

[a] Calculated values.
[b] Apparent.

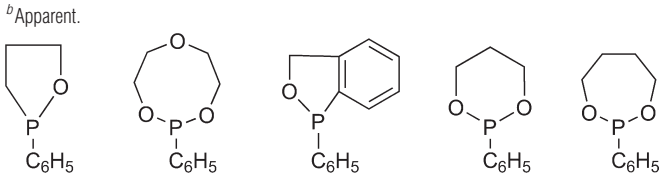

49 **63** **64** **67** **68**

Reproduced from Penczek and Lapienis[4] with permission of Copyright Clearance Center.

The nonisomerized structure of the polymer chain was obtained only in the polymerization initiated by alkyl chlorides,[117] whereas with alkyl bromides, iodides, and/or Lewis acid catalyst, the isomerized units were found in polymers.[21,33,35,93,97,98]

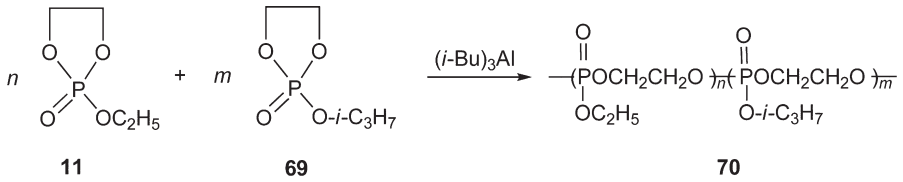

11 69 70 [31]

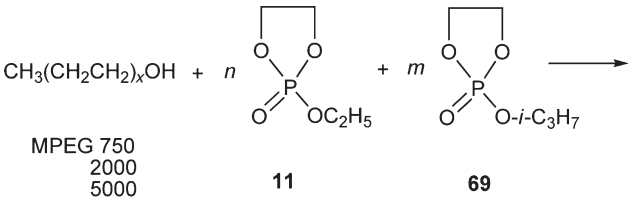

11 69 [32]

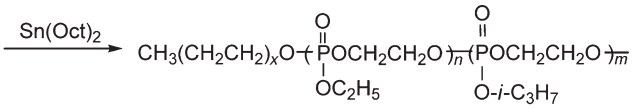

71

ratios equal to 2.23 and 0.48 were reported.[118] These two monomers were also copolymerized in the presence of MPEG as the initiator and $Sn(Oct)_2$ as the catalyst. The resulting thermoresponsive block copolymers (**71**) had various molar mass ($M_n \leq 3.5 \times 10^4$) and compositions.[56]

4.18.2.6 Copolymerization

The P-containing cyclic monomers undergo copolymerization with cyclic organophosphorus monomers as well as with other cyclic or unsaturated compounds. The published data (also the patent literature) devoted to this subject have been collected in previous review papers.[3,4,60]

Biodegradable **73** with $M_n = 1.2 \times 10^4$ was obtained in copolymerization of structure **69** with **72** (having ethyl methacrylate group) initiated by $(Bu^i)_3Al$. The calculated number of units of structure **72** in copolymer was ~2.[119–121] From structure **73** and 2-(methacryloyloxy)ethyl-phosphorylcholine (**74**), hydrogel was formed by radical polymerization.[119]

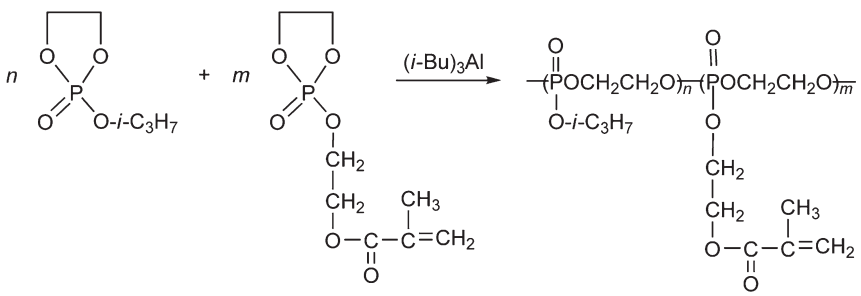

69 72 73 [33]

4.18.2.6.1 Copolymerization of cyclic phosphates

Fontaine *et al.*[42] studied the copolymerization of structure **15** with **14** and **12** (R = Et, cholesteryl). Molar mass of the resulting copolymers did not exceed 2×10^3. They also determined the reactivity ratios for the copolymerization of structure **14** with **15**, namely, $r_1 = 0.88$ and $r_2 = 0.51$ for the reaction in solution (CH_2Cl_2, r.t.) and $r_1 = 1.52$ and $r_2 = 0.89$ for copolymerization in bulk at 90 °C.

Thermoresponsive polyphosphoesters (**70**) were obtained in copolymerization of structures **11** and **69** and reactivity

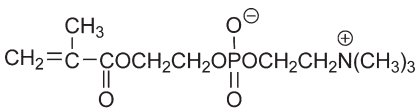

74

Copolymerization of structure **69** with five-membered cyclic phosphate bearing 2-bromoisobutyrate group (2-[(2-oxo-1,3,2-dioxaphosphoroyl)oxy]ethyl 2-bromois- obutyrate), (**75**),

using $(Bu^i)_3Al$ as an initiator was also reported. The resulting polyphosphates (76) had $M_w = 3.4 \times 10^4$ and 3.7×10^4 with 3.0 and 10.5 units of structure 75 per macromolecule.[43] Amphiphilic polyphosphate graft copolymers with hydrophilic graft chains were formed by grafting 74 from 75 sites in 76 by atom transfer radical polymerization (ATRP).[43,122]

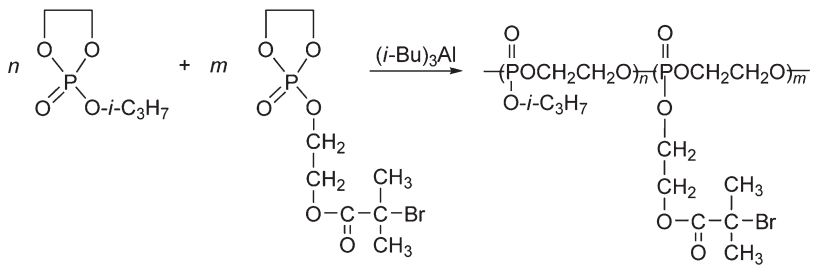

69 75 76

[34]

Terpolymers containing units derived from structures 69, 75, and 12 (R = cholesteryl) monomers were also obtained.[122]

4.18.2.6.2 Copolymerization with cyclic esters

Various cyclic phosphorus compounds, mainly 2-ethoxy-2-oxo-1,3,2-dioxaphospholane (11), were copolymerized with lactide (LA),[123,124] ε-caprolactone (CL),[51,52,54,125–127] and six-membered cyclic carbonates (77)[128,129] or 1,4-dioxan-2-one (78).[130] As a result, random and/or block copolymers were obtained. Aluminum alkoxides and/or $Sn(Oct)_2$ were usually applied as initiators. In some cases, polymerization of cyclic phosphates was initiated by hydroxy-terminated compounds: dodecanol,[52] MPEG,[65] poly-L-lactide (PLLA),[131] and poly(ε-caprolactone) (PCL)[51,132,133] with $Sn(Oct)_2$ as the catalyst.[54]

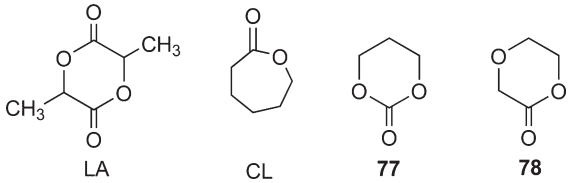

Well-controlled ROP of cyclic phosphates initiated by $(Pr^iO)_3Al$[125] or alcohol/$Sn(Oct)_2$[52,53,133] produces block copolymers with desired molecular structures, composition, and defined molar mass control of polyphosphate chain and possessing functional hydroxy end groups, which can be further modified for conjugation with bioactive molecules.[53]

When hydrophobic macroinitiators (e.g., PCL and PLA with hydroxyl end groups) were used as the initiators, the resulting amphiphilic block copolymers with polyphosphate chains can form various self-assemblies in aqueous solution.[53,57] On the other hand, when, for example, MPEG as a hydrophilic macroinitiator is used, the formed block copolymer is doubly hydrophilic.[56,59]

Amphiphilic triblock copolymers (79) of poly-11 and PCL with various block lengths of poly-11 ($M_n = 3–21 \times 10^3$) and PCL ($M_n = 1–7.5 \times 10^3$) were synthesized and characterized.[53,57]

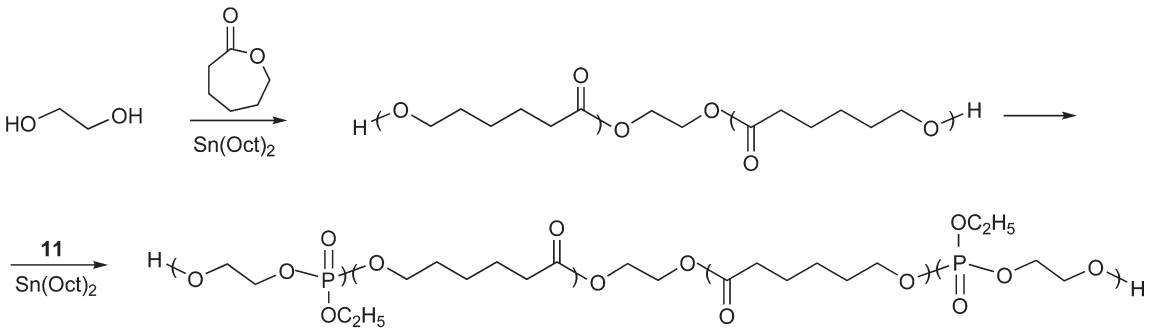

79

[35]

Amphiphilic and cationic triblock copolymers consisting of MPEG, PCL, and poly-12 (R = $CH_2CH_2NH_2$) were also obtained.[134] Cyclic phosphates (12) (R = Me, Et, Pr^i) were used to adjust the hydrophobic–hydrophilic balance of the copolymers and influence their thermosensitivity in a wide range.[133,135]

The analysis of the kinetics of propagation of five-membered cyclic phosphates, used as the second monomer in the synthesis of PCL–polyphosphate block copolymers, disclosed that the rate constants of propagation are affected by the structure of pendent group connected to phosphorus. Thus, the rate constant (in toluene) for structure 12 (R = Pr^i) was equal to 7.2×10^{-4} l mol^{-1} s^{-1} (90 °C) and it increased to 2.7×10^{-3} l mol^{-1} s^{-1} (50 °C) for structure 11.[126]

Polymerization of structure 12 (R = MPEG 750) on PCL block gave brush-coil diblock copolymer containing 62 monomer units of CL and up to 6 PEG brushes per polymer chain.[136]

The calculated reactivity ratios $r_1 = 1.27$ and $r_2 = 0.94$ in copolymerization of structure **11** with D,L-lactide (D,L-LA) in bulk in the presence of $(Pr^iO)_3Al$ as initiator denote that the active chain ends **11*** and LA* both have a greater tendency to react with **11** than with LA.[124]

The synthesis of four-armed biodegradable star block copolymers of PCL and poly-**11** using hydroxyl-terminated four-arm star PCL and a $Sn(Oct)_2$ co-initiation system was also reported.[137] Amphiphilic three ABC-miktoarm star terpolymers composed of PCL, MPEG, and poly-**11** were synthesized by a combination of ROP and 'click' chemistry.[138]

Block copolymers (poly-**12**-*block*-poly-**74**) were synthesized by ATRP of 2-(methacryloyloxy)ethyl-phosphorylcholine (**74**) by using poly-**12** (R = Pr^i) as a macroinitiator.[61]

The reactivity values $r_1 = 1.75$ and $r_2 = 0.34$ ($r_1 \times r_2 < 1$) were determined for the copolymerization of trimethylene carbonate (**77**) with 2-hydro-2-oxo-1,3,2-dioxaphosphorinane (**22**) using $(Bu^i)_3Al$ as the initiator.[139]

Enzymatic ring-opening copolymerization of structures **77** and **11** was performed in bulk at 100 °C using porcine pancreas lipase and/or *Candida rugosa* lipase as catalysts.[128]

Hydrolysis of the main chain of random copolymer of D,L-LA and **11** exhibited a higher rate compared with PLLA itself, obviously because of the increased hydrophilicity of the copolymer facilitating the diffusion of water molecules to the polymer chain.[124] Additionally, in acid environment the hydrolysis of the side chains proceeded faster than that of the main chain,[124] which agrees with the previously reported data.[140]

4.18.2.6.3 Zwitterionic copolymerization

Zwitterionic copolymerization was mostly developed by Saegusa and Kobayashi. A number of alternating copolymers, involving cyclic P-containing monomers, were prepared that way.[2,9,105,141–149] In these copolymerizations, two monomers form the donor–acceptor pair, with sufficiently strong delocalization of charges to induce the copolymerization. The role of 'initiator' is being played by one monomer toward the other. Copolymerization of that pair does not require any added initiator and can give an alternating copolymer simply by mixing the monomers at room or higher temperatures.

Zwitterionic copolymerization involves the reaction of a nucleophilic monomer (M_N) with an electrophilic monomer (M_E) to generate a zwitterion (**80**) ($^+M_N–M_E^-$) (generic zwitterion). The propagation is described by eqn [37], which starts with the reaction between 2 moles of generic zwitterions (**80**) (eqn [36]).

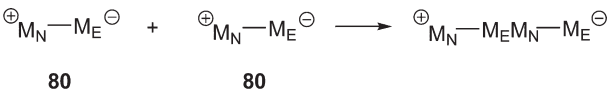

80 **80**

[36]

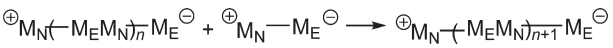

[37]

Saegusa studied a very broad spectrum of cyclic and acyclic trivalent phosphorus compounds as the M_N components in combination with many M_E monomers. Some of investigated cyclic P-containing monomers are shown in **Table 4**.

Zwitterionic copolymerization takes place at moderate temperatures (usually ≥ 80 °C). Spirophosphoranes (**1**) obtained at room temperature, undergoing thermally induced ROP at high temperatures.[143,153,154,164,172–178] The structures of the resulting copolymers were established by IR and by ^{1}H and ^{31}P NMR.

As an example, the alternating copolymerization of 2-phenyl-1,3,2-dioxaphospholane (**81a**) can be used. Thus, the copolymerization of structure **81a** with acrylic acid (**87**) and with β-propiolactone (**88**) gives the same alternating copolymer (**90**).[153] The M-A reaction is responsible for the appearance of the tetracoordinated phosphorus. The zwitterion **89** is assumed to be identical in both cases.

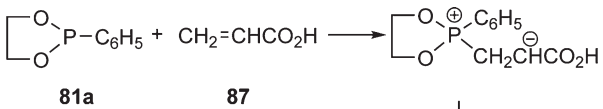

81a **87**

[38]

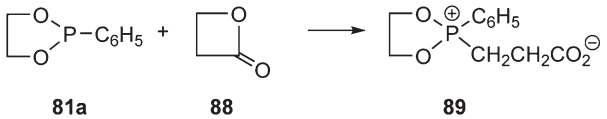

81a **88** **89**

[39]

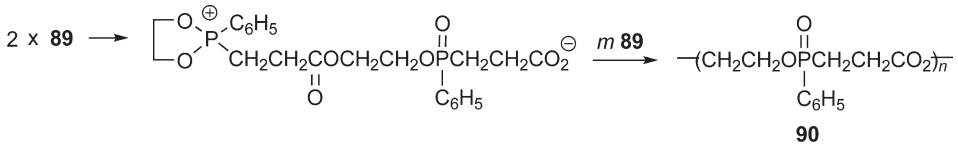

90

[40]

Table 4 M_N monomers giving a phosphonium site in zwitterionic copolymerization

M_N monomers	*References*
63	150
67	151, 152
81a	150, 153–163
81b	155–158, 164
82a	165
82b	165
83	166
84	167
85a	151, 163, 168–170
85b	161, 168, 170
86	171

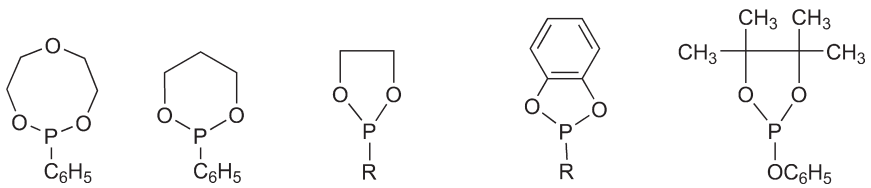

63 **67** **81** **82** **83**

a: R = C_6H_5
b: R = OC_6H_5

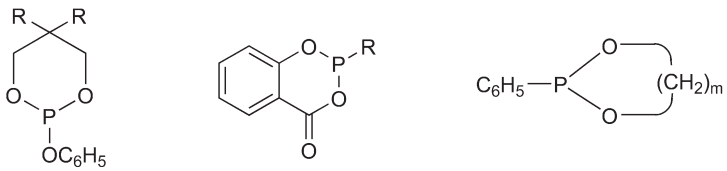

84 **85** **86**

a: R = C_6H_5
b: R = OC_6H_5

m = 2, 3, 4

This copolymerization takes place only above 100 °C, giving structure **90** with $M_n \leq 4.4 \times 10^3$.[143] At room temperature, the reaction of an equimolar mixture of structures **81a** and **87** in ether gives, in almost quantitative yield, a crystalline material (m.p. 80 °C) having the spirophosphorane structure (**91**).[146,153] At higher temperatures, the P–O–C(=O) bond in structure **91** undergoes heterolytic cleavage to give the zwitterion **89**, promoting polymerization (cf. eqn [40]).[9,146]

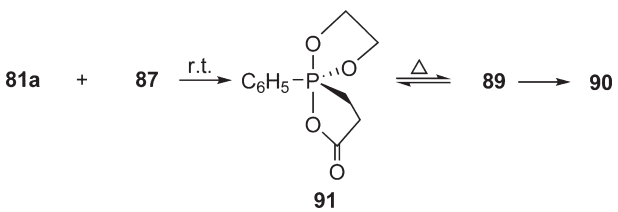

91

[41]

Polymers obtained by homopolymerization of spirophosphoranes have higher molar mass than their analogues from zwitterionic copolymerization, probably because of higher purity of the spiro monomers and an 'inherent stoichiometry'.[179]

Some monomers having an acid hydrogen such as acrylic acid,[153] α-keto acids,[164] and ethylenesulfonamide[158] undergo a hydrogen-transfer copolymerization (cf. eqn [42]).

In the case of copolymerization of vinylphosphonic acid monoethyl ester (**92**) with cyclic phosphonites (**86**), the alternating copolymer (**93**) having two kinds of phosphorus atoms in the main chain was formed. During the copolymerization, monomer **92** was reduced involving a hydrogen-transfer process and monomer **86** was oxidized; the oxidation state of the phosphorus atom of monomer **86** changed, therefore, from trivalent to pentavalent ('oxidation–reduction copolymerization').[171]

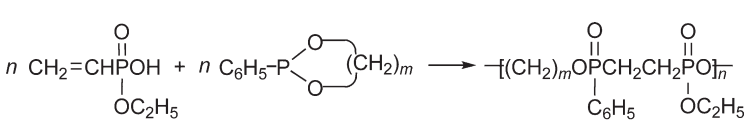

92 **86** **93**

m = 2, 3, 4

[42]

A similar structure to polymer **93** was observed when **92** was replaced by its *N*-propylamide derivative.[180]

Alternating copolymers by zwitterionic mechanism were also formed in group-transfer alternating copolymerization of 2-phenyl-1,3,2-dioxaphosphorinane (**67**) with trimethylsilyl 3-(acryloyloxy)propanoate.[152]

Kobayashi also elaborated a specific method of copolymerization called 'ring-opening-closing alternating copolymerization' (ROCAC). This method relies on the synthesis of alternating copolymers (**94**), having the structure of a ring-opened unit derived from a cyclic monomer **A** and a ring-closed unit formed from a noncyclic, bifunctional monomer **B**.[181–185] Cyclic phosphonites (**5**) as **A**-type (ring-opening) monomers and methacrylic and acrylic anhydrides,[181] muconic acid,[182,185] and/or dialdehydes[183,184] as **B**-type (ring-closing) monomers were used. The method of ROCAC is visualized schematically in eqn [43].

A **B** **94** [43]

4.18.3 Polyaddition

Models of TAs (naturally occurring constituents of cell walls of Gram-positive bacteria) were prepared by different methods:

1. Polycondensation of glycerol[186] or ribitol[187] with phosphorylating agent (e.g., $(PhO)_2POCl$ in the presence of tertiary amine).[188]
2. ROP of structure **17** (cf. eqn [3]).[66]
3. Polyaddition of H_3PO_4 (or its derivatives) and/or H_3PO_3 to diepoxides.[188–194]

In this section, only the synthesis of polyphosphates (**97**) prepared by direct addition of phosphoric acid (**95a**) and its silyl derivative (**95b**) to diepoxides (**96**) is discussed. The number of carbon atoms between two closest phosphate groups was varied depending on the structure of starting diepoxide.[190,192,194]

The oxirane rings, activated (through protonation or hydrogen binding to the P–OH groups), react with hydroxy groups and in this way propagation of oxiranes according to the activated monomer (AM) mechanism occurs (cf. Chapter 4.08).[190,192] The kinetics of –P(=O)OH oxirane addition is, however, much more complex than the simple kinetics of the AM polymerization, due to the possibility of formation of the intramolecular hydrogen bonds.

The simple polyaddition becomes shortly challenged by branching, either at the third acidic group or at the hydroxy C–OH group. Apparently, when all three acidic groups of the same P atom are engaged in addition, the network is formed.[190,191,195]

Under certain conditions, insoluble polymers, highly swelling in water, were obtained (the degree of swelling approached 10^3%). The idealized polyaddition of H_3PO_4 to diepoxides was possible if only two acidic functions were engaged (cf. eqn [44]).

In some reactions, in order to avoid branching and to increase the solubility of the resulting polymers, H_3PO_4 was reacted with diepoxides in the presence of a stoichiometric amount of the reagent blocking *in situ* formed hydroxy groups, for example, acetic anhydride and/or 3,4-dihydro-2*H*-pyran.[191–193]

Linear polymers (**99**) with much less branching were also prepared by polyaddition of diepoxides (**96**) to disilyl esters of methylphosphoric acid (**95b**), because the addition of the phosphoryl fragment to the epoxide ring is connected with the simultaneous blocking of the hydroxy groups by the trimethylsilyl moieties.[188,189,191,192]

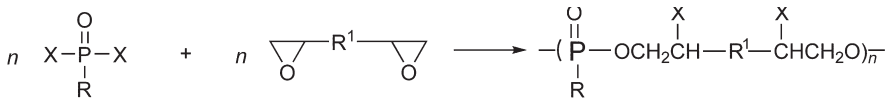

95 **96** **97** [44]

a: R = X = OH

b: R = OCH_3, X = $OSi(CH_3)_3$

c: R = H, X = OH

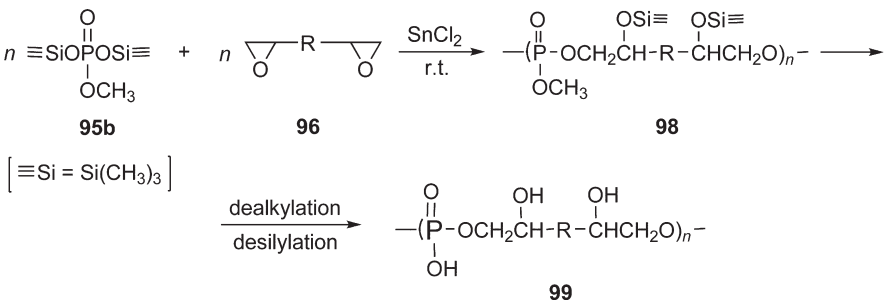

95b **96** **98** [45]

99

4.18.4 Transformation of Poly(alkylene phosphate)s

Poly(alkyl alkylene phosphate)s were converted into poly(alkylene phosphate)s (e.g., structure **100**). The dealkylation process was elaborated for poly(2-methoxy-2-oxo-1,3,2-dioxaphospholane) (poly-**12**, R = CH_3). Over 90% of methyl groups were removed and a slight decrease in molar mass of polymer (less than 30%) was observed.[75]

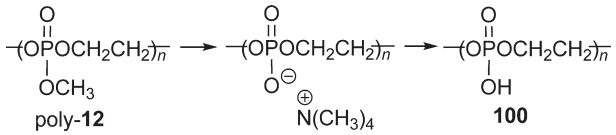

[46]

Some poly(alkylene phosphate)s were modified by introducing derivatives of imidazole,[196] amino acids,[197] and/or NA bases as side groups.[198–200]

4.18.5 Some Properties and Applications of Poly (alkylene phosphate)s

The properties and applications of poly(alkylene phosphate)s were described in more detail in the previous chapters.[7,82,188,201] In this chapter, only a few examples are mentioned.

Polyphosphates exhibit flame retardation and adhesive characteristics. As additives, they improve processability by increasing the solubility of the polymer in common solvents or by lowering the glass transition temperature.[123,124]

High molar mass poly(alkylene phosphate)s were obtained as models of biopolymers and bioanalogous polymers.[82,83,188,189] Poly(trimethylene phosphate) (**23**; model of TAs)[202,203] and other poly(alkylene phosphate)s[204–208] were used as components in the studies of active ion transport through liquid membranes. Simple poly(alkylene phosphate)s were used for studies of cation binding and conductivity measurements gave the binding sequence similar to that reported for DNA, namely, $Ca^{2+} > Mg^{2+} > K^{+} > Na^{+}$.[209] For some model polymers, their hydrolytic stability was also studied.[140] The rate constants of hydrolysis and the pH-rate profile for poly (trimethylene phosphate) (**23**) and poly(methyl ethylene phosphate) (poly-**12**, R = CH_3) were determined.[140,189]

The equilibrium constants of complexation of Na^{+} cations by poly(methyl ethylene phosphate) (poly-**12**, R = CH_3) were determined by using ^{23}Na NMR method. The numerical values are close to those known for PEG.[210]

Poly(alkylene phosphate)s form stable complexes with poly (pyridin-1-ium-1,4-diylethylene)[211] and conductive complexes with polyaniline.[212,213]

Biodegradable polyphosphates appear attractive for biological and pharmaceutical applications because of their biocompatibility and structural flexibility. They could be used for drug and gene delivery and in the field of tissue engineering as scaffolds carriers.[51,78,79,137,214–216]

Biocompatible and biodegradable hydrogels based on polyphosphoesters were also synthesized and applied in cell encapsulations[58,60,120,217,218] and as novel cellular matrices.[219] Amphiphilic random and block copolymers of phosphoesters, capable of self-assembling into micellar nanoparticles, were evaluated recently for drug and gene delivery.[43,53,57]

Addition of $LiClO_4$ to poly(poly(oxyethylene) methyl phosphate) causes the formation of polymer electrolyte. The influence of the complex composition on T_g and ionic conductivity has been studied.[220]

Some poly(alkylene phosphate)s are useful as additive flame retardants.[201]

4.18.6 Polymerization of Cyclic Inorganic P-Containing Compounds

4.18.6.1 Polyphosphazenes

Polyphosphazenes are high molar mass, essentially linear polymers, with main chains consisting of alternating phosphorus and nitrogen atoms and two side groups, attached to each phosphorus atom. There are known several hundred different polyphosphazenes (**101**), with a wide variety of different organic (e.g., alkoxy, aryloxy, amino, alkyl, and aryl), inorganic, or organometallic side groups (R). The inorganic backbone of alternating phosphorus–nitrogen bonds gives the polymer chain high flexibility and the side groups attached to the phosphorus atoms influence the overall properties (e.g., their size, shape, polarity, etc.) of the resulting polymer.

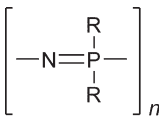

101

Three main methods exist for the synthesis of polymeric phosphazenes:

1. ROP of the cyclic trimers, hexachlorocyclotriphosphazene ($(NPCl_2)_3$; structure **102**) or $(NPF_2)_3$, followed by replacement of the halogen atoms in the polymer by organic or organometallic side groups (eqn [47]);
2. polymerization of phosphazene cyclic trimers that already bear the organic or organometallic side groups (eqn [48]); and
3. polycondensation of phosphoranimines (eqns [49] and [50]) (not discussed in this chapter).[221,222] The one-pot synthesis of linear polyphosphazenes should also be mentioned here, method elaborated by Allen and described by Peterson *et al.*[223]

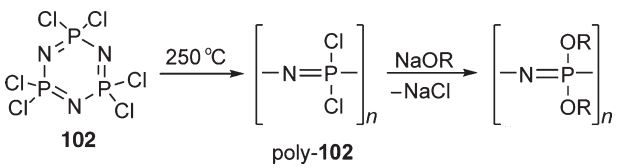

[47]

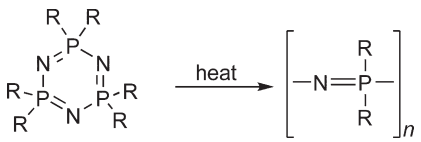

[48]

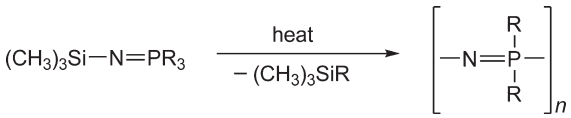

[49]

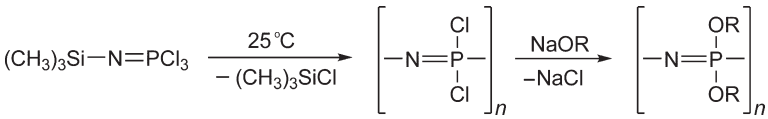

[50]

Stokes,[224] in the nineteenth century, was the first to obtain (by heating structure **102** in bulk) the rubberlike poly(dichlorophosphazene) (poly-**102**) that is called 'inorganic rubber' because of mechanical properties similar, in many aspects, to natural rubber.[225] Before 1965, thermal and/or catalyzed polymerization of $(NPX_2)_3$ (X = CI, F, Br, NCS) was carried out, giving mostly cross-linked $(NPX_2)_n$ at higher conversion.[226–229]

Allcock and Kugel,[230,231] reported in 1965 the preparation of linear high molar mass $(NPCl_2)_n$, completely soluble in common organic solvents. Polymerization was stopped at lower conversion (usually ≤ 70%), before any gelation occurred.

There are a huge number of papers describing the synthesis, chemistry, modifications, and properties of polyphosphazenes, but the earlier ones were mostly devoted to polymerization of cyclic monomers. In this chapter, only selected references are reported. More detailed data is available in many books[232–237] and the review papers published by Allcock[222,238–248] and others.[4,223,249–262]

4.18.6.1.1 Polymerization of $(NPCl_2)_3$

4.18.6.1.1(i) Polymerization in bulk

Polymerization of structure **102** (obtained in the reaction of phosphorus pentachloride and ammonium chloride and rigously purified) is usually carried out at ~250 °C in evacuated and sealed glass tubes for 24–72 h.[230,231,238,252,263–267] The molar mass of the polymer is often very high ($M_w \sim 10^6$), but with a broad molar mass distribution.[236] It is difficult to gain the repeatability of the results (characteristics of the polymerization products), namely, molar mass, dispersity, and degree of cross-linking.[242,268]

It has also been found that traces of water act as catalyst promoting polymerization, whereas some other impurities (e.g., PCl_5) are powerful inhibitors.[269,270] Thus, for example, a small amount of water (below 0.1 mol.%) was found to increase the rate of polymerization. On the other hand, larger amounts (> 0.2 mol.%) may suppress polymerization completely, or increase the formation of cross-linked polymer (> 1 mol.% water).[270]

Additives or impurities, which are able to remove chloride ions from monomer, accelerate the rate of polymerization, but some of them promote the cross-linking processes.[227,270–274] The degree of cross-linking increases with the increase in polymerization time and the reaction temperature.[242]

In the presence of catalysts, polymerization occurs at lower temperatures; for example, with BF_3 structure **102** polymerizes at 150 °C.[275] A lot of different compounds were tested as catalysts, namely, carboxylic acids, their salts and esters, ethers, ketones, alcohols, nitromethane, metallic zinc, tin, or sodium.[238,252,271,272] The best results were obtained with Lewis acids ($SbCl_5$, $AlCl_3$, BCl_3, BF_3).[252,256,275–277] Metal halides,[265] sulfur,[238,252] tetraphenyltin,[266] oxygen,[252,273] water,[252,270,272] tungsten and molybdenum silicates,[278] and phosphates[279] were also used.

Radiation-induced (^{60}Co γ-rays) polymerization of structure **102**[280] and cold plasma-initiated polymerization of $(NPCl_2)_3$, $(NPCl_2)_4$, and $(NPF_2)_3$ were investigated as well.[281–283] The reaction proceeded at lower temperatures than thermal process, for example, polymerization of $(NPCl_2)_4$ occurred at ~60 °C.[283]

$(NPCl_2)_3$ (**102**) polymerizes faster than tetramer $(NPCl_2)_4$ in both catalyzed and uncatalyzed reactions.[233,238] Although the thermal polymerization of structure **102** provides access to many derivatives of high molar mass polyphosphazenes (**101**), this route suffers from a number of drawbacks. High costs are associated with the synthesis of structure **102**, a high level of monomer purity is required to achieve reproducible polymerization and a high temperature of the reaction is required.[268]

4.18.6.1.1(ii) Polymerization in solution

$(NPCl_2)_3$ (**102**) was also polymerized to the high molar mass polymers in solution. Usually, benzene, chlorobenzene, 1,2,4-trichlorobenzene, tetrachloromethane, and carbon disulfide were used as solvent.[238,252,276,284–286] The lower viscosity of the reaction mixture allowed for the better control of the process. In a typical solution polymerization of structure **102**, lower molar mass and broader dipersity of poly-**102** were observed. The rates of polymerization were from one-half to one-third of those in the bulk.[237,286] Polyphosphoric,[252] sulfamic, toluenesulfonic and sulfobenzoic acids,[287,288] metal and quaternary ammonium salts of carboxylic, sulfonic, amidosulfonic, picric, or phosphorus acids,[252,287,288] sulfur,[252] and BCl_3[276,287] were used as initiators.

Recently, polymerization of structure **102** carried out in 1,2-dichlorobenzene at 25 °C with (trialkylsilyl)carboranes ($(R_3Si)CHB_{11}X$, where $X = Cl_{11}$, H_5Br_6, Me_5Br_6) as catalysts was reported. As a result, polymers with $M_w = 1.12 \times 10^5$ and dispersity (D_M) equal to 1.83 were obtained.[268]

4.18.6.1.1(iii) Solid-state polymerization

The cyclic trimer **102** was polymerized in the solid state when irradiated with X-rays[289] or ^{60}Co γ-rays.[281] Usually, cross-linked products were obtained. The presence of water, oxygen, solvents, and cyclic tetramer decreased the polymerization rate, and polymerization stopped at the relatively low (e.g., 10%) conversion.[289] This phenomenon has previously been observed in a number of the solid-state polymerizations and is due to the less perfect crystalline structures formed in the presence of some impurities.

4.18.6.1.2 Kinetics and mechanism of polymerization of $(NPCl_2)_3$

Polymerization of structure **102** occurs according to a cationic ring-opening mechanism involving dissociation of chloride ions from phosphorus,[245] and the progress of the reaction in solution[290] and in bulk[276,291] was followed by Raman spectroscopy and laser light scattering.

The following reactions (cf. eqns [51]–[55]) describe the process of formation of poly-**102**. The initiating species (**103**) are formed as a result of the endothermic P–Cl bond rupture in cyclic trimer (**102**) (eqn [51]).[233,251,269,292] Because of the lower electronegativity of phosphorus, the electrophilic center of the initiating species is located on phosphorus.

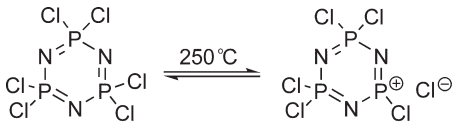

[51]

102 **103**

In the propagation step (eqn [52]), nitrogen atom from monomer ring attacks the electrophilic phosphorus center causing ring rupture.

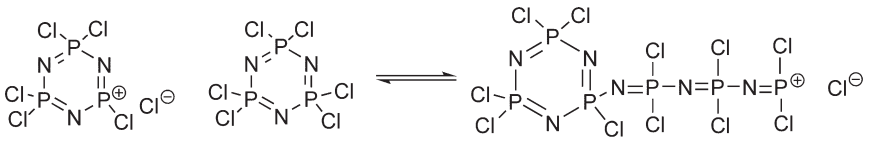

[52]

Dissociation of a chloride ion from a linear polymer segment also produces the propagating species, which are able to generate chain branching (eqn [53])

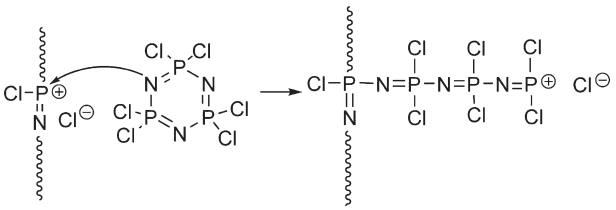

[53]

or cross-linking (eqn [54]).

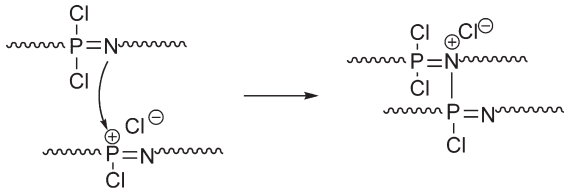

[54]

The reactions [53] and [54] become important at higher conversions (~70%) and are responsible for gel formation.

Termination (eqn [55]) occurs at lower temperatures, usually during cooling.

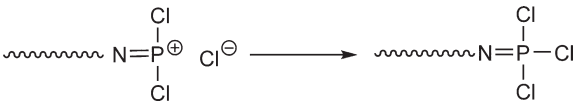

[55]

At longer polymerization times, the amount of cyclic homologs $(NPCl_2)_n$ $(n>3)$ slowly increases. Formation of cyclic oligomers (**104**) may simply proceed by the backbiting process (eqn [56]),[293] as in the cationic polymerization of other cyclic monomers, containing heteroatoms,[294]

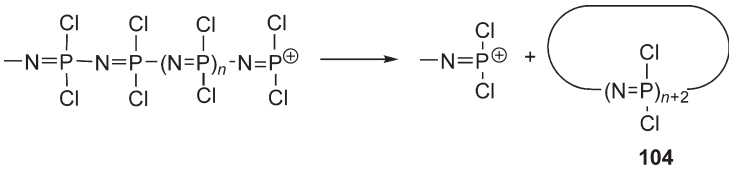

[56]

104

or by the four-center mechanism (cf. **Scheme 4**), proposed by Kireev *et al.*[295]

Polymerization without any intentionally added initiator is kinetically a second-order process, with activation enthalpy varying from 176 to 239 kJ mol^{-1}, [238,251,272] and the entropy of activation equal to 145 J mol^{-1} at 280 °C.[232] The rate of polymerization is markedly affected by the purity of the cyclic trimer (**102**). The depolymerization is a first-order process with an activation energy of 94 ± 8 kJ mol^{-1}.[293]

The mechanism of polymerization of structure **102** in 1,2,4-trichlorobenzene solution at 170–230 °C, catalyzed by BCl_3, has also been proposed (cf. **Scheme 5**).[276,277]

The respective kinetic and thermodynamic parameters at 170 °C, determined with some simplification of the kinetic

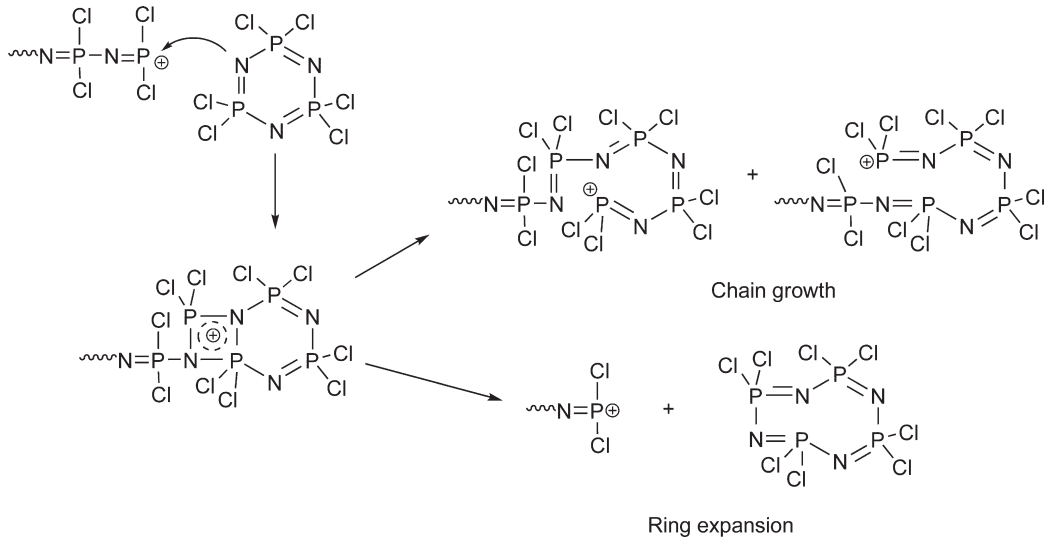

Scheme 4 Formation of cyclic oligomers by the four-center mechanism.

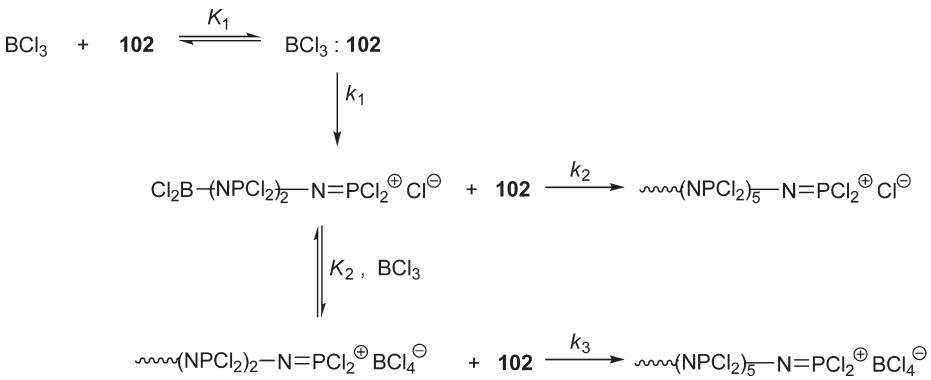

Scheme 5 The mechanism of polymerization of structure **102** catalyzed by BCl_3.

scheme, were also reported: ΔH_2 = −117 ± 17 kJ mol^{-1}, ΔS_2 = −234 ± 29 J K^{-1} mol^{-1}, K_2 = 33 ± 3 (kg of solution) mol^{-1}, and $\Delta H_3^{\neq}$ = 151 ± 17 kJ mol^{-1}. The reported activation energy equal to 151 ± 17 kJ mol^{-1} is lower than that for the uncatalyzed process.[238,251,272]

In the hydrolysis products of the trimer (**102**), thermally unstable hydroxycyclotriphosphazene (**105**) was found that may cause the ring opening and generate active species for either anionic or cationic chain propagation.[252,255,270]

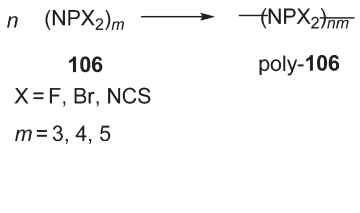

[58]

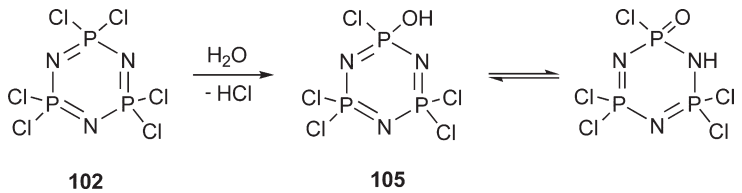

[57]

4.18.6.1.3 Synthesis of poly(halophosphazene)s

Cyclophosphazenes (**106**) substituted with fluoro, bromo, and isothiocyano groups also polymerize at 150–350 °C, giving rubbery polymers[232,233,238,296–301] with high molar mass ($M_w > 10^6$, poly-**106**; X = F).[300,301]

Polymerization of structure **106** (X = F) was performed in the way similar to that described for the synthesis of poly-**102**. Poly-**106** (X = F) is a white elastomeric material, hydrolytically unstable, and soluble only in perfluorinated solvents.[301]

4.18.6.1.4 Polymerization of substituted cyclophosphazenes

It has been found that cyclic trimers or tetramers ($(NPR_2)_m$, $m = 3,4$) wholly substituted with organic groups (e.g., alkyl, aryl, or fluoroalkoxy) undergo only ring–ring equilibration to other cyclic phosphazenes at higher temperatures (>150 °C), and do not form high polymers.[269,302,303] ROPs of cyclophosphazenes involve small but significant changes in enthalpy (the repeating units in the cyclic species and the polymer are the same, but the intramolecular interactions are different), but large changes in entropy since many small molecules are converted to far fewer macromolecules. Consequently, polymerization–depolymerization equilibria dominate in the thermal processes.[236,245] Allcock[233,238] suggests that the formation of the polymer is inhibited thermodynamically, because the bulky side groups, larger than chlorine or fluorine, are causing the intramolecular repulsion within a macromolecule. There are a few exceptions known (e.g., structures **107** and **108**).

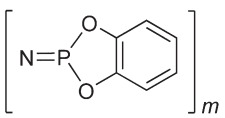

107

$m = 3, 4$

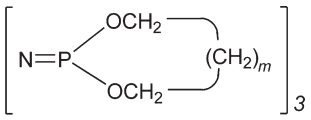

108

$m = 2, 3$

Monomer **107** ($m = 3$) at 300 °C gives a linear or macrocyclic polymer, and structure **108** polymerizes when heating at > 300 °C for a very short time.[233] On the other hand, linear high molar mass poly(organophosphazenes) easily depolymerize to a mixture of cyclics at higher temperatures (> 150 °C).[304,305]

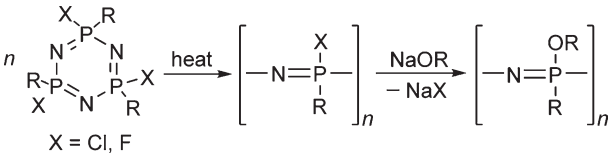

[59]

Progressive substitution of halogens by organic groups reduces the tendency for polymerization. On the other hand, it has been reported that the polymerization of $[NP(OR)_2]_3$ with equimolar amount of BCl_3 is possible and gives polymers with molar mass up to 7×10^4 and having ~50% of alkoxy groups replaced by chlorine atoms from BCl_3.[317] The kinetic study of polymerization of pentachloro(phenoxy)cyclotriphosphazene allowed to determine the rate constant of propagation, $k_p = 4 \times 10^{-7}\ s^{-1}$ (at 230 °C), and the activation energy 126 kJ mol^{-1}.[310]

Fluoro analogs also undergo ROP, but at higher temperatures. One of the most useful of these monomers is pentafluoro(phenyl) cyclotriphosphazene ($N_3P_3F_5Ph$), which yields a polymer that, unlike $(NPF_2)_n$, is soluble in common organic solvents and can thus undergo efficient polymer substitution reactions.[245]

The problem of the polymerization of trimers substituted with a different number of organic groups (especially with metallocenyl substituents) was discussed in some review papers.[245,261]

Fully substituted ferrocenylcyclophosphazenes (**109**) were also polymerized. A small amount of $(NPCl_2)_3$ (~1 mol.%) acts as polymerization initiator.[318]

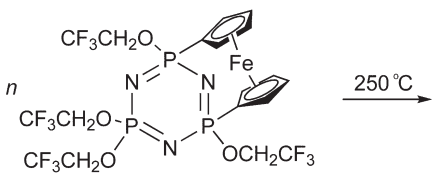

109

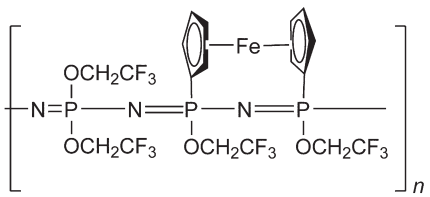

poly-**109**

[60]

The detailed description of polymerization of other metallocene derivatives was given previously.[222,261,318]

Fully substituted trimers with 2- and 4-pyridyloxy pendent groups were polymerized in bulk (in the absence of a catalyst) to high polymers at relatively low temperatures, above 200 °C and 150 °C, respectively.[319] On the other hand, the 3-pyridyloxy trimer did not polymerize even at temperature as high as 300 °C and in the presence of $(NPCl_2)_3$, $AlCl_3$, or water as catalyst. It means that only in monomers with nitrogen atoms in *ortho* or *para* to the phosphorus-bound oxygen stabilization of the cation formed by the initial loss of chloride is possible. This result supports the cationic mechanism for polymerization of small phosphazene rings.[261]

Only poly(organophosphazenes), obtained through the replacement of the highly reactive halogen atoms in poly-**102** and poly-**106** (X = F) by organic groups, can be applied as stable and useful materials. This is for some derivatives

relatively easy, for example, reaction of $(NPCl_2)_n$ with CF_3CH_2ONa yields $(NP(OCH_2CF_3)_2)_n$ after refluxing 20 h in THF solution.[320]

4.18.6.2 Poly(phosphazenylphosphazene)s

Poly(phosphazenylphosphazene)s (poly-**110** and poly-**111**), having short phosphazene branches linked to the phosphorus atoms, were synthesized by the ROP of cyclic phosphazenylphosphazenes **110** and **111**, respectively.[321] Because the reactivity of the P–Cl bonds in the side branches differs from those in the main chain, the selective introduction of two or more different organic substituents was possible.[245]

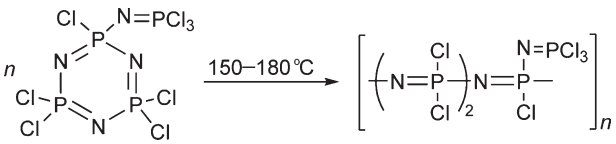

110 poly-**110**

[61]

Poly(chlorophosphazenylphosphazene) (poly-**111**) was prepared by the thermal polymerization of bis(trichlorophosphazenyl)tetrachlorocyclotriphosphazene (**111**) at 150 °C under reduced pressure for about 2 h.[322,323] Further reaction with alcoholates allowed structures **112** (R = Ph, $M_w = 9 \times 10^5$), **113** (R^1 = Ph, $M_w = 7 \times 10^5$), and **113** ($R^1 = CH_2CF_3$, $M_w = 1 \times 10^5$) to be obtained.[323]

The activation energy determined for the polymerization of structure **111** ~193 kJ mol^{-1} [322] is comparable to the values reported for $(NPCl_2)_3$ (176–239 kJ mol^{-1}).[238,251,272] The first-order rate constants $k = 9.93 \times 10^{-5}$ s^{-1} (at 150 °C) and $k = 2.44 \times 10^{-4}$ s^{-1} (at 157 °C) were also determined.[322]

4.18.6.3 Poly(carbophosphazene)s

Poly(heterophosphazene)s whose backbones comprise phosphorus, nitrogen, and another element – carbon or sulfur – were also synthesized.[324] In poly(carbophosphazene)s (poly-**114**), every third phosphorus atom is replaced by carbon.[325] Poly-**114** obtained in the thermal polymerization of a cyclic carbophosphazene was further transformed into white, solid, hydrolytically stable poly((aryloxy)carbophosphazene) (structure **115**; $M_w \sim 10^5$). The polymer backbone in structure **115** was less flexible than in classical polyphosphazenes.[257,325] The reaction of poly-**114** with alkylamines was also studied.[326]

Poly(carbophosphazene)s have higher glass transition temperatures than their classical polyphosphazene counterparts with the same side groups. The increased stiffness of the carbophosphazene backbone is attributed to the high torsional barrier of the 'organic' C = N π-bonds compared to the low barrier of the P = N π-bonds.[245]

4.18.6.4 Poly(thiophosphazene)s

Polymerization of thiophosphazene **116** was conducted in bulk in evacuated Pyrex tubes at 90 °C for 4 h. The resulting high polymers (poly-**116**) show more resemblance to classical polyphosphazenes, but are less stable.[245,257,261,327]

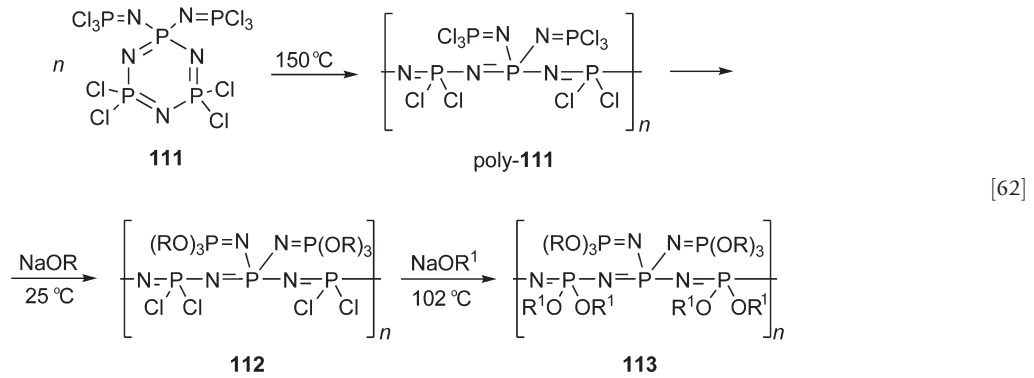

111 poly-**111** **112** **113**

[62]

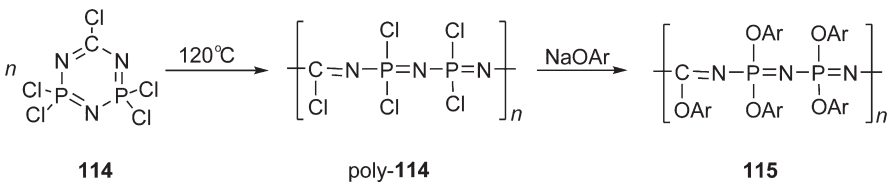

114 poly-**114** **115**

[63]

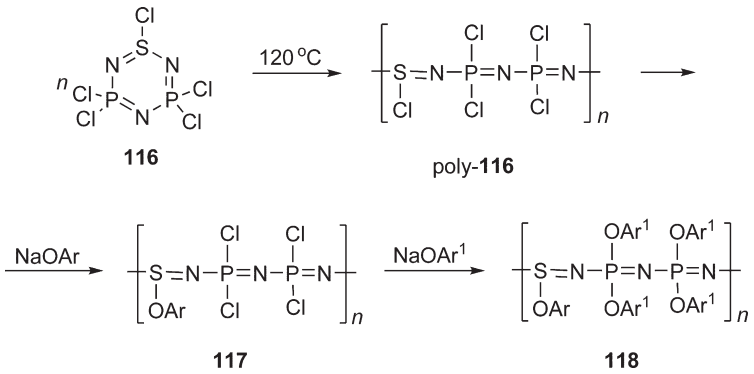

116 poly-116 117 118 [64]

An increase in viscosity over a period of several weeks was observed for structure **116**, even if it was stored at room temperature in evacuated ampoules.[261,328]

In poly-**116**, the S–Cl bonds are much more reactive than the P–Cl bonds. Thus, regioselective substitution at the sulfur center is possible to yield macromolecules (**118**) with different aryloxy substituents at sulfur and phosphorus.[257,327,329]

4.18.6.5 Poly(thionylphosphazene)s

Polymerization of thionylphosphazene (**119**), conducted in an evacuated Pyrex tubes at 165 °C for 4 h, gave a linear poly-**119** with chlorine at both sulfur and phosphorus in ~80% yield (eqn [65]).[257,261,329] Apart from polymer and unreacted monomer, 12-, 18-, 24-, 30-, and 36-membered rings ($[(NSOCl)(NPCl_2)_2]_n$, $n = 2–6$) were also formed.[235,257]

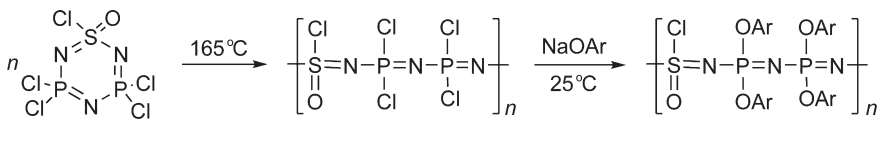

119 poly-119 120 [65]

Polymerization of the fluorinated thionylphosphazene $[(NSOF)(NPCl_2)_2]_3$ occurs at a slightly higher temperature (180 °C) than of its chlorinated analog.[261,330] The resulting structure **120** with S–F bonds is moisture stable.[261] It was postulated that the thermal polymerization of structure **119** or $[(NSOF)(NPCl_2)_2]_3$ proceeds by heterolytic dissociation of the sulfur–halogen bond as the initiation step, forming the highly reactive thionylphosphazene cation.[257]

Ambient temperature polymerization of structure **119** in methylene chloride and with $GaCl_3$, $AlCl_3$, or $SbCl_5$ as initiators was also reported.[331] Apart from the high molar mass poly(thionylphosphazene) $[(NSOCl)(NPCl_2)_2]_n$, 12-, 18-, 24-, and higher-membered macrocycles were formed. $GaCl_3$ is the most effective initiator and $AlCl_3$ the least one.[331]

4.18.6.6 Linear Polymers Containing Phosphorus and Transition Elements

Only a few examples of polymers are known that contain both transition metals and phosphorus atoms in the main chain. In 1989, the first synthesis of poly(metallaphosphazene)s (poly-**121**) was reported, where every third phosphorus atom of a classical phosphazene was replaced by a metal atom (M = Mo, W).[320]

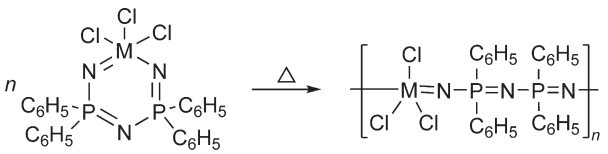

121 poly-121 [66]

Poly-**121** was inert to hydrolysis, even in boiling water, and did not decompose below ~300 °C, but detailed characterization of these materials was not reported.[257,320]

4.18.6.7 Poly(organophosphazene)s and Related Polymers

The synthesis of poly(organophosphazene)s (**101**) with a variety of substituents was described in many books and review papers, as mentioned already in Section 4.18.6.1. For example, Allcock[244,245] in his comprehensive reviews discussed various structures of polyphosphazenes and their diversity of properties.

Polyphosphazenes form amphiphilic block copolymers with organic polymers, such as poly(ethylene oxide), polystyrene, or poly(dimethylsiloxane).[244] Comb, star, and dendritic architectures were also obtained. There are also

known polymeric structures that consist of an organic polymer backbone with cyclophosphazene groups (122), the result of polymerization of vinyl- or allylcyclophoshazenes and/or norbornene derivatives by ring-opening metathesis polymerization.[244,245]

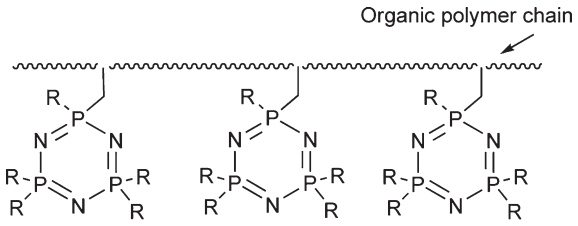

122

Apart from the mentioned polymers, there are also known cyclolinear (123)[244,245,252] and cyclomatrix polymers (124).[225,235,238]

Cyclolinear polyphosphazenes (123) were prepared by linking cyclophosphazene rings through difunctional organic groups (R^1). The synthesis of these polymers depends on the presence of blocking divalent groups, R^1, which prevent cross-linking and determine the properties (e.g., elastic or thermoplastic) of the resulting polymers. Cyclolinear phosphazene polymers are much more thermally stable than linear poly(organophosphazene)s.[238,258]

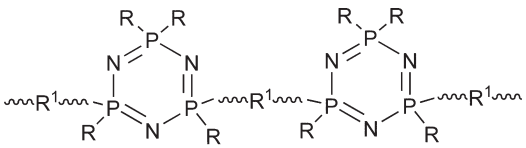

123

Cyclomatrix polymers with general structure 124 are formed by the extensive cross-linking of multifunctional ring systems, for example, by the reaction of $(NPCl_2)_n$ with diols or diamines.[224,238] Such completely cross-linked ring systems form tough materials with high melting points and high hardness.[238,258,332]

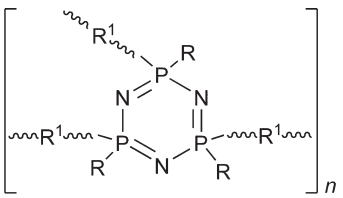

124

4.18.7 Some Properties and Applications of Linear Poly(organophosphazene)s

Properties of polyphosphazenes result from a high chain flexibility (their backbone is one of the most flexible known, being comparable to silicone polymers) and can be influenced by choosing the required substituents at phosphorus atoms at will.

Polymers are semicrystalline and thermoplastic, when only one type of substituent is present. Rubbery and amorphous materials, having high elasticity in a wide range of temperatures, were obtained when two or more different types of substituents were introduced into the chain.[235,236,238]

The variety of different properties and applications of phosphazenes were reported in many works.[5,222,244,245,257–260,333–335] In this chapter, only some selected information is given.

Glass temperatures for poly(organophosphazene)s are between −84 °C for $[NP(OCH_2CH_3)_2]_n$ and 100 °C for $[NP(NHPh)_2]_n$.[235]

Poly(alkoxyfluorophosphazene)s have advantages over organic elastomers or silicone rubber, because of their low transition temperatures and unusual resistance to oils, fuel, hydraulic fluids, and so on. Thus, for example, Firestone Tire and Rubber Company supplied different products from them, for example, O-rings, gaskets, hydrocarbon fuel hoses, and fire-resistant foam rubber devices.[239,245,251,269]

The polyphosphazene backbone is also transparent to radiation from the near infrared to 220 nm. That explains their stability to radiation in the visible and near-UV region and the interest in polyphosphazenes as optical and photonic materials.[245]

Polyphosphazenes have low inflammability, very high values of limiting oxygen index (LOI) equal to 24–65,[237,255] and evolve no toxic gases during burning. Most of them do not burn and some are used as additives to other polymers as flame retardants.[233,235,237,251,256]

Polyphosphazenes were used as solid polymer electrolytes for batteries, membranes for gas and liquid separations, and proton exchange membranes for fuel cells as well as for energy storage and energy generation applications.[236,244,333,336,337]

Biodegradability and biocompatibility of polyphosphazenes were studied as well as their degradation behavior *in vitro* and *in vivo*.[258,334] It was reported that their degradation products are also biocompatible.[244,258,335,338] Some reviews are devoted to using polyphosphazenes as hydrogel-forming materials.[235,244]

The surface of poly(alkoxyfluorophosphazene) films and nanofibers was modified with plasma to introduce new functional groups and alter the water contact angles.[244,283]

4.18.8 Outlook

The presented chapter consists of two parts. In the first part, the ROP of cyclic organophosphorus monomers is described, whereas the second part is devoted to polyphosphazenes and related polymers.

Cyclic monomers with phosphorus atoms at different level of oxidation, namely, pentavalent (P^V) and trivalent (P^{III}), were polymerized according to anionic and/or cationic mechanism, giving as a result polymers with various structures and properties. The mechanism, kinetics, and thermodynamics of polymerization were described for selected groups of monomers. The structures of active centers were established and the rate constants, activation parameter, and thermodynamic parameter were determined.

High molar mass poly(alkylene phosphate)s were obtained as models of biopolymers, namely, NA and TA.

Many papers are devoted to copolymerization of cyclic phosphates with cyclic esters, for example, CL and LA. Recently, enzymatic polymerization has received much attention as a new method of polymer syntheses.

The synthesis of P-containing polymers by polyaddition is discussed only for the reaction of phosphoric acid derivatives with diepoxides.

The future of polyphosphazenes, poly(alkylene phosphate)s, and their copolymers is mainly associated with their potential role in biomedical and pharmaceutical fields, such as drug/gene delivery and tissue engineering.

Acknowledgments

This chapter is based in large fragments on chapters: Phosphorus-Containing Polymers in Handbook of Polymer Synthesis (Ref. 4) and Poly(alkylene phosphate)s in Polymeric Materials Encyclopedia (Ref. 7) both coauthored by S. Penczek and G. Lapienis. The author of this chapter (GL) wishes to express his gratitude to Professor Stanislaw Penczek for the permission to use large fragments of the texts in the present paper.

References

1. Gefter, E. L. *Organophosphorus Monomers and Polymers*; Pergamon Press: Oxford, 1962.
2. Kobayashi, S.; Saegusa, T. In *Alternating Copolymers*; Cowie, J. M. G., Ed.; Plenum Press: New York, 1985; p 185.
3. Lapienis G.; Penczek, S. In *Ring-Opening Polymerization*; Ivin, K. J.; Saegusa, T., Eds.; Elsevier: New York, 1984; Vol. 2, p 919.
4. Penczek, S.; Lapienis, G. In *Handbook of Polymer Synthesis*; Kricheldorf, H. R., Ed.; Marcel Dekker: New York, 1992; Vol. 2, p 1077.
5. Sander, M.; Steininger, E. *J. Macromol. Sci., Rev.* **1967**, *C1*, 1; Sander, M.; Steininger, E. *J. Macromol. Sci., Rev.* **1968**, *C2*, 1.
6. Sandler, S. R.; Karo, W. *Polymer Synthesis*; Academic Press: New York, 1974; Vol. 1, p 367.
7. Penczek, S.; Lapienis, G. In *Polymeric Materials Encyclopedia*; Salamone, J. C., Ed.; CRC Press: Boca Raton, FL, 1996; Vol. 7, p 5361.
8. Wang, Y.-C.; Yuan, Y.-Y.; Du, J.-Z.; *et al. Macromol. Biosci.* **2009**, *9*, 1154.
9. Kobayashi, S.; Saegusa, T. *Pure Appl. Chem.* **1981**, *53*, 1663.
10. Dutasta, J. P.; Grand, A.; Guimaraes, A. C.; Robert, J. B. *Tetrahedron* **1979**, *35*, 197.
11. Dutasta, J. P.; Guimaraes, A. C.; Martin, J.; Robert, J. B. *Tetrahedron Lett.* **1975**, 1519.
12. Zwierzak, A. *Can. J. Chem.* **1967**, *45*, 2501.
13. Pudovik, A. N.; Evstaf'ev, T. V. *Vysokomol. Soedin.* **1964**, *5*, 886.
14. Nifanteev, E. E.; Nasonovskii, I. S.; Borisenko, A. A. *Zh. Obshch. Kim.* **1971**, *41*, 1876.
15. Lucas, H. J.; Mitchell, F. W., Jr.; Scully, C. N. *J. Am. Chem. Soc.* **1950**, *72*, 5491.
16. Pudovik, A. N.; Tcherkasov, R. A.; Kondrat'eva, R. M. *Vysokomol. Soedin.* **1967**, *9*, 1118.
17. Pudovik, A. N.; Evstaf'ev, T. V. *Vysokomol. Soedin.* **1964**, *6*, 2139.
18. Dutasta, J. P.; Martin, J.; Robert, J. B. *Heterocycles* **1980**, *14*, 1631.
19. Greenhalgh, R.; Newbery, J. E.; Woodcock, R.; Hudson, R. F. *J. Chem. Soc., Chem. Commun.* **1969**, 22.
20. Robert, J. B.; Weichmann, H. *J. Org. Chem.* **1978**, *43*, 3031.
21. Harwood, H. J.; Patel, N. K. *Macromolecules* **1968**, *1*, 233.
22. White, D. W. *Phosphorus* **1971**, *1*, 33.
23. Mukayama, T.; Fujisawa, T.; Tamura, Y.; Yokota, Y. *J. Org. Chem.* **1964**, *29*, 2572.
24. Bentrude, W. G.; Yee, K. C.; Bertrand, R. D.; Grant, D. M. *J. Am. Chem. Soc.* **1971**, *93*, 797.
25. Dutasta, J. P.; Guimares, A. C.; Robert, J. B. *Tetrahedron Lett.* **1977**, 801.
26. Dutasta, J. P.; Robert, J. B. *J. Am. Chem. Soc.* **1978**, *100*, 1925.
27. Dutasta, J. P.; Robert, J. B.; Vincens, M. *Tetrahedron Lett.* **1979**, 933.
28. Petrov, K. A.; Nifanteev, E. E.; Goltsova, R. G.; Solntseva, L. M. *Vysokomol. Soedin.* **1963**, *5*, 1691.
29. Lapienis, G.; Penczek, S. *Macromolecules* **1977**, *10*, 1301.
30. Lapienis, G.; Penczek, S. *J. Polym. Sci., Polym. Chem. Ed.* **1977**, *15*, 371.
31. Libiszowski, J.; Kaluzynski, K.; Penczek, S. *J. Polym. Sci., Polym. Chem. Ed.* **1978**, *16*, 1275.
32. Penczek, S. *Pure Appl. Chem.* **1976**, *48*, 363.
33. Kawakami, Y.; Miyata, K.; Yamashita, Y. *Polym. J.* **1979**, *11*, 175.
34. Sharov, V. N.; Klebanskii, A. L.; Bartashev, V. A. *Vysokomol. Sordin., Ser. A.* **1972**, *14*, 653.
35. Vogt, W.; Ahmad, N. V. *Makromol. Chem.* **1977**, *178*, 1711.
36. Yasuda, H.; Sumitani, M.; Lee, K.; Araki, T.; Nakamura, A. *Macromolecules* **1982**, *15*, 1231.
37. Vogt, W.; Pflüger, R. *Makromol. Chem., Suppl.* **1975**, *1*, 97.
38. Penczek, S.; Libiszowski, J. *Makromol. Chem.* **1988**, *189*, 1765.
39. Sosnowski, S.; Libiszowski, J.; Slomkowski, S.; Penczek, S. *Makromol. Chem., Rapid Commun.* **1984**, 5, 239.
40. Yasuda, H.; Sumitani, M.; Nakamura, A. *Macromolecules* **1981**, *14*, 458.
41. Vandenberg, E. J. *J. Polym. Sci., Part A-1: Polym. Chem.* **1971**, *9*, 2451.
42. Fontaine, L.; Derouet, D.; Brosse, J. C. *Eur. Polym. J.* **1990**, *26*, 865.
43. Iwasaki, Y.; Akiyoshi, K. *Macromolecules* **2004**, *37*, 7637.
44. Majoral, J. P.; Mathis, F.; Munoz, A.; *et al. Bull. Soc. Chim. France* **1968**, 4455.
45. Munoz, A.; Vives, J.-P. *C. R. Hebd. Seances Acad. Sci., Ser. C* **1961**, *253*, 1693.
46. Petrov, K. A.; Nifanteev, E. E.; Fedorchuk, L. V. *Vysokomol. Soedin.* **1960**, *2*, 417.
47. Navech, J.; Revel, M.; Vives, J.-P.; Munoz, A. *C. R. Hebd. Seances Acad. Sci., Ser. C* **1965**, *260*, 224.
48. Lapienis, G.; Penczek, S. *Macromolecules* **1974**, *7*, 166.
49. Cox, J. R., Jr.; Wall, R. E.; Westheimer, F. H. *Chem. Ind.* **1959**, 929.
50. Westheimer, F. H. *Acc. Chem. Res.* **1968**, *1*, 70.
51. Wang, Y.; Liu, X.; Sun, T.; *et al. J. Controlled Release* **2008**, *128*, 32.
52. Xiao, C. S.; Wang, Y. C.; Du, J. Z.; *et al. Macromolecules* **2006**, *39*, 6825.
53. Wang, Y. C.; Tang, L. Y.; Sun, T. M.; *et al. Biomacromolecules* **2008**, *9*, 388.
54. Wang, F.; Wang, Y.-C.; Yan, L.-F.; Wang, J. *Polymer* **2009**, *50*, 5048.
55. He, J.; Ni, P.; Wang, S.; *et al. J. Polym. Sci., Part A: Polym. Chem.* **2010**, *48*, 1919.
56. Wang, Y. C.; Tang, L. Y.; Li, Y.; Wang, J. *Biomacromolecules* **2009**, *10*, 66.
57. Yang, X. Z.; Wang, Y. C.; Tang, L. Y.; *et al. J. Polym. Sci., Part A: Polym. Chem.* **2008**, *46*, 6425.
58. Du, J. Z.; Sun, T. M.; Weng, S. Q.; *et al. Biomacromolecules* **2007**, *8*, 3375.
59. Xiong, M. H.; Wu, J.; Wang, Y. C.; *et al. Macromolecules* **2009**, *42*, 893.
60. Liu, J.; Huang, W.; Zhou, Y.; Yan, D. *Macromolecules* **2009**, *42*, 4394.
61. Iwasaki, Y.; Yamaguchi, E. *Macromolecules* **2010**, *43*, 2664.
62. He, F.; Zhuo, R. X.; Liu, L. J.; *et al. React. Funct. Polym.* **2001**, *47*, 153.
63. Wen, J.; Zhuo, R. X. *Makromol. Chem., Rapid Commun.* **1998**, *19*, 641.
64. Ivin, K. J. In *Reactivity, Mechanism and Structure in Polymer Chemistry*; Jenkins, A. D.; Ledwith, A., Eds.; Wiley: New York, 1974; p 514.
65. Penczek, S.; Kubisa, P.; Matyjaszewski, K. *Adv. Polym. Sci.* **1980**, *37*, 1.
66. Klosinski, P.; Penczek, S. *Macromolecules* **1983**, *16*, 316.
67. Lapienis, G.; Penczek S. *J. Polym. Sci., Polym. Chem. Ed.* **1990**, *28*, 1519.
68. Gehrmann, T.; Vogt, W. *Makromol. Chem.* **1981**, *182*, 3069.
69. Vogt, W.; Siegfried, R. *Makromol. Chem.* **1976**, *177*, 1779.
70. Gerlt, J. A.; Westheimer, F. H.; Sturtevant, J. M. *J. Biol. Chem.* **1975**, *250*, 5059.
71. Sharov, V. N.; Klebanski, A. L. *Vysokomol. Soedin., Ser. A* **1973**, *15*, 2453.
72. Korshak, V. V.; Gribova, I. A.; Andreeva, M. *Izv. Akad. Nauk SSSR, Ser. Khim.* **1957**, 631.
73. Korshak, V. V.; Gribova, I. A.; Andreeva, M.; Medved, T. A. *Vysokomol. Soedin., Geterotsepn. Vysokomol. Soedin.* **1964**, 117.
74. Kaluzynski, K.; Libiszowski, J.; Penczek, S. *Makromol. Chem.* **1977**, *178*, 2943.
75. Kaluzynski, K.; Libiszowski, J.; Penczek, S. *Macromolecules* **1976**, *9*, 365.
76. Biela, T.; Penczek, S.; Slomkowski, S.; Vogl, O. *Makromol. Chem., Rapid Commun.* **1982**, *3*, 667.
77. Wang, J.; Mao, H. Q.; Leong, K. W. *J. Am. Chem. Soc.* **2001**, *123*, 9480.
78. Wang, J.; Zhang, P. C.; Lu, H. F.; *et al. J. Controlled Release* **2002**, *83*, 157.
79. Huang, S. W.; Wang, J.; Zhang, P. C.; *et al. Biomacromolecules* **2004**, *5*, 306.
80. Wang, J.; Gao, S.-J.; Zhang, P.-C.; *et al. Gene Ther.* **2004**, *11*, 1001.
81. Biela, T.; Klosinski, P.; Penczek, S. *J. Polym. Sci., Polym. Chem. Ed.* **1989**, *27*, 763.
82. Penczek, S.; Klosinski, P. In *Models of Biopolymers by Ring-Opening Polymerization*; Penczek, S., Ed., CRC Press: Boca Raton, FL, 1990; p 291.
83. Penczek, S.; Klosinski, P. In *Biomimetic Polymers*; Gebelein, C. G., Ed., Plenum: New York, 1990; p 243.
84. Pretula, J.; Kaluzynski, K.; Penczek, S. *J. Polym. Sci., Polym. Chem. Ed.* **1984**, *22*, 1251.

85. Kałużyński, K.; Penczek, S. *Makromol. Chem.* **1987**, *188*, 1713.
86. Lapienis, G.; Pretula, J.; Penczek, S. *Macromolecules* **1983**, *16*, 153.
87. Munoz, A.; Navech, J.; Vives, J.-P. *Bull. Soc. Chim. France* **1966**, 2350.
88. Navech, J.; Vives, J.-P.; Munoz, A. *Bull. Soc. Chim. France* **1966**, 2355.
89. Revel, M.; Munoz, A.; Navech, J. *C. R. Hebd. Seances Acad. Sci., Ser. C* **1967**, *265*, 1053.
90. Shalaby, S. W.; Sifniades, S.; Klein, K. P.; Sheehan, D. *J. Polym. Sci., Polym. Chem. Ed.* **1974**, *12*, 2917.
91. Shalaby, S. W.; Sifniades, S.; Sheehan, D. *J. Polym. Sci., Polym. Chem. Ed.* **1976**, *14*, 2675.
92. Petrov, K. A.; Nifanteev, E. E.; Khorkhyanu, L. V.; *et al. Vysokomol. Soedin.* **1962**, *4*, 246.
93. Shimidzu, T.; Hakozaki, T.; Kagiya, T.; Fukui, F. *Bull. Chem. Soc. Jpn.* **1966**, *39*, 562.
94. Shimidzu, T.; Hakozaki, T.; Kagiya, T.; Fukui, F. *J. Polym. Sci., Part B* **1965**, *3*, 871.
95. Singh, G. *J. Org. Chem.* **1979**, *44*, 1060.
96. Kobayashi, S.; Huang, M. Y.; Saegusa, T. *Polym. Bull.* **1981**, *4*, 185.
97. Vogt, W. *Makromol. Chem.* **1977**, *178*, 3179.
98. Yamashita, Y. *J. Polym. Sci., Polym. Symp.* **1976**, *56*, 447.
99. Kobayashi, S.; Suzuki, M.; Saegusa, T. *Polym. Bull.* **1981**, *4*, 315; Kobayashi, S.; Suzuki, M.; Saegusa, T. *Polym. Bull.* **1982**, *8*, 417.
100. Kobayashi, S. In *Ring-Opening Polymerization*; McGrath, J. E., Ed., ACS Symposium Series 286; American Chemical Society: Washington, DC, 1985; p 293.
101. Kobayashi, S.; Suzuki, M.; Saegusa, T. *Macromolecules* **1984**, *17*, 107.
102. Kobayashi, S.; Suzuki, M.; Saegusa, T. *Macromolecules* **1986**, *19*, 462.
103. Fujisawa, T.; Yokota, Y.; Mukaiyama, T. *Bull. Chem. Soc. Jpn.* **1967**, *40*, 147.
104. Kobayashi, S.; Suzuki, M.; Saegusa, T. *Macromolecules* **1983**, *16*, 1010.
105. Ogata, N.; Saito, S. *Makromol. Chem.* **1973**, *164*, 95.
106. Liu, J.; Huang, W.; Pang, Y.; *et al. Biomacromolecules* **2010**, *11*, 1564.
107. Penczek, S. *J. Polym. Sci., Polym. Symp.* **1980**, *67*, 149.
108. Penczek, S.; Lapienis, G.; Klosinski, P. *Pure Appl. Chem.* **1984**, *56*, 1309.
109. Penczek, S.; Lapienis, G.; Klosinski, P. *Phosphorus Sulfur* **1986**, *27*, 153.
110. Penczek, S.; Biela, T.; Klosinski, P.; Lapienis, G. *Makromol. Chem., Macromol. Symp.* **1986**, *6*, 123.
111. Penczek, S.; Duda, A.; Kaluzynski, K.; *et al. Makromol. Chem., Macromol. Symp.* **1993**, *73*, 91.
112. Kałużyński, K.; Penczek, S. *Makromol. Chem.* **1979**, *180*, 2289.
113. Penczek, S. In *Phosphorus Chemistry Directed Towards Biology*; Stec, W. J., Ed.; Pergamon: Oxford, 1980; p 133.
114. Bone, S. A.; Trippett, S.; Whittle, P. J. *J. Chem. Soc., Perkin Trans. I* **1977**, 80.
115. Hamilton, W. C.; La Placa, S. J.; Ramirez, F. *J. Am. Chem. Soc.* **1965**, *87*, 127.
116. Kałużyński, K. Ph.D. thesis, Centre of Molecular and Macromolecular Studies Lodz, 1989.
117. Saegusa, T. *Makromol. Chem., Macromol. Symp.* **1988**, *13/14*, 111.
118. Iwasaki, Y.; Wachiralarpphaithoon, C.; Akiyoshi, K. *Macromolecules* **2007**, *40*, 8136.
119. Iwasaki, Y.; Nakagawa, C.; Ohtomi, M.; *et al. Biomacromolecules* **2004**, *5*, 1110.
120. Iwasaki, Y.; Komatsu, S.; Narita, T.; *et al. Macromol. Biosci.* **2003**, *3*, 238.
121. Wachiralarpphaithoon, C.; Iwasaki, Y.; Akiyoshi, K. *Biomaterials* **2007**, *28*, 984.
122. Iwasaki, Y.; Akiyoshi, K. *Biomacromolecules* **2006**, *7*, 1433.
123. Wen, J.; Kim, G. J. A.; Leong, K. W. *J. Controlled Release* **2003**, *92*, 39.
124. Wen, J.; Zhuo, R. X. *Polym. Int.* **1998**, *47*, 503.
125. Wang, Y. C.; Shen, S. Y.; Wu, Q. P.; *et al. Macromolecules* **2006**, *39*, 8992.
126. Chen, D. P.; Wang, J. *Macromolecules* **2006**, *39*, 473.
127. Chew, S. Y.; Wen, J.; Yim, E. K. F.; Leong, K. W. *Biomacromolecules* **2005**, *6*, 2017.
128. Feng, J.; Zhuo, R.; He, F. *Sci. China* **2003**, *46*, 160.
129. Wang, X. L.; Zhuo, R. X.; Liu, L. J. *Polym. Int.* **2001**, *50*, 1175.
130. Li, F.; Feng, J.; Zhuo, R. *J. Appl. Polym. Sci.* **2006**, *102*, 5507.
131. Yang, X. Z.; Sun, T. M.; Dou, S.; *et al. Biomacromolecules* **2009**, *10*, 2213.
132. Song, W. J.; Du, J. Z.; Liu, N. J.; *et al. Macromolecules* **2008**, *41*, 6935.
133. Wang, Y. C.; Li, Y.; Yang, X. Z.; *et al. Macromolecules* **2009**, *42*, 3026.
134. Sun, T. M.; Du, J. Z.; Yan, L. F. *et al. Biomaterials* **2008**, *29*, 4348.
135. Wang, Y. C.; Yuan, Y. Y.; Du, J. Z.; *et al. Macromol. Biosci.* **2009**, *9*, 1154.
136. Du, J. Z.; Chen, D. P.; Wang, Y. C.; *et al. Biomacromolecules* **2006**, *7*, 1898.
137. Cheng, J.; Ding, J. X.; Wang, Y. C.; Wang, J. *Polymer* **2008**, *49*, 4784.
138. Yuan, Y. Y.; Wang, Y. C.; Du, J. Z.; Wang, J. *Macromolecules* **2008**, *41*, 8620.
139. Hu, B.; Zhuo, R.; Fan, C. *Polym. Adv. Technol.* **1998**, *9*, 145.
140. Baran, J.; Penczek, S. *Macromolecules* **1995**, *28*, 5167.
141. Bolle, J.; Mileo, J. C.; Nicolas, L. *C. R. Hebd. Seances Acad. Sci., Ser. C* **1965**, *261*, 1852.
142. Inagaki, N.; Katsuura, K. *J. Appl. Polym. Sci.* **1979**, *24*, 249.
143. Saegusa, T.; Kobayashi, S. *J. Macromol. Sci., Chem.* **1979**, *A13*, 295.
144. Saegusa, T. *Pure Appl. Chem.* **1981**, *53*, 691.
145. Saegusa, T. *Makromol. Chem., Suppl.* **1981**, *4*, 73.
146. Saegusa, T. *Angew. Chem., Int. Ed. Engl.* **1977**, *16*, 826.
147. Saegusa, T.; Kobayashi, S. *J. Polym. Sci., Polym. Symp.* **1978**, *62*, 79.
148. Saegusa, T.; Kobayashi, S.; Kimura Y. *Pure Appl. Chem.* **1976**, *48*, 307.
149. Ibrahim, A. M.; Mahadevan, V.; Srinivasan, M. *Eur. Polym. J.* **1988**, *24*, 385.
150. Kobayashi, S.; Huang, M. Y.; Saegusa, T. *Polym. Bull.* **1982**, *6*, 389.
151. Kobayashi, S.; Chow, T. Y.; Saegusa, T. *Polym. Bull.* **1983**, *9*, 588.
152. Kobayashi, S.; Kadokawa, J.; Uyama, H. *Macromolecules* **1991**, *24*, 4475.
153. Saegusa, T.; Kimura, Y.; Ishikawa, N.; Kobayashi, S. *Macromolecules* **1976**, *9*, 724.
154. Saegusa, T.; Kobayashi, S.; Kimura, Y. *Macromolecules* **1977**, *10*, 64.
155. Saegusa, T.; Yokoyama, T.; Kobayashi, S. *Polym. Bull.* **1978**, *1*, 55.
156. Saegusa, T.; Kobayashi, S.; Furukawa, J. *Polym. Bull.* **1978**, *1*, 171.
157. Saegusa, T.; Kobayashi, S.; Furukawa, J. *Macromolecules* **1977**, *10*, 73.
158. Saegusa, T.; Kobayashi, S.; Furukawa, J. *Macromolecules* **1978**, *11*, 1027.
159. Saegusa, T.; Niwano, M.; Kobayashi, S. *Polym. Bull.* **1980**, *2*, 249.
160. Saegusa, T.; Yokoyama, T.; Kimura, Y.; Kobayashi, S. *Polym. Bull.* **1978**, *1*, 91.
161. Saegusa, T.; Kobayashi, T.; Kobayashi, S. *Polym. Bull.* **1979**, *1*, 259.
162. Saegusa, T.; Kobayashi, S.; Kimura, Y. *Macromolecules* **1977**, *10*, 68.
163. Saegusa, T.; Furukawa, J.; Kimura, Y.; Kobayashi, S. *Polym. Bull.* **1979**, *1*, 243.
164. Saegusa, T.; Yokiyama, T.; Kimura, Y.; Kobayashi, S. *Macromolecules* **1977**, *10*, 791.
165. Saegusa, T.; Kobayashi, S.; Kobayashi, T. *Macromolecules* **1981**, *14*, 463.
166. Kobayashi, S.; Yokoyama, T.; Kawabe, K.; Saegusa, T. *Polym. Bull.* **1980**, *3*, 585.
167. Kobayashi, S.; Yokoyama, T.; Saegusa, T. *Polym. Bull.* **1980**, *3*, 505.
168. Saegusa, T.; Kobayashi, T.; Kobayashi, S. *Polym. Bull.* **1979**, *1*, 535.
169. Kobayashi, S.; Okawa, M.; Niwano, M.; Saegusa, T. *Polym. Bull.* **1980**, *5*, 331.
170. Saegusa, T.; Kobayashi, T.; Chow, T. Y.; Kobayashi, S. *Macromolecules* **1979**, *12*, 533.
171. Kobayashi, S.; Kadokawa, J.; Yen, I. F.; Shoda, S. *Macromolecules* **1989**, *22*, 4390.
172. Kobayashi, S.; Kaku, M.; Saegusa, T. *Polym. Bull.* **1981**, *5*, 325.
173. Saegusa, T.; Miyamoto, M.; Kimura, Y. *Macromolecules* **1981**, *14*, 115.
174. Kobayashi, S.; Hashimoto, T.; Saegusa, T. *Macromolecules* **1980**, *13*, 1650.
175. Kobayashi, S.; Chow, T. Y.; Saegusa, T. *Macromolecules* **1982**, *15*, 202.
176. Kobayashi, S.; Narukawa, Y.; Mori, S.; *et al. Macromolecules* **1983**, *16*, 858.
177. Kobayashi, S.; Narukawa, Y.; Saegusa, T. *Macromolecules* **1984**, *17*, 134.
178. Kobayashi, S.; Kadokawa, J.; Uyama, H. *Polymer J.* **1992**, *24*, 699.
179. Kobayashi, S.; Narukawa, Y.; Hashimoto, T.; Saegusa, T. *Chem. Lett.***1980**, 1599.
180. Kobayashi, S.; Kadokawa, J.; Uyama, H.; Shoda, S. *Polymer J.* **1991**, *23*, 1099.
181. Lundmark, S.; Kadokawa, J.; Kobayashi, S. *Macromolecules* **1992**, *25*, 5873.
182. Kobayashi, S.; Kadokawa, J.; Uyama, H.; *et al. Macromolecules* **1992**, *25*, 5861.
183. Kobayashi, S.; Lundmark, S.; Kadokawa, J.; Albertsson, A. C. *Macromolecules* **1992**, *25*, 5867.
184. Kobayashi, S.; Lundmark, S.; Kadokawa, J.; Albertsson, A. C. *Macromolecules* **1991**, *24*, 2129.
185. Kobayashi, S.; Kadokawa, J.; Uyama, H.; *et al. Macromolecules* **1990**, *23*, 3541.
186. Michelson, A. M. *J. Chem. Soc.* **1959**, 1371.
187. Applegarth, D. A.; Buchanan, J. G.; Baddiley, J. *J. Chem. Soc.* **1955**, 1213.
188. Penczek, S.; Klosinski, P. In *Biomimetic Polymers*; Gebelein, C. G., Ed.; Plenum: New York, 1990; p 223.
189. Penczek, S.; Klosinski, P. In *Progress in Biomedical Polymers*; Gebelein, C. G.; Dunn, R. L., Eds., Plenum: New York, 1990; p 291.
190. Nyk, A.; Klosinski, P.; Penczek, S. *Makromol. Chem.* **1991**, *192*, 833.
191. Penczek, S.; Lapienis, G.; Kaluzynski, K.; Nyk, A. *Polish J. Chem.* **1994**, *68*, 2129.
192. Penczek, S.; Kubisa, P.; Klosinski, P.; *et al.* In *Catalysis in Polymer Synthesis*; Vandenberg E. J.; Salamone, J. C., Eds.; ACS Symposium Series 496; American Chemical Society: Washington, DC, 1992; p 248.
193. Kłosiński, P.; Penczek, S. *Makromol. Chem., Rapid Commun.* **1988**, *9*, 159.
194. Nyk, A.; Klosinski, P.; Penczek, S. In *Biophosphates and Their Analogues, Synthesis, Structure; Metabolism and Activity*; Bruzik, K. S.; Stec, W. J., Eds.; Elsevier: Amsterdam, 1987; p 231.
195. Penczek, S.; Klosinski, P.; Narebska, A.; Wodzki, R. *Makromol. Chem., Macromol. Symp.* **1991**, *48/49*, 1.
196. Pretula, J.; Kaluzynski, K.; Penczek, S. *Macromolecules* **1986**, *19*, 1797.
197. Kaluzynski, K.; Penczek, S. *Makromol. Chem. Phys.* **1994**, *195*, 3855.
198. Lapienis, G.; Penczek, S. In *Biophosphates and Their Analogues, Synthesis, Structure, Metabolism and Activity*; Bruzik, K. S.; Stec, W. J., Eds.; Elsevier: Amsterdam 1987; p 225.
199. Lapienis, G.; Penczek, S.; Aleksiuk, G. P.; Kropachev, V. A. *J. Polym. Sci., Part A: Polym. Chem. Ed.* **1987**, *25*, 1729.
200. Lapienis, G.; Penczek, S. *J. Polym. Sci., Polym. Chem. Ed.* **1990**, *28*, 1519.

201. Weil, E. D. In *Kirk-Othmer Encyclopedia of Chemical Technology*; 3rd edn.; Wiley Interscience: New York, 1980; Vol. 10, p 396.
202. Wodzki, R. *Eur. Polym. J.* **1986**, *22*, 841, 845.
203. Ostrowska-Czubenko, J.; Wodzki, R. In *Biophosphates and Their Analogues, Synthesis, Structure, Metabolism and Activity*; Bruzik, K. S.; Stec, W. J., Eds.; Elsevier: Amsterdam 1987; p 575.
204. Narebska, A.; Wodzki, R.; Wyszynska, A. *Makromol. Chem.* **1989**, *190*, 1501.
205. Wodzki, R.; Kaluzynski, K. *Makromol. Chem.* **1989**, *190*, 107.
206. Wodzki, R.; Klosinski, P. *Makromol. Chem.* **1990**, *191*, 921.
207. Wodzki, R.; Kaluzynski, K.; Kłosiński, P. *Macromol. Chem. Phys.* **1997**, *198*, 1809.
208. Wodzki, R.; Kaluzynski, K. *Makromol. Chem., Rapid. Commun.* **1984**, *5*, 385.
209. Ostrowska-Czubenko, J.; Wodzki, R. *Colloid Polym. Sci.* **1988**, *266*, 35.
210. Szymański, R.; Penczek, S. *Makromol. Chem.* **1993**, *194*, 1645.
211. Kabanov, V. A.; Kargina, O. V.; Mishustina, L. A.; *et al. Makromol. Chem., Rapid Commun.* **1981**, *2*, 343.
212. Kulszewicz-Bajer, I.; Pretula, J.; Pron, A. *J. Chem. Soc., Chem. Commun.* **1994**, 641.
213. Kulszewicz-Bajer, I.; Sobczak, J.; Hasik, M.; Pretula, J. *Polymer* **1996**, *37*, 25.
214. Zhao, Z.; Wang, J.; Mao, H. Q.; Leong, K. W. *Adv. Drug Delivery Rev.* **2003**, *55*, 483.
215. Wang, D. A.; Williams, C. G.; Yang, F.; *et al. Tissue Eng.* **2005**, *11*, 201.
216. Wan, A. C.; Mao, H. Q.; Wang, S.; *et al. Biomaterials* **2001**, *22*, 1147.
217. Wang, D. A.; Williams, C. G.; Li, Q. A.; *et al. Biomaterials* **2003**, *24*, 3969.
218. Li, Q.; Wang, J.; Shahani, S.; *et al. Biomaterials* **2006**, *27*, 1027.
219. Ilia, G. *Polym. Adv. Technol.* **2009**, *20*, 707.
220. Kim, D. Y.; Kim, J. K.; Kim, C. Y. *Synthetic Metals* **1995**, *69*, 567.
221. Neilson, R. H.; Wisian-Neilson, P. *J. Macromol. Sci., Chem.* **1981**, *A16*, 425.
222. Allcock, H. R. *J. Inorg. Organomet. Polym. Mater.* **2005**, *15*, 57.
223. Peterson, E. S.; Luther, T. A.; Harrup, M. K.; *et al. J. Inorg. Organomet. Polym. Mater.* **2007**, *17*, 361.
224. Stokes, H. M. *Am. Chem. J.* **1896**, *18*, 629.
225. Allcock, H. R. *Chem. Br.* **1974**, *10*, 118.
226. Seel, F.; Langer, J. *Angew. Chem.* **1956**, *68*, 461.
227. Konecny, J. O.; Douglas, C. M. *J. Polym. Sci.* **1959**, *36*, 195.
228. Gimblett, F. G. R. *J. Polym. Sci.* **1962**, *60*, S29.
229. Paddock, N. L. *Q. Rev., Chem. Soc.* **1964**, *18*, 168.
230. Allcock, H. R.; Kugel, R. L. *J. Am. Chem. Soc.* **1965**, *87*, 4216.
231. Allcock, H. R.; Kugel, R. L.; Valan, K. *J. Inorg. Chem.* **1966**, *5*, 1709.
232. Allcock, H. R. *Heteroatom Ring Systems and Polymers*; Academic Press: New York, 1967.
233. Allcock, H. R. *Phosphorus-Nitrogen Compounds*; Academic Press: New York, 1972.
234. Pantel, S.; Becke-Goehring, M. *Sechs – und achtgliedrige Ringsysteme in der Phosphor-Stickstoff-Chemie*; Springer-Verlag: Berlin, 1969.
235. Gleria, M.; de Jaeger, R., Eds., *Polyphosphazenes: A Worldwide Insight*; NOVA Science: Hauppauge, NY, 2004.
236. Allcock, H. R. *Chemistry and Applications of Polyphosphazenes*; Wiley: Hoboken, NJ, 2003.
237. Singler, R. E.; Hagnauer, G. L. In *Organometallic Polymers*; Canalier, C. E., Jr.; Sheats, J. E.; Pittman, C. U., Jr., Eds.; Academic Press: New York, 1978; p 257.
238. Allcock, H. R. *Chem. Rev.* **1972**, *72*, 315.
239. Allcock, H. R. *Science* **1976**, *193*, 1214.
240. Allcock, H. R. *Acc. Chem. Res.* **1979**, *12*, 351.
241. Evans, T. L.; Allcock, H. R. *J. Macromol. Sci., Chem.* **1981**, *A16*, 409.
242. Allcock, H. R. *Chem. Eng. News* **1985**, *63*, 22.
243. Allcock, H. R. *Makromol. Chem., Macromol. Symp.***1986**, *6*, 101.
244. Allcock, H. R. *Curr. Opin. Solid State Mater. Sci.* **2006**, *10*, 231.
245. Allcock, H. R. *J. Inorg. Organomet. Polym. Mater.* **2007**, *16*, 277.
246. Allcock, H. R. In *The Chemistry of Inorganic Ring Systems*; Steudel, R., Ed.; Elsevier: Amersterdam, 1992; p 145.
247. Allcock, H. R. *Polymer* **1980**, *21*, 673.
248. Allcock, H. R. In *Comprehensive Polymer Sciences*; Eastmond, G. C.; Ledwith, A.; Russo, S., Eds.; Pergamon: Oxford, 1989; Vol. 4, Part 2, p 585.
249. Allen, G.; Lewis, C. J.; Todd, S. M. *Polymer* **1970**, *11*, 31.
250. Tate, D. P. *J. Polym. Sci., Polym. Symp.* **1974**, *48*, 33.
251. Singler, R. E.; Schneider, N. S.; Hagnauer, G. L. *Polym. Eng. Sci.* **1975**, *15*, 321.
252. Hagnauer, G. L. *J. Macromol. Sci., Chem.* **1981**, *A16*, 385.
253. Kireev, V. V.; Astrina, V. I.; Tchernyshev, E. A. *Usp. Khim.* **1981**, *50*, 2270.
254. Kireev, V. V.; Mitropol'skaya, G. I.; Zinovitch, Z. K. *Usp. Khim.* **1982**, *57*, 266.
255. Tur, D. R.; Vinogradova, S. V. *Vysokomol. Soedin., Ser. A* **1982**, *24*, 2247.
256. Vinogradova, S. V.; Tur, D. R.; Minos'yants, I. I. *Usp. Khim.* **1984**, *53*, 87.
257. McWilliams, A. R.; Dorn, H.; Manners, I. *Top. Curr. Chem.* **2002**, *220*, 141.
258. Kumbar, S. G.; Bhattacharyya, S.; Nukavarapu, S. P.; *et al. J. Inorg. Organomet. Polym. Mater.* **2006**, *16*, 365.
259. Allen, C. W. *J. Inorg. Organomet. Polym. Mater.* **2006**, *16*, 273.
260. Andrianov, A. K. *J. Inorg. Organomet. Polym. Mater.* **2006**, *16*, 397.
261. Stewart, F. F.; Peterson, E. S. In *Handbook of Ring-Opening Polymerization*; Dubois, P.; Coulembier, O.; Raquez, J. M., Eds.; Wiley-VCH Verlag: Weinheim, 2009; p 97.
262. Neilson, R. H.; Wisian-Neilson, P. *Chem. Rev.* **1988**, *88*, 541.
263. MacCallum, J. R.; Tanner, J. *J. Polym. Sci., Part B* **1969**, *7*, 743.
264. Korshak, V. V.; Vinogradova, S. V.; Tur, D. R.; Kazarova, I. I. *Acta Polym. (Berlin)* **1980**, *31*, 669.
265. Devadoss, E.; Nair, C. P. R. *Ind. Eng. Chem. Prod. Res.* **1984**, *23*, 272.
266. Kireev, V. V.; Milashvili, M. V.; Rochev, V. Ya.; *et al. Vysokomol. Soedin. Ser. A* **1986**, *28*, 1589.
267. Ganapathiappan, S.; Dhathathreyan, K. S.; Krishnamurthy, S. S. *Macromolecules* **1987**, *20*, 1501.
268. Zhang, Y.; Huynh, K.; Manners, I.; Reed, C. A. *Chem. Commun.* **2008**, 494.
269. Allcock, H. R. *Angew. Chem., Int. Ed. Engl.* **1977**, *16*, 147.
270. Allcock, H. R.; Gardner, J. E.; Smeltz, K. M. *Macromolecules* **1975**, *8*, 36.
271. Jacques, J. K.; Mole, M. F.; Paddock, N. L. *J. Chem. Soc.* **1965**, 2112.
272. MacCallum, J. R.; Werninck, A. *J. Polym. Sci., Part A-1: Polym. Chem.* **1967**, *5*, 3061.
273. Colclough, R. O.; Gee, G. *J. Polym. Sci., Part C* **1968**, *16*, 3639.
274. Emsley, J.; Udy, P. B. *Polymer* **1972**, *13*, 593.
275. Horn, H.-G.; Kolkmann, F. *Makromol. Chem.* **1982**, *183*, 1833.
276. Sennett, M. S.; Hagnauer, G. L.; Singler, R. E.; Davies, G. *Macromolecules* **1986**, *19*, 959.
277. Potts, M. K.; Hagnauer, G. L.; Sennett, M. S.; Davies, G. *Macromolecules* **1989**, *22*, 4235.
278. Kajiwara, M. *Angew. Makromol. Chem.* **1985**, *129*, 71.
279. Kajiwara, M.; Saito, H. *Angew. Makromol. Chem.* **1985**, *132*, 197.
280. Liu, H. Q.; Stannett, V. T. *Macromolecules* **1990**, *23*, 140.
281. Osada, Y.; Hashidzume, M.; Tsuchida, E.; Bell, A. T. *Nature (London)* **1980**, *186*, 693.
282. Klein, J. A.; Bell, A. T.; Soong, D. S. *Macromolecules* **1987**, *20*, 782.
283. Vorac, Z.; Alberti, M.; Janca, J. *Plasma Process. Polym.* **2009**, *6*, 262.
284. Retuert, J.; Ponce, S.; Quijada, J. R. *Polym. Bull.* **1979**, *1*, 653.
285. Retuert, J.; Aguilera, C.; Martinez, F. *Polym. Bull.* **1982**, *6*, 535.
286. Scopelianos, A. G.; Allcock, H. R. *Macromolecules* **1987**, *20*, 432.
287. Mujumdar, A. N.; Young, S. G.; Merker, R. L.; Magill, J. H. *Macromolecules* **1990**, *23*, 14.
288. Mujumdar, A. N.; Young, S. G.; Merker, R. L.; Magill, J. H. *Macromol. Chem.* **1989**, *190*, 2293.
289. Caglioti, V.; Cordishi, D.; Mele, A. *Nature (London)* **1962**, *195*, 491.
290. Chu, B.; Lee, D. *Macromolecules* **1986**, *19*, 1592.
291. Lee, D.; Ford, J. R.; Fytas, G.; *et al. Macromolecules* **1986**, *19*, 1586.
292. Allcock, H. R.; Best, R. J. *Can. J. Chem.* **1964**, *42*, 447.
293. MacCallum, J. R.; Werninck, A. R. S. *J. Macromol. Sci., Chem.* **1971**, *A5*, 653.
294. Goethals, E. J. *Adv. Polym. Sci.* **1977**, *23*, 104.
295. Kireev, V. V.; Korshak, V. V.; Mitropol'skaya, G. I.; Sulkovsky, V. *Vysokomol. Soedin., Ser. A* **1979**, *21*, 100.
296. MacCallum, J. R.; Tanner, J. *J. Macromol. Sci., Chem.* **1970**, *A4*, 481.
297. Herring, D. L. *Chem. Ind.* **1960**, 111.
298. John, K.; Moeller, T. *J. Am. Chem. Soc.* **1960**, *82*, 2647.
299. Otto, R. J. A.; Audrieth, L. F. *J. Am. Chem. Soc.* **1958**, *80*, 5894.
300. Allcock, H. R.; Patterson, D. B.; Evans, T. L. *J. Am. Chem. Soc.* **1977**, *99*, 6095.
301. Allcock, H. R.; Patterson, D. B.; Evans, T. L. *Macromolecules* **1979**, *12*, 172.
302. Allcock, H. R.; Patterson, D. B. *Inorg. Chem.* **1977**, *16*, 197.
303. Allcock, H. R.; Schmutz, J. L.; Kosydar, K. M. *Macromolecules* **1978**, *11*, 179.
304. Allcock, H. R.; Cook, W. J. *Macromolecules* **1974**, *7*, 284.
305. Allcock, H. R.; Moore, G. Y.; Cook, W. J. *Macromolecules* **1974**, *7*, 571.
306. Ritchie, R. J.; Harris, P. J.; Allcock, H. R. *Macromolecules* **1979**, *12*, 1014.
307. Allcock, H. R.; Ritchie, R. J.; Harris, P. J. *Macromolecules* **1980**, *13*, 1332.
308. Allcock, H. R.; Moore, G. Y. *Macromolecules* **1975**, *8*, 377.
309. Prons, V. N.; Grinblat, M. P.; Klebanskii, A. L. *Vysokomol. Soedin., Ser. A* **1974**, *16*, 1620.
310. Volodin, A. A.; Burin, S. V.; Levin, M. D.; *et al. Vysokomol. Soedin., Ser. B* **1987**, *29*, 808.
311. Scopelianos, A. G.; O'Brien, J. P.; Allcock, H. R. *J. Chem. Soc., Chem. Commun.* **1980**, 198.
312. Allcock, H. R.; Scopelianos, A. G.; O'Brien, J. P.; Bemheim, M. Y. *J. Am. Chem. Soc.* **1981**, *103*, 350.
313. Allcock, H. R.; Brennan, D. J.; Graaskamp, J. M. *Macromolecules* **1988**, *21*, 1.
314. Allcock, H. R.; Riding, G. H.; Lavin, K. D. *Macromolecules* **1987**, *20*, 6.

315. Allcock, H. R.; Lavin, K. D.; Riding, G. H. *Macromolecules* **1985**, *18*, 1340.
316. Allcock, H. R.; McDonnell, G. S.; Desorcie, J. L. *Macromolecules* **1990**, *23*, 3873.
317. Horn, H.-G.; Kolkmann, F. *Makromol. Chem.* **1982**, *183*, 1843.
318. Allcock, H. R.; Dodge, J. A.; Manners, I.; Riding, G. H. *J. Am. Chem. Soc.* **1991**, *113*, 9596.
319. Cho, Y.; Baek, H.; Sohn, Y. S. *Macromolecules* **1999**, *32*, 2167.
320. Roesky, H. W.; Lücke, M. *Angew. Chem. Int. Ed. Engl.* **1989**, *28*, 493.
321. Allcock, H. R.; Kuharcik, S. E.; Morrissey, C. T.; Ngo, D. C. *Macromolecules* **1994**, *27*, 7556.
322. Allcock, H. R.; Ngo, D. C. *Macromolecules* **1992**, *25*, 2802.
323. Ngo, D. C.; Rutt, J. S.; Allcock, H. R. *J. Am. Chem. Soc.* **1991**, *113*, 5075.
324. Allcock, H. R.; Coley, S. M.; Manners, I.; *et al. Macromolecules* **1991**, *24*, 2024.
325. Manners, I.; Allcock, H. R.; Renner, G.; Nuyken, O. *J. Am. Chem. Soc.* **1989**, *111*, 5478.
326. Allcock, H. R.; Coley, S. M.; Morrissey, C. T. *Macromolecules* **1994**, *27*, 2904.
327. Dodge, J. A.; Manners, I.; Allcock, H. R.; *et al. J. Am. Chem. Soc.* **1990**, *112*, 1268.
328. Allcock, H. R.; Dodge, J. A.; Manners, I. *Macromolecules* **1993**, *26*, 11.
329. Liang, M.; Manners, I. *J. Am. Chem. Soc.* **1991**, *113*, 4044.
330. Ni, Y.; Stammer, A.; Liang, M.; *et al. Macromolecules* **1992**, *25*, 7119.
331. McWilliams, A. R.; Gates, D. P.; Edwards, M.; *et al. J. Am. Chem. Soc.* **2000**, *122*, 8848.
332. Zhang, T.; Cai, Q.; Wu, D.-Z.; Jin, R.-G. *J. Appl. Polym. Sci.* **2005**, *95*, 880.
333. Wycisk, R.; Pintauro, P. N. *Adv. Polym. Sci.* **2008**, *216*: 157.
334. Crommen, J. H. L.; Schacht, E. H.; Mense, E. H. G. *Biomaterials* **1992**, *13*, 511, 601.
335. Lakshmia, S.; Kattia, D. S., Laurencina, C. T. *Adv. Drug Delivery Rev.* **2003**, *55*, 467.
336. Allcock, H. R.; Wood, R. M. *J. Polym. Sci., Part B: Polym. Phys.* **2006**, *44*, 2358.
337. Tang, H.; Pintauro, P. N. *J. Appl. Polym. Sci.* **2001**, *79*, 49.
338. Allcock, H. R. In *Biodegradable Polymers as Drug Delivery Systems*; Chasin, M. R. Langer, R., Eds.; Marcel Dekker: New York, 1990; p163.

Biographical Sketch

Grzegorz Lapienis works in the Centre of Molecular and Macromolecular Studies, Polish Academy of Sciences, Lodz, Poland, as assistant professor. He received his MS (1970) and PhD (1975) degrees, both in polymer chemistry, from the Technical University of Lodz, and DSc (2010) degree in chemical sciences from the Centre of Molecular and Macromolecular Studies. From 1978–79, he held postdoctoral positions at the Department of Chemistry, The Queen's University of Belfast with Prof. K. J. Ivin. He worked for many years with Prof. S. Penczek on the ring-opening polymerization of cyclic phosphates and the synthesis of models of biopolymers. He obtained analogs of nucleic acids, polyesters of phosphoric acid, which did not contain sugar fragment and/or devoid of nitrogen bases. He received group awards of Scientific Secretary of Polish Academy of Sciences twice in the years 1977 and 1985. He has written over 60 articles and review papers, 3 chapters in books, and 3 patents. Recently, he elaborated a new method of the synthesis of star-shaped polymers with highly branched core formed from diepoxides. His current research interests are the synthesis, characterization, and application of star-shaped polymers, synthesis of derivatives of poly(ethylene oxide), and size-exclusion chromatography.

4.19 Radical Ring-Opening Polymerization

T Endo, Kinki University Iizuka, Japan

4.19.1 General

Radical ring-opening polymerization (radical ROP) is an intriguing method of polymerization from the viewpoints of its potential to afford polymers with heteroatom-containing main chains inherited from the corresponding heterocyclic monomers as well as its potential versatility in copolymerizations of such cyclic monomers with various vinyl monomers. In general, cyclic monomers that can undergo radical ROP are endowed with carbon–carbon double bonds such as vinyl and *exo*-methylene groups that can react with radical species, although there are some exceptions such as cyclic disulfides and bicyclobutanes. The addition of radical species to the vinyl group is followed by ring-opening reaction of the cyclic monomers to afford the corresponding radical at the propagating chain end. Therefore, in some cases, radical ROP is completed by radical chain-growth polymerization, which should be avoided by appropriate molecular designs of cyclic monomers.

There are four essential requirements, which should be fulfilled in designing the ideal cyclic monomers for achieving efficient radical ROP. (1) They should possess a C–C double bond that can accept radical species. (2) They should possess highly distorted ring structures. (3) Their ring-opening reactions should be accompanied by some isomerization processes that can afford thermodynamically stable functional groups. (4) These ring-opening reactions should be promoted by giving the corresponding radical species stabilized somehow. For a more specific explanation, the radical ROP of vinyl cyclopropanes is selected as an example and depicted in Scheme 1. The first step is the addition reaction of a radical species to the vinyl group. This step is followed by the ring-opening reaction of the three-membered ring with releasing its high distortion energy, leading to the formation of another type of radical stabilized by the substituents X and Y such as phenyl, ester, and cyano groups. This stabilization effect as well as the formation of internal olefin assists the smooth ring-opening reaction of the cyclopropane ring.

Scheme 2 depicts another example, that is, the radical ROP of cyclic ketene acetals. In this case, the *exo*-methylene group is the radical acceptor. The ring-opening reaction is accompanied by the formation of an acyclic ester linkage, which is thermodynamically much more stable than the original cyclic acetal. In addition, the resulting radical is stabilized by the adjacent phenyl group, and this stabilization contributes to the efficient ring-opening reaction.

Besides these monomers, several intriguing monomers and their radical ROP have been reported. Their structural characteristics, their polymerization behaviors, and the structures of the corresponding polymers are summarized below.

4.19.2 Cycloalkanes

In Scheme 3, the radical ROP of bicycloalkanes with highly distorted structures is shown. In spite of the lack of a C–C double bond that can accept radical species, these bicycloalkanes undergo radical ROP due to the sp^2 character of the carbon atoms consisting of the bicyclic system that allows the efficient addition of radical species on the monomers.[1–3] Introduction of substituents X such as cyano, esters, and sulfonates is essential for the efficient polymerization, because these substituents can promote the ring-opening reaction by stabilizing the resulting radical. The resulting polymers exhibit high thermal stability due to the presence of rigid cyclobutane rings.

In Scheme 4, the radical ROP of vinyl cyclopropanes is shown. The vinyl group acts as a radical acceptor. After accepting a radical, the cyclopropane ring undergoes the ring-opening reaction. Due to the high distortion energy of the cyclopropane ring, this ROP is free from chain-growth radical polymerization of the vinyl group. The introduction of functional groups X, such as halogens, esters, and cyano groups,[4–7] is one of the keys to the molecular design of this class of monomers, which can promote the ring-opening reaction by stabilizing the resulting radicals. In contrast to the chain-growth polymerizations of vinyl monomers such as styrene derivatives, acrylates, and methacrylates that suffer from large volume shrinkage, the radical ROP of some vinyl cyclopropanes is accompanied by much smaller volume shrinkage.[8] The main chain of the resulting polymers has carbon–carbon double bonds, which are potentially applicable as reactive sites for polymer reactions. In addition, as shown in Scheme 4, in some cases depending on substituents, cyclobutane rings are incorporated into the polymer, due to the backbiting of the terminal radical to the C–C double bond in the main chain.

A vinyl cyclopropane bearing trimethylsiloxy group is a useful monomer for synthesizing a versatile reactive polymer

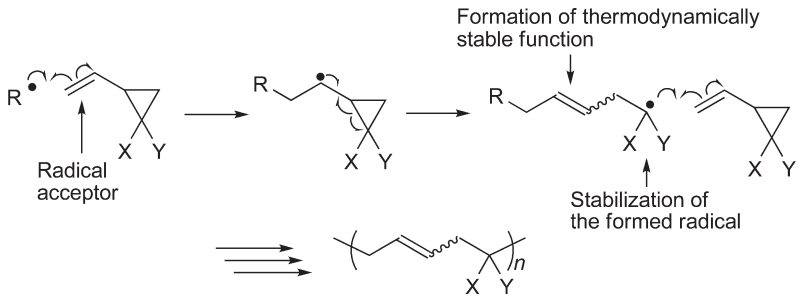

Scheme 1

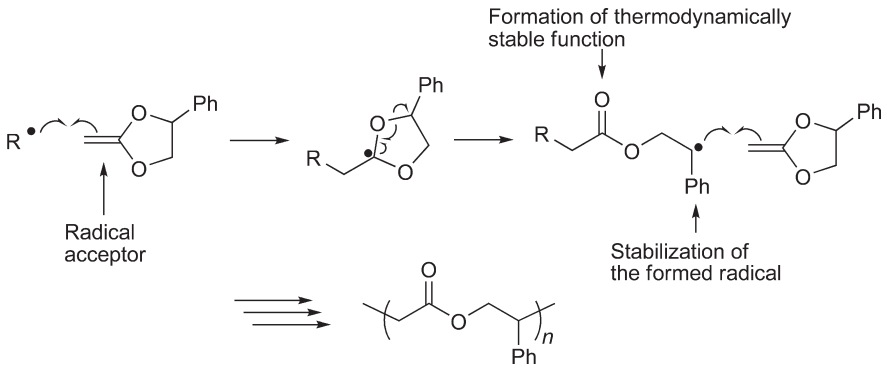

Scheme 2

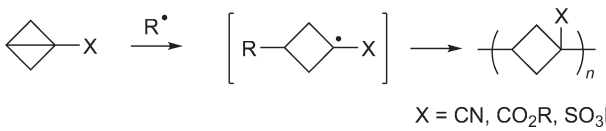

Scheme 3

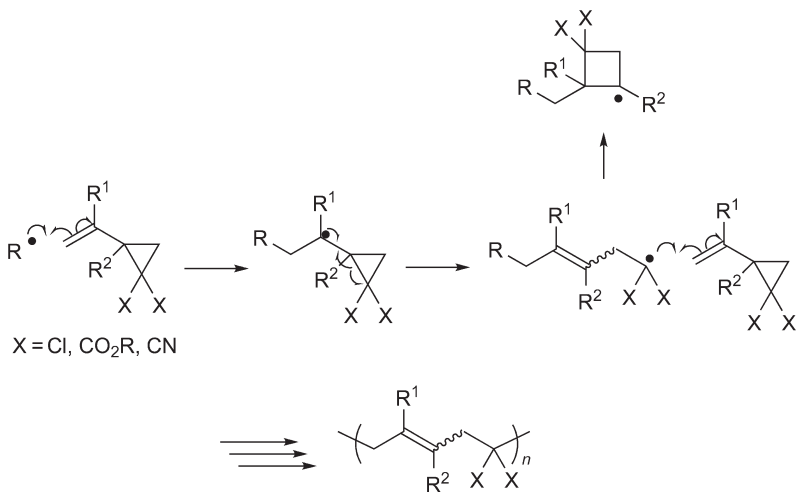

Scheme 4

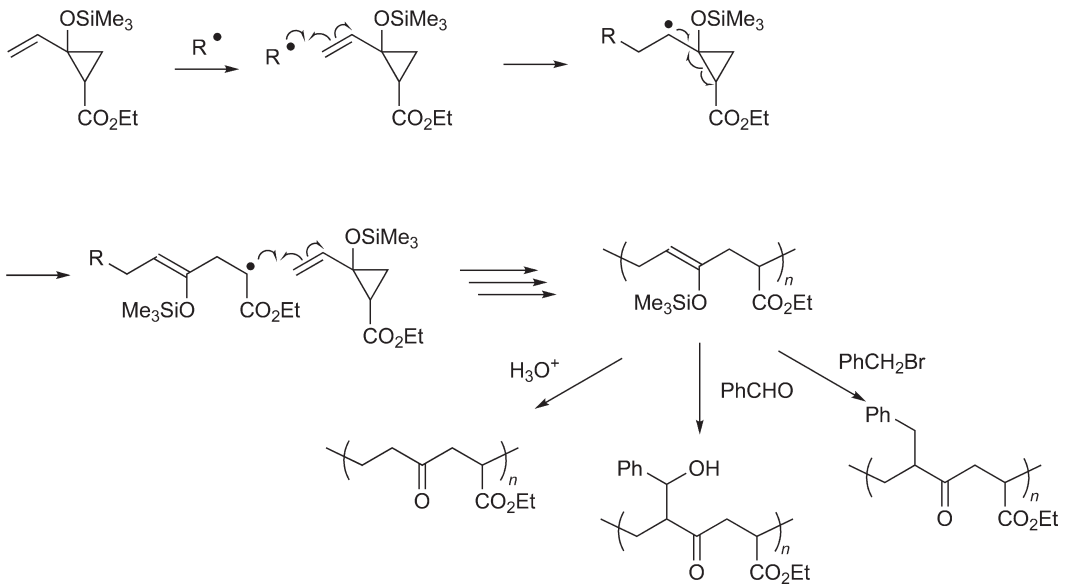

Scheme 5

(Scheme 5).[9] Its radical ROP gives the corresponding polymer bearing silyl enol ether, which is a nucleophilic functional group. Various electrophiles such as aldehydes and alkyl bromides can react with the silylenol ether in the main chain to permit versatile functionalization of the polymer.

Vinyl cyclopropanes undergo radical copolymerization with methyl methacrylate (MMA) (Scheme 6).[10] Quite interestingly, the copolymerization is accompanied by the formation of five- and six-membered rings in the main chain. The radical at the chain end formed by the ring-opening reaction of vinyl cyclopropanes attacks MMA preferably, and the resulting radical is located so that it can react with a C–C double bond in the main chain forming a five- or six-membered ring. The copolymerization parameters were evaluated to be $r_1 = 0.11$ and $r_2 = 21.51$ (M_1, vinyl cyclopropane; M_2, MMA) by nonlinear least-squares methods. The degree of volume shrinkage on the copolymerization decreases as the content of vinyl cyclopropane increases. A similar tendency was observed in the glass transition temperature of the copolymers.

It has been reported that 10-methylene-9,10-dihydroanthryl-9-spirocyclopropane undergoes the radical ROP efficiently (Scheme 7).[11] In the monomer design, π-conjugated system is properly inserted between the vinyl group and the cyclopropane moiety. The driving force for the ROP is not only the release of the distortion energy of the cyclopropane ring, but also the formation of anthracene moiety, an expanded π-conjugated system.

α-Cyclopropylstyrene also undergoes the radical ROP (Scheme 8).[12] The ring-opening reaction of the cyclopropyl moiety gives a relatively unstable radical; however, the styrene part in the monomer captures such a highly active radical immediately to suppress termination and chain transfer reactions. The resulting polymer has a repeating unit that consists of a styrene-derived part and a sequence of three methylene groups, which cannot be obtained by any other methods.

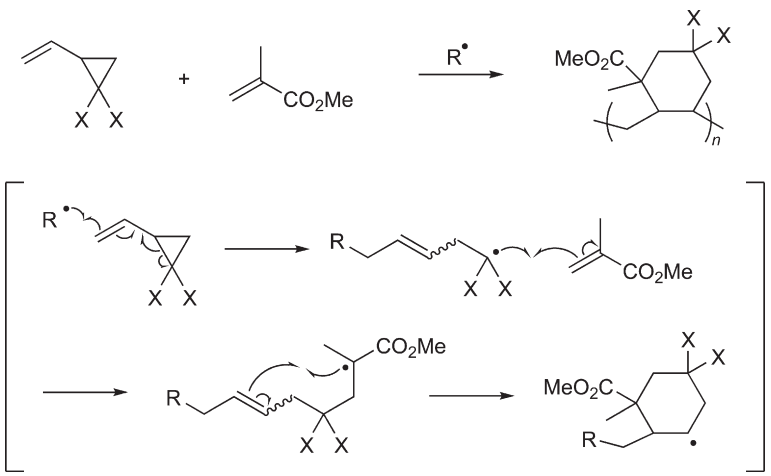

Scheme 6

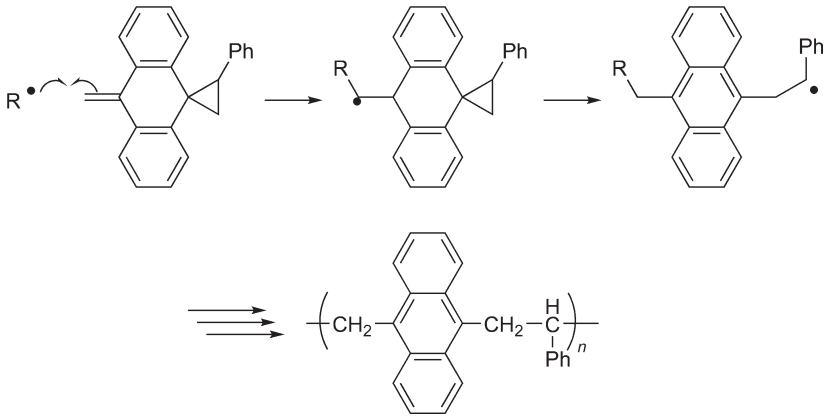

Scheme 7

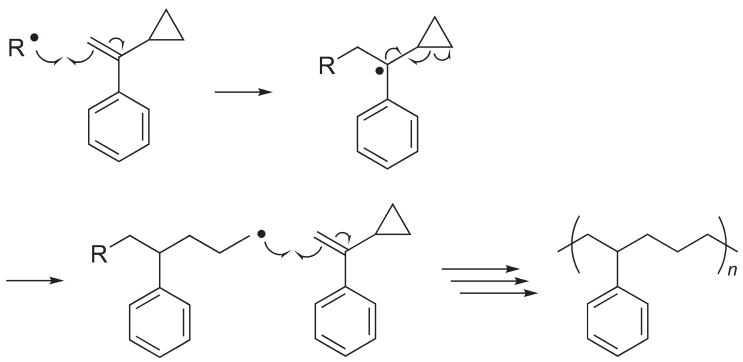

Scheme 8

Besides the examples of the chain-growth polymerizations, a step-growth polymerization has been also reported. In the presence of radical initiator, vinyl cyclopropane and thiol undergoes the addition reaction with ring-opening (Scheme 9). Based on this reaction, a polyaddition system has been developed.[13] In this system, bifunctional vinyl cyclopropanes and dithiols can be used as monomers, polyaddition of which gives the corresponding polysulfides bearing C–C double bonds in the main chain.

Not only the cyclopropane derivatives but also some cyclobutane derivatives undergo radical ROPs. Scheme 10 depicts the ROP of a vinyl cyclobutane.[14] Release of the distortion energy of four-membered ring and stabilization of the resulting radical by the adjacent ester group promote the polymerization.

Benzocyclobutene is also a highly distorted compound, which undergoes thermally induced ring-opening reaction to afford *o*-quinodimethane (Scheme 11).[15] The formed *o*-quinodimethane undergoes radical polymerization forming *o*-phenylene structure in the main chain. This process with 'aromatization' is one of the driving forces for the efficient polymerization. By introducing functional groups on the cyclobutene ring, the temperature for the polymerization can be controlled.[16] The methoxy-substituted monomer undergoes

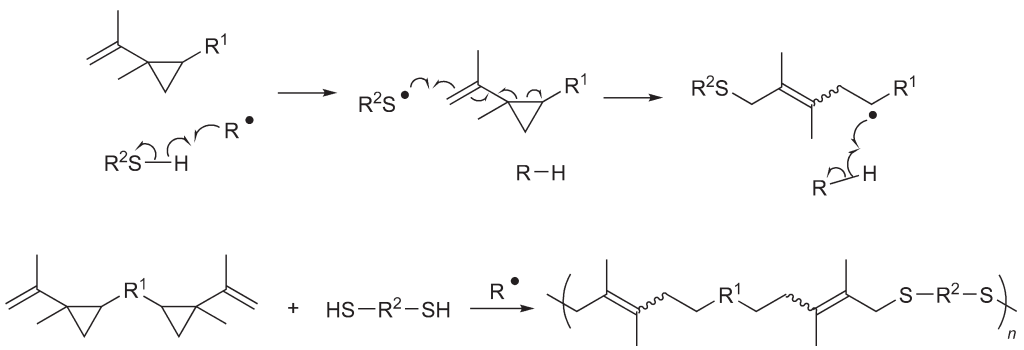

Scheme 9

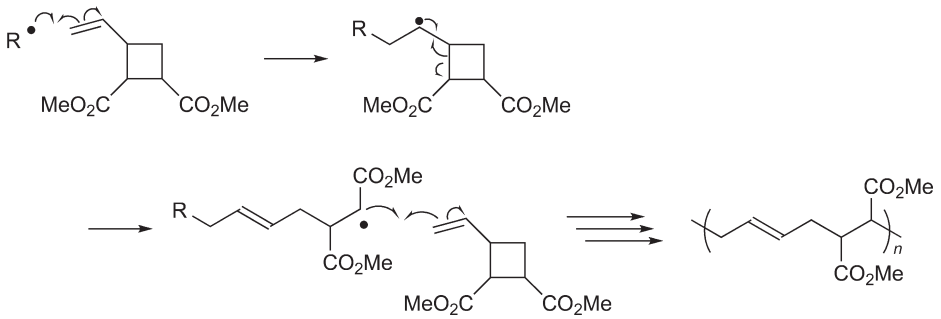

Scheme 10

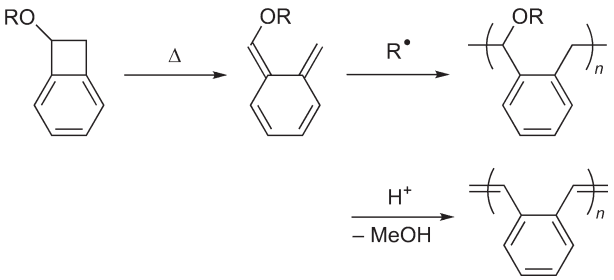

Scheme 11

the radical ROP at 120 °C to afford a methoxy-substituted poly (phenylene ethylene). By heating this polymer in the presence of *p*-toluenesulfonic acid, methanol can be eliminated to give poly(phenylene vinylene), a π-conjugated polymer. The benzocyclobutene-type monomer also undergoes copolymerization with various vinyl monomers such as MMA, methyl acrylate, and acrylonitrile. For example, the copolymerization with methyl acrylate with a feed ratio of 50:50 gives the corresponding copolymer with a composition ratio of 47:53.

A compound consisting of six-membered rings can undergo radical ROP, despite the less distorted nature of six-membered rings than that of the three- and four-membered rings (Scheme 12).[17] The *exo*-methylene group is the acceptor of radical. In this case, the ring-opening reaction of the center ring is promoted by the formation of *o*-phenylene unit, that is, aromatization of cyclohexadiene radical into phenyl group releasing benzyl radical. Another driving force of the ring-opening reaction is the formation of a relatively stable benzyl radical. The copolymer structure is quite interesting, since it can be regarded as an imaginary copolymer of benzyne and ethylene. Although copolymerization of this monomer with conventional vinyl monomers has been not reported yet, it would be an efficient strategy to synthesize polymers with enhanced thermal stability and mechanical strength due to the introduction of phenyl groups into the main chain.

4.19.3 Cyclic Ethers and Cyclic Sulfides

Oxiranes and thiiranes are cyclic monomers that can undergo cationic and anionic ROP. Attachment of vinyl groups to these highly reactive heterocycles can give a new class of monomers that undergo radical ROP. Vinyl oxiranes and vinyl thiiranes are heteroatom-containing analogues of vinyl cyclopropanes. Similar to vinyl cyclopropanes, these three-membered cyclic ethers and sulfides undergo radical ROPs (Scheme 13).[18–20] The first step is the addition of radical species to the C–C double bond of the monomers. This reaction is followed by the ring-opening reaction of the three-membered ring, which is driven by the release of the distortion energy of the three-membered ring. Introduction of a phenyl group on the three-membered ring is an essential point in the molecular design, because the phenyl group can stabilize the adjacent radical formed by the ring-opening reaction.

As shown in Scheme 14, the introduction of a spiro bicyclic structure is an interesting way of designing a new radical polymerization system.[21] Similar to other types of cyclic monomers

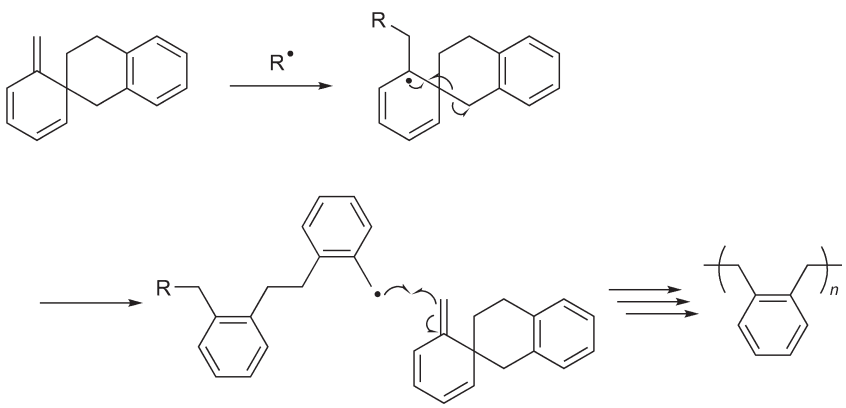

Scheme 12

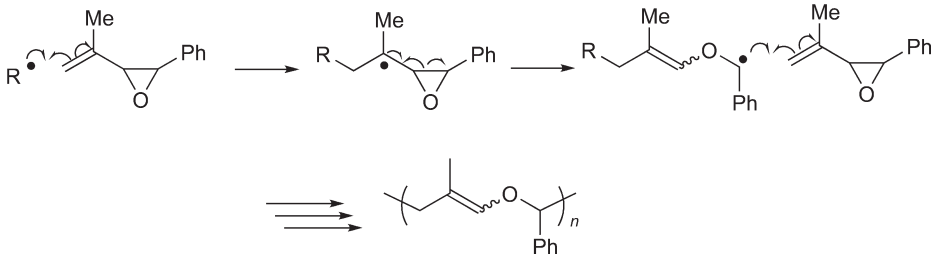

Scheme 13

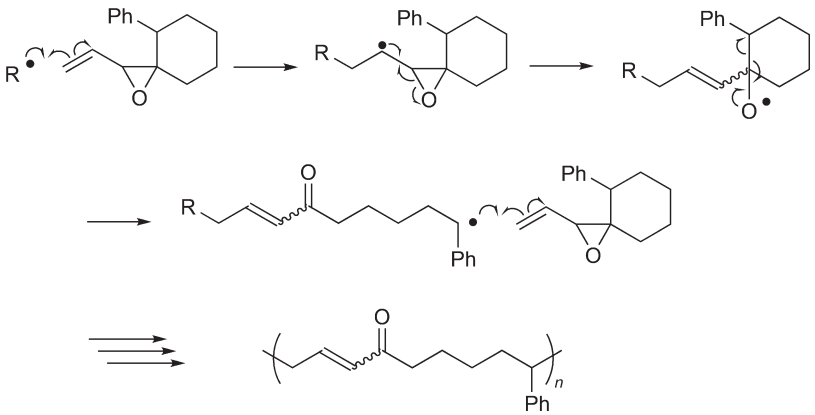

Scheme 14

that undergo radical ROP, this spiro bicyclic monomer accepts radical species at its vinyl group. One of the features of this polymerization system is that both the oxirane moiety and the cyclohexane ring in the spiro cyclic system undergo ring-opening reaction. The ring-opening reaction of the oxirane ring is followed by the ring-opening reaction of the cyclohexane ring. The latter ring-opening reaction is assisted by the formation of a benzyl radical. The resulting polymer has an α,β-unsaturated ketone structure in the main chain, which would be used as an electrophilic reactive group for functionalization of the polymer.

Analogous to the polyaddition of bifunctional vinyl cyclopropanes and dithiols, bifunctional vinyloxiranes also undergo polyaddition with dithiols to give the corresponding polysulfides bearing a vinylether structure in the main chain (Scheme 15).[22] An H radical can be abstracted from an SH group in the presence of a radical initiator, and the formed S radical reacts with the vinyl group. Then, the ring-opening reaction of the oxirane ring proceeds, and the resulting radical abstracts an H radical from another SH group. This polymerization can be conducted using a radical initiator such as azobisisobutyronitrile (AIBN) at 60 °C. In addition, the same polymerization proceeds under photo-irradiation at room temperature.

A methylene oxetane shown in Scheme 16 can be regarded as not only a cyclic monomer but also a vinyl ether-type monomer. Consequently, this monomer undergoes not only the radical ROP but also the chain-growth radical polymerization of the C–C double bond (Scheme 16).[23] The resulting polymer consists of ketone-containing units and oxetane-containing units in a ratio of 4:6. The *exo*-methylene group accepts a radical, and the resulting radical is transformed into a primary alkyl radical. The formed radical is not stabilized and thus

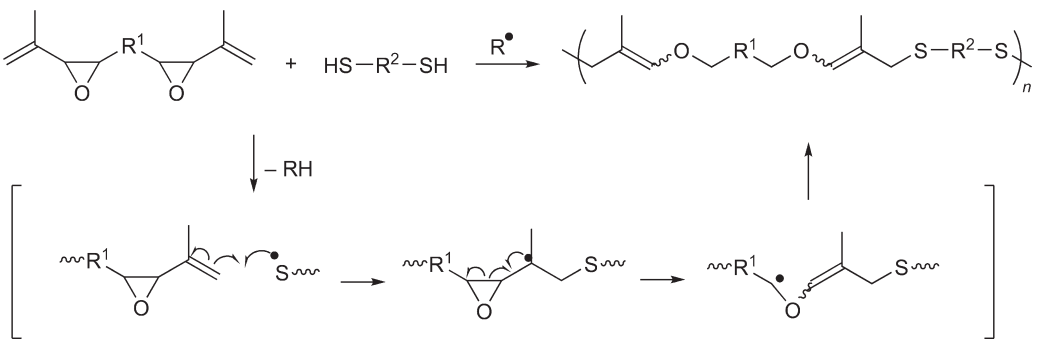

Scheme 15

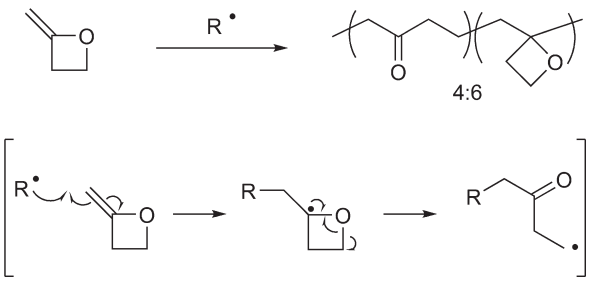

Scheme 16

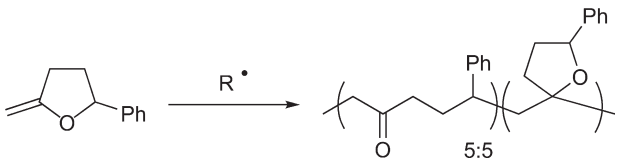

Scheme 17

relatively difficult to form; however, the formation of the thermodynamically stable ketone group can drive the ring-opening reaction.

A five-membered cyclic ether with an *exo*-methylene group is a monomer for radical ROP (Scheme 17).[24] The radically induced ring-opening reaction is promoted by two factors: (1) the formation of thermodynamically stable ketone group, and (2) that of relatively stable benzyl radical-type chain end. On the other hand, an analogous compound with a six-membered cyclic ether structure does not undergo ROP, but its *exo*-methylene group undergoes the chain-growth radical polymerization.

A seven-membered cyclic allyl sulfide shown in Scheme 18 is a monomer that was designed based on the high reactivity of allyl sulfide in various radical reaction systems.[25] It undergoes ROP selectively to afford the corresponding polysulfide. The first step is the addition reaction of the radical to the *exo*-methylene group of the monomer, leading to the formation of a radical at the β-position of the sulfur atom. This cyclic radical undergoes the ring-opening reaction forming a new acyclic allyl sulfide and thiyl radical. In general, thiyl radicals readily react with C–C bonds without the hydrogen abstraction that causes various side reactions. In fact, radical ROP of the seven-membered cyclic allyl sulfide proceeds smoothly at 70 °C to afford the corresponding polysulfide, the weight average molecular weight of which is more than 600 thousands. An analogous monomer with eight-membered ring also undergoes radical ROP smoothly.

Cyclic disulfides are also radically polymerizable monomers. Although they do not have a C–C double bond for accepting radicals, the homolysis of the S–S bond permits the formation of S radicals (Scheme 19).[26] The resulting biradical undergoes polyaddition to afford polydisulfide.

Lypoamide, a five-membered cyclic disulfide, is a coenzyme necessary for the oxidative acylation reactions in bioorganic systems. Although it does not undergo homopolymerization, it can be used as a comonomer for the radical polymerizations of vinyl monomers such as styrene, vinyl

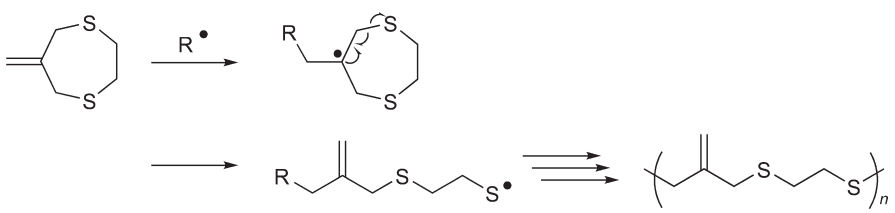

Scheme 18

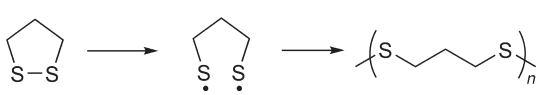

Scheme 19

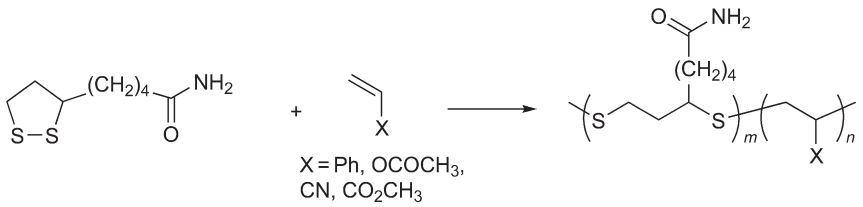

Scheme 20

acetate, and methyl acrylate (Scheme 20).[27] These copolymerizations gave the corresponding polymers with sulfide linkages in the main chain. By using 15 mol.% lypoamide as a comonomer, the copolymers with 8–25% content of lypoamide-derived unit can be obtained.

4.19.4 Cyclic Acetals

Cyclic ketene acetals, a class of monomers with highly nucleophilic nature, have been developed for the purpose of their efficient cationic ROP. Nevertheless, it has been clarified that these monomers also undergo radical ROP. The radical ROP behaviors of cyclic ketene acetals depend on two parameters: ring size and substituents (Scheme 21). These monomers can undergo not only ROP but also vinyl polymerization. Herein, 'ring-opening efficiency' is defined as a ratio of (number of units formed by ROP)/(total number of units including those formed by vinyl polymerization). In the polymerizations of the 5-, 6-, and 7-cyclic ketene acetals without substituents, the corresponding ring-opening efficiencies are 83%, 85%, and 100%, respectively, implying that ring distortion is a critical parameter.[28] On the other hand, by introducing substituents such as alkyl and phenyl groups, the ring-opening efficiency can be improved to 100% regardless of ring size, presumably due to the effects of these substituents to promote the ring-opening reaction by stabilizing the radicals formed at the chain end.[29–33] Particularly, one of the seven-membered cyclic ketene acetal listed in Scheme 21 undergoes radical ROP highly efficiently (Scheme 22). The C–C double bond accepts radical species to give the corresponding cyclic acetal-type radical. Due to the high distortion energy, the seven-membered ring undergoes the ring-opening reaction efficiently. The resulting radical is a benzyl radical, which is stabilized by delocalization.

Cyclic ketene acetals undergo radical copolymerization with various vinyl monomers (Scheme 23).[34] For example, in the case of the copolymerization of the five-membered cyclic ketene acetal bearing phenyl group and MMA, composition of the copolymer can be efficiently controlled in a range from 9:91 to 82:18 by varying the feed ratio of the monomers. This is a useful method for synthesizing degradable polymers bearing ester linkages in the main chains, which were derived from the cyclic monomers.

The polymerization behavior of a five-membered cyclic *O*, *S*-ketene acetal, a sulfur-containing analog of a cyclic ketene acetal, has been reported (Scheme 24).[35] The ring-opening efficiency of the polymerization was 45%, which was lower than that of the polymerization of the five-membered ketene acetal. The difference in ring-opening efficiency would be attributable to the difference in the thermodynamic stability between the resulting functional groups, ester and thioester. In general, ester is much more stable than thioester, and thus the formation of the ester function by the ROP of ketene acetal is more favorable than the formation of the thioester by the ROP of ketene *O*,*S*-acetal.

8-Methylene-1,4-dioxaspiro-[4.5]deca-6,9-diene is a five-membered cyclic ketene acetal that undergoes radical ROP selectively (Scheme 25).[36] Although it is more difficult for a five-membered ring to undergo ring-opening reaction than three-, four-, and seven-membered rings, the formation of aromatic ring in the main chain assists in the highly efficient ROP.

The combination of the two different monomer designs of vinyl cyclopropane and cyclic ketene acetal permits the creation of a new monomer that undergoes double ROP (Scheme 26).[37,38] Although the resulting polymer is contaminated by some other units such as those formed by the vinyl

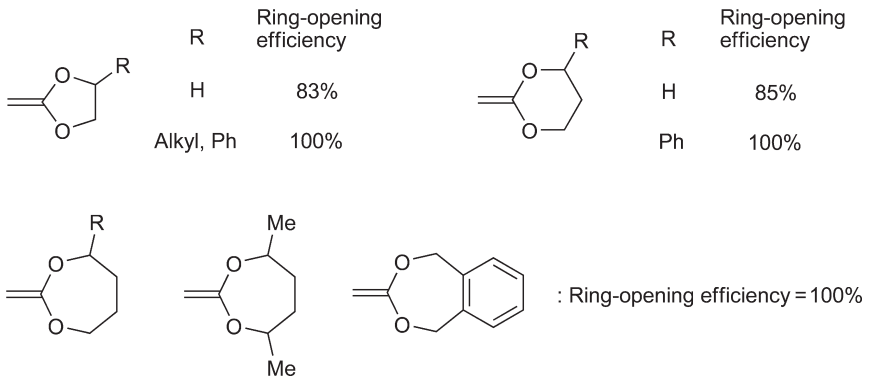

Scheme 21

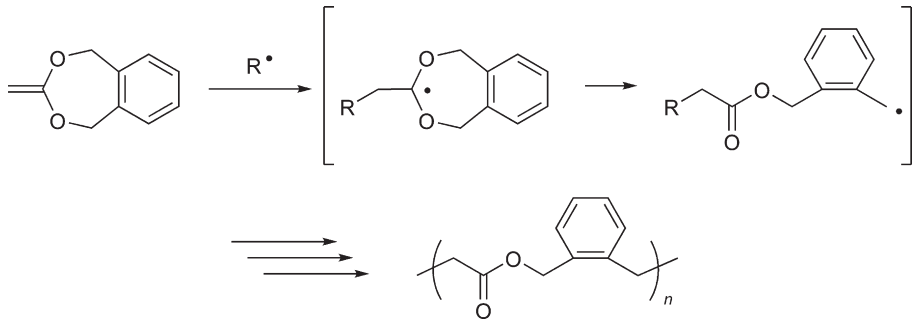

Scheme 22

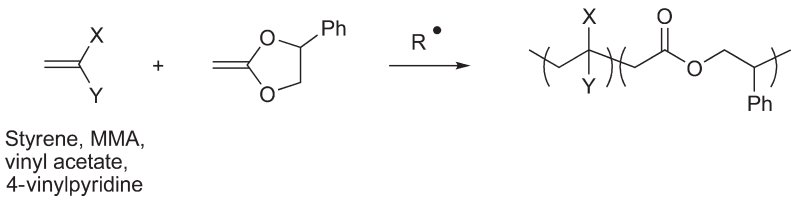

Scheme 23

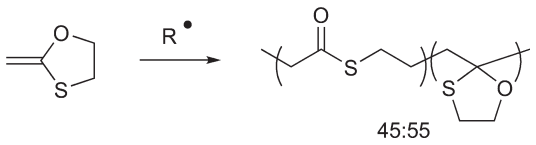

Scheme 24

polymerization and the ROP of the vinyl cyclopropane part without ring opening of the cyclic acetal part, the pathway dominating the system is the double ROP, which affords the corresponding polyester bearing C–C double bonds in the main chain. The high ring distortion energy of the seven-membered ring is essential for the double ROP. In the radical polymerization of an analogous monomer bearing five-membered cyclic acetal moiety, only the vinyl cyclopropane part undergoes radical ROP to afford the corresponding polymer that inherits the cyclic acetal moiety from the monomer. Even if the cyclic acetal part is a five-membered one, by introducing a phenyl group on it, the double ROP can be induced.

The radical polymerization behaviors of 4-methylene-1,3-dioxolane involve three polymerization modes (Scheme 27):[39–42] The first one is the chain-growth radical polymerization of the *exo*-methylene group, while the second one is the ROP. The third one is another mode of ROP to afford polyketone, which is accompanied by the elimination of the corresponding carbonyl compounds. The ratio of these modes depends on the substituents X and Y.

For example, when both of these substituents are phenyl groups, ROP in the third mode proceeds selectively with the elimination of benzophenone.[43] The high selectivity would be due to the smooth ring-opening reaction of the five-membered ring driven by the formation of a stable diphenyl methyl radical (X = Y = Ph). This is a new method for synthesizing polyketone. The introduction of a electron-withdrawing group at the *para* position of the phenyl ring results in the acceleration of the polymerization.[44] For example, the monomer bearing 4-cyanophenyl groups (X = Y = 4-cyanophenyl) does not undergo the polymerization at 60 °C using AIBN as an initiator, while the monomer bearing 4-methoxyphenyl groups (X = Y = 4-methoxyphenyl) undergoes the polymerization smoothly under the same conditions.

Copolymerizations of the five-membered cyclic acetal (X = Y = phenyl) bearing *exo*-methylene group and vinyl monomers have also been reported.[41] This cyclic monomer can undergo the copolymerizations with vinyl pyrrolidone, styrene, vinyl acetate, and MMA to afford the corresponding

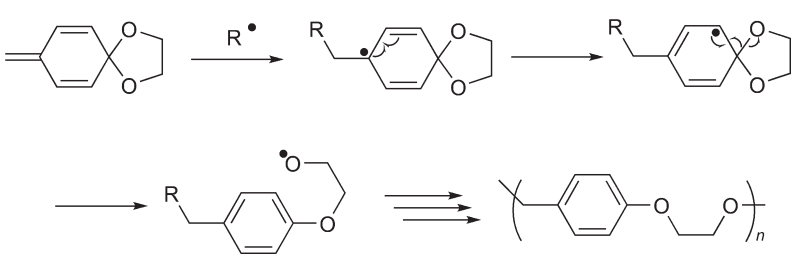

Scheme 25

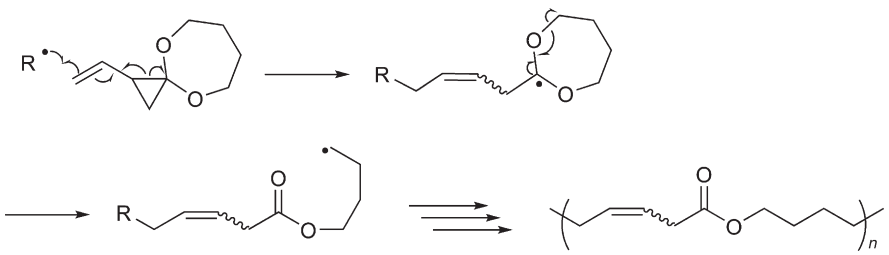

Scheme 26

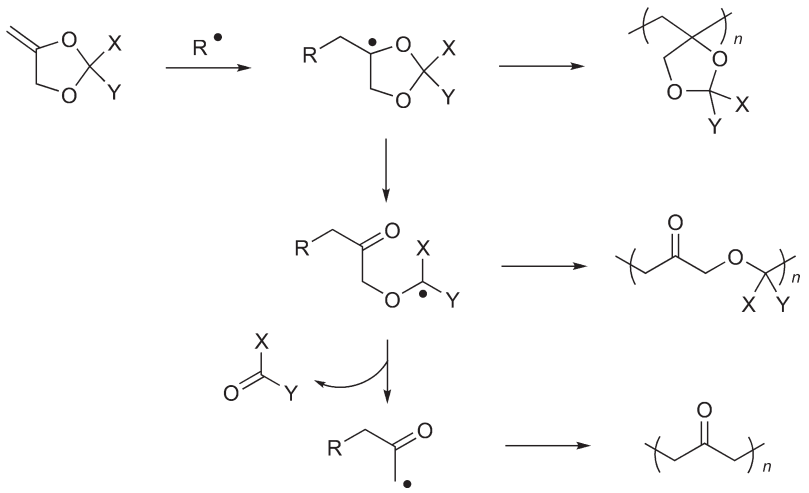

Scheme 27

copolymers bearing ketone moieties in the main chain. Except for the copolymerization with MMA, the copolymerizations proceed with the ring-opening reaction of the monomer releasing benzophenone selectively. The polymer composition can be controlled linearly to the feed ratio of the comonomers. Since ketone groups undergo some photo-induced reactions (Norrish-type reactions), the copolymers with ketone groups in the main chain are potentially photodegradable polymers.

There has been a report on the synthesis and utilization of an *exo*-methylene dioxolane bearing styryl group (Scheme 28).[45] The styryl group can be used for the copolymerization with other vinyl monomers such as styrene to obtain the corresponding polymers bearing *exo*-methylene dioxolane moieties in the side chains. This 'mother' polymer can produce a 'daughter' polyketone through the radical ROP of the *exo*-methylene dioxolane moieties.

4.19.5 Spiroorthocarbonates and Spiroorthoesters

Spiroorthocarbonates (SOCs) and spiroorthoesters (SOEs) have been known as cyclic monomers that can undergo

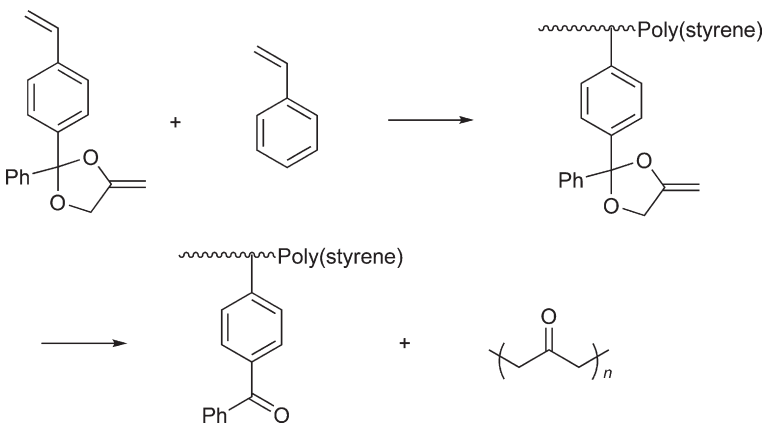

Scheme 28

Scheme 29

cationic ROPs (Scheme 29). Their cationic polymerizations are accompanied by volume expansion, because the highly compact structures of the monomers are transformed into acyclic structures that occupy a much larger space. These 'volume-expandable monomers' can be applied to sealants and adhesives, which are free from formation of voids and cracks caused by the volume shrinkage during the polymerizations of conventional monomers.

Based on the spirocyclic ether structures, several radically polymerizable cyclic monomers have been designed and synthesized. Such monomers are potentially applicable as volume-expandable monomers that can copolymerize with conventional vinyl monomers to suppress the volume shrinkage.

SOC bearing *exo*-methylene group undergoes radical ROP through double ring-opening reactions to give the corresponding polycarbonate (Scheme 30).[46] In the case of the polymerization of a monomer bearing a six-membered cyclic acetal moiety, the corresponding volume expansion degree is reported to be 4.5%.

SOC, consisting of two six-membered acetal moieties with an *exo*-methylene group, also undergoes radical ROP (Scheme 31).[46] It can undergo the copolymerization with styrene to give the corresponding polystyrene derivative bearing carbonate moieties in the main chain. On the other hand, an analogous SOC consisting of five-membered acetal moieties does not undergo ROP.[47] The *exo*-methylene groups can be used for radical copolymerizations with various vinyl monomers to afford the corresponding cross-linked polymers.

SOEs bearing *exo*-methylene group undergo radical ROP regardless of the ring size of the cyclic ether part (Scheme 32).[48,49]

In the radical ROP of a SOE bearing an aromatic ring, the propagating end is a benzyl radical (Scheme 33).[50]

4.19.6 α-*exo*-Methylene Lactones

Cyclic lactones bearing an *exo*-methylene group at the α-position have been designed so that (1) the acrylate-type structure involved in the monomer can accept radical, and (2) the resulting radical species can be transformed into a benzyl

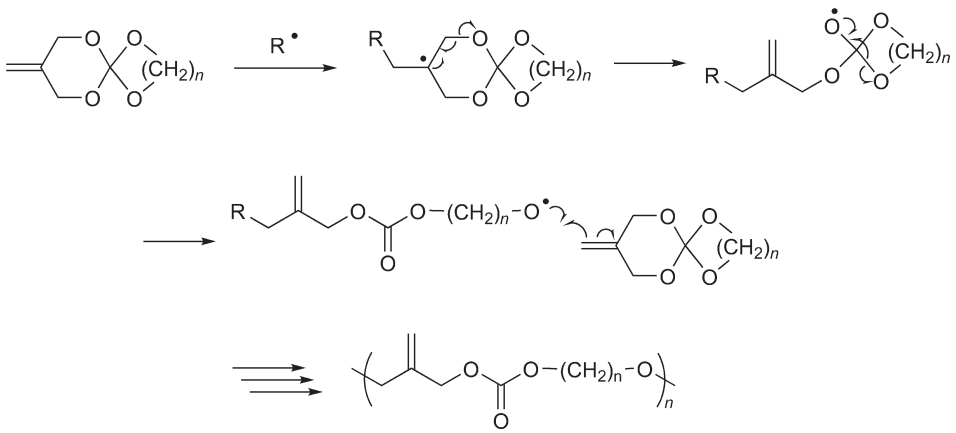

Scheme 30

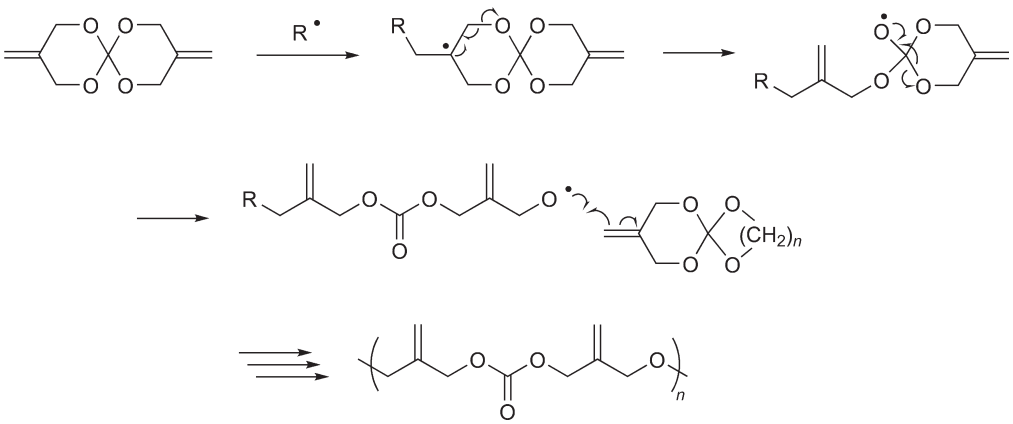

Scheme 31

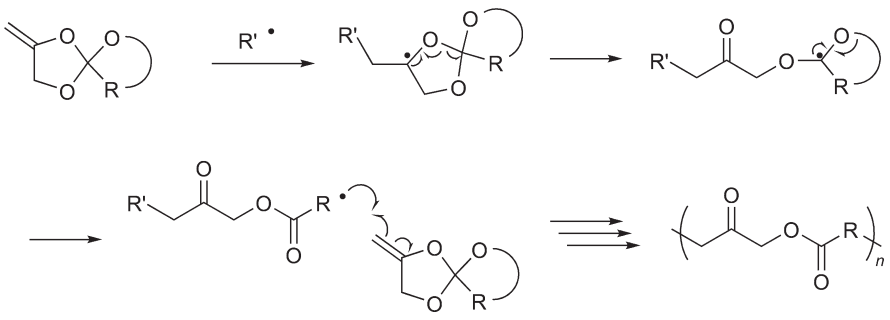

Scheme 32

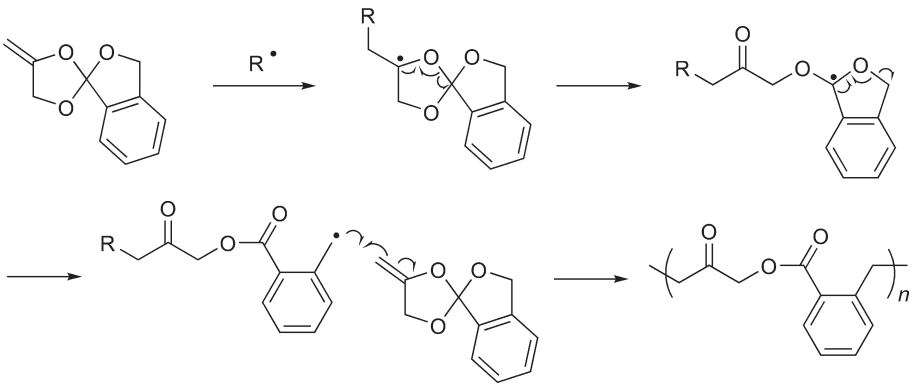

Scheme 33

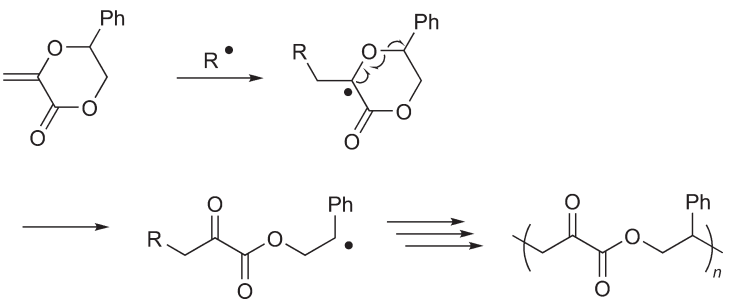

Scheme 34

radical. By virtue of this molecular design, a six-membered lactone undergoes radical ROP efficiently to give the corresponding polymer bearing α-ketoester linkage in the main chain, which exhibits photodegradability (Scheme 34).[51] In a similar manner, a five-membered lactone with *exo*-methylene group undergoes radical ROP to afford the corresponding polymer bearing α-ketoester linkage in the main chain.[52]

A seven-membered cyclic lactone with an *exo*-methylene group and sulfur atom also undergoes radical ROP (Scheme 35).[53] The ring-opening reaction gives thiyl radical, which can readily react with methacrylates and styrene to permit the successful copolymerizations of the cyclic monomer and the vinyl monomers.

4.19.7 Cyclic Sulfones with Vinyl Group

A five-membered cyclic sulfone with a vinyl group undergoes radical ROP selectively to give the corresponding polysulfone (Scheme 36).[54] On the other hand, the polymerization of an analogous six-membered one is accompanied by the radical chain-growth polymerization of the vinyl group (Scheme 37).[55] The polymerization of a six-membered cyclic disulfone bearing vinyl group proceeds with selective ROP (Scheme 38).[56]

4.19.8 Controlled Radical Ring-Opening Polymerization

The current progress in the field of controlled radical polymerization has allowed polymer chemists to control some of the radical ROPs. In the first example of such controlled radical ROPs, nitroxyl radical (2,2,6,6-tetramethyl-1-piperidinyloxy: TEMPO) was added to the ROP of 2-methylene-1,3-dioxepane.[57,58] The polymerization afforded the corresponding polyester with polydispersity (M_w/M_n) as low as 1.2. Addition of TEMPO was also effective to control the ROP of SOE bearing

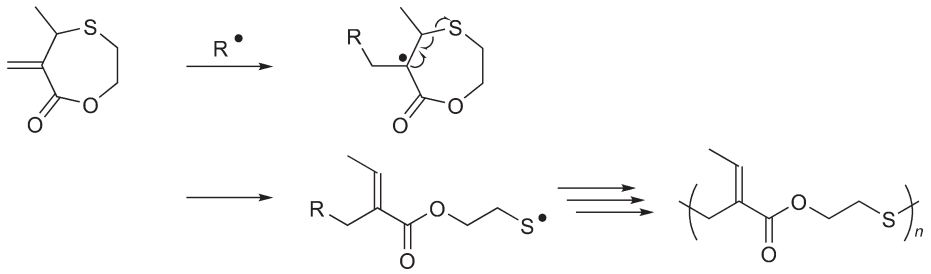

Scheme 35

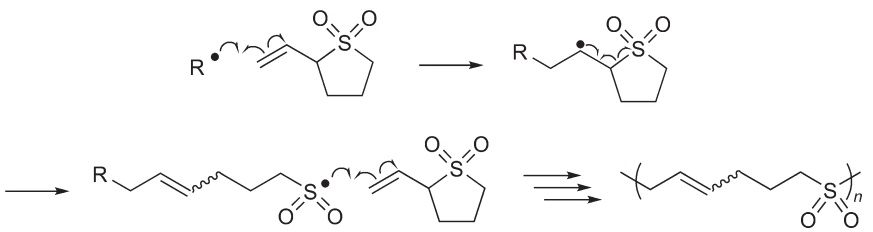

Scheme 36

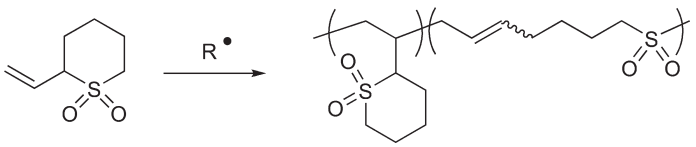

Scheme 37

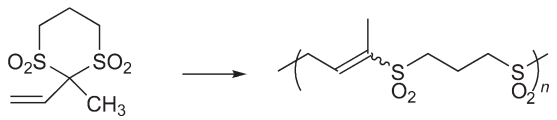

Scheme 38

an aromatic ring (Scheme 39).[59] In this case, the benzyl radical at the propagating end can be capped by a TEMPO radical into the corresponding dormant species.

Copper-mediated controlled radical polymerization, which is known as 'atom transfer radical polymerization (ATRP)', is also a useful tool to control ROP of several cyclic monomers. The copper-mediated ROP of 2-methylene-4-phenyl-1,3-dioxolane, a five-membered cyclic ketene acetal, has been reported.[60] By using an α-bromoester/CuBr/2,2′-bipyridine system, the ROP was successfully controlled to give the corresponding polyester with predictable molecular weights and low polydispersities. The ATRP technique was also effectively exploited to control the ROP of 5,6-benzo-2-methylene-1,3-dioxepane, a seven-membered cyclic ketene acetal (Scheme 40).[61]

The polymerization proceeds in a controlled manner, that is, the corresponding first-order kinetic plot is linear. The resulting polymer is a telechelic polyester: The initiating end is derived from the α-bromoester used as the initiator and the propagating end bears benzyl bromide-type structure. The molecular weight increases linearly to monomer conversion, and the molecular weight distributions are narrow.

Other examples of ATRP involve that of a vinylcyclopropane[62] and that of a five-membered lactone with *exo*-methylene group.[63] The latter example afforded a polymer bearing α-ketoester linkage in the main chain. In addition, the copolymerization of the lactone and MMA proceeded in a statistical manner to afford the corresponding copolymer with a poly(MMA) backbone, into which the α-ketoester units derived from the cyclic monomer are randomly distributed (Scheme 41). As a virtue of the photocleavable nature of α-ketoester, the copolymer is endowed with a photodegradable nature.

Another current trend in controlled radical ROP is the utilization of 'reversible addition–fragmentation chain transfer (RAFT)', which has been widely exploited as a powerful tool to control radical polymerizations of various vinyl monomers. The radical ROPs of 5,6-benzo-2-methylene-1,3-dioxepane, a seven-membered cyclic ketene acetal,[64] and those of 9,10-dihydroanthracene derivatives bearing *exo*-methylene and cyclopropane moieties[65,66] have been reported.

4.19.9 Summary

Radical ROP is expected to be a useful tool for constructing various polymers bearing heteroatom-containing functional groups, which are not attained by chain polymerization of vinyl monomers. Those functional groups incorporated into the polymers serve as cleavable points, leading to the

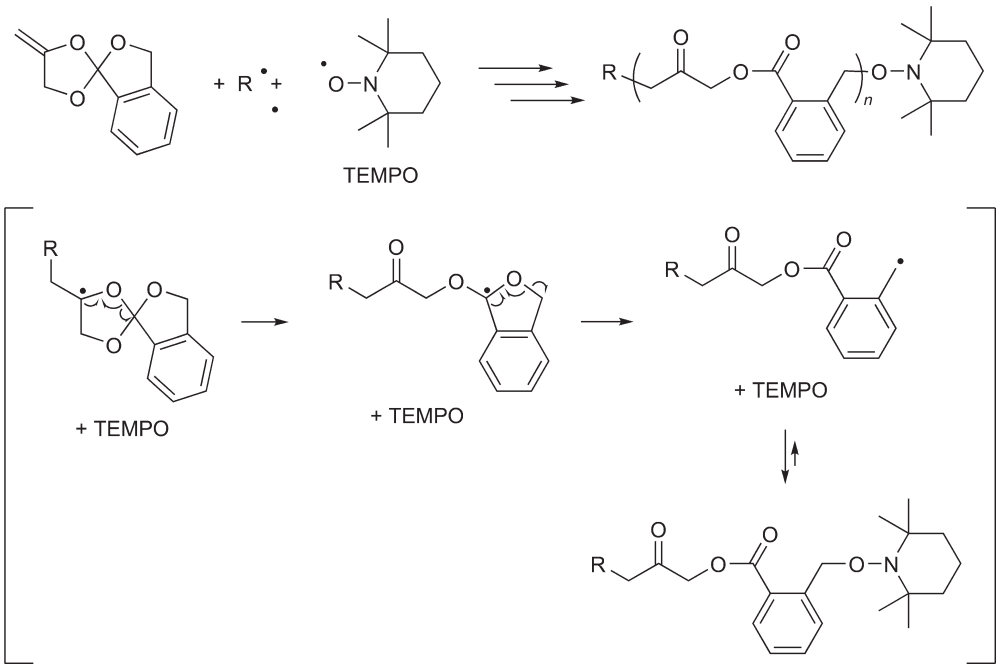

Scheme 39

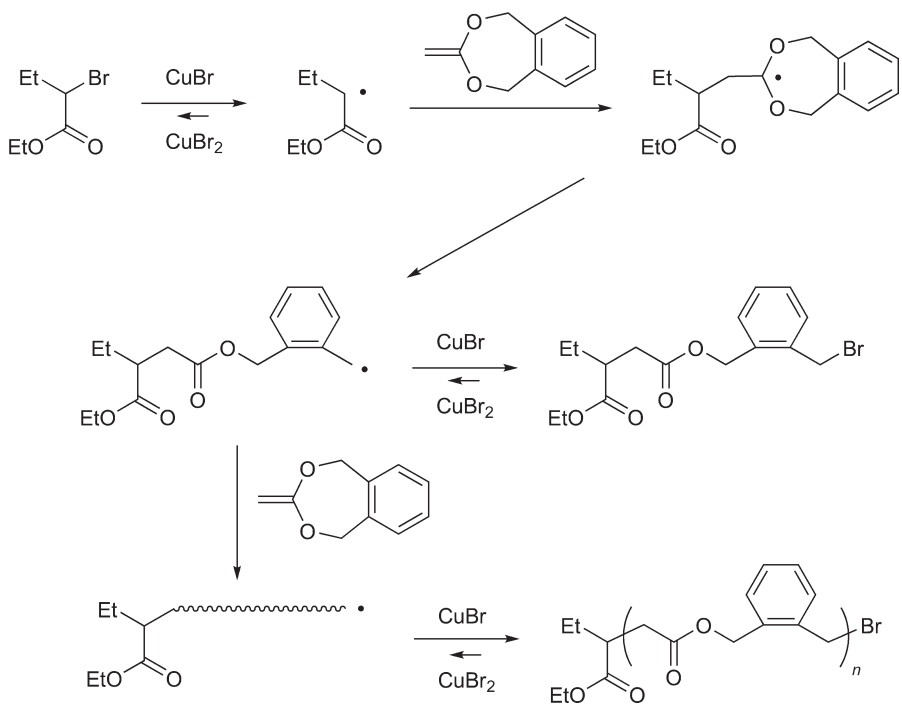

Scheme 40

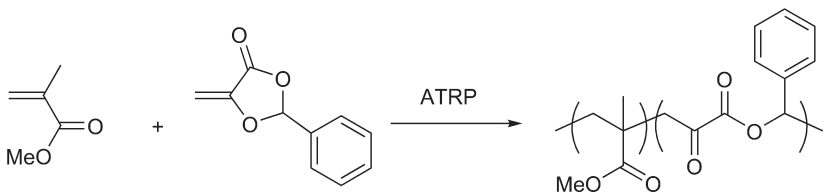

Scheme 41

development of various degradable polymers.[67–70] Furthermore, one of the features of radical ROP that has attracted much attention of polymer chemists is the opportunity for radical copolymerizations with a wide range of conventional vinyl monomers such as styrenics, acrylics, and methacrylics. By these copolymerizations, various functional groups derived from the cyclic monomers can be incorporated into the resulting main chains, which can be hydrolyzable and photodegradable. Another expectation for radical ROP is the inherent small volume shrinkage nature due to the ring-opening reactions involved in the polymerization systems.[8,71,72] In addition, recent advances in 'living'/controlled radical polymerization techniques have given the opportunity to control radical ROP leading to polymer chains having predictable molecular weights. For this purpose, nitroxy radical-mediated polymerization (NMP), radical addition–fragmentation transfer (RAFT), and ATRP are the systems that can be conveniently used. These controlled radical ROPs will give us the opportunities to construct various polymer architectures with functions such as block copolymers and graft copolymers. Some efforts to clarify the mechanisms of several radical ROP systems have also been reported.[73–75] A proper understanding of the mechanisms of radical ROP will guide us to new molecular designs of cyclic monomers, and the development of their controlled ROPs will result in the development of unprecedented polymer materials to support future industries.

References

1. Swartz, T. D.; Hall, H. K., Jr. *J. Am. Chem. Soc.* **1971**, *93*, 137.
2. Hall, H. K., Jr.; Ykman, P. *J. Polym. Sci., Polym. Symp.* **1976**, *54*, 373.
3. Drujon, X.; Riess, G.; Hall, H. K., Jr.; Padias, A. B. *Macromolecules* **1993**, *26*, 1199.
4. Takahashi, T. *J. Polym. Sci.: Part A-1* **1968**, *6*, 403.
5. Endo, T.; Suga, K. *J. Polym. Sci., Polym. Chem. Ed.* **1989**, *27*, 1831.
6. Cho, I.; Ahn, K.-D. *J. Polym. Sci., Polym. Chem. Ed.* **1979**, *17*, 3169.
7. Sanda, F.; Endo, T. *Macromolecules* **1992**, *25*, 6719.
8. Sanda, F.; Takata, T.; Endo, T. *Macromolecules* **1995**, *28*, 1346.
9. Mizukami, S.; Kihara, N.; Endo, T. *J. Am. Chem. Soc.* **1994**, *116*, 6453.
10. Takahashi, T. *J. Polym. Part A-1* **1970**, *8*, 739.
11. Cho, I.; Song, K. Y. *J. Polym. Sci., Part A: Polym. Chem.* **1994**, *32*, 1789.
12. Sanda, F.; Takata, T.; Endo, T. *Macromolecules* **1992**, *25*, 6719.
13. Sanda, F.; Komiya, T.; Endo, T. *Macromol. Chem. Phys.* **1998**, *199*, 2165.
14. Hiraguri, Y.; Endo, T. *J. Polym. Sci.: Part C: Polym. Lett.* **1989**, *27*, 333.
15. Chino, K.; Takata, T.; Endo, T. *Macromol. Rapid Commun.* **1996**, *17*, 339.
16. Chino, K.; Takata, T.; Endo, T. *Macromolecules* **1997**, *30*, 6715.
17. Errede, L. A. *J. Polym. Sci.* **1961**, *49*, 253.
18. Cho, I.; Kim, J.-B. *J. Polym. Sci., Polym. Lett. Ed.* **1983**, *21*, 433.
19. Endo, T.; Kanda, N. *J. Polym. Sci., Polym. Chem. Ed.* **1985**, *23*, 1931.
20. Koizumi, T.; Nojima, Y.; Endo, T. *J. Polym. Sci., Part A: Polym. Chem.* **1993**, *31*, 3489.
21. Koizumi, T.; Ando, T.; Kojima, Y.; Endo, T. *Macromolecules* **1998**, *31*, 9096.
22. Koizumi, T.; Sakamoto, J.; Moriya, O.; *et al. Macromolecules* **1995**, *28*, 5649.
23. Sidney, L. N.; Shaffer, S. E.; Bailey, W. J. *ACS Polym. Prepr.* **1981**, *22*, 373.
24. Bailey, W. J.; Chen, P. Y.; Chen, S.-C.; *et al. J. Macromol. Sci. Chem.* **1984**, *A21*, 1611.
25. Evans, R. A.; Rizzardo, E. *Macromolecules* **1996**, *29*, 6983.
26. Schoberl, A.; Grafje, H. *Justus Liebigs Ann. Chem.* **1958**, *614*, 66.
27. Suzuki, T.; Nambu, Y.; Endo, T. *Macromolecules* **1990**, *23*, 1579.
28. Bailey, W. J.; Ni, Z.; Wu, S.-R. *J. Polym. Sci., Polym. Chem. Ed.* **1982**, *20*, 3021.
29. Bailey, W. J.; Wu, S.-R.; Ni, Z. *Makromol. Chem.* **1982**, *183*, 1913.
30. Cho, I.; Gong, M. S. *J. Polym. Sci., Polym. Lett. Ed.* **1982**, *20*, 361.
31. Bailey, W. J.; Ni, Z.; Wu, S.-R. *J. Polym. Sci., Polym. Chem. Ed.* **1982**, *20*, 3021.
32. Schulze, T.; Klemm, E. *Angew. Makromol. Chem.* **1995**, *229*, 123.
33. Bailey, W. J.; Ni, Z.; Wu, S.-R. *Macromolecules* **1982**, *15*, 711.
34. Endo, T.; Yako, N.; Azuma, K.; Nate, K. *Makromol. Chem.* **1985**, *186*, 1543.
35. Sidney, L. N.; Shaffer, S. E.; Bailey, W. J. *ACS Polym. Prepr.* **1981**, *22*, 373.
36. Cho, I.; Song, K.-Y. *Makromol. Chem., Rapid Commun.* **1993**, *14*, 377.
37. Sanda, F.; Takata, T.; Endo, T. *J. Polym. Sci. Part A: Polym. Chem.* **1993**, *31*, 2659.
38. Sanda, F.; Takata, T.; Endo, T. *Macromolecules* **1994**, *27*, 1099.
39. Pan, C.-Y.; Wu, Z.; Bailey, W. J. *J. Polym. Sci.: Part C: Polym. Lett.* **1987**, *25*, 243.
40. Pan, C.-Y.; Wu, Z.; Zhu, Q. R.; Bailey, W. J. *J. Macromol. Sci. Chem.* **1988**, *A25*, 27.
41. Hiraguri, Y.; Endo, T. *J. Polym. Sci.: Part C: Polym. Lett.* **1989**, *27*, 1.
42. Gong, M. S.; Chang, S.-I.; Cho, I. *Makromol. Chem., Rapid Commun.* **1989**, *10*, 201.
43. Hiraguri, Y.; Endo, T. *J. Am. Chem. Soc.* **1987**, *109*, 3779.
44. Hiraguri, Y.; Sugizaki, T.; Endo, T. *Macromolecules* **1990**, *23*, 1.
45. Sugiyama, J.-I.; Yokozawa, T.; Endo, T. *Macromolecules* **1994**, *27*, 5536.
46. Endo, T.; Bailey, W. J. *J. Polym. Sci. Polym. Chem. Ed.* **1975**, *13*, 2525.
47. Tagoshi, H.; Endo, T. *J. Polym. Sci. Part A: Polym. Chem.* **1989**, *27*, 1415.
48. Endo, T.; Bailey, W. J. *J. Polym. Sci. Polym. Lett. Ed.* **1980**, *18*, 25.
49. Endo, T.; Okawara, M.; Yamazaki, N.; Bailey, W. J. *J. Polym. Sci. Polym. Chem. Ed.* **1981**, *19*, 1283.
50. Han, Y.-K.; Choi, S.-K. *J. Polym. Sci., Polym. Chem. Ed.* **1983**, *21*, 353.
51. Feng, P. *Chinese J. Polym. Sci.* **1993**, *11*, 153.
52. Bailey, W. J.; Feng, P.-Z. *ACS Polym. Prepr.* **1987**, *28*, 154.
53. Evans, R. A.; Moad, G.; Rizzardo, E.; Thang, S. H. *Macromolecules* **1994**, *27*, 7935.
54. Cho, I.; Kim, S.-K.; Lee, M. *J. Polym. Sci. Polym. Symp.* **1986**, *74*, 219.
55. Cho, I.; Lee, M.-H. *J. Polym. Sci.: Part C: Polym. Lett.* **1987**, *25*, 309.
56. Cho, I.; Choi, S. Y. *Makromol. Chem. Rapid Commun.* **1991**, *12*, 399.
57. Wei, Y.; Connors, E. J.; Jia, X.; Wang, C. *Chem. Mater.* **1996**, *8*, 604.
58. Wei, Y.; Connors, E. J.; Jia, X.; Wang, C. *J. Polym. Sci. Part A: Polym. Chem.* **1998**, *36*, 761.
59. Jia, X.; Li, M.; Han, S.; *et al. Mater. Lett.* **1997**, *31*, 137.
60. Pan, C.-Y.; Lou, X.-D. *Macromol. Chem. Phys.* **2000**, *201*, 1115.
61. Yuan, J.-Y.; Pan, C.-Y.; Tang, B. Z. *Macromolecules* **2001**, *34*, 211.
62. Singha, N. K.; Kavitha, A.; Sarker, P.; Rimmer, S. *Chem. Commun.* **2008**, *26*, 3049.
63. Chung, I. S.; Matyjaszewski, K. *Macromolecules* **2003**, *36*, 2995.
64. He, T.; Zou, Y.-F.; Pan, C.-Y. *Polym. J.* **2002**, *34*, 138.
65. Mori, H.; Masuda, S.; Endo, T. *Macromolecules* **2006**, *39*, 5976.
66. Mori, H.; Tando, I.; Tanaka, H. *Macromolecules* **2010**, *43*, 7011.
67. Bailey, W. J.; Chen, P. Y.; Chen, S. C.; *et al. Makromol. Chem., Macromol. Symp.* **1986**, *6*, 81.
68. Seema, A.; Liqun, R. *Macromolecules* **2009**, *42*, 1574.
69. Hiraguri, Y.; Tokiwa, Y. *J. Polym. Environ.* **2010**, *18*, 116.
70. Agarwal, S. *Polym. Chem.* **2010**, *1*, 953.
71. Evans, R. A. *Chem. Aust.* **1996**, *63*, 83.
72. Choi, K.; Chon, J. W. M.; Gu, M.; *et al. Adv. Funct. Mater.* **2009**, *19*, 3560.
73. Ochiai, B.; Endo, T. *J. Polym. Sci., Part A: Polym. Chem.* **2007**, *45*, 2827.
74. Coote, M. L.; Hodgson, J. L.; Krenske, E. H.; *et al. Aust. J. Chem.* **2007**, *60*, 744.
75. Coote, M. L.; Namazian, M.; Wild, S. B. *Aust. J. Chem.* **2010**, *63*, 1189.

Biographical Sketch

Takeshi Endo is a Professor at Kinki University and an Emeritus Professor of Chemical Resources Laboratory at Tokyo Institute of Technology (TIT). He is the Director of Molecular Engineering Institute at Kinki University and Vice President of Kinki University. He got his doctoral degree from TIT and became an Assistant Professor at TIT in 1969. He was promoted to Associate Professor in 1982 and then to Full Professor in 1986. From 1991 until 2000, he was the Director of Chemical Resources Laboratory at TIT. He moved to Yamagata University in 2000, and was Director of Faculty of Engineering at Yamagata University from 2001 to 2004, and Vice President of Yamagata University from 2004 until his retirement from Yamagata University in 2005. He moved to Kinki University in 2005. He was awarded the Award of the Society of Polymer Science, Japan (1984), the Chemical Society of Japan Award for Creative Work (1989), the Chemical Society of Japan Award for Technical Development (2000), SPSJ (the Society of Polymer Science, Japan) Award for Outstanding Achievement in Polymer Science and Technology (2007). In 2008, he became an Honorary Member of the Society of Polymer Science, Japan.

4.20 Architectures of Polymers Synthesized using ROMP

JP Moerdyk and CW Bielawski, The University of Texas at Austin, Austin, TX, USA

4.20.1 Introduction

Since its discovery in the 1950s and 1960s, olefin metathesis has burgeoned into a powerful transformation utilized in industry as well as academia. Among the first olefin metathesis methods to be utilized industrially, ring-opening metathesis polymerization (ROMP) has taken on a key role in numerous applications. Typically driven by the release of ring strain, ROMP is capable of producing functionally diverse and structurally complex polymers from a diverse range of monomers through the implementation of well-defined catalysts, namely the Schrock- and Grubbs-type precatalysts (Figure 1).[1]

4.20.2 Catalysts (Grubbs and Schrock Type)

Enhanced stability toward air and water as well as a toleration of a broad variety of functional groups often make Ru-based complexes the precatalysts of choice.[2] Within this family, the first- and third-generation Grubbs-type catalysts are the most widely used because their complete initiation leads to the most predictable molecular weights (MWs) and uniform products. The Hoveyda–Grubbs complexes are also capable precatalysts but suffer from poor initiation characteristics, and thus, are employed less frequently. The Schrock-type Mo catalysts are often more active than Grubbs-type catalysts, which makes them exceptionally powerful, but their use is tempered by a relatively functional group tolerance and high sensitivity to water and moisture. These catalysts are more commonly utilized for particularly challenging ROMP polymerizations not typically facilitated by the Grubbs-type catalysts (e.g., cycloalkynes) or when rapid conversions are required.

The catalysts mentioned above are the tools used to build various polymeric architectures via ROMP, ranging from the simplest linear homopolymer to intricate double helices. This chapter aims to delve into these architectures from the most basic to the most complex. In many cases, only representative examples are discussed and should only be used as a guide as the inclusion of all work from the field into a single chapter is not possible. Ultimately, this chapter aims to give its readers an appreciation and understanding of the structural opportunities already obtained through ROMP and a vision for its future.

4.20.3 Basic Categories

Polymers prepared using ROMP broadly into four basic categories (Figure 2). The simplest, linear homopolymers consist of a single repeating unit or monomer. Block copolymers, as indicated by the name are comprised of more than one monomer, with blocks or polymeric segments of one monomer attached to that of another in a linear fashion. Most commonly, this order is obtained through the complete polymerization of a given monomer, A, followed by the polymerization of a second monomer, B, to form an ordered polyA–polyB arrangement, called a diblock copolymer. This may be further expanded to a third monomer or a repetition of the first monomer and so on to access triblocks, tetrablocks, and so forth. In stark contrast to blocks, random copolymers consist of two or more different monomers but their ordering is statistical rather than controlled by the order of addition. This statistical mixture is commonly prepared by mixing two or more monomers of interest prior to addition of the catalyst. Constant, repetitive polymerization of a single monomer (A) followed by another

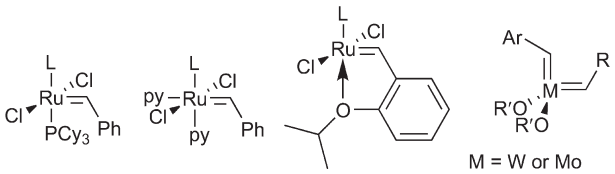

Figure 1 The structures of various precatalysts used to initiate ROMP reactions (PCy_3, tricyclohexylphosphine; py, pyridine). Reproduced with permission from Schwab, P.; Grubbs, R. H.; Ziller, J. W. *J. Am. Chem. Soc.* **1996**, *118*, 100.; Scholl, M.; Ding, S.; Lee, C. W.; Grubbs, R. H. *Org. Lett.* **1999**, *1*, 953.; Kingsbury, J. S.; Harrity, P. A.; Bonitatebus, P. J., Jr.; Hoveyda, A. H. *J. Am. Chem. Soc.* **1999**, *121*, 791.; Sanford, M. S.; Love, J. A.; Grubbs, R. H. *Organometallics.* **2001**, *20*, 5314.; Schrock, R. R.; DePue, R.; Feldman, J.; Schaverien, C. J.; Dewan, J. C.; Liu, A. H.; *et al. J. Am. Chem. Soc.* **1988**, *110*, 1423;. Schrock, R. R.; Depue, R. T.; Feldman, J.; Yap, K. B.; Yang, D. C.; Davis, W. M.; Park, L. Y.; DiMare, M.; Schofiled, M.; Anhaus, J.; Walborsky, E.; Evitt, E.; Krüger, C.; Betz, P.; *et al. Organometallics.* **1990**, *9*, 2262.; Schrock, R. R.; Hoveyda, A. H. *Angew. Chem. Int. Ed.* **2003**, *42*, 4592.[2]

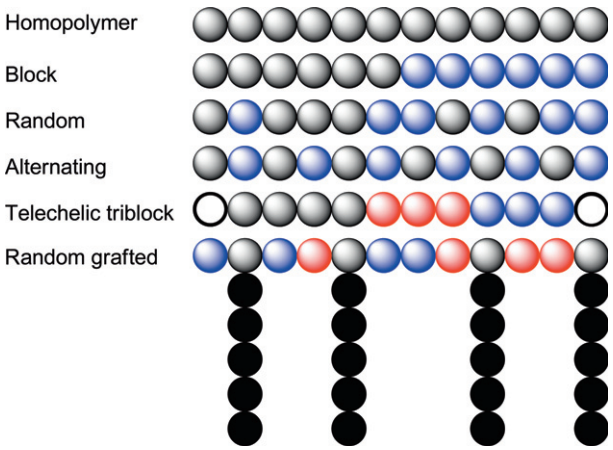

Figure 2 Representations of different polymer architectures.

monomer (B) may afford copolymers with alternating segments of polyA and polyB.

The aforementioned polymers can further be classified as telechelic if the ends (endcaps) of the polymer are functionalized so as to enable further chemical transformations (e.g., atom transfer radical polymerization (ATRP), S_N2 reactions, etc.) from that position. This is accomplished through the use of a functionalized chain transfer agent upon the completion of the polymerization or by using functionalized monomers, though the latter method is not regiospecific as it places the functionality throughout the entire polymer chain rather than solely at the end. Semitelechelic polymers are polymers where only one end is functionalized, while homotelechelic polymers have both ends equivalently functionalized. Recent work has now realized heterotelechelic polymers wherein the ends are differentially substituted so as to be recognizable as chemically separate entities. Finally, graft copolymers have a linear polymeric chain called the backbone from which another polymeric sequence is attached in an orthogonal fashion. The polymeric side chains may be formed postpolymerization of the backbone or incorporated into the monomer prior to polymerization, forming a macromonomer.

The architectures of polymers synthesized using ROMP generally fall under four broad categories: linear, cross-linked, branched, and dendritic. Linear polymers, as the name implies, possess chains that extend in one dimension, and encompass flexible coils, rigid rods, cycles, and polyrotaxanes, which can all be related to a string. Flexible coils may be imagined as a length of string that can be elongated, balled up, or exist anywhere in between these states. Stretching the string to its maximal elongation approximates the structure of a rigid rod that can rotate and move through space but cannot be readily contracted, bent, or looped. Most typically, this occurs due to extended conjugation along the polymeric backbone. Cyclic polymers and rotaxanes involve rings, where the polymer chains effectively has its 'ends' connected to form a cycle and polyrotaxanes are where cyclic, molecular 'rings' (which need not but can be polymeric in nature) surround a linear polymer strand. As will be discussed below, the flexible coil is by far the most common ROMP architecture whereas, while cyclic polymers and polyrotaxanes have been accessed via ROMP, the synthesis of these materials remain challenging (Section 4.20.5).

Cross-linking arises from the covalent attachment of one polymer chain to another. An obvious distinction, lightly cross-linked polymers have relatively few interchain attachments compared to densely cross-linked polymers. These are distinguished from the intertwining of two or more cross-linked polymers, which is labeled as an interpenetrating network. These functionalities are also accessible through ROMP, especially with the use of cyclopentadiene or other polyolefinic monomers.

Branched polymers can have long or short side chains (i.e., branches), which when randomly dispersed are called random short branches or random long branches. Well-ordered and defined branches of an elongated polymeric backbone are termed regular comb-branched polymers. Rather than forming an extended polymeric backbone, side chains may extend outward in all directions from a central core (polymeric or otherwise) like the arms of a starfish to form star polymers. Again, these forms have all been realized via ROMP, though many polymers from this class are formed from a combination of ROMP and other polymerization techniques such as ATRP, ring-opening polymerization (ROP), reversible addition-fragmentation chain transfer polymerization (RAFT), or others.

Dendrimers begin from a central point that branches repeatedly as it grows away from this center much like what one expects of a genealogical family tree. Random hyperbranched polymers lack any order or pattern to the branching. Dendrons exhibit ordered and identical splitting of each branch off of the core. Thus, the number of its endgroups is multiplied by a fixed value with each successive generation (denoted by the number of splits along a given branch). When ordered in a spherical shape, the name changes to dendrimer. Dendrons and

dendrimers have never, to the best of our knowledge, been formed solely through ROMP, though some of these polymerizations have used preformed dendritic cores. One form of this family ROMP does perform well in is with dendritic grafts, where dendrimers are appended to a polymeric backbone. These may be realized through a dendrimer-functionalized monomer or postpolymerization functionalization. An appreciation may be realized from this list about the broad scope of ROMP in accessing structurally diverse and important macromolecular structures from monomeric precursors.

4.20.4 Monomers

In theory, any cyclic olefin is a candidate for ROMP, but typically only those with large amounts of ring strain are used. Large rings are rarely utilized for this reason as they present synthetic challenges and are nearly strainless. Entropy-driven ROMP is possible by employing large ring systems but is much less common than those driven by the release of ring strain. Three- and four-membered cyclic alkenes possess some of the largest ring strains (**Table 1**),[3] but also pose problems in their synthesis and polymerization. Norbornadiene is likewise heavily strained but has a tendency to cross-link due to its two olefins and therefore is only sparingly employed. The vast majority of monomers used in ROMP are those that possess five- to eight-membered cycles or norbornene and their derivatives. Of these, norbornene and cyclooctadiene (COD) and their functionalized derivatives are preferred as their high ring strain and ease of synthesis make them attractive monomers.

Norbornene is the workhorse of ROMP. Its high degree of ring strain affords rapid polymerizations to polynorbornene (**Figure 3**) with a wide variety of catalysts under gentle conditions, but perhaps most importantly is one of the most easily derivatized monomers. Afforded by the [4 + 2]cycloaddition (Diels–Alder) of cyclopentadiene and an olefin, the side chain of the resultant polymer is determined by the substitution of the alkene moiety. Thus, accessing a plethora of functionality ranging from ionic, hydrophobic, liquid crystalline, radical, macromolecular, and nearly anything in between is relatively facile. COD possesses a sufficient degree of ring strain, but is not quite as easily functionalized as norbornene. Therefore, this monomer is most commonly utilized for forming hydrophobic blocks in copolymers. The scope of these two monomers will become apparent in the rest of the work discussed here.

4.20.5 Linear Architectures

Homopolymers are the simplest form of polymer and are readily obtainable through ROMP. Typically, in the absence of self-assembly or cross-linking, these polymers exist as flexible coils rather than rigid rods. A notable exception to this is polyacetylene, which is discussed later. Importantly, these polymers are relatively easy to prepare and often evenly distribute functionality throughout their backbone, which makes them useful for many applications (Section 4.20.6).

Electrochemically active materials can be accessed as metals and ions are well tolerated. For example, the homopolymerization of a norbornene monomer modified to include ferrocene linked through an alkyl quaternary ammonium salt affords

Table 1 Ring strain values for common ROMP monomers

Cyclic alkene	*Ring strain (kcal mol^{-1})*	*Cyclic alkene*	*Ring strain (kcal mol^{-1})*
Cyclopropene	54.5	1,4-Cyclohexadiene	2.2
1-Methylcyclopropene	54.5	Cycloheptene	6.7
1,2-Dimethylcyclopropene	51.0	1-Methylcycloheptene	6.3
Cyclobutene	30.6	1,3-Cycloheptadiene	3.9
1-Methylcyclobutene	29.7	1,3,5-Cycloheptatriene	–2.0
1,2-Dimethylcyclobutene	29.6	*cis*-Cyclooctene	7.4
Cyclopentene	6.8	*trans*-Cyclooctene	16.7
1-Methylcyclopentene	5.0	1,4-Cyclooctadiene	13.3
1-Ethylcyclopentene	5.9	1,3,5-Cyclooctatriene	2.4
Cyclopentadiene	2.9	Cyclooctatetraene	2.5
Cyclohexene	2.5	*cis*-Cyclononene	11.5
1-Methylcyclohexene	1.7	*trans*-Cyclononene	14.4
1-Ethylcyclohexene	1.8	Norbornene	27.2
1,3-Cyclohexadiene	1.9	Norbornadiene	34.7

Reproduced with permission from Schleyer, P. v. R.; Williams, J. E.; Blanchard, K. R. *J. Am. Chem. Soc.* **1970**, *92*, 2377.; Allinger, N. L.; Sprague, J. T. *J. Am. Chem. Soc.* **1972**, *94*, 5734.

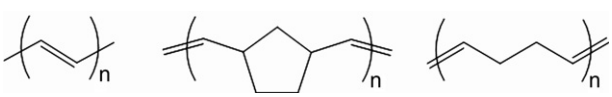

Figure 3 Polyacetylene, polynorbornene, and polybutadiene.

ambiphilic homopolymers. The inclusion of the ferrocenyl group combined with the solubility of the monomer and resultant polymer gives these polymers potential for use in electrochemically based diagnostic applications.[4] A separate group reported the ROMP of norbornene derivatives bearing one or two cationic iron units (η^6-(chlorobenzene)-η^5-cyclopentadienyliron hexafluorophosphate or η^6-(*p*-chlorotoluene)-η^5-cyclopentadienyliron hexafluorophosphate), which cleanly afforded analogous homopolymers.[5]

While most metal centers are incorporated into ROMP polymers as pendant side chains, they may also be included in the polymeric backbone. ROMP of *t*-butyl-functionalized ferrocenophane dienes afforded a fully conjugated, soluble polymer with ferrocene incorporated in the backbone. Bathochromic shifts in the UV–vis spectra of these materials confirmed the extended conjugation and two reversible peaks were observed electrochemically, indicating communication between the ferrocenyl units as would be expected if the system were conjugated.[6] Similar work several years later successfully polymerized ferrocenylenevinylene monomers bearing *t*-butyl groups via ROMP to yield the corresponding soluble, conjugated polymer with the ferrocenes incorporated into the backbone and spaced by only two carbon atoms (**Figure 4**). As observed previously, a two-wave reduction was observed, which suggests that this system may be conjugated.[7]

In another set of monomers studied for their electronic properties, cyclophosphazenes bearing one or more norbornenes attached to the phosphorus atoms successfully underwent ROMP, though the hexanorbornene derivative resulted in gelation.[8] Later work with these cyclotriphospazene-bearing polynorbornenes found them to have low T_g values and semiconductivities (10^{-5} S m^{-1}).[9] Thiophene oligomer or sexithiophene-modified norbornenes also undergo ROMP to give electrochemically active polymers.[10]

Boron carbides are of interest for their thermal stability, neutron capture capability, and high temperature thermoelectric properties. Appended to norbornenes, the monomers 6-(norbornenyl)decaborane and 6-(cyclooctenyl)decaborane underwent ROMP to afford their respective homopolymers with low polydispersity index (PDI) values (**Figure 5**).[11] The applications of these materials in boron carbide/carbon ceramics were explored.[12] An early attempt at biocompatible monomers, Schrock and Nomura formed homo and co-polymers with protected sugar-bearing norbornenes and successfully deprotected the sugars postpolymerization.[13]

While these aforementioned norbornene-derived monomers readily undergo polymerization, smaller rings like cyclopropenes and cyclobutenes are more challenging. It was not until 2006 that Schrock reported the first successful ROMP of cyclopropene using Schrock and Grubbs-type catalysts.[14] The ROMP of cyclobutene was found highly dependent on its alkene substituent. The esters of 1-cyclobutene-1-methanol and the secondary amides of the carboxylic acid undergo ROMP but esters and tertiary amides of the carboxylic acid derivative do not. This prompted the conclusion that the polymerization is dependent on sterics and electronics and would lead to the development of a method for alternating ROMP.[15] Sterically demanding olefins are also challenging substrates. Careful catalyst selection was required for the ROMP of 1,5-dimethyl-1,5-COD which done in the presence of the chain transfer unit *cis*-1,4-diacetoxy-2-butene afforded telechelic polyisoprene with well-defined regiochemistry.[16]

A showcase of the tolerance of ROMP is its ability to function in the presence of radical side chains (**Figure 6**). Masuda[17] polymerized 2,2,6,6,-tetramethylpiperidine-1-oxy (TEMPO) containing norbornene monomers, which they further extended to include the ROMP of mono- or di- 2,2,5,5-tetramethyl-1-pyrrolidinyloxy-bearing norbornene monomers. The resultant polymers exhibited little absorption over 400 nm and demonstrated reversible charge/discharge processes.[18] Unfortunately, the first report of TEMPO-containing norbornene monomers resulted in insoluble polymers, but later work involving the ROMP of a variety of other TEMPO-containing monomers provided two polymers that were soluble in common solvents, facilitating their study. Charge/discharge capacities were found to be dependent on the spatial arrangement of the TEMPO moieties off the backbone and had excellent cycle lifetimes.[19] Switching to oxanorbornene derivatives functionalized with TEMPO provided further solubility enhancement with soluble polymers up to 112 kDa in weight. The oxygenated backbone did not affect the radical sides as evidenced by the retention of good charge/discharge properties and cycle life.[20]

As mentioned earlier, ROMP is not limited to strained cyclic olefins. In an entropy-driven ROMP, the polymerization is propelled through the increase in entropy associated with ring opening. In an example, cyclodepolymerization of ester

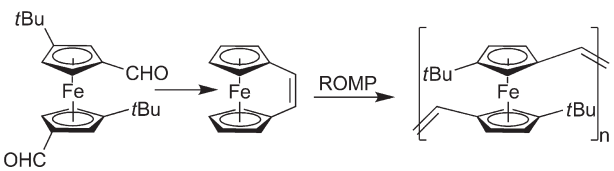

Figure 4 ROMP to a conjugated polymer incorporating ferrocene in the backbone. Reproduced with permission from Masson, G.; Lough, A. J.; Manners, I. *Macromolecules*. **2008**, *41*, 539.[7]

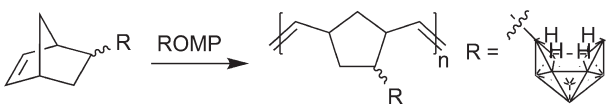

Figure 5 ROMP polymer containing decaborane side chains. Reproduced with permission from Wei, X.; Carroll, P. J.; Sneddon, L. G. *Chem. Mater.* **2006**, *18*, 1113.[12]

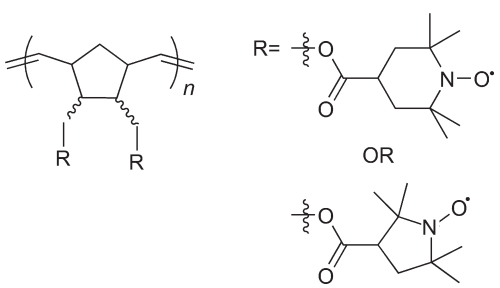

Figure 6 A homopolymer formed in the presence of the radical TEMPO group. Reproduced with permission from Katsumata, T.; Qu, J.; Shiotsuki, M.; *et al. Macromolecules* **2008**, *41*, 1175.[19]

polymers prepared via acyclic diene metathesis afforded strainless macrocyclic oligomers ranging in size from 21 to 84 members. In 50% w/v monomer solution, the ROMP polymer was obtained in high yield for various ring sizes.[21] Highly concentrated solutions are necessary in this method in order to bias the system toward polymerization rather than the competing ring-closing metathesis reaction.

A benefit of functionalized homopolymers is the ability to perform postpolymerization modifications. A norbornene bearing a methacroyl isocyanate efficiently underwent homopolymerization via ROMP to yield a cross-linked homopolymer, which upon ligand exchange with poly(methyl methacrylate) afforded a material with enhanced thermal stability over the original poly(methyl methacrylate).[22] The preparation of an oxanorbornene derivative bearing a 1,2-bis (3-thienyl)cyclopentene photochrome followed by ROMP accessed a polymer capable of the same reversible photoisomerization as the monomer.[23]

An advantage of the ruthenium ROMP catalysts is their ability to become hydrogenation catalysts in the presence of molecular hydrogen. Thus, completely saturated polymers may be obtained from unsaturated monomers through the use of a single precatalyst. The ROMP of cyclooctene or norbornene derivatives using the first generation Grubbs catalyst (G1) followed by the addition of base and 1 atm H_2 affords the corresponding saturated polymer (**Figure 7**). In addition, the hydrogenation catalyst can be cycled back to the alkylidene ROMP catalyst and polymerizations restarted.[24] Another polymerization and subsequent hydrogenation of cyclopentadiene yielded amorphous, cross-linked, transparent polymers with low water permeabilities.[25]

It would be reticent to ignore the importance of details from the choice of catalyst and solvent to minor monomer alterations on the polymerization and architecture of homopolymers. For instance, an aryl nitrile-functionalized oxanorbornene polymerizes using a Schrock catalyst gave predominantly *trans* selectivity, but failed to polymerize with a ruthenium catalyst.[26] Benzene-1,3,5-tricarboximides are known to form supramolecular polymers in dilute solutions and the solid state, and one study evaluated the use of ROMP for forming alkyl tethers between two of these molecules. The random ROMP of cyclooctene and 5-ethoxycyclooctene, telechelic endcapping with the tricarboximides, and hydrogenation afforded the desired alkyl-linked carboximides. The structure adapted was highly solvent dependent with helical aggregates formed in hydrocarbons while the polymer was unstable in more polar solvents like *tert*-butyl methyl ether.[27]

The ROMP of norbornene carboximides revealed thermal differences from differentially substituted phenyl groups. For example, the *ortho* substituted *N*-phenyl-*exo*-norbornene dicarboximide gave two exotherms in a range where the *para* and *meta* only gave one.[28] A seemingly innocuous alteration, *N*-cyclopentyl norbronene dicarboximides were found to yield polymers with higher T_g, density, and gas impermeability properties than the cyclohexyl derivative.[29] Finally, an intriguing difference in the polymerization method was observed for five- or six-membered carbonate cycles. ROMP caused a volume expansion whereas using other monomers or a vinyl polymerization of the same substrate did not result in swelling. Cationic polymerization also did not cause volume expansion leading to the conclusion that it was caused from the ROMP mechanism.[30] The list of homopolymers is nearly endless, and the range of functional groups makes them useful in numerous applications. There is one homopolymer that bears a closer look, not for its functionality but for the lack thereof.

4.20.6 Polyacetylene

Polyacetylene has garnered a significant amount of attention, particularly during the second half of the twentieth century as an alternative to metal semiconductors. The utility of this simple polyene was largely hampered by ill-defined and insoluble products. In 1958, Natta *et al.* polymerized acetylene with triethyl aluminum and titanium propoxide to access well-defined, high molecular weight polymers. However, these structures suffered from poor conductivity and it was not until Shirakawa's method of doping films of the polymers with halides or arsenic pentafluoride that conductivities rose to that of the transition metals.[31] Indeed, semiconductor devices were successfully formed from polyacetylene and found to store charge in soliton-like excitations of the chain induced by the presence of a surface electric field.[32]

In the 1980s, the use of ROMP for the preparation of polyacetylene was realized via two distinct routes. Though theoretically accessible from cyclobutadiene or benzene, the more direct route (developed second chronologically) to polyacetylene was realized using cyclooctatetraene as the monomer. This method is attractive due to the absence of the highly flammable acetylene used for the Ziegler–Natta polymerization or the extrusion process involved in the Durham route. The first reported ROMP of this monomer was accomplished using a tungsten catalyst. Unfortunately, the polymers obtained using this synthesis were exceedingly insoluble.[33] The polymerization of this slightly ring strained monomer (⊠2.5 kcal mol^{-1}) also required more active catalysts such that ruthenium catalysts were incapable of effecting this polymerization until the development of the second-generation Grubbs catalyst.[34]

Performing the ROMP of cyclooctatetraene in the neat monomer helped somewhat with the processing of the

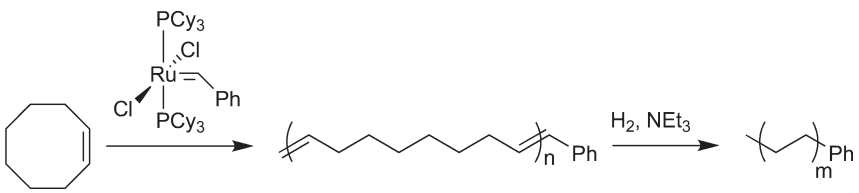

Figure 7 Formation of polyethylene utilizing one metal precatalyst. Reproduced with permission from Masson, G.; Lough, A. J.; Manners, I. *Macromolecules* **2008**, *41*, 539.[7]

product, affording silver films similar to those obtained from the Shirakawa method. Upon doping with iodine, the polymers had conductivities ranging from 50 to 350 $\Omega^{-1}\,cm^{-1}$, which were lower but on the order of magnitude for those prepared via the Shirakawa method. In addition, this method enabled the 'painting' of polyacetylene onto essentially any surface by dipping an object in the monomer/catalyst solution and then spreading it on another surface where the polymerization would afford the desired polymer. In the same report, copolymerization with COD resulted in random copolymers while using norbornene resulted in essentially a block copolymer due to the rapid rate of norbornene polymerization.[35]

Rather than proceeding to polyacetylene directly from a monomer, Feast championed a route (now called the Durham route after the locale of his work) wherein 7,8-bis (trifluoromethyl)tricyclo-[4.2.2.0]deca-3,7,9-triene undergoes ROMP with the exclusive ring opening of the four-membered ring (**Figure 8**). A prepolymer, thermal heating results in the retro-[4 + 2]cycloaddition (i.e., retro-Diels–Alder) and exudes hexafluoroxylene to access the polyacetylene polymer.[36] Advantages of this method are the minimization of impurities through the removal of the catalyst prior to forming the final polymer and, more importantly for the ROMP method, the prepolymer is soluble and able to be cast in contrast to the insoluble materials obtained by direct polymerizations using ROMP.[37] Soluble polyenes containing up to 15 consecutive double bonds were formed through this method.[38]

An alternative to the Durham route which extrudes hexafluoroxylene, benzvalene can be polymerized and upon heating or stress form polyacetylene without the exuding of any second molecule (**Figure 9**). Unfortunately, cross-linking was found to occur and cited as a reason for the shorter conjugation lengths of polyacetylene obtained through this method and so was not widely applied.[39] An extension of the classical Durham route, *p*-dimethoxybenzotricyclo[4.2.2.0] deca-3,7,9-triene can also be polymerized as a soluble polymer precursor and forms polyacetylene through the loss of dimethoxynaphthalene. Block copolymers of the triene and norbornene or a silyl ether norbornene derivative resulted in spherical, cylindrical, and lamellar morphologies dependent on the percent compositions and overall size. The morphologies were retained upon extruding the dimethoxynaphthalene providing self-assembled structures of polyacetylene, except for low-MW polymers that did not retain their structure.[40]

While cyclooctatetraene led to insoluble polymers, monosubstituted cyclooctatetraene led to fairly soluble polymers

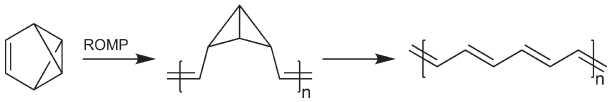

Figure 9 An atom-economical alternative to the Durham route. Reproduced with permission from Swager, T. M.; Dougherty, D. A.; Grubbs, R. H. *J. Am. Chem. Soc.* **1988**, *110*, 2973.[39]

with high MWs. The solubility was especially improved through the use of groups with secondary or tertiary centers adjacent to the backbone. These larger R-groups twist the main chain, disrupt conjugation, and consequently increase solubility. The amorphous polymers were found to absorb in the visible spectrum with initial preferences for the *cis* confirmation that thermally reverted to the *trans* product. Upon doping with iodine, the polymers were conductive but much less so than that of doped, unsubstituted polyacetylene due again to their shorter effective conjugation length.[41] Cyclic voltammetry performed on substituted polyacetylenes prepared from ROMP found the spin-cast films to exhibit well-defined electrochemical processes. The potential was tunable over 0.3 V depending on the substituent and the oxidative and reductive potentials were separated by 1.5–2 V. Coulombic measurements indicated a transfer of electrons for every 13–15 double bonds. Unlike the *trans* polymer, the *cis* polymer exhibited irreversible electrochemical processes that were attributed to the isomerization of the *cis*- to the more thermodynamically favored *trans*-linkage.[42]

A later effort to enhance the solubility of polyacetylene polymers formed polyenes through the Durham route that could be capped with aryl or alkyl endgroups; however, this only slightly enhanced the solubility of the polyacetylene chains.[43] Telechelic polyenes have also been formed from cyclooctatetraene in the presence of a chain transfer agent. The use of polystyrene, poly(methyl methacrylate), or poly (ethylene glycol) (PEG) chains terminated with an olefin enabled the formation of block copolymers with the polyacetylene though the polyene chain was much shorter than expected based on the stoichiometry of the starting materials and was attributed to back-biting into the polymer chain.

The use of solvents can be incompatible with certain chemical entities, and the capabilities of ROMP, which are broadly studied in solution can also be applied to solventless systems. In the case of polyacetylene, this can be used to circumvent its insolubility. Using soft lithography, Xu generated hydrophobic and hydrophilic patterns on the surface of either a gold or a

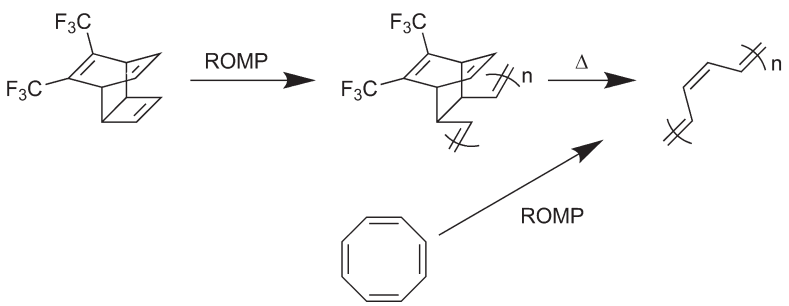

Figure 8 The Durham route (top) and a direct route from cyclooctatetraene accessing polyacetylene. Reproduced with permission from Edwards, J. H.; Feast, W. J. *J. Polym.* **1980**, *21*, 595;[36] Korshak, Y. V.; Kanischka, G.; Höcker, H. *Makromol. Chem. Rapid Commun.* **1985**, *6*, 685.[33]

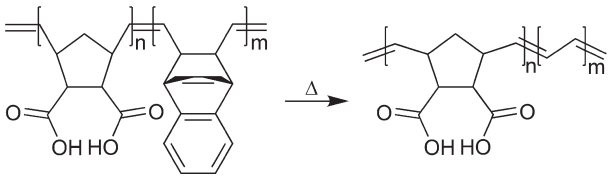

Figure 10 A block copolymer incorporating polyacetylene. Reproduced with permission from Royappa, A. T.; Saunders, R. S.; Rubner, M. F.; Cohen, R. E. *Langmuir* **1998**, *14*, 6207.[46]

silicon wafer. Dipping the surface into a solution of ruthenium catalyst resulted in adhesion of the catalyst to the hydrophilic portions. Placing this plate in a reduced-pressure chamber with gas-phase cyclooctatetraene resulted in the solventless ROMP of the monomer to yield well-defined patterns of polyacetylene. Pyrolysis of the resultant material afforded a diamond-like carbon film with a hardness of 65 GPa, which is an order of magnitude greater than that of a similarly pyrolyzed pattern generated in solution.[44] Nanopatterned polymer structures have also been synthesized by atomic force microscopy (AFM) anodization of a silicon wafer and surface ROMP from the silicon-functionalized surface. ROMP to polyacetylene (from cyclooctatetraene) or to polynorbornene were successful in the solution or gas phase and afforded a fast method for patterning.[45]

Ambiphilic block copolymers incorporating polyacetylene have also been synthesized via ROMP (**Figure 10**). The Durham route was followed to form the polyacetylene while a silyl ester protected dicarboxylic acid norbornene monomer was used to form the hydrophilic block. Employment of the Langmuir–Blodgett technique, which forms ordered molecular layers based on the hydrophilic–hydophobic interactions between the polymer and the surface, enabled the fabrication of films that exhibited superior conductivity over spin-coated or bulk cast films of the same composition.[46] Even electrochemically activated catalysts have been successfully used in the ROMP of cyclooctatetraene,[47] but in general the research into polyacetylene has diminished in recent decades relying more on other polyenes (e.g., polythiophene and polyphenylene) that exhibit the conductivity desired from polyacetylene as well as better solubilities and stabilities.

4.20.7 Diblocks/Triblocks

Multiblock polymeric networks are the logical extension of the homopolymer as it is essentially two or more homopolymers covalently attached in a linear fashion. For many applications, the result is rather simplistic in functionality.[48] An early example of block copolymers used a titanacyclobutane to effectuate the polymerization of norbornene, norbornadiene derivatives, and cyclopentadiene into diblock or triblock hydrocarbon copolymers with PDIs of 1.08–1.14. The ROMP of cyclobutadiene using a tungsten catalyst followed by hydrogenation yielded polyethylene or instead of hydrogenation, it can be used to form diblocks and triblocks with norbornadiene.[49] The ability to form block copolymers can be a test of the efficiency of a catalyst as was done with the third-generation Grubbs catalyst by Stelzer in which oligomeric norbornyl monomers were used to synthesize homopolymers, diblocks, and triblocks, in order to demonstrate that this catalyst initiates completely and gives narrow dispersities.[50] Besides the more commonly employed mononuclear catalysts, binuclear catalysts also perform well in the formation of block copolymers as demonstrated for molybdenum[51] and ruthenium[52] binuclear catalysts.

As with homopolymers, block copolymers may incorporate metals such as in the work of Chan and Schrock where palladium-containing norbornene moieties were copolymerized and the metal reduced below the T_g of the polymer to afford metal clusters whose size was modulated by the polymeric composition.[53] Even with fairly labile metals, the gentle reaction conditions of ROMP can incorporate them into polymeric networks. The ROMP of a variety of norbornene derivatives bearing cationic iron moieties was accomplished without loss of the iron, whereas heating above 100 °C resulted in loss of the iron without degradation of the polymer. The norbornene polymer sans iron was also realized via photolysis.[54]

The first reported ROMP of the zwitterionic sulfopropylbetaine- and carboxyethylbetaine-exo-7-oxanorbornene derivatives illustrates an advantage of ROMP over other techniques (**Figure 11**). Controlled polymerization via ROMP was performed in aqueous or organic solvents. Diblocks from these monomers were found to disperse in highly concentrated electrolyte solutions but self-assemble in its absence.[55] An interest in artificial muscle materials brought together the ROMP of a norbornenyl liquid crystal monomer and the ATRP of *n*-butyl acrylate off the initiator endcapped polynorbornene derivative to yield a liquid crystal/isotactic diblock adopting a lamellar structure.[56]

As with homopolymers, multiblock polymers have been synthesized for their photochemical properties. The ROMP of carbazoyl and phthalimide-derivatized norbornene monomers afforded fluorescent diblocks soluble in organic solvents. Hydrogenation of the backbone afforded similar results with enhanced thermal stability.[57] The polymerization of norbonene-functionalized tetradentate cyclometalated platinum(II) monomers with a bis(carbazolyl) norbornene monomer formed soluble copolymers with PDI values near 2.5, suggesting that the polymerization may not be well controlled. Compared to the starting monomers, the photophysical and electrochemical properties differed little. The processable polymers are highly luminescent in the green

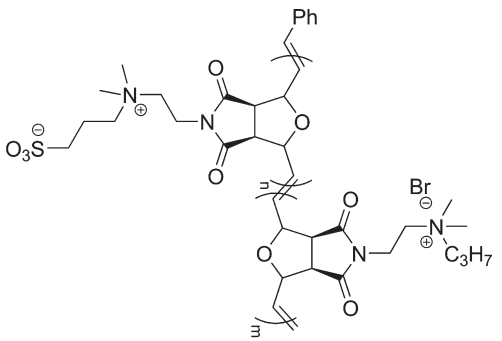

Figure 11 A zwitterionic polymer formed in aqueous or organic solutions. Reproduced with permission from Rankin, D. A.; Lowe, A. B. *Macromolecules* **2008**, *41*, 614.[55]

region of the spectrum, and thus are possibly of use in organic light-emitting diodes (OLEDs) or other optical devices.[58]

While monomeric structures may be similar (e.g., based on a norbornene scaffold), a given catalyst may work well for one monomer but not as well for a seemingly similar analog as demonstrated by Tanner *et al.* Using matrix-assisted laser desorption/ionization mass spectrometry, the kinetics were analyzed for different monomer and catalysts with special attention focused on the crossover reaction where the propagating polymer switches to a different monomer in block polymerizations. The results showed that this change is often inefficient though the fully initiating, third-generation Grubbs catalyst showed high activity throughout in one instance.[59] Thus, to get the optimal activity, catalysts should be screened, though for more basic monomers the differences are relatively minor.

A large amount of active catalyst is typically wasted upon monomer consumption as the catalyst lifetime exceeds that of the reaction. Aimed at forming more polymer from less catalyst, homopolymers and copolymers of norbornene derivatives of uniform MWs were obtained through pulsed-addition ROMP. The polymerization is terminated with *cis*-octene as a chain transfer agent, which due to the rapidity of the polymerization over the chain transfer process can be present throughout the polymerization. The transfer agent serves to both cap the living polymer and regenerate a precatalyst. Injection of fresh monomer and initiation forms identical polymer chains. Accounting for catalyst death in the addition of monomer, low polydispersities were maintained over 10 cycles. Due to the rapidity of the ROMP, diblocks could also be formed by carefully timing the addition of the second monomer so as to precede chain transfer but follow the polymerization of the first monomer.[60]

No one polymerization technique is capable of forming the array of polymeric strands that might be envisioned for block copolymers. Fortunately, the mixing and matching of separate techniques (sometimes at the same time) has been found very successful in accessing polymers not achievable through one polymerization technique alone. Endcapping COD with a homotelechelic trithiocarbonate moiety after ROMP can afford handles from which to polymerize styrene and acrylates via RAFT, ultimately affording ABA triblocks.[61] Combining the ROMP of COD and ROP of D,L-lactide, ABA triblocks may also be accessed as telechelic capping of the living ROMP polymer (**Figure 12**). An observed benefit of this reaction was increased elongation of the polymer due to the COD but retention of the high tensile strength characteristic of polyacrylates.[62] Linear poly(dichlorophospazene) was formed through a cationic polymerization and endcapped with either one or two norbornenylphosphoranimines. ROMP of the homotelechelic macromonomers afforded cross-linked polymers but the semitelechelic did not, presumably due to the lower number of active sites, leading instead to an poly(Monomer A)-poly(Monomer B)-poly(Monomer A) (ABA) triblock.[63] A one-pot synthesis of ABA triblocks was accomplished through the ROMP of COD, bistelechelic endcapping with a chain transfer agent bearing ATRP initiators and ATRP of styrene or methylmethacrylate from both ends.[64]

In an application to smart materials, norbornene and norbornadiene monomers were modified to include liquid crystal side chains attached by a 6- or 10-atom linker. A bimetallic Schrock catalyst was utilized for the polymerization and phase segregating ABA triblocks were formed with one of these monomers and methyltetracyclodecene as the A monomer. Small-angle X-ray scattering indicated the formation of smectic C* monolayers when using the six-carbon linker norbornene triblock but bilayers for the 10-atom-linked norbornene or norbornadiene triblocks. With an elastic plateau above the T_g, these polymers could possibly be utilized in shape memory applications.[65] An extension to include a nematic liquid crystal side chain resulted in the absence of a liquid crystalline phase for this polymer when using a polyoxyethylene spacer. With this same spacer, the smectic polymer (homopolymer or block copolymer) exhibited the expected liquid crystal transition.[66]

The use of the commerically-available Grubbs catalyst can be challenging for accessing telechelic polymers because the benzylidene moiety is relatively inert for postpolymerization events. Thus, only the propagating end of the polymer can be capped, or both ends of the polymer can be capped but only with the same functional group to give a homotelechelic polymer. As Weck and co-workers recently reported, the use of a functionalized benzylidene that becomes incorporated into the polymeric chain may be used to form one telechelic end and a chain transfer agent on the living polymer end realizes a heterotelechelic polymer. In their study, a 2,6-diamidopyridine or Hamilton receptor-modified styrene was used to form the precatalyst and subsequently incorporated into the chain. Capping the propogating end with a pyridyl derivative formed the desired heterotelechelic polymer. Addition of a polymer capped with thymine formed a diblock through its hydrogen bonding with the diamidopyridine moiety, and addition of a palladium-capped polymer formed the triblock as the pyridine coordinated to the metal center (**Figure 13**).[67]

An extension on the heterotelechelic polymer used the same Hamilton receptor-modified ruthenium catalyst, but the transfer agent incoporated diamidonapthyridine so as to have differentiated hydrogen bonding moieties. Through Hamilton receptor–cyanuric acid and diamidonapthyridine–ureidoguanosine pairing, a triblock polymer was formed in a single pot. The purpose of using the hydrogen bonding motif over covalent bonds was to afford a dynamic polymer capable of implementation into smart materials that could respond dynamically to an external stimulus yet in its absence return to the original state.[68]

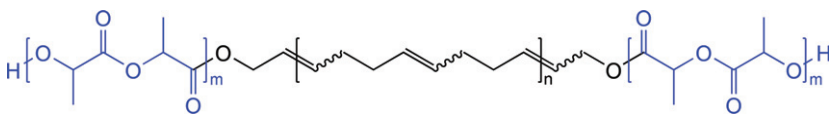

Figure 12 ABA triblock synthesized via ROMP and ROP. Reproduced with permission from Pitet, L. M.; Hillmyer, M. A. *Macromolecules* **2009**, *42*, 3674.[62]

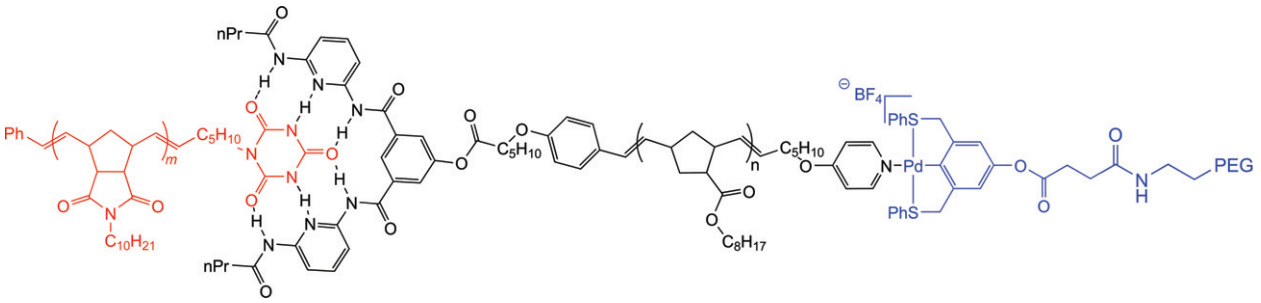

Figure 13 A triblock formed from a heterotelechelic polymer strand. PEG, poly(ethylene glycol). Reproduced with permission from Ambade, A. V.; Yang, S. K.; Weck, M. *Angew. Chem. Int. Ed.* **2009**, *48*, 2894.[67]

4.20.8 Random

Statistical mixtures of monomeric units can be afforded through the premixing of monomers before the addition of catalyst, and the resultant random copolymer often possesses very different properties from the respective block copolymer of the monomers. A study interested in these differences explored random and block copolymers from alkyl ester-, hydroxyl-, amino-, methacroyl-, or ammonium (protected during ROMP)-modified norbornene monomers. While the diblocks with the alkyl ester- and ammonium-bearing monomers self-assembled to nanoscale micelles, none of the random copolymers formed a micellular structure. The random copolymers simply lacked the driving force of separated, strongly hydrophobic and hydrophilic concentrations to self-assemble. In general, the structures of micelles or nanoparticles strongly depend on the hydrophilic–hydrophobic balance as well as the polymer concentration, salt concentration, temperature, solvent pH, and other matrix effects.[69]

More sparingly employed monomers, paracyclophan-1-enes were studied for the effect of polymerization on energy transfer. Homopolymers were prepared using a Schrock catalyst, and diblock and random copolymers were also formed with norbornene. These polymerizations placed stillbene (predominantly *cis*) in the polymer backbone acting as a potential chromophore. Studies of these polymers found a strong red-shift in the photoluminescence spectra, suggesting aggregation or chromophore cooperativity. This interaction was dependent on state for one polymer that only exhibited the shift as a film. The oxidation of the stilbenes to phenanthrene was also performed yielding a product absent of chromophore cooperativity and possessing a lower hydrodynamic volume.[70]

The use of random and block copolymers may be combined to gain benefits from both types. The ROMP of xanthene-functionalized norbornene with norbornene dimethyl ester was studied for its application as a sensor (Figure 14). The random copolymer was amorphous, but the further addition of an ethylene glycol-appended norbornene formed a block copolymer from the random copolymer precursor and provided the hydrophobic–hydrophilic interaction leading to self-assembly. The UV–vis active xanthene was irradiated to ionize the assembled polymer, which decreased the aggregate sizes presumably through the attraction of ion pairs generated.[71] Another example of the usefulness of mixing random and block polymerizations was also employed for its photochemical properties. A statistical, random copolymer of phosphorescent platinum

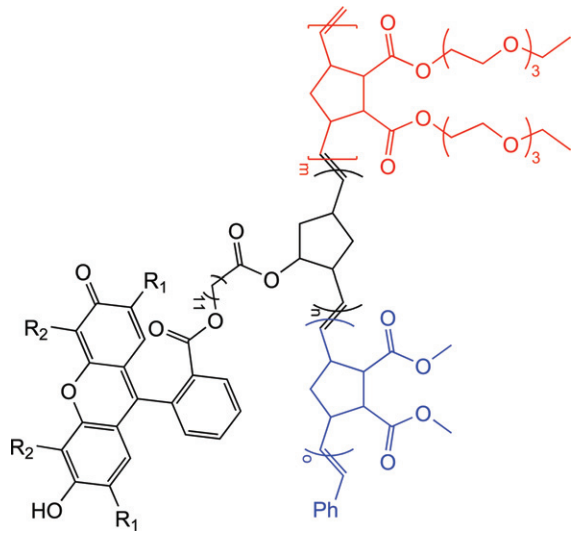

Figure 14 Self-assembling random block copolymer. Reproduced with permission from Sandholzer, M.; Slugovc, C. *Macromol. Chem. Phys.* **2009**, *210*, 651.[71]

and fluorescent carbazole-derivatized norbornenes was synthesized to disperse the platinum and carbazole centers so as to maximize the number of host–guest interactions which otherwise might be minimized if segregated in a block copolymer. The block copolymer strand of a norbornenyl ester yielded the potential for self-assembly. Unselective solvents saw only blue fluorescence but in selective solvents promoting aggregation and self-assembly, a red phosphorence indicative of energy transfer between the carbazole and platinum was observed. Besides the numerous host–guest interactions enhanced by the higher concentrations imposed by the covalent bonding over homogenous solutions of monomers, the polymer increased solvent compatibility for the photochemical process (i.e., the polymer was soluble in solvents which the Pt complex by itself is insoluble).[72] Though often a necessary driving force for self-assembly, a block copolymer of hydrophobic–hydrophilic monomers is not a prerequisite for self-assembly. Upon ROMP, a block copolymer incorporating a cyclooctene derivative functionalized with an ambiphilic phosphorylcholine group and an aryl azide-functionalized cyclooctene forms polymersomes (i.e., polymeric vesicals or lysosomes). However, the random block copolymer did so as well over a broad range of MWs.[73] It is important to note that not all random polymers are amorphous strands.

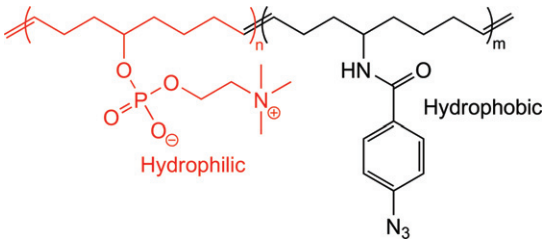

Figure 15 A random copolymer that self-assembles into polymersomes. Reproduced with permission from Kratz, K.; Breitenkamp, K.; Hule, R.; *et al. Macromolecules* **2009**, *42*, 3227.[73]

In addition to the macrostructure, physical properties can also be affected by functional group conformations as observed by Yang and Swager. The random ROMP of COD and alkene-bridged calix[4]arene monomers formed polymers wherein the conformation of the calixarene (three possibilities) was critical to its mechanical properties.[74] A demonstration of the applicability of random copolymers in optics, a polyimide was used to link copolymer strands of exo-7-oxanorbornene-5,6-dicarboxylic anhydride with a second oxanorbornene derivative. The resulting flexible, relatively transparent film was stable toward common solvents and incorporated into an OLED device that compared favorably with typical indium tin oxide-grown glass substrates (Figure 15).[75]

Shape memory polymers have the potential for application in 'smart' materials. Capable of changing shape in response to an external stimulus such as temperature or pH, these materials can react with programmed responses to changing environments. A limitation of many materials is their ability to only remember a single shape, the permanent shape, so that in the absence of the stimulus the material returns to this state. Kasi and co-workers have shown the application of ROMP to form a polymer that undergoes two-way shape memory cycles via thermal mechanisms at the glass transition temperature (T_g) and clearing temperature (T_{cl}). This enabled the storage of a permanent and one temporary shape. To realize this ability, a terpolymer was specifically designed to bear three types of functionality (Figure 16). Norbornenes bearing cholesterol side chains for liquid crystal properties, PEG for its plasticizing ability, and acrylate for the cross-linking necessary to form the 'memorized' permanent shape as well as to prevent chain slippage upon recovery were randomly polymerized. The stages of applying stress above the shape transition, fixation by cooling below that temperature, and recovery by heating above the transition temperature was observed at the T_g and T_{cl} temperatures, allowing the exchange between three shapes depending on the temperature. The temporary shapes were attributed to a highly interdigitated mesophase composed of the cholesterol units.[76]

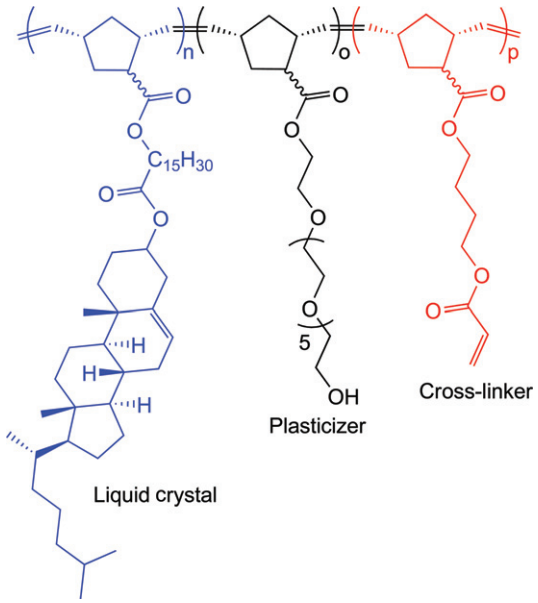

Figure 16 A random copolymer for shape memory applications. Reproduced with permission from Ahn, S.; Deshmukh, P.; Kasi, R. M. *Macromolecules* **2010**, *43*, 7330.[76]

4.20.9 Alternating

In principle, alternating polymerizations exhibit the strictest control of microstructure through the repetitive polymerization of two different monomers in an alternating fashion. A forerunner to this area, Waring and co-workers[77] used $ReCl_5$ as a ROMP catalyst with a racemic norbornene monomer and found instead of a random mixture of stereoisomers, exclusive head-to-tail couplings of monomers (i.e., alternating enantiomers). However, it was not until more than a decade later when Samak *et al.* discovered the alternating polymerization of cyclopentene and norbornene with $RuCl_3$ that alternating copolymers were accessed via ROMP. A steric cage effect around the metal center was invoked to rationalize the alternating preference for the two monomers polymerized, and the effect was highly specific as it only occurred with phenol as the solvent. Additionally the alternating copolymer required a large excess of the cyclopentene monomer to compensate for the much slower rate of ring opening for this less-strained monomer compared to norbornene.[78] The study was later expanded to demonstrate its applicability with either the well-defined Grubbs or Schrock-type catalysts.[79]

These reactions can also be strongly biased by the choice of monomer and catalyst. The polymerization of substituted, polar 7-oxanorbornene derivatives with apolar cycloalkenes by Coughlin and Ilker afforded up to 98% alternating monomer utilizing G1 while the more active catalyst G2 yielded at best 85% of the desired pattern. Similarly, use of COD or cyclooctene enable >90% alternation while this value plummeted to 40% when norbornene was used as the nonpolar monomer.[80]

Further work in catalyst development for this field has revolved around adapting the framework of ruthenium-based Grubbs-type catalysts to enhance advantageous steric interactions (Figure 17). A series of papers by Chen and co-workers outlined the development of a bisphospine complex wherein they incorporated a bischelating phosphine with an ether linker whose oxygen atom displaced a chloride on the catalyst. The differentially substituted phosphines modify the steric environment on both sides of the catalysts, and thus bias the reaction toward the monomer which will minimize steric interactions. Using this system, a copolymer with 76% alternation

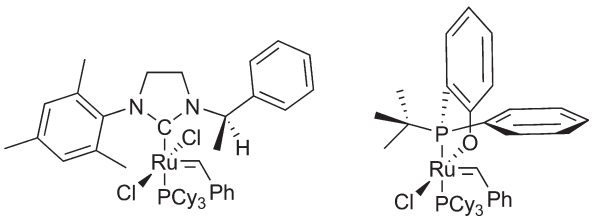

Figure 17 Two examples of catalysts designed for alternating ROMP based on steric parameters. Reproduced with permission from Bornand, M.; Chen, P. *Angew. Chem. Int. Ed.* **2005**, *44*, 7909; Bornand, M.; Torker, S.; Chen, P. *Organometallics* **2007**, *26*, 3585;[81] Vehlow, K.; Wang, D.; Buchmeiser, M. R.; Blechert, S. *Angew. Chem. Int. Ed.* **2008**, *47*, 2615.[83]

of cyclooctene and norbornene was obtained when a 200:1 mixture of cyclooctene/norbornadiene was used; random like copolymers were observed when the monomers were presenting in equimolar or even 10:1 ratios.[81,82] Upon integration of a chiral N-heterocyclic carbene (NHC) into G2, similarly effects the steric environment and was an improvement over the phosphine as it was found capable of 97% alteration between cyclooctene and norbornene at 50:1 mol. equiv.. Additionally, >70% alternation were observed for norbornadiene and octa-1,4-dieneoxide at equimolar concentrations and the scope of monomers employed was expanded to include functionalized norbornenes and substituted CODs.[83]

One of the more complex applications of alternating ROMP to date was performed with cyclooctene and norbornene monomers functionalized with *N*-alkyl thymine or diaminopyridine. While norbornenes typically polymerize much faster than cyclooctene, the bulky nature of the monomers employed disfavored homopolymerization, but once sterically decongested by the eight-carbon spacer from the cyclooctene, another norbornene monomer was readily added to the chain over the slower cyclooctene. When the two alternating copolymers were mixed together, noncovalent linking of the chains was effected through the hydrogen bonding of the thymine and diaminopyridines (**Figure 18**).[84] The zipper-like binding of these strands self-assembled into aggregates which bound in a 1:1 stoichiometry as determined by Job plots.

Another alternating copolymer was used to prepare a polymeric asymmetric hydrogenation catalyst via the ROMP of a chiral bisphosphine norbornene derivative. Whereas the sterically bulky norbornene monomer did not undergo homopolymerization, the addition of cyclooctene enabled copolymerization of the two monomers. The relatively slow homopolymerization of cyclooctene compared to the norbornene-derivative facilitated the formation of the alternating copolymer. The application of this polymeric catalyst afforded up to 83% enantiomeric excess in the hydrogenated products.[85] An improvement on this catalyst was reported by the same group three years later wherein a bisoxanorbornyl derivative with a diphenylphosphino-2,2′-bis(diphenylphosphino)-1,1′-binaphthyl (BINAP) moiety linker was synthesized and the phosphines coordinated to ruthenium. Alternating ROMP with cyclooctene yielded the reusable polymeric hydrogenation catalyst with up to 97% enantiomeric excess.[86]

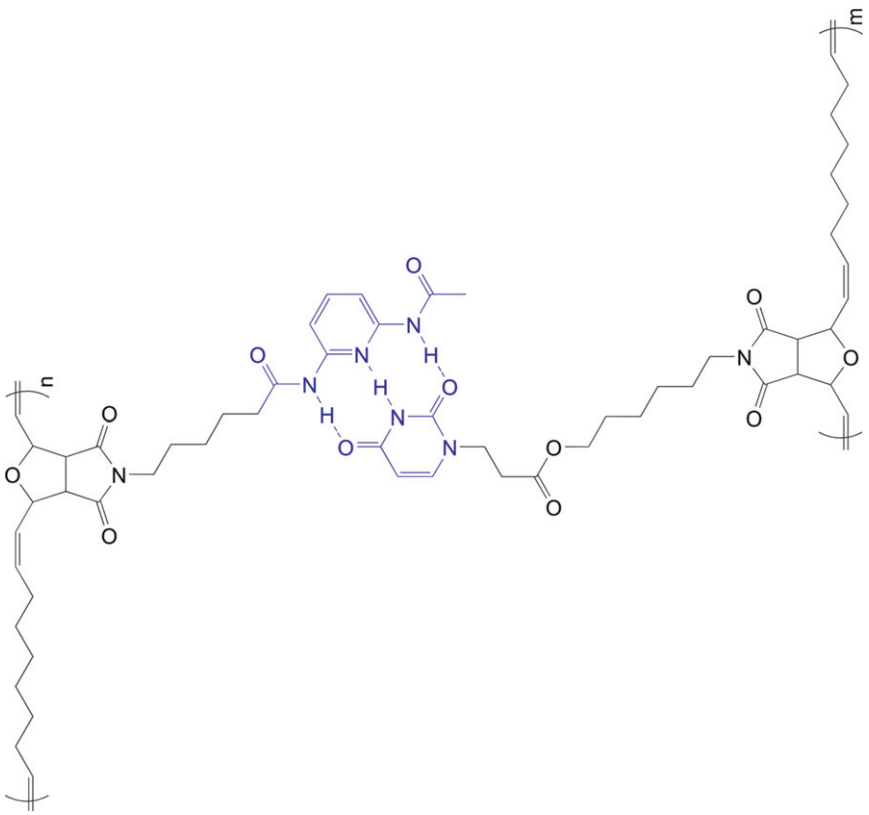

Figure 18 A double-stranded alternating copolymer held together through hydrogen bonding. Reproduced with permission from Nakade, H.; Ilker, M. F.; Jordan, B. J.; *et al. Chem. Commun.* **2005**, 3271.[84]

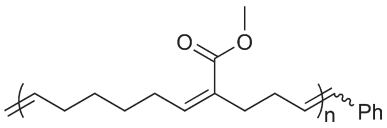

Figure 19 An alternating copolymer prepared from monomers incapable of homopolymerization via ROMP. Reproduced with permission from Song, A.; Parker, K. A.; Sampson, N. S. *J. Am. Chem. Soc.* **2009**, *131*, 3444.[87]

Recent work by Song *et al.* has demonstrated essentially complete control over the alternating polymerization of cyclohexene and cyclobutene 1-carboxylic esters at nearly 1:1 concentrations or higher by taking advantage of the monomeric matches rather than steric interactions.[87] The functionalized cyclobutene ring opens but does not polymerize and cyclohexene is only active in cross metathesis. Thus, homopolymerization of either monomer is eliminated while promoting the alternating copolymerization of the two monomers (Figure 19). Though unfortunately not applicable to common ring-strained ROMP monomers (e.g., norbornenes), this method opens the door to highly controlled structures using the equimolar concentrations rarely feasible with previous studies. Furthermore, switching from using G3 to a HG2 catalyst enabled access to the rare cyclic architecture of ROMP polymers.[88]

While the previously mentioned alternating ROMPs rely on differing concentrations of kinetically inequivalent monomers or the inability of the more strained monomer to homopolymerize (often for steric reasons), a third approach is the noncovalent preorganization of monomers. An example was performed using amino acid-functionalized norbornene monomers wherein one monomer terminated in the amine and the other in the carboxylic acid. Whether acid–base interactions of the monomers prior to polymerization place the monomers in an alternating order that the catalyst moves along stitching together or if the acid–base interaction occurs between the monomer and the propagating polymer was not determined.[89] This noncovalent organization holds promise in expanding the scope of alternating ROMP beyond that of exceptionally bulky or nonhomopolymerizable monomers as coulombic attraction, hydrogen bonding, and so on might be envisioned to form these highly ordered polymers.

4.20.10 Cyclic

Cyclic polymers are less viscous, exhibit higher T_g values, and have smaller hydrodynamic volumes and radii than their linear counterparts. They have also proven to be one of the more challenging architectures to access via ROMP for several reasons. Closure of a linear polymer to macrocyclic ring is entropically disfavored due to the organization of the chain (the reversal of which is used to open macrocyclic monomers and form polymers through entropy-driven ROMP). Secondly, with the elongation of the polymeric chain prior to the cyclization event, the nonliving polymer end must coordinate to the metal center of the living polymer, a declining probability as the chain length increases.

Overcoming the latter difficulty was accomplished by Bielawski and co-workers[90] through the use of a cyclic catalyst.

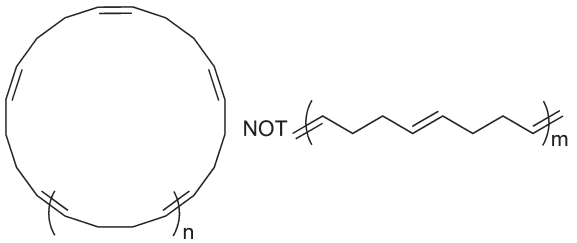

Figure 20 Cyclic polybutadiene prepared with a cyclic ROMP catalyst. Reproduced with permission from Bielawski, C. W.; Benitez, D.; Grubbs, R. H. *J. Am. Chem. Soc.* **2003**, *125*, 8424.[90]

Covalently attaching the alkylidene to the NHC ensured the proximity of this polymer end to the necessary metal center and enabled the ROMP of COD or dodecatriene to afford cyclic polybutadiene (Figure 20). Later, the same catalyst was also employed with dendritic norbornene derivatives to afford the corresponding cyclic polymer.[91] However, this area still remains challenging and a field for future improvements.

4.20.11 Grafted

Grafting occurs through one of three pathways. (1) A preformed polymer is attached to another polymer's side chain in a grafting to approach, (2) a macromonomer bearing a polymeric side chain is polymerized in a grafting through approach, or (3) a polymeric backbone has side chains functionalized with a catalyst or other polymerization initiator from which polymerization occurs in a grafting from approach.

As an example of grafting to for photochemical processes, a ditelechelic polybutadiene prepared via ROMP and a chain transfer agent featuring anhydride-terminated polystyrene was grafted to it, forming the respective triblock. Lamellar morphologies were observed and polystyrene functionalized with a fluorescent chromophore was also grafted to the polybutadiene polymer.[92] Using norbornene monomers bearing carbazoyl or alkyl bromides, copolymers were formed. Poly(methyl methacrylate) was grafted to this material which resulted in the formation of a highly fluorescent polymer.[93] An important method for separating chiral mixtures, high-performance liquid chromatography (HPLC) requires a chiral column. With the MW control and highly adaptable norbornene frameworks, ROMP can be used, though typically is not, to form these columns as demonstrated by Buchmeiser. Chiral norbornene derivatives with L-valine and phenylalanine were surface grafted to norbornene-derivatized silica- or poly(styrene-divinylbenzene)-based supports with Schrock or Grubbs catalysts, and one of the polymers formed was found suitable for performing chiral HPLC separations.[94] In a cross between block copolymers and graft copolymers, either norbornene- or norbornene-derivatized sugars (protected as the acetals) were polymerized by Nomura to either homopolymers or block copolymers. The resultant copolymers were endcapped with 4-$Me_3SiOC_6H_4CHO$ or 3,5-$(Me_3SiO)_2$-C_6H_3CHO to provide a second functional handle. The deprotected alcohols were used in the grafting to of PEG, which in the latter endcap formed a three-armed species with the deprotected dihydroxy arene ring serving as the center of the two arms branching off

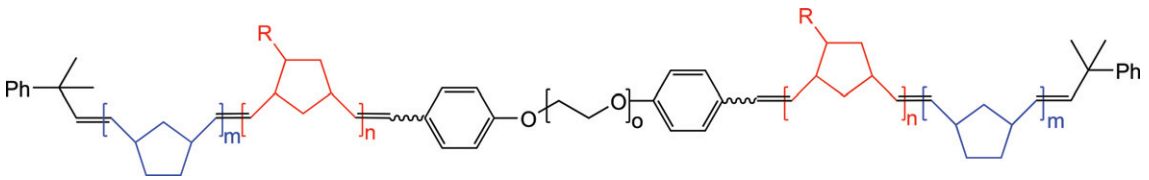

Figure 21 An ABCBA block copolymer by grafting together two AB chains. Reproduced with permission from Murphy, J. J.; Kawasaki, T.; Fujiki, M.; Nomura, K. *Macromolecules* **2005**, *38*, 1075.[95]

the original polymer (the third arm). This method was amenable to numerous architectures including linear (AB and ABC), branched (AB_2 and ABC_2), and ABA or ABCBA (wherein PEG served as an interpolymer linker between polynorbornenyl block copolymer chains) structures (**Figure 21**).[95]

Though grafting to can be used for forming graft copolymers, the approach is frequently hampered by incomplete reactions or the inability to remove excess homopolymer from the newly grafted copolymer. A way to avoid this problem is to graft through a macromonomer that needs no postpolymerization modifications. An extension of this work used norbornene carboxylic acid rather than PEG to functionalize the alcohol endcaps, forming a macromonomer for grafting through. After the ROMP of the macromonomer and termination with the same chain transfer agents, PEG could be grafted to the end of these extended polymers, providing even higher weight polymers. In this instance, with or without the PEG, micelles capable of encapsulating the dye Nile Red were formed as evidenced by tunneling electron microscopy.[96] In another grafting through approach, macromonomers bearing either polylactide or poly(*n*-butyl acrylate) were formed, and ROMP of these macromonomers afforded high MW random or block copolymers. With equimolar monomer ratios, the random copolymers had side chains that formed lamellar structures with 14–21 nm thicknesses, while nonequimolar polymers showed no ordered morphology. Noteworthy, the domain spacing of these structures was unaffected by the length of the backbone, while the block copolymers had lamellar domains of over 100 nm dependent on the backbone length.[97]

As in the formation of multiblock polymers, a combination of polymerization techniques may be employed for grafting. From a cyclobutene bearing an ATRP initiator, ATRP of styrene or acrylate derivatives followed by ROMP successfully formed well-defined graft copolymers with the polybutene backbone.[98] Rather than using ATRP from the polymeric backbone, graft copolymers of styrene and norbornene units were accessed through attachment of the polystyrene to the norbornene monomer unit and ROMP of the resultant macromonomer in another grafting through approach.[99]

Polyelectrolytes with a hydrophobic backbone and oligopeptide brushes have been prepared via ROMP in a grafting through approach. A lysine oligopeptide-functionalized COD monomer was used to form the homopolymer or mixed with PEG-appended COD to form a random copolymer. At 30% or more PEG, aggregates rather than extended structures were observed.[100] An extension of this work utilized a pentalysine-grafted polymer as effective transfection reagents of comparable or better activity than commercial alternatives with cell viabilities relative to untreated cells as high as 99%.[101]

While hydroxyl groups are commonly employed for the grafting of PEG, an alternative involves click chemistry

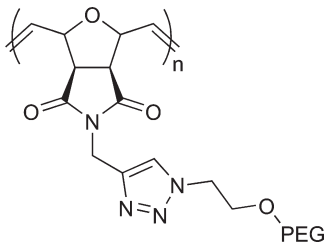

Figure 22 A brush polymer formed via the grafting through approach. Reproduced with permission from Le, D.; Montembault, V.; Soutif, J.; *et al. Macromolecules* **2010**, *43*, 5611.[102]

(Huisgen 1,3-dipolar addition) of azide endcapped PEG with an alkyne-functionalized monomer. Biocompatable brush and comb copolymers were synthesized in this manner by grafting through ω-oxanorbornenyl PEG monomers prepared using the click method. ROMP with G3 afforded the graft polymer which displayed excellent solubility attributed to the oxygenated backbone (**Figure 22**).[102] Like grafting to, grafting through also has its advantages and disadvantages. For example, a macromonomer for grafting through was synthesized by the ATRP of methyl acrylate from an α-oxanorbornenyl derivative. However, for this monomer, the ROMP did not proceed to completion. Presumably this was due to sterics, which is a common problem with macromonomers and dendritic monomers whose side chains are so large as to prevent the proximity of the two units around the metal center.[103]

A solution to the steric bulk of the macromonomers is grafting from where polymerizations occur from the functionalized side chains of the ROMP-generated backbone. The copolymerization of propylene with 4 mol% COD yielded terminal vinyl groups off the main polymer chain resulting from the addition of the COD. Attachment of the catalyst at the vinyl group via olefin metathesis enabled ROMP of norbornene derivatives from the polyolefin backbone.[104] In a grafting from approach, norbornene monomers with covalently attached ATRP initiators were copolymerized with ester-functionalized norbornenes to form the polymeric backbone. The ATRP of acrylic acid successfully yielded the brush polymer.[105]

In addition to using two polymerization techniques common to many graft polymers, others have used three. Comb-like block copolymers have been formed through a mixture of ROMP, ATRP, and ROP. ROMP of *exo*-norbornene monomers formed a copolymer backbone wherein one of the monomers contained an ATRP initiator and the other an alcohol. ATRP of styrene followed by ROP of lactide from the alcohol formed the comb's teeth. These polymers are some of the largest ROMP polymers with MWs exceeding 10 000 kDa

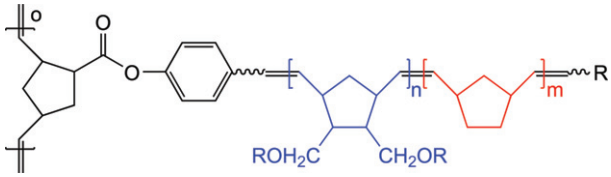

Figure 23 A brush copolymer formed through repetitive ROMP. Reproduced with permission from Nomura, K.; Takahashi, S.; Imanishi, Y. *Macromolecules* **2001**, *34*, 4712.[107]

and domain sizes > 100 nm.[106] While most brush polymers are formed through a combination of several different polymerization techniques, they may also be prepared through repetitive rounds of ROMP when appropriately terminated in a grafting through method. A homopolymer or block copolymer of norbornene and its derivatives was endcapped with *p*-$Me_3SiOC_6H_4$-CHO. The deprotection and reaction of the hydroxyl group with norbornene carboxylic acid chloride provided the macromoner which readily polymerizes via ROMP (**Figure 23**).[107] Rather than using endcaps to attach the norbornene unit in order to ROMP a second time, the post-functionalization of a ROMP polymer formed from maleimide-containing norbornene monomers also provides the necessary functional handle. The Diels–Alder reaction of the maleimide with cyclopentadiene provides a new norbornenyl group for ROMP. The subsequent addition of an α-chloroacetamide norbornene derivative and ROMP afforded the graft polymer along with some homopolymerization of the added monomer. With graft densities off the main chain less than 26%, no homopolymerization was observed and chain elongation was preferred over the intrachain cross-linking observed at higher graft densities.[108]

Besides relying on functionality of the backbone to provide sites for grafting polymer, ROMP can be incorporated into elegant and complex strategies for architectural control. Bowden *et al.* took an olefin-terminated monolayer on a silica wafer and reacted it with a ruthenium catalyst to establish the ROMP precatalyst at the termini. A polydimethylsilyl slab containing microchannels was placed on top of the monolayer and undecenoic acid added so as to undergo cross metathesis in the open channels bearing the ruthenium catalyst. Etching the walls of the channel with HF or Bu_4NF for monitored time periods enabled the controlled introduction of fresh catalyst from which carboxylic acid- or anhydride-bearing norbornenes were polymerized via ROMP. In this manner, polymer brushes ranging from 70 nm to several microns were prepared in a surface grafting from approach.[109] In another nontraditional method, dip-pen lithography has been used to fabricate ordered brush arrays on the nanometer scale. One technique applied thiol-functionalized norbornene to gold by coating the tip with the monomer and touching it to the surface at specified intervals. ROMP with norbornene-based monomers afforded various brush arrays and a wide variety of geometric shapes. A second method used a silicon wafer, 5-(bicycloheptenyl) trichlorosilane, and G1 to form a layer. An AFM tip was then coated with monomer and touched down at intervals, initiating ROMP at the contact point and effecting patterning with reproducible heights based on the tip's contact time.[110]

Some catalyst supporting polymers have been accessed through grafting. Norbornene-functionalized silica and

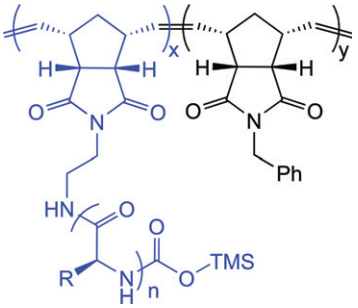

Figure 24 A random graft copolymer prepared in a one-pot synthesis. Reproduced with permission from Lu, H.; Wang, J.; Lin, Y.; Cheng, J. *J. Am. Chem. Soc.* **2009**, *131*, 13582.[113]

monolithic supports underwent copolymerizations with norbornene derivatives bearing two pyridine subunits. The pyridine enabled bischelation of $PdCl_2$ and the catalyst was subsequently used to perform Heck couplings.[111] An interesting analysis on the chain properties of graft polymers, a physical study used neutron diffractometry to determine the thickness of PEG and backbone regions of polynorbornene containing grafted PEG at the air–water interface. The backbone was found to have a constant thickness while the PEG increased as the surface concentration of the film increased.[112]

Generating less waste, 'one-pot' syntheses have attracted attention not only for environmental and economic concerns but also as a time and labor efficient method. The highly tolerant nature of the ROMP and its capability of forming ordered, complex structures makes it a shining candidate for this approach. Indeed, several of these reactions have been reported. In one example, a brush-like polymer was formed through the ROMP of aryl and TMS-protected amine norbornene moieties in the presence of *N*-carboxyanhydrides. Unmasking of the amine polymerizes the anhydride to form the brush-like structure (**Figure 24**).[113] The ability of ruthenium catalysts to facilitate both ROMP and ATRP at the same time, can make one-pot synthesis of a brush polymer nearly trivial as demonstrated by the use of norbornene functionalized with an ATRP initiator, which in the presence of acrylates and a ruthenium catalyst concomitantly polymerize by ATRP and ROMP.[114]

4.20.12 Polyalkynes

Historically, the inclusion of alkynes into the repertoire of ROMP has been extremely limited. Namely, the lack of capable catalysts and suitable substrates has severely hampered this area of research. Unlike the ROMP of norbornene where even some of the least active Grubbs and Schrock-type catalysts initiate ROMP, few catalysts are active enough for cyclic alkynes. Indeed, the ROMP of cyclic alkynes has been exceedingly challenging using ruthenium catalysts, and the few successful polymerizations have arisen from carefully chosen tungsten and molybdenum catalysts. The scope of substrates has been limited in part by the difficulty of incorporating the linear, *sp*-hybridized alkyne into a cyclic system with the ring strain required for ROMP, but also by the sensitivity of the employable catalysts to common functional

groups. An essence of the conundrum, cyclic alkynes with alcohols cannot undergo ROMP because the Schrock catalysts are sensitive to the functional group, and the ruthenium catalysts, which tolerate this functionality well, fail to polymerize the cyclic alkyne.

Though a challenging field, the first alkyne ROMP was realized fairly early by Schrock using a molybdenum catalyst and cyclooctyne. The characterization of the resulting chain was inhibited, however, as at greater than 250 equiv. of monomer, a gelatinous solid was obtained and had to be hydrogenated before being studied.[115] A subsequent report on this work expanded the catalysis to include tungsten, but the insolubility of the polymers continued to hamper its characterization. Broad PDIs were observed, and whether related to the hydrogenation, polymerization, or both, it brought into question the ability to perform the ROMP of cyclic alkynes in a living manner.[116] Five years would pass before the first living ROMP of an alkyne was performed using 1,2,5,6-tetrasilacycloocta-3,7-diyne whose resultant, soluble polymer of alternating disilanylene and acetylene units had a PDI of 1.4 (**Figure 25**). A more in-depth study found the ROMP to be regioselective regarding the two alkynes as differential substitution of the 1,2- versus the 5,6-positions and ^{29}Si NMR showed exclusively head-to-tail polymerization of the monomers.[117]

Another decade followed before Nuckolls, working off his previous ROMP of (5*Z*,11*E*)-dibenzo[*a*,*e*]cyclooctatetrane extended it to the ene-yne analog. Though the polymerization was deemed successful, the PDI was rather broad (2.4) and a multitude of products was obtained. Among these was a dewar-benzene derivative that prompted the authors to question the validity of extending the metallocarbene mechanism to this substrate.[118] More recently, the same group formed ring-strained dibenzo[*a*,*e*]-[8]annulenes that undergo ROMP with a Schrock catalyst (**Figure 26**). These monomers bear the additional advantage of facile functionalization and ease of synthesis though the limited choice of catalysts may temper its application.[119]

Coming full circle back to cyclooctyne, a report using a tungsten catalyst obtained narrow PDI values (1.2–1.4). The polymerization was highly concentration dependent with macrocycles composed of three to nine monomer units formed under dilute conditions and a mixture of linear polymer and cyclic oligomers at high substrate concentrations. However, medium-MW polymers were obtained when the polymerization was performed neat in cyclooctyne.[120] As can be inferred from the limited success in this area, the restrictions to date of substrate and catalyst development for alkynyl ROMP present challenges and opportunities for the field.

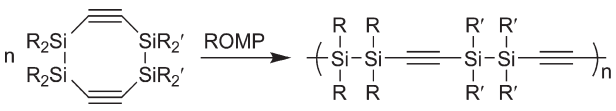

Figure 25 A living ROMP to a polyalkyne. Reproduced with permission from Zhang, X.-P.; Bazan, G. C. *Macromolecules* **1994**, *27*, 4627.[117]

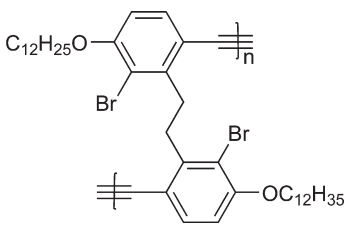

Figure 26 A polyalkyne synthesized via ROMP. Reproduced with permission from Fischer, F. R.; Nuckolls, C. *Angew. Chem. Int. Ed.* **2010**, *49*, 7257.[119]

4.20.13 Nano

Increasingly nanoscale particles, materials, and applications have been explored in all manners of disciplines from energy and communication to lithography and medicine. Decreased size has also brought along the necessity for well-defined reproducible products with an ever-increasing need for precision. Thus, it might not be surprising that the nearly monodisperse polymerizations obtained through living ROMP have found implementation in this field of study. An early foray into the incorporation of carbon nanoparticles, Wudl attempted the formation of a C_{60}-bearing polymer via ROMP. The cycloaddition of quadricyclane with the C_{60} formed the prerequisite olefinic compound and underwent ROMP with excess norbornene. Though electroactive, cross-linking at or above 80 °C led to an insoluble polymer which hampered its application.[121] An alternate approach used ruthenium catalysts with appended pyrene to anchor the catalyst to carbon nanotubes in a noncovalent fashion. Polymerization of norbornene was effected to obtain coatings of up to 20 nm. However, the layer diminished in size over time presumably due to release of the noncovalently bound anchor or dissolution of the polymer.[122]

A more recent incorporation of C_{60} has made strides toward its utility in energy applications. Through drop-casting or spin-coating, block-copolymer nanowires of C_{60} and zinc porphyrin-modified norbornenes were observed to undergo photoinduced charge transfer as indicated by fluorescence quenching of the porphyrin moiety (**Figure 27**). Importantly, the dimensions of the wire are tunable with the diameter dependent on the polymer length and the internal domain spacing based on the monomer's width.[123]

Azides are traditionally hard to incorporate into monomers for ROMP because of their adverse interactions with the catalyst. However, postfunctionalization of an alkyl bromide may be used. As an example, a norbornene bearing a dendrimer capped with an alkyl bromine was successfully used to form diblocks, which upon polymerization was substituted for the azide. 'Click chemistry' with C_{60} formed dendritic side chains bearing up to three C_{60} units though only half of the potential sites were found to be reactive: this was attributed to steric bulk of the C_{60} groups as similar chemistry with zinc porphyrins went to completion (**Figure 28**).[124]

Working with hexabenzocoronene amphiphiles, Aida reported the ability to form nanocoils at ambient conditions, while upon heating nanotubular structures were obtained. Covalent attachment of norbornene to the surface followed by ROMP enabled the locking of a given shape as heating of the polynorbornene nanocoil did not produce the thermally favored nanotube. Besides demonstrating the utility of ROMP to maintain substrate shapes through polymerization,

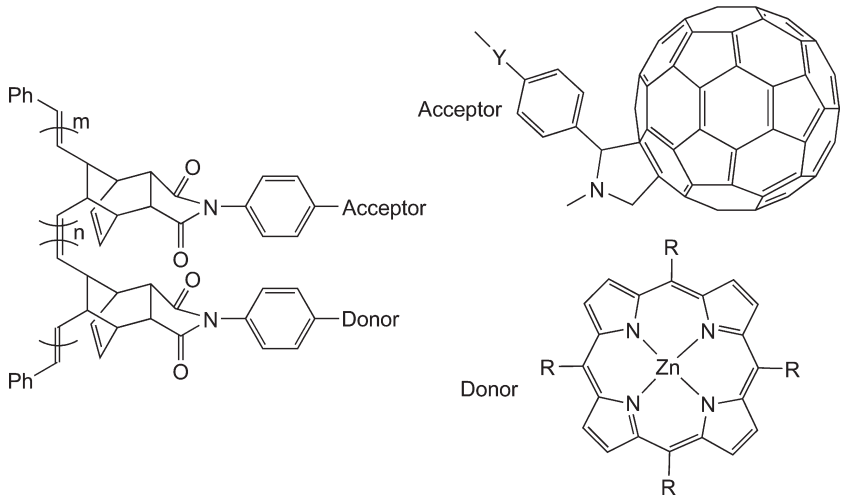

Figure 27 A random copolymer nanowire for photoinduced charge transfer. Reproduced with permission from Charvet, R.; Acharya, S.; Hill, H. P.; *et al. J. Am. Chem. Soc.* **2009**, *131*, 18030.[123]

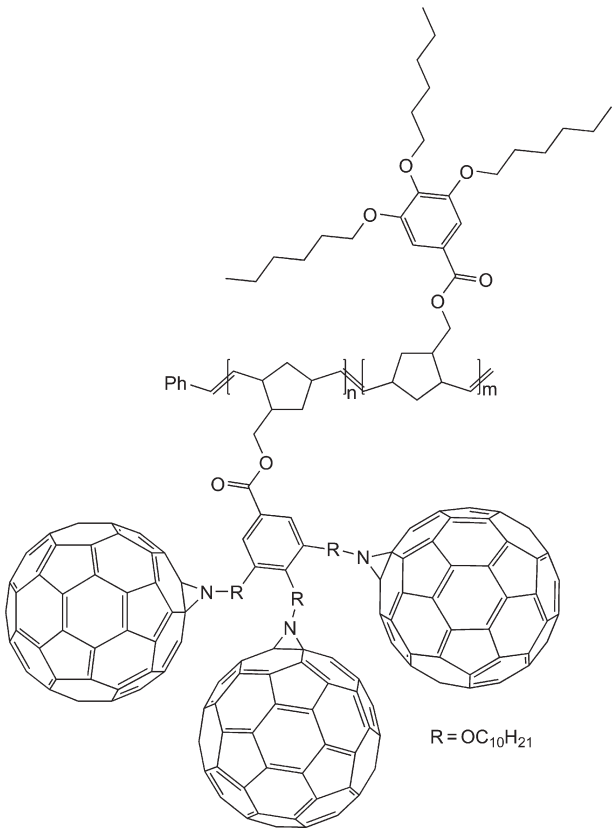

Figure 28 A diblock copolymer with dendritic and C_{60} side chain functionality. Reproduced with permission from Fiset, E.; Morin, J. *Polymer* **2009**, *50*, 1369.[124]

the work has application toward nanoscale solenoids as the nanocoils were conductive when doped with iodine.[125] Also, interested in the electronics of nanomaterials, Swager utilized ROMP copolymers and self-assembly properties to form conductive channels. Attaching phenylene through two carbons to norbornene and either two thiophines, bisthiophenes, or furans *para* to each other off the same phenylene, a conductive side chain parallel to the growth of the norbornene polymer was achieved. Resultant copolymers incorporating one of these monomers was followed with electropolymerization to connect the conductive side chains into a polymeric conductive channel paralleling the polynorbornene backbone. Doping of these channels formed stable, electroactive channels for potential usage in nanoelectrochemical devices.[126]

Differing work with pentadecafluorooctyl-5-norbornene-2-carboxylate polymerized from TiO_2 nanowires and other metals explored its potential as a protecting layer. Linked to the oxide surface via the catechol initiator L-3,4-dihydroxyphenylalanine for improved adhesion over the more commonly employed thiols, nanometer-thick norbornenyl sheaths around the nanowires were observed via TEM. High contact angles for both water and several organic solvents such as diiodomethane indicated strides toward a repellant coating for uses in antifouling or anticorrosion.[127] Rather than grafting to a nanosupport, formation of nanotubes or fibers from block copolymers and a mold have also been accomplished. Copolymers were melted at 150 °C for 48 h and allowed to fill preformed Al_2O_3 molds. The solidified polymer produced hollow nanotubes for large mold pore sizes (400 nm) and with high-MW polymers, whereas smaller pore sizes (180 nm) and lower MWs yielded solid nanofibers upon etching away of the Al_2O_3.[128]

4.20.14 Micelles

Polymeric nanomaterials need not be based on nanoscale supports. Micelles are spherical assemblies that differ from star polymers in the absence of a covalently linked core. Typically, this morphology arises from polymeric strands possessing hydrophobic and hydrophilic regions, which will self-aggregate and assemble based on similar polarities. In polar solvents, the

hydrophobic regions segregate in the center while the hydrophilic ends reach outward to the solution. For ROMP, diblocks are typically used to form the regions of hydrophobicity and hydrophilicity necessary for the self-assembly into micelles or nanoparticles. For example, a block copolymer formed from hydrophobic octanoate-substituted norbornene and hydrophilic ammonium salt (formed postpolymerization)-bearing norbornene monomers readily self-assemble into micelles. However, too much of the salt monomer (>80%) caused aggregation, presumably through hydrophobic cross-linking.[129] A study on the ratios of hydrophilic/hydrophobic monomers and MWs determined the following. At identical MWs and varying monomer ratios, the micelle size remained constant, while the core size decreased linearly with the increasing fraction of the lyophilic monomer. Alternatively, increasing MW with equivalent monomer ratios yielded similar core:shell ratios and linearly increasing bulk of the micelles. This clearly demonstrates the capability for tuning the micellular structure, though at too high or low lyophilic monomer concentration solubility problems do arise.[130]

An interesting one-step synthesis of composite nanoparticles <50 nm in size was performed in microemulsions of methyl methacrylate and norbornene with G1 which is capable of ATRP (though attenuated) and ROMP, forming graft or random copolymers (**Figure 29**).[131] A follow-up study concluded the block copolymer was more likely to form micelles than its random copolymer counterpart.[132] A one-pot synthesis of shell-funtionalized diblock micelles through the ROMP of a hydrophobic ester oxanorbornene and a bromine-appended norbornene derivative has also yielded 110–210 nm micelles stable over several days.[133] Postmodification of structures via photochemical methods prompted Slugovc and co-workers to look at cinnamic acid-derivatized norbornenes that in a block copolymer self-assembled into micelles. Irradiation resulted in cross-linking of the micellular structures via [2 + 2]cycloadditions of the cinnamic acids. Up to 78% conversion of the starting acid occurs as evidenced by integration of the IR signals for the ketone and double bond.[134]

The size of nanoparticles has profound biological importance. It has been observed that nanoparticles tend to aggregate in tumor cells preferentially over other healthy cells due to the increased pore size of the tumor cells. This has brought about numerous hypotheses for targeting diseases through the encapsulation of known drugs for release upon uptake into the targeted cells. In one example, the known drug indomethacin was appended to a norbornene for the purpose of polymerization. An amphiphilic diblock was obtained from this monomer and a second norbornene monomer with PEG

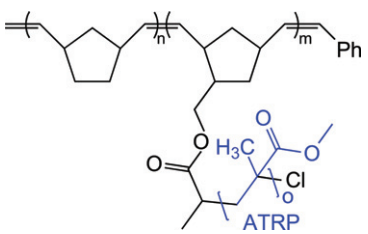

Figure 29 Nanoparticle-forming polymer formed in one step via simultaneous ROMP and ATRP. Reproduced with permission from Airaud, C.; Ibarboure, E.; Gaillard, C.; Héroguez, V. *J. Polym. Sci., Part A: Polym. Chem.* **2009**, *47*, 4014.[131]

chains for hydrophilicity resulted in the formation of micellular materials. Hydrolysis of the linked drug successfully released the active form under acidic conditions.[135] Similarly, from the same group, incorporation of the anticancer drug doxorubicin into the polymeric structure self-assembled into 230 ± 10 nm particles. Acidifying at pH 4 resulted in the release of almost 50% of the drug over 24 h.[136] While striking, the release does leave some challenges for practical application as the pH even of tumor cells which have been shown to be more acidic than that of healthy cells are above a pH 5 and therefore would release much less than 50% of the active drug.

Expanding on the endomethacin study, a block copolymer with the indomethacin-containing norbornene and tosylated hexaethylene glycol-appended norbornene monomers was studied for its binding properties. Upon self-assembly, the surface binding of single-stranded DNA antisense oligodeoxynucleotides (which have found application in fighting breast cancer) and/or antibodies targeting the transmembrane human epidermal growth factor receptor-2 were observed with the binding confirmed by the use of probes and subsequent TEM imaging.[137] Biotin groups have high binding affinities to numerous proteins including streptavidin. Taking advantage of this interaction, Sleiman and co-workers formed homopolymer and copolymers endcapped with biotin, which self-assembled in acetonitrile/water into luminescent micelles. Addition of streptavidin caused cross-linking of these micelles as the biotin groups bound to the bacterial protein.[138] Looking to form micelles for use in biological applications, three oxanorbornene bearing (1) luminescent Ir, Ru, or Os bipyridine complexes for sensing, (2) PEG for enhanced hydrophilicity as well as protection of the metal center, and (3) biocompatible groups for specific binding (e.g., biotin and streptavidin) were explored. The assembled triblocks formed micelles with the metals buried in the core (**Figure 30**).[139]

4.20.15 Polyrotaxanes and Polycatenane

Catenanes are two interlocked cycles, like two links in a chain, which cannot be separated without the breaking of a covalent bond. Rotaxanes are similar but are composed of a cycle encircling an acyclic molecule like a ring around a thread. A naturally occurring rotaxane, DNA polymerase III encircles DNA during replication. Polyrotaxanes and polycatenanes are well-defined repetitions of these interlocking structures and should not be confused with intertwined cross-linked polymers whose interconnectivity is random in nature. These intricate polymeric networks have posed challenges to synthetic chemists, and a few have utilized ROMP in their preparation.

In 2003, Rowan reported using a known host-guest interaction of a synthetic porphyrin and viologen interaction to form [3]rotaxanes and [4]rotaxanes (two and three cycles around a linear molecule, respectively). Relating it to ROMP, the use of a symmetrical [3]rotaxane possessing an internal double bond was found to be a suitable chain transfer agent in the ROMP of COD. Thus, a [3]rotaxane with a polybutene linker between the rotaxane functionalities was accessed.[140] Although strictly speaking a polyrotaxane was not obtained, this work does show the flexibility in chain transfer agent options. Five years later, Mayer employed a Sauvage-type [2]catenane with 1,10-phenanthroline-based cycles (**Figure 31**). These cycles

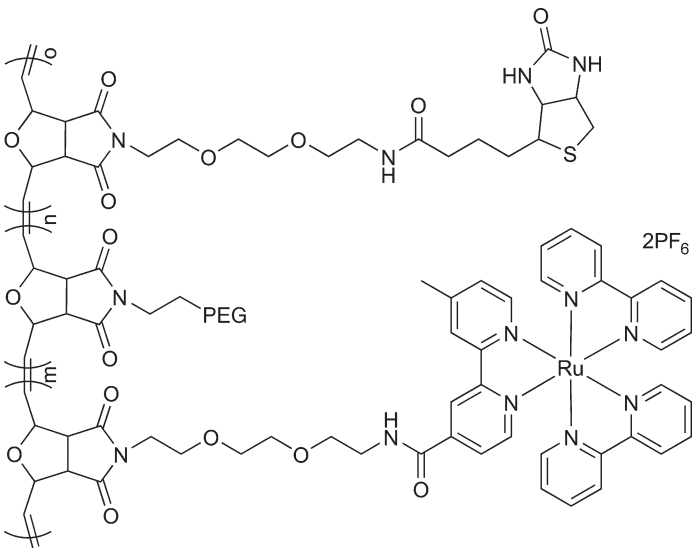

Figure 30 A self-assembling, random copolymer for biological sensing and binding applications. Reproduced with permission from Sankaran, N. B.; Rys, A. Z.; Nassif, R.; *et al. Macromolecules* **2010**, *43*, 5530.[139]

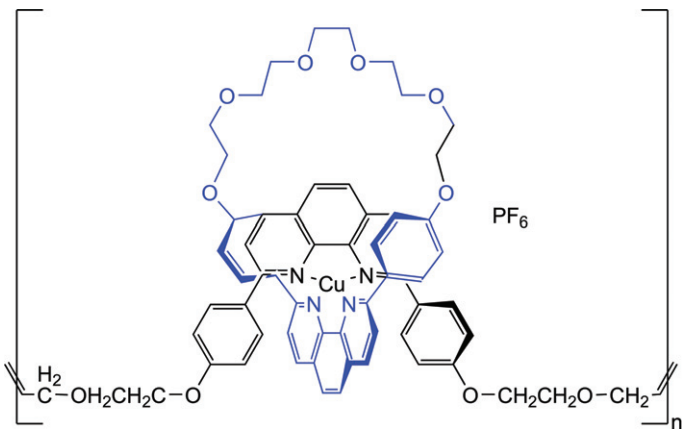

Figure 31 A polypseudo rotaxane. Reproduced with permission from Kang, S.; Berkshire, B. M.; Xue, Z.; *et al. J. Am. Chem. Soc.* **2008**, *130*, 15246.[141]

interlocked as they coordinated to a copper atom, and one of the cycles was functionalized to contain an internal alkene. Entropy-driven ROMP of this olefinic cycle resulted in the polypseudorotaxane, though unfortunately, treatment with potassium cyanide to remove the copper and access the corresponding polyrotaxane caused the cycles to slip off the polymeric strand.[141]

Recent work by Grubbs tackled the challenge of a polycatenane charm bracelet structure where numerous cyclic structures all encircle a single large cycle. To realize this structure the crown ether interaction with charged alkyl ammoniums was exploited. The role of ROMP was the polymerization of a nine-membered protected amine ring that was endcapped with an alkyl bromine on both ends. Substitution to the azide followed by click chemistry with a bisalkyne formed the large ring whose deprotection and alkylation formed a polyalkylammonium cycle. The introduction of acyclic crown ether analogs interacted so as to encircle the charged nitrogen and RCM of these acyclic analogs under dilute conditions afforded the desired charm bracelet.[142]

4.20.16 Dendrimers

Dendrimers have the distinct advantage of introducing multiples of a given functionality from a single center in a highly regular manner. However, branching at uniform and consistent lengths has been a drawback in the preparation of these structures using ROMP as it typically proceeds linearly or with random branching/cross-linking instead of controlled branching. However, this has not discouraged efforts in using ROMP to functionalize dendritic structures or to incorporate dendrimers into polymers via macrocyclic monomers. An early attempt, Stewart and Fox[143] performed the ROMP of a norbornenyl monomer bearing a second-generation naphthyl-capped dendron to give a fluorescent polymer (**Figure 32**). While the naphthalene excimer emission was not observed for the monomer, the naphthalene singlet and excimer emissions were observed for the polymer indicating a structural dependence of this excitation and a critical role of the secondary structure to the characteristics of individual units.

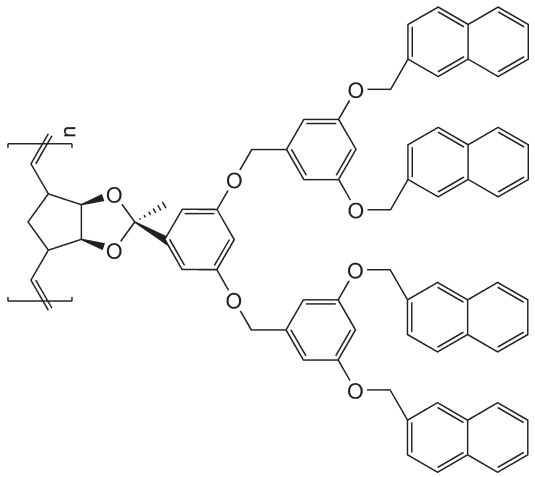

Figure 32 A fluorescent polymer bearing a second-generation dendrimer side chain. Reproduced with permission from Stewart, G. M.; Fox, M. A. *Chem. Mater.* **1998**, *10*, 860.[143]

Similarly, using macromonomers to which the dendrimer had already been appended, Holerca and Percec found a dependence of the polymer's shape on that of the dendrimer. Homopolymers were prepared from norbornene dendrimer derivatives where the dendrimer branch consisted of an aryl group with two or three ether chains extending outward. When both ether linkages were located in the *meta* positions, a cylindrical polymer structure was obtained. However, the addition of the third ether at the *para* position resulted in spheres or cylinders dependent on the number of monomers incorporated. The rationale for the differing outcomes was attributed to the greater planarity of the disubstituted dendrimer as opposed to the trisubstituted wherein the alkyl chains of the ether for steric reasons would not easily be contained in a plane. This would hinder the formation of a cylinder wherein the dendrimers would stack or lay on top of each other along the height of the cylinder.[144] Another effort investigating the ROMP of first- to fourth-generation dendrimers consisting of 2,2-bis(methylol)propionic acid pendant to a norbornene resulted in the desired homopolymers. Interested in their use as porous membranes, only the fourth-generation polymer formed a porous membrane that was successfully pulled into fibers (**Figure 33**).[145]

Taking advantage of the increasingly popular 'click chemistry' wherein an azide undergoes a formal [3 + 2]cycloaddition with an alkyne, Newkome dendrons with an azide were 'clicked' with a norbornenyl alkyne. Subsequent ROMP with PEG-modified norbornene, formed block copolymers capable of self-assembly into polyion complex micelles. Interested in toxicity toward diseased cells, the dendronized polymer showed a high binding affinity for pDNA, but was also found highly toxic against all cell lines tested, suggesting a need to dial back on the polymer's potency.[146] Rather than using one dendritic monomer, Fréchet used two differentially substituted dendritic monomers to form copolymer with vast steric bulk. For this process, *exo*- rather than *endo*-norbornene derivatives were necessary for the polymerization to occur (**Figure 34**). When depositing a block copolymer containing both aryl ether and polyester dendrimers on a mica surface, self-segregation was observed. The aryl ether dendron self-aggregated while the polyester dendrimer elongated for maximal surface contact, yielding a tadpole-like structure as imaged through AFM.[147]

ROMP has also been utilized to form a linker between dendritic ends. A pseudo-ABA triblock, the polymer core was constructed from COD and capped through its cross metathesis with a bisdendrimer chain transfer agent. Hydrogenation to the saturated and more flexible polyethylene bore out the ability to use ROMP for the installation of well-defined alkyl linkers

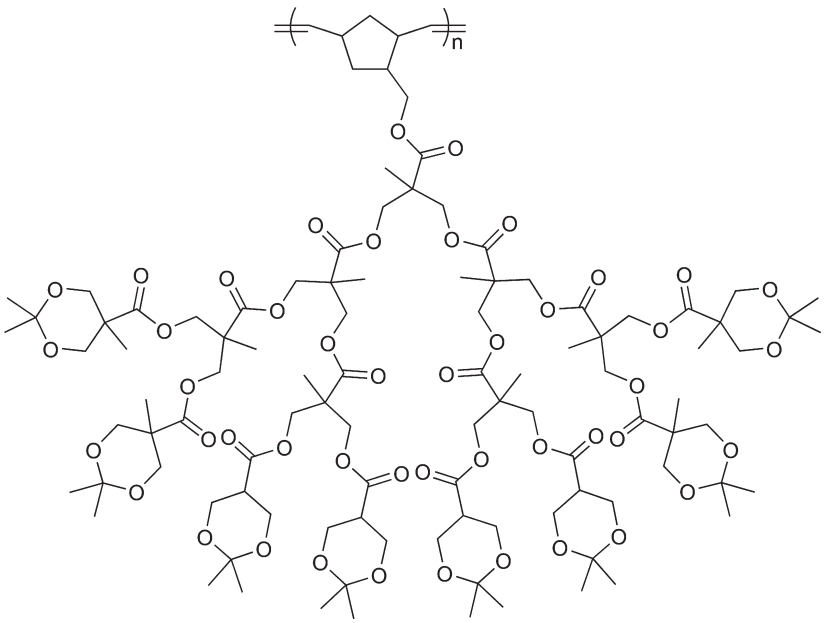

Figure 33 Dendritic homopolymer applied to the fabrication of a porous membrane. Reproduced with permission from Nyström, A.; Malkoch, M.; Furó, I.; *et al. Macromolecules* **2006**, *39*, 7241.[145]

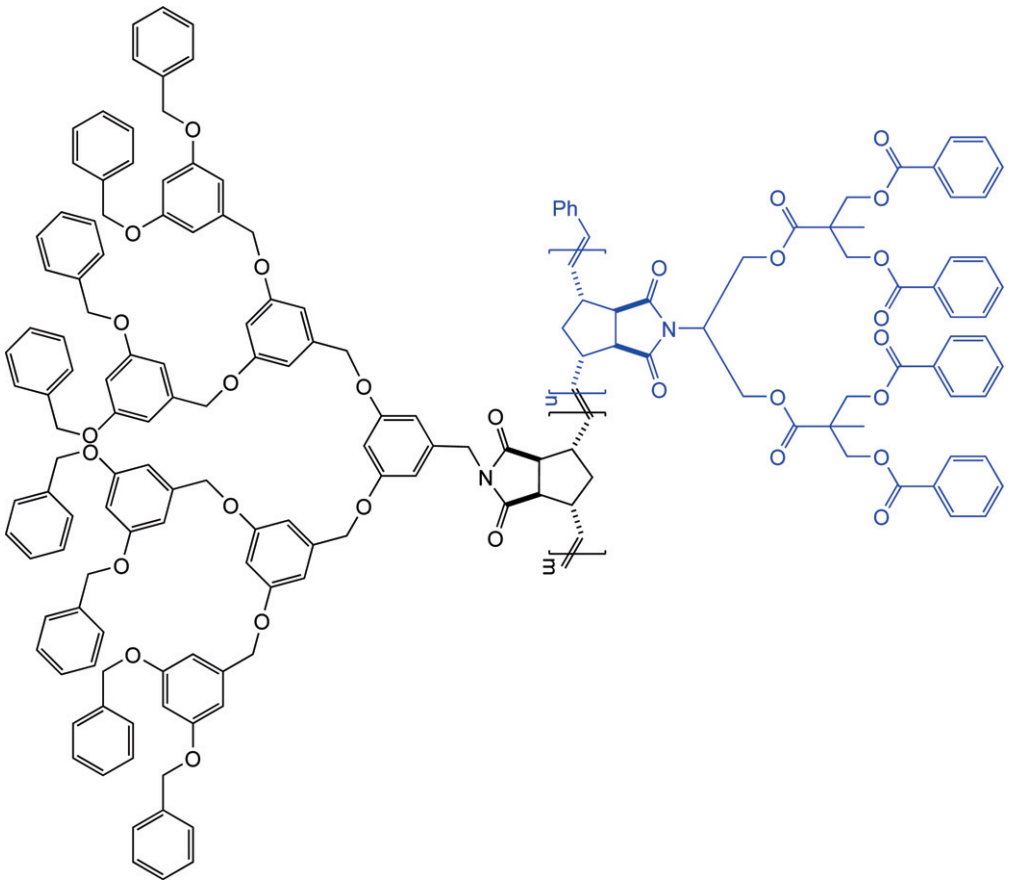

Figure 34 A dendritic graft copolymer. Reproduced with permission from Rajaram, S.; Choi, T.; Rolandi, M.; Fréchet, J. M. J. *J. Am. Chem. Soc.* **2007**, *129*, 9619.[147]

(Figure 35).[148] Another alternative to dendritic monomers involves the preparation of a dendritic core terminated in olefins which are available for metathesis with a catalyst's alkylidene such that the catalyst becomes incorporated at the ends of the dendrimer. From there, ROMP of monomers such as norbornene elongates the dendritic ends into linear arms to yield a star polymer with a dendritic core (Figure 36). Interestingly, prior to ROMP, the catalysts attached to the dendrimer reversibly dimerized at low temperatures and high concentrations.[149]

4.20.17 Star Polymers

Star polymers in general consist of a core unit, which may or may not be polymeric in nature, with long arms extending outward from that center (Figure 37), several of which were mentioned earlier. An early effort toward these morphologies placed four tungsten catalysts to a core silicon atom. The ROMP of norbornene caused intermolecular cross-linking of the catalytic sites, affording branched star polymers.[150] Star-like polymers were also prepared by the copolymerization of α-norbornenyl macromonomers and poly(methyl methacrylate)-bearing norbornene. The ATRP iniatiating norbrornene derivative could also be grafted with a fluorescent tag through ATRP.[151] Due to the potential for star polymers to possess polymeric cores as well as arms, multiple techniques may be employed to obtain this structural motif. Ma *et al.*[152] formed a star polymer consisting of a poly(norbornene) core (*via* ROMP) and polystyrene arms through RAFT. Considering the hydrophobic nature of most monomers, soluble star polymers are less common. An example of this involved the ROMP of norbornene that was subsequently cross-linked via 1,4,4a,5,8,8a-hexahydro-1,4,5,8-*exo-endo*-dimethanonaphthalene to form the core and terminal olefins. Further polymerization of norbornene to form the 'arms' and termination with a silylether carboxaldehyde or pyridinecarboxaldehyde gave the desired, soluble star polymer.[153]

4.20.18 Other

Besides directly combating tumors and other health issues with drug-containing polymers, block copolymers have found use in imaging. Fluorine-18, a label used in positron emission tomography for imaging tumors was studied by Grubbs. A random block of functional *exo*-norbornene-imides, one with cinnamoyl groups for cross-linking and the other with PEG capped by a mesolate for postpolymerization exchange with the radioactive fluorine was successfully synthesized for use as an *in vivo* imaging agent.[154] An alternative to radioactive imaging, iron oxide can be used for magnetic resonance imaging; however,

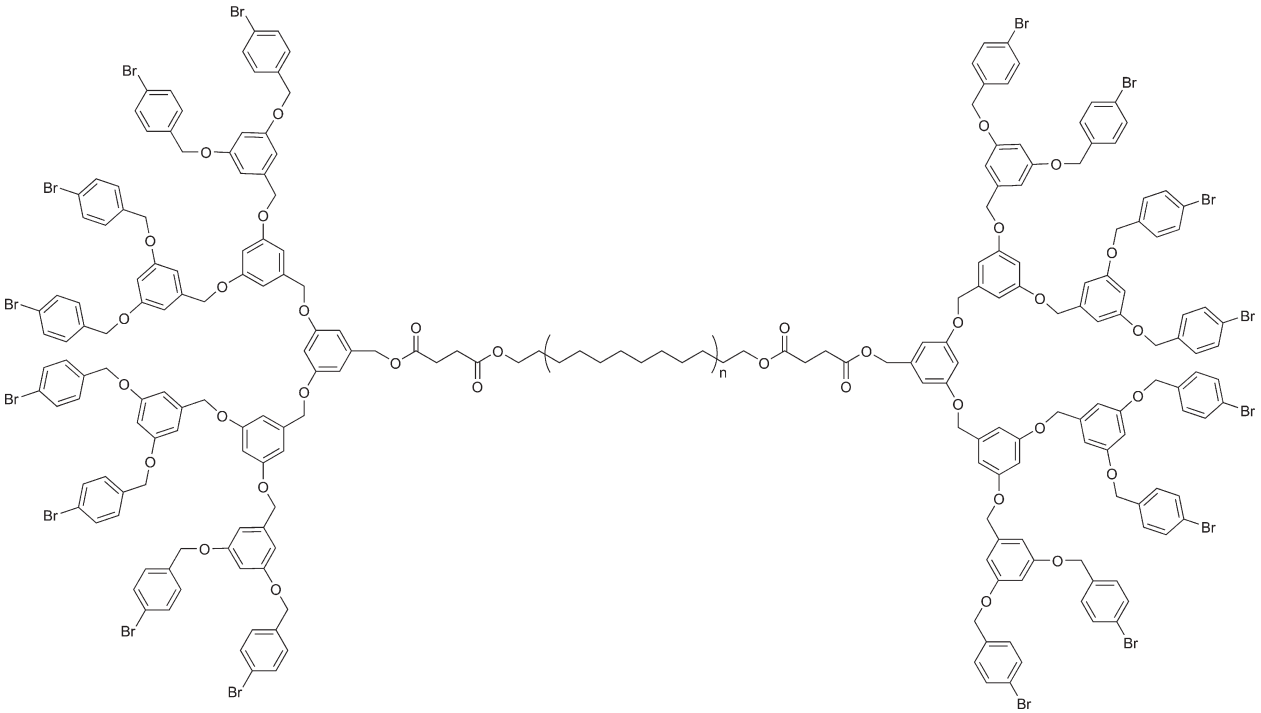

Figure 35 A homotelechelic linear polymer formed from a dendritic chain transfer agent. Reproduced with permission from Sill, K.; Emrick, T. *J. Polym. Sci., Part A: Polym. Chem.* **2005**, *43*, 5429.[148]

stability and aggregation are problematic with this agent. A block copolymer of norbornene carboxylic acid oxiranylmethyl ester for steric stabilization along with norbornene comonomer was found to act as a coating and stabilizer of the iron oxide, as well as reducing aggregation that hinders its use as a contrast agent.[155] A study highlighting the preference of polymers for tumor cells synthesized amphiphilic copolymers of norbornene-modified monomers. One monomer contained an ether for hydrophobicity, the second PEG for stability and solubility in water, and the third a folate or indocyanine green dye (or a mixture of both). High water solubility and nanometer self-assemblies were observed and accumulation was observed preferentially for tumor tissue over other organs providing a possible improvement for *in vivo* tumor selectivity and fluorescence imaging.[156]

Along with the self-assembly and beneficial size properties of polymeric structures, the relative low toxicity, amenable functionalization, and excellent mechanical properties of polynorbornene backbones have caused them to be considered as biomimics. Incorporation of saturated neoglycopolymers through the tandem ROMP hydrogenation of carbohydrate-functionalized norbornenes resulted in a polymeric alternative to commonly used animal-based sources. Used as collagen cross-linking agents and glycosaminoglycan mimics, the polymers possessed higher stability, enzymatic resistance, and permeability over control materials, but also much lower tensile strength that would necessarily need to be addressed before its implementation.[157] Monoterpenes have been extensively studied for their biological activities. However, many of them also possess cyclohexene rings suitable for metathesis reactions. The ROMP of cyclopentadiene with monoterpenes produced highly cross-linked polymers containing linear, terminal, dendritic, and semidendritic regions (**Figure 38**).[158] While useful for its synthesis of a variety of morphologies at once, a controlled form for obtaining one or more of these systems selectively would greatly enhance its allure. In another effort to make polymers more biocompatible and less reliant on petrochemical sources, new monomer syntheses incorporating biological roots have been undertaken. Interested in forming bioplastics, castor oil norbornene derivatives were prepared by reacting the norbornenyl acid chloride with the oil's alcohol groups. With multiple alcohols per castor oil molecule, multiple norbornenes could be appended, and as might be expected, the monomers with higher norbornene content produced more highly cross-linked polymers (**Figure 39**). These polymers also had the most improved thermal and mechanical stabilities.[159]

A series of studies headed by Trimmel has investigated the photochemical photo-Fries rearrangement as it pertains to postpolymerization modification of polymeric side chains. The initial study was performed with aryl esters wherein the rearrangement yielded a hydroxyketone that was subsequently converted to an ester, hydrazone, or fluorescent sulfonates (**Figure 40**). The modified materials were found to be applicable in lithographic patterning.[160] Applying this method to optics, bisnaphthyl norbornene derivatives formed homo and block copolymers with an aromatic chromophore upon ROMP. Photo-Fries rearrangement through UV–vis irradiation caused an increase in the refractive index of the polymer film, whereas further irradiation at a shorter 254-nm wavelength decreased the refractive index, and allowed some modular control over the refractive power through the absence or presence of specific wavelengths of light.[161] Switching to an aryl amide gave the corresponding amino ketone via the

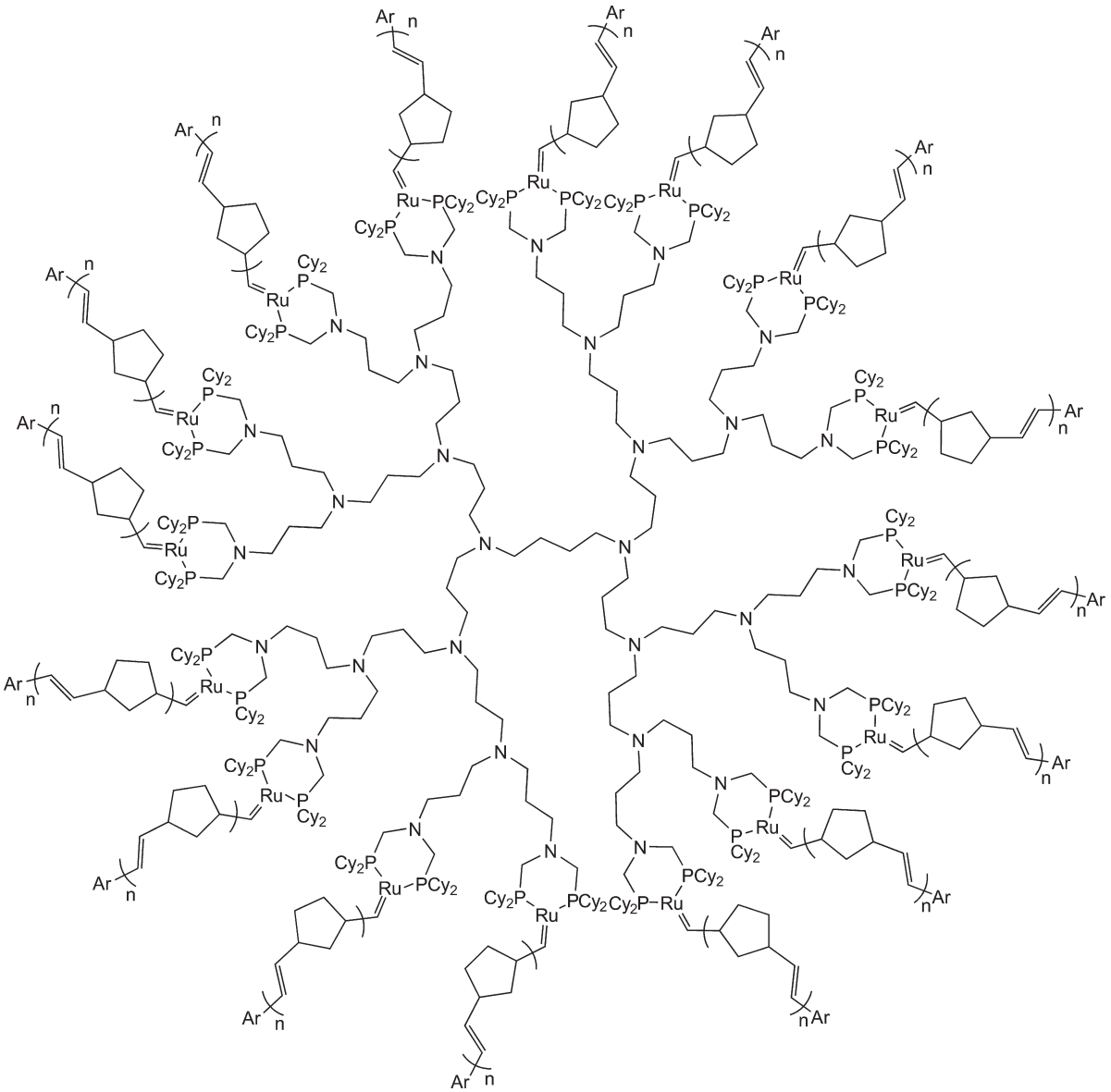

Figure 36 A dendrimer with end groups composed of polynorbornene. Reproduced with permission from Gatard, S.; Nlate, S.; Cloutet, E.; *et al. Angew. Chem. Int. Ed.* **2003**, *42*, 452.[149]

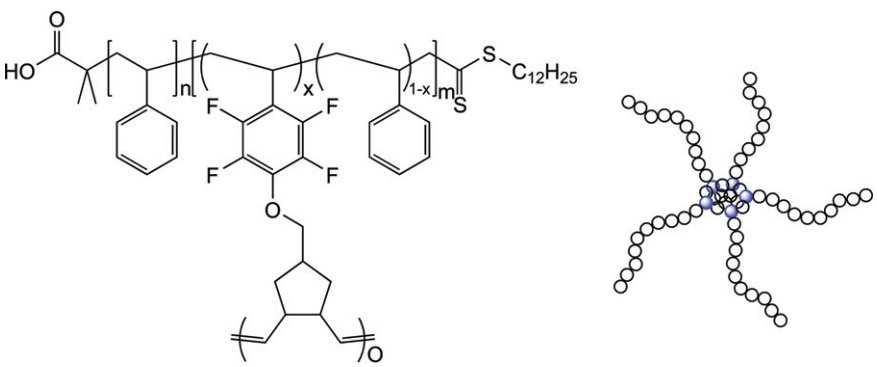

Figure 37 A self-assembling star polymer (left) and its generic representation (right). Reproduced with permission from Ma, J.; Cheng, C.; Wooley, K. L. *Aust. J. Chem.* **2009**, *62*, 1507.[152]

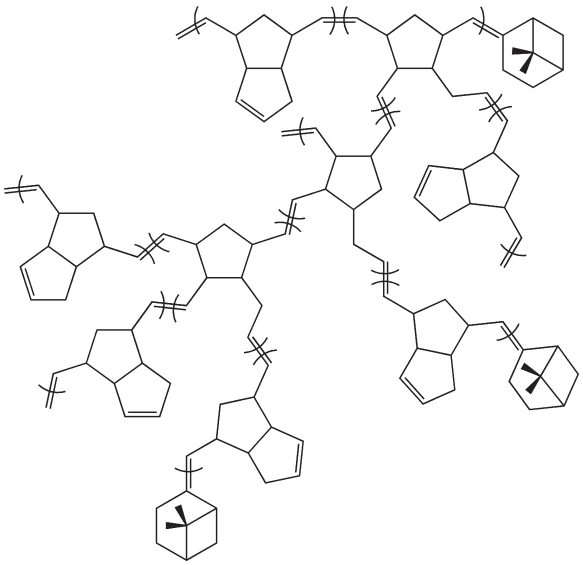

Figure 38 A highly cross-linked polymer from cyclopentadiene and monoterpenes. Reproduced with permission from Mathers, R. T.; Damodaran, K.; Rendos, M. G.; Lavrich, M. S. *Macromolecules* **2009**, *42*, 1512.[158]

photo-Fries rearrangement. An increased refractive index was also found with the added capability to further functionalize via acid chlorides and fluorescamine off the amine. Acid chloride-appended norbornene was grafted from the irradiated polymer as well, showing some modularity in the structure and composition of the polymer.[162]

As mentioned for iron oxide, ROMP has been of interest for the functionalization, stabilization, and structural modification of metals. While the range of metals that are potentially suitable is broad, much of the work has revolved around gold due to the affinity of this element for sulfur – a trait enabling

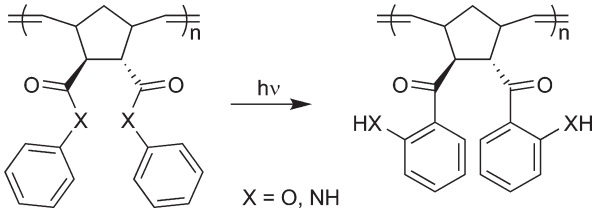

Figure 40 The photo-Fries rearrangement of a polymer via UV–vis irradiation. Reproduced with permission from Griesser, T.; Höfler, T.; Temmel, S.; *et al. Chem. Mater.* **2007**, *19*, 3011;[160] Griesser, T.; Kuhlmann, J.; Wieser, M.; *et al. Macromolecules* **2009**, *42*, 725[161].

the facile attachment of functional groups (like ring-strained olefins!) via thiol alkyl linkers. The first growth off a metal nanoparticle occurred right before the twenty-first century. A proof of concept paper, a thiol linkage attached norbornene to the metal which subsequently underwent ROMP in the presence of ferrocenyl-modified norbornenes.[163] The work was quantified the next following year, determining 11 polymer strands per gold particle and that the order of the ferrocenyl monomers was inconsequential to its electrochemical properties.[164] When attaching the monomer, the choice of linker can have significant effects on the stability of the polymer. A comparison of sulfide and sulfur linkers with comparable alkyl chains capped with norbornene, showed the ROMP proceeded for both but that the sulfide-linked polymers had poor solubility and underwent desorption from the surface.[165]

Cadmium selenide is also commonly studied. This metal was coordinated through the oxygen lone pairs of functionalized phosphine oxide. The exchange of an alkyl ligand for a styrene was used to coordinate a Grubbs catalyst, and COD, oxanorbornenes, or cyclopentadiene were polymerized outward to give the metal-centered star polymer.[166] Shortly thereafter, the polymerization of carbazoyl and hydroxyl containing monomers was successful off CdSe to form nanostructures for which energy

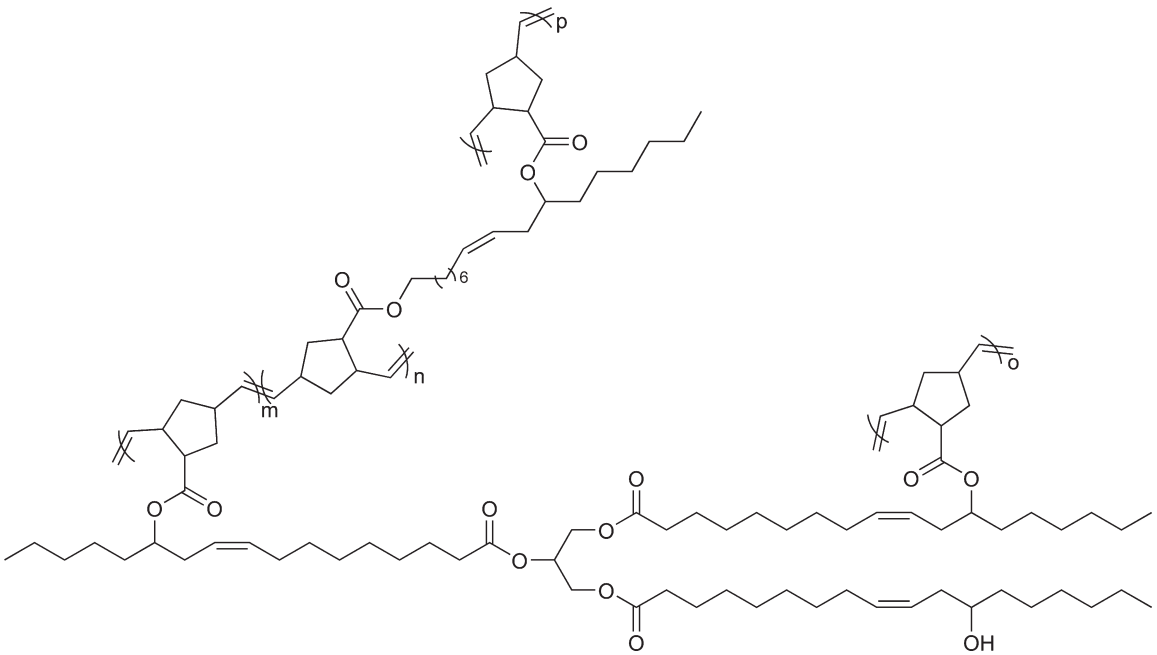

Figure 39 A biocompatible polymer derived from castor oil. Reproduced with permission from Xia, Y.; Larock, R. C. *Polymer* **2010**, *51*, 2508.[159]

transfer was observed through the blocks.[167] Cross-linking for norbornene-appended metals can also controllably occur under certain conditions. For norbornenes attached to gold nanoparticles, intramolecular cross-linking was afforded through high gold:norbornene ratios and working under dilute conditions (Figure 41). These polymers were found to afford higher thermal stabilities and resistance of the metal to etching. Removal of the metal centers induced precipitation of the organic framework as the polymer collapsed.[168]

ROMP from metals is not limited to only monophasic mixtures. A fluorescein containing two norbornenes was attached to ferritin, a 24-protein subunit, and CdSe nanoparticles in an oil–water mixture. Segregation to the toluene–water interface occurred, resulting in cross-linked, thin sheets at the interface upon ROMP.[169] While polymerization is frequently used to make metals more soluble in given solvents, the polymerization can also be used to exclude certain molecules. The ROMP of 5-(perfluoro-*n*-alkyl)norbornenes from gold shot, yielded polymer films of varied thicknesses. These exhibited enhanced hydrophobicity and oleophilicity as well as forming a barrier to aqueous ions.[170] Growing polynorbornene bearing perfluorinated *n*-butyl substituents from the surface of a platinum-coated gold electrode via a thiol alkyl linker found an increased resistance to proton transfer but improved partitioning of oxygen.[171]

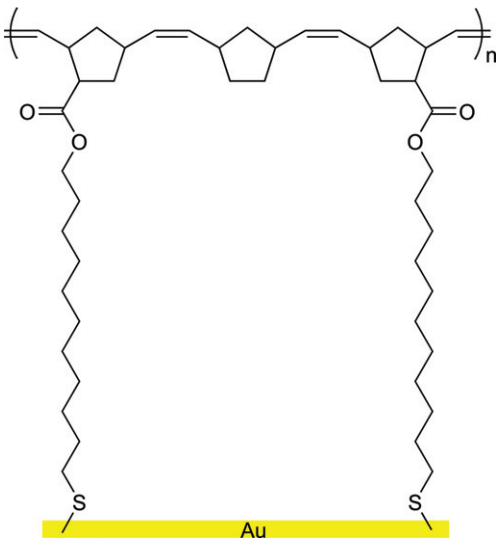

Figure 41 Resultant cross-linking from the ROMP of Au-appended norbornene derivatives and free norbornene. Reproduced with permission from Koenig, S.; Chechik, V. *Langmuir* **2006**, *22*, 5168.[168]

In another application of ROMP, several groups have formed membranes via this polymerization technique (Figure 42). An alkaline anion exchange membrane was prepared via the ROMP of an ammonium salt bearing norbornenes cross-linked with cyclopentadiene. A high resistance to swelling and a low methanol permeability coupled with high conductivities enhances the interest of these materials for use in methanol fuel cell applications, as methanol crossover resulting in catalyst death is currently a serious problem in these systems.[172] Similarly, interested in cutting down the permeability of methanol, an electrolyte membrane was prepared via a combination of ATRP and ROMP. Using norbornenylstyrene-s-styrene and *n*-propyl-*p*-styrenesulfonate monomers, the diblock was prepared by ATRP and followed by ROMP to cure the membrane through cross-linking the norbornenes. The resulting bicontinuous morphology had lower methanol crossover than Nafion, the current industrial standard for methanol fuel cells.[173]

Postpolymerization modification of polymeric structures is not limited to small molecules. A testament to the modularity of ROMP, hydroxyl-appended norbornenes were polymerized. Treatment of the polymer chain with 2-cyanoethyl tetraisopropylphosphorodiamidite provided the functionality to bind the 5′ end of DNA to the polymer. The formation of block copolymers extending off the DNA even when including ferrocenyl groups left the recognition capability of the DNA unaffected.[174] As an extension, two different ferrocenyl-bearing monomers with easily distinguished redox potentials were incorporated into a triblock and bound to DNA. Through the use of this triblock or multiple diblocks and its redox properties, single base pair changes could be detected. An additional advantage to the polymeric structure was a higher binding affinity than that associated with the oligonucleotides from which it was derived.[175]

An impressive example of the architectures accessible through ROMP, Luh and co-workers attempted the synthesis of a polymeric mimic of DNA. Viewing DNA as a double-stranded polymer twisted into a helix, the group synthesized a bisnorbornene derivative with a ferrocene at the center of the linker. This unit was employed for its ability to not only serve the role of the base pairs in holding the two strands together, but also help induce the twisting necessary for helical formation. Polymerization of this unit (Figure 43) did in fact access a helical, DNA-like morphology but also adopted supercoil and ladder secondary structures as evidenced by scanning tunneling microscopy (STM). Modeling of the system showed

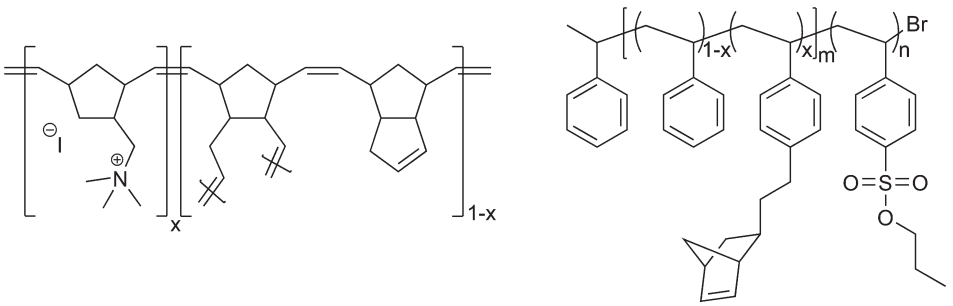

Figure 42 Polymers formed for use in membranes. Reproduced with permission from Clark, T. J.; Robertson, N. J.; Kostalik IV, H. A.; *et al. J. Am. Chem. Soc.* **2009**, *131*, 12988;[172] Chen, L.; Hallinan, D. T., Jr.; Elabd, Y. A.; Hillmyer, M. A. *Macromolecules* **2009**, *42*, 6075.[173]

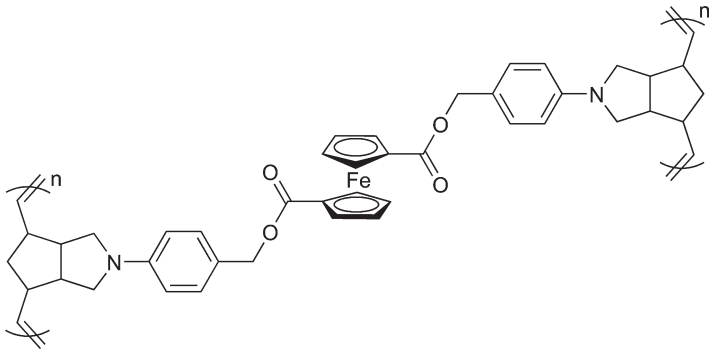

Figure 43 A double-stranded polymer prepared via ROMP capable of adapting helical, supercoil, or ladder morphologies. Reproduced with permission from Yang, H.; Lin, S.; Yang, H.; *et al. Angew. Chem. Int. Ed.* **2006**, *45*, 726.[176]

these three structures to be local minima on the energy plain with the supercoil most favored thermodynamically. As a further resemblance to DNA, hydrolysis of the double-stranded polymer produced two single-stranded polymers, mimicking the unzipping of double-stranded DNA prior to replication or transcription.[176]

Further pursuing the use of double-stranded polymers to form more complex architectures, Luh attempted the formation of a ladderphane where the polymer chain forms the outer supports and the rungs consist of aromatic compound stacked on top of each other. Beginning with a bisnorbornene monomers with aromatic linkers, ROMP formed a double-stranded polymer with aromatic or porphyrin linkers stacked orthogonal to the polymeric backbone and face to face with each other (**Figure 44**). The well-ordered STM image was used to rule against cross-linking. For aromatic linkers, decreased molar absorptivities were recorded while exciton coupling was evidenced for the porphyrin-linked polymers.[177]

All the examples given here have been confined to a size far too small for unaided visualization by the human eye. STM, AFM, or scattering techniques lead the way in determining shape and size. However, an application of ROMP worth noting here was used not for the ability of the monomer to form a given structure by itself but for its ability to maintain the shape of the matrix of which it was a part. Ferrofluids are colloidal magnetic nanoparticles and thus take the shape of any external magnetic field. In the absence of a field, it collapses back into a pool in the shape of its container. Bian and McCarthy, mixed COD with a ferrofluid. Exposure to a magnetic field followed by ROMP of the COD 'froze' the ferrofluid shape so that even upon the removal of the magnetic field, the field-induced shape was maintained. The ability to 'remember' a shape from the past holds promise that ROMP could enable the identification of a stimulus even after it is gone.[178]

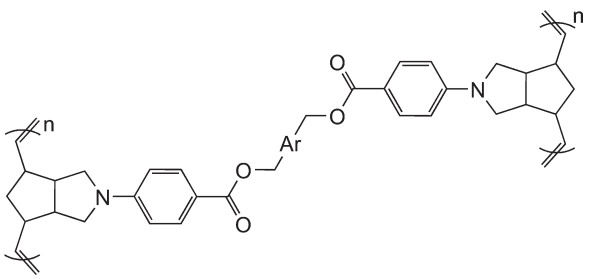

Figure 44 A polymeric ladderphane wherein the aromatic linkers (Ar) stack face-to-face. Reproduced with permission from Chou, C.-M.; Lee, S.-L.; Chen, C.-H.; *et al. J. Am. Chem. Soc.* **2009**, *131*, 12579.[177]

4.20.19 Conclusion

Though these examples are only a subset of the body of work already achieved in the field of ROMP, we hope that the scope and breadth of this transformation is appreciated. Structures from the simplest linear chain to architectures mimicking the very genetic makeup of our cells and materials capable of responding to stimuli have been achieved via ROMP. However, challenges still remain and new frontiers to be explored, which will continue to expand this method to enable access to new and useful materials.

References

1. Slugovc, C. *Macromol. Rapid Commun.* **2004**, *25*, 1283; Leitgeb, A.; Wappel, J.; Slugovc, C. *Polymer* **2010**, *51*, 2927; Vougioukalakis, G. C.; Grubbs, R. H. *Chem. Rev.* **2010**, *110*, 1746.
2. Schwab, P.; Grubbs, R. H.; Ziller, J. W. *J. Am. Chem. Soc.* **1996**, *118*, 100; Scholl, M.; Ding, S.; Lee, C. W.; Grubbs, R. H. *Org. Lett.* **1999**, *1*, 953; Kingsbury, J. S.; Harrity, P. A.; Bonitatebus, P. J., Jr.; Hoveyda, A. H. *J. Am. Chem. Soc.* **1999**, *121*, 791; Sanford, M. S.; Love, J. A.; Grubbs, R. H. *Organometallics* **2001**, *20*, 5314; Schrock, R. R.; DePue, R.; Feldman, J.; *et al. J. Am. Chem. Soc.* **1988**, *110*, 1423; Schrock, R. R.; Depue, R. T.; Feldman, C. J.; *et al. Organometallics* **1990**, *9*, 2262; Schrock, R. R.; Hoveyda, A. H. *Angew. Chem. Int. Ed.* **2003**, *42*, 4592.
3. Schleyer, P. v. R.; Williams, J. E., Jr.; Blanchard, K. R. *J. Am. Chem. Soc.* **1970**, *92*, 2377; Allinger, N. L.; Sprague, J. T. *J. Am. Chem. Soc.* **1972**, *94*, 5734.
4. Watson, K. J.; Nguyen, S. T.; Mirkin, C. A. *J. Organomet. Chem.* **2000**, *606*, 79.
5. Abd-El-Aziz, A. S.; May, L. J.; Hurd, J. A.; Okasha, R. M. *J. Polym. Sci., Part A: Polym. Chem.* **2001**, *39*, 2716.
6. Heo, R. W.; Park, J.-S.; Goodson, J. T.; *et al. Tetrahedron* **2004**, *60*, 7225.
7. Masson, G.; Lough, A. J.; Manners, I. *Macromolecules* **2008**, *41*, 539.
8. Allcock, H. R.; Laredo, W. R.; deDenus, C. R.; Taylor, J. P. *Macromolecules* **1999**, *32*, 7719.
9. Allcock, H. R.; Laredo, W. R.; Morford, R. V. *Solid State Ionics* **2001**, *139*, 27.
10. Zhao, C.; Zhang, Y.; Pan, S.; *et al. Macromolecules* **2007**, *40*, 1816.
11. Wei, X.; Carroll, P. J.; Sneddon, L. G. *Organometallics* **2004**, *23*, 163.
12. Wei, X.; Carroll, P. J.; Sneddon, L. G. *Chem. Mater.* **2006**, *18*, 1113.
13. Nomura, K.; Schrock, R. R. *Macromolecules* **1996**, *29*, 540.
14. Singh, R.; Czekelius, C.; Schrock, R. R. *Macromolecules* **2006**, *39*, 1316.
15. Song, A.; Lee, J. C.; Parker, K. A.; Sampson, N. S. *J. Am. Chem. Soc.* **2010**, *132*, 10513.

16. Thomas, R. M.; Grubbs, R. H. *Macromolecules* **2010**, *43*, 3705.
17. Katsumata, T.; Satoh, M.; Wada, J.; *et al. Macromol. Rapid Commun.* **2006**, *27*, 1206.
18. Qu, J.; Katsumata, T.; Satoh, M.; *et al. Macromolecules* **2007**, *40*, 3136.
19. Katsumata, T.; Qu, J.; Shiotsuki, M.; *et al. Macromolecules* **2008**, *41*, 1175.
20. Qu, J.; Katsumata, T.; Satoh, M.; *et al. Polymer* **2009**, *50*, 391.
21. Kamua, S. D.; Hodge, P.; Hall, A. J.; *et al. Polymer* **2007**, *48*, 6808.
22. Liaw, D.; Tsai, J.; Wu, P. *Macromolecules* **2000**, *33*, 6925.
23. Myles, A. J.; Zhang, Z.; Liu, G.; Branda, N. R. *Org. Lett.* **2000**, *2*, 2749.
24. Drouin, S. D.; Zamanian, F.; Fogg, D. E. *Organometallics* **2001**, *20*, 5495.
25. Kodemura, J.; Natsuume, T. *Polym. J.* **1995**, *27*, 1167.
26. Gangadhara, Campistron, I.; Thomas, M.; Reyx, D. *J. Polym. Sci., Part A: Polym. Chem.* **1998**, *36*, 2807.
27. Mes, T.; Smulders, M. M. J.; Palmans, A. R. A.; Meijer, E. W. *Macromolecules* **2010**, *43*, 1981.
28. Madan, R.; Anand, R. C.; Varma, I. K. *J. Polym. Sci., Part A: Polym. Chem.* **1997**, *35*, 2917.
29. Díaz, K.; Vargas, J.; del Castillo, L. F.; *et al. Macromol. Chem. Phys.* **2005**, *206*, 2316.
30. Hino, T.; Inoue, N.; Endo, T. *J. Polym. Sci., Part A: Polym. Chem.* **2006**, *44*, 395.
31. Feast, W. J.; Tsibouklis, J.; Pouwer, K. L.; Meijer, E. W. *Polymer* **1996**, *37*, 5017.
32. Burroughes, J. H.; Jones, C. A.; Friend, R. H. *Nature* **1988**, *335*, 137.
33. Korshak, Y. V.; Kanischka, G.; Höcker, H. *Makromol. Chem. Rapid Commun.* **1985**, *6*, 685.
34. Scherman, O. A.; Grubbs, R. H. *Synth. Met.* **2001**, *124*, 431.
35. Klavetter, F. L.; Grubbs, R. H. *J. Am. Chem. Soc.* **1988**, *110*, 7807.
36. Edwards, J. H.; Feast, W. J. *J. Polym.* **1980**, *21*, 595.
37. Edwards, J. H.; Feast, W. J.; Bott, D. C. *Polymer* **1984**, *25*, 395.
38. Knoll, K.; Schrock, R. R. *J. Am. Chem. Soc.* **1989**, *111*, 7989.
39. Swager, T. M.; Dougherty, D. A.; Grubbs, R. H. *J. Am. Chem. Soc.* **1988**, *110*, 2973.
40. Saunders, R. S.; Cohen, R. E.; Schrock, R. R. *Macromolecules* **1991**, *24*, 5599.
41. Gorman, C. B.; Ginsburg, E. J.; Grubbs, R. H. *J. Am. Chem. Soc.* **1993**, *115*, 1397.
42. Jozefiak, T. H.; Ginsburg, E. J.; Gorman, C. B.; *et al. J. Am. Chem. Soc.* **1993**, *115*, 4705.
43. Dounis, P.; Feast, W. J.; Widawski, G. J. *J. Mol. Catal. A: Chem.* **1997**, *115*, 51.
44. Gu, H.; Zheng, R.; Zhang, X.; Xu, B. *Adv. Mater.* **2004**, *16*, 1356.
45. Lee, W.-W.; Caster, K. C.; Kim, J.; Zauscher, S. *Small* **2006**, *2*, 848.
46. Royappa, A. T.; Saunders, R. S.; Rubner, M. F.; Cohen, R. E. *Langmuir* **1998**, *14*, 6207.
47. Karabulut, S. *Polym. J.* **2009**, *41*, 629.
48. Sundararajan, G.; Vasudevan, V.; Reddy, K. A. *J. Polym. Sci., Part A: Polym. Chem.* **1998**, *36*, 2601.
49. Cannizzo, L. F.; Grubbs, R. H. *Macromolecules* **1988**, *21*, 1961.
50. Slugovc, C.; Riegler, S.; Hayn, G.; *et al. Macromol. Rapid Commun.* **2003**, *24*, 435.
51. Schrock, R. R.; Gabert, A. J.; Singh, R.; Hock, A. S. *Organometallics* **2005**, *24*, 5058.
52. Weck, M.; Schwab, P.; Grubbs, R. H. *Macromolecules* **1996**, *29*, 1789.
53. Chan, Y. N. C.; Schrock, R. R. *Chem. Mater.* **1993**, *5*, 566.
54. Abd-El-Aziz, A. S.; Okasha, R. W.; May, L. J.; Hurd, J. *J. Polym. Sci., Part A: Polym. Chem.* **2006**, *44*, 3053.
55. Rankin, D. A.; Lowe, A. B. *Macromolecules* **2008**, *41*, 614.
56. Li, M.-H.; Keller, P.; Albuoy, P.-A. *Macromolecules* **2003**, *36*, 2284.
57. Liaw, D.-J.; Huang, C.-C.; Wu, P.-L. *Polymer* **2001**, *42*, 9371.
58. Feng, K.; Zuniga, C.; Zhang, Y.-D.; *et al. Macromolecules* **2009**, *42*, 6855.
59. Binder, W. H.; Pulamagatta, B.; Kir, O.; *et al. Macromolecules* **2009**, *42*, 9457.
60. Matson, J. B.; Virgil, S. C.; Grubbs, R. H. *J. Am. Chem. Soc.* **2009**, *131*, 3355.
61. Mahanthappa, M. K.; Bates, F. S.; Hillmyer, M. A. *Macromolecules* **2005**, *38*, 7890.
62. Pitet, L. M.; Hillmyer, M. A. *Macromolecules* **2009**, *42*, 3674.
63. Allcock, H. R.; de Denus, C. R.; Prange, R.; Laredo, W. R. *Macromolecules* **2001**, *34*, 2757.
64. Bielawski, C. W.; Morita, T.; Grubbs, R. H. *Macromolecules* **2000**, *33*, 678.
65. Gabert, A. J.; Verploegen, E.; Hammond, P. T.; Schrock, R. R. *Macromolecules* **2006**, *39*, 3993.
66. Singh, R.; Verploegen, E.; Hammond, P. T.; Schrock, R. R. *Macromolecules* **2006**, *39*, 8241.
67. Ambade, A. V.; Yang, S. K.; Weck, M. *Angew. Chem. Int. Ed.* **2009**, *48*, 2894.
68. Yang, S. K.; Ambade, A. V.; Weck, M. *J. Am. Chem. Soc.* **2010**, *132*, 1637.
69. Liaw, D.-J.; Chen, T.-P.; Huang, C.-C. *J. Polym. Sci., Part A: Polym. Chem.* **2005**, *43*, 4233.
70. Miao, Y.; Herkstroeter, W. G.; Sun, B. J.; *et al. J. Am. Chem. Soc.* **1995**, *117*, 11407.
71. Sandholzer, M.; Slugovc, C. *Macromol. Chem. Phys.* **2009**, *210*, 651.
72. Niedermair, F.; Sandholzer, M.; Kremser, G.; Slugovc, C. *Organometallics* **2009**, *28*, 2888.
73. Kratz, K.; Breitenkamp, K.; Hule, R.; *et al. Macromolecules* **2009**, *42*, 3227.
74. Yang, Y.; Swager, T. M. *Macromolecules* **2007**, *40*, 7437.
75. Choi, M.-C.; Hwang, J.-C.; Kim, C.; *et al. J. Polym. Sci., Part A: Polym. Chem.* **2010**, *48*, 1806.
76. Ahn, S.; Deshmukh, P.; Kasi, R. M. *Macromolecules* **2010**, *43*, 7330.
77. Hamilton, J. G.; Ivin, K. J.; Rooney, J. J.; Waring, L. C. *J. Chem. Soc., Chem. Commun.* **1983**, *4*, 159.
78. Samak, B. A.; Carvill, A. G.; Hamilton, J. G.; *et al. Chem. Commun.* **1997**, 2057.
79. Amir-Ebrahimi, V.; Rooney, J. J. *J. Mol. Catal. A* **2004**, *208*, 115.
80. Ilker, M. F.; Coughlin, E. B. *Macromolecules* **2002**, *35*, 54.
81. Bornand, M.; Chen, P. *Angew. Chem. Int. Ed.* **2005**, *44*, 7909; Bornand, M.; Torker, S.; Chen, P. *Organometallics* **2007**, *26*, 3585.
82. Torker, S.; Müller, A.; Chen, P. *Angew. Chem. Int. Ed.* **2010**, *49*, 3762.
83. Vehlow, K.; Wang, D.; Buchmeiser, M. R.; Blechert, S. *Angew. Chem. Int. Ed.* **2008**, *47*, 2615.
84. Nakade, H.; Ilker, M. F.; Jordan, B. J.; *et al. Chem. Commun.* **2005**, 3271.
85. Ralph, C. K.; Akotsi, O. M.; Bergens, S. H. *Organometallics* **2004**, *23*, 1484.
86. Ralph, C. K.; Bergens, S. H. *Organometallics* **2007**, *26*, 1571.
87. Song, A.; Parker, K. A.; Sampson, N. S. *J. Am. Chem. Soc.* **2009**, *131*, 3444.
88. Song, A.; Parker, K. A.; Sampson, N. S. *Org. Lett.* **2010**, *12*, 3729.
89. Sutthasupa. S.; Shiotsuki, M.; Masuda, T.; Sanda, F. *J. Am. Chem. Soc.* **2009**, *131*, 10546.
90. Bielawski, C. W.; Benitez, D.; Grubbs, R. H. *J. Am. Chem. Soc.* **2003**, *125*, 8424.
91. Boydston, A. J.; Holcombe, T. W.; Unruh, D. A.; *et al. J. Am. Chem. Soc.* **2009**, *131*, 5388.
92. Ji, S.; Hoye, T. R.; Macosko, C. W. *Polymer* **2008**, *49*, 5307.
93. Liaw, D.-J.; Huan, C.-C.; Kang, E.-T. *Polymer* **2006**, *47*, 3057.
94. Buchmeiser, M. R.; Sinner, F.; Mupa, M.; Wurst, K. *Macromolecules* **2000**, *33*, 32.
95. Murphy, J. J.; Kawasaki, T.; Fujiki, M.; Nomura, K. *Macromolecules* **2005**, *38*, 1075.
96. Murphy, J. J.; Furusho, H.; Pateon, R. M.; Nomura, K. *Chem. Eur. J.* **2007**, *13*, 8985.
97. Xia, Y.; Olsen, B. D.; Kornfield, J. A.; Grubbs, R. H. *J. Am. Chem. Soc.* **2009**, *131*, 18525.
98. Morandi, G.; Montembault, V.; Pascual, S.; *et al. Macromolecules* **2006**, *39*, 2732.
99. Khosravi, E.; Hutchings, L. R.; Kujawa-Welten, M. *Des. Monomers Polym.* **2004**, *7*, 619.
100. Breitenkamp, R. B.; Ou, Z.; Breitenkamp, K.; *et al. Macromolecules* **2007**, *40*, 7617.
101. Breitenkamp, R. B.; Emrick, T. *Biomacromolecules* **2008**, *9*, 2495.
102. Le, D.; Montembault, V.; Soutif, J.; *et al. Macromolecules* **2010**, *43*, 5611.
103. Morandi, G.; Mantovani, G.; Montembault, V.; *et al. New J. Chem.* **2007**, *31*, 1826.
104. Preishuber-Pflügl, P.; Podolan, R.; Stelzer, F. *J. Mol Catal. A: Chem.* **2000**, *160*, 53.
105. Kriegel, R. M.; Rees, W. S., Jr.; Weck, M. *Macromolecules* **2004**, *37*, 6644.
106. Runge, M. B.; Dutta, S.; Bowden, N. B. *Macromolecules* **2006**, *39*, 498.
107. Nomura, K.; Takahashi, S.; Imanishi, Y. *Macromolecules* **2001**, *34*, 4712.
108. Allen, M. J.; Wangkanont, K.; Raines, R. T.; Kiessling, L. L. *Macromolecules* **2009**, *42*, 4023.
109. Perring, M.; Mitchell, M.; Kenis, P. J. A.; Bowden, N. B. *Chem. Mater.* **2007**, *19*, 2903.
110. Liu, X.; Guo, S.; Mirkin, C. A. *Angew. Chem. Int. Ed.* **2003**, *42*, 4785.
111. Buchmeiser, M. R.; Lubbad, S.; Mayr, M.; Wurst, K. *Inorg. Chem. Acta* **2003**, *345*, 145.
112. Miller, A. F.; Richards, R. W.; Webster, J. R. P. *Macromolecules* **2000**, *33*, 7618.
113. Lu, H.; Wang, J.; Lin, Y.; Cheng, J. *J. Am. Chem. Soc.* **2009**, *131*, 13582.
114. Cheng, C.; Khoshdel, E.; Wooley, K. L. *Nano Lett.* **2006**, *6*, 1741.
115. Krouse, S. A.; Schrock, R. R.; Cohen, R. E. *Macromolecules* **1987**, *20*, 903.
116. Krouse, S. A.; Schrock, R. R. *Macromolecules* **1989**, *22*, 2569.
117. Zhang, X.-P.; Bazan, G. C. *Macromolecules* **1994**, *27*, 4627.
118. Carnes, M.; Buccella, D.; Siegrist, T.; *et al. J. Am. Chem. Soc.* **2008**, *130*, 14078.
119. Fischer, F. R.; Nuckolls, C. *Angew. Chem. Int. Ed.* **2010**, *49*, 7257.
120. Lysenko, S.; Haberlag, B.; Wu, X.; Tamm, M. *Macromol. Symp.* **2010**, *293*, 20.
121. Zhang, N.; Schricker, S. R.; Wudl, F. *Chem. Mater.* **1995**, *7*, 441.
122. Gómez, F. J.; Chen, R. J.; Wang, D.; *et al. Chem. Commun.* **2003**, 190.
123. Charvet, R.; Acharya, S.; Hill, H. P.; *et al. J. Am. Chem. Soc.* **2009**, *131*, 18030.

124. Fiset, E.; Morin, J. *Polymer* **2009**, *50*, 1369.
125. Yamamoto, T.; Fukushima, T.; Yamamoto, Y.; *et al. J. Am. Chem. Soc.* **2006**, *128*, 14337.
126. Kang, H. A.; Bronstein, H. E.; Swager, T. M. *Macromolecules* **2008**, *41*, 5540.
127. Ye, Q.; Wang, X.; Li, S.; Zhou, F. *Macromolecules* **2010**, *43*, 5554.
128. Pulamagatta, B.; Binder, W. H.; Yau, E.; *et al. Macromol. Symp.* **2010**, *293*, 58.
129. Liaw, D.; Chen, T.; Huang, C. *Macromolecules* **2005**, *38*, 3533.
130. Stubenrauch, K.; Moitzi, C.; Fritz, G.; *et al. Macromolecules* **2006**, *39*, 5865.
131. Airaud, C.; Ibarboure, E.; Gaillard, C.; Héroguez, V. *J. Polym. Sci., Part A: Polym. Chem.* **2009**, *47*, 4014.
132. Liaw, D.; Wang, K.; Chen, T.; *et al. Polymer* **2007**, *48*, 3694.
133. Zhang, L.; Song, C.; Yu, J.; *et al. J. Polym. Sci., Part A: Polym. Chem.* **2010**, *48*, 5231.
134. Sandholzer, M.; Bichler, S.; Stelzer, F.; Slugovc, C. *J. Polym. Sci., Part A: Polym. Chem.* **2008**, *46*, 2402.
135. Bertin, P. A.; Watson, K. J.; Nguyen, S. T. *Macromolecules* **2004**, *37*, 8364.
136. Bertin, P. A.; Smith, D.; Nguyen, S. T. *Chem. Commun.* **2005**, 3793.
137. Bertin, P. A.; Gibbs, J. M.; Shen, C. K.; *et al. J. Am. Chem. Soc.* **2006**, *128*, 4168.
138. Chen, B.; Metera, K.; Sleiman, H. F. *Macromolecules* **2005**, *38*, 1084.
139. Sankaran, N. B.; Rys, A. Z.; Nassif, R.; *et al. Macromolecules* **2010**, *43*, 5530.
140. Coumans, R. G. E.; Elemans, J. A. A. W.; Thordarson, P.; *et al. Angew. Chem. Int. Ed.* **2003**, *42*, 650.
141. Kang, S.; Berkshire, B. M.; Xue, Z.; *et al. J. Am. Chem. Soc.* **2008**, *130*, 15246.
142. Clark, P. G.; Guidry, E. N.; Chan, W. Y.; *et al. J. Am. Chem. Soc.* **2010**, *132*, 3405.
143. Stewart, G. M.; Fox, M. A. *Chem. Mater.* **1998**, *10*, 860.
144. Percec, V.; Holerca, M. N. *Biomacromolecules* **2000**, *1*, 6.
145. Nyström, A.; Malkoch, M.; Furó, I.; *et al. Macromolecules* **2006**, *39*, 7241.
146. Wigglesworth, T. J.; Teixeira, F., Jr.; Axthelm, F.; *et al. Org. Biomol. Chem.* **2008**, *6*, 1905.
147. Rajaram, S.; Choi, T.; Rolandi, M.; Fréchet, J. M. J. *J. Am. Chem. Soc.* **2007**, *129*, 9619.
148. Sill, K.; Emrick, T. *J. Polym. Sci., Part A: Polym. Chem.* **2005**, *43*, 5429.
149. Gatard, S.; Nlate, S.; Cloutet, E.; *et al. Angew. Chem. Int. Ed.* **2003**, *42*, 452.
150. Beerens, H.; Verpoort, F.; Verdonck, L. *J. Mol. Catal. A: Chem.* **2000**, *159*, 197.
151. Liaw, D.-J.; Huang, C.-C.; Ju, J.-Y. *J. Polym. Sci., Part A: Polym. Chem.* **2006**, *44*, 3382.
152. Ma, J.; Cheng, C.; Wooley, K. L. *Aust. J. Chem.* **2009**, *62*, 1507.
153. Nomura, K.; Watanabe, Y.; Fujita, S.; *et al. Macromoleules* **2009**, *42*, 899.
154. Matson, J. B.; Grubbs, R. H. *J. Am. Chem. Soc.* **2008**, *130*, 6731.
155. Biswas, S.; Belfield, K. D.; Das, R. K.; *et al. Chem. Mater.* **2009**, *21*, 5644.
156. Miki, K.; Oride, K.; Inoue, S.; *et al. Biomaterials* **2010**, *31*, 934.
157. Merrett, K.; Liu, W.; Mitra, D.; *et al. Biomaterials* **2009**, *30*, 5403.
158. Mathers, R. T.; Damodaran, K.; Rendos, M. G.; Lavrich, M. S. *Macromolecules* **2009**, *42*, 1512.
159. Xia, Y.; Larock, R. C. *Polymer* **2010**, *51*, 2508.
160. Griesser, T.; Höfler, T.; Temmel, S.; *et al. Chem. Mater.* **2007**, *19*, 3011.
161. Griesser, T.; Höfler, T.; Jakopic, G.; *et al. J. Chem. Mater.* **2009**, *19*, 4557.
162. Griesser, T.; Kuhlmann, J.; Wieser, M.; *et al. Macromolecules* **2009**, *42*, 725.
163. Watson, K. J.; Zhu, J.; Nguyen, S. T.; Mirkin, C. A. *J. Am. Chem. Soc.* **1999**, *121*, 462.
164. Watson, K. J.; Zhu, J.; Nguyen, S. T.; Mirkin, C. A. *Pure Appl. Chem.* **2000**, *72*, 67.
165. Li, X.; Huskens, J.; Reinhoudt, D. N. *Nanotechnology* **2003**, *14*, 1064.
166. Skaff, H.; Ilker, M. F.; Coughlin, E. B.; Emrick, T. *J. Am. Chem. Soc.* **2002**, *124*, 5729.
167. Gratt. J. A.; Cohen, R. E. *J. Appl. Polym. Sci.* **2003**, *88*, 177.
168. Koenig, S.; Chechik, V. *Langmuir* **2006**, *22*, 5168.
169. Tangirala, R.; Hu, X.; Joralemon, M.; *et al. Soft Matter* **2009**, *5*, 1048.
170. Faulkner, C. J.; Fischer, R. E.; Jennings, G. K. *Macromolecules* **2010**, *43*, 1203.
171. Berron, B. J.; Faulkner, C. J.; Fisher, R. E.; *et al. Langmuir* **2009**, *25*, 12721.
172. Clark, T. J.; Robertson, N. J.; Kostalik IV, H. A.; *et al. J. Am. Chem. Soc.* **2009**, *131*, 12888.
173. Chen, L.; Hallinan, D. T., Jr.; Elabd, Y. A.; Hillmyer, M. A. *Macromolecules* **2009**, *42*, 6075.
174. Watson, K. J.; Park, S.; Im, J.; *et al. J. Am. Chem. Soc.* **2001**, *123*, 5592.
175. Gibbs, J. M.; Park, S.; Anderson, D. R.; *et al. J. Am. Chem. Soc.* **2005**, *127*, 1170.
176. Yang, H.; Lin, S.; Yang, H.; *et al. Angew. Chem. Int. Ed.* **2006**, *45*, 726.
177. Chou, C.-M.; Lee, S.-L.; Chen, C.-H.; *et al. J. Am. Chem. Soc.* **2009**, *131*, 12579.
178. Bian, P.; McCarthy, T. J. *Langmuir* **2010**, *26*, 6145.

Biographical Sketches

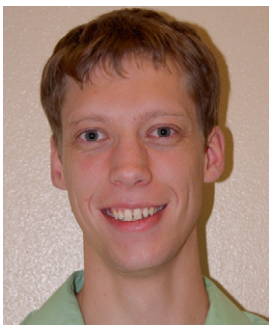

Jonathan P. Moerdyk is a PhD candidate from the University of Texas at Austin in the research group of Prof. Christopher W. Bielawski. He received his BS degree in chemistry from Hope College in 2009, where he conducted research under Prof. Jason G. Gillmore on the development of novel photochromic photooxidants for optical and materials applications. His current research interests include the tuning of nucleophilic carbene scaffolds and the development of carbene-supported transition metal-based catalysts.

Christopher W. Bielawski received a BS in chemistry from the University of Illinois at Urbana-Champaign (1996) and a PhD from the California Institute of Technology (2003) working under the mentorship of Prof. Robert H. Grubbs. After postdoctoral studies (also at Caltech), he launched his independent career at the University of Texas in Austin in 2004, where he is currently a professor of chemistry. Prof. Bielawski's research program lies at the interface of polymer science and materials chemistry, and focuses on the synthesis and study of unique organic and organometallic macromolecules, particularly those accessed via designer catalysts.

4.21 High-Molecular-Weight Poly(ethylene oxide)

I Dimitrov and CB Tsvetanov, Bulgarian Academy of Sciences, Sofia, Bulgaria

4.21.1 Introduction

Polyoxiranes (or poly(alkylene oxide)s) are well known and useful polyethers in a number of applications such as detergent and cleaner compositions, oil well drilling fluids, inks, metal working fluids, lubricants in paper-coating compositions, ceramics manufacturing, chemical intermediates for nonionic surfactants which in turn are used in cosmetics, textiles, and chemical processing, polyurethanes which are used as flexible foams and elastomers, chemical intermediates for esters which are used in textile spin finishes, cosmetic agents, and as foam control agents for a wide variety of processes, and in many other applications.

The most important representative of polyoxiranes, poly(ethylene oxide) (PEO), is a crystalline, thermoplastic polymer. It is an uncharged polyether with the chemical formula, $-(OCH_2CH_2)_n-$, which is the simplest structure of water-soluble polymers. Unlike most polymer systems, PEO is commercially available in an extraordinarily wide range of molecular weights (MWs) from 200 to several millions or more. The lower-MW members of this series, with MWs up to about 10 000, are known as poly(ethylene glycol)s (PEG). The higher members of the series are known as PEOs or poly(oxyethylene)s. At room temperature, PEO is completely soluble in water in all proportions for all degrees of polymerization. The water solubility of PEO is unlimited, at least up to temperatures slightly below 100 °C. In contrast to the complete water solubility of PEO, closely related polymers such as poly(oxymethylene), poly(trimethylene oxide), polyacetaldehyde, and poly(propylene oxide) (PPO) are water-insoluble under ordinary conditions.

High-MW PEO exhibits unique binding, thickening, lubricity, water retention, and film formation properties, as well as hydrogel products find a variety of applications, such as in body care, building materials, mining, papermaking, drug delivery, tablet binders, and polymer electrolytes.

4.21.2 Oxirane Polymerization

4.21.2.1 Investigations of an Early Date

Three-, four-, five-, or higher-membered ring systems with one cyclic ether oxygen form a series of related, reactive chemical intermediates that can polymerize to form polyethers. While all ring systems are opened by cationic or acid-initiated mechanisms, only the 1,2-epoxide oxirane (and in a few cases, oxetanes) can be polymerized by both anionic and cationic initiation. The ring of the most important representative, oxirane (ethylene oxide (EO)) has the estimated strain energy between 14 and 25 kcal mol^{-1}, which is the driving force for ring-opening polymerization to PEO. There are three principal ring-opening polymerization reactions of oxirane: acid-initiated, base-initiated, and coordination polymerizations.

The earliest reported preparation of solid poly(alkylene oxide)s was the polymerization of EO in the presence of a small amount of an alkali metal hydroxide or zinc chloride by Wurtz in 1878.[1] In 1929, Staudinger and Schweitzer studied the polymerization of EO using a number of basic or acid catalysts and separated the products obtained according to their molecular weights.[2] They prepared a high-MW PEO using oxides of calcium, strontium, or zinc as a catalyst. It is worth noting that the collaboration of Staudinger and Svedberg in characterizing the samples of PEO confirmed the macromolecular hypothesis, which established polymer science during the 1920s.

During the 1930s, poly(ethylene glycol)s were produced commercially through a base-initiated addition of EO to ethylene glycol. A number of applications of PEGs were developed

as in pharmaceuticals, cosmetics, textile lubricants and detergents, electroplating, and so on. In 1940, Flory studied the mechanism of base-initiated polymerization of oxiranes and predicted a narrow, Poisson distribution of molecular weights.[3] In the 1940s, the base-initiated polymerization of propylene oxide (PO) came into use to produce liquid polymers that are still employed nowadays as lubricants and hydraulic fluids.[4] In 1950s, the polymerization mechanism was studied to produce high-MW polyoxiranes with controlled stereoregularity of substituted alkylene oxides.[5] Calcium amides were found to be particularly effective in polymerizing EO into high-MW PEO.[6] The first report on the coordination polymerization of an epoxide, leading to a stereoregular (isotactic) polymer was about the polymerization of PO with ferric chloride/PO catalyst. The respective patent, registered by Pruitt and Baggett, appeared in 1955.[7]

4.21.2.2 Anionic Polymerization in Solution

Anionic polymerization of oxirane requires the use of nucleophilic initiators and involves mostly alkali metal compounds, which are characterized by a high nucleophilicity of the monomer-attacking agent and by low Lewis acidity of the positive counterion. Thus, nucleophilic initiation of the anionic polymerization does not require any monomer coordination to the metal, although interaction of the monomer with an electrophilic counterion is considered commonly to take place to some extent, as it will be discussed below.

Conventional sodium-, potassium-, or cesium-based initiators in an ether solvent, such as tetrahydrofuran (THF), or in polar media, such as dimethyl sulfoxide (DMSO) or hexamethylphosphortriamide (HMPTA), afford a controlled polymerization allowing the synthesis of end-functional PEO.[8] The chemical mechanism of EO polymerization is relatively simple in view of the well-known stability of alkoxide growing chains toward termination and transfer reactions. The standard method for producing low-MW PEO (PEG) is based on controlled addition of EO to water or alcohols in the presence of alkaline catalysts. The kinetics of EO polymerization, initiated by sodium methoxide in the presence of a small excess of methanol in dioxane involves a contact ion pair of the initiator. The reaction rate in the case of alkali/alkoxide initiation alone is slow, but increases with the concentration of excess alkanol.[9] Within the variation of excess alkanol concentration, the MW distribution (MWD) of the polymers produced remains narrow. Formation of an alkanol–alkoxide complex as an effective initiator is envisaged. The complex formation loosens the bonding of the tight alkoxide ion pair.

The mechanism of the anionic polymerization of EO and the physicochemical properties of the active centers in ether solvents were studied in more detail by Kazanskii *et al.*,[10–12] Sigwalt and Boileau,[13] Berlinova *et al.*,[14,15] and Tsvetanov *et al.*[16] The polymerization proceeds without termination or chain transfer through a living mechanism. We will mention the most important features of EO polymerization in solution. The oxygen atom on the charged end of the growing chain contributes to a considerable localization of the negative charge and in this way substantially increases the tightness of the ion pair. As a result, the role of the latter in the process of anionic polymerization of EO in solution becomes very significant. On the other hand, the growing ends are highly associated even in a very dilute solution. Moreover, systems based on Li derivatives are inactive under similar conditions due to the more covalent character of the lithium–alkoxide bond and the strong aggregation phenomena.[17,18] The presence of electron-rich ether oxygen atoms in the monomer and the polyether backbone makes it possible for both of them to compete with the solvent and the growing ends of other active PEO chains in the solvation of the ion-pair cation. The mobility of the formed PEO segments and the solvating properties of EO units favor self-solvation[10] and the formation of ion triplets.[14,15,19,20] The solvation ability and the activity of the growing ends are a function of the increasing number of EO units added (penultimate effect). Thus, the conductivity of short-chain living polymers $R–(CH_2CH_2O)_{n-1}–CH_2CH_2O^- M^+$ in THF is a function of chain length and tends to reach a steady-state value for n between 3 and 7.[10,14,15]

An increase in the polymerization rate in the initial reaction stages was also observed.[10] The activation energy for the EO addition to the growing end is in the 17.8 kcal mol^{-1} range. This, as well as the fact that the rate of propagation is almost insensitive to the influence of the solvent properties, is explained by the self-association 'shielding' effect of EO units, located near the growing end. An interaction between the cation and the EO monomer was also proposed.[16,21,22]

In conclusion, the characteristic features of the active centers in anionic polymerization of EO in ether solvents are: (1) tight ion pairs with extremely low dissociation constants (10^{-8}–10^{-12} mol l^{-1} in THF); (2) formation of ion triplets and higher associates; and (3) competitive interaction of the growing chains with monomer units sequences, monomer, and electron-pair donors such as crown ethers or cryptands. Thus, the complex character of the growing species is the fundamental problem in the anionic solution polymerization of EO, PO, and other oxiranes. An upper limit (up to 50 000) for the MWs has been reported.[9]

The main factors ensuring an effective polymerization process in ether solution are

- the use of alkoxide-enriched starting systems;
- primary hydroxy groups exhibit a higher reactivity in oxirane addition than the secondary ones;
- EO addition is considerably faster than that of PO (the monomer reactivity decreases with the increase in the substituent bulkiness);
- high-temperature and high-pressure polymerization; and
- the use of potassium- or cesium-based alkoxides, since they are less associated.

4.21.2.3 Role of Additives: Anionic Polymerization of Substituted Oxirane in Solution and Polymerization of PO

Improvements in a PO polymerization process and the ways of maintaining its living character have been the objects of significant research efforts ever since PPO found important applications, both as functional oligomers and as a high-MW elastomer. The anionic PO polymerization suffers from several important drawbacks due to the high basicity of propagating species generated by alkali metal alkoxide or hydroxide initiators. Thus, proton abstraction from the PO methyl group takes place leading to a chain-transfer reaction to monomer.[23] This side process results in the exclusive formation of PPO

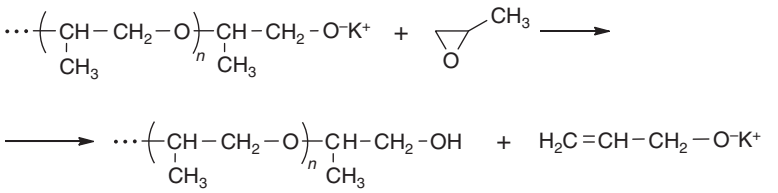

Figure 1 Proton abstraction reaction in anionic polymerization of PO.

oligomers, a large fraction of which possess a terminal allyl unsaturation. This chain-transfer reaction would be expected to terminate the polymer chain growth and to generate a new allyl alkoxide anion, which could initiate polymerization of PO (Figure 1).

The tendency of PO to isomerize to allyl alcohol decreases in the following order of alkali metal counterions:

$$Li^+ > Na^+ > K^+ > Rb^+ > Cs^+$$

Consequently, the above side reactions may be overcome to a great extent by using cesium-initiating systems.[24]

Becker and Wagner have found that the addition of crown ethers leads to an essential acceleration of the polymerization rate when potassium is used as counterion. However, there is an insignificant influence on the rate of chain-transfer reaction.[25] Although it has been stated that the average MW is limited to ~6000 at temperatures around 90 °C because of the high rate of chain-transfer ($k_p/k_{tr} \leq 100$)[26] studies by Price and coworkers have shown that number-average MWs as high as 13 000 can be obtained at 40 °C in neat PO in the presence of 18-crown-6 ether.[27]

Esswein and Möller showed that the addition of a strong Lewis base, for example, the phosphazene base *t*Bu-P$_4$, can strongly complex the Li^+ counterion and enable EO polymerization in THF.[28,29] The base *t*Bu-P$_4$ fulfills an important criterion of a cryptand: the polar amino groups are located inside the globular molecule, and the outer shell is formed by the alkyl substituents. The void volume inside the molecule is sufficient to host the rather compact Li^+ ion. The phosphazene base forms a [Li-*t*BuP$_4$]$^+$ complex that suppresses ion pair association of lithium alkoxides (Figure 2). The activation of lithium alkoxides by *t*Bu-P$_4$ for the polymerization of EO is rather remarkable in view of the negative results with the [2.1.1] cryptand. This approach has already been successfully applied to the synthesis of block copolymers.[30,31]

Deffieux *et al.* reported a very active initiating system for anionic PO polymerization based on the association of an alkali metal alkoxide or ammonium salt initiator with triisobutylaluminum as a catalyst.[32] The experimental PPO MWs

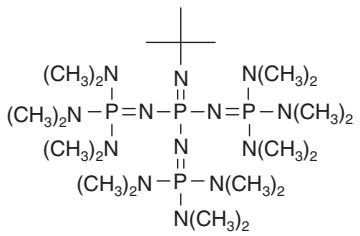

Figure 2 Structure of phosphazene base *t*Bu-P$_4$.

were close to theoretical values and the MWDs were narrow (1.1–1.3) suggesting a controlled PO polymerization without any significant contribution of the monomer chain-transfer reaction. Tsvetanov *et al.* originally studied the mechanism of oxirane polymerization initiated by 'ate' complexes.[16] The polymerization of EO initiated by NaAlBu$_4$ was shown to proceed upon initial complex formation of monomer and initiator. Polycentric polymerization mechanism was proposed. The very significant finding of Defieux *et al.* was the activating effect of the 'free' trialkylaluminum derivative.[32] When additional trialkylaluminum is added, a drastic enhancement of the reactivity and selectivity toward monomer insertion of the propagating species is observed, allowing a fast living-type ring-opening polymerization to proceed at 0 °C in nonpolar solvent. This is explained by the necessary formation of a second complex between the aluminum derivative in excess and the monomer (Figure 3). The latter is strongly activated toward nucleophiles and polymerizes rapidly. Thus, controlled polymerization proceeds only when the molar ratio $r = [i\text{-Bu}_3\text{Al}]/[i\text{-PrONa}]$ is higher than 1. At $r > 1$, the higher the fraction of trialkylaluminum, the faster is the polymerization. Moreover, at 0 °C, in the whole MW range examined, the experimental PPO MWs are close to the calculated theoretical values assuming the formation of one polymer chain per *i*-PrONa molecule.[33–36]

MWDs are narrow although a slight broadening can be noticed for PPO of MWs higher than 10 000. This suggests a living-like character for the PO polymerization or at least a significant decrease in the contribution of the monomer chain-transfer process, which is observed with alkali-metal-based initiators. These results are consistent with the strong activation of the polymerization by R$_3$Al present in excess with respect to *i*-PrONa and with a reaction mechanism in which the monomer is activated by an electrophilic aluminum compound prior to its insertion into the sodium poly[(1-methylethylene)]triisobutylaluminate growing chain end (see Figure 3). The strong reduction of the chain transfer to monomer can be assigned to the much larger electron-withdrawing effect of R$_3$Al complexation on the methylene and methine PO α-carbons (the two potential active sites in the ring-opening process) than on the β-methyl hydrogens involved in the chain-transfer reaction to monomer. Reduction of the basicity of alkali metal alkoxide species in aluminate complexes may also contribute to the reduction of the proton abstraction reaction yielding chain transfer to monomer.

4.21.2.4 Synthesis of Polyglycidol

Glycidol is a highly reactive monomer bearing both epoxy and hydroxy groups. Its composition and structure favor the primary

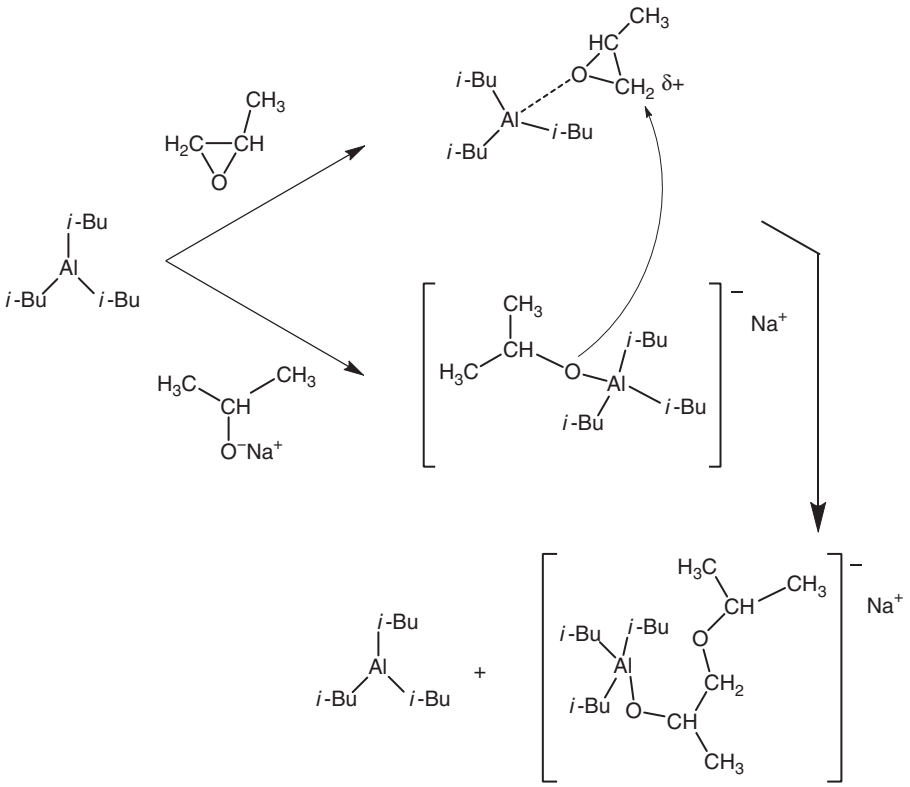

Figure 3 Polymerization mechanism involving monomer activation prior to insertion into the growing "ate" complex. Reprinted from Carlotti, S.; Billouard, C.; Gautriaud, E.; *et al. Macromol. Symp.* **2005**, *226*, 61.[34] with permission of John Wiley & Sons Ltd., UK.

to secondary transitions of the alkoxide active sites, as well as the intermolecular transfers during base-initiated polymerization.[37] The propagation may evoke side reactions. Generally, both the anionic and cationic polymerizations of glycidol lead to hyperbranched oligomers with numerous hydroxy end-groups. Hyperbranched polyglycidols combine several remarkable features, including a highly flexible aliphatic polyether backbone, multiple hydrophilic groups, and excellent biocompatibility. Within the past decade, intense efforts have been directed at the optimization of synthetic procedures affording glycidol homo- and copolymers with different MW characteristics and topology.[38] In 1990, Sunder *et al.* described the multibranching anionic polymerization of glycidol, carried out under slow monomer addition conditions (Figure 4).[37]

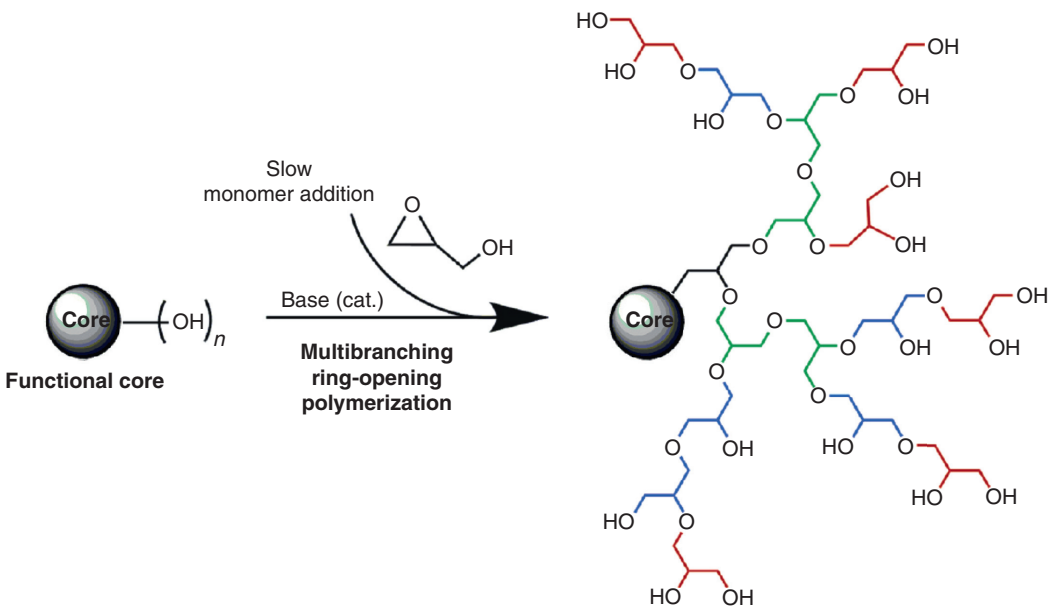

Figure 4 Synthesis of hyperbranched polyglycidol by anionic multibranching ring-opening polymerization. Reprinted from Wilms, D.; Stiriba, S.-E.; Frey, H. *Acc. Chem. Res.* **2010**, *43*, 129.[38] with permission of the American Chemical Society, USA.

Thus, they were able to avoid the broad MWD of the random AB_m-type polycondensation. Chiral hyperbranched polyether polyols have been prepared in a similar manner using enantiomerically pure glycidol monomer.[39] Furthermore, Huck *et al.* demonstrated the versatility of the same synthetic protocol through a surface-initiated polymerization of glycidol on Si/SiO_2 surfaces.[40] In 2006, Brooks *et al.* reported the synthesis of hyperbranched polyglycidol of very low polydispersity using dioxane as an emulsifying low-polar agent.[41] MWs up to 700 000 were reported.

Despite these important advances, the controlled preparation of branched polyglycidols with MWs exceeding 6000 has remained a challenge until very recently. A facile two-step approach via low-MW polyglycidol macroinitiators was developed by Frey *et al.*[42] The polyfunctionality of the macroinitiators affords higher concentrations of alkoxide active sites even at elevated degrees of polymerization. Thus, hyperbranched polyglycidols of MWs up to 24 000 were obtained under slow monomer addition conditions.

A different approach complementing the scope of accessible MWs for branched polyglycidol structures has been developed by Dworak *et al.*[43] It is based on the repeated polymerization and deprotection of a protected glycidol monomer yielding three generations of comb-burst polyglycidols with MWs of 82 000, 740 000, and 1 800 000, respectively.

Motivated by the preparation of well-defined hyperbranched polyglycidols, a variety of polyglycidol-based complex polymer architectures were synthesized. These include linear-dendritic block copolymers,[44–47] random copolymers,[48] and multiarm star copolymers.[49–52]

Recently, linear polyglycidol and its copolymers have drawn much attention due to their biocompatibility, high hydroxy functionality, and potential biomedical applications.[53–55] Furthermore, the hydroxy groups of polyglycidol are ideal precursors for the insertion of different other functionalities, leading, for example, to thermoresponsive polymers.[56,57] Moreover, glycidol can constitute a significant economical issue as far as it is readily obtained from glycerol, a byproduct of the synthesis of biodiesel.[58]

The synthesis of linear polyglycidols requires a protection of the monomer hydroxy function prior to the polymerization. The most generally used protection method, first reported by Spassky is the preparation of 1-ethoxyethyl glycidyl ether (EEGE) by the reaction of glycidol with ethyl vinyl ether.[59] The efficiency and ease of the monomer protection step and its subsequent deprotection by acid treatment make EEGE a good candidate as monomer for the synthesis of linear polyglycidols. Recently, other glycidol protecting groups have been reported, including the *tert*-butyl group.[60] The advantage of *tert*-butyl glycidyl ether (*t*BuGE) comes from the fact that it is commercially available, in contrast to EEGE.

Many polymerization studies of EEGE have been conducted using both anionic and coordination polymerizations.[31,60–65] Coordination polymerization using diethylzinc/water or calcium amide/alkoxide allows the synthesis of high-MW poly (2-ethoxyethyl glycidyl ether) (PEEGE), but with broad MWDs. Anionic processes involving the use of alkali metal salts and/or phosphazene base initiators enable the synthesis of PEEGE with MWs limited to 30 000 due to chain transfer to monomer, as confirmed recently.[65] Keul and Möller studied the polymerization of EEGE with regard to the occurrence of chain transfer to the monomer (**Figure 5**).

Despite this drawback, a series of block and random copolymers based on glycidol, EO,[64,66–69] and PO[70] have been synthesized to combine the hydrophilic behavior of PEO and the high functionality of polyglycidol. However, the polyglycidol block remained limited to low polymerization degrees. The synthesis of high-MW homo- and copolymers of glycidol with narrow MWD is of great interest. Recently, the preparation of polyglycidol combining high MW and a narrow MWD was successfully achieved by the anionic polymerization of protected glycidols (2-EEGE and *t*BuGE) in the presence of a binary initiating system consisting of tetraoctylammonium bromide $(Oct_4N^+)Br^-$ and an excess of triisobutylaluminum $(i\text{-}Bu)_3Al$.[71] This method allows the controlled syntheses of PEEGE and P*t*BuGE of high MWs, up to 85 000 in short reaction time, at 0 °C. The proposed formation of a 1:1 initiating or propagating complex of weak basicity suppresses chain-transfer reactions to monomer. Fast polymerizations at low temperatures indicate a high nucleophilicity of the system due to the monomer activation. An excess of Lewis acid is required to trigger the reaction and to obtain quantitative yields. After a clean and quantitative acid deprotection, polyglycidol as well as a variety of glycidol-based copolymers with controlled MWs can be obtained, offering new opportunities of applications, in particular in the field of biomaterials.

Glycidol was also used as a branching reagent in EO polymerization.[72] Initially, a linear triblock copolymer of EO and short flanking blocks of protected glycidol (1-EEGE) was synthesized. After deprotection, the short polyglycidol blocks were used as branching units for the next generation. The repeated step-by-step process leads to the 'pom–pom-like' branched poly(oxyethylene) macromolecules of MWs up to 2×10^5 and narrow MWD, enriched in hydroxy groups in the outer shell.

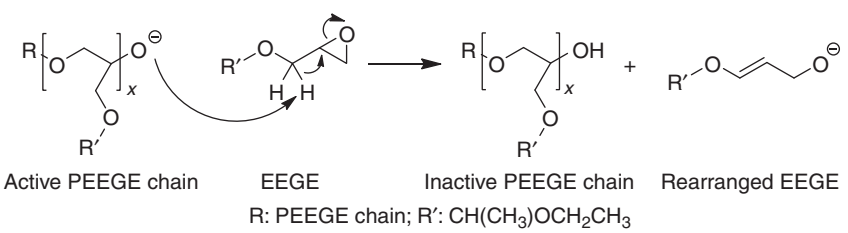

Figure 5 Mechanism of the chain transfer to the monomer in anionic polymerization of EEGE. Reprinted from Hans, M.; Keul, H.; Moeller, M. *Polymer* **2009**, *50*, 1103.[65] with permission of Elsevier Ltd., UK.

4.21.3 Anionic Coordination Polymerization

Most of the reported coordination catalysts are formed in binary or ternary systems consisting of an alkylmetal compound and a protic compound. Catalysts formed in such systems contain associated multinuclear species with the metal (Mt)–heteroatom (X) active bond (Mt–X → Mt, where Mt = Al, Zn, and Cd and X = O, S, and N) or nonassociated mononuclear species with the Mt–X active bond (Mt = Al and Zn, X = Cl, O, and S).

The anionic coordination polymerization of oxirane for the preparation of high-MW polyoxirane (or polyoxirane resins) has been studied for many years, and a large number of anionic initiators have been investigated to improve both the polymerization control and kinetics. Hill *et al.*,[6] Miller and Price,[73] Vandenberg,[74] Furukawa *et al.*,[75] Osgan and Teyssie,[76] Hsieh,[77] and Zhang and Shen[78] used alkaline earth carbonate, aluminum isopropoxide–zinc chloride, alkyl aluminum–water–acetylacetonate, diethyl zinc–aluminum oxide, bimetallic oxido–alkoxide catalyst $[(RO)_2Al\text{-}O\text{-}Zn\text{-}Al(OR)_2]$, trialkylaluminum–water–zinc acetylacetonate, trialkylaluminum–water, and rare earth metal acetylacetonate as catalysts to obtain high-MW PEO. Xie *et al.* found an active quaternary catalyst (trialkylaluminum–phosphoric acid–water–tertiary amine) for the polymerization of epichlorohydrin.[79] However, there are some serious problems regarding the catalyst's stability, required amounts, conversion, and so on.

The coordination has two effects: activation of the monomer for polymerization and providing an orientation of the reacting molecules leading to stereospecific polymerization as in the case of cyclic ethers other than EO. The most effective initiators are derivatives of divalent and trivalent metals. All the metals possess Lewis acidity. For industrial purposes, calcium- and zinc/aluminum-based catalysts are the most widespread.

It is worth noting that polymerizations and copolymerizations of heterocyclic monomers in the presence of coordination catalysts constitute a distinct group of coordination polymerization processes. Considering the polymerization mechanism, they differ essentially from coordination polymerization of unsaturated hydrocarbon monomers: the differences involve the mode of monomer coordination and enchainment in the coordinating monomer. With the exception of Ca-based catalysts, oxirane polymerizations involve monomer coordination at the catalyst active sites via σ-bond formation between the monomer heteroatom and the catalyst metal atom, followed by nucleophilic attack of the initiating group or polymer-chain active site on the coordinating monomer in the initiation or propagation step, respectively.

Calcium initiators are much weaker than the aluminum or zinc systems in forming oxirane complexes. As a result, they are particularly effective in polymerizing EO, which forms complexes more readily in comparison with the substituted oxiranes. Calcium initiators form weaker complexes with the substituted oxiranes, PO in particular, and initiate a low-rate polymerization.

4.21.3.1 Calcium-Based Catalyst Systems: Polymerization in Suspensions and Synthesis of High-MW PEO

Alkaline earth amides and amide-alkoxides are the most active catalysts for EO polymerization which have found application in the commercial production of high-MW PEO. They are active in the 0–50 °C temperature range, which is remarkable considering that alkaline earth carbonates and oxides require much higher temperatures, usually above 70 °C. The fact that calcium amide catalysts are very active at temperatures below the melting point of PEO has a considerable industrial significance. It would be technologically impractical to perform the polymerization in bulk or in solution due to the high viscosity and heat-transfer problems, as well as the rapid degradation of PEO in shear fields. The synthesis of PEO resins in the form of free-flowing white powders can be most effectively realized in a precipitant medium where the polymer is directly produced in the form of fine particles. The polymerization is a precipitation (dispersion) polymerization since the reaction medium (hydrocarbons) dissolves only the monomer. While PEO is insoluble in hydrocarbons, PPO, poly(1,2-epoxybutane) (PBO), and PEEGE form highly swollen gels.[74,75,80] Therefore hydrocarbons are considered as organic reaction diluents. Below the melting point, the polymer produced remains in granular form. The temperature is easily controlled by the rate of monomer feed. The main requirement for a successful dispersion polymerization is the presence of a nonionic surfactant or amphiphilic block copolymer to stabilize the polymer particles by forming a dissolved protective layer around them. The most efficient type of dispersant is based on a block or graft copolymer, which consists of two essential polymer components – one soluble in the liquid medium interspersed by short segments, usually called 'anchors' which are strongly adsorbed at the particle surface.

Some of the calcium-based catalysts are very active. Thus, the granular PEO contains only a small amount of catalysts as impurity and no special purification of the polymer is required. The granular polymer can therefore be recovered by filtration and used without further processing. The details of the techniques used to manufacture PEO resins have not been disclosed yet.

Various calcium-based catalysts have been discovered. Systematic studies on catalyst activity and polymerization mechanism are scanty. The synthesis of an effective catalyst is the manufacturer know-how. Most of the catalyst systems are published in patent literature. Given the large discrepancy observed in such polymerizations between the number of metal atoms contained in the catalyst charged to the reactor and the number-average MW of the polymer produced, one may conclude that only a small fraction of the metal centers present in the system are actually involved in the initiation and propagation of the polymerization. That makes the elucidation of the structure of catalyst active site extremely difficult. There are only three publications describing the synthesis of Ca catalysts in more detail.[8,81,82] Usually, the catalyst systems are poorly defined heterogeneous aggregates. In many cases, the catalyst is formed on silica carriers or even on modified hydrophobic silica carriers. The efficiency of these initiators is rather low: in most cases, only from 10^{-2} to 10^{-3} of the introduced initiator is consumed. The activity of the catalyst can be enhanced by the use of a scavenging agent with no activity in the polymerization process, which removes traces of oxygen and moisture from the polymerization mixture. Useful scavengers are R_3Al, $LiAlH_4$, *n*-BuLi, $ZnEt_2$, and so on. The mode of polymerization greatly differs from the olefin precipitation polymerization where extremely high catalyst efficiencies are achieved. Goeke and Karol from Union Carbide Corporation reported modified Ca catalysts that are exceptionally effective for EO polymerization yielding 1800 g of polymer per g Ca.[83] The main characteristics of EO suspension polymerization in the presence of different Ca catalysts systems are presented in Table 1.[8]

Table 1 Calcium catalytic systems for suspension polymerization of EO

Catalyst	*Solvent*	T *(°C)*	*Time (h)*	*Productivity (g PEO/g Ca)*	M_v *(× 10^{-6})*	*Reference*
$Ca(NH_2)_2$	Hydrocarbons	30	12	40	8	81
Calcium amide-alkoxide	Hydrocarbons	17	10	70	3	81
Calcium amide-alkoxide (modified)	Heptane	40	8	170	4.5	84
Ph_2Ca	Heptane	10	9.5	270	6	82
Union carbide Calcium amide catalyst	Heptane	31	4	1800	4	83

Reprinted from Tsvetanov, Ch.; Dimitrov, I.; Doytcheva, M.; *et al.* In *Applications of Anionic Polymerization Research*; Quirk, R., Ed.; ACS Symposium Series 696; American Chemical Society: Washington, DC, 1997; p 236.[8] with permission of the American Chemical Society, USA.

According to Kazanskii *et al.*,[82] the rate of EO polymerization initiated by Ph_2Ca in hydrocarbon media is a linear function of the monomer and catalyst concentrations:

$$R = k_{\text{eff}}[\text{Cat}]_0[\text{M}]_0$$

This means that the process is kinetically controlled and the growing centers are not blocked by the formation of partially crystalline polymer. A very important finding is that the effective activation energy is 7–8 kcal mol^{-1}, which is much lower than the typical values 18–20 kcal mol^{-1} for epoxide polymerization processes. The low activation energy is apparently the main factor responsible for the efficiency of the Ca amide-modified catalysts.

The rate constant in suspension polymerization is higher than the propagation rate constant for the free ions k_p. Kazanskii *et al.* gave a reasonable explanation for this unique difference in the activity.[82] According to them, the acceleration in suspension polymerization is due to both the effective coordination of EO to the active centers and the localization of the growing centers on the catalyst surface in contrast to the highly associated active centers in solution polymerization. The propagation rate constants for EO polymerization in solution and in suspension are presented in Table 2.

The MW of the polymer increases constantly during the first stage of the process (Table 3).[8] The polymers possess broad MWD in the 2–8 range. It narrows, along with the monomer consumption indicating a nonsimultaneous appearance of active centers as well as difference in their activity, obviously due to the different active sites on the catalyst surface.

The physicochemical mechanism of the polymer growth on catalyst particles is far from clear.[8,87,88] As already mentioned, the anionic dispersion polymerization of EO produces a polymer insoluble in polymer diluents. As a result, the catalyst particles transform into polymer particles rapidly, within a few minutes after the start of the reaction. The size of the initial catalyst particles is in the 1–50 μm range. Their shape is not well defined. The relatively broad particle size distribution is due to the formation of agglomerates. Therefore, during the polymerization process, some manufacturers successfully apply ultrasound technique or surface-active compounds as additives to destroy the aggregates and to enhance the catalyst productivity.

In contrast to similar radical processes, where the active species are distributed in the bulk polymer phase, the active centers in the case of EO suspension polymerization are located in the core of the PEO particle. They are localized on the surface

Table 2 Propagation rate constants of anionic and anionic coordination polymerizations of EO

Solvent diluent	T *(°C)*	$K_p^{\pm}$(l mol^{-1} s^{-1}) K^+	Cs^+	$k_{p,\,app}$ Ca^{++}	K_p^-	*References*
THF [2,2,2]	20	0.025			1.67	13b, 85
THF	20	0.05	0.12			13b, 85
HMPA	40		0.2		22.0	86
Heptane	10			2.8		82
Heptane	40			77 ± 10		8

Reprinted from Tsvetanov, Ch.; Dimitrov, I.; Doytcheva, M.; *et al.* In *Applications of Anionic Polymerization Research*; Quirk, R., Ed.; ACS Symposium Series 696; American Chemical Society: Washington, DC, 1997; p 236.[8] with permission of the American Chemical Society, USA

Table 3 PEO characteristics during the suspension polymerization

Time (h)	*Productivity (g PEO/g Ca)*	M_n *(× 10^{-6})*	M_w/M_n	*Crystallinity index*
0.25	5.0	0.2	8.3	0.39
0.5	11.5	0.84	6.0	0.56
1.0	20	1.57	4.2	0.62
2.0	39	1.80	4.0	0.64

of the catalyst core, placed under the polymer layer formed. As a result, the monomer contact with the growing chain takes place on the surface of catalyst encapsulated by the already formed PEO layer. Since the polymerization process is highly exothermal, a surface of enhanced temperature (hot zone) is created around the particle. In the hot zone, the polymer chain cannot start to crystallize immediately. Krusteva *et al.* assumed that the initial crystallization takes place at a distance of 30 μm from the catalyst surface. These authors present a model for the formation of the nascent PEO structure at different polymerization stages.[88]

The monomer diffusion is one of the most serious technological problems. The diffusion rate decreases with the accumulation of polymer, which limits the accessibility to the growing sites. The diffusion limitation inside the microparticles is mostly related to the density of the particle and the size of penetrating molecules. Thus, the morphology of the growing polymer particles becomes an important factor, particularly in view of the marked crystallization tendency of PEO. Microscopic examination of the texture and size of PEO grains show that they are macroporous aggregates of smaller particles.[8] The formation of void space between agglomerates creates penetrating channels, thus feeding the growing centers with monomer. The relatively small EO molecules rapidly diffuse into the pores and pass through the smallest aggregate particles. The polymerization rate remains constant for a long period of the reaction time, thus becoming independent of the particle size and particle number.

At the initial polymerization stages, the polymer is characterized by a substantially low crystallinity index (see **Table 3**), most probably due to the presence of a big portion of catalyst residue that hinders the crystallization process. According to Dubrovski and Kazanski, the degree of crystallinity of the polymer formed on the catalyst surface can also influence the activity of the growing species.[87] The authors suggested that a mechanical chain termination is likely to take place, due to diffusion blocking of the active centers located within the large crystallites. The crystallinity of the nascent PEO particles increases with the increase in polymer yield and particle size.

With the increase in the particle size, it is very difficult to control the reaction temperature within the active centers area. The process has to be carried out at temperatures considerably below the melting point of the polymer, for example, below 62 °C. At higher temperatures, the structure of the particle changes from porous to dense, leading to a constant decrease in the polymerization rate. For this purpose, hydrocarbon solvents with very low boiling points (such as isopentane) are preferable. Usually, EO is added at a rate consistent with the temperature limitation of the equipment.

Because of the difficult control over the polymer MW, current industrial processes for the production of PEO with MWs between 100 000 and 2 000 000 employ high-energy radiation to initiate radical chain scission in the polymer after it has left the reactor. This process is complex and costly, and may cause instability of the polymer leading to a continuous decrease in MW over time even in the presence of stabilizers.

4.21.3.2 Ca-Based Initiators in Copolymerization

In the last decade, a large number of high-MW amphiphilic ether copolymers have been prepared by suspension anionic polymerization using a calcium amide-alkoxide initiating system. The materials produced by such polymerization using that initiating system are typically not well defined: they are characterized by a broad MWD in accordance with the results presented in **Table 3** and composition heterogeneity. Those features, together with the ubiquitous clustering in solution, often complicate the investigations of high-MW-PEO-based materials and hamper the efforts to fully understand their behavior.

A high-MW poly(propylene oxide-*block*-ethylene oxide) diblock copolymer was prepared in heptane via sequential suspension anionic polymerization using a calcium amide-alkoxide initiating system.[89] In line with the extremely large MW of the copolymer, its aqueous solution properties are characterized by the existence of aggregates with the aggregation number in the range 2–3 at very low concentrations. Additionally, the aggregates exhibit an enhanced kinetic stability toward dilution below the critical aggregation concentration (CAC) and their disintegration took weeks. Light-scattering measurements of commercial PEO samples showed that the coils of very high-MW PEO undergo microgel formation and collapse into more compact structures most likely stabilized by intramolecular hydrogen bonding mediated through water molecules.[90]

Due to the much higher reactivity of EO compared to that of the other alkylene oxides, it is difficult to control the regular incorporation of the comonomer units into the PEO chain.[91] The reactivity of the monomers used decreases with the increase in their bulkiness, that is, EO is more reactive than PO. In order to increase the amount of incorporated PO, a new synthetic method for the preparation of high-MW EO–PO copolymers with block-like gradient structure was developed.[92,93] The strategy is based on repeating short-time feeds of EO to the reaction mixture in regular time intervals (feeding cycles) during the polymerization. The rate of monomer incorporation into the growing chains depends on both the monomer reactivity and the monomer concentration. Therefore, at the beginning of each cycle, when the system is saturated with EO, the significant difference in the reactivity of EO and PO will result in preferred incorporation of EO into the chain. The copolymer sequence will be enriched in EO units. At the end of each cycle, EO should be entirely consumed and the respective sequence should be enriched in PO units (**Figure 6**).

Using a Calcium-amide initiating system, novel high-MW PEO-*block*-poly(alkyl glycidyl ether) diblock copolymers with enhanced association properties in aqueous media were prepared.[94] The copolymers were synthesized via sequential suspension polymerization of epoxide monomers. The hydrophobic block was formed by the polymerization of monomers with a general structure shown in **Figure 7**, followed by EO polymerization. The homopolymerization of hydrophobically modified glycidyl ethers proceeded only at elevated temperatures.

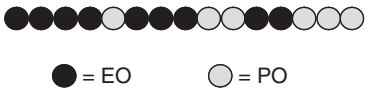

Figure 6 Schematic representation of the block-like gradient poly (ethylene oxide-*co*-propylene oxide) copolymers. Reprinted from Petrov, P.; Berlinova, I.; Tsvetanov, C.; *et al. Macromol. Mater. Eng.* **2008**, *293*, 598.[92] with permission of John Wiley & Sons Ltd., UK.

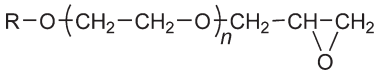

Figure 7 Structure of the Brij-type alkyl glycidyl ethers. Reprinted from Petrov, P.; Rangelov, S.; Novakov, C.; *et al. Polymer* **2002**, *43*, 6641.[94] with permission of Elsevier Ltd., UK.

Brij-type alkyl glycidyl ethers can be polymerized in heptane at the reflux with almost quantitative conversion, while at 40 °C the conversion is negligible. The results suggested a two-stage process when the hydrophobic glycidyl ether was polymerized at the reflux and then EO was copolymerized at 40 °C, the second block being practically pure PEO. It has been reported that a small difference in the oxyethylene chain length in $R(EO)_nOH$ strongly affects the formation of micelles in aqueous solution.[94] Therefore, copolymers with EO spacers of different length between the polymer backbone and the hydrophobic chains were obtained using monomers as n–$C_{18}H_{37}(EO)_2$–glycidyl ether and n–$C_{18}H_{37}(EO)_{10}$–glycidyl ether (Figure 7) for the hybrophobic block formation.

The synthesis of high-MW copolymers of EO and other oxiranes bearing polar functional groups is a very complicated problem. The latter undergo various side reactions involving either cationic or anionic polymerization making the propagation process complex and difficult to control.[95–98] On the other hand, the incorporation of various functional groups into a common high-MW PEO could yield interesting novel materials. They will exhibit most of the characteristic properties of PEO, and in addition, they could be designed through a selective chemical modification to meet the specific requirements of controlled drug delivery systems, nanoparticle formation, and rheology modifiers.

Dimitrov *et al.* reported the synthesis of novel high-MW copolymers of EO with glycidol as a second monomer via a suspension anionic mechanism using a calcium amide-alkoxide initiating system.[80] Thus, PEO-bearing hydroxy groups were obtained by a one-pot procedure that can be easily adopted for industrial purposes. It was possible to synthesize well-defined EO/1-EEGE copolymers under mild conditions, with significantly reduced side reactions (Figure 8).

A simple modification of the hydroxy groups on EO/glycidol copolymers by stearoyl moieties brought a significant change in the rheological properties of the aqueous polymer solutions. Hydrophobically modified PEO underwent self-aggregation at a CAC of 1.3 g l^{-1}. The hydroxy groups in the copolymer have been utilized for grafting *N*-isopropylacrylamide (NIPAAm) using ceric ion (Ce^{4+}) redox initiation (Figure 9).[99] As a result, the 'smart' thermoresponsive properties of poly(*N*-isopropylacrylamide) (PNIPAM) grafts were imprinted into a common high-MW PEO.

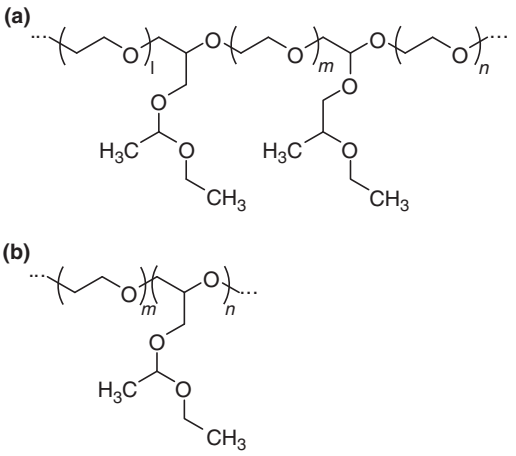

Figure 8 EO/EEGE copolymers: (a) poly(ethylene oxide-*co*-1-ethoxyethyl glycidyl ether); (b) poly(ethylene oxide-*block*-1-ethoxyethyl glycidyl ether). Reprinted from Dimitrov, Ph.; Hasan, E.; Rangelov, S.; *et al. Polymer* **2002**, *43*, 7171.[80] with permission of Elsevier Ltd., UK.

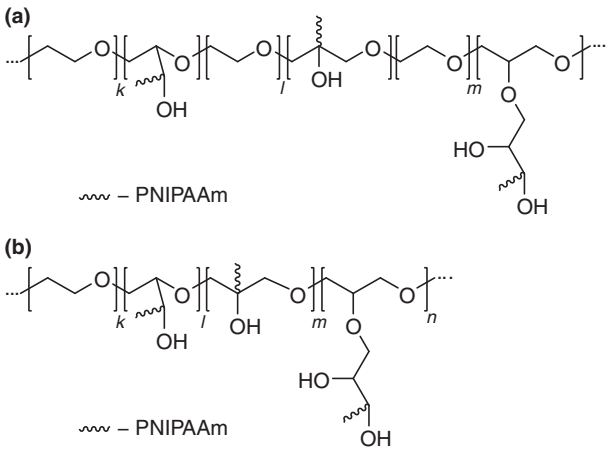

Figure 9 Water-soluble copolymers composed of: (a) poly(EO-*co*-glycidol) or (b) poly(EO-*block*-glycidol) backbone and PNIPAM grafts. Reprinted from Hasan, E.; Jankova, K.; Samichkov, V.; *et al. Macromol. Symp.* **2002**, *177*, 125.[99] with permission of John Wiley & Sons Ltd., UK.

4.21.3.3 Aluminum-Based Catalysts

The main representatives of multinuclear catalysts for oxirane polymerization are Al and Zn compounds, which are characterized by moderate nucleophilicity and relatively high Lewis acidity. The appropriate Lewis acidity of the metal and the appropriate nucleophilicity of the metal substituent in these catalysts make monomer coordination preferable to the nucleophilic attack. The difference between coordination polymerization initiated by Ca compounds and Zn and Al compounds lies in the covalent nature of the Al–O and Zn–O bonds, which activate the monomer by coordination, enhancing the nucleophilicity of the metal substituent simultaneously.

The trivalent aluminum complexes possess a combination of properties that makes them predisposed to catalyze the oxirane polymerization. Bearing basic groups such as alkyl or alkoxide fragments, these species are quite reactive toward electrophilic carbon atoms, while the open coordination site forms strong associations with the Lewis basic atoms. Aluminum compounds are also known to undergo ligand-exchange reactions. Therefore, it has been possible to construct mechanisms for oxirane ring opening involving activation of the epoxide ring by an aluminum atom, while another aluminum atom contributes the alkoxide, which attacks the ring. This reaction path, which may include the concomitant exchange of a charge-balancing ligand between

the two aluminum centers, was postulated by Vandenberg to be the route taken by aluminum-based epoxide polymerization catalysts.[100]

4.21.3.3.1 Bimetallic mechanism of oxirane polymerization

Vandenberg first demonstrated that a combination of trialkylaluminum species with water, ether, or pentane-2,4-dione is an effective catalyst for the ring-opening polymerization of EO and substituted oxiranes.[100–104] He proposed a bimetallic mechanism for the oxirane ring opening that involved the growing chain shift from one Al atom to an adjacent Al atom bearing a coordinating activated epoxide. It was also found that the addition of less than 1 equiv of a Lewis base per aluminum atom (e.g., NR_3) could significantly increase the activity of trialkylaluminum compounds in EO polymerization.[104] Later on, Teyssie *et al.* embarked on a systematic investigation of the structure of Al–Zn oxyalkoxides and concluded that a superior activity is achieved by the formation of bimetallic associates. Coordination bonds in the catalyst structure are required in order to make it possible to move the growing polymer chain from one metal atom to the adjacent one (**Figure 10**):

This 'flip–flop' mechanism, postulated by Vandenberg and Teyssie, as a multinuclear mechanism of oxirane growth, was the earliest explanatory attempt involving the formation of an intermediate that could accommodate the essentially linear, three-centered transition state necessary for inversion of configuration at the epoxide ring carbon atom where it was cleaved.[105–108]

The formation of epoxide polymers with very high MW and relatively broad MWD indicates the existence of various active sites.[108] This is due to the highly associated nature of the multinuclear species. Additionally, ligands bound to these atoms, having been involved in the formation of initiating and propagating polymerization species (Mt–X → Mt), can exhibit various reactivities. It was also found that only a fraction of the metal species in the catalyst is effective for the polymerization.

4.21.3.3.2 Aluminum porphyrin initiators

Aluminum porphyrins are excellent initiators for the living polymerizations of oxiranes affording the corresponding polymers of controlled MWs and narrow MWD.[109–112] Metalloporphyrins are characterized by a strongly conjugated, rigid, and planar macrocyclic ligand called 'porphyrin', which imparts to the central metal atom an unusual property, sterically as well as electronically. Therefore, when using metalloporphyrins as catalysts, their reactivity is expected to be controlled by the following factors: site isolation; excitation of the porphyrin ring by visible light; structure of the peripheral substituents of porphyrin; and the effect of external ligands coordinating to the central atom.[109]

Polymerization of PO with aluminum porphyrin was substantially accelerated (460 times) by the addition of an organoaluminum compound such as methylaluminum bis(2,4,6-tri-*tert*-butylphenolate). The basic concept of this high-speed living polymerization involves the coordinative activation of monomer by a bulky Lewis acid, which does not react directly with the growing species on the bulky aluminum porphyrin.[113] The sterically demanding Lewis acid organoaluminum complexes accelerate the coordination ring-opening polymerization (**Figure 11**).[113,114]

Braune and Okuda have shown the possibility to substitute porphyrin initiators by simpler systems based on the association of ammonium salts with a bulky aluminum bis(phenolate) electrophile.[115] According to their study, the ring-opening polymerization of PO cannot occur at simple Lewis acid centers, but that nucleophilic 'ate' complexes must be present at the same time. However, so far, only the synthesis of PPO oligomers with MWs less than 5000 has been reported for this system. The important contribution of Braune and Okuda is that they confirmed the Vandenberg binuclear mechanism earlier proposed for epoxide polymerization (see **Figure 12**).[100–103]

From the practical point of view, however, the synthesis of high-MW PEO based on these chelating systems suffers from low metal-based productivities (i.e., g polymer/g Al). Furthermore, the development of these catalytic systems is mostly focused on the polymerization of monomers other than EO.

4.21.3.3.3 Aluminum phenoxide initiators

Recent years have seen increasing attention paid to aluminum alkoxides as homogeneous catalysts (or cocatalysts)[113,116] for the polymerization of EO[114] and PO.[117–119] While almost all these catalysts are aluminum phenoxides, chelating aluminum 2,2′-methylenebisphenoxides and their derivatives have been particularly extensively studied.[117–126] There are two reasons for this interest. First, the catalysts form homogeneous solutions, allowing detailed *in situ* analysis of their structures. Second, the catalytic behavior reflects the structure of the precursor ligand environment, enabling correlations to be made between the ligand structure and polymer microstructure. It appears that bulky phenolate ligands impart a degree of resistance to formation of alkyl- or alkoxide-bridged aluminum cluster and influence the tacticity and regiospecificity of epoxide polymerization.

Recently, in a Union Carbide Corporation patent, it was shown that the aluminum phenoxide catalysts and particularly

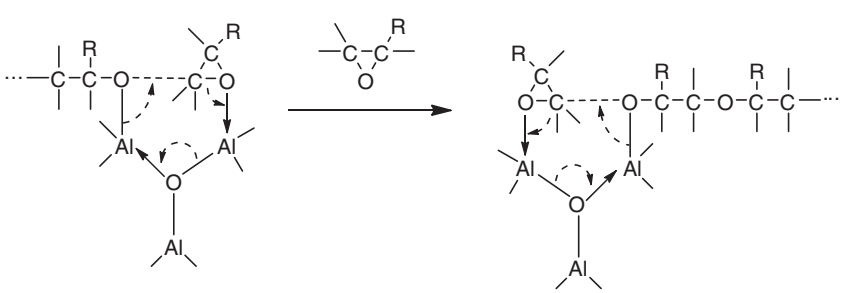

Figure 10 'Flip–flop' mechanism of anionic coordination polymerization of oxirane involving AlR_3.

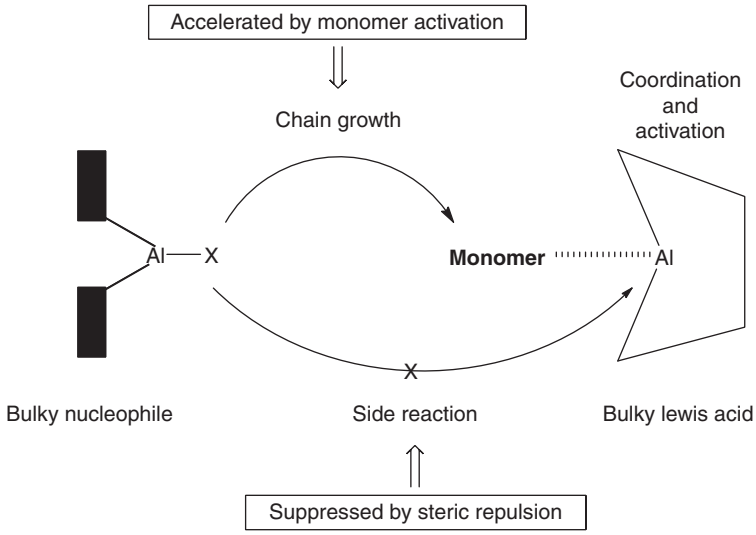

Figure 11 Schematic representation of the concept of "high-speed living polymerization" by aluminum porphyrin as a nucleophile. Reprinted from Sugimoto, H.; Kawamura, C.; Kuroki, M.; *et al. Macromolecules* **1994**, *27*, 2013.[116] with permission of the American Chemical Society, USA.

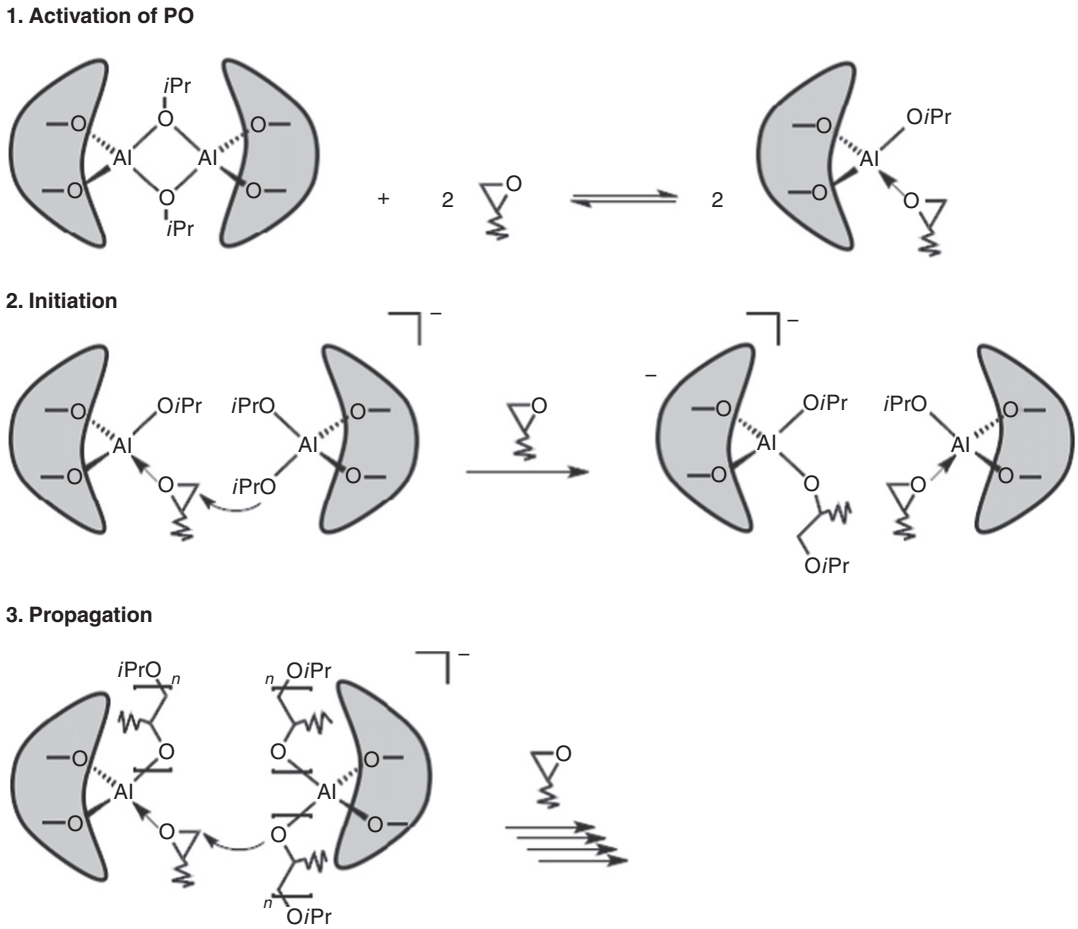

Figure 12 The concept of anionic coordination polymerization with chain transfer. Reprinted from Braune, W.; Okuda, J. *Angew. Chem. Int. Ed.* **2003**, *42*, 64.[115] with permission of John Wiley & Sons Ltd., UK.

the systems, bearing sulfur bridges between the phenolate groups, are highly active in the production of high-MW PEO and copolymers of EO with other oxiranes.[127] It was also found that the ligand structure has a profound influence on the catalyst behavior.

Wasserman *et al.* further developed this finding showing that aluminum complexes of sterically hindered sulfur-bridged bisphenols are highly active catalysts for EO polymerization.[128] The sulfur atom binds to aluminum in the solid-state structures of the catalyst precursors (Figure 13). Greater steric hindrance

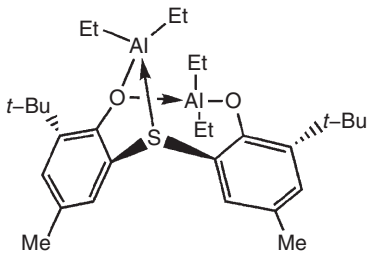

Figure 13 Structure of the aluminum complex of sterically hindered sulfur-bridged bisphenols.

at the *ortho* positions of the phenols and in the aluminum alkyl groups increases catalyst productivity.

In 2008, Tang *et al.* evaluated the efficiency of various combinations of trialkylaluminum compounds and phenols for producing high-MW PEO at room temperature in hexane (Figures 14 and 15).[129] Mixtures of certain phenols with trialkylaluminum compounds, especially with triisobutylaluminum, Al(*i*-Bu)$_3$, gave fairly high productivity. The focus of their study was on the use of aluminum tetraphenoxides as extremely high active catalysts for the ring-opening polymerization of both EO and PO in the presence of Lewis bases.

Certain ligands bearing four phenol groups form particularly active catalysts when combined with Al(*i*-Bu)$_3$ (2 equiv) and triethylamine (1 equiv) as initiator. Thus, immobilization of two metal centers in the same molecule takes place. Productivities of >4000 g polymer/g Al have been achieved in both EO and PO polymerizations using a

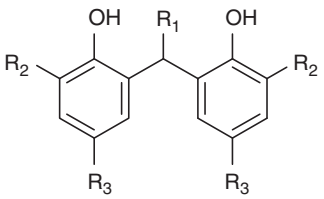

Figure 14 Hindered bisphenols used as ligands (Ligand 1, Table 4). Adapted from Tang, L.; Wasserman, E.; Neithamer, D.; *et al. Macromolecules* **2008**, *41*, 7306.[129] with permission of the American Chemical Society, USA.

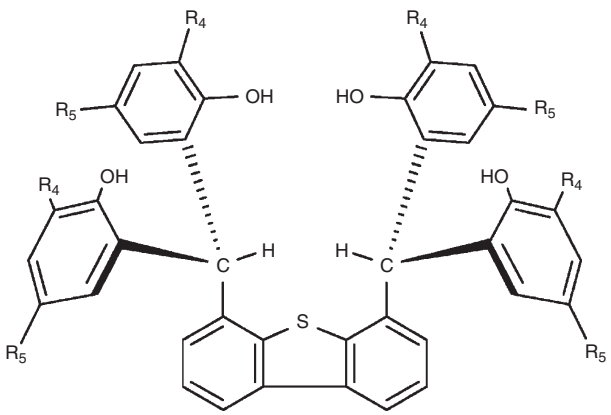

Figure 15 Thiophene-bridged tetraphenols used as highly active ligands for EO and PO polymerization (Ligands 2, Table 4). Adapted from Tang, L.; Wasserman, E.; Neithamer, D.; *et al. Macromolecules* **2008**, *41*, 7306.[129] with permission of the American Chemical Society, USA.

dibenzothiophene-bridged tetraphenol (Figure 15). The addition of alcohols such as propan-2-ol or benzyl alcohol as potential chain-transfer agents led to the expected reduction in polymer MW. Both alcohols were considered to be sufficiently bulky to disfavor the formation of strong alkoxide bridges between aluminum atoms. Addition of up to 3 equiv (relative to Al precursor) of *i*-PrOH lowered MW but did not broaden the MWD, suggesting an effective chain transfer.

A series of ligand variations with the structure presented in Figure 15 were prepared. The *ortho* and *para* substituents in the phenol rings were varied to maximize the catalyst productivity. These ligands were tested in polymerizations of EO under generally comparable conditions. The highest productivities and polymer MWs were obtained at low catalyst concentration and longer polymerization time. The effect of conditions in catalyst preparation was not clear. In general, catalyst activity increases with increasing bulkiness of *ortho* substituents. Mechanistic investigations support a binuclear insertion process. The most important results obtained by Tang *et al.* are summarized in Table 4.

The most active tetraphenol-based systems maintained high activity at very lower levels of catalyst (≤10 μmol Al).

The recent results of Wasserman *et al.* and Tang *et al.*[128,129] clearly show the potential of the systems tetraphenol derivatives/Al(*i*-Bu)$_3$/N(Et)$_3$ as powerful catalysts for production of high-MW polyoxirane. Based on these results, two patent applications of Dow Chemical were published in 2010.[130,131]

The main factors for effective anionic coordination polymerization initiated by aluminum compounds leading to high-MW polyoxiranes are:

1. Coordination of oxirane with the metal triggers the process which is followed by the insertion of the coordinated monomer molecule into the Al–alkoxy bond simultaneously with the opening of the CH_2–O bond in the monomer ring.
2. Multicenter mechanism with ligand-exchange reactions: oxirane ring opening involves the activation of the epoxide ring by one aluminum atom, while another aluminum atom is contributed by the alkoxide which attacks the ring. Thus, two Al atoms in an appropriate geometry are brought together for the growing polymer chain.
3. The rate of polymerization decreases with increasing polarity of the solvent, opposite to the behavior observed for the alkali alkoxides initiators. This observation implies that the monomer and the solvent compete for the active sites of the catalyst.
4. The combination chelating agent–aluminum compound–Lewis base leads to very high catalyst productivity. The significant role of Al(*i*-Bu)$_3$ as an additive is well known.
5. The catalyst systems are rigid. Varying the substituent groups can substantially modify the activity of the catalyst. The use of 'cluster' aluminum alkoxides with tetraphenol ligands and bulky substituents leads to effective synthesis of high-MW polyoxirane.

4.21.3.4 Double-Metal and Multimetal Cyanide Compounds as Initiators

Rapid and controlled PO polymerization has recently become effective for industrial application through the commercially available double-metal cyanide (DMC) compounds, whose

Table 4 Productivity of bis/tetraphenol ligands in Al(*i*-Bu)$_3$/N(Et)$_3$ catalyst systems. Conditions: hexane, 40 °C, reaction time 3 h, Al(*i*-Bu)$_3$/N(Et)$_3$ = 0.5

Ligand L	*L/Al(i-Bu)$_3$ (μmol/μmol)*	*Productivity (g polymer/g Al)*	M_n	M_w/M_n
None	0:20	1700	64 200	1.3
Bisphenol ligand (**1**) (**Figure 14**)	20:20	540	14 300	2.4
Tetraphenol ligands (**2**) (**Figure 15**)				
$R_1 = R_2 =$ *t*-Bu	1:2	7300	132 000	2.03
$R_1 =$ *t*-Bu; R_2 = Me	1:2	10 700	162 000	2.07
$R_1 = R_2 = C(Me)_2Ph$	1:2	15 000	227 000	2.27

structure and mechanism are, however, still unclear.[132,133] The catalytic system is based on $Zn_3[Co(CN)_6]_2$.[134,135] Compared with conventional potassium hydroxide (KOH) catalysts, DMC is much more active, producing polyethers with a much lower extent of unsaturation and much narrower MWD. DMC catalysts for epoxide polymerization are usually obtained by reacting a water-soluble metal salt ($ZnCl_2$) with a water-soluble metal cyanide salt (potassium hexacyanidocobaltate) in aqueous medium and then treating the water-insoluble DMC ($Zn_3[Co(CN)_6]_2$) with a low-MW complex ligand (ether or alcohol) (**Figure 16**). Despite its advantages, unlike KOH, DMC catalysts must be activated before monomer can be added to the reactor. Usually, a polyol initiator (or starter) and DMC are heated under vacuum prior to the addition of a small portion of monomer. The induction periods depend on reaction temperature, water content, and the type and amount of catalysts, regulators, and solvents. A series of DMC catalysts were synthesized by varying the type and amount of the co-complexing agents and were utilized for PO polymerization. The DMC catalyst prepared by using $K_3[Co(CN)_6]_2$ and $ZnCl_2$ in the presence of *tert*-BuOH as a complexing agent and poly(butane-1,4-diol) as the second agent showed a very high

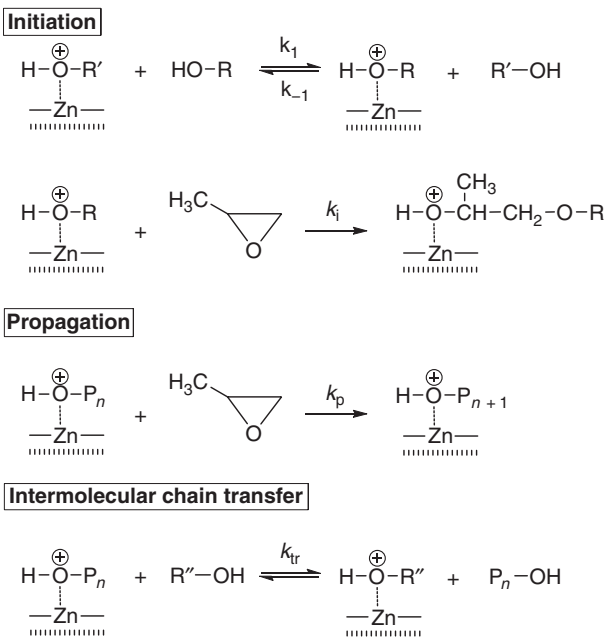

Figure 16 Mechanism of DMC-catalyzed ring-opening polymerization of PO.

activity (2672 g PPO/g cat). The resulting polymers exhibited a very low unsaturation level (0.003–0.006 meq g^{-1}) and narrow MWD (1.02–1.04). Some indirect evidence showed that the active sites in DMC and multimetal cyanide (MMC)-catalyzed polymerization of PO had both cationic and coordinative characters as shown in **Figure 16**.

Controlling the induction period is a great technical challenge because, once catalyst activation has been achieved, the PO initially introduced reacts very rapidly due to the consecutive, very high catalyst activity, with the evolution of a great amount of heat. Another problem associated with DMC catalysis is that, in a batch process, a previously propoxylated starter alcohol has to be used, since low-MW starter alcohols, such as propane-1,2-diol and glycerol, deactivate the DMC catalyst.

Lee *et al*. and Kim *et al*. synthesized a series of multimetal catalysts prepared by reacting $ZnCl_2$ with various metal cyanide compounds such as $K_3[Co(CN)_6]_2$, $K_4Fe(CN)_6$, $K_3Fe(CN)_6$, and $K_2Ni(CN)_4$ in the presence of *tert*-butyl alcohol and poly(butane-1,4-diol) as complexing agents.[136,137] All catalysts prepared from $K_3[Co(CN)_6]_2$ showed an extremely high activity once they were activated. The catalytic activity, induction period, polymer MW characteristics, and viscosity could be tuned by simply choosing different metal cyanide salts for the catalyst formulation.

4.21.4 Applications of High-MW Polyoxiranes

High-MW PEO, a polymer composed by a sequence of –(CH_2CH_2O)– monomer units, has many important technological applications, ranging from biocompatible materials to ion-conducting polymer electrolytes.[91,138–141]

4.21.4.1 High-MW PEO Polyelectrolytes and Lithium Batteries

The aggressive and growing market for portable electronic products, as well as the environmental necessity for zero-emission vehicles, i.e., electric vehicles, has motivated researchers to develop electrochemical power sources characterized by high energy density, long life-cycle, reliability, and safety. A recent breakthrough in the field was the commercialization of rechargeable lithium batteries, the lithium-ion batteries, which are now produced at a rate of about a million units per month.[142]

High-MW PEO was the earliest and most extensively studied polymer for the development of lithium batteries that has gained an unprecedented significance in the past three decades as the demand for portable telecommunication devices, computers, and eventually hybrid electric vehicles increased. Only a very few reports on other composite polymer electrolytes are available. Although Fenton *et al.*[143] discovered the ionic conductivity of high-MW PEO in 1973, its technical importance was recognized only in the early 1980s.[144–147] Classical examples of lithium polymer electrolytes are blends of a lithium salt, LiX, where X is preferably a large soft anion, such as ClO_4^- or $(CF_3SO_2)_2N^-$, and a high-MW PEO containing Li^+-coordinating groups. These electrolytes combine the advantages of solid state with the ease of casting as thin films.

The development of PEO electrolytes has passed through three stages (1) dry solid-state polymer, (2) gel/plasticized polymer electrolyte systems, and (3) polymer composites. The very first example of 'dry solid' polymer electrolyte is the high-MW-PEO-based systems that showed a very low ambient-temperature conductivities of the order of 10^{-8} S cm^{-1}. Because of their specific structural position the lithium ions can be released to transport the current only on unfolding the coordinating PEO chains. This type of polymer electrolytes requires local relaxation and segmental motion of the solvent (i.e., PEO) chains to allow fast lithium-ion transport. Thus, high conductivity is restricted to the amorphous state of the PEO component. At about 70 °C, the temperature at which the PEO the crystalline-to-amorphous transition occurs, the conductivity increases by several orders of magnitude to reach, at about 100 °C, the order 10^{-3} S cm^{-1}, the values that are of practical interest. This implies that the use of the PEO–LiX electrolytes is restricted to batteries with relatively high operating temperature limits. On the other hand, the relatively high operating temperature limits their overall practical output. Several attempts have been made to enhance the room-temperature performances of PEO-based systems either by using special salts[148] (highly ionized and acting as plasticizers) or by trying to reduce polymer matrix crystallinity.[149] The observation of amorphous PEO systems evidenced the importance of the repeating oxyethylene unit in dissociation and transport phenomena. Accordingly, many studies have been carried out aiming at improvement of the low-temperature conductivity of PEO-based polymer electrolytes. Various approaches have been considered in attempting to achieve this goal. For example, modified PEO polymer architectures were used to reduce the crystallinity at room temperature. These modifications include block copolymers, cross-linked polymer networks, and comb-shaped polymers bearing short oligo(oxyethylene) chains attached to the polymer backbone.[150–152]

The PPO systems were investigated by a few research groups in the early 1980s. The thermal stability and high-pressure electric conductivity,[153] the interfacial properties of lithium anode,[154] as well as ionic conductivity and nuclear magnetic resonance (NMR) spectra[155,156] of PPO hosts such as complexes with different lithium salts have been reported. It is a well-known fact that the dissolution of inorganic salts in polymer hosts is facilitated if the lattice energy of the salt is low and the dielectric permittivity (ε) of the polymer is high. Unfortunately, the ionic conductivity of amorphous mixtures of lithium salts with PPO is considerably lower than that of the equivalent mixture with PEO. This is due to a lower ε of PPO and the presence of a methyl group which hinders the segmental motion of the polymer chain and thus reduces its conductivity.[157]

PEO-based cross-linked gel polymer electrolytes were used in the fabrication of quasi-solid-state TiO_2 dye-sensitized solar cells (DSSCs).[158] The copolymerization of EO and other alkylene oxides is a suitable approach to obtain products of lower crystallinity. However, due to the much higher reactivity of EO compared to that of other alkylene oxides, it is difficult to control the regular incorporation of the comonomer units throughout the PEO chain.[91] Petrov *et al.* and Nelles *et al.* have found that the copolymerization of EO and PO initiated by the calcium amide/alkoxide system resulted in high-MW copolymers of decreased crystallinity compared to that of the PEO homopolymer.[92,93] It was found that the DSSCs based on the EO-*co*-PO copolymer containing small amounts of PO (17–21 mol.%) show higher efficiencies and longer lifetimes compared to both the EO-*co*-PO copolymer with high PO content (44 mol.%) as well as PEO- and PPO-based DSSCs. It seems that a small content of PO units in the copolymer is sufficient to introduce a certain degree of disorder in the polymer structure, which reduces significantly the crystallinity and increases the long-term stability. The good ion-diffusion properties in a polymer gel electrolyte of such copolymers are maintained. Importantly, the DSSCs based on chemically cross-linked P(EO-*co*-PO) gel electrolytes show much longer lifetime compared to physical P(EO-*co*-PO) gel electrolytes. This result can be attributed to the fact that the chemically cross-linked polymer gels show better mechanical stability in terms of ethylene carbonate/propylene carbonate leakage compared to the physical gel. This second category of polymer electrolyte called 'gel polymer electrolyte' or 'plasticized polymer electrolyte' is neither liquid nor solid or, conversely, both liquid and solid.[157] The gels possess both cohesive properties of solids and the diffusion property of liquids. This unique characteristic makes them ideal candidates for various important applications including polymer electrolytes.

It would be best to use 'solid plasticizers' that would promote amorphicity at ambient temperature without affecting mechanical and interfacial properties of the electrolyte. A result that approaches this ideal condition has been obtained by dispersing selected ceramic powders, such as TiO_2, Al_2O_3, and SiO_2, at the nanoscale particle size, in the PEO–LiX matrix.[159,160]

Wieczorek *et al.* discussed the effect of $AlBr_3$, $AlCl_3$, and α-Al_2O_3 inert fillers on ionic conductivity and ultrastructure of PEO–$LiClO_4$ solid electrolytes.[161] The results obtained were analyzed in terms of Lewis acid–base interactions occurring between various chemical groups of the composite electrolyte systems. It was demonstrated that aluminum halides interact with polyethers and form aluminum halide complexes, thus stiffening the polymer electrolytes. Aluminum halides also form complexes with CLO_4^- ions, acting as plasticizers for the polyether matrix. The addition of Lewis acid results in a decrease in the degree of crystallinity of PEO-based electrolytes, followed by an increase in ionic conductivity. DSC analyses also confirmed these results.

The dispersion of selected nanosized ceramics leads to the development of true solid-state PEO–LiX nanocomposite polymer electrolytes that, in the 30–80 °C range, possess excellent

mechanical stability (promoted by the network of the fillers in the polymer bulk) and high ionic conductivity (induced by the high surface area of the dispersed fillers). These electrolytes appear to be particularly suitable for use as separators in advanced rechargeable lithium batteries characterized by a long life-cycle and high power capabilities.

4.21.4.2 High-MW PEO in Drug Delivery Systems and Tissue Engineering

Among a variety of hydrophilic polymers, high-MW PEO is one of the most important materials used in the pharmaceutical industries mainly because of its nontoxicity, high water-solubility and swellability, insensitivity to the pH of the biological medium, and ease of production. Recently, the swelling and dissolution behavior of PEO tablets[162–165] and hydrogels,[166] as well as their influence on drug release characteristics have been studied. It was found that high-MW PEO tablets swell to a greater extent compared with the low-MW PEO, and the swelling of the polymer rather than its dissolution is the governing factor for drug release. The compression force applied during the manufacturing process, pH of the release medium, and the stirring rate do not affect the drug release behavior significantly. Incorporation of drugs in PEO hydrogel obtained after γ-irradiation cross-linking of high-MW PEO ensures their retarded release for a relatively longer period.[167] The release profiles were found to depend on the radiation dose, the network surface, and the drug nature.[168]

Apicella *et al*. investigated water-soluble PEOs of two MWs (600 000 and 4 000 000) and their blends as potential mucoadhesive drug delivery systems.[162] The mechanisms and rates of drug release were significantly affected by the polymer MW characteristics, swelling and dissolution rate, as well as the drug diffusivity in the polymer gel surrounding the tablet. The adhesion capacity depended heavily on the average MW. The *in vitro* test data indicated that maximum adhesion occurred at an average MW of 400 000 and a further increase in MW caused a decrease in adhesion. Nonetheless, the actual adhesion time measured for tablets placed in the buccal pouch of patients did not decrease once the polymer MW exceeded 400 000. The adhesion remained approximately constant once a critical chain length was reached. Di Colo *et al*. evaluated the application of high-MW (400 kDa) linear PEO in gel-forming erodible inserts for the controlled ocular delivery of ofloxacin *in vitro* and *in vivo*.[169,170]

In the field of synthetic blood-compatible materials, an increasing interest is devoted to surfaces bearing PEO chains. This interest stems from the unusual properties of PEO and PEO-covered surfaces, which exhibit strongly reduced adsorption of proteins and other biological species.[171,172] PEO coatings are highly effective in preventing the adsorption of plasma proteins like albumin, γ-globulin, and fibrinogen.[173] Moreover, PEO coatings generally reduce adhesion of many bacterial strains involved in biomaterial-centered infections, like *Staphylococcus epidermidis*, *Staphylococcus aureus*, and *Escherichia coli* by more than 90%.[174–176]

The physical basis of the properties of PEO-covered surfaces are as follows: mobility of PEO chains in aqueous environment, steric stabilization effects, structural fit of PEO repeating unit and water structure, and van der Waals interactions between PEO chains and formed blood elements. Spectral observations, mainly by electron spectroscopy for chemical analysis (ESCA) or NMR measurements under hydrated conditions, have shown that PEO chains project from a hydrated surface and move vigorously with coordinated water. This thermal mobility of PEO chains is much greater than that of other hydrophilic or water-soluble polymers such as poly(vinylpyrrolidone), poly (2-hydroxyethyl methacrylate), or polyacrylamide.[171] Kinetically, the process of plasma protein interactions with and irreversible absorption on the surface of a material to form a support for platelet adhesion is largely influenced by the dwelling time on the surface.[177] Microflows of water are induced on the surface of the PEO-coated material by the above-mentioned movements of hydrated PEO chains, and because plasma protein is prevented from dwelling on the surface, absorption is inhibited (Figure 17).

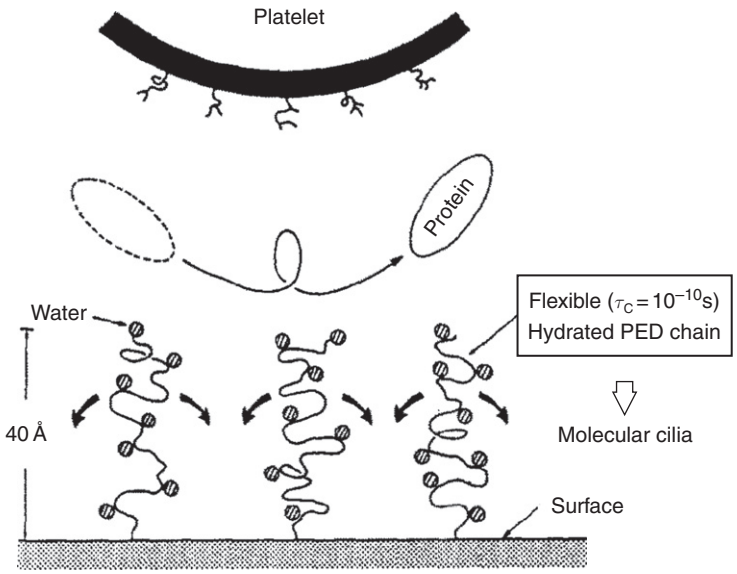

Figure 17 The interaction between blood components and hydrated PEO chains on the surface. Reprinted from Nagaoka, S.; Nakao, A. *Biomaterials* **1990**, *11*, 119.[177] with permission of Elsevier Ltd., UK.

For PEO coatings, both grafting density and chain length are of critical importance for their efficiency in preventing protein adsorption and bacterial adhesion.[178,179] If the grafting density is low, either penetration of the PEO coating can occur or parts of the bare substrate can be revealed. Furthermore, theories describing PEO layer–particle interaction predict stronger particle repelling for longer PEO chains, that is, with increasing thickness of the PEO layer at the surface.[180,181] The thicker PEO layer implies a larger separation between the surface and the incoming particles and hence a stronger attenuation of the long-range van der Waals attraction. It was demonstrated that PEO coatings are stable under sterile conditions[182] or for an extended exposure to phosphate-buffered saline.[183] Although an everlasting PEO coating for every application may be a utopia, a carefully developed and *in vitro* tested PEO coating could greatly reduce bacterial adhesion and, hence, the risk of biomaterial-centered infections.[184]

Perez *et al*. studied a two-layer composite material comprising a thin layer of corneal tissue and a synthetic PEO hydrogel.[185] The gels were synthesized by electron irradiation-induced cross-linking of an aqueous PEO solution on a thin layer of collagenous tissue substrate. Light microscopy studies indicated that the interface between the corneal tissue and PEO gel appeared well adherent with no gaps in the interface. SEM studies of the material surface showed architecture similar to that of normal corneal tissue.

Tsvetanov *et al*. described a film formation process involving the dissolution of PEO together with another water-soluble polymer (e.g., polysaccharide) in a solvent consisting of water, an organic solvent, or a mixture in any proportion of water and organic solvent, in the presence of an effective quantity of a photoinitiator or a cross-linking agent. The water-containing film was then irradiated by UV light in the 200–400 nm wavelength range. The resulting films are useful in the cosmetic or medical industry.[186] For PEO hydrogel application as a dressing, poly(vinyl alcohol) was added to improve its strength.[187] The blended hydrogel gave 80% of gel on 60-kGy electron beam irradiation. The hydrogel provides a wet environment for wounds, causing faster healing compared with the gauze dressing and dry environment. Mechanical properties of this hydrogel are satisfactory for a dressing material.

4.21.4.3 PEO Cross-linking: Hydrogels and Cryogels

High-MW PEO is composed of flexible polymer chains that on cross-linking and swelling in water produce a soft hydrogel. This hydrogel is inert and therefore suitable for various applications. It has been shown that cross-linked polymers derived from high-MW PEO find a number of applications (wound dressings,[188] controlled-release drug systems,[167,189] phase-transfer catalysts,[190–192] semipermeable membranes,[193] solid electrolytes for batteries,[194] etc.). PEO hydrogels are nontoxic and biocompatible materials. They meet all the requirements for strength, absorbency, flexibility, and adhesiveness in biomedical applications.

Cross-linked high-MW PEO was first obtained via γ-irradiation of degassed dilute polymer aqueous solutions.[195] Irradiation of polymers in aqueous solution can be used effectively for medical purposes, since such systems, containing neither monomers nor cross-linking agents, are easier to control and study. Moreover, a lower number of usually unwanted processes such as homografting of monomer on the polymer chain occurs, and, last but not least, hydrogels formed in this way are suitable for biomedical use with no need of further purification.[196,197] The process of chain cross-linking resulting in the formation of hydrogels upon γ-irradiation of aqueous solutions of polymers is initiated by water radiolysis transient products, mainly, hydroxyl radicals.[198] The interaction of OH radicals with PEO macromolecule leads to hydrogen atom abstraction followed by recombination of macroradicals. As a result, the polymer chains are cross-linked to form a three-dimensional network. Unfortunately, γ-irradiation processes have certain limitations because of the cost and safety requirements. Later on, methods based on chemical cross-linking were suggested.[199,200] Chemical cross-linking was reported for low-MW polymers by the reaction between the PEO end groups and multifunctional cross-linking agents. Sloop *et al*.[201] and Doytcheva *et al*.[202] have shown that PEO of MWs from 200 000 to 7 000 000 can be successfully cross-linked by irradiation with UV light in the presence of hydrogen-abstracting benzophenone (BP) as a photoinitiator. It should be mentioned that pure PEO cannot be UV cross-linked because of the absence of photosensitive chromophoric groups. The studies have shown that it is possible to control the network density by varying the irradiation temperature. The gel fraction amounts to more than 90%. The ease, relative safety, and low cost of UV-induced cross-linking provide significant advantages for many applications over the other methods. On the other hand, commercial powdery high-MW PEO can be heterogeneously cross-linked with multifunctional monomers like pentaerythritol triacrylate (PETA) using radical initiators.[203] This acrylate monomer is supposed to easily undergo photoinitiated radical polymerization. The polymer gels obtained were free from low-MW aromatic impurities, which are inevitable if photoinitiators are used. UV irradiation in the presence of PETA seems to be a simple method for obtaining films or powdery products of cross-linked PEO. Hydrogels of high-MW PEO have been obtained *in situ* applying a very simple procedure that involves UV cross-linking of PEO in aqueous solution. The efficiency of the photoactivated cross-linking of thin PEO layers in aqueous solution in the presence of (4-benzoylbenzyl) trimethylammonium chloride as a photoinitiator has been determined at room temperature and in the frozen state (−25 °C). It was found that the cross-linking efficiency varies with the concentration of PEO solution, the MW of PEO, and particularly with the temperature. In case the UV cross-linking was performed in the frozen state, porous hydrogels (cryogels) with a very high yield of gel fraction (above 90%) and high cross-linking density were obtained.[204] Petrov *et al*. have shown that the UV irradiation technique is a facile method for the synthesis of supermacroporous polymer cryogels. The combination of a H_2O_2 initiator and the high conversion allows preparation of green materials consisting of biocompatible polymer networks and water without any additional purification. All cryogels obtained possess macroporous structure, which impart a very rapid water uptake and, in the case of temperature-responsive polymers, ultrarapid volume phase transition. In general, different nano- and microsized particulates can be immobilized within the cryogels pores and/or walls.[205]

The UV irradiation technique was successfully used for the preparation of a new family of films from cross-linked polymers based on high-MW PEO in combination with

(1) water-soluble pH-sensitive[206] and temperature-responsive polymers;[207] (2) unsaturated quaternary ammonium salts;[208] (3) calcium hydroxyapatite[209] and other inorganic salts;[210] and (4) polysaccharide including cellulose polymers, pectins, carrageenans, and alginates.[211]

Networks of high-MW PEO were successfully obtained also in the presence of radical initiators. PEO with a MW of 2 000 000 was cross-linked in the molten state by *tert*-butyl peroxybenzoate or a difunctional peroxide such as 2,5-bis(*tert*-butylperoxy)-2,5-dimethylhexane (Luperox 101) at 145–160 °C.[212,213,214] Significant chain degradation occurs during heating as longer reaction times do not lead to cross-linking.

References

1. Wurtz, A. *C. R. Acad. Sci. Paris.* **1878**, *86*, 1176.
2. Staudinger, H.; Schweitzer, O. *Ber. Dtsch. Chem. Ges.* **1929**, *62*, 2395.
3. Flory, P. *J. Am. Chem. Soc.* **1940**, *62*, 1561.
4. Rife, H.; Roberts, F. U.S. Patent 2,520,612, 29 August 1950.
5. Ishii, Y.; Sakai, S. In *Ring Opening Polymerization*; Frisch, K.; Reegen, S., Eds.; Marcel Dekker: New York, 1969; p 1.
6. (a) Bailey, F.; Fitzpatrick, J. U.S. Patent 2,941,963, 21 June 1960. (b) Hill, F.; Bailey, F.; Fitzpatrick, J. U.S. Patent 2,969,402, 24 January 1961.
7. Pruitt, M.; Baggett, J. U.S. Patent 2,706,181, 12 April 1955.
8. Tsvetanov, Ch.; Dimitrov, I.; Doytcheva, M.; *et al.* In *Applications of Anionic Polymerization Research*; Quirk, R., Ed.; ACS Symposium Series 696; American Chemical Society: Washington, DC, 1997; p 236.
9. Wojtech, A. *Makromol. Chem.* **1963**, *66*, 180.
10. Kazanskii, K.; Ptitsyna, N.; Kazakevich, V.; *et al. Dokl. Akad. Nauk SSSR* **1979**, *234*, 858.
11. Ptitsyna, N.; Ovsyannikova, S.; Gel'fer, T.; Kazanskii, K. *Polym. Sci. U.S.S.R.* **1980**, *22*, 2779.
12. Kazanskii, K. *Pure Appl. Chem.* **1981**, *53*, 1645.
13. (a) Sigwalt, P.; Boileau, S. *J. Polym. Sci.* **1978**, *62*, 51. (b) Boileau S. In *Anionic Polymerization: Kinetics, Mechanisms and Synthesis*; Mc Grath J., Ed.; ACS Symposium Series 166; American Chemical Society: Washington, DC, 1981; p 283.
14. Berlinova, I.; Panayotov, I.; Tsvetanov, Ch. *Eur. Polym. J.* **1977**, *13*, 757.
15. Berlinova, I.; Panayotov, I.; Tsvetanov, Ch. *Vysokomol. Soedin. B* **1978**, *20*, 839.
16. Tsvetanov, Ch.; Petrova, E.; Panayotov, I. *J. Macromol. Sci. A* **1985**, *22*, 1309.
17. Hsieh, H.; Quirk, R. *Anionic Polymerization: Principles and Practical Applications*; Marcel Dekker: New York, 1996.
18. Mark, H.; Bikales, N.; Overberger, C.; *et al. Encyclopedia of Polymer Science and Engineering*; Wiley: New York, 1985; Vol. 21, 1–43.
19. Szwarc, M. *Carbanions, Living Polymers, and Electron-Transfer Processes*; Interscience Publishers: New York, 1968; p. 647.
20. Szwarc, M.; van Beylen, M. *Ionic Polymerization and Living Polymers*; Chapman & Hall: New York, London, 1993; p. 33.
21. Chang, C.; Kiesel, R.; Hogen-Esch, T. *J. Am. Chem. Soc.* **1973**, *95*, 8446.
22. Tsvetanov, Ch.; Dimov, D.; Petrova, E.; Dotcheva, D. *Makromol. Chem., Macromol. Symp.* **1992**, *60*, 297.
23. Price, C.; Carmelite, D. *J. Am. Chem. Soc.* **1966**, *88*, 4039.
24. Wegener, G.; Brandt, M.; Duda, L.; *et al. Appl. Catal. A Gen.* **2001**, *221*, 303.
25. Becker, H.; Wagner, G. *Acta Polym.* **1984**, *35*, 28.
26. Price, C. *Acc. Chem. Res.* **1974**, *7*, 294.
27. Ding, J.; Heatley, F.; Price, C.; Booth, C. *Eur. Polym. J.* **1991**, *27*, 895.
28. Esswein, B.; Möller, M. *Angew. Chem. Int. Ed.* **1996**, *35*, 623.
29. Esswein, B.; Molenberg, A.; Möller, M. *Makromol. Chem., Macromol. Symp.* **1996**, *107*, 331.
30. Quirk, R.; Lizarraga, G. *Macromol. Chem. Phys.* **2000**, *201*, 1395.
31. Toy, A.; Reinicke, S.; Müller, A.; Schmalz, H. *Macromolecules* **2007**, *40*, 5241.
32. Deffieux, A.; Billouard, C.; Carlotti, S.; Desbois, P. *Polym. Prepr.* **2004**, *45* (2), 571.
33. Billouard, C.; Carlotti, S.; Desbois, P.; Deffieux, A. *Macromolecules* **2004**, *37*, 4038.
34. Carlotti, S.; Billouard, C.; Gautriaud, E.; *et al. Macromol. Symp.* **2005**, *226*, 61.
35. Labbe, A.; Carlotti, S.; Billouard, C.; *et al. Macromolecules* **2007**, *40*, 7842.
36. Rejsek, V.; Sauvanier, D.; Billouard, C.; *et al. Macromolecules* **2007**, *40*, 6510.
37. Sunder, A.; Hanselmann, R.; Frey, H.; Mülhaupt, R. *Macromolecules* **1999**, *32*, 4240.
38. Wilms, D.; Stiriba, S.-E.; Frey, H. *Acc. Chem. Res.* **2010**, *43*, 129.
39. Sunder, A.; Mülhaupt, R.; Haag, R.; Frey, H. *Macromolecules* **2000**, *33*, 253.
40. Khan, M.; Huck, T. *Macromolecules* **2003**, *36*, 5088.
41. Kainthan, R.; Muliawan, E.; Hatzikiriakos, S.; Brooks, D. *Macromolecules* **2006**, *39*, 7708.
42. Wilms, D.; Wurm, F.; Nieberle, J.; *et al. Macromolecules* **2009**, *42*, 3230.
43. Walach, W.; Kowalczuk, A.; Trzebicka, B.; Dworak, A. *Macromol. Rapid Commun.* **2001**, *22*, 1272.
44. Istratov, V.; Kautz, H.; Kim, Y.-K.; *et al. Tetrahedron* **2003**, *59*, 4017.
45. Barriau, E.; García Marcos, A.; Kautz, H.; Frey, H. *Macromol. Rapid Commun.* **2005**, *26*, 862.
46. Wurm, F.; Nieberle, J.; Frey, H. *Macromolecules* **2008**, *41*, 1184.
47. Wurm, F.; Nieberle, J.; Frey, H. *Macromolecules* **2008**, *41*, 1909.
48. Sunder, A.; Türk, H.; Haag, R.; Frey, H. *Macromolecules* **2000**, *33*, 7682.
49. Knischka, R.; Lutz, P.; Sunder, A.; *et al. Macromolecules* **2000**, *33*, 315.
50. Burgath, A.; Sunder, A.; Neuner, I.; *et al. Macromol. Chem. Phys.* **2000**, *201*, 792.
51. Maier, S.; Sunder, A.; Frey, H.; Mülhaupt, R. *Macromol. Rapid Commun.* **2000**, *21*, 226.
52. Shen, Z.; Chen, Y.; Barriau, E.; Frey, H. *Macromol. Chem. Phys.* **2006**, *207*, 57.
53. Kainthan, R.; Gnanamani, M.; Ganguli, M.; *et al. Biomaterials* **2006**, *27*, 5377.
54. Klajnert, B.; Walach, W.; Bryszewska, M.; *et al. Cell Biol. Int.* **2006**, *30*, 248.
55. Kainthan, R.; Janzen, J.; Levin, E.; *et al. Bio Macromolecules* **2006**, *7*, 703.
56. Dworak, A.; Trzebicka, B.; Walach, W.; *et al. Macromol Symp.* **2004**, *210*, 419.
57. Utrata-Wesolek, A.; Trzebicka, B.; Dworak, A.; *et al. e-Polymer* **2007**, no. 019.
58. Tesser, R.; Santacesaria, E.; Di Serio, M.; *et al. Ind. Eng. Chem. Res.* **2007**, *46*, 6456.
59. Taton, D.; Le Borgne, A.; Sepulchre, M.; Spassky, N. *Macromol. Chem. Phys.* **1994**, *195*, 139.
60. Erberich, M.; Keul, H.; Möller, M. *Macromolecules* **2007**, *40*, 3070.
61. Dworak, A.; Baran, G.; Trzebicka, B.; Walach, W. *React. Funct. Polym.* **1999**, *42*, 31.
62. Li, Z.; Li, P.; Huang, J. *J. Polym. Sci., Part A: Polym. Chem.* **2006**, *44*, 4361.
63. Halacheva, S.; Rangelov, S.; Tsvetanov, C. *Macromolecules* **2006**, *39*, 6845.
64. Dimitrov, P.; Rangelov, S.; Dworak, A.; *et al. Macromol. Symp.* **2004**, *215*, 127.
65. Hans, M.; Keul, H.; Moeller, M. *Polymer* **2009**, *50*, 1103.
66. Kaluzynski, K.; Petrula, J.; Lapienis, G.; *et al. J. Polym. Sci., Part A: Polym. Chem.* **2001**, *39*, 955.
67. Penczek, S.; Petrula, J.; Kaluzynski, K. *J. Polym. Sci., Part A: Polym. Chem.* **2004**, *42*, 432.
68. Dimitrov, P.; Utrata-Wesolek, A.; Rangelov, S.; *et al. Polymer* **2006**, *47*, 4905.
69. Dimitrov, P.; Porjazoska, A.; Novakov, C.; *et al. Polymer* **2005**, *46*, 6820.
70. Dimitrov, P.; Rangelov, S.; Dworak, A.; Tsvetanov, C. *Macromolecules* **2004**, *37*, 1000.
71. Gervais, M.; Brocas, A.-L.; Cendejas, G.; *et al. Macromolecules* **2010**, *43*, 1778.
72. Walach, W.; Trzebicka, B.; Justynska, J.; Dworak, A. *Polymer* **2004**, *45*, 1755.
73. Miller, R.; Price, C. *J. Polym. Sci.* **1959**, *34*, 161.
74. Vandenberg, E. *J. Polym. Sci.* **1960**, *47*, 486.
75. Furukawa, J.; Saegusa, T.; Tsuruta, T.; Kakogawa, G. *Makromol. Chem.* **1959**, *36*, 25.
76. Osgan, M.; Teyssie, Ph. *Polym. Lett.* **1967**, *B5*, 789.
77. Hsieh, H. *J. Appl. Polym. Sci.* **1971**, *15*, 2425.
78. Zhang, Y.; Shen, Z. *Acta Polym. Sin.* **1998**, *6*, 469.
79. Xie, H.-Q.; Zhang, J.-H.; Cui, M.-H.; Xie, D. *J. Appl. Polym. Sci.* **2007**, *105*, 562.
80. Dimitrov, Ph.; Hasan, E.; Rangelov, S.; *et al. Polymer* **2002**, *43*, 7171.
81. Tarnorutskii, M.; Artamonova, S.; Grebenshchikova, V.; Filatov, I. *Polym. Sci. U.S.S.R.* **1972**, *14*, 2764.
82. Kazanskii, K.; Tarasov, A.; Paleyeva, I.; Dubrovskii, S. *Polym. Sci. U.S.S.R.* **1978**, *20*, 442.
83. Goeke, G.; Karol, F. U.S. Patent 4,193,892, 18 March 1980.
84. Panayotov, I.; Berlinova, I.; Bojilova, M.; et al. Bulg. Patent 25,142, 1978.
85. Deffieux, A.; Boileau, S. *Polymer* **1977**, *18*, 1047.
86. Nenna, S.; Figueruelo, J. *Eur. Polym. J.* **1975**, *11*, 511.
87. Dubrovskii, S.; Kazanskii, K. *Khim. Fiz.* **1982**, *12*, 1681.
88. Krusteva, M.; Nedkov, E.; Mihailov, M. *Bulg. J. Phys.* **1979**, *6*, 667.
89. Rangelov, S.; Petrov, P.; Berlinova, I.; Tsvetanov, C. *Polym. Bull.* **2004**, *52*, 155.
90. Rangelov, S.; Brown, W. *Polymer* **2000**, *41*, 4825.
91. Bailey, F.; Koleske, J. *Alkylene Oxides and Their Polymers*; *Surfactant Science Series Vol. 35*; Marcel Dekker Inc.: New York, 1990.
92. Petrov, P.; Berlinova, I.; Tsvetanov, C.; *et al. Macromol. Mater. Eng.* **2008**, *293*, 598.
93. Nelles, G.; Rosselli, S.; Miteva, T.; *et al.* EP 1 840 152 A1, Oct 03, 2007.
94. Petrov, P.; Rangelov, S.; Novakov, C.; *et al. Polymer* **2002**, *43*, 6641.
95. Tanford, C.; Nozaki, Y.; Rohde, M. *J. Phys. Chem.* **1977**, *81*, 1555.

96. Cantor, S.; Brindell, G.; Brett, T. Jr.*J. Macromol. Sci. A* **1973**, *7*, 1483.
97. Saegusa, T.; Kobayashi, T.; Kobayashi, S.; *et al. Polym. J.* **1979**, *11*, 463.
98. Lagarde, F.; Durand, C.; Reibel, L.; Franta, E. *Makromol. Chem., Macromol. Symp.* **1993**, *73*, 117.
99. Hasan, E.; Jankova, K.; Samichkov, V.; *et al. Macromol. Symp.* **2002**, *177*, 125.
100. Vandenberg, E. *J. Polym. Sci.* **1960**, *149*, 486.
101. Vandenberg, E. *J. Am. Chem. Soc.* **1961**, *83*, 3538.
102. Vandenberg, E. *J. Polym. Sci., Part B: Polym. Lett.* **1964**, *2*, 1085.
103. Vandenberg, E. *J. Polym. Sci., Part A: Polym. Chem.* **1969**, *7*, 525.
104. Kutner, A.; Vandenberg, E. U.S. Patent 3,186,958, 1 June 1965.
105. Osgan, M.; Teyssie, Ph. *J. Polym. Sci. B* **1967**, *5*, 789.
106. Kohler, N.; Osgan, M.; Teyssie, Ph. *J. Polym. Sci. B* **1968**, *6*, 559.
107. Osgan, M.; Teyssie, Ph. *J. Polym. Sci. B* **1970**, *8*, 319.
108. Kuran, W. *Prog. Polym. Sci.* **1998**, *23*, 919.
109. Aida, T.; Inoue, S. *Acc. Chem. Res.* **1996**, *29*, 39.
110. Sugimoto, H.; Inoue, S. *Adv. Polym. Sci.* **1999**, *146*, 39.
111. Aida, T.; Sanuki, K.; Inoue, S. *Macromolecules* **1985**, *18*, 1049.
112. Aida, T.; Mizuta, R.; Yoshida, Y.; Inoue, S. *Makromol. Chem.* **1981**, *182*, 1073.
113. Akatsuka, M.; Aida, T.; Inoue, S. *Macromolecules* **1994**, *27*, 2820.
114. Xie, H.-Q.; Guo, J.-S.; Yu, G.-Q.; Zu, J. *J. Appl. Polym. Sci.* **2001**, *80*, 2446.
115. Braune, W.; Okuda, J. *Angew. Chem. Int. Ed.* **2003**, *42*, 64.
116. Sugimoto, H.; Kawamura, C.; Kuroki, M.; *et al. Macromolecules* **1994**, *27*, 2013.
117. Kuran, W.; Listos, T.; Abramczyk, M.; Dawidek, A. *J. Macromol. Sci., Pure Appl. Chem. A* **1998**, *35*, 427.
118. Chisholm, M.; Navarro-Llobet, D.; Simonsick, W. *Macromolecules* **2001**, *34*, 8851.
119. Chisholm, M.; Gallucci, J.; Navarro-Llobet, D.; Zhen, H. *Polyhedron* **2003**, *22*, 557.
120. Zevaco, T.; Sypien, J.; Janssen, A.; *et al. Catal. Today* **2006**, *115*, 151.
121. Zevaco, T.; Sypien, J.; Janssen, A.; *et al. J. Organomet. Chem.* **2007**, *692*, 1963.
122. Ko, B.-T.; Lin, C.-C. *Macromolecules* **1999**, *32*, 8296.
123. Liu, Y.-C.; Ko, B.-T.; Lin, C.-C. *Macromolecules* **2001**, *34*, 6196.
124. Hsueh, M.-L.; Huang, B.-H.; Lin, C.-C. *Macromolecules* **2002**, *35*, 5763.
125. Chen, C.-T.; Huang, C.-A.; Huang, B.-H. *Macromolecules* **2004**, *37*, 7968.
126. Lewinski, J.; Horeglad, P.; Tratkiewicz, E.; *et al. Macromol. Rapid Commun.* **2004**, *25*, 1939.
127. Annis, L.; Wasserman, E. WO Patent WO2002098559, 12 December 2002.
128. Wasserman, E.; Annis, L.; Chopin, L.; *et al. Macromolecules* **2005**, *38*, 322.
129. Tang, L.; Wasserman, E.; Neithamer, D.; *et al. Macromolecules* **2008**, *41*, 7306.
130. Wasserman, E.; Cheng, Y.; Tang, L. U.S. Patent Application 20100197873, 5 August 2010.
131. Wasserman, E.; Galley, R.; Song, W.; Ghosh-Dastidar, A. U.S. Patent Application 20100190955, 29 July 2010.
132. Ooms, P.; Hofmann, J.; Steinlein, C.; Ehlers, S. WO Patent Application WO 0134297(A2), 17 May 2001.
133. Ostrowski, T.; Harre, K.; Zehner, P.; et al. WO Patent Application WO0162826(A1), 30 August 2001.
134. Wu, L.; Yu, A.; Zhang, M.; *et al. J. Appl. Polym. Sci.* **2004**, *92*, 1302.
135. Kim, I.; Ahn, J.-T.; Ha, C.; *et al. Polymer* **2003**, *44*, 3417.
136. Lee, S.; Byun, S.; Baek, S.; *et al. Catal. Today* **2008**, *132*, 170.
137. Kim, I.; Ahn, J.-T.; Lee, S.-H.; *et al. Catal. Today* **2004**, *93–95*, 511.
138. Johnson, J.; Saboungi, M.-L.; Price, D.; Ansell, S. *J. Chem. Phys.* **1998**, *109*, 7005.
139. Croce, F.; Persi, L.; Ronci, F.; Scrosati, B. *Solid State Ionics* **2000**, *135*, 47.
140. Sandí, G.; Carrado, K.; Joachin, H.; *et al. J. Power Sources* **2003**, *119–121*, 492.
141. Fischer, H. *Mater. Sci. Eng. C* **2003**, *23*, 763.
142. Croce, F.; Scrosati, B. *Ann. N.Y. Acad. Sci.* **2003**, *984*, 194.
143. Fenton, D.; Parker, J.; Wright, P. *Polymer* **1973**, *14*, 589.
144. Gray, F.; McCallum, J.; Vincent, C. *Solid State Ionics* **1986**, *18–19*, 282.
145. Gorecki, W.; Andreani, R.; Bertheir, C.; *et al. Solid State Ionics* **1986**, *18–19*, 295.
146. Kelly, I.; Owen, J.; Steele, B. *J. Power Sources* **1985**, *14*, 13.
147. Moulin, J.; Damman, P.; Dosiere, M. *Polymer* **1999**, *40*, 171.
148. Armand, M.; Gorecki, W.; Andreani, R. In *Second International Symposium on Polymer Electrolytes* Scrosati, B., Ed.; Elsevier: London, 1990; p 91.
149. Neat, R.; Kronfli, E.; Lovell, K. In *Second International Symposium on Polymer Electrolytes* Scrosati, B., Ed.; Elsevier: London, 1990; p 151.
150. Marchese, L.; Andrei, M.; Roggero, R.; *et al. Electrochim. Acta* **1992**, *37*, 1559.
151. Abraham, K.; Alamgir, M. *Chem. Mater.* **1991**, *3*, 339.
152. Nogueira, A.; Longo, C.; De Paoli, M. *Coord. Chem. Rev.* **2004**, *248*, 1455.
153. Fontanella, J.; Wintersgill, M.; Calame, J.; *et al. Solid State Ionics* **1986**, *18–19*, 253.
154. Bonino, F.; Scrosati, B.; Selvaggi, A. *Solid State Ionics* **1986**, *18–19*, 1050.
155. Roux, C.; Gorecki, W.; Sanchez, J.; Belorizky, E. *Electrochim. Acta* **1998**, *43*, 1575.
156. Bruce, P.; Evans, J.; Vincent, C. *Solid State Ionics* **1987**, *25*, 255.
157. Stephan, A. *Eur. Polym. J.* **2006**, *42*, 21.
158. Ren, Y.; Zhang, Z.; Fang, S.; *et al. Sol. Energy Mater. Sol. Cells* **2002**, *71*, 253.
159. Croce, F.; Appetecchi, G.; Persi, L.; Scrosati, B. *Nature* **1998**, *394*, 456.
160. Best, A.; Ferry, A.; McFarlane, D.; Forsyth, M. *Solid State Ionics* **1999**, *126*, 269.
161. Wieczorek, W.; Zalewska, A.; Raducha, D.; *et al. J. Phys. Chem.* **1998**, *102*, 352.
162. Apicella, A.; Cappello, B.; Nobile, M.; *et al. Biomaterials* **1993**, *14*, 83.
163. Kim, C. *J. Pharm. Sci.* **1995**, *84*, 303.
164. Kim, C. *Pharm. Res.* **1995**, *12*, 1045.
165. Maggi, L.; Segale, L.; Torre, M.; *et al. Biomaterials* **2002**, *23*, 1113.
166. Savas, H.; Gqven, O. *Int. J. Pharm.* **2001**, *224*, 151.
167. Lambov, N.; Stanchev, D.; Peikov, P.; *et al. Pharmazie* **1995**, *50*, 126.
168. Belcheva, N.; Stamenova, R.; Tsvetanov, C.; *et al. Macromol. Symp.* **1996**, *103*, 193.
169. Di Colo, G.; Burgalassi, S.; Chetoni, P.; *et al. Int. J. Pharm.* **2001**, *215*, 101.
170. Di Colo, G.; Burgalassi, S.; Chetoni, P.; *et al. Int. J. Pharm.* **2001**, *220*, 169.
171. Andrade, J.; Nagaoka, S.; Cooper, S.; *et al. ASAIO Transact.* **1987**, *33*, 75.
172. Mora, M.; Occhiello, E.; Garbassi, F. *Clin. Mater.* **1993**, *14*, 255.
173. Lee, J.; Oh, S. *J. Biomed. Mater. Res.* **2002**, *60*, 44.
174. Costerton, J.; Stewart, P.; Greenberg, E. *Science* **1999**, *284*, 1318.
175. Roosjen, A.; Kaper, H.; Van der Mei, H.; *et al. Microbiology* **2003**, *149*, 3239.
176. Razatos, A.; Ong, Y.; Boulay, F.; *et al. Langmuir* **2000**, *16*, 9155.
177. Nagaoka, S.; Nakao, A. *Biomaterials* **1990**, *11*, 119.
178. Gombotz, W.; Guanghui, W.; Horbett, T.; Hoffman, A. *J. Biomed. Mater. Res.* **1991**, *25*, 1547.
179. Ki, D.; Young, S.; Dong, K.; *et al. Biomaterials* **1998**, *19*, 851.
180. Jeon, S.; Lee, J.; Andrade, J.; Gennes, P. *J. Colloid Interface Sci.* **1991**, *142*, 149.
181. Leckband, D.; Sheth, S.; Halperin, A. *J. Biomater. Sci. Polym. Ed.* **1999**, *10*, 1125.
182. Lee, S.; Laibinis, P. *Biomaterials* **1998**, *19*, 1669.
183. Branch, D.; Wheeler, B.; Brewer, G.; Leckband, D. *Biomaterials* **2001**, *22*, 1035.
184. Roosjen, A.; de Vries, J.; van der Mei, H.; *et al. J. Biomed. Mater. Res., Part B: Appl. Biomater.* **2005**, *73B*, 347.
185. Perez, E.; Cima, W. *Mater. Res. Soc. Symp. Proc.* **1992**, *252T*, 375.
186. Tsvetanov, C.; Stamenova, R.; Riess, G.; et al. WO Patent Application WO 03054065(A1), 3 July 2003.
187. Yoshii, F.; Zhanshan, Y.; Isobe, K.; *et al. Radiat. Phys. Chem.* **1999**, *55*, 133.
188. (a) Lang, S.; Webster, D. UK Patent Application 2,093,702(A), Sep, 02, 1982. (b) Webster, D.; Lang, S. 2,093,703(A), 8 September 1982.
189. Graham, N.; McNeill, M. *Biomaterials* **1984**, *5*, 27.
190. Tsanov, T.; Stamenova, R.; Tsvetanov, C. *Polymer* **1993**, *34*, 617.
191. Tsanov, T.; Stamenova, R.; Tsvetanov, C. *Polym. J.* **1993**, *25*, 853.
192. Tsanov, T.; Vassilev, K.; Stamenova, R.; Tsvetanov, C. *J. Polym. Sci. Part A: Polym. Chem.* **1995**, *33*, 2623.
193. Dennison, K. Ph.D. thesis, Massachusetts Institute of Technology, 1988.
194. Hooper, A.; North, J. *Solid State Ionics* **1983**, *9–10*, 1161.
195. King, P.; Warwick, N. U.S. Patent 3,264,202, 2 August 1966.
196. Rosiak, J.; Ulanski, P. *Radiat. Phys. Chem.* **1999**, *55*, 139.
197. Ulanski, P.; Zainuddin; Rosiak, J. *Radiat. Phys. Chem.* **1995**, *46* (4–6), 913.
198. Zakurdaeva, O.; Nesterov, S.; Feldman, V. *High Energy Chem.* **2006**, *39*, 201.
199. Gnanou, Y.; Hild, G.; Rempp, P. *Macromolecules* **1984**, *17*, 945.
200. Melekaslan, D.; Kasapoglu, I.; Ito, K.; *et al. Polym. Int.* **2004**, *53*, 237.
201. Sloop, S.; Lerner, M.; Stephens, T.; *et al. J. Appl. Polym. Sci.* **1994**, *53*, 1563.
202. Doytcheva, M.; Dotcheva, D.; Stamenova, R.; *et al. J. Appl. Polym. Sci.* **1997**, *64*, 2299.
203. Doytcheva, M.; Dotcheva, D.; Stamenova, R.; Tsvetanov, C. *Macromol. Mater. Eng.* **2001**, *286*, 30.
204. Doycheva, M.; Petrova, E.; Stamenova, R.; *et al. Macromol. Mater. Eng.* **2004**, *289*, 676.
205. Petrov, P.; Petrova, E.; Tsvetanov, C. *Polymer* **2009**, *50*, 1118.
206. Doycheva, M.; Stamenova, R.; Tsvetanov, C.; *et al. Macromol. Mater. Eng.* **2001**, *286*, 151.
207. Dotcheva, D.; Tsvetanov, C. *Polym. Bull.* **1999**, *42*, 709.
208. Doytcheva, M.; Stamenova, R.; Zvetkov, V.; Tsvetanov, C. *Polymer* **1998**, *39*, 6715.
209. Banat, R.; Tincer, T. *J. Appl. Polym. Sci.* **2003**, *90*, 488.
210. Tsvetanov, C.; Stamenova, R.; Dotcheva, D.; *et al. Macromol. Symp.* **1998**, *128*, 165.
211. Tsvetanov, C.; Stamenova, R.; Riess, G.; *et al.* US Patent Application 20050043429 A1, 24 February 2005.
212. Emami, S.; Salovey, R.; Hogen-Esch, T. *J. Polym. Sci. Part A: Polym. Chem.* **2002**, *40*, 3021.
213. Emami, S.; Salovey, R.; Hogen-Esch, T. *J. Polym. Sci. Part A: Polym. Chem.* **2003**, *41*, 520.
214. Emami, S.; Salovey, R. *J. Appl. Polym. Sci.* **2003**, *88*, 1451.

Biographical Sketches

Dr. Ivaylo Dimitrov received his PhD in Polymer Chemistry from the Institute of Polymers, Bulgarian Academy of Sciences in 2001 under the supervision of Associate Professor Iliyana Berlinova in the area of associating amphiphilic copolymers. He held postdoctoral positions at the Max Planck Institute of Colloids and Interfaces, Germany with Dr. Helmut Schlaad working on peptide-based hybrid copolymers and at the University of Massachusetts at Lowell, USA with Professor Rudolf Faust working on kinetics of carbocationic polymerization of isobutylene. Since 2009, he has been associate professor at the Institute of Polymers of the Bulgarian Academy of Sciences. His research focuses on controlled polymerization methods, peptide-based hybrid copolymers of different architecture, and targeted drug delivery systems.

Christo B. Tsvetanov is full professor of polymer science at the Institute of Polymers, Bulgarian Academy of Sciences and head of the Scientific Council of the Institute of Polymers. A major focus of his research concerns controlled polymerization methods, water-soluble polymers and hydrogels, stimuli-responsive copolymers, and their self-assembly to polymeric nanoparticles. He is well known for his contributions to the area of anionic coordination polymerization of oxirane and the role of donor and acceptor additives on the mechanism of anionic polymerization. Since 2004, he has been a corresponding member of the Bulgarian Academy of Sciences.

4.22 Nonlinear Macromolecules by Ring-Opening Polymerization

C Schüll, D Wilms, and H Frey, Johannes Gutenberg University (JGU), Mainz, Germany

4.22.1 Introduction

Advances in nanotechnology and many areas of materials science require complex materials with well-defined architectures. The use of linear polymers limits functional and structural possibilities. Therefore, nonlinear polymers have become an important topic in polymer research during the past two decades, since they open a pathway to novel complex structures with exciting properties. Fritz Vögtle published a groundbreaking work on the synthesis of cascade-branched macromolecules in 1978, followed by seminal works by Tomalia, Newkome, and Hawker and Fréchet.[1] These dendritic (in Greek *dendros*, meaning tree) macromolecules are characterized by a branch-on-branch topology, resulting in a monodisperse, multivalent, and globular structure, which makes them interesting for a wide range of applications.[2] However, the perfectly branched structures of dendrimers are obtained using a multistep reaction approach. This is also their major drawback for large-scale production and subsequent applications.

Randomly branched macromolecular structures have been known since the 1930s, from natural polysaccharides such as glycogen, dextran, or amylopectin.[3] In a theoretical work from the 1950s, Flory theoretically described AB_m polycondensates, which are obtained by step-growth mechanisms, demonstrating that such 'random $AB_{(f-1)}$ polycondensates' show a random dendritic structure and very high polydispersities.[4] Pioneering work in the synthesis of such polymers was carried out by Kim and Webster in the 1990s, who coined the term 'hyperbranched' for random dendritic branching in polymers.[5] The outstanding advantage over dendrimers is the availability of hyperbranched polymers in one single reaction step. In addition, their multivalency and three-dimensional structure that usually shows no entanglements increase solubility and lower viscosity of the polymers compared to their linear analogs. This makes them interesting for a variety of current and future applications ranging from biomedicine to catalysis, being a serious rival for the synthetically challenging dendrimers.[6]

A large number of different monomers such as cyclic ethers, acetals, amides, esters, and siloxanes are used in ring-opening polymerizations (ROPs) to obtain linear polymers for a variety of everyday applications.[7] Nevertheless, ring-opening strategies have also been established as a versatile method for the synthesis of hyperbranched homopolymers as well as other complex macromolecular architectures in the recent years.

This chapter focuses on fundamental concepts of hyperbranching polymerizations, based on ring-opening strategies using single-monomer methodology (concepts for multimonomer approaches are covered in Chapter 6.05). The state of the art and mechanistic details in the synthesis of homopolymers as well as some selected applications and complex structures by core variation, terminal functionalization, and (block) copolymerization will be summarized as well. Furthermore, some of these concepts for the generation of more complex hyperbranched topologies, for example, linear-hyperbranched block copolymers (LHBCs) or multiarm star polymers will be presented at the end of the chapter. The details for the synthesis of macrocyclic polymers, which can also be considered as nonlinear, are treated in another chapter (see Chapter 6.02).

4.22.2 Background and History

4.22.2.1 General Concepts in Synthesis of Nonlinear Polymers by Ring-Opening Polymerization

As demonstrated in other chapters of this comprehensive, hyperbranched polymers were traditionally prepared by polycondensation of AB_m-type monomers.[8,9] In the mid-1990s, Fréchet *et al.* introduced the self-condensing vinyl polymerization (SCVP)[10,11] utilizing monomers containing a polymerizable vinyl group along with an initiating functionality, as highlighted in the preceding chapter (see Chapter 6.05). These monomers are often referred to as 'inimers', because they combine an initiating and a polymerizable moiety in one molecule. Even though a huge variety of hyperbranched polymers are accessible via both AB_m polycondensation and SCVP, broad

molecular weight distributions with polydispersities in the range of degree of polymerization (DP_n)/2 are always obtained, which is often undesirable.

In the late 1990s, Penczek and co-workers described the synthesis of highly branched (star) polymers by reacting oligomeric alcoholates obtained by ring-opening polymerization of ethylene oxide (EO) with various diepoxides.[12] One possible reaction sequence of the reaction is shown in **Scheme 1**. This approach can be seen as the first self-condensing ROP (SCROP) synthesis (see below) to obtain hyperbranched polymers.

Shortly after this, Hedrick *et al.* and Fréchet *et al.* almost simultaneously presented an analogous concept that relies on cyclic lactone inimers, which they called self-condensing (or self-condensation) ROP (SCROP).[13,14] It is interesting to note that this approach uses monomers containing a cyclic moiety that can generate a branching point by introducing a new functionality only upon ring opening during the polymerization reaction. Such monomers are often called 'latent AB_m monomers' (cf. general **Scheme 2**). The driving force for this type of polymerization is the ring-opening isomerization of the cyclic monomer unit driven by the ring strain of the cyclic inimer and the formation of thermodynamically and kinetically stable bonds in the polymer structure. Today, this method is also commonly referred to as ring-opening multibranching polymerization (ROMBP). The terms SCROP and ROMBP are equivalent at present.

Well in advance of these works and before hyperbranched polymers became a matter of broad scientific interest, Sandler and Berg,[15] as well as Vandenberg *et al.*[16] studied the polymerization of glycidol, a typical cyclic latent AB_2 monomer. Primarily they were aiming at linear polymer architectures, but in the course of their studies they also observed the formation of undesirable branched structures due to propagation of both the primary and secondary hydroxyl groups present after ring opening of glycidol. These polymers were chatracterized by Vandenberg *et al.* in a seminal paper published in 1985, which describes the generation of different chain units upon the base-catalyzed polymerization of glycidol.[16]

Subsequently, both cationic[17,18] and anionic[19–21] ROP techniques were applied to the polymerization of glycidol in the early 1990s by Penczek, Kubisa, and Dworak in important works in this field. The crucial prerequisite for the versatility of applicable polymerization techniques for glycidol is the oxygen heteroatom, which provides a reaction site in the ring for both nucleophilic and electrophilic attacks of initiating or propagating species. Further progress in this area was made by Frey *et al.*,[19] who established the slow monomer addition (SMA) technique in 1999, leading to polyglycerols (PGs) with moderate to narrow molecular weight distributions.

As early as 1992, Suzuki and Saegusa reported the palladium-catalyzed multibranching polymerization of a cyclic

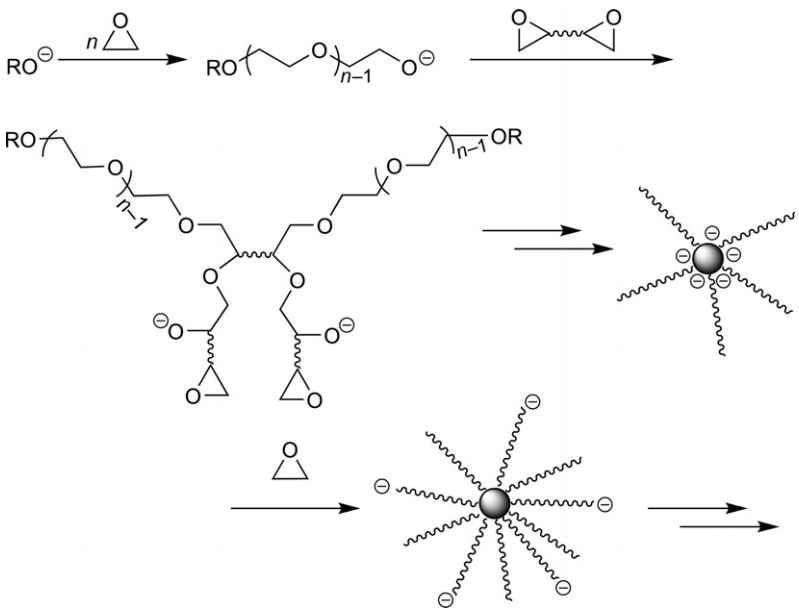

Scheme 1 Synthesis of highly branched polyethers by Penczek and co-workers.

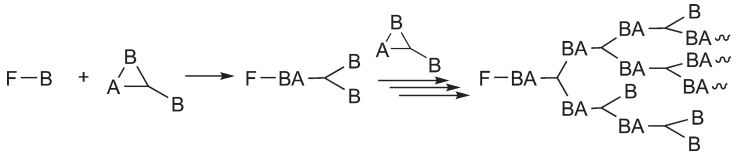

Scheme 2 General principle of ring-opening multibranching polymerizations (ROMBPs). F is the single focal unit, while B depicts the reactive groups of the cyclic inimer.

carbamate, another example for a latent cyclic AB_2 monomer, leading to hyperbranched polyamines.[22] It is important to note that Suzuki and Saegusa in their paper reported the first 'initiated' type of multibranching polymerization, that is, a chain-growth mechanism. The low polydispersity ($M_w/M_n = 1.35$) demonstrates the possibility to control the growth of the polymer chains in this system.

This type of polymerization reaction is usually initiated by a suitable molecule containing a focal unit F as well as reactive B groups that can react with the cyclic structure under ring opening. For each AB_2 monomer being incorporated into the growing polymer molecule, two new potential polymerization sites B are created, while only one is consumed. For the AB_2 system, the number of functional B-groups in the final polymer structure can be calculated easily as the sum of the number of initiating units F and the DP_n.

4.22.2.2 Degree of Branching

Besides the crucial parameters: (1) nature of the backbone, (2) chain-end functional groups, (3) chain length between the branching points, and (4) molecular weight distribution, the degree of branching (DB) is a crucial characteristic for hyperbranched polymers. It distinguishes linear structure in the absence of branching (linear polymer, DB = 0), random branching (hyperbranched polymer, ideally random, DB = 0.5), and perfect branching (dendrimer, DB = 1). Webster[23] and Fréchet *et al.*[24] suggested an equation for the calculation of the DB for AB_2-type hyperbranched polymers in the early 1990s, depending on the content of dendritic (D), terminal (T), and linear (L) units in the polymer structure, which are usually determined by NMR spectroscopy.

$$DB_{Fréchet} = \frac{T + D}{T + D + L} \quad [1]$$

Frey *et al.*[25] modified this equation on the basis of a systematic approach to

$$DB_{Frey} = \frac{2D}{2D + L} \quad [2]$$

For AB_2 systems, since eqn [1] fails for polymers with high DP_n and low DB, leading to DB > 0 for linear, low-molecular-weight polymers. Müller and Yan at the same time developed a systematic equation to calculate the DB for the SCVP.[26]

4.22.3 Specific Concepts in the Synthesis of Nonlinear Polymers by Ring-Opening Polymerization

Utilizing a variety of monomers, initiators and catalysts, ROMBPs have been carried out under various conditions. Regarding the reaction mechanism, basically all reported approaches are based on the principle illustrated in Scheme 2.

In the following sections, a detailed overview of the respective polymerization mechanisms, that is, cationic, anionic, and catalytic ROMBPs will be treated. The respective seminal works leading to their development, specific prerequisites, synthetic principles, and peculiarities for each method will be examined and discussed for heterocyclic monomers containing different ring sizes and different heteroatoms. Selected issues treated in this overview have also been considered in a recently published book on hyperbranched polymers coedited by H. Frey of this chapter.[27]

4.22.3.1 Cationic Ring-Opening

In cationic polymerizations, electron-deficient initiators (mostly Brønsted or Lewis acids) react with electron-rich monomers. The active chain end (ACE) bears a positive charge with the active sites being either carbenium or oxonium ions. Molecular weights are often limited by the inherent sensitivity to impurities, chain transfer, and rearrangement reactions. Suitable monomers for cationic polymerizations are vinyl monomers with electron-donating moieties or cyclic structures containing heteroatoms, while the latter case is termed cationic ROP. Eligible monomers include cyclic ethers, acetals, and amines as well as lactones and lactams (Scheme 3).

In 1969, Hauser first described the ROP of alkylene imines.[28] It was observed that the polymerization of aziridines (three-membered cyclic imines) leads to a product with extensive branching. Subsequently, Dick and Ham reported a random distribution of primary, secondary, and tertiary amino groups.[29] Branching results from the formation of tertiary amino groups upon intermolecular nucleophilic attack of secondary amine nitrogens in polymer repeating units on propagating iminium centers (Scheme 4). Thus, the long-known polymerization of aziridines is in fact the oldest known ROMBP, leading to hyperbranched poly(ethylene imine)s. The resulting materials have been available for more than three decades and are sold under the trade name Lupasol® on a scale of several 100 000 ton per year. They are used for paper modification as well as in sewage plants for removal of heavy metal ions. Substitution on the aziridine ring impedes polymerization.[30,31] The 1,2- and 2,3-disubstituted aziridines do not polymerize; 1- and 2-substituted aziridines undergo polymerization, but polymer yields and molecular weights are limited.

Azetidines, four-membered cyclic imines and their derivatives were also investigated regarding their cationic polymerization in the early 1980s.[32] In analogy to the polymerization of aziridine, hyperbranched structures are obtained by the same mechanism as described previously. Still, the difficult monomer preparation and the limitation of molecular weights due to rather low reactivity of the chain end compared to oxo-heterocycles limited the interest in these polymers. By using the derivative *N*-phenylazetidine (Scheme 3), the formation of linear chains can be favored. Branching termination reactions are suppressed because of the decreased

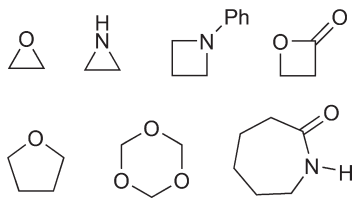

Scheme 3 Important monomers for cationic ring-opening polymerizations.

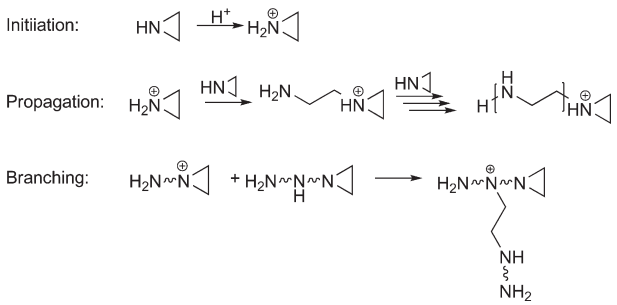

Scheme 4 Hyperbranching polymerization of ethylenimine (aziridine).

nucleophilicity, while propagation is supported by enhanced ring-opening reactivity.[33]

Compared to sulfur-[34] or nitrogen-containing heterocycles, oxygen-containing heterocycles are most widely used in cationic ROP. The high electronegativity of the oxygen heteroatom is beneficial for the ring opening, while the high nucleophilicity of the oxy anion leads to high propagation rates. Oxiranes or oxetanes with hydroxyl groups can potentially be polymerized by typical cationic initiators, for example, protic or Lewis acids such as trifluoromethanesulfonic acid (TfOH) or boron trifluoride etherate ($BF_3 \cdot OEt_2$). During the reactions, branching points are generated, which justifies the term 'cationic ROMBP'. In an important work, Dworak and Penczek[17] studied the coexistence of ACE and the activated monomer (AM) mechanisms in the cationic polymerization of glycidol (**Schemes 5** and **6**). In order to investigate the comparative relevance of both concurrent reaction pathways, hyperbranched polygylcerols with molecular weights of up to 10 000 g mol^{-1} were synthesized and characterized. It is obvious that only primary hydroxyl groups would be present as substituents of the polyether chain if the reaction proceeded exclusively by the ACE mechanism.

In contrast, propagation by the AM mechanism generates two different types of repeating units. R–OH in **Scheme 5** depicts either the chain end or the side group. In the latter case, branching occurs.

Characterizing the structure of the polymers, Dworak and Penczek found a significant contribution of the AM mechanism to the chain growth. Also within the scope of this elegant work, a direct correlation between the specific initiator and the percentage of secondary hydroxyl groups attached to the polymer backbone was verified.[17] Use of $SnCl_4$ or $BF_3 \cdot OEt_2$ as Lewis acid initiators in particular proved to promote the AM mechanism.

Crivello described the synthesis of linear and hyperbranched polyethers using alicyclic epoxy alcohols derived from cyclohexane scaffolds.[35] Kakuchi and co-workers recently presented the detailed characterization of these hydrophobic hyperbranched polyethers using 3,4-epoxycyclohexane-1-methanol and α-terpineol epoxide (**Scheme 7(a)**) as latent AB_2 monomers. While the latter one showed almost no polymerization reaction due to sterical hindrance of the tertiary alcohol group.[36] While matrix-assisted laser desorption ionization time of flight (MALDI-TOF) mass spectrometry indicates no side reactions, the molecular weights are in the range 2000–5000 g mol^{-1} with moderate polydispersities (M_w/M_n) of 1.4–2.1. Other poly(terpene alcohol)s were also synthesized using citronellol oxide and nopol oxide as cyclic inimers (**Scheme7(b)**).[37] Kakuchi *et al.* also described the synthesis of hyperbranched polyerythritol by ROMBP of 2,3-anhydroerythritol as a latent AB_3 monomer (**Scheme 7(c)**). The use of highly reactive

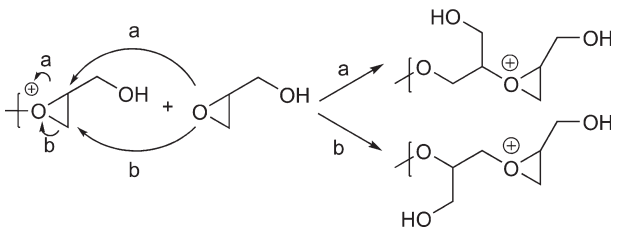

Scheme 5 Active chain-end mechanism in the cationic polymerization of glycidol: (a) α- and (b) β-ring opening preserves the CH_2OH substituent.

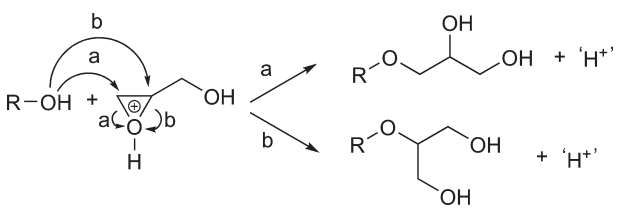

Scheme 6 Activated monomer mechanism in the cationic polymerization of glycidol: (a) β- and (b) α-ring opening preserves the CH_2OH substituent.

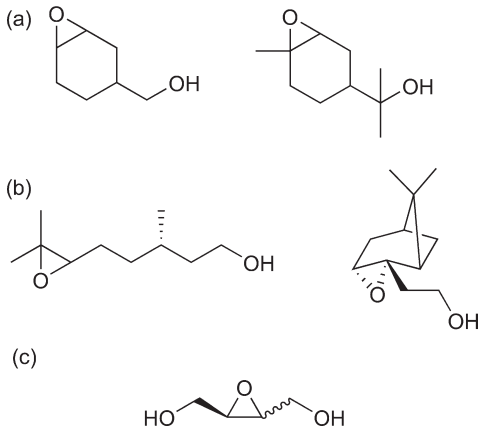

Scheme 7 Other hydroxyl-functional epoxide derivatives polymerized by Crivello *et al.* and Kakuchi *et al.*

oxiranes instead of 1,2-anhydroerythritol (five-membered ring) as monomer lead to polymers free from cyclic repeating units and almost random DB, which were obtained in the earlier works.[38]

Besides the oxiranes, the respective four-membered heterocyclic oxetanes have been studied as monomers in ROPs. Vandenberg *et al.* obtained a linear and highly crystalline polymer from oxetanes[39,40] and other authors detailed the synthesis of hyperbranched polyethers from hydroxyl-functional oxetanes.[41,42] Mostly cationic initiators have been used in the ROP of oxetanes, primarily because of the higher basicity compared to three-membered oxiranes, which are prevalently polymerized by anionic techniques.

In 1999, Hult *et al.*[43] published a study on the cationic ROP of 3-ethyl-3-(hydroxymethyl)oxetane (EHO). A convenient method for the preparation of the respective hyperbranched polyether by thermally induced bulk polymerization was introduced. The sulfonium salt initiator 1-benzyltetrahydrothiophen-1-ium hexafluoroantimonate was used in this approach (**Scheme 8**).

Surprisingly narrow molecular weight distributions ($M_w/M_n = 1.26–1.43$) at molecular weights up to 5000 g mol^{-1} were found. Detailed characterization of the hyperbranched polymers by proton-decoupled ^{13}C NMR experiments showed a correlation between monomer conversion and the DB. While at low conversions (< 30%), predominantly linear units were formed, increased conversion led to a higher fraction of dendritic units in the polymer structure. The possibility of tailoring the DB of these polymers by controlling the monomer conversion was later reported by the same authors.[44] Determination of the number of secondary and tertiary oxonium ions during the reaction provides the ratio of ACE and AM mechanisms in the polymerization of hydroxyl-functionalized oxetanes. A significant prevalence (90:10) of the AM mechanism was found, leading to highly branched polyethers. However, in no case a DB exceeding 0.4 was obtained, which is significantly lower than the theoretical value 0.5, for polymerizations under entirely random conditions. This observation leads to the assumption that upon ring opening of oxetanes, the coexistence of ACE and AM mechanisms adversely affects the generation of branching points.

By subsequent addition of glycidol monomer to the cationic ROP of EHO, Gao *et al.* obtained amphiphilic core–shell block copolymers with a complex branch-on-branch topology (**Scheme 9**).[45] The higher feed ratio of glycidol monomer corresponds to a better solubility of the polymer in water. This behavior was expected due to a higher hydrophilicity of glycidol compared to the EHO repeating units.

3,3-Bis(hydroxymethyl)oxetane (BHMO; **Scheme 10**), an AB_3-type cyclic monomer with an oxetane ring, can also be used for cationic ROP.

Farthing[46] and later Vandenberg *et al.*[39] polymerized BHMO by initiating with a trifluoromethanesulfonic acid catalyst, obtaining a weakly branched polymer of low molecular weight. Interestingly, a more crystalline product of higher molecular weight was obtained when using the trimethylsilyl ether of BHMO and i-Bu_3Al-0.7 · H_2O cationic catalyst as initiator. Characterization of all of these polymers with regard to the DB is unfortunately limited by the complexity of the respective ^1H and ^{13}C NMR spectra. In addition, the strong aggregation of the highly hydroxyl-substituted polymers is a severe limitation for further characterization since their solubility in all common solvents is low. However, BHMO appears to offer a potential for further efforts in the future that may rely on copolymerization with other cyclic comonomers and which might affect the solubility and branching topology of the resulting materials.

Monosubstituted derivatives of tetrahydrofuran (THF) have been known to be difficult to polymerize due to thermodynamic reasons.[47] Bednarek and Kubisa extended cationic multibranching polymerizations to the class of five-membered cyclic ethers containing hydroxyl groups as substituents.[48] They polymerized 2-(hydroxymethyl)tetrahydrofuran, using a trifluoromethanesulfonic acid initiator. MALDI-TOF mass

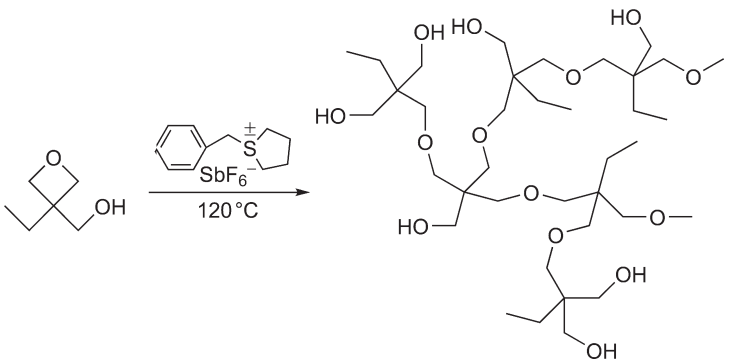

Scheme 8 Synthesis of hyperbranched polyethers via cationic ring-opening multibranching polymerization of EHO.

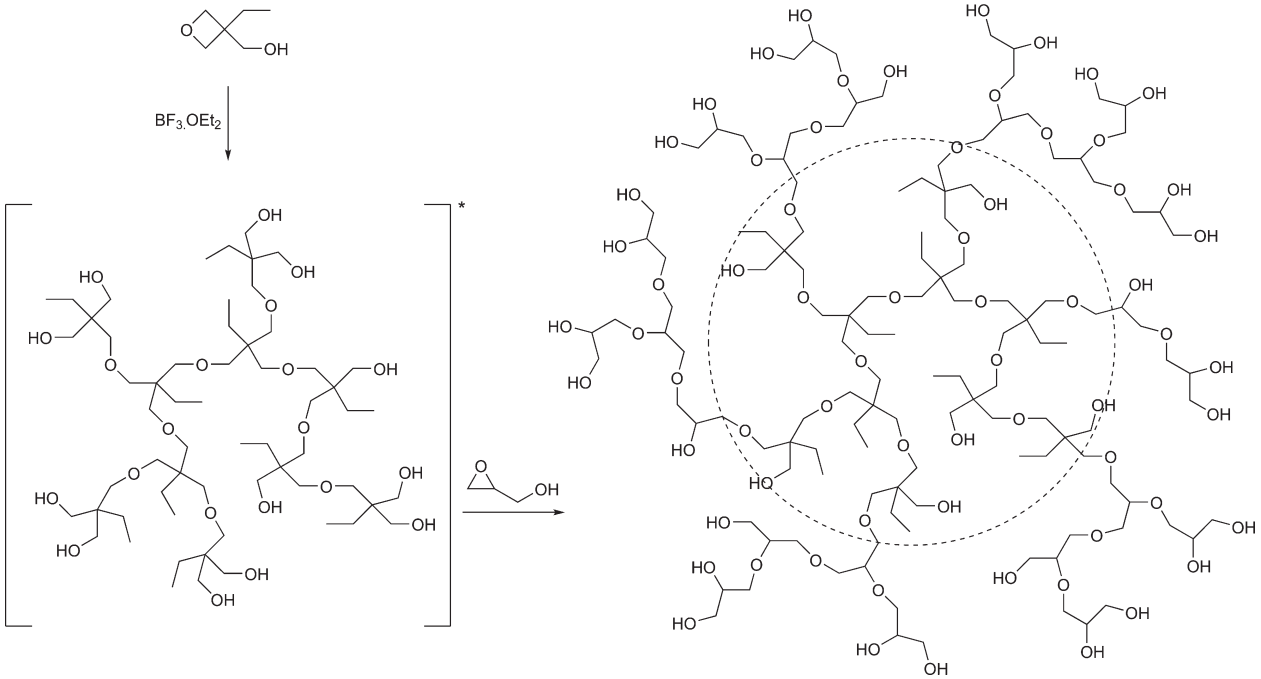

Scheme 9 Synthesis of an amphiphilic core–shell copolymer by cationic polymerization of EHO and subsequent addition of glycidol.[43]

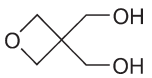

Scheme 10 3,3-Bis(hydroxymethyl)oxetane (BHMO).

spectrometry of the obtained oligomers indicated that elimination of water took place in the course of the polymerization. Scheme 11 shows this undesirable side reaction leading to unsaturated units in the polymer structure.

In order to understand whether this behavior can be ascribed to a more complex mechanism than formerly assumed, the authors studied the polymerization of other THF derivatives and observed elimination of water in all cases. Bednarek and Kubisa suggested a general reinvestigation of the polymerizability problems of five-membered cyclic ethers containing hydroxyl groups since the mechanistic details must still be evaluated to explain these results.

Multivalent glycopolymers as complex polymer architectures for biomedical applications are an emerging research field.[49] The polyol structure of carbohydrates obviously leads to the concept of using ROPs for the synthesis of highly branched sugars, which dates back to the late 1950s with works of Schuerch *et al.*[50] Kakuchi *et al.* presented several syntheses during the last decade, wherein several attempts toward a detailed characterization were performed.[38,51,52] In a recent interesting work, 17 kinds of D-glucopyranosyl and D-glucofuranosyl repeating units were assigned using ^{13}C NMR spectroscopy, which emerge when 1,6-anhydro-β-D-glucopyranose is polymerized by cationic ROMBP as a latent AB_4-monomer (Scheme 12).[53] A tremendous variety of repeating units make these materials interesting as viscosity modifiers, as suggested by the authors, but not for applications in biomedicine since the materials are not sufficiently well defined to investigate specific interaction with physiological systems. It is obvious that further progress in controlling the chemoselectivity in the synthesis of hyperbranched glycopolymers has to be achieved in the future.

Cationic ROMBPs for the synthesis of hyperbranched polymers are generally limited in terms of their potential for further investigation and commercial applications by the number of eligible monomers. Other methods have proven to be superior in terms of achievable molecular weights, control over the reaction and suppression of the formation of undesired side products.

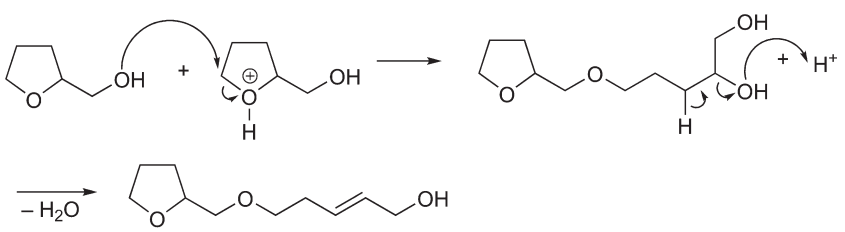

Scheme 11 Formation of unsaturated units in the acid-catalyzed polymerization of 2-(hydroxymethyl)tetrahydrofuran.

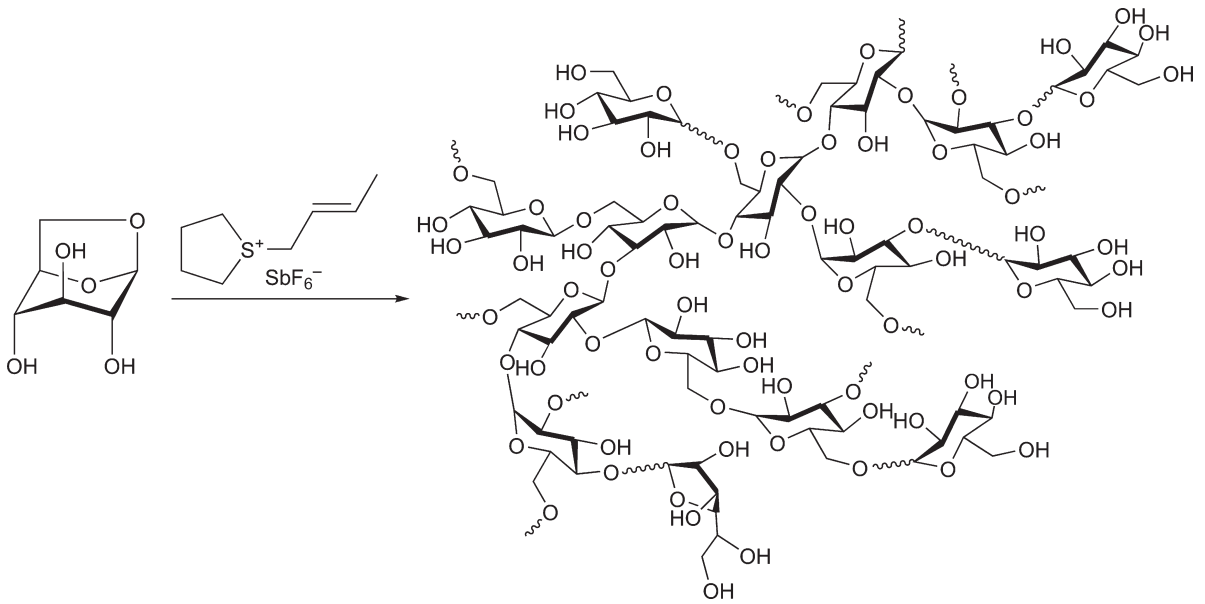

Scheme 12 Synthetic hyperbranched poly(D-glucan).

4.22.3.2 Anionic Ring-Opening Multibranching Polymerization

Various basic (nucleophilic) initiators can be used to initiate anionic polymerization, including covalent or ionic metal amides, alkoxides, hydroxides, cyanides, phosphines, amines, and organometallic compounds such as butyllithium. The polymerization is initiated by addition of the initiating species to the monomer, typically a vinyl compound with electron-withdrawing moieties. In anionic ROPs, cyclic monomers with electron-deficient carbon atoms such as amides (lactams) and esters (lactones), ethers (oxiranes), or Leuchs anhydrides are used as monomers (Scheme 13).

Glycidol (2,3-epoxy-1-propanol), a latent cyclic AB_2-type monomer containing a highly strained three-membered oxirane ring, can be polymerized by addition of a nucleophilic initiator. In an early work by Rider and Hill, it was casually mentioned that pyridine polymerized glycidol to a water-soluble black tar.[54] Sandler and Berg later observed by chance that glycidol polymerized vigorously in the presence of triethylamine. This motivated them to further investigation of the effect of basic catalysts on the rate of polymerization.[15] The assumption that the obtained product shows an exclusively linear structure (Scheme 14) was not challenged until Vandenberg *et al.* characterized a variety of protected and unprotected PGs in the mid-1980s in a systematic manner.[16] These polymers were prepared by polymerization of glycidol with KOH catalyst, aiming at a linear polymer structure.

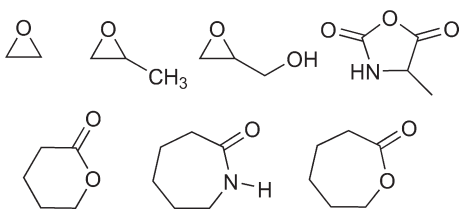

Scheme 13 Examples of monomers for anionic ring-opening polymerizations.

As a part of detailed investigations, the analysis of ^{13}C NMR spectra provided the authors with initial information about the actual branched structure of PG (Scheme 15) obtained by the polymerization of nonprotected glycidol.

It was concluded that a 1,4-polymerization involving proton transfer is predominant in the base-catalyzed polymerization of glycidol, giving poly(oxetan-3-ol). Hydroxyl groups (or trimethylsilyloxy groups in the case of protected PGs) are present on both the monomer and the polymer. Facile exchange with the propagating oxyanion was found to result in chain branching and chain transfer. The individual processes taking place upon growth of the polyether chains are illustrated in Scheme 16. Primary and secondary alkoxides are formed after the ring opening due to rapid intra- and intermolecular transfer. Further propagation of these species directly results in branching.

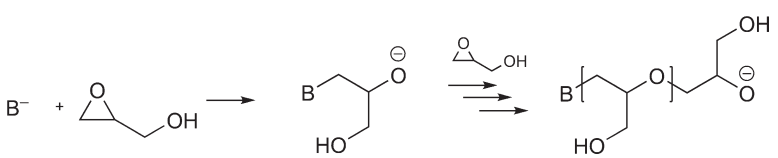

Scheme 14 Hypothetic formation of linear polyglycerol, as proposed by Sandler and Berg. The primary hydroxyl group was not considered by these authors.

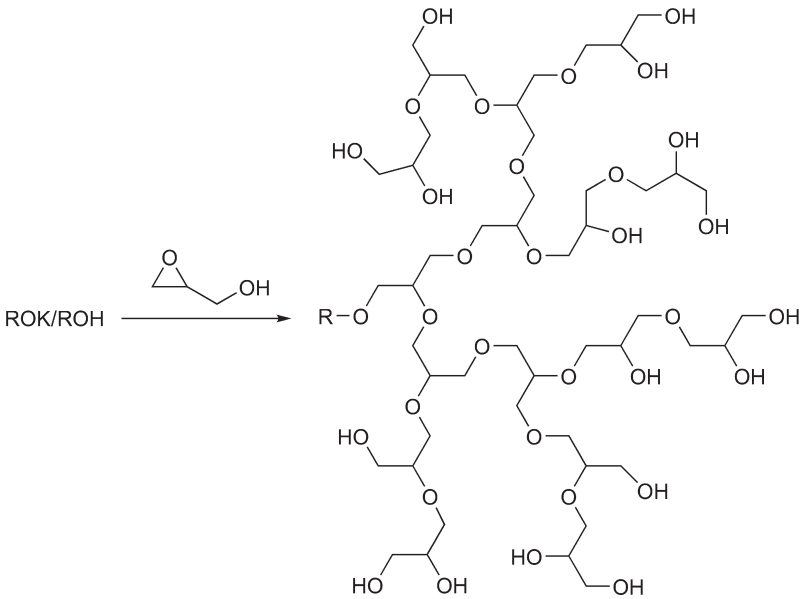

Scheme 15 Synthesis of hyperbranched polyglycerol via base-catalyzed polymerization of glycidol.

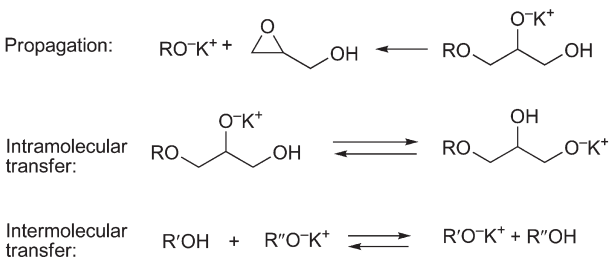

Scheme 16 Mechanism of the anionic polymerization of glycidol.

After that, no follow-up works were published on the anionic polymerization of glycidol, most probably since the formation of dendritic polymers was not a topic of major interest at that time. Extensive research on the synthesis, characterization, and structure of hyperbranched aliphatic polyethers has been carried out by Frey *et al.* since the late 1990s, which was motivated by the search for alternatives to the tediously prepared dendrimers.[19,20] In analogy to concepts developed for atom transfer radical polymerization (ATRP)[55] and the synthesis of poly(propylene oxide),[56] conventional base initiators were replaced by a partially deprotonated polyfunctional alcohol. Controlled polymerization of glycidol was achieved by applying the SMA approach. 1,1,1-Trimethylolpropane (TMP), bearing three OH-groups, has been widely used as a typical multifunctional initiator core for the synthesis of PG in the recent decade. Simultaneous chain growth is essential for obtaining well-defined hyperbranched PGs (hbPGs) with narrow molecular weight distributions ($M_w/M_n = 1.2–1.8$). Thus, the concentration of active sites in the polymerization (alkoxides) has to be controlled by deprotonating the initiator hydroxyl groups only partly, usually by 10%, upon addition of a strong base like potassium methylate as a deprotonating agent, followed by removal of excess methanol. Slow addition of the monomer (SMA) circumvents homopolymerization initiated by deprotonated glycidol as well as any undesired cyclization reactions. Hence this technique further promotes low polydispersities and complete control of the number-average molecular weight by adjustment of the monomer/initiator ratio, when – in the ideal case – every newly formed glycerol unit is attached to the polyfunctional cores or the branched polyols already present in the reaction. The polymerization reaction involves a reversible termination mechanism; nucleophilic attack of the alkoxide takes place at the unsubstituted end of the oxirane ring, leading to a secondary alkoxide. Due to fast proton transfer equilibria, also known from linear epoxide polymerizations,[56] the more stable and more reactive linear alkoxide is formed to a certain extent (**Scheme 16**). Both types of alkoxides represent ACEs and, therefore, lead to the formation of hyperbranched structures. The fundamental relevance of polyfunctional initiators and the SMA methodology for the formation of well-defined hyperbranched polymers was also shown in elegant theoretical work for SCVP[57] and by computer simulation.[58]

If the secondary hydroxyl group propagates, the polymer chain is attached to a glycerol unit and a linear 1,3-unit (L_{13}) is generated. A linear 1,4-unit (L_{14}) is formed, when the primary hydroxyl group undergoes propagation. Reaction of both hydroxyl groups with monomer leads to the incorporation of a highly branched, that is, dendritic unit (D). If a monomer

unit has been deactivated by proton exchange, a terminal unit (T) with two hydroxyl end groups is formed. A detailed structural investigation of these hbPGs was carried out by Frey *et al.* who analyzed inverse gated ^{13}C NMR spectra in order to calculate DBs and DP_n's.[19] Incorporation of the TMP core into the polymer and the amount of cyclization occurring during the reaction were studied by MALDI-TOF mass spectrometry. Polymers with molecular weights up to 10 000 g mol^{-1} (significantly higher M_n than those obtained from the previously discussed cationic polymerizations) were prepared. They exhibited narrow molecular weight distributions ($M_w/M_n < 1.5$, mostly < 1.3) due to the pseudo-chain-growth kinetics. The polydispersity was shown to be $1 + 1/n$, n being the functionality of the initiator polyol employed.[56]

The controlled synthesis of hbPGs of molecular weights exceeding 7000 g mol^{-1} was not possible by the 'classical' SMA protocol[19] until recently. Wilms *et al.* used hbPG of low molecular weight as a macroinitiator for the controlled synthesis of hbPG with molecular weights up to 24 000 g mol^{-1}.[59] In this two-step approach, the synthesis of polymers with elevated molecular weights under SMA conditions is possible, which results in controllable molecular weight and moderate polydispersity indices ($M_w/M_n < 1.8$). A very interesting work in this area was published by Brooks *et al.*, who modified the standard procedure by adding dioxane as an emulsifier. In this case, high-molecular-weight PGs with M_n up to 700 000 g mol^{-1} have been obtained.[60] These materials exhibit the highest molecular weights obtained for synthetic hyperbranched polymers reported to date. The reason for the formation of high-molecular-weight PGs possessing nevertheless low polydispersity is not yet clear. Brooks *et al.* tentatively explain the effect on molecular weight by the fast proton exchange in their system. In further studies, Brooks *et al.* have demonstrated excellent biocompatibility and low toxicity for hbPGs, similar as it has been known for a long time for poly(ethylene oxide) (PEO). This renders the material interesting for biomedical applications, potentially as a substitute for PEO.[61]

To facilitate the synthesis of hbPG for industrial processing, microreactor technology[62] can be used to obtain polymers with molecular weights up to 1500 g mol^{-1}.[63] In this approach, an efficient continuous process is used, which results in significantly reduced experimental effort, albeit with molecular weight limitations.

Within the last decade, there has been an increasing interest in highly branched chiral macromolecules. Supramolecular ordering and chiral recognition can be realized by chiral dendritic structures.[64] In the 1980s and 1990s, the stereospecific mechanisms of ROP were studied.[65] Nevertheless, only few works studied the properties of chiral hyperbranched polymers. If only one of the enantiomers of glycidol is used in the polymerization, chiral hbPGs can be obtained. In analogy to the previously discussed racemic PGs, the respective polymerization of both commercially available glycidol enantiomers has been investigated.[66] The obtained polymers exhibited specific optical rotation [α] per monomer unit when using only one enantiomer of glycidol for the polymerization. This is an important observation since it confirms the expectation that in anionic epoxide polymerization the nucleophilic attack occurs at the least substituted end of the epoxide ring.[28] In a recent work, Stiriba and co-workers realized chiroptical induction and molecular recognition by incorporating an inherently chiral benzophenone core into a chiral hbPG structure (**Scheme 17**).[67] They could show that the enaniomerically pure polymer 'shell' induces a preferred helical sense at the benzophenone core. Interestingly, the addition of further racemic glycidol leads to amplification of the chirality within the polymers. The incorporation of core molecules into nonlinear polymers will be discussed in more detail later.

Random copolymers are interesting as they combine different properties of several polymers within one material. In a

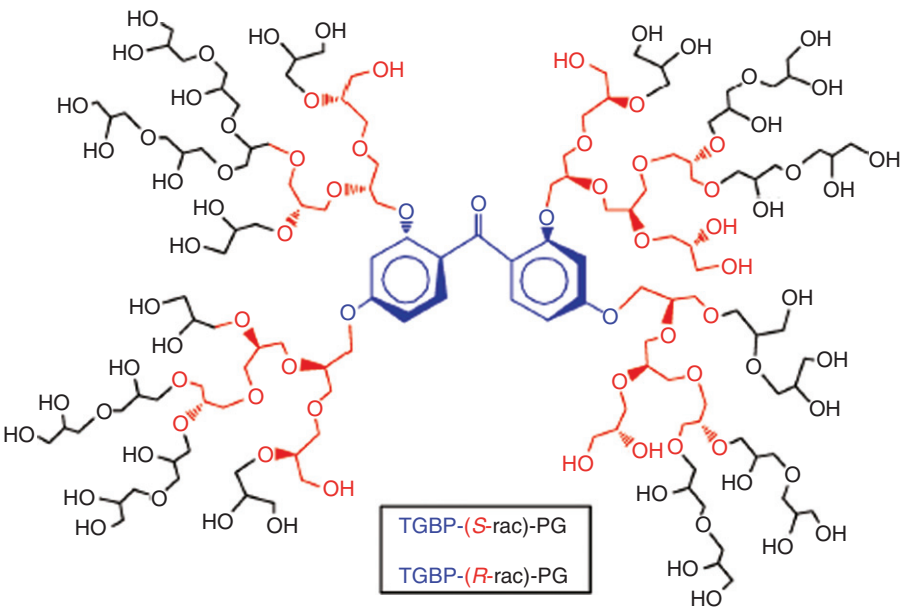

Scheme 17 Structure of chiral polyglycerol using 2,2′,4,4′-tetrahydroxybenzophenone as a initiating core molecule. Reprinted with permission from Pastor-Pérez, L.; Kemmer-Jonas, U.; Wurm, F.; *et al. Macromolecules* **2010**, *43*, 9583.[67] Copyright 2010 American Chemical Society.

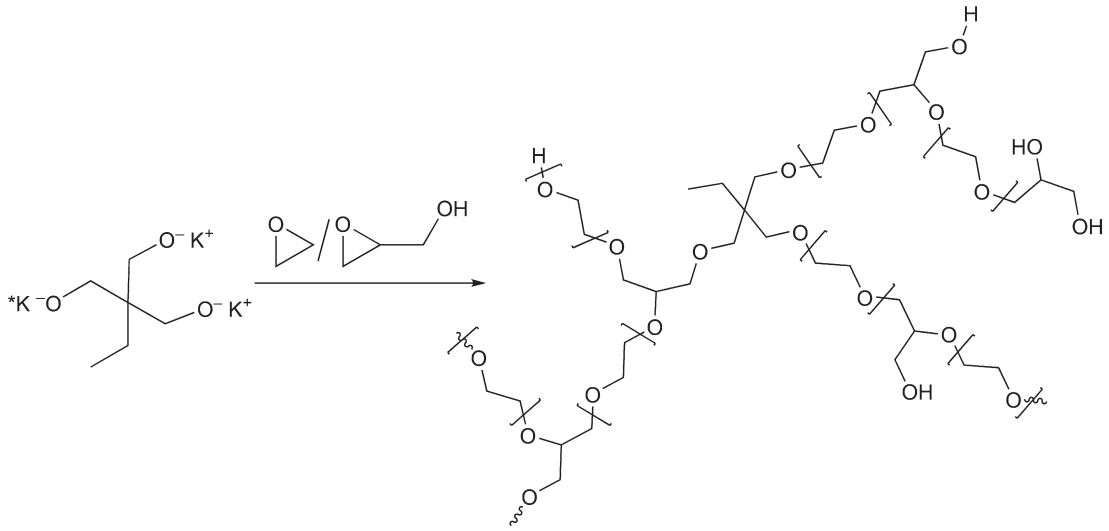

Scheme 18 Random copolymerization of ethylene oxide and glycidol.

recent work, Frey *et al.* developed random copolymers which show high biocompatibility. EO and glycidol were copolymerized in a one-step procedure using anionic ROMBP at 80 °C, where the length of the linear segments could be adjusted by the comonomer ratio (Scheme 18).[68] Polymers with molecular weights up to 50 000 g mol^{-1} and narrow polydispersities ($M_w/M_n < 1.8$) were prepared, which are currently under investigation for new battery and, in particular, biomedical applications since both constituents, poly(ethylene glycol) and PG, show high biocompatibility.[69,70]

The state of the art in the synthesis of hbPG and advanced structures using hbPG as building block was also covered in a recent review article.[71]

Rokicki *et al.*[72] recently reported a promising alternative synthesis of hbPG by ROMBP of glycerol carbonate, a benign monomer that can be obtained conveniently from the renewable materials glycerol and dimethyl carbonate. TMP was used as a trifunctional initiator core under SMA conditions, leading to the formation of branched polyethers upon CO_2 liberation. The attack of the alkoxide can occur at the carbonyl or alkyl carbon atoms of the cyclic carbonate group. The authors observed an additional ^{13}C NMR signal that did not appear in the spectra of the polymers obtained by glycidol polymerization. This signal can be attributed to the generation of terminal propane-1,3-diol units, which are the result of an intramolecular rearrangement that can take place in the course of the polymerization after formation of an intermediate linear carbonate (Scheme 19). The obtained polymers were of low molecular weight and their polydispersities ranged between 1.2 and 1.3.

In 1999, Fréchet and Chang presented a process called 'proton-transfer polymerization', which uses intermolecular proton transfer to obtain hyperbranched polymers.[73] This is in contrast to the anionic ROMBP of glycidol, where intramolecular counter-ion transfer is the crucial step to obtain branched structures. Scheme 20 shows the mechanistic details of this approach. The phenol bisepoxide monomer **1** combines several important aspects to make this mechanism possible: First, the high nuecleophilicity of the phenolate **2** compared with the secondary alkoxide **3** or **5** promotes fast proton-transfer activation of the phenolate and therefore comparatively slower epoxide ring opening. Secondly, the low pK_a of the phenolic group compared to the secondary alkoxide leads to chemoselective chain ends during propagation and, thirdly, the ring opening is preferred at one side of the epoxide because of steric hindrance. These three factors promote chemo- and regionselective growth of the polymer. Nevertheless, broad molecular weight distributions (M_w/M_n between 1.3 and 12) occur, characteristic for the polymers due to cyclization side reactions and unequal reactivity of focal groups as a result of their different steric environment. In a follow-up work, Fréchet *et al.* also applied the concept of proton-transfer polymerization to the synthesis of hyperbranched polyesters.[74]

Even though oxetanes have been classically considered as monomers for cationic polymerizations, some anionic

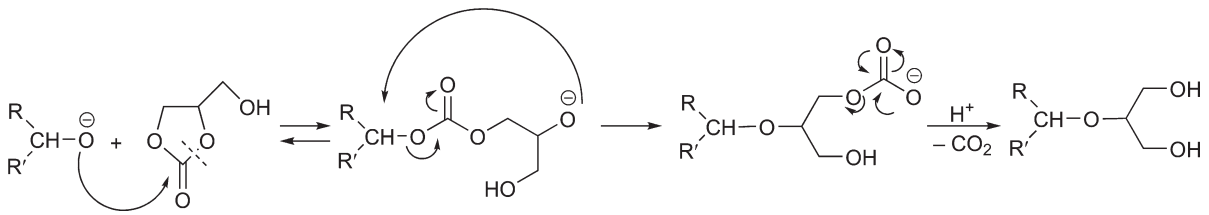

Scheme 19 Formation of terminal propane-1,3-diol units in the polymerization of glycerol carbonate.[32]

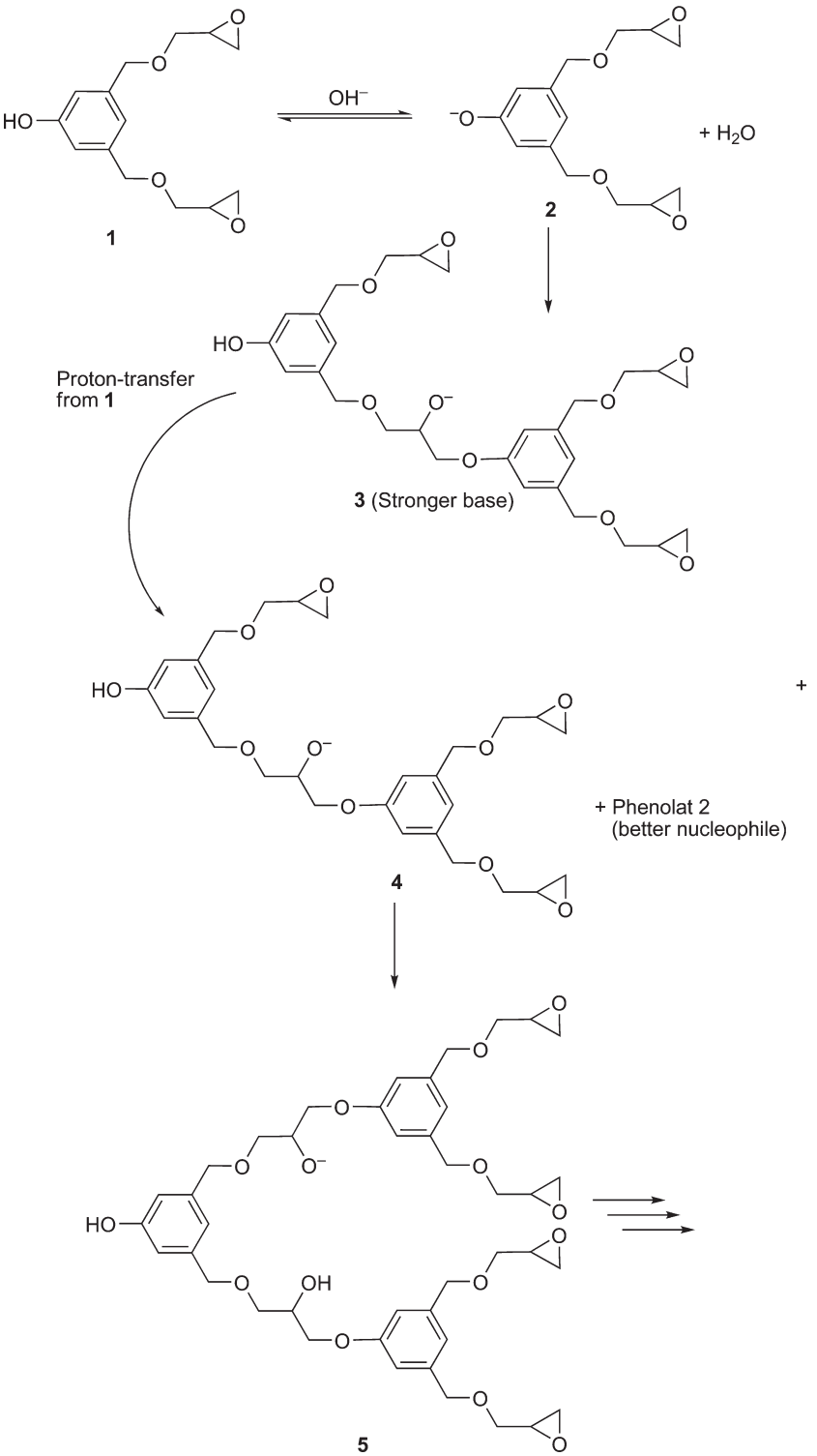

Scheme 20 Mechanism of the proton-transfer polymerization approach introduced by Fréchet *et al.*

polymerizations of unsubstituted oxetane using bulky aluminum-based catalysts with added Lewis acids have been reported.[75,76] It was shown that treatment of substituted oxetanes with strong nucleophiles, such as the azide anion,[77] or redox conditions with lithium 4,4´-di-*tert*-butylbiphenylide[78] result in ring opening, but do not promote polymerization.

Multifunctional oxetane derivatives undergo cationic ROPs resulting in hyperbranched polyether structures comparable to hbPGs. Smith and Mathias[79] first described the anionic ROP of EHO to a hyperbranched polyether polyol using sodium hydride as a strong base catalyst and TMP as a multifunctional initiator core. The polymerization was carried out under SMA

conditions at high temperatures above 100 °C because of the high activation energy of the ring opening.

The resulting hyperbranched polyols (Scheme 21) were of low molecular weight. Contrary to hbPGs, hyperbranched poly(EHO) could be dissolved in chloroform and benzene, but was insoluble in water, thus proving its lower polarity resulting from the additional ethyl groups in each repeating unit. A fraction of the polymers was soluble in acetone and had a higher DB (DB = 0.48) than the acetone-insoluble fraction (DB = 0.2).

In a different approach, EHO and MHO (3-(hydroxymethyl)-3-methyloxetane) were polymerized in *N*-methyl-2-pyrrolidone (NMP) using sodium *tert*-butoxide as deprotonation agent and 18-crown-6 to complex sodium counterions and enhance the reactivity of the oxy anions.[80] The authors investigated the influence of the degree of initial deprotonation, temperature, and reaction time on the resulting polymer properties. Even though high yields could be obtained, low DBs (DB < 0.3) and broad molecular weight distributions ($M_w/M_n < 5$) characterize most of the products. Still, using sodium *tert*-butoxide as initiator leads to conservation of the oxetane function. After acetylation of the OH-groups, the telechelic polymers of 1000 g mol^{-1} molecular weight were polymerized as macromonomers in cationic ROP initiated by $BF_3.OEt_2$ to obtain linear polyethers grafted with hyperbranched side chains which are obtained after removal of the protective groups (Scheme 22). This four-step approach leads to hyperbranched polyethers with molecular weights up to 7600 g mol^{-1} and reasonably narrow molecular weight distributions ($M_w/M_n = 1.4$).

The latent AB_3-monomer BHMO was also investigated using the same synthetic strategy as described before.[81] Here, higher DBs (up to 0.55) and molecular weights up to 4400 g mol^{-1} were achieved. Due to the higher DB, these polymers could not be polymerized by cationic ROP to obtain higher-molecular-weight branched polyethers, as described previously. This problem was solved by copolymerizing the macromonomers with 3-ethyl-3-phenoxyoxetane (EPO), which afforded polyethers with molecular weights up to 15 000 g mol^{-1} and low polydispersities ($M_w/M_n = 1.3$).

Sulfur-containing heterocycles have rarely been used in ROP even though they are interesting for a variety of biomedical applications.[34] Heterocycles higher than four membered cannot be polymerized by an anionic mechanism. While the cationic polymerization of thietanes leads to branched polymers or crosslinked networks, higher sulfur heterocycles were never used in the synthesis of hyperbranched polymers by ROP, since the synthesis of linear polymers is already challenging due to low reactivity of the ACEs and degradation processes during the synthesis of linear poly(sulfide)s.

In summary, anionic polymerization techniques are by far the most common approach in the synthesis of well-defined hyperbranched polymers by ROP at present, especially in the field of hyperbranched polyols. Numerous research groups are currently engaged in the preparation, modification, and characterization of such polymers for a wide variety of applications, ranging from biomedicine, advanced coatings, and rheological modifiers to novel catalyst supports.

4.22.3.3 Catalytic Ring-Opening Multibranching Polymerization

The Nobel Prizes in chemistry in 1963 for Ziegler and Natta for their stereoselective polymerization of α-olefins[82,84] and in 2005 for Chauvin, Grubbs, and Schrock for their achievements in the domain of ring-opening metathesis polymerization (ROMP)[85] shows the importance of the research in the field of catalytic polymerization techniques.

ROPs of cyclic lactides and lactones initiated by nucleophiles (alcohols and amines) in the presence of suitable organometallic promoters have been outlined in numerous publications.[86] The recent impressive progress in the catalytic polymerization of vinyl monomers leading to hyperbranched structures is detailed in Chapter 9 of this volume. The first ROMBP involving a transition metal catalyst was reported by Suzuki *et al.* in 1992.[22] Previous studies[87] provided the authors with a concept of combining the catalytic effect of a Pd(0) complex with a suitable monomer structure for ROP. The monomer of choice was the cyclic carbamate 5,5-dimethyl-6-vinyltetrahydro-1,3-oxazin-2-one. Benzylamine-initiated polymerization catalyzed by $Pd_2(dba)_3 \cdot CHCl_3$-2dppe as a catalyst at room temperature produced a hyperbranched polyamine consisting of primary, secondary, and tertiary amine moieties and concurrent CO_2 evolution. A simplified illustration of the reaction is given in Scheme 23.

Suzuki and co-workers proposed a detailed mechanism, which is depicted in Scheme 24. It involves the η^3-allylpalladium complex **2** as the key intermediate. The amine initiator is assumed to attack the electrophilic site of **2** to produce the diamine **3**, releasing carbon dioxide and regenerating a Pd(0) complex. Depending on which of the amino groups of **3** reacts, two different triamines, **4a** and **4b**, are possible.

A peculiarity of this work becomes obvious when the molecular weight distribution of the obtained polymer is

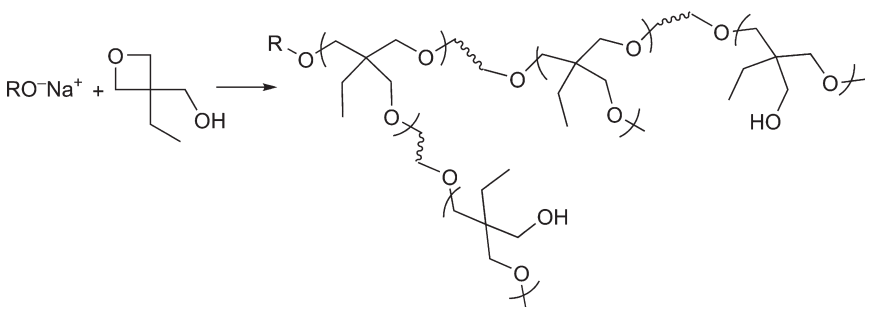

Scheme 21 Ring-opening multibranching polymerization of EHO.

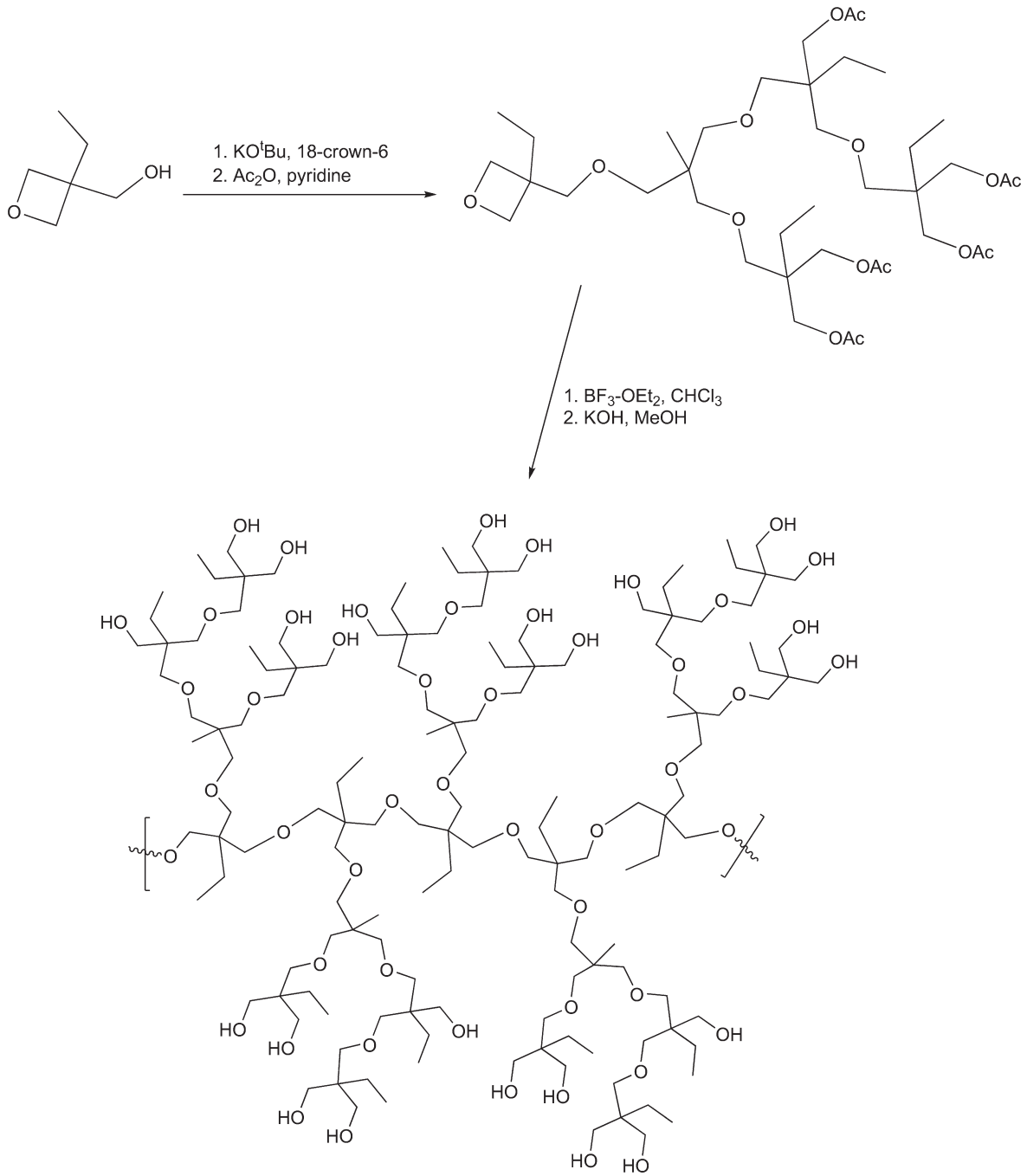

Scheme 22 Synthesis of a hyperbranched polyether by combination of cationic and anionic ROP.

considered. After transformation of secondary amino groups into carbamate groups (to prevent interaction with the polystyrene beads in the SEC column), a very low polydispersity (M_w/M_n) of 1.35 was found at a molecular weight of about 3000 g mol^{-1}. Since the amount of initiator employed determines the molecular weights obtained, Suzuki *et al.* in fact developed the first case of a controlled ROMBP, avoiding broad molecular weight distributions and undesirable side reactions. Paralleling this pioneering work, further studies were carried out utilizing a slightly varied cyclic carbamate structure (**Scheme 25**).[88] 5-Methylidenetetrahydro-1,3-oxazin-2-one was polymerized with a Pd(0) catalyst of very similar structure. Triphenylphosphine was found to be a better ligand than 1,2-bis(diphenylphosphino)ethane (dppe) in this case. Low-polydispersity (M_w/M_n = 1.3–1.5) and highly branched polymers with molecular weights between 2000 and 3000 g mol^{-1} were obtained in this work as well.

Stannous octoate ($SnOct_2$, **Scheme 26**) is a widely used transesterification catalyst in polylactide synthesis[89,90] as well as in the polymerization of lactones with alcohol initiators.[86,91,92]

The precise initiation mechanism presumably depends on the temperature and has not been entirely elucidated to date. Two basic types of mechanisms have been proposed in the

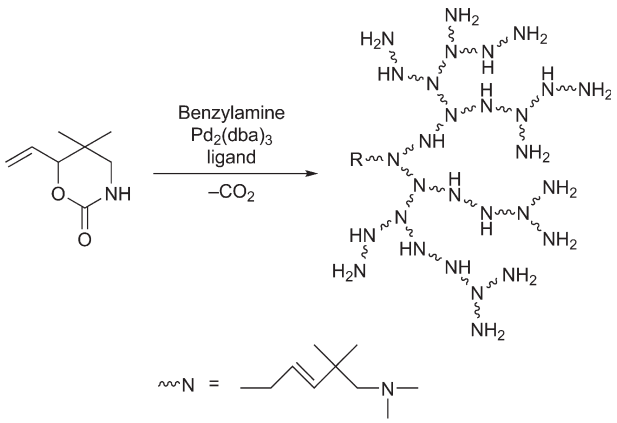

Scheme 23 Catalytic polymerization of 5,5-dimethyl-6-vinyltetrahydro-1,3-oxazin-2-one.

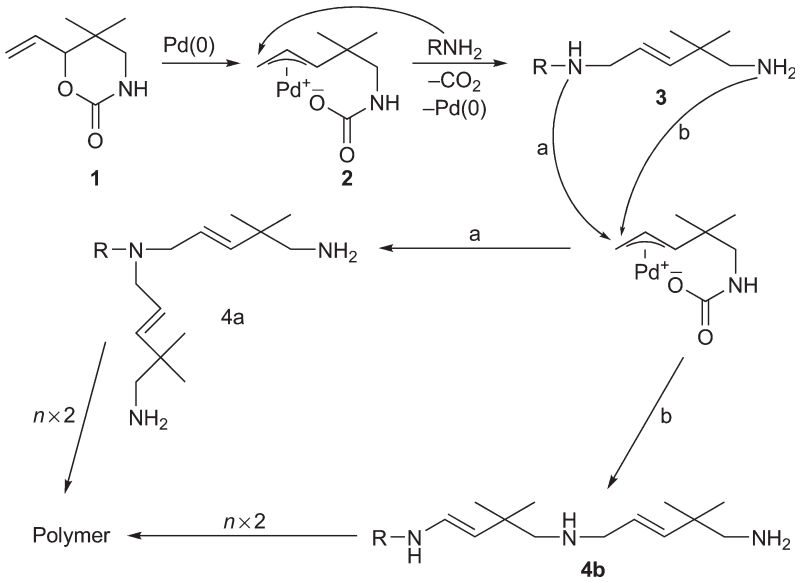

Scheme 24 Mechanism of the catalytic polymerization of 5,5-dimethyl-6-vinyltetrahydro-1,3-oxazin-2-one.

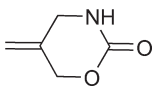

Scheme 25 5-Methylidenetetrahydro-1,3-oxazin-2-one.

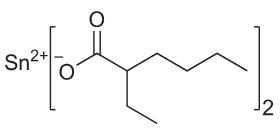

Scheme 26 Stannous octoate ($SnOct_2$).

literature: a direct catalytic type,[93,94] where the catalyst serves the activation of the monomer through coordination with its carbonyl oxygen, and monomer insertion type mechanisms,[95–101] involving the catalyst as a co-initiator along with either purposely added or adventitious hydroxyl impurities. In the latter case, polymerization proceeds through an activated stannous alkoxide bond.

Fréchet *et al.* reported an elegant approach to hyperbranched polyesters of high molecular weights in 1999, based on the ROP of a lactone-based inimer, that is, a monomer containing an ε-caprolactone ring as well as a primary alcohol moiety (4-(2-hydroxyethyl)-ε-caprolactone).[11] Bulk polymerization was carried out at elevated temperature in the presence of a catalytic amount of $SnOct_2$.[102] Scheme 27 depicts the pathway of this ROMBP leading to high-molecular-weight hyperbranched polymers ($M_w = 65\,000–85\,000\ g\,mol^{-1}$) with a polydispersity of 3.2. Like in SCVP, high polydispersities are in line with the expectation for a one-pot synthesis of this type.

The reaction was found to proceed faster when the amount of catalyst was increased. However, smaller amounts of catalyst tended to give polymers with elevated molecular weights. In agreement with other hyperbranched polymers possessing a large number of hydroxyl end groups, like the previously discussed PG, the obtained polyester was soluble in polar solvents such as dimethyl sulfoxide (DMSO), dimethylformamide (DMF), and methanol, but insoluble in THF, CH_2Cl_2 and $CHCl_3$. In order to determine the relative amount of linear,

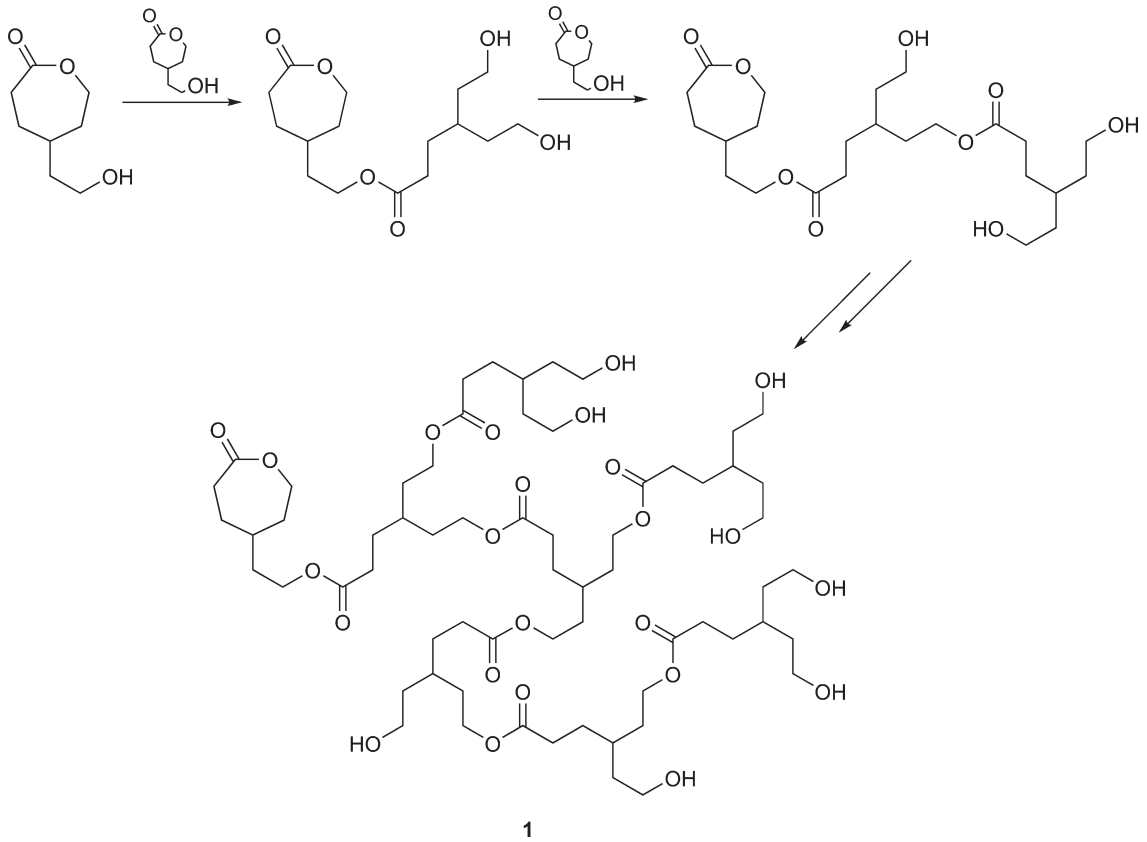

1

Scheme 27 Catalytic polymerization of 4-(2-hydroxyethyl)-ε-caprolactone.[59]

terminal and dendritic subunits, ^{13}C NMR spectra of the polymer were recorded and compared to the spectra obtained from suitable model compounds. The DB was then calculated to be 0.50 according to the definition established by Hawker, Lee, and Fréchet, confirming the hyperbranched structure.[4]

Almost at the same time, Hedrick *et al.* published a reaction based on the same concept, where the term 'self-condensing ring-opening polymerization' (SCROP) was introduced.[13] The inimer 4-{[2,2-bis(hydroxymethyl)propanoyl]oxy}hexano-6-lactone (Scheme 28) was reacted in the presence of a catalytic amount of $SnOct_2$ to yield hyperbranched polyesters.

Another hyperbranched polyester was prepared and characterized in an elegant work by Rokicki *et al.* in 2006.[103] They described the synthesis of 5-(hydroxymethyl)-1,4-dioxan-2-one (5-HDON) and its application in the preparation of hyperbranched polymers by ROMBP promoted by the $SnOct_2$ catalyst.

The theoretical structure of the obtained polymers and oligomers is shown in Scheme 29. Similar to the hyperbranched polyester prepared by Fréchet *et al.*, four main subunits are possible. The polymerization commences at the core unit A. Dendritic subunit B is completely substituted and therefore it is a branching point, while unit C depicts a linear fragment of the molecule. The terminal units D contain two unsubstituted hydroxymethyl groups.

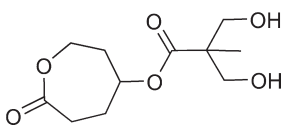

Scheme 28 Structure of 4-{[2,2-bis(hydroxymethyl)propanoyl]oxy} hexano-6-lactone.

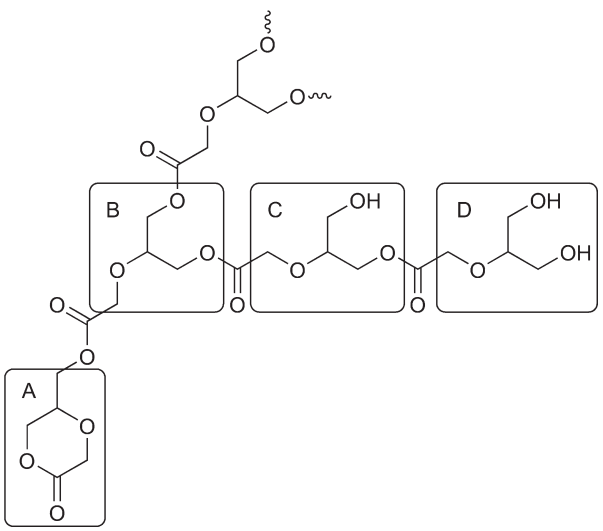

Scheme 29 Theoretical structure with four major main subunits of poly (5-HDON).

Characterization by MALDI-TOF mass spectrometry showed a small fraction of polymer containing either hydrolyzed 5-HDON or glycerol as the core unit. Comparably high molecular weights ($M_n = 25\,000–44\,000\,g\,mol^{-1}$) and low

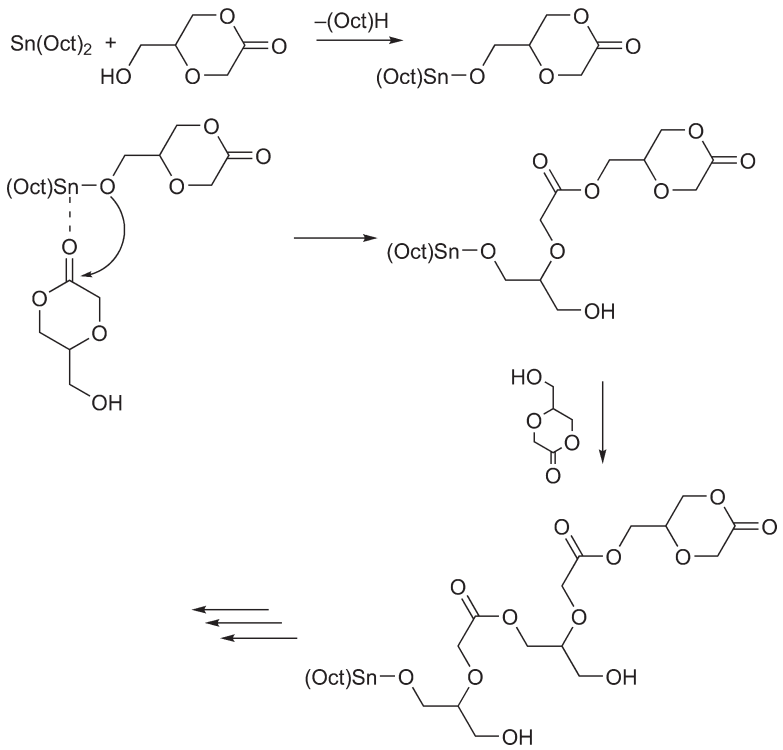

Scheme 30 Mechanism of the coordination-insertion polymerization of 5-HDON in the presence of $Sn(Oct)_2$.

polydispersities ($M_w/M_n = 1.7–2.0$) were found by GPC analysis. Detailed investigation by NMR spectroscopy revealed that the use of an anionic initiator (1,8-diazabicyclo[5.4.0]undec-7-ene (DBU)) lead to incorporation of a higher fraction of dendritic units into the polymer structure. However, extending the reaction time to 72 h instead of 24 h at increased temperature (110 °C instead of 75 °C) gave highly branched polymers with the $Sn(Oct)_2$ catalyst. These observations appear to confirm earlier assumptions about the temperature dependence of the mechanism. The authors, therefore, suggest the predominance of a coordination-insertion mechanism (**Scheme 30**) at lower temperatures. The respective reaction pathway favors the incorporation of linear subunits (C). Higher temperatures and longer reaction times, however, promote action of $Sn(Oct)_2$ as a transesterification catalyst and hence resulting in a larger amount of branched structures.

Yu *et al.* prepared a hyperbranched polyester of a closely related structure by using 6-(hydroxymethyl)-1,4-dioxan-2-one (6-HDON) as inimer and $Sn(Oct)_2$ as catalyst at elevated temperatures over periods of 1–8 days.[104] Molecular weights were found in the range of 7800–25 600 g mol^{-1} with polydispersities between 2.0 and 3.0. Polymers with high molecular weights were only obtained when the molar ratio catalyst/feed was fixed at 1/400. Increasing or decreasing the amount of catalyst resulted in lower molecular weights. The DBs (0.4) were determined by inverse gated ^{13}C NMR spectral analysis. The polymerization reaction and different units in the obtained polyesters are illustrated in **Scheme 31**. Terminal units A and B, linear units C and D, as well as dendritic units E are present in the polymer structure and can be assigned to the respective signals in the NMR spectra. This polymer consists of glycerol and glycolic acid units, which renders it biodegradable and biocompatible.

Since the Nobel Prize for chemistry in 2005 was awarded to Chauvin, Schrock, and Grubbs, ROMP has developed to a widely used tool in catalytic polymerization.[85] Even though, to the best of our knowledge, no homogenous hyperbranched polymer has been synthesized by ROMP of cyclic alkens yet, Lavrich *et al.*[105] presented an elegant way to obtain hyperbranched hydrocarbon polymers by using the monoterpenes *d*-limonene, β-pinene, or limonene oxides as the 'solvents' that were reported to be powerful chain transfer agents in ROMP, leading to branched structures.[106] The authors polymerized dicyclopentadiene (DCPD) in the presence of a second-generation ruthenium catalyst to produce materials without crosslinking, with high molecular weights, low polydispersities (M_w/M_n mostly < 2), and high DBs (0.40–0.60) (**Scheme 32**).

In a following work, the authors characterized the materials in more detail. They found a smaller hydrodynamic volume compared to the linear analogs and depicted the different linear, dendritic, semidendritic, and terminal units by NMR spectroscopy.[105]

Enzymes are biocatalysts that are becoming increasingly important in organic synthesis due to their high selectivity in various complex reactions. Enzyme-supported synthesis of polymers is an emerging field of research, which affords large-scale materials on large-scale and under mild conditions.[107] The enzymes can be easily removed from reaction mixtures not leaving heavy metal catalyst traces in the resulting products, which is a great advantage in biomedical applications. Even though enzymes were used as catalysts for the ROP of a variety of monomers to obtain linear polymers, only very limited works describe the synthesis of hyperbranched polymers using this strategy. Work in this field was carried out by Frey and co-workers, who combined the ROP

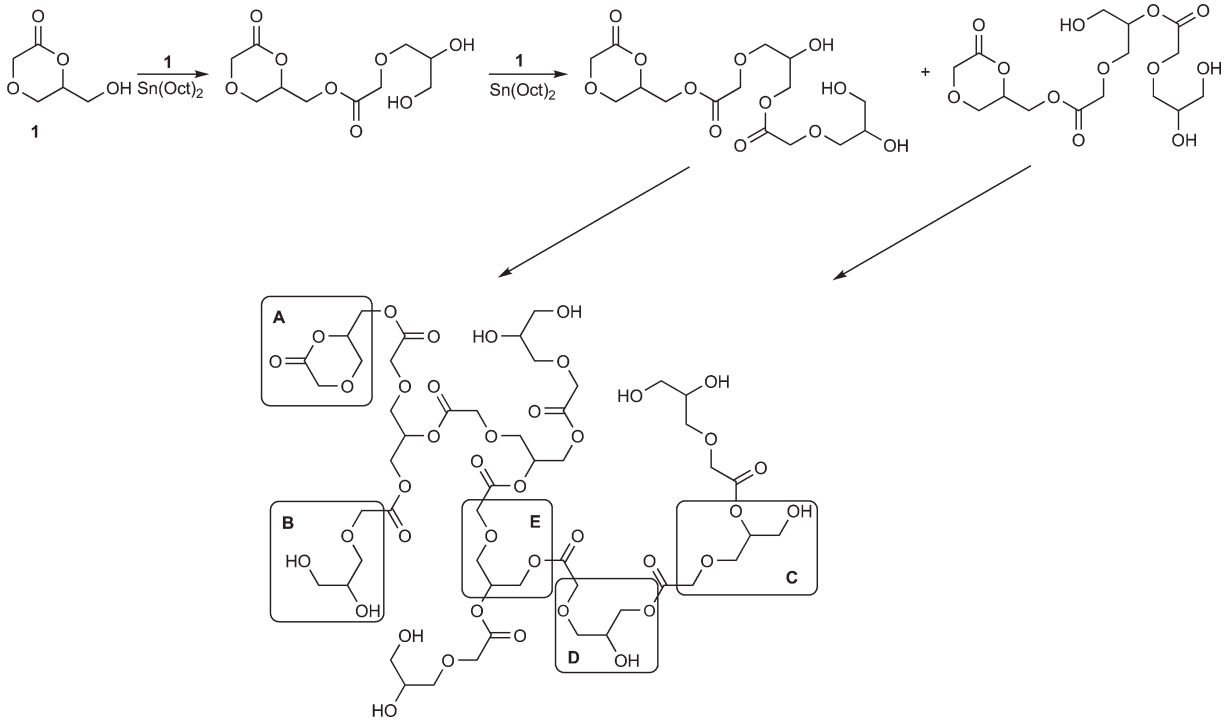

Scheme 31 Synthesis and structure of poly(6-HDON).

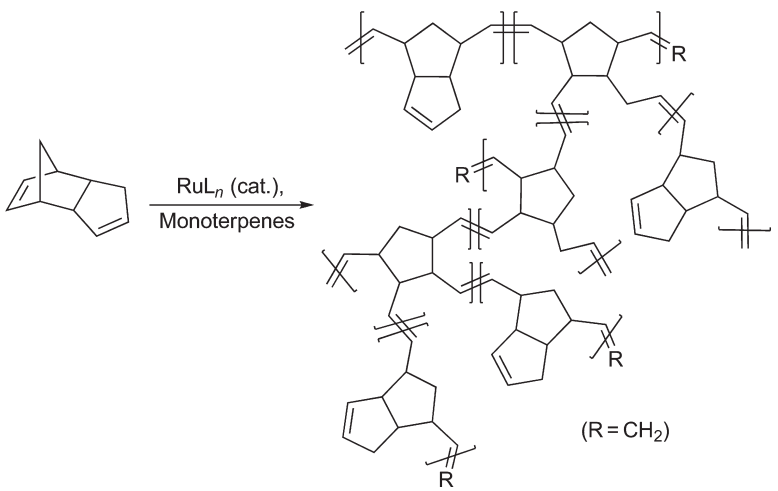

Scheme 32 ROMP of dicyclopentadiene (DCPD) in the presence of monoterpenes.

and AB_2 polycondensation of ε-caprolactone and 2,2′-bis (hydroxymethyl)butanoic acid (BHB) in the presence of immobilized Lipase B from *Candida antarctica* (Novozym 435) (Scheme 33).[108] Molecular weights up to 35 000 g mol^{-1} with low polydispersities ($M_w/M_n < 1.6$) were obtained. The DB was limited and never exceeded a value of 0.35. It is noteworthy that until today no work has been published using an enzymatic ROMBP to obtain hyperbranched homopolymers.

As an example of phosphorus-containing heterocyclic monomers, Yan *et al.* recently presented the first synthesis of a water-soluble hyperbranched polyphosphate by SCROP, using the new inimer 2-[(2-hydroxyethoxy)ethoxy]1,3,2-dioxaphospholan-2-one (HEEP).[109] Polymerization was carried out in bulk in absence of a catalyst. Therefore, this material is particularly interesting for biomedical applications due to its low toxicity and good biodegradability.[110] Scheme 34 shows the reaction, by which polymers with molecular weights of 5200 g mol^{-1}, low polydispersities ($M_w/M_n = 1.75$), and almost a statistical DB (DB = 0.47) were obtained.

Catalytic ROMBPs have become a fitting method for the preparation of hyperbranched polyesters with high DP_n's. The respective high molecular weights are often conveniently accessible because the sensitivity of the polymerization reactions to traces of impurities is less distinct than in cationic or anionic polymerization techniques. Clearly, enzymatic polymerizations,

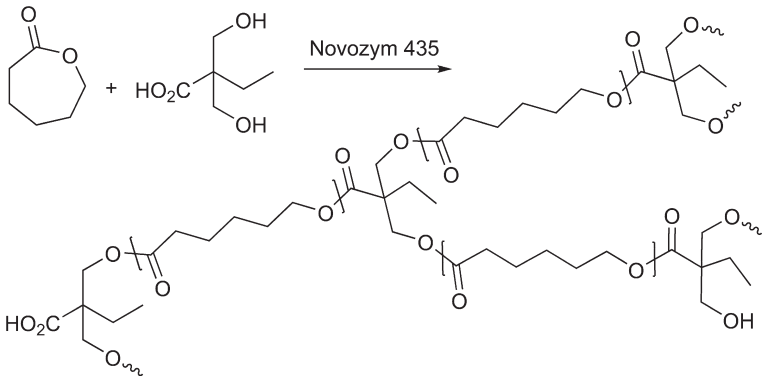

Scheme 33 Enzymatic synthesis of hyperbranched aliphatic polyesters by combining ROP and AB_2 polycondensation.

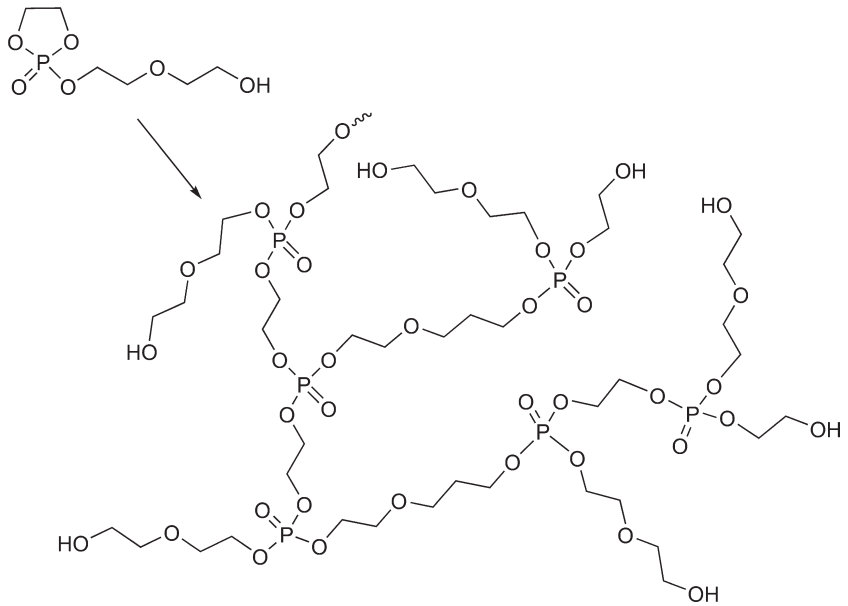

Scheme 34 ROMBP of HEEP for the synthesis of hyperbranched polyphosphates.[103]

an emerging field of interest in polymer synthesis, have not been applied to full success in ROMBP. Nevertheless, many advantages of this approach will certainly motivate ongoing research in this field.

4.22.4 Complex Polymer Architectures Containing Nonlinear Macromolecules Generated by ROP

In the following section, several complex polymer structures consisting of non-linear-hyperbranched polymer segments and their applications will be described. The structures are synthesized by ROP. Each of the following subsections forms a growing area of research, covered in Chapter 6.05 and other review articles in more detail. Selected examples in the particular fields will be covered, to complete the overview regarding the materials described in this chapter and to deepen the motivation for ongoing research on polymer architectures capitalizing on hyperbranched building blocks. Within all sections dealing with copolymers like LHBCs or hyperbranched-linear copolymers ('hyperstars'), only strategies using ROP in both block synthesizes will be covered to show how the different strategies within ROP can be combined. Also, in the 'core variation' and 'terminal functionalization' sections, only polymers obtained by ROMBP will be discussed. The synthesis of hyperbranched polymers by ROMBP from surfaces or nanoparticles is described in Chapter 6.05 of this volume.

4.22.4.1 Core Variation

Molecular encapsulation in dendritic and highly branched polymers has received increasing attention recently.[111] It was shown for dendrimers that the site isolation of a functional core unit in a dendritic scaffold is of great interest with respect to optical properties, catalysis, and other future applications. Detailed studies on dendrimers have revealed that at some critical dendrimer generation, the core is encapsulated by the sterically crowded and densely packed highly branched architecture.[112,114] Within this context, Fréchet *et al.* introduced 1-(*N*,*N*-dimethylamino)-4-nitrobenzene as a solvatochromic chromophore at the focal point of a poly(benzyl ether) dendrimer.[114] In other works, manganese and zinc porphyrins

coated with a dendritic structure exhibit better stability and improved regioselectivity in catalytic processes.[115,116] Additionally, dendritic encapsulation of an active core moiety has been proposed to serve as a model for the shielding of active centers in naturally occurring enzymes.[117]

Hyperbranched polymers containing an encapsulated single core moiety have qualified as an interesting alternative to dendrimers for analogous studies, since they resemble in a majority of their characteristics and are usually easily accessible by a convenient synthesis. Tian *et al.* used a modified triphenylamine as core for a conjugated hyperbranched polymer,[118] where a direct influence of the hyperbranched architecture on UV-absorption and fluorescence properties of the core was observed. Furthermore, postpolymerization modification of the nitrophenyl ester core, subsequent to the formation of the dendritic structure, has been reported.[119,120]

Competing homopolymerization of the branched monomer is an often disregarded reaction in the synthesis of core-containing hyperbranched polymers. For simple statistical reasons, a majority of the hyperbranched macromolecules are unlikely to possess a core unit in a conventional B_n/AB_m-type copolycondensation. In a very elegant study, Žagar and Žigon demonstrated this for commercially available hyperbranched polyesters (Boltorn®) obtained from an AB_2 monomer and B_3 functional core molecule.[121] Frey *et al.* studied the incorporation of different initiator cores into hbPGs under the previously described SMA conditions.[122] The employed cores were structurally different, including mono- and bifunctional *n*-alkylamines as well as photoactive cores, such as benzylamine and methyl (1-naphthyl)amine and a typical triplet photosensitizer, 2,2′,4,4′-tetrahydroxybenzophenone ($BP(OH)_4$). Twofold reaction of the amines with glycidol prior to polymerization (**Scheme 35**) was found to result in improved molecular weight control ($M_n = 1600–8400\ g\ mol^{-1}$) and moderate polydispersity ($1.5 < M_w/M_n < 2.5$).

Macromolecules obtained from polymerization of glycidol initiated by the tetra-hydroxybenzophenone $BP(OH)_4$ as a core were of low polydispersity ($M_w/M_n < 2$) and exhibited up to $5800\ g\ mol^{-1}$. The benzophenones substituted with a hyperbranched polyglycidol corona showed high photostability after prolonged irradiation times and therefore are promising materials as easily recoverable and reusable photocatalysts.[123] Also, by using pure glycidol enantiomers instead of racemic glycidol as monomers, chiroptical induction of the core can be obtained.[67]

Linear polymers with a short multifunctional initiator blocks have been used as core molecules to synthesize LHBCs by a three-step strategy. Frey *et al.* synthesized a linear macroinitiator by hydroxylation of a polystyrene-*block*-polybutadiene, which was attached to a hbPGs core (**Scheme 36**).[124]

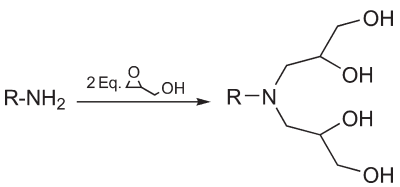

Scheme 35 Double hydroxyl functionalization of amine initiator cores with glycidol.

These polymers show well-defined micellar aggregation in atomic force microscopy (AFM), which proofs their amphiphilic structure. The aggregation may be regarded as surprising in view of the structural inhomogeneity of the hyperbranched block. LHBCs are interesting hybrid polymer architectures suitable for various applications. They will be discussed in more detail later.

4.22.4.2 Terminal Functionalization and Bioconjugation

A high number of functional groups in terminal and interior repeating units offer the possibility of further functionalization to prepare tailored functional materials with defined properties based on hyperbranched polymer scaffolds.

hbPG has been extensively studied in this context because the polyether structure shows high biocompatibility, which makes the material interesting in a variety of applications in nanomedicine.[61] This field of research was reviewed by Haag *et al.* in detail just recently.[70] In the following section, some selected examples will be described and discussed. Haag *et al.* also developed the synthesis of perfect PG dendrons and dendrimers,[125,126] which have been investigated in related projects.

In order to increase the blood circulation time and to improve immunogenicity of hydrophilic drugs, the development of molecular carriers for bioactive guest molecules based on branched macromolecules is a well-established field of research. The use of physical aggregates like liposomes as capsules is arguable, due to their instability under shear stress and because of physiological degradation processes. Covalent transporters based on biocompatible polymers are a promising alternative approach (see also Section 4.22.4.3). Hyperbranched PG can be employed as polymer scaffold for synthesis of inverted micelles (core–shell structures) by esterification[127] or acetalization[128] of the terminal OH-groups. The latter approach affords pH-dependent cleavage of the outer shell and controlled release of model compounds and drugs upon lowering pH (**Scheme 37**). It is noteworthy that also some catalysts were immobilized in hbPG core–shell structures to make them recoverable.[129–131] Further, temperature responsiveness was introduced by adding PNIPAM moieties.[132] Nontoxic core–multishell structures (CMSs) developed by Haag *et al.* offer the possibility to encapsulate hydrophilic and hydrophobic molecules in the carrier, with increased capacity and a variety of guest molecules compared to simple core–shell structures.[133,134] Furthermore, multi-allyl-functionalized hbPG scaffolds were crosslinked by ring-closing metathesis to obtain covalently closed shell systems with increased stability of the host–guest complex investigated using various dye solutions.[135] By introducing nitrobenzyl groups within the shell, light-triggered release of guest molecules from photodegradable nanocapsules is possible.[136]

The covalent conjugation of bioactive compounds to a biocompatible PG scaffold offers the possibility to increase the binding efficiency of target structures, to enhance solubility, and – in contrast to physical transporters – to attain total control over loading capacity. By using stimuli-responsive linkers, controlled release under specific conditions is possible. Haag *et al.* as well as other research groups conjugated drugs such as ibuprofen,[137] prodrugs of the chemotherapeutic agent

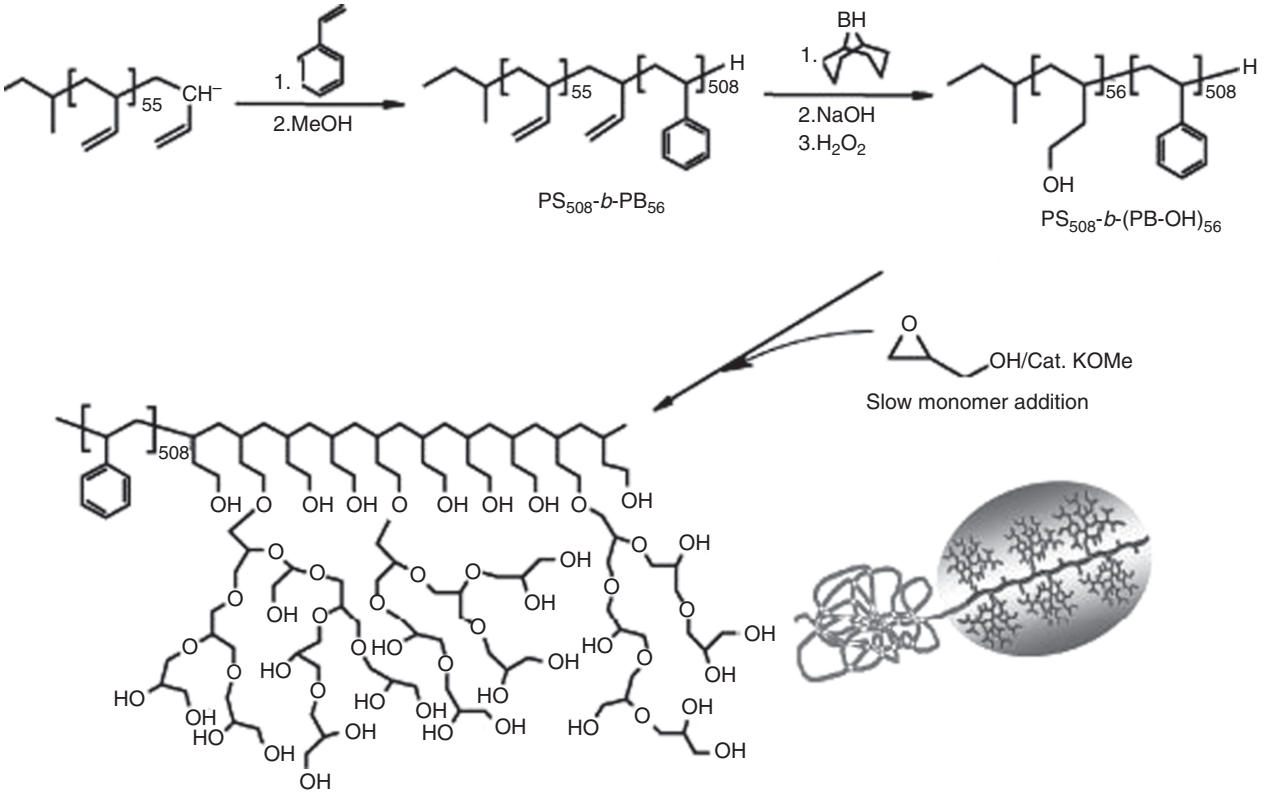

Scheme 36 Synthetic approach to a linear-hyperbranched block copolymer using polystyrene-*block*-poly[(hydroxyethyl)ethylene] (PS–*b*-(PB–OH)) as initiating 'core'. Reprinted with permission from Barriau, E.; García Marcos, A.; Kautz, H.; Frey, H. *Macromol. Rapid Commun.* **2005**, *26*, 862.[124] Copyright Weley-VCH Verlag GmbH & co. KGaA.

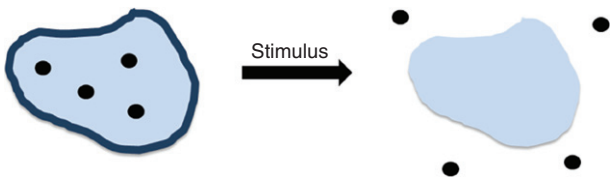

Scheme 37 Encapsulation and controlled release from hyperbranched core–shell nanocapsules.

doxorubicin,[138] sugar sulfates to hbPG to obtain heparin analogs with a higher lectin-binding efficiency than heparin itself,[139,140] or short peptides like arginine-glycine-aspartic acid (RGD sequence) with anti-inflammatory properties.[141] The attachment of Gd^{3+} chelators resulted in contrast agents for MRI diagnostics.[142] The immobilization of enzymes[143] is a key step toward specific biosensors based on hyperbranched polyether scaffolds. In addition, by coupling dithionic acid, self-assembled monolayers (SAMs) of hbPG on gold surfaces formed, which showed efficient prevention of protein adsorption.[144]

Besides the biomedical applications, terminal functionalization of hbPG can be used to change the thermal properties of the polymer. The attachment of mesogenic cyanobiphenyl end groups via spacers, results in liquid-crystalline hyperbranched polymers and increasey the glass transition to 40–50 °C.[145]

Hyperbranched polyethers synthesized by cationic ROMBP have barely been used as scaffolds for further functionalization because of limited control over the polymerization reaction. Low polydispersities and defined molecular weights are essential criteria for the development of materials, especially for biomedical applications. Only materials with these properties can systematically be investigated *in vivo* and *in vitro* because a clear structure–effect relationship can be developed to evaluate the polymers for these tasks. The same problem occurs for hyperbranched polyesters synthesized by catalytic ROMBP. Additionally, remaining catalyst residues can show toxic effects in living organisms. Still, recently developed biocompatible hyperbranched polyphosphates can be synthesized by ROMBP without catalysts and have successfully been conjugated to drugs. Release is possible due to biodegradability of the materials.[110]

Besides that, many new monomers have been developed just recently for ROMBP and the respective polymerization reactions are still under investigation. Given further progress in the years to come in polymer synthesis, a variety of new materials with well-defined properties will be available for further functionalization. Nevertheless, for many potential applications of the hyperbranched polymers like in coatings, catalyst immobilization or viscosity modification, there is no terminal functionalization necessary.

4.22.4.3 Multiarm Star Polymers or 'Hyperstars'

Various hyperbranched polymers prepared by ROMBP have been used as macroinitiators for the synthesis of multiarm star polymers, where multiple linear chains are attached to a multifunctional hyperbranched core. These structures are also referred to as 'hyperstars' or could be called 'hyperbranched-linear block copolymers'. They can be synthesized using a core-first approach (grafting by living polymerization from a multifunctional initiator core) or an arm-first approach by quenching a living polymerization of linear polymers with a multifunctional coupling agent. Again, a convenient one-step synthesis is the major advantage over dendrimers when hyperbranched polymers are used as macroinitiators. Nevertheless, low polydispersities are a crucial requirement for the synthesis of defined structures after the attachment of the linear chains. Therefore, mainly ionic and controlled radical polymerization techniques such as ATRP have been used for the attachment of the linear chains since these techniques provide low polydispersities. Based on this consideration, it is not surprising that the ROP of EO to attach PEO side chains has been studied extensively using various core molecules.[146] However, the major focus in this section is on the use of ROPs for the synthesis of the arms and the hyperbranched cores, respectively. Of course, many other polymers such as the commercially available Boltorn® polyester[147] or polyphenylenes[148] have been used to name only two. Depending on the chemical structure of the arms, polarity, solubility, flexibility, and functionality of the hyperbranched core can be modified.

hbPG synthesized by anionic ROMBP using the SMA technique (see previously) has been widely used as a macroinitiator, owing to its moderate to narrow molecular weight distributions. Frey's group as well as others used hbPG as initiator for the anionic ROP of EO or propylene oxide (PO) and for the catalytic ROP of L-lactide (LA), glycolide (GL), or ε-caprolactone (**Scheme 38**). Using the more hydrophobic PO, the glass transition temperatures (T_g) and melting temperatures (T_m) of the amorphous PG can be tailored.[149] Knischka *et al.* found that it was crucial to use hbPG-*b*-PPO stars instead of only hbPG as macroinitiator for the grafting-from of EO to attain control over molecular weight and polydispersity.[150] However, by modifying the reaction conditions, Doycheva *et al.* prepared hbPG-*b*-PEO copolymers.[151] Hyperstars with biodegradable polyester side chains such as poly(L-lactide)[152,153] or poly(ε-caprolactone)[154] lead to unimolecular micelles with a biodegradable hydrophobic shell and a biocompatible hydrophilic core, which are interesting as drug-delivery systems in biomedical applications. Due to its high crystallinity and poor solubility leading to problems in processing, glycolide is barely used as a lactone monomer for homo- or copolymers in ROP. By attaching polyglycolide (up to 91 wt.%) to a hbPG core by catalytic ROP, the solubility can be improved, which opens a road to a better processing of polyglycolide materials.[155] In addition,

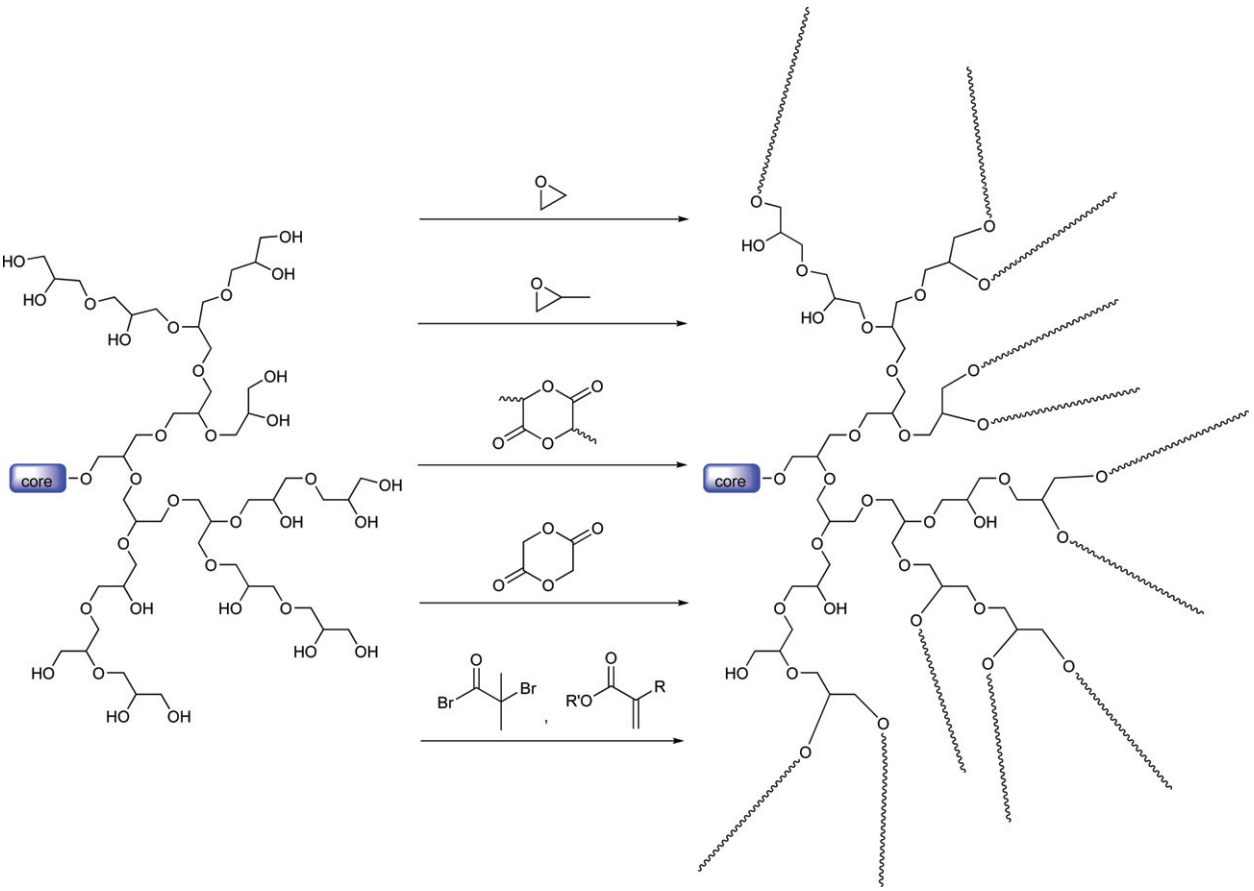

Scheme 38 Synthesis of various hyperstars using hbPG as multifunctional macroinitiating core.

hbPG was functionalized with multiple ATRP-initiating groups to polymerize several polymethacrylate and polyacrylate side chains from the hyperbranched core.[156,157]

Other multifunctional polyethers can be obtained by cationic ROMBP of 3-alkyl-3-(hydroxymethyl)oxetane (HMO) (vide supra). They possess a similar polyol structure as hbPG, therefore they are useful macroinitiators for the synthesis of hyperstars. After functionalization with isobutyryl bromide they were used in ATRP polymerizations as macroinitiators.[158] Hyperbranched poly(3-ethyl-3-hydroxy-2-methyloxetane), synthesized by cationic ROMBP was also used as a macroinitiator for the synthesis of PEO multiarm star polymers.[159] Using cationic ROP, Yan *et al.* synthesized hyperstars by multibranching polymerization of HMO in THF in a one-pot reaction. Due to different propagation rates, the hyperbranched core is formed first, followed by the attachment of the linear chains.[160]

In different approaches, Dworak and co-workers also synthesized other star architectures. They used a tetrafunctional initiator, grafted blocks of PEO as well as acetal-protected linear PG and removed the protective groups under acidic conditions. This macroinitiator can be used for the same reaction sequence again to obtain defined polymers with up to 200 terminal hydroxy units.[161] In a recent work, they also used other glycidol monomers to obtain multifunctional four-arm stars by ROP.[162]

4.22.4.4 Linear-Hyperbranched Block Copolymers

LHBCs are an emerging field of research in the polymer chemistry community, since they offer unusual polymer topologies both in the solid state and in solution. Three major synthetic strategies can be applied to obtain these interesting hybrid structures: (1) coupling strategy, (2) chain-first strategy, and (3) dendron-first strategy.[163] Use of ROP has opened the pathway for several novel structures with interesting properties, which were developed just recently.

Based on the SMA technique, which was described previously, Frey *et al.* described the first well-defined LHBC in 2003, where the hyperbranched block was synthesized by 'hypergrafting' of glycidol on a linear precursor in an anionic ROMBP.[164] Another example, polystyrene-*block*-hbPGs was described in an earlier section.[124]

Poly(ethylene glycol)-*block*-hyperbranched PG (PEO-*b*-hbPG) copolymers prepared using an analogous route are of special interest for biomedical applications due to their biocompatible polyether-only structure.[165] By using a protected amino function as initiator, α,ω_n-telechelic polymers can be synthesized, while the polyfunctionality ω_n can be adjusted by the DP_n of glycidol. The different functional groups can be addressed in different chemical reactions, providing orthogonal modifications. These polymers are interesting candidates for protein conjugation to increase blood circulation times, in analogy to the established PEGylation. Using a four-step protocol combining two anionic ROP steps and two deprotection steps (**Scheme 39**), these biocompatible LHBCs can be obtained with low polydispersities ($M_w/M_n < 1.3$) and molecular weights from 1000 up to 25 000 g mol^{-1} in a chain-first strategy.[166] EO and 2-ethoxyethyl glycidyl ether (EEGE) are polymerized by anionic ROP to obtain a linear PEG block with a short linear PG block attached, which functions as macroinitiator for the ROMBP of glycidol after cleavage of the acetal protective groups under acidic conditions.

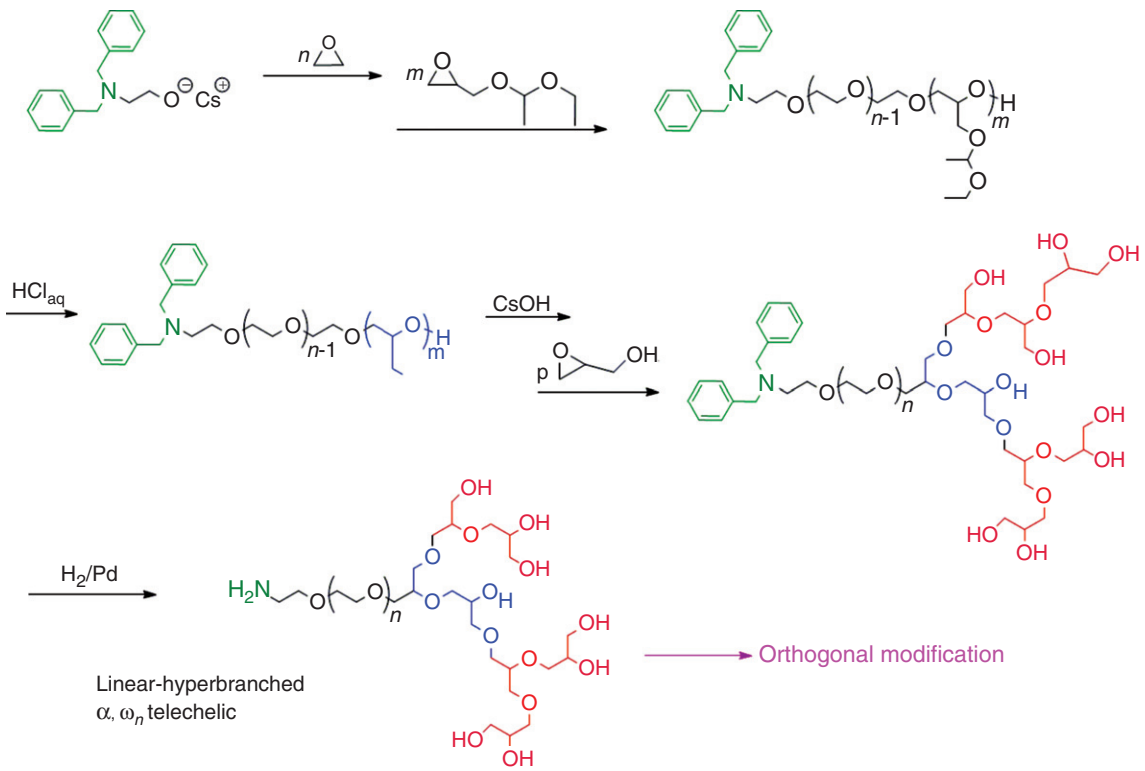

Scheme 39 Four-step synthesis of biocompatible α,ω_n-telechelic LHBCs. Reprinted with permission from Wurm, F.; Klos, J.; Räder, H. J.; Frey, H. *J. Am. Chem. Soc.* **2009**, *131*, 7954.[166] Copyright 2009 American Chemical Society.

The benzyl-protected terminal amino groups are cleaved in the final reaction step by catalytic hydrogenation without side reactions or degradation of the polyether structure.

By using aliphatic initiators such as cholesterol or glycerol ethers within the same synthesis concept, amphiphilic block copolymers can be synthesized which show micelle formation and are currently under evaluation as novel stealth liposomes for drug-delivery applications.[167]

Hyperbranched-linear-hyperbranched (ABA) triblock copolymers (HLHBCs) of hbPG-*b*-PEO-*b*-hbPG with molecular weights up to 45 000 g mol^{-1} have also been synthesized by anionic ROP of EO and EEGE and subsequent anionic ROMBP of glycidol.[168] In different approaches, Lim *et al.*[169] used a linear block of THF, polymerized by cationic ROP, and subsequent anionic ROMBP of glycidol and studied the micelle formation behavior of the polymers, while Malmström *et al.*[170] in an analogous grafting procedure synthesized a linear block of PEO by anionic ROP and two hyperbranched blocks by cationic ROMBP of HMO to obtain HLHBCs.

4.22.5 Conclusion and Perspectives

In this chapter, it has been demonstrated that ROMBP (also referred to as SCROP) are by now well established as a versatile and often preferential method for the controlled synthesis of well-defined hyperbranched polymers with moderate polydispersities. The heterocyclic monomers discussed earlier are generally latent AB_m monomers that are eligible for pseudo-chain-growth when using SMA conditions (polymerization by ring opening – chain growth, condensation of the pending B group with the heterocycle – step growth).

A major advantage of ROPs compared to conventional polycondensations is the general absence of polycondensation side products. This inherent characteristic allows for the application of cationic, anionic, and catalytic polymerization techniques in the initiated polymerization of suitable cyclic monomers, using functional initiators to achieve remarkable control over molecular weights and polydispersity. Employing SMA conditions, pseudo-chain-growth was realized for glycidol, permitting control over molecular weights. Understanding and controlling the branching pattern as well as molecular weight and polydispersity are an important issue both for the elucidation of structure–property relationships and the assembly of more complex polymer architectures using ROMBP. In this context, the synthetic principles other than ROP and detailed examples of the advantages of all basic strategies are presented in Chapter 4.11 of this volume.

In addition to the development of more efficient reaction systems for existing polymerization procedures such as the use of more efficient or recoverable catalysts or the use of enzymatic catalysis systems ('green chemistry'), future development of ROMBP reactions will certainly include novel cyclic monomers, leading to a variety of branched materials that can be obtained under controlled conditions.

Well-established materials, such as hyperbranched polyether polyols, have been used to develop exciting hybrid structures, from multiarm star polymers to LHBCs. Chemical modification of the core as well as the multiple terminal and interior groups leads to multifunctional materials for applications such as catalyst supports for bioconjugation and as photosensitizers. Unmodified hyperbranched polymers can contribute to applications in materials processing, for example, as rheology modifiers or coatings. The convenient synthesis of hyperbranched polymers in single reactions makes these materials highly interesting for industrial production. Further basic research in this field of polymer science will contribute to the development of complex polymer structures with a potential for academic and commercial specialty purposes.

References

1. Buhleier, E.; Wehner, W.; Vögtle, F. *Synthesis* **1978**, *2*, 155.
2. (a) Newkome, G. R.; Moorefield, C. N.; Vögtle, F. *Dendrons and Dendrimers: Concepts, Synthesis and Applications*; Wiley-VCH: Weinheim, 2001. (b) Fréchet, J. M. J.; Tomalia, D. A., Eds. *Dendrimers and Other Dendritic Polymers*; Wiley-VCH: New York, 2002. (c) Boas, U.; Heegard, P. M. H. *Chem. Soc. Rev.* **2004**, *33*, 43. (d) Lee, C. C.; MacKay, J. A.; Fréchet, J. M. J.; Szoka, F. C. *Nat. Biotechnol.* **2005**, *23*, 1517. (e) Mery, D.; Astruc, D. *Coord. Chem. Rev.* **2006**, *250*, 1965. (f) Calmark, A.; Hawker, C.; Hult, A.; Malkoch, M. *Chem. Soc. Rev.* **2009**, *38*, 352.
3. Staudinger, H.; Husemann, E. *Justus Liebigs Ann. Chem.* **1937**, *527*, 195.
4. Flory, P. J. *J. Am. Chem. Soc.* **1952**, *74*, 2718.
5. Kim, Y. H.; Webster, O. W. *J. Am. Chem. Soc.* **1990**, *112*, 4592.
6. (a) Kim, Y. H. *J. Polym. Sci., Part A: Polym. Chem.* **1998**, *36*, 1685. (b) Voit, B. J. *Polym. Sci., Part A: Polym. Chem.* **2000**, *38*, 2505. (c) Jikei, M.; Kakimoto, M. *Prog. Polym. Sci.* **2001**, *26*, 1233. (d) Gao, C.; Yan, D. *Prog. Polym. Sci.* **2004**, *29*, 183. (e) Voit, B.; Lederer, A. *Chem. Rev.* **2009**, *109*, 5924.
7. (a) Frisch, K. C.; Reegen, S. L., Eds. *Ring-Opening Polymerization*; Marcel Dekker: New York, 1969. (b) Saegusa, T.; Goethals, E., Eds. *Ring-Opening Polymerization*; American Chemical Society: Washington, DC, 1977. (c) Ivin, K. J.; Saegusa, T., Eds. *Ring-Opening Polymerization*; Elsevier: London, 1984; Vol. 1 & 2. (d) Sigwalt, P.; Spassky, N.; Sekiguchi, H. *Makromol. Chem., Macromol. Symp.* **1986**, *6*, 1.
8. (a) Voit, B. I. *Acta Polym.* **1995**, *46*, 87. (b) Kim, Y. H. *J. Polym. Sci. Part A, Polym. Chem.* **1998**, *36*, 1685.
9. Kim, Y. H.; Webster, O. W. *Polym. Prepr. (Am. Chem. Soc., Div. Polym. Chem.)* **1988**, *29*, 310.
10. Fréchet, J. M. J.; Henmi, M.; Gitsov, I.; *et al. Science* **1995**, *269*, 1080.
11. Hawker, C. J.; Fréchet, J. M. J.; Grubbs, R. B.; Dao, J. *J. Am. Chem. Soc.* **1995**, *117*, 10763.
12. (a) Lapienis, G.; Penczek, S. Pol. Patent Appl. 1998, P-328117. (b) Lapienis, G.; Penczek, S. *Macromolecules* **2000**, *33*, 6630.
13. Liu, M.; Vladimirov, N.; Fréchet, J. M. J. *Macromolecules* **1999**, *32*, 6881.
14. Trollsas, M.; Löwenhielm, P.; Lee, V. Y.; *et al. Macromolecules* **1999**, *32*, 9062.
15. Sandler, S. R.; Berg, F. R. *J. Polym. Sci., Part A: Polym. Chem.* **1966**, *4*, 1253.
16. Vandenberg, E. J. *J. Polym. Sci., Polym. Chem. Ed.* **1985**, *23*, 915.
17. Tokar, R.; Kubisa, P.; Penczek, S.; Dworak, A. *Macromolecules* **1994**, *27*, 320.
18. Dworak, A.; Walach, W.; Trzebicka, B. *Macromol. Chem. Phys.* **1995**, *196*, 1963.
19. Sunder, A.; Hanselmann, R.; Frey, H.; Mülhaupt, R. *Macromolecules* **1999**, *32*, 4240.
20. Sunder, A.; Frey, H.; Mülhaupt, R. *Macromol. Symp.* **2000**, *153*, 187.
21. Sunder, A.; Frey, H.; Mülhaupt, R. *Adv. Mater.* **2000**, *12*, 235.
22. Suzuki, M.; Ii, A.; Saegusa, T. *Macromolecules* **1992**, *25*, 7071.
23. Kim, Y. H.; Webster, O. W. *Macromolecules* **1992**, *25*, 5561.
24. Hawker, C. J.; Lee, R.; Fréchet, J. M. J. *J. Am. Chem. Soc.* **1991**, *113*, 4583.
25. Hölter, D.; Burgath, A.; Frey, H. *Acta Polym.* **1997**, *48*, 30.
26. Yan, D. Y.; Müller, A. H. E.; Matyjaszewski, K. *Macromolecules* **1997**, *30*, 7024.
27. Yan, D.; Gao, C.; Frey, H., Eds., *Hyperbranched Polymers: Synthesis, Properties, and Applications*; John Wiley & Sons: New York, 2011.
28. Hauser, M. In *Ring-Opening Polymerization*; Frisch, K. C.; Reegen, S. L., Eds.; Marcel Dekker: New York, 1969.
29. Dick, R. C.; Ham, G. E. *J. Macromol. Sci., Part A* **1970**, *A4*, 1301.
30. Van de Velde, M.; Goethals, E. J. *Macromol. Chem. Macromol. Symp.* **1986**, *6*, 271.
31. Baklouti, M.; Chaabouni, R.; Sledz, J.; Schue, F. *Polym. Bull.* **1989**, *21*, 243.
32. Goethals, E. J.; Schacht, E. H.; Bogaert, Y. E., *et al. Polym. J.* **1980**, *12*, 571.
33. Oike, H.; Washizuka, M.; Tezuka, Y. *Macromol. Chem. Phys.* **2000**, *201*, 1673.
34. (a) Prince, C. C.; Blair, E. A. *J. Polym. Sci., Part A: Polym. Chem.* **1967**, *5*, 171. (b) Goethals, E. J.; Trossaert, G. G.; Hartmann, P. J.; Engelen, K. *Makromol.*

Chem., Macromol. Symp. **1993**, *73*, 77. (c) Vo, C. D.; Kilcher, G.; Tirelli, N. *Macromol. Rapid Commun.* **2009**, *30*, 299.
35. Crivello, J. V.; Liu, S. *J. Polym. Sci., Part A: Polym. Chem.* **2000**, *38*, 389.
36. Kitajyo, Y.; Kinugawa, Y.; Tamaki, M.; *et al. Macromolecules* **2007**, *40*, 9313.
37. Satoh, T.; Kinugawa, Y.; Tamaki, M.; *et al. Macromolecules* **2008**, *41*, 5265.
38. (a) Imai, T.; Nawa, Y.; Katajyo, Y.; *et al. Macromolecules* **2005**, *38*, 1648. (b) Imai, T.; Satoh, T.; Kaga, H.; *et al. Macromolecules* **2004**, *37*, 3113.
39. Vandenberg, E. J.; Mullis, J. C.; Juvet, R. S., Jr. *J. Polym. Sci., Part A: Polym. Chem.* **1989**, *27*, 3083.
40. Vandenberg, E. J.; Mullis, J. C.; Juvet, R. S., Jr.; *et al. J. Polym. Sci., Part A: Polym. Chem.* **1989**, *27*, 3113.
41. Bednarek, M.; Biedron, T.; Helinski, J.; *et al. Macromol. Rapid Commun.* **1999**, *20*, 369.
42. Yan, D.; Hou, X.; Zhu, J.; *et al. Macromol. Rapid Commun.* **2000**, *21*, 557.
43. Magnusson, H.; Malmström, E.; Hult, A. *Macromol. Rapid Commun.* **1999**, *20*, 453.
44. Magnusson, H.; Malmström, E.; Hult, A. *Macromolecules* **2001**, *34*, 5786.
45. Xu, Y.; Gao, C.; Kong, H.; *et al. Macromolecules* **2004**, *37*, 6264.
46. Farthing, A. C. *J. Chem. Soc.* **1955**, *77*, 3648.
47. Dreyfuss, M. D.; Westphal, J.; Dreyfuss, P. *Macromolecules* **1968**, *1*, 437.
48. Bednarek, M.; Kubisa, P. *J. Polym. Sci., Part A: Polym. Chem.* **2006**, *44*, 6484.
49. (a) Turnbull, W. B.; Stoddart; J. F.; *Rev. Mol. Biotechnol.* **2002**, *90*, 231. (b) Spain, S. G.; Gibson, M. I.; Cameron, N. R. *J. Polym. Sci. Part. A: Polym. Chem.* **2007**, *45*, 2059. (c) Voit, B.; Appelhans, D. *Macromol. Chem. Phys.* **2010**, *211*, 727.
50. Carvalho, J. D. S.; Prins, W.; Schuerch, C. *J. Am Chem. Soc.* **1959**, *81*, 4054.
51. Satoh, T.; Imai, T.; Ishihara, H.; *et al. Macromolecules* **2003**, *36*, 6364.
52. Imai, T.; Satoh, T.; Kaga, H.; *et al. Macromolecules* **2003**, *36*, 6359.
53. Satoh, T.; Imai, T.; Ishihara, H.; *et al. Macromolecules* **2005**, *38*, 4202.
54. Rider, T. H.; Hill, A. J. *J. Am. Chem. Soc.* **1930**, *52*, 1521.
55. Patten, T. E.; Matyjaszewski, K. *Adv. Mater.* **1998**, *10*, 901.
56. Bailey, F. E.; Koleske, V. In *Surface Science Series*; Schick, M. J., Fowkes, F. M., Eds.; Marcel Dekker: New York, 1990; Vol. 35, p 35.
57. Radke, W.; Litvinenko, G.; Müller, A. H. E. *Macromolecules* **1998**, *31*, 239.
58. Hanselmann, R.; Hölter, D.; Frey, H. *Macromolecules* **1998**, *31*, 3790.
59. Wilms, D.; Wurm, F.; Nieberle, J.; *et al. Macromolecules* **2009**, *42*, 3230.
60. Kainthan, R. K.; Muliawan, E. B.; Hatzikiriakos, S. G.; Brooks, D. E. *Macromolecules* **2006**, *39*, 7708.
61. Kainthan, R. K.; Janzen, J.; Levin, E.; *et al. Biomacromolecules* **2006**, *7*, 703.
62. Wilms, D.; Klos, J.; Frey, H. *Macromol. Chem. Phys.* **2008**, *209* (4), 343.
63. Wilms, D.; Nieberle, J.; Klos, J.; *et al. Chem. Eng. Technol.* **2007**, *30*, 1519.
64. (a) Jansen, J. F. G. A.; Brabander-van den Berg, E. M. M.; Meijer, E. W. *Science* **1994**, *266*, 1226. (b) Percec, V.; Ahn, C. H.; Ungar, G.; *et al. Nature* **1998**, *391*, 161. (c) Peerlings, H. W. I.; Meijer, E. W. *Chem. Eur. J.* **1997**, *3*, 1563. (d) Cornelissen, J. J. L. M.; Rowan, A. E.; Nolte, R. J. M.; Sommerdijk, N. A. J. M. *Chem. Rev.* **2001**, *101*, 4039.
65. Spassky, N. *Makromol. Chem., Macromol. Symp.* **1991**, *42*, 15.
66. Sunder, A.; Mülhaupt, R.; Haag, R.; Frey, H. *Macromolecules* **2000**, *33*, 253.
67. Pastor-Pérez, L.; Kemmer-Jonas, U.; Wurm, F.; *et al. Macromolecules* **2010**, *43*, 9583.
68. Wilms, D.; Schömer, M.; Wurm, F.; *et al. Macromol. Rapid Commun.* **2010**, *31*, 1811.
69. Gref, R.; Minamitake, Y.; Peracchia, M. T.; *et al. Science* **1994**, *263*, 1600.
70. Calderon, M.; Quadir, M. A.; Sharma, S. K.; Haag, R. *Adv. Mater.* **2009**, *21*, 1.
71. Wilms, D.; Stiriba, E.-S.; Frey, H. *Acc. Chem. Res.* **2010**, *43*, 129.
72. Rokicki, G.; Rakoczy, P.; Parzuchowski, P.; Sobiecki, M. *Green Chem.* **2005**, *7*, 529.
73. Chang, H.-T.; Fréchet, J. M. J. *J. Am. Chem. Soc.* **1999**, *121*, 2313.
74. Gong, C.; Fréchet, J. M. J. *Macromolecules* **2000**, *33*, 4997.
75. Amass, A. J.; Perry, M. C.; Riat, D. S.; *et al. Eur. Polym. J.* **1994**, *30*, 641.
76. Takeuchi, D.; Aida, T. *Macromolecules* **1996**, *29*, 8096.
77. Nayak, U. G.; Whistler, R. L. *J. Org. Chem.* **1968**, *33*, 3582.
78. Mudryk, B.; Cohen, T.; *J. Org. Chem.* **1989**; *54*, 5657.
79. Smith, T. J.; Mathias, L. J. *Polymer* **2002**, *43*, 7275.
80. Morita, A.; Kudo, H.; Nishikubo, T. J. *Polym. Sci., Part A: Polym. Chem.* **2004**, *42*, 3739.
81. Morita, A.; Kudo, H.; Nishikubo, T. *Polym. J.* **2004**, *36*, 413.
82. Ziegler, K.; Holzkamp, E.; Breil, H.; Martin, H. *Angew. Chem.* **1955**, *67*, 426.
83. Ziegler, K. *Angew. Chem.* **1964**, *76*, 545.
84. Natta, G. *Science* **1965**, *147*, 261.
85. Grubbs, R. H. *Handbook of Metathesis*; Wiley-VCH: New York, 2003.
86. (a) Lundberg, R. D.; Cox, E. F. In *Ring-Opening Polymerization*; Risch, K. C., Reegen, S. L., Eds.; Marcel Dekker: New York, London, 1969; Vol. 6, p 266. (b) Löfgren, A.; Albertsson, A.-C.; Dubois, P.; Jérôme, R. *J. Macromol. Sci., Rev. Macromol. Chem. Phys.* **1995**, *35*, 379. (c) Kricheldorf, H. R.; Sumbel, M. *Eur. Polym. J.* **1991**, *25*, 585. (d) Kricheldorf, H. R.; Boettcher, C. *Makromol. Chem.* **1993**, *194*, 1653.
87. Suzuki, M.; Sawada, S.; Saegusa, T. *Macromolecules* **1989**, *22*, 1507.
88. Suzuki, M.; Yoshida, S.; Shiraga, K.; Saegusa, T. *Macromolecules* **1998**, *31*, 1716.
89. Leenslag, J. W.; Pennings, A. J. *Makromol. Chem.* **1987**, *188*, 1809.
90. Schwach, G.; Coudane, J.; Engel, R.; Vert, M. *J. Polym. Sci., Part A: Polym. Chem.* **1997**, *35*, 3431.
91. Schindler, A.; Hibionada, Y. M.; Pitt, C. G. *J. Polym. Sci., Part A: Polym. Chem.* **1982**, *20*, 319.
92. Kim, S. H.; Han, Y.; Kim, Y. H.; Hong, S. I. *Makromol. Chem.* **1992**, *193*, 1623.
93. Du, Y. J.; Lemstra, P. J.; Nijenhuis, A. J.; *et al. Macromolecules* **1995**, *28*, 2124.
94. Kricheldorf, H. R.; Kreiser-Saunders, I.; Boettcher, C. *Polymer* **1995**, *36*, 1253.
95. Storey, R. F.; Taylor, A. E.; *J. Macromol. Sci., Pure Appl. Chem.* **1998**, *35*, 723.
96. Kowalski, A.; Libiszowski, J.; Duda, A.; Penczek, S. *Polym. Prepr. (Am. Chem. Soc., Div. Polym. Chem.)* **1998**, *39*(2), 74.
97. Kowalski, A.; Duda, A.; Penczek, S. *Macromol. Rapid Commun.* **1998**, *19*, 567.
98. Kowalski, A.; Duda, A.; Penczek, S. *Macromolecules* **2000**, *33*, 689.
99. Duda, A.; Penczek, S.; Kowalski, A.; Libiszowski, J. *Macromol. Symp.* **2000**, *153*, 43.
100. Kowalski, A.; Libiszowski, J.; Duda, A.; Penczek, S. *Macromolecules* **2000**, *33*, 1964.
101. Kricheldorf, H. R.; Kreiser-Saunders, I.; Stricker, A. *Macromolecules* **2000**, *33*, 702.
102. (a) Trollsas, M.; Hedrick, J. L.; Mecerreyes, D.; *et al. Macromolecules* **1998**, *31*, 2756. (b) In´t Veld, P. J. A.; Velner, E. M.; van de Witte, P.; *et al. J. Polym. Sci., Part A: Polym. Chem.* **1997**, *35*, 219.
103. Parzuchowski, P. G.; Grabowska, M.; Tryznowski, M.; Rokicki, G. *Macromolecules* **2006**, *39*, 7181.
104. Yu, X.; Feng, J.; Zhuo, R. *Macromolecules* **2005**, *38*, 6244.
105. Mathers, R. T.; Damodaran, K.; Rendos, M. G.; Lavrich, M. S. *Macromolecules* **2009**, *42*, 1512.
106. Mathers, R. T.; McMahon, K. C.; Damodaran, K.; *et al. Macromolecules* **2006**, *39*, 8982.
107. (a) Kabayashi, S.; Ritter, H.; Kaplan, D., *Adv. Polym. Sci.* **2006**, *194*, 1. (b) Albertsson, A.-C.; Srivastava, R. K. *Adv. Drug Delivery Rev.* **2008**, *60*, 1077. (c) Kobayashi, S.; Makino, A. *Chem. Rev.* **2009**, *109*, 5288.
108. Skaria, S.; Smet, M.; Frey, H. *Macromol. Rapid Commun.* **2002**, *23*, 292.
109. Liu, J.; Huang, W.; Zhou, Y.; Yan, D. *Macromol. Rapid Commun.* **2009**, *42*, 4394.
110. Huang, J. L.; Pang, Y.; Zhu, X.; *et al. Biomacromolecules* **2010**, *11*, 1564.
111. (a) Newkome, G. R.; Moorefield, C. N.; Vögtle, F. In *Dendritic Molecules: Concepts, Synthesis, Perspectives*; VCH: Weinheim, **1996**. (b) Newkome, G. R.; He, E.; Moorefield, C. N. *Chem. Rev.* **1999**, *99*, 1689. (c) Fisher, M.; Vögtle, F. *Angew. Chem. Int. Ed.* **1999**, *38*, 885. (d) Bosman, A. W.; Jansen, H. M.; Meijer, E. W. *Chem. Rev.* **1999**, *99*, 1665. (e) Hecht, S.; Fréchet, J. M. J. *Angew. Chem. Int. Ed.* **2001**, *40*, 74. (f) Gorman, C. B.; Smith, J. C. *Acc. Chem. Res.* **2001**, *34*, 60. (g) Grayson, S. M.; Fréchet, J. M. J. *Chem. Rev.* **2001**, *101*, 3819. (h) Cameron, C. S.; Gorman, C. B.; *Adv. Funct. Mater.* **2002**, *12*, 17.
112. Tomalia, D. A.; Naylor, A. M.; Goddard, W. A. III *Angew. Chem. Int. Ed.* **1990**, *29*, 138.
113. Devadoss, C.; Bharati, P.; Moore, J. S. *Angew. Chem. Int. Ed.* **1997**, *6*, 1633.
114. Hawker, C. J.; Wooley, K. L.; Fréchet, J. M. J. *J. Am. Chem. Soc.* **1993**, *115*, 4375.
115. Bhyrappa, P.; Young, J. K.; Moore, J. S.; Suslick, K. *J. Am. Chem. Soc.* **1996**, *118*, 5708.
116. Vestberg, R.; Nyström, A.; Lindgren, M.; *et al. Chem. Mater.* **2004**, *16*, 2794.
117. Smith, D. K.; Diederich, F. *Chem. Eur. J.* **1998**, *4*, 1353.
118. Hua, J. L.; Li, B.; Meng, F. S.; *et al. Polymer* **2004**, *45*, 7143.
119. Gittins, P. J.; Alston, J.; Ge, Y.; Twyman, L. J. *Macromolecules* **2004**, *37*, 7428.
120. Gittins, P. J.; Twyman, L. J.; *J. Am. Chem. Soc.* **2005**, *127*, 1646.
121. Žagar, E.; Žigon, M. *Macromolecules* **2002**, *35*, 9913.
122. Pastor Pérez, L.; Barriau, E.; Berger-Nicoletti, E.; *et al. Macromolecules* **2008**, *41*, 1189.
123. Pastor-Perez, L.; Barriau, E.; Frey, H.; *et al. J. Org. Chem.* **2008**, *73*, 4680.
124. Barriau, E.; García Marcos, A.; Kautz, H.; Frey, H. *Macromol. Rapid Commun.* **2005**, *26*, 862.
125. Haag, R.; Sunder, A.; Stumbé. J.-F. *J. Am. Chem. Soc.* **2000**, *122*, 2954.
126. Wyszogrodzka, M.; Möws, K.; Kamlage, S.; *et al. Eur. J. Org. Chem.* **2008**, 53–63.
127. Sunder, A.; Krämer, M.; Hanselmann, R.; *et al. Angew. Chem. Int. Ed.* **1999**, *38*, 3552.
128. Krämer, M.; Stumbé, J.-F.; Türk, H.; *et al. Angew. Chem. Int. Ed.* **2002**, *41*, 4252.
129. Mecking, S.; Thomann, R.; Frey, H.; Sunder, A. *Macromolecules* **2000**, *33*, 3958.
130. Slagt, M. Q.; Stiriba, S.-E.; Gebbink, R. J. M. K.; *et al. Macromolecules* **2002**, *35*, 5734.

131. Stitiba, S.-E.; Slagt, M. Q.; Kautz, H.; *et al. Chem. Eur. J.* **2004**, *10*, 1267.
132. Kojima, C.; Yoshimura, K.; Harada, A.; *et al. Bioconjugate Chem.* **2009**, *20*, 1054.
133. Radowski, M. R.; Shukala, A.; von Berlepsch, H.; *et al. Angew. Chem. Int. Ed.* **2007**, *46*, 1265.
134. Küchler, S.; Radowski, M. R.; Blaschke, T.; *et al. Eur. J. Pharm. Biopharm.* **2009**, *71*, 243.
135. Zimmermann, S. C.; Quinn, J. R.; Burakowska, E.; Haag, R. *Angew. Chem.* **2007**, *119*, 8312.
136. Burakowska, E.; Zimmermann, S. C.; Haag, R. *Small* **2009**, *5*, 2199.
137. Kohle, P.; Khandare, J.; Pillai, O.; *et al. Pham. Res.* **2004**, 21, 2185.
138. Calderon, M.; Graeser, R.; Kratz, F.; Haag, R. *Bioorg. Med. Chem. Lett.* **2009**, 14, 3725.
139. Papp, I.; Dernedde, J.; Enders, S.; Haag, R. *Chem. Commun.* **2008**, *44*, 5851.
140. Türk, H.; Haag, R.; Alban, S. *Bioconjugate Chem.* **2004**, *15*, 162.
141. Zhang, J. G.; Krajden, O. B.; Kainthan, R. K.; *et al. Bioconjugate Chem.* **2008**, *19*, 1241.
142. Jászberényi, Z.; Moriggi, L.; Schmidt, P.; *et al. J. Biol. Inorg. Chem.* **2007**, *12*, 406.
143. Ramos-Fernandes, E. G.; de Queiroz, A. A. A.; Abraham, G. A.; Roman, R. J. *J. Mater. Sci.: Mater. Med.* **2006**, *17*, 105.
144. Sieger, C.; Biesalski, M.; Haag, R. *Chem. Eur. J.* **2004**, *10*, 2831.
145. Sunder, A.; Quincy, M. F.; Mülhaupt, R.; Frey, H. *Angew. Chem. Int. Ed.* **1999**, *38*, 2928.
146. Lapienis, G. *Prog. Polym. Sci.* **2009**, *34*, 852.
147. Claesson, H.; Malstrom, E.; Johannson, M.; Hult, A. *Polymer* **2002**, *43*, 3511.
148. Wang, F.; Rauh, R. D.; Rose, T. L. *J. Am. Chem. Soc.* **1997**, *119*, 11106.
149. Sunder, A.; Hanselmann, R.; Frey, H. *Macromolecules* **2000**, *33*, 309.
150. Knischka, R.; Lutz, P. J.; Sunder, A.; *et al. Macromolecules* **2000**, *33*, 315.
151. Doycheva, M.; Berger-Nicoletti, E.; Wurm, F.; Frey, H. *Macromol. Chem. Phys.* **2010**, *211*, 35.
152. Adeli, M.; Haag, R.; Zarnegar, J. *Nanopart. Res.* **2007**, *9*, 1057.
153. Gottschalk, C.; Wolf, F.; Frey, H. *Macromolecules* **2007**, *208*, 1657.
154. Burgath, A.; Sunder, A.; Neuner, I.; *et al. Macromol. Chem. Phys.* **2000**, *201*, 792.
155. Wolf, F. K.; Fischer, A. M.; Frey, H. *Beilstein J. Org. Chem.* **2010**, *6*, 1.
156. Meier, S.; Sunder, A.; Frey, H., Mülhaupt, R. *Macromol. Rapid. Commun.* **2000**, *21*, 226.
157. Shen, Z.; Chen, Y.; Barriau, E.; Frey, H. *Macromol. Chem. Phys.* **2006**, *207*, 57.
158. Calmark, A.; Vestberg, R.; Malström, E.; Johnson, M. *Polymer* **2002**, *43*, 4237.
159. Bednarek, M.; Kubisa, P. *Polimery (Warsaw)* **2004**, *49*, 719.
160. Hou, J.; Yan, D. *Macromol. Rapid Commun.* **2002**, *23*, 456.
161. Dworak, A.; Wa1ach, W. *Polymer* **2009**, *50*, 3440.
162. Libera, M.; Trzebicka, B.; Kowalczuk, A.; *et al. Polymer* **2011**, *52*, 250.
163. Wurm, F.; Frey, H. *Prog. Polym. Sci.* **2011**, *36*, 1.
164. Istratov, V.; Kautz, H.; Kim, Y. K.; *et al. Tetrahedron* **2003**, *59*, 4017.
165. Wurm, F.; Nieberle, J.; Frey H. *Macromolecules* **2008**, *41*, 1184.
166. Wurm, F.; Klos, J.; Räder, H. J.; Frey, H. *J. Am. Chem. Soc.* **2009**, *131*, 7954.
167. Hofmann, A. M.; Wurm, F.; Hühn, E.; *et al. Biomacromolecules* **2010**, *11*, 568.
168. Wurm, F.; Kemmer-Jonas, U.; Frey, H. *Polym. Int.* **2009**, *58*, 989.
169. Lim, S. H.; Cha, E. J.; Huh, J.; Ahn, C. H. *Macromol. Chem. Phys.* **2009**, *210*, 1734.
170. Rahm, M.; Westlund, R.; Eldsa, C.; Malmström, E., *J. Polym. Sci., Polym. Chem. Ed.* **2009**, *47*, 6191.

Biographical Sketches

Christoph Schüll (born 1985 in Frankfurt/Main, Germany) studied biomedical chemistry at the Johannes Gutenberg University of Mainz (Germany) with a temporary stay at the Department of Polymer Science and Engineering at the University of Massachusetts, Amherst (USA) in the group of Todd Emrick. After another research stay at the Department of Biotechnology and Bioprocess Engineering at the Technical University of Graz (Austria), he received his diploma degree in 2010. Currently, he is working on his PhD thesis at the Institute of Organic Chemistry at the University of Mainz in the group of Holger Frey. His major research interest is the synthesis of novel functional polymer architectures by anionic polymerization techniques.

Daniel Wilms (born 1981 in Mönchengladbach, Germany) studied chemistry at the Johannes Gutenberg University of Mainz (Germany) and the University of Massachusetts, Amherst (USA). He obtained his PhD from the University of Mainz in 2010 for his research at the Institute of Organic Chemistry on anionic polymerizations in continuous flow and novel branched macromolecules in the group of Holger Frey. He received a PhD fellowship of the 'Fonds der Chemischen Industrie' and the PhD award from the 'MAINZ' graduate school of excellence. Currently, he is working at BASF SE in Ludwigshafen (Germany).

Holger Frey (born 1965 in Ellwangen, Germany) studied chemistry at the University of Freiburg. Following a stay at Carnegie Mellon University in Pittsburgh (Kris Matyjaszewski), he obtained his PhD degree for research on polysilane copolymers at the University of Twente (NL) in the group of Martin Möller. After his habilitation at the University of Freiburg (1998) on polycarbosilanes, he moved to the Johannes Gutenberg University at Mainz in 2001. Since 2003, he has held a Full Professorship in organic and macromolecular chemistry. His research interests are directed at novel linear and branched functional polymer structures with unusual topology and biomedically relevant materials in general. He has published 200 peer-reviewed original publications and reviews and is a co-inventor of 12 patents.

4.23 Current and Forthcoming Applications of ROMP-Derived Polymers: Functional Surfaces and Supports

MR Buchmeiser, Universität Stuttgart, Stuttgart, Germany; Institut für Textilchemie und Chemiefasern (ITCF), Denkendorf, Germany

4.23.1 Introduction to Ring-Opening Metathesis Polymerization

Ring-opening metathesis polymerization (ROMP) is a polymerization process that is best accomplished by Schrock-type carbenes; that is, high-oxidation-state transition-metal alkylidenes in which cyclic olefins, whether mono-, bi-, or multicyclic, undergo ring opening and are concomitantly joined together to form a polymer chain. ROMP is thus a chain-growth polymerization and belongs, together with Ziegler-Natta-type polymerizations and group transfer polymerizations, to the family of polyinsertions. The mechanism is based on olefin metathesis.[1–4] The ring-opening process occurs at the most stable site of the monomer, that is, at the double bond (**Scheme 1**).[5]

It is important to note that, as with all metathesis reactions, all steps are in principle reversible. Furthermore, the double bond of the monomer is formally preserved, resulting in one double bond per repeat unit. This high unsaturation of the resulting ROMP-derived polymers affects the stability versus oxygen of the resulting polymers, particularly of poly(norborn-2-ene) (poly(NBE)). However, a significantly reduced propensity versus oxidation is observed for ROMP-derived polymers of mono- or disubstituted NBEs as well as of *cis*-cyclooctene (COE)-derived polymers. ROMP may therefore be regarded as a reversed ring-closing metathesis (RCM) reaction. It is driven by the thermodynamics that are entailed with the reduction in ring strain that occurs during incorporation of the monomer into the growing chain. In general, the ring opening of 3-, 4-, 8-, and larger-membered rings is energetically favored.[6] Consequently, mono-, bi-, or tricyclic ring structures with large ring strain, for example, NBEs, norbornadienes, COEs, cyclooctadienes (CODs), cyclobutenes, are favored. The overall ΔG° value for the ROMP process of 7-membered and in particular of 5- and 6-membered rings, that is, whether positive or negative, strongly depends on the concentration of the monomer, substituents at the ring, and the fact whether the cyclic olefins are part of a bi- or multicyclic ring system.[7] Finally, as another consequence of the large number of double bonds present in ROMP-derived polymers, backbiting processes may occur, leading to cyclic oligomers/polymers (**Scheme 2**).[8–10]

The extent of this process strongly depends on temperature, monomer concentration, *cis*/*trans* configuration of the double bonds within the polymer backbone, solvent, reaction time, and, probably most important, the steric bulk of the monomer used.

4.23.2 Initiators for ROMP

During the past 25 years, tremendous efforts have been put into the development of well-defined 'single-site' transition-metal alkylidenes.[7,11–21] Among all, the work of two groups deserves particular attention, a fact that was also recognized by awarding the 2005 Nobel Prize in chemistry to R. H. Grubbs[22–28] and R. R. Schrock.[29–36] They shared this award with Y. Chauvin,[5] honored for his fundamental work on metathesis chemistry. Mainly the work of Grubbs and Schrock led to the development of well-defined

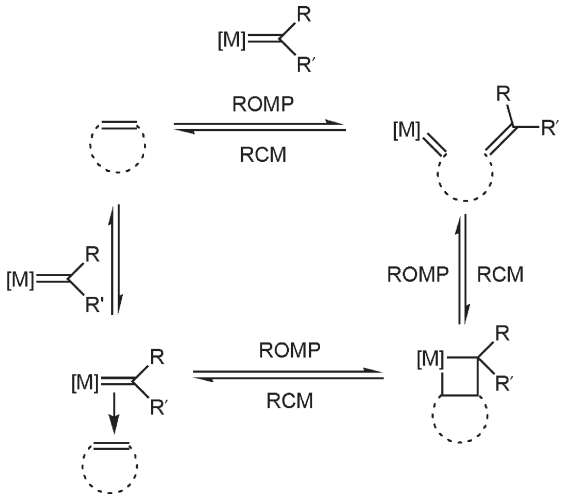

Scheme 1 Illustration of the ROMP process.

transition-metal alkylidenes that rapidly outrivaled the so far existing traditional initiator systems (Figure 1).

These initiators have the advantage of representing well-defined compounds and in particular of possessing preformed metal alkylidenes. Consequently, an *in situ* formation of the reactive species, that is, of the corresponding metal alkylidene, is not necessary. This dramatically reduces the load of metal salts and auxiliary ligands and thus does not only reduce the costs but also facilitate the purification of the final polymers.

'Schrock catalysts' are high-oxidation-state molybdenum (tungsten) alkylidenes and were first reported by Schrock *et al.*[37] in 1990. The systems possess the general formula $M(NAr')(OR')_2(CHR) \cdot L$, where M = Mo, W; Ar′ = phenyl, a substituted phenyl group or adamantyl; R = ethyl, phenyl, trimethylsilyl, CMe_2Ph, or *tert*-butyl; R′ = CMe_3, CMe_2CF_3, $CMe(CF_3)_2$, $C(CF_3)_2$, aryl, and so on; and L=quinuclidine, trialkylphosphane, tetrahydrofuran (THF), and so on. The most commonly used and also commercially available systems are based on the neopentylidene, the neophylidene, the 2,6-(2-Pr)$_2$-C_6H_3-imido, the adamantylimido, the *tert*-butoxide, the hexafluoro-*tert*-butoxide, and the (substituted) binaphtholate and biphenolate ligand.

Grubbs-type initiators are well-defined ruthenium alkylidenes,[38–41] however, with a more pronounced carbene character. The so-called 'first-generation Grubbs initiators' are based on phosphanes, while the 'second-generation Grubbs initiators' bear both an N-heterocyclic carbene (NHC) and a phosphane.[13–15,42,43] Finally, the 'third-generation Grubbs initiators' contain one NHC and one or two (substituted) pyridines.[44] Another milestone in catalyst activity was the development of Grubbs-type initiators with an internally oxygen-chelated ruthenium alkylidene (Figure 2).[20] They are usually referred to as Grubbs–Hoveyda catalysts and exhibit pronounced stability and longevity, for example, in RCM reactions. A release–return mechanism has been proposed for these systems;[45] however, more recent reports make this mechanism highly questionable.[46]

Finally, Ru-carboxylate[47] and bis(trifluoroacetate) derivatives of the general formula $Ru(CF_3COO)_2(NHC)(CHR)$ and $Ru(CF_3COO)_2(PCy_3)(NHC)(CHPh)$ (NHC = IMes, $IMesH_2$, 1,3-dimesityl-3,4,5,6-tetrahydropyrimidin-2-ylidene, 1,3-dimesityl-4,5,6,7-tetrahydro-1,3-diazepin-2-ylidenes; R = 2-(2-PrO)-C_6H_4, 2-MeO-5-NO_2-C_6H_3)[18,47–57] have to be mentioned. These catalysts are highly active in ROMP and also allow for the ('living') cyclopolymerization of 1,6-heptadiynes (Figure 3).[56–59]

4.23.2.1 ROMP with Schrock Initiators

Generally speaking, Schrock[60] initiators are highly active in the ROMP of a vast variety of cyclic alkenes such as substituted NBEs, norbornadienes, 7-oxanorbornenes, cyclooctatetraenes (COTs), 1,4-CODs, etc., or polycyclic alkenes such as certain quadricyclanes.[61] In addition, they may be used for 1-alkyne polymerization and the cyclopolymerization of 1,6-heptadiynes.[58,62] Despite the fact that they are highly sensitive

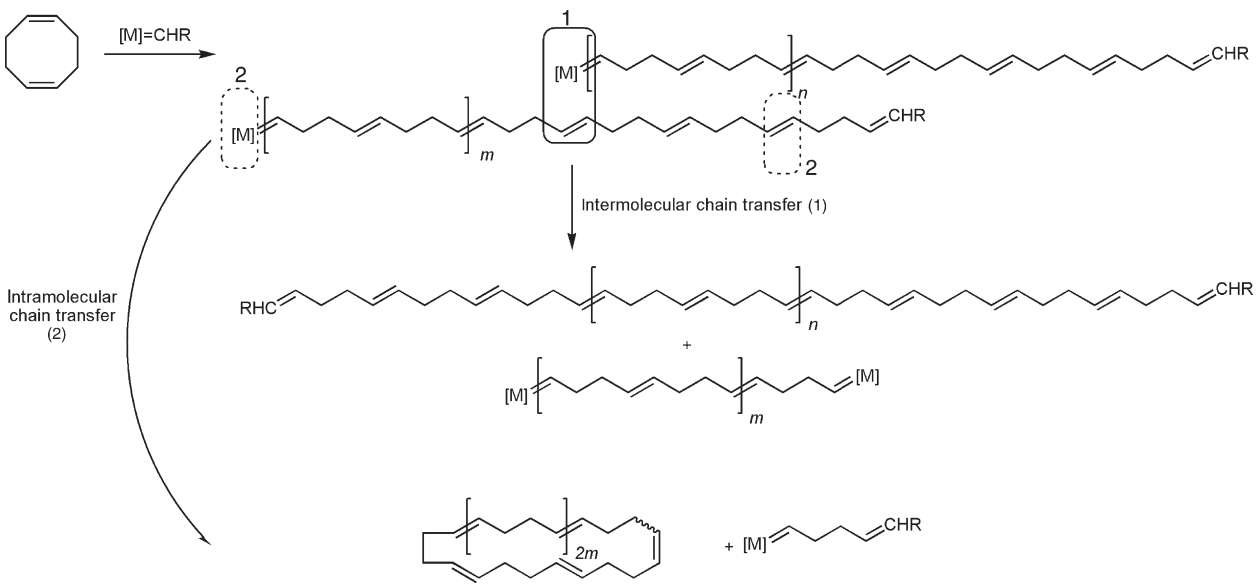

Scheme 2 Inter- (1) and intramolecular (2) chain transfer reactions in ROMP.

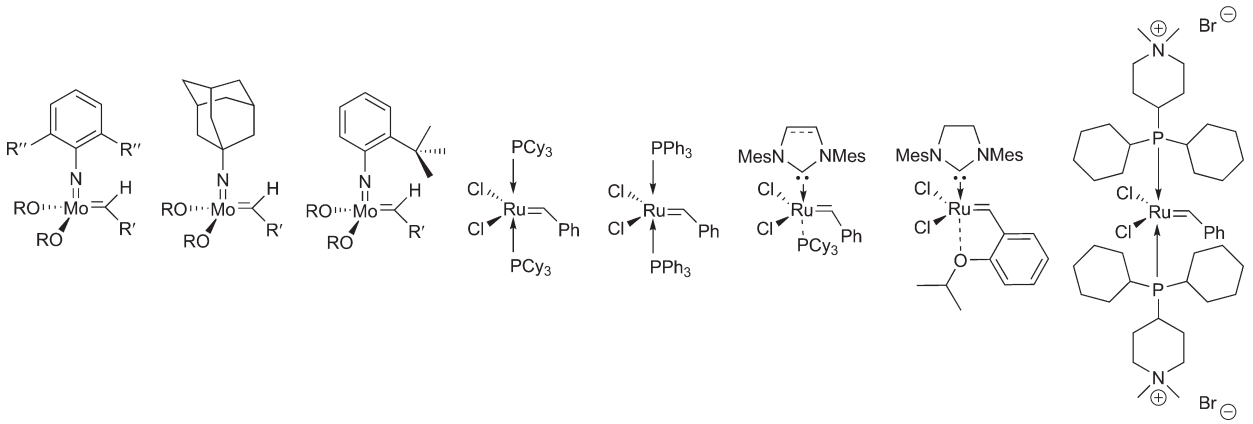

Figure 1 Selected examples of Grubbs- and Schrock-type initiators.

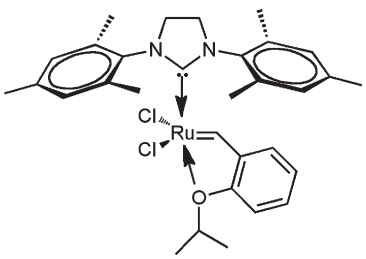

Figure 2 Second-generation Grubbs–Hoveyda catalyst.

toward traces of oxygen or moisture, they possess a remarkable stability versus various functionalities including cyano groups, esters, anhydrides, amides, ethers, amines, and so on.[31,63,64]

Schrock catalysts exist in form of two rotamers. The one compound in which the *tert*-butyl or CMe_2Ph group points toward the imido ligand is commonly called the *syn*-rotamer, while the second with the *tert*-butyl or CMe_2Ph group pointing away from the imido ligand is called the *anti*-rotamer (Figure 4).

These two rotamers, whose reactivity and relative ratio is governed by the electronic nature of the alkoxide ligand, are responsible for the structure of the final ROMP-derived polymer. The rates of interconversion between these two rotamers strongly depend on the alkoxide. The 'living' polymerizations triggered by Mo-bis(*tert*-butoxide)-derived initiators usually lead to the formation of all-*trans*, highly tactic polymers.[65] Tacticity of such polymers is believed to be controlled by the chirality of the alkylidenes, β-carbon (chain end control).[28–36,66] Living, Schrock initiator-triggered polymerizations are best

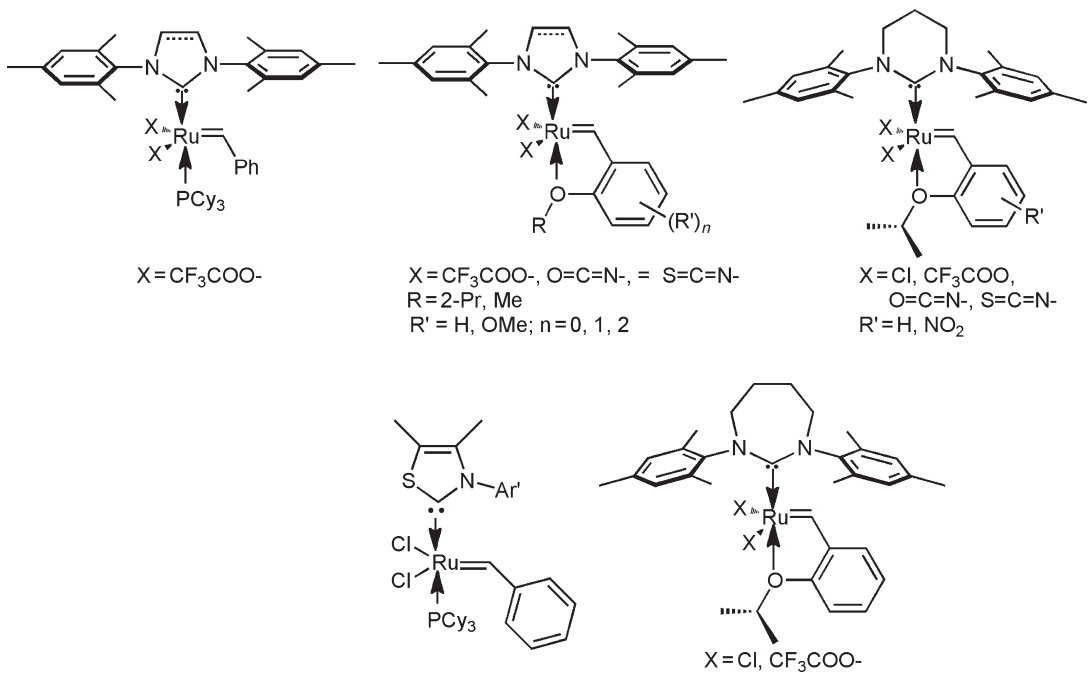

Figure 3 Selection of modified Grubbs-type initiators.

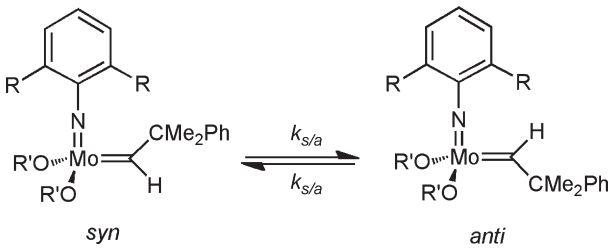

Figure 4 *syn*- and *anti*-rotamers of a Schrock catalyst. $k_{s/a}$ and $k_{a/s}$ are the rate constants for the interconversion of the *syn*- into the *anti*-rotamer and vice versa.

terminated by aldehydes in a Wittig-type reaction: polymer–CH=[Mo] + RCHO → polymer–CH=CHR + [Mo=O].[67]

4.23.2.2 ROMP with Grubbs-Type Initiators

Compared to molybdenum- or tungsten-based Schrock catalysts, the reactivity of ruthenium-based Grubbs catalysts is somewhat different. Reactivity in $RuCl_2(PR_3)_2(CHPh)$ may efficiently be tuned by the use of different phosphanes[68] rather than by the nature of the alkylidene moiety or by substitution of the chlorides by other, more electron-withdrawing groups.[69] The widely accepted dissociative mechanism[25,70,71] is shown in Scheme 3.

The stability as well as the reactivity order that can be deduced therefrom is $PPh_3 < PBz_3 < PCyPh_2 < PCy_2Ph < P\text{-}i\text{-}Bu_3 < P\text{-}i\text{-}Pr_3 < PCy_3$. Concerning the variation of the other ligands, an increase in reactivity in the order X=I<Br<Cl and R=H<Ph<alkyl<COOR for $RuX_2(PR_3)_2(CHR')$ is observed. Vice versa, in terms of initiation, an increase in the rate constant of initiation has been observed in the order X=Cl<Br<I, R′=H<Ph<alkyl<COOR, and PR_3=PCy<PPh_3. In terms of polymer structure, the ROMP of NBEs and norbornadienes using ruthenium-based systems generally results in the formation of polymers that predominantly contain *trans*-vinylene units. For a detailed discussion on the stereochemistry of ROMP-derived polymers and the determination of tacticity refer to the chapter by J. G. Hamilton in Ref. 25 and the references cited therein. Polymerizations initiated by Grubbs-type initiators are best terminated by the use of ethyl vinyl ether, yielding vinyl-terminated polymers and Ru-(ethoxymethylidenes) with very low ROMP activity.[72]

4.23.3 1-Alkyne Polymerization

The term 1-alkyne polymerization refers to a process in which a terminal alkyne undergoes, similar to the ROMP process of a cyclic olefin, a [2 + 2] cycloaddition to a metal carbene (alkylidene). This can proceed via α- or β-insertion of the alkyne into the metal–carbon double bond (Scheme 4). Both insertion mechanisms lead to conjugated polymers. With a few exceptions,[73–75] polymerizations based on α-insertion are the preferred ones, since they offer better control over molecular weights due to favorable values of k_i/k_p (k_i and k_p are the rate constants of initiation and propagation, respectively).

Despite some reports on a successful polymerization of terminal alkynes by Grubbs-type initiators, the efficient and living polymerization of these monomers is still the

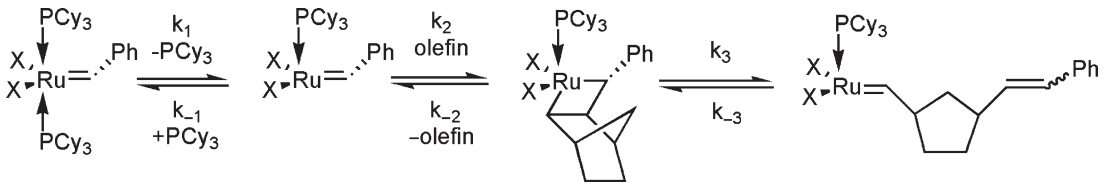

Scheme 3 Mechanism of ROMP initiated by Grubbs-type initiators.

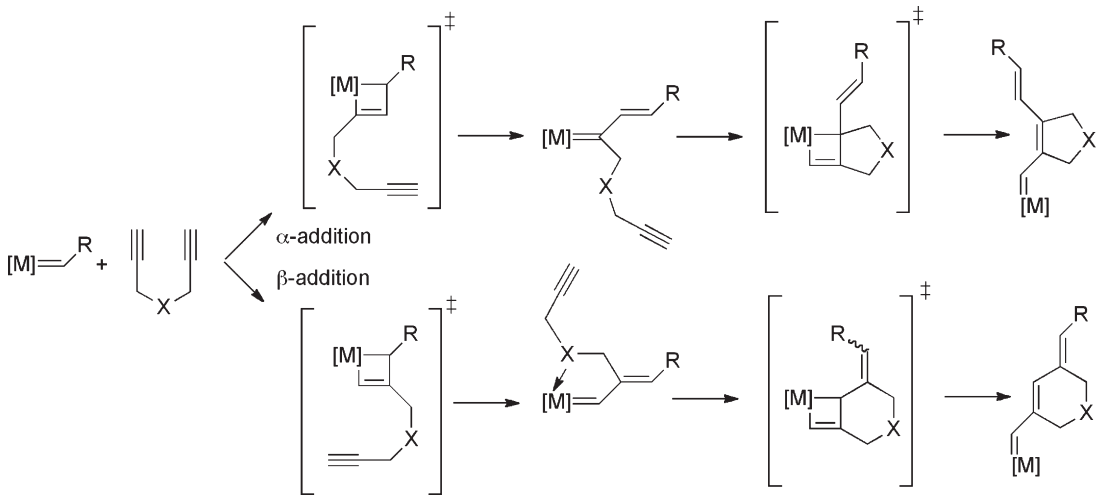

Scheme 4 α- and β-insertion of a terminal alkyne into a metal alkylidene.

domain of Schrock-type initiators.[49] Importantly, the careful tuning of both the steric and electronic properties of the catalysts can be used to generate polymerization systems where k_p is comparable to or larger than k_i, resulting in polymerizations characterized by the complete and instantaneous consumption of initiator. In case an initiator fulfills all these criteria, polymers with defined molecular weight and low polydispersity (polydispersity index (PDI), typically <1.15) are obtained. In addition, a stoichiometric design and the construction of block copolymers are possible. Finally, the formation of a certain backbone structure, that is, the relative orientation of one monomer unit to another, may be predetermined by the choice of a certain initiator. Nevertheless, to rely on these potential advantages, a careful investigation of the polymerization system is necessary for every single monomer used.

4.23.4 Supports

4.23.4.1 Inorganic Surfaces

4.23.4.1.1 Gold surfaces

The first surface modification using a 'grafting-from' approach aimed on the preparation of 1-mercapto-10-(*exo*-5-norborn-2-enoxy)decane-modified gold nanoparticles for the $RuCl_2(PCy_3)_2$(CHPh)-initiated grafting of ferrocene-containing NBEs to produce redox-active polymer-nanoparticle hybrids (Scheme 5)[76,77] The concept was later extended to insulating surfaces such as silicon using a synthetic protocol similar to the one described by Grubbs *et al.* and Buchmeiser *et al.* (see below).[78]

A similar approach for the modification of Au surfaces was reported by Grubbs and Weiss *et al.*, who used the more rigid tether molecule 4-(4-(norborn-5-ene-2-ylmethylenoxy) phenylethynyl)tolane-4′-thiol (Figure 5). *N*-Methyl-7-oxanorborn-5-ene-5,6-dicarbimide and 2,3-bis(*tert*-butoxydimethylsilyloxymethylene)-norborn-5-ene were used in a 'grafting-from' approach.[79] Similarly, surfaces of gold particles were modified with norborn-5-ene-2-ylmethanthiol and the surface-immobilized NBE groups were subsequently used for the grafting of NBE using a 'grafting-from' approach. The resulting material was used for the construction of a field-effect transistor.[80]

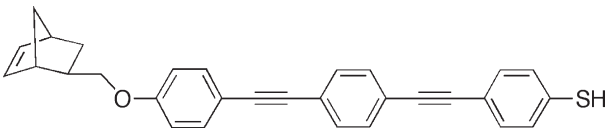

Figure 5 4-(4-(Norborn-5-ene-2-ylmethylenoxy)phenylethynyl)tolane-4′-thiol used as anchor group in a 'grafting-from' approach for the modification of Au surfaces.

Li *et al.*[81] utilized a norborn-5-en-2-yloxydodecan-1-thiol-modified gold cluster. Cross-linking of the core was accomplished with the first-generation Grubbs initiator $RuCl_2(PCy_3)_2$(CHPh). Both intra- and interparticle cross-linking was observed.[81] The latter could be avoided by using flat Au surfaces. Wu *et al.*[82] described the synthesis of nanometer-sized hollow polymer capsules from polymer-grafted gold particles. A metathesis-based route utilizing $RuCl_2(PCy_3)_2$(CHPh) was applied, where the terminal alkene groups of the tripodal Au-immobilized ligand shown in Figure 6 were cross-linked to form a three-dimensional polymer network. Dissolution of the gold particles with $KCN/K_2[Fe(CN)_3]$/THF yielded the desired hollow capsules.[82]

Finally, Samanta *et al.*[83] reported on the synthesis of Au nanoparticles carrying self-assembled monolayers (SAMs) with various functional groups including ferrocene and Fischer carbenes (Scheme 6).

4.23.4.1.2 Silicon-based surfaces

Juang *et al.* and Harada *et al.*[84,85] reported on the surface modification of Si (111). Conversion of the surface Si–H moieties into Si–allyl groups allowed to pursue the 'grafting-from' approach shown in Scheme 7. The thickness of the polymer layer could be varied up to 5500 nm by simple variation of the monomer, that is, the NBE concentration.

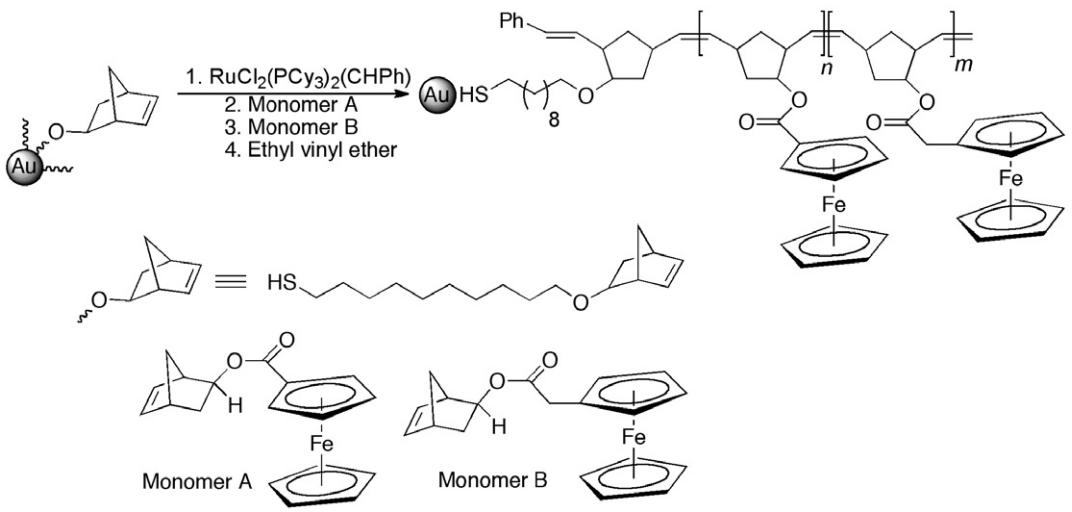

Scheme 5 Synthesis of Au-hybrid nanoparticles with electroactive copolymer shell structure.

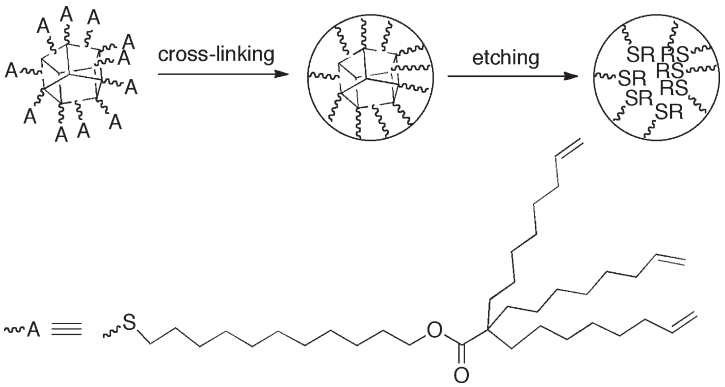

Figure 6 Synthesis of nanometer-sized hollow polymer capsules from polymer-coated Au particles.

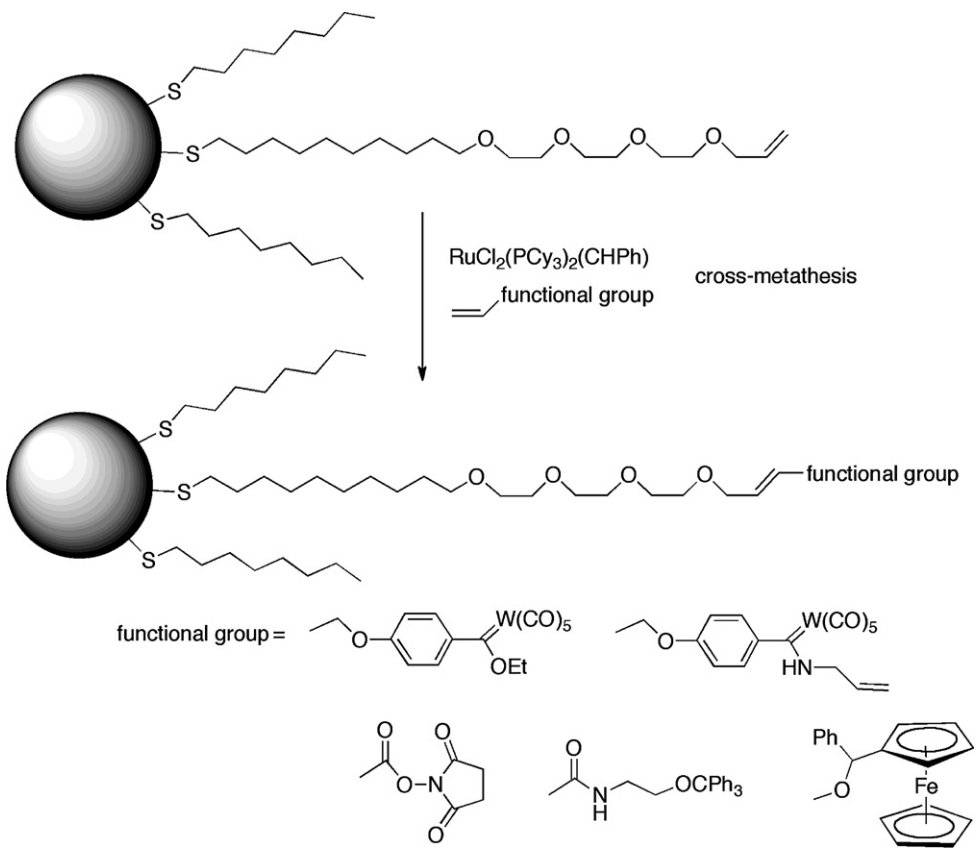

Scheme 6 Synthesis of Au nanoparticles bearing functional self-assembled monolayers (SAMs).

4.23.4.1.3 Silica-based surfaces

Many applications of surface-modified materials, for example, in separation science or heterogeneous catalysis applying continuous flow conditions, require the use of mechanically and pressure-stable carriers. Buchmeiser *et al.*[86–88] were the first to develop synthetic protocols for both a 'grafting-from' and a 'grafting-to' approach for the modification of micrometer-sized inorganic, that is, silica particles (Scheme 8).

Surface-immobilized norborn-5-ene-2-yl-groups were used as suitable anchoring groups for the preparation of graft copolymers using ROMP. These can easily be introduced in the case of silica materials using trichloronorborn-5-ene-2-ylsilane, chlorodimethylnorborn-5-ene-2-ylsilane, or trialkoxynorborn-2-ene-5-ylsilanes. To gain access to accurate surface analysis using elemental analysis, the former appears favorable, since all carbon found in norborn-5-ene-2-ylsilyl-derivatized silica can be clearly attributed to the surface-immobilized NBE groups. In contrary, the use of trialkoxynorborn-2-ene-5-ylsilanes results in the formation of additional surface-bound alkoxysilanes that impede accurate quantification of surface-bound NBE groups via elemental analysis.[89,90] Subsequent 'end capping' with a mixture of chlorotrimethylsilane and dichlorodimethylsilane followed by addition of absolute methanol leads to a sufficient derivatization of a major part of the surface silanol groups

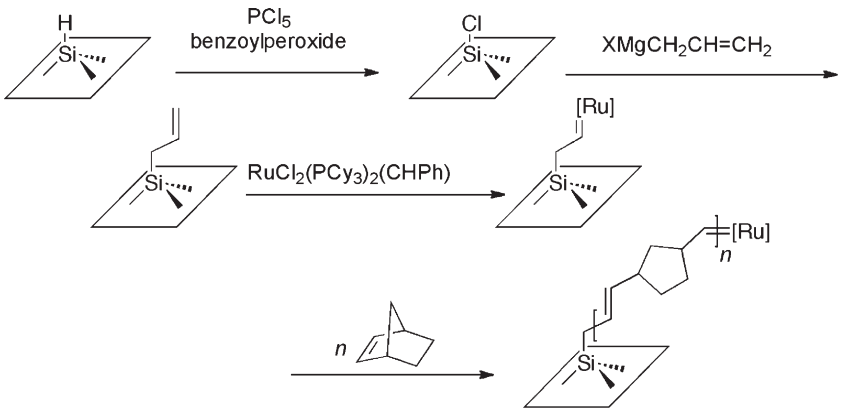

Scheme 7 Surface modification of Si using a 'grafting-from' approach.

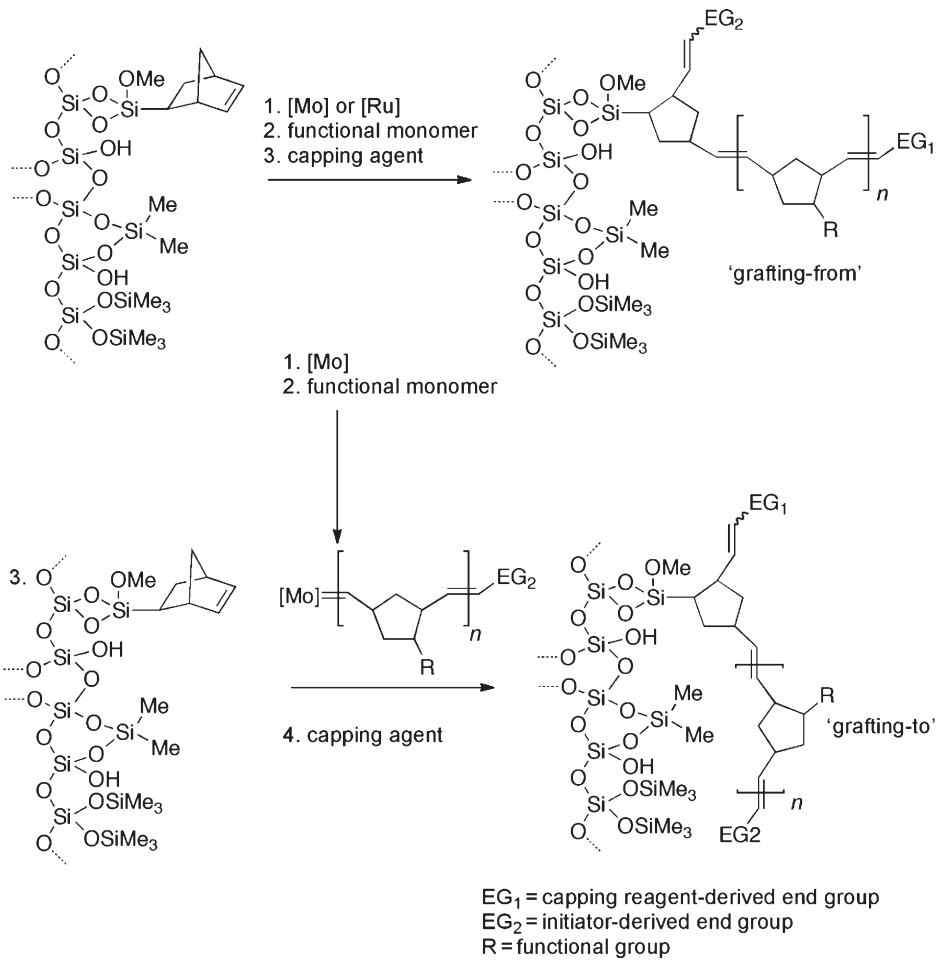

Scheme 8 Surface functionalization of silica via ROMP. 'Grafting-from' approach (top), 'grafting-to' approach (bottom).

(approximately 90%). For the 'grafting-to' approach, the monomer was transformed into a living polymer via ROMP and subsequently attached to the support by reaction with the surface NBE groups. This approach required at least class-IV living systems[91] and consequently leads to the formation of tentacle (brush)-type stationary phases with the linear polymer chains attached to the support. Alternatively, the initiator can first be reacted with the support to become heterogenized. Monomer is added consecutively and grafted onto the surface ('grafting-from' approach). While the first-generation Grubbs-type initiator $RuCl_2(PCy_3)_2(CHPh)$ could be used only for 'grafting-from' experiments, Schrock-type initiators are applicable to both methods.

With these methods in hand, various monomers including the chiral, enantiomerically pure monomer *N*-(norborn-5-ene-2-carboxyl)-phenylalanine ethylester was surface-grafted on porous 5 μm silica. Using Nucleosil 300-5, 60 mmol of this monomer was immobilized on the surface using a 'grafting-from' approach

and $RuCl_2(PCy_3)_2(CH\text{-}p\text{-}F\text{-}C_6H_4)$ as initiator.[86] With Mo(*N*-2,6-Me_2-C_6H_3)($CHCMe_2Ph$)($OCMe(CF_3)_2$)$_2$ as initiator, 40 mmol of this monomer could be grafted to the surface using either a 'grafting-from' or a 'grafting-to' approach. The resulting chiral stationary phase (CSP) was successfully used as high-performance liquid chromatography (HPLC) support in the separation of racemic dinitrobenzoyl-protected phenylalanine ethyl ester.[86] The broad applicability of this concept was demonstrated by immobilizing a series of β-cyclodextrin (β-CD) derivatives, 6-*O*-(norborn-2-ene-5-carboxyl)-β-CD, tetrakis(6-*O*-norborn-2-ene-5-carboxyl)-β-CD, 6-*O*-(7-oxanorborn-2-ene-5-carboxyl)-β-CD, 6-*O*-(6-(norborn-2-ene-5-carbonylaminohexoyl)-β-CD, 6-*O*-(norborn-2-ene-5-ylmethoxymethylsilyl)-β-CD, tris(6-*O*-norborn-2-ene-5-ylmethoxymethylsilyl)-β-CD, tetrakis (6-*O*-norborn-2-ene-5-ylmethoxymethylsilyl)-β-CD, and hexakis (6-*O*-norborn-2-ene-5-ylmethoxymethylsilyl)-β-CD, on Nucleosil 300-5.[92] A 'grafting-from' approach using $RuCl_2(PCy_3)_2(CHPh)$ as initiator was used throughout resulting in grafting densities of 11–34 mmol g^{-1}. The CSPs could be prepared with high reproducibility and used within a pH range of 2–10. With these stationary phases in hand, a series of β-blockers, dansyl (DNS)- or 9-fluorenylmethoxycarbonyl (Fmoc)-protected amino acids, and planar chiral ferrocene derivatives (Figure 7) could be separated.[92,93] Selected data on the separation efficiency, selectivity factor (α), and resolution (R_s) are provided in Table 1. Relative standard deviations (RSDs) (s_{n-1}) of the mean resolution (R_s) were in the range of 2–7% throughout. In a comparative study, poly(7-oxanorborn-5-ene-2,3-dicarboxylic acid)-grafted silica supports, again prepared via a 'grafting-from' approach, possessed superior separation behavior to the analogous coated separation media.[94]

Based on our studies on metallocenylalkynes,[73–75,95] poly (ethynylferricinium)-based anionic exchangers were prepared applying the 'grafting-to' concept described above.[96] Thus,

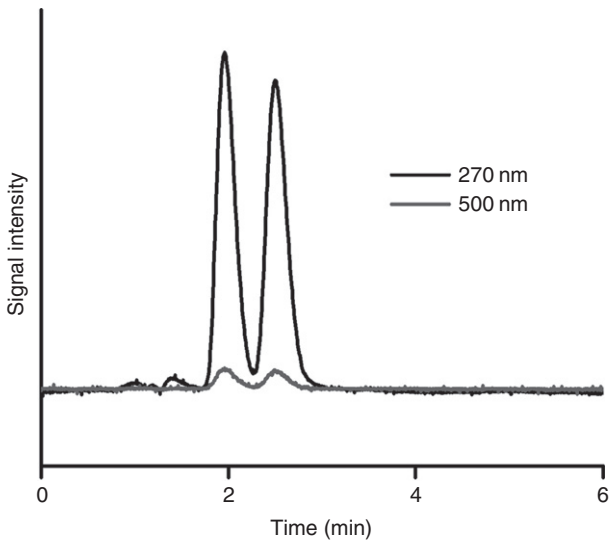

Figure 7 Separation of *rac*-ferroceno[2,3a]inden-1-ones on a poly (tetrakis(*endo/exo*-6-*O*-norborn-2-ene-5-ylmethoxymethylsilyl)-β-CD)-grafted column. Conditions: $T = 21.5$ °C, flow rate 0.5 ml min^{-1}, acetonitrile/MeOH/acetic acid/triethylamine (90:10:0.15:0.45), UV-detection. Reprinted from Mayr, B.; Schottenberger, H.; Elsner, O.; Buchmeiser, M. R. *J. Chromatogr. A* **2002**, *973*, 115–122. © Copyright 2002, with permission from Elsevier.

metathesis polymerization of 4-ethynyl-1-(octamethylferrocenylethenyl)benzene using the Schrock-type catalyst Mo(*N*-2,6-Me_2-C_6H_3)($CHCMe_2Ph$)($OCMe(CF_3)_2$)$_2$ and subsequent grafting of the living polymer onto a (norborn-5-ene-2-yl)-derivatized silica support resulted in the desired octamethylferrocene-grafted stationary phase (Scheme 9). Both porous, that is, Nucleosil 300-5, and nonporous silica supports, that is, Micra, were used. Oxidation with I_2 resulted in an octamethylferricinium-based anion exchanger that was successfully used for the separation of oligonucleotides (dT_{12}-dT_{18}).

As shown in preceding investigations, *N*,*N*-dipyrid-2-ylnorborn-2-en-5-ylcarbamide can be polymerized in a living manner using well-defined Schrock initiators.[97] Thus, a class-VI living system[91] was accomplished with Mo(*N*-2,6-*i*-Pr_2-C_6H_3)($CHCMe_2Ph$)($CMe(CF_3)_2$)$_2$. This monomer was grafted on NBE surface-functionalized silica, using a 'grafting-from' approach to generate tentacles of poly-(*N*,*N*-dipyrid-2-ylnorborn-2-en-5-ylcarbamide) with a controlled degree of polymerization (DP), typically <50 (Scheme 10).[98]

It is worth mentioning that the careful end capping of silica with a mixture of $ClSiMe_3$ and Cl_2SiMe_2 eliminates virtually any initiator deterioration potentially caused by the interaction with the silanol groups. In addition, complete reaction of the initiator with the support as evidenced by the absence of any soluble polymer was observed.[86] The loading of the supports with palladium was accomplished by reaction with H_2PdCl_4. Within a few hours, a quantitative reaction was observed resulting in slightly yellow-colored supports. Values of 0.28 and 0.08 mmol Pd/g, respectively, were achieved. Not surprising, $RuCl_2(PCy_3)_2(CHPh)$ was not capable of polymerizing *N*,*N*-dipyrid-2-ylnorborn-2-en-5-ylcarbamide or its 7-oxa analogue in a quantitative or living manner due to an irreversible coordination of the ligand to the ruthenium core. The palladium-loaded silica were successfully used in various Heck reactions including slurry reactions under standard as well as under microwave conditions where removal of the support was simply accomplished by filtration. In particular the use of microwave lead to a drastic reduction of reaction times, which is of particular interest for applications in high-throughput screening (HTS). Turnover frequencies (TOFs) were typically in the range of 0.1–0.3 s^{-1}. Alternatively, palladium-loaded silica was packed into stainless steel columns, which were subsequently loaded with monomers for Heck reactions and employed as reaction columns as in HTS machines. Alternatively, flow-through reactors were realized with surface-derivatized silica-packed stainless steel columns. With these columns, a constant conversion of iodobenzene with styrene (70–80%) was observed over several hours. TOFs were in the range of 0.07 s^{-1}. In all these experiments, irrespective of the application, only minor amounts of Pd, typically less than 2.5%, were leached into the reaction mixture.[98]

Grafting of 4′-(norborn-2-en-5-ylmethylenoxy)terpyridine was accomplished by ROMP, too. However, polymerization of this monomer by the Schrock initiator Mo(*N*-2,6-*i*-Pr_2-C_6H_3)($CHCMe_2Ph$)($CMe(CF_3)_2$)$_2$ only fulfilled the requirements of a class-V living system.[91] Consequently, the corresponding surface-grafted support had to be prepared applying a 'grafting-from' approach as described above[86] (Scheme 11).

Loading with Cu(I) afforded the desired atom transfer radical polymerization (ATRP) support.[99–101] Typical metal

Table 1 Separation of racemic DNS- and Fmoc-protected amino acids and drugs on 6-*O*-(norborn-2-ene-5-carboxyl)-β-CD-grafted Nucleosil 300-5

	k_L	k_D	a	R_S		k_L	k_D	a	R_S
DNS-Val[a]	2.03	5.07	2.50	4.75	DNB-Trp[a]	6.61	7.88	1.19	0.89
DNS-Trp[a]	3.52	5.35	1.52	2.12	DNB-Phe[a]	10.21	6.84	1.49	2.36
DNS-Thr[a]	0.47	1.44	3.08	2.38	Fmoc-Phe[a]	10.15	9.09	1.12	0.67
DNS-Ser[a]	0.86	1.59	1.85	1.08	Atenolol[b]	9.09	11.68	1.28	1.05
DNS-Phe[a]	3.10	5.02	1.62	2.50	Propranolol[b]	2.19	2.60	1.19	0.56
DNS-Met[a]	1.72	3.30	1.92	2.71	Metoprolol[b]	2.57	3.27	1.27	0.85
DNB-Val[a]	4.32	5.50	1.27	1.22	Proglumide[b]	2.08	3.54	1.70	2.57

[a]99.8:0.2:0.01:0.03, acetonitrile/MeOH/acetic acid/triethylamine.
[b]98:2:0.2:0.2, acetonitrile/MeOH/acetic acid/triethylamine.
Column dimensions: 150 × 2 mm; T = 0 °C; flow = 0.5 ml min^{-1}.

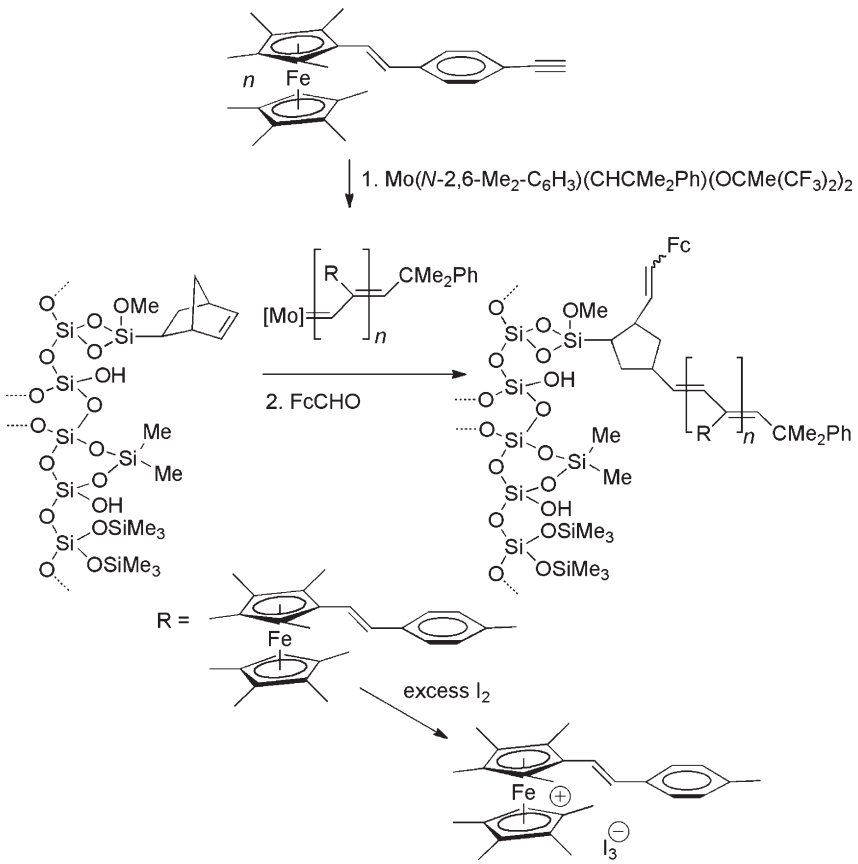

Scheme 9 Surface functionalization of silica via 1-alkyne polymerization using a 'grafting-to' approach.

loadings were in the range of 15 mmol g^{-1}. Polystyrene (PS) prepared under ATRP conditions with these supports showed comparably low polydispersities (PDI = 1.55–1.77). The ATRP system consisted of a metal center with one terpyridyl and presumably three acetonitrile ligands, which were at least in part substituted by monomer. Consequently, and in contrast to standard systems,[102] the equilibrium $M^{n+} \leftrightarrow M^{n+1}$ in this type of reaction did not require conformational changes or dissociation of a terpyridyl ligand. Therefore, polymerization proceeded comparably fast within 2 h, however, polymer yields were low (<35%).

The capability of ROMP of polymerizing even more complex functional monomers was demonstrated by the fact that the cationic NHC precursor 1,3-di(1-mesityl)-4-{[(bicyclo[2.2.1]hept-5-en-2-ylcarbonyl)oxy]methyl}-4,5-dihydro-1*H*-imidazol-3-ium tetrafluoroborate can be polymerized with the Schrock initiator Mo(*N*-2,6-*i*-Pr_2-C_6H_3)(CHCMe$_2$Ph)(OCMe$(CF_3)_2)_2$[103] at ambient temperature in CH_2Cl_2. The observed theoretical DP of 7 was in excellent accordance with a DP of 7 ± 1 found via end-group analysis using ^{1}H-NMR. The polymerization system fulfilled at least the requirements of a class-V living polymerization system,

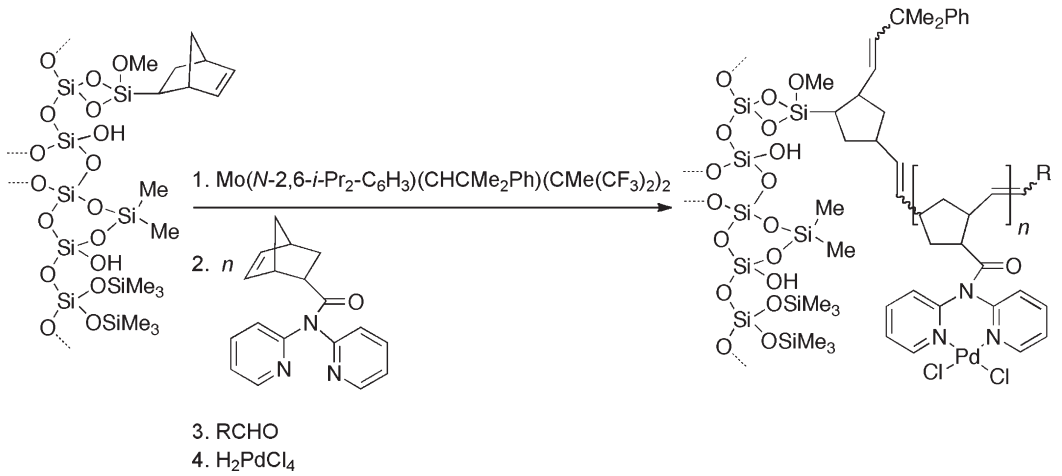

Scheme 10 Immobilization of norborn-5-ene-5-*N*,*N*-dipyrid-2-ylcarbamide on silica-60 using a 'grafting-from' approach.

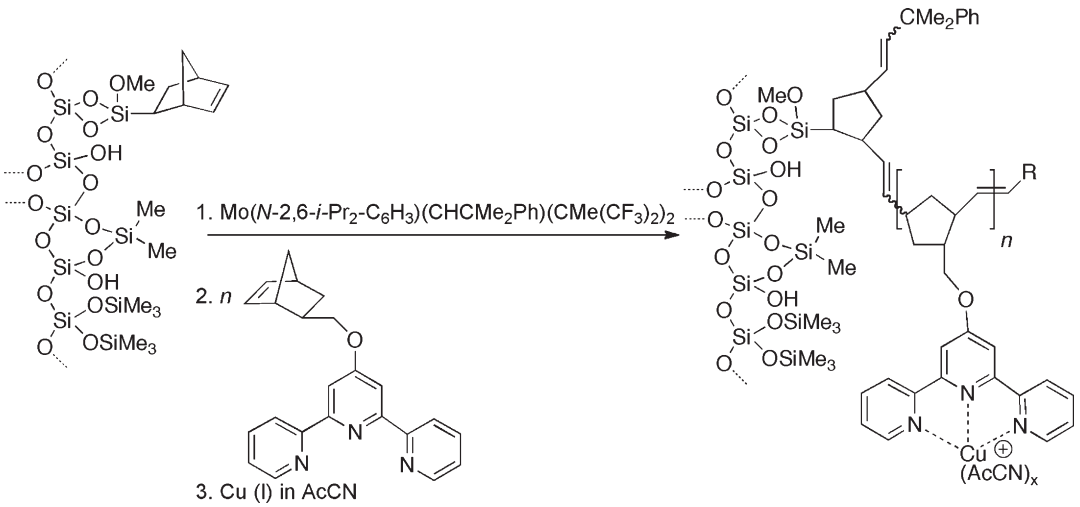

Scheme 11 Grafting of 4′-(norborn-2-en-5-ylmethylenoxy)terpyridine on silica and loading with Cu(I).

which allowed for a quantitative conversion into a telechelic polymer via reaction of the living polymer in a Wittig-type reaction with an excess of ω-(triethoxysilyl) propyl isocyanate (Scheme 12). This telechelic oligo-(1,3-di(1-mesityl)-4-{[(bicyclo[2.2.1]hept-5-en-2-ylcarbonyl)oxy] methyl}-4,5-dihydro-1*H*-imidazol-3-ium tetrafluoroborate) was then reacted with silica-60. Generation of the free carbene with KO-*t*Bu in THF at −30 °C and reaction with $RuCl_2(PCy_3)_2(CHPh)$ yielded the immobilized second-generation Grubbs catalyst.[104] The ruthenium content as measured by inductively coupled plasma-optical emission spectroscopy (ICP-OES) revealed catalyst loadings up to 0.5 wt.%. RCM carried out with diethyl diallylmalonate (DEDAM) as a benchmark gave turnover numbers (TONs) ≤80 for a stirred batch. No catalyst bleeding was observed (limit of detection for Ru by ICP-OES=0.1 ppm), thus offering access to virtually metal-free products.

In an alternative approach to supported Grubbs-type initiators (norborn-2-ene-5-yl-trichlorosilane or norborn-2-ene-5-yl-triethoxysilane) (both *exo*/*endo*-mixtures), surface-derivatized silica was reacted with $RuCl_2(PCy_3)_2(CHPh)$, followed by the addition of *exo*,*exo*-7-oxanorborn-2-ene-5,6-dicarboxylic anhydride and 7-oxanorborn-2-ene-5-carboxylic acid, respectively. By this 'grafting-from' approach, satisfactory amounts of both monomers were grafted onto the support. Thus, anhydride loadings of 0.22 mmol g^{-1} (LiChrospher 300-5) and 1.2 mmol g^{-1} (Nucleosil 300-7) were achieved. Conversion into the corresponding di- and mono-silver salts and reaction with $RuCl_2(PCy_3)(IMesH_2)(CHPh)$ gave the desired supported catalysts (Scheme 13). Catalyst loadings up to 63 mg catalyst per gram (LiChrospher) were achieved. RCM reactions carried out with these two silica-supported catalyst versions allowed TONs up to 520 for a series of simple α,ω-dienes.[47]

Identical protocols for the preparation of surface-bound thin polymer films using Si/SiO_2 surface-bound norborn-5-ene-2-ylsilanes were described by other groups, too.[105] Combining a 'grafting-from' approach with microcontact imprinting, patterned polymer films of variable thickness (5–500 nm) consisting of poly(5-triethoxysilylnorborn-5-ene)

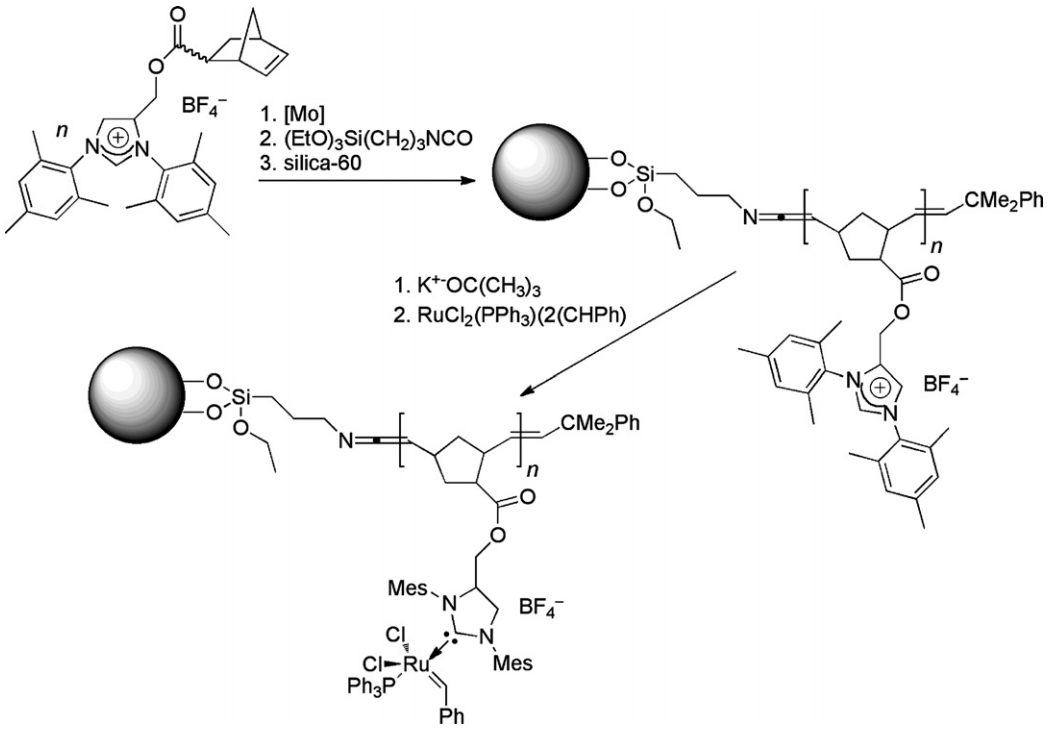

Scheme 12 Living polymerization of an *N*-heterocyclic carbene (NHC) precursor, formation of ω-(triethoxysilyl)-telechelic oligomer, and immobilization on silica.

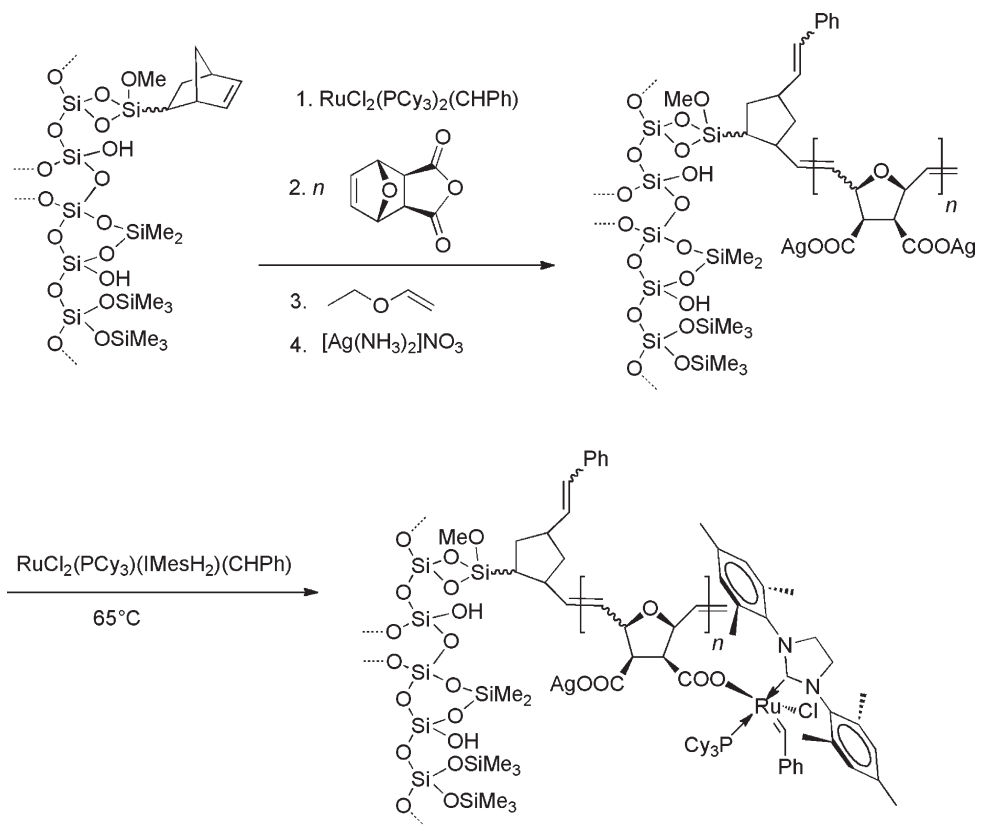

Scheme 13 Synthesis of silica-supported second-generation Grubbs-type initiators.

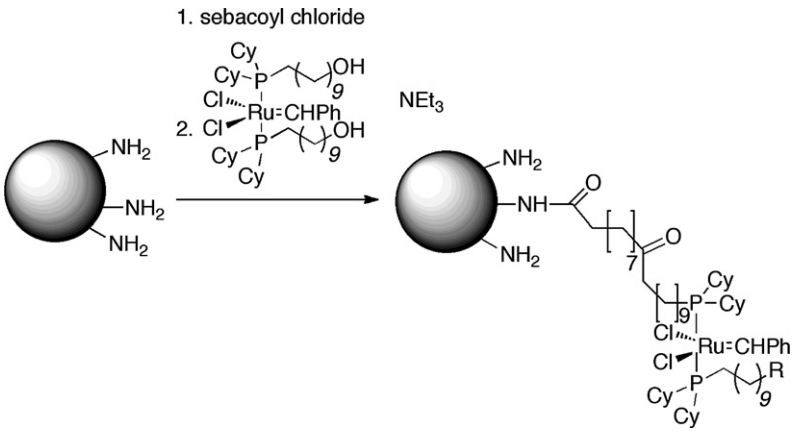

Scheme 14 Preparation of hybrid core-shell particles.

were prepared using $RuCl_2(PCy_3)_2(CHPh)$ as initiator. Lateral dimensions as small as 2 mm could be realized.[106] Recently, Mingotaud *et al.*[107] reported on the immobilization of the first-generation Grubbs-type catalyst, $RuCl_2(PCy_3R)_2(CHPh)$ ($R=(CH_2)_{10}$-OH) on amino-functionalized silica using sebacoyl chloride. The immobilized system was used for the preparation of hybrid core-shell particles using NBE as monomer[107] (Scheme 14).

4.23.4.1.4 Other inorganic surfaces

Skaff *et al.*[108] reported on the synthesis of CdSe–polymer composites. A vinylbenzyl-derivatized phosphine oxide was physisorbed onto cadmium selenide particles. Subsequent reaction with $RuCl_2(PCy_3)_2(CHPh)$ or $RuCl_2(IMes)(PCy_3)(CHPh)$ (IMes=1,3-dimesitylimidazol-2-ylidene) followed by addition of COE, 7-oxanorborn-5-ene-2,3-dicarboxylic anhydride (ONDCA), dicyclopentadiene, or *N*-methyl-7-oxanorborn-5-ene-2,3-dicarboxylimide resulted in the desired surface modification and formation of the composite, which were, without proof, proposed to possess interesting solution and electronic properties (Scheme 15).[108]

4.23.4.2 Organic Surfaces

4.23.4.2.1 Merrifield-type resins

Merrifield-type resins are among the most prominent organic supports for solid-phase synthesis, particularly in organic synthesis. The most straightforward methods for providing anchoring groups for the subsequent attachment of other groups or polymers are the chloromethylation of polystyrene-*co*-divinylbenzene (PS-DVB) or the substitution of styrene by chloromethylstyrene during synthesis of these supports. However, bromomethyl groups appear more favorable, since they exhibit enhanced reactivity as compared to their chloromethyl analogues. They can be generated by bromomethylation using trioxane, tin tetrabromide, and trimethylbromosilane[109] and, alternatively, via conversion of the chloromethyl groups into to the corresponding bromomethyl groups via halogen exchange.[110,111] For a ROMP-based grafting, the bromomethylated PS-DVB resins were converted into the norborn-2-ene-5-ylmethylethers via standard Williamson ether synthesis. Up to 2 mmol g^{-1} of norborn-5-ene-5,6-dicarboxylic anhydride was successfully grafted onto such norborn-5-ene-2-yl-derivatized Merrifield resins (2% cross-linked) using either a 'grafting-from' or a 'grafting-to' approach.

4.23.4.2.2 ROMP spheres

An alternative to Merrifield resins, that is, the synthesis of ROMP spheres for use in combinatorial chemistry, was reported by Barrett *et al.*[112] Here, surface functionalization was accomplished via reaction of vinyl-PS-DVB with a low degree of cross-linking with $RuCl_2(PCy_3)_2(CHPh)$ to form the immobilized catalytic species. Reaction with a

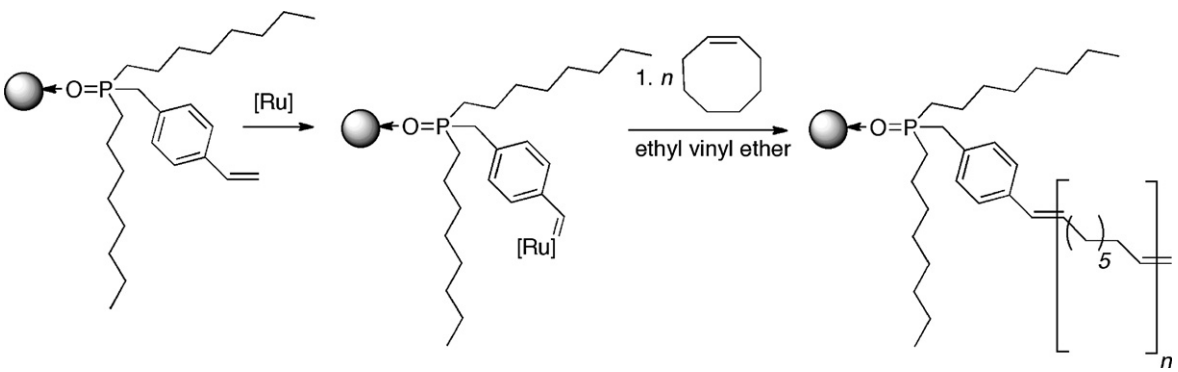

Scheme 15 Synthesis of CdSe–polymer composites.

functional monomer, for example, norborn-2-en-5-ylmethyl-4-bromobenzoate, gave the corresponding support with loadings up to 3 mmol of functional monomer per gram of resin (Scheme 16).[113]

The same group reported on the synthesis of ROMPGELs. There linear homopolymers of a functional monomer, usually NBE-based, were polymerized using a Ru-based initiator ($RuCl_2(PCy_3)_2(CHPh)$). Since these homopolymers were undiluted by cross-linkers, high capacities, that is, amounts of functional groups approaching 3 mmol g^{-1}, were obtained. Scheme 17 summarizes the reaction as well as the functional monomers used. In case the homopolymers were soluble in the solvent of choice, cross-linking was performed, for example, with the aid of norbornadiene or 1,4,4a,5,8,8a-hexahydro-1,4,5,8-*exo*,*endo*-dimethanonaphthalene (DMN-H6). Such ROMPGELs have been used in the Horner–Emmons synthesis of α,β-unsaturated esters,[114] as scavengers for the sequestration of amines and hydrazines (slightly cross-linked with norbornadiene),[115] for the preparation of homoallyl alcohols (DMN-H6 cross-linked),[116] and arene-catalyzed lithiations.[117]

4.23.4.2.3 Functional supports prepared via ring-opening metathesis precipitation copolymerization

- *Supports for solid-phase extraction*

Aiming on polymeric supports for solid-phase extraction (SPE), materials had to be created that were entirely pH-stable and recyclable. In addition, to be usable in standard SPE equipment, both a particle size and particle size distribution had to be realized that allowed for a simple removal of the support by filtration. In addition, the swelling in those solvents typically used in SPE (i.e., methanol, acetone, water) had to be kept within acceptable limits (typically <20%). This required a substantial degree of cross-linking in the final polymers. In contrast, the pressure stability, a key issue in HPLC, was not to the fore here. However, a maximum on well-defined 'working functionality' had to be present. For these purposes, norborn-5-ene-2,3-dicarboxylic anhydride (NDCA) was considered promising for the following reasons. First, the two *cis*-oriented dicarboxylic acid groups resulting from the hydrolysis of the anhydride would allow for the extraction of basic compounds, and, at the same time, also offer access to dipolar

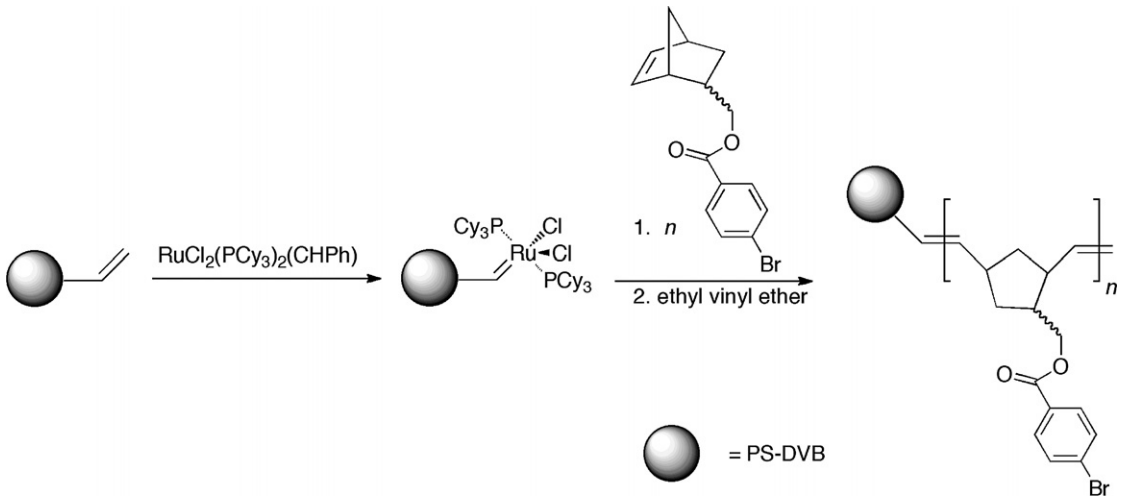

Scheme 16 Surface grafting of organic supports starting from surface-immobilized vinyl groups.

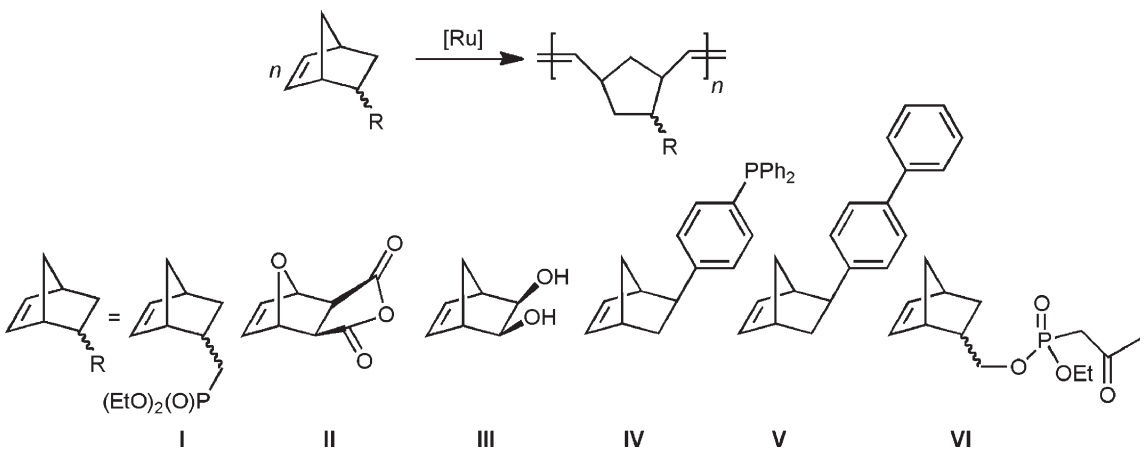

Scheme 17 Preparation of ROMPGELs and functional monomers used.

interactions or hydrogen bonding. Second, when focusing on trace analysis of organic compounds, the high polarity of this monomer would allow for a wetting of the resin by water alone. Finally, a significant amount of nonpolar sites as provided by the rest of the monomer was considered to be essential for the extraction of nonpolar compounds.

Keeping the above-mentioned prerequisites in mind, a ROMP-based precipitation copolymerization setup was created. In this setup, living homopolymers prepared from a functional monomer were finally cross-linked to form polymeric beads approximately 30–60 μm in size. For the synthesis of carboxylic acid-derivatized particles, DMN-H6 was used as a cross-linker and its copolymerization with NDCA using the well-defined Schrock initiator Mo(*N*-2,6-*i*-Pr_2-(C_6H_3)($CHCMe_2Ph$)($OCMe(CF_3)_2$)$_2$ was established for the synthesis of high-capacity, *vic*-dicarboxylic acid-derivatized resins (**Scheme 18**).

Due to the polymerization technique used, capacities of the different weak cation-exchangers (WCXs) could be reproducibly varied over many orders of magnitudes (up to 10 mequiv g^{-1}). The optimum COOH capacity was found to be within 2.0–4.0 mequiv COOH per gram. As a result of the polymerization setup and sequence, respectively, the new materials generally consisted of linear chains of the functional monomer attached to a cross-linked interior. While the entire backbone provided sufficient sites for hydrophobic (solvophobic) interactions, the functional groups guarantee sufficient wetting and represented the active sites for ion exchange as well as for any additional polar interaction. The new materials were applied to the enrichment of a large variety of organic compounds, such as phenols, alcohols, aldehydes, carboxylic acids, esters, nitrosamines, amines, anilines, lutidines, halogenated hydrocarbons, and polynuclear aromatic hydrocarbons, both in form of particles and membranes consisting of Teflon-embedded particles, from which suitable disks were cut out and used for extraction.[118,119] The new materials exhibited excellent extraction efficiencies for all kinds of basic, neutral, and even acidic analytes with a carbon content ≥C_5. The new resins also showed remarkable stability and were used more than 40 times without any loss of performance.

Following the synthetic protocol described above, *N*,*N*-dipyridyl amide-functionalized supports suitable for the SPE of metal ions from aqueous solutions were prepared, too.[97] Resins were synthesized via the copolymerization of *endo*-norborn-2-ene-5-yl-*N*,*N*-di-2-pyridyl carboxylic amide with DMN-H6 using Mo(*N*-2,6-*i*-Pr_2-C_6H_3)($CHCMe_2Ph$)($OCMe(CF_3)_2$)$_2$ as initiator. The polymer-bound dipyridyl amide ligand showed excellent selectivity toward Hg^{2+} and Pd^{2+} even under competitive conditions, allowing for the selective extraction of both divalent metal ions over a broad range of concentration from complex mixtures. Due to the stability of the resulting complexes, high loadings of the material with both metals, reaching 57 wt.%, were achieved.

Following the setup first described by Sinner *et al.*,[97,118,119] Årstad *et al.*[120] homopolymerized phosphane-containing monomers with the second-generation Grubbs initiator, cross-linked with *p*-di(norborn-2-ene-5-yl)benzene and used in the halogenation of alcohols. In a similar approach, an ethyl-1-diazo-2-oxopropylphosphonate-functionalized resin was prepared and used for the conversion of aldehydes into 1-alkynes.[121] Fuchter *et al.*[122,123] also developed a ROMP capture–release approach to the synthesis of porphyrazine derivatives (**Scheme 19**). Crossover Linstead macrocyclization of a bis(norborn-5-ene-2-methyloxy-*p*-phenylenmethyl)-functionalized dimercaptomaleonitrile with dipropyl maleonitrile yielded both the octapropyl-substituted and the bis-norborn-5-ene-2-yl-substituted species 1 and 2. Subsequent ring-opening metathesis copolymerization with a cross-linker (*p*-di(norborn-5-ene-2-yl)benzene) under the action of the second-generation Grubbs initiator $RuCl_2(PCy_3)(IMesH_2)(CHPh)$ resulted in an insoluble polymer that could easily be separated from soluble 1. Deprotection, removal of the Mg^{2+} ion, and reaction with $Ni(dppe)Cl_2$ and $Zn(OAc)_2$ finally gave the target compound (dppe=1,2-diphenylphosphinoethane).

Following this concept, bis(dimethylamino)-substituted porphyrins have been prepared, too.[122] Zn derivatives of the

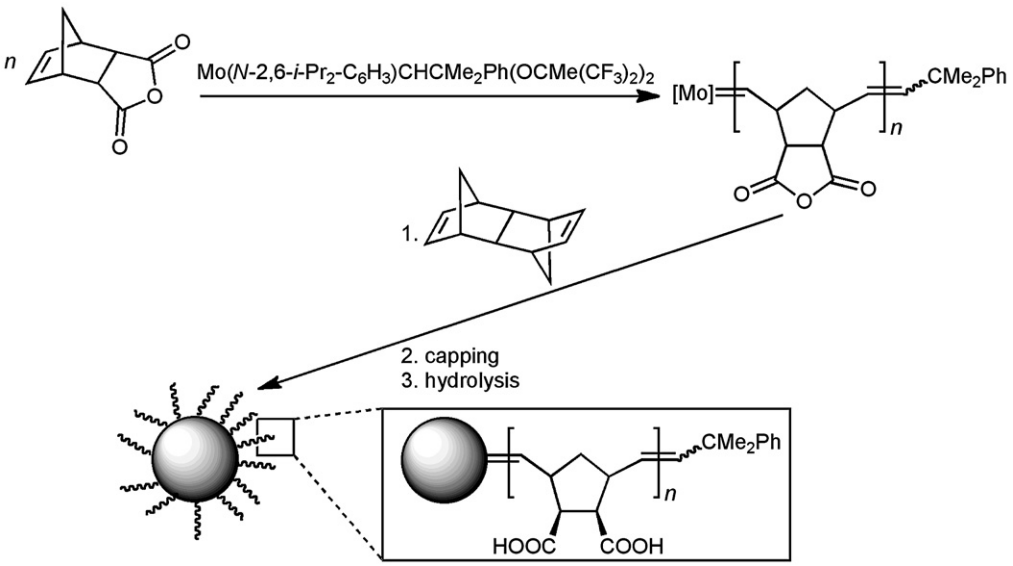

Scheme 18 Synthesis of functional polymers prepared via ring-opening metathesis precipitation polymerization.

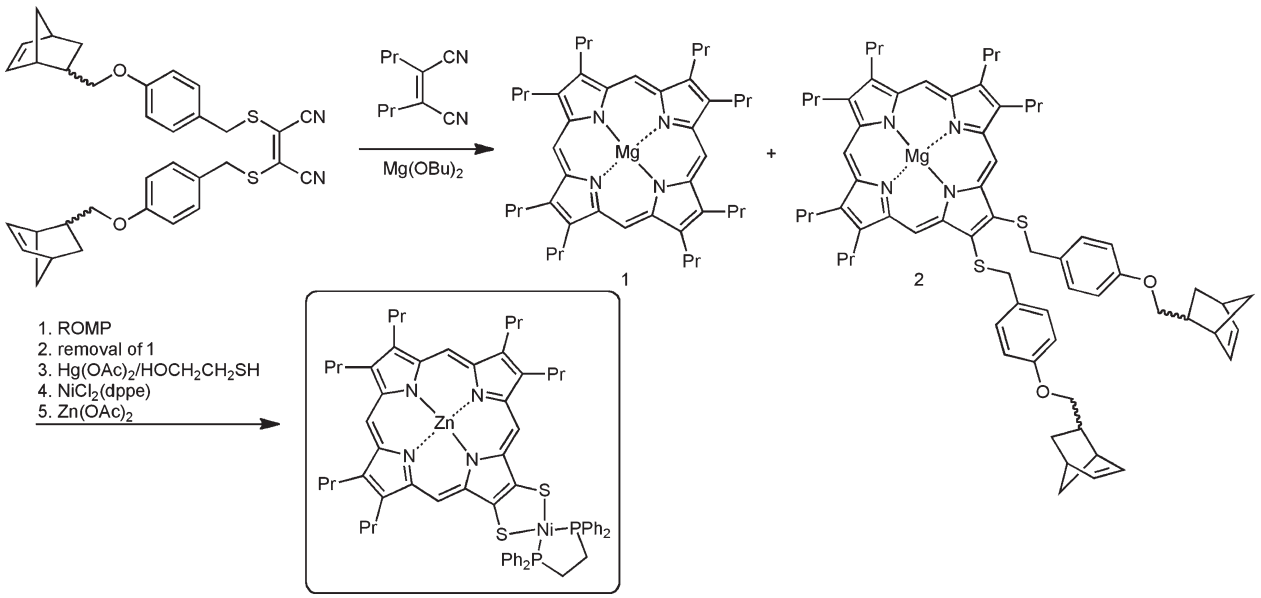

Scheme 19 ROMP capture–release approach to the synthesis of porphyrazine derivatives.

latter in their ROMP sphere-supported form were used for the sensitized production of singlet oxygen for the parallel synthesis of endoperoxides and ene-adducts.[124]

• *Catalytic supports*

Kröll *et al.*[125] reported on the synthesis of a supported version of a chiral Schrock catalyst prepared by ROMP. For precipitation polymerization, they prepared a bis(norborn-2-ene)-substituted chiral phenoxide, which could be polymerized without any protection/deprotection steps using $Ru(CF_3COO)_2(IMesH_2)(=CH\text{-}2\text{-}(2\text{-}PrO)\text{-}C_6H_4)$.[18,51] Reaction of the polymeric support with potassium hydride followed by addition of $Mo(N\text{-}2,6\text{-}i\text{-}Pr_2\text{-}C_6H_3)(CHCMe_2Ph(OTf)_2 \cdot DME$ resulted in the desired supported catalyst (Scheme 20).

Due to the low cross-linked nature of the support, which showed a swelling of 700%, resulting in a solvent uptake of 2000%, the catalytic sites showed excellent accessibility. Consequently, lower amounts of catalyst were required, while yields and the values for the enantiomeric excess (ee) were basically identical to those obtained with the supported system described above. Again, catalyst (molybdenum) leaching was <5%.

The Schrock and Hoveyda groups jointly reported on the synthesis of a set of poly(styrene)- and poly(NBE)-supported

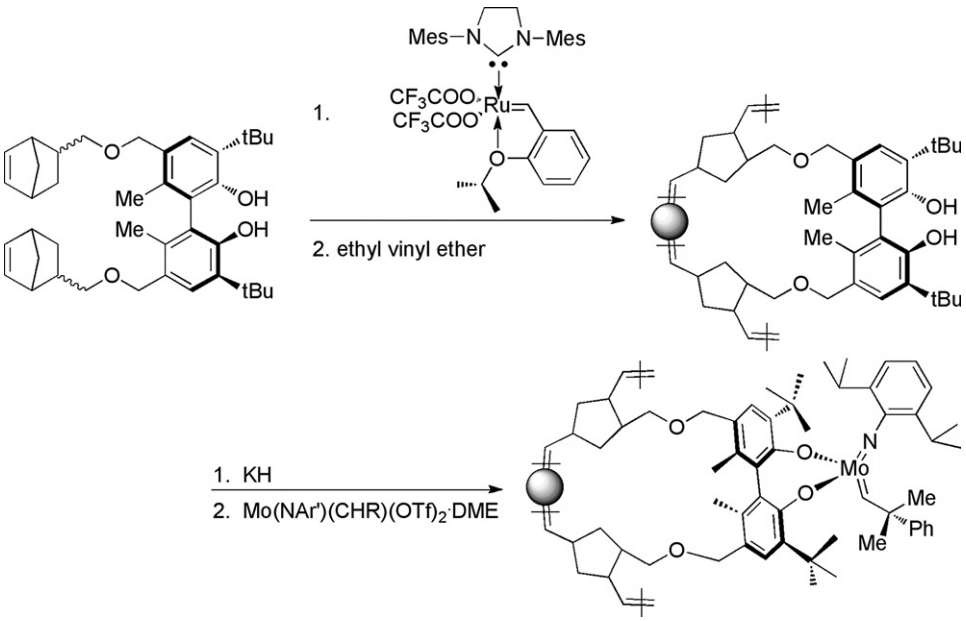

Scheme 20 Synthesis of a poly(norborn-2-ene)-supported, enantioselective Schrock catalyst via ROMP.

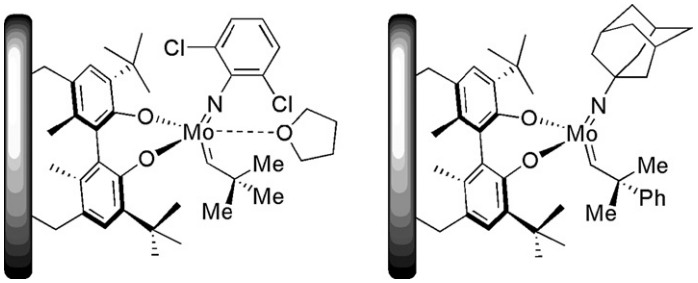

Figure 8 Polymer-supported, chiral 2,6-dichlorphenylimido- and adamantylimido-based Schrock catalysts.

Schrock-type catalysts. Following the synthetic route described for the synthesis of a polymer-supported chiral biphenyl-based Schrock catalyst,[126] analogous systems based on the 2,6-dichlorophenylimido and adamantylimido ligand were prepared (Figure 8).

Similarly, chiral binaphthyl-based Schrock catalysts containing the 2,6-dichlorophenylimido and adamantylimido ligand were synthesized (Scheme 21).[127]

Finally, in a synthetic protocol very similar to the one reported by Kröll *et al.*, the Schrock and Hoveyda groups also reported on supported, chiral Schrock catalysts prepared via ROMP. They used a bis(norborn-2-ene)-substituted, unprotected chiral biphenyl that they subjected to ROMP in the presence of a cross-linker, that is, DMN-H6,[128] and the catalyst precursor, that is, $Mo(NR')(CHCMe_2Ph)(OTf)_2 \cdot DME$ (R′=2,6-*i*Pr_2-C_6H_3, 2,6-Cl_2-C_6H_3, adamantyl; Scheme 22).[127] The desired catalyst formed immediately, initiated ROMP and the support formed. With all the systems reported by these two groups, the ee obtained in a series of asymmetric RCM, ROC, and desymmetrization reactions was in most cases very similar to the one obtained with the parent, unsupported ones, indicating that immobilization did not put any steric constraints onto the chiral center, since this might certainly well be expected to lead to significant changes in stereoselectivity.

4.23.4.2.4 ROMP-derived stationary phases prepared by coating techniques[129]

Coating is a straightforward way of preparing stationary phases[130–139] and the technique itself is well established. One can use virtually any carrier that is suitable in terms of particle size, pore size distribution, and pore volume, for example, silica, alumina, titania, or zirconia.[140] In principle, one can distinguish between dynamic and covalent coatings.[141,142] Among these two, dynamic coatings are the most convenient ones to perform. In a typical dynamic coating process, surface-active coating materials or surface modifiers are dissolved in a suitable solvent and deposited on a support. Coating materials most suitable for dynamic coating are strongly adsorbed to the support's surface via physical interactions. The only prerequisite for such coatings is that the polymer deposited onto the surface of the supports is insoluble in the mobile phase that is to be used later. However, though easy to perform, significant changes in pore volume and specific surface area entailed with such coating procedures and

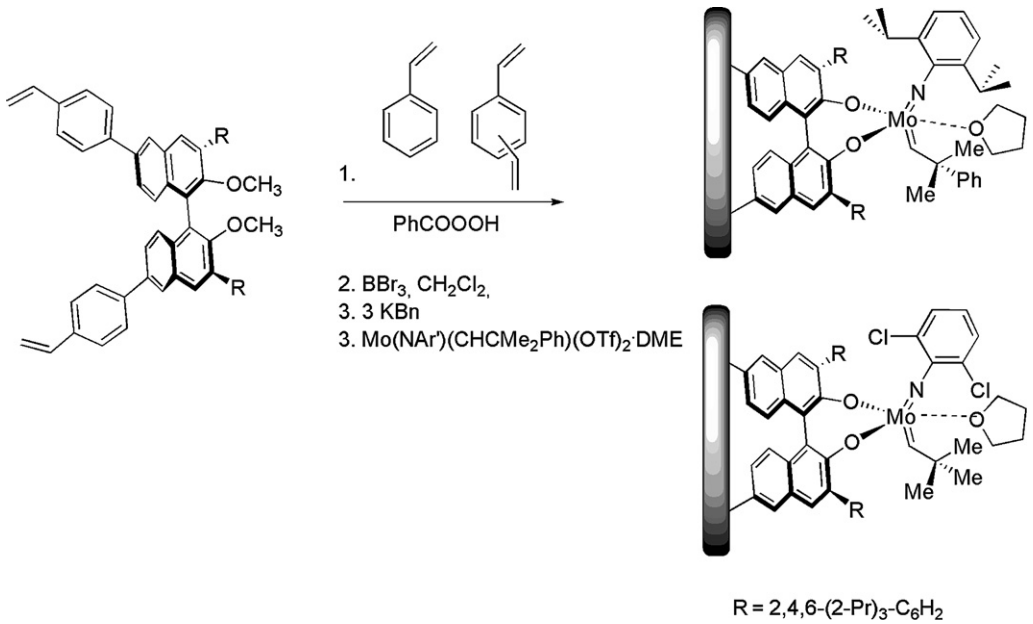

Scheme 21 Polymer-supported chiral binaphthyl-based Schrock catalysts.

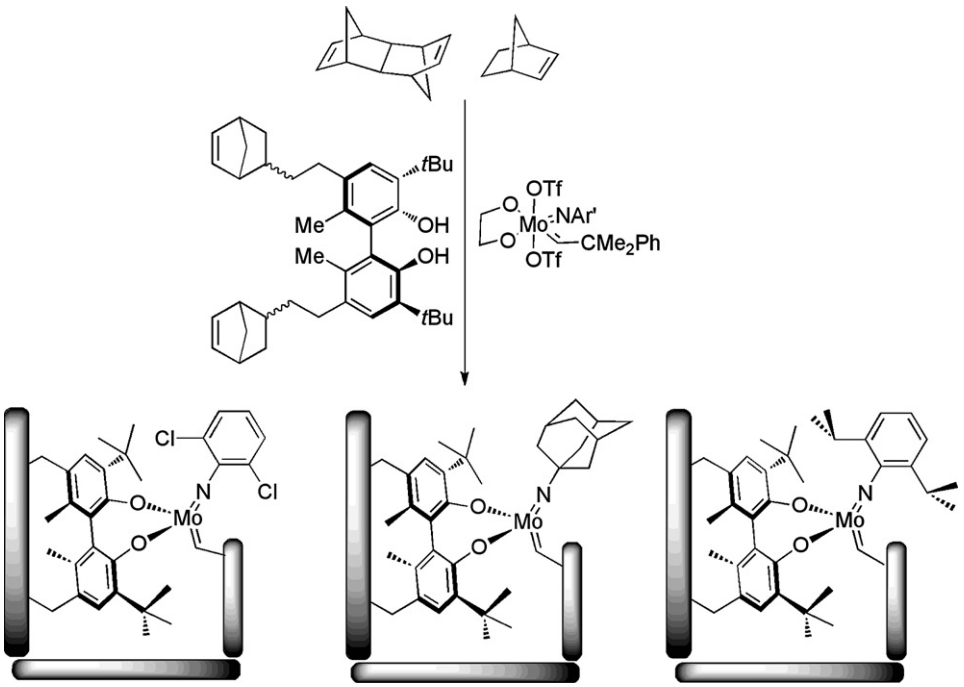

Scheme 22 Chiral biphenyl-based Schrock catalysts immobilized on ROMP-derived supports.

must certainly be considered as major drawbacks.[143] Consequently, despite their ease of manufacture, dynamic surface modifications are in many cases not the preferred ones since the coatings may eventually desorb from the stationary phase in course of the separation process. Therefore, coatings covalently bound to the support's surface have been developed.[141] We were particularly interested in the synthesis of ROMP-derived, coated, silica-based and hence pressure-stable supports based on ONDCA. Such supports were of considerable interest for numerous reasons. First, such stationary phases would withstand the high pressures used in HPLC. Second, unlike in poly(maleic acid), the two carboxylic acid moieties of the monomer would pertain their *cis*-orientation after polymerization (see below). Third, the oxygen in the repeat unit significantly enhanced the hydrophilicity compared to the parent poly(norborn-5-ene-2,3-dicarboxylic acid). And finally, unlike in conventional free radical polymerization, well-defined block copolymers with a nonpolar comonomer, for example, NBE, are available. The synthesis of the block copolymers is outlined in **Scheme 23**.

By variation of the block sizes, synergistic effects of the hydrophilic, poly(7-oxanorborn-5-ene-2,3-dicarboxylic acid)-functionalized part and the hydrophobic poly(NBE) part on separations were studied and the optimum copolymer composition for particular high-performance ion-chromatographic (HPIC) separations was determined. After hydrolysis, the resulting polymer backbone of the poly(ONDCA) block consisted of a vinylene-spaced poly(tetrahydrofuran) with each unit bearing two *vic*-, *cis*-configured carboxylic acids. The general quality of both the coating and the coating method was checked by applying the standard Engelhardt test to a poly (NBE)-coated material.[144] No polar interaction of the analytes with the stationary phase, indicating the absence of any free silanol groups, was detected. Not unexpected, a loss of pore volume and specific surface area was observed, particularly in case materials with smaller pores were used. Thus, the specific surface area (σ) of silica with 60 Å pore diameter was reduced by a factor of 2 while 100 or 300 Å materials showed only a loss in σ of approximately 20%.

Coated silica materials have also been used as stationary phases in the separation of isomeric anilines and lutidines. A typical separation achieved with these supports is shown in **Figure 9**. High selectivity was achieved, as demonstrated by the fast baseline separation of the analytes of interest, which

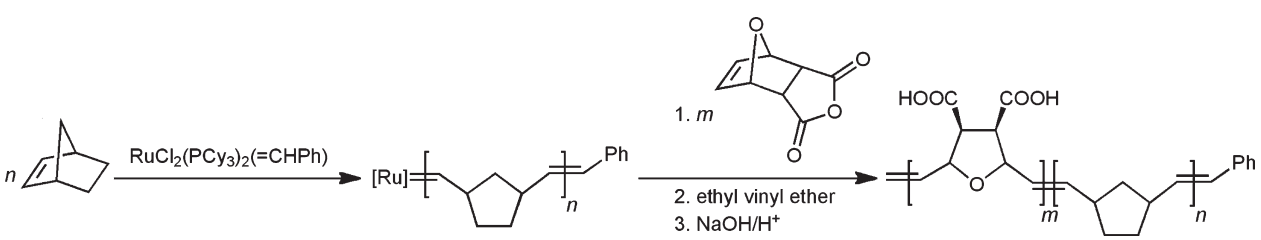

Scheme 23 Grubbs-type initiator triggered synthesis of ONDCA-*b*-NBE copolymers.

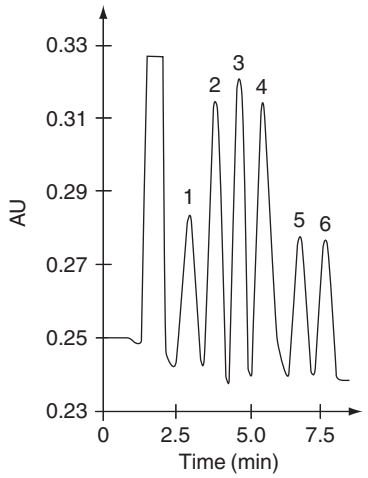

Figure 9 Separation of 2,6-dimethylaniline (1), *N*-methylaniline (2), pyridine (3), *N,N*-dimethylaniline (4), 2,6-lutidine (5), and 3,4-lutidine (6) on Polygosil 60-10 coated with a poly(NBE_{600}-*b*-$ONDCA_{500}$) copolymer. Mobile phase: water/acetonitrile 98:2, 10 mM acetic acid, 7 mM triethylamine, flow rate 1.0 ml min^{-1}, inj. vol. 5 µl (20 ppm each), UV 254 nm. Reprinted with permission from Buchmeiser, M. R.; Mupa, M.; Seeber, G.; Bonn, G. K. *Chem. Mater.* **1999**, *11*, 1533–1540.[129] © Copyright 1999 American Chemical Society.

were similar with regard to pK_a values, size, and chemical properties. Separation efficiency was positively influenced by the presence of the nonpolar sites from the poly(NBE) block. The importance of such sites suggests some additional hydrophobic interaction of the analytes with the material, the more, since separation of these analytes on a silica-based, poly(ONDCA) homopolymer-coated column was poor. Finally, isomeric hydroxyquinolines[129] as well as various flavones[145] were successfully separated on such columns. Particularly for the latter, the new stationary phases allowed fast separations even at extreme pH values. For further characterization of the analytes, a liquid chromatography (LC) system was coupled to a mass spectrometer via an electrospray ionization interface (ESI).

In the course of our investigations on the metal extraction capabilities of carboxylic acid-derivatized, ring-opening metathesis precipitation polymerization-derived SPE supports (see above), we found that these possessed excellent selectivity for lanthanides, even in the presence of other metal ions.[146,147] In a simple SPE setup, these allowed for concentrating rare earth elements (REEs) from various rock digests and their subsequent quantification by means of ICP-OES. However, irrespective of the excellent extraction capabilities, a pressure-stable functional support had to be developed to gain access to automated systems. The main objective was to finally develop a fast, on-line SPE-HPLC routine for the analysis of REEs. For the SPE (pre-) column, we utilized poly(NBE_{600})-*b*-poly($ONDCA_{500}$)-coated silica. For evaluation, GSR-3 basalt and GSR-1 andesite were used as certified REE-containing materials. To obtain some fundamental information about the extraction capability and selectivity, silica-60 coated with a ROMP-derived poly(NBE)-*b*-poly(ONDCA)[129] was used for the extraction of a mixture of two radioactive lanthanides, ^{152}Eu and ^{147}Pm.[148] The coated silica showed high extraction efficiencies for these two lanthanides as determined by standard SPE experiments using β-liquid scintillation counting for quantification. Extraction efficiencies, determined over a concentration range of 23 ng l^{-1} to 250 mg l^{-1}, thus covering a range of seven orders of magnitude, were virtually quantitative in all cases. A first important finding was that the pH for lanthanide extraction could be extended to a range of 3.5–5.5. This significantly improved complexation of the REEs by the ONDCA-derived ligand was attributed to the presence of the additional ether functionality in the ONDCA-derived repeat units, which was not present in the poly(norborn-5-ene-2,3--dicarboxylic acid)-derived system.[146] Recovery, HPLC as well as ICP-OES experiments confirmed the high selectivity of the new sorbent for lanthanides. The final design of the on-line SPE-HPLC system is shown in **Figure 10**. Rock digests were obtained from dissolving the corresponding rock sample in an $LiBO_2$ melt followed by dissolution in 1 N nitric acid. They were then modified with 5-sulfosalicylic acid to mask Fe^{3+} and

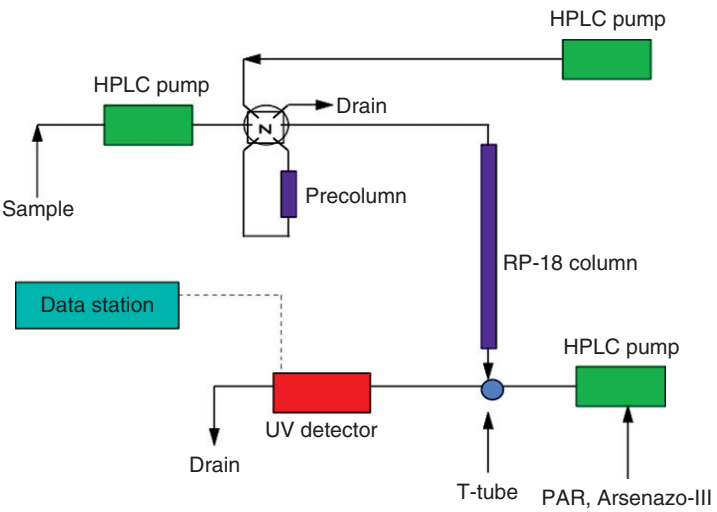

Figure 10 Schematic drawing of the on-line SPE-RP-ion-pair-HPLC system. Adapted from Buchmeiser, M.R.; Seeber, R.; Tessadri, R. *Anal. Chem.* **2000**, *72*, 2595–2602. © Copyright 2000 American Chemical Society.

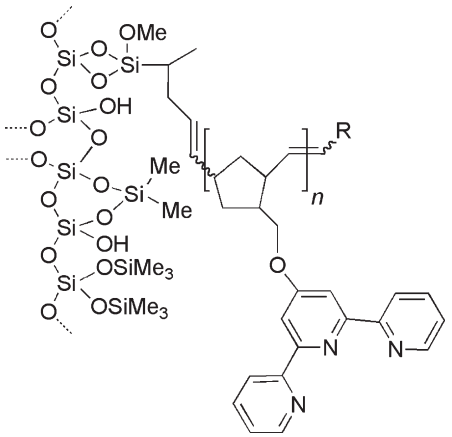

Figure 11 Structure of silica coated with a terpyridine-containing ROMP-derived polymer.

Al^{3+}.[146] Methanol was added to prevent the formation of polysilicic acid. The entire solution was adjusted to a pH of 4.0 and passed over precolumns (60 × 4 mm) packed with poly(NBE_{600})-*b*-poly($ONDCA_{500}$)-coated silica-60. The separation of REEs was accomplished using RP-ion-pair chromatography applying a gradient separation system consisting of hydroxyisobutyric acid (HIBA) and sodium octadecylsulfonate. REE concentrations prior to enrichment were typically in the range of 1–25 ng ml^{-1}; the total amount of each REE extracted by the precolumn was in the range of 8–270 ng. Quantitative recoveries (97–103%) were obtained for most REEs.

To obtain a silica-based, pressure-stable SPE support capable of extracting transition-metal ions, 4′-(norborn-2-en-5-ylmethylenoxy)terpyridine was block copolymerized with NBE using Mo(*N*-2,6-*i*-Pr_2-C_6H_3)($CHCMe_2Ph$)($OC(CH_3)(CF_3)_2$)$_2$ as initiator to give a poly(NBE_{900})-*b*-poly(4′-(norborn-2-en-5-ylmethylenoxy)terpyridine$_{60}$) block copolymer (**Figure 11**).

This block copolymer was used for the preparation of polymer-coated silica-60 (4.8 wt.% coating). While no main group elements were extracted by this support, the selectivity order under competitive conditions at pH < 0.6 was Pd ≈ Ag ≈ Au ≈ Pt > Re > Ir > Rh > Ru > Fe > Cr ≈ Mn ≈ Cd ≈ Zn. An even enhanced selectivity was observed at a pH of 3.5. Quantitative recoveries >97% were observed for all metal ions.[149]

4.23.4.2.5 Surface modification of polymeric fibers

Caster and Walls[150] described the surface modification of multifilament fibers such as nylon or Kevlar. Both coating techniques using preformed ROMP-based polymers and process contact metathesis polymerization (CMP), initially described by Klavetter and Grubbs,[151] were used. The latter comprises a procedure where the initiator is physisorbed onto the surface of a substrate and fed with a ROMP-active monomer that finally encapsulates the substrate. Such modified fibers were reported to display improved adhesion to natural rubber elastomers.

4.23.4.2.6 ROMP-derived monolithic supports

Monolithic separation media are an excellent example for a successful development in material science that strongly affected separation science. Based on theoretical reflections, the idea was to produce a support with a high degree of continuity that should meet the requirements for fast, yet highly efficient separations.[152,153] The first experiments into this direction were carried out in the 1960s and 1970s.[154,155] Yet it took some 20 years to fully establish this technology and to fully adapt these new supports to meet the demands of separations scientists and to carry this technology to other areas of chemistry, for example, to heterogeneous catalysis or tissue engineering. During their evolution, these supports, usually referred to as monolithic supports, continuous beds, or rigid rods,[155] were successfully used in LC, including microseparation techniques,[156–159] capillary electrochromatography, as well as SPE.[160] In these separation techniques, the focus was first on medium and high-molecular-mass biopolymers,[161] but was later extended to low-molecular-mass analytes.[162–165] Buchmeiser *et al.*[98,166–177] contributed to that area by developing a ROMP-based synthesis for these types of materials for use in separation science, heterogeneous catalysis, and tissue engineering.[178–180]

- *Basics and concepts*

The term 'monolith' applies to any single-body structure containing interconnected repeating cells or channels. Such materials may either be metallic or prepared from inorganic mixtures, for example, by a sintering process to form ceramics,[181] or from organic compounds, usually by a cross-linking polymerization.[182,183] Within the context discussed here, the term 'monolith' or 'rigid rod' shall comprise cross-linked, polymeric materials, which are characterized by a defined porosity and which support interactions/reactions between this solid and the surrounding liquid phase. Besides advantages such as lower back pressure and enhanced mass transfer,[184,185] the ease of fabrication as well as the many possibilities in structural alteration need to be mentioned. Furthermore, in capillary HPLC, the tedious and time-consuming manufacturing of the end frits can be omitted.

Until now, a considerable variety of functionalized and nonfunctionalized monolithic materials based on either organic or inorganic polymers are available. While inorganic monoliths are usually prepared from silica precursors, for example, $Si(OR)_4$, via sol-gel techniques,[162,164,165] organic continuous beds have mostly been prepared from methacrylates or poly(styrene)-*co*-poly(divinylbenzene)[182,186–189] applying almost exclusively free radical polymerization. However, polymerization techniques have been successfully used as well.[190]

A profound insight into the technology of both sol-gel and free radical polymerization-based monoliths may be found in books particularly dedicated to this subject.[191] Despite the comparably poor control over free radical polymerization-based systems, the porosity and microstructure of monolithic materials has successfully been varied.[182] In view of the general applicability of a transition-metal-based polymerization technique such as ROMP to the synthesis of functional supports and in view of the high definition of the resulting materials, Sinner and Buchmeiser[167] investigated to which extent ROMP could be used for the synthesis of monolithic polymers. They demonstrated that continuous matrices could in fact be generated via the ring-opening metathesis copolymerization of NBE and COE, respectively, with different cross-linkers in the presence of different porogenic solvents within a device (column). In addition, they elaborated different concepts for the surface grafting of

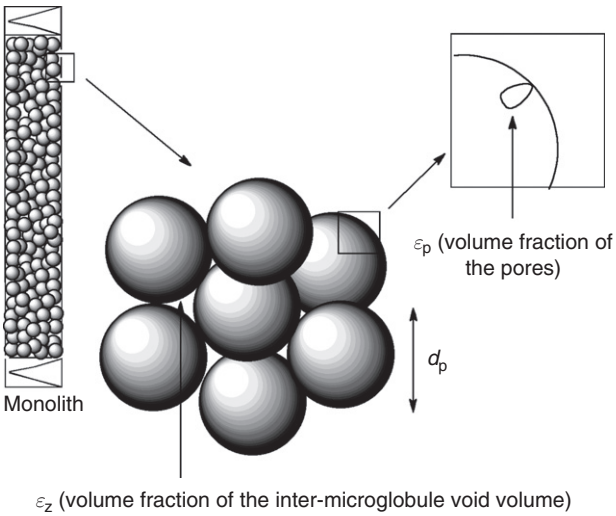

Figure 12 Construction of a monolith.

these monolithic supports. The concepts and applications shall be outlined in the following chapters.

• *Microstructure of metathesis-based rigid rods*

To understand monolithic supports and the effects of polymerization parameters, a brief description of the general construction of a monolith in terms of microstructure, backbone, and relevant abbreviations is given in Figure 12.[166,167] As can be deduced therefrom, monoliths consist of interconnected microstructure-forming microglobules, which are characterized by a certain diameter (d_p) and microporosity (ε_p). In addition, the monolith is characterized by an inter-microglobule void volume (ε_z), which is mainly responsible for the back pressure at a certain flow rate.

The volume fractions of both micropores (ε_p) and voids (inter-microglobule porosity, ε_z) represent the total porosity (ε_t). This value indicates a percentage of pores in the monolith. The pore size distribution can be calculated from inverse size exclusion chromatography (ISEC) data[192,193] or from mercury intrusion.[194] Together, these two values translate into a total pore volume V_p, expressed in ml g^{-1}.

The relative ratios of all components, that is, the monomers, the cross-linkers, the porogens, and the initiators, allow for broad variations in the microstructure of the monolithic material. Thus, the volume fractions of the interglobular void volume (ε_z) and total porosity (ε_t) have successfully been varied within a range of *c.* 30–70% and 50–90%, respectively. Figure 13 illustrates some of the microstructures that were generated.

•*Monolithic materials prepared from NBE-based monomers*

The choice of a suitable initiator represents an important step in the creation of a well-defined polymerization system in terms of initiation efficiency and control over propagation. Only in the case where a quantitative and fast initiation occurs, the entire system can be designed on a 'stoichiometric base'. This is of enormous importance, since for the control over the microstructure the composition of the entire polymerization mixture needs to be varied within quite small increments. The initiator needs to be carefully selected from both a chemical and a practical point of view. Generally, Schrock[31,32,60,66,195] and Grubbs systems,[27] both highly active in the ROMP of strained functionalized olefins, can be used. Since the preparation and in particular derivatization of ROMP-based rigid rods require some handling that can hardly be performed under an inert atmosphere, the less oxygen-sensitive and less reactive ruthenium-based Grubbs-type initiators were used first.[174] Thus, the first experiments on the suitability of ROMP for the synthesis of monolithic supports entailed the copolymerization of NBE with DMN-H6 in the presence of two porogenic solvents, that is, 2-propanol and toluene, with $RuCl_2(PCy_3)_2$(CHPh).[167] Such a setup in fact allowed for the realization of the first ROMP-derived monolithic supports (Scheme 24). By variation of the polymerization mixture in terms of monomer, cross-linker, and porogen content, the volume fraction of the interglobular void volume (ε_z) and the total porosity (ε_t) were successfully varied within a range of 0–50% and 50–80%, respectively. The addition of small amounts of triphenylphosphine in the low ppm range allowed for tuning the polymerization kinetics. NBE-based monoliths prepared by ROMP displayed linear plots of pressure versus flow rate, which confirmed that the monoliths were not compressed even at high linear flow velocities up to 20 mm s^{-1}. ICP-OES measurements on totally dissolved samples of various monoliths revealed that the ruthenium introduced into the monolithic matrix in form of the initiator could in fact be totally removed by the use of appropriate capping agents, for example, ethyl vinyl ether in dimethyl sulfoxide, resulting in Ru concentrations <0.1 μg g^{-1}, which corresponds to a metal removal >99.99%.[178]

Alternatively, monoliths can be prepared from NBE-based monomers with the aid of a Schrock initiator.[196] Here, the most 'inactive' Schrock initiator, that is, Mo(*N*-2,6-(2-Pr)$_2$-C_6H_3)(CHCMe$_2$Ph)(OC(CH$_3$)$_3$)$_2$, had to be used to avoid any unwanted exothermic reactions. Using various ratios of NBE and DMN-H6 in different mixtures of micro- with macroporogens, that is, 1,2-dichloroethane, toluene, and THF with hexane or pentane, monolithic polymeric materials with continuous, interconnected pores in the micrometer range as well as with micro- and mesopores in the 1.5–300 nm range could be synthesized within the confines of 3 × 100 mm glass columns. Hexane and pentane had to be used as porogens instead of

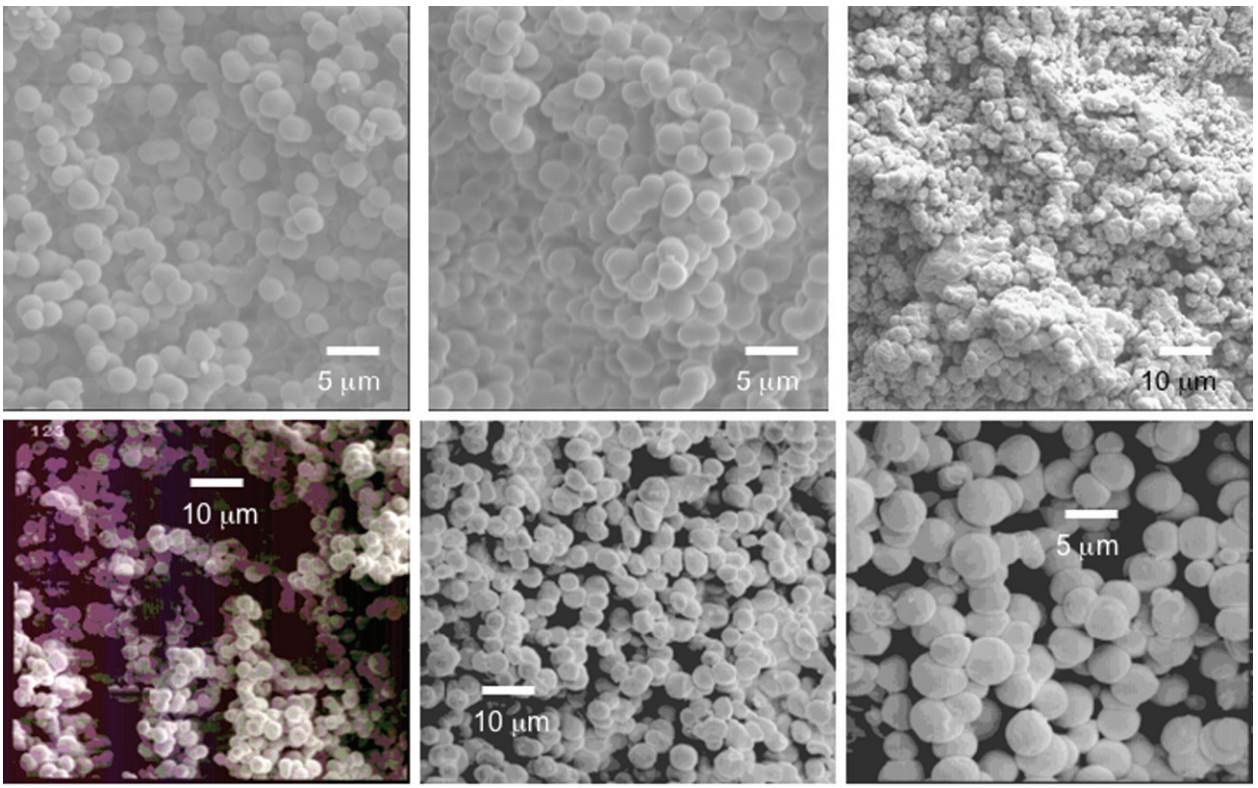

Figure 13 Structural variations in ROMP-derived monoliths.

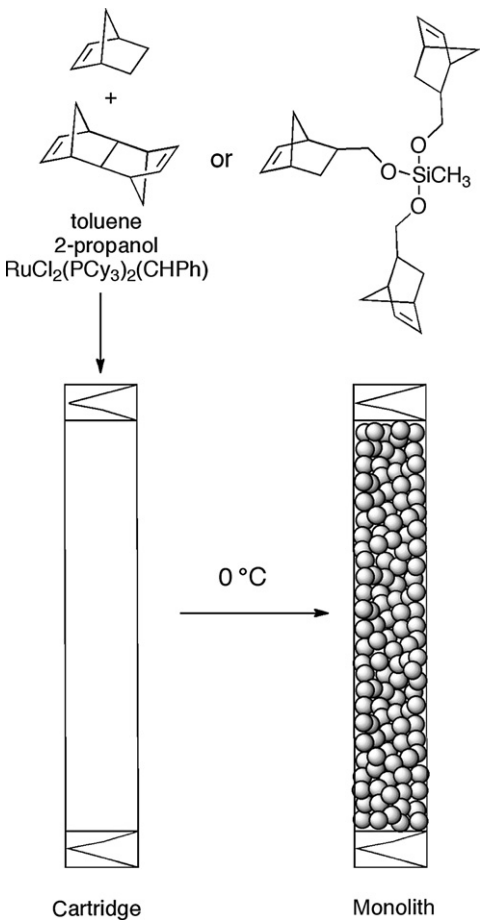

Scheme 24 Synthesis of a ROMP-derived monolith.

2-propanol since Schrock initiators, in contrast to the Ru-based initiators, do not tolerate the presence of the standard protic macroporogens. The resulting monoliths were, as evidenced by ISEC, characterized by a volume fraction of the pores (ε_p) of approximately 21% and a volume fraction of the inter-microglobule porosity (ε_z) of 68%, resulting in a monolithic structure with almost 90% total porosity. Consequently, the monoliths showed excellent flow-through characteristics with low back pressures at high flow rates and could be successfully used for the fast separation of proteins. Thus, ribonuclease A, insulin, cytochrome *c*, lysozyme, and albumin were separated in less than 140 s. Peak widths at half height were in the range of 1.4–3.1 s; resolution was in the range of 1–2.55. As a consequence of the large fraction of small pores (<2 nm, approximately 43%), low-molecular-weight analytes such as Fmoc-protected amino acids were successfully separated in less than 120 s.

• *Monolithic materials prepared from COE-based monomers*

In general, NBE-derived monomers result in polymer structures that comprise tertiary allylic carbons (**Figure 14**).

Despite the high mechanical and thermal stability of these structures,[168] which are by far sufficient for short- and medium-term analytical applications as well as applications in heterogeneous catalysis,[197–199] *tert*-allylic carbons located at the surface of a monolithic structure tend to be oxidized, resulting in a slow change of surface polarity of such monolithic columns. Consequently, the typical long-term stability of NBE-based, ROMP-derived columns is limited to less than 1000 injections. To solve this problem, a novel monomer/cross-linker system had to be introduced. For these purposes, Buchmeiser *et al*. developed a polymerization system based on

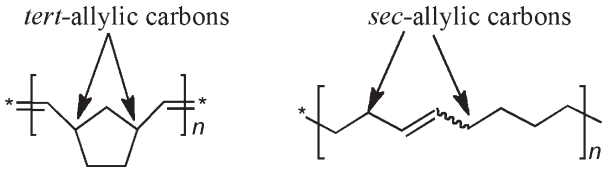

Figure 14 *tert*- vs. *sec*-allylic carbons in NBE- and COE-based polymers, respectively.

COE and a COE-based cross-linker, that is, tris(cyclooct-4-en-1-yloxy)methylsilane (TCOMS).[201] This development was guided by the idea that the polymer backbone of poly (COE)-derived materials consists of *sec*-allylic carbons and, therefore, presents a viable alternative to NBE-based systems. However, compared to NBE-based monomers, COEs are characterized by a significantly reduced ring strain, which makes the use of a more active initiator than the commonly used first-generation Grubbs initiator inevitable. These changes in monomer, cross-linker, and initiator required a comprehensive redesign of monolith synthesis. As a direct consequence of the reduced ring strain in COEs, the reactivity of the initiator had to be enhanced. First, the first-generation Grubbs initiator $RuCl_2(PCy_3)_2(CHPh)$ was replaced by a fast-initiating second-generation Grubbs initiator, that is, by $RuCl_2(Py)_2(IMesH_2)(CHC_6H_5)$ (Mes = mesityl, Py = pyridine).[200] To tune the reactivity in a way that the polymerization mixtures could be conveniently transferred into the compartments of interests (i.e., into the columns), small amounts of pyridine in the low ppm region were added. Similar to the NBE-based system, the final polymerization system consisted of various amounts of the monomer (COE), the cross-linker (TCOMS), the macroporogen (2-propanol), the microporogen (toluene), and the modulator (pyridine). An initiator loading of 0.2 wt.% was chosen throughout.

Some important differences between COE- and NBE-based, ROMP-derived monolithic supports were identified and need to be outlined. **Figures 15(a)** and **15(b)** illustrate the different structure of an NBE- and COE-based ROMP-derived monolith using the same amounts of monomers, cross-linkers, and porogens. **Figure 15(c)** illustrates the fast separation (<150 s) of a mix of proteins, that is, ribonuclease A, lysozyme, insulin,

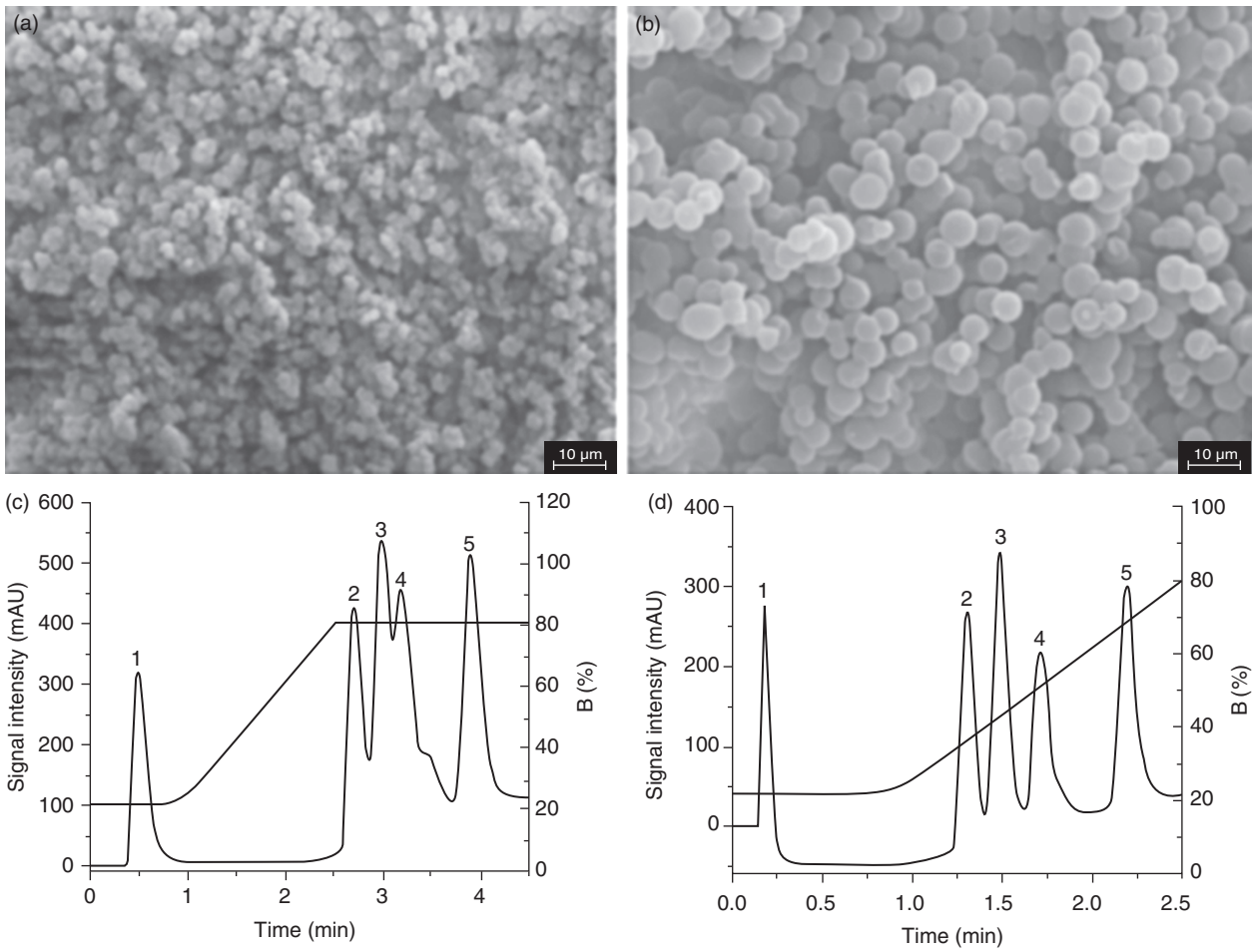

Figure 15 Structure of an NBE-based (a) and COE-based (b) monolith. NBE/DMN-H6/2-PrOH/toluene/initiator=COE/TCOOMS/2-PrOH/toluene/initiator=35:15:40:10:0.2. In both pictures, scale = 10 µm. Separation of a protein standard on an NBE- (c) and a COE-derived monolith (d). Column dimensions (3 × 100 mm). Mobile phase A: 95% water + 5% acetonitrile + 0.05% TFA; mobile phase B: 20% water + 80% acetonitrile + 0.05% TFA; linear gradient, 22–80% B in 2.5 min, then 80% B up to 4.5 min; flow rate = 3 ml min^{-1}; T = 25 °C; UV 200 nm. Peak order (1) lysozyme A, (2) ribonuclease, (3) insulin, (4) cytochrome *c*, and (5) myoglobin. Adapted with permission from Bandari, R.; Prager-Duschke, A.; Kühnel, C. *Macromolecules* **2006**, *39*, 5222–5229.[201]

cytochrome *c*, and myoglobin on a COE-based monolith applying gradient elution. Peak half widths ($\omega_{0.5}$) were <6 s and resolution (R_s) was >1.2 throughout. For purposes of comparison, an NBE-based monolith prepared from the same amounts of monomers, cross-linkers, and porogens was used for separation (**Figure 15(d)**). Applying the identical gradient, peak half widths ($\omega_{0.5}$) were <7 s and resolution (R_s) was >1.1 throughout. Some interesting aspects regarding the separation mechanism have been deduced from these experiments. Since lysozyme (M_w=14 307 g mol^{-1}) and ribonuclease (M_w = 13 700 g mol^{-1}) were well separated (R_s = 10.6), separation must be independent of the molecular weight, but dependent on the tertiary structure of these analytes. The most striking difference in separation behavior of both COE- and NBE-based columns is observed in the retention times of the analytes as well as in R_s and the values for the mean peak half width ($\omega_{0.5}$). These findings were related to the structural data obtained via ISEC[193] for both the COE- and the NBE-based monolith.[201]

• *Further applications in separation science*

Nonpolar, nonfunctionalized polymeric surfaces are widely used as stationary phases for both RP-HPLC and IP-RP-HPLC. While the former is the method of choice for high-resolution separations of peptides and proteins, the latter is eminently suited for the separation of single- and double-stranded nucleic acids. Using ROMP-derived, NBE-based monoliths, the separation of oligothymidylic acids $(dT)_{12\text{-}18}$ ranging in mass from 3638 D (dT_{12}) to 5456 D (dT_{18}) was accomplished on a semipreparative scale within 2 min (**Figure 16**).[168]

As one can see, the elution order of oligodeoxynucleotides strongly correlates with their molecular mass, suggesting that an increase in molecular mass directly translates into an increase in hydrophobic interaction of the corresponding analyte with the monolith. In addition, a mixture of eight proteins (ribonuclease A, insulin, cytochrome *c*, lysocyme, α-lactalbumin, α-chymotrypsinogen A, β-lactoglobulin B, and catalase) was separated in less than 90 s by RP chromatography.[168]

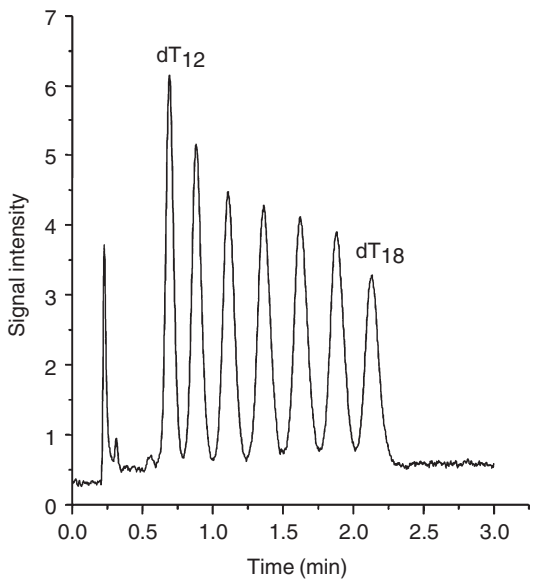

Figure 16 IP-RP-HPLC separation of an oligodeoxynucleotide $(dT)_{12–18}$ on a ROMP-derived NBE-based monolith (3 × 60 mm). Mobile phase: 100 mmol l^{-1} triethylammonium acetate at pH 7.0; linear gradient, 11–16% acetonitrile in 10 min; flow rate, 2 ml min^{-1}; T = 20 °C; detection, UV 264 nm; sample: $(dT)_{12–18}$, 0.1 µg of each oligodeoxynucleotide.

Similar high separation efficiency was obtained for double-stranded (ds) DNA.[171] The separation of pBR322 DNA-*Hae*III fragments could in fact be accomplished on monolithic systems using a two-step gradient (**Figure 17**). There, the amount of DNA material that could be loaded onto a 100 × 3 mm inner diameter (i.d.) column without serious loss in separation efficiency was about 2.5 µg.

• *Miniaturized systems: ROMP-derived monolithic capillary columns*[170]

Contributing to ongoing efforts toward the miniaturization of analytical devices and to develop systems applicable to the coupling to highly sensitive quantification methods such as mass spectroscopy, Buchmeiser *et al*. reported on an extension of the concept of ROMP-derived monolithic supports to the synthesis of capillary columns. Transferring the synthetic concepts, methods, and procedures elaborated for semipreparative scale separations to 0.2 mm i.d. capillaries, high resolution was achieved in the separation of the oligodeoxynucleotides $(dT)_{12\text{-}18}$ ($2.27 < R_s < 3.47$). In addition, four homologous oligodeoxynucleotides, ranging in length from 24 to 27 nucleotides and differing from each other by the insertion of one, two, and three thymidines after position 18 of the 24-mer were baseline separated within 7 min.[170] Investigations on the run-to-run precision revealed that, for example, for proteins (lysozyme A, ribonuclease, insulin, cytochrome *c*, and myoglobin), deviations in retention times were <1.4%.[202] **Figure 18** depicts the analysis of a mixture of dsDNA fragments obtained by digestion of the pBR322 plasmid with the restriction enzyme *Hae*III. The fragments ranging in size from 51 to 587 base pairs were separated by capillary IP-RP-HPLC. The excellent separation efficiency of ROMP-based monoliths for dsDNA was documented in peak widths at half height of 3.1–8.5 s for the fragments up to about 250 base pairs. Longer DNA fragments eluted with peak widths at half height around 10–12 s. These higher peak widths were a result of the shallower gradient required for total resolution.

Hydrophobic ROMP-derived monolithic stationary phases were also tested for the separation of some proteins by RP-HPLC. **Figure 19** illustrates the separation of six proteins (ribonuclease A, insulin, cytochrome *c*, lysocyme, α-chymotrypsinogen A, and catalase) by capillary RP-HPLC at a flow rate of 6 µl min^{-1}. The use of a steep gradient ensured for the rapid elution of the proteins as extremely sharp peaks with peak widths at half height between 1 and 2 s. The selectivity was high, allowing for the separation of all components to baseline within less than 5 min. Finally, it is worth mentioning that NBE-based monolithic supports were also found capable of separating diastereomeric phosphorothioates.[170]

Monolithic columns for capillary HPLC were also prepared via ROMP of COE, TCOMS, 2-propanol, toluene, and $RuCl_2(Py)_2(IMesH_2)(CHC_6H_5)$ within the confines of 200 µm i.d. fused silica columns.[203] For evaluation, a protein standard consisting of six proteins in the molecular weight range of 5800–66 000 g mol^{-1}, that is, ribonuclease A, insulin, albumin, lysozyme, myoglobin, and β-lactoglobulin, was used again.

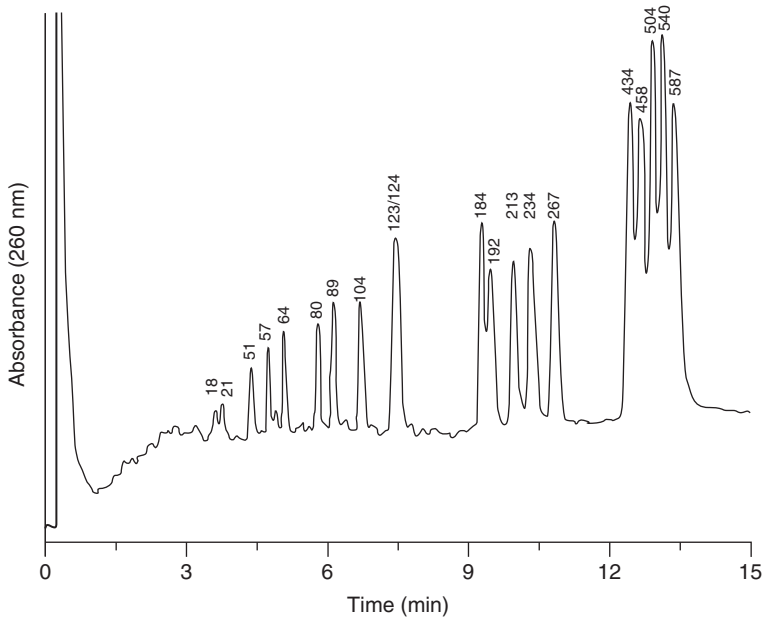

Figure 17 Separation of dsDNA fragments on an NBE-based monolith (3 × 100 mm). Mobile phase A: 0.1 mol l^{-1} triethylammonium acetate, pH 7.0, 4% glycerol; mobile phase B: 0.1 mol l^{-1} triethylammonium acetate, pH 7.0, 40% acetonitrile, 4% glycerol, gradient 10–25% B in 5 min, 25–45% B in 12 min, flow rate = 2.0 ml min^{-1}; T = 50 °C; UV 254 nm, sample, 0.75 µg pBR322 DNA-*Hae*III digest. Reprinted from Lubbad, S.; Mayr, B.; Huber, C.; Buchmeiser, M. R. *J. Chromatogr. A* **2002**, *959*, 121–129. [171] © Copyright 2002, with permission from Elsevier.

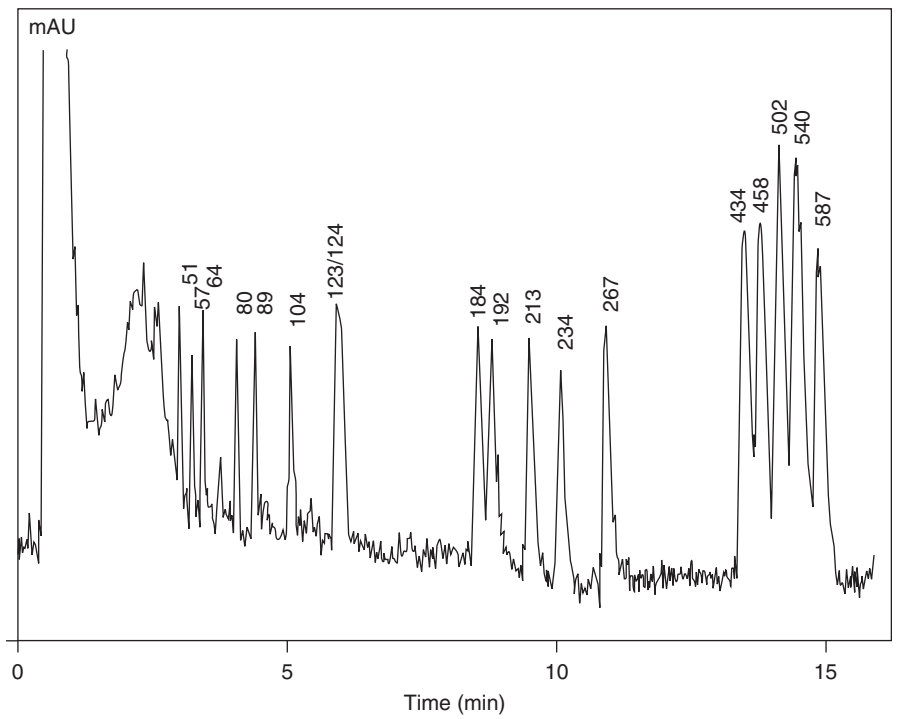

Figure 18 Separation of dsDNA on a monolith (0.2 × 60 mm); mobile phase 4–10% acetonitrile in 1 min, 10–16% ACN in 14 min in 0.1 M $Et_3NH^+OAc^-$, pH 7.0; 1% MeOH; flow rate 3 µl min^{-1}; UV 254 nm. Adapted with permission from Mayr, B.; Hölzl, G.; Eder, K.; *et al. Anal. Chem.* **2002**, *74*, 6080–6087.[170] © Copyright 2002 American Chemical Society.

Reproducibility of synthesis was checked by determining the RSD in retention times (t_R), which was found to be in the range of 2.9–3.9% for all analytes. The long-term stability of the COE-based monolithic columns was checked after more than 1000 runs at 50 °C and revealed excellent stability of the columns, thus proofing the concept of replacing NBE- by COE-based monomers and cross-linkers. No significant alteration in separation performance was observed; however,

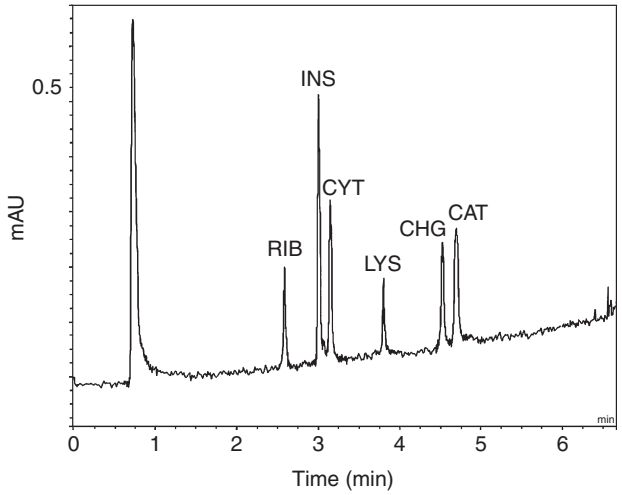

Figure 19 Separation of proteins (ribonuclease, insulin, cytochrome c, lysozyme, α-chymotrypsinogen A, catalase) on a monolith (0.2 × 220 mm). Mobile phase A, 0.05% aqueous TFA; mobile phase B, ACN + 0.05% TFA; linear gradient 10–100% B in 10 min; delay 2 min; RT, flow rate: 5.71 µl min^{-1} (400 ml min^{-1}+50/375/40 cm split); 180 bar; inj. vol. 500 nl; conc. 10 µg ml^{-1}, UV 218 nm. Adapted with Permission from Mayr, B.; Hölzl, G.; Eder, K.; *et al. Anal. Chem.* **2002**, *74*, 6080–6087. [170] © Copyright 2002 American Chemical Society.

retention times slightly decreased after 1200 injections (approximately 1.6–7.2% for all analytes). ROMP-derived capillary monoliths were also found applicable to separation problems common in medical research.[204] Thus, insulin and various insulin analogs used in diabetic treatment were analyzed. The monolithic column showed equivalent separation efficiency compared to Vydac C4- and Zorbax C3-based stationary phases. Moreover, the high permeability of monoliths enabled chromatographic separations at higher flow rates, thus shortening analysis times to about one-third without any loss in separation efficiency. For the analysis of insulin in human biofluid samples, enhanced sensitivity was achieved by using a 50 µm i.d. ROMP-derived monolith (**Figure 20**).

Finally, ROMP-derived, NBE-based columns have also been successfully applied in voltage-assisted capillary LC.[205]

• *Monolithic ROMP-derived columns for size-exclusion chromatography*[172]

Buchmeiser *et al*. also applied ROMP to the synthesis of monolithic supports for fast, nonaqueous gel permeation chromatography (GPC). This approach was characterized by some differences concerning the morphologies of monoliths used in HPLC and GPC. In contrast to monolithic HPLC supports, which allow for the fast separation of biomacromolecules because of the lack of micro- and mesoporosity, monolithic supports suitable for GPC required porous supports, preferably with a continuous pore size distribution. Therefore, the major task was to develop a ROMP-based polymerization system that allowed for the formation of the desired polymeric structure, that is, a monolith containing micro-, meso-, and macropores had to be synthesized. This task was accomplished by using a mixture of two cross-linkers, DMN-H6 and $(NBE\text{-}CH_2O)_3SiCH_3$, for monolith synthesis. Reproducibility in elution was confirmed by injecting standards 30 times. Excellent stability in terms of retention time t_R was observed. Thus, the average value for t_R was 4.499 ± 0.001 min, corresponding to an RSD of 0.031%. A third-order calibration curve with a good fit ($R^2 = 0.994$)

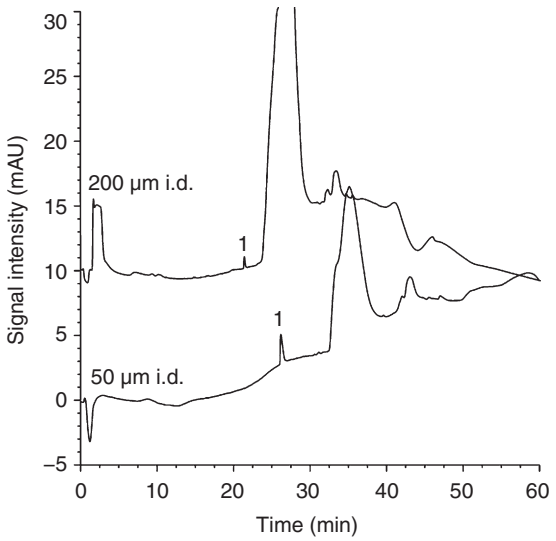

Figure 20 Analysis of human insulin in interstitial fluid samples using capillary monoliths of (a) 8 cm × 200 µm i.d. and (b) 8 cm × 50 µm i.d. Interstitial fluid samples diluted (a) 1:10 and (b) 1:160 and spiked with (1) human insulin (100 fmol $µl^{-1}$), injection volume 1 µl. Mobile phase: (A) 95% water, 5% acetonitrile, 0.05% TFA; (B) 20% water, 80% acetonitrile, 0.04% TFA; gradient: 0–30 min 0–60% B; 50–90% B within 5 min; flow rate (a) 1.5 µl min^{-1}, (b) 0.5 µl min^{-1}; $T = 25$ °C; UV 190 nm. Reprinted from Sinner, F. M.; Gatschelhofer, C.; Mautner, A.; *et al. J. Chromatogr. A* **2008**, *1191*, 274–281. © Copyright 2008, with permission from Elsevier.

was recorded for PS standards in a range of 2600–3 280 000 g mol^{-1}. To check the quality of the new GPC columns, different narrow PS standards ranging from 265 to 1 500 000 g mol^{-1} were applied as unknowns. Deviations in the calculated average molecular weight of these samples were significantly lower compared to a commercial column. The most important feature of the new supports, however, was the reduction in separation times to less than 5 min for molecular weights in the range of 2000–1 300 000 g mol^{-1}.

• *Functionalization and metal removal*

ROMP triggered with Schrock- or Grubbs-type initiators is a living polymerization process. The 'living' character[91,206–210] of ROMP catalyzed by both Grubbs- and Schrock-type initiators offers a perfect access to functionalization. In fact, the active ruthenium sites can be used for derivatization after rod formation is complete. ICP-OES-based investigations revealed that more than 98% of the initial amount of a first-generation Grubbs initiator is located at the microglobule surface once microstructure formation is complete.[169] This can be attributed to the highly polar character of the initiator, which preferably locates at the interface between the nonpolar, toluene-enriched microglobule and the polar, 2-propanol-enriched interface. In addition, microglobules are designed in a way that their pore size is <1.2 nm, which basically restricts functionalization to their surface.[172,211]

Using the active initiator covalently bound to the surface of the structure-forming microglobules after completed rod formation, various functional monomers have been grafted onto the monolith surface by simply passing solutions thereof through the mold (**Scheme 25**).[166,167] This way, linear polymer chains, that is, polymer brushes, were attached to the inner surface of the monolith. The degree of this graft polymerization of functional monomers varied within almost two orders of magnitude, depending on their ROMP activity. This approach generally offers some advantages. First, the structure of the 'parent' monolith is not affected by the functional monomer and can be optimized regardless of the functional monomer used later. Second, solvents other than the porogens, for example, methanol, methylene chloride, dimethylformamide, can be used for this '*in situ*' derivatization.[98] The versatility of this concept was demonstrated by grafting various ester-, amine-, phenol-, β-CD-, imidazolium salt-, carboxylic acid-containing NBE- or 7-oxanorborn-2-ene-based monomers onto the surface of monoliths. An overview over the different monomers that have already been grafted is given in **Figure 21**.

Using a β-CD-derivatized monolith, the chiral separation of proglumide was accomplished.[167] In extension to this chemistry, a postsynthesis grafting method was developed that offers access to high-capacity functionalized monolithic systems. By applying this method, the amounts of grafted monomers exceeded 1 mmol g^{-1}.[211] Such high-capacity monoliths are very vital for various applications such as catalysis, extraction of environmental contaminants, extraction of compounds for either pharmaceutical or clinical purposes, or, more general, separation techniques.[182]

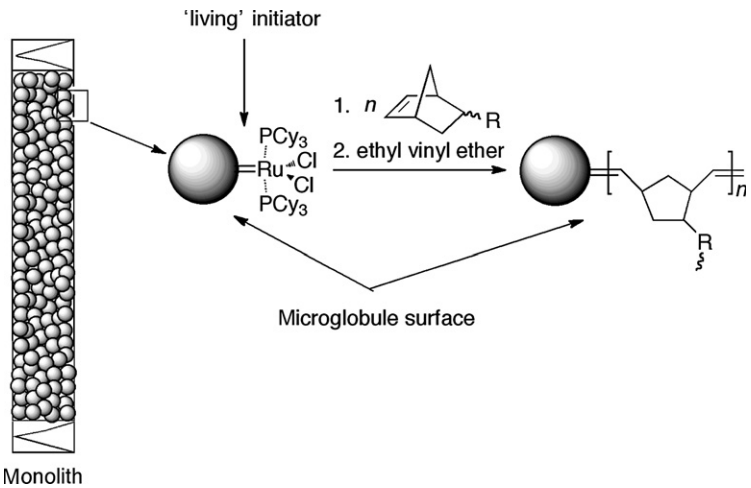

Scheme 25 '*In situ*' functionalization of a ROMP-derived monolith.

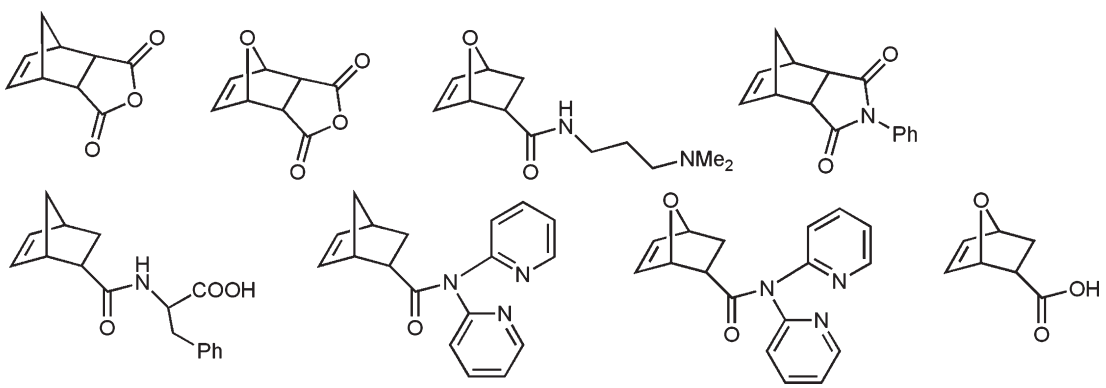

Figure 21 Overview over the functional monomers used.

Because the living initiator is almost quantitatively located at the surface of the microglobules, the efficiency of 'metal removal' from the monolith after polymerization is high. Typical residual metal contents are in the low ppm range. Noteworthy, Deleuze *et al.*[212] used the same approach for the synthesis and functionalization of emulsion-derived polymeric foams. ROMP-derived, NBE-based monoliths were also subjected to *in situ* surface functionalization using 2-(*N*, *N*-dimethylaminoethyl)norborn-5-ene-2-ylcarboxylic amide. The resulting functionalized monoliths were used in anion-exchange chromatography of oligodeoxynucleotides.[213] Good separation efficiency was achieved allowing for the baseline separation of these analytes. Peak half widths at half height were in the range of 8.4–11.4 s, peak resolution were 4.59 and 2.14, respectively. *In situ* functionalization of monolithic capillary columns with ONDCA gave access to weak anion-exchange capillary monoliths suitable for the separation of peptides.[214]

As an alternative to this grafting-from approach, ROMP-derived monoliths were prepared from 5-norborn-2-enemethyl bromide (NBE-CH_2Br) and tris(5-norborn-2-enemethoxy)methylsilane ($(NBE\text{-}CH_2O)_3SiCH_3$) within the confines of surface-silanized borosilicate columns (100×3 mm i.d.), applying Grubbs' first-generation catalyst $RuCl_2(PCy_3)_2(CHPh)$.[215] An investigation of the copolymerization kinetics of NBE-CH_2Br with the ones of $(NBE\text{-}CH_2O)_3SiCH_3$ revealed that the former was copolymerized slowly. This low copolymerization propensity results in relatively high concentrations of NBE-CH_2Br at a late stage of monolith formation and, therefore, larger amounts of this monomer are located at the surface of the microglobule. These surface-located NBE-CH_2Br groups were then converted into weak anion exchangers via reaction with diethyl amine. The resulting monolithic anion exchangers demonstrated a very good potential for the anion-exchange separation of nucleic acids applying a phosphate buffer (0.05 mol l^{-1}, pH 7) and NaCl (1.0 mol l^{-1}) as a gradient former. Fast and efficient separations, indicated by sharp and highly symmetric analyte peaks, were established. Except for the 267 and 298 base-pair fragments, the 11 fragments of a ds-pUC18 DNA *Hae*III digest were baseline separated within ~8 min. Nineteen fragments of a ds-pBR322 *Hae*III digest were separated within ~12 min. There, only the 192 and 213 base-pair fragments and the 458, 504, and 540 base-pair fragments coeluted. A ds-pUC18 DNA *Hae*III digest was used as a control analyte in evaluating the influence of organic additives on the mobile phase such as methanol and acetonitrile on nucleic acid separation.

ROMP has also been used for the postsynthesis functionalization of electron-beam curing-derived,[216–219] (meth) acrylate-based polymeric monolithic materials.[220] These were prepared via the copolymerization of norborn-2-ene-5-yl acrylate with trimethylolpropane triacrylate (TMPTA) and ethyl methacrylate (EMA). In contrast to the acrylate and methacrylate moieties, the NBE groups did not undergo free radical polymerization in course of the electron-beam triggered process and could thus, after monolith formation, be reacted with either $RuCl_2(PCy_3)_2(CHPh)$ or $RuCl_2(PCy_3)$ (1,3-dimesitylimidazolin-2-ylidene)(CHPh). After the surface attachment of the initiators was completed, a variety of functional monomers was successfully grafted onto the surface of these supports (**Scheme 26**). Grafting densities up to 290 µmol monomer per gram were realized. For purposes of completeness, a comparative study of the separation performance of ROMP-based NBE- and COE-derived monolithic columns with electron-beam curing-derived ones shall be mentioned.[219] All columns investigated allowed for the rapid separation of proteins; however, the novel electron-beam curing-derived polymeric columns allowed for the fastest separation of these analytes with sufficient peak resolution.

• *Applications of functionalized ROMP-derived monoliths in catalysis*

In heterogeneous catalysis, one wants to combine the general advantages of homogeneous systems such as high definition, activity, and so on, with the advantages of heterogeneous catalysis such as increased stability, ease of separation, and recycling. Traditionally, monolithic catalytic media are mostly composed of metal oxides, porous metals, and certain polysaccharides.[221] The first successful use of metathesis-based monolithic media for

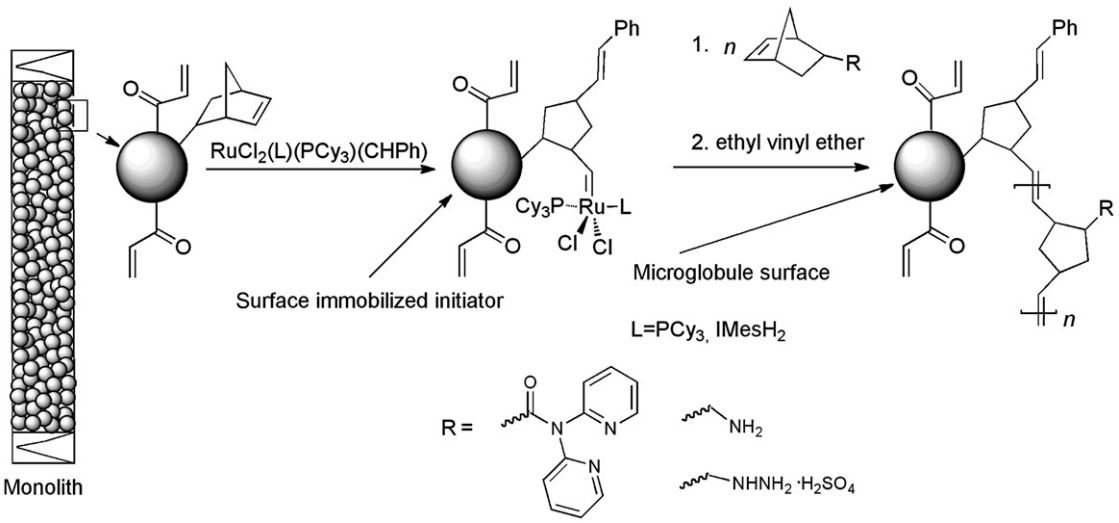

Scheme 26 Postsynthesis functionalization of electron-beam curing-derived monolithic supports via ROMP ($IMesH_2$=1,3-dimesitylimidazolin-2-ylidene).

heterogeneous catalysis was accomplished by using these supports as carriers for Grubbs-type initiators based on NHCs.[222,223] To generate sufficient porosity, monoliths with a suitable microporosity (40%) and microglobule diameter (1.5 ± 0.5 mm) were synthesized.

Consecutive '*in situ*' derivatization was successfully accomplished using a mixture of NBE and a polymerizable NHC precursor (**Scheme 27**).[169,224–226] The use of NBE drastically enhanced grafting yields for the functional monomer. Using this setup, tentacles of copolymer with a degree of oligomerization of the functional monomer of 2–5 were generated. The free NHC was generated with the aid of a base and reacted with $RuCl_2(PCy_3)_2(CHPh)$ to yield up to 1.4 wt.% of an immobilized second-generation Grubbs catalyst. Monolith-immobilized metathesis catalysts prepared by this approach showed high activity in various metathesis-based reactions such as ROMP and RCM. The *cis*/*trans* ratios of polymers (90%) exactly corresponded to the ones found with analogous homogeneous systems. In a benchmark reaction with DEDAM, these properties directly translated into high average TOFs of up to $0.5\ s^{-1}$.

Alternatively, monolith-supported second-generation Grubbs catalysts containing unsaturated (e.g., IMes = 1,3-dimesitylimidazol-2-ylidene) or saturated (e.g., $IMesH_2$ = 1,3-dimesitylimidazolin-2-ylidene) NHCs[28] were prepared by a synthetic protocol summarized in **Scheme 28**. Surface derivatization of a monolith was carried out with ONDCA followed by conversion of the grafted poly(anhydride) into the corresponding polysilver salt. This silver salt was used for the halogen exchange with a broad variety of second-generation Grubbs catalysts, leading to the desired catalytic species. In the benchmark reaction with DEDAM, TONs up to 830 were achieved.[47]

Model reactions revealed that only one chloride was exchanged by the silver carboxylate, while the second chloride remains unaffected. However, these systems benefit from the presence of free silver carboxylate groups, which actually act as a reversible scavenger for phosphine. Thus, the use of

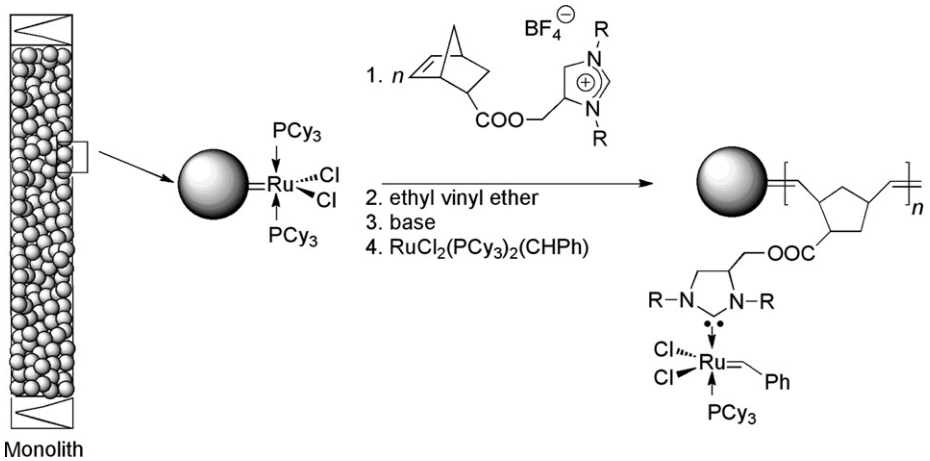

Scheme 27 Immobilization of an NHC precursor on a ROMP-derived monolith via *in situ* grafting.

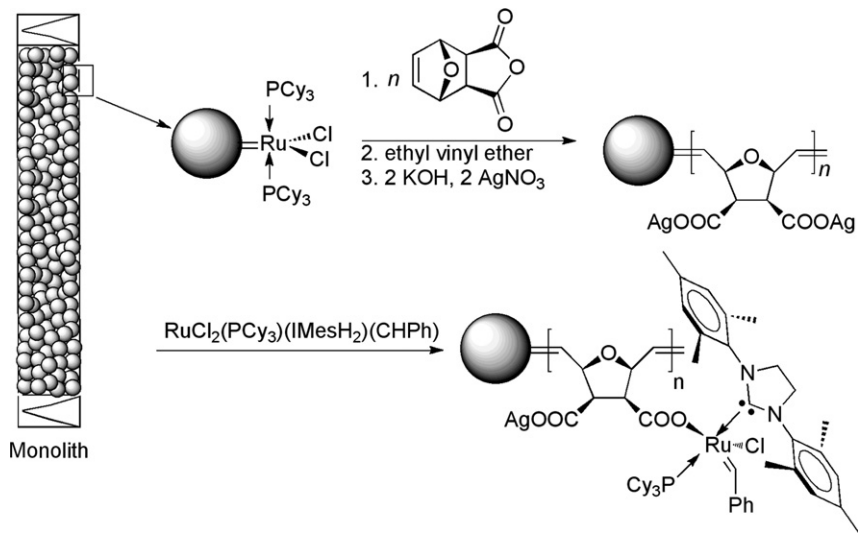

Scheme 28 Immobilization of a metathesis catalyst on a ROMP-derived monolithic support.

monocarboxylic acids such as 7-oxanorborn-2-ene-5-carboxylic acid instead of the ONDCA resulted in a supported catalyst that showed significantly reduced TONs in the RCM of DEDAM. In addition and in contrast to supported systems based on pendant silver carboxylates, high concentrations of phosphine were monitored in the effluent applying a continuous flow setup. Again, the use of silica as support results in low TONs around 120. This comparably low activity of silica-based systems was attributed both to the nonreversible scavenging of the phosphine by residual silanol groups and to diffusion-controlled reactions and can in fact be overcome by the use of the above-mentioned monolithic systems.

A monolith-supported version of the Grubbs–Hoveyda catalyst was prepared in an analogous approach using a perfluoroglutaric anhydride-derived ligand (**Scheme 29**). When used in continuous flow experiments, TONs were >500.[48,50]

It is worth mentioning that the TONs obtained with these two supported versions exceeded all published data on TONs of supported well-defined metathesis catalysts at that time. Equally important, the contamination of the products with ruthenium was (at that time) unprecedented low, that is, 1.8 ppm. The same group also reported on an extension of this work by immobilizing 1,3-dimesityltetrahydropyrimidin-2-ylidene-based on ROMP-derived monolithic supports.[17]

The above-described bis(norborn-2-ene)-functionalized, chiral biphenyl ligand has also been immobilized on monolithic supports. Monoliths were designed in a way that they could be cut into pieces and, after encasement, could be used for HTS (**Scheme 30**).

The high porosity (ca. 60% pore volume) of the monolithic supports guaranteed for a sufficient void volume to take up solutions of the corresponding educt. The monolithic supports thus served simultaneously as catalyst supports, reactions vessels, and filtration units. A series of asymmetric RCM reactions and desymmetrization reactions were carried out. Using the supported chiral Schrock catalyst, very similar enantioselectivity was found as for the parent homogeneous system.[227] Metal leaching was reported to be <3%.

A 'grafting-from' approach was also used for the immobilization of dipyridylamide ligands. To avoid any potential incompatibilities of the ruthenium-based initiator used with the pyridine-containing ligands, a completely new approach was elaborated for monolith functionalization with these ligands. Since the nitrogen lone pair needed to be protected to prevent coordinating to the ruthenium core, the catalytically active complex, *N,N*-dipyrid-2-yl-7-oxanorborn-5-en-2-ylcarbamido palladium dichloride, was synthesized and grafted onto a monolith using NBE as a comonomer (**Scheme 31**). Following this 'grafting-from' approach, monoliths containing 7 μmol (0.07%) Pd were prepared. In a model reaction between styrene and iodobenzene, TOFs of 1.2–1.6 s^{-1} were found. These figures clearly exceed those obtained with supports prepared by ring-opening metathesis precipitation copolymerization, which gave TOFs of 0.35 s^{-1} in an identical reactions.[228] Pd leaching was generally low (2.2% total over 10 h). Alternatively, if used as a cartridge, amounts of reactants typical in combinatorial chemistry (50–100 mg in total) were converted in satisfactory yields (<80%).[98]

- *Pore-size-selective functionalization of monoliths*

An approach to Pd(0)-mediated, ligand-free coupling reactions was developed by Bandari *et al.*[229] Electron-beam-triggered free radical polymerization-derived monolithic supports prepared from a mixture of glycidyl methacrylate and TMPTA in 2-propanol, 1-dodecanol, and toluene were prepared in a way that porous monolithic matrix that was characterized by large (convective) pores in the 30 μm range as well as of pores <600 nm, formed. The epoxy groups present within the

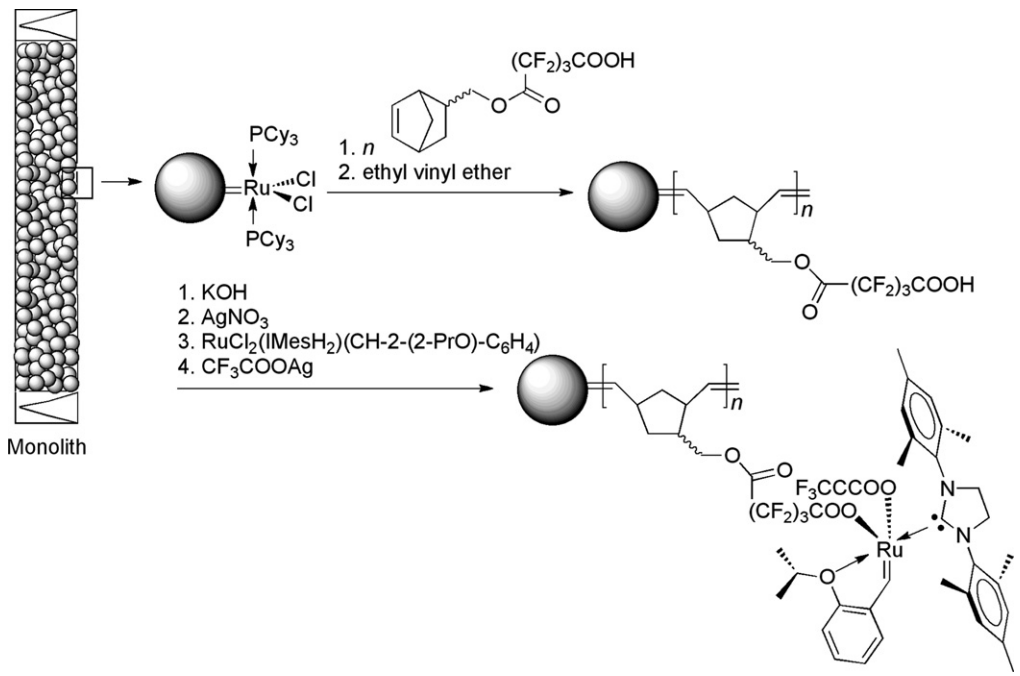

Scheme 29 Immobilization of a metathesis catalyst on a ROMP-derived monolithic support using fluorinated carboxylates.

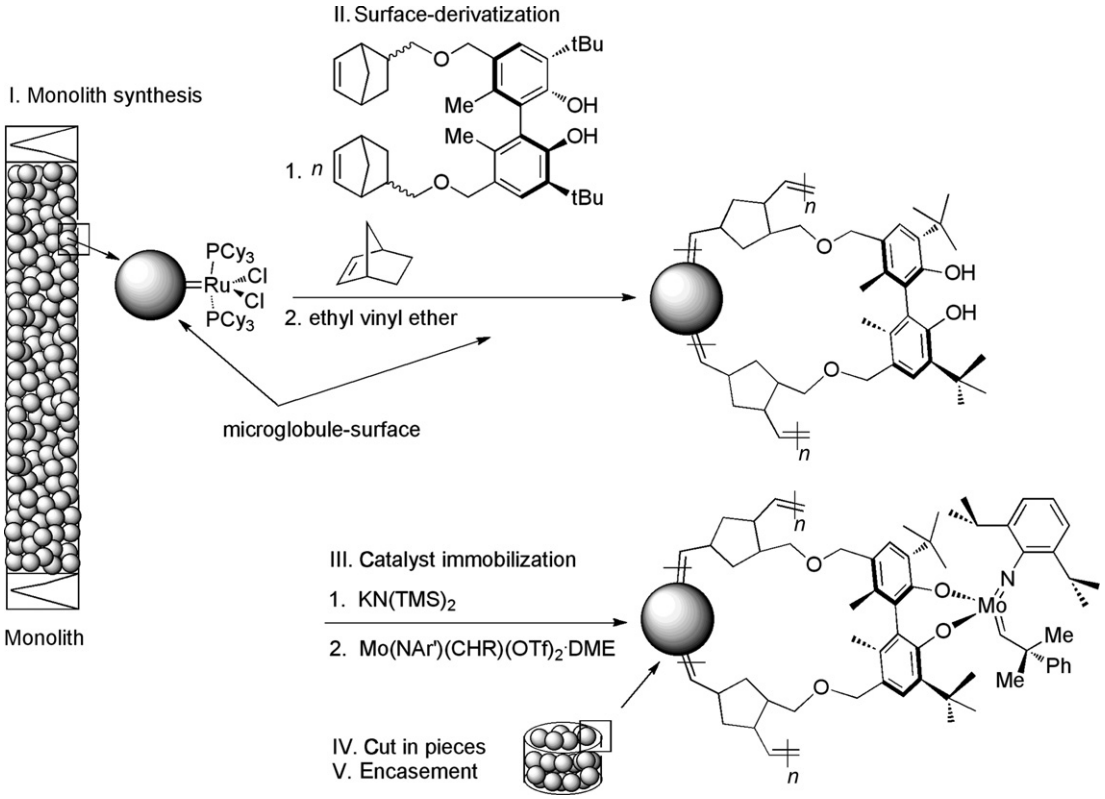

Scheme 30 Monolith-supported chiral Schrock catalyst.

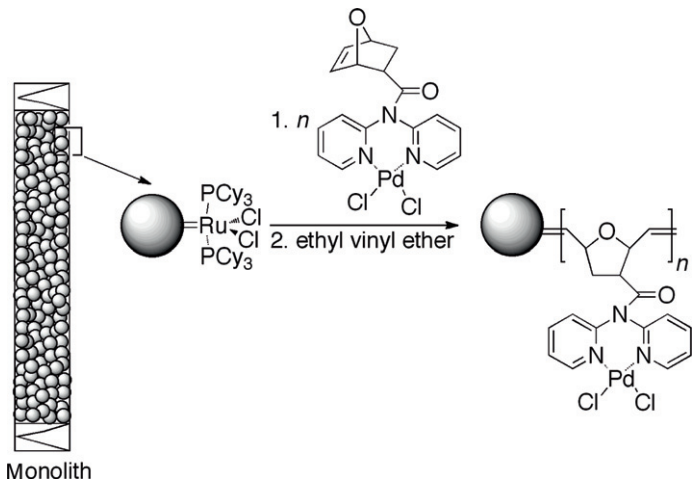

Scheme 31 Immobilization of a Heck catalyst on a ROMP-derived monolithic support.

entire monolith were hydrolyzed in pores >7 nm using poly (styrene sulfonic acid) (M_w = 69 400 g mol^{-1}, PDI = 2.4). The remaining epoxy groups inside pores <7 nm were subject to aminolysis with norborn-5-ene-2-ylmethylamine, providing covalently bound NBE groups inside these pores (Scheme 32). These NBE groups were then reacted with the first-generation Grubbs initiator $RuCl_2(PCy_3)_2(CHPh)$. The thus immobilized Ru-alkylidenes were further used for the surface modification of these small pores applying a grafting-from approach. Different monomers, for example, *N*,*N*-di(pyrid-2-yl)-7-oxanorborn-5-ene-2-ylcarboxylic amide were surface-grafted inside the small pores. The thus poly-5 grafted polymers were then used to permanently immobilize Pd^{2+} and Pt^{4+}, respectively, inside these pores. After reduction, metal nanoparticles approximately 2 nm in diameter were formed. Monoliths containing Pd nanoparticles inside the constrained geometries of the small pores were then used in both Heck- and Suzuki-type coupling reactions achieving TONs up

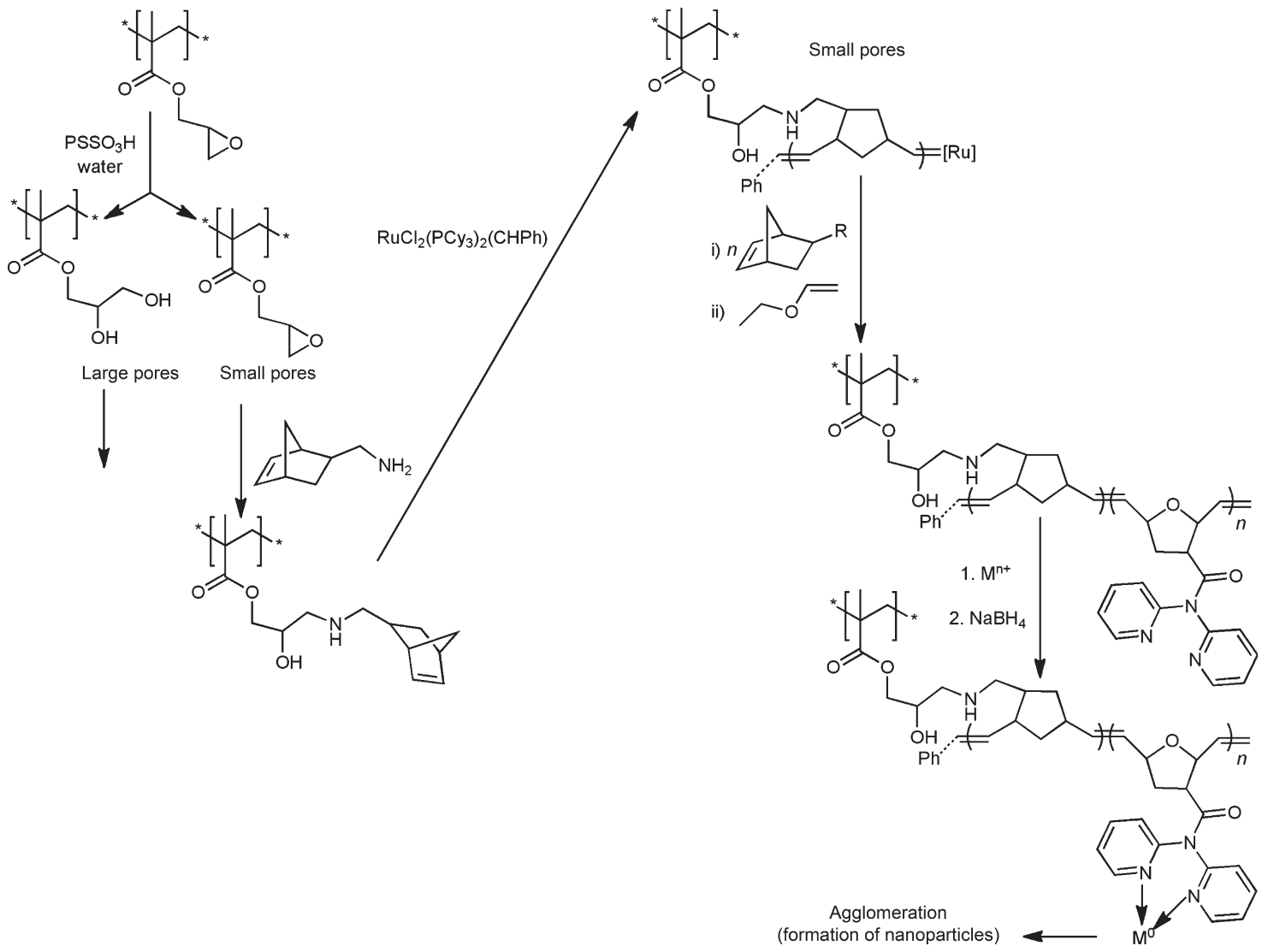

Scheme 32 Pore-size-selective functionalization of monolithic supports.

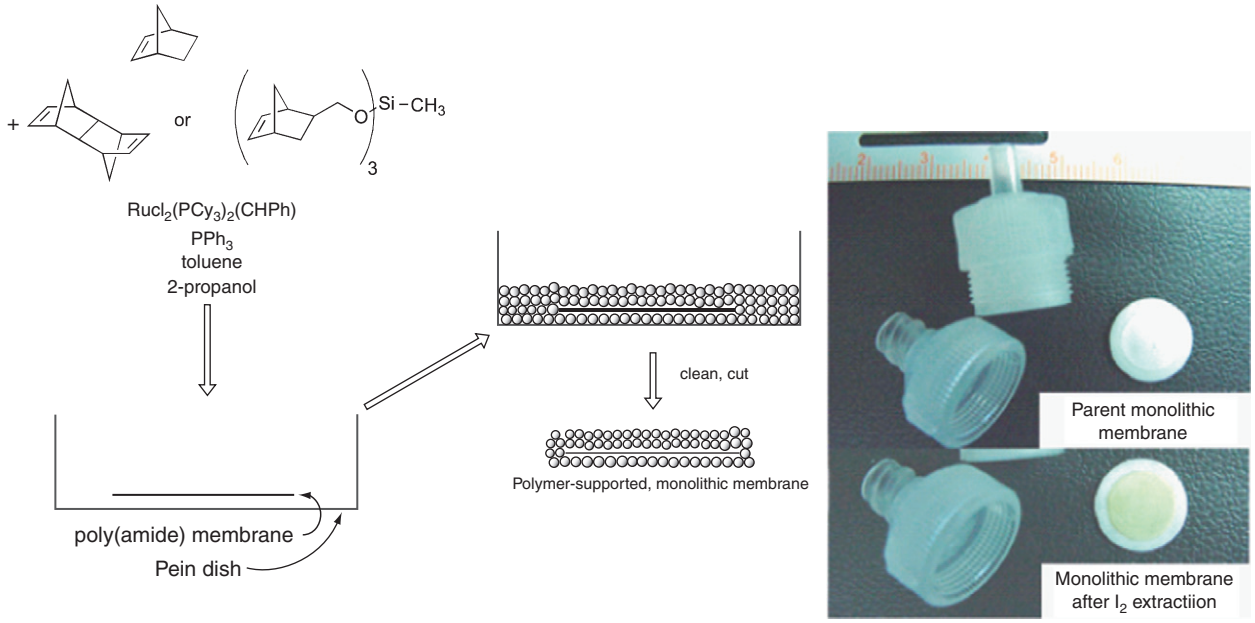

Scheme 33 Synthesis of ROMP-derived monolithic membranes (left) and monolithic membrane after I_2 extraction. Buchmeiser, M. R. *J. Sep. Sci.* **2008**, *31*, 1921. © Copyright Wiley-VCH Verlag GmbH & Co. KGaA. Reproduced with permission.

to 167 000 and 63 000, respectively. Due to the steric constraints, the nanoparticles did not significantly change in particle size.

• *Monolithic ROMP-derived disks*[230]

For monolithic disk synthesis, solutions of NBE, DMN-H6, and tris(norborn-5-ene-2-ylmethylenoxy)methylsilane, respectively, in 2-propanol and toluene (25:25:41:9, all wt.%) were subject to ROMP using the first-generation Grubbs initiator $RuCl_2(PCy_3)_2(CHPh)$ and triphenylphosphine (PPh_3) as modulator. To come up with disks with sufficient mechanical strength, poly (amide) membranes were soaked with the polymerization mixture (Scheme 33). This way, membrane-supported monolithic disks up to 2 mm in thickness were realized. These disks were successfully used for the preconcentration of iodine and selected organic solutes from dilute aqueous samples by SPE. Quantitative measurement of the extracted solutes was achieved by diffuse-reflectance spectroscopy (DRS) directly on the surface of the disk.

• *Monolithic materials for tissue engineering*[178,180,231]

In search of alternative scaffolds suitable for tissue engineering, we took advantage of the particular properties of monolithic supports, which are a tailor-made porosity and pore distribution as well as the possibility to create large transport pores in the micrometer region. In addition, the molding processes that are feasible thereby significantly reduce restrictions in shape. By using a 20:20 wt.% mixture of NBE and pentaglycerol bis(7-oxanorborn-5-ene-2-ylcarboxylate) acrylate (PGBA) in a microporogen (toluene) and a macroporogen (2-propanol, 5:10 wt.% ratio), monolithic structures were realized with the aid of $RuCl_2(pyridine)_2(IMesH_2)(CHPh)$ (0.03 wt.%) and low amounts (<100 ppm) of additional free pyridine as regulator.[78] Scheme 34 illustrates the basic polyreaction.

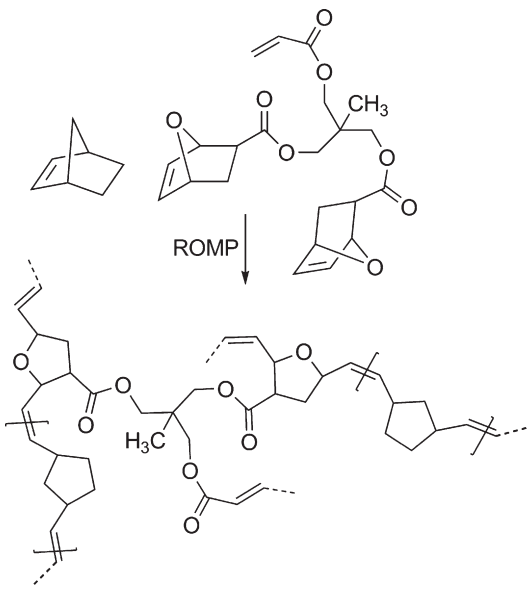

Scheme 34 Synthesis of 7-oxanorborn-2-ene-based, ROMP-derived monoliths.

Large transport pores up to 400 µm, which should facilitate neovascularization, could be created. Upon cultivation with adipose tissue mesenchymal stem cells and subsequent differentiation into adipose and osseous tissue, respectively, the novel supports in fact turned out to be biocompatible and biodegradable. Thus, excellent ingrowth of the cells into the monolithic support and cell proliferation was observed. However, the high porosity of these supports and the large pores were proposed to be responsible for the comparably low mechanical stability. To enhance the mechanical stability of the supports, nanoscaled inorganic particles, that is, $CaCO_3$

and hydroxylapatite, were added. Simultaneously, to enhance the compatibility of the organic support with the polar nanoparticles, NBE was replaced by *cis*-cyclooctene-5,6-diol. The Grubbs-type initiators used not only tolerated the presence of the inorganic nanoparticles, but, equally importantly, particle loadings up to 12 wt.% did not interfere with the phase separation process, allowing for the realization of monolithic nanocomposites.[232] Equally important, preliminary cell cultivation studies did not indicate any negative effects of the nanoparticles on cell adhesion and growth.

4.23.5 Summary

Metathesis-based polymerization techniques have found their place in many areas of materials science. This has been made possible by developing well-defined and tolerant initiators. With these catalytic systems in hand, particular ROMP and 1-alkyne polymerization have had an enormous impact on the development of surface-modified organic and inorganic materials. Applications in catalysis and separation science have been added to the more 'traditional' ones in optics and electronics. The ongoing developments in organometallic chemistry, that is, in initiator design, in polymer chemistry, and in particular in metathesis polymerization, will certainly result in the permanent improvement of existing systems and techniques as well as in new applications in many areas of chemistry and materials science. However, for some applications, the unsaturated nature of the polymers created by ROMP still represents a significant drawback as compared to functional surfaces prepared by other polymerization techniques. Here, intermediary saturation, for example, by hydrogenation, must be considered.

References

1. Calderon, N.; Chen, H. Y.; Scott, K. W. *Tetrahedron Lett.* **1967**, *34*, 3327.
2. Calderon, N. *J. Macromol. Sci. Rev. Macromol. Chem.* **1972**, *C7*, 105.
3. Calderon, N. *Acc. Chem. Res.* **1972**, *5*, 127.
4. Calderon, N.; Ofstead, E. A.; Judy, W. A. *Angew. Chem.* **1976**, *88*, 433.
5. Chauvin, Y. *Angew. Chem.* **2006**, *118*, 3824.
6. Ivin, K. J., Olefin Metathesis and Metathesis Polymerization Wiley Interscience: London, 1974.
7. Ivin, K. J.; Mol, J. C.*Olefin Metathesis and Metathesis Polymerization*; Academic Press: San Diego, CA, 1997.
8. Jacobson, H.; Stockmayer, W. H. *J. Chem.Phys.* **1950**, *18*, 1600.
9. Benedicto, A. D.; Claverie, J. P.; Grubbs, R. H. *Macromolecules* **1995**, *28*, 500.
10. Chen, Z.-R.; Claverie, J. P.; Grubbs, R. H.; Kornfield, J. A. *Macromolecules* **1995**, *28*, 2147.
11. Quignard, F.; Leconte, M.; Basset, J. M. *J. Chem. Soc. Chem. Commun.* **1985**, 1816.
12. Katz, T. *Angew. Chem.* **2005**, *117*, 3070.
13. Weskamp, T.; Schattenmann, W. C.; Spiegler, M.; Herrmann, W. A. *Angew. Chem.* **1998**, *110*, 2631.
14. Weskamp, T.; Kohl, F. J.; Herrmann, W. A. *J. Organomet. Chem.* **1999**, *582*, 362.
15. Weskamp, T.; Kohl, F. J.; Hieringer, W.; *et al. Angew. Chem.* **1999**, *111*, 2573.
16. Frenzel, U.; Nuyken, O. *J. Polym. Sci., Part A: Polym. Chem.* **2002**, *40*, 2895.
17. Yang, L.; Mayr, M.; Wurst, K.; Buchmeiser, M. R. *Chem. Eur. J.* **2004**, *10*, 5761.
18. Krause, J. O.; Wurst, K.; Nuyken, O.; Buchmeiser, M. R. *Chem. Eur. J.* **2004**, *10*, 777.
19. Chauvin, Y.; Hérisson, J.-L. *Macromol. Chem.* **1971**, *141*, 161.
20. Kingsbury, J. S.; Harrity, J. P. A.; Bonitatebus, P. J., Jr.; Hoveyda, A. H. *J. Am. Chem. Soc.* **1999**, *121*, 791.
21. Wache, S.; Herrmann, W. A.; Artus, G.; *et al. J. Organomet. Chem.* **1995**, *491*, 181.
22. Grubbs, R. H. In Wilkinson, G., Stone, F. G. A., Abel, E., Eds.; *Comprehensive Organometallic Chemistry*; Pergamon: Oxford, 1982; p 499.
23. Grubbs, R. H. *J. Macromol. Sci. Pure Appl. Chem.* **1994**, *A31*, 1829.
24. Grubbs, R. H.; Chang, S. *Tetrahedron* **1998**, *54*, 4413.
25. Grubbs, R. H., Ed. *Handbook of Metathesis*; Wiley-VCH: Weinheim, 2003.
26. Grubbs, R. H. *Angew. Chem.* **2006**, *118*, 3845.
27. Trnka, T. M.; Grubbs, R. H. *Acc. Chem. Res.* **2001**, *34*, 18.
28. Buchmeiser, M. R. *Chem. Rev.* **2000**, *100*, 1565.
29. Schrock, R. R. *J. Am. Chem. Soc.* **1974**, *96*, 6796.
30. Schrock, R. R. In *Ring-Opening Polymerization*; Brunelle, D. J., Ed.; Hanser: Munich, 1993; p 129.
31. Schrock, R. R. *Pure Appl. Chem.* **1994**, *66*, 1447.
32. Schrock, R. R. *Chem. Rev.* **2002**, *102*, 14.
33. Schrock, R. R.; Hoveyda, A. H. *Angew. Chem.* **2003**, *115*, 4740.
34. Schrock, R. R. *The Discovery and Development of High-Oxidation State Mo and W Imido Alkylidene Complexes for Alkene Metathesis*; Wiley-VCH: Weinheim, 2003.
35. Schrock, R. R. *Chem. Commun.* **2005**, 2773.
36. Schrock, R. R. *Angew. Chem.* **2006**, *118*, 3832.
37. Schrock, R. R.; Murdzek, J. S.; Bazan, G. C.; *et al. J. Am. Chem. Soc.* **1990**, *112*, 3875.
38. Schwab, P.; France, M. B.; Ziller, J. W.; Grubbs, R. H. *Angew. Chem.* **1995**, *107*, 2179.
39. Schwab, P.; Grubbs, R. H.; Ziller, J. W. *J. Am. Chem. Soc.* **1996**, *118*, 100.
40. Nguyen, S. T.; Johnson, L. K.; Grubbs, R. H. *J. Am. Chem. Soc.* **1992**, *114*, 3974.
41. Nguyen, S. T.; Grubbs, R. H. *J. Am. Chem. Soc.* **1993**, *115*, 9858.
42. Weskamp, T.; Böhm, V. P. W.; Herrmann, W. A. *J. Organomet. Chem.* **2000**, *600*, 12.
43. Huang, J.; Stevens, E. D.; Nolan, S. P.; Petersen, J. L. *J. Am. Chem. Soc.* **1999**, *121*, 2674.
44. Choi, T.-L.; Grubbs, R. H. *Angew. Chem.* **2003**, *115*, 1785.
45. Kingsbury, J. S.; Hoveyda, A. H. *J. Am. Chem. Soc.* **2005**, *127*, 4510.
46. Vorfalt, T.; Wannowius, K.-J.; Plenio, H. *Angew. Chem.* **2010**, *122*, 5665.
47. Krause, J. O.; Lubbad, S.; Nuyken, O.; Buchmeiser, M. R. *Adv. Synth. Catal.* **2003**, *345*, 996.
48. Krause, J. O.; Lubbad, S.; Mayr, M.; *et al. Polym. Prepr. (Am. Chem. Soc., Div. Polym. Chem.)* **2003**, *44*, 790.
49. Krause, J. O.; Zarka, M. T.; Anders, U.; *et al. Angew. Chem.* **2003**, *115*, 6147.
50. Krause, J. O.; Lubbad, S. H.; Nuyken, O.; Buchmeiser, M. R. *Macromol. Rapid Commun.* **2003**, *24*, 875.
51. Krause, J.O.; Mayr, M.; Lubbad, S.; et al. e-Polymers-conference papers section P_007 2003.
52. Krause, J. O.; Nuyken, O.; Buchmeiser, M. R. *Chem. Eur. J.* **2004**, *10*, 2029.
53. Krause, J. O.; Wang, D.; Anders, U.; *et al. Macromol. Symp.* **2004**, *217*, 179.
54. Halbach, T. S.; Mix, S.; Fischer, D.; *et al. J. Org. Chem.* **2005**, *70*, 4687.
55. Halbach, T. S.; Krause, J. O.; Nuyken, O.; Buchmeiser, M. R. *Macromol. Rapid Commun.* **2005**, *26*, 784.
56. Kumar, P. S.; Buchmeiser, M. R. *Organometallics* **2009**, *28*, 1785.
57. Kumar, P. S.; Wurst, K.; Buchmeiser, M. R. *Chem. Asian J.* **2009**, *4*, 1275.
58. Buchmeiser, M. R. *Adv. Polym. Sci.* **2005**, *176*, 89.
59. Kumar, P. S.; Wurst, K.; Buchmeiser, M. R. *J. Am. Chem. Soc.* **2009**, *131*, 387.
60. Schrock, R. R. *Acc. Chem. Res.* **1990**, *23*, 158.
61. Saunders, R. S. *Macromolecules* **1995**, *28*, 4347.
62. Buchmeiser, M. R. *Monatsh. Chem.* **2003**, *134*, 327–342.
63. Murdzek, J. S.; Schrock, R. R. *Macromolecules* **1987**, *20*, 2640.
64. Bazan, G. C.; Schrock, R. R.; Cho, H.-N.; Gibson, V. C. *Macromolecules* **1991**, *24*, 4495.
65. Bazan, G. C.; Khosravi, E.; Schrock, R. R.; *et al. J. Am. Chem. Soc.* **1990**, *112*, 8378.
66. Schrock, R. R. *Polyhedron* **1995**, *14*, 3177.
67. Fox, H. H.; Lee, J.-K.; Park, L. Y.; Schrock, R. R. *Organometallics* **1993**, *12*, 759.
68. Cucullu, M. E.; Li, C.; Nolan, S. P.; *et al. Organometallics* **1998**, *17*, 5565.
69. Wu, Z.; Nguyen, S. T.; Grubbs, R. H.; Ziller, J. W. *J. Am. Chem. Soc.* **1995**, *117*, 5503.
70. Sanford, M. S.; Ulman, M.; Grubbs, R. H. *J. Am. Chem. Soc.* **2001**, *123*, 749.
71. Sanford, M. S.; Love, J. A.; Grubbs, R. H. *J. Am. Chem. Soc.* **2001**, *123*, 6543.
72. Louie, J.; Grubbs, R. H. *Organometallics* **2002**, *21*, 2153.
73. Buchmeiser, M. *Macromolecules* **1997**, *30*, 2274.
74. Buchmeiser, M. R.; Schuler, N.; Kaltenhauser, G.; *et al. Macromolecules* **1998**, *31*, 3175.

75. Buchmeiser, M. R.; Schuler, N.; Schottenberger, H.; *et al. Des. Monomers Polym.* **2000**, *3*, 421.
76. Watson, K. J.; Zhu, J.; Nguyen, S. T.; Mirkin, C. A. *J. Am. Chem. Soc.* **1999**, *121*, 462.
77. Watson, K. J.; Zhu, J.; Nguyen, S. T.; Mirkin, C. A. *Pure and Appl. Chem.* **2000**, *72*, 67.
78. Liu, X.; Guo, S.; Mirkin, C. A. *Angew. Chem.* **2003**, *115*, 4933.
79. Weck, M.; Jackiw, J. J.; Rossi, R. R.; *et al. J. Am. Chem. Soc.* **1999**, *121*, 4088.
80. Rutenberg, I. M.; Scherman, O. A.; Grubbs, R. H.; *et al. J. Am. Chem. Soc.* **2004**, *126*, 4062.
81. Li, X.-M.; Huskens, J.; Reinhoudt, D. N. *Nanotechnology* **2003**, *14*, 1064.
82. Wu, M.; O'Neill, S. A.; Brousseau, L. C.; *et al. Chem. Commun.* **2000**, 775.
83. Samanta, D.; Faure, N.; Rondelez, F.; Sarkar, A. *Chem. Commun.* **2003**, 1186.
84. Juang, A.; Scherman, O. A.; Grubbs, R. H.; Lewis, N. S. *Langmuir* **2001**, *17*, 1321.
85. Harada, Y.; Girolami, G. S.; Nuzzo, R. G. *Langmuir* **2003**, *19*, 5104.
86. Buchmeiser, M. R.; Sinner, F.; Mupa, M.; Wurst, K. *Macromolecules* **2000**, *33*, 32.
87. Buchmeiser, M. R.; Sinner, F. M., in Functionalized Supporting Materials which can be obtained by means of metathesis graft polymerization; A 604/99; PCT/EO00/02846; WO 00/61288; Chem. Abstr. 1999, 133, 322561.
88. Buchmeiser, M. R. *High-Performance Materials for Separation Techniques via ROMP*; Kluwer: Dordrecht, NL, 2002.
89. Blümel, J. *J. Am. Chem. Soc.* **1995**, *117*, 2112.
90. Behringer, K. D.; Blümel, J. *J. Liq. Chromatogr. Relat. Technol.* **1996**, *19*, 2753.
91. Matyjaszewski, K. *Macromolecules* **1993**, *26*, 1787.
92. Mayr, B.; Sinner, F.; Buchmeiser, M. R. *J. Chromatogr. A* **2001**, *907*, 47.
93. Mayr, B.; Schottenberger, H.; Elsner, O.; Buchmeiser, M. R. *J. Chromatogr. A* **2002**, *973*, 115.
94. Mayr, B.; Buchmeiser, M. R. *J. Chromatogr. A* **2001**, *907*, 73.
95. Buchmeiser, M. R.; Schrock, R. R. *Macromolecules* **1995**, *28*, 6642.
96. Eder, K.; Reichel, E.; Schottenberger, H.; *et al. Macromolecules* **2001**, *34*, 4334.
97. Sinner, F.; Buchmeiser, M. R.; Tessadri, R.; *et al. J. Am. Chem. Soc.* **1998**, *120*, 2790.
98. Buchmeiser, M. R.; Lubbad, S.; Mayr, M.; Wurst, K. *Inorg. Chim. Acta* **2003**, *345*, 145.
99. Kröll, R.; Eschbaumer, C.; Schubert, U. S.; *et al. Macromol. Chem. Phys.* **2001**, *202*, 645.
100. Buchmeiser, M. R.; Kröll, R.; Wurst, K.; *et al. Macromol. Symp.*, **2001**, *164*, 187.
101. Schubert, U. S.; Weidl, C. H.; Eschbaumer, C.; *et al. Polym. Mater. Sci. Eng.* **2001**, *84*, 514.
102. Matyjaszewski, K.; Xia, J. *Chem. Rev.* **2001**, *101*, 2921.
103. Oskam, J. H.; Fox, H. H.; Yap, K. B.; *et al. J. Organomet. Chem.* **1993**, *459*, 185.
104. Mayr, M.; Buchmeiser, M. R.; Wurst, K. *Adv. Synth. Catal.* **2002**, *344*, 712.
105. Kim, N. Y.; Jeon, N. L.; Choi, I. S.; *et al. Macromolecules* **2000**, *33*, 2793.
106. Jeon, N. L.; Choi, I. S.; Whitesides, G. M.; *et al. Appl. Phys. Lett.* **1999**, *75*, 4201.
107. Mingotaud, A.-F.; Reculusa, S.; Mingotaud, C.; *et al. J. Mater. Chem.* **2003**, *13*, 1920.
108. Skaff, H.; Ilker, M. F.; Coughlin, E. B.; Emrick, T. *J. Am. Chem. Soc.* **2002**, *124*, 5729.
109. Itsuno, S.; Uchikoshi, K.; Ito, K. *J. Am. Chem. Soc.* **1990**, *112*, 8187.
110. Yoon, K. B.; Kochi, J. K. *J. Chem. Soc. Chem. Commun* **1987**, 1013.
111. Batler, J. H.; Spina, K. P. *Synth. Commun.* **1984**, *14*, 14.
112. Barrett, A. G. M.; Cramp, S. M.; Roberts, R. S. *Org. Lett.* **1999**, *1*, 1083.
113. Barrett, A. G. M.; Hopkins, B. T.; Köbberling, J. *Chem. Rev.* **2002**, *102*, 3301.
114. Barrett, A. G.; Cramp, S. M.; Roberts, R. S.; Zecri, F. J. *Org. Lett.* **1999**, *1*, 579.
115. Arnauld, T.; Barrett, A. G. M.; Cramp, S. M.; *et al. Org. Lett.* **2000**, *2*, 2663.
116. Arnauld, T.; Barrett, A. G. M.; Seifried, R. *Tetrahedron Lett.* **2001**, *42*, 7899.
117. Arnauld, T.; Barrett, A. G. M.; Hopkins, B. T. *Tetrahedron Lett.* **2002**, *43*, 1081.
118. Buchmeiser, M. R.; Atzl, N.; Bonn, G. K. *J. Am. Chem. Soc.* **1997**, *119*, 9166.
119. Buchmeiser, M. R.; Bonn, G. K. *Am. Lab.* **1998**, *11*, 16.
120. Årstad, E.; Barrett, A. G. M.; Hopkins, B. T.; Köbberling, J. *Org. Lett.* **2002**, *4*, 1975.
121. Barrett, A. G. M.; Hopkins, B. T.; Love, A. C.; Tedeschi, L. *Org. Lett.* **2004**, *6*, 833.
122. Fuchter, M. J.; Vesper, B. J.; Murphy, K. A.; *et al. J. Org. Chem.* **2005**, *70*, 2793.
123. Fuchter, M. J.; Hoffman, B. M.; Barrett, A. G. M. *J. Org. Chem.* **2005**, *70*, 5086.
124. Fuchter, M. J.; Hoffman, B. M.; Barrett, A. G. M. *J. Org. Chem.* **2006**, *71*, 724.
125. Kröll, R. M.; Schuler, N.; Lubbad, S.; Buchmeiser, M. R. *Chem. Commun.* **2003**, 2742.
126. Hultzsch, K. C.; Jernelius, J. A.; Hoveyda, A. H.; Schrock, R. R. *Angew. Chem.* **2002**, *114*, 609.
127. Dolman, S. J.; Hultzsch, K. C.; Pezet, F.; *et al. J. Am. Chem. Soc.* **2004**, *126*, 10945.
128. Stille, J. K.; Frey, D. A. *J. Am. Chem. Soc.* **1959**, *81*, 4273.
129. Buchmeiser, M. R.; Mupa, M.; Seeber, G.; Bonn, G. K. *Chem. Mater.* **1999**, *11*, 1533.
130. Kolla, P.; Köhler, J.; Schomburg, G. *Chromatographia* **1987**, *23*, 465.
131. Hanson, M.; Unger, K. K.; Schomburg, G. *J. Chromatogr.* **1990**, *517*, 269.
132. Dunlap, C. J.; Carr, P. W. *J. Liq. Chromatogr. Relat. Technol.* **1996**, *19*, 2059.
133. Nasal, A.; Haber, P.; Kaliszan, R.; *et al. Chromatographia* **1996**, *43*, 484.
134. Anazawa, T. A.; Jardim, C. S. F. *J. Liq. Chromatogr. Relat. Technol.* **1998**, *21*, 645.
135. Kobayashi, S.; Tanaka, I.; Shirota, O.; *et al. J. Chromatogr. A* **1998**, *828*, 75.
136. Machida, Y.; Nishi, H.; Nakamura, K. *J. Chromatogr. A* **1999**, *830*, 311.
137. Crini, G.; Morcellet, M.; Torri, G. *J. Chromatogr. Sci.* **1996**, *34*, 477.
138. Thuaud, N.; Leliévre, G.; Deratani, A.; Sebille, B. *Eur. Polym. J.*, **1987**, *33*, 1015.
139. Cassidy, R. M.; Elchuk, S. *Anal. Chem.* **1982**, *54*, 1558.
140. Buchmeiser, M. R. *J. Chromatogr. A* **2001**, *918/2*, 233.
141. Chambers, S. D.; Glenn, K. M.; Lucy, C. A. *J. Sep. Sci.* **2007**, *30*, 1628.
142. Hanai, T. *J. Chromatogr. A* **2003**, *989*, 183.
143. Kurganov, A.; Kuzmenko, O.; Davankov, V. A.; *et al. J. Chromatogr.* **1990**, *506*, 391.
144. Engelhardt, H.; Löw, H.; Götzinger, W. *J. Chromatogr.* **1991**, *554*, 371.
145. Huck, C. W.; Buchmeiser, M. R.; Bonn, G. K. *J. Chromatogr. A* **2001**, *941*, 33.
146. Buchmeiser, M. R.; Tessadri, R.; Seeber, G.; Bonn, G. K. *Anal. Chem.* **1998**, *70*, 2130.
147. Buchmeiser, M. R.; Tessadri, R., Bonn, G. K. *Austrian Pat. Appl.*, A 1132/97 (020797).
148. Seeber, G.; Brunner, P.; Buchmeiser, M. R.; Bonn, G. K. *J. Chromatogr. A* **1999**, *848*, 193.
149. Glatz, I.; Mayr, M.; Hoogenboom, R.; *et al. J. Chromatogr. A* **2003**, *1015*, 65.
150. Caster, K. C.; Walls, R. D. *Adv. Synth. Catal.* **2002**, *344*, 764.
151. Klavetter, F. L.; Grubbs, R. H. *J. Am. Chem. Soc.* **1988**, *110*, 7807.
152. Afeyan, N. B.; Gordon, N. F.; Mazsaroff, I.; *et al. J. Chromatogr.* **1990**, *519*, 1.
153. Afeyan, N. B.; Fulton, S. P.; Regnier, F. E. *J. Chromatogr.* **1991**, *544*, 267.
154. Kubín, M.; Špaček, P.; Chromeček, R. *Collect. Czech. Chem. Commun.* **1967**, *32*, 3881.
155. Hansen, L. C.; Sievers, R. E. *J. Chromatogr.* **1974**, *99*, 123.
156. Hosoya, K.; Ohta, H.; Yoshizoka, K.; *et al. J. Chromatogr. A* **1999**, *853*, 11.
157. Maruska, A.; Ericson, C.; Végvári, A.; Hjertén, S. *J. Chromatogr. A* **1999**, *837*, 25.
158. Gusev, I.; Huang, X.; Horváth, C. *J. Chromatogr. A* **1999**, *855*, 273.
159. Tang, Q.; Xin, B.; Lee, M. L. *J. Chromatogr. A* **1999**, *837*, 35.
160. Xie, S.; Švec, F.; Fréchet, J. M. J. *Chem. Mater.* **1998**, *10*, 4072.
161. Gerstner, J. A.; Hamilton, R.; Cramer, S. M. *J. Chromatogr.* **1992**, *596*, 173.
162. Tanaka, N.; Nagayama, H.; Kobayashi, H.; *et al. J. High Resolut. Chromatogr.* **2000**, *23*, 111.
163. Tanaka, N.; Kobayashi, H.; Ishizuka, N.; *et al. J. Chromatogr. A* **2002**, *965*, 35.
164. Rabel, F.; Cabrera, K.; Lubda, D. *Int. Lab.* **2001**, *01/02*, 23.
165. Cabrera, K.; Lubda, D.; Eggenweiler, H.-M.; *et al. J. High Resolut. Chromatogr.* **2000**, *23*, 93.
166. Sinner, F.; Buchmeiser, M. R. *Macromolecules* **2000**, *33*, 5777.
167. Sinner, F.; Buchmeiser, M. R. *Angew. Chem.* **2000**, *112*, 1491.
168. Mayr, B.; Tessadri, R.; Post, E.; Buchmeiser, M. R. *Anal. Chem.* **2001**, *73*, 4071.
169. Mayr, M.; Mayr, B.; Buchmeiser, M. R. *Angew. Chem.* **2001**, *113*, 3957.
170. Mayr, B.; Hölzl, G.; Eder, K.; *et al. Anal. Chem.* **2002**, *74*, 6080.
171. Lubbad, S.; Mayr, B.; Huber, C. G.; Buchmeiser, M. R. *J. Chromatogr. A* **2002**, *959*, 121.
172. Lubbad, S.; Buchmeiser, M. R. *Macromol. Rapid Commun.* **2002**, *23*, 617.
173. Buchmeiser, M.R.; Sinner, F. Eur. Pat. Appl. 409 095 (A 960/99, 310599), PCT/EP00/04 768, WO 00/73782 A1, EP 1 190244 B1.
174. Buchmeiser, M. R. *Macromol. Rapid. Commun.* **2001**, *22*, 1081.
175. Buchmeiser, M. R. *J. Mol. Catal. A: Chem.* **2002**, *190*, 145.
176. Buchmeiser, M. R.*Rigid Polymers Prepared by Ring-Opening Metathesis Polymerization*; Elsevier: Amsterdam, 2003.
177. Lubbad, S.; Mayr, B.; Mayr, M.; Buchmeiser, M. R. *Macromol. Symp.* **2004**, *210*, 1.
178. Löber, A.; Verch, A.; Schlemmer, B.; *et al. Angew. Chem.* **2008**, *120*, 9279.
179. Löber, A.; Scheibitz, B.; Frerich, B.; Buchmeiser, M. R. *Macromol. Symp.* **2010**, *293*, 48.
180. Buchmeiser, M. R. *J. Polym. Sci., Part A: Polym. Chem.* **2009**, *27*, 2219.
181. Ertl, G.; Knözinger, H.; Weitkamp, J. *Preparation of Solid Catalysts*; Wiley-VCH: Weinheim, 1999.
182. Peters, E. C.; Švec, F.; Fréchet, J. M. J. *Adv. Mater.* **1999**, *11*, 1169.
183. Buchmeiser, M. R. *Angew. Chem.* **2001**, *113*, 3911.
184. Rodrigues, A. E. *J. Chromatogr. B* **1997**, *699*, 47.
185. Xu, Y.; Liapis, A. I. *J. Chromatogr. A* **1996**, *724*, 13.
186. Sýkora, D.; Švec, F.; Fréchet, J. M. J. *J. Chromatogr. A* **1999**, *852*, 297.
187. Viklund, C.; Pontén, E.; Glad, B.; *et al. Chem. Mater.* **1997**, *9*, 463.
188. Viklund, C.; Švec, F.; Fréchet, J. M. J.; Irgum, K. *Chem. Mater.* **1996**, *8*, 744.

189. Wang, Q. C.; Švec, F.; Fréchet, J. M. J. *Anal. Chem.* **1993**, *65*, 2243.
190. Buchmeiser, M. R. *Polymer* **2007**, *48*, 2187.
191. Tennikova, B.; Deyl, Z., Švec, F.*Monolithic Materials: Preparation, Properties and Application, J. Chromatogr. Libr.* Elsevier: Amsterdam, 2001.
192. Halász, I.; Martin, K.. *Ber. Bunsenges. Phys. Chem.* **1975**, *79*, 731.
193. Halász, I.; Martin, K. *Angew. Chem.* **1978**, *90*, 954.
194. Leon y Leon, C. A.; Thomas, M. A. *GIT Lab. J.* **1997**, *2*, 101.
195. Schrock, R. R. *J. Chem. Soc., Dalton Trans.* **2001**, 2541.
196. Scheibitz, B.; Prager, A.; Buchmeiser, M. R. *Macromolecules* **2009**, *42*, 3493.
197. Buchmeiser, M. R. *New. J. Chem.* **2004**, *28*, 549.
198. Buchmeiser, M. R., Ed. *Metathesis-Based Polymers for Organic Synthesis and Catalysis*; Wiley-VCH: Weinheim, 2003.
199. Buchmeiser, M. R. In *Metathesis Polymerization From and To Surfaces*; Buchmeiser, M. R., Ed.; Springer: Berlin; Heidelberg; New York, 2005.
200. Love, J. A.; Morgan, J. P.; Trnka, T. M.; Grubbs, R. H. *Angew. Chem.* **2002**, *114*,4207.
201. Bandari, R.; Prager-Duschke, A.; Kühnel, C.; *et al. Macromolecules* **2006**, *39*, 5222.
202. Gatschelhofer, C.; Magnes, C.; Pieber, T. R.; *et al. J. Chromatogr. A* **2005**, *1090*, 81.
203. Schlemmer, B.; Gatschelhofer, G.; Pieber, T. R.; *et al. J. Chromatogr. A* **2006**, *1132*, 124.
204. Sinner, F. M.; Gatschelhofer, C.; Mautner, A.; *et al. J. Chromatogr. A* **2008**, *1191*, 274.
205. Sedláková, P.; Miksik, I.; Gatschelhofer, C.; *et al. Electrophoresis* **2007**, *28*, 2219.
206. Szwarc, M. *Makromol. Chem., Rapid Commun.* **1992**, *13*, 141.
207. Penczek, S.; Kubisa, P.; Szymanski, R. *Makromol. Chem., Rapid Commun.* **1991**, *12*, 77.
208. Johnson, A. F.; Mohsin, M. A.; Meszena, Z. G.; Graves-Morris, P. *J. Macromol. Sci. Rev. Macromol. Chem. Phys.* **1999**, *C39*, 527.
209. Szwarc, M. *J. Polym. Sci. A Polym. Chem.* **1998**, *36*, ix.
210. Webster, O. W. *Science* **1991**, *251*, 887.
211. Lubbad, S.; Buchmeiser, M. R. *Macromol. Rapid Commun.* **2003**, *24*, 580.
212. Deleuze, H.; Faivrea, R.; Herroguez, V. *Chem. Commun.* **2002**, 2822.
213. Eder, K. *Macromol. Rapid Commun.* **2007**, *28*, 2029.
214. Gatschelhofer, C.; Mautner, A.; Reiter, F.; *et al. J. Chromatogr. A* **2009**, *1216*, 2651.
215. Lubbad, S. H.; Buchmeiser, M. R. *J. Chromatogr. A* **2011**, *1218*, 2362.
216. Bandari, R.; Knolle, W.; Prager-Duschke, A.; Buchmeiser, M. R. *Macromol. Chem. Phys.* **2007**, *208*, 1428.
217. Bandari, R.; Knolle, W.; Buchmeiser, M. R. *Macromol. Symp.* **2007**, *254*, 87.
218. Bandari, R.; Elsner, C.; Knolle, W.; *et al. J. Sep. Sci.* **2007**, *30*, 2821.
219. Bandari, R.; Knolle, W.; Buchmeiser, M. R. *J. Chromatogr. A.* **2008**, *1191*, 268.
220. Bandari, R.; Knolle, W.; Buchmeiser, M. R. *Macromol. Rapid Commun.* **2007**, *28*, 2090.
221. Nandakumar, M. P.; Pålsson, E.; Gustavsson, P.-E.; *et al. Bioseparation* **2001**, *9*, 193.
222. Scholl, M.; Trnka, T. M.; Morgan, J. P.; Grubbs, R. H. *Tetrahedron Lett.* **1999**, *40*, 2247.
223. Scholl, M.; Ding, S.; Lee, C. W.; Grubbs, R. H. *Org. Lett.* **1999**, *1*, 953.
224. Mayr, M.; Mayr, B.; Buchmeiser, M. R. *Des. Monomers Polym.* **2002**, *5*, 325.
225. Mayr, M.; Mayr, B.; Buchmeiser, M. R. In *Studies in Surface Science and Catalysis: Scientific Bases for the Preparation of Heterogeneous Catalysts*; Gaigneaux, E., DeVos, D.E., Grange, P., *et al.*, Eds.; Elsevier: Amsterdam, 2002; p 305.
226. Buchmeiser, M. R. *Bioorg. Med. Chem. Lett.* **2002**, *12*, 1837.
227. Mayr, M.; Wang, D.; Kröll, R.; *et al. Adv. Synth. Catal.* **2005**, *347*, 484.
228. Buchmeiser, M. R.; Wurst, K. *J. Am. Chem. Soc.* **1999**, *121*, 11101.
229. Bandari, R.; Höche, T.; Prager, A.; *et al. Chem. Eur. J.* **2010**, *16*, 4650.
230. Lubbad, S.; Steiner, S. A.; Fritz, J. S.; Buchmeiser, M. R. *J. Chromatogr. A* **2006**, *1109*, 86.
231. Buchmeiser, M. R. In *NATO Science for Peace and Security Series A. Chemistry and Biology;* Khosravi, E., Yagci, Y., Savelyev, Y., Eds.; Kluwer: Dordrecht,2009.
232. Weichelt, F.; Frerich, B.; Lenz, S.; *et al. Macromol. Rapid Commun.* **2010**, *31*, 1540.

Biographical Sketch

Prof. Dr. Michael R. Buchmeiser is chair of Macromolecular Compounds and Fiber Chemistry in the Institute of Polymer Chemistry at Universität Stuttgart.

His research topics include the following:

- New catalysts for metathesis polymerization (ROMP, cyclopolymerization) of functional monomers. Catalysts for photopolymerization (ROMP, polyaddition, polycondensation)
- Catalytic olefin polymerization, synthesis of functional hybrid polymers by switchable transition-metal-based polymerization systems
- Surface-modification of meso- and macroporous supports, surface immobilization of organometallic catalysts, application in heterogeneous catalysis
- Synthesis of functional (monolithic) separation and support materials for the analysis of biologically and medically relevant compounds (DNA, proteins, oligonucleotides) and for the downstream processing
- Precursor polymers for carbon fibers, carbon fiber fabrication
- Fabrication of high-performance fibers
- Fibers for special applications (high modulus fibers, elastomeric fibers, carbon fibers, high temperature-resistant ceramic fibers)
- Chemical modification of natural and synthetic fibers.

Curriculum Vitae

Michael R. Buchmeiser received his PhD in inorganic chemistry in 1993 from the University of Innsbruck, Austria. He was then awarded an 'Erwin Schrödinger Fellowship' and spent 1 year at the Massachusetts Institute of Technology (MIT, Cambridge, MA) within the group of Professor Richard R. Schrock. In 1995, he accepted a position as an assistant professor at the University of Innsbruck where he finished his 'Habilitation' in macromolecular chemistry in 1998. From 1998 to 2004, he held a faculty position as associate professor. He was then offered faculty positions (full professor of polymer chemistry) at the Universities of Halle (Germany, 2004), Leoben (Austria, 2005), and Dresden (Germany, 2007), all of which he declined. Instead, in 2004, he accepted a faculty position (C-4 Professorship) at the University of Leipzig, Germany. In addition, from 2005 to 2009, he was vice director and member of board at the Leibniz Institute of Surface Modification, Leipzig, Germany. Since 2009 he has held a faculty position (full professor and chair of polymer chemistry) at the University of Stuttgart (Germany) and also serves as director of the Institute of Textile Chemistry and Artificial Fibers, Denkendorf. He received the '1998 Professor Ernst Brandl Research Award', the 'START Award-2001', the 'Novartis Award 2001', and the 'Otto-Roelen Medal' (2010).

4.24 Chain Extension by Ring Opening

TJA Loontjens, University of Groningen, Groningen, The Netherlands
EJ Goethals, Ghent University, Gent, Belgium

4.24.1 General

About 50 million tons of polyesters[1] and 7 million tons of polyamides[2] are produced worldwide annually. Although recycling of used plastic has become mandatory for environmental reasons, practically, it is still a challenge.[3] Successful reuse of plastics depends heavily on a well-organized waste management system. Of all plastics, the waste logistics of polyesters is the best organized. About 50% of all PET bottles are collected for reuse in the EU.[4]

A major problem of reusing polycondensates is their degradation (hydrolysis) during use and reprocessing, resulting in materials with inferior properties with respect to the virgin materials. In order to compete with virgin feedstocks, the molecular weight has to be restored to its original level. This is currently done in a solid-state postcondensation (SSP) process. To accomplish this, the granulate is heated for 20–50 h at 200 °C under vacuum in the solid state. This is obviously an expensive process preventing a massive reuse of polyester and polyamide waste.

In a chain extension reaction, the polymer end groups are coupled in a similar statistical way as during a polycondensation process. The difference with the (solid-state) postcondensation process is that the chain extenders couple the polymer end groups within minutes, instead of in hours. Chain extension is, therefore, a promising alternative, provided that it can be done during an existing compounding step, in order to avoid an additional processing step. Additionally, the chemistry should proceed unambiguously and be well controlled. Polyesters and polyamides possess hydroxyl, amino, and carboxylic end groups, which are useful linking units. The challenge is to design harmless chain extenders that react rapidly with these end groups without side reactions (e.g., branching) and without releasing harmful reaction products.

It is virtually unavoidable that coupling units will be incorporated into the polymer backbone. Nevertheless, no measurable influence on the properties is expected since the incorporated amounts of 'comonomers' are small (< 1 wt.%).

Chain extenders can be classified into two main groups. In one class the coupling proceeds with, and in the other class without, the release of a low molecular weight compound. Here, we will discuss the first class of compounds only briefly, whereas the focus will be on coupling agents without releasing volatiles. It appears that the latter is achievable via ring-opening reactions.

4.24.2 Chain Extension

The residence time during an extrusion step to produce end products is in the order of 1 min at temperatures of 250–300 °C. As a consequence, chain extenders should be quite reactive to accomplish the coupling within this short period of time. On the other hand, they have to be thermally stable to withstand these high temperatures. Chain extension of polycondensates like PET can also be done at lower temperatures, but then it has to be accomplished in the solid state (SSP)[5] due to the high melting point (255 °C). As a consequence, an additional processing step will be required.

Polyesters and polyamides have variable amounts of hydroxy, amine, or carboxylic end groups. Consequently, the chain extenders have to match with the type as well as with the concentrations of these end groups. In **Scheme 1**, an example is given of a chain extension reaction via carboxylic end groups of polyesters, which will not affect the concentration of the hydroxy groups.

In that case, the increase of the molecular weight will depend only on the concentration of the carboxylic end groups. This is of course a limitation, but in most cases a moderate increase of the number-average molecular weight from 15 000 to 20 000 Da is sufficient to restore the original material properties. The M_n of commodity polycondensates is approximately 20 000 Da. Synthesis of higher molecular weight polycondensates is technically not very feasible in existing commercial polycondensation equipments, due to viscosity limitations. If higher molecular weights are desired ($M_n > 20\,000$ Da), two types of chain extenders can be used (vide infra). Chain extension could therefore also be a useful alternative for making high-duty polycondensates.

Finally, the possibility to connect chains of two different polymers by this chain extension mechanism can also be applied to make block copolymers.

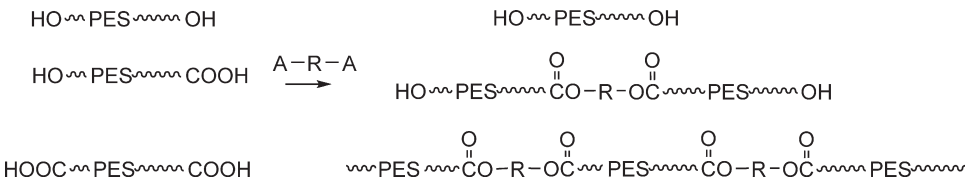

Scheme 1 General scheme of chain extension of polyesters with a chain extender that reacts only with acid end groups.

4.24.3 Diepoxides

Compounds containing two or more epoxy functions are well known as constituents of epoxy resins. Hence, a large number of diepoxides are commercially available. Figure 1 gives an overview of the most common ones.

The general procedure to prepare glycidyl compounds is from alcohols, phenols, or acids and epichlorohydrin. The reaction with bisphenol A, leading to diepoxide 5, is depicted in Scheme 2.

Most of these compounds have a low volatility which makes them suitable for coupling reactions in the melt. The highly reactive epoxy group reacts with a variety of functional groups: carboxylic acids, alcohols, amines, and so on. Many of the commercial compounds are glycidyl derivatives wherein the two epoxy groups are connected to a central unit. With these epoxides, ring opening can occur in two ways: attack either on the methylene carbon (α-position), producing a secondary alcohol, or on the methine carbon (β-position), producing a primary alcohol (Scheme 3). Generally the α-opening is the dominant reaction, but β-opening can happen in up to 20%.

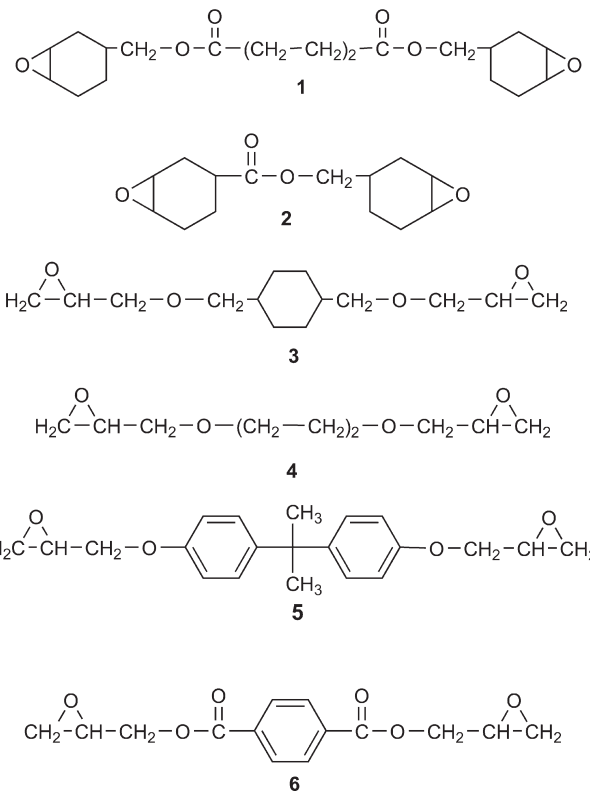

Figure 1 Examples of commercial diepoxides.

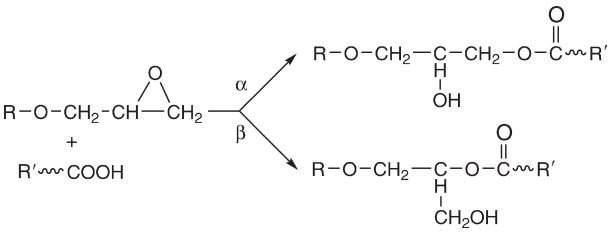

Scheme 3 Ring opening of glycidyl ether by carboxyl function.

The reaction of a diepoxide with a carboxylic acid-terminated polymer will, therefore, result in a coupling of two chains. This method has been proposed in a patent[6] as early as 1971. In the late 1990s, a comparative study of chain extension of PET by means of several commercial diepoxides has been reported.[7,8] The reactions were carried out at 270 °C for different periods of time. The diepoxides 1 and 2 of Figure 1, comprising aliphatic cyclohexyl moieties, gave chain extension reaction as evidenced by the increase in intrinsic viscosities and substantial decrease of carboxyl content of the end products. With the diglycidyl ether types (3, 4, and 5), however, decreased viscosity values, increased carboxyl content, and lower melting points were observed.

The negative results obtained with the glycidyl compounds were confirmed by another group.[9] The positive results described above for one of the diepoxides, comprising aliphatic cyclohexyl moieties, were partially confirmed: the molecular weight of the processed PET was increased but the value of the untreated original product was not attained. It is not clear why epoxy compounds comprising cyclohexyl moieties are more effective. One can speculate that the reverse reaction is sterically more hindered than with linear glycidyl moieties.

The chain extension reaction in poly(butylene terephthalate) (PBT) melt with diglycidyl tetrahydrophthalate has been reported in detail.[10] This chain extender was found to react with the hydroxyl and carboxyl end groups of PBT at a high reaction rate and relatively high temperature. The reaction time decreased with increasing temperature and above 250 °C, the

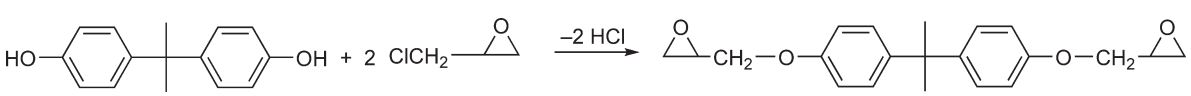

Scheme 2 Preparation of diepoxide of bisphenol A and epichlorohydrin.

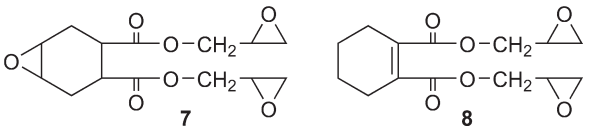

Figure 2 Epoxides used as chain extenders for PA1010.[11]

chain extension reaction could be completed within 2–3 min. Shear rate had some effect on the reaction rate, which might be due to improved mixing. The melt flow index of the chain-extended PBT dramatically decreased (from 35 to 3 g in 10 min) and the impact strength and elongation-at-break increased. The chain-extended PBT appeared to be more thermally stable than the virgin product. Compared with the conventional solid post-polycondensation method, this approach is reported to be simpler and cheaper to obtain high molecular weight PBT resins.

The chain extension of polyamide PA1010 with two diepoxides (Figure 2)[11] has been reported. The reactions were carried out at 240 °C and were monitored by viscosity using a Haacke viscosimeter. The results indicated that with epoxide 7 a higher torque (= viscosity) was obtained than with epoxide 8, although both increase dramatically the melt viscosity within several minutes. Here, the glycidyl groups are effective, which might be due to the lower reaction temperature (coupled product is thermodynamically more favorable at lower temperatures).

As compound 7 is trifunctional, it will lead to branched and ultimately to cross-linked products. This is sometimes beneficial, but mostly undesired.

Recently, unsaturated (oligomeric) polyesters (UPE) of molecular weights in the range of 500–700 Da have been chain-extended at temperatures between 130 and 160 °C using di- or multifunctional epoxy compounds.[12] The extenders were bisphenol A diglycidyl ether (5 in Figure 1), 1,2,7,8-diepoxyoctane, and epoxidized soybean oil. Different weight ratios were tried and solubilities, gel times, and mechanical and thermal properties of the chain-extended polyesters were examined. The study showed that di- or multifunctional epoxy compounds are effective chain extenders for UPEs. The molecular weights of the chain-extended polymers were in the same range as commercial UPEs. The use of these extenders decreases the production time and, as a result, increases the yield of polyesters equipment, without compromising its solubility in styrene or the mechanical and thermal properties of the final cured UPE–styrene materials. As viscosity limits do not impose any restriction on these low molecular weight UPEs, chain extension was carried out in a common polyester reactor and proceeds without formation of by-products. The diol loss due to evaporation, which is often encountered in the late stages of commercial UPE manufacture, is also eliminated.

In order to produce modified PET resins with improved rheology for applications requiring high viscosity and elasticity, a novel diimidodiepoxide (9, see Figure 3) was evaluated as chain extension agent.[13] Its reactivity was compared with that of an ethylene/glycidyl methacrylate copolymer. The diepoxide showed a higher reactivity than the copolymer and could be used at much lower concentrations. The complex chain extension/degradation reactions occurring in the melt were followed in a batch mixer. The preliminary results indicated an overall decrease in carboxyl content and increase in hydroxyl content, intrinsic viscosity, melt viscosity, and storage modulus depending on mixing time and type and concentration of the additives.

4.24.4 Cyclic Imino Ethers

All cyclic 1,3-oxaza compounds, depicted in Figure 4, are able to give ring-opening reactions and are, as a consequence, in potential all chain extender moieties. Despite all these options, only bisoxazines (1), bisoxazolines (2), and bisoxazolinones (3) are frequently described as chain extenders.

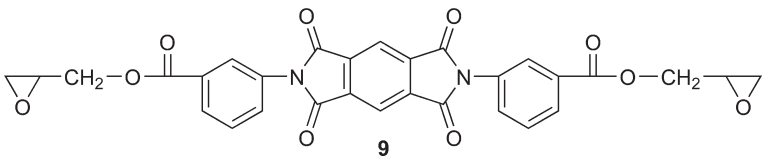

Figure 3 Structure of diimidodiepoxide used as chain extender of PET.[13]

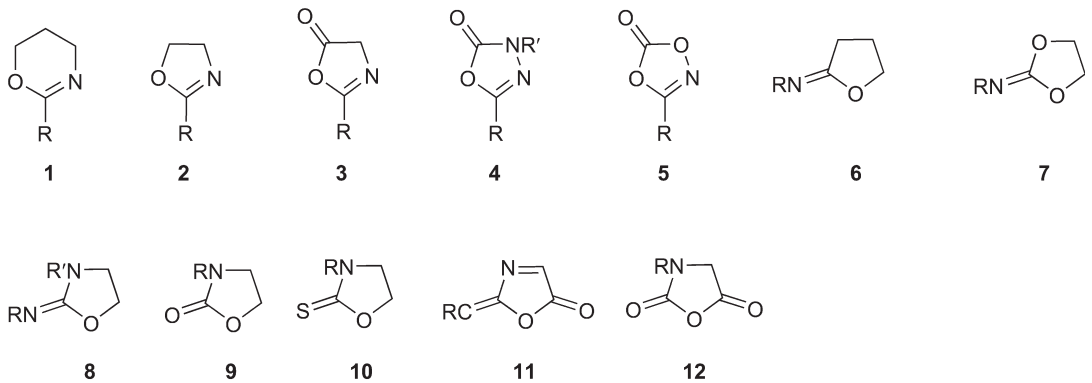

Figure 4 Cyclic 1,3-oxaza compounds[14] as potential chain extension moieties (depicts only half of the compounds).

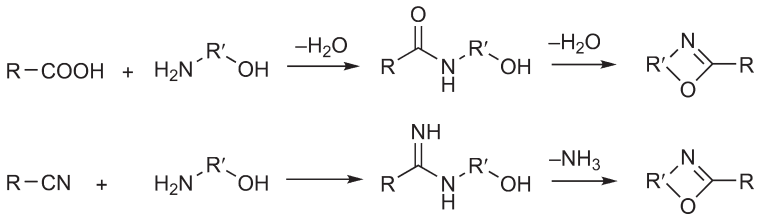

Scheme 4 Preparation of cyclic imino ethers from acids or nitriles (R′ = $(CH_2)_n$, n = 2–4).

Bisoxazolinones will be discussed in Section 4.24.6, whereas the bisoxazolines and bisoxazines will be discussed here.

After the pioneering work of Inata[15] in the late 1980s, particularly bisoxazolines were considered as the most promising compounds to increase molecular weights.

Oxazolines and oxazines are easily prepared from amino alcohols and carboxylic acids or nitriles, as was shown in an early work of Witte and Seeliger[16] (Scheme 4).

The synthetic route via nitriles is generally preferred as the reaction proceeds in high yields in a one-step procedure. The reaction between acids and hydroxy alkyl amines is rather slow. But, the preparation of the hydroxy alkyl amides proceeds fast and in high yields if acid chlorides are used instead of acids. Nevertheless, (di)acids are interesting starting materials due to their abundant availability.

Ring-opening reactions proceed after activation of the ring either by alkylation or by protonation of nitrogen, followed by a nucleophilic attack on the C5 carbon, as depicted in Scheme 5[17] for oxazolines. The driving force of the reaction is not so much to relieve ring strain but rather the isomerization of the iminoether structure into an amide.

Compounds for which the Brønsted acidity is high enough to protonate oxazolines and for which the corresponding anion is a suitable nucleophile to attack the C5 carbon can couple via a ring-opening reaction. Carboxylic acids fulfill these requirements and thus polyester or polyamide acid end groups will react with bisoxazolines or bisoxazines (Scheme 6).

Bisoxazoline chain extenders are most frequently reported, particularly in patents.[18] The reaction of carboxylic acid functional polymers with bisoxazolines proceeds well at temperatures up to about 200 °C.

Stanssens *et al.*[19] and others[20] have shown that the reaction between oxazolines and carboxylic acids is reversible. At higher temperatures, the equilibrium shifts, for entropic reasons, toward the starting products, limiting the efficacy of bisoxazolines at the processing temperature of most polycondensates (> 200 °C). It was shown that at temperatures[36] above 200 °C bisoxazines are more effective. This can be explained by the fact that unsaturated five-membered rings are more stable than the corresponding six-membered rings.

Inata and Matsumura[15] showed that 2,2′-bis(2-oxazoline) (BOZ), which is less inclined to give the reversed reaction, is the most effective oxazoline chain extender for PET. It can be used at high temperature, provided that PET is properly dried (BOZ is susceptible to hydrolysis). Intrinsic viscosities [η] ranging from 0.66 to 1.06 dl g^{-1} were obtained at 280 °C with up to 0.5 wt.% of BOZ. The melting temperature (T_m) decreased maximally from 255 to 248 °C. However, this is mainly due to the increase of the molecular weight, which results in a lower T_m. Figure 5 shows the relation between T_m and the intrinsic viscosity of pure PET and chain-extended PET. It can be estimated that the decrease of T_m due to chain extension is less than 2 °C.

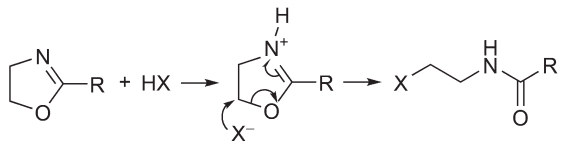

Scheme 5 Ring-opening reaction of an oxazoline by a compound comprising a dissociable proton.

4.24.5 Cyclic Anhydrides

Hydroxyl and amino groups react rapidly with anhydrides, forming esters or amides, respectively, with release of an acid. Cyclic anhydrides react similarly, yielding ester- or amide-acids. Accordingly, dicyclic anhydrides can couple two compounds and were, therefore, studied as chain extenders, particularly for polyesters.[21] Some examples of commercially available dicyclic anhydrides are given in Figure 6. Pyromellitic dianhydride (PMDA, 1) is probably the most important member of this group.

Dianhydrides can be prepared in a number of ways, for instance, by a selective oxidation of the corresponding alkyl compounds.[22]

Maleic anhydride copolymers comprise a number of cyclic anhydrides and are used as well.[23] However, these compounds will give branched or even cross-linked polyesters, due to the high functionality, and are outside the scope of this chapter.

Amino end groups of polyamides react with cyclic anhydrides to form the corresponding amide-acids, after which the reaction can continue forming stable imides, as depicted in Scheme 7.

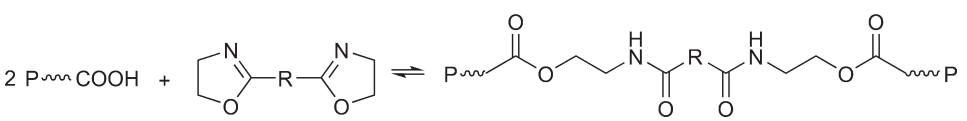

Scheme 6 Coupling of two polymer chains by using bisoxazolines.

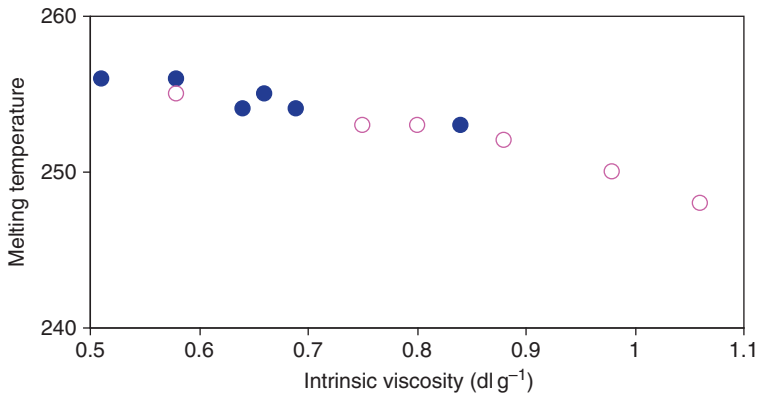

Figure 5 Relation between T_m and the intrinsic viscosity of PET (open circles) and of chain-extended PET (filled circles).[15]

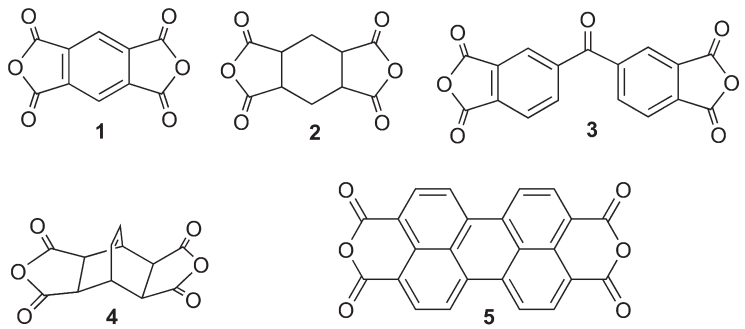

Figure 6 Some commercially available cyclic dianhydrides.

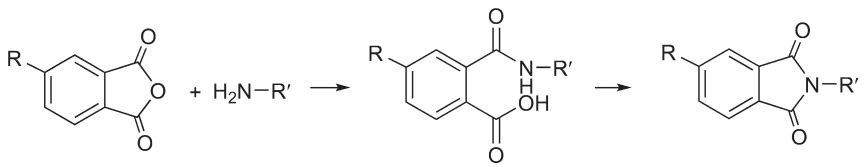

Scheme 7 Two-step reaction of an amine and a cyclic anhydride.

In contrast, the reaction of hydroxyl functional compounds with cyclic anhydrides, which yields ester-acids, is reversible (Scheme 8).[24]

Due to entropic reasons, the equilibrium depicted in Scheme 8 will shift to the left at higher temperatures. As a result, the reaction will not go to completion at processing temperatures of PET (about 300 °C). Nevertheless, high viscosities are obtained with pyromellitic anhydride (**1**, PMDA). Daver *et al.*[25] have studied the rise of the viscosity of PET after reaction with PMDA in detail. The relation between the intrinsic viscosity and the amount of PMDA is given in Figure 7.

The intrinsic viscosity of the starting PET was 0.75 and dropped to 0.67 dl g^{-1} after processing for 45 s. This is a common phenomenon of polyesters due to thermal and hydrolytic degradation. About 0.25 wt.% of PMDA is sufficient to compensate for the viscosity drop. Higher concentrations of PMDA will result in higher viscosities but also in a more pronounced branching and finally in cross-linking, due to the involvement of the acid groups. The acid side groups react via transesterification reactions. Transesterification reactions are rather slow and will consequently continue for a long time. As a result, the viscosity will be dependent on the residence time in the melt, which is generally undesired. Branched polymers are beneficial if high viscoelastic properties are required, for instance, for foams to prevent cell collapse.[26]

During the reaction of polyesters and cyclic dianhydrides, polymers with useless or even undesired acid side groups are formed. These acid groups can cause branching or catalyze hydrolytic degradation. However, one can take advantage of

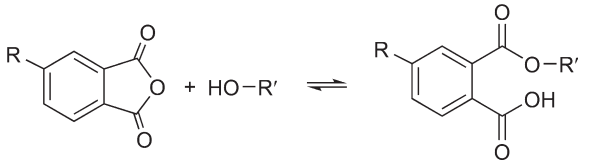

Scheme 8 Reversible reaction between a cyclic anhydride and a hydroxyl comprising compound.

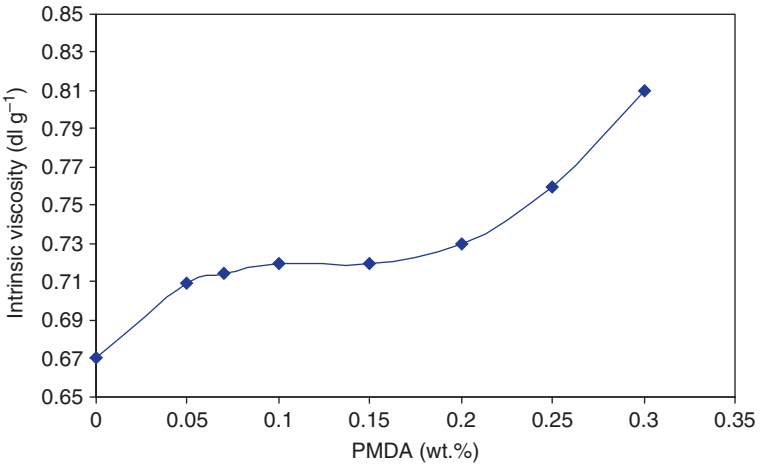

Figure 7 The relation between the intrinsic viscosity of chain-extended PET and the concentration of PMDA.[25]

these acid side groups to couple hereon useful side groups and introduce novel properties.[27,28] In general, however, acid side groups are not desired as linear polymers and processing time-independent viscosities are more preferred.

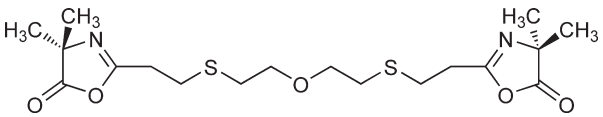

Figure 8 Structure of liquid bisoxazolinone described by Saint-Loup *et al.*[29]

4.24.6 Bisoxazolinones

5-Oxazolinones are five-membered azlactones (in some older publications referred to as oxazolones) that can be obtained from α-amino acids, for example, from α-amino isobutyric acid, and carboxylic acids (**Scheme 9**).

Oxazolinones react with both amino and hydroxyl groups forming amide or ester-amide linkages, respectively. **Scheme 10** shows the ring-opening reaction with an amine.

Bisoxazolinones are, therefore, possible chain extenders for polymers containing such end groups. Bisoxazolinones are preferentially prepared from amino acids and dicarboxylic acid dichlorides following the same route as shown in **Scheme 9**. An alternative method, leading to a liquid bisoxazolinone with structure shown in **Figure 8**, is the free radical di-addition of bis(mercaptoethyl) ether to a 2-ethenyl oxazolinone, as described by Saint-Loup *et al.*[29]

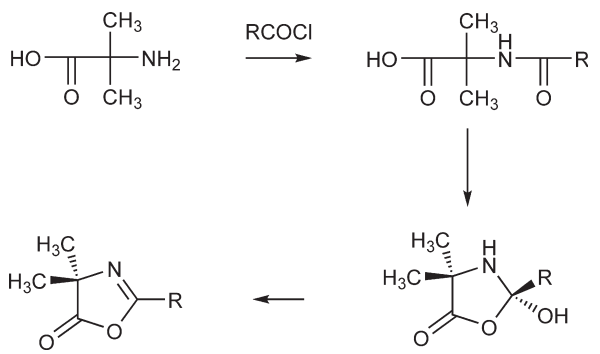

Scheme 9 Synthesis of 5-oxazolinone starting from α-amino acid and carboxylic acid.

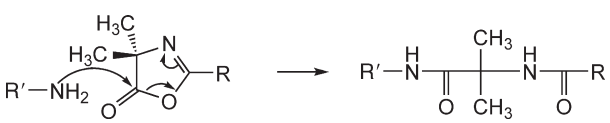

Scheme 10 Reaction of a 5-oxazolinone with an amine.

Acevedo and Fradet investigated the use of two bisoxazolinones, 2,2′-bis(4,4-dimethyl-5(4*H*)-oxazolinone) (**B1**) and 2,2′-(1,2-ethylene)-bis(4,4-dimethyl-5(4*H*)-oxazolinone) (**B2**), as chain extension agents for amine-terminated polyamide 12 of molar mass 1000 Da (**Figure 9**).[30] The coupling reactions were performed in bulk.

With **B2**, the coupling reaction was fast and high molar mass polymers were obtained within 10 min at 185 °C. A consecutive intramolecular side reaction, cyclodehydration of α-aminoisobutyryl moieties leading to imidazolinone cycles in the chains (see **Scheme 11**), has been observed, but the presence of these structures has no unfavorable consequence on the thermal and/or mechanical properties of the end products.

With coupling agent **B1**, side reactions of oxazolinone rings were observed, leading only to low molar mass polymers.

Reactions of polyamide-12 and amine-terminated polyether (Jeffamine ED-900) with the same coupling agents have been applied by the same authors for the synthesis of

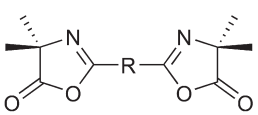

B1 : R= --; **B2** : R= –CH_2–CH_2–

Figure 9 Bisoxazolinones used by Fradet *et al.* for chain extension of amino-terminated polymers.

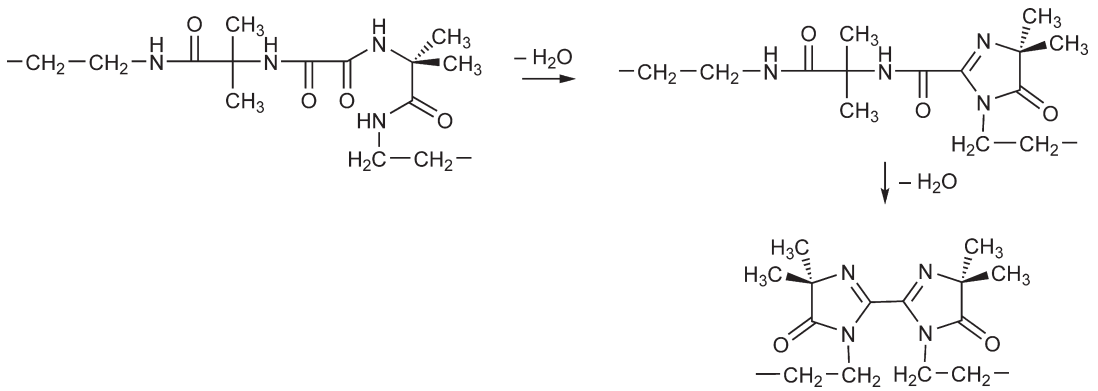

Scheme 11 Formation of imidazolinone groups by cyclodehydration of dipeptide-like moieties formed during amine–oxazolinone chain coupling.

polyether-*block*-polyamides.[31] High molar mass block copolymers were synthesized in bulk within 1 h at 200 °C and under atmospheric pressure, instead of several hours at 240 °C under vacuum for the usual reaction between dicarboxy polyamides and dihydroxy polyethers. No other side reactions than the formation of a small amount of imidazolinones have been found. DSC studies of the block copolymers showed the existence of phase separation between the soft (polyether) and hard (polyamide) blocks.

In their first papers on this topic, the authors stressed the fact that disubstitution at the 4 position of the oxazolinone ring was necessary since, in the presence of a base, a hydrogen atom abstraction at the 4 position was expected to cause the oxazolinone rings to undergo dimerization. Thermal or cationic polymerizations have also been reported for these compounds.

In later publications, however, the same authors reported that the reaction of bis(5(4*H*)oxazolinones) derived from naturally occurring α-amino acids, that is, with at least one hydrogen atom at the 4 position, with amine-terminated polyethers and polyamides in the bulk at 175–200 °C is also possible.[32] Scheme 12 shows the synthesis in which the bisoxazolinones derived from alanine, valine, phenylalanine, and methionine were obtained.

The chain coupling reactions were found to be extremely fast (much faster than with the 4,4-disubstituted reagents) leading from polymers to high molar mass copolymers containing peptide linkages in less than 5 min. Besides the chain extension reactions with polymers, model reactions were carried out using primary alkyl amines. The NMR spectra of model compounds and polymers showed that the oxazolinone/amine addition reaction proceeds in the expected way, without any noticeable side reaction. Owing to its very high rate, this coupling reaction successfully competes with the degradation or polymerization side reactions normally associated with the heating of 4-monosubstituted oxazolinones. The chain-extended polymers exhibit lower crystallinity, higher T_g, and a melting temperature close to or lower than that of the starting oligomers.

In the same line of research, Lefèbvre and Fradet[33] described the bulk chain extension reactions between hydroxy-terminated poly(oxytetramethylene), poly(oxyethylene), or poly(ε-caprolactone) and several bis(4-monosubstituted-5(4*H*)oxazolinones). These polyaddition reactions proceed rapidly and without side reactions in the case of poly(oxytetramethylene) or poly(ε-caprolactone) when a catalytic amount of $Ti(OBu)_4$ is used. The efficiency of the extension was much lower in the case of poly(oxyethylene). This was attributed to the coordination of poly(oxyethylene) oxygen atoms at the active sites of $Ti(OBu)_4$.

High molar mass block copolymers were synthesized by the reaction of mixtures of hydroxy-terminated poly(oxytetramethylene) and poly(ε-caprolactone) with the same bisoxazolinones. Differential scanning calorimetry (DSC) study of the block copolymers revealed phase separation between the two blocks when the starting polymers have M_n of 1000 Da or higher. Lower molar masses of the starting polymers yielded amorphous products.

Block copolymers could also be prepared by the bulk reaction of mixtures of amino-terminated aliphatic polyamides and polyethers using monosubstituted bisoxazolinones.[34] In the same paper, it was reported that the coupling also succeeded for mixtures of hydroxy-terminated polymers and amino-terminated polymers, making this synthetic method applicable to a large range of polymers.

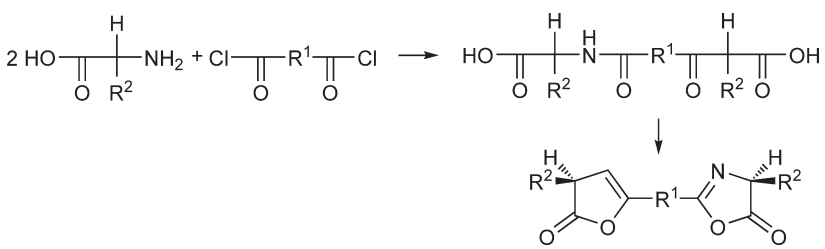

Scheme 12 Synthesis of 4-monosubstituted bisoxazolinones derived from natural α-amino acids.

4.24.7 Coupling with Release of Blocking Groups

Chain extenders that release low molecular compounds during coupling reactions do not fit in this ring-opening chapter. Nevertheless, they are discussed here as they are probably the most developed chain extenders and thus the benchmark. Among all potential chain extenders comprising releasing groups, bislactams are the most important ones, since they do not give side reactions and caprolactam, which is released, is hardly toxic. Hence, here, only bislactams will be discussed.

The most important bislactams are depicted in Figure 10. They are easily prepared in high yields from caprolactam and acid chlorides.

During the coupling reaction with hydroxy or amino functional polymers, bislactams release caprolactam (Scheme 13) that will remain as an inert, low molecular compound in the polymer matrix. Although this is obviously not desired, the amount is rather low as the usually required amount of chain extender is low (< 1 wt.%).

All the bislactams[35] depicted in Figure 10 behave quite similarly and their efficacy as chain extender will therefore be illustrated here with carbonyl biscaprolactam (CBC).[36] Figure 11 shows the increase of the relative viscosity of three commercial PET grades, with different starting viscosities (η_{rel} = 1.56, 1.72, and 1.99 dl g^{-1}, in *m*-cresol, 0.5 dl g^{-1}), after processing with various amounts of CBC. It can be seen that the viscosity increases regularly with the amount of CBC. It is worthwhile to mention that the Mark–Houwink coefficient of PET prepared by the SSP (0.69) was equal to that of the chain-extended product with the same molecular weight (0.68), indicating that no branching reactions took place.

In order to increase the reaction rate with polyesters, Loontjens[36] studied the influence of catalysts in a small-scale extruder (DSM micro-compounder). In Figure 12, it can be seen that the reaction rate is enhanced considerably by adding a titanium catalyst. As a result, the reaction times are now in the range of residence times of commercial extruders.

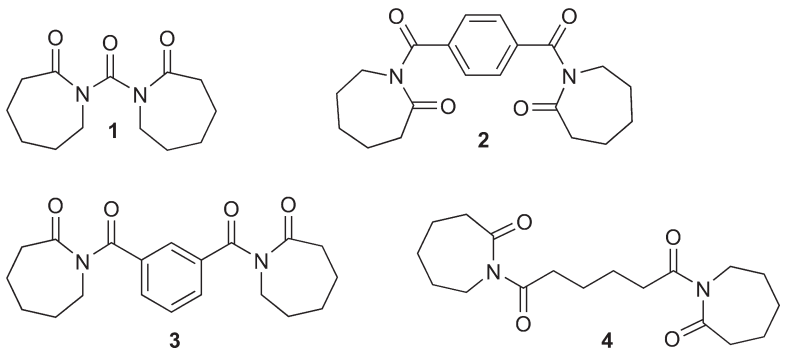

Figure 10 Structure of carbonyl biscaprolactam (**1**, CBC), isophthaloyl biscaprolactam (**2**, IBC), terephthaloyl biscaprolactam (**3**, TBC), and adipoyl biscaprolactam (**4**, ABC).

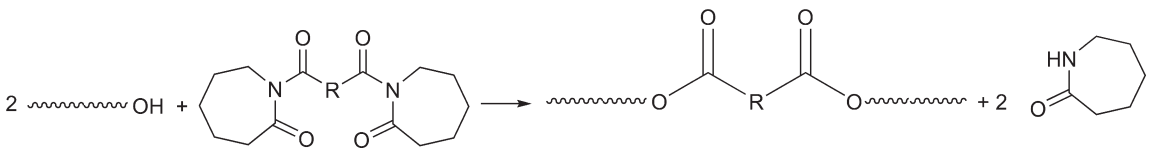

Scheme 13 Chain extension of polyesters with bislactams.

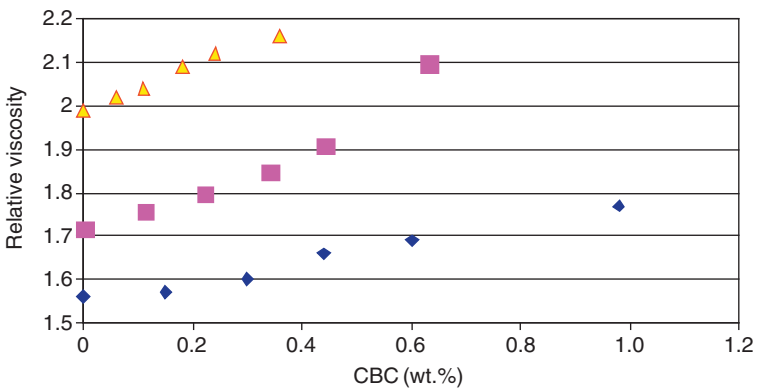

Figure 11 The relative viscosity of PET (in dl g^{-1}, in *m*-cresol) as function of the wt.% CBC.

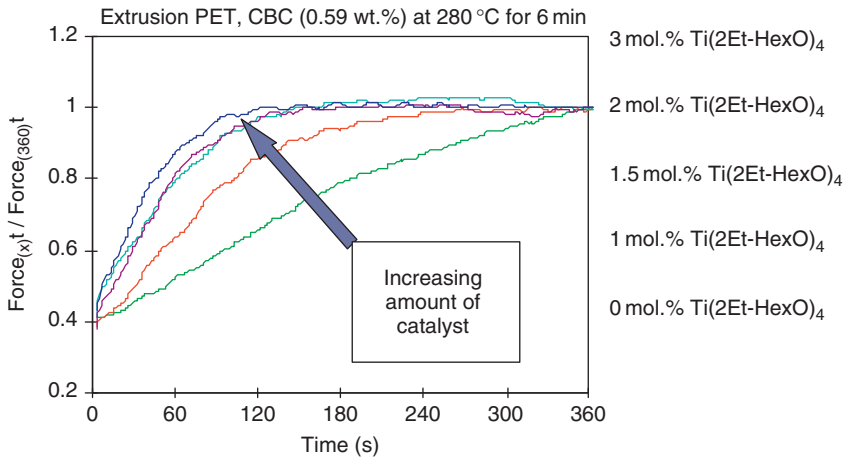

Figure 12 The normalized torque of the micro-compounder during the processing of PET with CBC in the presence of various concentrations of Ti(2Et-HexO)$_4$.

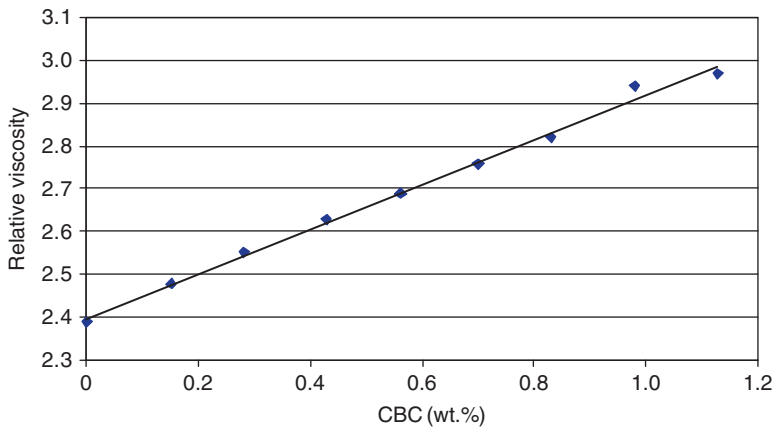

Figure 13 The relation between the relative viscosity (in dl g^{-1}, in formic acid/water 90/10 wt.%/wt.%) of nylon-6 (Akulon K123) and the amount of added CBC, after processing.

As amino groups are more reactive (more nucleophilic) than hydroxy groups, it is expected that the chain extension will be faster with nylons than with polyesters. The same authors showed that in the case of nylon-6 the reaction was almost finished within 45 s, indicating that the reaction with CBC is, indeed, very fast. The viscosity of chain-extended nylon-6 as a function of the amount of CBC used is shown in Figure 13.[36]

A further increase in viscosity is obtainable if, next to bislactams, bisoxazines or bisoxazolines are used that react with the carboxylic end groups, as will be discussed next.

4.24.8 Mixed Systems

With one type of chain extender, the impact on the molecular weight will be limited, since polyesters and polyamides have not only hydroxy or amino end groups but also carboxylic end groups. It seems obvious to use both types of end groups for optimal chain extension. But, hydroxy and amino groups react with acid groups. As a consequence, a chain extender that reacts with acids could react with the complementary chain extender that reacts with hydroxy or amino groups. So, if two chain extenders are used they should be selected in such a way that they react only with hydroxy, amino, and acid end groups, but not with each other. It was shown that the combination of CBC and bisoxazines or bisoxazolines fulfill these requirements. In Figure 14, an example is given of the change of the torque of PET in a micro-compounder in the presence of CBC and phenylene bisoxazoline (PBOX) or phenylene bisoxazine (PBO).[36] It can be seen that the influence on the torque, and thus on the molecular weight, is much more pronounced with two than with one chain extender. Moreover, it is clearly shown that under those conditions PBOX is much more effective than POB.

Böhme *et al.* prepared compounds comprising two different reactive groups in one molecule.[37,38] Compounds **1** and **2** have an oxazoline group that reacts with carboxylic groups and an oxazinone group that reacts with amino or hydroxy groups. The reactions are highly selective and were utilized in the chain extension of PA26 and in the synthesis of segmented PA12-polyether block copolymers. Using compound **1**, the synthesis of block copolymers based on amino-terminated PA12 and carboxy-terminated PBT was also investigated.

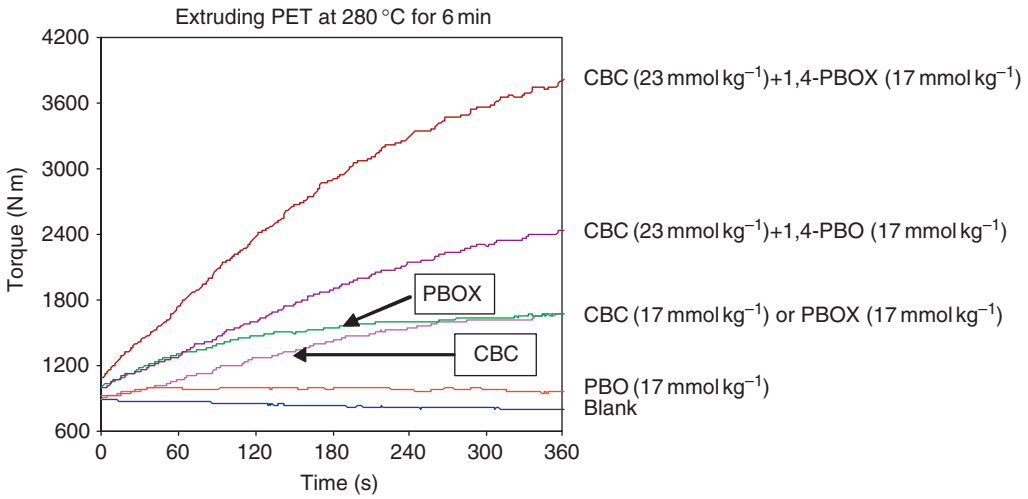

Figure 14 The torque of the micro-compounder during the processing of PET in the presence of CBC, 1,4-PBO, 1,4-PBOX, CBC + 1,4-PBO. or CBC + 1,4-PBOX.

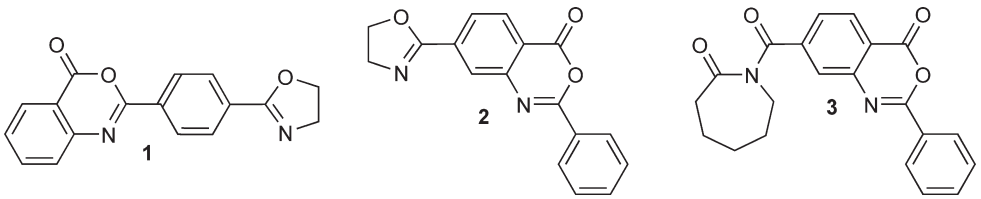

Figure 15 Dual chain extenders.[37,38]

Although the coupling efficiency has proven to be good, the molar masses were not high enough to ensure good mechanical properties. In particular, partial hydrolysis of the polyester blocks, probably catalyzed by residual carboxylic groups, could not be prevented completely (Figure 15).

Another example is bifunctional coupling agent 3 containing an oxazinone and a lactamate group in one molecule.[38] Model reactions showed that this coupling agent is highly selective. At 220 °C, the substitution of the lactamate group was about 90%. In a second reaction, the oxazinone group was converted with an aliphatic amino compound. This high selectivity was utilized in the synthesis of segmented polyester/polyamide block copolymers by sequential conversion of the coupling agent with hydroxy-terminated PBT or polycaprolactone (PCL) and amino-terminated polyamide 12 (PA12) under reactive extrusion conditions. In the case of the PA12/PBT block copolymer, ductile behavior was observed, whereas the PA12/PCL block copolymer showed elastic properties. Both polymers phase separated on the nanometer scale, as evidenced by AFM and SEM.

4.24.9 Conclusions

Chain extension is a beneficial process to improve the mechanical properties of polycondensates by increasing molecular weights during processing. Chain extenders are used in such a small amount (about 0.5%) that the crystallinity is not measurably disturbed. This makes chain extension an important enabling technology for upgrading polyesters and polyamides. During the preparation of polycondensates, the viscosities in these solvent-free processes raise enormously, making the synthesis of high molecular weight resins virtually impractical. It would be highly beneficial if in autoclaves only one low molecular weight grade could be produced and the higher molecular weight grades during extrusion. A second major advantage would be the upgrading of recycled polycondensates. During use, the molecular weight of polycondensates drops and, consequently, the mechanical properties will deteriorate. Restoration of the molecular weight would enable to reuse these polymers in their original applications.

The feasibility of chain extenders is unambiguously demonstrated. To achieve this, these compounds must be very reactive without giving side reaction. These challenging requirements are met by a few compounds. The coupling of carboxyl, amino, or hydroxyl end groups via ring-opening reactions is by far preferred, since no volatiles are liberated. However, most of these reactions are equilibriums, preventing sometimes complete conversions. Chain extension via substitution of releasing groups is feasible as well and might be even more preferred if the releasing compounds are harmless.

In summary, chain extension is a feasible technology to make high molecular polyesters and polyamides during common extrusion steps.

References

1. http://finance.yahoo.com/news/Polyester-PET-industry-bw-3736716467.html?x=0
2. http://www.chemsystems.com/about/cs/news/items/PERP%200708S6_Nylon%206.cfm
3. Awaja, F.; Pavel, D. *Eur. Polym. J.* **2005**, *41*, 1453.
4. http://www.europeanplasticsnews.com/subscriber/newsmail.html?id=1279700406&cat=1
5. Dias Nacimento, C. R.; Azuma, C.; Bretas, R.; *et al. J. Appl. Polym. Sci.* **2010**, *115*, 3177.
6. Dijkstra, A. J. US Patent 3553157, 1971.
7. Haralabakopoulos, A. A.; Tsiourvas, D.; Paleos, C. M. *Abstr. Papers Am. Chem. Soc.* **1997**, *213*, 94-POLY.
8. Haralabakopoulos, A. A.; Tsiourvas, D.; Paleos, C. M. *J. Appl. Polym. Sci.* **1999**, *71*, 2121–2127.
9. Fenouillot, F.; Hedreul, C.; Forsythe, J.; *et al. J. Appl. Polym. Sci.* **2003**, *87*, 1995–2003.
10. Guo, B. H.; Chan, C. M. *J. Appl. Polym. Sci.* **1999**, *71*, 1827–1834.
11. Qian, Z. Y.; Chen, X.; Xu, J.; *et al. J. Appl. Polym. Sci.* **2004**, *94*, 2347–2355 Schacker, O.; Braun, D.; Hellmann, G.P. *Macromol. Mater. Eng.* **2001**, *286*, 382.
12. Taylan, E.; Kusefoglu, S. H. *J. Appl. Polym. Sci.* **2009**, *112*, 1184–1191.
13. Xanthos, M.; Young, M. W.; Karayannidis, G. P.; *et al. Polym. Eng. Sci.* **2001**, *41*, 643–655.
14. Ivin, K. J.; Saegusa, T. *Ring-Opening Polymerizations*; Elsevier Applied Science Publisher: London, 1984.
15. (a) Inata, H.; Matsumura, S. *J. Appl. Polym. Sci.* **1985**, *30*, 3325; (b) Inata, H.; Matsumura, S. *J. Appl. Polym. Sci.* **1986**, *32*, 5193; (c) Inata, H.; Matsumura, S. *J. Appl. Polym. Sci.* **1986**, *32*, 4581; (d) Inata, H.; Matsumura, S. *J. Appl. Polym. Sci.* **1987**, *33*, 3069; (e) Inata, H.; Matsumura, S. *J. Appl. Polym. Sci.* **1987**, *34*, 2609; (f) Inata, H.; Matsumura, S. *J. Appl. Polym. Sci.* **1987**, *34*, 2769; (g) Karayamidis, G. P.; Psalida, E.A. *J. Appl. Polym. Sci.*, **2000**, *77*, 2206.
16. Witte, H.; Seeliger, W. *Liebigs Ann. Chem.* **1974**, 996.
17. Saegusa, T.; Aoi, K.; Mijamoto, M.; *et al. Macromol. Chem., Macromol. Symp.* **1991**, *47*, 163.
18. (a) Hüls, EP 541926; (b) Teijin, EP 0020944; (c) KRI international EP 0742258; (d) Takeda, EP 0140291; (e) Elf Atochem, EP 0581641; (f) DSM, WO96/34909; DSM WO05/21605.
19. Stanssens, D.; Hermanns, R.; Wories, H. *Progr. Org. Coat.* **1993**, *22*, 379.
20. Loontjens, J. A.; Pauwels, K.; Derks, F.; *et al. J. Appl. Polym. Sci.* **1997**, *65*, 1813.
22. (a) Ciba, WO 9523176; (b) Phobos, EP 422282; (c) Recherche, WP 9217519.
23. Samuel, P.; Maity, S.; Khan, S.; *et al. J. Sci. Ind. Res.* **2008**, *67*, 1051.
24. Paine, J. B. *J. Org. Chem.* **2008**, *73*, 4929.
25. Daver, F.; Awaja, F. *Polym. Eng. Sci.* **2004**, *44*, 1579.
26. Yamanak, T.; Kanomata, A.; Inoue, T. *Macromol. Symp.* **2003**, *199*, 73.
27. Yilmazer, U.; Xanthos, M.; Bayram, G.; *et al. J. Appl. Polym. Sci.* **2000**, *75*, 1371.
28. Ankola, D. D.; Kumsr, M. N. V. R.; Chiellini, F.; Solaro, R. *Macromolecules* **2009**, *42*, 7388.
29. Saint-Loup, R.; Robin, J. J.; Boutevin, B. *Macromol. Chem. Phys.* **2002**, *203*, 199.
30. Acevedo, M.; Fradet, A. *J. Polym. Sci. Part A, Polym. Chem.* **1993**, *31*, 817.
31. Acevedo, M.; Fradet, A. *J. Polym. Sci. Part A, Polym. Chem.* **1993**, *31* (6), 1579–1588.
32. Lefebvre, H.; Fradet, A. *Macromol. Chem. Phys.* **1998**, *199*(5), 815–824.
33. Lefebvre, H.; Fradet, A. *Macromol. Chem. Phys.* **1998**, *199*(12), 2747–2753.
34. Lefebvre, H.; Fradet, A. *J. Polym. Sci. Part A, Polym. Chem.* **1999**, *37*(23), 4412–4421.
35. Hong, J. H.; Choi, C. W.; Ramasundaram, S.; *et al. Polym. Degrad. Stab.* **2008**, *93*, 392.
36. (a) Loontjens, J. A. *J. Polym. Chem., Part A, Polym. Chem.* **2003**, *41*, 3198; (b) Loontjens, J. A., Ph.D. thesis, http://alexandria.tue.nl/extra2/200512318.pdf; (c) DSM, WO9847940; (d) DSM WO09634909.
37. Jakisch, L.; Komber, H.; Wursche, R.; *et al. J. Appl. Polym. Sci.* **2004**, *94*, 2170.
38. Jakisch, L.; Komber, H.; Böhme, F. *Macromol. Mater. Eng.* **2007**, *292*, 557.

Biographical Sketches

Ton Loontjens is principal scientist of macro-organic chemistry at DSM Research in the Netherlands and part-time professor at the University of Groningen. He started studying chemistry at the University of Nijmegen in 1969 and received in 1972 the Unilever award. He finished his study in 1975 (cum laude) and started at DSM research as leader of the polypropylene polymerization group. In 1980, he became workgroup leader on polypropylene, polyethylene, and unsaturated polyester research. From 1985 until 1995, he was head of a polymer chemistry department on coating resins, melamine resins, stabilization of polymers, polyesters, and nylons. Since 1995, he has held the position of principal scientist. In 2005, he received his PhD degree and in the same year he was appointed as part-time professor for polymer chemistry at the University of Groningen. Loontjens is the co-author of more than 55 publications and more than 65 patents.

Eric Goethals graduated from Ghent University (Belgium) in 1958 and obtained his PhD degree in organic chemistry at the same university in 1963. After a postdoctoral year at the Gütenberg University in Mainz (Germany), where he worked with professor Rolf Schulz, he returned to Ghent where he started a research group on polymer chemistry. He was appointed associate professor in 1970 and full professor in 1980. He was head of the department of organic chemistry from 1996 till 2002, the year of his retirement from university. He has lectured on organic chemistry to medical students and polymer science to chemists. His field of research was in polymer synthesis, cationic polymerization, ring-opening polymerization, telechelic polymers, polymer networks, and reactive polymers. He is the editor of four books and co-author of over 400 publications in international scientific journals.

4.25 Ring-Opening Dispersion Polymerization

S Slomkowski, Polish Academy of Sciences, Lodz, Poland

4.25.1 Introduction

Polymerizations in heterogeneous systems (suspension, dispersion, emulsion, and related polymerizations) have certain advantages over polymerizations in bulk and in solution. Polymers synthesized in heterogeneous systems can be easily isolated, most often by simple sedimentation or, in the case of polymers with the density lower than the density of continuous medium, by flotation. It is also worth noting that the viscosity of polymerization mixture is much lower for the heterogeneous polymerization than for the polymerizations in bulk or in solution. Low viscosity allows efficient mixing helping to maintain the uniform distribution of components of polymerization mixture and efficient heat transfer providing good control of temperature as well as convenient transport of reaction products.

Majority of studies of heterogeneous polymerizations were concentrated on radical processes, in particular on polymerizations of vinyl monomers in water-based media. Several important technologies are based on the knowledge gathered in these studies. On the other hand, the heterogeneous ring-opening polymerizations of heterocyclic monomers were investigated to much lesser extent, in spite that the first reports on such processes are about 40 years old.[1,2] Probably, the much slower development of studies on ionic and pseudoionic ring-opening polymerizations in dispersed systems, in comparison with similar studies on radical polymerizations of vinyl monomers, was related to experimental difficulties, because the intensively stirred polymerizing mixtures must be protected against contamination with moisture. However, recently, when microparticles from biodegradable polyesters obtained by polymerization of lactides and lactones found application in medicine as drug carriers and building blocks for scaffolds used in tissue engineering,[3–6] the direct synthesis of particles by the ring-opening polymerization attracted much more attention.

Generally, in polymerizations in dispersed systems, the suspension of particles can be stabilized either by electrostatic repulsion or by steric hindrance.[7] Sufficiently strong stabilizing repulsive forces occur only in highly polar media (e.g., in water) in which the ionic species are dissociated. Ionic and pseudoionic ring-opening polymerizations are usually carried out in media with the dielectric permittivities much lower than those of water. As a result, the ionic double layer at particle–organic continuous medium interface is very thin and therefore even at short distances between particles, the compensation of particle charge by small counterions effectively reduces the repulsive ionic interactions and does not prevent particle aggregation. Therefore, in the case of the ionic and pseudoionic ring-opening polymerizations, the stability of particle suspension can be assured only by steric stabilization. The mechanism responsible for steric stabilization of polymer colloids is illustrated in **Figure 1**.

Particles stabilized sterically are coated with nonionic surfactant strongly adsorbed or covalently immobilized onto the particle's surface. The molecules of surfactants contain segments efficiently solvated with molecules of the continuous medium. When two particles are in close contact, the entanglement of chains of surfactants leads to the higher local concentration of the chains. This increases the osmotic pressure inducing flux of solvent into the interparticle space, therefore preventing their irreversible aggregation. Moreover, the high local concentration reduces segmental motion of surfactant molecules, which leads to an unfavorable decrease in entropy. The above-mentioned events lead to the positive change of Gibbs energy accompanying reduction of the distance between particles and manifest themselves by repulsive forces preventing particle aggregation. The suspension is colloidally stable during synthesis and in the postpolymerization period, provided the surface-active agents were properly chosen for the particular polymer–continuous medium system. The general

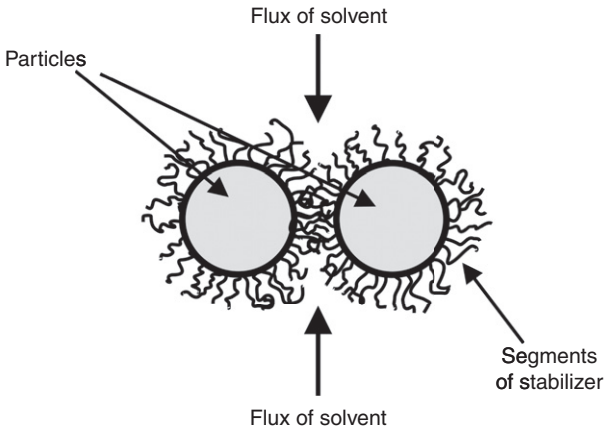

Figure 1 Schematic illustration of sterically stabilized particles in close contact.

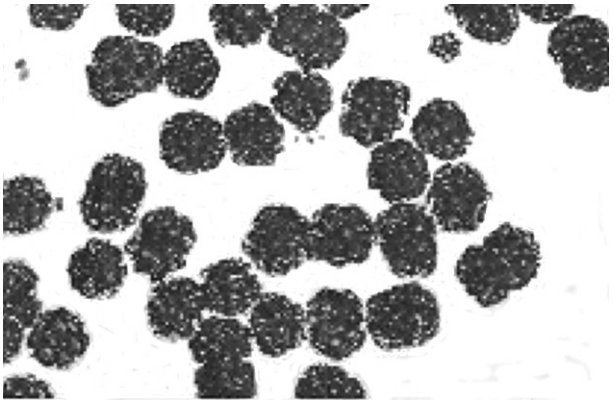

Figure 2 Copolymers obtained in copolymerization of 1,3,5-trioxane and 1,3-dioxolane carried out in the presence of poly(ethylene oxide) (M_n = 15 000). Initial concentrations of 1,3,5-trioxane and 1,3-dioxolane were equal to 7.0 and 0.35 mol kg^{-1}, respectively.

rule is to select the surfactant containing segments with a high affinity to the polymer particles (or the surfactant that is suitable for the covalent binding to the surface of the particles) and segments soluble in the continuous medium (at least at the polymerization conditions).

It is worth noting that chemical reactions responsible for polymer formation during the polymerizations in dispersed systems are the same as in the case of the polymerizations in the bulk or in solution. However, for the polymerizations in dispersed systems, the processes responsible for particle formation, transport of initiator and growing polymer into particles, and release of the growing chains into continuous medium are just as important. As a result, in dispersion polymerizations, significant differences in concentrations of monomer and propagating chains in the continuous medium and in the particles are very common. Thus, one may expect that the rates of polymerization in dispersed systems and in solution are different even if monomer and initiator concentrations are similar in both systems.

4.25.2 Cationic Ring-Opening Dispersion Polymerization

In the domain of the cationic ring-opening polymerization in dispersion, until now only one system has been investigated. In 1968, Penczek *et al.* published results of the studies of the cationic copolymerization of 1,3-dioxolane and 1,3,5-trioxane initiated with BF_3 and carried out in cyclohexane in the presence or the absence of poly(ethylene oxide). The initial concentration of 1,3-dioxolane in these studies was 20 times lower than the initial concentration of 1,3,5-trioxane. The former monomer was used with the purpose of protecting poly (1,3,5-trioxane) from depolymerization. It was found that depolymerization stops when 1,3-dioxolane monomeric unit is the terminal one.

Microscopic observations revealed that polymer formed during the above-mentioned process was shaped into the raspberry-like particles (see Figure 2). The diameters of particles formed in the absence of poly(ethylene oxide) were in the range of 25–100 μm, whereas the diameters of particles formed by polymerization in the presence of poly(ethylene oxide) (samples with M_n equal to 15 000 and 40 000 were used in the studies) were in the range of 8 to about 100 μm, depending on the content of polyether. It is worth noting that for the weight fraction of poly(ethylene oxide) ranging from 1% to 2.5% (relative to comonomers), the number-average diameter of particles was almost constant (within the range from 8 to 12 μm).

According to the authors, the cationic species present in the polymerization mixture participate in not only transacetalization but also transetherification reactions, yielding copolymers with the polyacetal and poly(ethylene oxide) blocks (see Scheme 1). These copolymers can function as the *in situ*-formed suspension stabilizers adsorbed onto the surface of polyacetal particles via the polyacetal blocks and with the poly(ethylene oxide) segments providing steric stabilization.

The initially formed primary particles are not sufficiently stabilized with attached surface-active copolymer and therefore aggregate into the larger ones. According to the basic laws of geometry, the ratio of surface to volume of the aggregates decreases with their increased size and eventually the amount of the adsorbed surface-active copolymer is sufficient to provide colloidal stabilization of suspension. It is worth noting, however, that the primary particles in aggregates do not lose their identity (see microphotograph in Figure 2). Probably, at the polymerization temperature equal to 60 °C, the copolymer rich in poly(1,3,5-trioxane) is crystalline. The softening temperature of poly(1,3,5-trioxane) is close to 180 °C,[8,9] which prevents fusion of particles.

Monitoring the dependence of the average diameter of particle aggregates on monomer conversion (shown in Figure 3) reveals the important difference between the copolymerization of 1,3,5-trioxane and 1,3-dioxolane in the presence and the absence of poly(ethylene oxide) used as a precursor of the surface-active suspension stabilizer with polyester and polyether blocks. For example, in the polymerization carried out in the absence of poly(ethylene oxide), the diameter of particle aggregates grows continuously with monomer conversion, whereas in the copolymerization carried out in the presence of poly(ethylene oxide), the diameter of particle aggregates after the initial growth reaches plateau (with D_n close to 10 μm) for monomer conversion exceeding 40%.

Because the initiation was completed below 40% of monomer conversion, the above-mentioned dependence could

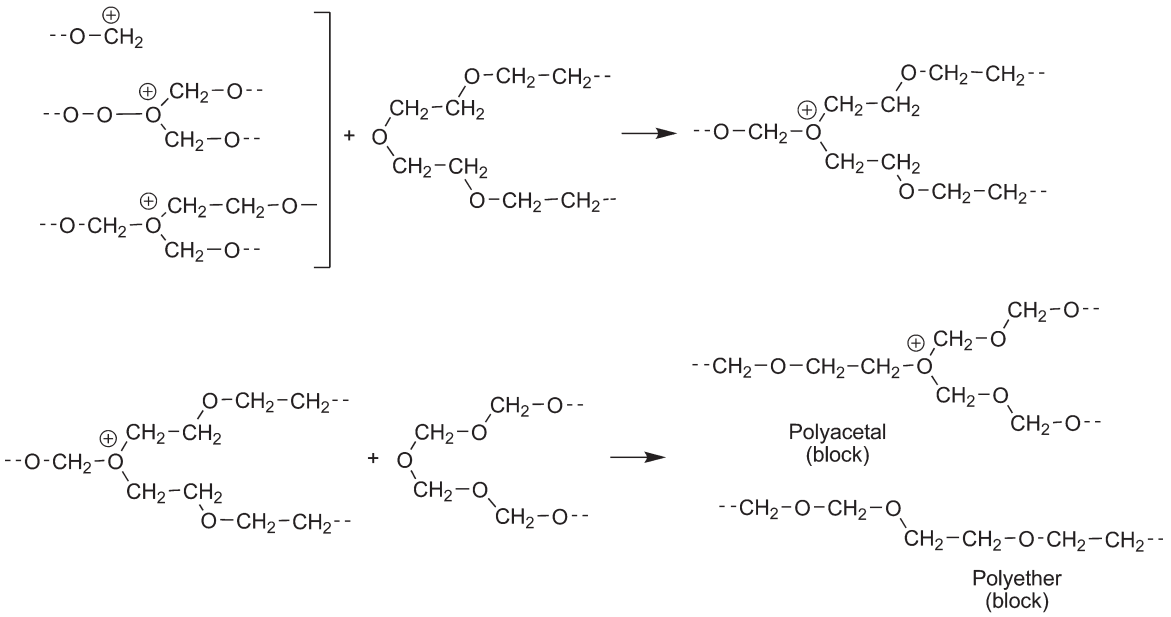

Scheme 1 Reaction of cationic species of 1,3,5-trioxane and 1,3-dioxolane copolymerization with poly(ethylene oxide) yielding polyacetal-*block*-polyether suspension stabilizing the block copolymer.

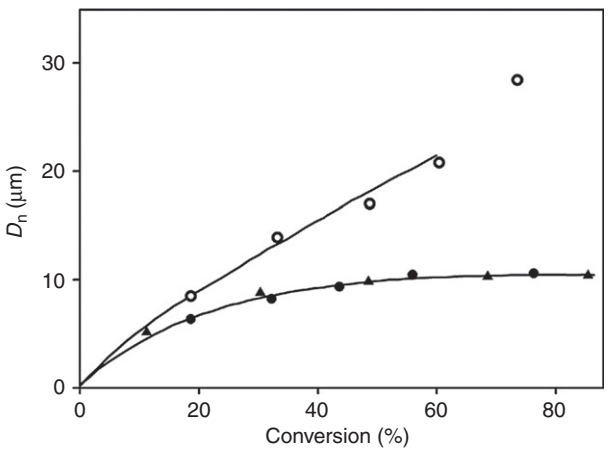

Figure 3 Influence of the average diameter of particles on concentration of poly(ethylene oxide) in the copolymerizing mixture of 1,3,5-trioxane ([1,3,5-trioxane] = 7.0 mol kg^{-1}) and 1,3-dioxolane ([1,3-dioxolane] = 0.35 mol kg^{-1}). Concentration of BF_3OBu_2 initiator was equal to: 1.75×10^{-3} mol kg^{-1} (○), 3.50×10^{-3} mol kg^{-1} (●), and 4.50×10^{-3} mol kg^{-1} (▲). Reproduced with permission from Penczek, S.; Fejgin, J.; Sadowska, A.; Tomaszewicz, M. *Makromol. Chem.* **1968**, *116*, 203.[1]

occur only in the system that was colloidally stable and allowed for the release of the propagating species from the aggregates. The released propagating species form new primary particles and eventually new aggregates. Presumably, the propagating copolymer chains with short polyacetal blocks can be desorbed from particles and in the subsequent reactions (see **Scheme 2**) form growing copolymer chains with longer polyacetal segments, the chains of which are able to assemble into the primary particles.

Combining all of the available experimental data leads to the scheme of 1,3,5-trioxane and 1,3-dioxolane copolymerization shown in **Figure 4**.

According to this scheme, after initiation in solution, when the propagating chains reach a critical length, the nucleation process begins by chain self-assembly (**Figures 4(a)–4(c)**). Because the primary nanoparticles are insufficiently stabilized by the attached poly(ethylene oxide) chains, they further aggregate into the large particles composed of the primary ones (**Figure 4(d)**). Since the surface-to-volume ratio for the large particles is smaller than that for the small particles, the stabilization of the former ones is easier. As a result, adsorption of the primary nanoparticles onto the large particles stops. In parallel to formation of particles, the transacetalization reactions in the particle interfacial layer yield growing chains with short polyacetal and with long poly(ethylene oxide) segments. These chains may be released by desorption and grow in solution until their polyacetal segments reach the critical length and, due to the lost solubility, nucleate and form new primary particles (**Figure 4(e)**). Thus, in the cationic dispersion copolymerization of 1,3,5-trioxane and 1,3-dioxolane, the poly(ethylene oxide) chains act as not only the chain transfer agents but also 'particle transfer agents', limiting size of polymer particles formed in the process (**Figure 4(f)**).

4.25.3 Anionic and Pseudoanionic Ring-Opening Dispersion Polymerization

The anionic and pseudoanionic ring-opening polymerizations were studied only for ε-caprolactone and for the cyclic dimers of lactic acid (L,L-lactide, D,D-lactide, and D,L-lactide).

The first reports on the dispersion polymerization of cyclic esters are related to the patent to Union Carbide (from 1972).[2] However, in this patent, the majority of fundamental problems were not clarified. Systematic studies of the dispersion polymerizations of ε-caprolactone and lactides were started only in 1994 by Penczek and co-workers.[10] Later the studies were

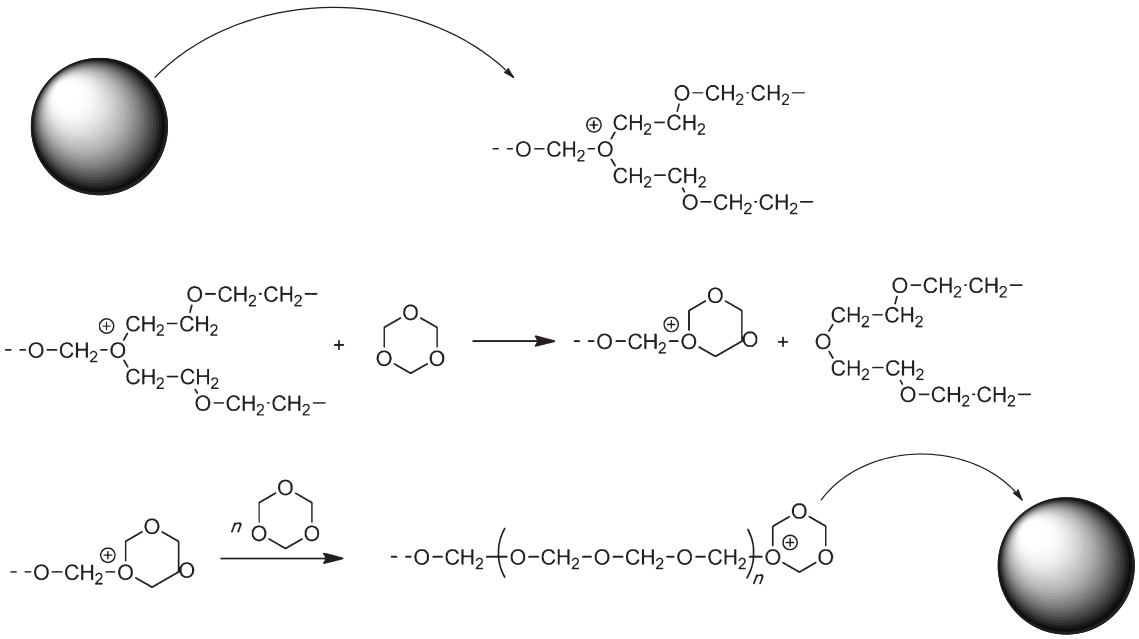

Scheme 2 Desorption of propagating chains and nucleation of new particles in the cationic copolymerization of 1,3,5-trioxane and 1,3-dioxolane carried out in presence of poly(ethylene oxide).

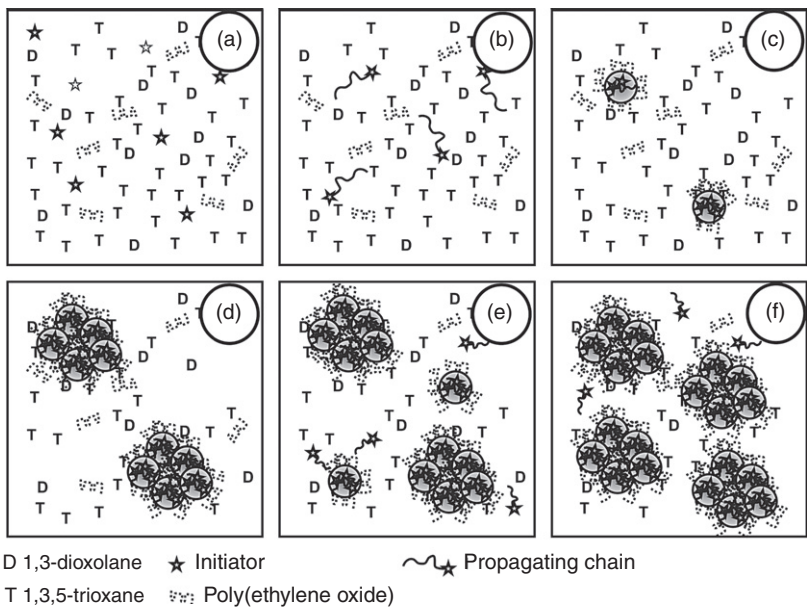

Figure 4 Schematic illustration of the cationic dispersion copolymerization of 1,3,5-trioxane and 1,3-dioxolane. (a) – solution before beginning of the polymerization, (b) – polymerization in solution, length of polymer chains is shorter than the critical one, (c) – chain-to-globule transition and formation of the primary particles, (d) – formation of aggregates of the primary particles, polymerization in aggregates, (e) – escape of growing species from particle aggregates to solution and formation of new primary particles, (f) – formation of new aggregates.

carried out by two research groups (S. Slomkowski, Centre of Molecular and Macromolecular Studies, Lodz, Poland, and H. Yoshizawa and T. Ono, Okayama University, Japan).

4.25.3.1 Continuous Media for the Anionic and Pseudoanionic Dispersion Polymerizations of ε-Caprolactone and Lactides

Continuous media for the anionic or pseudoanionic dispersion polymerization of cyclic esters should fulfill the following criteria. Monomers and initiators should be soluble in these liquids but polymers must remain insoluble. Moreover, the continuous media must be chemically inert toward initiators and propagating species. Active centers of the anionic and pseudoanionic polymerizations of cyclic esters are the ionic or covalent metal alkoxides with polarized metal–oxygen bond, respectively. These species react with various kinds of protic impurities (such as water, alcohols, and acids). Because aliphatic and aromatic hydrocarbons, as well as linear and cyclic ethers (with the exception of oxiranes), do not react

with metal alkoxides, these compounds were selected for preparation of continuous media for the dispersion polymerizations of cyclic esters. Unfortunately, no single compound of this group of liquids was a sufficiently good solvent for monomers and initiators, and nonsolvent for polymers. However, it was found that mixed solvents with properly tailored composition fulfilled the above-mentioned solubility/insolubility criteria. The dispersion polymerizations of ε-caprolactone were carried out in the heptane/1,4-dioxane (9:1, v/v) mixture.[10] For the polymerizations of lactides (D,L-lactide and L,L-lactide), the appropriate mixture was heptane/1,4-dioxane in the 4:1 (v/v) ratio.[10,11] Recently it has been found that the dispersion polymerization of D,L-lactide can be effectively carried out in the heptane/xylene 2:1 (v/v) mixture.[12,13] Traces of water in these liquids were removed either by treatment with molecular sieves[12] or with sodium–potassium alloy.[10]

4.25.3.2 Initiators

The dispersion polymerizations of ε-caprolactone and lactides were initiated with initiators used for initiation of polymerizations of the above-mentioned monomers in solution. Diethylaluminum ethoxide,[10,11,14] stannous 2-ethylhexanoate,[10,11] stannous 2-ethylhexanoate/polyalcohols,[12,13,15] and 2,2-dibutyl-2-stanna-1,3-dioxepane[16] were used for the dispersion polymerizations of lactides. The dispersion polymerizations of ε-caprolactone were initiated with diethylaluminum ethoxide[10] and sodium trimethylsilanolate.[17] Of the above-mentioned initiators, only the latter one initiated the anionic polymerization.

4.25.3.3 Suspension Stabilizers

Colloidal stability of polyester particles formed in the dispersion polymerization of ε-caprolactone and lactides was achieved by adding to the polymerizing mixture block or graft copolymers with tailored chemical structure and with molecular weight from a few thousands to about 50 000 or by producing such copolymers *in situ*, during polymerization. Copolymer stabilizers were built of segments that could be efficiently bound to the surface of growing particles (e.g., poly(ε-caprolactone) (PCL),[10,11,14,16] polylactide,[12,13,15] poly(dimethylsiloxane),[13] or poly(ethylene oxide)[13]) and blocks of polymers soluble in reaction medium (e.g., poly(dodecyl acrylate) (PDA),[10,11,14,16] poly(dodecyl methacrylate),[12,13,15] or a gradient copolymer such as poly{(octadecyl methacrylate)-*co*-(dimethylaminoethyl methacrylate)}[18]).

Poly(dodecyl acrylate)-*graft*-poly(ε-caprolactone), poly(dodecyl methacrylate)-*g*-poly(D,L-lactide), poly(dodecyl methacrylate)-*graft*-poly(dimethylsiloxane), and poly(dodecyl methacrylate)-*graft*-poly(ethylene oxide) stabilizers were obtained by radical copolymerization of dodecyl acrylate or dodecyl methacrylate with methacrylate-type macromonomers containing PCL, poly(L,L-lactide), poly(D,L-lactide), poly(ethylene oxide), or poly(dimethylsiloxane) chains according to Scheme 3.

Poly(dimethylsiloxane) and poly(ethylene oxide) macromonomers were commercial products.[13] PCL macromonomer was obtained in reaction of the terminal hydroxyl end-groups of PCL with methacryloyl chloride.[10] Poly(D,L-lactide) methacrylate was obtained by using 2-hydroxyethyl methacrylate as an initiator of the D,L-lactide polymerization and stannous acrylate as a catalyst.[12]

Poly(dodecyl acrylate)-*graft*-poly(D,L-lactide) could also be obtained *in situ* in dispersion polymerization of D,L-lactide initiated with stannous 2-ethylhexanoate and carried out in the presence of poly[(dodecyl methacrylate)-*co*-(2-hydroxyethyl methacrylate)] (see Scheme 4).[15]

4.25.3.4 Typical Recipes for Dispersion Polymerizations of ε-Caprolactone and Lactide

Since in dispersion polymerization of cyclic esters, some experimental details are crucial for obtaining product in the form of suspension of microspheres free of their aggregates, brief recipes for synthesis of poly(D,L-lactide) and PCL microspheres are given below. These recipes are based on experiments described in Reference 10.

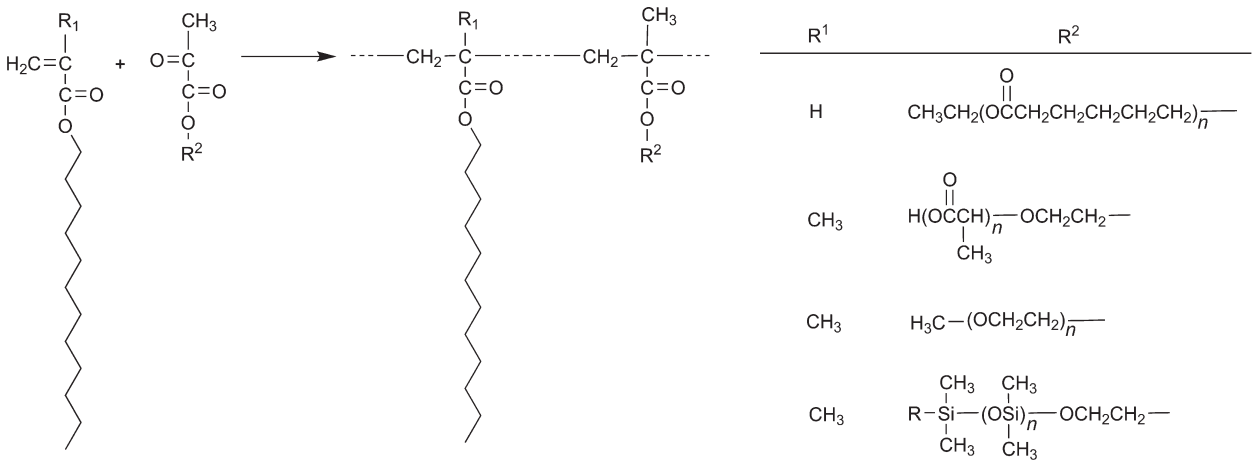

Scheme 3 Synthesis of stabilizers by copolymerization of dodecyl acrylates or dodecyl methacrylates with (methacrylic acid)-*graft*-poly(ε-caprolactone), (methacrylic acid)-*graft*-poly(D,L-lactide), (methacrylic acid)-*graft*-poly(ethylene oxide), and (methacrylic acid)-*graft*-polysiloxane.

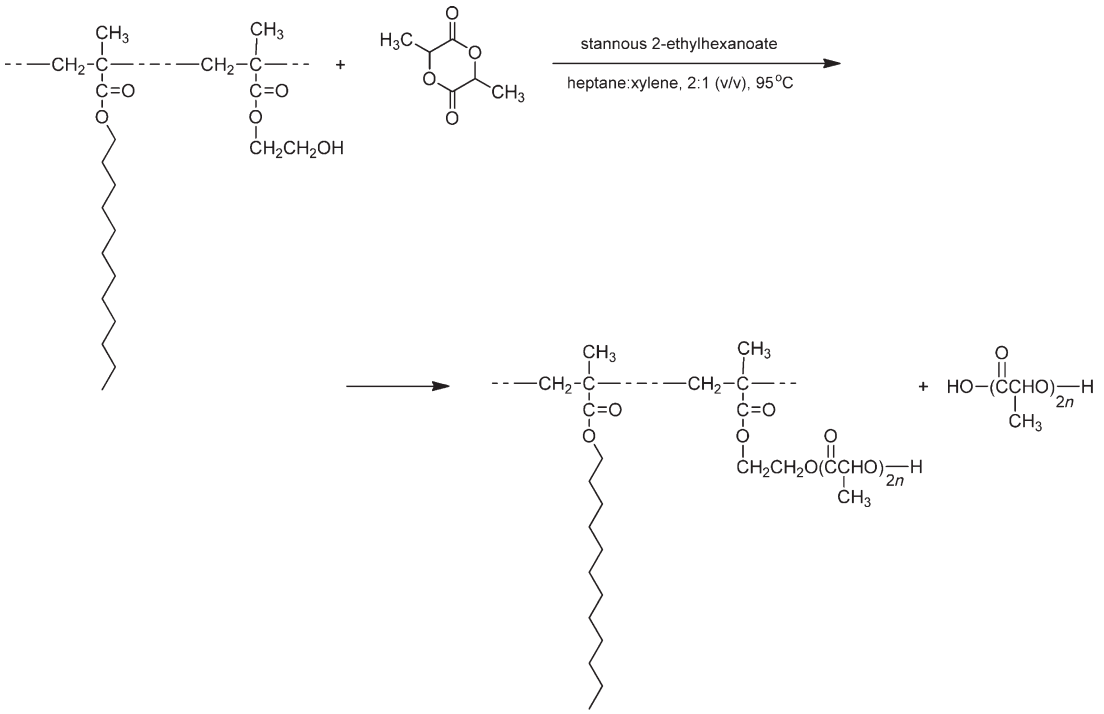

Scheme 4 *In situ* synthesis of poly[(dodecyl acrylate)-*co*-(2-hydroxyethyl methacrylate)]-*graft*-poly(D,L-lactide) by dispersion polymerization of D,L-lactide.

4.25.3.4.1 Dispersion polymerization of D,L-lactide

The polymerization mixture was prepared and dispersion polymerization carried out in argon atmosphere. D,L-Lactide (4 g) and poly(dodecyl acrylate)-*graft*-poly(ε-caprolactone) were dissolved in a mixture of 1,4-dioxane (18 ml) and heptane (72 ml). Molecular weight (M_n) of poly(dodecyl acrylate)-*graft*-poly(ε-caprolactone) used in this process was equal to 40 000. The number-average molecular weight (M_n) and dispersity (M_w/M_n) of PCL grafts were equal to 3100 and 1.19, respectively. The average number of grafts in one copolymer macromolecule was equal to 4.1 and the molar fraction of ε-caprolactone units was 0.25. The solution containing D,L-lactide and the stabilizer was placed in a reactor, stirred with magnetic stirrer, and heated to the reflux. Separately, a solution of stannous 2-ethylhexanoate (0.19 g) in a mixture containing 2 ml of 1,4-dioxane and 8 ml of heptanes was prepared. This solution was added to a boiling solution of D,L-lactide and the polymerization was carried out at 95 °C for 2 h. Then, the hot polymerization mixture was rapidly added to 100 ml of heptane precooled to 10 °C and the mixture was further cooled to 15 °C. The sedimented crude product was washed with small portions of heptane and then dispersed in heptane. The dispersion was cooled to 5 °C and left standing for crystallization of the remaining unreacted monomer. Because monomer crystals sedimented within about 2 min and poly(D,L-lactide) microspheres began to settle down only after about 15 min, the polymer particles were separated by fractional sedimentation. The yield of poly(D,L-lactide) microspheres (after purification) was 68%. The number and the weight average diameters of poly(D,L-lactide) microspheres were $D_n = 2.50$ μm and $D_w = 2.88$ μm. The diameter dispersity factor close to 1 ($D_w/D_n = 1.15$) indicated that microspheres were quite uniform with respect to their size. The number-average molecular weight M_n of poly(D,L-lactide) in microspheres was equal to 9400 and the molecular weight dispersity factor M_w/M_n was equal to 1.05.

It is known that the ring-opening polymerization of lactides is an equilibrium process and some monomers are present in the reaction mixture even at the very end of polymerization.[19–21] Depropagation (like side reactions if they do occur) results in broadening of the molecular weight distribution. Thus, the value of the dispersity close to 1 indicates that at the moment when the above-described dispersion polymerization of D,L-lactide was stopped, the system was still far from equilibrium.

4.25.3.4.2 Dispersion polymerization of ε-caprolactone

Dispersion polymerization of ε-caprolactone was carried out using the same suspension stabilizer (poly(dodecyl acrylate)-*graft*-poly(ε-caprolactone)) as the stabilizer used in the above-described dispersion polymerization of D,L-lactide. The polymerization mixture was prepared by dissolving 0.22 g of the stabilizer in a mixture containing ε-caprolactone (5.55 g), 1,4-dioxane (10 ml), and heptane (80 ml). To this solution, 0.1 g of diethylaluminum ethoxide dissolved in 10 ml of 1,4-dioxane was added. The polymerization was carried out for 1 h in argon atmosphere while stirring at the rate of 60 rpm. The polymerization was stopped by addition of 0.23 g of acetic acid dissolved in 100 ml of heptane. The PCL particles were isolated by decantation and then washed 10 times with small portions of heptane. Their number-average diameter and dispersity were equal to $D_n = 628$ nm and $D_w/D_n = 1.04$, respectively. The number-average molecular weight and dispersity of PCL in particles were equal to $M_n = 8200$ and $M_w/M_n = 1.11$. Thus, the above-described dispersion polymerization yielded particles with a narrow distribution of their diameters and a

narrow distribution of molecular weight of the polymer from which they were made.

4.25.3.5 Distribution of Diameters of Polyester Microspheres Synthesized in Dispersion Polymerization of Lactides

In the systems in which particle nucleation and aggregation of primary particles occur only in the initial period of the polymerization, all particles grow at the later stages simultaneously. As a result, the diameter distribution of particles formed in such polymerization processes must be narrow. Aggregation of colloidal particles strongly depends on the properties of stabilizers and on their concentration. Properties of the stabilizers are determined by their chemical structure. Therefore, in particular for the poly(dodecyl acrylate)-*graft*-poly(ε-caprolactone) and poly(dodecyl methacrylate)-*graft*-poly(D,L-lactide) stabilizers, the colloidal stability of polylactide microspheres should depend on the number and molecular weight of polyester grafts.

Comprehensive studies of the dispersion polymerization of L,L- and D,L-lactides carried out in the presence of poly(dodecyl methacrylate)-*graft*-poly(D,L-lactide) with M_n in the range of 21 800–32 300 and with the PCL content in copolymer equal to 21 ± 2 wt.% revealed that the distribution of diameters of microspheres strongly depends on the ratio of the number-average molecular weight of PCL grafts (M_n(PCL)) and the number-average molecular weight of the whole poly (dodecyl acrylate)-*graft*-poly(ε-caprolactone) copolymer (M_n (PDA-PCL)). The diameter distribution of microspheres was characterized using a parameter $\xi = D_n/(D_w - D_n)$. In the case of the very broad diameter distribution $D_w/D_n \gg 1$, the parameter ξ approaches D_n/D_w, whereas for the very uniform microspheres, for which $D_w - D_n$ approaches 0, the parameter ξ increases to infinity. The plot of ξ as a function of $\chi = M_n$ (PCL)/M_n(PDA-PCL) shown in Figure 5 reveals that the most uniform microspheres were obtained for χ close to 0.23. The average number of PCL grafts in one macromolecule of these stabilizers was equal to 1.3.

Probably, when molecular weight of PCL is too small, the anchoring of stabilizer molecules onto the surface of growing particles is too weak. However, when the M_n(PCL)/M_n (PDA-CL) ratio is much higher than 0.23, the length of PCL segments is sufficient for efficient binding, but the length of poly(dodecyl acrylate) blocks is too short to provide efficient stabilization.

One may expect that the dispersity of particle diameters formed in the ring-opening polymerization of lactides should depend on not only the structure of stabilizers but also their concentration. Therefore, it was rather surprising to notice that for the stabilizers with optimized structure, the dispersity of diameters of polyester particles did not change significantly in a rather broad range of stabilizer concentrations. For example, for the dispersion polymerization of D,L-lactide carried out in the presence of poly(dodecyl methacrylate)-*graft*-poly(D,L-lactide) stabilizers, the concentration of which was varied from 0.5 to 10 g l^{-1}, the coefficient of variation (CV) for diameters of synthesized particles in almost all experiments did vary quite randomly within the range of 15–33% (see Figure 6). Data characterizing the above-mentioned copolymers are given in Table 1. Particles with the lowest diameter dispersity were obtained for the copolymer G_3, which was less soluble in reaction medium and thus better adsorbed onto particles compared to the others used in these studies.[13]

Values M_w and M_w/M_n of stabilizers were obtained from gel permeation chromatography (GPC) traces using polystyrene standards.

Important information was obtained also from monitoring the dependence of yield of the poly(L,L-lactide) microspheres on the concentration of stabilizers.[22] Polymerizations were carried out in the presence of the poly(dodecyl acrylate)-*graft*-poly(ε-caprolactone) stabilizer with $M_n = 26\,400$ (M_n of PCL was equal to 4700). In these studies, it was found that for the stabilizer concentrations lower than 0.6 g l^{-1}, the yield of polyester microspheres suddenly decreased and almost the whole amount of poly(L,L-lactide) was obtained as the shapeless aggregates.

The above-described features of the dispersion polymerization of lactides allow for the following conclusions. The

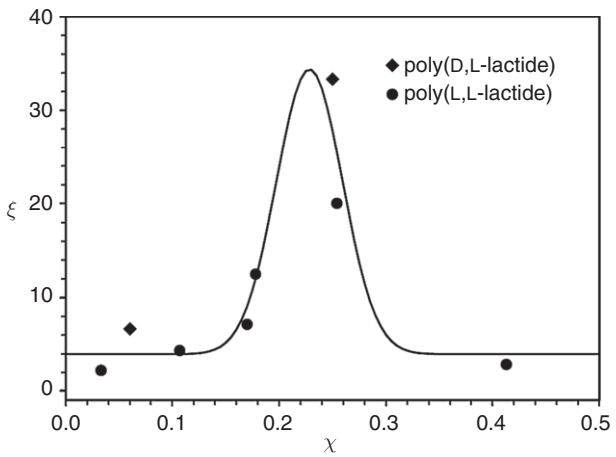

Figure 5 Dependence of parameter $\xi = D_n/(D_w - D_n)$ on the ratio $\chi = M_n$ (PCL)/M_n(PDA-PCL) for dispersion polymerization of L,L- and D,L-lactides initiated with stannous 2-ethylhexanoate. Reproduced with permission from Slomkowski, S.; Sosnowski, S.; Gadzinowski, M. *Polym. Degrad. Stabil.* **1998**, *59*, 153.[22]

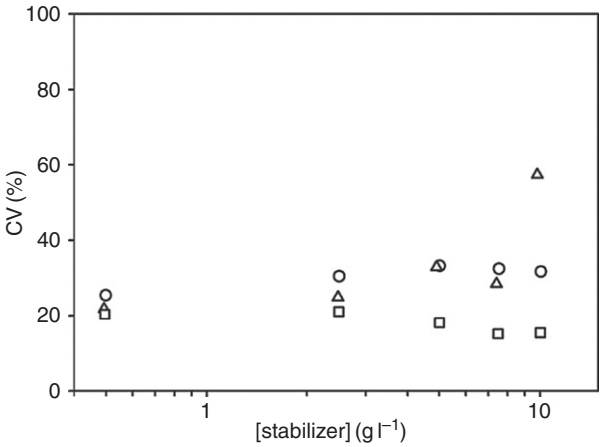

Figure 6 CV of the diameters of poly(D,L-lactide) microspheres synthesized by the ring-opening polymerization which was carried out at various concentrations in the presence of the poly(dodecyl methacrylate)-*graft*-poly(D,L-lactide) stabilizers: stabilizer G_1 (circle), G_2 (triangle), and G_3 (squares). The parameters characterizing the structure of stabilizers are given in Table 1.

Table 1 Poly(dodecyl methacrylate)-*graft*-poly(D,L-lactide) stabilizers used in ring-opening dispersion polymerization of D,L-lactide (based on data from Reference 13)

			Poly(D,L-lactide) graft		
Code	M_w *of stabilizer*	M_w/M_n *of stabilizer*	M_w	M_w/M_n	N
G_1	41 300	2.31	3 700	1.30	1.3
G_2	34 500	2.23	3 700	1.30	2.0
G_3	36 500	2.04	3 700	1.30	3.4
G_4	30 700	2.53	6 600	1.40	2.4

N denotes the average number of poly(D,L-lactide grafts) in poly(dodecyl methacrylate)-*g*-poly(D,L-lactide) molecule.

fraction of dodecyl acrylate and dodecyl methacrylate monomeric units in the stabilizers should be sufficiently high to provide steric stabilization of the polylactide microspheres in the hydrocarbon-rich (heptane and xylene) media. However, when this fraction is too high, the stabilizer prefers to remain in solution, because the blocks of poly(D,L-lactide) or PCL are too short or are present in a too small number in the stabilizer molecules to assure their effective adsorption. For a given concentration of polymer formed during the heterogeneous polymerization, there is a critical concentration of the stabilizer, below which the polymer particles are insufficiently stabilized and therefore aggregate and precipitate as a shapeless coagulum. Obviously, there is always a distribution of a number of the adsorbed stabilizer macromolecules in one formed polylactide particle. Thus, some particles could be sufficiently stabilized, remain in solution, and grow with a similar rate. Therefore, the distribution of the particle diameters could be still quite low, even if a significant part of polymer forms coagulum.

4.25.3.6 Control of Diameters of Polylactide Microspheres Formed in Ring-Opening Dispersion Polymerizations

It is well known that in dispersion radical polymerizations, the diameters of synthesized particles strongly depend on the concentration of stabilizer.[23] In all investigated systems, the increased concentration of stabilizer resulted in the formation of particles of smaller diameters. This is because the thermodynamically most favorable localization of good stabilizer molecules is in the interfacial layer of stabilized particles. Thus, for the systems with higher stabilizer concentrations, the total surface of particles should be larger to accommodate all stabilizer molecules. Assuming that the total mass of polymer microsphere is equal to m and that their diameters are equal to D, one could write

$$m = Nd\frac{1}{6}\pi D^3 \quad [1]$$

where N and d denote the number of particles and the polymer density, respectively.

Since the total surface of microspheres denoted S equals

$$S = N\pi D^2 \quad [2]$$

the following relation holds:

$$S = \frac{6m}{d}\frac{1}{D} \quad [3]$$

Thus, taking into account that the higher amount of stabilizer required for adsorption to the larger surfaces of particles, one could expect that for the higher stabilizer concentrations particles with smaller diameters are formed.

The above-described reasoning should be general and thus valid also for the ring-opening dispersion polymerization of lactides. Indeed, as one can see in **Figure 7**, in the dispersion polymerization of D,L-lactide carried out in the presence of the poly(dodecyl methacrylate)-*graft*-poly(D,L-lactide) stabilizer, the diameters of microspheres obtained at the higher stabilizer concentrations are smaller. It has to be noted, however, that the slopes of the plots in **Figure 7** are not equal to −1, as it should be for the constant surface concentration of stabilizer adsorbed on particles, but are equal to -0.57 ± 0.09. This discrepancy suggests that for a higher concentration of stabilizer in solution, its surface concentration on microspheres is also higher.

It is worth noting, however, that variation of stabilizer concentration, with the purpose to regulate particle diameters, has some limits. It was already mentioned in the previous section that when the concentration of stabilizer is too low instead of microspheres, the shapeless precipitate is obtained. Using the higher initial monomer concentrations with the purpose of obtaining larger microspheres also has some limits. For example, at concentrations of L,L-lactide exceeding 0.4 mol l^{-1}, the

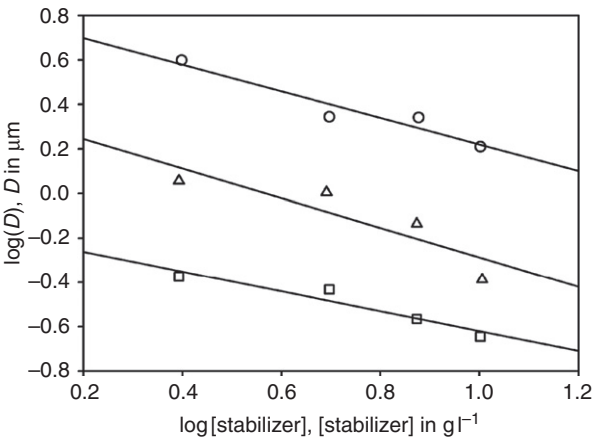

Figure 7 Dependence of the diameters of poly(D,L-lactide) microspheres synthesized by ring-opening polymerization on the concentration of the poly(dodecyl methacrylate)-*graft*-poly(D,L-lactide) stabilizers: stabilizer G_1 (circle), G_2 (triangle), and G_3 (squares). The stabilizers are described in **Table 1**.

monomer is not fully soluble in the heptane/1,4-dioxane mixed solvent (4:1, v/v) containing the poly(dodecyl acrylate)-*graft*-poly(ε-caprolactone) stabilizer.[24] When the polymerization mixture is inhomogeneous at the very beginning of the polymerization, it is impossible to obtain polymer in the form of regular microspheres. In such a system, the undissolved monomer particles with irregular shape and with the not controlled dimensions are coated with polymer.

Complications related to the limited monomer solubility were solved by addition of new monomer portions only when those added earlier were already polymerized. In this way, the total concentration of the monomer, which was added initially and later in the subsequent portions ($[M]_{tot} = [M]_1 + [M]_2 + \ldots$), was increased and poly(L,L-lactide) microspheres with diameters exceeding 6 μm were obtained.

In the above-described experiment, the total mass of polymer microspheres (m) is related to monomer conversion $[M]_{tot} - [M]_{tot,e}$ (where $[M]_{tot,e}$ denotes the equilibrium monomer concentration) in the following way:

$$m = VM_{PLA}([M]_{tot} - [M]_e) \quad [4]$$

where V is the volume of reaction mixture and M_{PLA} is the molecular weight of monomer.

Combination of eqns [1] and [4] leads to the following dependence of diameters of microspheres on the monomer conversion:

$$D = a([M]_{tot} - [M]_{tot,e})^{1/3} \quad [5]$$

where

$$a = \left(\frac{6VM_{PLA}}{\pi dN}\right)^{1/3}$$

Therefore, the dependence of the number-average diameter of poly(L,L-lactide) microspheres on $([M]_{tot} - [M]_{tot,e})^{1/3}$ should be described by the straight line passing through the origin of coordinate point, provided the coefficient a is constant. The dependence of particle diameter on the cubic root of monomer conversion is shown in Figure 8. The plot in Figure 8 is based on the experiment in which the polymerization of L,L-lactide initiated with stannous 2-ethylhexanoate was carried out in heptane/1,4-dioxane mixed solvent (4:1, v/v) containing the poly(dodecyl acrylate)-*graft*-poly(ε-caprolactone) stabilizer.[24,25] The number-average molecular weight of stabilizer was equal to 62 000. The ratio of the number-average molecular weight of the PCL grafts to the number-average molecular weight of the stabilizer was equal to 0.18. The concentrations of initiator and stabilizer were equal to 5.70×10^{-3} mol l^{-1} and 1.67 g l^{-1}, respectively. The initial monomer concentration was equal to 3.50×10^{-1} mol l^{-1}. Polymerization was carried out at 95 °C for 1.5 h. After that time the new portion of monomer was added and the total concentration of L,L-lactide introduced to the polymerization mixture was raised to 6.24×10^{-1} mol l^{-1}. Subsequently, when 1.5 h elapsed, a new monomer portion was added again and the total concentration of introduced L,L-lactide raised to 9.10×10^{-1} mol l^{-1}. Then, the polymerization was continued for another 1.5 h.

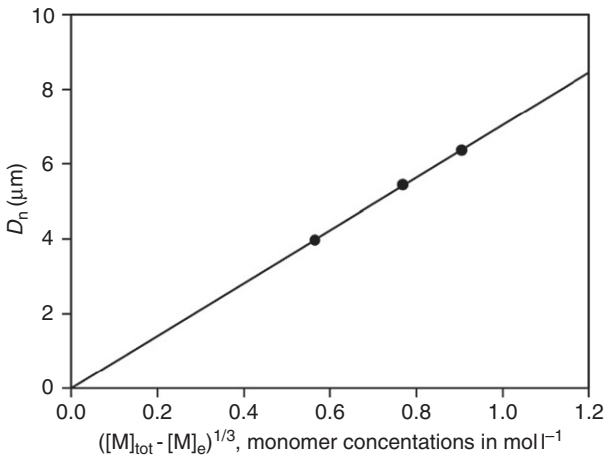

Figure 8 Dependence of the number-average diameter of poly(L,L-lactide) microspheres on $([M]_{tot} - [M]_{tot,e})^{1/3}$ for particles synthesized by dispersion ring-opening polymerization with three monomer additions (based on data from References 24 and 25).

After completion of each polymerization step, a sample of reaction mixture was analyzed. Diameters and diameter distributions of microspheres after the first polymerization step were equal to $D_n = 3.97$ μm and $D_w/D_n = 1.09$. The second step yielded particles with $D_n = 5.44$ μm and $D_w/D_n = 1.13$. The third monomer addition allowed to obtain particles with $D_n = 6.36$ μm and $D_w/D_n = 1.20$. Thus, the broadening of particle diameter distribution after each monomer addition is evident, but it is not very large.

It is worth noting that experimental points in Figure 8 fit very well to the straight line passing through the origin of coordinates. According to the discussion presented above, the straight line dependence indicates that concentration of microspheres was constant during the polymerization with the repeated (three times) monomer addition.

In summary, for a given stabilizer, there is a range within which the decreasing or the increasing of stabilizer concentration leads correspondingly to an increase or a decrease in the diameters of formed microspheres. When microspheres with the required large diameters cannot be obtained by decreasing the concentration of stabilizer (because the system is losing colloidal stability), still there is a chance for successful synthesis by the multistep monomer addition.

4.25.3.7 Mechanism of Particle Formation During Ring-Opening Dispersion Polymerization

Any mechanism proposed for the formation of microspheres in the anionic or the pseudoanionic ring-opening polymerizations of lactides and ε-caprolactone should conform to the following observations:

1. Shortly after beginning of the polymerization, all propagating macromolecules are localized in seeds of microspheres.[14]
2. During the main part of the polymerization (i.e., when monomer conversion exceeds 20%), the number of microspheres is constant.[14,16,17,26,27]
3. Partition of monomer between continuous and condensed (microspheres) phases favors the latter one. The concentration of monomer in microspheres is about 10 times higher than that in solution.[26]

4. The average number of propagating macromolecules per microsphere is independent of initiator concentration varying in quite a broad range.[16]

The mechanism that fulfills the above given requirements is proposed below. According to this mechanism, the polymerization is initiated in solution in a homogenous system. When growing chains reach a critical length, their conformation undergoes transition from coil to globule. In the globular form, they aggregate and create seeds of microspheres. In the case of dispersion polymerization of ε-caprolactone, the critical length at which the propagating chains undergo conformational changes and form seed particles lies in the range of 5–10 monomeric units.[14] After a very short period, the number of seed particles becomes so high that for the new chains that undergo the coil-to-globule transition, the probability for adsorption on seed particles becomes higher than the probability of formation of the new particle seeds.

The following considerations reveal that the mechanism described above also conforms to the requirement of independence of the average number of growing chains per particle on concentration of initiator. It is reasonable to assume that the rate at which the particle seeds are formed is proportional to the concentration of chains with length longer than the critical length. Let us assume that initiation of the polymerization is much faster than the seed formation. Thus, for the rate of the particle seed formation (dN/dt), the following equation could be written:

$$\frac{dN}{dt} = \frac{1}{2}k_a n^2 \qquad [6]$$

where n denotes the concentration of growing chains (defined as the number of chains in a unit volume) with at least the critical length (these chains have globular conformation) and k_a denotes the rate constant of chain aggregation. The coefficient 1/2 was introduced because when two oligomer chains aggregate, only one particle seed is formed.

The growing chains are incorporated into particles by one of the following two processes. The first one consists of formation of particle seeds as a result of chain aggregation and the second one consists of adsorption of oligomers onto the already existing particles. The rate at which oligomer chains are removed from solution during the particle seed formation (R_1) can be described by eqn [7]:

$$R_1 = -k_a n^2 \qquad [7]$$

The rate at which oligomer chains are adsorbed onto the earlier formed particles (R_2) should be proportional to chain concentration (n) and to the total surface of particles in a unit volume of the polymerizing mixture ($S_{total} = NS$, where N denotes the particle concentration and S denotes the average surface of a particle):

$$R_2 = -k_{ads} S n N \qquad [8]$$

Thus, the total rate at which the oligomer chains disappear from solution ($dn/dt = R_1 + R_2$) can be described as

$$\frac{dn}{dt} = -k_a n^2 - k_{ads} S N n \qquad [9]$$

The mass of all seeds of polymer microspheres in a unit volume of reaction mixture (m) is determined by their number-average molar mass (M_n) and the difference of the initial concentration of oligomer chains (n_0) and the chain concentration at a given time moment (n):

$$m = \frac{M_n}{N_A}(n_0 - n) \qquad [10]$$

where N_A denotes the Avogadro number.

The average volume of each microsphere seed equals $V = m/(Nd)$, where d denotes density, therefore

$$V = \frac{1}{6}\pi D^3 = \frac{M_n}{N_A N d}(n_0 - n) \qquad [11]$$

and the formula for S can be written as follows:

$$S = \pi^{\frac{1}{3}}\left[\frac{6M_n}{N_A N d}(n_0 - n)\right]^{2/3} \qquad [12]$$

Taking into account eqn [12], eqn [9] could be rewritten as

$$\begin{aligned}\frac{dn}{dt} &= -k_a n^2 - k_{ads} n \pi^{\frac{1}{3}}\left(\frac{6M_n}{N_A d}\right)^{\frac{2}{3}}\left[N(n_0 - n)^2\right]^{\frac{1}{3}} \\ &= -k_a n^2 - k_{ads}^{eff} n\left[N(n_0 - n)^2\right]^{1/3}\end{aligned} \qquad [13]$$

Numerical solution of a set of eqns [6] and [13] for $k_a = 100\,l\,s^{-1}$ and $k_{ads}^{eff} = 7.3 \times 10^5\,l\,s^{-1}$, and for the concentration of propagating species in the range of 10^{-3}–$5 \times 10^{-2}\,mol\,l^{-1}$ gave number of growing chains per particle (n/N) equal to 1.8×10^8; it is the value determined experimentally for one of the dispersion polymerizations of L,L-lactide.[16]

One must remember, however, that the above-discussed equations describing formation of particle seeds are valid only for the systems in which initiation is much faster than propagation; the oligomers with critical length are formed in the time period much shorter than the time period required for formation of particle seeds and particle nucleation is completed at the early stage of polymerization.

In the heterogeneous systems with different concentrations of reagents in various phases, the kinetics of chemical reactions strongly depends on the volume fraction of each phase. Thus, the above-discussed mechanism of particle formation should have an important influence on the kinetics of the dispersion ring-opening polymerization.

4.25.3.8 Kinetics of Dispersion Polymerization of ε-Caprolactone

In dispersion polymerization, the total volume of reaction mixture (V_t) is equal to the sum of volumes of microspheres (V_m) and of the continuous phase (V_c):

$$V_{tot} = V_m + V_c \qquad [14]$$

One must remember that each microsphere contains not only polymer but also monomer swelling the particle. Similarly, the total number of moles of monomer (m_{tot}) is equal to the sum of moles of monomer in microspheres (m_m) and in the continuous phase (m_c):

$$m_{tot} = m_m + m_c \qquad [15]$$

Thus, monomer concentration averaged over the whole volume of reaction mixture ($[M]_{tot}$) can be described by the following formula:

$$[M]_{tot} = \frac{m_t}{V_{tot}} = \frac{V_m}{V_{tot}}[M]_m + \frac{V_c}{V_{tot}}[M]_c \quad [16]$$

where $[M]_m$ and $[M]_c$ denote monomer concentrations in microspheres and in continuous phase, respectively.

For systems with fast rate of monomer exchange between the microspheres and the continuous phase

$$\frac{[M]_m}{[M]_c} = \beta \quad [17]$$

where β denotes the partition coefficient.

Denoting the volume fraction of microspheres as α ($\alpha = V_m/V_{tot}$), the volume fraction of the continuous phase (V_c/V_{tot}) is equal to $(1-\alpha)$. Thus, eqn [16] could be rewritten as follows:

$$[M]_m = \frac{\beta}{1+\alpha\beta}[M]_{tot} \quad [18]$$

Remembering that in dispersion polymerization, all propagating chains are localized exclusively in microspheres, one could write the equation for the rate at which polymer is formed in particles:

$$\frac{d[P]_m}{dt} = k_{p,m}^{app}[M^*]_m[M]_m \quad [19]$$

where $[P]_m$ and $[M^*]_m$ denote the concentrations of monomeric units in polymer chains and the concentration of propagating active species in microspheres, respectively, and $k_{p,m}^{app}$ denotes the apparent propagation rate constant for polymerization in microspheres. This constant is called 'apparent', because it is a function of the rate constants of propagation involving various kinds of active centers (e.g., ions, ion pairs and ionic aggregates in ionic polymerization, and monomeric and aggregated propagating species in the pseudoionic processes) and a function of the equilibrium constants between these species.

Multiplication of both sides of eqn [19] by $\alpha = V_m/V_{tot}$ leads to the equation describing the rate of polymerization averaged over the whole volume of reaction mixture:

$$\frac{d[P]_{tot}}{dt} = k_{p,m}^{app}[M^*]_{tot}[M]_m \quad [20]$$

where $[M^*]_{tot} = \alpha[M^*]_m$

Substituting the expression for $[M]_m$ from eqn [18] in eqn [20] yields

$$\frac{d[P]_{tot}}{dt} = \frac{\beta}{1+\alpha\beta}k_{p,m}^{app}[M^*]_{tot}[M]_{tot} \quad [21]$$

Remembering that the concentration of monomeric units in polymer (averaged over the whole volume of reaction mixture) equals $[P]_{tot} = [M]_{tot,0} - [M]_{tot}$ and introducing $k_{p,d}^{app} = \frac{\beta}{1+\alpha\beta}k_{p,m}^{app}$ (the apparent propagation rate constant in dispersion polymerization), the kinetic equation can be written as follows:

$$-\frac{d[M]_{tot}}{dt} = k_{p,d}^{app}[M^*]_{tot}[M]_{tot} \quad [22]$$

There are two limiting cases. When the volume fraction of microspheres is so small that $\alpha\beta \ll 1$ the coefficient $\beta/(1+\alpha\beta)$ in eqn [18] simplifies to β. On the other hand, when localization of monomer in particles is strongly favored ($\alpha\beta \gg 1$, which means that particles are constituted from monomer droplets containing small amount of polymer), this coefficient can be approximated by $1/\alpha$. For polymerization with reversible propagation, eqn [22] should be replaced with the modified one (eqn [23]). According to eqn [23] the polymerization process reaches an equilibrium at which the equilibrium monomer concentration ($[M]_{tot,e} = k_{d,d}^{app}/k_{p,d}^{app}$, where $k_{d,d}^{app}$ denotes the depropagation rate constant in dispersion polymerization) is different from zero:

$$-\frac{d[M]_{tot}}{dt} = k_{p,d}^{app}[M^*]_{tot}[M]_{tot} - k_{d,d}^{app}[M^*]_{tot} \quad [23]$$

Solution of eqn [23] gives a formula similar to that for the polymerization in solution:

$$\ln([M]_{tot,0} - [M]_{tot,e})/([M]_{tot} - [M]_{tot,e}) = k_{p,d}^{app}[M^*]_{tot}t \quad [24]$$

The slope of the plot of the left-hand side of eqn [24] versus time allows to determine denotes the depropagation rate constant $k_{p,d}^{app}$. An example of such plot for dispersion polymerization of ε-caprolactone initiated with diethylaluminum ethoxide is shown in **Figure 9**.

One has to remember that for the polymerization of ε-caprolactone, the equilibrium monomer concentration is very low and thus $[M]_{tot,e} \cong 0$.

Experimental points in the kinetic plot shown in **Figure 9** could be approximated with very good accuracy by the straight line with the slope $2.02 \times 10^{-3}\,s^{-1}$ for which the apparent propagation rate constant was $k_{p,d}^{app} = 1.25 \times 10^{-1}\,l\,(mol\,s)^{-1}$. The short induction period in this plot corresponds to the time during which nuclei become particles.

Figure 10 shows the dependence of the apparent propagation rate constants of the anionic and pseudoanionic dispersion polymerizations of ε-caprolactone ($k_{p,d}^{app}$) on the concentration of propagating species. In **Figure 10**, there are also given plots of the ratios of the apparent propagation rate constants for dispersion polymerization and for the polymerization in solution ($k_{p,d}^{app}/k_{p,s}^{app}$).

Plots in **Figure 10** show that the apparent propagation rate constants of the anionic and pseudoanionic dispersion

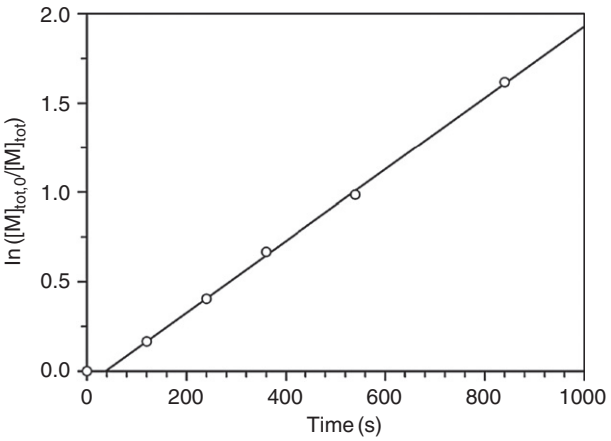

Figure 9 Kinetic plot for dispersion polymerization of ε-caprolactone. $[M_t]_{tot,0}$ and $[M]_{tot}$ denote monomer concentrations averaged over the whole polymerizing mixture, the initial concentration and concentration at a given time, respectively. Polymerization conditions: $[\varepsilon\text{-caprolactone}]_0 = 4.3 \times 10^{-1}\,mol\,l^{-1}$, $[(CH_3CH_2)_2AlOCH_2CH_3]_0 = 1.6 \times 10^{-2}\,mol\,l^{-1}$. Reproduced with permission from Gadzinowski, M.; Sosnowski, S.; Slomkowski, S. *Macromolecules* **1996**, *29*, 6404.[14]

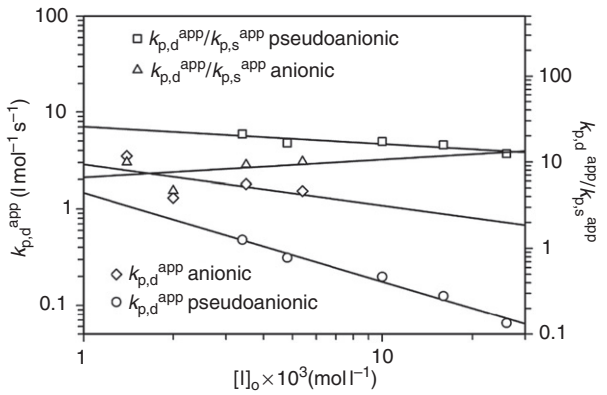

Figure 10 Dependence of the apparent propagation rate constants of the anionic and pseudoanionic dispersion polymerizations ($k_{p,d}^{app}$) and dependence of the ratio of the apparent propagation rate constants for dispersion polymerization and for the polymerization in solution ($k_{p,d}^{app}/k_{p,s}^{app}$) of ε-caprolactone on the concentration of propagating species. Conditions of the polymerization: $(CH_3CH_2)_2AlOCH_2CH_3$, initiator for the pseudoanionic polymerization; $(CH_3)_3SiONa$, initiator for the anionic polymerization; initial monomer concentration $[\varepsilon\text{-caprolactone}]_0 = 0.41 \pm 0.02$ mol l^{-1}; continuous medium for dispersion polymerization, 1,4-dioxane:heptane (1:9, v/v) mixture; for solution polymerization in THF. Reproduced with permission from Slomkowski, S.; Gadzinowski, M.; Sosnowski, S. *Macromol. Symp.* **1998**, *132*, 451.[17]

polymerizations decrease with increasing initiator concentration. This dependence indicates that like in the case of solution polymerizations, in dispersion polymerization, the higher the concentration of propagating species, the higher the fraction of the less reactive aggregates. It is worth noting also that $k_{p,d}^{app}/k_{p,s}^{app}$ ranges from 8 to 12. Remembering that partition of ε-caprolactone between reaction medium and microspheres is such that monomer concentration in particles is about 10 times higher than that in the continuous phase ($\beta \cong 10$),[26] that fraction of particles in reaction mixture $\alpha \cong 0.04$, and taking into account the relation $k_{p,d}^{app} = \frac{\beta}{1+\alpha\beta} k_{p,m}^{app}$, one could estimate the ratio $k_{p,d}^{app}/k_{p,m}^{app} \cong 7$. Thus, for the same initiator concentrations, the apparent propagation rate constants for polymerization of ε-caprolactone in microspheres and in solution are quite close. Their ratio ($k_{p,m}^{app}/k_{p,s}^{app}$) ranges from 1.1 to 1.7,

4.25.3.9 Control of Molecular Weight in Dispersion Polymerization of ε-Caprolactone

Polymerization of ε-caprolactone consists of a complex system of reactions including, in addition to propagation, intra- and intermolecular transesterification.[28] As a result, at equilibrium, the system is composed of a linear polymer with a broad molecular weight distribution and cyclic oligomers present in significant amounts.[28–30] Because the equilibrium concentration of cyclics depends very weakly on the initial monomer concentration, running the polymerization at high monomer concentration allows to decrease the fraction of cyclic oligomers in the final product. It has also been found that proper selection of initiators allows to separate the time periods during which linear macromolecules and cyclics are formed.[31–36] In such systems, polymerization could be stopped at high monomer conversion, before cyclics begin to appear in a significant concentration. The kinetic reduction in the formation of cyclic oligomers was achieved by using initiators yielding the less reactive active centers, which were still able to react with strained monomer but were much less reactive toward the unstrained linear polyesters. In accordance with the above-described principle, the kinetic suppression of the formation of cyclic oligomers was noticed for the pseudoanionic polymerizations with covalent active species, which are less reactive than those in the anionic polymerization.

It was interesting to find out whether the dispersion polymerization of ε-caprolactone with all active centers localized inside the monomer swollen particles allows for synthesis of polymers with narrow molecular weight distribution and with controlled molecular weight. Studies were performed for the polymerizations carried out in 1,4-dioxane:heptane (1:9, v/v) mixture using $(CH_3CH_2)_2AlOCH_2CH_3$ and $(CH_3)_3SiONa$ as initiators of the pseudoanionic and anionic polymerizations, respectively. Results of these studies are summarized in Figure 11.

The calculated number-average molecular weight (M_n (calcd)) was obtained assuming that the functionality of initiators of the anionic and pseudoanionic polymerizations was equal to 1 and that all the monomer was converted into polymer:

$$M_n(\text{calcd}) = M_{CL} \frac{[\varepsilon - \text{caprolactone}]_0}{[I]_0} \qquad [25]$$

where M_{CL} and $[I]_0$ denote molecular weight of monomer and concentration of initial initiator, respectively.

The plot in Figure 11 shows very good agreement between the calculated and experimentally determined molecular weight of PCL (the slope of the linear regression line was equal to 1.16). Such dependence is characteristic of polymerizations with absence of any chain transfer reactions. The low dispersity for the high-molecular-weight polymers (M_w/M_n close to 1.15) also indicates that chain transfer does not play an important role.

It is worth noting that with respect to transesterification, the anionic polymerizations of ε-caprolactone carried out in solution and in dispersion differ significantly. In the anionic

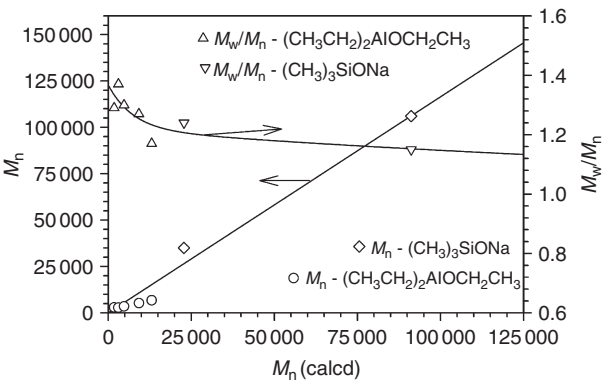

Figure 11 Relation between the experimentally determined molecular weight, dispersity (M_w/M_n), and calculated number-average molecular weight (M_n(calcd)) for the pseudoanionic and anionic polymerization of ε-caprolactone. Reproduced with permission from Slomkowski, S.; Sosnowski, S.; Gadzinowski, M.; *et al. Macromol. Symp.* **2000**, *150*, 259.[27]

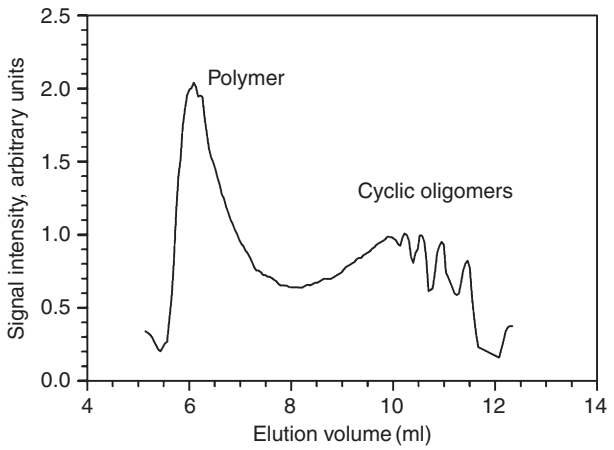

Figure 12 GPC trace of the product of the anionic solution polymerization of ε-caprolactone in THF. Conditions of polymerization: $[\varepsilon\text{-caprolactone}]_0 = 6.1 \times 10^{-1}$ mol l^{-1}, initiator $[(CH_3)_3SiONa]_0 = 6.1 \times 10^{-3}$ mol l^{-1}, and temperature 20 °C. Reproduced with permission from Sosnowski, S.; Slomkowski, S.; Penczek, S.; Reibel, L. *Makromol. Chem.* **1983**, *184*, 2159.[30]

polymerization in solution, transesterification yields product with the high content of cyclic oligomers (see Figure 12). On the contrary, the GPC trace of the product of the anionic dispersion polymerization indicates that the polymer does not contain cyclic oligomers in a measurable amount (see Figure 13). Whereas the absence of cyclics reveals the strong reduction of intramolecular transesterification, the narrow molecular weight distribution proves that intermolecular transesterification is also strongly reduced.

The reason for the very efficient reduction of transesterification in the anionic dispersion polymerization of ε-caprolactone is not yet fully clarified. However, it is possible that the high local viscosity inside of microspheres reduces the reactivity of the propagation centers and makes them more selective.

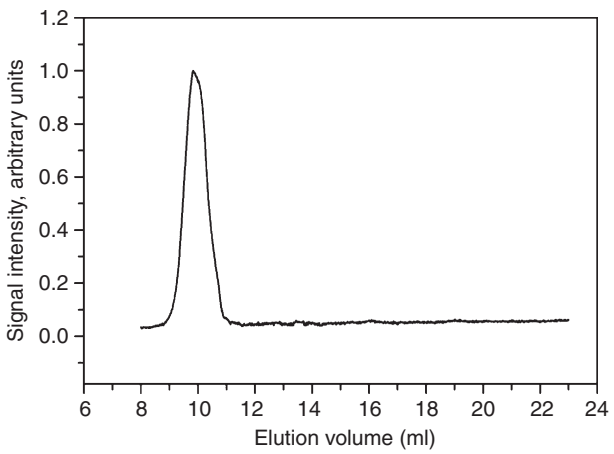

Figure 13 GPC trace of the anionic dispersion polymerization of ε-caprolactone in 1,4-dioxane:heptane (1:9 v/v) mixture. Polymerization conditions: $[\varepsilon\text{-caprolactone}]_0 = 4.0 \times 10^{-1}$ mol l^{-1}, initiator $[(CH_3)_3SiONa]_0 = 5.1 \times 10^{-4}$ mol l^{-1}, room temperature. From calibration on PCL samples with narrow molecular weight distribution $M_n = 106\,600$, $M_w/M_n = 1.15$. Reproduced with permission from Slomkowski, S.; Sosnowski, S.; Gadzinowski, M. *Colloids Surf. A Physicochem. Eng. Aspects* **1999**, *153*, 111.[26]

4.25.3.10 Mechanism of Dispersion Polymerization of ε-Caprolactone and Lactides

All experimental data collected in studies of the dispersion ring-opening polymerization of ε-caprolactone and lactides conform to the polymerization scheme shown in Figure 14.

According to this scheme, initially monomer, initiator, and stabilizer are dissolved in reaction medium. Initiation begins in solution (Figure 14(a)) and propagating chains grow until they reach the critical length (Figure 14(c)). In the case of ε-caprolactone, the critical chain length ranges from about 5 to 10 monomeric units. The oligomers with critical length undergo the coil-to-globule transition and aggregate forming the primary particles onto which the stabilizer is adsorbed. Monomer swells the colloidally stable particles and the polymerization proceeds inside the particles. These particles could be considered as microreactors.

It is worth noting that in the case of the dispersion ring-opening polymerizations of lactides and ε-caprolactone, the term living can be used in the traditional sense, describing processes in which after fast initiation the propagation proceeds without significant contribution of chain transfer and termination. The dispersion polymerization of lactides and ε-caprolactone also proceeds with rapid formation of particles, which after the initial period do not undergo aggregation and coalescence. Therefore, in the ring-opening polymerization of the above-mentioned monomers, both macromolecules and particles can be considered as living.

4.25.4 Practical Importance of Ring-Opening Dispersion Polymerization

Active species in the ring-opening dispersion polymerizations are sensitive to any compounds with carboxyl and hydroxyl groups. Thus, these processes are usually carried out in aprotic media, most often hydrocarbons and mixtures of hydrocarbons with cyclic ethers. Obviously, although the isolation of polymer in the form of precipitating particles is convenient, the need for recycling of volatile and flammable reaction medium makes these processes often inferior to the bulk polymerizations. However, there are some exceptions. The cationic dispersion polymerization of 1,3,5-trioxane is an example. This process is carried out at temperatures well below the melting temperature of the polymer (e.g., at 60 °C, whereas poly(1,3,5-trioxane) melts at 180 °C). Thus, the bulk polymerization in melt would require more energy for heating compared to the dispersion polymerization at the much lower temperature. Moreover, crystallization of poly (1,3,5-trioxane) shifts equilibrium between monomer and polymer to the side of the latter.

In the case of polylactides and PCL, the synthesis by dispersion polymerization does not provide any advantage over polymerizations in bulk. However, for preparation of materials for various medical applications, when biodegradable particles with the narrow diameter dispersity, composed of polymers with the narrow molecular weight distribution, are needed, the dispersion polymerization may be the choice.

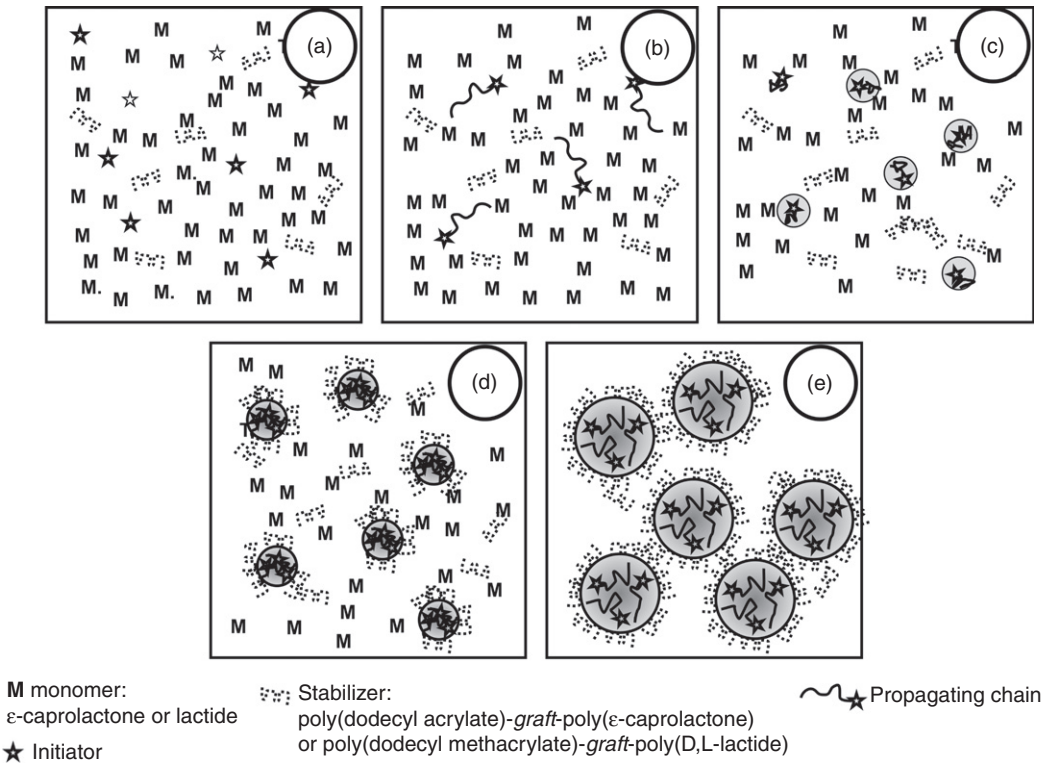

Figure 14 Schematic illustration of dispersion polymerization of ε-caprolactone and lactides. (a) – solution before beginning of the polymerization, (b) – polymerization in solution, length of polymer chains is shorter than the critical one, (c) – chain-to-globule transition and formation of the primary particles, all active centers in particles, (d) – propagation in momomer swollen microspheres, (e) – end of polymerization, microspheres contain still active propagation species.

The carefully controlled treatment of PCL and polylactide microspheres with KOH solution allows particles with interfacial layer rich in carboxyl and hydroxyl groups to be obtained.[37] These groups could be used for binding fluorescent labels, for example, 6-aminoquinoline and Lucifer yellow.[37,38] In biological and medical studies, the fluorescent particles are often used for monitoring an uptake of particulate material by cells and for its visualization in various intracellular compartments.

The polylactide and PCL microspheres obtained by the ring-opening dispersion polymerization can be used as well-defined carriers of biologically active compounds. The following strategies were developed for preparation of the drug-loaded polyester particles:

1. Incorporation of bioactive compound into the microspheres during dispersion ring-opening polymerization.
2. Synthesis of microspheres containing prodrug formed when the bioactive compound acts as the chain transfer agent and becomes covalently attached to polyester macromolecules in microspheres.
3. Adsorption of bioactive compounds onto the surface of microspheres.
4. Swelling of microspheres with liquid bioactive compound.

The first strategy can be used only in the case of drugs that are inert to any components of polymerizing mixture, in particular for drugs that do not react with propagation active centers. The above-mentioned method was used for synthesis of the omeprazole (5-methoxy-2-{[(4-methoxy-3,5-dimethylpyridyl)-methyl]sulfinyl}-1H-benzimidazole)-loaded poly(L,L-lactide) microspheres.[38,39] Omeprazole, an inhibitor of (H^+–K^+)ATPase,[40,41] is used as an active substance in drugs administered for reduction of HCl secretion in stomach (e.g., for treatment of gastric hyperacidity). The omeprazole-loaded poly(L,L-lactide) microspheres were synthesized by the dispersion polymerization of L,L-lactide initiated with stannous 2-ethylhexanoate and carried out at 95 °C in heptane/1,4-dioxane mixture (4:1 (v/v) ratio) containing dissolved poly(dodecyl acrylate)-*graft*-poly(ε-caprolactone) stabilizer. The polymerization was started according to the description given in Section 4.25.3.4.1. Shortly after nucleation of microspheres, when the polymerizing mixture became turbid, the solution of omeprazole in heptane was added dropwise and the polymerization was continued for 2 h. The number-average diameter of obtained microspheres (D_n) was 1.73 μm and the dispersity (D_w/D_n) was 1.17. The content of omeprazole in microspheres was equal to 11%. It is worth noting that GPC and ^{1}H nuclear magnetic resonance (NMR) analysis of microspheres dissolved in THF revealed that the process of encapsulation did not lead to decomposition of omeprazole.[38]

The second strategy was used for the synthesis of PCL microspheres containing *N*,*N*-bis(2-hydroxyethyl)isonicotinamide.[38] The microspheres were obtained by dispersion polymerization of ε-caprolactone carried out at room temperature in heptane/1,4-dioxane mixture (9:1, v/v). The

polymerization was initiated with $(CH_3)_3SiONa$. *N,N*-Bis (2-hydroxyethyl)isonicotinamide was present in the polymerizing mixture from the very beginning. The colloidal stability of produced microspheres was secured due to the presence of poly (dodecyl acrylate)-*graft*-poly(ε-caprolactone) stabilizer. During polymerization, the hydroxyethyl groups of *N,N*-bis(2-hydroxyethyl)isonicotinamide participated in chain transfer reactions, resulting in the incorporation of the drug into the polymer chain. It is worth noting, however, that any PCL macromolecule cannot contain more than one molecule of this drug. Thus, the drug content in obtained microspheres was very low (only up to 6.4%).

The usefulness of the third strategy, based on adsorption of bioactive compounds onto the surface of microspheres, was verified for preparation of poly(D,L-lactide) and PCL microspheres with adsorbed proteins.[10] The protein-loaded particles were obtained by incubation of poly(D,L-lactide) ($D_n = 2.50\,\mu m$) or PCL ($D_n = 0.63\,\mu m$) microspheres with human serum albumin or with human γ-globulin solutions. PCL microspheres with the maximal content of human serum albumin and γ-globulin equal to 9.0% and 23.6% (w/w), respectively, were obtained. In the case of much larger poly(D,L-lactide) microspheres, the maximal protein content was equal to 2.1% and 4.0% for human serum albumin and γ-globulin, respectively.

The model PCL microspheres swollen with lipophilic ethyl salicylate were obtained by incubation of particles (5.4 mg of microspheres with $D_n = 0.62\,\mu m$ and $D_w/D_n = 1.5$) with 1 ml of a mixture of ethanol–water (7:1, v/v) containing from 1.5 to 50 μl of ethyl salicylate. The incubation was carried out at room temperature for 48 h and particles were isolated by centrifugation. Partition of ethyl salicylate between PCL microspheres and continuous phase favoring the former yielded particles with drug content from about 9% to 34% (w/w).

Due to the relatively easy and precise control of diameters of polylactide microspheres obtained by ring-opening polymerization, these particles may also be considered as interesting candidates for building blocks of polymeric scaffolds used in tissue engineering. Recently, there were reports on the advantages of polylactide scaffolds for hard tissue engineering that were prepared by sintering of poly(lactide-*co*-glycolide) microspheres.[42–44] However, for these applications, particles with diameters close to 100 μm should be synthesized.

References

1. Penczek, S.; Fejgin, J.; Sadowska, A.; Tomaszewicz, M. *Makromol. Chem.* **1968**, *116*, 203.
2. Union Carbide. U.S. Patent 3,632,669, 1972.
3. Cohen, H.; Levy, R. J.; Gao, J.; *et al. Gene Ther.* **2000**, *7*, 1896.
4. Almeida, A. J.; Souto, E. *Adv. Drug Deliv. Rev.* **2007**, *59*, 478.
5. Borden, M.; Attawia, M.; Laurencin, C. T. *J. Biomed. Mater. Res.* **2002**, *61*, 421.
6. Borden, M.; El-Amin, S. F.; Attawia, M.; Laurencin, C. T. *Biomaterials* **2003**, *24*, 597.
7. Ottewill, R. H. In *Emulsion Polymerization and Emulsion Polymers*; Lovell, P. A.; El-Aasser, M. S., Eds.; Wiley: Chichester, UK, 1997; p 59.
8. Samon, J. M.; Schultz, J. M.; Hsiao, B. S.; *et al. Polymer* **2001**, *42*, 1547.
9. Takasa, K.; Miyashita, N.; Takeda, K. *J. Appl. Polym. Sci.* **2005**, *99*, 835.
10. Sosnowski, S.; Gadzinowski, M.; Slomkowski, S.; Penczek, S. *J. Bioact. Compatible Polym.* **1994**, *9*, 345.
11. Sosnowski, S.; Gadzinowski, M.; Slomkowski, S. *Macromolecules* **1996**, *29*, 4556.
12. Muranaka, M.; Kitamura, Y.; Yoshizawa, H. *Colloid Polym. Sci.* **2007**, *285*, 1441.
13. Muranaka, M.; Yoshizawa, H.; Ono, T. *Colloid Polym. Sci.* **2009**, *287*, 525.
14. Gadzinowski, M.; Sosnowski, S.; Slomkowski, S. *Macromolecules* **1996**, *29*, 6404.
15. Muranaka, M.; Ono, T. *J. Polym. Sci. A Polym. Chem.* **2009**, *47*, 5230.
16. Sosnowski, S.; Slomkowski, S.; Lorenc, A.; Kricheldorf, H. R. *Colloid Polym. Sci.* **2002**, *280*, 107.
17. Slomkowski, S.; Gadzinowski, M.; Sosnowski, S. *Macromol. Symp.* **1998**, *132*, 451.
18. Jakubowski, W.; Lutz, J.-F.; Slomkowski, S.; Matyjaszewski, K. *J. Polym. Sci.: Part A: Polym. Chem.* **2005**, *43*, 1498.
19. Leenslag, J. W.; Pennings, A. J. *J. Makromol. Chem.* **1987**, *188*, 1809.
20. Jamshidi, K.; Eberhart, R. C.; Hyon, S.-H.; Ikada, Y. *ACS Polym. Prep.* **1987**, *28* (1), 236.
21. Duda, A.; Penczek, S. *Macromolecules* **1990**, *23*, 1636.
22. Slomkowski, S.; Sosnowski, S.; Gadzinowski, M. *Polym. Degrad. Stabil.* **1998**, *59*, 153.
23. Cawse, J. L. In *Emulsion Polymerization and Emulsion Polymers*; Lovell, P. A.; El-Aasser, M. S., Eds.; Wiley: Chichester, UK, 1997; p 743.
24. Slomkowski, S.; Sosnowski, S. *ACS Polym. Prep.* **1998**, *39* (2), 212.
25. Slomkowski, S.; Sosnowski, S. In *Polymeric Drug and Drug Delivery Systems*; Ottenbrite, R. M., Kim, S. W., Eds.; CRC: Boca Raton, FL, 2001; Chapter 19, p 261.
26. Slomkowski, S.; Sosnowski, S.; Gadzinowski, M. *Colloids Surf. A Physicochem. Eng. Aspects* **1999**, *153*, 111.
27. Slomkowski, S.; Sosnowski, S.; Gadzinowski, M.; *et al. Macromol. Symp.* **2000**, *150*, 259.
28. Ito, K.; Hashizuka, Y.; Yamashita, Y. *Macromolecules,* **1977**, *10*, 821.
29. Ito, K.; Yamashita, Y. *Macromolecules* **1978**, *11*, 68.
30. Sosnowski, S.; Slomkowski, S.; Penczek, S.; Reibel, L. *Makromol. Chem.* **1983**, *184*, 2159.
31. Slomkowski, S.; Duda, A. In *Ring-Opening Polymerization*; Brunelle, D. J., Ed.; Carl Hanser Verlag: Munich; Viennna; New York, 1993; p 87.
32. Penczek, S.; Duda, A.; Szymanski, R. *Macromol. Symp.* **1998**, *132*, 441.
33. Penczek, S.; Cypryk, M.; Duda, A.; *et al. Prog. Polym. Sci.* **2007**, *32*, 247.
34. Hofman, A.; Slomkowski, S.; Penczek, S. *Makromol. Chem. Rapid Commun.* **1987**, *8*, 387.
35. Penczek, S.; Duda, A.; Slomkowski, S. *Makromol.Chem. Macromol.Symp.* **1992**, *54/55*, 31.
36. Baran, J.; Duda, A.; Kowalski, A.; *et al. Macromol. Symp.* **1997**, *123*, 93.
37. Gadzinowski, M.; Slomkowski, S.; Elaissari, A.; Pichot, Ch. *J. Biomater. Sci. Polym. Edn.* **2000**, *11*, 459.
38. Slomkowski, S. In *Colloidal Biomolecules, Biomaterials, and Biomedical Applications*; Elaissari, A., Ed.; Surfactant Science Series, Vol. 116; Marcel Dekker: New York, 2003; p 371.
39. Slomkowski, S.; Sosnowski, S.; Gadzinowski, M.; *et al.* In *Tailored Polymeric Materials for Controlled Delivery Systems*; McCulloch, I., Shalaby, W., Eds.; ACS Symp. Ser. 709; ACS: Washington, DC, 1998; p 143.
40. Sturm, E.; Kruger, U.; Senn-Bilfinger, J.; *et al. J. Org. Chem.* **1987**, *52*, 4573.
41. Senn-Bilfinger, J.; Kruger, U.; Sturm, E.; *et al. J. Org. Chem.* **1990**, *55*, 4163.
42. Borden, M.; Attawia, M.; Khan, Y.; Laurencin, C. T. *Biomaterials* **2002**, *23*, 551.
43. Borden, M.; El-Amin, S. F.; Attawia, M.; Laurencin, C. T. *Biomaterials* **2003**, *24*, 597.
44. Borden, M.; Attawia, M.; Khan, Y.; *et al. Bone Joint Surg.* **2004**, *86-B*, 1200.

Biographical Sketch

Stanislaw Slomkowski graduated from the Department of Physics of the Moscow State Lomonosov University (Russia) in 1968. Then, he worked at the Technical University in Lodz (Poland). In 1972 he moved to the Center of Molecular and Macromolecular Studies of the Polish Academy of Sciences (CMMS PAS) in Lodz. After receiving a Ph.D. under the guidance of Prof. Stanislaw Penczek he spent a year (1975/76) in the laboratory of Prof. Michel Szwarc at the New York State University at Syracuse as the post doctoral fellow. After returning to CMMS PAS he focused his studies on the ring-opening polymerization of cyclic esters, for which in 1988 he received the D.Sc. degree. In 1997 he obtained the Full Professor title. Currently he is the head of Department of Engineering of Polymer materials and Director of CMMS PAS. He worked as a research associate at the University of Toronto (Canada) in 1986 and as an invited professor at the University Paris Diderot (France). His major research interest are concentrated on fundamental and applied studies of polymer nano- and microobjects and related materials for medical diagnostics and drug delivery, in particular on dispersion ring-opening polymerization of cyclic esters.

4.26 Ring-Opening Metathesis Polymerization in the Synthesis of Conjugated Polymers

WJ Feast, Durham University, Durham, UK

4.26.1 Introduction

4.26.1.1 Preamble

Conjugated polymers are of considerable scientific and technological interest. They have a fairly long history as a subject of intellectual curiosity but, particularly during the past few decades, have become a matter of real interest in practical technologies. As will emerge, many of the materials of interest, which were initially made and investigated out of the scientific curiosity aroused by theoretical speculations, are beginning to offer hope of a major shift in the ease of manufacture and application of some useful technologies.

At the time of writing, summer 2010, it is clear that the world faces many major challenges and that there are great differences in the quality of life for different sections of the global population. Science and technology brings benefits to some that contribute to their ability to live increasingly healthy, interesting, and comfortable lives; by contrast, in some parts of the world, many people do not have either adequate food and shelter or access to clean water and medical care. The severe consequences of these problems are compounded by the predictions of possible damaging climate change, economic difficulties, and the world's limited finite material resources. Considerations of this kind make us all aware of the importance of providing wider access to new technologies as a small step toward improving quality of life; for example, through better and cheaper communications, displays, lighting, medical diagnostics and treatment devices; as presently formulated many of these things are expensive with regards to the use of resources and energy. To begin to tackle this challenge and make a contribution toward rectifying some of the current gross imbalances, low-cost manufacturing of useful technological products having low-energy running costs is essential. It has emerged that conjugated polymers, many of which are polymeric semiconductors, are key materials in realizing this objective. This applies to all the technologies listed above, and possibly many others. The materials involved are organic polymers or oligomers and so, in principle, capable of being relatively cheap; they allow large-scale manufacture of devices via well-established relatively inexpensive solution-processing or printing technologies and they have excellent electronic properties for device formulation. Conjugated polymers may also have a role to play in the generation of clean energy via solar cells and in other electrical technologies such as batteries.

4.26.1.2 Origins of Interest in Conjugated Polymers

Although it can be argued that conjugated polymers, in various manifestations of pyrolytic graphite, were in use as the filaments in the electric lights invented variously by Grove, Swan, and Edison during the nineteenth century, those technologies were undoubtedly empirically derived, expensive in labor and energy terms, and relatively short lived as useful technologies.[1–3] In chemistry, the development of competences in synthesis, together with structural and theoretical understanding, grew rapidly from the early years of the twentieth century. With this increasing understanding of chemical bonding came speculation concerning the likely properties of materials that were nonexistent at the time. For our present context, the 1931 publication of Hückel,[4] a theoretical physicist working on an

abstruse problem during economically constrained times, was a key step (the reader may find aspects of this paper instructive vis-à-vis the history of ideas and societal attitudes to the funding of science in economically stressed times). He postulated that sets of electrons in the same unsaturated hydrocarbon molecule could be considered to move orthogonally and, as a consequence, their behaviors and properties could be treated separately; chemists now classify these electrons as sigma (σ) and pi (π), and treat σ-electrons as if they were largely localized, providing the bonding of the molecular structural framework and π-electrons as less tightly bound, delocalized, and more mobile. Another 'scene setting' factor was the demonstration, by Staudinger,[5] that molecular weight was the major factor that distinguished the properties of the materials we now know as polymers from ordinary organic molecules. This early work led Lennard-Jones, in 1937,[6] to publish a theoretical consideration of the likely properties of the π-electrons in a long linear chain assembled from sp^2 hybridized carbons, each bonded to another sp^2 carbon and a single hydrogen atom using σ-electrons and having an electron in a 2p atomic orbital (AO) perpendicular to the σ-bond framework, that is, polyacetylene, undoubtedly the paradigm for our field. In his model, the carbon–carbon bonds would all have the same length and the π-molecular orbitals (MOs) would form a continuous band structure that was half filled with π-electrons. This band structure had similarities with the picture of bonding in electrically conducting metals; consequently, he concluded that polyacetylene could be expected to display metallic behavior. In the same University 19 years later, Longuet-Higgins and Salem repeated the calculation in a more sophisticated formalism and concluded that such a structure would experience a Peierls distortion and alternating carbon–carbon bond lengths rather than the equal bond lengths assumed by Lennard-Jones in his completely delocalized model. Consequently, they predicted that the π-MOs would form bonding and antibonding bands separated by a gap;[7] if this was the case, the size of the gap would determine whether the material was a semiconductor or an insulator. The obvious thing to do is to make some polyacetylene and do the appropriate electrical measurements; however, 'obvious things' are not necessarily easy things to do well. The obvious first choice route is, of course, the direct addition polymerization of acetylene (Figure 1).

Natta's group were the first to do this job properly; in 1958, they polymerized acetylene by bubbling the gas into a solution of a transition metal-based catalyst, such as $(C_2H_5)_3Al/Ti(OC_4H_9)_4$ in a hydrocarbon solvent; the dark, air-sensitive, insoluble, infusible powder that precipitated was shown, by X-ray diffraction, to be *trans*-polyacetylene.[8] As far as I have been able to discover from people who knew him, Natta thought it a fairly unattractive material and moved on to other things; indeed the properties listed were not encouraging despite the expectations based on the earlier theoretical calculations. The dark color, which varies with the prevalent geometry of the double bonds in the sample, is to be expected for any conjugated polyene of significant length that is able to adopt a fairly planar conformation; where there is any steric inhibition of planarity, the color lightens and, for example, poly(hexafluorobutyne) is an off-white, insoluble material in which we are led, by a combination of X-ray photoelectron spectroscopy (XPS) and MO calculations, to the conclusion that successive double bonds are perpendicular to each other due to the steric interactions between adjacent trifluormethyl groups on the backbone. Although this particular polymer is conjugated in the sense of having alternating single and double bonds, it is not conjugated in a π-electron delocalization sense.[9] Similarly, poly(*tert*-butylacetylene) has alternating single and double bonds that are perpendicular to each other and is colorless.

There are many ways of representing simple unsubstituted polyacetylene (see Figure 2). Most of the isomers are able to adopt a conformation that is fairly close to planar; however, it seems certain that an all *cis*-cisoid form will be forced to adopt a helical conformation. The predominant form obtained by conventional polymerization at or above room temperature is the *trans* structure; at lower temperatures, *cis* structures predominate. *Trans*-transoid or *cis*-transoid is how the structure is generally represented although other conformations and various defects can contribute. Thus, early electron spin resonance (ESR) spectroscopic investigation of the as-made material showed the presence of free spins, suggesting a material with bond alternation defects as shown at the bottom of Figure 2; also ^{13}C nuclear magnetic resonance (NMR) spectroscopy indicated the presence of sp^2 carbons in both *cis* and *trans* environments and sp^3 carbons suggesting cross-links due to carbon–carbon coupling. Thus, we can see that even this superficially simple polymer structure can exist in a number of interchangeable forms. The fact that the material is also air sensitive and thermally labile makes it quite a demanding material with respect to handling and sample reproducibility.

Ten years later, the polyacetylene story moved from Italian academe to American industry, when two chemists working for Cyanamid, Berets, and Smith took Natta's dark powder and compressed it into a disc that turned out to be a poor semiconductor, the conductivity of which increased in the presence of volatile oxidants like iodine and decreased in the presence of ammonia vapor.[10]

Following these early developments, there came a great stimulus to work on the material in 1971 when Ikeda and Shirakawa published their discovery that polymerization of

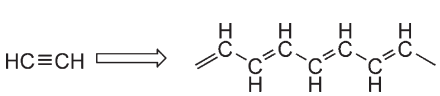

Figure 1 Addition polymerization of acetylene.

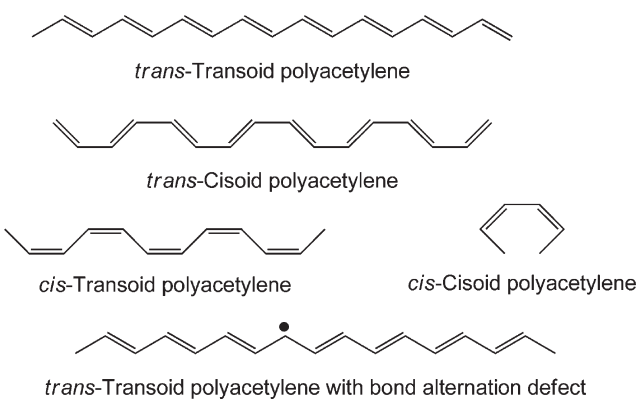

Figure 2 Segments of different forms of polyacetylene.

acetylene gas at the surface of a concentrated solution of a Ziegler–Natta catalyst in an hydrocarbon solvent leads to the formation of porous low-density mats of semicrystalline polyacetylene fibers that were in a suitable form for relatively easy handling and careful investigation of the physics and materials science of the material.[11] There was a tremendous explosion of activity and the field remained of interest to theoreticians, materials chemists, and physicists. The polyene structures indicated in Figure 2 are expected to be reactive organic chemicals and readily subject to reduction and oxidation (redox) chemistry, allowing mobile delocalized radicals, cations, anions, radical cations, and radical anions to be formed on the backbone and act as charge carriers. The low-density mats of polyacetylene fibrils allowed relatively easy access to reagents. It was soon shown that polyacetylene undergoes massive redox modification on exposure to chemical or electrochemical oxidation or reduction and the conductivity of this superficially simple polymer has been demonstrated to vary from that of a good insulator to that of a metallic conductor.[12] Thus, the Shirakawa route can lead to materials with a conductivity as low as $10^{-14}\,S\,cm^{-1}$, comparable to quartz, for *cis*-polyacetylene carefully prepared and handled at low temperature; whereas values of $10^{5}\,S\,cm^{-1}$ or higher have been obtained for stretch-aligned films heavily oxidized by iodine.[13] Clearly, a superficially simple organic polymer like this that can be manipulated by redox procedures to display electrical conductivity varying over 19–20 orders of magnitude is likely to attract intense interest and so it proved. Polyacetylene as generally obtained via the direct route has predominantly *trans* geometry at the vinylenes, often has saturated carbon structural defects (probably evidence of cross-links), and is electrically neutral, but ESR shows free spins, that is radicals, which are located in delocalized nonbonding MOs at the middle of the band gap and are associated with structural defects where the sense of the conjugation in the polyene chain is reversed (see Figure 2). Such electrons are mobile along the chain and can 'hop' between chains, thus accounting for the observed electrical conductivity; the other potential charge carriers mentioned above can move in a similar manner. The transport of such electronic charge carriers through films under the influence of fields is of interest in many of the semiconductor-based electronics-based technologies and in batteries; the transport of electronically excited states is important in light-emitting diode (LED) and photovoltaic technologies; and the transport of ions and small molecules has importance in membranes for fuel cells and batteries and in various biomedical technologies. Synthesis via ring-opening metathesis polymerization (ROMP) is finding uses in many such applications and they will occasionally be referred to in this section to aid 'joined-up thinking and awareness' for the reader.

As-made polyacetylenes are generally semiconductors that undergo increases in conductivity of several orders of magnitude when subject to redox chemistry. Structural changes are required to accommodate the counterions necessary to balance the charges created on the polyene chains. Pristine polyacetylene also displays a large third-order nonlinear optical effect. This is a remarkable combination of properties in one material. This is not the place for a detailed review of this work that led to an explosion of publications and the birth of specialist journals. Undoubtedly, polyacetylene became the paradigm for the field in that period, although it was soon superseded by other materials.[14] The work of Hideki Shirakawa, Alan Heeger, and, the late, Alan MacDiarmid inspired many to enter the field and their work and influence was recognized in 2000 by the award of the Nobel Prize for Chemistry to them jointly.

This section aimed to explain the reasons for the interest in conjugated polymers and the history of how that interest developed. In subsequent sections, we consider how ROMPs may be used to generate conjugated polymers and how such routes can lead to processing options. I wrote a review of this field a few years ago and saw little point in just duplicating the approach used then since the review is still readily available;[2] although there is always relevant new work appearing, the availability of various 'search engines' means that the interested reader can readily update even the most recent review. So, in this section, I will attempt to avoid the esoteric niceties that tend to fascinate protagonists and review the available data and 'state of the art' from a different, somewhat more general and detached viewpoint in order to meet the specifications of the publishers who said in their 'Aims and Scope' for this work: "…articles will be written at a level that allows students to understand the material, while providing active researchers with a ready reference resource for information in the field".

4.26.2 Ring-Opening Polymerization of Monocyclic Polyenes

4.26.2.1 General Considerations

Since we defined the paradigm for the field, polyacetylene, as "a linear chain assembled from sp^2 hybridized carbons each bonded to another sp^2 carbon and a single hydrogen atom and carrying one electron in a 2p AO," if we want to make it by a ring opening protocol, we can, in principle at least, start with any monocyclic structure constructed from the same elementary building blocks, namely, a ring of sp^2 hybridized carbons each bonded to another sp^2 carbon and a single hydrogen atom and carrying an electron in a 2p AO. The first few odd members of this family are cyclopropenyl, cyclopentadienyl, and cycloheptatrienyl radicals and the even members are cyclobutadiene, benzene, and 1,3,5,7-cyclooctatetraene and they and the hypothetical concept of using them as monomers for polyacetylene syntheses are shown in Figure 3. So far, in practice only one of these polymerizations has been realized, namely, that of cyclooctatetraene, although, with a bit of

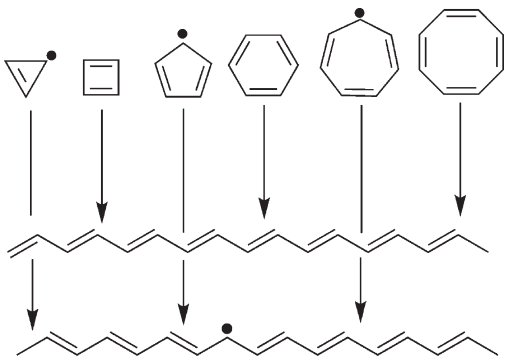

Figure 3 Hypothetical routes to polyacetylene via ring opening of cyclic polyenes.

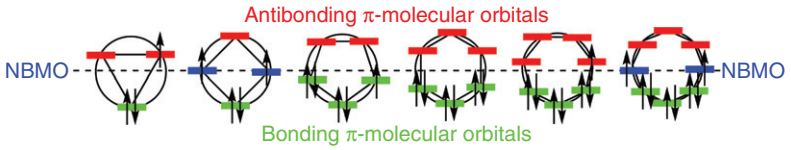

Figure 4 Mnemonic for π-MO energies in planar cyclic polyenes.

'special pleading', we will claim another two of the family as monomers for the task. Why do these potential monomers appear to be of so little use to us? The answer comes from a consideration of their π-bonding situations for which a simple mnemonic is shown in Figure 4.

To work out an approximate indication of the relative π-bonding energies in this structural series, we simply inscribe the appropriate regular polygons, with their points down, inside a set of circles of the same radius. Where the vertices of the polygons touch the circumference of the circles indicates, to a first approximation, where the energies of the associated π-MOs lie in relation to the energy associated with an isolated electron in a carbon 2p AO, that is, the energy of the nonbonding MO (NBMO); this mnemonic assumes that the polygons are planar. We can, in light of this, now work through our set of cyclic structures starting from the left-hand side considering each as a potential monomer.

4.26.2.2 Unsaturated Three-Membered Rings as Starting Materials

Cyclopropenes are predicted to have a favorable free energy of polymerization;[15,16] however, examination of the simple π-MO picture, shown in Figure 4, for cyclopropenyl radical predicts it to have two electrons in the π-bonding orbital and one in an antibonding orbital and this latter electron contributes to destabilizing the specie that is not available as a monomer. One-electron oxidation of cyclopropenyl radical to give a cyclopropenyl cation would be fairly easy. The synthesis and relative stability of cyclopropenyl cation has been the subject of many studies,[17] but, as far as I can establish, there have not been any attempts to use a cyclopropenyl cation salt as a ROMP monomer. 3,3-Disubstituted cyclopropenes undergo ROMP,[18,19] but the linear polymers obtained have not been used as precursors for the generation of conjugated polymers.

3,3-Diphenylcyclopropene has a place in ROMP history as its reactions with transition metal complexes can lead to the formation of allylidene complexes that are initiators for ROMP and, at a stretch of the imagination, can be seen as conjugated fragments (see Figure 5).[20]

Another possible application of cyclopropene ROMP in the investigation of conjugated polymers would be to use its dimer, bicycloprop-2-enyl (the structure on the extreme right in Figure 6), as a cross-linking comonomer in a polyacetylene synthesis.

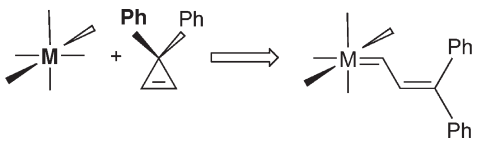

Figure 5 Allylidenes from 3,3-diphenylcyclopropene.

Bicycloprop-2-enyl is known and, although reactive, survives in solution in dichloromethane between −90 and −10 °C.[21] If it was copolymerized with another monomer for polyacetylene synthesis, through both of its cyclopropene rings it would give the cross-linking structure that has been postulated in conventionally prepared polyacetylene on the basis of ^{13}C NMR spectroscopy, thus confirming or contradicting the present view of one of the defects in the material. To the best of my knowledge, this experiment has not been tried. Neither methylenecyclopropene, an isomer of cyclobutadiene, nor any of its substituted derivatives, which could be considered as potential monomers for the ROMP synthesis of cross-conjugated polymers (see Figure 7) appears to have been considered for this purpose; indeed their existence appears to be transitory at best.

4.26.2.3 Unsaturated Four-Membered Rings as Starting Materials

4.26.2.3.1 General considerations

Cyclobutenes are known to undergo ROMP readily.[15] They have a favorable free energy for ring opening,[16] are stable under normal conditions, and are fairly readily available; however, referring to Figure 4, we see that for cyclobutadiene, the mnemonic predicts a diradical. This is an oversimplification, because the mnemonic was constructed on the assumption that the unsaturated compound being considered assumes the shape of a regular polygon and in practice this molecule avoids becoming a diradical because it distorts to become a rectangular cyclic diene rather than a square; the short sides being the double bonds and long sides the single bonds. The molecule exists and can be trapped as a 4π donor ligand on a metal or as a Diels–Alder adduct but is too reactive to be an effective monomer for our purposes since, when generated in the free state, it undergoes self-dimerization and oligomerization. However, this problem can be circumvented by one of the standard strategies of synthetic organic chemistry, namely, to hide a sensitive part of a molecule behind a protecting group while various synthetic manipulations that are potentially damaging to the sensitive unit are being performed and then removing the protecting group at the end of the synthesis. Protecting groups must be easily put in place and easily removed but stable to the reaction conditions and reagents used in the synthetic manipulations employed; there are libraries of protecting groups and their use has been crucial to the success of a great deal of synthetic organic chemistry. We established such routes to polyacetylene via protected precursor polymers; the approach is summarized in Figure 8.[22–24]

Figure 6 Benzene and its valence bond isomers.

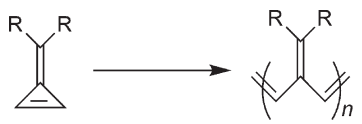

Figure 7 Hypothetical ROMP of substituted methylenecyclopropene.

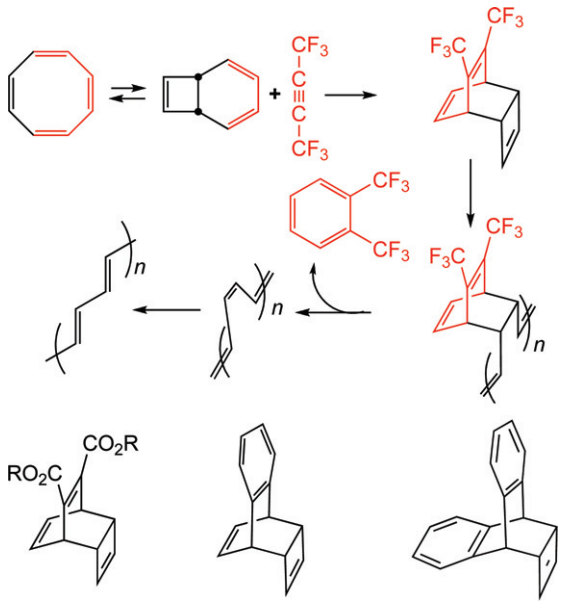

Figure 8 (Top) Durham precursor route to polyacetylene. (Bottom) Alternative starting monomers.

4.26.2.3.2 The Durham route to polyacetylene and related matters

The route involves synthesizing a substituted cyclobutene monomer that undergoes ROMP to give a soluble precursor that can be converted to polyacetylene *in situ* after processing. In the example shown in Figure 8, the monomer is made via a Diels–Alder reaction of hexafluorobut-2-yne with the cyclohexa-1,3-diene unit of the valence tautomer of cycloocta-1,3,5,7-tetraene. ROMP of this monomer occurs exclusively through the cyclobutene vinylene to give a soluble polymer of high molecular weight (M_w in the range 400–1000 kDa) which, with appropriate precautions to take account of its relatively low thermal stability, can be characterized by the standard techniques of polymer chemistry and, after solution processing, converted to a clean fully dense ($\rho = 1.05\,g\,cm^{-3}$ cf. 0.3–0.4 $g\,cm^{-3}$ for the Shirakawa route material) form of polyacetylene via a symmetry allowed thermal elimination of 1,2-bistrifluoromethylbenzene.[25]

The route summarized in the top part of Figure 8 is not 'atom efficient' in that a large part of the precursor polymer is 'waste' and in the colored version of this section the process is color coded to make it easier to follow. The conversion protocol (temperature, film thickness, pressure, and mechanical stress) determines the details of the product structure that is generally obtained as a pinhole-free continuous film.[26] The *cis*/*trans*-vinylene frequency and distribution in the soluble precursor polymer is a function of the ROMP initiator used; in the first experiments, the 'classical ill-defined initiator' WCl_6/Ph_4Sn was used and gave a roughly random 50:50 distribution, although subsequently we and others have used well-defined initiators successfully. During the thermal conversion to polyacetylene, each new vinylene formed in the polymer backbone is *cis* as-made as a consequence of the symmetry allowed nature of the process, which means that the nascent polyacetylene produced by this route has roughly 75% *cis*-vinylenes; however, depending on temperature and time, it will isomerize to a predominantly *trans* material. The eliminated 1,2-bistrifluoromethylbenzene initially plasticizes the polymer, then diffuses through the film and eventually evaporates; as expected, the rates of these processes depend on temperature and pressure and they overlap in time and space, so the process is complicated to disentangle in detail but not difficult to understand. However, control of the conversion protocol adopted allows good control of the form of the polyacetylene produced; typically, pristine polyacetylene obtained by this route has little or no order, has an electrical conductivity σ of approximately $3 \times 10^{-8}\,\Omega\,cm^{-1}$, which is 2 or 3 orders of magnitude lower than typical Shirakawa route material, suggesting somewhat greater purity with fewer adventitious defects or impurities giving rise to charge carriers. The value observed is similar to values obtained for the material by the Grubbs' route from cyclooctatetraene *vide infra*. Whatever route is adopted, most polyacetylene samples will undergo redox modification into similar conductivity regimes.

The process described above turns out to be the most effective of several variants tried and allows another potentially useful manipulation since, although the pristine precursor polymer is colorless when carefully manipulated and maintained at a temperature of 0 °C or below, at room temperature it begins to slowly convert, the partially converted material remaining soluble providing oxygen and light are excluded. Yellow-red thin films of the partially converted precursor, containing a distribution of short polyene sequences, can be spun cast and the polyene sections in these films are susceptible to cross-linking in the presence of air and UV light. Irradiation through a mask followed by heating under vacuum results in the formation of a negative image of the mask in the film in which the black areas are composed, after about 70% reduction in volume, of newly formed polyacetylene semiconductor embedded in insulating transparent areas of photo-cross-linked partially converted precursor that looses only about 30% of its volume; images with a resolution of about 0.3 μm were readily obtained; thus, structured patterns of an organic semiconductor in an insulating matrix of a cross-linked

fluorohydrocarbon polymer can be made in a fairly simple manner, although the image is bound to be under some stress.[27,28] The monomers shown at the bottom of Figure 8 are more stable (particularly the ones in the middle and on the right-hand side) than the bistrifluoromethyl-substituted triene, but can nevertheless be used to generate polyacetylene; reading from left to right, they result in the elimination of a dialkyl phthalate, naphthalene, and anthracene, respectively. All three of these eliminated units are less volatile than 1,2-bistrifluoromethylbenzene and consequently higher temperatures and lower pressures are required in the conversion step and lower quality polyacetylene films are produced.[23] The increased stability of the precursors derived from the monomers in the middle and on the right-hand side at the bottom of Figure 8 presumably reflects the smaller thermodynamic gain in going from precursor polymer to polyacetylene plus naphthalene and anthracene, respectively.

If the unconverted or partially converted precursor polymer is stretched prior to or during conversion, oriented polyacetylene is obtained, which displays increased order (X-ray diffraction) and anisotropy in its spectroscopic properties and electrical conductivity.[29] The investigation of the solid-state physics of the form of polyacetylene described above, generally known as 'Durham polyacetylene', was undertaken in the group of Friend[30,31] who prepared and characterized Schottky-barrier diodes, metal–insulator–semiconductor (MIS) diodes, and MISFET structures using polyacetylene derived from precursor polymer as the active semiconducting component of the device structure; these early experiments demonstrating the potential of the field that is now generally known as 'plastic electronics'. The material proved a useful learning vehicle for the beginning of what has become an important area of science and technology, but it has not found a place in the development and exploitation of the field that has followed; the devices demonstrated had carrier mobilities that were too low to be of practical use, *vide infra*, and, added to the cost and synthetic challenges, were soon abandoned in favor of other promising materials.

The observation of improved properties following stretch alignment of polyacetylene led to an attempt to achieve polyene alignment in material produced from thermally converted spun cast precursor polymers. This was an interesting objective since it was known that for amorphous organic semiconductors, there was a linear correlation between conductivity and carrier mobility;[32] device suitability depended on the combination of relatively low conductivity with relatively high mobility; since 'Durham polyacetylene', being clean, had low conductivity but, being highly disordered, had a low mobility. The objective of the exercise was to retain the low conductivity while increasing the carrier mobility via spontaneous ordering. An example of how this was attempted making use of improving precision and control of ROMP is summarized in Figure 9. The route shown in Figure 8 was followed but using the Schrock well-defined tetrahedrally substituted molybdenum carbene as initiator instead of the classical ill-defined WCl_6/Ph_4Sn system; this gives the living precursor polymer shown at the right hand of Figure 9. Using a well-defined initiator gives two advantages: first, the initiator-to-monomer ratio allows control of the molecular weight and second, the molybdenum carbene at the end of the chain allows further reaction; in the present case, the living precursor polymer was terminated by addition of 4-pentylbenzaldehyde that puts an oxygen on the molybdenum and the liquid crystal (LC) mesogen, 4-pentylphenyl, at the end of the polymer chain. Thermal conversion of these precursors gave polyacetylene films thar were interpreted, based on conductivity, mobility, and polarized UV spectroscopy measurements as consisting of a disordered array of ordered domains of polyacetylene. The conductivity remained low, as desired, and the carrier mobility increased by 2 or 3 orders of magnitude but, unfortunately, remained below the target value. Presumably, the observed changes in properties resulted from phase segregation of the chain-end mesogens in the precursor during or prior to conversion and the segregated 4-pentylphenyl domains nucleated partial orientation of the forming polyene sequences.[33,34]

Polymerization of 7,8-bis(trifluoromethyl)tricycle[*4.2.2.0*]deca-3,7,9-triene with well-defined initiators is further exemplified by work from, *inter alia*, the groups of Grubbs and Schrock.[35–39] Block copolymers of Durham precursor polymer (10–200 molecular equivalents) with norbornene or 9-methyltetracyclo[*6.2.1.1*]dodec-4-ene were prepared and spun from solution as submicron films for investigation of their third-order optical nonlinearity.[35] Interestingly, in the case of the norbornene block copolymers, there was a red shift with higher spin speeds during the film formation, suggesting better aligned and longer polyene sequences; the nonlinear optical susceptibility (χ^3) was probed with third harmonic generation and degenerate four-wave mixing and (χ^3) increased in

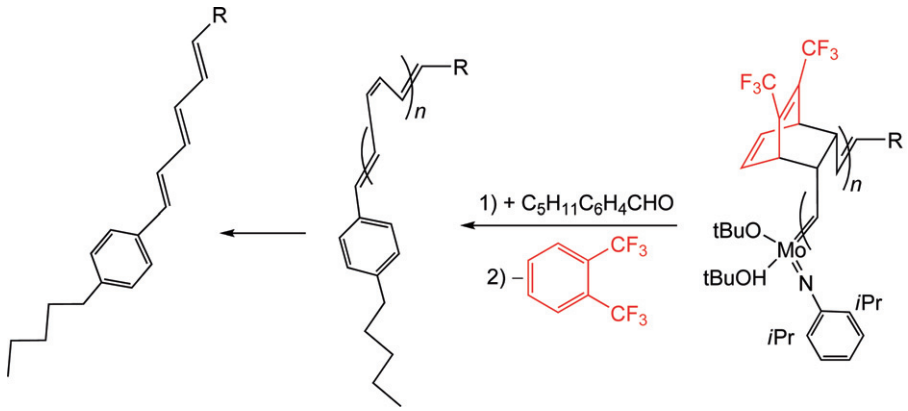

Figure 9 Durham route to mesogen-terminated polyacetylene.

magnitude with increasing polyene block length and were always greater in the norbornene copolymers. Schrock also used living polymerization with well-defined initiators for the preparation of oligopolyenes terminated with *t*-butyl groups, which were purified as single compounds by chromatograph for a study of the correlation of spectroscopic properties with chain length. The expected phase separation effects on block copolymers of the Durham precursor and norbornene leading to a distribution of microdots in a polynorbornene matrix have also been reported.[36–39]

As reported above, the precursor route summarized in Figure 8 gives material that undergoes slow conversion to polyacetylene at room temperature; although this presents no great problem, since most laboratories have access to refrigerators and even refrigerated transport is becoming common place, several attempts to make a more thermally stable precursor that, nevertheless, undergoes thermal conversion to good quality polyacetylene have been made since this might aid long-term storage and interlaboratory collaborations. In this last part of this section, considering routes from cyclobutene derivatives, the last case to be considered is that summarized in Figure 10.

This route involves photoisomerization of the monomer, 7,8-bis(trifluoromethyl)tricyclo[*4.2.2.0*]deca-3,7,9-triene, as indicated in the top left-hand part of the figure. The dotted lines are drawn in that way to aid the eye in recognizing what has been joined to what during this $2\pi + 2\pi$ intramolecular cycloaddition, but they represent full σ-bonds; the monomer is kinetically stable since the cycloreversion to starting material is symmetry forbidden in the ground state. As expected, this new monomer undergoes ROMP through the cyclobutene residue to give the precursor polymer shown in the top right-hand corner of the figure. This new precursor polymer is also kinetically stable and can be spun from solution into thin films that can be thermally converted to polyacetylene provided that only very thin films are used! The reason for this emphasis on caution is that although the precursor is kinetically stable, it has considerable stored strain energy per repeat unit, resulting from the two three-membered and one four-membered rings that are fused together. The strain energy amounts to roughly 20% of a TNT molecule per repeat unit, and although polyacetylene can be prepared from thin films, explosive decompositions have also occurred, so this route works but provides a hazard and cannot be recommended as practically useful in view of the risk involved.[40,41]

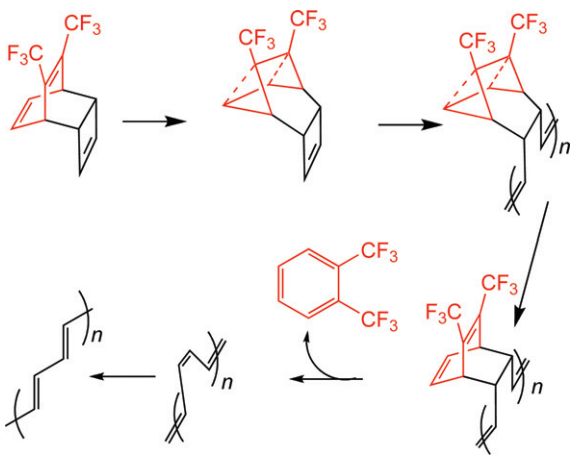

Figure 10 Durham route via a precursor photoisomer.

4.26.2.3.2(i) Hypothetic routes to conjugated polymers from cyclobutene derivatives

The route described in this section was reported by Novak and constitutes an ingenious attempt to improve the atom efficiency of the original Durham route.[42] The route investigated is summarized in Figure 11; the monomer shown on the left-hand side of the figure is formed via the Diels–Alder addition of an *N*-alkyl or *N*-aryl maleimide to the cyclohexadiene part of the valence tautomer of cyclooctatriene; this undergoes ROMP through the cyclobutene unit and the idea was to thermally eliminate the maleimide to give polyacetylene as shown below, using all the carbons from the cyclooctatetraene residue. In practice, the intended precursor proved to be much more thermally stable than anticipated ($300\,^{\circ}C < T_d < 344\,^{\circ}C$) and upon hydrogenation the methyl derivative showed even greater stability with a glass transition at 285 °C and a thermal stability enhanced by approximately 100 °C. Novak mentioned further work in progress to improve the effectiveness of the elimination required but, unfortunately, this came to naught.[43] We had similar experience with the analogous adduct formed from dimethylmaleate and cyclooctatetraene; this also polymerized readily via ROMP at the cyclobutene residue, but the putative polyacetylene precursor, which required a symmetry allowed thermal elimination of a cyclohexadiene derivative, yielded no polyacetylene below its decomposition temperature. Novak's route was, in part at least, derived from a successful precursor route based on the thermal elimination of a furan diester from poly(diethyl-7-oxabicyclo[*2.2.1*]hepta-2,5-diene-2,3-dicarboxylate), the left-hand structure in Figure 12, to give *trans*-polyacetylene at 100 °C. This precursor was derived from the 1,2-vinyl-polymerization of the 2,3-diethylester of a 7-oxanorbornadiene monomer initiated with a palladium (II) catalyst and, while it does not come strictly within the remit of this review, it is useful in that it demonstrates that furan derivatives are appropriate protecting groups for olefins in putative polyene syntheses.[44]

After these proposed precursors that were too thermally stable to be useful, the next example in this section involves speculation about a precursor route from a derivative of cyclobutene that exists but is definitely unstable. The hypothetical route is shown in Figure 13 below.

Cyclobutadiene was an elusive target for synthesis for several years and one extensively investigated starting material was 2-pyrone.[45–47] A solution of 2-pyrone in ether maintained below −10 °C can be photoisomerized in high yield to the

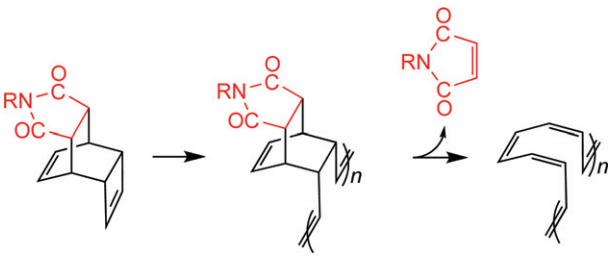

Figure 11 Novak's proposed route to polyacetylene.

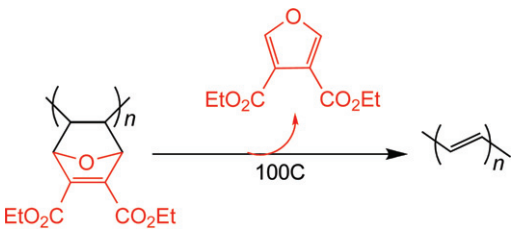

Figure 12 Precursor route to transpolyacetylene from a poly (7-oxanorbornene) derivative.

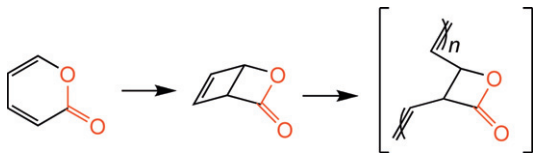

Figure 13 Hypothetical route to a polyacetylene precursor.

bicyclo[*2.2.0*]lactone shown in the middle of Figure 13. This compound can be purified and characterized (elemental analysis, spectroscopy) and is described as "a colorless, hygroscopic liquid which is pyrophoric in air at room temperature and which can explode on warming in air".[45] Nevertheless, with skill and caution it can be handled and it is established that the cyclobutene part can act as a dienophile with appropriately reactive dienes and that the molecule undergoes hydrogenation in two steps. Pirkle describes a reaction at 25 °C with methanol to give $CH_3OCH{=}CH{-}CH{=}CH{-}COOH$;[46] most work with this molecule appears to have been directed toward eliminating carbon dioxide to generate cyclobutadiene, often via irradiation in a frozen glassy matrix,[47] and the author has not discovered any attempt to use it as a ROMP monomer.

4.26.2.3.3 A cross-conjugated polymer via ROMP of a cyclobutene derivative

To close this section on cyclobutene ROMP routes, we consider an example that, while not a direct route to a conjugated polymer, involves the ROMP of an unsaturated four-membered ring and provides access to a semiconducting polymer system. The monomer 3,4-diisopropylidenecyclobutane (Figure 14) is polymerized by ROMP using a source of titanium carbene, $Cp_2Ti{=}CH_2$, as the initiator system.[48] The backbone of the product is constructed from sp^2 carbons but is cross-conjugated rather than conjugated. Nevertheless, oxidation of films of the pristine-insulating polymer with iodine vapor gives materials with conductivities up to 10^{-3} S cm^{-1}.

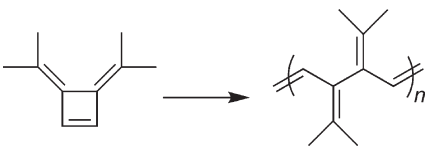

Figure 14 ROMP synthesis of a cross-conjugated polymer.

4.26.2.4 Unsaturated Five-Membered Rings as Starting Materials

4.26.2.4.1 General considerations

The free energy for ring opening of cyclopentene is considerably less favorable than that of cyclobutene and, depending on the position and kind of substitution on the ring, ΔG can be just positive or just negative.[15,16] Nevertheless, cyclopentene and many of its derivatives do undergo ROMP readily, polymer formation being favored by lower temperatures and higher monomer concentrations. At one point several years ago, the homopolymer from cyclopentene, polypentenamer, was under serious consideration as a substitute for commercial diene elastomer manufacture; indeed, it was reported that prototype vehicle tires were made and road tested before changes in economics and tire technology made the venture nonviable.

The mnemonic in Figure 4 indicates that the cyclopentadienyl radical is not a stable entity and will display a strong tendency to pick up an electron and become an aromatic cyclopentadienyl anion, as is indeed the case. So the direct route from cyclopentadienyl radical portrayed in Figure 3 is out of the question and routes to conjugated polymers involving ROMP of cyclopentene derivatives will inevitably involve other steps in the overall scheme. The ring-opening polymerizability of five-membered rings is enhanced by strain and this can be induced by making them part of a polycyclic structure, *vide infra*.

4.26.2.4.2 An atom-efficient route to polyacetylene from benzvalene

As was mentioned in Section 4.26.2.3.3, the Durham route to polyacetylene, while convenient experimentally, is not atom efficient and consequently there have been several proposals designed to circumvent this problem. Novak's attempt to overcome this deficiency did not meet with success, but the route summarized in Figure 15 provides a somewhat more effective attempt to solve this shortcoming. Benzvalene, one of the isomers of benzene (see Figure 6 above) constitutes a highly strained cyclopentene as a consequence of the two fused cyclopropane rings in its structure; not surprisingly, it readily undergoes ROMP to give the precursor polymer shown in the middle of Figure 15. This precursor can be isomerized in the presence of mercuric salts to give the desired conjugated polymer.[49,50] The material can be oxidized by iodine vapor into the low-conductivity semiconductor regime, but ^{13}C NMR spectroscopy indicates a significant content of residual saturated carbon. This route works as planned but, like the Durham photoisomer route summarized in Figure 10 above, it carries a hazard in that the high strain energy per repeat unit in the precursor is reported to make it prone to detonation; it should therefore only be handled on a small scale and with appropriate precautions.

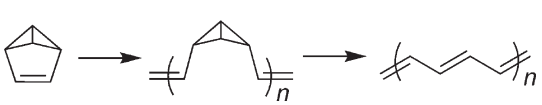

Figure 15 Benzvalene as a monomer for ROMP.

4.26.2.4.3 Real and hypothetical routes to conjugated polymers based on initial ROMP of five-membered rings

There are many potential routes to conjugated polymers and the increasing understanding of the correlation between polymer structure and physical properties, particularly electrical and optical properties, have, not unreasonably, stimulated the imaginations of synthetic organic chemists to design syntheses and join the worldwide plastic electronics activity to the benefit of all. In practice, some of the routes explored work well and some, which look equally viable 'on paper', do not work at all and it seems worth giving some time to considering why this is the case.

4.26.2.4.3(i) Consideration of the dehydrogenation route from norbornadiene

First, as an example, we will consider the generalized scheme shown as Figure 16. This potential route has been explored with varying degrees of success by various research groups. In essence it starts from the norbornadiene skeleton, ROMP through one ring leads to a precursor (middle structure in Figure 16), which then has to be converted to the desired conjugated structure shown on the right-hand side of the figure. This two-step approach to conjugated polymer synthesis can be regarded as an example of the standard protecting group strategy of synthetic organic chemistry. There is a potential drawback to this route in that the proposed precursor contains a cyclopentene ring and might undergo ROMP leading to cross-linking; however, the cyclopentene rings in the norbornadiene monomer are strained and considerably more reactive than those in the proposed precursor so this is not a great risk or problem; indeed, such polymers were made and characterized and are known to be very susceptible to oxidation, particularly when the double bond in the five-membered ring of the precursor is part of an aromatic ring.[51,52] Protecting groups, as mentioned in Section 4.26.2.3.1, must be stable during manipulation and must be easily and completely removed at the appropriate time. In the case outlined in Figure 16, the 'protecting group' consists of two tertiary and doubly allylic hydrogen atoms and the putative final step is a dehydrogenation; in this case, the problems resolve themselves into:

- the reactivity of the dehydrogenating reagent,
- the ease with which the dehydrogenating reagent and the by-products of its reactions can be removed from the scene,
- the nature and reactivity of the newly formed conjugated polymer, and
- the conformational requirements of the process.

We shall meet with these, or an analogous set of considerations, frequently in this section on five-membered ring routes and the next sections on six- and higher membered rings. Several groups have used 2,3-dichloro-5,6-dicyanoquinone (DDQ) as the dehydrogenation reagent and this is a potent and fairly undiscriminating reagent so the nature of the intended conjugated polymer and the possible workup procedures for the product are important determinants of success or failure. In the route summarized in Figure 16, the second step is a redox process, the precursor undergoes dehydrogenation (oxidation), and the DDQ is reduced from a quinone to the hydroquinone, its dihydro form, 2,3-dichloro-5,6-dicyanohydroquinone ($DDQH_2$). The products of reaction and any surplus reagent should be immediately removed because the nascent conjugated segments shown on the right-hand side of Figure 16 are inherently likely to be easily oxidized, possibly even more readily than the pristine precursor. This imposes experimental problems because neither DDQ or its reduction product is easily removed by evaporation and the nascent conjugated segment is a chemically reactive cyclopentadiene unit and its reactivity with itself and any reagent in the vicinity has to be taken into account. There is also a large conformational reorganization required on changing from a precursor system with two vinylene units in the 3 and 5 positions on the cyclopentene ring, which are *syn* to each other in the precursor, to the essentially planar structure of the conjugated polymer product. At first sight, this may not seem a great restriction because the precursor polymer will almost certainly be soluble so, if the conversion is attempted in solution, it ought to be able to adopt to the required conformational change; however, the product conjugated polymer will almost certainly not be soluble and as the conjugation, planarity, and insolubility of the forming product increase, the conformational flexibility of the polymer backbone will decrease and the dehydrogenation will be severely inhibited. These considerations help to explain the lack of significant success via this route; however, as will emerge in the section 4.26.2.5 *vide infra*, when the product of the dehydration step is a stable phenylene unit rather than a highly reactive cyclopentadiene entity, this approach meets with success.

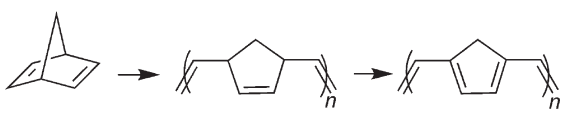

Figure 16 ROMP routes from norbornadiene derivatives.

4.26.2.4.3(ii) Consideration of the dehydrohalogenation route from norbornenes

Another essentially unsuccessful 'plausible paper chemistry' route to conjugated polymers via a precursor made by ROMP through a five-membered ring is summarized in Figure 17. The monomer is a halogenated norbornene prepared via Diels and Alder cycloaddition between a halogenated olefin, for example, 2,3-dichlorohexafluorobut-2-ene, $CF_3(Cl)C{=}C(Cl)CF_3$, and cyclopentadiene; this kind of molecule readily undergoes ROMP to give the proposed precursor polymer shown in the middle of the figure.[53,54]

Dehydrohalogenation of this putative precursor polymer was expected to be relatively easy because the hydrogens to be removed are tertiary and allylic and for the two 1,2-eliminations required the four atoms involved in each step are close to coplanar that is expected to favor elimination; the author is aware of several attempts to put this idea into practice, both in his laboratory and elsewhere but, to the best of his knowledge, all have failed so far. The proposed precursor polymers are easily made, characterized, and handled; they are soluble in a range of solvents and can be cast as films. A large number of polymers have been made and subjected to thermogravimetric analysis. Their physical properties have been investigated and some of the fluorohydrocarbon polymers display potentially interesting properties as pyro-, piezo-, and electrostrictive materials,[55] but all attempts to dehydrohalogenate them to give conjugated

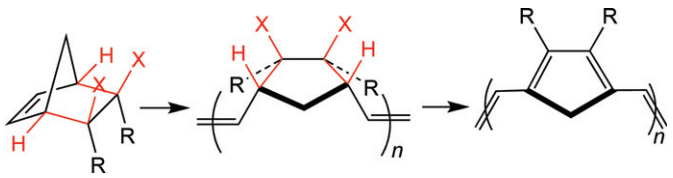

Figure 17 ROMP routes from norbornene derivatives.

polymers fail. Thermal and base-catalyzed reactions using a variety of bases and conditions, from aqueous through to non-nucleophilic hindered bases, eventually result in polymer degradation, but no structurally well-defined conjugated polymers were obtained (it has been known for authors to claim conjugated polymer synthesis on the basis of an organic polymer going black on pyrolysis, but in the author's view this hardly constitutes evidence). Similar strictures apply to attempts to make polyacetylene by dehydrochlorination of polyvinyl chloride (PVC). The route probably fails because the polymer films cannot accommodate the conformational strain imposed on going from the flexible precursor polymer to the rigid conjugated structure *vide supra* (Section 4.26.2.4.3(ii)) and because the hydrogen halide eliminated in the first step is a very effective catalyst for degradation and isomerization of the nascent conjugated segments.

4.26.2.4.3(iii) Consideration of potential routes from fulvene-derived monomers

The proposed route outlined in Figure 18 starts with a monomer, shown on the left-hand side, produced via a Diels–Alder reaction of an acetylene with a substituted fulvene; as expected, this monomer underwent ROMP to give the soluble transparent 'precursor' polymer shown in the middle of the figure.[56] The design intention was that photexcitation via the styryl chromophore would promote a 1,3-migration of one of the tertiary bis-allylic hydrogen atoms in the repeat unit, followed by a 1,2-hydrogen shift to give the conjugated polymer structure shown on the right-hand side of the figure.

Irradiation through a mask might then allow a conjugated polymer pattern to be photochemically written into the precursor; although plausible, the process did not work and the intended precursor polymer proved to be surprisingly photostable remaining transparent after UV irradiation. These last three plausible routes to conjugated polymers proving, yet again, if proof were needed, that "The best laid schemes o'mice an' men, gang aft agley."[57]

4.26.2.4.3(iv) Consideration of potential routes using the dichlorovinylene carbonate synthon

Figure 19 summarizes the work of Harper,[58] who took the Diels and Adler adduct of dichlorovinylene carbonate with cyclopentadiene and showed that it underwent ROMP with 'classical' ROMP initiator systems to give the chlorinated precursor polymer, shown in the middle of the figure, as a soluble film-forming material. Exposure of the surfaces of films of this precursor polymer to aqueous acids or bases resulted in the colorless, transparent films being converted to a lustrous 'metallic' film. Based on the fact that under the same conditions the monomer is converted to norbornene-5,6-diketone, and analysis of the IR and UV–Vis spectroscopic evidence, it was postulated that the lustrous film was a consequence of the formation of the conjugated polymer shown on the right-hand side of Figure 19. The extent of the conversion reaction was controlled by the conditions and duration of the hydrolysis. Partially converted films could be cross-sectioned and microscopic examination of the edge showed a layer of the postulated black conjugated polymer at the surfaces with a layer of the colorless, transparent insulating precursor in the middle, leading initially to optimism that oxidative modification of one surface would lead to the fabrication of MIS structures. However, this optimism was misplaced and the investigation was not pursued further since the lustrous film was extraordinarily susceptible to oxidation by atmospheric oxygen and very difficult to handle; indeed it was suggested that it might make a reasonable glove box oxygen scavenger. The molecular structure of the lustrous films was not completely established. However, more recently, Sleiman[59] has reported the use of the Grubbs' well-defined initiator, $Cl_2(PCy_3)_2Ru{=}CHPh$, together with the monomer shown in Figure 19 and its 7-oxa-norbornene analog, derived from Diels–Alder reaction with furan, to make well-defined homo- and block copolymers in well-regulated reactions. They report narrow molecular-weight distributions characteristic of living polymerization, phase segregation in the block copolymers, and hydrolytic conversion of the dichlorovinylene carbonate-derived segments to a low band gap (0.85 eV based on the location of the absorption band edge) semiconducting conjugated polymer.

4.26.2.4.3(v) Consideration of other routes involving an enolization step

The examples summarized in this section are related to the previous one since they involve quinone/hydroquinone

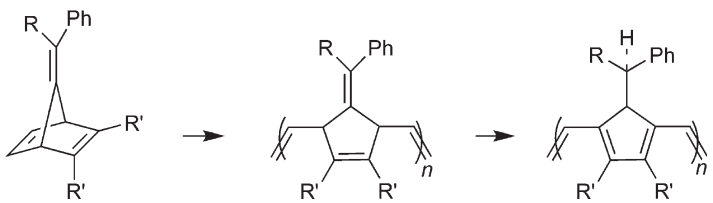

Figure 18 A potential route from a fulvene-derived monomer.

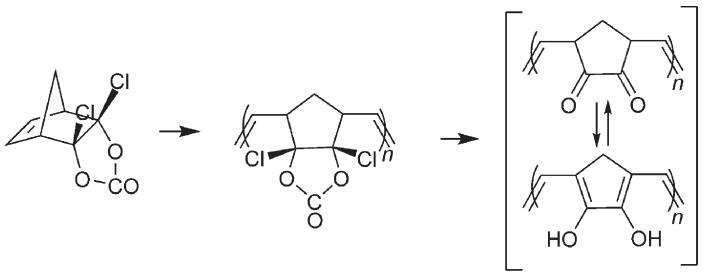

Figure 19 Route from a dichlorovinylene carbonate-derived monomer.

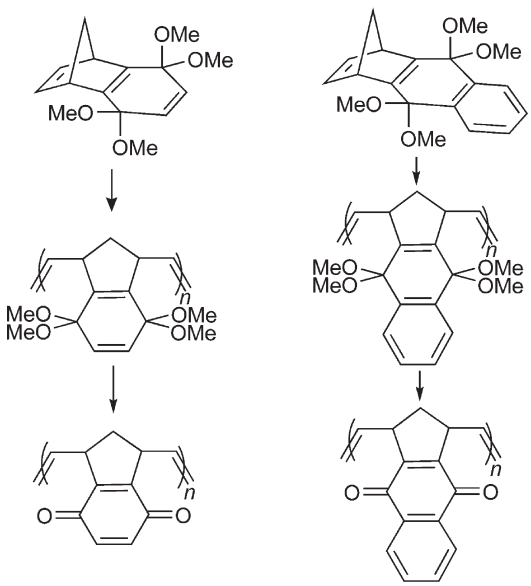

Figure 20 Initial stages of a route via quinones.

isomerization and enolization. Figure 20 records two quinone-derived monomers, both of which were readily polymerized under ROMP conditions.[60] The polymers were solution-processable precursors to insoluble conjugated polymers. As shown in Figure 20, hydrolysis results in conversion of the protected tetramethoxy precursor polymers to quinone derivatives that underwent enolization to give fully conjugated hydroquinone polymers displaying conductivities in the semiconductor regime. Quinone/hydroquinone systems in general have a fairly complex redox chemistry and, as expected, such systems have a complicated redox chemistry and electrochemistry. The behavior of these materials and of those reported in the previous section is also complicated by the presence of mobile ionizable protons; those at the doubly allylic tertiary carbons in the bottom structures in the figure being transferred to the quinone oxygens to form a fully conjugated polymer backbone carrying pendant hydroquinone units.

4.26.2.4.3(vi) Routes involving ROMP of five-membered ring systems carrying a conjugated oligomer substituent

The routes to conjugated polymers via ROMP discussed so far in this chapter have predominantly been concerned with incorporating some or all of the atoms in the monomer into the conjugated segments of the product; however, a ROMP monomer can be used as a processing aid or a scaffold in the syntheses of electroactive and conjugated polymers and this section records some of the many systems investigated. The generalized concept is shown in Figure 21; the systems of interest contain a ROMP polymerizable entity, a linking or spacer unit, and an oligomeric conjugated structure attached to the linker via a functional group at one end or in the middle of the conjugated oligomer. The initially formed polymer can be investigated and applied as made or subject to further modification (e.g., reactions linking the pendant oligomers into longer sequences) as summarized in Figure 21. There are many examples of this approach and it is an active area of synthesis at the time of writing; the interested reader would be well advised to use the journal indexes or contents pages or a search engine if interested in a specific structure.

Polymer brushes in which the frequency and distribution of functional surface attachment points can be controlled are of interest in several potential device technologies. Grubbs and coworkers have described a monomer based on oligo *p*-phenylene ethynylene, with a norbornene at one end and a thiol at the other. The thiol can be inserted into a self-assembled array dodecanethiol on a gold surface to provide isolated 'molecular wires' terminated by norbornene units which can then be used to initiate ROMP leading to single chain brushes formed from the surface.[61] Swager and Moon have used similar ideas in the investigation of biosensor design, establishing a methodology for making polymer brush structures in which poly(*p*-phenylene ethynylene) chains are directed to be perpendicular to the film surface by ROMP grafting from the surface. The aim is to ensure the rapid transport of excitons formed in the film to the film surface, thus speeding up the biomolecular recognition event in the device. The technique worked in that film in which poly(*p*-phenylene

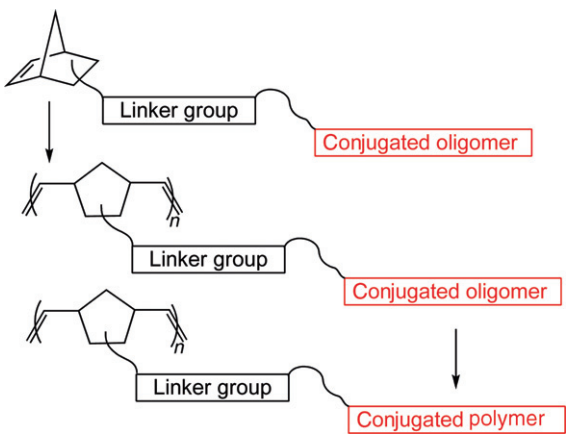

Figure 21 Routes using ROMP as a processing aid.

ethynylene) chains 71–110 Å thick were formed without aggregation that gave higher emission quantum yields than spun cast films.[62] Polythiophene has proved to be an interesting conjugated polymer and, in addition to the standard strategy of attaching solubilizing groups to the backbone or chain ends, several attempts have been made to overcome its intractability by attaching it to a ROMP monomer and either using the product polymer as made or subjecting it to chemical or electrochemical oxidiation to link up the oligomeric thiophene units into larger blocks.[63–67] The strategy outlined in Figure 21 has been used, *inter alia*, to make photochromic homopolymers based on the light-sensitive conjugated 1,2-bis(3-thienyl)cyclopentene side chain[68] and to make a range of conjugated conducting copolymers based on various arrangements of phenylene, thiphene, and furan side chains in a ROMP scaffold that can be chain extended by electrochemical oxidation and hydrogenated to increase stability;[69] Sleiman has reported using nucleobase-templated polymerization to copy the chain length and polydispersity of living ROMP polymers into conjugated poly(ethynylene phenylene)s;[70] and finally in this section we note Coates' use of ROMP to synthesize alkaline anion exchange membranes which, of course, conduct ions rather than electrons or electronic charge carriers.[71] (It is worth noting that this idea has recently been extended to eight-membered rings but these do not come within the remit of this chapter.)

4.26.2.5 Routes Involving ROMP of Six-Membered Ring Systems

Benzene, a six-membered ring of sp^2 carbons, each carrying a hydrogen and one π-electron in a 2p AO perpendicular to the σ-framework, is potentially an ideal monomer for ROMP, leading to conjugated polymers but, of course, it is aromatic and far too stable for the purpose (Figure 4). The only way to get a six-membered ring to undergo ROMP is to place it in a strained environment, such as the barralene structures shown in Figure 22.

In the example at the top of the slide, the monomers were hexyl- and undecyl-substituted benzobarrelenes and these side-chain-substituted systems are soluble and undergo ROMP readily using the Schrock molybdenum carbene initiators.[72–74] The *cis*/*trans* ratio in the product polymer and the molecular-weight distribution depended on the substituents at molybdenum in the initiator used and the conditions adopted. The well-defined Schrock initiator, $Mo(=CHC(CH_3)_2Ph)(=NAr)(OC(CH_3)(CF_3)_2)_2$, gave a relatively slow reaction to give the expected precursor polymer in good yield, a molecular weight of about $M_w \sim 60\,000$ kDa and relatively broad polydispersity.

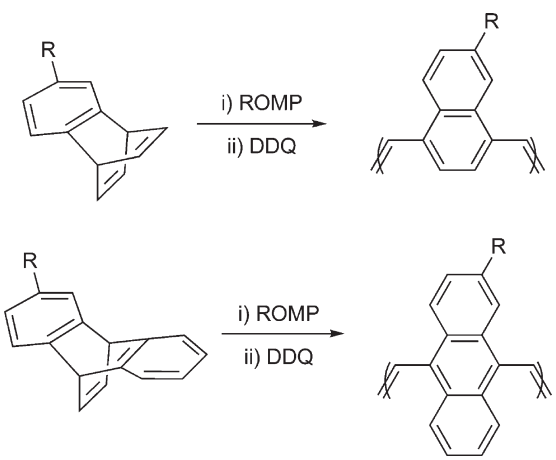

Figure 22 Successful ROMP and dehydrogenation routes to poly(arylene vinylenes).

The broad polydispersity is due to competition from termination reactions and/or slow initiation relative to propagation. Both the precursor polymers were dehydrogenated using DDQ to give solution–processable, relatively stable hexyl- and undecyl-poly(napthylene vinylene)s that were strongly fluorescent and could be oxidized with nitrosonium tetrafluoroborate to conductivities of about ~10 $\Omega\,cm^{-1}$, which was 2 orders of magnitude higher than those observed for the unsubstituted analogue. The solid-state photoluminescence of these materials was relatively modest – ~3% for the homopolymers and ~10% for blends with polystyrene; these materials are structurally regular and probably fairly well ordered as a consequence, face-to-face ordering of arylene vinylene segments being known to result in intermolecular quenching of the excited states in such materials. The bottom part of Figure 22 summarizes the analogous route reported by Stelzer and coworkers to poly(anthracenylene vinylene)s.[75] They used the same initiator and experimental conditions as the Grubbs group but obtained only a low-molecular-weight product with a mixture of *cis*- and *trans*-vinylenes rather than an all-*trans* system seen for the upper case. The monomer suffers two disadvantages in the lower case: first, it is more sterically hindered than that shown at the top of the figure and second, in the upper structure the monomer presents two double bonds to the growing polymer chain end, whereas in the Steltzer case only one hindered double bond is available for reaction. In the lower case, the initially formed precursor polymer was dehydrogenated with DDQ, but these workers found it very difficult to remove the $DDQH_2$ from the poly(anthracenylene vinylene) product; possibly because there were strong interactions between the anthracene residues, which are expected to be relatively easily oxidized, and the DDQ or $DDQH_2$, whatever the reasons the Stelzer group were unfortunate in their system, which serves to underline the validity of the earlier quotation from Reference 57. Another related monomer, 2,3-dicarboxybicyclo[*2.2.2*]octa-2,5,7-triene has been polymerized in benzene or methylene chloride using the same protocols and catalysts reported above. Addition of hexafluoro-*t*-butanol and tetrahydrofuran (THF) to the polymerization mixture had a marked accelerating effect on the rate. The precursor polymers obtained were successfully dehydrogenated with DDQ to give ester-substituted derivatives of poly(phenylene vinylene) (PPV). Hydrolysis of the esters allowed the synthesis of the anhydride and hence the disodium salt of the bis-carboxylate, thus giving rise to a water-soluble, fluorescent PPV derivative. Curiously at the time of publication, but now widely accepted, dehydrogenation of the precursor polymer to the extent of about 80% gave a significantly higher photoluminescence efficiency than the completely converted material, indicating an unexpected advantage, as far as photoluminescence is concerned, of having a disordered structure.

There being no examples of ROMP of seven-membered rings as routes to conjugated polymers known to the author, we now move directly to a consideration of eight-membered rings.

4.26.2.6 Unsaturated Eight-Membered Rings as Starting Materials

4.26.2.6.1 The direct route to polyacetylenes via ROMP of cyclooctatetraenes

The first thing to note when considering cycloocta-1,3,5,7-tetraene as a potential monomer is that our mnemonic (Figure 4) is of no help in this case because this molecule adopts a nonplanar conformation and it can be treated as, indeed, an alternating bond length cyclic polyene. There are planar cycloocta-1,3,5,7-tetraenes; two examples are the perfluoroalkylated and the fully bicyclo[*2.1.1*]hexa-2-ene-annelated derivatives, but to achieve planarity they have to be heavily substituted and this makes them unsuitable as monomers for ROMP.[76,77] It turns out that cyclooctatetraene does undergo ROMP effectively and since cyclobutadiene is too reactive, benzene is too stable, and the higher cyclic conjugated molecules are not readily available, it is the only unadorned cyclic polyene that can be used as a monomer for our purposes. This reaction, which is summarized in Figure 23, has been studied by several groups over the years.

Korshak *et al*. were the first to demonstrate the feasibility of this approach (Figure 23, R=H) and they obtained polyacetylene as a black powder using the 'classical' initiator system $WCl_6/Al(C_2H_5)_2Cl$ in toluene.[78] The product yield was only 6%. Subsequently, the same group improve the yield to 40%; this was achieved using the catalyst $W(OCH(CH_2Cl)_2)_n\ Cl_{6-n}/Al(C_2H_5)_2Cl$ as the initiator and condensing the cyclooctatetraene directly onto a layer of solid catalyst.[79]

They also reported that oligomeric side products were formed although they were identified by mass spectroscopy and not individually isolated; compounds identified included the cyclic polyenes $(CH{=}CH)_n$ where $n = 5–8$. This pioneering piece of work established the occurrence of backbiting reactions in competition with polymerization in this system. They also reported that the *cis* double bond content depended on the Al:W ratio in the catalyst; at an Al:W ratio of 1, a blue/black film with a *cis*-vinylene content of >80% was reported, whereas at an Al:W ratio of 2, the film had a golden hue and <40% *cis*-vinylene content.

The Grubbs group have reported a lot of work on this synthesis; in early experiments using the Schrock,[80] $W(=CHC(CH_3)_3)(=NAr)(OC(CH_3)(CF_3)_2)_2$, and the Osborn, $W(=CHC(CH_3)_3)(OCH_2C(CH_3)_3)_2Br_2.GaBr_3$,[81] well-defined catalysts, they were able to demonstrate much better control over the reaction.[82] Dissolution of such initiators in neat

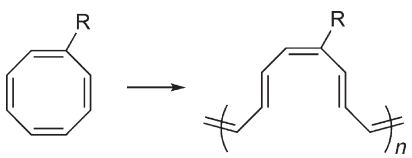

Figure 23 ROMP of cycloocta-1,3,5,7-tetraene and substituted analogues.

cyclooctatetraene gave high-quality lustrous films of polyacetylene within a few seconds; the films were silvery in color and had very smooth surfaces. This synthesis presented a protocol for the well-controlled generation of a sensitive conjugated polymer like polyacetylene *in situ*. Cyclooctatetraene has all *cis* double bonds and the nascent ROMP product must contain at least 75% *cis*-vinylene units; however, as discussed earlier, it is known that the thermodynamically stable configuration of polyacetylene that is of interest with respect to semiconducting behaviour is the *trans* transoid form (see Figure 2). Solid-state ^{13}C NMR is the most widely used analytical method for studying the isomerization and structure of solid polyacetylene. The exact shifts observed depend on *cis*/*trans*-vinylene geometry and the nature of the nearest neighbor vinylenes. The analysis is complicated but the evolution of chain microstructure can be followed quite well. In the nascent polymer, two peaks are observed; the more intense peak, corresponding to *cis*-vinylene units in all *cis* sequences, occurs at 126.4 ppm, with a weaker signal for the *trans*-vinylenes in *cis* sequences occurring at 132.2 ppm. The spectrum changes during thermal isomerization; the original signals decay and are eventually replaced by a dominant peak at 135.9 ppm, which are due to carbons in *trans* transoid sequences. The peak has a small upfield shoulder attributed to residual *cis* units between *trans* vinylenes. This study provided a useful improvement in the processing of polyacetylene since, while in the liquid stage of the synthesis, the liquid could be painted out onto substrates. The films of polyacetylene obtained were somewhat brittle, but they could be coated onto a rigid substrate and examined for both semiconducting (pristine material) and conducting (after exposure to volatile redox reagents) properties. This new form of polyactylene turned out to have structural features and physical properties similar to those of conventional Shirakawa polyacetylene (density, X-ray diffraction spacing, I_2-oxidized conductivity) but has a smoother surface and a lower intrinsic conductivity ($<10^{-8}–10^{-5}\ S\,cm^{-1}$), implying a significantly higher purity. It is also worth noting that working with a neat liquid, like cyclooctatetraene or its derivatives, has considerable advantages from the point of view of convenience and safety as compared to working with gaseous acetylene. The method also provides greater synthetic flexibility since derivatives of cyclooctatetraene are fairly readily made as are copolymers. As an example, copolymers with 1,5-cyclooctadiene and norbornene are easily made by this route and monomer feed ratio controls the distribution of polyene block lengths, allowing control of processability, film color, and conductivity. Thus, films of homo poly(cyclooctadiene) are colorless, but copolymers containing 20% of cyclooctatetraene are orange, 40% red, 80% red-black, and 100% silver.[83] Grubbs' group have studied this direct route from cyclooctatetraenes to conjugated polymers in considerable detail; various experimental conditions were investigated, a range of initiators was employed, and cyclooctatetra-1,3,5,7-ene and a variety of substituted cyclooctatetraenes were used either on their own or in conjunction with mono- and polycyclic olefins as comonomers. Some of the conclusions from this large volume of work, leading to the synthesis and characterization of many new materials, are reported briefly below.[84]

The simple homopolymer of cyclooctatetraene, obtained as described above, is formed as a smooth, shiny, but rather brittle film; this disadvantage could be overcome by the introduction

of substituents without serious reduction in the desired electronic properties. The polymerization of simple mono- and disubstituted acetylenes leads to polyenes in which there are alternating double and single carbon–carbon bonds along the polymer backbone, but there is no π overlap between adjacent double bonds; thus, for example, poly(*t*-butylacetylene) and poly(hexafluoro-2-butyne) are undoubtedly polyenes, but both are close to white in color because steric interactions between neighboring substituents twist the polyene backbone so that successive π bonds cannot be coplanar. When monosubstituted cyclooctatetraenes are polymerized, the substituents in the product can, formally, occur once on every eight carbons of the backbone; however, in practice in the case of neat monomer, backbiting reactions occur to the extent of 7–16%, resulting in the elimination of monosubstituted benzenes but no unsubstituted benzene. This means that no ROMP occurs at the substituted double bonds and that statistically the substituents will be on every fourth or fifth double bond in the chain, because reaction occurs at any of the unsubstituted double bonds in the monomer. The consequence of these considerations is that 1,2- and 1,3-placement of substituents, required for significant steric interaction leading to nonplanarity, is vanishingly small. Substituted polyenes formed by this route were generally soluble as made but, consistent with reasonable expectations concerning order/disorder effects on solubility, tended to become less soluble when the nascent *cis*-vinylene sequences were isomerized to the more ordered *trans* sequences either by prolonged storage at room temperature or by warming. A single methyl substituent on the monomer does not improve the product properties at all; it remains brittle and insoluble, but butyl or larger *n*-alkyl substituents give films that are flexible and very slightly soluble. Evidence for the postulated isomerization process is that, as made, the polymers give red-brown solutions that turn blue on prolonged standing at room temperature. These products resemble conventional Shirakawa polyacetylene in some respects; thus, they are oxidized into the metallic conductivity regime on exposure to iodine vapor. Branched chain or aromatic substituents give polymers that are completely soluble as made, but become insoluble as the *trans*-vinylene content and molecular order increase on standing. Really bulky substituents, such as *t*-butyl, provide access to a completely soluble but yellow materials because the steric bulk close to the polyene chain prevents extended backbone planarity; this polymer remains an insulator on exposure to iodine vapor that is also consistent with the steric inhibition of planarity.

Careful selection of substituents provides access to soluble and highly conjugated forms of substituted polyacetylene, for example, when R is trimethylsilyl.[84] The readily solution-processed polyenes prepared by this route were studied as active components in devices such as Schottky barrier structures and solar cells and advantages of polymeric semiconductors demonstrated.[85–87] These advantages stemming, at least in part, from the milder solution-based processing as compared to the conventional, highly energetic vacuum sputtering by which metals may be deposited. For solar cells fabricated by spin coating thin transparent films of trimethylsilyl-substituted polyacetylene from solution onto *n*-type silicon and subsequently oxidizing the semiconducting polymer layer with iodine vapor. These authors reported that the photovoltages much greater than those obtained from similar structures based on thin films of conventional vacuum deposited metals onto the same substrate; again the improvement was attributed to the mild solution-processing conditions. These early promising observations concerning the advantages of organic polymers in the fabrication of electronic devices have been fully born out in the subsequent development and exploitation of 'organic electronics' although, in the event, these early examples were not to be adopted as the materials of choice in the commercialization of the area. The area continues to be developed and the use of well-defined initiators has allowed the convenient synthesis of telechelic soluble, end-functionalized polyenes and polyacetylene block copolymers.[88] For full details of this extensive program of work, the reader is referred to the articles and reviews cited; but we will close this section with one further example. When the substituent R in **Figure 23** is chiral, soluble polyacetylenes are the products.[89] The $\pi - \pi^*$ transition of the conjugated backbone demonstrates a large CD effect, indicating that the backbone chain must be dissymmetric or in a dissymmetric environment. Consequently, we can conclude that the presence of a chiral substituent on the backbone results in twisting the chain predominantly in one sense rather than just electronically perturbing the chromophore. The exploration of the electronic and optical properties of substituted polyacetylenes derived from substituted cyclooctene ROMP continues to attract interest; for example, thick optical quality films of poly(cycloocta-1,3,5,7-tetraene) display large ultrafast third-order nonlinearities of use in the construction of ultrafast image correlation devices.[90] We can conclude that the route indicated by **Figure 23**, coupled to the developments in living ROMP, offers the best option for precision and control in the synthesis and manipulation of polymeric polyenes.

Finally, for this section we note Lonergan's work on the polymerization of ionically functionalized cyclooctatetraenes (syntheses and kinetics) and the nature of the product polymers as both ionic and electronic conductors.[91]

4.26.2.6.2 Other conjugated polymer syntheses starting from eight-membered ring monomers

ROMP of eight-membered rings has been used constructively to make processable block copolymers of regioregular poly(3-hexylthiophene) and polyethylene in which both blocks are crystalline. To introduce the conjugated segment, this method utilizes an allyl-functionalized poly(3-hexylthiophene) as a chain transfer during the living ROMP of cyclooctene; subsequent hydrogenation of the poly(octenamer) block giving a highly linear polyethylene block terminates with an oligothiophene (see **Figure 24**). Linear polyethylene is an excellent thermoplastic and this novel block copolymer offers the opportunity to explore new processing techniques, new morphologies, and the electrical and optical properties for conjugated polymers in which the conjugated part is distributed in high-quality insulating polymer whose dielectric properties have proved invaluable in many earlier technologies.[92]

The Nuckolls' group has recently described two novel metathesis polymerizations involving eight-membered ring monomers. The first is summarized in **Figure 25** and involves the nontrivial synthesis of helical (5Z,11E)-dibenzo[*a*,*e*]cyclooctatetranene via a double Wittig reaction with the 1,2-bis(triphenylphosphonium ylide) derived from *ortho*-phthalaldehyde with *ortho*-phthalaldehyde. The monomer is

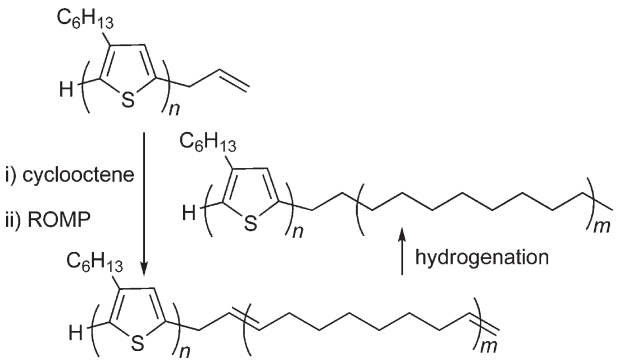

Figure 24 Synthesis of poly(3-hexylthiophene)-*block*-polyethylene.

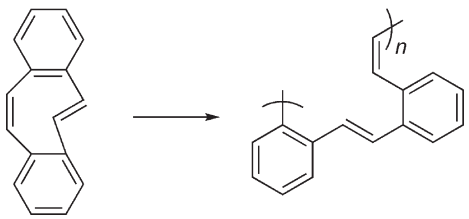

Figure 25 ROMP of a strained cyclooctadiene derivative.

strained and the density functional theoretical calculations indicate a strain energy of 18 kcal mol^{-1} compared to the *cis, cis*-vinylene analog. This monomer is described by the authors as 'spring loaded' which seems an appropriate metaphor since X-ray diffraction indicates that it adopts a helical conformation and indeed it is the associated strain that makes it polymerizable. The *cis,trans*-vinylene isomer shown in the figure undergoes living polymerization when initiated with the well-defined Grubbs' initiator, $Cl_2(PCy_3)_2Ru{=}CHPh$, whereas the *cis,cis*-isomer does not. This is the first example of a PPV in which all the phenylenes are 1,2-incorporated into the polymer chain.[93]

The second example from this group is summarized in Figure 26. In their initial work, the polymerization of 5,6-didehydrodibenzo[*a,e*]cyclooctatetraene (the totally unsubstituted version of the monomer shown in the figure) was described, but the monomer was unstable and high polydispersities in a nonliving polymerization were observed.[94] However, more recently they have developed syntheses of substituted analogs of 5,6-didehydrodibenzo[*a,e*]cyclooctatetraene and shown that with a mixture of [$(N(tBu)Ar)_3$-$Mo{\equiv}CCH_2CH_3$] and three equivalents of *ortho*-nitrophenol as initiator reliable living alkyne metathesis to gives high molecular weights and low polydispersities in polymers with alternating alkyne and alkane linkages along a poly(*ortho*-phenylene) backbone, as shown in the figure.

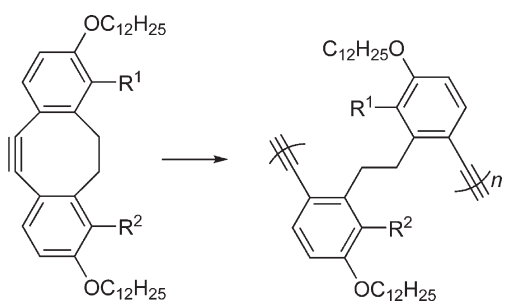

Figure 26 Cyclic alkyne ROMP.

4.26.2.7 Monomers with Larger than Eight-Membered Rings as Starting Materials

The events following the astute observation by Jeremy Burroughes of light emission from a layer of PPV held under an electrical potential that led to the description of the use of such materials as the electroluminescent layer in polymer-based LEDs,[95] and the enormous amount of research and development associated with this area has now entered the 'folk law' of the organic electronics field. [2.2]Paracyclophane-1,9-diene, the monomer shown on the left-hand side in Figure 27 (where R=H), is the obvious monomer to use in ROMP for the synthesis of such materials and Thorn-Csányi and coworkers were the first to show that this was possible.

They obtained PPV as an insoluble, yellow fluorescent powder; soluble copolymers were obtained with cyclopentene, cyclooctene, and cycloocta-1,5-diene as comonomers. In the UV–Vis spectra of the copolymers with cyclooctene, distinct absorption peaks are resolved that can be assigned to sequences of one, two and three paraphenylene vinylene repeat units; this shows that the polymer formation is not a straightforward chain-growth ROMP reaction since the presence of the units with one and three paraphenylene vinylene repeat units can only arise from secondary metathesis at the vinylenes.[96–98] Bazan showed that [2.2]paracyclophane-1-ene (the monohydrogenated monomer of Figure 27) is polymerized using the Schrock initiator $Mo(=CHC(CH_3)_2Ph)(=NAr)(OC(CH_3)(CF_3)_2)_2$ in toluene solution to give a soluble polymer that, as formed, has 98% *cis*-vinylenes. When the double bonds are isomerized to *trans* geometry, the polymer rapidly becomes insoluble, emphasizing the problems associated with processing the more ordered material. They developed a precursor route to circumvent the solubility problem by attaching $OSi(CH_3)_2C(CH_3)_3$ at one of the saturated carbons in [2.2]paracyclophane-1-ene; this gave a soluble polymer on ROMP even in all *trans*-vinylene structures and replacement of the silyl group by hydroxyl gave a precursor amenable to acid-catalyzed dehydration to PPV.[99] Bazan used this route to materials for an exploration of the effects of chain length and interchain contacts on fluorescence quantum yields.[100] The concept summarized in Figure 27 has been extensively exploited and extended. The Turner group has made block copolymers having a controlled distribution of 1,4- and 1,3-phenylene vinylene segments via living ROMP of the appropriately substituted

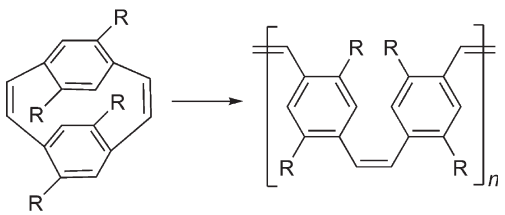

Figure 27 Phenylene vinylene ROMP.

cyclophanedienes and been able to use such structures to study luminescence and energy transfer in a range of systems; they synthesized a range of soluble monomers with various substituents (R in Figure 27).[101–104] ROMP of ferrocenophanes (ferrocenes with the cyclopentadienyls bridged by a vinylene) and ferrocenylenes (with diene bridges) has also been reported.[105–107]

Summary

The synthesis of conjugated polymers via ring ROMP was briefly discussed and the author has attempted to follow this brief without too many diversions. However, the reader whose interests are primarily in conjugated polymers and not necessarily in the way in which they are made should note that metathesis catalysts can be used in acyclic diene metathesis (ADMET) synthesis, alkyne metathesis, and ring-closing reactions of dipropargyl derivatives; these reactions having been extensively examined and shown to yield conjugated polymers in the conventional sense of 'conjugated'.[108] Some aspects of this were covered in Reference 2, and journal indexes and search engines will provide more data. Meanwhile, Chujo and others are exploring through-space conjugated polymers rather than conventional conjugation.

References

1. Bryson, B. In *The Story of Science and the Royal Society*; Bill B., Ed.; Harper Press: London, 9, ISBN 978-0-00-730256–7, 2010.
2. Feast, W. J. In *Handbook of Metathesis*; Grubbs, R. H., Ed.; Wiley-VCH: Weinheim, ISBN 3-527-30616–1, October 2003.
3. Clouth, D. *Joseph Swan*, Gateshead Metropolitan Borough Council, Department of Education: Gateshead, UK, 1979, ISBN 0 905977 07 6.
4. Huckle, E. *Z. für Phys.* **1931**, *70*, 204.
5. Staudinger, H. *Ber. Dtsch. Chem. Ges.* **1920**, *53*, 1073.
6. Lennard-Jones, J. F. *Proc. Roy. Soc.* **1937**, *A158*, 280.
7. Longuet-Higgins, H. C.; Salem, L. *Proc. Roy. Soc.* **1959**, *A251*, 172.
8. Natta, G.; Mazzanti, G.; Corradini, P. *Rend. Accad. Naz. Lincei Cl Sc. Fis. Mat. E Nat.* **1958**, *25*, 3.
9. Chambers, R. D.; Clark, D. T.; Kilcast, D.; Partington, S. *J. Pol. Sci: Polym. Chem. Ed.* **1974**, *12* (8), 1647.
10. Berets, D. J.; Smith, D. S. *Trans. Farad. Soc.*, **1968**, *64*, 823.
11. Shirakawa, H.; Ikeda, S. *Polym. J.* **1971**, *2*, 231.
12. Shirakawa, H.; Lewis, E. J.; MacDiarmid, A. G.; *et al. Chem. Commun.* **1977**, 578; Chiang, C. K.; Fincher, C. R.; Park, Y. W.; Heeger, A. J.; Shirakawa, H.; Lewis, E. J.; Gau, S. C.; MacDiarmid, A. G. *Phys. Rev. Lett.* **1977**, *39*, 1098.
13. Naarmann, H.; Theophilou, N. *Synth. Met.* **1987**, *22*, 1; Tsukamoto, J.; Takahashi, A.; Kawasaki, K. *Jpn. J. Appl. Phys.* **1990**, *29*, 125.
14. Kuzmany, H.; Mehring, M.; Roth, S., Eds. *Electronic Properties of Polymers and Related Compounds Springer Series in Solid-State Sciences*; Springer-Verlag: Berlin, Germany, 1985; Vol. 63 and continuations; Skotheim, T. A., Ed., *Handbook of Conducting Polymers*, 2 Vols., *Marcel Dekker, Inc: New York, 1986 and supplements; Billingham, N. C.; Calvert, P. D.* Electrically Conducting Polymers – A Polymer Science Viewpoint, *in* Adv. Polym. Sci.; Springer-Verlag: Berlin, Germany, **1989**, 90, 1–104; *Aldissi, M.* Inherently Conducting Polymers: Processing, Fabrication, Applications, Limitations, *Noyes Data Corporation, 1989*, 1–96; *Feast, W. J.; Friend, R. H. Synthesis and material and electronic properties of conjugated polymers, in* J. Mat. Sci. **1990**, 25, 3796–3805; *Zerbi, G., Ed.* Polyconjugated Materials*; North-Holland Press:* Amsterdam, 1992; *Bredas, J. L.; Silbey, R.* Conjugated Polymers*; Kluwer Academic Publishers:* Dordrecht, 1991; *Salaneck, W. R.; Lindström, I.; Rånby, B.* Conjugated Polymers and Related Materials: The Interconnection of Chemical and Electronic Structure*;* Oxford University Press: Oxford, 1993; *Feast, W. J.; Tsibouklis, J.; Pouwer, K. L.; Groenendaal, L.; Meijer, E. W. Synthesis, processing and material properties of conjugated polymers, a Review,* Polymer **1996**, *37*, 5017–5047.
15. Ivin, K. J. *Olefin Metathesis*; Academic Press: New York, 1983; Ivin, K. J.; Mol, J. C. *Olefin Metathesis and Metathesis Polymerisation*; Academic Press: New York, 1997.
16. Ivin, K. J. In *Reactivity, Mechanism and Structure in Polymer Chemistry*; Jenkins, A. D.; Ledwith, A., Eds.; Wiley/Interscience: London, 1974; Chapter 16.
17. Breslow, R.; Groves, J. T. *J. Am. Chem. Soc.* **1970**, *92*, 984.
18. Singh, R.; Czekelius, C.; Schrock, R. R. *Macromolecules* **2006**, *39*, 1316; Singh, R.; Schrock, R. R. *Macromolecules* **2008**, *41*, 2990.
19. Binder, W. H.; Kurzhals, S.; Pulamagatta, B.; *et al. Macromolecules* **2008**, *41*, 8405.
20. de la Mata, E. J.; Grubbs, R. H. *Organometallics* **1996**, *15*, 577; Johnson, L. K.; Grubbs, R. H.; Ziller, J. W. *J. Am. Chem. Soc.* **1993**, *115*, 8130.
21. Billups, W. E.; Haley, M. M. *Angew. Chem. Int. Ed. Eng* **1989**, *107*, 3736.
22. Edwards, J. H.; Feast, W. J. *Polymer* **1980**, *21*, 595.
23. Edwards, J. H.; Feast, W. J.; Bott, D. C. *Polymer* **1984**, *25*, 395.
24. Bott, D. C.; Chai, C. K.; Edwards, J. H.; *et al. J. de Physique* **1983**, *44*, C3–143.
25. Bott, D. C.; Brown, C. S.; Edwards, J. H.; *et al. Mol. Cryst. Liq. Cryst.* **1985**, *117*, 9.
26. Bott, D. C.; Brown, C. S.; Chai, C. K.; *et al. Synth. Met.* **1986**, *14*, 245.
27. Allen, P. C.; Bott, D. C.; Brown, C. S.; *et al.* In *Springer Series in Solid State Science*; Kusmany, H., Mehring, M., Roth, S., Eds.; Springer-Verlag, 1989; pp 91, 456.
28. Clemenson, P. I.; Feast, W. J.; Ahmad, M. M.; *et al. Polymer* **1992**, *33*, 4711.
29. Martens, J. H. F.; Pichler, K.; Marseglia, E. A.; *et al. Polymer* **1994**, *35*, 403.
30. Burroughes, J. H.; Jones, C. A.; Friend, R. H. *Nature* **1988**, *335*, 137.
31. Burroughes, J. H.; Friend, R. H. In *Conjugated Polymers*; Bredas, J. L., Silbey, R., Eds.; Kluwer Academic Publishers: Dordrecht, 1991; p 555.
32. de Leeuw, D. Technical University Eindhoven, Personal communication.
33. Widawski, G.; Feast, W. J.; Dounis, P. *J. Mater. Chem.* **1995**, *5*, 1847.
34. Dounis, P.; Feast, W. J.; Widawski, G. *J. Mol. Cat. A.* **1997**, *115*, 51.
35. Craig, G. S. W.; Cohen, R. E.; Schrock, R. R.; *et al. Macromolecules* **1995**, *28*, 2512.
36. Schrock, R. R. *Acc. Chem. Res.* **1990**, *23*, 158.
37. Klavetter, F. L.; Grubbs, R. H. *Synth. Met.* **1988**, *26*, 311.
38. Stelzer, F.; Leitner, O.; Pressl, K.; *et al. Synth. Met.* **1991**, *41–43*, 991.
39. Stelzer, F.; Grubbs, R. H.; Leising, G. *Polymer* **1991**, *32*, 1851.
40. Feast, W. J.; Winter, J. N. *Chem. Commun.* **1985**, *20*.
41. Jones, C. A.; Laurence, R. A.; Martens, J.; *et al. Polymer* **1991**, *32*, 1200.
42. Charvet, R.; Novak, B. M. *Macromolecules* **2001**, *34*, 7680.
43. Novak, B. M. North Carolina State University, Personal communication.
44. Safir, A. L.; Novak, B. M. *Macromolecules* **1993**, *26*, 4072.
45. Corey, E. J.; Streith, J. *J. Am. Chem. Soc.* **1964**, *86*, 950.
46. Pirkle, W. H.; McKendry, L. H. *J. Am. Chem. Soc.* **1969**, *91*, 1179, and references therein.
47. Lin, C. Y.; Krantz, A. *J.C.S. Chem. Comm.* **1972**, *1111*.
48. Swager, T. M.; Dougherty, D. A.; Grubbs, R. H. *J. Am. Chem. Soc.* **1987**, *109*, 894.
49. Swager, T. M.; Dougherty, D. A.; Grubbs, R. H. *J. Am. Chem. Soc.* **1988**, *110*, 2973.
50. Swager, T. M.; Dougherty, D. A.; Grubbs, R. H. *J. Am. Chem. Soc.* **1989**, *111*, 4413.
51. Feast, W. J.; Wilson, B. *J. Mol. Cat.* **1980**, *8*, 277.
52. El-Saafin, I. F. A. F.; Feast, W. J. *J. Mol. Cat.* **1982**, *15*, 61.
53. Alimuniar, A. B.; Blackmore, P. M.; Edwards, J. H.; *et al. Polymer* **1986**, *27*, 1281; Feast, W. J.; Shahada, L. A. H. *Polymer* **1986**, *27*, 1289; Blackmore, P. M.; Feast, W. J. *Polymer* **1986**, *27*, 1296.
54. Blackmore, P. M.; Feast, W. J. *J. Mol. Cat.* **1986**, *36*, 145.
55. Davies, G. R.; Hubbard, H. V. St. A.; Ward, I. M.; *et al. Polymer* **1995**, *36*, 235.
56. Feast, W. J.; Millichamp, I. S. *J. Mol. Cat.* **1985**, *28*, 331.
57. Burns, R.; **2005**. *To a Mouse*. The Complete Poems and songs of Robert Burns, Geddes and Grosset: New Lanark, Scotland, ISBN 10: 855349825.
58. Feast, W. J.; Harper, K. *J. Mol. Cat.* **1985**, *28*, 293; *Brit. Polymer J.* **1986**, *18*, 161.
59. Bazzi, S. H.; Sleiman, H. F. *Macromolecules* **2002**, *35*, 624.
60. Swager, T. M.; Rock, M. M.; Grubbs, R. H. *New Polymeric Mater.* **1990**, *2*, 1.
61. Weck, M.; Jackiw, J. J.; Rossi, R. R.; *et al. J. Am. Chem. Soc.* **1999**, *121*, 4088.
62. Moon, J. H.; Swager, T. M. *Macromolecules* **2002**, *35*, 6086.
63. Watson, K. J.; Wolfe, P. S.; Nguyen, S. T.; *et al. Macromolecules* **2000**, *33*, 4628.
64. Jang, S.-Y.; Stozing, G. A.; Marquez, M. *Macromolecules* **2002**, *35*, 7293.
65. Zhao, C.; Zhang, Y.; Pan, S.; *et al. Macromolecules* **2007**, *40*, 1816.
66. Kumar, A.; Jang, S.-Y.; Padilla, J.; *et al. Polymer* **2008**, *49*, 3686.
67. Nantalaksakui, A.; Krishnamoorthy, K.; Thayumanavan, S. *Macromolecules* **2010**, *43*, 37.
68. Myles, A. J.; Branda, N. R. *Macromolecules* **2003**, *36*, 298; Wigglesworth, T. J.; Branda, N. R. *Chem. Mater.* **2005**, *17*, 5473.

69. Kang, H. A.; Bronstein, H. E.; Swager, T. M. *Macromolecules* **2008**, *41*, 5540.
70. Lo, P. K.; Sleiman, H. F. *J. Am. Chem. Soc.* **2009**, *131*, 4182.
71. Clark, T. J.; Robertson, N. J.; Kostalik, H. A.; *et al. J. Am. Chem. Soc.* **2009**, *131*, 12888; See Kostalik, H. A.; Clark, T. J.; Robertson, N. J.; *et al. Macromolecules* **2010**, *43*, 7147.
72. Tasch, S.; Graupner, W.; Leising, G.; *et al. Adv. Mater.* **1995**, *7*, 903.
73. Pu, L.; Wagaman, M. W.; Grubbs, R. H. *Macromolecules* **1996**, *29*, 1138.
74. Wagaman, M. W.; Grubbs, R. H. *Macromolecules* **1997**, *30*, 3978.
75. Stelzer, F.; Muelner, R.; Schlick, H.; Leising, G. In *Ring Opening Metathesis Polymerization and Related Chemistry*; Khosravi, E., Szymanska-Buzar, T., Eds.; Kluwer Academic Publishers: Dordrecht, 2002; p 185.
76. Soulen, R. L.; Wirz, J. *J. Fluorine Chem.* **1985**, *29*, 245.
77. Matsuura, A.; Komatsu, K. *J. Am. Chem. Soc.* **2001**, *123*, 1768.
78. Korshak, Y. V.; Korshak, V. V.; Kanischka, G.; Höcker, H. *Macromol. Chem., Rapid Commun.* **1985**, *6*, 685.
79. Tlenkopachev, M. A.; Korshak, Y. V.; Orlov, A. V.; Korshak, V. V. *Dokl. Akad. Nauk SSSR* **1986**, *291*, 409.
80. Schaverien, C.; Dewan, J.; Schrock, R. R. *J. Am. Chem. Soc.* **1986**, *108*, 2771.
81. Kress, J.; Wesolak, M.; Osborn, J. A. *Chem.Commun.* **1982**, *514*.
82. Klavetter, F. L.; Grubbs, R. H. *J. Am. Chem. Soc.* **1988**, *110*, 7807; Klavetter, F. L.; Grubbs, R. H. *Synth. Met.* **1989**, *28*, D99–D108; *Polym. Mater. Sci. Eng.* **1988**, *58*, 855.
83. Ginsburg, E. J.; Gorman, C. R.; Grubbs, R. H.; *et al.* In *Conjugated Polymeric Materials: Opportunities in Electronics, Optoelectronics and Molecular Electronics*; Brédas, J.-L., Chance, R. R., Eds.; Kluwer Academic Publishers: Dordrecht, 1990; pp 65–81.
84. Ginsburg, E. J.; Gorman, C. R.; Marder, S. R.; Grubbs, R. H. *J. Am. Chem. Soc.* **1989**, *111*, 7621; Ginsburg, E. J.; Gorman, C. R.; Marder, S. R.; Grubbs, R. H. *Angew. Chem. Adv. Mater.* **1989**, *101*, 1604.
85. Sailor, M. J.; Klavetter, F. L.; Grubbs, R. H.; Lewis, N. S. *Nature* **1990**, *345*, 155.
86. Jozefiak, T. H.; Sailor, M. J.; Ginsburg, E. J.; *et al. Proc. SPIE* **1991**, *1463*, 8.
87. Sailor, M. J.; Ginsburg, E. J.; Gorman, C. R.; *et al. Science* **1990**, *249*, 1146.
88. Scherman, O. A.; Rutenberg, I. M.; Grubbs, R. H. *J. Am. Chem. Soc.* **2003**, *125*, 8518.
89. Moore, J. S.; Gorman, C. R.; Grubbs, R. H. *J. Am. Chem. Soc.* **1991**, *113*, 1704.
90. Chi, S.-H.; Hales, J. M.; Fuentes-Hermandes, C.; *et al. Adv. Mater.* **2008**, *20*, 3199.
91. Johnston, D. H.; Gao., L.; Lonergan, M. C. *Macromolecules* **2010**, *43*, 2676; Langsdorf, B. L.; Zhou, X.; Adler, D. H.; Lonergan, M. C. *Macromolecules* **1999**, *32*, 2796.
92. Radano, C. P.; Scherman, O. A.; Stingelin-Stutzmann, N.; *et al. J. Am. Chem. Soc.* **2005**, *127*, 12502.
93. Carnes, M.; Buccella, D.; Siegrist, T.; *et al. Chem. Int. Ed.* **2008**, *47*, 2982.
94. Carnes, M.; Buccella, D.; Decatur, J.; *et al. J. Am. Chem. Soc.* **2008**, *130*, 14078.
95. Burroughes, J. H.; Bradley, D. D. C.; Brown, A. R.; *et al. Nature* **1990**, *347*, 539.
96. Thorn-Csányi, E.; Höhnk, H.-D. *J. Mol. Cat.* **1992**, *76*, 101.
97. Thorn-Csányi, E.; Pflug, K. P. *Macromol. Chem.* **1993**, *194*, 2287.
98. Thorn-Csányi, E.; Kraxner, P.; Hammer, J. *J. Mol. Cat.* **1994**, *90*, 15.
99. Miao, Y.-J.; Bazan, G. C. *J. Am. Chem. Soc.* **1994**, *116*, 9379; Miao, Y.-J.; Sun, B. J.; Bazan, G. C. *Macromol. Symp.* **1995**, *95*, 185.
100. Bazan, G. C.; Miao, Y.-J.; Renak, M. L.; Sun, B. J. *J. Am. Chem. Soc.* **1996**, *118*, 2618.
101. Yu, C.-Y.; Turner, M. L. *Angew. Chem. Int. Ed.* **2006**, *45*, 7797.
102. Yu, C.-Y.; Kingsley, J. W.; Lidzey, D. G.; Turner, M. L. *Macromol. Rapid Commun.* **2009**, *30*, 1889.
103. Spring, A. M.; Yu, C.-Y.; Horie, M.; Turner, M. L. *Chem. Commun.* **2009**, *2676*.
104. Yu, C.-Y.; Horie, M.; Spring, A. M.; *et al. Macromolecules* **2010**, *43*, 222.
105. Stanton, C. E.; Lee, T. R.; Grubbs, R. H.; *et al. Macromolecules* **1995**, *28*, 8713.
106. Heo, R. W.; Somoza, F. B.; Lee, T. R. *J. Am. Chem. Soc.* **1998**, *120*, 1621.
107. Heo, R. W.; Park, J. S.; Goodson, J. T.; *et al. Tetrahedron* **2004**, *60*, 7225.
108. Morisaki, Y.; Chujo, Y. *Chem. Soc. Jpn.* **2009**, *82*, 1070.

Biographical Sketch

W. Jim Feast is a materials chemist with interests in, *inter alia*, semiconducting, piezoelectric, electroluminescent, electrostrictive, dendric, and hyperbranched polymers; self-assembly; and biomaterials and bacterial fouling. He was the director of the Leeds–Bradford–Durham Interdisciplinary Research Centre in Polymer Science and Technology from 1994 to 2002. He was elected a fellow of the Royal Society of Chemistry, the Institute of Materials, and the Royal Society. He was an undergraduate in Sheffield and postgraduate in Birmingham, spent most of his career in Durham, and reached pensionable age during 2003, but remained active as a research professor in Durham and in The Technical University of Eindhoven, where he was based during the writing of this chapter. He was President of the Royal Society of Chemistry from 2006 to 2008.

He was born in Birmingham (UK) in 1938 and grew up near Lichfield. He is married (Jenneke E.C. van der Kuijl, 1967) and has two adult daughters and four grandchildren. His pleasures include family, friends, science, fell walking (UK), cycling (Nl), reading, theater, and fine arts.

4.27 Oligomeric Poly(ethylene oxide)s. Functionalized Poly(ethylene glycol)s. PEGylation

I Dimitrov and CB Tsvetanov, Bulgarian Academy of Sciences, Sofia, Bulgaria

4.27.1 Introduction

PEGylation is the process of covalent attachment of poly(ethylene glycol) (PEG) to another molecule, in most cases a drug or therapeutic protein. It leads to the formation of prodrug – pharmaceutical substance administered in an inactive or significantly less active form. The covalent attachment of PEG to a drug or therapeutic protein involves 'stealth' effect (e.g., reduced immunogenicity and antigenicity), an increase in the hydrodynamic size of agents, which prolongs its circulatory time by reducing renal clearance. Importantly, PEGylation can also provide water solubility to hydrophobic drugs and proteins. ISI Web of Science database in the period 1995–2010 lists more than 1400 papers on 'PEGylation' as a keyword. Since the first PEGylated product was approved by the Food and Drug Administration (FDA) in 1990, PEGylation has been widely used for improving biomedical efficacy and physicochemical properties of therapeutic proteins.

The clinical value of PEGylation is now well established. PEGylation can impart several significant pharmacological advantages over the unmodified form, such as

- improved drug solubility;
- reduced dosage frequency, without diminished efficacy with potentially reduced toxicity;
- extended circulating life;
- increased drug stability; and
- enhanced protection from proteolytic degradation.

Even though nearly four decades of development in PEGylation technology has proven its pharmacological advantages and acceptability, the technology still lags in providing a commercially attractive, generic process to produce highly specific PEGylated therapeutic products at a high yield. As a multimillion dollar annual business with growing interest from both emerging biotechnology and established multinational pharmaceutical companies, there is great scientific and commercial interest in improving present methodologies and in introducing innovative process variations.

4.27.2 Properties of PEGs

PEG, which has the general formula $HO–(CH_2CH_2O)_n–H$ with typical molecular weights (MWs) of 500–20 000 Da, unlike other polyethers (general formula $[(CH_2)_xO]_m$, for PEG $x = 2$), is soluble both in common organic solvents, like the other members of the series, and in water. This characteristic behavior seems to be due to a crucial balance of the hydrophobic forces exerted by the ethylene units, $–CH_2–CH_2–$, with the hydrophilic interaction of the oxygens presented in the oxirane units and in the terminal groups. The latter play an important role in the shortest chains; their importance diminishes when the polymerization degree m increases. As a result of these two competitive forces (hydrophilic and hydrophobic), the PEG is soluble in water in all proportions at temperatures lower than the boiling point of solvents. As far as PEG molecular conformation is concerned, it is well stated that in the crystalline state PEG assumes a helical conformation (like other important biological macromolecules, e.g., DNA) that contains seven oxyethylene units, $–CH_2–CH_2–O–$, with two helical turns per fiber identity period (19.3 Å), that is, 7_2 helix structure.[1] Experimental evidences support the hypothesis that PEG retains some of its helicity even in dilute aqueous solutions,[2] assuming a more ordered conformation in the presence of water compared to the one in the melted state. Moreover, the similarity of the ether oxygen spacing (2.88 Å) with that of oxygen in water (2.85 Å) evidently provides a good structural

fit of the PEG coil to the hydrogen-bonding network in water. Furthermore, each oxyethylene PEG unit is able to coordinate 3–5 water molecules, thus increasing the polymer hydrodynamic volume by an approximately 5- to 10-fold greater amount than that predicted by the nominal MW.

PEGs above triethylene glycol range from white liquids to waxlike solids. Storage under an inert atmosphere is recommended since, although stable toward several chemical reagents, PEG is sensitive to oxidation that may cleave the chain. As with all the synthetic polymers, PEG is polydisperse; the M_w/M_n value is about 1.04 for polymers with MW ranging from 2 to 10 kDa, while reaching values up to 1.2 for higher-MW polymers.

PEGs are widely used as lubricants, solvents, binders, and intermediates in the rubber, food, pharmaceutical, cosmetic, agricultural, textile, paper, petroleum, and many other industries. The following is a brief listing of some properties of interest:

- amphipathic behavior – soluble in water, chloroform, methylene chloride, and benzene, and insoluble in diethyl ether and aliphatic hydrocarbons;
- nontoxic: PEG (MW = 1000–5000 Da) can be safely administered (*in vivo*) in 10% solutions to rats, guinea pigs, rabbits, and monkeys. FDA approval has been granted for internal consumption;
- poorly immunogenic;
- causes cell fusion (in high concentrations);
- forms two-phase systems with an aqueous solution of other macromolecules such as dextran or concentrated salt solution; and
- can be used to precipitate proteins and nucleic acids.

If PEG is covalently coupled with proteins, the conjugates may exhibit the following properties:

- enables solubilization of enzymes and bioactive substances in organic solvents or in aqueous solutions;
- renders proteins nonimmunogenic;
- prolongs the clearance time of PEG–protein drug *in vivo*;
- stabilizes the physiological function of bioactive substances;
- alters pharmacokinetics of various drugs; and
- separates biological macromolecules, membranes, cell particles, and cells.

The most important applications of PEG are biological since PEG is compatible with human blood and tissue.[3] Therefore, despite its apparent simplicity, PEG is the focus of much interest in biomedical and biotechnical communities.

4.27.3 Chemistry of PEGylation

PEG is synthesized by an anionic ring-opening polymerization of ethylene oxide initiated by a nucleophilic attack of an alkoxide ion on the epoxide ring. Having only one or two terminal functional groups, PEG has a limitation with a poor loading capacity. Most used PEGs for prodrug modification are either monomethoxy PEG (Figure 1, structure 1) or dihydroxy PEG (Figure 1, structure 2). High water solubility makes PEG

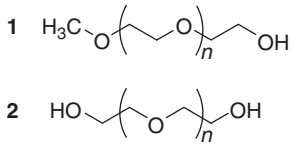

Figure 1 Structural formulas of PEG molecules.

polymer a versatile candidate for the prodrug conjugation. PEG is also considered to be somewhat hydrophobic due to its solubility in many organic solvents.

In order to couple PEG to another molecule such as polypeptide, polysaccharide, polynucleotide, or small organic molecule, activation of one or both termini is necessary. The activation of PEG involves introduction of various functional groups such as activated carbonates, activated esters, aldehydes, or alkyl 2,2,2,-trifluoroethanesulfonates (tresylates), depending on the type of the reactive group on the molecule that will be coupled. A variety of chemical modifications are used to obtain an activated functional PEG derivative.[4]

Most applications of PEG conjugation involve labile molecules. Therefore, the coupling reactions require mild chemical conditions. In the case of polypeptides, the most common reactive groups involved in coupling are nucleophiles, such as thiols, α-and ε-amino groups, carboxylates, or alcoholates. However, the thiol group is rarely present in proteins and is often involved in active sites. On the other hand, carboxylic groups are difficult to activate without intra- or intermolecular cross-linking reactions with the protein amino groups. Therefore, amino groups, namely, the α- or ε-amino groups of lysine residues, are the usual sites of PEG linking.[5] PEG succinimidyl ether or ester and PEG-aldehyde have proven very useful for conjugation to amino groups of lysine residues, while PEG-maleimide reacts with thiols of cysteine residues. Such reactions are also applicable to the conjugation of drug molecules where appropriate reactive functionality is available.

4.27.3.1 Activated PEG Derivatives for Conjugation with Amines

4.27.3.1.1 Alkylating PEGs

In their early work, Davis and co-workers used cyanuric chloride to activate PEG for coupling to proteins.[6,7] 2,4-Dichlorotriazine-activated OH groups of PEG (Figure 2, structure 3) are capable of reacting with various nucleophilic functional groups through displacement of one of the chlorine atoms. Although the reactivity of the remaining chlorine toward the nucleophilic protein residues is lower, it is still sufficient to allow cross-linking reactions. To avoid this problem, Matsushima *et al.*[8] synthesized 2,4-bis(methoxy-PEG)-6-chloro-1,3,5-triazine (Figure 2, structure 4). The lower reactivity of the single chlorine leads to a more selective coupling with lysine and cysteine residues and an absence of side reactions.

Another alkylating reagent for nonspecific modification of multiple amino groups through formation of secondary amine linkages to proteins, viruses, and liposomes is PEG-tresylate (Figure 2, structure 5).[9] Although the PEG-tresylate is more specific toward amino groups than dichlorotriazine-PEG, the conjugation products are not well defined and may contain degradable linkages.[10]

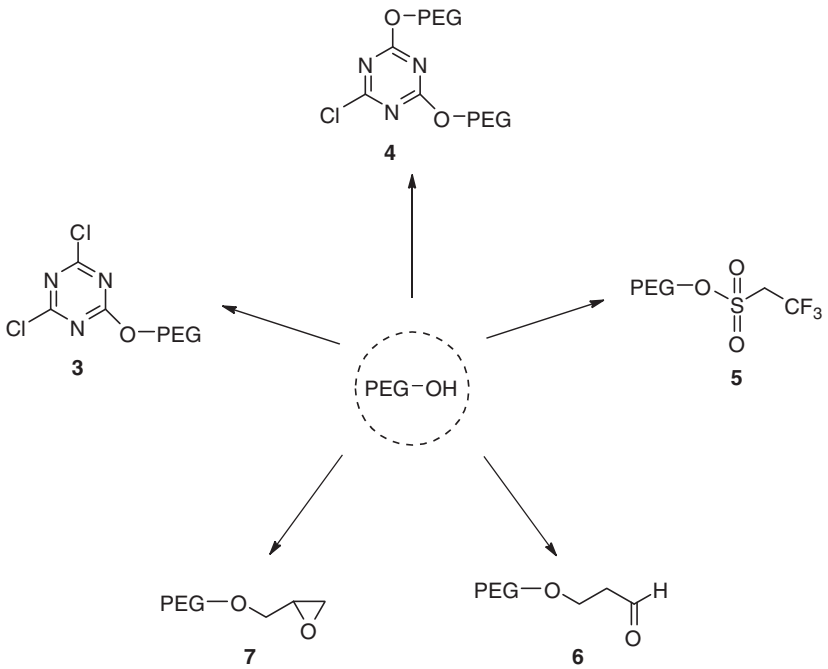

Figure 2 Alkylating PEGs: (**3**) 2,4-dichlorotriazine-PEG; (**4**) 2,4-bis(methoxy-PEG)-6-chloro-1,3,5-triazine; (**5**) trifluoromethanesulfonyl-PEG; (**6**) PEG-aldehyde; and (**7**) PEG-epoxide.

The use of activated PEG-aldehyde (Figure 2, structure 6) is a convenient way for conjugation that gives a permanent linkage after Schiff base formation followed by cyanoborohydride reduction.[11] However, the reaction rate for the Schiff base formation is quite slow with consequent inactivation of labile molecules.

The reaction of the hydroxyl group of PEG and epichlorohydrin allows a terminal epoxy moiety to be introduced, which can be subsequently employed for amine conjugation (Figure 2, structure 7).[12] Similar to PEG-aldehyde, the use of PEG-epoxide for conjugation suffers from low reactivity and lack of specificity since the formed hydroxy groups may also react.

4.27.3.1.2 Acylating PEGs

Most widely used PEG chemistries are those producing conjugates through acylation. Activated esters of PEG carboxylic acids can react with primary amines at nearly physiological conditions to form stable amides. A popular and extensively employed method for the activation of PEG toward amines is based on PEG succinimidyl (NHS) esters. The NHS ester can be introduced into the PEG chain end in two steps. Initially, PEG is acylated with succinic anhydride to yield an ester with a terminal carboxylic group. Important An important advantage of this method is that producing the carboxylic acid intermediate allows purification of the PEG derivative by removing unsubstituted or disubstituted PEG impurities.[13] The second reaction step is coupling of NHS ester to the succinylated PEG.[14] It is important to know that the spacer between the activated ester and the polyether chain may vary by up to three methylene units (Figure 3, structure 8).[15] Changing the distance between the ester group and the PEG backbone has a profound effect in terms of lowering the reactivity toward amines and water. The major drawback of this method is the possible hydrolysis of the ester bond to the succinylated PEG. A way to avoid this problem is coupling of NHS to PEG via carbonate (Figure 3, structure 9).[16,17] The carbamate group formed as a result of amine conjugation is stable to hydrolytic cleavage.

Other activated esters that have been used to couple PEG to proteins via acylation include PEG 4-nitrophenyl carbonate (Figure 3, structure 10), PEG 2,4,5-trichlorophenyl carbonate (Figure 3, structure 11), and PEG imidazol-1-yl carbonate (Figure 3, structure 12).[18,19] They are prepared by reacting chloroformates or carbonylimidazole with the PEG hydroxy end group. All these derivatives are less reactive than the above-mentioned succinimidyl carbonate. Generally speaking, however, the lower activity of the coupling moiety will result in a higher selectivity toward a specific amino acid residue within the protein.

4.27.3.1.3 Carbodiimide method

The PEG conjugation can also be accomplished directly by activating the polymer *in situ* with the use of a carbodiimide.[20] In this manner, the carboxylic group of succinylated PEG[14] is activated and coupled to various peptides.[21] When organic solvents are used, *N,N′*-diisopropylcarbodiimide (DIC) is the coupling agent of choice. The water-soluble 1-(3-dimethylaminopropyl)-3-ethylcarbodiimide hydrochloride (EDC) is suitable for reactions in the aqueous phase (Figure 4).

4.27.3.2 Activated PEG Derivatives for Thiol Conjugation

A few proteins possess thiol groups suitable for PEG binding. Usually, these are free cysteine residues in proteins and their PEGylation is the main approach to site-specific modification. In the absence of a free cysteine in a native protein, they can be introduced through genetic engineering.[22] In this way, it is possible to direct the site-specific PEGylation at protein areas that will minimize a loss in biological activity and, at the same

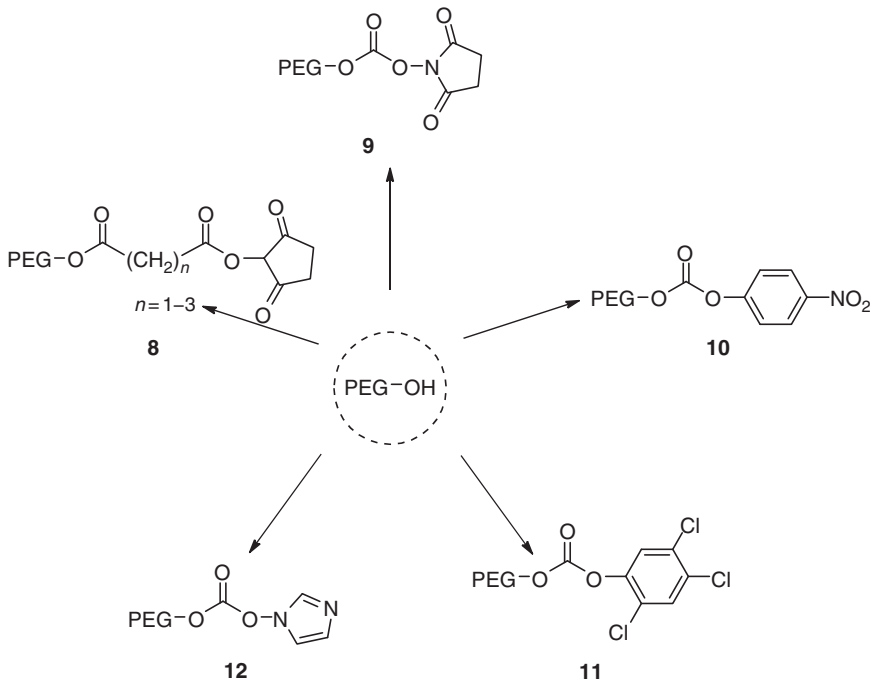

Figure 3 Acylating PEGs: (**8**) PEG 2,5-dioxocyclopentyl succinates; (**9**) PEG succinimidyl carbonate; (**10**) PEG 4-nitrophenyl carbonate; (**11**) PEG 2,4,5-trichlorophenyl carbonate; and (**12**) PEG imidazol-1-yl carbonate.

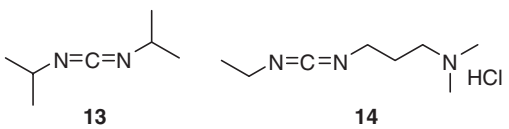

Figure 4 Structures of carbodiimides: (**13**) *N,N*′-diisopropylcarbodiimide (DIC) and (**14**) 1-(3-dimethylaminopropyl)-3-ethylcarbodiimide hydrochloride (EDC).

time, decrease the immunogenicity. On the other hand, the cysteine addition through genetic engineering increases the risk of unwanted disulfide formation and protein dimerization.

The PEG derivatives, such as PEG vinyl sulfone,[23] PEG-maleimide,[24] PEG-iodoacetamide,[25] and PEG 4-pyridyl disulfide,[26] which have been developed for PEGylation of cysteine residues are shown in **Figure 5**.

Each of the above-mentioned derivatives is characterized by its own advantages and disadvantages. PEG vinyl sulfone exhibits low reactivity toward thiols at slightly alkaline conditions (pH 7–8) and forms stable thioether linkage to the protein. The reactivity increases at elevated pH and PEG vinyl sulfone may react with lysine residues. PEG-maleimide, on the other hand, is more reactive to thiols even under slightly acidic conditions (pH 6–7), but is less stable in water. It can undergo ring

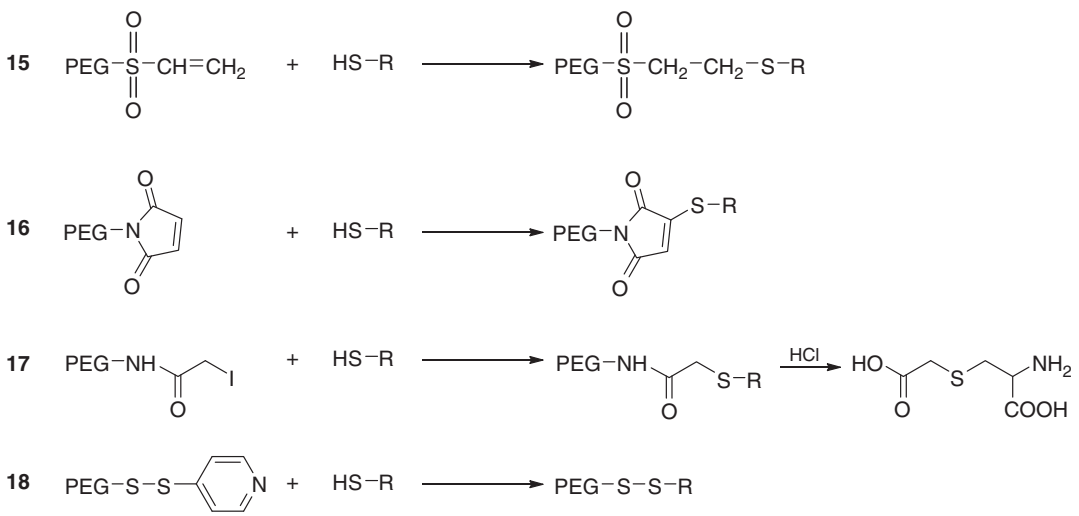

Figure 5 Thiol-reactive PEGs: (**15**) PEG vinyl sulfone; (**16**) PEG-maleimide; (**17**) PEG-iodoacetamide; and (**18**) PEG 4-pyridyl disulfide.

opening or the addition of a water molecule to the double bond. PEG-iodoacetamide reacts slowly with free thiols by nucleophilic substitution forming a stable thioether linkage. It is necessary to perform the reaction in the dark to avoid the release of free iodine, which is capable of reacting with other amino acids. Although the thioether linkage is stable, a slow cleavage of one of the amide bonds can take place through hydrolysis. PEG 4-pyridyl disulfide reacts specifically with thiol groups in wide pH interval (pH 3–10) to form disulfide linkages with the protein molecule. Disulfide bonds are also stable, except under reducing conditions when the linkage is broken to thiols. The advantage of the latter modification procedure is that by strong hydrolysis PEGylated cysteine quantitatively gives rise to carboxymethylcysteine. This stable derivative may be evaluated by standard amino acid analysis, offering a method to assess the cysteine conjugation.[25]

4.27.3.3 Activated PEG Derivatives for 'Click' Conjugation

Recent efforts geared toward expanding the scope of conjugation chemistry for proteins and small molecules include 'click' chemistry.[27] A click reaction is defined as one that has a wide scope of applications, gives high yields, and is chemo- and regiospecific. In addition, click reaction conditions should be mild, and the product should be isolated by facile methods such as recrystallization or distillation. A common example of click chemistry being introduced in bioconjugation is the 1,3-dipolar cycloaddition of alkynes and azides.[28,29] Typical PEG derivatives for click reactions are shown in Figure 6. For example, Deiters *et al.*[30] reported an elegant example of site-specific PEGylation of proteins using click chemistry. The methodology is based on the site-specific incorporation of 4-azidophenylalanine into proteins in yeast. The incorporated azide group was then used in a mild click reaction with an alkyne-derivatized PEG to produce selectively PEGylated protein. This strategy should be useful for the generation of selectively PEGylated proteins for therapeutic applications.

Hiki and Kataoka[31] recently reported the synthesis of heterobifunctional PEG derivatives, having a primary amine or carboxylic acid group at one chain end and an azide group at the other (Figure 6, structures 21 and 22). Such functional PEGs are expected to have significant versatility in click chemistry, due to the mild reaction conditions used (aqueous buffers) and the high degree of chemoselectivity of the reaction.

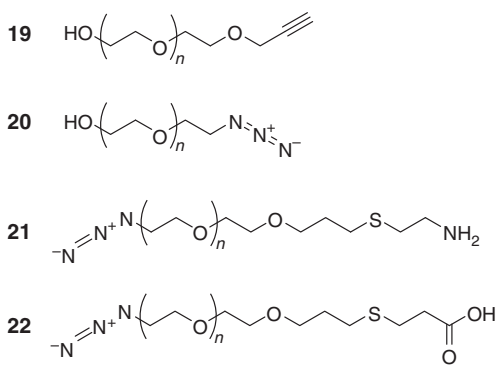

Figure 6 PEG derivatives for 'click' conjugation: (**19**) PEG-alkyne; (**20**) PEG-azide; (**21** and **22**) bifunctional PEG-azides.

Currently, there are a number of commercially available PEG derivatives of high quality.[32–34] Various kinds of activated PEG derivatives having great features such as narrow MW distribution and extremely low impurity profile are supplied. These include monofunctional linear-type, branched-type, multiarm/bifunctional-type, and heterofunctional-type structures that are conjugated with terminal end-groups, such as maleimide, aldehyde, and amine, in wide MW range. The products are suitable for numerous applications of drug delivery techniques, such as PEGylated protein drugs, PEGylated nanoparticles (NPs) like liposomes and polymer micelles, PEG hydrogels, and PEG linker for antibody-conjugated NPs. The most popular PEG oligomer derivatives available on the market are presented in Table 1.

The purity of functionalized PEG derivatives is very important, especially for the synthesis of PEG–biomolecule hybrids. High-purity PEG derivatives are obtained from polydisperse oligomers through fractionation procedures as shown in Figure 7.

4.27.4 PEG Conjugation to Peptides and Proteins

4.27.4.1 Importance of Peptide/Protein–Polymer Conjugation

Naturally produced peptides and proteins can be regarded as highly refined polymers. They are monodisperse and have a precisely defined primary amino acid sequence, which allows them to hierarchically fold and organize into three-dimensional structures. This permits them to exhibit biofunctional features such as catalysis or receptor recognition. As a downside to this delicate folding behavior, proteins are sensitive to temperature and pH changes. Furthermore, they have limited solubility in organic solvents, are susceptible to enzyme degradation, and their use in biomedical applications can be restricted by their possible toxicity and undesired elicited immune response.

The potential value of proteins as therapeutics has been recognized for years. More than 100 pharmaceutical biotech companies are working on the development of bioactive peptides. As a result, more than 70 therapeutic peptides are on the market. Unfortunately, the delivery of human proteins still suffers from a short blood circulation time and low stability, and therefore requires the use of high doses to maintain therapeutic efficacy. As peptide drugs can target metabolic diseases, the delivery requires few side effects to ensure compliance and high safety levels because the drug has to be taken for several years. In addition, peptide drugs are successful against cancer, which requires high selectivity and efficiency of drugs in life-threatening circumstances. The drawbacks in peptide/protein delivery can be overcome by backbone modification.

Peptide/protein–polymer conjugates are hybrid materials, which are designed either to benefit from the synergistic behavior of both components or to overcome shortcomings inherent to the components alone. Creating bioconjugates by combining polymers with peptides or proteins is an emerging multidisciplinary field of research that is enjoying increasing attention. The resulting bioconjugates can synergically combine the properties of the individual components and overcome their separate limitations. The protein or peptide element can impart biofunctional properties to the bioconjugate, whereas the polymer component can improve protein stability, solubility, and biocompatibility. It should be mentioned that in contrast to peptides and proteins,

Table 1 List of most popular commercially available functionalized PEGs

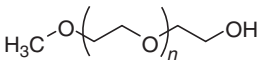	Methoxy-PEG	1 OH group per chain. Protein PEGylation
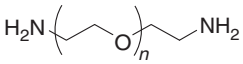	PEG-diamine	Highly appreciated function
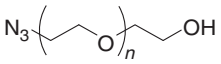	PEG-azide	'Click' chemistry
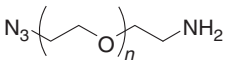	Azido-PEG-amine	
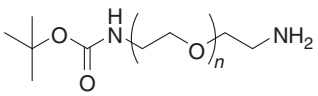	Boc-amino PEG amine	Protected amino group
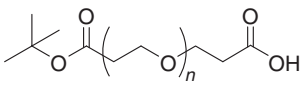	PEG *t*Bu-propionate	Activated ester group
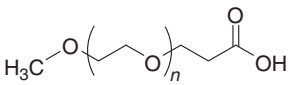	Methoxy-PEG acid	Conjugation reaction
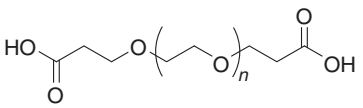	PEG diacid	
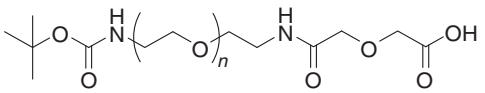	Boc-amino PEG diglycolic acid	Protected amino groups
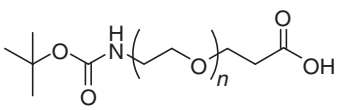	Boc-amino PEG propionic acid	
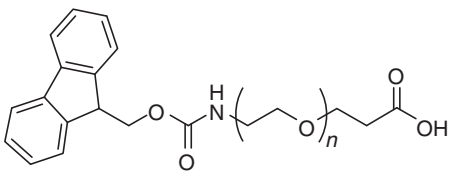	Fmoc-amino PEG propionic acid	
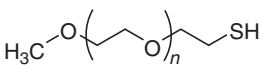	Methoxy-PEG thiol	Thiol group – strong nucleophile conjugation reactions
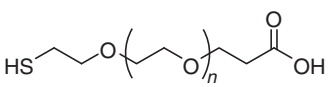	PEG thiol propionic acid	
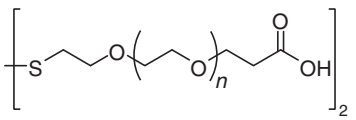	PEG acid disulfide	Reduction-sensitive groups
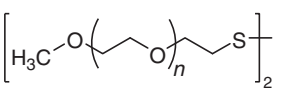	Methoxy-PEG disulfide	

(*Continued*)

Table 1 (*Continued*)

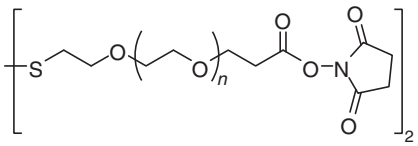	PEG succinimidylpropionate, disulfide	Conjugation chemistry
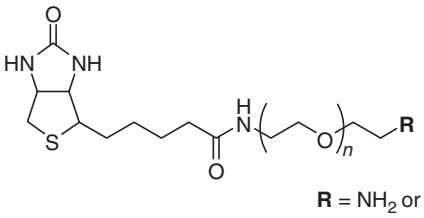 **R** = NH_2 or COOH	Biotin-PEG-amine; biotin-PEG acid	Affinity label toward avidin and streptavidin
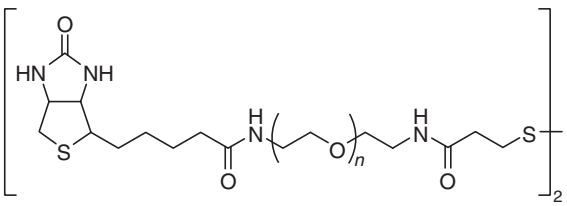	Biotin-PEG disulfide	
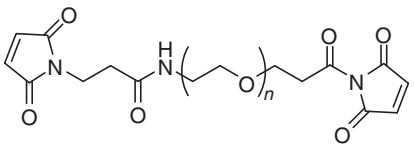	Maleimidopropionamido-propionylmaleimide-PEG	Conjugation chemistry

synthetic polymers are a mixture of many different macromolecules. The incorporation of synthetic polymers may introduce new important properties, such as self-assembly and phase behavior, and even modulate protein activity. Approaches such as PEGylation or lipidization allow increasing the stability (and accordingly require fewer administrations), which results in a more 'natural' level of the compound comparable with the endogenous system. This has opened the door to a wide range of applications, which have already been extensively reviewed in recent literature.[4,35–40] For a suitable conjugation to chemical and biopharmaceutical drugs, many polymers have been proposed as carriers, and among these PEG has gained particular importance.[41–43] In fact, PEGylation was the first major success of polymer–drug conjugates and one of the key technologies and critical elements that stimulated further development of nanocarriers for controlled drug delivery.[44]

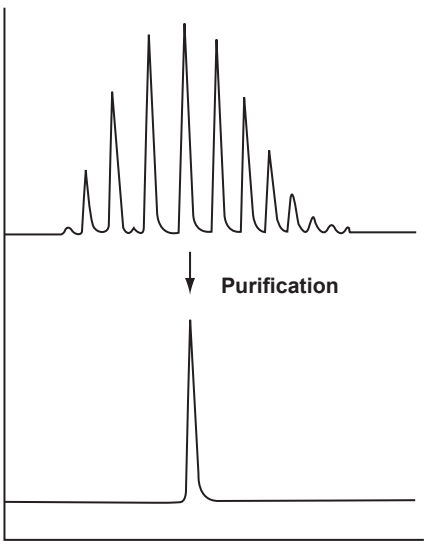

Figure 7 Polydisperse PEG fractionation into a single oligomer. Reprinted from http://www.polypure.com/technology/[32] with permission of Polypure AS, Norway.

4.27.4.2 PEGylated Protein Drugs

Peptide drugs functionalized with linear PEG have been studied extensively *in vitro* and *in vivo*, and the use of PEG for drug conjugation is now well established. The conjugation of monomethoxy poly(ethylene glycol) (mPEG) with the protein is accomplished mainly by reaction with the available amino groups. The primary amino groups are abundantly present on the surface of proteins in lysine residues and the N-terminus. This facilitates easy functionalization with activated PEGs both by alkylation, which maintains the positive charge of the protein at physiological pH, and by acylation, which is accompanied by loss of charge at the conjugation site. Such reactions usually result in formation of conjugates composed of a globular protein at its core to which several polymer chains are covalently linked. The composition of such a graft copolymer system is dependent on the number of available attachment sites (NH_2 and other nucleophilic groups), the reactivity of the mPEG, and reaction conditions. Due to the

polyfunctional nature of proteins and peptides, however, such approaches ultimately lead to a mixture of products.

PEG was initially chosen as the polymer for protein modification as it was already used as 'safe' in body care products and approved for use as excipient in many pharmaceutical formulations. Another advantage is that it could be synthesized by using anionic polymerization to have a MW of narrow polydispersity and also to have one terminal functional group (monosubstituted mPEG), making it ideal for protein modification without risk of cross-linking. Moreover, this highly hydrated PEG chain makes it theoretically ideal to 'mask' sites responsible for the immunogenicity of proteins to which it was bound. As already mentioned, PEG can impart several properties to the linked molecules, namely, increased half-life ($t_{1/2}$) due to reduced kidney clearance; protection against degrading enzymes or reduced uptake by reticuloendothelial system (RES), thanks to the polymer steric hindrance; increase in water solubility, particularly relevant for some anticancer drugs with low solubility; prevention of immunogenicity of proteins; and selective tumor accumulation. The covalently attached PEG chains form a shield against attacking proteases, which is further enlarged by the accumulation of water molecules by the polymer, which furthermore improves the water solubility of the compound.

Although there is evidence of limited *in vivo* chain degradation for very small PEGs by alcohol dehydrogenase,[45] aldehyde dehydrogenase,[46] and cytochrome P-450,[47] PEG is considered a non-biodegradable polymer, and for human use it is commonly used at MWs below its kidney clearance threshold. Therefore, one of the limitations is the accumulation of PEG in the liver, especially if high-MW PEG chains are employed.[48] So far, the highest PEG MW employed for a conjugate approved for human therapy (i.e., PEGASYS®) is 40 kDa. In fact, the threshold for an easy kidney filtration is about 40–60 kDa (a hydrodynamic radius of approximately 4.5 nm[49]) and over this limit the polymer remains in blood circulation for longer periods of time and accumulates in the liver. Of interest is the sigmoidal relationship between PEG MWs and their *in vivo* $t_{1/2}$, which fits the theoretical models of renal excretion of macromolecules based on the pore sizes of the glomerular capillary wall, in this case with a marked increase in circulation times in the range of 20–30 kDa.[50,51] This behavior implies that the influence of PEG on the $t_{1/2}$ of protein conjugates is not easily predictable and several cases in case studies were, therefore, carried out to determine the increases in the $t_{1/2}$.[52]

In terms of PEGylation parameters two different approaches can be identified based on the type of protein studied:

- *Heterologous protein*. Usually, the main limit of these proteins is the immunogenicity rather than a short pharmacokinetics. Therefore, both the PEG MW and coupling chemistry should ensure a wide shielding of the protein surface or, at least, the immunogenic sites. Basically, in these cases low-MW PEGs (5–10 kDa) and random amine coupling are used. Typical examples of this approach are the nonendogenous enzymes. It is important to note that all the enzymes studied react with small substrates; these can cross the PEG layer around the protein and easily reach the active site. Conversely, active site approach of large and hindered substrates would be prevented, thus compromising the enzyme activity. This would suggest that PEGylation may not be a suitable approach for immunogenic enzymes having big substrates.
- *Endogenous protein*. For these biopharmaceutical drugs, the prolongation of body circulation $t_{1/2}$ is the driving force in seeking a polymer conjugate. Most of the endogenous proteins act through a receptor-mediated activity. This dictates the strategy for an optimum PEGylation approach, namely, a site-specific conjugation to generate mono-PEGylated isomers. In particular, the site of polymer attachment must be far from the receptor recognition area. In this case, it is mandatory to use high-MW polymer.

The idea of protein PEGylation was first developed by F. Davis to enhance both the blood circulation time and the stability (against enzyme attack or immunogenic recognition) of the recombinant protein drugs.[53] In 1977, Abuchowski *et al.*[6] demonstrated that, as therapeutic agents, PEG-conjugated proteins are more effective than their corresponding unmodified parent molecules. Since then, several pharmaceutical proteins have been PEGylated and have been shown to have properties of use in clinical applications.

Davis and co-workers demonstrated that covalent attachment of PEG to serum albumin and catalase leads to the reduction of immunoreactivity toward respective antibodies.[6,7] Since then, many articles concerning the chemical modification of proteins by conjugation with PEG derivatives have been published. Inada *et al.*[54,55] performed protein modifications in order to reduce immunogenicity and suppression of immunoglobulin E (IgE) production in medical processes. Lee and Sehon[56] reported that the formation of IgE-class antibodies caused by ragweed pollen allergen *in vivo* is suppressed by the administration of PEG-allergen. PEGylated derivatives also exhibit passive tumor targeting by the enhanced permeability and retention (EPR) effect. This is a consequence of the highly active angiogenesis in many solid tumors, resulting in an increased tumor vascularization and blood flow.[57]

The most important classes of protein-based pharmaceuticals are shown in **Table 2**.

The utility of PEGylation has been translated into drug delivery of nonhuman proteins. Thus, PEGylated bovine adenosine deaminase (ADAGEN®) has been successfully commercialized by Enzon Inc. in replacement therapy to treat severe combined immunodeficiency disease.[59] The PEG-modified enzyme contains multiple chains of PEG5000 per molecule of enzyme, and has a $t_{1/2}$ about 6.4 times that of unmodified enzyme in rats.[60] Enzon Inc. has also utilized PEGylation for effective drug delivery of L-asparaginase. This PEGylated construct (ONCASPAR®) was shown to be as effective as the native drug in treating patients with acute lymphoblastic leukemia, but with much lower degree of immunogenicity than the native one.[61]

PEGylation has gained significant attention during the past years, with PEGASYS®[62] and PEG-INTRON®,[63] two α-interferon (α-IFN) derivatives used to treat chronic infection by hepatitis C in adults. The plasma circulation $t_{1/2}$ of PEG-INTRON® is about 8 times that of native IFN α-2b, allowing a weekly subcutaneous dosing of the conjugated protein. Another example is NEULASTA®, which is a PEGylated form of granulocyte colony-stimulating factor (G-CSF) and serves to treat neutropenia.[64] If the PEG chain is long enough

Table 2 Classes of protein-based medicines that can be improved by PEGylation. Reprinted from Choi *et al.*[58] with permission of Springer Science + Business Media, Germany

Protein type	*PEGylation need*	*Comment*
Replacement proteins	Half-life extension required for proteins that need frequent administration	Site-specific PEGylation would improve product homogeneity. There is a need for improved efficiency in production. Proteins include cytokines, growth factors, and blood factors
Peptides	Half-life extension required. Mask immunogenicity for nonendogenous proteins	Many peptides are in development. Site-specific PEGylation is required since the relative steric-shielding effects of PEG will be much greater than with larger MW polypeptides
Full antibodies	Half-life extension is not generally required. PEGylation could mask effector function	Full antibodies are expensive to produce at the doses required for clinical efficacy. Effector function is not required for many applications
Enzymes	Half-life extension may be required	Multisite, hyper-PEGylation of nonhuman proteins is preferred to avoid immunogenicity

(MW = 20 000 Da), renal clearance will be diminished, all of which leads to a much longer $t_{1/2}$ and, therefore, increased bioavailability of the peptide. Furthermore, allergic reactions are diminished because the immune system cannot attack PEG. Clinical results have been also reported for several other PEG-conjugated proteins, including IL-2.[65]

The peptide PEGylation has also generated interest in the drug delivery studies. Modification of recombinant (r)-hirudin (naturally occurring anticoagulant polypeptide) with two PEG chains through urethane bonds affords PEG-hirudin that exhibits a significantly prolonged $t_{1/2}$ resulting in enhanced antithrombotic activity and no observable immunogenicity.[66] Mono- and di-PEGylated species of salmon calcitonin (therapeutic polypeptide hormone) showed slightly enhanced pharmacokinetics and lower renal excretion compared to the unmodified polypeptide.[67]

The vast majority of PEGylated products are mixtures with PEG conjugated at different sites on the protein, leading to positional isomerism. In recent years, site-specific PEGylation has become a key goal because the issue of positional isomers has caused some questions to be asked about the nature of heterogeneous product mixtures. In particular, such mixed products can have a variety of biological activities and the physical and pharmacological properties of proteins are changed depending on the site and the number of PEG molecules conjugated to the protein. The search for more specific modification methods has been the topic of significant academic research during the past decade.[67,68] Well-defined peptide/protein–polymer conjugates are defined as hybrid constructs that combine (1) a defined number of peptide/protein segments with uniform chain lengths and defined monomer sequences (primary structure) with (2) a defined number of synthetic polymer chains. The constructs are obtained by coupling specific amino acid residues on the peptide/protein with specific functional groups located at defined positions on the synthetic polymers. Site-specific modifications would first of all help with the purification and characterization of the obtained products, because mixtures are avoided. Furthermore, if the modification is directed to a specific location, the protein activity might be better preserved. For instance, the site for polymer conjugation can be located far away from the active site to avoid interference with the biological functioning of the protein. Alternatively, it can also be located nearby, or even within the active site, in order to control the biological activity of the protein. Terminal amine conjugation is typically conducted by reductive amination and is considered to be a substantially site-specific PEGylation strategy.[69] The second successful approach is insertion of an unpaired cysteine as a PEGylation site.[58]

Block polymers of PEG-polycation (A–B) or PEG-polycation-PEG (A–B–A) have been used to condense a nucleic acid drug, to form PEGylated micelles, with the water-insoluble nucleic acid–polycation electrostatic complexes (polyplexes) forming the core of the PEGylated polymeric micelle.[70] In the 2000s, a number of companies (e.g., Alnylam, Roche, Merck, and Calando) have been involved in clinical trials for delivery of siRNA from similar lipoplexes and polyplexes.[71,72]

4.27.4.3 PEGylated Enzymes

A new approach in biotechnological processes is to prepare enzymes modified with PEG that has both hydrophilic and hydrophobic properties.[73] Generally, enzymes are used as suspended powders in organic solvents, and the dispersion degree may be a critical factor in the expression of catalytic activity. The activity of one enzyme depends on the number of productive encounters that occur between the enzyme and a substrate. As expected, due to diffusion limitations, dispersed enzymes in organic solvents were found to exhibit 10- to 1000-fold reduced catalytic activities in comparison with enzymes dissolved in aqueous solution.[74] Consequently, every method that may increase dispersion in organic solvents may improve the catalytic performance and those methods that will allow complete dissolution will be highly desirable. Among the proposed methods to solubilize enzymes, PEGylation is preferred because the amphiphilic polymer conveys its dissolution properties to the proteins. It was found that the solvent might influence enzyme stability, rate of reaction, and selectivity. Among the several enzymes that were PEGylated and studied in organic solvents so far, we will mention only a couple of examples that may illustrate the potentials and limitations of this procedure. *Candida rugosa* lipase treated with PEG 4-nitrophenyl chlroformate[75] and PEG-cyanuric chloride[76] were found to exhibit enhanced stability in isooctane, where the first conjugate was found to be more active than the second one. In both cases, however, they exhibited decreased lipase and esterase activities, compared to activity in aqueous systems although transesterification activity was improved.[77]

4.27.5 PEG Conjugation with Small Drugs

In contrast to the successful PEG modification of proteins for drug delivery, only a few examples of small organic drug conjugates with PEG have been prepared through permanent bond formation and they did not result in clinically improved compounds.[78] For example, PEG amide derivatives of doxorubicin (Dox) and amphetamine were prepared and tested only *in vitro*.[79] PEGylation of paclitaxel through carbamate derivative formation was also reported aiming at solubilization and delivery of this anticancer drug (**Figure 8**).[80] The water-soluble PEG-paclitaxel derivatives are nontoxic but as prodrugs 10^3 times less active *in vitro* than the native drug. Most likely this is due to the shielding effect of the PEG chain, which blocks the activity at the target cells or the insufficient PEG-paclitaxel concentration in the cells.

The prodrug design represents an optimization of drug delivery. As already mentioned, the prodrug is a biologically inactive drug derivative that releases the active substance usually as a result of enzymatic transformation within the body.[81–83] It has also improved delivery properties over the parent molecule. The stability of the drug conjugate linkage and its potential for controlled degradation determine the prodrug effectiveness. The most often employed prodrugs are usually based on hydrolyzable or enzymatically cleavable bonds such as esters, carbonates, carbamates, and hydrazones. In special cases, certain amides can be broken down by peptidases or cathepsins.

Several highly water-soluble PEG esters of paclitaxel were prepared and studied by Enzon Inc. researchers. They proved to function as prodrugs, that is, their breakdown occurred in a predictable manner.[84,85] Although a PEG-paclitaxel derivative entered phase I clinical trials, the company discontinued the development of this product.

Camptothecin is another active drug against many types of cancer. However, the poor water solubility and physiological instability hamper its clinical implementation. A PEGylated camptothecin was developed to improve both water solubility and blood circulation time *in vivo*. The PEGylated derivative consists of 40 000 Da PEG chain, with the drug attached at both chain ends through ester linkages (**Figure 9**).[85]

Functionalization of drugs with linear PEG suffers from the following drawbacks:

- The loading capacity of linear PEG is limited to the polymer chain ends, giving a maximum of two biologically active agents per polymer molecule.
- Drug release from linear polymer conjugates relies on degradation of the linker in a continuous process, rather than a precisely triggered event.
- Simple PEGylated drugs also lack targeting functionality that would enable specific interactions with diseased tissue.

The research efforts trying to overcome the above-mentioned limitations include drug linking to branched polymer architectures, including PEG-dendrimers, and hyperbranched and graft copolymers. For example, a few studies have been performed to overcome the low PEG loading through branching the chain end groups or coupling them with small dendron structures.[86–89] It seems that the use of multiarm PEGs is a promising approach to solve the problem with low PEG loading. Another advantage of this approach is that the linked drug molecules are quite distant from each other, thus overcoming the steric hindrance occurring with PEG dendrons.

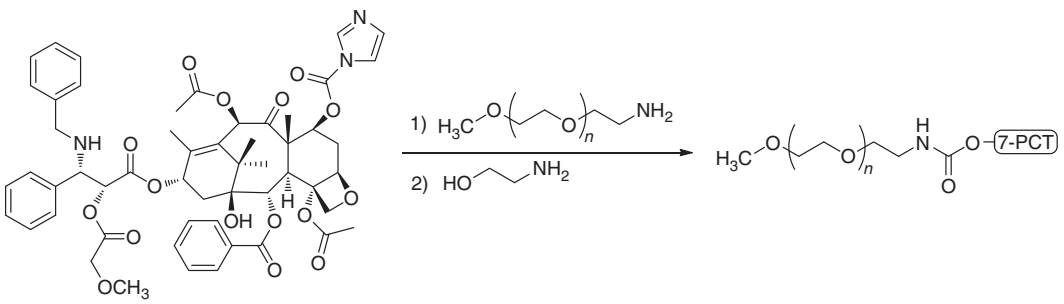

7-(Imidazole-1-carbonyl)-2′-(methoxyacetyl)taxol

Figure 8 Synthesis of PEG-carbamate-paclitaxel.

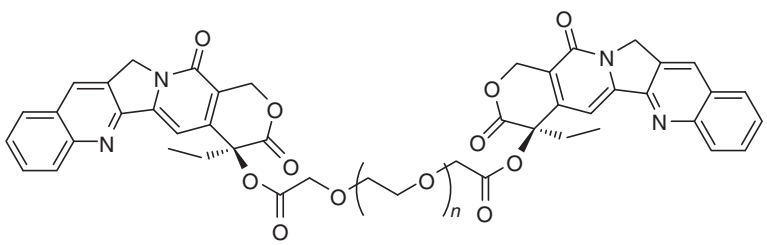

Figure 9 PEGylated camptothecin.

4.27.6 PEGylated Dendrimers as Drug Delivery Systems

Dendrimers possess important distinctions from linear polymers, namely, their MW and size are well defined. Indeed, many dendrimers have been prepared and purified as single 'monodisperse' macromolecules. This exquisite level of structure control is a function of the stepwise dendrimer synthesis that differs from the statistically dictated step- and chain-growth polymerization methods used to prepare more conventional linear and branched polymer architectures. Taken together, the monodispersity, degree of branching, and size control of dendrimers provide access to precise polymer materials that are expected to limit or eliminate undesirable effects of size variation in polymer drug delivery systems. Moreover, dendrimers as nanomaterials with multiple chain ends are also tunable in terms of functional group type and density. This multifunctional design provides an advantage over linear polymers for covalent attachment of drugs, imaging agents, targeting ligands, and other biologically relevant moieties.

Among the many types synthesized to date, poly(amidoamine) (PAMAM) dendrimers are used extensively in therapeutic research, benefiting from the convenience of commercial availability of a range of dendrimer sizes and chain-end functionality. PAMAM-based dendrimers have progressed considerably in drug and gene delivery, for example, as anti-HIV (VivaGel®) and diagnostic (Stratus®) agents, and as the gene delivery reagent SuperFect®.[90] The core-shell architecture of PEGylated PAMAM dendrimers is useful for encapsulation of hydrophobic small-molecule drugs, and the *in vivo* behavior of these systems as drug delivery agents has been evaluated.[91] Studies were performed on the PEGylated versus non-PEGylated PAMAM delivery carriers of the anticancer drug fluorouracil. The drugs were sequestered noncovalently into the dendritic core, and held there by hydrogen bonding. PEGylated PAMAM was seen to sequester an order of magnitude more fluorouracil than PAMAM itself, attributed in part to steric effects of the PEG corona that hinder drug release. The presence of the PEG coating led to a sixfold decrease in drug release rate and lower hemolytic toxicity, for a better overall performance relative to non-PEGylated PAMAM.

Bow-tie dendrimers functionalized with both PEG and Dox were prepared as drug delivery carriers to combine pH-dependent drug release with passive tumor targeting.[92] This sophisticated synthetic strategy, combining different polymer architectures and compositions in one structure, also provides a pH-triggered delivery of the drug. Each component of this polymer therapeutic plays a role in the delivery design that seeks to minimize side effects associated with Dox treatment. The dendritic polyester scaffold forms not only the delivery carrier, but is also biodegradable, such that following delivery of the therapeutic drug, the degraded dendrimer can clear from the bloodstream without accumulating in the liver or kidneys.

Recently, an amino acid-based dendrimer was PEGylated and conjugated to camptothecin in an effort to provide a new drug delivery platform. Fox *et al.*[93] synthesized a second-generation lysine dendron, which was subsequently functionalized with aspartic acid, providing two different functionalities at the periphery: an amine and a carboxylic acid. The amine was PEGylated, while the acid was coupled with a camptothecin derivative, yielding a 40 kDa PEGylated poly(L-lysine) (PLL) dendrimer–camptothecin conjugate, typically loaded with 4–6 wt.% camptothecin. The drug conjugate showed improved blood circulation time over the drug alone, as well as increased uptake in tumor tissue, and was shown to increase the survival rate of tumor-bearing mice.

PEGylation of the PLL dendrimers results in enhanced control over the pharmacokinetics and degradability of these materials, as well as the biodistribution, and rate of renal clearance.[94] The blood circulation $t_{1/2}$ of the dendrimer could be manipulated based on the MW of the peripheral PEG chains that are conjugated to the PLL core.

Xu *et al.*[95] reported the synthesis, uptake, and release profile of dendrimer–drug conjugates composed of a polyethyleneimine (PEI) core and PEG corona. Covalent PEGylation in this system was accomplished through imino groups. Imine lability at pH < 6 is thus expected to give polymer fragmentation within the acid regions associated with tumor vasculature and lysosomal compartments. The PEGylated dendrimers gave markedly enhanced drug loading, from 54 mmol per mole carrier for the PEI dendrimer to 440 mmol per mole carrier for the fully PEGylated PEI dendrimer.

4.27.7 PEGylated Inorganic–Organic Core-Shell Nanoparticles

Inorganic nanoparticles (INPs) are important in our lives because of their use as drugs, imaging agents, and antiseptics. Among the most promising INPs being developed are metal, silica, inorganic dendrimers, organic–inorganic hybrids, and bioinorganic hybrids. In this chapter, we focus on the most widely studied gold and silica NPs. Gold NPs are very important and promising in imaging, as drug carriers, and for thermotherapy of biological targets and useful in the fight against cancer. Metal NP contrast agents enhance magnetic resonance imaging and ultrasound results in biomedical applications of *in vivo* imaging. Silica NPs have been used in drug delivery and gene therapy. Nanometer-sized silica particles find outstanding applications in various industrial fields, such as electronic substrates, electrical and thermal insulators, and humidity sensors. Spherical mesoporous silica with high colloidal stability and a biocompatible external surface is especially desirable for biological applications such as drug delivery or diagnostics.

The functionalization of the external surface plays an important role in the colloidal stability of the INPs and their interactions with the environment, that is, with living cells and other biological substrates.[96,97] In particular, the functionalization of the outer NP surface with PEG was well developed[98–100] due to the remarkable ability of PEG to resist protein adsorption.[101,102] All these features increase the NP blood circulation time for *in vivo* applications.[103,104] PEGylated silica NPs produced through the sol–gel method have received great attention in recent years, as nanocarriers for biomedical applications.[105] The synthesis of the PEGylated NPs was carried out in two steps (**Figure 10(a)**).

In the first one, the PEG precursor was obtained by preparing an intermediate leaving group, poly(ethylene glycol) tosylate and then combining it with (3-aminopropyl)

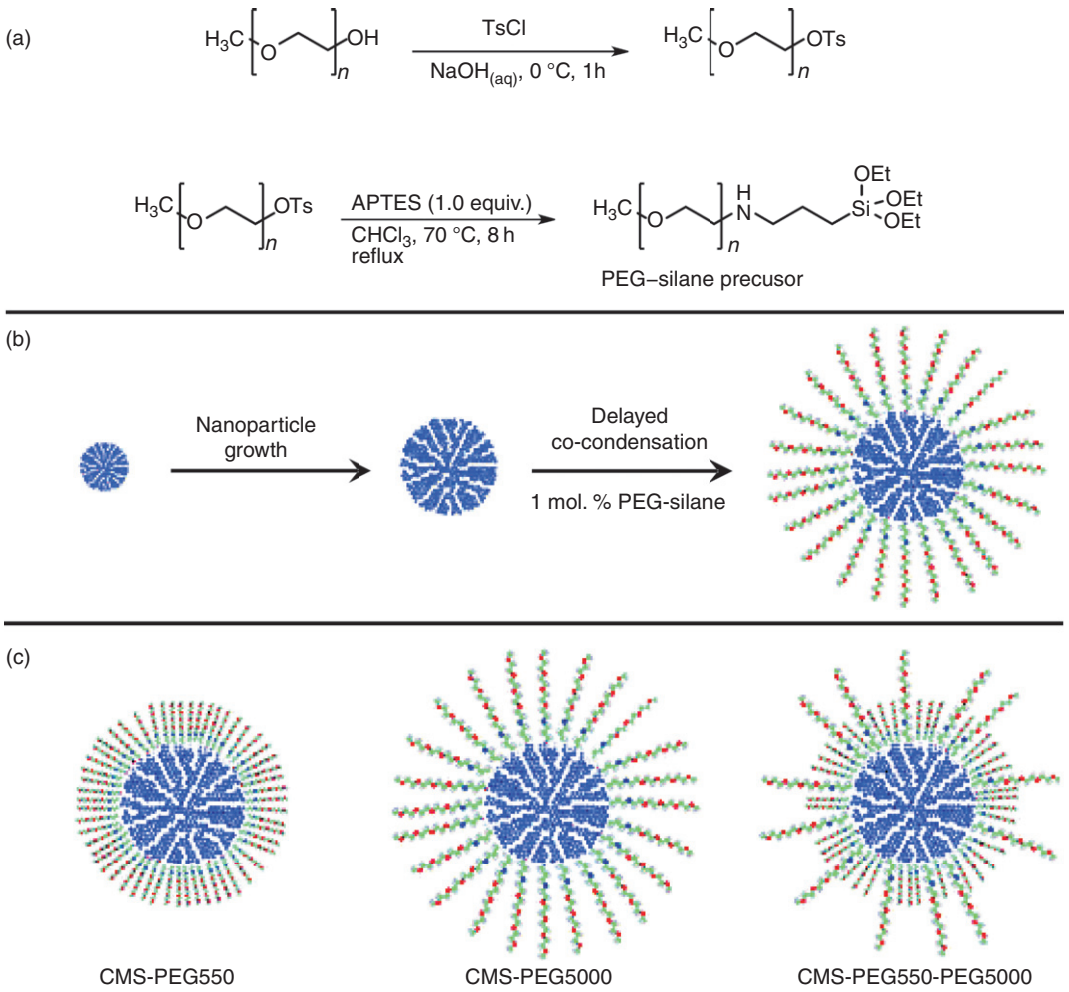

Figure 10 PEGylated colloidal stable mesoporous silica NPs (CMS NPs): (a) Synthesis of PEG-silane precursor; (b) scheme of PEGylated CMS NPs through the delayed co-condensation approach; and (c) scheme of different PEGylated NPs. Reprinted from Cauda, V.; Argyo, C.; Bein, T. *J. Mater. Chem.* **2010**, 20, 8693.[106] with permission of the Royal Society of Chemistry, UK.

triethoxysilane (APTES) to create the linear PEG-silane precursor. The tosylate-leaving group facilitates the modification of the long PEG chain (MW = 5000 Da). In the second step, the PEG-silane moiety was co-condensed with a small amount of silica precursor, tetraethyl orthosilicate (TEOS), at the outer surface of the growing colloidal mesoporous silica NPs in the colloidal mesoporous silica (CMS) synthesis batch[107] (Figure 10(**b**)). Specifically, three different PEGylated colloidal mesoporous silica CMS NPs were prepared (Figure 10(**c**)), thus co-condensing the mesoporous particles with short (MW = 550 Da) and long (MW = 5000 Da) PEG chains and also with a mixture of the two chains with 75 mol.% PEG550/25 mol.% PEG5000 (Figure 10).

The PEGylated mesoporous NPs are stable in simulated body fluid at 37 °C for 1 month. Longer and denser polymer shells are most efficient in slowing down the biodegradation kinetics in comparison with the unfunctionalized mesoporous NPs.

The stability of the PEGylated silica NPs as water colloidal suspensions depends on the PEG/silica mass ratio (Figure 11).[108] By properly selecting the PEG concentration, NPs smaller than 150 nm were obtained, stable to aggregation in water media up to 6 months. The stabilization is due

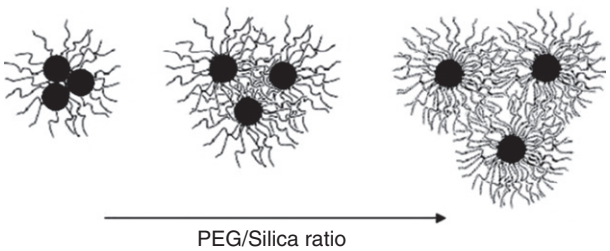

Figure 11 PEGylated silica cluster structure change with increasing the PEG/silica ratio.[108] Reprinted from Branda, F.; Silvestri, B.; Luciani, G.; *et al. Colloid Surf., A* **2010**, 367, 12.[108] with permission of Elsevier Ltd., UK.

to both steric and electrostatic effects. In this view, PEG is expected to play key role both in clusters formation and in their aggregation. As traditional micelles, derived from amphiphilic block copolymers, silica/PEG clusters can be regarded as nanosized molecular containers able to capture and concentrate in their small volume other species. The presence of functionalized silica NPs, of very high specific surface, promises to have new functionalities and open the

perspective to innovative applications, particularly in the biomedical field.

The use of gold nanoshells as imaging and therapeutic agents for cancer has been well documented in recent years. The main reason for their popularity lies in their unique core-shell nanostructure made up of a spherical dielectric core material such as silica or polystyrene that is surrounded by a gold layer.[109] The optical scattering properties of such structures coupled with their optical tunability have spurred the use of gold nanoshells as promising optical contrast agents, where their optical response can be adjusted to match the light source of different wavelengths used in different imaging modalities. Several *in vitro* studies[110,111] using gold nanoshells targeted on cancer cells have demonstrated effective destruction of the cancer cells upon exposure to near-infrared (NIR) radiation, with cell damage limited to the laser treatment spot.

PEGylation of gold nanoshells provides an effective means to reduce their RES clearance in body. Connor *et al.*[112] succeeded in preparing gold NPs circulating in the bloodstream for long periods using PEG modification. The PEGylation of gold nanoshells has been reported in several *in vivo* application studies.[113–117] PEGylated gold nanoshells were synthesized in a four-step process as shown in Figure 12.

The three factors that can affect the ability of macrophage to ingest gold nanoshells include the PEG surface density, PEG MW, and size of the gold nanoshells. It is also important to note that even though the effective PEGylation of gold nanoshells can minimize their RES uptake, the nonbiodegradability of gold nanoshells presents other issues regarding their clearance and toxicity of long-term accumulation.

Lipka *et al.*[119] studied 5 nm Au NPs, either stabilized with a ligand of phenylbis(4-sulfonatophenyl)phosphine (Phos) or surface-modified with PEG of different chain lengths of either 750 Da (PEG750) or 10 kDa (PEG10k) on top of a polymer shell (Figure 13).

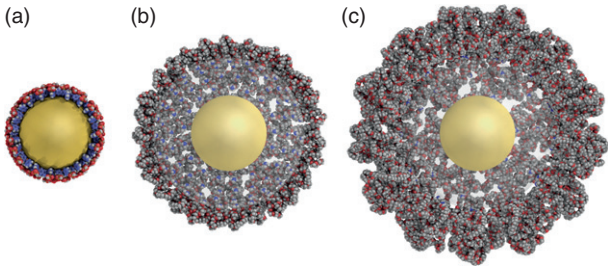

Figure 13 Symbolic illustration of (a) 5 nm Au-Phos nanoparticles; (b) 5 nm Au-PEG750 nanoparticles; and (c) 5 nm Au-PEG10k nanoparticles. NPs in b and c are coated with dodecane-1-thiol and amphiphilic polymer (light gray shell), to which PEG of different molecular weights is covalently bound. Reprinted from Lipka, J.; Semmler-Behnke, M.; Sperling, R.; *et al. Biomaterials* **2010**, 31, 6574.[119] with permission of Elsevier Ltd., UK.

Almost 40 years after the initial studies, PEGylation is now a well-established tool able to address the limitations of proteins, peptides, and oligonucleotides and, in addition, a number of PEG-drug conjugates have been tested clinically for both parenteral and oral administration. PEGylation is a mature and tested technology, which has already resulted in nine FDA-approved therapeutics, testifying to the safety and applicability of the methodology. Since its introduction, PEGylation has been focused mostly on existing therapeutic proteins and their life-cycle management. However, with the development of protein nanobodies and scaffolds, which are believed to represent the next-generation therapeutics but require $t_{1/2}$ extension to exert a clinically meaningful effect, even wider medical use can be expected.

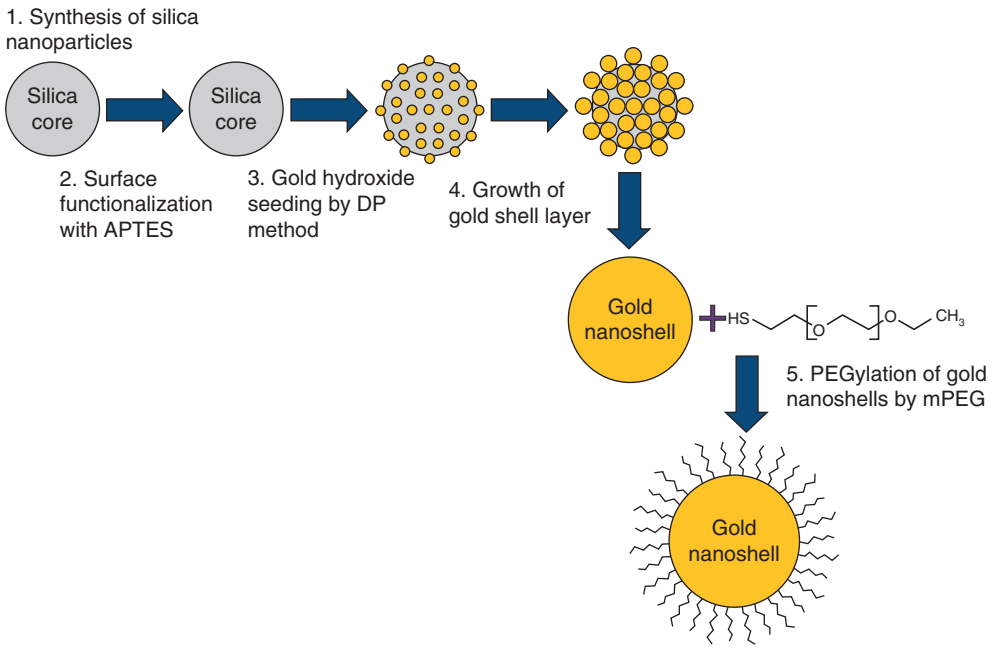

Figure 12 Synthesis and PEGylation of gold nanoshells. Reprinted from Kah, J.; Wong, k.; Neoh, k.; *et al. J. Drug Target.* **2009**, *17*, 181.[118] with permission of Taylor & Francis Ltd., UK.

References

1. Rabolt, J.; Johnson, K.; Zitter, R. *J. Chem. Phys.* **1974**, *61*, 504.
2. Matsura, H.; Fukuhara, K. *J. Mol. Struct.* **1985**, *126*, 251.
3. Harris, J., Ed. *Poly(Ethylene Glycol) Chemistry: Biotechnical and Biomedical Applications*; Plenum Press: New York, 1992.
4. Harris, M.; Chess, R. *Nat. Rev. Drug Discovery* **2003**, *2*, 214.
5. Zalipsky, S.; Lee, C. In *Poly(Ethylene Glycol) Chemistry: Biotechnical and Biomedical Applications*; Harris, J., Ed.; Plenum Press: New York, 1992; p 347.
6. Abuchowski, A.; van Es, T.; Palczuk, N.; Davis, F. *J. Biol. Chem.* **1977**, *252*, 3578.
7. Abuchowski, A.; McCoy, J.; Palczuk, N.; *et al. J. Biol. Chem.* **1977**, *252*, 3582.
8. Matsushima, A.; Nishimura, H.; Ashihara, Y.; *et al. Chem. Lett.* **1980**, *9*, 773.
9. Francis, G.; Fisher, D.; Delgado, C.; *et al. Int. J. Hematol.* **1998**, *68*, 1.
10. Gais, H.; Ruppert, S. *Tetrahedron Lett.* **1995**, *36*, 3837.
11. Harris, J.; Herati, R. U.S. Patent 5,252,714, Oct 12, 1993.
12. Bergström, K.; Holmberg, K.; Safranj, A.; *et al. J. Biomed. Mater. Res.* **1992**, *26*, 779.
13. Zalipsky, S.; Barany, G. *Polym. Prep.* **1986**, *27*, 1.
14. Abuchowski, A.; Kazo, G.; Verhoest, C.; *et al. Cancer Biochem. Biophys.* **1984**, *7*, 175.
15. Harris, J.; Kozlowski, A. U.S. Patent 5,672,662, Sept 30, 1997.
16. Zalipsky, S.; Seltzer, R.; Menonrudolph, S. *Biotechnol. Appl. Biochem.* **1992**, *15*, 100.
17. Miron, T.; Wilchek, M. *Bioconjugate Chem.* **1993**, *4*, 568.
18. Veronese, F.; Largajolli, R.; Boccu, E.; *et al. Appl. Biochem. Biotechnol.* **1985**, *11*, 141.
19. Beauchamp, C.; Gonias, S.; Menapace, D.; Pizzo, S. *Anal. Biochem.* **1983**, *131*, 25.
20. Valeur, E.; Bradley, M. *Chem. Soc. Rev.* **2009**, *38*, 606.
21. Atassi, M.; Manshouri, T. *J. Protein Chem.* **1991**, *10*, 623.
22. Goodson, R.; Katre, N. *Biotechnology* **1990**, *8*, 343.
23. Morpurgo, M.; Veronese, F.; Kachensky, D.; Harris, J. *Bioconjugate Chem.* **1996**, *7*, 363.
24. Ishii, Y.; Lehrer, S. *Biophys. J.* **1986**, *50*, 75.
25. Gard, F. *Methods Enzymol.* **1972**, *B25*, 424.
26. Woghiren, C.; Sharma, B.; Stein, S. *Bioconjugate Chem.* **1993**, *4*, 314.
27. Joralemon, M.; McRae, S.; Emrick, T. *Chem. Commun.* **2010**, *46*, 1377.
28. Rostovtsev, V.; Green, L.; Fokin, V.; Sharpless, K. *Angew. Chem., Int. Ed.* **2002**, *41*, 2596.
29. Tornøe, C.; Christensen, C.; Meldal, M. *J. Org. Chem.* **2002**, *67*, 3057.
30. Deiters, A.; Cropp, T.; Summerer, D.; *et al. Bioorg. Med. Chem. Lett.* **2004**, *14*, 5743.
31. Hiki, S.; Kataoka, K. *Bioconjugate Chem.* **2007**, *18*, 2191.
32. Polypure. http://www.polypure.com/ (accessed 10th December 2010).
33. NANOCS. http://www.nanocs.com/PEG.htm.
34. NOF Corporation. http://www.peg-drug.com/ (accessed 10th December 2010).
35. Opsteen, J.; van Hest, J. In *Macromolecular Engineering. Precise Synthesis, Materials Properties, Application*; Matyjaszewski, K., Gnanou, Y., Leibler, L., Eds.; Wiley: Weinheim, 2007; Vol. 4, p 2645.
36. Klok, H.-A. *J. Polym. Sci., Part A: Polym. Chem.* **2005**, *43*, 1.
37. Veronese, F.; Pasut, G. *Drug Discovery Today* **2005**, *10*, 1451.
38. Roberts, M.; Bentley, M.; Harris, J. *Adv. Drug Delivery Rev.* **2002**, *54*, 459.
39. Duncan, R. *Nat. Rev. Cancer* **2006**, *6*, 688.
40. Hoffman, A.; Stayton, P. *Macromol. Symp.* **2004**, *207*, 139.
41. Vellard, M. *Curr. Opin. Biotechnol.* **2003**, *14*, 444.
42. Pasut, G.; Veronese, F. *Prog. Polym. Sci.* **2007**, *32*, 933.
43. Veronese, F.; Harris, J. *Adv. Drug Delivery Rev.* **2002**, *54*, 453.
44. Hoffman, A. *J. Controlled Release* **2008**, *132*, 133.
45. Kawai, F. *Appl. Microbiol. Biotechnol.* **2002**, *58*, 30.
46. Friman, S.; Egestad, B.; Sjovall, J.; Svanvik, J. *J. Hepatol.* **1993**, *17*, 48.
47. Beranova, M.; Wasserbauer, R.; Vancurova, D.; *et al. Biomaterials* **1990**, *11*, 521.
48. Caliceti, P.; Veronese, F. *Adv. Drug Delivery Rev.* **2003**, *55*, 1261.
49. Petrak, K.; Goddard, P. *Adv. Drug Delivery Rev.* **1989**, *3*, 191.
50. Yamaoka, T.; Tabata, Y.; Ikada, Y. *J. Pharm. Sci.* **1994**, *83*, 601.
51. Yamaoka, T.; Tabata, Y.; Ikada, Y. *J. Pharm. Sci.* **1995**, *84*, 349.
52. Hamidi, M.; Azadi, A.; Rafiei, P. *Drug Delivery* **2006**, *13*, 399.
53. Davis, F. *Adv. Drug Delivery Rev.* **2002**, *54*, 457.
54. Inada, Y.; Yoshimoto, T.; Matsushima, A.; Saito, Y. *Trends Biotechnol.* **1986**, *4*, 68.
55. Inada, Y.; Furukawa, M.; Sasaki, H.; *et al. Trends Biotechnol.* **1995**, *13*, 86.
56. Lee, W.; Sehon, A. *Nature* **1977**, *267*, 618.
57. Goh, P.; Sze, D.; Roufogalis, B. *Curr. Cancer Drug Targets* **2007**, *7*, 743.
58. Choi, J.-W.; Godwin, A.; Balan, S.; *et al.* In *PEGylated Protein Drugs: Basic Science and Clinical Applications*; Veronese, F., Ed.; Birkhäuser Verlag: Basel, 2009; p 47.
59. Hershfield, M. *Semin. Hematol.* **1998**, *35*, 291.
60. Nucci, M.; Short, R.; Abuchowski, A. *Adv. Drug Delivery Rev.* **1991**, *6*, 133.
61. Kurtzberg, J. In *Cancer Medicine 4th Edition*; Holland, J., Bast, R., Jr., Morton, D., *et al.*, Eds.; Williams and Wilkins: Baltimore, 1997; p 1027.
62. Fried, M.; Shiffman, M.; Reddy, K.; *et al. New Engl. J. Med.* **2002**, *347*, 975.
63. Manns, M.; McHutchison, J.; Gordon, S.; *et al. Lancet* **2001**, *358*, 958.
64. Heil, G.; Hoelzer, D.; Sanz, M.; *et al. Blood* **1997**, *90*, 4710.
65. Yang, J.; Topalian, S.; Schwartzentruber, D.; *et al. Cancer* **1995**, *76*, 687.
66. Esslinger, H.; Haas, S.; Maurer, R.; *et al. Thromb. Haemostasis* **1997**, *77*, 911.
67. Yoo, S.; Jun, H.; Shin, B.; *et al. Chem. Pharm. Bull.* **2000**, *48*, 1921.
68. Gauthier, M.; Klok, H.-A. *Chem. Commun.* **2008**, *44*, 2591.
69. Lee, D.; Sharif, I.; Kodihalli, S.; *et al. J. Interferon Cytokine Res.* **2008**, *28*, 101.
70. Canalle, L.; Löwik, D.; van Hest, J. *Chem. Soc. Rev.* **2010**, *39*, 329.
71. Harada, A.; Kataoka, K. *Science* **1999**, *283*, 65.
72. Bumerot, D.; Manoharan, M.; Koteliansky, V.; Sah, D. *Nat. Chem. Biol.* **2006**, *2*, 711.
73. Inada, Y.; Takahashi, K.; Yoshimoto, T.; *et al. Trends Biotechnol.* **1986**, *4*, 190.
74. Carrea, G.; Riva, S. *Angew. Chem., Int. Ed.* **2002**, *39*, 222.
75. Yamamoto, Y.; Kise, H. *Biotechnol. Lett.* **1993**, *15*, 647.
76. Hernaiz, M.; Sanchez-Montero, J.; Sinisterra, J. *Biotechnol. Bioeng.* **1997**, *55*, 252.
77. DeSantis, G.; Jones, J. *Curr. Opin. Biotechnol.* **1999**, *10*, 324.
78. Greenwald, R.; Choe, Y.; McGuire, J.; Conover, C. *Adv. Drug Delivery Rev.* **2003**, *55*, 217.
79. Zalipsky, S.; Gilon, C.; Zilkha, A. *Eur. Polym. J.* **1983**, *19*, 1177.
80. Greenwald, R.; Pendri, A.; Bolikal, D. *J. Org. Chem.* **1995**, *60*, 331.
81. Stella, V.; Charman, W.; Naringrekar, V. *Drugs* **1985**, *29*, 455.
82. Bundgaard, H. *Drugs Future* **1991**, *16*, 443.
83. Sinhababu, A.; Thakker, D. *Adv. Drug Delivery Rev.* **1996**, *19*, 241.
84. Greenwald, R.; Pendri, A.; Bolikal, D.; Gilbert, C. *Med. Chem. Lett.* **1994**, *4*, 2465.
85. Greenwald, R.; Gilbert, C.; Pendri, A.; *et al. J. Med. Chem.* **1996**, *39*, 424.
86. Pasut, G.; Canal, F.; Dalla Via, L.; *et al. J. Controlled Release* **2008**, *127*, 239.
87. Schiavon, O.; Pasut, G.; Guiotto, A.; *et al. Eur. J. Med. Chem.* **2004**, *39*, 123.
88. Choe, Y.; Conover, C.; Wu, D.; *et al. J. Controlled Release* **2002**, *79*, 55.
89. Pasut, G.; Scaramuzza, S.; Schiavon, O.; *et al. J. Bioact. Compat. Polym.* **2005**, *20*, 213.
90. Tomalia, D.; Frechet, J. *Prog. Polym. Sci.* **2005**, *30*, 217.
91. Bhadra, D.; Bhadra, S.; Jain, S.; Jain, N. *Int. J. Pharm.* **2003**, *257*, 111.
92. Lee, C.; Gillies, E.; Fox, M.; *et al. Proc. Natl. Acad. Sci. U.S.A.* **2006**, *103*, 16649.
93. Fox, M.; Guillaudeu, S.; Frechet, J.; *et al. Mol. Pharmacol.* **2009**, *6*, 1562.
94. Kaminskas, L.; Boyd, B.; Karellas, P.; *et al. Mol. Pharmacol.* **2008**, *5*, 449.
95. Xu, S.; Krämer, M.; Haag, R. *J. Drug Target* **2006**, *14*, 367.
96. Slowing, I.; Trewyn, B.; Lin, V. *J. Am. Chem. Soc.* **2007**, *129*, 8845.
97. Slowing, I.; Vivier-Escoto, J.; Wu, C.-W.; Lin, V. *Adv. Drug Delivery Rev.* **2008**, *60*, 1278.
98. Zalipsky, S.; Harris, J. In *Poly(Ethylene Glycol): Chemistry and Biological Applications*; Harris, J., Zalipsky, S., Eds.; ACS Symposium Series 680; American Chemical Society: Washington, DC, 1997; p 1.
99. Lee, J.; Lee, H.; Andrade, J. *Prog. Polym. Sci.* **1995**, *20*, 1043.
100. Cauda, V.; Schlossbauer, A.; Bein, T. *Microporous Mesoporous Mater.* **2010**, *132*, 60.
101. Harder, P.; Grunze, M.; Dahint, R.; *et al. J. Phys. Chem. B* **1998**, *102*, 426.
102. Groll, S.; Elza, V.; Amirgoulova, E.; *et al. J. Am. Chem. Soc.* **2004**, *126*, 4234.
103. Ogris, M.; Brunner, S.; Schüuller, S.; *et al. Gene Ther.* **1999**, *6*, 595.
104. Kingshott, P.; Griesser, H. *Curr. Opin. Solid State Mater. Sci.* **1999**, *4*, 403.
105. Feng, S.-S.; Chien, S. *Chem. Eng. Sci.* **2003**, *58*, 4087.
106. Cauda, V.; Argyo, C.; Bein, T. *J. Mater. Chem.* **2010**, *20*, 8693.
107. Kecht, J.; Schlossbauer, A.; Bein, T. *Chem. Mater.* **2008**, *20*, 7207.
108. Branda, F.; Silvestri, B.; Luciani, G.; *et al. Colloid Surf., A* **2010**, *367*, 12.
109. Hirsch, L.; Gobin, A.; Lowery, A.; *et al. Ann. Biomed. Eng.* **2006**, *34*, 15.
110. Hirsch, L.; Stafford, R.; Bankson, J.; *et al. Proc. Natl. Acad. Sci. U.S.A.* **2003**, *100*, 13549.
111. Stern, J.; Stanfield, J.; Lotan, Y.; *et al. J. Endourol.* **2007**, *21*, 939.
112. Connor, E.; Mwamuka, J.; Gole, A.; *et al. Small* **2005**, *1*, 325.
113. James, W.; Hirsch, L.; West, J.; *et al. J. Radioanal. Nucl. Chem.* **2007**, *271*, 455.
114. Kah, J.; Phonthammachai, N.; Wan, R.; *et al. Gold Bull.* **2008**, *41*, 23.
115. O'Neal, D.; Hirsch, L.; Halas, N.; *et al. Cancer Lett.* **2004**, *209*, 171.
116. Wang, Y.; Xie, X.; Wang, X.; *et al. Nano Lett.* **2004**, *4*, 1689.
117. Gobin, A.; Lee, M.; Halas, N.; *et al. Nano Lett.* **2007**, *7*, 1929.
118. Kah, J.; Wong, K.; Neoh, K.; *et al. J. Drug Target.* **2009**, *17*, 181.
119. Lipka, J.; Semmler-Behnke, M.; Sperling, R.; *et al. Biomaterials* **2010**, *31*, 6574.

Biographical Sketches

Dr. Ivaylo Dimitrov received his PhD in polymer chemistry from the Institute of Polymers, Bulgarian Academy of Sciences in 2001 under the supervision of associate Professor Iliyana Berlinova in the area of associating amphiphilic copolymers. He held postdoctoral positions at the Max Planck Institute of Colloids and Interfaces, Germany with Dr. Helmut Schlaad working on peptide-based hybrid copolymers, and at the University of Massachusetts Lowell, USA with Professor Rudolf Faust working on kinetics of carbocationic polymerization of isobutylene. Since 2009 he has been associate professor at the Institute of Polymers of the Bulgarian Academy of Sciences. His research focuses on controlled polymerization methods, peptide-based hybrid copolymers of different architecture, and targeted drug delivery systems.

Christo B. Tsvetanov is a full professor of polymer science at the Institute of Polymers, Bulgarian Academy of Sciences and head of the Scientific Council of the Institute of Polymers. A major focus of his research concerns controlled polymerization methods, water-soluble polymers and hydrogels, and stimuli-responsive copolymers and their self-assembly to polymeric nanoparticles. He is well known for his contributions to the area of anionic coordination polymerization of oxirane and the role of donor and acceptor additives on the mechanism of anionic polymerization. Since 2004 he has been a corresponding member of the Bulgarian Academy of Sciences.

4.28 Current and Forthcoming Applications of ROMP Polymers – Biorelated Polymers

LL Kiessling and SL Mangold, University of Wisconsin–Madison, Madison, WI, USA

4.28.1 Bioactive Polymers from the Ring-Opening Metathesis Polymerization

4.28.1.1 Introduction

Synthetic polymers provide new opportunities to perturb or interrogate biological systems. Recent advances in polymer chemistry and catalyst design are providing the means to synthesize well-defined macromolecular architectures. The ability to precisely control parameters such as polymer architecture, ligand valency, and binding epitope orientation has facilitated the production of polymers with potent and unique biological activities. Indeed, one advantage of using synthetic polymers is that they can be optimized and customized for specific applications.

The macromolecular nature of bioactive polymers renders their properties distinct from those of small molecules (**Figure 1**), and these polymer attributes are being exploited. In diagnostic imaging, for example, polymers can exhibit enhanced sensitivity. The relaxivity of a magnetic resonance imaging (MRI) contrast agent can be augmented through its incorporation into a polymer.[1] Likewise, polymers can bear many copies of an imaging agent, such as dyes and radiotracers, which can lead to signal enhancement (**Figure 1(a)**).[2] Moreover, polymers have prolonged circulation half-lives,[3] a feature that has been used not only in cellular imaging but also for drug delivery. Indeed, there are many situations in which the bioactive species must have sufficient residence time to observe its localization or to deliver a chemotherapeutic agent. For instance, the larger pore size present in the tumor vasculature allows macromolecules to passively diffuse into the tumor, rendering polymers ideal delivery agents (**Figure 1(b)**).[4] An additional benefit of this strategy is that the lymphatic system is defective for most tumors; thus polymers have long residence times, a phenomenon referred to as the enhanced permeation and retention (EPR) effect.[3] These applications capitalize on the bulk properties of polymers.

The distinctive recognition properties of polymers can also be used to advantage. For example, polymers can function as potent inhibitors of biological interactions by occupying more than one binding site (**Figure 1(c)**). Through their ability to interact with subsites on a single receptor or with multiple sites on an oligomeric receptor, polymers can bind avidly to a target. Polymers interacting through this binding mode can act to block subsequent interactions not only through their avidity but also because their backbone can serve as a steric barrier (a phenomenon referred to as steric stabilization).[5] Their ability to bind multiple receptors also means that polymers can cluster proteins and thereby act as potent activators of biological signaling (**Figure 1(d)**).[6] Because polymer valency and length can be altered, signal output can be tuned. Thus, the attributes of polymers can be optimized to generate compounds that offer novel insights into biological mechanisms or have potent activity in disease prevention and treatment. These applications are predicated on the development of new methods for the controlled synthesis of these materials. Here, we focus on one powerful method for the synthesis of bioactive polymers, the ring-opening metathesis polymerization (ROMP).

A major advance in polymerization via metathesis occurred when Schwab *et al.*[7] and Schrock[8] unveiled well-defined transition metal catalysts. Molybdenum- and ruthenium-based catalysts are highly active in olefin metathesis reactions. The general mechanism that underlies their reactivity is outlined in **Figure 2**.[9] The catalyst reacts with the alkene via a [2 + 2] cycloaddition reaction to afford a metallocyclobutane intermediate. Cycloreversion with concomitant ring opening relieves strain and unleashes a new metal carbene that reacts with subsequent monomers to yield the polymer chain.

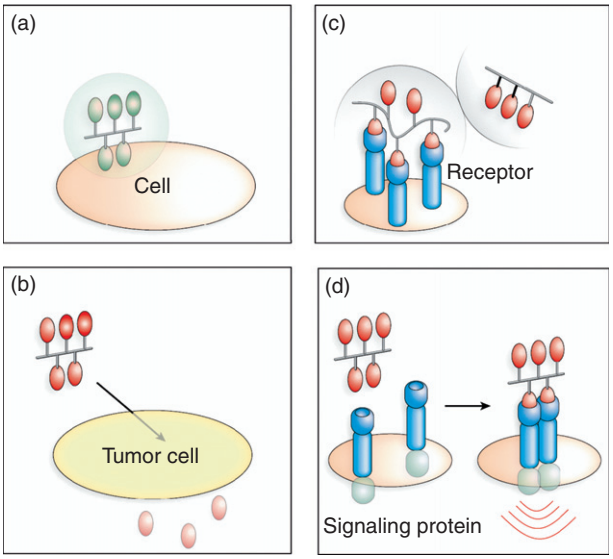

Figure 1 Applications of bioactive polymers. (a) Imaging: Polymers can incorporate multiple copies of a dye, radiotracer, or other reporter, which can lead to signal enhancement in imaging. (b) Tumor targeting and drug delivery: Macromolecules can preferentially accumulate in tumor tissue by enhanced permeation and retention. (c) Inhibition: Polymers can function as potent inhibitors of biological processes. (d) Activation of cell signaling: Polymers can act to cluster cell-surface receptors thereby activating cell signaling.

A critical feature of ROMP is that the polymerization can be living, such that chain termination and transfer events are much slower than chain propagation.[10] In this way, ROMP affords polymers or block copolymers with defined lengths and low polydispersity indexes (PDIs). By exploiting these mechanistic features, ROMP can be used to rapidly synthesize defined bioactive polymers with structural features optimized for the desired application.

4.28.1.2 Attributes of ROMP for Controlling Bioactive Ligand Incorporation

4.28.1.2.1 Functional group tolerance of metal carbene initiators

Alkene metathesis is especially attractive as a method for the assembly of biologically active polymers. The alkene functional group is rarely essential for a bioactive epitope, so a catalyst with high chemoselectivity for alkenes is invaluable for assembling polymers bearing bioactive groups. In the late 1980s, the finding that transition metal salts could be used to carry out ROMP in water[11,12] presaged the development of the aforementioned functional group-tolerant metathesis catalysts. One useful class of initiators is molybdenum alkylidenes, which are highly reactive toward alkenes and typically provide polymers with low PDI values.[13] These initiators can also be used to control the stereochemistry and tacticity of the polymer backbone.[8] Despite their advantages, they can be sensitive to some oxygen-containing functional groups, and trace amounts of oxygen and water in the reaction system can be problematic. The development of ruthenium carbene initiators was a major step forward for biological applications. They not only give rise to polymers with narrow PDI values,[14,15] but are also remarkably selective for alkenes even in the presence of polar functionality, such as hydroxyl, ester, and amide groups. Indeed, densely functionalized bioactive ligands, such as sulfated sugars,[16] peptides,[17] and small-molecule drugs,[18] have been used successfully in ruthenium-catalyzed ROMP.

4.28.1.2.2 Control over polymer length

The powerful ROMP initiators can be not only highly chemoselective but can also exert excellent control over polymer length. As mentioned above, these initiators can carry out living polymerizations, in which unwanted termination reactions do not effectively compete with propagation. For a living polymerization, when initiation rates exceed those of propagation,

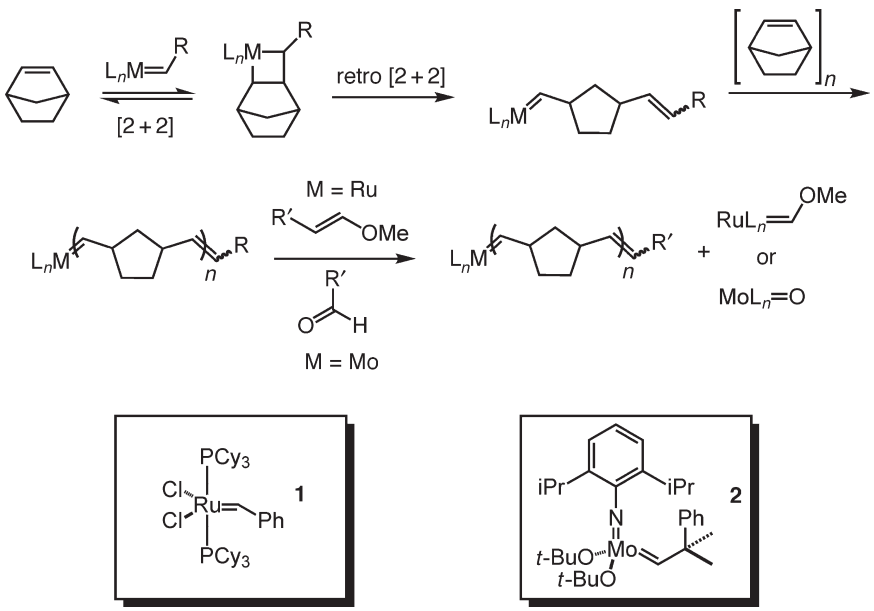

Figure 2 Mechanism of ROMP catalyzed by metal carbene initiators. Examples of ruthenium (**1**) and molybdenum (**2**) initiators are highlighted.

polymers of defined lengths and excellent PDIs are obtained. Thus, by varying the monomer-to-initiator (M:I) ratio, length and therefore ligand valency can be controlled. Polymers that vary in length and consequently in the number of recognition elements they display have been used in diverse biological applications including as inhibitors of protein–carbohydrate interactions,[19] as novel and selective antimicrobial agents,[20] and as effectors of biological responses.[21,22] Specific illustrations of how polymer length control can be used to enhance inhibition of biologically relevant processes are provided in Section 4.28.1.4.2.

4.28.1.3 Synthetic Strategies for Bioactive Ligand Incorporation

4.28.1.3.1 Homopolymers and random copolymers

Many biologically important epitopes (e.g., sugars, peptides, small molecules) have limited solubility in solvents that are compatible with ROMP. This problem has been addressed through modification of the monomers by introducing protecting or solubilizing groups.[23,24] The use of protected monomers, however, can give rise to problems with protecting-group removal subsequent to the polymerization reaction. Conditions successfully optimized for the monomer are often ineffective for the polymer. Moreover, when these problems are encountered, characterization of the resulting mixture of partially protected products is often challenging. Because the conditions for final protecting-group removal can be harsh, eliminating this step allows for the synthesis of materials containing sensitive bioactive epitopes. Consequently, the ability to synthesize substituted polymers utilizing both defined initiators and unprotected monomers constituted a critical advance in the synthesis of bioactive substituted polymeric displays via ROMP. Methods that have been used successfully for the incorporation of polar bioactive ligands are highlighted.

- *Polar catalysts for aqueous metathesis*

The introduction of ruthenium catalysts significantly broadened the scope of ROMP because of their high activity and functional group tolerance. After the demonstration that ROMP of 7-oxonorbornenes could be carried out in water using $RuCl_3$,[11,12] Mortell *et al.*[25] capitalized on this observation by using ROMP to prepare bioactive polymers (**Figure 3**). The application of well-defined ruthenium initiators under aqueous conditions is complicated by catalyst insolubility, prompting researchers to search for water-soluble ruthenium catalysts (**Figure 4**).[26,27] In early investigations, catalysts possessing water-soluble triaryl phosphines (**3**) were shown to catalyze the polymerization of norbornenes in water.[28] Although these catalysts initiated ROMP of norbornene monomers, the propagating species decomposed before polymerization was complete. Thus, control over the polymer products was limited. Alternative water-soluble catalysts for

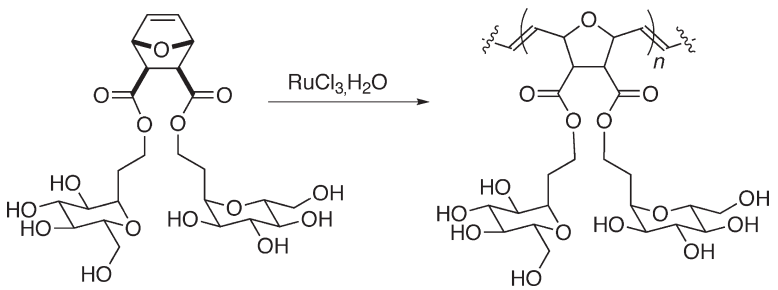

Figure 3 Synthesis of carbohydrate-substituted polymers under aqueous conditions.

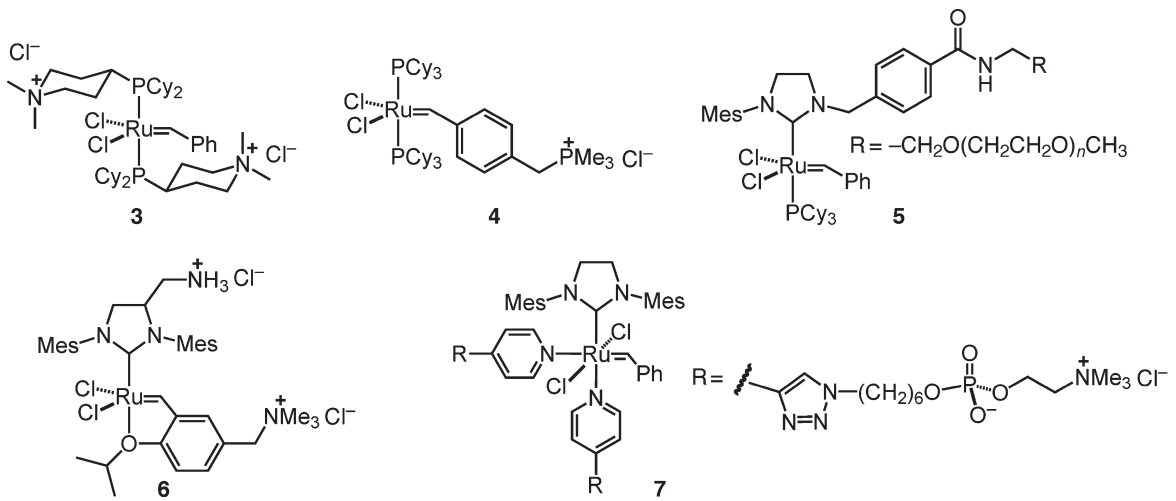

Figure 4 Examples of ruthenium catalysts for aqueous ROMP.

conducting living polymerizations have subsequently been sought. In particular, polar or ionic functional groups have been introduced via modifications to the N-heterocyclic carbene[29] or benzylidene ligands.[30,31] Modifications to the catalyst, however, can have deleterious effects on the kinetics of the polymerization. Accordingly, few examples have demonstrated that water-soluble versions of the ruthenium catalysts provide living polymerizations.[31,32] We anticipate that the design of new polar catalysts with favorable kinetics of polymerization will undoubtedly advance the utility of ROMP, especially for generating bioactive polymers and for expanding the utility of metathesis in complex biological milieu.

- *Emulsion conditions for polar monomers.*

The chemoselectivity of even early defined ruthenium carbene catalysts was readily apparent;[33] however, as mentioned above, the insolubility of these catalysts under aqueous conditions posed a problem for their use with polar monomers. To overcome solubility differences between the catalyst and the growing polymer chain, Fraser and Grubbs[34] utilized a mixed solvent system of water and dichloromethane that contained the cationic emulsifier dodecyltrimethylammonium bromide (DTAB) to polymerize carbohydrate-functionalized norbornenes (**Figure 5**(**a**)). These conditions afforded a glucose-substituted polymer in excellent yield. These data suggest that polymerization reactions conducted under these conditions can yield biological probes. Indeed, Manning *et al.*[35] applied emulsion conditions to generate potent ligands for carbohydrate-binding proteins (**Figure 5**(**b**)). When sulfated sugar-functionalized norbornene derivatives were subjected to polymerization in a mixture of dichloromethane and methanol, however, the reaction was incomplete and the polymer product precipitated. Under aqueous conditions with DTAB as a surfactant, however, the polymerization proceeded with complete and rapid consumption of the monomer. Emulsion conditions have been utilized for the polymerization of a variety of monomers containing bioactive groups including disaccharides,[36] sulfated monosaccharides,[37,38] trisaccharides,[39,40] and small molecules,[41] although the kinetics of the polymerization can be variable leading to broadened molecular weight distributions.

- *Polar mixed reaction solvents*

Although emulsion conditions facilitate the polymerization of highly functionalized monomers, homogeneous reactions afford more reproducible kinetics of polymerization and therefore more defined polymer products. To this end, Kanai *et al.*[42] devised homogeneous conditions for the polymerization of monomers bearing unprotected monosaccharides. Initiation was performed in a mixture of methanol, water, and dichloromethane; propagation was conducted by adding a mixture of water and methanol to dissolve the resulting oil (**Figure 6**(**a**)). These conditions resulted in polymers of narrow PDI (1.2) relative to standard emulsion conditions. Still, they did not afford polymers with a degree of polymerization (DP) greater than 50, although they did allow for the production of polymers of biologically relevant lengths that display unprotected carbohydrate residues.

Related conditions were used in the polymerization of carbohydrate-substituted cyclooctene monomers by Rawat *et al.*[43] (**Figure 6**(**b**)). They conducted polymerization reactions on monomers with pendent sulfated carbohydrates using a mixed solvent system of 1:5 methanol/dichloroethane to solubilize the monomer. Polymerization using a water-soluble version of the Grubbs–Hoveyda catalyst was unsuccessful; however, catalyst **9** provided glycopolymers with acceptable PDI values (1.3–1.6) and in good yields (51–88%). Under these conditions, polymers with a DP of 86 were obtained. Together, these examples highlight the range of conditions that can be used to afford carbohydrate-substituted polymers.

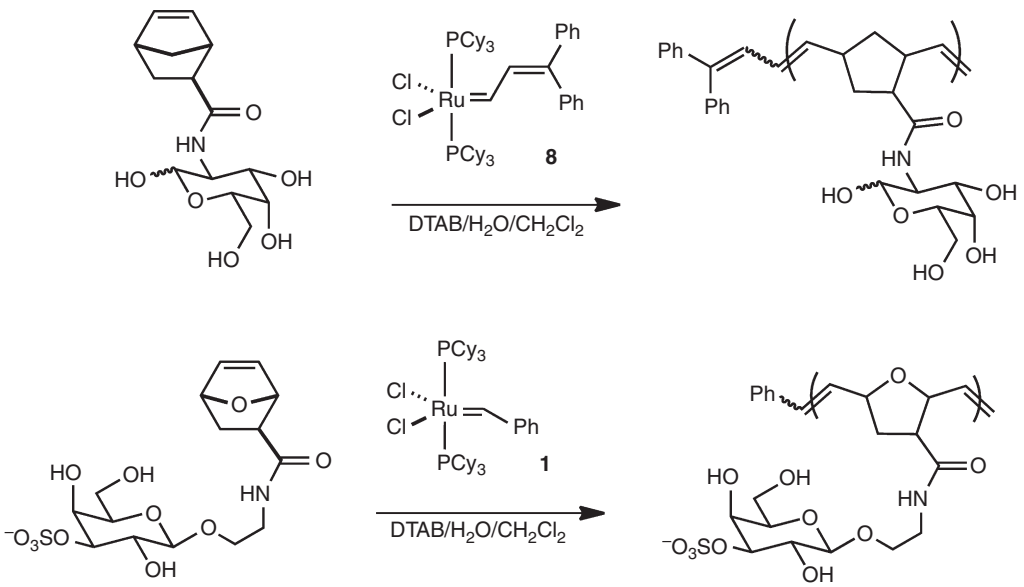

Figure 5 Polymerization of monomers bearing unprotected carbohydrates using emulsion conditions. (a) Monomers with unprotected carbohydrate groups can be polymerized using defined initiator **8**. (b) Bioactive polymers can be generated under emulsion conditions.

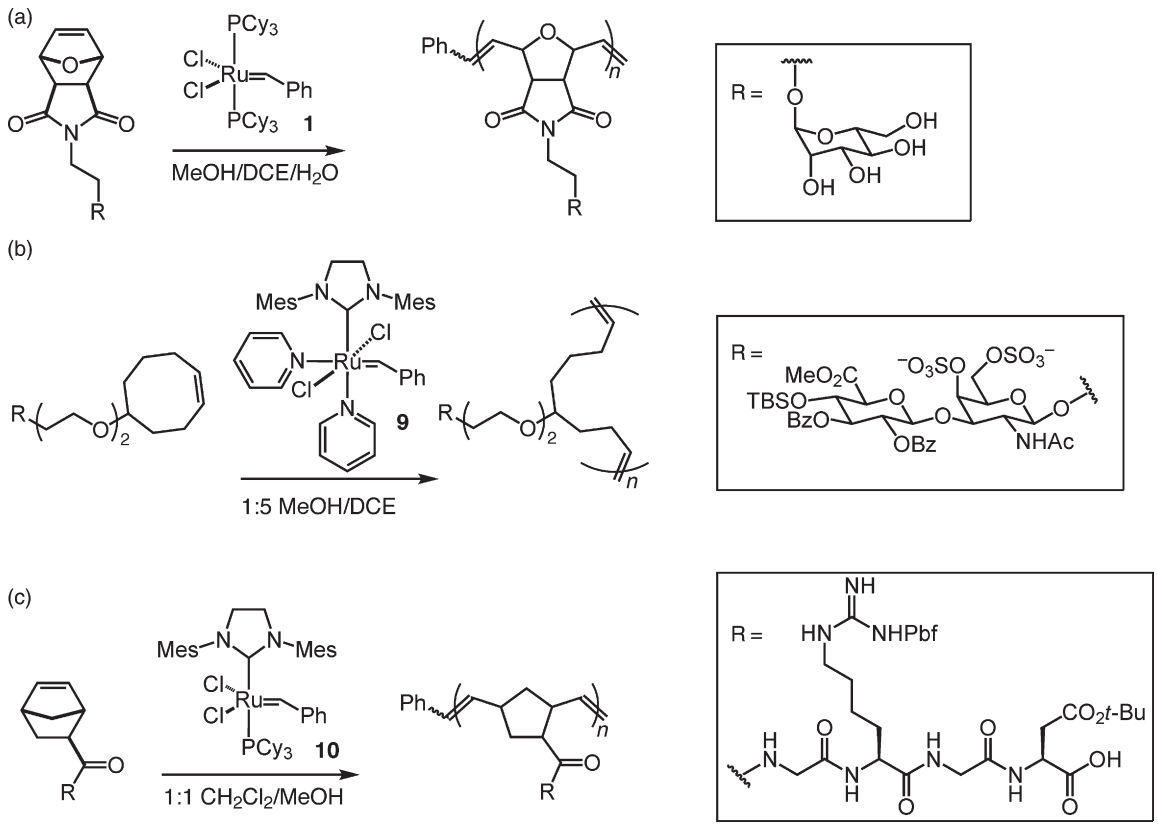

Figure 6 Polymerization of bioactive functionalized monomers using polar mixed reaction solvents. (a) Polymerization of unprotected carbohydrate-functionalized oxanorbornene monomers. (b) Polymerization of cyclooctene monomers bearing sulfated carbohydrates using highly active catalyst **9**. (c) Peptide-functionalized norbornene monomers were polymerized using defined catalyst **10**. DCE, 1,2-dichloroethane; Pbf, 2,2,4,6,7-pentamethyl-dihydrobenzofuran-5-sulfonyl.

Peptide-substituted monomers are also polar, so their polymerization raises issues similar to those encountered with carbohydrate-bearing substrates. Moreover, even with the chemoselective ruthenium catalysts, monomers bearing peptides are challenging and peptide side-chain protection is necessary, as amines, guanidinium groups, and other chelating functionality can result in deactivation of the catalyst or degradation of propagating intermediates.[44] Additionally, variability in PDI can result from aggregation of the growing polymer chain and therefore premature termination. To address these issues, polar solvent mixtures similar to those described for carbohydrates (i.e., dichloromethane and methanol) were employed to afford peptide-functionalized polymers in good overall yield (52–92%) and acceptable PDI (1.1–1.3) (Figure 6(c)).[45] The use of solvent mixtures can result in polymers of narrow PDI, which is beneficial for optimizing the biological activity of polymers.

• *Postpolymerization modification*

A complementary strategy for using ROMP to synthesize polymers that contain biologically important epitopes has been developed. This method does not rely on the polymerization of the epitope as part of the monomer unit. This postpolymerization modification (PPM) strategy utilizes a general monomer unit that contains a reactive functional group that can be modified subsequent to polymerization (Figure 7).[46,47]

By choosing a monomer with solubility in nonpolar solvents, the advantages of ROMP can be exploited to construct materials with defined lengths. Because the biological epitope is introduced after the polymerization, less-soluble molecules can be conjugated to the polymer in polar solvents such as dimethylsulfoxide or dimethylformamide, which are incompatible with the current polymerization catalysts.[48] This mode of synthesis offers the advantage that polymers of same length and polydispersity can be prepared and their biological activities directly compared. As a result, a desired biological response (e.g., inhibition, activation) can be optimized or structure–activity relationships for a given process can be derived. Examples of postpolymerization strategies for the investigation of signaling are highlighted in Section 4.28.1.4.4.

4.28.1.3.2 Block copolymers

The unique properties of block copolymers have led to their use in many biological applications including as therapeutics,[49] imaging agents,[50] and drug delivery platforms.[51–53] In general, each block can be endowed with specific properties. For example, blocks with disparate properties (e.g., hydrophilicity, hydrophobicity) can facilitate intermolecular interactions that result in macromolecular assemblies.[54] Alternatively, a relatively unexplored opportunity for block copolymers is to endow each block with a distinct biological function. For these and other applications, defined block copolymers can be produced by taking advantage of the kinetics of ROMP.

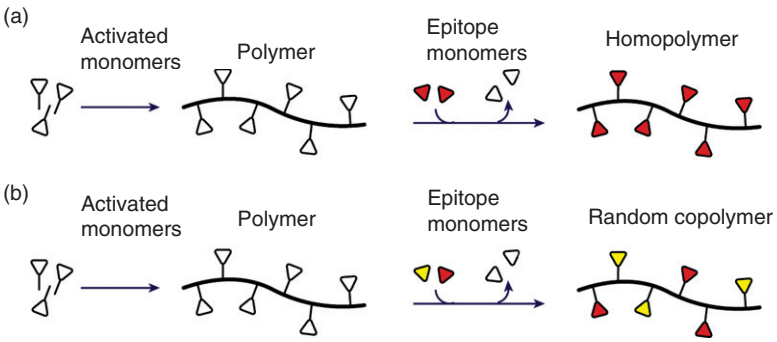

Figure 7 Bioactive ligands can be appended to a polymer using PPM to generate (a) homopolymers or (b) random copolymers.

There are two synthetic approaches that can be employed to generate block copolymers: coupling of two end-functionalized polymer chains or the sequential addition of monomers. The first synthetic method involves linking two end-functionalized polymer chains. In a typical example, monomers are polymerized using ROMP, and the propagating metal carbene is used to append the resulting polymer to another preformed polymer. This strategy has been used to prepare block copolymers through the reaction of end groups via Wittig-type reactions;[55] however, the utility of the resulting materials for biological applications has yet to be explored. By contrast, the second strategy is versatile and widely utilized. It has been used to synthesize block copolymers with a variety of architectures, including diblock and cyclic block copolymers (Figure 8(a)).[56] For example, monomers bearing different bioactive groups have been polymerized sequentially.[57] Alternatively, a general block copolymer template can be produced and then elaborated to install bioactive groups (Figure 8(b)). The latter method is powerful in that block copolymers with diverse properties can be accessed from a single scaffold composed of orthogonally reactive blocks.[58]

4.28.1.3.3 End-labeled polymers

The mechanistic features of ROMP provide opportunities to incorporate specific polymer end labels. The propagating metal center in ROMP can be used to introduce a distinct functional group at the polymer terminus (Figure 9(a)).[59] Molybdenum alkylidene intermediates can react with aldehydes to terminate the polymerization.[8] By contrast, polymerization reactions mediated through ruthenium carbene intermediates can be terminated with electron-rich alkenes to form less-reactive Fischer carbenes.[60,61] Electron-rich alkenes bearing groups that can undergo subsequent chemoselective reactions have been used in many applications. For instance, end labeling with substituted vinyl ethers bearing ketones has been used for the incorporation of bioactive ligands containing thiosemicarbazide[62] or alkoxylamine[63] functionality for the formation of acylhydrazones and oximes, respectively. Termination of the polymerization with vinyl carbonate or vinyl lactone moieties affords polymers bearing aldehyde and carboxylic acid end groups, respectively (Figure 9(b)).[64] All of these strategies provide a site for subsequent bioactive ligand incorporation.

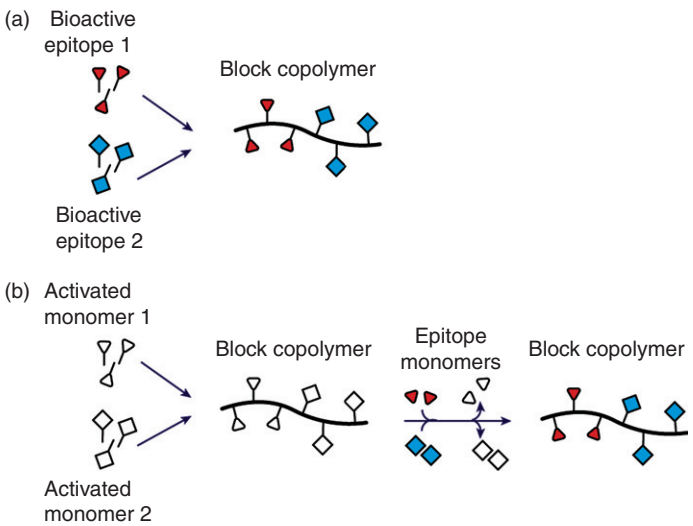

Figure 8 Strategies for synthesizing block copolymers displaying bioactive epitopes. (a) Sequential polymerization of monomers bearing a bioactive epitope. (b) PPM of two orthogonally reactive blocks.

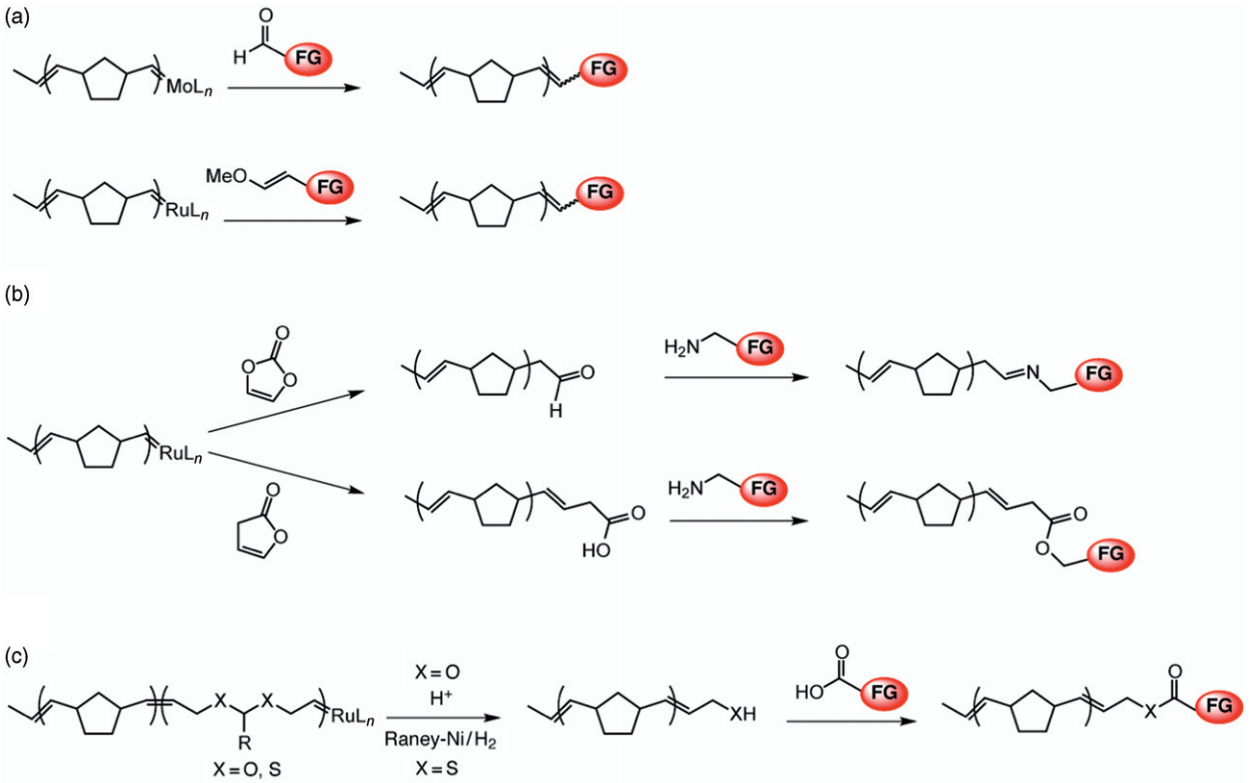

Figure 9 End-labeling strategies for the incorporation of bioactive epitopes. (a) Termination of the polymerization can be effected with aldehydes (molybdenum alkylidenes) or vinyl ethers (ruthenium carbenes) to install a single reporter group. (b) Termination of ruthenium carbenes with a vinyl carbonate or vinyl lactone leaves a terminal aldehyde or carboxylic acid that can be further derivatized. (c) Sacrificial synthesis: An acetal or thioacetal block can be unmasked to reveal a single terminal alcohol or thiol that can be modified selectively.

An alternative end-capping strategy is to employ sacrificial synthesis (Figure 9(c)).[65–67] In contrast to the aforementioned methods of end labeling, sacrificial synthesis utilizes an additional block of a cleavable monomer to polymerize onto the desired polymer. This block is then removed in a subsequent reaction, thereby liberating a functional group such as an alcohol or thiol, which can be used for further derivatization. While it would not be labeled 'atom economical' as an end-labeling strategy, the approach can be extremely efficient. In addition, the sacrificial block serves as a highly effective mask for reactive functional groups.

The utility of end-labeling strategies has been exploited to convert polymers into highly effective biological probes. Some examples of end labeling with fluorophores for imaging cellular internalization will be discussed in Section 4.28.1.4.3.

4.28.1.4 Applications of Biologically Active Polymeric Displays

4.28.1.4.1 ROMP-derived multivalent ligand design

An important advantage of using synthetic ligands to investigate biological interactions is that the effect of ligand structure on activity, such as binding affinity or biological signaling, can be determined. The opportunities that ROMP offers to vary ligand structure are valuable because multivalent ligands can engage in a range of different binding modes and these can contribute to potency and mechanism of action (Figure 10).[5] The ability of a multivalent ligand to utilize a given mechanism depends on its architecture and the receptor of interest. Variables such as the valency of the display and the density and orientation of the epitopes may have an influence. Indeed, multivalent ligands rarely utilize a single binding mechanism. Because ligand features can be varied using ROMP, the activities of the compounds that result can be optimized for the desired response. The examples that follow highlight the use of multivalent ligand design to either perturb or interrogate biologically relevant interactions.

4.28.1.4.2 Polymers from ROMP as inhibitors

As mentioned previously, the first protein ligands generated by ROMP were carbohydrate-substituted polymers.[68] These compounds inhibited the cell-binding activity of the tetrameric glucose-binding protein concanavalin A (ConA) with activities >1000-fold better than that of the monovalent glucose derivative. Their interactions with ConA were not only avid but also extremely selective.[69] These early studies demonstrated that ROMP could afford bioactive ligands. At the time, however, effective transition metal catalysts for ROMP were just being developed and not widely available; therefore, the original investigations used heterogeneous polymers. Still, their potencies and selectivities provided

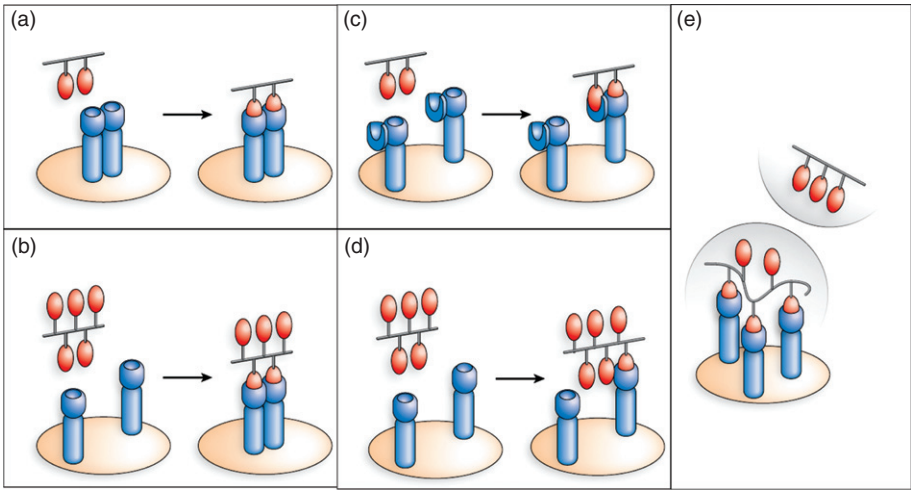

Figure 10 Binding modes of multivalent ligands. (a) Chelate effect: Simultaneous engagement of multiple ligands to multiple receptors. (b) Receptor clustering: Multivalent ligands can alter the proximity of ligand-bound receptors. (c) Subsite binding: Multivalent ligands can bind to a secondary binding site on the same receptor. (d) Statistical rebinding: Multivalent ligands have a higher local concentration of binding epitopes that can favor rebinding. (e) Steric stabilization: Once a multivalent ligand is bound to its target, the backbone can act as a steric impediment to subsequent binding events.

impetus to use ROMP to generate multivalent inhibitors of carbohydrate-binding proteins.

• *Polymers as inhibitors of leukocyte rolling*

Protein–carbohydrate interactions have been found to be important in the early stages of inflammation. The protein targets, the selectins (E-, P-, and L-selectin), bind anionic saccharides to mediate leukocyte rolling at sites of tissue damage.[70] Polymers generated by ROMP that display sulfated carbohydrates have been devised to block these protein–carbohydrate interactions. For example, ROMP was used to generate polymers presenting sulfated galactose derivatives as mimics of sulfated glycolipid (sulfatide) arrays.[38] The resulting materials can inhibit selectively the binding of HL60 cells (a leukocyte cell line) to selectin family members (**Figure 11(a)**). In a P-selectin adhesion assay, the monosulfated polymers were approximately as potent as the monomeric ligand sialyl Lewis^x (sLe^x), but the polymers substituted with 3,6-disulfogalactose residues were 40-fold more active. The potent polymeric ligand was not only effective at blocking P-selectin but it also exhibited 20-fold preference for P- over L-selectin. Interestingly, the method of polymer synthesis influenced the activity of the resulting products. Specifically,

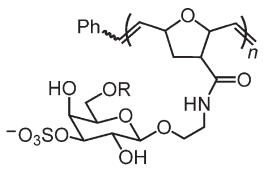

(a)

Compound	*P-selectin IC_{50} (mM)*	*L-selectin IC_{50} (mM)*	*E-selectin IC_{50} (mM)*
sLe^X	3.4	3.5	3.3
R = H	2.2	75% at 3.0	2.9
R = SO_3Na	0.084	0.17	90% at 3.0

(b)

Compound	*P-selectin IC_{50} (mM)*	*L-selectin IC_{50} (mM)*	*E-selectin IC_{50} (mM)*
R = H	7.8	0% at 20.0	20.0
R = SO_3Na	13% at 20.0	13% at 20.0	13% at 20.0

Figure 11 Polymers displaying sulfated galactose derivatives are inhibitors of selectin–ligand interactions. The ability of the polymers to inhibit the binding of HL60 cells to immobilized selectins is reported as the concentration required for 50% inhibition (IC_{50}). Polymers were generated using (a) homogeneous conditions or (b) emulsion conditions. For compounds for which IC_{50} values were not available, the percent inhibition at a particular concentration is reported.

polymers synthesized under emulsion conditions were less potent than those generated under homogeneous conditions (Figure 11(b)). The authors hypothesized that the highly charged monomers had broader molecular weight distributions under homogeneous conditions. Therefore, high-molecularweight polymers are likely to be potent inhibitors. These studies highlight that polymer valency can influence potency.

Multivalent ligands were used to mirror the features of another class of selectin ligands, the sulfated O-glycoprotein mucins. Naturally occurring ligands for L-selectin are highly glycosylated proteins that display many copies of the sulfated saccharides. These proteins bind to L-selectin and thereby facilitate leukocyte rolling.[71] It was envisioned that polymers generated by ROMP might serve as excellent mucin mimics. To assess whether multivalent ligands could block this rolling event, a series of sulfated carbohydrate polymers were synthesized bearing Le^x, sLe^x, and sulfatide epitopes to assess the importance of sulfation pattern for inhibition of L-selectin-mediated rolling (Figure 12(a)).[16,40] Polymers functionalized with the sulfated variants of the trisaccharide Le^x or the tetrasaccharide sLe^x were potent inhibitors of leukocyte rolling. Interestingly, the position of the pendent sulfo groups was found to be critical for polymer activity, suggesting that sulfation *in vivo* could have a dramatic effect on cell adhesion (Figure 12(b)). Unexpectedly, the potency of the sulfated polymers was enhanced under flow rates similar to those that occur in blood vessels. This finding is interesting as both the polymers and the O-glycoprotein mucins are expected to adopt an extended conformation under these conditions.

The ability of the polymers to block L-selectin was not due solely to their inhibition of natural ligand binding. These compounds were found to decrease the concentration of L-selectin on the cell surface by inducing its proteolytic release (or shedding) from the cell (Figure 12(c)).[16,39] The authors postulate that the polymers bind multiple copies of L-selectin at the cell surface, and it is the clustering of L-selectin that leads to protease activation and subsequent cleavage of L-selectin. Together, these studies foreshadow the power of ligands generated by ROMP for clustering receptors and thereby activating biological processes.

- *Polymers as inhibitors of neuronal growth*

Another important class of sulfated glycoconjugates is the glycosaminoglycans (GAGs). GAGs are sulfated, linear polysaccharides that are central components of the extracellular matrix (ECM). They are involved in myriad biological functions, including blood coagulation, angiogenesis, tumor growth and metathesis, and neurite outgrowth.[72] Chondroitin sulfate,

(a)

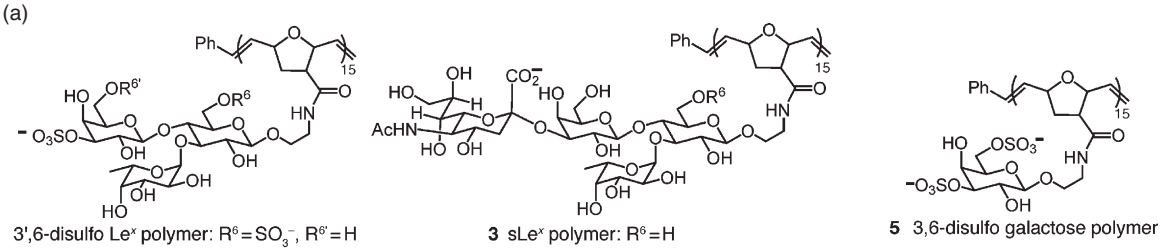

(b)

Compound	IC_{50} (mM) for L-selectin-mediated rolling
1	0.002
2	>5000
3	>60.0
4	0.022
5	121

(c)

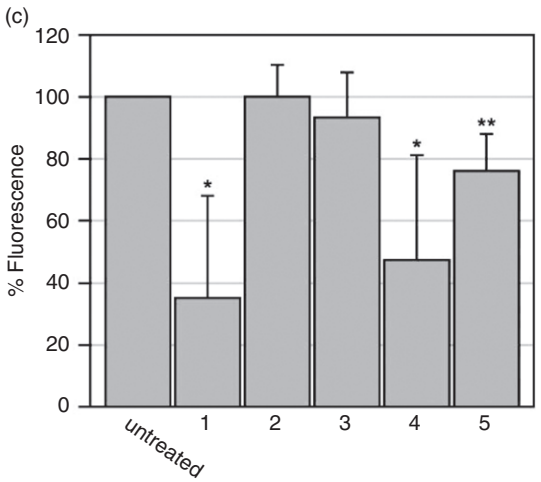

Figure 12 Synthetic multivalent compounds promote L-selectin shedding thereby inhibiting its function. (a) Polymers designed as mimics of the glycolipid sulfatides or the highly O-glycosylated mucins that display the oligosaccharides Le^x or sLe^x. (b) Data from an assay measuring L-selectin-mediated cell rolling. IC_{50} values are reported on a saccharide residue basis. (c) Assessment of ligand-induced shedding of L-selectin. Polymers **1, 4**, and **5** promote L-selectin shedding but polymers **2** and **3** do not. L-selectin shedding from human neutrophils was detected with a fluorophore-conjugated anti-L-selectin antibody using flow cytometry.

(a)

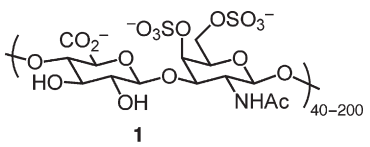

1

(b)

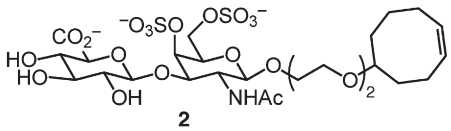

2

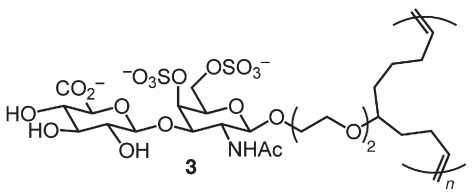

3

Compound	% Inhibition of neuronal outgrowth
Chondroitin Sulfate (**1**)	100
Disaccharide (**2**)	n.i.
Polymer **3**, n = 25	41
Polymer **3**, n = 80	86

Figure 13 Polymers that mimic chondroitin sulfate are inhibitors of hippocampal neuronal growth. (a) Structure of chondroitin sulfate. (b) Structure of the synthetic multivalent mimics of CS. The activity of the highest valency polymer was comparable to that of CS. n.i., no inhibition.

a polymer of repeating disaccharide units consisting of *N*-acetylgalactosamine and D-glucuronic acid (**Figure 13(a)**), is an important member of the GAG family. Chondroitin sulfate polysaccharides are linear and consist of 40–200 sulfated disaccharide units. Highly sulfated sequences within the chain serve as recognition sites for growth factors and other proteins.[73] GAG-mediated recruitment of essential growth factors can profoundly affect cell proliferation, motility, development, and proliferation.[74]

Rawat *et al.*[43] envisioned using ROMP to generate multivalent saccharide derivatives that mimic the features of chondroitin sulfate. Although such a polymer would not directly resemble the linear polysaccharide, the authors surmised that appending sulfated sugars to the polymer would yield a species capable of interacting with proteins that bind to highly sulfated saccharide substructures. To this end, they generated a series of disaccharide-substituted polymers using M:I ratios of 25–80. As soluble chondroitin sulfate can block neurite outgrowth, the resulting polymers were evaluated for this inhibitory activity. Although the disaccharide alone was unable to block the outgrowth of hippocampal neurons, a polymeric display of this epitope was effective. These results suggest that the polymers are distracting target proteins from binding to cell-surface chondroitin sulfate. The potency of the polymers depended on their lengths: polymers with 25 disaccharide units had moderate activity (41% inhibition relative to isolated chondroitin sulfate-E) while polymers with an M:I ratio of 80 were more potent (86% inhibition) (**Figure 13(b)**). These data indicate that the chondroitin sulfate chains act as scaffolds to assemble multiple proteins. In addition, they highlight the ability of polymers generated by ROMP to mimic linear GAGs. The authors postulate that the strategic placement of epitopes is sufficient to recapitulate many of the properties of natural GAGs. Thus, the ability to control both the density and placement of biological epitopes bodes well for using ROMP to generate mimics of other linear polysaccharides.

- *Polymers as inhibitors of integrin-mediated cell adhesion*

Integrins are a family of cell adhesion proteins that mediate critical physiological processes including cellular adhesion, proliferation, and trafficking, but they are also involved in pathological processes such as tumor cell invasion and inflammation.[75] Many integrins bind to the peptide motif arginine–glycine–aspartate (RGD) found within ECM proteins such as fibronectin and vitronectin. As a result, researchers have focused on developing RGD-based inhibitors that block the interactions between an integrin and its ligand.[76,77] Maynard *et al.*[78] used ROMP to generate a series of polymers that contain both the peptide sequences Gly-Arg-Gly-Asp-Ser (GRGDS) and Pro-His-Ser-Arg-Asn (PHSRN), the latter of which was suggested to bind synergistically with the RGD motif. These compounds were tested for their ability to block cell adhesion to fibronectin-coated surfaces. Specifically, fibroblasts, which use their cell-surface integrins to bind to ECM proteins like fibronectin, were treated with the monovalent peptide GRGDS or polymers displaying GRGDS, and cell adhesion was quantified (**Figure 14**). The concentration at which 50% inhibition was observed (IC_{50}) was found to be 1.33 mmol for the monovalent peptide but 0.18 mmol for the polymeric inhibitor, indicating that the latter is about sevenfold more active. A polymer displaying the PHSRN peptide, which binds with low affinity to integrins, was an ineffective inhibitor of adhesion; however, copolymers functionalized with GRGDS and PHSRN sequences blocked cell adhesion with an IC_{50} of 0.04 mmol (33-fold more potent than RGD alone). Thus, the multivalent display is critical for achieving sufficient avidity. These data highlight the benefit of using ROMP to generate effective ligands for integrins. Such compounds could be used to examine the role of integrins in specific processes or as targeting agents to bind to cells with upregulated levels of integrins.[79,80]

Peptide-functionalized polymers synthesized by ROMP have also been used to investigate the importance of integrins in fertilization. The β1 integrin on the surface of the egg is thought to play a key role in the fusion of gametes through recognition of the peptide sequences glutamate–cysteine–aspartate (ECD) and glutamine–cysteine–aspartate (QCD) within the integrin-binding domain on the sperm.[81] This initial binding event is thought to be critical for successful fertilization, but the role of β1 integrins in this process has been controversial. To investigate the importance of this interaction, Lee and Sampson[82] used ROMP to synthesize polymers equipped with the ECD and QCD peptide sequences to assess their ability to block gamete fusion. Short oligomers of QCD (M:I 2) had modest potency (IC_{50} of 500 μM), while longer polymers (M:I 100) were more active (IC_{50} of 4.1 μM). Control polymers with peptide sequences glutamate-serine-alanine

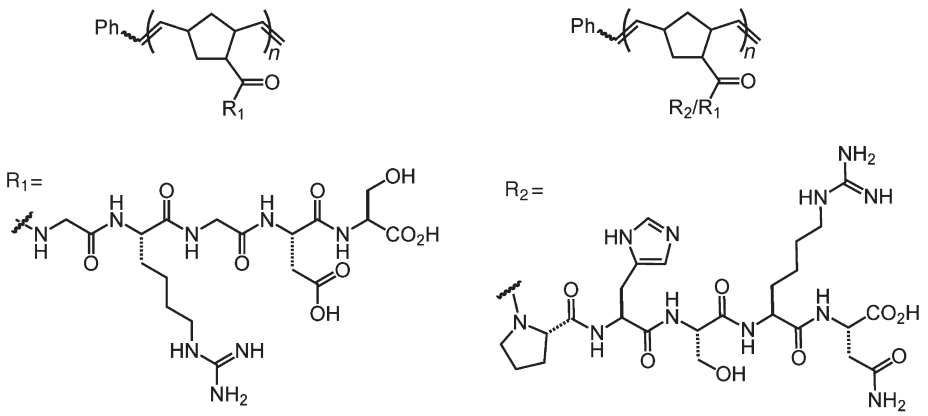

Compound	IC_{50} (mM)	Relative Potency
GRGDS	1.3	1
PHSRN	n.i.	–
GRGDS Polymer	0.18	7.4
GRGDS/PHSRN Polymer	0.04	33

Figure 14 Polymers that present the integrin-binding domain GRGDS and a sequence that binds synergistically, PHSRN, are inhibitors of fibroblast adhesion. IC_{50} values were determined by measuring the ability of each compound to block human fibroblasts from binding to fibronectin-coated surfaces. n.i., no inhibition.

(ESA) that do not interact with the protein showed no inhibition (Figure 15(a)). Interestingly, triblock copolymers consisting of terminal ECD and QCD peptide sequences with spacers that do not interact with the receptors had nearly the same inhibitory potency as homopolymers of the same length (Figure 15(b)). These results indicate that only a small percentage of peptides on the homopolymers are required for binding to the cell surface, suggesting that the size of the polymer plays a critical role in its inhibitory activity.

The relationship of polymer scaffold to potency in the gamete fusion assay was tested. Polymers of varying lengths were synthesized that incorporate a backbone derived from polyethylene glycol (PEG) or from norbornene polymerization. In all cases, the inhibitory potencies of the PEG backbones were diminished. The authors speculated that increased flexibility in the PEG backbone was responsible for lower binding affinities. This conclusion is logical, although it should be noted that the relative flexibilities of these polymer classes have not been determined. In summary, these studies highlight the importance of different polymer features in the inhibition of fertilization and may guide the design of future cell adhesion inhibitors.

4.28.1.4.3 ROMP to generate polymers for monitoring cellular internalization

Because of their high molecular weight and polarity, many polymers are cell impermeable. Strategies to promote polymer uptake have been explored to facilitate drug or gene delivery.[83] Specifically, polymeric micelles can be designed such that they are taken up into endosomes and, in these acidic compartments, release their cargo.[84] Additionally, many charged polymers display groups that both facilitate solubilization and promote Coulombic attraction to cell surfaces.[85,86] Alternatively, polymers can be decorated with groups that target internalizing cell-surface receptors.[17,87] A general strategy to facilitate polymer uptake into the cytoplasm could provide novel therapeutic strategies and illuminate signaling processes.

- *Artificial translocation domains*

Kolonko and Kiessling[63] devised a strategy to enhance polymer internalization using artificial translocation domains (ATDs). Specifically, they used PPM (see Section 4.28.1.3.1) to install guanidinium groups that facilitate uptake. Internalization is believed to occur through association of the guanidinium groups with the negatively charged sulfate groups of cell-surface GAGs such as heparan sulfate.[88] This association is followed by internalization via an energy-dependent endocytic pathway. To visualize internalization, polymers were terminated with a vinyl ether bearing a ketone, which was used for subsequent functionalization with a hydroxylamine-containing rhodamine dye via a hydrolytically stable oxime linkage.[89] Cell permeability of the polymers was assessed by confocal microscopy. Cellular internalization was rapid for polymers with an M:I ratio of 10, occurring in 5 min (Figure 16). As expected from studies using oligoarginine

(a)

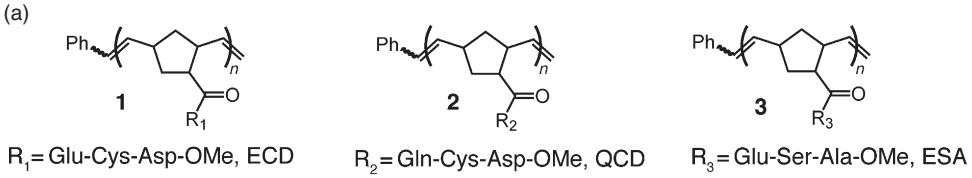

R_1 = Glu-Cys-Asp-OMe, ECD R_2 = Gln-Cys-Asp-OMe, QCD R_3 = Glu-Ser-Ala-OMe, ESA

Compound	*IC_{50} (μM) by FI*	*IC_{50} (μM) by FR*
QCD (**2**), $n=2$	496	492
QCD (**2**), $n=100$	4.1	5.7
ESA (**3**), $n=100$	n.i.	n.i.

(b)

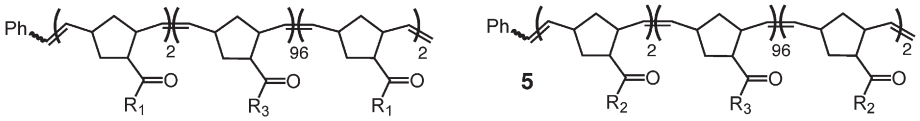

Compound	*% Inhibition of fertilization*
ECD homopolymer (**1**), $n=100$	52
ECD–ESA–ECD copolymer (**4**)	46
QCD homopolymer (**2**), $n=100$	30
QCD–ESA–QCD copolymer (**5**)	15

Figure 15 Polymers generated by ROMP inhibit fertilization. (a) The inhibitory potency of homopolymers conjugated with the peptide sequence QCD increases with polymer valency. Polymers functionalized with the noninteracting peptide ESA do not inhibit fertilization, as determined by the fertilization index (FI) and fertilization rate (FR). (b) A triblock copolymer consisting of terminal ECD and QCD peptide sequences and noninteracting peptide ESA inhibited fertilization with a potency similar to that of homopolymers of the same length. n.i., no inhibition.

peptides,[85] longer polymers (M:I 25) were internalized less efficiently. Given the ability to append other molecules to the polymer end group, these results demonstrate that ROMP can afford ATDs for delivering cargo to the interior of cells.

• *Receptor-mediated internalization of polymers*

The ability to track polymer movement within cells would constitute a critical advance in understanding and optimizing polymers as delivery agents. Ideally, imaging strategies that allow observation of polymer internalization should involve minimal sample manipulation to limit artifacts. Exploring how receptor-mediated uptake of polymers influences their trafficking in a complex physiological environment requires the synthesis of polymers possessing epitopes that bind to a specific receptor. Such compounds could be exploited to understand polymer internalization in live cells and also to direct polymers to specific cell types. To this end, ROMP has been used to generate polymers that display B-cell-receptor-specific epitopes. The incorporation of a masked terminal fluorophore[90] provides the means to visualize the process of polymer internalization in real time and in live cells.[91,92] The synthetic route utilizes a vinyl ether bearing an azide group as a terminator. The resulting end-functionalized polymer can undergo subsequent reaction with an alkyne-functionalized rhodamine dye using copper-catalyzed azide/alkyne cycloaddition (CuAAC, a reaction that is classified as click chemistry).[93,94]

To target the polymers to B cells that display a specific receptor, ROMP-derived polymers were functionalized with the immunogenic antigen 2,4-dinitrophenyllysine (DNP). These polymers bind to a cell line that displays a DNP-specific B-cell receptor (BCR).[95] Clustering of the BCR promotes B-cell activation and uptake of antigen. Binding and internalization of the polymer was shown to be receptor-mediated, as colocalization was observed with the polymer and a marker specific to the BCR (**Figure 17**). Because the fluorophore is masked until it encounters endosomal esterases,[91,92] fluorescence was observed only upon

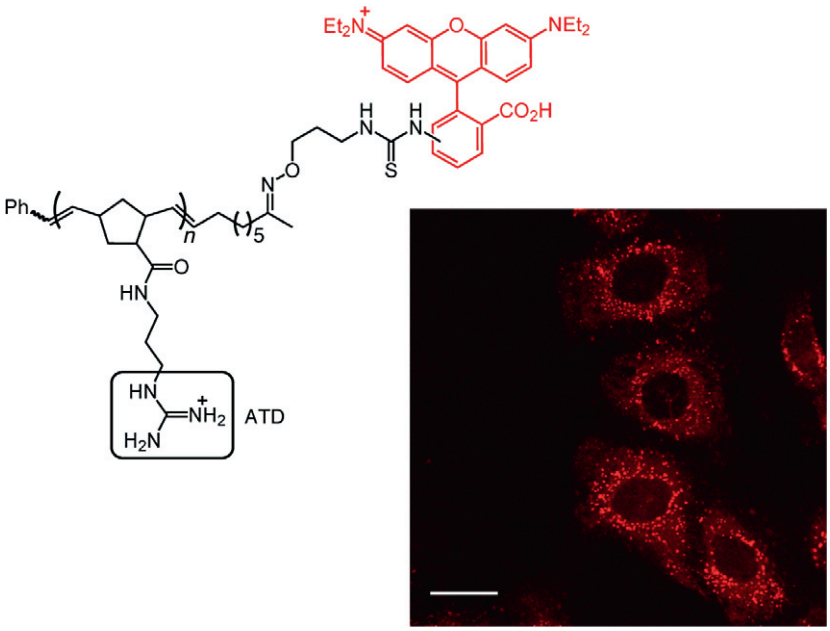

Figure 16 Polymers with ATDs can be generated by ROMP. The ATD promotes cellular internalization. HeLa cells were incubated with polymer and visualized by using confocal fluorescence microscopy. The polymeric ATD is seen in endocytic vesicles (punctate fluorescence) as well as in the cytoplasm (diffuse fluorescence). Scale = 25 μm.

polymer internalization. This feature of the probe eliminates the need for subsequent washing steps to eliminate background fluorescence. Thus, this strategy offers the benefit of monitoring polymer internalization and trafficking in real time and highlights the utility of end-capping strategies for incorporation of probes used in cellular imaging.

4.28.1.4.4 ROMP to generate polymers for probing cell signaling responses and mechanisms

- *Polymers as modulators of bacterial chemotaxis*

Polymers have been used to explore the sensory signaling cascade in bacteria that results in chemotaxis. The ability of a cell to sense and respond to extracellular signals is essential for its function and survival. Through 40 years of intensive study, the bacterial chemotaxis system has emerged as a paradigm for transmembrane signaling and molecular information processing.[96,97] In *Escherichia coli*, four primary ligand-binding membrane-bound chemoreceptors Tsr, Tar, Tap, and Trg mediate responses to a range of attractants including serine, aspartate, dipeptides, and glucose/galactose, respectively.[98,99] Upon binding their respective ligands, these receptors initiate a signaling process that ultimately controls whether bacteria move toward or away from the ligand. How bacteria can respond sensitively (e.g., to five molecules of attractant)[98] has been a mystery. A model was advanced proposing that bacterial chemoreceptors within the plasma membrane collaborate to amplify signals.[100] To test this hypothesis, Gestwicki *et al.*[101] synthesized a series of galactose-substituted polymers of increasing length. They postulated the galactose epitopes would serve as attractants and the polymer length variation would provide a means to cluster the chemoreceptors to different extents. The shortest polymer (M:I 10) had a potency similar to that of monovalent galactose but polymers generated using higher M:I ratios (e.g., 25:1) were about 100-fold more potent as attractants (Figure 18). These results imply that chemoreceptor–chemoreceptor interactions are important in signal transduction.

Bacteria cluster their chemoreceptors at the cell poles, and subsequent studies using polymers generated by ROMP revealed the importance of the chemoreceptor lattice.[102,103] Specifically, polymers were used to alter the organization of the chemoreceptor lattice. Interestingly, polymer treatment resulted in the amplification of signals to other attractants (serine or aspartate). These results emphasize that occupation of one receptor type can influence signaling from another. In *E. coli* this effect is important only for attractant and not for repellent signaling. When the repellent leucine is displayed on a polymer backbone (M:I of 50 or 100), it becomes an attractant (Figure 19(**a**)).[21] This intriguing result was hypothesized to result from loosening of the chemoreceptor lattice such that polymers functionalized with repellents disrupt preorganized lattice formation. Interestingly, monovalent repellents stabilize the chemoreceptor array (Figure 19(**b**)), but attractants appear to loosen it. Disrupting resting-state interactions present in unstimulated signaling complexes could be a general mechanism for activating cellular responses. Importantly, the ability of multivalent ligands to activate distinct signaling processes, relative to their monovalent counterparts, highlights the utility of ROMP-derived materials for exploring fundamental questions in cell biology.

- *Polymers as probes of immune signaling*

The ability of cell-surface receptors to recognize and respond to ligands provides impetus to discover natural or non-natural ligands that can be used to perturb or interrogate cell signaling. Because cells naturally encounter

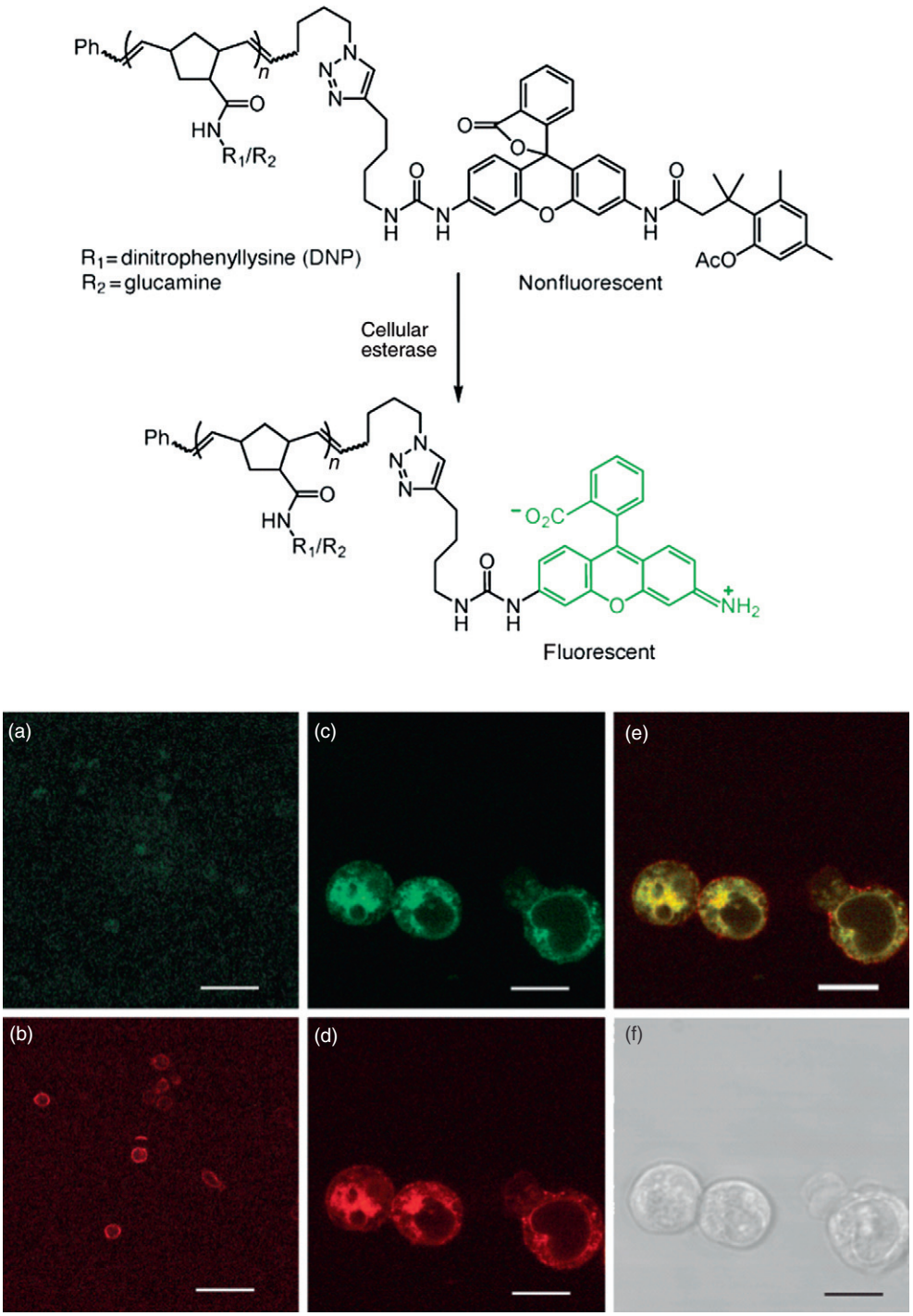

Figure 17 DNP-functionalized polymers synthesized by ROMP are taken up by cells via BCR-mediated endocytosis. To stain the DNP-specific BCR, cells were treated for 30 min with Cy3-conjugated anti-IgM. Rhodamine-labeled DNP-substituted polymer was added and images were acquired immediately without washing (a, b) or after 15 min (c, d). Panel (e) depicts data from the emission of both the Cy3 and rhodamine probes. Panel (f) is a bright field image of the B cells. Scale = 39 μm (a, b) and 10 μm (c–f).

multivalent displays in physiological settings, polymeric ligands can serve as excellent probes of biological responses. For example, the immune system employs multivalent interactions to initiate signaling events that lead to immunity or tolerance. B lymphocytes have a cell-surface receptor that senses antigen and directs responses toward antibody production (immunity) or anergy (tolerance).[102,104] B-cell responses to either foreign or self-antigens are elicited through a multiprotein complex containing a membrane-bound antibody termed the B-cell receptor (BCR). Engagement of the BCR by multivalent antigen can result in B-cell survival, proliferation, and differentiation or B-cell quiescence or programmed cell death.[105,106] A number of features of the antigen are thought to influence

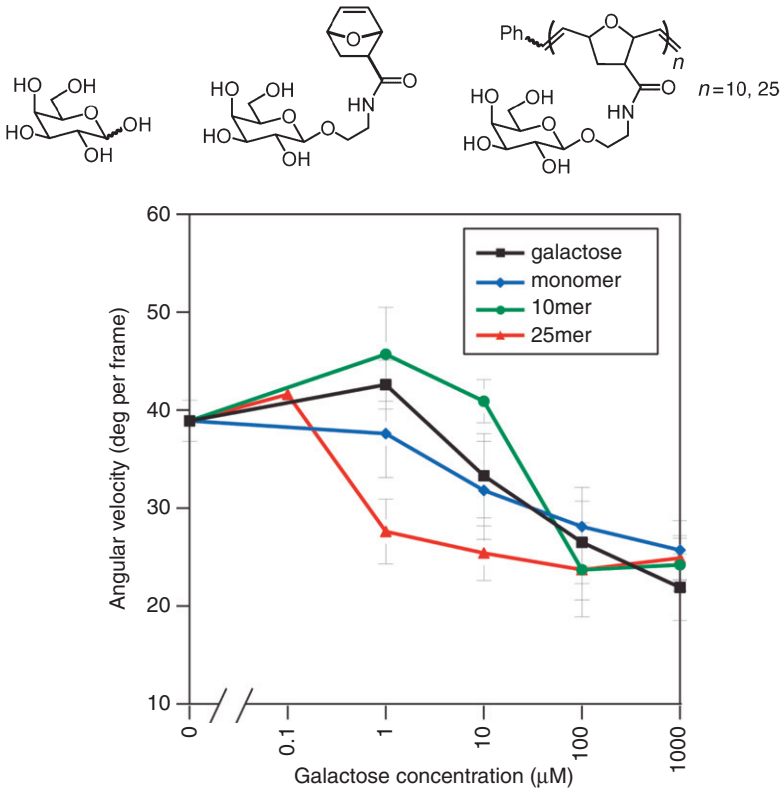

Figure 18 Galactose-substituted polymers generated by ROMP promote bacterial chemotaxis. Data are from *Escherichia coli* treated with galactose, monomer, or polymers (10mer or 25mer) at the given concentrations. A decrease in the mean angular velocity is indicative of a more potent chemoattractant.

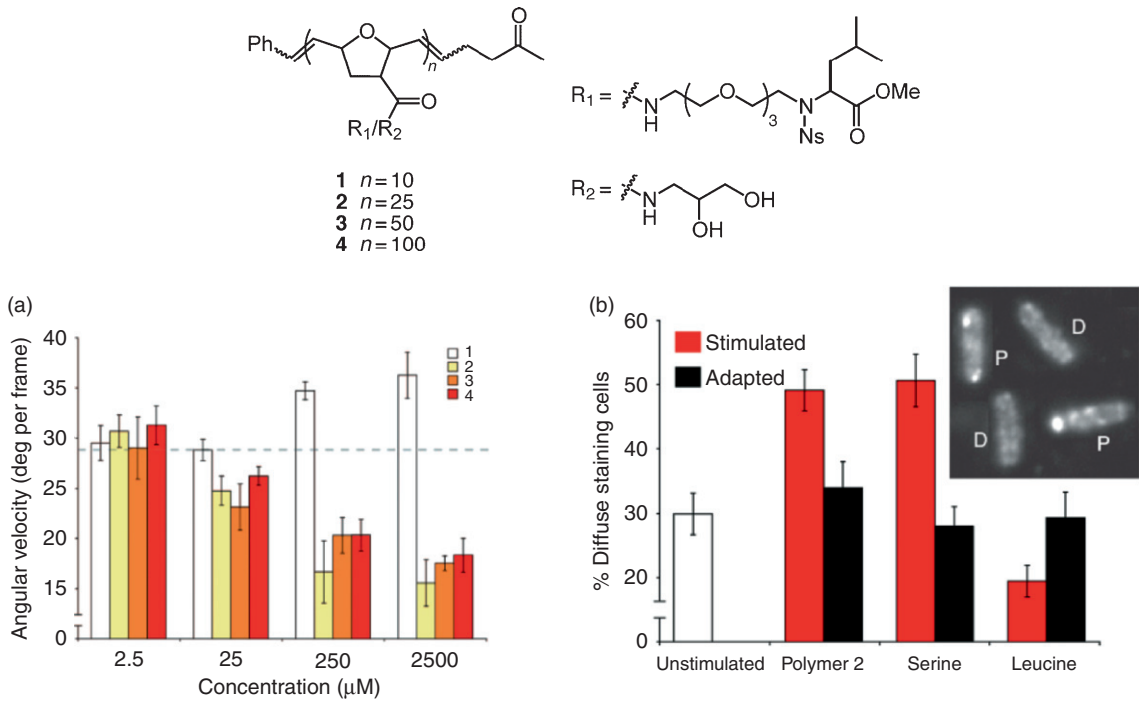

Figure 19 Polymers synthesized by ROMP to probe chemotactic responses of *Escherichia coli* to the repellent leucine. (a) Polymers **1** and **2** were sensed as repellents (increased angular velocity), but higher valency polymers (e.g., **3** and **4**) were sensed as attractants (lower angular velocity). The angular velocity of unstimulated cells is denoted by the dashed line. (b) Percentage of *E. coli* exhibiting diffuse staining when treated with chemostimulant addition. Adapted cells (black) were treated with 1 mM stimuli 5 min prior to fixation. The results indicate that leucine-substituted polymers induce a change in the localization of the chemoreceptors. By contrast, monovalent leucine stabilizes the chemoreceptor array. Inset: Example of cells displaying polar (P) or diffuse (D) staining of chemoreceptors.

signaling including its functional affinity (avidity), dose, and valency.

How antigen structure influences B-cell responses was examined using polymers synthesized by ROMP.[22] Polymers functionalized with the aforementioned DNP were evaluated for their ability to elicit anti-DNP antibody production in mice. Polymers of different valencies were used to interrogate the role of receptor clustering in B-cell activation. Animals treated with the highest valency polymer (M:I 500) exhibited DNP-specific antibody levels that were significantly higher than that achieved with the lower valency polymers (**Figure 20(a)**). These investigations indicate that polymers generated by ROMP could be used to activate signaling *in vivo* without causing toxicity.

One key manifestation of antigen-induced signaling in B cells is an increase in intracellular calcium ion concentration. Assessing the magnitude of changes in calcium ion concentration provides an insight into whether the observed valency-dependent differences in antibody production *in vivo* correlate with B-cell signaling. Accordingly, calcium flux was measured when cells were treated with polymers of different valency (**Figure 20(b)**). Intracellular calcium levels rose with longer length polymers, suggesting that higher valency polymers are more potent inducers of signaling. An unexpected finding of these studies, however, was that even the low-valency polymers activate signaling. Thus, differences in polymer activity cannot be attributed merely to whether they can contribute to signal amplification.[105]

The signal amplitude elicited by various multivalent ligands was related to their ability to promote BCR clustering (**Figure 21(a)**). A greater degree of clustering was observed in cells treated with the higher valency polymers (M:I 500) and the corresponding signal was high. Interestingly, the polymers could effect clustering of both occupied and unoccupied receptors, suggesting that BCR–BCR interactions can contribute to signal amplification (**Figure 21(b)**). Intriguingly, the influence of ligand valency on receptor clustering and the magnitude of output responses were similar in the unrelated processes of bacterial chemotaxis and B-cell signaling. These data suggest that there may be similarities in how responses to low concentrations of signals are amplified. Moreover, the data indicate that ROMP can be used to generate polymers that elicit specific cellular responses both *in vitro* and *in vivo*.

• *Signaling polymers that cluster multiple types of receptors*

B-cell signaling events critical for immune system regulation often rely not only on the BCR but also on coreceptors. Coreceptors add context to BCR responses to antigen by either augmenting or diminishing B-cell activation. They therefore are critical for the ability of cells to respond appropriately to foreign and self-antigens.[107,108] An important coreceptor on B cells is CD22 (Siglec-2), which acts to suppress B-cell activation. CD22 binds glycoconjugates possessing terminal sialic acid residues.[109] Glycoconjugates of this type are present on some antigens, and they are also abundant on the glycans that

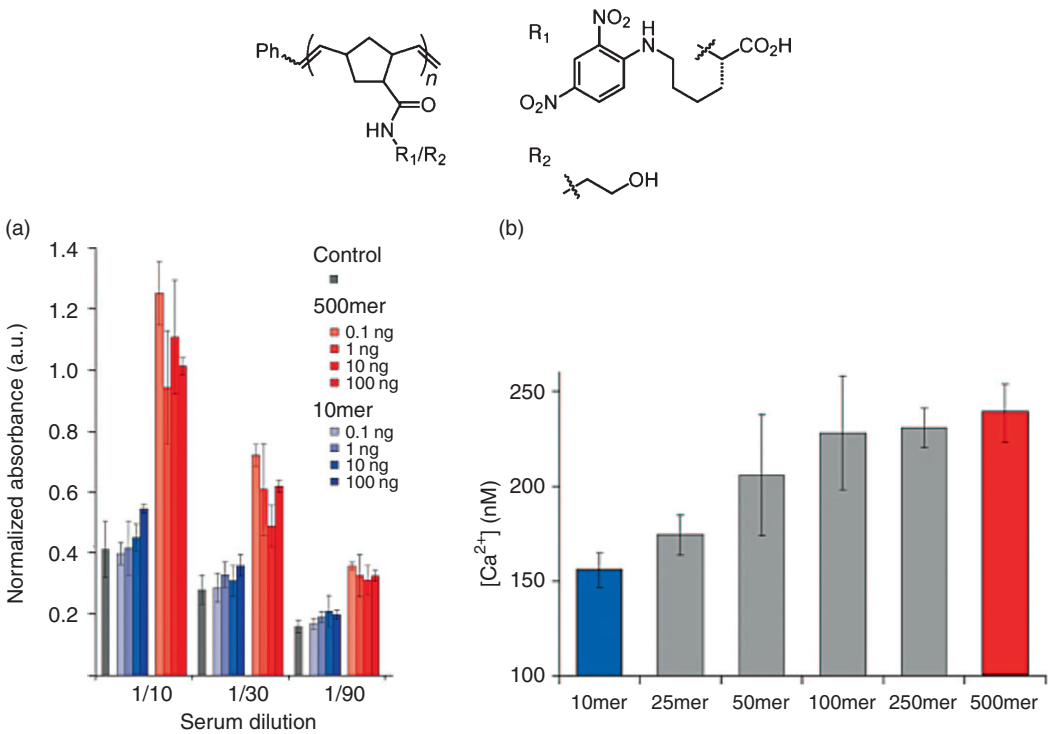

Figure 20 Polymers generated by ROMP elicit antibody production *in vivo*. (a) The levels of anti-DNP antibodies in BALB/c mice were determined 15 days after the injection of synthetic multivalent ligands. The higher valency polymer (500mer, red) induced production of DNP-specific IgM antibodies, but the 10mer (blue) did not. (b) Changes in calcium concentration induced by multivalent ligands. An increase in calcium flux was observed for higher valency polymers.

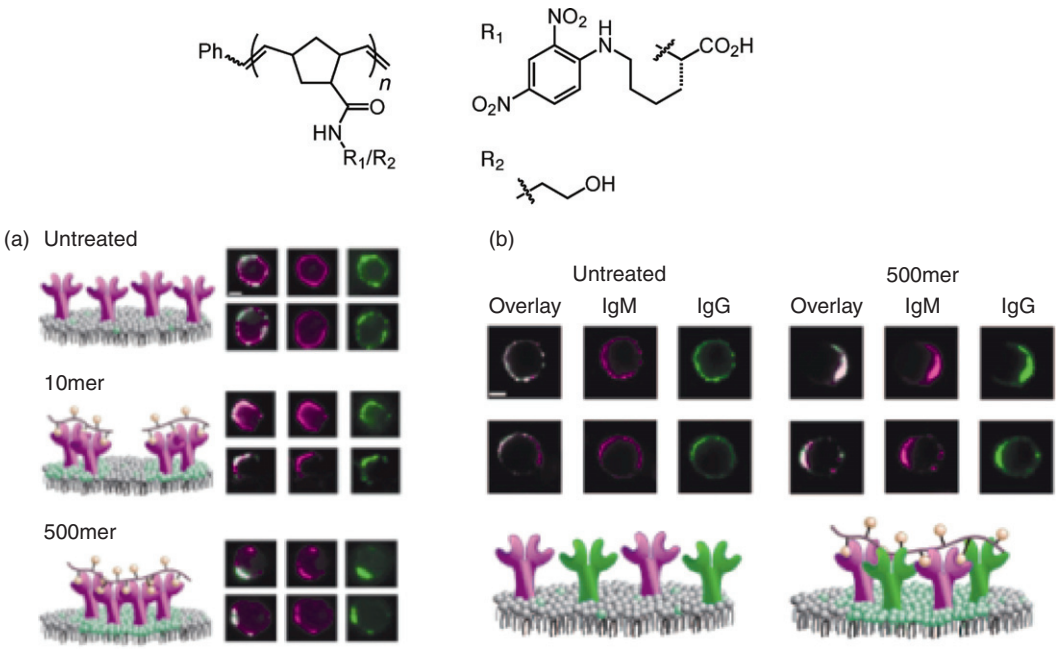

Figure 21 Bioactive polymers induce BCR clustering. (a) Visualization of B-cell receptor (BCR) in untreated cells or cells treated with DNP-substituted polymers (10mer or 500mer). BCR clustering is more pronounced in cells treated with high valency polymers. (b) Polymers cluster both ligated and unligated receptors. DNP-specific BCR (IgM) and unliganded BCR (IgG) colocalize and cluster in the presence of polymers.

reside on the B-cell surface.[110,111] Accordingly, interactions of CD22 with cell-surface glycoproteins (*cis* interactions) might sequester it from interacting with glycosylated antigens (*trans* interactions).

While the importance of *cis* interactions in the modulation of immunity has been established,[110] the functional role of *trans* interactions was unclear. Polymers generated by ROMP were used to investigate whether *trans* interactions could recruit CD22 to modulate BCR signaling.[112] As mentioned previously, a hallmark of B-cell activation and signaling is the increase in intracellular calcium ion concentration. As expected, homopolymers (M:I 250) decorated with DNP epitopes resulted in B-cell activation. Homopolymers presenting a trisaccharide CD22 ligand (M:I 250), however, did not bind because of masking by *cis* interactions (**Figure 22(a)**). By contrast, a copolymer consisting of DNP and CD22 could bind and colocalize both CD22 and the BCR. Interestingly, this copolymer attenuates B-cell signaling, indicating that CD22 can function in *trans* (**Figure 22(b)**). These findings suggest that immune responses to glycosylated antigens that can bind CD22 will be suppressed; therefore, they highlight a new role for antigen glycosylation. Together, these studies underscore the value and versatility of ROMP for generating polymers that can elicit biological responses by assembling multiple types of proteins.

4.28.1.4.5 Block copolymers

- *Potential for polymeric micelles in imaging*

Probes for optical imaging of tumor cells can facilitate the noninvasive diagnosis of cancer progression.[113] Polymers can be especially useful for imaging tumor cells because of their preferential accumulation in solid tumors due to the EPR effect.[4] The extent of polymer localization within the tumor microenvironment is dramatically affected by many factors including polymer charge,[53,114] molecular weight,[115,116] and solution conformation.[117] One effective strategy for targeting tumor cells has been to use amphiphilic assemblies, such as liposomes[118,119] or micelles,[120,121] suggesting that imaging agents with these architectures might be valuable.

To this end, the Grubbs group has used ROMP to generate amphiphilic block copolymers bearing fluorine-18 for positron emission tomography (PET) imaging.[2] Norbornene-imide monomers bearing a cinnamoyl group were used as building blocks because photo-cross-linking could be used after polymerization to impart stability to the micelle. Monomers bearing oligoethylene glycol units with terminal mesylate groups were used to generate a second block. The mesylate group serves as a reactive handle for subsequent fluorine-18 incorporation. The functionalized PEG chains are biocompatible and block copolymers were assembled using catalyst **9** to afford amphiphilic micelles. The hydrodynamic radius of the polymers was readily controlled by varying the monomer to catalyst ratios (**Figure 23**). Late-stage installation of fluorine-18 provided the means to generate polymers that can be used in PET imaging. This study highlights the versatility of ROMP for controlling the size of block copolymer assemblies. It will be interesting to determine the utility of the different-sized macromolecular aggregates in tumor imaging.

- *Polymers generated by ROMP localize to tumors*

Miki *et al.*[122] have implemented ROMP to generate amphiphilic copolymers equipped with near-infrared dyes for *in vivo* tumor imaging. Their probes are based on triblock copolymers consisting of hydrophobic, hydrophilic, and dye segments (**Figure 24**). Norbornadiene monomers were used in the polymerization, and the resulting polymers were rendered water soluble through subsequent dihydroxylation of the polymer

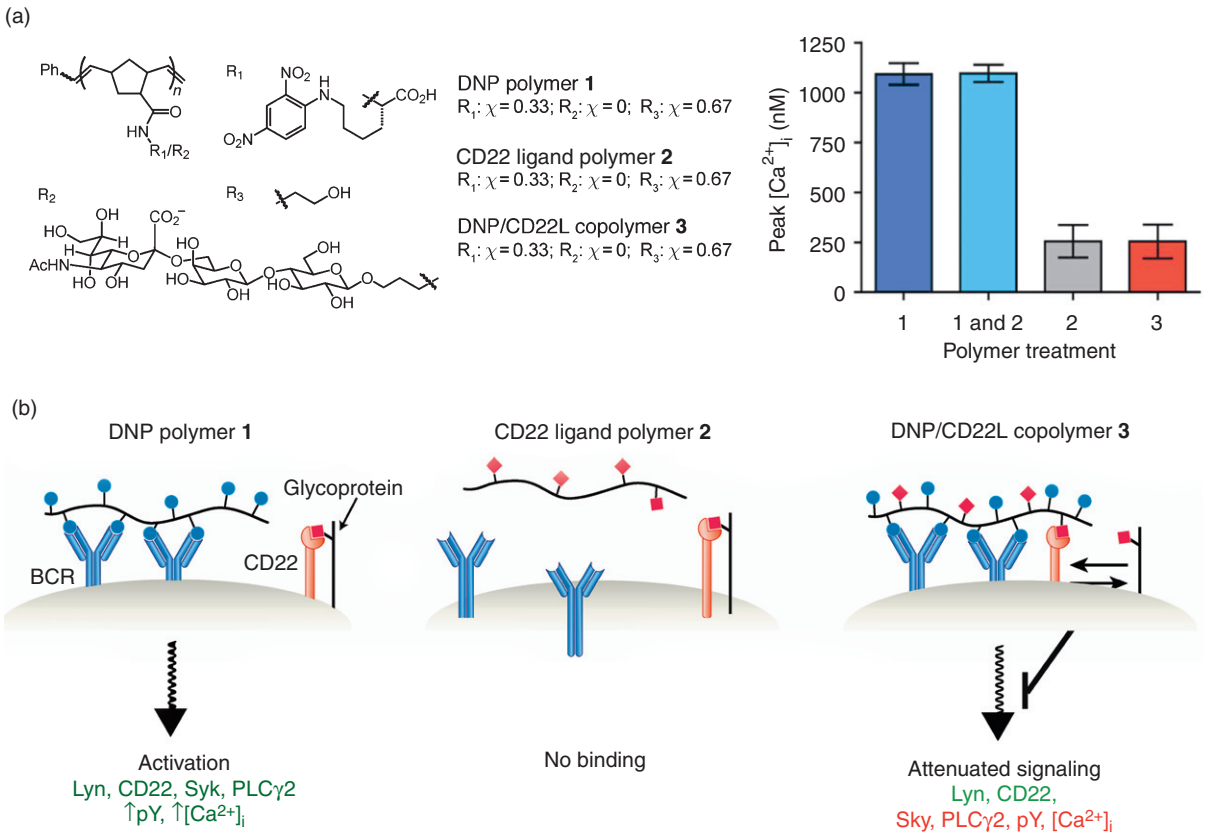

Figure 22 Polymers synthesized by ROMP can bind simultaneously to the BCR and the inhibitory coreceptor CD22 and attenuate cell activation. (a) The ability of polymers **1**–**3** to bind to the BCR and activate signaling (calcium flux, right). DNP homopolymers (1) activate signaling, but copolymers (3) that bind both the BCR and CD22 inhibit B-cell activation. (b) Schematic depiction of the recognition processes that lead to activation (green) or inhibition (red) of B-cell signaling. The activation process involves upregulation of intracellular Ca^{2+} and tyrosine phosphorylation (as represented by the upward arrow).

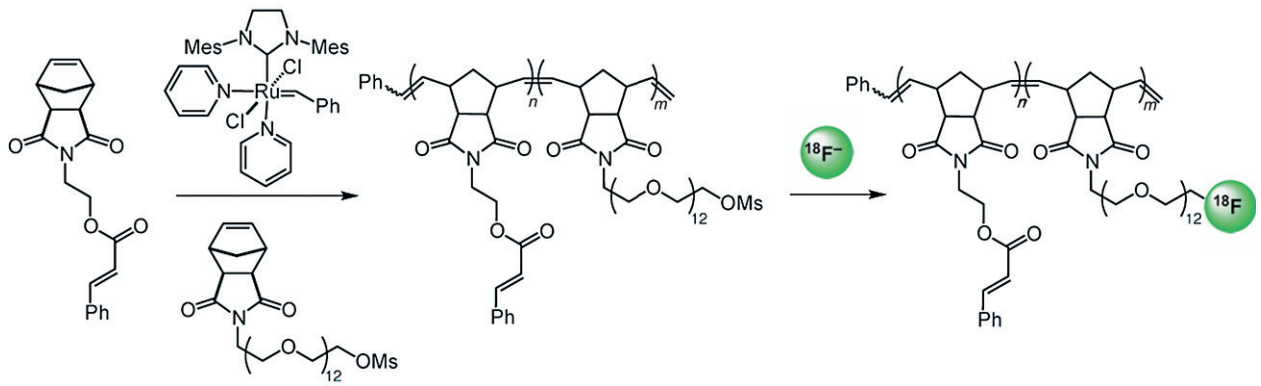

Figure 23 Amphiphilic block copolymers that incorporate fluorine-18 for PET imaging. Ms, mesylate.

backbone. The triblock copolymers form micelles with low critical micelle concentration values, indicating that the self-assembled block copolymers are stable in aqueous solution. When mice were injected with the copolymers, the imaging agents accumulated in the tumors and were observable for 2 weeks. The authors speculate that the long retention time in the tumor is a result of the stability of the polymer assemblies. This study provides another example of *in vivo* use for polymers generated by ROMP.

• *Block copolymers for drug delivery*

Bertin *et al.*[123] used ROMP to synthesize amphiphilic copolymers that function as both targeting and drug delivery agents. Copolymers were generated using a monomer possessing ethylene glycol units bearing tosyl groups and another conjugated to the nonsteroidal anti-inflammatory drug indomethacin. This drug has shown anticancer activity and the authors wanted to deliver it to tumor cells (**Figure 25**). The amphiphilic block copolymers produced form micelles in aqueous media, such

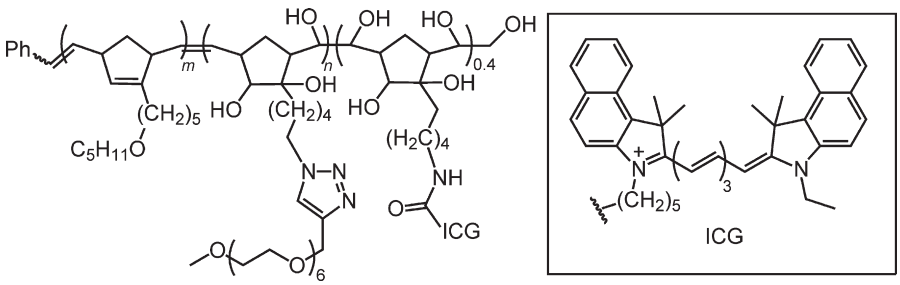

Figure 24 Triblock copolymer synthesized for *in vivo* tumor imaging. ICG, indocyanine green.

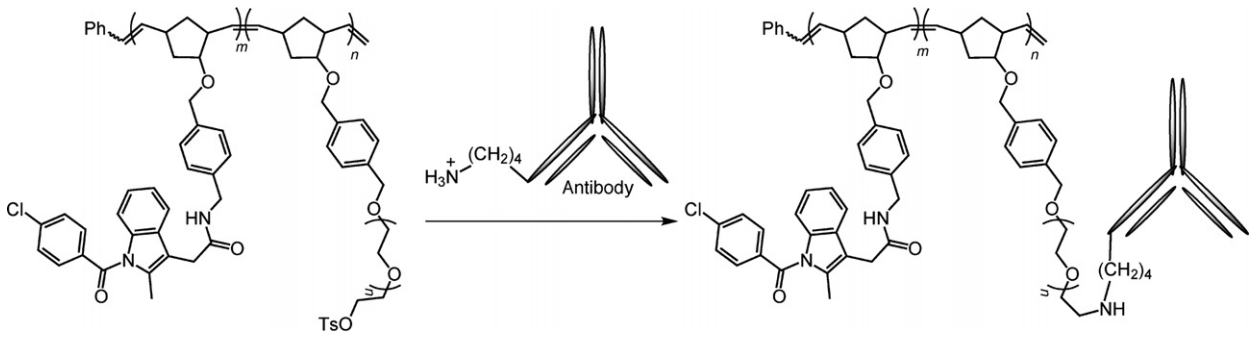

Figure 25 Amphiphilic copolymer for tumor targeting and drug delivery. Antibodies targeted to the human epidermal growth factor receptor-2 (HER-2) on cancer cells were appended to the polymer through conjugation of exposed lysine residues. The conjugates are taken up in cancer cells. Ts, tosyl.

that the hydrophobic drug is sequestered in the lipophilic core of the nanoparticle while the tosyl groups are exposed on the surface. The tosyl groups could be displaced to append antibodies that recognize the transmembrane human epidermal growth factor receptor-2 (HER-2), a receptor upregulated in cancer cells. The macromolecular conjugates were tested for internalization by the human breast carcinoma cell line SKBR3. The functionalized block copolymer assemblies were taken up efficiently, and internalization depended on antibody conjugation. These data indicate that the uptake of these micelles depended upon their ability to interact with an endocytic receptor. Thus, ROMP can be used to generate polymers that present both targeting groups and chemotherapeutic agents and such conjugates may lead to new types of polymer-based chemotherapeutics.

- *Copolymers as antimicrobial agents*

The ability of an organism to sense and respond to bacterial infection is an important line of defense in innate immunity. When organisms are invaded by pathogens, natural antimicrobial peptides (AMPs) are produced, which confer a level of protection for the host and are among the first class of compounds produced after infection.[124] A common feature of most antimicrobial peptides is their positive charge and facial amphiphilicity, which are thought to be important for insertion into the negatively charged membrane of various pathogenic organisms.[125] This insertion causes membrane reorganization and disruption, which ultimately leads to pore formation and cell lysis.[126] Because of the differences in the surfaces of bacterial and mammalian cells, AMPs can selectively attack bacteria within a host organism. Moreover, resistance to AMPs is much harder to evolve than antibiotic resistance;[127] consequently, the development of polymers that recapitulate the features of AMPs could yield antimicrobial agents.

Researchers have sought to mimic the molecular architecture and activity of AMPs using synthetic polymers.[128–131] Lienkamp *et al.*[128] have used ROMP to generate synthetic mimics of antimicrobial peptides (SMAMPs). Homopolymers functionalized with both hydrophobic and hydrophilic moieties were designed to mimic the natural amphiphilicity of AMPs. In addition, the effect of size and hydrophobicity of the polymers on their antibacterial activity and selectivity toward the growth of the bacteria *E. coli* and *Staphylococcus aureus* and on their hemolytic activity toward red blood cells was assessed (**Figure 26**). Homopolymers functionalized with the less hydrophobic methyl esters were inactive and nonhemolytic for *S. aureus* and *E. coli* as well as red blood cells. The highest antibacterial activity was obtained with polymers possessing propyl substituents; these compounds had a minimum inhibitory concentration for 90% bacterial killing (MIC_{90}) of 6.25 μm ml^{-1} for *E. coli* and 15 μm ml^{-1} for *S. aureus*. The activity of more hydrophobic polymers was decreased ($MIC_{90} > 200$ μm ml^{-1}). Hemolytic activity, however, increased with increasing hydrophobicity of the polymers ($HC_{50} < 50$ μg ml^{-1}). Interestingly, the molecular weight of the polymers was shown to affect the growth of *E. coli* and *S. aureus*. Oligomers and low-molecular weight polymers (3k) were shown to have antibacterial activity against *S. aureus* but little activity against *E. coli*. Conversely, higher molecular weight polymers (10k) were more active against *E. coli* than *S. aureus*. Thus, an optimal balance of amphiphilicity and

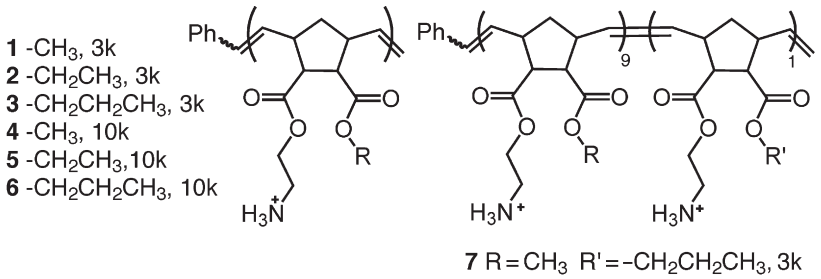

	MIC_{90} ($\mu g\,ml^{-1}$)		HC_{50} ($\mu g\,ml^{-1}$)	Selectivity	
Compound	*E. coli*	*S. aureus*		*E. coli*	*S. aureus*
1	>200	100	2000	<10	20
2	50	50	1400	28	28
3	6.25	15	50	8.3	3.3
4	>200	>200	50	<10	<10
5	>200	>200	1250	<6.3	<6.3
6	3.75	200	<50	13	<0.25
7	>200	<3.75	>200	10	>533

Figure 26 Polymers generated by ROMP can function as antimicrobial agents. The minimal inhibitory concentration that prevents 90% bacterial growth (MIC_{90}) and hemolytic activity toward red blood cells (HC_{50} = concentration that promotes lysis of 50% of red blood cells) were assessed for each compound. Selectivity is defined by the ratio of HC_{50}/MIC_{90}. 3k and 10k refer to polymers with molecular weights of 3000 and 10 000 g mol^{-1}, respectively.

molecular weight of the polymers influences their antibacterial activity and selectivity.

Greater selectivity for antimicrobial activity over hemolysis led to the synthesis of copolymers. The combination of an inactive and nonhemolytic block with an active and hemolytic block afforded copolymers that were 533-fold more selective for bacteria over red blood cells and 50-fold more selective for *S. aureus* over *E. coli*. Thus, tuning the overall hydrophobicity and charge density of the polymers afforded polymer selectivity. These results indicate that polymers generated by ROMP can function as potent and selective antimicrobial agents.

• *Copolymers possessing an intracellular delivery block*

Applications of block copolymers typically result from imbuing each block with distinct properties (e.g., hydrophobicity or hydrophilicity) such that the resulting polymer can form a macromolecular assembly. Biologically active block copolymers that could be designed in which each domain serves a distinct biological function would prove valuable. For instance, a strategy in which one block could serve as an internalization component for cellular uptake of polymers would be valuable. Kolonko *et al.*[132] devised a strategy in which one block was designed to function as an ATD (see Section 4.28.1.4.3). Specifically, they used ROMP to control block length and thereby installed a short block displaying guanidinium groups that facilitates uptake (Figure 27). The block copolymer was internalized with localization in both vesicles and the cytoplasm. A homopolymer lacking the ATD failed to undergo internalization. These data reveal that the ATD can promote uptake of block copolymers. This strategy can yield cell-permeable bioactive polymers.

4.28.1.5 Conclusions

ROMP can be used to construct polymers for diverse biological applications. Advances in design are affording new catalysts with exceptional chemoselectivity. Thus, even more complex polymers can be assembled. In addition, catalysts and conditions can be devised to vary polymer structure and thereby optimize polymer function. To date, ROMP has been used to generate polymers with diverse functions, including inhibitors of receptor–ligand interactions, novel drug delivery agents, innovative imaging agents, and incisive mechanistic probes of multivalent interactions. Ligands generated by ROMP have been applied to illuminate the role of receptor organization in bacterial chemotaxis and cell-mediated immunity. Indeed, applications of ROMP are providing new materials for understanding and tuning biological responses. Further advances in ROMP will undoubtedly fuel new and imaginative applications of bioactive polymers.

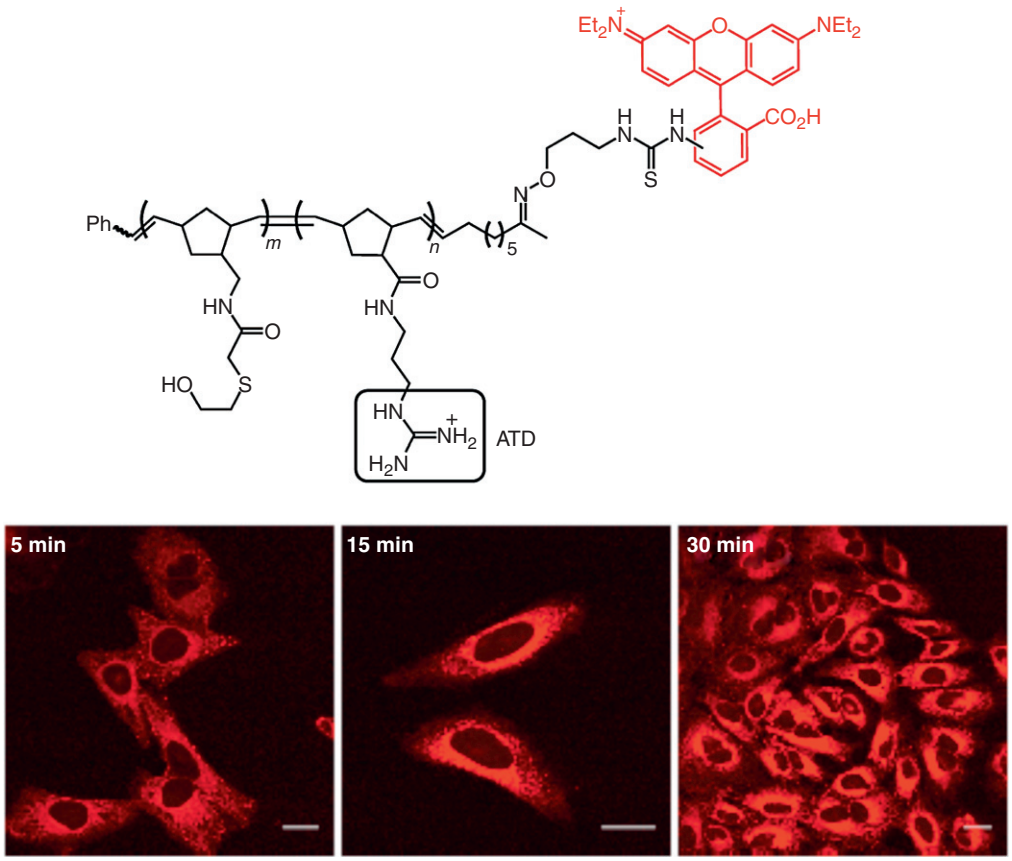

Figure 27 Block copolymers in which one block serves as an ATD can be internalized by cells. Fluorescence microscopic images of live HeLa cells incubated with the rhodamine-labeled polymer for varying time points at 37 °C are shown. The block copolymer localizes in both endocytic vesicles (punctate staining) and the cytoplasm (diffuse fluorescence). Scale = 25 μm.

References

1. Allen, M. J.; Raines, R. T.; Kiessling, L. L. *J. Am. Chem. Soc.* **2006**, *128*, 6534.
2. Matson, J. B.; Grubbs, R. H. *J. Am. Chem. Soc.* **2008**, *130*, 6731.
3. Duncan, R. *Nat. Rev. Drug Discov.* **2003**, *2*, 347.
4. Maeda, H.; Wu, J.; Sawa, T.; *et al. J. Control. Release* **2000**, *65*, 271.
5. Mammen, M.; Choi, S. K.; Whitesides, G. M. *Angew. Chem. Int. Ed.* **1998**, *37*, 2755.
6. Kiessling, L. L.; Gestwicki, J. E.; Strong, L. E. *Angew. Chem. Int. Ed.* **2006**, *45*, 2348.
7. Schwab, P.; Grubbs, R. H.; Ziller, J. W. *J. Am. Chem. Soc.* **1996**, *118*, 100.
8. Schrock, R. R. *Tetrahedron* **1999**, *55*, 8141.
9. Herisson, J.-L.; Chauvin, Y. *Makromol. Chem.* **1971**, *141*, 161.
10. Bielawski, C. W.; Grubbs, R. H. *Prog. Polym. Sci.* **2007**, *32*, 1.
11. Novak, B. M.; Grubbs, R. H. *J. Am. Chem. Soc.* **1988**, *110*, 7542.
12. Novak, B. M.; Grubbs, R. H. *J. Am. Chem. Soc.* **1988**, *110*, 960.
13. Schrock, R. R.; Hoveyda, A. H. *Angew. Chem. Int. Ed.* **2003**, *42*, 4592.
14. Camm, K. D.; Castro, N. M.; Liu, Y. W.; *et al. J. Am. Chem. Soc.* **2007**, *129*, 4168.
15. Trnka, T. M.; Grubbs, R. H. *Acc. Chem. Res.* **2001**, *34*, 18.
16. Mowery, P.; Yang, Z. Q.; Gordon, E. J.; *et al. Chem. Biol.* **2004**, *11*, 725.
17. Lee, Y.; Sampson, N. S. *Curr. Opin. Struct. Biol.* **2006**, *16*, 544.
18. Bertin, P. A.; Smith, D. D.; Nguyen, S. T. *Chem. Commun.* **2005**, 3793.
19. Kiessling, L. L.; Pohl, N. L. *Chem. Biol.* **1996**, *3*, 71.
20. Lienkamp, K.; Tew, G. N. *Chem. Eur. J.* **2009**, *15*, 11784.
21. Borrok, M. J.; Kolonko, E. M.; Kiessling, L. L. *ACS Chem. Biol.* **2008**, *3*, 101.
22. Puffer, E. B.; Pontrello, J. K.; Hollenbeck, J. J.; *et al. ACS Chem. Biol.* **2007**, *2*, 252.
23. Nguyen, S. T.; Grubbs, R. H.; Ziller, J. W. *J. Am. Chem. Soc.* **1993**, *115*, 9858.
24. Nomura, K.; Schrock, R. R. *Macromolecules* **1996**, *29*, 540.
25. Mortell, K. H.; Weatherman, R. V.; Kiessling, L. L. *J. Am. Chem. Soc.* **1996**, *118*, 2297.
26. Burtscher, D.; Grela, K. *Angew. Chem. Int. Ed.* **2009**, *48*, 442.
27. Zaman, S.; Curnow, O. J.; Abell, A. D. *Aust. J. Chem.* **2009**, *62*, 91.
28. Mohr, B.; Lynn, D. M.; Grubbs, R. H. *Organometallics* **1996**, *15*, 4317.
29. Gallivan, J. P.; Jordan, J. P.; Grubbs, R. H. *Tetrahedron Lett.* **2005**, *46*, 2577.
30. Binder, J. B.; Guzei, I. A.; Raines, R. T. *Adv. Synth. Catal.* **2007**, *349*, 395.
31. Roberts, A. N.; Cochran, A. C.; Rankin, D. A.; *et al. Organometallics* **2007**, *26*, 6515.
32. Lynn, D. M.; Mohr, B.; Grubbs, R. H.; *et al. J. Am. Chem. Soc.* **2000**, *122*, 6601.
33. Lynn, D. M.; Kanaoka, S.; Grubbs, R. H. *J. Am. Chem. Soc.* **1996**, *118*, 784.
34. Fraser, C.; Grubbs, R. H. *Macromolecules* **1995**, *28*, 7248.
35. Manning, D. D.; Strong, L. E.; Hu, X.; *et al. Tetrahedron* **1997**, *53*, 11937.
36. Pohl, N. L.; Kiessling, L. L. *Synthesis* **1999**, 1515.
37. Gordon, E. J.; Strong, L. E.; Kiessling, L. L. *Bioorg. Med. Chem.* **1998**, *6*, 1293.
38. Manning, D. D.; Hu, X.; Beck, P.; Kiessling, L. L. *J. Am. Chem. Soc.* **1997**, *119*, 3161.
39. Gordon, E. J.; Sanders, W. J.; Kiessling, L. L. *Nature* **1998**, *392*, 30.
40. Sanders, W. J.; Gordon, E. J.; Dwir, O.; *et al. J. Biol. Chem.* **1999**, *274*, 5271.
41. Arimoto, H.; Nishimura, K.; Kinumi, T.; *et al. Chem. Commun.* **1999**, 1361.
42. Kanai, M.; Mortell, K. H.; Kiessling, L. L. *J. Am. Chem. Soc.* **1997**, *119*, 9931.
43. Rawat, M.; Gama, C. I.; Matson, J. B.; Hsieh-Wilson, L. C. *J. Am. Chem. Soc.* **2008**, *130*, 2959.
44. Slugovc, C. *Macromol. Rapid Commun.* **2004**, *25*, 1283.
45. Maynard, H. D.; Okada, S. Y.; Grubbs, R. H. *Macromolecules* **2000**, *33*, 6239.
46. Barrett, A. G. M.; Hopkins, B. T.; Kobberling, J. *Chem. Rev.* **2002**, *102*, 3301.
47. Gauthier, M. A.; Gibson, M. I.; Klok, H. A. *Angew. Chem. Int. Ed.* **2009**, *48*, 48.
48. Pontrello, J. K.; Allen, M. J.; Underbakke, E. S.; Kiessling, L. L. *J. Am. Chem. Soc.* **2005**, *127*, 14536.
49. Haag, R.; Kratz, F. *Angew. Chem. Int. Ed.* **2006**, *45*, 1198.

50. Torchilin, V. P. *Pharm. Res.* **2007**, *24*, 1.
51. Farokhzad, O. C.; Langer, R. *ACS Nano* **2009**, *3*, 16.
52. Shenhar, R.; Norsten, T. B.; Rotello, V. M. *Adv. Mater.* **2005**, *17*, 657.
53. Christie, R. J.; Grainger, D. W. *Adv. Drug Deliv. Rev.* **2003**, *55*, 421.
54. Hadjichristidis, N.; Pitsikalis, M.; Iatrou, H. *Adv. Polym. Sci.* **2005**, *189*, 1–124.
55. Risse, W.; Grubbs, R. H. *Macromolecules* **1989**, *22*, 1558.
56. Yin, R.; Amis, E. J.; Hognesch, T. E. *Macromol. Symp.* **1994**, *85*, 217.
57. Smith, D.; Clark, S. H.; Bertin, P. A.; *et al. J. Mater. Chem.* **2009**, *19*, 2159.
58. Ladmiral, V.; Mantovani, G.; Clarkson, G. J.; *et al. J. Am. Chem. Soc.* **2006**, *128*, 4823.
59. Hilf, S.; Kilbinger, A. F. M. *Nat. Chem.* **2009**, *1*, 537.
60. Murphy, J. J.; Nomura, K. *Chem. Commun.* **2005**, 4080.
61. Owen, R. M.; Gestwicki, J. E.; Young, T.; Kiessling, L. L. *Org. Lett.* **2002**, *4*, 2293.
62. Yang, Z. Q.; Puffer, E. B.; Pontrello, J. K.; Kiessling, L. L. *Carbohydr. Res.* **2002**, *337*, 1605.
63. Kolonko, E. M.; Kiessling, L. L. *J. Am. Chem. Soc.* **2008**, *130*, 5626.
64. Hilf, S.; Grubbs, R. H.; Kilbinger, A. F. *J. Am. Chem. Soc.* **2008**, *130*, 11040.
65. Hilf, S.; Grubbs, R. H.; Kilbinger, A. F. M. *Macromolecules* **2008**, *41*, 6006.
66. Hilf, S.; Kilbinger, A. F. M. *Macromolecules* **2009**, *42*, 4127.
67. Perrier, S.; Wang, X. S. *Nature* **2007**, *445*, 271.
68. Mortell, K. H.; Gingras, M.; Kiessling, L. L. *J. Am. Chem. Soc.* **1994**, *116*, 12053.
69. Weatherman, R. V.; Mortell, K. H.; Chervenak, M.; *et al. Biochemistry* **1996**, *35*, 3619.
70. McEver, R. P. *Curr. Opin. Cell Biol.* **2002**, *14*, 581.
71. Rosen, S. D. *Annu. Rev. Immunol.* **2004**, *22*, 129.
72. Murrey, H. E.; Hsieh-Wilson, L. C. *Chem. Rev.* **2008**, *108*, 1708.
73. Deepa, S. S.; Umehara, Y.; Higashiyama, S.; *et al. J. Biol. Chem.* **2002**, *277*, 43707.
74. Esko, J. D.; Selleck, S. B. *Annu. Rev. Biochem.* **2002**, *71*, 435.
75. Miranti, C. K.; Brugge, J. S. *Nat. Cell Biol.* **2002**, *4*, E83.
76. Garanger, E.; Boturyn, D.; Coll, J. L.; *et al. Org. Biomol. Chem.* **2006**, *4*, 1958.
77. Mousa, S. A. *Curr. Opin. Chem. Biol.* **2002**, *6*, 534.
78. Maynard, H. D.; Okada, S. Y.; Grubbs, R. H. *J. Am. Chem. Soc.* **2001**, *123*, 1275.
79. Carlson, C. B.; Mowery, P.; Owen, R. M.; *et al. ACS Chem. Biol.* **2007**, *2*, 119.
80. Giancotti, F. G.; Ruoslahti, E. *Science* **1999**, *285*, 1028.
81. Cuasnicu, P. S.; Ellerman, D. A.; Cohen, D. J.; *et al. Arch. Med. Res.* **2001**, *32*, 614.
82. Lee, Y.; Sampson, N. S. *ChemBioChem* **2009**, *10*, 929.
83. Torchilin, V. P. *Adv. Drug Deliv. Rev.* **2006**, *58*, 1532.
84. Kazunori, K.; Glenn, K. S.; Masayuki, Y.; *et al. J. Control. Release* **1993**, *24*, 119.
85. Goun, E. A.; Pillow, T. H.; Jones, L. R.; *et al. ChemBioChem* **2006**, *7*, 1497.
86. Okuyama, M.; Laman, H.; Kingsbury, S. R.; *et al. Nat. Methods* **2007**, *4*, 153.
87. Qian, Z. M.; Li, H.; Sun, H.; Ho, K. *Pharmacol. Rev.* **2002**, *54*, 561.
88. Tyagi, M.; Rusnati, M.; Presta, M.; Giacca, M. *J. Biol. Chem.* **2001**, *276*, 3254.
89. Kalia, J.; Raines, R. T. *Angew. Chem. Int. Ed.* **2008**, *47*, 7523.
90. Mangold, S. L.; Carpenter, R. T.; Kiessling, L. L. *Org. Lett.* **2008**, *10*, 2997.
91. Lavis, L. D.; Chao, T. Y.; Raines, R. T. *ACS Chem. Biol.* **2006**, *1*, 252.
92. Lavis, L. D.; Chao, T. Y.; Raines, R. T. *ChemBioChem* **2006**, *7*, 1151.
93. Meldal, M.; Tornoe, C. W. *Chem. Rev.* **2008**, *108*, 2952.
94. Kolb, H. C.; Finn, M. G.; Sharpless, K. B. *Angew. Chem. Int. Ed.* **2001**, *40*, 2004.
95. Sato, K.; Ochi, A. *Immunol. Lett.* **1998**, *61*, 135.
96. Adler, J. *Annu. Rev. Biochem.* **1975**, *44*, 341.
97. Baker, M. D.; Wolanin, P. M.; Stock, J. B. *BioEssays* **2006**, *28*, 9.
98. Jasuja, R.; Lin, Y.; Trentham, D. R.; Khan, S. *Proc. Natl. Acad. Sci. U.S.A.* **1999**, *96*, 11346.
99. Mesibov, R.; Adler, J.*J. Bacteriol.* **1972**, *112*, 315.
100. Bray, D.; Levin, M. D.; Morton-Firth, C. J. *Nature* **1998**, *393*, 85.
101. Gestwicki, J. E.; Strong, L. E.; Kiessling, L. L. *Chem. Biol.* **2000**, *7*, 583.
102. Goodnow, C. C. *Proc. Natl. Acad. Sci. U.S.A.* **1996**, *93*, 2264.
103. Gestwicki, J. E.; Kiessling, L. L. *Nature* **2002**, *415*, 81.
104. Healy, J. I.; Goodnow, C. C. *Annu. Rev. Immunol.* **1998**, *16*, 645.
105. Dintzis, H. M.; Dintzis, R. Z.; Vogelstein, B. *Proc. Natl. Acad. Sci. U.S.A.* **1976**, *73*, 3671.
106. Goldsby, R. A.; Kindt, T. J.; Osborne, B. A. *Immunology (Kuby)*, 4th ed.; W.H. Freeman and Co.: New York, NY, 2000.
107. Crocker, P. R.; Paulson, J. C.; Varki, A. *Nat. Rev. Immunol.* **2007**, *7*, 255.
108. Iwasaki, A.; Medzhitov, R. *Science* **2010**, *327*, 291.
109. Nitschke, L. *Curr. Opin. Immunol.* **2005**, *17*, 290.
110. Razi, N.; Varki, A. *Proc. Natl. Acad. Sci. U.S.A.* **1998**, *95*, 7469.
111. Collins, B. E.; Blixt, O.; DeSieno, A. R.; *et al. Proc. Natl. Acad. Sci. U.S.A.* **2004**, *101*, 6104.
112. Courtney, A. H.; Puffer, E. B.; Pontrello, J. K.; *et al. Proc. Natl. Acad. Sci. U.S.A.* **2009**, *106*, 2500.
113. Weissleder, R. *Science* **2006**, *312*, 1168.
114. Snyder, E. L.; Dowdy, S. F. *Pharm. Res.* **2004**, *21*, 389.
115. Chen, B.; Jerger, K.; Frechet, J. M.; Szoka, F. C., Jr. *J. Control. Release* **2009**, *140*, 203.
116. Liu, Y.; Ibricevic, A.; Cohen, J. A.; *et al. Mol. Pharm.* **2009**, *6*, 1891.
117. Fox, M. E.; Szoka, F. C.; Frechet, J. M. *Acc. Chem. Res.* **2009**, *42*, 1141.
118. Lee, S. M.; Chen, H.; Dettmer, C. M.; *et al. J. Am. Chem. Soc.* **2007**, *129*, 15096.
119. Lila, A. S. A.; Ishida, T.; Kiwada, H. *Exp. Opin. Drug Deliv.* **2009**, *6*, 1297.
120. Gao, Z. G.; Fain, H. D.; Rapoport, N. *J. Control. Release* **2005**, *102*, 203.
121. Torchilin, V. P. *J. Control. Release* **2001**, *73*, 137.
122. Miki, K.; Kuramochi, Y.; Oride, K.; *et al. Bioconjug. Chem.* **2009**, *20*, 511.
123. Bertin, P. A.; Gibbs, J. M.; Shen, C. K.; *et al. J. Am. Chem. Soc.* **2006**, *128*, 4168.
124. Brogden, K. A. *Nat. Rev. Microbiol.* **2005**, *3*, 238.
125. Boman, H. G. *Immunol. Rev.* **2000**, *173*, 5.
126. Yang, L.; Gordon, V. D.; Mishra, A.; *et al. J. Am. Chem. Soc.* **2007**, *129*, 12141.
127. Zasloff, M. *Nature* **2002**, *415*, 389.
128. Lienkamp, K.; Madkour, A. E.; Musante, A.; *et al. J. Am. Chem. Soc.* **2008**, *130*, 9836.
129. Porter, E. A.; Wang, X.; Lee, H. S.; *et al. Nature* **2000**, *404*, 565.
130. Tew, G. N.; Liu, D.; Chen, B.; *et al. Proc. Natl. Acad. Sci. U.S.A.* **2002**, *99*, 5110.
131. Arnt, L.; Nusslein, K.; Tew, G. N. *J. Polym. Sci. Part A: Polym. Chem.* **2004**, *42*, 3860.
132. Kolonko, E. M.; Pontrello, J. K.; Mangold, S. L.; Kiessling, L. L. *J. Am. Chem. Soc.* **2009**, *131*, 7327.

Biographical Sketches

Laura L Kiessling received her undergraduate training in chemistry at the Massachusetts Institute of Technology. There she conducted undergraduate research in organic synthesis with Professor Bill Roush. She received her PhD in chemistry from Yale University where she worked with Stuart L Schreiber on the synthesis of antitumor natural products. Her postdoctoral training at the California Institute of Technology in the research group of Peter B Dervan led her to explore the recognition of duplex DNA through triple helix formation. She began her independent career in the Department of Chemistry at the University of Wisconsin-Madison in 1991.

Laura was recently inducted into the National Academy of Sciences. Her honors and awards include a Guggenheim Fellowship, an ACS Frances P. Garvan–John M. Olin Medal, a Harrison Howe Award, an Arthur C. Cope Scholar Award, and a Horrace S. Isabell Award.

Shane L Mangold received his undergraduate degree in chemistry at Montana State University-Bozeman. There, he conducted research in organic synthesis with Professor Mary Cloninger. He is currently a graduate student in the laboratory of Professor Laura Kiessling working on the synthesis of small molecules using metathesis.

4.29 Polyphosphoesters: Controlled Ring-Opening Polymerization and Biological Applications

J Wang, Y-Y Yuan, and J-Z Du, University of Science and Technology of China, Hefei, Anhui, People's Republic of China

4.29.1 Introduction and Historical Background

Polyphosphoesters (PPEs) represent a wide range of biodegradable polymers with phosphoester bonds in the backbone. Due to the pentavalency of the phosphorus atom, various side groups can be connected to the polymer backbone. Depending on the nature of the side groups, the PPEs can be described as polyphosphate, polyphosphonate, polyphosphite, or polyphosphoramidate, as shown in **Figure 1**. In this chapter, we focus on the introduction of polyphosphates with P–O linkage between the backbone and the side group.

Past interests in phosphorus-containing polymers have primarily concentrated on their flame-retardant properties. However, due to the high cost of synthesis of polymers in comparison to carbon analogs and their instability, research interest in PPEs faded in the 1960s. Thereafter, Prof. Penczek and his colleagues pioneered the research on PPEs in basic science and biological applications in the 1970s. They proposed that, as analogs of nucleic and teichoic acids, these polymers could represent interesting classes of biomacromolecules. They also extensively studied the synthesis of PPEs and elucidated the mechanisms of reactions, summarized in excellent reviews.[1–4] Based on these foundations, several representative groups such as Zhuo's and Leong's groups have explored the biomedical applications of PPEs since the 1980s. Initially, they synthesized polymers for controlled drug delivery[5–10] and subsequently expanded applications to tissue engineering and gene delivery.[11–13] Parts of these studies have been summarized in comprehensive reviews.[13–15]

In recent years, the development of PPEs has made great progress on aspects of both synthetic methods and biomedical applications. This is mainly attributed to the innovation in synthetic approaches of these polymers. Wang and his colleagues first found that, under the catalysis of stannous octoate ($Sn(Oct)_2$) or aluminum isopropoxide ($Al(O^iPr)_3$), one can obtain well-defined PPEs by controlled ring-opening polymerization (ROP) of five-membered cyclic phosphoester monomers.[16–18] Thereafter, Iwasaki's group reported the first example of ROP of PPEs using an organocatalyst such as 1,8-diazabicyclo[5.4.0]undec-7-ene (DBU) or 1,5,7-triazabicyclo [4.4.0]dec-5-ene (TBD), which further contributed to the preparation of PPEs.[19] Based on these methods, a series of PPE-containing polymers with different topological structures such as block copolymers, graft copolymers, miktoarm star polymers, and hyperbranched polymers have been developed. Novel properties of PPEs such as thermosensitivity have been discovered and the functionalization of PPEs through the side groups has become easy with these processes. More importantly, the biomedical applications of PPEs have been further advanced. For example, PPE-containing polymers have been fabricated as nanoparticle carriers for hydrophobic or hydrophilic drugs and even for small interfering RNAs (siRNA) in cancer therapy. The recent progress of PPEs in terms of synthesis and biomedical applications has been partially reviewed by Wang *et al.*[20] recently.

This chapter consists of three main parts. First, controlled ROPs of cyclic phosphoester monomers are elucidated. Second, the novel properties of PPEs such as thermosensitivity and

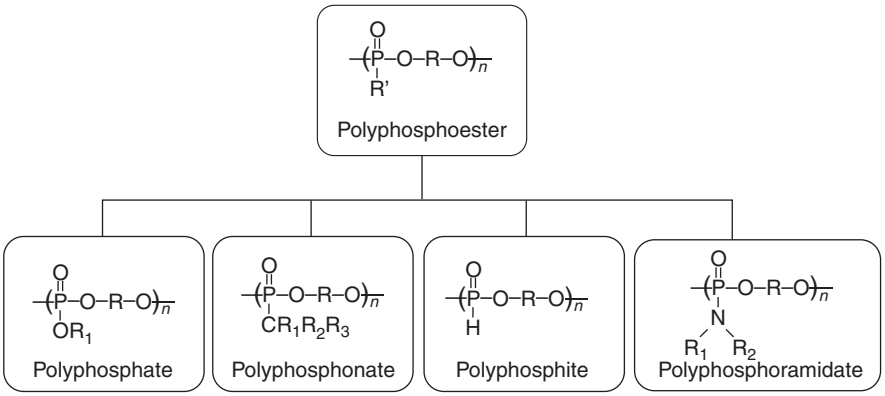

Figure 1 Structures of PPEs.

functionality are described. The final part is devoted to a summary of the biomedical applications of PPEs in drug and nucleic acid delivery as well as in the field of tissue engineering.

4.29.2 Controlled Syntheses of PPEs by Ring-Opening Polymerization

Syntheses of PPEs by ROP were pioneered by Prof. Penczek and his colleagues at the end of the 1970s, initially as analogs of nucleic and teichoic acids, later on as biomembranes designed as polymer–inorganic hybrids or for mimicking biomineralization.[21] They studied synthesis extensively and elucidated many of the mechanisms of different preparation methods, including anionic and cationic ROPs,[22,23] polycondensation,[24,25] and polyadditions.[26] These methods are still the main approaches for the syntheses of PPE-based biomaterials, although interfacial polymerization[27] and recently reported enzyme-catalyzed polymerization[28] are possibly alternative methods.

However, the polymerization methods described above always face difficulties when it is necessary to prepare PPEs with a well-defined structure, controlled composition, and tunable molecular weight. It is also difficult to synthesize block copolymers of PPEs with other biocompatible polymers for potential physicochemical property adjustment in biomedical applications.[13] Recently, Wang *et al.* and Iwasaki *et al.* reported, respectively, that some metal-containing catalysts and organocatalyst can efficiently catalyze the ROP of five-membered cyclic phosphoester monomers with controlled/living polymerization characteristics.[16–19] These processes remarkably enhance the ability to design and prepare PPE-containing polymers with well-defined structures. Thus, we plan to introduce these studies in the first part of this chapter. As reported recently, three different approaches have been employed to perform the controlled synthesis of homopolymer or block copolymers of PPEs. We will discuss the ROPs in the sequence of $Al(O^iPr)_3$, $Sn(Oct)_2$, and organocatalyst reactions.

4.29.2.1 Controlled Polymerization with $Al(O^iPr)_3$

$Al(O^iPr)_3$ has been used as an initiator and catalyst for the polymerization of aliphatic polyesters such as poly(ε-caprolactone) (PCL) and poly(lactic acid) (PLA) through the 'coordination–insertion' mechanism.[29] The polymerization process can be readily controlled, and it involves selective cleavage of the acyl–oxygen bond of the monomer, to make a hydroxyl end group after hydrolysis or acidolysis.[30] It has been reported that two main species, trimer (A_3) and tetramer (A_4) of $Al(O^iPr)_3$, react with ε-caprolactone (ε-CL) with different polymerization rates. A_3 initiates the polymerization of ε-CL efficiently and quantitatively, while A_4 cannot initiate polymerization.[31,32]

Although $Al(O^iPr)_3$ has showed high potency for ROP, it was not used for the controlled polymerization of cyclic phosphoester monomers before the year 2006. Wang *et al.* first investigated the ROP of a model five-membered cyclic phosphoester monomer, namely methoxyethyl ethylene phosphate (MOEEP) (eqn [1]). It was found that this monomer can be initiated with A_3 in tetrahydrofuran (THF). The linear dependence of $\ln\{([M]_0 - [M]_{eq})/([M] - [M]_{eq})\}$ on polymerization time shown in **Figure 2** is in agreement with first-order kinetic plots for polymerization, indicating living polymerization of the MOEEP monomer, where $[M]_0$, $[M]$, and $[M]_{eq}$ are concentrations of MOEEP at time 0, time t, and equilibrium.

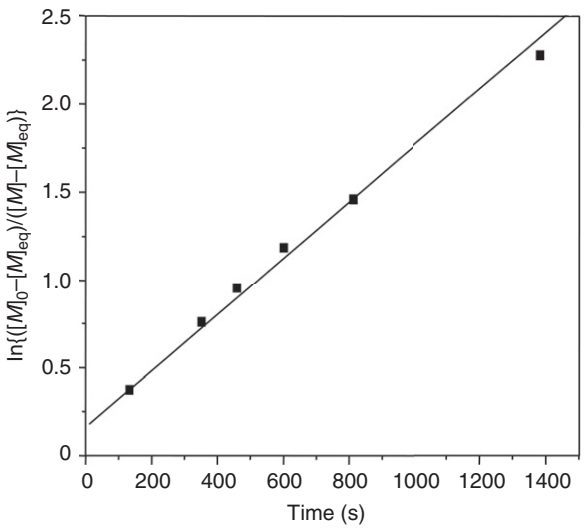

Figure 2 Kinetics of homopolymerization of MOEEP initiated with aluminum isopropoxide trimer (A_3). Conditions: 20 °C in THF, $3[A_3] = 5.0 \times 10^{-3}$ mol l^{-1}, initial concentration of MOEEP $[M]_0 = 0.25$ mol l^{-1}. $[M]$ and $[M]_{eq}$ are concentrations of MOEEP at time t and equilibrium. Reproduced with permission from Wang, Y. C.; Shen, S. Y.; Wu, Q. P.; *et al. Macromolecules* **2006**, *39*, 8992–8998.[17]

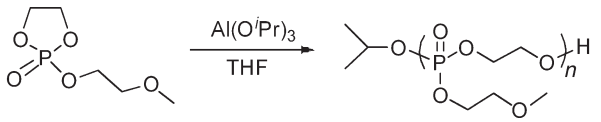

[1]

The structural similarity between the cyclic phosphoester monomer and lactone may suggest the same 'coordination–insertion' mechanism as shown in eqn [2].[17]

In addition, it has also been revealed that the rate of propagation of the PPE block is affected by the structure of the pendent group connected to the phosphorus. For example, when the side group is isopropoxy, the polymerization rate is much lower than that of the monomer with an ethoxy group.[16] The rate constant was 4.3×10^{-2} l mol^{-1} min^{-1} at 90 °C in toluene when the side group was isopropoxy group, while it increased to 1.6×10^{-1} l mol^{-1} min^{-1} at 50 °C in the same solvent when the side group was replaced by an ethoxy group. Nevertheless, this polymerization procedure will facilitate the synthesis of block copolymers of aliphatic polyesters and PPEs with defined molecular architectures and properties for potential biomedical applications.

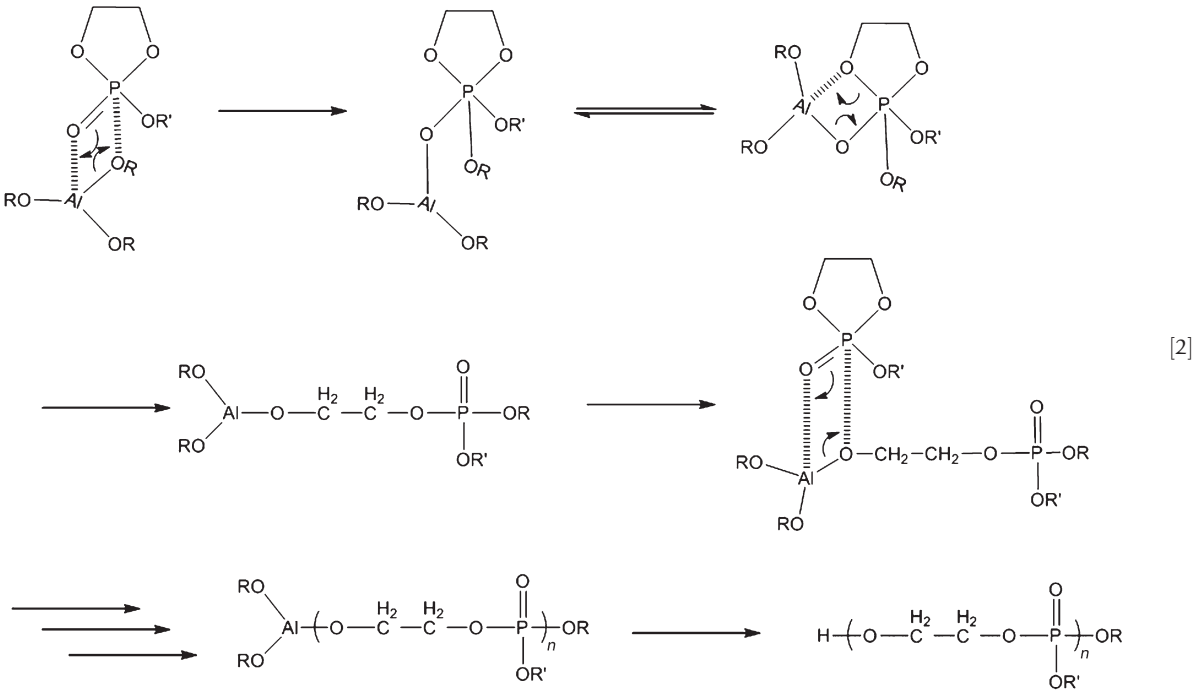

[2]

Block copolymerization of PCL and PPEs can be performed with the initiation of Al(O^{i}Pr)$_3$.[16,17] In a typical example, the polymerization of ε-CL was initiated by A_3 in THF, followed by the addition of phosphoester monomer (eqn [3]). The actual formation of the expected block copolymers was confirmed by nuclear magnetic resonance (NMR), Fourier transform infrared spectroscopy (FT-IR), and gel permeation chromatography (GPC). Kinetic studies revealed that the M_n of PPE follows a linear relationship with monomer conversion (up to 94.3%), and the molecular weight distribution remains narrow with dispersity (PDI) around 1.2, indicating that a limited amount of inter- or intramolecular transesterification reactions occurred. This enables the synthesis of block copolymers with narrow molecular weight distribution, controlled molecular weights, and adjustable compositions.

4.29.2.2 Controlled Polymerization with Sn(Oct)$_2$

As one of the most widely used catalysts for the polymerization of cyclic esters, Sn(Oct)$_2$ has been reported to catalyze the polymerization of ε-CL, lactide (LA), or analogs in bulk or in solution by the formation of stannous alcoholate active centers in the presence of ROH or RNH$_2$.[33,34] Polymer chain propagation has been described as simple monomer insertion into the –Sn–OR bond.[33] Polymerization of cyclic phosphoester monomers with the catalysis of Sn(Oct)$_2$ has been studied in

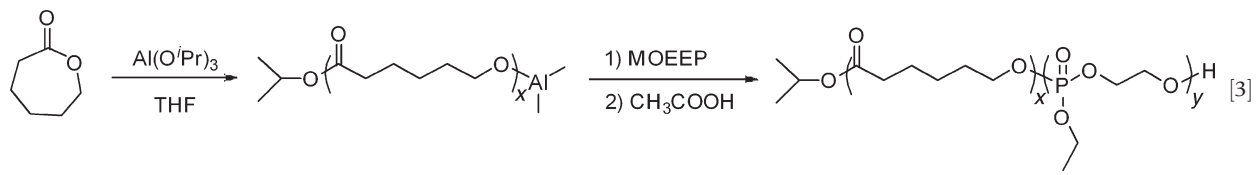

[3]

either THF or bulk with the co-initiation of $Sn(Oct)_2$ and alcohol or a macroinitiator containing a hydroxy end group.[18,35–38] Similar to the mechanism proposed for ε-CL and LA polymerization,[33,39–41] a stannous alkoxide species is produced between the alkoxy group and $Sn(Oct)_2$. The reaction of stannous alkoxide with monomers by means of coordination–insertion generates the first actively propagating chain end (1 mer*), consisting of both the initiating alkoxy fragment and the active propagating center derived from the first monomer unit and stannous alkoxide (eqn [4]).

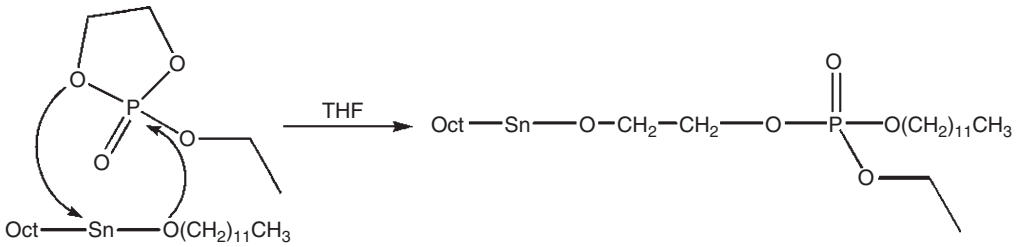

[4]

Figure 3 shows the first-order kinetic plots for the polymerization of monomer ethyl ethylene phosphate (EEP) at different temperatures, where $[M]_0$, $[M]$, and $[M]_{eq}$ are concentrations of EEP at time 0, time t, and equilibrium. The linearity of these plots demonstrated that the EEP consumption is in first order with reaction time and can be described by

$$R_p = \frac{d[EEP]}{dt} = k_{app}([EEP]-[EEP]_{eq})$$

where R_p is the rate of polymerization and k_{app} is the apparent propagation rate constant. Since the relationships shown in Figure 3(**a**) are linear, the slopes of these plots are equal to k_{app}. It has been found that k_{app} increases 20-fold on increasing the polymerization temperature from 0 to 40 °C, and an Arhennius analysis has revealed that the relationship between k_{app} and polymerization temperature is consistent with the following equation, where ln k_{app} is linearly dependent on $1/T$:

$$k_{app} = A\exp\left(-\frac{E_a}{RT}\right)$$

Figure 3(**b**) shows the conversion dependence of EEP on reaction time. Practically, at 40 °C, approximately 90% conversion of EEP can be achieved in 30 min, while only less than 40% conversion of EEP was observed at 0 °C under otherwise identical polymerization conditions.

The above kinetic studies revealed that the ROP reaction is first order and suggested the formation of active center stannous alkoxide as well as a coordination–insertion polymerization mechanism.[18] By this means, block copolymers of PPE with poly(ethylene glycol) (PEG) or aliphatic polyesters (e.g., PCL or polylactide) can be synthesized conveniently under the co-initiation of $Sn(Oct)_2$ with a hydroxyl group-ended polymer chain, while the block lengths of PPE can be well controlled.[35–38,43]

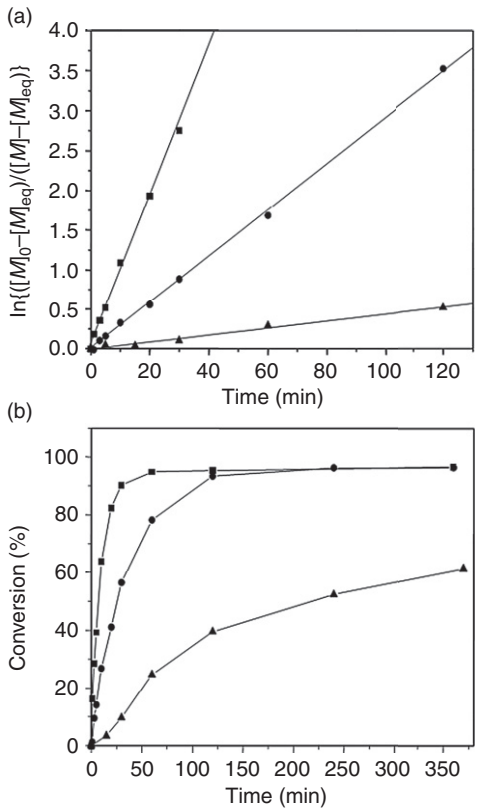

Figure 3 Kinetics of EEP ROP initiated with $Sn(Oct)_2$ and dodecanol. Conditions: $[EEP]_0 = 1.0$ mol l^{-1}, $[Sn(Oct)_2]_0 = 0.025$ mol l^{-1}, $[dodecanol]_0 = 0.05$ mol l^{-1}, THF solvent; (a) effect of reaction temperature 40 °C (■), 25 °C (●), 0 °C (▲); (b) EEP conversion at various reaction time, 40 °C (■), 25 °C (●), 0 °C (▲). Reproduced with permission from Xiao, C. S.; Wang, Y. C.; Du, J. Z.; *et al. Macromolecules* **2006**, *39*, 6825–6831.[18]

It is worth noting that significant side reactions may occur with prolonged reaction time; furthermore, it is possible to generate branched structures due to side chain transfer. Transesterification during the polymerization of cyclic aliphatic esters is known to cause the scission of the backbone chain and the formation of different structures.[44] Differing from tetravalent carbon atoms in aliphatic cyclic esters and polyesters, the phosphorus atom is pentavalent, and, therefore, the side chain transfer reaction may be more complicated. As illustrated in eqn [5]

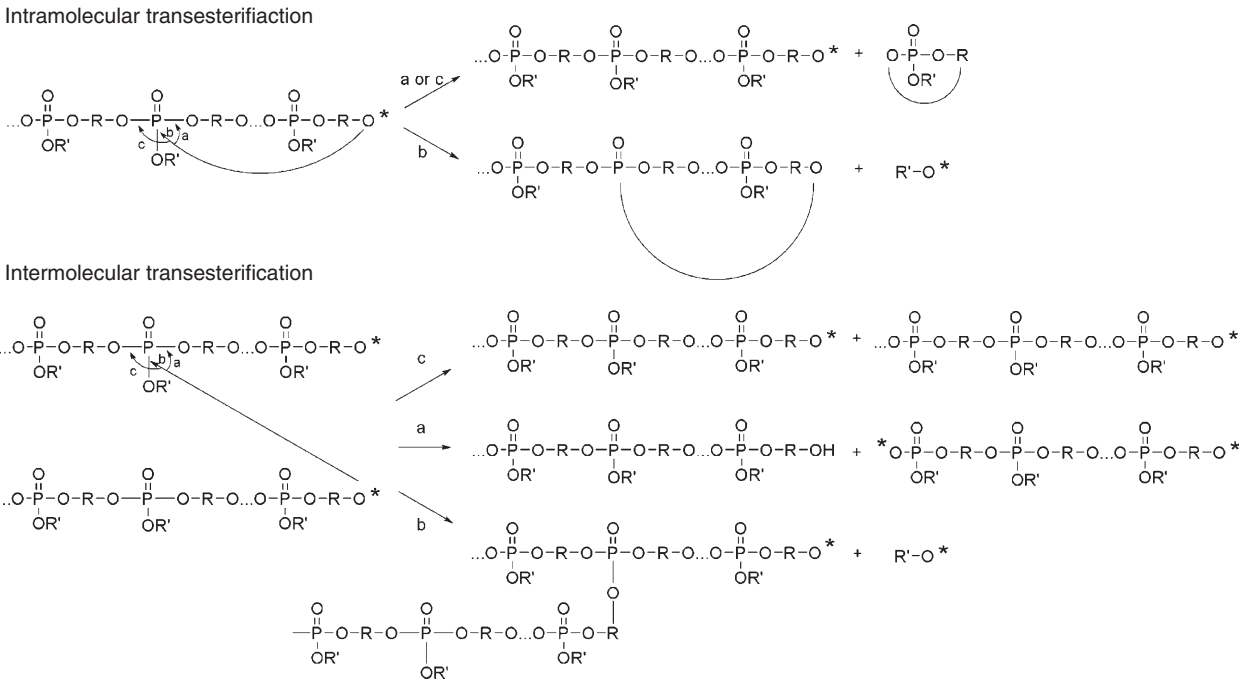

[5]

(* represents the active center), intramolecular and intermolecular chain transfer to the backbone or the pendant group may lead to homo, branched, or macrocyclic structures, particularly when the reaction time is extended after monomer consumption reaches equilibrium. However, by controlling the polymerization conditions or the reaction time, such side reactions can be suppressed to synthesize PPEs with a well-defined linear structure.

On the other hand, although it seems difficult to prepare homo- or block copolymer of PPEs with high molecular weight (e.g., number-average molecule weight (M_n) higher than 20 000) when performing polymerization in THF using $Sn(Oct)_2$ as the catalyst, higher molecular weights can be achieved by bulk polymerization. The molecular weights in bulk polymerization can achieve around 40 000–50 000 according to GPC analysis, and monomer conversions are above 70%. The molecular weight distributions of the block copolymers are around 1.50, which are slightly higher than those obtained in solution polymerization.[37,38,45–47]

4.29.2.3 Controlled Polymerization with Organocatalysts

The ROP process of cyclic phosphoesters using metallic compounds has been very successful, as described above. However, there is a concern with environmentally sensitive metal compounds, and it is also expected that there should be no metal contaminant in PPEs, particularly when they are synthesized for biomedical applications. In addition, although the synthesis of PPEs with high molecular weights using metallic catalysts has been successful,[37,38,48,49] there have been limitations on the molecular weight distributions. Taking advantage of organocatalysts in the syntheses of polyesters, polycarbonates, and silicones,[50] Iwasaki's group first prepared well-defined poly (2-isopropoxy-2-oxo-1,3,2-dioxaphospholane) (PIPP) using DBU or TBD as the organocatalyst.[19] PIPP with both a narrow molecular weight distribution and a high molecular weight was obtained. As shown in **Figure 4**, the plot of the average molecular weight (M_n) versus conversion of monomer IPP was linear

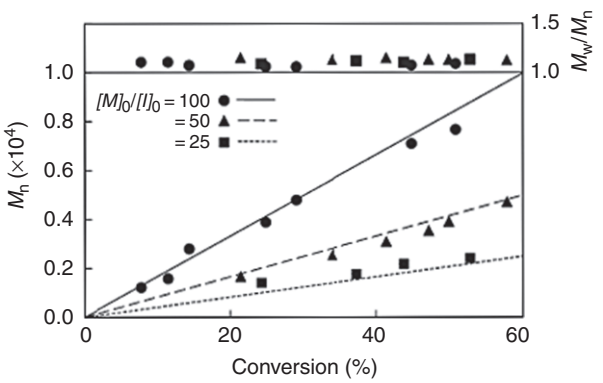

Figure 4 Plot of M_w/M_n and M_n vs. monomer conversion for the polymerization of 2-isopropoxy-2-oxo-1,3,2-dioxaphospholane (IPP) by using DBU as the catalyst. Broken lines suggest the theoretical amount of each polymerization condition. Reproduced with permission from Iwasaki, Y.; Yamaguchi, E. *Macromolecules* **2010**, *43*, 2664–2666.[19]

up to 60% conversion. The linearity of the plot suggested that the number of macromolecules in the reaction system was constant during polymerization. The molecular weight distributions of PIPPs are narrow and stable during the polymerization process. Iwasaki *et al.* indicated that DBU and TBD might form hydrogen bonds with the alcohol, similar to the mechanism of ROP of lactone and LA with organocatalysts proposed by Hedrick and co-workers.[51,52] Based on this hypothesis, ROP of IPP with DBU may occur through a quasi-anionic polymerization mechanism through activation of the alcohol, but TBD may serve as a dual activation catalyst for both the phosphoester monomer and the initiator. With this method, block copolymer of different PPEs has been reported using organocatalysts.[53]

4.29.3 Topological Structure of PPE

The development of PPE synthetic chemistry makes the synthesis of PPEs with various structures possible. Recently, PPE-based polymers with different topological structures including linear random copolymers, block copolymers, star polymers, miktoarm polymers, and brush and hyperbranched polymers have been synthesized. Among them, linear homopolymers or random copolymers of PPEs are perhaps the most studied. Different block copolymers with AB, ABA, and ABC architectures have been synthesized by controlled ROP. By the combination of ROP of PPE with other controlled polymerization methods, such as living radical polymerization, or 'click' chemistry, more complex architectures including miktoarm, comb, or graft copolymers can be synthesized. The richness of structures has allowed the convenient adjustment of material properties of PPE for biomedical applications.

4.29.3.1 Random Copolymers of PPE

Random copolymers of PPE with other polymers have been synthesized by ring-opening copolymerization of cyclic phosphate monomers with other monomers (e.g., ε-CL, D,L-LA, trimethylene carbonate, 2,2-dimethyl trimethylene carbonate, or dioxanone). Many random copolymers have been reported, such as poly[(ε-CL)-*co*-(MOEEP)],[17] poly[(D,L-LA)-*co*-(methyl ethylene phosphate)],[54] poly[(trimethylene carbonate)-*co*-(EEP)], poly[(2,2-dimethyl trimethylene carbonate)-*co*-(EEP)],[55] and poly[(*p*-dioxanone)-*co*-(EEP)].[56] The incorporation of phosphoester linkages into the polymer backbone increases the solubility of copolymers in common organic solvents and decreases the glass-transition temperature. As a result, the processability of copolymers can be greatly improved.[42]

4.29.3.2 Block Copolymers of PPE

One of the significant advantages of controlled ROP of PPE with $Al(O^iPr)_3$, $Sn(Oct)_2$, or organocatalysts over traditional methods relies on the syntheses of block copolymers of PPEs with other polymers, such as PEG and polyesters. Undoubtedly, the success of block copolymer (e.g., AB, ABA, ABC, or star-type block copolymers) synthesis is a significant development in PPE chemistry in recent years.[20]

Block copolymers of PCL and PPEs have been successfully synthesized through a two-step sequential ROP of CL and MOEEP, with a trimer of $Al(O^iPr)_3$ as the initiator.[17] The molecular architecture can be well controlled through adjusting the feed ratios between monomers and the initiator, while the side reactions on the other hand can be limited by properly ceasing the reaction. In addition, a series of biodegradable block copolymers of poly(ethyl ethylene phosphate) (PEEP) with varied PCL or poly(L-lactic acid) (PLLA) lengths (**1** and **2**) have been synthesized in solution or in bulk through ROP of EEP monomers under the co-initiation of $Sn(Oct)_2$ and PCL- or PLLA-bearing hydroxyl end groups.[35,36,38]

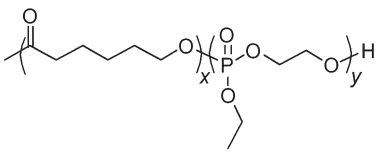

1

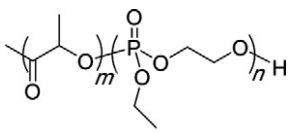

PLLA-*b*-PEEP

2

Similarly, diblock copolymers MPEG-*b*-PEEP (**3**) with different compositions that are composed of monomethoxy poly(ethylene glycol) (MPEG), copolymers of EEP, or isopropyl ethylene phosphate (PEP) have been synthesized by ROP in bulk.[37,46,47]

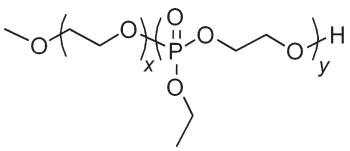

3

Pluronic analogs based on block copolymers of poly(propylene oxide) and PEEP (PEEP-*b*-PPO-*b*-PEEP) (**4**) have been synthesized by ROP of EEP using commercially available PPO as the macroinitiator and $Sn(Oct)_2$ as the catalyst. Interestingly, the aqueous solution of the polymers can form a thermoresponsive hydrogel, which can be used for sustained drug release in biomedical applications.[57]

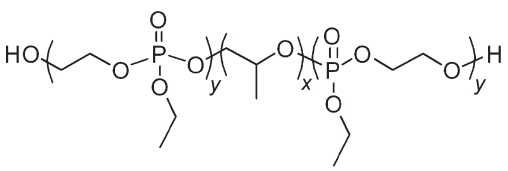

4

Iwasaki and his colleagues prepared block copolymers of PIPP-*b*-poly(2-methacryloyloxyethylphosphorylcholine) (PIPP-*b*-PMPC) (**5**) via the combination of organocatalyst ROP and atom transfer radical polymerization (ATRP) methods.[19] In that work, PIPP was prepared by ROP of cyclic phosphoester monomers using DBU or TBD as the organocatalyst. The resulting PIPP exhibited a narrow molecular weight distribution but a high

molecular weight. PIPP was further modified and used as a macroinitiator to initiate the polymerization of MPC in the presence of copper(I) bromide (CuBr) and 2,2′-bipyridine (bpy). With a well-defined structure, the polymer can form biocompatible nanomaterials with potential for biomedical applications.[19]

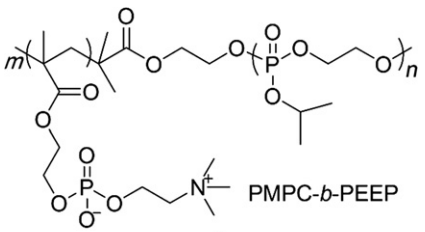

5

The linear block copolymer PEEP-*b*-PIPP (**6**) has been prepared by Liu *et al.*[53] The authors used a two-step ROP procedure of EEP and IPP, in turn using $Sn(Oct)_2$ and DBU as the initiators. First, propargyl alcohol and $Sn(Oct)_2$ were used as the initiator and the catalyst to prepare linear polyphosphate PEEP by the ROP of EEP in THF. Then, the PEEP was further used as the macroinitiator and DBU was used as the organocatalyst to carry out the ROP of IPP in bulk, producing the linear block copolymer PEEP-*b*-PIPP.

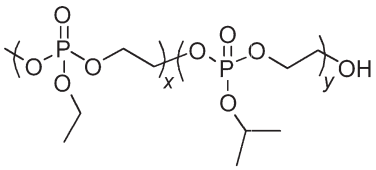

6

Ni and his colleagues prepared block copolymers of PEEP-*b*-poly[2-(dimethylamino)ethyl methacrylate] (PEEP-*b*-PDMAEMA) (**7**) via the combination of ROP and ATRP.[58] The PEEP block terminating with bromine (PEEP-Br) was first prepared by ROP of EEP using 2-hydroxyethyl 2-bromoisobutyrate as a bifunctional initiator and $Sn(Oct)_2$ as the catalyst. ATRP was then used to polymerize DMAEMA monomers in a methanol/water mixture with PEEP-Br as the macroinitiator, resulting in diblock copolymers of PEEP-*b*-PDMAEMA. These block copolymers are expected to have potential applications in gene therapy.

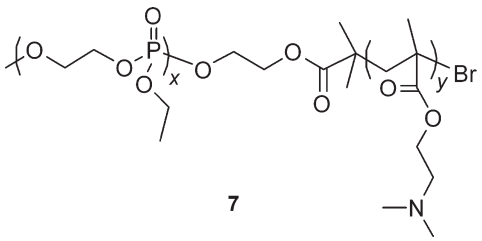

7

4.29.3.3 Star/Miktoarm Block Polymers of PPE

ROP has also been utilized for the preparation of star and miktoarm block copolymers containing PPEs. Biodegradable star block copolymers with four arms composed of hydrophobic PCL and hydrophilic PEEP (SS-PCL-*b*-PEEP) (**8**) have been successfully synthesized using a 'core-first' strategy. The copolymers were obtained by polymerization of CL, followed by ROP of EEP in the presence of $Sn(Oct)_2$.[59]

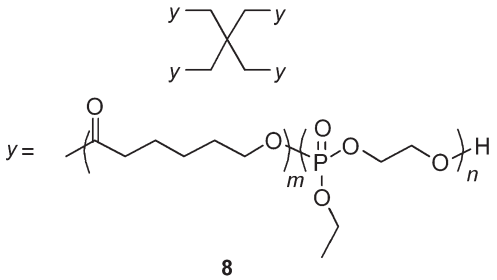

8

In another study, amphiphilic ABC 3-miktoarm star terpolymers composed of PCL, MPEG, and PEEP (**9**) have been synthesized by a combination of ROP and 'click' chemistry.[60]

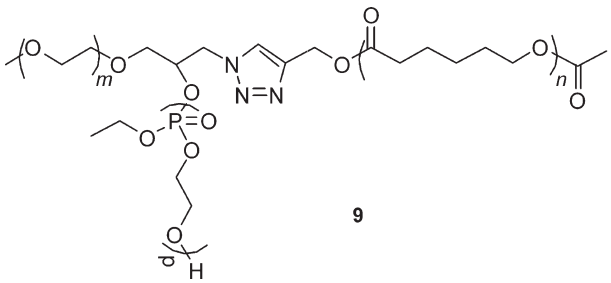

9

MPEG-armed PPE core-cross-linked nanogels have been prepared by a one-step ROP, using MPEG as the arm to polymerize a difunctional phosphate monomer, namely 3,6-dioxaoctan-1,8-diyl bis(ethylene phosphate) (TEGDP), to obtain the core-cross-linked star polymer.[61] This synthesis procedure is surfactant-free, and the core material is constituted of a PPE which has been demonstrated to be biodegradable[35,36] and which may have wide applications in drug delivery.[13]

4.29.3.4 Graft/Comb Polymers of PPE

Up to now, a variety of well-defined brush copolymers with various architectures have been synthesized by controlled/'living' polymerization methods, such as ATRP, ring-opening metathesis polymerization (ROMP), nitroxide-mediated free radical polymerization (NMP), ROP, reversible addition fragmentation chain transfer (RAFT) polymerization, as well as a combination of these polymerization techniques via various synthetic strategies. Three methods are usually applied for the preparation of graft/comb polymers, termed 'graft onto', 'graft through', and 'graft from' approaches.[62,63] The synthetic advancement in PPEs also provided helpful approaches to graft/comb PPE-containing polymers.

Novel biodegradable amphiphilic brush-coil block copolymers consisting of PCL and PEGylated PPEs (**10**) have been synthesized by ROP of a PEGylated phosphoester monomer with the initiation of PCL.[64] The composition and structure of the copolymer have been well characterized by ^1H NMR, ^{13}C NMR, and FT-IR, and the molecular weight and molecular weight distribution have been analyzed by GPC measurements to confirm the brush structure. The block copolymer is amphiphilic and forms micellar structures

in water, and the obtained brush copolymer micelles are biodegradable in the presence of *Pseudomonas* lipase.

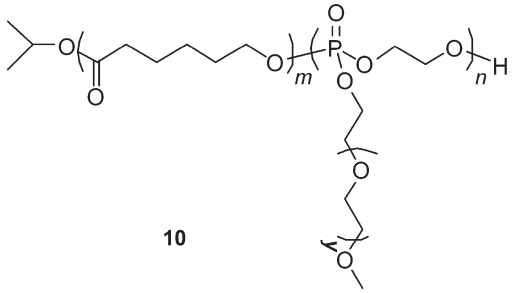

10

Amphiphilic centipede-like brush copolymers (**11**) with biodegradable PCL and PEEP as side segments have been prepared by a one-pot syntheses strategy.[65] The syntheses combined ROP of EEP through a 'grafting from' strategy and 'click' reaction with α-propargyl-ω-acetyl-PCL through a 'grafting to' strategy, using multifunctional poly(*tert*-butyl methacrylate)-*co*-poly (2-hydroxy-3-azidopropyl methacrylate) as the main chain, which bears hydroxyl and azide groups from the junction points. The reactions are controllable, and the structure of the obtained centipede-like brush copolymers has been well characterized.

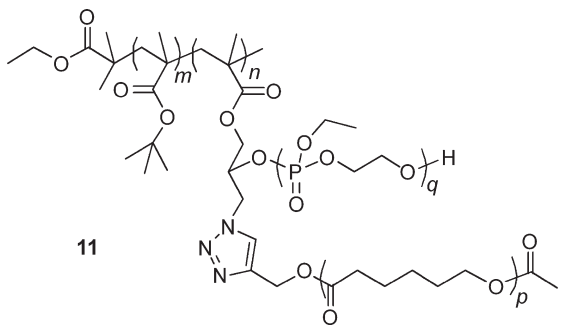

11

In another study, a series of biocompatible and biodegradable block copolymers of PCL with 'clickable' PPE (**12**) have been reported.[43] These block copolymers were synthesized through controlled ROP of five-membered cyclic phosphoester monomer, propargyl ethylene phosphate (PAEP), initiated with hydroxyl-ended PCL. The polymerization follows first-order kinetics; thus the molecular weight and composition of the copolymers are tunable by adjusting the feed ratio of the PAEP monomer to the macroinitiator. Azide-functionalized PEG has been grafted to the copolymer by Cu(I)-catalyzed 'click' chemistry of azides and alkynes, generating 'brush-coiled' polymers. The mild conditions associated with the click reaction are shown to be compatible with PCL and PPE backbones, rendering the click reaction a generally useful method for grafting numerous types of functionality onto block copolymers. The block copolymers also show good biocompatibility with cells, supporting their suitability for a range of biomaterial applications.

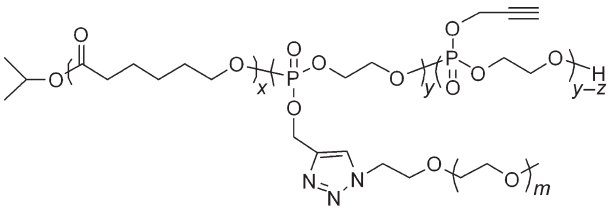

12

4.29.3.5 Hyperbranched Polymers of PPE

Hydroxyl functionalized five-membered cyclic phosphoester monomers, namely 2-(2-hydroxyethoxy)ethoxy-2-oxo-1,3,2-dioxaphospholane (HEEP), have been prepared for the synthesis of a water-soluble hyperbranched polyphosphate (HPHEEP) (**13**). The polymer was synthesized through a so-called self-condensation ROP (SCROP) in bulk without the addition of any catalyst.[53,66] The terminal hydroxyl groups potentially provide a unique opportunity for further modification and functionalization in biomedical applications.[67–70]

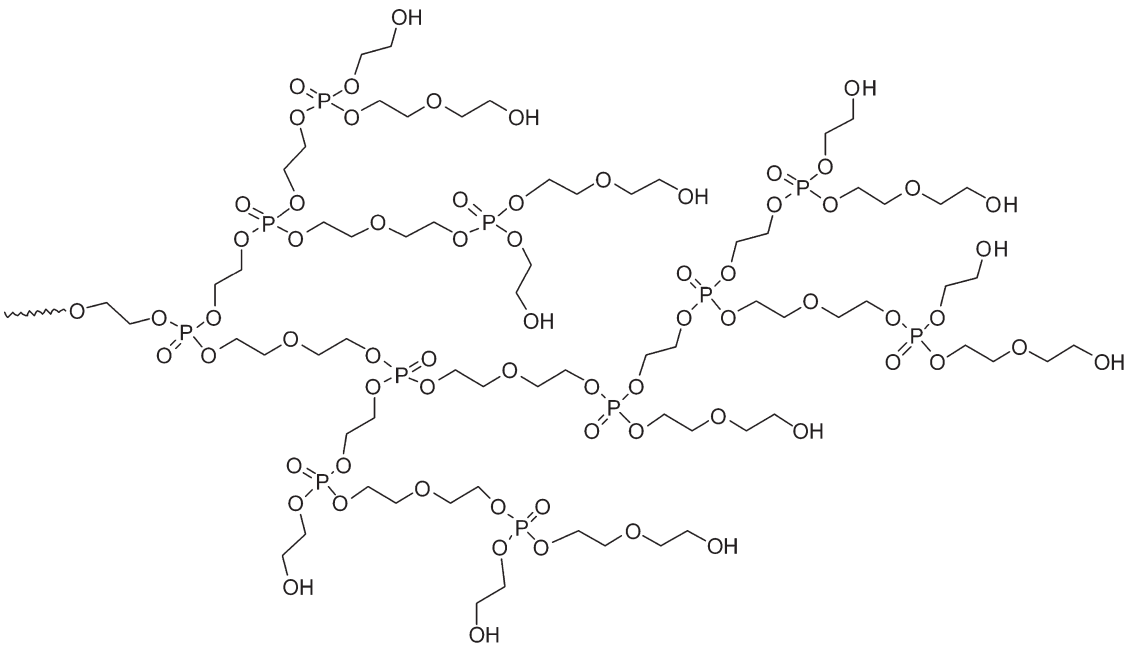

13

4.29.4 Thermoresponsive PPEs

Thermoresponsive polymers are promising for biomedical applications, including as smart drug/gene delivery systems, injectable tissue engineering scaffolds, and cell culture and separation sheets.[71,72] However, either the most frequently studied thermoresponsive polymers such as poly(*N*-isopropylacrylamide) (PNIPAAm), oligopoly(ethylene glycol), poly(*N*,*N*′-diethylacrylamide), and poly(2-carboxyisopropylacrylamide) are non-degradable or the lower critical solution temperature (LCST) cannot be tuned.

Iwasaki and co-workers first reported that PPEs with alkyl side groups are thermosensitive. Their LCSTs are tunable by adjusting the composition of polymers.[73] The possibility of varying the molecular designs and the changeable LCST of PPE polymers are significant advantages over conventional biodegradable polymers (e.g., aliphatic polyesters). This kind of biocompatible and thermoresponsive PPEs can be used as novel smart biomaterials.

The influence of molecular weights and compositions of PPE on thermoresponsiveness has been carefully investigated by Wang *et al.*, through the synthesis of block copolymers of PPE with either PCL or PEG.[37,38] Block copolymers of PEG with specific PPEs show thermo-induced self-assembly behavior in aqueous solution, resulting in micellar nanoparticles (MNPs) with a hydrophobic PPE core and a hydrophilic PEG shell when the temperature is higher than its LCST. These polymers are biocompatible and hydrolytically degradable. The molecular weight and compositions of block copolymers have been modulated through the controlled random ROP of EEP and IPP, using MPEG as the initiator and $Sn(Oct)_2$ as the catalyst (eqn [6]). It has been clearly demonstrated that the phase transition temperatures of polymer solutions can be finely adjusted by the molecular weights and the composition of PPE blocks.[37]

On the contrary, amphiphilic block copolymers of hydrophobic PCL and thermoresponsive PPEs form MNPs in aqueous solution with PCL as the core and PPE as the shell, when the temperature is lower than its LCST. The block copolymers were synthesized as described in eqn [7].[38] Cyclic phosphoester monomers with methyl, ethyl, and isopropyl side groups have been used for the random polymerization of PPE to balance the hydrophobic/hydrophilic properties. The thermo-induced transition of obtained micelles is reversible, and the thermosensitivity is also affected by the molecular weight and composition of the PPE block. It has also been observed that the concentration of sodium chloride in the medium affects the transition temperature, which in turn allows more convenient adjustment of their thermosensitivity.

When thermoresponsive diblock copolymers of MPEG and PPE are coated onto the surface of gold nanoparticles, the collapse temperature of coated nanoparticles can be finely adjusted, supporting their potential use in cancer diagnosis and therapeutics.[46] Three diblock copolymers composed of MPEG and PPE with different compositions have been prepared and thioctic acid has then been conjugated to the terminal hydroxyl group of the PPE block by esterification. Thermoresponsive diblock copolymer-coated gold nanoparticles were then prepared in the presence of thioctic acid-modified block copolymers. The clear core–shell structure of the coated gold nanoparticles was demonstrated by transmission electron microscopy, exhibiting an average gold core diameter of about 10 nm surrounded by a MPEG-*b*-P(EEP-co-PIPP) shell with a thickness of about 30 nm. The collapse temperature was tunable, ranging from 28.0 to 44.5 °C, depending on the relative ratio of the PIPP component.

However, unlike the block copolymer of thermoresponsive PPE with PCL or PEG, the ABC 3-miktoarm star terpolymer (MPEG)(PCL)(PPE) (**9**) self-assembles into nanoparticles in aqueous solution but changes its morphology with temperature variation.[74] The terpolymer (MPEG)(PCL)(PPE) is

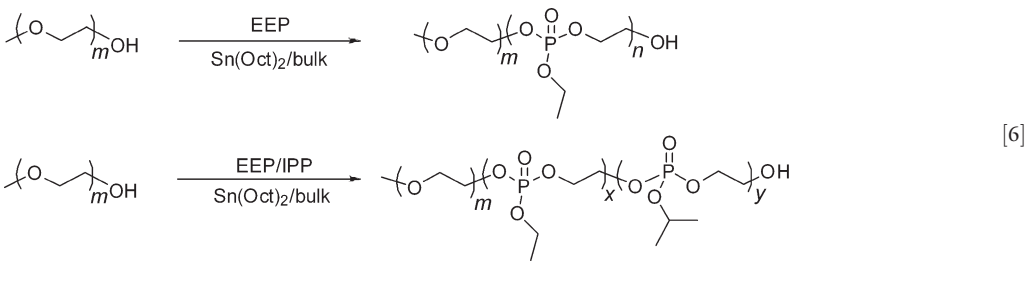

[6]

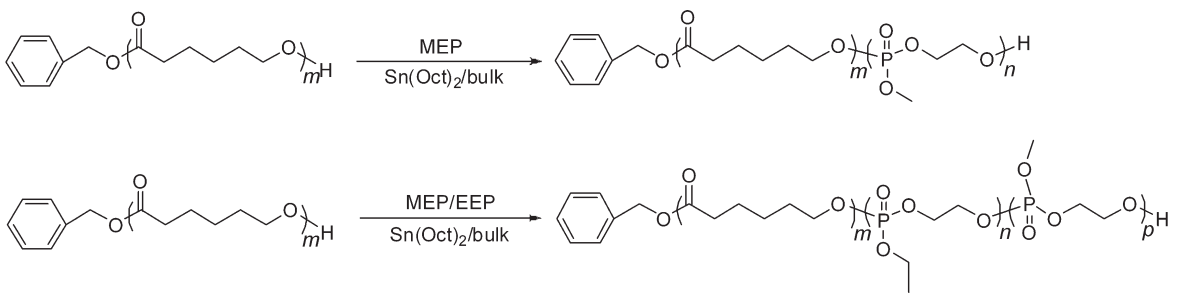

[7]

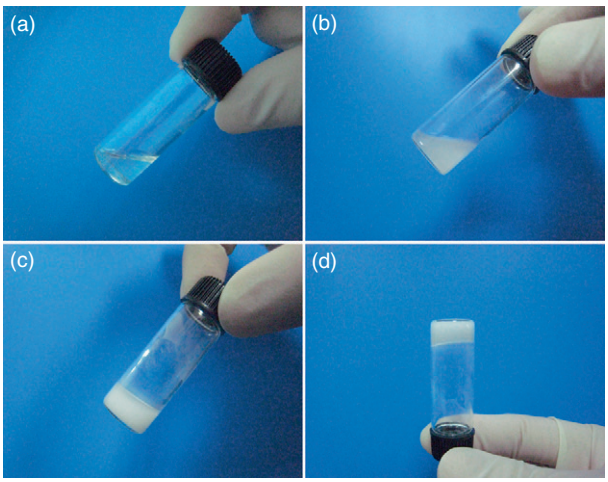

Figure 5 Phase transition of $PEEP_{14}$-PPO_{52}-$PEEP_{14}$ aqueous solution at 25 wt.%: (a) clear solution at 4 °C, (b) turbid solution at 17 °C, and (c and d) opaque gels at 25 °C. Reproduced with permission from Wang, Y. C.; Xia, H.; Yang, X. Z.; Wang, J. *J. Polym. Sci. Pol. Chem.* **2009**, *47*, 6168–6179.[57]

composed of hydrophilic MPEG, hydrophobic PCL, and thermoresponsive PPE chains, emanating from a central junction point. Such a terpolymer forms spherical micelles at lower temperatures, but it transits into a short nano-rod morphology at temperatures higher than its cloud point. This temperature-induced morphological transition may be used for stimulus-controlled drug delivery.

Block copolymers of poly(propylene oxide) and PEEP (PEEP-*b*-PPO-*b*-PEEP) have also been synthesized to mimic thermoresponsive Pluronic copolymers.[57] In addition to the thermo-induced gel formation property like thermoresponsive Pluronic copolymers, PEEP-*b*-PPO-*b*-PEEP is biodegradable and more biocompatible for potential biomedical applications. The aqueous solution of PEEP-*b*-PPO-*b*-PEEP at a concentration range from 20 to 40 wt.% undergoes thermo-induced phase transitions from a clear solution to a turbid solution, then to opaque gel and syneresis phases, depending on the molecular weights of the PEEP blocks (Figure 5). Such a thermoresponsive hydrogel can be utilized for sustained drug release and cell encapsulation.

The thermoresponsiveness of PPE with a specific chemical structure can also be used for the convenient fabrication of nanoparticles, which can be used as carriers of chemotherapeutic drugs for cancer therapy. Biodegradable nanogels based on PPEs with tunable sizes have been synthesized by a template-free method as potential carriers for drug delivery.[47] As shown in Figure 6, the nanogels were obtained by cross-linking thermo-induced PPE-based nanoparticles with subsequent swelling at low temperatures. The nanogels loaded with doxorubicin (DOX) were efficiently taken up by A549 tumor cells and the drug could be released intracellularly, resulting in enhanced growth inhibition activity to tumor cells in comparison with free DOX treatment.

Nanoparticles can even be cell-targetable with ligand modification. In another study, a versatile approach for the engineering of biodegradable nanogels with adjustable sizes for targeted drug delivery to hepatocytes has been reported.[75] Block copolymers of PEG and thermoresponsive PEEP have been synthesized and the end groups have been modified with acryl groups. Such polymers formed self-assemblies, induced by NaCl, while the sizes of the assemblies were dependent on the concentration of the polymer and salt. After photo-cross-linking, well-controlled nanogels with adjustable sizes have been engineered (Figure 7). With the integration of lactosyl moieties by mixing PEG-*b*-PEEP diblock copolymers, where the chain end of PEG is modified with a lactosyl group, the obtained nanogels can be targeted to HepG2 cells by receptor mediation. These nanogels can deliver drug molecules to cells more efficiently, resulting in enhanced cytotoxicity.

Liu *et al.* have reported pH- and temperature-responsive double hydrophilic diblock copolymers, PEEP-*b*-PDMAEMA.[58] In aqueous solution, these diblock copolymers show obvious pH- and temperature-responsive behavior, self-assembling into nanoparticles with different sizes and morphologies at different pH values. The LCSTs of the diblock copolymers depend on the degree of polymerization of each block. With a decrease in PDMAEMA units, increasing LCST can be observed. Additionally, the diblock copolymers can effectively condense plasmid DNA, resulting in small (about 95 nm in diameter) and positively charged complexes. These dual-responsive double hydrophilic diblock copolymers are expected to have potential applications in gene therapy.

4.29.5 Functional PPEs

Unlike commonly studied polyesters, the unique advantage of PPE is the functionalization ability owing to the pentavalent nature of the phosphorus atoms. However, previous reports on PPE functionalization were mainly performed through post-polymerization modification. Owing to the success in ROP of cyclic phosphoester monomers, functional PPEs can

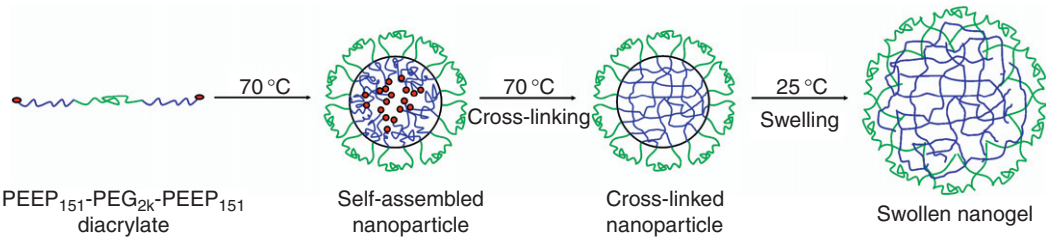

Figure 6 Schematic illustration of nanogel formation. Reproduced with permission from Wu, J.; Liu, X. Q.; Wang, Y. C.; Wang, J. *J. Mater. Chem.* **2009**, *19*, 7856–7863.[47]

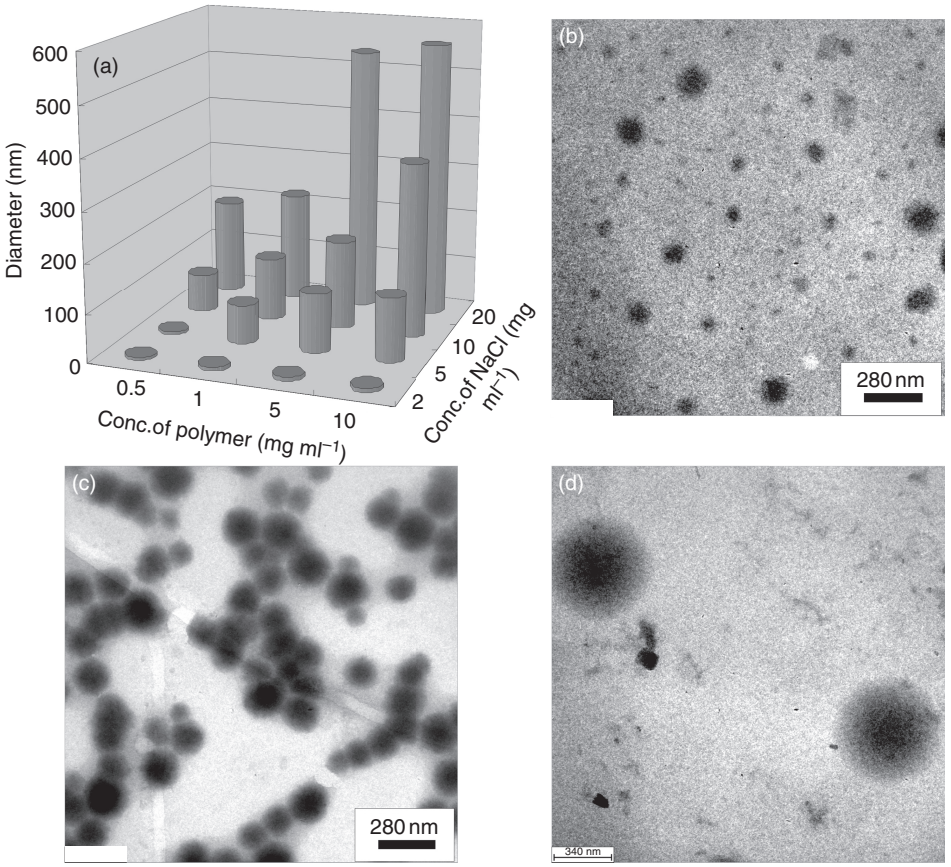

Figure 7 (a) Size dependence of Acr-PEEP$_{150}$-*b*-PEG$_{6K}$-*b*-PEEP$_{150}$-Acr assemblies on concentrations of polymer and NaCl; (b–d) representative transmission electron microscopic images of nanogels prepared under conditions of polymer (5 mg ml^{-1}) with NaCl at 5 mg ml^{-1} (b), 10 mg ml^{-1} (c), and 20 mg ml^{-1} (d). Reproduced with permission from Wang, Y. C.; Wu, J.; Li, Y.; *et al. Chem. Commun.* **2010**, *46*, 3520–3522.[75]

be obtained by direct polymerization of functionalized monomers. As reported, a series of functionalized monomers bearing reactive pendant groups including hydroxyl groups, amino groups, thiol groups, and so on (**14–18**) can be synthesized and functionalizable PPEs become available. These polymers can be applied in biomedical applications, particularly for the construction of novel controlled drug delivery systems.

methoxy)-2-oxo-1,3,2-dioxaphospholane (GEP) (**14**), using hydroxyl end-capped PCL and Sn(Oct)$_2$ as the macroinitiator and catalyst, respectively, followed by a deprotection process (eqn [8]).[45] Interestingly, these amphiphilic functionalized block copolymers can self-assemble into micellar or vesicular aggregates in aqueous solution, depending on the composition. Combining the advantages of PCL and PPE with

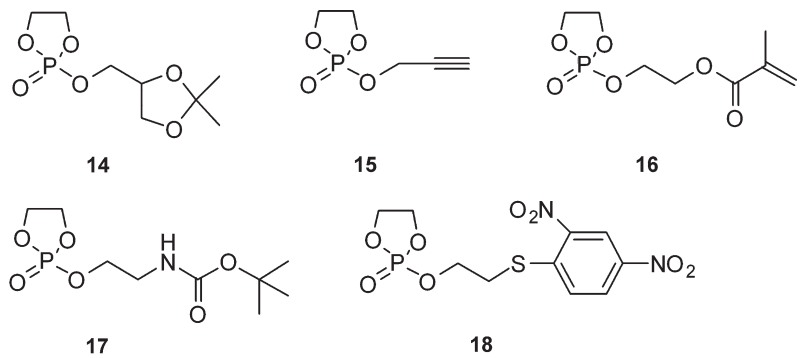

Block copolymers of PCL and PPE bearing functional hydroxyl pendant groups, denoted as PCL-*b*-PHEP, have been synthesized through the ROP of functionalized cyclic phosphoester monomer 2-(2,2-dimethyl-1,3-dioxolan-4-yl-

functional hydroxyl pendant groups for further biological modification, such amphiphilic block copolymers potentially provide novel opportunities for the design of drug delivery systems and therapeutic applications.

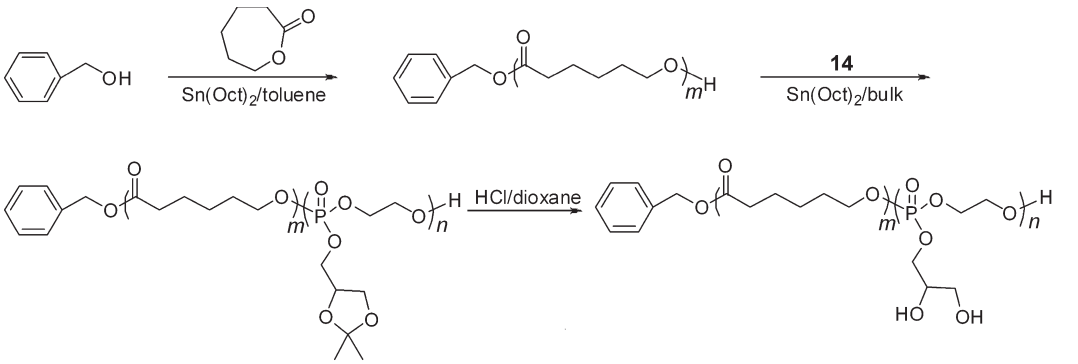

[8]

The side groups of PPE can also be 'clickable'. Biocompatible and biodegradable block copolymers of PCL with 'clickable' PPE have been synthesized through controlled ROP of PAEP (**15**).[43] Azide-functionalized PEG has been grafted to the copolymer to demonstrate the reactive feasibility by Cu(I)-catalyzed 'click' chemistry of azides and alkynes, generating 'brush-coil' polymers. The mild conditions associated with the click reaction have been shown to be compatible with PCL and PPE backbones, rendering the click reaction a generally useful method for grafting numerous types of functionality onto block copolymers. Block copolymers also show good biocompatibility with cells, suggesting their suitability for a range of biomedical applications.

The functionality of PPE has also been used to develop biocompatible hydrogels. A cyclic phosphate monomer 2-(2-oxo-1,3,2-dioxaphospholoyloxy) ethyl methacrylate (OPEMA) (**16**), bearing photo-cross-linkable double bonds, has been synthesized to prepare biodegradable hydrogels for cell encapsulation.[76] The polymers are synthesized by ROP using PEG as the initiator and $Sn(Oct)_2$ as the catalyst (eqn [9]). Further cross-linking of side methacrylate groups of PPE under photo-initiation results in various hydrogels with different cross-linking densities and degradation properties. These hydrogels are used for cell encapsulation and exhibit potential in tissue engineering.

To make amino-group functionalized PPEs, which will be positively charged and therefore have potential for nucleic acid delivery, the functional phosphoester monomer 2-(*N*-tert-butoxycarbonylamino)ethoxy-2-oxo-1,3,2-dioxaphospholane (PEEABoc) (**17**) has been synthesized. Based on the ROP of PEEABoc using hydroxyl-terminated MPEG-*b*-PCL as the macroinitiator, an amphiphilic and cationic triblock copolymer consisting of MPEG, PCL, and poly(2-aminoethyl ethylene phosphate) has been developed, which is denoted mPEG-*b*-PCL-*b*-PPE-EA (eqn [10]).[77] This amphiphilic polymer can self-assemble into nanoparticles in aqueous solution and absorb siRNA for RNAi-based therapy.

Functional PPE with thiol side groups can be used for the stabilization of nanoparticles, which potentially overcome the shortage of MNPs in drug delivery. A triblock copolymer of PCL-*b*-poly((2,4-dinitrophenyl)thioethyl ethylene

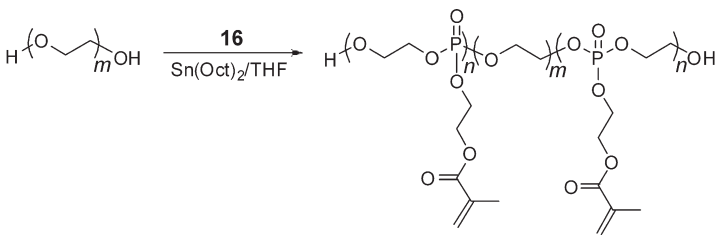

[9]

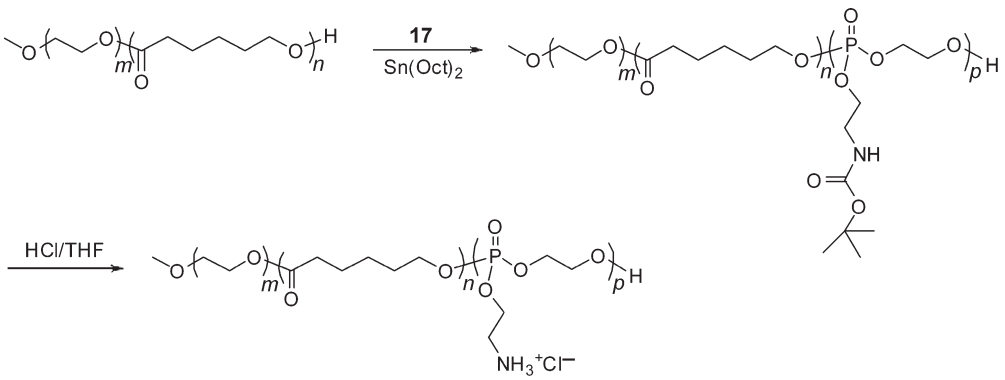

[10]

phosphate)-*b*-PEG) (PCL-*b*-PDNPTEP-*b*-PEG) has been synthesized through consecutive ROP of ε-CL and 2,4-dinitrophenylthioethyl ethylene phosphate (**18**), followed by the conjugation of PEG (eqn [11]).[78] After deprotection, the resultant triblock copolymer bearing free thiol groups forms core–shell–corona micelles in aqueous solution. Selective cross-linking of the shell layer of the micelle stabilizes the micellar structure against dilution. Thus, release of drug from the nanoparticles is retarded by the cross-linking and is accelerated under simulated intracellular reductive conditions, due to the degradation of disulfide bonds. The enhanced intracellular drug release behavior and enhanced cytotoxicity have been demonstrated in A549 cells.

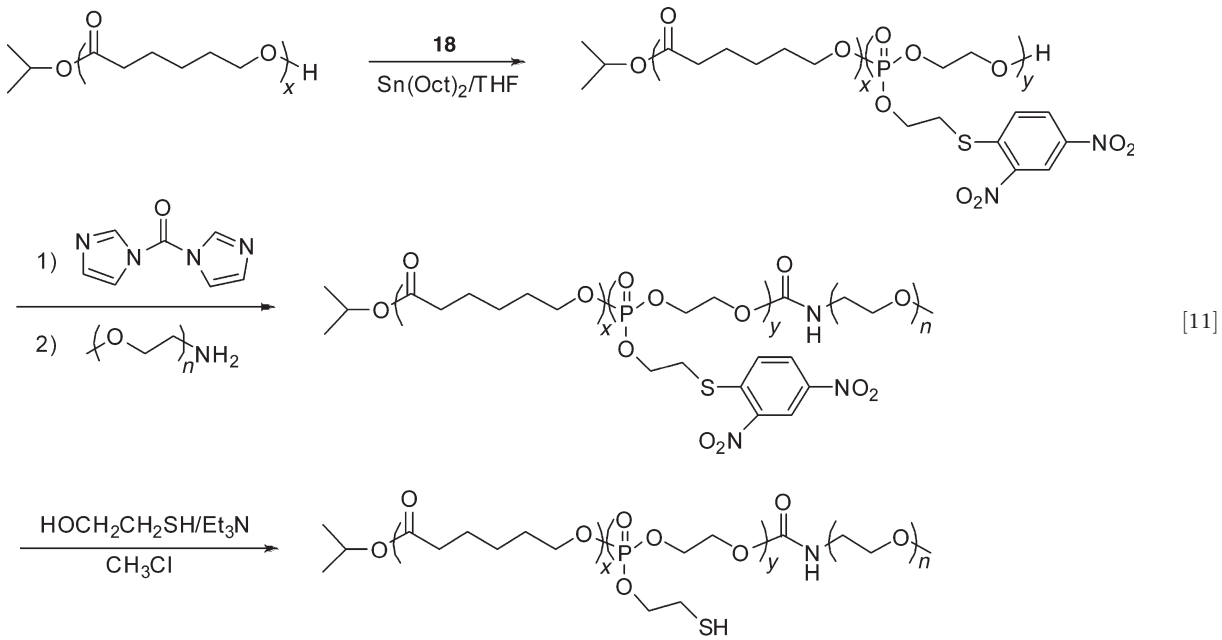

[11]

characteristics of the triblock copolymers showed that these copolymers are completely biodegradable under enzymatic catalysis of *Pseudomonas* lipase and phosphodiesterase I.[61,64,79,80] Paclitaxel has been successfully loaded into the micelles, and the *in vitro* release profile was correlative to the polymer composition.[35]

The functional end group and side chains of the PPE shell can be easily modified with biofunctional molecules or ligands for specific drug delivery.[81] Wang *et al.* reported that MNPs of a diblock copolymer PCL-*b*-PEEP can be surface conjugated with galactosamine to target the asialoglycoprotein receptor (ASGP-R) of HepG2 cells.[81] Such surface conjugation enhanced cell binding and internalization through specific recognition between galactose ligands with ASGPR. **Figure 8** shows the

4.29.6 Biomedical Applications of PPEs

4.29.6.1 Delivery of Therapeutic Small Molecules with PPE

The advancement of controlled polymerization of PPEs makes it feasible to combine PPE-containing block copolymers with other hydrophobic polyesters such as PCL and PLLA, and so on. During this process, it has been observed that PPEs with suitable side groups are hydrophilic; thus these kinds of copolymers self-assemble into core–shell nanoparticles in aqueous solution with PPEs as the protective shell. The core–shell structure renders these nanoparticles capable of encapsulating hydrophobic anticancer drugs and works as delivery systems.

To this end, Wang *et al.* have synthesized a series of amphiphilic triblock copolymers of PPE and PCL (PEEP-PCL-PEEP) using $Sn(Oct)_2$ as the catalyst. These amphiphilic block copolymers formed micelles with a hydrophobic core of PCL and a hydrophilic shell of PEEP in aqueous solution. It was found that the size and critical micelle concentration values of the micelles were dependent on both hydrophobic PCL block length and PEEP hydrophilic block length. The *in vitro* degradation

differential interference contrast (DIC), fluorescence, and merged images of HepG2 cells after 2 h incubation at 37 °C with rhodamine-123-loaded micelles with or without galactosamine conjugation. The intensity of fluorescence observed in HepG2 cells incubated with NP-Gal (nanoparticles with galactosamine modification) markedly increased compared with that of HepG2 cells incubated with nonmodified NP. This illuminated the preponderance of NP-Gal on cellular uptake due to the interaction between galactosyl moieties with ASGP-R on HepG2 cells. Moreover, paclitaxel-loaded MNPs with galactose ligands exhibited comparable activity to free paclitaxel in inhibiting HepG2 cell proliferation. At a paclitaxel dose of 0.3 μM, only 12% viable cells were observed following treatment with NP-Gal-PTX (nanoparticles with galactosamine modification and paclitaxel encapsulation), which was comparable to cells treated with free paclitaxel. In contrast, about 50% of the cells remained alive following treatment with NP-PTX (nanoparticles without galactosamine modification but with paclitaxel encapsulation) at the same paclitaxel dose due to the poor inhibition activity of MNPs without galactose ligands.[81]

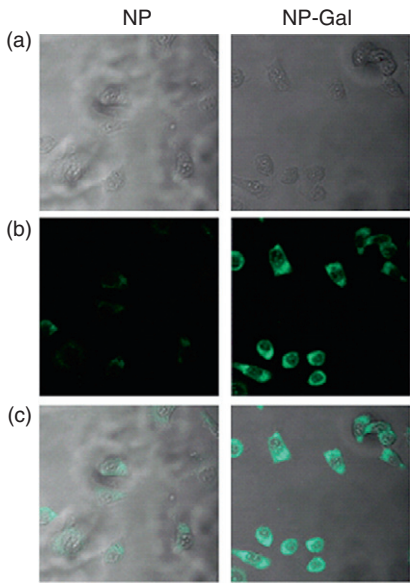

Figure 8 Differential interference contrast (DIC, a), fluorescence (b), and merged (c) images of HepG2 cells after 2 h incubation with nonmodified micelles (NP) or galactosamine-conjugated micelles (NP-Gal) at 37 °C. Reproduced with permission from Wang, Y. C.; Liu, X. Q.; Sun, T. M.; *et al. J. Control Release* **2008**, *128*, 32–40.[81]

To overcome the intracellular release barrier and maximize the delivery efficiency of anticancer drugs, promising approaches have been developed that allow carrier systems to release the drug by intracellular stimuli, such as pH,[82–85] glutathione (GSH),[86–89] and enzymes.[90] Upon reaching the targeted tissue, such carriers can be rapidly localized intracellularly and subsequently provoked by these stimuli to release the drug, hence inducing aggressive activity within tumor cells and leading to maximal therapeutic efficacy with reduced side effects. As an intracellular stimulus, GSH can reduce disulfide bonds in the cytoplasm due to the significantly high intracellular concentration of GSH (~10 mM) in comparison to the extracellular level (~2 μM).[91]

Based on these considerations, a single disulfide-linked biodegradable diblock copolymer of PCL and PEEP, named PCL-SS-PEEP (**19**), has been synthesized and used as a smart drug delivery carrier to accelerate intracellular drug release. The polymer forms biocompatible micelles in aqueous solution and can encapsulate the anticancer drug DOX in the PCL core. The main feature of this MNP is its rapid response to intracellular reductive stimuli such as GSH. Under GSH stimulus, the PEEP shell detaches from the nanoparticle and thus disassembles the core–shell micellar structure, resulting in rapid drug release. Based on the results from FACS and CLSM measurements, the GSH-sensitive micelles rapidly released DOX intracellularly and led to enhanced growth inhibition in A549 tumor cells.[92]

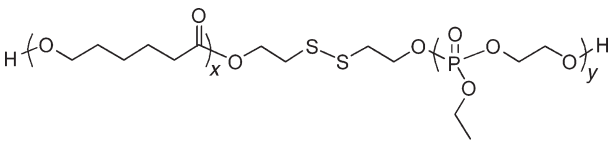

19

Although shell cross-linking of polymer micelles can increase the stability of MNPs against dilution in the blood circulation, it may also potentially prevent burst release of the drug from nanoparticles, and the ineffective release of drug in cells may hinder the efficiency of chemotherapy. It is expected that drugs encapsulated in micelles can be retained in nanoparticles during circulation but are specifically and more rapidly released in the interior of targeted cells.[93–95] Therefore, maintenance of cross-linkages of the micellar shell may indeed act as a barrier to intracellular drug release.[96]

To overcome this barrier, reversibly cross-linked core–shell–corona micelles based on a triblock copolymer composed of poly(aliphatic ester), PPE, and PEG have been synthesized (eqn [11]), and a responsive delivery system has been developed (**Figure 9**).[78] This amphiphilic polymer forms core–shell–corona micelles with free thiols in the shell. Cross-linking of the micelles within the shell reduces their critical micellization concentration and enhances their stability against severe conditions. The redox-sensitive cross-linkage allows the facilitated release of entrapped anticancer drugs in the cytoplasm in response to the intracellular reductive environment. DOX, an anthracycline drug widely used to treat various types of cancer, has been used as the model drug. DOX-loaded shell cross-linked micelles (SCMs) were incubated with 20×10^{-3} M GSH, and a rapid release of DOX was observed, reaching 30% at 24 h. However, the release of entrapped DOX was greatly retarded from the SCMs with a very minimal burst release in the absence of GSH.

From the viewpoint of nanogel development for enhanced therapeutic efficacy, the nanogel itself and the most desirable

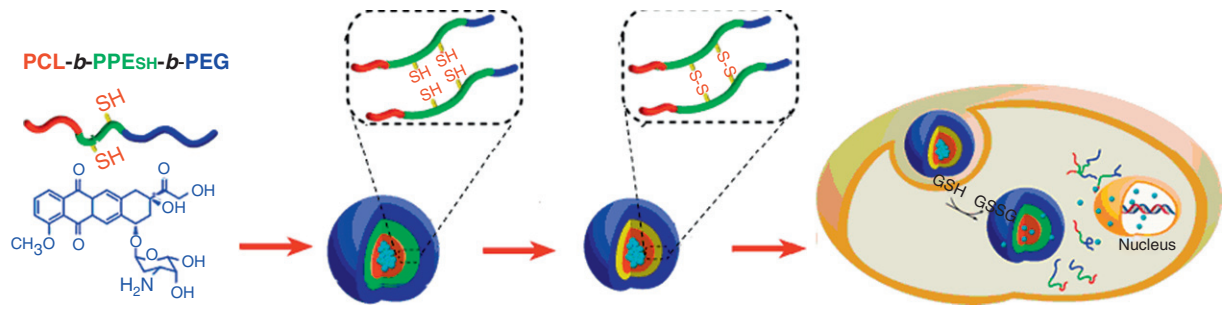

Figure 9 Schematic illustration of the formation of cross-linked micelles and intracellular drug release. Reproduced with permission from Wang, Y. C.; Li, Y.; Sun, T. M.; *et al. Macromol. Rapid Commun.* **2010**, *31*, 1201–1206.[78]

synthesis approaches are expected to meet the following requirements: (i) facile, controllable, and biocompatible synthesis methods; (ii) surface pegylation to achieve potential long circulation *in vivo*; (iii) active targeting ability to specific site or cells; and (iv) biocompatibility and biodegradability with a response to the intracellular environment in the cells.[75]

A smart nanogel based on PPE has been synthesized by a template-free process from a triblock copolymer $PEEP_{151}$-PEG_{2K}-$PEEP_{151}$ diacrylate consisting of PEG and biodegradable PEEP segments (**Figure 6**). It assembled into nanoparticles in aqueous solution at a temperature higher than its LCST. Such nanoparticles were further cross-linked and subsequently swelled into nanogels at physiological temperature that could be used as an efficient carrier for DOX delivery to A549 tumor cells.[47]

In another study, Wang *et al.* reported biodegradable nanoscopic hydrogels synthesized in a template-free method by photo-cross-linking salt-induced polymer assemblies and determined their applicability for targeted drug delivery to hepatocytes. As described above, the approach is based on block copolymers containing PEEP, which undergoes a salt-induced hydrophobic-to-hydrophilic transition. The functionalized block copolymers Acr-$PEEP_{150}$-*b*-PEG_{6K}-*b*-$PEEP_{150}$-Acr are soluble in water but self-assemble into core–shell structural nanoparticles upon the addition of salt. After UV cross-linking to fix the structure and dialysis to remove the salt, the nanoparticles become totally hydrophilic, generating nanogel particles with an inner reservoir for water-soluble drugs (**Figure 10**).[75]

Based on the unique core–shell structure, hyperbranched multiarm copolymers have been prepared as unimolecular micelles to overcome the disadvantages of classical micelles in recent years.[97–102] The unimolecular micelle does not disassemble in dilute solution and is stable to environmental changes *in vivo*. Meanwhile, the highly branched structure of hyperbranched multiarm copolymers can provide many nanocavities for drug encapsulation. Liu *et al.* have reported a series of hyperbranched PPEs for drug delivery applications which integrate the advantages of hyperbranched polymers and PPEs together.

A drug nanocarrier has been constructed through self-assembly of phospholipid-analogous hyperbranched polymers (HPHEEP-alkyls) which contain a polar hyperbranched polyphosphate head group and many aliphatic tails (eqn [12]). HPHEEP-alkyls have been synthesized by self-condensing ROP of HEEP and then capped with palmitoyl chloride. The size of the nanomicelles could be controlled conveniently from 98 to 215 nm by adjusting the capped fraction of the hydroxyl groups with hydrophobic palmityls. Confocal laser scanning microscopy and flow cytometry analysis demonstrated their good cell permeability. These nanomicelles were easily internalized by cells and were mainly located in the cytoplasm rather than in the nucleus. Chlorambucil-loaded micelles were investigated for proliferation inhibition of the MCF-7 breast cancer cell line *in vitro*.[67]

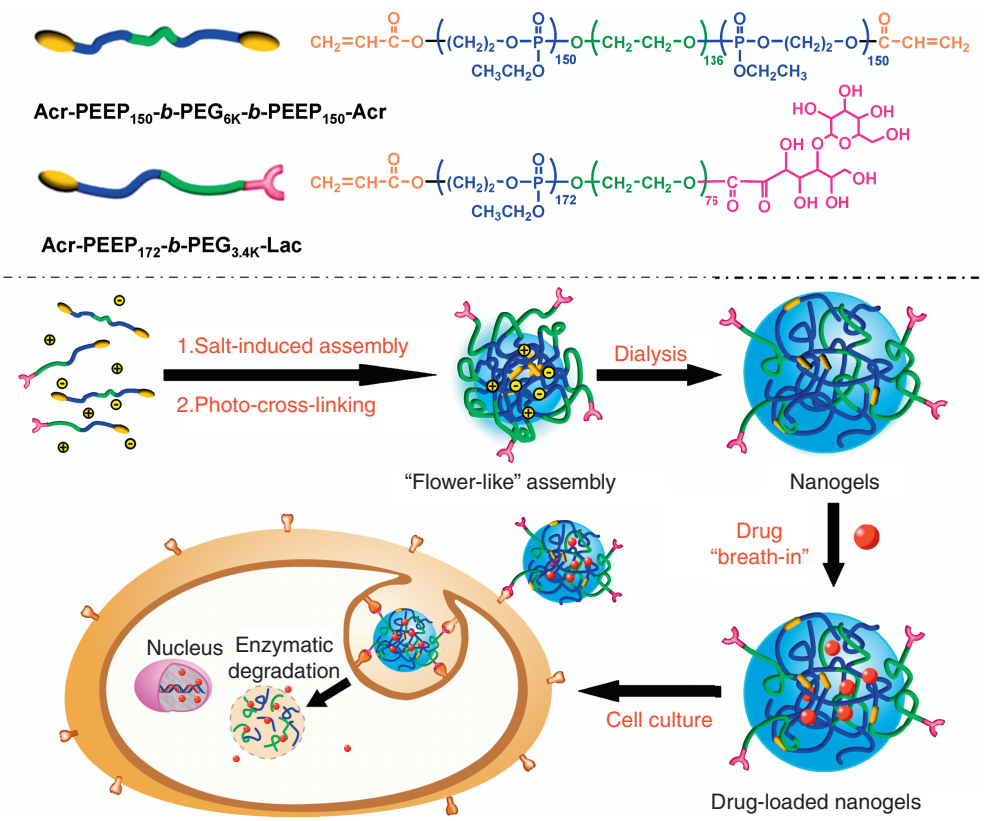

Figure 10 Schematic illustration of nanogel engineering by photo-cross-linking salt-induced polymer assembly for targeted drug delivery. Reproduced with permission from Wang, Y. C.; Wu, J.; Li, Y.; *et al. Chem. Commun.* **2010**, *46*, 3520–3522.[75]

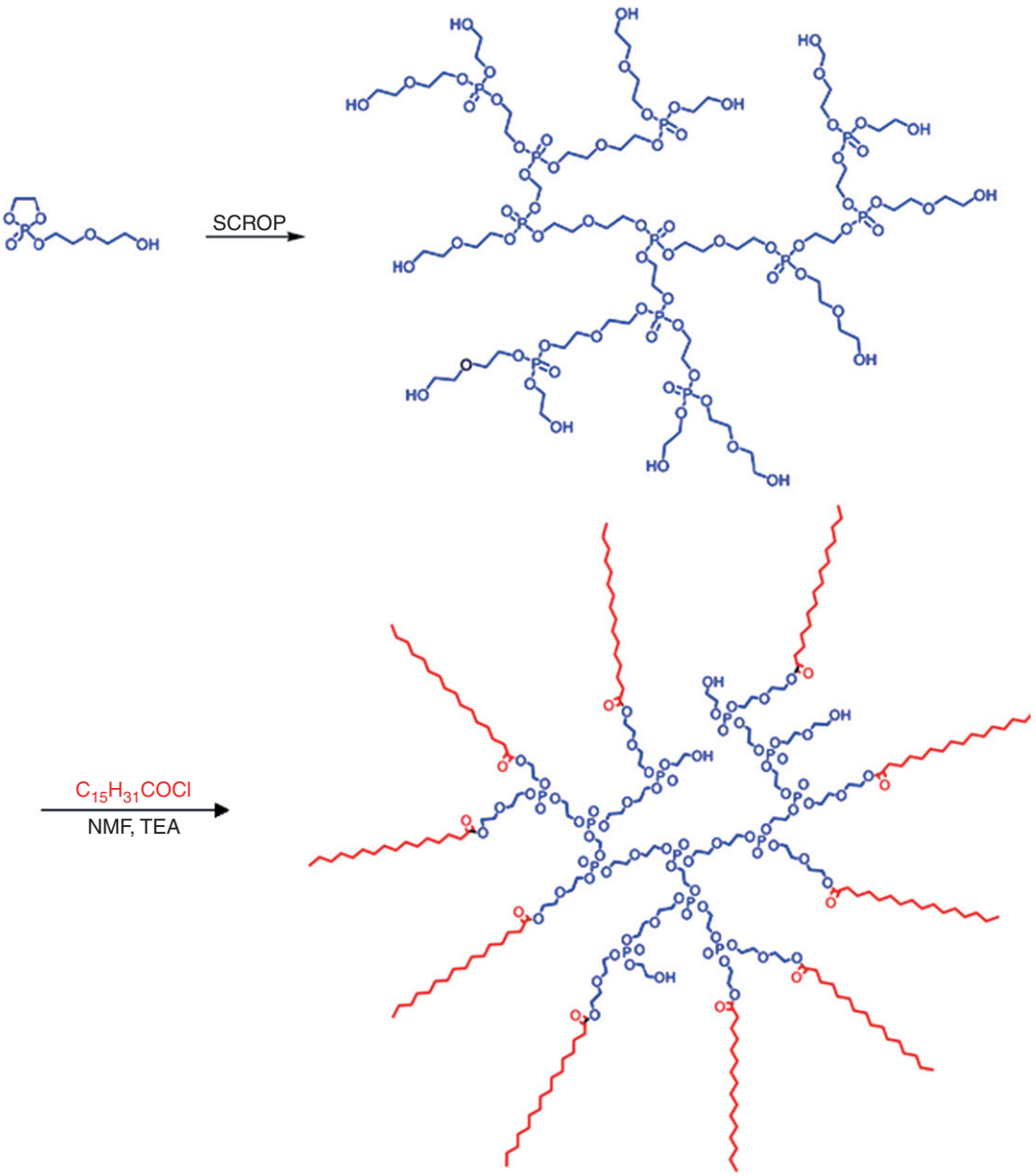

[12]

The potential of HPHEEP as a carrier for intracellular drug delivery has also been evaluated by conjugation of chlorambucil to HPHEEP (**Figure 11**). The IC_{50} value (dose required for 50% cellular growth inhibition) of the conjugated chlorambucil against the MCF-7 breast cancer cell line *in vitro* was found to be 75 μg/ml, measured by the MTT assay, which was only slightly higher than that of the free chlorambucil ($IC_{50} = 50\ \mu g\ ml^{-1}$). The significant activity of the conjugate could be attributed to the biodegradability of HPHEEP, which releases free chlorambucil in cells.[69]

A full-polyphosphate nanocarrier has been constructed through self-assembly of amphiphilic hyperbranched multiarm copolymers (denoted as HPHEEP-star-PPEPs) (eqn [13]). The hydrophilic core and hydrophobic multiarm of HPHEEP-star-PPEPs are composed of hyperbranched and linear polyphosphates, respectively. HPHEEP-star-PPEPs can self-assemble into nanocarriers in aqueous media with controlled sizes from 48 to 74 nm by adjusting the length of the hydrophobic arm. These nanocarriers possess excellent biocompatibility against NIH 3T3 cells and are easily internalized by live cells. Chlorambucil-loaded nanocarriers have been investigated for the proliferation inhibition of MDA-MB-231 breast cancer cell line *in vitro*.[68]

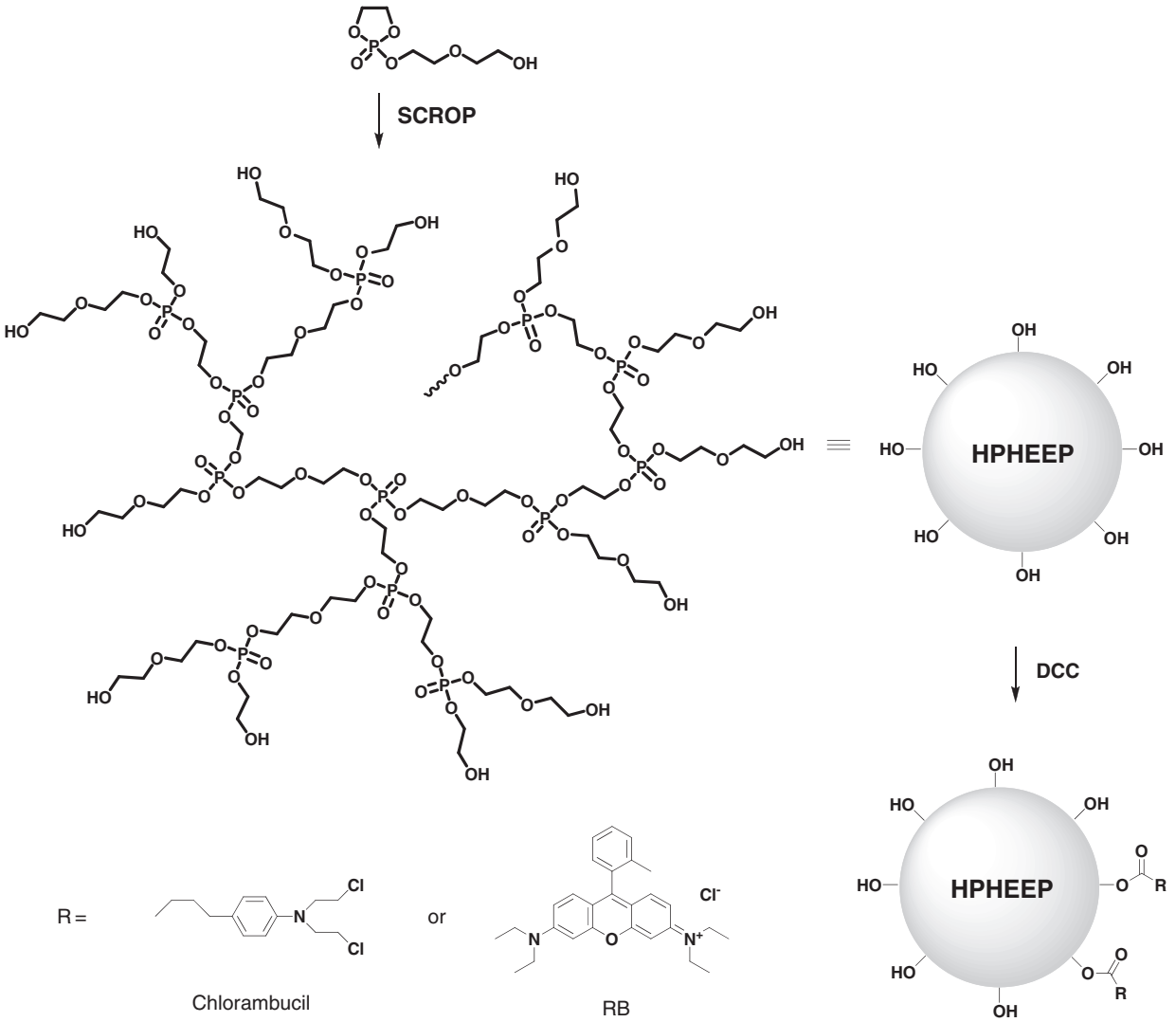

Figure 11 Synthesis route of HPHEEP–chlorambucil/RB conjugates. Reproduced with permission from Liu, J. Y.; Huang, W.; Pang, Y.; *et al.* *Biomacromolecules* **2010**, *11*, 1564–1570.[69]

In another study, an amphiphilic hyperbranched multiarm copolymer [H40-star-(PLA-*b*-PEP-OH)] was synthesized through a two-step ROP procedure (**Figure 12**). First, Boltorn H40 was used as the macroinitiator for the ROP of L-LA to form the intermediate (H40-star-PLA-OH). Then, the ROP of EEP was further initiated to produce H40-star-(PLA-*b*-PEP-OH). Benefiting from the amphiphilic structure, H40-star-(PLA-*b*-PEP-OH) was able to self-assemble into micelles in water with an average diameter of 130 nm. *In vitro* evaluation of these micelles demonstrated their excellent biocompatibility and efficient cellular uptake. DOX-loaded micelles were investigated for the proliferation inhibition of HeLa human cervical carcinoma cell line, and the DOX dose required for 50% cellular growth inhibition was found to be 1 μg ml^{-1}.[70]

4.29.6.2 Delivery of Plasmid DNA with PPE

Delivery of nucleic acids (e.g., plasmid DNA, siRNA, or antisense oligomers) is promising for the treatment of numerous diseases, including cancer.[103–106] Cationic polymers have been one of the most important kinds of nonviral carriers for nucleic acid delivery, due to their ability to bind negatively charged nucleic acids by electrostatic interactions.[106–112] Typical cationic polymers used in this field are poly(ethylene imine) (PEI) and polylysine (PLL).[113–115]

As biodegradable polymers, PPEs have shown great potential as carriers for drug delivery. In addition to their biodegradability, PPEs also have a pentavalent phosphorus atom in the backbone, which makes them readily modifiable and appropriate as vectors of nucleic acids. As the first example, Wang *et al.* designed and synthesized a degradable PPE, namely, poly(2-aminoethyl propylene phosphate) (PPE-EA) (**20**) as a gene delivery vector.[11] In the study, the authors synthesized a PPE-EA polymer with high molecular weight, which was able to efficiently condense DNA and also exhibited the ability to protect DNA from nuclease degradation. More importantly, PPE-EA mediated a higher level of gene expression when compared with PEI and PLL, which was due to the controlled release of plasmid DNA from the PPE-EA/DNA complexes, achieved as a result of PPE-EA degradation.

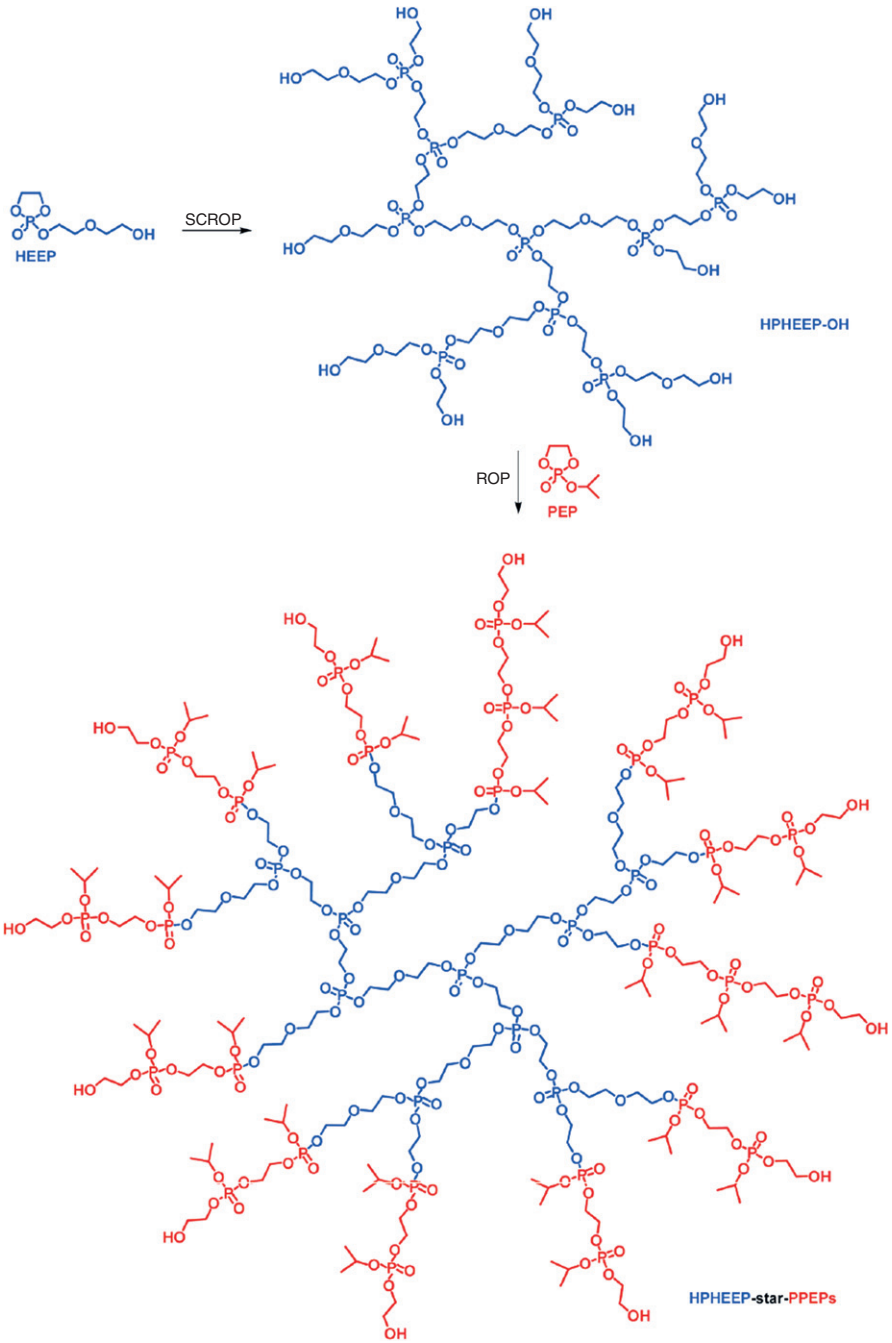

[13]

PPE-EA and its degradation products are biocompatible, rendering it a promising gene delivery vector.

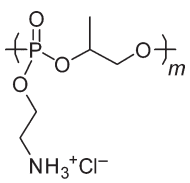

20

The efficiency of PPE-EA as the carrier of plasmid DNA has also been examined *in vivo*.[116] The *in vivo* gene transfer efficiency of the PPE-EA/DNA complexes was evaluated in mouse muscle following intramuscular injection using *LacZ* as a model gene. The expression levels of β-galactosidase encoded by *LacZ* gene in mice which received complexes with N/P ratios of 0.5 and 1, respectively, were compared with those given naked DNA injections. As shown in **Figure 13**, naked DNA injection showed a peak expression, and the expression leveled off between days 7 and 14. In contrast, PPE-EA/DNA complexes with an N/P ratio of 1 yielded a lower level of expression at day 3, peaked at day 7, and then decreased at day 14. This corresponded to 13-fold and 6-fold higher gene expression than naked DNA expression at days 7 and 14, respectively. It is interesting to note that the complexes with a lower N/P ratio, 0.5 versus 1, were more effective. Complexes with an N/P ratio of 0.5 gave 17-fold higher β-gal expression on day 7, and the level persisted until at least day 14.

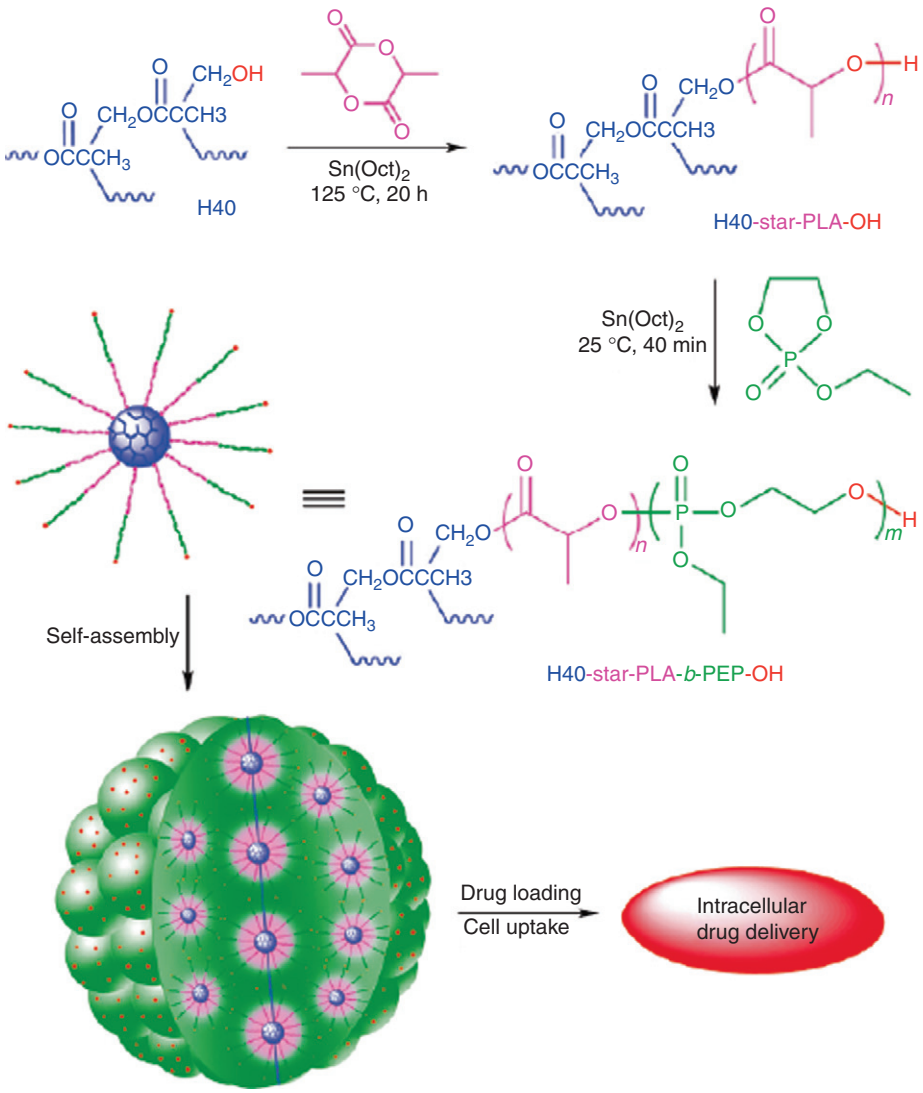

Figure 12 Schematic illustration of synthesis and self-assembly of H40-star-(PLA-*b*-PEP-OH) for drug delivery. Reproduced with permission from Liu, J. Y.; Huang, W.; Pang, Y.; *et al. Langmuir* **2010**, *26*, 10585–10592.[70]

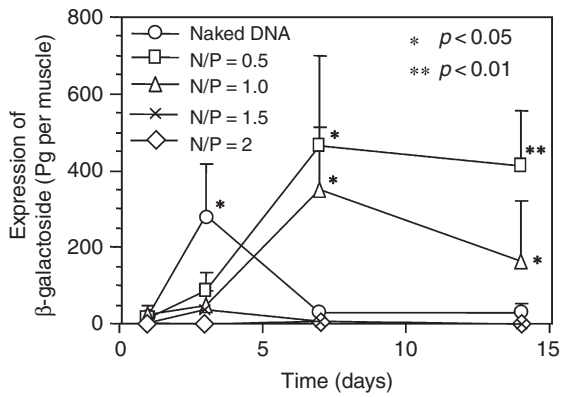

Figure 13 β-Galactosidase expression in mouse muscle after intramuscular injections of naked DNA and PPE-EA/DNA complexes with various N/P ratios. Mean ± SD ($n = 6$). Effect of N/P ratio on β-Gal expression level. Naked DNA and complexes (N/P, 0.5, 1.0, 1.5, 2.0) were given at a dose of 2 μg of DNA per muscle in 40 μl of saline. Reproduced with permission from Wang, J.; Zhang, P. C.; Mao, H. Q.; Leong, K. W. *Gene Ther.* **2002**, *9*, 1254–1261.[116]

Unexpectedly, the PPE-EA/DNA complexes with N/P ratios of 1.5 and 2 were ineffective. It is likely that the slow release of plasmid DNA in the muscle due to the degradation of PPE-EA resulted in this enhancement of gene expression.

Due to the potential of sustained release of plasmid DNA from PPE complexes, Wang *et al.* further investigated the effect of polymer structure of PPEs (mainly the side group) on their transfection performance as gene carriers.[117] They synthesized cationic PPEs with different side chain charge groups and compared their behaviors in terms of gene transfer. It was found that poly(*N*-methyl-2-aminoethyl propylene phosphate) (PPE-MEA) (**21**), with a secondary amino group ($-CH_2CH_2NHCH_3$) side chain, released DNA over several hours at N/P ratios from 0.5 to 5, whereas poly(6-aminohexyl propylene phosphate) (PPE-HA) (**22**), bearing $-CH_2(CH_2)_4CH_2NH_2$ groups on the side chain, did not release DNA in the same ratio range over 30 days. Hydrolytic degradation and DNA binding results suggested that side chain cleavage, besides polymer degradation, was the predominant factor which affected DNA release and transfection efficiencies. The side chain of PPE-MEA was cleaved faster than that of PPE-HA,

resulting in poor cellular uptake and no transgene expression for PPE-MEA/DNA complexes in COS-7 cells at charge ratios from 4 to 12. In contrast, PPE-HA/DNA complexes were stable enough to be internalized by cells and effected gene transfection (3400-fold higher than background at a charge ratio of 12). Interestingly, gene expression levels mediated by PPE-MEA and PPE-HA in mouse muscle following intramuscular injection of complexes showed a reversed order: PPE-MEA/DNA complexes mediated 1.5–2-fold higher luciferase expression in mouse muscle compared to naked DNA injection, while PPE-HA/DNA complexes induced delayed and lowered luciferase expression compared to naked DNA. These results suggested that the side chain structure is a crucial factor determining the mechanism and kinetics of hydrolytic degradation of PPE carriers, which in turn influences the kinetics of DNA release from PPE/DNA complexes and their transfection abilities *in vitro* and *in vivo*.

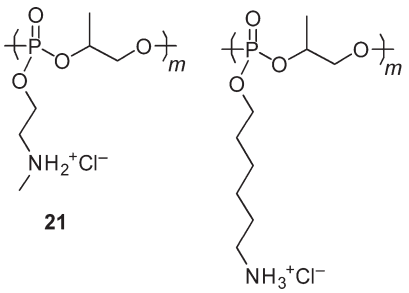

Gene transfer into the central nervous system (CNS) offers the prospect of manipulating gene expression for studying neuronal function and eventually for treating neurological disorders. The feasibility of using PPE-EA/DNA complexes for gene transfection in the CNS has been explored after intracisternal and intrastriatum injection in mice using luciferase as the reporter gene.[118]

It has also been demonstrated that sustained release of plasmid DNA from its complexes with PPE-EA facilitates gene expression in the mouse brain (**Figure 14**). Gene transfer efficiency increased with an N/P ratio from 0.2 to 2 and then dropped as the N/P ratio reached 10 (**Figure 14(a)**). The time course study shown in **Figure 14(b)** demonstrates prolonged gene expression in the mouse brain following intracisternal injection of PPE-EA/pCAG-Luc complexes. Although PEI/DNA provided the highest transgene expression at 2×10^5 RLU/brain at the first day after injection, about fourfold higher than that produced by PPE-EA/DNA at an N/P ratio of 2 and twofold higher than the expression mediated by naked DNA and PPE-EA/DNA at an N/P ratio of 0.5, by the third day after injection, the luciferase expression level of PPE-EA/DNA at an N/P ratio of 2 increased to 1.8×10^5 RLU/brain, while the expression levels of the other three groups remained unchanged. After 10 days, the expression level for PPE-EA/DNA at an N/P ratio of 2 was about the same as on day 3, while those of the other three groups began to drop. Up to 28 days, PPE-EA/DNA at an N/P ratio of 2 still provided a level of transgene expression at 8×10^4 RLU/brain, similar to that observed at previous time points. This level was significantly higher than those offered by PEI/DNA, naked DNA, and

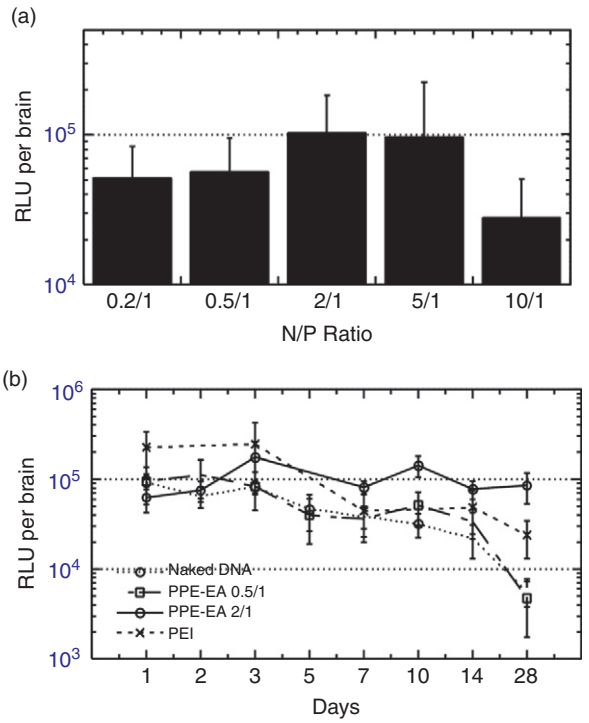

Figure 14 Luciferase expression in mouse brain after intracisternal injections of PPE-EA/pCAG-Luc complexes: (a) effects of N/P ratios; (b) time course study. Values are presented as mean ± SD ($n = 6$). Reproduced with permission from Li, Y.; Wang, J.; Lee, C. G. L.; *et al. Gene Ther.* **2004**, *11*, 109–114.[118]

PPE-EA/DNA at an N/P ratio of 0.5. This study demonstrated that biodegradable PPE-EA may mediate prolonged gene transfer in the CNS through sustained release of plasmid DNA, with an efficiency superior to naked DNA and its complexes with PEI.

The advantage of sustained release of plasmid DNA using PPE-EA as the carrier has also been demonstrated in a multi-layered membrane model. Wang *et al.* further fabricated a multilayer film by layer-by-layer assembly using PPE-EA and plasmid DNA as the pair of polyions,[119] aiming to sustain gene expression in the cells cultured on the surface of multilayer film. It was expected to modulate the behavior of 'seed' cells by prompting or prolonging specific protein expression by the cells, which could be beneficial for tissue engineering applications.

The multilayer film of PPE-EA and plasmid DNA degraded upon incubation in phosphate-buffered saline at 37 °C and sustained the release of bioactive plasmid DNA for up to 2 months. On the other hand, the surface of PPE-EA facilitated mouse osteoblast cell adhesion, and the sustained DNA release directly prolonged gene expression in osteoblast cells cultured on the surface. Osteoblast cells cultured on $(\text{pEGFP-N2/PPE-EA})_{10}$ film showed sustained expression of green fluorescence protein for up to 20 days in culture. The transfected cell ratio was 42.1% at day 5 and increased to 46.9% after 10 days in culture (**Figure 15**). However, when using non-degradable PEI to fabricate the multilayer film $(\text{pEGFP-N2/PEI})_{10}$, only about 10% cells cultured on the surface were positive, regardless of the observed cytotoxicity of such films. The study

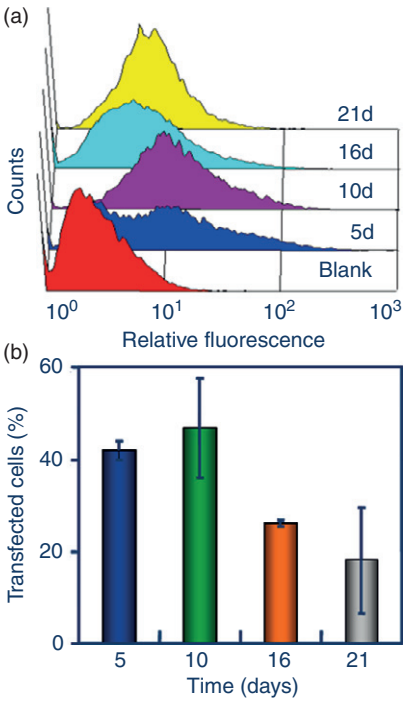

Figure 15 The local transfection efficiency of osteoblast cells on $(pEGFP\text{-}N2/PPE\text{-}EA)_{10}$ films at different times in physiological condition: (a) the histogram of the fluorescence intensity of the cells cultured on films; (b) the percentage of EGFP-positive cells. Values shown are averages ± SD ($n = 2$). Reproduced with permission from Lu, Z. Z.; Wu, J.; Sun, T. M.; *et al. Biomaterials* **2008**, *29*, 733–741.[119]

demonstrated that without any additional transfection reagent, films fabricated from biodegradable PPE-EA polycations and plasmid DNA are capable of sustained delivery of transcriptionally active DNA to cells cultured on the film. Such a multilayer system may be useful in the surface modification of tissue engineering scaffolds.

4.29.6.3 Delivery of siRNA with PPE

RNA interference (RNAi) has recently emerged as a powerful method for biological research and holds great potential for the treatment of human diseases.[103,105,120–122] Due to its fast degradation in the physiological milieu, poor cellular uptake, inefficient translocation into the cytoplasm, and lack of targeting ability, delivery of synthetic siRNA for disease treatment remains the major obstacle to its therapeutic application. Various delivery vehicles have been developed as carriers for siRNA delivery to treat human diseases, including cancer.[110,123]

Cationic PPE has shown superiority in delivering plasmid DNA, owing to its fast degradation at neutral pH or in cells.[11,116,117,119] Considering that the intracellular release of siRNA is indeed a very important barrier for the performance of gene silencing, cationic PPE can be used as the carrier for siRNA. It may facilitate the release of siRNA and hence improve the delivery efficiency. In 2008, Wang *et al.* reported the first PPE-containing polymer, namely poly(ethylene glycol)-*b*-poly(ε-caprolactone)-*b*-poly(2-aminoethyl ethylene phosphate) (mPEG-*b*-PCL-*b*-PPE-EA) (**23**) for efficient siRNA delivery.[77] The triblock copolymer was amphiphilic and self-assembled in aqueous solution to form tri-layered cationic MNPs. The rationale behind the design is that PCL block is hydrophobic, which could induce micellar core formation and stabilize the nanoparticles, while hydrophilic PEG can protect siRNA and extend blood circulation for systemic administration and the positively charged PPE-EA block serves as an siRNA binding site and is expected to release siRNA. These unique tri-layered MNPs allow siRNA loading after nanoparticle formation while maintaining uniformity and mediate gene expression silencing in the presence of serum while showing good biocompatibility in cells.

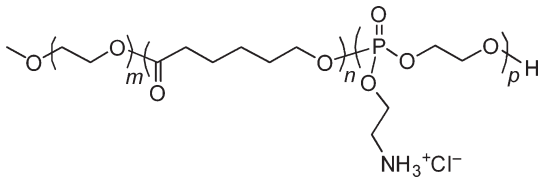

23

As shown in Figure 16, expression of GFP was significantly downregulated in HEK293 cells transfected with pEGFP-N2 (Figure 16(a)). FACScan analysis revealed that the number of GFP-expressing cells transfected with GFP22 siRNA/MNPs (N/P = 50:1) was comparable with those transfected with complexes of GFP22 siRNA using Lipofectamine 2000 transfection when increasing the siRNA dose (Figure 16(b)). Gene silencing efficiency using MNPs was dependent on the N/P ratio, as increasing the N/P ratio from 50 to 100 resulted in significantly enhanced inhibition of gene expression (Figure 16(c)). Such enhancement was possibly due to the improved siRNA internalization by cells when the N/P ratio was increased. It has been demonstrated that the relative geometrical mean fluorescence intensities (GMFI) of HEK293 cells incubated with MNPs/FAM-siRNA showed an N/P ratio-dependent increase when compared with those treated with free FAM-siRNA at the same siRNA dose, indicating that siRNA internalization by cells was improved with an increased N/P ratio (Figure 16(d)).

The potential of mPEG-*b*-PCL-*b*-PPE-EA as an siRNA carrier has been further evaluated *in vivo* for cancer therapy. Wang *et al.* studied *in vivo* cancer treatment using a complex of mPEG-*b*-PCL-*b*-PPE-EA with siRNA, termed a micelleplex, by targeting the acid ceramidase (AC) oncogene through systemic administration.[124] A tumor xenograft model was generated in female athymic (nu/nu) mice by injection with BT474 breast cancer cells. They compared the tumor growth inhibition efficacy of systemic administration of micelleplex$_{siAC}$ (si*AC* represents the specific siRNA targeting AC) with micelleplex$_{siN.C.}$ or blank vehicle administration. Mice were treated every day, beginning on the 10th day after xenografts were seeded. As shown in Figure 17, intravenous injection of micelleplex$_{siAC}$ in tumor-bearing mice showed particularly significant inhibition of tumor growth, whereas neither micelleplex$_{siN.C.}$ at the same siRNA dose nor blank MNP at the same concentration affected tumor growth, indicating that micelleplex$_{siAC}$-delivered si*AC* displays sequence-specific antitumor activity *in vivo*. Importantly, this delivery system does not activate the innate immune response, demonstrating its potential for systemic delivery of siRNAs for cancer therapy.

Cancer therapy relying on a single therapeutic strategy may remain suboptimal. The combination of two or more therapeutic approaches with different mechanisms can

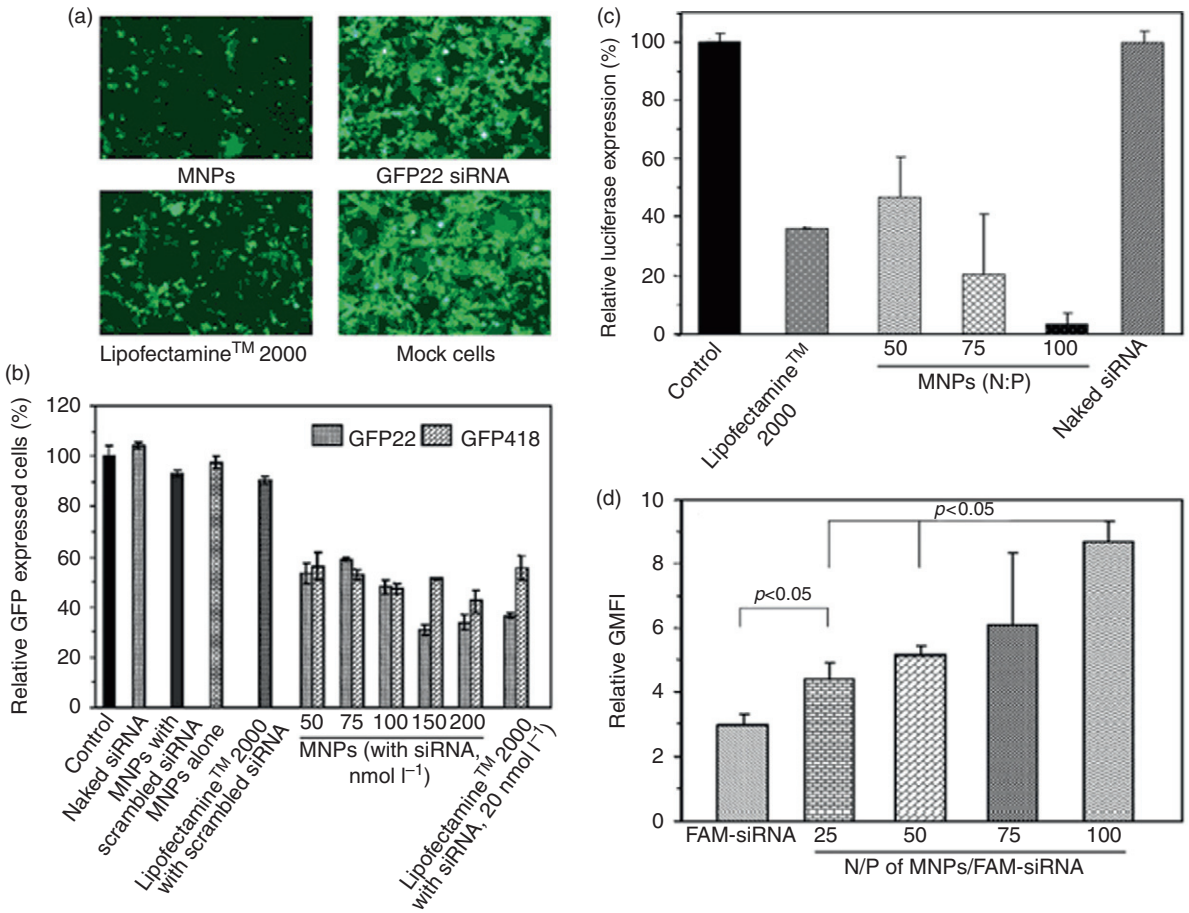

Figure 16 (a) Fluorescence images of HEK293 cells with GFP expression silenced by MNPs or Lipofectamine 2000 with GFP22 siRNA or with naked GFP22 siRNA or without treatment (mock cells). Dose of siRNA for MNPs and naked GFP22 siRNA was 150 nmol l^{-1}, while dose of siRNA for Lipofectamine 2000 was 20 nmol l^{-1}. (b) Relative gene silencing efficiency in GFP-expressed HEK293 cells. N/P ratios of MNPs to siRNA were fixed at 50:1. Dose of siRNA for Lipofectamine 2000 and naked siRNA was 20 and 100 nmol l^{-1}, respectively. (c) Effect of N/P ratios of MNPs to siRNA on gene silencing efficiency. Dose of siRNA for Lipofectamine 2000 and MNPs was 20 and 100 nmol l^{-1}, respectively. (d) Dependence of the relative geometrical mean fluorescence intensities (GMFI) of HEK293 cells to N/P ratio. Cells were treated with MNPs carrying FAM-siRNA at a dose of 100 nmol l^{-1}. Reproduced with permission from Sun, T. M.; Du, J. Z.; Yan, L. F.; *et al. Biomaterials* **2008**, *29*, 4348–4355.[77]

cooperatively prohibit cancer development and is a promising strategy for effective treatment of cancers with synergistic or combined effects.[108] Taking this into consideration, Wang *et al.* further developed the mPEG-*b*-PCL-*b*-PPE-EA system to form a 'two-in-one' micelleplex for simultaneous delivery of therapeutic siRNA and anticancer drug paclitaxel for synergistic cancer therapy (**Figure 18**).[125]

They first demonstrated that MNPs were capable of simultaneous encapsulation of both siRNA and paclitaxel to form a 'two-in-one' micelleplex. Thereafter, they confirmed both *in vitro* and *in vivo* that the 'two-in-one' micelleplex could effectively co-deliver the two cargos into the same tumor cells. They demonstrated that the 'two-in-one' micelleplex, $^{paclitaxel}micelleplex_{siPlk1}$, could synergistically inhibit tumor cell proliferation *in vitro*. They further assessed whether the synergistic effect of $^{paclitaxel}micelleplex_{siPlk1}$ on cell proliferation inhibition *in vitro* could also be achieved in terms of tumor growth inhibition following systemic administration. Mice bearing MDA-MB-435s xenografts were treated with $^{paclitaxel}micelleplex_{siPlk1}$ or various other formulations through i.v. injection every other day from the 12th day after xenograft implantation. As indicated (**Figure 19(a)**), the delivery of paclitaxel by $^{paclitaxel}micelleplex_{siNonsense}$ at a lower paclitaxel dose (0.667 μg kg^{-1} per injection) hardly affected tumor growth compared with PBS treatment. Delivery of siPlk1 (0.223 mg kg^{-1} per injection) by $micelleplex_{siPlk1}$ only moderately inhibited tumor growth. However, simultaneous delivery of the same doses of paclitaxel and si*Plk1* by $^{paclitaxel}micelleplex_{siPlk1}$ exhibited particularly significant inhibition of tumor growth compared with PBS treatment ($p < 0.0001$). More importantly, a synergistic inhibitory effect of the two therapeutic agents on tumor growth was demonstrated (combination index < 1). In contrast, combinatorial delivery of separate siPlk1 and paclitaxel by $micelleplex_{siPlk1}$ and $^{paclitaxel}micelleplex_{siNonsense}$ only showed moderate inhibition of tumor growth and no synergistic effect was observed, primarily due to the more separate internalization of the two micelleplexes by tumor cells as demonstrated above. Additionally, the co-delivery system $^{paclitaxel}micelleplex_{siPlk1}$ showed a more effective antitumor growth effect than Taxol at the same paclitaxel dose (**Figure 19(b)**).

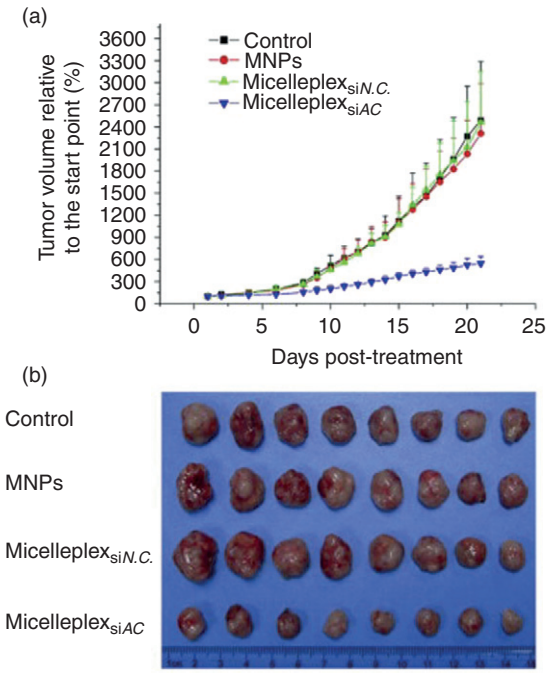

Figure 17 Antitumor growth by intravenous injection of various formulations. (a) Inhibition of BT474 xenograft tumor growth by micelleplex$_{siAC}$. Doses of siRNA and micelles for intravenous injection were 1 mg kg^{-1} and 19.5 μg kg^{-1} per injection, respectively. (b) Images of BT474 xenograft tumors at the end time point of the treatment. The control group received Phosphate Buffered Saline (pH 7.4, 0.01 M) (PBS) injections. Reproduced with permission from Mao, C. Q.; Du, J. Z.; Sun, T. M.; *et al. Biomaterials* **2011**, *32*, 3124–3133.[124]

4.29.6.4 PPE for Tissue Engineering Applications

Tissue engineering is a medical engineering technology that offers a promising new approach to create biological alternatives for regenerating different tissues.[126] An artificial extracellular matrix in which cells can proliferate and differentiate with subsequent new tissue generation is critical in tissue engineering. Scaffolds provide necessary substances on which cells can attach, and they regulate cell proliferation, differentiation, and function in tissue engineering applications. Both natural extracellular materials and synthetic biodegradable polymers have been used to fabricate scaffolds for tissue engineering.[127]

It is known that the properties of scaffolds including the surface properties, stiffness, and so on are critical for cell–scaffold interactions.[128] Therefore, structural variation of the components comprising the scaffold is required. Fortunately, PPEs are indeed structure adjustable; both the backbone and side chain groups can be readily manipulated to alter their physicochemical properties. Additionally, it has been shown that the phosphoester bond in the PPE backbone can be cleaved by water under physiological conditions and the ultimate hydrolytic breakdown products of the polymers are phosphate, alcohol, and diol. It is expected that the phosphate group can capture calcium ions in the medium, which help to produce abundant hydroxyapatite-like calcium phosphate deposits, which further promote their applications in tissue engineering. Due to the unique features of PPEs, a variety of PPE-containing scaffolds have been fabricated for tissue engineering.

4.29.6.4.1 PPE as a nerve guide conduit

The first example of PPEs used in tissue engineering was an elastic PPE copolymer.[12,14] The copolymer P(BHET-EOP/TC) (**24**) was obtained by polycondensation of bis(hydroxyethyl) terephthalate and ethyl ortho-phosphodichloridate (EOP), followed by chain extension with terephthaloyl chloride in a second polycondensation step.

The obtained copolymer P(BHET-EOP/TC) has been fabricated into conduits to guide nerve regeneration. One day after implantation, some of the nerve guide conduit chambers (three out of four type II conduits) became filled with a solid structure that bridged the two nerve stumps (**Figure 20(a)**). This structure appeared as a blood clot and was loosely attached to the stumps. On day 3, the solid structure was present in all tubes examined (**Figure 20(b)**). By microscopic examination, small threads dis-

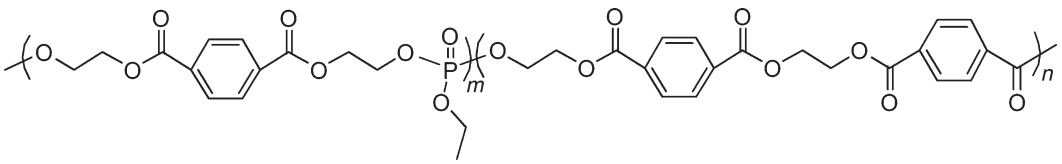

24

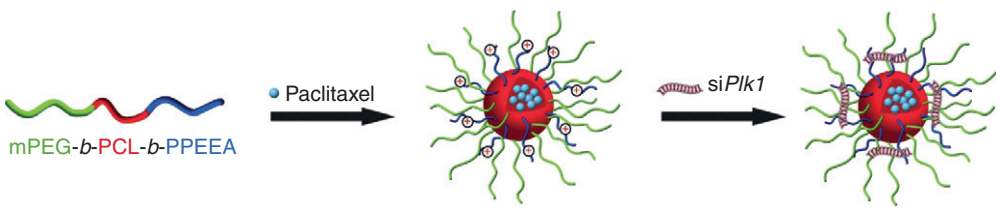

Figure 18 Schematic illustration of MNP formation and the loading of paclitaxel and siRNA. Reproduced with permission from Sun, T. M.; Du, J. Z.; Yao, Y. D.; *et al. ACS Nano* **2011**, *5*, 1483–1494.[125]

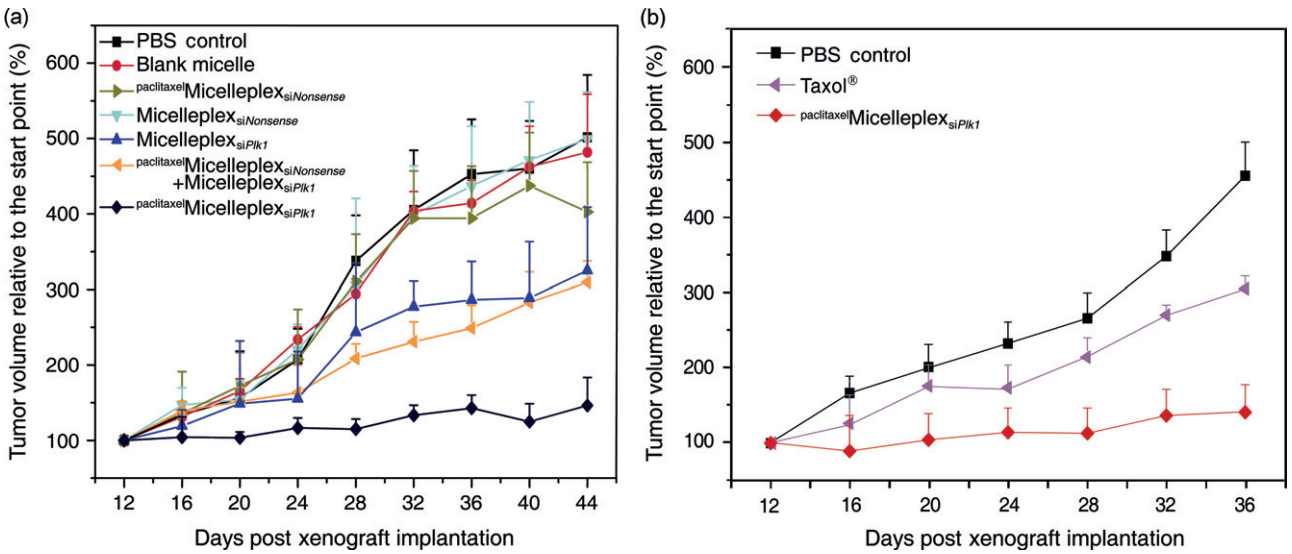

Figure 19 (a) Inhibition of MDA-MB-435s xenograft tumor growth by ^{paclitaxel}micelleplex$_{siPlk1}$ in comparison with various formulations ($n = 6$). (b) Comparison of tumor growth inhibition effect between i.v. injection of Taxol and ^{paclitaxel}micelleplex$_{siPlk1}$ with the same dose of paclitaxel ($n = 6$). MDA-MB-435s xenograft tumor-bearing mice received one i.v. injection every other day from the 12th day post xenograft implantation in all of the experiments. The dose of paclitaxel per injection was 0.667 μg kg^{-1} and the dose of siRNA was 0.223 mg kg^{-1}, if required. The tumor tissues were collected for western blot analyses 24 h after the last injection. Reproduced with permission from Sun, T. M.; Du, J. Z.; Yao, Y. D.; *et al. ACS Nano* **2011**, *5*, 1483–1494.[125]

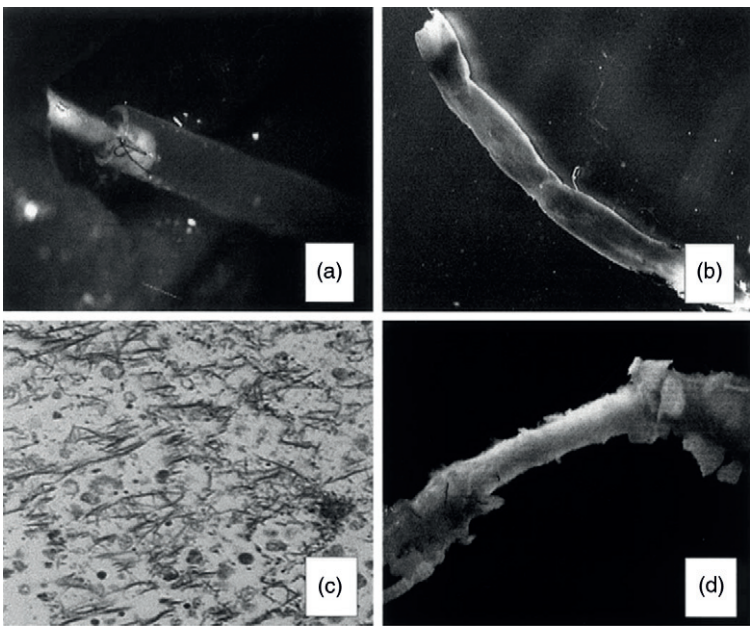

Figure 20 Macroscopic views of (a) the sciatic nerve repaired at the proximal stump with a type II PPE conduit prefilled with saline at the time of implantation. (b) A macroscopic picture of the matrix cable across 10 mm gap at 3 days in a type II PPE conduit. (c) Micrograph of a longitudinal section of the acellular fibrin matrix found at 3 days. The original magnification was × 200. (d) A regenerated nerve 3 months after surgery. A conduit, 14 mm in total length, was used to bridge a 10 mm gap. The obtained copolymer P(BHET-EOP/TC) has been fabricated into conduits to guide nerve regeneration.[12]

tributed with a predominantly longitudinal orientation were observed (Figure 20(c)), suggesting an accumulation of 'brain matrices'. The structure had become connected with the stumps 5 days post-implantation. Regenerated axons could be observed 2 weeks later in the proximal part of regenerated cables and 1 month later in the distal sciatic stump, 5 mm distal to the suture line. Most of them were unmyelinated and were present together with numerous Schwann cells. After 3 months, positive reflex responses were observed in 40% of the rats that were implanted with type I and 92% of those implanted with type II conduits when the nerve trunks distal to the conduits were pinched in anesthetized animals. All the rats had a regenerated cable inside the conduits, which had bridged a 10 mm gap between the nerve stumps (Figure 20(d)). The regenerated cables were centrally located within the conduits, surrounded by a fine epineurium. The cables contained numerous fascicles of myelinated as well as unmyelinated axons. Most of the axons in the distal nerve trunks were already myelinated.

4.29.6.4.2 PPE for bone tissue regeneration and osteogenesis

Recent research into PPE scaffolds for tissue engineering has been more focused on bone tissue regeneration because of the attractive osteoinductive potential of phosphate-containing polymers.[12,14,129]

Wang *et al.* have recently demonstrated that surface modification with PEEP can enhance osteoblast adhesion, proliferation, and function.[130] In this study, a diblock copolymer PLLA-*b*-PEEP was used to modify a PLLA surface by a spin-coating process. X-ray photoelectron spectroscopy measurements were used to demonstrate the enriched phosphorus atomic composition of the surface. Initial osteoblast attachment and proliferation on the modified surfaces were significantly enhanced. Moreover, cellular alkaline phosphatase activity and mineral calcium depositions were also promoted by PEEP modification (**Figure 21**). Gene expression determined by reverse transcription polymerase chain reaction further revealed that type I collagen and osteocalcin expression were upregulated in osteoblasts cultured on the modified surfaces, which indicated that PEEP modification might be potentially osteoinductive.[130]

Although the mechanism of the osteoinductive property of PPEs is still not clearly understood, it has been reported that phosphate groups may have a direct influence on osteogenesis.[131] Anseth and co-workers found that the tethered charged phosphate groups on the polymer scaffold directly affected the differentiation fate of human mesenchymal stem cells (hMSCs) and led to osteogenesis.[131] Penczek's group elaborated a transesterification method and prepared a number of related poly (alkylene phosphates).[21,132,133] These biorelated polymers have shown ability to bind cations[134] and to actively transport cations of biological importance (Mg^{2+},Ca^{2+}) through biomembranes.[135] Such interactions with cations mimicked the biomineralization processes. The hydrolysis of PPE generates phosphate groups, which might contribute to the osteoinductive property of PPEs.

Such an advantage of PPE-based scaffolds has also been demonstrated in a hydrogel for marrow-derived mesenchymal stem cell (MSC) encapsulation. Elisseeff and co-workers have synthesized a water-soluble macromer, PEG di-[ethyl phosphatidyl (ethylene glycol) methacrylate] (PhosPEG-dMA), which can be photopolymerized using UV light with 0.05% photoinitiator (**Figure 22**).[136,137] They observed that the polymer was hydrolytically degradable, and alkaline phosphatase, a bone-derived enzyme, accelerated degradation. Gene expression and protein analysis demonstrated that a hydrogel containing an intermediate concentration of the phosphoester promoted the gene expression of bone-specific markers with the encapsulation of MSC. Mineralization of the phosphoester-containing hydrogels increased in the presence of phosphorus because the degradation product, phosphoric acid, can capture calcium ions to produce abundant hydroxyapatite-like calcium phosphate deposits.

Wang *et al.* have explored therapeutic chondrogenesis with rabbit synovium-derived mesenchymal stem cells (SMSC) encapsulated in photopolymerized hydrogels. A non-degradable poly (ethylene glycol) diacrylate (PEGDA)-based hydrogel and a biodegradable phosphoester poly(ethylene glycol) (PhosPEG)-based hydrogel were both applied as three-dimensional scaffolds for mediation of SMSC chondrogenesis *in vitro*.[138]

Another phosphoester-containing and photo-cross-linkable hydrogel was obtained from acrylated PPE-HA, which was synthesized by the conjugation of acrylate groups to the side chains of PPE-HA.[139] Goat mesenchymal stem cells encapsulated in the gel maintained their viability when cultured in osteogenic medium for 3 weeks.

In addition, Wang's group developed a one-step method to synthesize photo-cross-linkable macromers based on copolymers of PEG and PPE and further photopolymerized them to form hydrogels, which were capable of cell encapsulation.[76] Qiu and co-workers have prepared a series of unsaturated PPEs (eqn [14]), which can be cross-linked. They have investigated the cross-linking, mechanical properties, degradation, and biocompatibility of these materials as injectable and biodegradable bone substitutes.[140–143]

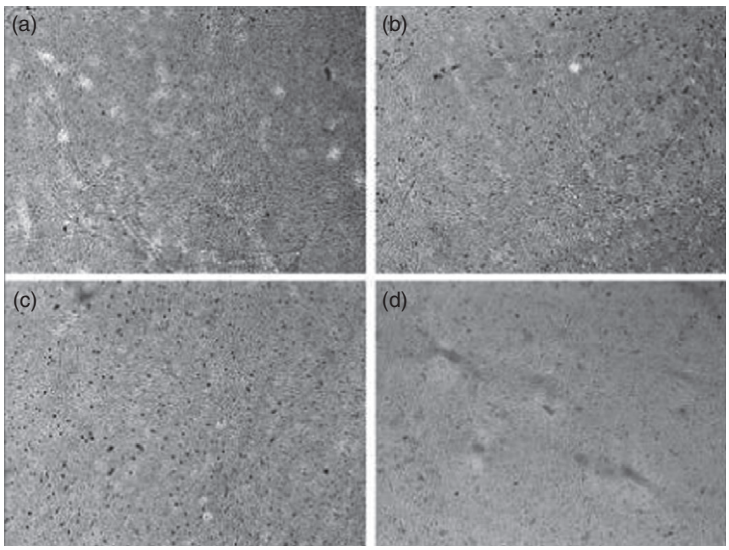

Figure 21 Von Kossa staining views of osteoblasts cultured for 14 days on different surfaces: (a) $PLLA_{85}$-*b*-$PEEP_{58}$; (b) $PLLA_{85}$-*b*-$PEEP_{110}$; (c) $PLLA_{85}$-*b*-$PEEP_{224}$; and (d) PLLA. Reproduced with permission from Yang, X. Z.; Sun, T. M.; Dou, S.; *et al. Biomacromolecules* **2009**, *10*, 2213–2220.[130]

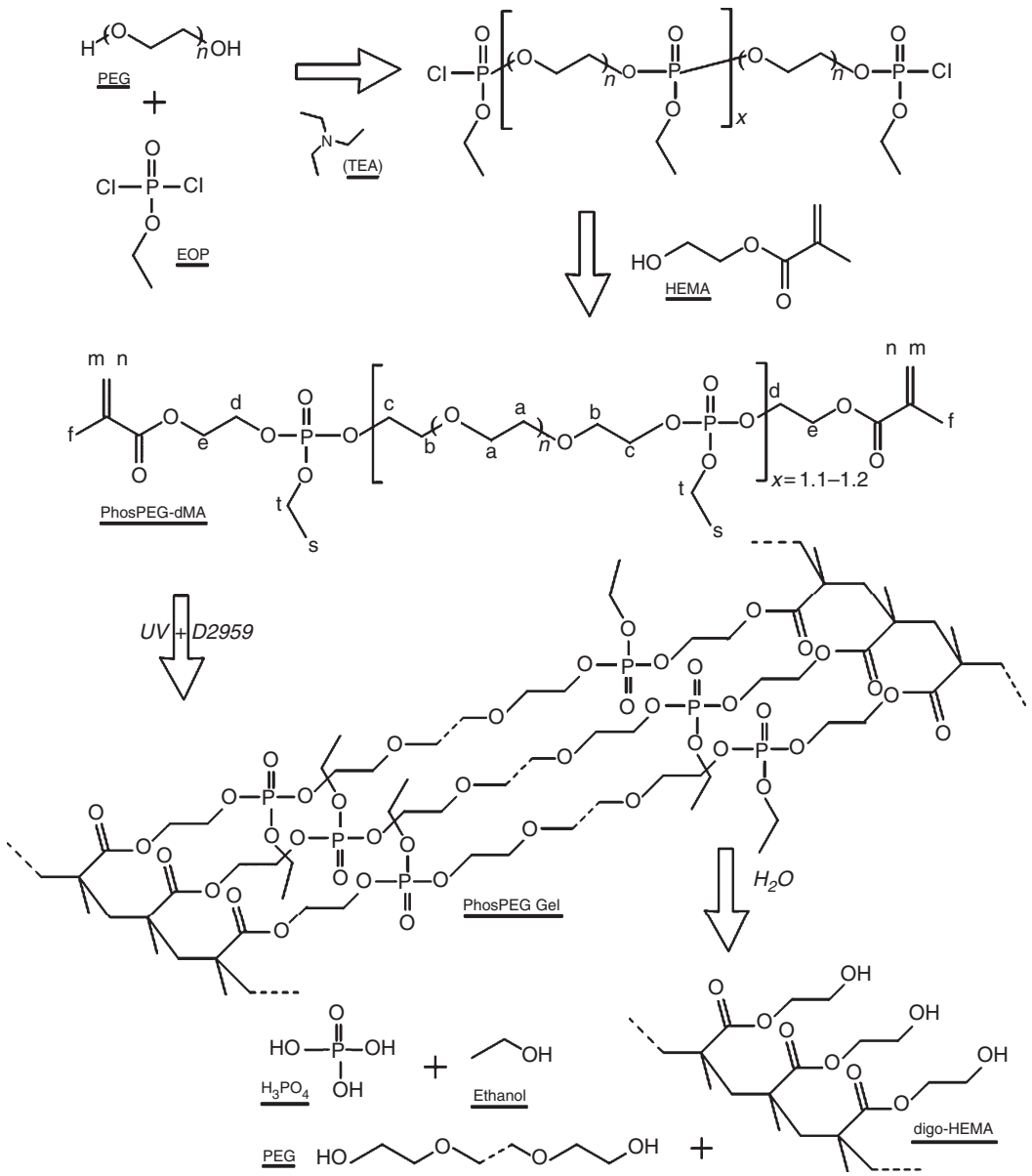

Figure 22 Schematic illustration for macromer PhosPEG-dMA synthesis, PhosPEG Gel photogelation, and degradation. Reproduced with permission from Wang, D. A.; Williams, C. G.; Li, Q. A.; *et al. Biomaterials* **2003**, *24*, 3969–3980.[137]

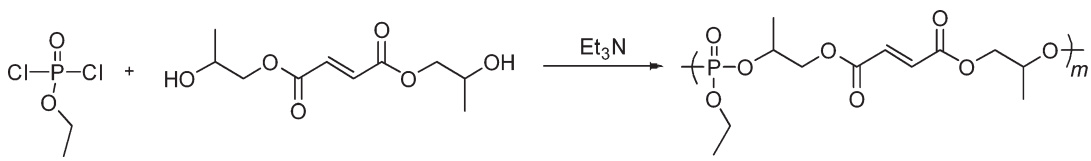

[14]

4.29.7 Conclusions and Outlook

The applications of PPE have expanded remarkably owing to significant improvements in controlled synthesis approaches, which make the synthesis of different macromolecular structures accessible. Furthermore, these materials show the capability of self-assembly to form nanostructures, a variety of functionalities, and a corresponding diversity of properties. Although PPEs have shown great potential in drug/gene delivery and cell-responsive tissue engineering, many aspects of investigation or optimization still need to be further detailed: (1) fundamental aspects of PPEs in chemistry need further studies to match the requirements for potential commercial developments; (2) the *in vivo* fate of PPEs still remain unclear, particularly when they are used for drug and gene delivery; (3) some PPEs have shown enhanced cell adhesion and/or proliferation function *in vitro*, but *in vivo* activities with respect to osteoinductiveness need further evaluation; and

(4) other aspects like the thermoresponsiveness of some PPEs and their applications still need detailed investigations. Although still under-researched, this class of materials with a biodegradable backbone is promising for biomedical applications.

References

1. Penczek, S.; Duda, A.; Kałużyński, K.; *et al. Makromol. Chem. Macromol. Symp.* **1993**, *73*, 91–101.
2. Penczek, S.; Lapienis, G.; Kałużyński, K.; Nyk, A. *Pol. J. Chem.* **1994**, *68*, 2129–2142.
3. Penczek, S.; Pretula, J.; Kałużyński, K. *Pol. J. Chem.* **2001**, *75*, 1171–1181.
4. Penczek, S.; Klosinski, P. *Models of Biopolymers by Ring-Opening Polymerization*; CRC Press: Boca Raton, FL, **1990**; 291–378.
5. Dahiyat, B. I.; Richards, M.; Leong, K. W. *J. Control. Release* **1995**, *33*, 13–21.
6. Luo, Y.; Zhuo, R. X.; Fan, C. L. *Chem. J. Chin. U* **1995**, *16*, 1633–1636.
7. Luo, Y.; Zhuo, R. X.; Fan, C. L. *Chin. Chem. Lett.* **1995**, *6*, 333–334.
8. Fu, J.; Zhuo, R. X.; Fan, C. L. *Chem. J. Chin. U* **1997**, *18*, 1706–1710.
9. Richards, M.; Dahiyat, B. I.; Arm, D. M.; *et al. J. Biomed. Mater. Res.* **1991**, *25*, 1151–1167.
10. Shi, F. Y.; Wang, L. F.; Tashev, E.; Leong, K. W. *ACS Symp. Ser.* **1991**, *469*, 141–154.
11. Wang, J.; Mao, H. Q.; Leong, K. W. *J. Am. Chem. Soc.* **2001**, *123*, 9480–9481.
12. Wang, S.; Wan, A. C. A.; Xu, X. Y.; *et al. Biomaterials* **2001**, *22*, 1157–1169.
13. Zhao, Z.; Wang, J.; Mao, H. Q.; Leong, K. W. *Adv. Drug Deliv. Rev.* **2003**, *55*, 483–499.
14. Wan, A. C. A.; Mao, H. Q.; Wang, S.; *et al. Biomaterials* **2001**, *22*, 1147–1156.
15. Leong, K. W.; Mao, H. Q.; Zhuo, R. X. *Chin. J. Polym. Sci.* **1995**, *13*, 289–314.
16. Chen, D. P.; Wang, J. *Macromolecules* **2006**, *39*, 473–475.
17. Wang, Y. C.; Shen, S. Y.; Wu, Q. P.; *et al. Macromolecules* **2006**, *39*, 8992–8998.
18. Xiao, C. S.; Wang, Y. C.; Du, J. Z.; *et al. Macromolecules* **2006**, *39*, 6825–6831.
19. Iwasaki, Y.; Yamaguchi, E. *Macromolecules* **2010**, *43*, 2664–2666.
20. Wang, Y. C.; Yuan, Y. Y.; Du, J. Z.; *et al. Macromol. Biosci.* **2009**, *9*, 1154–1164.
21. Penczek, S.; Pretula, J.; Kałużyński, K. *Biomacromolecules* **2005**, *6*, 547–551.
22. Lapienis, G. P.; Penczek, S. *J. Polym. Sci. Pol. Chem.* **1977**, *15*, 371–382.
23. Lapienis, G. P.; Penczek, S. *Macromolecules* **1977**, *10*, 1301–1306.
24. Pretula, J.; Penczek, S. *Makromol. Chem.* **1990**, *191*, 671–680.
25. Penczek, S.; Pretula, J.; Kałużyński, K. *J. Polym. Sci. Pol. Chem.* **2005**, *43*, 650–657.
26. Biela, T.; Kubisa, P.; Penczek, S. *Makromol. Chem.* **1992**, *193*, 1147–1164.
27. Richards, M.; Dahiyat, B. I.; Arm, D. M.; *et al. J. Polym. Sci. Pol. Chem.* **1991**, *29*, 1157–1165.
28. Wen, J.; Zhuo, R. X. *Macromol. Rapid Commun.* **1998**, *19*, 641–642.
29. Penczek, S.; Cypryk, M.; Duda, A.; *et al. Prog. Polym. Sci.* **2007**, *32*, 247–282.
30. Dubois, P.; Jacobs, C.; Jerome, R.; Teyssie, P. *Macromolecules* **1991**, *24*, 2266–2270.
31. Duda, A.; Penczek, S. *Macromol. Rapid Commun.* **1995**, *16*, 67–76.
32. Duda, A.; Penczek, S. *Macromolecules* **1995**, *28*, 5981–5992.
33. Kowalski, A.; Duda, A.; Penczek, S. *Macromolecules* **2000**, *33*, 7359–7370.
34. Kowalski, A.; Libiszowski, J.; Biela, T.; *et al. Macromolecules* **2005**, *38*, 8170–8176.
35. Wang, Y. C.; Tang, L. Y.; Sun, T. M.; *et al. Biomacromolecules* **2008**, *9*, 388–395.
36. Yang, X. Z.; Wang, Y. C.; Tang, L. Y.; *et al. J. Polym. Sci. Pol. Chem.* **2008**, *46*, 6425–6434.
37. Wang, Y. C.; Tang, L. Y.; Li, Y.; Wang, J. *Biomacromolecules* **2009**, *10*, 66–73.
38. Wang, Y. C.; Li, Y.; Yang, X. Z.; *et al. Macromolecules* **2009**, *42*, 3026–3032.
39. Kricheldorf, H. R.; Kreiser-Saunders, I.; Stricker, A. *Macromolecules* **2000**, *33*, 702–709.
40. Ryner, M.; Stridsberg, K.; Albertsson, A. C.; *et al. Macromolecules* **2001**, *34*, 3877–3881.
41. Storey, R. F.; Sherman, J. W. *Macromolecules* **2002**, *35*, 1504–1512.
42. Wen, J.; Zhuo, R. X. *Polym. Int.* **1998**, *47*, 503–509.
43. Wang, Y. C.; Yuan, Y. Y.; Wang, F.; Wang, J. *J. Polym. Sci. Pol. Chem.* **2011**, *49*, 487–494.
44. Penczek, S.; Szymanski, R.; Duda, A.; Baran, J. *Macromol. Symp.* **2003**, *201*, 261–269.
45. Song, W. J.; Du, J. Z.; Liu, N. J.; *et al. Macromolecules* **2008**, *41*, 6935–6941.
46. Yuan, Y. Y.; Liu, X. Q.; Wang, Y. C.; Wang, J. *Langmuir* **2009**, *25*, 10298–10304.
47. Wu, J.; Liu, X. Q.; Wang, Y. C.; Wang, J. *J. Mater. Chem.* **2009**, *19*, 7856–7863.
48. Kaluzynski, K.; Libisowski, J.; Penczek, S. *Makromol. Chem.* **1977**, *178*, 2943–2947.
49. Kaluzynski, K.; Libisowski, J.; Penczek, S. *Macromolecules* **1976**, *9*, 365–367.
50. Kamber, N. E.; Jeong, W.; Waymouth, R. M.; *et al. Chem. Rev.* **2007**, *107*, 5813–5840.
51. Pratt, R. C.; Lohmeijer, B. G. G.; Long, D. A.; *et al. J. Am. Chem. Soc.* **2006**, *128*, 4556–4557.
52. Nederberg, F.; Lohmeijer, B. G. G.; Leibfarth, F.; *et al. Biomacromolecules* **2007**, *8*, 153–160.
53. Liu, J. Y.; Pang, Y.; Huang, W.; *et al. Macromolecules* **2010**, *43*, 8416–8423.
54. Wen, J.; Kim, G. J. A.; Leong, K. W. *J. Control Release* **2003**, *92*, 39–48.
55. Wang, X. L.; Zhuo, R. X.; Liu, L. J. *Polym. Int.* **2001**, *50*, 1175–1179.
56. Li, F.; Feng, J.; Zhuo, R. X. *J. Appl. Polym. Sci.* **2006**, *102*, 5507–5511.
57. Wang, Y. C.; Xia, H.; Yang, X. Z.; Wang, J. *J. Polym. Sci. Pol. Chem.* **2009**, *47*, 6168–6179.
58. Liu, X.; Ni, P. H.; He, J. L.; Zhang, M. Z. *Macromolecules* **2010**, *43*, 4771–4781.
59. Cheng, J.; Ding, J. X.; Wang, Y. C.; Wang, J. *Polymer* **2008**, *49*, 4784–4790.
60. Yuan, Y. Y.; Wang, Y. C.; Du, J. Z.; Wang, J. *Macromolecules* **2008**, *41*, 8620–8625.
61. Xiong, M. H.; Wu, J.; Wang, Y. C.; *et al. Macromolecules* **2009**, *42*, 893–896.
62. Sheiko, S. S.; Sumerlin, B. S.; Matyjaszewski, K. *Prog. Polym. Sci.* **2008**, *33*, 759–785.
63. Zhao, B.; Brittain, W. J. *Prog. Polym. Sci.* **2000**, *25*, 677–710.
64. Du, J. Z.; Chen, D. P.; Wang, Y. C.; *et al. Biomacromolecules* **2006**, *7*, 1898–1903.
65. Yuan, Y. Y.; Du, Q.; Wang, Y. C.; Wang, J. *Macromolecules* **2010**, *43*, 1739–1746.
66. Liu, J. Y.; Huang, W.; Zhou, Y. F.; Yan, D. Y. *Macromolecules* **2009**, *42*, 4394–4399.
67. Liu, J. Y.; Pang, Y.; Huang, W.; *et al. Biomaterials* **2010**, *31*, 1334–1341.
68. Liu, J. Y.; Huang, W.; Pang, Y.; *et al. Biomaterials* **2010**, *31*, 5643–5651.
69. Liu, J. Y.; Huang, W.; Pang, Y.; *et al. Biomacromolecules* **2010**, *11*, 1564–1570.
70. Liu, J. Y.; Huang, W.; Pang, Y.; *et al. Langmuir* **2010**, *26*, 10585–10592.
71. Alarcon, C. D. H.; Pennadam, S.; Alexander, C. *Chem. Soc. Rev.* **2005**, *34*, 276–285.
72. Rapoport, N. *Prog. Polym. Sci.* **2007**, *32*, 962–990.
73. Iwasaki, Y.; Wachiralarpphaithoon, C.; Akiyoshi, K. *Macromolecules* **2007**, *40*, 8136–8138.
74. Yuan, Y. Y.; Wang, J. *Colloids Surf. B: Biointerfaces* **2010**, DOI: 10.1016/j.colsurfb.2010.10.044
75. Wang, Y. C.; Wu, J.; Li, Y.; *et al. Chem. Commun.* **2010**, *46*, 3520–3522.
76. Du, J. Z.; Sun, T. M.; Weng, S. Q.; *et al. Biomacromolecules* **2007**, *8*, 3375–3381.
77. Sun, T. M.; Du, J. Z.; Yan, L. F.; *et al. Biomaterials* **2008**, *29*, 4348–4355.
78. Wang, Y. C.; Li, Y.; Sun, T. M.; *et al. Macromol. Rapid Commun.* **2010**, *31*, 1201–1206.
79. Li, S. M.; Garreau, H.; Pauvert, B.; *et al. Biomacromolecules* **2002**, *3*, 525–530.
80. Li, S. M.; Pignol, M.; Gasc, F.; Vert, M. *Macromolecules* **2004**, *37*, 9798–9803.
81. Wang, Y. C.; Liu, X. Q.; Sun, T. M.; *et al. J. Control Release* **2008**, *128*, 32–40.
82. Zhang, L. Y.; Guo, R.; Yang, M.; *et al. Adv. Mater.* **2007**, *19*, 2988–2992.
83. Lee, Y.; Fukushima, S.; Bae, Y.; *et al. J. Am. Chem. Soc.* **2007**, *129*, 5362–5363.
84. Lee, E. S.; Gao, Z. G.; Bae, Y. H. *J. Control Release* **2008**, *132*, 164–170.
85. Gillies, E. R.; Frechet, J. M. J. *Bioconjugate Chem.* **2005**, *16*, 361–368.
86. Takae, S.; Miyata, K.; Oba, M.; *et al. J. Am. Chem. Soc.* **2008**, *130*, 6001–6009.
87. Koo, A. N.; Lee, H. J.; Kim, S. E.; *et al. Chem. Commun.* **2008**, *48*, 6570–6572.
88. Kim, S. H.; Jeong, J. H.; Lee, S. H.; *et al. J. Control Release* **2008**, *129*, 107–116.
89. Cerritelli, S.; Velluto, D.; Hubbell, J. A. *Biomacromolecules* **2007**, *8*, 1966–1972.
90. Thornton, P. D.; Mart, R. J.; Ulijn, R. V. *Adv. Mater.* **2007**, *19*, 1252–1256.
91. Saito, G.; Swanson, J. A.; Lee, K. D. *Adv. Drug Deliv. Rev.* **2003**, *55*, 199–215.
92. Tang, L. Y.; Wang, Y. C.; Li, Y.; *et al. Bioconjugate Chem.* **2009**, *20*, 1095–1099.
93. Kim, D.; Lee, E. S.; Oh, K. T.; *et al. Small* **2008**, *4*, 2043–2050.
94. Liu, S. Q.; Wiradharma, N.; Gao, S. J.; *et al. Biomaterials* **2007**, *28*, 1423–1433.
95. Bae, Y.; Kataoka, K. *Adv. Drug Deliv. Rev.* **2009**, *61*, 768–784.
96. Li, Y. T.; Lokitz, B. S.; Armes, S. P.; McCormick, C. L. *Macromolecules* **2006**, *39*, 2726–2728.
97. Kainthan, R. K.; Brooks, D. E. *Bioconjugate Chem.* **2008**, *19*, 2231–2238.
98. Mugabe, C.; Hadaschik, B. A.; Kainthan, R. K.; *et al. BJU Int.* **2009**, *103*, 978–986.
99. Kontoyianni, C.; Sideratou, Z.; Theodossiou, T.; *et al. Macromol. Biosci.* **2008**, *8*, 871–881.
100. Kitajyo, Y.; Kinugawa, Y.; Tamaki, M.; *et al. Macromolecules* **2007**, *40*, 9313–9321.
101. Ternat, C.; Ouali, L.; Sommer, H.; *et al. Macromolecules* **2008**, *41*, 7079–7089.
102. Kainthan, R. K.; Mugabe, C.; Burt, H. M.; Brooks, D. E. *Biomacromolecules* **2008**, *9*, 886–895.

103. Bumcrot, D.; Manoharan, M.; Koteliansky, V.; Sah, D. W. Y. *Nat. Chem. Biol.* **2006**, *2*, 711–719.
104. Fire, A. Z. *Angew. Chem. Int. Ed.* **2007**, *46*, 6967–6984.
105. de Fougerolles, A.; Vornlocher, H. P.; Maraganore, J.; Lieberman, J. *Nat. Rev. Drug Discov.* **2007**, *6*, 443–453.
106. Morille, M.; Passirani, C.; Vonarbourg, A.; *et al. Biomaterials* **2008**, *29*, 3477–3496.
107. Bilensoy, E. *Expert. Opin. Drug Deliv.* **2010**, *7*, 795–809.
108. Wang, Y.; Gao, S. J.; Ye, W. H.; *et al. Nat. Mater.* **2006**, *5*, 791–796.
109. Wiradharma, N.; Zhang, Y.; Venkataraman, S.; *et al. Nano Today* **2009**, *4*, 302–317.
110. Oh, Y. K.; Park, T. G. *Adv. Drug Deliv. Rev.* **2009**, *61*, 850–862.
111. Tseng, Y. C.; Mozumdar, S.; Huang, L. *Adv. Drug Deliv. Rev.* **2009**, *61*, 721–731.
112. Luten, J.; van Nostruin, C. F.; De Smedt, S. C.; Hennink, W. E. *J. Control Release* **2008**, *126*, 97–110.
113. Merdan, T.; Kopecek, J.; Kissel, T. *Adv. Drug Deliv. Rev.* **2002**, *54*, 715–758.
114. Shuai, X. T.; Merdan, T.; Unger, F.; *et al. Macromolecules* **2003**, *36*, 5751–5759.
115. Lee, S. K.; Han, M. S.; Asokan, S.; Tung, C. H. *Small* **2011**, *7*, 364–370.
116. Wang, J.; Zhang, P. C.; Mao, H. Q.; Leong, K. W. *Gene Ther.* **2002**, *9*, 1254–1261.
117. Wang, J.; Huang, S. W.; Zhang, P. C.; *et al. Int. J. Pharm.* **2003**, *265*, 75–84.
118. Li, Y.; Wang, J.; Lee, C. G. L.; *et al. Gene Ther.* **2004**, *11*, 109–114.
119. Lu, Z. Z.; Wu, J.; Sun, T. M.; *et al. Biomaterials* **2008**, *29*, 733–741.
120. Hannon, G. J. *Nature* **2002**, *418*, 244–251.
121. Chitwood, D. H.; Timmermans, M. C. P. *Nature* **2010**, *467*, 415–419.
122. Castanotto, D.; Rossi, J. J. *Nature* **2009**, *457*, 426–433.
123. Whitehead, K. A.; Langer, R.; Anderson, D. G. *Nat. Rev. Drug Discov.* **2009**, *8*, 129–138.
124. Mao, C. Q.; Du, J. Z.; Sun, T. M.; *et al. Biomaterials* **2011**, *32*, 3124–3133.
125. Sun, T. M.; Du, J. Z.; Yao, Y. D.; *et al. ACS Nano* **2011**, *5*, 1483–1494.
126. Langer, R.; Vacanti, J. P. *Science* **1993**, *260*, 920–926.
127. Shin, H.; Jo, S.; Mikos, A. G. *Biomaterials* **2003**, *24*, 4353–4364.
128. Jiao, Y. P.; Cui, F. Z. *Biomed. Mater.* **2007**, *2*, R24–R37.
129. Hacchou, Y.; Uematsu, T.; Ueda, O.; *et al. J. Dent. Res.* **2007**, *86*, 893–897.
130. Yang, X. Z.; Sun, T. M.; Dou, S.; *et al. Biomacromolecules* **2009**, *10*, 2213–2220.
131. Benoit, D. S. W.; Schwartz, M. P.; Durney, A. R.; Anseth, K. S. *Nat. Mater.* **2008**, *7*, 816–823.
132. Pretula, J.; Penczek, S. *Makromol. Chem. Rapid Commun.* **1988**, *9*, 731–737.
133. Pretula, J.; Kaluzynski, K.; Szymanski, R.; Penczek, S. *J. Polym. Sci. Pol. Chem.* **1999**, *37*, 1365–1381.
134. Szymanski, R.; Penczek, S. *Makromol. Chem.* **1993**, *194*, 1645–1651.
135. Wodzki, R.; Klosinski, P. *Makromol. Chem.* **1990**, *191*, 921–931.
136. Wang, D. A.; Williams, C. G.; Yang, F.; *et al. Tissue Eng.* **2005**, *11*, 201–213.
137. Wang, D. A.; Williams, C. G.; Li, Q. A.; *et al. Biomaterials* **2003**, *24*, 3969–3980.
138. Fan, J. B.; Ren, L.; Liang, R. S.; *et al. J. Biomater. Sci. Polym. Ed.* **2010**, *21*, 1653–1667.
139. Li, Q.; Wang, J.; Shahani, S.; *et al. Biomaterials* **2006**, *27*, 1027–1034.
140. Qiu, J. J.; Liu, C. M.; Hu, F.; *et al. J. Appl. Polym. Sci.* **2006**, *102*, 3095–3101.
141. Qiu, J. J.; He, Z. X.; Liu, C. M.; *et al. Biomed. Mater.* **2008**, *3*, 044107.
142. Qiu, J. J.; Bao, R.; Liu, C. M. *Phosphorus, Sulfur Silicon Relat. Elem.* **2008**, *183*, 815–816.
143. Zhang, Z. X.; Feng, X. L.; Mao, J.; *et al. Biochem. Biophys. Res. Commun.* **2009**, *379*, 557–561.

Biographical Sketches

Jun Wang received a joint BS in chemistry and cell biology at Wuhan University in 1993 and a PhD in polymer chemistry and physics from Wuhan University in 1999 under the direction of Prof. Ren-Xi Zhuo. He has been a postdoctoral fellow at Johns Hopkins Singapore and the Johns Hopkins University School of Medicine under the direction of Prof. Kam Leong. In 2004, he joined the faculty of University of Science and Technology of China as a professor of Life Sciences and Polymer Chemistry. He is a joint professor at the Hefei National Laboratory for Physical Sciences at the Microscale of China. He received the Capsugel Innovation Award in Controlled Drug Delivery from the Controlled Release Society in 2001. His main research interest is the development of biodegradable and biocompatible polymers for drug, gene delivery, and nanomedicine.

You-Yong Yuan, born in 1985 in Anhui, received his BS from Anhui University in 2007. He is currently in the PhD program at the Hefei National Laboratory for Physical Sciences at the Microscale, University of Science and Technology of China. His current interest is the synthesis of nonlinear PPE polymers and their applications in biomedical research.

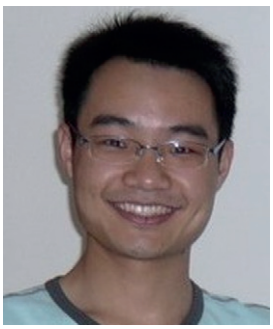

Jin-Zhi Du, born in 1983 in Anhui, received his BS from the Department of Polymer Science and Engineering, University of Science and Technology of China in 2006, where he is currently pursuing graduate studies on stimuli-responsive nanoparticles for drug and gene delivery.

4.30 Industrial Applications of ROMP

A Nickel and BD Edgecombe, Materia, Inc., Pasadena, CA, USA

4.30.1 Introduction

The introduction of novel polymer systems into the modern marketplace is a challenging endeavor. In the simplest terms, if a new material possesses the proper performance-to-cost ratio, it will achieve at least some degree of commercial success. However, both 'performance' and 'cost' are imprecise terms, as there are a number of factors that contribute to each of these designations for a given material.

The performance of a material is always judged relative to the benchmark of an existing technology. Whereas some applications may be underserved by the incumbent material regarding particular performance criteria, design solutions are frequently employed to compensate for such limitations in material properties. For example, 'low toughness' or 'low modulus' is solved through thicker parts, while 'poor abrasion resistance' can be mitigated through the use of matte surfaces. A new material can be successfully introduced to the marketplace when overall cost savings are possible through more efficient part manufacturing, even if the new material itself commands a higher unit price.

In some instances, the incumbent polymeric materials exceed the minimum property requirements for a given application. For example, DVDs, traditionally made of polycarbonate (PC), arguably do not require the high toughness and glass transition temperature provided by the polymer. In this scenario, a new polymer could compete on a 'low-cost' approach; although the new material does not match the performance of the incumbent product, it provides adequate properties at a lower price.

Cost is always a factor in the adoption of a new polymer. New materials invariably face two major challenges when comparing total cost versus incumbent technologies. First, it is difficult to compete against a mature material when the economies of scale for production of the new material have not yet been realized. The millionth kilogram of an existing product will always be cheaper to produce than the first kilogram of a new one. Not only does the new material need to undercut the existing product, but its entire raw material supply chain must also meet the increased demand while minimizing an increase in price. Second, the degree of cost savings to the material's end user must be sufficient to justify the risk of adopting a new product without a proven history in the application. This inherent reluctance to switch materials is more than just aversion to risk (which can be considerable, especially in the high-end biomedical and aerospace industries, where the price of failure is high), but extends to up-front costs like those associated with equipment reengineering and personnel training.

An additional challenge to the commercialization of new polymer products is the finite scope and depth of market knowledge in any technologically innovative company. For example, a company that holds market expertise in rubber products for tires will invariably struggle to introduce a polymer into the medical plastics market or the architectural coatings market. Therefore, a key requirement for successfully bringing new products to market is the coupling of technological

innovation with a thorough understanding of the decision drivers for materials selection in the target applications. Without this type of market research, a new polymeric material may find itself a 'solution in search of a problem' and commercially stagnant.

Since the 1950s, a number of research projects related to the preparation of polymers via ring-opening metathesis polymerization (ROMP) have been reported, some of which have resulted in products of commercial significance. The scope of this chapter is limited to those significant commercial products for which considerable development efforts have been demonstrated in the public domain. Although there are additional applications proposed in the open literature beyond those listed here, emphasis is placed on areas where the 'market pull' has been matched to some degree with the 'technology push' and commercialization resources have been deployed sufficiently to support the market interest.

4.30.2 Olefin Metathesis in the Petrochemical Industry

The compounded challenges of process and market development required in the introduction of a new polymeric material make for often low-yielding commercialization efforts. Accordingly, early successes for a given technology often come from 'direct replacement' applications, where the developer's process development expenses can be predictably recovered from sales into an existing merchant market. This was certainly the case for olefin metathesis, where several successful petrochemical processes were implemented to fill demand in existing markets. Two of these processes, OCT® and SHOP, have grown to million metric tons per year capacities, and their successes illustrate the competence of olefin metathesis in the context of large-scale commercial endeavors.

4.30.2.1 Phillips Triolefin Process and OCT®

The first commercial olefin metathesis process, known as the Phillips Triolefin Process, was implemented by Phillips Petroleum Company just a few years after their initial report on the conversion of propylene to 2-butenes and ethylene.[1] The process employed a heterogeneous WO_3/SiO_2 catalyst at a temperature of approximately 400 °C. The plant, operated by Shawinigan near Montreal, Quebec (Canada), opened in 1966 to convert excess propylene to butenes and polymer grade ethylene that were in short supply at the time. It operated at a capacity of 30 000 metric tons of butenes and 15 000 metric tons of ethylene per year until the early 1970s, when an increased demand for propylene rendered the process uneconomical. Production was halted in 1972.[2,3]

Because olefin metathesis is an equilibrium reaction, the Triolefin Process can be run in the reverse direction to produce propylene from 2-butene and ethylene. Lyondell licensed the Phillips Triolefin process and opened the first propylene plant based on this technology in 1984, eventually expanding capacity to 450 000 metric tons per year.[4] In 1997, Lummus Technology, who engineered the first two applications under license from Phillips, purchased the technology from Phillips. The metathesis of ethylene and butenes to propylene is now commercialized as Olefins Conversion Technology (OCT®) and represents the largest growing technology for on-purpose propylene production, with individual OCT® unit capacities of up to 800 000 metric tons per year.[5] Lummus Technology has licensed over 30 units worldwide with total propylene capacity exceeding 6.8 million metric tons per year, representing over 8% of the world's production of propylene.

4.30.2.2 SHOP

Next to OCT®, olefin metathesis finds its largest scale application as a component in the multistep Shell Higher Olefins Process (SHOP). Overall, SHOP converts ethylene into linear olefins. In the first step of the process, ethylene is oligomerized with a homogeneous nickel catalyst in 1,4-butanediol solvent to form a fixed distribution of linear alpha olefins with even carbon numbers from C4–C40. These olefins are immiscible with the polar solvent and are readily separated from the catalyst solution. The linear olefins then enter a distillation unit that isolates the highest value products (C6–C18). The heavier and lighter olefins are recombined in an isomerization unit that converts the terminal olefins to internal positions, providing a mixture comprised of linear internal olefins containing fewer than 6 carbons or greater than 18 carbons.

The metathesis process step occurs next. The mixed olefin stream from the isomerization unit is fed to a MoO_3/Al_2O_3 metathesis catalyst operating at 100–125 °C and 10 bar. The metathesized products are linear internal olefins with a broad chain-length distribution. Internal olefins between C11 and C18 are collected and the remaining heavy and light olefins are recycled back into the isomerization unit.[6] By reengineering the process, Shell can use SHOP to tailor its otherwise fixed product distribution to meet changes in market demand.

The initial SHOP capacity in 1977 was 104 000 mt yr^{-1} of linear olefins, which Shell currently markets under the trade name Neodene®. Following several expansions, the current SHOP operating capacity is 330 000 metric tons per year at Shell's Stanlow (UK) site, and 920 000 mt yr^{-1} at Geismar, Louisiana, giving an overall capacity of roughly 1.25 million mt of Neodene® per year.[7]

4.30.3 Polymer Modification

4.30.3.1 Hydrogenated Acrylonitrile-Butadiene Copolymers (Therban® AT)

Lanxess (then part of Bayer Materials Science AG) was an early adopter of the functional group-tolerant Grubbs ruthenium-based olefin metathesis catalysts, using them to produce a line of hydrogenated acrylonitrile-butadiene copolymers (HNBR).[8] HNBR is a specialty elastomer with excellent oil and heat resistance and is used in the automotive industry for belts, seals, and gaskets. It is made by hydrogenation of the workhorse acrylonitrile-butadiene copolymer (NBR). The saturated backbone accounts for the increased thermal and chemical stability relative to NBR, but also results in an increase in viscosity. Accordingly, HNBR poses processing challenges, especially for intricate parts, and often plasticizers are needed for adequate processibility.

The viscosity of HNBR is determined by acrylonitrile content, degree of hydrogenation, and molecular weight. Altering either of the first two characteristics can result in a change in the final material performance, whereas a decrease in molecular weight

results in a high-performing, low-viscosity product. Lanxess developed a process to make low-viscosity HNBR that involves the partial metathesis degradation of high-molecular-weight NBR with a second-generation Grubbs catalyst prior to hydrogenation. Importantly, the process accommodates a bulk commercial NBR feedstock to produce an intermediate NBR with reduced molecular weight. Upon ultimate hydrogenation, an HNBR with lower molecular weight and viscosity is produced.[9] Lanxess's Therban® AT line of reduced viscosity HNBR has product grades with Mooney viscosities of about 40, compared to > 60 Mooney units for conventional HNBR. The added production costs due to the metathesis step are offset by lower processing costs of the lower viscosity material. Furthermore, the reduced viscosity reduces or eliminates the need for added plasticizers, which can increase the operating lifetime of HNBR products. Lanxess continues to expand its Therban® AT product offerings, such as the trial product ULV Therban® AT 3400 VP that has viscosities between 100 and 1000 Pa s, providing flows of 1000–10 000 times faster than other low-viscosity Therban® AT grades.[8]

4.30.3.2 Hydrogenated Metathesized Soy Wax (NatureWax®)

Waxes made from hydrogenated or partially hydrogenated soybean oil have gained traction for use in candles and other applications as natural alternatives to petroleum-based paraffin waxes. These products can compete on a cost basis when crude oil prices are high, but even during periods of relatively low-cost petroleum, the soy-based waxes can capture a segment of the overall market that is willing to pay a premium for a 'natural' product.

Unmodified soybean oil is a triglyceride comprised of saturated, as well as mono-, di-, and tri-unsaturated fatty esters, containing an average of about 4.5 olefins per molecule. Partial hydrogenation results in a reduction of the overall unsaturation to provide soft wax. This soy wax suffers from a low melting point that causes excessive dripping in free-standing candle applications and wick drowning in jar candles. Fully hydrogenated soy wax has a higher melting point but tends to form microcrystalline regions upon solidification and accordingly produces a brittle wax not suitable for candles.[10]

Elevance Renewable Sciences offers a metathesis-modified soy wax in their NatureWax® product line. In a process codeveloped by Cargill and Materia, a second-generation Grubbs catalyst is added to soybean oil to form a mixture of triglyceride oligomers, with the concomitant release of the hydrocarbon tails (Scheme 1). Hydrogenation of the mixture yields a wax that is firmer than soft soy wax but less brittle than hydrogenated soy wax.[11,12] Applications for this metathesis-modified wax range from candle to personal care applications, as well as other traditional wax markets.

4.30.4 ROMP Polymers Based on Dicyclopentadiene

4.30.4.1 Raw Material Considerations

As the capacity for ethylene production grew during the latter half of the twentieth century, the supply of related olefin streams has also grown. Ethylene production from steam cracking of liquid petroleum feedstocks such as naphtha results in the formation of, among other by-products, a considerable quantity of species containing five carbon atoms, the 'C5 stream'. The supply of purified C5 products has steadily climbed as applications have been established for isoprene, piperlyene, and dicyclopentadiene (DCPD, formed from the spontaneous Diels–Alder dimerization of cyclopentadiene). By 2005, the global merchant market for DCPD had reached 500 000 metric tons per year, the largest fraction of which was used for chemical modification of unsaturated polyester resins. In the context of olefin metathesis, DCPD can be polymerized directly or cracked to its monomer, cyclopentadiene, and converted to any number of ROMP-active norbornenes.

Although DCPD is an inexpensive, readily-available raw material, the predominant merchant grade (85% nominal purity) contains levels of impurities that render it unsuitable for effective polymerization using any olefin metathesis catalysts developed to date. The use of high purity monomer streams is not unusual for polymer production, but in this context it meant that the early developers of ROMP-polymerized DCPD-based resin systems each needed to create a new supply chain around a previously unavailable high purity grade of DCPD.

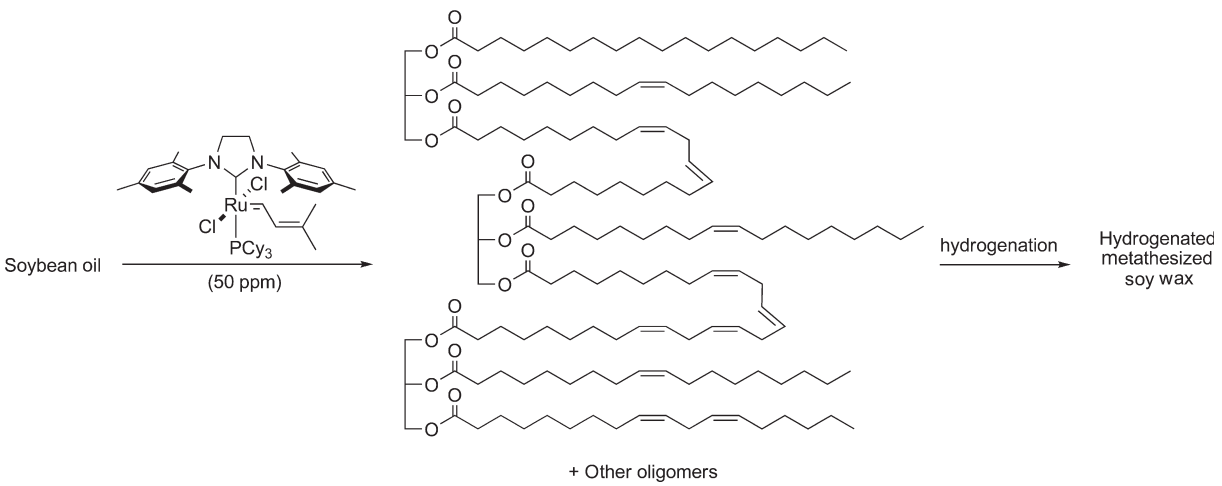

Scheme 1 Process for production of hydrogenated metathesized soy wax.

4.30.4.2 Polydicyclopentadiene Based on Traditional Catalysts (Telene®, Metton®, Pentam®)

During the 1980s, resin systems for the molding of polydicyclopentadiene (pDCPD) parts were introduced by the B.F. Goodrich Company (sold as Telene®) and by Hercules (sold as Metton®). Later, Goodrich licensed technology to Nippon Zeon that marketed the product under the Pentam® brand in Asia. These resin systems were based on ill-defined catalysts generated *in situ* from molybdenum or tungsten salts mixed with cocatalysts, promoters, and/or inhibitors (details of the chemistry can be found elsewhere).[13] Due to the exceptional reactivity of the strained bicyclic olefin in DCPD, these were formulated as two-part resin systems, with the monomer and catalyst kept separate until just prior to curing. Curing was effected by mixing the two complementary parts, typically in impingement or other in-line mixers. Unlike most thermoset resins, the fully cured pDCPD exhibited high toughness in addition to relatively high use temperature (> 100 °C). To some extent, these properties could be attributed to the combination of relatively low cross-link density and the steric bulk of the bicyclic structure (Scheme 2).

Maintaining an air-free, moisture-free environment is critical for traditional pDCPD catalyst systems to maintain good catalyst reactivity and high extent of curing. Due to this environmental sensitivity, the traditional pDCPD products have been closely tied to the reactive injection molding (RIM) process that allows for fast, in-line mixing of the two-part system before injection into the mold cavity under inert conditions. Fortunately, existing RIM processing equipment designed for molding polyurethane parts could be adapted readily for pDCPD resins. The RIM method of processing benefits from low tooling costs especially for large parts (up to 100 kg) because of the relatively low clamping pressures required. Also, the low viscosity of DCPD-based resin filling the part allows for a high degree of flexibility in part design unlike traditional injection molding of thermoplastics. However, production of plastic parts by the RIM process does have certain limitations. Production molding of pDCPD by RIM typically requires cycle times of 2–4 min, compared to the 5–30 second cycle times common in traditional injection molding. As a result, the RIM process is typically too costly for large volume part production (> 15 000 parts per year).

As a result of a complex array of business, regional branding, and licensing transactions, the ownership of these first pDCPD products has changed several times during the past few decades. However, pDCPD has established a continuous market presence, with an estimated global market for pDCPD in 2006 of approximately 25 000 metric tons per year for specialty parts, including hoods, wind deflectors, and fasciae for heavy truck and agricultural and industrial equipment. These types of parts benefit from the key characteristics of pDCPD such as high toughness/impact resistance, high heat distortion temperature, and good chemical resistance relative to alternative materials of construction.

The formulation and processing technology of traditional pDCPD has continued to progress. For example, filler-reinforced and flame-retardant resin systems are currently offered in addition to the standard resin. Furthermore, improvements have been made to reduce the odor caused by residual DCPD monomer through process improvements. However, these resin systems based on traditional catalysts have not expanded to molding outside of the RIM processing paradigm.

4.30.4.3 Early Applications of Grubbs Ruthenium Catalysts in pDCPD (Cyonyx®, Prometa®)

4.30.4.3.1 pDCPD in neat resin systems

Beginning in the 1990s, the new generations of well-defined olefin metathesis catalysts such as those developed by Prof. Robert Grubbs and Prof. Richard Schrock were beginning to be evaluated for commercialization in pDCPD materials. The first company to recognize the importance of the user-friendly characteristics of the Grubbs catalysts and license the technology for pDCPD molding from the California Institute of Technology was Advanced Polymer Technologies (APT). Although APT largely focused on the development of RIM-prepared or cast components for corrosion applications, typical of traditional pDCPD materials, it promoted new applications in other areas through licensing. In particular, the A.O. Smith Corporation launched a line of high-performance, corrosion-resistant composite pipe products under the trade name Cyonyx®. Compared with traditional steel or composite pipe products, Cyonyx® offered low weight, excellent impact resistance, and superior resistance to halogens (liquid bromine and chlorine gas). In creating Cyonyx®, Smith also developed novel composite technology[14] and demonstrated flame-retarding methodologies.[15] Unfortunately, shortly after the spin-off and merger of A.O. Smith's fiberglass piping division to form Smith Fibercast, this promising but not yet established product was discontinued.

In the early 2000s, APT entered into a joint venture with BF Goodrich, known as Cymetech, LLC, which within a few years became owned by an investment firm after BF Goodrich exited

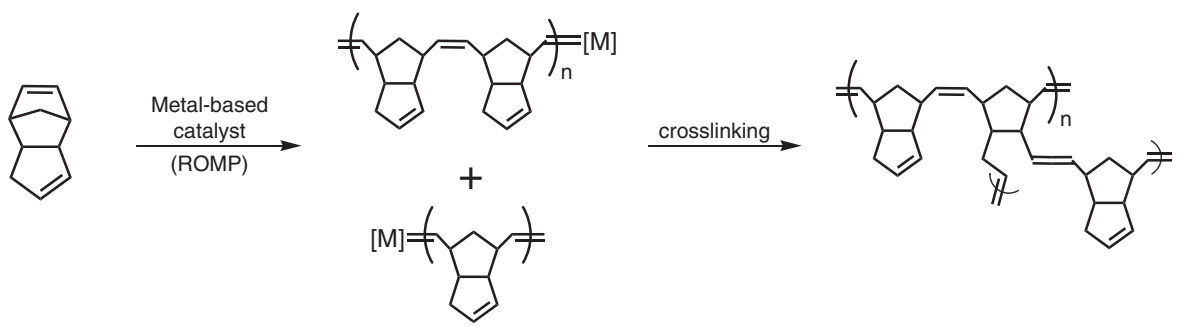

Scheme 2 Polymerization and cross-linking of DCPD.

the chemicals business. Cymetech retained its facilities in Huntsville, Texas, which supplied Telene® pDCPD product lines acquired from Goodrich and in Calvert City, Kentucky, which produced Ultrene® high purity DCPD. In 2003, Cymetech launched its Prometa® line of 'engineering' pDCPD resins based on the Grubbs ruthenium catalyst technology. Upon introduction, these new pDPCD resin systems were reported to meet or exceed the physical properties of the pDCPD products based on traditional catalysts while offering improvements of reduced sensitivity to impurities and significantly less odor evolution.[16] Four formulations of Prometa® pDPCD were introduced for various processes including RIM, rotational molding, resin transfer molding (RTM), and vacuum-assisted RTM (VARTM). The primary applications were molded parts for the corrosion industry, parts for agribusiness, tanks for aerospace, and various specialty industrial components. Cymetech also investigated the use of pDCPD in liners of composite tanks for cryogenic liquids, based on the work of Toplosky, demonstrating that pDCPD exhibits superior elongation at break at 77 K compared to epoxy and polyester.[17] In Asia, Cymetech formed a partnership with Hitachi Chemical, who promoted pDCPD technology under its Metathene™ designation. Hitachi developed a variety of electronic and consumer (e.g., bathroom fixtures) applications during the 2000s but currently appears to be inactive in this area.[18]

By the mid-2000s, Materia, Inc., a small company based in Pasadena, California, was demonstrating some success in the commercialization of various olefin metathesis catalyst technologies related to specialty chemicals and polymer materials. Combining the exceptional toughness and corrosion resistance offered by pDCPD with the facile processing of ruthenium-based catalysts, Materia had been evaluating a variety of applications including ballistics, blast containment, and high-performance composites (**Figure 1**). Some of the Materia technology in the area of sporting goods had been licensed to Easton Sports, a manufacturer of sports equipment based in Van Nuys, California. Materia and Easton codeveloped several materials for product lines in the areas of baseball, hockey, and archery equipment.

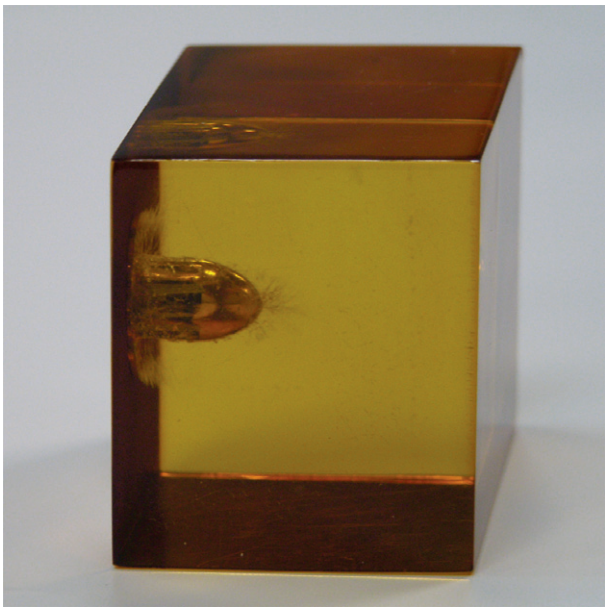

Figure 1 A full metal jacketed 9 mm bullet fired into a cast panel of pDCPD cured using the first-generation Grubbs catalyst, demonstrating the exceptional toughness of pDCPD (viewed on edge, thickness of 1.5 in).

Materia patented technology related to variable density composites[19] (including syntactic foam and metal-filled tooling and prototyping materials) and methods for adhering hydrocarbon resins such as pDCPD to various surfaces.[20] They have also demonstrated the infusion of very low-viscosity cycloolefin resins into porous substrates, such as wood, to make novel composite materials with enhanced mechanical performance, improved chemical and moisture resistance, and greater durability.[21] In 2004, Materia acquired from Cymetech the licensing and patent rights related to pDCPD, in addition to the Huntsville production facility. Since the acquisition, Materia has been active on the pDCPD front through its efforts to commercialize resins in the area of RIM parts, syntactic foam parts, and tooling block.

4.30.4.3.2 pDCPD in glass and carbon fiber composites

Fiber-reinforced polymer (FRP) materials are composite materials that represent a key application area for thermoset polymer systems. Typically, FRP composites are comprised of reinforcing fibers within a continuous matrix resin and provide excellent mechanical properties at relatively low weight. Therefore, composites based on fiberglass or carbon fibers are commonly used to make high-stiffness or high-strength parts for applications such as boat hulls, sports materials, shower surrounds, and wind turbine blades. Several processes are employed in the manufacture of fiber composite parts. One process for manufacturing large fiber composites, known as VARTM, has become increasingly common because of its low cost, versatility, and compatibility with the desire for low worker exposure to hazardous volatile organic compounds (VOCs). The VARTM process, sometimes referred to as vacuum infusion, involves sealing multiple layers of reinforcing fiber-based fabrics between a mold surface and a flexible film. After the system is placed under vacuum, resin is allowed to flow into the fabric, then heated through a prescribed curing protocol.

Due to the excellent toughness exhibited in nonreinforced pDCPD-molded parts, it was hypothesized that pDCPD-based composites would have high fracture toughness as well. Furthermore, the low viscosity of pDCPD-based systems appeared to be well suited for the VARTM process. However, several characteristics of pDCPD resins have traditionally presented processing challenges in composite applications using standard processing techniques such as VARTM. First, since infusion of the fabric with resin can be slow, especially in large parts, significant 'pot life' or working time is required for the resin/catalyst mixture (0.5–2.0 h) for most parts. For a successful process, the viscosity of the resin cannot change significantly during this period. Given the reactivity of DCPD in the presence of most olefin metathesis catalysts, the viscosity of such mixtures would typically increase too quickly to allow for complete filling of the part. In addition, the hydrophobic pDCPD does not inherently adhere to traditional commercial reinforcing fibers. Good adhesion must be achieved between the resin and the fiber (e.g., glass or carbon fiber) in order to

realize adequate properties including interlaminar shear strength (ILSS) and compression strength.

Thanks to undisclosed improvements in pDCPD resin formulation and processing techniques, Materia has recently announced the introduction of a resin designed for fiberglass and related composites that are compatible with VARTM.[22] In this system, pDCPD offers a number of performance advantages relative to traditional composite materials. Agastra and Mandell recently showed that pDCPD glass fiber laminates exhibited unusually high interlaminar fracture toughness in Mode I, also denoted as G_{Ic}, when compared to laminates based on traditional resin systems of unsaturated polyester, epoxy, and vinyl esters.[23] While these traditional laminates typically have values of 200–400 J m^{-2} for initial G_{Ic}, pDCPD laminates were measured to be in the range of 1500 J m^{-2}. This high level of toughness is typically associated with engineering thermoplastic polymers such as polyether ether ketone (PEEK).

In addition to superior toughness, pDCPD composites have high ductility in the nonfiber directions. For structural applications, anisotropic or unidirectional reinforcement fabrics are commonly used to provide maximum stiffness, but this can cause the parts to be rather brittle in the cross-fiber direction. Extra reinforcing fibers are typically used as 'cross-bracing' to compensate for the low strength. However, pDCPD, which has a high-strain deformation before breaking, can allow for design changes and efficiencies in the composite by reducing the amount of cross-bracing reinforcement required.

Independent of the performance characteristics, the low viscosity of DCPD provides pDCPD composites with a distinct processing advantage in vacuum infusion relative to traditional materials. Whereas typical resin systems for infusion processes have viscosities in the range of 200–400 cP, pDCPD systems have viscosities in the range of 10–40 cP. For vacuum infusion processes and RTM in general, this low viscosity translates directly into faster processing time. In addition, the low viscosity allows for process simplification through the reduction of peripherals such as flow aids.

For pDCPD-based glass and carbon fiber composites, the reported performance profiles and processing advantages provide the foundation for adoption into composite applications. Coupled with the relatively low monomer cost associated with purification of a well-known petrochemical by-product, a compelling case can be made that a successful polymer is on the horizon. The market will have the final word during the next few years on whether these attributes are indeed sufficient for a commercial success.

4.30.4.4 Polynorbornene (Norsorex®)

Polynorbornene, developed by CdF-Chimie, holds the distinction of being the first commercial ROMP polymer. It was originally introduced in France in 1976 under the trade name Norsorex®, and though it has since expanded into the global market, it remains a niche product. The monomer for this material, 2-norbornene, is the product of the Diels–Alder reaction between cyclopentadiene and ethylene. Polymerization proceeds in the presence of a $RuCl_3$/HCl/BuOH catalyst system, resulting in a material with an extremely high molecular weight (> 3 000 000 g mol^{-1}) and predominantly *trans* olefins. The high-molecular-weight and unsaturated microstructure impart the material with unusual properties, behaving as both elastomeric and thermoplastic. Norsorex® has a T_g of 37 °C that contributes to its remarkable damping properties in shock, vibration, and sound control applications.[24]

Due to its low polarity and high molecular weight, Norsorex® can absorb up to 10 times its dry weight in hydrocarbons, forming a gel that maintains reasonable mechanical properties. Accordingly, it has found some application for oil spill cleanup. In addition, hydrocarbon plasticizers can be added to form workable formulations containing > 400 phr of plasticizer, which allows for polynorbornene formulations with T_g as low as −60 °C.[25] This versatile product is now marketed by the Vienna-based company Astrotech.

4.30.4.5 Cylic Olefin Copolymers (Zeonex®, Zeonor®, Arton®)

Cyclic olefin polymers and cyclic olefin copolymers (COCs) are terms generally used when referring to a class of thermoplastic polymers with high optical clarity for use in optical and film applications. COCs are made by copolymerization of norbornene derivatives, by either ROMP or addition polymerization (Scheme 3). The addition polymers can be either homopolymers of one or more norbornenes (Avatrel® from Promerus) or copolymers with an additional olefin such as ethylene (Topas® from Ticona and Apel® from Mitsui). All have good optical transmittance over a broad wavelength and thermal range, and compete primarily with high-end PC and poly(methyl methacrylate) (PMMA).

Performance, rather than cost, has been the primary driver for the adoption of COCs into industry. With applications in lenses for laser printers, LCD screens, cell phone cameras, and other high-value products, only a small amount of polymer is required to produce valuable parts. Accordingly, the market can accommodate a relatively high price per pound for these materials. Due to the stringent purity requirements for optical applications, much of the cost associated with COC manufacturing is in contaminant removal and clean room handling. Taken together, the impact of raw material and polymerization costs is relatively small compared to other polymeric materials.

Development of the first commercial hydrogenated ROMP polymer, Zeonex®, began at Nippon Zeon in the early 1980s. Zeon was motivated primarily by upstream considerations, with an interest in norbornene chemistry grounded in the goal of fully utilizing the C5 by-products from Zeon's isoprene purification facility. Research began by making substituted norbornenes via Diels–Alder chemistry from cyclopentadiene and polymerizing them by ROMP. The resulting linear polymers were thermoplastic, but the residual backbone unsaturation resulted in poor thermal and oxidative stability, which complicated melt processing. In an effort to improve these properties, Zeon investigated the hydrogenation of these materials and found that in addition to improved stability, some hydrogenated polynorbornenes possessed excellent optical properties.[26]

The parent hydrogenated polynorbornene is an opaque crystalline product, but substitution of the norbornene backbone with cyclic groups tends to create amorphous materials. The optical properties of these amorphous COCs in the visible range are comparable to optical grades of PC and PMMA, but extend into the ultraviolet range better than competing

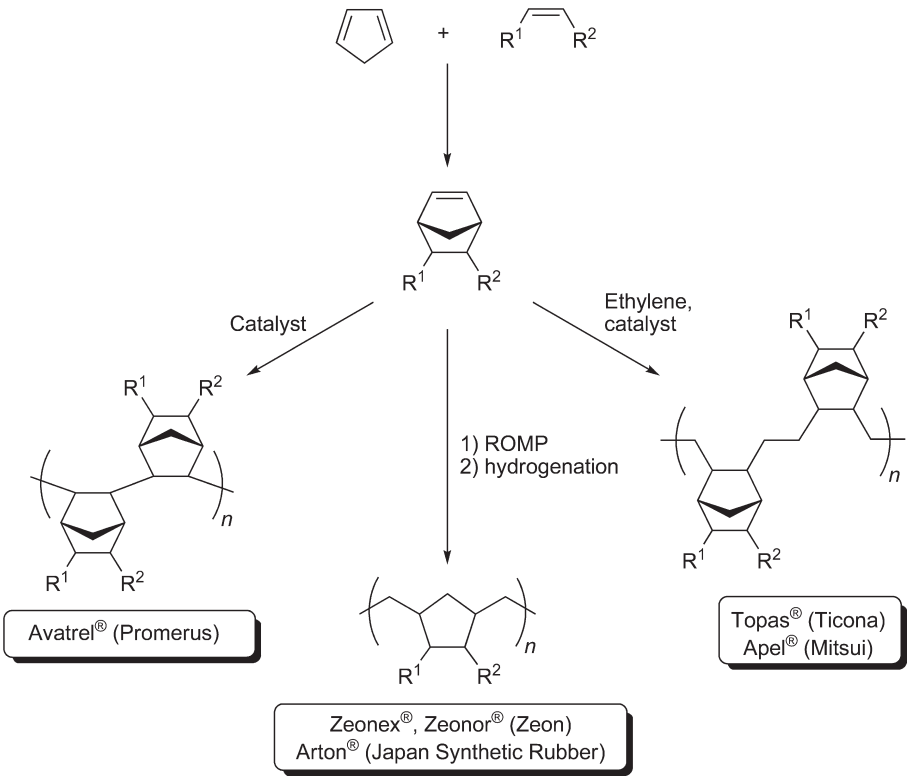

Scheme 3 Chemical structures and generic syntheses of marketed addition and ROMP COCs.

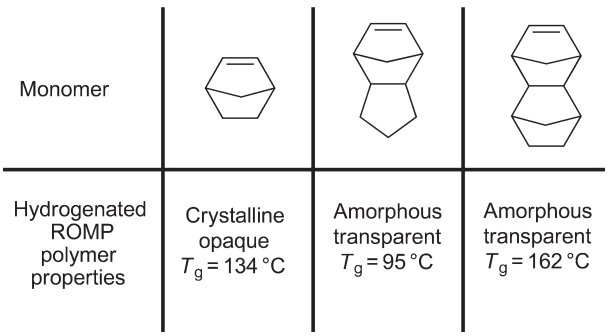

Figure 2 Select ROMP monomers for COCs and the impact of monomer structure on polymer properties.[26]

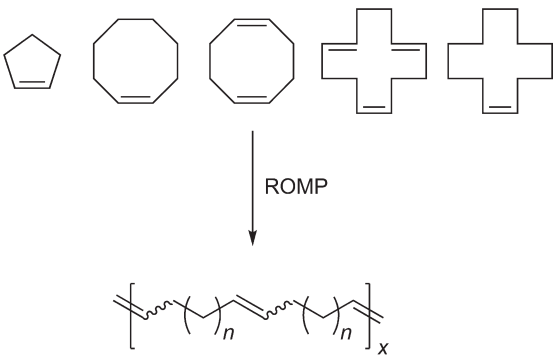

Scheme 4 Linear polyalkenamers

materials. Altering the norbornene substitution, especially with polycyclic groups, can provide materials with high T_g, which is critical for maintaining consistent optical properties at high operating temperatures or over wide temperature ranges (Figure 2).

4.30.5 Linear Polyalkenamers

ROMP of mono- or polyunsaturated monocyclic alkenes provides linear polymers containing unsaturation at regular intervals along the backbone, termed polyalkenamers (Scheme 4). The properties of these elastomers depend on the degree of unsaturation (as dictated by the monomer) and the *cis*/*trans* olefin ratio (as determined by the polymerization conditions). Only one polyalkenamer, polyoctenamer, has achieved commercialization, and its success relative to the related polymers discussed herein is due to a combination of material properties, process considerations, and feedstock economics.

4.30.5.1 Polybutenamer

Dimerization or trimerization of butadiene produces 1,5-cyclooctadiene (COD) or 1,5,9-cyclododecatriene (CDDT), respectively. Each of these monomers undergoes efficient

ROMP to provide polybutenamer, a product with the structure of a fully 1,4-polybutadiene. While this microstructure differs from polybutadiene prepared by radical, anionic, or Ziegler–Natta-type polymerizations, no compelling performance advantage has been reported. Due to the added relative monomer cost of COD and CDDT with respect to butadiene, there has been no motivation to develop a polybutenamer product.

4.30.5.2 Polypentenamer

The availability of cyclopentene as a petrochemical by-product served as the driving force for the development of polypentenamer. Cyclopentene will undergo ROMP, though because of minimal ring strain, single-pass complete conversions are difficult to obtain. Goodyear, Bayer, Nippon Zeon, and Japan Synthetic Rubber each had developmental programs focused on this elastomeric material, but a commercial product was never developed. The postvulcanization properties of polypentenamer are similar to polybutadiene, but despite the desire to utilize cyclopentene, the additional cost of monomer isolation and relatively inefficient ROMP made the overall process economics unattractive. The development of polypentenamer could potentially reactivate if the price imbalance between cyclopentene and butadiene becomes significant.[27]

4.30.5.3 Polyoctenamer (Vestenamer®)

The only commercially successful linear polyalkenamer is polyoctenamer. Hüls (now Evonik) has marketed this product with the trade name Vestenamer® since 1980. In the Vestenamer® process, cyclooctene is polymerized in the presence of a WCl_6 catalyst in hexane solvent at temperatures of less than 100 °C, producing a bimodal product distribution. The polymer is predominantly the expected linear product with a molecular weight of 50 000–100 000 g mol^{-1}, but at least 25% of the polyoctenamer consists of macrocyclic polymers arising from competitive polymer backbiting. Most of the cyclic components have lower molecular weights than the linear chains; the highest proportion has molecular weights around 15 000 g mol^{-1}, but cyclic polymers up to at least 100 000 g mol^{-1} are observed.[28] The olefins in Vestenamer® are predominantly *trans*, with the two commercially available grades of Vestenamer® possessing *cis*/*trans* ratios of 20:80 and 40:60.

The combination of high cyclic content, low branching, and *trans* unsaturation imparts Vestenamer® with an unusual combination of properties compared to other elastomeric materials. The high *trans* content causes it to be semicrystalline in the solid state. The mixture of cyclic and linear polymer chains results in relatively low-melt viscosity that makes Vestenamer® useful for certain applications such as asphalt modification.

The added raw material and production costs relative to other elastomers (polybutadiene, styrene-butadiene copolymers, etc.) have kept polyoctenamer from entering the realm of a commodity rubber, but Vestenamer® has achieved success as a minor component in numerous elastomer blends. Formulations containing 10–20% of Vestenamer® have lower melt viscosity and better green strength than their parent formulations, and can be vulcanized using traditional chemistries.[29]

4.30.5.4 Polydodecenamer

Concurrent to their polyoctenamer development efforts in the 1970s, Hüls thoroughly investigated polydodecenamer made from the ROMP of cyclododecene. The properties of this material are similar to those of polyoctenamer, and the ultimate commercialization of the latter rather than the former was not driven by material properties.

When research into ROMP began at Hüls around 1969, the company had been operating a butadiene trimerization plant to produce CDDT for 4 years, and though butadiene dimerization to cyclooctadiene COD was known, at the time there were no dedicated commercial sources for this feedstock. Accordingly, the cyclo-C12 feedstock was readily available and the cyclo-C8 feedstock was only available as a by-product from the Hüls trimer plant. This supply chain imbalance favored the development of the polydodecenamer.[30]

Despite the uncertain supply chain for its monomer, there were a number of practical processing advantages in favor of polyoctenamer. The polymerization of cyclo-C12 had a lower time yield due to a slower reaction rate (a function of monomer ring strain), and removal of any residual higher boiling C12 monomer by distillation was more energy- and time-intensive.[31]

Perhaps the most important factor that tipped the balance in favor of polyoctenamer over polydodecenamer had to due with the sensitivity of the tungsten catalyst and the details of monomer purification. Cyclooctene and cyclododecene are both made in two steps from butadiene via the partial hydrogenation of the cyclic diene and triene, respectively. It was found that residual dienes from this reduction can become isomerized into conjugation, leading to catalyst poisons. Accordingly, the partial reductions needed to be run to complete consumption of dienes, which in practice meant over-reduction of some feedstock to the saturated species. In the case of cyclooctadiene, the substantial difference in olefin reactivity allowed for selective reduction with $<5\%$ of over-reduction product. For cyclododecatriene, however, there is less ring strain and mono-olefin can only be obtained with 15–20% of over-reduced product. While this product could have been salvaged for other uses, the added expense, in addition to the aforementioned issues, shifted the balance of commercial appeal away from polydodecenamer in favor of polyoctenamer.[32]

4.30.5.5 End-Functional Polymers (Difol®)

In the presence of pure cycloolefin, ROMP can provide polymers with very high molecular weights, but if an acyclic olefin is introduced to the polymerization mixture, lower molecular-weight polymers are obtained. In this scenario, molecular weights are determined by the ratio of cyclic monomer to acyclic chain terminator. In the mid-1990s, Amoco (later BP Amoco) developed a chain-terminated ROMP process to make linear hydroxyl-terminated polybutenamer (HTPBD for hydroxyl-terminated polybutadiene). Their process used a $(RuCl_2(p\text{-cymene}))_2/PCy_3$ catalyst to polymerize COD in the presence of *cis*-1,4-diacetoxybutene in chlorobenzene

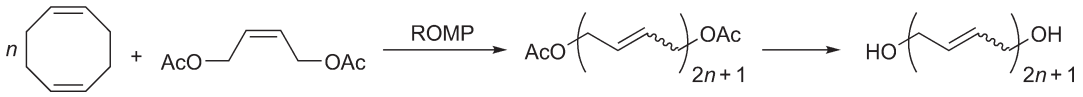

Scheme 5 Synthesis of HTPBD by ROMP of 1,5-cyclooctadiene in the presence of a functional chain transfer agent.

solvent.[33] The resulting telechelic diacetate was then hydrolyzed to give the HTPBD (Scheme 5).

HTPBD produced by BP Amoco entered development under the trade name Difol® and was marketed as a component in polyurethanes, in both cast elastomers and thermoplastic polyurethanes. Polyurethanes are prepared from diisocyanate prepolymers derived from long-chain diols or polyols. In traditional polyurethane systems, the long-chain polyol component is either polyether- or polyester-based with molecular weights in the range of 2000–10 000. When HTPBD in this range was used as the diol component, the resulting polyurethanes had differentiated properties with respect to traditional materials. The hydrophobic HTPBD backbone provided excellent hydrolytic stability, chemical resistance, and low-temperature elasticity. However, the high cost of HTPBD relative to already commoditized polyether and polyester polyols made it unlikely that HTPBD would displace the incumbent materials and its use would be restricted to only market segments where these properties were of critical importance. To date, this segment of the polyurethane market has been relatively small.

BP Amoco never commercialized their Difol® product line, perhaps because the moderate sized market was outside of BP Amoco's core area of expertise. In the late 1990s, Bayer Materials Science began development of a similar line of HTPBD utilizing the first-generation Grubbs catalyst in a process otherwise similar to Amoco's.[34] Bayer's sizeable presence in the polyurethane markets provided a decreased barrier to market penetration while also allowing Bayer to expand their existing product offerings.

In 1997, before Bayer reached the commercial stage with their HTPBD, direct competition emerged with the introduction of HTPBD produced by anionic polymerization of butadiene. This material was developed by the Czech company Kaucuk and was marketed under the trade name Krasol®.[35] The lower feedstock cost of butadiene versus cyclooctadiene gave Krasol® a cost advantage in this already cost-disadvantaged specialty polyurethane market segment. Bayer abandoned its line of ROMP-derived HTPBD before a commercial launch, whereas Krasol® was successfully commercialized and is now marketed by Cray Valley.

4.30.6 Conclusion

Due to the aforementioned commercial successes of polymeric materials based on ROMP chemistry, olefin metathesis deservedly holds a place among the short list of successful polymerization processes. In addition, a number of ROMP polymer systems have been developed that possess useful properties, but a combination of feedstock pricing, process challenges, and lack of market pull have limited their use. However, because the markets for raw materials are dynamic and new applications for materials are invented almost daily, it is quite possible that a previously abandoned polymer will find new life in the future. Furthermore, as olefin metathesis has become increasingly commonplace in academia over the past few decades, each new generation of practicing polymer chemists is ever more comfortable with this chemistry. New ROMP solutions to both existing and yet-to-be-discovered problems are surely on the horizon.

References

1. Banks, R. L.; Bailey, G. C. *Int. Eng. Prod. Dev.* **1964**, *3*, 170.
2. Dwyer, C. L. In *Metal-Catalysis in Industrial Organic Processes*; Chiusoli, G. P., Maitlis, P. M., Eds.; Royal Society of Chemistry: Cambridge, United Kingdom, 2006; pp 201–217.
3. Weissermel, K.; Arpe, H.-J. *Industrial Organic Chemistry*, 4th edn; Wiley-VCH Verlag GmbH & Co. KGaA: Weinheim, Germany, 2003; pp 85–90.
4. Witcoff, H. A.; Reuben, B. G.; Plotkin, J. S. *Industrial Organic Chemicals*, 2nd edn; John Wiley & Sons, Inc.: Hoboken, NJ, 2004; p 88.
5. Henni, A. *Downstream focus: Lummus Technology*, Feb 10, 2010. Arabian Oil and Gas Web site. http://www.arabianoilandgas.com/article-6909-downstream-focus-lummus-technology/ (accessed Sep 6, 2010).
6. Mol, J. C. *J. Mol. Catal. A: Chem.* **2003**, *213*, 39–45.
7. Shell chemical manufacturing locations Web site. http://www.shell.com/home/content/chemicals/products_services/our_products/alpha_olefins_detergent_alcohols/neodene/manufacturing_locations/geismar/ and http://www.shell.com/home/content/chemicals/products_services/our_products/alpha_olefins_detergent_alcohols/neodene/manufacturing_locations/stanlow/ (accessed Sep 62010).
8. Granson, E. *Process West* **2010**, 30–32.
9. Guérin, F. U.S. Patent No. 6,673,881, Jan 6, 2004.
10. Rezaei, K.; Wang, T.; Johnson, L. A. *J. Am. Oil Chem. Soc.* **2002**, *79*(*12*), 1241–1247.
11. (a) Murphy, T. A.; Tupy, M. A.; Abraham, T. W.; Shafer, A. Candle and Candle Wax Containing Metathesis and Metathesis-Like Products. WIPO International Patent Publication No. 2006/076364, Jul 20, 2006. (b) Murphy, T. A.; Tupy, M. J.; Abraham, T. W.; Shafer, A. Candle and Candle Wax Containing Metathesis and Metathesis-Like Products. U.S. Patents Application No. US 2009/0217568, Sep 3, 2009.
12. Tupy, M. J.; Amore, F.; Kaido, H.; Meng, X. Method of making hydrogenated metathesis products. WO 2007/081987, Jul 19, 2007.
13. Mol, J. C. *J. Mol. Catal. A: Chem.* **2003**, *213*, 39–45.
14. Warner, M. W.; Drake, S. D.; Giardello, M. A. U.S. Patent No. 6,040,363, Mar 21, 2000.
15. Warner, M.; Giardello, M. A. U.S. Patent No. 6,071,459, Jun 6, 2000.
16. Toner, S. A. M.; Leslie, P.;Frost, J. O. DCPD – The Promise Fulfilled. Presented at the Society for the Advancement of Material and Process Engineering 2004, Long Beach, California (USA), 16–20 May 2004.
17. Toplosky, V. J.; Walsh, R. P. Thermal and Mechanical Properties of Poly-Dicyclopentadiene (DCPD) at Cryogenic Temperatures. Presented at Advances in Cryogenic Engineering. *Advances in Cryogenic Engineering*, Transactions of the Cryogenic Engineering Conference, Keystone, Colorado (USA), Aug 29–Sep 2, 2005, Balachandran, U., Ed. AIP Conference Proceedings, Vol. 824, 2006, pp 219–224.
18. Aoki, T.; Yamazaki, H.; Kawai, H.; *et al.* Electronic Device, WIPO International Publication No. WO 00/51178, Aug 31, 2000.
19. Giardello, M. A.; Lasch, J. G.; Cruce, C. J.; *et al.* U.S. Patent No. 6,525,125, Feb 25, 2003.
20. Giardello, M. A.; Haar, C. M. U.S. Patent No. 6,409,875, Jun 25, 2002.
21. Cruce, C. J.; Filice, G. W.; Giardello, M. A.; *et al.* Infusion of Cyclic Olefin Resins into Porous Materials, WIPO International Publication No. WO 03/020504, Mar 13, 2003.
22. Edgecombe, B. D.; Cruce, C. J.; Stephen, A. R.; *et al.* Fatigue Performance of Defect-Tolerant Glass Composites based on a High-Toughness Resin.

Presented at High Performance Resins 2010, Schaumburg, Illinois (USA), Sep 23–24, 2010.
23. Agastra, P.; Mandell, J. F. Testing and Simulation of Damage Growth at Ply Drops in Wind Turbine Blade Laminates. Presented at the Society for the Advancement of Material and Process Engineering, Seattle, Washington (USA), May 17–20, 2010; Paper 398.
24. Marbach, A.; Hupp, R. *Rubber World,* **1989**, **30**.
25. Drăguţan, V.; Streck, R. *Catalytic Polymerization of Cycloolefins: Ionic, Ziegler-Natta and Ring Opening Metathesis Polymerization*; Elsevier Science BV: Amsterdam, The Netherlands, 2000; pp 1162–1172.
26. Yamakazi, M. *J. Mol. Catal. A: Chem.* **2004**, *213*, 81–87.
27. Streck, R. *J. Mol. Catal.* **1988**, *46*, 305–316.
28. Streck, R. In *Olefin Metathesis and Polymerization Catalysts*; Imamoglu, Y., Ed.; Kluwer Academic Press: Dordrecht, The Netherlands, 1990; pp 439–516.
29. Drăgutan, V.; Streck, R. In *Handbook of Polyolefins*; Vasile, C., Ed.; Marcel Dekker, Inc.: New York, 2000; pp 99–137.
30. Oenbrink, G.; Schiffer, T. In *Ullmann's Encyclopedia of Industrial Chemistry*; Wiley-VCH Verlag Gmbh & Co. KGaA, 2009, DOI: 10.1002/14356007.a08_205.pub2. Online edition, 15 Oct.
31. Streck, R. *J. Mol. Catal.* **1982**, *15*, 3–19.
32. Streck, R. *J. Mol. Catal.* **1992**, *76*, 359–372.
33. Nubel, P. O.; Yokelson, H. B.; Frye, W. H.; *et al.* U.S. Patent 6,060,570, May 09, 2000.
34. Peters, M. A. U.S. Patent No. 6,476,167, Nov 5, 2002.
35. Pytela, J.; Sufcak, M. Novel Thermoplastic Polyurethanes for Adhesives and Sealants, Jun 2, 2003. Adhesives Industry Web site. http://www.adhesivesmag.com/Articles/Feature_Article/83a1f29c59ac8010VgnVCM100000f932a8c0 (accessed Sept 19, 2010).

Biographical Sketches

Andrew Nickel received his BS from Temple University and his PhD from Yale University in 2005 in the field of natural product total synthesis. Nickel began his career in medicinal chemistry at Bristol-Myers Squibb, where he worked on novel small-molecule therapies for the hepatitis C virus. He joined Materia in 2008 as a research scientist and is currently engaged in the development of new applications for Materia's olefin metathesis catalyst technology.

Brian Edgecombe received his PhD in materials science and engineering in 1997 from Cornell University with a focus on the polymer chemistry of block copolymers. After graduation, he joined the Rohm and Haas Company in the research and product development group supporting Plexiglas® PMMA acrylic thermoplastics. Through a business acquisition, Edgecombe continued at Arkema in the development of new thermoplastic and core-shell modifier products. In 2006, Brian joined Materia and has been active in technology development of ruthenium-catalyzed pDCPD resins for various composite applications. He is Director of Materials R&D and is a coinventor of patents in the diverse areas of polymer toughening, surface gloss control, and novel functional polymers.

4.31 Ring-Opening Polymerization of Cyclic Esters: Industrial Synthesis, Properties, Applications, and Perspectives

J-M Raquez, R Mincheva, O Coulembier, and P Dubois, University of Mons, Mons, Belgium

4.31.1 Introduction

Biodegradable polymers make a significant contribution to sustainable development and, as defined by the Brundtland Commission, are "meeting the needs of the present generation without compromising the needs of future generations".[1] Biodegradable polymers are commonly defined as 'polymers that degrade in an acceptable period of time after their introduction in natural conditions (e.g., human body, soil, compost, sewage, or sludge) without references to the mechanism(s) of degradation involved'. In this respect, biodegradable polymers have attracted a lot of attention as biodegradable substitutes for commodity polymers such as polyethylene (PE) for short-time applications as well as in the biomedical realm.[2–8] In medicine, their functions are bonding (monofilament sutures, screws), closure (covering and occlusion), scaffold (cellular proliferation and tissue guide), separation (isolation and contact inhibition), and drug delivery devices.[9–10] They offer the advantage of being biocompatible and bioresorbable, for example, degrading in low-molecular-weight products, which are either excreted or metabolized.

Among them, aliphatic polyesters such as poly (ε-caprolactone) (PCL) and polylactides (PLAs) represent one of the most promising family and are up to date the most extensively investigated ones.[11] In addition to their biodegradability and biocompatibility, they are thermoplastic polymers with excellent thermomechanical properties. Moreover, PLAs are totally derived from renewable resources, representing a sustainable solution regarding environmental pollution, greenhouse gas emissions, waste disposal, and the depletion of fossil resources like oil.[6,7,12–16] The 'Green Chemistry' issue affords a platform to substitute partially, and to some extent totally, petroleum-based polymers through the design of bio-based polymers competing or even surpassing the existing petroleum-based materials on cost-performance basis with high eco-friendliness values.[17,18] In this respect, aliphatic polyesters are finding broad applications from packaging for industrial products to mulching films in agriculture or bioresorbable materials for hard tissue replacement and controlled drug delivery devices.[11] However, a precise control over properties like hydrophilicity, glass transition temperature (T_g), and crystallinity is of utmost importance for their thermomechanical properties, biodegradation rate, and bioadherence, and relies on the availability of an adequate synthetic pathway.

The traditional synthetic route to the preparation of aliphatic polyesters is the step-growth polymerization or polycondensation of diols with diacids (or diesters), or of hydroxyacids.[19] Despite its low cost, direct polycondensation suffers from several drawbacks such as the need for high temperature, the continuous removal of by-products (most often water), and long reaction times, favoring side reactions. Moreover, the resulting molar weights are typically lower than 30 000 g mol^{-1} with polydispersities close to 2,[20] yielding polyesters with poor mechanical properties.

In contrast to the limitations of the step-growth polymerization techniques, ring-opening polymerization (ROP) of cyclic esters may provide high-molecular-weight aliphatic polyesters (up to 100 kg mol^{-1}) under mild conditions.[21–25] ROP is the preferred synthetic pathway used in industry, and

can be performed in bulk (absence of solvent), in solution, or in emulsion.[26] Under given conditions (temperature, solvent, initiator, catalyst), ROP proceeds in a controlled manner. This affords a prediction of molecular weights for polyesters by controlling the initial monomer-to-initiator molar ratio, but also the synthesis of well-defined polyesters with a low degree of polydispersity. In this chapter, the industrial aspects to obtain these aliphatic polyesters by ROP as well as their properties and applications – existing and *in spe*, will be discussed with a special emphasis on the prominent examples of commercially available aliphatic polyesters, namely PLA, polyglycolide (PGA), PCL, and poly(1,4-dioxan-2-one) (PPDX). Prior to these different issues, some generalities about ROP of cyclic esters will be discussed through their industrial aspects.

4.31.2 ROP of Cyclic Esters: Generalities

Depending on the cyclic monomer, the catalytic/initiating system, and the nature of the resulting active species, ROP proceeds as free radical, coordinative, anionic (or cationic), or enzymatic polymerization.[27] Anionic and coordinative ROP allow reaching the highest polymerization yields and molecular weights in short reaction times.

Anionic ROP proceeds through nucleophilic compounds (organometallic compounds, metal amides, amines, alkoxides, alcohols, water, etc.) as initiators. The anionic ROP process has successfully been used for the synthesis of well-defined (co) polyesters made of 4- and 5-membered lactone rings such as β-butyrolactone initiated by metallic potassium and in presence of 18-crown-6 ether.[28,29] Depending on the nature of the initiator, either an alkyl-oxygen or an acyl cleavage occur, with the respective formation of a carboxylate or an alkoxide growing species (Figure 1).[30] In contrast to 4- and 5-membered lactone rings, ROP for higher ring sizes such as ε-caprolactone (CL) is exclusively initiated by metallic alkoxides instead of metallic carboxylates, which are not nucleophilic enough to open the lactone ring.[31]

Unfortunately, anionic ROP promoted by metal alkoxides is often accompanied by significant intra- and intermolecular transesterification and termination reactions, resulting in the formation of cyclic oligomers and broadening the molecular weight distribution. The occurrence of side reactions along anionic ROP is ascribed to the high ionicity of the metal alkoxide bond.

The side reactions have been depressed using graphite intercalated with alkaline metals (e.g., Na) as initiating system.[32] In this case, the polymerization takes place within the interlamellar spacing of graphite, preventing the growing polyester chains from adopting the conformation necessary to form

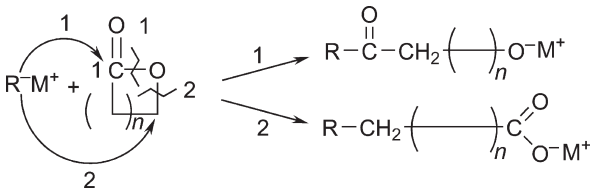

Figure 1 ROP of lactones by anionic initiation by either (1) O-acyl bond cleavage or (2) O-alkyl bond cleavage.

cyclics (by backbiting). Another way to avoid these side reactions is to take advantage of coordinative (pseudoanionic) ROP.

Coordinative ROP proceeds through initiators able to covalently bind the monomer, that is, forming covalently bound propagating species. This has been found to prevent inter- and intramolecular transesterification reactions by decreasing the reactivity of metal alkoxides and polymerization rate. Alkoxides of metals with free p or d orbitals (Mg, Sn, Al, Ti, Zr, Zn, etc.) have, therefore, become of significant interest. The nature of the metal forming the 'active covalent' bond is of utmost importance for the control over side reactions.[33] Within the limits of the studied initiators, the order of the relative reactivity increases as follows: $Al(O^iPr)_3 < Zn(O^nPr)_2 < Ti(O^nBu)_4 < Bu_3SnOMe < Bu_2Sn(OMe)_2 < K(OMe)$. The use of bulky coordinated groups enables a further decrease of side reactions, yielding linear high-molecular weight polyesters of narrow distribution and high stereoregularity.[34–36] In accordance with these results, 'selectivity parameters' γ (the ratio of propagation rate constant to the intermolecular transesterification rate constant) and β (the ratio of propagation rate constant to backbiting rate constant) have been defined for quantifying the extent of transesterification side reactions.[37,38] High selectivity with minimal side reactions have been found for aluminum and lanthanide initiators.[38,39] For example, propagation in presence of aluminum alkoxides is 100 times faster than bimolecular transesterification during ROP of L-lactide (L-LA) in tetrahydrofuran, and the molecular weight of the resulting polyester is usually controlled.[37] Moreover, both chain ends are predictable and well defined. An ester group 'RO–C=O' with an alkoxy group – RO – from the initiator is anchored in α-position, while hydrolysis of the propagating chains results in ω-hydroxy-terminated polyester. The exceptional control using aluminum alkoxides has logically been utilized as a synthetic platform for the preparation of aliphatic polyesters of desired macromolecular structure.[40] However, aluminum alkoxides, either trialkoxides ($Al(OR)_3$) or dialkyl alkoxide ($R_2Al(OR')$), are known to aggregate as dimers, trimers, and tetramers.[41–43] These aggregates play an important role in the kinetics of the polymerization of cyclic (di)esters. For instance, an induction period of time is observed before the initiation step, and is attributed to the rearrangement of the aggregated forms into the 'more active' initiating species.[44] Importantly, this rearrangement can also determine the initiation extent. For example, $Al(O^iPr)_3$ in toluene is a mixture of two aggregates (trimer (A_3) and tetramer (A_4)) in equilibrium (Figure 2). Depending on the cyclic (di)ester and reaction conditions, both species ($A_3 + A_4$) can act as initiators, for example, for the ROP of lactide (LA), while only the more reactive A_3 can be involved, for example, for the ROP of CL. This difference is attributed to the much lower reactivity of A_4 tetramer compared to A_3 trimer, so that in polymerization of CL initiated by a mixture of A_4 and A_3, only A_3 is completely consumed while A_4 species remains 'untouched'.

Other very often reported 'initiating systems' for coordinative ROP are covalent metal carboxylates, particularly tin(II) 2-ethylhexanoate ($Sn(Oct)_2$).[45] Indeed, $Sn(Oct)_2$ belongs to the most frequently used catalyst for the ROP of cyclic esters in industry (Figure 3). Such commercial catalysts can be readily handled (i.e., do not require high vacuum equipments) and are relatively easy to purify (at least down to ~2 mol.% of proton containing impurities) by distillation for semiquantitative synthetic work.[46] In contrast to aluminum derivatives, tin

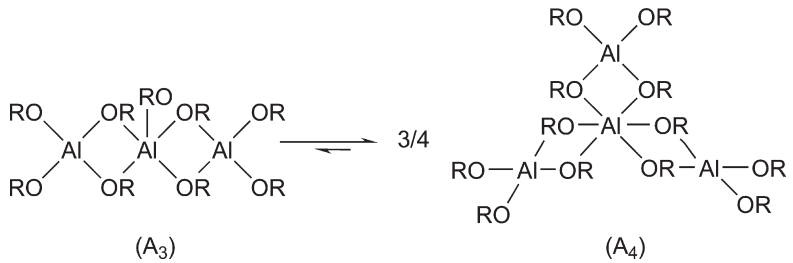

Figure 2 Dynamic equilibrium of aggregated A_4 and A_3 species derived from $Al(O^iPr)_3$ in toluene.

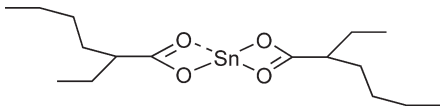

Figure 3 Molecular structure of tin(II) octoate.

carboxylates are accepted in food regulations by the Food and Drug Administration (FDA).

The most advocated mechanism[47,48] involves a direct catalytic action of $Sn(Oct)_2$. Actually, $Sn(Oct)_2$ was first proposed to activate the monomer forming a donor–acceptor complex, which further participates directly in the propagation step. $Sn(Oct)_2$ is liberated in every act of propagation. It results from this mechanism that Sn(II) atoms are not covalently bound to the polymer at any stage of polymerization. Interestingly, Penczek and co-workers[49–51] proposed another more reliable mechanism, proceeding through the 'active chain end' mechanism, that is, by the *in situ* formation of Sn-alkoxide bonds located at the chain ends as observed by matrix-assisted laser desorption ionization time of flight (MALDI-TOF) and fully confirmed by kinetic studies. Through a rapid exchange equilibrium $Sn(Oct)_2$, and most probably any other covalent metal carboxylates, are first converted by reaction with protic compounds (ROH) into tin (or other metal) alkoxides as active centers for the polymerization. ROP proceeds through a 'coordination-insertion' mechanism when promoted with these tin alkoxides similarly to the previously discussed covalent metal alkoxides such as aluminum alkoxides (**Figure 4**).

The investigated metal complexes finding applications in the ROP of cyclic lactones have recently been reviewed by several groups,[52–54] contributing to a better understanding of the factors governing this polymerization. Spectacular improvements in terms of molecular parameters and stereocontrol, activity, and productivity have therefore been achieved. In addition to these 'rather conventional' systems, newer metal-free catalysts have been developed and some of them have already found industrial applications. Metal-free ROP evoked a significant interest following the pioneering research of Hedrick *et al.* in 2001. Among the simplest ones, some selected enzymes, tertiary amines, urea- and iodine-based compounds, phosphines, and carbenes have proven efficient metal-free catalysts.[53,55,56] It is worth noting that the use of enzymes has several advantages over the conventional chemical methods: they need milder conditions, the use of organic solvents might be avoided, high enantio- and regioselectivities are achieved, and the catalyst is usually recyclable. Enzymatic reactions are reversible, demanding appropriate reaction conditions to control the equilibrium. Among all enzymes, lipases that are able to cleave ester bonds, and are also reversible catalysts in esterification and transesterification.[57,58] Moreover, some lipases have proven stable in organic solvents. The preferred system is the *Candida antarctica* (known as *Novozyme-435*).[57]

Whatever the free-metal initiating system, the mechanism of metal-free ROP is not completely understood yet, but the activated monomer mechanism, involving a transient monomer–catalyst complex (**Figure 5**) is somehow accepted.[53,55,59,60]

After the formation of the transient monomer–catalyst complex, the protic initiator will react to form the 'ring-opened adduct' with the simultaneous delivery of the catalyst. Analogously proceeds chain propagation. Accordingly, acid or ester functionality is expected in α-position, similarly to the 'coordination-insertion' mechanism described above. However, this metal-free ROP significantly differs from the classical coordinative ROP as the nucleophilic catalyst only activates the monomer, without remaining bound to the growing chain end. The recent advances in the controlled metal-free ROP of cyclic monomers have thoroughly been discussed by Dechy-Cabaret *et al.*[53]

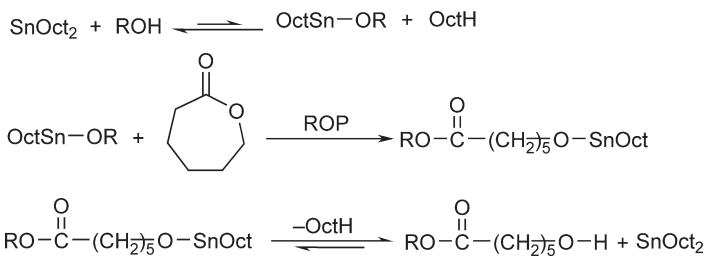

Figure 4 Proposed activation mechanism for the ROP of ε-CL promoted by $Sn(Oct)_2$ (only tin-monoalkoxide, Oct-Sn-OR, is shown even though the formation of tin dialkoxide cannot be ruled out).

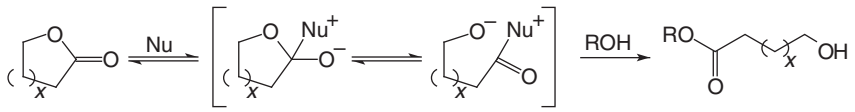

Figure 5 Schematic presentation of the metal-free nucleophilic ROP. Nu, nucleophilic transesterification catalyst; ROH, protic initiator or growing polyester chain. Adapted from Dechy-Cabaret, O.; Martin-Vaca, B.; Bourissou, D. *Chem. Rev.* **2004**, *104*, 147.[53]

4.31.3 Industrial Aliphatic Polyesters Implemented by ROP

The aliphatic polyesters implemented by ROP were the earliest and have been the most extensively studied polymers for their inherent biodegradability. Their uniqueness lies in their immense diversity. Most of them have already been industrialized and found applications in medicine, food, and agriculture. In Table 1, the structure of the industrialized monomers and the corresponding homopolymers are listed. PLA, PGA, and their associated copolymers, as well as PCL are the most investigated. The synthesis (related with industrial aspects), properties, applications, and perspective developments of these polyesters will be discussed hereafter.

4.31.3.1 Poly(lactide)

4.31.3.1.1 Generalities

Regarding the development of environmentally friendly processes and products, PLA represents one of the most auspicious candidate for the substitution of various petrochemical polymers as polystyrene (PS) and poly(ethylene terephthalate) (PET). The monomeric repeating unit of PLA is the lactic acid (2-hydroxypropionic acid), the simplest α-hydroxy acid containing an asymmetric carbon atom. Due to the chirality of the carbon atom, the lactic acid exists in two enantiomeric configurations – L(+) and D(−) stereoisomers (Figure 6).[61] Lactic acid is commercially produced by converting carbohydrates obtained from vegetable sources (e.g., corn, wheat, rice) using either bacterial fermentation or a petrochemical route, even if the first approach is more extensively used, since it is more eco-friendly.[62] Furthermore, the petrochemical synthesis yields an optically inactive 50:50 mixture of D- and L-forms, whereas the bacterial fermentation-derived lactic acid exists almost exclusively in the L-form.[62,63] The bacterial fermentation process uses homolactic organisms such as optimized or modified strains of the genus *Lactobacillus*.[61] These bacteria are classified as homofermentative and produce the lactic acid from the carbohydrates through the Embden–Meyerhof pathway. Various types of carbohydrates can be chosen depending on the particular strain of *Lactobacillus*. In general, most of the simple sugars obtained from agricultural by-products can be used: glucose, maltose, and dextrose from corn or potato starch, sucrose from cane or beet sugar, and lactose from cheese whey. Along with these carbohydrates, the bacteria require proteins and other complex nutrients such as B vitamins, amino acids, and nucleotides. Moreover, the fermentation approach has been found to be more 'eco-friendly'. Since 1990, it has been the more extensively used route toward the production of lactic acid.[63] Batch, continuous or cell recycle reactors, producing 4.5–76 g l^{-1} h of lactic acid have, therefore, been developed and are nowadays used by industry.[64] It is worth noting that recent research has shown the possibility of producing D-lactic acid starting from renewable resources with

Table 1 Industrialized cyclic ester monomers and corresponding homopolymers

Cyclic monomer		*Homopolymer*	
Name	*Chemical structure*	*Name*	*Chemical structure*
Lactide (LA)	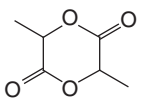	Poly(lactide) (PLA)	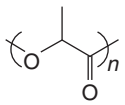
Glycolide (GA)	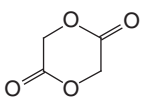	Poly(glycolide) (PGA)	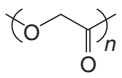
ε-Caprolactone (ε-CL)	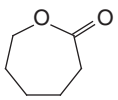	Poly(ε-caprolactone) (PCL)	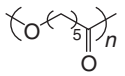
Dioxanone (PDX)	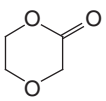	Poly(dioxanone) (PDX)	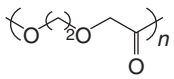

Reproduced from Nair, L.; Laurencin, C. *Prog. Polym. Sci.* **2007**, *32*, 762, with permission from Elsevier.

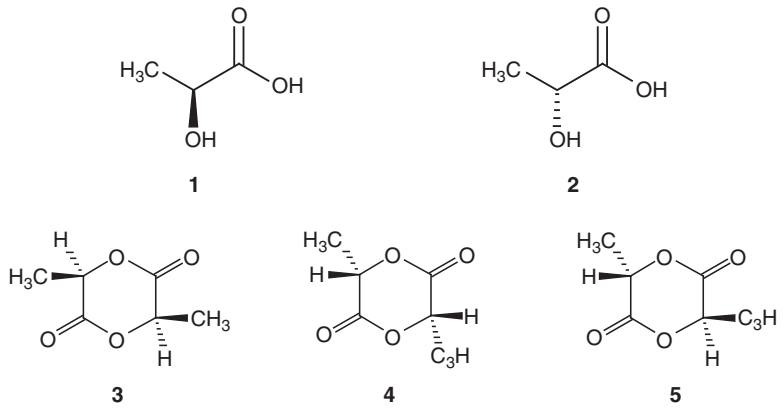

Figure 6 Chemical structures of the monomers for the synthesis of PLA: (**1**) L-lactic acid (m.p. 16.8 °C); (**2**) D-lactic acid (m.p. 16.8 °C); (**3**) D,D-lactide (m.p. 97 °C); (**4**) L,L-lactide (m.p. 97 °C), and (**5**) D,L-lactide (*meso*-lactide, m.p. 52 °C). m.p. = melting point.

high yields. For instance, the production of pure D-isomer is obtained by converting lignocellulosic materials into lactic acid through simultaneous saccharification and fermentation with *Lactobacillus coryniformis* (ssp.) *torquens*.[65]

Starting from lactic acid, PLA with elevated molecular weights may be produced by (1) 'direct polycondensation' or (2) 'azeotropic dehydrative polycondensation'.[66–68] The direct polycondensation (1) is the less expensive route. However, due to its reversibility, it requires removal of a by-product (i.e., water) and long reaction times with resulting polymers of only about 30 kg mol^{-1}. Chain coupling agents and additives are needed to increase the molecular weight of resulting PLA, therefore, adding cost and complexity to the polyester synthesis. The use of chain coupling and additivation can be avoided by performing 'solid-state polymerization' (SSP) by the indirect method. The latter is carried out by heating PLA prepolymers at a temperature just below their melting temperature (T_m), and by continuously removing the by-products (water) under reduced pressure or through a gaseous carrier.[69] Although the reaction time is much longer than of polymerizations carried out in melt or in solution, high-molecular-weight PLAs up to 500 kg mol^{-1} are readily obtained by this method. The main advantage of this technique is also that low reaction temperatures are utilized, reducing the incidence of side reactions such as thermal, oxidative, hydrolytic degradation, and, therefore, yielding the synthesis of PLA with high molecular weights up to 100 kg mol^{-1} and good thermomechanical properties. More directly, another method avoiding chain coupling and additivation is the (2) azeotropic condensation synthetic route.[70,71] The azeotropic dehydrative polycondensation (2) of lactic acid leads to the preparation of higher molecular weight PLA going up to 300 kg mol^{-1} in the presence of tin-based catalysts and azeotropic solvents such as diphenylether.[72] However, removing the by-product is still needed, together with the use of long reaction times (up to 40 h). In this respect, the best control over the molecular parameters (molecular weight, nature of chain ends, etc.) for the synthesis of PLA is successfully obtained by ROP of the lactic acid cyclic dimer –LA (see **Figure 6**).[73] Due to the presence of two chiral centers, LA exists as two optical isomers, D,D-lactide (D-LA) and L,L-lactide (L-LA). Two optically inactive LA are also available: *meso*-LA as well as the racemic mixture of L-LA and D-LA, called *rac*-LA.[74]

Although the first syntheses of PLA by ROP of LA were carried out by Carothers *et al.* in 1932,[75] the first industrial example was patented and published by NatureWorks (ex. Cargill Inc.) in 1992.[76,77] The Cargill process involves the continuous production of LA, followed by its direct ROP. The process starts from the fermentation of corn dextrose, leading to mainly L-lactic acid. The lactic acid is then condensed in order to obtain lactic acid oligomers, which is further catalytically depolymerized under reduced pressure to give pure LA containing minimum 95% of L-LA (**Figure 7**). In a batch reactor, ROP of resulting LA is subsequently carried out in the absence of solvent using tin octoate as catalyst to give high-molecular-weight PLA. Up to recently, NatureWorks has announced a production capacity of approximately 140 000 metric t year^{-1} of PLA under the name Ingeo™, mainly for commodity market.[72,78]

The NatureWorks™ process embodies the Green Chemistry principles by using a fermentation process for monomer production, replacing petroleum-based resources with annually renewable resources, performing the synthesis in the absence of solvents and other hazardous chemicals, reducing energy consumption and increasing yields by efficient catalysis, and completely recycling product and by-product streams.[19] Interestingly, due to its renewable origin, the overall production of PLA could even yield a negative greenhouse gas impact in comparison with petrochemical polymers (**Figure 8**).[78] This can be achieved by utilizing the lignin fraction of lignocellulosic feedstocks as stream of LA, as well as by replacing the grid electricity with wind power in the biorefinery, lactic acid, and PLA production facilities. Thanks to these sustainability and eco-friendly characteristics, PLA exhibits biodegradable, recyclability, and compostable properties, which make it an attractive biopolymer.[79] In this respect, there are several other Good Manufacturing Practice (GMP)-grade PLA, distributed under the trademarks Purasorb™ and Puralact™ (Purac Biomaterials, The Netherlands), Lactel™ (Birmingham Polymers, Alabama, USA), Resomer™ (Boehringer Ingelheim, Germany), Medisorb™ (Alkermes, USA), and Futerro™ PLA (Futerro, Belgium). However, a serious problem is caused by the proper choice of plant stock for the manufacture of PLA. The use of corn for the manufacture of PLA – justified from the purity and economical point of view – is hampered by its food applications. Purposeful growth of significant crops in poor soils has

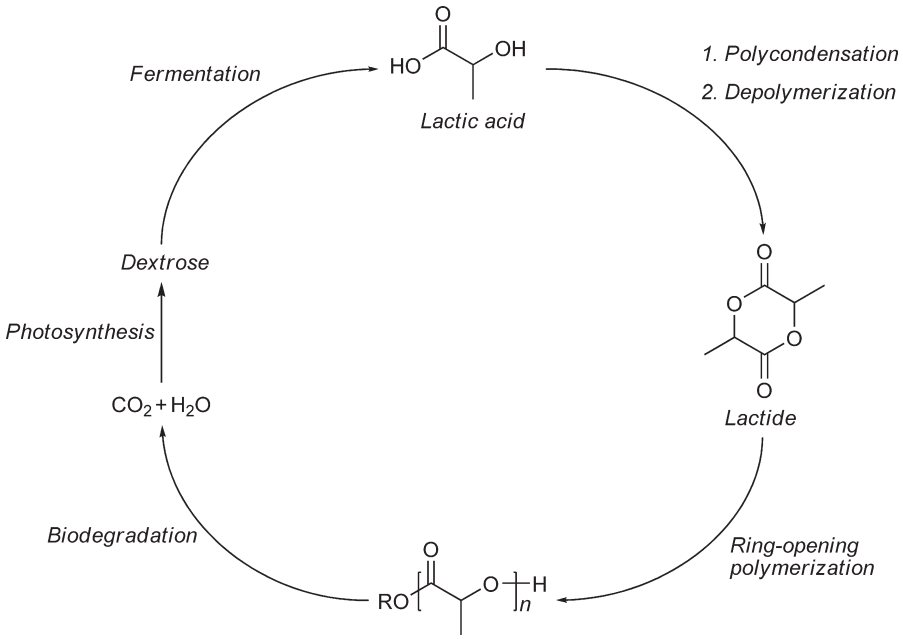

Figure 7 Schematic presentation of the current Cargill Dow LLC process for PLA production in Blair, Nebraska, USA. Reproduced from Kharas, G. B.; Sanchez-Riera, F.; Severson. D. K. Polymers of lactic acid. In *Plastics from Microbes;* Mobley, D. P., Ed.; Hanser Publishers: Munich, 1994; p 93.[64]

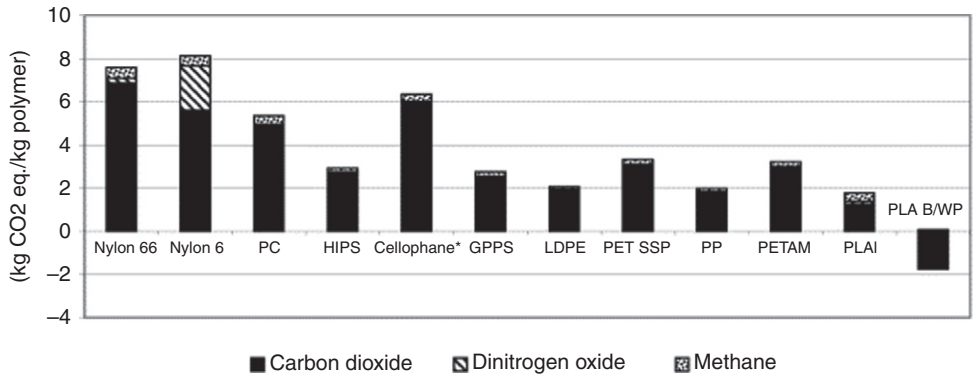

Figure 8 Contributions to global climate change for some petrochemical polymers and two PLA (PLA 1 = first-generation PLA; PLA B/WP = PLA derived from biomass and wind power scenario). Reproduced from Vink, E. T. H.; Rábago, K. R.; Glassner, D. A.; Gruber, P. R. *Polym. Degrad. Stab.* **2003**, *80*, 403,[78] Copyright Elsevier.

been proposed as an alternative.[80] By-products from hydrolysis of plant stock containing hexoses or agricultural wastes might be also useful.

Recent industrial developments provided by Futerro™ regarding the continuous production of PLA have emerged from adapted reactive extrusion (REX) processing.[81,82] REX is a continuous melt-processing technique used for the chemical modification and the *in situ* synthesis of polymers in the absence of solvent. This gives access to new polymeric materials that are cost competitive and friendly environmentally from the viewpoint of 'green chemistry'. REX polymerization of LA is currently carried out not only in the presence of tin octoate (II) complexed with an appropriate Lewis base, for example, triphenylphosphine, as catalytic system, but also with suitable stabilizers and antioxidants. Highly thermal stable PLA can be readily obtained by this REX process.

In the past decade, the lipase-catalyzed ROP of LA has become a very attractive and eco-friendly technique for the synthesis of PLA.[83] However, the obtained polyesters usually present low molecular weights, unusable in industrial applications. Much effort has been making to overcome this limitation. First, Matsumura *et al.*[84] reported on the enzymatic synthesis of poly(*meso*-LA) (P(*meso*-LA)) by lipase-catalyzed ROP (lipase from *Burkholderia cepacia* (former *Pseudomonas cepacia*), Lipase PS) at 80–130 °C, resulting in PLAs with weight-average molecular weight ($\overline{M}_W$) higher than 10^4. As an alternative to organic solvents, García-Arrazola *et al.*[85] have reported the synthesis of PLA by enzymatic ROP in supercritical CO_2. Very recently (in December 2009), a research team from KAIST University in Seoul (South Korea) and the Korean chemical company LG Chem announced the production of PLA through bioengineering – using enzymes from metabolically engineered strain of *Escherichia coli*, rather than fossil-based catalysts.[86] In this case, differing from the two-stage continuous process described above, a one-step fermentation process has accordingly been developed.

4.31.3.1.2 Properties

4.31.3.1.2(i) Thermomechanical properties

The configurational difference between the monomeric units (D(L)-LA and the *meso*-LA) has a significant influence over the thermomechanical properties of resulting PLA. For example, PLA homopolymers prepared from optically pure L-LA or D-LA arrange in isotactic manner,[87] giving semicrystalline polyesters with a T_m of about 175 °C and a T_g of approximately 55–60 °C.[87,88] It has been found that poly(L-LA) (P(L-LA)) crystallizes in three easily distinguished forms, namely, α-, β-, and γ-forms.[89,90] Similar crystalline structures but with the opposite (mirror-like) arrangement of the molecular chains in the crystal lattices are predicted for poly(D-LA) (P(D-LA)).[91] The PLA crystal structures have accurately been described in several reviews.[74,91] Their crystallinity and T_m have usually been found to decrease upon decreasing the degree of optical purity.[91] For pure P(L-LA), that is, containing 100% L-LA, the crystallinity can reach 30–50%, while for PLA containing more than 10% of optical impurities, the resulting PLAs are amorphous with a T_g of ~60 °C. The content of optical impurities has been found to significantly affect other physical properties of PLA. For instance, P(*meso*-LA) has lower tensile strength and higher ultimate elongation than P(L(D)-LA)s. In this respect, semicrystalline P(L-LA) is considered more for its mechanical properties by comparison with those of amorphous PLA. In the case of semicrystalline P(L-LA), the Young's modulus is around 3 GPa, the tensile strength is between 50 and 70 MPa with a elongation at break of approximately 4%, and an impact strength close to 2.5 kJ m^{-2}.[92]

By comparison with commodity polymers such as PE, polypropylene (PP), PS, and PET,[92,93] the mechanical properties of semicrystalline P(L-LA) are interesting, particularly its Young's modulus, considering PLA as an excellent substitute for commodity polymers in short-time packaging (**Table 2**). However, like PS, PLA behaves as a brittle material with low impact strength.[74] This is one of its main limitations for the development of PLA due to the low impact strength.

Interestingly, when optically pure PLA made of L-LA is combined with optically pure PLA made of D-LA, it results in the formation of a stereocomplex (sc). The T_m of these structures (called sc) can be about 50 °C higher (~230 °C) than that of the pure enantiomeric homopolymers.[94] The sc formation will enable the thermal resistance of non-stereocomplexed PLAs to be improved, especially heat-deflection temperature (HDT), broadening the polyester applications. Indeed, HDT for PLA-based materials is quite low (around 50 °C), limiting some applications such as electronics where heat resistance is required.[95] The formation of stereocomplexed PLA (sc-PLA) must afford the development of new durable applications for PLA-based materials.

4.31.3.1.2(ii) Optical properties

PLA homopolymers obtained from pure enantiomeric lactide (L-LA or D-LA) have shown to be equal in value but opposite in sign specific optical rotation.[96] Studies have shown that PLA does not transmit in the lower ultraviolet (UV) range (up to 225 nm), while significantly transmitting at higher wavelengths.[74] This might require the addition of UV light blockers in some specific applications. Moreover, within the visible light band ranges, the PLA possesses a yellowness index comparable to those of petroleum-based polymers as PS. This light yellow color might create a consumer perception for an old final material.[74]

4.31.3.1.2(iii) Solubility and barrier properties

PLA-based materials are hydrophobic polymers, dissolving in common organic solvents as chloroform, tetrahydrofuran, 1,4-dioxane, acetone, and the others.[64] The solubility depends mainly on their molecular weight and crystallinity.

These polyesters present rather acceptable barrier properties toward O_2, some organic compounds, and water vapor, comparable to those of PS and PET. However, barrier properties toward CO_2 are not good enough for PLA-based materials in comparison with PET when containers for sparkling water are considered.[97]

4.31.3.1.2(iv) Melt processing and thermal stability

PLA possesses rheological properties close to those of PS, allowing its melt processing through conventional systems including injection molding, extrusion, film blowing, sheet forming, and fiber spinning.[74] The majority of commercial PLA grades is made of a mixture of L-LA (>95%) and D-LA (<5%). The addition of this small fraction such as D-LA is to improve the processability of commercial PLA using conventional melt-processing techniques. However, during processing at temperatures close to 200 °C, the thermal degradation of PLA readily occurs through different mechanisms – hydrolysis, unzipping depolymerization reactions, oxidative degradation, and transesterification reactions – where hydrolysis is the predominant mechanism at these elevated temperatures. Therefore, processing conditions have to be adapted, for example, in the absence of atmospheric humidity, and use of appropriate stabilizers such as tris(nonylphenyl)phosphite is required, reducing the incidence of hydrolysis reactions.[98]

4.31.3.1.2(v) End-life properties

PLA may be considered as biodegradable when placed in compost. However, confusion must be avoided as its biodegradation actually proceeds in two stages: (1) ester bond hydrolysis, and (2) microbial attack. The first of them is autocatalyzed due to the release of acid compounds during the hydrolysis of PLA. During the hydrolytic degradation of PLA, this stage is predominant, is affected by temperature and

Table 2 Overview of mechanical properties for PE, PP, PS, and PET[92,93]

Properties	*PLA*	*LDPE*	*PP*	*PS*	*PET*
Young's modulus (MPa)	3000	100–300	1700	2000	1700
Break elongation (%)	4	100–800	>10	1–4	180
Impact strength (J m^{-2})	2.5	No fracture	50	20	90

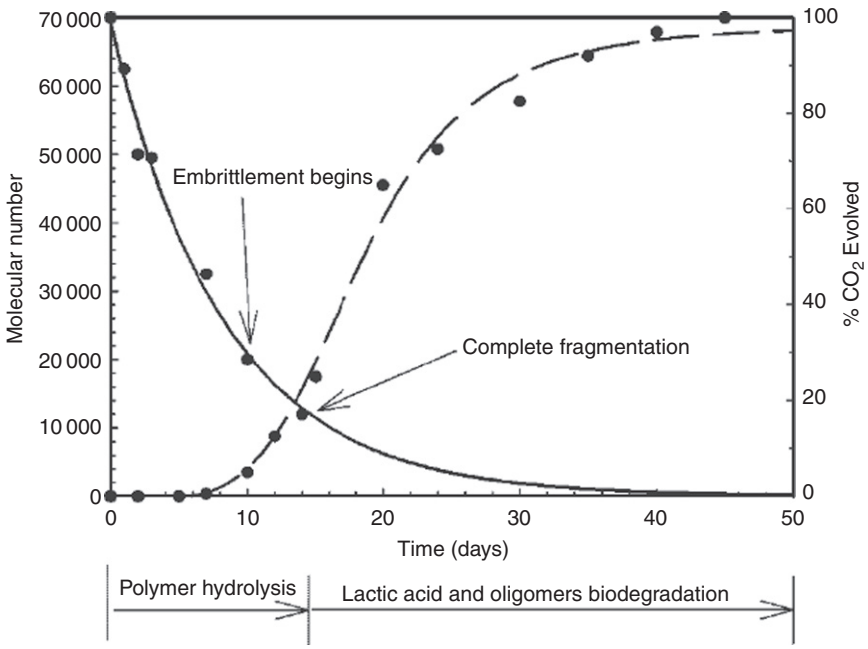

Figure 9 Biodegradation of PLA in compost at 60 °C. Adapted from Auras, R.; Harte, B.; Selke, S. *Macromol. Biosci.* **2004**, *4*, 835,[74] Copyright Wiley-VCH.

moisture levels,[76] and follows a first-order kinetics.[99] It is only after a certain time that the second degradation step occurs, reducing PLA to low-molecular-weight lactic acid oligomers, by the natural action of microorganisms (**Figure 9**).

Biodegradation and/or composting represent an interesting end-life management option, especially in the case of bio-sourced materials such as PLA. Recently, Galactic SA (Belgium) introduced the green patented LOOPLA® technology[100] (**Figure 10**). The LOOPLA® technology is a chemical recycling process that goes back from PLA to lactic acid by hydrolysis of PLA-based materials after use. The obtained lactic acid is the same starting ingredient to produce a new PLA with the exact properties. This technology does not need harmful chemicals, and enhances the eco-benefits toward composting. The main feature is to reduce the implementation of food resources used for the manufacture of PLA upon the Cargill process, and therefore the concern about the possible food shortage.

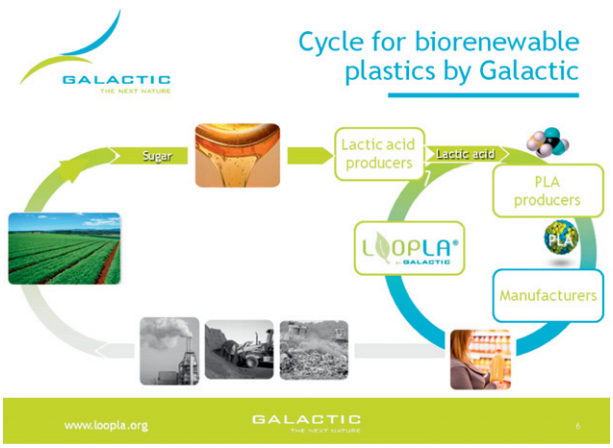

Figure 10 LOOPLA® cycle. Reproduced with permission from Galactic SA Mariage, P. A.; Hottois, D.; Coszach, P. BE Patent 1,018,247, 2010,[100] Copyright Galactic SA.

For *in vivo* applications, PLA has demonstrated its bioresorbability and biocompatibility. While biocompatibility is related to no harmfulness to the living host, the bioresorbability applies to natural or synthetic materials that degrade over time through hydrolysis into small fragments capable of being metabolized.[101] The main factors affecting bioresorbability are the manufacturing process, the sterilization technique, water uptake, pH, and crystallinity.[102] Due to these properties, PLA has found extensive applications in tissue repair, drug delivery systems, and tissue engineering as surgical implants.[88] The degradation rate of P(L-LA) is, however, very low and takes between 2 and 5.6 years for total resorption *in vivo*,[103] which is due to its hydrophobic nature and high degree of crystallinity. Even though the polymer is known to lose its strength in approximately 6 months when hydrolyzed, no significant changes in mass occur after a very long time. This leads to undesirable inflammatory responses in a certain number of clinical studies with the necessity to remove the implants afterward. In order to increase the degradation rate of P(L-LA), copolymers of L-LA and D,L-LA have, therefore, been prepared as well as glycolide (GA), trimethylene carbonate, and 1,4-dioxan-2-one (PDX) have been incorporated within the polyester chains.[104,105]

4.31.3.1.3 *Applications – existing and* in spe

The applications of PLA – existing and *in spe* – will be discussed upon both the biomedical field and the daily applications such as packaging. Interestingly, due to the depletion of petroleum resources, PLA is more and more considered as a valuable biosourced polymer substitute in durable applications such as electronics.

4.31.3.1.3(i) Biomedical applications

PLA achieved its first commercial success in medicine for the development of improved multifilament sutures in the 1980s.[74] This was due to its biocompatibility and bioresorbability in the human body as earlier approved[64,106–108] in 1971 by the FDA. Thanks to the high strength of multibraided fibers, PLA has been used as scaffolds for ligament replacement and for replacing the nonbiodegradable fibers such as Dacron™.[109,110] Some PLA fiber-based devices are also under investigation as long-term blood vessel conduits.[111,112]

Moreover, a number of different prosthetic devices based on PLA have been developed in orthopedic fixation or as bone substitution materials.[103,113] The choice of this PLA polymer is based on its high crystallinity degree, inducing slow degradation, good tensile strength, low extension, and a high modulus, thus making it an ideal biomaterial for load-bearing applications. Bone screws, plates, and pin structures made of PLA are not corrosive, do not require additional surgery for implant removal after bone healing, and are biocompatible.[114] However, in some cases, some inflammatory responses may occur due to the release of acidic products during the resorption of PLA-based materials. For resolving these acidic reactions and improving their mechanical properties, ceramic polyester materials have been proposed. Macro- and nanocomposites of PLA matrix containing hydroxyapatite, β-tricalcium phosphate, or $CaCO_3$ have been reported in the literature.[115–117] In comparison to pure PLA and microcomposites, the recently obtained nanocomposites have shown higher compressive strength and better cell affinity and compatibility.[117] Some of the PLA-based orthopedic products actually available on the market include the Phantom Soft Thread Soft Tissue Fixation Screws, Phantom Suture Anchors (DePuy), Full Thread Bio Interference Screws (Arthrex), BioScrews, Bio-Anchors, Meniscal Stingers (Linvatec), and the Clearfix Meniscal Dart (Innovasive Devices).[10]

As PLA materials present good collapse pressure, they have been studied for the production of biodegradable stents. The first of them, the so-called Duke stent, was based on PLA-woven strands and was developed in the 1980s at Duke Medical Center.[58] This stent was able to withstand a collapse pressure of 1.3 relative units, while maintaining its strength in saline buffer for about 30 days. Further studies have shown that the increase in PLA molecular weight from 3.22×10^5 to 10.6×10^5 does not significantly affect the collapse pressure.[118] Several patents also appeared[119,120] and implantation in humans has been reported.[121]

An injectable material made of PLA (Sculptra, B.T-Fill™) has been developed and approved by the FDA for the restoration or correction of facial fat loss or lipoatrophy in people with the human immunodeficiency virus.[10] Subcutaneous increase in volume of depressed areas, particularly to correct skin depressions such as in skin creases, wrinkles, folds, scars, eye rings and for skin aging, is also targeted.

Investigations on PLA applications as drug delivery systems have shown improved therapeutic effect, prolonged biological activity, controlled release rate, and decreased administration frequency.[122] This very important area of applications has been a subject of numerous scientific reviews.[58,123] Drug delivery vehicles and low-strength scaffolds for tissue regeneration based on PLA have accordingly been developed.[10] The amorphous PLA has been used in this case as it loses strength within 1–2 month(s) and undergoes mass loss within only 12–16 months.[124]

4.31.3.1.3(ii) From daily to durable applications

Besides its medical applications and due to its renewability, biodegradability, optical properties, processability, and mechanical properties, PLA has found various applications in packaging (cups, bottles, films, and containers).[74] However, due to its higher cost, the initial purpose was for high-value films, rigid thermoforms, food and beverage containers, and coated papers. Two of the pioneer companies using PLA as a packaging material were Danone and McDonald's in Germany in yogurt cups and cutlery, respectively.[125] Over the past years, the use of PLA as a packaging material has increased all over the world, mainly for packaging of fresh products with short shelf-life such as fruits and vegetables.[74,125] PLA is also used in compostable yard bags (Compostable Yard Bag, BioCycle, October 1996). It has been considered that the mechanical properties of PLA-based films dedicated to packaging are better than those of PS and comparable to those of PET.[74] It is worth noting that BASF is now manufacturing totally biodegradable plastics – Ecovio® – made of 35 wt.% PLA and 65 wt.% Ecoflex (a biodegradable polymer derived from petroleum).[74] Ecovio® finds different applications including carrier bags (e.g., Aldi® bags), compostable linters, mulch films, and food wrappings.[126]

Recently, PLA fibers have been considered as one of the largest potential development in nonwoven (Spanbond) applications.[19,80] Since the properties and temperature characteristics of PLA are comparable to those of the PP and polyamide, the filament processing equipment used for PLA fibers is also similar.[127] In the literature, solution- and melt-spun high-molecular-weight P(L-LA) fibers, typically of very high tensile strength (from 0.38 to 0.87 GPa) and modulus (up to 9.2 GPa), have been widely studied.[128–139] In most cases, significant losses in molar weight (up to 70%) and very low collection rates ($5\ m\ min^{-1}$) had been first observed. Interestingly, Schmack *et al.*[135] demonstrated the possibility to attain collection rates suitable for the textile industry ($\sim 1000\ m\ min^{-1}$), paving the way to large-scale production of PLA fibers (see below). The common process is an almost no-waste process and includes melt spinning (200–240 °C), thermal drawing, thermal relaxation, and final textile operations. In some cases, bulk dyeing using PET suitable disperse dyes before melt spinning may be performed.[80] Dyeing is conducted in the temperature range 98–110 °C. Special precautions are taken in terms of moisture content in PLA before fiber processing.[19] Typical drying conditions include 2–4 h in a hopper dryer at 40 °C, which result in moisture content of < 50 ppm. Some representative key properties of PLA fibers are listed in **Table 3**.

PLA fibers can be produced with a high degree of orientation, and usually have crystallinity degree of 60–80%. Their T_m falls between those of the PP and nylon fibers. The shrinkage in hot water depends upon the completeness of the relaxation processes in heat treatment.[80] They are water resistant, light resistant, and elastic. These properties allow creating PLA textiles for use as geotextiles, filters, soft containers, covers, fishing tackle, netting for vegetables, curtains, draperies, and furniture upholstery.

Up to the present time, several industrial plants for production of PLA fibers have been created all over the world.

Table 3 Properties of PLA fibers as compared to other synthetic polymers

	Fibers (filaments) properties			
Index	*PLA*	*PET*	*PP*	*Polyamide*
Strain modulus (GPa)	4–6	4–8	2–3.5	2–4
Strength (cN tex^{-1})	40–55	35–50	35–50	35–50
Elongation at break (%)	30–40	30–50	40–60	40–50
Elastic recovery (%)[a]	60–65	60–65	98–100	95–98

[a]For 10% initial deformation.
Reproduced from Perepelkin, K. E. *Fibre Chem.* **2002**, *34*, 85.

NatureWorks (ex-Cargill Dow (USA)) reported an output of up to 8000 t of NatureWorks™ fibers for a large assortment of articles.[80,140] The Japanese Shimadzu Corporation and Kanebo Goshen Ltd. also announced the beginning of PLA fiber production under the brands Lacty™ (Shimadzu) and Lactron™ (Kanebo).[141,142] Some current uses of PLA fibers include hollow fibers for pillows and comforters, bulk continuous filaments for carpets, filament and spun yarns for binders, and self-crimping fibers.[19] In addition, applications such as foamed articles and paper coatings[143–146] are being pursued.

In more added value applications, PLA has attracted much attention as biosourced material melt blended or not with petroleum-based polymers. For example, PLA-based masterbatches have recently been developed by Sukano for dispersion within engineering polymers such as PMMA, PC, and ABS to increase their mechanical performances as well as their biosourced content.[147] Fujitsu and NEC have recently commercialized green notebooks and cell phones based on PLA.[148] Pioneer Corporation has developed flame-retardant PLA resins for the front panel of its DVD drivers.[149]

Even if PLA displays good tensile strength and Young's modulus, it suffers from some shortcomings such as its brittleness, low thermal resistance, low heat-distortion temperature, and low rate of crystallization,[79] limiting its further commercial developments. In order to improve the properties of PLA, several strategies have been employed. The first one consists in tuning the molecular parameters of PLA such as molecular weight, crystallinity, and the stereochemistry. This allows the amorphous character to be changed, and, therefore, its mechanical properties.[150] The second one, largely used in industry, is the incorporation of additives into PLA matrix.[92] In this respect, plasticizers and polymers partially or totally miscible with PLA have been envisioned as additives. Plasticizers are added not only to increase the melt processing of PLA-based materials, but also to increase their flexibility and ductility. The current plasticizers are LA monomer itself, glycerol, citrate ester, poly(ethylene glycol) (PEG), and so on. The most cited plasticizer remains PEG, leading to very high break elongation with low tensile strength.[151] However, both Young's modulus and tensile strength of resulting PLA materials decrease upon the addition of any plasticizer. In order to maintain the ductility of PLA, impact modifiers are, therefore, preferred,[152–154] currently, commercial ethylene-based copolymers obtained by radical copolymerization of ethylene with functional/substituted acrylics. The most currently used impact modifiers are Biomax Strong® from DuPont, Biostrength® and Lotader® from Arkema, and Paraloid® from Rohm and Haas, resulting in a significant improvement of impact strength at low content (max. 5 wt.%). However, these impact modifiers are not biodegradable, leading also to a loss (or decrease) of transparency for the resulting materials. This represents a main drawback for certain applications such as packaging. Interestingly, Paraloid®[154] is the only impact modifier (commercialized by Rohm and Haas) that improves the impact strength, without affecting the transparency of PLA-based materials.

The low crystallization rate is also a significant issue concerning the properties and processability of PLA in more added value applications. For instance, improving the crystallinity of PLA-based materials will enhance, for example, its barrier properties against CO_2, leading to functional packaging for products with longer shelf-life. Therefore, various types of nucleating agents or crystallization-manipulating agents have been used to optimize the crystallization behavior and rate during the industrial processing of PLA. One can cite the addition of inorganic nucleating agents, such as talc and montmorillonite, and of low-molecular-weight organic compounds, such as amide and hydrazide.[155–165] Interestingly, Purac reported the industrial production of equimolar blending of P(L-LA) and P(D-LA), yielding the formation of previously discussed stereocomplexes (sc-PLA) with, for example, improved crystallinity and HDT.[165] Upon this formulation, PLA would be usable for fast-food goods, requiring no shape modification at high temperature (coffee cups). For the first time, PLA would be able to largely substitute commodity plastics such as poly(vinyl alcohol) (PVA), low-density polyethylene (LDPE), linear LDPE (LLDPE), PP, and PS.[166] Recently, Teijin has announced the launch of heat-resistant bioplastics derived from these sc under BIOFRONT™ trade name.[167] These bioplastics will be used for the manufacture of a high-quality, highly durable car-seat fabric made of 100% Biofront fibers in collaboration with Mazda. Other applications are envisioned in fields such as automotive, biomedical, and apparel textiles.

4.31.3.2 Polyglycolide

4.31.3.2.1 Generalities

Another environmentally friendly polymer attracting much attention is PGA. Its monomer unit is the glycolic acid – hydroxyacetic acid, the smallest α-hydroxy acid. Millions of kilograms of glycolic acid are produced annually by reacting chloroacetic acid with sodium hydroxide, followed by a reacidification step. It can be produced from renewable resources such as sugarcane, beets, and pineapple.[168] Moreover, it can be readily produced through an enzymatic process, actually a much less polluting and energy-consuming process than the traditional chemical process. The enzymatic synthesis of glycolic acid is carried out from the corresponding α-hydroxynitrile and a microorganism belonging to the genera *Acidovorax*,[169] *Corynebacterium*,[170] *Rhodococcus*, *Gordona*,[171] and so on.

Similar to the synthesis of poly(lactic acid), the polycondensation of glycolic acid is the simplest process available to prepare PGA, but it is not the most efficient one because it yields low-molecular-weight products. The procedure is as follows: glycolic acid is heated at atmospheric pressure and a temperature of about 175–185 °C during a time necessary for removing water. Subsequently, the reaction pressure is reduced

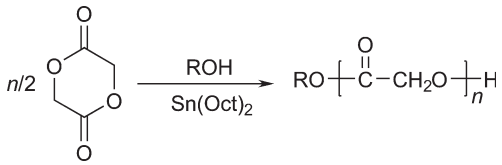

Figure 11 Ring-opening polymerization of GA promoted by hydroxyl compounds in presence of $Sn(Oct)_2$.

to 150 mm Hg, still keeping the temperature unaltered for about 2 h, yielding low-molecular-weight PGA.[172] In this respect, ROP of GA is preferred for the synthesis of PGA. Similar to the LA monomer, the GA cyclic dimer is prepared by first condensing glycolic acid into their low-molecular-weight condensation polymers, and thus thermally depolymerized. Ring-opening (co)polymerization of GA is currently carried out in bulk in the presence of tin- or zinc-based catalysts in order to prepare PGA (Figure 11).[173–175] Surprisingly, some further efforts are now providing an SSP starting from halogenated glycolic acid derivatives with the elimination of HX.[176–178] SSP leads to the synthesis of high-quality PGA because no catalyst and no solvent are used. According to the SSP principles, this last feature is successfully achieved because PGA is highly crystalline, leading to a poor solubility of PGA with its corresponding precursors.

4.31.3.2.2 Properties

PGA is highly crystalline (45–55%) with a melting point of approximately 225 °C and a T_g of 35 °C.[175] Because of its high degree of crystallinity, it is not soluble in most organic solvents except for highly fluorinated organics such as hexafluoroisopropanol. PGA is exclusively degraded by hydrolysis *in vitro* and *in vivo*.[104] The *in vivo* breakdown of PGA proceeds in a similar way as that of PLA and PCL shown schematically in Figure 12. The resulting products can be readily either metabolized or extracted. Furthermore, their biocompatibility has been recognized, and FDA has approved their use in biomedical field for a long time.[179]

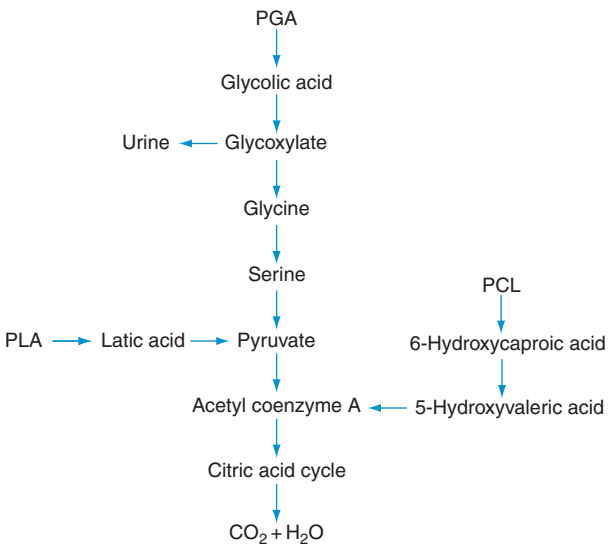

Figure 12 Breakdown of biodegradable/bioresorbable polymers. Adapted from Maurus, P. B.; Kaeding, C. C. *Oper. Tech. Sport. Med.* **2004**, *12*, 158.

4.31.3.2.3 Applications – existing and in spe

PGA was used to develop the first synthetic absorbable suture in the 1960s by Davis and Geck, Inc.[104] These PGA-based sutures became commercially available in the 1970s.[180] Due to its low solubility, PGA-based fibers are traditionally extruded into filaments with high degree of orientation, and, therefore, with high-strength properties.[181] These individual filaments are subsequently braided into multifilament yarns to give the final suture material.[182–184] These resulting fibers exhibit high tensile strength (from ~70 to 140 MPa) and modulus of elasticity (~6900 MPa). In order to reduce the stiffness of fibers, and also to modulate the degradation rate of PGA, GA can be copolymerized with other (di)lactones such as CL and LA.[185] For instance, an LA/GA ratio of 50:50 poly(LA-*co*-GA) (PLGA) degrades in 1–2 months, 75:25 in 4–5 months, and 85:15 in 5–6 months. Because of the ease of manufacture, controllable degradation rates and success in earlier suture materials progress have been made to further develop PLGA biomaterials as replaceable materials for controlled drug delivery systems and scaffolds for tissue engineering.[104,177,186,187] However, regarding PGA itself, the low solubility and high melting point of this polymer limit its interest in commodity applications such as in packaging.

Over the past decade, PGA-based materials have been gaining great interest in the development of temporary bone devices.[104,177] Like PLA, PGA provides some interesting characteristic features such as high strength, biocompatibility, and bioresorbability, making PGA-based materials interesting for internal bone fracture fixation.[177] However, despite their biocompatibility, the use of PGA is associated with inflammatory responses due to the release of acidic products during healing. Therefore, some efforts have been conducted by combination of PGA with bioceramics such as hydroxyapatite.[188–190] In bone-guided engineering, such PGA-based composite will open interesting opportunities to tailor their physical, biological, and mechanical properties, while maintaining the bioactivity of the bioceramics. In principle, these composite materials can be engineered in such a way that their resorption rate in the body matches with the formation rate of the new tissue.

4.31.3.3 Poly(ε-caprolactone)

4.31.3.3.1 Generalities

PCL was one of the earliest polymers synthesized by Carothers in the early 1930s through ROP of CL.[191] Due to its high polymerizability, ROP of CL has been the subject of numerous studies through anionic, enzymatic, cationic, and coordination-insertion mechanisms. We should also mention that PCL can be obtained by free radical ROP of 2-methylene-1-3-dioxepane.[192–194] However, high-molecular-weight PCL are more readily obtained by coordination-insertion ROP of CL as industrially catalyzed with, for example, $Sn(Oct)_2$ in the presence of heavy alcohol (initiator) such as 1-dodecanol (Figure 13).[23] Very interestingly, some of us have shown that three-arm PCL can be synthesized by REX ROP of CL promoted by aluminum *sec*-butanoxide [$Al(O^{sec}Bu)_3$].[195] Without using any solvent, this fast reactive process gives access to 'green' PCL

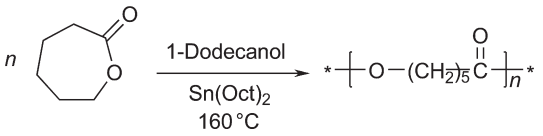

Figure 13 Industrial pathway to high-molecular-weight PCL.

with better mechanical and rheological properties at low production costs as compared with commercial PCL.

The CL monomer is obtained by the traditional Baeyer–Villiger reaction, starting from cyclohexanone as substrate. However, this synthetic route is not environmentally friendly, which has involved the development of two greener routes: (1) use of a peroxycarboxylic acid (such as 3-chloroperbenzoic acid or peracetic acid) in dichloromethane at 40 °C, and (2) use of hydrogen peroxide as oxidizer and zeolite/tin catalysis.[196] The second process is considered the greenest because the main by-product is exclusively water and the tin-impregnated zeolite is an environmentally friendly catalyst. Nowadays, CL is produced by several manufacturers like BASF (USA), Perstorp (UK), and Daicel Chemical Industries Ltd. (Japan).

4.31.3.3.2 Properties

PCL was thoroughly investigated because of the possibility of blending this aliphatic polyester with a number of miscible commercial polymers such as PVC and bisphenol A polycarbonate.[197] The solubility of PCL is established in chlorinated solvents (e.g., chloroform) and in aromatic solvents (e.g., toluene). This semicrystalline polyester with respective T_m and T_g of approximately 60 °C and -60 °C is highly hydrophobic, biodegradable, and biocompatible.[198] In addition to good water, oil solvent and chlorine resistance, PCL is a tough and semirigid material at room temperature with a modulus between those of LDPE and high-density polyethylene (HDPE).[22,72] To reduce the manufacturing costs, PCL may be blended with starch to produce trash bags as well as with fiber-forming polymers (such as cellulose) to make scrub suits, incontinence products, and bandage holders. In contrast to other commercial aliphatic polyesters such as PGA and PLA, PCL is highly thermally stable up to 250 °C.[199] Above this temperature, the thermal degradation of PCL occurs in a two-stage process: ester pyrolysis involving statistical ruptures of PCL chains (generating 5-hexenoic acid), followed by depolymerization of the PCL chains by unzipping reaction. PCL is known to undergo only microbial and enzymatic degradations under outdoor conditions.[200] Even though PCL is biocompatible, its bioresorbability is very slow, which is usually a disadvantage in medical applications except in drug delivery devices. This is due to its high permeability toward hydrophobic drugs.[201] Copolymerization of CL has been considered as a means to increase the degradation rate as well as the mechanical strength in orthopedic applications such as fixation of prosthetic devices. For instance, terpolymers of GA (60%), D,L-LA (30%), and CL were synthesized to obtain a material with a half-life in the range of 15–20 days.[23]

4.31.3.3.3 Applications – existing and in spe

Due to a high permeability to most hydrophobic drugs, PCL has been largely studied in drug delivery devices.[201] PCL acts like a reservoir, delivering drug molecules by physical diffusion. For instance, PCL-based suture materials (Maxon®) have been developed, remaining active for over 1 year. However, a low degradation rate of PCL has limited its biomedical applications except for PCL-based copolymers. For instance, as manufactured by Ethicon Ltd. under the trade name Monacryl®, (co)polymers made of PCL and PGA offer a reduced stiffness compared with pure PGA, while having an acceptable bioresorbability rate. Interestingly, recent works have shown that PCL has attractive features as shape-memory suture materials. In these systems, in combination with hard domains (see applications of PPDX in the next section), PCL is advantageously used as switching domains because low-molecular-weight PCL exhibits a T_m close to body temperature.[202] For instance, this concept has been demonstrated with degradable shape-memory sutures for wound closure in the case of injured rats (**Figure 14**).

Although the rather low T_m of PCL (at ~60 °C) is considered a shortcoming for its large-scale use, some people have taken advantage of this feature to develop heat-deformable prosthetics devices under trade name of X-lite® upon a PCL-based polyester urethane.[203] In contrast to common prosthetics, using a low heating source such as a hair dryer enables the reshaping of the prosthetics around the injured member to be healed. Within this type of polyester urethane products, some other applications such as theatre decors have also been found and commercialized.

Although mechanical properties are excellent, the low T_m of PCL, however, restricts its range of applications, for example, as biodegradable substitutes in short-time packaging as recently reviewed by Woodruff and Hutmacher.[198] Actually, the most current applications of PCL are not related to its biodegradability but rather to its low T_g. Low-molecular-weight α,ω-hydroxyl PCL are used as soft blocks in segmented polyurethanes such as adhesives and paints. Taking advantage of its low T_g, biodegradable PCL-based copolymers have been developed as impact modifiers in commercial PLA materials with satisfactory results.[204–206] This gives access to totally biodegradable PLA-based materials with good impact resistance. For example, when PCL-based copolymer such PLA-*b*-PCL-*b*-PLA triblock copolymers are used, a significant improvement is more likely to be achieved due to the formation of rubbery PCL-based nodules within the PLA matrix.

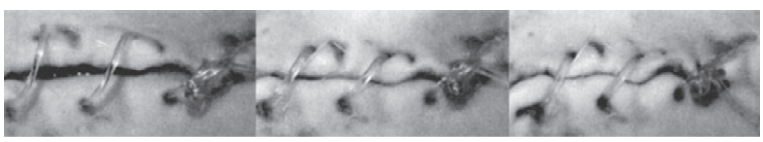

Figure 14 Degradable shape memory for wound closure in the case of injured rats. Reproduced from Lendlein, A.; Langer, R. *Science* **2002**, *296*, 1673.[202] Copyright © 2002, American Association for the Advancement of Science.

4.31.3.4 Poly(1,4-dioxan-2-one)

4.31.3.4.1 Generalities

PPDX represents an attractive biodegradable substitute for commodity polymers in short-time applications such as packaging. By comparison with the main commercial polyesters, that is, PCL and PLA, in terms of thermal transitions, this poly(ester-alt-ether) offers a good compromise between its processing temperature and its service temperature. Indeed, the T_m of PPDX is close to 110 °C with a T_g close to −10 °C. Although PPDX exhibits interesting thermomechanical properties, the synthesis of PPDX carried out by ROP of PDX and its properties have not been intensively investigated with respect to PCL and PLA.[207] The major reason was due to the noncommercial availability of PDX monomer in the past, until the development of one-step dehydrogenation starting from diethylene glycol using a copper(I)-based catalyst supported on silica particles[208] (Figure 15). Nowadays, Leap Labchem Co., Ltd. is the only supplier able to provide PDX monomer for academic and industrial purposes. Another reason could be related to the large amount of PDX monomer remaining during the synthesis of PPDX. This can be explained by the low ceiling temperature (235 °C), leaving, for example, 20 wt.% PDX monomer when polymerization of PDX is carried out at 110 °C. Some authors have tried to extend the polymerization degree upon a post-polymerization process treatment in the case of bulk ROP of PDX promoted with $Sn(Oct)_2$. This method involves crystallizing PPDX chains in the course of polymerization, while maintaining both polymerization rate and monomer conversion maximum as long as possible during the polymerization of PDX.[209] Although good yields are achieved, the major drawback rises when the polymerization temperature is above the T_m of PPDX, unzipping depolymerization reactions start, regenerating PDX monomer again.

ROP of PDX (Figure 16) is promoted with enzymes or organometallics such as lanthanum isopropoxide,[210] Zn(II) lactate, tin(II) octoate, cyclic tin(IV) alkoxides,[211] and aluminum alkoxides derivatives. Although aluminum species have shown to be the most efficient initiating system for ROP of PDX, $Sn(Oct)_2$ is industrially preferred because of its easy handlings and approval as food additives by FDA (*vide supra*). However, a fast single-stage process based on the (co)polymerization of PDX initiated with $Al(O^{sec}Bu)_3$ has been successfully developed using an REX process.[195,212,213] In this process, PDX is (co)polymerized with a limited amount of comonomer, that is, CL in order to limit the occurrence of unzipping depolymerization reactions during the synthesis and the melt processing of PPDX.[214] When 8 mol.% CL is initially added in the feed, the comonomer conversion is almost complete during this very fast reaction process. This behavior is explained by the fact that during the highly equilibrated polymerization of PDX, this comonomer shifts the equilibrium polymerization to copolymer chains rather than to comonomeric species with,

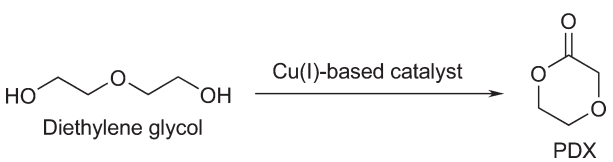

Figure 15 Catalytic dehydrogenation of diethylene glycol.

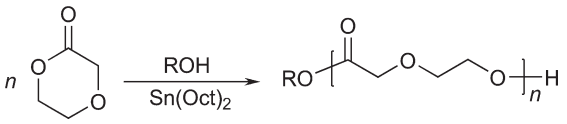

Figure 16 Ring-opening polymerization of PDX promoted by hydroxyl compounds in presence of $Sn(Oct)_2$.

therefore, their complete conversion. Interestingly, semicrystalline melt-stable PDX-based copolymers could be obtained, thanks to this REX process, paving the way to a more cost-competitive PDX polymerization process as well as the development of commercially viable PPDX. Some of us have reviewed the synthesis, properties, and applications of PPDX.[207] The following sections will summarize the main features about the properties and applications of PPDX, together with the recent inputs in the realm.

4.31.3.4.2 Properties

In addition to its biodegradability and biocompatibility, PPDX is a semicrystalline poly(ester-alt-ether) with a T_g at approximately −10 °C and T_m at around 110 °C. PPDX has shown to be tougher than PLAs and even HDPE with a tensile strength close to 50 MPa for an ultimate elongation ranging from 500 to 600% (Figure 17).[213] PPDX is poorly soluble expect in exotic solvents such as hexafluoroisopropyl, 1,1,2,2-tetrachloroethane, dimethyl sulfoxide, *N*,*N*-dimethyl formaldehyde, and 1,2-dichloroethane.[214]

The melt stability of PPDX is the main issue regarding its industrial exploitation, dictating the conditions of processing and application temperatures. This is related to its low ceiling temperature, leading to severe thermal degradations during the synthesis and melt processing of PPDX (e.g., melt molding).[215] Additives such as 4-benzoyl-3-methyl-1-phenyl-2-pyrazolin-5-one (BMP) used as catalyst deactivators or montmorillonite as (nano)fillers were studied in order to enhance the thermal stability of PPDX, but these results proved to be not totally satisfactory.[216,217] Chemical derivatizations of the hydroxyl end groups of PPDX with, for example, trichloroacetyl isocyanate, pyromellitic anhydride, and methylcyclohexene-1,2-dicarboxylic[215] were also carried out in order to suppress these unzipping depolymerization reactions under heating conditions. However, these chemically modified PPDX still exhibited a low thermal stability because of the occurrence of some chain scissions within the PPDX chains. This results in the formation of free ω-hydroxyl end groups from which unzipping can further proceed. The most suitable way to prevent or at least to limit the PPDX degradation by unzipping, while keeping its intrinsic thermal properties, is to randomly distribute a limited amount of, for example, CL[218] units all along the PPDX backbone. For instance and as aforementioned, thermally stable PPDX are readily obtained by simultaneously copolymerizing PDX and CL in bulk with PDX-rich starting feed compositions through one-step REX processing.[195,212] However, adding large amounts of comonomer can improve its thermal stability, but has an adverse effect on the thermal properties of PPDX by the formation of amorphous PPDX (co)polymer except for the work carried out by Jiang *et al.*[219] Jiang *et al.* prepared semicrystalline random poly(PDX-*co*-ω-pentadecalactone) copolymers by enzymatic ring-opening copolymerization of PDX with

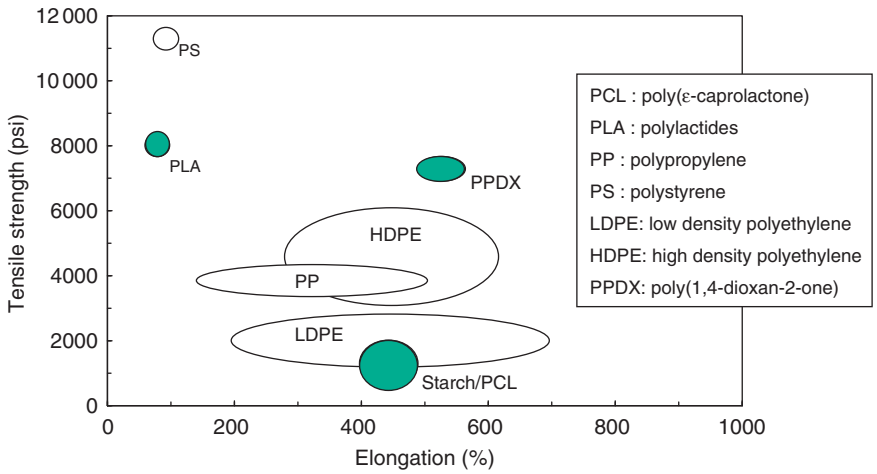

Figure 17 Physical properties map of commercial biodegradable polymers (shown in green) compared to commodity polymers.

ω-pentadecalactone. Interestingly, the microstructure of these resulting copolymers was random with a slight tendency toward alternating arrangement, yielding semicrystalline PDX-based copolyesters independent of the composition in comonomer. In general, random copolymers are expected to show a progressive decrease in crystallinity with increasing comonomer content and degree of randomness, unless the repeat units undergo isomorphous substitution. In contrast, wide-angle X-ray scattering and differential scanning calorimetry measurements show that PDX units can crystallize in the poly (ω-pentadecalactone) lattice as isodimorphism of the random copolymers, explaining the high crystalline content of all copolymers with PDX ≤ 57 mol.%. In addition, while being semicrystalline, copolymers of PDX with ω-pentadecalactone were found to remarkably enhance PPDX thermal stability at PDX content higher 30 mol.%. The works by Giammanco *et al.* also appear of high interest. They successfully prepared (co) polymers of cyclic oligo(hexamethylene terephthalate) composed of cycle sizes from 2 to 5 atoms and PDX in order to beneficially combine the properties of two parent homopolymers.[220] The aliphatic–aromatic copolyesters were obtained by entropically driven ring-opening (co)polymerizations of oligo (hexamethylene terephthalate) and PDX, resulting to aliphatic/aromatic (co)polymers with good thermomechanical properties and sensitivity to hydrolysis under physiological conditions. In addition, the resulting copolymers are semicrystalline when PDX content is maximum 31 mol.%.[220]

The biodegradability and biocompatibility of PPDX are well etablished.[221–224] The ether bond not only endows flexibility and hydrophilicity to PPDX, but also causes marked hydrolysis in air or in aqueous media. In water, the hydrolytic degradation of PPDX occurs through a two-stage autocatalytic random hydrolysis process such as PLA. In the first step, water diffuses faster to the less dense amorphous regions, and hydrolyzes the ester functions of PPDX chains. This is followed by the concomitant attack of compact crystalline regions. Some authors have modulated the hydrolytic degradation of PPDX by adding additives[225–227] such as PVA-*g*-PPDX graft copolymers or polycarbodiimide compounds and by (co)polymerizing with other cyclic monomers such as 5-benzyloxy-trimethylene carbonate. For instance, introducing hydrophobic 5-benzyloxy-trimethylene carbonate along PPDX chains reduces the water diffusion into polymeric matrix, and, therefore, the relative degradation rate. Microbial degradation of PPDX can also occur[228,229] in the presence of different microorganisms in natural environments.

PPDX fulfills the criteria of bioresorbability and biocompatibility, as assessed by cell adhesion and cell growth. In addition, the products as generated by hydrolytic degradation of PPDX did not provide any cytotoxicity, representing a crucial parameter in view of using degradable polymers such as PPDX for biomedical applications.[230]

4.31.3.4.3 *Applications – existing and* in spe

With outstanding biodegradability and bioresorbability, PPDX represents a candidate not only for medical use, but also for general uses as films, molded products, laminates, foams, nonwoven materials, adhesives, and coatings for more universal temporary uses.[207] In the biomedical realm, PPDX was the first clinically tested synthetic monofilament sutures manufactured by Ethicon Inc. under the trade name PDS®.[24] The presence of an ether bond endows great flexibility and hydrophilicity to PDS® suture with good tenacity and knotting behavior compared to traditional sutures based on GA/LA such as Vicryl®, Dexon®, and Polysorb®. Furthermore, the monofilament loses 50% of its initial breaking strength after 3 weeks of *in vivo* biomedical testing, and is totally absorbed within 6 months, providing an advantage over Dexon® or other products for slow-healing wound.[221] To prevent the bacterial attachment and growth on implanted sutures, PPDX filaments can be loaded with a hydrophobic drug with a well-demonstrated antimicrobial effect.[231] Copolymers of PDX with GA or trimethylene carbonate and/or D,L-methyl-1,4-dioxan-2-one[232] have also been reported for the preparation of sutures with improved properties as well as for the preparation of drug delivery systems.[233–235]

Recently, shape-memory PPDX-based polymers have been developed as smart degradable sutures. This enables bulky implants to be placed in the body through small incisions that are subsequently able to perform complex mechanical deformations under external stimuli such as temperature.[202] The first work dealing with the design of shape-memory

PPDX-based polymers consisted of covalently couple oligo-PPDX diols and oligo-PCL diols together in solution. This leads to multiblock copolymers with shape-memory properties adjustable on the composition of both macrodiols.[202] The segment oligo-PPDX forms hard domains, while the segment oligo-PCL forms the switching domains as previously mentioned (see Section 4.31.3.3.3). Other authors have recently explored the formation of amorphous polymer networks built of star-shaped LA-based macrotetrols containing PDX as comonomer.[105] Interestingly, PDX comonomer was able to tune up the switching temperature of this shape-memory system, without affecting the elastic properties of the polymer networks, and, therefore, the shape-memory properties. Behl *et al*. also reported the development on binary polymer blends made of two different multiblock copolymers through extrusion processing.[236] These multiblock copolymers respectively made of PPDX as hard segments and PCL as switching segments contain the same segment, that is, by incorporating poly(alkylene adipate) mediator segment. This poly (alkylene adipate) mediator segment provides some cohesion between these immiscible segments (PPDX and PCL). All polymer blends investigated showed excellent shape-memory properties due to the presence of this elastic poly(alkylene adipate) mediator segment.

4.31.4 Conclusions and Outlook

The sustainable concerns have driven considerable effort in the design of environmentally friendly polymeric materials. Aliphatic polyesters such as PCLs and PLAs are the most promising ones due to their biodegradability, biocompatibility, and excellent mechanical properties. In addition, PLA-based materials are environmentally friendly due to their renewable origins. This biosourced origin reduces their environmental impact when life-cycle assessment is concerned. These polyesters are readily obtained by ROP of their corresponding cyclic esters. This synthetic pathway enables a precise control over their properties such as hydrophilicity, T_g, and crystallinity. They have found different applications including packaging for industrial products to mulching films in agriculture or bioresorbable materials for hard tissue replacement and controlled drug delivery devices. However, in the past, most people considered only their biodegradable properties when using aliphatic polyesters as substitutes for commodity polymers in short-time applications such as in packaging. However, their properties, particularly their thermal properties, were not suitable in high-added value applications such as in automotive or electronic industries. Thanks to the recent progress achieved for improving their properties, aliphatic polyesters, particularly PLAs, are now finding new perspectives in durable applications. This is confidently based on its renewability, good physical properties, and easy melt processing using conventional processing equipments (thermoforming, etc.). Improving the PLA properties by, for example, the development of thermally resistant sc-PLA will enable PLA to be used under long-term and stringent conditions that are currently required in automotive and electronic applications. Interestingly, although the overall consumption of biopolymers such as PLA is relatively modest in 2011 (0.3 vol.% against petropolymers), a recent report would indicate a real breakthrough with PLA – a growth rate more than 40% a year – if they are integrated in automotive and electronics.[237] As a rough estimation, the overall production of PLA would be close to 830 000 t in 2020. This highlights the real potentiality to use PLA as a renewable substitute of petropolymers for durable applications.

Moreover, recent years have shown the development of new products or processes such as REX that are (more) environmentally friendly. REX represents a unique melt-processing tool to cost-effectively carry out different types of processes (melt blending, polymerization, grafting, etc.), enhancing the sustainability and future growth of aliphatic polyesters for broad range of applications going from packaging to electronics. Finally, similar to PLA, we can be confident that PCL and PPDX will be soon derived from renewable resources, making aliphatic polyesters one of the future materials in the twenty-first century as recently reported in the case of CL derived from renewable resources.[238]

References

1. Assessing the eco-efficiency of plastics packaging waste recovery 1998; Association of Plastics Manufacturers in Europe, see http://www.plasticseurope.org (consulted on 04/15/2011).
2. Karlsson, S.; Albertsson, A.-C. *Polym. Eng. Sci.* **1998**, *38*, 1251.
3. Reddy, C.; Ghai, R.; Rashmi, V. *Bioresour. Technol.* **2003**, *87*, 137.
4. Omichi, H. *Handbook of Polymer Degradation*; Dekker: New York, 1992; p 335.
5. Lynd, L.; Wyman, C.; Gerngross, T. *Biotechnol. Prog.* **1999**, *15*, 777.
6. Song, S. S.; Hein, S.; Steinbuchel, A. *Biotechnol. Lett.* **1999**, *21*, 193.
7. Gandini, A. *Macromolecules* **2008**, *41*, 9491.
8. Langer, R.; Peppas, N. A. *AIChE J.* **2003**, *49*, 2990.
9. Jagur-Grodzinski, J. *Polym. Adv. Tech.* **2006**, *17*, 395.
10. Nair, L.; Laurencin, C. *Prog. Polym. Sci.* **2007**, *32*, 762.
11. Lindblad, M. S.; Liu, Y.; Albertsson, A.-C.; *et al. Adv. Polym. Sci.* **2000**, *157*, 139.
12. Raquez, J.-M.; Nabar, Y.; Narayan, R.; Dubois, P. *Int. Polym. Process.* **2007**, *22*, 463.
13. Kummerer, K. *Green Chem.* **2007**, *9*, 899.
14. Raston, C. *Green Chem.* **2005**, *7*, 57.
15. Jenck, J. F.; Agterberg, F.; Droescher, M. J. *Green Chem.* **2004**, *6*, 544.
16. Frattini, S. *JEC Composites* **2008**, *38*, 32.
17. Stewart, R. *Plast. Eng.* **2008**, *64*, 16.
18. Kaplan, D. L. *Biopolymers from Renewable Resources*; Springer: New York, 1998.
19. Henton, D. E.; Gruber, P.; Lunt, J.; Randall, J. Polylactic Acid Technology. In: *Natural Fibers, Biopolymers and Biocomposites*; Mohanty, A. K.; Misra, M.; Drzal, L. T., Eds.; Taylor & Francis Group LLC: Boca Ration, FL, 2005; p 527.
20. Brunelle, D. J. Cyclic oligomers of polycarbonates and polyesters; In *Cyclic Polymers*; Semlyen, J. A., Ed.; Kluwer Academic Publishers: The Netherlands, 2000; p 185.
21. Gruber, P. R.; O'Brien, M. Polylactides "Nature Works™ PLA". In: *Biopolymers in 10 Volumes, Volume 4, Polyesters III Applications and Commercial Products*; Doi, Y.; Steinbüchel, A., Eds.; Wiley-VCH: Weinheim, 2002; pp 235–249.
22. Mohanty, A.; Misra, M.; Hinrichsen, G. *Macromol. Mater. Eng.* **2000**, *276/277*, 1.
23. Perrin, D.; English, J. In *Handbook of Biodegradable Polymers*; Domb, A. J.; Kost, J. and Wiseman, D. M., Eds.; Harwood Academic Publishers: Amsterdam, 1997; p 291.
24. Bezwada, R.; Jamiolkowski, D.; Cooper, K. In *Handbook of Biodegradable Polymers*; Domb, A.; Kost, J.; Wiseman, D., Eds.; Harwood Academic Publishers: Newark, NJ, 1997; p 29.
25. Lin, H. L.; Chu, C. C.; Grubb, D. *J. Biomed. Mater. Res.* **1993**, *27*, 153.
26. Sosnowski, S.; Gadzinowski, M.; Slowkowski, S. *Macromolecules* **1996**, *29*, 4556.
27. Duda, A.; Kowalski, A. Thermodynamics and kinetics of ring-opening polymerization. In *Handbook of Ring-Opening Polymerization*; Dubois, P.; Coulembier, O.; Raquez, J.-M., Eds.; Wiley-VCH: Weinheim, 2009; p 1.
28. Kurcok, P.; Dubois, P.; Sikorska, W.; *et al. Macromolecules* **1997**, *30*, 5591.
29. Duda, A. *J. Polym. Sci., Part. A-1: Polym. Chem.* **1992**, *30*, 21.
30. Hofman, A.; Slomkowski, S.; Penczek, S. *Makromol. Chem. Phys.* **1984**, *185*, 91.
31. Yamashita, Y.; Tsuda, T.; Ishida, H.; *et al. Makromol. Chem. Phys.* **1968**, *113*, 139.

32. Albertsson, A.-C.; Varma, I. K. *Adv. Polym. Sci.* **2000**, *157*, 1.
33. Kricheldorf, H. R.; Berl, M.; Scharnagl, N. *Macromolecules* **1988**, *21*, 286.
34. Shen, Y.; Shen, Z.; Shen, J.; *et al. Macromolecules* **1996**, *29*, 3441.
35. Shen, Y.; Shen, Z.; Zhang, Y.; Yao, K. *Macromolecules* **1996**, *29*, 8289.
36. Agarwal, S.; Mast, C.; Dehnicke, K.; Greiner, A. *Macromol. Rapid Commun.* **2000**, *21*, 195.
37. Baran, J.; Duda, A.; Kowalski, A.; *et al. Macromol. Rapid Commun.* **1997**, *18*, 325.
38. Baran, J.; Duda, A.; Kowalski, A.; *et al. Macromol. Symp.* **1997**, *123*, 93.
39. Dubois, P.; Degée, P.; Ropson, N.; *et al.* In *Macromolecular Design of Polymeric Materials*; Hatada, K.; Kitayama, T.; Vogl, O., Eds.; Marcel Dekker: New York, 1997; Vol. 14, p 247.
40. Mecerreyes, D.; Jérôme, R.; Dubois, P. *Adv. Polym. Sci.* **1999**, *147*, 1.
41. Duda, A.; Penczek, S. *Macromol. Rapid Commun.* **1994**, *15*, 559.
42. Wurm, B.; Keul, H.; Hocker, H. *Macromol. Chem. Phys.* **1994**, *195*, 3489.
43. Mole, T.; Jeffery, E. *Organoaluminum Compounds*; Elsevier: Amsterdam, 1972; p 205.
44. Baran, J.; Duda, A.; Kowalski, A.; *et al. Macromol. Symp.* **1998**, *128*, 241.
45. Jérôme, C.; Lecomte, P. *Adv. Drug Delivery Rev.* **2008**, *60*, 1056.
46. Penczek, S.; Duda, A.; Kowalski, A.; *et al. Macromol. Symp.* **2000**, *157*, 61.
47. Doi, Y.; Lemstra, P.; Nijenhuis, A.; *et al. Macromolecules* **1995**, *28*, 2124.
48. Kricheldorf, H.; Kreiser-Saunders, I.; Boettcher, C. *Polymer* **1995**, *36*, 1253.
49. Majerska, K.; Duda, A.; Penczek, S. *Macromol. Rapid Commun.* **2000**, *21*, 1327.
50. Libiszowski, J.; Kowalski, A.; Duda, A.; Penczek, S. *Macromol. Chem. Phys.* **2002**, *203*, 1694.
51. Kowalski, A.; Duda, A.; Penczek, S. *Macromolecules* **2000**, *33*, 689.
52. Wu, J. C.; Yu, T. L.; Chen, C. T.; Lin, C. C. *Coord. Chem. Rev.* **2006**, *250*, 602.
53. Dechy-Cabaret, O.; Martin-Vaca, B.; Bourissou, D. *Chem. Rev.* **2004**, *104*, 147.
54. Coulembier, O.; Degée, P.; Hedrick, J. L.; Dubois, P. *Prog. Polym. Sci.* **2006**, *31*, 723.
55. Gross, R. A.; Kumar, A.; Kalra, B. *Chem. Rev.* **2001**, *101*(7), 2097.
56. Coulembier, O.; Meyer, F.; Dubois, P. *Polym. Chem.* **2010**, *1*, 434.
57. Gotor, V. *Bioorg. Med. Chem.* **1999**, *7*, 2189.
58. Albertsson, A.-C.; Varma, I. K. *Biomacromolecules* **2003**, *4*, 1466.
59. Kamber, N.; Jeong, W.; Waymouth, R.; *et al. Chem. Rev.* **2007**, *107*, 5813.
60. Bourissou, D.; Moebs-Sanchez, S.; Martin-Vaca, B. *C. R. Chim.* **2007**, *10*, 775.
61. Platel, R. H.; Hodgson, L. M.; Williams, C. K. *Polym. Rev.* **2008**, *48*, 11.
62. Sawyer, D. J. *Macromol. Symp.* **2003**, *201*, 271.
63. Bogaert, J.; Coszach, P. *Macromol. Symp.* **2000**, *153*, 287.
64. Kharas, G. B.; Sanchez-Riera, F.; Severson. D. K. Polymers of lactic acid. In *Plastics from Microbes*; Mobley, D. P., Ed.; Hanser Publishers: Munich, 1994; p 93.
65. Yáñez, J. R.; Alonso, L.; Parajo, J. C. *J. Chem. Technol. Biotechnol.* **2005**, *80*, 76.
66. Kricheldorf, H. R.; Kreiser-Saunders, I.; Jurgens, C.; Wolter, D. *Macromol. Symp.* **1996**, *103*, 85.
67. Zhao, Y.; Wang, Z.; Wang, J.; *et al. J. Appl. Polym. Sci.* **2004**, *91*, 2143.
68. Moon, S. I.; Lee, C. W.; Taniguchi, I.; *et al. Polymer* **2001**, *42*, 5059.
69. Ajioka, M.; Enomoto, K.; Suzuki, K.; Kashima, T. *Polym. Degrad. Stab.* **1998**, *59*, 137.
70. Enomoto, K.; Ajioka, M.; Yamaguchi, A. U.S. Patent 310,865, 1994.
71. Gross, R.; Kalra, B. *Science* **2002**, *297*, 803.
72. Södergård, A.; Stolt, M. *Prog. Polym. Sci.* **2002**, *27*, 1123.
73. Leenslag, J. W.; Pennings, A. J. *Makromol. Chem.* **1987**, *188*, 1809.
74. Auras, R.; Harte, B.; Selke, S. *Macromol. Biosci.* **2004**, *4*, 835.
75. Carothers, W. H.; Dorough, G. L.; Natta, F. J. *J. Am. Chem. Soc.* **1932**, *54*, 761.
76. Drumright, R. E.; Gruber, P. R.; Henton, D. E. *Adv. Mater.* **2000**, *12*, 1841.
77. Gruber, P.R.; Hall, E.S.; Kolstad, J. H.; *et al.* U.S. Patent 5,142,023, 1992.
78. Vink, E. T. H.; Rábago, K. R.; Glassner, D. A.; Gruber, P. R. *Polym. Degrad. Stab.* **2003**, *80*, 403.
79. Rasal, R. M.; Janorkar, A. V.; Hirt, D. E. *Prog. Polym. Sci.* **2010**, *35*, 338.
80. Perepelkin, K. E. *Fibre Chem.* **2002**, *34*, 85.
81. Jacobsen, S.; Degee, P.; Fritz, H. G.; *et al. Polym. Eng. Sci.* **1999**, *39*, 1311.
82. Jacobsen, S.; Degee, P.; Fritz, H. G.; *et al. Ind. Crops Prod.* **2000**, *11*, 265.
83. Kobayashi, S.; Uyama, H. In *Biopolyesters*; Babel, W.; Steinbuchel, A., Eds.; Springer-Verlag: Heidelberg, 2001; p 241.
84. Matsumura, S.; Mabuchi, K.; Toshima, K. *Macromol. Rapid Commun.* **1997**, *18*, 477.
85. García-Arrazola, R.; López-Guerrero, D. A.; Gimeno, M.; Bárzana, E. *J. Supercrit. Fluids* **2009**, *51*, 197.
86. Yang, T. H.; Kim, T. W.; Kang, H. O.; *et al. Biotechnol. Bioeng.* **2010**, *105*, 150.
87. Jamshidi, K.; Hyon, S.-H.; Ikada, Y. *Polymer* **1988**, *29*, 2229.
88. Stridsberg, K.; Ryner, M.; Albertsson, A.-C. *Adv. Polym. Sci.* **2002**, *157*, 41.
89. Hoogsten, W.; Postema, A. R.; Pennings, A. J.; *et al. Macromolecules* **1990**, *23*, 634.
90. Cartier, L.; Okihara, T.; Ikada, Y.; *et al. Polymer* **2000**, *41*, 8909.
91. Pan, P.; Inoue, Y. *Prog. Polym. Sci.* **2009**, *34*, 605.
92. Kelly, S.; Kathleen, M.; Marc, A. *Polymer Reviews* **2008**, *48*, 85.
93. Mark, J. E. *Polymer Data Handbook*; Oxford University Press: London, 2002.
94. Ikada, Y.; Jamshidi, K.; Tsuji, H.; Hyon, S.-H. *Macromolecules* **1987**, *20*, 904.
95. Petersson, L.; Kvien, I.; Oksman, K. *Comp. Sci. Tech.* **2007**, *67*, 2535.
96. Pauly, S. Permeability and diffusion data. In *Polymer Handbook*; Brandup, J. I.; Grulke, E. H., Eds.; John Wiley & Sons Inc.: New York, 1999; p 547.
97. Tsuji, H.; Ikada, Y.; Hyon, S. H.; *et al. J. Appl. Polym. Sci.* **1994**, *51*, 337.
98. Burlet, J.; Heuzey, M. C.; Dubois, C.; *et al. ANTEC* **2005**, *2*, 1133.
99. Zhang, X.; Wyss, U. P.; Pichora, D.; Goosen, M. F. A. *J. Bioact. Compat. Polym.* **1994**, *9*, 80.
100. Mariage, P.A.; Hottois, D.; Coszach, P. BE Patent 1,018,247, 2010.
101. Fathi, M. H.; Doostmohammadi, A. *J. Mater. Process. Technol.* **2008**, *209*, 1385.
102. Capps, S. G. *BONEZone*, Fall *2006, p 54.*
103. Middleton, J. C.; Tipton, A. J. *Biomaterials* **2000**, *21*, 2335.
104. Yu, N. Y. C.; Schindeler, A.; Little, D. G.; Ruys, A. J. *J. Biomed. Mater. Res., Part B* **2010**, *93B*, 285.
105. Lendlein, A.; Zotzmann, J.; Feng, Y.; *et al. Biomacromolecules* **2009**, *10*, 975.
106. Doi, Y.; Fukuda, K. *Biodegradable Plastics and Polymers*; Elsevier: Amsterdam, 1994.
107. Scoot, G.; Gilead, D., Eds.; In *Biodegradable Polymers. Principles and Applications*; Chapman & Hall: London, 1995.
108. Vert, M.; Schwarch, G.; Coudane, J. *J. Macromol. Sci., Part A: Pure Appl. Chem.* **1995**, *32*, 787.
109. Lu, H. H.; Cooper, J. A.; Manuel, S.; *et al. Biomaterials* **2005**, *26*, 4805.
110. Cooper, J. A.; Lu, H. H.; Ko, F. K.; *et al. Biomaterials* **2005**, *26*, 1523.
111. Zilberman, M.; Nelson, K. D.; Eberhart, R. C. *J. Biomed. Mater. Res., Part B* **2005**, *74*, 792.
112. Agrawal, C. M.; Clark, H. G. *Invest. Radiol.* **1992**, *27*, 1020.
113. Dauner, M.; Planck, H.; Caramoro, L.; *et al. J. Mater. Sci. Mater. Med.* **1998**, *9*, 173.
114. Leenslag, J. W.; Pennings, A. J.; Bos, R. M.; *et al. Biomaterials* **1987**, *8*, 70.
115. Kikuchi, M.; Suetsugu, Y.; Tanaka, J.; Akao, M. *J. Mater. Sci.: Mater. Med.* **1997**, *8*, 361.
116. Kasuga, T.; Maeda, H.; Kato, K.; *et al. Biomaterials* **2003**, *24*, 3247.
117. Nejati, E.; Firouzdor, V.; Eslaminejad, M. B.; Bagheri, F. *Mater. Sci. Eng. C* **2009**, *29*, 942.
118. Venkatraman, S.; Poh, T. L.; Vinalia, T.; *et al. Biomaterials* **2003**, *24*, 2105.
119. Eury, E. P. U.S. Patent 5,443,458, 1995.
120. Buscemi, P.J.; Stejskl, E.A.; Palme, D.F.; Wang, L. X. U.S. Patent 5,968,092, 1999.
121. Tamai, H.; Igaki, K.; Kyo, E.; Kosuga, K. *Circulation* **2000**, *102*, 399.
122. Soppimath, K. S.; Aminabhavi, T. M.; Kulkarni, A. R.; Rudzinski, W. E. *J. Controlled Release* **2001**, *70*, 1.
123. Uhrich, K. E.; Cannizzaro, S. M.; Langer, R. S.; Shakeshelf, K. M. *Chem. Rev.* **1999**, *99*, 3181.
124. Maurus, P. B.; Kaeding, C. C. *Oper. Tech. Sport. Med.* **2004**, *12*, 158.
125. Baillie, J. *Packaging Week, 1997, p 13.*
126. Shopping bags – a big opportunity for bioplastics, *Bioplastics Magazine*, June 2002, *1*, 10.
127. Fourne, F. In *Synthetic Fibers Machines, Equipment, Manufacture, Properties*; Carl Henser Verlag: Munich-Vienna, 1999.
128. Horacek, I.; Kalisek, V. *J. Appl. Polym. Sci.* **1994**, *54*, 1751.
129. Leenslag, J. W.; Gogolewski, S.; Pennings; A. J. *J. Appl. Polym. Sci.* **1984**, *29*, 2829.
130. Gogolewski, S.; Pennings A. J. *J. Appl. Polym. Sci.* **1983**, *28*, 1045.
131. Fambri, L.; Pegoretti, A.; Mazzurana, M.; Migliaresi, C. *J. Mater. Sci. Med.* **1994**, *5*, 679.
132. Leenslag, J. W.; Pennings, A. J. *Polymer* **1987**, *28*, 1695.
133. Eling, B.; Gogolweski, S.; Pennings A. J. *Polymer* **1982**, *23*, 1587.
134. Fambri, L.; Pegoretti, A.; Fenner, R.; *et al. Polymer* **1997**, *38*, 79.
135. Schmack, G.; Tandler, B.; Vogel, R.; *et al. J. Appl. Polym. Sci.* **1999**, *73*, 2785.
136. Mezghani K.; Spruiell J. E. *J. Polym. Sci., Part B: Polym. Phys.* **1998**, *36*, 1005.
137. Yuan, X.; Mak, A. F. T.; Kwok, K. W.; Yung, B. K. O. *J. Appl. Polym Sci.* **2001**, *81*, 251.
138. Yao, K. *J. Appl. Polym Sci.* **2001**, *81*, 251.
139. Cicero, J. A.; Dorgan, J. R. *J. Polym. Environ.* **2001**, *9*, 1.
140. Ryan, C.; Buehler, U.; Gessner, S.; Brosch, A. U.S. Patent 6,506,873, 2003.
141. Matsui, M. *Chem. Fibers Int.* **1996**, *46*, 318.
142. Yamanaka, K. *Chem. Fibers Int.* **1999**, *49*, 501.
143. Sinha Ray, S.; Okamoto, M. *Macromol. Rapid Commun.* **2003**, *24*, 815.
144. Fang, Q.; Hanna, M. A. *Cereal Chem.* **2000**, *77*, 779.
145. Mikos, A. G.; Thorsen, A. J.; Czerwonka, L. A.; *et al. Polymer* **1994**, *35*, 1068.
146. Whiteman, N. *2000 Polymers, Laminations and Coatings Conference*, Chicago, USA, 2000.

147. Evans, J. *Plastics Eng.* **2010**, *66*(2), 15.
148. Darder, M.; Aranda, P.; Ruiz-Hitzky, E. *Adv. Mater.* **2000**, *19*, 309.
149. Muench, O. *Bioplastics Magazine, May 2008, 3*, p 10.
150. Perego, G. *J. Appl. Polym. Sci.,* **1996**, *59*, 37.
151. Nijenhuis, E.; Pennings, A. J. *Polymer,* **1996**, *37*, 5849.
152. Smillie, B. U.S. Patent (appl.) 2006084259, 2006.
153. Ness, J. KR Patent (appl.) 20070089135, 2007.
154. Stanislaus, C.; Spera, L.; Tullos, G.; Daly, A. U.S. Patent (appl.) 2004077784, 2004.
155. Thakur, K. A. M.; Kean, R. T.; Zupfer, J. M.; *et al. Macromolecules* **1996**, *29*, 8844.
156. Kolstad, J. J. *J. Appl. Polym. Sci.* **1996**, *62*, 1079.
157. Schmidt, S. C.; Hillmyer, M. A. *J. Polym. Sci., Part B: Polym. Phys.* **2001**, *39*, 300.
158. Nam, J. Y.; Ray, S. S.; Okamoto, M. *Macromolecules* **2003**, *36*, 7126.
159. Pluta, M. *Polymer* **2004**, *45*, 8239.
160. Krikorian, V.; Pochan, D. J. *Macromolecules* **2005**, *38*, 6520.
161. Moon, S. I.; Jin, F.; Lee, C. J.; *et al. Macromol. Symp.* **2005**, *224*, 287.
162. Tsuji, H.; Takai, H.; Fukuda, N.; Takikawa, H. *Macromol. Mater. Eng.* **2006**, *291*, 325.
163. Pan, P.; Liang, Z.; Cao, A.; Inoue, Y. *ACS Appl. Mater. Interfaces* **2009**, *1*, 402.
164. Nam, J. Y.; Okamoto, M.; Okamoto, H.; *et al. Polymer* **2006**, *47*, 1340.
165. Hideto, T.; Ayaka, O.; Satomi, Y. WO Patent (appl.) 2010JP64575, 2010.
166. Guerin, V. *L'usine nouvelle* **2005**, *2987*, 114.
167. Suzuki, H.; Ikegame, M. U.S. Patent (appl.) 2010130676, 2010.
168. Miltenberger, K. In *Hydroxycarboxylic Acids, Aliphatic in Ullmann's Encyclopedia of Industrial Chemistry*; Wiley-VCH: Weinheim, 2005.
169. DiCosimo, R.; Panova, A.; Thompson, J. S.; *et al.* US patent (appl.) 2006024767, 2006.
170. Chauhan, S.; Di Cosimo, R.; Fallon, R. D.; *et al.* U.S. Patent 6,416,980, 2002.
171. Nakamura, T. JP Patent (appl.) 09028390, 2009.
172. Lowe, C. E. U.S. Patent 2,668,162, 1954.
173. Dobrzynski, P.; Kasperczyk, J.; Bero, M. *Macromolecules* **1999**, *32*, 4735.
174. Kricheldorf, H. R.; Kreiser, I. *Makromol. Chem.* **1987**, *188*, 1861.
175. Barakat, I.; Dubois, P.; Grandfils, C.; Jérôme, R. *J. Polym. Sci., Part A-1: Polym. Chem.* **2001**, *39*, 294.
176. Zurita, R.; Puiggali, J.; Franco, L.; Rodriguez-Galan, A. *J. Polym. Sci., Part A-1: Polym. Chem.* **2006**, *44*, 993.
177. Epple, M.; Herzberg, O. *J. Biomed. Mater. Res., Part B* **1998**, *43*, 83.
178. Pinkus, A. G.; Subramanyam, R. *J. Polym. Sci., Polym. Chem. Ed.* **1984**, 22, 1131.
179. Vert, M.; Schwach, G.; Coudane, J. *J. Controlled Release* **1998**, *53*, 85.
180. Gilding, D. K.; Reed, A. M. *Polymer* **1979**, *20*, 1459.
181. Vert, M.; Chabot, F.; Leray, J.; Christel, P. *Makromol. Chem. Suppl.* **1981**, *5*, 30.
182. Ashammakhi, N.; Rokkanen, P. *Biomaterials* **1997**, *18*, 3.
183. Schmitt, E.E.; Polistina, R. A. U.S. Patent 3,463,146, 1969.
184. Vainionpaa, S.; Rokkanen, P.; Tormala, P. *Prog. Polym. Sci.* **1989**, *14*, 679.
185. Grijpma, D.; Pennings, A. *Macromol. Chem. Phys.* **1994**, *195*, 1633.
186. Jung, R. E.; Lecloux, G.; Rompen, E.; *et al. Clin. Oral Impl. Res.* **2009**, *20*, 151.
187. Ashammakhi, N. A. *J. Biomed. Mater. Res., Part B* **1996**, *33*, 297–303.
188. Linhart, W.; Peters, F.; Lehmann, W.; *et al. J. Biomed. Mater. Res.* **2001**, *54*, 162.
189. Xie, D.; Park, J.-G.; Zhao, J. *J. Appl. Polym. Sci.* **2007**, *103*, 2977.
190. Busch, S.; Schwarz, U.; Kniep, R. *Chem. Mater.* **2001**, *13*, 3260.
191. Van Natta, F. J.; Hill J. W.; Carothers, W. H. *J. Am. Chem. Soc.* **1934**, *56*, 455.
192. Bailey, W. J. In *Comprehensive Polymer Science, the Synthesis, Characterization and Application of Polymers*; Allen; G.; Bevington; J. C., Eds.; Pergamon Press: Oxford, 1989; Vol. 3, p 283.
193. Bailey, W. J.; Ou, J. M.; Zhou, L.-L. *ACS Polym. Prepr. Div. Polym. Chem.* **1990**, *31*, 24.
194. Bailey, W. J.; Wu, S.-R.; Ni, Z. *Makromol. Chem.* **1982**, *183*, 1913.
195. Raquez, J.-M.; Degée, P.; Dubois, P.; *et al. C. R. Chim.* **2006**, *9*, 1370.
196. Wilson, E. *Chem. Eng. News. Am. Chem. Soc.* **2001**, *79*, 14.
197. Brode, G.; Koleske, J. *J. Macromol. Sci. Chem.* **1972**, *A6*(6), 1109.
198. Woodruff, M. A.; Hutmacher, D. W. *Progr. Polym. Sci.* **2010**, *35*, 1217.
199. Persenaire, O.; Alexandre, M.; Degee, P.; Dubois, P. *Biomacromolecules* **2001**, *2*, 288.
200. Pitt, F.; Chasalow, Y.; Hibionada, D.; *et al. J. Appl. Polym. Sci.* **1981**, *26*, 3779.
201. Ponsart, S.; Coudane, J.; Vert, M. *Biomacromolecules* **2001**, *2*, 373.
202. Lendlein, A.; Langer, R. *Science* **2002**, *296*, 1673.
203. Hick, C.; Smits, J.F.; Allard, P.; Dubois, P. WO Patent (appl.) 2006079602, 2006.
204. Wang, L.; McCarthy, S. P. *Polym. Degrad. Stab.* **1998**, *59*, 161.
205. Broz, M. E. *Biomaterials,* **2003**, *24*, 4181.
206. Maglio, G. *Macromol. Rapid Commun.* **1999**, *20*, 236.
207. Raquez, J.-M.; Coulembier, O.; Duda, A.; *et al. Polimery* **2009**, *3*, 163.
208. Forschner, T. U.S. Patent 5,310,945, 1994.
209. Esteves, L. M.; Márquez, L.; Müller, A. J. *J. Appl. Polym. Sci.* **2005**, *97*, 659.
210. Zhu, X.-L.; Wu, G.; Qiu, Z.-C.; *et al. J. Polym. Sci., Part A-1: Polym. Chem.* **2008**, *46*, 5214.
211. Redin, T.; Fine, A.; Mathisen, T.; Albertsson, A.-C. *J. Polym. Sci., Part A-1: Polym. Chem.* **2007**, *45*, 5552.
212. Raquez, J.-M.; Degée, P.; Dubois, P.; *et al. Polym. Eng. Sci.* **2005**, **45**, 622.
213. Raquez, J.-M. Ph.D. thesis, University of Mons-Hainaut, 2003.
214. Yang, K.; Wang, X.; Wang, Y. Z. *J. Macromol. Sci.* **2002**, *C 42*, 373.
215. Raquez, J.-M.; Degée, P.; Narayan, R.; Dubois, P. *Polym. Degrad. Stab.* **2004**, *86*, 159.
216. Ding S. D.; Wang, Y. Z. *Polym. Degrad. Stab.* **2006**, *91*, 2465.
217. Huang, F. Y.; Wang, Y. Z.; Wang, X. L.; *et al. J. Polym. Sci., Part A-1: Polym. Chem.* **2005**, *43*, 2298.
218. Rodriguez, A.; Franco, N. L.; Puiggali, J. *J. Polym. Sci., Part A-1: Polym. Chem.* **2009**, *47*, 6758.
219. Jiang, Z.; Azim, H.; Gross, R.; *et al. Biomacromolecules* **2007**, *8*, 2262.
220. Giammanco, G.; de Ilarduya, A. M.; Alla, A.; Munoz-Guerra, S. *Biomacromolecules* **2010**, *11*(9), 2512.
221. Albuerne, J.; Marquez, L.; Müller, A. J.; *et al. Macromol. Chem. Phys.* **2005**, *206*, 903.
222. Sabino, M. A.; Sabater, L.; Ronca, G.; Muller, A. J. *Polym. Bull.* **2002**, *48*, 291.
223. Pekkin A. P. T., Duek E. A. R. *Polym. Degrad. Stab.* **2002**, *78*, 405.
224. Yang, K. K.; Wang, X. L.; Wang, Y. Z.; Huang, H. X. *Mater. Chem. Phys.* **2004**, *87*, 218.
225. Chen, S. C.; Zhou, Z. X.; Wang, Y. Z.; *et al. Polymer* **2006**, *47*, 32.
226. Liu, Z. P.; Ding, S. D.; Sui, Y. J.; Wang, Y. Z. *J. Appl. Polym. Sci.* **2009**, *112*, 3079.
227. Yoon, K. R.; Kim, W. J.; Choi, I. S. *J. Polym. Res.* **2004**, *11*, 265.
228. Nishida, H.; Konno, M.; Tokiwa, Y. *Polym. Degrad. Stab.* **2000**, *68*, 271.
229. Nishida, H.; Konno, M.; Tokiwa, Y. *Polym. Degrad. Stab.* **2000**, *68*, 205.
230. Sabino, M. A.; Feijoo, J. L.; Nunez, O.; Ajami, D. *J. Mater. Sci.* **2002**, *37*, 35.
231. Blanco, M. G.; Franco, L.; Puiggali, J.; Rodrıguez-Gala, A. *J. Appl. Polym. Sci.* **2009**, *114*, 3440.
232. Lochee, Y.; Bhaw-Luximon, A.; Jhurry, D.; Kalangos, A. *Macromolecules* **2009**, *42*, 7285.
233. Roby, M.; Bennett, S.; Liu, C. U.S. Patent 5,554,170, 1996.
234. Liu, C.; Ying, J.; Roby, M.; *et al.* U.S. Patent 557,8046, 1996.
235. Wang, H.; Dong, J.; Qiu, K.; Gu, Z. *J. Polym. Sci., Part A-1: Poly. Chem.* **1998**, *36*, 1301.
236. Behl, M.; Ridder, U.; Feng, Y.; *et al. Soft Matter* **2009**, *5*, 676.
237. Lunt, J. The World of Bioplastics. European Bioplastics. Plastics News Executive Forum, Tampa, Florida, March 7–10, 2010.
238. Buntara, T.; Noel, S.; Phua, P.; Melian-Cabrera, I.; de Vries, J.; Heeres, H. J. *Angewandte Chem. Int. Ed.* **2011**, *50*, 7083.

Biographical Sketches

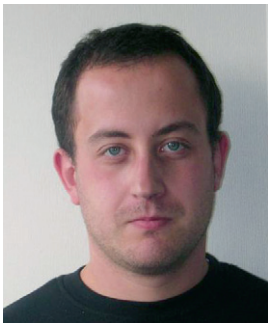

Jean-Marie Raquez received his PhD degree in polymer chemistry under the supervision of Professor Philippe Dubois (University of Mons-Hainaut – UMH). After a postdoctoral stay with Professor Ramani Narayan (Michigan State University, USA), he moved back to UMH as a FRS-FNRS postdoctoral researcher at UMONS (old-UMH). His research work focuses on the chemical modification and synthesis of polymer-based (nano)composites issued from renewable resource using reactive extrusion processing. In this realm, he has more than approximately 38 publications in international journals, 11 personal communications at conferences, and is coinventor of 7 patents. He coedited 1 book.

Rosica Mincheva was born in Sofia (Bulgaria) in 1979. She graduated in chemistry from the University of Sofia (Bulgaria) in 2002. Her master-degree thesis, supervised by Professor Iliya Rashkov and Professor Nevenka Manolova (Laboratory of Bioactive Polymers, Institute of Polymers-BAS, Sofia, Bulgaria), was awarded 'Best Master Degree Thesis', from 'Shimatzu' in Bulgaria. Under their supervision, she received a PhD degree in polymer chemistry on the topic dealing with the preparation of micro- and nanostructured materials from chitosan and its derivatives by different methods, including electrospinning. After 1 year of research with Professor Jérôme (University of Liège, Belgium), in 2007 she moved to a postdoctoral stay with Professor Philippe Dubois (University of Mons, Belgium) where she is now an associate researcher. Her research covers macromolecular chemistry and engineering, physicochemical and thermomechanical characterization, and melt processing of (nano)materials based on biosourced and/or biodegradable polymers. It is summarized in about 20 peer-reviewed scientific publications (including 2 book chapters), more than 20 personal communications at conferences, and is coinventor of 1 patent.

Olivier Coulembier received his PhD degree from the University of Mons-Hainaut (Belgium) in 2005 and joined the University of Stanford (United States) for his postdoctoral research in 2006. He is currently a research associate by Belgian FNRS in the Laboratory of Polymeric and Composite Materials (LPCM) of Professor Philippe Dubois at the University of Mons. His main activities are focused on the (non)organometallic ring-opening polymerization of cyclic monomers. He has (co)authored 50 scientific papers in international journals, 1 patent, and 1 book chapter.

Philippe Dubois, PhD in sciences, is a full professor at the University of Mons (UMONS, Belgium) and an honorary senior research associate of the Belgian FNRS. He is currently director of the Center of Innovation and Research in Materials and Polymers (CIRMAP, ~135 persons). He is scientific director at Materia Nova Research Center in Mons and past-president of the Belgian Royal Chemical Society. His expertise covers organic chemistry, macromolecular chemistry, catalysis in polymer materials, melt (reactive) processing/engineering, and physicochemical and thermomechanical characterization of nanocomposite and nanohybrid materials, including biodegradable polymers and biosourced polymers.

He has authored more than 450 peer-reviewed scientific publications (including ~40 reviews and book chapters and more than 80 papers in 'Macromolecules', #1 in polymer science), more than 220 personal communications at conferences, and is inventor of approximately 50 patents. He has edited seven books and special issues and is a member of the editorial board of eight leading journals in the field of polymers and composites. He is also associate professor at the University of Liège, invited professor at the University of Namur, and adjunct professor at the Michigan State University (Faculty of Chemical Engineering, USA). He is currently vice-rector of scientific research at UMONS and titular member of the Royal Academy of Belgium.

4.32 Polymerization Kinetic Modeling and Macromolecular Reaction Engineering

S Zhu and A Hamielec, McMaster University, Hamilton, ON, Canada

Nomenclature

A functional group or cross area of tubular reactor
AA difunctional monomer
AB difunctional monomer
A_{cw} Arrhenius constant of chain-walking reaction
$[A]_0$ initial concentration of functional group A
A_f *f*-functional monomer
A_p Arrhenius constant of propagation reaction or surface area of polymer particle
B functional group
$[B]_0$ initial concentration of functional group B
BB difunctional monomer
C transition metal complex
C_P polymer concentration
D axial dispersion coefficient
D_p particle diameter
D_r self-diffusion coefficient of chains having length *r*
D_s self-diffusion coefficient of chains having length *s*
E_A apparent activation energy
E_d activation energy of initiator decomposition
E_p activation energy of propagation
E_t activation energy of termination
F_i instantaneous copolymer composition
$\bar{F}_i$ cumulative copolymer composition
$\vec{F}_i$ feeding rate
ΔH_p heat of polymerization
I initiator molecule
$[I]_0$ initial initiator concentration
$[I]_{out}$ initiator concentration at reactor exit
K_{eq} equilibrium constant
L length of tubular reactor
M monomer molecule
$[M]_0$ initial monomer concentration
$[M]_{out}$ monomer concentration at reactor exit
$[M]_W$ moles of monomer per liter of water in emulsion polymerization
$dM/\Delta M$ mass fraction of chains generated under specific birth condition
Me^+ metal cation
$\bar{M}_w$ weight-average polymer molecular weight
N_1 number of moles of monomer 1
N_2 number of moles of monomer 2
$N_{1,0}$ fast monomer in semibatch policy I
$N_{2,0}$ slow monomer in semibatch policy I
N_{A0} moles of functional group A initially charged to reactor
N_A moles of functional group A
N_{Av} Avogadro's number
N_{B0} moles of functional group B initially charged to reactor
N_B moles of functional group B
N_I moles of initiator inside reactor
N_{M0} moles of monomer initially charged to reactor
N_M moles of monomer in reactor at present time
N_P moles of polymer chains inside reactor or number of polymer particles in emulsion polymerization
$[P]_{out}$ polymer chain concentration at reactor exit
PD polydispersity index
$P_r^\bullet$ radical chain having length *r*
P_r^- anionic chain having length *r*
$P_s^\bullet$ radical chain having length *s*
$\hat{P}_{r,s}$ adduct chain having two arms of *r* and *s* lengths
$Q_i^\bullet$ *i*th moment of radical polymer chains
Q_i *i*th moment of dead polymer chains
ϕ_i^X *i*th moment of dormant chains
$\hat{Q}_i$ *i*th moment of adduct chains
R gas constant
$R_0^\bullet$ primary radical
R_{cw} rate of chain-walking reaction
R_d rate of initiator decomposition
R_{fp} rate of chain transfer to polymer reaction
R_{fZ} rate of chain transfer to Z
$R_{I,W}$ rate of radical initiation per liter of water in emulsion polymerization
R_p rate of propagation reaction or rate of polymerization
R_t rate of radical termination
R_{tc} rate of radical termination by combination
R_{td} rate of radical termination by disproportionation
$[RX]_0$ initial initiator concentration in ATRP
S stable molecule
$[S]_{CMC}$ CMC of surfactant
SSH stationary-state hypothesis or steady-state hypothesis
T polymerization temperature
T_{gm} glass transition temperature of monomer
T_{gp} glass transition temperature of polymer
V reaction volume or reactor volume
X halogen atom
Z small molecule in chain transfer: monomer, solvent, chain transfer agent, or impurity
$Z^\bullet$ radical species
$[Z]_P$ chain transfer agent concentration inside particle
-ab- linkage in condensation
***a*PP** atactic polypropylene
a_s specific area of surfactant
comp(*y*/*r*) composition distribution
f initiation efficiency or functionality
f_i mole fraction of monomer i
f_m function in comb polymer
g_m function in comb polymer

***i*PP** isotactic polypropylene
k apparent rate constant
$\hat{k}_1$ pseudokinetic propagation rate constant of monomer 1 in semibatch control
$\hat{k}_2$ pseudokinetic propagation rate constant of monomer 2 in semibatch control
k_{br} rate constant of long-chain branching
k_C chemically controlled rate constant
k_{ac} rate constant of activation
k_{as} rate constant of adsorption
k_{cp} rate constant of primary cyclization
$k_{cs,a}$ rate constant of additional secondary cyclization
k_d rate constant of initiator decomposition
k_D diffusion-controlled rate constant
k_{de} rate constant of radical deactivation
k_f rate constant of fragmentation
k_{fM} rate constant of chain transfer to monomer
k_{fp} rate constant of chain transfer to polymer
k_{fZ} rate constant of chain transfer to small molecule Z
k_i rate constant of initiation
k_{iZ} rate constant of initiation of small molecule Z
k_p rate constant or pseudokinetic rate constant of propagation
k_p^- rate constant of propagation of free anion
$k_p^=$ pseudokinetic propagation rate constant for addition with pendant double bond
$k_p^\pm$ rate constant of propagation of ion pair
k_{p0} parameter in an expression for diffusion-controlled propagation rate constant
$k_{p,C}$ chemically controlled rate constant of propagation
$k_{p,D}$ diffusion-controlled rate constant of propagation
k_t rate constant of termination
k_{t0} parameter in an expression for diffusion-controlled termination rate constant
k_{tc} rate constant of termination by combination
$k_{t,C}$ chemical-controlled termination rate constant
k_{td} rate constant of termination by disproportionation
$k_{t,D}$ diffusion-controlled termination rate constant
k_x rate constant of cross-linking
k_β rate constant of β-hydride elimination
m monomer molecular weight
$\bar{n}$ number of radicals per particle in emulsion polymerization
n_A number of difunctional monomer A
n_B number of difunctional monomer B
$n(r)$ number-fraction polymer chain length distribution
$n^\bullet(r)$ number-fraction polymeric radical chain length distribution
$n^+(r)$ number-fraction cationic chain length distribution
$n^*(r)$ number-fraction active chain length distribution
q_i relative moments
r chain length
r_i reactivity ratio
$\bar{r}_N$ number-average chain length
$\bar{r}_{Np}$ number-average length of primary chains
$\bar{r}_N^\bullet$ number-average length of radical chains
$\bar{r}_N^X$ number-average length of dormant chains
$\bar{r}_W$ weight-average polymer chain length
$\bar{r}_W^\bullet$ weight-average length of polymer radical chains
$\bar{r}_W^X$ weight-average length of dormant chains
$\bar{r}_{Wp}$ weight-average length of primary chains
s chain length
***s*PP** syndiotactic polypropylene
t reaction time
t' birth time
$\bar{t}$ mean residence time
$t_{1/2}$ initiator half-lifetime
V reactor volume
$\vec{v}$ volumetric flow rate
w_g gel fraction
$w(r)$ weight-fraction chain length distribution
$w(r,\gamma)$ bivariate distribution of chain length and composition
$w_{cum}(r)$ weight-fraction distribution of cumulative chains
$w_p(r)$ chain length distribution of primary chains
w_s sol fraction
x monomer conversion
x_A functional group A conversion
x_B functional group B conversion
v_f free-volume fraction
α stoichiometric imbalance ratio
α_m differential thermal expansion coefficient of monomer
α_{mg} differential thermal expansion coefficient of monomer in glass state
α_{ml} differential thermal expansion coefficient of monomer in liquid state
α_p differential thermal expansion coefficient of polymer
α_{pg} differential thermal expansion coefficient of polymer in glass state
α_{pl} differential thermal expansion coefficient of polymer in liquid state
β ratio of combination termination rate to propagation rate as defined by eqn [57]
δ branching coefficient
ε empirical exponent
ζ parameter in free volume
θ birth conversion
κ parameter in cyclization or parameter in semibatch control
λ parameter in free volume
μ particle volumetric growth rate or parameter in metallocene polymerization with branching
ξ parameter in free-volume equation
ρ_m monomer density
ρ_p polymer density
ρ branching density
$\rho(\theta,\Theta)$ cross-link density distribution
$\rho_a(\theta,\Theta)$ additional cross-link density distribution
$\rho_c(\theta,\Theta)$ cyclization density
$\rho_{cs,a}(\theta,\Theta)$ additional secondary cyclization density
$\rho_{cp}(\theta)$ primary cyclization density
$\rho_{cs,i}(\theta)$ instantaneous secondary cyclization density
$\rho_i(\theta)$ instantaneous cross-link density
σ reaction radius of the reacting species
τ ratio of reaction rates as defined by eqn [56]
$\phi_i^\bullet$ number fraction of type-i radicals
ϕ_m monomer volume fraction
ϕ_p polymer volume fraction
$\phi_r^\bullet$ chain length r number fraction
$\phi_s^\bullet$ chain length s number fraction
Θ present conversion

4.32.1 Introduction

Macromolecular reaction engineering is a more recent synonym for polymer reaction engineering. The difference between the two names is that the new name puts more emphasis on science-based first principles; it is same as that between the terms 'macromolecule' and 'polymer'. The former is a scientific term derived from the work of Hermann Staudinger, who discovered that polymers are actually large molecules composed of small molecules joined together by covalent bonds. In contrast, the term 'polymer' was coined by Berzelius in 1833 when people did not actually understand what a polymer is in the modern sense.

Macromolecular reaction engineering originated from chemical reaction engineering.[1] It applies chemical reaction engineering principles to the production and processing of polymer materials. Chemical reaction engineering is one of the core subdisciplines in chemical engineering and is arguably the major subdiscipline that differentiates chemical engineering from other engineering disciplines.[2,3] Chemical engineering is concerned with the design and operation of industrial processes that convert raw materials to useful products. It involves activities in two major areas: reaction and separation. In both areas, there are three major questions to be answered, that is, 'how far?', 'how fast?', and 'how to?'

For each specific reaction, one examines with thermodynamics of the reaction in order to answer such questions as 'is this reaction possible?' and, if so, 'how far can it go?'[4] Following this, the kinetics of the reaction is analyzed to answer the question: 'how fast can the reaction go?'[5] This is the point where catalysis becomes a factor. A catalyst changes the reaction rate, but not its equilibrium. Using the collected kinetic data, one can then design and operate reactor systems for safe and cost-effective production of the useful product.[2,3] Similarly, when presented with a specific separation task, one begins by examining the thermodynamics to see if the separation (or the opposite, mixing) is possible and how thoroughly it can be carried out.[4] It is then necessary to turn the focus toward transport phenomena (mass transfer, heat transfer, and fluid dynamics) for the answer on how fast the separation can be implemented.[6] Finally, unit operations and their integrated process system are designed and constructed to carry out the separation task.[7]

The above core knowledge enables chemical engineers to work in various areas such as advanced materials including polymers, control and automation of chemical processes, biochemical and biomedical engineering, environment and safety, energy and fuels, sustainable resources, microelectronics, pharmaceuticals, nanotechnology, and so on. Chemical engineering requires a solid foundation of various chemistries and mathematical sciences. Chemical engineers typically have a strong background in the knowledge of process systems, which differentiates them from chemists. At the same time, chemical engineers must know chemistry quite well; this differentiates them from other engineers (mechanical, electrical, civil, etc.).

The human race is now living in the 'Materials World'. Humanity currently consumes more polymeric materials than all other types of synthetic materials combined. Polymers are chain molecules and their material properties are determined to a large extent by their chain microstructure properties; these properties include molecular weight distribution (MWD), copolymer composition distribution, chain sequence distribution, short-chain and long-chain branching, tacticities, chain topology, and other functionalities. In contrast to the branch of chemical reaction engineering that deals with small molecules, macromolecular reaction engineering is mainly concerned with industrial production of polymer materials. The major tasks of macromolecular reaction engineering involve the study of rates of polymerization and how to best design and operate polymer reactor systems. There are many commonalities with small-molecule chemical reaction engineering. However, macromolecular reaction engineering is generally more complicated because its products are macromolecules, which are not as well defined as small molecules. A small difference in chemical recipe and/or in reactor system design and operation can lead to totally different grades of materials. Also because of chain structure, there are many opportunities through innovation that can improve the properties of existing polymers or develop new polymer products. In this sense, polymers are products of process. In the manufacturing of small-molecule products, different processes can result in different productivities and costs, but the type of products remains the same as long as the same chemical recipe is used. In contrast, not only the productivity and cost but also the product type can vary from one process to another in the manufacture of polymers. For this reason, discussion of product engineering apart from process engineering makes no practical meaning in the polymer production. Rather, integration of the two provides the most powerful tool for the innovative design of new polymers and the improvement of existing polymers.

Macromolecular reaction engineering is a typical example of a multidisciplinary subject. It is concerned with industrial production of polymers. It provides the critical bridge between bench-scale chemistry performed in a laboratory and full-scale commercial production in industry. It covers a wide range of subjects from reaction mechanism and kinetics, to design of reactor systems and processes, scaling up, to process integration, optimization, and control, to safe operation, environment impact, sustainable engineering, and so on. Its fundamental approach is based on experimentation and modeling. The traditional task of polymer reaction engineers is to apply the lab discoveries of polymer chemists. As the scientific understanding of a polymer grows from discovery toward application, it becomes more and more dependent on reaction engineers for product and process innovations. For example, using the same chemical recipe, polymers produced from different reactors can have totally different material properties. The residence time distribution (RTD) of reactor, as well as flow, mass, and heat transport histories, to a large extent determines productivity and quality of polymer products.

Facing strong competition, polymer producers often need to change product grades to meet the market needs. However, such changes normally require years of development that begin with lab chemistry research before industrial implementation. Modeling and simulation of polymerization processes can greatly accelerate such a change in the product from years to months or even days, giving companies a strategic position in the marketplace. In addition, the designs of advanced polymer products are now application driven. Special applications require tailor-made materials with properties that can be

obtained only from specific polymer chain microstructures. Appropriate polymerization reactor systems and processes are then designed and operated accordingly. Mechanism-based process modeling, coupled with the data collected from industrial operations, provides a powerful tool for these types of application-driven designs. Furthermore, the recent developments in polymer nanoscience demand innovations in macromolecular reaction engineering for industrial production of the useful materials and chemicals.

Macromolecular reaction engineering covers a wide range of areas and indeed requires a comprehensive textbook to adequately describe its principles. In design and analysis of polymer production systems, we need to look into three dimensions:

1. *Polymerization mechanisms*: condensation, free radical, cationic, anionic, living anionic, controlled radical, Ziegler–Natta, metallocene, etc.
2. *Polymerization processes*: bulk, solution, precipitation, dispersion, suspension, emulsion, slurry, gas phase, etc.
3. *Polymerization reactors and systems*: stirred tank, tubular, fluidized-bed; batch, semibatch, continuous, etc.

This chapter by no means covers every detail of every area. It intends to introduce basic concepts and some recent advances. For readers who are interested in expanding knowledge, there are some textbooks and numerous review articles, as well as a specialized journal titled *Macromolecular Reaction Engineering*, available. To name a few, Biesenberger and Sebastian,[8] Ray,[9] Reichert and Moritz,[10] Hamielec and Tobita,[11] Dotson *et al.*,[12] Meyer and Keurentjes,[13] Asua,[14] and Schork *et al.*[15] Since there are many chapters in this book series covering almost every aspect of polymer chemistry in great detail, it is also assumed here that readers of this chapter have acquired a good understanding of polymer chemistry.[16–22] We emphasize quantitative analyses and discussions based on equations, with particular attention paid to the rate of polymerization and the polymer molecular weight.

4.32.2 Stepwise Polymerization

Beginning with the work of Bakelite in the early twentieth century, currently there are many types of polymers developed based on stepwise condensation or other stepwise polymerization mechanisms including polyphenols, polyesters, polyamides, polyurethanes, polyureas, polycarbonates, and polysiloxanes. A majority of engineering polymers are produced by stepwise polymerization. Polymer chains of these polymer products are made up through a series of steps. High-molecular-weight materials can be made only after many steps. Each step produces a linkage unit such as an ester –COO– and an amide –CONH–. Condensation polymerization is a form of stepwise polymerization. The two terms are used interchangeably in this chapter, though they can mean different things in some cases. Polyesters are produced via the condensation of diols and dicarboxylic acids and polyamides from diamides and dicarboxylic acids. In general, difunctional monomers AA and BB react to form –ab– linkage:

$$n_A\text{AA} + n_B\text{BB} \rightarrow \text{Aabba}\ldots\text{abB} \rightarrow \text{A(ab)}_{n-1}\text{B} \qquad [1]$$

where n_A and n_B are numbers of AA and BB, and it is stoichiometrically balanced if $n_A = n_B$. It is also possible for condensation to involve two functional groups on a single molecule and then AB monomers react to form –ab– linkage with an assured stoichiometric balance:

$$n\text{AB} \rightarrow \text{Ababa}\ldots\text{baB} \rightarrow \text{A(ab)}_{n-1}\text{B} \qquad [2]$$

In condensation reactions, monomer functionality is important. If a monomer is monofunctional, it becomes a chain stopper. If monomer has a functionality that is higher than two, it becomes a chain-branching agent.

4.32.2.1 Rate of Polymerization

The most fundamental question in reaction engineering is, how fast can the product be made? The condensation reaction rate is conventionally expressed with respect to how many moles of functional group A is consumed per unit of volume per unit of time. Since one B is required to react with one A, it is equivalent to how many moles of B consumed. At the same time, one –ab– linkage is generated by consuming one A and one B. We, therefore, have

$$-\frac{\mathrm{d}V[\mathrm{A}]}{V\,\mathrm{d}t} = -\frac{\mathrm{d}V[\mathrm{B}]}{V\,\mathrm{d}t} = \frac{\mathrm{d}V[\mathrm{ab}]}{V\,\mathrm{d}t} = k[\mathrm{A}][\mathrm{B}] \qquad [3]$$

The rates are proportional to the functional group concentrations. In general, when monomers are condensed to polymers, the polymerization system experiences some volume shrinkage. In practice, the volume shrinkage effect is often neglected for simplicity:

$$-\frac{\mathrm{d}[\mathrm{A}]}{\mathrm{d}t} = -\frac{\mathrm{d}[\mathrm{B}]}{\mathrm{d}t} = \frac{\mathrm{d}[\mathrm{ab}]}{\mathrm{d}t} = k[\mathrm{A}][\mathrm{B}] \qquad [4]$$

The rate constant k is a function of chain length of the reactants. However, it was demonstrated that the functional group reactivity does not vary much as long as chain length is greater than about 10 monomeric units. Most polymer chains are long except for those at the very beginning of polymerization. Therefore, k can be treated as a single value. This is an important finding, otherwise one would have tens of thousands of rate equations to deal with in any calculation.

In the stoichiometric balance case $[\mathrm{A}] = [\mathrm{B}]$, we can readily solve eqn [4] and have

$$\frac{1}{[\mathrm{A}]} - \frac{1}{[\mathrm{A}]_0} = kt \qquad [5]$$

In the general case where the stoichiometry is not balanced $[\mathrm{A}] \neq [\mathrm{B}]$, we have

$$\frac{1}{[\mathrm{A}]_0 - [\mathrm{B}]_0} \ln \frac{[\mathrm{A}][\mathrm{B}]_0}{[\mathrm{A}]_0[\mathrm{B}]} = kt \qquad [6]$$

As in practice we are mainly concerned with the monomer conversion, eqns [5] and [6] can be arranged as

$$\frac{1}{1 - x_A} = 1 + k[\mathrm{A}]_0 t \qquad [7]$$

$$\ln \frac{1 - x_A}{1 - \alpha x_A} = k[\mathrm{A}]_0 \left(1 - \frac{1}{\alpha}\right) t \qquad [8]$$

where the functional group A conversion is defined as $x_A = ([A]_0 - [A])/[A]_0$ and the stoichiometric imbalance ratio as $\alpha = [A]_0/[B]_0$. Equations [7] and [8] relate x_A to polymerization time t and other reaction conditions such as the initial functional group concentrations ($[A]_0$, $[B]_0$), temperature, and system viscosity. The functional group B conversion can be calculated from $x_B = \alpha x_A$, based on the mass balance of $[B]_0 - [B] = [A]_0 - [A]$. Equations [7] and [8] have been verified for many condensation polymerization systems and are often used to estimate k from conversion versus time experimental data.

4.32.2.2 Molecular Weight of Polymers

What makes a polymer so special and so different from monomers is its chain microstructure, which is evident in characteristics such as high molecular weight. Most industrial polymers have a molecular weight in the range of 10^4–10^7 g mol^{-1}. Low-molecular-weight polymers of 10^3–10^4 g mol^{-1} are often termed oligomers. It should be emphasized that polymer chains do not have the same molecular weight. This is in sharp contrast to some natural polymers such as polynucleotides and proteins. Scientists continue to make efforts toward the synthesis of polymers with precisely controlled molecular weight and composition for tailor-made properties. The task is challenging particularly for industrial polymers, and there are still many things that we can learn from nature about polymer synthesis.

Polymer chains do not have uniform molecular weights and thus there exists a MWD. Research in academia often struggles to achieve precisely controlled narrow MWD polymers. However, a narrow MWD is not necessarily better than a broad one in application. The opposite can be true in some industrial applications. High-molecular-weight chains provide strength and low-molecular-weight ones offer processability. Practical materials should have good application properties and at the same time good processing properties. From a fundamental point of view, narrow MWD polymers do have advantages over broad counterparts. The reason is simple: mixing is easier than separation. We can easily mix similar-type polymers having different molecular weights, but it is difficult to separate those polymers once mixed. The separation processes such as preparatory chromatography and solvent/nonsolvent refractionation are very time consuming and costly.

Take the AB-type monomer as an example for derivation of equations for molecular weight calculation. It should be clarified here that we use the terms 'chain length' and 'degree of polymerization' interchangeably, both being defined as the number of monomeric units in a polymer chain. The molecular weight of a polymer chain can be calculated from its chain length simply multiplied by the monomeric unit molecular weight (note, it can be different from unreacted monomer molecular weight because during condensation the reaction releases small molecules such as H_2O). For AA + BB type, the chain length counts for both monomeric units, that is, a repeating unit, –aabb–, is counted as two units. The monomeric molecular weight takes their average, possibly deducted by two condensation byproduct molecules if any.

Let us consider 10 monomers at the start. When $x_A = 0$, the average chain length is 1 because all are still monomers. When four As are reacted, the conversion $x_A = 0.4$ and the number-average chain length $\bar{r}_N = 10/6$ because each condensation step consumes one molecule. When six As are reacted, $x_A = 0.6$ and $\bar{r}_N = 10/4$. Similarly, when eight As are reacted, $x_A = 0.8$ and $\bar{r}_N = 10/2$, and so on. This derivation can be generalized for a population of N_{A0} monomers. The number-average chain length can be calculated by dividing the number of monomers initially charged to the reactor by the number of molecules (regardless of their sizes that include monomers, dimers, trimers, etc.) present in the system at time t.[23] For the stoichiometric balance case

$$\bar{r}_N = \frac{N_{A0}}{N_A} = \frac{1}{1-x} \quad [9]$$

and for the stoichiometric imbalance case

$$\bar{r}_N = \frac{(N_{A0} + N_{B0})/2}{(N_A + N_B)/2} = \frac{1+\alpha}{1+\alpha-2\alpha x_A} \quad [10]$$

Note that the number of chains can be counted either as the number of 'heads' in the AB case or half of the sum of 'heads' and 'tails' in the AA + BB case.

An examination of eqns [9] and [10] clearly shows that in order to produce high-molecular-weight polymers in condensation polymerization, we must have very high monomer conversion that requires removal of small molecular byproduct and very accurate control of the stoichiometric ratio α. The maximum chain length possibly achievable at $x_A = 1$ is $\bar{r}_N = (1+\alpha)/(1-\alpha)$. The system should be free of side reactions that consume A or B. Monomers and other raw materials should have very high purities. The polymerization rate must be reasonably high with little tendency toward cyclization reactions.

4.32.2.3 MWD of Polymers

The full MWD (also termed as chain length distribution) of a condensation polymerization product can be derived using a statistical approach. Take the AB case as an example. In statistics, the conversion x can be understood as the probability that a randomly selected functional group A has reacted.[16] The number-fraction chain length distribution $n(r)$ is the probability of having a chain randomly selected from a population that has the chain length r. This is equivalent to a chain that experiences $r-1$ step growth and 1 step stop:

$$n(r) = x^{r-1}(1-x) \quad [11]$$

The weight-fraction chain length distribution $w(r)$ can be calculated from $n(r)$ by

$$w(r) = rn(r)/\sum_{r=1}^{\infty} rn(r) = rx^{r-1}(1-x)^2 \quad [12]$$

The number- and weight-fraction chain length distributions are interchangeable. The former can also be calculated from the latter by $n(r) = (w(r)/r)/\sum_{r=1}^{\infty}(w(r)/r)$. The number-average chain length $\bar{r}_N$ is thus

$$\bar{r}_N = \sum_{r=1}^{\infty} rn(r) = \frac{1}{1-x} \quad [13]$$

which agrees with eqn [9]. The weight-average chain length is

$$\bar{r}_W = \sum_{r=1}^{\infty} rw(r) = \frac{1+x}{1-x} \quad [14]$$

and the polydispersity index

$$PD = \frac{\bar{r}_W}{\bar{r}_N} = 1 + x \quad [15]$$

At high conversions $x \to 1$, eqn [11] can be approximated by $n(r) = (\bar{r}_N)^{-1}\exp(-r/\bar{r}_N)$ and eqn [12] by $w(r) = (\bar{r}_N)^{-2} r \exp(-r/\bar{r}_N)$ because of $x^{r-1} \to (1-\delta)^{r-1} \approx \exp(-\delta r)$, where $r >> 1$ and $\delta = 1 - x$. $w(r)$ is a random distribution, also called Flory's most probable distribution, and it has polydispersity equal to 2.

Figure 1 shows the number- and weight-fraction chain length distributions at different monomer conversions. It should be pointed out that the weight-fraction distribution is more useful when polymers are used as bulk materials. It also corresponds to the data obtained by gel permeation chromatography (GPC, also called size exclusion chromatography, SEC). However, the number-fraction distribution is also helpful in product quality analysis and in some applications where the number of chains is important. Although they constitute negligible amount in terms of weight, short chains can experience unwanted release from bulk materials.

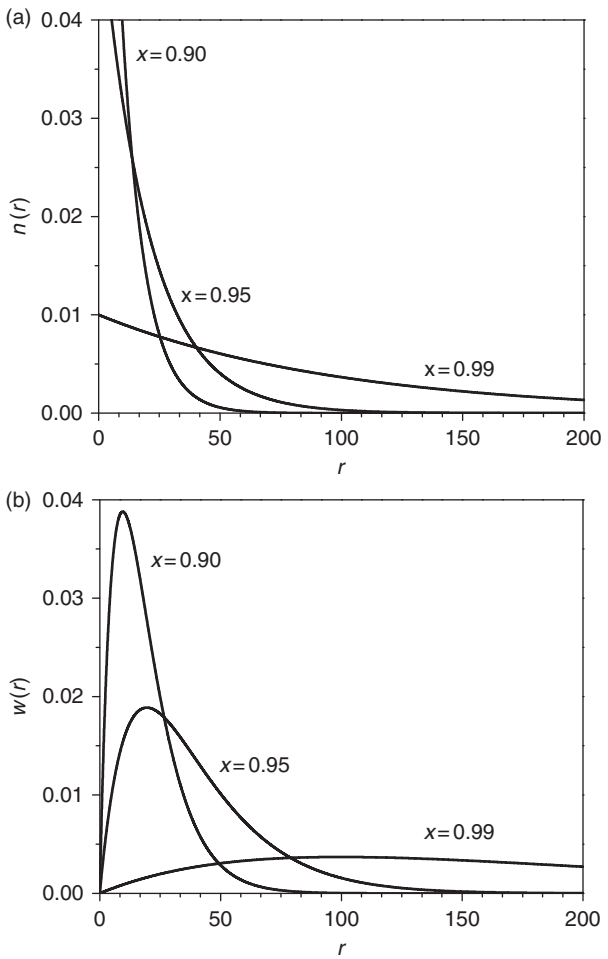

Figure 1 (a) Number-fraction chain length distribution $n(r)$ and (b) weight-fraction chain length distribution $w(r)$ of the polymers at different functional group conversions in condensation polymerization.

4.32.2.4 Nonlinear Condensation Polymerization

Polymers can be linear, branched, and cross-linked. In condensation polymerization, branched chains and cross-linked networks can be formed if the system contains some monomer molecules having three or more functionalities. Examples are thermosetting materials such as phenolics, glyptal polyesters, ureas, and siloxanes. In a broad sense, the terms of thermosetting, curing, cross-linking, gelation, and network formation all mean the same thing. Polymer chains are cross-linked and form a network structure called gel.[23] Gel molecules cannot dissolve in any solvent but can be swelled by good solvents. Thermosetting plastics, rubbers, and absorbents are typical examples of gel materials. In contrast to gel, linear and branched polymers are termed as sol molecules that are soluble in good solvents.

Gelation is an important phenomenon. During polymerization, there exists a critical point called gel point or gelation point or onset of gelation. In production of gel materials, it is important to cross this point, otherwise the produced materials are still soluble. However, if only branching is wanted, the polymerization system should be stopped before the gel point. Knowledge of the gel point is therefore critical.

Take the AA + BB + A_f case as an example for illustration. Because of the f-functional monomer A_f, chains become branched. Following Flory and Stockmayer,[16,24–27] we assume that all functional groups react independently of one another, all functional groups of the same type are equally reactive, and there are no intramolecular reactions in sol molecules. In addition to the monomer conversion $x_A = ([A]_0 - [A])/[A]_0$, stoichiometric ratio $\alpha = (2[AA]_0 + 3[A_3]_0)/(2[BB]_0)$, and functionality f, we define the fraction of A groups on A_f as $\rho = f[A_f]_0/(2[AA]_0 + f[A_f]_0)$. The branching coefficient δ, defined as the probability of one branching leading to another branching, can then be derived as follows: the probability for A_f to react with BB to form A_{f-1}abB is the conversion x_A. The probability for A_{f-1}abB to react with AA to form A_{f-1}abbaA is $x_A[\alpha x_A(1-\rho)]$. The probability for A_{f-1}abbaA to react with BB to form A_{f-1}abbaabB is $x_A[\alpha x_A(1-\rho)x_A]$. The probability of repeating n times of the last two steps to form A_{f-1}a(bbaa)$_n$bB is $x_A[\alpha x_A(1-\rho)x_A]^n$. The probability of this last molecule to react with A_f is $x_A[\alpha x_A(1-\rho)x_A]^n \alpha x_A \rho$. Since n can be any number from 0 to infinity, the branching coefficient is thus the sum of the probability $x_A[\alpha x_A(1-\rho)x_A]^n \alpha x_A \rho$:

$$\delta = \sum_{n=0}^{\infty} \alpha x_A^2 \rho[\alpha x_A^2(1-\rho)]^n = \frac{\alpha x_A^2 \rho}{1 - \alpha x_A^2(1-\rho)} \quad [16]$$

When the branching coefficient reaches the critical value of $1/(f\text{-}1)$, gelation occurs and gel molecules starts to form:

$$x_{A,gel} = \frac{1}{[\alpha + \alpha\rho(f-2)]^{1/2}} \quad [17]$$

Equation [17] shows that the gel point $x_{A,gel}$ is determined by three parameters: the functionality, the stoichiometric imbalance ratio, and the fraction of A groups on A_f. For a system to be gelable $x_{A,gel} < 1$, a minimum amount of multifunctional monomer is required to assure $\rho > (1-\alpha)/[\alpha(f-2)]$. Figure 2 shows the relationship between ρ and α at $f = 3$, 4, and 5. It should be pointed out that eqn [17] is applicable only to the AA + BB + A_f case. There are many different cases in

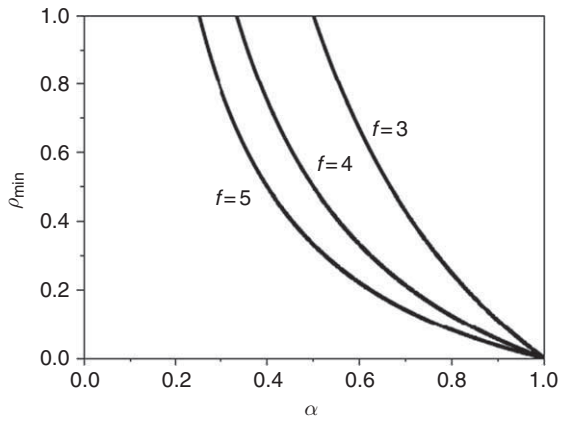

Figure 2 Minimum amount of multifunctional monomer A_f required to assure gelability in the condensation polymerization of AA + BB + A_f.

condensation polymerization that can lead to gelation.[28,29] However, their corresponding equations need to be derived based on specific conditions. Numerous advanced methods have been developed for modeling gelation in polycondensation.[30–38]

4.32.3 Free-Radical Polymerization

Free-radical polymerization is the most widely used mechanism and accounts for about 50% of the total polymer production. Major polymer types such as polyvinyl chloride (PVC), polystyrene (PS), polymethyl methacrylate (PMMA), polyvinyl acetate (PVAc), polytetrafluoroethylene (PTFE), low-density polyethylene (LDPE), as well as their copolymers, are all produced by free-radical polymerization. A typical free-radical polymerization system includes the following elementary reactions:

$$\text{Initiator decomposition: I} \xrightarrow{k_d} 2R_0^\bullet \qquad [18]$$

$$\text{Initiation: } R_0^\bullet + M \xrightarrow{f,k_i} P_1^\bullet \qquad [19]$$

$$\text{Propagation: } P_1^\bullet + M \xrightarrow{k_p} P_2^\bullet \qquad [20]$$

$$P_r^\bullet + M \xrightarrow{k_p} P_{r+1}^\bullet \qquad [21]$$

Termination (note: $k_t = k_{td} + k_{tc}$):

$$\text{by disproportionation: } P_r^\bullet + P_s^\bullet \xrightarrow{k_{td}} P_r + P_s \qquad [22]$$

$$\text{by combination: } P_r^\bullet + P_s^\bullet \xrightarrow{k_{tc}} P_{p+s} \qquad [23]$$

$$\text{Chain transfer: } P_r^\bullet + Z \xrightarrow{k_{fZ}} P_r + Z^\bullet \qquad [24]$$

where I is an initiator molecule such as peroxide or azo compound, which normally generates two primary radicals $R_0^\bullet$ upon decomposition with k_d as its decomposition rate constant. As the initiation step, the primary radical $R_0^\bullet$ reacts with monomer M and k_i is the initiation rate constant. However, in reality, not all the primary radicals initiate the growth of polymer chains. Some primary radicals experience various side reactions and are wasted. Thus, there is an initiation efficiency f.

Propagation reactions are responsible for chain growth. In general, a radical chain $P_r^\bullet$ having chain length r reacts with a monomer M and becomes $P_{r+1}^\bullet$. The propagation rate constant k_p is chain length independent because the propagation reaction involves a small molecule M, even though the other reactant is a macromolecular species $P_r^\bullet$. Most free radicals are high-energy species and terminate rapidly once two radical centers meet each other. There are two types of termination modes. Disproportionation termination yields two dead polymer chains, while combination termination generates one chain. Chain transfer reactions can occur to polymeric radicals. The molecule Z can be monomer, solvent, polymer, some impurities, and chain transfer agent purposely added for regulation of polymer molecular weight. Depending on its reactivity, Z can be an inhibitor if $Z^\bullet$ is incapable of reacting with M or a retarder if $Z^\bullet$ reacts with M at a slower rate than propagation. An ideal chain transfer agent should have a similar or larger rate constant to that of propagation k_p in

$$Z^\bullet + M \xrightarrow{k_{fZ} \approx k_p} P_1^\bullet \qquad [25]$$

Compared with condensation, free-radical polymerization has the following features. Only radical chains add monomers through propagation, individual polymer chains are formed almost instantaneously, monomer concentration decreases steadily throughout polymerization, and a long time is required for high polymer yield, but it can have a small effect on polymer molecular weight. While in condensation polymerization, any two molecular species can react, individual chains grow steadily throughout polymerization, monomer molecules disappear quickly at an early stage, and long polymerization time is essential for a high-molecular-weight polymer product to be obtained.

4.32.3.1 Initiation, Propagation, and Termination

4.32.3.1.1 Initiation

It should be pointed out that there are many methods for initiation of free-radical polymerization, though the most popular approach in industry is the use of chemical initiators such as peroxides and azo compounds. Thermal and radiation initiations are also employed in industry. For chemical initiation, the initiator thermal decomposition is a monomolecular reaction:

$$\frac{d[I]}{dt} = -k_d[I] \qquad [26]$$

where k_d is a first-order rate constant (units t^{-1}: s^{-1}, min^{-1}, h^{-1}). At an isothermal condition with constant k_d, we have

$$[I] = [I]_0 \exp(-k_d t) \qquad [27]$$

where $[I]_0$ is initial initiator concentration. During polymerization, the initiator concentration experiences an exponential decay with time. The time when half of initiator molecules are decomposed is termed as the initiator's half-lifetime or simply as lifetime, $t_{1/2} = (\ln 2)/k_d$. Due to the nature of exponential decay, the actual lifetime would theoretically be infinity. Most industrial initiators have half-lifetimes ranging from hours to tens of hours at the polymerization temperature.

The initiator efficiency is caused by a so-called cage effect.[17,39] Upon decomposition, the two primary radicals are trapped in an imaginary cage ($2R_0^\bullet$). Due to the proximity, the

trapped radicals can experience side reactions and convert to inert and stable molecules S or react with neighboring monomers M to start chain growth or escape from the cage and become 'free' primary radicals that can either terminate with other radicals or initiate with monomers for chain growth:

$$\mathrm{I} \xrightarrow{k_d} (2\mathrm{R}_0^{\bullet}) \quad [28]$$

$$(2\mathrm{R}_0^{\bullet}) \xrightarrow{k_D} 2\mathrm{R}_0^{\bullet} \quad [29]$$

$$(2\mathrm{R}_0^{\bullet}) \xrightarrow{k'_S} \mathrm{S} \quad [30]$$

$$2\mathrm{R}_0^{\bullet} \xrightarrow{k_S} \mathrm{S} \quad [31]$$

$$(2\mathrm{R}_0^{\bullet}) + \mathrm{M} \xrightarrow{k'_i} \mathrm{R}_0^{\bullet} + \mathrm{P}_1^{\bullet} \quad [32]$$

$$\mathrm{R}_0^{\bullet} + \mathrm{M} \xrightarrow{k_i} \mathrm{P}_1^{\bullet} \quad [33]$$

The initiator efficiency is therefore

$$f = \frac{k_D + k'_i[\mathrm{M}] + k_i[\mathrm{M}]}{k'_S + k_S[\mathrm{R}_0] + k_D + k'_i[\mathrm{M}] + k_i[\mathrm{M}]} \quad [34]$$

where f must be $0 \le f \le 1$ by definition and is typically in the range of 0.5–0.8 for most industrial initiators.[17,40–42]

4.32.3.1.2 Propagation

Vinyl monomers of $CH_2=CHR$ and $CH_2=CR_1R_2$ types are polymerizable by free-radical mechanism; however, the type of $R_1HC=CHR_2$ monomers do not normally polymerize to high molecular weight due to steric effects. Double bonds are in high-energy states. Propagation reactions are therefore exothermic with $-\Delta H_p$ values in the range of tens of kilocalories per mole (or 10^2–10^3 kcal kg^{-1}). For example, ethylene has $-\Delta H_p$ of 21 kcal mol^{-1}; propylene 19 kcal mol^{-1}; styrene 17 kcal mol^{-1}; vinyl chloride 26 kcal mol^{-1}; and MMA 13 kcal mol^{-1}.[17] The exothermic nature is often exploited for monitoring monomer conversion based on heat balance. Also because of the high $-\Delta H_p$, heat removal becomes a key concern in reactor design and operation. In a runaway reaction, reactor temperature can increase by hundreds of degrees and cause fires and explosions. Figure 3 shows how temperature can rise inside small ampoule reactors during the bulk radical polymerization of MMA that is set to an isothermal condition of 90 °C in a water or oil bath.

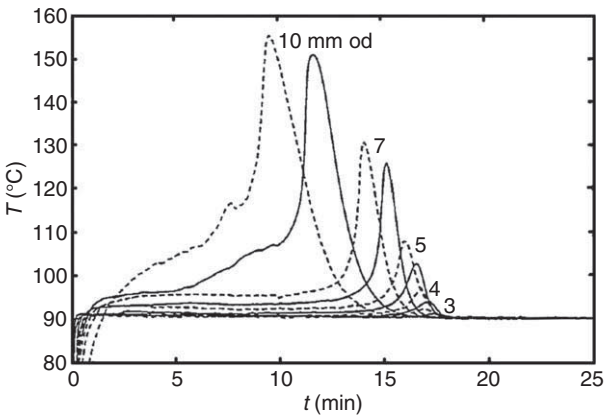

Figure 3 Temperature rises in the bulk radical polymerization of MMA with 0.5 wt.% 2,2'-azobis(2-methyl-propionitrile) (AIBN). Ampoules of 3, 4, 5, 7, 10 mm outer diameter (1.8, 2.4, 3.4, 5, 8 mm inner diameter) are immersed in water (solid lines) or in silicone oil (dotted lines) bath set to 90 °C.[43]

Individual chains in free-radical polymerization are generated in seconds. This is estimated as follows: the number of monomer molecules added to a growing chain per unit of time is $(N_{Av}k_p[\mathrm{M}][\mathrm{P}^{\bullet}])/(N_{Av}[\mathrm{P}^{\bullet}]) = k_p[\mathrm{M}]$. Equivalently, it takes a period of $1/(k_p[\mathrm{M}])$ to add one monomer molecule to the chain. Given $k_p = 10^3$ l mol^{-1} s^{-1} and $[\mathrm{M}] = 10$ mol l^{-1}, the time required to add one monomer is 10^{-4} s. For a chain of 10^4 units, it takes only 1 s. This is in sharp contrast to condensation polymerization where it takes hours for chains to fully grow. It should be emphasized that while individual chains take such short times to form, the free-radical polymerization process requires hours to obtain a high polymer yield.

Propagation reactions are responsible for the development of polymer chain microstructure that determines polymer material properties. For example, PVC chains can have 'head-to-tail' and 'head-to-head' structures. The 'head-to-tail' structure is favored for its low-energy state. However, the 'head-to-head' structure can also be formed particularly at high temperature.[44] PVC materials with significant 'head-to-head' structures have poor quality in application, are not stable, and are susceptible to polyene formation.

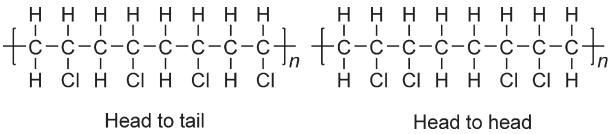

4.32.3.1.3 Termination

Radical termination is a bimolecular reaction that involves two polymeric radicals. Because of high reactivity ($k_t \sim 10^8$ l mol^{-1} s^{-1}) and extremely low concentration (10^{-7}–10^{-9} mol l^{-1}) of radicals, chain diffusion becomes critically important and often determines the magnitude of termination rate.[45–51] In general, radical termination involves three steps, as shown in Scheme 1. First, two radical chains approach each other by translational diffusion. Once in vicinity, two radical centers come together by segmental diffusion. Chemical activation of two radical centers takes almost no time to occur due to their reactive nature.

Radical termination is always diffusion controlled. At low monomer conversion or dilute polymer solution, it is controlled by segmental diffusion.[52–55] When the polymerization system becomes viscous, it is controlled by translational diffusion.[56–58] Both diffusions are chain length dependent.[41,59–61] However, segmental diffusion is a weaker function of chain length than is translational diffusion and it is often neglected or incorporated into the chemical activation term. The termination rate constant for two radicals having chain lengths r and s is $k_t(r,s)$ with their average rate constant as

$$k_t = \sum_{r=1}^{\infty}\sum_{s=1}^{\infty} k_t(r,s)\phi_r^{\bullet}\phi_s^{\bullet} \quad [35]$$

where $\phi_r^{\bullet}$ and $\phi_s^{\bullet}$ are respective number fractions. In practice, the termination rate constant is treated as a single value. The k_t data reported in literature are very diverse even for the same monomer under similar polymerization conditions. This lack of accuracy reflects the complication of chain length dependence.

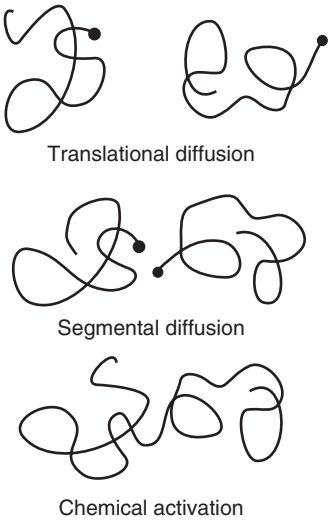

Scheme 1 Three steps involved in bimolecular termination of radicals: translational diffusion, segmental diffusion, and chemical activation. Radical termination is always diffusion controlled: segmental diffusion controlled at low conversions, and translational diffusion controlled at high conversions.[43]

Added to this is the extremely low radical concentration, which can be estimated from a mass balance of the total radical population:

$$\frac{d[P^\bullet]}{dt} = 2fk_d[I] - k_t[P^\bullet]^2 \approx 0 \qquad [36]$$

Applying the stationary-state or steady-state hypothesis (SSH),[62,63] we have the radical chain concentration

$$[P^\bullet] = (2fk_d[I]/k_t)^{1/2} \qquad [37]$$

Given the representative values of $[I] = 10^{-1}\,\text{mol}\,\text{l}^{-1}$, $f = 0.5$, $k_d = 10^{-5}\,\text{s}^{-1}$, and $k_t = 10^8\,\text{l}\,\text{mol}^{-1}\,\text{s}^{-1}$,[64] the total radical concentration is $10^{-7}\,\text{mol}\,\text{l}^{-1}$. The concentration of primary radicals can also be estimated by applying mass balance and SSH:

$$\frac{d[R_0^\bullet]}{dt} = 2fk_d[I] - (k_p[M] + k_t[P^\bullet])[R_0^\bullet] \approx 0 \qquad [38]$$

and is found to be at $[R_0^\bullet] = 2fk_d[I]/(k_p[M] + k_t[P^\bullet]) \approx 10^{-10}\,\text{mol}\,\text{l}^{-1}$.

4.32.3.2 Rate of Polymerization

In free-radical polymerization, monomer molecules are mainly consumed by propagation reactions with the rate of polymerization:

$$R_p = -\frac{d[M]}{dt} = k_p[P^\bullet][M] \qquad [39]$$

where $N_M = N_{M0}(1-x)$. N_{M0} and N_M are respective moles of monomer initially charged to reactor and at present time. In terms of monomer conversion x, eqn [39] becomes

$$\frac{dx}{dt} = k_p[P^\bullet](1-x) \qquad [40]$$

Combining eqn [40] with eqns [37] and [27] yields

$$\frac{dx}{dt} = \left(\frac{2fk_dk_p^2[I]_0}{k_t}\right)^{1/2}(1-x)\exp\left(-\frac{1}{2}k_dt\right) \qquad [41]$$

Assuming that all the rate constants in eqn [41] remain unchanged during polymerization and solving the equation with an initial condition of $x = 0$ at $t = 0$ result in

$$-\ln(1-x) = \left(\frac{8fk_p^2[I]_0}{k_dk_t}\right)^{1/2}\left[1-\exp\left(-\frac{1}{2}k_dt\right)\right] \qquad [42]$$

According to eqn [42], the maximum monomer conversion at $t \to \infty$ is

$$x_\infty = 1 - \exp\left[-\left(\frac{8fk_p^2[I]_0}{k_dk_t}\right)^{1/2}\right] \qquad [43]$$

Equation [43] shows that a dead-end polymerization can occur at low initiator concentration. In practice, an adequate initiator amount must be added to assure high monomer conversion.

From eqns [37] and [39], we can see that the rate of free-radical polymerization is determined by three parameters: temperature, initiator concentration, and monomer concentration:

$$R_p = k_p[P^\bullet][M] = \left(\frac{2fk_dk_p^2}{k_t}\right)^{1/2}[I]^{1/2}[M] \qquad [44]$$

that is, $R_p \propto e^{-(E_A/RT)}[I]^{1/2}[M]$. The apparent activation energy E_A is about 20 kcal mol^{-1}, estimated from the representative values of $E_p = 5$ kcal mol^{-1}, $E_d = 30$ kcal mol^{-1}, and $E_t = 1$ kcal mol^{-1}. This high activation energy suggests the polymerization rate has a strong temperature dependence. Raising the temperature can dramatically accelerate the polymerization. Increasing initiator concentration can also increase the rate. Doubling initiator amount increases the rate of polymerization by 41%. The monomer concentration is also effective in increasing the rate, but its variation is limited to many other parameters in design and operation of the polymerization system. It should be emphasized that there are trade-offs in promoting polymerization rate through the above means. Adjusting these parameters can also change polymer molecular weight, which will be discussed later.

4.32.3.3 Diffusion-Controlled Reactions

Reactions in free-radical polymerization can easily become diffusion controlled.[65,66] This is particularly true for those involving two polymeric radicals such as bimolecular termination. During polymerization, polymer chains can grow larger and polymer concentration increases. The system can experience many orders of magnitude change in viscosity that can dramatically affect the diffusion of reacting chain species. **Figure 4** shows the conversion versus time data of the bulk polymerization of MMA initiated with 0.5 wt.% AIBN at 70 °C. Equation [42] can fit only its low-conversion data points. The polymerization rate starts to accelerate at about 20% conversion. This autoacceleration phenomenon is rather common with acrylic and styrenic systems. It is termed as the 'gel effect', which is a misnomer because there are no gel molecules involved, or as 'the Trommsdorff effect' after the name of an early investigator.[67,68] Reaction autoacceleration can be damaging in practice. It imposes great challenges for heat removal

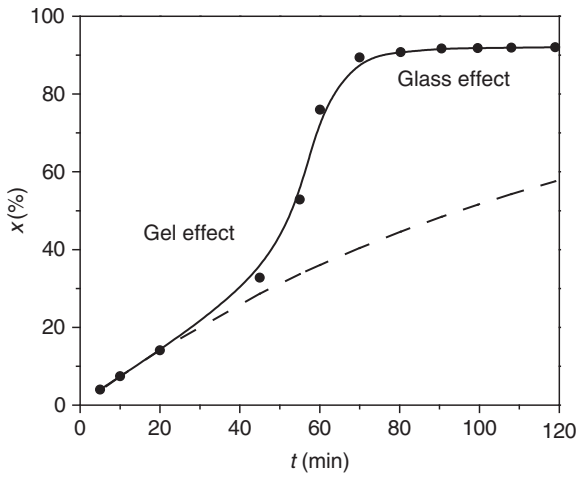

Figure 4 Conversion versus time data for the bulk polymerization of MMA with 0.5 wt.% AIBN at 70 °C. The dotted line is calculated using eqn [42].[69]

and temperature control. When a reactor system is designed or selected, it must meet the requirements for heat removal at the maximum polymerization rate. The effect of viscosity on the rate has been intensively studied for decades since the discovery of the autoacceleration phenomenon. Although there are still some fundamental questions to be answered, it is agreed that the autoacceleration is caused by diffusion-controlled polymeric radical termination. In essence, the corresponding task is to establish the relationships between various reaction rate constants with the diffusions of reacting species.

The starting point for such relationships is the Smoluchowski equation in its simplest form:[70]

$$k_D = \sigma(D_r + D_s) \quad [45]$$

where k_D is diffusion-controlled rate constant, σ is the reaction radius of the reacting species, and D_r and D_s are self-diffusion coefficients. Equation.[45] applies to small molecules. An equivalent equation valid for diffusion-controlled reactions between two macromolecules has not been derived to date. Nevertheless, the above equation has been used and σ is usually taken as proportional to chain length with an empirical exponential ε in treating diffusion-controlled radical termination reactions, $k_{t,D}(r,r) \propto r^{\varepsilon} D_r$, where D_r is self-diffusion coefficient of radicals having chain length r.

The next question is how the diffusion coefficient is related to the radical chain lengths and system viscosity. According to de Gennes' chain reptation theory[71–75]

$$D_r \propto r^{-2} C_P^{-7/4} \quad [46]$$

where C_P is the polymer concentration. According to chain entanglement and free-volume theory[76–80]

$$D_r \propto r^{-2.5} \exp(-A/v_f) \quad [47]$$

where v_f is free-volume fraction, which can be estimated from

$$v_f = [0.025 + \alpha_m(T - T_{gm})]\phi_m + [0.025 + \alpha_p(T - T_{gp})]\phi_p \quad [48]$$

where T is the polymerization temperature, T_{gm} and T_{gp} are monomer and polymer glass transition temperatures, respectively, $\alpha_m = \alpha_{ml} - \alpha_{mg}$ and $\alpha_p = \alpha_{pl} - \alpha_{pg}$ are differential thermal expansion coefficients of monomer and polymer between liquid and glass states, respectively, and ϕ_m and ϕ_p are monomer and polymer volume fractions, respectively. Both reptation and free-volume theories have achieved some levels of success in modeling free-radical polymerization kinetics. The apparent termination rate constant k_t is formulated as $k_t^{-1} = k_{t,C}^{-1} + k_{t,D}^{-1}$ or

$$k_t = \frac{k_{t,C} k_{t,D}}{k_{t,C} + k_{t,D}} \quad [49]$$

where $k_{t,C}$ is the chemical-controlled termination rate constant. Most reported k_t values in the literature are $k_{t,C}$ values. Because termination is always diffusion controlled and segmental, diffusion dominates at low conversion and $k_{t,C}$ is actually the low-conversion rate constant that has incorporated segmental diffusion effect.[81,82] A practical semiempirical expression for the diffusion-controlled termination rate constant $k_{t,D}$ in eqn [49] is

$$k_{t,D} = k_{t0}(\bar{M}_w)^{-n} \exp(-\lambda/v_f) \quad [50]$$

where $\bar{M}_W$ is the weight-average dead polymer molecular weight and k_{t0}, n, and λ are adjustable parameters to correlate experimental data.[42,61,83–89] There were many models proposed for quantitative description of chain length-dependent radical termination reactions.

At very high conversion in free-radical polymerization, not only radical termination but also monomer propagation can become diffusion controlled. If polymerization is carried out below polymer glass temperature $T < T_{gp}$, the reacting mixture reaches its glass state before complete monomer conversion, termed as 'glass effect'. The limiting conversion can be estimated from eqn [48] by setting the free-volume fraction v_f to its universal value of 0.025 at the glass state:

$$x \approx \phi_p = \alpha_m(T - T_{gm})/[\alpha_m(T - T_{gm}) + \alpha_p(T_{gp} - T)] \quad [51]$$

Under $T_{gm} < T < T_{gp}$, $x < 1$. For systems run below the polymer glass transition temperature, the polymerization temperature must be raised at its final stage for further polymerization. Figure 5 shows such an operation. MMA is first polymerized at 80 °C for high molecular weight. However, the polymerization stops at 95% conversion and is restarted by elevating the temperature to 100 °C. The final 5% polymer product has a lower molecular weight.[45]

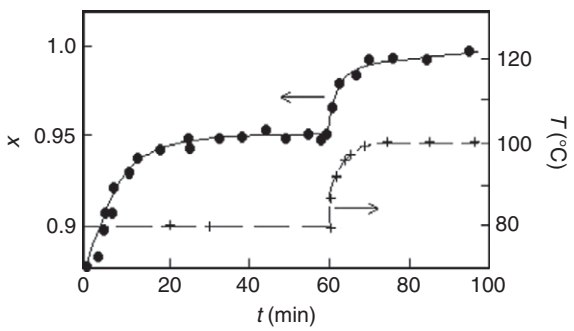

Figure 5 Glass effect – MMA polymerized at 80 °C stops at 95% conversion. Temperature is raised at the end of polymerization to complete the residual 5% monomer.[45]

The glass effect on propagation can also be described by free volume, $k_p^{-1} = k_{p,C}^{-1} + k_{p,D}^{-1}$ or

$$k_p = k_{p,C}k_{p,D}/(k_{p,C} + k_{p,D}) \quad [52]$$

where[42,90]

$$k_{p,D} = k_{p0}\exp(-\zeta/v_f) \quad [53]$$

k_{p0} and ζ are semiempirical adjustable parameters. $k_{p,D}$ is independent of chain length, though propagation involves chain species. In this bimolecular reaction, the diffusion of monomer dominates. At the vicinity of glass state, radical initiation is suppressed by severe cage effect. Although initiator decomposition is a monomolecular reaction and not affected by diffusion limitations, the initiator efficiency f decreases. Several terms in eqn [34] are diffusion dependent and this is particularly true for $(2R_0^\bullet) \xrightarrow{k_d} 2R_0^\bullet$. The primary radicals in the cage are trapped because of small k_D, favoring conversion to the inert S. Unfortunately, there is little quantitative work in the literature on the diffusion-controlled initiation. Another point worth mentioning at the glass state is the termination by 'propagation diffusion'. At this stage, chain species are effectively frozen. However, radical centers can still move because of propagation reactions. Adding a monomer molecule to a radical center moves the center a step further, which facilitates the radical termination. A residual term can be added to eqn [50] to account for this 'propagation diffusion' termination:[41]

$$k_{t,D} = k_{t0}(\bar{M}_W)^{-n}\exp(-\lambda/v_f) + \omega k_p[M] \quad [54]$$

with ω as an adjustable parameter. Figure 6 shows the orders of magnitude changes of propagation and termination rate constants with monomer conversion during bulk radical polymerization run below polymer glass temperature.[42,91]

4.32.3.4 Molecular Weight and Distribution of Polymers

In free-radical polymerization, there are two chain populations inside the reactor: radical chains and dead chains. Each population has a MWD. These distributions can be derived from mass balances of their respective species. For a radical chain having chain length r, we have

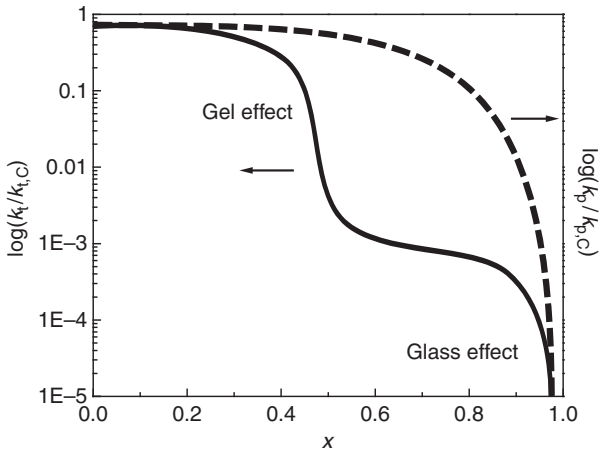

Figure 6 Change of propagation and termination rate constants during bulk free-radical polymerization.[43]

$$\frac{d[P_r^\bullet]}{dt} = k_p[M][P_{r-1}^\bullet] - (k_p[M] + k_t[P^\bullet] + k_{fZ}[Z])[P_r^\bullet] \quad [55]$$

Applying the SSH (i.e., $d[P_r^\bullet]/dt \approx 0$) and defining

$$\tau = \frac{k_{td}[P^\bullet]}{k_p[M]} + \frac{k_{fZ}[Z]}{k_p[M]} \quad [56]$$

$$\beta = \frac{k_{tc}[P^\bullet]}{k_p[M]} \quad [57]$$

we obtain

$$[P_r^\bullet] = \frac{[P_{r-1}^\bullet]}{1+\tau+\beta} = \ldots = \frac{[P_1^\bullet]}{(1+\tau+\beta)^{r-1}} = \frac{(\tau+\beta)}{(1+\tau+\beta)^r}[P^\bullet] \quad [58]$$

and finally the number-fraction chain length distribution of radical population

$$n^\bullet(r) = \frac{[P_r^\bullet]}{[P^\bullet]} = \frac{(\tau+\beta)}{(1+\tau+\beta)^r} \approx (\tau+\beta)\exp[-(\tau+\beta)r] \quad [59]$$

The radical chain population is very small compared with the dead-chain population ($[P^\bullet] \sim 10^{-7}$–10^{-9} mol l^{-1} vs. $[M] \sim 1$–10 mol l^{-1}). In terms of polymer product, the dead-chain population represents the total polymer. Equation [59] is important for polymer production, but not so for polymer applications.

Similarly, the chain length distribution of dead polymer population (equivalently, that of the total polymer) can be derived based on the mass balance of

$$\frac{d[P_r]}{dt} = k_{td}[P^\bullet][P_r^\bullet] + k_{fZ}[Z][P_r^\bullet] + \frac{1}{2}k_{tc}\sum_{s=1}^{r-1}[P_s^\bullet][P_{r-s}^\bullet] \quad [60]$$

Substituting eqn [58] for eqn [60], we can obtain the weight-fraction distribution after some mathematical manipulation ($r\,d[P_r]/dt)/(k_p[P^\bullet][M])$:[92–95]

$$w(r) = (\tau+\beta)\left[\tau + \frac{\beta}{2}(\tau+\beta)r\right]r\exp[-(\tau+\beta)r] \quad [61]$$

It should be emphasized that eqn [61] is an instantaneous distribution, that is, the distribution of the chains generated during the time interval from t to $t+\Delta t$. The parameters τ and β as defined in eqns [56] and [57] change during polymerization. The final product is thus the sum of all instantaneous populations accumulated inside a reactor:

$$w_{cum}(r) = \frac{1}{x}\int_0^x w(r)dx \quad [62]$$

Figure 7 shows the cumulative chromatograms of the polymer samples collected at different conversions from the bulk MMA polymerization initiated with 0.5% AIBN at 70 °C, as well as their average molecular weights. Theoretically, the instantaneous molecular weights can be obtained from derivatives of the cumulative data. However, the accuracy can be an issue in this practice.

The number- and weight-average chain lengths, as well as the polydispersity, of the instantaneous polymer population can be derived from eqn [61]

$$\bar{r}_N = 1/\int_0^\infty [w(r)/r]dr = \frac{1}{\tau+\beta/2} \quad [63]$$

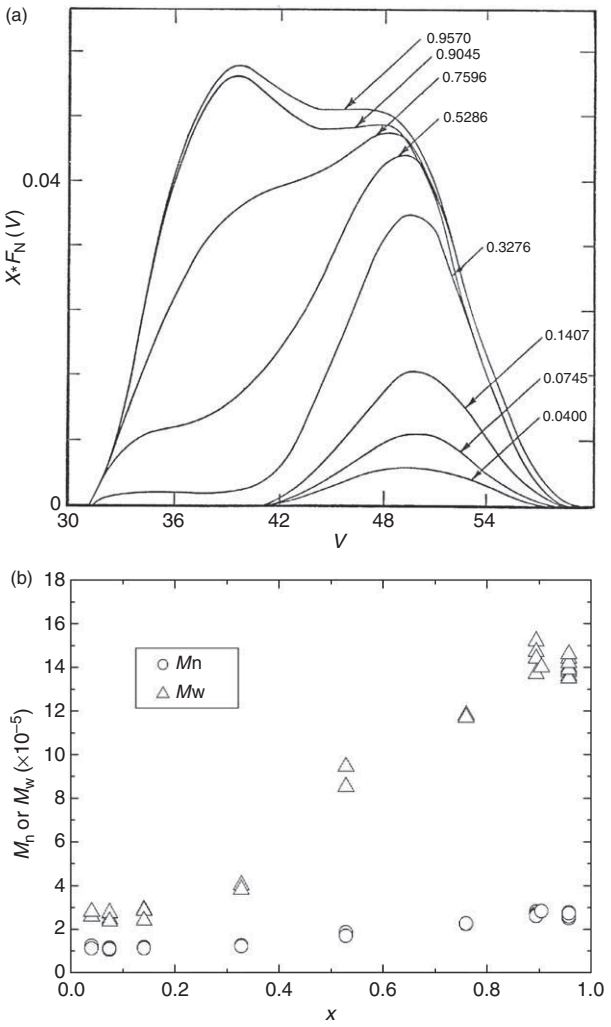

Figure 7 (a) Change of GPC curves with monomer conversion in bulk MMA polymerization at 70 °C and 0.5% AIBN and (b) their calibrated number- and weight-average molecular weights.[69]

$$\bar{r}_W = \int_0^\infty [rw(r)]dr = \frac{2\tau + 3\beta}{(\tau + \beta)^2} \quad [64]$$

$$PD = \bar{r}_W/\bar{r}_N = \frac{(\tau + \beta/2)(2\tau + 3\beta)}{(\tau + \beta)^2} \quad [65]$$

Their corresponding chain properties of the cumulative polymer are

$$\bar{r}_{N,cum} = x/\int_0^\infty (1/\bar{r}_N)dx \quad [66]$$

$$\bar{r}_{W,cum} = \left(\int_0^\infty \bar{r}_W\, dx\right)/x \quad [67]$$

$$PD_{cum} = \bar{r}_{W,cum}/\bar{r}_{N,cum} \quad [68]$$

The instantaneous polydispersities are between 1.5, if dominated by combination termination, and 2, if dominated by disproportionation termination and chain transfer reactions. Commercial polymer products are cumulative polymers and have polydispersity values higher than 2.

The key factors that determine polymer molecular weight are the initiator, monomer, and chain transfer agent concentrations, as well as temperature. In the absence of chain transfer agent, the relative influences of temperature, initiator concentration, and monomer concentration can be examined from

$$\bar{r}_N \sim R_p/R_t \propto \frac{k_p}{(k_d k_t)^{1/2}}[I^\bullet]^{-1/2}[M] \quad [69]$$

where the apparent activation energy for $k_p(k_d k_t)^{-1/2}$ is approximately $-10\,kcal\,mol^{-1}$. Comparing the polymer molecular weight $\bar{r}_N \propto \exp(10\,kcal\,mol^{-1}/RT)[I]^{-1/2}[M]$ to the rate of polymerization $R_p \propto \exp(-20\,kcal\,mol^{-1}/RT)[I]^{1/2}[M]$, it can be seen that the influences of temperature and initiator concentration are in the opposite directions. While raising temperature and initiator concentration increases rate of polymerization, it reduces polymer molecular weight. In practice, polymer productivity (rate) and product quality (molecular weight) must be compromised.

4.32.3.5 Branching and Cross-linking

Branching can occur in the presence of chain transfer to polymer reactions. For example, in ethylene polymerization, the radical centers backbite their own chains and form short-chain branches. It is these short-chain branches that limit chain crystallization and result in LDPE. Because of no control over backbiting sites, the branch lengths are ill defined and vary a lot from site to site and from chain to chain.

Backbiting is an intramolecular chain transfer reaction. If transfer reactions occur between different chains, long-chain branched polymers are formed. Well-known examples include ethylene and vinyl acetate. Vinyl acetate polymerization could lead to gel formation under certain conditions. It should be pointed out that chain transfer to polymer reaction alone generates only T-type branch structures that do not result in gel formation. Theoretically, some mechanism such as radical termination by combination that brings two chains together to form H-type branch structures is an essential condition for gelation.

The rate of chain transfer to polymer follows

$$R_{fp} = k_{fp}[P^\bullet]\sum_{r=1}^{\infty} rP_r = k_{fp}[P^\bullet][M]_0 x \quad [70]$$

The branching density ρ is defined as the ratio of the number of branching points to that of monomeric units and it can be estimated from

$$\frac{d(x\rho)}{dx} = \frac{k_{fp}}{k_p}\frac{x}{1-x} \quad [71]$$

Solving eqn [71] yields

$$\rho = -\frac{k_{fp}}{k_p}\left[1 + \frac{\ln(1-x)}{x}\right] \quad [72]$$

The branching density increases dramatically at high conversions because of the high polymer concentration that facilitates the chain transfer to polymer reactions.

Chain transfer to polymer reactions increases the weight-average molecular weight but not the number-average molecular weight. It can be clearly illustrated by two chains having the same chain length 10. Without chain transfer, their number- and weight-average chain lengths are both equal to

10. If one chain transfers to another at its half chain length, the two chains would have chain lengths 5 and 15. Their number-average chain length is still $(1 \times 5 + 1 \times 15)/(1 + 1) = 10$, but the weight-average chain length increases to $(5 \times 5 + 15 \times 15)/(5 + 15) = 12.5$.

4.32.3.6 Method of Moments

It is challenging to derive chain length distribution functions for branching and cross-linking systems. In such cases, we often resort to the use of the method of moments.[96,97] The ith moments of radical and dead polymer chains are defined as

$$Q_i^{\bullet} = \sum_{r=1}^{\infty} r^i [P_r^{\bullet}] \quad [73]$$

$$Q_i = \sum_{r=1}^{\infty} r^i [P_r] \quad [74]$$

The zeroth and first moments have clear physical meanings. $Q_0^{\bullet}$ (=$[P^{\bullet}]$) and Q_0 are the radical and dead polymer chain concentrations, respectively. $Q_1^{\bullet}$ and Q_1 (=$[M]_0 x$) are their monomeric unit concentrations. The number- and weight-average chain lengths of radical chains are thus

$$\bar{r}_N^{\bullet} = \sum_{r=1}^{\infty} r[P_r^{\bullet}] / \sum_{r=1}^{\infty} [P_r^{\bullet}] = Q_1^{\bullet}/Q_0^{\bullet} \quad [75]$$

$$\bar{r}_W^{\bullet} = \sum_{r=1}^{\infty} r^2[P_r^{\bullet}] / \sum_{r=1}^{\infty} r[P_r^{\bullet}] = Q_2^{\bullet}/Q_1^{\bullet} \quad [76]$$

Similarly, the number- and weight-average chain lengths of dead (or total) polymer chains are

$$\bar{r}_N = \sum_{r=1}^{\infty} r[P_r] / \sum_{r=1}^{\infty} [P_r] = Q_1/Q_0 \quad [77]$$

$$\bar{r}_W = \sum_{r=1}^{\infty} r^2[P_r] / \sum_{r=1}^{\infty} r[P_r] = Q_2/Q_1 \quad [78]$$

Adding the terms $+k_{fp}[P^{\bullet}]r[P_r] - k_{fp}Q[P_r^{\bullet}]$ to eqn [55] and $+k_{fp}Q_1[P_r^{\bullet}] - k_{fp}[P^{\bullet}]r[P_r]$ to eqn [60], we have the following moment equations after some algebra:[98,99]

$$\frac{dq_0}{dx} = \tau + \beta/2 \quad [79]$$

$$\frac{dq_1}{dx} = 1 \quad [80]$$

$$\frac{dq_2}{dx} = \frac{2(1 + c_{fp,2})}{\tau + \beta + c_{fp,1}} + \frac{\beta(1 + c_{fp,2})^2}{(\tau + \beta + c_{fp,1})^2} \quad [81]$$

where $c_{fp,i} = (k_{fp}Q_i)/(k_p[M])$ and $q_i = Q_i/[M]_0$ are dimensionless relative moments of Q_i scaled with the initial monomer concentration $[M]_0$. Equations [79]–[81] clearly show that the chain transfer reaction to polymer does not affect the number-average chain length but increases the weight-average chain length. From eqn [81], it can also be seen that such polymerization systems do not gel in the absence of radical termination by combination, that is, $\beta = 0$. Figure 8 shows the weight-average chain length during the bulk polymerization of vinyl acetate.[100] The solid line is calculated with $k_{tc} = 0$, while the dashed line is calculated with $k_{td} = 0$. The latter predicts a gel point at $x = 0.912$. At the gel point, the weight-average chain length goes to infinity.

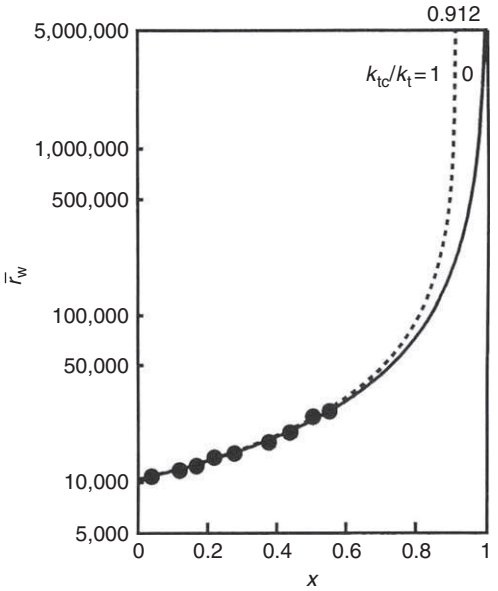

Figure 8 Increase of weight-average chain length with monomer conversion during the bulk polymerization of vinyl acetate at 60 °C.[99]

4.32.4 Ionic Polymerization

Depending on the charge type on the propagating center, ionic polymerization is further divided into anionic polymerization and cationic polymerization. Many aspects of ionic polymerization are similar to free-radical polymerization. Ionic polymerization consists of initiation, propagation, and termination, as well as chain transfer reactions. However, because like charges repel, there is little bimolecular termination that involves two growing chains. Ionic polymerization processes normally require high purification and low operation temperature to eliminate side reactions for high-molecular-weight products. They also have high polymerization rates and are very sensitive to the types of solvents used.

4.32.4.1 Cationic Polymerization

The type of monomers suitable for cationic polymerization are those containing an electron-donating substituent such as 1,1-dialkyl, alkene, alkoxy, and phenyl that stabilize the propagating cationic centers. Successful industrial examples include polyisobutylene and its copolymers with dienes such as butyl rubber. In ionic polymerization, initiator is conventionally called a catalyst. However, by definition, catalyst and initiator are two different types of reagents. Catalyst takes part in reactions but can be removed from the final product if necessary. On the other side, initiator molecules or their fragments become a part of the produced chains after polymerization. In cationic polymerization, a single catalyst is not sufficient and a cocatalyst is required. Typical catalysts are Lewis acids such as BF_3, $AlCl_3$, and $TiCl_4$ that must be used with a protonic cocatalyst such as H_2O and methanol:[17,101,102]

$$BF_3 + H_2O \overset{K_{eq}}{\longleftrightarrow} H^+ + BF_3OH^- \quad [82]$$

A total dissociation of the catalyst system is rare. There exists an equilibrium:

$$[H^+B^-] = K_{eq}[LA][H_2O] \quad [83]$$

where K_{eq} is the equilibrium constant, LA is Lewis acid, and B^- represents BF_3OH^- or counterion in general. The amount of cocatalyst added is critical. An optimum level is one that it is sufficient to shift equilibrium to promote H^+ formation, but not excessive to the point of terminating chains prematurely via chain transfer reactions. The optimum catalyst/cocatalyst ratio varies with the system employed and the solvent used. The electron-donating substituent R on M helps to stabilize the cationic center:

$$H^+B^- + M \xrightarrow{k_i} P_1^+B^- \quad [84]$$

where k_i is the initiation rate constant. The separation of the ion pairs depends on the reaction medium, particularly the type of solvent used. Free ions make monomer insertion easy and thus a high propagation rate constant k_p is possible:

$$P_r^+ + M \xrightarrow{k_p} P_{r+1}^+B^- \quad [85]$$

Chain transfer reactions are far more important for cationic polymerization. Propagating chains can be terminated by reactions of the cationic centers with cocatalyst or other protonic sources

$$P_r^+B^- + H_2O \xrightarrow{k_t} P_r + HB \quad [86]$$

or by chain transfer to monomer

$$P_r^+B^- + M \xrightarrow{k_{fM}} P_r + M^+B^- \quad [87]$$

The rate of initiation is

$$R_i = k_i[H^+B^-][M] = k_iK_{eq}[LA][H_2O][M] \quad [88]$$

and the rate of termination is

$$R_t = k_t[P^+][H_2O] \quad [89]$$

where $[P^+] = \sum_{n=1}^{\infty}[P_n^+B^-]$. If an SSH can be assumed, the total cationic center concentration $[P^+] = (k_iK_{eq}/k_t)[LA][M]$. The rate of polymerization is then

$$R_p = k_p[P^+][M] = (k_pk_iK_{eq}/k_t)[LA][M]^2 \quad [90]$$

and the number-average chain length is

$$\bar{r}_N = R_p/R_t = k_p[M]/(k_t[H_2O]) \quad [91]$$

Equation [90] shows that the rate of polymerization is proportional to the Lewis acid concentration and the square of monomer concentration but is not affected by H_2O concentration. This is sharply different from free-radical polymerization, $R_p \sim [I]^{1/2}[M]$. Equation [91] shows that the polymer chain length is proportional to monomer concentration and inversely proportional to H_2O concentration but no influence from Lewis acid as catalyst or initiator. This is also in contrast to free-radical process, where $\bar{r}_p \sim [I]^{-1/2}[M]$. In the cationic polymerization catalyzed by Lewis acid, the amount of protonic cocatalyst must be optimized. An adequate level is needed to initiate the polymerization, but an excess amount yields a low-molecular-weight polymer product.

The MWD functions for the polymers resulting from cationic polymerization can be easily derived based on the following mass balance equations for cationic propagating and dead chains:

$$\frac{d[P_r^+]}{dt} = k_p[M][P_{r-1}^+] - (k_p[M] + k_t[H_2O] + k_{fM}[M])[P_r^+] \quad [92]$$

$$\frac{d[P_r]}{dt} = (k_t[H_2O] + k_{fM}[M])[P_r^+] \quad [93]$$

Applying the SSH to eqn [92], we obtain the number-fraction chain length distribution for the cationic chains, $n^+(r) = [P_r^+]/[P^+] \approx \exp(-\tau r)$. Substituting this function into eqn [93] gives the weight-fraction chain length distribution of the total polymer:

$$w(r) = \tau^2 r \exp(-\tau r) \quad [94]$$

where

$$\tau = \frac{k_t[P^+]}{k_p[M]} + \frac{k_{fM}}{k_p} \quad [95]$$

Equation [94] is a random distribution or Flory's most probable distribution with polydispersity equal to 2. It is the same as in free-radical polymerization in the absence of termination by combination and as in condensation polymerization at high monomer conversions $x \to 1$.

It should be pointed out that cationic centers are very active and sensitive to polar impurities and that the SSH for the cationic concentration can be easily violated. Unexpected side reactions impose great challenges to quantitative analysis or modeling of cationic polymerization processes. The above equations should not be generalized as those in free-radical polymerization.

4.32.4.2 Anionic Polymerization

Anionic polymerization requires a type of monomer that contains an electron-withdrawing substituent such as phenyl, carboxyl, nitrile, and diene. Successful industrial examples are some styrenic products such as styrene–butadiene rubber (SBR) and styrene–butadiene–styrene (SBS) thermoplastic elastomer resins. Commonly used industrial catalysts are ethyl lithium (C_2H_5Li) and sodium naphthalide ($C_{10}H_8Na$), which quickly dissolves and dissociates in a proper solvent. The primary anion R^- reacts with monomer and initiates chain growth through successive propagation steps:

$$RMe \xrightarrow{k_d} R^-Me^+ \xrightarrow{k_{i,+M}} P_1^-Me^+ \xrightarrow{k_{p,+(r-1)M}} P_r^-Me^+ \quad [96]$$

where P_r^- is the anionic propagating chain and Me^+ is the metal cation. The mode of monomer addition to anionic centers depends on the distance between the centers and their counterions. The centers can be free anions if completely solvated and ion pairs if partially solvated. There exists an equilibrium:

$$(P_r^-Me^+) \overset{K_{eq}}{\longleftrightarrow} P_r^- + Me^+ \quad [97]$$

Reaction medium and counterion type have large effects on the rate of polymerization. The propagation rate constants of free ions k_p^- are at the level of $10^4\,l\,mol^{-1}\,s^{-1}$, while those of ion pairs $k_p^{\pm}$ are at $10^2\,l\,mol^{-1}\,s^{-1}$. Table 1 shows the effect of

Table 1 Propagation rate constants of free ions and ion pairs in anionic polymerization of styrene in THF at 25 °C.[103]

Counterion	$k_p^{\pm}$ ($l\,mol^{-1}\,s^{-1}$)	k_p^- ($l\,mol^{-1}\,s^{-1}$)	$K_{eq} \times 10^7$ ($mol\,l^{-1}$)
Li^+	160	6.5×10^4	2.2
Na^+	80	6.5×10^4	1.5
K^+	60–80	6.5×10^4	0.8
Rb^+	50–80	6.5×10^4	0.1
Cs^+	22	6.5×10^4	0.02

counterion on the propagation rate constants in the anionic polymerization of styrene in tetrahydrofuran (THF) at 25 °C.

While the free anion k_p^- remains the same with different counterions, the ion pair $k_p^{\pm}$ decreases significantly with the size of the metal cation. The equilibrium constant K_{eq} is also a strong function of the metal type with two orders of magnitude decrease from Li^+ to Cs^+. It is noted that K_{eq} have small values and the equilibria are in favor of ion pair formation. Most ions are thus in pairs. Take the system initiated by $10^{-3}\,mol\,l^{-1}$ sodium naphthalene as an example. Only about 1% of the ions, $1.2 \times 10^{-5}\,mol\,l^{-1}$, are free ions. However, it is this small percentage of free ions that consume the majority of monomer, $k_p^-[P^-]/k_p^{\pm}[P^{\pm}] \sim 10$. The rate of polymerization is

$$R_p = k_p^-[P^-][M] + k_p^{\pm}[P^{\pm}][M] \approx k_p^-[P^-][M] = \frac{1}{2}k_p^- K_{eq}[M](\sqrt{1+4[I]}-1) \approx k_p^- K_{eq}[I][M] \quad [98]$$

where [I] is the initial catalyst concentration. The free ion association and ion pair dissociation reactions are very fast and thus for individual chains, some segments are formed by free ions and others by ion pairs.

4.32.4.3 Living Anionic Polymerization

Like cationic polymerization, anionic polymerization also experiences various termination and chain transfer reactions such as hydride transfer and those to trace amounts of impurities such as O_2, CO_2, and H_2O. However, under appropriate conditions, these side reactions can be minimized or even eliminated. Such systems are termed as living anionic polymerization, first demonstrated by Szwarc in 1956.[104,105] The characteristics of living anionic polymerization include constant active center concentration and linear increase in polymer molecular weight during polymerization, complete monomer consumption, final product having molecular weight equal to $m_w \times [M]_0/[I]_0$ (m_w is monomer molecular weight), narrow MWD, chain extension with further monomer addition, and quantitative chain-end functionalization. Living anionic polymerization is particularly important for synthesis of block copolymers such as SBS thermoplastic elastomer.

Polymers produced by living anionic polymerization have Poisson distribution of molecular weight, which can be derived as follows. With instantaneous initiation, $[P_1^-] = [I]_0$ at $t = 0$. In the absence of termination and chain transfer reactions

$$\frac{d[P_1^-]}{dt} = -k_p[M][P_1^-] \quad [99]$$

$$\frac{d[P_r^-]}{dt} = k_p[M][P_{r-1}^-] - k_p[M][P_r^-] \quad [100]$$

where $r \geq 2, 3, \ldots$. Solving the above equations with the initial conditions $[P_r^-] = 0$ at $t = 0$ gives

$$n(r) = \frac{[P_r^-]}{[I]_0} = \frac{(\bar{r}_N)^r}{r!}\exp(-\bar{r}_N) \quad [101]$$

where the number-average chain length $\bar{r}_N = [M]_0/[I]_0$. Equation [101] is the Poisson distribution, which is very narrow and has polydispersity equal to $PD = 1 + (\bar{r}_N)^{-1}$. For high-molecular-weight polymers, PD approaches to unity. In practice, some broadening in the MWD is inevitable due to impurities and slow initiation.

4.32.5 Controlled Radical Polymerization

Since Szwarc's discovery of living anionic polymerization, there have been many developments in living polymerization processes over the past half a century. As of now, almost every type of polymerization has been made 'living' under appropriate conditions including living cationic polymerization, living ring-opening metathesis polymerization, living group-transfer polymerization, living Ziegler–Natta polymerization, and living free-radical polymerization. These living polymerization processes allow for the preparation of various polymers with narrow MWDs. Condensation polymerization is living by nature although it does not produce narrow MWD polymers. Compared to other types of polymerization, free-radical polymerization has clear advantages in its versatility of monomer types, mild reaction conditions, and ease in industrial implementation. However, due to the extreme active nature of free radicals, it is challenging to eliminate radical termination and to slow down monomer propagation. The strategy behind achieving 'livingness' in a free-radical system is to temporarily and frequently shield propagating radical centers from termination and other side reactions while allowing monomer insertions.[106] Currently, there is no truly living radical polymerization process. Some widely accepted alternative names are controlled radical polymerization or controlled/'living' radical polymerization.

Currently, there are several different controlled radical polymerization processes that have been developed. What makes free-radical polymerization living or controlled is the introduction of a reversible activation/deactivation process:

$$P^X \underset{k_{de}}{\overset{K_{eq}=k_{ac}/k_{de}}{\rightleftharpoons}} P^{\bullet} + X \quad [102]$$

Radical sources are typically from thermal activation of chemical initiators and propagate with monomers to be converted to polymer radicals $P^{\bullet}$, which can be deactivated by X to become dormant P^X. Here X acts as a mediator or a radical capping agent. This reversible activation/deactivation cycle is the key that minimizes radical termination and slows down propagation. The equilibrium is much in favor of the deactivation direction with very small ratios of $[P^{\bullet}]/[P^X]$. Radical species spend most of the time in their dormant state. The time interval between activation and deactivation is in the range of milliseconds, compared to seconds in conventional free-radical polymerization. In such a short lifetime, radical termination and transfer reactions are effectively suppressed, though not

totally eliminated. Individual chains grow in an on–off manner following the repeated activation and deactivation cycles. Due to the highly rapid and frequent on–off actions and few monomer molecules added in each cycle, all chains have virtually the same chance to grow. As a result, the radical centers are protected and molecular weight of the polymer continuously increases during polymerization. The final polymer product has a narrow MWD.

Among the developed controlled radical polymerization processes, stable free-radical polymerization (SFRP, also called nitroxide-mediated polymerization (NMP)),[107,108] atom transfer radical polymerization (ATRP),[109–112] and reversible addition–fragmentation chain transfer (RAFT) radical polymerization[113] are the most successful. **Figure 9** shows a typical example of their conversion versus time and molecular weight and polydispersity versus conversion curves. In literatures, these controlled radical polymerization systems are usually demonstrated by the following three sets of experimental data: (1) linear $-\ln(1-x) \sim t$, (2) linear $\bar{M}_N \sim x$, and (3) low polydispersity. The conversion–time relationship is based on the assumption that radical concentration remains unchanged during polymerization and thus integration of the rate equation $-dx/dt = k_p[P^\bullet](1-x)$ gives $-\ln(1-x) = k_p[P^\bullet]t$. The linear increase in number-average molecular weight with conversion comes from $\bar{M}_N = ([M]_0 - [M])/[I]_0 = m_w[M]_0 x/[I]_0$ and the low polydispersity is expected from a Poisson distribution $PD = 1 + 1/\bar{r}_N$. All of these relationships are analogous to living anionic polymerization because they satisfy the criteria of instantaneous chain initiation and absence of chain termination and transfer reactions. Unfortunately, this criterion is not strictly satisfied in controlled radical polymerization. Accurate correlations of kinetic data must resort to more detailed modeling.[114–122]

4.32.5.1 Stable Free-Radical Polymerization

SFRP is particularly suitable for styrene polymerization. Its elementary reactions are the same as in the conventional free-radical polymerization. All the reactions of eqns [18]–[25] can possibly occur. Peroxides are often used as the initiator. In addition, nitroxide is added as the mediator. The nitroxide molecule bears a stable free-radical center that can temporarily stabilize the propagating radical as[107,108,124–128]

$$P_r^X \overset{K_{eq}=k_{ac}/k_{de}}{\rightleftharpoons} P_r^\bullet + X \qquad [103]$$

where k_{ac} and k_{de} are activation and deactivation rate constants, respectively. An ideal living polymerization produces polymer chains having a Poisson distribution with polydispersity close to one. The molecular weight is therefore determined by the ratio of monomer concentration to that of initiator. The key requirement for an ideal SFRP process is a rapid initiation of

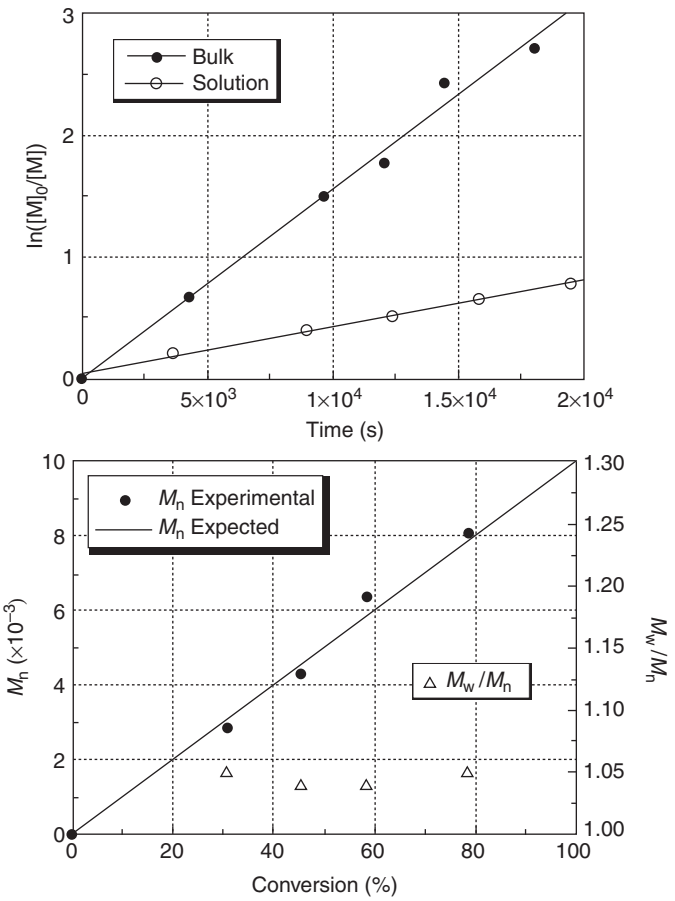

Figure 9 Monomer conversion versus time and polymer molecular weight and polydispersity versus conversion of the bulk and solution ATRPs of styrene at 110 °C. Bulk: 1 mol.% initiator 1-PEBr and catalyst CuBr/2 × dNbipy based on styrene. Solution: 50% (v/v) solution in diphenyl ether.[123]

primary radicals and a fast dynamic equilibrium between the active and dormant species. Unlike ionic polymerization where the initiation step is instantaneous through initiator dissolution, the initiation via the chemical initiator thermal decomposition can be rather slow. This slow initiation and side reactions of radical termination and transfer can give rise to broad MWDs.

A full MWD function that takes into account the slow initiation and various side reactions is yet to be developed. However, the average molecular weights can easily be obtained from mass balances.[115] For the radical chain species, eqn [55] becomes

$$\frac{d[P_r^\bullet]}{dt} = k_p[M][P_{r-1}^\bullet] + k_{ac}[P_r^X] - (k_p[M] + k_{de}[X] + k_t[P^\bullet] + k_{fZ}[Z])[P_r^\bullet] \quad [104]$$

For the dead chains, eqn [60] becomes

$$\frac{d[P_r]}{dt} = k_{td}[P^\bullet][P_r^\bullet] + k_{fZ}[Z][P_r^\bullet] + \frac{1}{2}k_{tc}\sum_{s=1}^{r-1}[P_s^\bullet][P_{r-s}^\bullet] \quad [105]$$

However, in an ideal SFRP, the dead chains P_r must be minimized and the dormant chains P_r^X should dominate:

$$\frac{d[P_r^X]}{dt} = k_{de}[X][P_r^\bullet] - k_{ac}[P_r^X] \quad [106]$$

On account of the activation and deactivation terms involved in the radical balances, eqn [104] is not a simple function as eqn [55] that gives the radical chain length distribution equation [58] by applying the SSH. We therefore resort to the use of the method of moments for average polymer chain properties. In addition to the radical and dead-chain moments defined by eqns [73] and [74], the dormant chain moments are

$$Q_i^X = \sum_{r=1}^{\infty} r^i[P_r^X] \quad [107]$$

The zeroth, first, and second moment equations can be easily derived from eqns [104]–[106]:

$$\frac{dQ_0^\bullet}{dt} = 2fk_d[I] - k_tQ_0^\bullet Q_0^\bullet + k_{ac}Q_0^X - k_{de}[X]Q_0^\bullet + k_{iZ}[Z^\bullet][M] - k_{fZ}[Z]Q_0^\bullet \quad [108]$$

$$\frac{dQ_0}{dt} = k_{td}Q_0^\bullet Q_0^\bullet + k_{fZ}[Z]Q_0^\bullet + \frac{1}{2}k_{tc}Q_0^\bullet Q_0^\bullet \quad [109]$$

$$\frac{dQ_0^X}{dt} = k_{de}[X]Q_0^\bullet - k_{ac}Q_0^X \quad [110]$$

$$\frac{dQ_1^\bullet}{dt} = k_p[M]Q_0^\bullet + k_{ac}Q_1^X - k_{de}[X]Q_1^\bullet - k_tQ_0^\bullet Q_1^\bullet - k_{fZ}[Z]Q_1^\bullet \quad [111]$$

$$\frac{dQ_1}{dt} = k_tQ_0^\bullet Q_1^\bullet + k_{fZ}[Z]Q_1^\bullet \quad [112]$$

$$\frac{dQ_1^X}{dt} = k_{de}[X]Q_1^\bullet - k_{ac}Q_1^X \quad [113]$$

$$\frac{dQ_2^\bullet}{dt} = k_p[M]Q_0^\bullet + 2k_p[M]Q_1^\bullet + k_{ac}Q_2^X - k_{de}[X]Q_2^\bullet - k_tQ_0^\bullet Q_2^\bullet - k_{fZ}[Z]Q_2^\bullet \quad [114]$$

$$\frac{dQ_2}{dt} = k_tQ_0^\bullet Q_2^\bullet + k_{fZ}[Z]Q_2^\bullet + k_{tc}Q_1^\bullet Q_1^\bullet \quad [115]$$

$$\frac{dQ_2^X}{dt} = k_{de}[X]Q_2^\bullet - k_{ac}Q_2^X \quad [116]$$

where the radical moments $Q_i^\bullet$ are much smaller than those of dormant and dead chains of the same order i (Q_i^X, Q_i). For successful SFRP, dead chain Q_i should also be smaller than dormant Q_i^X. The chain transfer agent Z follows the decay of

$$\frac{d[Z]}{dt} = -k_{fZ}[Z]Q_0^\bullet \quad [117]$$

while its radical species $Z^\bullet$ follows the decay of

$$\frac{d[Z^\bullet]}{dt} = k_{fZ}[Z]Q_0^\bullet - k_{iZ}[M][Z^\bullet] \quad [118]$$

If the SSH applies, the $k_{iZ}[M][Z^\bullet]$ term in eqn [108] can be replaced by $k_{fZ}[Z]Q_0^\bullet$. Equations [108]–[117] can be solved together with eqn [26], as well as the conservations of $Q_0^X + [X] = [X]_0$ and $Q_1^\bullet + Q_1^X + Q_1 + [M] = [M]_0$, given the initial concentrations of initiator $[I]_0$, stable free radical (nitroxide) $[X]_0$, monomer $[M]_0$, and chain transfer agent $[Z]_0$. The monomer conversion can be calculated from

$$x = (Q_1^\bullet + Q_1^X + Q_1)/[M]_0 \quad [119]$$

the number-average chain lengths from

$$\bar{r}_N^\bullet = \frac{Q_1^\bullet}{Q_0^\bullet},\ \bar{r}_N^X = \frac{Q_1^X}{Q_0^X},\ \bar{r}_N = \frac{Q_1}{Q_0},\ \bar{r}_{N,tot} = \frac{Q_1^\bullet + Q_1^X + Q_1}{Q_0^\bullet + Q_0^X + Q_0} \quad [120]$$

the weight-average chain lengths from

$$\bar{r}_W^\bullet = \frac{Q_2^\bullet}{Q_1^\bullet},\ \bar{r}_W^X = \frac{Q_2^X}{Q_1^X},\ \bar{r}_W = \frac{Q_2}{Q_1},\ \bar{r}_{W,tot} = \frac{Q_2^\bullet + Q_2^X + Q_2}{Q_1^\bullet + Q_1^X + Q_1} \quad [121]$$

and the respective polydispersities from the above number- and weight-average chain lengths.

4.32.5.2 Atom Transfer Radical Polymerization

ATRP is a catalyst-mediated process. It is versatile in the monomer type. Various acrylic and styrenic monomers have been successfully polymerized.[108,129–132] Initiators are normally alkyl halides. Propagating radicals $P^\bullet$ are generated through reversible redox process catalyzed by transition metal complex C (= Mt^n–Y/ligand, e.g., Cu^ICl ligated by bipyridines and multidentate amines), which undergoes one-electron oxidation and abstracts halogen atom X from dormant species P^X. The catalyst forms high-oxidation-state transition metal complex C^X (= X–Mt^{n+1}–Y/ligand). $P^\bullet$ can react with C^X and resume to P^X:

$$P_r^X + C \underset{}{\overset{K_{eq}=k_{ac}/k_{de}}{\rightleftharpoons}} P_r^\bullet + C^X \quad [122]$$

The molar concentrations of various species change with time and obey the following mass balance equations:

$$\frac{d[P_r^\bullet]}{dt} = k_p[P_{r-1}^\bullet][M] + k_{ac}[P_r^X][C] - (k_p[M] + k_{de}[C^X] + k_tQ_0^\bullet + k_{fZ}[Z])[P_r^\bullet] \quad [123]$$

$$\frac{d[P_r]}{dt} = k_{td}Q_0^\bullet[P_r^\bullet] + k_{fZ}[Z][P_r^\bullet] + \frac{1}{2}k_{tc}\sum_{s=1}^{r-1}[P_s^\bullet][P_{r-s}^\bullet] \quad [124]$$

$$\frac{d[P_r^X]}{dt} = k_{de}[P_r^\bullet][C^X] - k_{ac}[C][P_r^X] \quad [125]$$

With the moments defined by eqns [73], [74], and [107], the equations of moments corresponding to eqns [123]–[125] are as follows:[114]

$$\frac{dQ_0^\bullet}{dt} = k_{ac}[C]Q_0^X - k_{de}[C^X]Q_0^\bullet - k_t Q_0^\bullet Q_0^\bullet + k_{iZ}[Z^\bullet][M] - k_{fZ}[Z]Q_0^\bullet \quad [126]$$

$$\frac{dQ_0}{dt} = k_{td}Q_0^\bullet Q_0^\bullet + k_{fZ}[Z]Q_0^\bullet + \frac{1}{2}k_{tc}Q_0^\bullet Q_0^\bullet \quad [127]$$

$$\frac{dQ_0^X}{dt} = k_{de}[C^X]Q_0^\bullet - k_{ac}[C]Q_0^X \quad [128]$$

$$\frac{dQ_1^\bullet}{dt} = k_p[M]Q_0^\bullet + k_{ac}[C]Q_1^X - k_{de}[C^X]Q_1^\bullet - k_t Q_0^\bullet Q_1^\bullet - k_{fZ}[Z]Q_1^\bullet \quad [129]$$

$$\frac{dQ_1}{dt} = k_t Q_0^\bullet Q_1^\bullet + k_{fZ}[Z]Q_1^\bullet \quad [130]$$

$$\frac{dQ_1^X}{dt} = k_{de}[C^X]Q_1^\bullet - k_{ac}[C]Q_1^X \quad [131]$$

$$\frac{dQ_2^\bullet}{dt} = k_p[M]Q_0^\bullet + 2k_p[M]Q_1^\bullet + k_{ac}[C]Q_2^X - k_{de}[C^X]Q_2^\bullet - k_t Q_0^\bullet Q_2^\bullet - k_{fZ}[Z]Q_2^\bullet \quad [132]$$

$$\frac{dQ_2}{dt} = k_t Q_0^\bullet Q_2^\bullet + k_{fZ}[Z]Q_2^\bullet + k_{tc}Q_1^\bullet Q_1^\bullet \quad [133]$$

$$\frac{dQ_2^X}{dt} = k_{de}[C^X]Q_2^\bullet - k_{ac}[C]Q_2^X \quad [134]$$

Equations [126]–[134] can be solved together with eqns [117] and [118], as well as the conservations of $[C^X] + [C] = [C]_0$, $Q_0^X + [C^X] = [RX]_0$, and $Q_1^\bullet + Q_1^X + Q_1 + [M] = [M]_0$, given the initial concentrations of catalyst $[C]_0$, initiator $[RX]_0$ (i.e., initial Q_0^X value at $t = 0$), monomer $[M]_0$, and chain transfer agent $[Z]_0$. The monomer conversion and the average lengths of the various types of chains can be calculated from eqns [119]–[121].

4.32.5.3 Reversible Addition–Fragmentation Chain Transfer Radical Polymerization

RAFT polymerization process uses dithioester as the mediator. Propagating radical reacts with the dithio compound and becomes adduct radical that is not active for monomer propagation. This is an addition reaction that is equivalent to radical deactivation. The adduct radical is not stable and undergoes β-scission in either direction to generate a propagating radical, which is a fragmentation reaction.[113,133–135] These addition and fragmentation reactions are frequent and reversible:

$$P_r^\bullet + P_s^X \xrightarrow{k_{de}} \hat{P}_{r,s} \xrightarrow{k_{ac}} P_r^X + P_s^\bullet \quad [135]$$

where k_{de} and k_{ac} are addition and fragmentation rate constants, respectively. $P_r^\bullet$, P_s^X, and $\hat{P}_{r,s}$ are radical, adduct, and dormant chains, respectively. In addition to eqns [73], [74] and [107], the corresponding moments of adduct chains are defined as[119,122]

$$\hat{Q}_{i,j} = \sum_{r=1}^{\infty}\sum_{s=1}^{\infty} r^i s^j [\hat{P}_{r,s}] \quad [136]$$

$$\hat{Q}_i = \frac{1}{2}\sum_{r=2}^{\infty}\sum_{s=1}^{r-1} r^i [\hat{P}_{r-s,s}] = \frac{1}{2}\sum_{j=0}^{i}\binom{i}{j}\sum_{r=1}^{\infty}\sum_{s=1}^{\infty} r^{i-j}s^j[\hat{P}_{r,s}] = \frac{1}{2}\sum_{j=0}^{i}\binom{i}{j}\hat{Q}_{i-j,j} \quad [137]$$

From eqn [137], we have $\hat{Q}_0 = \hat{Q}_{0,0}/2$, $\hat{Q}_1 = \hat{Q}_{1,0}$, and $\hat{Q}_2 = \hat{Q}_{2,0} + \hat{Q}_{1,1}$. The mass balances for the four types of chain species (radical, adduct, dormant, and dead) are

$$\frac{d[P_r^\bullet]}{dt} = k_p[P_{r-1}^\bullet][M] + \frac{1}{2}k_{ac}\sum_{s=1}^{\infty}[\hat{P}_{r,s}] - (k_p[M] + k_{de}Q_0^X + k_t Q_0^\bullet + k_{fZ}[Z])[P_r^\bullet] \quad [138]$$

$$\frac{d[P_r]}{dt} = k_{td}Q_0^\bullet[P_r^\bullet] + k_{fZ}[Z][P_r^\bullet] + \frac{1}{2}k_{tc}\sum_{s=1}^{r-1}[P_s^\bullet][P_{r-s}^\bullet] \quad [139]$$

$$\frac{d[P_r^X]}{dt} = \frac{1}{2}k_{ac}\sum_{s=1}^{\infty}[\hat{P}_{r,s}] - k_{de}Q_0^\bullet[P_r^X] \quad [140]$$

$$\frac{d[\hat{P}_{r,s}]}{dt} = k_{de}[P_r^\bullet][P_s^X] + k_{de}[P_s^\bullet][P_r^X] - k_{ac}[\hat{P}_{r,s}] \quad [141]$$

After some lengthy but straightforward algebra, the following moment equations are obtained. The zeroth moments (i.e., the concentrations of the four types of chains) are

$$\frac{dQ_0^\bullet}{dt} = 2fk_d[I] - k_t Q_0^\bullet Q_0^\bullet + k_{ac}\hat{Q}_0 - k_{de}Q_0^\bullet Q_0^X + k_{iZ}[M][Z^\bullet] - k_{fZ}[Z]Q_0^\bullet \quad [142]$$

$$\frac{dQ_0}{dt} = k_{td}Q_0^\bullet Q_0^\bullet + k_{fZ}[Z]Q_0^\bullet + \frac{k_{tc}}{2}Q_0^\bullet Q_0^\bullet \quad [143]$$

$$\frac{dQ_0^X}{dt} = k_{ac}\hat{Q}_0 - k_{de}Q_0^\bullet Q_0^X \quad [144]$$

$$\frac{d\hat{Q}_0}{dt} = k_{de}Q_0^\bullet Q_0^X - k_{ac}\hat{Q}_0 \quad [145]$$

The first moments (i.e., the concentrations of monomer units incorporated into the four types of chains) are

$$\frac{dQ_1^\bullet}{dt} = k_p[M]Q_0^\bullet + \frac{1}{2}k_{ac}\hat{Q}_1 - k_{de}Q_0^X Q_1^\bullet - k_t Q_0^\bullet Q_1^\bullet - k_{fZ}[Z]Q_1^\bullet \quad [146]$$

$$\frac{dQ_1}{dt} = k_t Q_0^\bullet Q_1^\bullet + k_{fZ}[Z]Q_1^\bullet \quad [147]$$

$$\frac{dQ_1^X}{dt} = \frac{1}{2}k_{ac}\hat{Q}_1 - k_{de}Q_0^\bullet Q_1^X \quad [148]$$

$$\frac{d\hat{Q}_1}{dt} = k_{de}Q_1^\bullet Q_0^X + k_{de}Q_0^\bullet Q_1^X - k_{ac}\hat{Q}_1 \quad [149]$$

The second moments are

$$\frac{dQ_2^\bullet}{dt} = k_p[M]Q_0^\bullet + 2k_p[M]Q_1^\bullet + \frac{1}{2}k_{ac}\hat{Q}_{2,0} - k_{de}Q_2^\bullet Q_0^X - k_t Q_0^\bullet Q_2^\bullet - k_{fZ}[Z]Q_2^\bullet \quad [150]$$

$$\frac{dQ_2}{dt} = k_t Q_0^\bullet Q_2^\bullet + k_{fZ}[Z]Q_2^\bullet + k_{tc}Q_1^\bullet Q_1^\bullet \quad [151]$$

$$\frac{dQ_2^X}{dt} = \frac{1}{2}k_{ac}\hat{Q}_{2,0} - k_{de}Q_0^\bullet Q_2^X \quad [152]$$

$$\frac{d\hat{Q}_2}{dt} = k_{de}Q_2^{\bullet}Q_0^{X} + 2k_{de}Q_1^{\bullet}Q_1^{X} + k_{de}Q_0^{\bullet}Q_2^{X} - k_{ac}\hat{Q}_2 \qquad [153]$$

Since eqns [150] and [153] involve $\hat{Q}_{2,0}$, the following equation is required for closure:

$$\frac{d\hat{Q}_{2,0}}{dt} = k_{de}Q_2^{\bullet}Q_0^{X} + k_{de}Q_0^{\bullet}Q_2^{X} - k_{ac}\hat{Q}_{2,0} \qquad [154]$$

Equations [142]–[154] can be solved together with eqns [26], [117], and [118], as well as the conservations of $Q_0^X + \hat{Q}_0 = [\text{RAFT}]_0$ and $Q_1^{\bullet} + \hat{Q}_1 + Q_1^X + Q_1 + [M] = [M]_0$, given the initial concentrations of initiator $[I]_0$, RAFT agent $[\text{RAFT}]_0$ (i.e., the Q_0^X value at $t = 0$), monomer $[M]_0$, and chain transfer agent $[Z]_0$. The monomer conversion can be calculated from

$$x = (Q_1^{\bullet} + \hat{Q}_1 + Q_1^X + Q_1)/[M]_0 \qquad [155]$$

the number-average chain lengths from

$$\bar{r}_N^{\bullet} = \frac{Q_1^{\bullet}}{Q_0^{\bullet}},\ \bar{r}_N = \frac{\hat{Q}_1}{\hat{Q}_0},\ \bar{r}_N^X = \frac{Q_1^X}{Q_0^X},\ \bar{r}_N = \frac{Q_1}{Q_0},$$
$$\bar{r}_{N,tot} = \frac{Q_1^{\bullet} + \hat{Q}1 + Q_1^X + Q_1}{Q_0^{\bullet} + \hat{Q}_0 + Q_0^X + Q_0} \qquad [156]$$

the weight-average chain lengths from

$$\bar{r}_W^{\bullet} = \frac{Q_2^{\bullet}}{Q_1^{\bullet}},\ \bar{r}_W = \frac{\hat{Q}_2}{\hat{Q}_1},\ \bar{r}_W^X = \frac{Q_2^X}{Q_1^X},\ \bar{r}_W = \frac{Q_2}{Q_1},$$
$$\bar{r}_{W,tot} = \frac{Q_2^{\bullet} + \hat{Q}_2 + Q_2^X + Q_2}{Q_1^{\bullet} + \hat{Q}_1 + Q_1^X + Q_1} \qquad [157]$$

and the respective polydispersities from the above number- and weight-average chain lengths. It should be noted that the propagating and adduct radical chain moments $Q_i^{\bullet}$ and $\hat{Q}_i$ are much smaller than the dormant and dead chain moments Q_i^X and Q_i. A successful RAFT system should also have negligible amount of dead chains generated $Q_i < Q_i^X$. **Figure 10** shows the simulated results for the rates of various reactions, as well as the moments, average chain lengths, and polydispersities of different chain types in the RAFT polymerization.

4.32.5.4 Comparison of NMP, ATRP, and RAFT Polymerization

All three processes are very useful because of their efficiency and ease of use in a wide range of reaction types (bulk, solution, emulsion, and suspension) and their tolerance toward water and oxygen impurities. These are important advantages in industrial practice. Purification and separation are tedious and costly. ATRP and RAFT polymerization have been applied to the polymerization of a wide range of monomers (e.g., methacrylates, acrylates, styrenes, vinylpyridines, acrylonitrile, and acrylamides), while the range afforded by NMP has been more limited. NMP is best suited to styrenes and its copolymers, although new nitroxides have allowed the polymerization of methacrylates and acrylates.

While all three processes are easily carried out, the availability and the cost of the reactants required vary greatly. Nitroxides have only recently been made commercially available (Arkema SG1) and are generally expensive and difficult to synthesize. Much of the research focus in NMP has been on new efficient routes to nitroxide synthesis. RAFT agents (e.g., dithioesters) are also challenging since they are not commercially available and must be synthesized. NMP and RAFT polymerization are therefore hampered by synthesis workup time. In contrast, the reagents necessary for ATRP are widely available. Alkyl halides, ligands, and metal salts are easily procured from common suppliers.

Differences in the mediator to polymer ratio further widen the cost gap between ATRP and NMP or RAFT polymerization. In NMP, the ratio is 1:1, that is, for every polymer chain formed, one nitroxide is consumed. In RAFT polymerization, the ratio is 1:2. In its early days, ATRP also required a 1:1 ratio catalyst loading. Later, it was discovered that the 1:1 ratio was in excess. With the advent of more active catalysts being developed, metal salt amounts have been greatly reduced to parts per million (ppm) levels. This catalytic flexibility is the most attractive trait of ATRP. Polymer chains produced by controlled radical polymerization bear active chain ends. These residuals may cause difficulties in applications. Dithioesters in RAFT polymerization present a special problem as they are volatile and odiferous.

It is challenging to produce high-molecular-weight polymers from the above processes. Although there are some developments such as RAFT emulsion polymerization, controlled radical polymerization processes are generally good for low-molecular-weight specialty products. Unlike living anionic polymerization, radical termination and transfer reactions are inevitable. High monomer conversions are also difficult to achieve. Good control over molecular weight is usually before 80–90% conversions. Above 90% conversion, polydispersities increase significantly. This can be partly attributed to diffusion-controlled reactions.[118] At high conversions, mobilities of mediator molecules can be limited. Reduction in radical deactivation makes propagation steps out of control and the system behaves as conventional free-radical polymerization. Reactions that easily become diffusion controlled are those involving two chain species. In this regard, the addition reaction in RAFT polymerization is most vulnerable to increases in molecular weight and monomer conversion, and its rate constant decreases significantly.[119–121] Diffusion control easily affects fast reactions according to $1/k = 1/k_C + 1/k_D$, where k, k_C, and k_D are apparent, chemically, and diffusion-controlled rate constants, respectively. Quantitative descriptions for the effects of diffusion control on these mediation (deactivation) reactions can follow those for radical termination (eqn [50]) and monomer propagation (eqn [53]).

4.32.6 Ziegler–Natta Polymerization

Ethylene was first polymerized in 1930s by free-radical polymerization. Polyethylene chains thus made have short branches with uncontrolled chain lengths resulting from a backbiting mechanism. Because of the branch structure, the polymers contain low levels of crystallinity and thus are LDPE products that are good for film production. The free-radical process requires high temperature and high pressure. Catalysts were long sought after for lower pressure and lower temperature conditions. The discovery of Ziegler–Natta catalysts in the early 1950s and their rapid developments in the 1960s and 1970s truly revolutionized the polymer industry. Ethylene polymers produced by Ziegler–Natta catalysts are high-density

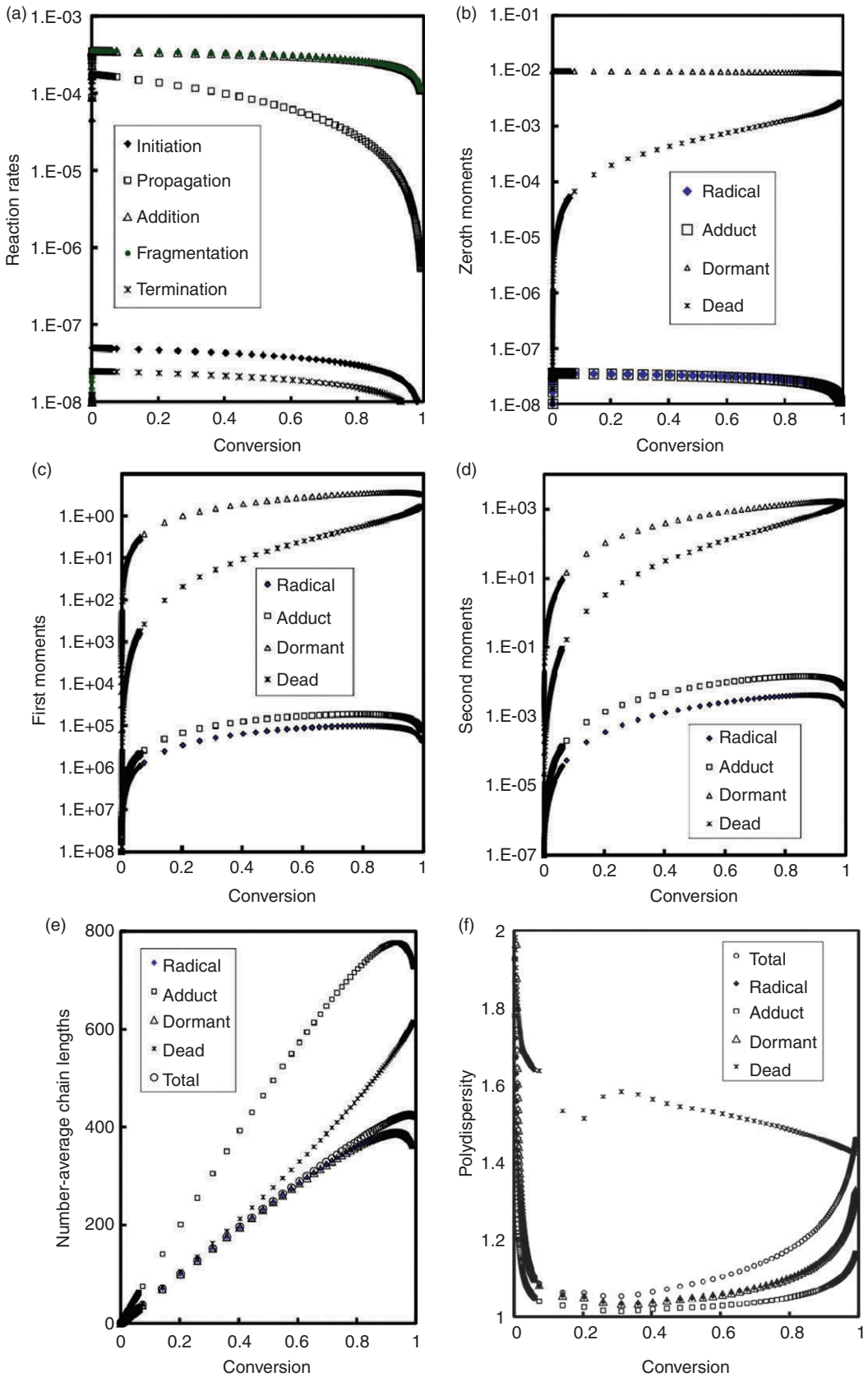

Figure 10 Simulated results of (a) the variation of reaction rates, and the development of (b) zeroth moments, (c) first moments, (d) second moments, (e) average chain lengths, and (f) polydispersities in RAFT polymerization.[136]

polyethylenes (HDPEs), which are linear chains and are easily crystallized. α-Olefin monomers such as butylene, hexene, and octene are added to ethylene to produce copolymers having well-controlled short branches. These polymers are linear low-density polyethylenes (LLDPEs).

As for propylene, Ziegler–Natta (and metallocene) polymerization is the only mechanism that can produce high-molecular-weight polypropylene (PP) products. For asymmetrical monomers like propylene, chain stereoregularity is an important factor that determines material properties. A PP chain having all meso diads with $-CH_3$ groups aligned to the same side of its backbone is an isotactic polypropylene (iPP). A chain having all racemo diads with the methyl groups alternating on each side of the backbone is a syndiotactic polypropylene (sPP). An atactic polypropylene (aPP) has the groups randomly aligned to both sides. Tactic polymers are easy to crystallize due to their chain stereoregularity and are totally different types of materials from their atactic counterparts. While iPP and sPP are good plastic materials, aPP is not as useful. Most commercial PP products are mainly iPP:

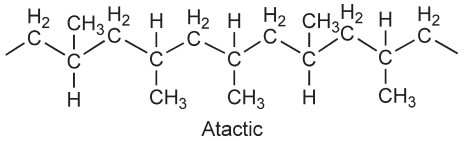
Atactic

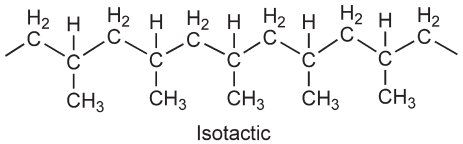
Isotactic

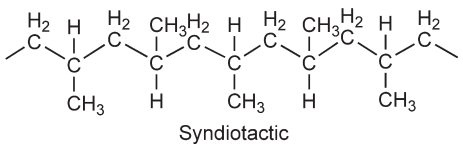
Syndiotactic

In theory, any asymmetric olefinic, as well as acrylic, styrenic, and vinylic, monomer can have tactic chain microstructures. However, it depends on the coordination power of catalysts. Free-radical polymerization processes do not have any coordination power and thus produce atactic polymers. Ionic polymerization processes have certain levels of coordination power, contributed by counterions. The counterion at the vicinity of a propagating center can coordinate the insertion of monomer molecules. Unfortunately, this coordination power is weak and yields a low degree of tacticity. As a result of the equilibrium between ion pairs and free ions, individual chains can have some tactic segments generated from the former with others atactic from the latter. In comparison, Ziegler–Natta catalysts possess strong coordination power for tactic polymer production.

4.32.6.1 Rate of Polymerization

Ziegler–Natta polymerization is heterogeneous in nature. A typical example is $TiCl_4$ supported on $MgCl_2$ packed into micropores of amorphous silica particles. The catalyst $TiCl_4$ is activated by a cocatalyst $Al(C_2H_5)_3$. An important feature of Ziegler–Natta catalysts is its multiple active site types. On each single site type, polymerization occurs in the following steps: monomer M adsorption to the active site A, propagation, and chain desorption:

$$M + A \xrightarrow{k_{as}} P_1^* \quad [158]$$

$$P_r^* + M \xrightarrow{k_p} P_{r+1}^* \quad [159]$$

$$P_r^* \xrightarrow{k_{ds}} P_r + A \quad [160]$$

where P_r^* is the growing chain with chain length r.

Invoking the SSH $k_{ds}[P^*] = k_{as}[M][A]$ and the conservation of active sites $[P^*] + [A] = [A]_0$, we have

$$[P^*] = K_s[A]_0[M]/(1 + K_s[M]) \quad [161]$$

where $K_s = k_{as}/k_{ds}$. The rate of polymerization is thus

$$R_p = -\frac{d[M]}{dt} = \frac{k_p K_s [A]_0 [M]^2}{1 + K_s[M]} \quad [162]$$

The dependence of the rate on monomer and catalyst (or initiator) concentrations (eqn [162]) is different from those of free-radical polymerization (eqn [44]), cationic polymerization (eqn [90]), and anionic polymerization (eqn [98]). Under desorption-controlled conditions, $k_{ds} << k_{as}$, $k_s[M] >> 1$, $[P^*] = K_s[A]_0[M]$, and thus $R_p = k_p[A]_0[M]$. Under adsorption control, $k_{ds} >> k_{as}$, $K_s[M] << 1$, $[P^*] = [A]_0$, and thus $R_p = k_p K_s [A]_0 [M]^2$. Ziegler–Natta polymerization processes are usually carried out in slurry or gas phase. Monomer vapors are pressurized in the reactor and their concentrations remain constant. However, the concentration of catalyst decays according to $d[A]_0/dt = -k_{de}[A]_0$, which is caused by various side reactions including impurity poisoning. Monomer molecules continuously diffuse into catalyst particles and polymerize inside them. The formed long chains hardly diffuse out from pores and fragmentation of particles results in replication of the catalyst particles.

4.32.6.2 Molecular Weight and Distribution of Polymer

The MWD function of polymer chains generated from a single site type can be derived from the following mass balances:

$$\frac{d[P_1^*]}{dt} = k_{as}[A][M] - k_p[M][P_1^*] - k_{ds}[P_1^*] \quad [163]$$

$$\frac{d[P_r^*]}{dt} = k_p[M][P_{r-1}^*] - k_p[M][P_r^*] - k_{ds}[P_r^*] \quad [164]$$

for $r \geq 2$. With the SSH applied to every $[P_r^*]$ and their sum

$$[P_1^*] = \frac{k_{as}[A][M]}{k_p[M] + k_{ds}} = \frac{k_{as}[A]}{k_p(1+\tau)} = \frac{\tau}{1+\tau}[P^*] \quad [165]$$

$$[P_r^*] = \frac{[P_{r-1}^*]}{1+\tau} = \cdots \frac{[P_1^*]}{(1+\tau)^{r-1}} = \frac{\tau'[P^*]}{(1+\tau)^r} \approx \tau[P^*]\exp(-\tau r) \quad [166]$$

where

$$\tau = \frac{k_{ds}}{k_p[M]} \quad [167]$$

The chain length distribution of active chains is thus

$$n^*(r) = \tau \exp(-\tau r) \quad [168]$$

The mass balances for dead-chain species are $d[P_r]/dt = k_{ds}[P_r^*]$. With the help of eqn [166], the MWD of the dead chains (equivalent to that of the total polymer) is obtained:

$$w(r) = \frac{d(r[P_r])dt}{k_p[P^*][M]} = \tau^2 r \exp(-\tau r) \quad [169]$$

which is the random distribution or the Flory's most probable distribution, similar to that in free-radical polymerization without combination termination, eqn [61] with $\beta = 0$, and to that in cationic polymerization, eqn [94]. The number-average chain length is $1/\tau$ with polydispersity equal to 2.

4.32.6.3 Multiple-Active-Site-Type Model

Due to multiple active site types, polymers produced by Ziegler–Natta polymerization have typical polydispersities between 4 and 20. The actual MWD is the sum of various chains generated from different site types:

$$w_{tot}(r) = \sum_i m_i w_i(r) \quad [170]$$

where m_i is the mass fraction of polymers that are generated from active site type *i*. For the same reason, the rate of polymerization is also a sum of eqn [162]:

$$R_{p,tot} = \sum_i R_{p,tot} = \sum_i k_{p,i} K_{s,i}[A]_{i,0}[M]^2/(1 + K_{s,i}[M]) \quad [171]$$

with all the rate constants and active site concentration associated with specific type of active sites, which decay as

$$d[A]_i/dt = -k_{de,i}[A]_i \quad [172]$$

Equation [170] can also be used for elucidating the number of active site types. The GPC curves of broad distributions can be deconvoluted into a series of Flory's most probable distributions.[136, 137] The mass fractions m_i are found from eqn [170] by fitting the GPC data, as shown in **Figure 11**.

4.32.7 Metallocene Polymerization

Single-site-type catalysts have been long sought for homogeneous olefin polymerization since 1950s. However, it was not until the discovery of metallocene catalysts by Walter Kaminsky in the early 1980s that significant impact on polyolefin production at an industrial scale was realized.[138–140] A representative example of metallocene catalysts is bis(cyclopentadienyl) zirconium dichloride (Cp_2ZrCl_2) activated with methylaluminoxane (MAO). These catalysts have very high activities and produce polymers having Flory's most probable distributions. Constrained geometry catalysts with monocyclopentadienyl ring such as $[C_5Me_4(SiMe_2N^tBu)]TiMe_2$ (Me, methyl; ^{t}Bu, *tert*-butyl; C_5, cyclopentadiene) activated with tris(pentafluorophenyl)boron give long-chain branched polyethylenes that have better melt strength and better shear thinning property than do their linear counterparts having the same molecular weight. Metallocenes with two cyclopentadienyl rings bridged together have good coordination power in chain stereoregularity and produce highly tactic polymers from prochiral monomers such as propylene.

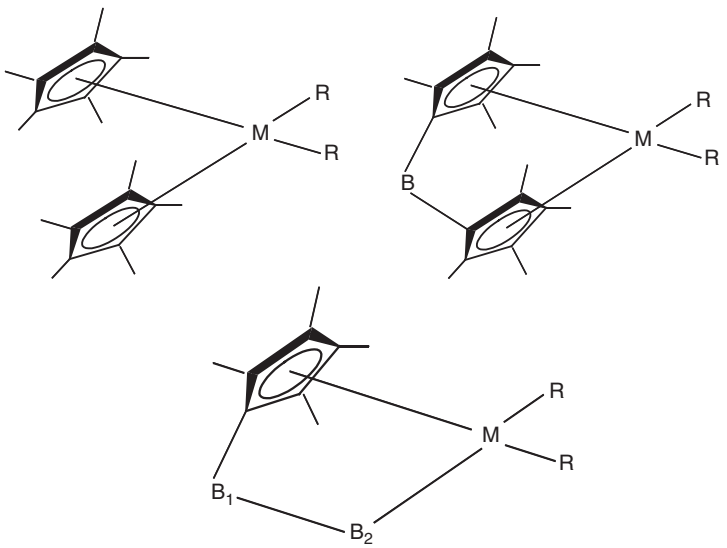

Metallocene catalysts

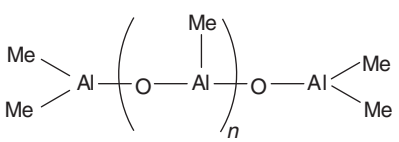

Methylaluminoxane (MAO)

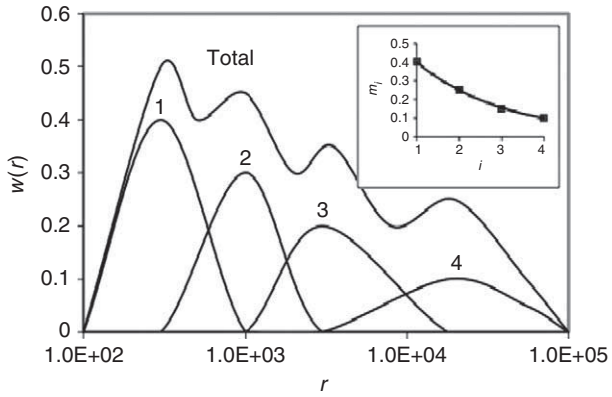

Figure 11 Deconvolution of GPC curve for multiple active site type of Ziegler–Natta catalyst.

4.32.7.1 Long-Chain Branching with Constrained Geometry Catalysts

The elementary reactions involved in metallocene polymerization include activation/reactivation, propagation, termination by β-hydride elimination, chain transfer (to hydrogen, monomer, MAO, etc.), and active site deactivation. β-Hydride elimination yields terminal double bond. These chains can act as vinyl macromonomers in further polymerization. Active centers of most metallocene catalysts have closed structures and are not accessible for macromonomers with high molecular weight. However, constrained geometry-type catalysts have rather open active centers and give reasonably high reactivities for incorporating high-molecular-weight macromonomers. Propagation with the macromonomers generated *in situ* from β-hydride elimination leads to long-chain branching. Such branched polymers have dendritic structures.[141–143]

Long-chain branched polymers have higher melt strength and better shear thinning than do their linear counterparts of the same molecular weight as shown in **Figure 12(a)**.[144] These polyethylene samples are prepared from high-temperature solution polymerization in a continuous stirred-tank reactor (CSTR) with constrained geometry catalyst (CGC) catalyst. The branching densities are at a level of several branches per 100 000 carbons, as evident from the nuclear magnetic resonance (NMR) spectrum in **Figure 12(b)**.[145–147]

The elementary reactions involved in this polymerization with branching are

$$\text{Activation/reactivation} \quad A + M \xrightarrow{k_{ac}} P^*_{1,0} \qquad [173]$$

$$\text{Propagation} \quad P^*_{r,m} + M \xrightarrow{k_p} P^*_{r+1,m} \qquad [174]$$

$$\beta\text{-Hydride elimination} \quad P^*_{r,m} \xrightarrow{k_\beta} P^=_{r,m} + A \qquad [175]$$

$$\text{Chain transfer} \quad P^*_{r,m} + Z \xrightarrow{k_{fZ}} P_{r,m} + A \qquad [176]$$

$$\text{Deactivation} \quad P^*_{r,m} \xrightarrow{k_{de}} P_{r,m} \qquad [177]$$

$$\text{Long-chain branching} \quad P^*_{r,m} + P^=_{s,n} \xrightarrow{k_{br}} P^*_{r+s,m+n+1} \qquad [178]$$

where $P^*_{r,m}$, $P^=_{r,m}$, and $P_{r,m}$ are propagating, macromonomer, and dead chains having chain length r and branch number m. Their respective moments are defined as

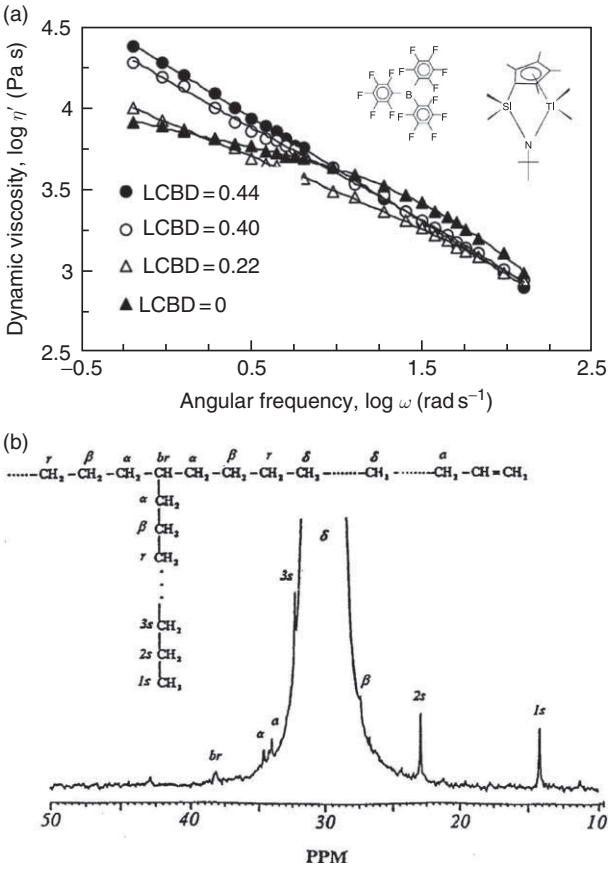

Figure 12 (a) Shear thinning and (b) NMR spectrum of polyethylene produced from solution polymerization with CGC catalyst in a CSTR.[144,145]

$$Q^*_0 = \sum_{r=1}^{\infty}\sum_{m=0}^{\infty} P^*_{r,m},\ Q^=_0 = \sum_{r=1}^{\infty}\sum_{m=0}^{\infty} P^=_{r,m},\ Q_0 = \sum_{r=1}^{\infty}\sum_{m=0}^{\infty} P_{r,m} \qquad [179]$$

The mass balances for these chain species are

$$\frac{d[P^*_{1,0}]}{dt} = k_{ac}[A][M] - (k_p[M] + k_f[Z] + k_\beta + k_{br}Q^=_0 + k_d)[P^*_{1,0}] \qquad [180]$$

$$\frac{d[P^*_{r,m}]}{dt} = k_p[M][P^*_{r-1,m}] + k_{br}\sum_{n=0}^{m-1}\sum_{s=1}^{r-1}[P^*_{s,n}][P^=_{r-s,m-n-1}] - (k_p[M] + k_f[Z] + k_\beta + k_{br}Q^=_0 + k_d)[P^*_{r,m}] \qquad [181]$$

$$\frac{d[P^=_{r,m}]}{dt} = k_\beta[P^*_{r,m}] - k_{br}Q^*_0[P^=_{r,m}] \qquad [182]$$

$$\frac{d[P_{r,m}]}{dt} = (k_{fZ}[Z] + k_d)[P^*_{r,m}] \qquad [183]$$

Applying SSH to propagating and macromonomer chains (eqns [180]–[182]) and treating r as continuous variable $d[P^*_{r,m}]/dr = [P^*_{r,m}] - [P^*_{r-1,m}]$ and its summation as integration, we have

$$\frac{d\phi^*_{r,m}}{dr} - \mu\phi^*_{r,m} = \eta\sum_{n=0}^{m-1}\int_0^r \phi^*_{s,n}\phi^*_{r-s,m-n-1}\,dr \qquad [184]$$

where

$$\mu = \frac{k_f[Z] + k_\beta + k_{br}Q_0^{=} + k_d}{k_p[M]} \quad [185]$$

$$\eta = \frac{k_\beta}{k_p[M]} \quad [186]$$

and $\phi^*_{r,m} = [P^*_{r,m}]/Q^*_0$ is the number fraction of chains having r monomeric units and m branches. Equation [184] has the following solution:[148–150]

$$\phi^*_{r,m} = \frac{\eta^m(\mu-\eta)^{m+1}}{m!(m+1)!} r^{2m} \exp(-\mu r) \quad [187]$$

$$\phi^*_r = \sum_{m=0}^{\infty} \phi^*_{r,m} = \frac{1}{r}\sqrt{\frac{\mu-\eta}{\eta}} \exp(-\mu r) I_1\left[2r\sqrt{\eta(\mu-\eta)}\right] \quad [188]$$

where $I_1\left(2r\sqrt{\eta(\mu-\eta)}\right)$ is the Bessel function of the first kind of imaginary argument of first order. The number-average chain length and the polydispersity of the distribution of eqn [188] are

$$\bar{r}^*_N = \frac{1}{\mu-2\eta} \quad \frac{\bar{r}^*_W}{\bar{r}^*_N} = \frac{2(\mu-\eta)}{\mu-2\eta} \quad [189]$$

From eqns [182] and [183], $\phi_{r,m} \equiv (d[P^*_r]/dt)/(dQ^*_0/dt) = \phi^*_{r,m} = \phi^{=}_{r,m}$. The number-fraction distributions and polydispersities of the instantaneous dead-chain population and that of macromonomers are also given by eqns [187]–[189]. **Figure 13(a)** shows the distributions calculated with $\mu = 0.001$ and $\eta = 0.0005$.

4.32.7.2 Binary Catalyst System for Long-Chain Branching

To maximize long-chain branching, binary metallocene systems can be employed. One of the catalysts mainly generates macromonomers via β-hydride elimination termination. It does not however propagate with terminal double bonds due to its closed metal active center and thus avoids the formation of dendritic polymers. On the other hand, the second catalyst must be constrained geometry type with an open metal active center. It polymerizes olefin monomers and incorporates the macromonomers, yielding *in situ* long chain branching (LCB) comb-structured chains.[146,151,152] Since $k_{br,2} >> k_{br,1}$ and $k_{\beta,2} << k_{\beta,1}$, $\phi_{r,m} = \phi^*_{r,m,2}$ and $\phi^{=}_{r,m} = \phi^*_{r,m,1}$, where subscripts 1 and 2 indicate the first and second catalysts, respectively. For the generation of macromonomers

$$\frac{d\phi^*_{r,m,1}}{dr} + \mu_1 \phi^*_{r,m,1} = 0 \quad [190]$$

which has a simple solution

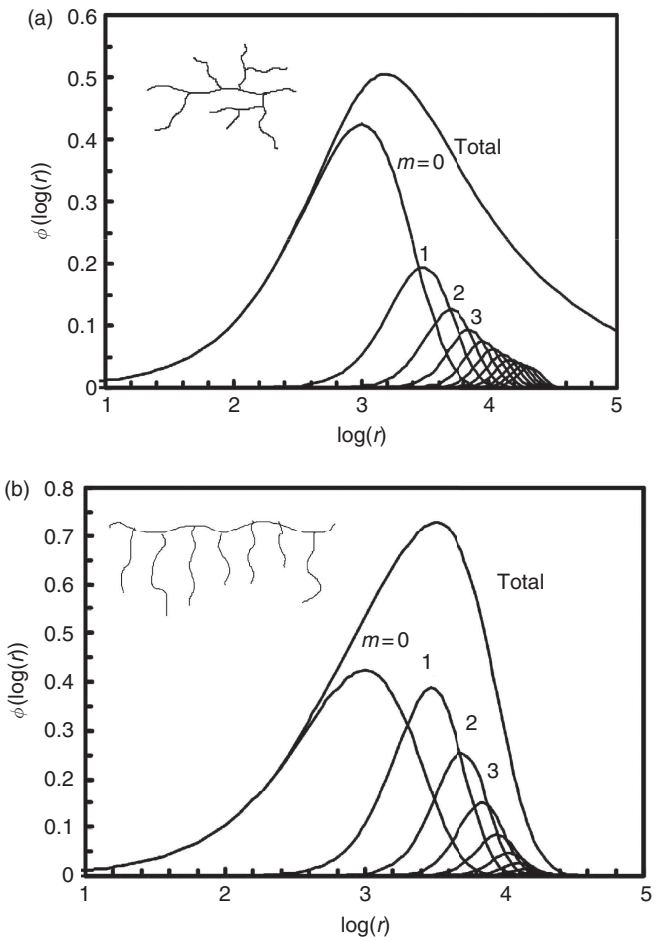

Figure 13 MWDs of polymer chains having m branching points and their total distribution of (a) dendritic polymer and (b) comb polymer.[150]

$$\begin{aligned}\phi^*_{r,0,1} &= \mu_1 \exp(-\mu_1 r)\\ \phi^*_{r,m,1} &= 0, m\geq 1\end{aligned} \quad [191]$$

These chains provide the teeth for comb polymers.

The polymerization of olefin monomers and the incorporation of the *in situ* macromonomers obey the following mass balance:

$$\frac{d\phi^*_{r,m,2}}{dr} + \mu_2\phi^*_{r,m,2} = \eta_2\int_0^r \phi^*_{s,m-1,2}\phi^*_{r-s,0,1}\, ds \quad [192]$$

which has the solution[150]

$$\phi^*_{r,m,2} = (-1)^m(\mu_2-\eta_2)\left[\frac{\mu_1\eta_2}{(\mu_1-\mu_2)^2}\right]^m [f_m(r)\exp(-\mu_2 r) - g_m(r)\exp(-\mu_1 r)] \quad [193]$$

where

$$f_m(r) = \sum_{n=0}^{m}\frac{(m-1+n)!}{n!(m-1)!}\frac{[(\mu_2-\mu_1)r]^{m-n}}{(m-n)!}$$

and

$$g_m(r) = \sum_{n=0}^{m-1}\frac{(m+n)!}{n!m!}\frac{[(\mu_1-\mu_2)r]^{m-n-1}}{(m-n-1)!}$$

In a special case when $\mu_1 = \mu_2$, eqn [193] becomes

$$\phi^*_{r,m,2} = \frac{\mu_2-\eta_2}{(2m)!}(\mu_2\eta_2)^m r^{2m}\exp(-\mu_2 r) \quad [194]$$

$$\phi^*_{r,2} = \sum_{m=0}^{\infty}\phi^*_{r,m,2} = (\mu_2-\eta_2)\exp(-\mu_2 r)\cosh(r\sqrt{\mu_2\eta_2}) \quad [195]$$

where $\cosh(x) = (e^x + e^{-x})/2$. The number-average molecular weight and the polydispersity of the distribution are

$$\bar{r}^*_{N,2} = \frac{\mu_2+\eta_2}{\mu_2(\mu_2-\eta_2)} \quad \frac{\bar{r}^*_{W,2}}{\bar{r}^*_{N,2}} = \frac{2\mu_2(\mu_2+3\eta_2)}{(\mu_2+\eta_2)^2} \quad [196]$$

The physical meaning of the condition of $\mu_1 = \mu_2$ is that the number-average length of tooth chains equal that of backbone segments, which are backbone portions between adjacent branching points.

Figure 13(b) gives the MWDs of polymer chains having m branching points and the total distribution calculated from eqn [195]. The parameters are $\mu_2 = 0.001$ and $\eta_2 = 0.0005$. The branched polymers, thus generated via *in situ* formation of macromonomers, are all comb type. Compared to the dendritic polymers in **Figure 13(a)**, the comb polymers have much narrow distributions with rather sharp truncation at the high-molecular-weight end. The average molecular weight and the branching density in **Figures 13(a)** and **13(b)**, respectively, are the same. This conclusion remains true for the whole range of μ and η values.

In addition to long-chain branching, binary metallocene systems are also used to construct bimodal MWDs for polyolefins that have better processability than narrow distribution materials.[153] The lower molecular weight chains reduce melt viscosities and thus make the materials easier to be processed. Another development is the tandem catalysis for LLDPEs. The current industrial practice involves two steps. Ethylene monomers are first oligomerized into α-olefins such as butene, hexene, and octene. The α-olefins are incorporated into polyethylene chains in a separate process. A tandem system integrates these two steps into one using two catalysts in one reactor with ethylene as the only monomer stock.[154–157] The oligomerization catalyst generates α-olefins that are incorporated into polyethylene chains *in situ* without purification. The current challenge is the matching of two catalysts under industrial conditions.

Metallocene polymers have improved toughness, higher clarity, lower heat seal initiation temperature, lower solvent extractive, as well as many other application properties better than Ziegler–Natta products. Metallocene polymers have replaced Ziegler–Natta in some high-end applications. However, they are not as competitive as Ziegler–Natta for general purposes. Traditional Ziegler–Natta products still dominate the polyolefin market. Among the main reasons are high costs of the cocatalyst MAO and the existing production technologies that have been developed and established for many decades based on heterogeneous catalysts. Initial investments to polymer production facilities such as Unipol reactor are substantial and it is unrealistic to build new facilities to accommodate new catalysts. Metallocene catalysts are homogeneous in nature and must be modified to suit for the established facilities. In most uses, they need to be supporting onto particles. Catalyst supporting adds further cost.

4.32.7.3 Post-Metallocene Development

Since metallocene catalysts have coordination power for chain stereoregularity, efforts are made to produce tactic polymers from nonolefin sources such as styrene, MMA, and vinyl chloride, which are normally polymerized using free-radical processes. Unfortunately, metallocenes based on early transition metals are too sensitive to polarity. Only styrene can be polymerized to high molecular weight. Syndiotactic PS was produced using half-sandwich metallocene in 1986 by Ishihara *et al.*[158,159] The materials have high melting temperature but are very brittle. Theoretical studies show that tactic vinyl, acrylic, and styrenic polymers possess many properties superior to their atactic products and are competitive with engineering materials. These added values of commodity polymers from chain tacticity have attracted and will continue to attract much attention from the research community. In addition to stereoregularity, catalyst polymerization is also much more effective than free-radical and ionic processes in terms of initiator/catalyst efficiency. One catalytic active site generates thousands of polymer chains, while one initiator molecule normally forms one or two chains.

Post-metallocene developments include Brookhart catalysts based on nickel and palladium. These catalysts can incorporate polar monomers such as methyl acrylate into polyethylene chains. They possess 'chain-walking' mechanisms that allow synthesis of various structures from HDPE to hyperbranched PE, as shown in **Scheme 2**.[160–165] Chain topology depends on the competition between chain walking and chain propagation. The chain-walking rate is a function of polymerization temperature:

$$R_{cw} = A_{cw}\exp(-E_{cw}/RT) \quad [197]$$

while the chain propagation rate is a function of both ethylene pressure and polymerization temperature:

$$R_p = A_p[M]\exp(-E_p/RT) \quad [198]$$

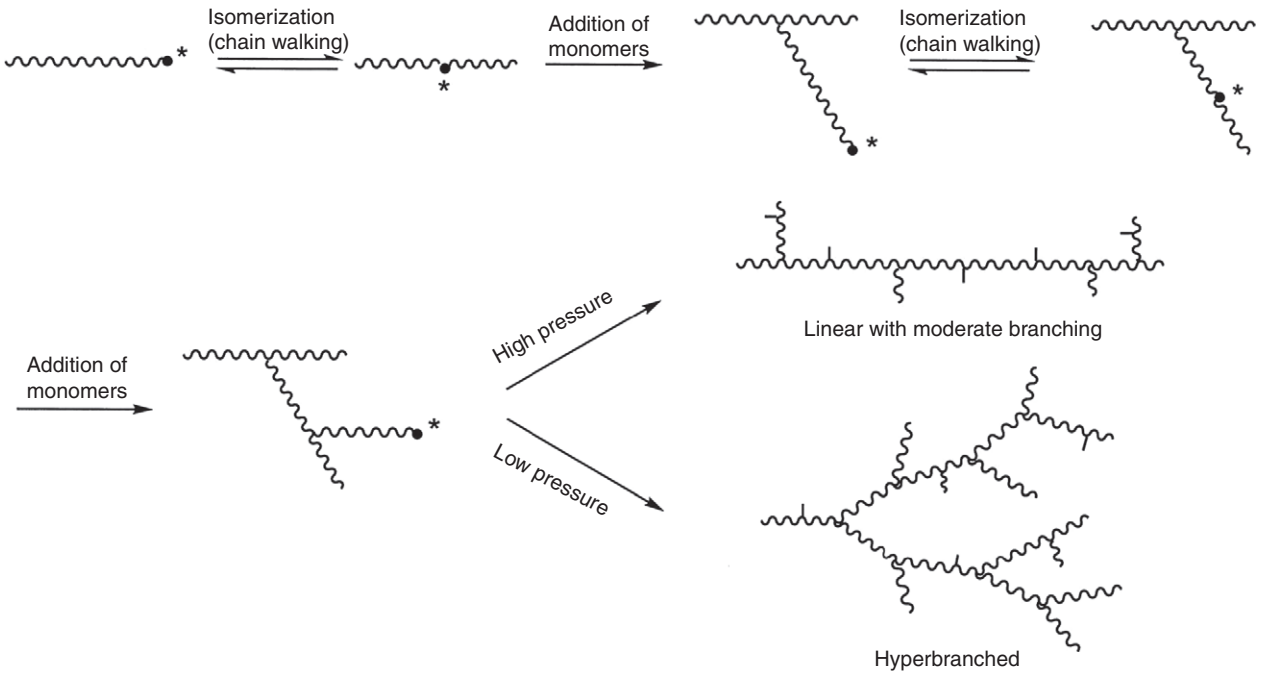

Scheme 2 Chain-walking mechanism of Brookhart catalyst. Low pressure produces linear chains and high pressure produces hyperbranched polymers.

Simple adjustment of temperature and pressure could easily control polymer chain topology. Brookhart catalysts are used in DuPont's Versipol system. Another class of post-metallocenes are Grubbs catalysts. These catalysts are good for incorporation of polar monomers and particularly suitable for production of specialty low-molecular-weight polymers with reactive functionalities.

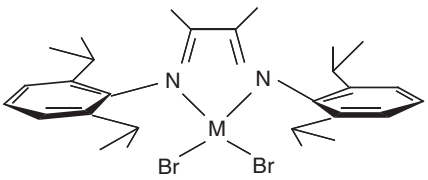

M = Ni, Pd
Brookhart catalyst

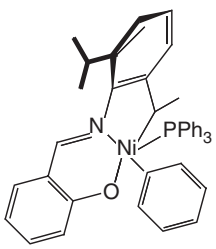

Grubbs catalyst

4.32.8 Emulsion Polymerization

All the above equation derivations and discussions of the rates of polymerization and the polymer chain properties are based on single-phase (homogeneous) polymerization such as bulk and solution. The theoretical developments in the single-phase polymerization provide solid foundation for their multiphase (heterogeneous) counterparts. However, in reality, more industrial polymers are produced using heterogeneous polymerization. There are various reasons for this. Among the most important considerations are agitation, heat removal, product separation, particle morphology, environment impact, as well as polymer solubility in monomer and/or solvents. The kinetics of heterogeneous processes is more complex than that of homogeneous ones. The complexity mainly arises from mass transports of reactants between the different phases involved.

Bulk polymerization eliminates solvents and suspending fluids other than monomer. It has the highest volume efficiency. However, the viscosity increases rapidly with the increase in polymer concentration and molecular weight, thereby reducing the mixing efficiency and heat transfer rate. Low heat transfer coefficient at high monomer conversions can cause safety problem with a runaway reaction. This is particularly true with the kinetics characteristic of significant gel effect due to diffusion-controlled bimolecular radical termination. In bulk polymerization, monomer conversions beyond 65% are unusual for stirred reactor vessels.

Solution polymerization uses a solvent for the monomer and polymer with a considerably high solvent-to-monomer ratio. The polymerization course is similar to bulk. Dilution of monomer and polymer with solvent reduces heat load and viscosity. But the output is also reduced by the diluents. Solution polymerization is advantageous only when the solution can be directly applied without separation such as in the manufacture of protective coatings. However, when the product is marketed in a solid form, the polymer must be separated from the solvent. Solvent separation often involves energy- and capital-intensive processes.

There have been many heterogeneous polymerizations developed over the decades. The main ones are precipitation, dispersion, suspension, emulsion, slurry, and gas-phase polymerization. In addition to the discussed chain properties, particle sizes and distribution are the important parameters that determine polymer product quality and reactor performance. Among the mentioned heterogeneous processes, emulsion polymerization has the best theoretical development. Scheme 3 shows schematic presentation of an emulsion polymerization that consists of three stages.

4.32.8.1 Particle Nucleation

Emulsion polymerization produces polymer latexes that are stable suspensions of polymer particles in water with particle sizes of tens to hundreds of nanometers and polymer particle concentrations of $N_p = 10^{14}$–10^{19} per liter. The particles are stabilized either by ionic (electrostatic) or nonionic (steric) emulsifiers to prevent coagulation. Emulsion polymerization can be carried out in batch, semibatch, and continuous reactors. Commercial uses of emulsion products are in either latex form, such as coatings and paints, or coagulated and dried rubber and plastic resin form. Due to the aqueous dispersion of polymer particles, emulsion and suspension polymerizations have some commonalities in terms of low viscosity, easy agitation, low level of wall fouling, good heat transfer capacity, and high polymerization rate. Emulsion polymerization is superior in the production of high-molecular-weight polymers due to its compartmentalization effect.

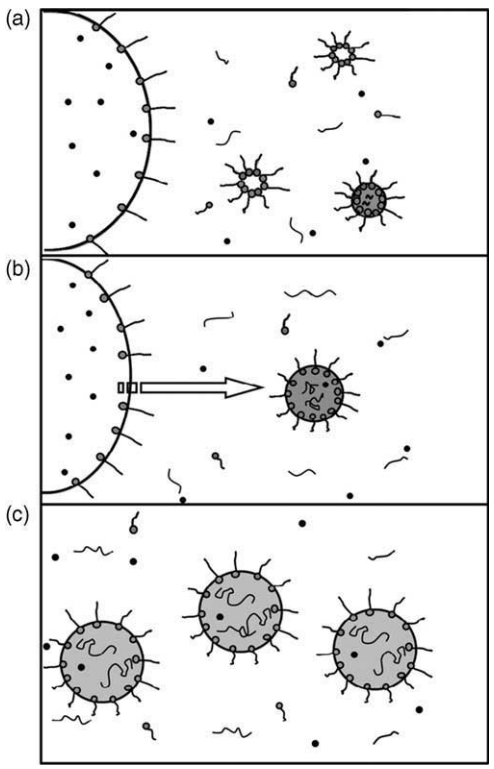

Scheme 3 Schematic presentation of emulsion polymerization that consists of three stages: (a) Stage I – particle nucleation; (b) stage II – particle growth; and (c) stage III – monomer depletion.

On the mechanistic side, emulsion polymerization is very different from suspension polymerization. Reactions do not normally occur in monomer droplets, but in water phase and polymer particles.[166–174] Water-soluble initiators are used. A typical recipe consists of 100 parts H_2O, 50–120 parts monomer, 0.5 part surfactant, 0.5 part initiator, and 0.5 part chain transfer agent. There are three stages in emulsion polymerization. In stage I, polymer particles are nucleated from micelles. This stage usually takes a few minutes and is completed at < 10% conversion. Monomer droplets having sizes about tens of micrometers are formed in continuous water phase by agitation and stabilized by surfactant. The added amount of surfactant must be adequate and above its critical micellar concentration (CMC) so that micelles can form.

By raising temperature, initiator molecules in the water phase decompose and generate primary radicals that propagate with a trace level of monomer present in water. When the chains grow to a critical length, they become insoluble in water and must enter organic phases. Although the large monomer droplets count for about half of the total mass, the small micelles dominate the total surface area. It is the surface area that determines which organic phase the radicals enter. The micelles are swollen with monomer molecules. Once a radical enters a micelle, it propagates with monomer and forms a radical chain. A polymer particle is thus nucleated. The radical chain terminates when another radical enters the polymer particle from the water phase. The consumed amount of monomer inside the particle is compensated for by the mass transfer from monomer droplets through the water phase. For an emulsion polymerization to be successful, a small solubility of monomer in water is required. Due to the small particle size, the polymer solubility in monomer (or monomer swellability in polymer) is about half. For an individual particle, the particle growth is in an on–off fashion with a step function of time. The particle grows in the presence of a radical center and the growth stops with the next radical entering the particle and terminating the chain. When radicals enter the particle at a very high on–off frequency and in a random manner, the particle appears to have a smooth growth with time. Radicals are continuously generated from the water phase and randomly captured by micelles or polymer particles. Stage I is completed when the micelles totally disappear. Not all micelles are converted to polymer particles. Some are dissolved to stabilize the growing polymer particles.

Although there are other nucleation mechanisms available such as homogeneous nucleation, most commercial emulsion polymerization uses micellar nucleation. The poor reproducibility of stage I in the commercial practice is responsible for poor batch-to-batch product quality control. To overcome this variability, polymer seed particles are often used. These small polymer particles at 30–50 nm are prepared by emulsion polymerization. Stage I is eliminated in the seeded emulsion polymerization.

The number of polymer particles per liter of water N_p is a function of surfactant and initiator concentrations, which can be derived as follows:

$$\frac{dN_p}{dt} = N_{Av} R_{I,w} \frac{A_m}{A_m + A_p} \quad [199]$$

where A_m and A_p are surface area of micelles and polymer particles, respectively, N_{Av} is the Avogadro's number, and $R_{I,w} = 2fk_d[I]_w$ is the initiation rate of radicals in the water phase. The radical termination in the water phase is neglected and all the radicals are captured by either micelles or polymer particles. The particle surface area is a function of its volume and age:

$$v(t,t') = \mu(t-t') \quad [200]$$

where t is the present time, t' is the birth time, $t-t'$ is the particle age, and μ is the volumetric growth rate

$$\mu = \frac{dv_p}{dt} = \frac{mk_p\bar{n}[M]_p}{N_{Av}\rho_p\phi_p} \quad [201]$$

where $\bar{n}$ is the number of radicals in the particle ($\bar{n} = 0.5$ in case II kinetics), $[M]_p$ is the polymer concentration in the particle, ϕ_p is the polymer volume fraction in the particle, ρ_p is the polymer density, and m is the monomer molecular weight. The surface area of a single particle is thus

$$a(t,\tau) = (36\pi\mu^2)^{1/3}(t-t')^{2/3} \quad [202]$$

and that of the total particles is

$$A_p = \int_0^t a(t,t')\frac{dN_p}{dt'}dt' \quad [203]$$

There are two approximations in relating the total particle surface area to time. The first approximation is to assume that all the radicals generated from the water phase purposely enter micelles at the constant rate $dN_p/dt = N_{Av}R_{I,w}$:

$$A_p = 2.9N_{Av}\mu^{2/3}R_{I,w}t^{5/3} \quad [204]$$

At the end of stage I, all surfactant molecules are consumed to cover the total polymer particle area, that is, $N_{Av}a_S[S]_w$, where $[S]_w$ is the surfactant concentration per liter of water and a_S is the specific area that each surfactant molecule can cover the particle surface. The time required for stage I can be found by equating A_p to $N_{Av}a_S[S]_w$, that is, $t_1 = 0.53\,\mu^{-2/5}(a_S[S]_w)^{3/5}\ R_{I,w}{}^{-3/5}$. The number of particles thus nucleated is[175]

$$N_p = N_{Av}R_{I,w}t_1 = 0.53N_{Av}(R_{I,w}/\mu)^{2/5}(a_S[S]_w)^{3/5} \quad [205]$$

The second approximation is to release the radical purpose entrance assumption but maintain the constant initiation rate, which is reasonable considering the short period of stage I and the initiator's long half-lifetime. Radicals have nonpreference of micelles over polymer particle but enter the organic phases randomly according to eqn [199]. With the assistance of $A_m + A_p = N_{Av}a_S([S]_w - [S]_{CMC}) \approx N_{Av}a_S[S]_w$, the total particle surface area is easily found from eqn [203]:

$$\frac{A_p}{N_{Av}a_S[S]_w} = 1 - \exp\left(-2.9R_{I,w}\frac{\mu^{2/3}t^{5/3}}{a_S[S]_w}\right) \quad [206]$$

Substituting eqn [206] into eqn [199] and integration with t from 0 to infinity gives[175]

$$N_p = 0.47N_{Av}(R_{I,w}/\mu)^{2/5}(a_S[S]_w)^{3/5} \quad [207]$$

The only difference between eqns [205] and [207] is their coefficients. The dependence of N_p on the initiator and surfactant concentration and the particle growth rate is the same, $N_p \sim [I]_w^{2/5}[S]_w^{3/5}\mu^{-2/5}$. Due to lack of accurate data for many of the parameters involved such as the surfactant specific area ($a_s \sim 30$–$100\,Å^2$ per molecule) and the polymer solubility in micelle, these equations do not give good estimates for the absolute number of particles nucleated, rather they are used as a scaling law for adjustment of recipes by surfactant and/or initiator loading under an isothermal conditions and with a constant monomer loading.

4.32.8.2 Rate of Polymerization

The rate of monomer consumption on a 1 l H_2O basis is

$$-\frac{d[M]_w}{dt} = k_p(\bar{n}N_p/N_{Av})[M]_p \quad [208]$$

where $[M]_w$ is mole of monomer per liter of water. In stage I, all the parameters in eqn [208] remain constant except for N_p, which changes with time. Using the first approximation

$$x = fk_dk_p\bar{n}[M]_p([I]_{w,0}/[M]_{w,0})t^2 \quad [209]$$

The x versus t relationship can also be obtained with the second approximation, but it involves a complex function.

Upon completion of particle nucleation, the polymerization process gets into stage II. Particles grow in the presence of monomer droplets. Monomers inside the particles are polymerized and are compensated by mass transfer from the monomer droplets through the water phase. The monomer concentration inside the particle remains constant at an equilibrium swelling. Radicals generated in the water phase continue to enter the growing particles. Stage II ends when the monomer droplets are consumed. This occurs at monomer conversions between 20% and 80%, for example, polyvinyl chloride (PVC) 75%, polyvinyl acetate (PVAc) 20%, polystyrene (PS) 30%, and polybutadiene 55%, which is determined by the polymer solubility in the particles.

The monomer concentration inside particle $[M]_p$ can be estimated from the polymer solubility ϕ_p, which is the polymer volume fraction in the particle: $[M]_p = (1-\phi_p)\rho_m/m$, where ρ_m is the monomer density. Neglecting the effect of surface energy on chemical potential, the volume fraction of polymer ϕ_p and the monomer concentration $[M]_p$ in the particle are independent of the particle size and are constant at constant temperature. The volumetric growth rate μ is thus constant and the particle size is a linear function of its age, $v_p = \mu t$. The rate of monomer consumption during stage II is also constant, giving a linear relationship for conversion versus time:

$$x = x_1 + k_p(\bar{n}N_p/N_{Av})([M]_p/[M]_{w,0})(t-t_1) \quad [210]$$

In practice, a small amount of additional surfactant is often added during stage II to prevent coagulation of polymer particles. At this stage, the particles are juicy and sticky and easily coagulate if their surfaces are not adequately protected by surfactant molecules. Gradual size reduction of the monomer droplets releases some surfactant molecules, but the growth of the huge number of particles demands more. However, caution must be exercised with the amount of additional surfactant. Excess amount forms new micelles and results in small polymer particles in the final product.

In case II kinetics, the number of radicals in individual particles is assumed to be $\bar{n} = 0.5$, that is, half of the time having one radical and the other half without a radical. The following estimate provides some justification. With a particle of 100 nm

diameter, its volume is $v_p = \pi D_p^3/6 = 5.24 \times 10^{-19}$ liter. If two radicals coexist, the radical concentration is $[P^\bullet] = 2/(N_{Av}v_p) = 6.34 \times 10^{-6}\,\text{mol l}^{-1}$ and their termination rate is $R_t = k_t[P^\bullet]^2 = 2.01 \times 10^{-3}\,\text{mol l}^{-1}\,\text{s}^{-1}$, given $k_t = 5 \times 10^7$ $\text{l mol}^{-1}\,\text{s}^{-1}$. The time required to consume two radicals is $2/(N_{Av}v_pR_t) = 3.15 \times 10^{-3}$ s. On the other hand, the rate of radicals entering individual particles is $2fk_d[I]_wN_{Av}/N_p = 6.02 \times 10^{-2}$ radicals per second, given $f = 0.5$, $k_d = 10^{-5}\,\text{s}^{-1}$, $[I] = 10^{-3}\,\text{mol l}^{-1}$, and $N_p = 10^{17}\,\text{l}^{-1}$. Therefore, a particle receives a radical from the water phase every 16.6 s. When another radical from the water phase enters the polymer particle that is already occupied by one radical, the two radicals are annihilated each other instantaneously. In other words, two radicals cannot coexist in a polymer particle.

Under some conditions, case II kinetics can be violated. These conditions can be large polymer particles, high radical entry rates into particles, high polymer concentrations inside particles, and so on. We then have case III kinetics with $\bar{n} > 0.5$. This is true particularly at the late stage of polymerization when the system reaches high conversions or in the presence of cross-linking. Styrene and acrylic polymerizations often run into case III kinetics. The opposite can also occur with $\bar{n} < 0.5$ when the radicals easily exit from particle to the water phase (case I kinetics). PVC and PVAc are outstanding examples that obey case I kinetics. Significant chain transfer reactions to small molecules can facilitate a radical's exit from polymer particles. For most emulsion polymerization systems, we assume $\bar{n} = 0.5$ at least for stages I and II when chain transfer to monomer is unimportant.

Disappearance of monomer droplets does not mean completion of the polymerization, rather it suggests the end of stage II. At this point, the residual monomers all reside in the polymer particles and are still in a large amount, depending on the monomer swellability in polymer $\phi_m = 1 - \phi_p$. The monomer conversion at the end of stage II is

$$x_2 = \frac{\phi_p \rho_p}{\phi_p \rho_p + \phi_m \rho_m} \quad [211]$$

which can be approximated by $x_2 \approx \phi_p$ if the difference between polymer and monomer densities is neglected. The duration of stage II is

$$t_2 - t_1 = \left(\frac{m[M]_{w,0}}{\rho_m}\right)\left(\frac{N_{Av}}{k_p \bar{n} N_p}\right)\left(\frac{x_2 - x_1}{1 - \phi_p}\right) \quad [212]$$

The term $m[M]_{w,0}/\rho_m$ is the initial monomer loading, that is, how many liters of monomer is originally charged to 1 l of water.

At the end of stage II, the sizes of polymer particles reach their maximum values and the particles experience volume shrinkage in stage III, according to

$$v_p = \frac{m[M]_{w,0}}{N_p \rho_m}[1 - (1 - \rho_m/\rho_p)x] \quad [213]$$

The kinetics of stage III is similar to that of the bulk polymerization. The polymer particles act as small reactors and there are no further mass transports between the different phases. The monomer inside the particle is gradually depleted with its concentration:

$$[M]_p = \frac{[M]_{w,0}(1 - x)}{N_p v_p} \quad [214]$$

Substituting eqn [214] into eqn [208] gives the rate of conversion:

$$\frac{dx}{dt} = \frac{k_p \bar{n}(1 - x)}{N_{Av} v_p} \quad [215]$$

which has an analytical solution of

$$(1 - \rho_m/\rho_p)(x - x_2) - (\rho_m/\rho_p)\ln\left(\frac{1 - x}{1 - x_2}\right) = \frac{\rho_m k_p \bar{n} N_p}{m[M]_{w,0} N_{Av}}(t - t_2) \quad [216]$$

Neglecting the difference in the monomer and polymer densities gives an explicit expression for the conversion versus time:

$$x = 1 - (1 - x_2)\exp\left[-\frac{\rho_p k_p \bar{n} N_p (t - t_2)}{m[M]_{w,0} N_{Av}}\right] \quad [217]$$

4.32.8.3 Molecular Weight Development of Polymers

Emulsion polymerization has the advantage of producing high-molecular-weight polymers due to its compartmentalization effect. Unlike homogeneous processes, radicals in emulsion polymerization are isolated from each other by nanosized particles. They terminate because other radicals enter the particles from the water phase. Molecular weight of polymer can be easily regulated by the radical initiation in the water phase and by chain transfer reactions inside the particles. The rate of polymerization is

$$R_p = k_p(\bar{n} N_p / N_{Av})[M]_p \quad [218]$$

The rate of generation of polymer chains is

$$R_t/2 + R_{fZ} = R_{I,w}/2 + R_{fZ} = fk_d[I]_w + k_{fZ}[Z]_p \bar{n} N_p / N_{Av} \quad [219]$$

where $[Z]_p$ is the transfer agent concentration in the particle. With an instantaneous termination, a small oligomer radical entering from the water phase contributes little to the polymer molecular weight. Therefore, no matter if the termination is by disproportionation or combination, the termination of two radicals produces one polymer chain. The instantaneous number-average molecular weight is thus

$$\bar{M}_N = \frac{R_p}{R_t/2 + R_{fZ}} = \frac{mk_p(\bar{n} N_p / N_{Av})[M]_p}{fk_d[I]_w + k_{fZ}[Z]_p(\bar{n} N_p / N_{Av})} \quad [220]$$

Due to the nature of random termination and/or transfer reactions, the instantaneous polymer has Flory's most probable MWD with polydispersity equal to 2. The cumulative average molecular weights can be found from their integrations with conversion, $\bar{M}_{N,cum} = x/(\int_0^x dx/\bar{M}_N)$ and $\bar{M}_{W,cum} = (\int_0^x \bar{M}_W\, dx)/x$. Figure 14 shows the development of monomer conversion and polymer particle size in the emulsion polymerization of styrene.

4.32.9 Dispersion and Suspension Polymerization

4.32.9.1 Dispersion Polymerization

Dispersion polymerization starts from a homogeneous solution where initiator, monomer, and solvent are totally miscible. However, the produced polymer is not soluble or

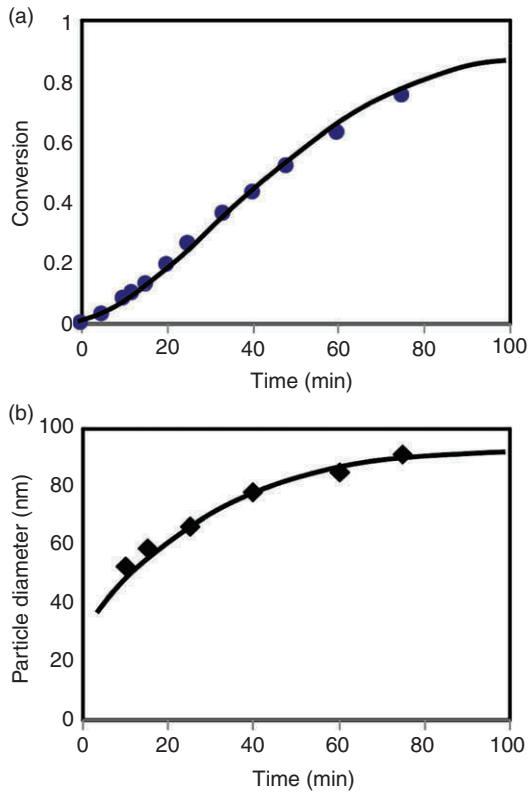

Figure 14 (a) Monomer conversion and (b) particle size in the emulsion polymerization of styrene with St 100, H_2O 190, potassium persulfate 0.31, and sodium lauryl sulfate on weight basis.[176]

has a limited solubility in the monomer or added solvent. Due to poor solvency of the reaction medium, radical and polymer chains form primary particles, resulting in phase separation at an early stage. There are two scenarios. If the primary particles are swollen with monomer and initiator molecules and become major loci for the polymerization to proceed, it is called dispersion polymerization. On the other side, if the primary particles do not swell with monomer and initiator but simply precipitate out from the solution and agglomerate with each other to become bigger particles, it is often called precipitation polymerization. In this case, the polymerization proceeds in the monomer phase and the primary particles are continuously nucleated and agglomerated. While dispersion polymerization produces spherical polymer particles, precipitation polymerization usually results in particles having broad size distributions and irregular shapes. The size and the shape of the particles are heavily influenced by the polymerization conditions such as temperature, reactant concentrations, and agitation. Adding steric stabilizers and providing effective agitation help provide control over the particle morphology. There is no clear-cut difference between dispersion and precipitation polymerizations. It depends on solvency of the reaction medium. In the literature, the two terms are used interchangeably.

An outstanding example is the production of PVC. The polymer is almost completely insoluble in its monomer. The solubility of the monomer in its polymer can be described by thermodynamic relations such as the Flory–Huggins equation. It is a two-phase polymerization. Initiation, propagation, and termination proceed simultaneously and in parallel in both monomer-rich and polymer-rich phases. Polymer chains formed in the monomer phase transfer to the polymer phase. Initiator and monomer concentrations in the two phases are in equilibrium. The monomer phase disappears at about 70% conversion as shown in **Figure 15**. The rate of total polymerization is contributed by the rates of both polymer and monomer phases:[177]

$$R_{p,total} = R_{p,m} + R_{p,p} = k_{p,m}[R^\bullet]_m[M]_m + k_{p,p}[R^\bullet]_p[M]_p \quad [221]$$

The polymers produced in the two phases have different molecular weights and the product is the result of both. The polymer particles are nucleated from the monomer phase through precipitation of polymer chains and grow by aggregations of primary particles, as well as propagation with monomer molecules in the polymer phase, as shown in **Scheme 4**.

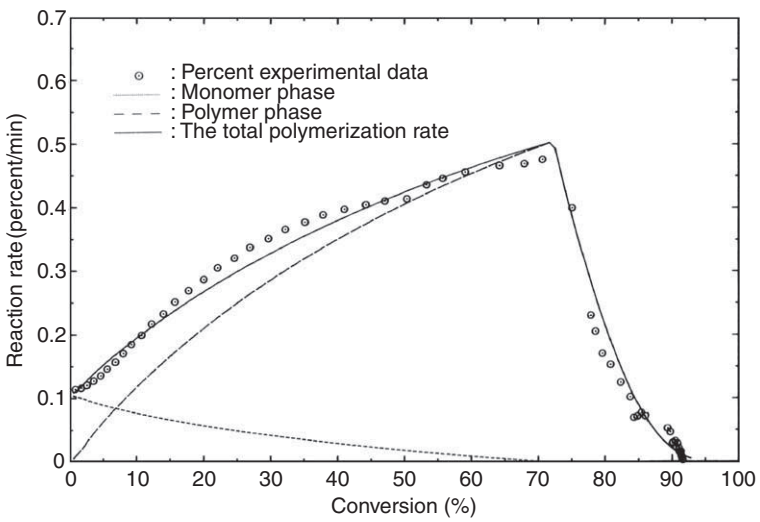

Figure 15 Variation of polymerization rate with conversion in the monomer and polymer phases of free-radical polymerization of vinyl chloride at 50 °C.[177]

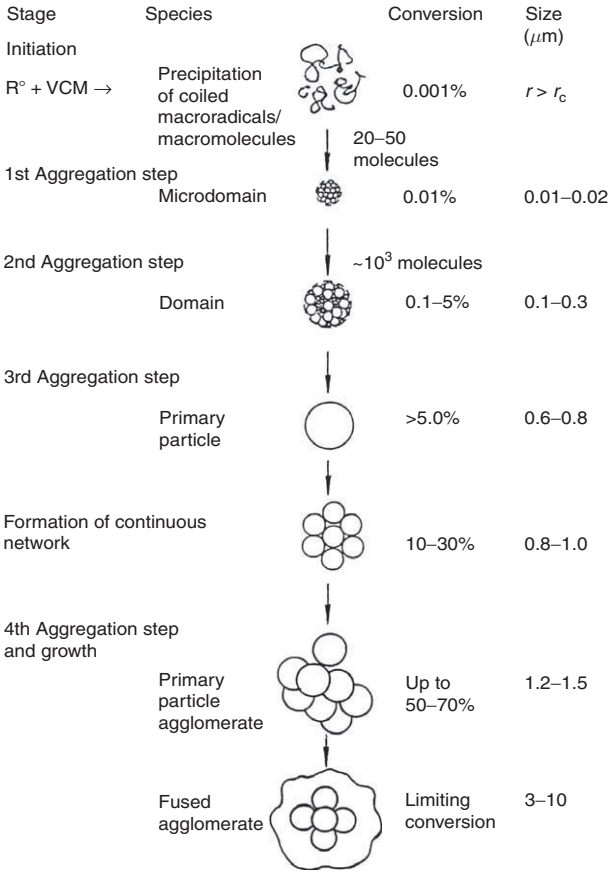

Scheme 4 Schematic presentation of particle formation in the precipitation polymerization of vinyl chloride.[177]

There are many other industrial examples such as acrylic fibers made from polyacrylonitrile (with 7% vinyl acetate). The monomer is fairly water soluble at about 5% and the polymerization occurs in the aqueous phase. However, the polymer is insoluble in water. The primary particles precipitate and agglomerate, forming larger particles that are stabilized by ionic initiator end groups. Butyl rubber (isobutylene + < 5% isoprene) is produced by cationic polymerization with aluminum trichloride catalyst in methyl chloride at about −100 °C. The polymer precipitates as fine polymer particles from the reaction medium.

4.32.9.2 Suspension Polymerization

In suspension polymerization, monomer droplets are dispersed in water and act as separate microreactors, as shown in Scheme 5. The polymerization is initiated with an organic initiator and proceeds as a miniature bulk polymerization. As monomer is converted to polymer, the droplets are transformed into sticky, viscous monomer/polymer particles that gradually become spherical solid polymer particles. Vigorous agitation and steric stabilizers are required. Produced polymer particles have sizes in hundreds of micrometers and settle out as soon as the agitation stops. Suspension polymerization is particularly useful in the production of polymers from reactive monomers via radical

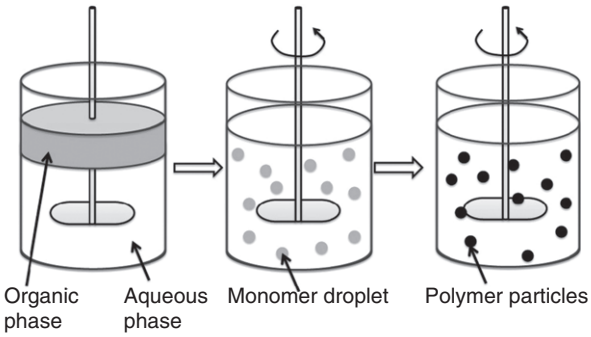

Scheme 5 Schematic presentation of suspension polymerization. Monomer droplets act as separate microreactors having the same kinetics as in bulk polymerization.

polymerization. Water as the continuous phase facilitates agitation and promotes heat transfer. The viscosity of the suspension remains relatively constant with monomer conversion. The polymer product must be separated from water for use. The volume fraction of dispersed phase is between 25% and 50%.

In suspension polymerization where controlled agglomeration is not used, the monomer droplet size distribution is the final polymer particle size distribution (PSD), except for some volume shrinkage. There is little mass transfer between particles. The PSD depends on the type and amount of steric stabilizer as well as agitation and vessel design. Controlled agitation and various types of steric stabilizers both inorganic and organic are used to maintain stable suspension and to obtain desired size, bulk density, and porosity of the particles.

There are two types of suspension polymerization. 'Beads' are nonporous polymer particles that are formed where the polymer is soluble in monomer such as PS and PMMA. 'Powders' are porous particles where the polymer is insoluble in monomer and precipitates during polymerization. The polymer powders are composed of many small primary particles. The powder particles are opaque and have substantial internal porosities. Control of particle porosity is very important for it controls absorption rate of plasticizers such as PVC. The production of PS beads and PVC powders by suspension polymerization will be described later as outstanding industrial examples.

The kinetics of suspension polymerization is similar to that of bulk or solution polymerization. The equations derived for polymerization rate and polymer molecular weight in bulk/solution apply to suspension with the lower reactor volume efficiency. The trade-off for the ease of agitation, heat removal, and product separation is the bulk reactor's volume efficiency. A real challenge in modeling suspension polymerization, as well as dispersion polymerization, is the PSD of the products, which is not well developed in an agitated vessel. The mechanisms of drop breakup and coalescence are not well understood.[178]

In addition to emulsion, dispersion, and suspension polymerization, there are other industrial heterogeneous polymerization processes (Table 2). Of particular importance are slurry and gas-phase processes for polyolefin production, which are also included in Section 4.32.13.

Table 2 Polymerization processes used for industrial production of some major polymers

	Polymerization process					
Polymer	*Bulk*	*Solution*	*Suspension*	*Emulsion*	*Slurry*	*Gas phase*
Free radical						
PVC			X	X		
LDPE	X					
PS	X	X	X			
PMMA	X					
Teflon				X		
ABS	X			X		
Ziegler-Natta						
HDPE		X			X	X
LLDPE		X			X	X
PP	X					X
Ionic						
Butyl rubber					X	
Condensation						
Nylon	X	X				
Polyester	X					
Polycarbonate		X				
Polyurethane	X	X				

4.32.10 Copolymerization

Material properties of polymers are determined by their chain microstructures. For polymers made from a single monomer type, the above-discussed molecular weight and distribution, chain stereoregularity, head–tail and *trans–cis* configurations, and so on all play important roles. For copolymers that contain multiple monomer types, chain composition, sequence, as well as their distributions, are added to the important microstructure property list. With these new parameters, almost unlimited number of polymer types can be produced for better balance of properties for commercial applications. Outstanding commercial examples include acrylonitrile–butadiene–styrene (ABS), SBS, Acrylan (acrylonitrile–vinyl acetate), styrene–butadiene (SBR), butyl rubber (isobutylene–isoprene), Vinylite (vinyl chloride–vinyl acetate), and styrene–maleic anhydride (SMA).

Depending on arrangements of the monomeric units along chain backbones, copolymers can be classified into three major categories:

Block	$M_1M_1M_1M_1M_1M_1M_1M_1M_2M_2M_2M_2M_2M_2M_2M_2$
Alternating	$M_1M_2M_1M_2M_1M_2M_1M_2M_1M_2M_1M_2M_1M_2M_1M_2$
Random	$M_2M_2M_1M_1M_2M_1M_1M_2M_1M_2M_2M_1M_1M_2M_1M_2$

Block copolymers are normally prepared by living anionic or controlled radical polymerization. AA + BB-type condensation products are alternating copolymers by definition. However, in the following, we deal with free-radical polymerization with all arguments easily extendable to other chain growth systems under general conditions. How monomeric units are arranged along chains is determined by the reactivities of radical chains toward different types of monomers. These reactivities can be described by either the terminal model or the penultimate model.

In the terminal model, the propagation rate constant is a function of the type of radical center and the type of monomer to be added. For example

$$\sim M_1M_2^{\bullet} + M_1 \xrightarrow{k_{p21}} \sim M_1M_2M_1^{\bullet}$$

In the penultimate model, the propagation rate constant is influenced by not only the types of radical center and monomer but also the neighboring monomeric unit adjacent to the radical center such as[179,180]

$$\sim M_1M_2^{\bullet} + M_1 \xrightarrow{k_{p121}} \sim M_1M_2M_1^{\bullet}$$

for most systems, the terminal model is adequate. However, when the two monomer types are very different from each other, it requires the penultimate model. In quantitative description of copolymerization system, both accuracy and simplicity need to be considered. For a binary monomer system, there are four propagation rate constants in the terminal model but eight in the penultimate model. With an increase in the monomer types, the difference in the number of parameters is substantial: four versus eight in copolymerization, nine versus twenty-seven in terpolymerization, sixteen versus sixty-four in tetrapolymerization, and so on. Estimation of these rate constants from polymerization kinetic data becomes daunting if not impossible. Analysis and discussion in this chapter focuses on the terminal model.

4.32.10.1 Terminal Model for Copolymer Compositions

There are four propagation reactions involved in copolymerization based on the terminal model:

$$P_{m,n,1}^{\bullet} + M_1 \xrightarrow{k_{p11}} P_{m+1,n,1}^{\bullet} \quad [222]$$

$$P_{m,n,1}^{\bullet} + M_2 \xrightarrow{k_{p12}} P_{m,n+1,2}^{\bullet} \quad [223]$$

$$P_{m,n,2}^{\bullet} + M_1 \xrightarrow{k_{p21}} P_{m+1,n,1}^{\bullet} \quad [224]$$

$$P_{m,n,2}^{\bullet} + M_2 \xrightarrow{k_{p22}} P_{m,n+1,2}^{\bullet} \quad [225]$$

where subscripts m and n are numbers of M_1 and M_2 incorporated into the chain, respectively. Majority of monomers are consumed by propagation reactions:

$$-\frac{d[M_1]}{dt} = k_{p11}[P_1^\bullet][M_1] + k_{p21}[P_2^\bullet][M_1] \quad [226]$$

$$-\frac{d[M_2]}{dt} = k_{p12}[P_1^\bullet][M_2] + k_{p22}[P_2^\bullet][M_2] \quad [227]$$

where

$$[P_1^*] = \sum_{m=1}^{\infty}\sum_{n=1}^{\infty}[P_{m,n,1}^*],\ [P_2^*] = \sum_{m=1}^{\infty}\sum_{n=1}^{\infty}[P_{m,n,2}^*] \quad [228]$$

The monomer fractions are defined as

$$f_1 = \frac{[M_1]}{[M_1]+[M_2]},\quad f_2 = \frac{[M_2]}{[M_1]+[M_2]} \quad [229]$$

and the polymer compositions as

$$F_1 = \frac{(-d[M_1]/dt)}{(-d[M_1]/dt)+(-d[M_2]/dt)},$$
$$F_2 = \frac{(-d[M_2]/dt)}{(-d[M_1]/dt)+(-d[M_2]/dt)} \quad [230]$$

Applying the long-chain assumption that the number of M_1 following M_2 approximately equals to that of M_2 following M_1 (with an error of ± 1, which is negligible for a long chain), that is

$$k_{p21}[P_2^\bullet][M_1] = k_{p12}[P_1^\bullet][M_2] \quad [231]$$

We have Mayo–Lewis equation:[181]

$$F_1 = \frac{r_1 f_1^2 + f_1 f_2}{r_1 f_1^2 + 2 f_1 f_2 + r_2 f_2^2},\ F_2 = \frac{r_2 f_2^2 + f_1 f_2}{r_1 f_1^2 + 2 f_1 f_2 + r_2 f_2^2} \quad [232]$$

where

$$r_1 = \frac{k_{p11}}{k_{p12}} \text{ and } r_2 = \frac{k_{p22}}{k_{p21}} \quad [233]$$

are the reactivity ratios.

The polymer compositions F_1 and F_2 defined by eqn [230] are instantaneous properties, that is, the compositions of those chains formed from t to $t+\Delta t$ from the monomer compositions f_1 and f_2 defined by eqn [229]. The compositions of accumulated copolymers are

$$\bar{F}_1 = \frac{[M_1]_0 - [M_1]}{[M]_0 - [M]} = \frac{f_{1,0} - (1-x)f_1}{x},$$
$$\bar{F}_2 = \frac{[M_2]_0 - [M_2]}{[M]_0 - [M]} = \frac{f_{2,0} - (1-x)f_2}{x} \quad [234]$$

where $[M] = [M_1] + [M_2]$ and $x = ([M]_0 - [M])/[M]_0$ with the subscript '0' indicating initial concentration.

Table 3 lists the reactivity ratios of some comonomer pairs in free-radical polymerization.[21] While the values of r_1 and r_2 can vary a lot, their products are close to or lower than 1, which is thermodynamically favored with entropic contributions. For a given pair of monomers, the reactivity ratios are very different in the different types of polymerization mechanisms. They are also temperature dependent because of different activation energies of the propagation reactions.

Figure 16(a) shows the relationships between polymer and monomer compositions for several sets of reactivity ratios. There are several limiting cases. When $r_1 = r_2 = 1$, radical centers do not discriminate monomer type and polymer composition is always the same as monomer's $F_1 = f_1$. When both r_1 and r_2 are very small and close to zero, the system tends to produce an alternating copolymer. In the opposite case, when both r_1 and r_2 are very large and approach infinity, the system produces two homopolymers or block copolymers. Such a system has not been found and is not thermodynamically favored because of the dramatic reduction in entropy. When $r_1 r_2 = 1$, $F_1 = r_1 f_1/(r_1 f_1 + f_2)$ and the curve is always at one side of the $r_1 = r_2 = 1$ line. When both r_1 and r_2 are smaller or larger than 1, there exists an azeotropic point at $F_1 = f_1 = (1-r_2)/(2-r_1-r_2)$. Only at the azeotropic point do polymers have the same composition as monomers. While the azeotropic points of r_1, $r_2 > 1$ are stable (but rarely found), those of r_1, $r_2 < 1$ are unstable. Any deviations in the monomer composition cause the polymer composition to drift away from the targeted value.

Table 3 Reactivity ratios and their products of some free-radical copolymerization systems

M_1	M_2	r_1	r_2	$r_1 r_2$
Acrylonitrile	Methyl vinyl ketone	0.61	1.78	1.09
	Methyl methacrylate	0.13	1.16	0.15
	α- Methyl strene	0.04	0.20	0.008
	Vinyl acetate	4.05	0.061	0.25
Methyl methacrylate	Styrene	0.46	0.52	0.24
	Methacrylic acid	1.18	0.63	0.74
	Vinyl acetate	20	0.015	0.30
	Vinylidence chloride	2.53	0.24	0.61
Styrene	Vinyl acetate	55	0.01	0.55
	Vinyl chloride	17	0.02	0.34
	Vinylidene chloride	1.85	0.085	0.16
	2-Vinyl pyridine	0.55	1.14	0.63
Vinyl acetate	1-Butene	2.0	0.34	0.68
	Isobutylene	2.15	0.31	0.67
	Vinyl chloride	0.23	1.68	0.39
	Vinylidene chloride	0.05	6.7	0.34

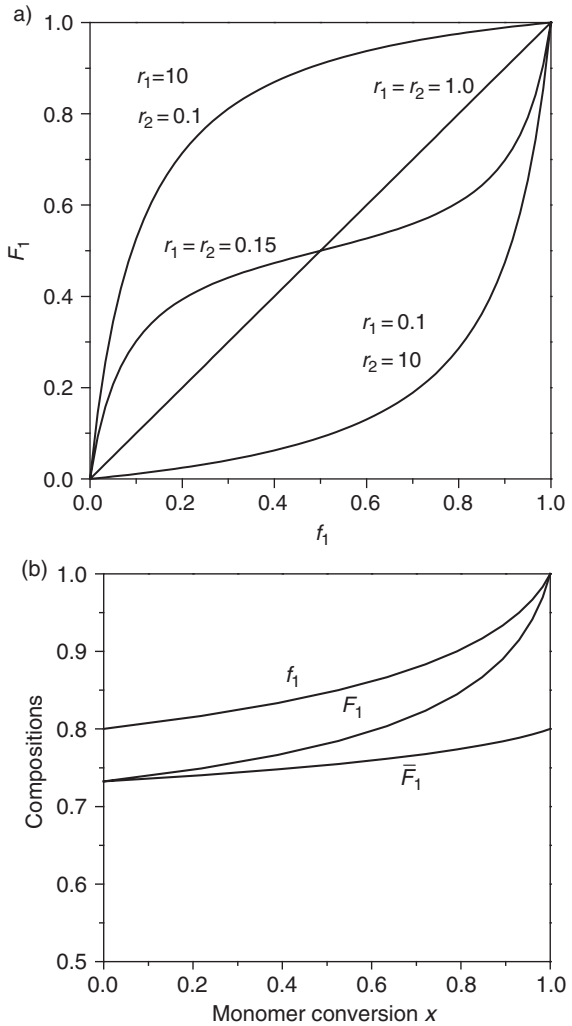

Figure 16 (a) Instantaneous copolymer composition versus comonomer composition with different reactivity ratios and (b) monomer composition, instantaneous copolymer composition, and cumulative copolymer composition as a function of monomer conversion with $r_1 = 0.53$, $r_2 = 0.56$, and $f_{1,0} = 0.8$.

Composition drifting in batch copolymerization presents a challenge to product quality control. This is true in particular for the cases when one reactivity ratio is large and the other is small such as styrene–vinyl acetate ($r_1 = 55$, $r_2 = 0.01$). If a copolymer product of 50% styrene is produced from free-radical mechanism, the batch gives a mixture of copolymer chains having a variety of compositions. Those chains generated at the beginning have >98% styrene, while those at the end are almost pure PVAc, estimated from eqn [232]. In order to have the homogeneous product of $F_1 = 0.5$, the monomer composition f_1 must remain at 0.0133 during the whole course of polymerization; this can be achieved only by semibatch or continuous processes. The direction of composition drifting is counterclockwise at reference of the $r_1 = r_2 = 1$ line.

The instantaneous copolymer composition F_1 is related to the monomer composition f_1 by Mayo–Lewis equation [232]. The cumulative copolymer composition $\bar{F}_1$ is related to not only the monomer composition f_1 but also the monomer conversion x. The monomer composition f_1 is further related to the conversion x by Meyer–Lowry equation, which can be easily derived based on Mayo–Lewis equation. From $[M] = [M_1]/f_1$ and $F_1 = d[M_1]/d[M]$, we have

$$\frac{df_1}{dx} = \frac{f_1 - F_1}{1 - x} \qquad [235]$$

Replacing F_1 by Mayo–Lewis equation and integrating eqn [235] with the initial condition of $f_1 = f_{1,0}$ at $x = 0$ give Meyer–Lowry equation:[182]

$$x = 1 - \left(\frac{f_1}{f_{1,0}}\right)^{\alpha}\left(\frac{1-f_1}{1-f_{1,0}}\right)^{\beta}\left(\frac{f_{1,0}-\delta}{f_1-\delta}\right)^{\gamma} \qquad [236]$$

where $\alpha = r_2/(1-r_2)$, $\beta = r_1/(1-r_1)$, $\gamma = (1-r_1r_2)/[(1-r_1)(1-r_2)]$, and $\delta = (1-r_2)/(2-r_1-r_2)$. **Figure 16(b)** shows variations of f_1, F_1, and $\bar{F}_1$ with x, calculated eqns [236], [232], and [234], respectively.

4.32.10.2 Pseudokinetic Rate Constant Method

The remaining question is how to relate the compositions, as well as polymer molecular weight information, to polymerization time through conversion. The rate of polymerization is

$$R_p = k_{p11}[P_1^\bullet][M_1] + k_{p21}[P_2^\bullet][M_1] + k_{p12}[P_1^\bullet][M_2] + k_{p22}[P_2^\bullet][M_2] \qquad [237]$$

If we define a pseudopropagation rate constant as[183–185]

$$k_p = k_{p11}\phi_1^\bullet f_1 + k_{p21}\phi_2^\bullet f_1 + k_{p12}\phi_1^\bullet f_2 + k_{p22}\phi_2^\bullet f_2 \qquad [238]$$

where $\phi_i^\bullet = [P_i^\bullet]/[P^\bullet]$ is the number fraction of type-i radicals, which can be calculated from the long-chain assumption $k_{p12}[P_1^\bullet][M_2] = k_{p21}[P_2^\bullet][M_1]$:

$$\phi_1^\bullet = \frac{k_{p21}f_1}{k_{p21}f_1 + k_{p12}f_2} \qquad [239]$$

In doing so, the rate of polymerization can be simplified as that of homopolymerization $R_p = -d[M]/dt = k_p[P^\bullet][M]$. Similarly, initiation, termination, and chain transfer reactions can be treated in the same way:

$$R_{in} = (k_{i1}[M_1] + k_{i2}[M_2])[R_0^\bullet] = k_i[M][R_0^\bullet] \approx 2fk_d[I] \qquad [240]$$

$$R_t = k_{t11}[P_1^\bullet][P_1^\bullet] + k_{t12}[P_1^\bullet][P_2^\bullet] + k_{t21}[P_2^\bullet][P_1^\bullet] + k_{t22}[P_2^\bullet][P_2^\bullet] = k_t[P^\bullet]^2 \qquad [241]$$

$$R_{fZ} = (k_{fZ1}[P_1^\bullet] + k_{fZ2}[P_2^\bullet])[Z] = k_{fZ}[P^\bullet][Z] \qquad [242]$$

where

$$k_i = k_{i1}\phi_1^\bullet + k_{i2}\phi_2^\bullet \qquad [243]$$

$$k_t = k_{t11}\phi_1^\bullet\phi_1^\bullet + k_{t21}\phi_2^\bullet\phi_1^\bullet + k_{t12}\phi_1^\bullet\phi_2^\bullet + k_{t22}\phi_2^\bullet\phi_2^\bullet \qquad [244]$$

$$k_{fZ} = k_{fZ1}\phi_1^\bullet + k_{fZ2}\phi_2^\bullet \qquad [245]$$

Using the above pseudokinetic rate constants, we can treat the kinetics of copolymerization as that of homopolymerization. The rate of polymerization can be calculated from eqns [39]–[41], with the total radical concentration from eqn [37] based on the SSH. The molecular weight and distribution functions of eqns [61]–[68] become directly applicable in copolymerization with τ and β defined by eqns [56] and [57]. In using the pseudokinetic rate constant method, it should always be kept in mind

that the so-defined rate constants do not have constant values during polymerization. Extra caution must be paid to integration of differential equations with time or conversion. The pseudokinetic rate constant can easily be extended to multicomponent polymerization systems. The only assumption involved is chain length independence of the radical fractions $\phi_i^\bullet$, which is valid for polymer chains having lengths higher than about 10 units.

Another point worth mentioning is the statistical broadening of copolymer composition. Strictly speaking, F_1 and F_2 are the average composition values of copolymer chains generated from t to $t+\Delta t$. Individual chains in the instantaneous population still vary in their compositions. Longer chains have compositions closer to these average values. But short chains can be significantly deviated. There exists a bivariate distribution of chain length and composition $w(r,\gamma)$, which is the product of weight-fraction chain length distribution $w(r)$ and composition distribution comp(γ/r), where γ is the difference between individual chain composition and F_1. The function comp(γ/r) is the conditional probability distribution given chain length r, originally formulated by Simha and Branson[186] and finally solved by Stockmayer,[26] as a Gaussian distribution:

$$\text{comp}(\gamma/r) = \frac{1}{\sigma\sqrt{2\pi}}\exp\left(-\frac{\gamma^2}{2\sigma^2}\right) \qquad [246]$$

where

$$\sigma^2 = (F_1F_2/r)\sqrt{1+4F_1F_2(r_1r_2-1)} \qquad [247]$$

The distribution broadness σ^2 is inversely proportional to chain length, suggesting smaller variations in longer chains. It is also a function of r_1r_2. Monomer pairs with small r_1r_2 values tend to produce alternating copolymers that have narrow composition distributions.

4.32.10.3 Vinyl/Divinyl Copolymerization

Highly branched or cross-linked polymer materials can be obtained through copolymerization of vinyl/divinyl monomers. Such products have applications as ion-exchange resins, chromatographic packings, superabsorbent materials, contact lenses, photoresists, and drug deliveries. Widely used divinyl monomers are divinylbenzene and ethylene glycol dimethacrylate.

When a polymer radical propagates with a double bond on a divinyl monomer, the unreacted double bond on the same monomer molecule becomes pendant on the chain. If a second radical adds to the pendant double bond, a H-type cross-linkage is formed and the chain is branched. Successive branching with H-type cross-linkages leads to gel formation. Gel molecules are three-dimensional networks that are not soluble but swellable in good solvents, as shown in Scheme 6.

Given a population of primary chains [P_r] having a total of Q_1 monomer units, the development of polymer molecular weight with cross-linking prior to gel formation can be followed by

$$\frac{d[P_r]}{dt} = -k_xQ_1r[P_r] + \frac{1}{2}k_x\sum_{s=1}^{r-1}s[P_s](r-s)[P_{r-s}] \qquad [248]$$

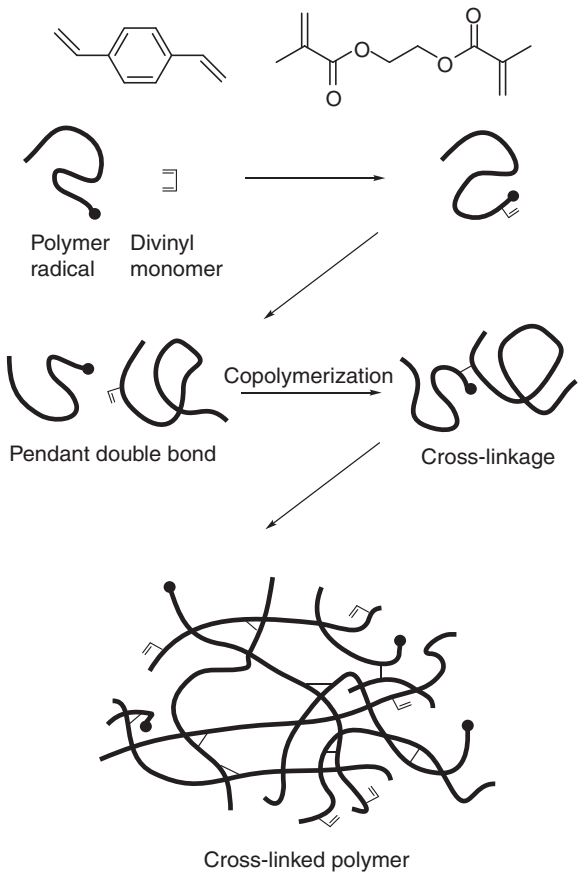

Scheme 6 Schematic presentation of cross-linking (gelation) in free-radical copolymerization of vinyl/divinyl comonomers.[43]

where k_x is the cross-linking rate constant. The cross-link density ρ (also called branch density) is defined as the ratio of the number of cross-link points to that of monomeric units (note: one H-type cross-linkage consists of two cross-link points). It is assumed that every monomeric unit in the primary chains has an equal probability to be cross-linked. Primary chains are rather imaginary and would exist if all cross-linkages were severed. The cross-link density can be calculated from

$$\frac{d(Q_1\rho)}{dt} = k_xQ_1Q_1 \qquad [249]$$

Applying the method of moments, we have

$$\frac{dQ_0}{dt} = -\frac{1}{2}k_xQ_1Q_1 \qquad [250]$$

$$\frac{dQ_1}{dt} = 0 \qquad [251]$$

$$\frac{dQ_2}{dt} = k_xQ_2Q_2 \qquad [252]$$

Solving eqns [249]–[252] gives the number- and weight-average chain lengths as

$$\bar{r}_N = \frac{\bar{r}_{Np}}{1-\frac{1}{2}\rho\bar{r}_{Np}} \qquad [253]$$

$$\bar{r}_W = \frac{\bar{r}_{Wp}}{1-\rho\bar{r}_{Wp}} \qquad [254]$$

where $\bar{r}_{Np}$ and $\bar{r}_{Wp}$ are number- and weight-average lengths of primary chains, respectively. With $w(r) = r[P_r]/Q_1$, eqn [248] can be easily rearranged into an integrodifferential form:

$$\frac{1}{r}\frac{dw(r)}{d\rho} = -w(r) + \frac{1}{2}\int_0^r w(s)w(r-s)ds \qquad [255]$$

which was solved by Saito, given primary chains having Flory's most probable distribution $w_p(r) = \tau^2 r \exp(-\tau r)$:[187]

$$w(r) = \tau^2 r \exp(-\tau r(1+\rho/\tau))\sum_{i=0}^{\infty}\frac{(\tau r)^{3i}(\rho/\tau)^i}{(1+i)!(1+2i)!} \qquad [256]$$

Equations [254] clearly shows that the polymerization system reaches the gel point when each primary chain has one cross-link point by its weight average, that is, $\rho\bar{r}_{Wp} = 1$. This conclusion is always true regardless of the type of primary chain distributions since no primary distribution is assumed in the equation derivation. At the gel point, the weight-average chain length approaches a theoretical infinity and gel molecules start to form. The gel fraction, that is, the ratio of the number of monomeric units in gels to that of total monomeric units, can be predicted by Flory's recursive equation:[16]

$$1 - w_g = \int_0^\infty w_p(r)(1-\rho w_g)^r dr \qquad [257]$$

where w_g is the gel fraction and $w_p(r)$ is the chain length distribution of primary chains. With $w_p(r) = \tau^2 r \exp(-\tau r)$, eqn [257] can be easily solved (hint: $(1-\rho w_g)^r \sim \exp(-\rho w_g r)$ with very small ρ), resulting in the widely used Charlesby–Pinner equation:[188]

$$w_s + \sqrt{w_s} = \frac{2}{\rho\bar{r}_{Wp}} \qquad [258]$$

where w_s is the sol fraction, $w_s = 1 - w_g$.

It should be pointed out that the above treatment and derivation of eqns [248]–[258] are based on a statistical argument that polymer networks are randomly assembled from primary chains at any cross-link density. It is also assumed that there are no chain cyclization reactions involved. In reality, gel molecules are gradually built up during polymerization, which is dependent on history. Realistic modeling of the gelation process must then resort to the use of kinetic approach based on mass balances of individual chains.

4.32.10.4 Cross-link Density Distribution

In conventional free-radical polymerization, it takes only seconds for individual primary chains to fully grow. In such a short period, chains are not fully relaxed and there is little time for diffusion either. Radicals can easily react with pendant double bonds on their own molecules to form cycles (not necessarily on their primary chains). These localized intramolecular reactions could lead to microgel formation and cause structural heterogeneity in network products, in which tight and rigid microgel domains are loosely connected. Slower chain growth such as controlled radical polymerization gives chains more time to relax and to diffuse, promotes intermolecular cross-linking, and thus reduces intramolecular cyclization. Statistical gelation theories usually work better for condensation and controlled radical processes than for conventional free-radical and Ziegler–Natta types.

Cyclization processes can be complex as shown in the Scheme 7.[189,190] At present conversion Θ, the cross-link density $\rho(\theta,\Theta)$ of primary chains of birth conversion θ ($\theta \le \Theta$) is the sum of instantaneous cross-link density $\rho_i(\theta)$ and additional cross-link density $\rho_a(\theta,\Theta)$:

$$\rho(\theta,\Theta) = \rho_i(\theta) + \rho_a(\theta,\Theta) \qquad [259]$$

The instantaneous cross-link points of an identified chain born at θ are formed during chain growth by propagation of its radical with pendant double bonds on those chains born earlier than θ. The additional cross-link points are formed by consumption of pendant double bonds on the identified chain by those chains born during the period from θ to Θ. Correspondingly, the density of cyclization density $\rho_c(\theta,\Theta)$ is the sum of primary cyclization density $\rho_{cp}(\theta)$, instantaneous secondary cyclization density $\rho_{cs,i}(\theta)$, and additional secondary cyclization density $\rho_{cs,a}(\theta,\Theta)$:

$$\rho_c(\theta,\Theta) = \rho_{cp}(\theta) + \rho_{cs,i}(\theta) + \rho_{cs,a}(\theta,\Theta) \qquad [260]$$

The primary cyclization occurs by propagation of a radical with pendant double bonds on the same chain. It is an intramolecular reaction that strongly depends on chain configuration. The instantaneous secondary cyclization occurs between the chains that are connected by instantaneous cross-linking. The additional secondary cyclization occurs between the chains that are connected by additional cross-linking. As the first approximation

$$\rho_{cp}(\theta) = k_{cp}F_2(\theta) \qquad [261]$$

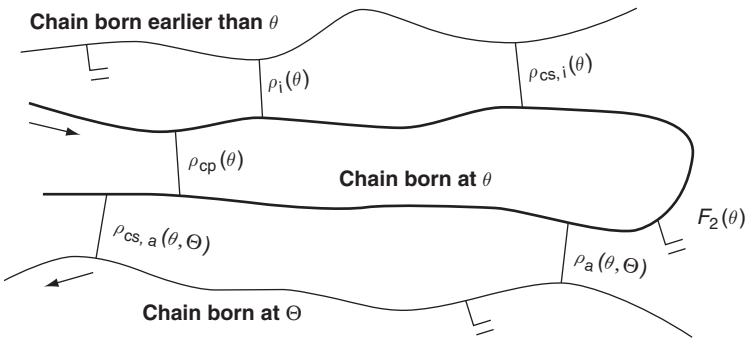

Scheme 7 Schematic representation of the polymer network formation in free-radical copolymerization of vinyl/divinyl monomers.[191]

$$\rho_{cs,i}(\theta) = k_{cs,i}\,\rho_i(\theta) \quad [262]$$

$$\rho_{cs,a}(\theta,\Theta) = k_{cs,a}\,\rho_a(\theta,\Theta) \quad [263]$$

where $F_2(\theta)$ is the mole fraction of divinyl monomer in the primary chain born at θ.

The formation of additional cross-link points is governed by[189,190]

$$\frac{\partial\rho_a(\theta,\Theta)}{\partial\Theta} = \frac{\bar{k}_p F_2(\theta) - \rho_{cp}(\theta) - \rho_{cs,a}(\theta,\Theta) - \rho_a(\theta,\Theta)}{k_p\,(1-\Theta)} \quad [264]$$

where k_p and $\bar{k}_p$ are pseudokinetic rate constants of the propagation with monomers and that with pendant double bonds. Since each additional cross-link needs one instantaneous partner, we have

$$\rho_i(\theta) = \int_0^\theta \frac{\partial\rho_a(\gamma,\theta)}{\partial\theta}\,d\gamma \quad [265]$$

Equations [259]–[265] can be solved numerically for the cross-link and cyclization density distributions $\rho(\theta,\Theta)$ and $\rho_c(\theta,\Theta)$ at the present conversion Θ as a function of the birth conversion θ. The average cross-link density is

$$\bar{\rho}(\Theta) = \frac{1}{\Theta}\int_0^\Theta \rho(\theta,\Theta)\,d\theta \quad [266]$$

$$\bar{\rho}_c(\Theta) = \frac{1}{\Theta}\int_0^\Theta \rho_c(\theta,\Theta)\,d\theta \quad [267]$$

Under azeotropic conditions and with low levels of divinyl monomers, $\bar{k}_p/k_p$ and $F_2(\theta)$ are weak functions of monomer conversion. The following analytical solutions are obtained:[192]

$$\rho(\theta,\Theta) = \kappa F_2\left\{\frac{\zeta}{1-\zeta}\left[(1-\theta)^{\zeta-1}-1\right] + \left[1-\left(\frac{1-\Theta}{1-\theta}\right)^{\zeta}\right]\right\} \quad [268]$$

$$\bar{\rho}(\Theta) = \frac{2\kappa F_2\left[1-\zeta\Theta-(1-\Theta)^{\zeta}\right]}{(1-\zeta)\Theta} \quad [269]$$

$$\rho_c(\theta,\Theta) = k_{cp}F_2 + \kappa F_2\left\{k_{cs,i}\frac{\zeta}{1-\zeta}\left[(1-\theta)^{\zeta-1}-1\right] + k_{cs,a}\left[1-\left(\frac{1-\Theta}{1-\theta}\right)^{\zeta}\right]\right\} \quad [270]$$

$$\bar{\rho}(\Theta) = k_{cp}F_2 + \frac{\kappa F_2(k_{cs,i}+k_{cs,a})\left[1-\zeta\Theta-(1-\Theta)^{\zeta}\right]}{(1-\zeta)\Theta} \quad [271]$$

where $\zeta = (\bar{k}_p/k_p)(1+k_{cs,a})$ and $\kappa = (1-k_{cp})/(1+k_{cs,a})$. Figure 17 shows such cross-link density distributions and clearly demonstrates that primary chains generated at different times during polymerization have different cross-link densities.

4.32.10.5 Kinetic Modeling of Gelation

The history-dependent molecular weight development prior to gel point can be derived from the following mass balances of the radical and dead-chain species:

$$\frac{d[P_1^\bullet]}{dt} = 2fk_d[I] + k_{fZ}[Z]Q_0^\bullet + k_{fp}[P_1]Q_0^\bullet - (k_p[M] + k_{fZ}[Z] + k_tQ_0^\bullet + k_{fp}Q_1 + \bar{k}_pQ_1)[P_1^\bullet] \quad [272]$$

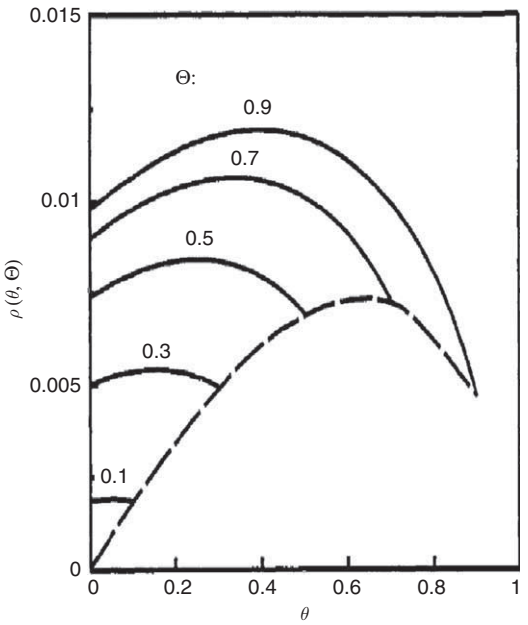

Figure 17 Cross-link density distribution of primary polymer chains with respect to their birth conversion.[43,97]

$$\frac{d[P_r^\bullet]}{dt} = k_p[M][P_{r-1}^\bullet] + k_{fp}r[P_r]Q_0^\bullet + \bar{k}_p\sum_{s=1}^{r-1}s[P_{r-s}^\bullet][P_s] - (k_p[M] + k_{fZ}[Z] + k_tQ_0^\bullet + k_{fp}Q_1 + \bar{k}_pQ_1)[P_r^\bullet] \quad [273]$$

The rate constants in eqns [272] and [273] are pseudokinetic rate constants. In addition to those defined by eqns [238], [243]–[245]:

$$k_{fp} = k_{fp11}\phi_1^\bullet\bar{F}_1 + k_{fp21}\phi_{21}^\bullet\bar{F}_1 + k_{fp12}\phi_1^\bullet\bar{F}_2 + k_{fp22}\phi_2^\bullet\bar{F}_2 \quad [274]$$

$$\bar{k}_p = (\bar{k}_{p13}\phi_1^\bullet + \bar{k}_{p23}\phi_2^\bullet)(\bar{F}_2 - \bar{\rho} - \bar{\rho}_c) \quad [275]$$

The corresponding moment equations of the radical chains are

$$\frac{dQ_i^\bullet}{dt} = 2fk_d[I] + k_{fZ}[Z]Q_0^\bullet + k_{fp}Q_0^\bullet Q_{i+1} + \bar{k}_p\sum_{j=1}^{i}\binom{i}{j}Q_{i-j}^\bullet Q_{j+1} + k_p[M]\sum_{j=0}^{i-1}\binom{i}{j}Q_j^\bullet - (k_{fZ}[Z] + k_tQ_0^\bullet + k_{fp}Q_1)Q_i^\bullet \quad [276]$$

for $i \geq 1$. Applying the SSH to eqn [276], we have

$$q_i^\bullet = \frac{\tau+\beta+c_{fp,i+1} + \sum_{j=1}^{i}\binom{i}{j}\bar{c}_{p,j+1}q_{i-j}^\bullet + \sum_{j=0}^{i-1}\binom{i}{j}q_j^\bullet}{\tau+\beta+c_{fp,1}} \quad [277]$$

where $q_i^\bullet = Q_i^\bullet/Q_0^\bullet$, $q_i = Q_i/[M]_0$, $c_{fp,i} = k_{fp}Q_i/k_p[M]$, and $\bar{c}_{p,i} = \bar{k}_pQ_i/k_p[M]$. τ and β are defined by eqns [56] and [57]. In general, $q_i^\bullet \geq 1 \gg \tau+\beta$. The first three moments of radical chains are

$$q_0^\bullet = 1 \quad [278]$$

$$q_1^\bullet = \frac{1+c_{fp,2}+\bar{c}_{p,2}}{\tau+\beta+c_{fp,1}} \quad [279]$$

$$q_2^\bullet = \frac{1+c_{fp,3}+\bar{c}_{p,3}}{\tau+\beta+c_{fp,1}} + \frac{2(1+\bar{c}_{p,2})(1+c_{fp,2}+\bar{c}_{p,2})}{(\tau+\beta+c_{fp,1})^2} \quad [280]$$

Similarly, the mass balances for dead chains are as follows:

$$\frac{d[P_r]}{dt} = (k_{fZ}[Z] + k_{td}Q_0^\bullet + k_{fp}Q_1)[P_r^\bullet] + \frac{1}{2}k_{tc}\sum_{s=1}^{r-1}[P_s^\bullet][P_{r-s}^\bullet] - (\bar{k}_p^= + k_{fp})r[P_r]Q_0^\bullet \quad [281]$$

Their moment equations are

$$\frac{dQ_i}{dt} = (k_{fZ}[Z] + k_t Q_0^\bullet + k_{fp}Q_1)Q_i^\bullet + \frac{1}{2}k_{tc}\sum_{j=1}^{i-1}\binom{i}{j}Q_j^\bullet Q_{i-j}^\bullet - (\bar{k}_p^= + k_{fp})Q_0^\bullet Q_{i+1} \quad [282]$$

which can be rewritten as

$$\frac{dq_i}{dx} = (\tau + \beta + c_{fp,1})q_i^\bullet + \frac{1}{2}\beta\sum_{j=1}^{i-1}\binom{i}{j}q_j^\bullet q_{i-j}^\bullet - \bar{c}_{p,i+1}^= - c_{fp,i+1} \quad [283]$$

Combining eqn [277] yields

$$\frac{dq_i}{dx} = \sum_{j=1}^{i-1}\binom{i}{j}\bar{c}_{p,j+1}^= q_{i-j}^\bullet + \sum_{j=0}^{i-1}\binom{i}{j}q_j^\bullet + \frac{1}{2}\beta\sum_{j=1}^{i-1}\binom{i}{j}q_j^\bullet q_{i-j}^\bullet \quad [284]$$

The first three moments of dead chains are[189,190,193]

$$\frac{dq_0}{dx} = \tau + \frac{\beta}{2} - \bar{c}_{p,1}^= \quad [285]$$

$$\frac{dq_1}{dx} = 1 \quad [286]$$

$$\frac{dq_2}{dx} = \frac{2(1 + \bar{c}_{p,2}^=)(1 + c_{fp,2} + \bar{c}_{p,2}^=)}{\tau + \beta + c_{fp,1}} + \beta\left(\frac{1 + c_{fp,2} + \bar{c}_{p,2}^=}{\tau + \beta + c_{fp,1}}\right)^2 \quad [287]$$

Figure 18 shows the model correlation with a set of experimental data.

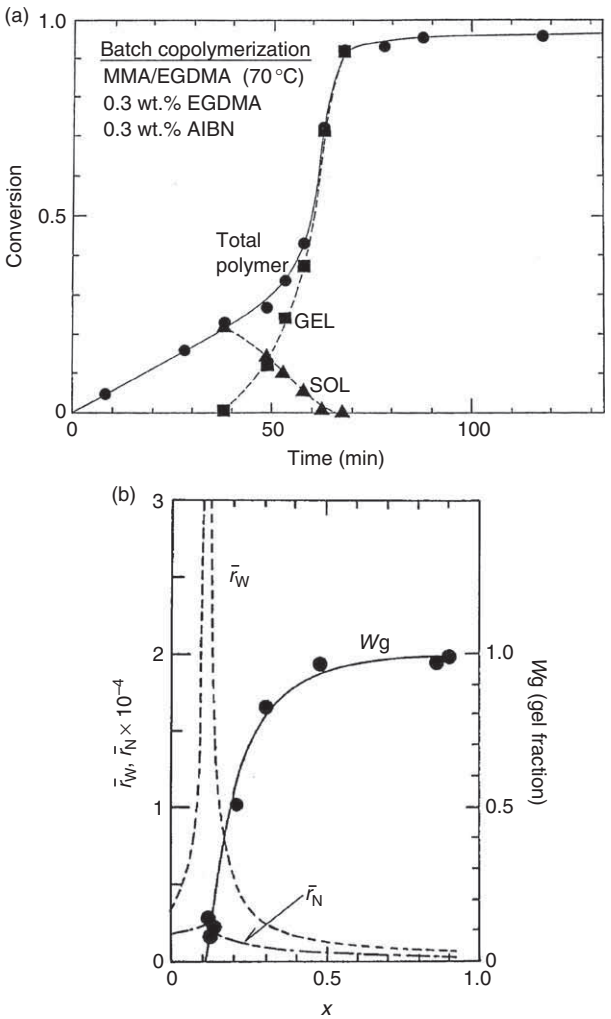

Figure 18 (a) Conversion versus time of sol, gel, and total polymers and (b) number- and weight-average chain lengths versus conversion, as well as gel development in bulk radical copolymerization of MMA/EGDMA at 70 °C with 0.3 wt.% ethylene glycol dimethacrylate (EGDMA) and 0.3 wt.% AIBN.[194,195]

4.32.11 Semibatch Control of Copolymer Composition

All the analysis and discussions so far are based on batch polymerization processes. All the derived equations are applicable to batch processes. In batch processes, all reagents are added to reactors at the beginning and remain in the reactors for the same length of times. The reactor must have capacity for rapid heating initially, adequate cooling capacity to accommodate maximum rate, and control to maintain desired temperature during polymerization. Batch processes are suitable for polymerization to be carried to high conversions. However, there are potential problems for runaway and for maintaining batch-to-batch product uniformity. Improved control systems are required to reduce these problems. In comparison, in semibatch processes, some reactants may be added incrementally or at intervals and some byproducts may also be removed during polymerization. The additions of catalyst, monomer, and other reagents can be programmed to provide improved control of the reaction. Semibatch processes are used in industry for various reasons.[196]

4.32.11.1 Monomer Feeding Policies for Uniform Copolymers

Semibatch processes with incremental monomer additions are particularly useful in copolymer production through free-radical polymerization when the reactivities of comonomers vary widely. For a binary copolymerization system, the mass balances for the two monomer types are

$$dN_1/dt = -\hat{k}_1[P^\bullet]N_1 + \overrightarrow{F}_{1,in} \quad [288]$$

$$dN_2/dt = -\hat{k}_2[P^\bullet]N_2 + \overrightarrow{F}_{2,in} \quad [289]$$

where the pseudokinetic propagation constants $\hat{k}_1 = k_{p11}\phi_1^\bullet + k_{p21}\phi_2^\bullet$ and $\hat{k}_2 = k_{p12}\phi_1^\bullet + k_{p22}\phi_2^\bullet$ with the radical fractions defined by eqn [239] based on the long-chain assumption.

There are two major policies in feeding monomers to the reactor.[184] The strategy is to achieve the constant copolymer composition by maintaining constant monomer composition during polymerization. In policy I, all of the slower reacting

monomer $N_{2,0}$ is charged to reactor at the start and there is no further addition during polymerization $\overrightarrow{F}_{2,\text{in}} = 0$. A sufficient amount of the faster monomer $N_{1,0}$ is also charged to the reactor at $t = 0$ to give a desired $f_1 = N_{1,0}/(N_{1,0} + N_{2,0})$ for the targeted $F_1 = (r_1 f_1^2 + f_1 f_2)/(r_1 f_1^2 + 2 f_1 f_2 + r_2 f_2^2)$. Additional amount of the faster monomer $(\Delta N = N_{2,0}(F_1/F_2) - N_{1,0})$ is added with a time-varying feed rate to maintain constant f_1 during polymerization. Applying $\mathrm{d}(N_1/N_2)/\mathrm{d}t = 0$ or equivalently $\mathrm{d}N_2/\mathrm{d}t = (N_2/N_1)\mathrm{d}N_1/\mathrm{d}t$ as a constraint to eqn [289], we have

$$\mathrm{d}N_1/\mathrm{d}t = -\hat{k}_2[\mathrm{P}^\bullet]N_1 \qquad [290]$$

Since f_1 and f_2 remain constant, $\hat{k}_1$ and $\hat{k}_2$ are also constant under an isothermal condition. If the radical concentration can be remained constant, eqn [290] has the analytical solution of

$$N_1 = N_{1,0}\exp(-\hat{k}_2[\mathrm{P}^\bullet]t) \qquad [291]$$

with the initial condition $N_1 = N_{1,0}$ at $t = 0$. Substituting eqns [290] and [291] into eqn [288] gives

$$\overrightarrow{F}_{1,\text{in}} = (\hat{k}_1 - \hat{k}_2)[\mathrm{P}^\bullet]N_{1,0}\exp(-\hat{k}_2[\mathrm{P}^\bullet]t) \qquad [292]$$

which is the required feed rate profile of the fast monomer. Equation [292] is a decay function with the maximum feeding rate at the start of polymerization. If the differences between monomer and polymer densities and their resulting volume shrinkage are neglected, the increase of volume during polymerization follows:

$$\mathrm{d}V/\mathrm{d}t = m_1\overrightarrow{F}_{1,\text{in}}/\rho_\mathrm{m} \qquad [293]$$

Substituting eqn [292] into eqn [293] gives

$$V = V_0 + V_{1,0}(\hat{k}_1/\hat{k}_2 - 1)[1 - \exp(-\hat{k}_2[\mathrm{P}^\bullet]t)] \text{ or}$$
$$V = V_{2,0}[1/F_2 - (F_1/F_2 - f_1/f_2)\exp(-\hat{k}_2[\mathrm{P}^\bullet]t)] \qquad [294]$$

where $V_{1,0} = m_1 N_{1,0}/\rho_\mathrm{m}$ and $V_0 = (m_1 N_{1,0} + m_2 N_{2,0})/\rho_\mathrm{m}$ are the initial volume of the faster monomer and that of the total monomers, m_1 and m_2 are monomer molecular weights, ρ_m is the monomer density, and note $\hat{k}_1/\hat{k}_2 = (F_1/F_2)(f_2/f_1)$. At $t \to \infty$, $V = V_{2,0}/F_2$.

To maintain constant radical concentration $d(N_\mathrm{I}/V) = 0$, additional initiator needs to be fed to the reactor to compensate the consumption by initiator decomposition $k_\mathrm{d}[\mathrm{I}]_0 V$, as well as the dilution by monomer addition $\mathrm{d}N_\mathrm{I}/\mathrm{d}t = [\mathrm{I}]_0(\mathrm{d}V/\mathrm{d}t)$, that is

$$\overrightarrow{F}_{\mathrm{I},\text{in}} = k_\mathrm{d}N_\mathrm{I} + \mathrm{d}N_\mathrm{I}/\mathrm{d}t = [\mathrm{I}]_0(k_\mathrm{d}V + \mathrm{d}V/\mathrm{d}t) \qquad [295]$$

Substituting eqn [294] into eqn [295] gives

$$\overrightarrow{F}_{\mathrm{I},\text{in}} = k_\mathrm{d}[\mathrm{I}]_0 V_{2,0}/F_2 + [\mathrm{I}]_0 V_{2,0}(F_1/F_2 - f_1/f_2)(\hat{k}_2[\mathrm{P}^\bullet] - 1)\exp(-\hat{k}_2[\mathrm{P}^\bullet]t) \qquad [296]$$

Policy I normally requires a separate feeding line for the initiator. However, if the initiator has a very long half-lifetime $t_{1/2} = \ln 2/k_\mathrm{d}$ (very small k_d), the ratio of $\overrightarrow{F}_{\mathrm{I},\text{in}}/\overrightarrow{F}_{1,\text{in}}$ becomes independent of time. The initiator can then be premixed with the monomer at $[\mathrm{I}]_0$ and fed to the reactor by a single line.

In policy II, parts of both monomers are charged to the reactor at $t = 0$ to give desired F_1 and rest of the monomers are added at time-varying feed rates to maintain constant monomer concentrations $[\mathrm{M}_1]$ and $[\mathrm{M}_2]$. The constraints are then $N_1/V = [\mathrm{M}_1]_0$ and $N_2/V = [\mathrm{M}_2]_0$, that is, $\mathrm{d}N_1/\mathrm{d}t = [\mathrm{M}_1]_0\mathrm{d}V/\mathrm{d}t$ and $\mathrm{d}N_2/\mathrm{d}t = [\mathrm{M}_2]_0\mathrm{d}V/\mathrm{d}t$. The volume increases as monomers are fed to the reactor:

$$\mathrm{d}V/\mathrm{d}t = (m_1\overrightarrow{F}_{1,\text{in}} + m_2\hat{F}_{2,\text{in}})/\rho_\mathrm{m} \qquad [297]$$

Combining eqns [288] and [289] with eqn [297], the constraints give

$$\mathrm{d}N_1/\mathrm{d}t = \hat{\kappa}[\mathrm{P}^\bullet]N_1 \quad \mathrm{d}N_2/\mathrm{d}t = \hat{\kappa}[\mathrm{P}^\bullet]N_2 \qquad [298]$$

where $\hat{\kappa} = (\phi_{\mathrm{w},1}\hat{k}_1 + \phi_{\mathrm{w},2}\hat{k}_2)/(1 - \phi_{\mathrm{w},1} - \phi_{\mathrm{w},2})$ and $\phi_{\mathrm{w},1} = m_1[\mathrm{M}_1]_0/\rho_\mathrm{m}$ and $\phi_{\mathrm{w},2} = m_2[\mathrm{M}_2]_0/\rho_\mathrm{m}$ are weight fractions of the two monomers (the rest are polymer and/or solvent). Substituting eqn [298] into eqns [288] and [289] gives

$$\overrightarrow{F}_{1,\text{in}} = (\hat{\kappa} + \hat{k}_1)[\mathrm{P}^\bullet]N_1$$
$$\overrightarrow{F}_{2,\text{in}} = (\hat{\kappa} + \hat{k}_2)[\mathrm{P}^\bullet]N_2 \qquad [299]$$

Solving eqn [298] under an isothermal condition and with constant radical concentration assumption, as well as $N_1 = N_{1,0}$ and $N_2 = N_{2,0}$ at $t = 0$ gives

$$N_1 = N_{1,0}\exp(\hat{\kappa}[\mathrm{P}^\bullet]t) \quad N_2 = N_{2,0}\exp(\hat{\kappa}[\mathrm{P}^\bullet]t) \qquad [300]$$

The monomer feeding rate profiles from eqn [299] are thus

$$\overrightarrow{F}_{1,\text{in}} = (\hat{\kappa} + \hat{k}_1)[\mathrm{P}^\bullet]N_{1,0}\exp(\hat{\kappa}[\mathrm{P}^\bullet]t)$$
$$\overrightarrow{F}_{2,\text{in}} = (\hat{\kappa} + \hat{k}_2)[\mathrm{P}^\bullet]N_{2,0}\exp(\hat{\kappa}[\mathrm{P}^\bullet]t) \qquad [301]$$

and the volume profile from eqn [297] is

$$V = V_0\exp(\hat{\kappa}[\mathrm{P}^\bullet]t) \qquad [302]$$

The feeding rate profile of additional initiator required to maintain constant radical concentration can be obtained from eqns [295] and [302]:

$$\overrightarrow{F}_{\mathrm{I},\text{in}} = [\mathrm{I}]_0 V_0(k_\mathrm{d} + \hat{\kappa}[\mathrm{P}^\bullet])\exp(\hat{\kappa}[\mathrm{P}^\bullet]t) \qquad [303]$$

From eqns [299] and [303], the feeding rates of initiator and monomers have the same time dependence with constant ratios. Therefore, only a single feeding line is needed in policy II for a premixed initiator and monomer stock.

4.32.11.2 Stability in Semibatch Operation

Compared to policy I, policy II has advantages in not only equipment setup but also operation. While the ratio of two monomers remains unchanged in policy I, the monomer concentration decreases and the polymer concentration increases during polymerization. The system becomes viscous and the rate of polymerization can either decrease due to monomer depletion or increase due to gel effect. The rate of heat generation varies and thus a reactor system having the capacity of heat removal at the highest rate is required. In policy II, the monomer concentration remains constant and so does the rate of polymerization and heat generation. The polymerization can be operated under different conditions.[184] Under the monomer-starved condition ($[\mathrm{M}_1] \sim 0$ and $[\mathrm{M}_2] \sim 0$), the system becomes self-regulated and thus stable. As shown in Figure 19, at the point P1, if turbulences in the feeding line cause an increase in the monomer concentration, the rate of

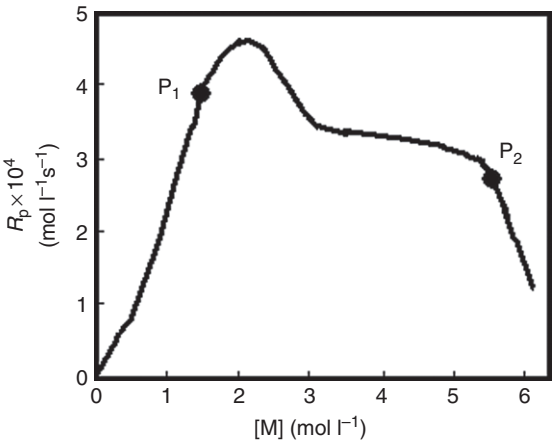

Figure 19 Stability in semibatch free-radical polymerization: P1 operated under monomer starving condition is stable, while P2 operated under monomer-rich condition is unstable.

polymerization increases and so does the heat generation that increases temperature. The increased temperature accelerates the rate of polymerization and thus consumes the excess monomers. On the other side, if turbulence leads to a reduced monomer concentration, the rate of heat generation is also reduced. Cooling the system slows down monomer consumption and balances the missed monomer amount. For the same reason, under the monomer-rich condition, the operation is unstable at the point P2. Any deviation in the monomer concentration from the feeding rate can be amplified and causes further deviation in the same direction that cannot be self-corrected by the reactor.

4.32.11.3 Semibatch Design of Gradient Copolymers

The batchwise free-radical copolymerization produces a copolymer product that is actually a blend of individual chains of various compositions. This composition drifting is caused by different reactivity ratios of the comonomers. As a consequence of the fact that one monomer is consumed faster than the other, the early produced chains are rich in the fast-reacting monomers and the later born chains contain more slow-reacting monomers. The characteristic feature of the conventional free-radical polymerization is slow initiation but fast propagation. Chains are continuously initiated throughout the whole course of polymerization that takes hours. Once initiated, individual chains take only seconds to grow to their full sizes. The duration of hours in the initiation facilitates control over the chain-to-chain composition, as demonstrated by the above semibatch policies for polymer products having uniform chain-to-chain compositions. However, the duration of seconds in the propagation does not permit any manipulation over the end-to-end composition along individual chains.

In contrast, in the 'living' types of controlled radical copolymerization such as SFRP, ATRP, and RAFT polymerization, individual chains are initiated in a relatively short period of time from seconds to minutes at the beginning but grow slowly and continuously by propagation for hours throughout the whole course of polymerization. All the chains thus have similar compositions but possess a composition profile from one end to the other. Such polymers having end-to-end composition variation are termed as 'gradient' copolymers.[197–201] The synthesis of gradient copolymers using batch-controlled radical processes has been well demonstrated. However, the obtained copolymer products have as-synthesized gradient compositions determined only by the comonomer reactivity ratios (**Scheme 8**).

There are several semibatch approaches of controlled radical copolymerization developed for targeting uniform copolymers. The simplest method is the use of policy I with constant feeding rates for the fast monomer. The produced copolymers have more uniform compositions compared to their batch products. Semibatch policies are powerful for making various types of gradient copolymers. Once a targeted profile of the composition versus chain length $F_1(\bar{r}_N)$ is defined, the constraint of N_1/N_2 in policy I becomes a function of polymerization time. The time-dependent monomer feeding rate $\overrightarrow{F}_{1,in}$ (note $\overrightarrow{F}_{2,in} = 0$) can be obtained by numerically solving eqns [288] and [289], provided the rate constants are given.[202,203] **Figure 20** shows the results of ATRP of MMA/*t*BMA.[204–206] The copolymers having various unprecedented gradient compositions are produced by regulating the monomer feeding pump by a computer programmed with the feeding rate

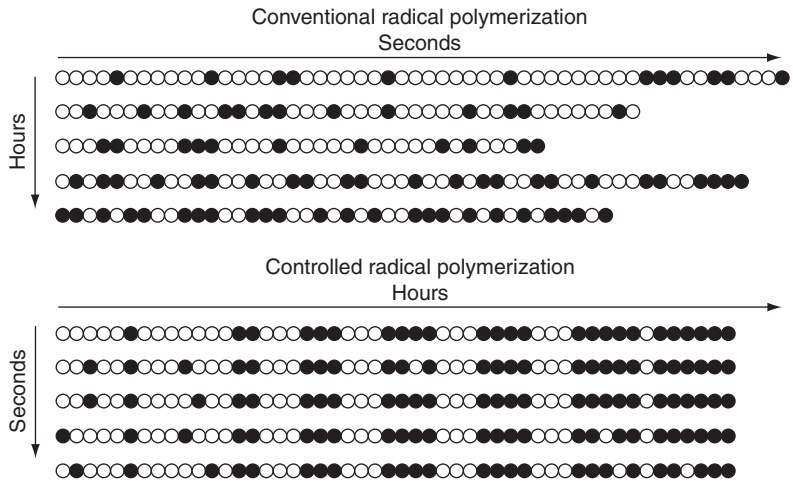

Scheme 8 Difference between conventional and controlled radical polymerization. The long period of chain growth time in controlled radical polymerization permits design and control over the composition along individual copolymer chains.

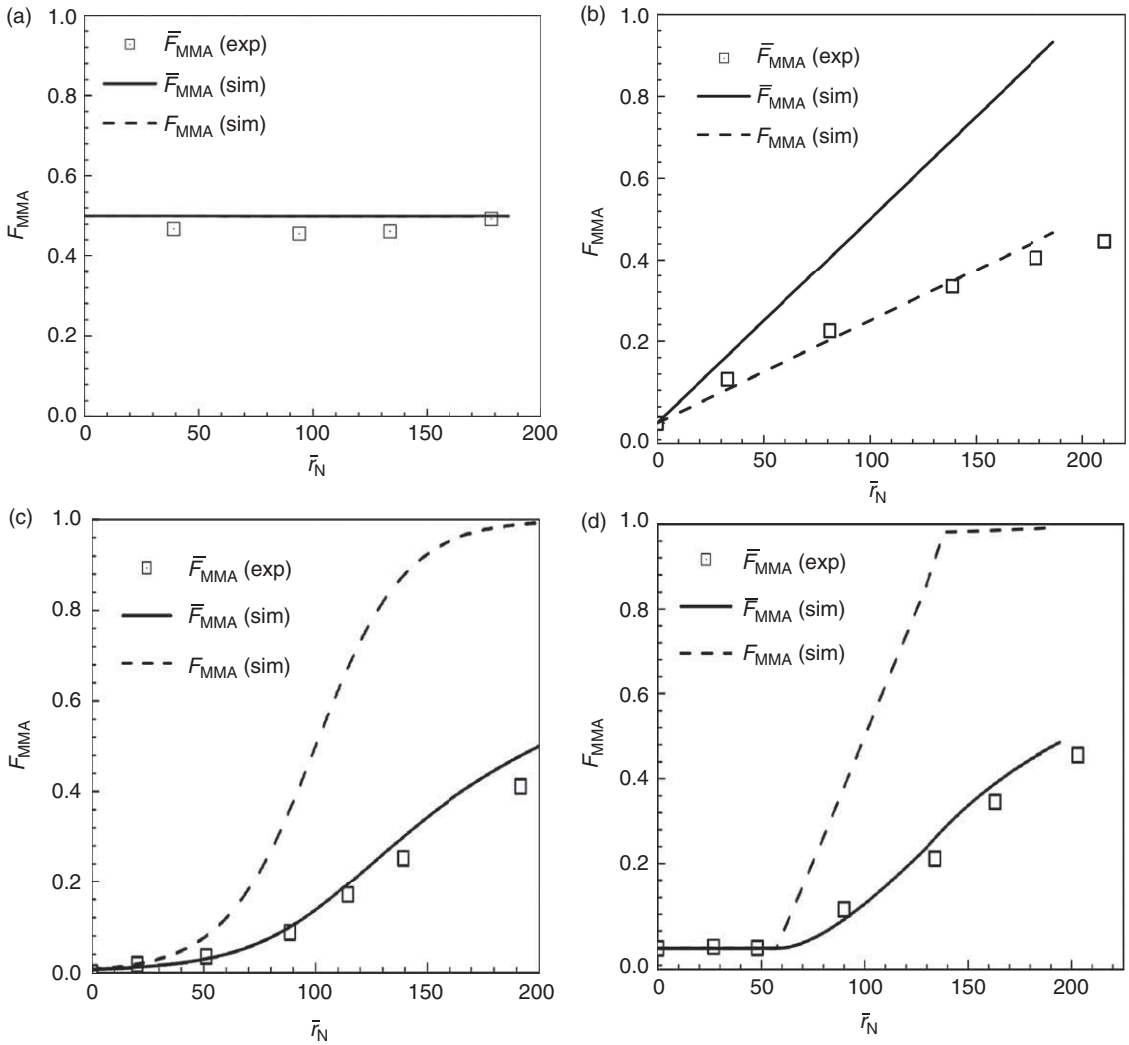

Figure 20 Gradient copolymers having (a) uniform, (b) linear, (c) hyperbolic, and (d) triblock with linear-gradient transition midblock.[206]

equations. The gradient profiles include uniform, linear gradient, hyperbolic tangent (tanh), and triblock with linear-gradient midblock, as illustrated in Scheme 9:

$$F_{1,\text{uniform}} = 0.5 \quad [304]$$

$$F_{1,\text{linear}} = \bar{r}_N/\bar{r}_{N,\text{final}} \quad [305]$$

$$F_{1,\text{hyperb}} = 0.5 + 0.5 \tanh \lambda(\bar{r}_N/\bar{r}_{N,\text{final}} - 0.5) \quad [306]$$

$$F_{1,\text{triblock}} = \begin{cases} 0, & \bar{r}_N \le 5\bar{r}_{N,\text{final}}/12 \\ 6\bar{r}_N/\bar{r}_{N,\text{final}} - 2.5, & 5\bar{r}_{N,\text{final}}/12 < \bar{r}_N \le 7\bar{r}_{N,\text{final}}/12 \\ 1, & \bar{r}_N > 7\bar{r}_{N,\text{final}}/12 \end{cases} \quad [307]$$

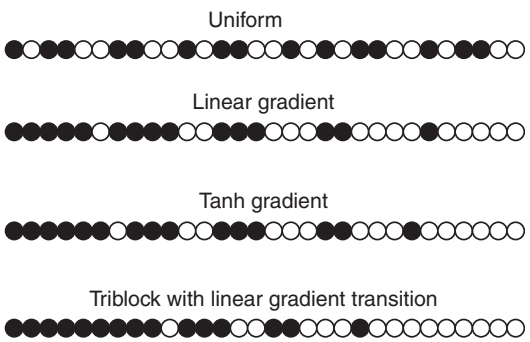

Scheme 9 Setup of semibatch reactor system for the designed gradient copolymers. Slow comonomer is fed through a metering pump controlled by a computer that is programmed with semibatch model.

4.32.12 Continuous Polymerization Processes

Most high-tonnage commodity polymers are produced in continuous processes. The feed is metered continuously into the reactor and the effluent is removed continuously from the reactor. When polymerization reaches a steady state in operation, the rate of heat generated at any point in the system is usually constant. Continuous processes have advantages of easy operation and low costs, particularly suitable for large-volume production. The mass balances of reactants and products are in a general form of 'accumulation = flow in – flow out + production – consumption'. For example, in the continuous free-radical polymerization, the mass balances for initiator, monomer and polymer, are

$$\frac{dN_I}{dt} = \vec{F}_{I,in} - [I]_{out}\vec{v}_{out} - R_d V \quad [308]$$

$$\frac{dN_M}{dt} = \vec{F}_{M,in} - [M]_{out}\vec{v}_{out} - R_p V \quad [309]$$

$$\frac{dN_P}{dt} = \vec{F}_{P,in} - [P]_{out}\vec{v}_{out} + (R_{td} + \tfrac{1}{2}R_{tc})V \quad [310]$$

where N_M, N_I, and N_P are moles of monomer, initiator, and polymer chains inside the reactor, respectively; $[M]_{out}$, $[I]_{out}$, and $[P]_{out}$ are monomer, initiator, and polymer chain concentrations at the exit, respectively; R_p, R_d, R_{td}, and R_{tc} are monomer propagation, initiator decomposition, radical disproportionation, and combination termination rates, respectively; $\vec{F}_{M,in}$, $\vec{F}_{I,in}$, and $\vec{F}_{P,in}$ are monomer, initiator, and polymer molar flow rates into the reactor, respectively; $\vec{v}_{out}$ is the volume flow rate out of the reactor; and V is the reaction volume. When $\vec{F}_{in} = \vec{v}_{out} = 0$, it becomes a batch process. When $\vec{F}_{in} = 0$ or $\vec{v}_{out} = 0$, it becomes a semibatch process. When $dN/dt = 0$, it becomes a steady-state continuous process.

4.32.12.1 Steady-State Operation

There are two major types of continuous reactors: plug-flow tubular reactor (PFTR) and CSTR. The polymerization kinetics with PFTR is similar to that of batch reactor. In PFTR, the concentrations of reactants and products vary with location but not with time. The rate equations derived for batch processes can be easily transformed into their corresponding equations for PFTR using

$$dl/dt = \vec{v}/A = \vec{v}L/V = L/\bar{t} \quad [311]$$

where L, A, and V are the length, the cross-sectional area, and the volume of the tubular reactor; and $\bar{t}$ is the mean residence time $\bar{t} = V/\vec{v}$. Simply replacing t by $(\bar{t}/L)l$ in the time functions gives the location functions applicable for PFTR. At the exit of PFTR, $l = L$ and the initiator concentration, the monomer conversion, and the polymer chain concentration are

$$[I] = [I]_0 \exp(-k_d\bar{t}) \quad [312]$$

$$-\ln(1-x) = \left(\frac{8fk_p^2[I]_0}{k_d k_t}\right)^{1/2}\left[1 - \exp\left(-\tfrac{1}{2}k_d\bar{t}\right)\right] \quad [313]$$

$$[P] = (2f[I]_0/k_t)(k_{td} + \tfrac{1}{2}k_{tc})[1 - \exp(-k_d\bar{t})] \quad [314]$$

In ideal CSTR, the concentrations of reactants and products inside the reactor are the same as those at the exit. The differential equations become algebraic equations, which can be easily solved:

$$[I]_{out} = [I]_{in}/(1 + k_d\bar{t}) \quad [315]$$

$$x = k_p[P^\bullet]\bar{t}/(1 + k_p[P^\bullet]\bar{t}) \quad [316]$$

$$[P]_{out} = (k_{td} + \tfrac{1}{2}k_{tc})\bar{t}[P^\bullet]^2 \quad [317]$$

where $[P^\bullet] \approx (2fk_d[I]_{out}/k_t)^{1/2}$. Scheme 10 shows CSTR, PFTR, CSTR in series, and PFTR with recirculation.

4.32.12.2 Reactor RTD

Reactors can be very different in structure and appearance. However, the most important reactor property is arguably its RTD. This is particularly true for polymerization where RTD has a great influence on polymer chain properties such as MWD. This influence can vary a lot, depending on the type of polymerization mechanism employed. PFTR and CSTR are two ideal cases. PFTR has a Dirac delta function, which is a pulse at $\bar{t}$ and zero elsewhere, while CSTR has an exponential decay function:

$$E_{PFTR}(t) = \delta(t - \bar{t}) \quad [318]$$

$$E_{CSTR}(t) = \bar{t}^{-1}\exp(-t/\bar{t}) \quad [319]$$

In reality, most reactors have RTDs between these ideal cases.[2,3,196] For example, backmixing (BM) is inevitable in tubular flow due to dispersion. With small extents of dispersion, the RTD of a tubular reactor can be described by

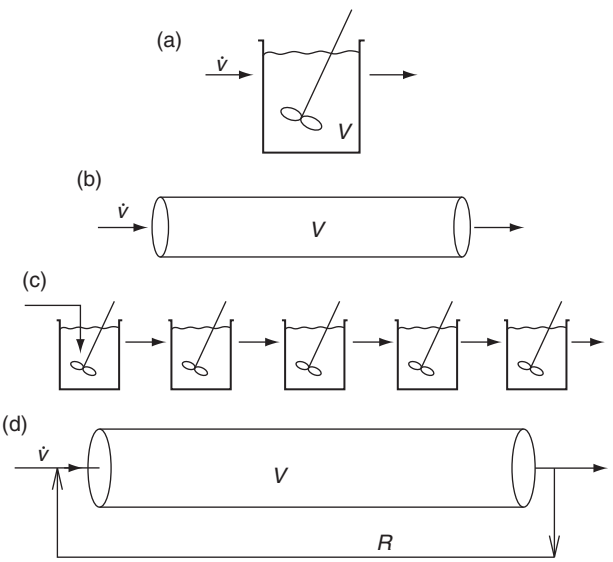

Scheme 10 (a) Single CSTR, (b) tubular reactor, (c) CSTR in series, and (d) tubular reactor with recirculation.

$$E_{\text{TR-SD}}(t) = \frac{1}{\sqrt{\pi\zeta\bar{t}}}\exp[-(t-\bar{t})^2/(\zeta\bar{t})] \quad [320]$$

where $\zeta = 4\bar{t}D/\overrightarrow{v}L$ and D is the axial dispersion coefficient. With large extents of dispersion, it is by

$$E_{\text{TR-LD}}(t) = \frac{1}{\sqrt{\pi\zeta t}}\exp[-(t-\bar{t})^2/(\zeta t)] \quad [321]$$

The RTDs of PFTR and CSTR can be interchangeable. A large number of CSTRs in series give an RTD of PFTR:

$$E_{n\text{CSTR}}(t) = \frac{n}{\bar{t}}\frac{(nt/\bar{t})^{n-1}}{(n-1)!}\exp(-nt/\bar{t}) \quad [322]$$

and a large circulation of PFTR gives an RTD of CSTR:

$$E_{\text{PFTR-R}}(t) = \frac{1}{R}\sum_{i=1}^{\infty}\left(\frac{R}{1+R}\right)^i\delta(t-i\bar{t}) \quad [323]$$

A combination of CSTR in series with recirculation gives an RTD of

$$E_{n\text{CSTR-R}}(t) = \frac{n}{\bar{t}}\exp(-nt/\bar{t})\sum_{i=1}^{\infty}\frac{(nt/\bar{t})^{\text{in}-1}}{(\text{in}-1)!} \quad [324]$$

Figure 21 shows the major types of reactors and their RTD's.

4.32.12.3 Effect of RTD on Polymer Chain Properties

Reactor RTD has a strong influence on polymer chain properties such as molecular weight, copolymer composition, and branching density. The level of RTD effect depends on the relative magnitudes of two characteristic times: the time that chains reside inside the reactor before coming out (chain residence time) and the time it takes for chains to grow (chain lifetime).[207–212] By this criteria, all the polymerization mechanisms can be classified into two major groups. Group I are those mechanisms in which individual chains are generated rapidly such as free-radical polymerization, cationic polymerization, and Ziegler–Natta polymerization. It takes only seconds for the individual chains to propagate thousands of monomers. Such a short-chain lifetime can be considered as instantaneous, as most industrial polymerization processes take hours to complete. Group II are the polymerizations in which chains continuously grow as long as they reside inside reactor. That is, the lifetimes of individual chains are as long as their residence times. Condensation polymerization, living anionic polymerization, controlled radical polymerization, and any other 'living' types of polymerization belong to this group.

Since the total polymer is comprised of chains having various residence times, the MWD at the exit of a reactor is therefore

$$w_{\text{exit}}(r) = \int_o^{\infty} w_{\text{cum}}(r)E(t)\text{d}t \quad [325]$$

where the chains having the same residence time are generated under various birth conditions that can vary with time and/or location inside the reactor:

$$w_{\text{cum}}(r) = \frac{1}{\Delta M}\int_0^{\Delta M} w(r)\text{d}M \quad [326]$$

where $\text{d}M/\Delta M$ is the mass fraction of the chains generated under a specific birth condition. The birth condition includes the concentrations of various reactants and polymerization temperature as reflected by the parameters τ and β in eqns [61], [94], and [169]. In batch polymerization, eqn [326] is the same as eqn [62].

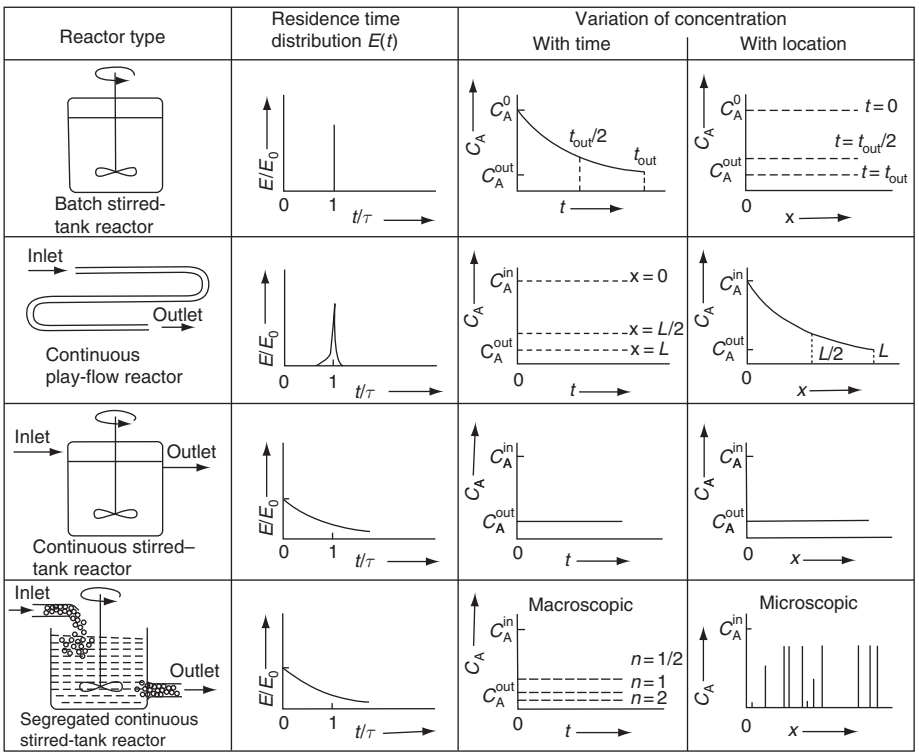

Figure 21 Schematic representation of the course of reaction in various reactor types.[11]

Because chain lifetimes are much shorter than chain residence times, the instantaneous MWD $w(r)$ of group I polymerization is determined only by the birth condition but not influenced by the residence time. In a steady-state homogeneous CSTR, there is only one single condition for chains to be generated, that is, under constant τ and β. The MWD of the total polymer $w_{exit}(r)$ represents a single instantaneous distribution and is therefore narrower than those of batch reactor and PFTR, which are cumulative of many instantaneous distributions at various τ and β values.

The molecular weight of polymer chains in group II polymerization is a strong function of their residence time. Chains continuously grow inside the reactor and are 'born' at the exit. Their birth times are thus the same as the residence times. With an ideal living system, the chain length r is proportional to the residence time t, as $dr/dt = k_p[M]$. This relationship is a linear function under ideal CSTR condition, $r = k_p[M]t$. The MWD of living polymers produced from the ideal CSTR is thus

$$n_{exit}(r) = E(t)/(dr/dt) = \bar{r}_N^{-1}\exp(-r/\bar{r}_N) \quad [327]$$

$$w_{exit}(r) = \bar{r}_N^{-2} r\exp(-r/\bar{r}_N) \quad [328]$$

which is the Flory's most probable distribution. Compared to the Poisson distribution equation [101] made from batch or PFTR processes, the CSTR gives a much broader MWD. Figure 22 shows the influence of RTD on MWD and polydispersity.[190]

RTD does influence not only the polymer MWD but also other chain microstructure properties such as copolymerization composition and branching density. Copolymers experience composition drifting in batch and PFTR processes due to different reactivities of comonomers. In an ideal CSTR process, the monomer composition remains constant and so does the copolymer composition. For reactions with polymer chains such as branching and cross-linking, CSTR has the advantage over batch reactor/PFTR. For example, the rate of branching via chain transfer to polymer is proportional to the polymer concentration and most branching occurs at high conversions. For the same final conversion, CSTR yields a higher branching density than do batch reactor/PFTR.

In addition to the polymerization kinetics, the selection of reactor also depends on satisfactory transport of mass and energy as well as the state of polymer product as marketed (solid, solution, or latex). The purpose is to increase polymer output and to improve product quality at the lowest costs. Scheme 11 shows some reactor designs for heat or mass removal purposes.[11]

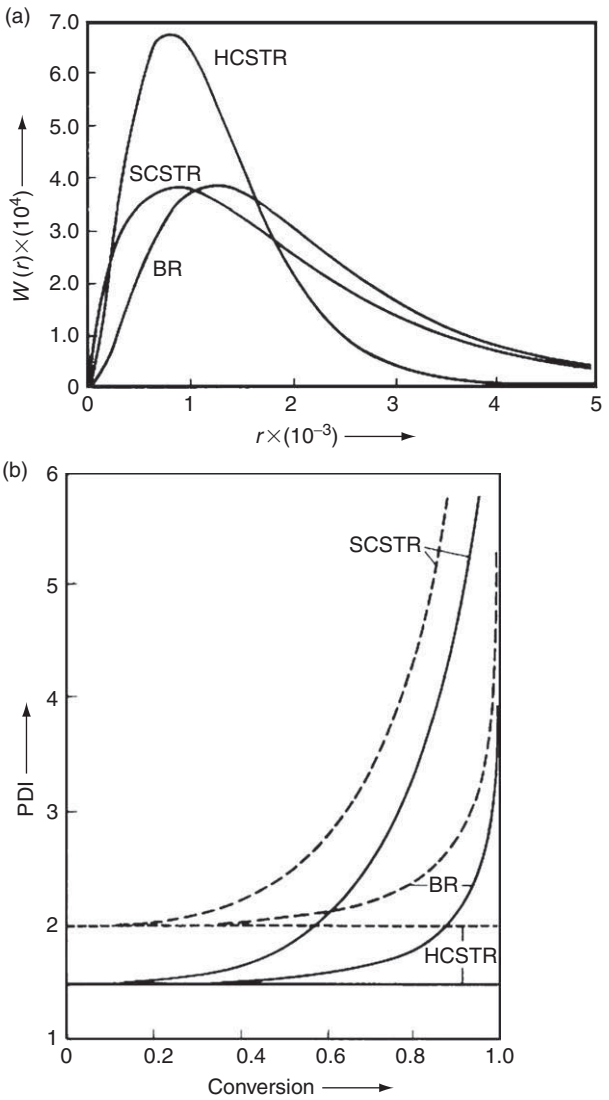

Figure 22 (a) MWD of free-radical polymerization in three different reactors and (b) change of polydispersity with conversion (solid lines, combination termination; dotted lines, disproportionation termination).

4.32.13 Industrial Examples of Polymer Production

The classical chemical reaction engineering textbooks by Levenspiel[2] and Fogler[3] are widely used by instructors at both undergraduate and graduate levels in chemical engineering. They are the first ones to illustrate the comprehensive use of chemical engineering principles including chemical reaction kinetics, heat, mass and momentum transfer, RTD, micromixing and segregated flow in the design, and operation and control of large-scale commercial reactors operating in batch, semibatch, and continuous modes of production. However, these textbooks do not focus on large-scale production of polymers.

Principles of Polymerization Engineering by Biesenberger and Sebastian[8] is the first to consider and expand chemical reaction engineering to include commercial-scale polymer production. Quoted directly from the text, the term 'reaction path' has at least two connotations. To chemists, it suggests a particular reaction mechanism. To chemical engineers, the term signifies the physical history experienced by a reaction as dictated by prevailing reactor dynamics. All continuous-flow vessels, whether of agitated or streamline type, are nonideal in the sense that neither the fluid elements in the vessel nor those in the effluent are of same age at any given time. The age distribution among elements in the vessel at any instant is called the internal age distribution $I(t)$ and that in the effluent leaving the vessel is the exit age distribution $E(t)$. Since the age of a fluid element in the effluent is equal to its RTD, to assess the effects of polymerization reactors, we must distinguish between

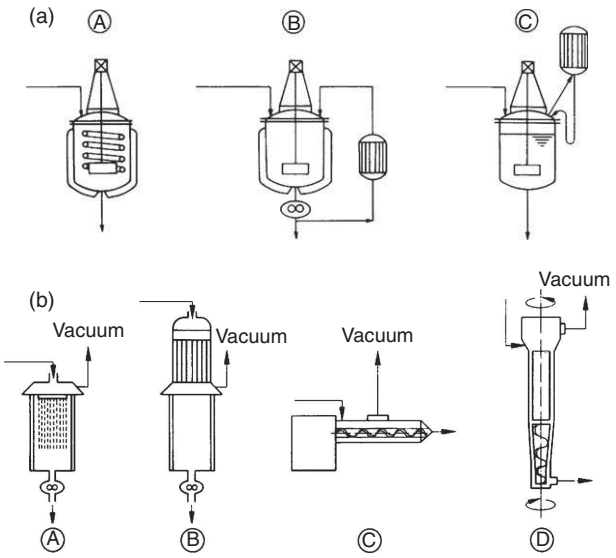

Scheme 11 Reactor designs for (a) heat removal and (b) mass removal.

transverse and longitudinal mixing and between macromixing and micromixing. An important characteristic of longitudinal macromixing is the RTD. A consequence of micromixing is the phenomenon of BM. The former describes the distribution among ages of fluid elements and is generally associated with macromixing. The latter describes the intermingling of molecules of different ages (micromixing) made possible by the action of macromixing. In other words, macromixing breaks up the fluid in chunks and, with increased surface area between chunks of different ages, molecules of different age intermix. In summary, macromixing should be avoided only when plug-like flows are feasible and desirable.

4.32.13.1 Low-Density Polyethylene

The commercial production of LDPE is by free-radical polymerization. Supercritical bulk ethylene is fed into a tubular reactor operated at steady state. The polymers experience both short- and long-chain branching. The short-chain branches are a consequence of backbiting and the long-chain branches are a consequence of chain transfer to polymers. The low density of the product is a consequence of short-chain branching.

Scheme 12 presents a schematic diagram of a tubular reactor with multiple feed points. The temperature profile along the reactor length is an important measurement. The rate of polymerization can double for every 10 °C rise in temperature. These are reactor safety concerns as well as polyethylene product quality concerns. Large heats of polymerization are common for chain growth polymerization, where carbon–carbon double bonds are converted to carbon–carbon single bonds. It has been observed that at temperature above 210 °C, molten polyethylene may tend to cross-link, while at temperature above 290 °C, chain scission may dominate.

Kinetic models to describe the polymerization rate and polymer properties, including copolymer composition, molecular weight, short- and long-chain branching, melt flow index, and polymer density, have been proposed. The model parameters were fitted to industrial data to give useful steady-state simulation software, allowing for multiple feed points, multiple initiators (including oxygen), and nonisothermal polymerization. The effects of the pulse valve and the product cooler are incorporated.

The reactor pressure affects both the rates of reaction and the thermodynamic properties of the reaction mixture. The reactor pressure decreases along the tubular reactor length to the pulse valve, where a larger pressure drop is experienced. Furthermore, the pulse valve helps to reduce reactor fouling. Pulsing causes the reaction mixture to heat up and cool down. Owing to changes in the reaction rate, the flow rate, and the heat transfer coefficient, the amount of accumulated fouling can be reduced. The pulse valve causes a large drop in pressure from the reactor to the product cooler section. This pressure drop can change the rate of any residual reaction and the temperature of the reaction mixture.

A precise knowledge of polymer properties is of great importance as more and more specialties are required for specific industrial applications. In order to predict the physical properties of a resin, it is essential to know the chain properties of the polymer. For this reason, properties such as MWD and branching frequencies, short and long, are very important in model calculations. From an industrial point of view, a reliable copolymerization model is capable of appraising synthesis conditions, as well as allowing studies on new copolymers prior to industrial tests. Thus, new polymer grades could be developed more easily and the existing ones may be optimized in order to supply consistently high-quality resins to customers.

Autoclave reactors are also employed in the production of LDPE. The mixing pattern in an autoclave reactor tends to be of a recirculating nature. The effect of mixing on reactor performance is very important, since an imperfectly mixed vessel requires more initiator per unit of polymer produced. The initiator tends to decompose near the feed points and not in the bulk of the reactor, which causes a reduction in productivity. Hence it is desired to improve mixing with concomitant increase in the production rate. The measurement of temperature profile along the reactor length can be used to establish goodness of mixing.

4.32.13.2 High-Impact PP

Polyolefins are among the most important commodity polymers with polyethylene and PP as today's major tonnage plastic materials worldwide. Most industrial processes for the production of polyolefins utilize heterogeneous Ziegler–Natta catalysts. Metallocene catalysts with aluminoxane and other cocatalysts are able to produce polyolefins at very high productivity with a degree of microstructure control not possible using conventional Ziegler–Natta catalysts. Heterogeneous Ziegler–Natta catalysts consist of porous secondary particles that are formed by loosely aggregated primary particles. During the polymerization, the growing polymer chains fragment these secondary particles, forming an expanding polymer particle containing primary particles and living and dead polymer chains. This catalyst fragmentation mechanism has been documented for most types of heterogeneous Ziegler–Natta catalysts. One of the consequences is the replication phenomenon with the PSD of the polymer particles that, at the end of polymerization, closely approximates the PSD of the catalyst. The replication phenomenon is very important in predicting

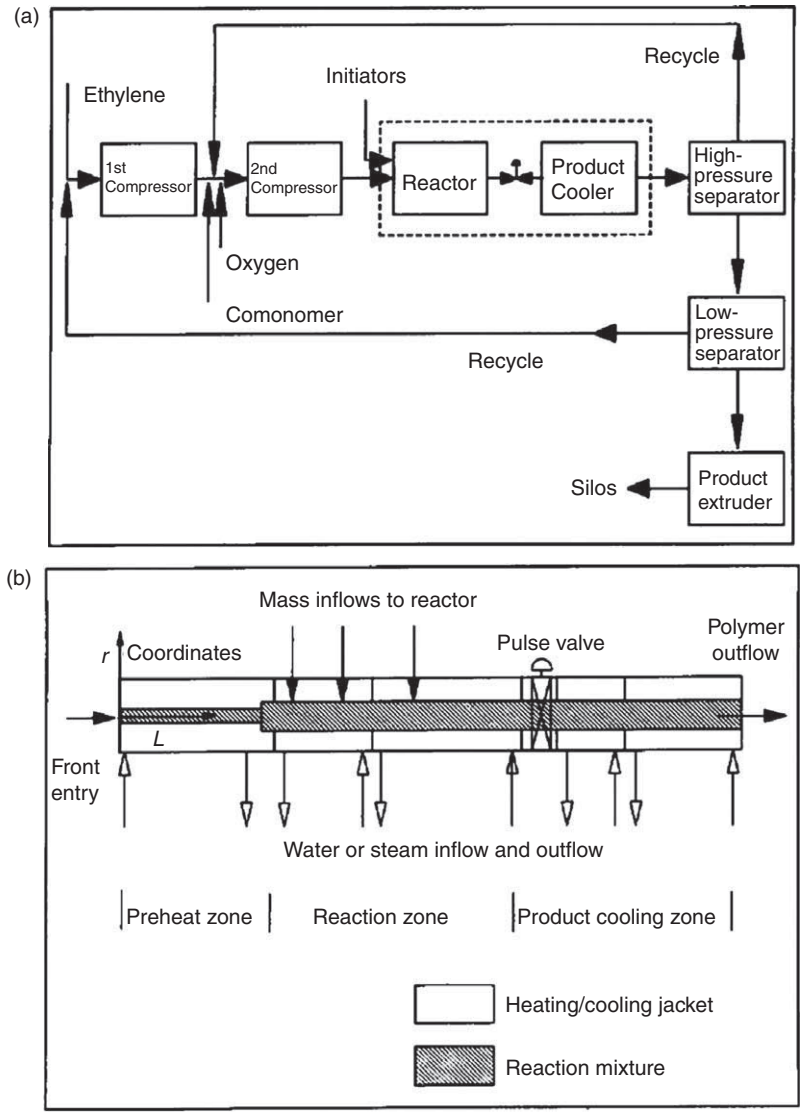

Scheme 12 (a) Process for production of high-pressure polyethylene and copolymers and (b) schematic diagram of tubular reactor with multiple feed points.[213–215]

the polymer PSD from a knowledge of the PSD of the catalyst. The PSD of the polymer particles is an important variable in designing and operating polymer recovery, treatment, and processing units. For a continuous polymerization process, the RTD of the polymerizing fluid may have a significant effect on the PSD of the polymer.[216,217]

The present commercial manufacture of high-impact polypropylene (HIPP) involves a continuous two-stage polymerization process.[218,219] In Stage-1, iPP particles are produced using a titanium-based Ziegler–Natta catalyst on an inorganic support. The preferred reactor/process type for stage 1 is one- or two-loop reactors in series for slurry-phase polymerization or one or more stirred or fluidized-bed reactors in series for gas-phase polymerization. The preferred reactor/process type for stage 2 is one or more gas-phase reactors in series. The RTDs in the two stages may be equivalent to one or more backmixed reactors in series. The PP particles leaving stage 1 enter stage 2 and experience an atmosphere of ethylene/propylene monomer mix. A rubbery ethylene/propylene copolymer is formed on the same active sites as those which polymerize iPP chains in stage 1.

4.32.13.3 Linear Low-Density and High-Density Polyethylene

Scheme 13 is a schematic of an industrial fluidized-bed polyethylene reactor using a multiple-active-site Ziegler–Natta catalyst. The copolymerization of ethylene with butene-1 and hexene-1 produces short-chain branches. When modeling a single-pass fluidized-bed reactor or a recycle reactor with high conversion per pass, one must account for gas-phase concentration gradients between the bottom and the top of the bed and for mass transfers between bubble and emulsion phases. Since the industrial fluidized-bed reactor system under consideration has a sizeable recycle stream and a low conversion per pass through the bed, the vertical concentration gradient through the bed is very small and can be neglected. BM of

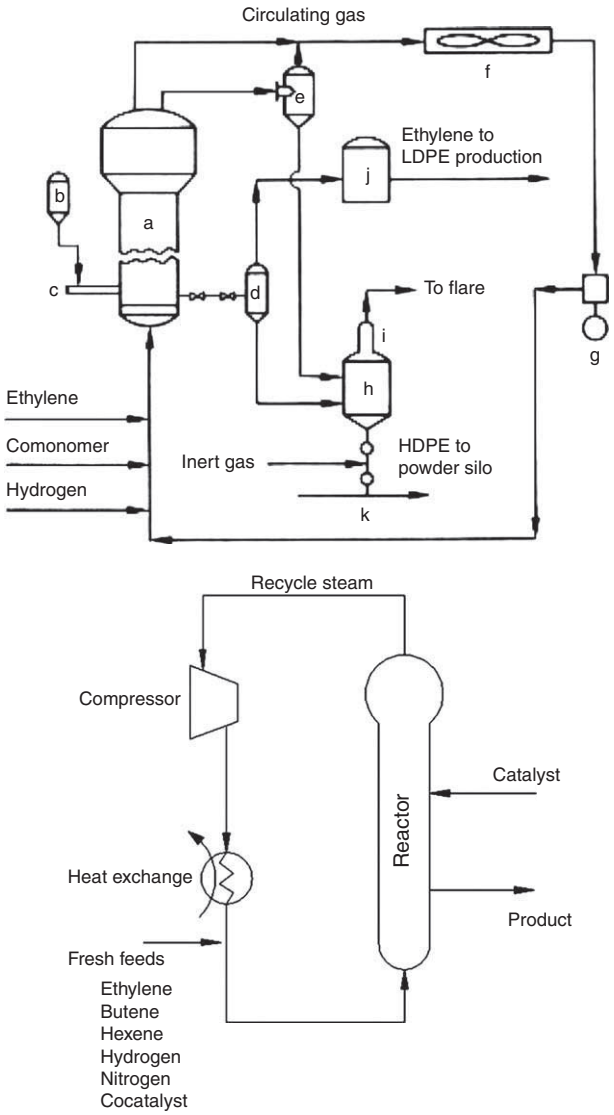

Scheme 13 Schematic diagram of the Union Carbide gas-phase process for manufacturing HDPE:[221,222] (a) fluidized-bed reactor; (b) catalyst transfer tanks; (c) catalyst feeders; (d) product discharge tanks; (e) multiclone dust separator; (f) air coolers; (g) compressor; (h) product degassing tank; (i) filter; (j) ethylene tank; and (k) pneumatic transport system.

both gas and solid phases of the fluidized bed does occur. Thus, modeling the fluidized-bed reactors plus recycle system as a CSTR containing a well-mixed solid phase interacting with a well-mixed gas phase is justified.[220]

The feed to the reactor comprises ethylene, comonomer (1-butene or 1-hexene), hydrogen, and nitrogen. These gases provide the fluidization and heat transfer media and supply reactants for the growing catalyst/polymer particles. A Ti-based heterogeneous ZN catalyst and a triethyl aluminum cocatalyst are fed continuously to the reactor. The fluidized particles disengage from the reactant gas in the expanded top section of the reactor. The unreacted gases are combined with fresh feed streams and recycled to the base of the reactor. Since the polymerization is highly exothermic, heat must be removed from the recycle gas before it is returned to the reactor. The conversion per pass through the bed is very low at about 2–3%. Thus, the recycle stream is much longer than the fresh feed stream. Periodically, the product discharge valve near the base of the reactor opens and fluidized product flows into a surge tank. The unreacted gas is recovered from the product, which proceeds to the finishing area of the plant for additive incorporation and pelletization. In normal industrial reactor operation, the recycle to fresh fed ratio is approximately 40:1. Thus, modeling the fluidized-bed reactor plus recycle system as a CSTR containing a well-mixed solid phase interacting with a well-mixed gas phase is adequate.

Thermocouples at different vertical positions in the reactor indicate that vertical temperature gradients are small in the reaction zone. A rise of less than 3 °C between the gas distribution plate, located below the reaction zone and the top of the bed, is typical. For modeling purposes, it is assumed that the effects of any small radial or vertical temperature gradients can be neglected. The next topic worth considering is the relative importance of gas-phase concentrations versus concentrations of species at the active sites when polymerization rates and polymer molecular properties are calculated. When new catalyst particles are injected into a gas-phase reaction, the active sites are quickly covered by the growing polymer chains. Thus, reaction rates are controlled by the concentrations of reactants dissolved in the polymer surrounding the sites rather than by bulk concentrations in the gas phase. In general, the solubility of gaseous substances in olefin polymers depends on the degree of crystallinity. Gases are absorbed only into the amorphous regions of the polymers. Since polymer chains grow away from the catalyst surface, the polymer at the active sites is in a nascent amorphous state. Thus, the crystallinity or the density of the polymers being produced is not expected to affect monomer concentrations at the catalyst active sites. Since diffusional resistances can usually be neglected, the concentrations of species at the active sites are assumed to be the equilibrium concentrations in the amorphous polymers.

4.32.13.4 Polystyrene

Continuous solution polymerization is the most important process for the commercial production of PS, although suspension polymerization is used for the manufacture of expandable PS. Actual commercial processes may have up to five reactors in series, although only one reactor is sometimes used. Styrene, solvent, and occasionally radical initiators are fed to the first reactor. Solvent is used primarily for viscosity control with the amount determined by the exact configuration of the reactor and the polymer molecular weight desired. A secondary function of solvent is control of molecular weight by chain transfer to solvent, although more effective chain transfer agents are also used. The reactors are run at successively increasing temperatures with 180 °C in the last reactor. The first reactor is run at 120 °C for thermal-initiated polymerization but at 90 °C when initiator is used in the feed stream. Both single- and two-initiator systems are used. Final conversions of 60–90% are achieved in the last reactor. The reaction mixture is passed through a vacuum devolatilizer to remove solvent and residual monomer that are condensed and recycled to the first reactor. The devolatilized PS (at 220–260 °C) is fed to an extruder and pelletized. Commercial PS has molecular weights in the range of 50 000–150 000 g mol^{-1} and polydispersities in the range

of 2–4. Although completely amorphous ($T_g = 85\,^{\circ}C$), its bulky rigid chains (due to phenyl–phenyl interactions) impart good strength with high dimensional stability with only 1–3% elongation. PS is a typical rigid plastic and is a very good electrical insulator. It has excellent optical clarity, possesses good resistance to aqueous acids and bases, and is easy to fabricate into products since only T_g must be exceeded for the polymer to flow. However, PS has some limitations. It is attacked by hydrocarbon solvents, has poor weatherability (UV, oxygen, and ozone attack) due to the labile benzylic hydrogens, is somewhat brittle, and has poor impact strength due to the stiff polymer chains. The upper temperature limit for PS applications is low because of lack of crystallinity and low T_g. In spite of these problems, styrene polymers are used extensively with almost tens of billions of pounds of styrene plastics and billions of pounds of styrene elastomers produced annually.

4.32.13.5 Polyvinyl Chloride

PVC products are mainly made using suspension polymerization processes. A typical recipe includes 180 parts water, 100 parts vinyl chloride monomer (VCM), and small amounts of dispersants (< 1 part), monomer-soluble initiator, and chain transfer agent (e.g., trichloroethylene). All components except monomer are charged into the reactor, which is then partially evacuated. VCM is drawn into the reactor, sometimes by pressurized oxygen-free nitrogen gas. The reactants are then heated in the closed system to about 50 °C and the pressure rises to about 0.5 MPa. The temperature is maintained at about 50 °C as the polymerization proceeds. When the pressure is about 0.05 MPa, corresponding to 90% VCM conversion, residual monomer is vented off to be recycled. Removal of the residual monomer typically involves passing the reaction mixture through a countercurrent of steam. The reaction mixture is then cooled and the polymer separated, dried in hot air at about 100 °C, sieved to remove any oversized particles, and stored. Typical molecular weights for commercial PVC are in the range of 30 000–80 000 g mol^{-1}. PVC has very low crystallinity but achieves strength because of the bulky polymer chains, which is a consequence of the large Cl groups on every other carbon atom in the chain. PVC is relatively unstable to light and heat with the evolution of HCl, which can have deleterious effects on the properties of nearby objects (e.g., electrical components) and can have negative physiological effects on humans.

The commercial importance of PVC would be greatly reduced were it not for the fact that this instability can be controlled by blending with appropriate additives such as metal oxides and carbonates as well as fatty acid salts. These additives stabilize PVC by slowing down the dehydrochlorination reaction and absorption of the evolved HCl. PVC is a very tough and rigid material with extensive applications. Its range of utilization is significantly expanded by plasticization, which converts rigid PVC to flexible PVC. Plasticization involves blending PVC with plasticizers such as dioctyl phthalate, tritolyl phosphate, and epoxidized oils. Tens of billions of pounds of PVC products about equally divided between rigid and flexible goods are produced annually.

The case of PVC has been chosen because mixing plays a particularly important role in the suspension polymerization of VCM. This is true because PVC is insoluble in VCM and almost immediately precipitates as the polymerization of VCM in the suspended VCM droplets begins. PVC particles swollen with VCM are suspended in a continuous phase of almost pure VCM inside the droplets. As the polymerization continues with free radicals via initiator being generated in both VCM phase and PVC/VCM phase, the PVC/VCM particles grow in number and size until the VCM phase is consumed. At this point, the reactor pressure begins to fall. Agglomeration of the suspended polymer particles in an aqueous continuous phase may result in an average polymer particle size of about 150 μm.[223]

Large VCM suspension polymerization reactors can vary in size from 60 000 to 200 000 l with diameters in the range of 2.4–3.6 m. The final polymer particle size obtained is determined mainly by the agglomeration process. This is strongly dependent on the temperature, the type of suspending agent, and the vessel volume. An important consideration is the maintenance of PVC particle porosity. For many applications of PVC, the T_g of pure PVC is too high and a plasticizer must be incorporated into the PVC particles to improve processability. Another important consideration is PVC reactor productivity. To achieve maximum productivity, it is important that heat generation by polymerization be as close as possible to reactor heat removal capacity. This can be done using two or more free-radical initiators with different half-lives.

4.32.13.6 Nylon 66

In the step growth polymerization, high-molecular-weight polymers are usually not produced until the final stage of monomer conversion so that thermal control and mixing of the polymerizing mixture do not present serious problems in the earlier stages. However, the final stage of polymerization is very important for the production of high-molecular-weight polymers. Newer high-capacity plants offer use of continuous processes. The first approximation for the continuous process is a reactor system that consists of plug-flow reactors (PFRs) and CSTR in various combinations, although various nonideal effects such as flow patterns in the reactor, mass and heat transfer limitations, and RTD must be considered for a detailed understanding of the performance of the real reactor system. An important feature of the step growth polymerization is that the variance of the molecular weight distribution is smallest in a batch reactor or a PFR and is largest in a homogeneous CSTR. This result may be surprising since it is in principle impossible to produce polymers whose polydispersity index is smaller than 2 at sufficiently high monomer conversions.

Nylon 66 is manufactured by polycondensation of hexamethylenediamine and adipic acid usually in a multistage process. First, nylon salt hexamethylene diammonium adipate is prepared from stoichiometric quantities of hexamethylenediamine and adipic acid in water. The salt can easily be separated by precipitation with methanol:

$$H_2N(CH_2)_6NH_2 + HOOC(CH_2)_4COOH \rightarrow \begin{bmatrix} {}^{-}O_2C(CH_2)_4CO_2^{-} \\ {}^{+}H_3N(CH_2)_6{}^{+}NH_3 \end{bmatrix}$$

The use of nylon salt guarantees the presence of equimolar amounts of $-NH_2$ and –COOH groups. The control of diamine–diacid balance is critically important to have high molecular weights and reactive end groups of the final polymers. Nylon 66 is fairly unstable at high temperatures in the

presence of oxygen. Not only degradation but also cross-linking of polymer chains may occur. Complete elimination of oxygen has made it possible to carry out continuous polymerization. The aqueous nylon salt solution is heated to above 200 °C at >17 bar in an oxygen-free atmosphere. Thereafter, the pressure is reduced to atmospheric and the vapor is separated from the polymer to promote polymerization to the desired high molecular weight. It has also been possible to polymerize hexamethylenediamine and adipic acid directly.

4.32.14 Conclusion and Outlook

Macromolecular reaction engineering is concerned with the industrial production of polymers. It bridges bench-scale polymer chemistry to industry-scale commercial polymer production. It involves many areas from polymerization mechanism and kinetics to reactor and process to safety and environment impact. In design and analysis of polymer production, reaction engineers must acquire good knowledge and skills in polymer chemistry, reaction kinetics, flow, mass transfer, heat transfer, reactor design, process control, and system engineering. This chapter provides some basic concepts with its emphasis on modeling and quantitative analysis.

Macromolecular reaction engineering (or previously called 'polymer reaction engineering') combines chemical reaction engineering with polymer chemistry. Macromolecular reaction engineers have a dual citizenship in the two disciplines. In a traditional sense, reaction engineers take recipes developed by chemists and scale up for production. It has not been fully appreciated by chemists that engineers can do much more than that. The reason is simple: polymers are products by process. Different reactors and process designs can yield totally different products even with the same recipe. They can have different chain microstructures, different particle morphologies, and different applications. Nowadays, engineers play more and more important roles in development of new polymer products through process innovation.

Macromolecular reaction engineering as a discipline started in the 1960s. A rapid growth was experienced in the 1970s and 1980s. In the recent two decades, there were many new developments in polymer chemistry. Take homogeneous metallocene catalysts as an example. Polyolefin production was well established based on heterogeneous Ziegler–Natta catalysts. It would be too costly to design and build brand new reactor systems and processes to fit the new catalysts. Reaction engineers must be innovative in developing various support systems for the catalysts to fit the existing production facilities. The recent development of controlled radical polymerization is another example. With the timescale for chain growth extended to tens of minutes or hours, reaction engineers could excise reactor design skills and produce polymers having tailor-made chain microstructure needed in special applications.

Macromolecular reaction engineering is a very dynamic discipline. Recent developments in nano and bio areas require innovations for production of specialty polymers. Market-driven commodity products, such as vinyl, acrylic, styrenic, and olefinic polymers, also require continuous improvement through innovations for better application properties. There will be more challenges ahead and there are more successes ahead for macromolecular reaction engineers.

Acknowledgment

S.Z. would like to thank his graduate students, Mr. Bin Yang, Ms. Meng Li, Mr. Hongyu Lu, Ms. Rummana Syeda, Mr. Nels Graumen-Neander, and Ms. Helen Gu, for their assistance in preparation of the figures and tables of this chapter.

References

1. Felder, R. M.; Rousseau, R. W. *Elementary Principles of Chemical Processes*, 3rd ed.; Wiley: New York, 2005.
2. Levenspiel, O. *Chemical Reaction Engineering*, 3rd ed.; Wiley: New York, 1999.
3. Fogler, H. S. *Elements of Chemical Reaction Engineering*, 4th ed.; Prentice Hall, 2005.
4. Smith, J. M.; Van Ness, H. C.; Abbott, M. M. *Introduction to Chemical Engineering Thermodynamics*, 7th ed.; McGraw Hill, 2005.
5. Smith, J. M. *Chemical Engineering Kinetics*, 3rd ed.; McGraw Hill: New Delhi, 1981.
6. Bird, R. B.; Stewart, W. E.; Lightfoot, E. N. *Transport Phenomena*, Revised 2nd ed.; Wiley: New York, 2007.
7. McCabe, W.; Smith, J.; Harriott, P. *Unit Operations of Chemical Engineering*, 7th ed.; 2004.
8. Biesenberger, J. A.; Sebastian, D. H. *Principles of Polymerization Engineering*; Wiley, 1983.
9. Ray, W. H. In *Chemical Reactor Theory*; Lapidus, L.; Amundson, N. R., Eds.; Prentice Hall: Englewood Cliffs, NJ, 1977; p 532.
10. Reichert, K. H.; Moritz, H. U. *Polymer Reaction Engineering*, *Comprehensive Polymer Science*; Pergamon Press: Oxford, 1989; Vol. 3, p 327.
11. Hamielec A. E.; Tobita, H. *Ullmann's Encyclopedia of Industrial Chemistry*; VCH, 1992.
12. Dotson, N. A.; Galvan, R.; Laurence, R. L.; Tirrell, M. *Polymerization Process Modeling*; VCH, 1996.
13. Meyer, T.; Keurentjes, J., Eds. *Handbook of Polymer Reaction Engineering*; Wiley–VCH, 2005.
14. Asua, J. M., Ed. *Polymer Reaction Engineering*; Blackwell, 2007.
15. Schork, F. J.; Deshpande, P. B.; Leffew, K. W. *Control of Polymerization Reactors*; Mercel Dekker, 2003.
16. Flory, P. J. *Principles of Polymer Chemistry*; Cornell University Press, 1953.
17. Odian, G. G. *Principles of Polymerization*, 4th ed.; Wiley: Hoboken, NJ, 2004.
18. Carraher, Jr. *Introduction to Polymer Chemistry*, 8th ed.; CRC Press, 2010.
19. Allcock, H. R.; Lampe, F. W.; Mark, J. E. *Contemporary Polymer Chemistry*, 3rd ed.; Prentice Hall: NJ, 2003.
20. Stevens, M. P. *Polymer Chemistry: An Introduction*, 3rd ed.; Oxford University Press: New York, 1999.
21. Hiemenz, P. C.; Lodge T. P. *Polymer Chemistry*, 2nd ed.; Tayler & Francis, 2007.
22. Rudin, A. *The Elements of Polymer Science and Engineering*, 2nd ed.; Academic Press, 1998.
23. Carothers, W. H. *Trans. Faraday Soc.* **1936**, *32*, 39.
24. Flory, P. J. *J. Am. Soc.* **1941**, *63*, 3083, 3091, 3096.
25. Stockmayer, W. H. *J. Chem. Phys.* **1944**, *12*, 125.
26. Stockmayer, W. H. *J. Chem. Phys.* **1945**, *13*, 199–207.
27. Stockmayer, W. H. *J. Polym. Sci.* **1952**, *9*, 69; *J. Polym. Sci.* **1953**, *11*, 11.
28. Gupta, S. K.; Kumar, A. *Reaction Engineering of Step Growth Polymerization*; Plenum Press: New York, 1987.
29. Solomon, D. H., Ed. *Step-Growth Polymerization*; Marcel Dekker: New York, 1972.
30. Gordon, M. *Proc. R. Soc. Lond. A.* **1962**, *268*, 240.
31. Gordon, M.; Malcom, G. N. *Proc. R. Soc. Lond. A.* **1966**, *292*, 29.
32. Gordon, M.; Ross-Murphy, S. B. *Pure Appl. Chem.* **1975**, *43*, 1.
33. Durand, D.; Bruneau, C. M. *Polymer* **1983**, *24*, 587, 592.
34. Durand, O.; Bruneau, C. M. *Makromol. Chem.* **1982**, *83*, 1007, 1021.
35. Macosko, C. W.; Miller, D. R. *Macromolecules* **1976**, *9*, 199.
36. Miller, D. R.; Macosko, C. W. *Macromolecules* **1976**, *11*, 656.
37. Miller, D. R.; Macosko, C. W. *Macromolecules* **1976**, *9*, 206.
38. Miller, D. R.; Macosko, C. W. *J. Polym. Sci. Polym. Phys.* **1988**, *26*, 1.

39. Noyes, R. N. In *Encyclopedia of Polymer Science and Technology*; Wiley-Interscience: New York, 1965; Vol. 2, p 796.
40. Moad, G.; Solomon, D. H. *The Chemistry of Radical Polymerization*, 2nd ed.; Elsevier, 1995.
41. Russell, G. T.; Napper, D. H.; Gilbert, R. G. *Macromolecules* **1988**, *21*, 2141.
42. Zhu, S.; Hamielec, A. E. *Macromolecules* **1989**, *22*, 3093–3098.
43. Zhu, S. P. Ph.D. thesis, McMaster University, Hamilton, Ont., 1991.
44. Talamini, G.; Vidotto, G. *Makromol. Chem.* **1967**, *100*, 48.
45. Stickler, M.; Panke, D.; Hamielec, A. E. *J. Polym. Sci. Polym. Chem.* **1984**, *22*, 2243.
46. Schulz, G. V. Haborth, G. *Makromol. Chem.* **1948**, *1*, 106.
47. North, A. M. In *Reactivity, Mechanism and Structure in Polymer Chemistry*; Jenkins, A. D., Ledwith, A., Eds.; Wiley–Interscience: New York, 1974; Chapter 5.
48. O'Driscoll, K. F.; Davis, T. P. *Polym. Commun.* **1989**, *30*, 317.
49. Mita, I.; Horie, K. *J. Macromol. Sci. Rev. Macromol. Chem. Phys.* **1987**, *C27*, 91.
50. Hui, A. W.; Hamielec, A. E. *J. Polym. Sci. Polym. Symp.* **1968**, *25*, 167–189.
51. Hui, A. W.; Hamielec, A. E. *J. Polym. Sci., Part C* **1968**, *25*, 167.
52. North, A. M. *The Kinetics of Free Radical Polymerization*; Pergamon Press: London, 1966; p 94.
53. Benson, S. W.; North, A. M. *J. Am. Chem. Soc.* **1959**, *81*, 1339.
54. Olaj, O. F.; Bitai, I.; Hinkelmann, F. *Makromol. Chem.* **1987**, *188*, 1689.
55. Mahabadi, H. K.; O'Driscoll, K. F. *J. Macromol. Sci. Chem.* **1977**, *A11*, 967.
56. Balke, S. T.; Hamielec, A. E. *J. Appl. Polym. Sci.* **1973**, *17*, 905–949.
57. Tuiig, T. J.; Tirrell, M. V. *Macromolecules* **1981**, *14*, 1501.
58. Stickler, M. *Makromol. Chem.* **1983**, *184*, 2563.
59. Cardenas, J.; O'Driscoll, K. F. *J. Polym. Sci. Chem. Ed.* **1977**, *15*, 1883, 2097.
60. Broadhead, T. O.; Hamielec, A. E.; MacGregor, J. F. *Die Makromol. Chem. Suppl.* **1985**, *10/11*, 105–128.
61. Soh, S. K.; Sundberg, D. C. *J. Polym. Sci. Chem. Ed.* **1982**, *20*, 1299, 1315, 1331, 1345.
62. Bamford, C. H.; Barb, W. G.; Jenkins, A. D.; Onyon, P. F. *Kinetics of Vinyl Polymerization by Radical Mechanisms*; Butterworth: London, 1958.
63. Bamford, C. H., Radical Polymerization, In *Encyclopedia of Polymer Science and Engineering*; Mark, H. F.; Bikales, N. M.; Overberger, C. G.; and Menges, G., eds.; Wiley-Interscience: New York, 1988; Vol. 13, pp. 708–867.
64. Brandrup, J.; Immergut, E. H.; McDowell, W. *Polymer Handbook*, 2nd ed.; Wiley-Interscience: New York, 1975.
65. Tulig, T. J.; Tirrell, M. V. *Macromolecules* **1982**, *15*, 459.
66. Kloosterboer, J. G. *Adv. Polym. Sci.* **1988**, *84*, 1.
67. Trommsdorff, E.; Kohle, H.; Lagalry, P. *Makromol. Chem.,* **1948**, *1*, 169.
68. Trommsdorff, E. *Makromol. Chem.* **1954**, *13*, 76–89.
69. Balke, S. T. Ph.D. thesis, McMaster University, Hamilton, Ont., 1972.
70. Smoluchowski, M. V. *Z. Phys. Chem.* **1918**, *92*, 129–168.
71. de Gennes, P. G. *J. Chem. Phys.* **1971**, *55*, 572.
72. de Gennes, P. G. *Macromolecules*, **1976**, *9*, 587–594.
73. de Gennes, P. G. *Scaling Concepts in Polymer*; Cornell University Press: Ithaca, NY, 1979; p 139.
74. Doi, M.; Edwards, S. F. *J. Chem. Soc. Faraday Trans. 2,* **1978**, *74*, 560–570.
75. Doi, M.; Edwards, S. F. *The Theory of Polymer Dynamics*; Clarendon Press: Oxford, 1986.
76. Dolittle, A. K. *J. Appl. Phys.* **1951**, *22*, 1471–1475.
77. Dolittle, A. K. *J. Appl. Phys.* **1952**, *23*, 236–239.
78. Doolittle, A. K., *J. Appl. Phys.*, **1951**, *22*, 1471.
79. Bueche, F. *Physical Properties of Polymer*; Interscience, 1962.
80. Vrentas, J. S.; Duda, J. L. *J. Polym. Sci. Polym. Phys.* **1977**, *15*, 403–416,
81. Buback, M. *Makromol. Chem.* **1980**, *181*, 373.
82. Buback, M.; Lendle, H. *Makromol. Chem.* **1983**, *184*, 193.
83. Marten, F. L.; Hamielec, A. E. *ACS Symp. Ser.* **1979**, *104*, 43.
84. Chiu, W. Y.; Carratt, G. M.; Soong, D. S. *Macromolecules* **1983**, *16*, 348.
85. Achillias, D.; Kiparissides, C. *J. Appl. Polym. Sci.* **1990**, *35*, 1303.
86. Cardenas, J.; O'Driscoll, K. F. *J. Polym. Sci. Chem. Ed.* **1976**, *14*, 883.
87. Penlidis, A.; MacGregor, J. F.; Hamielec, A. E. *AIChE J.* **1985**, *31*, 881–889.
88. Gao, J.; Penlidis, A. *J Macromol. Sci. Rev.* **1996**, *C36*, 199–404.
89. Gao, J.; Penlidis, A. *J Macromol. Sci. Rev.* **1998**, *C38*, 651–780.
90. Ballard, M. J. *Macromolecules* **1986**, *19*, 1303.
91. Beuermann, S.; Buback, M. *Progr. Polym. Sci.* **2002**, *27*, 191–254.
92. Biesenberger, J. A. *AIChE J.* **1965**, *11*, 369, 371–373.
93. Ray, W. H. *J. Macromol. Sci. Rev. Macromol. Chem.* **1972**, *C8*, 1.
94. Peebles, L. H., Jr. In *Polymer Handbook*; Brandrup, J.; Immergut, E. H., Eds.; Wiley-Interscience: New York, 1975; Vol. II.
95. Tompa, H. In *Comprehensive Chemical Kinetics*; Bamford, C. H.; Tipper, C. F. H., Eds.; Elsevier: Amsterdam, 1976; Chapter 7.
96. Bamford, C. H.; Tompa, H. *J Polymer Sci.* **1953**, *10*, 345.
97. Bamford, C. H.; Tompa, H. *Trans. Faraday Soc.* **1954**, *50*, 1097.
98. Tobita, H. Ph.D. thesis, McMaster University, Hamilton, Ont., 1990.
99. Zhu, S.; Hamielec, A. E. *J. Polym. Sci. Polym. Phys.* **1994**, *32*, 929–943.
100. Graessley, W. W.; Mittelhauser, H.; Maramba, R. *Makromol. Chem.* **1965**, *86*, 129.
101. Olaj, O. F. *Angew. Makromol. Chem.* **1975**, *47*, 1–14.
102. Hungenberg, K. D. In *Handbook of Polymer Reaction Engineering*; Meyer; Keurentjes, Ed.; Wiley–VCH, 2005.
103. Bhattacharyya, D. N.; Smid, J.; Szwarc, M. *J. Phys. Chem.* **1965**, *69*, 624.
104. Szwarc, M.; Levy, M.; Milkovich, R. *J. Am. Chem. Soc.* **1956**, *78*, 2656.
105. Szwarc, M. *Living Polymers* in *Encyclopedia of Polymer Science and Technology*; Wiley–Interscience: New York, 1968; Vol. 8, p 303.
106. Otsu, T.; Yoshida, M. *Makromol. Chem. Rapid Commun.* **1982**, *3*, 127–132.
107. Solomon, D. H.; Rizzardo, E.; Cacioli, P. U.S. Patent 4,581,429, **1986**, p 28.
108. Georges, M. K.; Veregin, R. P. N.; Kazmaier, P. M.; Hamer, G. K. *Macromolecules* **1993**, *26*, 2987–2988.
109. Wang, J. S.; Matyjaszewski, K. *J. Am. Chem. Soc.* **1995**, *117*, 5614–5615.
110. Wang, J. S.; Matyjaszewski, K. *J. Am. Chem. Soc.* **1995**, *117*, 5614–5615.
111. Wang, J. S.; Matyjaszewski, K. *Macromolecules* **1995**, *28*, 7901–7910.
112. Kato, M.; Kamigaito, M.; Sawamoto, M.; Higashimura, T. *Macromolecules* **1995**, *28*, 1721–1723.
113. Chiefari, J.; Chong, Y. K.; Ercole, F.; *et al. Macromolecules.* **1998**, *31*, 5559–5562.
114. Matyjaszewski 1995.
115. Zhu, S. *J. Polym. Sci. Polym. Phys.* **1999**, *37*, 2692–2704.
116. Barner-Kowollik, C.; Quinn, J. F.; Morsley, D. R.; Davis, T. P. *J Polym Sci. Polym. Chem.* **2001**, *39*, 1353–1365.
117. Zhang, M.; Ray, W. H. *J. Appl. Polym. Sci.,* **2002**, *86*, 1630–1662
118. Delgadillo-Velazquez, O.; Vivaldo-Lima, E.; Quintero-Ortega, I. A.; Zhu, S. *AIChE J.* **2002**, *48*, 2597–2608.
119. Wang, A. R.; Zhu, S. *J. Polym. Sci. Polym. Chem.* **2003**, *41*, 1553–1566.
120. Wang, A. R.; Zhu, S. *Macromol. Theory Simul.* **2003**, *12*, 196–208.
121. Wang, A. R.; Zhu, S. *Macromol. Theory Simul.* **2003**, *12*, 663–668.
122. Monteiro, M. J. *J. Polym. Sci. A* **2005**, *22*, 5643–5651.
123. Matyjaszewski, K.; Patten, T. E.; Xia, J. H. *J. Am. Chem. Soc.* **1997**, *119*, 674–680.
124. Georges, M. K.; Veregin R. P. N.; Kazmaier, P. M.; *et al. Macromolecules* **1994**, *27*, 7228–7229.
125. Georges, M. K.; Veregin, R. P. N.; Hamer, G. K.; Kazmaier, P. M. *Macromol. Symp.* **1994**, *88*, 89–103.
126. Veregin, R. P. N.; Georges, M. K.; Kazmaier, P. M.; *et al. Macromolecules* **1993**, *26*, 5316–5320.
127. Veregin, R. P. N.; Georges, M. K.; Hamer, G. K.; *et al. Macromolecules* **1995**, *28*, 4391–4398.
128. Kazmaier, P. M.; Daimon, K.; Georges, M. K. *Macromolecules* **1997**, *30*, 2228–2231.
129. Patten, T. E.; Xia, J. H.; Abernathy, T.; Matyjaszewski, K. *Science* **1996**, *272*, 866–868.
130. Patten, T. E.; Matyjaszewski, K. *Adv. Mater.* **1998**, *10*, 901.
131. Matyjaszewski, K.; Xia, J. H. *Chem. Rev.* **2001**, *101*, 2921–2990.
132. Braunecker, W. A.; Matyjaszewski, K. *Progr. Polym. Sci.* **2007**, *32*, 93–146.
133. Chong, Y. K.; Le, T. P. T.; Moad, G.; *et al. Macromolecules* **1999**, *32*, 2071–2074.
134. Moad, G.; Chiefari, J.; Chong, Y. K.; *et al. Polym. Int.* **2000**, *49*, 993–1001.
135. Moad, G.; Rizzardo, E.; Thang, S. H. *Aust. J. Chem.* **2005**, *58*, 379–410.
136. Anantawaraskul, S.; Bongsontia, W.; Soares J. B. P. *Macromol Symposia* **2009** *282*, 167–174.
137. Alghyamah, A. A.; Soares J. B. P. *Macromol Symposia,* **2009** *265*, 81–89.
138. Kaminsky, W.; Miri, M.; Sinn, H.; Woldt, R. *Macromol Chem. Rapid Commun.* **1983**, *4*, 417–421.
139. Kaminsky, W.; Bark, A.; Arndt, M. *Makromol. Chem. Macromol. Symp.* **1991**, *47*, 83–93.
140. Kaminsky, W.; Arndt, M. *Polym. Catal. Adv. Polym. Sci.* **1997**, *127*, 143–187.
141. Lai, S. Y.; Wilson, J. R.; Knight, G. W.; *et al.* U.S. Patent 5, 272,236, 1993.
142. Knight, G. W.; Lai, S. *Polyolefins VIII. Technol. Pap. Reg. Technol. Conf. Soc. Plast. Eng., 1993;* Vol. 28.
143. Swogger, K.; Kao, W. C. I. *Polyolefins VIII. Technol. Pap. Reg. Technol. Conf. Soc. Plast. Eng., 1993;* Vol. 14.
144. Yan, D.; Wang, W. J.; Zhu, S. P. *Polymer* **1999** *40*, 1737–1744.
145. Wang, W.-J.; Yan, D.; Zhu, S.; Hamielec, A. E. *Macromolecules,* **1998**, *31*, 8677–8683.
146. Wang, W.-J.; Yan, D.; Zhu, S.; Hamielec, A. E. *Polym. React. Eng.* **1999**, *7*, 327–346.
147. Park, S.; Wang, W. J.; Zhu, S. P. *Macromol. Chem. Phys.* **2000**, *201*, 2203–2209.
148. Tobita, H. *Macromol Theory Simulation* **1996**, *5*, 129–144.
149. Soares, J. B. P.; Hamielec, A. E. *Macromol. Theory Simul.* **1996**, *5*, 547–572.
150. Zhu, S.; Li, D. *Macromol. Theory Simul.* **1997**, *6*, 793–803.

151. Kolodka, E.; Wang, W.-J.; Zhu, S.; Hamielec, A. E. *Macromolecules* **2002**, *35*, 10071–10086.
152. Ye, Z.; Alsyouri, H.; Zhu, S.; Lin, Y. S. *Polymer* **2003**, *44*, 969–980.
153. Soares, J. B. P.; Kim, J. D. *J. Polym. Sci. A Polym. Chem.* **2000**, *38*, 1408–1416.
154. Ye, Z.; Alobaidi, F.; Zhu, S. *Ind. Engr. Chem. Res.* **2004**, *43*, 2860–2870.
155. Ye, Z.; Alobaidi, F.; Zhu, S. *Macromol. Chem. Phys.* **2004**, *205*, 897–906.
156. Alobaidi, F.; Ye, Z.; Zhu, S. *J. Polym. Sci. Polym. Chem.* **2004**, *42*, 4327–4336.
157. Alobaidi, F.; Ye, Z.; Zhu, S. *Polymer* **2004**, *45*, 6823–6829.
158. Ishihara, N.; Seimiya, T.; Kuramoto, M.; *et al. Macromolecules* **1986**, *19*, 2464–2465.
159. Tomotsu, N.; Ishihara, N.; Newman, T. H. *J. Mol. Catal. A Chem.* **1998**, *128*, 167–190.
160. Guan, Z.; Cotts, P. M.; McCord, E. F.; McLain, S. J. *Science* **1999**, *283*, 2059.
161. Guan, Z.; Cotts, P. M. *Polym. Mater. Sci. Eng.* **2001**, *84*, 382.
162. Guan, Z. *Chem. Eur. J.* **2002**, *8*, 3086.
163. Cotts, P. M.; Guan, Z.; McCord, E.; McLain, S. *Macromolecules* **2000**, *33*, 6945.
164. Ye, Z.; Zhu, S. *J. Polym. Sci. Polym. Chem.* **2003**, *41*, 1152–1159.
165. Ye, Z.; Zhu, S. *Macromolecules* **2003**, *36*, 2194–2197.
166. Fikentscher, H. *Angew. Chem.* **1938**, *51*, 433.
167. Fikentscher, H.; Gerrens, H.; Schuller, H. *Angew. Chem.* **1960**, *72*, 856–864.
168. Harkins, W. D. *J. Chem. Phys.* **1945**, *13*, 381–382.
169. Harkins, W. D. *J. Chem. Phys.* **1946**, *14*, 47–48.
170. Harkins, W. D. *J. Am. Chem. Soc.* **1947**, *69*, 1428–1444.
171. Ugelstad, J.; El-Aasser, M. S.; Vanderhoff, J. W. *J. Polym. Sci. Polym. Lett. Ed.* **1973**, *11*, 503–513.
172. Brooks, B. W. In *Polymer Reaction Engineering*; Reichert, K. H.; Geiseler, W., Eds.; VCH: New York, 1989; p 3.
173. Napper, D. H.; Gilbert, R. G. *Polymerizations in Emulsions Comprehensive Polymer Science*; Vol. 4.
174. Ugelstad, J. *J. Macromol. Sci. Chem. A* **1977**, *11*, 1281–1305.
175. Smith, W. V.; Ewart, R. H. *J. Chem. Phys.* **1948**, *16*, 592–599.
176. Campbell, D. Ph.D. thesis, McMaster University, Hamilton, Ont., 1985.
177. Xie, T. Ph.D. thesis, McMaster University, Hamilton, Ont., 1990.
178. Yuan, H. G.; Kalfas, G.; Ray, W. H. *J. Macromol. Sci. Rev. Macromol. Chem. Phys.* **1991**, *C31*, 215–299.
179. Burke, A. L.; Duever, T. A.; Penlidis, A. *Chem. Eng. Sci.* **1995**, *50*, 1619–1634.
180. Burke, A. L.; Duever, T. A.; Penlidis, A. *Ind. Eng. Chem. Res.* **1997**, *36*, 1016–1035.
181. Mayo, F. R.; Lewis, F. M. *J. Am. Chem. Soc.* **1944**, *66*, 1594.
182. Meyer, V. E.; Lowry, G. G. *J. Polym. Sci. A* **1965**, *3*, 2843.
183. Hamielec, A. E.; MacGregor, J. F. In *Polymer Reaction Engineering*; Reichert, K. H.; Geiseler, W.; Eds. Hanser Publishers: New York, 1983; p. 21.
184. Hamielec, A. E.; MacGregor, J. F.; Penlidis, A. *Makromol Chemie - Macromol Symp.* **1987**, *10*, 521–570.
185. Tobita, H.; Hamielec, A. E. *Polymer,* **1991**, *32*, 2641–2647.
186. Simha, R.; Branson, H. *J. Chem. Phys.* **1944**, *12*, 253–267.
187. Saito, O. *J. Phys. Soc. Jpn.* **1958**, *13*, 198.
188. Charlesby, A.; Pinner, S. H. *Proc. R. Soc. Lond. A* **1959**, *249*, 367.
189. Tobita, H.; Hamielec, A. E. *Macromolecules* **1989**, *22*, 1989.
190. Tobita, H.; Hamielec, A. E. *Polymer,* **1992**, *33*, 3647–3657.
191. Tobita, H.; Hamielec, A. E. *ACS Symp series,* **1991**, *404*, 242–255.
192. Zhu, S.; Hamielec, A. E. *Macromolecules,* **1992**, *25*, 5457–5464.
193. Zhu, S.; Hamielec, A. E.; Pelton, R. H. *Makromol. Chemie Theory Simul,* **1993**, *2*, 587–604.
194. Li, W. H.; Hamielec, A. E. *Polymer* **1989**, *30*, 1513–1517.
195. Tobita, H.; Hamielec, A. E. In *Polymer Reaction Engineering*; Reichert, K. H.; Geiseler, W.; Eds. Berlin, 1989; p. 43–83.
196. Biesenburger 1983.
197. Matyjaszewski, K.; Coca, S.; Gaynor, S. G.; *et al. Macromolecules* **1998**, *31*, 5967–5969.
198. Matyjaszewski, K.; Ziegler, M. J.; Arehart, S. V.; *et al. J. Phys. Org. Chem.* **2000**, *13*, 775–786.
199. Davis, K.; Matyjaszewski, K. *Adv. Polym. Sci.* **2002**, *159*, 1–13.
200. Kim, J.; Mok, M. M.; Sandoval, R. W.; *et al. Macromolecules* **2006**, *39*, 6152–6160.
201. Beginn, U. *Colloid Polym. Sci.* **2008**, *286*, 1465–1474.
202. Wang, R.; Luo, Y. W.; Li, B. G.; Sun, X. Y.; Zhu, S. P. *Macromol. Theory Simul.,* **2006** *15*, 356–368.
203. Wang, R.; Luo, Y. W.; Li, B. G.; Zhu, S. P. *AIChE J,* **2007**, *53*, 174–186.
204. Sun, X. Y.; Luo, Y. W.; Wang, R.; Li, B. G.; Zhu, S. P. *Macromolecules,* **2007**, *40*, 849–859.
205. Sun, X. Y.; Luo, Y. W.; Wang, R.; Li, B. G.; Zhu, S. P. *AIChE J,* **2007**, *54*, 1073–1087.
206. Zhao, Y.; Luo, Y. W.; Ye, C. H.; Li, B. G.; Zhu, S. P. *J Polym. Sci. A Polym. Chem.,* **2009**, *47*, 69–79.
207. Denbigh, K. G. *Trans. Faraday Soc.* **1944**, *40*, 352–373.
208. Denbigh, K. G. *Trans. Faraday Soc.* **1947**, *43*, 648–660.
209. Denbigh, K. G. *J. Appl. Chem.* **1951**, *1*, 227–236.
210. Denbigh, K. G. *Chemical Reactor Theory*; Cambridge University Press: Cambridge, **1965**.
211. Biesenberger, J. A.; Tadmor, Z. *J. Appl. Polym. Sci.* **1965**, *9*, 3409–3416.
212. Biesenberger, J. A.; Tadmor, Z. *Polym. Eng. Sci.* **1966**, *6*, 299–305.
213. Zabisky, R. C. M.; Chan, W.-M.; Gloor, P. E.; Hamielec, A. E. *Polymer* **1992**, *33*, 2243.
214. Zabisky, R. C. M.; Chan, W. M.; Gloor, P. E.; Hamielec, A. E. *Polymer* **1992**, *33*, 2243–2262.
215. Chan, W. M.; Gloor, P. E.; Hamielec, A. E. *AIChE J.* **1993**, *39*, 111–126.
216. Kawai, H.; Hamielec, A. E. *Polym. React. Eng.* **1999**, *7* (4), 501–529.
217. Zhu, S.; Wang, W.-J. *Macromol. Theory Simul.* **1999**, *8*, 594–602.
218. Simonazzi, T.; Cecchin, G.; Mazzullo, S. *Progr. Polym. Sci.* **1991**, *16*, 303–329.
219. Debling, J. A.; Zacca, J. J.; Ray, W. H. *Chem. Eng. Sci.* **1997**, *52*, 1969–2001.
220. McAuley, K. B.; MacGregor, J. F.; Hamielec, A. E. *AIChE J.* **1990**, *36*, 837–850.
221. Rasmussen, D. M. *Chem. Eng.* **1972**, *79*, 104–105.
222. Rasmussen, D. M. *Chem. Eng.* **1972**, *79*, 104.
223. Xie, T. Y.; Hamielec, A. E.; Wood, P. E.; Woods, D. R. *J. Appl. Polym. Sci.* **1991**, *43*, 1259–1269.

Biographical Sketches

Dr. Shiping Zhu received BEng from Zhejiang University in 1982 and PhD from McMaster University in 1991 under the supervision of Archie Hamielec. He is currently a professor and chair of the Department of Chemical Engineering at McMaster University. He held a Canada Research Chair in 2001–2010 and was a Cheung Kong Scholar Chair in 2005–2008. He works in the fields of controlled radical polymerization, catalytic polymerization of olefins, surface modification through polymer grafting, polymer branching and cross-linking, and modeling of polymerization kinetics and processes. His group has published over 220 original technical papers in refereed journals. He is a registered professional engineer in Ontario (PEng), an elected fellow of Chemical Institute of Canada (FCIC), fellow of Engineering Institute of Canada (FEIC), and Fellow of Canadian Academy of Engineering (FCAE). He received an Ontario Premier Research Excellence Award in 2000 and CIC's Macromolecular Science and Engineering Award in 2011.

Dr. Archie Hamielec received his BEng from the University of Toronto in 1957, his MASc in 1958, and his PhD in 1961 under the supervision of Ab Johnson. He joined the Department of Chemical Engineering at McMaster University in 1963. He was trained in the area of fluid mechanics and his early research was about bubbles, drops, and particles. Today, he is best known as one of the founding fathers of polymer reaction engineering. In 1982, he founded the McMaster Institute for Polymer Production Technology (MIPPT). He took an early retirement in 1993 and is now professor emeritus of McMaster University. He has published over 300 refereed journal papers. He has received numerous recognitions and was elected as a Fellow of Chemical Institute of Canada (FCIC) and Fellow of Royal Society of Canada (FRSC) in 1987.

4.33 Template Polymerization

S Połowiński, Technical University of Lodz, Lodz, Poland

4.33.1 Introduction

In literature, the concept of matrix or template polymerization is used in multiple ways. Template polymerization is usually defined as a process in which "polymer chains are able to propagate along template macromolecules during most of their lifetime".[1]

Tan[2] defined template (or matrix or replica) polymerization as "any reaction implying propagation of polymer chains along template macromolecules during at least part of its lifetime".

Papisov[3] writes: "Matrix polymerization, also termed template polymerization, is the polymerization of monomers or oligomers in which formation of macromolecules whose structure and the rate of formation are determined by the information recorded in the structure of other macromolecules matrices or templates".

Strictly speaking, in 'replica polymerization', the template polymer and the polymer originating in the presence of that template must be identical.

The term 'replica polymerization' was first used by Szwarc[4] and variously termed 'matrix' or replica polymerization later by Bamford.[5] The polymer formed, sometimes called 'daughter polymer', is, in most cases, complexed with the template and can be separated by an additional process.

The term 'replica polymerization' shows some analogies between natural biological processes known as replication or transcription.

The well-known interaction between complementary bases adenine (A) and thymine (T) or cytosine (C) and guanine (G) plays an important role in DNA replication.

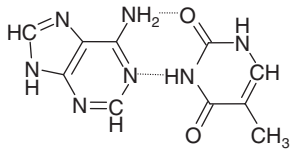

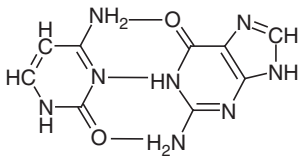

The scope of this chapter will be reduced to templates from synthetic polymers and processes known in polymer chemistry as polymerization, polycondensation, or polyaddition.

Nevertheless, the criteria by which a process can be recognized as a template process are not very clearly defined. Sometimes the experimental criterion is a 'template effect'.

The template effects can be expressed as: (1) kinetic effect – usually an enhancement of the reaction rate and change in kinetics equation; (2) molecular effect – consisting of an influence of the template on the molecular weight and molecular weight distribution of daughter polymer; (3) effect on tacticity – the daughter polymer can have the complementary structure to the structure of the template used; and (4) in the case of template copolymerization, the template effect – deals with the composition and sequence distribution of units.

On the other hand, template polymerization is a particular case of a more general group of processes such as polymerization in organized systems.[6]

Many factors may affect the organization of monomer units during polymerization. For example, polymerization in solid state proceeds when molecules of monomer are surrounded by molecules already organized in a crystal lattice. A specific type of polymerization occurs on the surface of solids. Montmorillonite, especially, can be used for polymerization of amino acid derivatives. This is connected with the fact that montmorillonite binds proteins so strongly that they cannot be washed out without being destroyed.

Numerous monomers with long hydrocarbon chains can form monolayers at the gas–water interface and are also oriented at the surface of the water. Polymerization of such organized systems leads to the preparation of polymers with peculiar morphologies and properties. It is a method for polymer synthesis in ultrathin films in different forms, for instance, polymerization in ultrathin films deposited using the 'layer-by-layer' method. By this method, polymeric microspheres containing drugs can be produced.

The most articles published in scientific journals, many reviews, and chapters of encyclopedias[7–13] deal with template polymerization proceeding at least part of its lifetime in a one-phase system. In this chapter, the term matrix or template polymerization will be used mainly to refer to one-phase systems. Only at the end of this chapter will some examples of polymerization proceeding in a confined space be discussed.

4.33.2 Mechanism of Template Polymerization

Template polymerization can proceed according to the mechanism of a chain reaction as radical, ionic, or ring-opening polymerization or as a step-growth process like polycondensation.

A mathematical model for template polymerization similar to the biological process was elaborated by Simha and co-workers.[14] The purpose of their paper was to explore mathematical consequences of alternative kinetic routes to the formation of polymer chains on polymer templates. However, since then, nobody has tried to use this theory for the description of template processes.

The most important phenomenon influencing the mechanism of template polymerization is connected with a type of interaction between the monomer and the template. This interaction can be of various types: hydrogen bonding, ionic interactions, donor–acceptor interactions, or covalent bonding.

For instance, hydrogen bonding exists between oxygen atom in poly(ethylene glycol) (PEG) and the carboxylic group in acrylic acid (AA) or methacrylic acid (MAA). However, in this case, the stability of the complex depends strongly on the degree of ionization, changing equilibrium (**Scheme 1**):

It was shown by Papisov and co-authors, examining polymerization of AA and MAA in the presence of PEG, that on reaching a certain length, all chains of polyacids growing in solution associate with PEG molecules.[15] Later on, this type of template polymerization was named 'pick up' mechanism.

Analogically, the well-known interaction between carboxyl groups leads to hydrogen bridges between poly(acrylic acid) (PAA) (template) and AA (monomer).

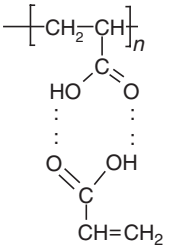

In template polymerization in which strong electrostatic interactions take place, it can be assumed that all the monomeric couterions are rigidly attached to the template as described in Reference 6.

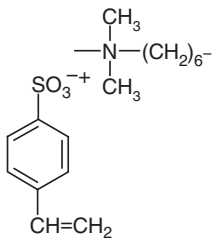

The mechanism of template polymerization depends on the degree of monomer adsorption or complexation by the template. Usually, it is assumed that an equilibrium exists according to the equation

$$M + T \leftrightarrow M_T \qquad [1]$$

where T signifies template site, M free monomer, and M_T monomer absorbed onto template. The absorption equilibrium constant $K_T = [M_T]/[M][T]$ depends on a number of factors such as the mode of interaction, temperature, solvent, and pH.

It is possible to distinguish three basic cases:

1. Interaction between the monomer and the template is too weak for stable adsorption of the monomer onto template. However, adsorption occurs if 'daughter' oligomers, created in the bulk solution reach a proper length, and then complex with the template, due to the cumulating effect.
2. Interaction between the monomer and the template leads to the creation of a stable complex. In other words, K_T is high. In some cases, template may be insoluble in a solvent in the absence of monomer.
3. Monomer and template are connected with covalent bonds.

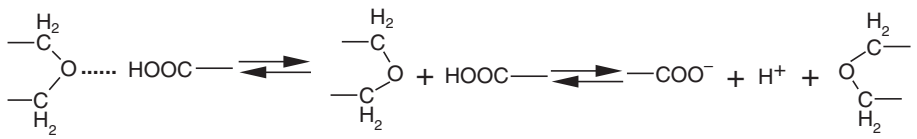

Scheme 1 Equilibrium between oxygen atom in PEG and carboxylic group.

The first and the second cases were deeply elaborated for radical template polymerization by Challa and co-workers[1,2,7,8] and are called 'pick-up mechanism' and 'zip mechanism', respectively.

A template can be a simple polymer containing a single type of group that interacts with only one type of monomer. However, in general, the template is a series of groups that interact specifically with a set of monomers.

A quantitative value of interaction between template and monomer in solution can be preferential solvation.[16] If the interaction between monomer and template is stronger than that between template and solvent, monomer molecules are associated with macromolecules of the template. Preferential solvation measured by interferometric and dialysis experiments was defined as an enrichment of monomer around the template. For instance, for MAA in dimethylformamide (DMF) in the presence of poly(2-vinylpyridine) (P2VP), it was found that the preferential solvation is 0.4.[16] Not only synthetic but also natural polymers can be applied as templates.

AA and sodium 4-styrenesulfonate were polymerized onto chitosan as a template.[17] The degree of acetylation for chitosan under investigation was 0.24. The reaction was carried out in water, initiated by $K_2S_2O_8$ at 50 °C. In all cases, insoluble interpolymer complex was obtained as a product of the reaction.

Chitosan for polymerization of sodium 4-styrenesulfonate was transformed to hydrochloride in order to cause strong ionic interaction between the monomer and the template. By the dilatometric technique, it was found that the reaction rate increases with increasing [T]/[M] ratio within the range 0–0.25 up to about 2.5 and then is stable. On the basis of this observation, the authors assumed a 'pick-up' mechanism for this process.

The only example dealing with the template polymerization of simple monomers in the presence of two sorts of templates was described by Papisov *et al.*[18] Polymerization of MAA in the presence of a mixture of poly(ethylene oxide) (PEO) and poly (*N*-vinylpyrrolidone) of sufficient chain lengths was examined. It was found that the rate of polymerization is determined by the template forming the stronger complex with a daughter polymer.

Depending on the basic mechanism of the template process, secondary reactions can take place. For instance, in polycondensation, there are such well-known reactions as cyclization, decarboxylation, dehydration, oxydation, and hydrolysis.

In radical polymerization usually in addition to the main elementary processes (initiation, propagation, and termination), we have the usual chain transfer to the monomer or to the solvent – changing the molecular weight of the product obtained – and also chain transfer to the polymer leading to the branched polymer. In ring-opening polymerization, many additional reactions can take place between monomer, solvent, and template depending on the chemical structure of the substrates.

4.33.3 Radical Template Polymerization and Copolymerization

4.33.3.1 Models and Examples

The majority of papers published in the field of template polymerization deals with the chain process initiated by radicals.

The most complete model of chain template polymerization was published by Tan and Alberda van Ekenstein.[19] Assuming that the polymerization goes also outside the template (blank reaction) and onto the template, the process consists of

1. Blank reaction: initiator decomposition, initiation, propagation, and termination;
2. Complexation: monomer adsorption, radical complexation, and polymer complexation; and
3. Reaction onto the template: propagation, template–template termination, and cross-termination.

The type of mechanism depends not only on the chemical structure of the template and the monomer, but also on the type of solvent, pH, and temperature.

This case, generally called 'pick-up mechanism' is illustrated in **Scheme 2**.

The next case, when absorption of monomer is strong and polymerization occurs according to the 'zip mechanism' is illustrated in **Scheme 3**.

The fact that PAA and poly(methacrylic acid) form complexes with poly(vinylpyrrolidone) (PVP) and PEG was a starting point for examination of template polymerization in different systems (**Table 1**).

The polymerization of AA in the presence of PEG is an example of this case. Hydrogen bonds between AA and PEG

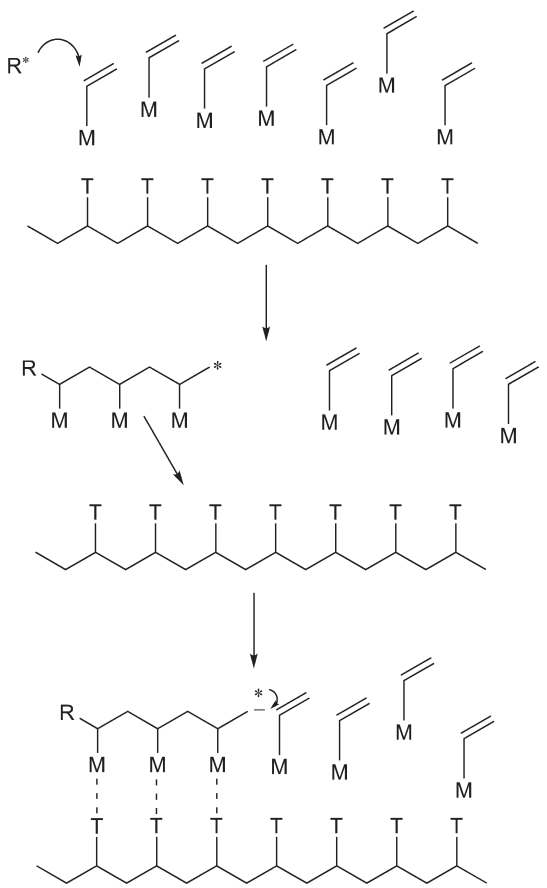

Scheme 2 Pick-up template polymerization. T, template unit; M, monomer interacting with the template.

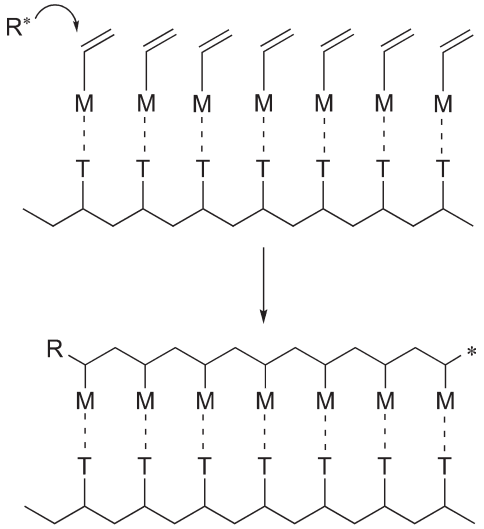

Scheme 3 Zip mechanism of template polymerization.

Table 1 Examples of template polymerization of acrylic acid (AA) and methacrylic acid (MAA)

Monomer	*Template*	*Solvent*	*Initiator*	*References*
AA	PVP	H_2O	$K_2S_2O_8$	20–22
AA	PEI	H_2O	$K_2S_2O_8$	23
AA	PEG	H_2O	$K_2S_2O_8$	15
AA	PEG	H_2O/methanol	$K_2S_2O_8$	15
AA	PEI	H_2O/aceton	AIBN + *hν*	24
AA	P(4VPy)	Methanol	AIBN	25, 26
MA	PEG	H_2O	$K_2S_2O_8$	15
MA	PEG	H_2O/methanol	$K_2S_2O_8$	15
MA	PEG	H_2O	$K_2S_2O_8$ + *hν*	27
MA	PVP	H_2O	UO_2SO_4 + *hν*	28
MA	P(4VPy)	Methanol	AIBN	25, 26
MA	P(2VPy)	Methanol	AIBN	29, 30

are week. However, a strong complex can be obtained only if the growing radical from PAA reaches a critical length. Such cooperative interaction was studied in Reference 15.

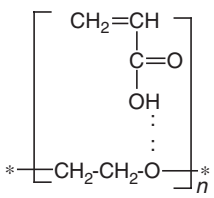

It is well known that polymerization of itaconic acid is more difficult than that of AA or MAA. However, template polymerization of itaconic acid in the presence of PEG was described.[31] The structure of the complex obtained was compared with the complex formed by mixing poly(itaconic acid) with PEG. It was found that complexes prepared by template polymerization have a stronger hydrogen bonding and more ordered structure.

The next case, where absorption of monomer is strong and polymerization occurs according to the 'zip mechanism', can be observed in the system examined by Blumstein and Kakivaya.[32]

Low-molecular-weight ionenes are used as a template for template polymerization of strong acidic monomers.

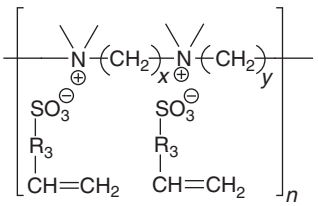

Electrostatic attraction leads to the stable complex between the template and the monomer.

The template polymerization of methacrylate monomers containing nucleic acid base was studied in the presence of the template polymer containing complementary nucleic acid bases.[33,34] Four monomers *N*-β-methacryloylethyl derivatives of adenine (MAOA), thymine (MAOT), uracil (MAOU), and theophylline (MAOThe) were synthesized. Atactic polymers were obtained from these monomers by radical polymerization initiated by azobisiso butyronitrile (AIBN) in dimethylsulfoxide (DMSO) solution and used as templates.

The rate of polymerization was found to accelerate when the complementary polymer was present. For instance, the rate of polymerization MAOA in pyridine solution in the presence of poly-MAOT is about 4 times higher than that in the absence of the template.

For the template polymerization of monomer containing uracil on the polymer containing adenine, it was found that interaction between adenine and uracil is not strong and monomer cannot interact with the polymer, but growing oligomer and the polymer containing uracil can form the complex with the template polymer containing adenine (pick-up model).

It was found that stereoregularity of the template plays an important role in the process. In a set of experiments, it was shown that the template effect is dependent on the tacticity of the template and also on the solvent used.

Polymerization of monomers containing nucleic acid bases groups was examined in the case where block copolymer was used as a template.[35]

Methacrylates with adenine (MA) and thymine (MT) groups connected with propyl spacer were synthesized. Copolymer with blocks of methacrylate with thymine units (MT) and blocks of polyethylene glycol was obtained by atom transfer radical polymerization (ATRP). Copolymer (PEG-*b*-oligo MT) was used as a template in polymerization of thymine monomer and adenine monomer. Polymerization was carried out using ATRP method with DMSO as a solvent. As expected, monomer with thymine groups did not show polymerization enhancement when copolymer with thymine groups was present. A significant enhancement of polymerization rate was observed when monomer with adenine groups was used. This template effect connected with well-known interaction between adenine–thymine groups was stronger for higher template to monomer concentration ratio. The rate acceleration in this case is, according to the authors, a result of a specific interaction between adenine and thymine moieties.

In some cases, the template has the same chemical composition as daughter polymer. In the first case with the polymerization of methyl methacrylate (MMA) onto isotactic poly(methyl methacrylate) (PMMA), it was found that daughter polymer is preferentially syndiotactic.[36–38] This interesting fact was explained by earlier known possibility of stereocomplex formation between iso- and syndiotactic PMMAs. Moreover, very interesting kinetic effects were observed in this system. Comparison of results obtained for blank and template

polymerizations leads to the conclusion that the most important difference is in radical lifetime of radicals, which is almost 8 times longer for a template process than a blank one. It leads to 2 orders of magnitude lower termination constant.

Polymerization of MMA in the presence of syndiotactic PMMA was also reported.[39] It was found that interaction between growing chains and the template is, in this case, not so strong and template influence is not as pronounced as in the case of isotactic template.

Matsuzaki *et al.*[40] used deuterated syndiotactic PMMA as a template for polymerization of MMA. In this case, measurements of tacticity of daughter polymer by ^{1}H NMR spectroscopy leads to the conclusion that the stereoeffect is negligible.

Other examples were described by Chapiro and Delieu.[41] The authors paid attention to the unusual behavior of polymerization of AA in different solvents. It is well known that organic acids form dimeric complexes by hydrogen bonds. The authors assumed that molecules of AA can take four forms as free monomer, cyclic dimer, linear oligomer, and monomer associated with polymeric template, depending on the nature of the solvent used, temperature, and concentration.

In pure AA and in water, dioxane, and methanol, which the authors call the first group of solvents, linear oligomers are stabilized by selective hydrogen bonds. In toluene, chloroform, and CCl_4 (second group of solvents), equilibrium of association is shifted from linear oligomers to cyclic dimers. Linear oligomer structure, appearing in pure monomer and in solvents of the first group, facilitates organization of monomer molecules by polymer formed in the very early stages of polymerization. It leads to a structure organized below.

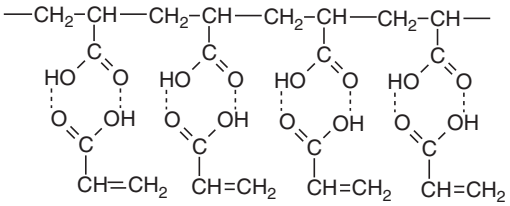

It was shown that the autoaccelerated character of AA polymerization is strictly correlated with such a form of monomer organization. The authors assumed that in such structures, a fast 'zip-up' propagation takes place along oriented double bonds.

A similar phenomenon was found for bulk polymerization of acrylonitrile initiated by gamma radiation and was described by Chapiro *et al.*[42]

The template mechanism was suggested by the authors for polymerization carried out above 60 °C. Polyacrylonitrile accumulated in the early stages of the reaction acts as a template to which monomer associates by dipole–dipole interaction. It is illustrated in the following formula:

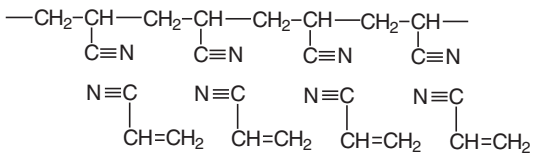

In the associates, polymerization occurs according to the zip-up propagation mechanism, and autoacceleration takes place. In the range of temperatures from 10 to 60 °C, the system gradually changes from one dominated by occlusion to one where template effect determines the kinetic behavior. In this temperature range, a significant posteffect occurs.[42]

4.33.3.2 Multimonomers as Templates

A special type of template polymerization takes place if monomer is connected with a template by covalent bonding. Initiation, propagation, and termination proceed in close contact with the template.

Kämmerer and co-workers were the pioneers in this investigation.[43–45] A multimonomer with the following structure was prepared:

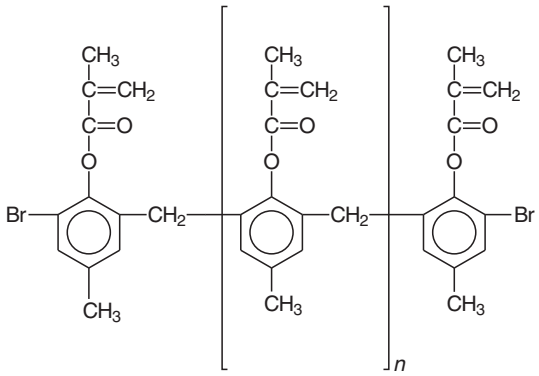

Polymerization of the multimonomer obtained was carried out in a very diluted benzene solution with a high concentration of AIBN used as an initiator. Such a procedure was used to minimize intermolecular reaction. The high concentration of the initiator leads to a preferential reaction between primary radicals with growing chains. It was proved that every oligomeric molecule was terminated from both sides by cyanopropyl groups. The structure predicted by the authors was as follows:

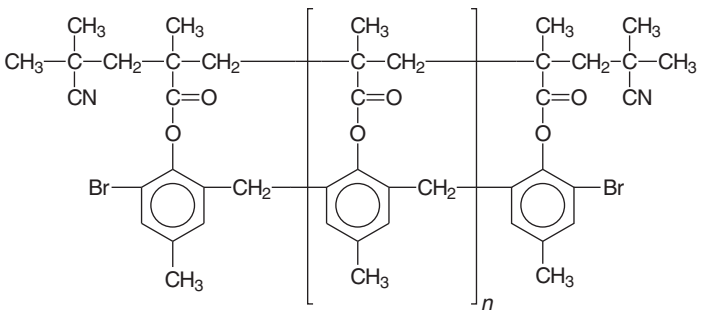

Hydrolysis of obtained products was carried out and oligomeric polyacids with the number of units predicted were found. Since then, many multimonomers have been synthesized using the following general formula (Table 2):

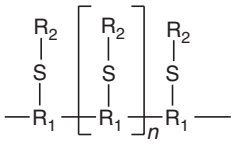

where R_1 is frame group, S the spacer, and R_2 the active group.

Another example is the synthesis of a ladder polymer suggested by Bamford,[5] but never realized in practice. According to his concept, active radicals in multimonomer, poly(vinyl methacrylate), would be created from CCl_3 end groups, in the presence of manganese carbonyl $Mn_2(CO)_{10}$, by UV irradiation. The radicals are expected to initiate selectively at one end of the template. It is shown in Scheme 4.

A similar system was examined afterward by Jantas.[47] Poly (vinyl methacrylate) was obtained by esterification of poly (vinyl alcohol) with methacrylic chloride and was used as a template. The polymerization can be represented by the reaction shown in Scheme 5.

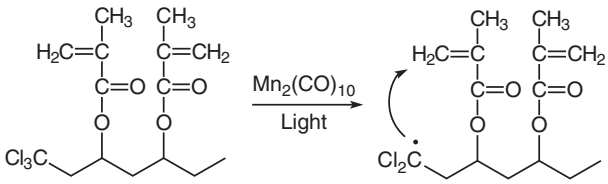

Scheme 4 Synthesis of ladder polymer suggested by Bamford.

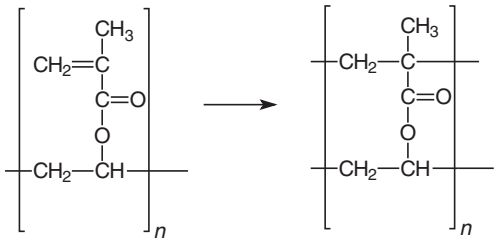

Scheme 5 Polymerization of poly(vinyl methacrylate).

The polymerization can begin at any of the groups present and may proceed in any direction. In other words, since the reactive groups are independent of one another and initiation occurs randomly, polymerization (zipping) leads to isolated

Table 2 Types of multimonomers

R_1	S	R_2	References
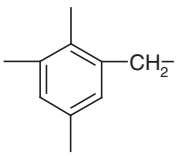	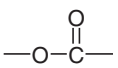		43, 44
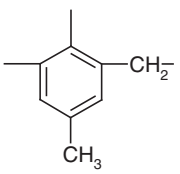	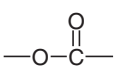		43, 44
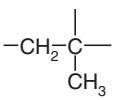	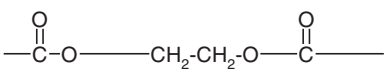		46–48, 54, 55
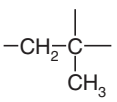	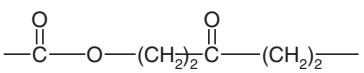		49
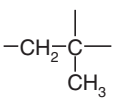	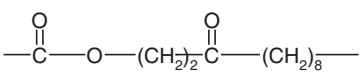		50
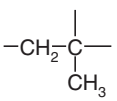	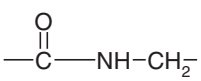		51
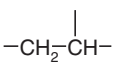	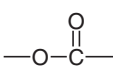		52, 53

reactive groups that are both potential crosslinking sites and breaks in the ladder structure. Crosslinking, as an intermolecular reaction, can be minimized by conducting the reaction at an appropriate dilution. If, however, the initiation is not random, but starts at one end of the template, we might expect to obtain a very regular ladder structure.

Another type of multimonomer, poly(methacryloyloxyethyl methacrylate) (PMOEM), has been synthesized and examined.[48] Selecting appropriate dilution, concentration of initiator, and temperature – even if initiation is random – polymerization leads to the ladder-type structure of the product as shown in the example of template polymerization of multimethacrylates according to the reaction presented in **Scheme 6**.

Recently,[54] PMOEM was synthesized in two methods: one was proposed by Jantas and Połowiński[52] and the other was by esterification of poly(2-hydroxyethyl methacrylate) (PHEMA) with methacrylic anhydride.[50] These two methods were compared. In both the cases, PHEMA was synthesized by ATRP.

Latterly, ladder-like polymers were synthesized by template polymerization of poly(2-methacryloyloxyethyl methacrylate) with different degrees of ladder. The process was carried out also by ATRP.[54]

In the next paper,[55] architectural effects of ladder-like polymer on glass transition temperature (T_g) were examined. Also in this case, the template (PHEMA) was synthesized by ATRP and was converted to multimonomer (PMOEM) by esterification with methacryloyl chloride. PMOEM was then polymerized by ATRP method and ladder-type polymer was obtained with a different percentage of ladder-type units dependent on the time of reaction. Additionally, the product with maximum ladder-type units (more than 70%) was hydrolyzed. It was found that glass transition temperature increases substantially when the degree of ladder in the product of template polymerization is more than 60%. According to the authors, the formation of a ladder-type sequence in the polymer was effective for improving the thermal stability with a small fraction of ladder-like sequence.

Polymerization of multimonomers can be discussed in terms of more general problems. Inter- or intramolecular reaction can takes place when the monomer has more than one double bond. Intermolecular reaction leads to the ladder structure and intermolecular reaction leads to the crosslinked or branched structure. Moreover, in the latter case, a part of the double bonds is unreacted. From the amount of double bonds and end-groups analysis,[48,49] a contribution of template reaction can be estimated. The value depends on the polymerization conditions the structure and molecular weight of multimonomer. This value seems to be a good measure for 'multimonomer ability' to template polymerization.

If the concentration of monomer used is very low, below the critical concentration, and concentration of initiating radicals is rather high, one can expect intramolecular polymerization leading to the product with ladder-type structure.

It was found[52] that polymerization of multiacrylates and multimethacrylates in dilute solutions leads to ladder-type polymer. Both, average molecular weight and distribution of molecular weights did not change up to quite a high degree of conversion.

A specific class of template polymerization is connected with polymerization of monomers included into cyclodextrin (CD). This type of polymerization leads in between classical template polymerization and polymerization in confined space, which will be discussed at the end of this chapter. From the other side, this type of polymerization is similar to polymerization of multimonomers described previously.

In a set of papers,[56–60] this type of atom transfer radical template polymerization was described. A unique template was synthesized by introduction of methacryloyl groups into cyclic compounds like β-CD. Synthesis of β-CD with methacrylic groups and polymerization of the monomer are presented in **Scheme 7**.

According to the authors,[59] the arrangements of vinyl groups in the template monomer (macromonomer) of β-CD is stricter than that in a template synthesis with a linear polymer. β-CD is a macrocyclic compound with seven primary hydroxyl groups and 14 secondary hydroxyl groups on both sides of a ring. If 14 vinyl groups are introduced to 14 secondary hydroxyl groups of β-CD, the vinyl groups will exist along one side of the ring of β-cyclidextrin. Since the maximum number of vinyl groups in the template monomer (macromonomer) of β-CD is 14, this template monomer will be suitable for the synthesis of oligomers.

When AIBN was used, the degree of polymerization (DP) of the methacryloyl group in the template monomer was polydispersed. When p-xylyl *N*,*N*-dimethyldithiocarbamate (XDC) or α-bromo-*p*-xylyl *N*,*N*-dimethyldithiocarbamate (BXDC), which are controlled/living radical initiators, were used at 25 °C, the values of DP of the methacryloyl group were 13 and 14, respectively, despite the fact that the average number of methacryloyl groups in the template monomer was 10.9. The main purpose of study[59] was to investigate the effects of the solvent and polymerization temperature with the 1,3-dibromobutane/HMTEMA/CuBr. ATRP initiator system on the template monomer.[58] It was found that the inclusion of toluene to the

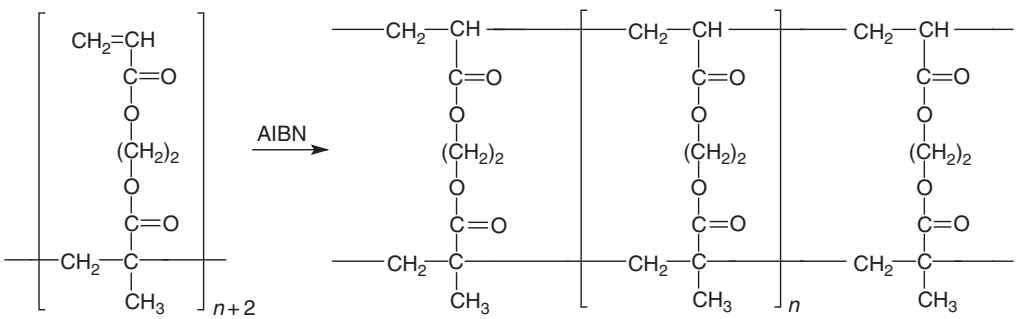

Scheme 6 Polymerization of poly(methacryloyloxyethyl methacrylate).

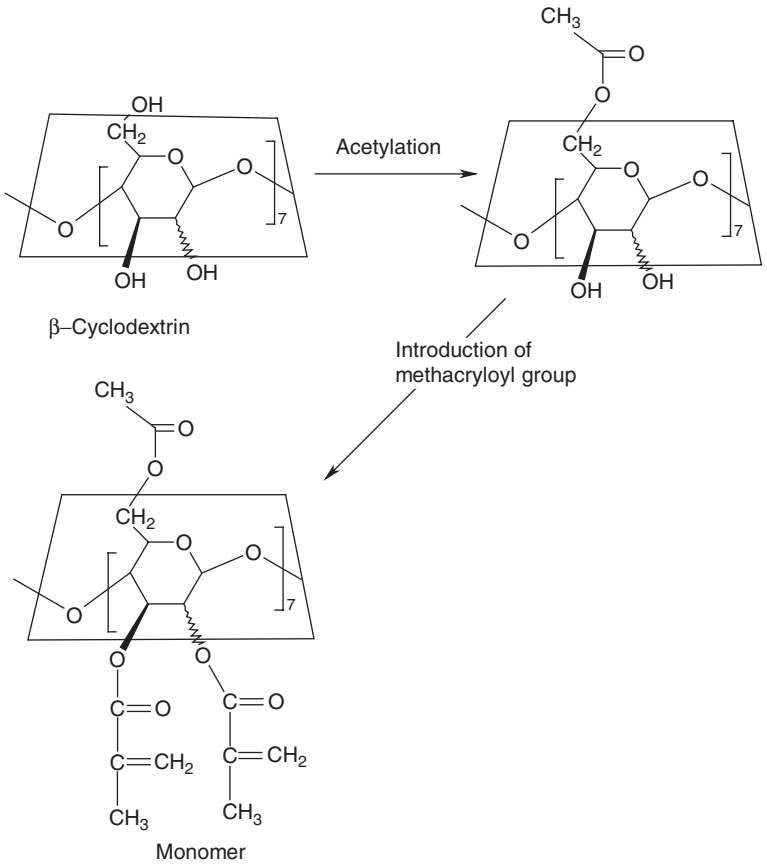

Scheme 7 Synthesis and polymerization of β-cyclodextrin with methacrylic groups.

template monomer with 10,6-vinyl groups improved the conversion due to the prevention of the inclusion of vinyl groups into the β-CD ring of the template monomer. In the next article,[64] a multivinyl template monomer with 20,4-methacryloyl groups was synthesized with β-CD by esterification of hydroxyl groups with methacrylic anhydride. ATRP of the template monomer was carried out. In the optimal case, the conversion of the vinyl groups was 21.1%. ATRP with methyl 2-bromopropionate – 2,2′-dipyridyl and CuBr as initiators, a ligand and a catalyst, respectively – was carried out. It was found that the molecular weight distribution of MAA oligomers obtained after hydrolysis was bimodal. DPs of the oligomers were 7 and 14. To strictly control the polymerization, the number of vinyl groups in the template monomer should be monodispersed. However, it was stereochemically difficult to synthesize the β-CD template monomer with 7.0 and 14.0 vinyl groups introduced into primary and secondary hydroxyl groups, respectively, in a good yield. Also, it was impossible to obtain the template monomer with 21 vinyl groups. The template monomer with 20.4 vinyl groups would be a mixture of template monomer with 21 vinyl groups and the template monomer with less than 20 vinyl groups.

Luck of the distribution of number of vinyl groups in the template monomer is important to clarify the effect of the template structure on the template polymerization.

In the next paper,[59] synthesis of cyclic poly(methacrylic acid) oligomers was described. Cyclization of oligo(methacryloyl) groups in template monomer of β-CD was investigated. It was found that cyclization by 1,3-diaminopropane oligomers obtained by ATRP with 1,3-dibromopropan as an initiator leads to cyclic oligomers.

In the next paper,[60] cyclic novolac with 24 OH groups, called 'Noria', was used as a template. As in previous papers, OH groups were estrificated in order to have multivinyl monomer. The average number of vinyl groups per molecule determined by ^{1}H NMR spectroscopy was 23.8. Polymerization of such prepared multimonomer was carried out by ATRP technique in methanol using methyl 2-bromopropionate, tris[2-(dimethylamino)ethyl]amine and CuBr. After hydrolysis, oligo(methacrylic acid) was analyzed by matrix associated laser desorption ionisation with time of flight (MALDI-TOF) technique. It was found that the polymerized product was a mixture of oligomers with different DP. However, it was unusual that DPs were only odd numbers. This unusual phenomenon would be connected with the specific structure of the template used.

4.33.3.3 Kinetics of the Radical Template Polymerization

Many factors that can influence the kinetics of the template polymerization can lead to effects similar to the 'template effect'. The increase of the reaction rate is known as the 'Tromsdorff effect' or 'gel effect'. The polymerization classified as the 'template process' often proceeds in a nonhomogeneous system, for instance, with precipitation of the complex formed. Some authors explain the 'template effect'[21,26] by a

change in 'local concentration' only. As was demonstrated,[61] if the monomer is distributed into two parts – inside template coils and in a 'free' volume – the kinetic equation can be transformed into the conventional form, providing that the concentration of the template is lower than the critical concentration. Quite a different polymerization mechanism may exist in a given template system above and below the critical template polymer concentration. In the latter case, polymerization can proceed inside the template coil and in a 'free' solution.

A critical inspection of the kinetic results in template polymerization is very important. The rate of template polymerization should be compared not only to the polymerization rate of the same monomer in the same solvent, but also with the system in which the low-molecular-weight analog of the template is present. The presence of an 'additional' substance (such as a template) in the polymerizing system can influence many processes as a chain transfer to polymer, which leads to grafting, selective sorption of initiating system, or changing monomer–dimmer equilibrium in the case of monomeric acids. It seems necessary to apply methods other than kinetics to ensure that the template influences the polymerization process on the 'molecular level', to compare the process with the low-molecular-weight analog and analyze all additional effects.

Nevertheless, an enhancement of the reaction rate is, in fact, the most pronounced effect of template polymerization. For many systems, a conventional kinetic equation has been applied.

$$-\frac{d[M]}{dt} = K_{ov}[I]^n[M]^n \qquad [2]$$

However, it was found that, in many cases, the template influences not only the rate constant (K_{ov}) but also n and m in the kinetic equation. It is illustrated in **Table 3**.

In order to estimate kinetic constants for elementary processes in template polymerization, two general approaches can be applied. The first one is based on the measurement of photopolymerization rate in a nonstationary state by rotating sector procedure.[64] The second one is based on the polymerization generalized by kinetic model,[65,66] results of such experiments for polymerization of MAA are presented in the **Table 4**

As we can see, the presence of template influences the rate constants of elementary processes k_p and k_t. In comparison with the polymerization without template (blank reaction), k_t for template polymerization is lower to a few orders of

Table 3 Examples of *n* and *m* for template polymerization acrylic or methacrylic acid

Monomer	*Template*	*Solvent*	*Initiator*	n	m	*Reference*
Acrylic acid	Poly(ethylene glycol)	H_2O	$K_2S_2O_8$	0.7	1.1	15
Acrylic acid	Poly(ethylene glycol)	H_2O + 50% methanol	$K_2S_2O_8$	0.7	-	15
Acrylic acid	Poly(vinyl pyrrolidone)	H_2O	$K_2S_2O_8$	1	1.5	20
Acrylic acid	Poly(vinyl pyrrolidone)	H_2O	$K_2S_2O_8$			22
Acrylic acid	Poly(vinyl pyrrolidone)	H_2O	$K_2S_2O_8$	0.5	1.9	21
Acrylic acid	Poly(ethylene imine)	H_2O	$K_2S_2O_8$	1	1	23
Methacrylic acid	Poly(ethylene glycol)	H_2O	$K_2S_2O_8$	0.7	1	15
Methacrylic acid	Poly(ethylene glycol)	H_2O + 50% methanol	$K_2S_2O_8$			15
Methacrylic acid	Poly(ethylene glycol)	H_2O	$Na_2S_2O_8^P$	0.5	1	27
Methacrylic acid	Poly(vinyl pyrrolidone)	H_2O	$UO_2SO_4^P$	0.5	1	28
Methacrylic acid	Poly(vinyl pyrrolidone)	H_2O	$K_2S_2O_8$	0–0.5	1.5	62
Methacrylic acid	ionene	H_2O	$K_2S_2O_8$	0.8	0.3–0.9[C]	63
p-styrene sulfonic acid	ionene	H_2O+ isopropanol	AIBN	1	1	32

P, photoinitiation; C, dependent on the concentration.

Table 4 Rate constants of elementary processes for methacrylic acid template polymerization

Solvent	*Temp. (°C)*	*Template*	*Initiator*	k_p *(l mol.$^{-1}$ s)*	k_t *(l mol.$^{-1}$ s)*	$k_p/(k_t)^{0.5}$	*Reference*
Water	25	Blank	Photo	22.6×10^2	3.2×10^6	1.2	65
Water	25	PDMA[a]	Photo	52.5	2.2×10^3	1.1	65
Water	25	PVP[b]	Photo	24.7	4.3×10^2	1.2	65
Water	25	PVP[c]	Photo	29.2	2.4×10^2	1.9	65
DMF	30	Blank	AIBN	70.0	5.0×10^6	0.03	66
DMF	30	P2VPy	AIBN	50.0*	$1.1 \times 10^{2**}$	1.5	66
Methanol	60	Blank	AIBN	30×10^3	40×10^6	4.7	61
Methanol	60	P4VPy	AIBN	$22.5 \times 10^{3*}$	$20 \times 10^{4**}$	50.3	61

[a]PD = 50.
[b]PD = 52.
[c]PD = 8860.
*for 'pick up' reaction;
**for template–template termination.

magnitude. Also k_p is lower in the examined systems, but k_p^2/k_t is sometimes almost the same as for polymerization without template. This example leads to the conclusion that even if the ratio of overall rate of template polymerization to blank polymerization is unity, template mechanism of reaction can be accepted.

Kinetics of template polymerization of multimonomers seems to be more complicated.

Assuming that it is possible to apply classical kinetic equation for polymerization of multiacrylates and multimethacrylates, exponents '*m*' and '*n*' were found to be 1 and 0.25, respectively.

Quite unusual reaction order in respect to initiator suggests that termination reaction is more complicated than that in conventional polymerization. The process of radical termination by electron paramagnetic resonance (EPR) technique.[68,69] EPR spectra for multimethacrylate in dioxane, after illumination of UV for 5 min and then switching off the light source were recorded.

It was found that radicals are very stable. After 1 h, there were still 60% of radicals. The calculated rate constant for termination reaction was found to be $11.8\,\mathrm{l\,mol.^{-1}\,s}$. Accepting this value and assuming a stationary state, k_p and k_t can be calculated. The results are compared with the values for MMA polymerization.

The results presented in Table 5 show the same tendency as presented in Table 4. Both k_p and k_t are much lower in template polymerization. However, presented calculations are very simplified. It is difficult to accept a stationary state in this process as well as a conventional kinetic equation. Moreover, it was found[67] that the reaction is not a second order, but in order to describe the kinetics a dispersive kinetic equation should be applied. On the basis of these data, we can conclude that in template polymerization, both rate constants, for propagation and termination, are lower than that in a conventional process.

It is probably connected with the fact that conformational rotation is needed for propagation as well as for radicals termination onto template.

Recently, Oral and Pepas[69] described the investigation of template polymerization in the system 2-hydroxyethyl methacrylate (PEG) with glucose as an imprinting compound. In the course of the crosslinking, reaction occurs. Effects of template concentration on the conversion and polymerization rate were investigated. The polymerization kinetics of networks imprinted with glucose and nonimprinted networks were examined, and a significant effects on the conversion and polymerization rate of imprinted polymers were observed and were compared to nonimprinted ones. An initial decrease in rate was observed followed by a slight autoacceleration effect in the polymerization of imprinted polymers prepared with fast-curing initiator and a mixture of fast-curing initiator and iniferter. The influence of various possibilities of hydrogen bonding between components of the examined system was discussed. From the presented results, one can see how many factors influence the kinetics of template polymerization.

Table 5 Rate constants for methyl methacrylate and multimethacrylate polymerization

Monomer	k_p	k_t	$k_p/(k_t)^{1/2}$
Methyl methacrylate	310	66×10^6	3.8×10^{-2}
Multimethacrylate	0.427	11.8	12.4×10^{-2}

4.33.3.4 Radical Template Copolymerization

In the literature, there is less information about template copolymerization than about template homopolymerization. However, the process seems to be very interesting on account of the fact that a template can influence not only the molecular weight and tacticity of the daughter polymer but also the composition and distribution of units in the copolymer macromolecule.

In principle, template copolymerization can be realized according to different reaction types as template copolycondensation, template copolyaddition, ring-opening copolymerization, and radical or ionic copolymerization. However, radical template copolymerization is slightly more elaborated. The process of template copolymerization can be classified from the point of view of structure of the template. We can make a distinction between two cases: whether the template is a homopolymer or a copolymer. An important role in the process of template copolymerization plays a difference in interactions between the template and two comonomers.

It is known that the composition and the distribution of units in simple copolymerization is controlled mainly by the propagation process. From this point of view, equations have been formulated[70] concerning how the reactivity ratios depend on the template concentration and individual reactivity rate constants of monomers taking part in the template copolymerization process.

These equations take into consideration the concentrations of radicals bonded with the template (denoted by $[A^*]$ and $[B^*]$) and nonbonded ($[A^\circ]$ and $[B^\circ]$). The equations were formulated with the assumption that the process sorption–desorption of radicals onto template is reversible with equilibrium constants K_A and K_B:

$$A^\circ + T \leftrightarrow A^* \quad K_A = \frac{[A^*]}{[A^\circ][T]} \qquad [3]$$

$$B^\circ + T \leftrightarrow B^* \quad K_B = \frac{[B^*]}{[B^\circ][T]} \qquad [4]$$

$$r_1^* = \frac{k_{AA} + K_A[T]k_{A^*A}}{k_{AB} + K_A[T]k_{A^*B}} \qquad [5]$$

$$r_2^* = \frac{k_{BB} + K_B[T]k_{B^*B}}{k_{BA} + K_B[T]k_{B^*A}} \qquad [6]$$

These equations indicate that the reactivity ratios are dependent on the concentration of template used [T], as well as on the interactions between the templates and monomers (K_A and K_B). The interactions are dependent on the solvent used in the process of copolymerization. It seems that this statement can be generalized.[71] Consequently, the template influences the average number of units in a sequence $\overline{l_A}$ and $\overline{l_B}$. From the general rules concerning radical copolymerization:

$$\overline{l_A} = r_A x + 1 \text{and} \overline{l_B} = \frac{x + r_B}{x} \qquad [7]$$

In many papers,[70,72] it was found that the presence of template changes the sequence length in the copolymer obtained. The simplest case is when both monomers are interacting with the template, forming the complex (Scheme 8).

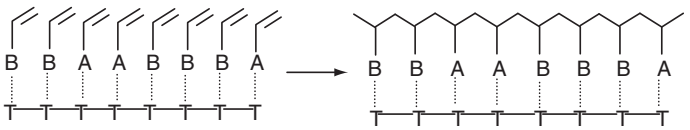

Scheme 8 Template copolymerization when both monomers are interacting with the template.

For copolymerization of AA with MAA in the presence of PEG in toluene and in benzene, the template effect was described in Reference 73. Template copolymerization was carried out with the equimolar quantity of acid groups present in the reaction mixture and PEG units. For different molar ratios of MAA to AA, it was found that the relation proposed by Kelen–Tüdös equation was fulfilled. Reactivity ratios change from 2.12 and 0.42 (without the template) to 2.64 and 0.2 (with template) for toluene and 2.77 and 0.29 for benzene used as a solvent, respectively.

In the next paper,[74] copolymerization of MAA with MMA was carried out in the presence of PEG. In this case, according to the authors, both monomers can create hydrogen bonds with the template. Reactivity ratios r_1 (for MMA) and r_2 (for MAA) were 0.10 and 2.10, respectively. For copolymerization without template, $r_1 = 0.55$ and $r_2 = 1.50$.

Copolymerization of acrylamide with MAA in the presence of poly(alkylammonium chloride) as a template was described by Liu and co-workers.[75] Microstructure of copolymer obtained by template polymerization, containing also phenoxy acrylate, was examined by ^{1}H NMR spectroscopy. Copolymerization was carried out in aqueous solutions with different pH. Dependence of hydrogen bonds between acrylamide blocks and MAA blocks on pH value of the solution was discussed in detail.

It was observed[76] that in the copolymerization AA with HEMA, the AA reaction rate is greater in the presence of PVP) compared with blanc copolymerization while the HEMA reaction rate is slightly lower. It can be stated that for the same conversion, the content of AA will be higher and anyway the medium length of sequences of HEMA will be shorter in the copolymer obtained in the presence of the template.

In conclusion, the obtained results clearly show that the presence of PVP as a template in the reaction environment influences the reactivity of the two monomers and therefore the structure of the produced copolymer.

An example of the case that the interaction with the template differs substantially for two comonomers is illustrated in Scheme 9.

This case was described by O'Driscoll and Capek.[77] Examining copolymerization of MMA with styrene in the presence of isotactic PMMA, it was found that a small amount of styrene destroys any template effect.

The next example deals with copolymerization of MAA with styrene in the presence of PEG.[70] It was assumed that, in this case, only MAA can interact with the template.

However, intermediate cases were described in which the conventional Mayo–Lewis equation is fulfilled, but reactivity ratios r_1 and r_2 depend on the template concentration.

Template copolymerization of styrene and MAA was examined by Frisch and Xu.[72] As a template, P2VP was used. Using ^{1}H NMR and ^{13}C NMR compositions, sequence lengths and sequence distribution for copolymer obtained with various feed composition were determined. It was found that the template had little, if any, effect on the molecular weight, composition, or glass transition temperature of the copolymers. However, copolymers with significantly longer block lengths of both styrene and MAA units were created with comparison with copolymerization without template. The influence of solvents on apparent reactivity ratios was described by Chapiro.[78] The author found that in the case of polar monomers, copolymerization reactivity ratios strongly depend on the type of solvent. It can be explained by assumption that the copolymer formed takes the template into further steps of the copolymerization.

It is shown in the case of AA that a solvent mixture that enhanced the 'matrix effect' in the homopolymerization of this monomer also favors its introduction in the copolymer with methyl acrylate. It was also found that the apparent reactivity ratios are particularly sensitive to solvent in copolymerizations involving acrylamide.

Template phenomena in synthesis of block and graft copolymers were discussed in Reference 79. The authors paid attention to 'template effects' observed in the case of synthesis of block and graft copolymers with cooperatively interacting polymer components. Grafting of MAA onto starch, initiated by a redox system with Ce^{IV}, described in Reference 80 is an example. The rate of the graft propagation was found to be 10 times higher than that of MAA homopolymerization. Later publications dealing with kinetic investigation of grafting acrylamide onto poly(vinyl alcohol) initiated in the presence of Ce^{VI} confirm, according to the authors, the hypothesis about the template character of the graft copolymerization.

Very few systems, beyond the polymerase chain reaction (PCR) method mention in the 'introduction' have been studied in which two comonomers are polymerized in the presence of copolymer template. It is illustrated in Scheme 10.

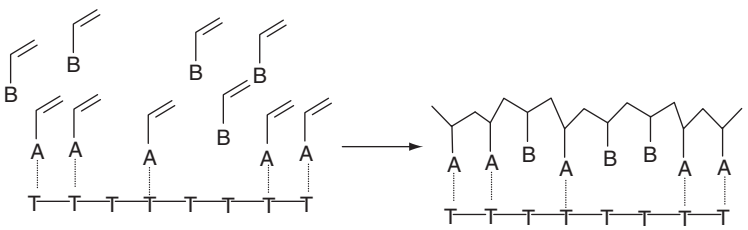

Scheme 9 Template copolymerization when only monomer A is interacting with the template.

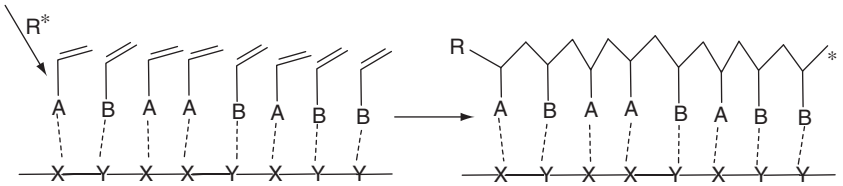

Scheme 10 Template copolymerization when monomer A is interacting with unit X and monomer B with unit Y.

Monomer A is interacting with unit X and monomer B with unit Y.

Ferguson and McLeod[81] described polymerization in which copolymer with interacting and noninteracting groups was used as a template, but only one monomer – AA – was used.

The separate category of template copolymerization is when at least one of the comonomers is a multimonomer (i.e., reacting units are connected with the template by covalent bonds).

The early work on the copolymerization of multimonomers with vinyl monomers employed *p*-cresol formaldehyde resins, esterified by methacryloyl chloride or acryloyl chloride as one of the comonomers, and simple vinyl monomer such as styrene,[82] acrylonitrile,[83] *p*-cresyl methacrylate,[84] and other monomers. Multimonomers were fractionated in order to have sharp fractions with a number of units 3 (molecular weight 334 g mol.$^{-1}$) (M3) and 8 units (mol. weight 960 g mol.$^{-1}$) (M8). Copolymerization of the multimonomers with styrene was carried out for different compositions of reacting mixture, and reactivity ratios were calculated and compared with reactivity ratios for copolymerization styrene with *p*-cresyl methacrylate (analog with one 'unit'). The obtained product was hydrolyzed, and, after treating, diazomethane copolymer poly(methyl methacrylate-*co*-styrene) was obtained and analyzed. It is presented in **Scheme 11**.

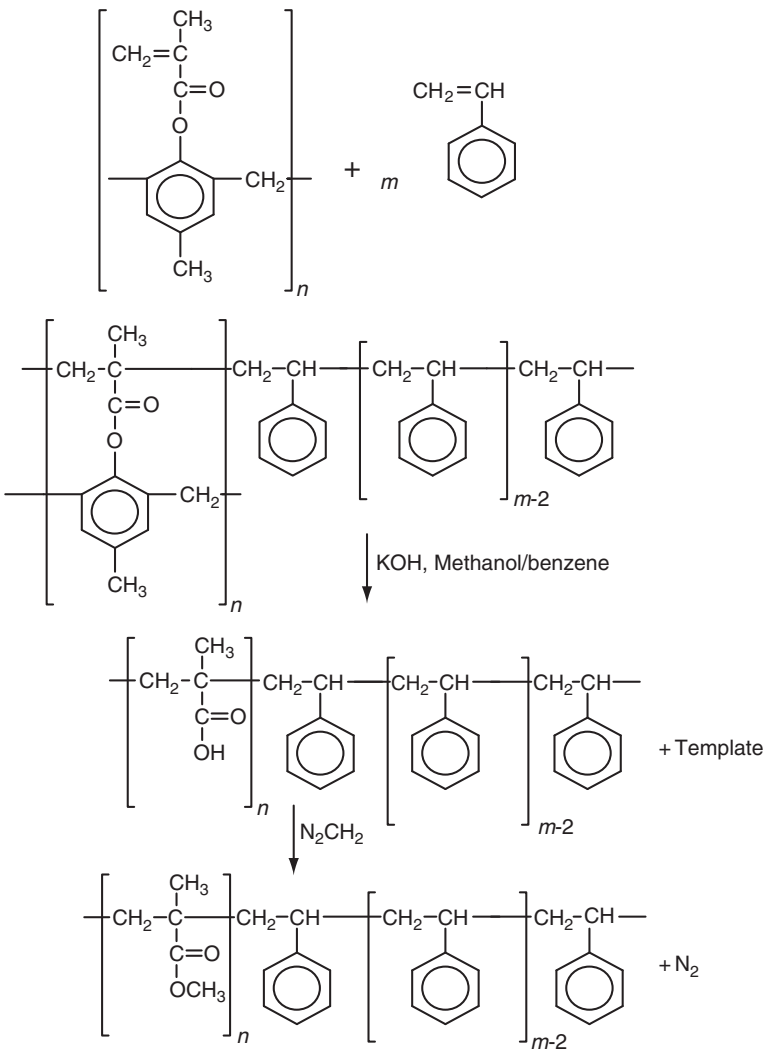

Scheme 11 Synthesis of poly(methyl methacrylate-*b*-styrene).

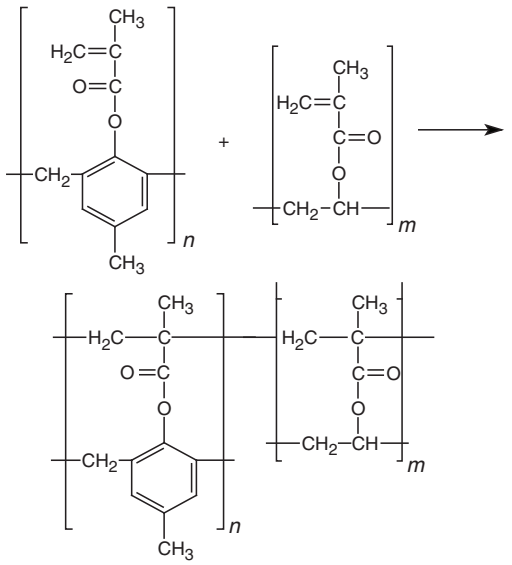

Scheme 12 Synthesis of ladder block copolymer.

Another case occurs if there are two different templates connected by covalent bonds with monomeric units. In other words, it is a copolymerization of two different multimonomers, described in Reference 85. One multimonomer was prepared from poly(vinyl alcohol) and the another one from cresyl-formaldehyde resin (Scheme 12).

Copolymerization of the multimonomers was carried out in a dilute solution in DMF at 90 °C using AIBN as an initiator. The copolymerization product was soluble in DMF and in chloroform. Hydrolysis of the copolymer obtained, followed by separation and analysis showed that one of the products of the hydrolysis is poly(vinyl alcohol) with a molecular weight similar to that of the initial PVA.

All these findings lead to the conclusion that by the copolymerization of two different multimonomers, a copolymer with two ladder-type blocks can be obtained.

4.33.4 Template Polycondensation

Conventional high-temperature polycondensation makes ordering of monomers along the template difficult. However, the interesting possibility of template polycondensation has been connected with a set of monomers synthesized by Ogata and co-workers.[86,87] Diesters with β-heteroatoms (X) like O, S, SO_2, N, and P or nuclei like furan, tiophen, pyridine, and pyrazine with a general formula: R′OOCCH$_2$CH$_2$X–R–XCH$_2$CH$_2$COOR′ were obtained. Polycondensation of such diesters with hexamethylenediamine proceeds in solution under mild conditions at relatively low temperature.

Template polycondensation of such monomers in the presence of P2VP and poly(4-vinylpyridine) (P4VP),[88] poly (vinylpyrrolidone), poly(vinyl alcohol), and others was described.[89–91] The most interesting results obtained were by examining the template polycondensation of two monomers: diethyl tartrate (A) and dimethyl mucate (B) or diethyl mucate (DEM).

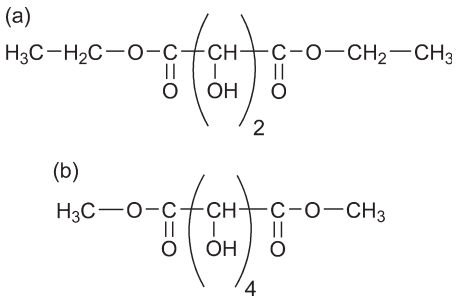

Results described in Reference 88 indicate that the rate of polycondensation of DEM with hexamethyldiamine (HMD) was rarely enhanced by the presence of P4VP. Similarly, the rate of polycondensation of DEM with HMD in the presence of P4VP was only slightly higher than that in the absence of the template. However, in this case, it was found that polymerization yielded a polyamide with much higher molecular weight than those in the presence of P2VP or in the absence of P4VP.

In Reference 89, polycondensation of dimethyl teartrate (DMT) with HMD in the presence of various templates was described.

In the case where poly(vinylpyrrolidone) (PVP) was used as template, it was observed that the polycondensation rate was higher than that in the presence of *N*-methyl-2-pyrrolidone (low molecular analog) and in the absence of a template. It was also found that the rate enhancement due to the PVP templates becomes more pronounced with an increase in the molecular weight of PVP. Experiments carried out at various concentrations of PVP lead, according to the authors, to the conclusion that in this case the effect of excluded volume might be negligible. Interesting results were obtained by examination of polysaccharides' influence on the rate of the process. Linear polysaccharide (Pullulan) PF with molecular weight $\overline{M_w}$ = 10 000 and 30 000, for β-CD and saccharose, respectively, was used. The results indicated that the polycondensation reaction in DMSO was greatly accelerated by the addition of templates in the following order:

$$\mathrm{PF}(\overline{M_w} = 30000) > \mathrm{PF}(\overline{M_w} = 10000) > \text{saccharose} > \beta\text{–CD} > \text{none}$$

Polycondensation of diethyl tartrate (A) and dimethyl mucate (B) in dimethyl sulfoxide in the presence of poly (vinyl alcohol) was slightly enhanced in comparison to the reaction in the presence of low molecular compounds such as glycerol or izopropanol.

In a separate paper,[91] molecular weight control in polycondensation of hydroxyl diesters with hexamethylenediamine by poly(vinylpyridine) was described. It was found that addition of P4VP increased the molecular weight of the resulting polyamide to a higher extent than P2VP and the molecular weight of the resulting polyamides could be controlled according to the molecular weight of P4VPy. Using copolymer 4-vinylpyridine-*co*-styren as a template, it was found that the presence of this copolymer also affected the molecular weight of the polyamide, which increased with increasing pyridine groups in the copolymer.

In the next paper in this set,[90] polymerization of diethyl chelidonate (DEC) with diamines in the presence of

high-molecular-weight ($M_n = 1.3 \times 10^6$) polyvinylcarbazole (PVK) was described.

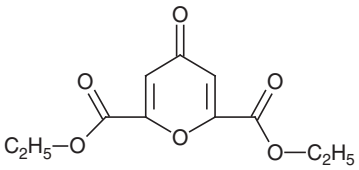

DEC

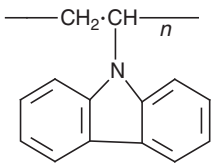

PVK

It was expected that DEC forms a charge transfer complex with poly(vinylcarbazole). Indeed, a significant increase in the template polycondensation rate was observed. The reaction was carried out in dioxane at 30 °C and it was found that the rate of reaction increased with template concentration. An interesting retardation effect was observed if *N*-ethylcarbazole (EK) (a low-molecular-weight analogue) was present. This effect can be explained, according to the authors, by the formation of a strong and stable charge transfer complex between DEC and EC.

Moreover, it was found that polycondensation of DEC with HMD in the presence of PVK was accelerated by the UV radiation probably owing to the transfer of light energy.

A new type of polycondensation by means of phosphorus compounds in mild conditions was described by Higashi and co-workers[92–95] and template effects were observed. The synthesis of polyamidation of polyamides by direct polyamidation of terephthalic acid with 4,4′-diaminodiphenylmethan was examined. P2VP, P4VP, poly(vinylpyrrolidone), and PEO were used as templates. For example, it was found that poly (terephthalamides) prepared from *p*-phenylenediamine and 4,4′-diaminodiphenylsulfone in the presence of PVP have much higher molecular weight than the same polymer obtained by a direct polycondensation reaction.

Several aromatic polyamides from aromatic dicarboxylic acids and diamines were prepared by polycondensation in the presence of P2VP, P4VP, and PEO and it was found that the template increased the molecular weight of the polymer obtained.

This type of template polycondensation was applied to the preparation of polypeptides directly from free amino acids. It was found, for instance, that an increase in the amount of PVP template in polycondensation of L-leucine lead to the increase of molecular weight of polyleucine obtained. Also, increasing the molecular weight of the template from 1×10^4 to 3.6×10^5 increased the obtained molecular weight of polyleucine more than 30 times.

An interesting method of polycondensation was described by Hattori *et al.*[96] Di-*p*-nitrophenyl methylsuccinate with thymine or theophylline groups was condensed with piperazine. The reaction was carried out in a pyridine/methylene chloride mixture or DMF in the presence of a copolymer of styrene and styrene derivatives with adenine groups as a template. The strong interaction between complementary groups – adenine in the template and thymine in the monomer – was confirmed by IR and the NMR techniques.

It was found that depending on the percentage of adenine groups in the copolymer, the rate of reaction was different. For a monomer with thymine groups, the maximum acceleration appears in about 50% of adenine groups in the template copolymer and in the ratio of 1:1 monomer to the template.

A template polycondensation of urea with formaldehyde in the presence of AA was published by Papisov and Litmanovich.[97] The authors suggested that a complex with polyacid is formed during the reaction. The complex has a different structure than urea-formaldehyde resin mixed with PAA. If during the reaction the pH is kept below 3.7, NH_2 groups are present in the obtained polycomplex. The presence of NH_2 groups was confirmed by the presence of 3440 cm^{-1} in the IR spectrum. In the absence of PAA, polycondensation leads to the structure –CH_2–NH–CO–NH–. The authors explained the mechanism of the template reaction by assuming an interaction between carboxylic groups and urea. Indeed, it is known that hydrogen bonds are formed in such a system, and the reaction shown in **Scheme 13** is obtained.

In our work,[98] the process of template copolycondensation was the subject of an investigation using urea and thiourea as co-reagents. It was expected that, similar to the reaction described by Papisov, copolycondensation in the presence of PAA would proceed according to **Scheme 14**.

A set of experiments was carried out at 25 °C. The reacting mixture after stirring for 4 h was kept for 7 days. The precipitated complex was centrifuged, washed a few times with water and dried in vacuum. From the results of the elemental analysis, the percent of thiourea in the product was calculated. As can be seen from the results, the percentage of thiourea in the product was similar to the percentage of thiourea in the monomer mixture. From the elemental analysis and IR spectrometry, it was proved that the thiourea is incorporated into the product; however, the thiourea percentage in the product is slightly lower than that in the monomer mixture.

The hydrolysis and then condensation of tetraacetoxysilane in the presence of PEG as a template were examined.[99] Stable interpolymer complex of poly(silicic acid) with PEG was obtained.

The template polymerization of the monomers, containing nucleic acid bases on the complementary template polymer was examined by Shimidzu *et al.*[100] The crosslinked P4VP containing adenine or thymine groups was used as a template.

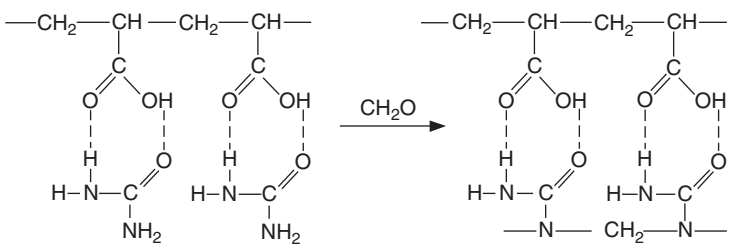

Scheme 13 Template polycondensation of urea.

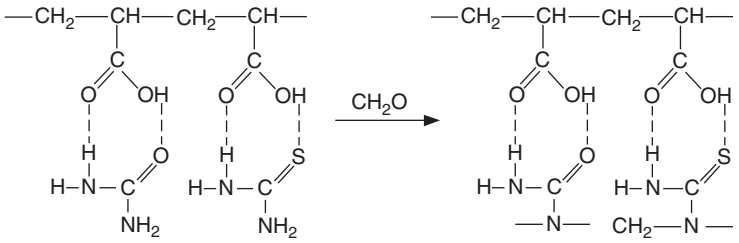

Scheme 14 Template copolycondensation of urea and thiourea.

Complementary nucleotides as quaternized pyridine derivatives were used as monomers. As a product of a template reaction, oligonucleotides were obtained with the structure complementary to the structure of the template used.

An unique template process leading to the synthesis of ladder-like polymethylsiloxanes was proposed by Tang and co-workers.[101] In the first step of the synthesis, *N,N′*-bis (4-[3-(diethoxymethylsilyl)propoxy]-phenyl]terephthalamide was obtained, named by the authors monomer (M). In the next step, diethoxymethylsilyl groups were hydrolyzed in order to obtain silanol groups. Such a prepared compound can be assembled into a stable complex through the interaction of amido bonding (C=O…NH) and silanol bonding (H…OH). Then, via a dehydration condensation reaction, an oligomer was formed and further condensed using concentrated H_2SO_4 into an ordered ladder-like polymethylsiloxane. The last state of the process is illustrated in Scheme 15.

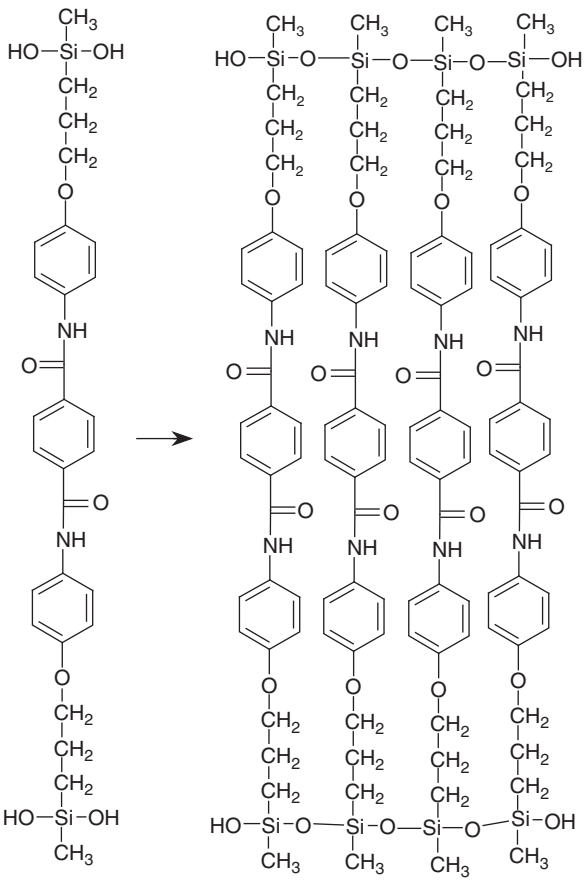

Scheme 15 Synthesis of ladder-type oligosiloxanes.

The product obtained was soluble in DMSO and analyzed in order to confirm the structure shown in Scheme 15.

A variety of characterization techniques such as ^{1}H NMR, ^{29}Si NMR, FT-IR spectrometry, and others confirm the structure.

A similar type of reaction was described by Guo and co-workers.[102] The ladder-type polymethylsiloxane was synthesized on the basis of hydroquinone H-bond-induced self-assembling as presented in Scheme 16.

Recently, the synthesis of a similar type of ladder polysiloxanes described in Reference 102 was reported,[103] but hydroquinone groups were changed to 9,10-diphenylanthryl groups.

4.33.5 Ring-Opening Template Polymerization

The application of template ring-opening polymerization for polypeptide synthesis was reported by Ballard and Bamford.[104] The substrate for the synthesis was *N*-carboxy-α-amino acid anhydrides (NCA).

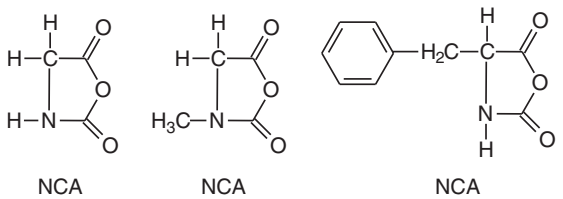

NCA NCA NCA

For instance, the first step consists of the reaction of phenylalanine NCA with secondary amine. In the course of the reaction, decarboxylation occurs (Scheme 17).

The product containing the amine group is an initiator for the next NCA molecule. The ring-opening process and the elimination of CO_2 proceed as a chain reaction yields the polypeptide. If a polypeptide containing a terminal base group with secondary amine is used as initiator with the NCA of different α-amino acid, the product is a block copolymer.

Unusual features were reported in Reference 104 when polysarcosine dimethylamide with the formula: $H[N(CH_3)CH_2CO)]_nN(CH_3)_2$ was used to initiate polymerization of DL-phenylalanine NCA. The initial rate of reaction in nitrobenzene solution at 15 °C was found to depend on the chain length (n) of the initiating polymer. For instance, for $n = 30$, the rate was more than 10 times higher than that for $n = 1$ (low-molecular-weight analog). This statement leads to the conclusion that the process is a template polymerization connected to the interaction between polysacrosine unit and molecule of phenylalanine NCA. This interaction can be illustrated as follows:

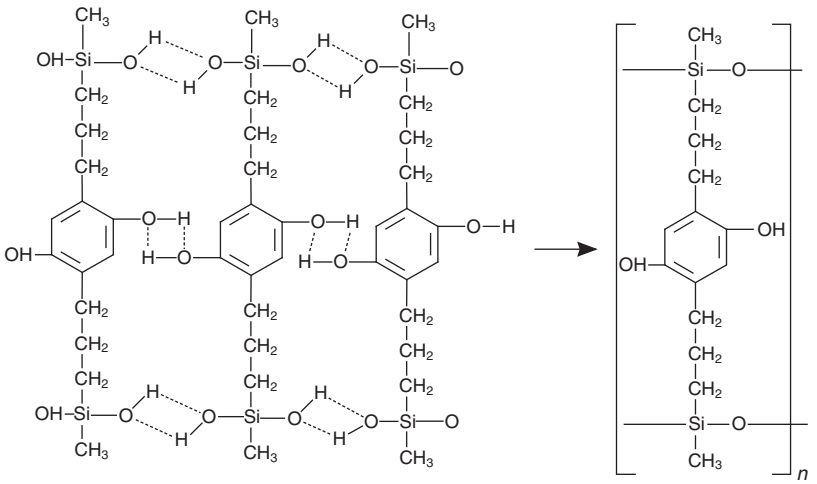

Scheme 16 Polycondensation of methylosiloxanes with hydroquinone groups.

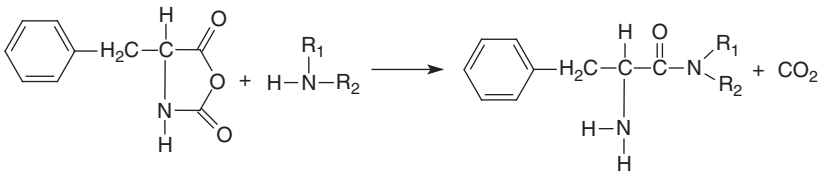

Scheme 17 Reaction of phenylalanine NCA with secondary amine.

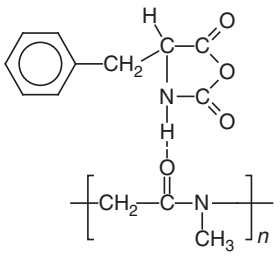

These types of interactions were confirmed by IR analysis by examination of the N–H stretching vibrations in monomer end C=O stretching vibrations of the polysarcosine groups. In any step of the reaction, the monomer molecule was adsorbed onto polysacrosine. It was proved by the authors that the rate of the reaction depended on the type of solvent used. The smaller the interaction, for instance, in *N*,*N*-DMF, the smaller the chain effect.

Valuable experimental material about polymerization of many different *N*-carboxyanhydrides initiated by many different polypeptides[105–107] as well as by poly (vinylpyridine)[108,109,110] was accumulated by Imanishi *et al.*

Using polysarcosine with a different DP as an initiator, and a template, of polymerization of DL-phenylalanine NCA, the authors found that the rate of reaction was much faster than those initiated by corresponding low-molecular-weight amines. Moreover, it was found that the rate of polymerization depended on the DP of polysarcosine and on the solvent used. The replacement of phenylanyl units for sarcosyle units in the polypeptide initiator lowered the initiator efficiency.

In continuation of the investigation on the chain-effect polymerization, stereoselectivity of this process was examined.[106,107] The set of polymerizations were conducted with polypeptide initiator with similar composition but different chiral structure. Obtained results indicated that the activated NCA-type polymerization is stereoselective.

Sugiyama *et al.*[111,112] reported a template process by the ring-opening polymerization induced by radicals. The polyethylene template was connected with 2,2-diphenyl-4-methylene-1,3-dioxolane groups by covalent bonds.

In the course of the polymerization, elimination of the benzophenone group occurs as does an opening of the dioxolane ring. As a result of these reactions, benzophenone groups remain connected with the main chain, while a new polymer is formed. The process can be illustrated by the reaction shown in Scheme 18.

On the contrary to the template processes described below, the daughter polymer is not up to that point connected with the template either by hydrogen or by covalent bonds. The authors have also noted an interesting phenomenon, namely, that when using styrene copolymer and the same monomer, the polymerization efficiency is even higher than that for the homopolymer.

4.33.6 Special Kinds of Template Polymerization

4.33.6.1 Spontaneous Template Polymerization

Spontaneous template polymerization of vinylpyridine in the presence of PAA was first observed by Kargin and Kabanov.[113–115] In initial papers, it was assumed that polymerization of vinylpyridine proceeds similarly to conventional

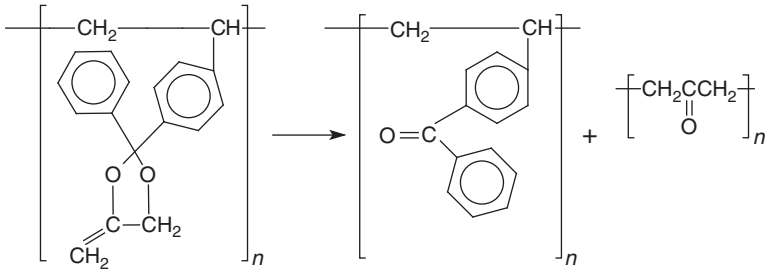

Scheme 18 Template polymerization with elimination of benzophenone groups.

polymerization of vinyl monomers by vinyl groups. However, Salamone[116] and then Kabanov *et al.*[117] drew the conclusion that, at least partially, 1–6 addition occurs, which leads to the daughter polymer with a mixture structure connected with the template.

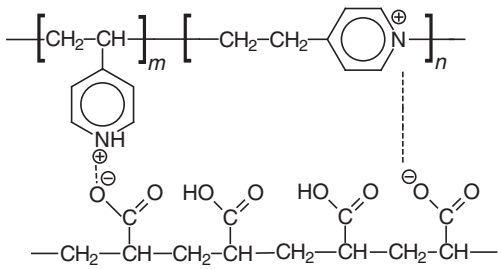

Furthermore, spontaneous polymerization was observed in the case of polymerization of maleic anhydride in the presence of poly(vinylpyridine).[118] The authors found that polymerization proceeds without any initiator in chloroform or nitromethane, although oxygen from air must be present. The authors explain the spontaneous polymerization by charge transfer interaction between the template and the monomer; however, the mechanism of the reaction is not fully clear.

The reverse system was the object of an investigation by Shima *et al.*[119] The polymerization of 2-vinylpyridine, 4-vinylpyridine, and dimethylaminostyrene was carried out in the presence of poly(maleic anhydride). The polymerization proceeds spontaneously without any initiator at 50 °C in DMF or acetone. In order to separate the poly(vinylpyridine) from the template, the reaction product was passed through a column packed with Dowex, and analyzed by IR spectrometry. The molecular weight of daughter polymer was low (DP = 14), but the DP of template used was also low and almost the same (DP = 12). It suggests that because strong-change transfer-interaction monomer is fully adsorbed, polymerization proceeds as type I (zip) reaction.

Polymerization of 4-vinylpyridine onto alternating styrene-maleic anhydride copolymer leads to similar results. Very low molecular weight (500) was found for poly(vinylpyridine) obtained onto template with molecular weight 4640. The authors explain the results in terms of the unfavorable location of the monomer units on the copolymer template.

It was found that the composition of the complex obtained was equimolar in the case of both 2-vinylpyridine and 4-vinylpyridine, whereas, in the case of dimethylaminostyrene, there is 0.4 unit of the latter for every one unit of the template. The polymerization mechanism suggested by the authors assumed adsorption of monomer units onto the template, while the initiation mechanism was not clear.

4.33.6.2 Oxidative Template Polymerization

Horseradish peroxidazed polymerization has been extensively studied in recent years. For instance, enzymatic polymerization of tyrosine derivatives was examined.[120] The reaction mechanism is known to involve free radical processes. Oligomerization of bifunctional phenols in the presence of β-CD was studied.[121] Recently, the role of synthetic polymers used as templates in this process has been studied.[122,123]

The simplest and most important phenolic compound in the industrial field, a soluble polyphenol consisting of a mixture of phenylene and oxyphenylene units, was synthesized by a voltammetry-catalyzed polymerization in a mixture of methanol and phosphate buffer and PEG as a template.[122]

In the polymerization in the absence of template, control of the coupling selectivity (regioselectivity) is often very difficult. The authors[122] pay attention to the role of PEG in the polymerization. Phenol was polymerized using horseradish peroxidase (HRP) as a catalyst in phosphate buffer in the presence of PEG at room temperature under air. The PEG amount greatly affected the reaction behaviors.

The change in the UV spectra of phenol was observed in the presence and absence of PEG ($M_n = 2 \times 10^3$) in phosphate buffer (pH 7.0). After adding PEG to the buffer containing phenol, a specific peak around 270 nm increased, suggesting the formation of a PEG–phenol complex by hydrogen-bonding interaction.

The intensity of this absorption increased with an increase in the weight ratio of PEG to phenol until 1.0 suggesting the hydrogen-bonding interaction of PEG with the hydroxyl group of phenol through a zip template mechanism.

Increasing the molar ratio of monomer units of PEG for phenol from 0 to 2.3 yield increased the polyphenol units to oxyphenol units (R%) from < 3% to 96%. The phenylene unit ratio R(%) depends on the molecular weight of PEG. R% increased from very low value from $2–3 \times 10^2$ up to 95–95% in the range of $10–200 \times 10^2$ and then decreased in the range $1000–3000 \times 10^2$. The authors explained this phenomenon by the large increase of the solution viscosity, which was observed by the addition of high-molecular-weight PEG solution to phenol, which prevented the efficient polymer production.

Synthesis and characterization of poly(catechol) catalyzed by tetrapyridyl porphyrin and HRP were examined.[123] The

oxidative polymerization was carried out in the presence of polystyrene sulfonate (PSS) as a template. It was proved that the complex between PSS and poly(catechol) was formed. TGA data show that the porphyrine-catalyzed poly(catechol) has more thermal stability compared to the enzymatic-catalyzed one. Moreover, by gel permeation chromatography (GPC) analysis it was shown that the polymerization with porphyrine generated higher-molecular-weight poly(catechol) than that obtained by polymerization in the presence of HRP. Cyclic voltammetry measurements showed that the synthesized polymers had convenient electroactivity. By the same method, poly (methyl catechol) and poly(methoxy catechol) were synthesized. It was found that all polymers obtained showed low electrical conductivity.

An oxidative polymerization of aniline in the presence of poly(2-acrylamido-2-methyl-1-propanesulfonic acid) (PAMPSA) as a template was described in Reference 124. The process was carried out in water, and ammonium persulfate was used as initiator. The synthesis was performed at room temperature. In similar conditions, but with benzenesulfonic acid instead of AMPSA, polymerization of aniline does not occur. According to the authors, the localization and protonization of aniline takes place along the chain of AMPSA. Adding sodium chloride to the reaction solution, considerably decreased in both the process rate and the polyaniline yields. What was interesting was that the system remained phase-homogeneous on all stages of conversions. Kinetics examination lead to the conclusion that the process is of a pronounced autocatalytic character. Electroconductivity of the film formed from polyaniline–PAMPSA complex has rather low conductivity of about $10^{-3}\,S\,cm^{-1}$.

4.33.7 Products of Template Polymerization and Potential Applications

The most promising applications of template polymerization seem to be the production of materials in which the daughter polymer and the template together form a final product, because the template synthesis of polymers requiring further separation of the product from the template is not acceptable for industry.

Many polymer–polymer complexes can be obtained by template polymerization. The hydrogen bonding in the complexes obtained by template polymerization is usually stronger than that obtained by mixing the components, and becomes stronger as the molecular weight of the template increases.

Applications of polyelectrolyte complexes are in biomedical materials, membranes, pharmaceutical applications, and many others.[125]

The original structure of polymer–polymer complexes obtained in the process of polymerization in such systems like AA, poly(vinylpyrolidone), or poly(ethylen glycol) leads to properties like sorption different in comparison with similar complexes obtained by mixing substrates.

Such parameters as type and proportion of various hydrogen bonds, amount of water (or another solvent) combined into the complex structure depends not only on the method of preparation but also on changes in time during precipitation, drying, and so on.

It can be predicted that the potential application of template polymerization products lies in obtaining membranes with a better ordered structure than that formed by mixing the components.

Examples of membranes from crosslinked PEG and PAA were described by Nishi and Kotaka.[126] The membranes can be used as so-called chemical valves for medical application. The membranes are permeable or impermeable for bioactive substances, depending on pH.

Properties of composites obtained by template polycondensation of urea and formaldehyde in the presence of PAA were described by Papisov *et al.*[127]

Products of template polycondensation obtained for 1:1 ratio of template to monomers are typical glasses, but elastic deformation of up to 50% at 90 °C is quite remarkable. This behavior is quite different for composites: mixture of PAA and urea-formaldehyde polymer. Introduction of PAA into the reacting system – urea formaldehyde – even in a very small quantity (2–5%) leads to fibrilization of the product structure. Materials obtained have a high compressive strength ($30–100\,kg\,cm^{-3}$).

Further polycondensation of the excess of urea and formaldehyde results in fibrillar structure composites. The structure and properties of such composites can be widely varied by changing the initial composition and reacting conditions.

Mucoadhesive complexes of PEG with PAA were obtained and an application for developing a transmucosal drug delivery systems was suggested.[128]

It was found that the glass transition temperature of PAA in the complexes was shifted to a lower temperature than that of the components blend.

In the next paper by the authors,[129] new polymer complexes were prepared by polymerization of AA using silk sericin as a template. Also in this case, the T_g of sericin and PAA in the complex was shifted compared with the T_g of sericin and PAA themselves. The measurements of the complexes obtained showed a strong adhesive force and limited aqueous solubility and an application for developing a transmucosal drug delivery systems was suggested.

Interpolymer complexes of poly(itaconic acid) and PEG were prepared by template polymerization of itaconic acid in the presence of PEG.[130] The complexes were compared with complexes obtained by mixing preformed poly(itacinic acid) with PEG. It was found that complexes prepared by template polymerization have a stronger hydrogen bonding and hence more ordered structure and better mucoadhesive properties.

Template polymerization of multimonomers is another example of obtaining materials, which cannot be obtained in the conventional way. For instance, oligomers with a ladder-type structure.[43]

A ladder-type polymer can be obtained as a result of template polymerization of poly(vinyl methacrylate) and others multimonomers. It is interesting that the polymers are soluble common solvents such as DMF, DMSO, chloroform, or toluene. Copolymers containing two different ladder-type blocks that were soluble in chloroform were also reported.[131]

Copolymers with one block of ladder-type and another of conventional structure were investigated.[132–134] Thermal properties and supermolecular structure were investigated by differential scanning calorimetry (DSC), small-angle X-ray scattering (SAXS), and wide angle X-ray scattering (WAXS) methods.

It was found that multimonomers polymerized in dilute solution, which are quite stable in dilute solutions, become insoluble after drying. Examination by X-ray diffraction shows that the polymers are amorphous.

Thermal properties of ladder-type polymers obtained from multimonomers were described.[135] The results obtained showed that ladder polymer obtained with poly (2-acryloxyethyl methacrylate) has a considerably higher thermal stability than that of their linear analog.

The polymerization of multimonomers in concentrated state leads to crosslinking. Copolymerization in bulk multimethacrylates with MMA or AA leads to networks. The networks have different swelling properties in comparison with the networks, with random distributed crosslinking points, obtained by using classical crosslinkers like dimethacrylates.

Unique ladder-like polysiloxanes described earlier,[102] with double-chain structure, have good film-forming abilities, excellent thermal stability, and good mechanical properties and it seems to be a interesting material for many applications.

Recently, the synthesis of similar type of ladder polysiloxanes described in Reference 103 was reported.[104] Changing the hydroquinone groups to 9,10-diphenylanthryl groups, the authors synthesized ladder polymers that can emit blue light with great stability and high efficiency in both solution and solid films. The polymers obtained have good thermal stability. This type of materials could have interesting practical applications.

Template effects in the reduction of metal salts, such as nickel, were described by Papisov and co-workers.[136] As template aqueous solutions of PEG, poly(*N*-vinylpyrrolidone), and copolymers acrylamide with AA were used. It was found that reduction of $NiSO_4$ lead to metallic nickel in the form of nanoparticles.

Another form of application connected with properties of template polymerization products is imaging,[137,138] which is based on the formation of insoluble polycomplexes or crosslinked polymers. A thin coating of a polymer used as template in a mixture of monomer and photoinitiator is applied onto a transparent film carrier. On UV irradiation through a mask, the exposed parts become insoluble polycomplex or crosslinked copolymer. The unexposed areas are removed by washing and immersion in a dye bath produces the final image.

4.33.8 Polymerization in Confined Space

4.33.8.1 Introduction

As it was mentioned at the beginning of this chapter, the term 'template' polymerization refers to one-face systems. However, sometimes the term 'template' has a very wide meaning. For instance, according to Hentze and Antonietti,[139] the most general definition of template is a structure directing agent. In the case of direct, or true 'templating', the templated material is a 1:1 copy of the template structure. During synthesis, no changes in order or length scale of the template structure occur. In contrast to direct templating, indirect templating results in metamorphic reconstruction, for example, by phase separation during synthesis.

The authors present the following techniques of template synthesis: molecular imprinting, colloid crystal templating, micellar imprinting, polymerization within sponge phases, and so on.

In the following section, some selected examples will be presented dealing with most general understanding of the term 'template', particularly dealing with polymerization in confined space.

On the other hand, polymerization in confined space is a particular case of polymerization in organized systems. Polymerization in organized systems includes polymerization of monomer crystals, of mono and multilayers, on surfaces, of mesomorphic phases, in micelles and onto macromolecules in solution.

Polymerization in confined space usually includes polymerization of inclusion compounds (clathrates), polymerization of monomer crystals, polymerization in nanolayers, or in dispersed systems.

4.33.8.2 Polymerization in Clathrates

Adducts can be formed with high- and low-molecular-weight molecules, in particular monomers, and polymerization carried out inside inclusion compounds.

As mentioned earlier, a specific class of template polymerization connected with polymerization of monomers included into CD leads in between classical template polymerization and polymerization in confined space and was partially described in section 4.33.3.2.

However, many articles and the reviews[140] devoted to polymerization of included monomers and the behavior of resulting polymers were published recently. Preparation and structural analysis of several types of complexes, CD with monomers like pyrole, fluorinated monomers, styrene, and many others have been described.[141]

Polymerization in clathrates was revived by Di Silvestro and Sozani.[142] More than 50 examples of polymerization of different monomers in clathrates were described.

Clathrates, or inclusion components (host), pack the molecules of second component (guest) into lattice, generating a definite crystalline structure. The most important aspect of polymerization in clathrates deals with possible topochemical control.

The space effect on inclusion polymerization was first recognized in the form of the stereocontrol of the addition polymerization of diene monomers. Clasen[143] applied the channels of thiourea to a polymerization reaction for the first time.

Brown and White confirmed the formation of highly stereoregular polymers from 1,3-butadiene and 2,3-dimethyl-1,3-butadiene. Since then, many monomers have been polymerized in clathrates.[145] In many cases, at least partially syndiotactic or isotactic polymers have been obtained.

Polymerization within a molecular scale porous template has been described in Reference 144 using thiourea as a 'host'. 2,3-Dichloro-1,3-butadiene-thiourea complex was obtained and polymerization was induced by γ-irradiation. It was found that polymerization occurs in single crystals, and takes place without destroying the original single-crystal habit. Furthermore, it was demonstrated that the highly 1,4-*trans*-tactic polymer was obtained.

A set of 1,4-*trans*-polybutadienes and several copolymers obtained by inclusion polymerization in perhydrotriphenylene have been described.

All obtained polymers and copolymers were precisely characterized by ^{13}C NMR spectrometry.

The application of cyclophosphazenes as host molecules provides the opportunity to describe an unusual range of interesting examples of polymerization in clathrates.[145]

The occlusion of a variety of molecules within tunnels of clathrate system derived from tri(*o*-phenylenedioxy) cyclotriphosphazene (TPDCTP) was reported.[145] Crystalline product with following formula forms tunnels with hexagonal lattice, and was used as a host for a set of vinyl monomers.

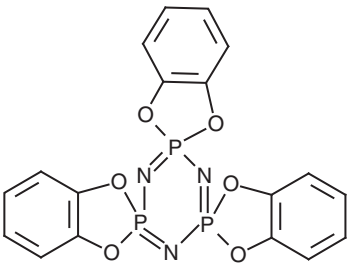

Acetylene, phenylacetylene, butadiene, isobutadiene, divinylbenzene styrene, and 4-bromobenzene have been trapped within a tunnel clathrate system of TPDCTP. However, irradiation of the clathrates by γ-rays leads to polymers only for butadiene, isobutylene divinylbenzene, and bromostyrene. Irradiated of the styrene, acetylene, or phenylacetylene adducts did not result in the formation of polymer.

In the next paper,[146] the same method was applied for polymerization of vinyl monomers such as AA, acrylic anhydride, acrylonitrile, methyl acrylate, MMA, and methyl vinyl ketone, and, in all cases, stereoregular polymers were obtained. The molecular weight of the clathrate-synthesized polymers were similar to those of polymers prepared in the bulk phase. The overall experimental approach was as follows: the monomer molecules were absorbed into the crystal framework of the pure host. Polymerization of the clathrated monomer was induced by γ-irradiation at low temperature (−29 °C or −78 °C). After irradiation, unreacted monomer was removed *in vacuo* and any polymer external to the host crystals was removed by washing with solvent. Then, included polymer was removed by extraction and purified. As a result, isotactic poly(acrylonitrile), poly(methyl acrylate), and poly (vinyl ketone) and syndiotactic PAA and PMMA were obtained.

Many different types of clathrates can be obtained from deoxycholic acid (DOCA).[142]

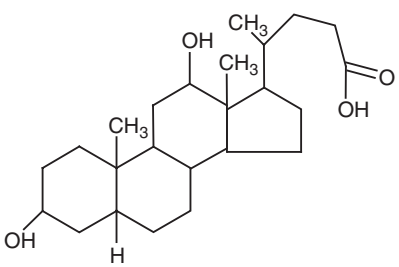

DOCA

DOCA forms inclusion compounds with a number of different organic molecules. For this ability to include almost any type of molecule, DOCA is not size selective as other host matrices are; but for the purposes of inclusion polymerization, it has a very wide application.

Recently, examination of radiation-induced polymerization of 2,3-dimethyl-1,3-butadiene (DBM) in the presence of DOCA was published.[147]

A lower degree of regularity and crystallinity has been found on the poly(2,3-dimethyl-1,3-butadiene) (PDMB) ample prepared as inclusion compound in DOCA in comparison to the reference PDMB obtained by inclusion polymerization in thiourea. However, 1,4-*trans* form of PDMB was higher (74.2%) for polymerization with DOCA in comparison to PDMB polymerized in emulsion with free radical initiator. (40.1%).

The next interesting 'host' compound for various types of monomers is perhydrotriphenylene (PHTP).

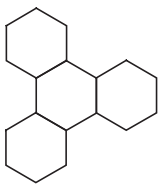

PHTP

In a set of papers, Farina and co-workers described polymerization of dienes including (PHTP).[148–150]

The stereoisomer of PHTP forms channel-like inclusion compounds both with low-molecular-weight substances and with linear macromolecules.

Radiation polymerization of *cis*- and *trans*-1-3-pentadiene[148,149] *trans*-2-methyl-1,3-pentadiene, *trans*-3-methyl-1,3-pentadiene, 4-methyl-1,3-pentadiene, *cis,cis*- and *cis, trans*-2,4-hexadiene[150] was carried out. Obtained products were characterized by Ir spectrometry, NMR and X-ray analysis. It was found that the polymers obtained have head-to-tail *trans*-1,4 structures and in some cases show crystallinity and stereoregularity.

4.33.8.3 Compartmentalization

The term 'compartmentalization' in dispersed polymerization systems refers to the effects of the isolation of radical species in particles ('compartments'). There are two distinct and opposite effects of compartmentalization.[151,152]

1. Radicals located in different particles are unable to react with each other (segregation effect).
2. The reaction rate between two radicals located in the same particle increases with decreasing particle size (confined space effect). The segregation effect on propagating radicals is the reason that higher molecular weight polymer is usually formed at higher rates in conventional emulsion polymerization than the corresponding bulk polymerizations.[12]

Recently, a set of papers about polymerization in nanoparticles of emulsion appeared.[151,152] Compartmentalization in ATRP in dispersed systems was investigated and the synthesis of polymers by intercalating monomers in layered inorganic hosts, mainly layered silicates, was described.

Compartmentalization can be realized in nanoporous systems. An example of this process is inclusion polymerization of aniline.

Grafting of polymers in well-defined nanoporous media has recently been published.[153]

ATRP was used to graft uniform layers of polyacrylonitryle, poly(2-dimethylamino)ethyl methacrylate, and polystyrene. The grafting process was carried out in cylindrical mesopores of diameter about 10 nm and spherical mesopores of diameter about 15 nm. It was found that the grafted polymer forms a uniform layer of thickness tailorable in the range from several 10ths of nanometer to at least 2 nm.

Polymerization of aniline in zeolite channels was examined and described in Reference 154.

Zeolites are crystalline open framework oxide structures (classically aluminosilicates) with pore sizes between 0.3 and 1.2 nm and exchangeable cations compensating for the negative charge of framework. In this work, zeolite Y was used, which is characterized by a three-dimensional open framework structure, composed of interconnected 'sodalite' and supercages, with pore openings of ~8 Å and cage diameter of ~13 Å.

The intrazeolite polymerization of aniline is believed to proceed in analogy to bulk chemical synthesis in *n*-hexane at 2 °C initiated by $(NH_4)_2S_2O_8$. It was found that different oxidation conditions for the intrazeolite polymerization of aniline allow one to control the level of polymer purity and level of intrazeolite acidity required for reaction. The intrazeolite polymers presented in this work are, according to the authors, a new family of molecular wires.

In an interesting paper, You and Pan[155] described the production of superbranched polymers. The first monomer was obtained from α-bromobutyric chloride and glycerol. The second monomer was obtained in porous resin treated with NaOH and then by CS_2, and was in the form of a CS_2^{2-} ion. By polycondensation of a trifunctional monomer (with three Br atoms in the molecule) and a CS_2^{2-} group after repeated procedures, hyperbranched polymer was obtained. The polymer was soluble in tetrahydrofurane (THF). In contrast, polymerization of the same tribromo compound with trithiocarbonate anion lead to the crosslinked, insoluble polymer.

Polymerization in confined space in layered clay systems was a subject of many papers and reviews. The synthesis of polymers by intercalating monomers in layered inorganic hosts, mainly layered silicates was described.

Polymer–clay nanocomposites are applied in packing, transport, sports equipment, and other industries. However, mechanical, thermal, and other physicochemical properties of clay-containing polymeric nanocomposites are still a subject of many investigations.[156–159]

Several types of synthetic or semisynthetic layered materials have been described,[160] partially applied to polycondensation or polymerization inside confined space in layered nanofillers. Model systems for confined polymers and polymer brushes were presented in Reference 160. Polymeric nanocomposites based on polyamides can be obtained by polycondensation of monomers (by homo- or heteropolycondensation) with fluorohectorite in interlayer spacing of 1–2 nm.

Epoxy polymers were prepared using preintercalated fluoromica. Upon intercalation, the interlayer spacing increased from 0.94 nm to 1.74 nm and then upon polymerization of reagents to 6.79 nm.

Synthetic clays prepared in a reaction between Mg, Li, and Na-silicate salts (Laponite) were used by Shemper *et al.*[161] for examination of photopolymerization methyl hydroxyl methyl acrylate. It was found that the clay autoaccelerated the reaction.

Well-known layered nanofiller – montmorillonite – was applied as template for polymerization of diglycidyl ether of bisphenol A (epoksy resin $M_w = 360$) with phenylenediamine.[162]

It was found that intergallery polymerization and clay layers exfoliation can be regulated by a proper procedure.

Polycondensation of ε-aminocapronic acid intercalated into α-zirkonium phosphate was described.[163] ε-Aminocapronic acid was intercalated into α-zirkonium phosphate to give expanded phases enclosing the amino acid monolayer. Polycondensation was carried out at 260 °C in N_2 atmosphere for 1 h. After destroying the inorganic part by hydrofluoric acid, polymer was water-washed and analyzed.

Polymerization within a molecular scale porous template was described in Reference 164.

It was shown that macromolecularly porous ultrathin film fabricated by a single assembly step can be used for the highly efficient stereoregular template polymerization of methacrylates through stereocomplex formation. The precursor films were fabricated using the layer-by-layer method. Syndiotactic and isotactic PMMAs were used as components in order to prepare ultrathin stereocomplex film. Then syndiotactic PMMA was extracted from the film in an aqueous alkaline solution, resulting in a macromoleculary porous isotactic PMMA film. Extraction of the precursor film from chloroform leads to porous film from isotactic PMMA. Polymerization carried out in such prepared films lead to PMMA with complementary stereoselectivity.

Oxidative polymerization of pyrrole and *N*-methlpyrrole in pores of diameter 5–1.2 μm and length 14–9 μm was carried out.[165] Such porous structure was produced by irradiation of poly(ethylene terephthalate) film by accelerated xenon ions. It was found that the rate of polymerization is dependent on the porous diameter.

4.33.9 Conclusion

The special polymerization process in which specific interactions between template macromolecules and growing chains exist is called template polymerization. The process, as described in the chapter, can proceed by the mechanism of a chain reaction as radical, ionic, or ring-opening polymerization or as a step-growth process like polycondensation.

It was shown that the template can influence the kinetic, molecular weight, molecular weight distribution, and chemical structure of the polymer formed. Special types of products obtained in template polymerization such as interpolymer complexes, ladder-type polymers, and copolymers seem to be interesting materials. Potential applications of such materials have been discussed. Polymerization processes dealing with most general understandings of the term 'template', particularly dealing with polymerization in confined space were also discussed.

References

1. Tan, Y. Y.; Challa, G. *Encyclopedia of Polymer Science and Engineering*; Mark, H. F., Bikales, N. M., Overberger, C. G., Menges, G., Eds.; Wiley: New York, 1989; Vol. 16, p 554.
2. Tan, Y. Y. In *Comprehensive Polymer Science*; Allen, G., Bevington, J. C., Ed.; Oxford, 1989; Vol. 3, p. 245.
3. Papisov, I. M. In *Polymeric Materials Encyclopedia*; Salamone, J. C., Ed; CRC: Boca Raton, 1996, Vol. **6**, p 4038.
4. Szwarc, M. *J. Polym. Sci.* **1954**, *13*, 317.
5. Bamford, C. H. In *Developments in Polymerization*; Haward, R. N., Ed.; Applied. Science Publishers: London, 1979, pp 215–277.
6. Elias, H. G. (Ed.) *Polymerization of Organized Systems*; Gordon and Breach Science Publishers: New York, 1977.
7. Challa, G.; Tan, Y. Y. *Pure Appl. Chem.* **1981**, *53*, 627.
8. Tan, Y. Y.; Challa, G. *Macromol. Chem. Macromol. Symp.* **1987**, *10/11*, 215.
9. Tan, Y. Y. *Prog. Polym. Sci.* **1994**, *19*, 561.
10. Połowiński, S. In *The Encyclopaedia of Advanced Materials*; Bloor, D., Brook, R. J., Flemings, M. C., Mahajan, S., Eds.; Pergamon Press: Oxford, 1994; p 2784.
11. Połowiński, S. In *Polymeric Materials Encyclopedia*; Salamone, J. C., Ed; CRC: Boca Raton, 1996; Vol. 11, p 8280.
12. Połowiński, S. *Template Polymerization*; ChemTec Pub.: Toronto-Scarborough, 1997.
13. Połowiński, S. *Prog. Polym. Sci.* **2002**, *27*, 537.
14. Simha, R.; Zimmerman, J. M.; Moacanin, J. *J. Chem. Phys.* **1961**, *19*, 1239.
15. Papisov, I. M.; Kabanov, V. A.; Osada, E.; *et al. Vysokomol. Soj.* **1972**, *14*, 2462.
16. Smid, J.; Tan, Y. Y.; Challa, G. *Eur. Polym. J.* **1983**, *19*, 853.
17. Cerrai, P.; Guerra, G. D.; Tricili, M.; *et al. Macromol. Chem. Phys.* **1996**, *1*, 197.
18. Papisov, I. M.; Nedialkova, Ts. I.; Avramchuk, N. K.; Kabanov, V. A. *Vysokomol. Soedin.* **1973**, *15*, 2259.
19. Tan, Y. Y.; Alberda van Ekenstein, G. O. R. *Macromolecules* **1991**, *24*, 1641.
20. Ferguson, J.; Shah, S. A. O. *Eur. Polym. J.* **1968**, *4*, 343.
21. Muramatsu, R.; Shimidzu, T. *Bull. Chem. Soc. Jpn.* **1972**, *45*, 2538.
22. Rainaldi, I.; Cristallini, C.; Ciardelli, G.; Giusti, P. *Polym. Int.* **2000**, *49*, 63.
23. Ferguson, J.; Shah, S. A. O. *Eur. Polym. J.* **1968**, *4*, 611.
24. Bamford, C. H.; Shikii, Z. *Polymer* **1968**, *9*, 596.
25. Ferguson, J.; McLeod, C. *Eur. Polym. J.* **1974**, *10*, 1083.
26. Fujimori, K.; Trainor, G. T.; Costigan, M. J. *J. Polym. Sci., Polym. Chem. Ed.* **1984**, *22*, 2472.
27. Matuszewska-Czerwik, J.; Połowiński, S. *Eur. Polym. J.* **1988**, *24*, 791.
28. Matuszewska-Czerwik, J.; Połowiński, S. *Eur. Polym. J.* **1990**, *26*, 549.
29. Smid, J.; Tan, Y. Y.; Challa, G. *Eur. Polym. J.* **1982**, *19*, 853.
30. Smid, J.; Tan, Y. Y.; Challa, G.; Speelman, J. *Eur. Polym. J.* **1985**, *21*, 141.
31. Lj, S.; Tomić, J.; Filipović, M. *Polym. Bull.* **2004**, *52*, 355.
32. Blumstein, A.; Kakivaya, S. In *Polymerization of Organized Systems*; H. G. Elias Ed.; Gordon and Breach Science Publishers: New York, **1977**; p 189.
33. Akashi, M.; Takeda, H.; Inaki, Y.; Takemoto, K. *J. Polym. Sci., Chem. Ed.* **2004**, *17*, 747.
34. Takemoto, K.; Inaki, Y.; Akashi, M. *J. Macromol. Sci.* **1979**, *A13*, 519.
35. Spijker, H. J.; Dirks, A. T. J.; van Hest, J. C. M. *Polymer* **2005**, *46*, 8528.
36. Buter, R.; Tan, Y. Y.; Challa, G. *J. Polym. Sci.* **1972**, *A1 10*, 1031.
37. Buter, R.; Tan, Y. Y.; Challa, G. *J. Polym. Sci.* **1973**, *11*, 1003, 1013.
38. Gons, J.; Vorenkamp, E. J.; Challa, G. *J. Polym. Sci.* **1975**, *13*, 1699.
39. Buter, R.; Tan, Y. Y.; Challa, G. *J. Polym. Sci.* **1973**, *11*, 2975.
40. Matsuzaki., K.; Kanai., T.; Chikara, I.; Makoto, Y. *Makromol. Chem.* **1984**, *185*, 2291.
41. Chapiro, A.; Delieu, J. *Eur. Polym. J.* **1977**, *13*, 563.
42. Chapiro, A.; Mankowski, Z.; Schmitt, N. *Eur. Polym. J.* **1985**, *21*, 1005.
43. Kämmerer, H.; Jung, A. *Makromol. Chem.* **1966**, *101*, 284.
44. Kämmerer, H.; Ozaki, S. *Makromol. Chem.* **1966**, *91*, 1.
45. Kämmerer, H.; Shukla, I.; Önder, N.; Schurmann, G. *J. Polym. Sci., Polym. Symp.* **1967**, *22*, 213.
46. Jantas, R. *J. Polym. Sci., Part A: Polym. Chem.* **1990**, *28*, 1973.
47. Jantas, R.; Szumilewicz, J.; Strobin, G.; Połowiński, S. *J. Polym. Sci., Part A: Polym. Chem.* **1994**, *32*, 295.
48. Jantas, R.; Strobin, G.; Połowiński, S. *Polym. Int.* **1995**, *37*, 315.
49. Jantas, R.; Draczyński, Z. *Polimery (Pol)* **2002**, *47*, 813.
50. Jantas, R.; Szocik, H. *Polym. Bull.* **2002**, *48*, 105.
51. Jantas, R.; Połowiński, S.; Podešva *J. Polym. Sci., Part A: Polym. Chem.* **1989**, *27*, 475.
52. Jantas, R.; Połowiński, S. *Acta Polym.* **1984**, *35*, 150.
53. Jantas, R.; Połowiński, S. *J. Polym. Sci., Part A: Polym. Chem.* **1986**, *24*, 1819.
54. Saito, R.; Iijima, Y.; Yokoi, K. *Macromolecules* **2006**, *39*, 6838.
55. Saito, R.; Iijima, Y. *Polym. Adv. Technol.* **2009**, *20*, 280.
56. Saito, R.; Kobayashi, H. *Macromolecules* **2002**, *35*, 7207.
57. Saito, R.; Okuno, Y.; Kobayashi, H. *J. Polym. Sci., Part A: Polym. Chem.* **2001**, *39*, 3539.
58. Saito, R.; Yamagushi, K. *Macromolecules* **2003**, *36*, 9005.
59. Saito, R.; Kobayashi, H. *J. Inclusion Phenom. Macrocyclic Chem.* **2002**, *44*, 303.
60. Saito, Y.; Saito, R.; Kudo, H.; Nishikubo, T. *Macromolecules* **2008**, *41*, 3755.
61. Połowiński, S.; Ferguson, J. *Polymer Yearbook (Glasgow)* **1995**, *12*, 53.
62. Shavit, N.; Cohen, J. In *Polymerization of Organized Systems*; Elias, H. G., Ed.; Gordon and Breach Science Publishers: New York, 1977; p 213.
63. Tsuchida, E.; Osada, Y. *J. Polym. Sci., Polym. Chem. Ed.* **1975**, *13*, 559.
64. Matuszewska-Czerwik, J.; Połowiński, S. *Eur. Polym. J.* **1975**, *27*, 1335.
65. Smid, J.; Speelman, C.; Tan, Y. Y.; Challa, G. *Eur. Polym.J.* **1985**, *21*, 2141.
66. Fujimori, K.; Trainor, G. T.; Costigan, M. J. *J. Polym. Sci.* **1984**, *22*, 2479. (Recalculated in: Y.Y. Tan, G.O.R. Alberda van Ekenstein, Macromolecules **1991** *24* 1641).
67. Błasińska, A. Thesis. Technical University of Lodz, Lodz, 2000.
68. Połowiński, S.; Jantas, R.; Błasińska, A. *Struktur and Kinetic Effects in Template Polymerization*; World Polymer Congress: Gold Coast, Australia, 1998 Prep; 656.
69. Oral, E.; Pepas, A. *Polymer* **2004**, *45*, 6163.
70. Połowiński, S. *J. Polym. Sci., Polym. Chem. Ed.* **1984**, *22*, 2887.
71. Połowiński, S. *Polimery* **1994**, *39*, 417.
72. Frisch, H. I.; Xu, Q. *Macromolecules* **1992**, *25*, 5145.
73. Połowiński, S. *Acta Polym.* **1992**, *43*, 99.
74. Połowiński, S. *Eur. Polym. J.* **1983**, *19*, 679.
75. Liu, A.-H.; Mao, S.-Z.; Liu, M.-L.; *et al. Colloid Polym. Sci.* **2007**, *285*, 381.
76. Rinaldi, C.; Cristallini, C.; Ciardelli, G.; Giusti, P. *Macromol. Chem. Phys.* **2000**, *201*, 2424.
77. O'Driscol, K. F.; Capek, I. *J. Polym. Sci., Polym. Lett. Ed.* **1981**, *19*, 401.
78. Chapiro, A. *Eur. Polym. J.* **1989**, *25*, 713.
79. Zheltonozhskaya, T.; Permyakova, N.; Momot, L. *Hydrogen-Bonded Interpolymer Complexes*; World Sci: New Jersey, London, **2009**.
80. Aravindakshan, P.; Bhatt, A.; Kumar, V. G. *J. Appl. Polym. Sci.* **1997**, *66*, 397.
81. Ferguson, J.; McLeod, C. *Eur. Polym. J.* **1974**, *10*, 1083.
82. Połowiński, S. IUPAC Conference, Budapeszt 1969, Vol. 3, p.171.
83. Połowiński, S.; Janowska, G. *Polimery* **1972**, *17*, 464.
84. Połowiński, S. *Eur. Polym. J.* **1978**, *14*, 563.
85. Jantas, R.; Połowiński, S. *J. Polym. Sci., Part A: Polym. Chem.* **1986**, *24*, 1819.
86. Ogata, N.; Sanui, K.; Okouchi, K. *Polym. J.* **1986**, *5*, 186.
87. Ogata, N.; Shimamura, K. *Polym. J.* **1975**, *7*, 72.
88. Ogata, K.; Sanui, H.; Nakamura, H.; Kishi, H. *J. Polym. Sci., Polym. Chem. Ed.* **1980**, *18*, 933.
89. Ogata, N.; Sanui, K.; Nakamura, H.; Kishi, H. *J. Polym. Sci., Polym. Chem. Ed.* **1980**, *18*, 939.
90. Ogata, N.; Sanui, K.; Abe, M. *J. Polym. Sci., Polym. Chem. Ed.* **1981**, *19*, 1361.
91. Ogata, N.; Sanui, K.; Tanaka, H.; *et al. J. Polym. Sci., Polym. Chem. Ed.* **1981**, *19*, 2609.
92. Higashi, F.; Nakano, Y.; Goto, M.; Kakimoto, H. *J. Polym. Sci., Polym. Chem. Ed.* **1980**, *18*, 1099.
93. Higashi, F.; Nakano, Y.; Goto, M.; Kakimoto, H. *J. Polym. Sci., Polym. Chem. Ed.* **1980**, *18*, 851.
94. Higashi, F.; Taguchi, Y. *J. Polym. Sci., Polym. Chem. Ed.* **1980**, *18*, 2875.
95. Yamazaki, N.; Higashi, F. *Adv. Polym. Sci.* **1980**, *38*, 1.
96. Hattori, M.; Nagagawa, H.; Kinoshita, M. *Makromol. Chem.* **1980**, *181*, 2325.
97. Papisov, I. M.; Litmanovich, A. A. *Adv. Polym. Sci.* **1980**, *90*, 139.
98. Machnicka,, M. Thesis, Technical University of Lodz, Lodz, **2002**.
99. Boliachevskaya, K. I.; Litmanovich, A. A.; Papisov, I. M. *Polym. Sci.* **1995**, *B37*, 424.
100. Shimidzu, T.; Murakami, A.; Konishi, Y. *J. Chem. Soc., Perkin Trans. 1, 1979,* 20, 215–277.
101. Tang, H.; Sun, J.; Zhou, X.; *et al. Macromol. Chem. Phys.* **2003**, *204*, 155.
102. Guo, G.; Zhang, Y.; Li, H.; *et al. Macromol. Rapid Commun.* **2002**, *23*, 366.
103. Zhang, J.; Chen, Z.; Fu, W.; *et al. J. Polym. Sci., Part A: Chem. Ed.* **2010**, *48*, 2391.
104. Ballard, D. G. H.; Bamford, C. H. *Proc. R. Soc.* **1956**, *A 236*, 384.
105. Bamford, C. H. In *Developments in Polymerization 2*; Howard, R. N., Ed.; Applied Science Publishers: London, **1979**.
106. Imanishi, Y.; Sugihar, T.; Higashimura, T. *Biopolymers* **1973**, *12*, 1505.
107. Imanishi, Y.; Kugimiya, K.; Higashimura, T. *Biopolymers* **1973**, *12*, 2643.
108. Imanishi, Y.; Kugimiya, K.; Higashimura, T. *Biopolymers* **1974**, *13*, 1205.
109. Suzuoki, K.; Imanishi, Y.; Higashimura, K. T. *Biopolymers* **1969**, *7*, 925.
110. Imanishi, Y.; Nagaoka, S.; Suzuoki, K. K.; Higashimura, T. *Biopolymers* **1973**, *12*, 181.
111. Sugiyama, J.; Yokozawa, T.; Endo, T. *J. Am. Chem. Soc.* **1993**, *115*, 2041.

112. Sugiyama, J.; Yokozawa, T.; Endo, T. *Macromolecules* **1994**, *27*, 5536.
113. Kargin, V. A.; Kabanov, V. A.; Kargina, O. V. *Dokl. Akad. Nauk SSSR* **1965**, *161*, 1131.
114. Kabanov, V. A.; Aliev, K. V.; Kargina, O. V.; *et al. J. Polym. Sci.* **1967**, *C16*, 1079.
115. Kabanov, V. A. *Pure Appl. Chem.* **1967**, *15*, 391.
116. Salamone, J. C.; Snider, B.; Fitch, W. L. *J. Polym. Sci. Part B* **1971**, *9*, 13.
117. Kabanov, V. A.; Kargina, O. V.; Petrovskaia, V. A. *Vysokomol. Soj.* **1971**, *13*, 348.
118. Papisov, I. M.; Garina, E. S.; Kabanov, V. A.; Kargin, V. A. *Vysokomol. Soj.* **1969**, *B11*, 614.
119. Shima, K.; Kakui, Y.; Kinoshita, M.; Imoto, M. *Makromol. Chem.* **1972**, *154*, 247.
120. Fukuoka, T.; Tachibana, Y.; Tonami, H.; *et al. Biomacromolecules* **2002**, *3*, 768.
121. Rehmann, M. H.; Ritter, H. *Macromol. Chem. Phys.* **2000**, *201*, 798.
122. Kim, Y.-J.; Uyama, H.; Kobayashi, S. *Macromolecules* **2003**, *36*, 5058.
123. Nabid, M. R.; Sedghi, Z. Z.; Nazzari, S. *Polym. Bull.* **2010**, *64*, 855.
124. Ivanov, V. F.; Gribkova, O. L.; Chebryako, K. V.; *et al. Russian J. Electrochem.* **2004**, *40*, 299.
125. Kutoryanskiy, V. V. In *Hydrogen-Bonded Interpolymer complexes*; Kutoryanskiy, V. V., Staikos, G. Eds.; World Sci.: New Jersey, London, **2009**; pp 235–258.
126. Nishi, S.; Kotaka, T. *Macromolecules* **1985**, *18*, 1519.
127. Papisov, I. M.; Kuzovleva, O. E.; Markov, S. V.; Litmanovich, A. A. *Eur. Polym. J.* **1984**, *20*, 195.
128. Choi, H.-K.; Kim, O.-J.; Chung, C.-K.; Cho, C.-S. *J. Appl. Polym. Sci.* **1999**, *73*, 2749.
129. Ahn, J.-S.; Choi, H.-K.; Lee, K.-H.; *et al. J. Appl. Polym. Sci.* **2001**, *80*, 274.
130. Tomić, S. Lj.; Filipović, J. M. *Polym. Bull.* **2004**, *52*, 355.
131. Jantas, R.; Połowiński, S. *J. Polym. Sci., Part A: Polym. Chem.* **1986**, *24*, 1819.
132. Rabiej, S.; Włochowicz, A. *Eur. Polym. J.* **1988**, *24*, 177.
133. Rabiej, S.; Włochowicz, A. *Eur. Polym. J.* **1988**, *24*, 183.
134. Włochowicz, A.; Rabiej, S. *Eur. Polym. J.* **1988**, *24*, 585.
135. Jantas, R.; Janowska, G.; Szocik, H.; Połowiński, S. *J. Thermal Anal.* **2000**, *60*, 371.
136. Papisov, I. M.; Yablokov, Yu. S.; Prokofiev, A. I. *Vysokomol. Soedin.* **1994**, *36*, 352.
137. Rätzsch, M. 30th IUPAC Symposium on Macromolecules. The Hague, Netherlands, **1985**; abstracts p. 37.
138. Turner, S. R.; Daly, R. C. In *Comprehensive Polymer Science*; Allen, G.; Bevington, J. C., Eds.; Pergamon Press: Oxford, **1988**; Vol. 6, p 193.
139. Hentze, H.; Antonietti, P. *Solid State Mater. Sci.* **2001**, *5*, 343.
140. Wenz, G.: *Adv. Polym. Sci.* **2001**, *222*, 1.
141. Choi, S. W.; Amajjahe, S.; Ritter, H. *Adv. Polym. Sci.* **2001**, *222*, 175.
142. Di Silvestro, G.; Sozani, P. In *Comprehensive Polymer Science*; Allen, G.; Bevington, J. B., Eds.; Pergamon Press: Oxford, **1989**; Vol. **4**, p 303.
143. Clasen, H. *Z. Electrochem.* **1956**, *60*, 982.
144. Brown, J. F.; White, D. M. *J. Am. Chem. Sci.* **1969**, *82*, 5671.
145. Chatani, Y.; Nakatani, S. *Macromolecules* **1972**, *5*, 597.
146. Allcoock, H. R.; Levin, M. L. *Macromolecules* **1985**, *18*, 1324.
147. Cataldo, F.; Ursini, O.; Ragni, P.; Rosati, A. *J. Radioanal. Nucl. Chem.* **2009**, *280*, 99.
148. Farina, M.; Pedretti, U.; Gramegna, M. T.; Audisio, G. *Macromolecules* **1970**, *3*, 475.
149. Farina, M.; Audisio, G.; Gramegna, M. T. *Macromolecules* **1971**, *4*, 265.
150. Farina, M.; Audisio, G.; Gramegna, M. T. *Macromolecules* **1972**, *5*, 617.
151. Zetterlund, P. B.; Okubo, M. *Macromol. Theory Simul.* **2007**, *16*, 221.
152. Kagawa, Y.; Zetterlund, P. B.; Minami, H.; Okubo, M. *Macromol Theory Simul.* **2006**, *15*, 608.
153. Kruk, M.; Dufour, B.; Celer, E. B.; *et al. Macromolecules* **2008**, *41*, 8584.
154. Bein, T.; Enzel, P. *Mol. Cryst. Liq. Cryst.* **1990**, *181*, 315.
155. You, Y.-Z.; Pan, C.-Y. *J. Polym. Sci., Part A: Polym. Chem.* **2008**, *46*, 1730.
156. Utracki, L. A. *Eur. Polym. J.* **2009**, *45*, 1891.
157. Okada, A.; Usuki, A. *Macromol. Mater. Eng.* **2006**, *291*, 1449.
158. Utracki, L. A. *J. Polym. Sci., Part B: Polym. Phys.* **2009**, *47*, 299 and 966.
159. Utracki, L. A.; Sepehr, M.; Boccaleri, E. *Polym. Adv. Technol.* **2007**, *18*, 1.
160. Giannelis, E. P.; Krishnamoorti, R.; Manias, E. *Adv. Polym. Sci.* **1999**, *138*, 107.
161. Shemper, B. S.; Morizur, J. F.; Alirol, M.; *et al. J. Appl. Polym. Sci.* **2004**, *93*, 1252.
162. Lan, T.; Padmananda, D.; Kaviratna, D.; Pinnavaia, T. J. *Chem. Mater.* **1995**, *7*, 2144.
163. Ding, Y.; Jones, J.; Maireles-Torres, P. R. *Chem. Mater* **1995**, *7*, 562.
164. Serizawa, T.; Hamada, K.-I.; Akashi, M. *Nature* **2004**, *429*, 6987.
165. Dobretsova, L. Y.; Ermolaev, S. V.; Jitariouk, N. I.; Milinchuk, V. K. *High Energy Chem.* **2005**, *39*, 10.

Biographical Sketch

Połowiński Stefan was born on 26 May 1931 in Wilno (Poland). In 1957, he received his MSc degree in polymer technology from the Technical University of Lodz, Poland. At the Technical University of Lodz, in the Department of Physical Chemistry of Polymers, he was an assistant (1957–60), senior assistant (1960–62), lecturer (1962–66), assistant professor (1966–87), and professor (1987–2006). In 2006, he retired, and has since worked in various research projects.

He has been Senior Visiting Fellow at the Strathclyde University in Glasgow (UK) (1966–67); member of experts group in radical polymerization, Polish Academy of Sciences (1974–78); Head of the Department of Physical Chemistry of Polymers (1993–2001); Vice Dean of Faculty Textile Engineering; National Representative in IUPAC Macromolecular Division (1996–97).

He has authored a book, *Template Polymerization* in 1997, various chapters in encyclopedias, and more than 120 articles in professional journals.

4.34 Mechanistic Aspects of Solid-State Polycondensation

SN Vouyiouka and CD Papaspyrides, National Technical University of Athens, Zographou, Athens, Greece

4.34.1 Introduction

For most commercial step-growth polymers, such as polyamides (PAs) and polyesters (PESs), the molecular weight (MW) builds via an equilibrium reaction between difunctional reactants, which is accompanied by the formation of a low-molecular-weight condensate C (eqn [1]):

$$P_n + P_m \rightarrow P_{n+m} + C \qquad [1]$$

where P_i represents a polymer molecule of degree of polymerization *i*. C is water in the case of PAs, and glycols and water in the case of PESs, while polymerization yield depends on removing essentially the condensate, thus avoiding depolymerization. In **Figure 1**, the reaction schemes for the formation of three typical condensation polymers are presented.

Beyond a certain MW, ~15 000–25 000, the application of the melt polymerization technique is not feasible due to thermal degradation, melt viscosity increase, and stirring restrictions, thus difficulty in heat and mass transfer dissipation and reactor handling. To achieve higher MW (>30 000), solid-state polycondensation (SSP) is used. It involves heating of the solid starting material to a temperature high enough to initiate and propagate polymerization reactions, but lower than the product melting point, so as to retain the solid phase. The first SSP patents were issued by Flory (1939)[1] and Monroe (1962);[2] since then, extensive academic and industrial research has been performed, as evidenced by a number of articles in scientific journals, as well as of patents (**Figure 2**).

Starting materials of SSP can be both crystalline monomers (direct SSP) and semicrystalline polymers (post-SSP).[3–5] Direct SSP is mainly applied on laboratory scale, presenting however considerable practical interest, since polymerization occurs from the beginning in the solid state. Consequently, all the problems associated with the high temperatures of melt technology, for example, energy consumption and polymer degradation, as well as the use of any solvent, are completely avoided.[3,6,7] On the other hand, in post-SSP, widely applied on industrial scale, a low-molecular-weight base polymer (prepolymer or precursor), which is derived from solution–melt polymerization technique, reacts to further increase the MW; the relevant step is often stated in overall polymerization layouts as 'post-SSP', 'drying,' or 'finishing'.

The overall SSP rate can be controlled by chemical and physical steps, since both reaction kinetics and transport phenomena play a key role in the process. In particular, the rate-determining steps can be the following:[4,5]

- *The chemical reaction*. It is defined by the reactant chemical affinity and composition
- *The diffusion of the functional groups*. It occurs through movement of a low-molecular-weight oligomer, through motion of terminal segments (segmental diffusion), and through exchange reactions (chemical diffusion). The latter comprises a few reaction steps, permitting a reactive group to move all over an amorphous domain and to approach another group to react.
- *The condensate removal through diffusion*. It is divided into interior diffusion, that is, inside the solid reacting particle, and surface diffusion, that is, from the reacting particle surface to the ambient atmosphere.

A number of parameters are reported to affect the overall rate of SSP and to define the relevant rate-determining step. Reaction temperature, initial end-group concentration, particle geometry, gas flow rate, crystallinity, and catalysts are listed as the most important and their effect on the controlling mechanism is presented briefly in **Table 1**, assuming negligible gas-phase resistance.[8,9]

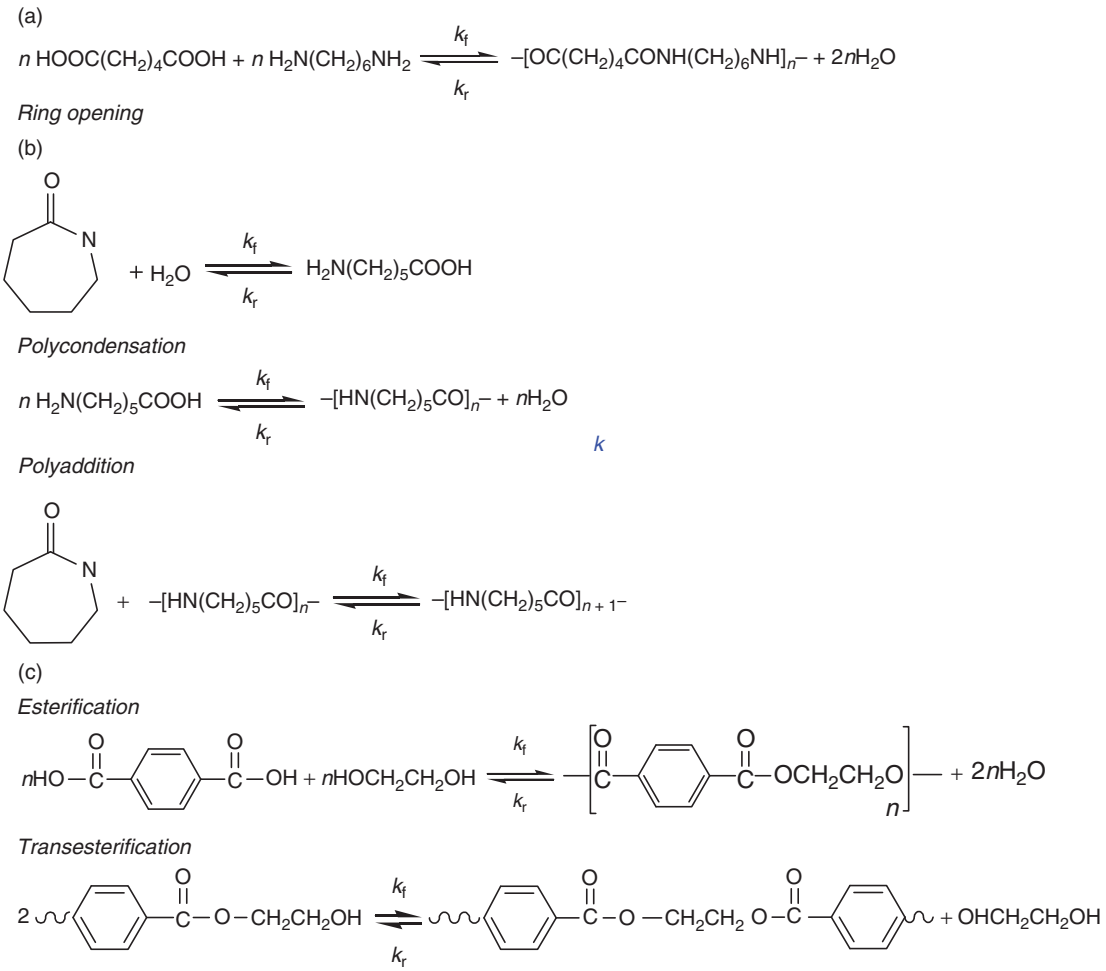

Figure 1 Reaction schemes for three typical condensation polymers: PA 66, PA 6, and poly(ethylene terephthalate) (PET). (a) Reaction scheme for PA 66; (b) reaction schemes for PA 6; (c) Reaction schemes for PET.

In the following sections, the prevailing mechanisms in direct and post-SSP are discussed, focusing on two of the most commercially important condensation polymers, that is, polyamide 66 (PA 66) and poly(ethylene terephthalate) (PET), as well as on poly(lactic acid) (PLA), which is widely considered as a very promising bioplastic.

4.34.2 Direct Solid-State Polycondensation

In direct SSP, the reaction takes place at a temperature below the melting point of both monomer (PA salt, amino acid) and polymer, under flowing nitrogen, in vacuum or at high pressure;[10–17] in many cases, the reactions are topotactic and the monomer crystals can be converted to polycrystalline polymer aggregates, permitting the preparation of highly oriented polymers.[16,17]

Volokhina *et al.*[18] studied the SSP kinetics for three aliphatic ω-amino acids, 7-aminoheptanoic (enanthoic), 9-aminononanoic (pelargonic) and 11-aminoundecanoic and three hexane-1,6-diamine (hexamethylenediamine) (HMD) salts of adipic, 5,5′-sulfanediylbis(pentanoic acid) (5,5′-thiodi (pentanoic acid)), and terephthalic acid at various temperatures. The investigation of the amino acid polyamidation process led to the conclusion that the reaction is 'distinctly autocatalytic'. Another Russian group arrived at the same conclusion by studying the SSP of 7-aminoheptanoic acid.[19] They suggested that the "autocatalytic acceleration of this reaction is due to increased reaction of the surface of the monomer–polymer boundary." This autocatalysis feature is also supported by Khripkov *et al.*[20] for HMD salt of adipic acid polymerized in the solid state in the presence of boric acid as catalyst. The activation energy of the polycondensation in solid phase was found to be 251 kJ mol^{-1} for 11-aminoundecanoic acid, 385 kJ mol^{-1} for 7-aminoheptanoic acid, and 752 kJ mol^{-1} for 9-aminononanoic acid. In liquid phase, the activation energy is much lower, being 180 kJ mol^{-1} for 7-aminoheptanoic acid and 159 kJ mol^{-1} for 9-aminononanoic acid.[21]

In many studies of direct SSP, polymerization is considered to follow the nucleation and growth model along the crystallographic directions of the monomer.[3] Accordingly, the kinetics comprises two steps and the respective curves are S shaped. In the following section, mechanistic aspects of SSP of PA 66 salt are discussed in detail, since it is the most promising monomer for direct SSP.

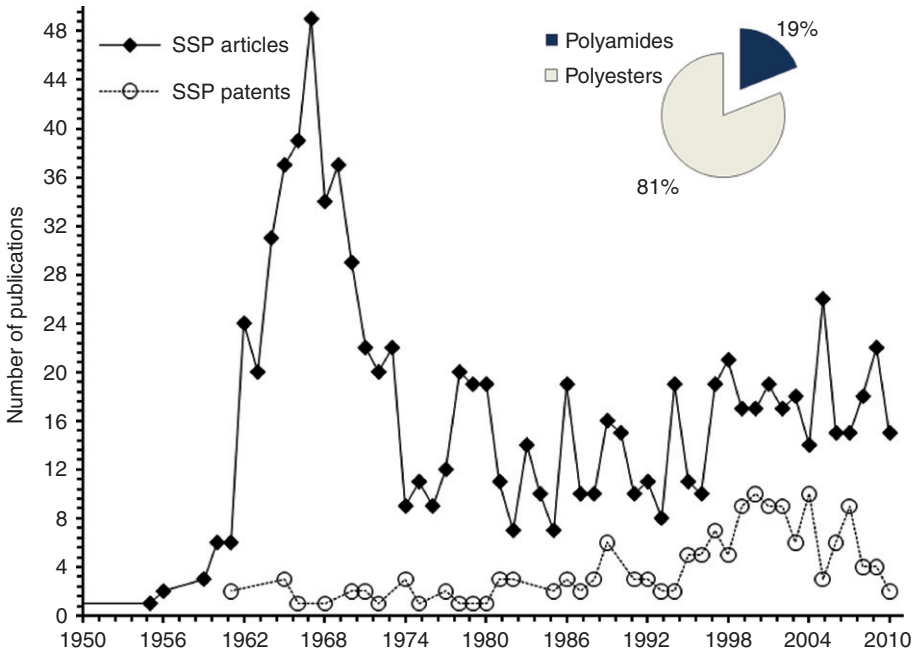

Figure 2 The number of publications (patents and scientific journals) on solid-state polymerization. Data from SciFinder Scholar 2010.

Table 1 The effect of most important variables on the rate-controlling mechanisms of SSP (in the absence of gas-phase resistance)[8]

	Reaction temperature (T)				
Process	*Low T*	*High T*	*Particle size*	*Initial MW and crystallinity*	*Catalyst concentration*
Chemical reaction	Yes (strong influence)	Yes (weak influence)	No	No	Yes
End-group diffusion	Yes (weak influence)	Yes (strong influence)	No	Yes	No
Condensate diffusion	Yes (weak influence)	Yes (strong influence)	Yes (strong influence)	Yes	Yes

4.34.2.1 The Role of Hexane-1,6-Diamine Volatilization

A critical feature of PA salt polymerization is the loss of the readily volatile diamine from the reacting material and the need to compensate for it so as to not disturb the stoichiometric equivalence of functional end-groups. Accordingly, the volatilization of HMD has been observed in the SSP of PA 66 and 610 salts[20,22,23] and also of different aromatic PA monomers.[24] Several measures have been adopted in PA 66 production to treat HMD loss, such as the introduction of the diamine at the beginning of the polycondensation reaction in an amount sufficient to balance diamine loss,[25] the use of nitrogen gas containing HMD, and finally a decrease in the reaction temperature in order to minimize the HMD loss.[26]

However, the HMD escape was found to play a key role in the direct SSP mechanism. In particular, SSP of PA 66 salt was examined in the temperature range of 160–190 °C under dry static or flowing (50 ml min^{-1}) nitrogen.[22] The runs were performed in a thermogravimetric analysis (TGA) chamber, where the reaction progress was evaluated by continuous monitoring of the weight of the reaction mixture and the effluent gas composition; the latter was analyzed by IR spectroscopy and titration.

The IR analysis of the TGA effluent gas provided an insight into the volatilization of HMD and the formation of polycondensation water. It was then discovered that the diamine escaped earlier than water. Regarding SSP at 180 °C, **Figure 3(a)** shows that after 30 min of SSP, the diamine was detected and its quantity increased rapidly, reaching the highest value at the reaction time of 40 min. On the other hand, based on **Figure 3(b)**, the polycondensation water escaped at a low rate during the first 50 min, after which the water loss was more intense and reached the highest value at 60 min. Thus, the HMD loss dominated early in the reaction; then, the reaction accelerated as it is evident from the rapid increase in the water loss.

Quantitative analysis of the effluent gas permitted the determination of polymerization conversion (p_t) through eqns [2] and [3]. The plots of p_t against time (**Figure 4(a)**) show that the kinetics of the process was characterized by two stages, namely induction and propagation. The S-shaped curves at each reaction temperature are indicative of the nucleation

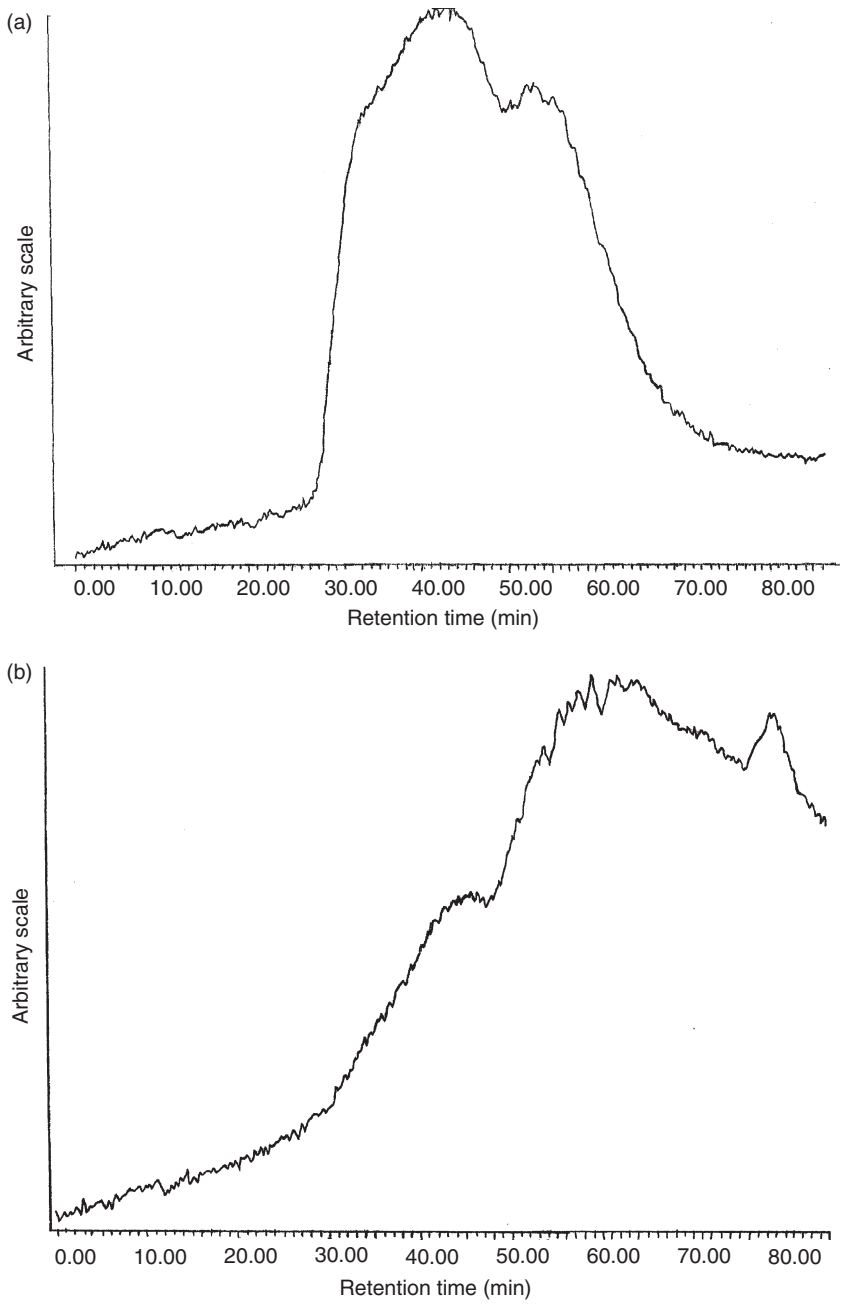

Figure 3 Evolution of (a) HMD and (b) water during SSP of PA 66 salt at 180 °C under flowing nitrogen. From Papaspyrides, C.; Vouyiouka, S.; Bletsos, I. *Polymer* **2006**, *47* (4), 1020–1027,[22] by permission of Elsevier.

growth model.[11,27] More importantly, at 180 °C, the duration of the nucleation stage (40 min) (**Figure 4(b)**) coincided with the HMD loss, as can be observed in **Figure 3(a)**:

$$p_t = \frac{m_{H_2O,t}}{18[NH_2]_0\, m_t} \quad [2]$$

$$m_t = m_0 - 10^{-3} m_{H_2O,t} - m_{HMD,t} \quad [3]$$

where $m_{H_2O,t}$ is the amount of water (g) escaped at any given time t, $m_{HMD,t}$ the amount of diamine (kg) escaped at any given time t, m_0 the initial weight of the salt (kg), and $[NH_2]_0$ the initial concentration of amine ends (mol kg^{-1}).

Combining the early evolution of HMD, as observed through IR analysis, and the theory of the nucleation growth model, which seems to prevail based on the two-stage character of the process, an SSP mechanism can be suggested. According to the nucleation growth model, the crystal lattice and its characteristics, such as the size of crystals, the number and type of lattice defects, and the presence of impurities, may significantly influence the polymerization in the solid state. For instance, crystal edges and defects may in some cases inhibit the propagation of polymerization through physical separation of the polymerizing units, while in other cases, they may act as active centers, since the orientation of the

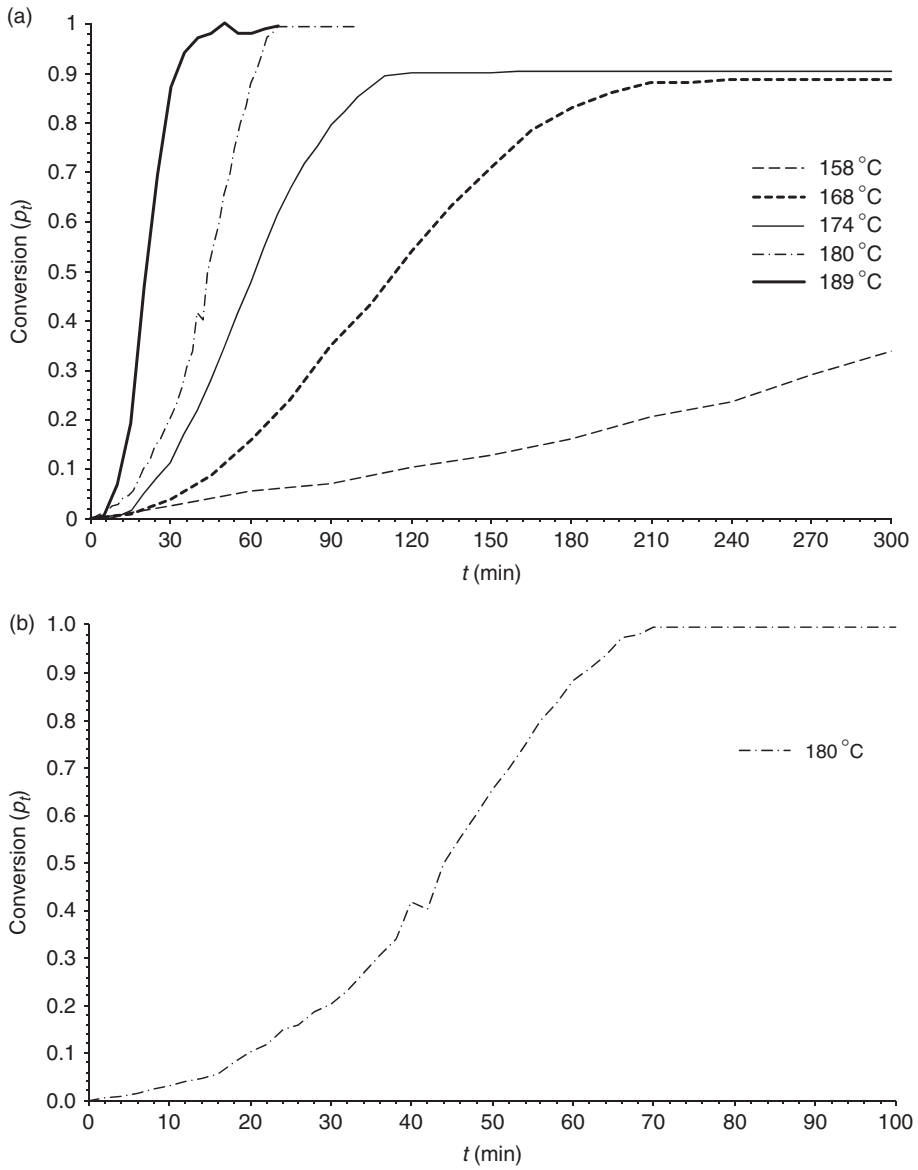

Figure 4 (a) Polymerization conversion (p_t) versus reaction time and temperature during SSP of PA 66 salt under nitrogen. (b) Conversion (p_t) versus reaction time at 180 °C. From Papaspyrides, C.; Vouyiouka, S.; Bletsos, I. *Polymer* **2006**, *47* (4), 1020–1027,[22] by permission of Elsevier.

reacting species at the defective surfaces within the crystallites may differ and promote the nucleation of the polymer phase (initiation stage). Impurities may act by creating lattice defects, which subsequently affect polymerization, may act as a physical diluent to impede polymerization, or may facilitate molecule mobility and assist in the polymerization.[10]

Based on these well-known principles of solid-state chemistry, the early evolution of HMD may be associated with the nucleation stage: the diamine volatilization results in creating new defective surfaces in the crystal lattice and in increasing the active centers for the nucleation of the generated polymer phase, which further grows following water formation.

4.34.2.2 The Role of Polycondensation Water

During the direct SSP of PA 66 salt, growth follows nucleation and often proceeds unexpectedly. In cases of highly hygroscopic monomers, depending on reaction temperature, a transition from the solid to the melt state has been observed, dominating in the moderately organized salt structures after quite a short reaction time. This phenomenon has been explained by Papaspyrides *et al.*[3,12–15] and correlated with the condensation water accumulating in the reacting mass.

More specifically, the SSP of different PA salts was investigated by dispersing the monomer particles in an inert nonsolvent and using a glassware assembly, which provided continuous monitoring of the physical form of the reacting mass. It was then observed that the SSP was accompanied, depending on the reaction conditions, by a distinct transition of the process from the solid to the melt state (solid–melt transition, SMT), where a very fast agglomeration of the reacting particles took place. The phenomenon was readily observed macroscopically, since stirring failed to keep the particles in suspension, while microscopically the

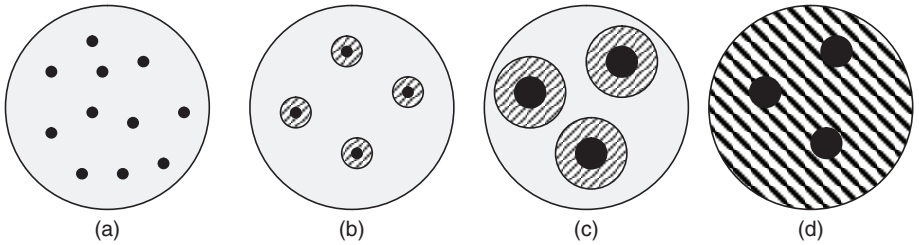

Figure 5 Schematic diagram of the SMT phenomenon. ●, Defects of the monomer crystalline structure; dark area, polymer nuclei insoluble in water; shaded area, 'Highly hydrated' and eventually melt area. From Kampouris, E.; Papaspyrides, C. *Polymer* **1985**, *26*, 413–417,[6] by permission of Elsevier.

transformation of sharp-edged crystals to nearly spherical particles was evident.

Taking into account these experimental findings and the hygroscopic nature of the PAs, a generalized mechanism for the effect of polycondensation water on the reaction behavior has been proposed for the growth stage of SSP of the salts (Figure 5). The reaction begins at the defective sites of the monomer crystalline structure, being the active centers of the reaction (Figure 5(**a**)). For active centers up to or very near to the grain surface, the water formed can be easily removed to the surrounding heating medium, without affecting the reacting mass. On the contrary, in the grain interior, the water hydrates the polar hydrophilic groups of the salt structure, and in the case of low reaction rates (i.e., low rates of water formation), an organized accommodation of the by-product within the crystal structure is taking place. As the accumulated amount of water increases, a 'highly hydrated' area of the monomer surrounds the active centers. This area has a lower melting point and soon falls into the melt state (Figure 5(**b**)). After the formation of these melt areas, the reaction proceeds mainly in the melt and the rate considerably increases, while the water accumulation leads to an increase in the total melt area (Figure 5(**c**)). Eventually an overlapping of these melt areas occurs, which explains the observed transition of the reaction from the solid state to the melt state (Figure 5(**d**)).

As the reaction proceeds further, the MW increases, the hygroscopicity of the reacting system decreases, and finally the solid character of the system is restored. At high reaction rates, it is proposed that the time available for controlled accommodation of the water formed is very limited, resulting in a more rapid breakdown of the salt structure and, subsequently, in a much faster appearance of the SMT phenomenon. This proposed model of water accumulation–hydration–transition to the melt was found to predominate in PA salts of moderate structure organization, while when the network of coordinating polar groups becomes more rigid (e.g., ethylenediammonium fumarate), a deviation from this model may occur.

4.34.2.3 The Role of Catalysts

The practical disadvantage of the direct SSP is the inevitable SMT occurring whenever the reaction proceeds at reasonable rates (Section 4.34.2.2). To overcome this problem, catalysts have been used to increase the reaction rate and favor keeping the process in the solid state. Boric, phosphoric, and sulfuric acids were studied as catalysts for the SSP of PA salts.[12,13] The results showed a considerable acceleration of the reaction, especially in the presence of boric acid, while the solid character of the process was maintained throughout the total course of the reaction, keeping the water accumulation parameter (D_t, eqn [4]) at low values (Figure 6):

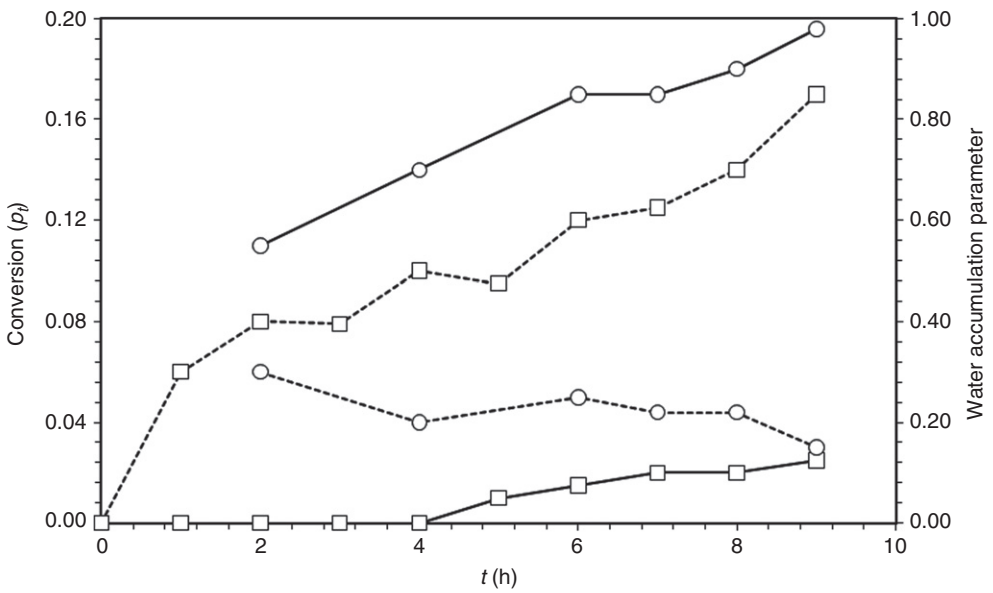

Figure 6 SSP of PA 66 salt at 142 °C. ———, Pure salt; - - -, salt containing 1.60 wt.% boric acid; □, conversion; ○ water accumulation parameter.

$$D_t = \frac{w}{\text{initial moisture} + \text{water formed}} \quad [4]$$

where w is the reacting mass.

It was proposed that the presence of a good catalyst in the reacting mixture contributes to an easier removal of the water formed, away from the reacting sites. In other words, hydration seems restricted and the diffusion of water is favored so that the reaction equilibrium is shifted to the right. This finding of easier water removal was also verified when using TGA as an SSP reactor and examining the effect of flowing and static nitrogen on the rate.[22] In particular, in the catalyzed process, the process-limiting step was not the by-product diffusion, since there was no difference in the rate of the reduced weight loss under either flowing or static nitrogen, as it was in the noncatalytic case.

4.34.2.4 Low-Temperature Prepolymerization Process

The aforementioned SMT occurring during SSP of PA salts can be exploited, instead of being avoided, through the development of a suitable prepolymerization process, as applied at DuPont Laboratories. More specifically, in the works of Papaspyrides *et al.*,[28,29] dry balanced salt has been converted to PA 66 prepolymer by a low-temperature autogenous process operating in the vicinity of the melting point of the salt. In fact, operating even far below the salt initial melting temperature, the melting point is reduced due to the SMT phenomenon and the salt grains turn to a semimelt mass (Figure 7). The lower temperatures used are beneficial, since undesirable side reactions cannot occur and degradation is minimized.

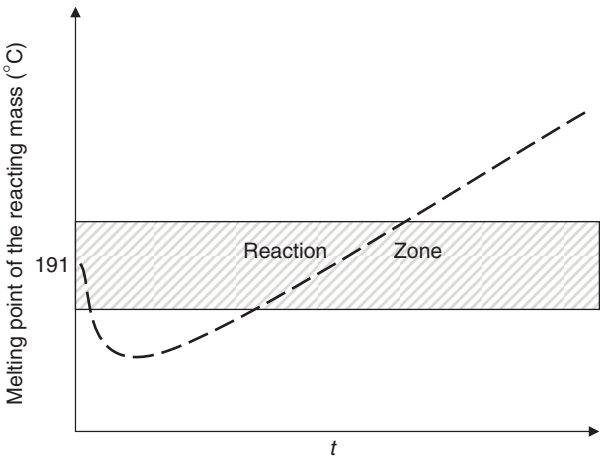

Figure 7 Decrease in the melting point of reacting mass during SSP of PA 66 salt.

Furthermore, in the suggested prepolymerization process, the diamine loss was avoided through an autogenous route; the use of a closed, intensively stirred vessel under autogenous pressure during initial stages of the polymerization was appropriate to ensure that a feed consisting of dry salt with balanced end-groups would result in stable and balanced prepolymer, without the need for an elaborate control strategy to maintain the proper stoichiometry. The autogenous condition was maintained up to or beyond the point where diamine end-groups had reacted, and then water vapor was vented from the vessel.

This autogenous route allowed the production of a balanced prepolymer without detectable thermal degradation products and without the need for HMD recovery. The PA prepolymers formed solutions of relative viscosity (RV, 8.4 wt.% in 90% formic acid at 25 °C) between 8.5 and 27.1 (weight-average MW 12 500–25 500) and a low water content (0.79–3.70%). The quality of these products ensured safe solid-state finishing at higher temperatures and much higher MWs.

Finally, it should be mentioned that on a large scale, the transitions between solid and melt require careful design of the experimental apparatus and the problem of an appropriate reactor arises. In particular, the equipment should be capable of handling (stirring and agitating) all these physical forms for an adequate period of time. The same reactor should be capable of keeping the reacting mass from hardening into a bulk mass and therefore producing a granular prepolymer. These requirements can be effectively satisfied through the use of a screw-type extruder.[28]

4.34.3 Post-Solid-State Polycondensation

It is generally accepted that reactions during post-SSP take place in the amorphous regions where, due to a temperature well above glass transition, the chain mobility is high enough to allow reactions to occur [30,31] (Figure 8). Any formed condensate is also transferred into the amorphous polymer phase along with end-groups and oligomers, and is preferably removed through convection caused by passing inert gas or by maintaining reduced pressure during the SSP process.

The post-SSP of various condensation polymers can be characterized by specific features, which are discussed in the text below, regarding PA 66, PET, and PLA.

4.34.3.1 Polyamide 66

PA 66 and PA 6 are the most popular PAs, corresponding to more than 90% of PA uses, namely in textiles, carpets, rugs and home textiles, technical fibers, engineering plastics, and films.

PA 66 prepolymer is prepared through a solution-melt polymerization technique, starting from the aqueous PA 66

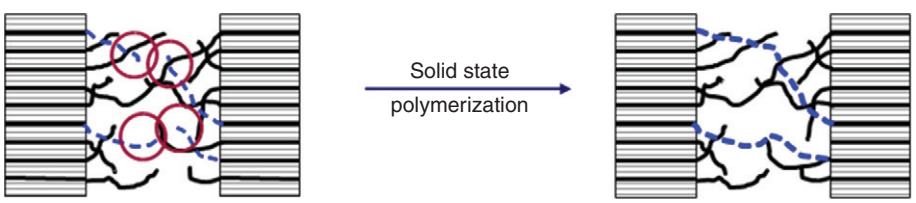

Figure 8 Schematic of solid-state polymerization reactions in the amorphous regions of prepolymers.

salt.[32] The precursors exhibit MWs equal to 15 000–25 000 and are suitable for textile applications. SSP follows in order to further increase the MW for injection or blow molding applications, avoiding in this way any thermal degradation and gel formation (eqn [5]), which can drastically impair the quality of the end product:[33–36]

$$R_1{-}NH_2 + H_2N{-}R_2 \underset{-NH_3}{\rightleftharpoons} R_1{-}\underset{\underset{H}{|}}{N}{-}R_2 \underset{-H_2O}{\rightleftharpoons} R_1{-}N{-}R_2 \quad \text{with} \quad + \begin{matrix} O{=}C{-}R_3 \\ | \\ OH_2 \end{matrix} \quad \text{and} \quad R_3{-}C{=}O \qquad [5]$$

where R_1, R_2, and R_3 are PA backbones of different polymerization degree.

The kinetics of PA 66 post-SSP has been studied by a number of researchers who developed proper kinetic equations in order to describe the process. More specifically, Vouyiouka *et al.*[37] used the Flory equations for second- and third-order kinetics and integrated them based on the polymerization conversion (p_t) (eqns [6] and [7]):

$$\frac{1}{D_0}\left(\ln\frac{1}{[COOH]_0} + \ln\frac{[COOH]_0 - [NH_2]_0\,p_t}{1-p_t}\right) = k_2 t \qquad [6]$$

$$\frac{1}{D_0^2}\ln\frac{[COOH]_0 - [NH_2]_0\,p_t}{[COOH]_0(1-p_t)} - \frac{1}{D_0}\left(\frac{1}{[COOH]_0 - [NH_2]_0\,p_t} - \frac{1}{[COOH]_0}\right) = k_3 t \qquad [7]$$

where $[COOH]_0$ and $[NH_2]_0$ are the initial concentrations of the carboxyl and amino end-groups (mmol kg^{-1}), k_2 (kg mmol^{-1} h^{-1}) and k_3 (kg^2 mmol^{-2} h^{-1}) the rate constants, and D_0 the initial carboxyl end-group excess (mmol kg^{-1}).

The third-order kinetics presented a slightly better fit under specific SSP conditions (160–200 °C, 0–4 h) and the rate expression of SSP was found as in eqn [8]:

$$k = 4.8 \times 10^{-6}\exp\left[\frac{70.41}{R}\left(\frac{1}{423} - \frac{1}{T}\right)\right] \qquad [8]$$

where k is the rate constant (kg^2 mmol^{-2} h^{-1}), T the reaction temperature (K), and R the universal gas constant (kJ mol^{-1} K^{-1}).

Composition effects on the kinetics of SSP of PA 66 have also been examined and are discussed below, revealing different process mechanisms. In particular, three additive categories were studied:

1. A comonomer, used for enhancing PA dyeability.
2. Phosphorus-containing antioxidants, tested as candidates for catalysts.
3. An organomodified clay, used for producing nanocomposites.

4.34.3.1.1 The role of sulfur-containing comonomer

The effect of sodium 5-sulfoisophthalic acid (NaSIPA) was examined with respect to the kinetics of post-SSP of PA 66.[38] As an aromatic dicarboxylic acid (**Figure 9(a)**), NaSIPA reacts with the free amine groups of PA structure and an anionically modified copolymer (ionomer) is formed (**Figure 9(b)**). The main attribute of the NaSIPA-containing copolymers is the improvement of polymer dyeability with cationic dyes, resulting in fibers or films with deep and brilliant colors and resistance to stains, fading, and yellowing throughout their life cycle. In addition, NaSIPA incorporation contributes to minimizing operation problems related to the use of pigments and stabilizers, as well as to avoiding problems during spinning. The preferred amount of NaSIPA to be used is 1–2 wt.% (added at the salt stage, i.e., prior to polymerization) for most combinations of pigments and copper, meanwhile above 4 wt.%, the additive itself begins to lower the relative viscosity of the polymer and gives poorer operability.[39–43]

The effect of NaSIPA on SSP of PA 66 was thoroughly examined, considering the importance of the additive on industrial scale and that its presence affects a majority of nylon production lines. NaSIPA-containing copolyamides (1–3 wt.% NaSIPA) were submitted to SSP runs under flowing and static nitrogen in the temperature range of 160–200 °C.[38] It was shown that, at every reaction temperature, the copolyamides exhibited reduced SSP rates; more specifically, the rate constant decreased by 11–57% as the amount of NaSIPA increased (**Figure 10**).

The observed retardation was correlated first with the morphology of the sulfonated ionomers. According to the model proposed by Eisenberg *et al.*[44] for random ionomers, the NaSIPA ionic moieties aggregate into 'multiplets', which, in turn, aggregate into clusters, creating finally a phase of restricted mobility in the polymer mass. During the SSP of the NaSIPA-containing copolyamides, the ionic groups are localized in the amorphous regions and create a low-mobility area, which obviously impedes the diffusion of the functional end-groups and/or the water escape, thus slowing down the SSP reaction.

A reason for critical retardation also proved to be the partial deactivation of the PA amine ends by the NaSIPA sulfonate units, which exist in the amorphous regions of the copolyamides. Through this reaction, NaSIPA improves the polymer resistance to acid stains, since the amine groups are no longer available for absorbing them (e.g., wine and soft drinks), which is really important for applications such as flooring covers.[41–43] However, during SSP in the presence of NaSIPA, this interaction leads to two types of end-groups, namely active and inactive amine ends. The former are able to participate in the polymerization reaction and their concentration in the copolyamides is lower compared with that of

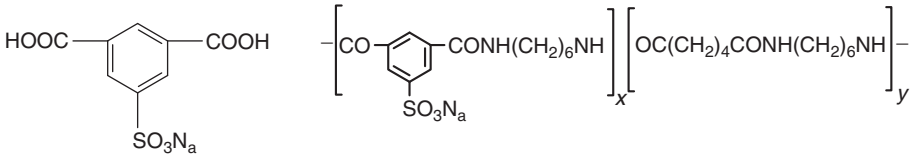

Figure 9 (a) NaSIPA and (b) PA 66 copolyamide with NaSIPA (x, 0.01–0.05; y, 0.95–0.99).

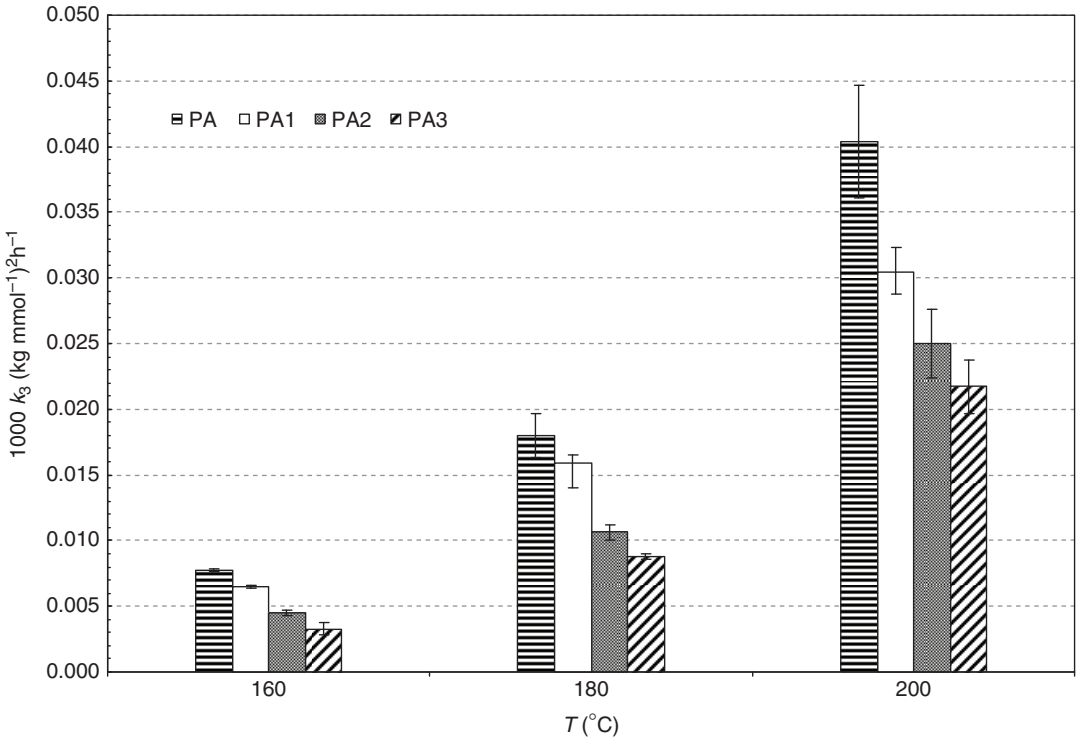

Figure 10 Rate constants (k_3) during PA 66 post-SSP under nitrogen. PA, PA 66 homopolymer; PA1, PA 66 containing 1 wt.% NaSIPA; PA2, PA 66 containing 2 wt.% NaSIPA; PA3, PA 66 containing 3 wt.% wt NaSIPA. From Vouyiouka, S.; Papaspyrides, C.; Weber, J.; Marks, D. *Polymer* **2007**, *48* (17), 4982–4989,[38] by permission of Elsevier.

PA 66 homopolymer, which results in reducing the reactant concentration and thus the reaction rate. The inactive amine groups are attached to SO_3^- in the restricted mobility domains (clusters) and their constant concentration in SSP is assumed to be a fraction of the total amine ends, depending on the SO_3^- concentration (C_s), the reaction temperature (T), and the morphology of the ionomer. The effect of the two last parameters is demonstrated on a deactivation factor denoted as $1/J$ (eqn [9]):

$$k_{cop} = k_{hom}\left(1 - \frac{C_s}{J}\right) \quad [9]$$

The assumption of the inactive amine-end mechanism was tested through examining the fitting of SSP experimental data to eqn [9], which shows a correlation between the SSP rate constants of homopolymer (k_{hom}) and copolymer (k_{cop}). Indeed, the k_{cop}/k_{hom} was found proportional to C_s ($R^2 = 0.9538$), verifying the validity of the suggested mechanism. Furthermore, C_s/J can be considered as the fractional decrease in the total amine ends in the copolyamide grades; that is, for PA1, the active amine ends make 82% of the experimentally measured value, for PA2 65%, and for PA3 47%.

Finally, the SSP kinetics was properly modified through eqn [10] to include the composition effect of NaSIPA on the apparent rate constant of SSP:[45]

$$k_{cop} = 4.8 \times 10^{-6}\exp\left[\frac{70.41}{R}\left(\frac{1}{423} - \frac{1}{T}\right)\right] \times \left\{1 - 6 \times 10^{-3}\exp\left[\frac{-4.587}{R}\left(\frac{1}{423} - \frac{1}{T}\right)\right] \times C_s\right\} \quad [10]$$

where k_{cop} is the SSP rate constant for the copolyamides (kg^2 mmol^{-2} h^{-1}), C_s the sulfonate group content (mmol kg^{-1}), T the reaction temperature (K), and R the universal gas constant (kJ mol^{-1} K^{-1}).

4.34.3.1.2 The role of phosphorus-containing additives

The effect of hydroxyphenylalkylphosphonic esters was investigated in post-SSP of PA 66.[46,47] In particular, the additives studied were Irgamod® 195 (**Figure 11(a)**) and Irgamod® 295 (**Figure 11(b)**) (formerly Ciba Specialty Chemicals, now BASF), which are used as antioxidants. Two approaches were examined regarding the additive incorporation: in the first one, the additive was mixed in concentrations of 0.1% and 0.5% with the prepolymer through melt blending in a single-screw extruder, meanwhile, in the second case, the compounds at a concentration of 0.1% were added during the prepolymer preparation through a low-temperature process starting from solid PA 66 salt (Section 4.34.2.4).

SSP runs were conducted at 160 and 200 °C under nitrogen flow, resulting in process acceleration when the phosphonates were present, especially at the high SSP temperature. Indicatively, the solution relative viscosity of the products increased by up to 288% (200 °C, 4 h, 0.5% Irgamod® 195), while the relevant value for pure PA 66 was 144%. The SSP kinetics was estimated using a linear correlation of relative viscosity vs. reaction time and the calculated rate constants are shown in **Figure 12**.

The catalytic activity of SSP of PA 66 was found to be dependent on the incorporation technique: the additive performance was improved when they were added in the

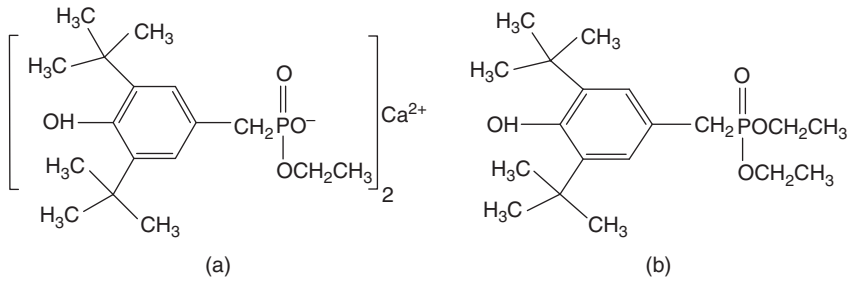

Figure 11 Molecular structures of (a) Irgamod® 195 (calcium bis[(3,5-di-*tert*-butyl-4-hydroxybenzyl)ethylphosphonate]) and (b) Irgamod® 295 (diethyl (3,5-di-*tert*-butyl-4-hydroxybenzyl)phosphonate).

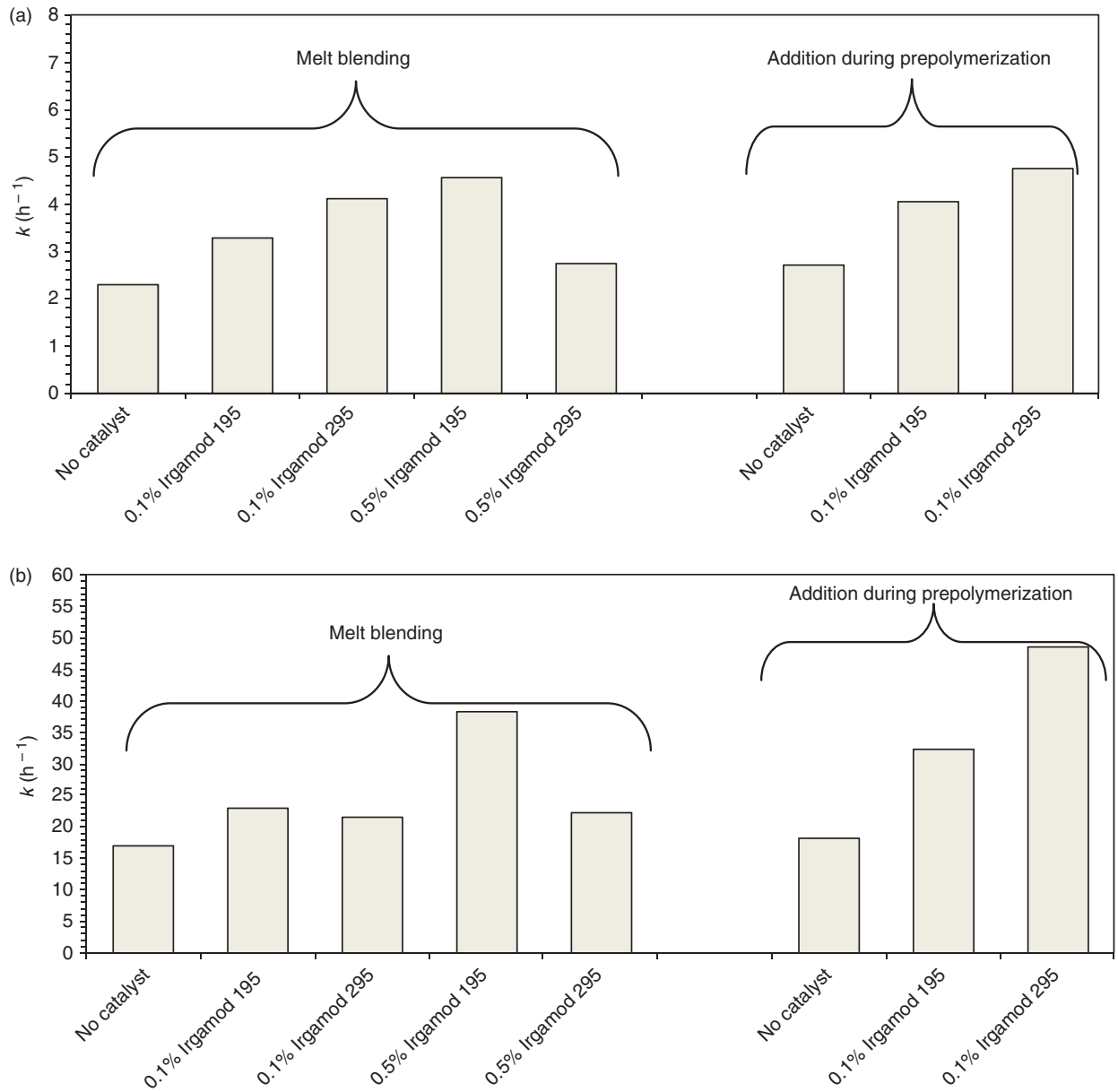

Figure 12 SSP rate constants in the presence of phosphorus-containing additives. (a) 160 °C and (b) 200 °C.

prepolymerization stage. The latter can be attributed to a more homogenous catalyst distribution in the reacting mass, without excluding the possibility of partial attachment of the catalyst to the PA backbone, thus rendering the pertinent segment more functional. A similar suggestion has also been made by Duh[48] for the catalyzed (Sb_2O_3) SSP of PET,

according to which antimony glycolate is attached to the end-group of a polymer chain, thus imparting catalytic activity to the polymer. Then, the catalyst containing the end-groups can react with a normal end-group to form a diester and regenerate glycolate, which continues to participate in the catalytic reaction.

Another phosphorus-containing antioxidant, (Irganox® B 1171, former Ciba Specialty Chemicals, now BASF), a 1:1 blend of a sterically hindered phenolic amide (*N*,*N*′-hexane-1,6-diylbis[3-(3,5-di-*tert*-butyl-4-hydroxyphenyl)propanamide]) and a phosphite (tris(2,4-di-*tert*-butylphenyl) phosphite), also exhibited strong catalytic action at a concentration of 1 phr (melt blending) in SSP of PA 66.[49] The relevant process yielded an SSP product of number-average MW equal to 37 300 (vs. 21 800 in noncatalyzed process) after 4 h of reaction at 200 °C, while the reaction rate constant increased by almost 450%. It is interesting to note that the modified prepolymer showed a high reaction rate even at long SSP times, unlike in a typical SSP kinetics, which is characterized by lower final rates due to limitations of end-group diffusion. The latter indicated the 'immunity' of the catalyzed system to such limitations, implying that the phosphorus additive seems to promote both chemical reaction and diffusion of end-groups.

Finally, the catalytic action of the above-tested antioxidant was attributed to its triphenyl phosphite parent compound. In particular, phosphite esters, such as triaryl phosphites, have been reported as SSP catalysts, but the relevant literature is restricted and patented.[47,50] On the other hand, the action of triaryl phosphites in solution and/or melt polycondensation has been shown by several groups,[51–56] mainly in the formation of aromatic PAs in solution at moderate temperatures. As an example, Aharoni *et al.*[54–56] studied polyamidation in the presence of triaryl phosphites in solution[55] and in the melt during extrusion.[54] They suggested that triaryl phosphites serve as chain extenders for the polyamidation reaction.

4.34.3.1.3 The role of nanomaterials

Recent publications indicate the catalytic effect of nanomaterials, as a result of morphological changes and/or of chemical interaction between the filler and the polymer matrix. In particular, Yu *et al.*[57] studied the SSP of PET in the presence of 2.5 wt.% clay. They reported an acceleration effect based on intrinsic viscosity (IV) measurements, with the pertinent increase ranging from 2% to 8% at 230 °C for up to 25 h. This rate increase was attributed to clay nucleation action, which led to more amorphous regions both on the crystal surfaces and between them, and thus to easier by-product diffusion. Bikiaris *et al.*[58] studied SSP kinetics in PET-activated carbon black (ACB) nanocomposites. A reaction scheme was suggested according to which ACB catalyzed the esterification reaction, while the transesterification rate decreased at low temperatures and remained the same at higher ones. The same group studied SSP kinetics of PET–silica (SiO_2) nanocomposite.[59,60] They found that the reaction rate depended on SiO_2 concentration: in small amounts (< 1 wt.%), both esterification and transesterification were enhanced, while at higher SiO_2 contents (1–5 wt.%), branching was observed due to side reaction of PET hydroxy groups with the nanosilica particles.

Regarding PA 66, the catalytic efficiency of nanoclays was proved in the solution–melt technique, being however strongly dependent on the extent of nanofiller exchange.[61] More specifically, clays fully organomodified by exchange at a concentration of 1 phr caused an almost ≈ 75% increase in relative viscosity of the polymers; this nanocatalysis was attributed to the clay action as a substrate for polyamidation, by forming an active intermediate between its SiOH groups and PA COOH ones, as it will be discussed later. On the other hand, in the case of clays partially organomodified, the MW was found almost equal to the reference grade. The latter observation was attributed to Na^+ cations present in the clay, the strong hydrophilic character of which renders them water 'traps' for the produced polycondensation water, thus enabling the reversible polycondensation.

Solid-state polymerization of PA 66 nanocomposites was thoroughly examined by the same group of researchers,[62] in the perspective of promoting the nanofiller incorporation not only for the modification and/or improvement of materials properties but also for exploring their performance as SSP 'multifunctional' catalyst systems. The SSP runs were carried out at temperatures of 160–200 °C and reaction times up to 8 h at a filler concentration of 1 phr (natural montmorillonite modified with benzyl dimethyl(octadecyl)ammonium chloride). The SSP rate constant was found increased by 20–50% depending on the reaction temperature, and MW up to 26 500 was reached, while the prepolymer value was 14 000. The Arrhenius equation was deduced for the SSP of PA 66 nanocomposites (eqn [11]), with a significantly increased pre-exponential factor at 848.1 ($kg^2\,mequiv^{-2}\,h^{-1}$) versus 33.5 for pristine PA:

$$k = 3.94 \times 10^{-6} \exp\left(\frac{-67.42}{R}\left(\frac{1}{T} - \frac{1}{423}\right)\right) \qquad [11]$$

where k is the SSP rate constant of the nanocomposite ($kg^2\,mmol^{-2}\,h^{-1}$), T the reaction temperature (K), and R the universal gas constant ($kJ\,mol^{-1}\,K^{-1}$).

A nanocatalysis mechanism of SSP of PA 66 was suggested based on chemical reactivity enhancement and thermal protection, induced by the presence of clay. In particular, the clay action as nucleation agent for PA 66 crystallization resulted in the creation of a very large number of small-size spherulites. This crystal morphology is anticipated to increase the end-group concentration in the amorphous regions and 'force' them to react, since the distance that these groups needed to diffuse was essentially lower. In other words, a higher number of total collisions were permitted, as expressed also by the high Arrhenius pre-exponential factor for the nanograde.

At the same time, clay was suspected to facilitate the amidation reaction, acting as chain extender due to the SiOH groups on the edges of its surface. It is a well-known fact that clays contain reactive SiOH groups on the edges of their surface,[63,64] which may be used as catalysts/chain extenders of amidation in peptide formation through activated intermediates.[65–67] The peptide reaction proceeds via the condensation of SiOH groups with amino acid COOH groups to form Si–O–CO ester/anhydride, which is then attacked by an NH_2 group to form amide. Accordingly, during SSP, clay can act as a substrate to promote amidation and chemical diffusion of end-groups, and this may explain the enhanced nanocomposite polymerizability (**Figure 13**).

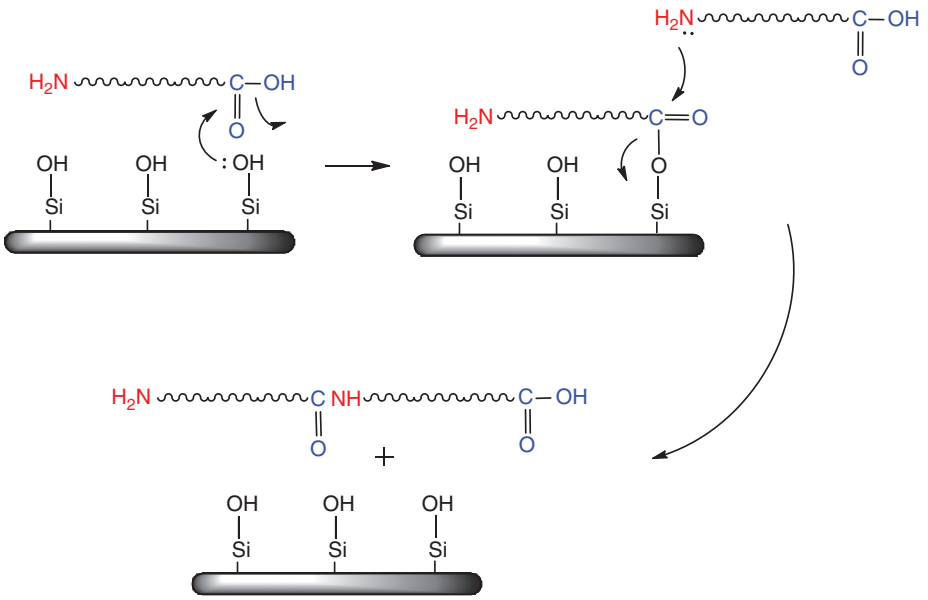

Figure 13 Action of clay substrate in polyamidation during SSP of PA 66 nanocomposite. From Boussia, A.; Konstantakopoulou, M.; Vouyiouka, S.; Papaspyrides, C. *Macromol. Mater. Eng.* **2011**, *296* (2), 168–177,[62] by permission of John Wiley & Sons, Inc.

Another rate enhancement factor was the absence of thermal degradation reactions, as clay was found to provide thermal protection to the PA matrix. Side reactions were thus inhibited, while the contrary would significantly affect the SSP by disturbing end-group balance.

Finally, in the case of SSP of PA 66, when combining a phosphorus-containing antioxidant and clay, reduced antioxidant catalytic performance was observed, which was ascribed to significant counteractions between them: clay hydrophilicity acted as a polycondensation water 'trap', hindering the escape of the by-product. The latter effect was also related to clay barrier properties, while the occurrence of adsorption phenomena on the surface of the nanofillers was also assumed to reduce the catalytic performance of the antioxidant.[49]

4.34.3.2 Poly(ethylene terephthalate)

PET is widely used for production of bottles. It is based on a copolymer of ethylene terephthalate and ethylene isophthalate, and constitutes an important family of commodity plastics, especially for packaging applications. In order to produce PET with IV of 0.6 dl g^{-1}, melt polymerization processes are normally employed, involving the bulk reaction of ethylene glycol with dimethyl terephthalate or purified terephthalic acid. PET resins with higher IV (> 0.7 dl g^{-1}) are produced through SSP processes at 200–240 °C for 10–30 h under inert gas flow or in vacuum. Among its many advantages, SSP also favors the simultaneous removal of acetaldehyde, which can be formed at high reaction temperatures.[68]

4.34.3.2.1 The role of water content in the carrier gas

As in all SSP processes, mass transfer phenomena also affect the PET reactions in the solid state, where the main volatile by-products are ethylene glycol, diethylene glycol, acetaldehyde, and water. The rate of polycondensation can thus be limited by the rates of by-product removal, which depends on the diffusion coefficients within the polymer phase and on mass transfer coefficients from the particle surface to ambient atmosphere.

There is extensive literature on the investigation of rate-controlling steps of SSP of PET. Most published studies regard them as models and analyze the diffusion phenomena inside the polymer particles,[9,69–81] neglecting mass transfer limitations on the particle surface, which can be associated with the properties of the gas phase. However, the proper understanding of the resistance of gas-side by-product to mass transfer may be of significant commercial importance in the PET business. Most PET plants perform closed-loop recycling of the gas phase, usually nitrogen, and even after gas purification, it may still contain small amounts of contaminant volatiles, such as water.

In particular, the presence of water can be detrimental to the quality of the SSP product. As pointed out by Whitehead,[82] the hydrolytic degradation of PET causes a loss of IV, an increase in the carboxyl content, a change of color, etc., even at postreaction stages, such as granulation, spinning, drying, and storage. PET studies performed in humid environment also reported the plasticizing role of water,[83–85] which leads to reduction of the glass transition temperature,[85] decrease in the mechanical performance,[85] swelling of the resin,[82] and modification of the resin morphology.[83]

Therefore, in a recent paper of Filgueiras *et al.*,[86] the effects caused by variable water vapor content of the carrier gas (0–8 wt.%) on the course of the SSP of PET were analyzed, with emphasis on the IV. When humid nitrogen was used as the carrier gas, its water content exerted a pronounced effect on the course of the polymerization and on the final properties of the obtained polymer (**Figure 14**). The effects were more pronounced when the water content of the carrier gas, the reaction temperature, and the reaction time increased, indicating that the observed effects can be explained in terms of the

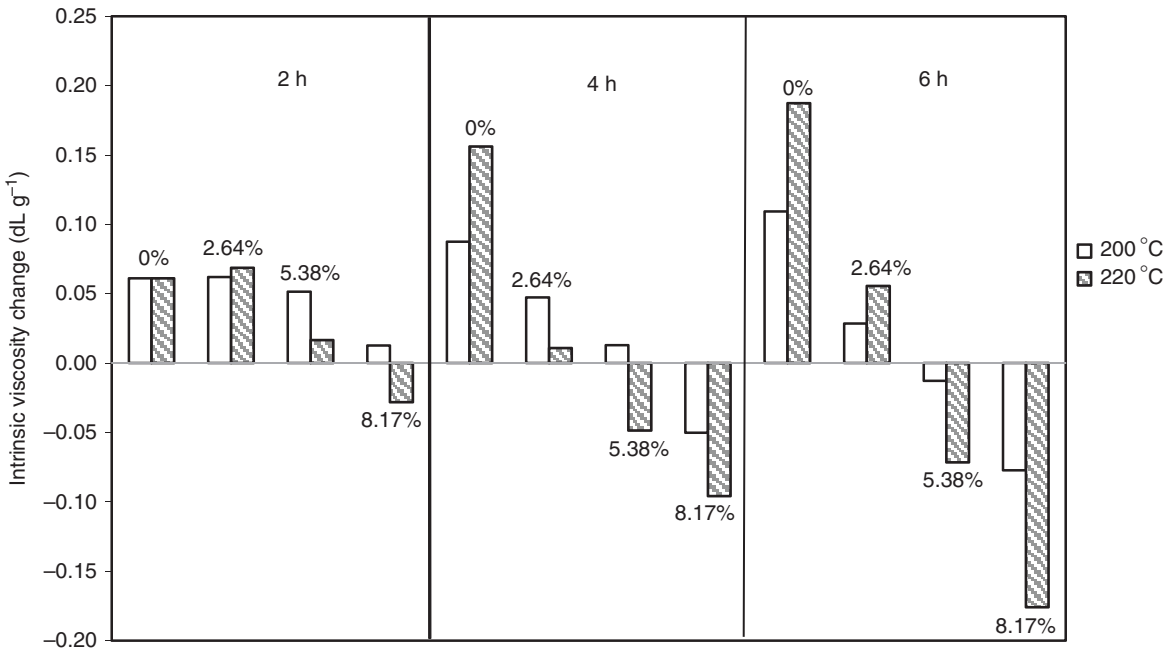

Figure 14 Intrinsic viscosity change ($\Delta IV = IV_t - IV_0$) as a function of the reaction time, reaction temperature, and water content during SSP of PET. From Filgueiras, V.; Vouyiouka, S.; Papaspyrides, C.; *et al. Macromol. Mater. Eng.* **2011**, *296*, 113–121,[86] by permission of John Wiley & Sons, Inc.

degradative reaction steps, specifically related to the hydrolysis of the ester groups. In particular, when the water content was equal to or higher than 2.64 wt.%, the solid-state polymerization of amorphous PET pellets did not lead to any significant increase in the intrinsic viscosities of the final products. On the contrary, it resulted in products with reduced MW compared with the initial value.

4.34.3.2.2 The role of crystallization

On industrial scale, cold crystallization usually precedes SSP of PET, in order to avoid sticking or sintering of prepolymer particles. Obviously, crystallization also takes place during SSP, since particles are heated at temperatures higher than glass transition (T_g); however, the crystallinity of the SSP product (preform) designated for bottle applications should be kept low, as higher T_m values lead to higher injection molding temperatures and higher acetaldehyde contents in the preforms.[68]

Existing literature focuses primarily on the crystallinity degree and crystallizability of the final SSP product of PET or PET grades produced through long reaction times. In other words, the evolution of these properties at early stages of SSP, where the main crystallization phenomena are anticipated to occur, is neglected. The reported crystallinity values (x_c) range from 25 to 67 wt.% for number-average MWs ($\overline{M_n}$) up to 50 000, SSP temperatures ranging from 180 to 245 °C and reaction times up to 20 h (**Table 2**). It is also interesting to note that different dynamic x_c trajectories have been reported during the SSP: x_c has been found to remain constant,[75] increasing significantly in the first few hours of the reaction before final stabilization [8,87] and even decreasing during the SSP.[88] The distinct x_c behavior has been attributed to different reaction parameters, such as the used catalysts, the presence of contaminants, and the thermal history of the prepolymer, among others.[57]

On the other hand, a part of the literature on SSP of PET focuses on the effects of initial and increasing polymer crystallinity on the observed reaction rates.[89,90] First, the increase in crystallinity leads to higher concentration of end-groups in the amorphous phase and thus to an increase in the reaction rate.[9,76] On the other hand, the mobility of polymer chains is believed to decrease with the degree of crystallinity,[91] which can lead to simultaneous reduction of reaction rates and removal of by-products from the reacting mass.[92] Duh[87] reviewed the works in the field and highlighted that SSP rates can increase with the degree of crystallinity at 220 °C in both pellets and powder, due to an increase in the concentration of active end-groups in the amorphous phase.

In a recent paper,[93] the evolution of crystal morphology and polymer crystallinity was investigated during the initial SSP stages (0–2 h) under typical reaction conditions (180–230 °C, nitrogen flow). Short reaction times were selected in order to minimize the effects of MW buildup on the crystallization process even at low SSP temperatures and to distinguish between primary and secondary crystal formation. The pertinent work resulted in multiple melting behavior for most SSP grades (**Figure 15**), where low melting peaks were attributed to secondary crystallization (SC) occurring since the early stages of crystal growth.

The size and shape of secondary crystals was found to be strongly dependent on SSP temperature: at low temperature, SC rates were low and low-melting secondary crystals were formed. At higher SSP temperatures, SC was accelerated due to enhanced segmental mobility, leading to thickening and larger amounts of pertinent crystals and change of the behavior from two to one melting endotherm. This observed melting behavior of PET samples was also correlated with the attained

Table 2 The effect of conditions of SSP of PET on crystallinity (x_c) and number-average MWs ($\overline{M_n}$)

References	SSP conditions	x_c (%)	$\overline{M_n}$
89[a]	230 °C		
	20 h	0.63	19 800
75	215–245 °C		
	12 h	0.42[b]	
8[a]	12 h		
	180 °C	0.42[b]	21 900
	190 °C	0.43[b]	25 800
	200 °C	0.44[b]	29 400
	210 °C	0.46[b]	32 600
	220 °C	0.53[b]	38 200
	230 °C	0.57[b]	46 000
87[a]	220 °C	0.57[b]	40 600
	20 h	0.59[b]	42 300
		0.62[b]	45 300
		0.67[b]	48 400
57	230 °C		
	0 h	0.34[c]	14 400
	4 h	0.31[c]	20 000
	10 h	0.30[c]	22 900
	20 h	0.25[c]	24 600

[a] Estimation is based on figures.
[b] Volume fraction crystallinity (x_v) was converted to mass fraction crystallinity (x_c) through the formula x_c $x_c = \left(\frac{\rho_c \rho_a}{\rho} - \rho_c\right)/(\rho_a - \rho)$, where ρ is the polymer density (g cm^{-3}), $\rho_c = 1.455$ g cm^{-3} the density of the crystalline phase, and ρ_a=1.355 g cm^{-3} the density of the amorphous phase.
[c] $\Delta H_0 = 135$ J g^{-1}.[73]

MWs: the higher the MW of PET, the greater the rejection of chain sections in interlamellar regions. This rejection lead to larger secondary nucleation sites and supported the SC model, which involved the formation of an intermediate crystalline structure in-between two parent crystals.[94]

The SSP time also exerted a positive effect on solid-phase perfection of secondary crystals. An empirical equation for melting point assessment as a function of SSP time and temperature was successfully constructed and applied (eqn [12]). It can be used to control the melting point of the SSP products at plant site, for the benefit of subsequent processing stages:

$$T_m = 0.10 \times t + 2544.27 \times \exp\left(\frac{-9845.44}{RT}\right) \qquad [12]$$

where T_m is the melting point due to SC (°C), T the SSP temperature (K), t the SSP time (min), and R the universal gas constant (J mol^{-1} K^{-1}).

4.34.3.2.3 The role of contaminants: recycling

SSP serves as a recycling technique for PET packaging materials, such as bottles and films.[95–97] In particular, both the processing of virgin pellets to PET bottles and the remelting of used bottle flakes are accompanied by reductions in IV, coloration, and formation of by-products, such as acetaldehyde, diethylene glycol, vinyl end-groups, and excess acid end-groups. PET bottle flakes can be subjected to SSP for upgrading IV and achieving acceptable quality in terms of color, lower acetaldehyde, and absence of contaminants. The recycling involves collection of the used PET bottles, crushing into flakes, sorting, and washing. Then, the flakes may be directly subjected to crystallization and SSP, or be melted and pelletized prior to crystallization and SSP. While the former process offers the advantage of a fast SSP rate, eliminates melting/pelletizing, and the associated costs and polymer degradation, the latter process employs melt filtration to reduce contamination, reduces the SSP equipment size (lower bulk of pellets), and reduces the heterogeneity in the final product.

It should be emphasized that despite a MW increase, SSP also serves as a highly efficient decontamination technique in PET bottle recycling industry.[98,99] More specifically, decontamination is the removal of all possible alien chemical substances (contaminants) that have penetrated into bottle wall through diffusion during the service life and waste disposal. This removal is an indispensable step in PET recycling because of (a) a variety of contaminants derived from the introduction of PET material to nearly all kinds of commonly used liquids, such as edible oil, household chemicals, detergents, and health-care products, and (b) the required

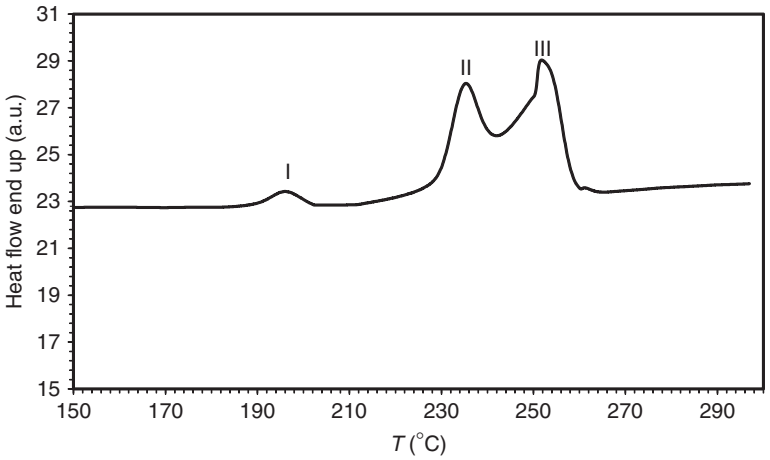

Figure 15 Typical DSC scan of PET presenting multiple melting behavior (endotherms I–III).

high food-grade purity when the recycled material is designated to be used in packaging applications.

Especially for the direct food contact applications, PET grade should meet strict requirements issued by Food and Drug Administration (FDA), for example, the limit of migration to the foodstuff packed in recycled PET is < 0.5 ppb. There is a wide range of relevant decontamination techniques, while the solid-state treatments, such as crystallization, drying, and SSP, belong to the most efficient ones. They are used to efficiently remove volatile substances from the recycled material, for example, acetaldehyde to trace concentration of < 1 ppm, with typical SSP temperatures for contaminant removal at 190–220 °C under vacuum (1 mbar) or using nitrogen flow along with high residence times (6–12 h).

In the industrial recycling practice, SSP is usually applied in combination with other decontamination techniques, such as vacuum extrusion, supercritical extraction, and vacuum melt polymerization. An example is the Buhler's bottle-to-bottle recycling, which involves in-house or market PET flakes, melt decontamination via vacuum extrusion, pellet crystallization and then their SSP. Another example is the Kornes process, which involves bottle sorting by mass spectroscopy, washing, and SSP of the flakes.[98]

Finally, the effectiveness of decontamination and validation of industrial recycling processes is achieved through the 'challenge test' procedure,[100] specified by FDA. A large number of possible contaminants are simulated through selection of chemical substances covering the following descriptions: (1) a volatile, nonpolar organic substance, (2) a volatile, polar organic substance, (3) a nonvolatile, nonpolar substance, and (4) a nonvolatile, polar organic substance. A substantial amount of test flakes is contaminated with a cocktail of the selected chemicals: the flakes and a surrogate cocktail blend are stored at 40 °C for 2 weeks under frequent agitation. After this treatment, the surrogate cocktail is separated, the flakes are rinsed with clean water, centrifuged, and then they are ready to be used in the decontamination test, determining which trace analysis of the contaminants is conducted.

4.34.3.3 Poly(lactic acid)

PLA is a semicrystalline biodegradable aliphatic PES that can be obtained from renewable resources. PLA has a glass transition temperature between 50 and 80 °C and a melting temperature between 170 and 180 °C depending on the amount of residual monomer. It is expected to have wide applications because of its excellent mechanical and biodegradable properties, as well as its adjustable hydrolyzability.[101]

The synthesis of high-molecular-weight PLA is generally carried out by the ring-opening polymerization of lactide or by direct polycondensation of lactic acid. Tin-based catalysts are typically used in both cases, either alone or in combination with *p*-toluenesulfonic acid.[102]

In the methods using lactide, the final product of the melt polymerization usually contains a certain amount of the cyclic monomer, which increases with polymerization temperature. This residual lactide has been known to deteriorate mechanical properties of the polymer to cause corrosion of the processing machines and to increase the degradation rate of PLA. Solid-state polymerization has been applied to PLA as a method for monomer removal, considering that during SSP, crystallization also occurs, which may result in excluding reactive ends and monomer in the amorphous regions, thus reaching polymerization conversion to 100%.[103] In the pertinent study, a two-step method and a one-step method were carried out in the presence of stannous 2-ethylhexanoate (octoate) as catalyst. In the former technique, melt polymerization of lactide was first performed at 140 and 170 °C for 1 h and then the postpolymerization continued for 9 h at the crystallization temperature of PLA, which was predetermined by DSC to be 120–140 °C. Optimum reaction conditions were found for the two stages in order to obtain crystalline PLA free of monomer. In the one-step process, a mixture of monomer and catalyst was subjected to polymerization at a constant temperature around the crystallization point of PLA to allow the system to transform into the solid state during the reaction. Indeed, this was achieved at temperatures up to 140 °C, while a further increase did not induce crystallization and monomer conversion. In both techniques, however, the MW of PLA did not increase due to the ester interchange reactions and the formation of oligomers.

A two-step method was also applied to the direct polycondensation of lactic acid,[104,105] where again a ring-chain equilibrium with the formation of cyclic monomer can occur and may reduce the product yield during the melt polymerization. In the pertinent studies, a binary catalyst system comprising tin dichloride hydrate and *p*-toluenesulfonic acid was used in a process comprising melt polymerization, prepolymer crystallization, and the solid-state polymerization. In particular, melt polycondensation was performed at 180 °C for 5 h, crystallization at 105 °C for 1 or 2 h, and SSP at 140 or 150 °C for 10–30 h. The suggested route resulted in high MW, above 500 000, and again crystallization of the prepolymer was a key process step and the crystallinity of the PLA product was well correlated with the increase in the MW.

Regarding the MW, the effect of crystallization on the SSP of PLA has been investigated when the starting form was lactic acid.[106] In particular, the crystallization temperature was set at 105 °C for various times (15–90 min) and SSP was then performed *in vacuo* at 135 °C for 15–50 h. The optimum conditions for a prepolymer of MW 18 000 were found, namely a crystallization time of 30 min at 105 °C and then the solid-state polymerization at 135 °C for 35 h. Higher crystallization times for the prepolymer had a negative effect on the SSP rate due to the formation of large crystals and thus to the higher limitation to by-product diffusion. On the other hand, higher SSP times were detrimental to MW due to the occurrence of degradation reactions.

Finally, in a very recent publication, PLA nanocomposites have been prepared through solid-state polymerization.[107] A prepolymer was first synthesized from both lactic acid and lactide in the presence of different organoclays and SSP followed. In the former case, a MW of 138 000 was reached after 10 h of SSP at 150 °C, while the presence of hydroxy groups in the organoclay modification inhibited a MW increase due to prepolymer end-groups binding to clay surface. When using lactide, an lactide–clay intercalated mixture was prepared by ring-opening polymerization and MW was further increased to 127 000 through SSP.

4.34.4 Conclusions

SSP processes are widely used in the production of PAs and PESs, in order to increase the degree of polymerization and to improve the quality of the end product. Recycling purposes are also highlighted, according to which SSP serves as an efficient decontamination technique in order to prepare food contact polymer. The most important commercial advantages of SSP focus on the use of easy and inexpensive equipment and on avoiding some of the drawbacks of conventional polymerization processes. This chapter provides insight into the prevailing mechanisms in direct SSP and post-SSP, focusing on two of the most commercially important condensation polymers, that is, PA 66 and PET, as well as on PLA, which is widely considered as a very promising bioplastic.

References

1. Flory, P. *Polymerization Process (E.I. Du Pont de Nemours and Company).* U.S. Patent 2,172,374, 1939.
2. Monroe, G. *Solid Phase Polymerisation of Polyamides (E.I. Du Pont de Nemours and Company).* U.S. Patent 3,031,433, **1962**.
3. Papaspyrides, C. In *The Polymeric Materials Encyclopedia*; Salamone, J. C., Ed.; CRC Press: Boca Raton, FL, 1996; pp 7819–7831.
4. Vouyiouka, S.; Karakatsani, E.; Papaspyrides, C. *Prog. Polym. Sci.* **2005**, *30*, 10–37.
5. Papaspyrides, C.; Vouyiouka, S. In *Solid State Polymerization*; Papaspyrides, C., Vouyiouka, S., Eds.; John Wiley & Sons: Hoboken, NJ, 2009.
6. Kampouris, E.; Papaspyrides, C. *Polymer* **1985**, *26*, 413–417.
7. Papaspyrides, C. *Polymer* **1988**, *29*, 114–117.
8. Kim, T.; Lofgren, E.; Jabarin, S.. *J. Appl. Polym. Sci.* **2003**, *89*, 197–212.
9. Ravindranath, K.; Mashelkar, R.*J. Appl. Polym. Sci.* **1990**, *39*, 1325–1345.
10. Grabar, D.; Hsia, C.; Catherine, S. *J. Polym. Sci. C* **1963**, *3*, 105–107.
11. Frayer, P.; Lando, J. *Mol. Cryst. Liq. Cryst. A* **1969**, *A1*, 465–483.
12. Papaspyrides, C. *Polym. Int.* **1992**, *29*, 293–298.
13. Katsikopoulos, P.; Papaspyrides, C. *J. Polym. Sci. A Polym. Chem.* **1994**, *32*, 451–456.
14. Papaspyrides, C. *Polymer* **1990**, *31*, 490–495.
15. Papaspyrides, C.; Kampouris, E. *Polymer* **1984**, *25*, 791–796.
16. Ikawa, T. In *The Polymeric Materials Encyclopedia*; Salamone, J. C., Ed.; CRC Press: Boca Raton, FL, 1996; Vol. 6, pp 4689–4694.
17. Ikawa, T. In *Solid State Polymerization*; Papaspyrides, C., Vouyiouka, S., Eds.; John Wiley & Sons: Hoboken, NJ, 2009; Chapter 6.
18. Volokhina, A.; Kudryavtsev, G.; Skuratov, S.; Bonetskaya, A. *J. Polym. Sci.* **1961**, *53*, 289–294.
19. Bagramyants, B.; Bonetskaya, A.; Enikolopyan, N.; Skuratov, S. *Vysokomol. Soedin.* **1966**, *8*, 1594–1598.
20. Khripkov, E.; Kharitonov, V.; Kudryavtsev, G. *Khim. Volokna* **1970**, *6*, 63–65.
21. Korshak, V.; Frunze, T. *Synthetic Hetero-Chain Polyamides*; IPST: Jerusalem, **1964***; pp 90–95, 119, 128.*
22. Papaspyrides, C.; Vouyiouka, S.; Bletsos, I. *Polymer* **2006**, *47*, 1020–1027.
23. Oya, S.; Tomioka, M.; Araki, T. *Kobunshi Kagaku* **1966**, *23*, 415–421.
24. Volokhina, A.; Kudryavtsev, G.; Raeva, M.; *et al. Khim. Volokna* **1964**, *6*, 30–33.
25. Kosinski, L.; Soelch, R. *Low Temperature Nylon Polymerization Process.* U.S. Patent 5,403,910, **1995**.
26. Wiloth, F. *Solid State Preparation of Polyamides.* U.S. Patent 3,379,696, **1968**.
27. Zeng, H.; Feng, L. *Gaofenzi Tongxun* **1983**, *5*, 321–327.
28. Tynan, D.; Papaspyrides, C.; Bletsos, I. *Polymer Mixing and Apparatus.* U.S. Patent 5,941,634, **1999**.
29. Papaspyrides, C.; Vouyiouka, S.; Bletsos, I. *J. Appl. Polym. Sci.* **2004**, *92*, 301–306.
30. Zimmerman, J.; Nylon, K. M. *J. Polym. Sci. A Polym. Chem.* **2001**, *39*, 2565–2570.
31. Zimmerman, J. *J. Polym. Sci. B Polym. Lett.* **1964**, *2*, 955–958.
32. Dujari, R.; Cramer, G.; Marks, D. *Method for Solid Phase Polymerization (E.I. Du Pont de Nemours and Company).* WO Patent 98/23666, 1998.
33. Heinz, H.; Schulte, H.; Buysch, H. *Process for the Manufacture of High Molecular Weight Polyamides (Bayer AG).* EP Patent 410,230/91 A2, 1991.
34. Shimizu, K.; Ise, S. *Polyhexamethyleneadipamide with Restricted Three-Dimensional Formation and Process for the Manufacture (Asahi Chemical Industry Ltd.).* JP Patent 4-93323, 1992.
35. Gaymans, R.; Sikkema, D. In *The Comprehensive Polymer Science*; Eastmon G, Ledwith A, Russo S, Sigwalt P, Ed.; Pergamon Press: Oxford, 1989; Vol. 5, pp 357–373.
36. Gaymans, R.; Van Utteren, T.; Van Den Berg, J.; Schuyer, J. *J. Polym. Sci. Polym. Chem. Ed.* **1977**, *15*, 537–545.
37. Vouyiouka, S.; Papaspyrides, C.; Weber, J.; Marks, D. *J. Appl. Polym. Sci.* **2005**, *97*, 671–681.
38. Vouyiouka, S.; Papaspyrides, C.; Weber, J.; Marks, D. *Polymer* **2007**, *48* (17), 4982–4989.
39. Po, R. In *The Polymeric Materials Encyclopedia*; Salamone, J. C., Ed.; CRC Press: Boca Raton, FL, 1996, pp 6100–6106.
40. Muller, H.; Rossbach, V. *Text Res. J.* **1977**, *47*, 44–51.
41. Flamand, C.; Pensacolz, F. *Basic Dyeable Acid Dye Resistive Polyamides Containing Terminal Aryl Disulfonated Groups (Monsanto Company).* U.S. Patent 3,542,743, 1970.
42. Studholme, M. *Acid Dye Stain-Resistant Fiber-Forming Polyamide Composition Containing Masterbatch Concentrate, Containing Reagent and Carrier (Prisma Fibers).* U.S. Patent 6,117,550, 2000.
43. Caldwell, J. *Sulfonated Polyamides (Eastman Kodak Company).* U.S. Patent 3,296,204, 1967.
44. Eisenberg, A.; Hird, B.; Moore, R. *Macromolecules* **1990**, *23*, 4098–4107.
45. Vouyiouka, S.; Papaspyrides, C. In Solid State Polymerization; Papaspyrides, C.; Vouyiouka, S., Eds.; John Wiley & Sons: Hoboken, NJ, 2009.
46. Vouyiouka, S.; Papaspyrides, C.; Pfaendner, R. *Macromol. Mater. Eng.* **2006**, *291*, 1503–1512.
47. Pfaendner, R.; Fink, J.; Simon, D.; et al. *Process for the Preparation of Polyamides in the Presence of a Phosphonate (Ciba Specialty Chemicals, Lampertheim GmbH).* WO2007/006647, 2007.
48. Duh, B. *Polymer* **2002**, *43*, 3147–3154.
49. Boussia, A.; Konstantakopoulou, M.; Vouyiouka, S.; Papaspyrides, C. *J. Appl. Polym. Sci.*, submitted
50. Brignac, E.P.; Duke, B.H.; Nunning, W.J.; Snook, R. J. *Method for Spinning Polyamide Yarn of Increased Relative Viscosity.* U.S. Patent 5,116,919, 1992.
51. Ogata, N.; Tanaka, H. *Polym. J.* **1971**, *2*, 672–674.
52. Yamazaki, N.; Higashi, F. *Tetrahedron* **1974**, *30*, 1323–1326.
53. Yamazaki, N.; Matsumoto, M.; Higashi, G. *J. Polym. Sci. Polym. Chem. Ed.* **1975**, *13*, 1373–1380.
54. Aharoni, S.; Hammond, W.; Szobota, J.; Masilamani, D. *J. Polym. Sci. Polym. Chem. Ed.* **1984**, *22*, 2567–2577.
55. Aharoni, S.; Hammond, W.; Szobota, J.; Masilamani, D. *J. Polym. Sci. Polym. Chem. Ed.* **1984**, *22*, 2579–2599.
56. Aharoni, S. *Int. J. Polym. Mater.* **1994**, *26*: 9–17.
57. Yu, H.; Han, K.; Yu, M. *J. Appl. Polym. Sci.* **2004**, *94*, 971–976.
58. Bikiaris, D.; Achilias, D.; Giliopoulos, D.; Karayannidis, G. *Eur. Polym. J.* **2006**, *42*, 3190–3201.
59. Bikiaris, D.; Karavelidis, V.; Karayannidis, G. *Macromol. Rapid Commun.* **2006**, *27*, 1199–1205.
60. Achilias, D.; Bikiaris, K. V.; Karayannidis, G. *Eur. Polym. J.* **2008**, *44*, 3096–3107.
61. Boussia, A.; Vouyiouka, S.; Papaspyrides, C. *Macromol. Mater. Eng*, submitted.
62. Boussia, A.; Konstantakopoulou, M.; Vouyiouka, S.; Papaspyrides, C. *Macromol. Mater. Eng.* **2011**, *296*, 168–177.
63. Wan, C.; Bao, X.; Zhao, F.; *et al. J. Appl. Polym. Sci.* **2008**, *110*, 550–557.
64. Park, C.; Smith, J.; Connell, J.; *et al. Polymer* **2005**, *46*, 9694–9701.
65. Lambert, J. *Origins Life Evol. Biosphere* **2008**, *38*, 211–242.
66. Bujdak, J.; Rode, B. *J. Mol. Evol.* **1997**, *45*, 457–466.
67. White, D.; Kennedy, R.; Macklin, J. *Origins Life* **1984**, *14*, 273–278.
68. Bashir, Z.; Al-Aloush, I.; Al-Raqibah, I.; Ibrahim, M. *Polym. Eng. Sci.* **2000**, *40*: 2442–2455.
69. Chang, T. *Polym. Eng. Sci.* **1970**, *10*: 364–368.
70. Chen, S.; Chen, F. *J. Polym. Sci A Polym. Chem.* **1987**, *25*, 533–549.
71. Devotta, I.; Maskelkar, R. *Chem. Eng. Sci.* **1993**, *48*, 1859–1867.
72. Yoon, K.; Kwon, M.; Jeon, M.; Park, O. *Polym. J.* **1993**, *25*, 219–226.
73. Zhi-Lian, T.; Gao, Q.; Nan-Xun, H.; Sironi, C. *J. Appl. Polym. Sci.* **1995**, *57*, 473–485.
74. Gao, Q.; Nan-Xun, H.; Zhi-Lian, T.; Gerking, L. *Chem. Eng. Sci.* **1997**, *52*, 371–376.
75. Wu, D.; Chen, F.; Li, R.; Shi, Y. *Macromolecules.* **1997**, *30*, 6737–6742.
76. Mallon, F.; Ray, W. *J. Appl. Polym. Sci.* **1998**, *69*, 1233–1250.
77. Kang, C. *J. Appl. Polym. Sci.* **1998**, *68*, 837–846.
78. Wang, X.; Deng, D. *J. Appl. Polym. Sci.* **2002**, *83*, 3133–3144.

79. Kim, T.; Jabarin, S. *J. Appl. Polym. Sci.* **2003**, *89*, 213–227.
80. Lee, E.; Yeo, Y.; Choi, K.; Kim, H. *J. Chem. Eng. Jpn.* **2003**, *36*, 912–925.
81. Goodner, M.; DeSimone, J.; Kiserow, D.; Roberts, G. *Ind. Eng. Chem. Res.* **2000**, *39*, 2797–2806.
82. Whitehead, B. *Ind. Eng. Chem. Process. Des. Dev.* **1977**, *6*, 341–346.
83. Lapkovskii, V.; Geller, Y.; Geller, B. *Fibre Chem.* **2006**, *38*, 7–12.
84. Toi, K. *J. Polym. Sci. Polym. Phys. Ed.* **1973**, *11*, 1829–1839.
85. Ishisaka, A.; Kawagoe, M. *J. Appl. Polym. Sci.* **2004**, *93*, 560–567.
86. Filgueiras, V.; Vouyiouka, S.; Papaspyrides, C.; *et al. Macromol. Mater. Eng.* **2011**, *296*, 113–121.
87. Duh, B. *J. Appl. Polym. Sci.* **2006**, *102*, 623–632.
88. Jabarin, S. *J. Appl. Polym. Sci.* **1987**, *34*, 85–96.
89. James, N.; Ramesh, C.; Sivaram, S. *Macromol. Chem. Phys.* **2001**, *202*, 1200–1206.
90. Medellin-Rodriguez, F.; Lopez-Guillen, R.; Waldo-Mendoza, M. *J. Appl. Polym. Sci.* **2000**, *75*, 78–86.
91. Fakirov, S.; Avramova, N. *Acta Polym.* **1982**, *33*, 271–275.
92. Li, L.; Huang, N.; Liu, Z.; *et al. Polym. Adv. Technol.* **2000**, *11*, 242–249.
93. Vouyiouka, S.; Filgueiras, V.; Papaspyrides, C.; *et al. J. Appl. Polym. Sci.*, submitted.
94. Medellin-Rodriguez, F.; Phillips, P.; Lin, J.; Campos, R. *J. Polym. Sci. B Polym. Phys.* **1997**, *35*, 1757–1774.
95. Wadekar, S.; Agarwal, U.; Boon, W.; Nadkarni, V. In *Solid State Polymerization*; Papaspyrides, C., Vouyiouka, S., Eds.; John Wiley & Sons: Hoboken, NJ, 2009; Chapter 8.
96. Cruz, S.; Zanin, M. *J. Appl. Polym. Sci.* **2006**, *99*, 2117–2123.
97. Karayannidis, G.; Kokkalas, D.; Bikiaris, D. *J. Appl. Polym. Sci.* **1993**, *50*, 2135–2142.
98. Thiele, U. *4th China International Recycled Polyester Fiber Market & Tech Forum Sept. 2008*; Hangzhou, China.
99. http://www.buhlergroup.com/global/downloads/Bottle_to_Bottle_Recycling_PD.pdf
100. Papaspyrides, C.; Voultzatis, Y.; Pavlidou, S.; *et al. Prog. Rubber Plast. Recycling Technol.* **2005**, *21*, 243–260.
101. Pilati, F.; Toselli, M. In *Solid State Polymerization*; Papaspyrides, C., Vouyiouka, S., Eds.; John Wiley & Sons: Hoboken, NJ, 2009; Chapter 3.
102. Maharana, T.; Mohanty, B.; Negi, Y. *Prog. Polym. Sci.* **2009**, *34*, 99–124.
103. Shinno, K.; Miyamoto, M.; Kimura, Y.; *et al. Macromolecules* **1997**, *30*, 6438–6444.
104. Moon, S.; Lee, C.; Taniguchi, I.; *et al. Polymer* **2001**, *42*, 5059–5062.
105. Moon, S.; Taniguchi, I.; Miyamoto, M.; *et al. High Perform. Polym.* **2001**, *13*, 189–196.
106. Xu, H.; Luo, M.; Yu, M.; *et al. J. Macromol. Sci. B Phys.* **2006**, *45*, 681–687.
107. Katiyar, V.; Nanavati, H. *Polym. Compos.* **2011**, *32*, 497–509.

Biographical Sketches

STAMATINA N. VOUYIOUKA is elected Lecturer in the School of Chemical Engineering at the National Technical University of Athens, Greece. She has been a research fellow in the "Plastic Additives Segment, Polymer Design" of Ciba Specialty Chemicals Lampertheim GmbH (Lampertheim, Germany). Her activity is documented in a number of papers published in Scientific Journals and presented in International and National Conferences. She is the joint editor (with Prof. C.D. Papaspyrides) of the book titled "Solid State Polymerization", which was published by John Wiley & Sons, Inc., in 2009.

CONSTANTINE (COSTAS) D. PAPASPYRIDES is Professor and Director of the Laboratory of Polymer Technology in the School of Chemical Engineering at the National Technical University of Athens, Greece. He has been President and Vice-President of the School and Visiting Professor/Consultant in Massachusetts Institute of Technology (MIT), Eidgenoessische Technische Hochschule Zuerich (ETH), E.I. du Pont de Nemours & Company, Inc. / Invista, Inc., and CIBA Lampertheim GmbH. He serves on the editorial board of International Editions on Polymers and he holds over 250 refereed publications in International Scientific Journals, presentations in International Scientific Events and US Patents with Industry. Recent Publications include also a book on "Solid State Polymerization" (C. D. Papaspyrides, S. N. Vouyiouka, Editors. John Wiley & Sons, 2009).

4.35 Radical Polymerization at High Pressure

S Beuermann, University of Potsdam, Potsdam/Golm, Germany
M Buback, Georg-August-Universität Göttingen, Göttingen, Germany

4.35.1 Introduction

Radical polymerizations are carried out on a technical scale at pressures up to about 3000 bar and temperatures up to 300 °C. Approximately 20 million tons of low-density polyethylene (LDPE) are produced worldwide per year. The continued interest in high-pressure ethene polymerization is due to the enormous flexibility of this reaction, which proceeds under supercritical (sc) conditions with respect to the monomer. Illustrated in Figure 1 is the continuous variation in density that may be achieved above the critical temperature T_c. The density of the symbols reflects the mass density of the fluid. As polymerization and polymer properties are determined by the properties of the reaction medium, polymerization in sc fluid phase allows for widely tuning polymerization rate and polymer properties by varying p and T. Further advantages of polymerization in the sc range consist in the tunability of solvent properties such that homogeneity is achieved for reaction and two-phase behavior may be selected for product separation. Moreover, heat and mass transfer processes are very efficient under sc conditions. Because of these many favorable aspects, high-pressure ethene polymerization, with T_c of ethene being at 9.5 °C, may be looked upon as the archetype of sc fluid-phase processes. The special signature of ethene high-pressure polymerization is that the monomer acts as both reactant and tunable sc fluid medium.

In order to fully exploit this tuning potential and also to adequately describe these high-pressure polymerizations, simulations of both monomer conversion and product properties are required. Modeling studies have been performed chiefly by the groups of Hamielec,[2] Villermaux,[3,4] Luft,[5,6] and Kiparissides.[7] It has become clear that restrictions for these simulations mainly result from the limited availability of reliable kinetic data. As is to be expected, the situation is even worse with kinetic data for copolymerization processes. Kinetic studies into high-pressure ethene polymerization have been pioneered by Ehrlich and his group[8] and by Thies and Schoenemann,[9] Szabo *et al.*,[10] Feucht *et al.*[11] The earlier work was mainly concerned with studies on overall polymerization rate.

With the exception of very few data at small degrees of monomer conversion,[12,13] individual rate coefficients of propagation k_p and termination k_t have not been reported as a function of pressure, temperature, and monomer conversion. In addition to k_p and k_t, transfer rates to monomer and to polymer, β-scission rates, and initiator decomposition rates as well as initiator efficiencies are required for the simulation of ethene homopolymerization. The lack of kinetic information is no signature of high-pressure polymerizations. Even for ambient pressure and moderate temperatures, k_p and k_t data of some common monomers are fairly uncertain. This situation has significantly improved upon introducing pulsed lasers as a powerful tool for precise and detailed analysis of free-radical polymerization kinetics. The accurate determination on the basis of pulse laser experiments for ethene polymerization has been pioneered by Schweer.[14] A large body of information on propagation and termination rate coefficients at high pressure has emerged from the investigations that use laser pulse initiation in conjunction with analysis of the molecular mass distribution (MMD) of the so-produced polymer and with highly time-resolved detection of the monomer conversion induced by a laser single pulse (SP), respectively. These methods have also been applied to high-pressure polymerizations of acrylates, methacrylates, styrene, and a few other monomers.[15]

It comes as no surprise that attempts have been made to use the benefits of tuning reaction conditions on a broader scale also for monomers that are below their critical temperature at typical

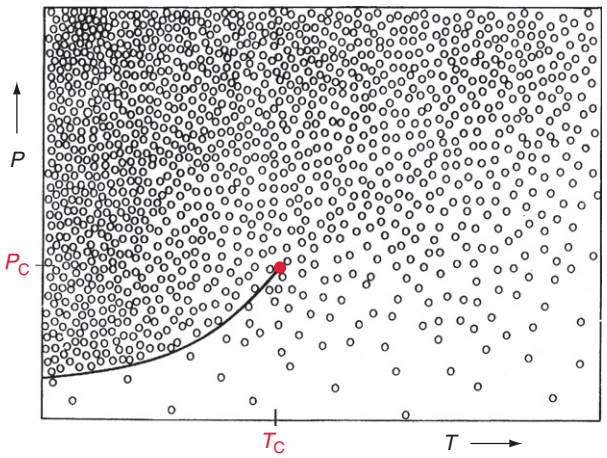

Figure 1 *P–T* diagram of a pure fluid. The full line represents the vapor pressure curve, which extends up to the critical point with critical temperature T_c and critical pressure p_c. Above the critical temperature, the density of the medium may be continuously tuned between gas-like and liquid-like densities. From Buback, M. *Angew. Chem. Int. Ed. Engl.* **1991**, *30*, 641.[1]

polymerization conditions. To achieve fluid-phase behavior, a wide range of monomers have been polymerized in $scCO_2$, mostly as dispersion polymerizations, but also as reactions in homogeneous solution.[16–21] The particular advantages of CO_2 are associated with a pronounced lowering of viscosity, with the ease by which this solvent may be separated from the polymeric product and with the inertness of CO_2 that includes the absence of chain-transfer-to-solvent reactions.[22] The nontoxicity of CO_2 and its easy removal resulted in studies on the synthesis of polymers for medical applications.[23] Further, $scCO_2$ is a comparably good solvent for fluoropolymers,[24,25] which are insoluble in most common organic solvents. Thus, $scCO_2$ is an attractive alternative to reaction in emulsion with fluorinated stabilizers or in fluorinated solvents. The methods of controlled radical polymerizations that allow for tailoring polymer architectures were applied to polymerizations in $scCO_2$ in heterogeneous[17,26] and homogeneous phases.[27] Moreover, $scCO_2$ has a high potential for applications in polymer processing.[28] For example, the solutions of the polymeric product in $scCO_2$ may be directly used for the generation of well-defined particle size distributions.[29] For this purpose, techniques such as particles from gas-saturated solution (PGSS), rapid expansion from supercritical solution (RESS), or others may be applied.[30] The pressures used for polymerization in $scCO_2$ are typically around 300 bar and thus about 1 order of magnitude below those used for LDPE production.

Beyond the interest in identifying new high-pressure processes and improving existing ones, applying high pressure with polymerization reactions allows for providing mechanistic evidence and for deducing rate coefficients of the relevant steps of radical polymerization, for example, on initiation, propagation, termination, and chain transfer (CT). These rate coefficients are also of relevance for controlled/living polymerizations, which according to IUPAC nomenclature should be referred to as reversible deactivated polymerization.

The intention of this chapter is to present the current state of scientific analysis of the kinetics of high-pressure radical polymerization. In Section 4.35.2, techniques for measuring rate coefficients up to 3 kbar will be illustrated. In Section 4.35.3, selected examples of initiation, propagation, and termination rate coefficients obtained as a function of pressure for homopolymerizations will be presented. Section 4.35.4 addresses high-pressure ethene polymerization. Section 4.35.5 deals with ethene copolymerizations and Section 4.35.6 illustrates examples of reversible deactivated polymerization up to high pressure. In Section 4.35.7, the applicability of $scCO_2$ as a reaction medium for homogeneous-phase polymerizations of conventional nonfluorinated monomers and of fluoroolefins is demonstrated and in Section 4.35.8, the focus is on the polymerization kinetics in the presence of $scCO_2$.

4.35.2 Experiments and Data Treatment

Detailed studies on high-pressure polymerization kinetics require the measurement of concentrations under reaction conditions. Particularly, valuable insight comes from highly time-resolved measurements of monomer concentration after instantaneous laser-induced photoinitiator decomposition, which produces an intense burst of free radicals.

Quantitative in-line spectroscopic analysis of polymerization processes depends on the availability of autoclaves equipped with windows that are transparent to the probing light and, for pulsed laser-induced studies, also to excimer laser light. A survey of such optical cells for vibrational spectroscopic online measurements up to kilobar pressures is given elsewhere.[1,31]

Spectroscopy in the infrared (IR) and near-infrared (NIR) regions is particularly useful for quantitative analysis. The majority of fundamental vibrational modes together with overtones and combination modes of low-wavenumber fundamentals occur in the IR at wavenumbers from 400 to 4000 cm^{-1}, whereas the NIR range between 4000 and 14 000 cm^{-1} is exclusively due to overtone and combination modes. Other than expected, the NIR range is not overly crowded but consists of a limited number of bands that are first and second overtones or binary and tertiary combination modes of A–H vibrations, for example, of C–H, O–H, and N–H. The disadvantage of NIR spectroscopy for detecting a multitude of characteristic bands is more than compensated by the lower absorption cross section, which allows even pure materials to be measured at optical layer thicknesses of millimeters and centimeters. As a rule of thumb, the layer size may be increased by 1–2 orders of magnitude in passing from a first to a second overtone and from a second to a third overtone.

In addition to measuring concentrations at widely differing optical path lengths and thus reactor dimensions, advantage of the enormous decay of absorption cross section toward higher overtone and combination modes may also be taken by simultaneously measuring the IR and NIR ranges at fixed path length. Such measurements, for example, for the wavenumber range 2000–10 000 cm^{-1}, which may be routinely performed on a Fourier transform (FT) instrument within less than 1 s, enable quantitative analysis over a wide concentration range. Monomer and polymer concentrations may be accurately monitored during the entire course of a polymerization reaction from very low polymer contents, for example, of 50–100 ppm, to almost full conversion where polymer is ubiquitous and only small amounts of residual monomer are present. The low polymer content in the initial polymerization period and the low content of residual monomer at high

conversion are measured by IR, whereas the high concentrations of monomer, in the early polymerization period, and of polymer, in the final stage of the polymerization, are determined via a higher overtone mode. Using this strategy, of course, depends on the availability of characteristic IR and NIR modes for both monomer and polymer. The enormous dynamic range associated with the simultaneous measurement of IR and NIR regions also allows for measuring the very low concentrations of initiator and initiator-derived species in the presence of high monomer and polymer concentrations.[32] The aspects and procedures of IR/NIR quantitative spectroscopy on fluids at pressures up to 5 kbar and partly up to 7 kbar have been presented in quite some detail elsewhere.[1,31,33] Detailed surveys of optical high-pressure cells are also given in the books by Isaacs[34] and by Sherman and Stadtmuller.[35] Within the subsequent text, only a brief account of optical high-pressure cells and of miniplant devices for studies on high-pressure polymerization including reactions in $scCO_2$ will be given.

Shown in Figure 2 is a transmission-type cell for experiments up to 3500 bar and 350 °C. The probing light penetrates the cell along the cylindrical axis. Each of the two windows is mounted on a steel ram and sealed according to Bridgman's unsupported area principle. The rams are pressed against the cell body, each by means of a flange secured by six bolts. The optical path length is determined by the distance between the internal surfaces of the high-pressure windows. The sample material is introduced into the cell through holes at right angle to the cylindrical axis of the autoclave. Through these borings also, the connections to the pressure-generating and pressure-monitoring equipment are made and sheathed thermocouples are introduced into the pressurized fluid. The cell is heated electrically from the outside by a resistance wire that is mounted onto a brass support.

For spectroscopic studies at wavenumbers between 2000 and 50 000 cm^{-1}, sapphire is unrivalled as high-pressure, high-temperature window material. Thus both the IR/NIR probing light and the excimer laser light at wavelengths of 248, 308, and 351 nm may be transmitted through the cell. The stainless-steel materials used for the construction of cells as in Figure 2 are W.St.-Nr. 2.4668 for the cell body and flange and W.St.-Nr. 2.4969 for the steel ram and bolts, with these numbers referring to the German standard. These steels contain significant amounts of nickel, cobalt, and other materials of potential catalytic activity. To eliminate or at least to reduce catalytic activity, the stainless-steel W.St.-Nr. 1.4122 has been used for construction of the cell body. For dimensions as in Figure 2, by this change, the maximum operating temperature and pressure are reduced to 200 °C and 2000 bar, respectively.

An efficient way of avoiding catalytic action of the metal walls consists of isolating the system under investigation from the steel parts. One such strategy is illustrated in Figure 3, where an internal cell that sits in between the windows of the high-pressure cell is shown. This particular internal cell consists of a poly(tetrafluorethylene) tube (inner diameter 9 mm, outer diameter 10 mm, and length about 12 mm) and two cylindrical CaF_2 windows (diameter 10 mm and height 5 mm). The tube is widened before inserting the CaF_2 windows so that a tight fit is achieved. The system under investigation is exclusively contained inside the internal cell. An obvious advantage of this device beyond eliminating catalytic action of the metal walls is that the entire sample volume can be irradiated by the incident light in photochemical (laser-induced) studies. In addition, the internal cell allows for easy collection of the product and easy cleaning of the device.

The setup with the internal cell can only be used for batch-type polymerizations, whereas the optical cell in Figure 2 may also be operated as a flow-through cell for quantitative in-line analysis before and/or after penetrating a continuously operated reactor, for example, a tubular reactor or a continuous stirred tank reactor (CSTR) as shown in Figure 4.

The CSTR for operation up to 3 kbar and 300 °C allows for investigations into high-pressure homo- and copolymerizations.[36] The internal volume may be monitored through the sapphire window of 34 mm diameter. The stirrer is magnetically driven from outside. Different geometries of the stirring device have been used; among them were stirrer types that leave significant free internal space that may be transmitted by laser light. The reactor thus also allows for photochemically induced high-pressure polymerization. Concentrations inside the CSTR are measured by IR/NIR spectroscopy using a transmission-type

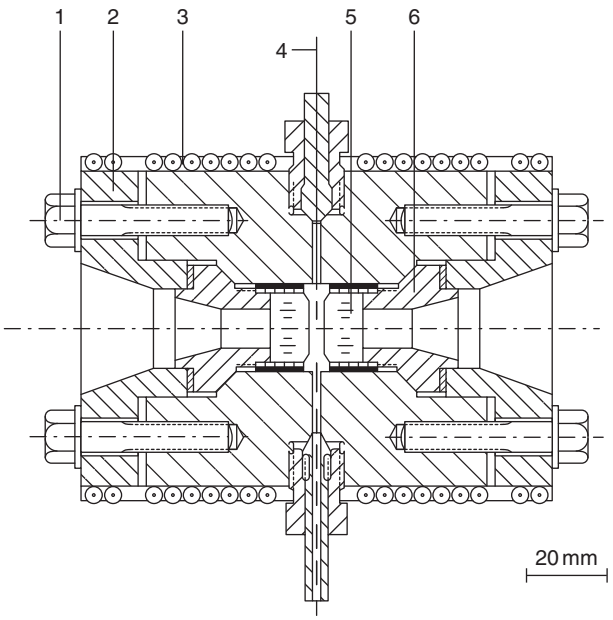

Figure 2 Optical high-pressure cell: bolt (1), flange (2), heating mounted onto a brass jacket (3), thermocouple (4), optical window (5), and plug (6). From Buback, M. *Angew. Chem. Int. Ed. Engl.* **1991**, *30*, 641.[1]

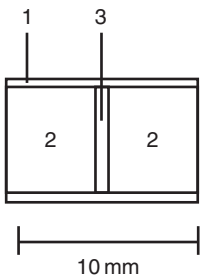

Figure 3 Internal cell consisting of Teflon tubing (1) and optical windows (2); (3) represents the reaction volume. From Buback, M.; Hinton, C. In *High-Pressure Techniques in Chemistry and Physics: A Practical Approach*; Isaacs, N. S.; Holzapfel, W. B., Eds.; Oxford University Press: Oxford, UK, 1997.[31]

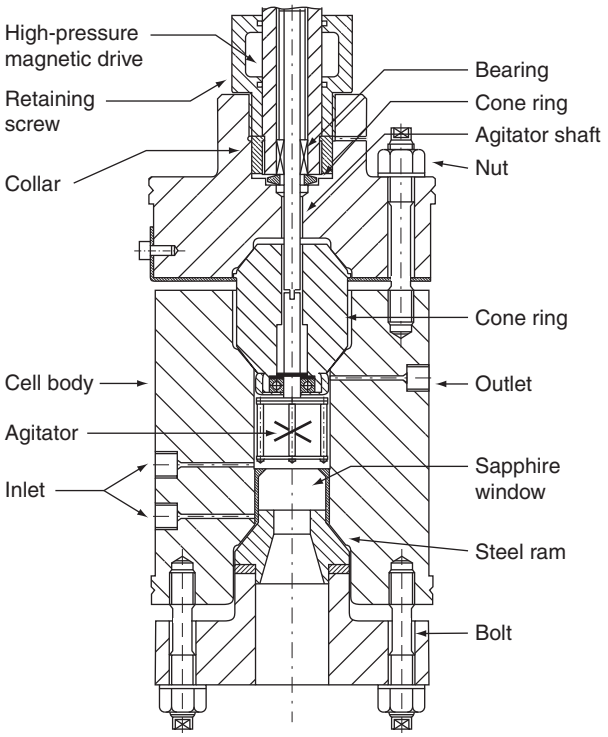

Figure 4 CSTR for operation up to 3 kbar and 300 °C. From Buback, M.; Busch, M.; Lovis, K.; Mähling, F.-O. *Chem. Ing. Tech.* **1994**, *66*, 510.[36]

cell as in Figure 2 that is positioned directly behind the exit of the CSTR. Through this optical cell also the residence time distribution of the reactor may be measured. For this purpose, a very short CO_2 pulse is added to the feed before entering the CSTR and the residence time distribution is found by spectroscopic measurement of the intense CO_2 absorption behind the CSTR.[37]

Information about the phase behavior of the polymerizing system is essential, as the situation of the reacting mixture directly affects polymer properties. An experimental device for measuring cloud-point pressures is presented in Reference 38.

Presented in Figure 5 is a series of NIR spectra in the region of the first C–H stretching overtones recorded during an ethene polymerization at 200 °C and 2500 bar. The polymerization reaction may be quantitatively monitored by the decrease of the ethene (E) bands, with maxima above 5900 cm^{-1}, and by the increase of the polyethylene (PE) bands, with maxima below 5900 cm^{-1}. The arrows indicate the direction of spectral changes with time.

Ethene homopolymerization may also be followed via the absorbance spectra taken in the region of C–H stretching second overtones. Illustrated in Figure 6 is a series of spectra recorded during an ethene polymerization at 190 °C and 2630 bar. The bands around 8730 and 8960 cm^{-1} are due to ethene. PE absorption occurs around 8260 cm^{-1}. The polymerizations in Figures 5 and 6 proceed at fairly high degrees of monomer conversion exceeding 75%. The optical path lengths are 1 and 20 mm for the spectral series in Figures 5 and 6, respectively.

4.35.2.1 Single Pulse-Pulsed Laser Polymerization

Monomer conversion in pulsed laser polymerization (PLP) induced by an SP is measured at a fixed wavenumber using an NIR light source, a monochromator, and a fast detection unit for recording NIR intensity as a function of time.[40]

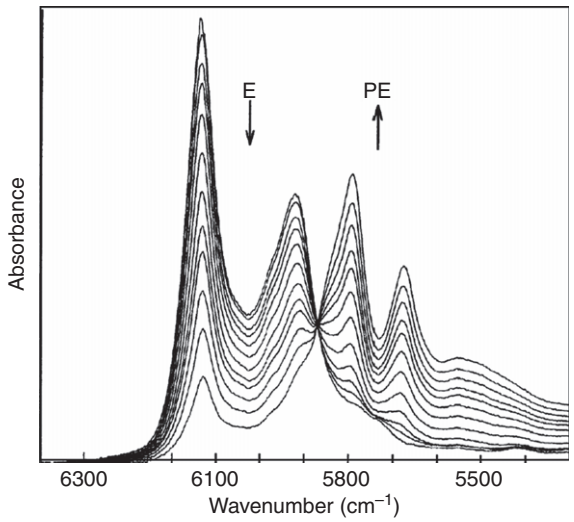

Figure 5 NIR spectra recorded during an ethene polymerization at 200 °C and 2500 bar. From Beuermann, S.; Buback, M. *High Press. Res.* **1997**, *15*, 333.[39]

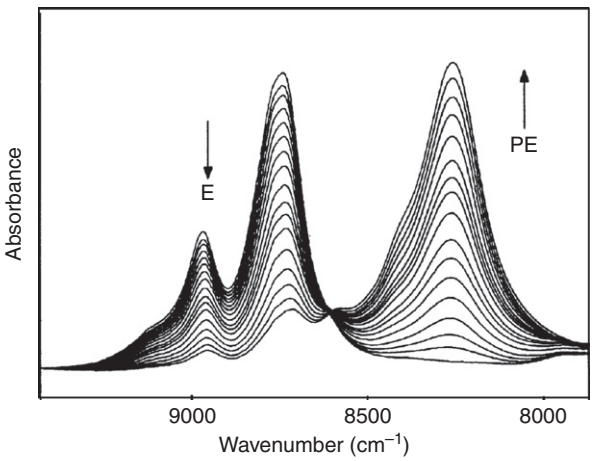

Figure 6 NIR spectra recorded during an ethene polymerization at 190 °C and 2630 bar. From Beuermann, S.; Buback, M. *High Press. Res.* **1997**, *15*, 333.[39]

Figure 7 illustrates this time-resolved procedure for a homopolymerization of butyl acrylate (BA) at 40 °C and 1000 bar in solution with CO_2. Relative concentration c_M/c_M^0 is plotted versus time t with c_M^0 referring to monomer concentration at $t = 0$, when the particular laser pulse is fired. Monomer conversion induced by an SP is relatively small, which allows, by carrying out a series of successive such SP experiments, to map out the conversion dependence of the termination rate coefficient. As the size of the radical grows linearly with time t after applying the pulse, the so-called SP-PLP (SP-PLP-NIR) experiment in Figure 7 provides access to chain-length-dependent termination rate coefficients. The coupled kinetic parameters k_t/k_p and $k_t \cdot c_R^0$ are obtained by fitting eqn [1] to the monomer concentration versus time profile measured after applying a single laser pulse to the system:

$$\frac{c_M(t)}{c_M^0} = (2 \cdot k_t \cdot c_R^0 \cdot t + 1)^{-k_p/2k_t} \quad [1]$$

where c_R^0 denotes radical concentration generated by the laser pulse. If monomer propagation is slow, which results in a weak

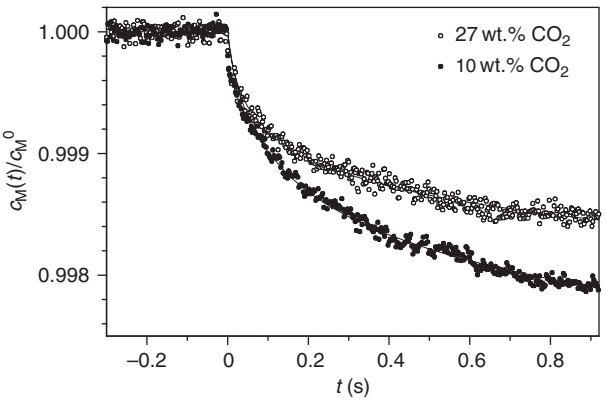

Figure 7 Change in relative monomer concentration during BA polymerizations at 40 °C, 1000 bar, and 38% overall monomer conversion at two CO_2 contents. From Beuermann, S.; Buback, M.; Schmaltz, C. *Ind. Eng. Chem. Res.* **1999**, *38*, 3338.[41]

SP-PLP-NIR signal, data analysis may be performed on the signal obtained by coadding c_M versus t traces measured for a few subsequent laser pulses. SP-PLP-NIR yields the ratio of propagation to termination rate coefficients (k_p/k_t) as one of the primary experimental quantities. From this ratio, k_t is obtained in conjunction with the PLP–size exclusion chromatography (SEC) method, which provides direct access to k_p. The SP-PLP-NIR method has been extensively used for measuring chain-length-averaged rate coefficients of termination for a series of monomers as a function of pressure, temperature, and degree of monomer conversion.[15]

Recently, the SP-PLP-electron paramagnetic resonance (EPR) technique has been introduced as a direct method for k_t measurement, in which EPR detection is used to trace the decay of radicals after laser pulse initiation.[42,43] This novel technique has however not yet been applied at high pressures.

4.35.2.2 Pulsed Laser Polymerization-Size Exclusion Chromatography

The measurement of propagation rate coefficients k_p by PLP in conjunction with SEC analysis of the polymeric product has been pioneered by Olaj *et al.*[44,45] The technique is the IUPAC-recommended method for k_p determination.[46] PLP-SEC has been used extensively for studies on k_p of a large number of monomers.[47–52] The PLP-SEC method is well suited for measuring k_p at high pressures, as only laser pulsing has to be carried out under high pressure, whereas the molecular mass analysis, which yields k_p, is performed by SEC at standard conditions. Polymerization is initiated by short laser pulses applied to the monomer/photoinitiator system at fixed repetition rate ν so as to allow for some small initial monomer conversion, typically of 1–2%. Due to the almost instantaneous production of photoinitiator-derived radicals, an increased termination probability for radicals from preceding pulses results upon application of each successive laser pulse. Repetitive laser pulse initiation at constant repetition rate is reflected by structured MMDs of the resulting polymer (see further below). A detailed discussion of the PLP-SEC procedure is given elsewhere.[48]

The accuracy of k_p determination by PLP-SEC is essentially determined by the quality of molecular mass analysis. In particular, the position of inflection points needs to be precisely known. SEC analysis is straightforward in cases where narrow molecular mass standards are available for calibration.

4.35.3 Initiation, Propagation, and Termination Rate Coefficients of Radical Polymerization up to High Pressure

4.35.3.1 Decomposition of Peroxide Initiators at High Pressure

Two pieces of kinetic information are essential with respect to applying chemical initiators in radical polymerization: the decomposition rate coefficient k_d defined as the loss in initiator concentration with time and the efficiency of initiation f, which refers to the fraction of primary radicals that actually start chain growth. As initiator decomposition rates are mostly deduced from independent experiments, by monitoring initiator decay in (inert) solution, it is recommended to select the solvent as close as possible to the monomer system of interest. The solvent material in which the k_d measurements have been performed needs to be stated when efficiencies f are presented. For use with ethene polymerization, k_d from experiments in solution of heptane should be well suited.

Quantitative IR spectroscopy has turned out to be very useful for measuring the decay of peroxide concentration or, alternatively, the increase in the concentration of products from decomposition. Two types of discontinuous procedures have been used: at lower reaction temperatures, the peroxide solution is contained in an internal cell (see **Figure 3**), which is filled and assembled in a glove box under an argon atmosphere. The internal cell is positioned into the optical high-pressure cell and pressurized with *n*-heptane acting as the pressure-transmitting medium. The assembly is heated to the reaction temperature and the collection of IR spectra is started. In the case that decomposition rate becomes too fast and a major fraction of the peroxide is decomposed before reaction conditions of constant T and p are reached, the peroxide solution is directly fed into a preheated autoclave. The solution is then quickly pressurized and the collection of IR spectra is started.

Kinetic analysis under conditions where decomposition is fast, for example, reaction half-lives are well below 1 min, has been performed using a tubular reactor, which essentially consists of a high-pressure capillary of 10 m (or even larger) length and 0.5 mm internal diameter.[53] The IR spectroscopic analysis is performed at reaction pressure, but at lower temperature, in an optical cell such (as the one in **Figure 2**) that is positioned directly behind the tubular reactor.

The decomposition kinetics of several classes of peroxides, such as dialkyl peroxides, diacyl peroxides, peroxyesters, peroxycarbonates, peroxydicarbonates, but also of a few multifunctional peroxides, has been studied. Among them, peroxyesters play an important role for high-pressure ethene polymerization. This group of peroxides will be discussed in some detail in the subsequent text.

A wide variety of peroxyesters of general structure R(CO)OOC$(CH_3)_2$R* (**Scheme 1**) are commercially available:[54] where R and R* may be primary (e.g., methyl and ethyl), secondary (e.g., *iso*-propyl), or tertiary (e.g., *tert*-butyl) alkyl groups.

Within the primary reaction step of thermally induced initiator decomposition, the O–O bond is broken. Depending on the rate at which successive bond scission of the

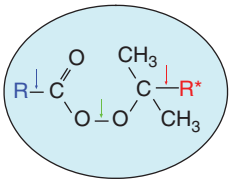

Scheme 1 Structure of peroxyesters.

initiator-derived primary radical species occurs, the overall decomposition rate coefficient k_d may be affected. The follow-up reaction of the primary radicals may be relatively fast in cases where the radical produced by β-scission, that is, scission of the bond in β-position to the radical functionality, is relatively stable, for example, is a *tert*-butyl radical.

The k_d values for primary peroxyesters, that is, the ones where R is CH_3 or CH_2R', are more or less identical, whereas in the cases of secondary and tertiary peroxyesters, the type of R moiety plays a significant role. This difference is best interpreted as being due to fast or even almost instantaneous β-scission with secondary and tertiary peroxyesters and to slow β-scission with primary peroxyesters. Within the latter group of initiators, the R–O bond is not rapidly broken and the R group in R(CO)O is too far off the peroxy linkage to affect primary decomposition kinetics. The opposite is true with tertiary peroxyesters, where the stable tertiary radical is immediately formed and the specific type of R moiety thus affects decomposition kinetics.

This interpretation is supported by inspection of measured activation energies of the observed decomposition rate coefficient. In **Figure 8**, numbers for the activation energy at low pressure E_A(0 bar) are plotted against bond dissociation energy of the R–H bond (BDE(R–H)), which serves as a measure for the stability of radical R. For primary peroxyesters, the activation energy is insensitive toward BDE(R–H), whereas for secondary and tertiary peroxyesters, where the radical R is produced early after primary O–O bond dissociation, the

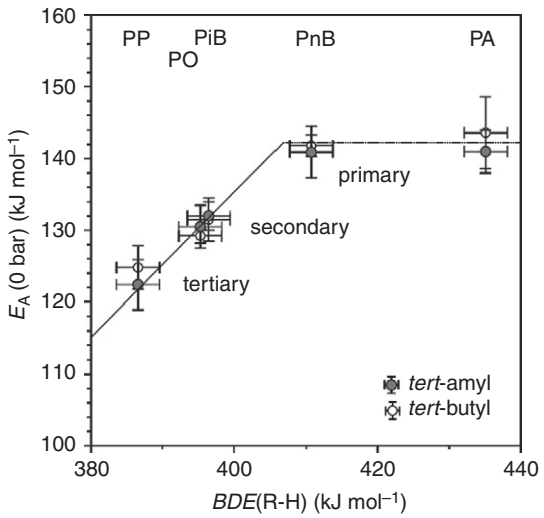

Figure 8 Activation energy E_A of the decomposition rate coefficient k_{obs} for *tert*-amyl (filled circles) and *tert*-butyl (open circles) peroxyesters plotted vs. the BDE of the associated alkane (BDE(R–H)). For explanation of the abbreviations, see **Table 3**. From Buback, M.; Nelke, D.; Vögele, H.-P. *Z. Phys. Chem.* **2003**, *217*, 1169.[55]

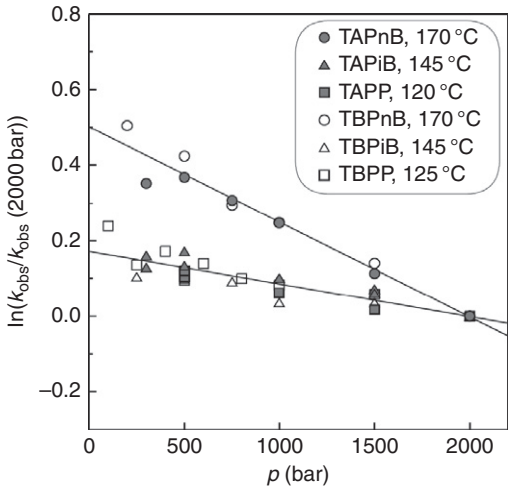

Figure 9 Pressure dependence of relative (with respect to the 2000 bar value) rate coefficients for *tert*-amyl peroxyesters (filled symbols) and *tert*-butyl peroxyesters (open symbols) at constant temperatures (between 120 and 170 °C). For explanation of the abbreviations, see **Table 3**. From Buback, M.; Nelke, D.; Vögele, H.-P. *Z. Phys. Chem.* **2003**, *217*, 1169.[55]

stability of R clearly matters. The increase in E_A(0 bar) is linearly correlated with BDE(R–H). The data for *tert*-butyl and *tert*-amyl show the same trend, which indicates that they essentially reflect the impact of the decarboxylation (β-scission) reaction on the observed decomposition rate coefficient.

The pressure dependence of k_{obs} for primary peroxyesters is clearly different from that for secondary and tertiary peroxyesters. Plotted in **Figure 9** are relative decomposition rate coefficients k_{obs}/k_{obs}(2000 bar). Secondary and tertiary peroxyesters show a similar type of behavior with only a modest decrease of the decomposition rate coefficient toward higher pressure, whereas primary peroxyesters exhibit a pronounced such decrease. This clear difference is assigned to single-bond scission in the case of primary peroxyesters, which is associated with a pronounced increase in molar volume of the activated state. Secondary and tertiary peroxyesters undergo almost concerted bond scission with the immediate production of the linear CO_2 molecule giving rise to only a weak increase in molar volume of the activated state, although two bonds are broken rather than one in the case of primary peroxyesters.

The rate parameters for decomposition of peroxides up to high pressure and temperatures may be calculated according to eqns [2] and [3]. The pressure dependence of the decomposition rate coefficient of aliphatic *tert*-butyl peroxyesters is given by eqn [2]:[56]

$$k(p,T)\ (\mathrm{s}^{-1}) = C_1 \exp\left(-\frac{C_2 + p\ (\mathrm{bar})(C_3 - C_4 \cdot p\ (\mathrm{bar}))}{T\ (\mathrm{K})}\right) \quad [2]$$

with the constants C_1–C_4 listed in **Table 1** and that of aliphatic *tert*-amyl peroxyesters by eqn [3]:[55]

$$k_{obs}(p,T)\ (\mathrm{s}^{-1}) = A \cdot \exp\left(\frac{E_A(0\ \mathrm{bar}) + \Delta V^{\#} \cdot p\ (\mathrm{bar})}{RT\ (\mathrm{K})}\right) \quad [3]$$

with the parameters A, E_A(0 bar), and $\Delta V^{\#}$ being listed in **Table 2**.

Table 1 Constants C_1, C_2, C_3, C_4 related to eqn [2] for estimating initiator decomposition rate coefficients of *tert*-butyl peroxyesters as a function of p and T[56]

	C_1	C_2	C_3	C_4
tert-Butyl peroxy-*neo*-decanoate(TBPD)	1.22×10^{14}	14 011	0.0208	0
TBPP	6.10×10^{14}	15 011	0.0367	0
tert-Butyl peroxy-2-ethylhexanoate (TBPO)	4.10×10^{14}	15 541	0.0433	0
tert-Butyl peroxy-2-methylbutanoate (TBPMB)	4.84×10^{14}	15 792	0.0481	0
TBP*i*B	4.03×10^{14}	15 809	0.0267	0
tert-Butyl peroxy-3,5,5-trimethylhexanoate (TBPN)	4.44×10^{15}	17 465	0.208	5.36×10^{-5}
tert-Butyl peroxy-*n*-butanoate (TBP*n*B)	2.78×10^{15}	17 381	0.162	1.95×10^{-5}
tert-Butyl peroxypropionate (TBPProp)	1.42×10^{15}	17 087	0.145	2.03×10^{-5}
TBPA	6.78×10^{15}	17 714	0.2471	3.336×10^{-5}

For explanation of the abbreviations, see **Table 3**.

Table 2 Parameters A, E_A (0 bar), and $\Delta V^{\#}$ related to eqn [3] for estimating initiator decomposition rate coefficients as a function of p and T[55]

	A (s^{-1})	E_A (0 bar) ($kJ\,mol^{-1}$)	$\Delta V^{\#}$ ($cm^3\,mol^{-1}$)
TAPA	1.52×10^{15}	141.2	12.5
TAP*n*B	1.03×10^{15}	139.6	8.2
TAP*i*B	7.53×10^{14}	132.9	2.6
tert-Amyl peroxy-2-ethylhexanoate (TAPO)	7.27×10^{14}	130.5	2.8
TAPP	4.11×10^{14}	122.7	2.4

For explanation of the abbreviations, see **Table 3**.

The kinetic information on single-bond scission (with primary peroxyesters) and close-to-concerted two-bond scission with secondary and tertiary peroxyesters is of relevance for initiator efficiency. In case of concerted two-bond scission, the primary radical fragments from decomposition may react with each other, by termination or disproportionation, within the solvent cage. These follow-up reactions consume radicals and thus lower initiator efficiency. In case of single-bond scission, combination of the primary fragments from peroxyester decomposition yields the initiator back, which may form radical species in a successive reaction step. Thus, the initiation efficiency of primary peroxyesters should be above that of secondary and tertiary peroxyesters, where radical–radical reactions after secondary bond scission irreversibly destroy radical functionality. The question may be asked, whether the less efficient secondary and tertiary peroxyesters are used at all. The answer to this question may be found from **Figure 8**, which illustrates the lower activation energy and thus higher decomposition rate of secondary and tertiary peroxyesters, thus allowing for initiation of polymerization at lower temperatures. As ethene conversion is associated with a significant enhancement of temperature, by about 11 °C per 1% conversion under adiabatic conditions, it is important to have a wide temperature range available to reach higher monomer conversion in technical polymerization processes.

The kinetically relevant quantity for modeling initiation in radical polymerization is r_i, the rate by which primary initiator-derived radicals add to a monomer molecule and thus start chain growth. This rate r_i is related to initiator decomposition rate r_d via the initiator efficiency f:

$$r_i = n \cdot f \cdot r_d \qquad [4]$$

where r_d is $-dc_i/dt$, with c_i being the initiator concentration, t the reaction time, and n the number of free radicals produced from the initiator. With monofunctional peroxides, n equals 2, whereas with bifunctional and trifunctional initiators, n is 4 and 6, respectively. By definition, f is in the range of 0 to unity. The fraction $(1-f)$ refers to radicals that are consumed in reactions other than propagation and recombination to the initiator molecule.

Initiator efficiency within ethene high-pressure polymerization has been measured for a wide range of organic peroxyesters.[57] Determination of f has been carried out via the quantity 'reduced peroxide-induced monomer conversion' (ΔX_r) presented in Reference 58. ΔX_r has been determined under stationary conditions in a CSTR (**Figure 4**) from the concentration of initiator decomposed in the CSTR under polymerization conditions $c_{I,dec}$ and monomer conversion ΔX. The quantity ΔX_r is related to the rate coefficients of propagation k_p and termination k_t, respectively, to CSTR residence time τ and to initiator efficiency f via eqn [5]:

$$\Delta X_r = \Delta X / c_{I,dec}^{0.5} = k_p \times k_t^{-0.5} \times f^{0.5} \times \tau^{0.5} \qquad [5]$$

Due to the imprecise knowledge of k_p and k_t under polymerization conditions, it is recommended to estimate initiator efficiency f via eqn [5] by using a reference initiator system of known f.

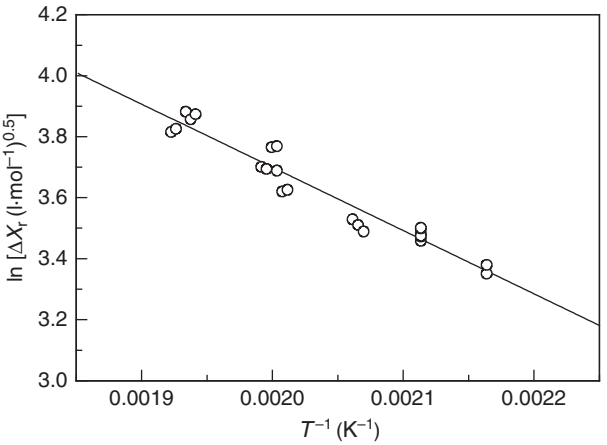

Figure 10 Arrhenius plot of reduced monomer conversion ΔX_r for di-*tert*-butyl peroxide (DTBP)-induced ethene polymerizations carried out at 2000 bar in the miniplant device equipped with a CSTR (see **Figure 4**). From Buback, M.; Fischer, B.; Hinrichs, S.; *et al. Macromol. Chem. Phys.* **2007**, *208*, 772.[57]

Shown in **Figure 10** is an Arrhenius plot of ΔX_r for DTBP-induced ethene polymerizations at 2000 bar. According to the discussion in Reference 58, the initiator efficiency f_{DTBP} of DTBP in ethene high-pressure polymerization is close to unity. The initiator efficiency f of an arbitrary peroxyester may be estimated from the ΔX_r value measured for ethene high-pressure polymerization initiated by this particular initiator. Using the known decomposition rate coefficients of this initiator, comparison of the measured ΔX_r value with the reference ΔX_r value of DTBP-induced ethene polymerization (for $f = 1$) obtained at a given temperature and otherwise identical reaction conditions directly yields the efficiency f for the initiator of interest.

The initiator efficiencies of 16 peroxides collated in **Table 3** have been determined. Both alkyl groups R and R* of the *tert*-alkyl peroxyesters R*–C(CH$_3$)$_2$–O–O–CO–R (see also **Scheme 1**) have been varied. The initiators were used as supplied from AkzoNobel Polymer Chemicals B.V., Deventer (The Netherlands). Ethene of 99.8% purity (Linde) has been freed from oxygen by passing ethene through a catalyst tower equipped with the BASF copper catalyst R 3-11.

The efficiency values of the peroxyesters under investigation listed in **Table 4** are in the range of $0.4 < f < 0.9$. With the exception of the data for *tert*-Butyl peroxy-2-ethylhexanoate (TBPEH) and *tert*-Butyl peroxypivalate (TBPP), no literature values for f have been reported so far. Luft and co-workers[59,60] measured the initiator consumption of TBPEH and TBPP in ethene polymerization at 1700 bar and found that of TBPEH to

Table 4 Initiator efficiencies f of peroxyesters in high-pressure ethene polymerization at 2000 bar[57]

Peroxyester	f
TBPA	0.79 ± 0.06
TBPPent	0.85 ± 0.05
TBP*i*B	0.66 ± 0.08
TBPEH	0.62 ± 0.03
TBPP	0.37 ± 0.04
TAPA	0.69 ± 0.08
TAP*n*B	0.73 ± 0.07
TAP*i*B	0.56 ± 0.08
TAPEH	0.61 ± 0.10
TAPP	0.48 ± 0.06
TMBPA	0.76 ± 0.06
TMBPEH	0.61 ± 0.07
TMBPP	0.50 ± 0.05
TMPPA	0.50 ± 0.05
TMPPP	0.50 ± 0.02

Table 3 Peroxyesters used within the polymerization experiments

Peroxyester	*R**	*R*	*Abbreviation*	*Purity (%)*
tert-Butyl peroxyacetate	Methyl	Methyl	TBPA	99.4
tert-Butyl peroxypentanoate	Methyl	*n*-Butyl	TBPPent	93.5
tert-Butyl peroxy-*iso*-butanoate	Methyl	*iso*-Propyl	TBP*i*B	98.1
tert-Butyl peroxypivalate	Methyl	*tert*-Butyl	TBPP	99.0
tert-Butyl peroxy-2-ethylhexanoate	Methyl	2-Heptyl	TBPEH	98.7
tert-Amyl peroxyacetate	Ethyl	Methyl	TAPA	98.9
tert-Amyl peroxy-*n*-butanoate	Ethyl	*n*-Propyl	TAP*n*B	98.0
tert-Amyl peroxy-*iso*-butanoate	Ethyl	*iso*-Propyl	TAP*i*B	98.0
tert-Amyl peroxy-2-ethylhexanoate	Ethyl	2-Heptyl	TAPEH	98.0
tert-Amyl peroxypivalate	Ethyl	*tert*-Butyl	TAPP	98.0
1,1,3,3-Tetramethylbutyl peroxyacetate	*neo*-Pentyl	Methyl	TMBPA	50
1,1,3,3-Tetramethylbutyl peroxy-2-ethylhexanoate	*neo*-Pentyl	2-Heptyl	TMBPEH	90.9
1,1,3,3-Tetramethylbutyl peroxypivalate	*neo*-Pentyl	*tert*-Butyl	TMBPP	75
Tetramethylpropyl peroxyacetate	*tert*-Butyl	Methyl	TMPPA	96.8
Tetramethylpropyl peroxypivalate	*tert*-Butyl	*tert*-Butyl	TMPPP	90.9
Di-*tert*-butyl peroxide	–	–	DTBP	99.0

The type of substituent, R and R*, refers to the notations in **Scheme 1**. All peroxyesters have been kindly provided by AkzoNobel functional chemicals in high purity.

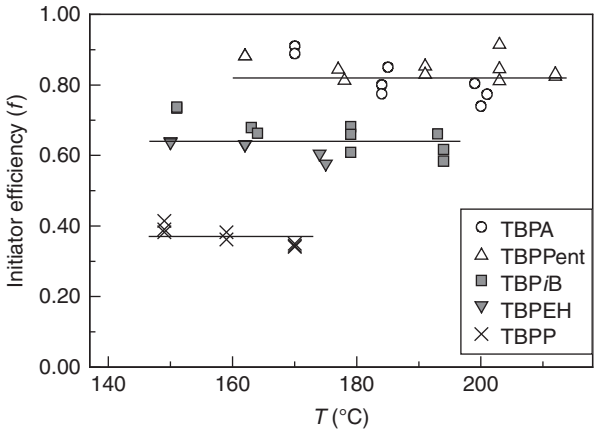

Figure 11 Initiator efficiency *f* of *tert*-butyl peroxyesters in high-pressure ethene polymerization at 2000 bar. The upper, middle, and lower lines indicate the arithmetic mean values of *f* for primary, secondary, and tertiary peroxyesters, respectively. For explanation of the abbreviations, see **Table 3**. From Buback, M.; Fischer, B.; Hinrichs, S.; *et al. Macromol. Chem. Phys.* **2007**, *208*, 772.[57]

be lower than that of TBPP, which is consistent with the result in **Table 4** saying that f_{TBPEH} exceeds f_{TBPP}. Van der Molen *et al.*[61] deduced the same result from investigations into the initiator consumption of TBPEH and TBPP.

The efficiencies of several *tert*-butyl peroxyesters are plotted in **Figure 11**. The size of *f* largely depends on the type of R moiety, that is, on the carbon atom in α-position to the carbonyl group being primary, secondary, or tertiary. In passing from primary to tertiary peroxyesters, the initiator efficiency clearly decreases. The less pronounced effects of varying the R* moiety for a given R group are illustrated and explained in Reference 57.

The initiator efficiency data demonstrate the strong impact on *f* of in-cage reactions that result in irreversible loss of radicals. Of relevance is whether successive β-scission reactions of primary radical species from initiator decomposition occur within the short time interval, of about 1 ns duration, during which the radicals $R^*C(CH_3)_2O\cdot$ and $RCOO\cdot$ remain in the caged situation. The two dominant follow-up reactions are decarboxylation of $RCOO\cdot$ and 'deacetonization' of $R^*–C(CH_3)_2O\cdot$ radicals. With primary peroxyesters, for example, with *tert*-butyl peroxyacetate, decarboxylation is relatively slow, as the methyl radical is too high in energy to be formed on the very short timescale of 1 ns. The significantly lower energy of tertiary radicals, for example, of *tert*-butyl, makes decarboxylation of the associated $R–COO\cdot$ species very fast. Thus, primary peroxyesters predominantly undergo out-of-cage decarboxylation, whereas secondary and tertiary peroxyesters undergo in-cage decarboxylation.

The β-scission rate of the $R^*–C(CH_3)_2O\cdot$ species follows similar trends. DFT calculations in conjunction with unimolecular rate theory indicate that the β-scission rate coefficient k_β for such isolated species strongly depends on the type of R substituent.[62] In passing from the *tert*-butoxy radical to the 1,1,2,2-tetramethylpropyloxy radical, k_β increases by about 4 orders of magnitude. The results from DFT calculation indicate that 'deacetonization' occurs as an in-cage process with 1,1,2,2-tetramethylpropyloxy radicals, whereas with *tert*-butoxy, *tert*-amyloxy, and 1,1,3,3-tetramethylbutyloxy radicals, this reaction most likely occurs as out-of-cage process.

4.35.3.2 Pressure Dependence of Homopropagation Rate Coefficients

Propagation rate coefficients k_p for a monomer A at a particular pressure *p* are deduced from the MMD measured by SEC on a poly(A) sample produced by PLP with repetition rate *v* at pressure *p*. The characteristic points of inflection are determined from the first-derivative curve of the MMD. Of particular interest is the degree of polymerization L_0 on the low molecular mass side of the MMD peak maximum. L_0, which reflects the number of propagation steps between two successive laser pulses, is correlated with k_p via eqn [6]:

$$L_0 = k_p \cdot c_M \cdot \nu^{-1} \qquad [6]$$

where c_M is the monomer concentration during the PLP experiment. Mostly, c_M is determined as the arithmetic mean of the initial monomer concentration prepared by weighing and c_M is measured after applying a sequence of laser pulses at constant *v*. The reliability of the PLP-SEC method is checked by monitoring higher order inflection points that occur at twice or even thrice the value of L_0. The characteristic position, for example, of $2L_0$ is assigned to termination being induced by the next but one laser pulse.

The PLP-SEC technique has been applied toward the study of k_p for a wide variety of monomers.[15] Literature reflects the excellent agreement of PLP-SEC data obtained by different groups. In what follows, a brief overview will be given on k_p data for homopolymerizations up to high pressure.

Illustrated in **Figure 12** is a series of MMDs for polystyrene samples obtained by PLP of styrene at 30 °C and pressures up to 2800 bar. A laser pulse repetition rate of $\nu = 9.9$ Hz has been applied for the entire set of polymerizations. With increasing pressure, the MMD peak shifts to higher molecular mass, as does the first point of inflection L_0, which serves for k_p determination. The variation of peak position with pressure directly reflects the increase of k_p with pressure. The intense peak corresponds to termination of propagating radicals after a growth period within the time interval $t = \nu^{-1}$. At lower pressure, the PLP-induced structure on the MMD is particularly clear, whereas at higher pressure, only the first-derivative spectra

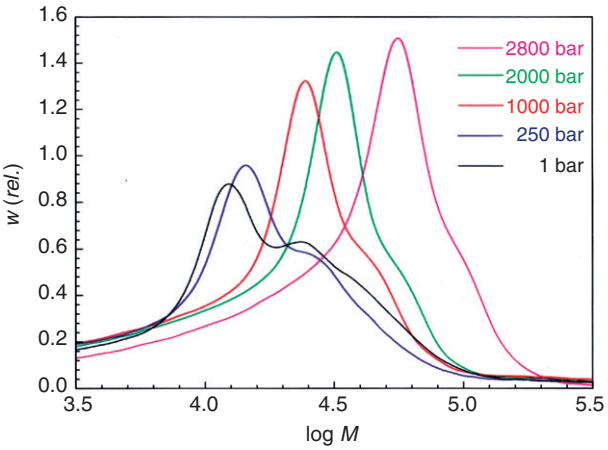

Figure 12 MMDs for polystyrene samples from PLP experiments on styrene at 30 °C and pressures up to 2800 bar; laser pulse repetition rate $\nu = 9.9$ Hz. From Buback, M.; Kuchta, F.-D. *Macromol. Chem. Phys.* **1995**, *196*, 1887.[63]

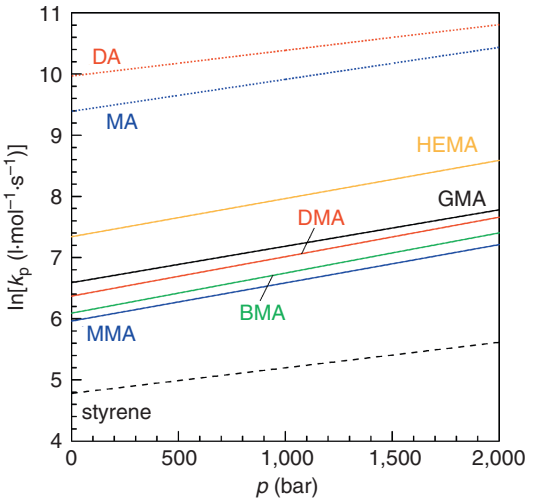

Figure 13 Pressure dependence of k_p for a range of monomers based on literature data. From Buback, M.; Kuchta, F.-D. *Macromol. Chem. Phys.* **1995**, *196*, 1887; Beuermann, S.; Buback, M.; Russell, G. T. *Macromol. Rapid Commun.* **1994**, *15*, 351; Buback, M.; Geers, U.; Kurz, C. H. *Macromol. Chem. Phys.* **1997**, *198*, 3451; Buback, M.; Kurz, C. H. *Macromol. Chem. Phys.* **1998**, *199*, 2301; Buback, M.; Kurz, C. H.; Schmaltz, C. *Macromol. Chem. Phys.* **1998**, *199*, 1721.[63–65,67,68]

give clear indication of 'overtone' peaks located at about iL_0 ($i = 2, 3, 4, \ldots$). The consistency criteria of reliable k_p determination are fulfilled by the styrene experiments.

Plotted in Figure 13 is the pressure dependence of k_p for polymerization of styrene, methyl acrylate (MA), and dodecyl acrylate (DA) as well as for several methacrylic acid esters at 30 °C. The k_p value of linear alkyl esters increases in passing from methyl methacrylate (MMA)[64] to dodecyl methacrylate (DMA).[65] The reason behind this trend is seen in the reduced internal friction of the transition state structure with DMA, where the dipolar interactions of the carbonyl moieties are better shielded than in case of MMA.[66]

Monomers with cyclic ester groups, such as glycidyl methacrylate (GMA) and cyclohexyl methacrylate (CHMA),[67] exhibit even higher k_p. For 2-hydroxyethyl methacrylate (HEMA), a particularly large k_p value is found.[67] Although the methacrylate k_p values clearly differ in size, for example, by a factor of 4 between MMA and HEMA, the activation volumes $\Delta V^{\neq}(k_p)$, calculated according to eqn [7], are identical within experimental accuracy: $\Delta V^{\neq}(k_p) = -(16.7 \pm 1.1)$ and $-(15.8 \pm 1.1)$ cm^3 mol^{-1}, respectively:

$$\left(\frac{\partial \ln(k_p/k^0)}{\partial p}\right)_T = -\frac{\Delta V^{\#}(k_p)}{R \cdot T} \qquad [7]$$

The individual activation volumes for methacrylate k_p, as deduced from PLP–SEC studies at 30 °C, are listed in Table 5. This entire set of activation volumes may be represented by $\Delta V^{\neq}(k_p) = -(16 \pm 2)$ cm^3 mol^{-1}. In addition, Table 5 contains values for MA and DA[68] as well as for styrene,[63] which are distinctly below methacrylate $\Delta V^{\neq}(k_p)$.

A clear family behavior is seen for both acrylates and methacrylates. The pressure dependence follows the general trend that larger steric hindrance at the reaction site is associated with the activation volume being larger in absolute value. The α-methyl group of the methacrylates is primarily responsible for this enhanced hindrance. The acrylate k_p values were measured at fairly low temperatures in order to avoid interference by the 1,5-hydrogen shift (backbiting) reaction, which transforms a secondary chain-end radical into a tertiary mid-chain radical. The k_p value associated with the latter radical is by 2–3 orders of magnitude below that of secondary chain-end radicals. The backbiting process has an important impact on acrylate kinetics at typical polymerization conditions. This aspect is described in more detail elsewhere.[51,69–71]

Table 5 Activation volumes $\Delta V^{\neq}(k_p)$ deduced from PLP-SEC experiments for methacrylates and styrene at 30 °C, for MA at –15 °C, and for DA at 15 °C[15]

Monomer		$\Delta V^{\#}$ (cm^3 mol^{-1})
Methacrylates	MMA	$-(16.7 \pm 1.1)$
	Butyl methacrylate (BMA)	$-(16.5 \pm 1.8)$
	DMA	$-(16.0 \pm 3.0)$
	GMA	$-(15.0 \pm 0.7)$
	CHMA	$-(16.2 \pm 1.1)$
	HEMA	$-(15.8 \pm 1.1)$
Acrylates	MA	$-(11.3 \pm 0.7)$
	DA	$-(11.7 \pm 1.8)$
Styrene		$-(12.1 \pm 1.1)$

4.35.3.3 Pressure Dependence of Homotermination Rate Coefficients

An essential difference between propagation and termination kinetics relates to the fact that propagation is chemically controlled, whereas termination proceeds under diffusion control. The latter effect is clearly seen from the pressure dependence of the termination rate coefficient k_t. Termination by combination occurs as a bond-forming reaction. Thus, as with propagation, one would expect k_t to be enhanced upon increasing pressure. The opposite is true. The observed decrease in k_t results from the enhancement of viscosity with pressure, which slows down diffusive motion.

The understanding of pressure-dependent k_t is difficult because of different types of diffusion control operating during polymerization to high degrees of monomer conversion X. Illustrated in Figure 14 is the variation of chain-length-averaged k_t with X, as observed with MMA bulk polymerization.

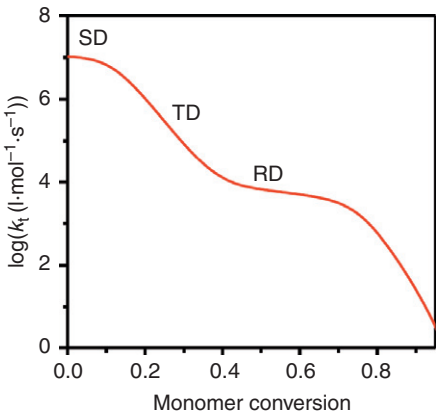

Figure 14 Chain-length-averaged termination rate coefficient of MMA as a function of the degree of monomer conversion.

The initial plateau region of constant k_t is followed by a significant decrease of k_t. Above 40% conversion, further decrease in k_t with conversion becomes less prominent but is more pronounced again at high X. The line in **Figure 14** is constructed from eqn [9] discussed further below. The low-conversion regime is assigned to segmental diffusion (SD), which basically says that segmental mobility of entangled macroradicals rather than diffusional motion of entire macroradicals controls k_t. The rate-controlling step consists of segmental reorientation such that the radical sites of two entangled macroradicals approach each other to undergo chemical reaction. In this initial range, both the motion of small, nonentangled radicals and the segmental reorientation of entangled macroradicals experience the friction provided by the viscosity of the solvent medium. In the case of bulk polymerization, this viscosity is essentially the one brought upon by the monomer. Toward higher conversion, center-of-mass diffusion controls termination rate. Under these higher conversion conditions, chemical reaction after segmental reorientation occurs once the macroradicals have approached each other by center-of-mass diffusion and have become entangled. The relevant viscosity in this translational diffusion (TD) regime is that of the monomer–polymer system but no longer the viscosity of the monomer. The steep decrease in k_t (**Figure 14**) is thus understood as resulting from the large increase in bulk viscosity of the monomer–polymer mixture with conversion.

The interpretation of termination behavior in the TD region is far more complicated, as monomer conversion is no sufficient measure for characterizing radical mobility. Average polymer size or, even better, size distribution and the extent of branching should additionally be known. The situation may be referred to as 'history-dependent' kinetics,[72] which basically says that k_t depends on the characteristics of the polymerizing system, in particular on the properties of the polymer. These properties are determined by the specific mode of polymerization by which a particular conversion has been reached. The pathway thus affects k_t under TD conditions via the polymeric structure given by the preceding polymerization.

Toward even higher conversion, bulk viscosity becomes too large so as to allow for significant center-of-mass diffusion of large polymeric species on the timescale of polymer growth. Under such conditions, a third mechanism comes into play. Termination occurs via propagation of macroradicals embedded into a monomer-containing environment. Radical functionalities thus may approach each other via propagation, the process of which is assisted by segmental motion of parts of the macroradicals, for example, of the sections in between entanglement nodes. This mechanism, which has been put forward by Schulz[73] and has been extended by several other groups,[74–76] is referred to as reaction diffusion (RD). In the RD regime, k_t is proportional to k_p and to monomer content. At very high degrees of monomer conversion, even k_p may come under diffusion control and, perhaps even more importantly, monomer content becomes very low, which leads to a significant drop in k_t at the highest degrees of monomer conversion. With C_{RD} as the reaction diffusion constant, the rate coefficient under reaction diffusion control $k_{t,RD}$ may be expressed by eqn [8]:

$$k_{t,RD} = C_{RD} \cdot k_p \cdot (1-X) \qquad [8]$$

where $1 - X$ is the fraction of (nonreacted) monomer.

As has been discussed in detail elsewhere,[75] the individual diffusion mechanisms may be put together into an equation for overall chain-length-averaged k_t:

$$k_t = \frac{1}{k_{SD}^{-1} + \eta_r / k_{TD}^0} + \frac{C_{RD} \cdot (1-X)}{k_{p,0}^{-1} + \eta_r / k_{p,D}^0} \qquad [9]$$

in which k_{SD}, k_{TD}^0, and $k_{p,0}$ denote the rate coefficients of SD, TD at zero conversion, and propagation at low conversion, respectively. $k_{P,D}^0$ refers to the diffusion-controlled propagation at zero conversion and η_r is the relative bulk viscosity: $\eta_r = \eta / \eta_0$, with η_0 referring to the viscosity of the pure monomer. The second term on the r.h.s. of eqn [9] essentially is $k_{t,RD}$, with, however, k_p being written as a diffusion-controlled quantity. With diffusion control of propagation being restricted to extremely high X, it is mostly sufficient to use eqn [9] with the second term on the r.h.s. being replaced by $C_{RD}\ k_{p,0}\ (1-X)$. The first term on the r.h.s. of eqn [9] accounts for diffusion control of k_t by SD and by TD, with $k_{TD} = k_{TD}^0 / \eta_r$ (for details, see Reference 74).

One way of testing the mechanistic concept, in particular the effect of viscosity on k_t, is by varying laser pulse repetition rate. Higher repetition rate shifts the MMD to lower molecular mass. The effect is demonstrated in **Figure 15** for MMA bulk polymerizations at 30 °C, 1000 bar, and laser pulse repetition rates of 0.21 and 13.5 Hz.[77] No significant effect of pulse repetition rate on k_t may be detected in the plateau region at low degrees of conversion, but a significant effect occurs at higher conversion. At lower repetition rates, the gel effect, associated with a clear drop in k_t, is seen at around 20% conversion, whereas at higher repetition rate and thus at smaller molecular mass of the radical species, the transition from SD to TD control of k_t is shifted to about 30% or even 35%. These results indicate that the variation of radical size has only a small influence on k_t under conditions of SD control, where

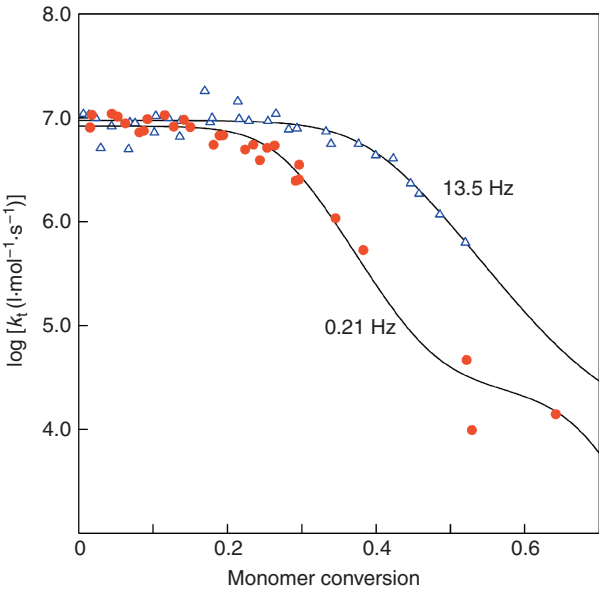

Figure 15 Variation of termination rate coefficient with monomer conversion in laser-induced MMA bulk polymerizations at 30 °C and 1000 bar carried out at laser pulse repetition rates of 0.21 and 13.5 Hz; the lines are fits to eqn [9]. From Beuermann, S. Ph.D. thesis, Cuvillier Verlag, Göttingen, 1994.[77]

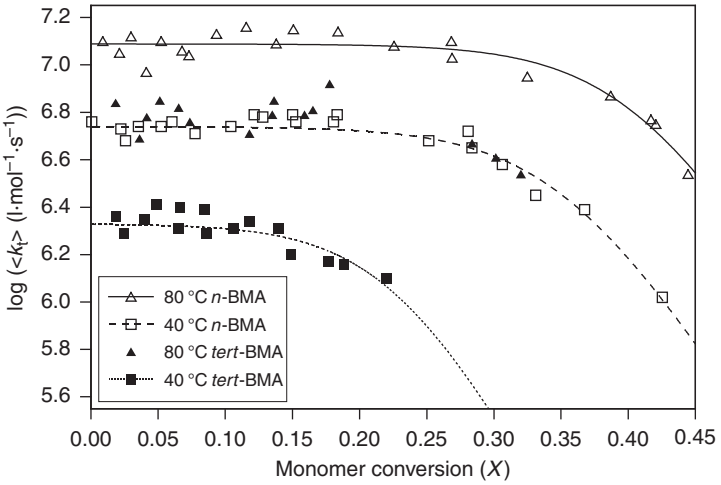

Figure 16 Comparison of log <k_t> as a function of monomer conversion X for n-BMA (open markers) and *tert*-BMA (full markers) bulk homopolymerizations at 2000 bar and 40 and 80 °C, respectively. From Buback, M.; Junkers, T. *Macromol. Chem. Phys.* **2006**, *207*, 1640.[78]

monomer viscosity controls termination rate. In the TD region, on the other hand, bulk viscosity matters and thus a pronounced dependence of both polymer concentration and polymer size is observed.

Even minor structural differences between monomers may largely affect termination behavior, as is illustrated for n-BMA and *tert*-BMA bulk homopolymerizations in Figure 16, where chain-length-averaged termination rate coefficients <k_t> are plotted for 2000 bar and temperatures of 40 and 80 °C. At identical p and T, <k_t> of n-BMA is well above the value of *tert*-BMA. This difference is assigned to higher flexibility of n-BMA macroradicals. The n-alkyl group acts as a better solubilizing moiety and the *tert*-butyl group may even enhance chain stiffness. This argument also accounts for the higher k_p value of n-BMA as compared to *tert*-BMA under otherwise identical conditions. Enhanced flexibility of poly(n-BMA) chains is also indicated by the lower glass transition temperature T_G, which is 20 °C for poly(n-BMA) as compared to 118 °C for poly(*tert*-BMA).[79] The steep decrease in <k_t> occurs at a higher degree of monomer conversion with n-BMA than with *tert*-BMA, which is also consistent with assuming a better chain-fluidizing action of n-butyl as compared to *tert*-butyl ester groups. It is known that upon addition of a solvent, the onset of gel-effect behavior of <k_t> is shifted toward higher degrees of monomer conversion or may even disappear.[15,41] Figure 16 tells that <k_t> of *tert*-butyl methacrylate (BMA) at 80 °C is close to <k_t> of n-BMA at 40 °C. The effect of reduced mobility on <k_t> of *tert*-BMA may thus be compensated by increasing temperature.

Reaction diffusion constants have been estimated from primary experimental <k_t>/k_p data at higher X (not shown in Figure 16) to be about 550 for n-BMA and close to 370 for *tert*-BMA. That C_{RD} is larger for n-BMA is consistent with the assumption of a higher segmental mobility of n-BMA as compared to *tert*-BMA macroradicals. Enhanced chain flexibility allows for a more efficient screening of the molecular environment and provides better opportunities for chain-end encounter and thus for termination. C_{RD} values reported for bulk homopolymerizations of other monomers are 800 for styrene (at 2000 bar), 700 for ethene (at 2550 bar), 100 for MMA, and 1200 for BA (both at ambient pressure).[75] As is

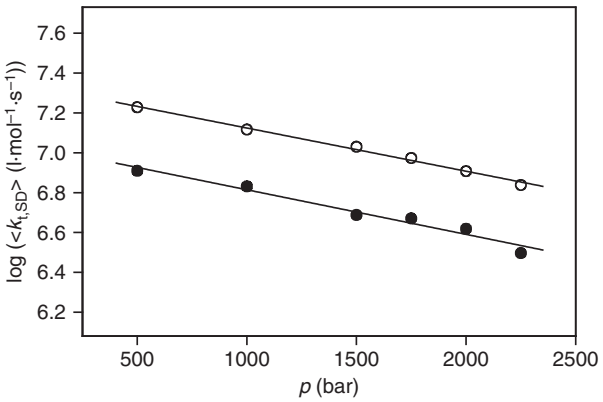

Figure 17 Pressure dependence of <$k_{t,SD}$> in the initial plateau region for n-BMA (open circles) and *tert*-BMA (full circles) bulk homopolymerizations at 60 °C. From Buback, M.; Junkers, T. *Macromol. Chem. Phys.* **2006**, *207*, 1640.[78]

to be expected, the C_{RD} values for n-BMA and *tert*-BMA are in between the ones reported for MMA and BA, with the number for *tert*-BMA being closer to the MMA value.

The effect of pressure on termination rate has been primarily investigated for the initial conversion range. Plotted in Figure 17 is the variation of the low-conversion plateau value <k_t> with pressure for *tert*-BMA and n-BMA bulk homopolymerizations at 60 °C.[78]

Within experimental uncertainty, the activation volumes associated with <$k_{t,SD}$> are almost identical for the two monomers: $\Delta V^{\#}(\langle k_{t,SD}\rangle) = (13.8 \pm 1.2)$ and $(14.3 \pm 2.6)\,\mathrm{cm^3\,mol^{-1}}$ for n-BMA and *tert*-BMA, respectively. The $\Delta V^{\#}(\langle k_{t,SD}\rangle)$ values are listed together with activation volumes for other (meth) acrylates and styrene in Table 6. The $\Delta V^{\#}(\langle k_{t,SD}\rangle)$ values for the entire series of monomers are rather similar.

The activation volume of styrene and MMA fluidity ($\Delta V^{\#}(\eta^{-1})$) amounts to 14.6 and 14.0 $\mathrm{cm^3\,mol^{-1}}$, respectively,[80] which are well within the range of the $\Delta V^{\#}(\langle k_{t,SD}\rangle)$ values listed in Table 6. This finding provides further evidence for the pressure dependence of <$k_{t,SD}$> being close to that of fluidity, η^{-1}.

Table 6 Activation volumes $\Delta V^{\#}(<k_{t,SD}>)$ for the initial polymerization period of various (meth)acrylates and styrene. The reaction conditions of the underlying experiments are given in Reference 15

	MMA	*n-BMA*	*tert-BMA*	*STY*	*MA*	*n-BA*	*DA*
$\Delta V^{\#}$ ($cm^3\,mol^{-1}$)	15 ± 5	13.8 ± 1	14.3 ± 3	15.4 ± 2	20 ± 6	16 ± 3	21 ± 6

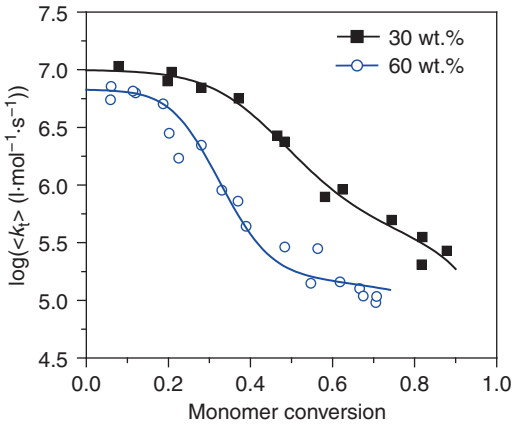

Figure 18 Dependence of the chain-length-averaged termination rate coefficient <k_t> on monomer conversion for MAA polymerizations at 50 °C and 2000 bar for initial monomer concentrations of 30 and 60 wt.% MAA, respectively. From Beuermann, S.; Buback, M.; Hesse, P.; *et al. Macromolecules* **2008**, *41*, 3513.[81]

Free-radical termination kinetics up to high pressure has also been studied for solution polymerizations. Illustrated in Figure 18 is the dependence of the chain-length-averaged termination rate coefficient <k_t> on monomer conversion for polymerization of nonionized methacrylic acid (MAA) in aqueous solution.[81] The SP-PLP-NIR experiments have been carried out at 50 °C and initial MAA concentrations of 30 and 60 wt.%. As with MMA bulk polymerization, <k_t> exhibits a plateau region at low degrees of monomer conversion, which is followed by the translational diffusion range with a steep decrease of <k_t> toward higher conversion. This decrease is rather pronounced at the higher MAA concentration, whereas the initial plateau values of <$k_{t,SD}$> at the two MAA contents are close to each other. The minor difference in <$k_{t,SD}$> is most likely due to the viscosity of the aqueous monomer solution with 60 wt.% MAA being clearly above that with 30 wt.% MAA. At even higher conversion, which becomes particularly clear from the data for 60 wt.%, termination runs into control by reaction diffusion.

The rate coefficient for termination under translational diffusion control k_{TD}, which primarily affects the section where the steep decrease of <k_t> occurs, may be expressed as $k_{TD} = k^0_{TD}/\eta_r$ (see first term on the r.h.s. of eqn [9]). Although η_r depends on both polymer content and the type of polymer produced, it has turned out in preceding studies on bulk (meth)acrylate[74] and MMA solution polymerizations[82] that η_r may be represented by the simplifying expression:

$$\ln \eta_r = C_\eta \cdot X \qquad [10]$$

The parameter C_η may be looked upon as an adjustable parameter, which determines the conversion dependence of <k_t> under conditions where k_{TD} controls termination rate. The C_η parameter may be found from the slope of the straight line, which intersects the ordinate at $\log(k^0_{TD})$ and passes through the inflection point of the sigmoidal $\log(<k_t>)$ versus X curve. The so-obtained C_η values are 12.8 and 21.2 for polymerization of 30 and of 60 wt.% MAA, respectively. That C_η at 60 wt.% MAA is above C_η at 30 wt.% MAA by a factor of about 2 may be understood as a consequence of twice the amount of polymer being present at initial contents of 60 wt.% MAA and identical X. Plotting the <k_t> data from Figure 18 against weight fraction of poly(methacrylic acid) rather than against conversion results in the two curves from Figure 18 sitting more or less on top of each other in the TD range.[81]

4.35.4 High-Pressure Ethene Polymerization

A kinetic scheme for high-pressure ethene polymerization includes propagation, termination, chain transfer (CT) to monomer, CT to polymer, CT to chain-transfer agents (CTAs), intramolecular CT (backbiting), and β-scission rate coefficients (Scheme 2). Initiation, propagation, and termination steps primarily determine monomer conversion, whereas the entire set of reactions needs to be known for simulation of MMD and polymer architecture.

4.35.4.1 Propagation and Termination

As mentioned above, diffusion-controlled kinetics depends on the history of the (preceding) polymerization. Thus, physical properties of the polymerizing medium, such as bulk viscosity and diffusivity as a function of chain length, should be known to fully understand polymerization kinetics. This information is mostly not available. Fortunately, under typical polymerization conditions, the impact of transport processes is not that all-invasive and it is essentially termination that is significantly affected. This dependence may, however, be very complicated and may largely vary with monomer conversion.

Among the pulsed laser techniques described in Section 4.35.3, only SP-PLP-NR could be successfully applied to ethene polymerization.[40] The primary parameters from SP-PLP are the coupled quantities k_p/k_t and $k_t \cdot c^0_R$ (and thus also $k_p \cdot \varphi_i$), where φ_i is the initiating quantum efficiency. φ_i should be close to unity, the assumption of which is supported by $k_p \cdot \varphi_i$ being almost identical to the k_p value reported by Lim and Luft[12] for 200 °C/1750 bar and extrapolated to the p and T conditions of the SP-PLP-NIR experiment (230 °C and 2550 bar). The extrapolation is based on the experimental activation parameters from Reference 83. Adopting $\varphi_i = 1$ for the entire range of high-temperature, high-pressure experiments allows for deducing both k_t and k_p from SP-PLP-NIR. According to this procedure, Schweer[14] obtained the correlations for k_t (eqn [11]) and k_p (eqn [12]) as a function of temperature, pressure, monomer conversion, and viscosity from his

$I_2 \xrightarrow{k_d} 2I\cdot$	initiation
$I\cdot + E \xrightarrow{k_p} R_1$	primary propagation step
$R_s + E \xrightarrow{k_p} R_{s+1}$	propagation
$R_s + R_r \xrightarrow{k_{t,comb}} P_{s+r}$	termination by combination
$R_s + R_r \xrightarrow{k_{t,disp}} P_s + P_r$	termination by disproportionation
$R_s + E \xrightarrow{k_{tr,M}} P_s + R_1$	chain transfer to monomer
$R_s + CTA \xrightarrow{k_{tr,X}} P_s + R_1$	CT to a CTA
$R_s \xrightarrow{k_{bb}} R_{r,sec}$	backbiting
$R_s + P_r \xrightarrow{k_{tr,P}\cdot r} P_s + R_{r,sec.}$	CT to polymer
$R_{r,sec.} \xrightarrow{k_\beta} P_{r-s} + R_s$	β-scission
$R_{r,sec.} + M \xrightarrow{k_{p,sec}} R_{r+1,LCB}$	propagation of a branched radical
$R_{r,sec(from\ bb).} + M \xrightarrow{k_{p,sec}} R_{r+1} + SCB$	monomer addition to a secondary radical from backbiting

Scheme 2 Kinetic steps of ethene homopolymerization (*r, s* characterize chain length).

measurements at temperatures between 190 and 230 °C and pressures between 1950 and 2900 bar:

$$k_t(T,p,X,\eta) = \left(0.832 \times \frac{1}{\eta_r} + 8.04 \times 10^{-6} \times (1-X) \times \frac{k_p^0}{1+\frac{k_p^0}{1.13\cdot 10^{10}}\cdot\eta_r}\right)\cdot k_t^0 \quad [11]$$

$$k_p(T,p,X,\eta) = \frac{k_p^0}{1+\frac{k_p^0}{1.13\cdot 10^{10}}\cdot\eta_r} \quad [12]$$

where η_r indicates relative bulk viscosity and $\eta_r = \eta/\eta_0$, with η_0 referring to pure ethene viscosity at identical p and T. The notations k_t^0 and k_p^0 refer to the termination and propagation rate coefficients at very low conversion, respectively. These two quantities were also deduced from SP-PLP experiments:

$$k_t^0\ (\mathrm{mol^{-1}\ s^{-1}}) = 8.11 \times 10^8 \cdot \exp\left(\frac{-553 - 0.190\cdot p\ (\mathrm{bar})}{T\ (\mathrm{K})}\right) \quad [13]$$

$$k_p^0\ (\mathrm{mol^{-1}\ s^{-1}}) = 1.88 \times 10^7 \cdot \exp\left(\frac{-4126 + 0.33\cdot p\ (\mathrm{bar})}{T\ (\mathrm{K})}\right) \quad [14]$$

4.35.4.2 CT to Monomer

CT to monomer occurs between the same reaction partners as does propagation:

$$R_s + E \xrightarrow{k_{tr,M}} P_s + R_1 \quad [15]$$

with R_s and P_s referring to radicals and polymer of chain length s, respectively; E is ethene; and R_1 is a small free radical of similar size to ethene.

According to the standard procedure, the inverse (average) degree of polymerization P_N^{-1} from experiments at low initiation rate, and thus also low termination levels, is used to estimate the CT to monomer constant $C_{tr,M}$:

$$P_N^{-1} = C_{tr,M} = k_{tr,M}/k_p \quad [16]$$

Plotted in Figure 19 is P_N^{-1} against inverse temperature for ethene homopolymerizations at 2000 bar and very low initiation rates.[84,85] Arrhenius-type behavior of $C_{tr,M}$ is clearly seen. The slope to the straight line yields the difference in the activation energies for CT to monomer and propagation. With $E_A(k_p)$ being known from Schweer's work,[14] the experimental value of $E_A(C_{tr,M})$ yields $E_A(k_{tr,M}) = (74 \pm 8)\ \mathrm{kJ\ mol^{-1}}$, which is remarkably close to $E_A(k_{tr,M}) = 83\ \mathrm{kJ\ mol^{-1}}$ estimated by Heuts *et al.*[86] from *ab initio* quantum mechanical calculations for the transfer reaction between an ethyl radical and ethene.

Fitting the entire set of experimental P_N^{-1} data measured as a function of p and T yields the following expression for $C_{tr,M}$:[84,85]

$$\ln C_{tr,M} = 2.90 - (T\ (\mathrm{K}))^{-1}\cdot\left(5524 + 0.257\cdot\left((p\ (\mathrm{bar})) - 2000\right)\right) \quad [17]$$

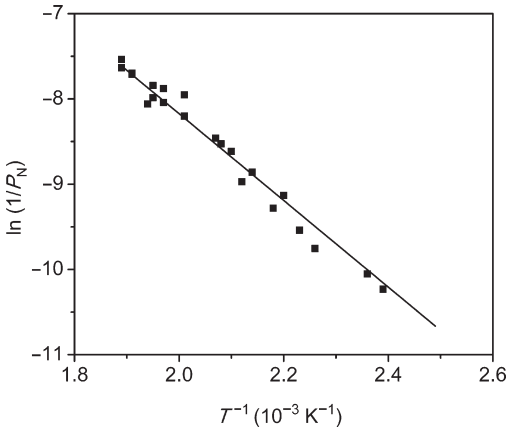

Figure 19 Variation of P_N^{-1} with inverse temperature for ethene polymerizations at 2000 bar and low initiation rates with data from Buback, M.; Choe, C.-R.; Franck, E. U. *Makromol. Chem.* **1984**, *185*, 1685; Buback, M.; Choe, C.-R.; Franck, E. U. *Makromol. Chem.* **1984**, *185*, 1699.[84,85]

4.35.4.3 CT to Polymer and β-Scission

Intramolecular CT (backbiting), intermolecular transfer to polymer, and β-scission largely affect polymer structure. Backbiting occurs by 1,5-H shift and results in the formation of short-chain branches, mostly *n*-butyl side groups. The backbiting reaction has been thoroughly studied by Goto *et al.*[87] and rate coefficients are available as a function of pressure and temperature.

Secondary macroradicals from intermolecular CT may either propagate to form long-chain branches (LCBs) or undergo β-scission. It should be noted that LCBs significantly contribute to the very specific and attractive structure of LDPE. No generally accepted view of the transfer-to-polymer process has emerged so far. Feucht *et al.*[11] treated this process as a single reaction step characterized by the rate coefficient $k_{tr,P}$. The increasing probability for CT of a larger molecule is taken into account by multiplying $k_{tr,P}$ with the chain length r of the polymer molecule, which reacts with radical R_s:

$$R_s + P_r \xrightarrow{k_{tr,P}\cdot(a+(1-a)\cdot r)} P_s + R_{r,LCB}, \quad a \in [0, \ldots, 1] \qquad [18]$$

An alternative description of the transfer-to-polymer process has been put forward by Goto *et al.*[87] These authors also assume transfer-to-polymer rate to scale with polymer chain length r (eqn [19]). By introduction of the β-scission step (eqn [20]) for branched macroradicals, the steep rise in M_W toward high conversion is avoided:

$$R_s + P_r \xrightarrow{k_{tr,P}\cdot r} P_s + R_{r,LCB} \qquad [19]$$

$$R_s + (P_q) \xrightarrow{k_\beta} P_s + R_r + (P_{q-r}) \qquad [20]$$

As a third alternative, Lorenzini *et al.*[3,4] envisaged the transfer-to-polymer process as a reaction sequence that starts with the formation of a secondary macroradical (eqn [21]) and is followed by either β-scission (eqn [22]) or propagation (eqn [23]):

$$R_s + P_r \xrightarrow{k_{tr,P}\cdot r} P_s + R_{r,sec} \qquad [21]$$

$$R_{r,sec} \xrightarrow{k_\beta} P_{r-s} + R_s \qquad [22]$$

$$R_{r,sec} + M \xrightarrow{k_{p,sec}} R_{r+1,LCB} \qquad [23]$$

Both the Goto *et al.* and the Lorenzini *et al.* models afford for a good fit of the experimentally observed long-chain branching index I_{LCB}, that is, of the number of branches per 1000 chain atoms, of measured M_W, and also of the full MMD. The Goto *et al.* scheme has the advantage of a reduced stiffness of the differential equations associated with this approach. In case that the type and the concentration of branched macroradicals need to be specified, the kinetic scheme of Lorenzini *et al.* appears to be more suitable.

The difficulties met in deducing chain-transfer and β-scission rate coefficients from experimental quantities are due to the fact that the individual kinetic steps contribute in a complex fashion to polyethylene properties. A brief survey on the correlation of fundamental polymerization kinetics to process design and to the prediction of polymer properties has been presented by Bauer *et al.*[88]

Several additional engineering aspects need to be considered with high-pressure ethene polymerizations carried out in tubular or autoclave reactors, including phase behavior and safety aspects.[89–91]

4.35.5 High-Pressure Ethene Copolymerization

Via high-pressure copolymerization, the properties of ethene-based materials may be significantly modified and adjusted to special applications. Frequently used comonomers are vinyl acetate and (meth)acrylic acid esters. Of primary importance is the knowledge of reactivity ratios r_i, which are defined as $r_i = k_{ii}/k_{ij}$, that is, the ratio of homopropagation k_{ii} to cross-propagation k_{ij} rate coefficients. The notation k_{ij} refers to addition of monomer j to a radical chain end with the terminal unit resulting from species i. Under ideal polymerization conditions, the mole fraction F_i of monomer units i contained in the copolymer is given by eqn [24], which holds for both the terminal and the implicit penultimate models.[92]

$$F_i = \frac{r_i \cdot f_i^2 + f_i \cdot (1-f_i)}{r_i \cdot f_i^2 + 2 \cdot f_i \cdot (1-f_i) + r_j \cdot (1-f_i)^2} \qquad [24]$$

In eqn [24], f_i is the mole fraction of monomer i in the monomer mixture. In the penultimate models, two monomer-derived segments at each radical chain end are taken into account, for example, by the rate coefficient k_{iij}, which refers to addition of a monomer molecule j to a radical chain end where both terminal and penultimate units consist of species i. Equation [24] is used to derive r_i and also $r_j = k_{jj}/k_{ji}$ from measured compositions of monomer mixture and copolymer, f_i and F_i, respectively.

Plotted in **Figure 20** is the copolymer mole fraction F_{MA} versus monomer mole fraction f_{MA} for E–MA copolymerizations carried out in a continuously operated reactor at 2000 bar and temperatures of 220, 250, and 290 °C. By visual and/or spectroscopic monitoring of the copolymerizing system, it is ensured that the reaction takes place in homogeneous phase. Copolymerization is associated with a significant increase in MA content. The two reactivity ratios are strongly correlated, which is best taken into account by calculating 95% confidence

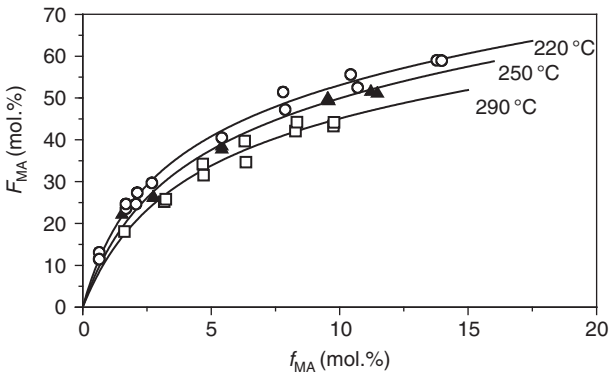

Figure 20 MA content of the copolymer F_{MA} (in mol.%) plotted against the MA content of the monomer mixture f_{MA} for E–MA copolymerizations at 2000 bar and temperatures of 220, 250, and 290 °C. The curves are fits of the experimental data to eqn [24]. From Buback, M.; Dröge, T. *Macromol. Chem. Phys.* **1997**, *198*, 3627.[93]

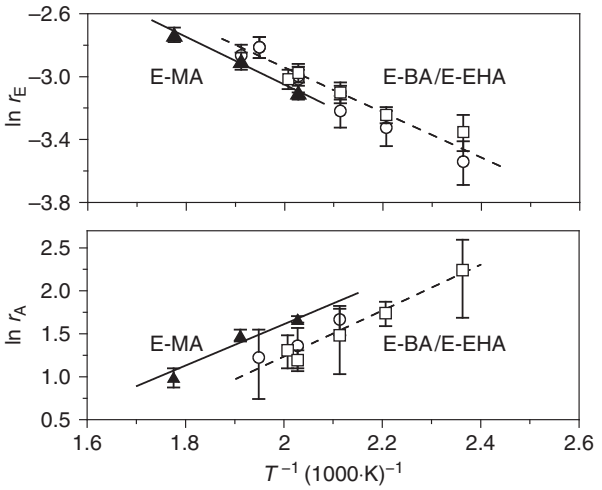

Figure 21 Arrhenius plots of ethene and acrylate reactivity ratios r_E and r_A, respectively, for copolymerization of the binary systems E–MA (triangles), E–BA (squares), and E–EHA (circles) at 2000 bar. The dashed lines represent the fit to the combined data set for E–BA and E–EHA. From Buback, M.; Dröge, T.; van Herk, A.; Mähling, F.-O. *Macromol. Chem. Phys.* **1996**, *197*, 4119.[95]

intervals for these quantities according to the procedure suggested by van Herk.[94]

Arrhenius plots of ethene and acrylate reactivity ratios r_E and r_A, respectively, for the E–MA, E–BA, and E–EHA (ethylhexyl acrylate) copolymerizations at 2000 bar are shown in Figure 21. The r_E values of the three systems are rather similar, whereas r_A of E–MA is slightly, but significantly, above the corresponding values for the E–BA and E–EHA systems. The fitted lines in Figure 21 are given by the following Arrhenius-type relations (referring to 2000 bar):

E–MA system:[93]

$$\ln r_E\,(\mathrm{MA}) = -0.0202 - 1516 \times \left(T\,(\mathrm{K})\right)^{-1} \qquad [25]$$

$$\ln r_A\,(\mathrm{MA}) = -3.170 - 2406 \times \left(T\,(\mathrm{K})\right)^{-1} \qquad [26]$$

($p = 2000$ bar; 220 °C ≤ Θ ≤ 290 °C).

E–BA and E–EHA systems:[95]

$$\ln r_E\,(\mathrm{BA/EHA}) = -0.0834 - 1431 \times \left(T\,(\mathrm{K})\right)^{-1} \qquad [27]$$

$$\ln r_A\,(\mathrm{BA/EHA}) = -4.135 - 2670 \times \left(T\,(\mathrm{K})\right)^{-1} \qquad [28]$$

($p = 2000$ bar; 150 °C ≤ Θ ≤ 250 °C).

Ethene high-pressure copolymerization studies have also been carried out for the systems E–MMA,[96] E–BMA,[97] E–acrylic acid, and E–methacrylic acid.[98,99] Whereas the comonomer reactivity ratios turn out to be slightly different, the ethene reactivity ratios for the entire set of (meth)acrylates and for (meth)acrylic acid are remarkably close to each other. The similarity of $r_E = k_{EE}/k_{EX}$ is probably due to the cross-termination propagation rate coefficient rate k_{EX} being dominated by the highly reactive ethene-terminated radical.[99]

Arrhenius equations such as eqns [25]–[28] and/or the corresponding expressions presented in References 96 and 99 allow for estimating ethene and comonomer reactivity ratios for 2000 bar, which is a typical pressure. Further information about reactivity ratios in ethene copolymerization may be found in the pioneering article by Ehrlich and Mortimer,[100] which contains a wealth of detailed information on all aspects of ethene homo- and copolymerization.

The variation of reactivity ratios with pressure is minor, as it is the difference between the activation volumes for homopropagation and cross-propagation that determines the formal activation volume of r: $\Delta V^{\neq}(r_i) = -(\partial \ln r_i/\partial p)_T RT$. As a consequence, the accurate measurement of the resulting small activation volumes poses problems, which is especially true for $\Delta V^{\neq}(r_X)$, as the comonomer content of the feed is mostly rather low. On the other hand, because of the small size of $\Delta V^{\neq}(r)$, this number need not be known overly accurately. Moreover, the pressure range of ethene copolymerizations is not very extended, as pressure is limited toward high p for technical reasons and toward low p by inhomogeneity of the reaction mixture.

A few experiments, in which pressure was changed during the course of continuous copolymerizations under otherwise constant reaction conditions, have been carried out to estimate $\Delta V^{\neq}(r_E)$.[93] The numbers obtained for the E–MA and E–EHA systems are $\Delta V^{\neq}(r_E) = -(7.4 \pm 4.1)$ and $-(8.2 \pm 3.5)\,\mathrm{cm^3\,mol^{-1}}$, respectively. For ethene–BMA copolymerizations, the value $\Delta V^{\neq}(r_E) = -(6.0 \pm 3.9)\,\mathrm{cm^3\,mol^{-1}}$ has been reported.[97] These negative $\Delta V^{\neq}(r_E)$ values indicate that r_E slightly increases with pressure.

Simulation of polymerization and copolymerization kinetics requires additional information about the phase behavior of the monomer–polymer system. Cloud-point studies on copolymer–ethene as well as copolymer–ethene–comonomer systems have been carried out over wide p and T ranges under visual inspection of the reaction mixture.[38,101] Part of the measured cloud-point curves have been modeled by perturbed chain - statistical associating fluid theory (PC-SAFT) theory.[102]

4.35.6 Reversible Deactivated Radical Polymerization

Reversible deactivated radical polymerization processes, which have been referred to as living/controlled radical polymerizations, allow for producing polymeric materials with controlled molecular masses, low dispersities, and complex macromolecular architectures, such as block and comb-like copolymers as well as star-shaped (co)polymers. In addition to nitroxide-mediated polymerization (NMP)[103] and atom-transfer radical polymerization (ATRP),[104] reversible addition fragmentation chain-transfer (RAFT) polymerization is an attractive new method.[105]

One type of RAFT agents are dithioesters, Z–C(=S)S–R, which have been developed in great structural variety. RAFT polymerization proceeds via a degenerative chain-transfer mechanism in which two equilibria (see Scheme 3) are embedded into a conventional radical polymerization scheme with the elementary initiation, propagation, and termination steps remaining unaffected. In the pre-equilibrium, addition of a propagating radical to the sulfur–carbon double bond of the RAFT agent **1** produces a carbon-centered intermediate RAFT radical **2**, which may undergo β-scission either yielding back the reactants or releasing an initiating radical $R^{\bullet}$ plus a polymeric dithioester compound **3** that constitutes the dormant species. A similar set of reactions is operating under main-equilibrium conditions, where growing macroradicals

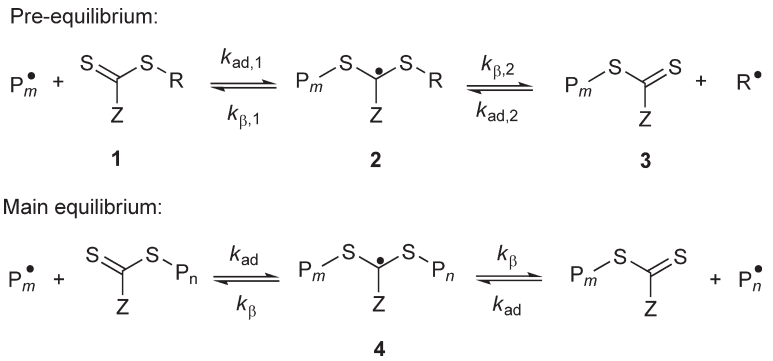

Scheme 3 Pre-equilibrium and main-equilibrium species occurring in dithiobenzoate-mediated RAFT polymerization.

react with polymeric RAFT agent **3** to produce the intermediate radical **4**. Repeated RAFT events result in the living/controlled characteristics of the polymerization.

High pressure may provide deeper insight into the RAFT mechanism and may also be interesting because of potential applications. Propagation rate should be enhanced by pressure, whereas termination rate should decrease. A first study on RAFT polymerization at high pressure (1.8 kbar) has been carried out on styrene.[106] Rzayev and Penelle[107,108] performed dithioester-mediated polymerizations of methyl ethacrylate and MMA under high pressure and succeeded in producing controlled polymer of high molecular mass.

Online NIR spectroscopy has been used to measure conversion versus time traces for cumyl dithiobenzoate (CDB)-mediated styrene bulk polymerizations up to 2.5 kbar. MMDs of the resulting polymer were determined by SEC.[109]

Polymerization rate is decreased with increasing RAFT concentration (**Figure 22**), which is a specific feature of CDB mediation that will not be addressed here. Irrespective of RAFT content, overall polymerization rate increases by a factor of 3 in passing from ambient pressure to 2.5 kbar.

In addition to favorably affecting rate, high pressure is advantageous with respect to molecular mass control. Dispersity, PDI, of polystyrene generated via CDB-mediated polymerization could be improved, for example, has been reduced in styrene bulk polymerization at 70 °C from 1.28 at ambient pressure to 1.12 at 2000 bar. Illustrated in **Figure 23** is the accompanying decrease in half-width of the MMD for polystyrene produced under CDB control at 1 and 2000 bar.

The beneficial action of high pressure on reversible deactivated radical polymerization is not restricted to RAFT systems

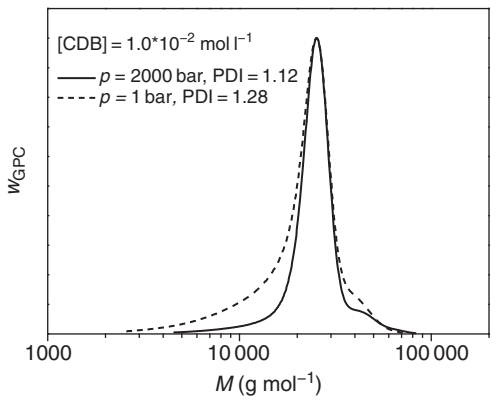

Figure 23 MMDs of polystyrene generated via CDB-mediated styrene bulk polymerization at 70 °C and two pressures, 1 and 2000 bar. The other reaction parameters were kept constant. From Arita, T.; Buback, M.; Janssen, O.; Vana, P. *Macromol. Rapid Commun.* **2004**, *25*, 1376.[109]

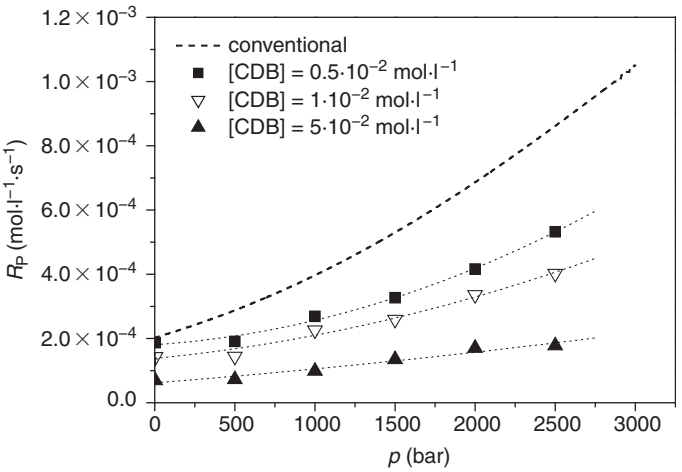

Figure 22 Pressure dependence of the rate of polymerization at 70 °C for CDB-mediated styrene bulk polymerization at three CDB levels; initiator azobisisobutyronitrile concentration: 1×10^{-2} mol l^{-1}. The dashed line represents conventional polymerization, that is, without CDB, under otherwise identical conditions. From Arita, T.; Buback, M.; Janssen, O.; Vana, P. *Macromol. Rapid Commun.* **2004**, *25*, 1376.[109]

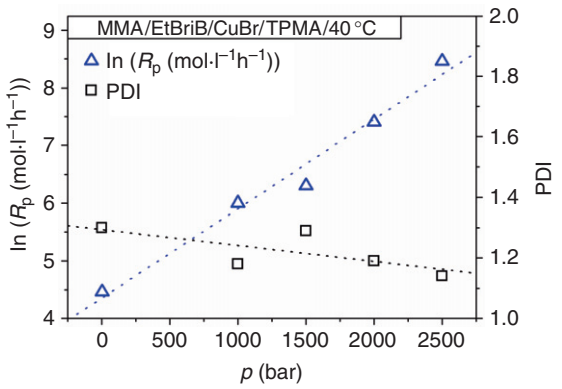

Figure 24 MMA polymerization under ATRP control by TPMA with EtBr*i*B as the initiator at 40 °C and several pressures; solvent, acetonitrile. From Morick, J. Ph.D. thesis, Georg-August-Universität Göttingen, Göttingen, 2011.[110]

but occurs also with ATRP. This is exemplified by data for MMA solution polymerization in acetonitrile with ethyl-2-bromo-*iso*-butyrate (EtBr*i*B) being the initiator and Cu^I complexed by *tris* [(2-pyridyl)-methyl]amine (TPMA) being the catalyst. The measured pressure-induced increase in polymerization rate and decrease in dispersity are plotted in Figure 24.[110]

4.35.7 Homogeneous-Phase Polymerization in $scCO_2$

The solubility of polymers in $scCO_2$ depends strongly on pressure and temperature, which alter inter- and intramolecular forces between solvent molecules and polymer segments and affect the free-volume difference between polymer and CO_2. Important parameters are the chemical nature of the repeat units, polymer crystallinity, molecular mass, and polymer architecture.[24] The presence of acetate and ether moieties,[111] Si atoms, and in particular of fluorocarbon pendent groups on a hydrocarbon backbone has a positive influence on polymer–$scCO_2$ phase behavior.[112–114]

Despite the fact that most nonfluorinated polymers show poor solubility in $scCO_2$, polymerizations may be carried out in homogeneous phase in the presence of significant amounts of $scCO_2$. In contrast to solubility measurements, in which a polymer has to be dissolved by the sc fluid, a polymerizing system initially consists of monomer and CO_2. Then, conversion occurs and polymer concentration increases, while monomer serving as cosolvent is still present. Depending on the CO_2 content, molecular masses, and type of polymer, solution polymerizations are feasible. For example, it was shown that even polystyrene, which is considered as the archetype of a polymer being insoluble in $scCO_2$,[115] may be obtained from single-phase polymerization in CO_2, provided that low-molecular-mass material is generated.[116] Moreover, the choice of pressure and CO_2 content strongly affects the styrene conversion that may be reached in homogeneous phase. If the CO_2 content is sufficiently low, CO_2 will diffuse into a polymer melt, leading to a homogeneous system consisting of a CO_2-swollen polymer melt.

With respect to technical applications, integral processes that combine polymer synthesis with formulation and polymer processing are particularly attractive. If all three steps benefit from $scCO_2$ as the common reaction and process medium, an integral process requires only one pressurization step in contrast to isolated individual process steps. In particular for high-pressure conditions, continuous processes are favorable, since the pressurized volume may be relatively small and still large quantities of product may be obtained. As an example for homogeneous-phase reactions, the synthesis of binder materials for coating applications is considered. In an effort to decrease the amount of solvents and to obtain products of high-solid contents, modern acrylic binders are of rather low molecular mass around 2000 g mol^{-1}. The actual coating is formed *in situ* on the surface via cross-linking reactions.[117] Synthesis of styrene–methacrylate copolymers that serve as model compounds for binder materials in solution with $scCO_2$ is discussed below. Other attractive monomers for homogeneous-phase polymerizations in $scCO_2$ are vinyl acetate and silica- and fluorine-containing monomers. In particular, fluorinated systems were investigated in $scCO_2$. The fluoropolymer synthesis in solution with $scCO_2$ is reported for fluorinated olefins, that is, vinylidene fluoride (VDF) and hexafluoropropene (HFP).

4.35.7.1 Styrene–Methacrylate Copolymers

Copolymers consisting of styrene, MMA, and functional methacrylates are applied as low-molecular-mass binder materials. Functional methacrylates such as GMA or hydroxyethyl methacrylate containing epoxy or hydroxyl groups are considered as cross-linkers. To study the feasibility of $scCO_2$ as reaction medium for binder synthesis, model copolymerizations containing initial monomer mole fractions of 0.07, 0.51, and 0.42 for styrene, MMA, and GMA, respectively, were carried out. In a first step, batch polymerizations were performed in optical high-pressure cells equipped with sapphire windows. This setup allows for visual inspection of the reaction mixture and for FT-NIR monitoring of monomer conversion during polymerization. Moreover, information on the phase behavior may be obtained from the NIR spectral series. Heterogeneity is detected from NIR light scattering, which results in an increase of the spectrum baseline, whereas a constant baseline indicates polymerization in homogeneous phase.[116] Single-phase copolymerizations were carried out with 20 wt.% CO_2 at temperatures ranging from 80 to 160 °C and pressures around 350 bar.[20] It should be noted that at temperatures above 120 °C, depropagation comes into play and limits the final conversion as well as affects copolymer composition.[118,119] Up to 120 °C, complete monomer conversion was obtained in homogeneous phase.

The molecular masses were controlled by either initiation rate or the use of CTAs. Because of the targeted low molecular masses, high amounts of initiator or conventional CTAs, such as dodecyl mercaptan, were required. In case that a catalytic CTA, such as bis(borondifluoro diphenylglyoximato) cobaltate (CoPhBF), is used for molecular mass control, only parts per million (ppm) amounts of CTA are required.[120] Molecular mass control via initiation leads to high-dispersity material. Because of the low CO_2 contents and consequently the high monomer concentrations, conventional peroxide initiators, for example, TBPP or TBPO, of known decomposition kinetics and efficiency (see Section 4.35.3.1) could be used. No special fluorinated initiators were required.

A tubular reactor setup was developed for the synthesis of the above-mentioned model copolymer for acrylic binder materials. The tubular reactor essentially consists of capillaries with an internal diameter of 3.8 mm and a length of either 4 or 8 m, which are wound up to a coil of 15 cm diameter. The two reactor lengths allow for adjusting residence times between 5.5 and 44 min. The maximum pressure of the setup is 500 bar at 200 °C.[120] Typically, a premixed solution containing the monomers, initiator, and, if applicable, the CTA, was pressurized and fed into the reactor via a membrane pump. Liquid CO_2 was fed by a pneumatic high-pressure liquid chromatography (HPLC) pump. A constant CO_2 flow of up to 8 ml min^{-1} was maintained by means of an electric HPLC pump. After bringing the monomer–initiator or the monomer–initiator–CTA solution and CO_2 together, a mixing chamber was passed to generate a homogeneous mixture. The homogenized mixture was pumped through the thermostated tubular reactor. Behind the reactor, the mixture was depressurized and the polymeric product was collected. For monomer conversions above 95%, a white powder was obtained during expansion. Expansion of the reaction mixture is accompanied by significant cooling and an oversaturation of polymer in the surrounding CO_2 phase. Consequently, particle formation occurs. Further details are contained in References 119 and 120.

Beneficial aspects for homogeneity are the required low molecular masses and the low CO_2 content of 20 wt.%. The latter is also important for process productivity. Moreover, the presence of $scCO_2$ leads to a reduction in viscosity compared to polymerizations in bulk or organic solvents, which is advantageous for a continuous process.

4.35.7.2 Fluorinated Olefins

Fluorinated polymers exhibit unique properties leading to advanced applications, which were outlined in a recent review by Ameduri.[121] VDF homo- and copolymers are of particular interest, because in addition to high stability, they show ferro-, pyro-, and piezoelectric behavior for use in transducers, sensors, or switches.[122] Being insoluble in common organic solvents, fluoropolymers are mostly synthesized in emulsion polymerization using fluorinated stabilizers, which, however, may accumulate in the environment.[123] Because of the fair solubility of amorphous fluoropolymers in common solvents, $scCO_2$ is considered as an attractive alternate reaction medium for the production of fluoropolymers. In their pioneering work on polymerizations in $scCO_2$, the group of DeSimone[124] studied homogeneous-phase polymerizations of tetrafluoroethene and semi-fluorinated acrylates (e.g., 1,1-dihydroperfluorooctyl acrylate or 2-(*N*-ethylperfluorooctanesulfonamido)ethyl acrylate) and styrene with fluorinated substituents, for example, perfluoroethyleneoxymethyl styrene. For tetrafluoroethene, the use of $scCO_2$ does not only provide a nonfluorinated reaction medium but also add to the safety of the process. Moreover, acid end groups frequently formed in aqueous phase are not seen.[125,126]

Most studies using $scCO_2$ in VDF polymerizations deal with heterogeneous-phase reactions, either dispersion or precipitation polymerizations.[127–131] In precipitation polymerization, bimodal MMDs were obtained, which was explained by different loci of polymerization.[132] Homogeneous-phase reactions in the absence of any fluorinated solvents or stabilizers yield rather narrow monomodal MMDs.[21,126,133–136] Additionally, a stabilizer influence on product properties is avoided. For kinetic investigations, homogeneous-phase conditions are desirable since no mass transfer processes over phase boundaries have to be considered and in-line FT-IR or FT-NIR spectroscopy may be applied to monitor monomer conversion throughout the reaction.

Poly(vinylidene fluoride) (PVDF) is only poorly soluble in $scCO_2$ despite the high degree of fluorination. The reason is seen in the semicrystallinity of PVDF.[114] With M_n values being limited to 10 000 g mol^{-1}, homogeneity may be obtained at 120 °C and 1500 bar in the presence of 77 wt.% CO_2 up to complete VDF conversion.[134] If chain length was controlled by the initiation rate, broad MMDs with dispersities ≥3 were obtained. When DTBP is used, a high concentration of 0.3 mol l^{-1} is required, which corresponds to 10% of the monomer concentration. To avoid the use of such high initiator concentrations, molecular mass was controlled by CTAs. With respect to phase behavior, fluorinated CTAs are interesting. Particularly attractive is the use of perfluorinated alkyl iodides, for example, $C_6F_{13}I$, because, as pointed out by Ameduri and co-workers,[137–139] fluorinated iodides such as $C_6F_{13}I$ do not only effectively control molecular masses but also enable so-called iodine transfer polymerizations (ITPs), which exhibit living polymerization behavior. ITP of VDF with $C_6F_{13}I$ has been carried out in $scCO_2$.[135] The availability of this technique is important for the fluorinated olefins, as other CRP techniques, such as ATRP, RAFT, and NMP, are not easily applied to this class of monomers.[121] ITP employing $C_6F_{13}I$ is based on the equilibrium between free radicals and I-end-capped radicals as the dormant species:

$$P_n^{\bullet} + P_m - I \rightleftharpoons P_n - I + P_m^{\bullet}$$

The prerequisite of the equilibrium is the rather labile C–I bond of the CH_2–CF_2–I end group. This labile end group may also be used for modification of the polymer, for example, to an azide end group, which may subsequently be used for reactions with alkynes or for functionalization of carbon black nanoparticles.[140,141]

As described above for styrene–methacrylate copolymers, PVDF is collected as a dry white powder after expansion of the reaction mixture containing $scCO_2$. Scanning electron micrographs of the particulate material show that porous structures are obtained. The molecular mass and polymer end groups originating from either initiator or CTA strongly influence the PVDF morphology, the degree of crystallinity, and the type of crystal phase.[133] In addition, the size distribution of PVDF nanoparticles obtained from RESS experiments strongly depends on M_n and polymer end groups.[142]

Despite the fluorination of the VDF units, rather high temperatures and pressures are required for homogeneous-phase polymerizations of VDF in $scCO_2$. Addition of HFP to the reaction mixture leads to a lowering of cloud-point pressures, because it is known that VDF–HFP copolymers are amorphous at HFP contents, F_{HFP}, above 0.20.[121] Due to the pending CF_3 group, the free volume of the polymer is increased and the entropy of mixing with CO_2 is enhanced. A reduction in polymer segment–segment interactions will favor the interchange energy.[143] Moreover, it was shown that HFP not only acts as a comonomer but also affects the phase behavior and reduces cloud-point pressures significantly.[144]

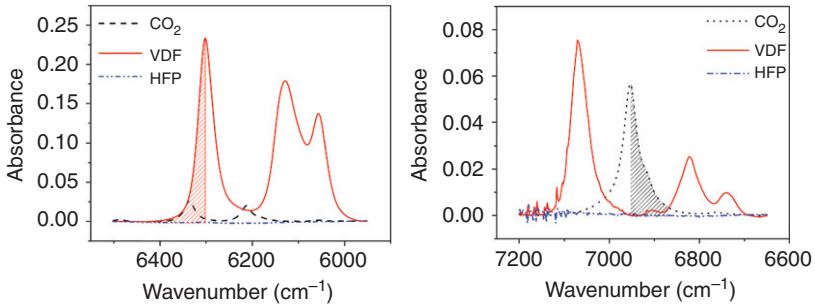

Figure 25 NIR (left)[145] and MIR (right) spectra of VDF, HFP, and CO_2 recorded at 100 °C and 800 bar. The crisscrossed area was integrated.

To explore the conditions for homogenous-phase VDF–HFP copolymerizations, monomer feed composition and CO_2 content were varied over a wide range. Performing the reactions in optical high-pressure cells allows for in-line monitoring of phase behavior and monomer conversion. As described above, the olefinic CH-stretching vibration of VDF is associated with a prominent peak at 6303 cm^{-1}. As shown in **Figure 25**, HFP shows no absorbance in the wavenumber range assigned to CH-stretching vibrations. CO_2 absorbs weakly at 6214 and 6332 cm^{-1}. Contributions of CO_2 were eliminated by subtraction of reference spectra recorded at the same temperature and pressure, since CO_2 has an intense peak at 6953 cm^{-1}, which is not superimposed by absorptions of either VDF or HFP. HFP is characterized by an absorption in the mid-infrared (MIR) range at 2095 cm^{-1}. The higher wavenumber half-band is not significantly superimposed by absorptions of VDF or CO_2. Monitoring of both monomers during a copolymerization requires the use of silicon windows, because the transparency of sapphire windows at and below 2100 cm^{-1} is unsatisfactory.

VDF–HFP copolymerizations with in-line monitoring of the NIR and the MIR region provide access to conversion of both monomers as a function of time, as is illustrated in **Figure 26(a)**. Since reacted monomer is converted into copolymer units, information on copolymer composition as a function of monomer feed composition is available. With one reactivity ratio value being below unity and the other one above unity, copolymer composition always differs from comonomer feed.

Copolymer composition data derived from four experiments are given in **Figure 26(b)**. The major advantage of this procedure is that a few experiments are sufficient to derive the reactivity ratios, in contrast to the classical approach where a large number of low-conversion experiments have to be carried out. The composition data obtained at reaction conditions may be used to derive the reactivity ratios according to the Lewis–Mayo equation, eqn [24].

The resulting reactivity ratios are $r_{VDF} = 4.3$ and $r_{HFP} = 0.12$. These values indicate, as can be seen in **Figure 26**, that VDF is preferentially built into the copolymer. Since HFP does not homopolymerize, HFP concentration is not further diminished once VDF is consumed. The reactivity ratios are within the expected range: $r_{VDF} = 3.3–5.13$ and $r_{HFP} = 0–0.09$.[19,131,146] It should be noted that the experimental composition data agree very well with values calculated from the reactivity ratios reported by Ahmed *et al.*[19,146] for reaction in the presence of $scCO_2$ at around 400 bar and 35–40 °C.

In-line FT-NIR spectroscopy was also used to detect phase separation. Shown in **Figure 27** are two NIR spectral series recorded during VDF–HFP copolymerizations at 100 °C in 70 wt.% CO_2 with equimolar amounts of both monomers in the feed at initial pressures of 900 and 510 bar. The two peaks at 6214 and 6332 cm^{-1} marked by the asterisk symbols are due to CO_2. The spectra recorded at 900 bar clearly show that the peak assigned to the CH-stretching vibration of VDF disappears completely and that the baseline of the spectra is not significantly varied, indicating a homogeneous-phase reaction. The VDF peak at 6303 cm^{-1} recorded during the copolymerization at 510 bar also disappears completely. However, contrary to the reaction at higher pressure, a strong baseline shift is observed at 510 bar. The numbers 1–5 refer to the chronological order of

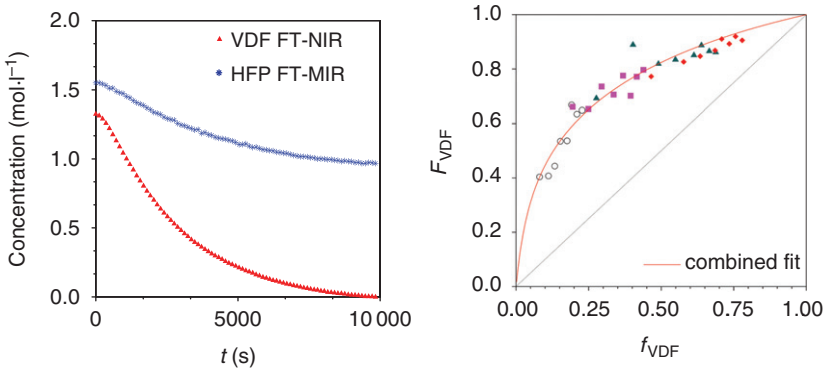

Figure 26 (a) Concentration vs. time curves for VDF–HFP copolymerization with $f_{VDF} = 0.46$ at 100 °C, 900 bar, and 70 wt.% CO_2. (b) Copolymer composition data derived from four VDF–HFP copolymerizations with in-line IR monitoring. From Möller, E.; Schreiber, U.; Beuermann, S. *Macromol. Symp.* **2010**, *289*, 52.[145]

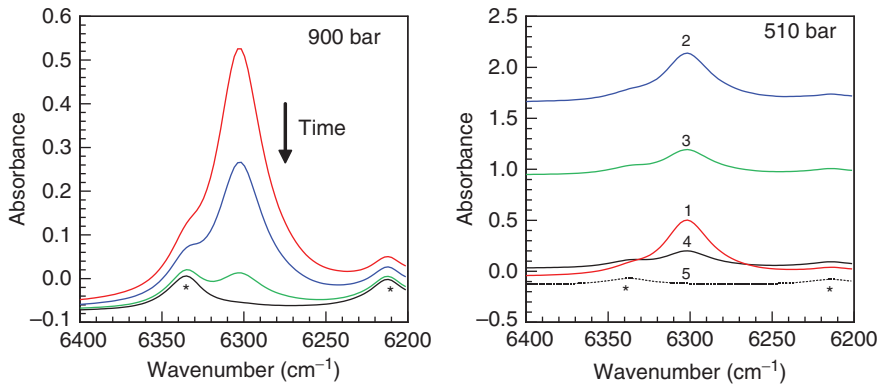

Figure 27 NIR spectra of a reaction mixture at 100 °C containing 70 wt.% CO_2 with $f_{HFP} = 0.5$ and $c_{DTBP} = 0.27$ mol l–1. *, CO_2 absorbance; the arrow indicates variation in absorbance with time. From Möller, E.; Beuermann, S. *Macromol. React. Eng.* **2011**, *5*, 8.[21]

spectra recording: 1 is the first spectrum and 5 the final one. After some conversion is reached, the system turns heterogeneous and the NIR light is scattered, which is reflected by a shift of the baseline to higher absorbance. With increasing conversion, the baseline moves back to lower absorbances, indicating that the heterogeneity disappears. When full VDF conversion is reached, the NIR baseline suggests that the reaction mixture is homogeneous again.[21]

Heterogeneity in VDF–HFP copolymerizations mostly occurs in the beginning of the reaction. With increasing conversion, the polymer content in the mixture increases and swelling of the copolymer with CO_2 becomes important, rather than dissolution of polymer in the monomer–CO_2 mixture. The extent of the heterogeneous behavior depends strongly on F_{HFP}: the more HFP is contained in the copolymer, the smaller is the heterogeneous-phase region. At high HFP content, VDF–HFP copolymerizations were feasible even in bulk due to the cosolvent action of HFP.[21] Roberts and DeSimone reported on VDF–HFP copolymerizations in a CSTR in homogeneous phase for HFP-rich systems. Typical conversions were around 10%.[19]

4.35.8 Kinetics of Radical Polymerization in Homogeneous Mixture with $scCO_2$

In the previous section, it was shown that homogeneous-phase polymerizations of conventional and fluorinated monomers may be carried out in $scCO_2$. The phase behavior is strongly determined by polymer properties, such as molecular masses and copolymer composition. To identify suitable reaction conditions and to optimize polymerization processes, kinetic modeling of the high-pressure reactions with sc carbon dioxide is important. The rate coefficients for the individual reaction steps need to be known for polymerization in the presence of $scCO_2$. Diffusion-controlled termination should be strongly affected, as CO_2 leads to a significant reduction of viscosity.[147] It is thus to be expected that termination rate coefficients are clearly enhanced compared to reactions in bulk or in organic solvents. For the chemically controlled propagation reaction, only a modest influence of CO_2 is anticipated. Nevertheless, it is important to know the impact of different amounts of CO_2 on k_p, because termination and transfer coefficients are commonly determined from parameters coupled to k_p, for example, from $k_p/\langle k_t \rangle$, $k_p^2/\langle k_t \rangle$, or k_{tr}/k_p. It goes without saying that accurate k_p is also required for estimates of the properties of polymer produced in $scCO_2$.

The decomposition kinetics of various peroxide initiators were described in Section 4.35.3.1 with particular emphasis on initiators used in high-pressure, high-temperature ethene homo- and copolymerizations. Since the reaction medium may affect decomposition kinetics,[148] it was tested whether $scCO_2$ influences k_d. For this purpose, the peroxyesters TAPP, TBPP, and TBPA as well as the diacyl peroxides dioctanoyl peroxide (DOP) and bis(3,5,5-trimethylhexanoyl) peroxide (BTMHP) were investigated.[149] For both peroxypivalates, a minor variation in k_d by about 10% was observed. While k_d of TBPP in the presence of CO_2 is slightly lower than that in *n*-heptane solution, k_d of TBPA is slightly enhanced. The opposite effect of CO_2 on decomposition rate is understood by differences in the mechanism: TBPP undergoes rapid successive two-bond scission accompanied by almost instantaneous production of CO_2. Decomposition of TBPA proceeds via single-bond scission to form a *tert*-butoxy radical and a methylcarbonyloxy radical. The low-viscosity environment of $scCO_2$ enables faster out-of-cage diffusion with TBPA, which in turn reduces the importance of back reaction and is identified as an enhancement of decomposition rate. A more detailed discussion is presented in Reference 150.

The CO_2 influence on the decomposition kinetics of BTMHP is somewhat larger. Plotted in **Figure 28** is the temperature dependence of k_d in $scCO_2$ and *n*-heptane. The data for decomposition in $scCO_2$ represent the experimental data points,[149] while the *n*-heptane data are calculated according to the pressure and temperature dependencies reported in the original work.[148] The slopes of the Arrhenius lines are very similar. Absolute k_d in $scCO_2$ is above the associated numbers in *n*-heptane by 40%. Similarly, k_d for DOP is enhanced by 40% in $scCO_2$ compared to *n*-heptane. A strong impact of solvent environment on the decomposition of BTMHP has been reported and correlated with the E_T^N parameter of the solvent, which provides a measure for polarity.[151] k_d is enhanced toward higher E_T^N.[152] As E_T^N of $scCO_2$ is above the *n*-heptane value, the polarity of CO_2 may contribute to the 40% increase in k_d.

The studies on peroxide decomposition kinetics in $scCO_2$ reveal that only minor differences compared to decomposition

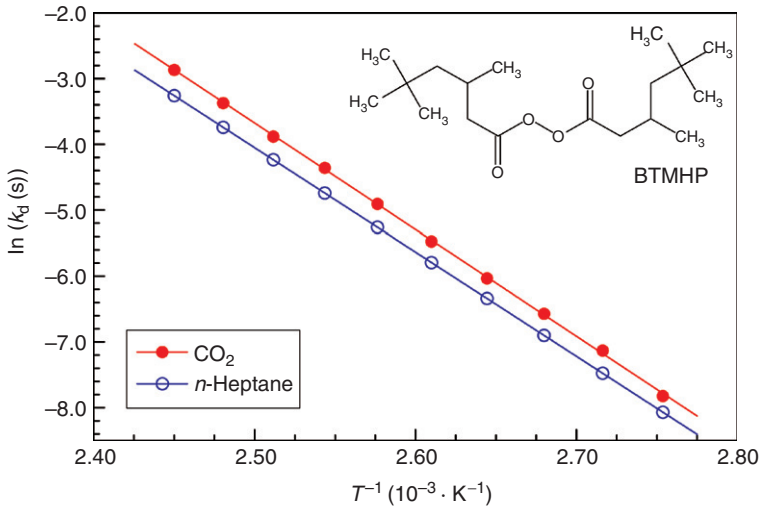

Figure 28 Decomposition rate coefficients k_d for BTMHP determined in solution of CO_2 and *n*-heptane at 500 bar. From Beuermann, S.; Buback, M. In *Supercritical Carbon Dioxide in Polymer Reaction Engineering*; Kemmere, M. F.; Meyer, T., Eds.; Wiley–VCH: Weinheim, 2005, pp 55–80.[150]

rate in *n*-heptane occur. Thus, with the exception of BTMHP, the large literature database available for peroxide decomposition in *n*-heptane up to high pressure may be used for estimates of k_d values for polymerizations of nonpolar monomers in the presence of $scCO_2$.

Phase behavior is determined by copolymer composition. Thus, control of the copolymer composition is of importance. Due to the nonideality of most systems, copolymer composition drift may occur during polymerization to high degrees of monomer conversion. To estimate the effect of CO_2 on copolymer composition, low-conversion polymerizations with varying monomer feed composition were carried out at constant temperature, pressure, and CO_2 content. Resulting copolymer was analyzed by ^{1}H-NMR spectroscopy. The reactions were carried out at 60 °C and 300 bar in bulk and in 40 wt.% CO_2. For styrene–BA systems as well as for styrene–alkyl methacrylate systems, it turned out that the reactivity ratios were not affected by the presence of $scCO_2$.[153] This finding, which is equivalent to stating that the *r* values are independent of CO_2 content, allows for using the large body of data already available for styrene–(meth)acrylate reactivity ratios to describe copolymerization in sc CO_2.

As described in Section 4.35.3.2, k_p data are derived from PLP-SEC. The experimentally accessible quantities are the time period between two successive laser pulses t_0 and the number of propagation steps between two subsequent laser pulses L_1 as obtained from SEC. In systems where solubility is no problem, for example, in many bulk polymerizations, c_M is easily identified with overall monomer concentration. However, in solution polymerizations, local monomer concentration in the vicinity of the propagating radical chain end $c_{M,loc}$ may differ from the analytic overall monomer concentration $c_{M,a}$. In particular for systems in which the solvent power of monomer and solvent (e.g., of $scCO_2$) are markedly different, $c_{M,loc}$ and $c_{M,a}$ may not be the same. If the addition of $scCO_2$ to a polymerizing system leads to a variation in the product $k_p \cdot c_M$, which is the quantity directly accessible from PLP-SEC, two limiting situations may occur:

$$k_p \cdot c_M = k_{p,app} \cdot c_{M,a} = k_{p,kin} \cdot c_{M,loc} \quad [29]$$

First, the relevant monomer concentration is given by $c_{M,a}$. Consequently, differences in $k_p \cdot c_M$ from the bulk value may be assigned to changes in the propagation rate coefficient, given by $k_{p,app}$. Second, the propagation rate coefficient is the same for bulk and solution polymerization, $k_p = k_{p,kin}$, and variations in $k_p \cdot c_M$ are due to changes in effective monomer concentration with the solution value being assigned as $c_{M,loc}$. Since only $c_{M,a}$ is known in what follows, the experimentally derived propagation rate coefficients are designated as $k_{p,app}$.

First, kinetic data derived for BA and MMA PLP with varying CO_2 content at otherwise identical conditions are presented in Figure 29.[154] The propagation rate coefficients and monomer concentrations c_M are given relative to the corresponding bulk values to facilitate comparison. Despite the fact that the monomers exhibit largely differing absolute k_p values, $k_{p,bulk}$ (BA) = 28 000 l mol^{-1} s^{-1} and $k_{p,bulk}$(MMA) = 648 l mol^{-1} s^{-1} at 50 °C, the variation with CO_2 content or with c_M is not

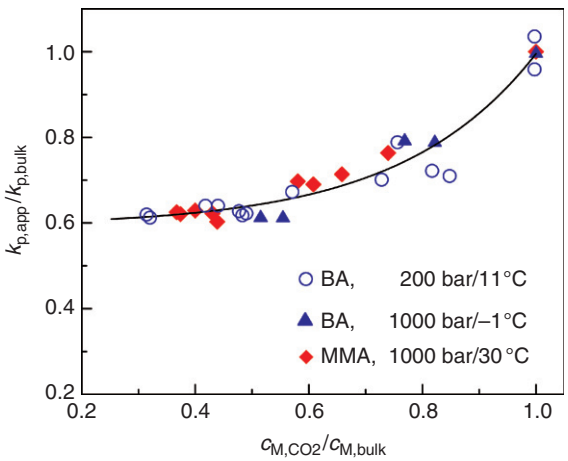

Figure 29 Variation of $k_{p,app}$ with monomer concentration for BA and MMA homopolymerizations at the indicated pressures and temperatures. The kinetic coefficients $k_{p,app}$ and monomer concentrations c_{MCO_2} are given relative to the corresponding bulk values $k_{p,bulk}$ and $c_{M,bulk}$. From Beuermann, S.; Buback, M.; Kuchta, F.-D.; Schmaltz, C. *Macromol. Chem. Phys.* **1998**, *199*, 1209.[154]

Table 7 The ratio of $k_{p,app}/k_{p,bulk}$ with $k_{p,app}$ referring to polymerizations in 40 wt.% CO_2[155]

Monomer		$k_{p,app}/k_{p,bulk}$
Methyl acrylate	MA	0.60 ± 0.10
Butyl acrylate	BA	0.65 ± 0.05
Dodecyl acrylate	DA	0.75 ± 0.05
Methyl methacrylate	MMA	0.65 ± 0.05
Butyl methacrylate	BMA	0.78 ± 0.05
Dodecyl methacrylate	DMA	0.83 ± 0.05
Glycidyl methacrylate	GMA	0.87 ± 0.05
Cyclohexyl methacrylate	CHMA	0.75 ± 0.05
iso-Bornyl methacrylate	iBoMA	0.60 ± 0.05
Styrene	S	1 ± 0.05
Vinyl acetate	Vac	1 ± 0.05
Hydroxypropyl methacrylate	HPMA	1 ± 0.05

significantly different. Moreover, PLP of BA at 11 °C and 200 bar or at −1 °C and 1000 bar does not show any difference in the relative k_p values plotted on the ordinate. Reduction of monomer concentration to 60% of the bulk value decreases k_p by 40%. Further lowering of monomer concentration does not result in an additional decrease in k_p. Additional monomers were studied in the plateau region at 40–60% of $c_{M,bulk}$. It turned out that a reduction in k_p compared to $k_{p,bulk}$ occurred in many cases, with the exception of vinyl acetate, styrene, and hydroxyl propyl methacrylate, where no impact of CO_2 on k_p was found.[150,155]

The extent by which k_p is lowered correlates with the size and structure of the ester group. Within the alkyl acrylate and alkyl methacrylate families, the decrease is most pronounced for the monomer with the smallest ester alkyl group. For monomers with dodecyl ester groups, the lowering is only by 17% and 25% for the methacrylates and acrylates, respectively. The data are summarized in Table 7. For methacrylates with the cyclic ester groups, the lowering is between 13% for glycidyl and 40% for *iso*-bornyl methacrylate. At first sight, polymer solubility is not the determining factor, because no influence of CO_2 is seen on styrene and vinyl acetate k_p, although polystyrene and poly(vinyl acetate) solubility in $scCO_2$ is known to be very different.[111,115]

To check whether CO_2-induced variations in k_p are of kinetic origin, the temperature and pressure dependence of k_p from PLP in $scCO_2$ was compared with the bulk data. As an example, the pressure dependence of BA k_p at 11 °C and of CHMA k_p at 40 °C for polymerizations in bulk and in 40 wt.% CO_2 is shown in Figure 30.[155,156] Whereas the data for polymerizations in $scCO_2$ are below the corresponding bulk data, the lines representing linear fits of the individual data sets in bulk or in $scCO_2$ are more or less parallel. Significant differences in the slopes are not seen. Thus, the activation volumes $\Delta V^{\#}$ are not affected by the presence of CO_2. The same is true for the activation energies.[150,155]

With MAA radical polymerization, the activation energy of k_p has been found to be insensitive to the solvent environment (MAA or MAA/water). This was assigned to changes in the pre-exponential and thus to a purely kinetic effect.[157] The question, whether the same argument applies to propagation in $scCO_2$, cannot be safely answered so far. The variation here may be due to the contribution of local monomer concentrations, but this should be checked by direct local concentration measurement.

To control molecular mass, CTAs may be used. The chemically controlled transfer reaction of dodecyl mercaptan in homo- and copolymerizations of styrene and MMA is not influenced by the presence of up to 40 wt.% CO_2.[158] On the other hand, the diffusion-controlled catalytic chain-transfer reaction of Co complexes was enhanced by up to 1 order of magnitude depending on the reaction conditions, in particular on CO_2 content and the Co complex used.[158,159]

Particular emphasis has been paid to studies on the influence of CO_2 on termination kinetics. The SP-PLP-NIR technique described in Section 4.35.2 has been applied to MA and DA polymerizations in 40 wt.% CO_2 and in bulk. The experimentally accessible quantity $k_p/\langle k_t \rangle$ is used to calculate $\langle k_t \rangle$ with k_p being known from PLP-SEC. The conversion dependence of chain-length-averaged termination rate coefficients $\langle k_t \rangle$ is plotted in Figure 31. DA $\langle k_t \rangle$ stays constant up to at least 60% conversion, but MA $\langle k_t \rangle$ stays constant only up to about 15% conversion. DA $\langle k_t \rangle$ shows the expected increase due to the presence of $scCO_2$, which amounts to almost 1 order of magnitude at 40 °C and 1000 bar. In contrast, for MA$\langle k_t \rangle$, no significant variation is found. At first sight, the latter result is surprising, as for both systems, comparable amounts of CO_2 are used and thus in both cases, a significant reduction in viscosity occurs.

The difference in CO_2 influence on $\langle k_t \rangle$ suggests that termination kinetics is not exclusively determined by viscosity η. For DA and MA, differences in shielding were discussed to have a

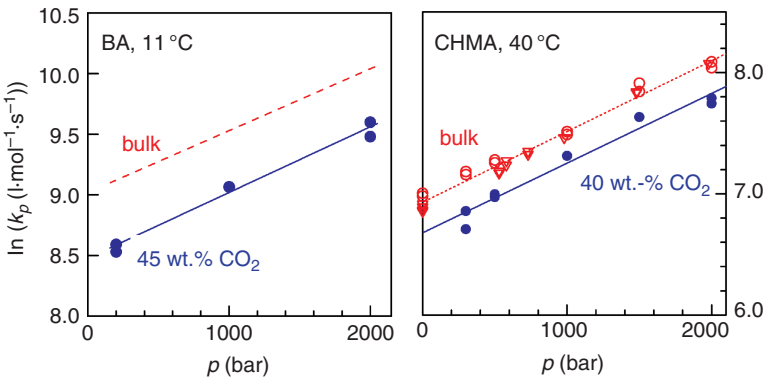

Figure 30 Pressure dependence of BA and CHMA propagation rate coefficients determined in bulk and in homogeneous mixture with $scCO_2$ at 11 and 40 °C, respectively. From Beuermann, S.; Buback, M.; El Rezzi, V.; *et al. Macromol. Chem. Phys.* **2004**, *205*, 876.[155]

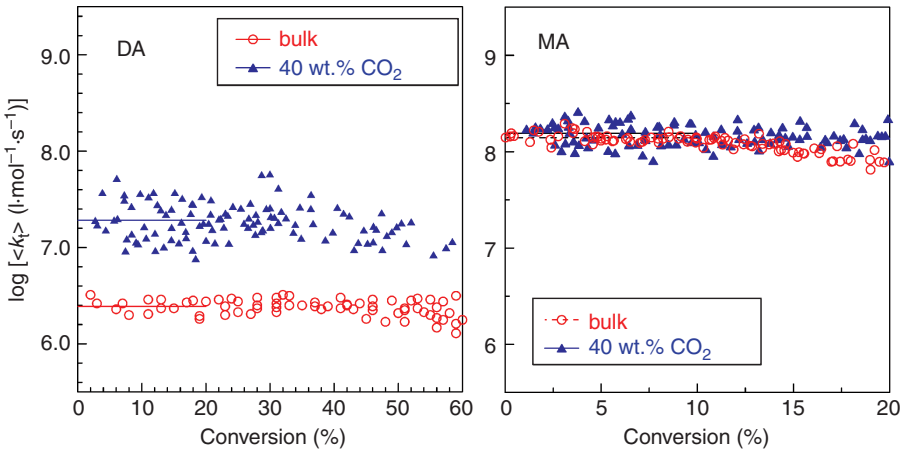

Figure 31 Conversion dependence of DA and MA termination rate coefficients derived from SP-PLP-NIR experiments at 40 °C and 1000 bar in bulk and in 40 wt.% CO_2. From Beuermann, S.; Buback, M. *Prog. Polym. Sci.* **2002**, *27*, 191.[15]

significant impact on the termination kinetics.[150] In the case of DA, each monomer unit carries a long dodecyl ester group, which provides shielding of the radical chain end. Thus, entanglement of two DA macroradicals does not necessarily lead to chain termination. The radicals may become separated before the two radical functionalities have approached each other. Thus, several encounters are required before two radicals actually react with each other. Addition of CO_2 and consequently a lowering of the intracoil viscosity, which is relevant for termination under SD control, strongly enhances chain-end mobility.[150] The potential of the entangled radical for screening its immediate environment and to bring the radical functionalities into close contact for termination is enhanced by the addition of CO_2, and termination may occur faster. For MA, on the other hand, no effective shielding is provided by the small alkyl ester groups. As a consequence, even in MA bulk systems, entanglement of two MA macroradicals results in termination. This may explain why $\langle k_t \rangle$ for MA bulk polymerizations is significantly higher than that for monomers with longer ester groups. Thus, as termination occurs anyway, the lowering of intracoil viscosity, which is associated with the addition of CO_2, does not result in any further significant enhancement of termination probability.

DMA and MMA polymerizations in $scCO_2$, in contrast to MA and DA, exhibit a very similar increase in $\langle k_t \rangle$ compared to the situation with bulk DMA and MMA polymerizations. This observation is explained by the dominant shielding action of the α-methyl group in close proximity to the radical functionality rather than to effects of the size of the alkyl ester group.[150] The influence of CO_2 content on termination kinetics has also been studied for styrene polymerizations.[116] Whereas E_A and $\Delta V^{\#}$ of $\langle k_t \rangle$ are not affected by the presence of CO_2, a large increase in $\langle k_t \rangle$ by about 1 order of magnitude has been seen. This effect may be due to the poor solubility of polystyrene in $scCO_2$, which can be associated with the occurrence of more tightly coiled polystyrene macroradicals that terminate at a much higher rate. Similar arguments were put forward to discuss the termination kinetics in conventional solvents.[160]

References

1. Buback, M. *Angew. Chem. Int. Ed. Engl.* **1991**, *30*, 641.
2. Hamielec, A. E.; Ray, W. H. *J. Appl. Polym. Sci.* **1969**, *13*, 1317.
3. Lorenzini, P.; Pons, M.; Villermaux, J. *Chem. Eng. Sci.* **1992**, *47*, 3969.
4. Lorenzini, P.; Pons, M.; Villermaux, J. *Chem. Eng. Sci.* **1992**, *47*, 3981.
5. Luft, G.; Kämpf, R.; Seidl, H. *Angew. Makromol. Chem.* **1982**, *108*, 203.
6. Luft, G.; Kämpf, R.; Seidl, H. *Angew. Makromol. Chem.* **1983**, *111*, 133.
7. Kiparissides, C.; Verros, G.; MacGregor, J. F. *J. Macromol. Sci. Rev. Macromol. Chem. Phys.* **1993**, *C33*, 437.
8. Ehrlich, P.; Woodbrey, J. C. *J. Appl. Polym. Sci.* **1969**, *13*, 117.
9. Thies, J.; Schoenemann, K. *Chem. Ing. Tech.* **1972**, *44*, 1072.
10. Szabo, J.; Luft, G.; Steiner, R. *Chem. Ing. Tech.* **1969**, *41*, 1007.
11. Feucht, P.; Tilger, B.; Luft, G. *Chem. Eng. Sci.* **1985**, *40*, 1935.
12. Lim, P.-C.; Luft, G. *Makromol. Chem.* **1983**, *184*, 849.
13. Takahashi, T.; Ehrlich, P. *Macromolecules* **1982**, *15*, 714.
14. Schweer, J. Ph.D. thesis, Georg-August-Universität Göttingen, Göttingen, 1988.
15. Beuermann, S.; Buback, M. *Prog. Polym. Sci.* **2002**, *27*, 191.
16. Kendall, J. L.; Canelas, D. A.; Young, J. L.; DeSimone, J. M. *Chem. Rev.* **1999**, *99*, 543.
17. Zetterlund, P. B.; Aldabbagh, F.; Okubo, M. *J. Polym. Sci. A Polym. Chem. Ed.* **2009**, *47*, 3711.
18. Davidson, T. A.; DeSimone, J. M. In *Chemical Synthesis Using Supercritical Fluids*; Jessop, P. G.; Leitner, W., Eds.; Wiley–VCH: Weinheim, 1999; p 297.
19. Ahmed, T. S.; DeSimone, J. M.; Roberts, G. W. *Macromolecules* **2008**, *41*, 3086.
20. Beuermann, S.; Buback, M.; Jürgens, M. *Ind. Eng. Chem. Res.* **2003**, *42*, 6338.
21. Möller, E.; Beuermann, S. *Macromol. React. Eng.* **2011**, *5*, 8.
22. Romack, T. J.; Maury, E. E.; DeSimone, J. M. *Macromolecules* **1995**, *28*, 912.
23. Tai, H.; Howard, D.; Takae, S.; *et al. Biomacromolecules* **2009**, *10*, 2895.
24. Kirby, C. F.; McHugh, M. A. *Chem. Rev.* **1999**, *99*, 565.
25. Rindfleisch, F.; DiNoia, T. P.; McHugh, M. A. *J. Phys. Chem.* **1996**, *100*, 15581.
26. Thurecht, K. J.; Howdle, S. M. *Aust. J. Chem.* **2009**, *62*, 786.
27. Arita, T.; Beuermann, S.; Buback, M.; Vana, P. *Macromol. Mater. Eng.* **2005**, *290*, 283.
28. Nalawade, S. P.; Picchioni, F.; Janssen, L. P. B. M. *Prog. Polym. Sci.* **2006**, *31*, 19.
29. Tomasko, D. L.; Li, H.; Liu, D.; *et al. Ind. Eng. Chem. Res.* **2003**, *42*, 6431.
30. Yeo, S.-D.; Kiran, E. *J. Supercrit. Fluids* **2005**, *34*, 287.
31. Buback, M.; Hinton, C. In *High-Pressure Techniques in Chemistry and Physics: A Practical Approach*; Isaacs, N. S.; Holzapfel, W. B., Eds.; Oxford University Press: Oxford, UK, 1997.
32. Buback, M.; Huckestein, B.; Kuchta, F.-D.; *et al. Macromol. Chem. Phys.* **1994**, *195*, 2117.
33. Buback, M. In *Supercritical Fluids—Fundamentals for Application*; Kiran, E.; Levelt-Sengers, J. M. H., Eds.; Kluwer: Dordrecht, Boston, London, 1994.
34. Isaacs, N. S. *Liquid Phase Pressure Chemistry*; Wiley: New York, 1981.
35. Sherman, W. F.; Stadtmuller, A. A. *Experimental Techniques in High-Pressure Research*; Wiley: Chichester, 1987.

36. Buback, M.; Busch, M.; Lovis, K.; Mähling, F.-O. *Chem. Ing. Tech.* **1994**, *66*, 510.
37. Buback, M.; Busch, M.; Panten, K.; Vögele, H.-P. *Chem. Ing. Tech.* **1992**, *64*, 352.
38. Buback, M.; Latz, H. *Macromol. Chem. Phys.* **2003**, *204*, 638.
39. Beuermann, S.; Buback, M. *High Press. Res.* **1997**, *15*, 333.
40. Buback, M.; Hippler, H.; Schweer, J.; Vögele, H.-P. *Makromol. Chem. Rapid Commun.* **1986**, *7*, 261.
41. Beuermann, S.; Buback, M.; Schmaltz, C. *Ind. Eng. Chem. Res.* **1999**, *38*, 3338.
42. Buback, M.; Müller, E.; Russell, G. T. *J. Phys. Chem. A* **2006**, *110*, 3222.
43. Barth, J.; Buback, M. *Macromol. React. Eng.* **2010**, *4*, 288.
44. Olaj, O. F.; Bitai, I.; Hinkelmann, F. *Makromol. Chem.* **1987**, *188*, 1689.
45. Olaj, O. F.; Schnöll-Bitai, I. *Eur. Polym. J.* **1989**, *25*, 635.
46. Buback, M.; Gilbert, R. G.; Russell, G. T.; *et al. J. Polym. Sci. Polym. Chem. Ed.* **1992**, *30*, 851.
47. Buback, M.; Gilbert, R. G.; Hutchinson, R. A.; *et al. Macromol. Chem. Phys.* **1995**, *196*, 3267.
48. Beuermann, S.; Buback, M.; Davis, T. P.; *et al. Macromol. Chem. Phys.* **1997**, *198*, 1545.
49. Beuermann, S.; Buback, M.; Davis, T. P.; *et al. Macromol. Chem. Phys.* **2000**, *201*, 1355.
50. Beuermann, S.; Buback, M.; Davis, T. P.; *et al. Macromol. Chem. Phys.* **2003**, *204*, 1338.
51. Asua, J. M.; Beuermann, S.; Buback, M.; *et al. Macromol. Chem. Phys.* **2004**, *205*, 2151.
52. Beuermann, S.; Buback, M.; Hesse, P.; *et al. Pure Appl. Chem.* **2007**, *79*, 1463.
53. Buback, M.; Klingbeil, S. *Chem. Ing. Tech.* **1995**, *67*, 493.
54. Crosslinking Elastomers and Thermoplastics, Organic Peroxides and Auxiliaries, Akzo-Nobel, 2010.
55. Buback, M.; Nelke, D.; Vögele, H.-P. *Z. Phys. Chem.* **2003**, *217*, 1169.
56. Buback, M.; Sandmann, J. *Z. Phys. Chem.* **2000**, *214*, 583.
57. Buback, M.; Fischer, B.; Hinrichs, S.; *et al. Macromol. Chem. Phys.* **2007**, *208*, 772.
58. Becker, P.; Buback, M.; Sandmann, J. *Macromol. Chem. Phys.* **2002**, *203*, 2113.
59. Luft, G.; Bitsch, H.; Seidl, H. *J. Macromol. Sci. Chem.* **1977**, *A11*, 1089.
60. Seidl, H.; Luft, G. *J. Macromol. Sci. Chem.* **1981**, *A15*, 1.
61. Van der Molen, T.; Koenen, A.; Oosterwijk, H.; van der Bend, H. *Ing. Chim.* **1982**, *18*, 7.
62. Buback, M.; Kling, M.; Schmatz, S. *Z. Phys. Chem.* **2005**, *219*, 1.
63. Buback, M.; Kuchta, F.-D. *Macromol. Chem. Phys.* **1995**, *196*, 1887.
64. Beuermann, S.; Buback, M.; Russell, G. T. *Macromol. Rapid Commun.* **1994**, *15*, 351.
65. Buback, M.; Geers, U.; Kurz, C. H. *Macromol. Chem. Phys.* **1997**, *198*, 3451.
66. Buback, M. *Macromol. Symp.* **2009**, *275–276*, 90.
67. Buback, M.; Kurz, C. H. *Macromol. Chem. Phys.* **1998**, *199*, 2301.
68. Buback, M.; Kurz, C. H.; Schmaltz, C. *Macromol. Chem. Phys.* **1998**, *199*, 1721.
69. Barth, J.; Buback, M.; Hesse, P.; Sergeeva, T. *Macromolecules* **2010**, *43*, 4023.
70. Wang, W.; Nikitin, A. N.; Hutchinson, R. A. *Macromol. Rapid Commun.* **2009**, *30*, 2022.
71. Junkers, T.; Barner-Kowollik, C. *J. Polym. Sci. A Polym. Chem.* **2008**, *46*, 7585.
72. Buback, M.; Egorov, M.; Gilbert, R. G.; *et al. Macromol. Chem. Phys.* **2002**, *203*, 2570.
73. Schulz, G. V. *Phys. Chem. (Munich)* **1956**, *8*, 290.
74. Buback, M. *Makromol. Chem.* **1990**, *191*, 1575.
75. Buback, M.; Huckestein, B.; Russell, G. T. *Macromol. Chem. Phys.* **1994**, *195*, 539.
76. Russell, G. T.; Napper, D. H.; Gilbert, R. G. *Macromolecules* **1988**, *21*, 2141.
77. Beuermann, S. Ph.D. thesis, Cuvillier Verlag, Göttingen, 1994.
78. Buback, M.; Junkers, T. *Macromol. Chem. Phys.* **2006**, *207*, 1640.
79. Brandrup, J.; Immergut, E. H. *Polymer Handbook*, 3rd ed.; Wiley: New York, NY, 1989.
80. Ogo, Y.; Kyotani, T. *Macromol. Chem.* **1978**, *179*, 2407.
81. Beuermann, S.; Buback, M.; Hesse, P.; *et al. Macromolecules* **2008**, *41*, 3513.
82. Beuermann, S.; Buback, M.; Russell, G. T. *Macromol. Chem. Phys.* **1995**, *196*, 2493.
83. Buback, M.; Schweer, J. *Z. Phys. Chem. N. F.* **1989**, *161*, 153.
84. Buback, M.; Choe, C.-R.; Franck, E. U. *Makromol. Chem.* **1984**, *185*, 1685.
85. Buback, M.; Choe, C.-R.; Franck, E. U. *Makromol. Chem.* **1984**, *185*, 1699.
86. Heuts, J. P. A.; Sudarko; Gilbert, R. G. *Macromol. Symp.* **1996**, *111*, 147.
87. Goto, S.; Yamamoto, K.; Furui, S.; Sugimoto, M. *J. Appl. Polym. Sci. Appl. Polym. Symp.* **1981**, *36*, 21.
88. Bauer, C.; Becker, K.; Herrmann, T.; *et al. Macromol. Chem. Phys.* **2010**, *211*, 510.
89. Meyer, T.; Keurentjes, J., Eds. *Handbook of Polymer Reaction Engineering*; Wiley: Weinheim, 2005.
90. Kiparissides, C.; Krallis, A.; Meimaroglou, D.; *et al. Chem. Eng. Technol.* **2010**, *33*, 1754.
91. Mähling, F.-O.; Klimesch, R.; Schwibach, M.; *et al. Chem. Ing. Tech.* **1999**, *71*, 1301.
92. Fukuda, T.; Kubo, K.; Ma, Y.-D. *Prog. Polym. Sci.* **1992**, *17*, 875.
93. Buback, M.; Dröge, T. *Macromol. Chem. Phys.* **1997**, *198*, 3627.
94. van Herk, A. M. *J. Chem. Educ.* **1995**, *72*, 138.
95. Buback, M.; Dröge, T.; van Herk, A.; Mähling, F.-O. *Macromol. Chem. Phys.* **1996**, *197*, 4119.
96. Buback, M.; Dietzsch, H. *Macromol. Chem. Phys.* **2001**, *7*, 1173.
97. Buback, M.; Dröge, T. *Macromol. Chem. Phys.* **1999**, *200*, 256.
98. Buback, M.; Wittkowski, L. *Macromol. Chem. Phys.* **1999**, *200*, 1935.
99. Buback, M.; Wittkowski, L. *Macromol. Chem. Phys.* **2000**, *201*, 419.
100. Ehrlich, P.; Mortimer, G. A. *Adv. Polym. Sci.* **1970**, *7*, 386.
101. Buback, M.; Busch, M. In *Thermodynamic Properties of Complex Fluid Mixtures*; Maurer, G., Ed.; DFG Research Report; Wiley–VCH: Weinheim, 2004; p 451.
102. Becker, F.; Buback, M.; Latz, H.; *et al. Fluid Phase Equilib.* **2004**, *215*, 263.
103. Hawker, C. J.; Bosman, A. W.; Harth, E. *Chem. Rev.* **2001**, *101*, 3661.
104. Braunecker, W. A.; Matyjaszewski, K. *Prog. Polym. Sci.* **2007**, *32*, 93.
105. Chiefari, J.; Chong, Y. K.; Ercole, F.; *et al. Macromolecules* **1998**, *31*, 5559.
106. Monteiro, M. J.; Bussels, R.; Beuermann, S.; Buback, M. *Aust. J. Chem.* **2002**, *55*, 433.
107. Rzayev, J.; Penelle, J. *Macromolecules* **2002**, *35*, 1489.
108. Rzayev, J.; Penelle, J. *Angew. Chem.* **2004**, *116*, 1723.
109. Arita, T.; Buback, M.; Janssen, O.; Vana, P. *Macromol. Rapid Commun.* **2004**, *25*, 1376.
110. Morick, J. Ph.D. thesis, Georg-August-Universität Göttingen, Göttingen, 2011.
111. Kilic, S.; Michalik, S.; Wang, Y.; *et al. Macromolecules* **2007**, *40*, 1332.
112. Kazarian, S. G.; Vincent, M. F.; Bright, F. V.; *et al. J. Am. Chem. Soc.* **1996**, *118*, 1729.
113. McHugh, M. A.; Garach-Domech, A.; Park, I.-H.; *et al. Macromolecules* **2003**, *35*, 6479.
114. DiNoia, T. P.; Conway, S. E.; Lim, J. S.; McHugh, M. A. *J. Polym. Sci. B Polym. Phys.* **2000**, *38*, 2832.
115. McHugh, M. A.; Krukonis, V. *Supercritical Fluid Extraction: Principles and Practice*, 2nd ed.; Butterworths Publishers: Stoneham, MA, 1993.
116. Beuermann, S.; Buback, M.; Isemer, C.; Wahl, A. *Macromol. Rapid Commun.* **1999**, *20*, 26.
117. Wicks, Z. W., Jr.; Jones, F. N.; Pappas, S. P. *Organic Coatings*; Wiley–Interscience: New York, NY, 1999.
118. Li, D.; Li, N.; Hutchinson, R. A. *Macromolecules* **2006**, *39*, 4366.
119. Beuermann, S.; Buback, M.; Gadermann, M.; *et al. Macromol. Symp.* **2004**, *206*, 229.
120. Beuermann, S.; Buback, M.; Gadermann, M.; *et al. J. Supercrit. Fluids* **2006**, *39*, 246.
121. Ameduri, B. *Chem. Rev.* **2009**, *109*, 6633.
122. Davis, G.; Broadhurst, M. G.; Lovinger, A. J.; Furukawa, T. *Ferroelectrics* **1984**, *57*, 73.
123. Giesy, J. P.; Kannan, K. *Environ. Sci. Technol.* **2001**, *35*, 1339.
124. Romack, T. J.; Combes, J. R.; DeSimone, J. M. *Macromolecules* **1995**, *28*, 1724.
125. Romack, T. J.; DeSimone, J. M.; Treat, T. A. *Macromolecules* **1995**, *28*, 8429.
126. Wells, S. L.; DeSimone, J. *Angew. Chem. Int. Ed.* **2001**, *40*, 518.
127. Saraf, M. K.; Gerard, S.; Wojcinski, L. M.; *et al. Macromolecules* **2002**, *35*, 7976.
128. Galia, A.; Caputo, G.; Spadaro, G.; Filardo, G. *Ind. Eng. Chem. Res.* **2002**, *41*, 5934.
129. Mueller, P. A.; Storti, G.; Morbidelli, M.; *et al. Macromolecules* **2005**, *38*, 7150.
130. Beginn, U.; Najjar, R.; Ellmann, J.; *et al. J. Polym. Sci. A Polym. Chem.* **2006**, *44*, 1299.
131. Tai, H.; Wang, W.; Howdle, S. M. *Macromolecules* **2005**, *38*, 9135.
132. Costa, L. I.; Storti, G.; Morbidelli, M. *Macromolecules* **2010**, *43*, 1714.
133. Imran-ul-haq, M.; Tiersch, B.; Beuermann, S. *Macromolecules* **2008**, *41*, 7453.
134. Beuermann, S.; Imran-ul-haq, M. *J. Polym. Sci. A Polym. Chem.* **2007**, *45*, 5626.
135. Beuermann, S.; Imran-ul-haq, M. *Macromol. Symp.* **2007**, *259*, 210.
136. Du, L.; Kelly, J. Y.; Roberts, G. W.; DeSimone, J. M. *J. Supercrit. Fluids* **2009**, *47*, 447.
137. David, G.; Boyer, C.; Tonnar, T.; *et al. Chem. Rev.* **2006**, *106*, 3936.
138. Boyer, C.; Valade, C.; Sauguet, L.; *et al. Macromolecules* **2005**, *38*, 10353.
139. Ameduri, B. *Macromolecules* **2010**, *43*, 10163.
140. Imran-ul-haq, M.; Förster, N.; Vukicevic, R.; *et al.* In *Controlled/Living Radical Polymerization: Progress in RAFT, DT, NMP & OMRP*; Matyjaszewski, K., Ed.; ACS Symposium Series; American Chemical Society: Washington, DC, 2009; Vol. 1024, p 233.
141. Vukićević, R.; Hierzenberger, P.; Hild, S.; Beuermann, S. *J. Polym. Sci. A Polym. Chem.* **2010**, *48*, 4847.
142. Breininger, E.; Imran-ul-haq, M.; Türk, M.; Beuermann, S. *J. Supercrit. Fluids* **2009**, *48*, 55.

143. Mertdogan, C. A.; DiNoia, T. P.; McHugh, M. A. *Macromolecules* **1997**, *30*, 7511.
144. Fahmy, S. M. Ph.D. thesis, Rheinisch-Westfälische Technische Hochschule Aachen, Aachen, 2005.
145. Möller, E. ; Schreiber, U. ; Beuermann, S. *Macromol. Symp.* **2010**, *289*, 52.
146. Ahmed, T. S.; DeSimone, J. M.; Roberts, G. W. *Macromolecules* **2006**, *39*, 15.
147. Gerhardt, L. J.; Gulari, E.; Manke, C. W. *J. Polym. Sci. B Polym. Phys.* **1997**, *35*, 523.
148. Buback, M.; Hinton, C. *Z. Phys. Chem. (Munich)* **1996**, *193*, 61.
149. Barner, Y. L. Ph.D. thesis, Georg-August-Universität Göttingen, Göttingen, 1997.
150. Beuermann, S.; Buback, M. In *Supercritical Carbon Dioxide in Polymer Reaction Engineering*; Kemmere, M. F.; Meyer, T., Eds.; Wiley–VCH: Weinheim, 2005, pp 55–80.
151. Reichardt, C. *Solvents and Solvent Effects in Organic Chemistry*, 2nd ed.; Wiley–VCH: Weinheim, 1990.
152. Buback, M.; Hinton, C. *Z. Phys. Chem.* **1997**, *199*, 229.
153. Beuermann, S.; Buback, M.; Isemer, C.; Wahl, A. *Proceedings of the 6th Meeting on Supercritical Fluids, Chemistry and Materials*, Nottingham, 1999, p 331.
154. Beuermann, S.; Buback, M.; Kuchta, F.-D.; Schmaltz, C. *Macromol. Chem. Phys.* **1998**, *199*, 1209.
155. Beuermann, S.; Buback, M.; El Rezzi, V.; *et al. Macromol. Chem. Phys.* **2004**, *205*, 876.
156. Beuermann, S.; Buback, M.; Schmaltz, C. *Macromolecules* **1998**, *31*, 8069.
157. Beuermann, S.; Buback, M.; Hesse, P.; Lacík, I. *Macromolecules* **2006**, *39*, 184.
158. El Rezzi, V. Ph.D. thesis, Georg-August-Universität Göttingen, Göttingen, 2001.
159. Forster, D. J.; Heuts, J. P. A.; Lucien, F. P.; Davis, T. P. *Macromolecules* **1999**, *32*, 5514.
160. Dionisio, J.; Mahabadi, H. K.; O'Driscoll, K. F.; *et al. J. Polym. Sci. Polym. Chem. Ed.* **1979**, *17*, 1891.

Biographical Sketches

Sabine Beuermann studied chemistry and received a Ph.D. in physical chemistry in the group of Michael Buback at the Georg-August-University of Göttingen. After working as a visiting scientist at the DuPont Experimental Station in Wilmington/DE, she returned to Göttingen to work on her habilitation, which was finalized with the venia legendi for technical and macromolecular chemistry. Since 2006 she has been professor of polymer chemistry at the University of Potsdam. Current research interests include synthesis, characterization, and modification of VDF polymers; polymerizations in supercritical carbon dioxide or ionic liquids; controlled radical polymerizations; functionalization of nanoparticles or fullerenes with fluorinated polymers; and detailed investigations into the kinetics of radical polymerizations. Since 1996, she has been a member of the IUPAC Subcommittee on 'Modeling of Kinetics and Processes of Polymerization'.

Michael Buback studied chemistry at the University of Karlsruhe, where he received his PhD in 1972. After Habilitation in 1978, he was awarded a Heisenberg fellowship by the German Science Foundation (DFG). In 1981, he became professor for applied physical chemistry at the University of Göttingen. He is currently full professor for technical and macromolecular chemistry and member of the Göttingen Academy of Sciences. Michael Buback received the Dechema Prize, the Bunsen-Denkmünze, and the Herman F. Mark Medal. He has published over 250 peer-reviewed papers. His research interests cover the entire field of radical polymerization with a focus on detailed kinetic studies via pulsed laser initiation carried out in conjunction with highly time-resolved IR, near-IR, and EPR spectroscopy. Further activities address the kinetics and the phase behavior of chemical processes in extended ranges of pressure and temperature. Special expertise centers around the quantitative monitoring, via in-line vibrational spectroscopy, of concentrations during chemical transformations at pressures up to 7000 bar.

4.36 Electroinitiated Polymerization

C Jérôme, University of Liège, Liège, Belgium

4.36.1 Introduction

Monomers can be polymerized electrochemically, i.e., by electrons that travel from (or to) the polymerization medium to (or from) a solid electrode of an electrolytic cell as schematized in Figure 1. Practically, two solid electrodes, usually made of a metal, are immersed in a solvent that contains the monomer and an electrolyte and they are polarized by an external power supply.

Polymerization in this case, occurs at one of the two electrodes, which is designated as the working electrode, whereas the second one, which is oppositely charged, is the counterelectrode.

Similar to conventional polymerization of vinyl monomers, electropolymerization can be initiated by radical, cationic, or anionic species, depending on the cell constituents and the polarization conditions. As defined by Michael Faraday, the cathode is the electrode to which cations flow for being reduced by reaction with electrons given by the electrode. Conversely, the anode is the electrode where the oxidation occurs by accepting the electrons from the reactant. Therefore, either a radical or an anionic polymerization can occur when the working electrode is the cathode whereas polymerization can be radical or cationic at the anode. Step-growth polymerization, for example, based on oxidative coupling reactions, can also be sustained electrochemically provided that the working electrode is properly polarized.

Whenever vinyl monomers are electropolymerized, two situations must be distinguished depending on whether the vinyl monomer is the precursor of the initiating species or not. Either the polymerization is directly initiated by the activated monomer or the initiation is indirect whenever the active species (radical, anion, or cation) is generated by a compound other than the monomer (conducting salt, solvent, or properly selected additives). Besides these electroinitiated polymerization processes, a very recent report[1] also demonstrated that electrochemistry is a valuable tool to mediate atom transfer radical polymerization (ATRP). Indeed, an externally applied electrochemical potential can activate the copper catalyst by a one-electron reduction of an initially added air-stable cupric species (Cu^{II}/ligand) allowing control of the polymerization kinetics in real time by tuning the position of the dormant to active species equilibrium by varying the magnitude of the applied potential.

In contrast to propagating species that can be identified by reaction with appropriate compounds, the number and life time of the initiating species are so low during the whole process that only sophisticated electrochemical techniques can provide reliable pieces of information about their nature.

The next section focuses on a representative example of electroinitiated polymerization of vinyl monomers, with the purpose of introducing basic concepts and some tools dedicated to the analysis of the process.

4.36.2 Electroinitiated Polymerization of Vinyl Monomers for Promoting Coatings Adhesive to Metals

Metals are currently protected against corrosion by deposition of preformed synthetic polymers by electrophoresis. This technique is more effective than the spray application of paints whenever the shape of a metal frame is highly complex, as may be the case in the car industry. Then, parts of the metal can be hidden from a direct line of sight and thus of protection by spraying paints. It is the reason why corrosion resistance is maximized by the electrodeposition of a primer coating by electrophoresis. For this purpose, the metal is electrically charged and immersed in a bath that contains oppositely charged polymer particles. Once they are in contact with the metal surface, these particles are electrically neutralized, and after curing at an appropriate temperature, they coalesce, ideally into a tough homogeneous film. Because the current practice is to have the metal frame cathodically polarized – which minimizes steel corrosion – the process is referred to as cataphoresis.

Despite recognized advantages, metal protection by electrophoresis suffers limitations because of the need of (1) high potential differences for preformed polymer particles to migrate to and be deposited on the metal, (2) high curing

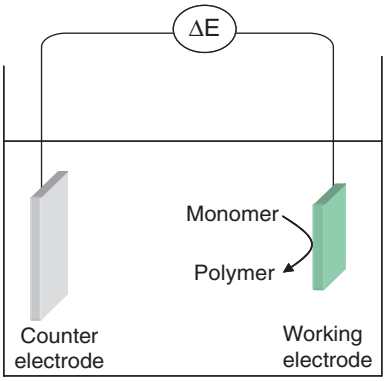

Figure 1 Schematic representation of an electrochemical cell used for electropolymerization.

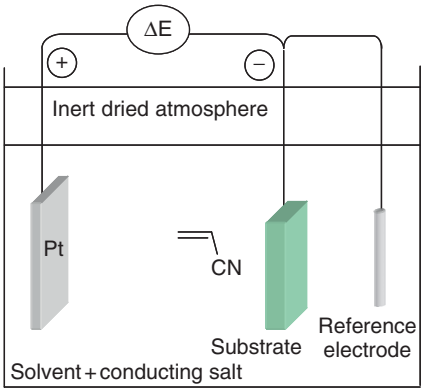

Figure 2 Conventional electrochemical cell used for electrografting.

temperature, and (3) strong adhesion to the metal that is usually not the case, because of lack of molecular interactions between the polymer particles and the metal.

Direct deposition of the protecting film by electroinitiating polymerization in the electrolyte bath is an alternative to the electrodeposition of preformed polymers. Compared to cataphoresis, this strategy does not need high electrical potentials, whereas the film adhesion may be improved to some extent. Early contributions to this technique of deposition of *in situ* electropolymerized acrylic and vinyl monomers in organic and aqueous media have been already reviewed elsewhere by Mengoli *et al.*[2]

In the 1980s, a paper by Lécayon *et al.*[3] aroused not only curiosity but also optimistic prospects for the permanent coating of metal and thus for their very effective protection against atmospheric agents. Indeed, these authors reported on the chemisorption, rather than on the mere deposition, of polyacrylonitrile (PAN) onto metals, such as copper and nickel.[3] This one-step electrografting technique relies on the electroinitiation of the acrylonitrile (AN) polymerization in acetonitrile (ACN) under well-controlled cathodic polarization. This pioneering work is discussed hereafter in terms of basic concepts, requirements, and advantages.

4.36.2.1 Implementation of the Electrografting of AN

The remarkable observation by Boiziau and Lécayon[4,5] was that a PAN film formed by cathodic electroinitiation of the AN polymerization in ACN was strongly adhering onto nickel, i.e., a common metal, used as the cathode. This so-called electrografting reaction was conducted in a very standard electrochemical cell (Figure 2). Nevertheless, it was mandatory to use an oxygen- and water-free solution of AN and a conducting salt in ACN, and to keep the whole system under a dry and inert atmosphere. Under these conditions, a strongly adhering thin film was deposited on the immersed part of the cathode a few seconds after the application of an appropriate cathodic potential. The working electrode was then passivated by this insulating organic film. For the potential applied to the working electrode to be controlled, a third electrode had to be used (Figure 2), the reference electrode, which was endowed with a stable and well-known potential. The calomel electrode is the well-known reference used in water. In contrast, the availability of a reference electrode suitable to organic solvents is quite a problem, which is circumvented by the use of a pseudo-reference electrode, such as a platinum wire. Nevertheless, although unknown, the electrode potential remains stable as long as the composition of the monomer/conducting salt solution is constant, which is a reasonable assumption in the herein reported experiments that consume a minute amount of monomer. It is, therefore, relevant to investigate the electrografting process by voltammetry, which is a potentiodynamic method in which the current at the working electrode is measured while the potential between the working electrode and the reference electrode is scanned linearly. Oxidation or reduction of species is recorded as a peak or a wave in the current signal at the potential at which the species starts to be oxidized or reduced. This technique was applied to the AN reduction on a Ni working electrode in a solution of tetraethylammonium perchlorate (TEAP; 0.05 M) in ACN. This solvent is very well suited to this type of reaction because (1) it dissolves monomers and most of the polymers, (2) it dissolves salts with ionic dissociation, (3) it is non-protic, (4) it is easily dried over calcium hydride, and (5) it is stable in a large window of cathodic potentials.

The choice of TEAP as a conducting salt was justified by electrochemical stability and ionic dissociation in organic solvents in relation to delocalization of the charge of both the cation and the anion over a large number of atoms. The voltammogram did not show any reduction peak below −2.2 V versus Pt (Figure 3). This observation is indirectly consistent with the effective elimination of water and oxygen from the electrolytic solution, otherwise their reduction peaks would have been recorded at potentials less cathodic than 2.2 V.

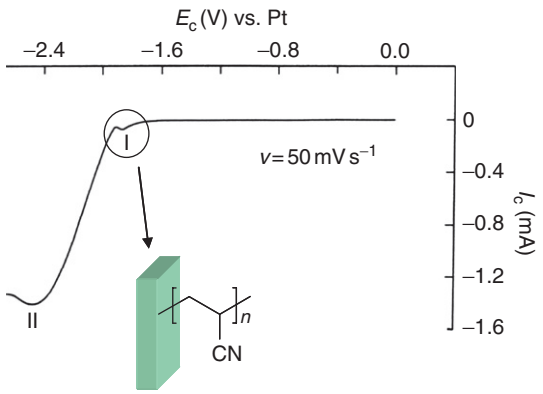

Figure 3 Voltammogram of the acrylonitrile reduction in acetonitrile containing tetraethylammonium perchlorate (0.05 M) on a Ni working electrode. The potential scanning rate was 20 mV s^{-1}. I, grafting peak; II, diffusion peak.

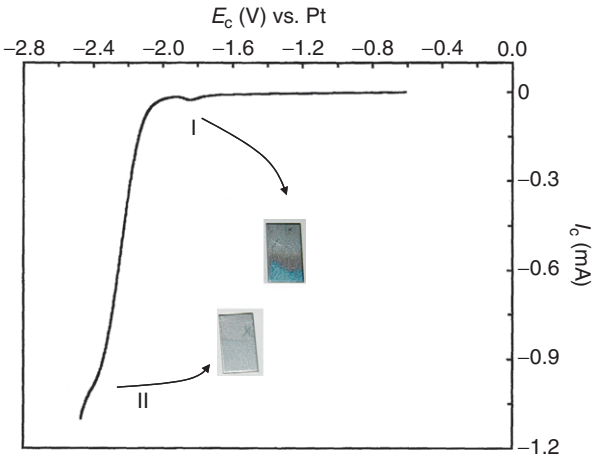

Figure 4 Voltammogram of the acrylonitrile reduction in DMF containing tetraethylammonium perchlorate (0.05 M) and AN (0.2 M) on Ni. The potential scanning rate was 20 mV s. Inset refers to a steel electrode and a scanning until the potential of peak I (PAN chemisorbed on the cathode area dipped in solution) and peak II (degrafting of PAN), respectively.

Two electrochemical waves were, however, observed beyond −2.2 V, which was not the case in the absence of monomer. They must thus be assigned to the monomer reduction. When the surface of the electrode was observed by the naked eye after the potential scanning until the one of peak I and peak II, respectively, the deposition of an organic layer identified as PAN was reported. The macroscopic aspect of the deposition was, however, different, being a very thin iridescent film when the potential was scanned until the less cathodic peak and a thicker yellowish layer in the second case, which was easily dissolved by a good solvent for PAN (dimethylformamide (DMF)), in contrast to the former film that resisted DMF washing. A tentative explanation is that the PAN chains electroinitiated at the cathode are chemisorbed onto the surface at the potential of peak I, whereas they are detached from the cathode at a more cathodic potential. However, ACN being a nonsolvent for PAN, these chains precipitate onto the electrode without any adhesion to the surface.

In order to give credit to this scenario, DMF was substituted for ACN in the voltammetry experiment. Again, two distinct reduction phenomena were observed on various metals such as Ni, Fe, and Pt (Figure 4, full line).[6] Scanning the potential to the maximum of the first cathodic peak (peak I, Figure 4) resulted in the deposition of a PAN film onto the cathode (see inset in Figure 4, peak I, in case of steel electrode). Scanning down to the second reduction wave (peak II, Figure 4), restored the original surface of the electrode as a result of release of the previously chemisorbed chains that grew in the electrolytic solution (see inset in Figure 4, peak II, in the case of a steel electrode). This preliminary voltammetric study in two organic solvents combined with the visual aspect of the working electrode in relation to the applied potential provided strong evidence that the PAN chains are electrografted at the potential of the first reduction peak, whereas this benefit is lost at more cathodic potentials.

4.36.2.2 Investigation of the Electrografting Process

In addition to conventional electrochemical methods, such as voltammetry, some more sophisticated and powerful techniques are available for the *in situ* investigation of electrochemical reactions at the surface of a polarized electrode. Quartz crystal microbalance (QCM)[7] is one of these techniques well suited for discriminating two situations in which electroinitiated chains either remain adsorbed or are not adsorbed onto the surface of the electrode. QCM actually measures a mass per unit area by recording the change in frequency of a quartz crystal resonator. Whenever this acoustic resonator is used as an electrode, the resonance is disturbed by the electrodeposition (or removal) of matter on the surface. The technique is then designated as 'electrochemical QCM (EQCM)' because voltammogram and frequency variation of the vibrating electrode are recorded simultaneously, which provides a unique tool for investigating any electrochemical reaction, that either form or do not form products at the surface of the working electrode. Indeed, according to the Sauerbrey relationship ($\Delta f = -K\Delta m$), a decrease of the electrode frequency (Δf) is consistent with a mass increase (Δm) of the electrode, and vice versa.

Figure 5 shows the two curves recorded by EQCM for the AN electropolymerization in DMF.[8] The voltammogram (full line) expectedly shows the two reduction waves, I and II, on the Pt sensor. Moreover, the vibration frequency of this cathode (dotted line) decreases at the potential of the first peak, in accordance with PAN chemisorption responsible for an increase in the sensor mass. Consistent with previous observations (Section 4.36.2.1), the initial frequency is restored at the potential of the second reduction wave (at −3.25 V, $\Delta f = 0$), which confirms that the previously chemisorbed/grafted chains are released from the cathode surface and grow in the electrolytic solution.

Because the PAN chains that are electroinitiated in a good solvent (DMF) at the potential of peak I are strongly adsorbed onto the cathode, this peak is currently designated as the 'grafting peak'. The very low intensity of this peak is accounted for by the very rapid passivation of the surface by the chemisorbed chains. In contrast, at the potential of peak II, the monomer reduction is merely controlled by the monomer diffusion to the cathode whose surface remains active; this more cathodic peak is referred to as the 'diffusion peak'.

Although of great interest, data provided by EQCM are not quantitative, including the amount of chains electrografted at

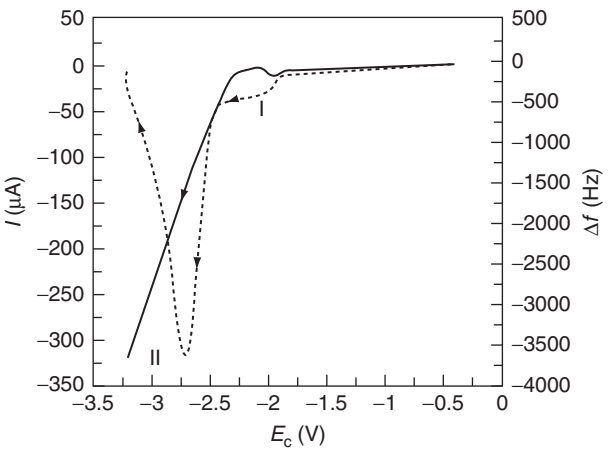

Figure 5 Potential dependence of the AN reduction current (voltammogram, full line) and the quartz crystal frequency (dotted line), in DMF containing tetraethylammonium perchlorate (0.05 M) and AN (0.2 M) on a Pt-coated quartz crystal vibrating electrode. The potential scanning rate was 20 mV s^{-1}.

the potential of peak I, because solvation of the grafted chains by DMF (a good solvent) makes the Sauerbrey equation invalid. Indeed, validity holds strictly only for rigid coatings.

4.36.2.3 Investigation of the Electrografting Mechanism

Despite the valuable and reliable experimental data collected by classical voltammetry and EQCM in poor and good solvents for the reaction product (PAN), the basic mechanism of the AN electrografting was a topic of debate.

According to the way the AN electropolymerization was conducted, the initiation of the process must be direct. Indeed, the conducting salt (Et_4NClO_4) is known for stability in the cathodic regime. All the constituents, that is, monomer, salt, solvent, and argon, were carefully dried (water content less than 5–10 ppm) such that indirect initiation by H• formed by water reduction (unobserved on the voltammogram) may be precluded. The oxygen content was also lower than 5 ppm consistent with lack of an O_2 reduction peak (expected at a potential less cathodic than the AN reduction), which allows indirect initiation by reduction by-product (O_2^{-}) to be disregarded. Lécayon and co-workers[9,10] proposed a mechanism that consists of the transfer of one electron from the cathode to the monomer together with the bonding of the accordingly formed radical-anion to the metal. Chain initiation is thus an electrochemical event in contrast to chain propagation that proceeds through the repeated addition of the monomer to the chemisorbed active species [$Ni–CH_2CH(CN)^{*}$].

The crucial question is the nature of this species. A series of experiments were devised and carried out in order to decide whether it is a radical or an anion.[11,10] Diphenylpicrylhydrazyl (DPPH), an electrochemically stable radical scavenger, was added to the electropolymerization medium. However, the PAN chains formed at the potential of peak I were not end-capped by a DPPH residue, as would be expected in the case of a radical process. AN was then tentatively copolymerized, respectively, with ε-caprolactone (a monomer that polymerizes anionically but not by radicals) and with vinyl acetate (a monomer that polymerizes radically but not by anions). Neither of these two comonomers were incorporated in the PAN chains electrografted at the potential of peak I, which may merely indicate that these comonomers were not part of the electrical double layer of the cathode. In a third experiment, a potential radical transfer agent ($CDCl_3$) was added to the electrolytic solution. The PAN chains formed at the less cathodic potential were selectively end-capped by –D to the exclusion of $–CCl_3$ as shown by secondary ion mass spectrometry (SIMS). This observation strongly suggested that $CDCl_3$ reacted as an acid with anionic species consequently capped by D^{+}. Finally, methyl methacrylate (MMA) was substituted for AN. Part of the poly(methyl methacrylate) (PMMA) chains were growing in solution at the potential of peak I (strong overlap of the two reduction peaks). They were analyzed by thermal gravimetric analysis because the thermogravimetric analysis (TGA) profile depends on the polymerization mechanism (anionic vs. radical). The one-step degradation profile that was observed is actually typical of anionically prepared PMMA. From this series of experiments, it may be reasonably concluded that the electrografting of AN proceeds through an anionic mechanism. As schematized in Figure 6, the acrylic monomer would be reduced in the potential range of peak I into an anion-radical that would then be chemisorbed (after some monomer additions or not) onto the cathode through the radical. As mentioned in the previous section, the very low intensity of peak I is the signature of the electrodeposition of a passivating polymer film. At a more cathodic potential, the chemisorption of the anion-radical species is no longer effective, the intensity of the reduction peak II increases rapidly, and the fast coupling of the radical-anions into anionic dimers sustains the chains propagation in solution. The general picture is, thus, that of an equilibrium between chemisorbed radical-anions and unbound radical-anions, whose position strongly depends on the cathodic potential.

4.36.2.4 Effect of Solvent on the Electrografting of AN

Until now, voltammetry has shown that AN could be electrografted onto usual metal in ACN (a nonsolvent for PAN) and in DMF (a good solvent for PAN) provided that the potential is kept in the range of the first reduction peak. Clearly, the 'grafting peak' is a passivation one, which means that the process is very rapidly stopped and that the thickness of the chemisorbed film cannot be increased further by keeping the potential constant as soon as it reaches the maximum of peak I. Nevertheless, the question must be addressed in order to know whether the actual reaction time (thus intensity of peak I) depends on both the solvent and the monomer concentration. Therefore, the current density of the electrografting peak (peak I) was measured at different monomer concentrations in several solvents. Table 1 clearly shows that the current density of peak I decreases when the monomer concentration is increased whatever the solvent may be.[12] This behavior, which is quite unusual for a faradic reaction, has been accounted for by the faster chain propagation at higher monomer concentration, which results in the more rapid passivation of the electrode. Coming back to the comparison of a nonsolvent (ACN) and a good solvent (DMF) for PAN, ellipsometry displayed strong differences in the film thickness and its dependence on the AN concentration (Figure 7). In DMF, the film thickness increases from 25 to 150 nm when the monomer concentration is

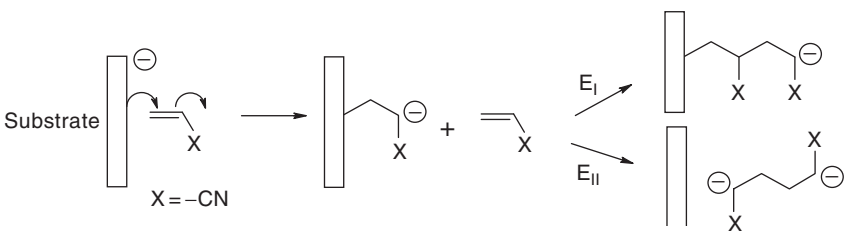

Figure 6 Proposal of mechanism for the electroreduction of acrylonitrile at the potentials of peak I and peak II, respectively.

Table 1 Intensity of peak I (I_{pI}) at different AN concentrations in solvents of different dielectric constants (ε) and donor numbers ($v = 20\ mV\ s^{-1}$)

Solvent	*ε*	*Donor number*	*[AN] 0.05 M (μA)*	*[AN] 0.1 M (μA)*	*[AN] 0.5 M (μA)*	*[AN] 2 M (μA)*
Acetonitrile	38	14.1	-	370	30	25
Propylene carbonate	65	15.1	-	650	90	60
Pyridine	12.3	33.1	25–30	15–20	Weak	Weak
Hexamethylphosphoramide	30	38.8	30–35	15–17	Weak	Weak

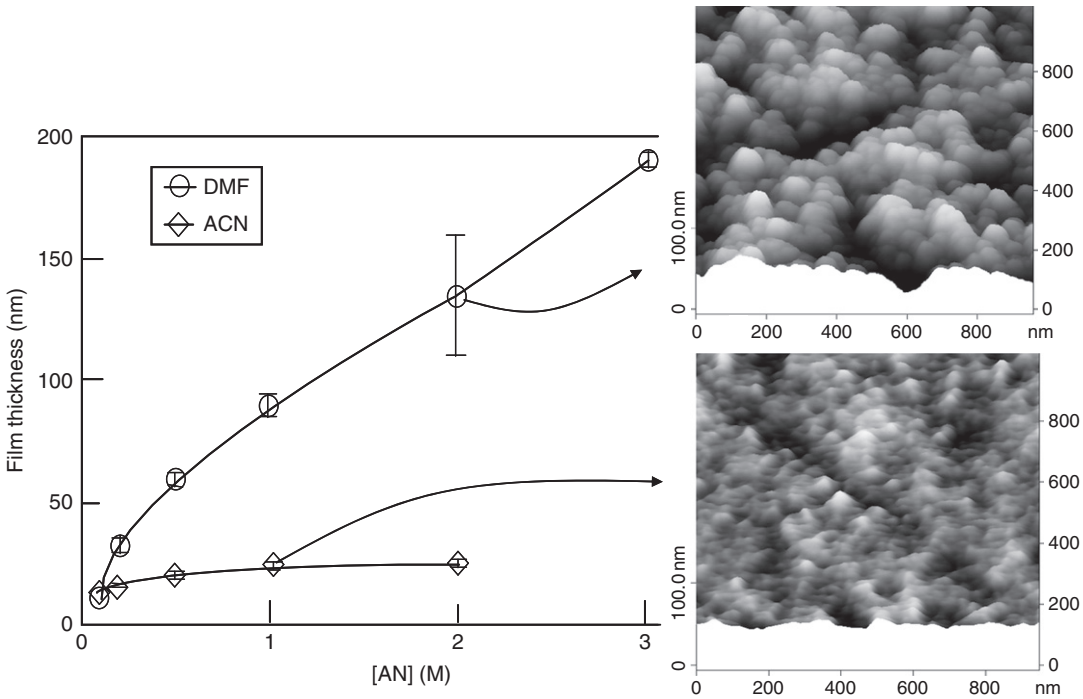

Figure 7 Film thickness vs. acrylonitrile (AN) concentration for polyacrylonitrile (PAN) films electrografted onto Ni in dimethylformamide (DMF) and acetonitrile (ACN). Inset: atomic force micrographs of electrografted PAN films.

increased from 0.1 to 2 M.[12] Because the chains are solvated in DMF, they can grow for a longer time and reach higher molecular weight at higher monomer concentration. The film thickness is basically independent of the AN concentration in ACN (less than 25 nm), merely because the growing PAN chains precipitate on the electrode as soon as their length exceeds a critical value and they do not propagate anymore whatever be the monomer concentration. Consistently, the morphological features of the cathode surface[13] can be seen by atomic force microscopy (AFM) (inset in **Figure 7**) beneath the film deposited in ACN, which is no longer the case when the film is formed in DMF at high monomer concentration. Thus the choice of both the solvent and the monomer concentration has an impact on the electrografted films.

Additional comparisons can be made on the basis of the I_{pI} data collected at the same AN concentration in different solvents (**Table 1**).[14] The current density of peak I at [AN] = 0.1 M is typically much lower in hexamethylphosphoramide (HMPA) than in ACN, which is of a comparable polarity (ε = dielectric constant) but of a much higher donor number (DN, a qualitative measure of the Lewis basicity developed by V. Gutmann) than HMPA. Obviously, passivation and thus electrografting are much more effective in the solvent of a higher DN in agreement with the deposition of a thicker film (ellipsometric data) in this solvent. The same conclusion holds when pyridine (Py) and ACN are compared, although the comparison is not straightforward because of an additional difference in polarity between the two solvents (cfr. infra). A reasonable explanation that will be discussed further in Section 4.36.2.5 may be found in a competition between the monomer and the solvent for adsorption to the electrode surface. Solvents of high DN (Py and HMPA) have a low propensity of adsorbing onto metals, which means that all the potential initiating sites on the surface are occupied by the monomer, which is then electrografted under 'ideal' conditions. In contrast, ACN and propylene carbonate (PC) of low DN are effective competitors for the monomer toward adsorption onto the cathode. As a result, electrografting and passivation are slower and less efficient.

Finally, when solvents of similar DN are compared at the same [AN] (ACN/PC and Py/HMPA), I_{pI} depends on the polarity of the solvent only in case of solvents of low DN (ACN and PC). Then, the more polar solvent is a better competitor for the monomer with regard to adsorption onto the electrode, which is detrimental to the polymer electrografting (PC in **Table 1**).

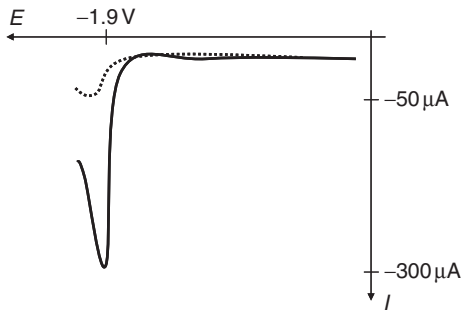

Figure 8 Voltammogram for the reduction of AN in DMF on Ni ($v = 20\,mV\,s^{-1}$): first scan, full line; second scan, dotted line.

Whenever solvents are poor competitors because of a high DN, a difference in polarity has no significant impact on I_{pI} and the electrografting (HMPA vs. Py in Table 1). Thus solvent donicity has a key effect on the electrografting process. As a rule, a solvent of high DN is recommended for the AN to be selectively adsorbed onto the working electrode and for the electrografted film to be thicker and more passivating.

As a rule, the homogeneity of the PAN film can be improved by increasing the grafting density. For this purpose, the scanning of the cathodic potentials until the maximum of peak I has to be repeated until passivation is complete, thus I_{pI} is negligible (Figure 8).

4.36.2.5 Extension of the Electrografting Process to Monomers Other than AN

For a long time, AN was the only monomer that could be electrografted onto a common metal. It might be argued that AN is the monomer best suited to an anionic-type polymerization because nitrile is the strongest electron-withdrawing substituent of the double bond in the family of vinyl monomers. For this reason, the DN of AN is low, which allows it to be adsorbed onto the cathode preferably to most of the organic solvents stable in the cathodic regime. As a rule, the other acrylate monomers, such as ethyl acrylate (EA), have a DN higher than that of ACN, which may explain why their electrografting failed in this solvent. An illustration can be found in Figure 9(a) showing only one reduction peak of EA, which is a diffusion peak typical for the polymer growth in solution (peak II). The trick is thus to use a solvent with a DN higher than that of the monomer. This is the case with DMF with respect to EA, because then the typical grafting peak of very low intensity is observed before polymerization in solution takes place as assessed by the diffusion peak (Figure 9(b)). The basic requirement for an anionically polymerizable monomer to be cathodically electrografted onto a metal is thus to use an organic solvent, easy to dry, stable in the cathodic regime, and above all having a DN higher than that of the monomer, and, therefore, unable to compete with it for adsorption to the metal.

This rule of competitive adsorption to the metal was illustrated by electroinitiating the EA polymerization in ACN/DMF mixtures of various compositions.[14] It must be noted that density functional theory (DFT) calculations ranked the affinity of EA, ACN, and DMF toward Ni as follows: ACN > EA > DMF.[15] Figure 10 shows the progressive increase of the peak I intensity when the relative content of ACN in the solvent mixture is increased, consistent with the increasingly more effective displacement of the monomer from the metal surface by ACN.

So, the best guideline for the cathodic electrografting of vinyl monomers to be successful is a scale of donicity of monomers and organic solvents stable in the cathodic regime. However,

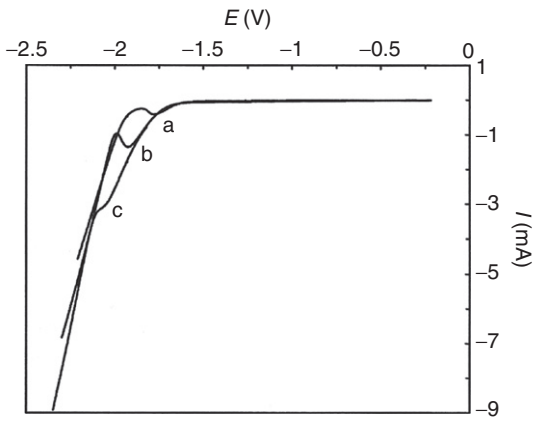

Figure 10 Voltammograms for the electroreduction of EA (1 M) on Ni in DMF added with increasing amounts of ACN: (a) pure DMF, (b) 3 vol.% ACN, and (c) 12 vol.% ACN.

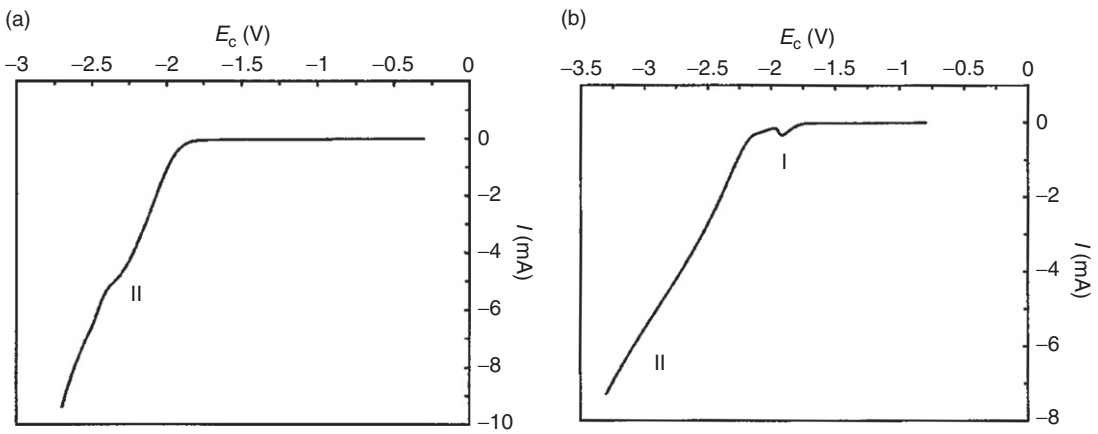

Figure 9 Voltammograms for the reduction of ethyl acrylate (EA) onto a Ni electrode: (a) in acetonitrile; and (b) in dimethylformamide. Et_4NClO_4 was the conducting salt (5×10^{-2} M) and the scanning rate was $20\,mV\,s^{-1}$.

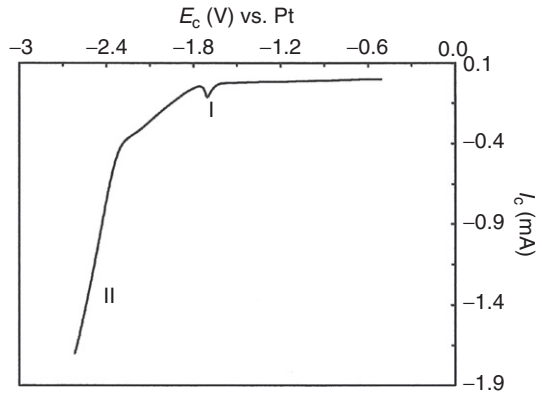

Figure 11 Voltammogram for the electroreduction of MMA (3 M) on Ni in DMF.

when DN of both the monomer and the solvent is comparable, the preferential adsorption of the monomer to the cathode can be enhanced by increasing the monomer concentration. This approach was illustrated in the case of a less activated monomer, that is, MMA, that could not be successfully electrografted in DMF at low concentration (0.2 M). Upon a tenfold increase in monomer concentration (2–3 M), the situation was considerably improved as illustrated by **Figure 11**.

Once the rule of the game was properly understood, a series of commercially available (meth)acrylics were successfully electrografted, including monomers with functional electron-withdrawing substituents (protected or not), making the surface hydrophilic and/or reactive toward various topcoats (epoxy, protected carboxylic acid, and hydroxyl groups),[14] or highly hydrophobic (partly fluorinated film) and the precursor of anti-adhesive coatings.[16]

As a rule, DMF appears to be the organic solvent best suited to the electrografting of (meth)acrylate derivatives, including macromonomers, because it affords a good compromise in terms of drying, handling, solvent power, electrochemical stability, and donicity. **Figure 12** shows a series of (macro) monomers that were electrografted onto common metals in DMF with good success.

These compounds were designed with the purpose (1) of increasing the thickness of the adhering organic film, which is systematically smaller than 200 nm, and (2) of increasing the range of the chemical properties and reactivity of the grafted films. For instance, the electrografting of the inimers **1** and **2** is a strategy for initiating a second generation of chains from the surface by controlled radical polymerization (ATRP or nitroxide-mediated polymerization (NMP)) (Chapter **3.05**).[17,18] Electrografted films were used to initiate the living ring-opening polymerization of lactones and norbornene (from structure **3**) in the presence of appropriate catalysts.[19–21] The activated ester substituent of *N*-succinimidyl acrylate (NSA; structure **4**) and related electrografted films were used to anchor amino derivatives similar to a molecular Velcro.[22,23] Dual monomers **5** and **6** were electrografted for the opportunity for the heteroaromatic ring to be anodically copolymerized with monomer precursor of conducting polymers, to which strong adhesion was accordingly imparted (see also Section 4.36.4).[24]

Finally, the successful electrografting of macromonomers generated strongly adhering films with specific properties, such as

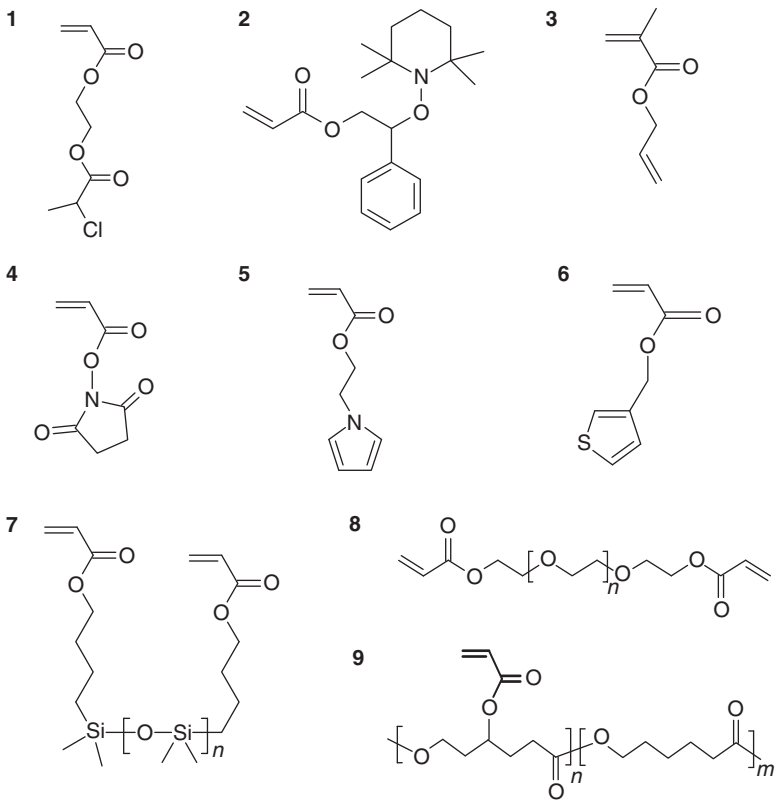

Figure 12 Examples of acrylic monomers and macromonomers that were designed for successful electrografting in DMF and that were able to fit specific applications.

lubricating properties (silicone derivative, structure 7), protein repellent properties (polyethylene oxide derivative, structure 8), and degradability (poly-ε-caprolactone derivative, structure 9).[25,26] The large variety of available electrografted coatings, their properties, and specific applications were recently reviewed elsewhere.[27] Application of electrografting to build efficient and permanent bactericidal coatings is exemplified in Box 1.

Box 1 Development of Antibacterial Coatings by Electrografting

A valuable approach for preventing surface-mediated infection consists in coating the surface with an intrinsically bactericidal polymer. Polycationic chains with long alkyl chain quaternary ammonium (octyl or dodecyl) constitutive units were found to be very efficient in eliminating bacteria as a result of increased hydrophobicity and cidal activity.[74,75] It is now widely accepted that the target site of these cationic polymers is the cytoplasmic membrane of bacterial cells and that the crucial step of their lethal action is the disruption of the membrane – penetrated by the ammonium alkyl chain – followed by the rapid release of K^+ ions and other cytoplasmic constituents.

Interestingly enough, coating of metals by strongly adhering bactericidal polymers, by the combination of electrografting and controlled radical polymerization (see Section 4.36.2.5), is an efficient strategy to obtain a long-term bioactive surface. For example, an alkoxyamine-containing acrylate (**Figure 12** (structure **2**)) can be first electrografted to the surface of a polarizable substrate, so making nitroxides available at this surface, that are effective for the controlled radical polymerization (NMP mechanism) of styrene (St) (or *n*-butyl acrylate (BuA)) and 2-(dimethylamino ethyl)acrylate (DAEA).[76] Finally, the DAEA comonomer units can be quaternized. The antibacterial activity of the quaternized copolymers was highlighted against Gram-positive bacteria (*Staphylococcus aureus*) and Gram-negative bacteria (*Escherichia coli*). For example, the efficiency of quaternized copolymers to kill *E. coli* bacteria was measured by the commonly reported viable cells counting method. This test, applied to poly(St_{62}-*co*-$DAEA_{38}$) quaternized by 1-bromooctane or bromododecane, shows that after 30 min all the bacteria are dead when the alkyl chain of the quaternary ammonium is octane for two different DAEA concentrations in the incubation medium (i.e., 288 and 1415 μg ml^{-1}) while there is a need for incubation between 1 and 2 h to kill completely the bacteria with the same quaternized copolymer but bearing dodecane chains for a concentration of DAEA of 1415 μg ml^{-1}.

A similar two-step 'grafting-from' method was successfully carried out by combining the electrografting of polyacrylate chains with an ATRP initiator in the ester groups (**Figure 12** (structure **1**)) and the atom transfer radical polymerization (ATRP) of 2-(*tert*-butylamino)ethyl methacrylate (TBAEMA).[77] By using the 2-(2-bromopropionate)ethyl acrylate inimer in the 'grafting-from' step by ATRP, hyperbranched polymer brushes were prepared with a high density of bromide groups, which were finally quaternized by an amine.[78] The positively charged hyperbranched polymer brush was preventing both protein adsorption and bacterial adhesion as a result of high hydrophilicity and high density of cationic groups.

In an alternative strategy, hyperbranched polymer brushes with a high density of quaternary ammonium groups were prepared by combining electrografting of poly(*N*-succinimidyl acrylate) (**Figure 12** (structure **3**)) onto stainless steel with the 'grafting-onto' method[22] of preformed hyperbranched polyethyleneimine.[78] Again, quaternization of the constitutive amines of the hyperbranched polymer was at the origin of antibacterial properties.

Because chitosan is a natural polymer known for bactericidal properties, chitosan-containing multilayered films were prepared by layer-by-layer deposition of polyanions and polycations, the very first layer being a polyanion or a polycation electrografted onto the solid substrate.[52,53]

The development of these bactericidal coatings is a representative example of how combining electrografting with more conventional controlled polymerization and deposition processes might be a powerful tool to confer long-term and specific surface properties to metals.

4.36.2.6 Microstructure of the Electrografted Chains

The analysis of the microstructure of electrografted chains is quite challenging. Although these chains are completely desorbed from the surface when the metal is immersed in an electrolytic solution (without monomer) and cathodically polarized in the potential range of the second voltammetric peak, the amount of chains to be recovered is so small that conventional analytical methods, such as size-exclusion chromatography and nuclear magnetic resonance (NMR), have to be precluded. Because the released material appears to be soluble (in DMF), poly(ethyl acrylate) (PEA), or PAN chains would not be cross-linked as might have been assumed in case of anionic polymerization and possible nucleophilic attack of the ester group of the monomer and/or the polymer by the propagating anions.

For PAN, the absence of cross-linking was confirmed by Fourier transform infrared (FTIR) analysis.[28] Nevertheless, depending on the experimental conditions, some azine intermolecular bonds were detected by Raman spectroscopy at the very first stage of electrografting.[28] For these bonds to be formed by nucleophilic addition of the nitrile groups, the latter have to be aligned, parallel to the electrode surface, which might be possible in the electrical double layer of the cathode, and liable in case of isotactic PAN. Isotacticity of PAN was experimentally confirmed by dynamic mechanical thermal analysis (DMTA) and near edge X-ray Absorption fine structure (NEXAFS)[29] analysis. These preliminary observations provide hints for a brush-like conformation of the electrografted chains.

Recent advances in AFM make this technique a unique tool for collecting pertinent information about length and conformation of the electrografted chains. In addition to topographic details, force–distance curves can be recorded by AFM as illustrated in **Figure 13**. This technique can be used to measure long-range attractive or repulsive forces between the probe tip and the sample surface, to elucidate local chemical and mechanical properties, such as adhesion and elasticity, and even to measure thickness of adsorbed molecular layers and bond rupture lengths.

The inset in **Figure 13** is the curve recorded when a gold-coated AFM tip is approaching a surface electrografted by poly(*N*-succinimidyl acrylate) (PNSA).[30,31] The compression profile of the chain that makes a bridge between the AFM tip and the surface directly depends on the monomer concentration used for the electrografting of NSA. Would this solution be diluted (0.05 M), the recorded profile is typical of the isolated chain regime, where the behavior of a tethered chain is independent of the neighboring ones as result of a low grafting density. In case of a more concentrated NSA solution (1 M), a monotonous increase in the repulsive forces is observed as the tip approaches the surface, which is characteristic of a brush regime when the grafting density is high enough. This situation was confirmed by topographic AFM imaging. The chain length was estimated from the tip–surface distance when the brush started to be compressed. A chain length of approximately 80 and 250 nm was reported for PNSA chains electrografted onto silicon nitride in a monomer solution in DMF of 0.5 and 1 M, respectively. These data directly confirm that the length of the grafted chains increases with the monomer concentration. In this example, the average degree of polymerization of the PNSA chains was estimated at 320 and 1000, respectively.

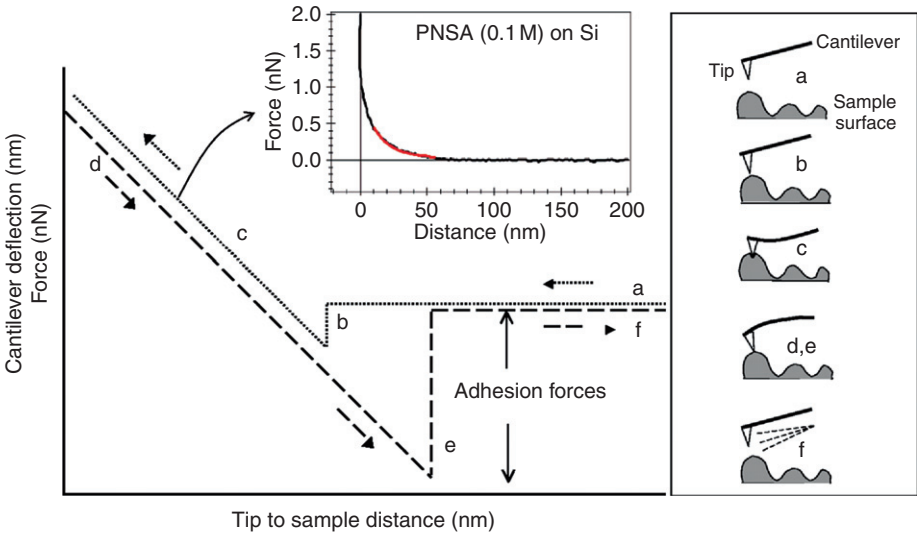

Figure 13 Idealized force–distance curve describing a single approach–retraction cycle of the AFM tip. Modified from Shahin, V. *et al. J. Cell. Sci.* 2006,*119*, 23–30. The AFM tip is approaching the sample surface (a). The initial contact between the tip and the surface is mediated by the attractive van der Waals forces (contact) that lead to an attraction of the tip toward the sample (b). Hence, the tip applies a constant and default force upon the sample surface that leads to sample indentation and cantilever deflection (c). Subsequently, the tip tries to retract and to break loose from the surface (d). Various adhesive forces between the sample and the AFM tip, however, hamper tip retraction. These adhesive forces can be taken directly from the force–distance curve (e). The tip withdraws and loses contact with the sample upon overcoming the adhesive forces (f). Inset: experimental approach curve recorded for a silicon surface electrografted by poly(*N*-succinimidyl acrylate) (PNSA) (from a 0.1 M NSA solution in DMF) with a silicon nitride tip.

The surface grafting of PNSA onto doped silicon was also analyzed by AFM. A grafting density of ~1 chain per 100 nm^2 was determined from the compression profile recorded for a surface electrografted in DMF ([NSA] = 1 M), i.e., in a brush regime (Chapter **1.15**). The tip–surface distance at which the chain rupture occurred in the retraction mode was the length of the chain fully stretched between the grafting point on the surface and the tip (**Figure 14**). The average degree of polymerization was accordingly estimated at 1016.[30]

Last but not least, the good fit of the shape of the compression profiles and the function based on the Alexander-de Gennes scaling concept that describes the compression forces of polymer brushes, together with the good agreement between the bridging profiles and models for a wormlike chain and freely jointed chain under tension, are strong indications that the grafted chains are essentially linear with few branching points.

In addition to providing strong evidence that the electrografted polyacrylate chains are tethered to the surface and form a brush as soon as the grafting density is high enough, AFM was also useful for investigating the adhesion forces of the grafted chains.

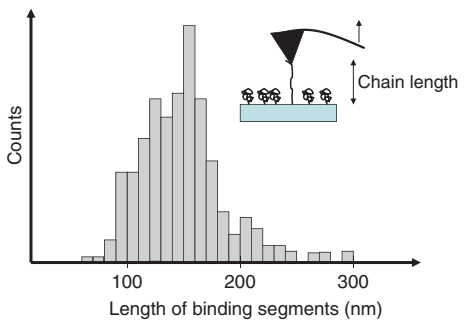

Figure 14 Distribution of the rupture distances obtained from the bridging interactions in DMF between a PNSA electrografted onto silicon, from a 0.1 M monomer solution, and from a gold-coated AFM tip.[30]

As illustrated by Lee *et al.*,[32] the adhesion force (Chapter **2.24**) of a polymer chain onto a solid surface can be extracted from retraction curves (**Figure 13**). This technique was applied to polymers electrografted onto gold and doped silicon[33,34] in order to confirm the chemisorption of the chains that was an assumption until then. These two solid substrates were electrografted by PNSA, which is highly reactive toward nucleophiles. In parallel, an AFM silicon tip was chemically grafted by an amino-containing organosilane. The tip was approached very closely to the electrografted surface, in DMF, a good solvent for PNSA. Individual chains were chemically captured by the tip as result of the spontaneous reaction between amino groups of the tip and NSA units of the electrografted film. Depending on the substrate onto which PNSA was grafted, rupture forces of 1.1 and 2.4 nN were measured for gold and silicon, respectively. These forces, which correspond to the rupture of the weakest bond of the bridged system, actually fit the strength of C–Au and C–Si bonds, respectively.

These data are in line with more conventional spectroscopic studies, particularly X-ray photoelectron spectroscopy (XPS), of the electrografting of 2-butenenitrile onto Ni.[35] Deniau *et al.* observed the bonding of monomeric, dimeric, and trimeric species by XPS at 283.6 eV, typical of carbon–nickel bonds. The higher acidity of this monomer compared to the methacrylate counterpart dramatically restricts the anionic propagation of the chains such that the deposition was thin enough for the bonding to Ni to be observed by XPS.

4.36.2.7 Variety of Substrates Suitable for Electrografting

Being a cathodic process, electrografting is an ideal coating process not only for 'noble' metals, that is, metals that resist

oxidation in the anodic regime, but also for common metals, such as Fe, Ni, and Cu, provided that they have been pretreated by removing any superficial oxides.[35] Actually, superficial oxides can be cathodically reduced in an ACN–conducting salt solution followed by the quick transfer of the reduced metal to the electrochemical cell, under inert atmosphere. Because Zn and Al oxides resist electrochemical reduction, electrografting onto these metals remains quite a problem.[36]

The metal used as the working electrode has a clear influence on the thickness of the electrografted film. For instance, the thickness of PAN films electrografted under the same conditions, except for the substrate, decreases as follows: Pt > Ag > Cu > Au. Interestingly enough, theoretical models showed that AN would be physisorbed onto gold[37] but chemisorbed onto copper,[38] silver,[39] and platinum,[37] thus in qualitative agreement with both the poor results observed whenever gold is the cathode and the preferential adsorption of the monomer to the surface that is the prerequisite of successful electrografting. Of course, the theoretical models did not take the environment into account (solvent, monomer concentration, polarization), whose optimization can provide the surface with a suitable coating. In addition to metal, various metallic alloys, for example, stainless steel, brass, nitinol, and shape-memory alloys, were also successfully electrografted by polyacrylates.

Semiconductors, such as n- and p-doped silicon, are quite valuable substrates in microelectronics. Their oxide layer can be removed by an appropriate chemical pretreatment with fluorhydric acid. These activated surfaces are then well suited to electrografting, i.e., to chemisorption of polymer chains through quite stable Si–C bonds.[33] It was also shown that depending on the solvent and the monomer, the electrografting potential changes with the conductivity of the substrate. According to **Table 2**, the passivation peak observed in the electroreduction of MMA in DMF is shifted toward more cathodic potentials when the silicon conductivity is decreased. In case of AN, the passivation potential is, however, independent of the electrode conductivity, more likely because the quantum states in the energy bands of the semiconductor and the electronic levels of the monomer nearly overlap,[40] making the electron transfer for the electroreduction of the monomer quite easy.

Electrografting onto the native oxide layer of doped silicon is also feasible,[41] because this layer is thin enough to allow for the tunneling electron transfer from silicon to the adsorbed monomer. However, the Si–O–C bond that is formed is hydrolytically unstable, and the polymer film can be dissolved by extensive washing of the surface with a good solvent (from the shelf) for the polymer.

Table 2 Potential of the peak I for the electroreduction of MMA and AN depending on the electrode conductivity using various doped silicon as substrates

	5×10^{-3}	0.1	10
Si resistivity (ohm cm)	*Potential of the grafting peak (V)*		
MMA 1 M	−2	−2.8	−3
AN 1 M	−2	−2	−2

In the field of microelectronics, electrografting appears as a cheap one-step technique for the localized modification of a composite conducting surface. This process is based on the concept that the local work function of electrons can be easily tuned by patterning the substrate with materials of different conductivity. In a typical example, silicon wafers (bearing an oxide top layer) have been locally coated with a thin film of gold by classical vacuum deposition through a mask (with a thin adhesion interlayer of chromium).[42] When such a composite conducting substrate is used as a cathode in the electrografting process, a polymer coating is observed only on the gold areas and no polymer is detected on the silicon oxide regions. This is observed whatever be the polarization contact area, that is, gold or silicon wafer. This locally selective grafting results from the electron transfer that is intrinsically more favorable from gold than from silicon oxide to the monomer. Selectivity is thus of a kinetic origin. This technology has been applied to submicrometer patterns, the lateral resolution being limited only by the thickness of the grafted polymer layer. This localized electrografting has also been extended to silicon wafer locally doped by ion implantation. The implantation pattern is clearly revealed by the polymer coating without use of any mask for deposition. This process opens up new prospects for the one-step local functionalization of various electronic devices, such as transistors, sensors, and memories.

Interestingly, several carbon allotropic forms[43] (at least semiconducting carbon objects) have been successfully electrografted by (meth)acrylates. The polymer is then chemisorbed to the surface through a carbon–carbon bond, which provides the organic coating with the best adhesion to the substrate. The extension of this process to carbon fibers[44] is thus a strategy for the sizing technology of carbon fibers.

In contrast to bulk materials, including fibers, that can be easily polarized, the situation is more complex when powdery or nanoparticulate conducting materials are concerned. Three main strategies were reported so far.

Electrically conducting powders were placed in a zinc container immersed in (and filled by) the electrochemical bath and used as a cathode. As long as the particles percolate and are in contact with the polarized container, they can be electrografted by poly(meth)acrylates provided that the cathodic potential and the solvent are properly chosen. An additional and critically important requirement must be pointed out, that is, the inability of the container to be electrografted. Otherwise, it would be rapidly passivated, and the process would be stopped possibly before the powdery material is coated as desired. Zinc fulfills this condition. Voltammograms on various carbon black and multiwalled carbon nanotubes (MWNTs) were recorded, and the electrografting potential was determined for each of them.[45] The electrografting of the individual particles, particularly carbon nanotubes (CNTs), is essential when they are intended to be extensively dispersed in a polymer matrix for preparing composites with high performances. For this purpose, the powdery or particulate conducting material was maintained under mechanical dispersion within the monomer and conducting salt solution, which resulted in the intermittent but repeated contact of the carbon particles with a zinc grid used as the working electrode.[45] Upon contact with the zinc grid, particles are instantaneously polarized, and the electrografting is accordingly initiated. Chain propagation, which does not require polarization, then occurs even in the absence

of contact. Although depending on the suspension stirring time and efficiency, the particles may hit the electrode frequently enough to be modified to the point where they are prevented from settling on the bottom of the flask when the stirring is stopped even for a long time. Particles inadequately modified, if any, can then be eliminated by filtration or centrifugation. Finally, taking advantage of the production of MWNTs by aerosol-assisted catalytic chemical vapor deposition,[46] the accordingly prepared carpet of aligned CNTs standing from the solid surface was cathodically polarized and the constitutive nanotubes were modified by electrografting.[47] Immobilization of polymerizable ferrocene derivatives by electrografting onto CNTs of high surface area is very interesting for sensoring or catalytic applications. Glucose sensors were recently prepared according to this strategy.[48]

4.36.2.8 Implementation of Electrografting in Aqueous Media

The implementation of electrografting on a large scale is severely limited by the use of an organic solvent together with the very demanding experimental conditions of dryness and absence of oxygen. It is thus highly desirable to conduct electrografting in nontoxic, cheap, and environmentally friendly media, which means substituting water for the organic solvent.

4.36.2.8.1 Direct initiation of amphiphilic acrylates

The major issues raised by the electrografting of acrylic derivatives in water are the rapid adsorption of water onto the electrode and the poor cathodic stability of water. A possible way of increasing the electrochemical window of water is to perform electrochemistry in emulsions. Indeed, a positively charged amphiphile added to water is expected to be adsorbed onto the cathode, so creating a protective hydrophobic barrier against water whose reduction would be shifted toward more cathodic potentials.[49] Based on this consideration, an amphiphilic acrylic monomer that consists of an acrylic unsaturation attached to the end of a hydrophobic tail, that is, [(10-acryloyloxy)decyl] trimethylammonium bromide (acry-C_{10}) (**Figure 15**), was synthesized. This purposely designed monomer was electropolymerized in water at the surface of a glassy carbon cathode and the chains were chemisorbed to carbon.[50]

In close relation to the molecular structure, the amphiphilicity of the monomer is of prime importance. On the basis of voltammetric and ellipsometric data, a three-step mechanism was proposed to explain the successful electrografting. The positively charged micelles formed by the monomer in water diffuse toward the cathode and spread out on the solid surface as a bilayer. At an appropriate cathodic potential, the acrylic double bonds of the double layer, which are close enough to the carbon surface, are reduced and grafted as radical species that propagate the polymerization. The electroreduction of water molecules that regularly migrate to the cathode in spite of the hydrophobic barrier results in hydrogen radicals that initiate polymerization as long as the potential is applied. Although they grow in the micelles, part of these chains can transfer to the electrografted chains whose lifetime is short because of irreversible chain termination. The electroinitiation is also limited in time as a result of the surface saturation. These chain transfer reactions have a beneficial effect on the film thickness that continues growing beyond the electroinitiating step. **Figure 16** is an illustration of films of poly(acry-C_{10}) electrografted onto carbon in DMF and in water. No macroscopic difference is noted between these two solvents (**Figures 16(b)** and **16(c)**). The substantial increase in the film thickness shown by **Figures 16(c)** and **16(d)** merely results from the repetition of the potential scanning.

Electrografting is thus possible in water, with formation of a strongly adhering polycationic coating. This type of positively charged film can impart specific properties to the surface, for example, bactericidal properties associated to the quaternary ammonium groups.[51] Moreover, they are highly desirable anchoring layers for building up multilayered films by the well-known layer-by-layer deposition of polyelectrolytes of opposite charges[52,53] (Chapter **7.09**).

4.36.2.8.2 Indirect electroinitiation of vinyl monomers by diazonium salts

As shown in the previous section, amphiphiles are effective in widening the narrow cathodic window of water, so making possible cathodic reactions that could not be achieved otherwise. An alternative to this direct electroinitiation method consists of an indirect electroinitiation process, based on the electroreduction of water-soluble aromatic diazonium salts (**Figure 17**). These molecules can be electrochemically cleaved at potentials less cathodic than water reduction, and the radical compounds that are accordingly generated can eventually form a covalent bond with the carbon electrode.[54] The concomitant release of nitrogen keeps the reactive species formed by electron transfer neutral, such that polyaddition reaction cannot occur as was the case for the electroreduction of acrylic monomers. The high stability of nitrogen formed as a by-product is the driving force of the reaction.

It must be noted that the thickness of the deposited layer exceeds that of a monolayer as a result of radical reaction of reduced species with the very first grafted layer as shown by XPS and scanning tunnelling microscopy (STM).

When aryl diazonium salts are electrochemically activated in water at low pH in the presence of vinyl monomers,[55]

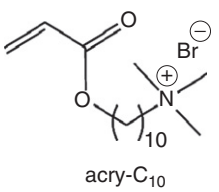

Figure 15 Amphiphilic acry-C_{10} monomer well suited to electrografting in water.

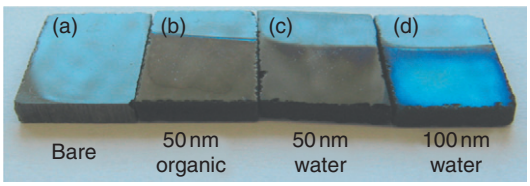

Figure 16 Photographs of carbon electrode (a) uncoated (b) coated by poly(acry-C_{10}) in DMF, and (c–d) coated by poly(acry-C_{10}) in aqueous medium after one (c) and several potential scans (d). Film thickness was determined by ellipsometry.

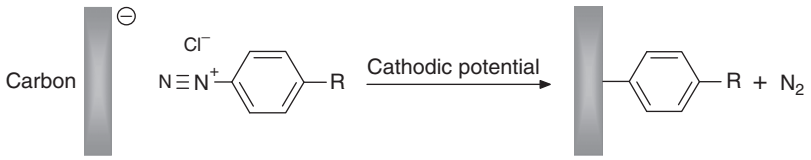

Figure 17 Electrochemical reduction of diazonium salt.

polyvinyl chains are chemisorbed onto the cathode. Indeed, in addition to the electrografting of an organic layer to the substrate (Figure 17), the radical polymerization of the vinyl monomer is initiated in solution. The radical growing chains can transfer to the electrografted organic layer, which is the basic mechanism of chemisorption of a thin polyvinyl film. This indirect electrografting process of vinyl monomers has been extended to the permanent coating of carpets of CNTs.[56] Resistance of the coating to long ultrasonic treatment in a good solvent of the polymer was reported.

4.36.3 Electropolymerization of Conjugated Polymers as Active Layers in Advanced Devices

If economical and ecological considerations have triggered the reviving interest for cathodic electrografting processes carried out in water for protective paints and coatings, the unique electronic properties of conjugated polymers that can be prepared by anodic electrodeposition are at the origin of the recent developments in anodic electrodeposition processes. Indeed, poly(hetero)aromatic compounds, such as polyaniline (PANI), polypyrrole (PPy), polythiophene (PThi), and their derivatives, are conductive polymers easily prepared by electrooxidation of the parent aromatic monomer[57] schematized in Figure 18. A conjugated π-electron system provides these polymers with high rigidity and strong intermolecular interactions, responsible for insolubility in both organic solvents and water. Doping occurs simultaneously to the anodic growth of the chains that precipitate onto the anode. Therefore, the coated electrode remains remarkably conductive during the whole electrochemical process and the film thickness can be easily tuned by coulometry (at least up to several tens of micrometers), in agreement with the mechanism of oxidative radical coupling polymerization that requires the withdrawal of two electrons for a new bond to be formed (Figure 18). This anodic electropolymerization can be carried out in organic solvents as well as in water at low pH provided that the heteroaromatic ring of the monomer is oxidized at a lower potential than the aqueous medium, which is the case for pyrrole and aniline. The polymerization is enhanced under acidic conditions.

The anodic polymerization herein discussed must be conducted with a noble metal as anode, i.e., a metal that is not oxidatively dissolved in the anodic regime. Pt, Au, stainless steel, carbon, and conductive oxides (ITO, etc.) are examples of commonly used anodes. Interestingly enough, these substrates are common constituents of devices, such as actuators, sensors, solar cells, and electrochromic windows, in which thin films of conjugated polymers are desirable active layers. Last but not least, conjugated polymers can also be electrodeposited onto common metals (iron and copper) for sake of protection against corrosion, provided that the composition of the electrolytic medium is properly controlled.[58]

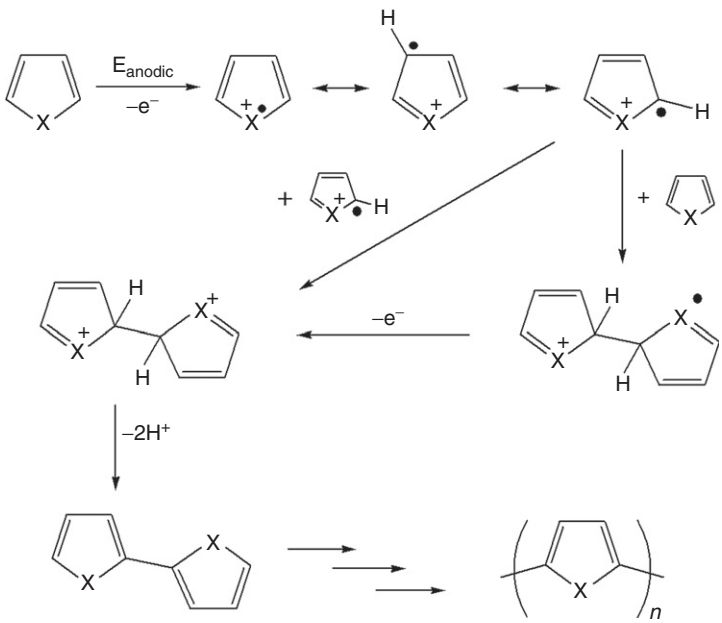

Figure 18 Oxidative coupling mechanism for the electropolymerization of an heteroaromatic monomer.

Interestingly enough, poly(*p*-phenylene vinylene) (PPV) films can be cathodically prepared by electroreduction of α,α,α′,α′-tetrabromo-*p*-xylene[59] in DMF using tetraethylammonium tetrafluoroborate as the conducting salt. The reductive coupling reactions in electrochemical polymerization of PPV studied by *in situ* UV–vis spectroscopy, by *in situ* UV–vis–ESR spectroscopy, and by the rotating ring-disk electrode technique show that the reduction of brominated monomer takes place in two steps.[60] The first step is a two-electron reduction process, leading to formation of intermediates that stay in solution without precipitation onto the electrode surface. The second two-electron reaction of these intermediates produces oligomers that precipitate onto the surface of the electrode. It was observed that the electrode material, cell design, and temperature have a marked influence on the value of the peak potential of the second reduction reaction. Resonance Raman spectroscopy, optical absorption spectroscopy, and electron spin resonance (ESR) spectroscopy led to the conclusion that in this reaction the quinoid structure is formed rather than the benzenoid structure.[61] FTIR spectroscopy and EQCM experiments[62] obtained from the charging–discharging reaction are consistent with movement of countercations during n-doping. In presence of fullerene,[63] such units can even be incorporated in the polymer main chain, leading to promising donor–acceptor systems.

The conjugated polymers under consideration are smart or responsive materials, because many of their properties (color, conductivity, volume, hydrophilicity, permeability, etc.) directly depend on their oxidation state and can thus be reversibly controlled by the applied potential (Chapter 8.06). As an example, smart windows[64] are organic–inorganic multilayers that consist of a conjugated polymer layer sandwiched between two ITO-coated glass sheets. These devices take advantage of the electrochromism of the polymer coating, thus the reversible switching between dark and colorless aspect in direct relation to the redox state of the polymer. The intensity of the light transmitted through such a window can be tuned at will by external electrical stimuli.

Surprisingly enough, the redox responses of these conjugated polymers change with the deposition conditions, which is an additional parameter for modulating the properties in relation to the envisioned applications. In the wide field of sensors (Chapter 8.05), electrodeposited conjugated polymers play a major role as a transducer layer. Their easy (bio)functionalization, high sensitivity and selectivity toward electroactive species, fast and accurate response, compactness, and cheapness make them highly competitive to construct diversified sensoring electrodes. They already have an active role in, for example, clinical analysis or environmental monitoring.

Quite interestingly, the conductive conjugated polymers can be shaped at the nanoscale by anodic electrodeposition onto properly designed electrodes.[65] For example, one side of porous membranes was coated by a metal (Au) to make them anodically polarizable. PPy nanotubules were then grown electrochemically into the pores and collected upon dissolution of the membrane (Figure 19).

Many books and reviews have been devoted to the electrochemical synthesis and applications of conductive conjugated polymers. Only for reasons of limited space, just few of them are cited herein.[58,66,67]

4.36.4 Electrografting of Conjugated Polymers

Although electrooxidation of heteroaromatic monomers, such as pyrrole, thiophene, and their derivatives, is a classical technique to prepare intrinsically conducting polymer,[68] a drawback of this method is the poor adhesion of the films to the substrate. The polymer chains are indeed merely deposited by precipitation on the electrode without creating specific mutual interactions. A way of tackling this problem is to combine anodic electropolymerization with cathodic electrografting.

In a first strategy, dual monomers, i.e., acrylates that contain a pyrrole or a thiophene unit in the ester group, such as *N*-(2-acryloyloxyethyl) pyrrole (PyA) and 3-(2-acryloyloxyethyl) thiophene (ThiA), were synthesized. The parent polyacrylates were easily chemisorbed under cathodic polarization, followed by a polarization inversion that resulted in the polymerization of the pyrrole or thiophene substituents, so making the electrically conducting film adhere strongly to the electrode. Pyrrole or thiophene can be added to the electrochemical bath for the purpose of increasing the thickness of the electrically conducting film, which was confirmed by the voltammetric analysis of the conjugated polymer electroactivity.[24,69]

In an alternative approach, PyA and ThiA were polymerized by conventional or controlled radical polymerization. Prior to electrooxidation of PyA or ThiA, the preformed polyacrylates, polyPyA and polyThiA, were either dissolved in the

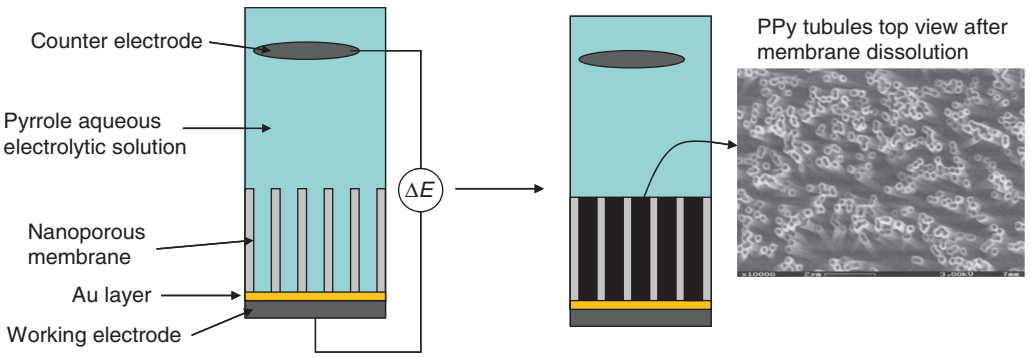

Figure 19 Template electrodeposition of Ppy and transmission electron microscopy (TEM) micrographs of the collected PPy nanotubules.

electrochemical bath or cast onto an electrode onto which PyA or ThiA was previously electrografted. Depending on the anodic polarization time, electroactive films of a controlled thickness (up to several micrometers) were prepared. This substantial progress can be instrumental in improving the performances of various high-tech devices, such as light-emitting diodes (Chapter 8.10), anticorrosion coatings, electrochromic windows, and electrochemical sensors, which depend on the stability and adherence of a conjugated polymer coating on a conducting solid surface.

In a second strategy, binary polymer films consisting of an insulating polymer and a conducting polymer were prepared by sequential electropolymerization of the parent monomers.[70] The insulating polymer (PAN or PEA) was electrografted under cathodic polarization, onto nickel and carbon, respectively. The conducting polymer (polybithiophene or PPy) was anodically deposited in a second step by electrooxidation of the related monomer in a good solvent for the electrografted chains. The main advantages of this strategy are the use of commercially available monomers and a substantial improvement of the adhesion of the conducting polymer, more likely by a chain entrapment effect. Finally, a solvent-responsive film was prepared as a result of the proper combination of both the insulating and the conducting polymers (e.g., PEA and PPy). Indeed, the electroactivity of PPy strongly depended on the extent of swelling of the electrografted PEA chains. The anodic polarization time was controlled for growing PPy nuclei smaller than the tethered PEA chains. Whenever the electroactivity of the binary film was recorded in a good solvent for the PEA chains, the ions could diffuse through the PEA coating and a strong redox signal typical of PPy was observed. However, in a poor solvent for PEA, the PPy nuclei were screened by the insulating polymer, and the electroactivity of PPy completely disappeared. These films thus have a potential in solvent sensoring devices.

Finally, under specific conditions, the grafted layer of an insulating polymer can act as a template for the growth of PPy nanowires. The conjugated polymer was synthesized under galvanostatic rather than potentiostatic conditions, and long filaments of conjugated polymers were formed as observed by SEM (Figure 20).[65,71,72] The proposed mechanism for the wire formation relies on the continuous electrooxidation of the pyrrole monomer at vicinity of the electrode, that is, beneath the PEA chains. The already polymerized PPy is simultaneously rejected from the surface through a channel left in the insulating layer that plays the role of template. The length of the nanowires depends only on the polarization time, whereas the diameter is mainly dictated by the characteristic features of the electrografted coating. Polyacrylate brushes of higher density are responsible for wires with a smaller diameter.[73]

4.36.5 Conclusion

The greatest potential of electroinitiated polymerization falls in coating technology. In this field, electrochemical methods may compete with conventional polymerization methods even though developed on a large scale. Provided that the solid substrate is (semi)conducting, the relevance of electroinitiated polymerization provides an unique opportunity to impart permanent functionality/reactivity to a variety of surfaces. Among possible achievements, let us mention the following:

- Homogeneous coating of surfaces with complex structures.
- Strongly adhesive polymer coatings onto (semi)conducting surfaces to be used as primer coating reactive toward various top coats.
- Electrochemical tuning of the thickness of coatings.
- One-step process of selective decoration of composite surfaces even at the nanoscale.

Protection of metals against corrosion remains, however, a major potential achievement as long as the electrografting can be conducted in aqueous media, which is a restriction on the choice of the monomer. Further improvements remain highly desirable, which is a strong driving force for future efforts.

The permanent coating of electrodes by a layer of an electroactive polymer is an effective strategy for providing it with functionalities very specific to various application fields, including sensors, actuators, batteries, electrochromic windows, light-emitting diodes, and solar cells.

It may be recalled that the electrografting of polymers onto surface plasmon resonance chips and the resonator sensor of QCM improved very advantageously by the analytical performances of those sensoring techniques.

The very fast development of nanotechnologies and microelectronics can also take advantage of electroinitiated polymerization, as was exemplified by the production of nano-objects of well-defined shape and dimensions by using properly designed template electrodes. A clever combination of AFM and electroinitiated polymerization is also looking very promising for manipulating macromolecules at the molecular level.

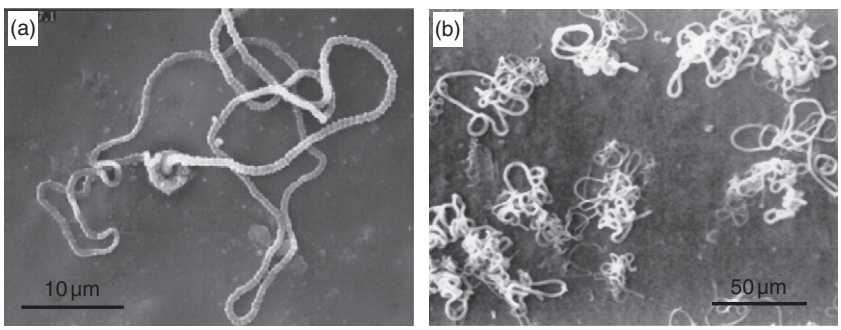

Figure 20 Polypyrrole wires anodically grown from (a) poly(ethyl acrylate)-coated carbon and (b) a poly(*t*-butyl acrylate)-coated carbon.

Last but not least, the anodic deposition of electroconductive conjugated polymers can benefit from the cathodic electrografting process for improving the intrinsically poor adhesion of these highly cohesive polymers. The great potential of the electrochemical polymerization techniques as a whole could be exploited in the future to face challenges raised by economical and ecological pressure, on the one hand, and by high level performances required by rapidly expanding top technologies, on the other hand.

References

1. Magenau, A. J. D.; Strandwitz, N. C.; Gennaro, A.; Matyjaszewski, K. *Science* **2011**, *332* (6025), 81.
2. Mengoli, G.; Subramanian, R. V.; Williams, G.; Block, H. *Advances in Polymer Science*; Springer Verlag: Berlin,1979.
3. Lécayon, G.; Bouizem, Y.; Le Gressus, C.; *et al. Chem. Phys. Lett.* **1982**, *91* (6), 506.
4. Boiziau, C.; Lécayon, G. *Recherche* **1988**, *19* (201), 888.
5. Boiziau, C.; Lécayon, G. *Surf. Interface Anal.* **1988**, *12* (1–12), 475.
6. Baute, N.; Calberg, C.; Dubois, P.; *et al. Macromol. Symp.* **1998**, *134 (Electron Transfer Processes and Reactive Intermediates in Modern Chemistry)*, 157.
7. Buttry, D.; Ward, M. *Chem. Rev.* **1992**, *92*, 1355.
8. Baute, N.; Martinot, L.; Jérôme, R. *J. Electroanal. Chem.* **1999**, *472* (1), 83.
9. Boiziau, C.; Leroy, S.; Reynaud, C.; *et al. J. Adhes.* **1987**, *23* (1), 21.
10. Bureau, C.; Deniau, G.; Viel, P.; Lécayon, G. *Macromolecules* **1997**, *30* (2), 333.
11. Calberg, C.; Mertens, M.; Jerome, R.; *et al. Thin Solid Films* **1997**, *310* (1-2), 148.
12. Mertens, M.; Calberg, C.; Baute, N.; *et al. J. Electroanal. Chem.* **1998**, *441* (1-2), 237.
13. Calberg, C.; Mertens, M.; Jérôme, R.; *et al. Thin Solid Films* **1997**, *310* (1-2), 148.
14. Baute, N.; Teyssié, P.; Martinot, L.; *et al. Eur. J. Inorg. Chem.* **1998**, (11), 1711.
15. Crispin, X.; Lazzaroni, R.; Geskin, V.; *et al. J. Am. Chem. Soc.* **1999**, *121* (1), 176.
16. Baute, N.; Jérôme, C.; Martinot, L.; *et al. Eur. J. Inorg. Chem.* **2001**, (5), 1097.
17. Claes, M.; Voccia, S.; Detrembleur, C.; *et al. Macromolecules* **2003**, *36* (16), 5926.
18. Voccia, S.; Jérôme, C.; Detrembleur, C.; *et al. Chem. Mater.* **2003**, *15* (4), 923.
19. Voccia, S.; Bech, L.; Gilbert, B.; *et al. Langmuir* **2004**, *20* (24), 10670.
20. Voccia, S.; Claes, M.; Jérôme, R.; Jérôme, C. *Macromol. Rapid Commun.* **2005**, *26* (10), 779.
21. Detrembleur, C.; Jérôme, C.; Claes, M.; *et al. Angew. Chem., Int. Ed.* **2001**, *40* (7), 1268.
22. Ameur, S.; Bureau, C.; Charlier, J.; Palacin, S. *J. Phys. Chem. B* **2004**, *108* (34), 13042.
23. Jérôme, C.; Gabriel, S.; Voccia, S.; *et al. Chem. Commun. (Cambridge, U. K.)* **2003**, (*19*), 2500.
24. Labaye, D. E.; Jérôme, C.; Geskin, V. M.; *et al. Langmuir* **2002**, *18* (13), 5222.
25. Gabriel, S.; Dubruel, P.; Schacht, E.; *et al. Angew. Chem., Int. Ed.* **2005**, *44* (34), 5505.
26. Lou, X.; Jérôme, C.; Detrembleur, C.; Jérôme, R. *Langmuir* **2002**, *18* (7), 2785.
27. Gabriel, S.; Jérôme, R.; Jérôme, C. *Prog. Polym. Sci.* **2010**, *35* (1-2), 113.
28. Easter, P. A.; Taylor, D. M. *J. Polym. Sci., Part A: Polym. Chem.* **2009**, *47*, 1685.
29. Tourillon, G.; Garrett, R.; Lazarz, N.; *et al. J. Electrochem. Soc.* **1990**, *137* (8), 2499.
30. Cuenot, S.; Gabriel, S.; Jérôme, R.; *et al. Macromolecules* **2006**, *39* (24), 8428.
31. Gabriel, S.; Jérôme, C.; Jérôme, R.; *et al. J. Am. Chem. Soc.* **2007**, *129* (27), 8410.
32. Lee, H.; Scherer, N. F.; Messersmith, P. B. *Proc. Natl. Acad. Sci. U. S. A.* **2006**, *103* (35), 12999.
33. Duwez, A.-S.; Cuenot, S.; Jérôme, C.; *et al. Nat. Nanotechnol.* **2006**, *1* (2), 122.
34. Cuenot, S.; Gabriel, S.; Jérôme, C.; *et al. Macromol. Chem. Phys.* **2005**, *206* (12), 1216.
35. Deniau, G.; Azoulay, L.; Jegou, P.; *et al. Surf. Sci.* **2006**, *600* (3), 675.
36. Fredriksson, C.; Lazzaroni, R.; Bredas, J. L.; *et al. Chem. Phys. Lett.* **1996**, *258* (3-4), 356.
37. Parent, P.; Laffon, C.; Tourillon, G.; Cassuto, A. *J. Phys. Chem.* **1995**, *99* (14), 5058.
38. Geskin, V. M.; Lazzaroni, R.; Mertens, M.; *et al. J. Chem. Phys.* **1996**, *105* (8), 3278.
39. Xue, G.; Dong, J.; Zhang, J.; Sun, Y. *Polymer* **1994**, *35* (4), 723.
40. Charlier, J.; Ameur, S.; Bourgoin, J.-P.; *et al. Adv. Funct. Mater.* **2004**, *14* (2), 125.
41. Charlier, J.; Baraton, L.; Bureau, C.; Palacin, S. *ChemPhysChem* **2005**, *6* (1), 70.
42. Charlier, J.; Clolus, E.; Bureau, C.; Palacin, S. *J. Electroanal. Chem.* **2009**, *625* (1), 97.
43. Mertens, M.; Martinot, L.; Jérôme, R. PCT Int. Appl. WO 9,902,614, 1999, 27 pp.
44. Jérôme, R.; Martinot, L.; Mertens, M. PCT Int. Appl. WO 9,920,697, 1999, 30 pp.
45. Petrov, P.; Lou, X.; Pagnoulle, C.; *et al. Macromol. Rapid Commun.* **2004**, *25* (10), 987.
46. Pinault, M.; Mayne-L'Hermite, M.; Reynaud, C.; *et al. Diamond Relat. Mater.* **2004**, *13* (4-8), 1266.
47. Defever, T.; Deniau, G.; Palacin, S.; *et al. J. Electroanal. Chem.* **2006**, *589* (1), 46.
48. Mesnage, A.; Esnouf, S.; Jégou, P.; *et al. Chem. Mater.* **2010**, *22*, 6229.
49. Mackay, R. A.; Texter, J. *Electrochemistry in Colloids and Dispersions*. VCH: New York,1992.
50. Cécius, M.; Jérôme, R.; Jérôme, C. *Macromol. Rapid Commun.* **2007**, *28* (8), 948.
51. Voccia, S.; Ignatova, M.; Jerome, R.; Jerome, C. *Langmuir* **2006**, *22* (20), 8607.
52. Charlot, A.; Gabriel, S.; Detrembleur, C.; *et al. Chem. Commun. (Cambridge, U. K.)* **2007**, (44), 4656.
53. Cécius, M.; Jérôme, C. *Prog. Org. Coat.* **2011**, *70* (4), 220.
54. Pinson, J.; Podvorica, F. *Chem. Soc. Rev.* **2005**, *34* (5), 429.
55. Mevellec, V.; Roussel, S.; Tessier, L.; *et al. Chem. Mater.* **2007**, *19* (25), 6323.
56. Tessier, L.; Chancolon, J.; Alet, P.-J.; *et al. Phys. Status Solidi A Appl. Mater. Sci.* **2008**, *205* (6), 1412.
57. Sabouraud, G.; Sadki, S.; Brodie, N. *Chem. Soc. Rev.* **2000**, *29*, 283.
58. Cosnier, S.; Karyakin, A. *Electropolymerization: Concepts, Materials and Applications*. Wiley: Weinheim, 2010.
59. Damlin, P.; Kvarnstrom, C.; Ivaska, A. *Electrochim. Acta* **1999**, *44* (23), 4087.
60. Damlin, P.; Kvarnstrom, C.; Petr, A.; *et al. Macromolecules* **2002**, *35* (15), 5789.
61. Damlin, P.; Kvarnstrom, C.; Petr, A.; *et al. J. Solid State Electrochem.* **2002**, *6* (5), 291.
62. Damlin, P.; Kvarnstrom, C.; Neugebauer, H.; Ivaska, A. *Synth. Met.* **2001**, *123* (1), 141.
63. Kvarnstrom, C.; Kulovaara, H.; Damlin, P.; Ivaska, A. *Synth. Met.* **2003**, *135–136*, 783.
64. Mortimer, R. J. *Chem. Soc. Rev.* **1997**, *26*, 147.
65. Jerome, C.; Demoustier-Champagne, S.; Legras, R.; Jerome, R. *Chem.– Eur. J.* **2000**, *6* (17), 3089.
66. Kumar, D.; Sharma, R. C. *Eur. Polym. J.* **1998**, *34*, 1053.
67. Li, C.; Bai, H.; Shi, G. *Chem. Soc. Rev.* **2009**, *38*, 2937.
68. Jerome, C.; Maertens, C.; Mertens, M.; *et al. Synth. Met.* **1996**, *83* (2), 103.
69. Labaye, D. E.; Jérôme, C.; Jérôme, R. *Polym. Mater. Sci. Eng.* **1999**, *80*, 10.
70. Jérôme, C.; Geskin, V.; Lazzaroni, R.; *et al. Chem. Mater.* **2001**, *13* (5), 1656.
71. Jérôme, C.; Jérôme, R. *Angew. Chem., Int. Ed.* **1998**, *37* (18), 2488.
72. Jérôme, C.; Labaye, D.; Bodart, I.; Jérôme, R. *Synth. Met.* **1999**, *101* (1-3), 3.
73. Jérôme, C.; Labaye, D. E.; Jérôme, R. *Synth. Met.* **2004**, *142* (1-3), 207.
74. Ikeda, T.; Tazuke, S.; Watanabe, M. *Biochim. Biophys. Acta* **1983**, *735*, 380.
75. Ikeda, T.; Yamaguchi, H.; Tazuke, S. *Antimicrob. Agents Chemother.* **1984**, *26*, 139.
76. Ignatova, M.; Voccia, S.; Gilbert, B.; *et al. Langmuir* **2004**, *20*, 10718.
77. Ignatova, M.; Voccia, S.; Gilbert, B.; *et al. Langmuir* **2006**, *22*, 255.
78. Ignatova, M.; Voccia, S.; Gabriel, S.; *et al. Langmuir* **2009**, *25*, 891.

Biographical Sketch

Christine Jérôme, born in 1971 in Belgium, completed her PhD in 1998 at the University of Liege, Belgium and then worked as a postdoctoral researcher at the same university. In 2000, she joined the University of Ulm in Germany as a recipient of the Humboldt scholarship. She returned to the University of Liege in 2001 as a research associate of the National Foundation of the Scientific Research in the group of Professor R. Jérôme, where she became assistant professor in 2006 and director of the Center for Education and Research on Macromolecules in 2007. Her research interests include electropolymerization, polymer functionalized nanoparticles, and biomaterials.

4.37 Photopolymerization

JV Crivello, Rensselaer Polytechnic Institute, Troy, NY, USA

4.37.1 Introduction

Within the constraints of a single chapter, it is not feasible to provide a detailed or comprehensive coverage of all aspects of the topic of photopolymerization chemistry. Accordingly, several relevant books and book chapters[1–6] are recommended to the reader as general resources on the topic of photopolymerization chemistry. In addition, key references are provided in each section of this chapter to allow the reader to pursue a further in-depth exploration of the specific material presented herein.

It is difficult to overstate the present and growing importance of photopolymerization chemistry both as a research area and with respect to the present and future technological impact of this field. Indeed, photopolymerizations have already changed our lives in manifold ways. Only a few examples will be given here. Without doubt, the electronic and microelectronic technology that pervades our lives would simply not be possible without the use of photopolymers. The application of photopolymerization chemistry is also responsible for the rapid curing printing inks used in our magazines and packaging materials, in the floor coatings and wallpaper used in our homes, and the simulated wood that is used in furniture, cabinetry, and paneling. The photopolymerization technology has provided these and a myriad of similar items at lower cost, with less environmental consequences and reduced energy consumption than would be obtainable by the traditional means used in their manufacture. Photocurable dental composites, dental coatings, and orthodontic retainers are another area where this technology is being applied to improve human health and welfare. Using computer-aided design and employing such three-dimensional imaging techniques as digital imaging, stereolithography, and ink-jet printing together with photopolymerization chemistry have revolutionized the entire design, engineering, and manufacturing process of many industries.

As the word implies, photopolymerizations are polymerization reactions that take place under the specific stimulus of light. From an organizational point of view, the various types of photopolymerizations can be classified according to the classical mechanistic and kinetic designations that are used to distinguish between polymerization reactions in general. Figure 1 shows a schematic representation of the basic classifications of photopolymerizations. These basic classifications form the outline for the major divisions within this chapter.

4.37.2 Photochemical Condensation Reactions

Photochemical condensation reactions that have been applied to the formation of polymers are of two basic types: (1) those in which the direct irradiation of a monomer species leads to its polymerization; and (2) those that are mediated by a photogenerated catalyst.

4.37.2.1 Direct Photochemical Condensation Reactions

Organic photochemical processes that result in the joining together, that is, condensation, of two or more molecules

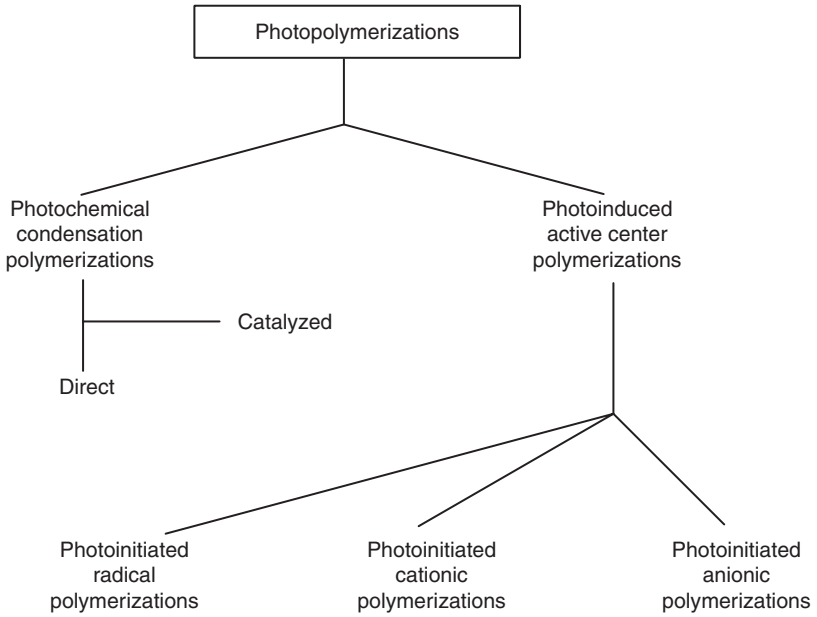

Figure 1 Categories of photopolymerization reactions.

were the first class of reactions to be utilized to make polymers. As has been previously documented,[7] the hardening of bitumen of Judea on exposure to light was used by ancient peoples to provide waterproof coatings for boats and for the preservation of Egyptian mummies. In the eighteenth and nineteenth centuries, the same reactions and materials were used by Niépce and others for photographic purposes to record images. The development of modern organic chemistry and its extension into the more specialized field of photochemistry provided a plethora of new types of reactions that could be harnessed to produce polymers. Let us consider, as a prototypical example, the photochemically allowed $2\pi + 2\pi$ cycloaddition of carbon–carbon double bonds to form cyclobutanes. A schematic representation of this reaction is shown in eqn [1] of **Scheme 1**.

Application of the $2\pi + 2\pi$ cycloaddition reaction to the formation of a linear polymer as shown in eqn [2] would require the use of a diene, such as represented by **1**, as a monomer. However, there are several difficulties with such a scheme. First, the quantum yields for such cycloaddition reactions with simple alkenes are very low ($\Phi = \sim 0.04$–0.10).[8] This is due to the fact that there are many pathways

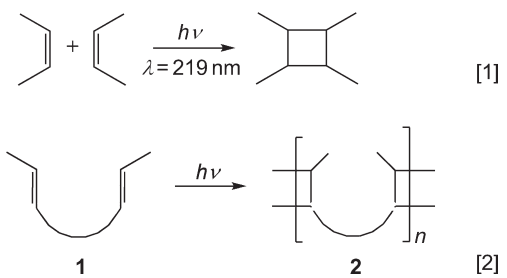

Scheme 1 Photopolymerization via $2\pi + 2\pi$ cycloaddition reaction of alkenes.

available by which photochemically generated excited states can be deactivated and is also due to the presence of a wide range of side reactions.[9] Even though the quantum yields for photocycloaddition of conjugated alkenes and for enones are considerably higher than for simple alkenes, these reactions are still unsuitable for the stringent selectivity and conversion requirements for the production of high-molecular-weight linear polymers, **2**. It is also worth noting that under optimal conditions for the photoinduced cycloaddition of **1**, a minimum absorption of a photon of light is required for each monomer incorporated within the polymer chain. This implies that these photochemical condensation reactions to make polymers are inherently highly energy-consumptive processes.

Despite the abovementioned drawbacks, photochemical condensation reactions have found considerable application in polymer chemistry. During the early development of integrated circuit (IC) technology in the 1960s to the mid-1970s, this chemistry was extensively used in the production of negative-tone photoresists.[10–12] Two typical examples are given below. Rather than using these photoinduced condensation reactions to prepare linear polymers, they were employed to carry out crosslinking reactions of appropriately functionalized oligomers and polymers. There are considerably fewer constraints in carrying out these types of reactions than for the synthesis of high-molecular-weight linear polymers. To achieve the differential solubility required to distinguish between the irradiated and nonirradiated regions of these photoresists, only a few crosslinks per chain are required. In the first instance, a poly(vinyl alcohol) backbone polymer is fitted with pendant photosensitive cinnamate groups.[13] As shown in eqn [3], the $2\pi + 2\pi$ cycloaddition occurs on ultraviolet (UV) irradiation to produce network polymers joined together by crosslinks containing cyclobutane units.

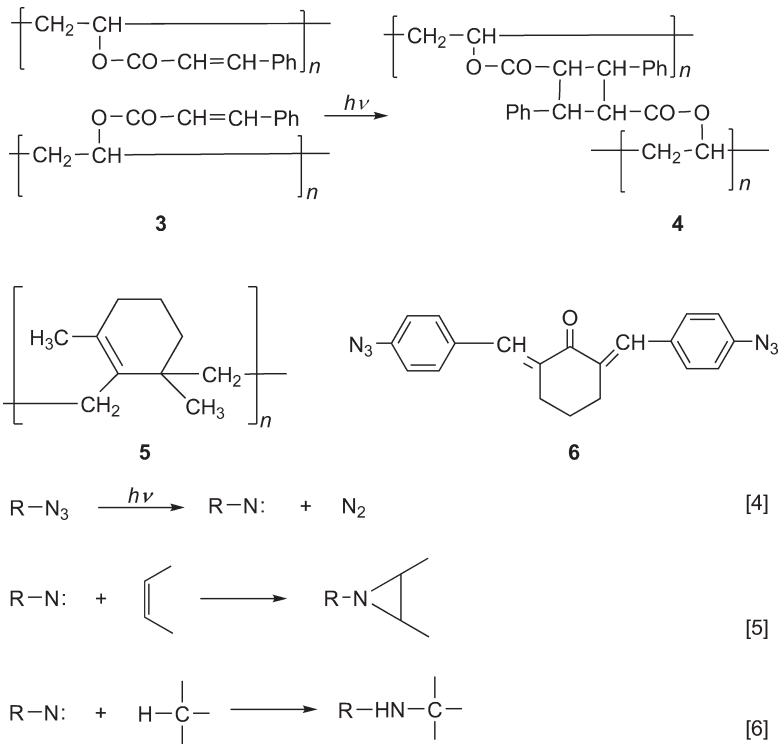

Scheme 2 Photoinduced generation of nitrenes and their addition to alkene double bonds.

Another approach that has been used in photoimaging is exemplified in eqn [4].[14] Cyclized *cis*-1,4-polyisoprene, **5**, containing residual double bonds is irradiated in the presence of a diazide such as compound **6**. As can be seen in the mechanism in eqns [4]–[6] of **Scheme 2**, the resulting bisnitrene that is produced inserts into the double bonds (eqn [5]) along the polymer chains crosslinking the polymer. Additionally, the highly active nitrenes can also undergo insertion into carbon–hydrogen bonds (eqn [6]) to give amine crosslinks.

Due partly to the rather low photosensitivity and resolution capabilities ($\gtrsim$2 mm) of negative photoresists based on condensation types of photoreactions, they are no longer in use for microelectronic applications. However, currently they do find some use in the fabrication of printed wiring boards and in photolithographic printing plates.

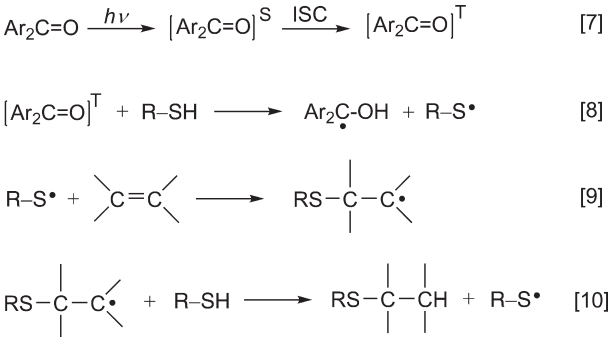

Scheme 3 Photoinitiated radical-catalyzed thiol–ene reaction.

4.37.2.2 Photocatalyzed Condensation Polymerization Reactions

Unlike the condensation reactions described above that depend on the direct absorption of light by chromophores present in the monomers or functionalized oligomers, the use of condensation reactions that proceed in the presence of photogenerated catalysts is an area of current active development. Several examples are presented here. The first is the well-known thiol–ene reaction. The mechanism of this reaction is shown in **Scheme 3**.[15–18] Irradiation of a diaryl ketone initially produces the singlet excited state (eqn [7]) that undergoes intersystem crossing (ISC) to the excited triplet. The latter species is capable of abstracting hydrogen atoms from a thiol (eqn [8]). Other photochemical sources of radicals can also be employed to initiate this reaction. In some cases, direct UV–vis irradiation is sufficient to induce the reaction in the absence of a photoinitiator. The resulting sulfur-centered thiyl radicals add to terminal double bonds (eqn [9]) generating carbon-centered radicals that subsequently abstract hydrogen atoms from the thiol (eqn [10]). This sets up a chain reaction (eqns [9] and [10]) that results in the quantitative addition of a sulfur–hydrogen group to a carbon–carbon double bond. Thus, this reaction has some aspects of both condensation and addition types of polymerizations. It is worth noting that unlike typical radical-mediated reactions, thiol–ene polymerizations show little sensitivity toward inhibition by

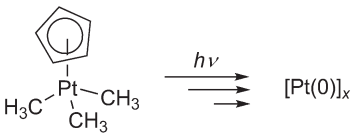

7 [11]

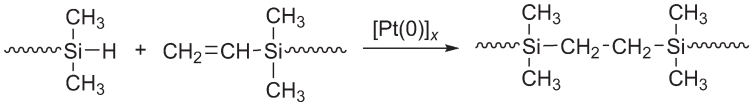

[12]

Scheme 4 Hydrosilylation reaction catalyzed by a photogenerated platinum colloid.

molecular oxygen. Although thiol–ene photopolymerizations are commonly carried out using a multifunctional thiol together with a multifunctional 'ene' to produce crosslinked polymers, they can also be used to prepare linear, block, or graft polymers. In recent years, thiol–ene chemistry has seen a resurgence of publication activity.[19,20] Two recent extensive reviews on this topic are especially recommended.[21,22]

As with all condensation reactions, thiol–ene polymerizations are sensitive to the stoichiometry of the thiol- and ene-containing monomer substrates. Typically, the best results are obtained when there is a molar equivalent concentration of thiol and double bonds present. Recently,[23,24] there has been a considerable effort to extend the photoinduced radical addition of thiols to alkynes (the so-called thiol–yne reaction).

Another polymerization that proceeds under the influence of a photogenerated catalyst is the hydrosilylation reaction. In a patent, Drahnak[25] described the photoinduced addition of Si–H functional silanes to poly(dimethylsiloxane)s containing pendant and terminal vinyl double bonds. This reaction is catalyzed by the *in situ* generation of a colloidal platinum hydrosilylation catalyst, $[Pt(0)]_x$, by the photolysis of η-cyclopentadienyl(trimethyl)platinum complex, **7**. The proposed mechanism is shown in eqns [11] and [12] of **Scheme 4**.[26] Reportedly, this chemistry has been used to generate crosslinked silicone elastomers.[27]

Amine bases generated by the photolysis of carbamates, *O*-acyloximes, ammonium salts, formanilides, aminoimides, α-aminoketones, and amidines[28–31] have been used to catalyze a wide range of different condensation polymerization reactions.[32,33] **Scheme 5** shows a mechanism for the photolysis of an *O*-acyloxime, **8**, as a photolatent base to produce benzylamine.

When the photolysis of photolatent base, **9**, is carried out in the presence of the photosensitizer, 2-isopropyl-9*H*-thioxanthen-9-one (ITX) as shown in eqn [13], the strong amidine base, 1,5-diazabicyclo[4.3.0]non-5-ene (DBN), is generated. DBN strongly catalyzes the condensation of isocyanates with polyols to produce urethanes (eqn [14] in **Scheme 6**).

Similarly, photolatent base, **9**, can be used to catalyze the addition of thiols, amines, and carboxylic acids to epoxide monomers. Oftentimes, the irradiation is followed by a brief thermal treatment as well to complete the polymerization reaction. The conjugate addition of thiols to electron-deficient acrylate double bonds has been successfully conducted under UV irradiation conditions through the use of a photolatent base such as **9** as a catalyst.[34] An unusual type of Michael polymerization reaction explored by Dietliker and co-workers[32,35] is depicted in eqn [15]. Photogenerated DBN is a sufficiently strong base to remove a proton from the multifunctional malonate monomer, **10**, and the corresponding malonate carbanion adds to the acrylate monomer, **11**.

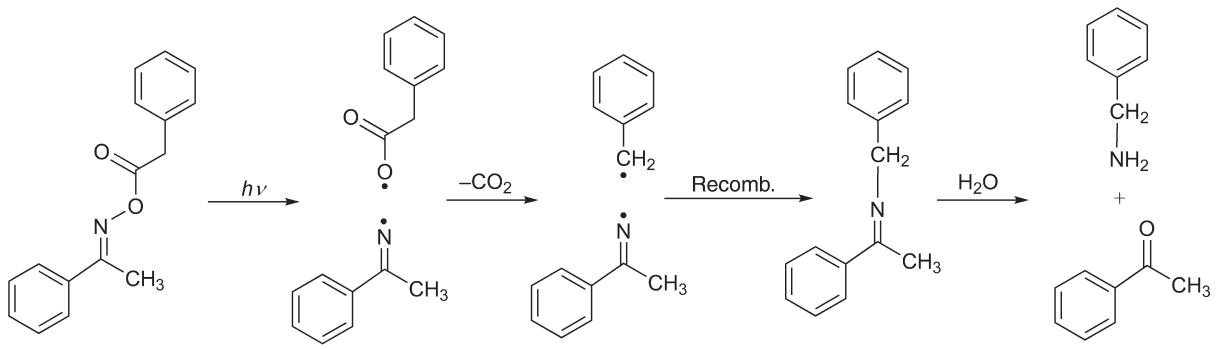

8

Scheme 5 Mechanism of the photogeneration of benzylamine from an *O*-acyloxime.

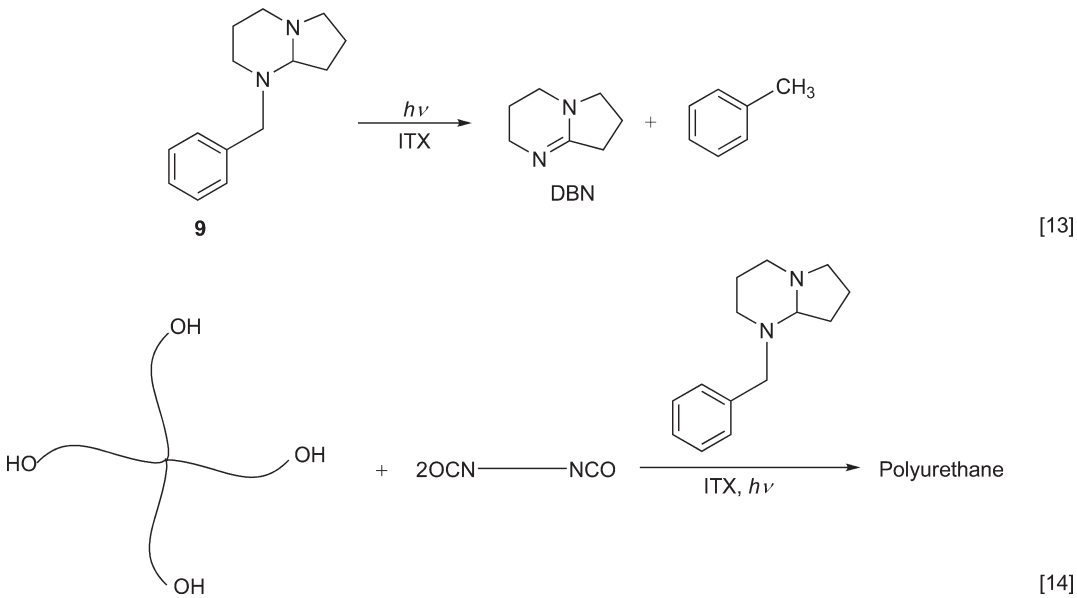

Scheme 6 Mechanism of the photobase-catalyzed urethane reaction.

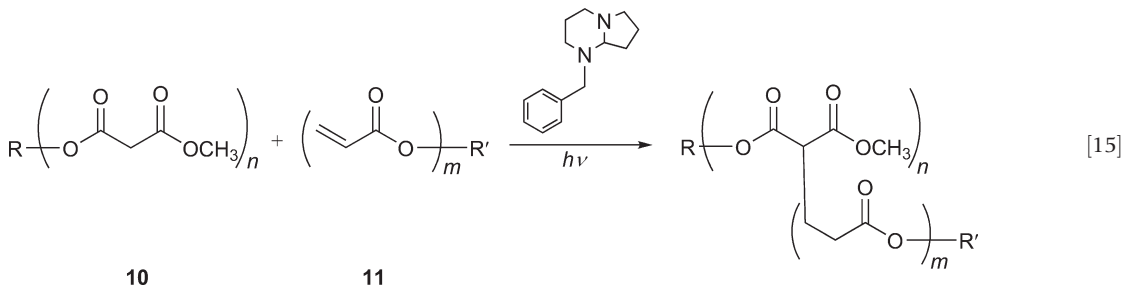

Sol–gel condensation polymerizations have also been carried out using either photogenerated acids or bases as catalysts. For example, Hanson and Jensen[36] employed a (diphenylmethyl)trimethylammonium salt as a photolatent source of trimethylamine to conduct the sol–gel condensation of tetraethoxysilane (**Scheme 7**). Postirradiation heating at 65 °C was necessary to drive the reaction to completion. Crivello and Mao[37] and Croutxe-Baghorn[38] have reported similar sol–gel condensation polymerizations of alkoxysilanes conducted using diaryliodonium salts as photoacid generators.

4.37.3 Photoinduced Active Center Polymerizations

These addition polymerizations occur by means of a chain reaction mechanism involving the propagation of an active center by interaction with the monomer. The active center consists of reactive species, typically, a radical, a cation, or an anion. In the simplest case, a photoinitiated addition polymerization can be represented as shown in eqns [16]–[18] of **Scheme 8**.

In the first step (eqn [16]), the active species is generated by the absorption of light by a photoinitiator, A, and the

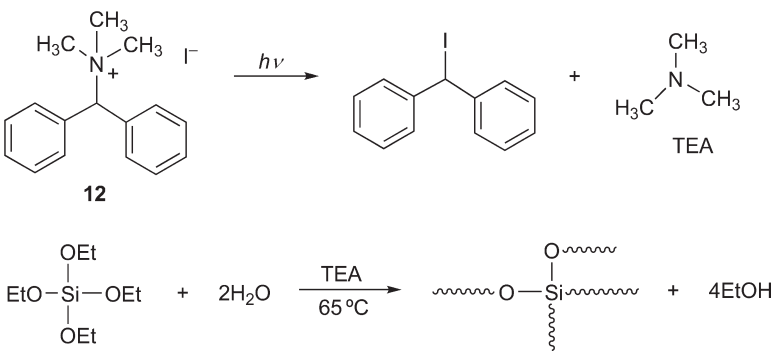

Scheme 7 Sol–gel condensation polymerization of tetraethoxysilane conducted using a photolatent base.

$$A \xrightarrow{h\nu} [A]^{\ddagger} \longrightarrow R^{*} \qquad [16]$$

$$R^{*} + M \longrightarrow RM^{*} \qquad [17]$$

$$RM^{*} + nM \longrightarrow R(M)_{n}M^{*} \qquad [18]$$

Scheme 8 General mechanism for photoinduced active center addition polymerizations.

subsequent decay of the excited species, $[A]^{\ddagger}$, by a homolytic or a heterolytic bond cleavage to generate the active center, R*. Again, R* represents a radical, a cation, or an anion. R* is the 'true' initiator that induces polymerization of the monomer, M, usually by opening a multiple bond or a ring (eqn [17]). During this process, the active center is conserved by producing a new reactive species, RM*. In the subsequent reaction of the latter species with monomer (eqn [18]), the polymer chain lengthens as monomer molecules are added to the active center located at the chain end. Depending on the type of active center present in the polymerization and the reaction conditions, a variety of chain termination or transfer processes may also occur that stop or disrupt the progress of the growing chain.

Consideration of the mechanism depicted above leads to the realization that the only factor that distinguishes an active center photopolymerization from classical radical, cationic, or anionic polymerizations is the use of light as a stimulus to break bonds present in the photoinitiator to generate the active center. Thereafter, the usual initiation, propagation, termination, and chain transfer processes are identical. Consequently, the design and synthesis of specific, high-quantum-yield photoinitiators with specific wavelength sensitivities to achieve each of the three different classes of photoinduced active center polymerizations is one of the major foci of photopolymerization technology.

Although it may be technically possible to conduct the large-scale synthesis of linear polymers using active center photopolymerizations, it is probably impractical to do so. The main considerations are the complex logistics of supplying UV light to a reaction vessel while simultaneously meeting the requirements of agitation and efficient removal of the heat of reaction. Instead, photoinitiated cationic ring-opening polymerizations find their main use with multifunctional monomers in crosslinking polymerizations. These photopolymerizations are part of a related group of technologies collectively denoted by the term 'UV curing' or 'radiation curing'.[1,2] It should be pointed out that photoinduced active center crosslinking polymerizations are inherently attractive from several practical points of view. Since they proceed by a chain reaction mechanism, they are highly efficient processes requiring the absorption of only a small quantity of light energy for the conversion of a large mass of monomer to polymer. Likewise, only a small amount, usually less than 5%, of the photoinitiator is required for this purpose. Most photopolymerizations used in UV curing applications are carried out as bulk processes without the use of solvents. This means that commercial products employing such technology have minimal adverse environmental consequences. UV curing is a so-called 'line-of-sight' technology with the prime requirement that exposure of the monomer–photoinitiator mixture to light must take place for polymerization to occur. This means that the best applications of this technology involve polymerizations carried out on thin liquid monomer films deposited on simple flat or curved surfaces. More complex surfaces can be accommodated with the aid of lenses and reflectors to bend and focus the light, although polymerizations on convoluted surfaces that are inaccessible to light are not possible. The photopolymerizations of highly filled, opaque, or heavily pigmented monomer mixtures are likewise problematic. Polymerizations of unfilled monomers can be carried out to provide appreciable thicknesses of crosslinked polymers of the order of several centimeters given the use of a long-wavelength, high-intensity light source and employing sufficiently long irradiation times. Most commercial applications, however, involve carrying out polymerizations in thin layers (<0.5 mm) at high rates (very short irradiation times). If a final thick polymeric object is desired, it is oftentimes advantageous to apply and photopolymerize multiple layers one on top of the other. This strategy is used in three-dimensional imaging processes such as stereolithography and ink-jet printing to build up solid polymer objects for modeling and prototyping purposes.

4.37.3.1 Photoinitiated Radical Polymerizations

Without question, the photoinitiated radical polymerizations of acrylates and methacrylates comprise the most well-studied and commercially important class of active center photopolymerizations. Contributing significantly to the commercial and academic success of this chemistry has been the development of a wide range of highly sensitive radical photoinitiators. A photoinitiator is a compound that becomes electronically excited through absorption of light within a given spectral range, and undergoes subsequent reactions to afford reactive species capable of inducing an addition polymerization reaction.

While the use of light to break bonds in organic, inorganic, and organometallic compounds to form radicals is a very common process, most of these reactions are inefficient. Two basic types of radical photoinitiators are currently in widespread use due to their high quantum yields of photolysis and because their simple synthesis makes them relatively inexpensive compounds.[28] The first type of radical photoinitiators is unimolecular photoinitiators based on aryl ketones that undergo facile α-cleavage reactions on irradiation with light. An example is shown in **Scheme 9** for the compound benzil dimethyl ketal (2,2-dimethoxy-1,1-diphenylethan-1-one). Irradiation of benzil dimethyl ketal results in the initial formation of a benzoyl, **13**, and α,α-dimethoxybenzyl, **14**, radical pair. Further fragmentation of **14** results in the formation of a methyl radical, **15**, along with methyl benzoate. Species **13** and **15** are credited with initiating the subsequent radical polymerizations.

A wide range of α-cleavage photoinitiators have been prepared and are commercially available. Not only have these photoinitiators been optimized to provide high quantum yields for radical production at specific irradiation wavelengths, but they have also been structurally modified to tailor their solubility and to provide nonyellowing characteristics in the final polymer product. The structures of some additional examples of α-cleavage photoinitiators that illustrate the versatility of these efficient photochemical radical sources are shown below:

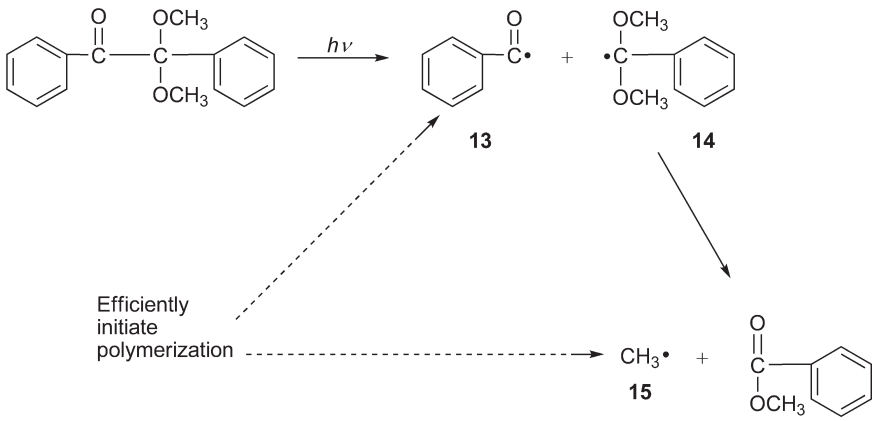

Scheme 9 Mechanistic pathway for the photolysis of benzil dimethyl ketal.

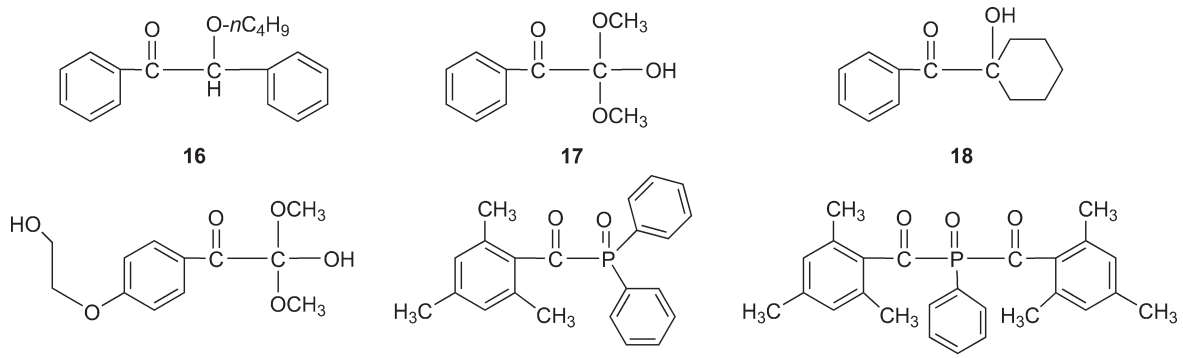

The second type of radical photoinitiators is the so-called bimolecular photoinitiators that consist of a diaryl ketone together with a compound that provides easily abstractable hydrogen atoms. The most common of these photoinitiators consists of benzophenone or a substituted benzophenone in combination with an aliphatic tertiary amine. A proposed mechanism for the formation of radicals by these bimolecular photoinitiators is depicted in Scheme 10. Photoexcitation of benzophenone results in the formation of triplet-state benzophenone that forms a charge transfer complex, 22, with triethanolamine. Formal electron transfer takes place with the subsequent formation of a radical cation–radical anion pair. Proton transfer then occurs with the formation of a carbon-centered radical, 23, and the hydroxy(diphenyl) methyl radical, 24. Radical species 23 initiates polymerization, while 24 primarily undergoes dimerization to form benzopinacol.

Since the diaryl ketone is the light-absorbing species in bimolecular photoinitiator systems, the selection of the appropriate ketone determines the wavelength sensitivity of the system. Besides benzophenone and substituted benzophenones, 25–27, a variety of thioxanthones (9*H*-thioxanthen-9-ones) and substituted thioxanthones, 28–30, are also commonly used.

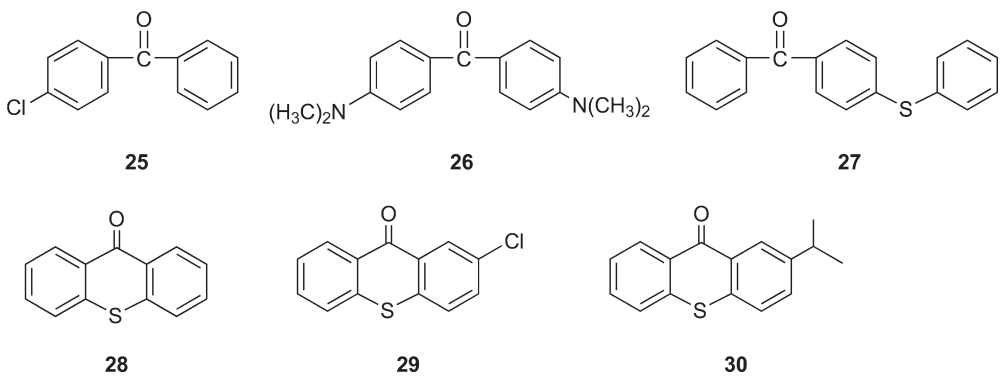

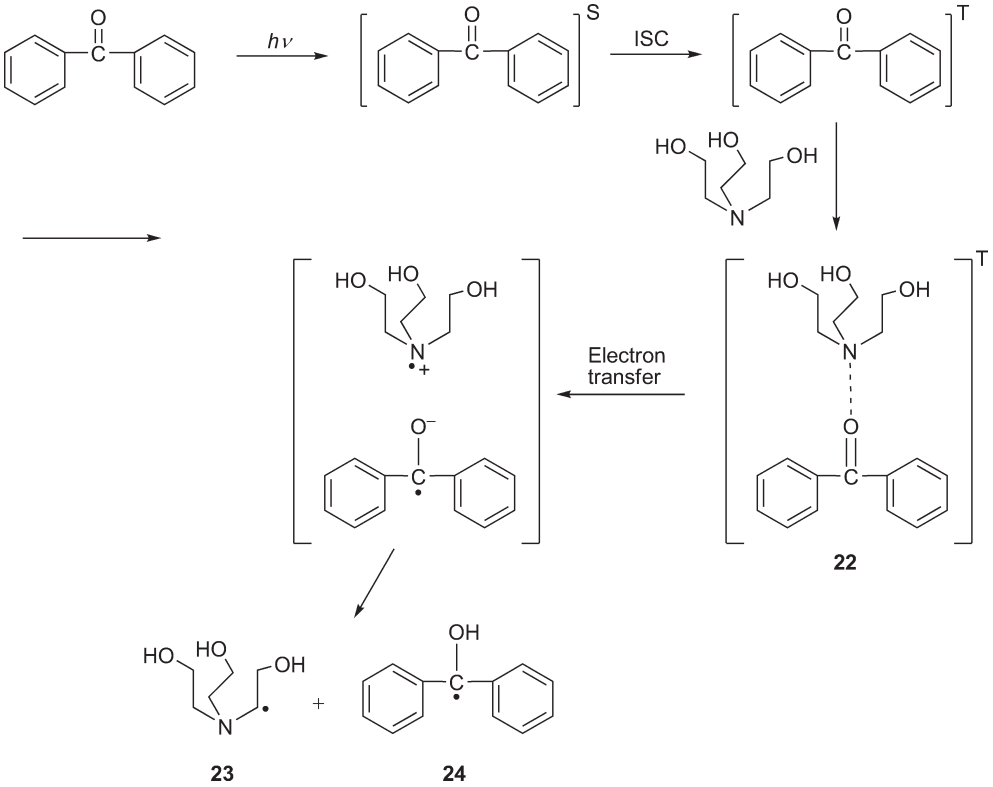

Scheme 10 Mechanism of the formation of radicals by bimolecular photoinitiator systems.

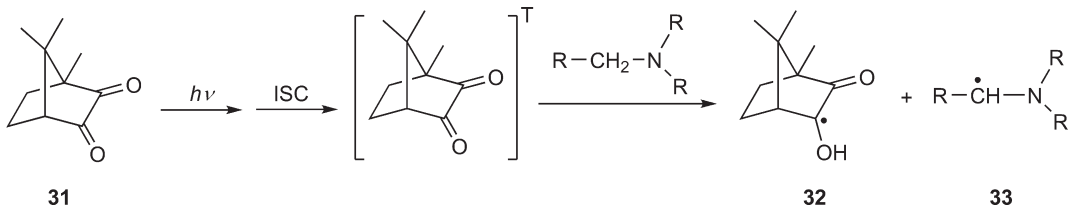

Scheme 11 Radical formation by the photolysis of camphorquinone in the presence of tertiary amines.

1,2-Diketones, benzil, biacetyl, and camphorquinone (bornane-2,3-dione) have strong absorption bands in the mid- and long-wavelength UV regions, which makes them valuable for use in bimolecular radical photoinitiator systems. Of particular note is the use of camphorquinone, **31**, shown in **Scheme 11**, which is extensively used together with various tertiary amines for the photocure of acrylate-based dental composites using visible light ($\lambda = 400–500$ nm). Both radicals **32** and **33** initiate the polymerization of the acrylate monomers.

A variety of amine-containing hydrogen donors are commonly employed. Besides triethanolamine (tris(2-hydroxyethyl)amine), methyldiethanolamine (bis(2-hydroxyethyl) methylamine), triisopropylamine, and ethyl-4-(dimethylamino)benzoate are commercially available and widely used for that purpose. Especially interesting is 4-[2-(diethylamino) ethoxy]benzophenone, **34**, which, due to the presence of both the amine and ketone functional groups in the molecule, forms an intramolecular excited-state charge transfer complex.

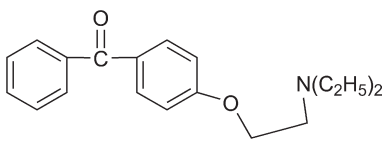

34

In addition to the above two classes of commonly used radical photoinitiators, a wide assortment of azo, sulfur, and heterocyclic compounds, organometallic compounds, and charge transfer complexes are known to generate radicals on irradiation with light. These systems are also occasionally used to initiate radical photopolymerizations and may have advantages in specific applications due to their long-wavelength absorption.

Advances in the field of radical photopolymer chemistry have been facilitated by the availability of a broad range of highly reactive monomers and functional oligomers. In particular, the use of well-established synthetic methodology to

prepare multifunctional acrylate and methacrylate monomers and to tailor them for specific end uses has been especially valuable in promoting this technology.

Several examples of the structures of typical multifunctional acrylic monomers (35–40) used in photoinduced radical cross-linking polymerizations are depicted below:

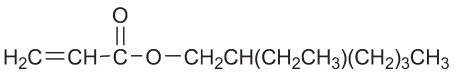

35

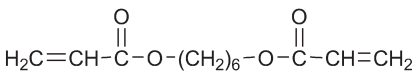

36

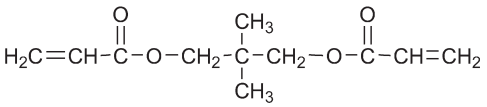

37

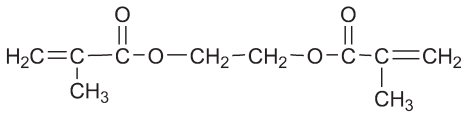

38

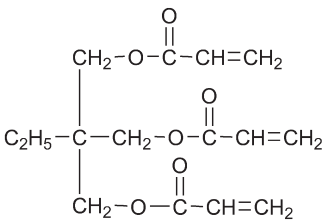

39

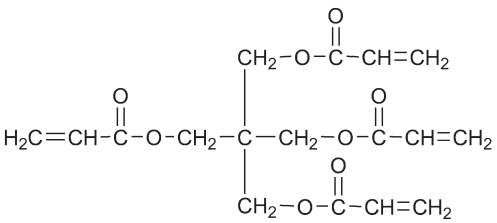

40

In addition, the reactions of acrylic and methacrylic acid and their derivatives with di- and multifunctional hydroxy-, amino-, epoxy-, anhydride-, and isocyanate-containing substrates give rise to a wide variety of acrylic functional oligomers with useful properties. For example, as shown in eqn [19], 2-hydroxyethyl acrylate undergoes facile condensation with 2,4-toluenediisocyanate (4-methyl-1,3-phenylene diisocyanate) to yield urethane-containing diacrylate oligomer, 34. More complex acrylate-terminated polyurethanes are similarly produced by the reaction of isocyanate-functional linear and branched short-chain polyurethanes with 2-hydroxyethyl acrylate. These are used to produce photocurable tough polyurethane floor coatings that display outstanding resistance to staining and abrasion.

In a similar manner, extended-chain oligomeric polyesters, polyethers, and poly(dimethylsiloxane)s have been fitted with acrylate or methacrylate functional groups, and these materials find a multitude of practical uses such as UV-curable coatings and adhesives. The photoinitiated radical polymerizations of acrylic monomers and oligomers proceed very rapidly in the absence of oxygen. However, the rates of polymerization are markedly reduced in the presence of oxygen due to its well-known inhibiting effects.

In the early 1990s, Decker and Moussa[39,40] described several classes of novel acrylic monomers that display enhanced rates of radical photopolymerization together with reduced sensitivity toward oxygen inhibition. Examples of the structures of several of these monomers are shown below. The presence of highly polar cyclic carbonate (41), cyclic urethane (42), or open-chain urethane (43) groups within the molecule appears to be required for the enhanced reactivity of these monomers. A number of theories[41,42] have been set forth to account for the results, but a fully definitive explanation is still not available.

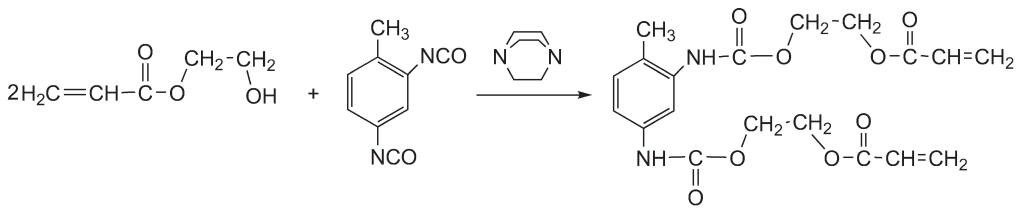

34 [19]

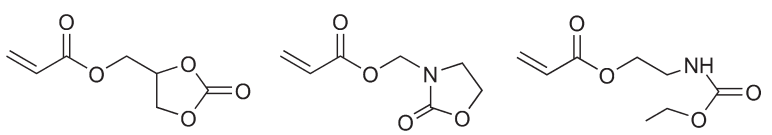

41 42 43

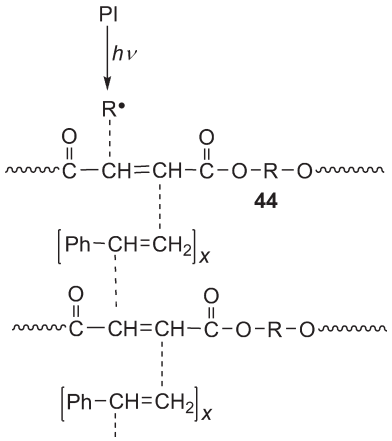

Scheme 12 Pathway for the crosslinking polymerization of styrene–unsaturated polyester systems.

An additional class of photoinitiated radical polymerizations in wide use is composed of a combination of a styrenic monomer together with a polyester oligomer bearing unsaturated double bonds arrayed along the backbone. Such systems are, in fact, photoinitiated copolymerizations that have a strong tendency toward alternation. A graphical representation of the mechanism involved in these chemistry systems is Shown in Scheme 12.

Unsaturated polyesters 44 containing multiple electron-deficient maleate and/or fumarate double bonds along the polymer chain are readily prepared by the reaction of maleic anhydride or fumaric acid with a diol. In many cases, other diacids or dianhydrides are also included as comonomers to improve the final mechanical properties. The polyester is combined with styrene monomer and photopolymerization is carried out using a radical photoinitiator. Due to the reactivity ratios of the two vinyl components, there is a tendency toward alternation. However, the length of crosslinks between the polymer chains can be controlled by the amount of excess styrene present. This allows appreciable control over the structure of the network polymer formed, and this has a considerable impact on its mechanical and chemical properties. Photocurable unsaturated polyester–styrene systems have found numerous uses, but the major applications are in wood finishing as UV-curable fillers/sealers and topcoats for particleboard.

Thermally initiated radical ring-opening polymerizations were first pioneered by Stansbury and Bailey.[43] Stansbury[44] has shown that the spiro orthocarbonate monomers such as 45 undergo facile ring-opening photopolymerization in the presence of radical photoinitiators (Scheme 13) and has suggested that they may be useful in low-volume-shrinkage photocurable dental composites. In addition to the polycarbonate repeating units, 46, formed by the double ring-opening reaction, simple vinyl polymerization of 45 and fragmentation of the radical intermediates also take place to give a polymer with a complex backbone structure.

4.37.3.2 Photoinitiated Cationic Polymerizations

Nearly 35 years have elapsed since the first practical onium salt cationic photoinitiators were reported.[45,46] During this period, the field of cationic photopolymerization has advanced rapidly propelled by both the considerable academic interest and their increasing use in industrial applications. A recent SciFinder search on this topic returned more than 1 660 000 citations, reflecting the past and present activities of a large number of researchers engaged in this field. It is well beyond the scope and intent of this chapter to summarize all these activities. Rather, the approach that will be taken in this chapter is to provide the reader with an overview of the essential aspects of various cationic photoinitiation processes as they apply to the design and function of the photoinitiators and to discuss the main applications of cationic photoinitiation, especially in the ring-opening crosslinking polymerizations of mono- and multifunctional heterocyclic monomers. For further reading, the reader is referred to several previously published summaries and reviews on this topic.[28,47,48]

Cationic vinyl and ring-opening polymerizations are a well-studied area of polymer chemistry.[49–53] A wide assortment of electrophilic agents have been documented as initiators for these polymerizations. Many such agents are routinely used both in the laboratory and for commercial purposes to prepare polymers by cationic polymerization. So, the question immediately arises, why use photochemical methods to conduct these polymerizations? There are two main reasons that can be cited to justify the use of photoinitiation: (1) photoinitiation provides access to electrophilic initiators that are otherwise

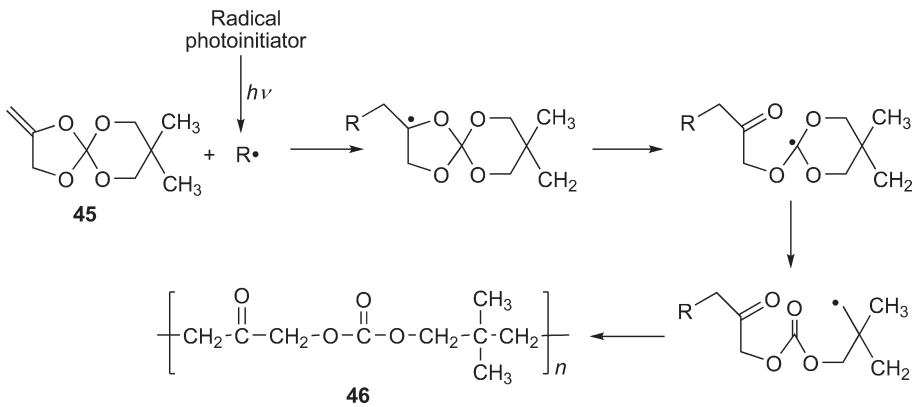

Scheme 13 Photoinitiated radical ring-opening polymerization of spiro orthocarbonate 45.

difficult or inconvenient to generate and to use; and (2) photoinitiation makes it possible to conduct the rapid, homogeneous formation of network polymers. There are many additional secondary benefits that derive from these two main rationales, and these will be further discussed and elaborated on in subsequent portions of this chapter.

4.37.3.2.1 Brønsted acids as initiators in cationic polymerizations

Among the simplest and broadest classes of initiators for the cationic polymerization of vinyl and heterocyclic monomers are protonic or Brønsted acids. The respective mechanisms for the initiation and subsequent polymerization by a Brønsted acid, HX, for these two types of monomers are depicted in Schemes 14 and 15. Only the initiation and propagation processes are depicted. Many additional termination and chain transfer processes may also occur depending on the specific Brønsted acid, monomer, and conditions used. The polymerization of a vinyl compound is straightforward consisting first of the protonation of the monomer (eqn [20]) followed by propagation of the carbocation, 47, that is formed (eqn [21]). The mechanism for cationic ring-opening polymerization involves a three-step process with four different rate constants. As shown in eqn [22], initiation involves the reversible electrophilic attack by a proton on the nucleophilic heteroatom, Z, of the monomer to afford the secondary onium ion 48. In subsequent steps (eqns [23] and [24]), 48 reacts further to give the tertiary onium species 49 and 50. The ability of a given acid to protonate a specific monomer is, therefore, directly related to its inherent acidity as well as the basicity of the monomer. Since heterocyclic monomers are only weakly basic and vinyl monomers even less so, strong acids are required to shift the equilibrium of eqns [20] and [22] significantly to the right.

The Hammett acidity scale shown in Table 1 provides a comparative ranking of the strengths of a number of the strongest inorganic and organic acids.[54] Some, but not all, of these acids are employed as initiators in cationic ring-opening polymerizations. It is important to note that the H_o values given in Table 1 are based on a logarithmic scale and that acids with strengths over a range of 25 orders of magnitude are represented. Brønsted acids with H_o values more negative than −12 (sulfuric acid) are classified as 'superacids'. Only 'superacids' with Hammett acidities of −14 to −30 are useful as initiators for the ring-opening polymerizations of heterocyclic monomers. Perfluoroalkanesulfonic acids ($H_o = -14$) are sometimes used for the polymerization of heterocyclic oxygen-containing monomers but are generally regarded as rather weak initiators

Table 1 Hammett acidities of Brønsted acids

Acid	H_o
H_3PO_4	−4.7
HNO_3	−6.3
H_2SO_4	−12.0
$HClO_4$	−13.0
$ClSO_3H$	−13.8
$CF_3CF_2SO_3H$	−14.0
CF_3SO_3H	−14.1
H_2SO_4–SO_3	−14.5
FSO_3H	−15.0
HBF_4	−16.6
$HTaF_6$	−18.9
HPF_6	~−20 to −25
$HAsF_6$	~−20 to −25
$HSbF_6$	~−30

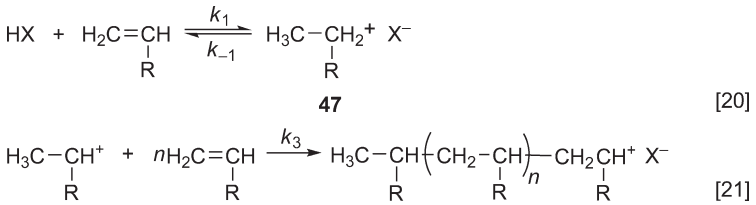

Scheme 14 General mechanism for Brønsted acid-catalyzed vinyl polymerizations.

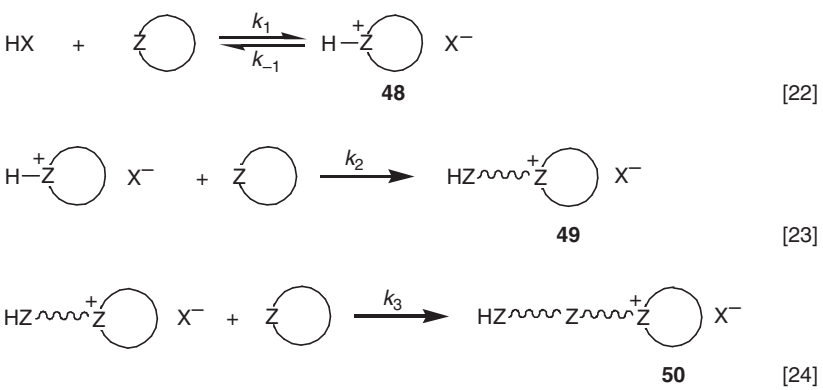

Scheme 15 General mechanism for Brønsted acid-catalyzed ring-opening polymerizations.

due to termination reactions with the propagating oxonium end groups to form stable fluoroalkanesulfonate esters. The most powerful acids and cationic initiators lie at the bottom of Table 1 and are represented by the complex fluorinated compounds HBF_4, HPF_6, and especially $HSbF_6$. Within the latter group, there is a very large range in acidity (13 orders of magnitude). Hexafluoridoantimonic acid, $HSbF_6$, is reputed to be the strongest acid known with an estimated H_o value of −30. Thus, $HSbF_6$ will protonate even nonpolar compounds such as methane as well as other aliphatic hydrocarbons.[55] All three pure complex fluorinated acids will efficiently and quantitatively initiate the polymerization of virtually all types of heterocyclic monomers. It is clear that the reason for the high acidities of HBF_4, HPF_6, $HAsF_6$, and $HSbF_6$ lies in the low nucleophilic character of the corresponding anion that is associated with the proton. Within the anion series, BF_4^-, PF_6^-, AsF_6^-, and SbF_6^-, the nucleophilic character decreases dramatically as the size of the complex anion increases, and this is probably related to dispersal of the negative charge over an increasingly larger spherical surface area. Similarly, anions such as TaF_6^- and $(C_6F_5)_4B^-$ are large and non-nucleophilic, and consequently, their corresponding protonic acids are also very strong.

Returning to the mechanisms shown in Schemes 14 and 15, it is important to note that the nucleophilic character of the anion of a Brønsted acid not only impacts the initiation step, but also plays a role in the subsequent respective propagation steps. In the latter steps, the lower the nucleophilic character of the anion, the higher the electrophilic character (i.e., reactivity) of the corresponding carbocation, 47, and secondary and tertiary onium ions 48–50 that are formed.

Having established that Brønsted superacids such as HBF_4, HPF_6, $HAsF_6$, and $HSbF_6$ are powerful initiators for cationic ring-opening polymerizations, it must also be acknowledged that they are very rarely employed either for academic studies or for industrial use. The reasons for this are apparent when one considers the general method used for their synthesis. Anhydrous HBF_4, HPF_6, $HAsF_6$, and $HSbF_6$ are prepared by reaction of gaseous HF with the corresponding Lewis acid. For example, as shown in eqn [25], $HSbF_6$ is produced by the reaction of HF with liquid SbF_5. The safe handling and storage of highly corrosive and exceedingly toxic HF, SbF_5, and $HSbF_6$ are problematic and require special equipment and techniques that are generally unavailable in the typical laboratory or in a commercial polymer synthesis facility. Such considerations have precluded the use of these Brønsted superacids as initiators for most ring-opening polymerizations.

$$HF + SbF_5 \rightarrow HSbF_6 \qquad [25]$$

There are additional factors that have militated against the use of the same initiators. Cationic ring-opening polymerizations of small-ring heterocyclic monomers are typically highly exothermic processes, especially when carried out under bulk reaction conditions. To maintain control over such polymerizations, the use of less active initiators is advisable. It is also generally impractical to use Brønsted superacids as initiators for the ring-opening polymerizations of multifunctional monomers. Since initiation with these acids is nearly instantaneous and quantitative and because the subsequent network formation is exceedingly rapid, it is not possible to achieve complete dispersion of the initiator in the monomer or solutions of the monomer even under intensive mixing conditions. Typically, when such acids are added to multifunctional monomers, a substantial portion of the initiator becomes encapsulated within the crosslinked gel particles that are formed. This leads to inhomogeneous reaction conditions with the formation of a correspondingly inhomogeneous product.

Nevertheless, network polymers based on vinyl monomers, and especially heterocyclic monomer systems such as di- and multifunctional epoxides and multifunctional oxetanes, are important for a multitude of applications ranging from potting and encapsulating compounds to composites. In addition to homogeneous reaction products, these applications require a considerable delay period before polymerization sets in to allow for processing. Both these requirements are currently met through the use of very weakly acidic initiating systems such as amine–Lewis acid complexes that are thermally dissociated at relatively high temperatures over long times during use.

Many of the above-described deficits surrounding the use of Brønsted superacids as initiators for cationic polymerization have been offset through the use of onium salt cationic photoinitiators.

4.37.3.2.2 Arenediazonium salts

The first effective onium salt cationic photoinitiators were arenediazonium salts. As early as 1949, Roe[56] showed that when arenediazonium salts bearing complex anions of the type BF_4^- were irradiated with light in the long-wavelength UV region, they are efficiently decomposed to yield an aryl fluoride, nitrogen gas, and the Lewis acid, BF_3. Noting that in the presence of a trace amount of water, BF_3 is a good initiator of cationic polymerization, Schlessinger,[57] Watt,[58] and Feinberg[59] irradiated arenediazonium tetrafluoroborates in the presence of various epoxide monomers and observed their cationic polymerization. Equations [26] and [27] of Scheme 16 depict this sequence of reactions. Unfortunately, monomer solutions of arenediazonium tetrafluoridoborates and especially the corresponding analogue salts containing the PF_6^-, SbF_6^-, and other similar anions tend to be thermally unstable and are subject to spontaneous polymerization even when stored in the absence of light. Moreover, the formation of nitrogen gas during irradiation of arenediazonium salts is a serious impediment for their use in most practical applications.

4.37.3.2.3 Diaryliodonium salts

Dialkylhalonium ions are highly reactive species and have been detected only as reactive intermediates in organic reactions.[60] In contrast, diarylhalonium salts are colorless, crystalline compounds that are quite stable at room temperature and above. These compounds can be prepared by straightforward electrophilic aromatic substitution chemistry. They are generally insoluble in water but freely soluble in common organic solvents from which they can be purified by the usual chromatographic and crystallization techniques.

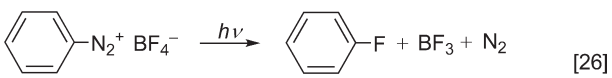

[26]

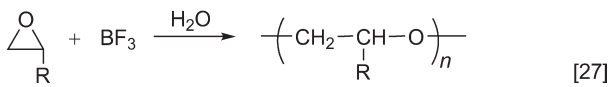

[27]

Scheme 16 Photoinitiated cationic polymerization by arenediazonium salts.

The discovery of diaryliodonium salts, **51**, as a class of highly photosensitive and thermally stable cationic photoinitiators in the early 1970s[43,44,61–64] marked the onset of the practical use of the photoinitiated cationic ring-opening polymerization of heterocyclic monomers. It may generally be stated that all diaryliodonium salts independent of the presence or absence of electron-donating or electron-withdrawing substituents are photosensitive. These include cyclic diaryliodonium salts such as **52**. These compounds undergo fragmentation reactions when irradiated with UV light, leading to the formation of Brønsted acids. In addition, the analogous diarylchloronium (**53**) and diarylbromonium (**54**) salts bearing non-nucleophilic anions, X^-, were subsequently prepared although in modest yields and were also observed to be excellent photoinitiators for cationic polymerization.[65] The latter diarylhalonium salts are somewhat less thermally stable than their diaryliodonium salt counterparts and more difficult to prepare; consequently, they have received little further attention.

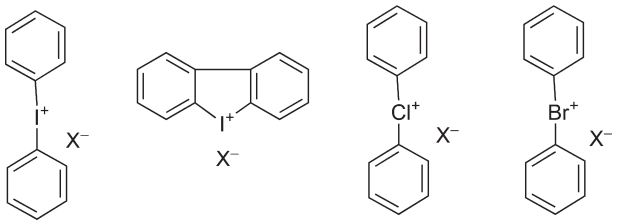

51 **52** **53** **54**

In recent years, there has been a considerable effort to expand the range of iodonium salts that can be employed as photoinitiators for cationic polymerizations. Stable iodonium salts can be obtained when one of the aryl groups in **51** is replaced by a moiety that can provide resonance stabilization to the positively charged iodine atom. For example, Koser *et al.*[66] prepared stable aryl(phenylethynyl)iodonium salts, **55**, that were shown by Kitamura *et al.*[67] and by Höfer and Liska[68] to exhibit good activity as cationic photoinitiators. Similarly, iodonium salts, **56**, in which the positively charged iodine atom is attached to the central carbon of a resonance-stabilized 1,3-diketone moiety such as dimedone are also isolable compounds that display the ability to serve as photoinitiators for cationic polymerization.[69] Finally, it has been reported[70] that diaryl(oxo)iodonium salts, **57**, can be readily prepared by the base-catalyzed self-condensation of diaryliodyl compounds. Replacement of the initial hydroxide anion by acidification with HBF_4 results in the formation of the desired tetrafluoridoborate salt as shown in **Scheme 17**.

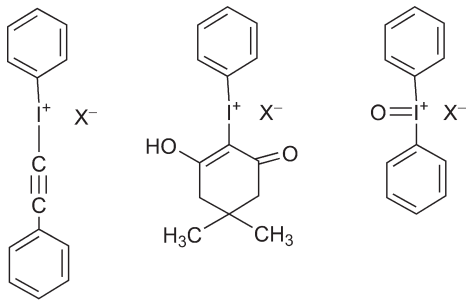

55 **56** **57**

4.37.3.2.3(i) Photochemistry of diaryliodonium salts

Scheme 18 shows the details of the complex mechanism that has been proposed for the photolysis of diaryliodonium salts.[71,72] UV irradiation of a diaryliodonium salt into its primary absorption band at 230–250 nm (depending on substitution) leads to the initial formation of the excited singlet state. Subsequent ISC results in conversion of the excited singlet to the excited triplet state. Fragmentation of the molecule with the formation of various reactive species including radicals, cations, and cation-radicals evolves from the respective excited singlet and triplet states by both in-cage and out-of-cage processes. For diaryliodonium salts, the fragmentation takes place predominantly by a homolytic pathway that results in the formation of aryl radicals and aryliodine cation-radicals. As noted in **Scheme 18**, no matter which pathway is followed, Brønsted acids are produced by reaction of the reactive primary fragmentation products of the diaryliodonium salt with traces of water, solvent, monomer, or other protonic species (RH) present in the reaction medium. A correspondingly wide range of organic photolysis products were identified. Similar results were obtained from the study of the photolysis of diarylchloronium and diarylbromonium salts.[66] The mechanisms for the photolysis of iodonium salts **55–57** have yet to be determined.

In most respects, diaryliodonium salts are nearly ideal as cationic photoinitiators for the ring-opening polymerizations of heterocyclic monomers. The photolysis of diaryliodonium salts is highly efficient with quantum yields of the order of 0.7 based on the amount of acid generated.[73,74] Not only are they

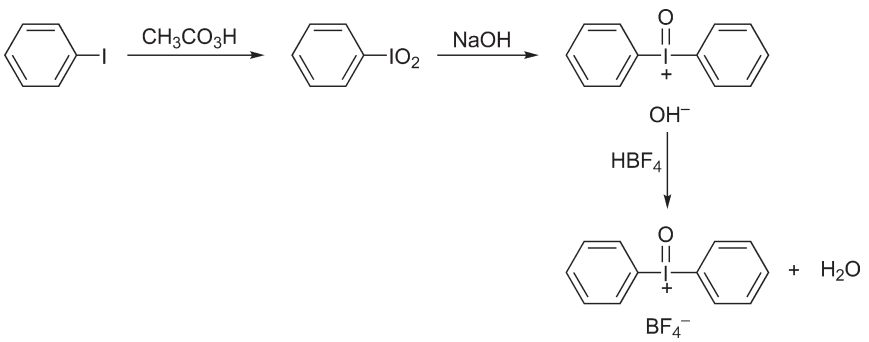

Scheme 17 Synthesis of diaryl(oxo)iodonium salt photoinitiators.

$$Ar_2I^+ X^- \xrightarrow{h\nu} [Ar_2I^+ X^-]^S \longrightarrow [Ar_2I^+ X^-]^T$$

Scheme 18 Mechanism of the photolysis of diaryliodonium salts.

very efficient photochemical sources of Brønsted superacids, but their photolysis also yields by-products that do not significantly interact during the subsequent cationic addition polymerizations of the monomers to cause inhibition, retardation, or chain transfer. An additional benefit derives from the fact that these photoinitiators can be prepared in good to excellent yields by a number of straightforward synthetic routes that allow great flexibility in the design of unique photoinitiators for specific end uses.[75,76] Several of these synthetic methods have been adapted for the industrial-scale synthesis of these photoinitiators on the multikilogram scale. Generally, these halonium salts are isolated as colorless, crystalline compounds that may be rigorously purified by common techniques such as crystallization and column chromatography. While they are highly sensitive to light in the short-wavelength UV region of the spectrum, they can be readily synthesized and handled for short times under laboratory lighting conditions with only minimal losses. Finally, these two classes of photoinitiators are indefinitely stable in the pure state when stored in the absence of light. Samples of diaryliodonium salt photoinitiators have been maintained under these conditions in this laboratory for over 25 years without appreciable degradation.

4.37.3.2.3(ii) Design and synthesis of diaryliodonium salts

It is useful to consider that diaryliodonium as well as other photosensitive onium salts as being composed of two discrete components, namely, the cation and the anion. These two essential components can be viewed as having different functions in the overall photoinitiation process of cationic polymerization. Most conveniently, each component can be manipulated more or less independently to optimize those functions. For example, in the case of a diaryliodonium salt, Table 2 outlines the functions ascribed to the respective cation and anion. The cation is the photosensitive component of the onium salt. The structure of the cation determines not only the position of the absorption wavelength maximum and its intensity but also the quantum yield of photolysis. In later portions of this chapter, it will also be shown that the magnitude of the redox potential of the diaryliodonium cation plays an important role in the electron transfer photosensitization of this class of photoinitiators. The cation is also the prime determinant responsible for the thermal stability and ultimately the latency of a diaryliodonium salt photoinitiator. Finally, manipulation of the structure of the cation through substitution on one or both of the aromatic rings allows tailoring of the solubility characteristics as well as permits the introduction of other useful functional groups. Whereas the photochemistry of a diaryliodonium salt is controlled by its cation, the anion, as noted previously, is the ultimate determinant of the type and strength of the Brønsted acid that is generated on photolysis. For this reason, the kinetics of both the initiation and the subsequent propagation processes, as pointed out previously, are determined by the character of the anion. In those cases where termination occurs by ion-splitting reactions, the rate and extent of this reaction are also controlled by the type of anion. For example, shown in eqn [28] is a schematic representation of the ion-splitting termination reaction that can occur during a cationic ring-opening polymerization with the BF_4^- anion. Similarly, if, for example, a diaryliodonium triflate is used as a photoinitiator, chain termination can occur by collapse of the propagating ion pair to form a stable, covalently bound triflate ester.

Table 2 Functions of the cation and anion of a diaryliodonium salt photoinitiator

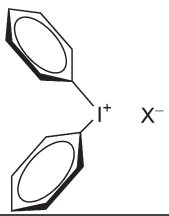

Cation function	*Anion function*
Absorption wavelength	Acid strength
Molar absorption coefficient	Ion pairing
Quantum yield	Anion stability
Photosensitization	Initiation efficiency
Thermal stability	Propagation rate constants
Solubility/crystallinity	Solubility/crystallinity

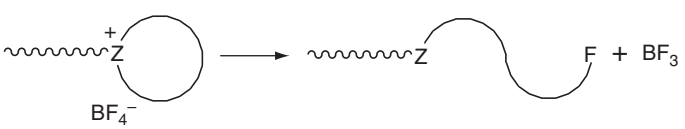

[28]

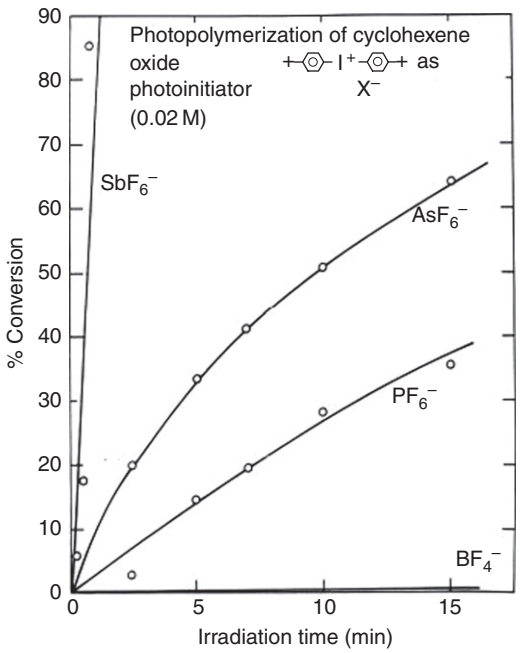

Figure 2 Comparison of the effects of different anions on the rate of ring-opening photopolymerization of cyclohexene oxide.

The ability to prepare photosensitive onium salts with different types of anions permits a direct comparison of the reactivity of the corresponding strong Brønsted acids in various ring-opening polymerizations. An example is shown in Figure 2. In this instance, the photoinitiated cationic polymerizations of cyclohexene oxide (1,2-epoxycyclohexane) using bis(4-*tert*-butylphenyl)iodonium salts bearing, respectively, the BF_4^-, PF_6^-, AsF_6^-, and SbF_6^- anions are compared at the same molar concentration and under identical UV irradiation conditions. Since the cations are the same in all cases, this also implies that identical amounts of the respective Brønsted acids are generated per unit irradiation time. The results are in good agreement with the prediction based on the Hammett acidities (Table 1) of the respective four acids that are generated. The rate of the polymerization using the SbF_6^--containing photoinitiator is almost too high to measure at room temperature. Although also very rapid, polymerizations carried out with the corresponding AsF_6^- and PF_6^- salts are slower and less vigorous than those with the SbF_6^- salt. In contrast, the polymerization rate of cyclohexene oxide using the tetrafluoridoborate salt is comparatively slow. Over the years, many similar comparisons of diaryliodonium and triarylsulfonium salts bearing different anions with various heterocyclic monomers have been made with the same results.

Many attempts have been made to find alternatives to the most reactive onium salt photoinitiators bearing the AsF_6^- and SbF_6^- anions. These efforts have mainly been in response to the perception of toxicity and/or the possibility heavy metal contamination due to arsenic- and antimony-containing residues that are of concern in certain applications. In recent years, there has been considerable progress in the development of novel anions with weakly coordinating (i.e., low nucleophilic) character.[77] For example, Castellanos *et al.*[78] have introduced diaryliodonium salt photoinitiators with the tetrakis(pentafluorophenyl)borate ($(C_6F_5)_4B^-$) anion. Following closely on this work, Neckers and co-workers[79,80] have reported on additional members of this class of photoinitiators with group III anions of low nucleophilic character as indicated in structure 58.

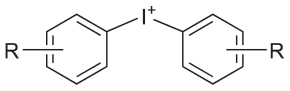

$^-M(C_6F_5)_4$

M = B, Al, Ga, In **58**

On a weight percentage basis, these photoinitiators generally display comparable, although slightly less, reactivity on a molar basis than the corresponding SbF_6^--containing onium salts.[81] One very conspicuous additional benefit of onium salts containing the ($(C_6F_5)_4M^-$) anion is their good solubility even in nonpolar monomers and oligomers. Ren *et al.*[82] have reported that diaryliodonium salts bearing the exceedingly non-nucleophilic hexabromocarborane anion ($CB_{11}H_6Br_6^-$) are similar to analogs bearing the SbF_6^- with respect to their activity as photoinitiators in cationic ring-opening polymerizations of epoxy-functional silicone polymers. However, it should be cautioned that when these or other photoinitiators are compared in such monomers or oligomers that are very poor solvents, the effects of solubility of the onium salt photoinitiators rather than their reactivity may dominate the results that are obtained.

4.37.3.2.3(iii) Tailoring the solubility and crystallinity of diaryliodonium salts

Diaryliodonium salts are ionic compounds. For this reason, crystalline mono- and disubstituted diphenyliodonium salts display good solubility in polar monomers, but rather poor solubility in nonpolar monomers. Consequently, the onium salt-catalyzed photopolymerizations of the latter substrates are often problematic. From Table 2, it may be noted that the solubility and related crystalline characteristics of a diaryliodonium salt are listed as being determined by the structures of both the cation and the anion. Generally, as one progresses from a diaryliodonium salt with a small anion such as a halide to a complex nonmetal halide such as PF_6^-, the solubility increases. However, for many nonpolar substrates, this is not sufficient. For example, due to the very nonpolar characteristics of linear and cyclic epoxy-functional poly(dimethylsiloxane)s, developing a photoinitiator for the photocrosslinking polymerization for these substrates was a particularly challenging problem. The solution required the synthesis of diaryliodonium salts that were specifically tailored for this application. Two different synthetic approaches were successfully developed and are presented here to illustrate general methods employed for the preparation of diaryliodonium salts. The first approach used by Eckberg and LaRochelle[83] and shown in Scheme 19 involves the synthesis of a symmetrical diaryliodonium SbF_6^- salt bearing long, highly branched alkyl groups. This synthesis employs dodecylbenzene as a starting material in which the dodecyl group is highly branched consisting of numerous positional and stereoisomers. Reaction in the presence of potassium iodate, sulfuric acid, and acetic anhydride directly yields the diaryliodonium hydrogensulfate salt, 59.[84] Replacement of the hydrogensulfate anion by a straightforward anion exchange with sodium hexafluoridoantimonate affords the desired bis(dodecylphenyl)iodonium SbF_6^-

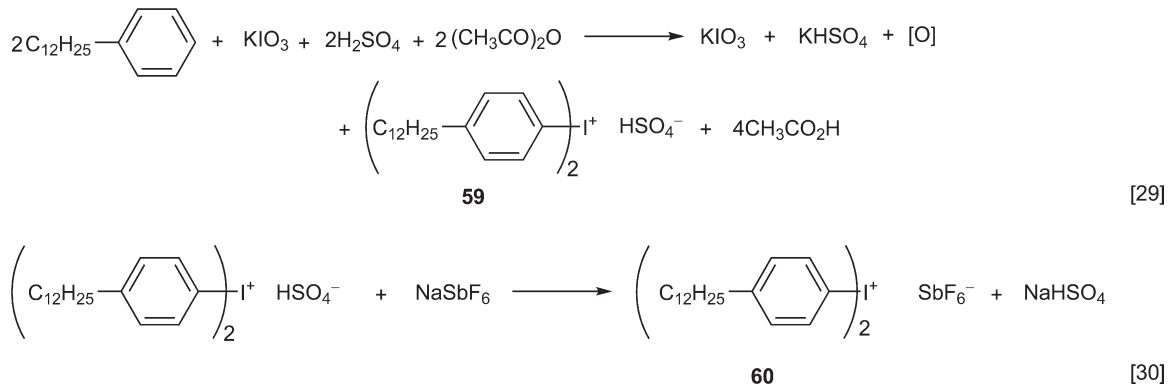

Scheme 19 Synthesis of bis(dodecylphenyl)iodonium hexafluoridoantimonate.

salt as a noncrystalline oil consisting of a complex mixture of isomeric salts. The *p,p′*-disubstituted isomers are formed preferentially in this synthetic method, although minor amounts of *o,p′*- and *o,o′*-substituted isomers are also produced. Hexafluoridoantimonate salt (**60**) is produced commercially using the reaction sequence shown in **Scheme 19**. It is freely soluble in epoxy-functional silicone oligomers and used to photocrosslink them at line speeds in excess of 500 m min^{-1}. These photopolymerizations are carried out on a large industrial scale for the production of release coatings.

A somewhat different approach shown in **Scheme 20** is used by the Rhône-Poulenc company to synthesize Rhodorsil 2746 for the photocrosslinking polymerization of epoxy-functional silicones.[85] Solubility is achieved by the synthesis of an unsymmetrical diaryliodonium cation together with the use of the large tetrakis(pentafluorophenyl)borate anion. As shown in **Scheme 20**, the unsymmetrical diaryliodonium tosylate, **61**, is obtained by the electrophilic attack of hydroxy(4-tolyl) iodonium tosylate on isopropylbenzene. Thereafter, **61** is subjected to a metathesis with $KB(C_6F_5)_4$ to give the desired Rhodorsil 2746, **62**, as a colorless crystalline powder.

The preparation of a hydroxy-functional diaryliodonium salt is shown in **Scheme 21**.[86] Phenol is first condensed with 1,2-epoxytetradecane in the presence of a basic catalyst. The resulting 2-hydroxyalkyl phenyl ether, **63**, is thereafter reacted with hydroxy(4-tolyl)iodonium tosylate under acid conditions to give the iodonium tosylate, **64**. Further anion exchange of **64** with an alkali salt bearing the desired anion yields the active

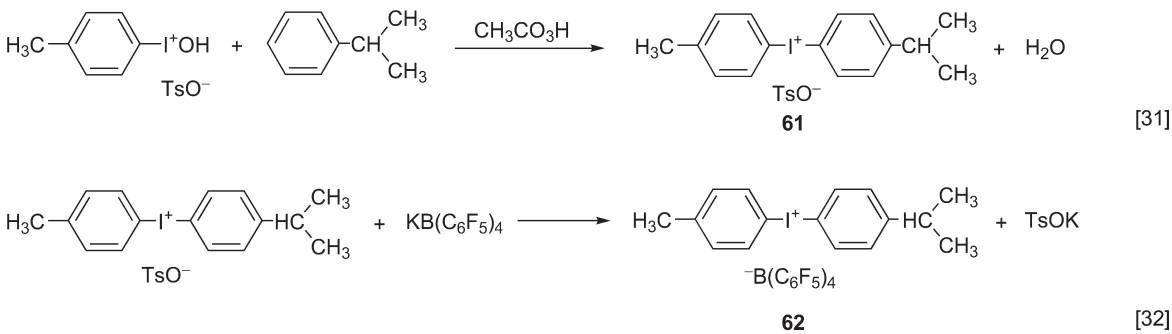

Scheme 20 Synthesis of Rhodorsil 2746.

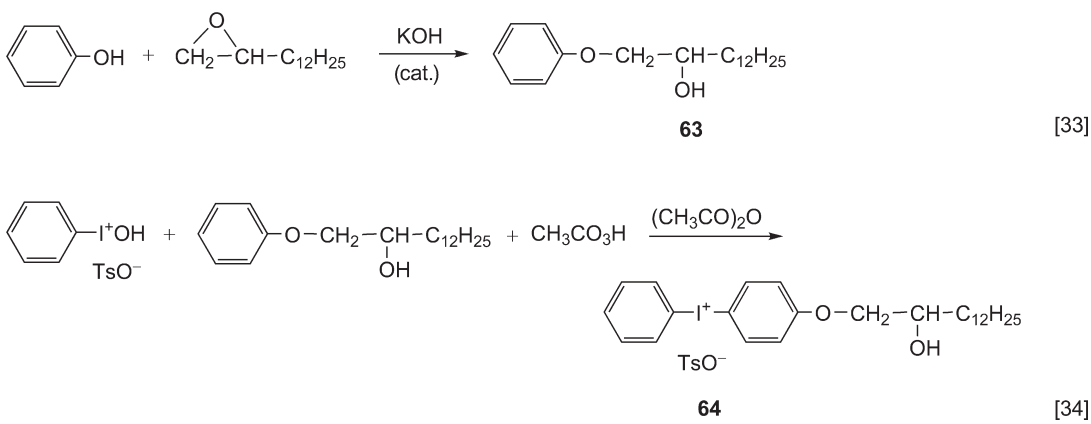

Scheme 21 Synthesis of an unsymmetrical diphenyliodonium salt bearing a hydroxy group.

photoinitiator. The presence of the long-chain alkoxy group together with the unsymmetrical substitution provides good solubility characteristics, while the hydroxy functional group allows fragments of the photoinitiator to be bound into a cross-linked matrix during ring-opening photopolymerization. The presence of the substituted alkoxy group also serves to activate the benzene ring toward attack by weakly electrophilic hydroxy (4-tolyl)iodonium tosylate. Subsequent further functionalization of the diaryliodonium salt can also be carried out by reaction at the hydroxy group. A series of related diaryliodonium salts with different alkyl chain lengths and anions were prepared analogously by varying the 1,2-epoxyalkane used in eqn [33].

4.37.3.2.3(iv) Photosensitization of diaryliodonium salts

As indicated in **Table 2**, the cation is responsible for determining all the parameters associated with the light absorption of a diaryliodonium salt and its resultant photosensitivity. Generally, it is desired to overlap as closely as possible the absorption characteristics of a photoinitiator with the emission bands produced by a given light source. Depending on the specific application, a wide variety of light sources with different emission characteristics are currently in use. These include high- and low-intensity mercury and xenon arc lamps, tungsten–halogen lamps, lasers, and light-emitting diodes (LEDs), among others. **Figure 3** shows the relationship between various different applications and the preferred wavelength range that is used. As may be noted, cationic photoinitiators have applications that require photosensitivity at wavelengths that span the electromagnetic spectrum from the extremely short-wavelength UV all the way into the visible region.

Unsubstituted diphenyliodonium salts and those bearing simple substituents absorb in the UV region with their λ_{max} from 230 to 250 nm. For this reason, they are well suited for high-performance photolithographic applications such as those used for the manufacture of ICs. Increasingly, shorter-wavelength irradiation is being used to define ever smaller features for this application. To achieve a reasonable irradiation flux requires the use of various laser light sources. Mercury arc lamps are the light sources of choice for carrying out ring-opening polymerizations used in so-called UV curing processes. These lamps have their most intense emission bands in the region 365–433 nm. While diaryliodonium salts can be used for UV curing applications, their efficiency is somewhat limited due to their poor absorption characteristics at these wavelengths. Similarly, the direct use of these onium salts in stereolithography,[87] in graphic arts imaging, and in a variety of biomedical and dental applications is precluded since all require sensitivity at wavelengths greater than 400 nm.

The need for long-wavelength-absorbing cationic photoinitiators to address the above targeted applications has provided the incentive for considerable synthetic activity focused on expanding the range of spectral sensitivity of diaryliodonium salts through manipulating the structure of their cations. Unfortunately, the introduction of various numbers and types of electron-donating and electron-withdrawing substituents onto the benzene rings produces only modest long-wavelength shifts in the absorption spectra of the basic diphenyliodonium chromophore. Consequently, alternative measures for broadening the spectral sensitivity of these compounds were sought.

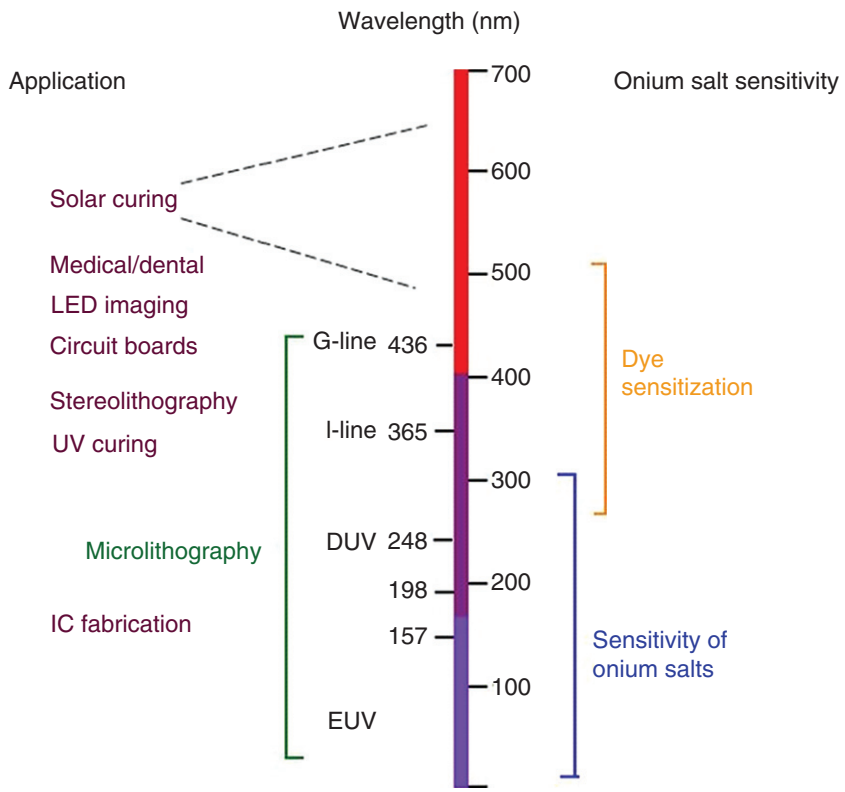

Figure 3 Relationship between the wavelength sensitivity of onium salts and their application as cationic photoinitiators. DUV, deep UV; EUV, extreme UV.

$$PS \xrightarrow{h\nu} [PS]^* \quad [35]$$

$$[PS]^* + Ar_2I^+ MtX_n^- \longrightarrow [PS \cdots Ar_2I^+ MtX_n^-]^* \quad \text{Exciplex} \quad [36]$$

$$[PS \cdots Ar_2I^+ MtX_n^-]^* \longrightarrow [PS]^{+\bullet} MtX_n^- + Ar_2I\bullet \quad [37]$$

$$Ar_2I\bullet \longrightarrow ArI + Ar\bullet \quad [38]$$

$$[PS]^{+\bullet} MtX_n^- + \text{Monomer} \longrightarrow \text{Polymer} \quad [39]$$

Scheme 22 Mechanism of the electron transfer photosensitization of diaryliodonium salts.

Specifically, direct and indirect methods of photosensitization were investigated to extend the range of spectral sensitivity of diaryliodonium salts. Much of the initial effort was concentrated on classical triplet energy transfer as a direct photosensitization method.[88,89] However, this type of photosensitization proved to be rather inefficient and, consequently, the direction of the focus of the research turned toward electron transfer photosensitization. Electron transfer photosensitization provides a practical means to extend the photosensitivity of diaryliodonium salts from the mid-UV well into the visible region of the spectrum. Shown in Scheme 22 is the proposed generalized mechanism for photosensitization as applied to diaryliodonium salts.

The photosensitizer, PS, is excited by the absorption of the irradiating light as shown in eqn [35]. Then, the excited photosensitizer interacts with the diaryliodonium salt to form an intermediate excited-state complex (exciplex) as depicted in eqn [36]. The latter transient species undergoes formal electron transfer (eqn [37]) to give a photosensitizer cation-radical, $[PS]^{+\bullet}$, and a diaryliodine radical. The process is rendered irreversible by the further fragmentation of the diaryliodine radical (eqn [38]) to give an aryl radical and an aryl iodide. It should be noted that the overall process can be considered a photoinduced redox reaction in which the diaryliodonium salt undergoes reduction while the photosensitizer is oxidized. The driving force (i.e., Gibbs free energy, ΔG) for an electron transfer photosensitization is expressed by the Rehm–Weller equation[90] shown in eqn [40], where E^{ox}_{sens} is the oxidation potential of the photosensitizer, E^{red}_{onium} the reduction potential of the diaryliodonium salt, and E^* the excitation energy of the photosensitizer. The magnitudes of the E^{ox}_{sens} and E^* parameters are known for many common photosensitizers, and the E^{red}_{onium} values have been measured by polarography for many different onium salt photoinitiators.

$$\Delta G = (E^{ox}_{sens} - E^{red}_{onium}) - E^* \quad [40]$$

For facile electron transfer photosensitization to occur, ΔG must have a value of at least $-10\,kcal\,mol^{-1}$. The magnitude of E^{red}_{onium} for diaryliodonium salts is of the order of $-5\,kcal\,mol^{-1}$, indicating that these compounds are easily reduced (i.e., they are good oxidizing agents). The low value of the reduction potential also suggests that it should be energetically possible to use dyes as electron transfer photosensitizers for diaryliodonium salts that absorb at long wavelengths, even those in the low-energy visible region. This has been verified as will be described below.

A wide assortment of electron transfer photosensitizers for diaryliodonium salts have been described in the journal and patent literature. Among these are polynuclear aromatic hydrocarbons with three or more rings such as anthracene,[91] alkoxyanthracenes,[92] pyrene, and perylene;[93] heterocyclic compounds of low basicity such as carbazoles[94] and phenothiazines;[95] aromatic ketones such as benzophenone,[96] Michler's ketone,[94] and thioxanthone and substituted thioxanthones;[97,98] coumarins;[99] phenanthrene-9,10-quinone;[100] Mannich bases;[101] and (dimethylamino)benzylidyne compounds.[102] In addition, the use of dyes such as eosine,[101] acridine orange, acridine red, and benzoflavin[103] has been employed to provide photosensitization in the visible region of the spectrum.

A particularly interesting and useful photosensitizer for diaryliodonium salts in the visible region of the spectrum is the naturally occurring dye, curcumin, **65**.[104] The source of curcumin is the spice, turmeric, which is widely used as a food flavoring and coloring agent. As a result of the extended conjugation present in this molecule, curcumin has a strong absorption band at 427 nm ($\varepsilon = 55\,000$) with a tail absorption that extends to at least 540 nm. Curcumin is readily available at low cost; it is highly soluble in a wide assortment of polar and nonpolar monomers, functional oligomers, and polymers.

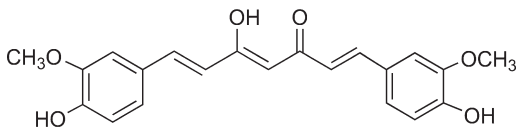

65

It is notable that according to the mechanism depicted in eqn [37] of Scheme 22, a key product formed during the photosensitization process is the photosensitizer-derived cation-radical, $PS^{+\bullet}$. The formation of this intermediate was readily confirmed for many different types of electron transfer photosensitizers. For example, the exposure of a mixture of a diaryliodonium salt and perylene in an inert solvent to UV light results in the immediate formation of an intensely deep blue solution. UV absorption spectra confirmed the formation of the comparatively stable perylene cation-radical. These results suggest, as shown in eqn [39], that in the case of photosensitized cationic polymerization systems, the primary initiating species is the cation-radical derived from photosensitizer. It should additionally be pointed out that such cation-radicals have been shown to initiate polymerization by a series of complex pathways, including a number that result in the formation of Brønsted superacids.[105,106] A further implication of this mechanism is that, like the diaryliodonium salt, the photosensitizer is also consumed by various reactions during and after the irradiation process. The 'bleaching' that occurs during these photosensitization reactions is important to many imaging applications.

Another indirect method by which spectral broadening of the sensitivity of diaryliodonium salts can be achieved is by the so-called free radical-promoted photosensitization. It has already been noted that diaryliodonium salts are oxidants with low

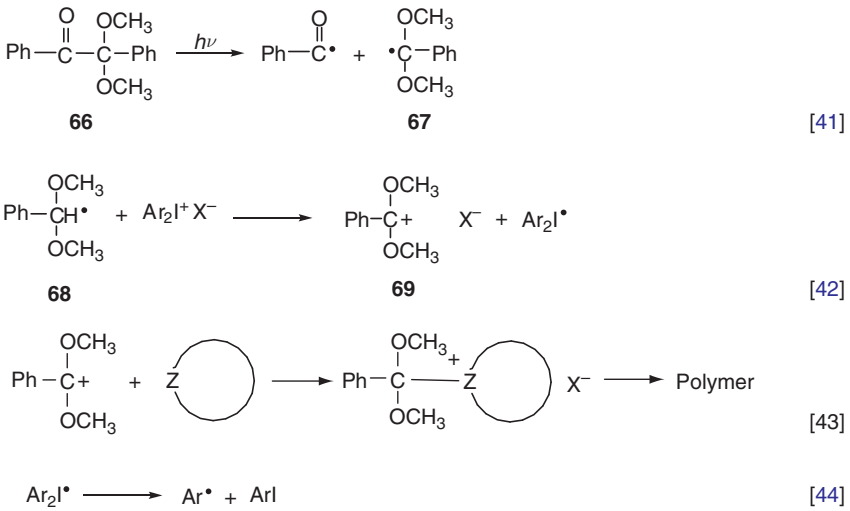

Scheme 23 Proposed mechanism for the radical-promoted photosensitization of diaryliodonium salts.

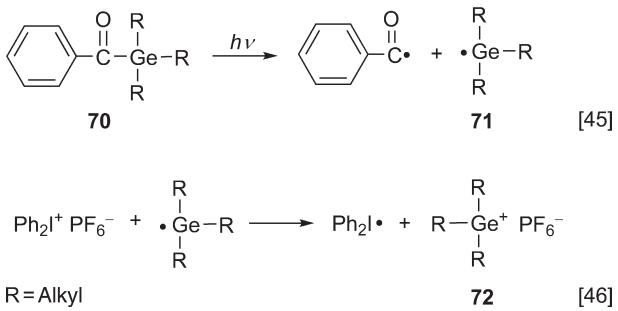

Scheme 24 Radical-promoted photosensitization of diaryliodonium salts.

oxidation–reduction potentials. Several research groups[107–112] have taken advantage of this fact by using easily oxidized radicals generated by both Norrish type I and type II photoreactions to release a cationic initiating species by the chemical reduction of a diaryliodonium salt. For example, unimolecular radical photoinitiators such as 2,2-dimethoxy-2-phenylacetophenone undergo efficient photolysis by a Norrish type I α-cleavage reaction as shown in eqn [41] of **Scheme 23** to afford the benzoyl (**66**) and α,α-dimethoxybenzyl radicals (**67**). Radical **67** can subsequently reduce a diaryliodonium salt (eqn [42]) to give the dimethoxybenzyl carbocation (**68**). Carbocation **68** initiates cationic ring-opening polymerization as shown in eqn [43] by direct electrophilic attack on the heterocyclic monomer. The diphenyliodine radical, **69**, which is also formed, irreversibly fragments to give a phenyl radical and iodobenzene (eqn [44]). By selection of a radical photoinitiator with the appropriate absorption characteristics, it is possible to conduct the polymerization of heterocyclic monomers using long-wavelength UV and even visible light.

Recently, Durmaz *et al.*[113] have described several interesting radical-promoted cationic photoinitiator systems based on the same general principles outlined above. One of the most interesting shown in **Scheme 24** involves the use of acylgermanes, **70**, as photochemical sources of radicals. These compounds conveniently absorb in the region 350–420 nm and undergo an α-cleavage (eqn [45]) to form the benzoyl and germyl radicals, **71**. In subsequent steps, **71** is oxidized by the diaryliodonium salt to form the germanium-centered cation, **72** (eqn [46]). The latter species initiates the polymerization of the monomer (cyclohexene oxide) by a direct electrophilic attack similar to that shown in eqn [43]. Another class of free radical photoinitiators that the Yagci group has employed together with diaryliodonium salts for radical-promoted cationic polymerization is diacylphosphine oxides **73**.[114] In this case, it was proposed that a photogenerated phosphorus-centered radical reduces the diaryliodonium salt.

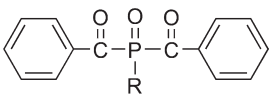

73

An example of a bimolecular photoinitiator that generates radicals by a Norrish type II hydrogen abstraction process is the combination of camphorquinone with a benzyl alcohol (eqn [47]).[115] The carbon-centered radical, **74**, is capable of reducing a diaryliodonium salt in a similar manner as shown previously in **Scheme 24**.

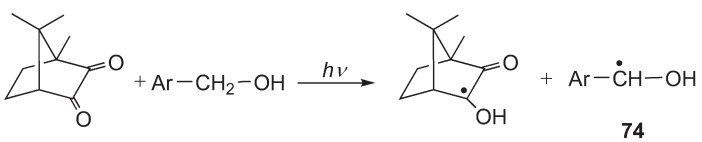

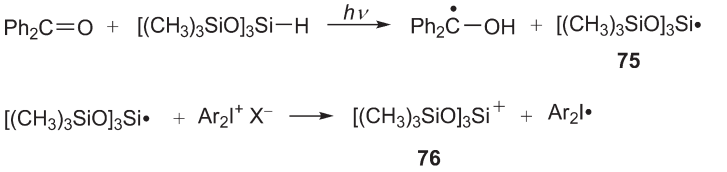

Scheme 25 Silyl radical-promoted cationic photopolymerization.

Recently, Lalevée *et al.*[116,117] have reported analogous Norrish type II systems involving the use of aromatic oxo compounds such as benzophenone, thioxanthone, camphorquinone, or eosine together with a silane or germane as a hydrogen donor.[118] For example, as depicted in eqn [48] of **Scheme 25**, the photolysis of benzophenone in the presence of tris[(trimethylsilyl)oxy]silane generates the silyl radical **75**. The latter species is oxidized by a diaryliodonium salt (eqn [49]) to yield the silylium cation **76** that then can initiate cationic ring-opening polymerization. The wavelength sensitivity of this system is determined by the choice of a specific ketone. A study of the ring-opening polymerizations of epoxide monomers was conducted using these silane-mediated initiator systems.

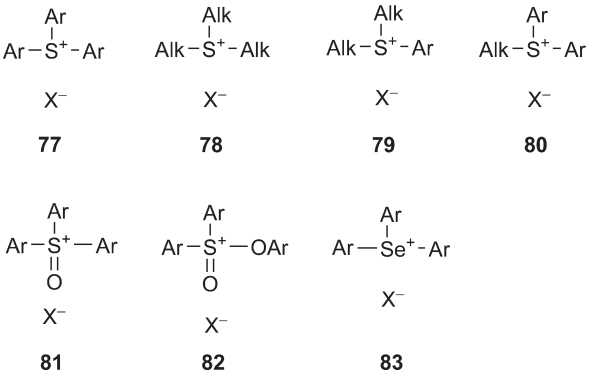

4.37.3.2.4 Triarylsulfonium salts

The initial development of diaryliodonium salt cationic photoinitiators was quickly followed by the nearly parallel discovery of triarylsulfonium salts as a second general class of highly efficient and thermally stable cationic photoinitiators.[119] Along with triarylsulfonium salts, **77**, their *S*-aryl sulfur-heterocyclic analogs display good photosensitivity and function well in photoinitiated cationic polymerizations.[120,121] In contrast, trialkylsulfonium salts, **78**, do not absorb in the UV spectrum and are not useful photoinitiators. As might be expected, dialkyl(aryl)sulfonium salts, **79**, and alkyl(diaryl)sulfonium salts, **80**, are progressively better photoinitiators but are less photoactive as well as less thermally stable and more difficult to prepare than their triarylsulfonium salt counterparts.[122] There have also been several reports of the use of triarylsulfoxonium salts, **81**,[123,124] and diaryl(aryloxy)oxosulfanylium salts, **82**,[125] as photoinitiators for cationic polymerization. In general, the latter classes of related sulfonium salts are more difficult to prepare and also less thermally stable than triarylsulfonium salts. Consequently, they have received less attention in the literature and are not used for commercial purposes. Triarylselenonium salts, **83**, while excellent cationic photoinitiators, are impractical for general use due to the relative rarity and expense of the starting materials required for their preparation.[126] Among the first-generation onium salts, triarylsulfonium salts remain the cationic photoinitiators of choice for academic studies as well as for use in industrial applications due to their outstanding thermal stability in solutions of highly reactive monomers.

4.37.3.2.4(i) Synthesis of triarylsulfonium salts

A variety of well-established synthetic schemes for the preparation of triarylsulfonium and related compounds appear in the literature. They were employed with appropriate modifications for the synthesis of these onium salt cationic photoinitiators. These methods will not be presented in this chapter and, instead, the reader is referred to the extensive literature that appears in several dated but still relevant review articles on the topic of sulfonium salts.[127,128] In recent years, the previous preparative methods for triarylsulfonium salts have been augmented by the development of several novel highly useful synthetic methods that will be briefly described here. The first of these involves the copper(I)-catalyzed arylation of diaryl sulfides with a diaryliodonium salt. An example is depicted in eqn [50] for the synthesis of *S*-phenyldibenzothiophenium salt, **84**.[63] The method is especially useful for simple substituted triphenylsulfonium salts and affords the desired active onium salt photoinitiator in nearly quantitative yields. This synthesis has been used for the preparation of compounds containing multiple triarylsulfonium salt moieties in the same molecule as well as for the facile arylation of sulfur-containing heteroaromatic compounds such as dibenzothiophene, thioxanthene, and thianthrene. An extension and modification of the above method involves the double arylation of benzenethiols for the synthesis of triarylsulfonium salts.[129] It should be noted that if an appropriate diaryliodonium salt bearing the desired anion is used, the triarylsulfonium salt obtained is directly ready for use when isolated as a cationic photoinitiator.

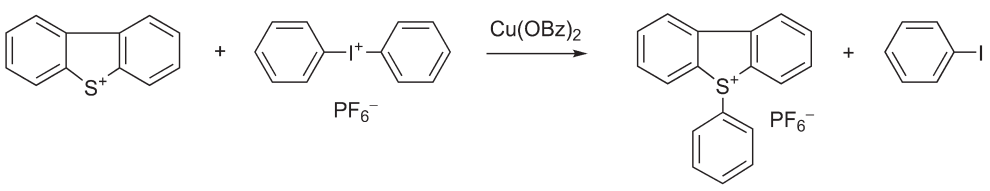

84 [50]

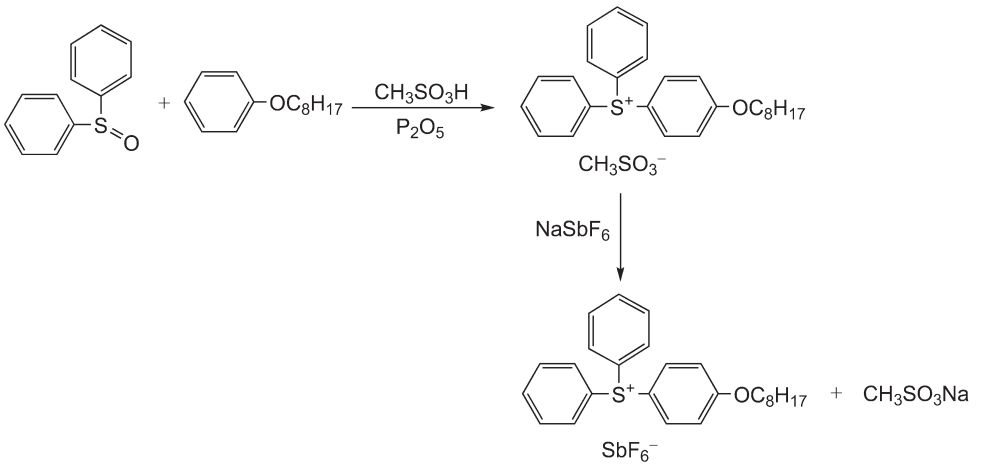

85 [51]

Scheme 26 Preparation of [4-(octyloxy)phenyl]diphenylsulfonium hexafluoridoantimonate.

A second general and highly useful method involves the acid-catalyzed condensation of a diaryl sulfoxide with an electron-rich aromatic compound.[130] The reaction is typically carried out using Eaton's reagent, a mixture of methanesulfonic acid and phosphorus pentoxide, as a catalyst and dehydrating agent. The reaction can be applied to a broad spectrum of diaryl sulfides, including both open-chain and cyclic compounds. An example is shown in eqn [51] of **Scheme 26** in which this method is used for the preparation of [4-(octyloxy)phenyl] diphenylsulfonium hexafluoridoantimonate, **85**. The reaction is usually carried out at 25–40 °C in the absence of a solvent. In all cases, the initially formed sulfonium salt bearing the methanesulfonate anion must be subjected to anion exchange. Yields of triarylsulfonium salts from this method are generally quite high (80–90%).

Employing both old and newly developed synthetic methods, the preparation of triarylsulfonium salts with a wide variation in their structures has been achieved. **Table 3** lists a sampling of some of these photoinitiators along with the appropriate literature references. Identical considerations with respect to the tailoring of the structures of the cations and anions for specific applications as were discussed for diaryliodonium salts (**Table 2**) apply to triarylsulfonium salt cationic photoinitiators as well.

4.37.3.2.4(ii) Photochemistry of triarylsulfonium salts

The mechanism of the photolysis of triarylsulfonium salts is very similar to that of diaryliodonium salts (**Scheme 18**), though with minor differences.[136] The major photolysis pathway involves the excitation of the triarylsulfonium salt with the formation of the excited singlet. The latter species undergoes heterolytic cleavage at a carbon–sulfur bond to generate an aryl cation and a diaryl sulfide pair. ISC from the excited singlet to the corresponding triplet does occur but is inefficient. However, radical products resulting from the decay of the excited triplet are always observed. Subsequent reaction of these primary species with themselves and with solvents or monomers leads to the formation of diaryl sulfides, coupled diaryl sulfides,[137,138] and aromatic hydrocarbons as well as small amounts of a variety of additional organic products. Brønsted acids are also generated. A shorthand representation of the mechanism of photolysis of triarylsulfonium salts is given in eqn [52].

$$Ar_3S^+\,X^- \xrightarrow{h\nu} \left[Ar_3S^+\,X^-\right]^* \longrightarrow \begin{bmatrix} Ar_2S^+_{\bullet}\,X^- + Ar\bullet \\ Ar^+\,X^- + Ar_2S \end{bmatrix} \rightarrow HMtX_n \quad [52]$$

Quantum yields for triarylsulfonium salts are in the range of 0.5–0.7.[139] It is notable that triarylsulfonium salts are highly photosensitive compounds, with quantum yields that are similar to those measured for diaryliodonium salts. However, diaryliodonium salts are more efficient photoinitiators of vinyl and cationic ring-opening polymerizations. The difference in the two classes of photoinitiators lies in the nature of the products produced as a result of their photolysis. As indicated previously, the organic products of diaryliodonium salts are chiefly aromatic hydrocarbons, biarenes, and various iodoaromatic compounds. These compounds do not interact with the monomers, initiators, or propagating species during a ring-opening polymerization. In contrast, the diaryl sulfides and the biarene sulfide products of triarylsulfonium salt photolysis are weakly nucleophilic and have been demonstrated to display both inhibiting and retarding effects in cationic ring-opening polymerizations.[140]

4.37.3.2.4(iii) Photosensitization of triarylsulfonium salts

While possessing marginally longer-wavelength absorption than diaryliodonium salts, the primary absorption bands of unsubstituted and monosubstituted triphenylsulfonium salts (λ_{max} = 240–305 nm) still lie in the short- to mid-wavelength region of the UV spectrum. As with their diaryliodonium salt counterparts, broadening of the spectral sensitivity of these cationic photoinitiators is necessary to enable their use in many different applications (e.g., **Figure 3**). Electron transfer photosensitization is again the most effective available method for extending the range of

Table 3 Structures of triarylsulfonium salt cationic photoinitiators

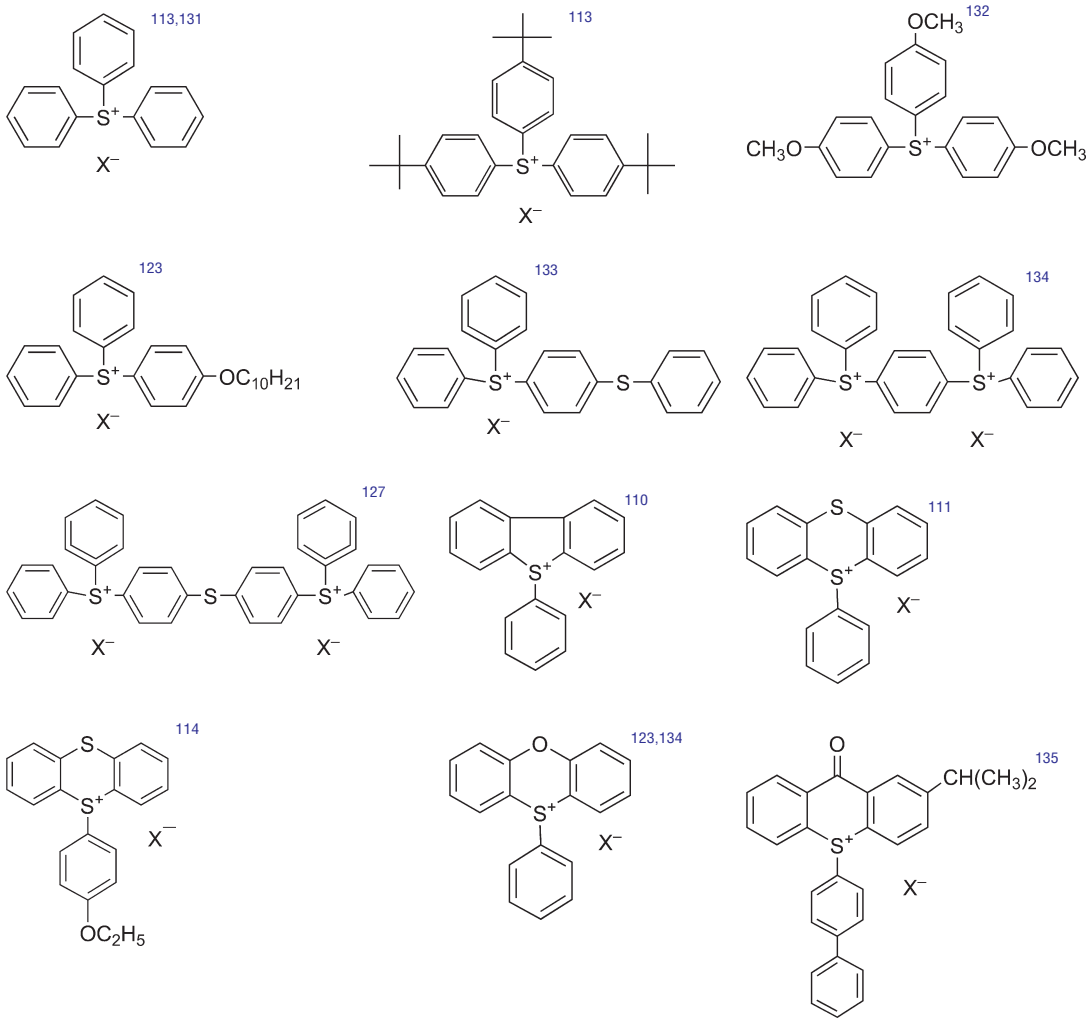

X^- is a non-nucleophilic anion.

spectral sensitivity of triarylsulfonium salts into the long-wavelength UV and visible regions. According to the Rehm–Weller equation, the ability of a triarylsulfonium salt to undergo electron transfer photosensitization depends on its reduction potential. The value of E^{red}_{onium} for a triphenylsulfonium salt is $-28\,kcal\,mol^{-1}$,[141] suggesting that triarylsulfonium salts are also more difficult to photosensitize by an electron transfer mechanism than the corresponding diaryliodonium salts. This has been confirmed experimentally. Nevertheless, there are several classes of 'crossover' photosensitizers that are capable of working with both types of onium salt photoinitiators. For example, some crossover photosensitizers are perylene,[142] anthracene and substituted anthracenes,[92] carbazoles,[94,143] phenothiazines, benzophenothiazines, and benzophenoxazines.[115] On the other hand, thioxanthones and dye photosensitizers, curcumin, benzoflavin, and acridine orange, which are effective for diaryliodonium salts, do not photosensitize the decomposition of triarylsulfonium salts. Despite many attempts, the radical-promoted photosensitization, which is so effective for diaryliodonium salts, also fails in the case of the triarylsulfonium salts. Again, this is due to the more than fivefold greater magnitude of the reduction potentials for the latter compounds, which makes them poorer oxidants for radicals.

The synthesis of sulfonium salts that incorporate a photosensitizing anthracene moiety in the same molecule was successfully undertaken by Pappas *et al.*[144] Details of the synthesis of an anthracene-containing sulfonium salt, **86**, are exhibited in eqn [53]. It was the objective of this work to improve the efficiency of electron transfer photosensitization since it was proposed that an intramolecular interaction between the photosensitizing moiety and the sulfonium groups would be more facile in these compounds than in an intermolecular one. Indeed, **86** bearing the tetrafluoridoborate anion was observed to exhibit excellent activity in the 300 nm region due to the presence of the strongly absorbing anthracene chromophore.

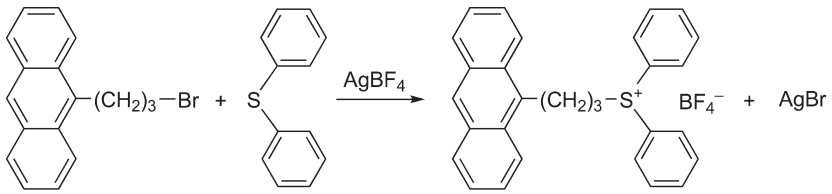

86 [53]

4.37.3.2.5 Other sulfonium salt photoinitiators

Although, as mentioned above, most of the academic and, in particular, the commercial development has been focused on triarylsulfonium salts, there have been a number of investigations of other types of sulfonium salt photoinitiators. The most notable of these are briefly discussed here.

4.37.3.2.5(i) S,S-Dialkyl-S-phenacylsulfonium salts

Probably, *S,S*-dialkyl-*S*-(phenacyl)sulfonium salts[145,146] have received the most attention as novel cationic photoinitiators for ring-opening polymerizations. One of their main attractive features is the very simple and broadly applicable synthesis shown in eqn [54] that has been developed for their preparation.[147] The general, one-pot synthesis is illustrated for one of these compounds, **87**, bearing the SbF_6^- anion. In addition, photoinitiator **87** incorporates a dodecyl group that provides excellent solubility of the photoinitiator in various nonpolar monomers. The reaction is typically carried out at room temperature in acetone or butan-2-one (ethyl methyl ketone). During the reaction, sodium bromide precipitates from the solution driving the reaction in the forward direction to form the desired sulfonium salt in excellent yields.

Studies of the mechanism of photolysis of *S,S*-dialkyl-*S*-(phenacyl)sulfonium salts showed that irradiation at 248 nm produces Brønsted acids by a reversible intramolecular Norrish type II hydrogen abstraction process as shown in **Scheme 27**.[148] Ylides are also formed as by-products. However, once the light is extinguished, the two photolysis products recombine to regenerate the starting sulfonium salt. Estimates of the quantum yields for these photoinitiators are 0.4–0.5.[93]

Despite the reversibility of the photolysis of *S,S*-dialkyl-*S*-(phenacyl)sulfonium salts, these compounds are quite good photoinitiators for the ring-opening polymerizations of epoxides, oxetanes, thiiranes, vinyl ethers, and 1,3,5-trioxane. It is also worth pointing out that the intermediate ylides generated during the photolysis can react as nucleophiles with the growing polymer chain as shown in eqn [55] resulting in termination. However, the macromolecular sulfonium salts, **88**, that are formed are capable of further dissociation on continued irradiation by the same photolysis mechanism.

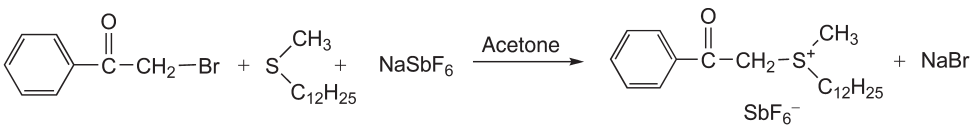

87 [54]

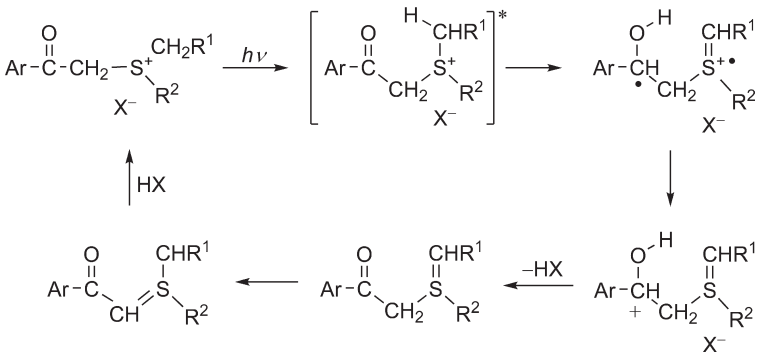

Scheme 27 Mechanism of the photolysis of *S,S*-dialkyl-*S*-(phenacyl)sulfonium salts.

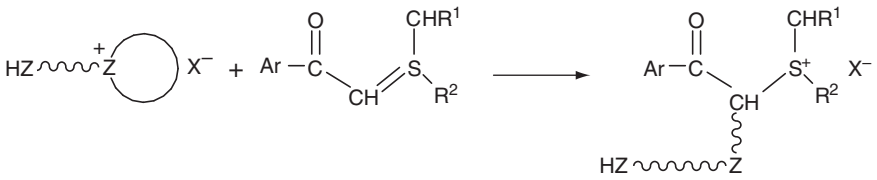

88 [55]

The E^{red}_{onium} values for *S,S*-dialkyl-*S*-(phenacyl)sulfonium salts have been measured and found to be −14.5 kcal mol^{-1}.[149] This suggests that these sulfonium salts might be expected to undergo more facile electron transfer photosensitization than reported to function well as cationic photoinitiators. While there appears to have been no additional information regarding these compounds, the authors suggest similar mechanisms for the photolysis of these oxosulfonium salts.

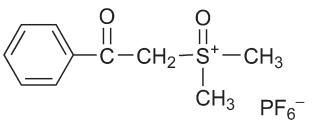

89

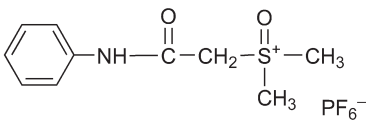

90

triarylsulfonium salts. Indeed, polynuclear aromatic hydrocarbons, carbazoles, and phenothiazines are good photosensitizers for *S,S*-dialkyl-*S*-(phenacyl)sulfonium salts.[150]

In analogy with triarylsulfonium salts, higher-oxidation-state analogs of *S,S*-dialkyl-*S*-(phenacyl)sulfonium salts and dialkyl(2-anilino-2-oxoethyl)sulfonium salts, **89** and **90**, respectively, have been described.[66] These compounds also appear to have appreciable photosensitivity and are

4.37.3.2.5(ii) S,S-Dialkyl-S-(4-hydroxyphenyl)sulfonium salts

An additional class of sulfonium salt photoinitiators that have received some attention is *S,S*-dialkyl-*S*-(4-hydroxyphenyl) sulfonium salts (**91**) and *S,S*-dialkyl-*S*-(2-hydroxyphenyl) sulfonium salts (**92**).[145] These compounds are readily prepared as illustrated in eqn [56] of **Scheme 28** by the room-temperature condensation of a phenol with a dialkyl sulfoxide in the presence of dry hydrogen chloride gas in

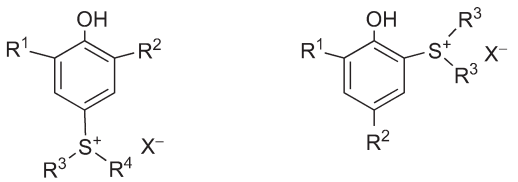

91

92

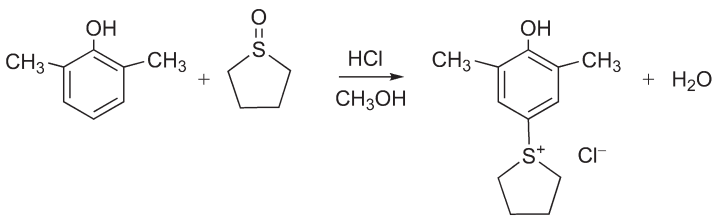

93 [56]

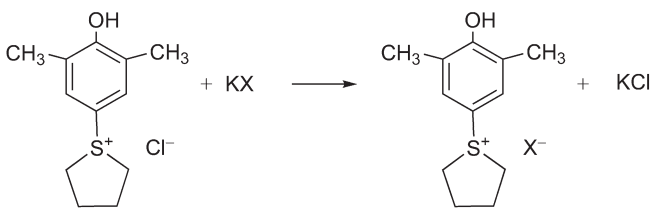

94 [57]

Scheme 28 Synthesis of *S,S*-dialkyl-*S*-(4-hydroxyphenyl)sulfonium salts.

methanol. Anion exchange (eqn [56]) in the sulfonium chloride, **93**, with an alkali or alkaline earth salt bearing a non-nucleophilic anion completes the synthesis of the active photoinitiator, **94**. An alternative synthetic procedure is to condense a dialkyl sulfide with a phenol in the presence of a mixture of methanesulfonic acid and phosphorus pentoxide (Eaton's reagent).[151]

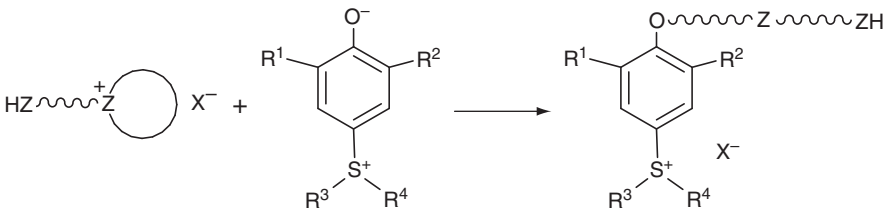

[59]

Irradiation of *S,S*-dialkyl-*S*-(4-hydroxyphenyl)sulfonium salts (eqn [58]) results in the reversible formation of the resonance-stabilized betaine, **95**, together with the Brønsted acid, HX. On standing in the dark, these two products recombine to form the starting sulfonium salt. The quantum yields based on the quantity of acid generated for these photoinitiators were found to range from 0.12 to 0.31 depending on the substitution and position of the sulfonium group relative to the hydroxy group.[152] *S,S*-Dialkyl-*S*-(2-hydroxyphenyl)sulfonium salts (**92**) have higher quantum yields than their *S,S*-dialkyl-*S*-(4-hydroxyphenyl)sulfonium salt (**91**) isomers.

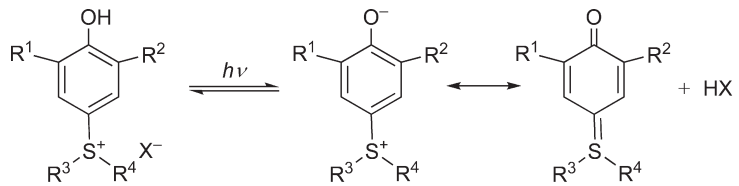

95

[58]

S,S-Dialkyl-*S*-(hydroxyphenyl)sulfonium salts are active photoinitiators for the cationic ring-opening polymerizations of a wide variety of heterocyclic monomers, including tetrahydrofuran, ε-caprolactone, epoxides, oxetanes, thiiranes, and 1,3,5-trioxane. It has been suggested that ring-opening polymerizations induced by these photoinitiators have an inherent chain termination reaction shown in eqn [59] that is analogous to that reported for *S,S*-dialkyl-*S*-(phenacyl) sulfonium salts (eqn [55]).

The reduction potentials for *S,S*-dialkyl-*S*-(hydroxyphenyl) sulfonium salts do not appear to have been measured. These sulfonium salts do not undergo electron transfer photosensitization. Rather, photosensitization has been achieved using typical diaryl ketones such as benzophenone, Michler's ketone, and thioxanthone as photosensitizers.[97] Strongly acidic solutions are produced during photosensitized photolysis, suggesting the formation of a protonic acid as one of the products.

4.37.3.2.5(iii) Thiopyrylium salts

The use of thiopyrylium salts, **96** and **97**, and pyrylium salts, **98**, bearing the BF_4^- anion (X = BF_4^-), as cationic photoinitiators was reported some years ago[153–155] and applied principally to the polymerization of epoxides.[156] Pyrylium salts such as **98** were less efficient as photoinitiators than their thiopyrylium counterparts. There are a number of straightforward routes to the synthesis of thiopyrylium salts.[80] Perhaps, the most general route is depicted in eqn [60] for the synthesis of thiopyrylium salt, **96**.

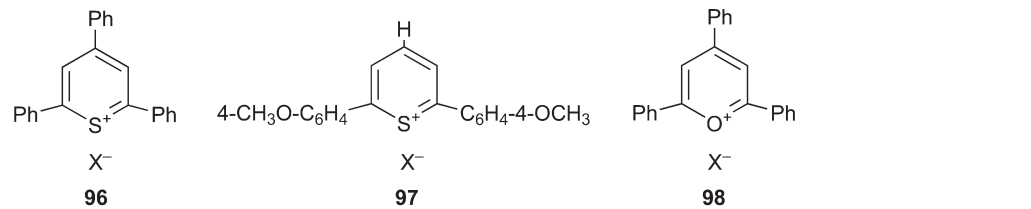

96 **97** **98**

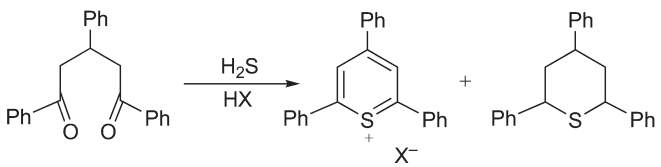

[60]

In general, thiopyrylium salts have currently seen little use as photoinitiators for cationic ring-opening polymerizations mainly due to their comparatively low initiation efficiency and poor thermal stability. In recent years, however, there appears to have been a resurgence of interest by Morlet-Savary *et al.*,[157] who have conducted a detailed study of the photophysics of their photolysis. This group has pointed out that thiopyrylium salts are particularly interesting due to their inherent long-wavelength absorption characteristics. For example, thiopyrylium salt, **96**, has major absorption bands at 232 and 475 nm with respective molar absorption coefficients of 16 100 and 29 200. More recent studies by El-Roz *et al.*[158] have shown that together with silanes bearing Si–H groups, thiopyrylium salts can be used in the radical-promoted photosensitization of diaryliodonium salts. Apparently, the photoexcited thiopyrylium salt interacts with silane to generate silyl radicals that subsequently reduce diaryliodonium salts. The polymerization of an epoxide monomer using this system was studied.

4.37.3.2.6 N-*Alkoxypyridinium and* N-*phenacylpyridinium salt photoinitiators*

A third major class of photoinitiators for cationic ring-opening polymerizations is *N*-alkoxypyridinium salts. The structures, **99–103**, are representative of this class of cationic photoinitiators. A comprehensive review of chemistry of these photoinitiators by Yagci and Endo was published in 1997.[159]

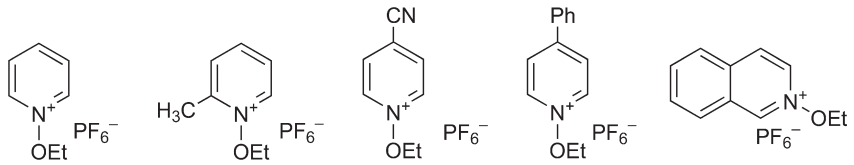

99 **100** **101** **102** **103**

Although a wide variety of substituted *N*-alkoxypyridinium salts have been prepared and evaluated as cationic photoinitiators, the simplest and most useful alkoxypyridinium salt is *N*-ethoxypyridinium hexafluoridophosphate, **99**. This photoinitiator is prepared by the reaction of pyridine-*N*-oxide with a triethyloxonium salt bearing a non-nucleophilic anion such as PF_6^- as depicted in eqn [61]. The preparations of photoinitiators **100–103** shown earlier were carried out in a similar manner.

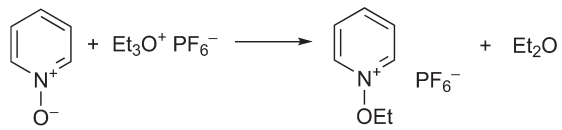

99

[61]

The proposed mechanism of photolysis and subsequent initiation of cationic ring-opening polymerization is displayed in **Scheme 29**.[160] During photolysis, *N*-alkoxypyridinium salts undergo homolytic cleavage of the nitrogen–oxygen bond to form the pyridine cation-radical, **104**, and an alkoxy radical, **105**. Quantum yields for this reaction have not been reported. The initiation of cationic polymerization proceeds either by the direct interaction of the pyridine cation-radical with the monomer or through the formation of a Brønsted acid by reaction with a hydroxy group or other proton donor (R–H). Subsequent studies[161] of the pyridinium cation-radicals by flash photolysis showed them to react very rapidly with monomers such as cyclohexene oxide and with vinyl ethers. Due to the formation of basic pyridines and pyridine-containing photolysis products, *N*-alkoxypyridines are chiefly useful for the photopolymerization of the most reactive, highly strained heterocyclic monomer systems.

The structural variations represented by compounds **99–103** provide spectral sensitivity from approximately 260 to 340 nm. Further sensitivity at longer wavelengths can be achieved by various photosensitization strategies. The half-wave oxidation–reduction potential ($E_{red}^{1/2}$) determined by polarography for **99** is −0.7 V (−16 kcal mol^{-1}), whereas the corresponding value for diphenyliodonium hexafluoridophosphate measured by the same technique is −0.2 V. This indicates that *N*-alkoxypyridinium salts should undergo facile reduction. Indeed, electron transfer photosensitization by typical excited-state electron donors such as anthracene, perylene, thioxanthene,[162] and trimethoxybenzene[163] has been reported. **Scheme 30** depicts the mechanism of the electron transfer photosensitization of **99** by excited anthracene. As shown in eqn [65], the alkoxypyridine radical, **106**, undergoes irreversible decomposition to give pyridine and an alkoxy radical.

The Yagci group has also demonstrated that the decomposition of *N*-alkoxypyridinium salts can be promoted using a variety of radical photoinitiators.[164] Among the radical photoinitiators that have been employed are benzoin

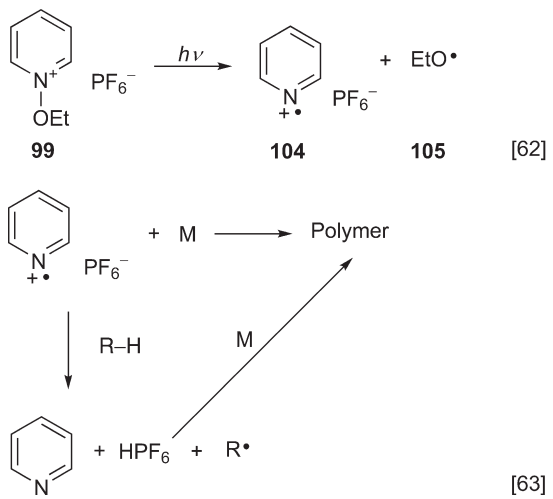

99 **104** **105** [62]

[63]

Scheme 29 Photolysis of *N*-ethoxypyridinium salts and cationic initiation.

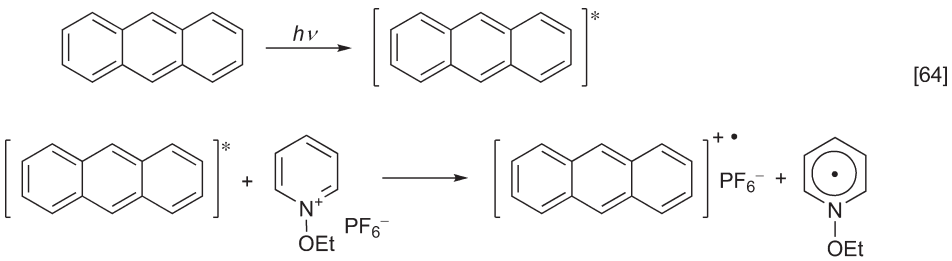

[64]

[65]

Scheme 30 Photosensitization of **99** by anthracene.

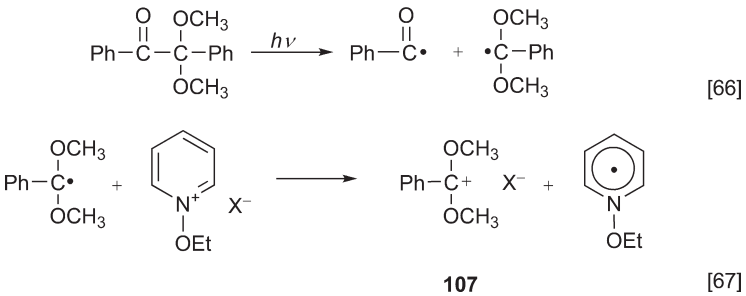

[66]

[67]

Scheme 31 Mechanism of the radical-promoted photosensitization of *N*-alkoxypyridinium salts.

derivatives, (phenylazo)triphenylmethane, 2,2-dimethoxy-2-phenylacetophenone, and acylphosphine oxides. As was the case with diaryliodonium salts and shown in **Scheme 31**, the mechanism involves the photolytic dissociation of the radical initiator into a pair of radicals. This is followed by oxidation of one or both of the radicals formed to the corresponding carbocation by the *N*-alkoxypyridinium salt. It has been proposed that the carbocation, **107**, initiates cationic ring-opening polymerization.

A number of additional photoinduced radical-promoted systems incorporating *N*-alkoxypyridinium salts were also described by the Yagci group. These include the use of photoexcited phthalaldehyde[165] and polysilanes[166] to generate reducible carbon- and silicon-centered radicals, respectively, by hydrogen abstraction and cleavage of silicon–silicon bonds.

N-Phenacylpyridinium salts, **108**, were briefly reported along with phenacyltriphenylphosphonium salts, **109**, to be good photoinitiators for cationic ring-opening polymerizations.[167] The photochemistry of these compounds has not been further investigated.

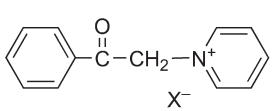

108

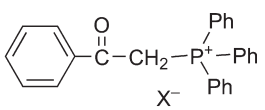

109

4.37.3.2.7 η^5-Cyclopentadienyl salt photoinitiators

η^5-Cyclopentadienyl(arene)iron(II) salts have been reported in a series of publications and patents as cationic photoinitiators for the ring-opening polymerizations of epoxides.[168–171] It is worth noting that the technical literature refers to this class of cationic photoinitiators as 'ferrocenium salts'. A prototypical example of these photoinitiators is η^5-cyclopentadienyl(η^6-isopropylbenzene)iron(II) hexafluoridophosphate, **110**. This compound was commercialized as a cationic photoinitiator by the Ciba-Geigy Corporation.

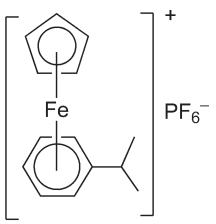

110

The general synthesis for this class of metallocene compounds is illustrated in **Scheme 32** for the preparation of **110**. Ferrocene undergoes η^5-cyclopentadienyl ligand replacement with the aromatic hydrocarbon in the presence of aluminum, aluminum chloride, and titanium tetrachloride to afford the desired η^5-cyclopentadienyl(isopropylbenzene)iron(II) chloride. Anion exchange with KPF_6 in aqueous solution gives the PF_6^- salt **110**.

η^5-Cyclopentadienyl(arene)iron(II) salts are deeply colored compounds with strong absorption bands in the long-wavelength UV and visible regions of the spectrum. The mechanism for the photolysis of η^5-cyclopentadienyliron(II) salts along with their initiation of the ring-opening polymerization of epoxides was investigated by Meier and Rihs[172] and by Hendrickson and Palazzotto.[173] The proposed mechanism is given in **Scheme 33**.

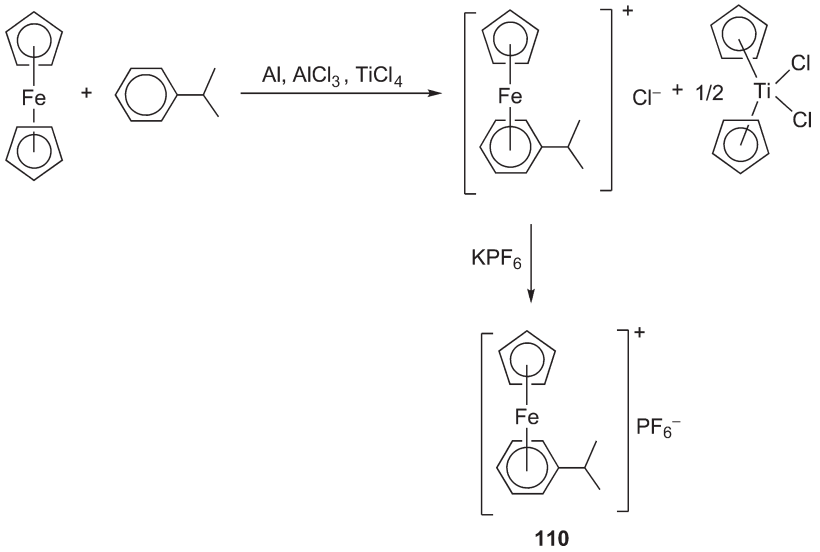

110

Scheme 32 Synthesis of η^5-cyclopentadienyl(η^6-isopropylbenzene)iron(II) hexafluoridophosphate photoinitiator.

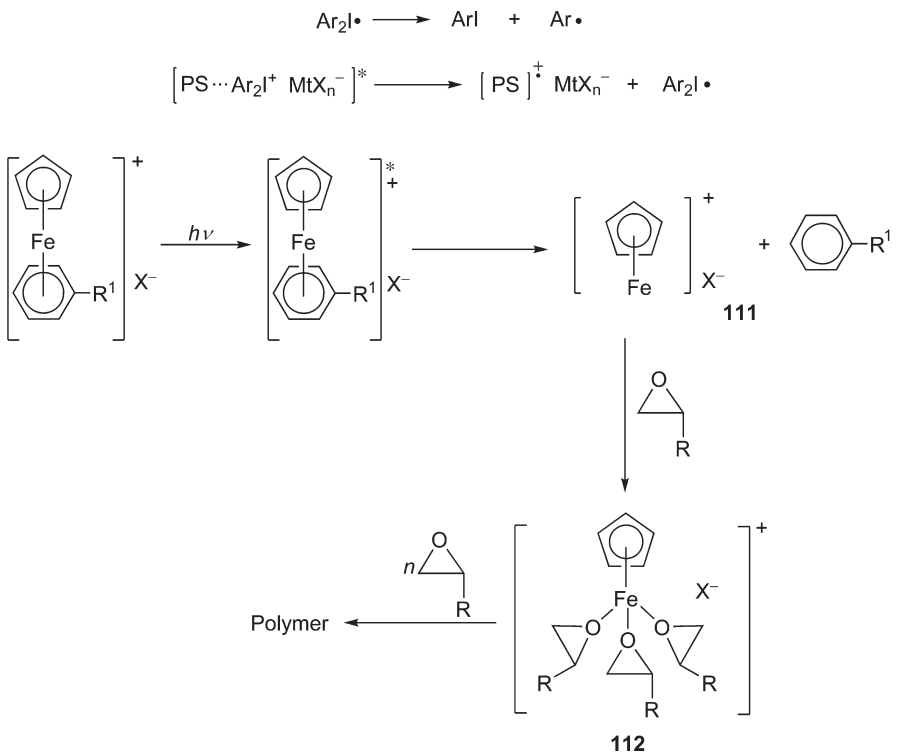

112

Scheme 33 Mechanism of the photolysis of η^5-cyclopentadienyliron(II) salts and subsequent initiation of epoxide polymerization.

On irradiation, the arene ligand is lost and the coordinatively unsaturated complex, **111**, is formed. If the photolysis takes place in the presence of an epoxide monomer, **111** ligates to three molecules of the monomer to form **112**. Epoxide polymerization begins within the coordination sphere of the iron atom of **112** and then proceeds outward. Experimental evidence[174] using ethylene oxide as a monomer appears to confirm this conclusion. The quantum yields for the photolysis of these η^5-cyclopentadienyliron(II) salts do not appear to have been measured.

In recent years, the range of η^5-cyclopentadienyliron(II) salts has been expanded by replacement of the isopropylbenzene in **110** with a wide assortment of arene ligands. For example, **113** bearing a fluorene ligand was described by Hendrickson and Palazzotto[173] while Wang and co-workers prepared analogs containing the carbazole (**114**),[175] diphenylmethane (**115**),[176] and benzophenone (**116**) ligands.[177] These modifications were all intended to enhance the photosensitivity of those respective η^5-cyclopentadienyliron(II) salts at long wavelengths.

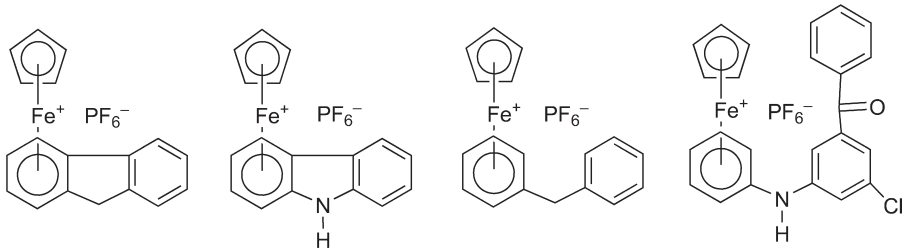

113 114 115 116

η^5-Cyclopentadienyliron(II) salts have been used primarily for the polymerization of epoxide monomers. Since the photolysis of η^5-cyclopentadienyliron(II) salts produces a relatively weak iron-based Lewis acid, their reactivity as photoinitiators in cationic polymerization is lower than typical Brønsted superacid producing diaryliodonium and triarylsulfonium salts. To improve the reactivity of these systems, oxidants such as cumene (isopropylbenzene) hydroperoxide, *tert*-butyl hydroperoxide,[178] or dibenzoyl peroxide[125] are often added. It is believed that these agents oxidize the η^5-cyclopentadienyliron(II) salts to the corresponding Fe(III) analogs and that the resulting photogenerated iron(III) intermediates are more powerful Lewis acid catalysts for cationic epoxide ring-opening polymerizations. Studies were also reported in which the effects of different superacid anions of a η^5-cyclopentadienyliron(II) salt were determined on the rates of the photopolymerization of the same epoxy monomer.[121] The rates were in the order $SbF_6^- > AsF_6^- > PF_6^- > BF_4^-$.

It was reported that the photolysis of η^5-cyclopentadienyliron(II) salts can be photosensitized.[179] The use of electron donor (polynuclear aromatic) compounds as photosensitizers suggests that the mechanism may involve electron transfer photosensitization.

4.37.3.2.8 Photoinitiated cationic polymerizations

Having presented the chemistry of the main classes of onium salt cationic photoinitiators, this section will be used to further elaborate on their use in cationic polymerizations. Those onium salts that generate Brønsted superacids on photolysis are technically capable of initiating the cationic polymerizations of all known polymerizable electron-rich vinyl and heterocyclic monomers. **Figure 4** provides an overview of the photopolymerizations of some of the more commonly used classes of monofunctional vinyl and heterocyclic monomers and is not intended to be inclusive.

Included among the many types of vinyl monomers that have been subjected to photoinitiated cationic polymerization are styrene,[46] substituted styrenes,[180] α-methylstyrenes,[181] *N*-vinylcarbazole,[182] alkyl vinyl ethers,[183] prop-1-en-1-yl ethers,[184,185] ketene acetals,[186] and alkoxyallenes.[187] Most useful in the crosslinking photopolymerizations employed for UV curing applications are multifunctional vinyl ethers and multifunctional prop-1-en-1-yl ethers. A number of multifunctional vinyl ether monomers are available from commercial sources, while multifunctional prop-1-en-1-yl ethers can be readily prepared by catalytic isomerization from their corresponding allyl ether precursors.[185,186] The photoinitiated cationic

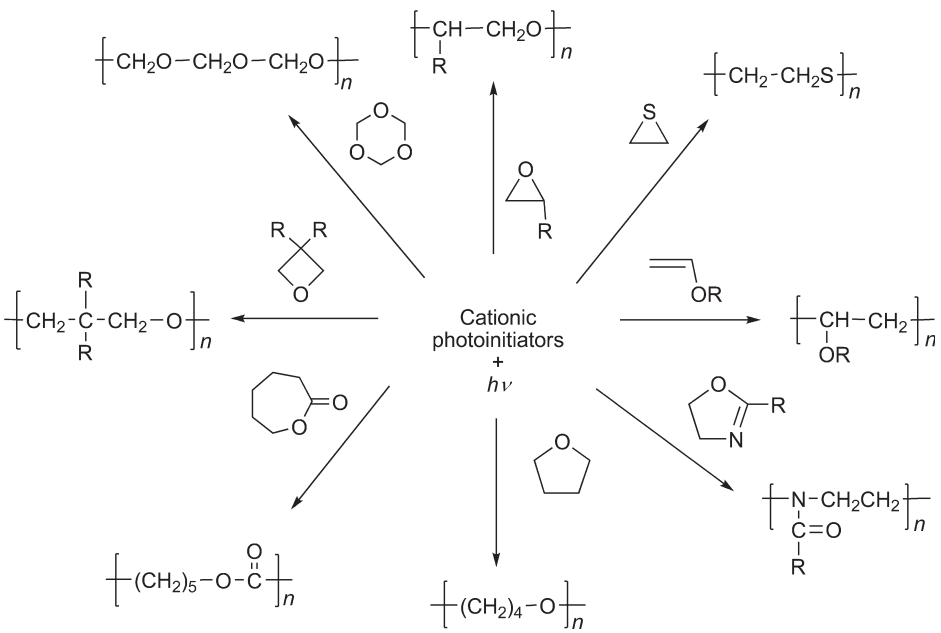

Figure 4 Range of monomers that can be cationically photopolymerized.

polymerizations of both of the latter classes of vinyl monomers are exceptionally fast and exothermic.

Monomers that undergo photoinitiated cationic ring-opening polymerization broadly encompass prop-1-en-1-yl-substituted small, medium, and large heterocycles as well as bi- and spirocyclic compounds incorporating one, two, and three or more heteroatoms. The same factors such as the influence of ring strain and the contributions of steric and electronic factors, which must be taken into account in determining the cationic polymerizability of a given monomer under thermally initiated conditions, also apply to its photopolymerization. The very extensive literature on cationic ring-opening polymerizations is comprehensively summarized in several monographs on this topic to which the reader is referred.[53,54,188,189]

Although it is possible to use onium salt photoinitiators to conduct the cationic photopolymerizations of many different types of heterocyclic monomers, it is evident that they are not all equal in this regard. As mentioned previously, diaryliodonium salts display the highest efficiency as cationic photoinitiators due to the inertness of the organic by-products of their photolysis toward the propagating species in the polymerizations. In confirmation of this, the photoinitiated cationic photopolymerizations of monomers such as tetrahydrofuran with diaryliodonium salts display classical 'living' behavior.[190] This implies that no chain transfer and no termination takes place. Triarylsulfonium salts are less efficient than diaryliodonium salts due to the slight nucleophilic character of their diaryl sulfide photoproducts. Triarylsulfonium salt photoinitiators are most effective when there is a large difference between the nucleophilicities of the photolysis by-products and the monomer undergoing polymerization. The same considerations also apply to *S,S*-dialkyl-*S*-(phenacyl)sulfonium salts and to *N*-alkoxypyridinium salts that respectively generate even more nucleophilic ylides and pyridines during photolysis. For the latter photoinitiators, the best polymerization results are obtained with the most highly reactive heterocyclic monomers. The relatively weak nature of the Fe^{2+} and Fe^{3+} electrophiles that are produced by the direct and peroxide-assisted photolysis of η^5-cyclopentadienyliron(II) salt photoinitiators also makes them suitable primarily for the most highly reactive heterocyclic monomers, that is, epoxides. Even so, η^5-cyclopentadienyliron(II) salts are not commonly employed in rapid, in-line industrial epoxide photopolymerizations such as for photocurable coatings, printing inks, and adhesives.

4.37.3.2.9 Fundamental studies of cationic ring-opening polymerizations

Onium salt cationic photoinitiators present many unique and interesting opportunities for basic studies of cationic ring-opening polymerizations. Since they are latent photochemical sources of strong Brønsted acids, they can be dissolved in the subject monomers and then precisely triggered on demand by the application of light. Mixing problems and the use of complex stopped-flow devices and other apparatuses required to overcome them are thus avoided. Only the rate of initiation is different in a photoinitiated cationic polymerization as compared to a conventional thermally initiated polymerization. The rate of initiation for an onium salt-photoinitiated cationic polymerization (eqn [68]) is determined by its quantum yield of photolysis, ϕ, and the absorbed light intensity, I_a. I_a is a function of the molar absorption coefficient of the photoinitiator and its concentration. The rate of a photochemically induced polymerization (R_p) follows the regular and well-known kinetic expression shown in eqn [69].[191] Therefore, knowing these parameters, one can very accurately determine the photopolymerization rate of a given monomer.

$$R_p = \phi I_a \quad [68]$$

$$R_p = k_p[M]\left(\frac{\phi I_a}{2k_t}\right)^{1/2} \quad [69]$$

Many different methods have been used to monitor the kinetics of cationic ring-opening photopolymerizations. Among the most commonly used techniques are real-time infrared spectroscopy,[192,193] differential scanning photocalorimetry,[194] thin-film calorimetry,[195] and optical pyrometry.[196]

A particularly important use of photoinitiated cationic polymerizations is the determination of the comparative reactivity of various related monomers. For example, epoxides (oxiranes) are a highly diverse class of cationically polymerizable monomers. While almost all epoxy compounds appear to undergo facile cationic ring-opening polymerizations, their rates are vastly different and dependent on various structurally related parameters such as ring strain, steric hindrance, and the polar and electronic effects of various substituents. Although much anecdotal information exists with respect to the relative reactivity of various members of this class of monomers, no published scientific ranking or explanation exists for the observed reactivity differences. Accordingly, Crivello and co-workers[197,198] undertook such a study, analyzed the results, and offered a rationalization for the behavior of individual epoxy monomers within the framework of the general cationic ring-opening polymerization mechanism shown in **Scheme 15**. During the course of that work, it was observed that the slowest and rate-determining step of the mechanism is the reaction of the secondary oxiranium ion with the monomer (eqn [23], **Scheme 15**). Those factors that tend to decrease the reactivity of the secondary oxiranium ion slow the polymerization, while those that increase its reactivity tend to accelerate the overall ring-opening polymerization. Insights into these structure–reactivity relationships are highly germane to the design of novel epoxy monomer systems. Parenthetically, the generation of oxiranium ions by acids generated by the photolysis of onium salts also provides a means for the direct spectroscopic detection of the metastable secondary oxonium intermediates. The extension of this type of study to other classes of heterocyclic monomers would also appear to afford an opportunity to gather valuable information concerning their structure–reactivity relationships.

In principle, onium salt cationic photoinitiators are capable of photochemically generating any desired Brønsted acid by simply selecting the appropriate anion of the salt. If individual members of a series of onium salts in which only the anion is varied are irradiated at a constant light intensity, the same quantity of Brønsted acid per unit time will be produced in every case. When the photolysis is carried out in a suitable heterocyclic monomer, a Brønsted acid can then be ranked

with others in terms of its efficiency as an initiator in that specific monomer. If pure onium salts and monomers are employed in such a study, the acid-lowering effects of water and protonic impurities can be minimized or eliminated. Given the difficulties of generating many pure Brønsted acids as outlined earlier in this chapter, there does not seem to be a suitable alternative means for accomplishing the same result.

4.37.3.2.10 Applications of photoinitiated cationic ring-opening polymerizations

Photoinitiated cationic ring-opening polymerization shares all of the benefits inherent in UV curing technologies. Among these are large energy savings as compared to traditional thermally induced polymerizations. This is achieved due to the nature of the chain reaction polymerizations that take place, which require the absorption of only a small number of photons to release a catalytic amount of an electrophilic agent (a Lewis or Brønsted acid or a cationic iron species) to initiate polymerization. Thus, a large polymer mass can be realized for the expenditure of a small amount of energy. In most cases, the photopolymerizations used in UV curing are conducted without the use of solvents. This means that UV curing does not release volatile organic compounds into the environment. Cationic UV curing is especially attractive in that ring-opening polymerizations do not exhibit inhibition due to the presence of oxygen. It is likewise fortunate that the excited states generated upon the irradiation of onium salts are not appreciably quenched by molecular oxygen. For these reasons, the use of inerting gases, as is necessary for many radical UV curing applications, is not required in the corresponding cationic photopolymerizations. Unlike photoinitiated radical polymerizations that generally quickly cease due to bimolecular termination reactions once irradiation is stopped, the corresponding photoinitiated cationic ring-opening polymerizations display a considerable 'dark' polymerization character. This means that while there may be extensive chain transfer taking place, these polymerizations are essentially nonterminating and that once photoinitiated will proceed further even in the absence of light.

In most commercial cationic UV curing applications, including high- and low-volume applications such as coatings, adhesives, printing inks, and stereolithography, the monomers of choice are multifunctional epoxides for these applications is the requirement for a high polymerization rate. Epoxide monomers undergo the most rapid polymerizations of all simple heterocyclic monomer systems due to their inherent high ring strain. In addition, photocured epoxy polymers possess excellent thermal capabilities, mechanical properties, solvent resistance, and adhesion to a wide variety of substrates. A broad spectrum of multifunctional epoxide monomers is available on a commercial scale. However, it should be cautioned that these monomers were developed primarily for use in condensation polymerizations with, for example, multifunctional amines as reaction partners. For this reason, many commercially available monomers may or may not be of insufficient purity to meet the requirements for a catalytic cationic photopolymerization. The observation of a long induction period prior to the onset of a polymerization is often indicative of the presence of inhibiting impurities. Additionally, and more significantly, currently available multifunctional epoxide monomers are not optimally designed for cationic ring-opening polymerizations. Consequently, there is a considerable opportunity for the development of novel, multifunctional epoxide monomers specifically for use in cationic UV curing. In recent years, some attempts have been made to bridge this gap with the synthesis of several new classes of epoxide monomers. Worthy of note is the synthesis of bis-cycloaliphatic epoxide monomers by Carter and Jupina[199] and by Sasaki[200] as well as the development of high-reactivity di- and multifunctional silicone–epoxide monomers by Crivello and co-workers.[201,202]

While photoinitiated cationic ring-opening polymerizations used in UV curing applications are most often applied to multifunctional epoxide monomers, these systems are often modified in many ways. For example, a common strategy is to combine epoxide monomers with long-chain poly(alkylene oxide) and poly(ε-caprolactone) polyols in UV-curable formulations to improve the fracture toughness and flexibility of crosslinked epoxy network polymers that are formed.[203,204] As has been described by Penczek *et al.*,[53] the addition of such polyols results in a changeover in the polymerization from an active chain end to an activated monomer mechanism. This is accompanied by a significant change in the kinetics of the photopolymerization reaction. Similarly, a number of authors[205–208] have investigated hybrid systems in which photoinitiated cationic and radical polymerizations are conducted concurrently. These hybrid systems produce interpenetrating networks with useful, unique, and interesting properties.

Oxetanes are slightly more basic than epoxides and have similar ring-strain energies. For this reason, oxetane monomers are also excellent candidates for use in UV curing applications. However, only monofunctional oxetane monomers were known and these were available only in small quantities from chemical supply houses. Crivello and Sasaki[209,210] and Sasaki *et al.*[211] used novel synthetic methods to prepare a series of mono- and difunctional 3,3-disubstituted oxetane monomers that are now available on a commercial scale. In many cases, the oxetane monomers are used in combination with epoxide monomers in UV curing applications.[212]

The use of onium salt photoinitiators to carry out cationic ring-opening polymerizations is an enabling technology that is currently finding a myriad of uses in many high-performance applications. Only a very few examples will be given here. Many of these exciting new applications rely on the design and synthesis of tailored, functional substrates that are fitted with polymerizable epoxide or oxetane groups. One of the major themes being investigated is the use of cationic photopolymerizations for biorenewable monomers intended for use in coatings, printing inks, adhesives, and composites. To that end, Crivello and co-workers[213,214] explored the synthesis and photopolymerization of epoxidized vegetable oils. Soucek and co-workers[215,216] and Lu and Wool[217] have pursued the use of epoxidized vegetable oils in UV-curable composites. Other biorenewable monomers derived from epoxidized terpenes have also been investigated.[218] The use of photoinitiated cationic ring-opening polymerizations to carry out three-dimensional imaging using stereolithography has already been mentioned.[219,220] Other computer-aided solid modeling and rapid prototyping technologies such as those offered commercially by Envisiontec and Objet Geometries, Ltd., also employ photopolymers based on epoxides. Thick (up to

2 mm) negative-tone photoresists based on highly functional novolak, epoxy, or bisphenol A glycidyl ether epoxy resins are employed for the fabrication of ink-jet printer heads and other MEMS (microelectromechanical systems) applications due to the excellent vertical side walls and high aspect ratios (>20:1) that can be obtained.[221] Other imaging processes that are also being researched include step and flash imprint lithography,[222,223] holographic image recording,[224] and holographic data storage.[225] The success of flexible plastic electronics will likely rely on the application and photopolymerization of monomers or oligomers bearing electroactive components that will serve various electronic functions such as conductors, insulators, and transistors.[226] Similarly, organic solar cells are being designed in which the photoactive electron donors and acceptors that will be rendered photopolymerizable by virtue of oxetane or epoxide functional groups that are appended to them.[227] Epoxy-based optical adhesives used for bonding lens and optical fibers are also in wide use. An important ongoing effort is being directed toward the development of photopolymerizable dental composites with reduced or no shrinkage during UV cure. Ge *et al.*[228] have investigated the photoinitiated double ring-opening cationic polymerization of spirobicyclic orthoesters and carbonates for this application.

4.37.3.3 Photoinitiated Anionic Polymerizations

Along with the photochemical generation of bases, Crivello and Dietliker[28] have reviewed the field of photoinitiated anionic polymerizations. Until this point in time, there has been no report of the photochemical generation of carbanionic species equivalent to those obtained from organometallic compounds that are broadly capable of initiating the anionic polymerizations of simple alkenes and conjugated dienes. Consequently, this area still remains as an academic challenge to future researchers. From a practical point of view, there may be few applications of such technology given the well-known sensitivity of most carbanionic polymerizations toward even traces of oxygen, water, alcohols, all acids, and a wide range of carbonyl compounds.

There are, however, several highly reactive vinyl monomers such as 2-(trifluoromethyl)acrylates and 2-cyanoacrylates that undergo anionic polymerizations in the presence of even weak bases. The photoinitiated anionic polymerizations of these monomers have been achieved using a number of photosensitive metal complexes.[229] For example, the irradiation of alkali salts containing the *trans*-$[Cr(NH_3)_2(NCS)_4]^-$ anion at wavelengths in the range of 350–532 nm releases the thiocyanate anion (SCN^-). As depicted in **Scheme 34**, the thiocyanate anion is capable of initiating the anionic chain polymerization of ethyl 2-cyanoacrylate.[230,231]

As described by the Kutal research group,[232] another approach to the photoinitiated anionic polymerization of ethyl 2-cyanoacrylate involves the photolysis of the platinum bis(acetylacetonate) complex, **117**. The irradiation of **117** at wavelengths above 300 nm results in the liberation of the acetylacetonate anion (**118**, **Scheme 35**) that is capable of initiating the polymerization of the monomer in a manner similar to the thiocycanate anion as shown in **Scheme 34**.

Further examples of the use of metal–organic complexes as photoinitiators for 2-cyanoacrylates are iron(II) and ruthenium(II) cyclopentadienyl complexes.[233]

Inoue and co-workers have been active in the study of immortal polymerizations conducted in the presence of

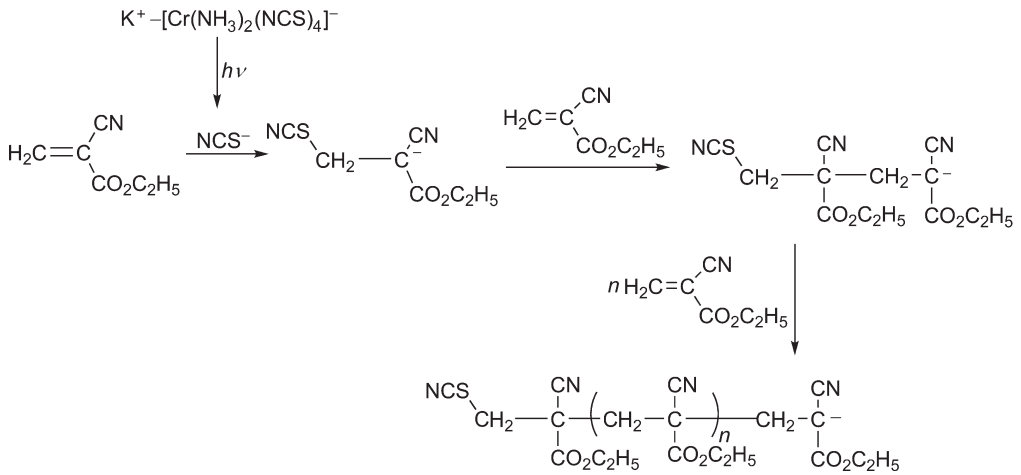

Scheme 34 Photoinitiated anionic polymerization of ethyl 2-cyanoacrylate by $K^+[Cr(NH_3)_2(NCS)_4]^-$.

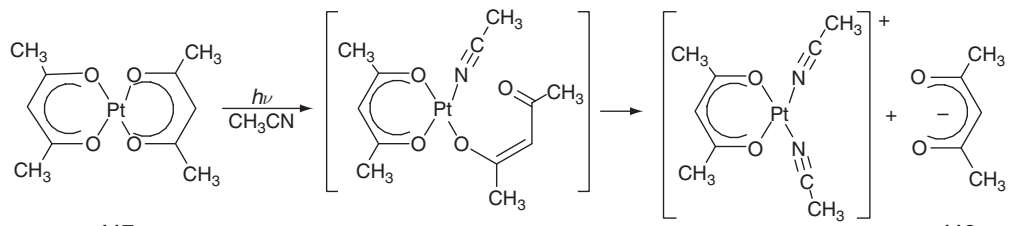

117 **118**

Scheme 35 Mechanism for the photogeneration of the acetylacetonate anion by photolysis of **117**.

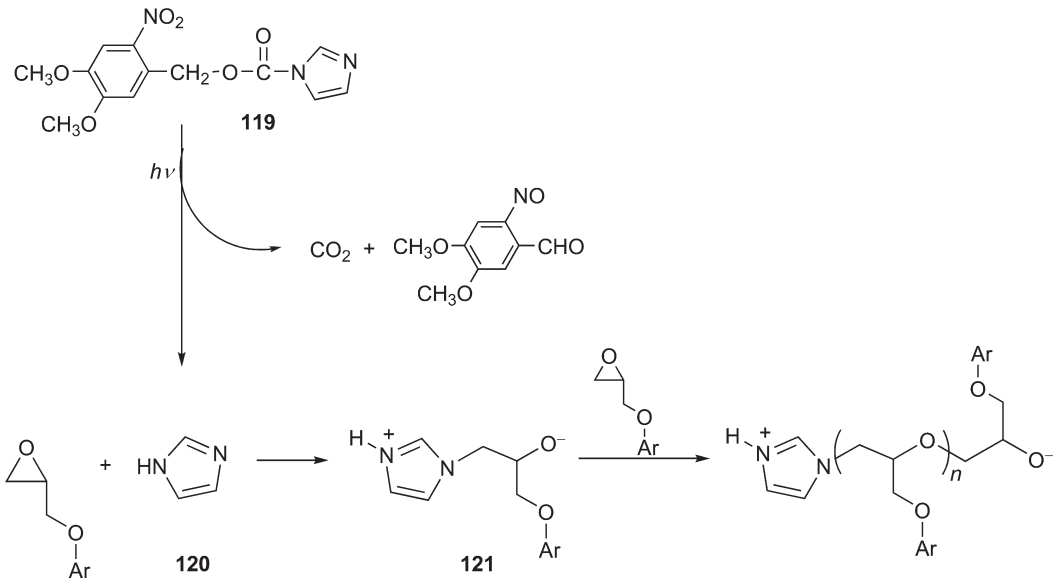

Scheme 36 Mechanism of the photoinitiated polymerization of aryl glycidyl ethers.

aluminum or zinc porphyrins. More recently, this group has reported that methyl methacrylate undergoes polymerization when irradiated in the presence of aluminum methyltetraphenylporphyrin coordination complex.[234] Evidence was offered that this polymerization takes place by an anionic mechanism. The Inoue group has reported that the polymerization, while anionic, does not appear to be photoinitiated. Continuous irradiation is required for the polymerization to proceed.

The ring-opening polymerizations of heterocyclic monomers take place under milder conditions than the corresponding carbanionic polymerizations of alkenes and dienes. For this reason, several examples of the photoinitiated anionic polymerizations of the former monomers have been successfully conducted. The Inoue group[235] has employed a modified zinc methyltetraphenylporphyrin as a photoinitiator to carry out the ring-opening polymerization of propylene oxide and other epoxides. The reaction, once initiated using light, proceeds further in the dark.

Imidazole is a well-known initiator for the anionic ring-opening polymerization of epoxides. The photogeneration of imidazole and its subsequent use as an initiator for the polymerization of multifunctional epoxy-novolak resins have been reported by Nishikubo *et al.*[236] Photolysis of the nitrobenzyl derivative **119** as shown in **Scheme 36** generates imidazole, **120**, which forms zwitterionic intermediate, **121**, by reaction with the epoxide. The latter species is a rather weak nucleophile and the application of heat (120 °C) was required to drive the polymerization to completion.

4.37.4 Conclusions

The rapid development of a variety of photopolymerization reactions has resulted in a proliferation of this technology that has been driven primarily by its implementation in a burgeoning number of high-volume and specialty applications. As the uses have expanded, the need for still other additional classes of thermally stable, highly efficient radical, cationic, and anionic photoinitiators with tailored wavelength sensitivities has also correspondingly increased. Parallel developments have taken place in the design and synthesis of novel photopolymerizable monomer and reactive oligomer systems that are targeted to meet the specific demands of the emerging applications. A further strong impetus for the development of the field is the increasing need to replace outdated solvent-based thermal cure coating, adhesive, and printing ink systems with more environmentally acceptable photopolymerization technologies. For all of these reasons, it would appear that the field of photopolymerization chemistry is well positioned to experience a continued future growth.

References

1. Pappas, S. P., Ed. *UV Curing: Science and Technology*; Technology Marketing Corp.: Stamford, CT, 1978.
2. Pappas, S. P., Ed. *Radiation Curing*; Plenum Press: New York, 1992.
3. Randall, D. R., Ed. *Radiation Curing of Polymers*; Royal Society of Chemistry: London, UK, 1987.
4. *Radiation Curing of Polymeric Materials*; Hoyle, C. E., Kinstle, J. F., Eds.; ACS Symposium Series 417; American Chemical Society: Washington, DC, 1990.
5. Fouassier, J. P.; Rabek, J. F. *Radiation Curing in Polymer Science and Technology*; Elsevier Applied Science: New York, 1993; Vols. I and II.
6. *Photoinitiated Polymerization*; Belfield, K. D., Crivello, J. V., Eds.; ACS Symposium Series 847; American Chemical Society: Washington, DC, 2003.
7. Stewart, M. D.; Wilson, C. G. In *Encyclopedia of Materials: Science and Technology*; Kremer, E. J.; Hadziannou, G., Eds.; Elsevier: Amsterdam, 2001; p 6973.
8. Gilbert, A.; Baggott, J. *Essentials of Molecular Photochemistry*; Blackwell Science: Oxford, UK, 1991; p 270.
9. Turro, N. J. *Modern Molecular Photochemistry*; Benjamin Cummings: Menlo Park, CA, 1978; pp 414–417.
10. *Introduction to Microlithography*; Thompson, L. F., Wilson, C. G., Bowden, M. J., Eds.; ACS Symposium Series 219; American Chemical Society: Washington, DC, 1983.
11. *Materials for Microlithography*; Thompson, L. F., Wilson, C. G., Fréchet, J. M., Eds.; ACS Symposium Series 266; American Chemical Society: Washington, DC, 1984.
12. *Polymers in Electronics*; Davidson, T., Ed.; ACS Symposium Series 242; American Chemical Society: Washington, DC, 1984.

13. Minsk, L. M. U.S. Patent 2,725,372, 1955 (to Eastman Kodak Co.).
14. Thompson, L. F.; Kerwin, R. E. *Annu. Rev. Mater. Sci.* **1976**, *6*, 267.
15. Morgan, C. R.; Magnotta, F.; Ketley, A. D. *J. Polym. Sci., Part A: Polym. Chem.* **1997**, *15*, 627.
16. Jacobine, A. T. In *Radiation Curing in Polymer Science and Technology*; Fouassier, J. P., Rabek, J. F., Eds.; Elsevier Applied Science: New York, 1993; p 219.
17. Gush, D. P.; Ketley, A. D. *Mod. Paint Coat.* **1978**, *68*, 54–62.
18. Hoyle, C. E.; Cole, M.; Bachemin, M.; *et al.* In *Photoinitiated Polymerization*; Belifield, K. D., Crivello, J. V., Eds.; ACS Symposium Series 847; American Chemical Society: Washington, DC, 2003.
19. Lee, T. Y.; Roper, T. M.; Jönsson, S. E.; *et al. Polymer* **2003**, *44*, 2859.
20. Campos, L. M.; Killops, K. L.; Saki, R.; *et al. Macromolecules* **2008**, *41*, 7063.
21. Bowman, C. N.; Hoyle, C. E. *Angew. Chem., Int. Ed.* **2010**, *49*, 1540.
22. Lowe, A. B. *Polym. Chem.* **2010**, *1*, 17.
23. Fairbanks, B. D.; Scott, T. F.; Kloxin, C. J.; *et al. Macromolecules* **2009**, *42*, 211.
24. Konkolewicz, D.; Gray-Weale, A.; Perrier, S. *J. Am. Chem. Soc.* **2009**, *131*, 18075.
25. Drahnak, T. J. U.S. Patent 4,600,484, 1986 (to 3M Corp.).
26. Boardman, L. D. *Organometallics* **1992**, *11*, 4194.
27. Butts, M. D. U.S. Patent 6,451,869, 2002 (to GE Corp.).
28. Crivello, J. V.; Dietliker, K. *Photoinitiators for Free Radical, Cationic and Anionic Polymerization*, 2nd ed.; Wiley: New York, 1998; p 479.
29. Suyama, K.; Shirai, M. *Prog. Polym. Sci.* **2009**, *34*, 194.
30. Frèchet, J. M. J. *Pure Appl. Chem.* **1992**, *64*, 1239.
31. Shirai, M.; Tsunooka, M. *Prog. Polym. Sci.* **1996**, *21*, 1.
32. Dietliker, K.; Jung, T.; Benkhoff, J.; *et al. Macromol. Symp.* **2004**, *217*, 77.
33. Dietliker, K.; Jung, T.; Benkhoff, J. In *e/5 2004 RadTech USA, Technical Conference Proceedings*, Charlotte, NC, 2–5 May 2004.
34. Shen, J.; Matsushima, H.; Comer, C. M.; *et al. Chem. Mater.* **2010**, *22*, 2616.
35. Blank, W. J. *Macromol. Symp.* **2002**, *187*, 261.
36. Hanson, J. E.; Jensen, K. H. In *ICPS '96: The Physics and Chemistry of Imaging Systems*, Proceedings of IS&T's 49th Annual Conference, Minneapolis, MN; Society for Imaging Science and Technology: Springfield, VA, 1996; p 5087.
37. Crivello, J. V.; Mao, Z. *Chem. Mater.* **1997**, *9*, 1554.
38. Croutxe-Baghorn, C. In *Proceedings of RadTech 2010*, Baltimore, MD, 23–27 May 2010.
39. Decker, C.; Moussa, K. *Makromol. Chem., Rapid Commun.* **1990**, *11*, 159.
40. Moussa, K.; Decker, C. *J. Polym. Sci., Part A: Polym. Chem.* **1993**, *31*, 2191.
41. Jansen, J. F. G. A.; Dias, A. A.; Dorschu, M.; Coussens, B. *Macromolecules* **2003**, *36*, 3861.
42. Berchtold, K. A.; Nie, J.; Stansbury, J. W.; *et al. Macromolecules* **2008**, *41*, 9035.
43. Stansbury, J. W.; Bailey, W. J. *J. Dent. Res.* **1986**, *65*, 219.
44. Stansbury, J. W. *J. Dent. Res.* **1992**, *71*, 1408.
45. Crivello, J. V.; Lam, J. H. W. *J. Polym. Sci., Polym. Symp.* **1976**, *56*, 383.
46. Crivello, J. V.; Lam, J. H. W. *Macromolecules* **1977**, *10*, 1307.
47. Crivello, J. V. In *UV Curing: Science and Technology*; Pappas, S. P., Ed.; Technology Marketing Corp.: Stamford, CT, 1978; p 24.
48. Crivello, J. V. In *Ring-Opening Polymerization*; Brunelle, D. J., Ed.; Hanser: Munich, Germany, 1992; p 157.
49. Gandini, A.; Cheradame, H. *Adv. Polym. Sci.* **1980**, *34/35*, 1–285.
50. Goethals, E. J., Ed. In *Cationic Polymerization and Related Processes*; Academic Press: New York, 1984.
51. Kennedy, J. P. *Cationic Polymerization of Olefins: A Critical Inventory*; Wiley-Interscience: New York, 1975.
52. Penczek, S.; Kubisa, P.; Matyjaszewski, K. *Adv. Polym. Sci.* **1980**, *37*, 8–34.
53. Penczek, S.; Kubisa, P.; Matyjaszewski, K. *Adv. Polym. Sci.* **1985**, *68/69*, 52–64.
54. Olah, G. A.; Surya Prakash, G. K.; Sommer, J. *Superacids*; Wiley: New York, 1985.
55. Olah, G. A.; Molnár, A. *Hydrocarbon Chemistry*, 2nd ed.; Wiley-Interscience: New York, 2003.
56. Roe, A. *Org. React.* **1949**, *5*, 193.
57. Schlessinger, S. J. U.S. Patent 3,826,650, 1972; U.S. Patent 3,708,926, 1973; *Photogr. Sci. Eng.* **1974**, *18*, 387.
58. Watt, W. R. U.S. Patent 3,721,617, 1973; U.S. Patent 3,721,616, 1973; U.S. Patent 3,794,576, 1974; U.S. Patent 3,816,280, 1974; U.S. Patent 3,815,278, 1974.
59. Feinberg, J. H. U.S. Patent 3,816,281, 1974; U.S. Patent 3,711,391, 1973; U.S. Patent 3,711,390, 1973.
60. Olah, G. A. *Halonium Ions*; Wiley: New York, 1975.
61. Smith, G. H. Belg. Patent 828,841, 1975.
62. Nemcek, J. Belg. Patent 837,782, 1976.
63. Crivello, J. V.; Lam, J. H. W. *J. Polym. Sci., Polym. Lett.* **1978**, *16*, 2441.
64. Crivello, J. V.; Lam, J. H. W.; Volante, C. N. *J. Radiat. Curing* **1977**, 2–24.
65. Crivello, J. V.; Lam, J. H. W. *J. Polym. Sci., Polym. Lett.* **1978**, *16*, 563.
66. Koser, G. F.; Rebrovich, L.; Wettach, R. H. *J. Org. Chem.* **1981**, *46*, 4324.
67. Kitamura, T.; Nagata, K.; Taniguchi, H. *Tetrahedron Lett.* **1995**, *36*, 1081; *Chem. Lett.* **1992**, *21*, 2245.
68. Höfer, M.; Liska, R. *J. Polym. Sci., Part A: Polym. Chem.* **2009**, *49*, 3419.
69. Nieland, O. Ya.; Karele, B. Ya. *J. Org. Chem. U.S.S.R. (Engl. Transl.)* **1980**, *6*, 889.
70. Irving, E. Eur. Pat. Appl. 104144, 1982; U.S. Patent 4,482,679, 1984.
71. Dektar, J. L.; Hacker, N. P. *J. Org. Chem.* **1990**, *55*, 639; *J. Org. Chem.* **1991**, *56*, 1838.
72. DeVoe, R. J.; Sahyun, M. R. V.; Serpone, M.; *et al. Can. J. Chem.* **1987**, *65*, 2342.
73. Pappas, S. P.; Gatechair, L. R. *Proc. Soc. Photogr. Sci. Eng.* **1982**, *46*, 77–84.
74. Baumann, H.; Timpe, H.-J.; Böttcher, H. *Z. Chim.* **1983**, *23*, 102.
75. Banks, D. F. *Chem. Rev.* **1966**, *66*, 243.
76. Beringer, F. M.; Falk, R. A. *J. Am. Chem. Soc.* **1959**, *81*, 2997.
77. Strauss, S. *Chem. Rev.* **1993**, *93*, 927.
78. Castellanos, F.; Fouassier, J. P.; Priou, C.; *et al.* U.S. Patent 5,668,192, 1997.
79. Ren, K.; Malpert, J. H.; Gu, H.; *et al. Tetrahedron* **2002**, *58*, 5267.
80. Ren, K.; Mejiritski, A.; Malpert, J.; *et al. Tetrahedron Lett.* **2000**, *41*, 8669.
81. Gu, H.; Ren, K.; Grinevich, O.; *et al. J. Org. Chem.* **2001**, *66*, 4161.
82. Ren, K.; Malpert, J. H.; Li, H.; *et al. Macromolecules* **2002**, *35*, 1632.
83. Eckberg, R. P.; LaRochelle, R. W. U.S. Patent 4,529,490, 1981; U.S. Patent 4,421,904, 1983.
84. Berry, D. A.; Greenlee, R. W.; Ellis, W. C.; *et al.* Presented at the 12th International Congress of Pure and Applied Chemistry, New York, NY, 10–13 September 1950; Abstr. p 465.
85. Castellanos, F.; Fouassier, J. P.; Priou, C.; *et al. J. Appl. Polym. Sci.* **1998**, *60*, 705.
86. Crivello, J. V. U.S. Patent 5,073,643, 1991.
87. Jacobs, P. F. *Stereolithography and Other RP&M Technologies*; Society of Manufacturing Engineers: Dearborn, MI, 1996.
88. Pappas, S. P.; Jilek, J. H. *Photogr. Sci. Eng.* **1979**, *23*, 140.
89. Welsh, K. M.; Dektar, J. L.; Hacker, N. F.; *et al. Polym. Mater. Sci. Eng. Prepr.* **1989**, *61*, 181.
90. Eberson, L. *Electron-Transfer Reactions in Organic Chemistry*; Springer-Verlag: Berlin, Germany, 1987; p 36.
91. Crivello, J. V.; Lam, J. H. W. *J. Polym. Sci., Part A: Polym. Chem.* **1979**, *17*, 1059.
92. Crivello, J. V.; Jang, M. *J. Photochem. Photobiol., A* **2003**, *159*, 173.
93. DeVoe, R. J.; Sahyun, M. R. V.; Schmidt, E. *J. Imaging Sci.* **1989**, *33*, 39.
94. Crivello, J. V. In *Photoinitiated Polymerization*; Belifield, K. D., Crivello, J. V., Eds.; ACS Symposium Series 847; American Chemical Society: Washington, DC, 2003; p 219.
95. Gomurashvili, Z.; Crivello, J. V. *J. Polym. Sci., Part A: Polym. Chem.* **2001**, *39*, 1187.
96. Dektar, J. L.; Hacker, N. P. *J. Org. Chem.* **1990**, *55*, 639.
97. Manivannan, G.; Fouassier, J. P. *J. Polym. Sci., Part A: Polym. Chem.* **1991**, *29*, 1113.
98. Fouassier, J. P.; Burr, D.; Crivello, J. V. *J. Photochem. Photobiol., A* **1989**, *49*, 317.
99. Fouassier, J. P.; Chesneau, E. *Makromol. Chem., Rapid Commun.* **1988**, *9*, 223.
100. Baumann, H.; Oertel, U.; Timpe, H.-J. *Eur. Polym. J.* **1986**, *22*, 313.
101. DeVoe, R. J.; Mitra, S. *Polym. Prepr.* **1988**, *29*, 522.
102. Ichimura, K.; Kameyama, A.; Hayashi, K. *J. Appl. Polym. Sci.* **1987**, *34*, 2747.
103. Crivello, J. V.; Lam, J. H. W. *J. Polym. Sci., Part A: Polym. Chem.* **1978**, *16*, 2441.
104. Crivello, J. V.; Bulut, U. *J. Polym. Sci., Part A: Polym. Chem.* **2005**, *43*, 5217.
105. Gandini, A.; Cheradame, H. *Adv. Polym. Sci.* **1980**, *34/35*, 215–218.
106. Bard, A. J.; Ledwith, A.; Shine, H. J. *Adv. Phys. Chem.* **1976**, *13*, 155.
107. Ledwith, A. *Polymer* **1978**, *19*, 1217.
108. Yagci, Y.; Ledwith, A. *J. Polym. Sci., Part A: Polym. Chem.* **1988**, *26*, 1911.
109. Klemm, E.; Flammersheim, H.-J.; Märtin, R.; *et al. Angew. Makromol. Chem.* **1985**, *135*, 131.
110. Crivello, J. V.; Liu, S.. *Chem. Mater.* **1998**, *10*, 3726.
111. Mowers, W. A.; Crivello, J. V.; Rajaraman, S. *RadTech Rep.* **2000**, March/April, 34–40.
112. Hua, Y.; Crivello, J. V. In *Photoinitiated Polymerization*; Belifield, K. D., Crivello, J. V., Eds.; ACS Symposium Series 847; American Chemical Society: Washington, DC, 2003; p 178.
113. Durmaz, Y. Y.; Moszner, N.; Yagci, Y. *Macromolecules* **2008**, *41*, 6714.
114. Dursun, C.; Degrimenci, M.; Yagci, Y.; *et al. Polymer* **2003**, *44*, 7389.
115. Crivello, J. V. *J. Polym. Sci., Part A: Polym. Chem.* **2008**, *46*, 3820.
116. Lalevée, J.; El-Roz, M.; Dirani, A.; *et al. Macromolecules* **2007**, *40*, 8527.
117. Lalevée, J.; El-Roz, M.; Allonas, X.; *et al. Macromolecules* **2008**, *46*, 2008.
118. Lalevée, J.; Dirani, A.; El-Roz, M.; *et al. J. Polym. Sci., Part A: Polym. Chem.* **2008**, *46*, 3042.
119. Crivello, J. V.; Lam, J. H. W. *J. Polym. Sci., Part A: Polym. Chem.* **1979**, *17*, 977.

120. Crivello, J. V.; Lam, J. H. W. *J. Org. Chem.* **1978**, *43*, 3055.
121. Crivello, J. V.; Ma, J.; Jiang, F. *J. Polym. Sci., Part A: Polym. Chem.* **2002**, *40*, 3465.
122. Shelnut, E.; Chakraborty, R.; Crivello, J. V. *J. Macromol. Sci., Part A: Pure Appl. Chem.* **2006**, *43*, 1339.
123. Stark, B. P.; Irving, E. *Ind. Chem. Bull.* **1982**, *5*, 164.
124. Chalkley, G. R.; Snowden, D. J.; Stevens, G.; Whitey, M. C. *J. Chem. Soc. (C)* **1970**, 683–687.
125. Green, G. E.; Irving, E. Eur. Patent 22081, 1980; U.S. Patent 4,299,938, 1981; U.S. Patent 4,339,567, 1982.
126. Crivello, J. V.; Lam, J. H. W. *J. Polym., Sci., Part A: Polym. Chem. Ed.* **1979**, *17*, 1047.
127. Price, C. C.; Oae, S. *Sulfur Bonding*; The Ronald Press: New York, 1962; pp 149–163.
128. Lowe, P. A. In *The Chemistry of the Sulphonium Group*; Stirling, C. J. M., Patai, S., Eds.; Wiley: New York, 1981; p 267.
129. Crivello, J. V.; Lam, J. H. W. *Synth. Commun.* **1979**, *9*, 157.
130. Akhtar, S. R.; Crivello, J. L.; Lee, J. L.; *et al. Chem. Mater.* **1990**, *2*, 732.
131. Wildi, D. S.; Taylor, S. W.; Potratz, H. A. *J. Am. Chem. Soc.* **1951**, *73*, 1965.
132. Hahn, W.; Stroh, R. U.S. Patent 2,833,827, 1958.
133. Crivello, J. V.; Lam, J. H. W. *J. Polym. Sci., Part A: Polym. Chem.* **1980**, *18*, 2677.
134. Crivello, J. V.; Lee, J. L. *Polym. Photochem.* **1982**, *2*, 219.
135. Herlihy, S. L.; Rowatt, B.; Davidson, R. S. In *Proceedings of RadTech Europe Conference*, Basel, Switzerland; Radtech Europe: Hannover, Germany, Oct 8-10 2001; p 545.
136. Dektar, J. L.; Hacker, N. P. *J. Chem. Soc., Chem. Commun.* **1987**, 1591–1592.
137. Dektar, J. L.; Hacker, N. P. *J. Am. Chem. Soc.* **1990**, *112*, 6004.
138. Tilley, M. G. Ph.D. thesis, North Dakota State University, Fargo, ND, 1988; Dissert. Abstr. No. AAC8826980.
139. Crivello, J. V. *Adv. Polym. Sci.* **1984**, *62*, 1.
140. Falk, B.; Zonca, M. R., Jr.; Crivello, J. V. *J. Polym. Sci., Part A: Polym. Chem.* **2005**, *43*, 2504.
141. Crivello, J. V.; Lee, J. L. *Polym. J.* **1985**, *17*, 73.
142. Crivello, J. V.; Lam, J. H. W. *J. Polym. Sci., Part A: Polym. Chem.* **1979**, *17*, 1059.
143. Crivello, J. V.; Hua, Y.; Gomurashvili, Z. *Macromol. Chem. Phys.* **2001**, *202*, 2133.
144. Pappas, S. P.; Tilley, M. G.; Pappas, B. C. *J. Photochem. Photobiol., A* **2003**, *159*, 161.
145. Crivello, J. V.; Lam, J. H. W. *J. Polym. Sci., Part A: Polym. Chem.* **1979**, *17*, 2877.
146. Crivello, J. V.; Lam, J. H. W. *J. Polym. Sci., Part A: Polym. Chem.* **1980**, *18*, 1021.
147. Crivello, J. V.; Kong, S. *Macromolecules* **2000**, *33*, 825.
148. Crivello, J. V.; Lee, J. L. *Macromolecules* **1983**, *16*, 864.
149. Saveant, J. M. *C. R. Hebd. Seances Acad. Sci., Ser. C* **1964**, *258*, 585.
150. Crivello, J. V.; Lee, J. L. *Macromolecules* **1981**, *14*, 1141.
151. Crivello, J. V.; Ahn, J. *J. Polym. Sci., Part A: Polym. Chem.* **2003**, *41*, 2556.
152. Crivello, J. V.; Ahn, J. *J. Polym. Sci., Part A: Polym. Chem.* **2003**, *41*, 2570.
153. Ketley, A. D.; Tsao, J. H. *J. Radiat. Curing* **1979**, *6*, 22.
154. Ledwith, A. *Polym. Prepr.* **1982**, *23*, 323.
155. Tsao, J. H. U.S. Patent 4,139,655, 1979.
156. Abadie, M. J. M.; Chia, N. K.; Boey, F. *J. Appl. Polym. Sci.* **2002**, *86*, 1587.
157. Morlet-Savary, F.; Parret, S.; Fouassier, J.-P.; *et al. J. Chem. Soc., Faraday Trans.* **1998**, *94*, 745.
158. El-Roz, M.; Lalevée, J.; Morlet-Savary, F.; *et al. J. Polym. Sci., Part A: Polym. Chem.* **2008**, *46*, 7369.
159. Yagci, Y.; Endo, T. *Adv. Polym. Sci.* **1997**, *127*, 61.
160. Yagci, Y.; Kornowski, A.; Schnabel, W. *J. Polym. Sci., Part A: Polym. Chem.* **1992**, *30*, 1987.
161. Yagci, Y.; Schnabel, W. *Macromol. Rep. A* **1993**, *30* (Suppls. 3 and 4), 175.
162. Yagci, Y.; Lukac, I.; Schnabel, W. *Polymer* **1993**, *34*, 1130.
163. Hizal, G.; Yagci, Y.; Schnabel, W. *Polymer* **1994**, *35*, 2428.
164. Bøttcher, A.; Hasebe, K.; Hizal, G.; *et al. Polymer* **1991**, *32*, 2289.
165. Johnen, N.; Kobayashi, S.; Yagci, Y.; *et al. Polym. Bull.* **1993**, *30*, 279.
166. Yagci, Y.; Kminek, I.; Schnabel, W. *Eur. Polym. J.* **1992**, *28*, 387.
167. Crivello, J. V. U.S. Patent 4,069,056, 1978.
168. Lohse, F.; Zweifel, H. *Adv. Polym. Sci.* **1986**, *78*, 61.
169. Meier, K.; Bühler, N.; Zweifel, H.; *et al.* Eur. Pat. Appl. 094915, 1983.
170. Meier, K.; Zweifel, H. *Polym. Prepr.* **1985**, *26*, 347.
171. Meier, K.; Zweifel, H. *J. Imaging Sci.* **1986**, *30*, 174.
172. Meier, K.; Rihs, G. *Angew. Chem.* **1985**, *97*, 879.
173. Hendrickson, W. A.; Palazzotto, M. C. *Adv. Chem. Ser.* **1994**, *238*, 411.
174. Meier, K.; Rihs, G. *Angew. Chem.* **1985**, *97*, 879.
175. Wang, T.; Chen, J. W.; Li, Z. Q.; Wan, P. Y. *J. Photochem. Photobiol., A* **2007**, *189*, 389.
176. Wang, T.; Li, Z. Q.; Zhang, Y.; *et al. Prog. Org. Coat.* **2009**, *65*, 251.
177. Li, M.; Chen, Y.; Zhang, H.; *et al. Prog. Org. Coat.* **2009**, *65*, 251.
178. Meier, K.; Eugster, G.; Schwarzenbach, F.; *et al.* Eur. Pat. Appl. 126712, 1986.
179. Gaube, G. G. In *Proceedings of RadTech Europe Conference*, Baltimore, MD, 3–10 May, Association for Finishing Processes, 1986; p 15.
180. Crivello, J. V.; Carter, A.; Ramdas, A.; Suh, D.-H. *J. Macromol. Sci., Part A: Pure Appl. Chem.* **1994**, *31*, 1807.
181. Crivello, J. V.; Ramdas, A. *J. Macromol. Sci., Part A: Pure Appl. Chem.* **1992**, *29*, 753.
182. Hua, Y.; Crivello, J. V. *J. Polym. Chem., Part A: Polym. Chem.* **2000**, *38*, 3697.
183. Crivello, J. V.; Lee, J. L.; Conlon, D. A. *J. Radiat. Curing* **1983**, *10*, 6.
184. Crivello, J. V.; Jo, K. D. *J. Polym. Sci., Part A: Polym. Chem.* **1993**, *31*, 1473.
185. Crivello, J. V.; Suh, D.-H. *J. Polym. Sci., Part A: Polym. Chem.* **1993**, *31*, 1847.
186. Crivello, J. V.; Malik, R.; Lai, Y.-L. *J. Polym. Sci., Part A: Polym. Chem.* **1996**, *34*, 3091.
187. Crivello, J. V.; Yoo, T.; Dougherty, J. A. *J. Polym. Sci., Part A: Polym. Chem.* **1995**, *33*, 2493.
188. Dubois, P.; Coulembier, O.; Raquez, J.-M., Eds. In *Handbook of Ring-Opening Polymerization*; Wiley-VCH: Weinheim, Germany, 2009.
189. Ivin, K. J.; Saegusa, T., Eds. In *Ring-Opening Polymerization*; Elsevier: Barking, Essex, UK, 1984; Vols. 1 and 2, pp 185–297.
190. Crivello, J. V.; Lee, J. L. *Macromol. Synth.* **1985**, *9*, 43.
191. Odian, G. *Principles of Polymerization*, 4th ed.; Wiley-Interscience: New York, 2004; p 221.
192. Decker, C.; Moussa, K. *Eur. Polym. J.* **1990**, *26*, 393.
193. Decker, C.; Moussa, K. *Makromol. Chem.* **1990**, *191*, 963.
194. Moore, J. E. In *UV Curing: Science and Technology*; Pappas, S. P., Ed.; Technology Marketing Corp.: Stamford, CT, 1978; p 134.
195. Roper, T. M.; Lee, T. Y.; Guymon, C. A.; *et al. Macromolecules* **2005**, *38*, 10109.
196. Falk, B.; Vallinas, S. M.; Crivello, J. V. *J. Polym. Sci., Part A: Polym. Chem.* **2003**, *41*, 579.
197. Bulut, U.; Crivello, J. V. *Macromolecules* **2005**, *38*, 3584.
198. Crivello, J. V. In *Basics and Applications of Photopolymerization Reactions*; Fouassier, J.-P., Allonas, X., Eds.; Research Signposts: Trivandrum, India, 2010; Vol. 2, pp 101–117.
199. Carter, W.; Jupina, M. In *Proceedings of RadTech Europe Conference*, 3–5 November 2003; Berlin, Germany; Radtech Europe: Hannover, Germany, Vol. 1, p 243.
200. Sasaki, H. *Prog. Org. Coat.* **2007**, *58*, 227.
201. Crivello, J. V.; Lee, J. L. In *The UV Cure of Epoxy-Silicone Monomers*; ACS Symposium Series; Hoyle, C. J.; Kinstle, J. F., Eds.; 417; American Chemical Society: Washington, DC, 1989; p 398.
202. Crivello, J. V.; Jang, M. In *Science and Technology of Silicones and Silicones-Modified Materials*; Clarson, S. J.; Fitzgerald, J. J.; Owen, M. J.; Smith, S. D., Eds.; ACS Symposium Series, 729; American Chemical Society: Washington, DC, 2007; p 27.
203. Koleske, J. V. U.S. Patent 4,593,051, 1986; U.S. Patent 4,892,894, 1990.
204. Smith, G. H. U.S. Patent 4,256,828, 1981.
205. Crivello, J. V.; Lam, J. H. W. *J. Polym. Sci., Polym. Lett.* **1979**, *17*, 759.
206. Pappas, S. P. *Radiat. Phys. Chem.* **1977**, *25*, 633.
207. Timpe, H.-J. *Pure Appl. Chem.* **1988**, *60*, 1033.
208. Oxman, J. D.; Jacobs, D. W.; Rom, M. X.; *J. Polym. Sci., Part A: Polym. Chem.* **2005**, *43*, 1747.
209. Sasaki, H.; Crivello, J. V. *J. Macromol. Sci., Part A: Pure Appl. Chem.* **1992**, *29*, 915.
210. Crivello, J. V.; Sasaki, H. *J. Macromol. Sci., Part A: Pure Appl. Chem.* **1993**, *30*, 189.
211. Sasaki, H.; Kuriyama, A.; Kakuchi, T. *J. Macromol. Sci., Part A: Pure Appl. Chem.* **1995**, *32*, 1699.
212. Sasaki, H.; Rudzinnski, J. M.; Kakuchi, T. *J. Polym. Sci., Part A: Polym. Chem.* **1995**, *33*, 1809.
213. Crivello, J. V.; Narayan, R. *Chem. Mater.* **1992**, *4*, 692.
214. Crivello, J. V.; Narayan, R.; Sternstein, S. S. *J. Appl. Polym. Sci.* **1997**, *64*, 2073.
215. Zou, K.; Soucek, M. D. *Macromol. Chem. Phys.* **2004**, *205*, 2032.
216. Chen, J.; Soucek, M. D.; Simonsick, W. J.; Celikay, R. W. *Polymer* **2002**, *43*, 5379.
217. Lu, J.; Wool, R. P. *J. Appl. Polym. Sci.* **2006**, *99*, 2481.
218. Crivello, J. V.; Narayan, R.; Bratslavsky, S. A.; *et al. Makromol. Chem., Macromol. Symp.* **1996**, *107*, 75.

219. Jacobs, P. F., Ed. In *Rapid Prototyping & Manufacturing: Fundamentals of Stereolithography*; Society of Manufacturing Engineers: Dearborn, MI, 1992.
220. Corcione, C. E.; Greco, A.; Maffezzoli, A. *J. Therm. Anal. Calorim.* **2003**, *72*, 687.
221. Gelorme, J. D.; Cox, R. J.; Guitierrez, S. A. R. U.S. Patent 4,882,245, 1989.
222. Gates, B. D.; Xu, Q.; Love, C.; *et al. Annu. Rev. Mater. Res.* **2004**, *34*, 339.
223. Crivello, J. V. *J. Photopolym. Sci. Technol.* **2007**, *20*, 599.
224. Chung, D.; Kim, J. P.; Kim, D.; *et al. J. Ind. Eng. Chem.* **2006**, *12*, 793.
225. Ingwall, R. T.; Waldman, D. A. *Springer Ser. Opt. Sci.* **2000**, *76*, 176.
226. Muller, D. C.; Falcou, A.; Reckefuss, N.; *et al. Nature* **2003**, *421*, 829.
227. Lazauskaite, R.; Grazulevicius, J. V. *Adv. Polym. Technol.* **2005**, *16*, 571.
228. Ge, J.; Trujillo-Lemon, M.; Stansbury, J. W. *Macromolecules* **2006**, *3*, 8968.
229. Kutal, C.; Sarpone, N. *Adv. Chem. Ser.* **1993**, *238*, 1–250.
230. Wang, Z.; Kutal, C. *Inorg. Chim. Acta* **1994**, *226*, 285.
231. Kutal, C.; Grutsch, P. A.; Yang, D. B. *Macromolecules* **1991**, *24*, 6872.
232. Gamble, G.; Grutsch, P. A.; Lavalee, R. J.; *et al. 15th Conf. Coord. Chem.* **1995**, *239*; *Chem. Abstr.* **1995**, *124*, 56811.
233. Sanderson, C. T.; Quinlan, J. A.; Conover, R. C.; *et al. Inorg. Chem.* **2005**, *44*, 3283.
234. Kuroki, M.; Aida, T.; Inoue, S. *J. Am. Chem. Soc.* **1987**, *109*, 4737.
235. Watanabe, Y.; Aida, T.; Inoue, S. *Macromolecules* **1990**, *23*, 2612.
236. Nishikubo, T.; Kameyama, A.; Toya, Y. *Polym. J.* **1997**, *29*, 450.

Biographical Sketch

Dr. James V. Crivello received his BS degree in chemistry from Aquinas College in Grand Rapids, Michigan, in 1962 and his PhD degree in organic chemistry from the University of Notre Dame in 1966. He joined the General Electric Corporate Research and Development Center in 1966 and was for several years a research project manager. His fields of activity include organic nitrations, oxidations, arylations, polyimides, silicones, and new photo- and thermal initiators for cationic and free radical polymerizations. In 1980, he was elected a Coolidge Fellow by the staff at the GE Corporate Research and Development Center and spent the 1986–87 year as a visiting scientist at the University of Mainz in the Federal Republic of Germany with Prof. Helmut Ringsdorf. He joined the faculty at the Rensselaer Polytechnic Institute in 1988 as professor, and currently, he directs a number of graduate students and postdoctoral associates in various aspects of research in the synthesis of polymers and copolymers by cationic, free radical, and transition metal catalysis.

4.38 Frontal Polymerization

JA Pojman, Louisiana State University, Baton Rouge, LA, USA

4.38.1 What Is Frontal Polymerization?

Frontal polymerization (FP) is a polymerization process in which polymerization occurs directionally in a localized reaction zone. There are three types of FP. The first is photofrontal polymerization in which the front is driven by the continuous flux of radiation, usually UV light.[1–7] The second is isothermal frontal polymerization (IFP), which is based on the 'gel effect' to create a localized reaction zone to propagate slowly from a polymer seed. The last type is thermal frontal polymerization,

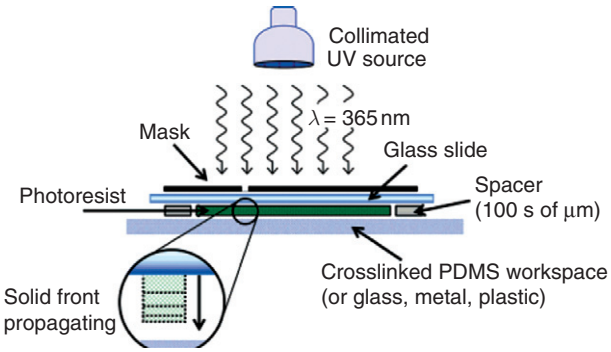

Figure 1 A schematic of photofrontal polymerization method used to prepare microfluidic chips. Reprinted with permission from Cabral, J. T.; Hudson, S. D.; Harrison, C.; Douglas, J. F. *Langmuir* **2004**, *20*, 10020–10029.[7] Copyright 2004 American Chemical Society.

and it results from the coupling of thermal transport and the Arrhenius dependence of the reaction rate of an exothermic polymerization (Figure 1).

Photofrontal polymerization produces fronts whose positions depend logarithmically on time if the initiator continues to absorb light and linearly on time if the initiator is photobleached. It is limited in application to unfilled systems. IFP propagates on the order of 1 cm day^{-1} and only for total distances of about 1 cm. Thermal frontal polymerization has the widest range of velocities and types of chemistries that can be used.

4.38.2 Photofrontal Polymerization

Photofrontal polymerization requires a continuous input of radiation, usually UV light, to create a propagating front. Koike *et al.*[8] and Ohtsuka and Koike[9] used photofrontal polymerization to create gradient optical materials (see next section). Briskman[4] and Righetti *et al.*[10] studied photopolymerization of acrylamide in weightlessness. The reaction mixture was composed of 18% aqueous solution of acrylamide with methylenebisacrylamide (0.46%), catalyst (tetramethylenediamide, 0.01%), and riboflavin (4.9×10^{-4}%) as the initiator. The illumination was provided by a lamp with a maximum intensity at 4450 Å. The experiment was performed in weightlessness (on the *Mir* space station) because buoyancy-driven convection was generated by the temperature and concentration gradients. In the absence of convection, the front position increased with the logarithm of illumination time. This reflects the exponential distribution of illumination in the sample caused by the absorption of the riboflavin.

Cabral *et al.*[7] developed a beautiful application of photofrontal polymerization for producing microfluidic chips. By illuminating through a glass plate in contact with a polymerizable resin, they created patterns that grew from the surface. If the polymer possessed the same absorption properties as the resin, then the front propagation was proportional to the logarithm of the dose (Figure 2). However, if the polymer absorbed more light than the resin, the position versus the logarithm of the dosage exhibits curvature. Warren *et al.*[11] analytically solved the phase-field model of the process.

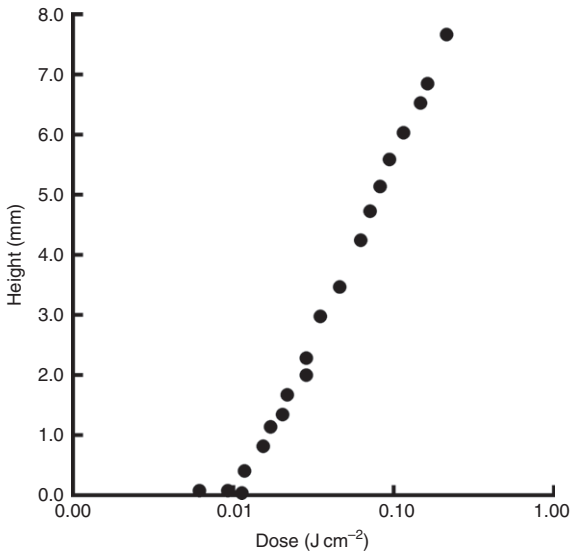

Figure 2 'Photoinvariant' polymerization: frontal kinetics of resist material whose transmission remains constant upon UV exposure. Adapted from Cabral, J. T.; Hudson, S. D.; Harrison, C.; Douglas, J. F. *Langmuir* **2004**, *20*, 10020–10029.[7]

If the photoinitiator is bleached, then a front with a constant velocity can be created. Terrones and Pearlstein[5] considered a model of free-radical photopolymerization with a photobleaching initiator. They derived an analytical expression for the front speed of the localized traveling wave

$$\text{Front speed} = \frac{\phi I_0}{C_{A,0}}$$

where ϕ, I_0, and $C_{A,0}$ are the quantum yield of the photoinitiator, incident intensity, and photoinitiator concentration, respectively. They predicted and confirmed numerically that front velocity does not depend on the absorption coefficient of the initiator, as long as it is sufficiently large. However, the front profile is a function of the coefficient.

4.38.3 Isothermal Frontal Polymerization

IFP is a slow process in which a localized polymerization propagates from a solid polymer piece into a solution of its monomer and a thermal radical initiator. The typical experiment requires placing a piece of high-molecular-weight poly (methyl methacrylate) (PMMA), the 'seed' in a solution of methyl methacrylate and azobisisobutyronitrile (AIBN). The monomer-initiator solution dissolves the polymer seed, creating a highly viscous 'gel' region (Figure 3). The initiator is decomposing throughout the system and initiating

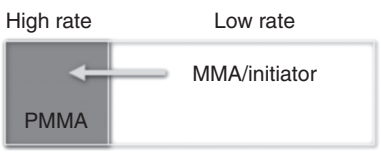

Figure 3 Schematic of isothermal frontal polymerization.

polymerization but because of the Norrish–Trommsdorff effect (gel effect),[12,13] the rate of polymerization is higher in the gel region than that in the rest of the solution.

Koike *et al.*[14] first discovered this process and called it 'interfacial gel polymerization'. He was interested in producing Gradient Refractive INdex (GRIN) optical materials.[14–24] GRIN materials are formed by dissolving a dopant in the monomer. Usually, the dopant possesses a higher refractive index than the polymer. As the front propagates, the dopant is partially incorporated in the polymer such that the dopant's concentration increases in the bulk solution. If the front is performed in a cylindrical geometry with the polymer seed in the form of an annulus, then as the front propagates toward the center, the dopant concentration increases. When all the monomer finally polymerizes, a gradient in dopant concentration remains, which creates a gradient in refractive index. As we can observe in **Figure 4**, the flat disk of PMMA magnifies the letters because of the gradient of naphthalene that was created.

Such GRIN cylinders are useful because they can be used in optics.[8,25] More importantly, such cylinders can be drawn into GRIN optical fibers, which have a higher bandwidth for data transmission than step-index fibers.[16,26]

For all the work carried out on polymeric GRIN materials via interfacial gel polymerization in the 1980s and 1990s, little work was performed on the actual front propagation process. Golubev *et al.*[27] proposed a mechanism in 1992. Gromov and Frisch[28] proposed a mathematical model that was flawed. Ivanov *et al.* did work with IFP in 1997[29] and 2002.[30]

Lewis *et al.*[31] used the deflection of a sheet of laser light to measure the position of the front and measure the magnitude of the gradient between the monomer and polymer. In 2005, they confirmed the proposed mechanism of IFP from experiments and numerical modeling.[32,33] Evstratova *et al.*[34] confirmed that the process is indeed isothermal and there exists a minimum molecular weight required for the seed.

The fronts propagate a short distance because polymerization is occurring throughout the solution, and the fronts stop propagating when the monomer has bulk polymerized.

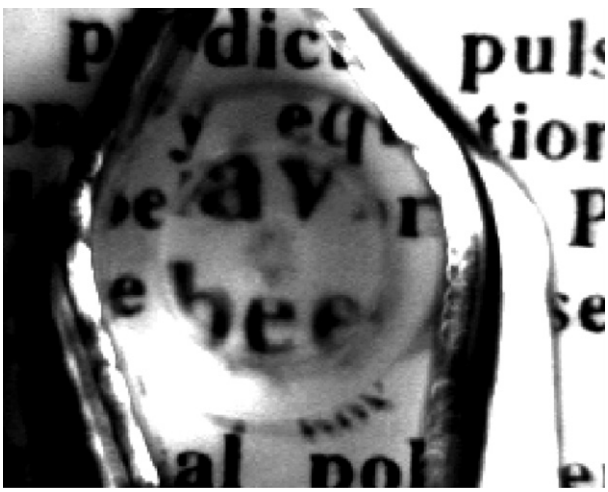

Figure 4 An image of a GRIN lens created by a radically propagating front of methyl methacrylate polymerization from an annulus (1.5 cm) of PMMA. Naphthalene was initially present in the monomer and accumulated as the front propagated inward.

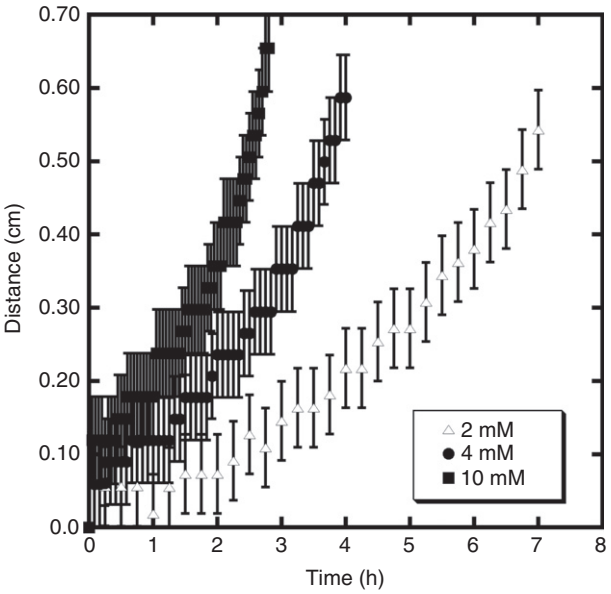

Figure 5 The front position versus time for three different concentrations of AIBN in methyl methacrylate at 50 °C. Data courtesy of L. Lewis.

Because of the slow bulk polymerization, the front accelerates (**Figure 5**). This is because as the front propagates, it enters region of higher and higher conversion, which means it takes less time for the reaction in the front to reach high viscosity and thus high reaction rate. This is analogous to smoldering.[35] If a piece of paper is uniformly heated until smoldering commences and then a flame is ignited at one end, the flame will accelerate as it propagates. The temperature is analogous to the conversion in the polymer case.

Volpert and his colleagues have performed mathematical analysis of IFP,[32,36,37] and modeled how the nonuniform dopant distribution arises.[38]

Short front propagation is adequate for many applications, but propagation over greater distances than a centimeter is possible. Masere *et al.*[39] used IFP to create gradients of dyes over several centimeters by performing the experiments at 4 °C with trioctylmethyl ammonium persulfate.[40] Ivanov *et al.*[29] used a polymeric inhibitor that would not diffuse into the gel region but did prevent polymerization in the bulk solution.

IFP is a useful technique for producing gradient optical materials but it is limited to free-radical systems that exhibit the gel effect and whose polymers are soluble in their monomers.

4.38.4 Cryogenic Fronts

A fascinating mode of frontal polymerization at temperatures of 77 K and below was developed at the Institute of Chemical Physics in Chernogolovka, Russia.[41–47] Many systems can be polymerized by this method, including acetaldehyde, formaldehyde, cyclopentadiene, and methyl methacrylate. Filled polymers, such as acetaldehyde and alumina, can also be prepared.[48]

The mechanism of propagation is via a non-Arrhenius mechanism. The monomer is frozen at a temperature from

4 to 77 K and then irradiated with gamma radiation. A monomer such as methyl methacrylate is cooled in liquid nitrogen or even liquid helium. Fronts are started by heating the surface. Temperature and density gradients arising in the reaction are responsible for further layer-by-layer disruption of the solid sample and creation of the surface on which the reaction continues. Because of this positive feedback between the solid-phase chemical reaction and the cracking of the frozen reagents, the polymerization proceeds in a layer-by-layer fashion and propagates through the entire sample as a front.

For example, epichlorohydrin can be rapidly cooled to 77 K and then irradiated with 680 kGy dose of gamma radiation.[43] A polymerization front with a velocity of 1.3 cm s^{-1} propagated after fracturing a small region of the sample. Cations formed by the irradiation were released by the cracking and a wave of polymerization resulted.

4.38.5 Thermal Frontal Polymerization

Thermal frontal polymerization is a process in which a localized reaction zone propagates from the coupling of thermal diffusion and the Arrhenius dependence of reaction rate of an exothermic polymerization. Thermal frontal polymerization was discovered at the Institute of Chemical Physics in Chernogolovka, Russia by Chechilo and Enikolopyan. They studied methyl methacrylate polymerization under 3500 atm pressure.[49–52] (We will consider later why these extreme conditions were used.) The literature from that Institute was reviewed in 1984.[53] Pojman[54] rediscovered what he called 'traveling fronts of polymerization' in 1991. Pojman *et al.*[55] reviewed the field in 1996. There have been other focused reviews.[56,57]

Thermal frontal polymerization is by far the most commonly studied form of FP, so we will henceforth refer to it as 'FP'. We will first consider the necessary conditions for FP and give an overview of the types of systems that have been studied.

4.38.5.1 Origins

Thermal fronts have been used in a process discovered in 1967 by Merzhanov and co-workers[58] called self-propagating high-temperature synthesis (SHS) to prepare ceramics and intermetallic compounds.[59–64] Secondly, such fronts demonstrate a variety of dynamical behavior, including planar fronts, spin modes,[65–68] and chaotically propagating fronts.[69]

Chechilo *et al.*[52] were the first to study FP. They studied methyl methacrylate polymerization with benzoyl peroxide as the initiator. **Figure 1** is taken from their original data. They performed the reactions in closed metal reactors under pressure so they were unable to directly observe the front.

Chechilo and Enikolopyan[51] studied the effect of pressure on the velocity. Raising the pressure (up to 5000 atm) increased the velocity by effectively increasing the concentration of the monomer and increasing the polymerization rate constant. They reported that drops of polymer descended from the front, which underwent a convective breakdown. By increasing the pressure to > 3500 atm, the instability was eliminated by possibly reducing the density difference between monomer and polymer and/or increasing the monomer/polymer viscosities.

In bulk polymerizations, as the viscosity increases, the rate of termination decreases causing autoacceleration, which is called the gel effect.[12,13] For a monomer such as methyl methacrylate, the gel effect can play a significant role in the kinetics. Davtyan *et al.*[70] examined the influence of the gel effect on the kinetics of radical polymerization in a front.

4.38.5.2 Attempts at Frontal Polymerization Reactors

A natural early goal of FP researchers was to develop a reactor in which the monomer–initiator solution was pumped in such that the product would continuously flow out, without the input of heat. Attempts were made with reactors of cylindrical and spherical geometries. Zhizhin and Segal[71] performed a linear stability analysis of a reactor consisting of two concentric cylinders. A radial, axisymmetric front was supposed because the monomer/initiator would be pumped through the permeable inner cylinder. The viscous reacted polymer was supposed to flow out through the outer permeable cylinder. No buoyancy-driven convection was included. They found that if the resistance of the outer boundary was small, the front would become hydrodynamically unstable. They also considered a reactor with concentric spheres and found similar results.

Volpert and Volpert and their colleagues in Chernogolovka continued these analytical and numerical studies.[72–77] They found cases where the front would become unstable and develop spin modes and multiple steady states, which we will discuss in detail later. More numerical studies were performed for the spherical case by Solovyov *et al.*[78] They found that the front could be unstable, and chaotic oscillations with low frequency could result.

All the studies ignored the difference in density between reactants and product, which meant they could not consider how buoyancy-driven convection would affect the reactor performance. From work, we will consider shortly, convective instabilities are a major interference when using monomers that form molten polymer.

4.38.5.3 Requirements for Frontal Polymerizations

For a system to support FP, it must have a low rate of reaction at the initial temperature but have a very high rate of reaction at a temperature between the initial temperature and the adiabatic reaction temperature. What we mean by the 'adiabatic reaction temperature' is the temperature reached if the reaction went to completion without heat loss. Clearly, the reaction must be exothermic. The essential criterion for FP is that the system must have an extremely low rate at the initial temperature but a high rate of reaction at the front temperature such that the rate of heat production exceeds the rate of heat loss. In other words, the system must react slowly or not at all at room temperature, have a large heat release, and have a high energy of activation. For free-radical polymerization, the peroxide or nitrile initiator provides the large activation energy. As we will discuss later, it is not possible to create a system that has a long pot life at room temperature and a rapid reaction at any arbitrary temperature if the system follows Arrhenius kinetics.

Thermal polymerization fronts can exhibit a wide range of interesting dynamical behavior.[79,80] Fronts do not have to propagate with a constant velocity or constant shape but can be affected by buoyancy-driven convection and/or intrinsic

thermal instabilities. Some of these phenomena significantly affect FP and must be considered; others are of more interest to those collecting nonlinear phenomena.[80]

4.38.5.4 Starting Fronts

Fronts can be started by any process that will raise the starting materials to a temperature high enough that the rate of heat production will exceed heat loss. Three methods have been used. The most common is to use a thermoelectric heater such as a soldering iron. With benzoyl peroxide as the initiator, *N*,*N*-dimethylaniline can be added to cause the peroxide to rapidly decompose in the location in which it is added. The other method is to use a UV light with a system that contains both photoinitiator and thermal initiator. Ritter *et al.*[81] analytically considered the necessary conditions for ignition. Heifetz *et al.*[82] performed numerical simulations determining how the temperature of a constant temperature heat source affected the ability to initiate a front with heat loss.

Nason *et al.*[83] examined the conditions for photoinitiation of FP of trimethylolpropane triacrylate with Luperox 231 as the thermal initiator and Darocur 4265 as the photoinitiator. They found that there was an optimal concentration of photoinitiator to achieve the shortest start time for the front (**Figure 6**).

4.38.5.5 Free-Radical Frontal Polymerization

Free-radical chemistry is the most amenable to FP because the reactions can be rapid, very exothermic, and with a high energy of activation controlled by the type of initiator. A number of radical polymerization reactions are highly exothermic and able to support the FP regime. A free-radical polymerization with a thermal initiator can be approximately represented by a three-step mechanism. First, an unstable compound, usually a peroxide or nitrile, decomposes to produce radicals:

$$I \rightarrow f2R\bullet \qquad [1]$$

where f is the efficiency, which depends on the initiator type and the solvent. A radical can then add to a monomer to initiate a growing polymer chain:

$$R\bullet + M \rightarrow P_1\bullet \qquad [2]$$

$$P_n^{\bullet} + M = P_{n+1}^{\bullet} \qquad [3]$$

The propagation step [3] continues until a chain terminates by reacting with another chain (or with an initiator radical):

$$P_n^{\bullet} + P_m^{\bullet} \rightarrow P_n + P_m(\text{or } P_{n+m}) \qquad [4]$$

The major heat release in the polymerization reaction occurs in the propagation step. However, the propagation step does not have a sufficiently high activation energy to permit a front. FP autocatalysis is controlled by the energy of activation of the initiator decomposition. The steady-state assumption in the polymerization model gives an approximate relationship between the effective activation energy of the entire polymerization process and activation energy of the initiator decomposition reaction:

$$E_{\text{eff}} = E_{\text{p}} + \left(\frac{E_{\text{i}}}{2}\right) - \left(\frac{E_{\text{t}}}{2}\right) \qquad [5]$$

where E_{p} is the activation energy of the propagation step, E_{i} is that for the initiator decomposition, and E_{t} is that for the termination step.

The second term in the right-hand side of eqn [5] depends on the initiator. Because it has the largest magnitude, this value mostly determines the effective activation energy. Because of this, the initiator plays a significant role in determining if a front will exist, and if so, temperature profile in the front and how fast the front will propagate.

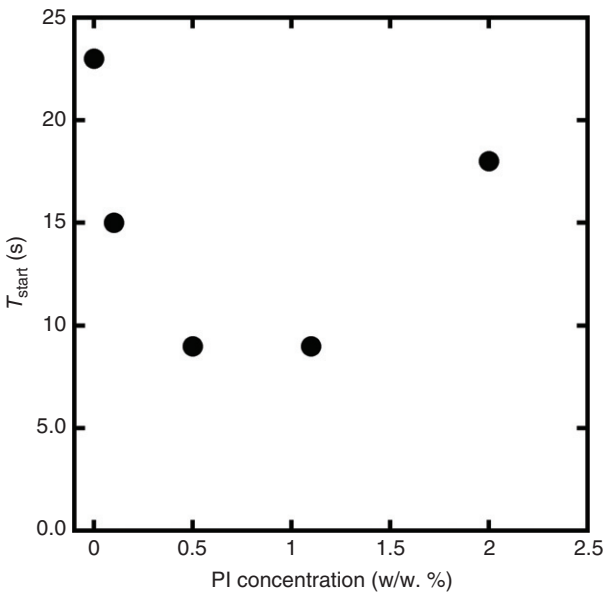

Figure 6 The time until front ignition as a function of photoinitiator concentration for irradiance of 5.9 mW cm^{-2} with 0.4 wt.% Luperox 231 for trimethylolpropane triacrylate. Adapted from Nason, C.; Roper, T.; Hoyle, C.; Pojman, J. A. *Macromolecules* **2005**, *38*, 5506–5512.[83]

4.38.5.6 Properties of Monomers

Some requirements on the physical properties of the polymerization medium itself must also be met. In the early papers on FP, the authors[49–52] applied very high pressure (up to 5000 atm) to eliminate monomer boiling (methyl methacrylate) and the reaction zone decay due to the density gradient in the reaction zone (Rayleigh-Taylor instability). They also managed to observe only downward traveling fronts because natural convection rapidly removed heat from the reaction zone of an ascending front leading to extinction. However, at pressures less than 1500 atm, descending fronts decayed because the polymer was denser than the monomer. Thus, unless a sufficiently high pressure is applied, it is not possible to obtain a polymerization front with methyl methacrylate (**Figure 7**).

We describe cases when FP is expected to be observed. The first case is the polymerization of crosslinking monomers (thermosets). The second group of monomers form polymers that are insoluble in the monomer. Good examples are acrylic and methacrylic acids.[54,84,85] Insoluble polymer particles adhere to each other during their formation and stick to the reactor or test tube walls, forming a mechanically stable phase and discernible polymer–monomer interface. Nonetheless, Rayleigh–Taylor and double-diffusive instabilities, which we will discuss

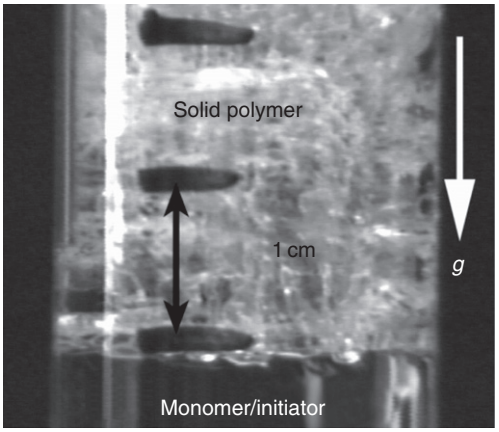

Figure 7 A descending front of triethylene glycol dimethacrylate polymerization with benzoyl peroxide as the initiator.

in Section 4.38.5.16.1, partially develop in such systems and manifest themselves as fingering.[54,86] How well the front sustains itself depends on conversion, the polymer glass transition temperature, and molecular weight distribution. Indeed, these properties themselves depend on the initial reactant temperature, initiator type, and concentration.[84]

Nagy and Pojman developed a technique to suppress fingering with methacrylic acid fronts in which the tube was rotated around the axis of front propagation.[87] The front velocity depended on the fourth power of the rotational frequency, and the amplitude of the front curvature was proportional to the square of the frequency.

The third group of monomers includes all highly reactive monomers that produce thermoplastic polymers, which are molten at the front temperature. Such fronts decay due to the Rayleigh–Taylor instability. Although these polymers are soluble in their monomers (given sufficient time), on the time scale of the front the polymer is effectively immiscible with the monomer. Adding inert filler such as ultrafine silica gel or a soluble polymer increases the viscosity and eliminates the front collapse. Some monomers such as styrene and methyl methacrylate require moderate pressure (20–30 atm) to eliminate monomer boiling. Higher-boiling-temperature monomers like butyl acrylate support the frontal regime at ambient pressure in test tubes. FP of the third group of monomers can be realized in any orientation because the large viscosity (of the monomer-Cabosil system) suppresses natural convection.

All FP monomers should be highly reactive to maintain the reaction in the presence of heat losses that always occur, and are especially important in narrow tubes. The frequency factor for the propagation rate coefficient should be at least $A_p \geq 10^5 \,\mathrm{l\,mol^{-1}\,s^{-1}}$, based on experience with reactions in the test tubes with less than 3 cm diameter at ambient temperature. A polymerization front is a thermal wave having existence conditions with respect to the heat loss intensity. In some cases, the problem of quenching can be solved by using larger diameter test tubes or preheating the initial reactants. Preheating will not work with a fast decomposing initiator, for example, AIBN, because of the homogeneous reaction in the bulk monomer.

4.38.5.7 Frontal Polymerization in Solution

FP of several reactive monomers can be performed in high boiling point solvents.[88] Acrylamide polymerization will propagate in water (with some vaporization of water),[89,90] in dimethyl sulfoxide (DMSO)[91] and in dimethyl formamide (DMF) with several initiators, including sodium persulfate, potassium persulfate, ammonium persulfate, and benzoyl peroxide. Interestingly, no gas bubbles are observed with acrylamide/persulfate in DMSO. (The persulfates do not produce volatile side products.) Several other monomers also work in these solvents, including acrylic acid, sodium methacrylate, and zinc dimethacrylate.[88]

For a monomer to support FP in a solvent, the enthalpy of the reaction must be sufficiently high that dilution does not lower the front temperature below a front-sustaining value. Dimethylbenzene can be used with polyurethane synthesis.[92]

Fronts of acrylamide in DMSO (1:1) are not destroyed by the Rayleigh–Taylor instability ('fingering') because the polyacrylamide gels. However, a monomer such as acrylic acid, which does not gel in DMSO, exhibits rampant fingering and will not propagate without the addition of a few percent of bisacrylamide (a difunctional monomer), which produces a crosslinked and solid product. The same is true for acrylamide in DMF.

4.38.5.8 Temperature Profiles

A polymerization front has a very sharp temperature profile, and profile measurements can provide much useful information. The temperature profiles help elucidate the reasons for incomplete conversion and the structure of the front. Two temperature profiles measured during FP of methacrylic acid are shown in Figure 8. The first profile is for benzoyl peroxide in methacrylic acid at different initial temperatures. The other profile was obtained for the same monomer with *tert*-butyl peroxide (*t*BPO). Conversion is directly proportional to the

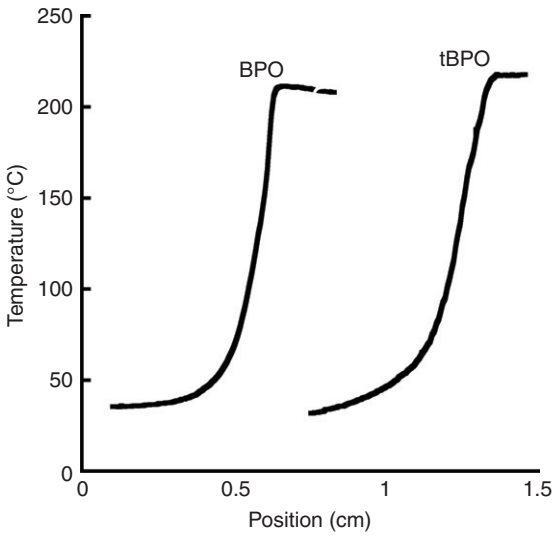

Figure 8 Spatial temperature profiles for methacrylic acid polymerization fronts: 2% w/v of benzoyl peroxide (BPO), 12.5% v/v of *tert*-butyl peroxide (*t*BPO). Adapted from Pojman, J. A.; Ilyashenko, V. M.; Khan, A. M. *J. Chem. Soc. Faraday Trans.* **1996**, *92*, 2825–2837.[55]

difference between the maximum and initial temperatures. The *t*BPO profile reflects the use of a more stable initiator, which led to the highest conversion and widest heat conductivity zone. All these facts point to initiator burn out, that is, when the initiator has been exhausted before the reaction has been completed, more stable initiators give higher conversion. The methacrylic acid front with *t*BPO was significantly slower in spite of having the highest reaction temperature. This means that the effective activation energy of a polymerization front is directly correlated to the activation energy of the initiator decomposition, as was expected.

4.38.5.9 Velocity Dependence on Initiator Concentration

Chechilo *et al.*[52] studied methyl methacrylate polymerization with benzoyl peroxide as the initiator. By placing several thermocouples, they could infer the front velocity and found a 0.36 power dependence for the velocity on the benzoyl peroxide concentration. More detailed studies for several initiators showed 0.223 for *t*BPO, 0.324 for BPO, and 0.339 for cyclohexylperoxide carbonate.[50]

Pojman *et al.* reported a detailed study of Triethylene glycol dimethacrylate (TGDMA) FP.[84] The power functional dependence for velocity versus initiator concentration was different for all three: AIBN (0.20), BPO (0.23), and LPO (0.31).

Khanukaev *et al.*[93,94] considered the theory of front propagation in terms of conversion and velocity as a function of initial temperature. Because of the high front temperature, all the initiator can decompose before all the monomer has reacted. The result is initiator 'burn out', which decreases conversion and velocity. High initial temperatures exacerbate this effect. Using their theory, they correctly predicted the conversion for one experiment with methyl methacrylate (46%) and a velocity of $0.12\,\mathrm{cm\,min^{-1}}$.

The most careful study of velocity as a function of experimental parameters was performed by Goldfeder *et al.*[95] They considered the FP of butyl acrylate containing fumed silica (to suppress convection) in a custom-built reactor that allowed temperature control at 50 atm pressure (to suppress bubbles). They developed analytical solutions for the front velocity as a function of initiator concentration and initial temperature.

4.38.5.10 Front Velocity as a Function of Temperature

The front velocity is a function of the initial temperature and the ΔT of the reaction, where ΔT is determine by the $|\mathrm{DH}| \times M_0/C_p$. The value of ΔT is also affected by the presence of any inert material. Goldfeder *et al.*[95] derived an expression for the front velocity in terms of the parameters for a free-radical polymerization. The velocity is a function of κ, the thermal diffusivity ($0.0014\,\mathrm{cm^2\,s^{-1}}$), T_b, k_d^0 = the preexponential factor for the initiator decomposition ($4 \times 10^{12}\,\mathrm{s^{-1}}$), $E_1 = E_d$ = the energy activation for the dissociation constant for the initiator = 27 kcal mol^{-1}, R_g is the ideal gas constant.

$$u^2 = \frac{\kappa R_g T_b^2}{2E_1(T_b - T_0)} k_d^0 e - E_d/R_g T_b \qquad [6]$$

The model worked well for butyl acrylate. Figure 9 shows the results for the experiment and analytical solution as well as numerical simulations with the complete model. This model does not work with multifunctional monomers.

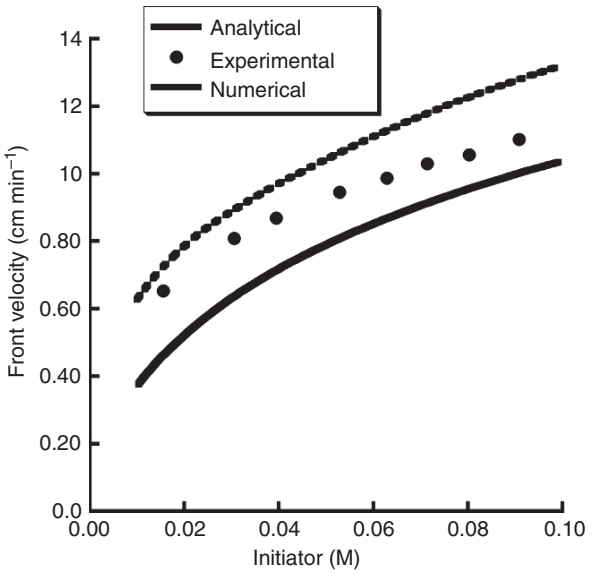

Figure 9 Comparison of the velocity dependence on the AIBN concentration for the frontal polymerization of butyl acrylate at 278 K, determined experimentally, numerically and analytically. Adapted from Goldfeder, P. M.; Volpert, V. A.; Ilyashenko, V. M.; *et al. J. Phys. Chem. B* **1997**, *101*, 3474–3482.[95]

4.38.5.11 The Effect of Type of Monomer and Functionality on Front Velocity

Fronts with methacrylates propagate more slowly than with acrylates, as would be expected from the lower reactivity of the methacrylate. Nason *et al.*[83] studied the velocity for many different acrylates and methacrylates (Figure 10). In Figure 11, we can see how the front velocity varies with the inverse of the molecular weight per acrylate group. Front velocities can reach as high as $50\,\mathrm{cm\,min^{-1}}$ for both triacrylates and tetraacrylates with high concentrations of initiator.

The high velocity is consistent with the behavior of multifunctional acrylates. Once gelation occurs, the rate of termination decreases and so the overall rate of polymerization increases. Thus, the multifunctional acrylates exhibit an extreme gel effect that causes them to polymerize very rapidly. This crosslinking also affects the manner of front propagation, as we will discuss in section 4.38.5.16.4.

4.38.5.12 Solid Monomers

Pojman *et al.*[96] demonstrated that acrylamide could be polymerized frontally without solvent. Using a rock tumbler, they ground acrylamide and various solid initiators, including benzoyl peroxide, AIBN, potassium persulfate, ceric ammonium nitrate, ceric ammonium sulfate, bromate/malonic acid, lead dioxide, and lithium nitrate. The conversion was determined by adding bromine[97] and titrating the excess iodimetrically.[98] The number of growing chains that are terminated by an initiator radical (primary termination) increases with higher concentrations of initiator, decreasing conversion. The degree

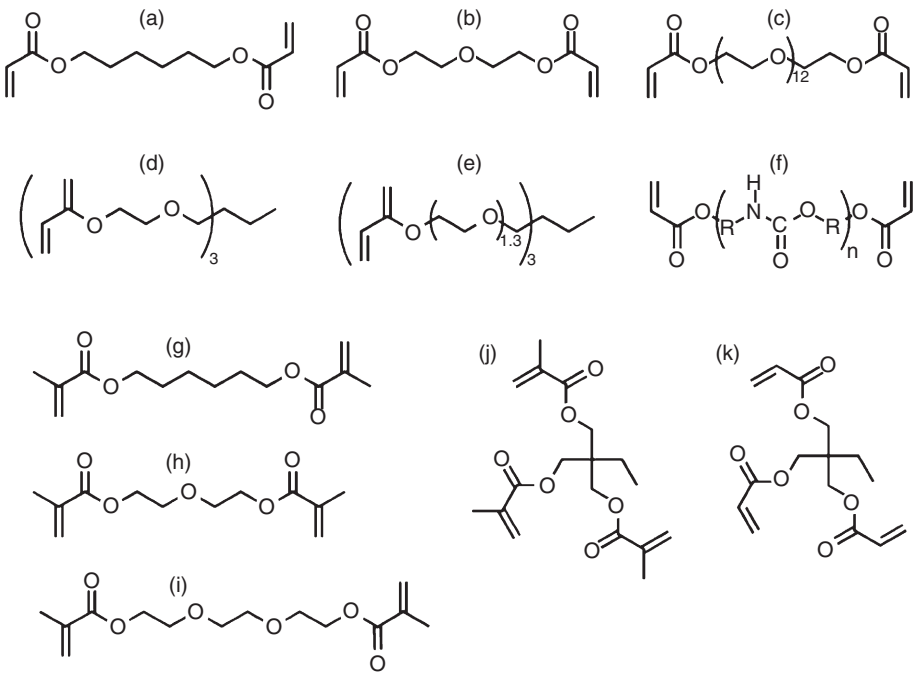

Figure 10 Chemical structures of some acrylate and methacrylate monomers: (a) hexanediol diacrylate (HDDA), (b) diethylene glycol diacrylate (DEGDA), (c) poly(ethylene glycol) diacrylate (PEGDA), (d) trimethylolpropane ethoxy triacrylate (TMPEOTAI), (e) trimethylolpropane ethoxy triacrylate (TMPEOTA-II), (f) difunctional urethane acrylate (Ebecryl 8402), (g) hexanediol dimethacrylate (HDDMA), (h) diethylene glycol dimethacrylate (DEGDMA), (i) triethylene glycol dimethacrylate (TREGDMA), (j) trimethylolpropane trimethacrylate (TMPTMA), (k) trimethylolpropane triacrylate (TMPTA). Reprinted with permission from Nason, C.; Roper, T.; Hoyle, C.; Pojman, J. A. *Macromolecules* **2005**, *38*, 5506–5512.[83] Copyright 2005 American Chemical Society.

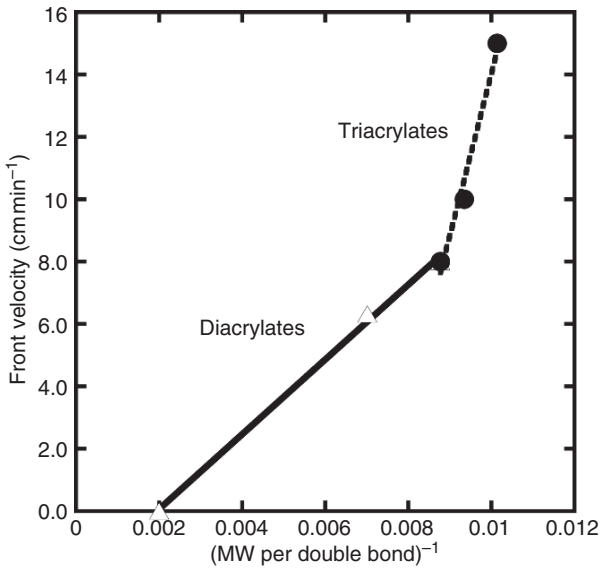

Figure 11 Velocity versus MW per double bond; 1 wt.% Luperox 231, 2 wt.% Darocur 4265; In air: Monomers and MW per double bond; PETA-K, 91; TMPTA, 99; DPHA, 105; DEGDA, 107; HDDA, 113; DPGDA, 121; TMPEOTA, 143; TMPEOTA, 201; PEGDA, 350; Ebecryl 8402, 500; irradiance of 5.9 mW cm^{-2}. Adapted from Nason, C.; Roper, T.; Hoyle, C.; Pojman, J. A. *Macromolecules* **2005**, *38*, 5506–5512.[83]

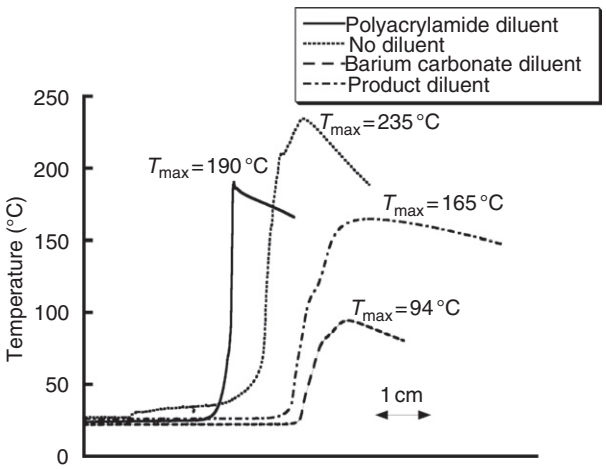

Figure 12 Temperature profiles for the frontal polymerization of undiluted acrylamide, of acrylamide diluted with commercial polyacrylamide, of acrylamide diluted with barium carbonate, and of acrylamide diluted with frontally polymerized acrylamide. Adapted from Fortenberry, D. I.; Pojman, J. A. *J. Polym. Sci. Part A: Polym. Chem.* **2000**, *38*, 1129–1135.[99]

of monomer conversion with AIBN was strongly dependent on the initiator concentration, with 0.8% AIBN, 95% of the monomer reacted but only 50% reacted with 2% AIBN.

The front velocities were about on the order of 10 cm min^{-1}. The higher velocities compared to monoacrylates resulted from high front temperatures (272 °C compared to 190 °C) and the greater reactivity of acrylamide.

Fortenberry and Pojman[99] studied FP of acrylamide in detail.Synthesis of polyacrylamide via FP resulted in a cross-linked, insoluble product. Figure 12 shows that the maximum

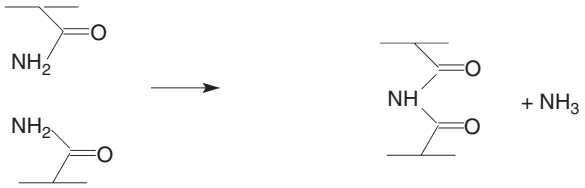

Figure 13 The scheme for intermolecular imidization, as occur in the frontal polymerization of acrylamide.

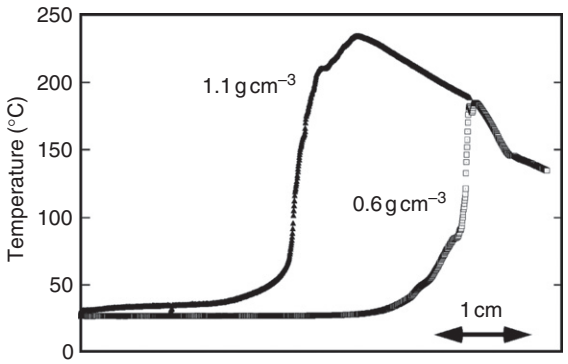

Figure 14 Temperature profiles of the frontal polymerization of acrylamide with potassium persulfate as the initiator, at two different initial densities. Adapted from Fortenberry, D. I.; Pojman, J. A. *J. Polym. Sci. Part A: Polym. Chem.* **2000**, *38*, 1129–1135.[99]

front temperature reached during polymerization was 235 °C. The presence of ammonia was detected by scent and litmus paper, which indicated imidization occurred (Figure 13). Analogous crosslinking by anhydride formation was observed in the FP of methacrylic acid (see section 4.38.5.14).[100] They calculated that the frontally produced samples were only 6% imidized. Imidization was prevented by adding an inert filler, either barium carbonate or polyacrylamide. Fronts propagated with front temperatures as low at 97 °C (Figure 14).

Foretenberry and Pojman[99] found that the front velocity was not a function of the particle size of the ground acrylamide but was a function of the green (unreacted) density. The velocity increased with the increased green density because the front temperature was higher and the thermal diffusivity larger. Fronts can even propagate if the sample is immersed in liquid nitrogen, provided a change of temperature of 400 K (Figure 15).

Pomogailo and his co-workers studied interesting solid systems that require no added initiator but proceed by a free-radical mechanism.[101–109] Using transition-metal complexes with acrylamide, they achieved FP with the solid monomers.

4.38.5.13 Effect of Pressure

Pojman *et al.*[55] performed experiments in a custom-built reactor that allowed isobaric and isothermal conditions. They found that the front velocity was a function of the applied pressure, even at low values of less than 30 atm. As the pressure is increased, the velocities decrease, exactly opposite the behavior observed by Chechilio and Enikolopyan at high pressures!

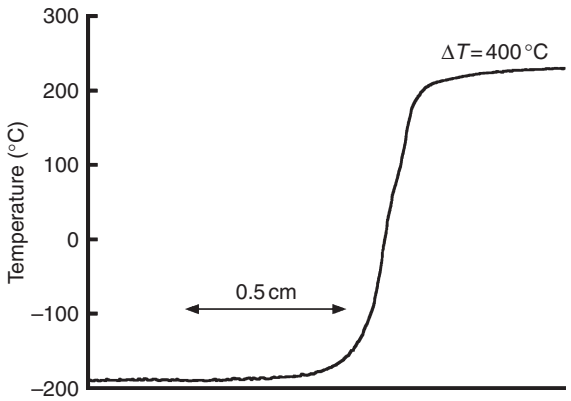

Figure 15 The temperature profile of frontal polymerization of acrylamide immersed in liquid nitrogen. Adapted from Pojman, J. A.; Ilyashenko, V. M.; Khan, A. M. *J. Chem. Soc. Faraday Trans.* **1996**, *92*, 2825–2837.[55]

At the low pressures we employ, we are not affecting the rate constants of polymerization but suppressing bubbles.

There are three sources of bubbles. All thermal initiators (except for persulfates), produce volatile byproducts, such as CO_2, methane, or acetone. It is an inherent problem with all commercially available peroxide or nitrile initiators.

Another source of bubbles is dissolved gas and water in the monomer. Gases can be removed under vacuum but water is extremely difficult to remove from methacrylic acid and TGDMA. Less than 1 mg of water will result in 2 cm^3 of water vapor at the front temperature of 200 °C and 1 atm of pressure. The only certain solution to all three sources is to perform reactions under pressure.

Bubbles can increase the velocity of fronts in standard closed test tubes initially at ambient pressure by as much as 30% compared to fronts free of bubbles under high pressure. The expansion of bubbles is part of the velocity by forcing unreacted monomer up and around the cooling polymer plug that is contracting; poly(methacrylic acid) is about 25% more dense than its monomer. This means that the pressure increases during the reaction because the tube is sealed, except for leakage around the initial polymer plug.[86]

Figure 16 shows the front velocity as a function of the inverse of the applied pressure. As the pressure was increased the velocity decreased because the volume of the bubbles was decreased, following Boyle's law.

We can write the velocity as

$$\text{vel}\,(p) = \text{vel}_0 + \frac{\text{Const}}{p} \qquad [7]$$

where the constant is a function of the number of moles of gas produced in the front. Therefore, the higher the initiator concentration, the higher is the applied pressure necessary to obtain the true front velocity.

To determine the true front velocity dependence on initiator concentration requires that the effect of bubbles be eliminated. Different initiators can yield different amounts of gas. Thus, the velocity depends not only on the kinetics of the initiator decomposition, but also on the amount of gas produced and on the applied pressure.

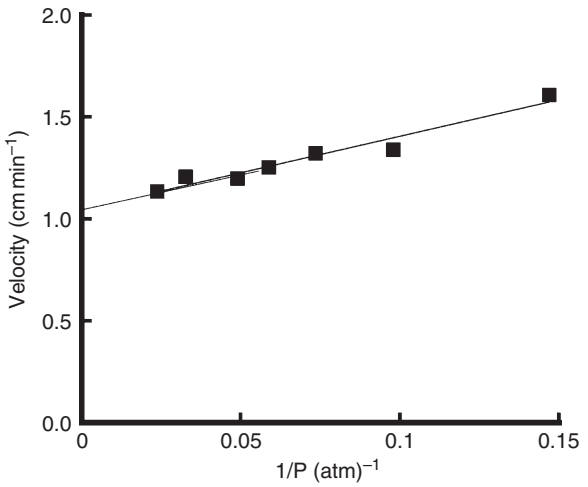

Figure 16 Front velocity of butyl acrylate polymerization as a function of applied pressure with AIBIN as the initiator (1.7% w/w) and 5.7% fumed silica. Adapted from Pojman, J. A.; Ilyashenko, V. M.; Khan, A. M. *J. Chem. Soc. Faraday Trans.* **1996**, *92*, 2825–2837.[55]

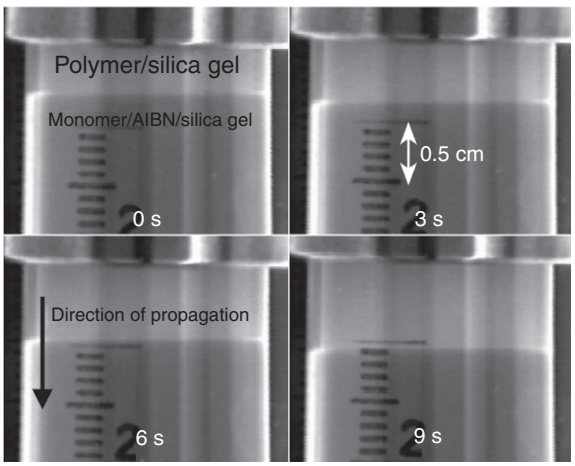

Figure 17 A front of butyl acrylate polymerization with fumed silica (to prevent convection) and with 4% AIBN, under 50 atm pressure. Adapted from Pojman, J. A.; Ilyashenko, V. M.; Khan, A. M. *J. Chem. Soc. Faraday Trans.* **1996**, *92*, 2825–2837.[55]

Poly(methacrylic acid) formed in a front in a test tube initially at ambient pressure is opaque but translucent when produced under at least 34 atm pressure. Very small bubbles scatter light and make the material opaque when in fact, the polymer itself is clear. This is also true with butyl acrylate fronts. Cabosil has a refractive index close enough to poly (butyl acrylate) that the initial solution and product are translucent, as can be seen in Figure 17.

If TGDMA was partially reacted to produce a gel before front initiation, no bubbles appear as the front propagates. (Gelling was accomplished by allowing TGDMA/initiator to sit at room temperature for several days or by heating to 40 °C until gelation occurs.) In ungelled TGDMA, copious bubble production occurs. It seems that the gel prevents nucleation of bubbles before complete crosslinking makes it impossible to form bubbles.

To reduce bubble formation, there are several approaches besides using applied pressure. Some peroxides produce less gas. Let us consider more about why peroxide and nitriles produce volatile compounds. The decomposition of a peroxide is endothermic and reversible. To make the production of radicals irreversible, initiators fragment (Figure 18). For example, AIBN decomposes to produce N_2 and organic radicals, making the overall reaction exothermic and irreversible. Benzoyl peroxide decomposes into the benzoyl radical, which fragments into carbon dioxide and a phenyl radical. Dicumyl peroxide breaks into peroxy radicals that undergo beta scission to produce acetophenone and methyl radicals. 1,1-Di-(*tert*-butylperoxy)-3,3,5-trimethylcyclohexane (Luperox 231) is a room-temperature stable liquid that readily dissolves in acrylates. Upon decomposition and beta scission, it produces acetone and methyl radicals and a diperoxy radical.

Persulfate does not produce bubbles. Pojman *et al.*[88] used ammonium persulfate in the solution polymerization of acrylamide in DMSO. Persulfate salts are not soluble in organics; so Masere *et al.*[40] synthesized trioctylmethyl ammonium persulfate, which is a room temperature ionic liquid. Mariani *et al.*[110] synthesized phosphonium-based persulfate ionic liquids, which had less of a plasticization effect because of their lower molecular weight.

4.38.5.14 Molecular Weight Distribution

Pojman *et al.*[100] examined the molecular distribution of two systems: methacrylic acid and butyl acrylate. Previously Pojman *et al.*[86] had determined the molecular weight of poly (methacrylic acid) produced frontally and reported very high molecular weight (about 10^6 g mol^{-1}), which did depend on the radial position in the sample. Methacrylic acid can undergo anhydride formation, leading to branched polymers of higher molecular weight than expected. Using morpholine to selectively cleave the anhydride linkages, they determined that the degree of polymerization was about 100 and that about 20% of the carboxyl groups were in the anhydride form. After cleavage, the molecular weight was in the expected range (Figure 19). Poly(butyl acrylate) prepared frontally produced the expected molecular weight ranges (Figure 20).

Fortenberry and Pojman[99] determined by light scattering that polyacrylamide prepared frontally with barium carbonate as an inert diluent had a molecular weight average on the order of 10^6.

Enikolopyan *et al.*[111] analytically considered the problem of the molecular weight distribution when the consumption of initiator was included. Not surprisingly, the distributions were more broad than observed in an isothermal polymerization, but no supporting experimental data were presented.

In order to produce the poly(butyl acrylate), silica gel was added to increase the viscosity and avoid convective mixing.[100] (We will discuss convective instabilities in section 4.38.5.16.1). Because high viscosity leads to high molecular weight via the gel effect, Pojman *et al.*[112] sought to prepare poly(butyl acrylate) frontally but without added silica. In order to accomplish this, they flew an experiment on a sounding rocket in order to avoid buoyancy-driven convection. They found that the molecular weight distribution was the same as that prepared in the lab using silica gel. Thus, they concluded that the silica increased the macroscopic viscosity but did not affect the molecular-level viscosity.

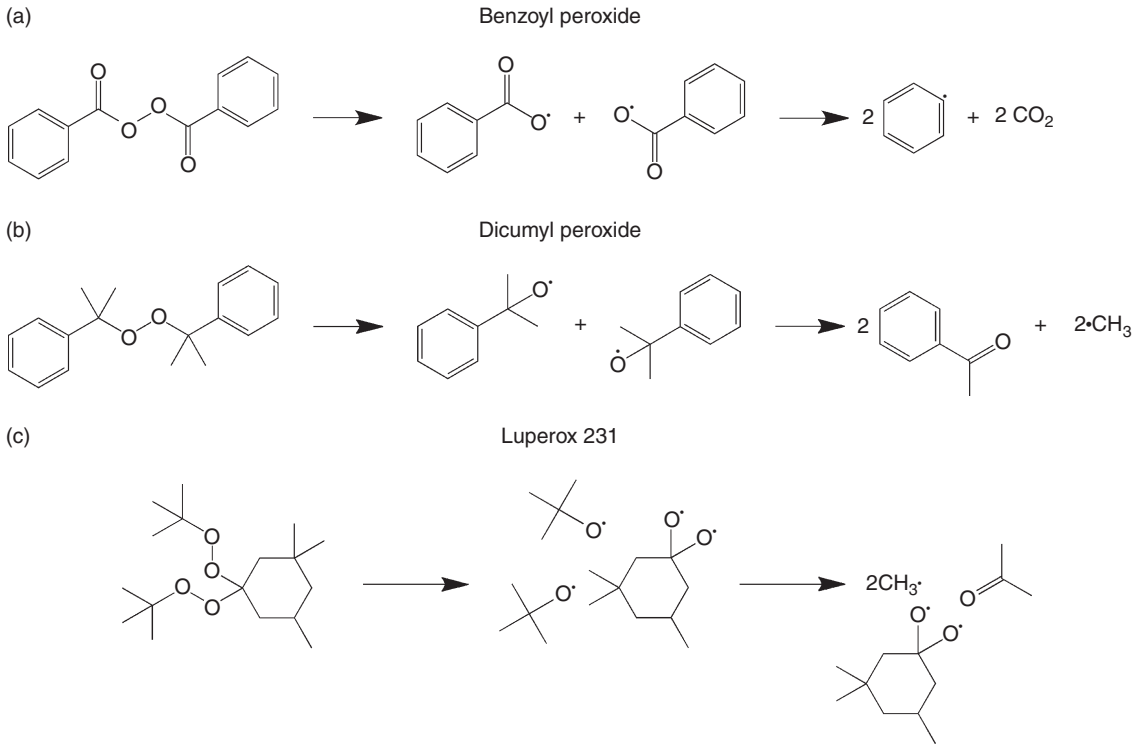

Figure 18 The decomposition schemes for three different initiators.

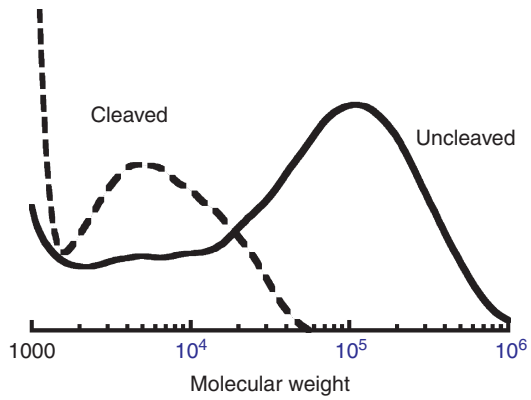

Figure 19 The molecular weight distribution for frontally prepared poly (methacrylic acid) and after the anhydride linkages were cleaved with morpholine. Adapted from Pojman, J. A.; Willis, J. R.; Khan, A. M.; West, W. W. *J. Polym. Sci. Part A: Polym. Chem.* **1996**, *34*, 991–995.[100]

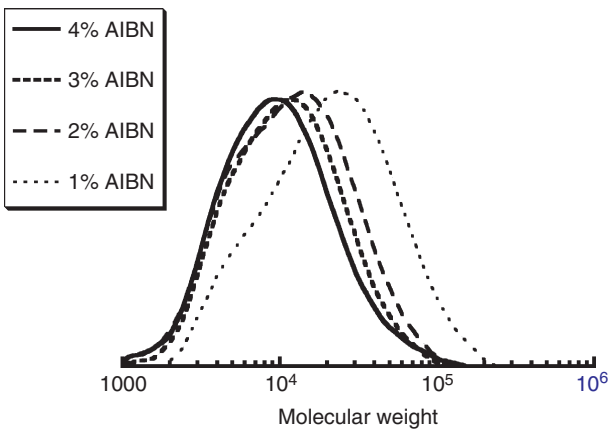

Figure 20 The molecular weight distributions for poly(butyl acrylate) produced frontaly. Adapted from Pojman, J. A.; Willis, J. R.; Khan, A. M.; West, W. W. *J. Polym. Sci. Part A: Polym. Chem.* **1996**, *34*, 991–995.[100]

4.38.5.15 Conversion

An important issue for using FP for polymer synthesis is conversion. We will consider in Section 4.38.5.26 the advantages of FP, some of which will be rapid conversion without the use of solvent. However, if conversion is low and the product must be purified, those advantages will be nonexistent. Initiator 'burn out' occurs when the all the initiator has decomposed before the monomer has been completely reacted.[93,94] For methacrylic acid polymerization with benzoyl peroxide as the initiator, conversion ranged from 80% to below 70% in a 2.2-cm tube (Figures 21 and 22).[84] The conversion was higher in a 1.5-cm diameter tube (85–80%) because the front temperature was lower due to greater heat loss in a narrower tube. With the more stable *t*BPO as the initiator in a 2.2-cm tube, conversion was significantly higher (92%) but the front velocity was lower, by as much as a factor of 2. Tredici *et al.*[113] found conversion around 90% for a copolymerization.

By combining the two peroxides, the conversion could be obtained as high as for *t*BPO alone with a velocity close to that with BPO alone. The front velocity was determined by the less stable peroxide, BPO, with the more stable *t*BPO finishing the reaction. However, the velocity was lower than for BPO alone, and the authors proposed that the radicals from the BPO decomposition could induce decomposition of the *t*BPO.

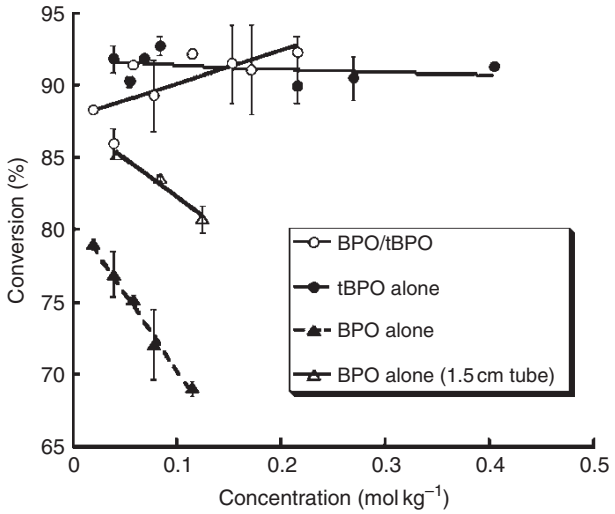

Figure 21 The conversion of methacrylic acid frontal polymerization as a function of benzoyl peroxide (BPO) and/or *tert*-butyl peroxide (*t*BPO). Adapted from Pojman, J. A.; Willis, J.; Fortenberry, D.; *et al. J. Polym. Sci. Part A: Polym. Chem.* **1995**, *33*, 643–652.[84]

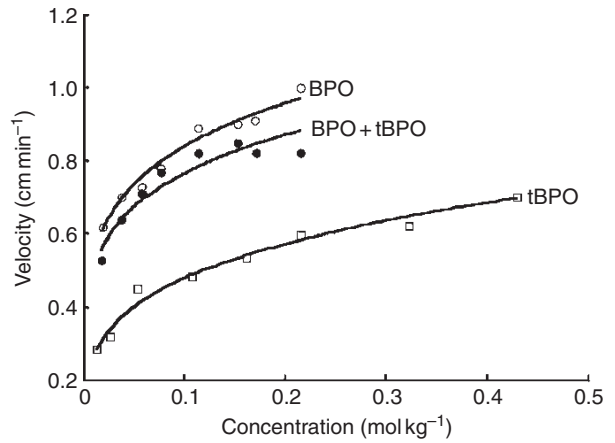

Figure 22 The velocity for methacrylic acid frontal polymerization with benzoyl peroxide (BPO) and *tert*-butyl peroxide (*t*BPO). Adapted from Pojman, J. A.; Willis, J.; Fortenberry, D.; *et al. J. Polym. Sci. Part A: Polym. Chem.* **1995**, *33*, 643–652.[84]

Conversion can also be limited by thermodynamics. Because the polymerization reactions are exothermic, the equilibrium conversion decreases with increasing temperature.[114] A relationship between temperature and the equilibrium monomer concentration (assuming unit activity coefficients) can be derived,[55] in which $[M]_0$ is the standard monomer concentration used to calculate the ΔS^0 and ΔH^0.

$$T = \frac{\Delta H_0}{\Delta S^0 + R \ln([M]_{eq}/[M]^0)} \quad [8]$$

For an adiabatic polymerization, the maximum conversion is uniquely determined by the ΔH^0 and ΔS^0 of polymerization. As the temperature increases, the equilibrium conversion is reduced and can be related by

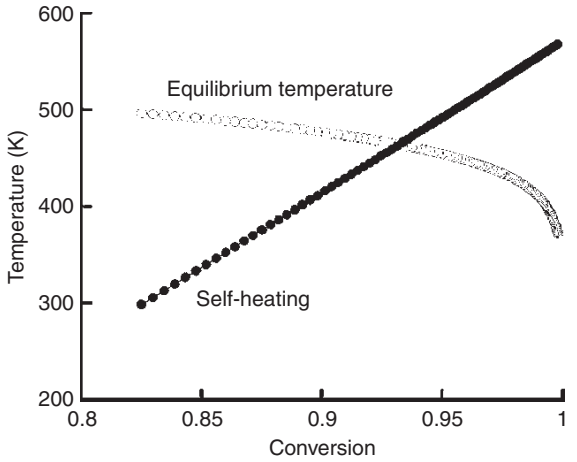

Figure 23 The relationship between the extent of conversion and the ceiling temperature for methyl methacrylate. $[M]_{initial} = 9.36$ M, $\Delta H^0 = -56$ kJ mol^{-1}, $\Delta S^0 = 117$ J K^{-1}, $C_p = 205.3$ J mol^{-1} K^{-1}, $T_i = 25$ °C. Adapted from Pojman, J. A.; Ilyashenko, V. M.; Khan, A. M. *J. Chem. Soc. Faraday Trans.* **1996**, *92*, 2825–2837.[55]

$$\alpha = 1 - \frac{1}{[M]_{initial}} \exp\left(\frac{\Delta H^0 - T\Delta S^0}{RT}\right) \quad [9]$$

The relationship for the temperature and conversion for adiabatic self-heating is

$$T = T_i + \frac{\alpha \Delta H^0}{C_p} \quad [10]$$

The solution of eqns [8] and [9] provides the conversion achieved in adiabatic polymerization. Figure 23 shows the results for methyl methacrylate with an initial temperature of 25 °C, using thermodynamic data from Odian.[115] The conversion is 0.93, which means that independent of initiator burnout, complete conversion can never be achieved because of the high front temperature. This value is very sensitive to the exact values of the thermodynamic parameters so the calculated value may not correspond precisely to experiment. Nonetheless, thermodynamics must be considered when selecting candidates for FP. Similar monomers may exhibit very different conversions at the same temperature. For example, zero conversion will be obtained at 310 °C with styrene but α-methylstyrene will not react above 61 °C.[115]

4.38.5.16 Interferences with Frontal Polymerization

4.38.5.16.1 Buoyancy-driven convection

Because of the large thermal and concentration gradients, polymerization fronts are highly susceptible to buoyancy-induced convection. Garbey *et al.*[116–118] performed the linear stability analysis for the liquid–liquid and liquid–solid cases. The bifurcation parameter was a 'frontal Rayleigh number'

$$R = \frac{g\beta q \kappa^2}{\nu c^3} \quad [11]$$

where g is the gravitational acceleration, β the thermal expansion coefficient, q the temperature increase at the front, κ the thermal diffusivity, ν the kinematic viscosity, and c the front velocity.

Let us first consider the liquid–solid case. Neglecting heat loss, the descending front is always stable because it

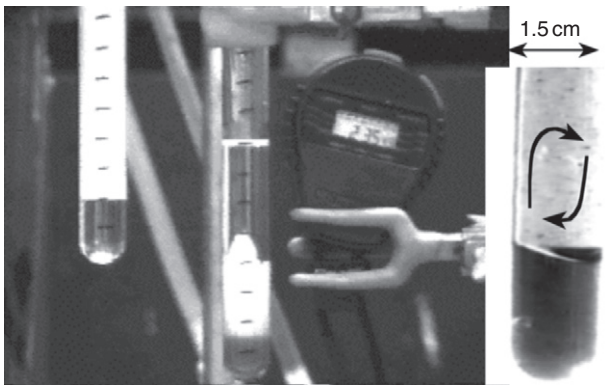

Figure 24 Left: The front on the left is descending and the one on the right ascending with an axisymmetric mode of convection. Right: An antisymmetric mode of an ascending front. The system is the acrylamide/bis-acrylamide polymerization in DMSO with persulfate initiator. Adapted from Bowden, G.; Garbey, M.; Ilyashenko, V. M.; *et al. J. Phys. Chem. B* **1997**, *101*, 678–686.[119]

corresponds to heating a fluid from above. The front is always flat. If the front is ascending, convection may occur depending on the parameters of the system. Bowden *et al.*[119] experimentally confirmed that the first mode is an antisymmetric one, followed by an axisymmetric one. **Figure 24** shows a flat descending front as well as axisymmetric and antisymmetric modes of ascending fronts. **Figure 25** shows the stability diagram in the viscosity-front velocity plane. Most importantly, they confirmed that the stability of the fluid was a function not only of the viscosity but also of the front velocity. This means that the front dynamics affects the fluids dynamics. McCaughey *et al.*[120] tested the analysis of Garbey *et al.* and found the same bifurcation sequence of antisymmetric to axisymmetric convection in ascending fronts as seen with the liquid–solid case.

If the reactor is not vertical, there is no longer a question of stability – there is always convection. Bazile *et al.*[121] studied descending fronts of acrylamide/bis-acrylamide polymerization in DMSO as a function of tube orientation. The fronts remained nearly perpendicular to the vertical but the velocity

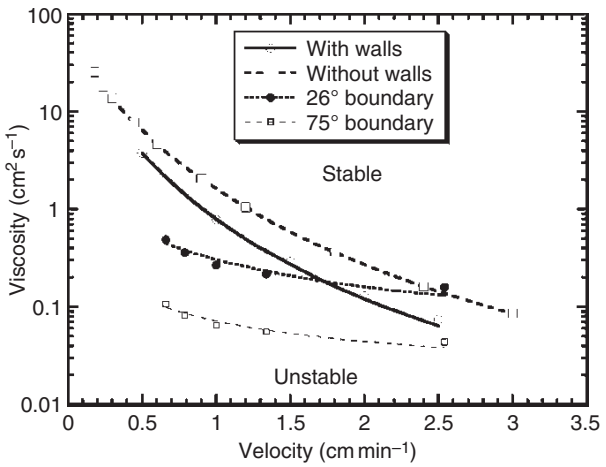

Figure 25 The stability diagram for the system in **Figure 24**. Adapted from Bowden, G.; Garbey, M.; Ilyashenko, V. M.; *et al. J. Phys. Chem. B* **1997**, *101*, 678–686.[119]

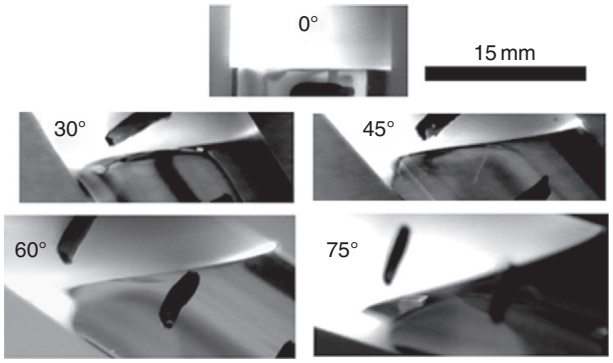

Figure 26 The dependence of the front shape for descending fronts of acrylamide polymerization in DMSO with persulfate initiator. Adapted from Bazile, M., Jr.; Nichols, H. A.; Pojman, J. A.; Volpert, V. *J. Polym. Sci. Part A: Polym. Chem.* **2002**, *40*, 3504–3508.[121]

projected along the axis of the tube increased with 1/cos of the angle (**Figure 26**).

Liquid–liquid systems are more complicated than the previous case because a descending front can exhibit the Rayleigh–Taylor instability. The product is hotter than the reactant but is more dense (**Figure 27**), and because the product is a liquid, fingering can occur. Bidali *et al.*[122] described the phenomenon as the 'rainstorm effect'. Such front degeneration is shown in **Figure 28**. The Rayleigh–Taylor instability can be prevented using high pressure,[52] adding a filler,[95] using a dispersion in salt water,[123] or performing the fronts in weightlessness.[123]

Texier-Picard *et al.*[124] analyzed a polymerization front in which the molten polymer was immiscible with the monomer and predicted that a front could exhibit the Marangoni instability even though the comparable unreactive fluids would not exhibit the instability. However, no liquid–liquid frontal system with an immiscible product has been identified. Even if such a system could be found, the experiment would have to be performed in weightlessness to prevent buoyancy-induced convection from interfering.

We note a significant difference between the liquid–liquid and the liquid–solid cases. For the liquid–solid case, convection in ascending fronts increases the front velocity but in the liquid–liquid case, convection slows the front. However, convection increases the velocity of pH fronts and Belousov-Zhabotinsky reaction waves.[125,126] Why is the difference between liquid–liquid FP and other frontal systems? In liquid–liquid systems, the convection also mixes cold monomer into the reaction zone, which lowers the front temperature. The front velocity depends more strongly on the front temperature than on the effective transport coefficient of the autocatalyst. Convection does not mix monomer into the reaction zone of a front with a solid product but rather increases thermal transport so the velocity is increased.

4.38.5.16.2 Effect of surface tension-driven convection

If there is a free interface between fluids, gradients in concentration and/or temperature parallel to the interface cause gradients in the surface (interfacial) tension, which cause convection.[127] This convection, also known as Marangoni convection, is especially noticeable in thin layers (or weightlessness) in which buoyancy-driven convection is greatly reduced.

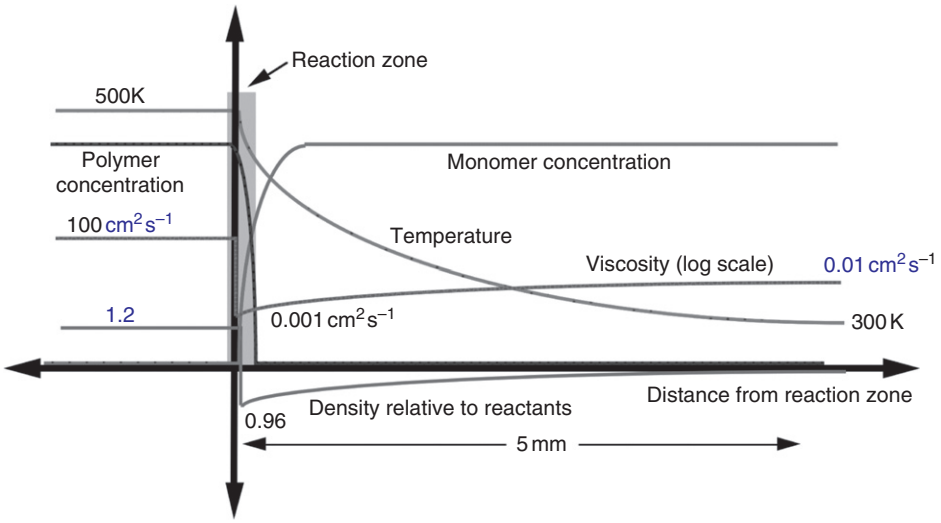

Figure 27 Schematic diagram showing changes in properties across a propagating polymerization front that produces a thermoplastic. Courtesy of Paul Ronney.

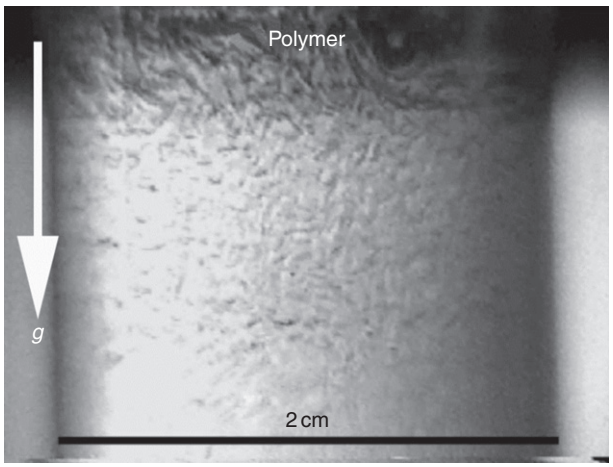

Figure 28 Rayleigh–Taylor instability with a descending front of butyl acrylate polymerization.

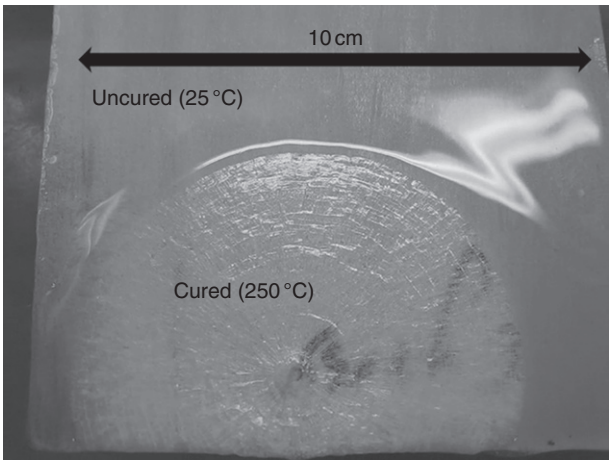

Figure 29 A front of pentaerythritol tetraacrylate propagating in a thin layer on wood.

Asakura *et al.*[128] recently explained that FP was not applied to thin layers because it was thought that FP could not occur in thin layers. In fact, interfacial tension-driven convection can cause so much heat loss that fronts are quenched. Figure 29 shows a front propagating in a thin layer (about 1 mm) of a tetraacrylate in which fumed silica is dispersed. The large temperature gradient created by the reaction 'pushes' monomer ahead but not enough to quench the front.

For a given surface, three variables affect whether a front will propagate, specifically, the viscosity (determined by the amount of fumed silica), the initiator concentration, and the thickness of the layer. For a fixed layer thickness, we determined that for trimethylolpropane triacrylate, with 2 phr silica, no front would propagate with 1 phr Luperox 231 but would propagate with 1.1 phr. (phr stands for 'parts per hundred resin'.) Figure 30 shows how complicated patterns can arise when the amount of silica was increased to 4 phr.

4.38.5.16.3 Dispersion polymerization

Pojman *et al.* overcame the Rayleigh–Taylor instability by dispersing benzyl acrylate in a salt water solution whose density was greater than that of the polymer,[123] an approach that had been considered theoretically.[129] Fronts reached 200 °C, the same temperature as benzyl acrylate fronts with a diacrylate to prevent fingering. This indicated that the dispersion broke relatively quickly, leaving the monomer to polymerize in bulk and the salt water to settle to the lower section of the tube. The polymer was insoluble in tetrahydrofuran (THF) and in DMSO, and so they concluded that the acrylic acid formed then formed anhydride crosslinks.

4.38.5.16.4 Thermal instabilities

Fronts do not have to propagate as planar fronts. Analogously to oscillating reactions, a front can exhibit periodic behavior, either as pulsations or as 'spin modes' in which a hot spot propagates around the reactor as the front propagates, leaving a helical pattern. This mode was first observed in SHS.[130] This

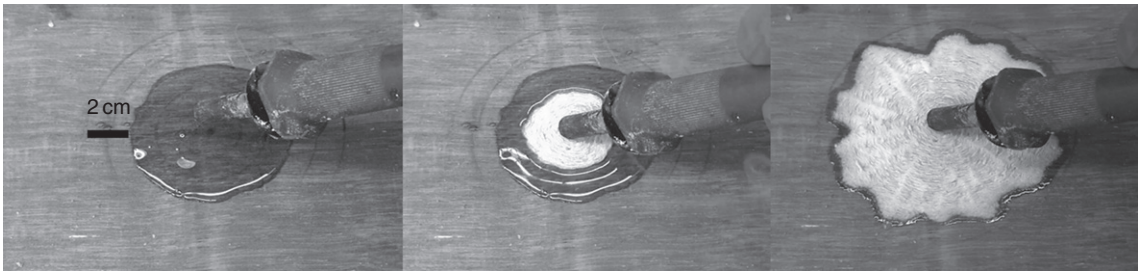

Figure 30 A front propagating in a thin layer of a triacrylate with 4 phr fumed silica and 2.1 phr Luperox 231, a peroxide initiator.

general issue nonlinear behavior in FP has been considered in great detail.[55,79,131,132]

The linear stability analysis of the longitudinally propagating fronts in the cylindrical adiabatic reactors with one reaction predicted that the expected frontal mode for the given reactive medium and diameter of the reactor is governed by the Zeldovich number

$$Z = \frac{T_m - T_0}{T_m}\frac{E_{eff}}{RT_m} \qquad [12]$$

For FP, lowering the initial temperature (T_0), increasing the front temperature (T_m), and increasing the energy of activation (E_{eff}) all increase the Zeldovich number. The planar mode is stable if $Z < Z_{cr} = 8.4$. By varying the Zeldovich number beyond the stability threshold, subsequent bifurcations leading to higher spin mode instabilities can be observed. Second, for a cylindrical geometry, the number of spin heads or hot spots is also a function of the tube diameter. We point out that polymerization is not a one-step reaction, so that the above form of the Zeldovich number does not directly apply. However, estimates of the effective Zeldovich number can be obtained from the overall energy of activation with the steady-state assumption for free-radical polymerization.

The most commonly observed case with FP in tube is the spin mode in which a 'hot spot' propagates around the front. A helical pattern is often observed in the sample. The first case was with the FP of ε-caprolactam,[133,134] and the next case was discovered by Pojman *et al.*[135] in the methacrylic acid system in which the initial temperature was lowered.

Spin modes have also been observed in the FP of transition metal nitrate acrylamide complexes,[107,109] which are solid, but were not observed in the frontal acrylamide polymerization system.[99]

The single-head spin mode was studied in detail by Ilyashenko and Pojman.[136] They were able to estimate the Zeldovich number by using data from the initiator and the methacrylic acid. The value at room temperature was about 7, less than the critical value for spin modes. In fact, fronts at room temperature were planar and spin modes only appeared by lowering the initial temperature. However, spin modes could be observed by increasing the heat loss from the reactor by immersing the tube in water or oil.

4.38.5.16.5 Effect of complex kinetics

Solovyov *et al.*[137] performed two-dimensional numerical simulations using a standard three-step free-radical mechanism. They calculated the Zeldovich number from the overall activation energy using the steady-state theory and determined the critical values for bifurcations to periodic modes and found that the complex kinetics stabilized the front.

Shult and Volpert[138] performed the linear stability analysis for the same model and confirmed this result. Spade and Volpert[139] studied linear stability for nonadiabatic systems. Gross and Volpert[140] performed a nonlinear stability for the one-dimensional case. Commissiong *et al.*[141] extended the nonlinear analysis to two dimensions. They confirmed that, unlike in SHS,[142] uniform pulsations are difficult to observe in FP. In fact, no such one-dimensional pulsating modes have been observed.

An interesting problem arises in the study of fronts with multifunctional acrylates. At room temperature, acrylate like 1,6-hexanediol diacrylate (HDDA) and TGDMA exhibit spin modes. In fact, if an inert diluent, such as DMSO is added, the spin modes are more apparent even though the front temperature is reduced. Masere and Pojman[143] found spin modes in the FP of a diacrylate at ambient conditions. Thus, although the mechanical quality of the resultant polymer material can be improved by using multifunctional acrylates, spin modes may appear and a nonuniform product results. This observation implicates the role of polymer crosslinking in front dynamics. In that same work, Masere and Pojman showed that pH indicators could be added to act as dyes that were bleached by the free radicals, making the observation of the spin pattern readily apparent (Figure 31).

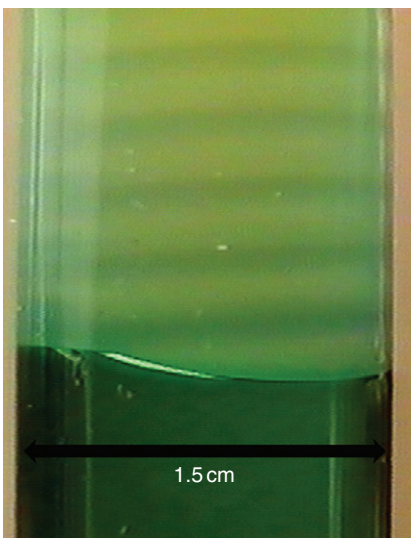

Figure 31 A single-head spin mode propagating around a front of 1,6-hexanediol diacrylate (40%) in diethyl phthalate with Luperox 231 as the initiator.[144] Tube diameter was 1.5 cm.

Tryson and Schultz[145] studied the energy of activation of photopolymerized multifunctional acrylates and found it increased with increasing conversion because of crosslinking. Gray found that the energy of activation of HDDA increased exponentially during the reaction.[146] Applying the steady-state theory of polymerization to Gray's results, Masere *et al.*[144] calculated the effective energy of activation for thermally initiated polymerization (photoinitiation has no energy of activation) by including the energy of activation of a typical peroxide. They calculated that the energy of activation of HDDA polymerization increased from 80 kJ mol^{-1} at 0% conversion, the same as methacrylic acid, to a 140 kJ mol^{-1} at 80% conversion. This can explain how spin modes appear at room temperature with multifunctional acrylates but not monoacrylates. The Zeldovich number of methacrylic acid polymerization at room temperature is below the stability threshold. Using the activation energy at the highest conversion that can be obtained with HDDA, Masere *et al.* estimated a Zeldovich number of 12.

Masere *et al.*[144] studied fronts with a peroxide initiator at room temperature and used two bifurcation parameters. They added an inert diluent, diethyl phthalate, to change the front temperature and observed a variety of modes. More interestingly, they also varied the ratio of a monoacrylate, benzyl acrylate, to HDDA, keeping the front temperature constant. Changing the extent of crosslinking changed the effective energy of activation, which revealed a wide array of interesting spin modes. Using trimethylol propane triacrylate in DMSO, they observed complex modes (**Figure 32**).

The three-dimensional nature of the helical pattern was studied by Manz *et al.*[147] using Magnetic Resonance Imaging (MRI). Pojman *et al.* observed zigzag modes in square reactors[148] and bistability in conical reactors.[149]

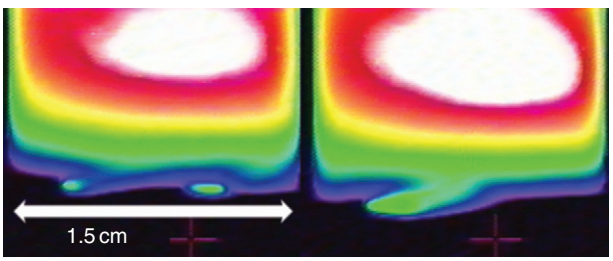

Figure 32 Complex modes of propagation observed with an IR camera in a 1.5 cm tube with trimethylol propane triacrylate in DMSO with Luperox 231.

4.38.5.16.6 Effect of bubbles

Pojman *et al.*[135] found an unusual mode of propagation when there are large amounts of very small bubbles that can occur when a linear polymer precipitates from its monomer. In studying fronts of methacrylic acid polymerization, they observed convection that periodically occurred under the front at the same time as the front deformed and undulated. The period of convection was about 20 s and remained constant during the entire front propagation.

Volpert *et al.*[150] analyzed the effect of the thermal expansion of the monomer on the thermal stability and concluded that the reaction front becomes less stable than without thermal expansion. The effective thermal expansion can be increased because of the bubbles, and it can considerably affect the stability conditions.

4.38.5.16.7 Effect of buoyancy

The first experimental confirmation that gravity plays a role in spin modes in a liquid–solid system came in the study of descending fronts in which the viscosity was significantly increased with silica gel. Masere *et al.*[144] found that silica gel significantly altered the spin behavior, as predicted by Garbey *et al.*[116] Pojman *et al.*[148] made a similar observation in square reactors. Pojman *et al.*[79] studied the dependence of spin modes on viscosity with the FP of HDDA with persulfate initiator. They found that the number of spins was independent of the viscosity until a critical viscosity was reached, when the spins vanished.

The issues arises why the analysis of Ilyashenko and Pojman worked so well for the methacrylic acid system, even though they did not consider the effect of convection. They induced spin modes by reducing the initial temperature to 0 °C – below the melting point of methacrylic acid. Thus, the system was a solid–solid system and so hydrodynamics played only a small role.

McFarland *et al.*[151,152] observed that spin modes did not occur when the initiator was microencapsulated. Not only were spin modes not observed, the material was 10 times stronger, which the authors attributed to the absence of spin modes.

4.38.5.16.8 Three-dimensional frontal polymerization

FP allows the study of spherically propagating fronts. Binici *et al.*[153] developed a system that was a gel created by the base-catalyzed reaction of a trithiol with a triacrylate. The gel was necessary to suppress convection. However, it turned out to be difficult to find a system that would exhibit spin modes in a gel. They succeeded and were able to create waves on the surface of the expanding polymerization front (**Figure 33**).

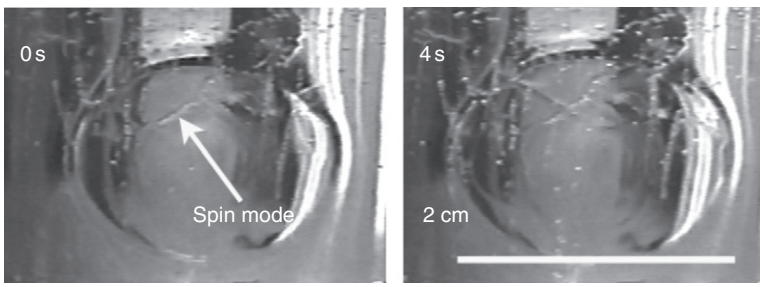

Figure 33 A spin mode on the surface of a spherically expanding front of triacrylate polymerization. Adapted from Binici, B.; Fortenberry, D. I.; Leard, K. C.; *et al. J. Polym. Sci. Part A: Polym. Chem.* **2006**, *44*, 1387–1395.[153]

4.38.5.17 The Effect of Fillers

Fillers are added to frontal systems to prevent convection, to modify the rheology of the unreacted formulation and to affect the mechanical properties of the product. Nason *et al.*[154] studied the effect of inorganic fillers on the photoinduced FP of a triacrylate. Not surprisingly, the front velocity decreased with increased loading of calcium carbonate or kaolin clay.

Pojman *et al.*[155] developed a system for studying Snell's Law of refraction in FP. Using trimethylolpropane triacrylate with 47% by mass kaolin clay (Polygloss 90), they created a formulation with the consistency of a putty, which could be molded into desired shapes. Viner *et al.*[156] used fillers that were inert but melted, so-called 'phase change materials', in an attempt to lower the front temperature without significantly reducing the front velocity.

Fumed silica was used by Bowden *et al.*[119] and McCaughey *et al.*[120] to precisely control the viscosity for convection studies. For acrylates, about 4 phr fumed silica will create a gel. For kaolin clay, about 40 phr is necessary to create moldable putty.

4.38.5.18 Encapsulation of Initiators

McFarland *et al.*[151,152] studied the effect of encapsulating the initiator cumene hydroperoxide. They found that the front velocity was consistently slower than when the peroxide was dissolved. However, the particles do not need to be extremely small. The front velocity is 25% slower for 400-μm capsules than for fronts with a dissolved initiator but almost the same with 50-μm capsules. These systems hold the promise of creating fronts that propagate rapidly at moderate temperatures by coupling the encapsulated initiator with a redox system (**Figure 34**).

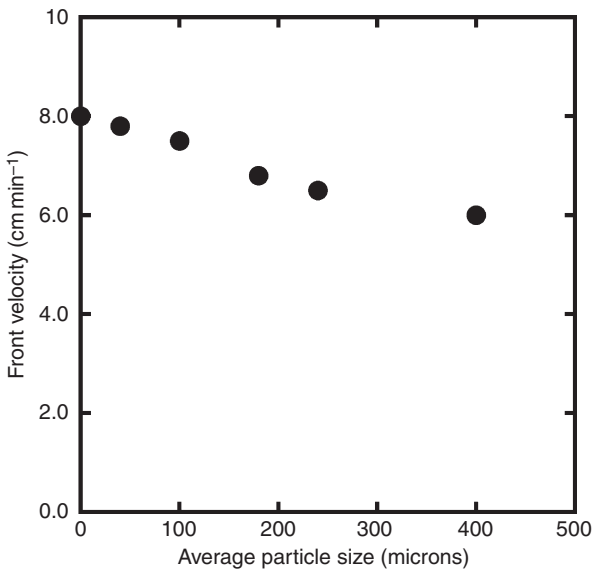

Figure 34 The frontal polymerization velocity for TMPTA polymerization with encapsulated dicumyl peroxide. Image courtesy of Chris Bounds.

4.38.5.19 Copolymerizations

Tredici *et al.*[113] studied the frontal copolymerization of acrylic acid–methacrylic acid, methyl methacrylate–methacrylic acid and styrene–methacrylic acid. They studied the velocity dependence on initiator concentration. They claimed that the elevated temperature of the front created a more random copolymer because the reactivity ratios were closer to one than under typical polymerization conditions. They performed numerical simulations for the velocity dependence and conversion on initiator concentration but strangely neither in experiments nor simulations did they study any dependence on monomer feed ratios.

Perry *et al.*[157] did study front velocity as a function of the monomer feed composition and the reactivity ratios. Frontal copolymerization experiments were performed with three different monomer systems. They are (1) methacrylic acid and acrylic acid (MAA-AA), (2) acryloyloxyethyltrimethylammonium chloride and acrylamide (AETMA-acrylamide), and (3) acrylic acid and acrylamide (AA-acrylamide). They chose these pairs because of their different reactivity ratios. The most significant result they found was that adding a highly reactive monomer could significantly increase the front velocity for a system that would propagate slowly or not at all. For example, AETMA in water would not support FP but could frontally copolymerize with acrylamide. For methacrylic acid, the velocity increased (from 2 cm min^{-1}) with 40% MAA to 4 cm min^{-1} at 10% MAA.

Thiols can be used in two ways with free-radical polymerization.[158] Thiols react with electron-rich enes (allyl ethers) via a step-growth mechanism to create a polymer only if both ene and thiol have functionalities of at least two. The allyl ethers cannot homopolymerize. If thiols are present, the acrylate can homopolymerize and copolymerize with the thiol.[159] Pojman *et al.*[160] studied frontal thiol-ene polymerization using pentaerythrytoltriallyl ether (PTE) and trimethylolpropanetris (3-mercaptopropionate) (95%) (TT1). Not surprisingly, the front velocity was a maximum at a 1:1 thiol:ene ratio (**Figure 35**).[161]

4.38.5.20 Atom Transfer Radical Polymerization

Bidali *et al.*[162] performed frontal atom transfer radical polymerization (ATRP) with tri(ethylene glycol dimethacrylate). They used CBr_4, tris(2-aminoethyl)amine, and CuBr. When the components were dissolved in the monomer, the solution was cooled to 0 °C to prevent bulk polymerization, which did not react for at least 3 h. Samples were heated to 25 °C before fronts were then initiated, which propagated with velocities of about 0.5 cm min^{-1}. The major advantage of this system compared to a typical peroxide-based system was the lack of bubbles. However, because the system reacted relatively quickly at room temperature, the system has limited applicability.

4.38.5.21 Ring-Opening Metathesis Polymerization

Mariani *et al.*[163] first demonstrated that FP could be achieved with the ring-opening metathesis polymerization (ROMP) of dicyclopentadiene. In a typical run, a glass test tube already containing suitable amounts of solid Grubbs catalyst (GC) and PPh_3 was filled with liquid dicyclopentadiene at 35 °C. After the reagents dissolved, the reaction mixture was cooled to 27 °C in order to permit solidification of the solution.

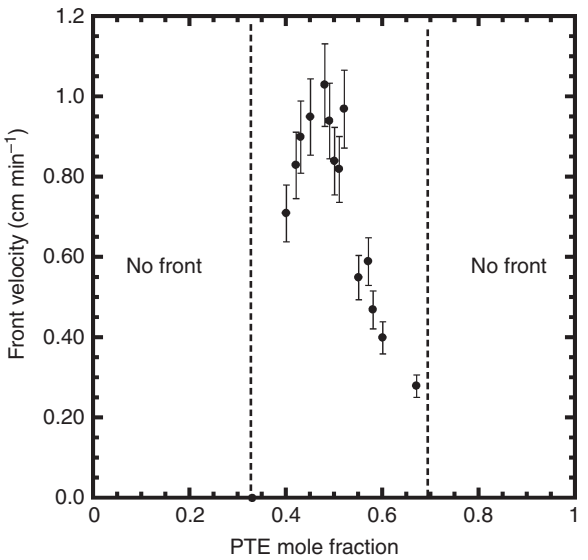

Figure 35 The front velocity as a function of the mole ratio between pentaerythrytoltriallyl ether (PTE) and trimethylolpropanetris(3-mercaptopropionate). Adapted from Pojman, J. A.; Varisli, B.; Perryman, A.; *et al. Macromolecules* **2004**, *37*, 691–693.[160]

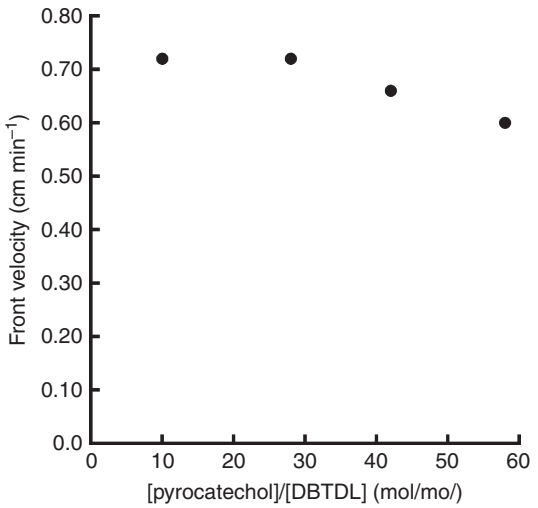

Figure 36 Front velocity vs [pyrocatechol]/[DBTDL] ratio. Experimental conditions: [DBTDL]/[HDI] = 9.4×10^{-4} mol mol^{-1}, DMSO = 18 wt.%, Cabosil = 3 wt.%. Adapted from Fiori, S.; Mariani, A.; Ricco, L.; Russo, S. *Macromolecules* **2003**, *36*, 2674–2679.[164]

A problem with this system is that it has a relatively short pot life. The authors found that by using PPh_3 the pot life was extended to 20 min. To overcome this drawback, they dissolved all components at 35 °C and quickly cooled them to 27 °C. This means that frontal ring opening metathesis polymerization runs were performed on solid mixtures, which melted immediately before being reached by the front. If stored at 7–8 °C, the samples could support a front after 3 weeks.

4.38.5.22 Polyurethanes

Fiori *et al.*[164,165] were the first to perform frontal urethane polymerization. They used 1,6-hexamethylene diisocyanate, ethylene glycol, and the catalyst dibutyltin dilaurate in DMSO with fumed silica. Pyrocatechol was added to extend the pot life up to 25 min (**Figure 36**). The front velocities were less than 1 cm min^{-1}.

Texter and Ziemer[166] created polyurethanes via FP in microemulsions. Chen *et al.*[167] created epoxy-polyurethane hybrid networks frontally. Pot lives were on the order of hours. Hu *et al.*[168] frontally prepared urethane–acrylate copolymers in DMSO using persulfate as the initiator. Chen *et al.*[92] studied FP of poly(propylene oxide) glycol, 2,4-toluene diisocyanate, and 1,4-butanediol with the catalyst stannous caprylate in dimethylbenzene. At room temperature, bulk polymerization did not occur quickly, and the pot life could be extended to 6 h if the solution was cooled to 10 °C. Mariani *et al.*[169] prepared diurethane diacrylates.

4.38.5.23 Epoxy Curing

In 1975, Arutiunian demonstrated frontal epoxy curing with amines using resins based on bisphenol A.[170] Chekanov *et al.*[171] studied the frontal curing of diglycidyl ether of bisphenol F (DGEBF), which was cured by the aliphatic amine curing agent Epicure 3371 in a stoichiometric ratio both frontally and in a batch-cure schedule. The pot life for the system was about 60 min. Glass transition temperatures (T_g) were determined using differential scanning calorimetry (DSC) and dynamic mechanical analysis (DMA). The properties of the frontally cured epoxy resin were found to be very close to that of batch-cured epoxy resin. They achieved 90% of the mechanical strength in 10% of the time for a sample 2.2 cm in diameter by 25 cm in length. The front temperatures were about 250 °C with front velocities of 4 cm min^{-1}. The maximum percentage of filler in the epoxy resin allowing propagation was 30%. Frulloni *et al.*[172] and Mariani *et al.*[173] studied a similar system and developed a phenomenological model of the front propagation.

Because the reaction between the amine curing agent and the epoxy is stoichiometric, the front velocity cannot be varied by changing the amount of curing agent without significantly affecting the conversion and mechanical properties of the product. Another significant difference between these systems and free-radical cured fronts is the relatively short pot life.

Mariani *et al.* combined FP and radical-induced cationic polymerization to cure thick samples of an epoxy monomer bleached by UV light. They used 3,4-Epoxycyclohexylmethyl-3′,4′-epoxycyclohexanecarboxylate (CE), benzoyl peroxide (BPO), and {4-[(2-hydroxytetradecyl)oxy]phenyl}phenyliodonium hexafluoroantimoniate (HOPH). The effect of the relative amounts of cationic photoinitiator and radical initiator was investigated and was related to the front's velocity and its maximum temperature.

Scognamillo *et al.*[174] studied the cationic curing of a triepoxy using latent BF_3–amine catalysts.

4.38.5.24 Binary Systems

If two noninteracting polymerization systems are mixed together, a binary FP can be created. Pojman *et al.*[175,176] studied the binary system composed of triethyleneglycol dimethacrylate with Luperox 231 as the free-radical initiator and diglycidyl ether of bisphenol A (DGEBA II), using the dual curing system

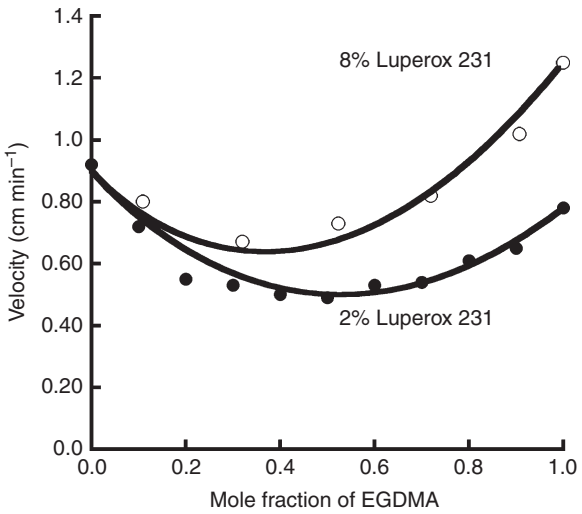

Figure 37 The front velocity as a function of the ethyleneglycol dimethacrylate mole fraction in the binary frontal polymerization with diglycidyl ether of bisphenol F. Adapted from Pojman, J. A.; Griffith, J.; Nichols, H. A. *e-Polymers* **2004**, *13*, 1–7.[176]

of an alkyl amine (Epicure 3271) and a boron trichloride/amine (BC13-NR3). Figure 37 shows how the front velocity exhibits a minimum as a function of the mole fraction of the two reactants.

4.38.5.25 Patents

In 1980, Dixon[177] received the first patent on FP, entitled *In Depth Curing of Resins Induced by UV Radiation*. He produced curing to depths of 500 mils (500/1000 in.) using a combination of a photoinitiator, thermal initiator, and multifunctional acrylate resin. The UV light caused a photopolymerization on the surface, which then triggered a propagating front. To increase the reactivity, he also added an accelerator such as a tertiary amine.

Scranton *et al.*[178] patented *Thick, Composite Parts Made from Photopolymerizable Compositions and Methods for Making Such Parts*, in which photopolymerization was combined with thermal FP.

In 2000 and 2001, Pojman and McCardle[179,180] received two patents on *Functionally Gradient Polymeric Materials*. Functionally gradient materials possess spatially varying properties. By creating an ascending front into which reagents were flowed at a rate sufficient to maintain a layer thin enough to significantly reduce buoyancy-driven convection, spatial variations of properties could be created. Chekanov and Pojman[181] discussed the process in detail.

Pfeil *et al.*[182] received a patent in 2003 on *Mortar Composition, Curable by Frontal Polymerization, and a Method for Fastening Tie Bars*. Chemical anchors are adhesives, usually based on epoxy chemistry that are used to secure rods in holes drilled in concrete. Their approach is to use multifunctional acrylates with silica and quartz fillers and thermal initiators as the frontally cured chemical anchor.

Bürgel and Böck[183] patented a further development in chemical anchors. They used a two-part formulation with one consisting of a monomer with an organic substituted ammonium salt and the other consisting of the monomer with ammonium persulfate. When the two components are mixed, the organic substituted ammonium salt exchanges with the ammonium persulfate to form an organic soluble persulfate, which does not produce gas during decomposition.

Gregory[184] patented *Ultraviolet Curable Resin Compositions Having Enhanced Shadow Curing Properties* in 2001. This patent has the same idea as Dixon's patent, that is, use photopolymerization at the surface of a filled resin to trigger a thermal front. Gregory went beyond using peroxide-cured vinyl resins. He used dialkyl iodonium salts, sensitized by α-hydroxy ketones, that produced Lewis acids upon UV irradiation. The Lewis acid triggered cationic polymerization of epoxy resins and vinyl ethers. The heat from the photoinitiated process decomposes peroxides into radicals that react with the iodonium salts to produce Lewis acids.

Crivello[185] patented *Command-Cure Adhesive* that is activated by UV light and then propagates thermally.

Pojman *et al.*[186] have a patent pending on FP microencapsulated monomers.

4.38.5.26 Applications of Thermal Frontal Polymerization

These patents demonstrate some possible applications of thermal FP but none have been commercialized. So we now consider if FP is more than a laboratory curiosity or an interesting way to study nonlinear phenomena in polymeric systems.

4.38.5.26.1 Solventless processing

The ability to prepare thermoplastics rapidly without solvent is a potential advantage.[54,95,187–190] Two problems were present in all these works, namely, lack of complete conversion and the necessity to add a component to suppress convection.

4.38.5.26.2 Energy savings

Numerous early publications included the claim that FP required less energy than conventional processing methods.[53,56] This was based on the observation that once the reaction was begun, no additional energy input was required. However, no detailed energy balance has been performed to verify this claim. Moreover, unless the conversion of a monofunctional monomer is 100%, some purification is required, which would reduce the energy advantage.

4.38.5.26.3 Rapid synthesis of materials

For all of the chemistries studied, a clear advantage over bulk polymerization is the speed at which materials can be prepared. The high temperature increases the rate of reaction but because that reaction is localized, the process can be carried out safely. For monoacrylates, the high temperature leads to relatively low molecular weights but this may be acceptable for some applications.

4.38.5.26.4 Preparation of hydrogels

Frontal preparation of hydrogels is a promising area. The first example was performed by Washington and Steinbock in 2001 with *N*-isopropylacrylamide.[191] They were able make a polymer with the expected temperature-dependent properties but in much less time than with a batch polymerization.

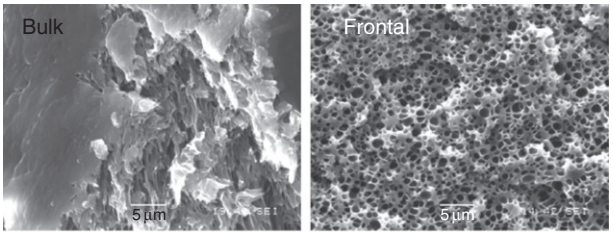

Figure 38 A comparison of porous polyacrylamide prepared by bulk polymerization and by frontal polymerization. Adapted from Lu, G. D.; Yan, Q. Z.; Ge, C. C. *Polym. Int.* **2007**, *56*, 1016–1020.[192]

Lu *et al.*[192] shows that porous polyacrylamide could be prepared frontally using $NaHCO_3$ as a foaming agent. The frontal samples (**Figure 38**) exhibited higher swelling rate and swelling ratio than the bulk polymerized samples. Pujari *et al.*[193] studied a series of glycidyl methacrylate-ethylene dimethacrylate copolymers synthesized by FP and by dispersion polymerization. They found that the frontal samples had higher internal pore volume and surface area than those prepared by dispersion polymerization but they had inferior surface morphologies.

Tu *et al.*[194] prepared amphiphilic gels in *N*-methyl-2-pyrrolidone as the solvent. They found the gels had good swelling capacity in water and organic solvents but could be prepared more rapidly than via bulk polymerization. Fang *et al.*[195] frontally prepared *N*-vinyl pyrrolidinone-based thermosensitive hydrogels in glycerol. Feng *et al.*[196] prepared macroporous polyacrylamide and poly (*N*-isopropylacrylamide) monoliths using FP.

Yan *et al.*[197–199] studied the FP of starch-grafted hydrogels. They used partially neutralized acrylic acid in water containing starch and bisacrylamide with persulfate as the initiator and determined that they hydrogels produced were spatially homogeneous.

All the investigators Mariani and his co-workers prepared poly(*N,N*-dimethylacrylamide) hydrogels[91] and super water absorbent hydrogels frontally.[200] Gavini *et al.*[89] evaluated FP to prepare drug controlled release systems based on polyacrylamide. They tested the sodium salt of diclofenac as the drug to be released and found that it survived the FP process. They also found that the samples showed comparable drug release characteristics to those of the batch polymerized samples.

4.38.5.26.5 Consolidation of stone

Proietti *et al.*,[201] Mariani *et al.*,[202] and Vicini *et al.*[203] have studied FP to consolidate stone. The idea is to allow an acrylate–initiator solution to infuse into a stone structure and then start a front to cure the monomer. The advantage over two-part formulations is that the resin would have a long time to infuse before curing. The advantage over autoclave curing is the material can be prepared in place and not moved to a lab.

4.38.5.26.6 Autoclaveless curing of large composites

White explored the idea of using the frontal curing of large composite parts as a means to avoid the charring that can occur when heat released from the curing causing a thermal runaway.[204,205] This approach is worth further exploration.

4.38.5.26.7 Cure-on-demand repair and adhesives

A promising application of FP is cure-on-demand repair and adhesives. The concept is to use a system with a very long pot life that can be used as a putty to fill a hole (**Figure 39**) in a floor, wall, or wood, which can be locally heated to start a front that rapidly cures the resin. The approach can also be applied to creating a wood adhesive. It would be especially exciting it if could be applied to the rapid repair of composites.

4.38.6 Conclusions

The three modes of FP have proven to offer advantages for different applications. Photofrontal polymerization is driven by a continuous flux of energy and has been applied to the preparation of microfluidic chips. It can be applied to any photopolymerization. IFP relies on the gel effect to create a slowly moving localized polymerization through monomers like methyl methacrylate. This method can be used to prepare gradient refractive index materials.

Thermal frontal polymerization can be applied to the widest range of materials. Any polymerization that follows

Figure 39 Cure-on-demand repair of a stone floor using an acrylate-based putty filled with kaolin. The coin is a US quarter.

Arrhenius kinetics and is highly exothermic can support localized polymerizations that propagate. Frontal polymerization has been studied with many different polymerization mechanisms but free-radical polymerization is the most studied. Most of the work has focused on the dynamics of the process, but recently applications have been studied. Hydrogels have been prepared frontally, which have superior properties to those prepared by conventional methods.

The major advantage of thermal frontal polymerization is the high rate of conversion. Cure-on-demand applications appear to be the most promising use for this approach.

References

1. Pearlstein, A. J. *J. Phys. Chem.* **1985**, *89*, 1054–1058.
2. Pearlstein, A. J.; Harris, R. M.; Terronesq, G. *J. Fluid. Mech.* **1989**, *202*, 443–465.
3. Terrones, G.; Pearlstein, A. J. *Phys. Fluids A* **1989**, *1*, 845–853.
4. Briskman, V. A. In *Polymer Research in Microgravity: Polymerization and Processing*; Downey, J. P.; Pojman, J. A., Eds.; ACS Symposium Series No. 793; American Chemical Society: Washington, DC, 2001; pp 97–110.
5. Terrones, G.; Pearlstein, A. J. *Macromolecules* **2001**, *34*, 3195–3204.
6. Terrones, G.; Pearlstein, A. J. *Macromoleules* **2004**, *37*, 1565–1575.
7. Cabral, J. T.; Hudson, S. D.; Harrison, C.; Douglas, J. F. *Langmuir* **2004**, *20*, 10020–10029.
8. Koike, Y.; Hatanaka, H.; Otsuka, Y. *Appl. Opt.* **1984**, *23*, 1779–1783.
9. Ohtsuka, Y.; Koike, Y. *Appl. Opt.* **1984**, *23*, 1774–1778.
10. Righetti, P. G.; Bossi, A.; Giglio, M.; *et al. Electrophoresis* **1994**, *15*, 1005–1013.
11. Warren, J. A.; Cabral, J. T.; Douglas, J. F. *Phys. Rev. E* **2005**, *72*, 021801.
12. Norrish, R. G. W.; Smith, R. R. *Nature* **1942**, *150*, 336–337.
13. Trommsdorff, E.; Köhle, H.; Lagally, P. *Makromol. Chem.* **1948**, *1*, 169–198.
14. Koike, Y.; Takezawa, Y.; Ohtsuka, Y. *Appl. Opt.* **1988**, *27*, 486–491.
15. Koike, Y.; Nihei, E.; Tanio, N.; Ohtsuka, Y. *Appl. Opt.* **1990**, *29*, 2686–2691.
16. Koike, Y. *Polymer* **1991**, *32*, 1737–1745.
17. Koike, Y. In *Polymers for Lightwave and Integrated Optics*; Hornak, L. A., Ed.; Marcel Dekker: New York, NY, 1992; pp 71–104.
18. Koike, Y.; Nihei, E. U.S. Patent 5,253,323, 1993.
19. Ishigure, T.; Nihei, E.; Koike, Y. *Appl. Opt.* **1994**, *33*, 4261–4266.
20. Koike, Y.; Asakawa, A.; Wu, S. P.; Nihei, E. *Appl. Opt.* **1995**, *34*, 4669–4673.
21. Sasaki, K.; Koike, Y. U. S. Patent 5,450,232, 1995.
22. Wu, S. P.; Nihei, E.; Koike, Y. *Polymer J.* **1995**, *27*, 21–25.
23. Nihei, E.; Ishigure, T.; Koike, Y. *Appl. Opt.* **1996**, *35*, 7085–7090.
24. Tagaya, A.; Teramoto, S.; Nihei, E.; *et al. Appl. Opt.* **1997**, *36*, 572–578.
25. Koike, Y.; Hidaka, H.; Ohtsuka, Y. *Appl. Opt.* **1985**, *24*, 4321–4325.
26. Koike, Y.; Koike, K. *J. Polym. Sci. Part B: Polym. Phys.* **2011**, *49*, 2–17.
27. Golubev, V. B.; Gromov, D. G.; Korolev, B. A. *J. Appl. Polym. Sci.* **1992**, *46*, 1501–1502.
28. Gromov, D. G.; Frisch, H. L. *J. Appl. Polym. Sci.* **1992**, *46*, 1499–1500.
29. Ivanov, V. V.; Stegno, E. V.; Pushchaeva, L. M. *Chem. Phys. Rep.* **1997**, *16*, 947–951.
30. Ivanov, V. V.; Stegno, E. V.; Pushchaeva, L. M. *Polym. Sci. Ser. A* **2002**, *44*, 1017–1022.
31. Lewis, L. L.; DeBisschop, C. A.; Pojman, J. A.; Volpert, V. A. In *Nonlinear Dynamics in Polymeric Systems*; Pojman, J. A.; Tran-Cong-Miyata, Q., Eds.; ACS Symposium Series No. 869; American Chemical Society: Washington, DC, 2003; pp 169–185.
32. Lewis, L. L.; DeBisschop, C. S.; Pojman, J. A.; Volpert, V. A. *J. Polym. Sci. Part A Polym. Chem.* **2005**, *43*, 5774–5786.
33. Lewis, L. L.; Massey, K. N.; Meyer, E. R.; *et al. Opt. Laser. Eng.* **2008**, *46*, 900–910.
34. Evstratova, S. I.; Antrim, D.; Fillingane, C.; Pojman, J. A. *J. Polym. Sci. Part A: Polym. Chem.* **2006**, *44*, 3601–3608.
35. Ohlemiller, T. J. *Prog. Energy Combust. Sci.* **1985**, *11*, 277–310.
36. Spade, C. A.; Volpert, V. A. *Math. Comp. Model.* **1999**, *30*, 67–73.
37. Spade, C. A.; Volpert, V. A. *Macromol. Theory Simul.* **2000**, *9*, 26–46.
38. Schult, D. A.; Spade, C. A.; Volpert, V. A. *Appl. Math. Lett.* **2002**, *15*, 749–754.
39. Masere, J.; Lewis, L. L.; Pojman, J. A. *J. Appl. Polym. Sci.* **2001**, *80*, 686–691.
40. Masere, J.; Chekanov, Y.; Warren, J. R.; *et al. J. Polym. Sci. Part A: Polym. Chem.* **2000**, *38*, 3984–3990.
41. Barelko, V. V.; Barkalov, I. M.; Goldanskii, V. I.; *et al. Adv. Chem. Phys.* **1988**, *74*, 339–385.
42. Barelko, V. V.; Barkalov, I. M.; Kiryukhin, D. P. *Russ. Chem. Rev.* **1990**, *59*, 205–217.
43. Kiryukhin, D. P.; Barelko, V. V.; Barkalov, I. M. *High Energy Chem.* **1999**, *33*, 133–144.
44. Volodin, J. E.; Zvyagin, V. N.; Ivanova, A. N.; Barelko, V. V. *Adv. Chem. Phys.* **1990**, *77*, 551–606.
45. Barelko, V. V.; Kiryukhin, D. P. *Russ. Chem. Rev.* **1994**, *63*, 491.
46. Kiryukhin, D. P.; Barkalov, I. M. *Polym. Sci. Ser. B* **2000**, *42*, 244–253.
47. Kiryukhin, D. P.; Barkalov, I. M. *Russ. Chem. Rev.* **2003**, *72*, 217–231.
48. Kiryukhin, D. P.; Kichigina, G. A.; Barelko, V. V. *Polym. Sci. Ser. B* **2010**, *52*, 221–226.
49. Chechilo, N. M.; Enikolopyan, N. S. *Dokl. Phys. Chem.* **1974**, *214*, 174–176.
50. Chechilo, N. M.; Enikolopyan, N. S. *Dokl. Phys. Chem.* **1975**, *221*, 392–394.
51. Chechilo, N. M.; Enikolopyan, N. S. *Dokl. Phys. Chem.* **1976**, *230*, 840–843.
52. Chechilo, N. M.; Khvilivitskii, R. J.; Enikolopyan, N. S. *Dokl. Akad. Nauk SSSR* **1972**, *204*, 1180–1181.
53. Davtyan, S. P.; Zhirkov, P. V.; Vol'fson, S. A. *Russ. Chem. Rev.* **1984**, *53*, 150–163.
54. Pojman, J. A. *J. Am. Chem. Soc.* **1991**, *113*, 6284–6286.
55. Pojman, J. A.; Ilyashenko, V. M.; Khan, A. M. *J. Chem. Soc. Faraday Trans.* **1996**, *92*, 2825–2837.
56. Khan, A. M.; Pojman, J. A. *Trends Polym. Sci. (Cambridge, U.K.)* **1996**, *4*, 253–257.
57. Washington, R. P.; Steinbock, O. *Polym. News* **2003**, *28*, 303–310.
58. Merzhanov, A. G.; Borovinskaya, I. P. *Dokl. Nauk SSSR* **1972**, *204*, 336–339.
59. Merzhanov, A. G. *Archiv. Comb.* **1981**, *1*, 23.
60. Varma, A.; Lebrat, J.-P. *Chem. Eng. Sci.* **1992**, *47*, 2179–2194.
61. Puszynski, J.; Degreve, J.; Hlavacek, V. *Ind. Eng. Chem. Res.* **1987**, *26*, 1424–1434.
62. Anselm-Tamburini, U.; Munir, Z. A. *J. Appl. Phys.* **1989**, *66*, 5039–5045.
63. Merzhanov, A. G. *Int. J. SHS* **1993**, *2*, 113–157.
64. Merzhanov, A. G. *Combust. Sci. Tech.* **1994**, *98*, 307–336.
65. Dvoryankin, A. V.; Strunina, A. G.; Merzhanov, A. G. *Combust. Explos. Shock Waves* **1982**, *18*, 134–139.
66. Merzhanov, A. G.; Dvoryankin, A. V.; Strunina, A. G. *Dokl. Phys. Chem.* **1982**, *267*, 869–872.
67. Sivashinsky, G. I. *SIAM J. Appl. Math.* **1981**, *40*, 432–438.
68. Volpert, A. I.; Volpert, V. A.; Volpert, V. A. *Traveling Wave Solutions of Parabolic Systems*; American Mathematical Society, Providence, RI, 1994.
69. Strunin, D. V.; Strunina, A. G.; Rumanov, E. N.; Merzhanov, A. G. *Phys. Lett. A* **1994**, *192*, 361–363.
70. Davtyan, S. P.; Surkov, N. F.; Rozenberg, B. A.; Enikolopyan, N. S. *Dokl. Phys. Chem.* **1977**, *232*, 64–67.
71. Zhizhin, G. V.; Segal, A. S. *Z. Prikl. Meh. Tehn. Fiz.* **1988**, 62–71.
72. Babadzhanyan, A. S.; Volpert, V. A.; Volpert, V. A.; *et al. Combust. Explos. Shock Waves* **1988**, *24*, 711–719.
73. Babadzhanyan, A. S.; Volpert, V. A.; Volpert, V. A.; *et al. Combust. Explos. Shock Waves* **1989**, *25*, 23–31.
74. Megrabova, I. N.; Volpert, V. A.; Volpert, V. A.; Davtyan, S. P. *Dokl. Phys. Chem.* **1990**, *307*, 618–620.
75. Megrabova, I. N.; Volpert, V. A.; Volpert, V. A.; Davtyan, S. P. *Combust. Explos. Shock Waves* **1991**, *26*, 413–417.
76. Babadzhanyan, A. S.; Volpert, V. A.; Davtyan, S. P. *Dokl. Phys. Chem.* **1987**, *293*, 357–360.
77. Zhizhin, G. V.; Segal, A. S.; Babadzhanyan, A. S.; *et al. Kinet. Katal.* **1986**, *27*, 1310–1314.
78. Solovyov, S. E.; Volpert, V. A.; Davtyan, S. P. *SIAM J. Appl. Math.* **1993**, *53*, 907–914.
79. Pojman, J. A.; Popwell, S.; Fortenberry, D. I.; *et al.* In *Nonlinear Dynamics in Polymeric Systems*; Pojman, J. A.; Tran-Cong-Miyata, Q., Eds.; ACS Symposium Series No. 869; American Chemical Society: Washington, DC, 2003; pp 106–120.
80. Pojman, J. A.; Tran-Cong-Miyata, Q. Eds. *Nonlinear Dynamics with Polymers: Fundamentals, Methods and Applications*; Wiley-VCH Verlag GmbH & Co KGaA: Weinheim, Germany, 2010.
81. Ritter, I. R.; Olmstead, W. E.; Volpert, V. A. *SIAM J. Appl. Math.* **2003**, *63*, 1831–1848.
82. Heifetz, A.; Ritter, L. R.; Olmstead, W. E.; Volpert, V. A. *Math. Comput. Model.* **2005**, *41*, 271–285.
83. Nason, C.; Roper, T.; Hoyle, C.; Pojman, J. A. *Macromolecules* **2005**, *38*, 5506–5512.
84. Pojman, J. A.; Willis, J.; Fortenberry, D.; *et al. J. Polym. Sci. Part A: Polym. Chem.* **1995**, *33*, 643–652.
85. Pojman, J. A.; Khan, A. M.; West, W. *Polym. Prepr. (Am Chem. Soc. Div. Polym. Chem.)* **1992**, *33*, 1188–1189.

86. Pojman, J. A.; Craven, R.; Khan, A.; West, W. *J. Phys. Chem.* **1992**, *96*, 7466–7472.
87. Nagy, I. P.; Pojman, J. A. *J. Phys. Chem.* **1996**, *100*, 3299–3304.
88. Pojman, J. A.; Curtis, G.; Ilyashenko, V. M. *J. Am. Chem. Soc.* **1996**, *118*, 3783–3784.
89. Gavini, E.; Mariani, A.; Rassu, G.; *et al. Eur. Polym. J.* **2009**, *45*, 690–699.
90. Alzari, V.; Mariani, A.; Monticelli, O.; *et al. J. Polym. Sci. Part A: Polym. Chem.* **2010**, *48*, 5375–5381.
91. Caria, G.; Alzari, V.; Monticelli, O.; *et al. J. Polym. Sci. Part A: Polym. Chem.* **2009**, *47*, 1422–1428.
92. Chen, S. H.; Sui, J.; Chen, L. *Colloid Polym. Sci.* **2005**, *283*, 932–936.
93. Khanukaev, B. B.; Kozhushner, M. A.; Enikolopyan, N. S. *Combust. Explos. Shock Waves* **1974**, *10*, 562–568.
94. Khanukaev, B. B.; Kozhushner, M. A.; Enikolopyan, N. S. *Dokl. Phys. Chem.* **1974**, *214*, 84–87.
95. Goldfeder, P. M.; Volpert, V. A.; Ilyashenko, V. M.; *et al. J. Phys. Chem. B* **1997**, *101*, 3474–3482.
96. Pojman, J. A.; Nagy, I. P.; Salter, C. *J. Am. Chem. Soc.* **1993**, *115*, 11044–11045.
97. Siggia, S.; Hanna, J. G. *Quantitative Organic Analysis Via Functional Groups*; Wiley: New York, NY, 1979.
98. Kolthoff, I. M.; Sandell, E. B.; Meehan, E. J.; Bruckenstein, S. *Quantitative Chemical Analysis*; Macmillan: London, UK, 1969; pp 842–847.
99. Fortenberry, D. I.; Pojman, J. A. *J. Polym. Sci. Part A: Polym. Chem.* **2000**, *38*, 1129–1135.
100. Pojman, J. A.; Willis, J. R.; Khan, A. M.; West, W. W. *J. Polym. Sci. Part A: Polym. Chem.* **1996**, *34*, 991–995.
101. Sówka, E.; Leonowicz, M.; Ka´zmierczak, J.; *et al. Physica B* **2006**, *384*, 282–285.
102. Kholpanov, L. P.; Zakiev, S. E.; Pomogailo, A. D. *Polym. Sci. Ser. A* **2006**, *48*, 11–17.
103. Pomogailo, A. D.; Dzhardimalieva, G. I. *Polym. Sci. Ser. A* **2004**, *46*, 250–263.
104. Kholpanov, L. P.; Zakiev, S. E.; Pomogailo, A. D. *Dokl. Phys. Chem.* **2004**, *395*, 84–87.
105. Dzhardimalieva, G. I.; Golubeva, N. D.; Pomogailo, A. D. *Diffus. Defect Data Pt. B* **2003**, *94*, 323–328.
106. Dzhardimalieva, G. I.; Pomogailo, A. D.; Volpert, V. A. *J. Inorg. Organomet. Polym.* **2002**, *12*, 1–21.
107. Barelko, V. V.; Pomogailo, A. D.; Dzhardimalieva, G. I.; *et al. Chaos* **1999**, *9*, 342–347.
108. Pomogailo, A. D.; Savost'yanov, V. S.; Dzhadimarlieva, G. I.; *et al. Russ. Chem. Bull.* **1995**, *44*, 1056–1061.
109. Savostyanov, V. S.; Kritskaya, D. A.; Ponomarev, A. N.; Pomogailo, A. D. *J. Polym. Sci. Part A: Polym. Chem.* **1994**, *32*, 1201–1212.
110. Mariani, A.; Nuvoli, D.; Alzari, V.; Pini, M. *Macromolecules* **2008**, *41*, 5191–5196.
111. Enikolopyan, N. S.; Kozhushner, M. A.; Khanukaev, B. B. *Dokl. Phys. Chem.* **1974**, *217*, 676–678.
112. Pojman, J. A.; Khan, A. M.; Mathias, L. J. *Microgravity Sci. Technol.* **1997**, *X*, 36–40.
113. Tredici, A.; Pecchini, R.; Morbidelli, M. *J. Polym. Sci. Part A: Polym. Chem.* **1998**, *36*, 1117–1126.
114. Sawada, H. *Thermodynamics of Polymerization*; Marcel Dekker: New York, NY, 1976.
115. Odian, G. *Principles of Polymerization*, 4th ed.; Wiley: New York, NY, 2004.
116. Garbey, M.; Taik, A.; Volpert, V. *Quart. Appl. Math.* **1998**, *56*, 1–35.
117. Garbey, M.; Taik, A.; Volpert, V. *Prepr. CNRS* **1994**, *187*, 1–42.
118. Garbey, M.; Taik, A.; Volpert, V. *Quart. Appl. Math.* **1996**, *54*, 225–247.
119. Bowden, G.; Garbey, M.; Ilyashenko, V. M.; *et al. J. Phys. Chem. B* **1997**, *101*, 678–686.
120. McCaughey, B.; Pojman, J. A.; Simmons, C.; Volpert, V. A. *Chaos* **1998**, *8*, 520–529.
121. Bazile, M., Jr.; Nichols, H. A.; Pojman, J. A.; Volpert, V. *J. Polym. Sci. Part A: Polym. Chem.* **2002**, *40*, 3504–3508.
122. Bidali, S.; Ducrot, A.; Mariani, A.; Rustici, M. *e-Polymers* **2004**, *44*, 1–20.
123. Pojman, J. A.; Gunn, G.; Owens, J.; Simmons, C. *J. Phys. Chem. Part B* **1998**, *102*, 3927–3929.
124. Texier-Picard, R.; Pojman, J. A.; Volpert, V. A. *Chaos* **2000**, *10*, 224–230.
125. Pojman, J. A.; Epstein, I. R. *J. Phys. Chem.* **1990**, *94*, 4966–4972.
126. Pojman, J. A.; Epstein, I. R.; Karni, Y.; Bar-Ziv, E. *J. Phys. Chem.* **1991**, *95*, 3017–3021.
127. Ostrach, S. *Annu. Rev. Fluid Mech.* **1982**, *14*, 313–345.
128. Asakura, K.; Nihei, E.; Harasawa, H.; *et al.* In *Nonlinear Dynamics in Polymeric Systems*; Pojman, J. A.; Tran-Cong-Miyata, Q., Eds.; ACS Symposium Series No. 869; American Chemical Society: Washington, DC, 2003; pp 135–146.
129. Gusika, P. L. *Khim. Fiz.* **1982**, *7*, 988–993.
130. Maksimov, Y. M.; Pak, A. T.; Lavrenchuk, G. V.; *et al. Comb. Expl. Shock Waves* **1979**, *15*, 415–418.
131. Pojman, J. A. In *Chemomechanical Instabilities in Responsive Materials (NATO Science for Peace and Security Series A: Chemistry and Biology)*; Borckmans, P.; De Kepper, P.; Khokhlov, A. R. Métens, S., Eds.; Springer: Dordrecht, The Netherlands, 2009; pp 221–240.
132. Pojman, J. A. In *Nonlinear Dynamics with Polymers: Fundamentals, Methods and Applications*; Pojman, J. A.; Tran-Cong-Miyata, Q., Eds.; Wiley-VCH Verlag GmbH & Co. KGaA: Weinheim, Germany, 2010; pp 45–68.
133. Begishev, V. P.; Volpert, V. A.; Davtyan, S. P.; Malkin, A. Y. *Dokl. Akad. Nauk SSSR* **1973**, *208*, 892.
134. Begishev, V. P.; Volpert, V. A.; Davtyan, S. P.; Malkin, A. Y. *Dokl. Phys. Chem.* **1985**, *279*, 1075–1077.
135. Pojman, J. A.; Ilyashenko, V. M.; Khan, A. M. *Physica D* **1995**, *84*, 260–268.
136. Ilyashenko, V. M.; Pojman, J. A. *Chaos* **1998**, *8*, 285–287.
137. Solovyov, S. E.; Ilyashenko, V. M.; Pojman, J. A. *Chaos* **1997**, *7*, 331–340.
138. Shult, D. A.; Volpert, V. A. *Int. J. SHS* **1999**, *8*, 417–440.
139. Spade, C. A.; Volpert, V. A. *Combust. Theory Model.* **2001**, *5*, 21–39.
140. Gross, L. K.; Volpert, V. A. *Stud. Appl. Math.* **2003**, *110*, 351–376.
141. Commissiong, D. M. G.; Gross, L. K.; Volpert, V. A. In *Nonlinear Dynamics in Polymeric Systems*; Pojman, J. A.; Tran-Cong-Miyata, Q., Eds.; ACS Symposium Series No. 869; American Chemical Society: Washington, DC, 2003; pp 147–159.
142. Shkadinsky, K. G.; Khaikin, B. I.; Merzhanov, A. G. *Combust. Explos. Shock Waves* **1971**, *1*, 15–22.
143. Masere, J.; Pojman, J. A. *J. Chem. Soc. Faraday Trans.* **1998**, *94*, 919–922.
144. Masere, J.; Stewart, F.; Meehan, T.; Pojman, J. A. *Chaos* **1999**, *9*, 315–322.
145. Tryson, G. R.; Shultz, A. R. *J. Polym. Sci. Polym. Phys. Ed.* **1979**, *17*, 2059–2075.
146. Gray, K. N. Master's Thesis, University of Southern Mississippi, 1988.
147. Manz, B.; Masere, J.; Pojman, J. A.; Volke, F. *J. Polym. Sci. Part A: Polym. Chem.* **2001**, *39*, 1075–1080.
148. Pojman, J. A.; Masere, J.; Petretto, E.; *et al. Chaos* **2002**, *12*, 56–65.
149. Huh, D. S.; Kim, H. S. *Polym. Int.* **2003**, *52*, 1900–1904.
150. Volpert, V. A.; Volpert, V. A.; Pojman, J. A. *Chem. Eng. Sci.* **1994**, *14*, 2385–2388.
151. McFarland, B.; Popwell, S.; Pojman, J. A. *Macromolecules* **2004**, *37*, 6670–6672.
152. McFarland, B.; Popwell, S.; Pojman, J. A. *Macromolecules* **2006**, *39*, 53–63.
153. Binici, B.; Fortenberry, D. I.; Leard, K. C.; *et al. J. Polym. Sci. Part A: Polym. Chem.* **2006**, *44*, 1387–1395.
154. Nason, C.; Pojman, J. A.; Hoyle, C. *J. Polym. Sci. Part A: Polym. Chem.* **2008**, *46*, 8091–8096.
155. Pojman, J. A.; Viner, V.; Binici, B.; *et al. Chaos* **2007**, *17*, 033125.
156. Viner, V. G.; Pojman, J. A.; Golovaty, D. *Physica D* **2010**, *239*, 838–847.
157. Perry, M. F.; Volpert, V. A.; Lewis, L. L.; *et al. Macromol. Theory Simul.* **2003**, *12*, 276–286.
158. Hoyle, C. E.; Lee, T. Y.; Roper, T. *J. Polym. Sci. Part A: Polym. Chem.* **2004**, *52*, 5301–5338.
159. Okay, O.; Bowman, C. N. *Macromol. Theory Simul.* **2005**, *14*, 267–277.
160. Pojman, J. A.; Varisli, B.; Perryman, A.; *et al. Macromolecules* **2004**, *37*, 691–693.
161. Devadoss, D. E.; Pojman, J. A.; Volpert, V. A. *Chem. Eng. Sci.* **2006**, *61*, 1257–1271.
162. Bidali, S.; Fiori, S.; Malucelli, G.; Mariani, A. *e-Polymers* **2003**, *060*, 1–12.
163. Mariani, A.; Fiori, S.; Chekanov, Y.; Pojman, J. A. *Macromolecules* **2001**, *34*, 6539–6541.
164. Fiori, S.; Mariani, A.; Ricco, L.; Russo, S. *Macromolecules* **2003**, *36*, 2674–2679.
165. Mariani, A.; Bidali, S.; Fiori, S.; *et al. e-Polymers* **2003**, *044*, 1–9.
166. Texter, J.; Ziemer, P. *Macromolecules* **2004**, *37*, 5841–5843.
167. Chen, S.; Tian, Y.; Chen, L.; Hu, T. *Chem. Mater.* **2006**, *18*, 2159–2163.
168. Hu, T.; Chen, S.; Tian, Y.; *et al. J. Polym. Sci. Part A: Polym. Chem.* **2006**, *44*, 3018–3024.
169. Mariani, A.; Fiori, S.; Bidali, S.; *et al. J. Polym. Sci. Part A: Polym. Chem.* **2008**, *46*, 3344–3352.
170. Arutiunian, K. A.; Davtyan, S. P.; Rozenberg, B. A.; Enikolopyan, N. S. *Dokl. Akad. Nauk SSSR* **1975**, *223*, 657–660.
171. Chekanov, Y.; Arrington, D.; Brust, G.; Pojman, J. A. *J. Appl. Polym. Sci.* **1997**, *66*, 1209–1216.
172. Frulloni, E.; Salinas, M. M.; Torre, L.; *et al. J. Appl. Polym. Sci.* **2005**, *96*, 1756–1766.
173. Mariani, A.; Bidali, S.; Fiori, S.; *et al. J. Polym. Sci. Part A: Polym. Chem.* **2004**, *42*, 2066–2072.
174. Scognamillo, S.; Bounds, C.; Luger, M.; *et al. J. Polym. Sci. Part A: Polym. Chem.* **2010**, *48*, 2000–2005.
175. Pojman, J. A.; Elcan, W.; Khan, A. M.; Mathias, L. *J. Polym. Sci. Part A: Polym. Chem.* **1997**, *35*, 227–230.
176. Pojman, J. A.; Griffith, J.; Nichols, H. A. *e-Polymers* **2004**, *13*, 1–7.
177. Dixon, G. D. U.S. Patent 4,222,835, 1980.
178. Scranton, A. B.; Rangarajan, B.; Coons, L. S. U.S. Patent 5,855,837, 1999.
179. Pojman, J. A.; McCardle, T. W. U.S. Patent 6,313,237, 2001.
180. Pojman, J. A.; McCardle, T. W. U.S. Patent 6,057,406, 2000.
181. Chekanov, Y. A.; Pojman, J. A. *J. Appl. Polym. Sci.* **2000**, *78*, 2398–2404.
182. Pfeil, A.; Burgel, T.; Morbidelli, M.; Rosell, A. U.S. Patent 6,533,503, 2003.
183. Bürgel, T.; Böck, M. U.S. Patent 6,815,517, 2004.
184. Gregory, S. U.S. Patent 6,245,827, 2001.

185. Crivello, J. V. *J. Polym. Sci. Part A: Polym. Chem.* **2007**, *45*, 4331–4340.
186. Pojman, J. A.; McFarland, B.; Popwell, S. US Patent pending.
187. Pojman, J. A.; Fortenberry, D.; Lewis, L. L.; *et al.* ; ACS Symp. Ser. (Solvent-Free Polymerization and Processes), *Solvent-Free Synthesis by Free-Radical Frontal Polymerization*; Vol. 713; American Chemical Society: Washington, DC, 1998; 140–153.
188. Hu, T.; Chen, S.; Tian, Y.; *et al. J. Polym. Sci. Part A: Polym. Chem.* **2007**, *45*, 873–881.
189. Cai, X.; Chen, S.; Chen, L. *J. Polym. Sci. Part A: Polym. Chem.* **2008**, *46*, 2177–2185.
190. Chen, S.; Hu, T.; Yu, H.; *et al. J. Polym. Sci. Part A: Polym. Chem.* **2007**, *45*, 4322–4330.
191. Washington, R. P.; Steinbock, O. *J. Am. Chem. Soc.* **2001**, *123*, 7933–7934.
192. Lu, G. D.; Yan, Q. Z.; Ge, C. C. *Polym. Int.* **2007**, *56*, 1016–1020.
193. Pujari, N. S.; Vishwakarma, A. R.; Pathak, T. S.; *et al. Polym. Int.* **2004**, *53*, 2045–2050.
194. Tu, J.; Chen, L.; Fang, Y.; *et al. J. Polym. Sci. Part A: Polym. Chem.* **2010**, *48*, 823–831.
195. Fang, Y.; Yu, H.; Chen, L.; Chen, S. *Chem. Mater.* **2009**, *21*, 4711–4718.
196. Feng, Q.; Yan, Q.-z; Ge, C.-c *Chin. J. Polym. Sci.* **2009**, *27*, 747–753.
197. Yan, Q. Z.; Su, X. T.; Zhang, W. F.; Ge, C. C. *Chem. J. Chin. Univ.* **2005**, *26*, 1363–1365.
198. Yan, Q.-Z.; Zhang, W.-F.; Lu, G.-D.; *et al. Chem. Eur. J.* **2005**, *11*, 6609–6615.
199. Yan, Q.; Zhang, W. F.; Lu, G. D.; *et al. Chem. Eur. J.* **2006**, *12*, 3303–3309.
200. Scognamillo, S.; Alzari, V.; Nuvoli, D.; *et al. J. Polym. Sci. Part A: Polym. Chem.* **2011**, n/a-n/a.
201. Proietti, N.; Capitani, D.; Cozzolino, S.; *et al. J. Phys. Chem. B* **2006**, *110*, 23719–23728.
202. Mariani, A.; Bidali, S.; Cappelletti, P.; *et al. e-Polymers* **2006**.
203. Vicini, S.; Mariani, A.; Princi, E.; *et al. Polym. Adv. Technol.* **2005**, *16*, 293–298.
204. Kim, C.; Teng, H.; Tucker, C. L.; White, S. R. *J. Comp. Mater.* **1995**, *29*, 1222–1253.
205. White, S. R.; Kim, C. *J. Reinf. Plast. Compos.* **1993**, *12*, 520–535.

Biographical Sketch

John A. Pojman is a professor in the Macromolecular Science Division of the Department of Chemistry at Louisiana State University. He earned his doctorate in chemical physics from the University of Texas at Austin. Dr. Pojman was a faculty member at the University of Southern Mississippi for 18 years. He has published over 100 peer-reviewed publications and coedited three monographs and coauthored another one. His interests include nonlinear dynamics with polymers, cure-on-demand polymerizations, nonequilibrium thermodynamics of miscible fluids, microgravity research, and the aquatic salamanders of Louisiana. He also claims the world's largest collection of pocket protectors.

4.39 Microwave-Assisted Polymerization

D Bogdal, Politechnika Krakowska, Krakow, Poland

Microwave irradiation is a rapid means of heating materials for domestic, industrial, and medical purposes. Microwaves offer a number of advantages over conventional heating such as noncontact heating (reduction of overheating of material surfaces), energy transfer instead of heat transfer (penetrative radiation), material-selective and volumetric heating, fast start-up and stopping, and, last but not least, reverse thermal effect. Moreover, the reduced time of processing under microwave conditions found for a great number of chemical reactions was the main reason that microwave techniques became so attractive for chemists, who, in the last two decades, have begun to apply this technique as a routine in their everyday practice.[1]

The fundamentals of electromagnetic heating and processing of polymers, resins, and related composites are summarized in a book chapter.[2] An overview of the application of microwaves in polymer synthesis can be found in review articles[3,4] and in comprehensive reviews with over 600 references cited in recently published books and chapters.[5,6] Therefore, the purpose of this chapter is to provide some representative examples concerning the application of microwave irradiation to polymer chemistry.

4.39.1 Interaction of Microwaves with Materials

Microwaves are part of the electromagnetic spectrum with frequencies of 300 GHz to 300 MHz, which corresponds to wavelengths of 1 mm to 1 m, respectively (**Figure 1**).[7] Depending on whether they are used for transmission of information (telecommunication) or transmission of energy, their major applications fall into two categories. In fact, the application of microwaves in telecommunication (mobile phones, radar, and radar-line transmissions) has caused only specially assigned frequencies to be allocated for energy transmission, that is, for industrial, scientific, or medical applications. For example, the most common microwave applicators (i.e., domestic microwave ovens) utilize the frequency of 2.45 GHz, which corresponds to the wavelength of 12.2 cm. For this reason, commercially available microwave reactors devoted for chemical use operate at the same frequency; however, some other frequencies are also available for heating.[8]

To apply microwaves to carry out chemical processes, it is most important to find at least one reagent component that is polarizable and whose dipoles can reorient (couple) rapidly in response to changing electric field of microwave radiation. In fact, the electric field component of microwave radiation is responsible for dielectric heating mechanisms since it can cause molecular motion either by migration of ionic species (conduction mechanism) (**Figure 2(a)**) or by rotation of dipolar species (dipolar polarization mechanism) (**Figure 2(b)**). At 2.45 GHz, the field oscillates 4.9×10^9 times per second, and the strong agitation, provided by cyclic reorientation of molecules, can result in an intense internal heating, which can lead to heating rates in excess of 10 °C per second when microwave radiation of a kilowatt-capacity source is used.[9]

Fortunately, a number of organic compounds and solvents fulfill these requirements and are the best candidates for microwave applications. These materials are characterized by dielectric properties, among which dielectric constant (ε_r), sometimes called electric permeability, is of the greatest importance. Dielectric constant (ε_r) is defined as the ratio of the electric permeability of the material to the electric permeability of free space (i.e., vacuum). Dielectric constants for some common materials are given in **Table 1**.

Nonpolar organic solvents (i.e., benzene, carbon tetrachloride, *n*-hexane) have low value of ε_r and, in fact, show negligible heating effects under microwave irradiation. Polar organic solvents (i.e., water, acetonitrile, ethyl alcohol) are characterized by relatively high values of ε_r, and, in turn, can be heated by dielectric heating mechanism under microwave irradiation. Most plastics range in the low values of ε_r (i.e., between 2 and 3); therefore,

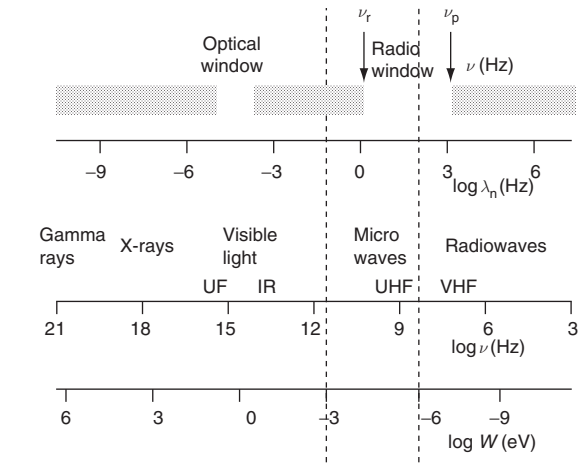

Figure 1 Spectrum of electromagnetic radiation: ν_r, lowest resonance frequency in the rotational spectrum of water; ν_p, plasma frequency of the ionosphere. Reproduced with permission from Kaatze, U. *Radiat. Phys. Chem.* **1995**, *45*, 539.[7]

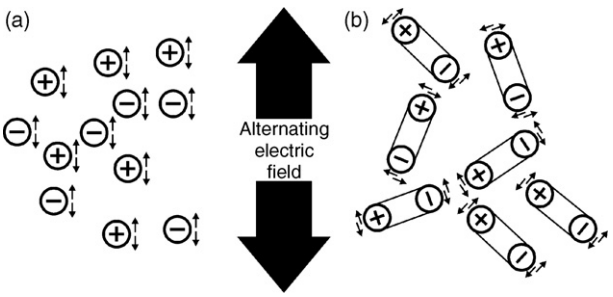

Figure 2 Interaction of charge particles and dipolar molecules with electromagnetic radiation: (a) space charge polarization and (b) orientation polarization.

some of these materials besides glass and quartz glass are used to manufacture reaction vessels for microwave application due to their good chemical as well as temperature resistance (e.g., polytetrafluoroethylene (Teflon), polyether ether ketone (PEEK)).

Heating a material in microwave ovens is based upon the ability of some liquids as well as solids to absorb and transform electromagnetic energy into heat. However, in the case of highly oscillating electric fields (ca. 10^9 Hz), dielectric constant (ε_r) is turned into complex permeability: $\varepsilon^* = \varepsilon' - j\varepsilon''$. The real permeability (ε') component characterizes the ability of the material to be polarized by the electric field and thus the ability of microwaves to propagate into the material. The imaginary part of the complex electric permeability (ε'') is usually called the loss factor and indicates the ability of the material to dissipate the energy, that is, the efficiency of conversion of electromagnetic radiation into heat (**Box 1**).

The ratio of ε'' and ε', which is commonly called loss tangent ($\tan\delta = \varepsilon''/\varepsilon'$), is another parameter used for characterization of material absorption and heating under microwave irradiation

Box 1 Thermal runaway and temperature nonuniformity.

The loss tangent and loss angle as well as real permeability (ε') and the loss factor (ε'') are always dependent on working frequency and temperature. The effect of frequency and temperature on complex permeability is shown in **Figure 3**. According to the frequency of the electromagnetic field, three general changes can be observed in the dielectric properties as the temperature changes: (1) real permeability (ε') and the loss factor (ε'') decrease with temperature; (2) real permeability (ε') and/or the loss factor (ε'') pass through a maximum; and (3) real permeability (ε') and the loss factor (ε'') increase with temperature. As in case (1), some materials (i.e., water) become poorer microwave absorbers with rising temperature, but other 'lossy' materials can become better microwave absorbers with rising temperature as in case (2). The rate at which the temperature of such lossy materials rises is proportional to the increase of the loss factor (ε''), that is, 'the hotter they get, the quicker they get hotter'. The rapid rise in the loss factor (ε'') with temperature is therefore a major factor in thermal runaway and temperature nonuniformity.[10]

Table 1 Dielectric constants (ε_r) of some common materials at 20 °C

Material	*Dielectric constant (ε_r)*	*Material*	*Dielectric constant (ε_r)*
Vacuum	1	Titanium dioxide	100
Air (1 atm)	1.000 59	Water	80
Air (100 atm)	1.0548	Acetonitrile	38
Glass	5–10	Liquid ammonia (– 78 °C)	5
Quartz glass	5	Ethyl alcohol	25
Porcelain	5–6	Benzene	2
Mica	3–6	Carbon tetrachloride	2
Rubber	2–4	Hexane	2
Nylon	3–22	Plexiglas	3
Paper	1–3	Poly(vinyl chloride)	3
Paraffin	2–3	Polyethylene	2
Soil (dry)	2.5–3	Teflon	2
Wood (dry)	1–3	Polystyrene (foam)	1.05

Reproduced with permission from Bogdal, D. *Microwave-Assisted Organic Synthesis, One Hundred Reaction Procedures;* Elsevier: Amsterdam, The Netherlands, 2005.

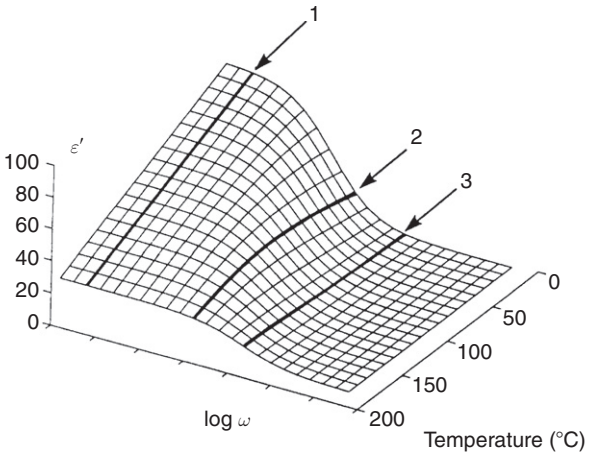

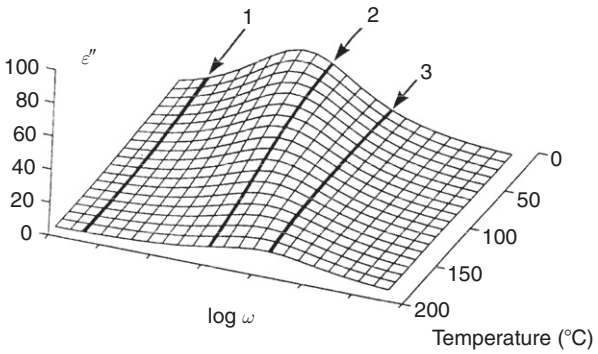

Figure 3 Change of complex dielectric permeability (i.e., ε' and ε'') with frequency and temperature. Reproduced with permission from Stuerga, D.; Delmotte, M. In *Microwaves in Organic Synthesis;* Loupy, A., Ed).; Wiley-VCH: Weinheim, Germany, 2003.[10]

and it even better describes the ability of a material to absorb microwave energy.

Loss tangent ($\tan\delta$) of some common solvents and materials is presented in Table 2, while $\tan\delta$ of water together with ε' and ε'' as a function of frequency is shown in Figure 4. It is apparent that appreciable values of $\tan\delta$ exist over a wide frequency range.

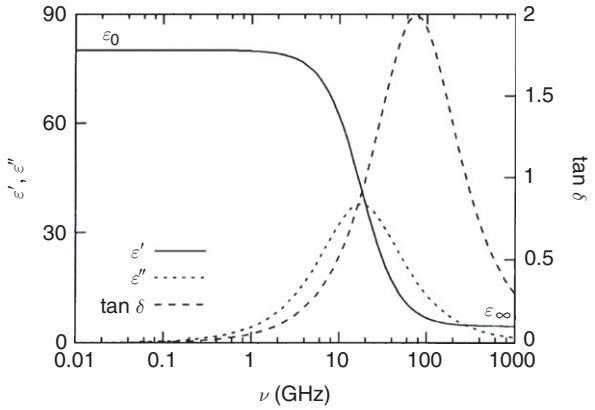

Figure 4 The loss tangent of water ($\tan\delta$) as a function of frequency together with ε' and ε''. Reproduced with permission from Gabriel, C.; Gabriel, S.; Grant, E. H.; *et al. Chem. Soc. Rev.* **1998**, *27*, 213.[9]

For instance, for water, the most effective heating as measured by $\tan\delta$ reaches its maximum at about 80 GHz, while most microwave ovens operate at a much lower frequency, that is, 2.45 GHz. A practical reason for the application of lower frequency is to heat the material throughout its interior – at a lower frequency, the radiation is not totally absorbed by the first layer of the material that it encounters and may penetrate further into the material, heating it more evenly. In other words, if the frequency is optimal for maximum heating rate, the microwaves are absorbed in the outer region of the material and penetrate only a short distance ('skin effect').[9]

The penetration depth is defined as the distance from the sample surface where the absorbed power is $1/e$ of the absorbed power at the surface. Beyond this depth, volumetric heating due to absorption of microwave energy is negligible. The penetration depth (D_p) is proportional to the wavelength of the radiation and depends on the dielectric properties of the material. For lossy dielectrics ($\varepsilon''/\varepsilon' << 1$), the penetration depth (D_p) can be calculated from the equation[11]

$$D_p = \lambda_0/2\pi * (\varepsilon')^{1/2}/\varepsilon''$$

where λ_0 is the length of electromagnetic wave.

Table 2 Loss tangents ($\tan\delta$) of different materials at 25 °C (2.45 GHz)

Solvent	*Loss tangent (tan δ)*	*Material*	*Loss tangent (tan δ)*
Water	0.12	Fused quartz	0.000 06
Ice	0.0009	Porcelain	0.001
Ethanol	0.94	Borosilicate glass	0.001
Butanol	0.57	Phosphate glass	0.0046
Acetic acid	0.17	Teflon	0.000 15
DMF	0.16	Polyethylene	0.0003
Acetonitrile	0.062	Polystyrene	0.0003
Acetone	0.054	Polycarbonate	0.0006
THF	0.047	Plexiglas^{R}	0.005
Methylene chloride	0.042	Polyamide	0.005
Hexane	0.021	Poly(vinyl chloride)	0.005
Vaseline	~0.0007	ABS (plastics)	0.006–0.019

Reproduced with permission from Bogdal, D. *Microwave-Assisted Organic Synthesis, One Hundred Reaction Procedures;* Elsevier: Amsterdam, 2005.[12]

Table 3 Microwave (2.45 GHz) penetration depth (D_p) in some common materials

Material	*Temperature (°C)*	*Penetration depth (D_p) (cm)*
Water	25	1.4
Water	95	5.7
Ice	−12	1100
Paper, cardboard	25	20–60
Wood	25	8–350
Rubber	25	15–350
Glass	25	35
Porcelain	25	56
Poly(vinyl chloride)	20	210
Epoxy resin (Araldite)	25	4100
Teflon	25	9200
Quartz glass	25	16 000

Reproduced with permission from Kubel, E. *Ind. Heating* **2005**, 43.[174]

Materials with relatively high values of the loss factor (ε'') are characterized by low values of the penetration depth (D_p), and, therefore, microwaves can be totally absorbed within the outer layers of these materials. For example, the penetration depth of water is 1.4 and 5.7 cm at 25 and 95 °C, respectively (Table 3). This means that during the experiments in a water solution on larger scales, only some parts (outer layers) of the reaction mixture interact with microwaves to generate heat, which is then transported into the rest of the mixture conventionally (i.e., by heat convection and/or conduction mechanism). On the other hand, microwaves can penetrate and pass through samples of materials with low values of the loss factor (ε'').[12]

Under microwave irradiation, the heating rate (i.e., temperature increase) of the material depends also on the shape and size of the sample. For instance, the study of the thermal behavior of alumina indicates that the temperature of the sample during microwave irradiation depends on the amount of the sample (Figure 5). In a multimode cavity, the maximum temperature was obtained for about 200 g of alumina since it had a larger surface and in turn could absorb more of the microwave energy per weight unit than, for example, 100 g of alumina. In contrast, a 500 g sample of alumina was heated with a lower heating rate than the 200 g sample, but in this case the most probable explanation is that 500 g of alumina consumed the entire microwave energy provided by the reactor, which in fact could be less per weight unit than for 200 g of alumina. Most likely, the amount of sample that would be heated most efficiently by microwaves under such experimental conditions was somewhere between 200 and 500 g of alumina. In turn, 4 g of alumina appeared as about the minimum amount for an appreciable thermal effect to be observed, while 1 g sample of alumina was unable to reach 100 °C even after a relatively long irradiation time (ca. 20 min).[13]

It is worth stressing that microwaves in comparison with conventional heating methods are the means of volumetric heating of the material, which gives rise to a very rapid energy transfer into the material being heated. In conventional heating, heat flow is initiated on the material surface and the rate of heat flow into the center is dependent on the material's thermal properties and temperature differentials. A conventional oven is required to be heated to temperatures much higher than is required by the material itself (Box 2).

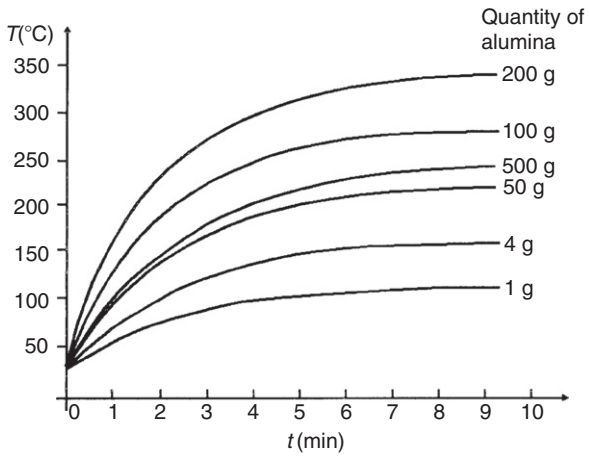

Figure 5 Thermal behavior of neutral alumina as a function of irradiation time and quantity. Reproduced with permission from Bram, G.; Loupy, A.; Majdoub, M.; Gutierrez, E.; Ruiz-Hitzky, E. *Tetrahedron* **1990**, *46*, 5167.[13]

Recently, microwave technology applied to polymer processing and particularly to polymerization process has become a subject of a great deal of academic and industrial research with a number of scientific and patent literature being generated.[1–3,15] Microwave technology has become a widely accepted and popular unconventional technology in polymer chemistry as an alternative to, and often improvement on, conventional heating.

The relationship between the loss factor (ε'') and the ability of some common materials to absorb microwave energy is shown in Figure 6.[16]

Materials with a high conductance and a low capacitance (such as metals) have a high loss factor (ε'') and the penetration depth approaches zero. Thus, these materials are considered as reflectors of microwave irradiation. In contrast,

Box 2 Temperature control.

Temperature control during microwave irradiation is a major problem that one faces during microwave-assisted chemical reactions. In general, temperature in a microwave field can be measured by means of

- fiber-optic thermometer
- shielded thermocouple
- pyrometer (IR sensor)

Maintaining good thermal contact with the material being heated is crucial when heating using microwave irradiation. Optical pyrometers and thermocouples are often used, but pyrometers measure only surface temperatures, which in fact can be much lower than the interior temperature in reaction mixtures. Application of thermocouples, which in the case of microwaves are metallic probes, screened against microwaves, can result in arcing between the thermocouple shield and the cavity walls leading to failures in a thermocouple performance.[12]

There is a general agreement that the application of fiber-optic thermometers is a reliable way to determine temperature under microwave conditions. However, according to some studies in which the reaction mixture was also monitored with a thermovision camera, it was shown that for the reactions in heterogeneous systems under microwave irradiation, the temperature measurement with a fiber-optic thermometer can lead to serious errors like pyrometry; in particular, this is observed in those experiments that are planned without any attention being paid to temperature homogeneity of the reaction mixture.[14]

Therefore, before considering the increase of reaction rates by special microwave effects (thermal or nonthermal), first we need to consider all the factors that might influence chemical reactions under microwave conditions like a reaction mechanism, diffusion of reagents, temperature profiles (gradients), and, in particular, proper design of our experiments.

Box 3 Specific microwave effects?

A sudden growth of interest in the application of microwave irradiation in almost all fields of chemistry was seen at the end of the 1980s. From the very beginning, it was realized that a number of chemical processes can be carried out with a substantial reduction in the reaction time in comparison to conventional processes. Reactions that usually take many hours or days can be run in a considerably shorter time of several minutes under the influence of microwave irradiation. These phenomena are not fully understood yet; however, there are two groups of theories that are proposed to explain the reduction of the reaction time under microwave conditions.

According to the first group, in spite of the fact that the course of the reactions is considerably shorter under microwave conditions than under conventional conditions, the kinetics and mechanism of the reactions are still the same. The time reduction is the result of sudden and, sometimes, uncontrollable temperature gradients under microwave irradiation, which in turn lead to an increase of reaction rates following common kinetics laws.[14]

The second group supposes that during microwave irradiation a specific effect of microwave activation appears that leads to an increase of reaction rates for which the bulk temperature of the reaction mixture is inadequate to explain. Such effects are the so-called the nonthermal microwave effect or specific microwave effect.

Recent critical reviews concerned with both groups of theories can be found in the literature.[12,17–19]

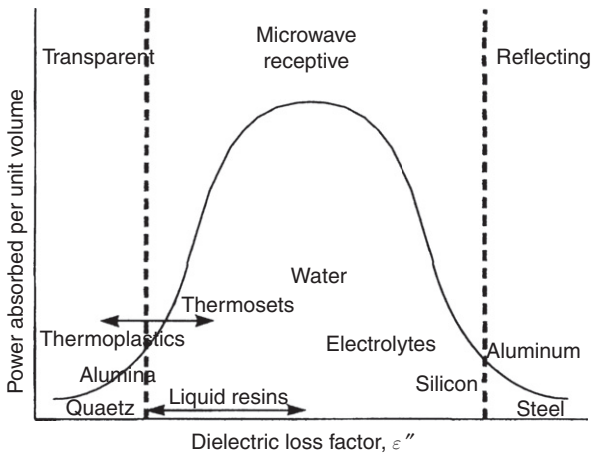

Figure 6 Relationship between the loss factor (ε'') and the ability of some common materials to absorb microwave energy. Reproduced with permission from Thostenson, E. T.; Chou, T. W. *Compos.: Part A* **1999**, *30*, 1055.[16]

materials with low values of the loss factor (ε'') have a large penetration depth. As a result, very little energy is absorbed in the material, and it is transparent to microwave irradiation like quartz glass. Because of such behavior, microwaves transfer energy most effectively to materials that possess loss factor (ε'') in the middle of conductivity range (**Figure 6**). In contrast, conventional heating transfers heat most efficiently to materials with high conductivity.[16] It is worth stressing that most of the polymers, that is, thermoplastics, thermosets as well as liquid resins, are in the microwave receptive region for a given frequency (**Figure 6**); however, a strict distinction between nonpolar and polar polymers, that is, polymers with nonpolar pendant groups and polar pendant groups, respectively, has to be kept in mind (**Box 3**).

4.39.2 Chain-Growth Polymerization Reactions

As a rapid method of heating and melting of neat and mineral-filled plastics, microwave irradiation has been employed for the synthesis and processing of polymeric materials since the late 1960s, which included polymerization of vinyl monomers, fast curing of thermosetting resins and composites, rapid drying of aqueous solutions or dispersion of polymers and resins, and heat drawing of polymer rods and tubings.[20] Emulsion polymerization of various vinyl monomers, that is, styrene, acrylic and methacrylic esters, and acrylic and methacrylic acids, was also described for the radio- and microwave frequency range.[21] In turn, microwave irradiation was applied to cure epoxy resins[22] and the use of microwave irradiation for bulk polymerization of dental materials was also reported.[23]

4.39.2.1 Free-Radical Polymerization

Microwave irradiation has been applied to free-radical polymerization and copolymerization reactions of various unsaturated monomers. In the 1980s, the bulk polymerization of 2-hydroxyethyl methacrylate (HEMA), which is a polar species that bears ester as well as alcohol functions capable of interacting and absorbing microwaves, was investigated.[24] Thus, the reactions were carried out without any radical initiator, and the liquid monomer polymerized to form a solid material that was insoluble in all the common solvents;

however, the material showed swelling behavior in water. In a similar case, it was shown that in the case of bulk copolymerization of HEMA with methyl methacrylate (MMA), microwave-assisted polymerizations gave copolymers with twice higher molecular weight and narrower molecular weight distribution than copolymers obtained under conventional thermal conditions.[25]

Using a variable power of microwave irradiation, the bulk polymerization of MMA was also investigated. It led to a reaction rate enhancement of about 130–150% when compared to the conventional methods.[26] However, thermal polymerization of MMA in the temperature range of 69–88 °C displayed a limiting conversion of about 90%, while limiting conversion of microwave polymerization declined in the following order: 200 W, 88% > 300 W, 84% > 500 W, 78%. Finally, the NMR analysis proved that the tacticities of the polymers for thermal and microwave polymerization are similar, suggesting that the polymerization process followed the same mechanism under microwave conditions.[26] In the next paper, a significant correlation between the reaction rate enhancements and the level of microwave power was found.[27] Even though the comparable temperature at variable power was the same, 52 °C, the reaction rate enhancement increased with the increase in microwave power. Compared to thermal method, the reaction rate enhancement of microwave polymerization was as follows: 500 W, 275%; 300 W, 220%; and 200 W, 138%.

Recently, free-radical homopolymerizations and copolymerizations of styrene were performed in toluene and *N*,*N*-dimethylformamide (DMF) as solvents in the presence of different initiators (i.e., *tert*-butyl perbenzoate (*t*BPB), dibenzoyl peroxide (DBPO), di-*tert*-peroxide (D*t*BP), dicumyl peroxide (DCP), and lauryl peroxide (LP) (**Figure 7**)).[28]

Under microwave irradiation, only the homopolymerization of styrene in DMF with DBPO showed an enhanced styrene conversion of about 46%; however, it was lower than the conversion under conventional conditions (i.e., an oil bath), which reached about 50%. Other initiators resulted in a slight increase in styrene conversions under microwave irradiation, that is, in the range of 2–20%. In any case, DMF was required to achieve an increase in styrene conversion under microwave irradiation, which is quite obviously caused by the higher energy absorption by DMF as compared to toluene in a given amount of time. It is interesting that significantly higher monomer conversions were observed under otherwise comparable conditions in the copolymerization of styrene and MMA. In this case, a monomer conversion of about 92% was observed under microwave irradiation in comparison to about 37% without microwave irradiation when *t*BPB was used as an initiator in DMF. However, for the copolymerization with DBPO as an initiator, conversions of 75% and 71% were obtained for the reactions under microwave and conventional conditions, respectively. Again, the use of toluene did not result in any enhancement by microwave irradiation. It was found that number-average molecular weights of polystyrene samples and the copolymers were dependent on the initiator and dropped in the range of 7600–199 000 and 13 000–369 000 g mol^{-1} for the homopolymerization and compolymerization experiments, respectively.[28]

By applying solvent-free conditions, a number of methacrylamides were synthesized from methacrylic acid and aliphatic and aromatic amines under microwave irradiation.[29] Then it was found that an addition of polymerization initiator (i.e., 2,2′-azobisisobutyronitrile (AIBN)) to the reaction mixture led directly to polymethacrylamides in a single reaction step (**Figure 8**).

Later, it was demonstrated that under microwave conditions it was possible to obtain chiral (*R*)-*N*-(1-phenyl-ethyl) methacrylamide directly from methacrylic acid and (*R*)-1-phenylethylamine. An addition of AIBN led again in a single-step reaction to the formation of an optically active polymer that contained both methacrylamide and imide moieties (**Figure 9**).[30,31] It was found that microwave irradiation accelerates considerably the process of condensation between the acid and the amine, which is also more selective in comparison to thermal heating. The one-pot polymerization under microwave conditions at 120 °C afforded polymers with relatively high yields (80%), which depended on applied power. The yield under classical heating conditions (an oil bath) was only 40%.

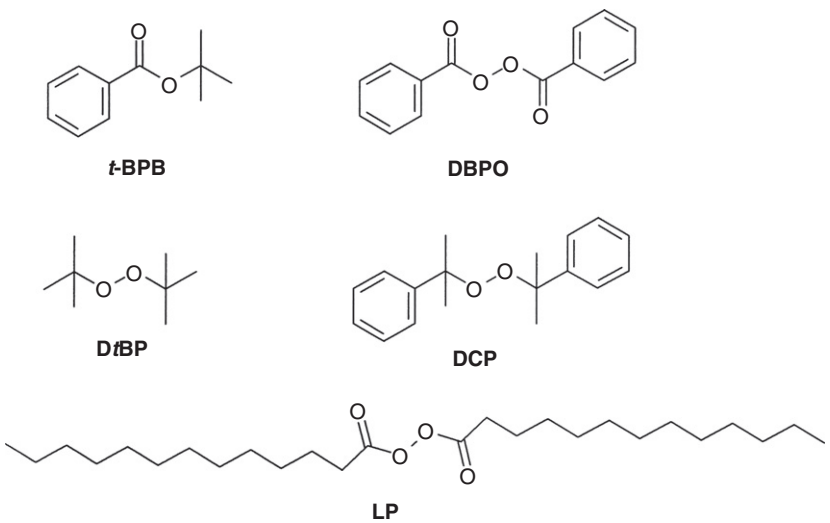

Figure 7 Chemical structures of initiators (i.e., *t*BPB, DBPO, D*t*BP, DCP, and LP) used for radical polymerization.

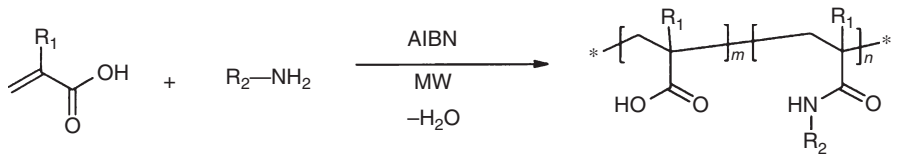

Figure 8 Formation of polymethacrylamides from the reaction of methacrylic acid and various amines.

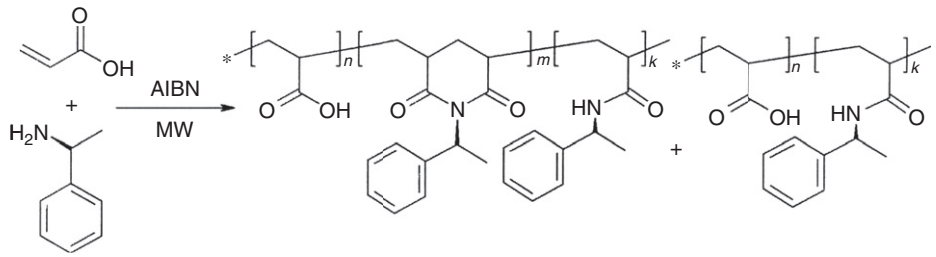

Figure 9 Synthesis of chiral polymers from (*R*)-*N*-(1-phenyl-ethyl)methacrylamide and methacrylic acid and (*R*)-1-phenylethylamine.

Recently, the bulk polymerization of *N*-phenylmaleimide, which was prepared from maleic anhydride and aniline prior to the reaction, under microwave irradiation was presented.[32] The final yield of the polymer was 57%, while the bulk homopolymerization under conventional conditions (an oil bath preheated to 95 °C) afforded the polymer with a relatively low yield of about 19%.

Free-radical polymerization of carbazole-containing monomers, that is, *N*-vinylcarbazole (NVC) and 2-(9-carbazolyl) ethyl methacrylate, under microwave irradiation was also carried out (Figure 10).[33] The reactions were run in pressure-resistant tubes in a solution by applying different solvents such as toluene, hexane, nitromethane, and diethylene glycol (DEG). After the precipitation, the polymers characterized by weight-average molecular weights of 20 000–50 000 g mol^{-1} were afforded in high yields of 80–99%. Interestingly, in the experiments under conventional conditions (a preheated oil bath), the polymers were obtained in very low yields of about 1%.

The bulk polymerization of NVC in the presence of fullerene C_{60} as a charge-transfer initiator as well as initiator

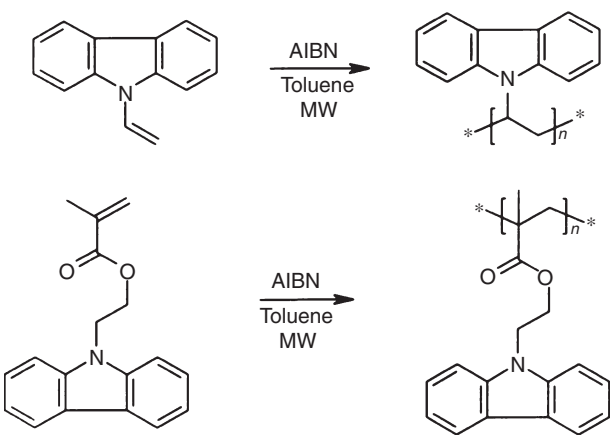

Figure 10 Polymerization of carbazole-containing monomers, that is, *N*-vinylcarbazole and 2-(9-carbazolyl)ethyl methacrylate.

was studied.[34] In comparison with polymerization under conventional conditions (water bath, 70 °C), microwave polymerization was found to be advantageous due to the decrease in the reaction time and considerable improvement in the yield of poly(*N*-vinylcarbazole) (PVK) – 70% as opposed to 8% after 10 min of conventional heating.[34] In fact, during microwave experiments, temperature was not measured or even evaluated, so it is hard to make any yield comparison between these two techniques. For example, in spite of different heating methods, the molecular weights and polydispersity index (PDI) of the resultant polymers were similar.

More recently, the polymerization of isoprene in the presence of organolanthanide catalysts under microwave irradiation was presented.[35] The main power values of microwave reactor necessary to reach and maintain temperature were 15, 32, 55, and 95 W for 60, 80, 100, and 120 °C, respectively. The study showed an enhancement in reactivity under microwave condition in comparison with conventional conditions, while the selectivity was only slightly modified. The highest yields (85–94%) of polyisoprene were obtained within 2 h of reaction time at 80 °C to afford the polymer with number-average molecular weight in the range of 17 000–27 000 g mol^{-1} and PDI in the range of 1.6–2.5. Interestingly, the reaction at 120 °C afforded polyisoprene with higher yield under conventional conditions, which was explained by a depolymerization reaction under microwave irradiation at high temperatures.

4.39.2.2 Controlled Radical Polymerization

For obtaining polymers with predetermined molecular weights, low PDI, specific functionalities, and diverse architecture than in conventional free-radical polymerization, controlled radical polymerization (CRP) methods were developed.[36] There are a number of reports that enhanced rates and low polydispersity indices were observed for atom transfer radical polymerization (ATRP) under microwave conditions; similarly, significant rate enhancements were reported for reversible addition–fragmentation chain transfer (RAFT) and nitroxide-mediated polymerization (NMP).

Table 4 Conversion of MMA for ATRP under microwave irradiation at various ratios of $[MMA]_0/[AIBN]_0$

$[MMA]_0/[AIBN]_0/[CuCl]_0/[BPY]_0$	*Time (min)*	*Conversion (%)*	$M_{n,GPC}$ *(g mol^{-1})*	M_w/M_n	$M_{n,th}$ *(g mol^{-1})*
200/0.1/1/3	3	14.1	30 400	1.48	14 100
	5	19.1	30 800	1.50	19 100
	10	31.1	36 500	1.49	31 100
	15	38.0	43 900	1.61	38 000
	25	47.4	44 100	1.89	47 500
	35	49.3	44 800	1.82	49 300
200/0.03/1/3	5	16.5	30 600	1.42	33 000
	8	22.2	36 700	1.46	44 500
	10	24.3	40 600	1.61	48 600
	15	30.0	44 600	1.76	60 100
	30	33.9	42 600	1.57	67 800
200/0.05/1/3	5	9.9	42 300	1.35	33 100
	8	19.4	42 400	1.47	64 900
	10	21.3	53 500	1.51	71 200
	15	21.5	59 900	1.69	71 600

Condition: $T = 69\,°C$; $[MMA]_0 = 9.46\,M$; microwave power 450 W; $M_{n,th} = [MMA]_0/[AIBN]_0 \times (1/2) \times M_{w\,MMA}$.
GPC, gel permeation chromatography.
Reproduced with permission from Chen, G.; Zhu, X.; Cheng, Z.; *et al. Radiat. Phys. Chem.* **2004**, *69*, 129.[38]

Thus, ATRP of MMA under microwave irradiation was described in a number of reports.[37–39] The reactions were run with different activator–initiator systems including benzyl chloride and bromide/CuCl/2,2′-bipyridine,[37] AIBN/$CuBr_2$/2,2′-bipyridine (**Table 4**),[38] and α,α′-dichloroxylene/CuCl/*N*,*N*,*N*′,*N*″,*N*″-pentamethyldiethylenetriamine.[40] In all the cases, microwave irradiation enhanced the rate of polymerization and gave polymers with narrower molecular weight distributions. Moreover, linear first-order rate plots, linear increase of the number-average molecular weight with conversion, and low polydispersities were observed, which indicated that ATRP of MMA was controlled under microwave conditions (**Figure 11**).

In a similar paper, ATRP of MMA under microwave irradiation was also studied in a solution in the presence of a small amount of CuCl, *N*,*N*,*N*′,*N*″,*N*″- pentamethyldiethylenetriamine, and ethyl 2-bromobutyrate (i.e., activator–initiator system).[41,42] Linear first-order rate plots, linear increase of the number-average molecular weight with conversion, and low polydispersities were observed. It was found that microwave irradiation enhanced the rate of polymerization; for example, after 150 min of microwave irradiation, the monomer conversion reached 27%, and the polymers were afforded with a number-average molecular weight of 57 300 g mol^{-1} and a PDI of–1.19, while under conventional conditions a similar conversion was achieved after 16 h, and the polymers were characterized by a number-average molecular weight of 64 000 g mol^{-1} and a PDI of –1.19 (**Figure 12**). Similar results were obtained for ATRP of *n*-octyl acrylate in an acetonitrile solution in the presence of 2-bromobutyrate, CuBr, and 2,2′-pyridine under microwave conditions.[43]

In contrast, it was also reported that under microwave conditions the ATRP of MMA in a *p*-xylene solution did not give any rate enhancement in comparison with conventional conditions.[44] The polymerization reaction exhibited a good

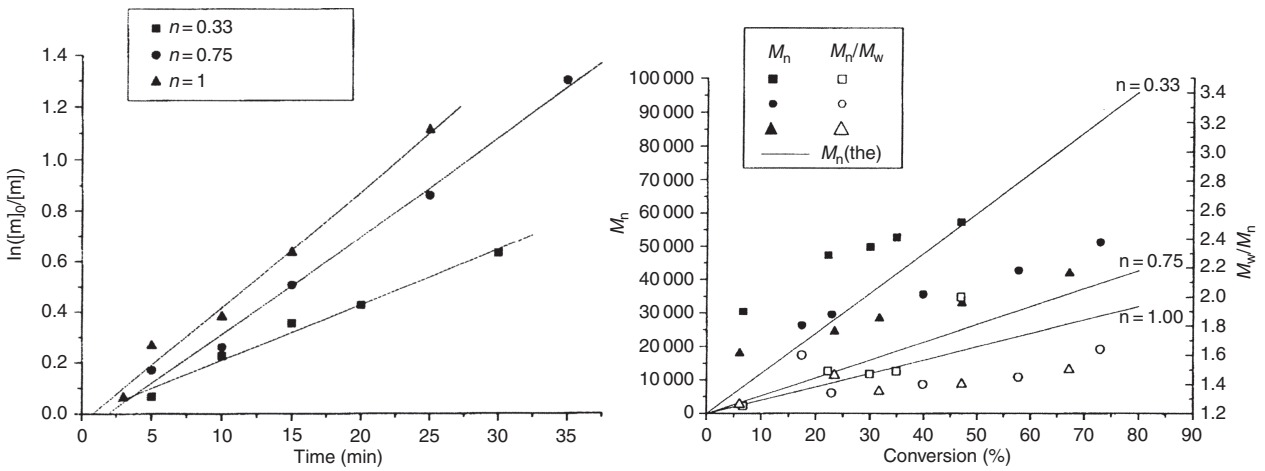

Figure 11 Kinetics of ATRP of MMA at different initiator concentrations and dependency of M_n and M_w/M_n on conversion for ATRPT of MMA.
Reproduced with permission from Lu, X.; Zhu, X.; Cheng, Z.; *et al. J. Appl. Polym. Sci.* **2004**, *92*, 2189.[40]

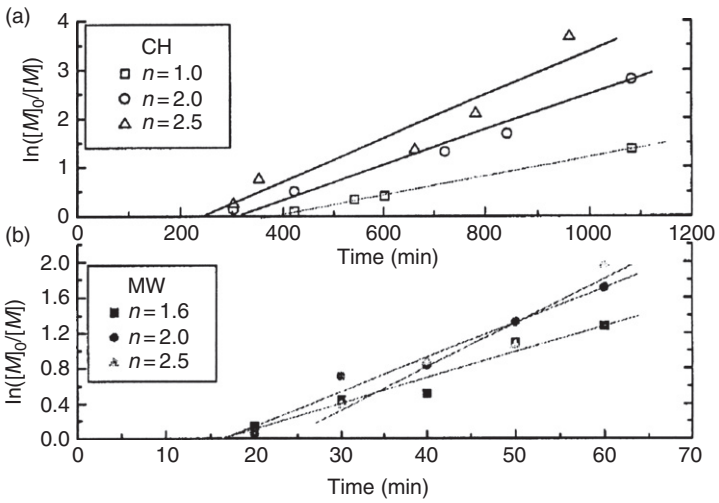

Figure 12 Kinetics of MMA polymerization in DMF under microwave (a) and conventional conditions (b) at different initiator concentrations. CH, conventional heating; MW, microwave irradiation. Reproduced with permission from Cheng, Z.; Zhu, X.; Zhang, L.; *et al. Polym. Bull.* **2003**, *49*, 363.[41]

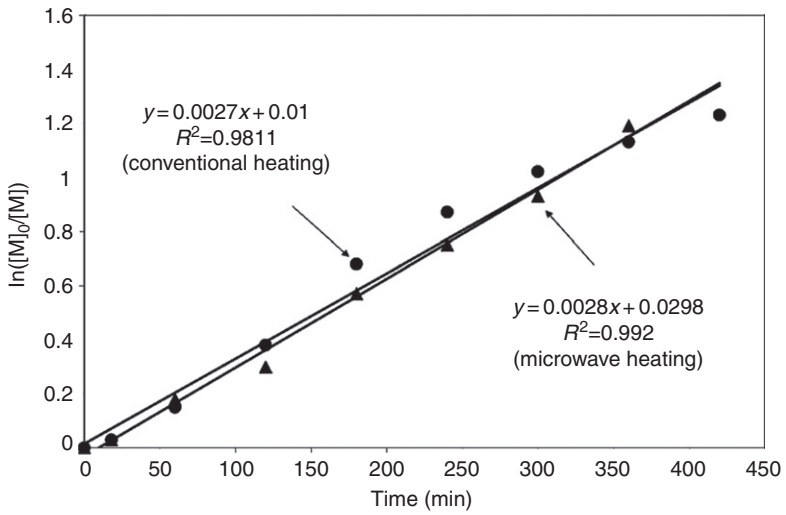

Figure 13 Comparison of the kinetics plot of the ATRP of MMA in DMF under conventional and microwave conditions. Reproduced with permission from Zhang, H.; Schubert, U. S. *Macromol. Rapid Commun.* **2004**, *25*, 1225.[44]

control in terms of linear first-order rate plots, linear increase of the number-average molecular weight with conversion, and low polydispersities; however, the reactions provided almost the same results as those performed under conventional conditions (Figure 13).

By applying microwave conditions, it was possible to obtain bromo-double-terminated polystyrene (Br-PS-Br) and poly(methyl methacrylate) (Br-PMMA-Br) with predesigned molecular weight and narrow polydispersity prepared by ATRP. The polymers were reacted with excess amounts of fullerene C_{60} in the presence of CuBr/bipyridine (CuBr/bipy) catalyst system under microwave irradiation. As a result, telechelic C_{60} end-capped polymers were obtained (Figure 14).[45]

The reaction mixture was irradiated under nitrogen atmosphere in a microwave oven for 20 min with a constant power of 300 W. Under conventional conditions, the same amount of substrates and solvents was heated in an oil bath for 8 h at 110 and 90 °C for styrene and MMA, respectively (Table 5).

The results showed that microwave irradiation could significantly increase the rate of fullerenation reactions of

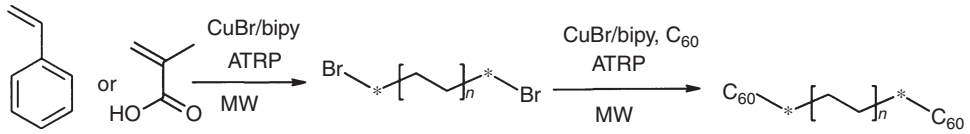

Figure 14 Synthesis of telechelic C_{60} end-capped polymers.

Table 5 Results of the telechelic C_{60} end-capped products

Product	*Reaction time*	M_n ($\times 10^4$ g mol^{-1})	M_w/M_n	*C_{60} content (wt.%)*	T_g (°C)
C_{60}–PSt–C_{60}(MI)	20 min	1.129	1.150	10.03[a] 10.25[b] (12.75)	97.7
C_{60}–PMMA–C_{60}(MI)	15 min	2.511	1.532	6.35[a] 5.51[b] (5.73)	124.4
C_{60}–PSt–C_{60}(CH)	8 h	1.195	1.311	11.55[a] 12.41[b] (12.05)	98.0
C_{60}–PMMA–C_{60}(CH)	8 h	2.457	1.502	4.88[a] 5.41[b] (5.86)	123.9

[a]Calculated on the basis of UV absorbance at 330 nm.

[b]Measured by TGA on the parent polymers and the C_{60} end-capped polymers; the data in parentheses are theoretical values based on M_n and telechelic C_{60}-monoadduct structure.

Reproduced with permission from Wu, H.; Li, F.; Lin, Y.; *et al. J. Appl. Polym. Sci.* **2006**, *99*, 828.[45]

bromo-end-capped polymers, while the physical properties and structure of the C_{60} end-capped polymers were not modified.

(2,2,6,6-Tetramethyl-piperidin-1-yl)oxyl (TEMPO)-mediated bulk radical polymerizations of styrene were successfully performed under microwave irradiation.[46] The polymerizations were well controlled in terms of linear kinetics plots, linear increase of molecular weight with increasing conversion, and narrow PDI (1.16–1.38) (**Table 6**).

The polymerization rates at appropriate power of microwave irradiation were faster than that under conventional heating conditions at the same reaction temperature with or without benzoyl peroxide. Furthermore, it was proved by successful chain extension polymerization and NMR spectrum analysis that the nitroxide moiety did exist at the end of polymeric chain.[46]

Solid-supported TEMPO-mediated controlled polymerization was also described for the preparation of novel high-loading functionalized styrenyl resins.[47] The resin was prepared in a neat reaction of TEMPO-methyl resin with styrene derivatives. The resin with a 7.25-fold increase in the mass was obtained. It was stressed that the microwave procedure was 150-fold faster in comparison to those described in literature under conventional conditions.

NMPs of methyl and *tert*-butyl acrylate in the presence of 2-methyl-2-[*N*-*tert*-butyl-*N*-(1′-diethylphosphono-2′,2′-dimethylpropyl)aminoxyl]propanoic acid (MAMA) and the radical *N*-*tert*-butyl-*N*-(1-diethylphosphono-2,2-dimethylpropyl) nitroxide (SG1) as initiators were performed under microwave irradiation (**Figure 15**).[48]

For the polymerization of *tert*-butyl acrylate, the monomer consumption followed the first-order kinetics, while that of MMA could be described with a kinetics model that includes the persistent radical effect. The control over the reaction could be preserved for monomer conversions of up to 90%, and poly(methyl methacrylate)s (PMMAs) with narrow molecular weight distributions (PDI below 1.3) were obtained. Conventional experiments with an oil bath showed a limited reproducibility and furthermore failed to yield polymers with similar narrow molecular weight distributions (for high conversions). This observation was refereed to the superiority of the uniform, noncontact, and internal heating mode of microwave irradiation.

Microwave irradiation was employed for the synthesis of well-defined homopolymers and block copolymers of acrylamido and acrylate monomers via RAFT polymerization. Homopolymerizations of *N*,*N*-dimethylacrylamide (DMA) and *N*-isopropylacrylamide (NIPAM) were conducted in the presence of 2-dodecylsulfanylthiocarbonylsulfanyl-2-methylpropionic acid as a chain-transfer agent (CTA) and AIBN as an initiator at ratios [DMA]/[CTA]/[AIBN] = 100/1/0.05 and 200/1/0.05 under microwave conditions

Table 6 Experimental results of thermal-initiated polymerization of styrene under microwave and conventional heating at 125 °C

Heating method	*Power (W)*	*Time (h)*	*Conversion (%)*	M_n (g mol^{-1})	M_w/M_n
Thermal	–	3	0	–	–
Thermal[a]	–	3	16	4400	1.25
Thermal	–	6	9	4650	1.18
MW	–	9	18	8100	1.23
MW[a]	100	3	3	2570	1.14
MW	100	3	41	9700	1.26
MW[a]	200	2	8	4600	1.15
MW	200	2	66	13 600	1.38
	200	3	37	11 100	1.38

[a]Conditions: $[\text{styrene}]_0 = 8.7$ M; $[\text{BPO}]_0 = 0.0305$ M; $[\text{OH-TEMPO}]_0 = 0.0366$ M. Others without BPO.

MW, microwave.

Reproduced with permission from Li, J.; Zhu, X.; Zhu, J.; Cheng, Z. *Radiat. Phys. Chem.* **2006**, *75*, 253.[46]

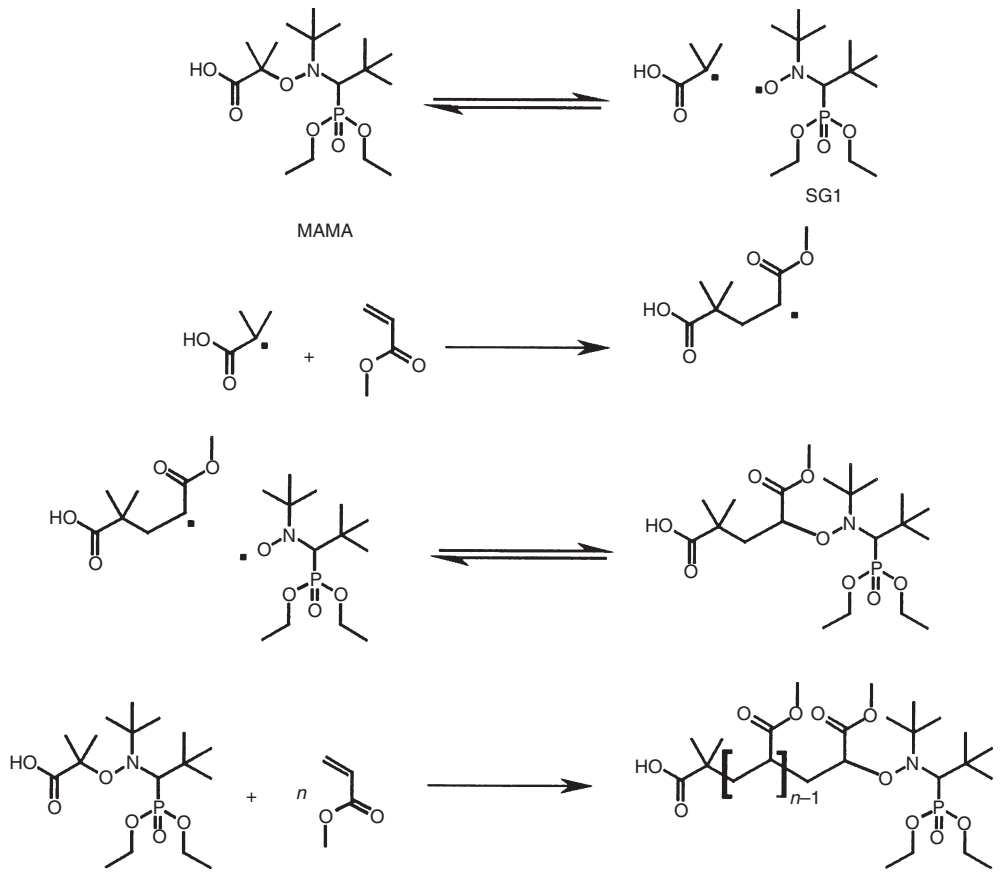

Figure 15 Nitroxide-mediated polymerizations of methyl and *tert*-butyl acrylate.

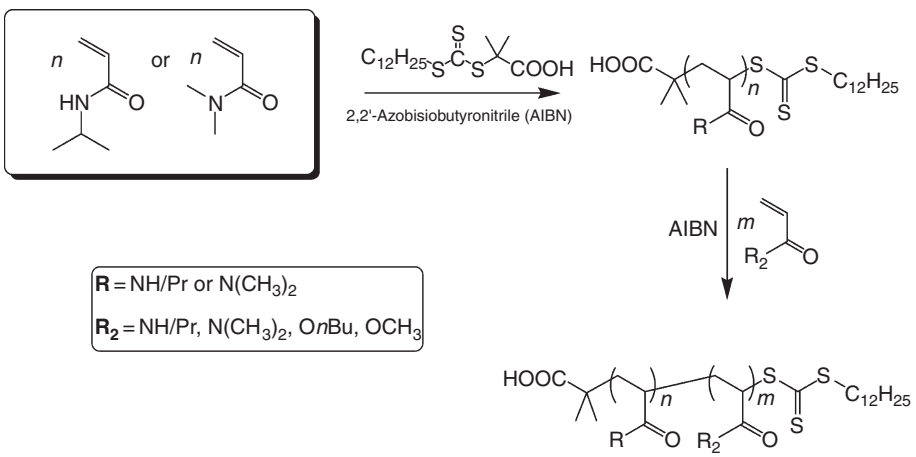

Figure 16 Microwave-assisted reversible addition–fragmentation chain-transfer homopolymerization of DMA or NIPAM and subsequent block copolymerization with NIPAM, DMA, butyl acrylate, or methyl acrylate.

(Figure 16). The rates of polymerization of DMA and NIPAM were significantly higher than those observed under conventional heating condition.[49] For instance, the polymerization with [DMA]/[CTA]/[AIBN] = 100/1/0.05 showed no monomer conversion after 30 min with conventional heating, but a conversion of 73% was obtained in 2 min with microwave irradiation.

In all the reactions, the pseudo-first-order rate plots remained relatively linear, with only a slight amount of deviation being observed at high conversion, which allowed calculation of apparent rate constants of propagation (k_p^{app}) with a variety of stoichiometric ratios and heating conditions. For example, for [DMA]/[CTA]/[AIBN] = 100/1/0.05, the relative values of k_p^{app} for polymerizations with conventional heating and microwave irradiation were 0.4×10^3 and 1.2–$6.6 \times 10^3\ s^{-1}$, respectively, which means that the rates of polymerization under microwave conditions might be up to 15 times faster (Table 7).[49]

Table 7 Apparent rate constants of propagation (k_p^{app}) as a function of heating method

Monomer	[M]/[CTA]/[I][a]	Temp.[b] (°C)	k_p^{app} ($\times 10^3\ s^{-1}$) EMW	MW	CH
DMA	[100]/[1]/[0.05]	70	6.6 ± 0.01	1.2 ± 0.1	0.4 ± 0.01
DMA	[200]/[1]/[0.05]	70	4.0 ± 0.04	0.7 ± 0.01	0.3 ± 0.47
DMA	[400]/[1]/[0.05]	70	1.2 ± 0.03		0.2 ± 0.01
DMA	[100]/[1]/[0.005]	70	1.1 ± 0.02		0.1 ± 0.01
NIPAM	[100]/[1]/[0.05]	60	1.4 ± 0.16	0.3 ± 0.02	0.1 ± 0.01
NIPAM	[200]/[1]/[0.05]	60	0.6 ± 0.05	0.2 ± 0.02	

[a]Molar ratio of [monomer (M)]/[chain-transfer agent (CTA)]/[initiator (I)].
[b]Programmed temperature of the microwave instrument.
CH, conventional heating; EMW, enhanced microwave heating; MW, standard microwave heating.
Reproduced with permission from Roy, D.; Ullah, A.; Sumerlin, B. S. *Macromolecules* **2009**, *42*, 7701.[49]

In turn, the homopolymers prepared under microwave conditions were employed as macro-chain-transfer agents (macroCTAs) for subsequent block copolymerization. The polymerization of the second monomer was also achieved via microwave irradiation, which allowed significantly accelerated access to block copolymers with with low PDI and unimodal molecular weight distributions. For instance, when poly(*N*, *N*-dimethylacrylamide) (PDMA, $M_n = 6300\ g\ mol^{-1}$, PDI = 1.16) prepared in just 1 min (56% conversion) under microwave conditions was employed as a macroCTA for the polymerization of NIPAM ([NIPAM]/[PDMA macroCTA]/[AIBN] = [100]/[1]/[0.05]), 71% conversion was obtained in 30 min, resulting in a polymer with $M_n = 12\,500\ g\ mol^{-1}$ (PDI = 1.17) (Figure 17(a)). Similarly, PNIPAM macroCTAs prepared by the microwave approach were also successfully utilized to copolymerize DMA. For instance, a PNIPAM homopolymer ($M_n = 7000\ g\ mol^{-1}$, PDI = 1.18) prepared in just 12 min (68% conversion) under microwave conditions was employed as a macroCTA for the polymerization of DMA ([DMA]/[PNIPAM macroCTA]/[AIBN] = [62]/[1]/[0.01]). In just 15 min (55% conversion), PNIPAM-*b*-PDMA block copolymer with $M_n = 12\,000\ g\ mol^{-1}$ was synthesized (Figure 17 (**b**)).

Other examples of RAFT polymerization reactions under microwave irradiation can be found in the literature.[50,51]

4.39.2.3 Ring-Opening polymerization

Ring-opening polymerization (ROP) reactions were investigated for a number of monomers like ε-caprolactone (ε-CL), D,L-lactide, and oxazoline derivatives. For example, ROP of ε-CL under microwave irradiation was carried out at different temperatures ranging from 80 to 210 °C in the presence of $Sn(Oct)_2$ and zinc powder as catalysts (Figure 18).[52]

Poly(ε-caprolactone) (PCL) with a weight-average molecular weight of 124 000 g mol^{-1} and a yield of 90% was obtained

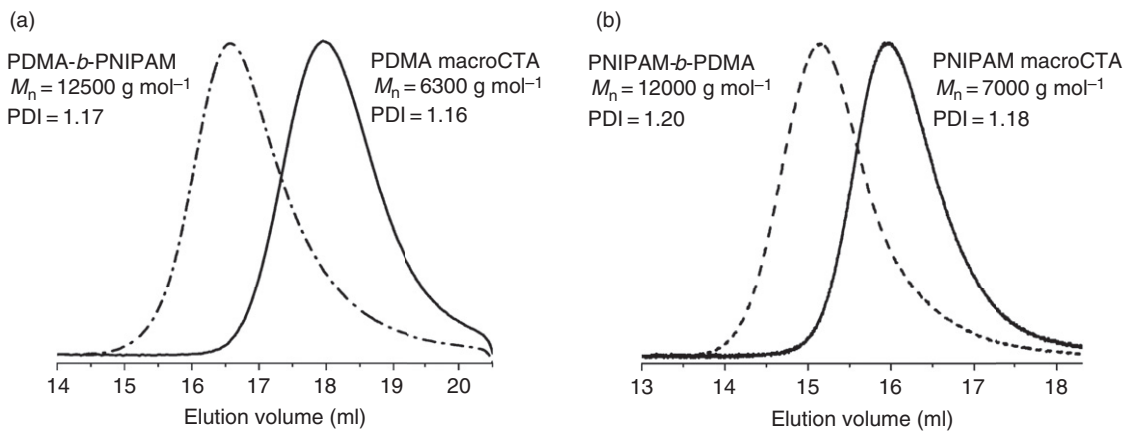

Figure 17 Size-exclusion chromatography traces of macroCTAs and block copolymers prepared by the enhanced microwave (EMW) approach. (a) PDMA macroCTA and PDMA-*b*-PNIPAM block copolymer; (b) PNIPAM macroCTA and PNIPAM-*b*-PDMA block copolymer. Reproduced with permission from Roy, D.; Ullah, A.; Sumerlin, B. S. *Macromolecules* **2009**, *42*, 7701.[49]

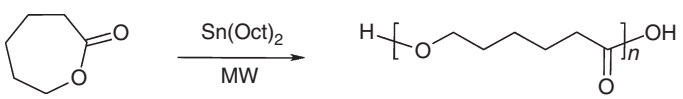

Figure 18 ROP of ε-CL in the presence of $Sn(Oct)_2$ and zinc powder as catalysts.

after 30 min of irradiation using 0.1% (mol/mol) of $Sn(Oct)_2$, whereas the polymerization catalyzed by zinc powder afforded PCL with a weight-average molecular weight of 92 300 g mol^{-1} after 30 min of irradiation using 1% (mol/mol) of zinc powder. Without microwave irradiation, the polymerization rate was considerably slower: at 120 °C, PCL was afforded with a weight-average molecular weight of 60 000 g mol^{-1} with Sn $(Oct)_2$ after 24 h and 27 000 g mol^{-1} with zinc powder after 48 h. A similar protocol was applied for the metal-free synthesis of PCL in the presence of benzoic acid.[53] The molar ratios of ε-CL to benzoic acid were in the range of 5–25, and the reaction mixture was heated up to 240 °C in a microwave reactor. The advantage of microwave protocol was an enhancement of propagation rate; however, above 240 °C, degradation of PCL became significant. With the metal-free method, the weight-average molecular weight was about 40 000 g mol^{-1}.

Recently, ROP of ε-CL in the presence of lanthanide halides as catalysts under microwave irradiation was also presented.[54] The highest number-average molecular weight of polymers was obtained when the mixture of the monomer and catalyst was intensively heated in a microwave reactor so that the boiling point of ε-CL was reached in about 1 min (i.e., 200–230 °C). The number-average molecular weight of the polymers was between 2900 and 14 100 g mol^{-1} (**Table 8**). Compared to conventional thermal processes, under microwave conditions the polymers gained higher molecular weight and lower PDI.

ROP of D,L-lactide in the presence of $Sn(Oct)_2$ under microwave irradiation was carried out in a similar manner.[55] It was found that the polymerization of D,L-lactide proceeded quickly; however, no comparison to a conventional procedure was made. Poly(D,L-lactide) (weight-average molecular weight 400 000 g mol^{-1}) was obtained with 90% yield after 10 min under optimal conditions. In a similar paper, poly(D,L-lactide) was obtained with an average molecular weight over 200 000 g mol^{-1} and a yield over 85% provided that appropriate reaction conditions such as carborundum (SiC) as heating medium, 0.15% catalyst, lactide with purity above 99.9%, 450 W microwave power, and 30 min irradiation time were applied.[56]

Oxazoline derivatives became the next group of cyclic monomers that were studied for ROP under microwave irradiation. For instance, 2-phenyl-2-oxazoline mixed with methyl tosylate in an acetonitrile solution was irradiated in a microwave reactor for

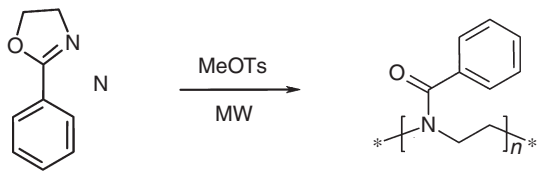

Figure 19 ROP of oxazoline derivatives.

30–150 min at 125 °C (**Figure 19**). A comparison with thermal heating experiments showed a great enhancement in the reaction rates while the living character of the polymerization was conserved. Under microwave irradiation after 90 min, the monomer conversion was nearly quantitative, that is, 98%. In contrast, the polymerization under conventional conditions showed only 71% conversion after 90 min. Interestingly, the reaction rate coefficient under conventional conditions was the same for the reaction in open and closed vessels, that is, 1.1×10^{-2} min^{-1}, while for the microwave experiments the reaction rate coefficient was different for the reaction in open and closed reaction vessels, that is, 3.6×10^{-2} and 4.2×10^{-2} min^{-1}, respectively.[57]

Then ROP reactions of a number of 2-substituted 2-oxazolines (i.e., 2-methyl, 2-ethyl, 2-nonyl, and 2-phenyl) in the presence of methyl tosylate as a catalyst were studied in the temperature range from 80 to 200 °C (**Figure 18**).[3,58,59] While the reaction rate was enhanced by a factor of 400 going from 80 to 200 °C (**Figure 20**), activation energies for the polymerization (E_A: 73–84 kJ mol^{-1}) were within the range of values obtained with conventional heating (**Table 9**). The first-order kinetics of the monomer conversion and livingness of the polymerization were maintained. A maximum number of 300 monomers can be incorporated into the polymer chains under such conditions. Moreover, the polymerization can be carried out in concentrated solutions or even bulk conditions to afford well-defined monomers (PDI < 1.20). Recently, it was observed that ROP of 2-oxazolines with fluorinated aromatic substituents was strongly accelerated (ca. 10 times) by *o*-fluoro substituents. This observed acceleration is due to an interaction of the cationic reaction center on nitrogen atom with the *ortho*-fluorine substituent which overcompensates the negative electron-withdrawing effect and due to the increased nucleophilic character of the monomer due to the nonplanarity of the oxazoline and the phenyl substituent.[60]

Table 8 Results of ε-caprolactone polymerization

Heating method	*Catalyst (mg)*	*Temp. (°C)*	*Time (min)*	M_n *(g mol^{-1})*	M_w/M_n
Thermal	$SmBr_3$, $6H_2O$ (15)	200	30	3600	1.94
Thermal	$SmCl_3$, $6H_2O$ (11)	200	15	2300	2.00
MW	$SmCl_3$, 3THF (10)	200	45	14 100	2.20
MW	$SmCl_3$, 3THF (10)	230	3	13 500	2.91
MW	$YbCl_3$, 3THF (15)	230	3	11 300	2.57
MW	$YbCl_3$, 3THF (10)	200	15	11 800	1.82

MW, microwave.

Reproduced with permission from Barbbier-Baudry, D.; Brachais, L.; Cretu, A.; *et al. Environ. Chem. Lett.* **2003**, *1*, 19.[54]

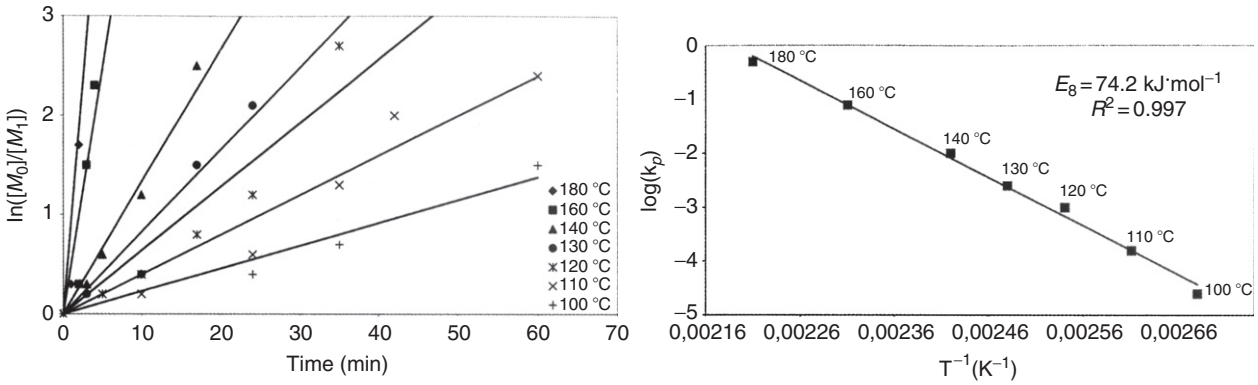

Figure 20 Monomer conversion against time plot for the polymerization of 2-nonyl-2-oxazoline at different temperatures. Reproduced with permission from Hoogenboom, R.; Wiesbrock, F.; Leenen, M. A. M.; *et al. J. Comb. Chem.* **2005**, *7*, 10.[58]

Table 9 Activation energy E_A and frequency factor A for the polymerization of 2-methyl-, 2-ethyl-, 2-phenyl-, and 2-nonyl-2-oxazoline

Monomer	*Frequency factor (A) ($\times 10^8$ l mol^{-1} s^{-1})*	*Activation energy (E_A) (kJ mol^{-1})*
2-Methyl-2-oxazoline	5.00 ± 1.20	75.4 ± 0.5
2-Ethyl-2-oxazoline	1.99 ± 0.85	73.4 ± 0.5
2-Phenyl-2-oxazoline	14.9 ± 2.8	84.4 ± 0.5
2-Nonyl-2-oxazoline	7.58 ± 1.15	76.3 ± 0.5

Reproduced with permission from Wiesbrock, F.; Hoogenboom, R.; Leenen, M. A. M.; *et al. Macromolecules* **2005**, *38*, 5025.[59]

A library of diblock copoly(2-oxazoline)s was prepared by applying the same technique of ROP under microwave irradiation. A total number of 100 (50 + 50) monomer units were incorporated into the polymer chains.[61] The reactions were initiated by methyl tosylate and carried out in an acetonitrile solution at 140 °C. After polymerization of the first monomer, the second monomer was added, and the reaction mixture was again irradiated in a microwave reactor. As a result, 16 polymers were obtained with narrow PDI < 1.30 (Table 10).

Recently, a similar method was used for the preparation of a library of 30 triblock copolymers from 2-methyl-, 2-ethyl-, 2-nonyl-, and 2-phenyl-2-oxazoline in a microwave reactor. The polymers exhibited narrow molecular weight distributions (PDI < 1.33) and showed only minor deviations from the targeted monomer ratio of 33:33:33 (Table 11). The glass transition temperature of the triblock copolymers spanned the range from 50 to 100 °C depending on the incorporated monomers.[62] More recently, the successful synthesis of 2-(3-ethylheptyl)-2-oxazoline and polymerization under microwave conditions were reported. The corresponding homopolymer was the first poly(2-oxazoline) that is amorphous and exhibits a low glass transition temperature at −6 °C. The significant differences in properties compared with its linear analogue 2-(3-nonyl)-2-oxazoline polymer are caused by the branching of the side chain resulting in a lower packing density, which is consistent with an easier molecular motion of the polymer. Thermal investigations of random copolymers revealed a linear dependency of the T_g with the weight percent of 2-(3-ethylheptyl)-2-oxazoline monomer, allowing simple fine-tuning of the T_g from −6 to 59 °C for specific applications.[63]

There is also an example of the combination of cationic ring ROP and ATRP, which resulted in the synthesis of block

Table 10 (Theoretical) number-average molecular weight M_n^{th} ($\times 10^3$ g mol^{-1}) and PDI for the four chain-extended and the 16 diblock copoly(2-oxazoline)s[a]

	Second monomer			
First monomer	*2-Methyl- 2-oxazoline*	*2-Ethyl-2-oxazoline*	*2-Nonyl-2-oxazoline*	*2-Phenyl-2-oxazoline*
2-Methyl-2-oxazoline	M_n^{th} = 8.5 PDI = –/1.16	M_n^{th} = 9.2 PDI = –/1.17	M_n^{th} = 14.2 PDI = –/–	M_n^{th} = 11.6 PDI = –/1.25
2-Ethyl-2-oxazoline	M_n^{th} = 9.2 PDI = –/1.18	M_n^{th} = 9.9 PDI = 1.12/1.16	M_n^{th} = 14.8 PDI = 1.15/-	M_n^{th} = 12.3 PDI = 1.27/1.19
2-Nonyl-2-oxazoline	M_n^{th} = 14.2 PDI = –/–	M_n^{th} = 14.8 PDI = 1.64/-	M_n^{th} = 19.7 PDI = 1.14/-	M_n^{th} = 17.2 PDI = 1.24/-
2-Phenyl-2-oxazoline	M_n^{th} = 11.6 PDI = –/1.18	M_n^{th} = 12.3 PDI = 1.35/1.19	M_n^{th} = 17.2 PDI = 1.28/-	M_n^{th} = 14.7 PDI = 1.27/1.16

[a]In each cell, the first (second) entry for the PDI results from measurements in chloroform (*N,N*-dimethylformamide).
Reproduced with permission from Wiesbrock, F.; Hoogenboom, R.; Van Nispen, S. F. G. M.; *et al. Macromolecules* **2005**, *38*, 7957.[61]

Table 11 Number of incorporated monomer units into the 30 triblock copoly(2-oxazoline)s resulting from combined ^{1}H NMR analyses (top) of the model (A and AB (block-co)polymers) and final polymers as well as the measured number-average molecular weights ($M_{n,GPC}$/PDI; bottom)[a]

	Third block (ratio)			
First–second block	*MeO$_X$* M$_n$ (× 10^3 g mol^{-1})/ M$_w$/M$_n$	*EtO$_X$* M$_n$ (× 10^3 g mol^{-1})/ M$_w$/M$_n$	*PhO$_X$* M$_n$ (× 10^3 g mol^{-1})/ M$_w$/M$_n$	*NoO$_X$* M$_n$ (× 10^3 g mol^{-1})/ M$_w$/M$_n$
MeO$_X$–EtO$_X$	33:28:33		33:33:32	33:31:33
	10.2/1.21		11.7/1.24	5.5/1.44
MeO$_X$–PhO$_X$	33:31:33	33:33:36		33:30:32
	14.1/1.22	13.9/1.15		10.2/1.21
MeO$_X$–NoO$_X$	33:28:33	33:30:37	33:29:29	
	9.9/1.20	10.0/1.21	10.6/1.27	
EtO$_X$–MeO$_X$		33:33:33	33:29:27	33:34:31
		10.9/1.32	12.4/1.23	9.5/1.28
EtO$_X$–PhO$_X$	33:31:30	33:30:33		33:30:36
	16.2/1.20	15.3/1.24		11.4/1.22
EtO$_X$–NoO$_X$	33:33:37	33:33:33	33:33:31	
	10.1/1.27	9.9/1.22	11.3/1.25	
PhO$_X$–MeO$_X$		33:35:35	33:27:33	33:31:31
		15.3/1.21	15.2/1.19	9.1/1.23
PhO$_X$–EtO$_X$	33:35:34		33:42:33	33:38:38
	17.2/1.32		19.1/1.28	14.1/1.21
PhO$_X$–NoO$_X$	33:38:34	33:45:37	33:36:33	
	9.7/1.21	8.8/1.21	11.6/1.22	
NoO$_X$–PhO$_X$	33:23:27	33:26:24		33:32:33
	7.2/1.40	7.8/1.33		10.3/1.38[b]

[a]1H NMR spectra were recorded in CDCl3 or CD2Cl2 (PhOX-containing polymers), and GPC analyses were performed using DMF (with 5 mM NH4PF6) as eluent. Mn,GPC was calculated utilizing PMMA standards.
[b]GPC measurement with CHCl3:Net3:2-PrOH (94:4:2) as eluent (PS calibration).
Reproduced with permission from Hoogenboom, R.; Wiesbrock, F.; Huang, H.; *et al. Macromolecules* **2006**, *39*, 4719.[62]

copolymers of 2-ethyl-2-oxazoline (EtOx) and styrene. Initially, poly(2-ethyl-2-oxazoline) homopolymers with controlle d molecular weights and narrow polydispersity were synthesized in the presence of α-bromoisobutyrylbromide at different polymerization temperatures ranging from 100 to 180 °C under microwave irradiation. Polymers with relatively high molar masses and low polydispersity indices (M_n = 48 500 g mol^{-1}, PDI = 1.29) could also be obtained. Following the synthesis of macroinitiator (i.e., homopolymers with M_n = 3700 g mol^{-1}, PDI = 1.09), the ATRP of styrene was performed with CuBr and tris[2-(dimethylamino)ethyl]amine (Me_6Tren) as catalytic system (Figure 21).[64]

4.39.2.4 Metathesis Polymerization

Metathesis polymerization under microwave irradiation of phenylacetylenes was carried out in the presence *in situ*-generated (arene)M(CO)$_3$ complexes (Figure 22).[65] The reaction were run in a microwave oven in a specially designed long-necked round-bottom flask that could withstand elevated pressure. The catalyst/monomer ratio was kept at a 1:50 level in a 1,2-dichloroethylene solution and irradiated for 5 min at time intervals of 10 min. The reaction time was reduced to 1 h in contrast to refluxing conditions of 24 h. W(CO)$_6$ was found to be the best catalyst precursor among the group VIB metal carbonyls, while phenol showed the highest activity among

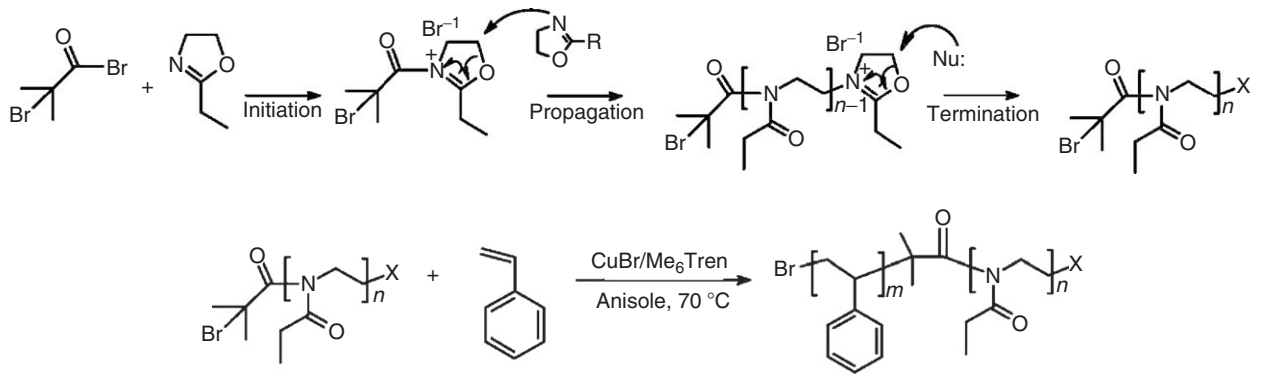

Figure 21 Schematic representation of the cationic ROP followed by ATRP of styrene initiated by a macroinitiator.

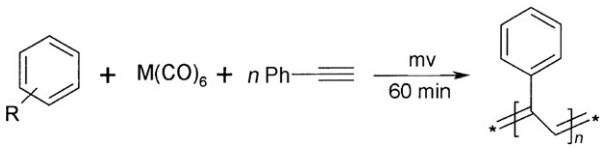

Figure 22 Metathesis polymerization of phenylacetylenes in the presence of *in situ*-generated (arene)$M(CO)_3$ complexes.

arenes. Under such conditions, poly(phenylacetylene) was obtained in 67–75% yield.

A new synthetic method to prepare soluble phenylenevinylene polymers by the ring-opening metathesis polymerization (ROMP) of 4,7,12,15-tetraoctyloxy-[2.2]paracyclophane-1,9-diene was also presented under microwave irradiation (Figure 23).[66] The polymerization showed a living character and gave polymers of controlled molecular weight, with a narrow polydispersity, fewer chain defects, and an alternating *cis,trans*-microstructure.

As it was shown, 4,12-di-20-ethylhexyloxy-7,15-dimethoxy-[2.2]paracyclophane-1,9-diene (**1**) was polymerized by the third-generation Grubbs catalyst when heated by microwave irradiation in anhydrous 1,2-dichloroethane. The optimum reaction conditions were found to be heating at 80 °C for 1 h. This compares with reaction times of up to 36 h required for complete monomer consumption using conventional heating in a THF solution. Under microwave irradiation, the polymers with a range of molecular weights were prepared by varying the initial monomer to catalyst ratio and the polydispersities were all low and in the range of 1.18–1.28 (Figure 24). Then the polymers were isomerized from the *cis*- to *trans*-vinylene form by prolonged irradiation at 365 nm in a THF solution (20 mg in 10 ml).[66]

Recently, ROMP was applied for the synthesis of maleimide-containing polymers from norbornene and maleimide in the presence of Grubbs catalyst.[67] Via Diels–Alder reaction with cyclopentadiene, the resulting maleimide side chain polymers were converted efficiently to the norbornene units of the polymer, which in turn were grafted by ROMP again (ROMP from ROMP) (Figure 25) under microwave irradiation.

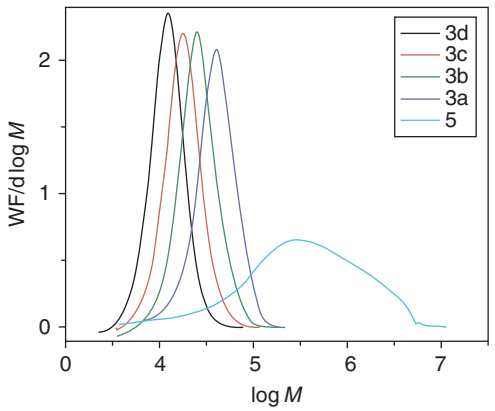

Figure 24 Molecular weight distributions of MEH-PPV prepared by microwave-assisted ROMP (3) and that prepared by the Gilch route (5) using calculated Mark–Houwink parameters. Reproduced with permission from Spring, A. M.; Yu, C.-Y.; Horie, M.; Turner, M. L. *Chem. Commun.* **2009**, 2676.[66]

4.39.3 Step-Growth Polymerization Reactions

4.39.3.1 Thermoplastic Polymers

A number of polymers obtained in step-growth polymerization reactions (i.e., polyethers, polyesters, polyamides) are accounted to functionally terminated thermoplastics, which combine the toughness of thermoplastics and the resistance of thermosets. The challenge during the synthesis and processing of these polymers is that temperature is often very close to their thermal degradation temperature, making temperature control crucial under both conventional and microwave conditions. Therefore, reduction of the timescale of processing under microwave irradiation in comparison with conventional conditions can be beneficial during synthesis and processing of these polymers.

For instance, a number of linear polyethers from either isosorbide or isoidide (important by-products of corn starch industry) and disubstituted alkyl bromides or methanesulfates were synthesized by using microwave irradiation under solid–liquid phase-transfer catalysis (PTC) conditions (Figure 26).[68,69]

In the case of isosorbide, the microwave-assisted synthesis proceeded more rapidly, compared with conventional heating, and was reduced to 30 min with the yield of approximately 69–78%. Under conventional conditions, the polyethers were afforded with 28–30% yield within 30 min. Similar yields of the polyethers were obtained while the reaction time was extended to 24 h. These yields remained practically unchanged even though the synthesis was carried out for another 7 days (Table 12).

Later, the same protocol was applied to the polycondensation of aliphatic diols of isosorbide with 1,8-dimesyloctane and other dibromo- and disulfonated alkylating agents

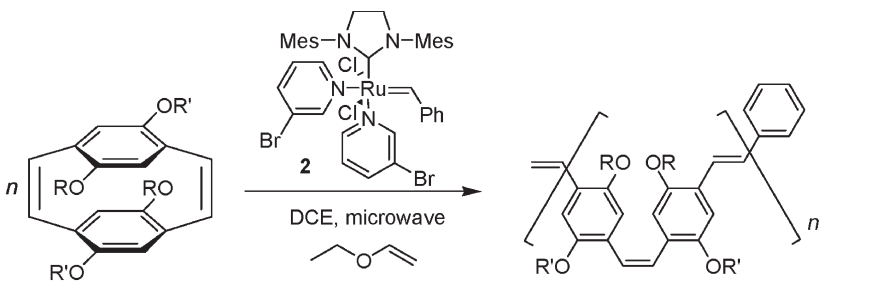

1 R = methyl, R' = 2-ethylhexyl **3a** (n = 50), **3b** (n = 40), **3c** (n = 30), **3d** (n = 20)

Figure 23 Synthesis of poly[[[(2-ethylhexyl)oxy]methoxy-1,4-phenylene]-1,2-ethenediyl] (MEH-PPV) by microwave-assisted ROMP.

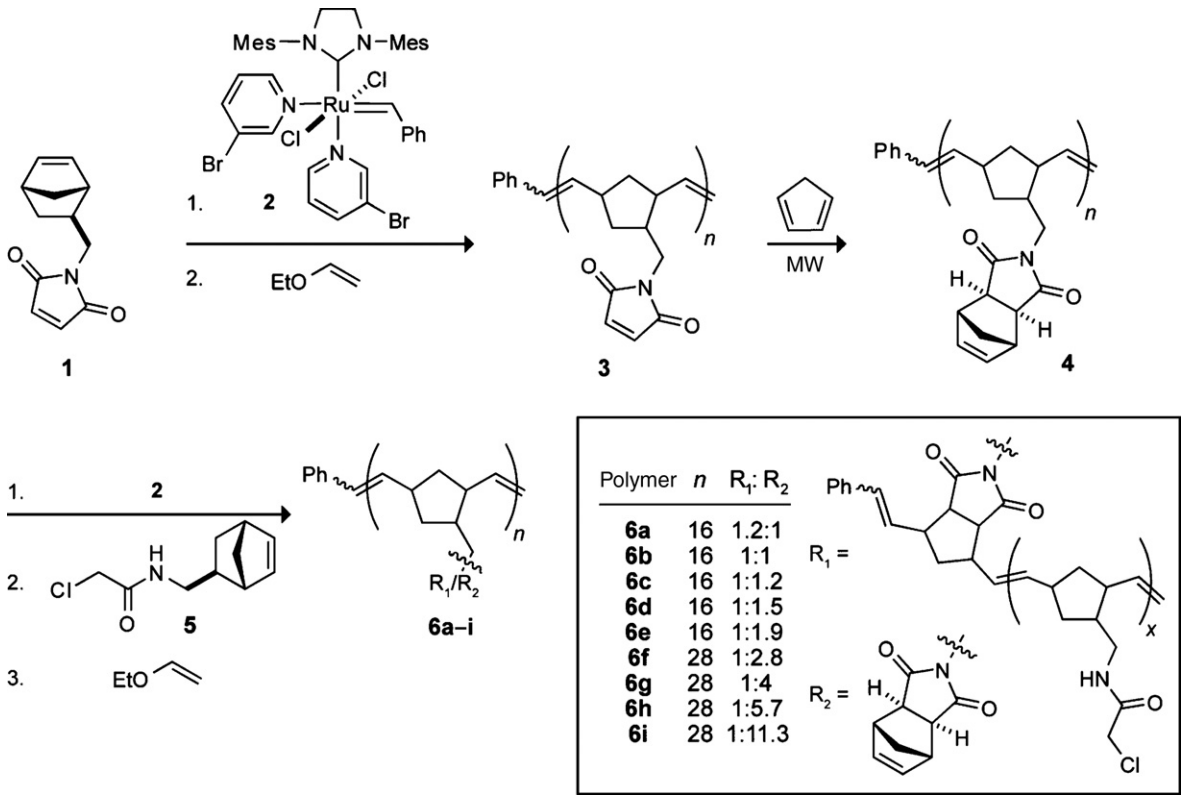

Figure 25 Synthetic route to graft copolymers (the *n* values refer to the degree of polymerization determined for the polymers by ^{1}H NMR analysis).

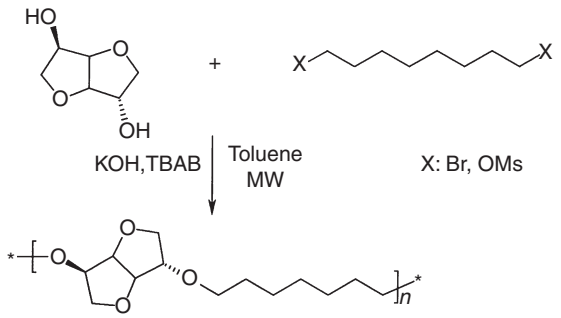

Figure 26 Synthesis of linear polyethers from either isosorbide or isoidide and disubstituted alkyl bromides or methanesulfates.

(Figure 27).[70] In all the cases, it was found that microwave-assisted polycondensations proceeded more efficiently compared with conventional heating; the reaction time was reduced from 24 h to 30 min. The polycondensation under microwave irradiation afforded polyethers with relatively high weight-average molecular weights up to 7000 g mol^{-1} with 63% yields.

It was demonstrated that the application of previously synthesized ethers of isosorbide was beneficial and allowed preparing polyethers in better yields than the polyethers obtained in direct reactions of isosorbide and dibromo- or dimesylalkenes. Recently, a novel group of polyamides were synthesized by the microwave-assisted polycondensation of an optically active isosorbide-derived diamine with different

Table 12 Influence of reaction time on the yields of high-molecular-weight fraction (FP MeOH) and low-molecular-weight fraction (FP Hex) of polyethers

Time	*Mode of activation*	*FP MeOH (%)*	*FP Hex (%)*	*Total yield (%)*
30 min	MW	67	18	85
60 min	MW	71	19	90
30 min	Thermal	12	81	93
1 day	Thermal	64	25	89
1 week	Thermal	83	5	88
1 month	Thermal	91	0	91

FP MeOH and FP Hex, fractions precipitated from methanol and then from *n*-hexane, respectively; MW, microwave irradiation.

Reproduced with permission from Chatti, S.; Bortolussi, M.; Loupy, A.; *et al J. Appl. Polym. Sci.* **2003**, *90*, 1255.[69]

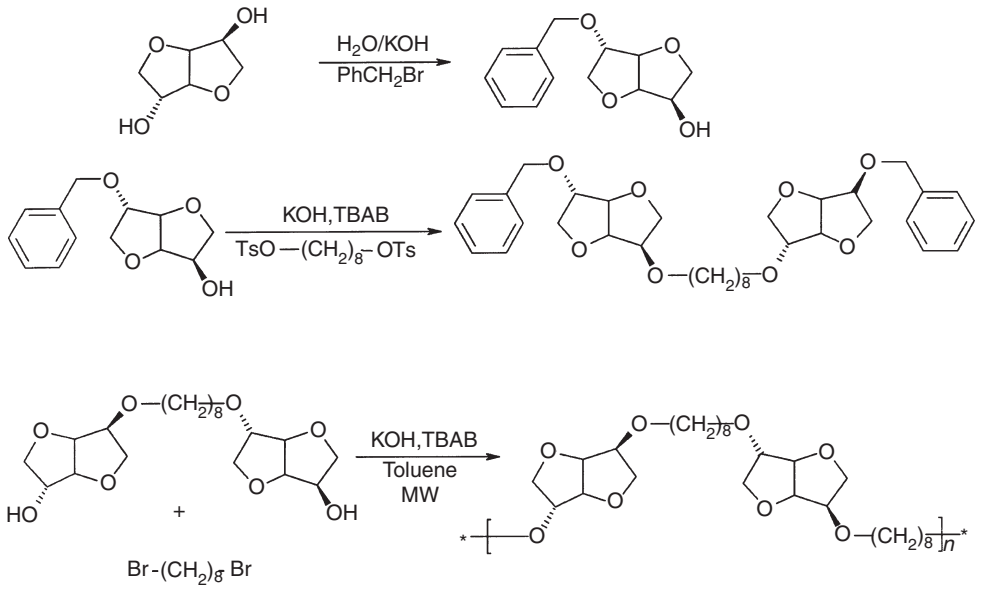

Figure 27 Polycondensation of aliphatic diols of isosorbide with 1,8-dimesyloctane and other dibromo- and disulfonated alkylating agents.

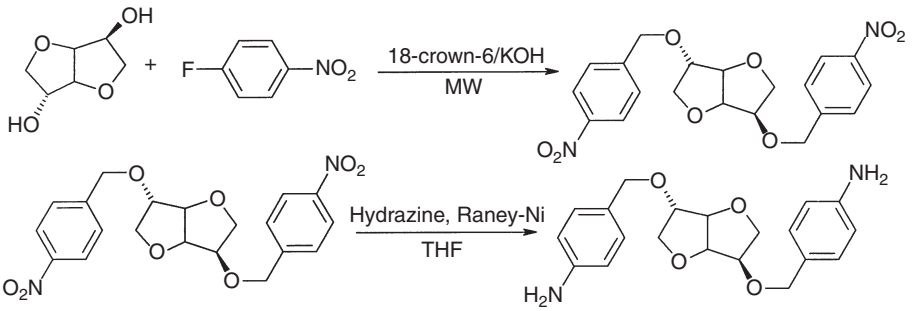

Figure 28 Reaction of isosorbide with *p*-fluoronitrobenzene and further reduction into isosorbide-derived diamine.

diacyl chlorides in the presence of a small amount of *N*-methylpyrrolidone (Figure 28).[71]

Polycondensation led to the formation of the polyamide with inherent viscosities in the range of 0.22–0.72 dl g^{-1}, which corresponded to rather higher molecular weights up to 140 000 g mol^{-1} (Figure 29). By applying interfacial polymerization under conventional heating conditions, lower molecular weight polyamides were obtained with inherent

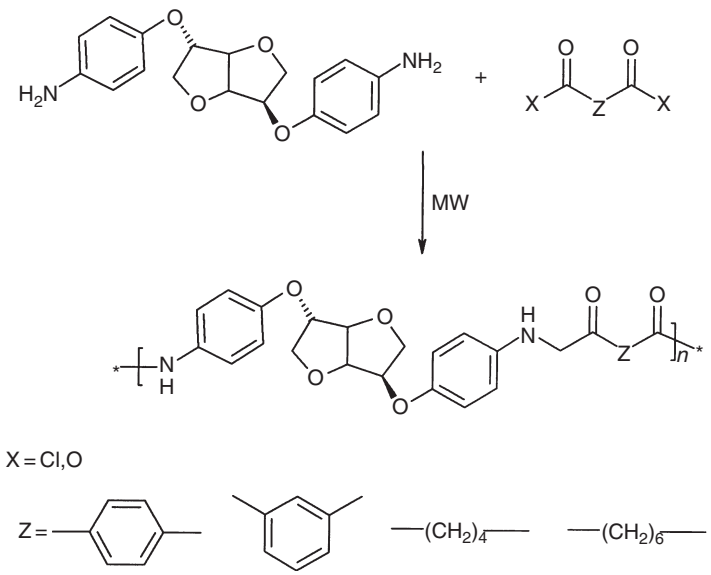

Figure 29 Polycondensation of acid dichlorides and the diamino derivative of isosorbide.

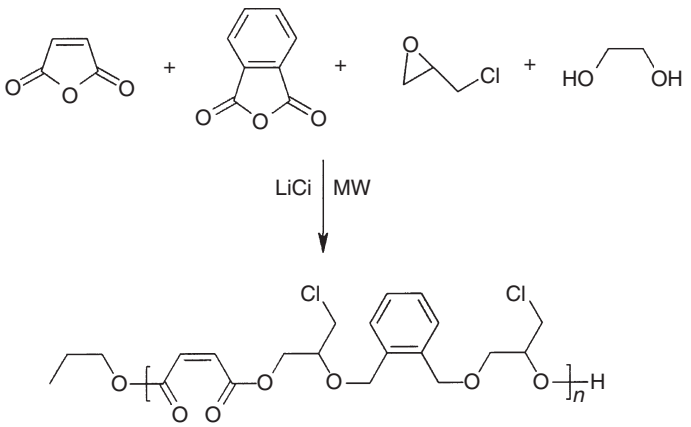

Figure 30 Synthesis of polyesters in the polyaddition reactions of alkylene oxides (i.e., epichlorohydrin) and acid anhydrides.

viscosities in the range of 0.04–0.36 dl g^{-1}, which was related to the maximum molecular weight of about 29 000 g mol^{-1}.[71]

The preparation methods for the synthesis of unsaturated and saturated polyester resins were also elaborated for microwave conditions. In the polyaddition reactions of alkylene oxides (i.e., epichlorohydrin) and acid anhydrides (i.e., maleic and phthalic anhydrides), unsaturated polyesters were prepared in the presence of lithium chloride as a catalyst (Figure 30).[72,73] In comparison with polycondensation reactions of acid anhydrides with diols, these reactions proceed without the release of by-products.

The polymerization reactions were run in the temperature range of 120–140 °C and continued until acid number value of polyesters dropped below 50 mg KOH g^{-1}. At the same time, the polyaddition reactions were performed under conventional thermal conditions, applying a similar set of reaction conditions. In comparison with these experiments, twofold reduction of reaction times was observed under microwave conditions while other parameters like number-average molecular weight and PDI were comparable.

The polycondensation of acid anhydrides (i.e., maleic and phthalic anhydrides) with diols (i.e., ethylene glycol) under microwave irradiation was also applied for the synthesis of unsaturated polyesters.[72] In addition to the previous protocol, the reaction temperature was increased to 200 °C, and a Dean–Stark trap was applied to remove water from the reaction mixture. It was found that the reaction times for microwave and conventional protocols were comparable and depended on the rate of removing water from the reaction system.

In turn, the synthesis of saturated polyesters by the step-growth polymerization reaction under microwave irradiation was presented for polycondensation of 1,4-butanediol and succinic acid in the presence of 1,3-dichloro-1,1,3,3-tetrabutyldistannoxane as a catalyst. The reaction mixtures were heated up to 200 °C in a microwave reactor, and, for comparison, polymerization under conventional conditions was carried out for 5 h in an oil bath preheated to 200 °C (Figure 31).[74]

Under microwave irradiation, poly(butylene succinate) (PBS) was obtained within 20 min with weight-average molecular weight M_w of 10 300 g mol^{-1}, while under conventional conditions, a similar value of weight-average molecular weight M_w of 10 200 g mol^{-1} was obtained after 5 h.

The synthesis of aliphatic polyamides under microwave irradiation has already been reported in a number of papers.[75–79] Polyamides were prepared from both ω-amino acids and diamines together with dicarboxylic acids (i.e., the nylon salt-type monomers) in the presence of a small amount of a polar organic medium (Figure 32).

The microwave-assisted polycondensation proceeded rapidly and was completed within 5 min for the polyamides with inherent viscosity around 0.24–0.63 dl g^{-1}.[77] For example, the solvent effect on the inherent viscosity of the polyamide

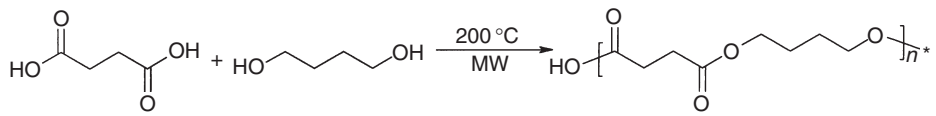

Figure 31 Polycondensation of 1,4-butanediol and succinic acid in the presence of 1,3-dichloro-1,1,3,3-tetrabutyldistannoxane as a catalyst.

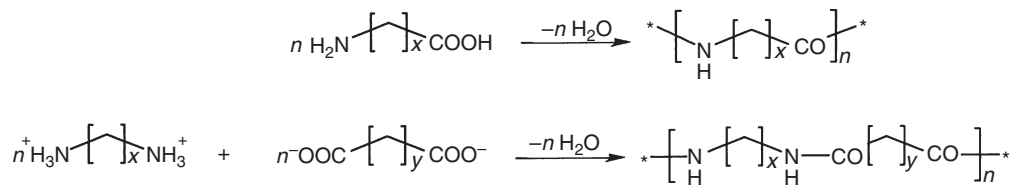

Figure 32 Synthesis of aliphatic polyamides from ω-amino acids as well as diamines and dicarboxylic acids.

Table 13 Solvent effect on microwave-assisted polycondensation of 12-aminododecanoic acid[a]

Solvent type	*Solvent* ε_r	*Boiling point (°C)*	*Ft*[b] *(°C)*	*Reaction time (min)*	*Ft*[c] *(°C)*	*Polymer* η_{inh}[d] *(dl g*$^{-1}$*)*
Water	78	100	97	5	220	0.35
Dimethyl sulfoxide	47	189	172	4	259	0.24
Dimethylacetamide	38	166	163	5	281	0.23
N-Methylpyrrolidone	32	202	179	4	267	0.39
Nitrobenzene	35	211	198	5	264	0.42
Ethanediol	38	197	193	5	317	0.59
1,4-Butanediol	31	229	189	5	242	0.24
Diphenyl ether	4	258	66	5	109	–

[a]The polymerization was carried out with 2 g of monomer and 2 ml of the solvent under microwave irradiation.
[b]Final temperature of the solvent alone after 2 min of microwave irradiation.
[c]Final temperature of the reaction mixture.
[d]Measured at a concentration of 0.5 d dl^{-1} in *m*-cresol at 30 °C.
Reproduced with permission from Imai, Y.; Nemoto, H.; Watanabe, S.; Kakimoto, M. *Polym. J.* **1996**, *28*, 256.[77]

formed by the polycondensation of 12-aminododecanoic acid under microwave irradiation is summarized in Table 13.

In a similar way, the synthesis of aromatic polyamides from aromatic diamines (*m*-phenylenediamine (*m*PDA), *p*-phenylenediamine, bis(4-aminophenyl)methane, and bis (4-aminophenyl)ether) and dicarboxylic acids such as isophthalic and terephthalic was performed.[80] The polycondensation was carried out in an NMP solution in the presence of triphenyl phosphite (TPP), pyridine, and lithium chloride as condensing agents. Polyamides with moderate inherent viscosities of 0.21–0.92 dl g^{-1} within 30–50 s were obtained; however, no marked differences in molecular weight distribution and inherent viscosities between the polyamides produced by conventional (60 s, 220 °C) and microwave methods were found.[80]

Recently, the synthesis of polyamides from linear nonaromatic dicarboxylic acids (i.e., adipic, suberic, sebacic, and fumaric acid) and aromatic diamines such as *p*-phenylenediamine or 2,5-bis(4-aminophenyl)-3,4-diphenylthiophene under microwave conditions was performed (Figure 33).[81]

The polyamides with inherent viscosity in the range of 0.1–0.8 dl g^{-1} were obtained in medium to high yield (60–100%); however, temperature was not detected during the microwave experiments.

Later, microwave irradiation was applied to the synthesis of copolymers, that is, poly(ε-caprolactam-*co*-ε-caprolactone) (PAE) directly from two cyclic monomers, ε-caprolactam and ε-CL, by anionic-catalyzed ROP.[82] ε-Caprolactam and ε-CL in the molar ratio of 2:1 were mixed together with solid LiAl[OC$(CH_3)_3]_3$H (1–3 mol% of total reactants), and the mixture was irradiated up to 140–180 °C for 1 h. The same ratio of reactants and catalyst were used for the conventional synthesis in an oil bath. Compared with the corresponding thermal products, the microwave-synthesized copolymers gave higher yield, higher amide composition, higher glass transition temperature, and equivalent molecular weights (Table 14).[82]

4.39.3.2 Thermosetting Resins

Microwave-assisted curing of thermosetting polymers represents the most widely studied area and is one of the first applications in polymer chemistry and technology. As thermosetting resins are cured, their dielectric loss factor decreases significantly because of the formation of crosslinked structures, increase of viscosity, and, finally, decreased motion of polymer molecules. Thus, thermosetting resins absorb less and less microwaves when they are being cured and the reactions can be self-quenched.[83] Some examples of thermosetting resins are presented in this chapter.

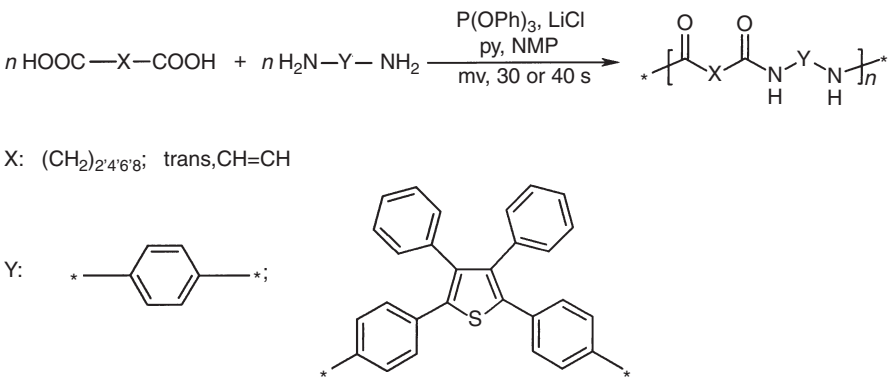

Figure 33 Synthesis of polyamides from linear nonaromatic dicarboxylic acids (i.e., adipic, suberic, sebacic, and fumaric acid) and aromatic diamines.

Table 14 Comparison of microwave and thermal activation in copolymerization reactions

Variable	Δ – PAE, 1%,[a] 160 °C– 30 min	Δ – PAE, 2%, 160 °C– 30 min	Δ – PAE, 3%, 160 °C– 30 min	MW – PAE, 1%, 160 °C– 30 min	MW – PAE, 2%, 160 °C– 30 min	MW – PAE, 3%, 160 °C– 30 min
Starting materials						
Ester/amide	1:2	1:2	1:2	1:2	1:2	1:2
Yield (%)	51.2	52.7	57.0	61.9	70.1	78.2
T_g (°C), tan δ, Dynamic Mechanical Thermal Analysis (DMTA) (1 Hz)	– 25.0	– 18.5	– 14.5	– 14.0	– 7.5	6.0
T_g (°C), from Fox equation	29	12	9	15	8	4
M_w ($\times 10^3$ g mol^{-1}), GPC	25.4	19.8	17.1	22.0	21.3	16.2
M_w/M_n	1.4	1.5	1.6	2.1	2.0	1.5

[a]Catalyst level.

Reproduced with permission from Fang, X.; Hutcheon, R.; Scola, D. A. *J. Polym. Sci. Part A: Polym. Chem.* **2000**, *38*, 1379.[82]

4.39.3.2.1 Epoxy resins

During the early investigation of epoxy systems, it was found that a pulse in comparison with continuous microwave irradiation could lead to an improvement in the mechanical properties of epoxy resins[84] and the fastest heating of the resins[85] at the same microwave energy level. These systems consisted of diglycidyl ether of bisphenol A (DGEBA) together with 4,4′-methylenedianiline (DDM) or 4,4′-diaminodiphenyl sulfone (DDS) (**Figure 34**). For example, the gel point for DGEBA–DDM system was 19 min using the pulse with a length of 0.25 ms and an average power of 40 W, while the gel point for continuous microwave irradiation at 40 W was reached in 21 min.[85]

Furthermore, it was shown that a computer-controlled pulsed microwave processing of epoxy systems could successfully eliminate the exothermic temperature peak and maintain the cure temperature to the end of the reaction.[86] Thus, it was possible to cure the epoxy systems under pulsed microwave irradiation at higher temperatures and faster without thermal degradation when compared to a continuous microwave or conventional processing. It was possible to measure the loss factor (ε'') of the samples during the controlled pulse microwave irradiation, and it was shown that the loss factor (ε'') decreased as the reaction progressed (**Figure 35**).

The study of the dielectric properties during the curing process has both fundamental and practical applications because dielectric properties provide information about the stage of curing reactions; thus, nondestructive testing methods to monitor the curing processes were developed. For the frequency range of 10^3–10^{10} Hz, the dielectric properties of the epoxy system consisting of DGEBA (EPON 828 EL) and ethylenediamine (EDA) were measured.[87,88] The results confirmed the possibility of utilizing dielectric quantities to obtain information on relevant parameters such as conversion, viscosity change, sol–gel transition, and glass transition temperatures. Moreover, the basic parameters such as static dielectric constant (ε_r) and dielectric permeability ($\varepsilon^* = \varepsilon' - j\varepsilon''$), which are important for microwave processing, can be found in these works. The loss factor (ε'') and permeability (ε') increase with the reaction temperature and decrease with the extent of cure, which can be attributed to the higher and lower mobility of molecular dipoles during heating and crosslinking, respectively (**Figure 36**).[89,90]

Dielectric properties of other curing epoxy resin systems, that is, DGEBA (DER 332) and DDS, Jeffamine D-230, or *m*PDA, at a frequency of 2.45 GHz in the temperature range of 20–100 °C can also be found in the literature together with the theoretical model for calculation of permeability (ε') and the loss factor (ε'') during curing epoxy systems under microwave irradiation.[91]

Curing of epoxy systems in thin films was also studied while thermal mechanical analysis (TMA) was used to determine the glass transition temperatures directly from the cured thin-film samples.[92] The epoxy systems consisted of DGEBA with different curing agents (i.e., DDS and *m*PDA), and the samples were prepared by casting stoichiometric mixtures of DGEBA/DDS

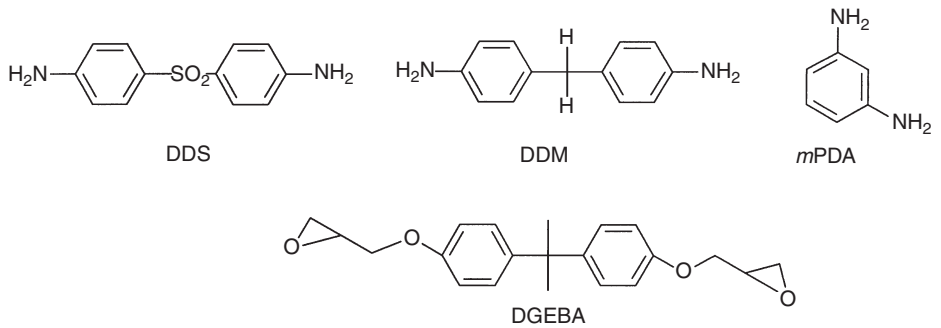

Figure 34 Diglycidyl ether of bisphenol A (DGEBA), 4,4′-methylenedianiline (DDM), 4,4′-diaminodiphenyl sulfone (DDS), and *m*-phenylenediamine (*m*PDA).

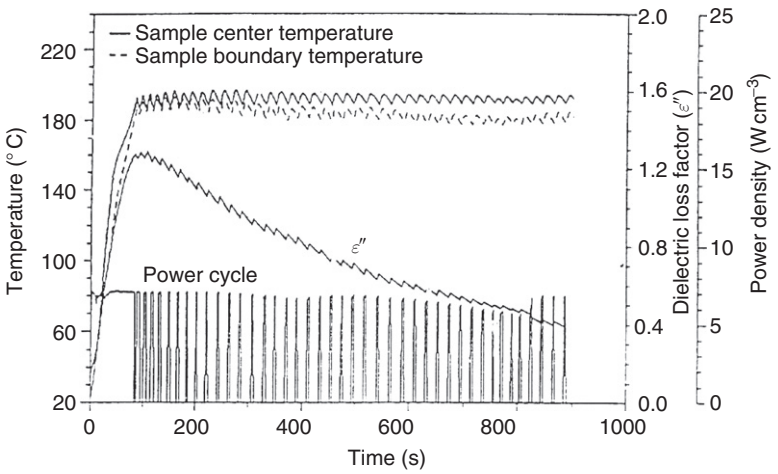

Figure 35 Temperature, loss factor, and input power density measurements during controlled pulsed microwave curing of DGEBA/DDS resins. Reproduced with permission from Jow, J.; DeLong, J. D.; Hawley, M. C. *SAMPE Quart.* **1989**, *20*, 46.[86]

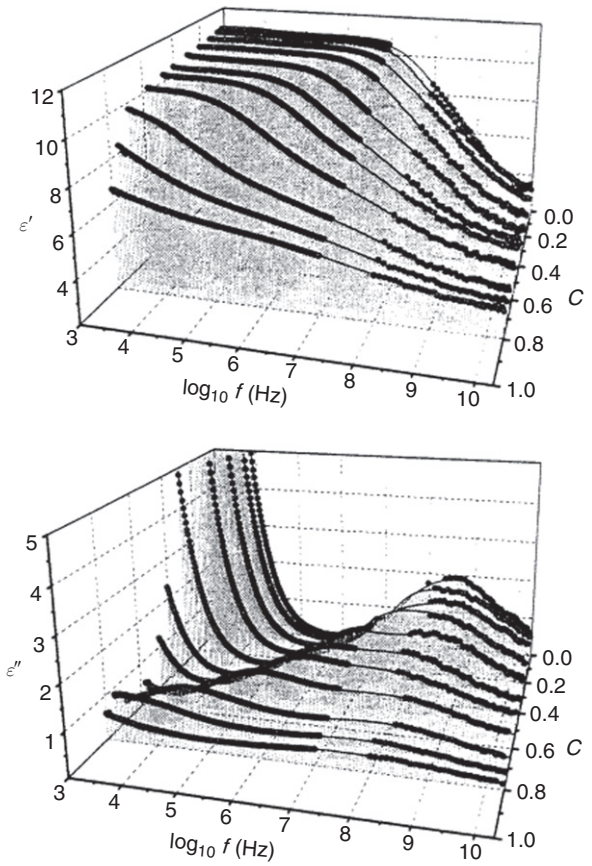

Figure 36 Three-dimensional plot of ε' and ε'' vs. conversion C and $\log_{10}$ of frequency for the DGEBA/EDA 1:1 system cured at 25 °C. The black spheres are from experimental data; contour lines of the shaded areas are from fit equations. Reproduced with permission from Casalini, R.; Corezzi, S.; Livi, A.; *et al. J. Appl. Polym. Sci.* **1997**, *65*, 17.[88]

and DGEBA/*m*PDA onto 13 mm diameter and 1 mm thick potassium bromide disks to form approximately 10 μm thick films. The thin-film samples were cured under microwave irradiation, while the temperature was measured directly from the thin epoxy films. The effects of microwave irradiation on the cure of epoxy systems depended on curing agents. Microwaves had a stronger effect on epoxy/DDS than epoxy/*m*PDA systems, and, consequently, the magnitude of increases in glass transition temperatures was much larger for DGEBA/DDS than for DGEBA/*m*PDA. Moreover, significantly higher ultimate extents of cure and faster reaction rate were observed in the microwave cure when compared to thermal cure.[92]

The effect of microwave curing of the epoxy system consisting of DGEBA and cycloaliphatic diamine (i.e., 4,4′-diamino-3,3′-dimethyldicyclohexyl methane (3DCM)) was also investigated for thicker samples and compared with conventional thermal cure samples.[93] The epoxy systems (ca. 13 g) were poured into molds (96 mm × 16 mm × 8 mm), which were irradiated in a microwave applicator. The sample temperature was measured continuously to give the surface and bulk temperature. It was found that microwaves did not have direct influence on the mechanical processing of the polymer network, and the only parameter that influenced the mechanical properties was the extent of the reaction. Under microwave processing conditions, it was not possible to obtain fully cured DGEBA/3DCM network. The fully cured samples were obtained by either thermal (140 °C, 1 h + 190 °C, 14 h) or combined processing (microwave 200 W, 15 min + thermal 190 °C, 14 h) (**Table 15**).[93]

Table 15 Comparison of epoxy compositions cured under both microwave and microwave/conventional conditions

Curing cycle	*MW*	*MW + thermal*
Power (W)	200	200
Temperature (°C)		190
Time	15 min	15 min + 14 h
Compression modulus (GPa)	3.15	2.9
Poisson's ratio	0.36	0.36
Glass transition temperature (°C)	131	186
Extent of reaction (%)	89	100

MW, microwave irradiation.

Reproduced with permission from Jordan, C.; Galy, J.; Pascault, J. P.; *et al. Polym. Eng. Sci.* **1995**, *35*, 233.[93]

On the other hand, the reaction rate enhancement under microwave conditions was reported when microwave irradiation and thermal curing were performed on the epoxy systems, too.[94] Three types of curing agents were used, that is, DDS, DDM, and *m*PDA together with DGEBA (Araldite GY6010). After the radiation, the samples were removed and the specimen temperature (T_{spec}) was measured by the thermocouple; then the samples were stored in a freezer. Finally, the percentage cure of the resin mixtures at selected time intervals was calculated from the heat of reaction of the exotherm curve obtained during the differential scanning calorimetry (DSC) run of the samples.

For the DDM and *m*PDA systems, full curing was achieved at all power levels, but the cure of the DDS system could not reach 100% at lower power levels. For instance, under microwave conditions, at a low power level (i.e., 200 W), the DDM and *m*PDA systems appeared to give shorter curing times of 10 and 8 min, respectively, in comparison with the DDS system, which cured after 15 min. However, at higher power levels (i.e., 400 and 600 W), the curing time was almost the same: 2 min 30 s for *m*PDA and 3 min for both DDS and DDM systems (Table 16).[94]

Table 16 Maximum of specimen temperature (T_{spec}) of microwave-treated epoxy/amine systems

Microwave curing temperature (°C)	T_{spec} *(°C)*	*Cure time (min)*
DGEBA/DDS		
200	141	15
300	165	10
400	184	5
500	225	5
600	235	3
DGEBA/DDM	111	10
200	137	5
400	174	3
600	135	8
DGEBA/*m*PDA	150	4
200	212	2.5
400		
600		

Reproduced with permission from Boey, F. Y. C.; Yap, B. H.; Chia. L. *Polym. Test.* **1999**, *18*, 93.[94]

According to the next report, the observed rate enhancement of curing of epoxy systems was the result of the decrease in the lag time prior to incitation of crosslinking and, in consequence, the decrease in the overall effective cure time.[95] Since a shortening of cure time is not different from a shortening achieved by a higher curing temperature, by comparison of the curing processes under both microwave and thermal conditions, it was possible to obtain temperature equivalent values for the microwave cure, which are only virtual ones and are prepared for the purpose of analysis of the cure kinetics. The regression plot of the effective cure time for thermal curing to obtain the equivalent temperatures for microwave curing is presented in Figure 37 and Table 17.

It is worth indicating that the equivalent temperatures obtained in all the cases were consistent and significantly higher than the maximum temperature measured in the samples, providing further support that the microwave curing is not merely thermal based.[95]

In turn, the synthesis of high-molecular-weight (solid) epoxy resins under PTC conditions was described.[96,97] The method was based on the polyaddition of bisphenol A (PBA) to a low-molecular-weight epoxy resin or DGEBA in the presence of ammonium or phosphonium salts as well as imidazole derivatives as a catalyst (Figure 38).

The main advantage of the microwave process is twofold reduction of reaction time in comparison to conventional conditions. It was found that the molecular weight distribution and degree of branching of the solid epoxy resins synthesized under microwave irradiation were comparable with those obtained under conventional heating and were not influenced by the reduction in reaction time (Table 18).[97]

During the synthesis, the surface temperatures of the solid epoxy resin samples were monitored by means of a thermovision camera in order to observe the temperature distribution under microwave and conventional conditions for both stirred and nonstirred reaction mixtures (Figure 39).

The experiments were carried out at 160 °C, and, as was expected for an exothermic reaction, the highest temperatures were observed in the center of the reaction vessel for all the processes (Figures 38(a)–38(d)). Furthermore, for both microwave and conventional processes, the stirring of the reaction mixture resulted in more uniform temperate profiles (Figures 38(a) and 38(c)), while for the nonstirred reaction mixture, the maximum surface temperature under microwave irradiation was much higher (approximately 200 °C) than the bulk temperature of the reaction mixture. Moreover, for

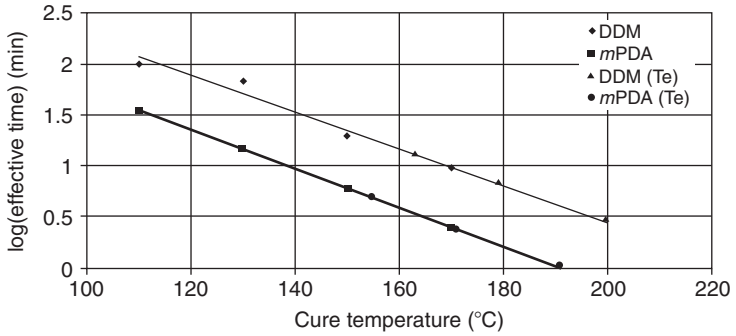

Figure 37 Regression plot of the effective cure time for thermal curing to obtain the equivalent temperatures for microwave curing. Reproduced with permission from Boey, F. Y. C.; Rath, S. K. *Adv. Polym. Technol.* **2000**, *19*, 194.[95]

Table 17 Equivalent cure temperature for microwave processing of epoxy/amine systems

Microwave power (W)	*Maximum temperature (°C)*	*Lag time (s)*	*Effective cure time (s)*	*Total cure time (s)*
DGEBA/DDM system				
200	120	144	163	154
400	130	170	179	173
600	162	181	196	190
DGEBA/*m*PDA system				
200	135	150	153	152
400	151	171	172	170
600	178	193	190	191

Reproduced with permission from Boey, F. Y. C.; Rath, S. K. *Adv. Polym. Technol.* **2000**, *19*, 194.[95]

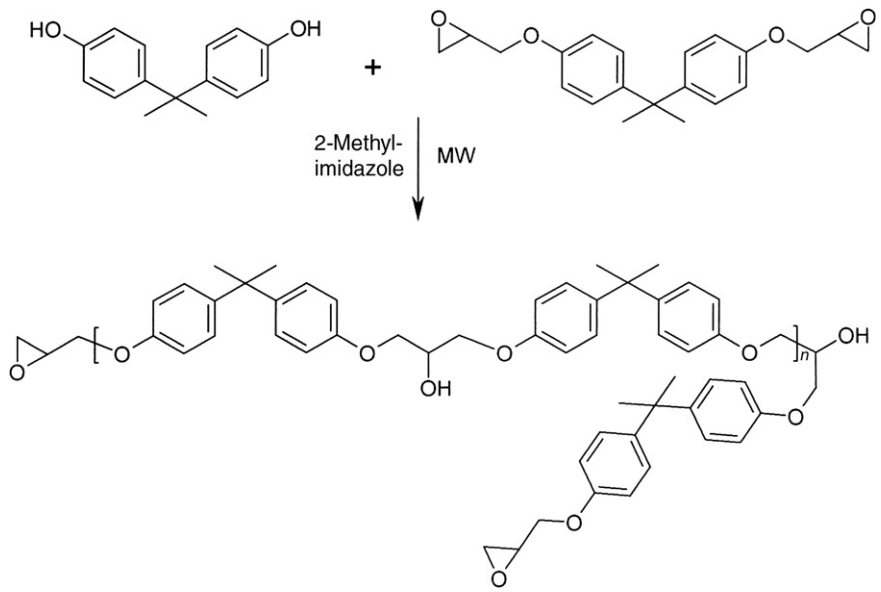

Figure 38 Synthesis of high-molecular-weight (solid) epoxy resins.

Table 18 The results and analysis of the molecular-weight distribution of (solid) epoxy resins by GPC.

Epoxy resinsample	*Condition*	*Reaction temp. [°C]*	*Catalystcontent [mol× 10^3]*	*Reaction time [min.]*	*Epoxy value [mol/100 g]*	*GPC*		
						M_n (g mol^{-1})	M_w (g mol^{-1})	$\bar{M}_w/\bar{M}_n$
1			0.5	150	0.114	1810	3260	1.80
2	MW	140	1.0	90	0.112	1470	2580	1.75
3			5.0	25	0.110	1950	3780	1.94
4			0.5	65	0.110	2140	3780	1.77
5	MW	160	1.0	40	0.113	1850	3390	1.83
6			5.0	20	0.104	2470	3390	1.83
7			0.5	65	0.109	2380	4340	1.85
8	MW	180	1.0	30	0.109	2180	3990	1.83
9			5.0	16	0.105	2420	4580	1.89
10			0.5	280	0.114	1380	2860	2.08
11	Δ	140	1.0	150	0.114	2020	3760	1.86
12			5.0	55	0.113	2170	3640	1.68
13			0.5	120	0.106	1790	3130	1.75
14	Δ	160	1.0	80	0.111	2180	4000	1.84
15			5.0	35	0.100	2380	5010	2.10
16			0.5	80	0.101	2180	4000	1.84
17	Δ	180	1.0	50	0.105	2250	4250	1.89
18			5.0	35	0.100	2320	4420	1.91

MW, microwave irradiation; Δ, conventional heating (i.e., electric heating mantle).
Reproduced with permission from Bogdal, D.; Gorczyk, J. *J. Appl. Polym. Sci.* **2004**, *94*, 1969.[97]

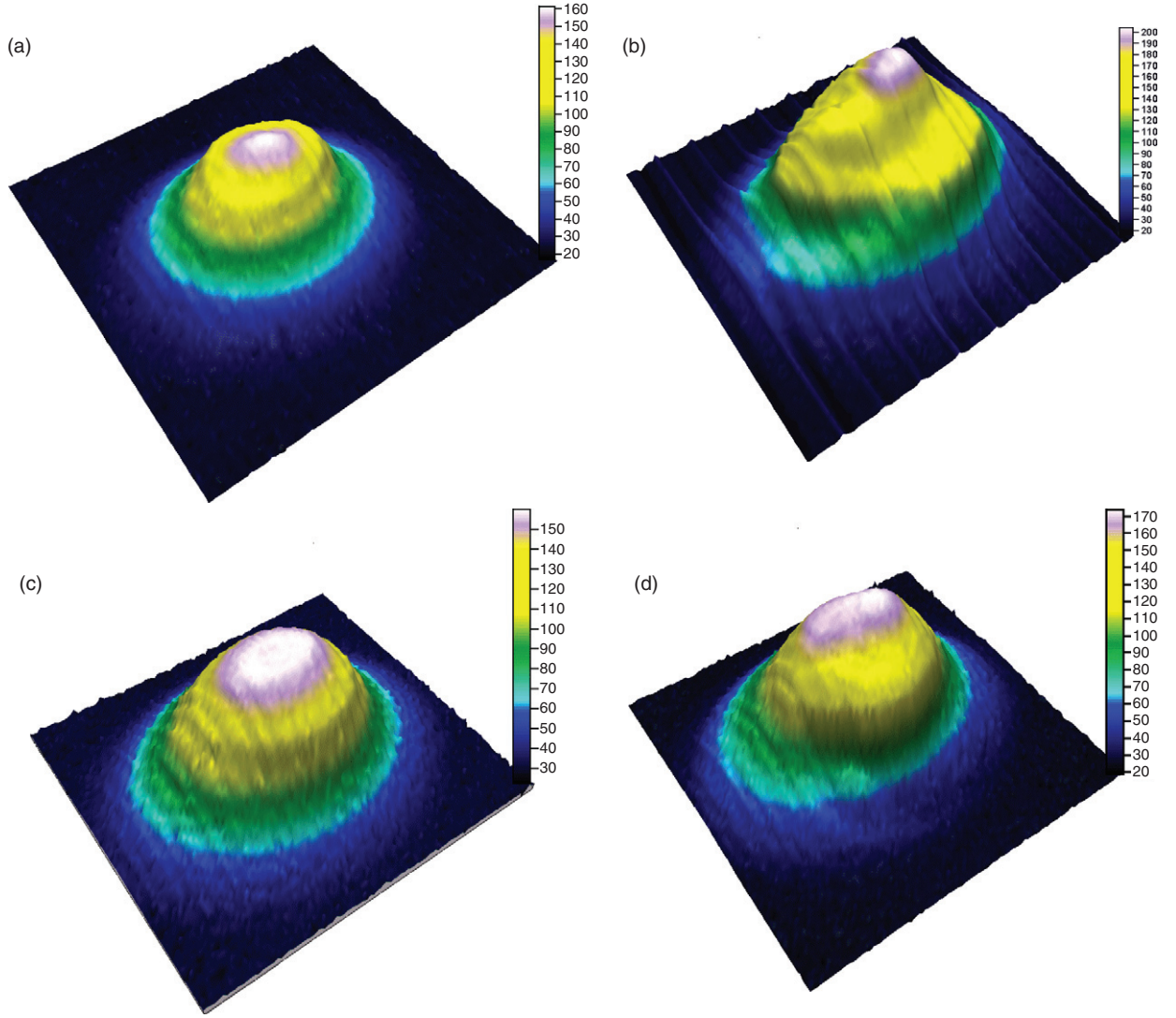

Figure 39 Surface temperature of the solid epoxy resin samples monitored by means of a a thermovision camera: a) microwave conditions with stirring b) microwave conditions no stirring c) conventional conditions with stirring d) conventional. Reproduced with permission from Bogdal, D.; Gorczyk, J. *J. Appl. Polym. Sci.* **2004**, *94*, 1969.[97]

the nonstirred samples prepared under microwave irradiation, high-temperature heterogeneity was observed (**Figure 38**(**b**)), which, in turn, led to crosslinking of resins. It was opposite to the reaction under conventional conditions, in which the temperature for the nonstirred reaction mixture was, however, more inhomogeneous than for the stirred mixture, but the maximum surface temperature reached only 170 °C (**Figure 38**(**d**)).[96]

Lately, the same approach for the synthesis of solid epoxy resins with reduced flammability was presented.[98] For this purpose, PBA was either substituted or partially substituted with 1,1-dichloro-2,2-bis(4-hydroxyphenyl)ethylene, and the synthesis of solid epoxy resins was realized in the same manner as described previously.

Other epoxides such as 3,4-epoxycyclohexylmethyl, 3,4-epoxycyclohexylcarboxylate were cured in the presence of diaryliodonium or triarylsulfonium salts (**Figure 40**) as a catalyst under microwave conditions.[99] The extent of the polymerization was determined by means of DSC and Fourier transform infrared (FTIR) spectroscopy and compared with samples cured under conventional conditions.

The study performed revealed some polymerization phenomena such as polymerization selectivity, polymerization

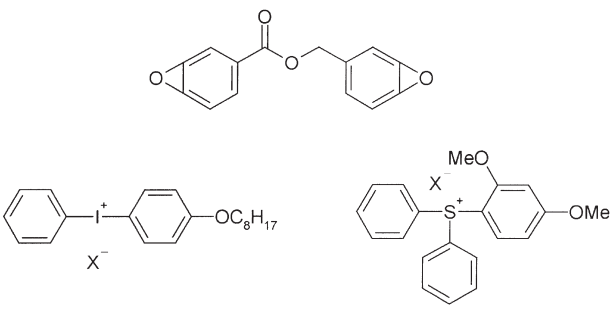

Figure 40 Polymerization 3,4-epoxycyclohexylmethyl, 3,4-epoxycyclohexylcarboxylate initiated by diaryliodonium or triarylsulfonium salts.

temperature shift, and polymerization temperature shift by microwave power setting under microwave irradiation in comparison with conventional conditions. To explain the phenomena, it was proposed that a new dipole partition function exists in the microwave field, so the values of thermodynamic properties such as internal energy and Gibbs free energy of the material with permanent dipole moments changed under microwave conditions, which in turn led to shifts in the reaction equilibrium and kinetics compared to conventional conditions at the same temperature.[44]

In turn, the application of microwave irradiation to cure isocyanate/epoxy resins in the presence of *N*-(2-hydroxyalkyl) trialkylammonium halides was also claimed to impart accelerations to both curing and postcuring kinetics with respect to conventional hot-air heating.[100] As a consequence, a new class of catalysts that endow aromatic isocyanate/epoxy and aliphatic or cycloaliphatic epoxy/anhydride systems with a particular efficiency for microwave processability was developed.[101] The catalysts belong to the family of *N*-(cyanoalkoxyalkyl)trialkylammonium halides (**Figure 41**), and their evaluation of the microwave enhancements was performed via isothermal comparative curing experiments under hot-air and microwave heating.[102]

As a result, the strong reaction enhancements of the specific catalysts were imparted under microwave heating to all of the reactive systems examined. The gelation and vitrification times were reduced by a factor of 8–10 of those under hot-air heating with the same catalyst and under the same concentration (**Table 19**), which was attributed to an ion-hopping conduction mechanism as the dominant source of the microwave absorption capacities of these catalysts.[102]

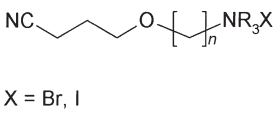

Figure 41 *N*-(Cyanoalkoxyalkyl)trialkylammonium halides.

4.39.3.2.2 Polyurethanes

Owing to high versatility of the polyurethane raw materials, a variety of products with diverse structures and polymer matrix from flexible to rigid, especially cellular materials, are manufactured. In the middle of the 1980s, crosslinking of polyurethane resins was performed by means of pulsed microwave irradiation.[103] The thermal behavior of an ethyl acetate solution of two prepolymers, triisocyanate (Desmodur L75) and polyester–polyalcohol (Desmophen 800), was investigated together with the formation of polyurethane coatings from the same mixture and film hardness as a function of different pulse regimes. The average power of microwave irradiation was 30 W and the pulse period varied from 2 to 200 ms so that the pulse time was varying from 50 μs to 30 ms.

The variations of the maximum temperature (T_{max}) with peak power were reported where each curve was related to a pulse period. All curves were issued from the same point, corresponding to the reference continuous wave, that is, power 30 W with T_{max} 70 °C. Starting from this point, T_{max} always increases with pulse power (**Figure 42**). Thus, it was concluded that the energy transfer by pulse microwaves is more efficient than by continuous irradiation, and microwave-cured polyurethane films were very much harder than oven-cured materials.

The crosslinking of polyurethane resin composed of diisocyanate derived from 4,4′-diisocyanate diphenylmethane and a low-viscosity polyethertriol was also investigated under microwave conditions.[104] The reactions were carried out without a catalyst and led to final networks with mechanical properties least equivalent to those prepared under conventional conditions. For example, the average elasticity modulus determined from uniaxial compression with samples (25 mm of height and 12.5 mm of diameter) was equal to 3120 MPa for curing under

Table 19 Isothermal curing times of aromatic isocyanate/epoxy and aliphatic epoxy/anhydride resin systems under conventional and microwave heating

Resin system Curing type (temperature)	*Catalyst concentration (mmol 100^{-1} g)*	*Curing time*	
		Gelation	*Vitrification*
System A: I-MDI/DGEBA 70:30 w/w	I-1[a]		
Conventional (66 °C)	1.90	40 min	>80 min
Microwave (66 °C)	1.90	–	15–20 min
System B: ERL-4299/(SA/Me-HHPA) 1:1 w/w	I-2[b]	3 h 40 min	14 h 30 min
Conventional (90 °C)	1.08	50 min	1 h 50 min
Microwave (90 °C)	1.08		
System C: ERL-4234/DDSA	I-3[c]		
Conventional (70 °C)	1.09	25 h 30 min	63 h
Microwave (70 C)	1.09	3 h	6 h
System C: ERL-4234/DDSA	I-4[d]		
Conventional (85 °C)	1.14	4 h 30 min	7 h 30 min
Microwave (85 °C)	1.14	30 min	60 min
	TBAI[e]		–
Microwave (85 °C)	1.52	3 h 30 min	

[a]*N*-[3-[2-Cyanoethoxy]propyl]-*N*,*N*-dimethyldecylammonium iodide.
[b]4-[3-[2-Cyanoethoxy]ethyl]-4-butylmorpholinium iodide.
[c]*N*-[2-[2-Cyanoethoxy]propyl]-*N*,*N*-dimethyldecylammonium iodide.
[d]4-[3-[2-Cyanoethoxy]ethyl]-4-butylmorpholinium iodide.
[e]*tetra*-Butylammonium iodide.
Reproduced with permission from Parodi, F. In *Polymers and Liquid Crystals*; Wlochowicz, A., Ed., Proceedings of SPIE – The International Society for Optical Engineering, 1999.[102]

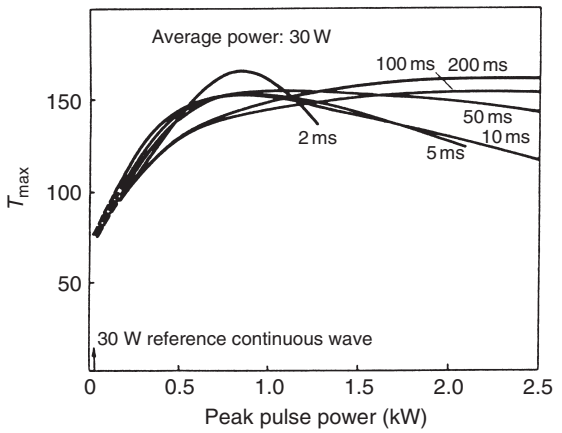

Figure 42 Peak pulse power dependence of the maximum temperature T_{max} (second parameter: pulse period). Reproduced with permission from Jullien, H.; Valot, H. *Polymer* **1985**, *26*, 506.[103]

microwave conditions (1 h at 20 W) and 2810 MPa for conventional curing in an oven (60 °C for 8 h).

The application of microwave irradiation is expected to help in the preparation of environmentally benign renewable components for polyurethane foams.[105,106] The vegetable oil-based polyols are examples of such components that can be used to obtain rigid polyurethane foams that possess satisfied properties for use as thermal insulating materials.

For this purpose, for the preparation of rapeseed and linseed oil-based polyols a two-step process was applied.[107] In the first step, the double bonds of the unsaturated triglycerides were transformed into oxirane rings with acetate peroxyacid to form epoxidized oil. In the second step, the ring opening reactions of the epoxy groups with monoethylene glycol (MEG) or DEG afforded the oil-based polyols. For rapeseed and linseed oils, it was reported that microwave irradiation can be applied for both steps of the process. In comparison to the processes under conventional conditions, reduction of the reaction time of epoxidation reaction (ca. 60%) and, then, the hydroxylation step (ca. 75%) was observed.

In turn, blowing and curing processes of rigid polyurethane foams under microwave irradiation were also investigated.[108] The polyurethane foams were blown inside a microwave reactor with continuous microwave power regulation. The foams were prepared in one step, that is, isocyanate was added to polyol premix with additives, and the mixtures were stirred for 10 s. The foaming processes were carried out as a free rise in the open mold and the mixtures were expanded freely in the vertical direction on a square area of 20 cm × 20 cm in polypropylene molds at ambient temperature (ca. 20 °C). In the second case, the polypropylene molds were placed inside a microwave reactor. The results reflected the dependence of foam properties on such parameters of microwave irradiation as power and time, and the application of lower power for longer time periods resulted in rigid foams with more beneficial properties (**Figure 43**)

In general, better mechanical properties were observed with the increase of apparent density of rigid polyurethane foams. However, in this case, it must be stressed that an increase of apparent density of about 20% increases compressive strength by more than 100% (**Figure 44**).

Eventually, the application of microwave irradiation for blowing of polyurethane foams led to reduction in the amount of amine catalysts required by half. The possibilities of the application of partially decomposed cellular polyurethane waste under microwave irradiation to formulate modern ecological systems for manufacturing heat-insulating foams were also presented.[109]

4.39.3.2.3 Polyimides

The preparation of polyimides is one of the most often attempted applications of microwave irradiation in polymer chemistry. The presented works can be divided into four main areas:

- polycondensation of salt monomers composed of diamines and pyromellitic acid;
- dehydration of poly(amic acid)s as polyimide precursors;
- polymerization of nadic end-capped or phenyl ethynyl-terminated imide oligomers; and
- polycondensation of imide diacid chlorides with aliphatic and aromatic amines (poly(amide imide)).

During polycondensation of salt monomers, polyimides were obtained from salts of aliphatic diamines and pyromellitic acid or its diethyl ester in the presence of a small amount of a polar organic medium (**Figure 45**).[75]

Under microwave irradiation, the polycondensation proceeded rapidly within 2 min for the polyimides with inherent

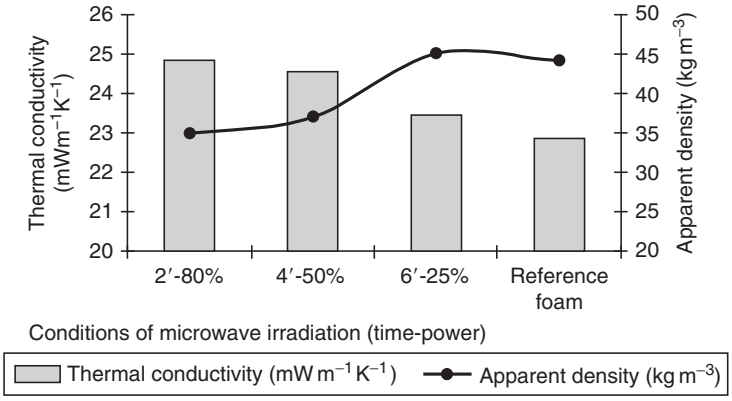

Figure 43 Thermal conductivity and apparent density of polyurethane foams. Reproduced with permission from Prociak, A.; Bogdał, D.; Pielichowski, J.; Dziadczyk, J. In *Rigid Polyurethane Foams Blown under Microwave Irradiation*, Proceedings of the 8th International Conference "Blowing Agents and Foaming Processes 2006, Munich", 2006.[108]

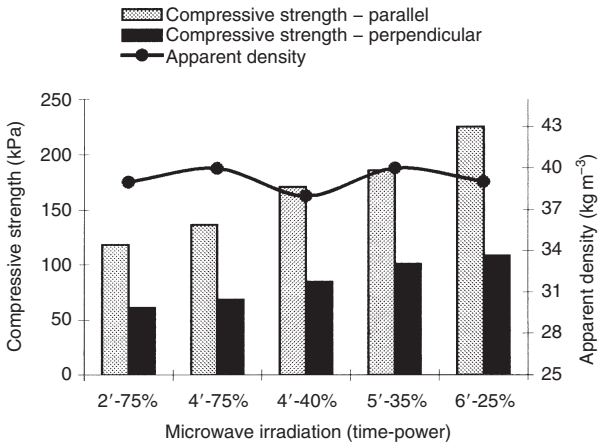

Figure 44 Apparent density and compressive strength of polyurethane foams measured in parallel and perpendicular rise directions. Reproduced from Bogdal, D.; Prociak, A.; Pielichowski, J. In *Application of Microwave Irradiation for Chemical Recycling of Polyurethanes*, Proceedings of Global Symposium on Recycling, Waste Treatment and Clean Technology, REWAS, Madrid, 2004.[109]

viscosity above 0.5 dl g^{-1}.[76] The rate of polymerization of salt monomers under various conditions was found to decrease in the following order: microwave-induced polycondensation > solid-state thermal polymerization > high-pressure thermal polycondensation.[86]

In the case of dehydration reactions of poly(amic acid)s, the kinetics study of imidization under microwave irradiation of poly(amic acid) prepared from 3,3′,4,4′-benzophenontetracarboxylic acid dianhydride (BTDA) and DDS was performed in a 20 wt.% solution of NMP and cyclohexylpyrrolidone (CHP) used as an azeotroping agent to remove water and prevent scission during imidization (Figure 46).[110]

It was observed that depending on the reaction temperature, microwave irradiation led to 20–34 times higher rates of

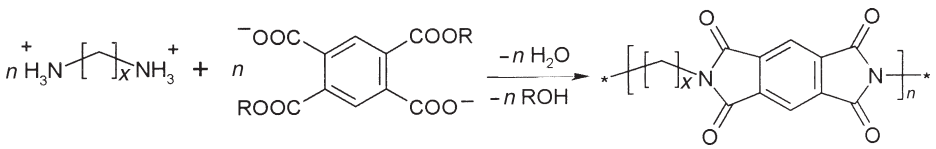

Figure 45 Preparation of polyimides from salt monomers composed of aliphatic diamines and pyromellitic acid or its diethyl ester.

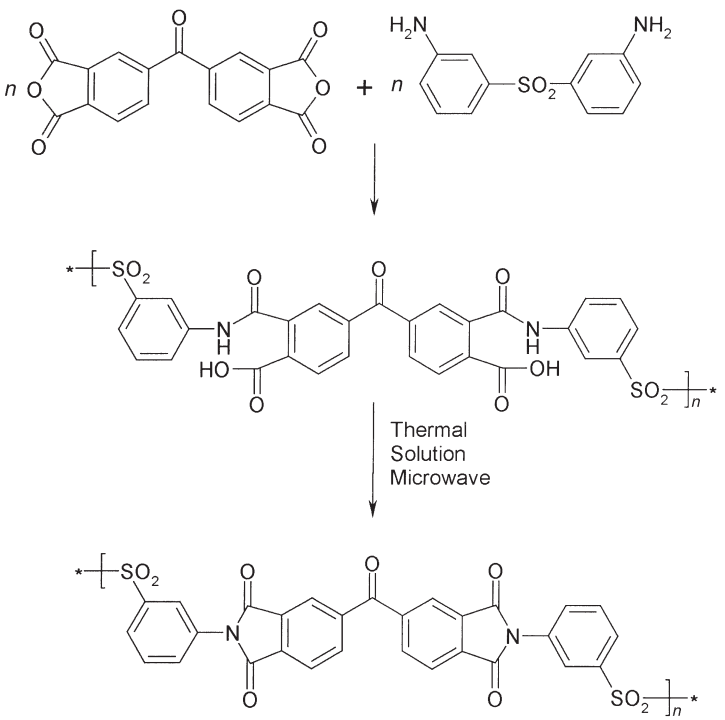

Figure 46 Imidization of poly(amic acid) prepared from 3,3′,4,4′-benzophenontetracarboxylic acid dianhydride (BTDA) and 3,3′-diaminodiphenyl sulfone (DDS).

Table 20 Rate constant for solution imidization

Temperature (°C)	$k_{thermal}$ *(min^{-1})*	$k_{microwave}$ *(min^{-1})*
130		0.030
140	0.0014	0.076
149	0.0022	0.103
150	0.0055	0.169
160	0.011	
161		
170		
175		

Reproduced with permission from Lewis, D. A.; Summers, J. D.; Ward, T. C.; McGrath, J. E. *J. Polym. Sci. Part A: Polym. Chem.* **1992**, *30*, 1647.[110]

imidization in comparison with conventional treatment. From an Arrhenius analysis, it was found that the apparent activation energy determined was reduced from 105 to 55 kJ mol^{-1} when microwave activation was utilized rather than conventional heating (Table 20).

Poly(amic acid) imidization was studied in a solid state under microwave irradiation as well.[111] Polyether-ester poly (amic acid) was prepared by the polycondensation of poly (tetramethylene oxide)glycol di-*p*-aminobenzoate (Polymine-650) with acid dianhydride (PMDA) in a DMF solution at room temperature. Then the prepolymer solution was cast on polytetrafluoroethylene (PTFE) plates to form 200 μm thin films, which were imidized in a microwave oven at 60 °C. The results showed that microwave irradiation reduced both the reaction temperature and time.[111]

Recently, side chain polymers of poly(amic acid) were obtained by polycondensation of benzoguanamine and pyromellitic dianhydride under microwave irradiation.[112–114] The synthesis was performed in a microwave oven in which a DMF solution of benzoguanamine and an equimolar amount of pyromellitic dianhydride were irradiated for 1 h at 60 °C (Figure 47). The resulted poly(amic acid) was precipitated from the solution and then modified in order to obtain side chain polymers with fluorescent as well as third-order non-linear optical (NLO) properties.

Subsequently, the crosslinking reaction of nadic end-capped imide, that is, *N*,*N*′-(oxydi-3,4′-phenylene)bis(5-norbornene-2,3-dicarboximide) under both conventional and microwave conditions was investigated (Figure 48).[115] The starting resin (RP-46) consisted of polyimide precursors, 3,3′,4,4′-benzophenontetracarboxylic acid methyl ester (BTDE), 3,4′-oxydianiline (3,4′-ODA), and the end-capping reagent 5-norbornene-2,3-dicarboxylic acid monomethyl ester (NE). The process proceeded in two stages: imidization (1) and a thermal-induced (reverse Diels–Alder) decomposition–recombination crosslinking step (2) (Figure 48).

The kinetics studies of a model compound under conventional and microwave conditions were carried out in order to simulate the crosslinking reaction of polyimide RP-46. The microwave cure was performed in the temperature range of 230–325 °C, and the results at 230–280 °C were used to determine the kinetics parameters. The microwave cure was rapid and led to the conversion to the crosslinked structure about 10 times faster than during a conventional heating (Table 21). The apparent activation energy for the thermal cure was estimated to be 94 kJ mol^{-1}, whereas for the microwave cure the value of activation energy fell in the range of 74–84 kJ mol^{-1}, which suggests that the microwave process is a more efficient energy process (Figure 49).[115]

The kinetics of the microwave cure of phenylethynyl-terminated imide oligomer (PETI-5, M_n = 5000 g mol^{-1}) and a model compound, 3,4′-bis[(4-phenylethynyl)phthalimido] diphenyl ether (PEPA-3,4′-ODA) (Figure 50), were also studied.[116]

The microwave cure of PEPA-3,4′-ODA and PETI-5 oligomer was performed in the temperature range of 300–330 and 350–380 °C, respectively.

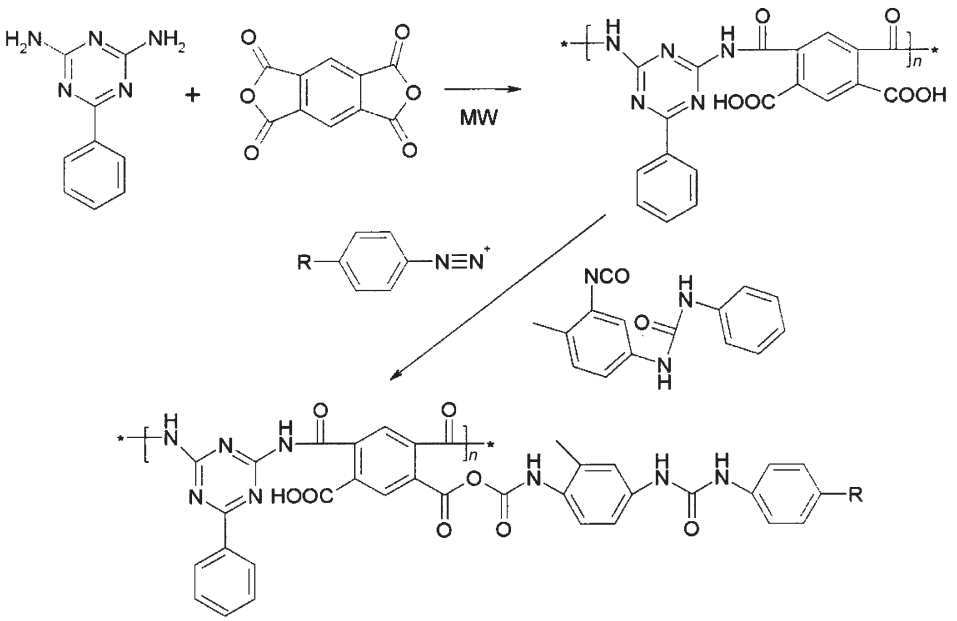

Figure 47 Side chain polymers of poly(amic acid) obtained by polycondensation of benzoguanamine and pyromellitic dianhydride.

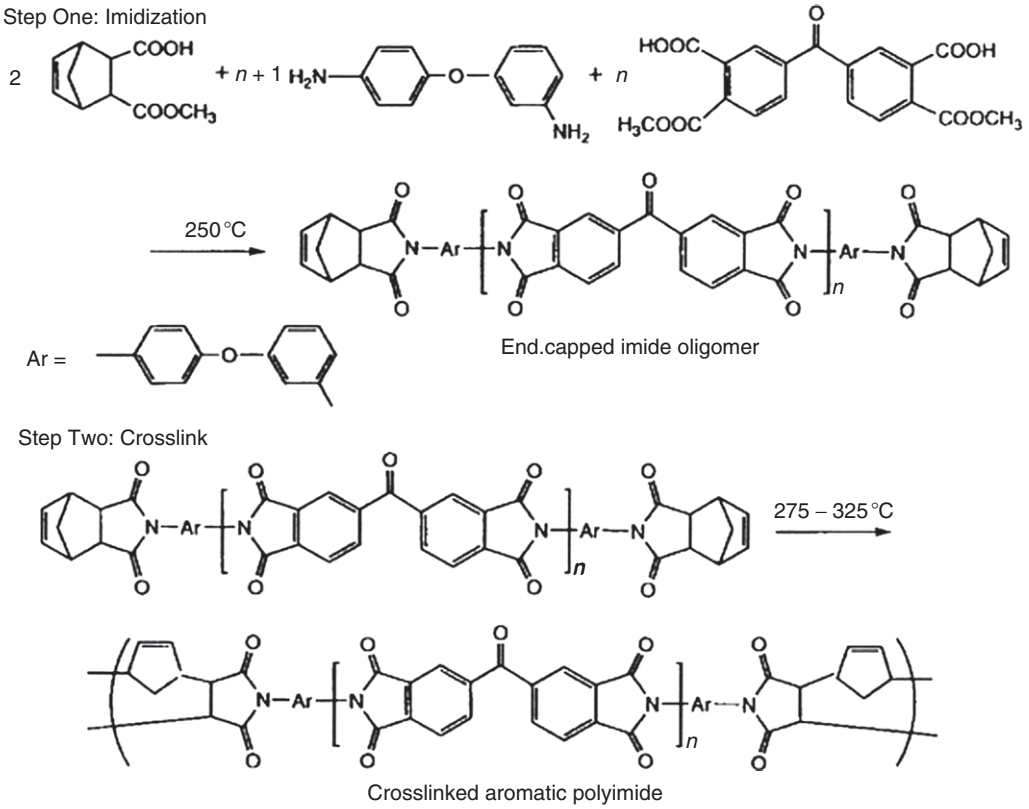

Figure 48 Crosslinking reaction of nadic end-capped imides.

Table 21 Rate constants for the thermal and microwave cure processes

Temperature (°C)	*Thermal process* k *(min^{-1})*	*Microwave process K (min^{-1})*
230	0.003	0.028
280	0.011	0.140
300	0.030	84
325	0.128	
Activation energy ($kJ\,mol^{-1}$)	94	

Reproduced with permission from Liu, Y.; Sun, X. D.; Xie, X. Q.; Scola, D. A. *J. Polym. Sci. Part A: Polym. Chem.* **1998**, *36*, 2653.[115]

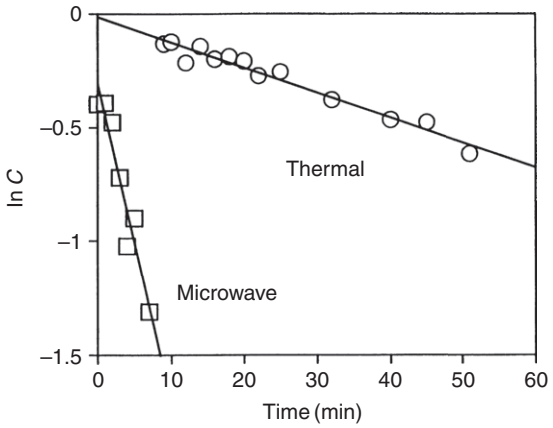

Figure 49 Comparison of the reaction rate for microwave and thermal cure of the bisnadimide model compounds at 280 °C. Reproduced with permission from Liu, Y.; Sun, X. D.; Xie, X.Q.; Scola, D. A. *J. Polym. Sci. Part A: Polym. Chem.* **1998**, *36*, 2653.[115]

In comparison with conventional thermal cure of PEPA-3,4′-ODA and PETI-5, microwave cure gave higher rate constants for both. For PEPA-3,4′-ODA, the reaction followed first-order kinetics, yielding an activation energy of 27.6 kcal mol^{-1}, which was 68% that of the thermal cure. For PETI-5, the reaction followed 1.5 order, yielding an activation energy of 17.1 kcal mol^{-1}, which was 51% that of the thermal cure for PETI-5.

Finally, the kinetics studies showed that in the same temperature range microwave irradiation provided a faster cure compared to conventional heating, or the same cure rate can be achieved at adequately lower temperature under microwave irradiation (**Table 22**).[117]

Poly(amide imide)s were also obtained by the polycondensation of a number of diacid chlorides such as [*N*,*N*′-(4,4′-carbonyldiphthaloyl)] bisalanine diacid chloride[118–120] and 4,4′-(hexafluoroisopropylidene)-*N*,*N*′-bis (phthaloyl-L-leucine) diacid chloride[121,122] with certain aromatic amines (**Figure 51**).

Prior to the reaction, diacid chloride was ground with an equimolar amount of an aromatic amine or diphenol and a small amount of a polar high-boiling solvent (e.g., *o*-cresol) that acted as a primary microwave absorber. Under microwave irradiation, the polycondensation reactions proceeded rapidly (6–12 min) compared with conventional conditions (reflux for

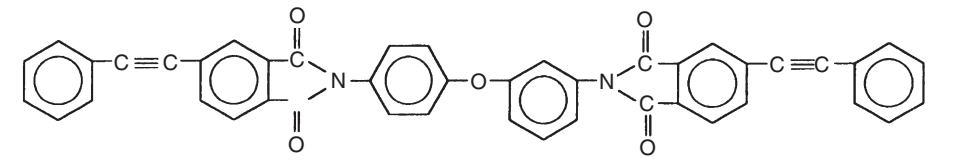

3,4′-Bis[4-(phenylethynyl)phthalimido]diphenyl ether
(PEPA-3,4′-ODA)

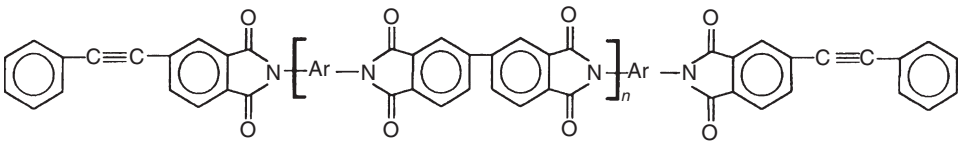

Where : Ar = (15%) + (85%)

Phenylethynyl-terminated imide oligomer (MW 5000 g mol^{-1})
(PETI-5)

Figure 50 Chemical structures of PEPA-3,4′-ODA and PETI-5.

Table 22 Comparison of activation energies of microwave and thermal cure reactions.

Sample	*MW*	*Thermal*
PEPA-3,4′-ODA	27.6 ± 2.3 (kcal mol^{-1})	40.7 ± 2.7 (kcal mol^{-1})
	1.20 ± 0.10 (eV)	1.77 ± 0.12 (eV)
PETI-5	17.1 ± 0.7 (kcal mol^{-1})	33.8 ± 2.0 (kcal mol^{-1})
	0.74 ± 0.03 (eV)	1.47 ± 0.09 (eV)

MW, microwave.
Reproduced with permission from Fang, X.; Hutcheon, R.; Scola, D. A. *J. Polym. Sci. Part A: Polym. Chem.* **2000**, *38*, 1379.[82]

12 h in chloroform, then for another 12 h in dimethylacetamide solutions) to give polymers with higher inherent viscosities of 0.36–1.93 dl g^{-1} (Table 23).[122]

For the polycondensation of 4,4′-(hexafluoroisopropylidene)-*N*,*N*′-bis(phthaloyl-L-leucine) diacid chloride with aromatic amines, higher glass transition temperatures (ca. 19–82 °C) were reported.[122] A similar series of poly(amide imide)s were obtained by the polycondensation of diacid chlorides such as [*N*,*N*′-(4,4′-carbonyldiphthaloyl)] bis-isoleucine diacid chloride,[123] *N*,*N*′- (4,4′-carbonyldiphthaloyl)-bis-*l*-phenylalanine) diacid chloride,[124] and *N*,*N*′- (4,4′--sulfonediphthaloyl)-bis-*l*-phenylalanine) diacid chloride[125] with certain aromatic amines and diacid chlorides derived from Epiclon B-4400 and phenylalanine[126] or *l*-leucine[127] with aromatic amines as well (Figure 52).

Poly(amide imide)s were also obtained by polycondensation of hydantoins and thiohydantoin derivatives of pyromellitic acid chlorides with [*N*,*N*′- (4,4′-carbonyldiphthaloyl)] bisalanine diacid chloride,[128] *N*,*N*′-(pyromellitoyl)-bis-*l*-phenylalanine diacid chloride,[129] and *N*,*N*′-(4,4′-diphenylether) bistrimellitide diacid chloride[130] (Figure 53). The polymerization reactions were run in a microwave oven for 10 min without temperature control, while a diacid chloride was mixed together with an equimolar amount of hydantoin derivatives in the presence of *o*-cresol. The resulting poly(amide imide)s were obtained in good yields with inherent viscosities of about 0.28–0.66 dl g^{-1}.

Likely, poly(amide imide) poly(ester imide)s were obtained by the polycondensation of a number of diacid chlorides such as [*N*,*N*′-(4,4′-carbonyldiphthaloyl)] bisalanine diacid chloride,[118] 4,4′-(hexafluoroisopropylidene)-*N*,*N*′-bis(phthaloyl-L-leucine) diacid chloride[121] as well as [*N*,*N*′-(pyromellitoyl)-bis-*l*-leucine diacid chloride[122] with certain bisphenols (Figure 54).

The synthesis of poly(ether imide)s in the condensation of disodium salt of PBA and bis(chlorophthalimide)s was also described under microwave irradiation (Figure 55).[131] The polymerization reactions were performed under PTC conditions in an *o*-dichlorobenzene solution. The polymerization reactions, in comparison with conventional heating polycondensation, proceeded rapidly (25 min vs. 4 h at 200 °C), and polymers with inherent viscosities in the range of 0.55–0.90 dl g^{-1} were obtained.

4.39.4 Polymer Composites and Nanocomposites

4.39.4.1 Polymer Composites

Composite materials are applied owing to their enhanced mechanical properties, which were found especially for such polymers as epoxies, polyesters, polyurethanes, and their derivatives. Usually during the preparation processes, heat is applied to materials to liquefy thermoplastic polymers and cure monomers or prepolymers. Radiation processing, which includes microwave irradiation, can be considered as an economical and applicable method of modification of composite materials (Table 25).

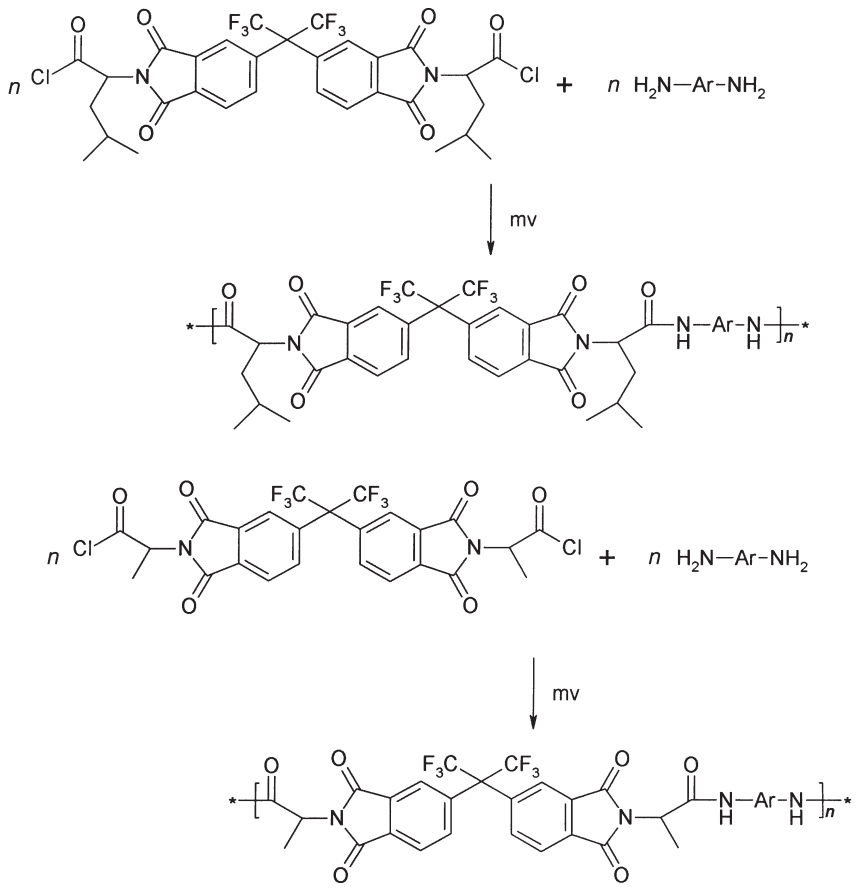

Figure 51 Polycondensation of diacid chlorides with certain aromatic amines.

Table 23 Inherent viscosity (η_{inh}) of the polymers (differences between the solution[a] and microwave methods)

Reagent	*Solution* – η_{inh} ($dl\,g^{-1}$)	*Microwave* – η_{inh} ($dl\,g^{-1}$)
Benzidine	0.22	1.22
4,4′-Diaminodiphenylmethane	0.29	1.32
1,5-Diaminoanthraquinone	0.09	1.73
4,4′-Sulfonyldianiline	0.09	0.50
3,3′-Diaminobenzophenone	0.22	1.26
p-Phenylenediamine	0.15	1.04
2,6-Diaminopyridine	0.12	1.44

[a]One equimolar of diacid chloride and diamines was refluxed for 12 h in $CHCl_3$ and then heated for 12 h at 120 °C in dimethylacetamide.
Reproduced with permission from Mallakpour, S. E.; Hajipour, A. R.; Khoee, S. *J. Polym. Sci. Part A: Polym. Chem.* **2000**, *38*, 1154.[123]

Microwave irradiation was tested as an alternative to conventional processing techniques for a glass/epoxy laminate.[132] A numerical simulation was developed to predict the one-dimensional transient temperature profile of the composite during both microwave and conventional heating for a glass/epoxy laminate with a thickness of 25 mm. As raw materials for the experimental investigation a bisphenol F/epichlorohydrin epoxy resin (Shell Epon 862) and an aromatic diamine (Shell Epi-Cure W) as a curing agent were used. The microwave power was varied continuously from 0 to 6 kW to show that it was possible to cure thick glass/epoxy composites uniformly and eliminate temperature excursions because of exothermic reactions during cure. Owing to continuous feedback power control and through more efficient energy transfer of the microwave irradiation, it was possible to monitor the cure of the composites and increase the quality of thick-section composites.[132]

In the next paper, a calorimetric analysis (DSC) of the cure kinetics of the same glass/epoxy composite was conducted for thermally and microwave curing samples.[133] Both numerical and experimental results showed that microwaves promoted an inside-out cure of the thick laminates due to volumetric heating, which dramatically reduced the overall processing time. Under conventional thermal conditions, to reduce thermal gradients, thick laminates were processed at lower cure temperature and heated with slow heating rates, resulting in excessive cure times. Outside-in curing of the autoclave-processed composite resulted in visible matrix cracks, while cracks could not be seen in the microwave-processed composite. The formation of cure gradients within the two composites cured under both microwave and conventional conditions was observed (**Figure 56**).[134]

Although cure gradients existed in both composites treated under microwave and thermal conditions, differences in the solidification behavior were notified. In the conventionally processed composite, the outside-in cure gradients were most significant during the early stages of the cure cycle, and the maximum cure rate for this epoxy resin system occurred at the

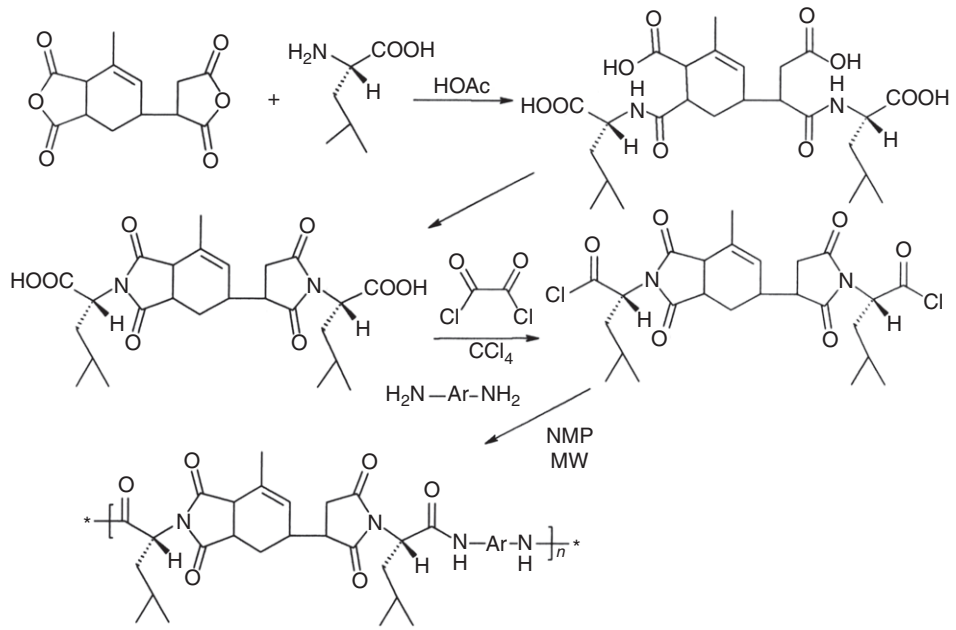

Figure 52 Polycondensation of diacid chlorides with some aromatic amines.

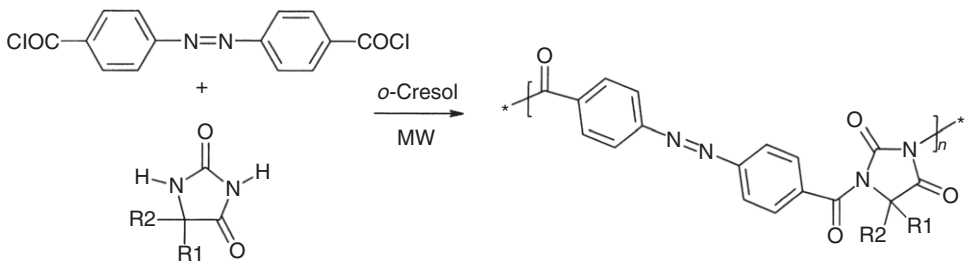

Figure 53 Polycondensation of hydantoin and thiohydantoins derivatives of pyromellitic acid chlorides.

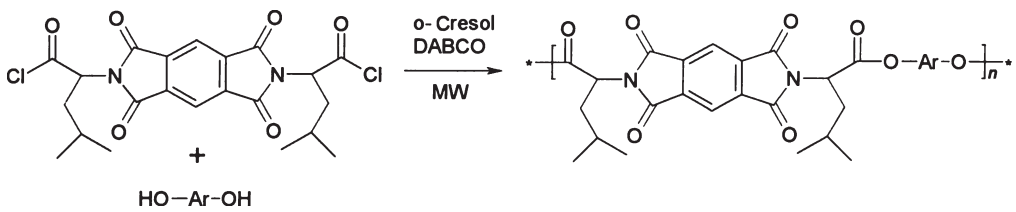

Figure 54 Polycondensation of diacid chlorides with certain biphenols.

beginning of cure. Therefore, it is critically important to initiate an inside-out cure at the beginning of the cure cycle. Reduced thermal gradients during the early stages of microwave curing allowed for better control over solidification behavior of the resin. In conventional processing, very slow heating rates were required to reduce the thermal lag and heat the composite up to a temperature where additional heat was generated by the chemical reaction. Once additional heat is generated, it will help to promote the desired inside-out cure. To obtain an inside-out cure in conventional processing, the required cycle time was almost 3 times longer than in the case of microwave processing. Thus, the processing time can be drastically reduced to achieve the desired inside-out cure through the use of microwaves.[134]

In another example, the fiberglass/epoxy (Dow-Derakane 411-350) composite panels with 15 layers of glass fiber mats were cured under microwave irradiation. The final panels (approximately 1.5 cm thick) were placed perpendicularly between a microwave source and receiver used to monitor the microwave energy absorption by the composite during the cure cycle. It was demonstrated that the application of microwave-assisted cure techniques reduced material degradation and residual stress in the composite.[135]

Preliminary studies on the microwave curing of a polyester resin and composite material used in marine yacht industry showed that the microwave curing was an alternative method for the faster processing of laminated materials for structural applications. Laminates (10 cm × 10 cm) made by three layers of fiberglass and polyester resin were prepared by manual layup and cured under a microwave irradiation power output of 1800 W. When the samples were heated less than 11–12 s, the

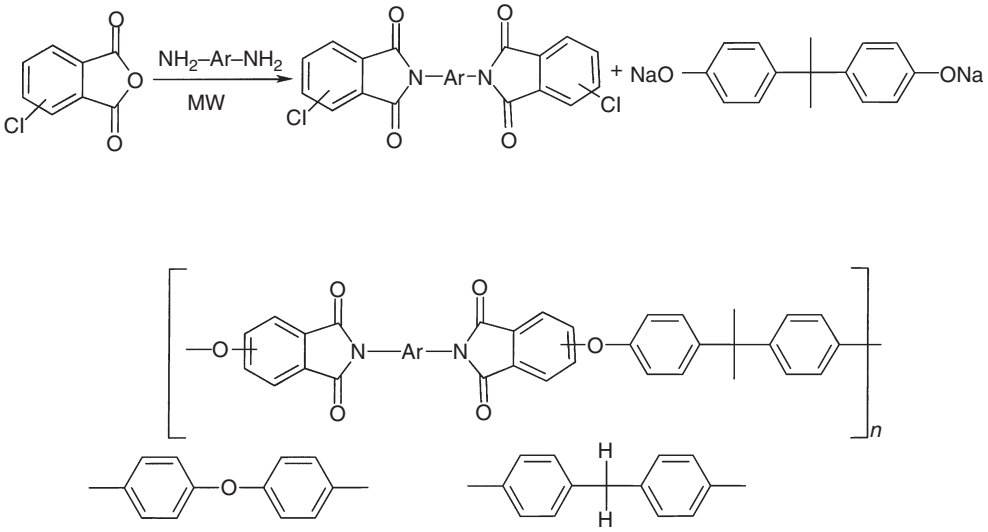

Figure 55 Polycondensation of disodium salt of bisphenol A and bis(chlorophthalimide)s.

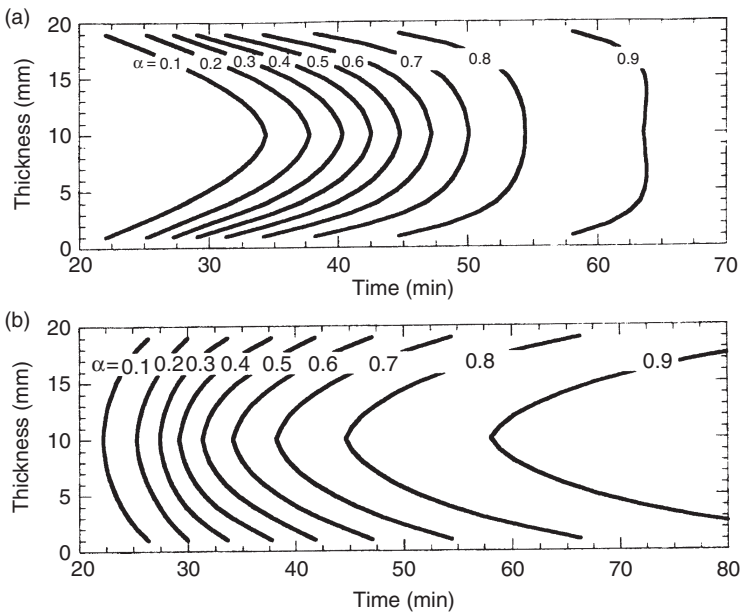

Figure 56 Formation of cure gradients with two laminates during (a) conventional and (b) microwave cures. Reproduced with permission from Thostenson, E. T.; Chou, T.-W. *Polym. Composites* **2001**, *22*, 197.[134]

mechanical properties of resins were not influenced by the microwave treatment, because the absorbed energy was sufficient enough to only activate the curing process but the resins were not full cured. At longer time periods, the resins quickly solidified and their maximum stress values were close to that of the resin cured at room temperature for 10 days. Curing time longer than 15 s caused a rapid cure process, which resulted in the appearance of ripples and bubbles in the sample. Finally, long radiation time of the resin showed negative effects with a rapid decrease of the mechanical properties reaching that of the not fully cured material. Moreover, it was found that the use of high power of microwave irradiation during a short time induces fast crosslinking and generates residual stress in the cured resin, which can cause matrix cracking.[136]

Glass fiber (70 wt.%) composites with diallyl phthalate polyester as matrix material were used in the investigation of composites. The prepreg was in the form of a 1.6 cm wide and 0.3 cm thick tape and it was prepared from vinyltoluene (30 wt.%) used as a crosslinking monomer and benzoyl peroxide serving as an initiator. Also, the kinetics study of a thin film showed that microwaves could initiate the reaction at a lower bulk temperature and shorter time than thermal heating to avoid large temperature gradients. Samples prepared on KBr disks were isothermally microwave cured at 85, 100, and

115 °C, while the extent of cure was monitored by means of FTIR spectroscopy. As a result, higher reaction rates were observed in microwave curing as compared to thermal curing. At lower polymerization temperatures, such as 85 °C, the ultimate extent of cure was higher under microwave than under conventional thermal conditions.[137]

Microwave irradiation was also used to enhance pultrusion process in the manufacture of glass fiber-reinforced composites. The main benefits of MAP (microwave-assisted pultrusion) over conventional process include faster line speeds, reduced pulling forces, greater uniformity of cure, and reduced floor area in the case of simple profiles. Microwave heating may be used to preheat a pultrusion precursor upstream of the main pultrusion die or it may be used in conjunction with a microwave transparent die as a direct replacement. This process is used to manufacture solid cylindrical profiles based on glass fiber and a number of resins, including unsaturated polyester, urethane, acrylate, vinyl ester, and epoxy and phenolic resins.[138]

Microwave irradiation was applied to process nadic end-capped polyimide precursor (RP-46 resin) and glass–graphite–RP-46 composites. Processing of thick sections by conventional thermal process requires slow ramp rates and a long processing time. Therefore, the composite material containing conducting fibers could be heated by the microwave process to achieve inside to outside heating patterns and quick heat ramp rate. Additionally, the microwave process may enhance the bonding strength between resin and fiber matrix.[139]

Both neat resin and composite with glass and graphite cloth were obtained and the effects of various parameters such as microwave power level, mold material, and pressure were studied. Depending on the conditions, cure of glass and glass–graphite hybrid composites was accomplished in 36–130 min under microwave irradiation, and the imidization of neat resin and composites was complete. Resin specimens containing only 0.057 wt.% chopped graphite fibers resulted in complete imidization in 6 min. However, glass and glass–graphite composites were fabricated by microwave irradiation with flexural strength and moduli equivalent to 50–80% of the properties of composites fabricated by conventional thermal processes.

It was shown that the sample size and geometry were important factors in microwave processes. For example, changing the sample size from 5 to 15 g caused a temperature increase of 32 °C in 10 min at the same power level. Essentially, no coupling occurred between a sample of 5 g

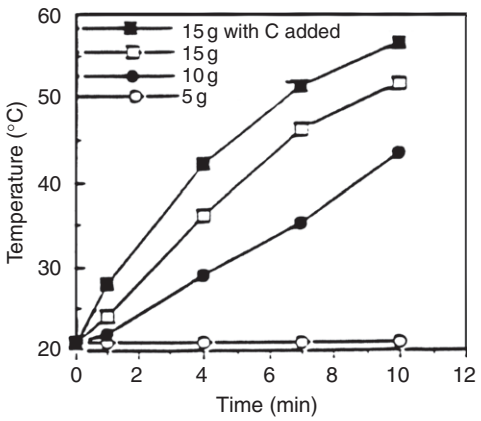

Figure 57 The effect of sample size on the microwave absorption of undried RP-46 resin. Reproduced with permission from Liu, Y.; Xiao, Y.; Sun, X.; Scola, D. A. *J. Appl. Polym. Sci.* **1999**, *73*, 2391.[139]

polyimide resin and microwave energy, proving that a critical mass was required to absorb the microwave energy with a high efficiency (Figure 57).[139]

The application of microwave irradiation to the processing of carbon fiber-reinforced phenylethynyl-terminated polyimide composites (PETI-5/IM7) was evaluated. A microwave process was demonstrated that fabricated unidirectional polyimide–(carbon fiber) composites with superior thermal and mechanical properties relative to the thermal process in half the time required for the thermal process.[140]

The glass transition temperature and modulus of functionally graded materials (FGMs) were investigated for 'epoxy–polyurethane elastomer' (EP/PUR) system that were cured with DDM under conventional and microwave conditions. For this purpose, a solution containing 65 wt.% of EP/PUR/DDM mixture in dichloromethylene was poured into the PTFE mold and was then irradiated at 200 W of microwave power for 20 min. Then the film was submitted for the next casting. After each layer was poured in, the whole sample was successively irradiated at 400 W for 30 min. By applying this procedure, the materials varying gradually in the glass transition temperature from – 54 up to 162 °C and modulus from 0.069 to 3.20 GPa were obtained (Table 24). Although the curing time of the specimen cured under microwave irradiation at 400 W was shorter, the material possessed better mechanical properties in comparison with the sample cured conventionally. The

Table 24 Properties along the thickness direction in the FGMs composed of EP/PUR elastomer

Thickness direction in the FGM											
Layer	1	2	3	4	5	6	7	8	9	10	11
PUR/EP (w/w)	10/0	10/2	10/4	10/6	10/8	10/10	8/10	6/10	4/10	2/10	0/10
Tensile strength (MPa)	4.65	5.84	11.6				27.4	32.5	45.8		
T_g (°C)	–54	–9.3	25.4	15.2	20.8	25.8	109.2	113.2	139.6	75.9	64.8
E (GPa)	0.069	0.078	0.245			99					
				45.7	83.2	60	39.4	1.585	2.62	145	162
				0.86	44.8	1.01	1.438			2.72	3.20
					0.99						

Microwave curing cycle: 200 W/20 min + 400 W/30 min.
Reproduced with permission from Liu, X. Q.; Wang, Y. S.; Zhu, J. H. *J. Appl. Polym. Sci.* **2004**, *94*, 994.[141]

properties of the sample were only related to the microwave power setting, and prolonging the irradiation time did not influence the tensile strength, modulus, and elongation.[141]

4.39.4.2 Nanocomposites

Polymer nanocomposites are defined as polymers in which small amounts of nanofillers (in the size range from 1 to 100 nm) are homogeneously distributed by only several weight percentages. Nowadays, different kinds of nanofillers are classified depending on size and shape. They are grouped into four categories: zero-dimensional (e.g., embedded clusters), one-dimensional (1D; e.g., nanotubes), two-dimensional (2D; nanoscale coatings, layered materials such as clays, metal oxides, metal phosphates), and three-dimensional (3D; framework systems such as zeolites).

Nanocomposites based on polymer–clay systems are of considerable interest for the development of new structural and functional materials. Recently, there has been much research into polymer/clay nanocomposites such as epoxy,[142] acrylic,[143] polystyrene,[144] and polyamide-6,[145] owing to their unique and improved properties. For instance, compared to polyamide-6, polyamide-6/clay nanocomposites at 5 wt.% clay loading level had the heat distortion temperature 87 °C higher. Also the tensile strength and tensile modulus were 49% and 68% higher, while the impact strength was almost unchanged.[146]

During conventional processing to fabricate polycarbonate/montmorillonite (PC/MMT) nanocomposites, the processing temperatures are often far too high for organophilic groups in the gallery of MMT to endure. Thus, microwave irradiation was applied for solid-state polymerization of PC prepolymer for the preparation of PC/MMT nanocomposites.[147] PC prepolymers were prepared by melt polymerization of BPA with diphenyl carbonate (DPC), and they were intercalated with modified montmorillonite (m-MMT) by melt mixing and solution mixing methods. The prepolymers were further polymerized in a microwave oven with various irradiation times (6–12 s) at 220 °C to obtain MMT/PC nanocomposites in the solid state. PC/MMT nanocomposites prepared by microwave irradiation contain a more advanced dispersion of MMT silicate in the polymer matrix, in comparison with the nanocomposites polymerized by oil-bath heating, as shown by X-ray diffraction (XRD) patterning. Subsequently, wide-angle X-ray diffraction (WAXD) revealed that microwave solid-state polymerization converted the preintercalated nanocomposite into the exfoliated nanocomposite. Thus, microwave-assisted solid-state polymerization was more effective in achieving uniform dispersion of clay in the polymer matrix than the conventional methods.[147]

Poly(ethylene oxide) (PEO)-based nanocomposites with MMT, hectorite, and laponite were prepared by a melting intercalation procedure induced by microwave irradiation. The microwave method takes advantage of smectic clays to absorb microwave energy, which activates water molecules in the hydration shell of the clay interlayer cations. This phenomenon makes possible the entry of PEO chains to coordinate the interlayer cations (Figure 58).

Variables such as the time of irradiation, microwave power, total amount of the mixture, and relative ratio of the components were examined. It was found that intercalations were not

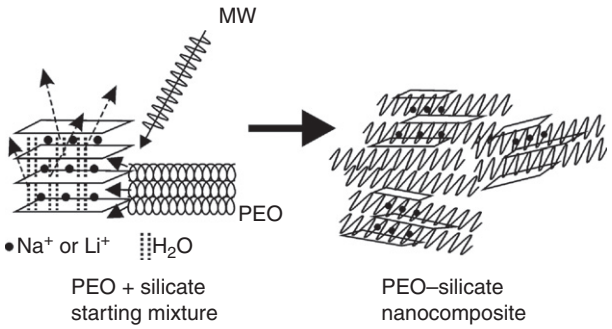

Figure 58 Scheme of the microwave (MW)-assisted melt-intercalation reaction. Reproduced with permission from Aranda, P.; Mosqueda, Y.; Perez-Cappe, E.; Ruiz-Hitzky, E. *J. Polym. Sci. Par B: Polym. Phys.* **2003**, *41*, 3249.[148]

produced for irradiation times shorter than 5 min. In the case of longer irradiation times, the XRD patterns confirmed the PEO intercalation, showing interlayer spacing of around 1.8 nm and a different degree of disorder in the stacking of the clay particles depending on the time of irradiation. Longer periods of irradiation gave materials with a better stacking order.[148]

Microwave irradiation proved to be an efficient method for the preparation of PCL/clay nanocomposites and the research indicated that PCL/clay nanocomposites had demonstrated many improved properties compared with pure PCL.[149–151] PCL/MMT nanocomposites were synthesized by microwave-assisted *in situ* ring-opening polymerization (MROP) of ε-CL in the presence of either unmodified or modified MMT within only 60 min.[152] In the presence of unmodified MMT (Cloisite®Na^+), PCL with a number-average molar weight (M_n) above 60 000 g mol^{-1} was obtained, showing an intercalated structure. Using a hydroxyl group-containing alkylammonium cation-modified MMT (Cloisite®30B), PCL/MMT nanocomposites with a predominantly exfoliated structure were obtained for 0.5–5 wt.% MMT loading levels with M_n of PCL ranging from 16 300 to 66 100 g mol^{-1} (Table 25).

In another paper, tin(II) 2-ethylhexanoate ($Sn(Oct)_2$)- and zinc powder-catalyzed ROP of ε-CL was investigated in a microwave oven. PCL with a high weight-average molar weight (M_w) of 124 000 and 92 300 g mol^{-1} was produced via the $Sn(Oct)_2$- and zinc powder-catalyzed ROP at 680 W for only 30 min, respectively.[153] The morphologies of the nanocomposites showed a predominantly exfoliated structure. A study on the heating characteristics of the MROP of ε-CL has indicated that the thermal effect of microwave energy had a significant influence on the polymerization yield and weight-average molar weight (M_w) as shown in Figure 59.[153,154]

Under microwave irradiation, *in situ* polymerization constitutes an alternative method for preparing poly(ethylene terephthalate) (PET)/layered double hydroxide (LDH) nanocomposites. LDHs are also known as anionic clays or hydrotalcite-like compounds. To overcome the lack of compatibility between PET and LDHs that contain purely inorganic anions, LDHs were modified with dodecyl sulfate prior to sample preparation. The preparation time was considerably reduced, and the inorganic filler was well dispersed and exfoliated in the polymer matrix. The nanocomposites thus obtained were thermally more stable than original PET,

Table 25 Ring-opening polymerization of ε-caprolactone

Heating	Filler type	Concentration (wt.%)	Temperature (°C)	Conversion (%)	M_n (g mol^{-1})	PDI
MW	30B	0.5	120	98	66 100	1.5
	30B	3	120	97	34 800	1.7
	30B	3	100	93	43 900	1.5
	30B	5	120	95	16 300	1.8
	Na^+	3	120	98	60 400	1.5
	-	0	120	85	44 300	1.7
Thermal (oil bath)	Na^+	3	120	1	1000	1.1
	30B	3	120	1	1300	1.2
	–	0	120	17	6500	1.1

MW, microwave irradiation.
Reproduced with permission from Liao, L.; Zhang, C.; Gong, S. *Macromol. Rapid Commun.* **2007**, *28*, 1148.[152]

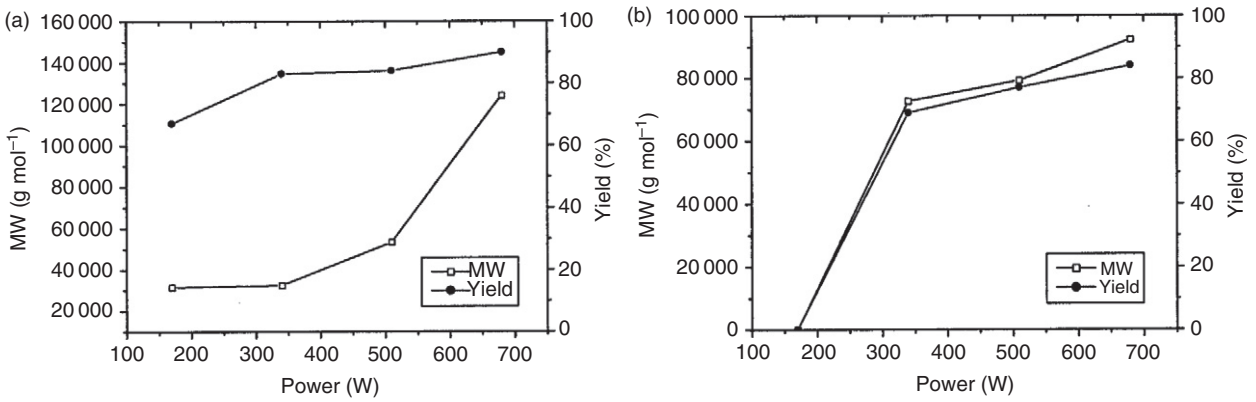

Figure 59 Effect of irradiation power on polymerization: (a) 0.1% $Sn(Oct)_2$, 30 min; (b) 1% zinc powder, 270 min. Reproduced with permission from Liao, L.; Liu, L.; Zhang, C.; *et al. J. Polym. Sci. Part A: Polym. Chem.* **2002**, 40, 1749–1755.[52]

especially for the low-loaded nanocomposites (**Figure 60**). Exfoliation and dispersion seem to be complete for LDH loadings up to 5 wt.%. Larger loadings lead to LDH aggregates in the composite. Curing under vacuum of the composite can be skipped, as neither the structure or properties of the nanocomposites are modified nor the thermal stability is enhanced.[155]

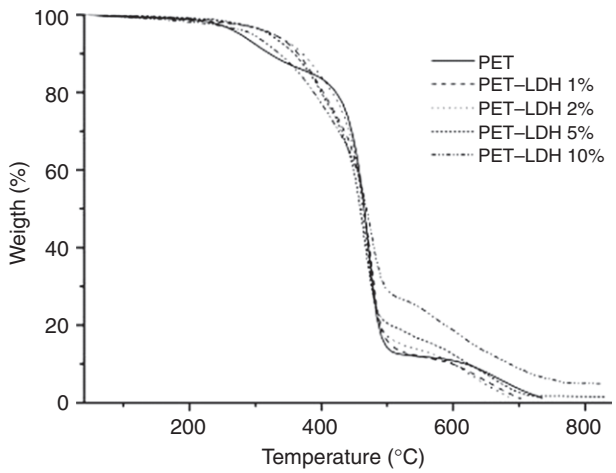

Figure 60 TG curve for PET and PET–LDH nanocomposites. Reproduced with permission from Martínez-Gallegos, S.; Herrero, M.; Rives, V. *J. Appl. Polym. Sci.* **2008**, *109*, 1388.[155]

Because of the engineering performance of epoxies, epoxy nanocomposites, which are prepared by incorporation of the layered inorganic components to the epoxies, were studied.[156,157] When the nanoparticles are dispersed in the polymer matrix, competition for curing reaction between the intragallery and extragallery epoxies resulted in two types of nanocomposite structures. If the former cures faster than the latter, the intragallery epoxy can cure fully before extragallery epoxy reaches its gel point. During microwave irradiation, a rapid curing reaction and curing speed of intragallery relative to that of the extragallery epoxy occurred, which was an important factor in influencing the exfoliation of clay.[156,157]

Favorable features of microwave curing were also utilized to demonstrate the effect of various surface-active clay modifier agents and the silicone acrylate (PDMS V-Si21) on the physical and mechanical properties of epoxy–MMT nanocomposites. These epoxy nanocomposites were synthesized by microwave curing using sodium montmorillonite modified by dodecylamine, hexadecylamine, octadecylamine, and hexcadecyltrimethyl ammonium bromide (HTAB). The microwave curing was very effective because of the fast reaction technique for supporting intragallery epoxy curing. Activation of the clay surface before reaction with the organic modifier influenced

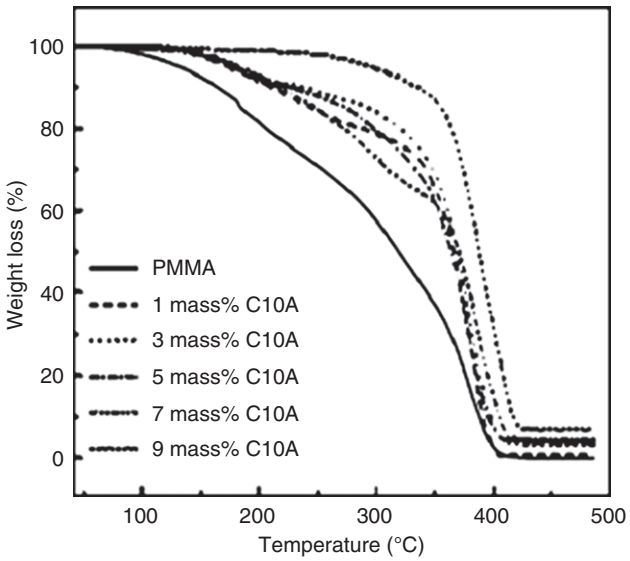

Figure 61 TGA curves of PMMA/C10A nanocomposites. Reproduced with permission from Kim, S. W.; Lee, J. J.; Yoon, S. Y.; Lim, K. T. *Int. J. Thermophys. Online First*™, 23 June 2009.[159]

the exfoliation of clay in the polymer nanocomposite and also prevented agglomeration in the matrix providing a uniform structure.[158]

Microwave irradiation was applied for *in situ* polymerization of PMMA/clay (C10A) layered nanocomposites. The polymerizations were carried out using a microwave reactor at 70 °C with 200 W of irradiation power. An intercalated/exfoliated structure was observed by both XRD and transmission electron microscopy (TEM) analyses. Thermogravimetry analysis (TGA) of pure PMMA and PMMA/clay nanocomposites showed the same decomposition onset temperature, which is 170 °C for all the samples (**Figure 61**).

The transition temperature of the synthesized PMMA/C10A nanocomposites increased continuously with the C10A content, until a content of 5 mass% was reached and decreased after that. Then PMMA chains were fixed inside the sheets of the clay, and the layers of the clay effectively suppressed fast heat transfer and segmental motions of the polymer chains.[159]

Novel polyaniline (PANI) nanocomposites were synthesized through the polymerization initiated by chemical oxidants. First, aniline was introduced into the interlayers of HNb_3O_8, $HTiNbO_5$, and $HSr_2Nb_3O_{10}$ and then the PANI nanocomposites were prepared by polymerization under microwave irradiation in the presence of oxidants. Orientation of the aromatic rings and the extent of oxidation and protonation of the interlayered PANI were closely related to the properties of different layers. The nanocomposites were used as porous electrolytes and analyzed by equivalent circuit, cyclic voltammetry, and charge-discharge measurements. Compared with the nanocomposites in which the aromatic rings are parallel with the inorganic slabs, the nanocomposites in which the aromatic rings are perpendicular to the slabs demonstrate higher conductivity, electroactivity, and discharge capacity. Thus, the nanocomposite with an enough interlayer space can provide a good Li^+ transition and act as a good reservoir to store ions (**Figure 62**).[160]

Metal nanostructures have been extensively studied because of their use in applications such as catalysis, optics, electronics, and optoelectronics. Different methods were applied to obtain the composites with nanocrystals. Previously prepared nanocrystals may be dispersed in polymers, and the other is the generation of nanocrystals in polymers *in situ*.

For instance, microwave irradiation was used in the synthesis of semiconductor–polymer nanocomposites of PVK with

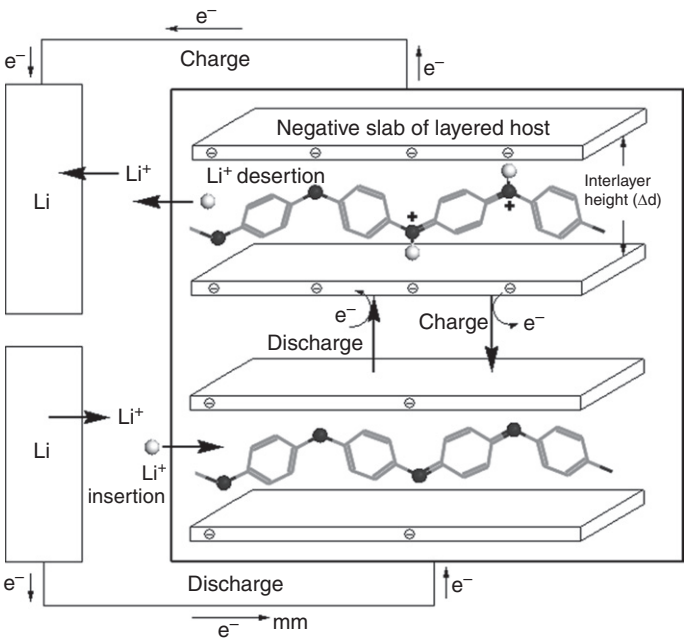

Figure 62 A charge/discharge mechanism for the electrochemical reaction in the Li/nanocomposite cell. Reproduced with permission from Yang, G.; Hou, W.; Feng, X.; *et al. Adv. Funct. Mater.* **2007**, *17*, 401.[160]

nanocrystalline CdS. Pyridine was applied as a solvent due to its dipole moment to promote NVC polymerization and formation of CdS nanoparticles. The polymerization reactions were carried out in the presence of AIBN, thiourea, and cadmium acetate under nitrogen atmosphere. Finally, a convenient one-step method for fabrication of nanocomposites was developed, in which crystalline inorganic nanoparticles are homogeneously dispersed in the polymer matrix.[161]

A facile protocol to achieve a crosslinking reaction of poly (vinyl acetate) (PVAC) with metallic and bimetallic systems using microwave irradiation was elaborated. Nanocomposites of PVAC-crosslinked metallic systems such as Pt, Cu, and In and bimetallic systems such as Pt–In, Ag–Pt, Pt–Fe, Cu–Pd, Pt–Pd, and Pd–Fe were prepared with various shapes such as nanospheres, nanodendrites, and nanocubes. In a typical procedure, Pt-crosslinked PVAC nanocomposites were prepared by reacting PVAC with an aqueous solution of inorganic salts such as $Na_2PtCl_6 \cdot 6H_2O$ at 100 °C for 1 h under microwave irradiation. It is known that PVAC chains can be crosslinked at an elevated temperature (250 °C); however, in this process, crosslinking of PVAC with Pt, In, and Cu metal ions occurred at a relatively low temperature (ca. 100 °C). The homogeneous microwave irradiation provided uniform nucleation and growth conditions, leading to homogeneous nanomaterials with small sizes.[162–164]

In a novel method, methacrylate monomers containing well-dispersed silver nanoparticles were *in situ* synthesized under microwave irradiation. The particles were spherical in shape with a narrow size distribution ranging from 1.0 to 5.5 nm and with a mean diameter of 2.8 nm. In contrast to conventional heating, the synthesis of Ag nanoparticles proceeded uniformly throughout the reaction vessel only under microwave irradiation, reaching completion of the reaction simultaneously in the whole reaction solution. Successive polymerization of the monomer containing the resulting nanoparticles successfully produced Ag nanoparticles dispersed in the polymer matrix.[165]

A novel combined procedure of sol–gel and microwave-assisted emulsion polymerization was developed to prepare TiO_2/polystyrene core–shell nanospheres with nanoscale TiO_2 core and smooth and well-defined polystyrene shell.[166] Typically, two solutions of tetra-*n*-butyl titanate ($Ti(OC_4H_9)_4$) in ethanol and deionized water with a pH of 9 adjusted by adding a solution of NaOH were stirred in the ratio 1:13. The reaction was carried out at 40 °C for 40 min in the microwave reactor (800 W), resulting in light white and transparent TiO_2 colloids which were then heated up to 70 °C. Immediately, sodium dodecyl sulfonate, ammonium persulfate, and varying amounts of freshly distilled styrene monomer were added into the flask to initiate emulsion polymerization on the surface of TiO_2 colloids. The microwave-assisted polymerization reaction was continued for 1.5 h, followed by centrifugation, washing, and vacuum drying, resulting in core (TiO_2)–shell (polystyrene) nanospheres. The diameter and the diameter distribution of the core–shell nanoparticles prepared under different concentrations of styrene monomer were measured with a submicron particle size analyzer (**Figure 63**). It is clearly shown that the average diameter of the particles increases with the concentration of styrene monomer in the emulsion solution, which is 123, 161, and 175 nm when a monomer concentration of 2.0, 3.5, and 5.0 vol.% was employed, respectively.

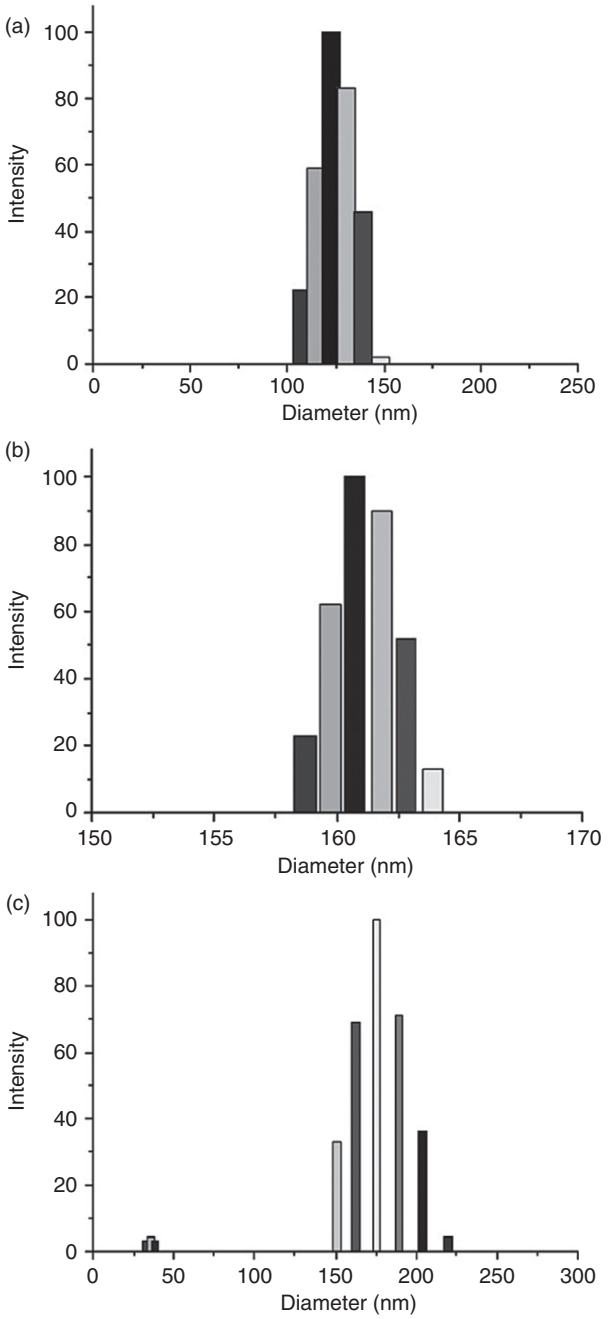

Figure 63 Diameter and the diameter distribution of TiO_2/polystyrene nanospheres synthesized under varying concentrations (by volume) of styrene monomer (a) 2.0%, (b) 3.5%, (c) 5%. Reproduced with permission from Luo, H. L.; Sheng, J.; Wan, Y. Z. *Mater. Lett.* **2008**, *62*, 37.[166]

Microwave irradiation was successfully used to prepare nanocomposites of polystyrene/silica (PS/SNs) with different contents of inorganic nanofillers by *in situ* bulk radical copolymerization of styrene with methacryloxypropyl silica nanoparticles (MPSNs).[167] Under optimized condition, 33% of grafting could be achieved with 98% conversion of styrene. In a typical experiment, MPSNs were mixed with styrene and a certain amount of AIBN with ultrasonic vibrations for 30 min. Then the mixture was irradiated in a microwave oven (700 W) for 10 min with a different power.[167]

Recently, atom transfer radical emulsion polymerization (ATRP) of styrene using chloro-terminated poly(ethylene glycol) (PEG-Cl) as macroinitiator under microwave irradiation was successfully conducted and monodispersed nanoparticles were prepared. In the typical procedure used for ATRP in the presence of CuCl and 2,2′-bipyridine (bipy), styrene, PEG-Cl, and Tween-20 (5 wt.%) were dispersed in deionized water, and the mixture was polymerized under microwave irradiation at 75 °C, while a stable dispersion was obtained after 1 h. It was found that the diameters of PEG-*b*-PS nanoparticles prepared under microwave irradiation were smaller (< 50 nm) and more monodispersed than those prepared with conventional heating.

Moreover, with the increase in the ratio of St/PEG-Cl, the hydrodynamic diameters (D_h) of the nanoparticles increased and the poly index decreased; both D_h and poly dispersity index of the nanoparticles prepared under microwave irradiation were smaller than those prepared with conventional heating; as the concentration of catalyst increased, the D_h of the nanoparticles decreased and the poly index of the nanoparticles increased. The effect of the ratio of St/PEG-Cl and the effect of the ratio of (CuCl/bipy)/PEG-Cl were studied (**Figure 64**).

Magnetic nanoparticles were also dispersed in a polymer matrix with the use of microwave irradiation,[168] and monodisperse magnetic Fe_3O_4/poly(styrene-*co*-acrylamide) (Fe_3O_4/poly(St–AAm)) nanoparticles were prepared by an emulsion polymerization. The polymerization of styrene and acrylamide monomers was carried out in a water solution in the presence of well-dispersed magnetic fluid solution. The reaction mixture was irradiated in a microwave reactor at 75 °C for 3 h. TEM results showed that magnetic Fe_3O_4/poly(St–AAm) microspheres prepared by microwave irradiation were smaller and more uniform than those obtained with conventional heating. The size of the magnetic Fe_3O_4/poly(St–AAm) nanoparticles prepared by emulsion polymerization with microwave irradiation increased as the initial St and AAm concentrations increased, while the size decreased with increasing ferrofluid content, which can be attributed to surfactant effects (**Figure 65**).[168]

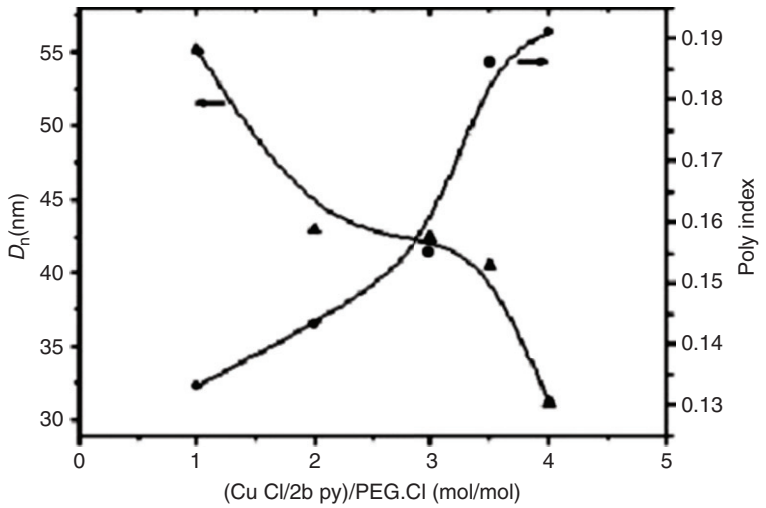

Figure 64 Effects of the ratio of (CuCl/bipy)/PEG-Cl on the size of nanoparticles. Reproduced with permission from Xu, Z.; Hu, X.; Li, X.; Yi, Ch. *J. Polym. Sci.: Part A* **2008**, *46*, 481.

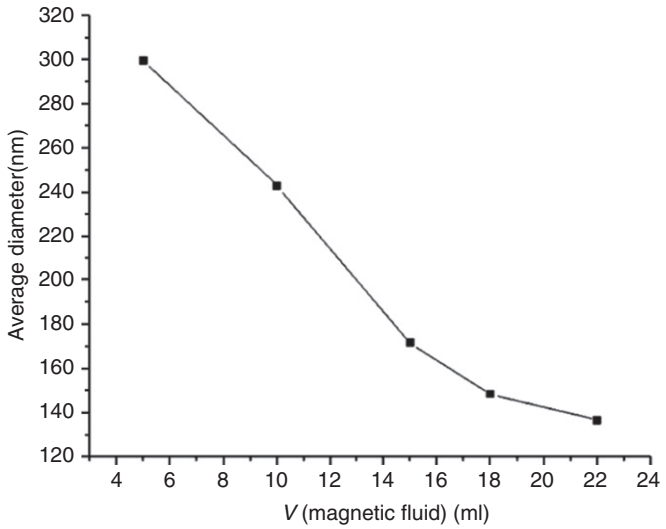

Figure 65 Effects of ferrofluid content on the average particle diameter of magnetic Fe_2O_3/poly(styrene-*co*-acrylamide) microspheres. Reproduced with permission from Huang, J.; Pen, H.; Xu, Z.; Yi, Ch. *React. Funct. Polym.* **2008**, *68*, 332.[168]

Table 26 PTFE loading and BET surface area of PTFE/C nanocomposites synthesized under microwave irradiation

PTFE/C composite	*Carbon powder*	*PTFE/C-15 s*	*PTFE/C-20 s*	*PTFE/C-25 s*	*PTFE/C-30 s*
PTFE loading (%)	0	36.8	27.9	16.7	14.8
BET surface area ($m^2 g^{-1}$)	232.6	50.8	101.2	142.2	161.2

BET surface is related to the specific surface area according to Brunauer-Emmett-Teller theory

Reproduced with permission from Tian, Z. Q.; Wang, X. L.; Zhang, H. M.; *et al. Electrochem. Commun.* **2006**, *8*, 1158.[169]

Carbon black-supported PTFE (PTFE/C) nanocomposite was synthesized by an intermittent microwave irradiation (IMI) method for polymer electrolyte fuel cells (PEFCs), using PTFE emulsion as the precursor.[169] The synthesized PTFE/C composite is characterized by uniformly distributed and nano-sized PTFE/C particles without additional high-temperature treatment and mechanical milling under liquid nitrogen frozen conditions, and the particle size of the PTFE/C composite is in the 10–50 nm range (Table 26). The PTFE/C nanocomposite was then mixed with Pt/C/Nafion to form a Pt/C/Nafion–PTFE/C composite catalyst. The incorporation of PTFE/C nanocomposite in the Pt/C/Nafion catalysts leads to a significant improvement in the mass transportation without any adverse effect on the electrochemical activity of the Pt electrocatalysts. The power output of the cell with a Pt/C/Nafion–PTFE/C composite cathode is 0.66 W cm^{-2}, which is 32% higher than that obtained for the cell with a Pt/C/Nafion cathode.[169]

PANI/multiwalled carbon nanotube (PANI/MWNT) composite was synthesized by microwave-assisted polymerization as well. For this purpose, purified MWNTs and aniline were dispersed in a H_2SO_4 solution together with ammonium persulfate and irradiated using a microwave oven for 3 min. The resulting powders were filtered and rinsed with deionized water and ethanol, and then dried at 50 °C overnight under vacuum. The highest specific capacitance for the nanocomposite (322 F g^{-1}) was almost 12 times higher than that of MWNTs (25.4 F g^{-1}) at 1 mA cm^{-2}. Compared with the specific capacitance (360 F g^{-1}) of the composite obtained by the oxidative polymerization method, the result of the experiment is little lower. However, the microwave-assisted method is simpler and more efficient, and the two values are still comparable (Table 27).[170,171]

Nanocomposites of poly(vinyl alcohol) (PVAL) crosslinked with single-walled carbon nanotubes (SWNTs), MWNTs, and buckminsterfullerene (C-60) were prepared by reacting an aqueous solution of PVAL (3 wt.%) with dispersed SWNTs in a microwave reactor at 100 °C for 1 h; the same procedure was maintained with MWNT and C-60. In order to understand the surface morphology of the crosslinked SWNT, MWNT, and C-60, scanning electron microscopy (SEM) and TEM measurements were conducted. For example, when 25 mg of SWNTs was used for 8 ml of 3 wt.% aqueous solution of PVAL, spherical sphere-shaped structures were formed where all carbon nanotubes (CNTs) were crosslinked with the PVAL matrix. Increasing the composition of SWNT to 50 mg resulted in the formation of porous structures. A further increase in the composition to 75 mg resulted in the generation of membrane-like structures where the CNTs were knitted together to form a porous structure (Figure 66).[172]

Microwave protocol was also described to accomplish alignment and decoration of noble metals on CNTs wrapped with carboxymethyl cellulose (CMC). CNTs such as SWNTs and MWNTs and buckminsterfullerene (C-60) were well dispersed using the sodium salt of CMC, and the addition of respective noble metal salts then generated noble metal-decorated CNT composites in a microwave reactor at 100 °C under irradiation for 5 min. The average size of the Ag particles was estimated at 50 nm. Moreover, the influence of the reaction time on the size of Ag clusters on SWNTs, MWNTs, and C-60 was observed, that is, longer reaction times caused the formation of larger particles. These results indicate that the particle nucleation on nanotubes was fast and ceased in the initial 30 s, after which particle growth, rather than further nucleation, dominated.[173]

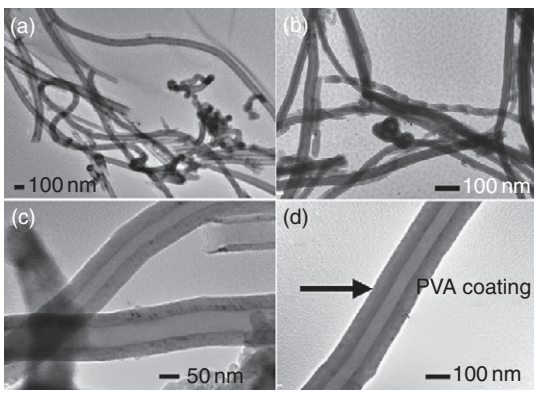

Figure 66 TEM images of (a) pure SWNTs obtained from Bucky Inc., USA, and (b) 25, (c) 50, (d) 75 mg SWNT crosslinked with PVAL nanocomposites. Reproduced with permission from Nadagouda, M. N.; Varma, R. S. *Macromol. Rapid Commun.* **2007**, *28*, 465.[164]

Table 27 The specific capacitances of MWNT and PANI/MWNT composite electrodes at different currents evaluated from charge–discharge tests

Current density (mA cm^{-2})		*1*	*2*	*3*	*4*	*5*
Specific capacitance (F g^{-1})	MWNTs	25.4	24.2	23.6	22.8	22.2
	PANI/MWNTs	322	310	300	292	280

Reproduced with permission from Tian, Z. Q.; Mi, H.; Zhang, X.; *et al. Electrochem. Commun.* **2007**, *9*, 2859.[169]

4.39.5 Scaling-Up Reactions under Microwave Irradiation

As shown above, synthesis of polymers as well as their processing under microwave conditions has been already developed for many successful laboratory-scale applications and can greatly benefit from the unique nature of microwave irradiation. These can include such issues as shorter processing time, increased process yield, and temperature uniformity during polymerization and crosslinking, thereby enhancing the properties of prepared polymeric materials. To fully understand all the advantages and limitation of microwave processing, a cross-disciplinary approach has to be taken since not all materials are good microwave absorbers and, therefore, suitable for microwave applications. Proper understanding and use of microwave power can bring even greater benefits than it can be expected; however, a unique treatment of every process that has to be matched for microwave application is necessary.

In fact, microwaves do not provide a universal solution to every process but in particular should be considered for those processes in which treated materials must be of high quality, so that the cost of microwave processing can be justified. Magnetron efficiencies are between 50 and 72% for 2.45 GHz compared to 80 and 87% for high power (922 or 915 MHz). Thus, the study of efficiency should also include a detailed analysis of a conventional process, of which the user often has a very vague idea (**Box 4**).[8]

Regarding the industrial applications of microwave irradiation, characteristics that have been suggested to be potentially attractive for microwave processing are[177]

- the size or thickness of the material should be large,
- the cost of the material should be high,
- improvements in properties obtainable from microwave processing are significant,
- plant space is limited,
- electricity is cheap, and
- minimizing handling is advantageous.

Other characteristics may include

- heat from the combustion of coal, oil, or natural gas is not practical (i.e., electricity is the only power source), and
- maintaining a very clean, controlled processing environment is important.

In summary, the economic benefits of microwave processing are difficult to define in a general way. Important factors include the location of the processing facility; the product requirements; possible property improvements; alternative sources of energy; availability of capital; and the balance between energy costs, labor costs, capital costs, and the value added to the product.[177]

Application of microwave irradiation for the continuous vulcanization of extruder rubbers was a remarkable achievement of the late 1960s.[178–180] Since 1970s, the microwave-assisted vulcanization of rubber compounds was used industrially, and it is still the most important application of microwave heating to polymeric materials in a number of plants, which at the beginning of the 1990s reached over 600 for microwave vulcanization of extruded rubber weather stripping for the automotive and construction industries.[181] Microwave processing offered significant advantages over conventional rubber processing, including improved product uniformity, reduced extrusion-line length, reduced scrap, and improved cleanliness and environmental sustainability compared with steam autoclaves, hot air, or fluid bed heating processes (**Box 5**).[177]

Box 4 Microwave reactors.

A number of most commonly used microwave reactors belong to two main types:

- multimode reactor
- single-mode reactor

A multimode reactor is in the shape of a rectangular metal box that can accommodate the target material. While microwaves are applied to such a box via a waveguide, the microwaves undergo multiple reflections from the walls. The reflected waves interfere and, in so doing, their superposition establishes a distribution of electrical field strengths within the internal space (including the material), which within the band of frequencies covered by a magnetron corresponds to many different possible modes of oscillations. For this reason such a metal box (cavity) is called a multimode microwave applicator (cavity) (**Figure 67**).

By far a very efficient applicator, particularly for syntheses on a small scale (≤ 50 ml), is a single-mode reactor, in which only one mode of microwave propagation is permitted and hence the field pattern is well defined and the material can be positioned accordingly (**Figure 68**).

Every efficient microwave reactor to perform chemical syntheses requires reliable temperature measurement as well as continuous power feedback control. Most of the reactors are equipped with temperature monitoring systems, which enable heating of reaction mixtures to a desired temperature without thermal runaways. Moreover, power feedback control systems that are operated in most of the microwave reactors enable a synthesis to be carried out without knowing the dielectric properties and/or conductive properties of all the components of the reaction mixture in detail. An overview of microwave equipment manufacturers[6,174] and detailed descriptions of microwave reactors[175,176] can be found in recent review papers and chapters.

Box 5 Scale of microwave processing.

For nearly 40 years following the invention of the microwave oven in 1945 during the RADAR project, industrialists and microwave equipment manufactures predicted a rosy future for microwave processing while very few expected that microwave ovens would become popular home appliances and reality was quite different. In fact, industrial microwave food processing has never achieved the success of domestic microwave ovens in which speed and convenience of reheating not cooking appliances were powerful driving forces for consumers.

For example, microwave heating was rapidly adopted by the food industry in the early 1950s. The first means of conveying materials through a microwave cavity was patented in 1952.[181] In 1984, the food industry applied 19 MW of microwave heating units installed worldwide.[182] Compared with the 5.1 MW of microwave heating units in use in 1978,[183] the annual growth in the years 1978–84 was on the order of 2.5 MW per year or an average increase of 20%. In addition, the number of industrial installations built by users for their own processes were not included in this statistic. In absolute terms, the 19 MW of industrial microwave power was equivalent to 32 thousands of 600 W domestic microwave ovens, which is derisory by comparison to the about 7 million units in domestic services in 1984 in the United States, where they used to show the highest growth rate in the electric domestic appliances sector between 1976 and 1986.[8]

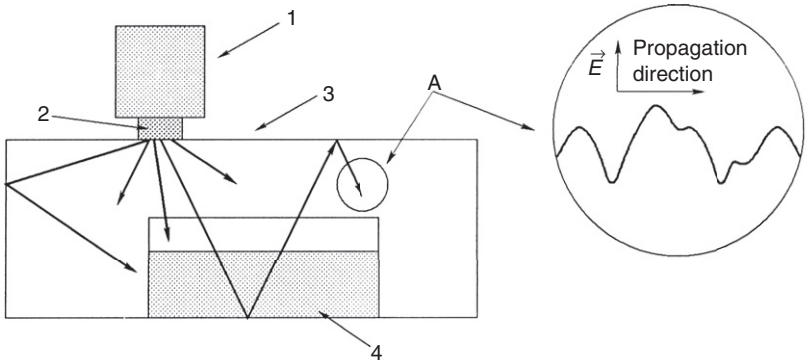

Figure 67 Multimode microwave reactor: 1, magnetron; 2, rotating reflector; 3, multimode cavity; 4, reaction vessel; A, nonregular shape of electromagnetic waves as a superposition of a number of waves.

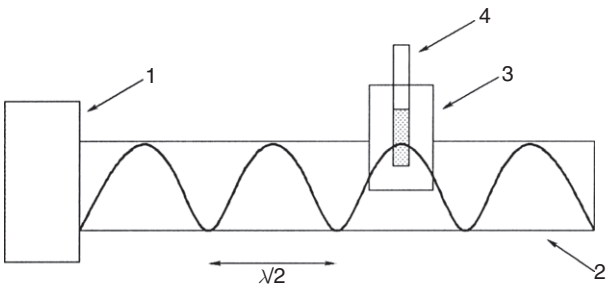

Figure 68 Single-mode microwave reactor: 1, magnetron; 2, waveguide; 3, single-mode microwave cavity; 4, reaction vessel.

At the moment, the microwave equipment manufacturers offer microwave equipment that are designed for automobile type profile and big industrial type profile. Present implementations are characterized by the 3–10 kW applied power, shifting velocity in the range of 0.75–45 m min^{-1}. Treated profile of about 50 × 50 mm passes the 3 m long microwave chamber followed by hot-air 15 kW, 7 m long space followed by a cooling section of approximately 4 m. The resultant processing capacity is about 500 kg h^{-1}, enabling processing of profiles with metal frames, skeletons, and reinforcements. However, profile section, properties of a given type of rubber, and required production capacity affect the speed of profile advance; control of the process, and especially the extent of installed microwave output heat, is typically 1 kW per approximately 30 kg of the product per hour (Figure 69).[184]

The temperature in the extruder rises to 80–90 °C and microwave preheating, placed before the input of the vulcanization tunnel, is set approximately to 130 °C. After entering the tunnel, the material is quickly heated to the vulcanization temperature (e.g., 180 °C) depending on the mix composition. After passing through the microwave tunnel, the material is maintained for 60–90 s at the required temperature by hot-air system and cooled. Microwave vulcanization under atmospheric pressure allows universal design and processing of various profiles without fundamental modification of lines, the construction of which is mostly similar.[184]

For processing of polymeric materials and composites, a number of industrial microwave equipment manufacturers offer equipment for the production of continuous cast-resin components, in which the microwave unit (3.6 or 7.2 kW) processes high-viscosity resin systems with flow rates up to 5.0 kg min^{-1}. The control system provides easy integration into other and/or existing systems. Several furnaces can be switched in cascades to achieve an increase in temperature difference between feeding flow and drain flow and/or an increase in the flow quantity of the medium to be treated. The microwave flow heater is available, which can also be applied in other fields, for example, food, plastic, and chemical

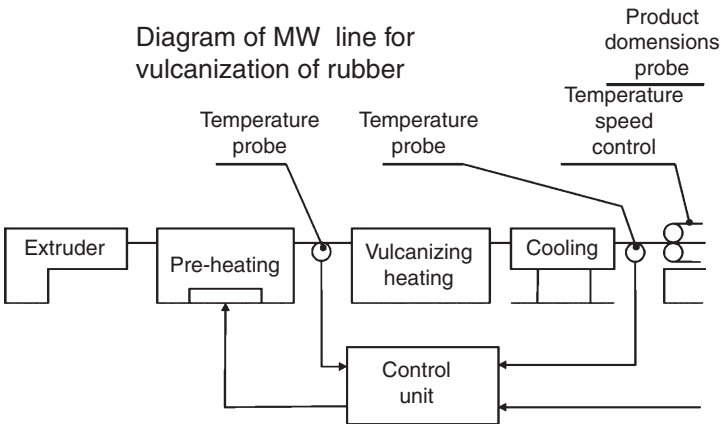

Figure 69 Diagram of microwave line for vulcanization of rubber. Reproduced with permission from Romill. http://www.romill.cz, 4 July 2010.[184]

industry. There is a microwave continuous heating chamber for glass fiber cables, glass fiber-reinforced plastics, and reinforced optical fibers (0.8, 1.6, and 2.4 kW).[185]

There are also available continuous microwave belt furnaces, in which the microwave generators are arranged in a spiral around the longitudinal axis of the cylindrical chamber to achieve a more uniform energy distribution. The conveyor belt passes over floor plates which are fitted with secondary radiators to provide a higher microwave concentration. The furnaces can be operated with a microwave power output of up to 200 kW. The power control system allows each magnetron to be switched on and off if necessary, which offers the advantage that power consumption is reduced compared to continuous power control. The size of channel opening is adapted to a process (**Figure 70**).[185]

Recently, an industrial microwave system HEPHAISTOS-CA2 (high electromagnetic power heating autoclaveless injected structures oven system) for curing of carbon fiber-reinforced plastics is being developed. The system is especially optimized for processes like injection molding or curing of that matrix and a modular system technology in connection with 'autoclaves' fabrication processes.[186]

The second segment in the microwave chemistry market is for instruments for laboratory use in chemical synthesis and analysis that target customers at academic working groups and laboratories in the chemical, pharmaceutical, and biochemical industries. Detailed descriptions of such instruments can be found in recent review papers and chapters.[12,175,176]

The synthesis of high-molecular-weight (solid) epoxy resins from PBA and a low-molecular-weight epoxy resin in a continuous microwave system that consists of four microwave cavities with a rotating quartz tube (2.0 m × 0.12 m) was tested and developed (**Figure 71**).

All the microwave cavities are equipped with a continuous power regulation and temperature control, while each magnetron can be separately switched on and off if necessary, which offers the advantage of reduced power consumption compared to continuous power control. The speed of the quartz tube rotation is also continuously adjustable. It was shown that by applying the continuous microwave reactor it was possible to obtain high-molecular-weight epoxy resins with an epoxy value of 0.11 mol of epoxy group per 100 g of resin by maintaining the flow of the substrates through the reactor at 8 kg h^{-1}.

In one set of experiments, the product (epoxy resin) was not removed from the reactor during the run; that is, the reaction mixture was 'frozen' in the tube. Then, the resin samples were taken from different parts of the tube and analyzed for the conversion, that is, epoxy values. It was found that the planned epoxy (i.e., 0.11 mol per 100 g) value was reached in the middle distance from the tube beginning, which means that the reactor can even work at flow rates higher than 8 kg h^{-1}.[187]

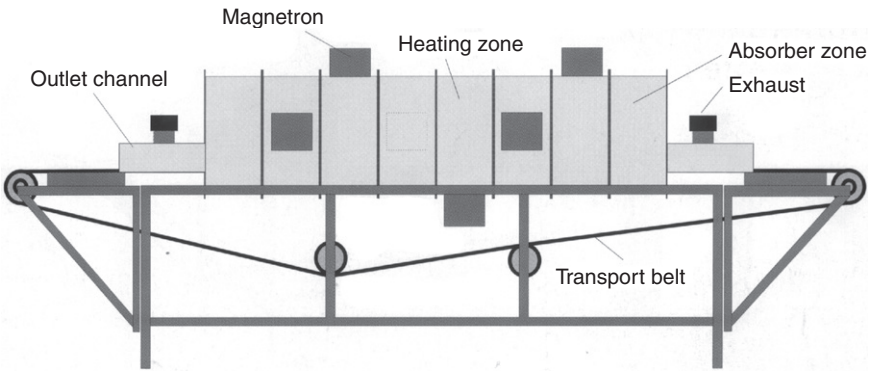

Figure 70 Continuous microwave belt furnace. Reproduced with permission from Linn High Therm. http://www.linn.de, 19 December 2010.[185]

Figure 71 Continuous microwave reactor with rotating quartz tube for the synthesis of high-molecular-weight epoxy resin (Ertec, Poland).

An extensive discussion on scaling-up reactions and different microwave systems can be found in recently published reviews.[188,189]

References

1. Bogdal, D.; Penczek, P.; Pielichowski, J.; *et al. Adv. Polym. Sci.* **2003**, *163*, 193.
2. Parodi, F.; Russo, S. In *Comprehensive Polymer Science*, 2nd supplement volume; Aggarwal, S. L., Ed.; Pergamon-Elsevier: Oxford, 1996.
3. Wiesbrock, F.; Hoogenboom, R.; Schubert, U. S. *Macromol. Rapid. Commun.* **2004**, *25*, 1739.
4. Bardts, M.; Gonsior, N.; Ritter, H. *Macromol. Chem. Phys.* **2008**, *209*, 25.
5. Bogdal, D.; Matras, K. In *Microwaves in Organic Synthesis*; Wiley-VCH: Weinheim, Germany, 2006; pp. 653–684.
6. Bogdal, D.; Prociak, A. *Microwave-Enhanced Polymer Chemistry and Technology*; Blackwell-Wiley: Ames, USA, 2007.
7. Kaatze, U. *Radiat. Phys. Chem.* **1995**, *45*, 539.
8. Thuery, J. *Microwaves: Industrial, Scientific, and Medical Applications*; Artech House: Boston, MA, London, 1992.
9. Gabriel, C.; Gabriel, S.; Grant, E. H.; *et al. Chem. Soc. Rev.* **1998**, *27*, 213.
10. Stuerga, D.; Delmotte, M. In *Microwaves in Organic Synthesis*; Loupy, A., Ed.; Wiley-VCH, 2003; pp. 1–33.
11. Metaxas, A. C.; Meredith, R. J. *Industrial Microwave Heating*; Peter Perigrinus: London, 1983.
12. Bogdal, D. *Microwave-Assisted Organic Synthesis, One Hundred Reaction Procedures*; Elsevier: Amsterdam, The Netherlands, 2005.
13. Bram, G.; Loupy, A.; Majdoub, M.; *et al. Tetrahedron* **1990**, *46*, 5167.
14. Bogdal, D.; Bednarz, S.; Lukasiewicz, M. *Tetrahedron* **2006**, *62*, 9440.
15. Hoogenboom, R.; Schubert, U. S. *Macromol. Rapid Commun.* **2007**, *28*, 368–386.
16. Thostenson, E. T.; Chou, T. W. *Compos.: Part A.* **1999**, *30*, 1055.
17. Perreux, L.; Loupy, A. *Tetrahedron* **2001**, *57*, 9199.
18. Nuchter, M.; Ondruschka, B.; Bonrath, W.; *et al. Green Chem.* **2004**, *6*, 128.
19. de la Hoz, A.; Diaz-Ortiz, A.; Moreno, A. *Chem. Soc. Rev.* **2005**, *34*, 164.
20. Parodi, F. *Chim. Ind.* **1998**, *80*, 55.
21. Vanderhoff, J. W. U.S. Patent 3,432,413, 1969.
22. Williams, N. H. *J. Microwave Power* **1968**, *123*, 2.
23. Nishii, M. *J. Osaka Dent. Univ.* **1968**, *2* 23.
24. Teffal, M.; Gourdenne, A. *Eur. Polym. J.* **1983**, *19*, 543.
25. Palacios, J.; Sierra, M.; Rodriguez, P. *New Polym. Mater.* **1992**, *3*, 273.
26. Chia, L. H. L.; Jacob, J.; Boey, F. Y. C. *J. Mater. Proc. Technol.* **1995**, *48*, 445.
27. Jacob, J.; Chia, L. H. L.; Boey, F. Y. C. *J. Appl. Polym. Sci.* **1997**, *63*, 787.
28. Stange, N.; Ishaque, M.; Niessner, N.; *et al. Macromol. Rapid Commun.* **2006**, *27*, 156.
29. Goretzki, Ch.; Krlej, A.; Steffens, Ch.; *et al. Macromol. Rapid Commun.* **2004**, *25*, 513.
30. Iannelli, M.; Alupei, V.; Ritter, H. *Tetrahedron* **2005**, *61*, 1509.
31. Iannelli, M.; Alupei, V.; Ritter, H. *Macromol. Chem. Phys.* **2005**, *206*, 349.
32. Bezdushna, E.; Ritter, H. *Macromol. Rapid Commun.* **2005**, *26*, 1087.
33. Pajda, M.; Bogdal, D.; Orru, R. In *Modern Polymeric Materials for Environmental Applications*; Pielichowski, K., Ed.; Teza: Krakow, Poland, 2004.
34. Chen, Y.; Wang, J.; Zhang, D.; *et al. Polymer* **2000**, *41*, 7877.
35. Zinck, P.; Barbier-Baudry, D.; Loupy, A. *Macromol. Rapid Commun.* **2005**, *26*, 46.
36. Matyjaszewski, K.; Xia, J. *Chem. Rev.* **2001**, *101*, 2921.
37. Zhu, X.; Chen, J.; Zhou, N.; *et al. Eur. Polym. J.* **2003**, *39*, 1187.
38. Chen, G.; Zhu, X.; Cheng, Z.; *et al. Radiat. Phys. Chem.* **2004**, *69*, 129.
39. Lu, J.; Wu, J.; Wang, L.; *et al. J. Appl. Polym. Sci.* **2004**, *97*, 2072.
40. Lu, X.; Zhu, X.; Cheng, Z.; *et al. J. Appl. Polym. Sci.* **2004**, *92*, 2189.
41. Cheng, Z.; Zhu, X.; Zhang, L.; *et al. Polym. Bull.* **2003**, *49*, 363.
42. Cheng, Z.; Zhu, X.; Chen, M.; *et al. Polymer* **2003**, *44*, 2243.
43. Xu, W.; Zhu, X.; Cheng, Z.; *et al. Eur. Polym. J.* **2003**, *39*, 1349.
44. Zhang, H.; Schubert, U. S. *Macromol. Rapid Commun.* **2004**, *25*, 1225.
45. Wu, H.; Li, F.; Lin, Y.; *et al. J. Appl. Polym. Sci.* **2006**, *99*, 828.
46. Li, J.; Zhu, X.; Zhu, J.; *et al. Radiat. Phys. Chem.* **2006**, *75*, 253.
47. Wisnoski, D. D.; Leister, W. H.; Strauss, K. A.; *et al. Tetrahedron Lett.* **2003**, *44*, 4321.
48. Leenen, M.; Wiesbrock, F.; Hoogenboom, R.; *et al. e-Polymers* **2005**, *071*.
49. Roy, D.; Ullah, A.; Sumerlin, B. S. *Macromolecules* **2009**, *42*, 7701.
50. Hou, C.; Qu, R.; Wang, C.; *et al. J. Appl. Polym. Sci.* **2008**, *107*, 2646.
51. Brown, S. L.; Rayner, C. M.; Graham, S.; *et al. Chem. Commun.* **2007**, 2145.
52. Liao, L. Q.; Liu, L. J.; Zhang, C.; *et al. J. Polym. Sci. Part A: Polym. Chem.* **2002**, *40*, 1749.
53. Yu, Z. J.; Liu, L. J. *Eur. Polym. J.* **2004**, *40*, 2213.
54. Barbbier-Baudry, D.; Brachais, L.; Cretu, A.; *et al. Environ. Chem. Lett.* **2003**, *1*, 19.
55. Zhang, Ch.; Liao, L.; Liu, L. *Macromol. Rapid Commun.* **2004**, *25*, 1402.
56. Jing, S.; Peng, W.; Tong, Z.; *et al. J. Appl. Polym. Sci.* **2006**, *100*, 2244.
57. Sinnwell, S.; Ritter, H. *Macromol. Rapid Commun.* **2005**, *26*, 160.
58. Hoogenboom, R.; Wiesbrock, F.; Leenen, M. A. M.; *et al. J. Comb. Chem.* **2005**, *7*, 10.
59. Wiesbrock, F.; Hoogenboom, R.; Leenen, M. A. M.; *et al. Macromolecules* **2005**, *38*, 5025.
60. Lobert, M.; Kohn, U.; Hoogenboom, R.; *et al. Chem. Commun.* **2008**, 1458.
61. Wiesbrock, F.; Hoogenboom, R.; Van Nispen, S. F. G. M.; *et al. Macromolecules* **2005**, *38*, 7957.
62. Hoogenboom, R.; Wiesbrock, F.; Huang, H.; *et al. Macromolecules* **2006**, *39*, 4719.
63. Kempe, K.; Jacobs, S.; Lambermont-Thijs, H. M. L.; *et al. Macromolecules* **2010**, *43*, 4098.
64. Becer, C. R.; Paulus, R. M.; Hoppener, S.; *et al. Macromolecules* **2008**, *41*, 5210.
65. Sundararajan, G.; Dhanalakshmi, K. *Polym. Bull.* **1997**, *39*, 333.
66. Spring, A. M.; Yu, C.-Y.; Horie, M.; *et al. Chem. Commun.* **2009**, 2676.
67. Allen, M. J.; Wangkanont, K.; Raines, R. T.; *et al. Macromolecules* **2009**, *42*, 4023.
68. Chatti, S.; Bortolussi, M.; Loupy, A.; *et al. Eur. Polym. J.* **2002**, *38*, 1851.
69. Chatti, S.; Bortolussi, M.; Loupy, A.; *et al. J. Appl. Polym. Sci.* **2003**, *90*, 1255.
70. Chatti, S.; Bortolussi, M.; Bogdal, D.; *et al. Eur. Polym. J.* **2004**, *40*, 561.
71. Caouthar, A.; Loupy, A.; Bortolussi, M.; *et al. J. Polym. Sci. Part A: Polym. Chem.* **2005**, *43*, 6480.
72. Pielichowski, J.; Bogdal, D.; Wolff, E. *Przem. Chem.* **2003**, *82*, 8.
73. Pielichowski, J.; Penczek, P.; Bogdal, D.; *et al. Polimery* **2004**, *49*, 763.
74. Velmati, S.; Nagahata, R.; Sudiyama, J.; *et al. Macromol. Rapid Commun.* **2005**, *26*, 1163.
75. Imai, Y. In *Step-Growth Polymers for High Performance Materials: New Synthetic Methods*; Hendrick, J. L., Labadie, J. W., Eds.; ACS, Series No. 624; Washington, DC, 1996.
76. Imai, Y.; Nemoto, H.; Kakimoto, M. *J. Polym. Sci. Part A: Polym. Chem.* **1996**, *34*, 701.
77. Imai, Y.; Nemoto, H.; Watanabe, S.; *et al. Polymer. J.* **1996**, *28*, 256.
78. Y. *React. Funct. Polym.* **1996**, *30*, 3.
79. Y. *Adv. Polym. Sci.* **1999**, *140*, 1.
80. Park, K. H.; Watanabe, S.; Kakimoto, M.; *et al. Polym. J.* **1993**, *25*, 209.
81. Pourjavadi, A.; Zamanalu, M. R.; Zohurian-Mehr, M. J. *Angew. Makromol. Chem.* **1999**, *269*, 54.
82. Fang, X.; Hutcheon, R.; Scola, D. A. *J. Polym. Sci. Part A: Polym. Chem.* **2000**, *38*, 1379.
83. Chen, M.; Siochi, E. J.; Ward, T. C.; *et al. Polym. Eng. Sci.* **1993**, *33*, 1110.
84. Thuillier, F. M.; Jullien, H. *Makromol. Chem. Macromol. Symp.* **1989**, *25*, 63.
85. Beldjoudi, N.; Gourdenne, A. *Eur. Polym. J.* **1988**, *24*, 265.
86. Jow, J.; DeLong, J. D.; Hawley, M. C. *SAMPE Quart.* **1989**, *20*, 46.
87. Levita, G.; Livi, A.; Rolla, P. A.; *et al. J. Polym. Sci. Part B: Polym. Phys.* **1996**, *34*, 2731.
88. Casalini, R.; Corezzi, S.; Livi, A.; *et al. J. Appl. Polym. Sci.* **1997**, *65*, 17.
89. Marand, E.; Baker, H. R.; Graybeal, J. D. *Macromolecules* **1992**, *25*, 2243.
90. Delmotte, M.; Jullien, H.; Ollivon, M. *Eur. Polym. J.* **1991**, *27*, 371.
91. Zong, L.; Kempel, L. C.; Hawley, M. C. *Polymer* **2005**, *46*, 2638.
92. Wei, J.; Hawley, M. C.; DeLong, J. D.; *et al. Polym. Eng. Sci.* **1993**, *33*, 1132.
93. Jordan, C.; Galy, J.; Pascault, J. P.; *et al. Polym. Eng. Sci.* **1995**, *35*, 233.
94. Boey, F. Y. C.; Yap, B. H.; Chia, L. *Polym. Test.* **1999**, *18*, 93.
95. Boey, F. Y. C.; Rath, S. K. *Adv. Polym. Technol.* **2000**, *19*, 194.
96. Bogdal, D.; Gorczyk, J. *Polymer* **2003**, *44*, 7795.
97. Bogdal, D.; Gorczyk, J. *J. Appl. Polym. Sci.* **2004**, *94*, 1969.
98. Brzozowski, Z. K.; Staszczak, S. K.; Hadam, L. K.; *et al. J. Appl. Polym. Sci.* **2006**, *100*, 3850.
99. Zhang, D.; Crivello, J. V.; Stoffer, J. O. *J. Polym. Sci. Part B: Polym. Phys.* **2004**, *42*, 4230.
100. Parodi, F.; Belgiovine, C.; Zannoni, C. U.S. Patent 5,288,833, 1994.
101. Parodi, F.; Gerbelli, R.; De Meuse, M. U.S. Patent 5,489,664, 1996.
102. Parodi, F. *Proceedings of SPIE – The International Society for Optical Engineering* **1999**, *4017*, 2.
103. Jullien, H.; Valot, H. *Polymer* **1985**, *26*, 506.
104. Silinski, B.; Kuzmycz, C.; Gourdenne, A. *Eur. Polym. J.* **1987**, *23*, 73.
105. Randall, D.; Lee, S. *The Polyurethanes Book*; Wiley & Sons: New York, USA, 2002.
106. Prociak, A. In *Modern Polymeric Materials for Environmental Applications*; Pielichowski, K., Ed.; Teza: Krakow, Poland, 2004.
107. Prociak, A. In Rigid Polyurethane Foams Modified with Vegetable Oil-Based Polyols, Proceedings of UTECH 2006 Conference, Maastricht, 2006.

108. Prociak, A.; Bogdał, D.; Pielichowski, J.; et al. In *Rigid Polyurethane Foams Blown under Microwave Irradiation*, Proceedings of the 8th International Conference "Blowing Agents and Foaming Processes 2006, Munich", 2006.
109. Bogdal, D.; Prociak, A.; Pielichowski, J. In *Application of Microwave Irradiation for Chemical Recycling of Polyurethanes*, Proceedings of Global Symposium on Recycling, Waste Treatment and Clean Technology, REWAS, Madrid, 2004.
110. Lewis, D. A.; Summers, J. D.; Ward, T. C.; *et al. Polym. Sci. Part A: Polym. Chem.* **1992**, *30*, 1647.
111. Chen, J.; Chen, Q.; Yu, X. J. *Appl. Polym. Sci.* **1996**, *62*, 2135.
112. Lu, J.; Yao, S.; Tang, X.; *et al. Opt. Mat.* **2004**, *25*, 359.
113. Li, N.; Lu, J.; Yao, S.; *et al. Mater. Lett.* **2004**, *58*, 3115.
114. Li, N.; Lu, J.; Yao, S. *Macromol. Chem. Phys.* **2005**, *206*, 559.
115. Liu, Y.; Sun, X. D.; Xie, X. Q.; *et al. J. Polym. Sci. Part A: Polym. Chem.* **1998**, *36*, 2653.
116. Fang, X.; Hutcheon, R.; Scola, D. A. *J. Polym. Sci. Part A: Polym. Chem.* **2000**, *38*, 2526.
117. Fang, X.; Hutcheon, R.; Scola, D. A. *J. Polym. Sci. Part A: Polym. Chem.* **2000**, *38*, 1379.
118. Mallakpour, S. E.; Hajipour, A. R.; Faghihi, K. *Polym. Int.* **2000**, *49*, 1388.
119. Mallakpour, S. E.; Hajipour, A. R.; Faghihi, K. *Eur. Polym. J.* **2001**, *37*, 119.
120. Mallakpour, S. E.; Hajipour, A. R.; Zamanlou, M. R. *J. Polym. Sci. Part A: Polym. Chem.* **2001**, *39*, 177.
121. Mallakpour, S. E.; Hajipour, A. R.; Khoee, S. *J. Appl. Polym. Sci.* **2000**, *77*, 3003.
122. Mallakpour, S. E.; Hajipour, A. R.; Khoee, S. *J. Polym. Sci. Part A: Polym. Chem.* **2000**, *38*, 1154.
123. Mallakpour, S.; Shahmohammadi, M. H. *J. Appl. Polym. Sci.* **2004**, *92*, 951.
124. Mallakpour, S.; Hajipour, A. R.; Zamanlou, M. R. *Eur. Polym. J.* **2002**, *38*, 475.
125. Mallakpour, S.; Kowsari, E. *J. Polym. Sci. Part A: Polym. Chem.* **2003**, *41*, 3974.
126. Mallakpour, S.; Zamanlou, M. R. *J. Appl. Polym. Sci.* **2004**, *91*, 3281.
127. Mallakpour, S.; Hajipour, A. R.; Zamanlou, M. R. *J. Polym. Sci. Part A: Polym. Sci.* **2003**, *41*, 1077.
128. Faghihi, K.; Zamani, K.; Mirsaamie, A.; *et al. Eur. Polym. J.* **2003**, *39*, 247.
129. Faghihi, K.; Zamani, K.; Mirsaamie, A.; *et al. J. Appl. Polym. Sci.* **2004**, *91*, 516.
130. Faghihi, K.; Hajibeygi, M. *J. Appl. Polym. Sci.* **2004**, *92*, 3447.
131. Gao, Ch.; Zhang, S.; Gao, L.; *et al. J. Appl. Polym. Sci.* **2004**, *92*, 2414.
132. Thostenson, E. T.; Chou, T.-W. *Proceedings of 12th Annual Meeting of the American Society Composites*, Dearborn, 1997.
133. Thostenson, E. T.; Chou, T.-W. In *Proceedings of 13th Annual Meeting of the American Society Composites*, Baltimore, 1998.
134. Thostenson, E. T.; Chou, T.-W. *Polym. Compos.* **2001**, *22*, 197.
135. Shull, P. J.; Hurley, D. H.; Spicer, J. W. M.; *et al. Polym. Eng. Sci.* **2000**, *40*, 1157.
136. Bonnacorsi, L.; Calabrese, L.; Proverbio, E.; et al. 10th International Conference on Microwave and RF Heating, Modena, Italy, 2005.
137. Hottong, U.; Wei, J.; Dhulipala, R.; *et al. Proceedings of the 93rd Annual Meeting of the American Ceramic Society, Cincinnati, USA, 1991.*
138. Methven, J. *Mat. Tech. Adv. Perf. Mat.* **1999**, *14*, 183.
139. Liu, Y.; Xiao, Y.; Sun, X.; *et al. J. Appl. Polym. Sci.* **1999**, *73*, 2391.
140. Fang, X.; Scola, D. A. *J. Polym. Sci. Part A: Polym. Chem.* **1999**, *37*, 4616.
141. Liu, X. Q.; Wang, Y. S.; Zhu, J. H. *J. Appl. Polym. Sci.* **2004**, *94*, 994.
142. Burnside, S. D.; Giannelis, E. P. *Adv. Mater.* **1995**, *7*, 154.
143. Sikka, M.; Cerini, L. N.; Ghosh, S. S.; *et al. J. Polym. Sci. Part B. Polym. Phys.* **1996**, *34*, 1443.
144. Lee, D. C.; Jang, L. W. *J. Appl. Polym. Sci.* **1996**, *61*, 1117.
145. Yano, K.; Usuki, A.; Kawasumi, M. *J. Appl. Polym. Sci.* **1993**, *49*, 1259.
146. Wang, D. Y.; Parlow, D.; Yao, Q.; *et al. J. Vinyl Add. Technol.* **2001**, *7*, 203.
147. Yoo, Y.; Choi, K.-Y.; Lee, J. H. *Macromol. Chem. Phys.* **2004**, *205*, 1863.
148. Aranda, P.; Mosqueda, Y.; Perez-Cappe, E.; *et al. Polym. Sci. Part B: Polym. Phys.* **2003**, *41*, 3249.
149. Schmidt, D.; Sinha Ray, S.; Bousmina, M. *Prog. Mater. Sci.* **2005**, *50*, 962.
150. Karaman, V. M.; Privalko, E. G.; Privalko, V. P.; *et al. Polymer* **2005**, *46*, 1943.
151. Chen, B.; Evans, R. G. *Macromolecules* **2006**, *39*, 747.
152. Liao, L.; Zhang, C.; Gong, S. *Macromol. Rapid Commun.* **2007**, *28*, 1148.
153. Liao, L.; Liu, L.; Zhang, C.; *et al. Polym. Sci. Part A: Polym. Chem.* **2002**, *40*, 1749.
154. Liao, L.; Liu, L.; Zhang, C.; *et al. J. Appl. Polym. Sci.* **2003**, *90*, 2657.
155. Martínez-Gallegos, S.; Herrero, M.; Rives, V. *J. Appl. Polym. Sci.* **2008**, *109*, 1388.
156. Chin, I. J.; Albrechta, T. T.; Kima, H. C.; *et al. Polymer* **2001**, *42*, 5947.
157. Jiankun, L.; Yucai, K.; Zongneng, Q.; *et al. J. Polym. Sci. Part B: Polym. Phys.* **2001**, *39*, 115.
158. Uyanik, N.; Erdem, A. R.; Can, M. F.; *et al. Polym. Eng. Sci.* **2006**, *46*, 1104.
159. Kim, S. W.; Lee, J. J.; Yoon, S. Y.; *et al. Int. J. Thermophys. Online First™, 23 June 2009.*
160. Yang, G.; Hou, W.; Feng, X.; *et al. Adv. Funct. Mater.* **2007**, *17*, 401.
161. He, R.; Qian, X.; Yin, J.; *et al. Mater. Lett.* **2003**, *57*, 1351.
162. Wu, W.; Wang, Y.; Shi, L.; *et al. Nanotechnology* **2005**, *16*, 3017.
163. Kong, H.; Jang, J. *Chem. Commun.* **2006**, *28*, 3010.
164. Nadagouda, M. N.; Varma, R. S. *Macromol. Rapid Commun.* **2007**, *28*, 465.
165. Y. *Polymer* **2007**, *48*, 1441.
166. Luo, H. L.; Sheng, J.; Wan, Y. Z. *Mater. Lett.* **2008**, *62*, 37.
167. Liu, P.; Su, Z. *Mater. Chem. Phys.* **2005**, *94*, 412.
168. Huang, J.; Pen, H.; Xu, Z.; *et al. React. Funct. Polym.* **2008**, *68*, 332.
169. Tian, Z. Q.; Wang, X. L.; Zhang, H. M.; *et al. Electrochem. Commun.* **2006**, *8*, 1158.
170. Mi, H.; Zhang, X.; An, S.; *et al. Electrochem. Commun.* **2007**, *9*, 2859.
171. Khomenko, V.; Frackowiak, E.; Beguin, F. *Electrochim. Acta* **2005**, *50*, 2499.
172. Nadagouda, M. N.; Varma, R. S. *Macromol. Rapid Commun.* **2007**, *28*, 842.
173. Nadagouda, M. N.; Varma, R. S. *Macromol. Rapid Commun.* **2008**, *29*, 155.
174. Kubel, E. *Ind. Heat.* **2005**, 43.
175. Kappe, O.; Stadler, A. *Microwave in Organic and Medical Chemistry*; Wiley-VCH: Weinheim, Germany, 2005.
176. Ondruschka, B.; Bonrath, W.; Stuerga, D. In *Microwaves in Organic Chemistry*; Loupy, A., Ed.; Wiley-VCH: Weinheim, Germany, 2006; pp. 62–107.
177. *Microwave Processing of Materials*; The National Academy Press: Washington, D.C., USA, 1994.
178. Akyel, C.; Bilgen, E. *Energy* **1989**, *14*, 839.
179. Krieger, B. *Polym. Mater. Sci. Eng.* **1992**, *66*, 339.
180. Krieger, B. *Mater. Res. Soc. Symp. Proc.* **1994**, *347*, 57.
181. Spencer, P. L. U.S. Patent 2,605,383, 1952.
182. Decareau, R. *Food Technol.* **1986**, *40*, 99.
183. Bengtsson, N.; Ohlsson, T. In *Food Process Engineering*; Linko, P., Malkki, Y., Olkko, J., Larinkari, J., Eds.; Applied Science Publishers: London, United Kingdom, 1980.
184. Romill. http://www.romill.cz, 4 July 2010.
185. Linn High Term. http://www.linn.de, 19 December 2010.
186. Feher, L.; Thumm, M.; Drechsler, K. *Adv. Eng. Mater.* **2006**, *8*, 26.
187. Bogdal, D.; Loupy, A. *Org. Process Res. Dev.* **2008**, *12*, 710.
188. Strauss, C. R. *Org. Process Res. Dev.* **2009**, *13*, 915.
189. Jankowski, J.; Reszke, E.; Burnett, N. W. *Microwave Induced Plasma Analytical Spectrometry*; RSC Publishing: Cambridge, 2011.

Biographical Sketch

Professor Dariusz Bogdal graduated from Cracow University of Technology (Krakow, Poland) and obtained his PhD diploma from Jagiellonian University (Krakow, Poland) and DSc diploma from Warsaw University of Technology (Warsaw, Poland). He has over 25 years of research experience in organic and polymer chemistry. He has carried out extensive studies on the application of phase-transfer catalysis (PTC) and microwave irradiation for organic and polymer synthesis as well as polymer modification and recycling. Prof. Bogdal has applied microwave-assisted reactions to polymer chemistry, for example, reactions on polymer matrices, preparation and modification of polymers with active pendant groups, and preparation and investigation of polymers for dental materials as well as optical devices. He has worked as a research fellow in Clemson University (Clemson, USA), Imperial College (London, UK), Napier University (Edinburgh, UK), and Karolinska Institute (Stockholm, Sweden). Prof. Bogdal is the author and coauthor of books published by Elsevier and Blackwell-Wiley (*Microwave-Assisted Organic Synthesis: One Hundred Reaction Procedures* (2005) and *Microwave-Enhanced Polymer Chemistry and Technology* (2007)), four book chapters, and over 90 papers and review articles. The profile of Prof. Bogdal can be viewed at http://www.cyfronet.pl/~pcbogdal.